ENCYCLOPEDIA OF

CONTROLED DRUG DELIVERY

VOLUMES 1 & 2

Edith Mathiowitz
Brown University
Providence, Rhode Island



A Wiley-Interscience Publication
John Wiley & Sons, Inc.
New York / Chichester / Weinheim / Brisbane / Singapore / Toronto

This book is printed on acid-free paper. ♾

Copyright © 1999 by John Wiley & Sons, Inc. All rights reserved.

Published simultaneously in Canada.

No part of this publication may be reproduced, stored in a retrieval system or transmitted in any form or by any means, electronic, mechanical, photocopying, recording, scanning or otherwise, except as permitted under Sections 107 or 108 of the 1976 United States Copyright Act, without either the prior written permission of the Publisher, or authorization through payment of the appropriate per-copy fee to the Copyright Clearance Center, 222 Rosewood Drive, Danvers, MA 01923, (978) 750-8400, fax (978) 750-4744. Requests to the Publisher for permission should be addressed to the Permissions Department, John Wiley & Sons, Inc., 605 Third Avenue, New York, NY 10158-0012, (212) 850-6011, fax (212) 850-6008, E-Mail: PERMREQ @ WILEY.COM.

For ordering and customer service, call 1-800-CALL-WILEY.

Library of Congress Cataloging-in-Publication Data:

Mathiowitz, Edith, 1952–
Encyclopedia of controlled drug delivery / Edith Mathiowitz.
p. cm.
Includes index.
ISBN 0-471-14828-8 (set : cloth : alk. paper).—ISBN 0-471-16662-6 (vol 1 : alk. paper).—ISBN 0-471-16663-4 (vol 2 : alk. paper)
1. Drugs—Controlled release Encyclopedias. I. Title.
[DNLM: 1. Drug Delivery Systems Encyclopedias—English. 2. Drug Carriers Encyclopedias—English. QV 13 M431e 1999]
RS201.C64M38 1999
615.7—dc21
DNLM/DLC
for Library of Congress 99-24907
CIP

Printed in the United States of America.

10 9 8 7 6 5 4 3 2 1

To my loving husband, George

To my dear children, Daphne and Ariel

CONTRIBUTORS

Patrick Aebischer, *University of Lausanne Medical School, Lausanne, Switzerland,* Immunoisolated Cell Therapy

V. Baeyens, *University of Geneva, Geneva, Switzerland,* Mucosal Drug Delivery, Ocular

Roland Bodmeier, *Freie Universität Berlin, Berlin, Germany,* Nondegradable Polymers for Drug Delivery

Nicholas Bodor, *University of Florida, Gainesville, Florida,* Chemical Approaches to Drug Delivery

Clarissa Bonnano, *Health Advances, Inc., Wellesley, Massachusetts,* Economic Aspects of Controlled Drug Delivery

Lisa Brannon-Peppas, *Biogel Technology, Indianapolis, Indiana,* Microencapsulation

Henry Brem, *Johns Hopkins University School of Medicine, Baltimore, Maryland,* Central Nervous System, Drug Delivery to Treat

Steve Brocchini, *University of London, London, United Kingdom,* Pendent Drugs, Release from Polymers

P. Buri, *University of Geneva, Geneva, Switzerland,* Mucosal Drug Delivery, Ocular

Martin Burke, *Johns Hopkins University School of Medicine, Baltimore, Maryland,* Central Nervous System, Drug Delivery to Treat

Paul A. Burke, *Amgen, Inc., Thousand Oaks, California,* Characterization of Delivery Systems, Magnetic Resonance Techniques

Gerardo P. Carino, *Brown University, Providence, Rhode Island,* Vaccine Delivery

F.J. Lou Carmichael, *Hemosol, Inc., Toronto, Canada,* Blood Substitutes: A Review of Clinical Trials

Pravin R. Chaturvedi, *Vertex Pharmaceuticals, Cambridge, Massachusetts,* Pharmacokinetics

Donald Chickering, *Brown University, Providence, Rhode Island,* Bioadhesive Drug Delivery Systems

Kadriye Ciftci, *Temple University, Philadelphia, Pennsylvania,* Veterinary Applications

Paolo Colombo, *University of Parma, Parma, Italy,* Mucosal Drug Delivery, Nasal

Nora E. Cutcliffe, *Hemosol, Inc., Toronto, Canada,* Blood Substitutes: A Review of Clinical Trials

Wenbin Dang, *Guilford Pharmaceuticals, Baltimore, Maryland,* Biodegradable Polymers: Poly(phosphoester)s; Fabrication of Controlled-Delivery Devices

M.C. Davies, *University of Nottingham, Nottingham, United Kingdom,* Characterization of Delivery Systems, XPS, SIMS and AFM Analysis

Fanny De Jaeghere, *University of Geneva, Geneva, Switzerland,* Nanoparticles

Arati A. Deshpande, *University of Geneva, Geneva, Switzerland,* Mucosal Drug Delivery, Intravitreal

Eric Doelker, *University of Geneva, Geneva, Switzerland,* Nanoparticles

Ruth Duncan, *University of London, London, United Kingdom,* Pendent Drugs, Release from Polymers

Elazer R. Edelman, *Massachusetts Institute of Technology, Cambridge, Massachusetts,* Cardiovascular Drug Delivery Systems

David A. Edwards, *Advanced Inhalation Research (AIR), Cambridge, Massachusetts,* Respiratory System Delivery

Jonathan D. Eichman, *University of Michigan Medical School, Ann Arbor, Michigan,* Mucosal Drug Delivery, Vaginal Drug Delivery and Treatment Modalities

Suzanne Einmahl, *University of Geneva, Geneva, Switzerland,* Mucosal Drug Delivery, Intravitreal

James P. English, *Absorbable Polymer Technologies, Pelham, Alabama,* Fabrication of Controlled-Delivery Devices

O. Felt, *University of Geneva, Geneva, Switzerland,* Mucosal Drug Delivery, Ocular

Gregory T. Fieldson, *ALZA Corporation, Palo Alto, California,* Characterization of Delivery Systems, Spectroscopy

Joseph Fix, *Yamanouchi Shaklee Pharmaceutical Research Center, Palo Alto, California,* Oral Drug Delivery, Small Intestine & Colon

Virginia Fleming, *ALZA Corporation, Palo Alto, California,* Pumps/Osmotic—ALZET® System

Achim Göpferich, *University of Regensburg, Regensburg, Germany,* Biodegradable Polymers: Polyanhydrides

Robert Gale, *ALZA Corporation, Palo Alto, California,* Transdermal Drug Delivery, Passive

A. Gerson Greenburg, *The Miriam Hospital and Brown University, Providence, Rhode Island,* Blood Substitutes: A Review of Clinical Trials

Gregory Gregoriadis, *University of London School of Pharmacy, London, United Kingdom,* Liposomes

M.J. Groves, *University of Illinois at Chicago, Chicago, Illinois,* Parenteral Drug Delivery Systems

Suneel K. Gupta, *ALZA Corporation, Palo Alto, California,* In Vitro–In Vivo Correlation

Robert Gurny, *University of Geneva, Geneva, Switzerland,* Mucosal Drug Delivery, Intravitreal; Mucosal Drug Delivery, Ocular; Nanoparticles; Poly(ortho esters)

Jorge Heller, *Advanced Polymer Systems, Redwood City, California,* Poly(ortho esters)

Benjamin A. Hertzog, *Brown University, Providence, Rhode Island,* Cardiovascular Drug Delivery Systems

Mohammad Ashlaf Hossain, *Nagasaki University School of Medicine, Nagasaki, Japan,* Infectious Disease, Drug Delivery to Treat

Eric Kai Huang, *Brown University, Providence, Rhode Island,* Microencapsulation for Gene Delivery

James Hunt, *ALZA Corporation, Palo Alto, California,* Transdermal Drug Delivery, Passive

Stephen S. Hwang, *ALZA Corporation, Palo Alto, California,* In Vitro–In Vivo Correlation

Jules S. Jacob, *Brown University, Providence, Rhode Island,* Bioadhesive Drug Delivery Systems; Characterization of Delivery Systems, Microscopy

OluFunmi L. Johnson, *Alkermes Incorporated, Cambridge, Massachusetts,* Peptide and Protein Drug Delivery

Yong Shik Jong, *Brown University, Providence, Rhode Island,* Microencapsulation for Gene Delivery

Irina Kadiyala, *The Johns Hopkins University School of Medicine, Baltimore, Maryland,* Biodegradable Polymers: Poly(phosphoester)s

James J. Kaminski, *Schering-Plough Research Institute, Kenilworth, New Jersey,* Chemical Approaches to Drug Delivery

Hyun D. Kim, *Genetics Institute, Andover, Massachusetts,* Protein Therapeutics for Skeletal Tissue Repair

Christopher J. Kirby, *Cortecs Research Laboratory, London, United Kingdom,* Liposomes

Shigeru Kohno, *Nagasaki University School of Medicine, Nagasaki, Japan,* Infectious Disease, Drug Delivery to Treat

Joseph Kost, *Ben-Gurion University, Beer-Sheva, Israel,* Intelligent Drug Delivery Systems

Mark R. Kreitz, *Brown University, Providence, Rhode Island,* Microencapsulation; Synthetic Vascular Grafts and Controlled-Release Technology

Connie Kwok, *University of Washington Engineered Biomaterials (UWEB), Seattle, Washington,* Characterization of Delivery Systems, Surface Analysis and Controlled Release Systems

Robert Langer, *Johns Hopkins University School of Medicine, Baltimore, Maryland,* Central Nervous System, Drug Delivery to Treat

Kathleen J. Leach, *University of Washington, Seattle, Washington,* Cancer, Drug Delivery to Treat—Local & Systemic

Kam W. Leong, *The Johns Hopkins University School of Medicine, Baltimore, Maryland,* Biodegradable Polymers: Poly(phosphoester)s

Robert J. Levy, *Children's Hospital of Philadelphia and the University of Pennsylvania, Philadelphia, Pennsylvania,* Calcification, Drug Delivery to Prevent

Suming Li, *Centre de Recherche sur les Biopolymères Artificiels, Montpellier, France,* Biodegradable Polymers: Polyesters

Anthony M. Lowman, *Drexel University, Philadelphia, Pennsylvania,* Hydrogels

Michael J. Lysaght, *Brown University, Providence, Rhode Island,* Immunoisolated Cell Therapy

Fiona C. MacLaughlin, *Valentis, Inc., The Woodlands, Texas,* Polymeric Systems for Gene Delivery, Chitosan and PINC Systems

Shigefumi Maesaki, *Nagasaki University School of Medicine, Nagasaki, Japan,* Infectious Disease, Drug Delivery to Treat

Judy Magruder, *ALZA Corporation, Palo Alto, California,* Pumps/Osmotic—VITS Veterinary Implant

Henry J. Malinowski, *U.S. Food and Drug Administration, Rockville, Maryland,* Food and Drug Administration Requirements for Controlled Release Products

Surya K. Mallapragada, *Iowa State University, Ames, Iowa,* Release Kinetics, Data Interpretation

Hai-Quan Mao, *The Johns Hopkins University School of Medicine, Baltimore, Maryland,* Biodegradable Polymers: Poly(phosphoester)s

Patrick J. Marroum, *U.S. Food and Drug Administration, Rockville, Maryland,* Food and Drug Administration Requirements for Controlled Release Products

Edith Mathiowitz, *Brown University, Providence, Rhode Island,* Bioadhesive Drug Delivery Systems; Microencapsulation

C. Russell Middaugh, *University of Kansas, Lawrence, Kansas,* Oligonucleotide Delivery

Geoffrey Moodie, *Brown University, Providence, Rhode Island,* Tissue–Implant Interface, Biological Response to Artificial Materials with Surface-Immobilized Small Peptides

Balaji Narasimhan, *Rutgers University, Piscataway, New Jersey,* Release Kinetics, Data Interpretation

Padma Narayan, *Drexel University, Philadelphia, Pennsylvania,* Diagnostic Use of Microspheres

Patrea Pabst, *Arnall Golden & Gregory, LLP, Atlanta, Georgia,* Patents and Other Intellectual Property Rights in Drug Delivery

Clarisa Peer, *ALZA Corporation, Palo Alto, California,* Pumps/Osmotic—ALZET® System

Nicholas A. Peppas, *Purdue University, West Lafayette, Indiana,* Hydrogels; Release Kinetics, Data Interpretation

Lorri Perkins, *ALZA Corporation, Palo Alto, California,* Pumps/Osmotic—ALZET® System

S.C. Porter, *Colorcon, West Point, Pennsylvania,* Coatings

Mary E. Prevo, *ALZA Corporation, Palo Alto, California,* Transdermal Drug Delivery, Passive

Venkatesh Raman, *Massachusetts Institute of Technology, Cambridge, Massachusetts,* Cardiovascular Drug Delivery Systems

Suneel K. Rastogi, *University of Minnesota, Minneapolis, Minnesota,* Characterization of Delivery Systems, X-Ray Powder Diffractometry

Michael J. Rathbone, *InterAg, Hamilton, New Zealand,* Mucosal Drug Delivery, Vaginal Drug Delivery and Treatment Modalities; Veterinary Applications

Buddy D. Ratner, *University of Washington Engineered Biomaterials (UWEB), Seattle, Washington,* Characterization of Delivery Systems, Surface Analysis and Controlled Release Systems

C.T. Rhodes, *PharmaCon, Inc., West Kingston, Rhode Island,* Coatings

C.J. Roberts, *University of Nottingham, Nottingham, United Kingdom,* Characterization of Delivery Systems, XPS, SIMS and AFM Analysis

Joseph R. Robinson, *University of Wisconsin, Madison, Wisconsin,* Mucosal Drug Delivery, Vaginal Drug Delivery and Treatment Modalities

Alain P. Rolland, *Valentis, Inc., The Woodlands, Texas,* Polymeric Systems for Gene Delivery, Chitosan and PINC Systems

G.J. Russell-Jones, *Biotech Australia Pty Ltd., Roseville, NSW, Australia,* Carrier-Mediated Transport, Oral Drug Delivery

J. Howard Rytting, *University of Kansas, Lawrence, Kansas,* Characterization of Delivery Systems, Differential Scanning Calorimetry

Maryellen Sandor, *Brown University, Providence, Rhode Island,* Cardiovascular Drug Delivery Systems

Camilla A. Santos, *Brown University, Providence, Rhode Island,* Bioadhesive Drug Delivery Systems; Characterization of Delivery Systems, Gel Permeation Chromatography; Fertility Control

K.M. Shakesheff, *University of Nottingham, Nottingham, United Kingdom,* Characterization of Delivery Systems, XPS, SIMS and AFM Analysis

Robert G.L. Shorr, *United Therapeutics, Washington, D.C.,* Cancer, Drug Delivery to Treat—Prodrugs

Jürgen Siepmann, *Freie Universität Berlin, Berlin, Germany,* Nondegradable Polymers for Drug Delivery

Pierre Souillac, *University of Kansas, Lawrence, Kansas,* Characterization of Delivery Systems, Differential Scanning Calorimetry

Mark Speers, *Health Advances, Inc., Wellesley, Massachusetts,* Economic Aspects of Controlled Drug Delivery

Cynthia L. Stevenson, *ALZA Corporation, Palo Alto, California,* Pumps/Osmotic—Introduction; Pumps/Osmotic—DUROS™ Osmotic Implant for Humans

Gregory R. Stewart, *ALZA Corporation, Palo Alto, California,* Pumps/Osmotic—DUROS™ Osmotic Implant for Humans

Raj Suryanarayanan, *University of Minnesota, Minneapolis, Minnesota,* Characterization of Delivery Systems, X-Ray Powder Diffractometry

Robert M. Swift, *Brown University and the VA Medical Center, Providence, Rhode Island,* Alcoholism and Drug Dependence, Drug Delivery to Treat

Cyrus Tabatabay, *University of Geneva, Geneva, Switzerland,* Mucosal Drug Delivery, Intravitreal

Kanji Takada, *Kyoto Pharmaceutical University, Kyoto, Japan,* Oral Drug Delivery, Traditional

Janet Tamada, *Cygnus, Inc., Redwood City, California,* Transdermal Drug Delivery, Electrical

S.J.B. Tendler, *University of Nottingham, Nottingham, United Kingdom,* Characterization of Delivery Systems, XPS, SIMS and AFM Analysis

Chris Thanos, *Brown University, Providence, Rhode Island,* Cardiovascular Drug Delivery Systems

Mark A. Tracy, *Alkermes Inc., Cambridge, Massachusetts,* Characterization of Delivery Systems, Particle Sizing Techniques; Peptide and Protein Drug Delivery

Robert F. Valentini, *Brown University, Providence, Rhode Island,* Protein Therapeutics for Skeletal Tissue Repair; Tissue–Implant Interface, Biological Response to Artificial Materials with Surface-Immobilized Small Peptides

Michel Vert, *Centre de Recherche sur les Biopolymères Artificiels, Montpellier, France,* Biodegradable Polymers: Polyesters

Narendra R. Vyavahare, *Children's Hospital of Philadelphia and the University of Pennsylvania, Philadelphia, Pennsylvania,* Calcification, Drug Delivery to Prevent

K.L. Ward, *Alkermes, Inc., Cambridge, Massachusetts,* Characterization of Delivery Systems, Particle Sizing Techniques

Wendy Webber, *Brown University, Providence, Rhode Island,* Mucosal Drug Delivery, Buccal

Margaret A. Wheatley, *Drexel University, Philadelphia, Pennsylvania,* Diagnostic Use of Microspheres

Leonore Witchey-Lakshmanan, *Schering-Plough Research Institute, Kenilworth, New Jersey,* Veterinary Applications

Jeremy C. Wright, *ALZA Corporation, Palo Alto, California,* Pumps/Osmotic—Introduction; Pumps/Osmotic—DUROS™ Osmotic Implant for Humans; Pumps/Osmotic—Ruminal Osmotic Bolus

Hiroshi Yoshikawa, *Toyama Medical and Pharmaceutical University, Toyama, Japan,* Oral Drug Delivery, Traditional

Zhong Zhao, *Guilford Pharmaceuticals, Inc., Baltimore, Maryland,* Biodegradable Polymers: Poly(phosphoester)s; Fabrication of Controlled-Delivery Devices

M. Zignani, *University of Geneva, Geneva, Switzerland,* Mucosal Drug Delivery, Ocular

FOREWORD

Drug delivery systems that can precisely control drug release rates or target drugs to a specific body site, although a relatively recent technology, have had an enormous medical and economic impact. New drug delivery systems impact nearly every branch of medicine and annual sales of these systems are far in excess of 10 billion dollars. However, to intelligently create new delivery systems or to understand how to evaluate existing ones, much knowledge is needed. Dr. Edith Mathiowitz of Brown University has, in this encyclopedia, successfully put together a remarkable amount of information to achieve that goal of knowledge.

The *Encyclopedia of Controlled Drug Delivery* provides an up-to-date analysis of critical areas in this promising field. New approaches in treating diseases such as alcoholism, cancer, heart disease, and infectious diseases are examined. Delivery of vaccines, contraceptive agents, anticalcification agents, orthopedic agents, and veterinary agents is discussed. Novel polymeric materials including polyanhydrides, chitosan polyesters, polyphosphates, polyphosphazenes, hydrogels, bioadhesive materials, and poly(ortho esters) are evaluated. Extensive characterization approaches including differential scanning calorimetry, gel permeation chromatography, spectroscopy, X-ray photoelectron spectroscopy, X-ray powder diffraction, and surface characterization are explored.

New areas related to drug delivery such as gene therapy, blood substitutes, food ingredients, and tissue engineering are discussed. An analysis of various routes of administration including parenteral, intravitreal, oral, rectal, ocular, nasal, buccal, vaginal, and the central nervous system is provided. Different controlled release designs such as osmotic pumps, pendent-chain systems, membrane systems, nanoparticles, and liposomes are examined. Finally, patents, regulatory issues, manufacturing approaches, economics, in vitro–in vivo correlations, pharmacokinetics, release kinetics, assays, diagnostics, and related issues are considered.

This encyclopedia is a very complete compendium of the state-of-the-art of this burgeoning field and should be of considerable value for those who wish to enter it.

ROBERT LANGER
Massachusetts Institute of Technology

PREFACE

The two-volume *Encyclopedia of Controlled Drug Delivery* will provide extensive, yet easily accessible, A–Z coverage of state-of-the-art topics in drug delivery systems. The encyclopedia can be used by research departments in industry, research institutes, universities, libraries, and consultants. The readers may range from undergraduate and graduate students to professional engineers, biologists, chemists, and medical researchers. In addition, research managers, as well as business venturers, will find this encyclopedia a very useful source of information. Scientists unfamiliar with the field of drug delivery will find a good introduction to the field, while experts will find the book to be a good, current source of information. The contents of these two volumes provide coverage of many aspects of drug delivery systems, including:

- The history and development of the field from 1975 to date
- Advantages and disadvantages of controlled release technology as compared to conventional delivery systems (pharmaceutical as well as veterinary applications)
- Detailed descriptions of the various systems for achieving controlled drug release, including nonerodible reservoir and matrix devices, bioerodible polymers, pendent drug substitutes, and osmotic pumps
- Pharmaceutical applications of drug delivery systems, approaches to achieve zero-release kinetics, development of pulsatile delivery systems including approaches to develop self-regulated systems by using responsive hydrogels or encapsulated live cells
- Stabilization and release characterization of proteins
- Characterization of specific delivery systems such as oral, nasal, ocular, and other routes of administration
- Methods to fabricate controlled delivery systems, including microencapsulation, liposome preparation, film casting, and membrane formation
- Factors affecting regulatory considerations
- Economic aspects of controlled drug delivery devices
- Patents and other intellectual property rights in drug delivery
- Oligonucleotides and gene delivery
- Specific topics in polymer technology which are peculiar to drug delivery systems, including polymer synthesis, structure, morphology, amorphous polymers, glassy and rubbery states, polymer networks, and a variety of methods to characterize polymers and drug delivery systems

The encyclopedia can easily be used as an advanced text or reference book for a drug delivery system course. It is written by some of the greatest experts and most diligent educators in the field. These volumes should constitute an important research reference tool, a desktop information resource, and supplementary reading for teaching professionals and their students.

ACKNOWLEDGMENT

The idea to start this two-volume book came from Hannah Ben-Zvi, of John Wiley and Sons, and caught me by surprise. I had been thinking for many years that there was no encyclopedia for the field of drug delivery systems, which has emerged since the 1970s. The encouragement to start this project came from my students. It was with the help of Kathleen Leach (Pekarek), Wendy Webber, and Camilla Santos that this project was born. I am also extremely thankful to the editorial board for the time and effort they contributed to this endeavor. I would like particularly to mention Howard Bernstein, Robert Gurny, and Nicholas Peppas, who contributed above and beyond to the success of this project. I would also like to thank Pierre Galletti, whose untimely death prevented him from seeing the completion of the encyclopedia. Special thanks to Jules Jacob, Jong Yong, Ben Hertzog, Mark Kreitz, Gerardo Carino, Chris Thanos, MaryEllen Sandor, and Don Chickering. I am also grateful to Glenn Collins of John Wiley, who was always there to help and comfort, to Susan Hirsch, who always kept me on track, and perhaps most importantly to the team of authors who put an enormous amount of time into writing this book. To my husband, who helped with graphics, I am eternally grateful for always being patient, even during the days when he hardly saw me.

EDITH MATHIOWITZ
Brown University

CONVERSION FACTORS, ABBREVIATIONS AND UNIT SYMBOLS

SI Units (Adopted 1960)

The International System of Units (abbreviated SI), is being implemented throughout the world. This measurement system is a modernized version of the MKSA (meter, kilogram, second, ampere) system, and its details are published and controlled by an international treaty organization (The International Bureau of Weights and Measures) (1).

SI units are divided into three classes:

BASE UNITS		SUPPLEMENTARY UNITS	
length	meter† (m)	plane angle	radian (rad)
mass	kilogram (kg)	solid angle	steradian (sr)
time	second (s)		
electric current	ampere (A)		
thermodynamic temperature‡	kelvin (K)		
amount of substance	mole (mol)		
luminous intensity	candela (cd)		

DERIVED UNITS AND OTHER ACCEPTABLE UNITS

These units are formed by combining base units, supplementary units, and other derived units (2–4). Those derived units having special names and symbols are marked with an asterisk in the list below.

Quantity	Unit	Symbol	Acceptable equivalent
*absorbed dose	gray	Gy	J/kg
acceleration	meter per second squared	m/s^2	
*activity (of a radionuclide)	becquerel	Bq	1/s
area	square kilometer	km^2	
	square hectometer	hm^2	ha (hectare)
	square meter	m^2	
concentration (of amount of substance)	mole per cubic meter	mol/m^3	
current density	ampere per square meter	$A//m^2$	
density, mass density	kilogram per cubic meter	kg/m^3	g/L; mg/cm^3
dipole moment (quantity)	coulomb meter	$C \cdot m$	
*dose equivalent	sievert	Sv	J/kg
*electric capacitance	farad	F	C/V
*electric charge, quantity of electricity	coulomb	C	$A \cdot s$
electric charge density	coulomb per cubic meter	C/m^3	
*electric conductance	siemens	S	A/V
electric field strength	volt per meter	V/m	
electric flux density	coulomb per square meter	C/m^2	
*electric potential, potential difference, electromotive force	volt	V	W/A
*electric resistance	ohm	Ω	V/A

†The spellings "metre" and "litre" are preferred by ASTM; however, "-er" is used in the encyclopedia.

‡Wide use is made of Celsius temperature (t) defined by

$$t = T - T_0$$

where T is the thermodynamic temperature, expressed in kelvin, and $T_0 = 273.15$ K by definition. A temperature interval may be expressed in degrees Celsius as well as in kelvin.

Quantity	Unit	Symbol	Acceptable equivalent
*energy, work, quantity of heat	megajoule	MJ	
	kilojoule	kJ	
	joule	J	$N \cdot m$
	electronvolt†	eV†	
	kilowatt-hour†	$kW \cdot h$†	
energy density	joule per cubic meter	J/m^3	
*force	kilonewton	kN	
	newton	N	$kg \cdot m/s^2$
*frequency	megahertz	MHz	
	hertz	Hz	1/s
heat capacity, entropy	joule per kelvin	J/K	
heat capacity (specific), specific entropy	joule per kilogram kelvin	$J/(kg \cdot K)$	
heat-transfer coefficient	watt per square meter kelvin	$W/(m^2 \cdot K)$	
*illuminance	lux	lx	lm/m^2
*inductance	henry	H	Wb/A
linear density	kilogram per meter	kg/m	
luminance	candela per square meter	cd/m^2	
*luminous flux	lumen	lm	$cd \cdot sr$
magnetic field strength	ampere per meter	A/m	
*magnetic flux	weber	Wb	$V \cdot s$
*magnetic flux density	tesla	T	Wb/m^2
molar energy	joule per mole	J/mol	
molar entropy, molar heat capacity	joule per mole kelvin	$J/(mol \cdot K)$	
moment of force, torque	newton meter	$N \cdot m$	
momentum	kilogram meter per second	$kg \cdot m/s$	
permeability	henry per meter	H/m	
permittivity	farad per meter	F/m	
*power, heat flow rate, radiant flux	kilowatt	kW	
	watt	W	J/s
power density, heat flux density, irradiance	watt per square meter	W/m^2	
*pressure, stress	megapascal	MPa	
	kilopascal	kPa	
	pascal	Pa	N/m^2
sound level	decibel	dB	
specific energy	joule per kilogram	J/kg	
specific volume	cubic meter per kilogram	m^3/kg	
surface tension	newton per meter	N/m	
thermal conductivity	watt per meter kelvin	$W/(m \cdot K)$	
velocity	meter per second	m/s	
	kilometer per hour	km/h	
viscosity, dynamic	pascal second	$Pa \cdot s$	
	millipascal second	$mPa \cdot s$	
viscosity, kinematic	square meter per second	m^2/s	
	square millimeter per second	mm^2/s	
volume	cubic meter	m^3	
	cubic diameter	dm^3	L (liter) (5)
	cubic centimeter	cm^3	mL
wave number	1 per meter	m^{-1}	
	1 per centimeter	cm^{-1}	

†This non-SI unit is recognized by the CIPM as having to be retained because of practical importance or use in specialized fields (1).

In addition, there are 16 prefixes used to indicate order of magnitude, as follows:

Multiplication factor	Prefix	Symbol
10^{18}	exa	E
10^{15}	peta	P
10^{12}	tera	T
10^{9}	giga	G
10^{6}	mega	M
10^{3}	kilo	k
10^{2}	hecto	h[a]
10	deka	da[a]
10^{-1}	deci	d[a]
10^{-2}	centi	c[a]
10^{-3}	milli	m
10^{-6}	micro	μ
10^{-9}	nano	n
10^{-12}	pico	p
10^{-15}	femto	f
10^{-18}	atto	a

[a]Although hecto, deka, deci, and centi are SI prefixes, their use should be avoided except for SI unit-multiples for area and volume and nontechnical use of centimeter, as for body and clothing measurement.

For a complete description of SI and its use the reader is referred to ASTM E380 (4).

A representative list of conversion factors from non-SI to SI units is presented herewith. Factors are given to four significant figures. Exact relationships are followed by a dagger. A more complete list is given in the latest editions of ASTM E380 (4) and ANSI Z210.1 (6).

CONVERSION FACTORS TO SI UNITS

To convert from	To	Multiply by
acre	square meter (m^2)	4.047×10^{3}
angstrom	meter (m)	1.0×10^{-10}†
are	square meter (m^2)	1.0×10^{2}†
astronomical unit	meter (m)	1.496×10^{11}
atmosphere, standard	pascal (Pa)	1.013×10^{5}
bar	pascal (Pa)	1.0×10^{5}†
barn	square meter (m^2)	1.0×10^{-28}†
barrel (42 U.S. liquid gallons)	cubic meter (m^3)	0.1590
Bohr magneton (μ_B)	J/T	9.274×10^{-24}
Btu (International Table)	joule (J)	1.055×10^{3}
Btu (mean)	joule (J)	1.056×10^{3}
Btu (thermochemical)	joule (J)	1.054×10^{3}
bushel	cubic meter (m^3)	3.524×10^{-2}
calorie (International Table)	joule (J)	4.187
calorie (mean)	joule (J)	4.190
calorie (thermochemical)	joule (J)	4.184†
centipoise	pascal second (Pa · s)	1.0×10^{-3}†
centistokes	square millimeter per second (mm^2/s)	1.0†
cfm (cubic foot per minute)	cubic meter per second (m^3/s)	4.72×10^{-4}
cubic inch	cubic meter (m^3)	1.639×10^{-5}
cubic foot	cubic meter (m^3)	2.832×10^{-2}
cubic yard	cubic meter (m^3)	0.7646
curie	becquerel (Bq)	3.70×10^{10}†
debye	coulomb meter (C · m)	3.336×10^{-30}
degree (angle)	radian (rad)	1.745×10^{-2}

†Exact.

CONVERSION FACTORS TO SI UNITS

To convert from	To	Multiply by
denier (international)	kilogram per meter (kg/m)	1.111×10^{-7}
	tex‡	0.1111
dram (apothecaries')	kilogram (kg)	3.888×10^{-3}
dram (avoirdupois)	kilogram (kg)	1.772×10^{-3}
dram (U.S. fluid)	cubic meter (m^3)	3.697×10^{-6}
dyne	newton (N)	1.0×10^{-5}†
dyne/cm	newton per meter (N/m)	1.0×10^{-3}†
electronvolt	joule (J)	1.602×10^{-19}
erg	joule (J)	1.0×10^{-7}†
fathom	meter (m)	1.829
fluid ounce (U.S.)	cubic meter (m^3)	2.957×10^{-5}
foot	meter (m)	0.3048†
footcandle	lux (lx)	10.76
furlong	meter (m)	2.012×10^{-2}
gal	meter per second squared (m/s^2)	1.0×10^{-2}†
gallon (U.S. dry)	cubic meter (m^3)	4.405×10^{-3}
gallon (U.S. liquid)	cubic meter (m^3)	3.785×10^{-3}
gallon per minute (gpm)	cubic meter per second (m^3/s)	6.309×10^{-5}
	cubic meter per hour (m^3/h)	0.2271
gauss	tesla (T)	1.0×10^{-4}
gilbert	ampere (A)	0.7958
gill (U.S.)	cubic meter (m^3)	1.183×10^{-4}
grade	radian	1.571×10^{-2}
grain	kilogram (kg)	6.480×10^{-5}
gram force per denier	newton per tex (N/tex)	8.826×10^{-2}
hectare	square meter (m^2)	1.0×10^{4}†
horsepower (550 ft · lbf/s)	watt (W)	7.457×10^{2}
horsepower (boiler)	watt (W)	9.810×10^{3}
horsepower (electric)	watt (W)	7.46×10^{2}†
hundredweight (long)	kilogram (kg)	50.80
hundredweight (short)	kilogram (kg)	45.36
inch	meter (m)	2.54×10^{-2}†
inch of mercury (32°F)	pascal (Pa)	3.386×10^{3}
inch of water (39.2°F)	pascal (Pa)	2.491×10^{2}
kilogram-force	newton (N)	9.807
kilowatt hour	megajoule (MJ)	3.6†
kip	newton (N)	4.448×10^{3}
knot (international)	meter per second (m/S)	0.5144
lambert	candela per square meter (cd/m^3)	3.183×10^{3}
league (British nautical)	meter (m)	5.559×10^{3}
league (statute)	meter (m)	4.828×10^{3}
light year	meter (m)	9.461×10^{15}
liter (for fluids only)	cubic meter (m^3)	1.0×10^{-3}†
maxwell	weber (Wb)	1.0×10^{-8}†
micron	meter (m)	1.0×10^{-6}†
mil	meter (m)	2.54×10^{-5}†
mile (statute)	meter (m)	1.609×10^{3}
mile (U.S. nautical)	meter (m)	1.852×10^{3}†
mile per hour	meter per second (m/s)	0.4470
millibar	pascal (Pa)	1.0×10^{2}
millimeter of mercury (0°C)	pascal (Pa)	1.333×10^{2}†
minute (angular)	radian	2.909×10^{-4}
myriagram	kilogram (kg)	10

†Exact.

‡See footnote on p. xvi.

CONVERSION FACTORS TO SI UNITS

To convert from	To	Multiply by
myriameter	kilometer (km)	10
oersted	ampere per meter (A/m)	79.58
ounce (avoirdupois)	kilogram (kg)	2.835×10^{-2}
ounce (troy)	kilogram (kg)	3.110×10^{-2}
ounce (U.S. fluid)	cubic meter (m^3)	2.957×10^{-5}
ounce-force	newton (N)	0.2780
peck (U.S.)	cubic meter (m^3)	8.810×10^{-3}
pennyweight	kilogram (kg)	1.555×10^{-3}
pint (U.S. dry)	cubic meter (m^3)	5.506×10^{-4}
pint (U.S. liquid)	cubic meter (m^3)	4.732×10^{-4}
poise (absolute viscosity)	pascal second (Pa · s)	0.10†
pound (avoirdupois)	kilogram (kg)	0.4536
pound (troy)	kilogram (kg)	0.3732
poundal	newton (N)	0.1383
pound-force	newton (N)	4.448
pound force per square inch (psi)	pascal (Pa)	6.895×10^3
quart (U.S. dry)	cubic meter (m^3)	1.101×10^{-3}
quart (U.S. liquid)	cubic meter (m^3)	9.464×10^{-4}
quintal	kilogram (kg)	1.0×10^2†
rad	gray (Gy)	1.0×10^{-2}†
rod	meter (m)	5.029
roentgen	coulomb per kilogram (C/kg)	2.58×10^{-4}
second (angle)	radian (rad)	4.848×10^{-6}†
section	square meter (m^2)	2.590×10^6
slug	kilogram (kg)	14.59
spherical candle power	lumen (lm)	12.57
square inch	square meter (m^2)	6.452×10^{-4}
square foot	square meter (m^2)	9.290×10^{-2}
square mile	square meter (m^2)	2.590×10^6
square yard	square meter (m^2)	0.8361
stere	cubic meter (m^3)	1.0†
stokes (kinematic viscosity)	square meter per second (m^2/s)	1.0×10^{-4}†
tex	kilogram per meter (kg/m)	1.0×10^{-6}†
ton (long, 2240 pounds)	kilogram (kg)	1.016×10^3
ton (metric) (tonnee)	kilogram (kg)	1.0×10^3†
ton (short, 2000 pounds)	kilogram (kg)	9.072×10^2
torr	pascal (Pa)	1.333×10^2
unit pole	weber (Wb)	1.257×10^{-7}
yard	meter (m)	0.9144†

†Exact.

BIBLIOGRAPHY

1. The International Bureau of Weights and Measures, BIPM (Parc de Saint-Cloud, France) is described in Appendix X2 of Ref. 4. This bureau operates under the exclusive supervision of the International Committee for Weights and Measures (CIPM).
2. *Metric Editorial Guide (ANMC-78-1),* latest ed., American National Metric Council, 5410 Grosvenor Lane, Bethesda, Md. 20814, 1981.
3. *SI Units and Recommendations for the Use of Their Multiples and of Certain Other Units (ISO 1000-1981),* American National Standards Institute, 1430 Broadway, New York, 10018, 1981.
4. Based on *ASTM E380-89a (Standard Practice for Use of the International System of Units (SI)),* American Society for Testing and Materials, 1916 Race Street, Philadelphia, Pa. 19103, 1989.
5. *Fed. Reg.,* Dec. 10, 1976 (41 FR 36414).
6. For ANSI address, see Ref. 3.

R. P. LUKENS
ASTM Committee E-43 on SI Practice

Contents

Contributors vii

Foreword xi

Preface xiii

Conversion Factors, Abbreviations and Unit Symbols xv

Alcoholism and Drug Dependence, Drug Delivery to Treat **1**

Alcoholism and Drug Dependence, Drug Delivery to Treat 1

Key Words 1

Outline 1

Addictive Disorders and Their Treatment 1

Treatment for Nicotine Dependence (Smoking) 2

Treatments for Opioid Dependence 4

Treatments for Alcohol Dependence 6

Summary 6

Bibliography 6

Bioadhesive Drug Delivery Systems *to* Blood Substitutes: a Review Ofclinical Trials **9**

Bioadhesive Drug Delivery Systems 9

Key Words 9

Outline 9

Background of Bioadhesion 9

Development of Bioadhesive Microspheres:a Case Study - Part 1 16

Development of Bioadhesive Microspheres:a Case Study - Part 2 31

Acknowledgments 42

Bibliography 42

Biodegradable Polymers: Poly(Ortho Esters) 45

This page has been reformatted by Knovel to provide easier navigation.

Biodegradable Polymers: Poly(Phosphoester)S 45
Key Words 45
Outline 45
Background of Poly(Phosphoester)S 46
Properties of PPEs with a Bisphenol a Backbone 46
Design, Synthesis, and Physicochemical Properties of PPEs 47
Example 1 48
Example 2 51
Example 3 52
Storage Stability and Sterilization Stability 53
In Vivo Degradation, Biocompatibility, and Cytotoxicity 53
Drug Release Properties 55
Summary 59
Bibliography 59
Biodegradable Polymers: Polyanhydrides 60
Key Words 60
Outline 60
Historical Development and Significance of Polyanhydridesas Biodegradable Polymers 60
Survey of the Various Types of Polyanhydrides 61
Polyanhydride Synthesis and Characterization 62
Polyanhydride Degradation and Erosion 65
Drug Delivery Systems Made of Polyanhydrides 68
Drug Release Kinetics 70
Summary and Outlook 70
Bibliography 70
Biodegradable Polymers: Polyesters 71
Key Words 71
Outline 71
Introduction 71
Synthesis 72
Manufacturing Methodology 75
Degradation Mechanisms 77
Factors Influencing Polymer Degradation and Drug Delivery 80
Conclusion 90
Bibliography 90
Blood Substitutes: a Review Ofclinical Trials 94
Key Words 94

This page has been reformatted by Knovel to provide easier navigation.

Outline 94
Introduction 94
Historical Perspective 94
The Need for Red Cell Substitutes 95
Purpose, Scope, and Methods 95
Results 95
Discussion 109
Acknowledgments 110
Bibliography 110

Calcification, Drug Delivery *to* Prevent *to* Coatings 113

Calcification, Drug Delivery to Prevent 113
Key Words 113
Outline 113
Background 113
Treatment Strategies 115
Future Directions 117
Conclusions 118
Bibliography 118
Cancer, Drug Delivery to Treat - Local & Systemic 119
Key Words 119
Outline 119
Introduction 119
Local Delivery 121
Locally Implanted Controlled-Release Systems 128
Systemic Delivery 131
Cancer Immunotherapy 139
Summary 141
Bibliography 141
Cancer, Drug Delivery to Treat—Prodrugs 143
Key Words 143
Outline 143
Introduction 143
The Problem 143
The Solution: Tumor Targeting Strategies 144
Bibliography 159
Cardiovascular Drug Delivery Systems 161
Key Words 161

This page has been reformatted by Knovel to provide easier navigation.

Outline 161
Introduction 162
Classifications 162
Catheter-Based Systems 162
Drug Delivery from Stents 165
Delivery from Polymer Devices 169
Bibliography 171
Carrier-Mediated Transport, Oral Drug Delivery 173
Key Words 173
Outline 173
Introduction 173
Carrier-Mediated Transport Systems 174
Receptor-Mediated Endocytosis of Transferrin and the Uptake of Fe 179
Use of the Vitamin B-12-Mediated Transport System for Uptake of Pharmaceuticals 179
Future Directions 182
Conclusions 183
Bibliography 183
Central Nervous System, Drug Delivery to Treat 184
Key Words 184
Outline 184
Introduction 184
Barriers to CNS Drug Delivery 185
Strategies for Enhanced Cns Drug Delivery 188
Interstitial CNS Drug Delivery Using Controlled-Release Polymer Systems 193
Conclusion 209
Acknowledgments 210
Disclosure Statement 210
Bibliography 210
Characterization of Delivery Systems, Differential Scanning Calorimetry 212
Key Words 212
Outline 212
Introduction 212
DTA and DSC 212
Modulated Differential Scanning Calorimetry 221
Heat Conduction Calorimetry 222
Thermogravimetry 223
Isoperibol Calorimetry 223

This page has been reformatted by Knovel to provide easier navigation.

Conclusions 225
Bibliography 225
Characterization of Delivery Systems, Gel Permeation Chromatography 227
Key Words 227
Bibliography 228
Characterization of Delivery Systems, Magnetic Resonance Techniques 228
Key Words 228
Outline 229
Introduction 229
Principles and Spectroscopic Methods 229
Applications 230
Summary 233
Bibliography 233
Characterization of Delivery Systems, Microscopy 234
Key Words 234
Outline 234
Introduction 234
Optical Microscopy 234
Transmission Electron Microscopy 236
Scanning Electron Microscopy 242
Summary 249
Bibliography 249
Characterization of Delivery Systems, Particle Sizing Techniques 250
Key Words 250
Outline 250
Introduction 250
Sieving Methods 250
Microscopy Methods 250
Electrical Sensing Zone (Coulter Principle) Method 252
Laser Light Scattering Methods 252
Comparing Results from Different Particle Sizing Methods 254
Bibliography 255
Characterization of Delivery Systems, Spectroscopy 255
Key Words 255
Outline 256
Introduction 256
Infrared Spectroscopy 256

This page has been reformatted by Knovel to provide easier navigation.

Techniques 256
Analysis of Infrared Spectra 257
Applications 258
Bibliography 259
Characterization of Delivery Systems, Surface Analysis and Controlled Release Systems 261
Key Words 261
Outline 261
Introduction 261
A Historical Consideration 263
A Short Overview of Methods 263
Some Examples from the Literature 265
Concluding Remarks 268
Acknowledgments 268
Bibliography 268
Characterization of Delivery Systems, XPS, SIMS and AFM Analysis 269
Key Words 269
Outline 269
Introduction 270
SIMS Process and Instrumentation 270
General Comments on SIMS Spectra of Pharmaceutical Materials 270
Application of TOF-SIMS to the Analysis of Pharmaceutical Delivery Systems 272
Concluding Remarks 274
Bibliography 274
Characterization of Delivery Systems, X-Ray Powder Diffractometry 275
Key Words 275
Outline 275
Introduction 275
Phase Identification 276
Determination of Crystallinity 277
Quantitative Analysis 279
Phase Transitions Induced During Processing or Storage 281
Characterization of Drug Delivery Systems 282
Other Applications 283
Summary 283
Bibliography 284
Chemical Approaches to Drug Delivery 285
Key Words 285

This page has been reformatted by Knovel to provide easier navigation.

Outline 285
Introduction 285
SD Design 286
Chemical Delivery Systems (CDSS) 291
Conclusions 297
Bibliography 297
Coatings 299
Key Words 299
Outline 299
Fundamental Requirements 300
Manufacturing Methods for the Application of Coating Materials for Controlled Release 302
Trends in the Formulation and Manufacture of Coated, Controlled-Release Products 303
Materials Used in Controlled-Release Products 306
Bibliography 309

Diagnostic Use of Microspheres 313

Diagnostic Use of Microspheres 313
Key Words 313
Outline 313
X-Ray Contrast Agents 313
MRI Contrast Agents 317
Ultrasound CA 325
Conclusion 336
Bibliography 336
Color Plates 332a

Economic Aspects of Controlled Drug Delivery 341

Economic Aspects of Controlled Drug Delivery 341
Key Words 341
Outline 341
Overview 341
Sources of Economic Value 341
Prioritizing Reformulation Candidates 345
The Future 347
Bibliography 347

This page has been reformatted by Knovel to provide easier navigation.

Fabrication of Controlled-Delivery Devices *to* Food and Drug Administration Requirements for Controlled Release Products **349**

Fabrication of Controlled-Delivery Devices 349
Key Words 349
Outline 349
Applications 349
Regulatory Considerations 351
Manufacturing Processes 351
Bibliography 362
Fertility Control 364
Key Words 364
Outline 364
Background and History 365
Contraceptive Devices 367
Abortifacients 379
Summary 379
Bibliography 379
Food and Drug Administration Requirements for Controlled Release Products 381
Key Words 381
Outline 381
Introduction 381
Types of Controlled-Release Products 381
Definitions 381
Laws, Regulations and Guidances for Controlled-Release Products 382
Information to Characterize the Drug Entity 383
Information to Characterize the Dosage Form 384
Bibliography 394

Hydrogels **397**

Hydrogels 397
Key Words 397
Outline 397
Structure and Properties of Hydrogels 398
Diffusion In Hydrogels 402
Classifications 406
Applications 409
Bibliography 415

This page has been reformatted by Knovel to provide easier navigation.

Immunoisolated Cell Therapy *to* Intelligent Drug Delivery Systems **419**

Immunoisolated Cell Therapy 419
Key Words 419
Outline 419
Introduction 419
Biomaterials and Cells for Immunoisolation 419
Therapeutic Applications of Immunoisolation 421
Concluding Perspectives 425
Acknowledgments 425
Additional Reading 425
In Vitro-in Vivo Correlation 425
Key Words 425
Outline 425
Introduction 425
USP Definition of Correlation 426
In Vivo Evaluation 426
In Vitro Evaluation 430
Correlation between the in Vivo and the in Vivo Profiles 430
Examples 430
Application of in Vitro/in Vivo Correlations 433
Conclusions 434
Bibliography 434
Infectious Disease, Drug Delivery to Treat 435
Key Words 435
Outline 436
Introduction 436
Liposomal Antimicrobial Agents against the Cytozoic Microorganisms Salmonella Typhimurium, Listeria Monocytogenes 437
Liposomal Antimicrobial (Piperacillin or Tobramycin) Agents Against Bacteria 437
Liposome-Encapsulated Antimycobacterial Agents 438
Liposome-Encapsulated Antifungal Agents 440
Liposome-Encapsulated Antiviral Agents 443
Liposome-Encapsulated Antiparasitic Agents 444
Bibliography 444
Intelligent Drug Delivery Systems 445
Key Words 445
Outline 446

This page has been reformatted by Knovel to provide easier navigation.

Pulsatile Systems 446
Responsive Systems 449
Systems Utilizing Enzymes 452
Systems Utilizing Antibody Interactions 456
Systems Utilizing Chelation 457
Concluding Remarks 457
Bibliography 457

Liposomes 461

Liposomes 461
Key Words 461
Outline 461
Introduction 461
Molecular Aspects of Liposome Formation 462
Liposomes as Drug Delivery Systems 463
Preparation of Liposomes in the Laboratory 466
Scale-Up and Industrial Manufacture of Liposomes 472
Characterization 474
Fate of Liposomes in Vivo and Its Control 475
Tailoring of Liposomes 477
Applications for Liposomes 482
Bibliography 489

Microencapsulation *to* Mucosal Drug Delivery, Vaginal Drug Delivery and Treatment Modalities 493

Microencapsulation 493
Key Words 493
Outline 493
Introduction 493
Background 493
Solvent Evaporation 504
Complex Coacervation: Gelatin and Gum Arabic 512
Organic Phase Separation: Coacervation 513
Interfacial Polymerization 515
Thermal Denaturation 520
Gelation: Alginate 523
Gelation Agarose 525
Hot Melt Microencapsulation 525

This page has been reformatted by Knovel to provide easier navigation.

Solvent Removal 528
Spray-Drying 531
One-Step Formation of Double-Walled Microspheres 537
Novel Encapsulation Techniques 541
Applications of Microencapsulation 541
Bibliography 543
Microencapsulation for Gene Delivery 546
Key Words 546
Outline 546
Introduction 546
Background 548
Fabrication Techniques 550
In Vivo Applications 551
Conclusion 552
Bibliography 552
Additional Reading 553
Mucosal Drug Delivery, Buccal 553
Key Words 553
Outline 553
The Structure of the Oral Mucosae 553
Delivery to the Systemic Circulation 555
Local Delivery to the Mouth 558
Bibliography 562
Mucosal Drug Delivery, Intravitreal 564
Key Words 564
Outline 564
Introduction 564
Vitreoretinal Diseases 565
Drug Delivery Systems 569
Conclusion 586
Acknowledgments 588
Bibliography 588
Mucosal Drug Delivery, Nasal 592
Key Words 592
Outline 592
Introduction 593
Nasal Delivery: Historical and Behavioral Use 593

This page has been reformatted by Knovel to provide easier navigation.

Anatomy and Physiology of the Nose 593
Toxicological Considerations 594
Dosage Forms and Materials 594
Metering and Insufflators 595
Qualitative and Quantitative Aspects of Nasal Dose Delivery 596
Penetration Enhancers and Bioadhesion 598
Drugs Developed for Nasal Administration 600
The Insulin Case and Future Developments: Vaccines and Brain Targeting Through the Nose 602
Acknowledgments 603
Bibliography 603
Mucosal Drug Delivery, Ocular 605
Key Words 605
Outline 605
Introduction 605
Hydrogels 606
Dispersed Systems 613
Inserts 616
Conclusion 622
Bibliography 622
Mucosal Drug Delivery, Vaginal Drug Delivery and Treatment Modalities 627
Key Words 627
Outline 627
Introduction and Overview 627
Vaginal Anatomy and Physiology 627
Desirable Features of a Vaginal Drug Delivery System 629
Reproductive System Pathologies and Treatment 630
Topical Contraceptives 633
Other Vaginal Drug Delivery Systems 634
Veterinary Applications 634
Design Factors in Controlled Release Intravaginal Veterinary Drug Delivery Systems 637
Intravaginal Veterinary Drug Delivery Systems 637
Future Demands and Requirements of Intravaginal Veterinary Drug Delivery Systems 637
Bibliography 637

This page has been reformatted by Knovel to provide easier navigation.

Nanoparticles *to* Nondegradable Polymers for Drug Delivery **641**

Nanoparticles 641
Key Words 641
Outline 641
Manufacture of Nanoparticles 641
Modulation of the in Vivo Fate of Nanoparticles 654
Characterization of Nanoparticles 659
Applications of Nanoparticles 659
Conclusion 661
Bibliography 662
Nondegradable Polymers for Drug Delivery 664
Key Words 664
Outline 664
Ethyl Cellulose 665
Cellulose Esters: Cellulose Acetate, Cellulose Acetate Butyrate, and Cellulose Acetate Propionate 670
Acrylic Polymers 674
Silicones 679
Poly(Ethylene Oxide) 684
Bibliography 685

Oligonucleotide Delivery *to* Oral Drug Delivery, Traditional **691**

Oligonucleotide Delivery 691
Key Words 691
Outline 691
Bibliography 696
Oral Drug Delivery, Small Intestine & Colon 698
Key Words 698
Outline 698
Small Intestine 699
Colon 717
Bibliography 726
Oral Drug Delivery, Traditional 728
Key Words 728
Outline 729
Tablets 729
Capsules 734
Microgranules/Spheroids 735

This page has been reformatted by Knovel to provide easier navigation.

Beads 735
Pellets 736
Stabilization of Drug 736
Control of the Absorption Process 738
Bibliography 740

Parenteral Drug Delivery Systems *to* Pumps/Osmotic—Ruminal Osmotic Bolus 743

Parenteral Drug Delivery Systems 743
Key Words 743
Outline 743
Introduction 743
Methods of Sterilization of Parenteral Drug Delivery Systems 745
Sterile Implants 752
Production of Macro-, Micro- and Nanoparticulate Systems - Part 1 754
Production of Macro-, Micro- and Nanoparticulate Systems - Part 2 768
Conclusions 774
Bibliography 775
Patents and Other Intellectual Property Rights in Drug Delivery 777
Key Words 777
Outline 777
Patents 778
Trade Secrets, Copyrights, and Trademarks 784
Exploiting Intellectual Property Rights 785
Summary 785
Bibliography 785
Pendent Drugs, Release from Polymers 786
Key Words 786
Outline 786
Introduction 786
Biological Rationale for Design 787
Soluble Polymeric Carriers 789
Pendent Chain Linkers 794
Clinical Progress 808
Conclusions 811
Bibliography 811
Peptide and Protein Drug Delivery 816
Key Words 816
Outline 816

This page has been reformatted by Knovel to provide easier navigation.

Introduction 816
Protein and Peptide Stability 817
Protein Release from Polymeric Delivery Systems 821
Processes for Making Polymeric Delivery Systems 823
Process Scale-Up, Manufacturing, and Regulatory Considerations 826
Administration of Microsphere Delivery Systems 828
Sustained-Release Formulations of Peptides and Proteins 828
Conclusions 831
Acknowledgments 831
Bibliography 831
Pharmacokinetics 833
Key Words 833
Outline 833
Introduction 834
Background 834
Overview of the Theoretical Principles of Pharmacokinetics 835
Classic Linear Compartmental Models 841
Assessment of Drug Input Rate from Controlled Drug Delivery Systems 844
Conclusions 850
Bibliography 850
Poly(Ortho Esters) 852
Key Words 852
Outline 852
Poly(Ortho Ester) I 852
Poly(Ortho Ester) II 853
Poly(Ortho Ester) III 865
Acknowledgments 872
Bibliography 873
Polymeric Systems for Gene Delivery, Chitosan and Pinc Systems 874
Key Words 874
Outline 874
Protective Interacting Noncondensing Systems 875
Chitosan 881
Bibliography 887
Protein Therapeutics for Skeletal Tissue Repair 889
Key Words 889
Outline 889
Introduction 889

This page has been reformatted by Knovel to provide easier navigation.

Growth and Morphogenetic Factors for Bone Repair 890
Mesenchymal Stem Cells 891
Mechanisms of Bone Repair 892
Carriers for Growth and Morphogenetic Factors 892
Summary 894
Bibliography 894
Pumps/Osmotic 896
Pumps/Osmotic—Introduction 896
Key Words 896
Outline 896
Early Osmotic Systems 896
Characteristics of Osmotic Systems 896
Osmotic System Theory 897
System Design Considerations 898
Current Osmotic Pump Applications 898
Bibliography 899
Pumps/Osmotic—Alzet® System 900
Key Words 900
Outline 900
Background 900
System Design and Function 901
Applications 904
Conclusions 905
Bibliography 905
Additional Reading 905
Pumps/Osmotic—VITS Veterinary Implant 906
Key Words 906
Outline 906
Background 906
System Design and Function 907
Applications 908
Conclusions 908
Bibliography 908
Pumps/Osmotic—Duros® Osmotic Implant for Humans 909
Key Words 909
Outline 909
Background 910
System Design 910

This page has been reformatted by Knovel to provide easier navigation.

System Performance 911
Formulation Capabilities 911
Duros® Leuprolide Implant 912
Disease State 912
Formulation Stability 912
In Vitro Performance 913
In Vivo Performance 913
In Vivo-in Vitro Release Rate and Stability Correlation 914
Implantation and Explanation 914
Clinical Experience 915
Conclusions 915
Acknowledgments 915
Bibliography 915
Pumps/Osmotic—Ruminal Osmotic Bolus 915
Key Words 915
Outline 916
Background 916
System Design and Function 916
Products 917
Conclusions 920
Bibliography 920

Release Kinetics, Data Interpretation *to* Respiratory System Delivery 921

Release Kinetics, Data Interpretation 921
Key Words 921
Outline 921
Diffusion in Drug Delivery Systems 921
Release Kinetics from Diffusion-Controlled Systems 922
Swelling-Controlled Systems 930
Chemically Controlled Systems 930
Other Aspects of Release Kinetics Modeling 932
Conclusions 934
Bibliography 934
Respiratory System Delivery 936
Key Words 936
Outline 936
Introduction 936
Lung Morphology and Physiology 936

This page has been reformatted by Knovel to provide easier navigation.

Aerosol Delivery to the Respiratory Tract 936
Fast-Acting Inhalation Therapies 937
Sustained Drug Delivery 938
Summary 940
Bibliography 940

Synthetic Vascular Grafts and Controlled-Release Technology 943

Synthetic Vascular Grafts and Controlled-Release Technology 943
Key Words 943
Outline 943
Introduction 943
Early Investigations 943
The Introduction of Synthetic Vascular Grafts 944
Small-Diameter Synthetic Graft Success or Failure 945
Cell Seeding and Other Graft Modifications 948
Polymeric Controlled Release 949
Tissue-Engineered Vascular Grafts 950
Summary 951
Bibliography 951

Tissue-Implant Interface, Biological Response to Artificial Materials with Surface-Immobilized Small Peptides *to* Transdermal Drug Delivery, Passive 955

Tissue-Implant Interface, Biological Response to Artificial Materials with Surface-Immobilized Small Peptides 955
Key Words 955
Outline 955
Introduction 955
Integrins 955
Application to Bone-Contacting Prostheses 956
Specific Immobilization Chemistries 957
Bibliography 964
Transdermal Drug Delivery, Electrical 966
Key Words 966
Outline 966
Introduction 966
Iontophoresis 967
Electroporation 971
Bibliography 972

This page has been reformatted by Knovel to provide easier navigation.

Transdermal Drug Delivery, Passive 975
Key Words 975
Outline 975
Introduction 976
Structure, Composition, and Function of Skin 976
Permeability of Human Skin 976
Permeability Models for Stratum Corneum 980
Animal Models for Percutaneous Absorption 981
Toxicology 982
Transdermal Drug Delivery 983
Marketed Transdermal Systems 985
Summary 990
Bibliography 990

Vaccine Delivery *to* Veterinary Applications 993

Vaccine Delivery 993
Key Words 993
Outline 993
Vaccine Immunology 994
Particle Uptake by Intestinal M Cells 995
Liposome Uptake 996
Liposome-Based Vaccines 996
Polymer-Based Devices 1000
Comparison between Liposomes and Microspheres 1004
Future Directions 1004
Bibliography 1005
Veterinary Applications 1006
Key Words 1006
Outline 1006
Introduction 1007
Factors Influencing Controlled Drug Delivery in Animals 1007
Comparison of Human and Animal Controlled Drug Delivery 1008
Veterinary Controlled-Release Drug Delivery and Delivery Systems 1010
Recent Initiatives 1026
Concluding Remarks 1034
Bibliography 1034

Index 1039

This page has been reformatted by Knovel to provide easier navigation.

ALCOHOLISM AND DRUG DEPENDENCE, DRUG DELIVERY TO TREAT

ROBERT M. SWIFT
Brown University and the VA Medical Center
Providence, Rhode Island

KEY WORDS

Addictive disorders
Alcoholism
Buprenorphine
Clonidine
Disulfiram
Drug abuse
Naltrexone
Nicotine
Opioids

OUTLINE

Addictive Disorders and Their Treatment
Treatment for Nicotine Dependence (Smoking)
  Nicotine Replacement
  Other Medications for Smoking Cessation
Treatments for Opioid Dependence
  Opioid Detoxification: Clonidine
  Opioid Maintenance
Treatments for Alcohol Dependence
  Disulfiram
  Naltrexone
Summary
Bibliography

ADDICTIVE DISORDERS AND THEIR TREATMENT

Addictive disorders, including alcoholism, drug dependence, and nicotine dependence, afflict over 30% of Americans (1) and are associated with considerable morbidity, mortality, social problems, and health care costs (2,3). Addiction is characterized by impaired control over drinking or drug use, increased tolerance to the effects of alcohol and drugs, preoccupation with alcohol and drugs, and use despite adverse consequences (4).

One way to reduce the impact of addictive disorders is through effective drug and alcohol treatment. Treatment consists of medical, psychological, and social interventions to reduce or eliminate the harmful effects of substances on the individual, his or her family and associates, and others in society. The treatment consists of two components: detoxification and rehabilitation. Detoxification refers to the removal of the drug from the body and the treatment of physiological withdrawal signs and symptoms that may occur with drug discontinuation. Rehabilitation provides the patient with strategies and techniques to avoid psychoactive substances, to develop better methods of coping with stress and distress, and to improve self-esteem and self-efficacy.

Medications are frequently used as a component of both detoxification treatment and rehabilitation treatment, along with psychosocial therapies, such as counseling and self-help groups (e.g., Alcoholics Anonymous). Pharmacotherapies can treat alcohol and drug dependence through several mechanisms that may reduce some of the impetus for drug use. These mechanisms and the medications that may operate through these mechanisms are depicted in Table 1.

Controlled drug delivery systems are particularly applicable to the treatment of addictive disorders. Several advantages of controlled drug delivery systems are as follows:

- They mimic the pharmacokinetics of the abused drug, including the rise and fall of plasma drug concentrations.
- They facilitate the attainment of constant plasma concentrations of drug to prevent intoxication symptoms caused by high plasma concentrations and to prevent the development of withdrawal caused by low plasma drug concentrations.
- They improve therapeutic medication bioavailability.
- They improve therapeutic medication compliance in drug and alcohol treatment.

For a medication used as a substitution treatment, a controlled delivery system can be used to mimic the pharmacokinetics of the abused drug, without the dangers as-

Table 1. Medications Used for Addiction Treatment

Medication property	Example
Substitution treatment with a cross-tolerant medication	Methadone maintenance treatment for opioid dependence; transdermal nicotine or nicotine gum for smoking cessation
Administration of agents to block the signs and symptoms of withdrawal	Transdermal clonidine in opioid detoxification and withdrawal
Administration of a medication to block drug intoxication	Depot naltrexone for opioid dependence
Aversive therapy	Depot disulfiram treatment in alcoholism
Administration of a medication to suppress craving	Depot naltrexone in alcohol dependence

sociated with the usual mode of administration. For example, several methods of controlled administration of nicotine can keep plasma nicotine levels high enough to prevent nicotine withdrawal, without the inherent dangers of smoking. Two of these nicotine delivery methods can actually induce the rise and fall of plasma nicotine levels that occurs with smoking. Patients with addictive disorders are frequently noncompliant with medications and may either overuse or underuse therapeutic medications. Controlled drug delivery systems offer methods for controlling drug use and plasma concentrations to improve compliance. This chapter discusses use of controlled drug delivery in the treatment of addictive disorders, the putative mechanisms of action of the medications, and the evidence for their efficacy.

TREATMENT FOR NICOTINE DEPENDENCE (SMOKING)

The treatment of nicotine dependence provides several examples of the therapeutic use of controlled medication delivery systems in treatment. Nicotine is an alkaloid drug present in the leaves of the tobacco plant, *Nicotiana tabacum*, used for centuries by Native Americans in rituals and folk medicine. Today, nicotine has become one of the most commonly used psychoactive drugs. Over 50 million persons in the U.S. are daily users of cigarettes (one-third of adults), and 10 million use another form of tobacco (5). Although the overall number of Americans who smoke has declined, the numbers of young women who smoke, and the use of other tobacco products such as smokeless tobacco, has increased. Tobacco use is increasing in developing countries.

The medical consequences of nicotine use are common and constitute a significant public health problem. These include coronary artery disease, vascular disease, respiratory disease, and cancer, particularly of the lung, oral cavity, and pharynx. Many deleterious effects of tobacco are not due to nicotine, but are due to other toxic and carcinogenic compounds present in tobacco extract or smoke.

To maximize the absorption of nicotine, tobacco products are usually smoked in pipes, cigars, or cigarettes, or instilled intranasally or orally as snuff or smokeless tobacco. Following absorption from the lungs or buccal mucosa, nicotine levels peak rapidly and then decline with a half-life of 30 to 60 minutes.

Nicotine has several effects on the peripheral autonomic and central nervous systems. It is an agonist at nicotinic cholinergic receptors in parasympathetic and sympathetic autonomic ganglia. Nicotine produces salivation, increases gastric motility and acid secretion, and releases catecholamines, resulting in cardiac stimulation and peripheral vasoconstriction. Nicotine is a central-nervous-system stimulant, producing increased alertness, increased attention and concentration, and appetite suppression. The fact that tobacco use can prevent weight gain makes the drug especially attractive to young women.

Repeated use of nicotine produces tolerance and dependence. The degree of dependence is considerable, as over 70% of dependent individuals relapse within one year of stopping use. Cessation of nicotine use in dependent individuals is followed by a withdrawal syndrome characterized by increased irritability, decreased attention and concentration, an intense craving for and preoccupation with nicotine, anxiety, and depression (6,7). Withdrawal symptoms begin within several hours of cessation of use or reduction in dosage, and typically last about a week. Increased appetite with weight gain occurs in the weeks and months following cessation of chronic nicotine use.

The treatment of nicotine dependence consists of reducing or stopping use of tobacco use and minimizing nicotine withdrawal symptoms. Brief education and advice on smoking cessation provided by physicians has been shown to be effective in helping patients stop smoking, and it is now recommended that all physicians provide their patients with smoking cessation tools (8,9). The most successful treatment programs use cognitive-behavioral techniques to educate patients about the health hazards of tobacco and provide the patient with behavioral methods of coping with urges. Such programs can achieve 25–45% abstinence rates at 6 to 12 months. Although some programs use gradual reduction in tobacco use over days to weeks (nicotine fading) for detoxification, others suggest abrupt discontinuation (cold turkey).

Nicotine Replacement

Pharmacologic therapy with nicotine replacement is increasingly popular in the treatment of nicotine dependence. The principle of nicotine replacement therapy is to provide the nicotine-dependent patient with nicotine in a form not associated with the carcinogenic and irritant elements in tobacco products. The substitution of tobacco with alternative nicotine delivery systems allows the patient to address behavioral aspects of the habit without having to experience nicotine withdrawal. At a later time, plasma nicotine levels can be reduced and eventually discontinued in a slow and controlled fashion. Several systems of controlled nicotine delivery have been developed and introduced into clinical practice.

Transdermal Nicotine. Thin film impregnated with various doses of nicotine (7 mg, 14 mg, and 21 mg) are made into adhesive patches for transdermal administration. Nicotine patches deliver a predictable amount of nicotine and achieve steady-state plasma nicotine levels in the ranges achieved by smoking 10 to 30 cigarettes per day. The labeled dose refers to the amount of nicotine delivered rather than the amount of nicotine present in the patch. Transdermal nicotine is well absorbed, but the peak plasma concentrations are delayed by up to 10 hours after patch application.

Placebo-controlled clinical trials with transdermal nicotine show efficacy in smoking cessation treatment. Nicotine replacement therapy with transdermal nicotine significantly reduces nicotine withdrawal symptoms and increases the likelihood of successful smoking cessation (10,11). A recent meta-analysis of 17 studies involving over 5,000 patients indicated that transdermal nicotine patches produced quit rates of 27.1% at end of treatment and 21.8% at 6 month follow-up, compared to 13.1% and 8.4% for placebo groups, respectively.

Transdermal nicotine is used as follows. After stopping tobacco use, one patch is applied to uncovered skin each 24-hour period and the previous patch discarded. Some patches are labeled for use during the daytime only and are not worn while the patient is asleep. Typical transdermal nicotine treatment involves applying a high-dose patch to skin for 2 to 4 weeks, an intermediate dose patch for 2 to 4 weeks, and then the smallest dose patch for 2 to 4 weeks. Side effects include irritation from the patch and nicotine effects (nausea, cardiac effects, etc.). It is important that patients not use tobacco products or other nicotine replacement methods while using the patch, as toxic nicotine blood levels may occur. It is also important that patients receive behavior-oriented treatment while using the patch.

Nicotine Gum. This gum is a sweet, flavored polacrilex resin containing 2 or 4 mg of nicotine that is released slowly when the resin is chewed. Up to 90% of the nicotine in the resin is released into the saliva, although the amount of release and the rate of release depends upon the rate and duration of chewing. Nicotine is absorbed across the buccal mucosa, with a time to peak concentration of 15 to 30 minutes after start of chewing. The gum is marketed as Nicorette® and has recently been made available as an over-the-counter medication, as well as being available by prescription.

Patients must be instructed in the proper use of the gum, which is chewed slowly and intermittently whenever the individual feels the need for tobacco. When tingling of the mouth or tongue is perceived, chewing should cease for a short time, while still holding the gum in the mouth. Rapid chewing releases excess nicotine and may cause nausea and other side effects of nicotine toxicity. The gum is chewed for 20 to 30 minutes and then discarded. This method reduces tobacco craving and withdrawal discomfort with nicotine blood levels that rise and fall, mimicking smoking (12). Nicotine gum has been shown to be more effective than placebo in most clinical trials of its use in smoking cessation (13). Recent studies suggest that the 4 mg nicotine gum is more effective than the 2-mg gum in high nicotine-dependent smokers (14). Side effects of gum use include symptoms of nicotine toxicity and occlusive injuries of the teeth and dental appliances.

Most patients achieve stable gum use within a few days if they can stop smoking. A schedule for tapering gum use is planned after the daily maintenance dose is established. For example, a patient using 15 pieces of gum each day during the first week of treatment gradually reduces the number to 10 per day by the end of the first month and 5 per day by the end of the second month. Patients are typically able to discontinue nicotine gum after 3 to 6 months of treatment.

Nicotine Nasal Spray. Nicotine has recently become available in a solution for intranasal administration, to be used as source of nicotine replacement during smoking cessation treatment. The medication is administered in a concentration of 0.5 mg nicotine per 50 μL of metered spray vehicle. The recommended nicotine nasal dose is 1–2 mg (2–4 sprays) per hour, with a maximum recommended daily dose of 40 mg. When nicotine is administered intranasally, the time to peak plasma concentration is 4 to 15 minutes. The bioavailability of nicotine nasal spray solution is approximately 53%, although peak plasma concentrations achieved vary considerably due to individual differences in absorption and variations in usage. Rhinitis or other nasal abnormalities may reduce absorption, reduce peak plasma nicotine concentrations, and increase the time to peak plasma concentrations. Side effects of the spray include irritation of the nasal and pharyngeal cavities, in addition to the physiological side effects of nicotine. It is recommended that tapering of nasal nicotine doses begin after 2–4 weeks and that use not exceed 8 weeks to minimize the chances of developing dependence on the nicotine spray.

Nicotine Inhaler. Nicotine replacement using a nicotine inhaler (sometimes called a smokeless cigarette) to deliver nicotine orally by inhalation through a plastic tube has recently become available and is marketed as the Nicotrol® Inhaler. An active, disposable nicotine cartridge consisting of a porous plug impregnated with 10 mg of nicotine is placed in the plastic tube, and the patient inhales through a plastic mouthpiece as if smoking a cigarette. The device delivers a dose of 13 μg nicotine per puff, for up to 400 puffs. The delivered nicotine is primarily absorbed through the buccal mucosa. This method most mimics smoking, as it involves bringing the device to the mouth and inhaling to obtain nicotine dosing. In a study of 247 smokers who had previously failed other nicotine replacement therapy, continuous abstinence rates were 28% with the active drug, compared to 18% with the placebo inhaler (15). Common side effects include dyspepsia, transient coughing, and mouth irritation.

Other Medications for Smoking Cessation

Clonidine: Oral and Patch. Clonidine has been found to be effective in the treatment of smoking cessation and the amelioration of nicotine withdrawal symptoms, reducing cigarette craving and other symptoms of nicotine withdrawal in dependent cigarette smokers who stopped cold turkey (16). Several other investigators have confirmed the efficacy of clonidine in reducing nicotine withdrawal and improving quitting rates. However, in other studies on the treatment of nicotine withdrawal, the effects of clonidine have been more equivocal.

A transdermal clonidine therapeutic system, marketed as Catapres-TTS®, was developed for the treatment of hypertension and is approved by the U.S. FDA for that indication. The medication is incorporated into a transdermal delivery device designed to adhere to the skin (a patch) and to provide stable therapeutic levels of drug for period of one week. A microporous membrane controls the rate of clonidine delivery to the skin surface, whereupon the drug diffuses into the skin. The dose received is proportional to the patch surface area. Bioavailability and efficacy studies demonstrate comparability to oral clonidine preparations (17). However, due to cutaneous compartmental pharmacokinetics, there is a delay of 48 to 72 hours before the therapeutic blood levels are achieved and a similar persis-

tence in clonidine levels after the patch is removed. A large multicenter clinical trial used transdermal clonidine combined with behavioral treatment for smoking cessation (18). The clonidine doses used in this study were 0.1 to 0.2 mg per day. Although there was some decrease in nicotine withdrawal symptoms with clonidine, there was no significant increase in quit rates, compared with placebo. Nevertheless, the reduction in nicotine withdrawal symptoms with clonidine may have benefits in selected patients (19). Some investigators have found an improved response in female smokers.

Side effects of clonidine include hypotension and sedation. Clonidine is usually prescribed for a period of 3 to 4 weeks, with the dose gradually reduced over the detoxification period. As with other forms of treatment for nicotine dependence, clonidine should be used in conjunction with a behavioral recovery program.

TREATMENTS FOR OPIOID DEPENDENCE

Opioid abuse and dependence are significant social and medical problems in the U.S., with an estimated opioid addict population of greater than 500,000. These patients are frequent users of medical and surgical services because of the multiple medical sequelae of intravenous drug use, including infections (especially human immunodifficiency virus) and overdose. The crime and violence associated with the addict lifestyle engenders serious injuries to the addicts and to others.

Opiate drugs affect organ systems due to stimulation of receptors for endogenous hormones, enkephalins, endorphins, and dynorphins. There exist at least three distinct opioid receptors, which are designated by the Greek letters μ, κ, and δ (20). Drugs that act primarily through μ-receptor effects include heroin, morphine, and methadone; such drugs produce analgesia, euphoria, and respiratory depression. Drugs mediated through the κ-receptor include the so-called mixed agonist-antagonists, buprenorphine, butorphanol, and pentazocine, which produce analgesia, but less respiratory depression. The δ-receptor appears to bind endogenous opioid peptides.

The treatment of opioid dependence includes detoxification, followed by long-term rehabilitation. Several medications that use the principles of controlled drug delivery systems are used clinically for detoxification and rehabilitation of the opioid-dependent patient.

Opioid Detoxification: Clonidine

Opiate withdrawal, although rarely life threatening, is subjectively distressing. It is marked by increased sympathetic activity, intestinal hyperactivity, hypersensitivity to pain, and an intense craving to use more opiates. The peak period of acute withdrawal depends on the opiate used: for short-acting opiates such as morphine, heroin, or meperidine, the peak withdrawal is 1–3 days and duration is 5–7 days. For longer-acting opiates, such as methadone, the peak is 3–5 days and the duration 10–14 days.

Clonidine hydrochloride is an imidazoline derivative originally approved as an antihypertensive medication. Clonidine is an agonist at presynaptic α-2 adrenergic receptors and blocks the release of central and peripheral norepinephrine. Noradrenergic neurons in the locus ceruleus of the brain show increased neuronal activity during opiate withdrawal and this effect can be blocked by α-2 adrenergic agonists such as clonidine (21). On the basis of this observation, clonidine was tested clinically as a blocker of opioid withdrawal signs and symptoms (22,23). Subsequent double-blind clinical trials confirmed that clonidine was more effective than placebo and slightly less effective then a slow methadone taper in reducing signs and symptoms of opiate withdrawal in both inpatients and outpatients. Clonidine was found to be effective in patients withdrawing from either short-acting opioids, such as heroin, or long-acting opioids, such as methadone. However, clonidine was never formally approved by the FDA for the treatment of withdrawal in opioid-dependent patients.

Although most studies have been performed using oral clonidine, clonidine is available as a transdermal delivery system (described earlier), and this modality has been used successfully to treat opioid withdrawal (24). Advantages of the clonidine transdermal system include attainment of more constant plasma levels of clonidine (i.e., the avoidance of peaks and troughs) and the psychological benefit of an addicted patient not taking pills to relieve discomfort. A disadvantage of transdermal clonidine is a lag time of up to 72 hours for medication effect after applying the patch to the skin. Because of the lag time application of the clonidine transdermal patch and the attainment of new steady-state blood levels, supplementation of the patch with the more rapidly absorbed oral clonidine may be required to treat emergent withdrawal symptoms. Likewise, hypotension from overmedication with transdermal clonidine will take several hours to resolve after dose reduction.

When used clinically to treat opioid withdrawal, clonidine suppresses approximately 75% of opioid withdrawal signs and symptoms, especially autonomic hyperactivity (tremor, piloerection, tachycardia), anxiety, and gastrointestinal symptoms (cramps and diarrhea). Clonidine is administered in increasing doses such that opioid withdrawal signs and symptoms are decreased but blood pressure is maintained. A typical schedule for transdermal clonidine uses 0.1 mg on day 1 following discontinuation of opiates, 0.2 mg on day 2, 0.3 mg on day 3, and 0.4 mg on day 4. This maximal dose is continued for 5–7 additional days for short-acting opioids and 10–14 additional days for long-acting opioids.

Opioid withdrawal symptoms not significantly ameliorated by clonidine include drug craving, insomnia, and arthralgias and myalgias. Insomnia is best treated with a short-acting hypnotic such as chloral hydrate, and pain may respond to nonnarcotic analgesics such as a nonsteroidal antiinflammatory medication or acetaminophen. Side effects of clonidine include dry mouth, sedation, and orthostatic hypotension. Clonidine should be used cautiously in hypotensive patients and in those receiving other antihypertensive, antidepressants, stimulants, or antipsychotics.

Opioid Maintenance

The most widely used pharmacological treatments for opioid-dependent individuals include pharmacological

maintenance treatments with the opiate agonists methadone and L-α-acetylmethodol (LAAM), maintenance with the partial opiate agonist buprenorphine, and opiate antagonist therapy with naltrexone. All of these medications are best used in the setting of a structured, maintenance treatment program, which includes monitored medication administration; periodic, random urine toxicological screening to assess compliance; and intensive psychological, medical, and vocational services. Maintenance treatments reduce use of illicit opiates by increasing drug tolerance, thereby decreasing the subjective effects of illicitly administered opiates, and by stabilizing mood, thereby decreasing self-medication. Maintenance treatments also provide an incentive for treatment so that they may be exposed to other therapies.

Methadone Maintenance. Methadone is a synthetic opiate, which is orally active, possesses a long duration of action, produces minimal sedation or high, and has few side effects at therapeutic doses. A single daily dose of methadone will prevent the onset of withdrawal for at least 24 hours. Since its introduction in 1965, methadone maintenance has become a major modality of long-term treatment of opioid abuse and dependence (25). Currently, over 100,000 individuals are maintained on methadone in the U.S.

Although orally administered, an elaborate medication delivery system has evolved to ensure the controlled administration of this medication. Methadone is dissolved in small aliquots of a sweetened, flavored liquid vehicle and stored in single-dose plastic bottles. Each dose of methadone is dispensed daily and must be consumed under the direct observation of the dispensing nurse or pharmacist to ensure compliance. Frequent urine samples are obtained at randomly determined intervals for toxicological screening to confirm the presence of methadone and the lack of other illicit drugs. In addition, patients receive counseling, medical, and social services to assist them in achieving a drug-free lifestyle. Long-standing program participants are allowed contingency take-home doses of methadone, which patients may self-administer. However, these are withdrawn for missing appointments or for evidence of illicit drug use. Doses of methadone usually range from 20 mg per day to over 100 mg per day. Higher doses are shown to be generally associated with better retention in treatment.

Many studies have shown the efficacy of methadone maintenance in the treatment of addicts who are dependent on heroin and other opiates. Methadone-treated patients show increased treatment retention, improved physical health, decreased criminal activity, increased employment, and decreased chance of becoming HIV positive (26). Methadone is most effective in the context of a program that provides intensive psychosocial and medical services, and adequate methadone dosing. The use of methadone for maintenance is highly regulated by government agencies. Senay (27) provides an excellent recent review of the theory and practice of methadone maintenance.

L-α-Acetylmethodol Acetate (LAAM). A long-acting, orally active opiate, the pharmacological properties of LAAM are similar to methadone. Studies on LAAM have shown it to be equal or superior to methadone maintenance in reducing IV drug use, when used in the context of a structured maintenance treatment program (28). The advantages of LAAM include a slower onset of effects and a longer duration of action than methadone. This allows LAAM to be administered only 3 times per week, reducing the cost of preparation and monitoring of medication and reducing the use of take-home medications that may be diverted to illicit use. Patients treated with LAAM should be started on 20 mg administered 3 times weekly, with the dose increased weekly in 10 mg increments as necessary. Doses up to 80 mg 3 times weekly are safe and effective.

Sublingual Buprenorphine. Buprenorphine is a partial agonist opiate medication (mixed agonist-antagonist), originally used medically as an analgesic. It has high affinity for the μ opioid receptor and the κ receptor. Buprenorphine possesses both agonist and antagonist properties—agonist properties predominate at lower doses and antagonist properties predominate at higher doses. Cessation in buprenorphine in dependent individuals results in a withdrawal syndrome that is much milder than that observed with pure opioid agonists. These properties of the drug suggested its use as a maintenance medication in the treatment of chronic opioid dependence. However, oral buprenorphine has poor bioavailability and only parenteral preparations of the medication are used.

Sublingual (SL) administration is an effective way of administering medication that may not be orally active. SL administration of buprenorphine results in effective medication plasma levels and was therefore tested in the treatment of opioid dependence. In the setting of a structured treatment program, daily dosing of SL buprenorphine was found to effective in the maintenance treatment of narcotics addicts, reducing illicit drug use (29–31). Buprenorphine may also reduce concomitant cocaine use in opiate addicts (32).

Buprenorphine doses usually range from 4 mg per day to up to 16 mg per day, administered sublingually. Advantages of buprenorphine include a milder withdrawal syndrome upon discontinuation and less potential for abuse, as agonist effects diminish at higher doses. Opioid-dependent patients may be started on 2 to 4 mg buprenorphine immediately after opiates are discontinued, and the dose of buprenorphine titrated to 8 to 16 mg over several days (33).

Naltrexone. Opioid antagonist therapy reduces the use of illicit drugs by blocking the effect of the drugs at neurotransmitter receptors, leading to decreased use. There is some evidence that opiate antagonists may block craving for opiates as well. Naltrexone (Trexan®) is a long-acting, orally active opioid antagonist, which when taken regularly, entirely blocks μ opioid receptors and thus blocks the euphoric, analgesic, and sedative properties of opioids (34). Oral naltrexone is administered either daily to detoxified opioid users at a dose of 50 mg, or 3 times weekly at doses of 100 mg, 100 mg, and 150 mg. Although naltrexone is quite effective when taken as prescribed, most studies have demonstrated poor medication compliance among

subjects. The drug appears to be most effective in motivated individuals with good social support and appears less helpful for heroin addicts or less motivated individuals.

Because of the low compliance with oral naltrexone formulations, there has been interest in the development of alternative drug delivery systems to improve medication compliance. Two parenteral depot formulations of naltrexone have been developed; injectable naltrexone microspheres coated with poly(DL-lactic acid) (35) and an implantable biodegradable copolymer polylactic/glycolic matrix delivery system (36,37). The injectable microspheres have been tested on animals and humans and found to result in plasma naltrexone levels that would effectively block exogenous opioids and that are stable for at least 30 days. Problems with residual organic solvent used in the microsphere preparation have delayed FDA approval of this method; however, new preparation techniques avoid the problem with organic solvents, and the injectable microspheres are being tested again. Both of these methodologies remain experimental but are undergoing continued testing.

TREATMENTS FOR ALCOHOL DEPENDENCE

Disulfiram

An irreversible inhibitor of the enzyme acetaldehyde dehydrogenase, disulfiram (Antabuse®) is used as an adjunctive treatment in selected alcoholic patients (38,39). If alcohol is consumed in the presence of disulfiram, the toxic metabolite acetaldehyde accumulates in the body, producing tachycardia, skin flushing, diaphoresis, dyspnea, nausea, and vomiting. Hypotension and death may occur if large amounts of alcohol are consumed. This unpleasant and potentially dangerous reaction provides a strong deterrent to the consumption of alcohol. Patients using disulfiram must be able to understand its benefits and risks. Alcohol present in foods, shaving lotion, mouthwashes, or over-the-counter medications may also produce a disulfiram reaction and must be avoided.

As increased disulfiram compliance improves treatment success, there has been interest in the development of long-lasting depot formulations of disulfiram to improve medication compliance (40). Several methods for depot disulfiram administration have been developed, including the implantation of disulfiram surrounded by a semipermeable membrane to retard absorption, direct tablet implantation, and the subcutaneous injection of disulfiram in vehicles such as methylcellulose or polysorbate 80. Unfortunately, most clinical studies have shown an inability of implanted forms of disulfiram to induce a significant disulfiram–alcohol reaction when subjects are challenged with alcohol (41).

Naltrexone

In clinical trials with recently abstinent human alcoholics, subjects treated with the opioid antagonist naltrexone had lower rates of relapse to heavy drinking, and more total abstinence, than did a placebo group (42,43). Subjects receiving naltrexone also report decreased craving and decreased high from alcohol. Naltrexone is thought to act by blocking the alcohol-induced release of dopamine in the nucleus accumbens and other brain areas that control the reinforcing properties of drugs and alcohol.

One factor that appears important for the efficacy of naltrexone is medication compliance. Two placebo-controlled clinical trials with oral naltrexone demonstrated significant efficacy in reducing drinking only in subjects that showed high compliance with medication ingestion (44,45). Thus, there is interest in the development of alternative drug delivery systems for naltrexone that will enhance compliance and optimize medication effects to improve treatment.

A recent report comparing oral naltrexone with injectable sustained-release naltrexone microspheres (35) in 20 patients found comparable effects of the two different preparations in reducing alcohol consumption (46). Side effects of the oral and sustained-release preparations were also similar. More research needs to be conducted on the sustained-release forms of naltrexone; however, the initial results are encouraging.

SUMMARY

Controlled drug delivery systems have been applied to the treatment of several addictive disorders, including nicotine dependence, opioid dependence, and alcohol dependence. In the case of nicotine dependence, several commercial products are available, giving clinicians and patients considerable flexibility in drug dosing. Controlled drug delivery systems are currently being studied in the maintenance treatment of alcoholism and opioid dependence.

BIBLIOGRAPHY

1. D.A. Regier, M.E. Farmer, and D.S. Rae, *J. Am. Med. Assoc.* **264**, 2511–2518 (1990).
2. D.P. Rice, *Alcohol Health Res. World* **17**, 10–11 (1990).
3. J.M. McGinnis and W.H. Foege, *J. Am. Med. Assoc.* **270**, 2201–2212 (1993).
4. American Psychological Association, *Diagnostic and Statistical Manual*, 4th ed., APA Press, Washington, D.C., 1994.
5. Centers for Disease Control, *Morbid. Mortal. Wkly. Rep.* **43**, 342–346 (1994).
6. J.R. Hughes and D.K. Hatsukami, *Arch. Gen. Psychiatry* **43**, 289–294 (1986).
7. N. Breslau, M. Kilbey, and P. Andreski, *Am. J. Psychiatry* **149**, 464–469 (1992).
8. H.L. Greene, R. Goldberg, and J.K. Ockene, *J. Gen. Intern. Med.* **3**, 75–87 (1988).
9. Agency for Health Care Policy and Research, *Clin. Pract. Guideline* **18B**, 1–10 (1996).
10. J.L. Tang, M. Law, and N. Wald, *Br. Med. J.* **308**, 21–26 (1994).
11. Transdermal Nicotine Study Group, *J. Am. Med. Assoc.* **266**, 3133–3138 (1991).
12. N.G. Schneider, *Addict. Behav.* **9**, 149–156 (1984).
13. M.G. Goldstein and R.S. Niaura, in J.A. Cocores, ed., *Clinical Management of Nicotine Dependence*, Springer-Verlag, New York, 1991, pp. 181–195.
14. N. Herrera et al., *Chest* **108**, 447–451 (1995).

15. A. Hjalmarson, F. Nilsson, L. Sjostrom, and O. Wiklund, *Arch. Intern. Med.* **157**, 1721–1728 (1997).
16. A.H. Glassman, F. Stetner, B.T. Walsh, and P.S. Raizman, *J. Am. Med. Assoc.* **259**, 2863–2866 (1988).
17. D.T. Lowenthal et al., *Am. Heart J.* **112**, 893–900 (1986).
18. A.V. Prochazka et al., *Arch. Intern. Med.* **152**, 2065–2069 (1992).
19. J.J. Green and D.H. Cordes, *West. J. Med.* **151**, 79–80 (1989).
20. T. Reisine and G. Pasternack, in J.G. Hardman and L.E. Limbird, eds., *Goodman and Gilman's The Pharmacological Basis of Therapeutics*, 9th ed., McGraw-Hill, New York, 1996, pp. 521–555.
21. G. Aghajanian, *Nature (London)* **276**, 186–187 (1978).
22. D.S. Charney et al., *Arch. Gen. Psychiatry* **38**, 1273–1278 (1981).
23. M.S. Gold, A.C. Pottash, D.R. Sweeney, and H.D. Kleber, *J. Am. Med. Assoc.* **234**, 343–344 (1979).
24. L. Spencer and M. Gregory, *J. Substance Abuse Treat.* **6**, 113–117 (1989).
25. V.P. Dole and M. Nyswander, *J. Am. Med. Assoc.* **93**, 646–650 (1965).
26. J.C. Ball, W.R. Lange, C.P. Myers, and S.R. Friedman, *J. Health Soc. Behav.* **29**, 214–226 (1988).
27. E. Senay, *Int. J. Addict.* **20**, 803–821 (1985).
28. W. Ling, R.A. Rawson, and P.A. Compton, *J. Psychoact. Drugs* **26**, 119–128 (1994).
29. P.A. Compton, D.R. Wesson, V.C. Charuvastra, and W. Ling, *Am. J. Addict.* **5**, 220–230 (1996).
30. R.E. Johnson, J.J. Jaffe, and P.J. Fudala, *J. Am. Med. Assoc.* **267**, 2750–2755 (1992).
31. T.R. Kosten, C. Morgan, and H.D. Kleber, *Am. J. Drug Alcohol Abuse* **17**, 119–128 (1991).
32. T.R. Kosten, H.D. Kleber, and C. Morgan, *Biol Psychiatry* **26**, 637–639 (1989).
33. T.R. Kosten, C. Morgan, and H.D. Kleber, *NIDA Res. Monogr.* **121**, 101–119 (1992).
34. R.B. Resnick, E. Schuyten-Resnick, and A.M. Washton, *Annu. Rev. Pharmacol. Toxicol.* **20**, 463–470 (1980).
35. E.S. Nuwayser, D.J. DeRoo, P.D. Balskovich, and A.G. Tsuk, *NIDA Res. Monogr.* **105**, 532–533 (1991).
36. R.H. Reuning et al., *J. Pharmacokinet. Biopharm.* **11**, 369–387 (1983).
37. A.C. Sharon and D.L. Wise, *NIDA Res. Monogr.* **28**, 194–213 (1981).
38. C. Brewer, *Alcohol Alcohol.* **28**, 383–395 (1993).
39. J. Chick, K. Gough, and W. Falkowski, *Br. J. Psychiatry* **161**, 84–89 (1992).
40. M.D. Faiman, K.E. Thompson, and K.L. Smith, in C.A. Naranjo and E.M. Sellers, eds., *Novel Pharmacological Interventions for Alcoholism*, Springer-Verlag, New York, 1992, pp. 267–272.
41. J.C. Hughes and C.C. Cook, *Addiction* **92**, 381–395 (1997).
42. S.S. O'Malley et al., *Arch. Gen. Psychiatry* **49**, 881–887 (1992).
43. J.R. Volpicelli, A.I. Alterman, M. Hayashida, and C.P. O'Brien, *Arch. Gen. Psychiatry* **49**, 876–880 (1992).
44. J. Chick, *10th World Psychiatry Conf.*, Madrid, Spain, Aug. 24, 1996.
45. J.R. Volpicelli et al., *Arch. Gen. Psychiatry*, **54**, 737–742 (1997).
46. H.R. Kranzler, V. Modesto-Lowe, and E.S. Nuwayser, *Alcohol Clin. Exp. Res.* **22**, 1074–1079 (1998).

BIOADHESIVE DRUG DELIVERY SYSTEMS

EDITH MATHIOWITZ
DONALD CHICKERING
JULES S. JACOB
CAMILLA SANTOS
Brown University
Providence, Rhode Island

KEY WORDS

Adsorption theory
Bioadhesion
Bioadhesive drug delivery systems
Bioadhesive polymers
Electronic theory
Fracture theory
Mucus
Oral delivery
Wetting theory

OUTLINE

Background of Bioadhesion
- Introduction
- Mucus and the Mucosal Layer
- Bioadhesion and Mucoadhesion
- Mechanisms of Bioadhesion
- Theories on Bioadhesion
- Methods to Evaluate Bioadhesive Interactions
- Bioadhesive Polymers
- Applications of Bioadhesive Polymers

Development of Bioadhesive Microspheres: A Case Study
- A Novel Electrobalance-Based Tensiometer
- Bioadhesive Measurements
- Characterization of Potential Bioadhesive Polymers
- GI Transit and Bioavailability of Low-Molecular-Weight Drugs
- Bioadhesive Microspheres for Oral Delivery of Proteins and Genes
- Concluding Remarks

Acknowledgments
Bibliography

The goals of this article are to give a general introduction to the field of bioadhesion, to discuss some specific theories of bioadhesion as well as methods involved in its quantification, and end with an overview of general applications of bioadhesion in the medical field. The current literature contains an enormous amount of material on bioadhesion, preventing us from including all the information available in the field, so we advise interested readers desiring further information to consult general books on bioadhesion (1–3).

Our approach to discussing the current trends in bioadhesion in this article is a bit unusual; we first cover the general concepts of bioadhesion and discuss current applications of bioadhesive polymers. Then we deviate from the norm and discuss what we know best: our work in bioadhesion over the past six years. We thought it more worthwhile to introduce, as a case study, the target of research in our laboratory. Thus, in the following section we discuss the general concept of bioadhesion, and in the section after that, "Development of Bioadhesive Microspheres: A Case Study," we describe in more detail several aspects of our research, including where appropriate the work of others as well. Our research covers five main focal points: (*1*) the development of an accurate and reproducible method to analyze the bioadhesive interaction between individual polymer microspheres and soft tissues in a controlled environment closely mimicking in vivo conditions; (*2*) the quantification of the bioadhesive properties of hydrogel and thermoplastic microspheres, including the characterization of a series of polymers suitable for bioadhesive drug delivery systems; (*3*) the use of several in vitro characterization techniques to gain insight into the mechanism and forces responsible for bioadhesion; (*4*) the determination of the effects bioadhesive polymers have on in vivo drug delivery by measuring gastrointestinal (GI) transit time; and (*5*) the evaluation of the bioavailability of encapsulated drugs such as dicumarol, insulin, and plasmid DNA.

BACKGROUND OF BIOADHESION

Introduction

Over the past 20 years, interaction among the fields of polymer and material science and the pharmaceutical industry has resulted in the development of what are known as drug delivery systems (DDSs), or controlled-release systems (4–7). The advantages of using polymer-based devices over traditional dosage forms include (*1*) the ability to optimize the therapeutic effects of a drug by controlling its release into the body; (*2*) lower and more efficient doses; (*3*) less frequent dosing; (*4*) better patient compliance; (*5*) flexibility in physical state, shape, size, and surface; (*6*) the ability to stabilize drugs and protect against hydrolytic or enzymatic degradation; and (*7*) the ability to mask unpleasant taste or odor (4–7).

DDSs are already in widespread use, and their applications seem limited only by the imaginations of their inventors. They have been designed in the forms of reservoirs, homogeneous matrices, emulsions, capsules, rods, tablets, patches, and pumps (7–13). Systems have been engineered to release in response to pH, ultrasonic, magnetic, photochemical, or thermal stimulation (7,14–16). Ad-

ministration routes, selected to target specific absorption pathways, have included oral, rectal, transdermal, subcutaneous, inhalatory, intrauterine, intravaginal, and intravenous (4).

Owing to the fact that intimate contact between a delivery device and the absorbing cell layer will improve both effectiveness and efficiency of the product, many researchers have recently focused on developing bioadhesive drug delivery systems (BDDSs) (17). The term *bioadhesion* refers to either adhesion between two biological materials or adhesion between some biological material (including cells, cellular secretions, mucus, extracellular matrix, and so on) and an artificial substrate (metals, ceramics, polymers, etc.). Bioadhesive materials have found numerous applications in the medical field. For example, cyanoacrylates (commonly known as "super glues") have frequently been used for both orthopedic and dental applications. In terms of the pharmaceutical industry, bioadhesion generally refers to adhesion between a polymer-based delivery system and soft tissue in the presence of water (18). Possible means of administration for BDDSs include the ocular, respiratory, buccal, nasal, GI, rectal, urethral, and vaginal routes (17–21). GI bioadhesive devices that can be administered orally are of considerable interest owing to the ease of administration and targeted contact with the absorbing intestinal epithelium (1,4,22,23).

Systemic drug delivery via absorption into the bloodstream through the GI epithelium can be limited by drug degradation during the first pass through the liver; however, the GI mucosa offers several advantages as an administration site over other mucus membranes. These advantages include the following: (*1*) the oral administration route is familiar, convenient, and an accepted means of dosing for most people; (*2*) the GI epithelium offers a large surface area for absorption; and (*3*) the GI epithelium provides a close connection with a vast blood supply. The development of efficient orally delivered BDDSs could enable the following four important effects: (*1*) enhanced bioavailability and effectiveness of drug due to targeted delivery to a specific region of the GI tract, (*2*) maximized absorption rate due to intimate contact with the absorbing membrane and decreased diffusion barriers, (*3*) improved drug protection by polymer encapsulation and direct contact with absorbing cell layers, and (*4*) longer gut transit time resulting in extended periods for absorption (23–25).

Many researchers have developed various techniques for determining and evaluating bioadhesion. Each of these systems has typically been tailored to the needs of a particular experiment (see "Methods to Evaluate Bioadhesive Interactions"). For this reason, the experimental conditions and resulting data have varied greatly between studies. It has been very difficult to compare one set of experimental findings with another. Also, owing to variations in mucus, tissue, tissue preparation techniques, polymers (their molecular weight, degree of cross-linking, degree of hydration, etc.), and polymer geometry, many of the experiments have lacked reproducibility and shown statistically high variations in data (26,27). Surprisingly, our lab has been the only group to attempt to mimic both physiological conditions and final delivery device geometries in a single in vitro experiment (28).

In developing orally administered BDDSs, it is important to realize that the targeted GI tissue is coated with a continuous layer of protective secretions known as mucus. With this in mind, BDDSs must be designed to either penetrate this boundary layer and bind to the underlying epithelium or adhere directly to the mucus (29). In either event, because mucus and epithelial cells are continuously sloughed off and replaced, it is unrealistic to expect a delivery device to adhere permanently to the luminal surface of the digestive system (30,31). Instead, a more feasible goal for oral bioadhesive systems should be delayed transit through the gut, during which time intimate contact is achieved between bioadhesive and target tissue. Once adhesion has occurred, the device can deliver its bioactive contents directly to the absorbing cell layer, minimizing losses to the luminal environment.

Mucus and the Mucosal Layer

The epithelium of the gut is protected by a continuous coating of mucus, which is secreted by a number of different cells: (*1*) mucus neck cells, from the necks of the gastric glands in the stomach, produce soluble mucus; (*2*) surface epithelial goblet cells produce visible mucus in the stomach as well as in the small and large intestines; (*3*) cells collectively known as Brunner's glands produce mucus in the proximal duodenum; and (*4*) goblet cells lining the crypts of Lieberkühn produce mucus in both the large and small intestines (32,33). Once produced, mucus is stored in large granules and then released either by exocytosis or exfoliation of the entire cell (32). Mucus in the GI tract functions mainly as a lubricant, protecting against abrasive, mechanical damage from food. It also creates a barrier against destruction of the epithelial cell layer by harsh gastric pH conditions and digestive enzymes (34–36). Mucus secretion is directly stimulated by even the smallest mechanical or chemical irritation of the mucosa (32).

Both the composition and thickness of the mucus layer vary with location, degree of GI activity, sex, and state of health (37,38). In general, it can be as thick as 1 mm in humans and consists mainly of water (up to 95%), electrolytes, proteins, lipids, and glycoproteins (29,39,40).

The glycoprotein mucins (molecular weight of approximately 2 million) give mucus its unique gel-like characteristics. These glycoproteins consist of a protein core (≅18.6–25.6% by weight) with covalently attached carbohydrate side chains (≅81.4–74.4% by weight) (39,41–43). Although specific composition varies with location (44), in general there are about four times as many amino acid groups in the protein core as there are side chains (Fig. 1) (29,42). Each of the side chains is anywhere from 2 to 20 sugars in length and terminates with either L-fucose or sialic acid. Mucus glycoproteins in solution are anionic polyelectrolytes at pH greater than 2.6. Disulfide, electrostatic, and hydrophobic interactions help to entangle mucin chains to produce the gel-like properties characteristic of mucus (18,43,45).

A pH gradient exists in the mucus layer from the cell surface to about 750 μm into the center of the lumen that varies with location along the gut (46). The pH at the epithelial surface is maintained around 7 in all areas of the

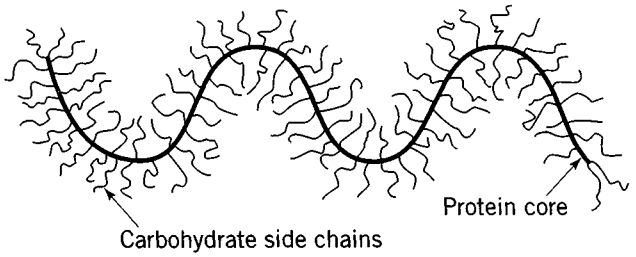


Figure 1. Schematic diagram of a glycoprotein mucin, showing protein core with carbohydrate side chains.

GI tract owing to alkaline fluids that are secreted along with mucus, while luminal pH may range anywhere from 2.0 (stomach) to 7.6 (duodenum) (32,36).

Below the mucus layer of the intestine are the cellular layers of the gut wall, consisting of epithelium, lamina propria, and muscularis mucosa. These tissues and mucus layers are collectively known as mucosa. The epithelium is a single layer of columnar cells that are arranged into fingerlike projections called villi. Each epithelial cell is blanketed with a coating of microvilli on its apical surface, known as the brush border. Within the lamina propria are numerous capillaries and lymphatic vessels or lacteals as well as mucus-secreting glands (32,47). Drugs and other molecules must first pass the barriers of the mucus layer, brush border, and epithelium before reaching the capillaries of the lamina propria. The muscularis mucosa is a thin, smooth muscle layer that produces folds in the epithelium known as valves or folds of Kerckring. The folds help to increase the absorbing surface area of the gut (33,47). In fact, the total absorptive area of the small intestine is approximately 250 m^2, which is about the size of a tennis court (33).

Bioadhesion and Mucoadhesion

Although the term *bioadhesion* can refer to any bond formed between two biological surfaces or a bond between a biological and synthetic surface, in this article it will specifically be used to describe the adhesion between polymer samples, either synthetic or natural, and soft tissue (GI mucosa). Although the target of orally administered BDDSs may be the epithelial cell layer, the actual adhesive bond may form with either the cell layer, the continuous mucus layer, or a combination of the two. In the instances when the bond involves the mucus coating and the polymer device, many authors use the term *mucoadhesion* (48,49). In this article, *bioadhesion* is meant to include all three possible adhesive conditions, and *mucoadhesion* is used only when describing a bond between polymer and mucus.

Mechanisms of Bioadhesion

The mechanisms involved in the formation of a bioadhesive bond are not completely clear. To develop ideal BDDSs, it is important to try to describe and understand the forces that are responsible for adhesive bond formation. Most research has focused on analyzing the bioadhesive bond between polymer hydrogels and soft tissue. The process involved in the formation of such bioadhesive bonds has been described in three steps: (*1*) wetting and swelling of polymer to permit intimate contact with biological tissue, (*2*) interpenetration of bioadhesive polymer (BP) chains and entanglement of polymer and mucin chains, and (*3*) formation of weak chemical bonds (17,19). In the case of hydrogels, it has been determined that several polymer characteristics are required to obtain adhesion: (*1*) sufficient quantities of hydrogen-bonding chemical groups (-OH and -COOH), (*2*) anionic surface charges, (*3*) high molecular weight, (*4*) high chain flexibility, and (*5*) surface tensions that will induce spreading into the mucus layer (49). These characteristics favor the formation of bonds that are either mechanical or chemical in nature.

Mechanical or Physical Bonds. Mechanical bonds can be thought of as a physical connection of polymer and tissue, similar to interlocking puzzle pieces. On a macroscopic level, they can be caused by the inclusion of one substance into the cracks or crevices of another (50). On a microscopic scale, they involve the physical entanglement of mucin strands with flexible polymer chains and the interpenetration of mucin strands into the porous structure of a polymer substrate. The rate of penetration of polymer strands into the mucin layer is dependent on chain flexibility and diffusion coefficients of each. The strength of the adhesive bond is directly proportional to the depth of penetration of the polymer chains. Other factors that influence bond strength include the presence of water, the time of contact between the materials, and the length and flexibility of the polymer chains (18).

Chemical Bonds. Chemical bonds can include strong primary bonds (i.e., covalent bonds) as well as weaker secondary forces such as ionic bonds, Van der Waals' interactions, and hydrogen bonds. Although it is possible to develop polymers with reactive functional groups that could theoretically form permanent covalent bonds with proteins on the surface of the epithelial cells, there are several reasons why investigators have not focused on such systems. First, the mucus barrier may inhibit direct contact of polymer and tissue. Second, permanent chemical bonds with the epithelium may not produce a permanently retained delivery device because the epithelial cells are exfoliated every three to four days. Third, biocompatibility of such binding has not been thoroughly investigated and could pose significant problems (18). For these reasons, most researchers have focused on developing hydrogel, mucoadhesive systems that bond through either Van der Waals' interactions or hydrogen bonds. Although these forces are very weak, strong adhesion can be produced through numerous interaction sites. Therefore, polymers with high molecular weights and greater concentrations of reactive polar groups (such as -COOH and -OH) tend to develop more intense mucoadhesive bonds (26,51).

Theories on Bioadhesion

Several theories have been developed to describe the processes involved in the formation of bioadhesive bonds. These theories have been used as guidelines in engineering

possible BDDSs. Some are based on the formation of mechanical bonds, while others focus on chemical interactions.

The Electronic Theory. The electronic theory is based on an assumption that the bioadhesive material and the glycoprotein mucin network have different electronic structures. On this assumption, when the two materials come in contact with each other, electron transfer will occur in an attempt to balance Fermi levels, causing the formation of a double layer of electrical charge at the interface. The bioadhesive force is believed to be due to attractive forces across this electrical double layer. This system is analogous to a capacitor, where the system is charged when the adhesive and substrate are in contact and discharged when they are separated (52). The electronic theory has produced some controversy regarding whether the electrostatic forces are an important *cause* or the *result* of the contact between the bioadhesive and the biological tissue (53).

The Adsorption Theory. This theory states that the bioadhesive bond formed between an adhesive substrate and intestinal mucosa is due to Van der Waals' interactions, hydrogen bonds, and related forces (54,55). The adsorption theory is the most widely accepted theory of adhesion and has been studied in depth by both Kinloch and Huntsberger (50,56,57).

The Wetting Theory. The ability of bioadhesive polymers or mucus to spread and develop intimate contact with their corresponding substrate is one important factor for bond formation. The wetting theory, which has been used predominantly in regards to liquid adhesives, uses interfacial tensions to predict spreading and, in turn, adhesion (49,58–60).

Figure 2 schematically represents a BP spreading over soft tissue. The contact angle (ϕ), which should be zero or near zero for proper spreading, is related to interfacial tensions (γ) through Young's equation:

$$\gamma_{tg} = \gamma_{bt} + \gamma_{bg} \cos\phi \quad (1)$$

where the subscripts t, g, and b stand for tissue, gastrointestinal contents, and bioadhesive polymer, respectively. For spontaneous wetting to occur, ϕ must equal zero and, therefore, the following must apply (49):

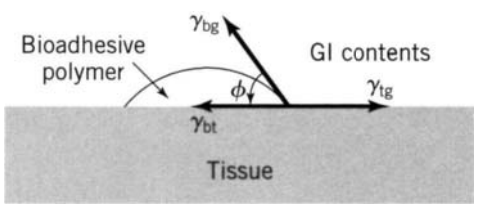


Figure 2. Schematic diagram showing the interfacial tensions involved in spreading.

$$\gamma_{tg} \geq \gamma_{bt} + \gamma_{bg} \quad (2)$$

The spreading coefficient, $S_{b/t}$, of a bioadhesive over biological tissue in vivo can be used to predict bioadhesion and can be determined as follows:

$$S_{b/t} = \gamma_{tg} - \gamma_{bt} - \gamma_{bg} \quad (3)$$

For the bioadhesive to displace GI luminal contents and make intimate contact with the biological tissue (i.e. spreading), the spreading coefficient must be positive. Therefore, it is advantageous to maximize the interfacial tension at the tissue/GI contents interface (γ_{tg}) while minimizing the surface tensions at the other two interfaces (γ_{bt} and γ_{bg}) (49).

It is theoretically possible to determine each of the parameters that make up the spreading coefficient. The interfacial tension of the tissue/GI contents interface (γ_{tg}) can be determined in vitro using classical Zisman analysis (61,62), although it has not been done. The interfacial tension at the BP/GI contents interface (γ_{bg}) can be experimentally determined using traditional, surface tension–measuring techniques such as the Wilhelmy plate method. Lastly, it has been shown that the BP/tissue interfacial tension (γ_{bt}) can be calculated as follows (63,64):

$$\gamma_{bt} = \gamma_b + \gamma_t - 2F(\gamma_b\gamma_t)^{1/2} \quad (4)$$

where values of the interaction parameter (F) can be found in previously published papers (65,66). Extensive studies have been conducted to determine the surface tension parameters for several biological tissues (γ_t) and many commonly used biomaterials (γ_b) (67).

The BP/tissue interfacial tension (γ_{bt}) has been shown to be proportional to the square root of the polymer–polymer Flory interaction parameter (c):

$$\gamma_{bt} \sim c^{1/2} \quad (5)$$

When c is small, the bioadhesive and biological components are similar structurally. This results in increased spreading and, therefore, greater adhesive bond strength (68,69).

Besides the spreading coefficient, another important parameter that may indicate the strength of an adhesive bond is the specific work of adhesion (W_{bt}). According to the Dupré equation, this is equal to the sum of the surface tensions of the tissue and bioadhesive, minus the interfacial tension (70):

$$W_{bt} = \gamma_b + \gamma_t - \gamma_{bt} \quad (6)$$

Thus, using the wetting theory, it is possible to calculate spreading coefficients for various bioadhesives over biological tissues and predict the intensity of the bioadhesive bond. By measuring surface and interfacial tensions, it is possible to calculate work done in forming an adhesive bond. Both spreading coefficients and bioadhesive work directly influence the nature of the bioadhesive bond and therefore provide essential information for development of BDDSs.

The Diffusion Theory. The diffusion theory suggests that interpenetration and entanglement of BP chains and mucus polymer chains produce semipermanent adhesive bonds (Fig. 3), and bond strength is believed to increase with the depth of penetration of the polymer chains (71).

Penetration of BP chains into the mucus network, and vice versa, is dependent on concentration gradients and diffusion coefficients. Obviously, any cross-linking of either component will tend to hinder interpenetration, but small chains and chain ends may still become entangled. It has not been determined exactly how much interpenetration is required to produce an effective bioadhesive bond, but it is believed to be in the range of 0.2–0.5 μm. It is possible to estimate penetration depth (l) with the following equation:

$$l = (tD_b)^{1/2} \tag{7}$$

where t is time of contact and D_b is the diffusion coefficient of the biomaterial in mucus. The maximum achievable bioadhesive bond for a given polymer is believed to occur when the depth of penetration is approximately equal to the end-to-end distance of the polymer chains (72,73).

For diffusion to occur, it is important to have good solubility of one component in the other; the BP and mucus should be of similar chemical structure. Therefore, the strongest bioadhesive bonds should form between those biomaterials whose solubility parameters (δ_b) are similar to those of mucus glycoproteins (δ_g) (50). Thus, the diffusion theory states that interpenetration and entanglement of polymer chains are responsible for bioadhesion. The more structurally similar a bioadhesive is to mucus, the greater the mucoadhesive bond will be.

The Fracture Theory. The most useful theory for studying bioadhesion through tensile experiments has been the fracture theory, which analyzes the forces required to separate two surfaces after adhesion. The maximum tensile stress (σ_μ) produced during detachment can be determined by dividing the maximum force of detachment, F_m, by the total surface area (A_o) involved in the adhesive interaction:

$$\sigma_m = F_m/A_o \tag{8}$$

In a uniform single-component system, fracture strength (σ_f), which is equal to the maximum stress of detachment (σ_m), is proportional to fracture energy (γ_c), Young's modulus of elasticity (E), and the critical crack length (c) of the fracture site, as described in the following relationship (74):

$$\sigma_f \sim (\gamma_c E/c)^{1/2} \tag{9}$$

Fracture energy (γ_c) can be obtained from the sum of the reversible work of adhesion, W_r (i.e., the energy required to produce new fracture surfaces) and the irreversible work of adhesion, W_i (i.e., the work of plastic deformation at the tip of the growing crack), where both values are expressed per unit area of the fracture surface (A_f):

$$\gamma_c = W_r + W_i \tag{10}$$

The elastic modulus of the system (E) is related to stress (σ) and strain (ϵ) through Hooke's law:

$$E = \left[\frac{\sigma}{\epsilon}\right]_{\epsilon \to 0} = \left[\frac{F/A_0}{\Delta l/l_0}\right]_{\Delta l \to 0} \tag{11}$$

In this equation, stress is equal to the changing force (F) divided by the area (A_0), and strain is equal to the change in thickness (Δl) of the system divided by the original thickness (l_0) (75).

One critical assumption in equation 11 is that the system being investigated is of known physical dimensions and composed of a single uniform-bulk material. Considering this, equations 9 and 11 cannot be applied to analyze the fracture site of a multicomponent bioadhesive bond between a polymer microsphere and either mucus or mucosal tissue. For such analysis, the equations must be expanded to accommodate dimensions and elastic moduli of each component (76). Furthermore, to determine fracture properties of an adhesive union from separation experiments, failure of the adhesive bond must be assumed to occur at the bioadhesive interface (73). However, it has been demonstrated that fracture rarely, if ever, occurs at the interface but instead occurs close to it (75,77).

Although these limitations exist, because the fracture theory deals only with analyzing the adhesive force required for separation, it does not assume or require entanglement, diffusion, or interpenetration of polymer chains. Therefore, it is appropriate to use equation 8 to calculate fracture strengths of adhesive bonds involving hard, bioadhesive materials in which the polymer chains may not penetrate the mucus layer (though one must be aware that the measurement may be the fracture strength of the cohesive properties of the mucus instead of the fracture strength of the adhesive bond). Other theories that could be applicable to such a system are the wetting, electronic, and adsorption theories, so long as it is assumed that Van der Waals' interactions and hydrogen bonds can form between flexible mucin chains and presumably rigid polymer chains of hard, bioerodible surfaces.

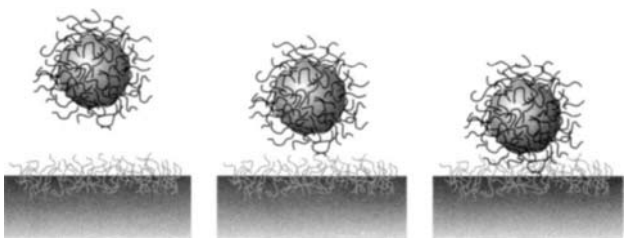


Figure 3. Interpenetration of bioadhesive and mucus polymer chains.

Methods to Evaluate Bioadhesive Interactions

Most researchers in the field of bioadhesion have developed their own techniques, which suit their particular systems and interests, for measuring and evaluating the interactions between BPs and biological substrates.

However, no attempt has been made to develop a standardized method of evaluation. Each technique has its own set of experimental conditions, and, therefore, it has been difficult to compare experimental findings among investigators. The following sections highlight some of the more significant methods that have been used in the past.

In Vitro Techniques. In vitro techniques have involved testing BPs against synthetic mucus, natural mucus, frozen tissue samples, or freshly excised tissue samples. For mucoadhesion studies, there have been two common techniques: the Wilhelmy plate technique and a shear test (26).

The Wilhelmy plate technique has traditionally been used for dynamic contact-angle measurement and involves a microbalance or tensiometer. A glass slide is coated with the polymer of interest and then dipped into a beaker of synthetic or natural mucus (Fig. 4a). The surface tension, contact angle, and adhesive force can be automatically measured using available software (78,79).

The shear test measures the force required to separate two polymer-coated glass slides joined by a thin film of natural or synthetic mucus (Fig. 4b) (80). The results of this technique often correlate well with in vivo test results (26).

A majority of the in vitro experiments have been variations of a simple tensile test that use either large tensile machines, modified tensiometers, or electrobalances (Fig. 5). Either a slab of polymer or a polymer-coated stopper is brought in contact with a section of biological tissue (either fresh or previously frozen). The samples are left in contact for a certain adhesion time, and the force required to break the adhesive bond is measured. These types of studies have been conducted with both hydrogels and thermoplastics, in air and various physiological buffers, and with varying temperatures and pH (2,24,48,51,81–85). The major flaw with most of these techniques is that they fail to incorporate both physiological conditions and delivery device geometries in a single, controlled experiment.

Some attempts have been made to mimic in vivo conditions in an in vitro environment. One such system consists of a unique flow chamber (Fig. 6) (73,86,87) in which a polymer microsphere is placed on the surface of a layer of natural mucus. Fluid, moving at physiologic rate, is introduced to the chamber, and the movement of the microsphere is monitored using video equipment. By measuring the size and speed of the microsphere, it was possible to calculate the bioadhesive force.

In Vivo Techniques. Most in vivo measurements of GI bioadhesive performance involve administering BPs to laboratory animals and monitoring their transit rate through the gut. Experiments have varied in both administration routes and tracking techniques. Bioadhesives have been orally force-fed by gavage (88–90), surgically implanted in the stomach (24) and infused with a perfusion pump through an in situ loop of the small intestine (48). Investigators have monitored transit using radiopaque markers (90,91), radioactive elements (92,93), and fluorescent labeling techniques (24).

Bioadhesive Polymers

From current scientific literature, two classes of polymers appear to be of interest for bioadhesion: hydrophilic polymers and hydrogels. Recent studies have suggested that in the large class of hydrophilic polymers, those containing carboxyl groups exhibit the best bioadhesive properties (75,94). Therefore, tremendous effort has been made to develop polyacrylic acid–based BDDSs (27,80,82,83,95–99). In other studies (51,78,82,100,101), promising bioadhesive polymers have included sodium alginate, methylcellulose, carboxymethylcellulose, hydroxymethylcellulose, and cationic hydrogels such as chitosan. In general, hydrogels have most often been used for bioadhesive drug delivery because of the belief that polymer–mucin chain entangle-

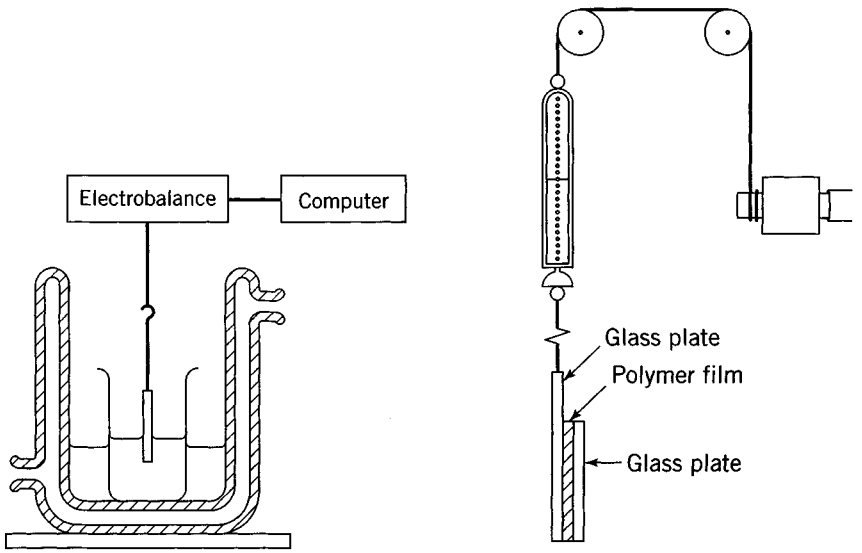


Figure 4. The Wilhelmy plate method (**a**) and the shear test for mucoadhesion studies (**b**).

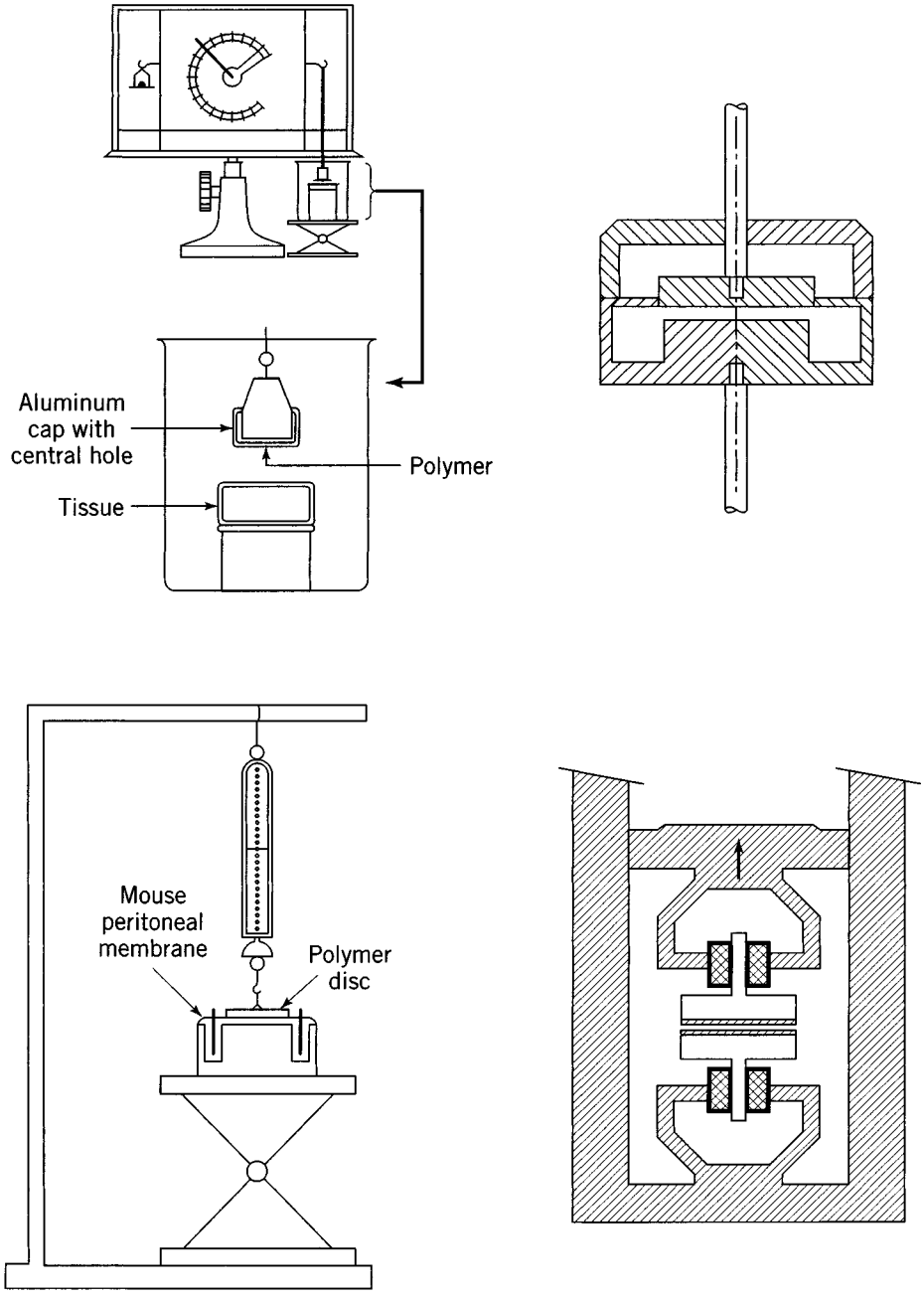


Figure 5. Tensile experiments for bioadhesive force measurements.

ment is an essential component in bioadhesive bond formation. However, other factors, such as surface energy, surface texture, electrical charge, and hydrophilic functional groups, may be equally important. It has recently been shown that nonhydrogel polymers that are high in hydrophilic functional groups can also produce intense bioadhesive interactions (25,28,102) and can be utilized to improve bioavailability of orally administered compounds (91). The case studies detailed in the following sections will describe this avenue of research in further detail.

Applications of Bioadhesive Polymers

The bioadhesive polymers discussed in the previous section have been used in various forms as drug delivery vehicles. It has been hypothesized that bioadhesive contact with an absorptive cell layer could improve drug transport, thereby increasing delivery efficiency. Furthermore, adhesives provide a means of securing DDSs to specific sites and localizing administration to targeted tissues. Common BDDS shapes and forms used in current research efforts have included tablets, powders, gels, patches, liposomes, and microspheres (1,21,23,73,103,104).

Bioadhesive tablets have been proposed for buccal, gingival, and vaginal delivery of such drugs as fluoride, miconazole, lidocaine, metronidazole, and morphine (17,99,105–116). These systems are usually produced by compressing a dry mixture of drug and polymer (most often polyacrylic acid). The tablets are administered by pressing

Next Page

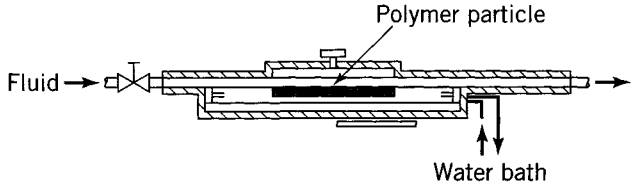


Figure 6. Fluid flow chamber for bioadhesive microsphere studies.

against a dried area in the mouth, and as saliva swells the polymer hydrogel, drug is released. Sustained release and adhesion are typically maintained for 8–10 h.

One group has investigated the possibility of delivering drug-containing bioadhesive powders to the mouth (117). The systems, designed to form an adhesive gel coating in situ, were shown to improve buccal retention and prolong delivery compared with systems delivered initially as a gel.

Bioadhesive gels have been investigated as drug carriers for delivery to the eye (12,95,118), mouth (2,12,117,119,120), rectum (121), vagina (13,110,122,123), and open wounds (124). As with bioadhesive tablets, polyacrylic acid (namely polycarbophil and Carbopol 934) has been the most commonly used polymer, most likely owing to its biocompatibility, strong adhesive characteristics, and U.S. FDA approval.

Other forms of bioadhesive systems have included patches, liposomes, and microspheres. Adhesive patches being developed by 3M, are intended for transdermal as well as buccal drug delivery (125,126). Bioadhesive liposomes, based on phosphatidylcholine, collagen, and hyaluronic acid, have been investigated as a means to enhance topical drug delivery (127–129). Microspheres, although widely studied as DDSs and often used as model systems for bioadhesive analysis (3,18,25,28,48,87,91,130–132), have thus far found fewer applications than other forms of BDDSs, with investigations focusing mainly on nasal (133,134) and GI administration (10,48,82,135–137). The following sections describe in depth our ongoing research efforts to utilize bioadhesive polymer microspheres as DDSs to the GI tract.

DEVELOPMENT OF BIOADHESIVE MICROSPHERES: A CASE STUDY

A Novel Electrobalance-Based Tensiometer

Although bioadhesive microspheres have been investigated as DDSs (18,82,87,131,133,138,139), only two methods have been reported for the measurement of bioadhesive interactions between individual polymer microspheres and soft tissues. One technique took advantage of the relationships between directional contact angles and physical forces to estimate strength of mucoadhesive bonds (131), whereas the other utilized a flow channel and basic fluid mechanic principles to calculate adhesive forces between microspheres and mucus (87,138). Neither of these systems was capable of directly measuring bioadhesive forces, and neither mimicked physiologic conditions by using viable tissue.

By modifying the operation of a sensitive microbalance, originally designed to measure dynamic contact angles, we developed a simple and reproducible method for measuring bioadhesion of microspheres. The system allows microspheres to be tested with freshly excised tissue while maintaining specific physiologic conditions, such as pH and temperature. Eleven parameters can be derived from the load-versus-deformation curves generated with each experiment, including fracture strength, deformation to failure, and tensile work.

Experimental Design and Methods ***Microbalance.*** A Cahn Dynamic Contact Angle Analyzer (Model DCA-322; CAHN Instruments, Inc.; Cerritos, CA) was modified to perform adhesive measurements (28,140). Although this piece of equipment is designed for measuring contact angles and surface tensions using the Wilhelmy plate technique, it is also an extremely accurate microbalance. The DCA-322 system includes a microbalance stand assembly, a Cahn DACS IBM-compatible computer, and an Okidata Microline 320 dot matrix printer (Fig. 7). The microbalance unit consists of stationary sample and tare loops and a z-translation stage powered by a stepper motor. The balance can be operated with samples weighing up to 3.0 g and has a sensitivity rated at 1×10^{-5} mN. The stage speed can be varied from 20 to 264 μm/s.

To develop an automated, reproducible method for bioadhesion measurements, it was necessary to modify the operation of the balance and stage. The standard DACS IBM-compatible computer system was replaced with an Apple Macintosh II computer. The computer–microbalance interface was through the modem port, with an -10 V signal supplied by an external power supply (DC Power Supply 1630; BK Precision, Chicago, IL), hardwired through the RS-232 connection. Labview II software was used to write a user-friendly, menu-driven package to automatically run tensile experiments, with easily adjustable settings for stage speed, applied load, and time of adhesion. After each run, graphs of load versus stage position and load versus time were plotted, and 11 parameters were automatically calculated: (*1*) compressive deformation, (*2*) peak compressive load, (*3*) compressive work, (*4*) yield point, (*5*) deformation to yield, (*6*) returned work, (*7*) peak tensile load, (*8*) deformation to peak tensile load, (*9*) fracture strength, (*10*) deformation to failure, and (*11*) tensile work (28,140).

Tissue Chamber. To maintain physiological temperature and pH throughout experiments, a temperature-controlled tissue chamber was constructed (Fig. 8). The chamber was fabricated of plexiglass and consisted of a 3-mL tissue cell jacketed by a circulating water bath connected to a Fisher Scientific Isotemp refrigerated circulator (model 9000). Two stainless-steel clamps with thumbscrews were used to secure tissue samples to the bottom of the tissue cell.

Mounting Microspheres. To attach microspheres to the microbalance, it was necessary to first mount microspheres on rigid support wires. Thermoplastic microspheres were melt-mounted by piercing with red-hot, 280-μm-diameter, iron wires (Leeds & Northrup Company, Philadelphia, PA) cut to $\approx$2 cm in length (although this technique could alter

Previous Page

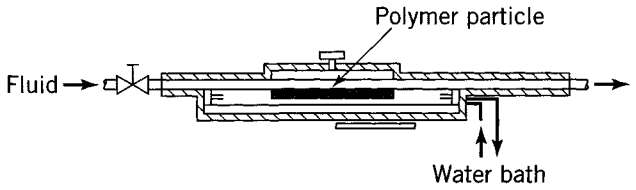


Figure 6. Fluid flow chamber for bioadhesive microsphere studies.

against a dried area in the mouth, and as saliva swells the polymer hydrogel, drug is released. Sustained release and adhesion are typically maintained for 8–10 h.

One group has investigated the possibility of delivering drug-containing bioadhesive powders to the mouth (117). The systems, designed to form an adhesive gel coating in situ, were shown to improve buccal retention and prolong delivery compared with systems delivered initially as a gel.

Bioadhesive gels have been investigated as drug carriers for delivery to the eye (12,95,118), mouth (2,12,117,119,120), rectum (121), vagina (13,110,122,123), and open wounds (124). As with bioadhesive tablets, polyacrylic acid (namely polycarbophil and Carbopol 934) has been the most commonly used polymer, most likely owing to its biocompatibility, strong adhesive characteristics, and U.S. FDA approval.

Other forms of bioadhesive systems have included patches, liposomes, and microspheres. Adhesive patches being developed by 3M, are intended for transdermal as well as buccal drug delivery (125,126). Bioadhesive liposomes, based on phosphatidylcholine, collagen, and hyaluronic acid, have been investigated as a means to enhance topical drug delivery (127–129). Microspheres, although widely studied as DDSs and often used as model systems for bioadhesive analysis (3,18,25,28,48,87,91,130–132), have thus far found fewer applications than other forms of BDDSs, with investigations focusing mainly on nasal (133,134) and GI administration (10,48,82,135–137). The following sections describe in depth our ongoing research efforts to utilize bioadhesive polymer microspheres as DDSs to the GI tract.

DEVELOPMENT OF BIOADHESIVE MICROSPHERES: A CASE STUDY

A Novel Electrobalance-Based Tensiometer

Although bioadhesive microspheres have been investigated as DDSs (18,82,87,131,133,138,139), only two methods have been reported for the measurement of bioadhesive interactions between individual polymer microspheres and soft tissues. One technique took advantage of the relationships between directional contact angles and physical forces to estimate strength of mucoadhesive bonds (131), whereas the other utilized a flow channel and basic fluid mechanic principles to calculate adhesive forces between microspheres and mucus (87,138). Neither of these systems was capable of directly measuring bioadhesive forces, and neither mimicked physiologic conditions by using viable tissue.

By modifying the operation of a sensitive microbalance, originally designed to measure dynamic contact angles, we developed a simple and reproducible method for measuring bioadhesion of microspheres. The system allows microspheres to be tested with freshly excised tissue while maintaining specific physiologic conditions, such as pH and temperature. Eleven parameters can be derived from the load-versus-deformation curves generated with each experiment, including fracture strength, deformation to failure, and tensile work.

Experimental Design and Methods ***Microbalance.*** A Cahn Dynamic Contact Angle Analyzer (Model DCA-322; CAHN Instruments, Inc.; Cerritos, CA) was modified to perform adhesive measurements (28,140). Although this piece of equipment is designed for measuring contact angles and surface tensions using the Wilhelmy plate technique, it is also an extremely accurate microbalance. The DCA-322 system includes a microbalance stand assembly, a Cahn DACS IBM-compatible computer, and an Okidata Microline 320 dot matrix printer (Fig. 7). The microbalance unit consists of stationary sample and tare loops and a z-translation stage powered by a stepper motor. The balance can be operated with samples weighing up to 3.0 g and has a sensitivity rated at 1×10^{-5} mN. The stage speed can be varied from 20 to 264 μm/s.

To develop an automated, reproducible method for bioadhesion measurements, it was necessary to modify the operation of the balance and stage. The standard DACS IBM-compatible computer system was replaced with an Apple Macintosh II computer. The computer–microbalance interface was through the modem port, with an -10 V signal supplied by an external power supply (DC Power Supply 1630; BK Precision, Chicago, IL), hardwired through the RS-232 connection. Labview II software was used to write a user-friendly, menu-driven package to automatically run tensile experiments, with easily adjustable settings for stage speed, applied load, and time of adhesion. After each run, graphs of load versus stage position and load versus time were plotted, and 11 parameters were automatically calculated: (*1*) compressive deformation, (*2*) peak compressive load, (*3*) compressive work, (*4*) yield point, (*5*) deformation to yield, (*6*) returned work, (*7*) peak tensile load, (*8*) deformation to peak tensile load, (*9*) fracture strength, (*10*) deformation to failure, and (*11*) tensile work (28,140).

Tissue Chamber. To maintain physiological temperature and pH throughout experiments, a temperature-controlled tissue chamber was constructed (Fig. 8). The chamber was fabricated of plexiglass and consisted of a 3-mL tissue cell jacketed by a circulating water bath connected to a Fisher Scientific Isotemp refrigerated circulator (model 9000). Two stainless-steel clamps with thumbscrews were used to secure tissue samples to the bottom of the tissue cell.

Mounting Microspheres. To attach microspheres to the microbalance, it was necessary to first mount microspheres on rigid support wires. Thermoplastic microspheres were melt-mounted by piercing with red-hot, 280-μm-diameter, iron wires (Leeds & Northrup Company, Philadelphia, PA) cut to $\approx$2 cm in length (although this technique could alter

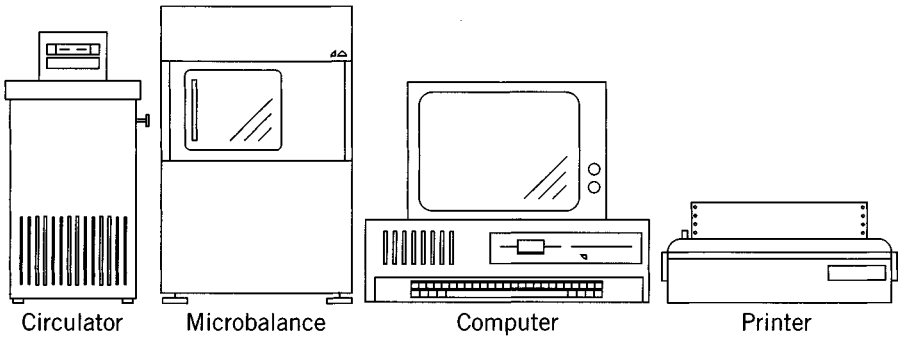


Figure 7. Cahn DCA 322 dynamic contact angle analyzer.

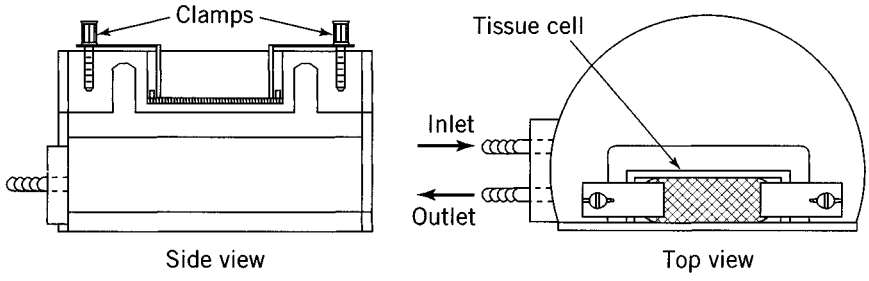


Figure 8. Tissue chamber showing tissue clamps and inlet and outlet flow ports for temperature control.

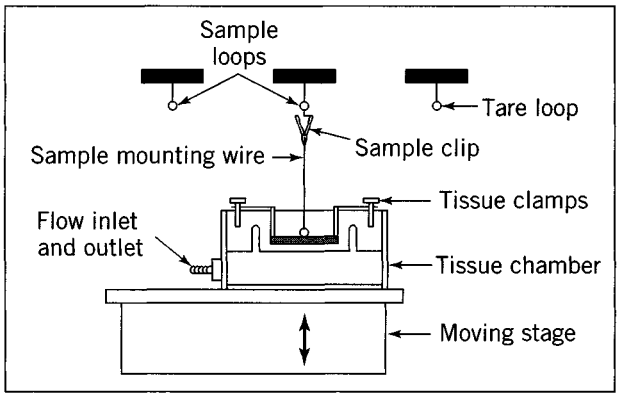


Figure 9. Microbalance enclosure with tissue chamber and polymer sample. The mobile stage can be raised and lowered at controlled rates while monitoring the load on the balance and the displacement of the stage. *Source:* Reproduced with permission from *Journal of Controlled Release* (Ref. 28).

the surface morphology of some materials, SEM analysis, not reported here, showed that the structure of the microspheres remained unchanged on the hemisphere intended for intestinal contact). Hydrogel microspheres were attached to the same wires using cyanoacrylate glue (Super Glue Corp., Hollis, NY). After mounting, wires were suspended from a sample clip in the microbalance enclosure (Fig. 9).

Microbalance Operation. Operation of the Cahn system is simple. The circulating water bath is adjusted to physiologic temperature (37°C), freshly excised tissue is placed in the chamber and submerged in phosphate-buffered saline (PBS), and the microsphere is suspended from the sample loop. The computer program is started, and the stage rises until the applied load between microsphere and tissue reaches the preprogrammed set point. At this position, motion stops for the duration of adhesion time, and then the stage is lowered. Once the stage returns to its initial position, parameters are calculated and graphs are plotted.

Results and Discussion ***Interpretation of the Microbalance Recordings.*** Figure 10 shows a typical load-versus-deformation graph obtained using the Cahn microbalance where the stage position and the mass exerted on the microbalance are represented by the horizontal and vertical axes, respectively. Letters have been added to Figure 10 to

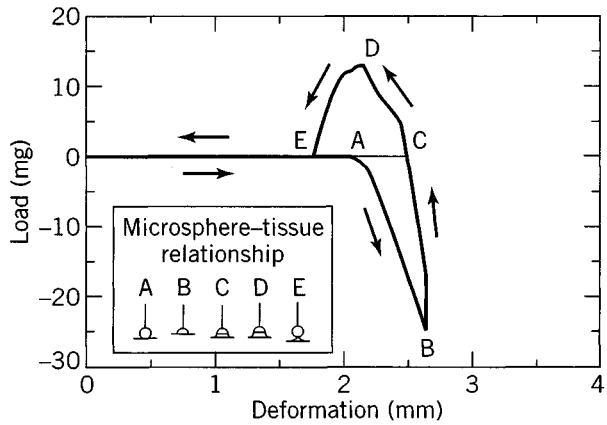


Figure 10. Typical load-versus-deformation curve: arrows indicate direction of tracing, and inset depicts relationship between tissue and microspheres at each lettered point. *Source:* Reproduced with permission from *Journal of Controlled Release* (Ref. 28).

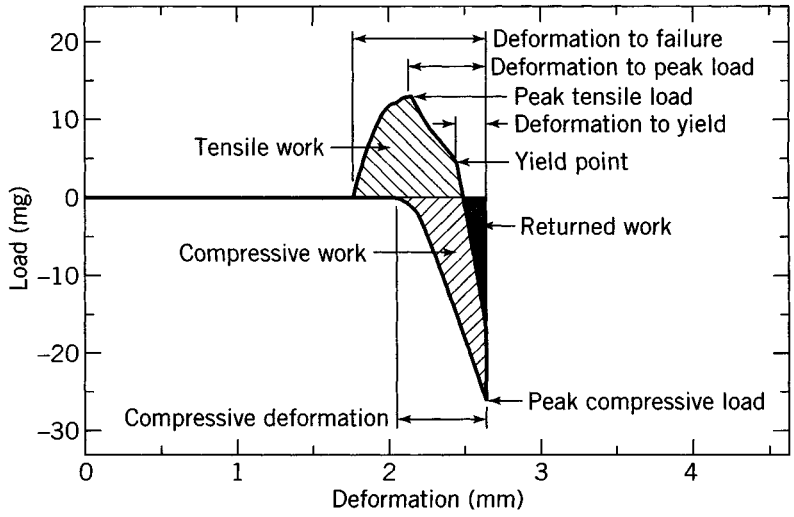


Figure 11. Typical load-versus-deformation curve indicating parameters of interest for bioadhesive analysis. *Source:* Reproduced with permission from *Journal of Controlled Release* (Ref. 28).

aid in description, and arrows have been added to indicate the order in which the curve is drawn over time. Experimental measurements have been indicated on Figure 11. The curve is a plot of the recorded forces (presented as a load) detected by the sample loop holding the microsphere as the stage holding the tissue is raised to contact the microsphere. Deformation is the distance the stage has moved. The initial state of the experiment begins with zero applied load and zero deformation. The stage then rises (increase deformation) to point A, the initial point of contact between the microsphere and tissue. The stage continues to rise until the set applied load (-25 mg) is recorded, point B, peak compressive load. The region from A to B represents the compressive deformation of the system. The stage position is held at point B for the set time of the experiment (usually seven minutes), during which the tissue often relaxes and the force decreases. This is seen as a completely vertical line in the plot just above point B. During this time the microsphere and mucus form an adhesive bond. After seven minutes, the stage is slowly stepped down, and the experiment enters the tensile region. The compressive load is released as the stage begins to move away from the microsphere. The recorded forces pass through point C, indicating zero applied force on the tissue. The stage continues to pull the tissue away from the microsphere, and a maximum force of adhesion is recorded, point D. In between points C and D, however, is the yield point of the system, which is identified by a change in slope of the curve from C to D. The initial slope of the curve above point C is linear and is indicative of the stiffness of the bioadhesive bond. The force increases during this time, and we assume that the contact area remains the same and that the earliest disruption of the bioadhesive bond between the microsphere and tissue is at the yield point. The distance from B to the yield point is the deformation to yield. As the stage continues to move, the adhesive bond is further disrupted, and the maximum adhesive force is measured, the peak tensile load (point D). The deformation to peak load is the distance from point B to point D. As the stage continues to move away, the recorded forces decrease as the adhesive contact between microsphere and tissue is completely disrupted and no force reading can be detected, point E. Point E is considered to be the point of failure. During the stage movement from point D to point E, we assume the adhesive contact area is decreasing until final separation is achieved. In some microsphere–tissue interactions, this region of the data plot is elongated and marked by several peaks and valleys, indicating existence of several individual adhesive bonds. Some bonds are stretched until the breaking point, causing the "peak" to appear, and then the curve drops momentarily as the load is transferred to other bonds (forming the "valley" on the data plot). Figure 12 schematically depicts the disruption of the adhesive union where several focal attachments may be responsible for the adhesive bond strength. In Figure 10, the distance from point B to point E is known as the deformation to failure. A large deformation to failure indicates the adhesive contact is extremely plastic and compliant and less susceptible to outside disruptions. The stage continues to move downward until its home position is reached (the point at which there is zero deformation on the y axis).

Three different work values can be obtained from these curves. Compressive work is the work done in joining the two surfaces and is calculated as the area between the compressive region of the curve and the zero load line (upward cross-hatched area in Fig. 11). Returned work is the work done by the tissue on the microsphere when the compressive load is released. This component is the area bounded by the negative region of the tensile curve and the

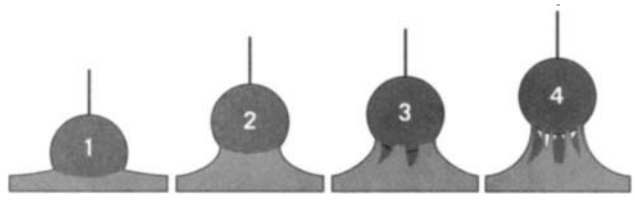


Figure 12. Schematic diagram showing the progression of bioadhesive fracture.

zero load line (dotted area in Fig. 11). Tensile work is the work done in separating the two surfaces and is the area between the positive portion of the tensile curve and the zero load line (downward cross-hatched area in Fig. 11).

To compute fracture strength (F_m/A_o) of a bioadhesive bond, the contact area has to be determined. The area of contact between the microsphere and mucosa was estimated to be the projected surface area of the spherical cap defined by the depth of penetration of the microsphere below the surface level of the tissue (Fig. 13). [Area = $A_o = \pi R^2 - \pi(R - a)^2$, where R is the microsphere radius and a is the depth of penetration. The depth of penetration, a, was visually estimated to be approximately equal to the microsphere radius for microspheres between 710 and 850 μm. Thus, $A_o = \pi R^2$.] Fracture strengths were obtained by normalizing peak load by the projected area of this cap.

Limitations of the System. The microbalance-based system has several limitations: (*1*) microspheres smaller than 300 μm are difficult to mount, (*2*) overshoot of the applied load must be accounted for, (*3*) very small and very large applied loads are difficult to control, and (*4*) changes in applied load over time due to tissue relaxation or contraction are not accounted for once the stage has stopped moving.

First, because of the mounting method, it is difficult to attach microspheres smaller than 300 μm to the microbalance. A more sophisticated method using micropipettes and a micropositioner (141) could possibly be employed to mount microspheres as small as 10 μm. However, estimations in contact area for fracture strength calculations would be difficult.

Second, since the sampling rate of the microbalance is 1 Hz, stage motion commands can be sent only every second. Therefore, once the microbalance reaches the applied load set point, there is a 1-s delay between when the computer commands the stage to stop moving and when the motion actually ceases. This results in overshoot of the applied load in the range of 5–50%. For moderate applied loads (i.e., 10–50 mg), the overshoot is easily adjusted for and is rarely greater than 20%.

Third, very small and very large applied loads are difficult to control due to response time of the microbalance and the nature of the motor controlling the stage movement. The stepper motor supplied with the DCA 322 moves in incremental jumps (as opposed to smooth motion). When an attempt is made to apply very small loads, a small amount of overshoot can be greater than 100% of the intended value. When very large loads are attempted, the slope of the load-versus-deformation curve is so steep that the overshoot is always very large. Therefore, moderate forces (10–50 mg) are most easily attained.

Fourth, in many cases the applied load changes while the stage is not in motion. This occurs due to relaxation or contraction of the smooth muscle in the tissue. Because of unsuitable response time and relatively large incremental movements of the stepper motor, accurate adjustments can not be made in the stage position to account for these small dynamic effects.

In summary, the microtensiometer described in this section offers many advantages over previous bioadhesion measurement devices. The setup enables determination of bioadhesive forces between a single microsphere and intestinal mucosa. This technique allows measurement of bioadhesive properties of a candidate material in the exact geometry of the proposed microsphere delivery device. The use of a physiological tissue chamber mimics temperature and pH conditions of a living animal and maintains viable tissue. Because experiments are conducted in an aqueous environment, problems in distinguishing surface tension forces at the air/liquid interface from forces at the microsphere/mucus interface are eliminated.

Eleven parameters relating to the bioadhesive event can be computed from every experiment. Although some are independent of the material studied, we believe that three may be direct predictors of bioadhesive potential: fracture strength, deformation to failure, and tensile work (28). The following section details a thorough analysis of adhesion data collected with the Cahn machine on various bioadhesive polymer microspheres.

Bioadhesive Measurements

Traditionally, two classes of polymers have been of interest for use as bioadhesives: hydrogels (21,101,142,143) and other hydrophilic polymers containing carboxylic groups [e.g. poly[acrylic acid]) (23,48,75,94)]. The formation of bioadhesive bonds between soft tissue and these materials has been described in three steps: (*1*) wetting and swelling of the polymer to permit intimate contact with the biological tissue, (*2*) interpenetration of bioadhesive polymer chains and entanglement of polymer and mucin chains, and (*3*) formation of weak chemical bonds (17,19). Because

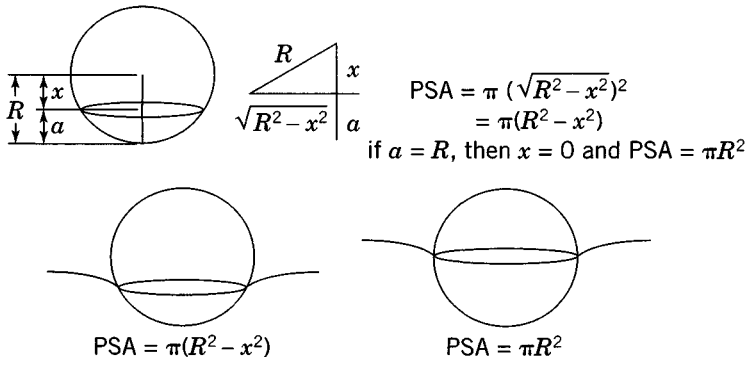


Figure 13. Calculation of projected surface area.

water-insoluble, bioerodible materials are often hydrophobic and typically do not exhibit highly flexible chains, swelling and chain entanglement appear unlikely to occur. Hence, investigation of these materials for bioadhesive applications has been neglected.

However, realizing that hydrogen bonding between surface carboxyl groups and mucus or epithelial cell glycoproteins could be a key contributor to nonspecific bioadhesion as dictated by the adsorption theory of adhesion, we hypothesized that some bioerodible thermoplastic materials might exhibit bioadhesive interactions. When polymers such as polyesters and polyanhydrides hydrolytically degrade, carboxylic acid groups are formed at the transected polymer chain ends. Rapidly degrading materials may quickly form surfaces rich in carboxylic acid ideally suited for bioadhesion. To test this concept, we used the Cahn microbalance (described in the previous section) to compare the bioadhesive properties of one hydrogel and five bioerodible thermoplastics.

Polymer Samples. Polymers investigated in this study were selected based on properties believed to favor bioadhesion (i.e., carboxylic acid) (23,26,51) and can be separated into two distinct categories: a natural hydrogel (alginic acid); and synthetic, degradable, thermoplastic polymers (polyesters, polyanhydrides). Figure 14 shows the chemical structures of the polymers. Powdered, medium-viscosity alginate (Kelgin® MV) was obtained from Kelco, Division of Merck & Co., Inc. (Chicago, IL). Low-molecular-weight (2K) polylactic acid (PLA) was purchased through Polysciences (Warrington, PA). The polyanhydrides studied were a copolymer of 1,3-bis(*p*-carboxyphenoxy)-propane (CPP) and sebacic acid (SA) (molar ratio of 20:80), and copolymers of fumaric acid (FA) and SA (molar ratios of 20:80 and 50:50). P(CPP:SA) 20:80, P(FA:SA) 50:50, and some P(FA:SA) 20:80 were obtained as a gift from Nova Pharmaceutical Corporation (Baltimore, MD). Other P(FA:SA) 20:80 was synthesized in our laboratory.

P(FA:SA) 20:80 Synthesis. P(FA:SA) 20:80 was synthesized according to the methods established by Domb and Langer (144,145). FA and SA monomers (Sigma Chemical Company, St. Louis, MO) (Fig. 15) were purified by recrystallization from 95% ethanol or 100% ethanol, respectively, and drying with vacuum in a calcium chloride desiccator.

Prepolymers (PP) were produced by refluxing purified monomer in acetic anhydride (FA:172 mmol/250 mL, 1 h; SA: 148 mmol/100 mL, 30 min), evaporating 80–90% at 50–60°C (Buchi RE-111 Rotavapor and 461 Water Bath system), and recrystallizing at −20°C. Precipitates were filtered, dissolved in toluene (100 mL or 30 mL, for FAPP or SAPP, respectively) with heat, precipitated overnight at room temperature, and then further recrystallized in an ice bath for 10 h. Precipitates were filtered, washed (in 200 mL petroleum ether or 1:1 volume ratio of ethyl/petroleum ether, for FAPP or SAPP, respectively), and dried under vacuum.

For polymerization, prepolymers (8 mmol SAPP, 2.288 g, and 2 mmol FAPP, 0.4 g) were melted under reduced pressure and periodically purged with nitrogen gas to remove acetic anhydride. After 30 min, the resulting viscous polymer was cooled, dissolved in methylene chloride, filtered, precipitated in hexane, dried, and stored at −20°C. Molecular weight was determined with gel permeation chromatography (GPC) to be between 5,000 and 15,000, depending on the batch.

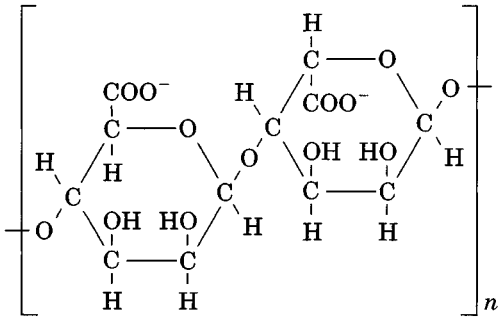
Microsphere Preparation ***Hydrogel Microspheres.*** Microspheres made of alginate were produced through a standard ionic gelation technique (146). The polymer was first dissolved in an aqueous solution (2% w/v) and then extruded through a microdroplet-forming device, which employed a flow of nitrogen gas to break off the droplet. A slowly stirred (≈100–170 rpm) calcium chloride bath (1.3% w/v) was positioned below the extruding device to catch the forming microdroplets. Microspheres were left to incubate in the bath for 20–30 min to allow sufficient time for gelation to occur. Microsphere particle size was controlled by using various size extruders or by varying either the nitrogen gas or polymer solution flow rates.

Bioerodible Thermoplastic Microspheres. Several methods for preparation of bioerodible microspheres exist (147–152). Certain methods are more appropriate for particular polymers. The two methods used in this study were hot-melt microencapsulation and solvent evaporation microencapsulation.

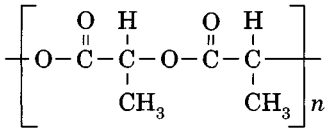
In hot-melt microencapsulation (147), 2 g of polymer (either PLA, P[CPP:SA] 20:80, P[FA:SA] 20:80, or P[FA:SA] 50:50) were melted in a crucible on a hot plate (melting points ranged from 60–125°C). The molten polymer was added to 250 mL of rapidly stirred silicon oil (200 Fluid; Dow Corning, Midland, MI), heated to ≈10°C above the melting point of the polymer, to form an emulsion. The emulsion was allowed to stabilize and was then rapidly cooled with an ice jacket until polymer particles solidified. The resulting microspheres were washed with petroleum ether to produce free-flowing beads. Microspheres with diameters between 10 and 1,000 μm were obtained with this method. External surfaces of spheres prepared with this technique ranged from very smooth to somewhat pitted, depending on the polymer used (148,153).

Solvent evaporation was used to manufacture PLA microspheres (154,155). Polymer solutions were produced by dissolving PLA in methylene chloride. A 20% (w/v) solution of PLA was suspended as an emulsion in 300 mL of 1% (w/v) poly(vinyl alcohol) (Sigma Chemical Co., St. Louis, MO). The solution was vigorously stirred at a rate of 1,200 rpm using a Caframo (Wiarton, Ontario) overhead stirrer. One drop of octanol (Sigma Chemical Company, St. Louis, MO) was added to the solution to reduce foaming. After 4 h of stirring to allow for evaporation of the organic solvent, resulting microspheres were collected, washed with water, and lyophilized (Lyph-Lock 6; Labconco, Kansas City, MO). Microspheres obtained with this technique ranged in size from 10 to 1,000 μm.

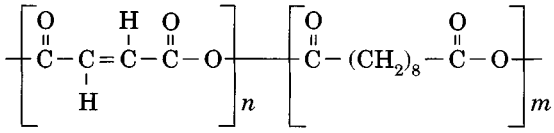
Tissue Collection and Handling. Unfasted, male, VAF, CD® rats (250–350 g, Charles River Labs, Wilmington, MA) were anesthetized by ip injection of nembutal (sodium pentobarbital, 55 mg/kg) and perfused transcardially with ice cold, 0.9% NaCl. Approximately 10–15 cm of jejunum



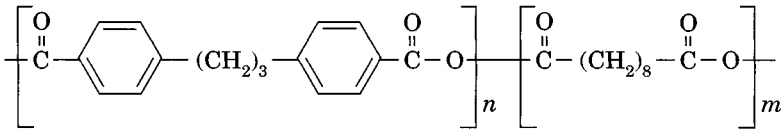
Alginate



Polylactic acid

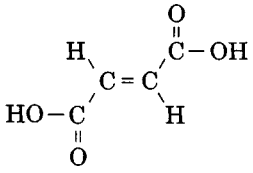


P(FA:SA)

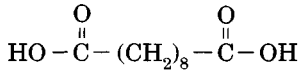


P(CPP:SA)

Figure 14. Chemical structures of polymers.



Fumaric acid



Sebacic acid

Figure 15. Chemical structures of monomers.

were excised, flushed with Dulbecco's phosphate-buffered saline containing 100 mg/dL of glucose (DPBSG), and stored in DPBSG at 4°C for no more than 3 h.

Bioadhesive Measurements. Adhesive forces between polymer microspheres and segments of rat jejunum were measured using the previously described microbalance. Polymers were evaluated for their bioadhesive properties using microspheres that were sieved to diameters ranging from 710 to 850 μm. Sections of rat jejunum (≈2 cm in length) were cut longitudinally (to expose the lumen), submerged at the bottom of a 9-mm layer (≈3 mL) of DPBSG, and clamped at their edges inside the tissue chamber. The chamber was subsequently placed on the moving stage below a suspended microsphere. The stage was raised manually until microspheres were completely submerged in buffer, but still 1–2 mm above the surface of the mucosa. At this point the microbalance was tared and data collection began. The stage was raised at a rate of 50.2 μm/s until contact was made between microsphere and tissue. Microspheres were left in contact with the tissue for 7 min with an applied force of ~0.25 mN and then pulled vertically away from the tissue sample (at 50.2 μm/s) while recording the required force of detachment. For each experiment, buffer was replaced with fresh DPBSG, and a new microsphere was brought in contact with a different site along the tissue. Tissue sections were used for three experiments and then replaced with fresh segments.

Data Analysis. As described previously, five theories of adhesion have been adapted and developed to analyze

bioadhesive interactions: electronic (52,53), adsorption (50,54–56), wetting (49,68,69), diffusion (49,50,68,69, 71,72), and fracture (74,75). Though these theories involve independent mechanisms, they are not mutually exclusive of one another. For analyzing the results of the tensile experiments we have applied the fracture theory; in the discussion that follows, we will assert that the adsorption and wetting theories of adhesion are most appropriate for explaining the observed bioadhesive phenomena.

Load-versus-Deformation Curve Morphology. Careful study of the load-versus-deformation curves produced from the microbalance tensile experiments can reveal many important phenomena. If the interaction between two materials is completely nonadhesive and both materials behave elastically, the curve would retrace itself and no adhesive force would be measured. There would be no hysteresis, and the compressive work imparted on the system would be returned completely as the stage was lowered to its original position (i.e., the interaction would be totally reversible). All materials investigated in this study showed positive adhesive forces, and therefore some form of adhesion occurred between the mucosa and the polymers. Representative load-versus-deformation curves for the six microsphere types studied are displayed in Figure 16. Although the recordings from the tensile experiments all have a similar general shape, three common trends were observed for the different materials investigated.

Some materials, such as PLA, exhibited adhesions that fractured in what appeared to be a brittle manner. In these instances, the resultant load-versus-deformation curves rose quickly during the descent of the stage but then returned sharply to zero as separation occurred (Fig. 16).

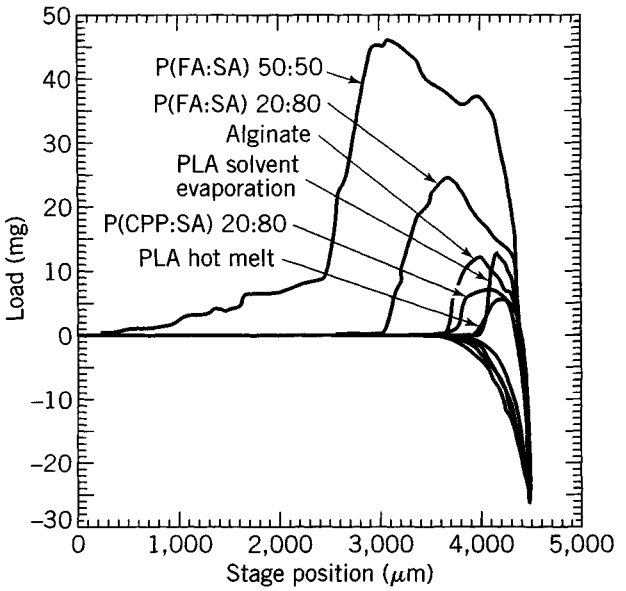


Figure 16. Characteristic load-versus-deformation curves generated with the microbalance for each of the six microsphere types studied. All curves have been scaled identically to emphasize the differences between them. *Source:* Reproduced with permission from *Journal of Controlled Release* (Ref. 28).

Failure took place at nearly the same stage position as the point of initial contact (i.e., deformation to failure = compressive deformation). The fracture strengths were low to moderate, depending on the microsphere fabrication technique, but the interaction between the microsphere and mucus seemed weak. We believe that the forces produced were mainly due to either mechanical engulfment of the microspheres by the mucus or by mechanical penetration of the mucus into crevices of the microspheres (in the solvent evaporation case). When fracture occurred, the microspheres almost "popped" out of the mucus layer as if the mucin was not actually bound to the microspheres.

Other materials, such as P(CPP:SA) 20:80, produced load curves that were more rounded in shape (Fig. 16). Again, no difference was observed between the deformation to failure and the compressive deformation. In these cases, we believe that some bioadhesive interaction occurred between the microsphere and the mucosal layer; however, the fracture strengths produced by these materials were only moderate at best. The bonds produced with the mucus appeared to be weaker than the adhesion of the mucus to the epithelial cell layer. The eventual fracture was witnessed to occur at the mucus/microsphere interface, and SEM examination revealed no mucus adherent to the microsphere surfaces.

In the final group of curves, both the peak load and deformation to failure were large. Copolymers of FA and SA (both P[FA:SA] 20:80 and 50:50) exhibited such load-versus-deformation curves (Fig. 16). In these cases, the bond between the microsphere and the mucosal layer was observed to be very strong. The deformation to failure was larger than the deformation due to the compressive load. In other words, the intensity of the bond was great enough to deform the adhesive site and elongate the mucus/mucosal surface beyond its original position. Prior to fracture, strands of mucin were observed bridging the gap between the microsphere and the mucosa. Fracture after peak load almost always occurred in a brittle manner, but the load rarely returned to zero. The fact that the load did not return to zero suggests that some mucin or cellular material was transferred from the tissue's surface to the microsphere and that the site of fracture occurred either within the mucus layer or at the mucus/epithelium interface instead of at the mucus/microsphere interface. Therefore, we believe that the weak link in the adhesive system is due to the properties of the biological substrate and not the bioadhesive interaction.

While overlapping of the compressive region of the six curves helped to support the repeatability of the experiment, size and shape of the tensile regions of the curves indicated there were differences between polymers. The most striking differences were found between both of the P(FA:SA) copolymers and all of the other materials; however, further statistical analysis was necessary to confirm these differences.

Comparison of Bioadhesive Parameters. Of the 11 parameters measured from the load-versus-deformation curves, 9 were tabulated (Tables 1 and 2) and compared: compressive deformation, deformation to yield, deformation to peak load, deformation to failure, yield force, fracture

Table 1. Mean Deformations (±SEM) Calculated from Load-versus-Deformation Plots Generated during the Electrobalance Tensile Experiments

Polymer	Compressive deformation (mm)	Deformation to yield (mm)	Deformation to peak load (mm)	Deformation to failure (mm)
PLA hot melt (n = 9)	0.656 ± 0.058	0.155 ± 0.022	0.335 ± 0.034	0.583 ± 0.054
P(CPP:SA)20:80 (n = 9)	0.647 ± 0.071	0.238 ± 0.030	0.459 ± 0.053	0.647 ± 0.063
PLA solvent evaporation (n = 6)	0.516 ± 0.087	0.202 ± 0.043	0.381 ± 0.067	0.625 ± 0.140
Alginate (n = 10)	0.957 ± 0.134	0.256 ± 0.052	0.649 ± 0.144	0.835 ± 0.189
P(FA:SA)20:80 (n = 23)	0.635 ± 0.037	0.256 ± 0.039	1.219 ± 0.185	1.859 ± 0.173
P(FA:SA)50:50 (n = 7)	0.866 ± 0.176	0.376 ± 0.137	1.367 ± 0.264	2.020 ± 0.198

Source: Ref. 140.

Table 2. Mean Yield Force, Fracture Strength, and Work Values (±SEM) Calculated from Load versus Deformation Plots Generated during the Electrobalance Tensile Experiments

Polymer	Yield force (μN)	Fracture strength (mN/cm^2)	Compressive work (nJ)	Returned work (nJ)	Tensile work (nJ)
PLA hot melt (n = 9)	40.77 ± 4.41	11.39 ± 0.97	46.01 ± 5.77	2.25 ± 0.78	17.37 ± 2.80
P(CPP:SA)20:80 (n = 9)	64.09 ± 4.31	17.89 ± 1.09	70.14 ± 11.34	10.99 ± 4.69	25.86 ± 4.39
PLA solvent evaporation (n = 6)	70.66 ± 18.03	24.30 ± 3.13	47.62 ± 5.74	5.43 ± 1.86	34.88 ± 12.65
Alginate (n = 10)	90.23 ± 15.23	30.16 ± 4.18	78.67 ± 21.82	6.21 ± 2.37	62.81 ± 14.50
P(FA:SA)20:80 (n = 23)	138.57 ± 9.51	51.63 ± 3.38	64.01 ± 5.21	7.45 ± 1.70	255.45 ± 33.04
P(FA:SA)50:50 (n = 7)	196.78 ± 71.44	76.85 ± 13.53	53.91 ± 5.50	3.18 ± 1.05	366.01 ± 64.07

Source: Ref. 140.

strength, compressive work, returned work, and tensile work.

The outcome of a detailed statistical analysis is discussed thoroughly in previous reports (28,132), and demonstrates that fracture strength, deformation to peak load, deformation to failure, and tensile work are the most important factors in characterizing bioadhesive materials.

Deformations. Table 1 compares four deformation parameters for the six varieties of microspheres investigated. Because the microbalance measures the interaction of the microsphere–tissue composite, the deformations are functions of the material properties of both the tissue and the microspheres. The system cannot distinguish between the elastic moduli of the composite's components. Microspheres with higher elastic moduli (i.e., hard, bioerodible materials) will undergo insignificant deformations under the loads used in this experiment. Therefore, we hypothesized that compressive deformations measured for these materials would depend on the mechanical properties of the tissue alone, while tensile deformations (i.e., deformation to yield, deformation to peak load, and deformation to failure) would depend on mechanical properties of the tissue and the adhesive bond. This would result in similar compressive deformations for all thermoplastics but different tensile deformations. In contrast, we believed that the low modulus of elasticity of alginate would contribute to both tensile and compressive deformations.

As hypothesized, compressive deformations of bioerodible microspheres were not statistically different, indicating that for those materials with considerably high moduli, this parameter is not a function of polymer or bioadhesive interaction but instead is a function of mucus and tissue moduli. However, alginate, which can be expected to have a low modulus compared to the bioerodible materials, produced a compressive deformation statistically different from P(FA:SA) 20:80 ($P \leq .005$). In this instance, the measured value for compressive deformation consists of the deformation of the tissue plus the deformation of the microsphere.

Deformation to yield represents the distance the stage travels before the tensile portion of the curve changes slope and indicates the point at which the adhered surfaces initially start to yield. Because nearly all of deformations to yield were statistically identical (excluding PLA hot melt), we concluded that the change in slope was caused by yielding of the biological component, not yielding of the microsphere or the adhesive union. Thus, we believe that within the microsphere/adhesive-bond/mucus/tissue composite, the component with the lowest modulus is most likely the mucus. In the case of PLA hot melt, however, deformation to yield was significantly less than other materials tested. In this instance, we believe the adhesive interaction may have been the first component to give way. The explanation for this effect may be found in the absence of surface texture of PLA hot-melt microspheres, which limits the degree of mechanical bonding.

Analysis of deformation to peak load and deformation to failure showed that copolymers of FA and SA were statistically different from all other materials (deformation to peak load: $P \leq .05$, deformation to failure: $P \leq .005$). These results clearly demonstrated that interactions formed between P(FA:SA) polymers and intestinal tissue were strong and unlike any other materials investigated. The adhesive bonds were resistant enough to elongate the bioadhesive/tissue composite to a length greater than twice that of any other materials studied.

Fracture Strengths. Fracture strengths of the microspheres are compared in Table 2 and were obtained by di-

viding the peak load by the projected contact area of adhesion, which for microspheres between 710 and 850 μm was estimated to be approximately 0.00487 cm^2. Polymers with the greatest bioadhesive fracture strengths were P(FA:SA) copolymers and alginate. All fracture strengths were statistically different from one another except for PLA solvent evaporation compared to alginate (Table 2). P(FA:SA) copolymers were different from nearly all other materials, with a confidence level of $P \leq .0005$. These results support the hypothesis that polymers with high concentrations of carboxylic acid groups, such as alginate and polyanhydrides, produce strong bioadhesive bonds. The extremely high fracture strengths obtained for P(FA:SA) 20:80 and P(FA:SA) 50:50 (51.63 mN/cm^2 and 76.85 mN/cm^2, respectively) suggest that bioerodible polymers could be promising bioadhesive delivery systems.

In analyzing fracture strengths, we also observed that fabrication technique influenced the bioadhesive properties of a material. PLA microspheres made by solvent evaporation produced greater fracture strengths than PLA microspheres made by hot-melt microencapsulation (24.30 $\pm$ 3.13 mN/cm^2 versus 11.39 $\pm$ 0.97 mN/cm^2, $P \leq .0005$). This effect could be attributed to increased surface texture of solvent evaporation microspheres (see "Characterization of Potential Bioadhesive Polymers"). Greater texture promotes mechanical bond formation and enlarges effective surface area, increasing sites for chemical bonding.

Works. The three work values analyzed in this study were compressive work, returned work, and tensile work (Table 2). Compressive work represents the work done in joining the microsphere and tissue together. This component is a function of the applied load and compressive deformation. Because an attempt was made to exert a consistent applied load of 25 mg and compressive deformation for bioerodible microspheres was shown to be a function of tissue property, compressive work was expected to be identical for all bioerodible materials. Statistical analysis proved that compressive works measured for all materials in this study were not significantly different [excluding PLA hot melt compared to P(FA:SA) 20:80, which showed weak statistical difference: $P \leq .05$].

During the initial tensile region of the curve (i.e., when compressive force is first released), elastic properties of the tissue respond by exerting a force upward on the microsphere. Work done by the tissue on the microsphere is what we have termed returned work. If the tissue and microsphere are completely elastic, returned work would equal compressive work. However, in our experiments energy was lost through plastic deformation, most likely as heat, and returned work was considerably less than compressive work for all materials (Table 2). Analysis of variance on returned work showed no statistical difference among the means ($.10 \leq P \leq .25$), indicating that returned work was dependent on tissue properties and not on microspheres.

Conversely, polymer type did affect tensile work (Table 2). As expected, tensile work was very large for those polymers that displayed high fracture strengths and large deformations to failure. P(FA:SA) 20:80 and 50:50 produced mean tensile works of 255.45 nJ and 366.01 nJ, respectively. These values were 4 to 20 times higher than any other material tested and statistically different.

Two explanations can be given for these results. One theory is that interfacial energies favor spreading of the mucus layer over the surface of the polymer microspheres, and the adhesive interaction is a function of polymer wettability by mucus, as suggested by Lehr (156,157). The other is that numerous surface carboxyl groups on the P(FA:SA) copolymers form hydrogen bonds with the mucin or epithelial cell layer during the compressive portion of the experiment. The intensity of the interaction would be dependent on the concentration of carboxylic acid. As anhydride bonds are degraded through hydrolysis, more carboxylic acid is produced, thus enhancing the bonding capacity of the microspheres. Both of these explanations probably contribute to the unique bioadhesion seen with these materials.

Summary. Using the microbalance as a microtensiometer, we were able to evaluate bioadhesive performance of both hydrogel and bioerodible microspheres. Although hard, bioerodible materials have not previously been studied for bioadhesive applications, we identified one group of polyanhydrides [P(FA:SA)] that exhibits high fracture strengths (>50 mN/cm^2), long deformations to failure (>1.7 mm), and large tensile works (>250 nJ). These findings strongly support the existence of bioadhesion between soft tissue and hard, bioerodible, thermoplastic polymers. In spite of the fact that in these experiments every attempt was made to use freshly excised, viable tissue under physiologic conditions, we should note that this method is an in vitro technique and therefore results may not exactly reflect bioadhesive properties of these materials in vivo. Correlation between these findings and in vivo performance is investigated later in this article.

Although hydrogels and hydrophilic polymers have been traditionally thought of as ideal BDDSs, new results suggest that novel materials with greater bioadhesive properties may exist (156). The findings in this study show that certain bioerodible polyanhydrides produce strong bioadhesive interactions, in vitro, compared to other thermoplastic and hydrogel materials. In bioerodible polymers lacking chain flexibility, bioadhesion could largely be a result of surface energy effects and/or hydrogen bonding between mucin and carboxyl groups. Thus, as suggested by Lehr et al. (83,156,157), chain flexibility and interpenetration of polymer and mucin chains should not be considered prerequisites for bioadhesion.

Characterization of Potential Bioadhesive Polymers

To gain a better understanding of the mechanisms responsible for bioadhesive phenomena observed with polyanhydride microspheres, three common polymer characterization techniques were employed. First, surface morphology and morphological changes produced through polymer degradation were investigated and documented using scanning electron microscopy (SEM). Second, bulk chemical analysis was conducted with Fourier transform infrared spectroscopy (FTIR). Our intent was to determine whether a correlation could be observed between high carboxylic acid content and high bioadhesive properties. Also, we were interested in determining if chemical composition

was affected by degradation and how these changes could alter a material's bioadhesive performance. Third, because interfacial forces are believed to play a large role in bioadhesion (58–60,64,67,156,157), both water and mucus contact angles were measured with a goniometer. Correlation between tensile experiment measurements and mucus contact angles was investigated (140).

Morphological Characterization Using SEM. To assess the effects of surface morphology on bioadhesive properties, microsphere samples were lyophilized and analyzed under SEM at both 150× and 1,000×. We analyzed both thermoplastics and hydrogels in the same manner even though we realize that alginate microspheres in the lyophilized state may appear quite different than those in the hydrated state. Although free of pores, surfaces of the alginate microspheres were marked with distinct arrays of raised stripes (Figs. 17a and 17b). The origin of these structures is unknown, but we believe that they may be a mechanical stretching artifact of the freeze-drying process. At 150× both P(CPP:SA) 20:80 and PLA microspheres, appeared fairly smooth in appearance (Figs. 17c and 17e), but closer examination (1,000×) revealed some differences. High-magnification analysis of P(CPP:SA) 20:80 microspheres demonstrated a granular texture as well as a few scattered, shallow pockmarks (Fig. 17d). PLA hot-melt microspheres were mostly smooth and uniform even at high power (Fig. 17f). Though some dispersed particulate matter could be found, surfaces were completely free of any pits or indentations. This smooth texture could account for the weak bioadhesive performance of these microspheres including the significantly low deformation to yield.

Among bioerodible microspheres, four were manufactured using a hot-melt technique: PLA, P(CPP:SA) 20:80, P(FA:SA) 20:80, and P(FA:SA) 50:50. Owing to the nature of this fabrication procedure, we expected the resulting microspheres to be generally smooth and dense in appearance. However, depending on the polymer employed, surfaces ranged from very smooth to highly pitted. SEMs of the two P(FA:SA) copolymers (Fig. 18a–d) demonstrated different surface morphologies. P(FA:SA) 20:80 copolymer microspheres possessed a granular topography and were riddled with deep pits approximately 10 μm in diameter and approximately 30–50 μm apart (Fig. 18b). We believe these structures developed through growth of spherulites during solidification of the microspheres, although fine lamellar morphologies could not be seen, and that the pits are actually crevices between adjacent spherulites. These structures were found on all P(FA:SA) 20:80 microspheres analyzed. However, P(FA:SA) 50:50 microspheres showed no sign of spherulite formation or pock marks but instead displayed a fine granular texture very similar to P(CPP:SA) 20:80 (compare Figs. 17d and 18d). This difference in spherulite development could be attributed to different cooling rates during the fabrication procedures and/or different glass transition temperatures.

PLA microspheres were also manufactured using a solvent evaporation technique. Because this process involves the removal of a solvent from the bulk of the polymer, we expected to find more porous microspheres than those created with the hot-melt technique. Examination of the surfaces did indeed reveal a highly porous morphology (Fig. 18e). At 1,000×, spherulites could be clearly seen with distinct lamellar structures (Fig. 18f). The irregular pores and channels, created as the solvent evaporated from the system, were approximately 3–10 μm in diameter and spaced 6–10 μm apart. This structure was completely different from the smooth surface observed on the hot-melt PLA microspheres (compare Figs. 17f and 18f). We believe this difference in surface morphology is the main explanation for the difference in bioadhesive properties measured using the microbalance (as discussed in "Bioadhesive Measurements".). Coarser surface texture improved adhesion of solvent evaporation microspheres through stronger mechanical interactions.

Morphological Characterization of Short-Term Degradation Using SEM. Because the polyanhydrides are known for their rapid hydrolytic degradation and our in vitro bioadhesion analysis is performed in an aqueous bath, it was important to study the morphological surface changes occurring on the polymers when incubated in buffer. All three polyanhydrides were degraded for 0, 7, 15, 30, and 60 min in PBS and analyzed by SEM (Figs. 19 and 20). The most obvious result was the change in surface texture of the P(FA:SA) 50:50 microspheres after only 7 min. The entire surface of the microspheres became porous and flaky (Fig. 19a) as compared to the nondegraded samples (Fig. 18d). After 15 min, the surfaces had further changed, looking more uniform but displaying small cracks and fissures (Fig. 19b). Thus, as degradation proceeded, the original flakes and scurf were swept away, and surface cracks developed. After 30 min, the cracks enlarged, and by 60 min more pieces of polymer had crumbled away from the surface (Figs. 19c and 19d). Cross sections of these microspheres showed a solid and relatively intact core, with only the outer 50 microns showing signs of degradation (158,159).

Analysis of the other two polyanhydrides showed less significant changes (Fig. 20). After 7 min we observed an increase in the size and number of pores or pits on the surface of P(FA:SA) 20:80 microspheres (Fig. 20a). These pits continued to grow in number and dimensions as degradation proceeded, but no cracks developed as was observed in the 50:50 copolymer (Fig. 20b). These microspheres may have degraded more slowly than the P(FA:SA) 50:50 microspheres owing to higher crystallinity, as indicated by pockmarks in the nondegraded samples. P(CPP:SA) 20:80 exhibited even fewer changes than the P(FA:SA) 20:80. At 1,000× there was no discernable difference between the microspheres at time zero and the microspheres after 7 min degradation. After 30 min, scattered pores developed across the surface, and granulation that was observed in nondegraded samples either degraded or washed away (Fig. 20c). By 60 min, very small cracks appeared (Fig. 20d). However, these changes were minimal compared to those shown by copolymers of P(FA:SA).

The results of SEM analysis may indicate one possible explanation for the tremendous adhesive interactions measured for some polyanhydride materials. The rapid surface degradation of copolymers of FA and SA may im-

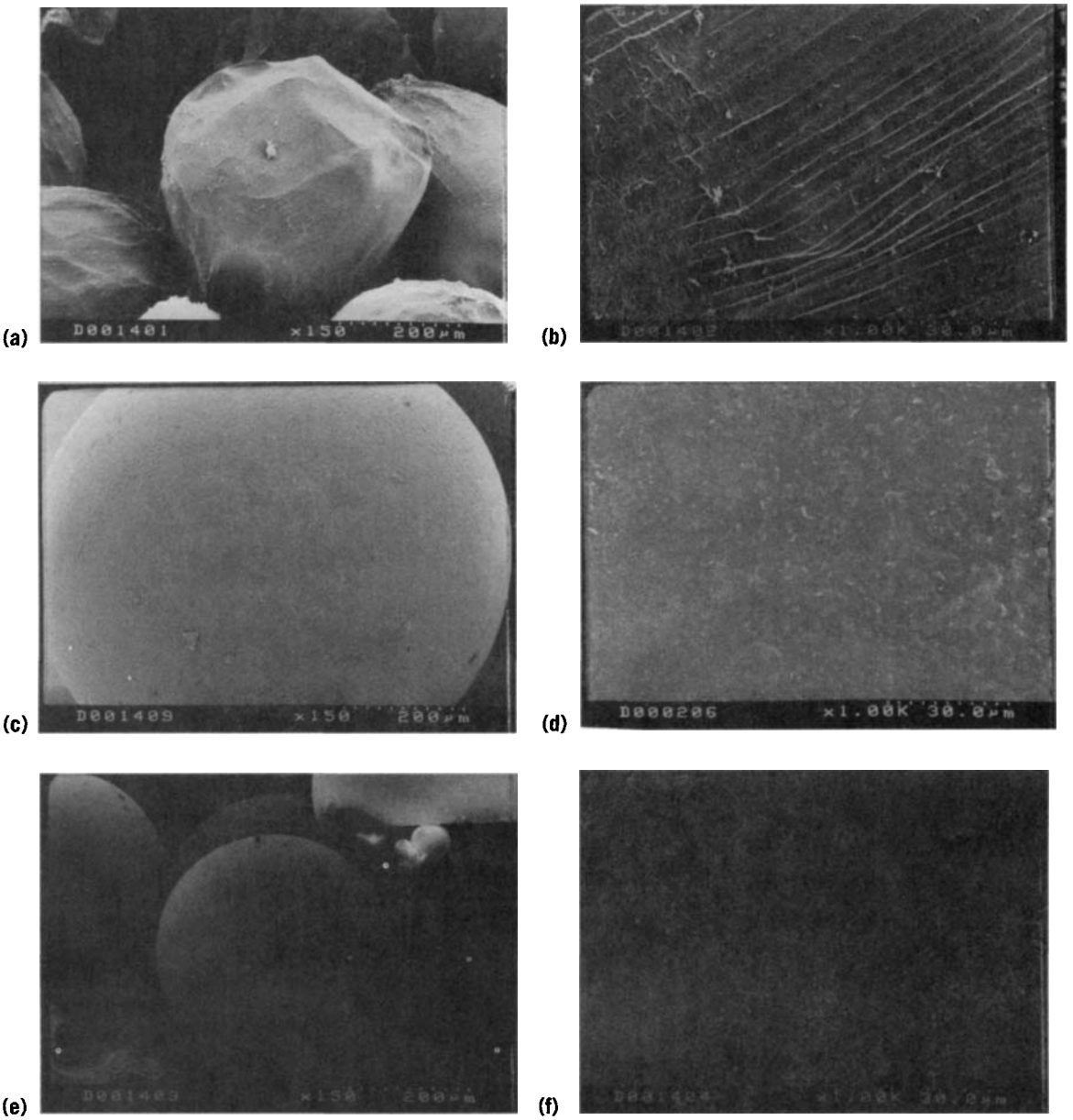


Figure 17. Scanning electron micrographs of three polymer microspheres. (**a**) Lyophilized alginate microsphere (150×). The nonspherical shape is an artifact of the lyophilization process; (**b**) higher magnification (1,000×) of (**a**) showing artifactual striations generated during the freeze-drying process; (**c**) P(CPP:SA) 20:80 microsphere made by hot melt (150×); (**d**) higher magnification (1,000×) of the microsphere in (**c**) showing a dense structure with a slightly granular surface. (**e**) PLA microsphere made by the hot-melt fabrication technique (150×); (**f**) higher magnification (1,000×) of the microsphere in (**e**) showing a very dense surface free of any pores. *Source:* Reproduced with permission from *Reactive Polymers* (Ref. 140).

prove their bioadhesive properties. As each anhydride bond is cleaved, two carboxylic acid groups are produced. These hydrophilic functional groups are then able to form hydrogen bonds with surrounding mucin strands that can in turn penetrate newly created surface cracks. The result is the formation of both chemical and mechanical bonds between the biological tissue and microsphere. Further degradation renews the surface carboxyl concentration, allowing for even greater adhesion.

FTIR Analysis. FTIR transmission spectra of polymer microspheres were taken to verify the presence of functional carboxyl groups believed to play a role in the formation of hydrogen bonds with biological tissues. Figure 21 shows transmission data from 2,000 cm^{-1} to 1,500 cm^{-1} for the polymers investigated in this study.

Peaks present in the spectrum for alginate were very broad, indicating an amorphous structure, but make it difficult to pinpoint specific chemical compo-

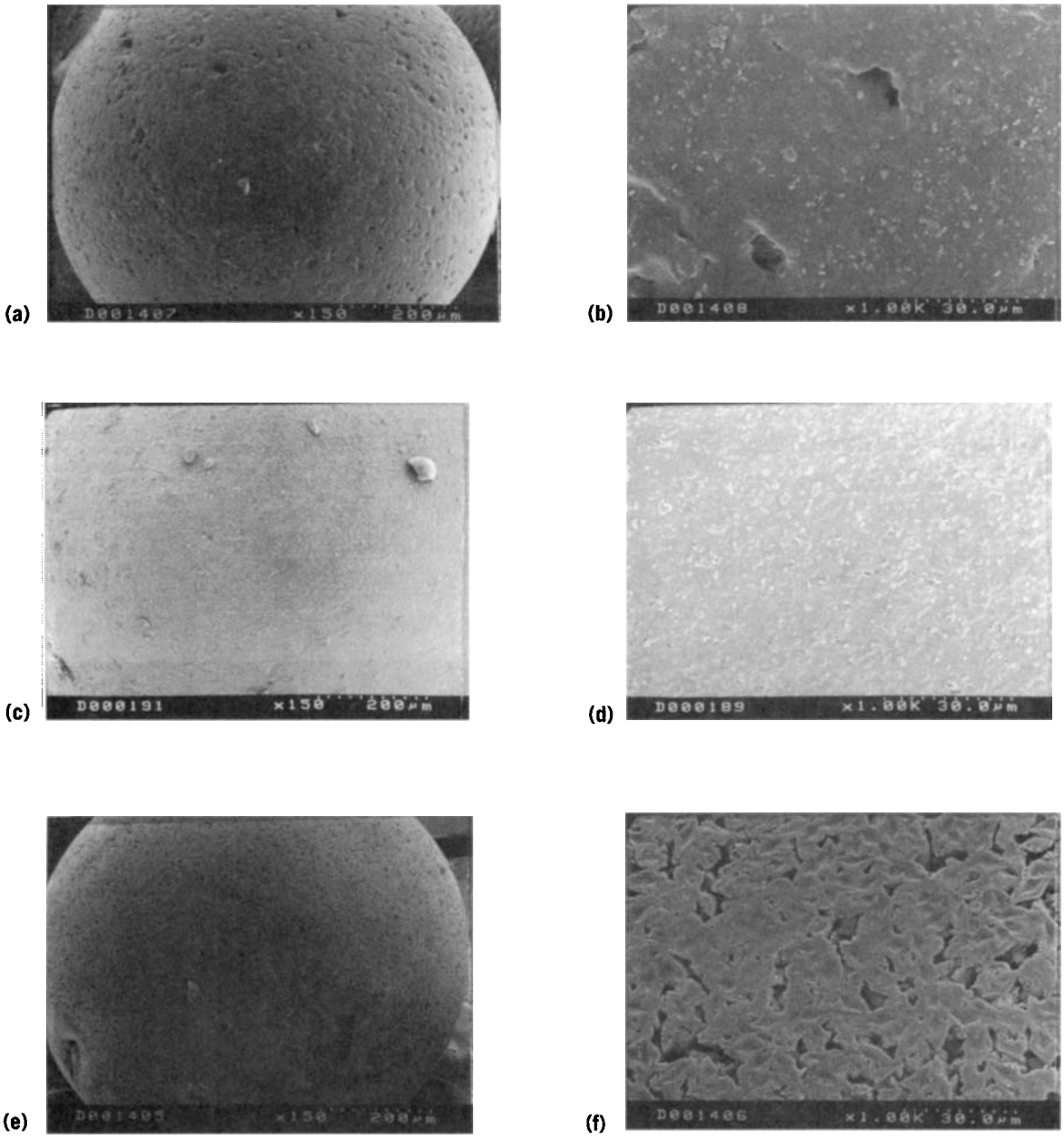


Figure 18. Scanning electron micrographs of three polymer microspheres. (**a**) P(FA:SA) 20:80 microsphere made by hot melt (150×); (**b**) higher magnification (1,000×) of the microsphere in (**a**) showing several large pits, which most likely represent spaces between adjacent spherulites; (**c**) P(FA:SA) 50:50 microsphere made by hot melt (150×); (**d**) higher magnification (1,000×) of the microsphere in (**c**); note that the external surface of this microsphere bears a closer resemblance to the P(CPP:SA) 20:80 (Fig. 17d) than it does to the P(FA:SA) 20:80 in (**b**); (**e**) PLA microsphere made by the solvent evaporation technique (150×); (**f**) higher magnification (1,000×) of the microsphere in (**e**) revealing the highly porous and corallike structure of the PLA. *Source:* Reproduced with permission from *Reactive Polymers* (Ref. 140).

nents. The broad band at 1630 cm^{-1} is typical of carboxyl groups.

Both PLA preparations showed distinct peaks around 1,760 cm^{-1} characteristic of the ester linkage as well as subtle bands at 1,625 cm^{-1} that we attribute to the presence of carboxylic acid. The occurrence of carboxylic acid in PLA is due to end-group contribution. Each hydrolytically degraded ester linkage results in the formation of one carboxyl and one hydroxyl end group (Fig. 22). The PLA used in this study was a low-molecular-weight material (M_r = 2K), and therefore the concentration of end groups appears as a significant fraction of the entire polymer sam-

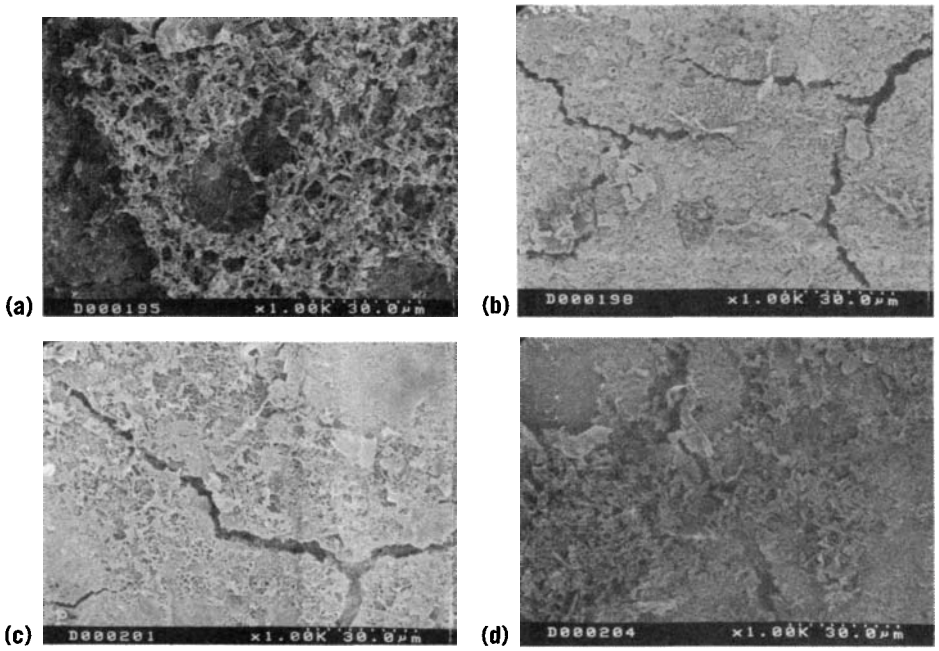


Figure 19. Scanning electron micrographs (1,000×) of the external surfaces of the poly(fumaric-*co*-sebacic anhydride) 50:50 microspheres after incubation in 37°C PBS (pH 7.4). (**a**) 7-min incubation, (**b**) 15-min incubation (note the crack formation), (**c**) 30-min incubation, (**d**) 60-min incubation. *Source:* Reproduced with permission from *Reactive Polymers* (Ref. 140).

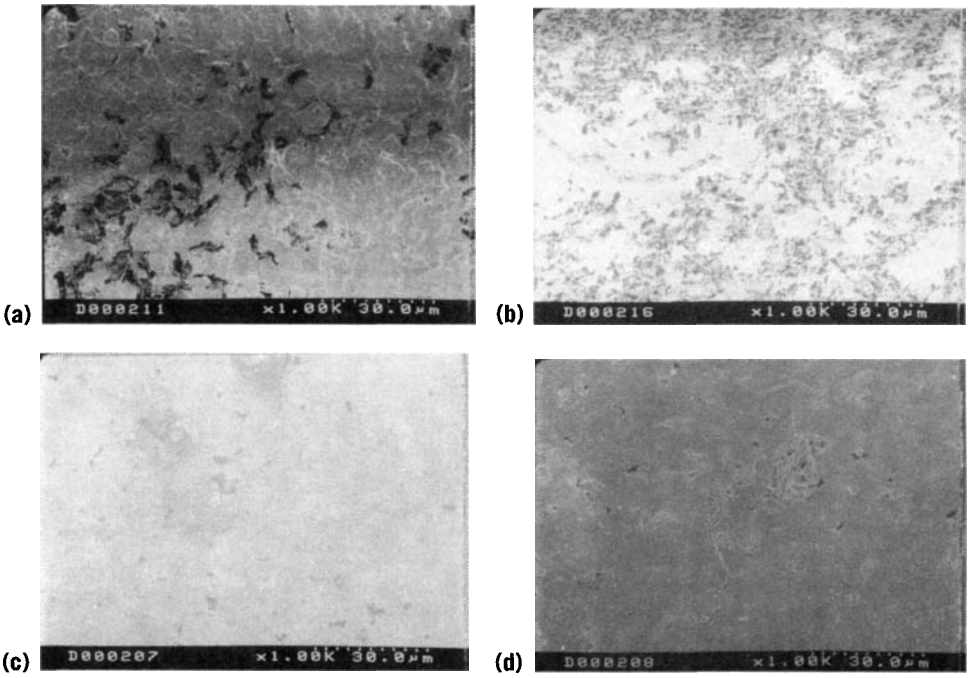


Figure 20. Scanning electron micrographs (1,000×) of the external surfaces of the poly(fumaric-*co*-sebacic anhydride) 20:80 and poly[1,3-bis(*p*-carboxyphenoxy)-propane-*co*-sebacic anhydride] 20:80 microspheres after incubation in 37°C PBS (pH 7.4). (**a**) P(FA:SA) 20:80 microsphere after a 7-min incubation, (**b**) P(FA:SA) 20:80 microsphere after a 60-min incubation. (**c**) P(CPP:SA) 20:80 microsphere after a 30-min incubation, (**d**) P(CPP:SA) 20:80 microsphere after 60-min incubation. *Source:* Reproduced with permission from *Reactive Polymers* (Ref. 140).

ple. In high-molecular-weight PLA, decrease in the relative number of end groups may make carboxylic acid undetectable by FTIR and reduce its bioadhesive properties.

All three polyanhydrides (P[CPP:SA] 20:80, P[FA:SA] 20:80, and P[FA:SA] 50:50) displayed multiple peaks from 1,840 cm^{-1} to 1,680 cm^{-1}, which are typical of anhydride linkages (159). Particular peaks correspond to either SA–SA, SA–CPP, CPP–CPP, FA–SA, or FA–FA diads or a combination of these. The small peak around 1,710 cm^{-1} is due to the presence of carboxylic acid (161) and is believed to increase as anhydride bonds degrade. Figure 23 depicts the the reaction scheme for hydrolytic degradation of polyanhydrides.

Spectra generated after short-term degradation experiments of P(FA:SA) 20:80 (Fig. 24) helped confirm the hypothesis that the peak at 1,710 cm^{-1} becomes more pronounced with degradation. The rapid hydrolytic degradation characteristic of polyanhydrides is believed to predominantly be a surface rather than bulk phenomenon. In fact, the degradation is often characterized by an erosion zone, made of high-molecular-weight, crystalline polymer containing carboxylic acid end groups (159). The hy-

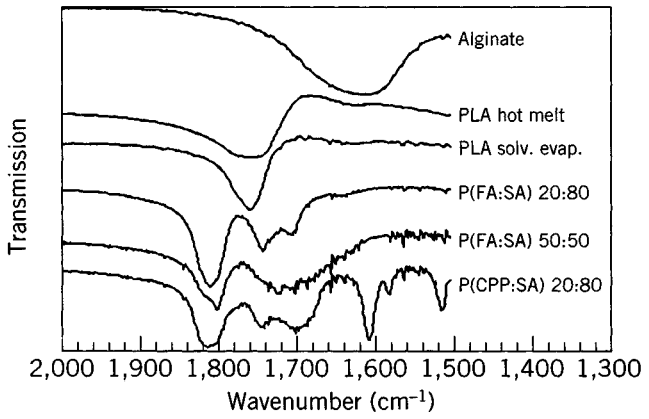
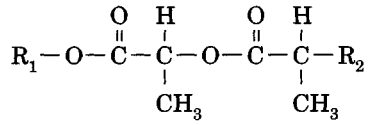


Figure 21. FTIR transmission spectra, from 2,000 to 1,500 cm^{-1}, of the polymers investigated in this study. *Source:* Reproduced with permission from *Reactive Polymers* (Ref. 140).

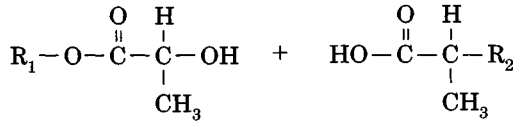
drolysis of each anhydride bond results in the formation of two carboxylic acid groups (Fig. 23). Figure 24 shows transmission spectra from 2000 to 1,200 cm^{-1} collected for P(FA:SA) 20:80 at four degradation times. In all three polyanhydrides (P[FA:SA] 20:80, P[FA:SA] 50:50 and P[CPP:SA] 20:80), the peak at 1,710 cm^{-1} increased in size proportional to other anhydride peaks at 1,800 and 1,734 cm^{-1} suggesting an increase in carboxyl end-group concentration as anhydride bonds are hydrolyzed (Fig. 24).

Another peak of interest was found at 1,260 cm^{-1}. Single-bond stretching and bending deformation associated with carboxylic acid are known to produce strong absorptions at this wavelength (160). Although this peak was nearly undetectable in the nondegraded sample of P(FA:SA) 20:80, after 7 min in buffer a distinct peak emerged that persisted throughout the degradation study (Fig. 24). Because this peak could not be found in either of the pure monomers or pure polymers of FA or SA (158), we suspect that it may have arisen as the ratio of ordered to



Polylactic acid

Water H_2O

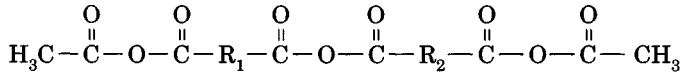


Degraded polymer chains with newly formed hydroxyl and carboxyl end groups

Figure 22. Degradation of polylactic acid.

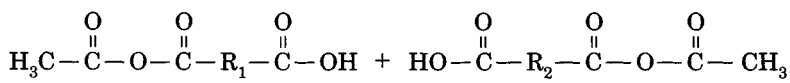
nonordered regions increased in the degrading polymer. As amorphous areas were rapidly degraded, crystalline regions were uncovered. These erosion-resistant zones may contain high-molecular-weight polymer chains as well as smaller chains, such as trimers, tetramers, pentamers, and so on, all with carboxylic end groups (158,159).

We believe that rapid degradation of P(FA:SA) copolymers resulting in carboxylic acid production plays an important role in the formation of the intense bioadhesion exhibited during the in vitro studies. For a material to form strong bioadhesive interactions through carboxyl group hydrogen bonding, carboxylic acid must be present as polymer end groups and not free monomer (which could not provide the necessary mechanical strength). The narrow



Polyanhydride

Water H_2O



Degraded polymer chains with newly formed carboxylic end groups

Figure 23. Hydrolytic degradation of polyanhydrides.

Next Page

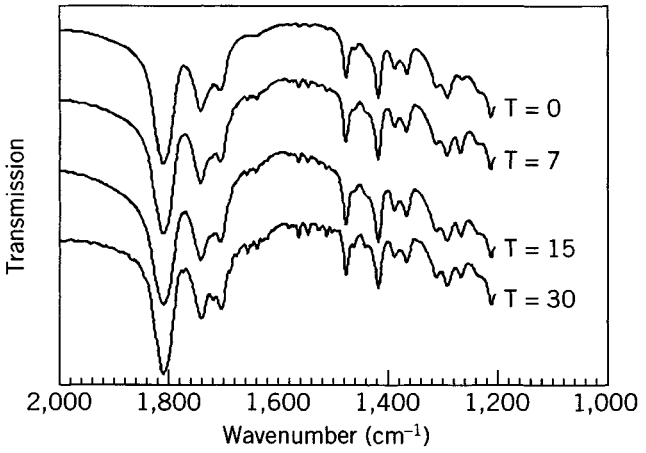


Figure 24. FTIR transmission spectra of P(FA:SA) 20:80 microspheres during the course of hydrolytic degradation (time T_0 to 30 min). Entire microspheres were ground with KBr and formed into pellets. Note the increasing prominence of peaks at 1,710 and 1,260 cm^{-1}. *Source:* Reproduced with permission from *Reactive Polymers* (Ref. 140).

shape of the peak at 1,710 cm^{-1} is a strong indication of carboxylic end groups because free acids typically appear as a broad band (158).

The Role of FA in Polyanhydride Copolymers. We suggest that bioadhesion of these hard, bioerodible materials is not due to chain entanglement, as required by the diffusion theory of bioadhesion, but due to numerous hydrogen bonds generated between hydrophilic functional groups (-COOH) and mucus glycoproteins. In addition, we found a strong correlation between the amount of fumaric acid and the adhesive forces, summarized in Table 3. Larger amounts of FA in the polymer result in larger tensile work measurements as well as higher fracture strength measurements. All experiments were performed as described in "Bioadhesive Measurements" using rat jejunum. Statistical analysis using the unpaired t-test is summarized in Table 3. As seen, the formulation made of P(FA:SA) 70:30 is statistically different from any formulation composed of 10 or 20% FA but not different from those containing higher concentrations of FA. The same trend is found for P(FA:SA) 60:40 and 50:50 (Tables 4a and 4b).

Everted Sac Experiments. We initiated a new study aimed at mapping the exact amount of microspheres adhering to the GI tract using the everted sac bioassay, which provides important information about the relative bioadhesion of different formulations at potentially any location along the length of the gut. The everted sac experiments were performed using viable segments of rat jejunum. Unfasted rats (300–400 g, male, CD strain) were sacrificed, and the tissue was excised and flushed with 10 mL of ice-cold pBS, pH 7.2, containing 200 mg/dL glucose (PBSG). Six-centimeter segments of jejunum were everted using a stainless steel rod and lightly washed with PBSG to remove the contents. Ligatures were placed at both ends of the segment, and the sac was filled with 1.0–1.5 mL of

Table 3. Tensile Work and Fracture Strength of Microspheres As Determined by Cahn Force Measurements for Different P(FA:SA) Copolymer Ratios

Polymer	Diam. (μm)	Tensile wk. (nJ)	Fract. str. (mN/cm^2)
	P(FA:SA)10:90 (n = 11)		
Average	784.45	82.99	31.58
stdev	43.14	40.35	17.61
	P(FA:SA)20:80 (n = 15)		
Average	775.67	32.95	17.46
stdev	48.02	20.27	6.64
	P(FA:SA)30:70 (n = 10)		
Average	788.90	66.89	24.26
stdev	44.42	60.10	15.29
	P(FA:SA)50:50 (n = 23)		
Average	737.26	315.29	58.04
stdev	68.91	208.93	22.11
	P(FA:SA)60:40 (n = 21)		
Average	763.10	319.53	67.44
stdev	49.63	209.96	31.92
	P(FA:SA)70:30 (n = 4)		
Average	781.75	453.23	99.71
stdev	66.77	82.67	30.06

Table 4a. Fracture Strength Statistics Using the Unpaired T-Test (Alternate Welch T-test); Two-Tailed *P* Value Reported

P(FA:SA)	10:90	20:80	30:70	50:50	60:40	70:30
10:90	n.s.	*	n.s.	***	***	*
20:80	—	—	n.s.	***	***	*
30:70	—	—	—	***	***	*
50:50	—	—	—	—	n.s.	n.s.
60:40	—	—	—	—	—	n.s.
70:30	—	—	—	—	—	—

* = significant, $P < .05$; ** = very significant, $P < .01$; *** = extremely significant, $P < .001$; n.s. = not significant.

Table 4b. Tensile Work Statistics Using the Unpaired T-Test (Alternate Welch T-Test); Two-Tailed *P* Value Reported

P(FA:SA)	10:90	20:80	30:70	50:50	60:40	70:30
10:90	—	**	n.s.	***	***	**
20:80	—	—	n.s.	***	***	**
30:70	—	—	—	***	***	**
50:50	—	—	—	—	*	n.s.
60:40	—	—	—	—	—	*
70:30	—	—	—	—	—	—

* = significant, $P < .05$; ** = very significant, $P < .01$; *** = extremely significant, $P < .001$; n.s. = not significant.

PBSG. Tissue was maintained at 4°C prior to incubation. The sacs were incubated with 60 mg of spheres and 5 mL of PBSG at 37°C. The incubated sacs were agitated end over end. After 30 min, the sacs were removed, and the solution of PBSG and unbound microspheres was centrifuged for 30 min. The supernatant fluid was discarded, the remaining spheres were washed with 5.0 mL distilled water, centrifuged, the water discarded, and the microspheres frozen and dried via lyophilization for 24–48 h. The weight of the bound spheres was determined by subtraction of the tared weight of the tube and lyophilized beads from the initial tare weight and is reported as percent binding.

One of the most interesting results was that the amount of binding is strongly related to the amount of FA in the polymer. Table 5 demonstrates this relationship for hot melt microspheres.

We found that spray-dried polyanhydride microspheres [P(FA:SA)20:80] showed tremendous bioadhesion to segments of small and large intestine in vitro. Spray-dried microspheres also display a much rougher surface and tend to be smaller in diameter than hot-melt microspheres. As much as 65% of the initial dose (100 mg microspheres/g wet weight of tissue) adhered to the mucosa after a 30-min incubation (data not shown). Additionally, the microspheres were found to adhere to mechanically damaged sites on the intestine (161).

Cahn and Everted Sac Correlation. To validate the results of our unique Cahn system to determine bioadhesion between individual microspheres and intestinal tissue in vitro, we correlated the results of these measurements to the everted sac bioassay for several polymers. Microspheres were prepared by the hot-melt method, collected by filtration, washed with petroleum ether, and sieved into two size ranges, 600 μm and below for everted sac measurements and 600–850 μm for Cahn measurements.

As seen in Figure 25, polymers that exhibit a high binding percentage in the everted sac assay also demonstrate high fracture strengths as determined by the Cahn microbalance. Specifically, [P(FA:SA)50:50]:FAPP (poly[fumaric-*co*-sebacic anhydride] blended with FA prepolymer) PCL:FAPP (a blend of polycaprolactone and FA prepolymer), and SAPP:FAPP (SA prepolymer and FA prepolymer) all show high bioadhesion in each method. In the everted sac assay [P(FA:SA) 50:50]:FAPP shows 71 ± 9% (mean ± SEM) binding, PCL:FAPP shows 82 ± 15% binding, and SAPP:FAPP shows 64 ± 4% binding. In the Cahn assay, the fracture strengths for each of these microspheres is 185 ± 45, 255 ± 37, and 333 ± 72 mN/cm^2, respectively. Interestingly, polymers such as PCL that show low percentage binding from everted sac experiments also demonstrate low fracture strengths in Cahn measurements. Everted sac experiments with PCL result in 2 ± 3% binding, and the Cahn assay shows a fracture strength of 15 ± 2 mN/cm^2, both of which are relatively low compared to the other polymers tested. These studies demonstrate for the first time a good correlation between the two methods.

Table 5. Percent Binding of Hot-Melt Microspheres As Determined by Everted Sac Experiments

Polymer	M_r (weight average)	% binding ± SEM	No. of sacs
P(FA:SA)20:80	10,000	19.9 ± 8.3	6
P(FA:SA)50:50	3,000	10.8 ± 7.4	6
P(FA:SA)70:30	3,000	61.3 ± 17.1	5

Contact Angle Measurements with Water and Mucus. Static contact measurements between polymer films and rat intestinal mucus (Pel Freeze, Rogers, AR) were made using a goniometer. Interestingly, water contact angle for the series of polymers studied gave similar hydrophobic readings (between 97° to 68°), while the mucus reading showed very low contact angle, which is a strong indication of high adhesive forces as dictated by the wetting theory of adhesion. Moreover, the series indicate that higher FA concentrations within the copolymer result in lower contact angles (Table 6). These results strongly correlate with the Cahn data described previously.

Static contact-angle measurements were measured for several polymers (Table 7). As expected, water contact-angle measurements for the bioerodible materials all gave similar hydrophobic readings (~64°), while the hydrated alginate sample showed zero (0°) contact angle (i.e., complete wetting).

Mucus measurements provided the most notable results. Though no correlation was seen between water contact angles and mucus contact angles, an interesting trend was observed between mucus contact angle and bioadhesive force. Both alginate and P(FA:SA) copolymers produced very low contact angles with mucus and produced strong bioadhesive interactions (see "Bioadhesive Measurements"), whereas P(CPP:SA) 20:80 produced a contact angle of 35° and weaker bioadhesive interactions. This supports the wetting theory of adhesion, which states that strong adhesive forces result from sufficient wetting of the two components, and these results further advocate the notion of bioadhesion between hard, bioerodible materials and soft tissue.

It is possible that surface energetics could promote bioadhesion in thermoplastic materials. All thermoplastics studied were rather hydrophobic (≥60°), suggesting a driving force away from water. Hydrogels, on the other hand, are naturally hydrophilic. Although both P(FA:SA) 50:50 and alginate produced similar mucus contact angles owing to the hydrophobic property of P(FA:SA), it may experience a greater driving force towards mucus. Figure 26 depicts a schematic representation of two microspheres in the GI lumen. Assuming the center of the lumen to be most like pure water and the edge of the lumen to be most like pure mucus, vectors are indicated representing the driving forces produced by interfacial energies. Alginate is both hydrophilic and mucophilic and thus experiences opposing driving forces, whereas P(FA:SA) 50:50 is hydrophobic and mucophilic and is thus driven towards the mucosal surface. Although this pure water/pure mucus condition does not exist in vivo, mucus concentration gradients are found in the GI lumen, and therefore similar driving forces may in-

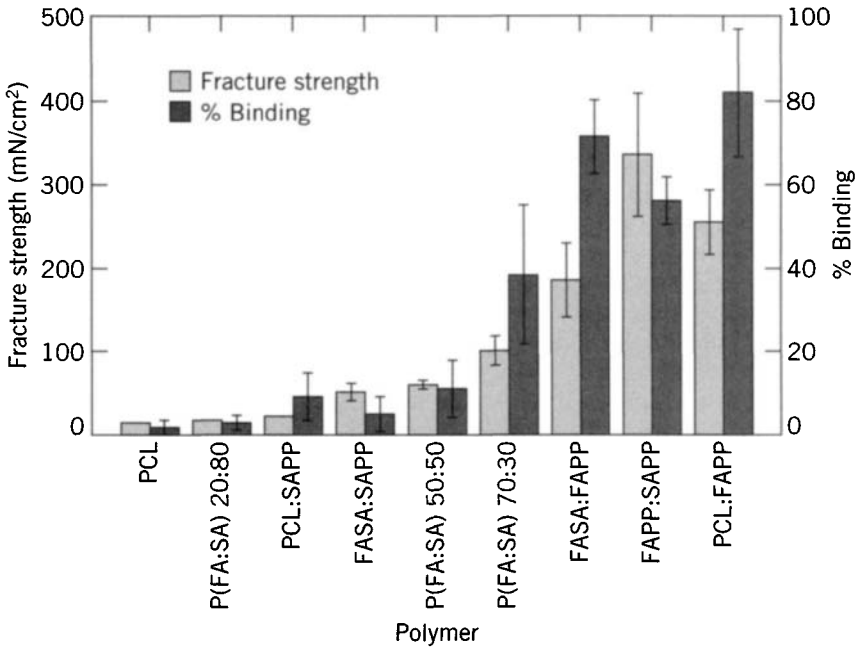


Figure 25. Correlation between Cahn and everted sac measurements. *Note:* FASA:SAPP and FASA:FAPP denote [P(FA:SA)50:50]:SAPP and [P(FA:SA)50:50]:FAPP.

Table 6. Contact Angle Measurements on Melt-Cast Films Made of P(FA:SA) Copolymers

P(FA:SA)	20:80	30:70	40:60	50:50	60:40	70:30
Water	97	89	81	88	71.5	68.5
Mucus	34	28	19	20	20	29

Table 7. Water and Mucus Static Contact Angles Measured on Polymer Films Cast on Glass Slides

Polymer	Water contact angle (°)	Mucus contact angle (°)
P(CPP:SA)20:80	64	35
PLA (solvent evaporation)	63	20
Alginate	0	14

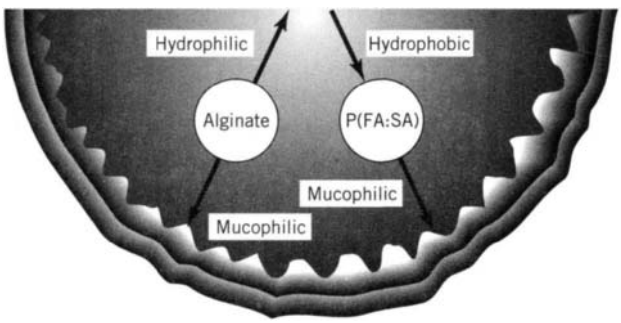


Figure 26. Proposed surface energy theory.

duce contact of P(FA:SA) microspheres with the mucosal layer.

In papers by Lehr et al. (156,157) and Baszkin et al. (60), a more sophisticated captive bubble technique was employed to measure contact angles and interfacial energies of hydrated bioadhesives. Lehr et al. found a strong correlation between mucus wetting of bioadhesives and bioadhesive bond strength. Furthermore, they suggested that interpenetration and chain entanglement was not a necessity for bioadhesion. In light of their analysis and the results of our study, we agree that mucus contact angle and surface energy analysis can be strong predictors of bioadhesive potential, and we believe that mechanisms other than chain entanglement are responsible for the bioadhesive properties of copolymers of P(FA:SA).

To summarize this section, we have shown that fracture theory analysis of the microbalance experiments clearly showed that copolymers of FA and SA produced bioadhesive bonds with rat intestine in vitro. Both the fracture strengths and tensile works calculated for these bioerodible microspheres indicated stronger adhesive interactions than those observed for any other material in this study, including alginate microspheres. We believe interactions between P(FA:SA) copolymers and intestinal tissue rely on more than simple physical entrapments. Furthermore, because these materials lack flexible polymer chains, it seems unlikely that polymer–mucin chain entanglement plays a significant role in bioadhesion. The results of our studies suggest that adhesion of these materials to mucus is due to surface energy effects and secondary bonding phenomena, but other mechanisms, yet to be determined, may also play a role.

SEMs of P(FA:SA) microspheres confirmed their ability to erode rapidly in the presence of water. Visible surface changes were observed after even very short incubation

periods (7 min). Degradation of melt-cast polyanhydrides has been shown to be a surface rather than bulk phenomena, characterized by a unique erosion zone (158,159). The remaining polymer in the eroding surface layer, although porous and fragile in appearance, is highly crystalline and contains specific spherulitic structures (158,159). We believe that rapid degradation of these materials may enhance their bioadhesive properties by not only creating a rougher and more porous surface but also by increasing the quantity of surface carboxylic acid.

An interesting trend was noted between bioadhesive fracture strengths and mucus contact angles. Those materials with low mucus contact angles (i.e., alginate and P[FA:SA] 50:50) produced strong adhesive interactions. These results support the wetting theory of adhesion, which states that strong bioadhesive bond formation is dependent on favorable spreading and wetting of the biological component on the polymer or vice versa. It should also be noted here that water contact angle seemed to have no correlation with mucoadhesive properties.

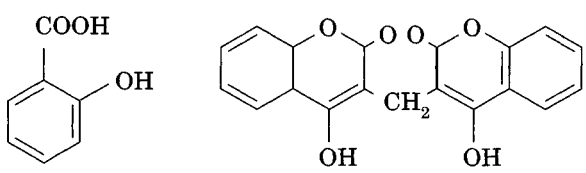
GI Transit and Bioavailability of Low-Molecular-Weight Drugs

Having established P(FA:SA) as a strong BP and realizing that polyanhydrides are well suited for drug delivery, we set out to determine if its bioadhesive properties could positively effect GI transit and bioavailability of two model drugs. Alginate was selected as a comparison polymer owing to its moderate adhesive performance, ease of microsphere fabrication, low cost, and the fact that it is a hydrogel.

To determine effects on transit through the gut, radiopaque barium sulfate was encapsulated in both polymers. After administration to rats, serial feces collections were made, feces were x-rayed, and microspheres were counted to determine GI residence time.

For bioavailability studies, two drugs were investigated: salicylic acid (an analgesic and nonsteroidal anti-inflammatory drug [NSAID] rapidly absorbed by the stomach and duodenum) and dicumarol (an anticoagulant that is poorly absorbed in the small intestine) (Fig. 27). To determine bioavailability, serum concentration-time curves were generated and maximum serum concentration (C_{max}), time to maximum serum concentration (T_{max}), and area under the serum-concentration-time curves (AUC) were compared to unencapsulated controls.

Material Selection and Animal Models. Bioadhesive polymers investigated in this study were alginate and P(FA:SA) 20:80 and were chosen based on in vitro results. A commercially available formulation of 95% w/w barium sulfate (Tonopaque) was chosen as a radiopaque marker for GI transit studies. Two model drugs [salicylic acid and 3,3′-methylene-bis(4-hydroxy-coumarin) (dicumarol)] were selected for bioavailability studies based on absorption characteristics and assessability using simple spectrophotometric techniques. Polyvinylphenol (PVP; Polysciences, Warrington, PA) was used to coat salicylic acid, as a barrier to dissolution, prior to encapsulation in P(FA:SA).



Salicylic acid Dicumarol

Figure 27. Chemical structures of salicylic acid and dicumarol.

Preparation of Drug-Loaded Microspheres ***Drug Preparation.*** To produce proper DDSs and controls for those systems, processing of the stock drugs was required. A LabPlant SD-4 spray-drier (Virtis, Gardiner, NY) equipped with a 1.0-mm nozzle was used to micronize dicumarol particles to improve dissolution and to coat salicylic acid particles with PVP to inhibit dissolution. Dicumarol was dissolved in methylene chloride (0.5% w/v) and sprayed with an inlet temperature of 90°C. Resulting particles were less than 5 μm in diameter, porous, and very fragile. Equal amounts of salicylic acid and PVP were dissolved in acetone (10% w/v for each component) to give a 1:1 ratio and sprayed at 65°C. Resulting particles were less than 5 μm in diameter, spherical, and dense.

Microsphere Fabrication and Ionic Gelation. Alginate microspheres were fabricated according to a modified method of Lim (146,162). Powdered drug (4, 25, or 50%, w/v of dicumarol, salicylic acid, or Tonopaque, respectively) was added to a 2% alginate solution. Each mixture was vigorously blended with a Virtis 23 microhomogenizer (Virtis, Gardiner, NY) for 3 min. The alginate suspension was loaded into a 10-cc syringe and pumped through the inner lumen (18 gauge) of a double-lumen spinneret at a rate of 0.8 mL/min using a syringe pump (model 22; Harvard Apparatus, South Natick, MA). Droplet size was adjusted by controlling the flow of nitrogen gas (30 psi) through the spinneret's outer lumen. Droplets were collected and allowed to gel for 20 min in a slowly stirred calcium chloride bath (1.3% w/v). Resulting microspheres were wet-sieved and collected into two size ranges (drug loaded: $d < 212$ μm and Tonopaque loaded: 600 μm $< d <$ 850 μm). Microspheres were stored damp in sealed vials. Final drug concentrations were assayed to be 16 and 25% weight/wet weight microspheres for dicumarol and salicylic acid, respectively.

Hot-Melt Microencapsulation. Hot-melt microencapsulation (147), was used to form large, radiopaque microspheres of P(FA:SA) for transit studies. P(FA:SA) was melted in a crucible over low heat (<100°C), and powdered Tonopaque was mixed with the polymer (50% w/w). The mixture was poured into a beaker containing 200 mL of silicon oil (200 Fluid; Dow Corning Inc., Midland, MI) at 80°C and stirred to produce droplets of molten P(FA:SA) containing barium sulfate. The oil system was cooled, causing droplets to solidify into microspheres. Microspheres were collected, washed with petroleum ether, and seived to a range of 600–850 μm.

Phase Inversion. To produce drug-loaded polyanhydride microspheres, a phase-inversion microencapsulation technique was developed. Briefly, the polymer was dissolved in

a good solvent (5% w/v in methylene chloride); drug (40 and 16% w drug/w polymer for dicumarol and spray-dried salicylic acid/PVP, respectively) was added to the solution; and the mixture was poured into a strong nonsolvent (petroleum ether) that was highly miscible with the solvent (solvent to nonsolvent ratio was 1:20). The result was spontaneous production of microparticles ($0.5\ \mu m < d < 5\ \mu m$) through phase inversion. The microparticles were filtered, briefly washed with petroleum ether, and dried with air. The advantages of this technique over methods that could produce similar-sized particles (spray-drying or solvent evaporation) are very low polymer loss, low drug loss (for dicumarol), simplicity, and speed.

In Vitro Dissolution and Release Studies. Drug and bioadhesive drug formulations (40 and 5 mg drug for salicylic acid and dicumarol, respectively) were incubated in 10 mL PBS in polypropylene centrifuge tubes at 23°C for 10 h. Periodically, 100-μL samples of the aqueous solution were removed from each tube and centrifuged through a 0.2-μm filter to eliminate particulates. Samples were analyzed to determine dissolved drug concentrations. After each sampling, tubes were shaken to resuspend drug and microspheres.

Animal Studies ***GI Transit of Radiopaque Microspheres.*** Prior to administration, ≈200-mg microspheres (either barium-loaded P[FA:SA] 20:80 made by hot-melt or barium-loaded alginate) were suspended in 1 mL 0.9% sodium chloride. Male, VAF, CD® rats (250–350 g, Charles River Labs, Wilmington, MA) that had been fasted overnight, were anesthetized with methoxyfurane, and a silicone feeding tube (2-mm o.d.) was used to deliver microsphere suspensions directly into their stomachs. Following administration, rats were allowed to recover from anesthesia.

Animals were reanesthetized and x-rayed using a Hitachi model DGC-1010 mobile X-ray unit (Hitachi Co., Tokyo, Japan) and Kodak Ready Pak II Type M X-ray film (Kodak, Rochester, NY), thereby verifying the presence of microspheres in the stomach lumen. From these X rays it was possible to determine the number of microspheres initially administered to each animal.

After x-raying to determine initial dose, animals were placed in metabolic cages positioned above a custom-designed, automatic, feces-collecting machine. Feces were separated from the urine and collected at 2 h–50 min intervals over a three-day period. During this time the animals were provided with food and water ad libitum. Feces were x-rayed, and microspheres were counted to determine their rate of passage from stomach to anus as well as the percentage of microspheres remaining in the animal at each time point.

Excel 5.0 (Microsoft, Redmond, WA) was used to perform one-tailed student t-tests (unpaired, equal variance) on raw data at each collection point to assess statistical differences between the groups.

Bioavailability of Drug and Encapsulated Drug Formulations. Catheters were required for repeated blood sampling during the bioavailability study. Male, VAF, CD® rats (250–350 g, Charles River Labs, Wilmington, MA) were anesthetized with an ip injection of sodium pentobarbital (60 mg/kg), and with the animals supine, a midline incision was made from the top of the neck to the clavicle. Blunt dissection was used to locate and isolate the external jugular vein. Three ligatures were placed around the vessel. One ligature was used to tie off the cranial end of the isolated segment, a small incision was made in the side of the vessel, and a silicone catheter (Bio-Sil medical grade silicone tubing (500-μm i.d., 940-μm o.d., 53-cm length); Sil-Med Corporation, Taunton, MA) filled with heparin (666 U/mL) was inserted into the vessel lumen and fed towards the heart. The other two ligatures were tied off around the vessel and catheter, caudal to the point of insertion, while being careful not to deform and restrict the catheter.

Next, animals were turned prone, and a second incision was made from the base of the skull to the midpoint between the scapulae. Forceps were used to tunnel subcutaneously to the opening of the ventral incision. The free end of the catheter was pulled beneath the skin to emerge from the dorsal incision at the base of the neck. The ventral incision was sutured. The free end of the catheter was fed through a 30.5-cm-long stainless steel spring tether with 22-gauge swivel (Harvard Apparatus, South Natick, MA). The button-end of the tether was sutured to the fascial covering of the muscles in the back of the neck, and a purse-string stitch was used to close the dorsal incision.

Tall cages were constructed to allow for untangled movement of the tether. To produce an enclosure 33 cm high, two rat cages (36 cm × 30 cm × 16 cm) were joined, one inverted on top of the other, with 4 delrin spacers (1 cm thick) to allow adequate air flow. Additional air holes were drilled, and a delrin collar was glued into the center of the top cage. The swivel-end of the tether was passed through the top of the upper cage and secured in the collar with a set screw. A three-way stopcock was attached to the swivel on the outside of the cage with a small section of silicone tubing (≈8 cm) to facilitate syringe changes without breaking the closed-catheter system. This setup allowed blood samples to be drawn from outside the cages without handling or anesthetizing the animals. Additionally, animals have near normal mobility.

On the day following surgery, the animals were anesthetized with methoxyfurane and a flexible silicone feeding tube was introduced via the esophagus to the stomach. Either microspheres or drug (25 or 200 mg drug weight/kg rat body weight for dicumarol or salicylic acid, respectively) were suspended in 1.5 mL of maple syrup (Camp Inc., Plessisville, Canada) and administered to the animals via the silicon tube. A positive displacement plunger was passed through the tube to ensure proper dosage.

Following drug administration, blood samples were drawn from the animals approximately 1 h for the first 4 h and approximately every 4 h after that point for the next 68 h. Samples were centrifuged, 100 μL of serum was removed, and blood cells were resuspended in 100 μL of saline (0.9% NaCl) and returned to the animals. Catheters were flushed with saline and plugged with heparin (1000 U/ml) after returning blood cells.

Salicylic acid concentrations were measured using a colorimetric assay (163). One hundred microliters of serum was diluted with 600 μL of distilled water and reacted with 1 mL 1.0% ferric nitrate in 0.07 N nitric acid. The presence

of salicylate was revealed by a change in color from faint yellow to deep purple. The samples were measured spectrophotometrically at 530 nm using a Beckman model DU65 spectrophotometer (Beckman Instruments, Inc.; Fullerton, CA).

Dicumarol concentrations were assayed spectophotometrically in the UV range (164). One hundred microliters of serum was acidified with 20 μL of 3 M HCl. Dicumarol was extracted from the aqueous phase into 700 μL of *n*-heptane. Six hundred microliters of the heptane phase was mixed with 900 μL of 2.5 M NaOH to back-extract the dicumarol. Dicumarol concentration in NaOH was measured spectrophotometrically (315 nm) in quartz cuvettes.

Readings from individual time points were averaged to produce mean concentrations with standard errors for graphical analysis. Pharmacokinetic software (R-Strip; Micromath Scientific Software, Salt Lake City, UT) was used to perform least-squares regression on the average values to produce exponential curve fits. Raw data points were analyzed with a students *t*-test (one-tailed, unpaired, equal variance) to determine statistical significance at each sampling time. C_{max}, T_{max}, and AUC were compared for statistical differences using a students *t*-test (two-tailed, unpaired, equal variance) on raw data for T_{max} and on logarithmically transformed values for C_{max} and AUC.

Results and Discussion. The effects of bioadhesive polymers on delaying microsphere transit and on bioavailability of encapsulated drugs have been studied. Two polymers were chosen for this study based on our in vitro bioadhesive strength measurements (see "Bioadhesive Measurements" through "GI Transit and Bioavailability of Low-Molecular-Weight Drugs"): alginate and poly(fumaric-*co*-sebacic anhydride) [P(FA:SA)]; calcium alginate microspheres were shown to have weak-to-moderate bioadhesive properties, whereas P(FA:SA) microspheres were shown to be very strong bioadhesives.

Radiopaque Microspheres. To provide a means of tracking microsphere transit through the GI tract, radiopaque barium sulfate was encapsulated in the polymers. Encapsulation was performed using ionic gelation (alginate) and hot-melt [P(FA:SA]20:80) methods. Because barium sulfate is a heavy powder that is insoluble in aqueous solutions and oil, encapsulation by these techniques was straightforward and nearly 100% efficient.

Drug Encapsulation. The hot-melt technique, which typically produces very dense microspheres larger than 100 μm in diameter (147) could have been used to encapsulate salicylic acid and dicumarol in P(FA:SA) 20:80, but preliminary investigations revealed that microspheres of this size and morphology produced inappropriate delivery profiles (lasting several days to several weeks, depending on size and loading). To speed release kinetics, a phase-inversion microencapsulation technique was used to produce very small, quick-releasing microparticles (Fig. 28). This procedure worked well for encapsulating dicumarol (initial loading: 40% w/w, final loading: 38% w/w), because dicumarol is soluble in methylene chloride and only partially soluble in petroleum ether. Also, because dicumarol is poorly soluble in neutral to acid aqueous solutions, the small particle size may help dissolution in vivo or enhance uptake.

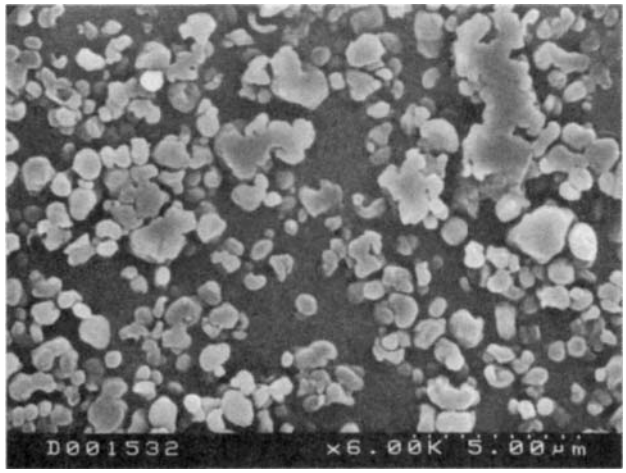


Figure 28. SEM of P(FA:SA) particles formed by the phase inversion method. Microparticles are very small (0.5 μm < d < 5 μm) and dense.

On the other hand, salicylic acid is quite soluble in petroleum ether and aqueous solutions. These two properties resulted in poor encapsulation (<1% w/w final loading) and extremely rapid release. Therefore, a double encapsulation technique was employed; salicylic acid was first spray-dried with PVP (from a 10% w/v of solution of both components in acetone), and then the spray-dried particles were encapsulated in P(FA:SA) using the phase-inversion technique. PVP was chosen because it has a common solvent with salicylic acid (acetone) and because it is nonsoluble in both methylene chloride and petroleum ether. The result of the double encapsulation was a much higher loaded final product (9% w/w) with a longer release profile.

Drug Controls. Appropriate controls were needed to assess the effect of bioadhesive polymers on bioavailability. It was essential to provide controls that had similar solubility and absorptivity as each bioadhesive system. No special controls were required for either of the salicylic acid–containing devices, because stock salicylic acid is known to be freely absorbed in the stomach.

Dicumarol, as received from Sigma, was in the form of particulate crystals (ranging in size from 10 to 200 μm) and was poorly soluble in neutral-to-acid aqueous solutions (165). Because drug particle size was unchanged by alginate encapsulation, stock dicumarol was determined to be an appropriate control for that system. However, to obtain a suitable control for the 0.5–5 μm, P(FA:SA)-encapsulated dicumarol-loaded microspheres produced through phase inversion, we felt it was necessary to reduce particle size and thereby improve dissolution. Dicumarol was micronized by dissolving in methylene chloride (0.5% w/v) and spray-drying. The resulting particles were less than 5 μm in diameter, porous, and very fragile.

In Vitro Dissolution. In vitro dissolution and release experiments were performed on all drugs and polymer-encapsulated drugs to investigate the effects of processing techniques and particle size on drug solubility and release. Figures 29 and 30 show dissolution and release profiles for salicylic acid and dicumarol formulations, respectively. In

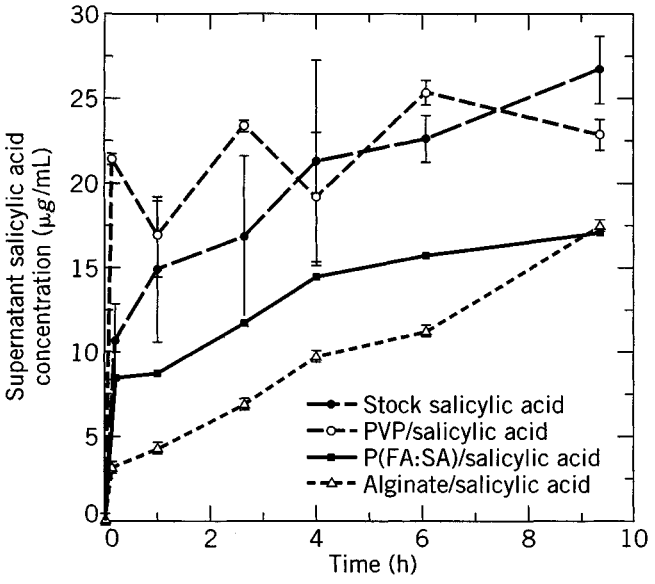


Figure 29. In vitro dissolution of stock salicylic acid and release curves for spray-dried salicylic acid/PVP, salicylic acid encapsulated in alginate, and salicylic acid/PVP encapsulated in P(FA:SA). Stock salicylate was chosen as the in vivo control for both alginate and P(FA:SA)-encapsulated forms.

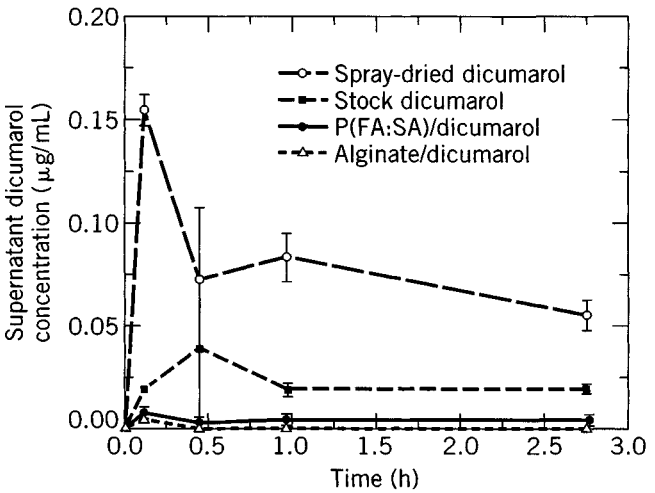


Figure 30. In vitro dissolution of stock dicumarol, spray-dried dicumarol, dicumarol encapsulated in alginate, and dicumarol encapsulated in P(FA:SA). Stock dicumarol was used as control for the alginate-encapsulated system, while spray-dried dicumarol served as control for the P(FA:SA) encapsulated system.

both graphs, controls (unencapsulated forms) result in equal or faster dissolution than polymer encapsulated formulations.

Of the dissolution and release curves for salicylic acid, stock salicylic acid and spray-dried PVP–salicylic acid produced the fastest release rates. The spray-dried material was released quickly owing to its very small particle size. However, release was significantly decreased by encapsulating PVP–salicylic acid in P(FA:SA) using the phase-inversion technique.

Dicumarol is normally insoluble in neutral-pH solutions. Dissolution and release curves for stock dicumarol, dicumarol encapsulated in alginate, and dicumarol encapsulated in P(FA:SA) supported this fact (Fig. 30). However, an interesting dissolution profile was observed with spray-dried dicumarol. After 5 min incubation, supernatant concentrations rose to 11 μg/mL, corresponding to approximately 2.2% dissolution. As the incubation continued, more drug became insoluble; the supernatant concentration dropped in half after 3 h. A possible explanation is that spray-drying not only reduces particle size and increases surface area but also creates an amorphous soluble structure. Although initially soluble with agitation, dicumarol quickly crystallizes as it precipitates around scattered drug particles acting as nucleation sites. We believe that in the living animal, the soluble material may be absorbed into the circulation prior to having the opportunity to recrystallizing. These results and beliefs are in agreement with others (165).

Alginate encapsulation appears to limit drug release for both salicylic acid and dicumarol even though alginate is a loose hydrogel network offering a poor diffusion barrier. However, the curves are misleading. During the ionic gelation fabrication process, most of the freely soluble drug is lost to the supernatant. Drug that remains encapsulated is of larger particle size and mainly crystalline. Therefore, dissolution of this material is slower than stock samples, and release rates of these devices tend to be less than expected.

In Vivo Transit. A simple and straightforward procedure using radiopaque markers, feces collection, and X rays was designed to monitor GI passage in vivo. By encapsulating 50% Tonopaque in polymer microspheres (using hot melt for P[FA:SA] and ionic gelation for alginate) and sieving the spheres to a fairly large size ($600 > d \geq 850$), we were able to produce polymer devices that were easily traced with X rays. Not only could microspheres be identified in feces, but immediately following oral administration they could also be clearly observed and counted in the lumen of the GI tract. Feces collection and X ray inspection provided us with a noninvasive method of monitoring total GI residence time without affecting normal GI motility. Designing and constructing an automated feces-collection machine (Figs. 31 and 32) simplified retrieval of the passed microspheres.

Twelve animals were used in this study. Each animal was used twice (once for alginate and once for P(FA:SA) 20:80), with greater than 1 week rest period between experiments. The mean percentages of microspheres retained in the animals at each time point with standard errors are shown in Figure 33.

Distinct differences were observed between the two polymers. Alginate spheres were eliminated quickly, appearing after 8.5 h; P(FA:SA) spheres never appeared before 11 h 20 min. By 17 h, only 27.41 ± 7.19% of the alginate microspheres remained in the animals, whereas 53.93 ± 11.14% remained for the P(FA:SA) 20:80. Although percentages beyond 27 h were not statistically different, the time required for 90% passage was about 20 h

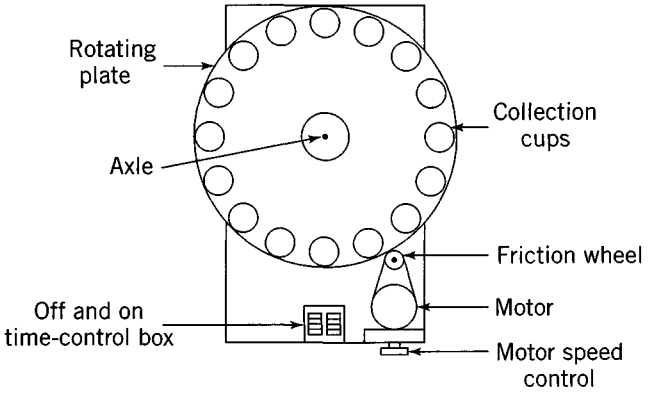


Figure 31. Automatic feces-collecting machine. Top view: shows arrangement of collection cups. *Source:* Reproduced with permission from *Journal of Controlled Release* (Ref. 91).

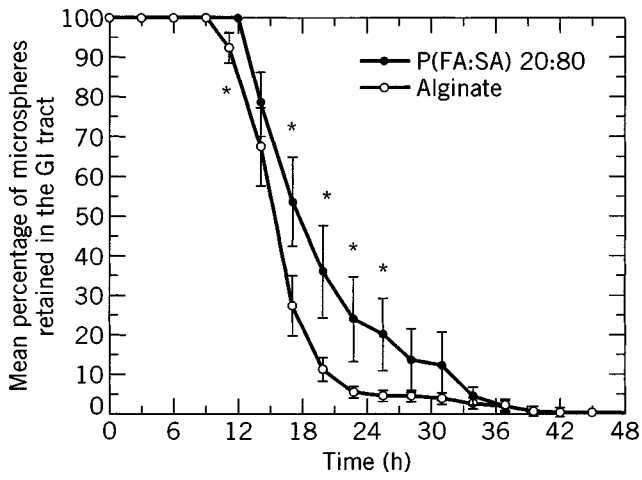


Figure 33. Percentage of microspheres retained over time for radiopaque alginate and P(FA:SA) 20:80. Time points marked by asterisks (*) indicate points that were statistically different in the two curves ($P \leq .05$). *Source:* Reproduced with permission from *Journal of Controlled Release* (Ref. 91).

for alginate and nearly 34 h for P(FA:SA) 20:80. These results clearly demonstrate the ability of bioadhesive P(FA:SA) 20:80 to slow GI transit in the rat.

Bioavailability Studies. Both plain drugs and BDDS microspheres were administered orally as either solutions or suspensions in maple syrup. A thick fluid, such as maple syrup, was required to prevent the microspheres from packing in the feeding tube during administration. Table 8 outlines the delivery systems and controls used in this study.

Catheters were implanted in the jugular veins to facilitate remote blood sampling without anesthetizing the animals and to provide a means of reinjecting sampled blood. To protect the fragile catheters from the animals, armored-steel spring tethers were used, requiring the fabrication of

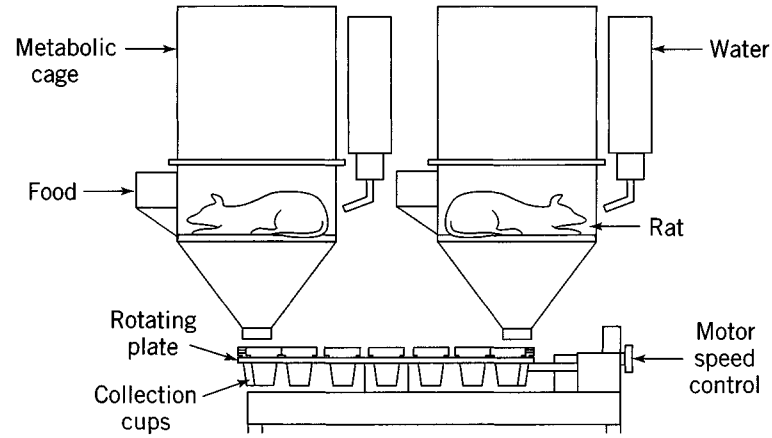


Figure 32. Automatic feces-collecting machine. Side view: shows position of collection cups, rotating wheel, and metabolic cages. *Source:* Reproduced with permission from *Journal of Controlled Release* (Ref. 91).

Table 8. Bioavailability Experiment Layout Showing Controls for Each Experimental Group

Drug	Experiment	Control
Salicylic acid (200 mg/kg)	Stock salicylic acid encapsulated in alginate suspended in maple syrup (25%, $d \leq 212$ μm)	Stock salicylic acid suspended in maple syrup
	Stock salicylic acid spray-dried with PVP encapsulated in P(FA:SA) 20:80 suspended in maple syrup (9%, d = 1–15 μm)	Stock salicylic acid suspended in maple syrup
Dicumarol (25 mg/kg)	Stock dicumarol encapsulated in alginate suspended in maple syrup (16%, $d \leq 212$ μn)	Stock dicumarol suspended in maple syrup
	Spray-dried dicumarol encapsulated in P(FA:SA) 20:80 suspended in maple syrup (38%, d = 0.5–5 μm)	Spray-dried dicumarol suspended in maple syrup

Note: Drug-loading per percentages and microsphere diameters are given in parentheses.

unusually tall cages to ensure untangled movement of the animals (Fig. 34). Blood samples were taken at regular intervals (every 3–5 h) not only to obtain data but also to reduce the chance of irreversible clot formation. After reinjecting resuspended cells, the catheters were flushed with saline and plugged with a heparin solution (1,000 U/mL) to minimize intraluminal coagulation. However, several catheters did clot, and, therefore, data for those animals were collected only up until that point.

Salicylic Acid. Salicylic acid is rapidly absorbed following protonation in the acid environment of the stomach. When orally administered in an unencapsulated form, most absorption occurs in the first 20–30 min, prior to gastric emptying. Once the drug passes through the duodenum into the higher pH of the lower segments of the small intestine, very little absorption takes place (166,167).

Figure 35 shows the serum-concentration-time curves for the three salicylic acid formulations. Both alginate- and P(FA:SA)-encapsulated formulations showed statistically lower AUC than the control ($P \leq .002$) and P(FA:SA) showed statistically lower C_{max} than the control ($P \leq .05$). No statistical differences were observed for T_{max}. Statistical differences for individual time points are displayed on the graph (Fig. 35).

In both encapsulated formulations we observed less salicylate entering the systemic circulation than in controls. This could be explained by the following: If the encapsulated formulations slow the release of salicylic acid, as observed by in vitro dissolution and release profiles, and gastric emptying occurs prior to the majority of release, then very little drug is available for absorption. The result is lower systemic concentrations. Thus, DDSs known to adhere to the small intestine have little effect on improving bioavailability of drugs that are rapidly absorbed in the stomach and duodenum, such as salicylates.

Dicumarol. Dicumarol is widely used clinically as an anticoagulant. Its mode of action is attributed to competitive inhibition of vitamin K, thus limiting the production of vitamin K-dependent coagulation factors VII, IX, X, and II (168). As received from Sigma Chemicals, it was a white, crystalline powder that was poorly soluble in all but very basic aqueous solutions. When given orally, dicumarol is taken up mainly in the small intestine, and its absorption has been characterized as poor and erratic (165,168,169). It was our hypothesis that a bioadhesive delivery system designed to adhere to the intestinal lining and deliver its contents over 4- to 8-h would improve absorption of dicumarol.

Bioavailability plots of stock dicumarol and alginate encapsulated dicumarol are compared in Figure 36. None of the concentrations were statistically different at any of the sampling points, and no statistical differences were observed for the C_{max}, T_{max}, and AUC. The two formulations produced identical results. The reason for this may be twofold: In vivo dissolution and release profiles of the formulations may not be significantly different, and physical properties of alginate (e.g., unfavorable surface energy for

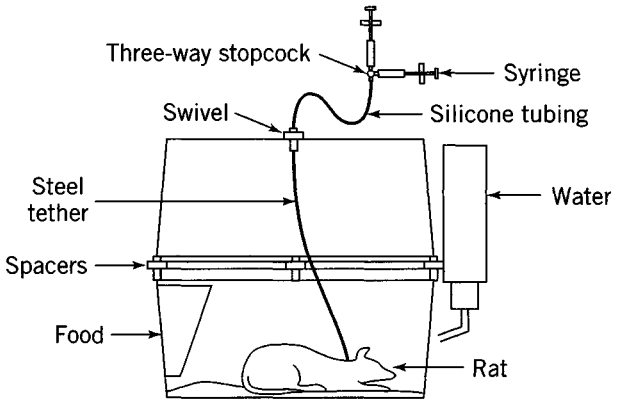


Figure 34. Diagram of catheterized rats. Tall cages were constructed to allow for untangled movement of animals. This system allowed blood to be sampled and returned to the animals without need for handling or anesthetizing. *Source:* Reproduced with permission from *Journal of Controlled Release* (Ref. 91).

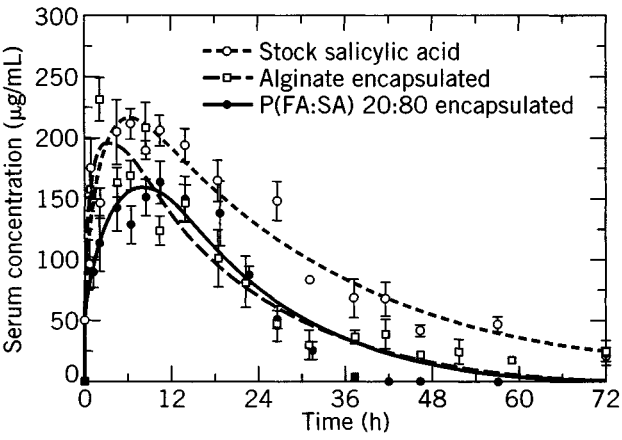


Figure 35. Mean salicylic acid serum concentrations (±SEM) versus time. Neither encapsulated form resulted in improved bioavailability.

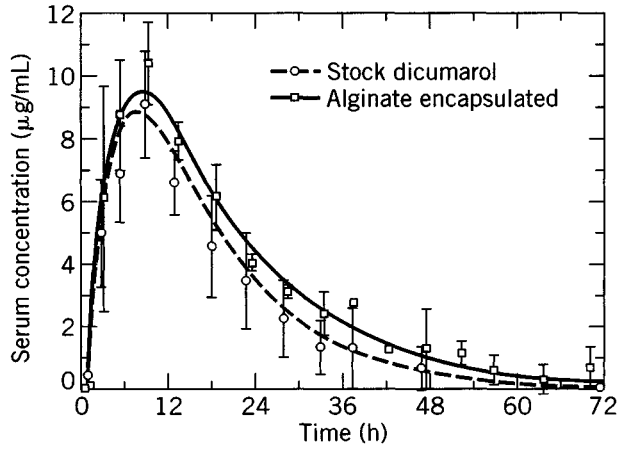


Figure 36. Mean dicumarol serum concentrations (±SEM) versus time for stock dicumarol and dicumarol encapsulated in alginate. No effect was observed on bioavailability. *Source:* Reproduced with permission from *Journal of Controlled Release* (Ref. 91).

spontaneous mucoadhesion) may produce bioadhesive interactions that are too weak to improve drug delivery and bioavailability.

Dicumarol encapsulated in P(FA:SA) 20:80 produced strong support for bioadhesion (Fig. 37). Although no significant increase was observed in C_{max} and T_{max}, the AUC for P(FA:SA)-encapsulated dicumarol was statistically higher than controls ($P \leq .05$). In fact, a 56.6% increase in mean AUC was observed for the bioadhesive device (363.6 and 232.1 μg h/mL for experimental and controls, respectively). Furthermore, beyond the first 12 h, 9 out of 13 time points showed statistically higher serum concentrations compared to spray-dried controls. Detectable serum dicumarol levels were maintained for at least 72 h in animals given bioadhesive formulations, while those given unencapsulated controls exhibited undetectable serum levels after 48 h.

Observation that controls exhibit more rapid dissolution profiles than encapsulated forms (Fig. 30) eliminates the possibility that improved bioavailability of bioadhesive dosage forms is a result of faster solubilization of the drug. If encapsulated dosages show slower dissolution rates, then improvements in bioavailability must be due to other mechanisms such as increased absorption rate through intimate contact with absorbing tissues or increased residence time at the site of absorption, both of which can be attributed to bioadhesion.

These results indicate that bioadhesive P(FA:SA) improves bioavailability by either enhancing absorption through intimate contact, minimizing drug degradation prior to absorption, or increasing residence time in the absorbing portion of the GI tract. Although statistical differences were measured, degradation, dissolution, and release characteristics of P(FA:SA) DDSs could possibly be tailored to produce even stronger effects.

Overview of Bioadhesive Performance. We have utilized four methods to assess bioadhesion: in vitro mechanical testing, polymer characterization techniques, measurement of in vivo transit, and assessment of in vivo bioavailability of encapsulated drugs. In all evaluations we observed better performance from P(FA:SA) 20:80 microspheres compared to calcium alginate microspheres. Table 9 outlines some relevant measurements. P(FA:SA) produced significantly greater deformation to failure, fracture strength, and tensile work than alginate as measured by the Cahn technique; significantly longer GI retention times compared to alginate; and increases in blood serum C_{max}, T_{max}, and AUC as compared to controls. P(FA:SA) polymers appear to offer promise for oral BDDSs.

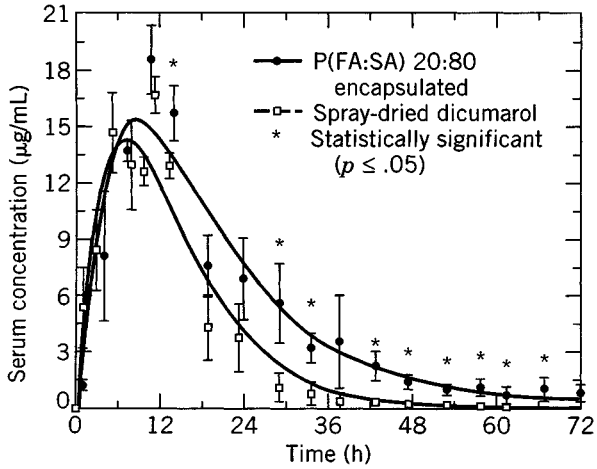


Figure 37. Mean dicumarol serum concentrations (±SEM) versus time for spray-dried and encapsulated dicumarol. Both formulations were administered orally via a silicone feeding tube. Encapsulation resulted in a 56% improvement in AUC compared to controls. *Source:* Reproduced with permission from *Biotechnology & Bioengineering* (Ref. 25).

Conclusions. The retention times obtained using noninvasive technique (the oral feeding of radioopaque microspheres) correlate well with in vitro results obtained previously using a Cahn microbalance to measure bioadhesion between microspheres and rat intestinal epithelium and with the properties measured using polymer characterization techniques. P(FA:SA) 20:80 showed greater fracture strength and tensile work than alginate, indicating stronger bioadhesive properties. This pattern was repeated in the in vivo transit study, where a significant delay in GI transit was observed for P(FA:SA) 20:80 microspheres when compared to alginate microspheres of a similar size. The results support the hypothesis that bioadhesive materials can prolong GI residence.

Even though no improvement was observed in salicylic acid absorption, dicumarol delivery was improved by encapsulating in P(FA:SA) 20:80. In light of these findings and based on known absorption properties of salicylic acid and dicumarol, we could assume a scenario where bioadhesive polyanhydride DDSs retained significant quantities of drug while in the stomach, delayed intestinal transit, and released most of their contents while adhered to the intestinal mucosa. We believe adhesion and the resulting increased residence time was most likely a result of hydrogen bond formation between surface carboxylic acid and mucosal glycoproteins. Through bioadhesion, intimate contact with absorptive epithelium may have reduced diffusion distances and drug loss, resulting in improved delivery.

Our findings show that bioadhesive, controlled-release systems are a potential solution for improving bioavailability of orally delivered drugs. To bring bioadhesive systems to practical use, each particular bioactive agent will require a well-engineered vehicle providing proper release kinetics as well as appropriate adhesive characteristics.

Table 9. Comparison of Bioadhesive Properties (±SEM) of Alginate and P(FA:SA) 20:80

Parameter	Alginate	P(FA:SA)20:80
Deformation to failure (mm)	0.649 ± 0.144	1.219 ± 0.185
Fracture strength (mN/cm^2)	30.16 ± 4.18	51.63 ± 3.38
Tensile work (nJ)	62.18 ± 14.50	255.45 ± 33.04
% remaining @ 11 h 20 min	90.68 ± 3.83	100.0 ± 0.00
% remaining @ 17 h	27.41 ± 7.19	53.93 ± 11.14
% remaining @ 25 h 30 min	4.82 ± 1.72	20.59 ± 9.44
$\%\Delta$ in C_{max} (dicumarol)		+38
$\%\Delta$ in T_{max} (dicumarol)	−26.9	+12.7
$\%\Delta$ in AUC (dicumarol)	+23.5	+56.6

Source: Ref. 91.

Site-specific targeting of the devices will be paramount to improving delivery efficiency. Overall, the findings of this study show that materials that have been proven to exhibit strong bioadhesive interactions in vitro may perform well as bioadhesive delivery systems in vivo. By fine-tuning the release kinetics of the vehicles, it should be possible to further improve bioavailability. We believe that bioadhesive polyanhydrides, such as P(FA:SA), will eventually find clinical use for the oral delivery of bioactive agents.

Bioadhesive Microspheres for Oral Delivery of Proteins and Genes

Previous investigators overlooked the possibility that hard thermoplastic materials may be suitable bioadhesives, based on the notion that diffusion and chain entanglement were essential to bioadhesion. However, our work proves that other factors, such as hydrogen bonding, surface texture, and surface energy, can play equally important roles in the formation of bioadhesive interactions and that thermoplastic, bioadhesive, controlled-release systems can be used to improve bioavailability of orally delivered drugs. We have found that polyanhydride copolymers of FA and SA [P(FA:SA)] demonstrated the highest bioadhesive properties (140) using two in vitro techniques—the Cahn microbalance and the everted sac technique (161). In vivo radiographic studies on P(FA:SA) microspheres showed longer residence times in the stomach as compared to that of other polymers (36 versus 18 h) (25). All these results suggest that strong bioadhesive interactions delay microspheres passage through the gastrointestinal system. Intrigued by this data, we then wondered what would happen if the bioadhesive microspheres were manufactured at a very small size. Others have demonstrated that small microspheres of polystyrene (PS), poly-lactide-*co*-glycolide (PLGA), and polycyanoacrylate could be taken up by lymphoid tissue associated with the Peyer's patches (PP) of the GI tract (170–178).

To explore the potential of uptake of our formulations in rats, we used optical microscopy to follow the fate of orally administered P(FA:SA) 20:80 microspheres (0.1–10 μm) fabricated using the phase-inversion (PIN) method. As early as 1 h postfeeding of a single dose, microspheres were observed to traverse both the mucosal epithelium (through and between individual cells) and the follicle-associated epithelium (FAE) covering the lymphatic elements of the PP. Microspheres were also observed within goblet cells. In addition, spheres were seen crossing through FAE and into the PP. After 3 and 6 h, an intense uptake was observed in absorptive cells and PP. The same observations were made 12 to 24 h postfeeding. Both spleen and liver tissue samples, with apparently normal-looking hepatocytes, showed a large number of microspheres. Similar patterns were never observed in sections of tissue from untreated control animals.

Transmission electron microscopy (TEM) experiments using an electron-opaque, 5-nm colloidal gold tracer that had been PIN-encapsulated with P(FA:SA) 20:80 were also conducted (137). The range of particle sizes observed in the cytoplasm of cells was 40–120 nm, well below the resolution of normal light optics. Colloidal gold-labeled nanospheres were visualized in the cytoplasm, inside Golgi apparatus and in secretory vesicles predominantly in the supranuclear (apical) portion of the absorptive cells. The mechanism of entry was not elucidated as relatively few pinocytotic vesicles were observed to account for the uptake. Microspheres were often found between microvilli, in vesicles near the lateral borders of the cell, in the intercellular spaces and in the basal aspects of the cells, in lymphatics, and also in Goblet cells (137). Unequivocal identification of the particles was difficult because the microspheres had different appearances depending upon their location in the cell or the intercellular spaces. This may have resulted from degradation or processing of the polymer in the various environments. However, in each case the particles were identified on the basis of the colloidal gold tag. Microspheres were never observed in control tissues from untreated animals (137). These findings suggest that translocation of polymer particles via the transcellular route as well as via paracellular transport occurred. Similar work, conducted with colloidal gold-labeled PS showed high uptake.

Oral Insulin Delivery. To evaluate the possibility of orally delivered insulin, three groups of fasted rats were injected subcutaneously with an initial glucose load (179) and then fed either (*1*) a suspension of P(FAO-PLGA) microspheres containing 20 IU zinc–insulin with micronized FeO included as an electron dense transmission electron microscopy (TEM) tracer in saline ($n = 6$), (*2*) 24 IU of soluble insulin in saline ($n = 8$), or (*3*) saline without insulin as controls ($n = 7$). (*Note*: FAO is fumaric anhydride oligomer, also known as fumaric acid prepolymer, FAPP.) The control animals showed the expected response to the glucose load (137). In saline-fed animals, blood glucose levels (BGL) rose by 46 mg/dL after 3 h and then slowly started to return toward baseline. Rats fed soluble insulin reached a maximum BGL of 36 mg/dL above baseline at 1.5 h postfeeding. At all timepoints, the BGL of animals receiving the insulin solution were not significantly different from those of control animals receiving saline only. In contrast, the BGL of animals fed the PIN-encapsulated insulin formulation never increased above the fasting levels and were statistically lower than both control groups at all four time points (137). Clearly, animals fed the P(FAO-PLGA)-encapsulated insulin preparation were better able to regulate the glucose load than the controls, suggesting that the insulin crossed the intestinal barrier and was released from the microspheres in a bioactive form.

Formulations of blends of PLA and FAO, up to ratios of 1:3 (w/w) and loaded with the same amount of insulin (with similar drug release kinetics, bioactivity and particle size), did not show any effect in the glucose tolerance test. This observation correlated well with the low level of PLA particle uptake. The differences observed between the two polymer formulations may be due to either the lesser bioadhesive properties or slower degradation rate of the blends of P(FAO-PLA) polymers.

To study the bioavailability of the insulin formulation, two normal rats, weighing 300 g each, were fed 20 IU of insulin in the P(FAO-PLGA) blend containing 1.6% insulin. Both rats had critically low BGLs (<60 mg/dL) at 4 h

and then began to return to normal at about 6 h. When lower doses were administered, we could not see the same effect. The results can be used to calculate the oral bioavailability by the following equation:

$$f = \frac{\mathrm{AUC}_{0\text{–}6\ \mathrm{oral}}}{\mathrm{AUC}_{0\text{–}6\ \mathrm{ip}}} \times \frac{(weight\ dose)_{\mathrm{oral}}}{(weight/dose)_{\mathrm{ip}}}$$

$$= \frac{118\%}{257\%} \times \frac{300_g/20_{IU}}{270_g/4_{IU}} = 10.2\% \qquad (12)$$

Information on the ip serum levels was obtained from Touitou (180). Thus, for the rats fed the microspheres orally, the calculated bioavailability is 10.2%.

These are only preliminary results, but further study indicated that in that particular formulation 25% of the microspheres were smaller than 4 μm and 10% were smaller than 1.6 μm (size distribution was determined by volume). If we take those numbers into consideration, the estimated bioavailability numbers rise to 40% for the 4 μm cutoff and to 100% for the 1.6 μm cutoff. These numbers seem extremely high; however, they indicate that transmucosal delivery of only a small population of insulin-loaded nanoparticles is necessary to reduce BGL. Furthermore, we believe that if we can shift the microsphere size range below 2 μm, then we can dramatically improve the oral bioavailability of insulin to levels above 50%.

Now if we remember that the oral bioavailability of dicumarol in the microspheres was estimated as 19% and the microspheres were loaded with 40% (w/w) dicumarol, up to 47% of the microparticles were estimated to be absorbed in the rats in the study. Again, the results between the oral insulin and the oral dicumarol are very intriguing, and more work will be done to further evaluate those systems.

Oral Gene Delivery. Perhaps the most surprising results were found when we applied the system to the delivery of plasmid DNA for in vivo gene transfer (137). Because "naked" plasmid DNA transfection efficiencies are generally low owing to inefficient uptake as well as rapid degradation of the DNA, encapsulation of plasmid DNA might serve to protect DNA and promote cellular uptake following oral administration. A bioadhesive polymer delivery system composed of P(FA:SA) 20:80 was used to encapsulate pCMV/β-gal (0.1% w/w), a commercially available reporter plasmid with bacterial β-galactosidase gene activity. The migration pattern of plasmid DNA extracted from the microspheres was identical to stock unencapsulated DNA, indicating that the fabrication process did not alter its structural integrity.

Five days following a single oral dose of either plasmid-loaded PIN microspheres or unencapsulated pCMV/β-gal, β-galactosidase activity was quantified in the stomach, small intestine, and liver (137). Animals fed encapsulated pCMV/β-gal showed increased levels of β-galactosidase activity in both the small intestine and the liver compared with those receiving unencapsulated material as well as unfed animals. The reporter gene activity measured in intestinal tissue of animals that received the encapsulated pCMV/β-gal was highest (>54 mU versus 24 mU for the unencapsulated plasmid and 18 mU for the background levels in untreated control animals; however, nsd for the three groups). These same animals averaged 11 mU of activity in the liver versus < 1 mU for plain CMV-fed ($P <$ .045) or untreated control animals ($P <$ .025). Reporter gene expression in stomach homogenates was generally low (<11 mU) in all groups.

Visual localization of transfected cells following oral administration was performed using X-gal histochemical staining techniques on whole tissue and frozen sections (181). Because epithelial cells on villi have endogenous lactase activity that can mask the bacterial β-galactosidase (182), we focused on the PP, which do not contain background activities.

The serosal surface of small intestine from encapsulated pCMV/β-gal-fed rats showed intensely stained cells in areas containing PP (137). Frozen sections of PP revealed that although there were a few β-galactosidase positive cells within the central lymphoid tissue mass (137), the majority of transfected cells were located in the muscularis mucosae and adventitia below the PP (137). This distribution of staining was consistent with previous studies that showed retention of microspheres in the PP. Neither the animals receiving unencapsulated pCMV/β-gal nor unfed normal rats showed any false-positive β-galactosidase staining in the PP region. Histological examination showed no evidence of mucosal damage or inflammation. This study confirmed that plasmid DNA can be delivered by the oral route using PIN formulations, with the encapsulated DNA incorporated into cells lining the small intestine and hepatocytes and expressing functional gene products at levels detectable using common histological and luminometric techniques.

In conclusion, when using the PIN system in combination with bioerodible bioadhesive polymers, the enhanced bioavailability of dicumarol might be explained by the delay in the dissolution of the drug caused by the encapsulation process (25), the increased absorption rate resulting from more intimate contact with the intestinal epithelium, or an increased residence time at the local absorption site—all of which can be attributed to bioadhesion. However, the increased bioactivity of insulin and plasmid DNA might also be due to the uptake of the microspheres into the circulation by the cells lining the GI tract. The results with insulin, a 6-kDa protein susceptible to proteolytic degradation by GI enzymes and having limited mucosal uptake, support this hypothesis. Clearly, the same uptake pathways can be used as a platform for a variety of therapeutic agents with poor oral absorption including nucleic acids and plasmids.

Concluding Remarks

Traditionally, bioadhesive researchers have stated that bioadhesion in hydrogels is mainly a function of chain entanglement (75,78,183). Recent findings, however, have indicated that other components, such as surface energies, may play major roles in the formation of bioadhesive interactions (156,157). Thus far, the study of bioadhesion in bioerodible polymers has been overlooked owing to the fact that these materials lack sufficient chain flexibility for in-

terpenetration. The results of our studies suggest that bioadhesion of bioerodible polymers lacking chain flexibility could largely be a result of secondary bond formation, such as hydrogen bonding between mucin and carboxyl groups. Rapid degradation of P(FA:SA) polymers may enhance their bioadhesive nature through production of carboxylic acid and increases in surface roughness. In light of our findings, we believe that bioadhesive analysis using the diffusion theory of chain entanglement may be inappropriate for hard, bioerodible materials. Presently more work is needed to clarify the exact mechanisms of bioadhesion in thermoplastics, but the results here suggest that bioerodible, bioadhesive polymers may be excellent candidates for the development of orally administered DDSs. Selection of the appropriate delivery system, with proper release kinetics as well as appropriate adhesive characteristics, is essential to producing desired effects. Not every drug will benefit from bioadhesive delivery, but if targeted bioadhesive systems can be developed many pharmaceutical agents may be administered more efficiently than by conventional means. This field is still in its infancy, but with decades of research ahead, it is sure to have an impact on future drug delivery systems.

ACKNOWLEDGMENTS

We would like to thank the National Institutes of Health and NSF for supporting this research.

BIBLIOGRAPHY

1. V. Lenaerts and R. Gurny, *Bioadhesive Drug Delivery Systems*, CRC Press, Boca Raton, Fla., 1990.
2. R. Gurny, J.M. Meyer, and N.A. Peppas, *Biomaterials* **5**, 336–340 (1984).
3. E. Mathiowitz, D.E. Chickering, and C.M. Lehr, *Bioadhesive Drug Delivery Systems: Fundamentals, Novel Approaches, and Development*, Dekker, New York, 1999.
4. W.J. Passl, *Prog. Polym. Sci.* **14**, 629–677 (1989).
5. R. Langer, *Methods Enzymol.* **73**, 57–75 (1981).
6. R. Langer and N. Peppas, *Biomaterials* **2**, 201–214 (1981).
7. R. Langer, *Science* **249**, 1527–1532 (1990).
8. S.S. Davis and L. Illum, in F.H. Roerdink and A.M. Kroon, eds., *Drug Carrier Systems*, Wiley, Chichester, England, 1989, pp. 131–153.
9. R. Langer, L.G. Cima, J.A. Tamada, and E. Wintermantel, *Biomaterials* **11**, 738–745 (1990).
10. G. Ponchel, J.M. Irache, C. Durrer, and D. Duchêne, *Proc. Int. Symp. Controlled Release Bioact. Mater.* **21**, 31–32 (1994).
11. W.D. Rhine, D.S.T. Hsieh, and R. Langer, *J. Pharm. Sci.* **69**, 265–268 (1980).
12. D.H. Robinson and J.W. Mauger, *Am. J. Hosp. Pharm.* **48**, S14–S23 (1991).
13. J.R. Robinson, *Proc. Int. Symp. Controlled Release Bioact. Mater.* **18**, 75–76 (1991).
14. J. Kost and S. Shefer, *Biomaterials* **11**, 695–698 (1990).
15. J. Kost, K. Leong, and R. Langer, *Proc. Nat. Acad. Sci. U.S.A.* **86**, 7663–7666 (1989).
16. E.R. Edelman, J. Kost, H. Bobeck, and R. Langer, *J. Biomed. Mater. Res.*, **19**, 67–83 (1985).
17. G. Ponchel and D. Duchêne, in M. Szycher, ed., *High Performance Biomaterials*, Technomic Publishing, Lancaster, Pa., 1991, pp. 231–242.
18. K.V. Ranga Rao and P. Buri, in M. Szycher, ed., *High Performance Biomaterials*, Technomic Publishing, Lancaster, Pa., 1988, pp. 259–268.
19. D. Duchêne, F. Touchard, and N.A. Peppas, *Drug Dev. Ind. Pharm.* **14**, 283–318 (1988).
20. D. Duchêne and G. Ponchel, *Biomaterials* **13**, 709–715 (1992).
21. J.D. Smart, *Adv. Drug Delivery Rev.* **11**, 253–270 (1993).
22. V. Lenaerts, P. Couvreur, L. Grislain, and P. Maincent, in V. Lenaerts and R. Gurny, eds., *Bioadhesive Drug Delivery Systems*, CRC Press, Boca Raton, Fla., 1990, pp. 93–104.
23. J.M. Gu, J.R. Robinson, and S.-H.S. Leung, *CRC Crit. Rev. Ther. Drug Carrier Syst.* **5**, 21–67 (1988).
24. H.S. Ch'ng, H. Park, P. Kelly, and J.R. Robinson, *J. Pharm. Sci.* **74**, 399–405 (1985).
25. D.E. Chickering, J. Jacob, and E. Mathiowitz, *Biotechnol. Bioeng.* **52**, 96–101 (1996).
26. J.L. Chen and G.N. Cyr, in R.S. Manly, ed., *Adhesion in Biological Systems*, Academic Press, New York, 1970, pp. 163–181.
27. C.-M. Lehr et al., *J. Controlled Release* **18**, 249–260 (1992).
28. D.E. Chickering and E. Mathiowitz, *J. Controlled Release* **34**, 251–262 (1995).
29. C. Marriot, *Proc. Int. Symp. Controlled Release Bioact. Mater.* **18**, 67–68 (1991).
30. C.-M. Lehr, F.G.J. Poelma, H.E. Junginger, and J.J. Tukker, *Int. J. Pharm.* **70**, 235–240 (1991).
31. A. Rubinstein and B. Tirosh, *Pharm. Res.* **11**, 794–799 (1994).
32. R.M. Berne and M.N. Levey, *Physiology*, Mosby, St. Louis, Mo., 1988.
33. A.C. Guyton, *Textbook of Medical Physiology*, Saunders, Philadelphia, 1986.
34. K.R. Bhaskar et al., *Nature (London)* **360**, 458–461 (1992).
35. A. Allen, L.A. Sellers, and M.K. Bennet, *Scand. J. Gastroenterol., Suppl.* **128**, 6–13 (1987).
36. A. Garner, G. Flemstrom, and A. Allen, *Scand. J. Gastroenterol.* **19**, 78–80 (1984).
37. B. Sandzén, H. Blom, and S. Dahlgren, *Scand. J. Gastroenterol.* **23**, 1160–1164 (1988).
38. L. Szentkuti et al., *Histochem. J.* **22**, 491–497 (1990).
39. R.G. Spiro, *Annu. Rev. Biochem.* **39**, 599–638 (1970).
40. J. Labat-Robert and C. Decaeus, *Pathol. Biol.* **24**, 241 (1979).
41. M. Scawen and A. Allen, *Biochem. J.* **163**, 363–368 (1977).
42. M.I. Horowitz and W. Pigman, *The Glycoconjugates*, Academic Press, New York, 1977.
43. W. Pigman and A. Gottschalk, in A. Gottschalk, ed., *Glycoproteins: Their Composition, Structure and Function*, Elsevier, Amsterdam, 1966, pp. 434–445.
44. S. Ohara, K. Ishihara, and K. Hotta, *Comp. Biochem. Physiol.* **106B**, 147–152 (1993).
45. P. Johnson and K.D. Rainsford, *Biochem. Biophys. Acta* **286**, 72–78 (1972).
46. G. Flemstrom and E. Kivilaakso, *Gastroenterology* **84**, 787–794 (1983).

47. P.R. Wheater, G.H. Burkitt, and V.G. Daniels, *Functional Histology*, Churchill-Livingstone, Edinburgh, 1987.
48. C.M. Lehr, J.A. Bouwstra, J.J. Tukker, and H.E. Junginger, *J. Controlled Release* **13**, 51–62 (1990).
49. N.A. Peppas and P.A. Buri, *J. Controlled Release* **2**, 257–275 (1985).
50. A.J. Kinloch, *J. Mater. Sci.* **15**, 2141–2166 (1980).
51. H. Park and J.R. Robinson, *J. Controlled Release* **2**, 47–57 (1985).
52. B.V. Derjaguin and V.P. Smilga, *Adhes.: Fundam. Pract.* **1**, 152–163 (1966).
53. B.V. Derjaguin, Y.P. Toporov, V.M. Muller, and I.N. Aleinikova, *J. Colloid Interface Sci.* **58**, 528–533 (1977).
54. R.J. Good, *J. Colloid Interface Sci.* **59**, 398–419 (1977).
55. D. Tabor, *J. Colloid Interface Sci.* **58**, 2–13 (1977).
56. J.R. Huntsberger, in R.L. Patrick, ed., *Treatise on Adhesion and Adhesives*, Dekker, New York, 1966, pp. 119–149.
57. J.R. Huntsberger, *J. Paint Technol.* **39**, 199–211 (1967).
58. A.G. Mikos and N.A. Peppas, *Int. J. Pharm.* **53**, 1–5 (1989).
59. R.T. Spychal, J.M. Marrero, S.H. Saverymuttu, and T.C. Northfield, *Gastroenterology* **97**, 104–111 (1989).
60. A. Baszkin, J.E. Proust, P. Monsenego, and M.M. Boissonnade, *Biorheology* **27**, 503–514 (1990).
61. C.T. Reinhart and N.A. Peppas, *J. Memb. Sci.* **18**, 227–239 (1984).
62. R.P. Campion, *J. Adhes.* **7**, 1–23 (1974).
63. L.A. Girifalco and R.J. Good, *J. Phys. Chem.* **61**, 904–909 (1957).
64. B.O. Bateup, *Int. J. Adhes. Adhes.*, 233–239 (July 1981).
65. R.J. Good, *J. Colloid Interface Sci.* **52**, 308–313 (1975).
66. S. Wu, *J. Phys. Chem.* **74**, 632–638 (1970).
67. D.H. Kaelble and J. Moacanin, *Polymer* **18**, 475–482 (1977).
68. E. Helfand and Y. Tagami, *J. Chem. Phys.* **57**, 1812–1813 (1972).
69. E. Helfand and Y. Tagami, *J. Chem. Phys.* **56**, 3592–3601 (1972).
70. P.C. Hiemenz, *Principles of Colloid and Surface Chemistry*, Dekker, New York, 1986.
71. S.S. Voyutskii, *Autohesion and Adhesion of High Polymers*, Wiley, New York, 1963.
72. A.G. Mikos and N.A. Peppas, *Proc. Int. Symp. Controlled Release Bioact. Mater.* **13**, 97–98 (1986).
73. A.G. Mikos and N.A. Peppas, *S.T.P. Pharmacol.* **2**, 705–716 (1986).
74. H.W. Kammer, *Acta Polym.* **34**, 112 (1983).
75. G. Ponchel, F. Touchard, D. Duchêne, and N. Peppas, *J. Controlled Release* **5**, 129–141 (1987).
76. D.H. Kaelble, *J. Appl. Polym. Sci.* **18**, 1869–1889 (1974).
77. J.J. Bikerman, *The Science of Adhesive Joints*, Academic Press, New York, 1968.
78. J.D. Smart, I.W. Kellaway, and H.E.C. Worthington, *J. Pharm. Pharmacol.* **36**, 295–299 (1984).
79. A.P. Sam, J.T.M. van der Heuij, and J.J. Tukker, *Int. J. Pharm.* **79**, 97–105 (1992).
80. M. Ishida, N. Nambu, and T. Nagai, *Chem. Pharm. Bull.* **31**, 1010–1014 (1983).
81. M. Ishida, Y. Machida, N. Nambu, and T. Nagai, *Chem. Pharm. Bull.* **29**, 810–816 (1981).
82. C.-M. Lehr and V.H.L. Lee, *Proc. Int. Symp. Controlled Release Bioact. Mater.* **19**, 94–95 (1992).
83. C.-M. Lehr, J.A. Bowstra, H.E. Boddé, and H.E. Junginger, *Pharm. Res.* **9**, 70–75 (1992).
84. M.F. Saettone, S. Burgalassi, L. Panichi, and B. Giannaccini, *Proc. Int. Symp. Controlled Release Bioact. Mater.* **21**, 559–560 (1994).
85. F.J. Otero-Espinar et al., *Proc. Int. Symp. Controlled Release Bioact. Mater.* **21**, 700–701 (1994).
86. N.A. Peppas, L. Achar, and N. Wisniewski, *Proc. Int. Symp. Controlled Release Bioact. Mater.* **21**, 581–582 (1994).
87. L. Achar and N.A. Peppas, *J. Controlled Release* **31**, 271–276 (1994).
88. D.E. Chickering, J.S. Jacob, and E. Mathiowitz, *Proc. Int. Symp. Controlled Release Bioact. Mater.* **20**, 244–245 (1993).
89. D.E. Chickering et al., *Proc. Mater. Res. Soc. Fall Meet. Biomater. Drug Cell Delivery*, Boston, March 31, 1993, pp. 67–71.
90. E. Mathiowitz et al., *Proc. Int. Symp. Controlled Release Bioact. Mater.* **21**, 27–26 (1994).
91. D.E. Chickering et al., *J. Controlled Release* **48**, 35–46 (1997).
92. S.S. Davis, J.G. Hardy, and J.W. Fara, *Gut* **27**, 886–892 (1986).
93. S.S. Davis, F. Norring-Christensen, R. Khosla, and L.C. Feely, *J. Pharm. Pharmacol.* **40**, 205–207 (1988).
94. N.A. Peppas, ed., *Hydrogels in Medicine and Pharmacy*, CRC Press, Boca Raton, Fla., 1987.
95. C.-M. Lehr, Y.-H. Lee, and V.H.L. Lee, *Invest. Ophthalmol. Visual Sci.* **35**, 2809–2814 (1994).
96. D.Q.M. Craig, S. Tamburic, G. Buckton, and J.M. Newton, *J. Controlled Release* **30**, 213–223 (1994).
97. D.R. Mack, P.L. Blain-Nelson, and J.W. Mauger, *J. Biomed. Mater. Res.* **27**, 1579–1583 (1993).
98. S. Anlar, Y. Capan, and A.A. Hincal, *Pharmazie* **48**, 285–287 (1993).
99. M. Ishida, N. Nambu, and T. Nagai, *Chem. Pharm. Bull.* **30**, 980–984 (1982).
100. H. Park and J.R. Robinson, *Pharm. Res.* **4**, 457–464 (1987).
101. K. Park, S.L. Cooper, and J.R. Robinson, in N.A. Peppas, ed., *Hydrogels in Medicine and Pharmacy*, CRC Press, Boca Raton, Fla., 1987, pp. 151–175.
102. D.E. Chickering, J.S. Jacob, and E. Mathiowitz, *Proc. Int. Symp. Controlled Release Bioact. Mater.* **21**, 776–777 (1994).
103. M.R. Jimenez-Castellanos, H. Zia, and C.T. Rhodes, *Drug Dev. Ind. Pharm.* **19**, 143–194 (1993).
104. M. Helliwell, *Adv. Drug Delivery Rev.* **11**, 221–251 (1993).
105. K. Satoh et al., *Chem. Pharm. Bull.* **37**, 1366–1368 (1989).
106. P. Bottenberg et al., *Proc. Int. Symp. Controlled Release Bioact. Mater.* **18**, 631–632 (1991).
107. P. Bottenberg et al., *J. Pharm. Pharmacol.* **44**, 684–686 (1992).
108. S. Bouckaert et al., *J. Pharm. Pharmacol.* **44**, 684–686 (1992).
109. S. Bouckaert, M. Temmerman, M. Dhont, and J.P. Remon, *Proc. Int. Symp. Controlled Release Bioact. Mater.* **21**, 585–586 (1994).
110. S. Bouckaert, R. Van WeissenBrauch, H. Nelis, and J.P. Remon, *Proc. Int. Symp. Controlled Release Bioact. Mater.* **21**, 543–544 (1994).
111. S. Miyazaki et al., *Biol. Pharm. Bull.* **17**, 745–747 (1994).
112. T. Nagai and R. Konishi, *J. Controlled Release* **6**, 353–360 (1987).

113. H.E. Boddé, M.E. de Vries, and H.E. Junginger, *J. Controlled Release* **13**, 225–231 (1990).
114. J. Voorspoels and J.P. Remon, *Proc. Int. Symp. Controlled Release Bioact. Mater.* **21**, 539–540 (1994).
115. E. Beyssac et al., *Proc. Int. Symp. Controlled Release Bioact. Mater.* **21**, 553–554 (1994).
116. E. Beyssac et al., *Proc. Int. Symp. Controlled Release Bioact. Mater.* **21**, 891–892 (1994).
117. C. Charrueau et al., *J. Controlled Release* **32**, 9–15 (1994).
118. F. Thermes, A. Rozier, B. Plazonnet, and J. Grove, *Proc. Symp. Controlled Release Bioact. Mater.* **18**, 627–628 (1991).
119. M.E. de Vries, H.E. Boddé, H.J. Busscher, and H.E. Junginger, *J. Biomed. Mater. Res.* **22**, 1023–1032 (1988).
120. H.L. Luessen et al., *J. Controlled Release* **29**, 329–338 (1994).
121. H. Umejima et al., *J. Pharm. Sci.* **82**, 195–199 (1993).
122. L.E. Nachtigall, *Fertil. Steril.* **61**, 178–180 (1994).
123. J.R. Robinson and W.J. Bologna, *J. Controlled Release* **28**, 87–94 (1994).
124. N. Celebi, N. Erden, B. Gönül, and M. Koz, *J. Pharm. Pharmacol.* **46**, 386–387 (1994).
125. J.-H. Guo, *Proc. Int. Symp. Controlled Release Bioact. Mater.* **21**, 545–546 (1994).
126. J.-H. Guo, *Proc. Int. Symp. Controlled Release Bioact. Mater.* **21**, 547–548 (1994).
127. N. Yerushalmi and R. Margalit, *Biochim. Biophys. Acta* **1189**, 13–20 (1994).
128. N. Yerushalmi, A. Arad, and R. Margalit, *Arch. Biochem. Biophys.* **313**, 267–273 (1994).
129. R. Margalit, M. Okon, N. Yerushalmi, and E. Avidor, *J. Controlled Release* **19**, 275–288 (1992).
130. A.G. Mikos, and N.A. Peppas, *J. Controlled Release* **12**, 31–37 (1990).
131. A.G. Mikos, E. Mathiowitz, N.A. Peppas, and R. Langer, *Proc. Int. Symp. Controlled Release Bioact. Mater.* **18**, 109–110 (1991).
132. D.E. Chickering, W.P. Harris, and E. Mathiowitz, *13th Ann. Meet. Expo. American Association of Medical Instrumentation*, Anaheim, Calif., 1995.
133. N.F. Farraj, B.R. Johansen, S.S. Davis, and L. Illum, *J. Controlled Release* **13**, 253–261 (1990).
134. P. Vidgren et al., *Proc. Int. Symp. Controlled Release Bioact. Mater.* **18**, 638–639 (1991).
135. C.-M. Lehr, W. Kok, and J. Koninkx, *Proc. Int. Symp. Controlled Release Bioact. Mater.* **21**, 344–345 (1994).
136. N. Hussain, P.U. Jani, and A.T. Florence, *Proc. Int. Symp. Controlled Release Bioact. Mater.* **21**, 29–30 (1994).
137. E. Mathiowitz et al., *Nature (London)* **386**, 410–416 (1997).
138. A.G. Mikos, E. Mathiowitz, R. Langer, and N.A. Peppas, *J. Colloid Interface Sci.* **143**, 367–373 (1991).
139. C. Pimienta et al., *Pharm. Res.* **7**, 49–53 (1990).
140. D.E. Chickering, J.S. Jacob, and E. Mathiowitz, *React. Polym.* **25**, 189–206 (1995).
141. W.H. Guilford and R.W. Gore, *Am. J. Physiol.* **263**, C700–C707 (1992).
142. C.M. Lehr et al., *J. Pharm. Pharmacol.* **44**, 402–407 (1992).
143. J.D. Smart, B. Carpenter, and S.A. Mortazavi, *Proc. Int. Symp. Controlled Release Bioact. Mater.* **18**, 629–630 (1991).
144. A.J. Domb, F.C. Gallardo, and R. Langer, *Macromolecules* **22**, 3200–3204 (1989).
145. A. Domb and R. Langer, *J. Polym. Sci.* **25**, 3373–3386 (1987).
146. F. Lim and D. Moss, *J. Pharm. Sci.* **70**, 351–354 (1981).
147. E. Mathiowitz and R. Langer, *J. Controlled Release* **5**, 13–22 (1987).
148. E. Mathiowitz, M.D. Cohen, and R. Langer, *React. Polym.* **6**, 275–283 (1987).
149. E. Mathiowitz et al., *J. Appl. Polym. Sci.* **35**, 755–774 (1988).
150. E. Mathiowitz, D. Kline, and R. Langer, *Scanning Microsc.* **4**, 329–340 (1990).
151. E. Mathiowitz, P. Dor, C. Amato, and R. Langer, *Polymer* **31**, 547–555 (1990).
152. E. Mathiowitz et al., *J. Appl. Polym. Sci.* **45**, 125–134 (1992).
153. E. Mathiowitz, E. Ron, G. Mathiowitz, and R. Langer, *Macromolecules* **23**, 3212–3218 (1990).
154. L.R. Beck et al., *Fertil. Steril.* **31**, 545–551 (1979).
155. L.R. Beck et al., *Am. J. Obstet. Gynecol.* **135**, 419–426 (1979).
156. C.-M. Lehr, H.E. Boddé, J.A. Bowstra, and H.E. Junginger, *Eur. J. Pharm. Sci.* **1**, 19–30 (1993).
157. C.-M. Lehr, *J. Pharm. Pharmacol.* **44**, 402–407 (1992).
158. E. Mathiowitz, J. Jacob, D. Chickering, and K. Pekarek, *Macromolecules* **26**, 6756–6765 (1993).
159. E. Mathiowitz, M. Kreitz, and K. Pekarek, *Macromolecules* **26**, 6749–6755 (1993).
160. D.J. Pasto and C.R. Johnson, *Organic Structure Determination*, Prentice-Hall, Englewood Cliffs, N.J., 1969.
161. J. Jacob et al., *Proc. Int. Symp. Controlled Release Bioact. Mater.* **22**, 312–313 (1995).
162. N.N. Salib, M.A. El-Menshawy, and A.A. Ismail, *Pharm. Ind.* **40** (11A), 1230 (1978).
163. P. Trinder, *Biochem. J.* **57**, 301–303 (1954).
164. J. Axelrod, J.R. Cooper, and B.B. Brodie, *Proc. Soc. Biol. Med.* **70**, 693–695 (1949).
165. H. Sekikawi et al., *Chem. Pharm. Bull.* **31**, 1350–1356 (1983).
166. S. Goodman et al., *J. Appl. Biomater.* **6**, 161–165 (1995).
167. R.J.L. Davidson, *J. Clin. Pathol.* **24**, 537–541 (1971).
168. E.S. Vesell and J.G. Page, *J. Clin. Invest.* **47**, 2657–2663 (1968).
169. L.S. Goodman and A. Gilman, eds., *The Pharmacological Basis of Therapeutics*, Macmillan, New York, 1975.
170. E. Sanders and C.T. Ashworth, *Exp. Cell Res.* **22**, 137–145 (1961).
171. T.H. Ermak et al., *Cell Tissue Res.* **279**, 433–436 (1995).
172. A. Florence and P.U. Jani, *Drug. Saf.* **10**, 233–266 (1994).
173. A.T. Florence, A.M. Hillery, N. Hussain, and P.U. Jani, *J. Controlled Release* **36**, 39–46 (1995).
174. M.E. LeFevre, R. Olivo, J.W. Vanderhoff, and D.D. Joel, *Proc. Soc. Exp. Biol. Med.* **159**, 298–302 (1978).
175. M.E. Lefevre, D.D. Joel, and G. Schidlovsky, *Proc. Soc. Exp. Biol. Med.* **179**, 522–528 (1985).
176. P. Jani, G.W. Halbert, J. Langridge, and A.T. Florence, *J. Pharm. Pharmacol.* **42**, 821–826 (1990).
177. A.M. Hillery, P.U. Jani, and A.T. Florence, *J. Drug Target.* **2**, 151–156 (1994).
178. D.E. Bockman and M.D. Cooper, *Am. J. Anat.* **136**, 455–478 (1973).
179. G.F. Tutwiler, T. Kirsch, and G. Bridi, *Diabetes* **27**, 856–867 (1978).
180. E. Touitou and A. Rubinstein, *Int. J. Pharm.* 95–99 (1986).
181. J.A. Wolff et al., *BioTechniques* **11**, 474–85 (1991).
182. C. Lau et al., *Hum. Gene Ther.* **6**, 1145–1151 (1995).

Next Page

183. S.-H.S. Leung and J.R. Robinson, *J. Controlled Release* **12**, 187–194 (1990).

See also MUCOSAL DRUG DELIVERY, BUCCAL; MUCOSAL DRUG DELIVERY, INTRAVITREAL; MUCOSAL DRUG DELIVERY, NASAL; MUCOSAL DRUG DELIVERY, OCULAR; MUCOSAL DRUG DELIVERY, VAGINAL DRUG DELIVERY AND TREATMENT MODALITIES.

BIODEGRADABLE POLYMERS: POLY(ORTHO ESTERS).

See POLY(ORTHO ESTERS).

BIODEGRADABLE POLYMERS: POLY(PHOSPHOESTER)S

HAI-QUAN MAO
IRINA KADIYALA
KAM W. LEONG
The Johns Hopkins University School of Medicine
Baltimore, Maryland
ZHONG ZHAO
WENBIN DANG
Guilford Pharmaceuticals, Inc.
Baltimore, Maryland

KEY WORDS

Biocompatibility
Biodegradable polymers
Controlled delivery
Degradation
Drug and protein delivery
Microspheres
Poly(phosphoesters)
Synthesis
Viscous liquid

OUTLINE

Background of Poly(phosphoester)s
Properties of PPEs with a Bisphenol A Backbone
Design, Synthesis, and Physicochemical Properties of PPEs
- PPEs Based on Poly(Ethylene Terephthalate)
- PPEs Based on Chain Extension of Oligomeric Lactides by Phosphates
- PPEs Based on Cyclohexane-1,4-Dimethyl Phosphate Backbone

Storage Stability and Sterilization Stability
In Vivo Degradation, Biocompatibility, and Cytotoxicity
Drug Release Properties
- Controlled Release through PPE Microspheres
- Controlled Release through Poly(Terephthalate-*co*-Phosphate) Film
- Controlled Release through P(*trans*-CHDM-HOP) Viscous Liquid

Summary
Bibliography

In controlled drug delivery, a biodegradable drug carrier may offer features difficult to attain with nonbiodegradable systems (1,2). Other than obviating the need to remove the drug-depleted devices, a biodegradable system is also applicable to a wider range of drugs. For nonbiodegradable matrices, drug release in most cases is controlled by diffusion through the polymer phase (3,4). Biomacromolecules with low permeability through polymers are released only through pores and channels created by the dissolved drug phase. Proteins might sometimes aggregate and precipitate in the matrix, clogging the channels for diffusion. A matrix-degradation–controlled drug release mechanism can leach out the entire drug content provided that there is no strong interaction between the drug and the degrading matrix. A diffusion-controlled release mechanism would yield a drug release rate that exponentially decays with time; a matrix-degradation–controlled mechanism in many cases would produce a more steady release.

Several classes of synthetic polymers, including polyesters (5–7), poly(amino acid)s (8,9), polyamides (10), polyurethanes (11), poly(orthoester)s (12), poly(anhydride)s (13,14), poly(carbonate)s (15,16), poly(iminocarbonate)s (17,18), and poly(phosphazene)s (19–23), have been proposed for controlled drug delivery; the poly(lactide-*co*-glycolide) copolymers still dominate the field (5,24). There is justification for continuing to develop new biodegradable drug carriers, however, because carriers may be required for more than just passive delivery. The widening scope of applications may require the carrier to assume different configurations, and the carrier may need to serve additional functions. For instance, active targeting would involve conjugation of ligands to the carriers, requiring the polymeric carrier to contain functional groups for derivatization. Applying the controlled-release device as more than just a monolithic matrix—for example, as a coating material for a drug-eluting stent—may require the polymer to have elastomeric properties. In the new and exciting field of tissue engineering, where local and sustained delivery of growth factors may influence the course of tissue development, the drug carrier may also need to perform the double duty of providing structural support or scaffolding functions. With such a broad use for these biodegradable drug carriers, no one single material can be expected to satisfy all of the requirements of different applications. In recognizing that there is still room for new biodegradable drug carriers with distinct characteristics, in the past decade we have been studying polymers with a phosphoester linkage in the backbone. In this article we describe our initial effort to assess the structure–property relationship of these polymers with a bisphenol A backbone (25–28), and we describe our most recent effort in developing these polymers with three different types of

Previous Page

183. S.-H.S. Leung and J.R. Robinson, *J. Controlled Release* **12**, 187–194 (1990).

See also MUCOSAL DRUG DELIVERY, BUCCAL; MUCOSAL DRUG DELIVERY, INTRAVITREAL; MUCOSAL DRUG DELIVERY, NASAL; MUCOSAL DRUG DELIVERY, OCULAR; MUCOSAL DRUG DELIVERY, VAGINAL DRUG DELIVERY AND TREATMENT MODALITIES.

BIODEGRADABLE POLYMERS: POLY(ORTHO ESTERS). See POLY(ORTHO ESTERS).

BIODEGRADABLE POLYMERS: POLY(PHOSPHOESTER)S

HAI-QUAN MAO
IRINA KADIYALA
KAM W. LEONG
The Johns Hopkins University School of Medicine
Baltimore, Maryland
ZHONG ZHAO
WENBIN DANG
Guilford Pharmaceuticals, Inc.
Baltimore, Maryland

KEY WORDS

Biocompatibility
Biodegradable polymers
Controlled delivery
Degradation
Drug and protein delivery
Microspheres
Poly(phosphoesters)
Synthesis
Viscous liquid

OUTLINE

Background of Poly(phosphoester)s
Properties of PPEs with a Bisphenol A Backbone
Design, Synthesis, and Physicochemical Properties of PPEs
- PPEs Based on Poly(Ethylene Terephthalate)
- PPEs Based on Chain Extension of Oligomeric Lactides by Phosphates
- PPEs Based on Cyclohexane-1,4-Dimethyl Phosphate Backbone

Storage Stability and Sterilization Stability
In Vivo Degradation, Biocompatibility, and Cytotoxicity
Drug Release Properties
- Controlled Release through PPE Microspheres
- Controlled Release through Poly(Terephthalate-*co*-Phosphate) Film
- Controlled Release through P(*trans*-CHDM-HOP) Viscous Liquid

Summary
Bibliography

In controlled drug delivery, a biodegradable drug carrier may offer features difficult to attain with nonbiodegradable systems (1,2). Other than obviating the need to remove the drug-depleted devices, a biodegradable system is also applicable to a wider range of drugs. For nonbiodegradable matrices, drug release in most cases is controlled by diffusion through the polymer phase (3,4). Biomacromolecules with low permeability through polymers are released only through pores and channels created by the dissolved drug phase. Proteins might sometimes aggregate and precipitate in the matrix, clogging the channels for diffusion. A matrix-degradation–controlled drug release mechanism can leach out the entire drug content provided that there is no strong interaction between the drug and the degrading matrix. A diffusion-controlled release mechanism would yield a drug release rate that exponentially decays with time; a matrix-degradation–controlled mechanism in many cases would produce a more steady release.

Several classes of synthetic polymers, including polyesters (5–7), poly(amino acid)s (8,9), polyamides (10), polyurethanes (11), poly(orthoester)s (12), poly(anhydride)s (13,14), poly(carbonate)s (15,16), poly(iminocarbonate)s (17,18), and poly(phosphazene)s (19–23), have been proposed for controlled drug delivery; the poly(lactide-*co*-glycolide) copolymers still dominate the field (5,24). There is justification for continuing to develop new biodegradable drug carriers, however, because carriers may be required for more than just passive delivery. The widening scope of applications may require the carrier to assume different configurations, and the carrier may need to serve additional functions. For instance, active targeting would involve conjugation of ligands to the carriers, requiring the polymeric carrier to contain functional groups for derivatization. Applying the controlled-release device as more than just a monolithic matrix—for example, as a coating material for a drug-eluting stent—may require the polymer to have elastomeric properties. In the new and exciting field of tissue engineering, where local and sustained delivery of growth factors may influence the course of tissue development, the drug carrier may also need to perform the double duty of providing structural support or scaffolding functions. With such a broad use for these biodegradable drug carriers, no one single material can be expected to satisfy all of the requirements of different applications. In recognizing that there is still room for new biodegradable drug carriers with distinct characteristics, in the past decade we have been studying polymers with a phosphoester linkage in the backbone. In this article we describe our initial effort to assess the structure–property relationship of these polymers with a bisphenol A backbone (25–28), and we describe our most recent effort in developing these polymers with three different types of

backbones, affording drug carriers with a wide range of physicochemical properties.

BACKGROUND OF POLY(PHOSPHOESTER)S

The general chemical structure of poly(phosphoester)s (PPEs) is shown in this section. Depending on the nature of the side chain connected to the phosphorus, these polymers are conventionally called polyphosphates (P-O-C), polyphosphonates (P-C), or polyphosphites. Interests in phosphorus-containing polymers in the past have primarily been centered on their flame-retardant property (29). Because of a combination of factors—their high cost of synthesis as compared with the carbon analogs and their perceived hydrolytic instability—research interest has faded since the 1960s. Our optimism on these polymers stems from the following considerations:

1. *Adjustable properties.* The versatility of these polymers comes from the versatility of the phosphorus atom, which is known for its multiplicity of reactions. Its bonding can involve the 3p orbitals or various 3s–3p hydrids; spd hybrids are also possible because of the accessible d orbitals. Examining the general structure of the PPEs (Scheme 1), one can see that their physicochemical properties can be readily altered by varying either the R or R′ group. The biodegradability of the polymer is due to the physiologically labile phosphoester bond in the backbone. By manipulating the backbone or the side chain, a wide range of biodegradation rates should be attainable.

2. *Favorable physicochemical properties.* The speculation that these polymers would have favorable physical properties is based on the fact that high molecular weights, which should yield good mechanical strength, have been reported for these polymers. Average molecular weights (M_r) of over 100,000 have been reported for a polyphosphate obtained by a ring-opening polymerization. Considering the high reactivity of the phosphoryl chloride, there is reason to believe that through optimization of the polymerization process, these polymers can be obtained in high molecular weights. In addition, the P-O-C group in the backbone is known to provide a plasticizing effect. This would lower the glass transition temperature of the polymer and most importantly confer the polymer solubility in common organic solvents (30,31). Although not immediately apparent, this is highly desirable so that the polymers can be easily characterized and processed.

3. *Biocompatibility.* The issue of biocompatibility is less amenable to prediction. However, in principle, the ultimate hydrolytic breakdown products of a polyphosphate are phosphates, alcohols, and diols, all of which have the potential to be nontoxic (Scheme 1). Naturally, the intermediate oligomeric products of the hydrolysis might have different properties, and the toxicology of a biodegradable polymer built from even innocuous monomeric structures can be determined only by careful in vivo studies.

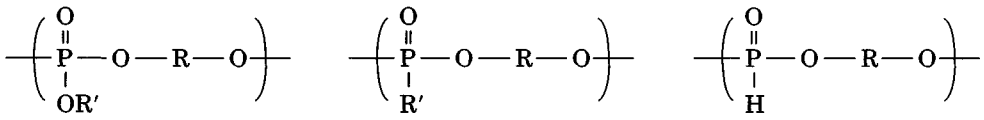
An additional feature of these polymers is the availability of functional side groups. This is a unique advantage of the phosphorus atom, which can be pentavalent, allowing the chemical linkage of drug molecules or other agents to the polymer (32). For instance, drugs with hydroxyl groups may be coupled to phosphorus via an ester bond, which is hydrolyzable. There are only a handful of pendent delivery systems based on a carbon–carbon backbone and even fewer with a heteroatom backbone. These PPEs are natural candidates for a completely biodegradable pendant delivery system.

PROPERTIES OF PPES WITH A BISPHENOL A BACKBONE

To perform a systematic study, we initially focused our attention on a series of bisphenol A–based PPEs shown in Scheme 2, the poly(oxyphosphoryl-oxy-1,4-phenyleneisopropylidene-1,4-phenylenes) (25,33): poly(bisphenol A-ethyl phosphate) (BPA-EOP), poly(bisphenol A-phenyl phosphate) (BPA-POP), poly(bisphenol A-phenyl phosphonate) (BPA-PP), and poly(bisphenol A-ethyl phosphonate) (BPA-EP). Bisphenol A (BPA), is chosen for this study because of the high reactivity of its phenoxide group and its relative hydrolytic stability, allowing the possibility of obtaining reasonable molecular weight with interfacial polymerization.

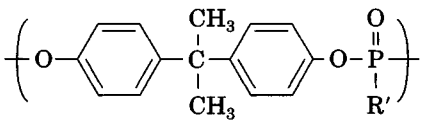
The polymers are obtained by interfacial polycondensation in methylene chloride–water, with potassium hydroxide as the acid receptor and cetyltrimethyl ammonium bromide as the phase transfer catalyst. With the parameters of the interfacial polycondensation optimized, the polymers have a M_r in the range of 30,000–50,000 (33). Degradation is observed for the four polymers studied under both in vitro and in vivo conditions and is affected by polymer side-chain structure. The ethyl side-chain polymer (BPA-EOP) degrades faster than its phenyl counterparts. Weight loss of this polymer in the intramuscular space of rabbits reaches more than 80% in 70 weeks. The most hydrophobic polymer in the series, BPA-PP, shows approximately 12% loss of mass in the same period, but the mass does not change significantly after week 5, suggesting that after the low molecular weight fragments are leached out, the polymers become quite stable. Tissue response to the PPEs in rabbits is characterized by slight or no lymphocyte, giant cell, or macrophage activity (25).

The swelling behavior of the polymers follows the relative hydrophobicity of the side chains, in the order of EOP > EP > POP > PP (25,27). The BPA-EOP swells up to the dimensions of the container and exhibits large voids and pores observable upon gross examination. For the other polymers, further water uptake ceases after 250 days in the absence of drug but continues beyond that when loaded with *p*-nitroaniline. Relative in vitro mass loss of the four polymers also matches the swelling trend. BPA-EOP degrades the most and BPA-PP the least, most likely because increased water uptake by the more hydrophilic polymers leads to increased hydrolytic cleavage of the polymer backbone and leaching of degradation products. Blank sample of BPA-EOP shows 10% mass loss after 150 days, while BPA-EP, BPA-POP, and BPA-PP degrade by 5, 2, and 1%, respectively (Fig. 1). The values increase to 22, 7, 3, and 2%, respectively, after 222 days. Cleavage of polymer chains is confirmed by gel permeation chromatography (GPC) in all cases.



Polyphosphate Polyphosphonate Polyphosphite

Scheme 1. General structure of PPEs.



R′ = $-OC_2H_5$ (BPA-EOP), $-OC_6H_5$ (BPA-POP), $-C_2H_5$ (BPA-EP), $-C_6H_5$ (BPA-PP)

Scheme 2. Structures of Bisphenol A–based PPEs.

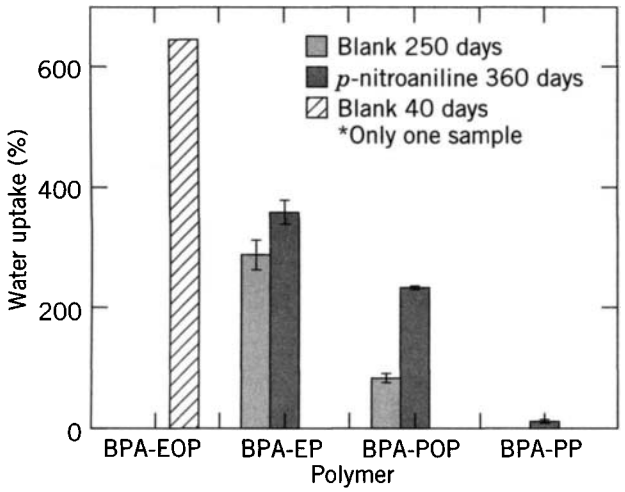


Figure 1. In vitro swelling of blank and *p*-nitroaniline–loaded PPE discs in phosphate-buffered saline at 37°C. Assay was carried out according to ASTM-D570 method.

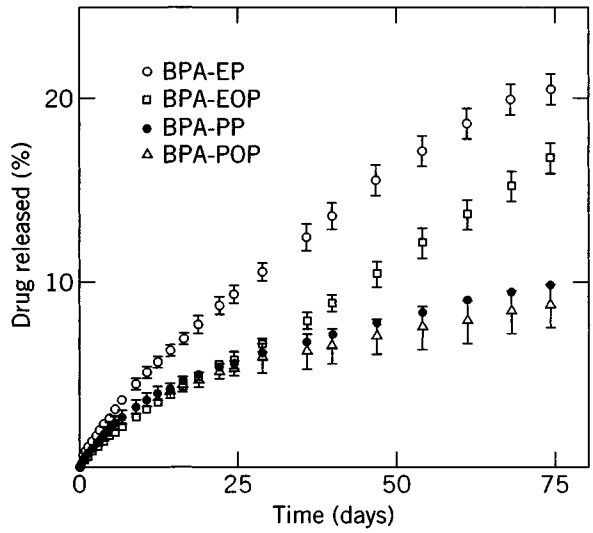


Figure 2. In vitro release of cortisone acetate from BPA-based PPE matrices at 37°C and pH 7.4.

To assess the effect of the chemical structure of the carriers on release behavior, two drugs of aqueous solubilities differing by a factor of 20 are examined against the four polymers (26). Release rates of cortisone acetate from the PPEs vary from about 25 to 75 $\mu g/day/cm^2$ for the nearly linear portion of the release curves (Fig. 2). Except for BPA-EOP, whose release profile over two and a half months is nearly linear with time (correlation coefficient 0.9995), the other three polymers, BPA-PP, BPA-POP, and BPA-EP, follow the square-root time kinetics typical of diffusion-controlled release.

Release of *p*-nitroaniline, a compound more hydrophilic than cortisone acetate and 20 times more soluble in phosphate buffer, is far more rapid except in the case of BPA-PP (Fig. 3). Release of *p*-nitroaniline from BPA-EOP and BPA-EP follows root-time kinetics for the first 60% of release and shows complete release after 20 and 360 days, respectively. Faster drug transport is likely due to higher water uptake and, to a lesser extent, greater degradation of these aliphatic side-chain polymers. A mass balance on BPA-EP shows an 11% degradation of the matrix by the end of drug release. It appears that in this case, release is predominantly controlled by the swelling of the matrices.

This initial structure–property relationship study confirms the influence of the side-chain structure on the swelling and degradation behavior of the polymers, which in turn regulates the drug release kinetics. It also suggests the polyphosphate might be the most promising to study because of its complete biodegradability. Subsequent studies therefore focused on the polyphosphates and with backbone structures that are potentially more likely to be innocuous for biocompatibility considerations.

DESIGN, SYNTHESIS, AND PHYSICOCHEMICAL PROPERTIES OF PPES

PPEs Based on Poly(Ethylene Terephthalate)

Poly(ethylene terephthalate) (PET) is one of the most commonly used biomedical polymers, as in vascular graft ap-

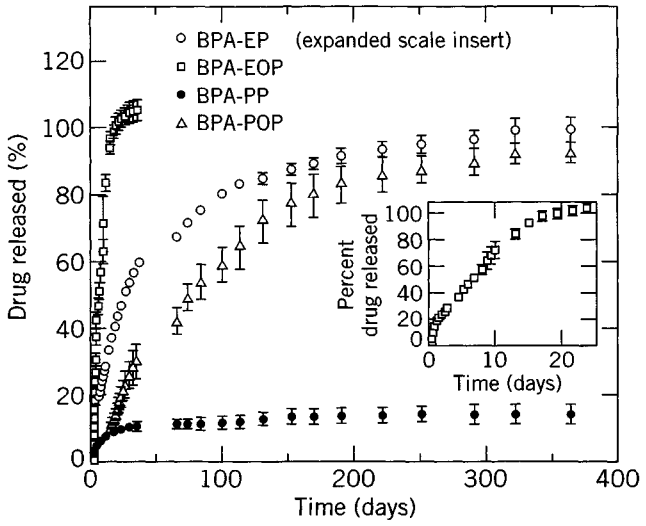


Figure 3. In vitro release of *p*-nitroaniline from BPA-based PPE matrices at 37°C and pH 7.4.

plications (34,35). Its appeal partly lies in its superb mechanical properties, which are derived from the liquid crystalline characteristics of the ethylene terephthalate structure. Hypothesizing that a biodegradable polymer with good mechanical properties can be built on this structure, we introduce phosphate units into PET (36). The general structure of poly(terephthalate-*co*-phosphate) is shown in Scheme 3 and Tables 1a and 1b. This series of PPEs can be synthesized by a two-step polycondensation. A diol such as 1,4-bis(hydroxyethyl)-terephthalate (BHET) is first reacted with ethyl phosphorodichloridate (EOP) to yield a hydroxyl-terminated prepolymer, which is further polymerized with the more energetic terephthaloyl chloride (TC). A typical synthetic procedure for P(BHET-EOP/TC, 80/20) is given in Example 1 (the numbers refer to the molar ratio of EOP to TC). The addition sequence and the ratio of reactive chlorides (EOP and TC) are crucial to obtain a polymer with high molecular weight and good solubility in common organic solvents. Adding the TC first or adding the two reactive dichlorides at the same time yields a polymer (T_m = 184°C) that is only slightly soluble in dimethylformamide (DMF) and dimethyl sulfoxide (DMSO) but not in chloroform or methylene chloride. As the chain extension is achieved more efficiently in the second step by the reactive TC, the molecular weight is increased but the solubility in chloroform or methylene chloride decreases because of the lower phosphate content. When the terephthalate unit is equimolar with the ethyl phosphoester unit, the polymer P(BHET-EOP/TC, 50/50) becomes insoluble in chloroform.

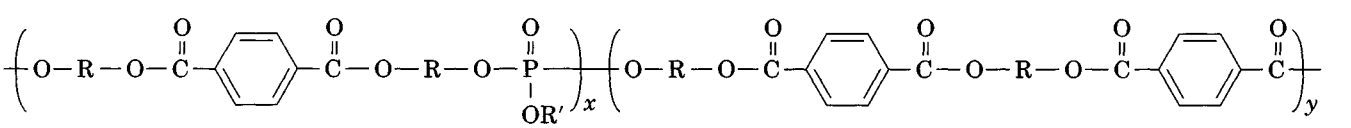
The composition of poly(terephthalate-*co*-phosphate) (contents of TC and phosphoester units) as calculated from the nuclear magnetic resonance (NMR) spectrum is consistent with the charging ratio. The relative molecular weights (using polystyrene as standards) of poly(terephthalate-*co*-phosphate)s increase with the TC content, which is also confirmed by the intrinsic viscosity data. This confirms that the reaction of the extended diol with terephthaloyl chloride is more energetic than that with ethyl phosphorodichloridate.

EXAMPLE 1

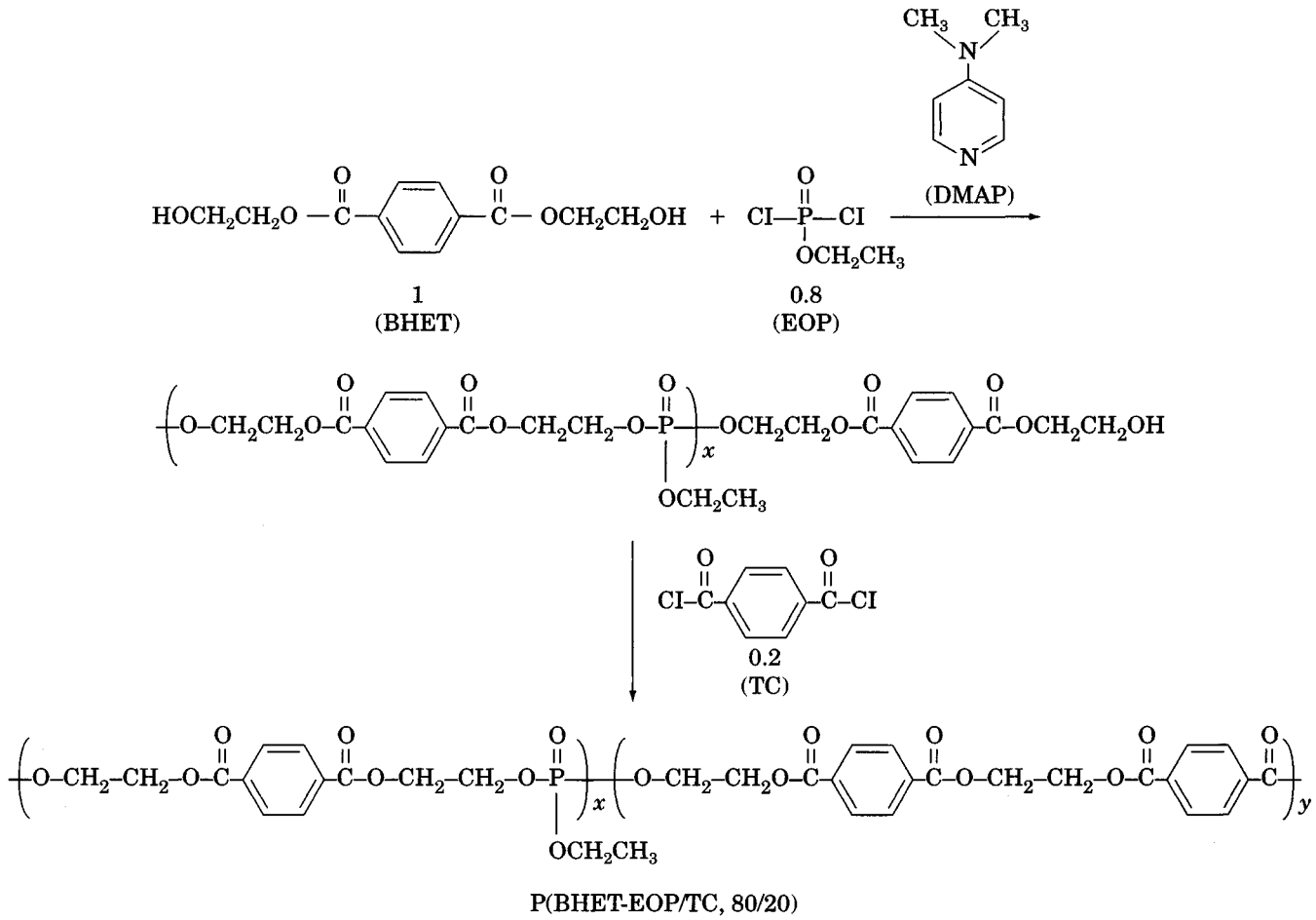
Synthesis of P(BHET-EOP/TC, 80/20) (Scheme 4).

Under an argon stream, a two-neck round-bottom flask (1 L) fitted with a condenser and addition funnel was charged with a solution of 50.85 g of 1,4-bis(hydroxyethyl) terephthalate (BHET, 0.2 mol). 48.9 g of 4-dimethylaminopyridine (DMAP, 0.4 mol) in 400 mL of methylene chloride. The mixture in the flask was cooled down to −40°C in a dry ice–acetone bath. A solution of 26.7 g of EOP (0.164 mol, 2.4% excess) in 50 mL of methylene chloride was added dropwise to the flask through the funnel. Following the addition of the EOP, the mixture was refluxed for 4 h, and then a solution of 8.12 g of TC (0.04 mol) in 20 mL of methylene chloride was added to the flask through the addition funnel. The temperature was gradually brought up to 50°C and allowed to react overnight. The mixture was cooled down to room temperature, washed three times with 0.1 N HCl solution saturated with NaCl (300 mL each time) and once with saturated NaCl solution (300 mL). The organic layer was dried over anhydrous sodium sulfate and filtered. The filtrate was concentrated and quenched with ether. The precipitate was collected and reprecipitated twice by methylene chloride–ether quenching. The precipitate was dried under vacuum at 60°C overnight to give a polymer (51 g, 73%) as a white, tough, chunky solid, with M_r = 14,910 and M_n = 5810 (by GPC measured in chloroform at 40°C using polystyrene as standards). It was found that a 2–5% excess of phosphorodichloridate yields a higher molecular weight polymer. This might be due to the high susceptibility of ethyl phosphorodichloridate to moisture.

Dacron (PET) is a highly crystallized polymer (T_m = 265°C, T_g = 69°C) (37). Introduction of an ethyl phosphate bond into the backbone significantly changes the polymer's thermal properties. In the P(BHET-EOP/TC) series, when the EOP/TC ratio is higher than 1, the PPEs are amorphous with no melting point (T_m) observable from differential scanning calorimetric (DSC) analysis; the polymers begin to soften at around 150°C. When the EOP/TC charging ratio is reduced to 1, crystalline phase begins to form in the polymer (T_m = 201°C for P[BHET-EOP/TC, 50/50]). As expected, the glass-transition temperature (T_g) increases as the charging ratio of EOP/TC decreases (Fig. 4). To evaluate the effect of a more sterically hindered diol on



Scheme 3. Structures of poly(terephthalate-*co*-phosphate)s.



Scheme 4. Synthesis of P(BHET-EOP/TC, 80/20).

Table 1a. Structural Variation of Poly(terephthalate-*co*-phosphate)s: Diol in the Backbone

R (R′ = CH_3CH_2-)		Polymer[a]
-CH_2-CH_2-	EG	P(BHET-EOP/TC)
-CH_2-CH_2-CH_2-	PD	P(BHPT-EOP/TC)
-CH_2-CH(-CH_3)-CH_2-	MPD	P(BHMPT-EOP/TC)
-CH_2-C(CH_3)$_2$-CH_2-	DMPD	P(BHDPT-EOP/TC)

[a]Numbers in the parentheses appearing in the text refer to the molar ratio of the two chloride monomers, ethyl phosphorodichloridate to terephthaloyl chloride.

Table 1b. Structural Variation of Poly(terephthalate-*co*-phosphate)Side Chains

R′ (R = -CH_2-CH_2-	Ratio[b]	Polymer
CH_3-CH_2-	80	P(BHET-EOP/TC, 80/20)
CH_3CH_2- and CH_3-	60/20	P(BHET-EMOP/TC, 60/20/20)
CH_3CH_2- and CH_3-	40/40	P(BHET-EMOP/TC, 40/40/20)
CH_3CH_2- and Na	60/20	P(BHET-ENaOP/TC, 60/20/20)
CH_3CH_2- and Na	40/40	P(BHET-ENaOP/TC, 40/40/20)

[b]Molar ratio of EOP to MOP.

the polymer biodegradation and physical properties, we have also synthesized a series of copolymers by substituting ethylene glycol (EG) with propylene diol (PD), 2-methylpropylene diol (MPD), or 2,2-dimethylpropylene diol (DMPD), respectively. Comparison of the aliphatic diol component indicates that the polymer chain rigidity decreases in the order of EG > DMPD > MPD > PD.

The relative hydrophobicity of the P(BHET-EOP/TC) series has been assessed by measuring the water-in-air contact angle. The contact angle decreases dramatically from 65° for P(BHET-EOP/TC, 80/20) to 8° for P(BHET-EOP). While the charging molar ratio of EOP/TC is maintained at 4 (or 80/20), substituting the ethoxy side chain with methoxy side chain (MOP) would also increase the hydrophilicity (Table 2). At the ratio of EOP/MOP/TC of 40/40/20, the contact angle decreases to a value close to that of P(BHET-EOP). Furthermore, converting the meth-

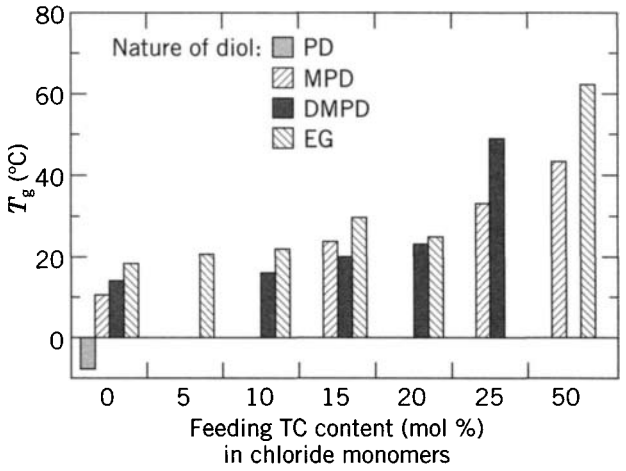


Figure 4. Glass-transition temperatures of poly(terephthalate-*co*-phosphate)s with different structures. Poly(terephthalate-*co*-phosphate)s were synthesized using propylene diol (PD), 2-methylpropylene diol (MPD), 2,2-dimethylpropylene diol (DMPD), or ethylene glycol (EG) as the initial diol (Scheme 1). The EOP/TC content is consistent with the charging ratio, calculated according to their NMR spectra.

oxy groups into sodium salt renders the polymer insoluble in chloroform and methylene chloride. The negatively charged P(BHET-ENaOP/TC)s become more hydrophilic by gross observation. As expected, the methoxy group substituted P(BHET-EOP/TC) and the negatively charged poly(terephthalate-*co*-phosphate)s have a much higher T_g than their parent polymers (Table 2). P(BHET-NaOP/TC, 80/20) has a clear sharp melting peak at 180°C as determined by DSC.

The poly(terephthalate-*co*-phosphate) shows typical tensile properties for plastics with low degrees of crystallinity. At compositions with an EOP/TC charging ratio of 80/20 to 85/15, the P(BHET-EOP/TC)s could form thin elastomeric films from solvent casting. At an EOP/TC ratio higher than 90/10, the film becomes brittle. Substituting EOP with MOP (P[BHET-EMOP/TC]s, see Table 2) does not affect the film formation. However, the film becomes more brittle and less ductile. Fibers could be drawn from polymer melts at 160–180°C from all the polymers with a 20% molar ratio of TC, even for the negatively charged P(BHET-ENaOP/TC)s (Table 3).

The in vitro degradation rates of solvent-cast films of P(BHET-EOP/TC, 80/20) and P(BHET-EOP/TC, 85/15), with relative molecular weights (M_r polystyrene as a standard) in the range of 5,000 to 7,000, lose 21 and 43%, respectively, of their original weight in 18 days when incubated in 0.1 M PBS at 37°C (Fig. 5). Higher molecular weight PPEs with the same composition degrades at a slower rate. P(BHET-EOP/TC, 80/20) with a M_r of 14,300 shows only a 5% weight loss in 14 days of incubation under the same condition. Increasing the TC content in the polymer would also retard the degradation rate.

As discussed above, in the P(BHET-EOP/TC, 80/20) series, substituting the ethoxy with a methoxy group yields polymers with higher hydrophilicity, which in turn accelerates the in vitro degradation as demonstrated in Figure 6. Furthermore, converting the methoxy group to a sodium salt dramatically increases the degradation rate.

Table 2. Glass-Transition Temperatures and Water-in-Air Contact Angles of Some Poly(terephthalate-*co*-phosphate)s

Poly(terephthalate-*co*-phosphate)	T_g (°C)	Water-in-air contact angle
P(BHET-EOP/TC, 80/20)	25	65°
P(BHET-EOP/TC, 85/15)	28	54°
P(BHET-EOP/TC, 95/5)	21	10°
P(BHET-EOP/TC, 100/0)	19	8°
P(BHET-EMOP/TC, 60/60/20)	32	14°
P(BHET-EMOP/TC, 40/40/20)	39	9°
P(BHET-NaOP/TC, 80/20)	58 (T_m = 180)	N.D.
P(BHET-ENaOP/TC, 60/20/20)	52	N.D.
P(BHET-ENaOP/TC, 40/40/20)	63	N.D.

PPEs Based on Chain Extension of Oligomeric Lactides by Phosphates

Poly(lactide-*co*-glycolide)s (PLGAs) remain the most popular and well-characterized biodegradable polymeric biomaterials. Their regulatory approval and extensive database of human use render them an obvious choice in medical applications that range from controlled drug delivery to tissue engineering (38). This series of PPEs contains phosphate bonds distributed between oligomeric blocks of lactides in the backbone. The rationale for designing such a structure is to explore the possibility of extending the physicochemical properties of the most commonly used PLGA polymers. The inclusion of the phosphate linkage in the backbone offers an extra degree of freedom to fine-tune the properties of the polymers (Scheme 5) (39). The degradation rate of a poly(lactide-*co*-phosphate) thus constructed is mainly controlled by the percentage of phosphate component introduced into the backbone. This has the effect of eliminating the biphasic degradation behavior typically exhibited by the crystalline polylactic acid (PLA). The higher the phosphate content in the backbone, the faster the degradation rate of the polymers. An additional factor that plays an important role in

Table 3. Tensile Properties of Poly(terephthalate-*co*-phosphate)s

Poly(terephthalate-*co*-phosphate)	Tensile stress at yield (psi)	Elongation at break (%)	Modulus of elasticity (MPa)
P(BHET-EOP/TC, 80/20)	230.89 ± 1.44	113.5 ± 42.3	13.35 ± 0.32
P(BHET-EMOP/TC, 60/20/20)	370.27 ± 67.95	74.6 ± 8.7	26.77 ± 2.19
P(BHET-EMOP/TC, 40/40/20)	404.22 ± 145.87	48.9 ± 1.6	27.59 ± 9.36

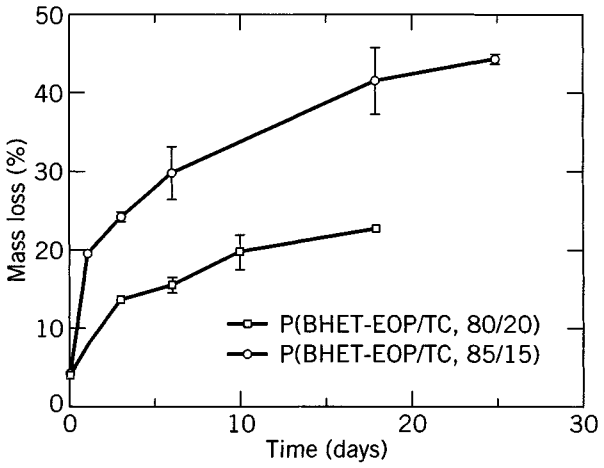


Figure 5. In vitro degradation of P(BHET-EOP/TC) discs in 0.1 M PBS at 37°C. The numbers in parentheses refer to the molar ratio of EOP to TC.

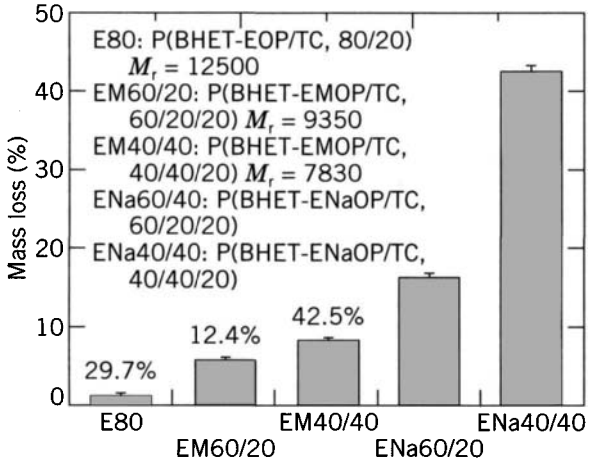


Figure 6. In vitro mass loss of P(BHET-EMOP/TC) discs in two weeks in 0.1 M PBS at 37°C. Numbers on top of the bars represent the average M_r decreases.

determining the overall degradation rate is the stereoisomerism of the lactide, with the D,L-lactide (DLLA) producing polymers with lower crystallinity, lower T_g, and faster degradation rate than polymers synthesized from L-lactide (LLA).

The synthesis of poly(lactide-*co*-phosphate)s starts with the ring opening of lactide with an aliphatic diol (Scheme 6). This step is accomplished by thermal ring opening either in the absence or presence of a tin catalyst. The resulting macromonomer diol is further chain extended by phosphorodichloridate carried out in melt. An example of the synthetic protocol is given in Example 2. Propylene glyol (PG) has also been used as the initiator of the ring-opening reaction because it has a better safety profile than EG. L-lactide can be substituted by D,L-lactide to afford a more rapid degradation profile of the final polymer. Small amount of stannous octoate (200 ppm) can be added to the prepolymerization to shorten the reaction time and result in a more uniform molecular weight distribution of the prepolymer. We have explored different molar ratios between DLLA and PG such as 5:1, 10:1, and 20:1, etc. to create prepolymers of different molecular weights and subsequently different degradation rates of the final polymers. This section will focus on two polymers in this series (Scheme 6), P(LAEG-EOP) and P(DAPG-EOP).

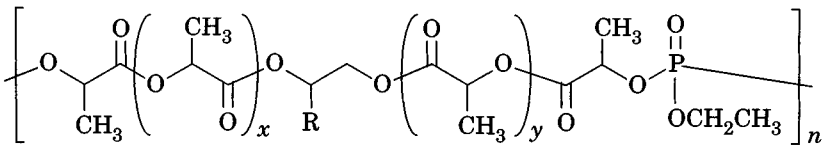
EXAMPLE 2

Synthesis of P(LAEG-EOP) Through Bulk Polymerization (Scheme 6).

To a 250-mL round-bottom flask flushed with dried argon, 20 g (0.139 mol) of (3S)-*cis*-3,6-dimethyl-1,4-dioane-2,5-dione (L-lactide) and 0.432 g (6.94 mmol) of EG were added. The flask was closed under vacuum, placed in a 140°C oven, and kept in the oven for 2 to 4 days with occasional shaking. Then it was filled with dried argon and placed in a 135°C oil bath. Under argon stream, 1.13 g of EOP was added through a funnel with stirring. A low vacuum (~20 Torr) was applied to the system after 1 h of stirring and let stand overnight, and a high vacuum (0.05 Torr) was applied for at least 2 h. The polymer was cooled down and dissolved in 250 mL of chloroform. The solution was quenched into 1 L of ether. The dissolving–quenching step was repeated twice. The polymer was dried under vacuum to yield a white or slightly yellowish powder, yield 72–80%. Parameters tested: M_r = 33,000, M_n = 4,800. [η] = 0.315 (chloroform, 40°C); T_g = 52°C.

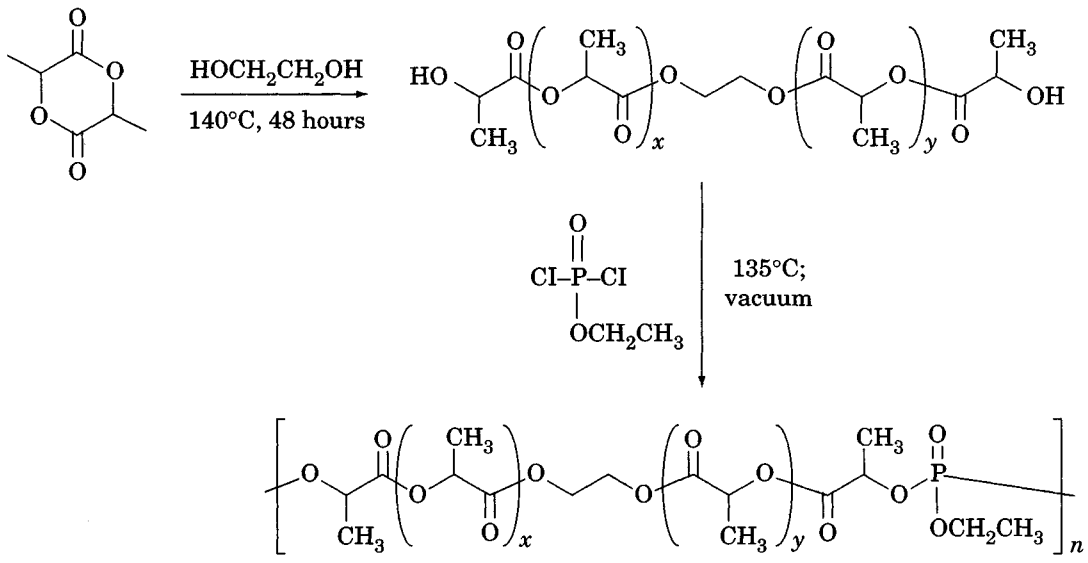
The poly(lactide-*co*-phosphate)s have excellent solubility in a broad range of organic solvents including ethyl acetate and acetonitrile, which are poor solvents for PLGA. Changing the initiation diol does not significantly change the physicochemical properties. As expected, P(DAPG-EOP) with a D,L-lactide block has an even higher solubility in common organic solvents.

The in vitro degradation has been studied in phosphate-buffered saline (PBS) at 37°C using microspheres prepared by the solvent evaporation method (40). The degradation rate is quite sensitive to the composition and molecular weights of the polymers. The feeding ratio of lactide to



P(LAEG-EOP); R = H, all L-lactide
P(DAPG-EOP); R = CH_3, D,L-lactide

Scheme 5. Structures of poly(lactide-*co*-phosphate)s.



Scheme 6. Synthesis of P(LAEG-EOP).

initiation diol or phosphorodichloridate determines the length of the oligomeric lactide block. Lowering the molecular weight and increasing the phosphate content of the PPEs will increase the degradation rate of microspheres, owing to the higher hydrophilicity of the polymers. Polymers with D,L-lactide oligomers as the repeating unit degrade faster than those prepared from the L-lactide oligomers. Molecular weight also plays an important role in the degradation. At the same DLA/PG feeding ratio of 10:1, polymer with M_r 7,900 degrades much faster than that with M_r 12,000 by about 20% mass loss in two months (Fig. 7). Polymers with a faster degradation rate could in principle be custom designed by increasing the phosphate content and lowering the molecular weight.

PPEs Based on Cyclohexane-1,4-Dimethyl Phosphate Backbone

The third series of PPEs are obtained from the polycondensation of aliphatic diols and aliphatic phosphorodichloridates, one of the simplest structures possible for PPEs. In contrast to the other PPEs described earlier, these polymers contain neither aromatic rings nor crystallizable blocks, and owing to a combination of the flexible phosphate and alkane structures, they have flowing points significantly below room temperature. The rationale of developing this series is to examine if these polymers, which exist as viscous liquids, would be useful as drug carriers, particularly for protein delivery, and may be applied with minimal fabrication processing. In principle, drugs can be blended into these polymers at a wide range of loading levels at room temperature and can be applied topically or injected into anatomical sites such as corneas and joints. In the case of proteins, the absence of any contact with organic solvents, low temperature, and possibility of inclusion of protein stabilizers in a simple loading process might be favorable for preserving the bioactivity of the proteins.

We focus on a cyclohexane dimethanol (*cis* or *trans*, or a mixture of both) backbone with different aliphatic side chains (39,41) (Scheme 7). A typical protocol of preparing P(*trans*-CHDM-HOP) is described in Example 3. These aliphatic polyphosphates are obtained as clear colorless or pale yellow liquids with M_n ranging from 3,000 to 10,000. Polymers can be obtained without a catalyst if the polymerization is conducted at high temperatures, but the molecular weights are generally lower. Side reactions such as transesterification involving the side chain may also lead to cross-linking. The viscosity profile of the P(*trans*-CHDM-HOP) as a function of temperature and frequency sweep is shown in Figure 8. Although viscous at room temperature with a viscosity of 327 Pas, the liquid can be injected with a gauge needle of 20 and below. The viscosity of the polymer is decreased if the backbone is composed of a mixture of *cis* and *trans* instead of the pure *trans* cyclic diol.

EXAMPLE 3

Synthesis of P(*trans*-CHDM-HOP) By Solution Polymerization (Scheme 8).

Under an argon stream, 10 g of *trans*-1,4-cyclohexane dimethanol (CHDM), 0.847 g of 4-dimethylaminopyridine (DMAP), 15.25 mL (14.03 g) of *N*-methyl morpholine (NMM) and 50 mL of methylene chloride were transferred into a 250 mL flask equipped with a funnel. The solution in the flask was cooled down to −40°C with stirring. A solution of 15.19 g of hexyl phosphorodichloridate (HOP) in 20 mL of methylene chloride was added through the funnel (10 mL of methylene chloride was used to flush through the funnel), and then the mixture was brought to boiling temperature gradually. It was kept refluxing for 4 h and was filtered. The filtrate was evaporated and redissolved in 100 mL of chloroform. This solution was washed twice with 0.5 M of HCl NaCl solution and once with saturated NaCl solution, dried over Na_2SO_4, and quenched into an ether–petroleum (1:5) mixture. The precipitate (oily) was collected and dried under vacuum. A clear, pale yellow, viscous liquid was obtained.

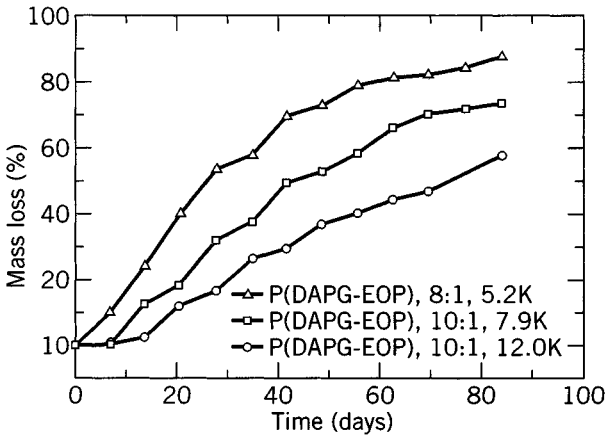


Figure 7 . In vitro degradation of microspheres made from P(DAPG-EOP) with different M_r and compositions. Ratios refer to DLLA/PG, followed by M_r of the polymers.

The polymers degrade in vitro as a function of the alkyl chain length in the side chain (39). Following the trend of the lipophilicity of the side chains, the degradation rate of the polymers decreases in the order of P(CHDM-EOP) > P(CHDM-BOP) > P(CHDM-HOP) (Figure 9). Higher degradation rates can be obtained by substituting CHDM with the linear aliphatic 1,6-hexane diol. The degradation rate would be even further enhanced if 1,4-butane diol is used. Poly(ethylene glycol) (PEG) of different molecular weights have also been studied as the backbone. These linear aliphatic PPEs become water soluble with low molecular weights of PEG and waxy with PEG of molecular weights above 8,000. In the series of PPEs with hexyl side chains, the viscosity of these linear aliphatic PPEs is in general lower than that of P(CHDM-HOP).

STORAGE STABILITY AND STERILIZATION STABILITY

Designed to be biodegradable, the PPEs are naturally susceptible to hydrolysis even in air. When stored in air at room temperature, their molecular weights decline slightly (42). However, all three series of polymers are reasonably stable in a desiccator at room temperature, without the need for storage under inert gas, as monitored by GPC and intrinsic viscosity. For example, the molecular weight of a P(LAEG-EOP) stored in a dessicator remains unchanged throughout a 3-month period (Fig. 10), but in contrast, the molecular weight drops about 70% when the same sample is placed in air.

Sterilizability of a biomedical polymer is an important parameter (43). These PPEs have been placed in an aluminum foil pouch, heat sealed, packed with dry ice, and γ-irradiated at 18.3–25.0 KGy. Both the structure and molecular weight are unaffected, as monitored by GPC, intrinsic viscosity measurement, and Fourier transform infrared spectroscopy (FTIR) (36,44).

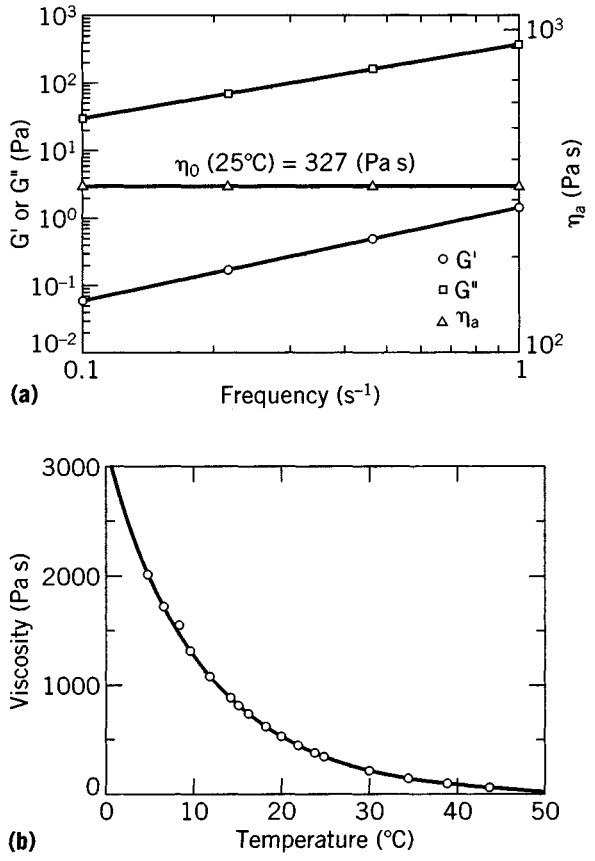
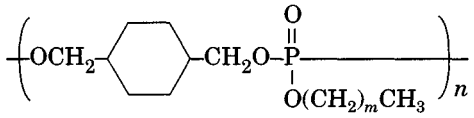


Figure 8. (**a**) Apparent viscosity (η_a), storage modules (G′) and loss modules (G″) of P(*trans*-CHDM-HOP) as a function of frequency; (**b**) temperature dependency of apparent viscosity (η_a) of P(*trans*-CHDM-HOP) at 25°C at a frequency of 1 s^{-1}.

The effect of γ-irradiation on the stability of a PPE/paclitaxel microsphere formulation has also been investigated by sterilizing the microspheres containing 10% Paclitaxel under the same condition (45). Neither the polymer molecular weights nor the microsphere characteristics are affected by the irradiation process, and paclitaxel in PPE microspheres remains stable during γ-irradiation. Furthermore, paclitaxel release profiles are comparable before and after γ-irradiation, suggesting that it can be used to sterilize paclitaxel/PPE microspheres.

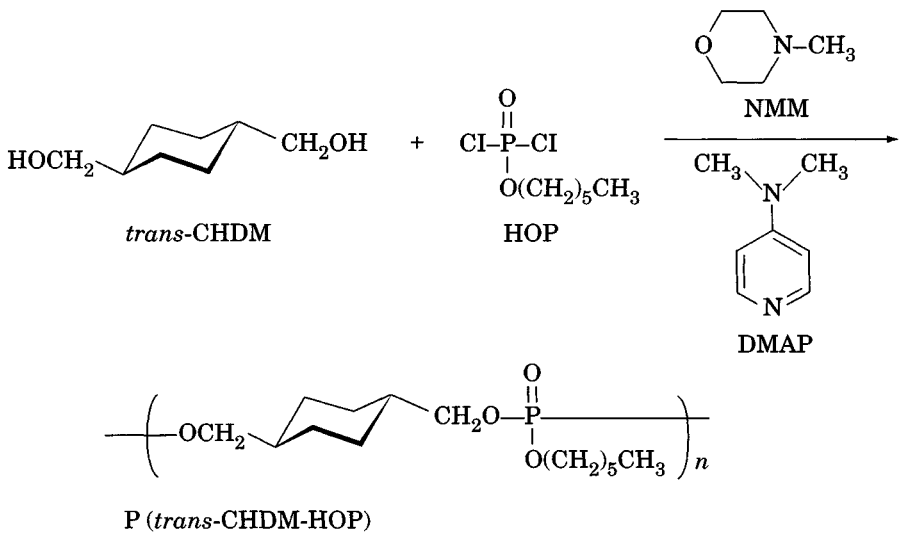
IN VIVO DEGRADATION, BIOCOMPATIBILITY, AND CYTOTOXICITY

The biodegradation and biocompatibility of these PPEs have been evaluated in an SPF Sprage-Dawley rat model.



m = 5, P(CHDM-HOP)
m = 3, P(CHDM-BOP)
m = 1, P(CHDM-EOP)

Scheme 7. Structures of CHDM-based PPEs.



Scheme 8. Synthesis of P(CHDM-HOP).

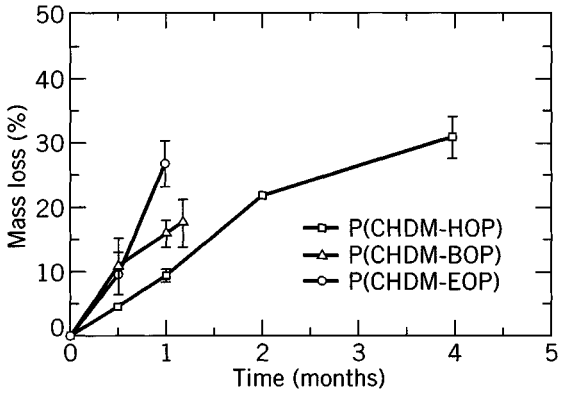


Figure 9. In vitro degradation of PPEs with different side chains in PBS at 37°C. Refer to Scheme 7 for the symbols.

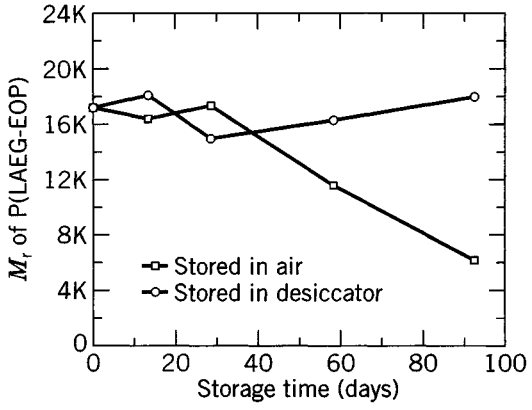


Figure 10. Changes in M_r of P(LAEG-EOP) samples stored at room temperature with or without desiccation.

P(BHET-EOP/TC, 80/20), P(LAEG-EOP), and P(CHDM-HOP) have been investigated as the representatives for each class of PPEs, compared with PLGA (75:25, RG755). PPE discs are fabricated by compression molding at 200 MPa or by a film-casting method and sterilized by γ-irradiation at 25 KGy on dry ice. The discs and viscous liquid are implanted into the muscles at the right hind limb of the adult rat. The reaction surrounding the implantation site is characterized as slight to mild for up to 4 months for all four polymers. At the 4- and 6-month time points, all tissue reactions to the four groups are characterized as only slightly irritating (Table 4). Hematology data, differential leukocyte counts, cellular morphology findings, and clinical chemistry values are overall unremarkable and comparable among the four groups at each interval. No histomorphological change in all major organs at the 6-month time point is observed (42).

The analysis of polymer discs retrieved at different time points shows a continuous mass loss of the P(LAEG-EOP) discs with time, compared with the typical biphasic degradation behavior of PLGA (Fig. 11). P(BHET-EOP/TC, 80/20), on the other hand, shows approximately 20% mass loss in 2 weeks and remains unchanged for up to 4 months (42). As discussed earlier for the in vitro degradation rate of the P(BHET-EOP/TC)s, it is expected that their in vivo degradation rates would be accelerated by increasing the phosphate content in the backbone.

The cytotoxicity of P(BHET-EOP/TC, 80/20) has been assessed by culturing human embryonic kidney cells (HEK293) on a polymer-coated cover slip. Cells exhibit a normal morphology and proliferate at a rate comparable to those cultured on tissue culture polystyrene (TCPS) surface. The proliferation assay on human gastric carcinoma cells (GT3TKB) showed no inhibition of cell growth for either P(BHET-EOP/TC, 80/20) or P(LAEG-EOP) microspheres at up to at least 0.5 mg/mL and 1.0 mg/mL concentration, respectively. The Ames test and International

Table 4. Tissue Reaction Score for PPE Discs and Viscous Liquid Implanted between the Muscle Layers of the Hind Limb of Male Sprague-Dawley Rats

	Time after the implantation[a] (d = days, m = months)						
PPE	3 d	7 d	14 d	1 m	2 m	4 m	6 m
P(LAEG-EOP)	SI (130)	SI (123)	SI (180)	SI (198)	SI (106)	SI (99)	SI (30)
P(BHET-EOP/TC, 80/20)	SI (151)	SI (116)	SI (163)	SI (98)	SI (60)	SI (35)	SI (52)
P(CHDM-HOP)	MI (226)	SI (197)	SI (196)	MI (225)	MI (207)	MI (122)	SI (40)
PLGA (RG755)	SI (148)	SI (98)	SI (137)	SI (105)	SI (94)	SI (43)	SI (44)

Note: The extent of inflammatory response at the implantation sites has been assessed by an independent pathologist. The number of monocytes and macrophages under 400× microscopic field are counted. The arithmetic mean of four different fields is used to grade the tissue reaction according to the following system: NI, no irritation (0); SI, slight irritation (1–200); MI, mild irritation (201–400); MOI, moderate irritation (401–600); SEI, severe irritation (>601).
[a]Numbers in parentheses represent average monocyte/macrophage count/fields at 400×.

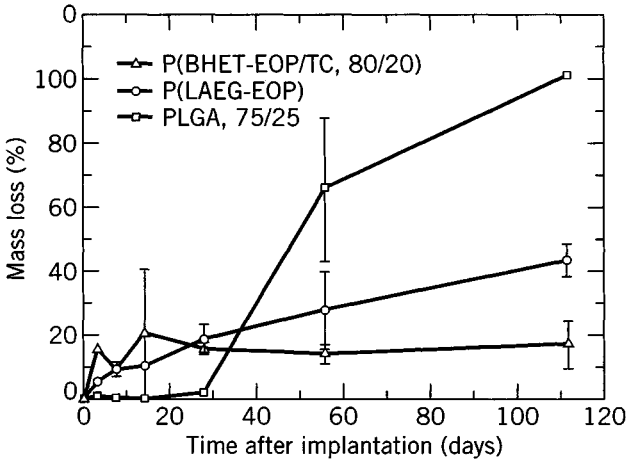


Figure 11. Degradation profiles of PPEs in rat muscle compared with PLGA (75/25).

Organization for Standardization (ISO) agarose overlay tests suggest that all three classes of polymers are neither mutagenic nor cytotoxic (36,39).

DRUG RELEASE PROPERTIES

Controlled release of several low-molecular-weight drugs, proteins, and plasmid DNA with different physicochemical properties have been studied in the forms of microspheres, thin films, or viscous liquids as described in this section.

Controlled Release through PPE Microspheres

Controlled Release of Paclitaxel, Cisplatin and Lidocaine. Most of our effort of delivering low-molecular weight drugs using PPE microspheres has been concentrated on two types of drugs, chemotherapeutic agents (Paclitaxel and cisplatin) and analgesics (lidocaine). All microspheres have been prepared by a solvent evaporation method.

The effect of side-chain length on drug release has been investigated using two poly(terephthalate-*co*-phosphate)s as a model system (45). Lidocaine encapsulated into P(BHDPT-EOP/TC, 50/50) or P(BHDPT-HOP/TC, 50/50) at a loading level of 5 wt % yields microspheres with a size range of 20 to 100 μm. PPE with a longer side chain P(BHDPT-HOP/TC, 50/50) causes a slower release kinetics for lidocaine (Fig. 12), consistent with the relative degradation rates of the polymers.

The correlation between degradation of and drug release from the PPE microspheres has been demonstrated in a P(DAPG-EOP) microsphere system (40). High encapsulation efficiency can be achieved greater than 96% with an average drug-loading level of 10 wt %. Paclitaxel release rate is the fastest for microspheres with 5:1 lactide-to-PG ratio, followed by polymer microspheres with 8:1 and 10:1 ratios. A continuous decrease in molecular weight and weight loss for all the PPE microspheres are observed (Figs. 7 and 13). Paclitaxel release from microspheres has shown similar kinetics.

Microspheres containing cisplatin or lidocaine have also been studied (43,46). The sizes of microspheres are generally between 3 and 50 μm with a loading level of 2.4 wt % for cisplatin or 5 wt % for lidocaine. A burst release of cisplatin (45%) is observed, followed by slower release for 3 days (Fig. 14). A near-zero-order release is found for lidocaine from the microspheres for the first 7 days, and the release reaches about 81% after 13 days.

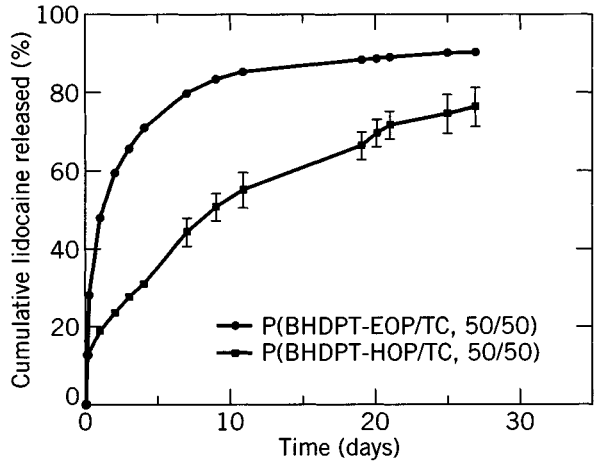


Figure 12. In vitro release of lidocaine from P(BHDPT-EOP/TC, 50/50) and P(BHDPT-HOP/TC, 50/50) microspheres in PBS at 37°C. Lidocaine was microencapsulated at 5 wt % loading in the microspheres. Both polymers were synthesized using DMPD as the initial diol, and the EOP/TC ratio was 50/50.

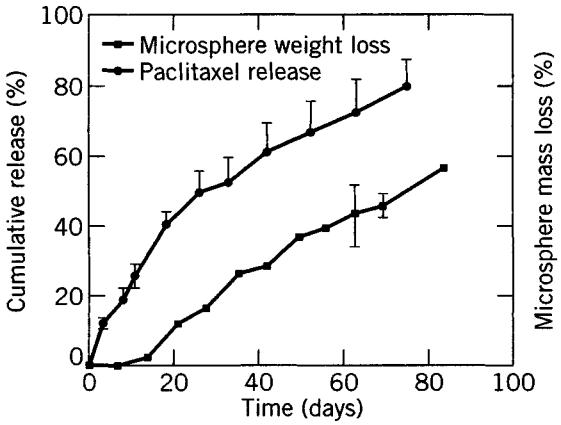


Figure 13. In vitro release of Paclitaxel from P(DAPG-EOP) microspheres (10 wt % loading) and mass-loss profile of these drug-loaded microspheres in PBS at 37°C. P(DAPG-EOP) used in this study had M_r 12,000 and a D,L-lactide–EOP ratio of 10:1.

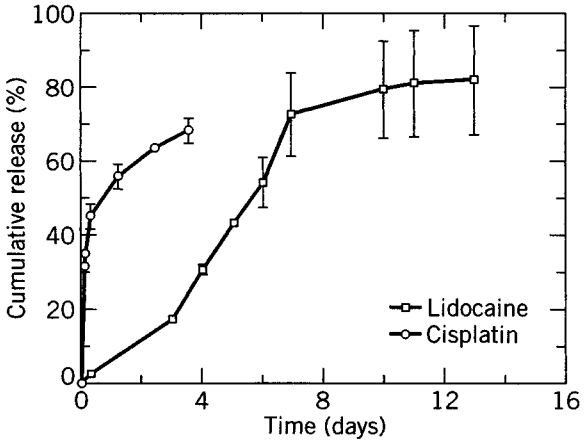


Figure 14. In vitro release of lidocaine (5 wt % loading) and cisplatin (2.4 wt % loading) from P(LAEG-EOP) microspheres in PBS at 37°C.

Controlled Release of Fluorescence-Labeled Bovine Serum Albumin (FITC-BSA) As a Model Protein Drug. FITC-BSA has been used as a model protein drug to study the controlled release properties of these PPEs (36,43). Microspheres are prepared from either poly(terephthalate-*co*-phosphate) or poly(lactide-*co*-phosphate) by the double-emulsion technique. A wide range of protein-loading levels (1.5–22.8 wt %) could be achieved with an encapsulation efficiency of 70–90%. The average size of PPE microspheres prepared by this method ranges from 2 to 20 μm with a smooth surface morphology.

The in vitro release of FITC-BSA from P(BHET-EOP/TC, 80/20) microspheres is relatively fast. As expected, higher loading levels result in increased release rates. More than 80% of the protein is released within the first 24 h for microspheres with 14.1 and 22.8 wt % loading levels, whereas nearly 75% is released from 1.5 wt % protein-loaded microspheres (Fig. 15a).

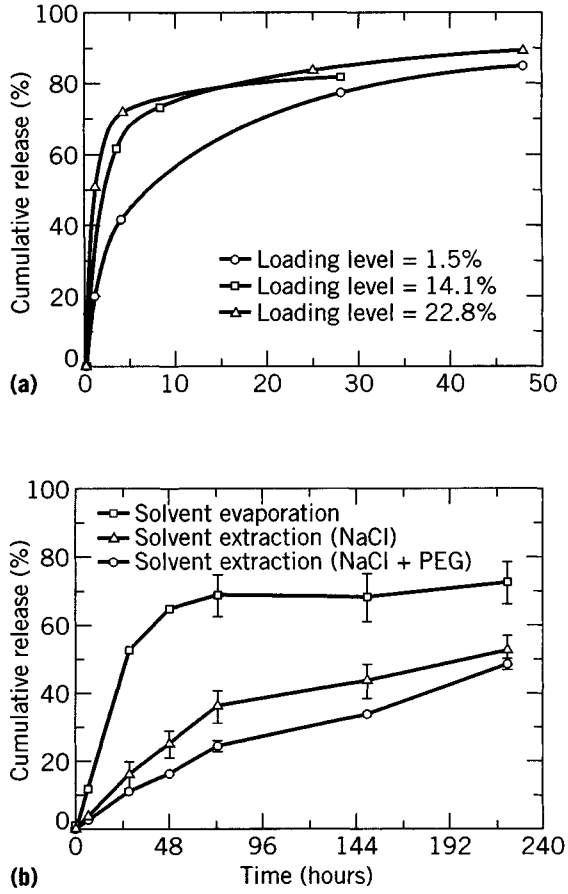


Figure 15. (**a**) Effect of loading level of FITC-BSA in P(BHET-EOP/TC, 80/20) microspheres on its in vitro release. (**b**) In vitro release of FITC-BSA from P(LAEG-EOP) microspheres prepared by different protocols. Microspheres were prepared by a solvent evaporation method (open square), a solvent extraction method using 0.3% poly(vinyl alcohol) (PVA) solution containing 5% sodium chloride as the second aqueous phase (open triangle), or 0.3% PVA–5% NaCl–1% $PEG_{8,000}$ solution (open circle).

The formulation method significantly affects the protein-release kinetics. The second aqueous phase in the double-emulsion method is of the major factor. Using a 5% sodium chloride solution containing 1% $PEG_{8,000}$ as the second aqueous phase yields microspheres the most linear release profile for FITC-BSA (Figure 15b).

Controlled Release of Plasmid DNA. Genetic immunization using naked DNA has spawned intense interest because of the promising immune responses that can be generated against different antigens in various animal models. It has also been argued that in gene therapy, the exogenous gene should be increasingly viewed as a drug for practical considerations (47). As such, many of the pharmaceutical issues confronting the successful application of delicate proteins are also relevant for nonviral gene delivery. Conceivable advantages of the controlled-release approach may include improving the bioavailability of the DNA to the target tissue and prolonging the expression of the gene product in the transfected cells. We have therefore

evaluated the feasibility of delivering plasmid DNAs using these PPEs in both the microsphere and the viscous liquid configurations.

Microspheres containing plasmid DNA have been prepared using a double-emulsion method (48,49). Two polymers that have been studied are P(DAPG-EOP) (M_r = 13.6 K), with the D,L-lactide oligomer as the building block, and P(LAEG-EOP) (M_r = 33 K), with the L-lactide oligomer as the macromonomer. With a typical double-emulsion protocol, microspheres containing 0.9–2% plasmid DNA are obtained with an encapsulation efficiency of 88–95%. A typical batch of microspheres has an average size of 8–10 μm and average volume of 42–57 μm. At such a low loading level, the release mechanism is almost purely matrix degradation controlled, which is quite slow. Bovine or mouse serum albumin (BSA or MSA, 8.5–10% w/w) has therefore been coencapsulated with the DNA to increase the DNA release rate. Confocal microscopic images of microspheres containing plasmid with a fluorescent dye suggest that the majority of DNA is concentrated in the core.

The in vitro release shows that microspheres prepared from P(DAPG-EOP) containing both DNA and MSA have an average DNA release rate of 380 ng/day/mg of microspheres, compared with 125 ng/day/mg of microspheres released from microspheres containing DNA alone (Fig. 16). Both rates are much higher than the microspheres made from higher-molecular-weight P(LAEG-EOP), which releases DNA at a rate of 20–29 ng/day/mg of microspheres. DNA released from these microspheres is intact as revealed by electrophoretic mobility analysis (Fig. 17).

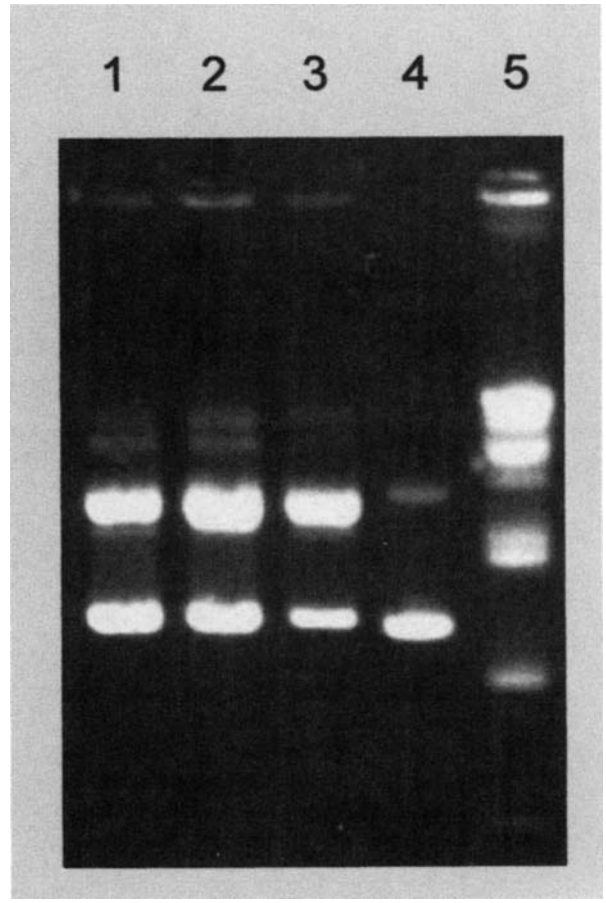


Figure 17. Electrophoretic mobility of DNA released from P(DAPG-EOP) microspheres. Supernatant of a microsphere–PBS suspension collected after 1 h (lane 1), 2 days (lane 2), or 6 days of incubation at 37°C (lane 3) was run on a 0.8% agarose gel, as compared with the original plasmid (lane 4). Lane 5 is the molecular-weight marker (λDNA *Hin*dIII digested).

Controlled Release through Poly(Terephthalate-*co*-Phosphate) Film

Paclitaxel (10 wt %) has been embedded in P(BHET-EOP/TC, 80/20) during solvent casting (50). The film is flexible with a smooth surface. DSC and X-ray analyses fail to show any crystallinity of the drug in the polymer. This formulation can deliver paclitaxel over a period of several months (Fig. 18). Less than 30% mass loss of the polymer is observed in this period. The degradation profile approximates that of the release profile of paclitaxel, indicating degradation controlled release mechanism. The unreleased paclitaxel remains stable in the film during the degradation of the polymer.

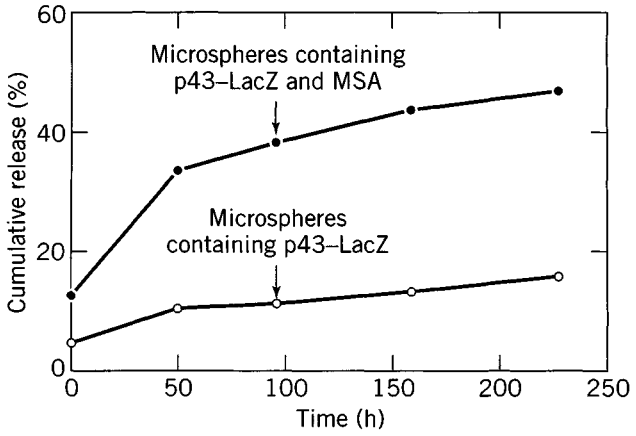


Figure 16. In vitro release of plasmid DNA from P(DAPG-EOP) microspheres containing 1.84–2% p43–LacZ plasmid coencapsulated with 8.9% MSA (filled circle) or without MSA (open circle) in PBS at 37°C.

Controlled Release through P(*trans*-CHDM-HOP) Viscous Liquid

Release of Lidocaine and Doxorubicin. Lidocaine (25 wt %) or doxorubicin (10 wt %) has been incorporated into the PPE viscous liquid by blending the drugs with P(*trans*-CHDM-HOP) viscous liquid until homogeneity is achieved. As shown in Figure 19, lidocaine is almost completely released in 1 week. The rapid release is expected of such a low molecular weight compound. Doxurubicin, which is more hydrophobic, unexpectedly produces a near linear release rate over 18 days (39). Initially it was thought that such a viscous liquid would not be able to provide a prolonged release for low-molecular-weight drugs. Apparently the P(*trans*-CHDM-HOP) is hydrophobic enough to retard

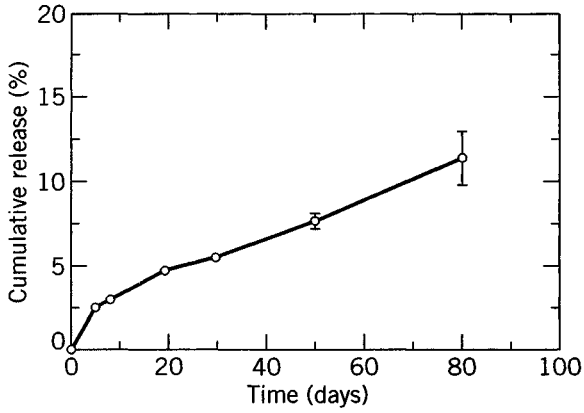


Figure 18. In vitro release of Paclitaxel from P(BHET-EOP/TC, 80/20) film (10 wt % Paclitaxel loading) in PBS at 37°C.

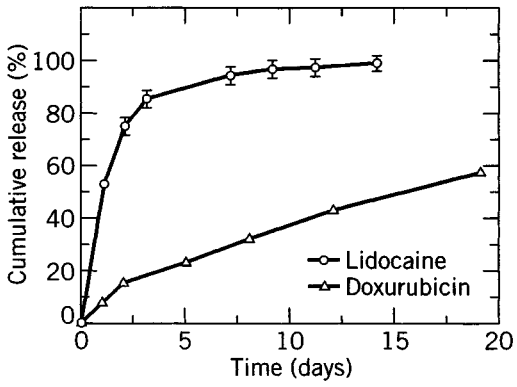


Figure 19. In vitro release of lidocaine (25 wt % loading) and doxorubicin (10 wt % loading) from P(*trans*-CHDM-HOP) in PBS at 37°C.

rapid penetration of water, and when a lipophilic drug is embedded, sustained release over several weeks is possible.

Release of FITC-BSA and Interleukin 2 (IL-2). The effect of loading level of FITC-BSA on the release kinetics is shown in Figure 20. With a 30% loading, the hydrophilic protein would strongly attract water absorption into the sample. Not surprisingly, over 80% of the protein is released in 1 week (39). In protein delivery by the nonbiodegradable poly(ethylene-vinyl acetate) (EVAc), a loading level above 30% is required to effect a complete release (51). Protein powder exposed to the surface leads to pores and channels for subsequently dissolved protein molecules to diffuse out. It is not clear if a similar mechanism is at work here because the P(*trans*-CHDM-HOP) is so much more fluid that any channel should collapse after the dissolution of the protein. Protein diffusion through its matrix is evident by the release of the 1% loaded sample. The release mechanism for such a low loading level may be dominantly matrix degradation controlled. However, because the matrix-degradation rate is low and lagged behind the release rate significantly, it suggests that the protein can also permeate through the polymer phase. The effect of the side chain of the P(*trans*-CHDM-phosphate) series on the protein release kinetics is shown in Figure 21. When the loading level is kept constant at 10 wt %, the relative release rate, more clearly so at the early time points, decreases with the lipophilicity of the side chain (39).

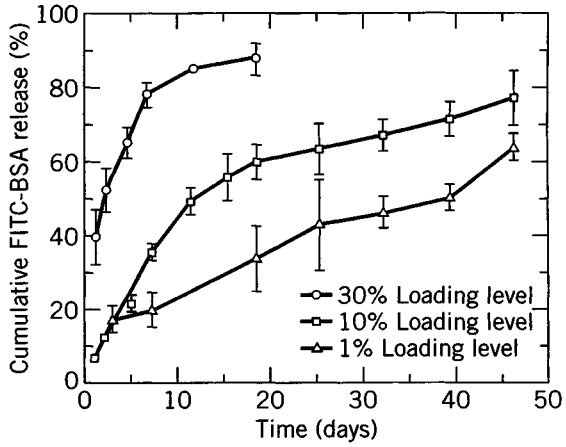


Figure 20. Effect of loading levels of FITC-BSA on its in vitro release from P(*trans*-CHDM-HOP) in PBS at 37°C.

To assess whether the bioactivity of the released protein is preserved, IL-2 release from P(*trans*-CHDM-HOP) has been studied (Fig. 22). The bioactive concentration of IL-2 is determined by a cellular assay where the NSF-60 cells proliferate in a dose-dependent manner in the presence of IL-2. Correlation of this biological concentration with the total IL-2 concentration measured by ELISA yields the retention of the bioactivity. The bioactive portion ranges from 16 to 35%. Because there is a finite time interval, ranging from hours to days, before a released IL-2 molecule is measured, the degradation of the protein while sitting in the PBS at 37°C may be the main source of loss of bioactivity.

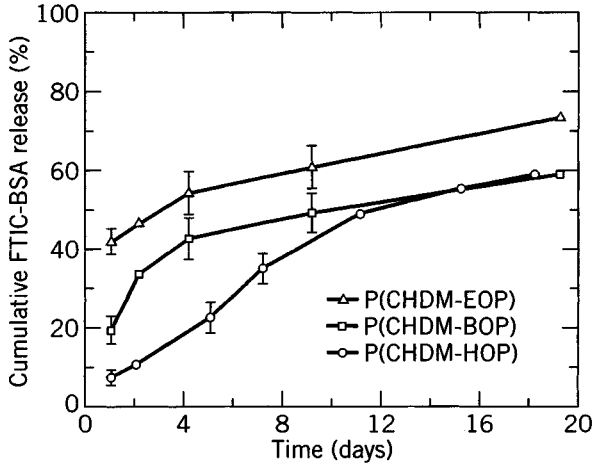


Figure 21. Effect of side-chain structure on the in vitro release kinetics of FITC-BSA from PPE in PBS at 37°C. Refer to Scheme 7 for the symbols.

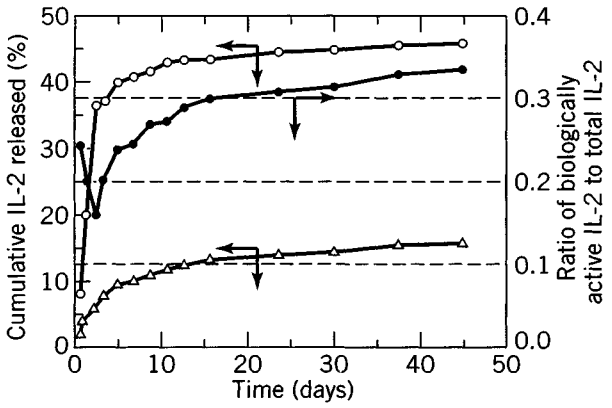


Figure 22. In vitro release of IL-2 from P(*trans*-CHDM-HOP) in RPMI-1640 medium at 37°C. Bioactive IL-2 (open triangle) was determined by NSF-60 cell proliferation assay, whereas total IL-2 released (open circle) was measured by ELISA. Bioactivity retention (filled circle) was defined as the ratio of the two.

The values presented are therefore the lower limit that can be expected of IL-2 delivery by such a system.

Release of Plasmid DNA. A viscous liquid containing plasmid DNA has been prepared by physically blending the lyophilized DNA–mannitol powder (1:10 or 1:50 weight ratio) with P(CHDM-HOP) at room temperature until the sample reaches homogeneity. The in vitro release of DNA has been studied on two batches of gels with a 1% DNA loading level. Mannitol can be used as an excipient (10 and 33 wt % loading in the gel, respectively) to help disperse the DNA throughout the gel and increase the release rate. As shown in Figure 23, 70 and 90% of the DNA is released within 2 weeks from PPE viscous liquids coloaded with 10 and 33 wt % mannitol, respectively.

SUMMARY

This article suggests that PPEs may be added to the list of biodegradable polymers for controlled drug delivery. The versatility of the polyphosphates should prove advantageous in different therapeutic applications. Matrix properties can range from viscous to crystalline to elastomeric. Device configurations of viscous liquids, wafers, microspheres, and flexible coatings are possible. Controlled release of bioactive agents spanning a wide range of molecular weights from doxurubicin and IL-2 to plasmid DNA has been demonstrated. The potential of this new class of drug carriers needs to be defined in animal and eventually clinical studies, and work is proceeding toward that end.

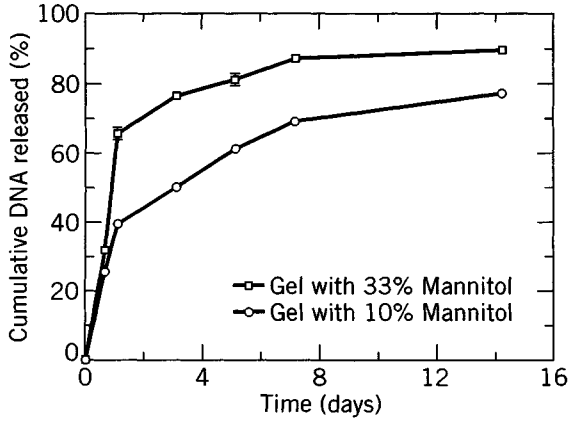


Figure 23. In vitro release of p43-LacZ (1 wt % loading) from P(*trans*-CHDM-HOP) in PBS at 37°C. Mannitol was coloaded with DNA at a loading level of 10 wt % (open circle) or 33 wt % (open square).

BIBLIOGRAPHY

1. R. Langer, *Science* **249**, 1527–1533 (1990).
2. K.W. Leong, in P. Tarcha, ed., *Synthetic Polymeric Drug Delivery Systems*, CRC Press, Boca Raton, Fla., 1991.
3. W.M. Saltzman and M.L. Radomsky, *Chem. Eng. Sci.* **46**(10), 2429–2444 (1991).
4. K.L. Leong and R. Langer, *Adv. Drug Delivery Rev.* **1**, 199 (1987).
5. R. Jain, N.H. Shah, A.W. Malick, and C.T. Rhodes, *Drug Dev. Ind. Pharm.* **24**(8), 703–727 (1998).
6. B. Buntner et al., *J. Controlled Release* **56**(1–3), 159–167 (1998).
7. T.W. Atkins and S.J. Peacock, *J. Biomater. Sci., Polym. Ed.* **7**, 1065–1073 (1996).
8. Y. Ogawa, *J. Biomater. Sci., Polym. Ed.* **8**, 391–409 (1997).
9. J. Kohn and R. Langer, *J. Am. Chem. Soc.* **109**, 817–820 (1987).
10. I. Gachard, S. Bechaouch, B. Coutin, and H. Sekiguchi, *Polym. Bull.* **38**(4), 427–431 (1997).
11. B.I. Dahiyat, E. Hostin, E.M. Posadas, and K.W. Leong, *J. Biomater. Sci., Polym. Ed.* **4**(5), 529–543 (1993).
12. J. Heller, R.V. Sparer, and G.M. Zentner, in M. Chasin and R. Langer, eds., *Biodegradable Polymers as Drug Delivery Systems*, Dekker, New York, 1990, pp. 121–162.
13. K.W. Leong et al., in J.I. Kroschwitz, ed., *Encyclopedia of Polymer Science and Engineering*, Wiley, New York, 1989.
14. M. Chasin et al., in M. Chasin and R. Langer, eds. *Biodegradable Polymers as Drug Delivery Systems*, Dekker, New York, 1990, pp. 43–70.
15. T. Kojima, M. Nakano, and K. Juni, *Chem. Pharm. Bull.* **33**, 5119–5125 (1985).
16. S.J. Shieh, M.C. Zimmerman, and J.R. Parsons, *J. Biomed. Mater. Res.* **24**, 789–808 (1990).
17. S. Pulapura, C. Li, and J. Kohn, *Biomaterials* **11**, 666–678 (1990).
18. S. Pulapura and J. Kohn, *Biopolymers* **32**, 411–417 (1992).
19. S.M. Ibim et al., *Pharm. Dev. Technol.* **3**(1), 55–62 (1998).
20. C.T. Laurencin et al., *J. Biomed. Mater. Res.* **30**(2), 133–138 (1996).
21. F. Langone et al., *Biomaterials* **16**(5), 347–353 (1995).
22. H.R. Allcock, in M. Chasin and R. Langer, eds., *Bioerodible Polymers as Drug Delivery Systems*, Dekker, New York, 1990, pp. 163–194.
23. H.R. Allcock, S.R. Pucher, and A.G. Scopelianos, *Biomaterials* **15**(8), 563–569 (1994).
24. C.G. Pitt et al., *J. Appl. Polym. Sci.* **26**, 3779–3787 (1981).
25. M. Richards et al., *J. Biomed. Mater. Res.* **25**, 1151–1167 (1991).

Next Page

26. B.I. Dahiyat, M. Richards, and K.W. Leong, *J. Controlled Release* **33**(1), 13–21 (1995).
27. S. Kadiyala, H. Lo, M.S. Ponticiello, and K.W. Leong, in J.O. Hollinger, ed., *Biomedical Application of Synthetic Biodegradable Polymers*, CRS Press, 1995, pp. 33–57.
28. S. Kadiyala, P. Axtel, J.D. Michelson, and K.W. Leong, *Annu. Meet. Soc. Biomater.* Birmingham, Ala., 1993, p. 321.
29. H.W. Coover, R. McConnel, and M. McCall, *Ind. Eng. Chem.* **52**, 409 (1960).
30. M. Sander and E. Steininger, *J. Macromol. Sci., Rev. Macromol. Chem.* **C1**(1), 91 (1967).
31. F. Ignatious, A. Sein, I. Cabasso, and J. Smid, *J. Polym. Sci., Part A: Polym. Chem.* **31**(1), 239–247 (1993).
32. J.C. Brosse, D. Derouet, L. Fontaine, and S. Chairatanathavorn, *Makromol. Chem.* **190**, 2339–2345 (1989).
33. M. Richards et al., *J. Polym. Sci., Part A: Polym. Chem.* **29**, 1157–1165 (1991).
34. A. Tunstall, R.C. Eberhart, and M.D. Prager, *J. Biomed. Mater. Res.* **29**(10), 1193–1199 (1995).
35. M.S. Aronoff, *J. Biomater. Appl.* **9**(3), 205–261 (1995).
36. H.-Q. Mao et al., *Proc. Am. Inst. Chem. Eng. Top. Conf. Biomater., Carriers Drug Delivery Scaffolds Tissue Eng.*, Los Angeles, Nov. 17–19, 1997, p. 141.
37. J. Brandrup and E.H. Immergut, eds., *Polymer Handbook*, 2nd ed., Wiley-Interscience, New York, 1975.
38. M. Chasin and R. Langer, eds., *Biodegradable Polymers as Drug Delivery Systems*, Dekker, New York, 1990.
39. H.-Q. Mao et al., *Pharm. Res.* **14**(11), Suppl., 601 (1997).
40. H. Wang et al., *Proc. Am. Assoc. Pharm. Sci. Annu. Meet.*, San Francisco, Nov. 15–19, 1998, p. 140.
41. I. Shipanova-Kadiyala, H.-Q. Mao, and K.W. Leong, *Proc. Am. Inst. Chem. Eng. Top. Conf. Biomater. Carriers Drug Delivery Scaffolds Tissue Eng.*, Los Angeles, Nov. 17–19, 1997, p. 40.
42. Z. Zhao et al., *Pharm. Res.* **14**(11), Suppl., 293 (1997).
43. W. Dang et al., *Proc. Am. Assoc. Pharm. Sci. Annu. Meet.*, San Francisco, Nov. 15–19, 1998, p. 419.
44. H.-Q. Mao et al., *Proc. Am. Inst. Chem. Eng. Top. Conf. Biomater., Carriers Drug Delivery Scaffolds Tissue Eng.*, Los Angeles, Nov. 17–19, 1997, p. 193.
45. A. Kader et al., *Proc. Am. Assoc. Pharm. Sci. Annu. Meet.*, San Francisco, Nov. 15–19, 1998, p. 413.
46. W. Dang et al., *Pharm. Res.* **14**(11), Suppl., 287–288 (1997).
47. R.G. Crystal, *Nat. Med.* **1**, 15–17 (1995).
48. H.-Q. Mao, B.S. Hendriks, K.Y. Lin, and K.W. Leong, *Proc. Int. Symp. Controlled Release Bioact. Mater.* **25**, 203 (1998).
49. H.-Q. Mao et al., *Proc. Int. Symp. Controlled Release Bioact. Mater.* **26** (1999).
50. A. Kader et al., *Proc. Am. Assoc. Pharm. Sci. Annu. Meet.*, San Francisco, Nov. 15–19, 1998, p. 413.
51. W.M. Saltzman and R. Langer, *Biophys. J.* **55**(1), 163–172 (1989).

See also BIODEGRADABLE POLYMERS: POLYANHYDRIDES; BIODEGRADABLE POLYMERS: POLYESTERS; POLY(ORTHO ESTERS).

BIODEGRADABLE POLYMERS: POLYANHYDRIDES

ACHIM GÖPFERICH
University of Regensburg
Regensburg, Germany

KEY WORDS

Bulk erosion
Degradation
Drug stability
Erosion
Erosion-controlled release
Erosion zone
Modeling
Polyanhydride
Polycondensation
Porosity
Pulsatile drug release
Surface erosion

OUTLINE

Historical Development and Significance of Polyanhydrides as Biodegradable Polymers
Survey of the Various Types of Polyanhydrides
- Monomers
- Aliphatic Polyanhydrides
- Aromatic Polyanhydrides
- Cross-linked and Branched Polyanhydrides

Polyanhydride Synthesis and Characterization
- Synthesis
- Physicochemical Characterization of Polyanhydrides
- Biocompatibility

Polyanhydride Degradation and Erosion
- Kinetics of Degradation
- Polyanhydride Erosion
- Theoretical Description of Polyanhydride Erosion

Drug Delivery Systems Made of Polyanhydrides
- Considerations Regarding the Kinetics of Drug Release
- Drug Stability
- Drug Delivery Systems Made of Polyanhydrides

Drug Release Kinetics
Summary and Outlook
Bibliography

HISTORICAL DEVELOPMENT AND SIGNIFICANCE OF POLYANHYDRIDES AS BIODEGRADABLE POLYMERS

When polymers are used for the parenteral administration of drugs, the most important advantage is the circumvention of the postapplication removal of the material. Deg-

26. B.I. Dahiyat, M. Richards, and K.W. Leong, *J. Controlled Release* **33**(1), 13–21 (1995).
27. S. Kadiyala, H. Lo, M.S. Ponticiello, and K.W. Leong, in J.O. Hollinger, ed., *Biomedical Application of Synthetic Biodegradable Polymers*, CRS Press, 1995, pp. 33–57.
28. S. Kadiyala, P. Axtel, J.D. Michelson, and K.W. Leong, *Annu. Meet. Soc. Biomater.* Birmingham, Ala., 1993, p. 321.
29. H.W. Coover, R. McConnel, and M. McCall, *Ind. Eng. Chem.* **52**, 409 (1960).
30. M. Sander and E. Steininger, *J. Macromol. Sci., Rev. Macromol. Chem.* **C1**(1), 91 (1967).
31. F. Ignatious, A. Sein, I. Cabasso, and J. Smid, *J. Polym. Sci., Part A: Polym. Chem.* **31**(1), 239–247 (1993).
32. J.C. Brosse, D. Derouet, L. Fontaine, and S. Chairatanathavorn, *Makromol. Chem.* **190**, 2339–2345 (1989).
33. M. Richards et al., *J. Polym. Sci., Part A: Polym. Chem.* **29**, 1157–1165 (1991).
34. A. Tunstall, R.C. Eberhart, and M.D. Prager, *J. Biomed. Mater. Res.* **29**(10), 1193–1199 (1995).
35. M.S. Aronoff, *J. Biomater. Appl.* **9**(3), 205–261 (1995).
36. H.-Q. Mao et al., *Proc. Am. Inst. Chem. Eng. Top. Conf. Biomater., Carriers Drug Delivery Scaffolds Tissue Eng.*, Los Angeles, Nov. 17–19, 1997, p. 141.
37. J. Brandrup and E.H. Immergut, eds., *Polymer Handbook*, 2nd ed., Wiley-Interscience, New York, 1975.
38. M. Chasin and R. Langer, eds., *Biodegradable Polymers as Drug Delivery Systems*, Dekker, New York, 1990.
39. H.-Q. Mao et al., *Pharm. Res.* **14**(11), Suppl., 601 (1997).
40. H. Wang et al., *Proc. Am. Assoc. Pharm. Sci. Annu. Meet.*, San Francisco, Nov. 15–19, 1998, p. 140.
41. I. Shipanova-Kadiyala, H.-Q. Mao, and K.W. Leong, *Proc. Am. Inst. Chem. Eng. Top. Conf. Biomater. Carriers Drug Delivery Scaffolds Tissue Eng.*, Los Angeles, Nov. 17–19, 1997, p. 40.
42. Z. Zhao et al., *Pharm. Res.* **14**(11), Suppl., 293 (1997).
43. W. Dang et al., *Proc. Am. Assoc. Pharm. Sci. Annu. Meet.*, San Francisco, Nov. 15–19, 1998, p. 419.
44. H.-Q. Mao et al., *Proc. Am. Inst. Chem. Eng. Top. Conf. Biomater., Carriers Drug Delivery Scaffolds Tissue Eng.*, Los Angeles, Nov. 17–19, 1997, p. 193.
45. A. Kader et al., *Proc. Am. Assoc. Pharm. Sci. Annu. Meet.*, San Francisco, Nov. 15–19, 1998, p. 413.
46. W. Dang et al., *Pharm. Res.* **14**(11), Suppl., 287–288 (1997).
47. R.G. Crystal, *Nat. Med.* **1**, 15–17 (1995).
48. H.-Q. Mao, B.S. Hendriks, K.Y. Lin, and K.W. Leong, *Proc. Int. Symp. Controlled Release Bioact. Mater.* **25**, 203 (1998).
49. H.-Q. Mao et al., *Proc. Int. Symp. Controlled Release Bioact. Mater.* **26** (1999).
50. A. Kader et al., *Proc. Am. Assoc. Pharm. Sci. Annu. Meet.*, San Francisco, Nov. 15–19, 1998, p. 413.
51. W.M. Saltzman and R. Langer, *Biophys. J.* **55**(1), 163–172 (1989).

See also BIODEGRADABLE POLYMERS: POLYANHYDRIDES; BIODEGRADABLE POLYMERS: POLYESTERS; POLY(ORTHO ESTERS).

BIODEGRADABLE POLYMERS: POLYANHYDRIDES

ACHIM GÖPFERICH
University of Regensburg
Regensburg, Germany

KEY WORDS

Bulk erosion
Degradation
Drug stability
Erosion
Erosion-controlled release
Erosion zone
Modeling
Polyanhydride
Polycondensation
Porosity
Pulsatile drug release
Surface erosion

OUTLINE

Historical Development and Significance of Polyanhydrides as Biodegradable Polymers
Survey of the Various Types of Polyanhydrides
  Monomers
  Aliphatic Polyanhydrides
  Aromatic Polyanhydrides
  Cross-linked and Branched Polyanhydrides
Polyanhydride Synthesis and Characterization
  Synthesis
  Physicochemical Characterization of Polyanhydrides
  Biocompatibility
Polyanhydride Degradation and Erosion
  Kinetics of Degradation
  Polyanhydride Erosion
  Theoretical Description of Polyanhydride Erosion
Drug Delivery Systems Made of Polyanhydrides
  Considerations Regarding the Kinetics of Drug Release
  Drug Stability
  Drug Delivery Systems Made of Polyanhydrides
Drug Release Kinetics
Summary and Outlook
Bibliography

HISTORICAL DEVELOPMENT AND SIGNIFICANCE OF POLYANHYDRIDES AS BIODEGRADABLE POLYMERS

When polymers are used for the parenteral administration of drugs, the most important advantage is the circumvention of the postapplication removal of the material. Deg-

radation and erosion processes the polymers into oligomers and monomers that can be metabolized and excreted. One of the major goals in the past decades of research on degradable polymers in medicine and pharmacy has been to obtain materials that allow controlled drug release to be controlled by polymer erosion. The development of polyanhydrides and poly(ortho esters) paved the way to understand under which circumstances this goal might be reached. Concomitantly, the tremendous efforts to synthesize new polymers in both classes led to a better understanding of polymer erosion in general and finally to new drug delivery systems on the market.

All degradable polymers consist of monomers that are connected to one another by functional groups that break down during the degradation process. Hydrolysis is the major cause for degradation (1) and can be investigated by following the loss of molecular weight. Degradation induces the subsequent erosion of the material, which is defined as the mass loss of the material. The degradation velocity depends amongst other factors on the type of hydrolyzable functional group that the polymer is built from and determines how a polymer erodes (2). Slowly degrading polymers such as poly(α-hydroxy esters) have been reported to be bulk eroding, while fast-degrading polymers have been reported to be surface eroding (3) (see "Polyanhydride Erosion"). Polyanhydrides have been reported to be surface eroding (1), which is not surprising since carboxylic acid anhydrides are among the functional groups that hydrolyze the most rapidly. The correlation between erosion and drug release that exists for some drugs allows the use of polyanhydrides for a number of very sophisticated drug delivery applications (4,5). Historically, polyanhydrides were first made for other reasons than obtaining a biomaterial: the manufacture of fibers. The work originated in 1909 with the synthesis of the first polyanhydrides (6). Extensive efforts were made in the 1930s and the 1950s to synthesize aliphatic and aromatic polyanhydrides with enhanced chemical stability (7–9). However, due to their rapid hydrolysis, these turned out to be too unstable to be used as a raw material for the manufacture of fibers. In the 1980s polyanhydrides were finally discovered for the purpose of drug delivery (10). Since then, a number of monomers were identified that can be used to synthesize a variety of biocompatible polyanhydrides. The general structure of polyanhydrides is shown in Figure 1.

SURVEY OF THE VARIOUS TYPES OF POLYANHYDRIDES

Monomers

It is obvious that the monomers used for the synthesis of polyanhydrides are bifunctional with at least two carboxylic acid groups per molecule. Figure 2 lists some of some molecules that have been used for the manufacture of polyanhydrides. The IUPAC names of some polymers made of these monomers would have rather long names. Therefore, the abbreviations given in parenthesis in Figure 2 are used in the literature to shorten polymer names for convenience. A copolymer made of 1,3-bis-(*p*-carboxyphenoxy)propane (CPP) and sebacic acid (SA), for example, is abbreviated p(CPP-SA). The monomer ratio is given by the figures after the abbreviation. p(CPP-SA) 20:80, for example, contains 20% (w/w) CPP and 80% (w/w) SA. A homopolymer such as poly(fumaric acid) is abbreviated p(FA).

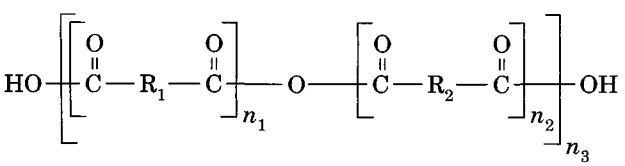


Figure 1. General polyanhydride structure.

A glance at Figures 1 and 2 illustrates that there is a substantial variability regarding the design of polyanhydrides. They can be manufactured as aliphatic or aromatic homopolymers and copolymers as well as cross-linked or branched polymers. As some of the homopolymers have poor mechanical properties and an undesired stability or instability against degradation, copolymers have been used for most medical and pharmaceutical applications (11).

Aliphatic Polyanhydrides

A group of polyanhydrides that were synthesized for drug delivery purposes are aliphatic polyanhydrides (12,13). One class of aliphatic polyanhydrides that proved to be useful for drug delivery purposes is p(FAD-SA) (14). Many other aliphatic polyanhydrides, however, have properties that are not of advantage for the manufacture of drug delivery systems. p(SA), for example, is highly crystalline and very brittle. p(FAD), on the other hand, is a liquid and not well suited for the manufacture of solid drug delivery systems. Aliphatic polyanhydrides hydrolyze on average much faster than aromatic ones due to the better accessibility of the bonds to water.

Aromatic Polyanhydrides

Aromatic polyanhydrides erode slower than aliphatic ones (15), which is due to their increased hydrophobicity and the hindered approach of water to the anhydride bond (16). The erosion rate can be increased by copolymerization with aliphatic monomers. p(CPP-SA) can serve as a good example (Fig. 3). Copolymerization allows the adjustment of erosion rates and, therefore, the duration of drug release in drug delivery applications. Depending on the composition, p(CPP-SA) erodes within weeks or months, whereas p(CPP) homopolymer has been reported to be stable for years (15). Aromatic polyanhydrides that have been under investigation for drug delivery applications are p(CPP) and p(CPP-IPA). In the form of homopolymers, however, some of these polymers cannot be processed at all. p(CPP) for example cannot be melt-processed as it has a high melting point at which it also begins thermal degradation. Furthermore, the solubility in common solvents is very low. This illustrates why tremendous efforts have been undertaken to improve the properties of polyanhydrides by copolymerization.

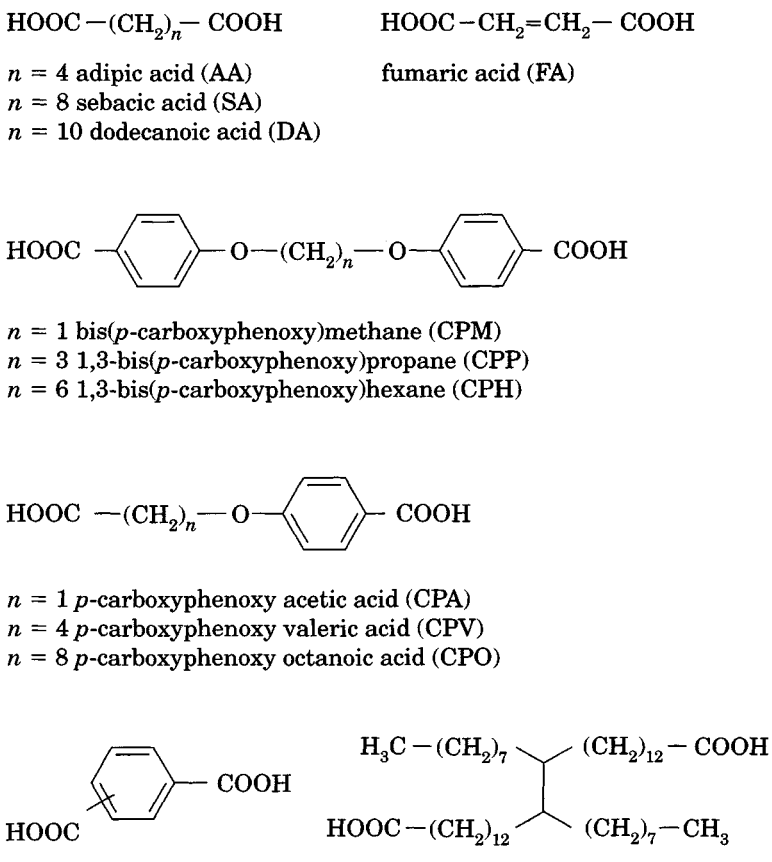


Figure 2. Monomers that have been used for the manufacture of polyanhydrides.

Cross-linked and Branched Polyanhydrides

The intention to manufacture cross-linked polyanhydrides was to increase the mechanical stability of polyanhydrides. This can be important for their use as load-bearing biomaterials in orthopedic applications. Cross-linked polyanhydrides can be obtained after introducing double bonds into the polymer backbone. A monomer that has been used for that purpose is FA in combination with SA.

The goal that was pursued with the manufacture of branched polyanhydrides was to improve the mechanical and film-forming properties, especially for the crystalline polyanhydrides. When p(SA) was compared with branched p(SA), an impact on drug release was noticeable but there was little change in physical and mechanical properties (17). By increasing the amount of branching agent benzenetricarboxylic acid from 0 to 2% it was possible to reduce the release of morphine from approximately 70% to approximately 40% within 8 days.

POLYANHYDRIDE SYNTHESIS AND CHARACTERIZATION

Synthesis

There are numerous ways to synthesize polyanhydrides from carboxylic acid monomers (18). The most frequently used technique for the manufacture of linear polyanhydrides is melt polycondensation. A common method of initiation of polycondensation is the activation of the carboxylic acids using acetic acid anhydride (19,20). For the manufacture of copolymers all individual monomers are activated separately. The resulting mixed anhydrides, i.e., the so-called prepolymers, are first purified and isolated. They usually consist of a few monomers that are connected to one another via anhydride bonds and form a mixed carboxylic anhydride group with acetic acid at each end of the molecule. For the actual polymerization these prepolymers are heated to 180°C under vacuum. For the synthesis of copolymers two types of prepolymer are mixed prior to the polycondensation. The oligomers polymerize under acetic anhydride formation, which is removed by distillation during the reaction. The advantage of polycondensation is the high molecular weight that can be obtained. A disadvantage of the method is the thermal stress to which the monomers are subjected. An alternative method for the synthesis of polyanhydrides is the use of phosgene or trichloromethyl chloroformate, which is a liquid diphosgene derivative (21). Both reagents activate the carboxylic acid group, which is reacted with nonactivated monomer under anhydride formation. This method of synthesis has the advantage that it allows the synthesis of polyanhy-

drides under mild conditions. However, the molecular weights that were reported for polyanhydrides synthesized by this method are only approximately 14,000 (21) compared to over 100,000 when prepared by melt polycondensation (20).

The manufacture of cross-linked polyanhydrides requires the manufacture of linear polyanhydrides that contain unsaturated carbon–carbon bonds in their backbone. For reasons of biocompatibility fumaric acid is one of the preferred compounds but also other unsaturated bicarboxylic acids such as such as 1,4′-stilbendicarboxylic acid have been used as model compounds for the synthesis of unsaturated polyanhydrides (22). These unsaturated polyanhydrides are cross-linkable by a radical mechanism. p(FA-SA) 50:50, for example, was cross-linked either in CH_2Cl_2 or in bulk by adding 2% (w/v) comonomer, 2% (w/v) catalyst, and 0.2% (w/v) accelerator. Styrene and methylmethacrylate were used as comonomers, benzoyl peroxide or 2-butanon peroxide as catalyst and dimethyltoluidine or cobalt naphtanoate as accelerator (22). As the cross-linked products are insoluble in most organic solvents, their use for pharmaceutical applications and especially drug delivery applications is limited. It is, however, possible that they might be used as biomaterials with enhanced mechanical stability for a limited period of time.

Branched polyanhydrides have been synthesized using either multifunctional carboxylic acids such as 1,3,5-benzenetricaboxylic acid or poly(acrylic acid) (17). Branched polymers made of these compounds and sebacic acid have also been synthesized by melt polycondensation. The components were again activated using acetic anhydride, which yields the necessary prepolymers. The molecular weights that were obtained using such multifunctional components in combination with sebacic acid were 250,000 compared to 80,000 for pure p(SA) (17).

Physicochemical Characterization of Polyanhydrides

The careful characterization of a biodegradable polymer is essential for the successful investigation of its erosion mechanism. The understanding of the latter is a must for the successful application of these materials in drug delivery applications. For that reason polyanhydrides have been characterized extensively (23).

One of the most important properties is crystallinity. The crystallinity of polyanhydrides was investigated by wide angle X-ray diffraction (WAXD). Some of the homopolymers such as p(SA), p(CPP), and p(FA) were found to be partially crystalline (24); others such as p(FAD) were found to be amorphous (25). Crystallinities as high as 60% have been recorded. The crystallinity of copolymers was shown to depend on the monomer ratio. As shown in Figure 4(a), the lowest degree of crystallinity is reached at a copolymer composition of 1:1 for many polyanhydrides. Polyanhydrides derived from monomers such as FAD or CPH in combination with SA are an exemption. As p(CPH) is almost amorphous the crystallinity of p(CPH-SA) increases only with increasing SA content. The same can be observed for p(FAD-SA) (Fig. 4(b)). When copolymers are made of one crystallizable type of monomer such as SA and one that does not form crystallites such as FAD, its crys-

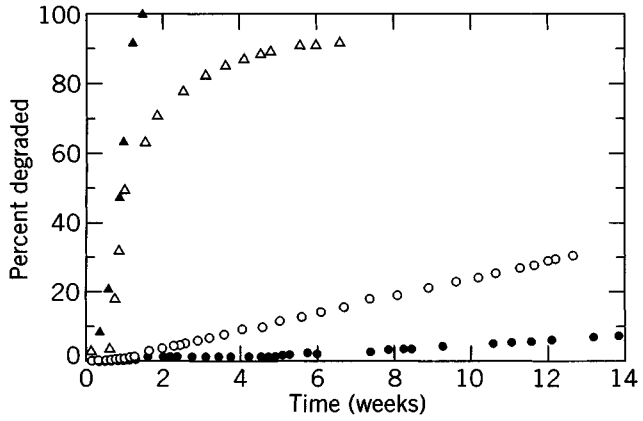


Figure 3. Degradation profiles of compression molded poly[bis(*p*-carboxyphenoxy)propane anhydride] and its copolymers with sebacic acid in 0.1 M pH 7.4 phosphate buffer at 37°C. ●, p(CPP); ○, p(CPP-SA) 85:15; △, p(CPP-SA) 45:55; ▲, p(CPP-SA) 21:79. *Source:* Reproduced with permission from Ref. 15.

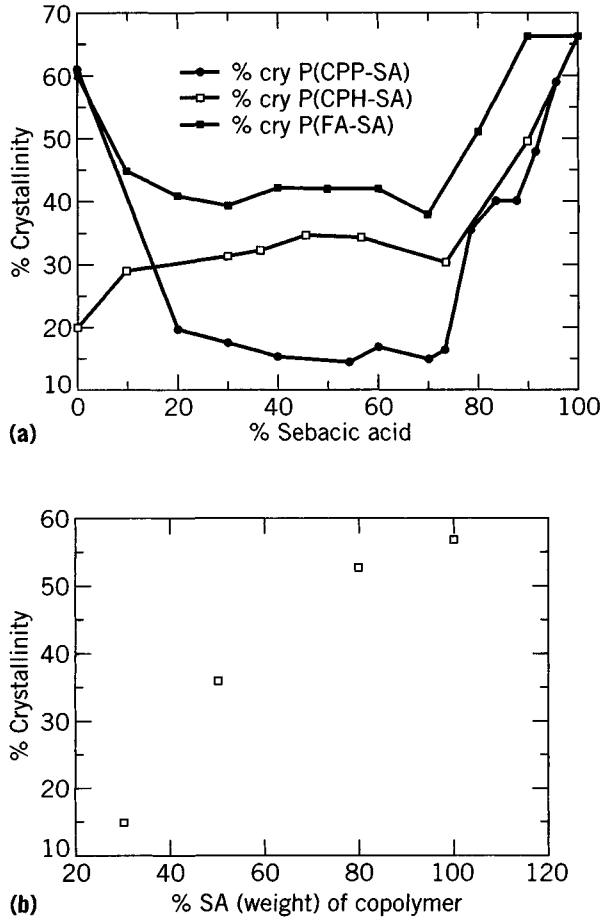


Figure 4. (**a**) Crystallinity of p(CPP-SA), p(CPH-SA), and p(FA-SA) as a function of the SA content. *Source:* Reproduced with permission from Ref. 24. (**b**) Crystallinity of p(FAD-SA) as a function of the SA content. *Source:* Reproduced with permission from Ref. 25.

tallinity has also been calculated from its heat of fusion data measured by differential scanning calorimetry (DSC). In addition to the melting enthalpy of the copolymer, the melting enthalpy of the homopolymer made of the crystallizable monomer has to be known (25).

Besides the melting point and the heat of fusion, which are related to the crystalline phase of a polymer, the glass-transition temperature, T_g, of the amorphous phase also can be determined by DSC. The melting points were found to be as high as 246°C for p(FA), 240°C for p(CPP), and 143°C for p(CPH). The melting points drop substantially after copolymerization. For all homopolymers made of SA, FA, CPP, and CPH and all copolymers made of SA in combination with FA, CPP, and CPH, T_g values ranged from 2°C to 60°C. Only p(CPP) is the exception with a T_g of 90°C. The lowest values were obtained for the copolymers with equal molar composition (24). More detailed data is shown for some polyanhydrides in Tables 1 and 2.

The distribution of monomers inside copolymer chains was investigated by NMR. The results differentiate between randomly distributed monomers in the polymer backbone and a more block-like structure. For copolymers made of SA in a combination with CPP or CPH, it was found that the monomers are mainly randomly distributed when the content of both monomers was equal (26) (Fig. 5). The extent of randomness in the distribution is important with respect to erosion. A block-like arrangement of the monomers inside the polymer chain might lead to the discontinuous erosion of the material when the two blocks exhibit different resistance against degradation and erosion.

Table 1. Melting Point, Glass-Transition Temperature, and Heat of Fusion

Polymer	T_m (°C)	T_g (°C)	Heat of fusion (cal/g)
p(SA)	86.0	60.1	36.6
p(CPH-SA) 10:90	74.4	58.3	17.8
p(CPH-SA) 18:82	66.4		13.1
p(CPH-SA) 27:73	57.2	45.0	9.3
p(CPH-SA) 44:56	52.7	6.1	7.2
p(CPH-SA) 55:45	49.5	11.5	3.2
p(CPH-SA) 64:36	43.3	11.8	2.5
p(CPH-SA) 70:30	110.5	14.5	3.0
p(CPH-SA) 10:90	133.1	34.8	7.3
p(CPH-SA) 80:20	136.2	26.0	18.4
p(CPH-SA) 90:10	143.1	47.0	1.7
p(FA)	246.2	41.2	16.0
p(FA-SA) 90:10	213.0	56.0	13.8
p(FA-SA) 80:20	185.7	58.0	22.8
p(FA-SA) 70:30	106.0	46.0	5.7
p(FA-SA) 60:40	94.7	—	4.7
p(FA-SA) 50:50	69.0	—	12.5
p(FA-SA) 40:60	68.0	47.0	9.0
p(FA-SA) 30:70	67.0	46.0	7.9
p(FA-SA) 20:80	73.9	—	21.9
p(FA-SA) 10:90	83.0	55.0	25.8
p(CPP)	240.0	96.0	26.5
p(CPP-SA) 4:96	76.0	41.7	24.9
p(CPP-SA) 9:91	78.0	—	25.7
p(CPP-SA) 13:87	75.0	47.0	20.7
p(CPP-SA) 17:83	72.0	47.0	19.3
p(CPP-SA) 22:78	66.0	47.0	15.3
p(CPP-SA) 27:73	66.0	44.0	10.2
p(CPP-SA) 31:69	66.0	40.0	5.1
p(CPP-SA) 41:59	178.0	4.2	2.0
p(CPP-SA) 46:54	185.0	1.8	3.1
p(CPP-SA) 60:40	200.0	0.2	6.0
p(CPP-SA) 80:20	205.0	15.0	8.2

Source: From Ref. 24.

Table 2. Molecular Weight and Viscosity of p(FAD-SA)

Polymer	M_r	M_n	T_m (°C)	Viscosity (η)
p(SA)	133,000	21,600	80–82	0.88
p(FAD-SA) 10:90	110,000	17,500	76–78	0.90
p(FAD-SA) 20:80	92,000	22,000	72–77	0.85
p(FAD-SA) 30:70	175,200	16,900	70–76	1.10
p(FAD-SA) 40:60	54,044	14,300	64–68	0.42
p(FAD-SA) 50:50	235,000	25,600	62–66	1.12
p(FAD-SA) 60:40	34,800	12,800	45–52	0.38
p(FAD-SA) 70:30	22,500	7,100	35–42	0.35
p(FAD-SA) 80:20	21,500	7,000	—	0.33
p(FAD-SA) 90:10	18,910	5,900	—	0.29
p(FAD)	37,000	12,500	—	0.25

Source: From Ref. 14.

Biocompatibility

The biocompatibility of polyanhydrides was investigated extensively. Early studies assessed the biocompatibility of p(CPP), p(TA), p(CPP-SA), and p(PTA-SA) as well as the toxicity of their monomers (27). The monomers were tested nonmutagenic, were nontoxic, and were found to have a low teratogenic potential in vitro. The polymers did not lead to inflammatory responses after 6 weeks of implantation into rabbit cornea and showed no signs of inflammation after subcutaneous implantation into rats. The encapsulation by fibrous tissue that was observed is not unusual for an implanted biomaterial (28). The biocompatibility of p(CPP-SA) 20:80 was tested subcutaneously

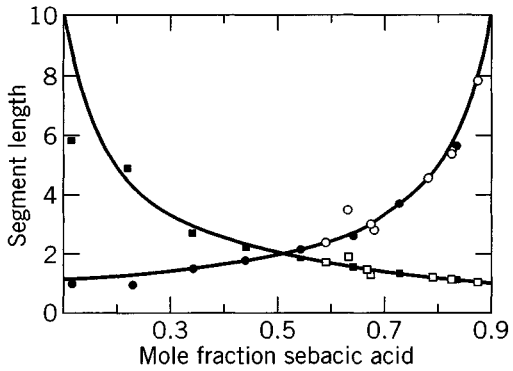


Figure 5. Comparison of block length as measured by NMR to that predicted by a random copolymer distribution for p(CPH-SA) and p(CPP-SA). For p(CPH-SA): ●, SA-SA; ■, CPH-CPH. For p(CPP-SA): ○, SA-SA; □, CPP-CPP. *Source:* Reproduced with permission from Ref. 16.

in rats. The polymer showed excellent biocompatibility in doses to rats of 2,400 mg/kg (29). The biocompatibility of p(CPP-SA) 20:80 in the brain was first assessed in rodent models (30,31). There was a slight transient inflammatory response to the polymer but it was comparable to the response provoked by Surgicel, an oxidized regenerated cellulose and established hemostatic agent used routinely in neurosurgery. Similar results were obtained for p(CPP-SA) 50:50 in rabbits. The polymer showed again no signs of toxicity and a tissue reaction comparable to Gelfoam, a resorbable gelatin sponge. The brain compatibility of p(FAD-SA) was also assessed in rats. It showed an acute inflammatory response after 3–6 days comparable to p(CPP-SA) and Surgicel, but was nontoxic as well (32). Finally the brain biocompatibility was verified in a monkey model (33). In the same animal model carmustine-loaded implants made of p(CPP-SA) 20:80 were found to be a safe dosage form.

POLYANHYDRIDE DEGRADATION AND EROSION

One of the most important characteristics of a biodegradable polymer is its degradation and erosion behavior. Degradation, which is the process of chain cleavage, can be investigated by following the molecular weight change of a substance. Erosion is the sum of all processes leading to the loss of mass from a polymer matrix. It should be kept in mind that degradation is not mandatory for a polymer matrix to erode. If the polymer is at least partially soluble inside the erosion medium, for example, dissolution processes might contribute to erosion as well. Conversely, if the polymer has degraded completely, it does not necessarily erode. In the case of polyanhydrides the polymers are not water-soluble and must, therefore, degrade at least to water-soluble oligomers prior to erosion.

Kinetics of Degradation

Polymer degradation is usually followed by investigating the loss of molecular weight. This was also done in the case of poly(anhydrides). When p(CPP-SA) 20:80 matrix discs with 8 mm diameter and 1.6 mm height were degraded in phosphate buffer solution pH 7.4 at 37°C it was found that the molecular weight drops exponentially during the first 24 hours (34). Such investigations reveal the time scale on which degradation occurs and, therefore, yields precious information on the expected time over which drugs may be released. However, the result of investigating large matrix discs does not allow the assessment of the degradation properties of a material unequivocally. With increasing dimensions, the result depends on other processes in addition to degradation, such as the diffusion of water into the polymer bulk. If water diffusion is slow, the degradation of the polymer matrix disc is affected tremendously because the lack of water prevents the degradation inside the polymer matrix. From the resulting molecular weight changes one would, however, draw the conclusion that polyanhydrides degrade across their entire cross section for geometries of reasonable size. Other aspects that have to be considered are autocatalytic effects that stem from the free monomers created during degradation. More recently, NMR investigations were performed to monitor the degradation of individual bonds in polyanhydride copolymers (35). Studies on p(CPP-SA) confirmed that bonds in which SA is involved are cleaved faster than bonds between CPP molecules.

The fast degradation of polyanhydrides is their strength and concomitantly their weakness. This is illustrated by experiments with polyanhydrides in solution. Even when dissolved in anhydrous chloroform they have been reported to lose molecular weight. p(CPV) M_r 18,500 and p(CPO) M_r 25,950 lost 50% of their molecular weight within approximately 1.5 hours (36). These examples illustrate that polyanhydrides have to be stored under anhydrous conditions.

Polyanhydride Erosion

Besides its biocompatibility the erosion of a degradable polymer is perhaps the most crucial property with respect to its performance as a carrier material for drug delivery. When research on degradable polymers for drug delivery intensified, a basic classification was proposed for degradable polymers. Bulk-eroding or homogeneously eroding polymers were distinguished from surface-eroding or heterogeneously eroding ones (37). The difference is illustrated in Figure 6. While a bulk-eroding polymer degrades and erodes over its entire cross section, a surface-eroding polymer erodes mainly from its surface. An essential condition for a water-insoluble polymer to undergo surface erosion is the fast degradation of its polymer backbone (38). It is not surprising that polyanhydrides and poly(ortho esters) are among the few polymer groups that have been reported to be surface eroding, since they are assembled from fast-hydrolyzing functional groups. However, one must bear in mind that surface erosion and bulk erosion are ideal cases. For most polymers, erosion has features of both mechanisms, which is also the case for most polyanhydrides. As a general rule one can assume that surface-eroding polymers erode faster than bulk-eroding ones. The differences in erosion between polyanhydrides and crystalline poly(lactides) might serve as an example:

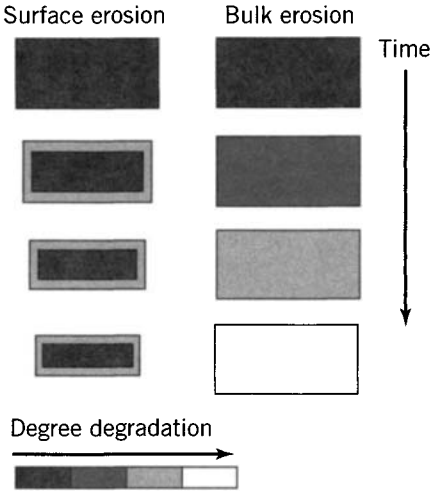


Figure 6. Schematic illustration of surface erosion and bulk erosion of polymers.

erosion is a matter of weeks for 2-mm thick p(CPP-SA) 20:80 and p(FAD-SA) 20:80 wafers. For poly(L-lactic acid), which is a partially crystalline bulk-eroding polymer, it is a matter of several months. However, some polyanhydrides such as those containing aromatic monomers such as p(CPP) have been reported to be extremely erosion-resistant as well.

The erosion of most of the clinically relevant polyanhydrides has been investigated extensively and revealed useful information for the manufacture of drug delivery systems. Originally erosion was followed by the determination of monomer release from the polymers (23) and the mass loss of polymer matrices during erosion (39). Figures 7 and 8 illustrate that such data can be very confusing. Although the mass loss of p(CPP-SA) matrix discs is almost linear (Fig. 7) as one would expect from a surface-eroding polymer, the release profiles of the monomers do not follow the same kinetics (Fig. 8). The two monomers CPP and SA are not only released in a nonlinear way, but also with marked differences regarding their overall kinetics. To solve this paradox, one must take into account other factors with an impact on erosion besides degradation. The microstructure of a polymer is one of them. The microstructure of a polymer and its changes due to erosion have to be assessed using physicochemical techniques. This information is essential to understand how polymers erode. For p(CPP-SA) the crystallinity changes were investigated using DSC, WAXD, scanning electron microscopy (SEM) (39,40), and solid-state NMR (D.L. McCann, F. Heatley, and A. D'Emanuelle, personal communication). It was found that these polymers do not erode according to a perfect surface erosion mechanism. The amorphous polymer parts were found to erode substantially faster than the crystalline ones (19, 39, D.L. McCann, F. Heatley, and A. D'Emanuelle, personal communication). As a consequence erosion zones form in which the amorphous polymer disappears first and is replaced by a network of pores that stretch through the crystalline areas of noneroded polymer. The foremost line of eroded polymer, the erosion front, moves from the surface of the polymer matrix into its center (39). Figure 9(a) illustrates schematically the changes that p(CPP-SA) polymers undergo during erosion. This erosion mechanism, which creates porous erosion zones, has a marked impact on the release of substances. A good example are the two monomers that are released during erosion.

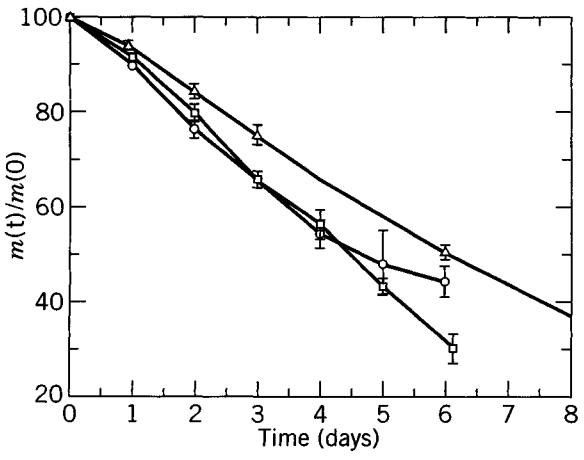


Figure 7. Mass loss of polyanhydride matrix discs (diameter 7 mm, height approximately 2 mm) during erosion. ○, p(SA); □, p(CPP-SA) 20:80; △, p(CPP-SA) 50:50. *Source:* Reproduced with permission from Ref. 39.

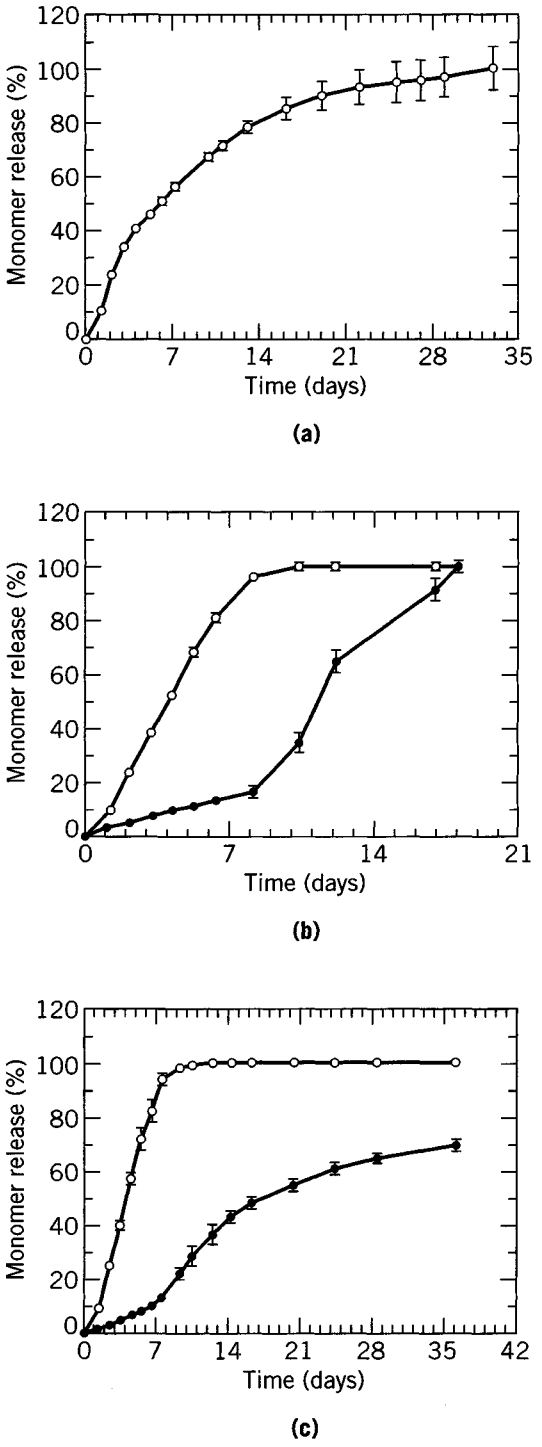


Figure 8. SA (○) and CPP (●) release polyanhydride matrix discs during erosion: (**a**) p(SA), (**b**) p(CPP-SA) 20:80, (**c**) p(CPP-SA) 50:50. *Source:* Reproduced with permission from Ref. 39.

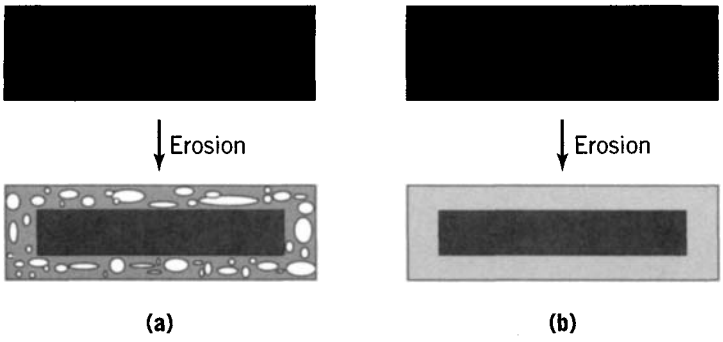


Figure 9. Schematic illustration of (**a**) p(CPP-SA) erosion and (**b**) p(FAD-SA) erosion.

Other investigations of the erosion mechanism of polyanhydrides focused on the characterization of the erosion zones and the chemical conditions that prevail within them. Investigations by confocal fluorescence microscopy using pH-sensitive fluorescent probes revealed that the pH on the surface of p(CPP-SA) 20:80 matrices is one unit lower than in the surrounding pH 7.4 buffer (39). From these results in combination with findings by DSC and WAXD, which indicate that both monomers crystallize inside the erosion zone, it was concluded that the pH inside the erosion zone is about 5 (39). These assumptions were confirmed more recently by spectral spatial electron paramagnetic resonance imaging using pH-sensitive spin probes (41). The effect that this pH microclimate has on the release of substances can again be seen from the release profiles of the monomers. The profile for SA is rapid concave downward as one would expect for a monolithic device. The profile of CPP, in contrast, exhibits a slow leakage before its rapid release. This can be explained with the solubility of the two compounds. In the pH range of interest, the solubility of SA was found to be 10 times higher than that of CPP (39). Given that both monomers are created at the same velocity by degradation, and that they have similar pKa values one can assume that SA determines the pH and keeps the solubility of CPP even lower while it is created in the erosion zone. Once SA is released completely, the solubility of CPP increases and so does its release velocity. These results confirm that even though the mass loss kinetics appear to be simple, the individual processes of erosion can become quite complicated.

That the erosion kinetics are an individual characteristic of a polymer group can be seen when comparing these results obtained for p(CPP-SA) with the erosion mechanism of p(FAD-SA) (25) (Fig. 9(b)). Although p(FAD-SA) polymers are also partially crystalline, their erosion mechanism is different from that of p(CPP-SA) (25,42). One major reason is the nature of FAD, a water-insoluble liquid. During the erosion of p(FAD-SA), FAD precipitates on the surface of polymer matrix discs while SA is released (25). The erosion zones are a semisolid layer of FAD and its salt and are less well defined as in the case of p(CPP-SA).

The erosion zones that are created during polyanhydride erosion may have some effect on the release of low molecular weight substances besides their impact on monomer release. p(CPP-SA) and p(FAD-SA) can serve again as a good example. Comparing the release of SA from both polymers the release is slightly faster from p(CPP-SA) compared to p(FAD-SA). Most likely the different nature of the erosion zones account for this effect. Whereas in one case SA can diffuse through a network of pores, it has to pass through an amorphous lipid layer in the other. The impact of the erosion zones on drug or monomer release from p(CPP-SA) has also been illustrated by applying diffusion theory (43). Under the assumption that a saturated solution of SA, which is in equilibrium with suspended SA, exists at the erosion front, a diffusion model simulates the release of SA through the porous and tortuous erosion zone. Assuming further that SA controls the solubility of CPP, the sigmoid release profile for CPP was confirmed by this modeling approach. The poor solubility of the monomers is also reflected by the fast release of drugs from p(CPP-SA) matrix discs. Indometacin, for example, was found to be released faster than SA (44).

Theoretical Description of Polyanhydride Erosion

There have been a number of approaches to describe the erosion of biodegradable polymers in the past. For bulk-eroding polymers this is very complicated, because their erosion mechanism is still not completely understood (45). For surface-eroding polymers early approaches assume that erosion fronts move at linear speed leaving no erosion zones behind (46,47). Such assumptions work well if erosion zones have no impact on the erosion kinetics, which is, however, not the case for most polyanhydrides. In order to take into account the effect of such zones on erosion, two-dimensional models were developed (48) similar to the ones used previously for modeling erosion-controlled drug release (49). For the simulation of erosion the matrices are first represented using two-dimensional rectangular grids such as the one shown schematically in Figure 10(a). The

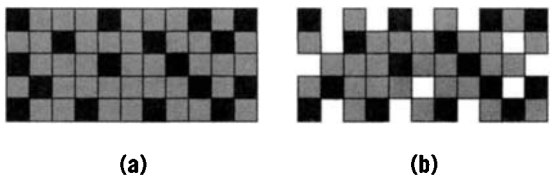


Figure 10. Theoretical representation of a cylindric polymer matrix cross-section by a two-dimensional grid (black pixels represent amorphous polymer; white pixels, amorphous polymer): (**a**) prior to erosion, (**b**) during erosion.

grid covers the cross-section through a cylindrical polyanhydride matrix disc and consists of a multitude of small polymer parts (pixels). The partial crystallinity of the polymer is taken into account by assigning some of the pixels the quality of being crystalline and others the quality of being amorphous. In the easiest case this can be done at random by simply taking the overall crystallinity of the material into account. To simulate erosion it is then necessary to define an erosion algorithm. In the case of p(CPP-SA) this required two basic assumptions:

1. A polymer pixel can only erode after it has contacted the erosion medium (at time 0 these are only the pixels located on the "surface" of the grid). After this contact is established, the lifetime of a pixel is calculated.
2. The lifetimes of all polymer pixels are distributed according to a first order Erlang distribution (equation 1). Lifetimes are determined at random from this distribution and once the lifetime expired the pixels are taken from the grid and are considered eroded (Fig. 10(b)). Amorphous polymer pixels have higher chances to erode at early times than crystalline ones. This is accounted for by a higher erosion rate constant, λ.

$$e(t) = \lambda \cdot e^{-\lambda t} \quad (1)$$

where e(t) is the probability that a pixel has the lifetime t. When this algorithm is applied to a large grid, simulations such as the one shown in Figure 11 are obtained. The appearance of these cross-sections is typical for eroding p(CPP-SA) and matches exactly the appearance of cross-sections of this material when observed by SEM (39). There is an erosion front that moves from the surface towards the center of the matrix and separates a noneroded polymer core from a highly porous erosion zone. The erosion zone consists mainly of crystalline pixels, which is in agreement with experimental findings. Such models have two advantages. First they provide a better understanding of how polymer surface erosion can be envisioned to proceed, and second, they can be used to predict certain parameters such as the porosity of the polymers during erosion and under certain conditions of drug release.

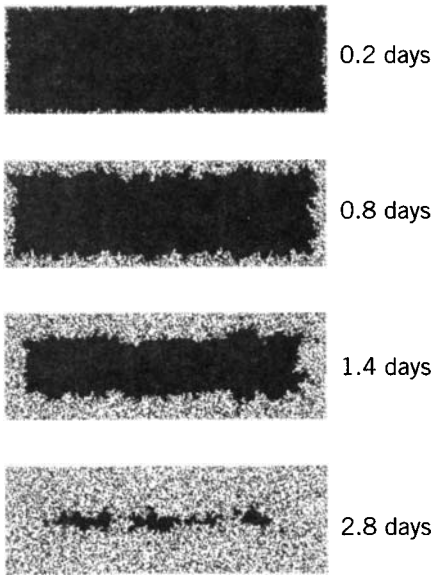


Figure 11. Simulation of the erosion of a p(CPP-SA) 20:80 matrix using discrete two-dimensional models. (Black pixels represent noneroded polymer; white pixels, eroded polymer.) *Source:* Reproduced with permission from Ref. 50.

DRUG DELIVERY SYSTEMS MADE OF POLYANHYDRIDES

Considerations Regarding the Kinetics of Drug Release

The fast erosion of polyanhydrides makes them attractive candidates for the purpose of drug delivery. There are three major mechanisms by which drugs can be released from polymers. Release can be controlled by diffusion, swelling, or erosion. In the case of a biodegradable polymer the three mechanisms compete against one another, and it will be the slowest of these processes that will control the release of drugs. If the three processes proceed at similar speed, drug release will be controlled by all three simultaneously. In order to have optimal control over drug release from degradable polymers, it is desirable that it be mainly erosion controlled. The only way that this can be achieved is by using fast-eroding polymers, which is the case for polyanhydrides. In some cases polyanhydrides have been reported to release drugs by perfect erosion control (15,51). An example is shown in Figure 12.

Drug Stability

The fast erosion of polyanhydrides can be attributed to the fast hydrolysis of the carboxylic anhydride bonds in the polymer chain. Water is, however, not the only nucleophile that might react with carboxylic anhydrides. Primary amines might react as well under irreversible amide formation. Although such reactions pose a potential threat to the stability of incorporated drugs, systematic investigations have shown that amide formation is strongly pH dependent (52). Whereas the interaction was reported to be strong at pH 7.4, it was most effectively suppressed at pH 5. From these results one can expect that the stability of drug-carrying amines could, on the other hand, be minimized, as the pH inside the erosion zones of polyanhydrides was found to be below 5 (39,41). The impact of polyanhydrides on the stability may not be too severe as evidenced by studies of encapsulated enzymes. It was found that polyanhydrides can even protect such systems from inactivation (53).

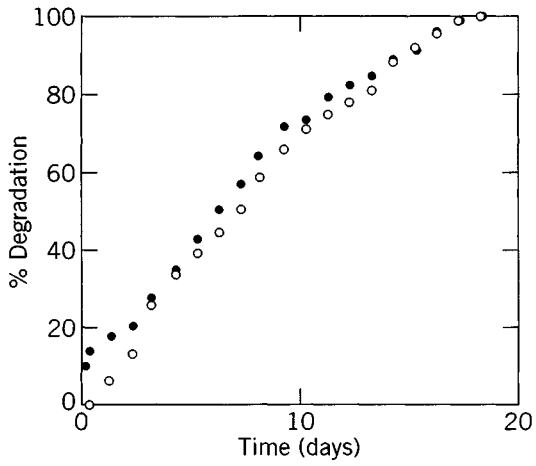


Figure 12. Release of *p*-nitroaniline (10% loading) from injection-molded poly[bis(*p*-carboxyphenoxy)propane anhydride] in 0.1 M pH 7.4 phosphate buffer at 37°C. (○) polymer degradation; (●) drug release. *Source:* Reproduced with permission from Ref. 51.

Drug Delivery Systems Made of Polyanhydrides

Polyanhydrides have been used for the manufacture of a number of challenging drug delivery applications involving the manufacture of new drug delivery systems (54) as well as new types of therapy (4,55). It is beyond the scope of this chapter to give a complete survey on all drug delivery applications for which polyanhydrides have been used. It is instead the intention to give some examples that illustrate how one can take advantage of the specific properties of polyanhydrides. More information on polyanhydride drug delivery systems can be found in chapters on CENTRAL NERVOUS SYSTEM, DRUG DELIVERY TO TREAT and MICROENCAPSULATION.

Although many of the applications already mentioned require the use of polyanhydrides for their quick erosion, which coincides with the goal of short-term drug delivery, some applications depend on the exact performance of these polymers. An example is the development of pulsatile drug delivery systems. The simulation shown in Figure 10 illustrates that polyanhydrides are surface eroding. If a polyanhydride matrix disc was made of several layers of polymer carrying different doses of the same drug, the drugs should be released one after another. This principle could be used for a number of drug delivery applications such as vaccination or local tumor therapy. Early investigations showed that such release behavior can indeed be achieved. In the simplest case, a composite matrix, such as the one shown in Figure 13(a), could be used to release drugs one after another. The drug release profile for two model compounds is shown in Figure 14(a). The drug release behavior can completely be understood on the basis of the erosion mechanism of polyanhydrides. When the erosion front moves into the core of the polymer matrix discs, the drug in the areas that are located inside the erosion zone are liberated by the process. As the erosion profiles move parallel to the matrix surface, first the drug from the perimeter is liberated and then from the core of the composite. Figure 14(a) also shows, however, that the possibilities to postpone the release of the second dose are limited. The lag period between the start of erosion and the release of the second dose depend on the geometry of the device. To postpone the release of the second drug for 10 days, the perimeter would have to be unreasonably thick. Therefore, the combination of polyanhydrides with slow-eroding polymers such as poly(lactic acid) was shown to be a useful alternative as illustrated in Figure 13(b). When

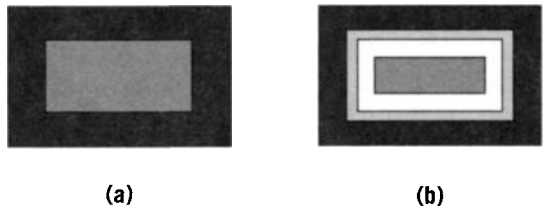


Figure 13. (**a**) Cross-section through a composite polyanhydride matrix cylinder, (**b**) Cross-section through a complex composite matrix cylinder made of polyanhydrides and poly(lactic acid). ■, drug-carrying polyanhydride perimeter; ■, drug-carrying polyanhydride core; □, drug-free polyanhydride layer; ▒, drug-free bulk-eroding polymer (e.g., PLA).

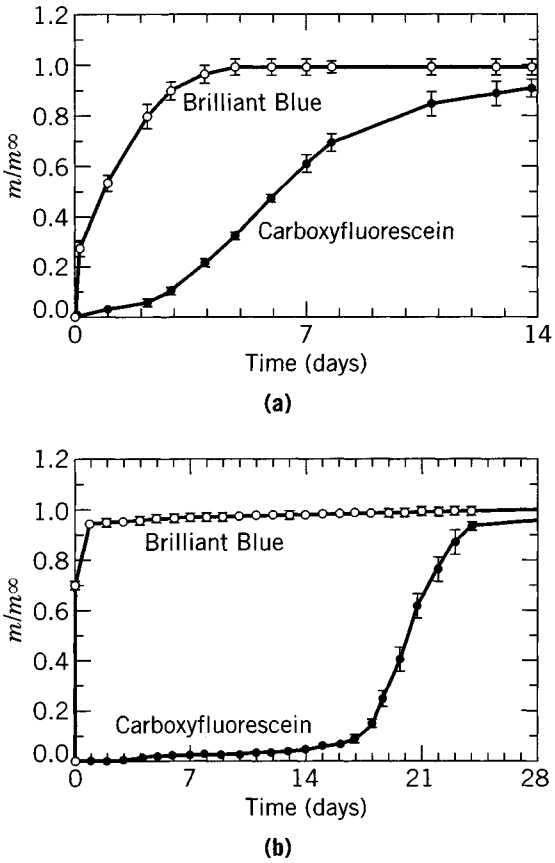


Figure 14. (○) Brilliant blue (perimeter) and (●) carboxyfluorescein (core) release from composite polymer matrix discs. (**a**) composite polyanhydride cylinder (see Fig. 13a). (**b**) composite polyanhydride cylinder in combination with poly(lactic acid) (see Fig. 13b). *Source:* Reproduced with permission from Ref. 50.

drugs are released from such a composite device, release profiles such as the one shown in Figure 14(b) can be obtained (50).

DRUG RELEASE KINETICS

The release kinetics depend on several factors. One of them is certainly the nature of the polyanhydride that is used as a drug carrier. The slower the erosion of the material, the slower the release of drug. Another aspect is the nature of the incorporated drug. Lipophilic drugs tend to be released more slowly from the polymers than hydrophilic ones (56). As many drugs possess some acid or base functionality the microclimate inside the eroding polymer can affect the property of a drug tremendously. The solubility of carboxylic acids, for example, will be decreased during the erosion of polyanhydrides, because the pH values inside these polymers are low.

SUMMARY AND OUTLOOK

Polyanhydrides are a very versatile and interesting group of polymer. The most important characteristic is their fast degradation, which is followed by the rapid erosion of the material. Polyanhydrides are ideal candidates for drug delivery applications that last from days to weeks. The clean-cut erosion mechanism makes polyanhydrides a family of polymer the erosion behavior of which can readily be understood. Therefore, polyanhydrides have been used for a number of drug delivery applications: the encapsulation of proteins and peptides, the treatment of osteomyelitis, and the treatment of brain tumors. They have been shown to be effective and safe, and one can assume that polyanhydrides will have their place in the family of biodegradable polymers for parenteral applications in the future.

BIBLIOGRAPHY

1. K. Park, W.S.W. Shalaby, and H. Park, *Biodegradable Hydrogels for Drug Delivery*, Technomic Publishing, Lancaster, Pa., 1993.
2. A. Göpferich, *Biomaterials* **17**, 103–114 (1996).
3. A. Göpferich and R. Langer, *AIChE J.* **41**, 2292–2299 (1995).
4. C.T. Laurencin et al., *J. Orthop. Res.* **11**, 252–262 (1993).
5. H. Brem, K.A. Walter, and R. Langer, *Eur. J. Pharm. Biopharm.* **39**, 2–7 (1993).
6. J.E. Bucher and W.C. Slade, *J. Am. Chem. Soc.* **31**, 1319–1321 (1909).
7. J.W. Hill, *J. Am. Chem. Soc.* **52**, 4110–4115 (1930).
8. J.W. Hill and W.H. Carothers, *J. Am. Chem. Soc.* **54**, 1569–1579 (1932).
9. A. Conix, *J. Polym. Sci.* **29**, 343–353 (1958).
10. H.B. Rosen et al., *Biomaterials* **4**, 131–133 (1983).
11. A. Domb, E. Ron, and R. Langer, in H.F. Mark et al., eds., *Encyclopedia of Polymer Science and Engineering*, 2nd ed., suppl. vol., Wiley, New York, 1989, pp. 648–665.
12. A.J. Domb and R. Nudelman, *Biomaterials* **16** 319–323 (1995).
13. M. Davies et al., *J. Appl. Polym. Sci.* **42**, 1597–1605 (1991).
14. A.J. Domb and M. Maniar, *J. Polym. Sci., Part A* **31**, 1275–1285 (1993).
15. K.W. Leong, B.C. Brott, and R. Langer, *J. Biomed. Mater. Res.* **19**, 941–955 (1985).
16. J. Tamada and R. Langer, *J. Biomater. Sci., Polym. Ed.* **3**, 315–353 (1992).
17. M. Maniar, X. Xie, and A.J. Domb, *Biomaterials* **11**, 690–694 (1990).
18. K.W. Leong, V. Simonte, and R. Langer, *Macromolecules* **20**, 705–712 (1987).
19. A.-C. Albertsson and S. Lundmark, *Br. Polym. J.* **23**, 205–212 (1990).
20. A.J. Domb and R. Langer, *J. Polym. Sci., Part A* **25**, 3373–3386 (1987).
21. A.J. Domb, E. Ron, and R. Langer, *Macromolecules* **21**, 1925–1929 (1988).
22. A.J. Domb et al., *J. Polym. Sci., Part A* **29**, 571–579 (1991).
23. J. Tamada and R. Langer, *Proc. Natl. Acad. Sci. U.S.A.* **90**, 552–556 (1993).
24. E. Mathiowitz et al., *Macromolecules* **23**, 3212–3218 (1990).
25. L. Shieh et al., *J. Biomed. Mater. Res.* **28**, 1465–1475 (1994).
26. E. Ron et al., *Macromolecules* **24**, 2278–2282 (1991).
27. K.W. Leong, P.D'Amore, M. Marletta, and R. Langer, *J. Biomed. Mater. Res.* **20**, 51–64 (1986).
28. D. Bakker, C.A. van-Blitterswijk, S.C. Hesseling, and J.J. Grote, *Biomaterials* **9**, 14–23 (1988).
29. C. Laurencin et al., *J. Biomed. Mater. Res.* **24**, 1463–1481 (1990).
30. R. Tamargo et al., *J. Biomed. Mater. Res.* **23**, 253–266 (1989).
31. H. Brem et al., *Select. Cancer Ther.* **5**, 55–65 (1989).
32. H. Brem et al., *J. Controlled Release* **19**, 325–330 (1992).
33. H. Brem, *Biomaterials* **11**, 699–701 (1990).
34. A. D'Emanuelle et al., *Pharm. Res.* **9**, 1279–1283 (1992).
35. F. Heatley, M. Humadi, R.V. Law, and A. D'Emanuele, *Macromolecules* **31**, 3832–3838 (1998).
36. A.J. Domb and R. Langer, *Makromol. Chem. Macromol. Symp.* **19**, 189–200 (1988).
37. R. Langer and N. Peppas, *J. Macromol. Sci., Rev. Macromol. Chem. Phys.* **C23**, 61–126 (1983).
38. A. Göpferich, *Eur. J. Pharm. Biopharm.* **42**, 1–11 (1996).
39. A. Göpferich and R. Langer, *J. Polym. Sci., Part A*: **31**, 2445–2458 (1993).
40. E. Mathiowitz, J. Jacob, K. Pekarek, and D. Chickering, III, *Macromolecules* **26**, 6756–6765 (1993).
41. K. Mäder et al., *Polymer* **38**, 4785–4794 (1997).
42. A. Göpferich, L. Schedl, and R. Langer, *Polymer* **37**, 3861–3869 (1996).
43. A. Göpferich and R. Langer, *J. Controlled Release* **33**, 55–69 (1995).
44. A. Göpferich, D. Karydas, and R. Langer, *Eur. J. Pharm. Biopharm.* **41**, 81–87 (1995).
45. A. Göpferich, *Macromolecules* **30**, 2598–2604 (1997).
46. D.O. Cooney, *AIChE J.* **18**, 446–449 (1972).
47. H.B. Hopfenberg, *ACS Symp. Ser.* **33**, 26–32 (1976).
48. K. Zygourakis, *Chem. Eng. Sci.* **45**, 2359–2366 (1990).
49. A. Göpferich and R. Langer, *Macromolecules* **26**, 4105–4112 (1993).

Next Page

50. A. Göpferich, *J. Controlled Release* **44**, 271–281 (1997).
51. A.J. Domb, C.F. Gallardo, and R. Langer, *Macromolecules* **22**, 3200–3204 (1989).
52. A.J. Domb, L. Turovsky, and R. Nudelman, *Pharm. Res.* **11**, 865–868 (1994).
53. Y. Tabata, S. Gutta, and R. Langer, *Pharm. Res.* **10**, 487–496 (1993).
54. K.J. Pekarek, J.S. Jacob, and E. Mathiowitz, *Nature (London)* **367**, 258–260 (1994).
55. H. Brem et al., *Lancet* **345**, 1008–1012 (1995).
56. L. Shieh et al., *J. Controlled Release* **29**, 73–82 (1994).

See also BIODEGRADABLE POLYMERS: POLY(PHOSPHOESTER)S; BIODEGRADABLE POLYMERS: POLYESTERS; POLY(ORTHO ESTERS).

BIODEGRADABLE POLYMERS: POLYESTERS

SUMING LI
MICHEL VERT
Centre de Recherche sur les Biopolymères Artificiels
Montpellier, France

KEY WORDS

Aliphatic polymer
Biodegradation
Biomaterial
Crystallinity
Degradation
Drug delivery
Hydrolysis
Lactic acid polymer
Lactic acid–glycolic acid copolymer
Poly(ϵ-caprolactone)
Polyglycolide
Polylactide
Stereocopolymer

OUTLINE

Introduction
Synthesis
  Monomer Synthesis
  Polymer Synthesis
Manufacturing Methodology
  Implantable Drug Delivery Devices
  Injectable Drug Delivery Devices
Degradation Mechanisms
  Enzymatic Degradation
  Hydrolytic Degradation
  Microbial Degradation
Factors Influencing Polymer Degradation and Drug Delivery
  Polymer Morphology
  Chemical Composition and Configurational Structure
  Molar Mass and Molar Mass Distribution
  Size and Porosity
  Drug Load and Drug/Polymer Interactions
  γ Irradiation
  pH and Ionic Strength
  Comparison Between in Vitro and in Vivo Behaviors
Conclusion
Bibliography

INTRODUCTION

During the past 50 years, synthetic polymers have changed the everyday life of humans due to the possibility of covering a wide range of properties by modification of macromolecular structures and introduction of additives (fillers, plasticizers, etc.). In the meantime, surgeons and pharmacists tried to use these materials as biomaterials (1,2). About 30 years ago, distinction was made between permanent and temporary therapeutic uses. The former requires biostable polymeric materials, and the main problem is resistance to degradation in the body. In contrast, the latter needs a material only for a limited healing time. In this regard, degradable polymers became of great interest in surgery as well as in pharmacology. The first degradable synthetic polymer was poly(glycolic acid) (PGA), which appeared in 1954 (3). This polymer was first discarded because of its poor thermal and hydrolytic stabilities, which precluded any permanent application. Later on, people realized that one could take advantage of the hydrolytic sensitivity of PGA to make polymeric devices that can degrade in a humid environment and, thus, in a human body. This led to the first bioabsorbable suture material made of a synthetic polymer (4,5). It is worth noting that terminology is one of the sources of confusion in the field. Nowadays, people tend to use the word *degradable* as a general term and reserve *biodegradable* for polymers that are biogically degraded by enzymes introduced in vitro or generated by surrounding living cells. The possibility for a polymer to degrade and to have its degradation by-products assimilated or excreted by a living system is thus designated as *bioresorbable* (6).

Most of the degradable and biodegradable polymers identified during the past 20 years have hydrolyzable linkages, namely ester, orthoester, anhydride, carbonate, amide, urea, and urethane in their backbone (7,8). The ester bond–containing aliphatic polyesters are the most attractive because of their outstanding biocompatibility and versatility regarding physical, chemical, and biological properties (9–11). The main members of the aliphatic polyester family are listed in Table 1. Only a few have reached the stage of clinical experimentations as bioresorbable devices in drug delivery. This is primarily due to the fact that being degradable or biodegradable is not sufficient. Many other prerequisites must be fulfilled for clinical use and commercialization (Table 2) (10).

The delivery of drugs to a human body can be achieved through oral, transdermal, topical, and parenteral admin-

Previous Page

50. A. Göpferich, *J. Controlled Release* **44**, 271–281 (1997).
51. A.J. Domb, C.F. Gallardo, and R. Langer, *Macromolecules* **22**, 3200–3204 (1989).
52. A.J. Domb, L. Turovsky, and R. Nudelman, *Pharm. Res.* **11**, 865–868 (1994).
53. Y. Tabata, S. Gutta, and R. Langer, *Pharm. Res.* **10**, 487–496 (1993).
54. K.J. Pekarek, J.S. Jacob, and E. Mathiowitz, *Nature (London)* **367**, 258–260 (1994).
55. H. Brem et al., *Lancet* **345**, 1008–1012 (1995).
56. L. Shieh et al., *J. Controlled Release* **29**, 73–82 (1994).

See also BIODEGRADABLE POLYMERS: POLY(PHOSPHOESTER)S; BIODEGRADABLE POLYMERS: POLYESTERS; POLY(ORTHO ESTERS).

BIODEGRADABLE POLYMERS: POLYESTERS

SUMING LI
MICHEL VERT
Centre de Recherche sur les Biopolymères Artificiels
Montpellier, France

KEY WORDS

Aliphatic polymer
Biodegradation
Biomaterial
Crystallinity
Degradation
Drug delivery
Hydrolysis
Lactic acid polymer
Lactic acid–glycolic acid copolymer
Poly(ϵ-caprolactone)
Polyglycolide
Polylactide
Stereocopolymer

OUTLINE

Introduction
Synthesis
  Monomer Synthesis
  Polymer Synthesis
Manufacturing Methodology
  Implantable Drug Delivery Devices
  Injectable Drug Delivery Devices
Degradation Mechanisms
  Enzymatic Degradation
  Hydrolytic Degradation
  Microbial Degradation
Factors Influencing Polymer Degradation and Drug Delivery
  Polymer Morphology
  Chemical Composition and Configurational Structure
  Molar Mass and Molar Mass Distribution
  Size and Porosity
  Drug Load and Drug/Polymer Interactions
  γ Irradiation
  pH and Ionic Strength
  Comparison Between in Vitro and in Vivo Behaviors
Conclusion
Bibliography

INTRODUCTION

During the past 50 years, synthetic polymers have changed the everyday life of humans due to the possibility of covering a wide range of properties by modification of macromolecular structures and introduction of additives (fillers, plasticizers, etc.). In the meantime, surgeons and pharmacists tried to use these materials as biomaterials (1,2). About 30 years ago, distinction was made between permanent and temporary therapeutic uses. The former requires biostable polymeric materials, and the main problem is resistance to degradation in the body. In contrast, the latter needs a material only for a limited healing time. In this regard, degradable polymers became of great interest in surgery as well as in pharmacology. The first degradable synthetic polymer was poly(glycolic acid) (PGA), which appeared in 1954 (3). This polymer was first discarded because of its poor thermal and hydrolytic stabilities, which precluded any permanent application. Later on, people realized that one could take advantage of the hydrolytic sensitivity of PGA to make polymeric devices that can degrade in a humid environment and, thus, in a human body. This led to the first bioabsorbable suture material made of a synthetic polymer (4,5). It is worth noting that terminology is one of the sources of confusion in the field. Nowadays, people tend to use the word *degradable* as a general term and reserve *biodegradable* for polymers that are biogically degraded by enzymes introduced in vitro or generated by surrounding living cells. The possibility for a polymer to degrade and to have its degradation by-products assimilated or excreted by a living system is thus designated as *bioresorbable* (6).

Most of the degradable and biodegradable polymers identified during the past 20 years have hydrolyzable linkages, namely ester, orthoester, anhydride, carbonate, amide, urea, and urethane in their backbone (7,8). The ester bond–containing aliphatic polyesters are the most attractive because of their outstanding biocompatibility and versatility regarding physical, chemical, and biological properties (9–11). The main members of the aliphatic polyester family are listed in Table 1. Only a few have reached the stage of clinical experimentations as bioresorbable devices in drug delivery. This is primarily due to the fact that being degradable or biodegradable is not sufficient. Many other prerequisites must be fulfilled for clinical use and commercialization (Table 2) (10).

The delivery of drugs to a human body can be achieved through oral, transdermal, topical, and parenteral admin-

Table 1. Main Members of the Aliphatic Polyester Family

Polymer	Structure
Poly(glycolic acid)	$-(-O-CO-CH_2-)_n-$
Poly(lactic acid)	$-(-O-CO-CH(CH_3)-)_n-$
Poly(ϵ-caprolactone)	$-(-O-CO-(CH_2)_5-)_n-$
Poly(*para*-dioxanone)	$-(-O-CO-(CH_2)_2-O-CH_2)_n-$
Poly(hydroxybutyrate)	$-(-O-CO-CH(CH_3)-CH_2-)_n-$
Poly(β-malic acid)	$-(-O-CO-CH(COOH)-CH_2)_n-$

Table 2. Prerequisites for Biomedical Applications of Degradable Polymers

Prerequisite	Polymer properties
Biocompatibility	Leachables (e.g., residual oligomers and monomers, degradation products)
	Shape
	Surface
Biofunctionality	Physical
	Mechanical
	Biological
Stability	Processing
	Sterilization
	Storage
Bioresorbability	Degradability
	Resorption of degradation products

istrations (12). A great deal of work has been done during the past two decades to develop degradable, controlled drug delivery systems adapted to these various routes. Large-size implants require surgery, whereas needle-like implants can be injected subcutaneously (s.c.) or intramuscularly (i.m.) using a trochar. Microparticles can also be injected s.c. and i.m. and behave as tiny implants. Intravenous (i.v.) injection is possible with microparticles, the size of which must be below 7 μm to avoid lung capillary embolization. However, microparticles can be taken up very rapidly by the macrophages of the reticuloendothelial system to finally end up in Kupffer cells in the liver. Although nanoparticles have been proposed to overcome the size limitation imposed by capillary beds; they can also be taken up by macrophages. Stealth nanoparticles with a surface covered by a brush of poly(ethylene oxide) (PEO) have been proposed to avoid macrophage uptake (13). In any event, nanoparticles, as well as microparticles, can hardly leave the vascular compartment. Recently, colloidal particles have been considered in the form of macromolecular micelles of amphiphilic biblock copolymers (14,15) or of aggregates of hydrophilic polymers bearing hydrophobic side chains (16). These systems can serve as a drug carrier via physical entrapment of a lipophilic drug within the hydrophobic microdomains formed by the core of micelles or aggregates. Macromolecular prodrugs, where a drug molecule is temporarily attached to a polymeric carrier, have also been proposed (17). Last but not least, the next century might see the development of polymeric drugs, because any synthetic polymer can advantageously interact with elements of living systems, such as molecules, cell membranes, viruses, and tissues (18).

So far, only drug delivery devices based on polymers and copolymers deriving from lactic acid (LA) enantiomers, glycolic acid, and ϵ-caprolactone (abbreviated as PLA, PGA, and PCL, respectively) have been commercialized. The prospective applications include devices to treat cancer, drug addiction, and infection, as well as drugs for contraception, vaccination, and tissue regeneration. A number of products are commercially available such as Decapeptyl®, Lupron Depot®, Zoladex®, Adriamycin®, and Capronor® (12).

High molar mass PLA, PGA, PCL, and their copolymers are obtained by ring-opening polymerization of cyclic esters, i.e., lactides, glycolide and ϵ-caprolactone, respectively (19,20). The direct polycondensation of corresponding hydroxy acids leads to low molar mass oligomers only (21–23). In the case of LA-containing polymer chains, chirality of LA units provides a worthwhile means to adjust bioresorption rates as well as physical and mechanical characteristics (24–26). The use of the PGA homopolymer is limited to suture material because of its high crystallinity and of the absence of practical solvent. In contrast, PLAGA copolymers have been largely used to make implants, microparticles, and nanoparticles.

For the sake of simplicity, PLA stereocopolymers and PLAGA copolymers are identified in this paper by the acronyms PLA_X or PLA_XGA_Y, where X is the percentage of L-LA units present in the monomer feed, Y is that of glycolic acid (GA) units, the rest being the percentage of D-LA units (Table 3). Similarly, copolymers of lactides and ϵ-caprolactone (CL) can be denoted as PLA_XCL_Y where X and Y represent the percentages of L-LA and CL units, respectively. This nomenclature presents the advantage of reflecting clearly the chemical and configurational compositions of the polymers, the average polymer chain composition being generally close to that of the feed (27). Nevertheless, it is far from being standardized. In fact, many other acronyms are used in the literature.

The properties of degradable polyesters depend on many factors, including those related to polymer synthesis and device processing (11). Therefore, the first part of this chapter recalls the various routes available to synthesize polymers and to fabricate drug delivery devices. In the second part, the various mechanisms by which an aliphatic polyester can degrade in a living environment are discussed. Thereafter, the various factors that can affect the degradation and release characteristics of the devices are examined. The discussion is largely based on recent advances in the field. Convergences and discrepancies are outlined when it is reasonably possible.

SYNTHESIS

From the practical aspect of drug delivery, users rarely prepare polymers themselves. This is particularly true nowadays because various PLA, PLAGA, and PCL compounds are marketed as raw materials.

Table 3. Homo- and Copolymers Deriving From Lactides and Glycolide

Polymer and acronym	Structure
	Poly(glycolic acid)
PGA	-(-O-CO-CH_2-)$_n$-
	Poly(L-lactic acid)
PLA_{100}	-(-O-CO-C(H)(-CH_3)-)$_n$-
	L-LA/D-LA stereocopolymers
PLA_X {X = $100n/(n + p)$}	-(-O-CO-C(H)(-CH_3)-)$_n$-O-CO-C(-CH_3)(H)-)$_p$-
	L-LA/D-LA/GA terpolymers
PLA_XGA_Y {X = $100n/(n + p + q)$} {Y = $100q/(n + p + q)$}	-(-O-CO-C(H)(-CH_3)-)$_n$-O-CO-C(-CH_3)(H)-)$_p$-O-CO-CH_2-)$_q$-

There are two main routes to synthesize these aliphatic polyesters: polycondensation of bifunctional hydroxy acids and ring opening polymerization of cyclic ester monomers.

Lactic acids, glycolic acid, or hydroxycaproic acid can be condensed at low pressure and high temperature, according to a step-growth mechanism. This route generally leads to low molar mass chains (M_r < 5,000 daltons) terminated by equimolar amounts of OH and COOH end-groups.

PLA compounds with rather high molar masses issued from step-growth polycondensation are mentioned in literature (28,29). Hiltunen et al. reported obtaining PLA with $\bar{M}_n$ (NMR) up to 30,000 by polycondensation of L-lactic acid in the presence of different catalysts at high temperatures (180–220°C). The best catalyst was found to be sulfuric acid, which yielded the highest molar masses (28). Compounds obtained by the postcondensation of PLA oligomers using a coupling reagent such as dicyclohexyl carbodiimide (DCC) were also reported (29).

The main route to high molar mass PLA, PLAGA, and PCL is the ring opening polymerization of heterocyclic monomers, namely lactide, glycolide, or ϵ-caprolactone (19,20).

Monomer Synthesis

In practice, the synthesis of lactides and glycolide consists of two steps as shown in Figure 1. Lactic acid or glycolic acid is first polycondensed to yield low molar mass oligomers. Then, the oligomers are thermally depolymerized to form the corresponding cyclic diester, which is recovered by distillation at low pressure (30). Catalysts such as zinc metal or zinc oxide are used in the second step to improve the yield (31).

Glycolide is an achiral molecule, whereas the lactide cycle bears two asymmetric carbon atoms. Therefore, there exist three diastereoisomeric forms of lactides, namely L-lactide (L,L cyclic dimer), D-lactide (D,D cyclic dimer) and meso-lactide (D,L cyclic dimer) as shown in Figure 2.

The equimolar mixture of L- and D-lactides, namely racemic- or DL-lactide, is also commercially available and largely used. Both lactides and glycolide need to be purified prior to polymerization if one wants to obtain well-defined, high molar mass polymers. Purification is generally achieved by sublimation or by recrystallization from acetone or ethyl acetate solutions.

ϵ-Caprolactone is generally manufactured by oxidation of cyclohexanone with peracetic acid in an efficient continuous process (32), as shown in Figure 3. It needs to be dried by distillation in the presence of either diphenylmethane 4,4′-diisocyanate (33), calcium hydride (34–36), or sodium metal (36) prior to polymerization.

Polymer Synthesis

A great deal of work has been done to investigate the ring opening polymerization of lactides and lactones. Carothers et al. were the first to polymerize lactides by heating at high temperature (250–270°C) (37). Only low molar mass compounds were obtained. In 1954, high molar mass PGA was obtained from the polymerization of glycolide in the presence of zinc chloride as initiator. The procedure included purification of monomer by recrystallization and degassing of the reaction mixture prior to bulk polymerization under vacuum (38,39). The same procedure was patented for lactides.

The conversion of cyclic monomers to polymer chains requires the use of initiators or catalysts. Many initiation systems have been reported in literature during the past two decades. Among them, two compounds are used industrially, namely tin(II) 2-ethyl hexanoate (stannous octoate or $SnOct_2$) and Zn metal. Stannous octoate has been approved by the U.S. FDA for surgical and pharmacological applications, although it is very unstable and usually contains impurities. This compound is the most widely used initiator. It provides high reaction rate, high conversion ratio, and high molar mass even under relatively mild conditions. However, the use of tin derivatives in the biomedical field remains dubious. In fact, it has been shown that stannous octoate is slightly cytotoxic (40). On the other hand, the presence of residues has been suspected and indirectly shown, such as octanoyl moieties combined to some of the alcoholic chain ends, octanoic acid and hydroxy tin octoate (41). Zn metal was retained as an alternative because Zn is an oligoelement with daily allowance for the metabolism of mammalian bodies. Zn ions are also regarded as bacteriostatic compounds. The use of Zn leads to slower polymerization as compared with stannous octoate. Nevertheless, no modification of chain ends has been detected so far. This feature is a source of difference of polymer properties.

From the structural viewpoint, the ring opening polymerization of cyclic dimers such as lactide and glycolide

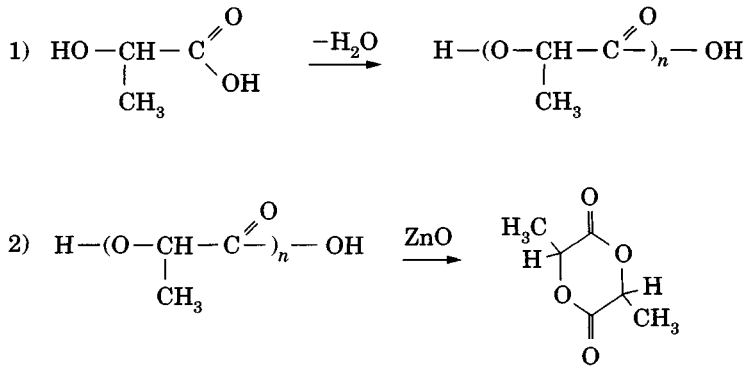


Figure 1. Synthesis of lactide by polycondensation of lactic acid and cyclization.

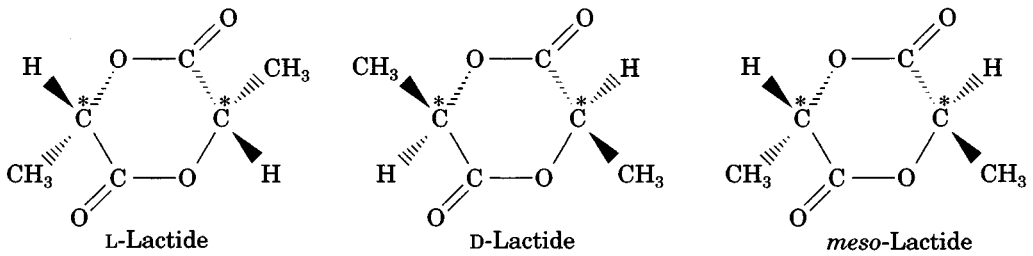


Figure 2. Diastereoisomeric forms of lactide: L-lactide, D-lactide, and *meso*-lactide.



Figure 3. Synthesis of ϵ-caprolactone by oxidation of cyclohexanone with peracetic acid. *Source:* From Ref. 76.

proceeds via pair addition of repeat units. Thus, nonrandom copolymer and stereocopolymer chains are obtained, depending on the composition of the feed (27). The case of ϵ-caprolactone is simpler since it contains only one repeat unit in the cycle. Transesterification reactions can be promoted by certain initiators at high temperatures. These reactions tend to randomize the distribution of repeat units issued from the pair addition mechanism (42).

The polymerization of lactones can proceed through anionic, cationic, or coordination routes. A great deal of work has been devoted to the understanding of these mechanisms because they determine the chain end structures, and to some extent, the degradability. However, many unknowns still remain in the literature due to the complexity of the lactone polymerization chemistry.

Anionic Polymerization. Anionic polymerization is generally conducted in solution under mild reaction conditions as compared with other methods. Anionic-type initiators such as calcium carbonate and lithium hydride had been used early in the 50s and 60s for the polymerization of lactides and glycolide (31,43). Later on, many other initiators were reported, mainly in the form of acetate, carbonate, or octoate salts of calcium, sodium, magnesium, potassium, and lithium metals (44–48).

The active species for the chain propagation have been identified. They are alcoholate or carboxylate groups resulting from the opening of lactone rings after nucleophilic substitution. In the case of strong nucleophilic attacks of basic alcoholate-type on the carbonyl, the ring is opened by cleavage of *O*-acyl bonds. Retention of configuration is thus observed during lactide polymerization. In contrast, initiation by weak nucleophiles of the carboxylate-type seems to lead to *O*-alkyl scission after attack on the methylated carbon, leading to racemization (49). The propagation step depends on the nature and size of the counterion, a pair of ions being formed at the active chain end. The stronger the interaction, the slower the chain propagation. The propagation kinetics are also influenced by the solvatation phenomena affecting both monomer and polymer.

Anionic polymerization is considered as a living process, chain growth continuing until the monomer is exhausted.

The living nature of the reaction is of interest since it allows functionalization and the obtainment of various block copolymers (50–52). From the structural viewpoint, anionic polymerization leads to polymers with various chain ends depending on initiation and termination mechanisms. Transesterification reactions, which are usually very limited due to the mild reaction conditions, can contribute to chain end modifications too.

Cationic Polymerization. Various initiators have been used for the cationic polymerization of lactones: strong acids (53–55), Lewis acids (56–58), acylating or alkylating agents (59,60). Some of them can promote rapid degradation of the polymers. However, cationic polymerization is a means to yield otherwise inaccessible copolymers.

During the initiation step, active species of the oxonium or carbocation-type are formed. The oxonium cycles which are stabilized by inductive effects have been observed by NMR (61). In contrast, carbocation cycles are generally instable. In the absence of other strong nucleophiles (e.g., water, alcohols), the propagation step consists in a nucleophilic attack of the active species by the endocyclic oxygen of another monomer molecule. For the lactide oxonium active species, the attack occurs on the carbonyl rather than on the methine due to the presence of the bulky methyl group. The attack is of S_N2-type, with cleavage of *O*-acyl bonds and retention of configuration. If the attack happens on the methine, racemization can be observed to various extents. For the carbenium one, the attack is considered to be of S_N1-type on the methine, leading to *O*-alkyl bond cleavage and racemization. Termination reactions are generally caused by an external agent or by the intra- or interchain nucleophilic attack of the active species by endochain oxygen atoms. Transesterification reactions have been reported (61).

Most of the mechanisms described in literature are based on coinitiation by impurities such as water, lactic acid, or lactoylactyl acid. Introduction of an alcohol is a means to insure reproductibility, but the molar mass is consequently decreased. Anyhow, one must keep in mind that the coinitiated polymerizations lead to polymers with different chain ends depending on the coinitiator.

Insertion-Coordination Polymerization. The insertion–coordination polymerization mechanism have been proposed for a class of initiators deriving from transition metals such as Zn, Al, Ti, Zr, Sn, Y, and lanthanides (62–68). This is regarded as the most versatile and efficient method to prepare PLA, PGA, PCL, and various copolymers. High molar mass and high conversion ratio can be easily achieved. As in the case of anionic polymerization, the product is a living polymer. In some cases, it has been shown that trace amounts of water or other nucleophiles are the initiator, the coordination compounds serving as catalyst.

The coordination–insertion mechanism can be considered as an intermediate between anionic and cationic ones. A coordination between lactide and the metal with vacant p or d orbitals occurs via the carbonyl oxygen, followed by a concerted attack by an endocyclic oxygen, which leads to the insertion of lactide into the initiator. Nevertheless, this mechanism has been demonstrated for few initiators only, and was derived from chain end modifications. Moreover, distinction from ionic mechanisms is not clear, especially in the case of stannous octoate.

No racemization has been observed with these initiators because the ring opening occurs by *O*-acyl cleavage. Transesterification reactions can be detected to variable extents depending on the polymerization conditions and on the nature of the initiator (69).

Recently, Schwach et al. carried out a systemic study on the ring opening polymerization of DL-lactide using stannous octoate or Zn metal as initiators (41,70–72). Data collected for low monomer–initiator ratios showed that the opening of lactide ring led to octoate-terminated chains. None of the experimental findings agreed with the coordination–insertion mechanism. A cationic-type mechanism coinitiated by 2-ethyl hexanoic acid was proposed with *O*-acyl cleavage and retention of lactyl configuration. This mechanism involves the formation of esterified alcohol chain ends in the form of octoate and the formation of hydroxy tin(II) octoate (41). In the presence of lactic acid, hydroxy tin(II) octoate gives rise to a side-product, hydroxy tin(II) lactate, which also initiates the lactide polymerization. This double initiation mechanism well accounted for the poor correlation between obtained molar masses and theoretical ones. In the case of Zn metal, it has been shown that the active species was Zn lactate. The initiation was also of cationic-type, with coinitiation by lactic acid. Use of Zn lactate was suggested instead of Zn metal since the former yielded higher conversion ratios in shorter times (69,70).

The initiation mechanisms by tin octoate (or hydroxy tin(II) lactate) and Zn metal (or Zn lactate) led to polymers with different chain ends. The presence of purification-resistant C8 hydrophobic derivatives was detected in the case of tin initiation. These hydrophobic compounds seemed to dramatically affect the general behavior of the PLA matrices (71,72). In contrast, Zn-based initiators led only to hydroxylated chain ends without hydrophobic residues.

Therefore, the variety of synthetic routes provides a means to modify the molecular characteristics of polymers such as molar mass, molar mass distribution, endgroup nature, configuration of lactyl units, and chain structure. These characteristics greatly determine the physicochemical properties, especially the degradability. On the other hand, the manufacturing methods used to make drug delivery devices can also be the source of structural modifications.

MANUFACTURING METHODOLOGY

Various PLA, PLAGA, and PCL polymers have been used to prepare controlled drug delivery devices. These devices present a number of advantages such as variable release rates and profiles, targeting of recipients, protection of immediate environment, increasing stability, separation of incompatible components, conversion of liquids to free-flowing solids, masking of odor, taste, and activity (73).

The various drug delivery devices can be divided in two types: (*1*) monolithic, the therapeutic agents being dis-

solved or dispersed in a polymeric matrix, and (2) reservoir, the active agents forming a core surrounded by a polymeric barrier (73–78). Macromolecular prodrugs where the active agent is covalently bound to a macromolecule constitute a more sophisticated type of drug delivery system. So far, no such system derived from PLA, PLAGA, and PCL has been reported because of the lack of pendent functional groups to attach drug molecules.

A wide variety of monolithic and reservoir drug delivery systems exist in the form of microspheres, nanospheres, fibers, films, discs, pellets, cylinders, and gels. These devices can be classified into two categories: implantable and injectable devices.

Implantable Drug Delivery Devices

Implantable large devices such cylinders, pellets, slabs, discs, and films thicker than 0.1 mm are usually prepared by compression molding an intimate polymer-drug mixture (79–82). However, there is risk of thermal degradation. Tubings and needle-like implants can be obtained by extrusion (76,83,84). The temperature of compression molding or extrusion depends on the morphological characteristics of the polymer. For crystalline polymers, the processing temperature has to be above the melting temperature (T_m). In the case of amorphous polymers, temperatures above the glass transition (T_g) are usually sufficient. Prior to processing, the polymer should be thoroughly dried to prevent thermal and/or hydrolytic degradation.

Thin films can be prepared by casting a polymer-drug solution (85–90). Hollow fibers of highly crystalline PLA_{100} can be prepared by using a "dry-wet" coagulation spinning process (91,92). The use of different spinning systems (i.e., different solvent–nonsolvent pairs and with or without additive) leads to hollow fibers with varying asymmetric membrane structures. PCL fibers containing tetracycline hydrochloride, with an outer diameter of 0.5 mm, have been prepared by melt spinning at 161°C (93). When organic solvents are used, the elimination of residual solvents is of major importance because they can generate toxicity regardless of the polymer matrix. Implantable mesh sheets were also reported (94).

Implantable systems provide various advantages such as prolonged release of drugs, reproductibility of drug release profiles, and ease of fabrication. However, implantation of such systems requires surgery with risk of infection.

Injectable Drug Delivery Devices

Injectable systems have been largely investigated in recent years because they circumvent the need for a surgical incision. Shah et al. used PLAGA copolymers in a formulation that forms a gel matrix immediately on contact with aqueous fluids (95). Prolonged release of drugs for up to months was achieved. Miyamoto and Takaoka developed composite delivery systems for bone morphogenetic protein (BMP) by mixing semipurified BMP and low molar mass PLA-poly(ethylene glycol) copolymer (96).

Among the various injectable drug delivery systems, microparticles are the most widely investigated. There are basically three methods to manufacture monolithic microparticles: grinding, phase separation, and solvent evaporation. Grinding can be applied to solid matrices issued from fusion of polymer-drug blends or from drying of polymer-drug solutions (97). The presence of residual solvents depends on drying and grinding temperatures. The thermal unstability of some drugs may render solvent removal difficult. This method is suitable for the preparation of monolithic microparticles containing a water-soluble drug because the drug is totally entrapped in the matrix.

The phase separation method consists in emulsifying an aqueous drug solution (dispersion phase) in an organic solvent solution of polymer (continuous phase). A second organic solvent, which is a nonsolvent of the polymer but miscible with the first organic solvent, is then added under vigorous stirring. The resulting particles precipitate, inserting the droplets of the aqueous drug solution (phase separation). Thereafter, the nonsolvent is extracted with an appropriate solvent to harden the spherical precipitate, and then the organic and the appropriate solvents are removed, leaving the microspheres (78). The first application of this technique was to produce microspheres that released drugs such as enzymes, hormones, and vaccines over a prolonged period (98). A great deal of effort has been devoted to the encapsulation of highly water-soluble drugs because of the total entrapment. Typical nonsolvents are silicone oil and alkanes such as *n*-hexanes and *n*-heptanes. Tice et al. (99) and Sanders et al. (100) successfully used this method for the microencapsulation of highly water-soluble peptides into PLAGA copolymers. They used methylene chloride as the solvent of the polymer, silicone oil as the nonsolvent, and a large volume of *n*-heptane or *n*-hexane as the solvent to extract the silicone oil. The major disadvantage of this method is the large amounts of *n*-alkanes that have to be used and cannot be totally removed from the matrix. The microencapsulation of hydrophobic or lipophilic drugs by this technique has also been described (101,102).

The solvent evaporation method has been largely used to encapsulate lipophilic drugs (103–106). The preparation of microspheres by this method consists of two steps. First, the drug and the polymer are dissolved or dispersed in a water-immiscible solvent, and then the solution is poured into an aqueous medium while being stirred to form small polymer droplets containing the drug. In the second step, the droplets are hardened to yield microspheres. The hardening process is achieved by solvent evaporation under normal or reduced pressure. Hardening of droplets can also be achieved by solvent extraction using a third solvent that is a precipitant for the polymer and miscible with both water and the first organic solvent. The latter is usually methylene chloride, chloroform, or some other relatively volatile solvent that is a good solvent for PLA, PLAGA, and PCL polymers but difficult to remove completely. Solvent removal by extraction is generally much faster than evaporation (<1 h versus 4–20 h, respectively). Furthermore, solvent extraction can lead to microspheres that are more porous than can solvent evaporation. A combination of both methods is often preferred. Emulsification usually requires the use of a surfactant in rather large amounts. The most commonly used surfactants are

poly(vinyl alcohol), poly(vinylpyrrolidone), alginates, and gelatins. The surfactant molecules attached to the surface of microspheres are very difficult to eliminate and thus remain as an uncontrolled component in the formulation. Carrio et al. reported preparation of surfactant-free microspheres based on a $PLA_{37.5}GA_{25}$ copolymer, amphiphilic PLA_{50} oligomers being used for emulsification (107).

In the case of more or less water soluble drugs, the oil-in-water (O/W) emulsion system leads to poor entrapment. To solve this problem, the solvent evaporation method has been adapted to the cases of oil-in-oil (O/O) and of water-in-oil-in-water (W/O/W)–types emulsions. Tsai et al. were the first to describe an O/O emulsion technique to entrap mitomycin-C (108). A polar organic solvent dissolving a water-soluble drug and the polymer constitutes the dispersed phase, whereas a nonsolvent oil such as liquid paraffin dissolving a low hydrophilic-lipophilic-balanced value (HLB) emulsifier constitutes the continuous phase. Subsequently, the polar solvent is evaporated to yield a suspension of microspheres in the nonsolvent. After filtration, the microspheres are washed with an appropriate solvent to eliminate the residual oil. Tsai et al. (108) and Jalil and Nixon (109) used acetonitrile as the polar solvent, liquid paraffin as the nonsolvent, and Span 65 or 41 as the emulsifier. Ikada et al. used dimethylformamide as the polar solvent, caster oil or liquid paraffin as the nonsolvent, and lecithin or Span 80 as the emulsifier, to prepare PLA microspheres containing cisplatin by the O/O emulsion technique (110,111). These methods can also introduce pollutants, especially the nonsolvent as it is slightly soluble in the polar organic solvent. The presence of these pollutants must be taken into account as they may affect the properties of microspheres.

An alternative to these methods is spray-drying (112,113). This technique is very convenient for the incorporation of highly water-soluble drugs. Large scale production under mild conditions is possible as it is rapid and sequential. Nevertheless, agglomerates can be formed during the spray process, which require the use of surfactants. Another disadvantage is the possible contamination by minute particles of alien substances.

When one deals with degradable drug delivery devices, the first question is to know whether the manufacturing process affected the structural characteristics of polymers and whether solvents and surfactants were present. As mentioned earlier, the properties of the polymeric matrix can be dramatically changed during the manufacturing process.

DEGRADATION MECHANISMS

According to literature, the degradation of polymeric materials in a living environment can result from either enzymatically mediated or chemically mediated cleavages. The two mechanisms can act separately or simultaneously. Although in vivo environments are different from outdoor ones, there is no fundamental difference between the biodegradation of a polymer by animal cells and that by microorganisms. Both involve water, enzymes, metabolites, and ions that interact with the material (114). Under these conditions, one can distinguish enzymatic, hydrolytic, and microbial degradations.

Enzymatic Degradation

It is now well identified that biopolymers such as proteins, polysaccharides, polynucleotides, and even bacterial poly(β-alkanoates) degrade enzymatically (115–118), in agreement with the two main characteristics of living systems (i.e., degradation and recycling). The situation is totally different in the case of synthetic polymers. In fact, there has been much debate about the involvement of enzymes in the in vivo degradation of PLA, PGA, and PCL homo- and copolymers. Some authors argued in favor of a substantial enzymatic degradation (117,119,120), whereas most relegated the enzymatic involvement to a second role (116,121–124). The secondary differences between parenteral and outdoor conditions further increased the confusion. In some cases, enzymatic degradation was shown from differences between the behaviors of samples in the presence and in the absence of living organisms. In the case of in vitro studies, comparison was generally made between data in the presence and in the absence of enzymes. However, the observation of such differences is not conclusive because there are many other factors that may interfere with polymer degradation when experimental conditions are not similar (10). Therefore, the demonstration of enzymatic degradation (biodegradation) must be based on the concordance of data issued from different analytical methods and from a careful monitoring of the generation and the fate of the degradation products.

Various enzymes have been investigated in attempts to clarify their effect on the degradation of PLAGA polymers. Among them, bacterial proteinase K was shown to be able to strongly accelerate the degradation rate of PLA stereocopolymers (21,125–128), L-LA units being preferentially degraded as compared to D-LA (127,128). Enzymes such as tissue esterases, pronase, and bromelain also affect PLA degradation (120,125). In contrast, many other enzymes seem to be inactive. Pitt et al. investigated the in vivo degradation of a series of elastomeric homo- and copolymers of PCL and poly(valerolactone) cross-linked with biscaprolactone. These compounds were subject to bioerosion involving immediate attack at the surface (129,130). This finding was inferred by the rubbery nature of the materials, polymer chains having enough freedom to take on chain conformations convenient for enzymatic attack. The authors also noted that for degradable polymers in the glassy state, this conformation could hardly be achieved and thus small (if any) enzymatic degradation could occur. Mochizuki et al. examined the enzymatic degradation of PCL fibres by Lipase (131). Scanning electron microscopy (SEM) photographs showed that the enzyme preferentially attacked amorphous regions rather than crystalline ones. As enzymatic degradation proceeded, the diameter of the fibers became gradually slimmer.

It should be noted that enzymes can be inactive on high molar mass material and become active at the later stages of degradation when the chain fragments become small and soluble in surrounding fluids. Once formed during degradation, tiny crystalline particles can be phagocytosed

and undergo intracellular degradation (132). Microspheres can also be easily phagocytosed (133).

In conclusion, it is now generally admitted that in the case of glassy aliphatic polyesters such as PLA, PGA, and their copolymers, enzyme involvement is unlikely at the early stages of degradation in vivo or under outdoor conditions. However, enzymes contribute at the later stages, especially when soluble by-products are released. In contrast, for rubbery polymers like cross-linked PCL, enzymes seem to be active from the very beginning via surface erosion phenomena (129,130). Actually, enzymatic degradation of aliphatic polyesters should not be claimed unless mass loss and dimensional changes without molar mass decrease are shown, and nonenzymatic degradation is excluded. So far, one can hardly consider that the biodegradation of linear PCL in the presence of enzymes has been clearly depicted.

Hydrolytic Degradation

Basically, the hydrolytic degradation of aliphatic polyesters proceeds through ester bond cleavage according to the reaction:

$$R{\sim}COO{\sim}R' + H_2O \longrightarrow R{\sim}COOH + HO{\sim}R'$$

From the macroscopic viewpoint, degradation of aliphatic polyesters has been regarded as homogeneous, although surface erosion was claimed occasionally. Ginde and Gupta investigated the in vitro degradation of PGA pellets and fibers in aqueous media at different pH values (134). The authors found that pellets showed considerable surface degradation, whereas fibers showed little surface changes. Singh et al. studied a drug delivery system based on PLA_{50} microcapsules and concluded erosion-based degradation, the hydrolytic cleavage of ester bonds in the polymer backbone at the surface of microcapsules leading to the formation of lactic acid monomers (135). Kimura et al. investigated the in vitro and in vivo degradations of fibers deriving from a copoly(ester-ether) composed of PLA_{100} and polyoxypropylene blocks (136). Surface erosion was observed in both cases and the authors concluded that hydrolysis was limited to the surface.

In contrast, many authors argued either explicitly or implicitly in favor of autocatalyzed bulk degradation. Hutchinson investigated the in vitro and in vivo release of polypeptides ($633 < \bar{M}_n < 22{,}000$ Da) from PLAGA copolymer matrices containing from 25% to 100% DL-lactic acid. The degradation process of the polymer matrix was considered as homogeneous (137). Sanders et al. studied a $PLA_{22}GA_{56}$ microsphere-based delivery system and observed a homogeneous (bulk) rather than heterogeneous (surface) degradation (138). This conclusion was derived from the biological response and from changes in microsphere aspects in vivo. Kenley et al. examined a series of PLAGA copolymers representing a range of monomer ratios and molar masses, with the goal of studying polymer degradation kinetics in vivo and in vitro (139). Hydrolysis was supposed to proceed throughout the bulk of the polymer structure because the onset of mass loss lagged behind molar mass decrease. Schakenraad et al. (140) and Helder et al. (141) investigated a series of glycine/DL-lactic acid copolymers in vivo and in vitro. Bulk hydrolysis was described as the degradation mechanism in both cases, molar mass decreasing continuously with the aging time. Cohen et al. used a PLAGA (75/25) copolymer for long-term delivery of high molar mass water-soluble proteins (142). At all times, molar mass distribution displayed a unimodal pattern, suggesting homogeneous degradation. St. Pierre and Chiellini reviewed the degradability of synthetic polymers for pharmaceutical and medical uses. These authors concluded that hydrolysis of PLAGA polymers was a bulk process with random cleavage of ester functions (143). In another review concerning the controlled release of bioactive agents from PLAGA polymers, Lewis concluded that degradation of aliphatic polyesters occurred in the bulk (144).

Pitt et al. studied the in vivo degradation of films of PLA_{50}, PCL, and corresponding copolymers. The authors suggested that the first stage of degradation was confined to a molar mass decrease due to random hydrolytic ester cleavage autocatalyzed by the carboxyl endgroups, the second stage being characterized by the onset of mass loss and a decrease in the rate of chain scission (82,145).

The kinetics of the autocatalyzed hydrolytic degradation proposed by Pitt et al. were derived according to the following equations:

$$d[E]/dt = -d[COOH]/dt = -k[COOH] \cdot [H_2O] \cdot [E] \quad (1)$$

where [COOH], $[H_2O]$, and [E] represent, respectively, carboxyl endgroup, water, and ester concentrations in the polymer matrix. By using the following relationships:

$$[COOH] = M/(\bar{M}_n \cdot V) = \rho/\bar{M}_n$$

$$[COOH] = [E]/(\overline{DP}_n - 1)$$

$$\bar{M}_n = m \cdot \overline{DP}_n$$

where M is the polymer matrix mass, V its volume, ρ its mass volume unit, $\bar{M}_n$ the number average molar mass, $\overline{DP}_n$ the number average degree of polymerization and m the repeat unit mass, one obtains equation 2:

$$d(1/\overline{DP}_n)/dt = k(\rho/m)[H_2O](\overline{DP}_n - 1)\overline{DP}_n^{-2} \quad (2)$$

Integration of equation 2 leads to equation 3:

$$\ln\{(1 - \overline{DP}_n)/(1 - \overline{DP}_{n0})\} = k't \quad (3)$$

where $k' = k(\rho/m)[H_2O]$, and $\overline{DP}_{n0}$ is the $\overline{DP}_n$ at time zero. This kinetic expression is valid before the onset of mass loss. If $\overline{DP}_n \gg 1$, equation 3 can be simplified to equation 4:

$$\ln(\overline{DP}_n/\overline{DP}_{n0}) = \ln(\bar{M}_n/\bar{M}_{n0}) = -k't \quad (4)$$

According to this relationship, semilog plots of $\overline{DP}_n$ or of $\bar{M}_n$ versus hydrolysis time should be linear prior to the onset of mass loss, a feature that was observed experimentally (145).

Next Page

A few years ago, the discovery of a faster degradation inside large-size PLA_{50} specimens greatly changed the understanding of the hydrolytic degradation of PLAGA polymers (146). The heterogeneous degradation was assigned to diffusion-reaction phenomena. Typically, the polymer matrix is initially homogeneous in the sense that the average molar mass is the same throughout the matrix. Once placed in an aqueous medium, water penetrates into the specimen leading to hydrolytic cleavage of ester bonds. Each ester bond cleavage forms a new carboxyl endgroup that, according to autocatalysis, accelerates the hydrolytic reaction of the remaining ester bonds (147). At the very beginning, degradation occurs in the bulk and is macroscopically homogeneous. However, the situation becomes totally different when soluble oligomeric compounds are generated in the matrix. The soluble oligomers that are close to the surface can escape from the matrix before total degradation, whereas those located inside the matrix can hardly diffuse out of the matrix. This difference results in a higher acidity inside than at the surface. When the aqueous medium is buffered at neutral, as is the case in vivo, the neutralization of carboxyl endgroups present at the surface can also contribute to decrease the surface acidity. Therefore, autocatalysis is larger in the bulk than at the surface, thus leading to a surface-interior differentiation. As the degradation proceeds, more and more carboxyl endgroups are formed inside to accelerate the internal degradation and enhance the surface-interior differentiation. Bimodal molar mass distributions are observable due to the presence of two populations of macromolecules degrading at different rates (Fig 4). Finally, hollow structures are formed when the internal material, which is totally transformed to soluble oligmers, dissolves in the aqueous medium (Fig. 5). Similar features were observed for other amorphous polymers like $PLA_{62.5}$, PLA_{75}, and $PLA_{37.5}GA_{25}$ (148–153). In contrast, in the case of crystallizable polyesters like $PLA_{87.5}$, PLA_{96}, PLA_{100}, $PLA_{75}GA_{25}$, and $PLA_{85}GA_{15}$, no hollow structures were obtained due to the crystallization of degradation products (Fig. 6), although degradation was faster inside than outside (148–153).

The faster internal degradation of PLA and PLAGA polymers is now regarded as a general phenomenon. It was confirmed by many authors (154–160), and for PLACL copolymers (161), lactide-glycine copolymers (140,141), lactide-1,5-dioxepan-2-one copolymers (162), poly(trimethylene carbonate) (163), and poly(*para*-dioxanone) as well (164). According to diffusion-reaction phenomena, small devices should degrade more slowly (*i.e.*, at the surface rate) than large ones since thinness favors the elimination of soluble oligomeric compounds and minimizes the autocatalytic effect. This trend was confirmed by comparing the degradation rates shown by submillimetric microparticles and films and millimeric plates made from the same PLA_{50} (165). As expected, the plates degraded faster than the microparticles and films.

In the case of PCL, hydrolytic degradation is very slow. However, the degradation mechanism is the same as that of PLAGA polymers. Typically, degradation of PCL begins

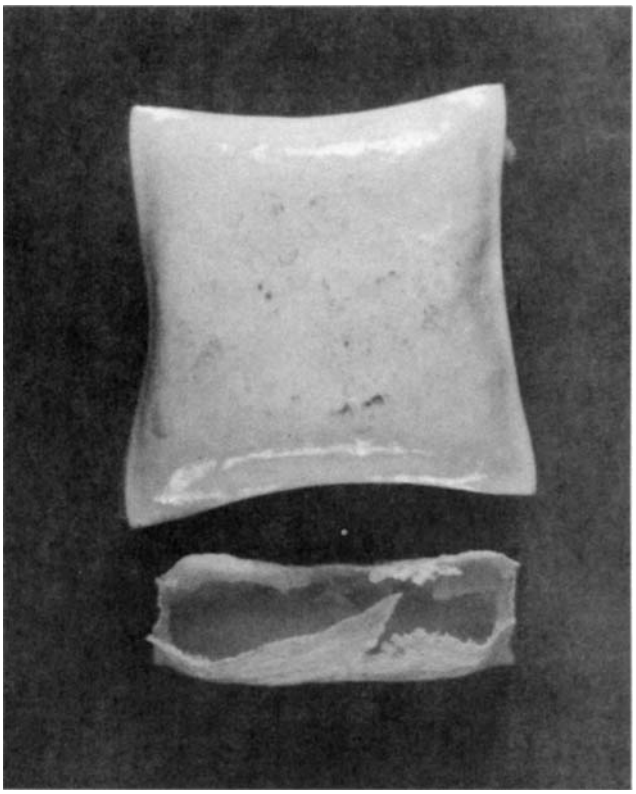


Figure 5. Hollow structure and cross section of a PLA_{50} plate after 17 weeks in a pH 7.4 phosphate buffer at 37°C. *Source:* From Ref. 182.



Figure 6. Cross section of a PLA_{96} plate after 40 weeks in a pH 7.4 phosphate buffer at 37°C. *Source:* From Ref. 150.

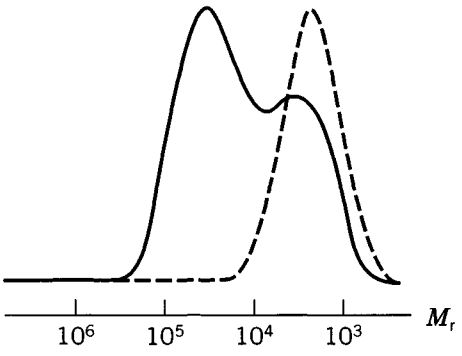


Figure 4. SEC chromatograms of PLA_{50} plates after 7 weeks in saline at 37°C: ——— (surface), --- (interior). *Source:* From Ref. 146.

Previous Page

with random hydrolytic cleavage of the ester linkages autocatalyzed by the carboxyl endgroups. The molar mass decreases continuously, but there is no weight loss during this first stage of degradation. The second phase is characterized by the onset of weight loss due to the formation of low molar mass fragments small enough to diffuse out of the bulk (82,161,166). No faster internal degradation has been reported for the PCL homopolymer so far, probably because of the combination of high crystallinity, hydrophobicity, and low degradation rate.

Therefore, the hydrolytic degradation of aliphatic polyesters is a complex process involving four main phenomena, namely water absorption, ester cleavage, diffusion of soluble oligomers, and solubilization of fragments (167). These phenomena depend on many factors such as matrix morphology, chemical composition and configurational structure, molar mass, size, distribution of chemically reactive compounds within the matrix, and nature of the degradation media (11). Considering the interdependence of degradation and drug release in controlled drug delivery systems, all the factors listed here can affect the characteristics of drug release, as will be shown later.

Microbial Degradation

More and more attention is paid to aliphatic polyesters of the PLA, PGA, and PCL types with respect to the problems of solid waste accumulation, delivery of chemicals to plants, and seed protection. Whether these polymers can biodegrade in a wild environment or whether it is the by-products generated by abiotic hydrolysis that can be bioassimilated by fungi or bacteria are two currently investigated questions, particularly in the area of composting.

Torres et al. studied the ability of some microorganisms to use lactic acids, PLA oligomers and polymers, and PLAGA copolymers as sole carbon and energy sources under controlled or natural conditions (168–170). Among the 14 filamentous fungal strains tested, two strains of *Fusarium moniliforme* and one strain of *Penicillium roqueforti* were identified as able to totally assimilate L- and DL-lactic acids as well as PLA_{50} oligomers (168,169). In contrast, PLA_{100} oligomers appeared biostable because of the crystallinity. A synergistic effect was observed when both microorganisms were present in the same culture medium containing PLA_{50} oligomers.

High molar mass polymers were also considered via degradation tests in soil and in selected culture media. *Fusarium moniliforme* filaments were found to grow on the surface of a $PLA_{37.5}GA_{25}$ copolymer and through the bulk. On the other hand, five strains of different filamentous fungi were isolated from the soil as capable of bioassimilating PLA_{50} soluble oligomers in mixed cultures. Based on the results obtained by SEM, size exclusion chromatography (SEC), pH, and water absorption measurements, the authors proposed a mechanism including abiotic hydrolysis of macromolecules followed by bioassimilation of soluble oligomers (170). Therefore, when a PLA material is placed in a degradation medium in the presence of microorganisms, only abiotic hydrolytic degradation occurs unless the few enzymes mentioned already as capable of degrading high molar mass PLA are present. Whether the degradation is homogeneous or heterogeneous depends on the size of the material and on the physical state of the medium (liquid or moisture). In a liquid medium, degradation is heterogeneous due to larger internal autocatalysis for large-size devices, whereas in the case of a humid environment, degradation has to be homogeneous since the soluble oligomers cannot diffuse out of the matrix. Anyhow, sooner or later, low molar mass assimilable oligomers are formed throughout the polymer matrix. The bioassimilation process then takes place. At this time, fungal filaments penetrate the partially degraded mass to take advantage of the internal oligomers, thus turning the abiotic degradation to a biotic one. Under wild conditions, this should happen after a long lag period. However, PLA polymers are definitely degraded and assimilated because the ultimate degradation products (L- and D-lactic acids) have been shown to be metabolized by some common microorganisms (170). In particular, it is now well known that PLA polymers degrade completely and rather rapidly in compost where the temperature is usually between 50 and 60°C.

Jarrett et al. investigated the microbial degradation of cross-linked PCL films and of PCL single crystals in the presence of a yeast, *Cryptococcus laurentii*, and a fungus, *Fusarium*. Data were compared with those obtained for the chemical degradation in a 40% methyl amine aqueous solution (171). These microorganisms produced both endo- and exoenzymes and a cofactor (surfactant), which worked together in the degradation of the polymer. In the absence of the cofactor, the access of enzyme to the hydrophobic polymer was limited. Lefebvre et al. examined the biodegradation of hydroxy- or methoxy-terminated PCL samples by mixed cultures of microorganisms issued from a suspension of compost, and also by a pure culture of an actinomycete isolated from compost (172). The authors suggested that the initiation of degradation took place in the vicinity of the chain ends. Methylation of the chain ends did not affect the biodegradability. Akahori and Osawa investigated the biodegradability of PCL-paper composites by outdoor exposure and outdoor soil burial (173). All the samples crumbled within 6 months. Molar mass of residual PCL was found to decrease slowly, suggesting the contribution of hydrolytic degradation.

FACTORS INFLUENCING POLYMER DEGRADATION AND DRUG DELIVERY

In the preceding paragraphs, we have underlined some of the main structural, physical, chemical, and biological characteristics of PLAGA and PCL polymers. Let us now consider the various factors that can affect the degradation of aliphatic polyesters as well as the drug delivery profiles. For the sake of clarity, these factors will be discussed separately, although most of them are interdependent.

Polymer Morphology

The morphology of a polymeric material (i.e., amorphousness or semicrystallinity) plays a critical role in both the enzymatic and nonenzymatic degradation processes. It is now known that degradation of semicrystalline polyesters

in aqueous media occurs in two stages. The first stage consists of water diffusion into the amorphous regions with random hydrolytic scission of ester bonds. The second stage starts when most of the amorphous regions are degraded. The hydrolytic attack then progresses from the edge towards the center of crystallites (174–176). This phenomenon was first observed by Fischer et al. who investigated the structure of solution-grown crystals of PLA stereocopolymers by means of chemical reactions (174). Disordered regions of single crystals were found to be selectively degraded by methanolic sodium hydroxide. In the case of a $PLA_{92.5}$ stereocopolymer, the authors obtained a trimodal molar mass distribution with three distinct peaks corresponding respectively to onefold, twofold, and threefold the crystalline lamellae thickness. Later on, many authors reported a preferential degradation of amorphous areas in the case of semicrystalline Vicryl® pellets or sutures (175–177), Dexon® sutures (177,178), and PLA_{100} plates and rods (179,180). An increase of crystallinity was often detected (175–180). On the other hand, Miller et al. observed that fast-cured PGA degraded more rapidly than slow-cured one (26), the in vivo half-lives being 0.85 and 5 months, respectively. The difference was related to the higher crystallinity of the latter. Gutwald et al. also observed a faster resorption of amorphous PLA_{100} implants as compared to crystalline ones (181). Last but not least, the degradation rate of PGA pellets was found to be much faster than that of fibers with similar crystallinity (134). This feature was assigned to the presence of long range order in fibers. Therefore, chain orientation could also play an important role in the hydrolytic degradation.

Recent systemic investigation on the in vitro degradation of PLAGA polymers well agreed with the preferential degradation in amorphous zones of semicrystalline PLA_{100}. Bimodal molar mass distributions were detected at the later stages of degradation, the two peaks corresponding to onefold and twofold the thickness of crystalline lamellae, respectively (149). On the other hand, crystallization was observed in the case of initially amorphous PLA_{100} and PLA_{96} obtained by quenching (149,150), as shown in Figure 7. Crystallization mainly resulted from low molar mass chains whose T_g was lower than that of longer chains. With the plasticizing effect of absorbed water, which further decreased the T_g, these short chains were mobile enough to crystallize under the degradation conditions. The resulting crystallites were more resistant to further degradation. As a consequence, a very narrow peak corresponding to low molar mass crystalline zones was detected by SEC (Fig. 8).

Among the various PLA_x stereocopolymers, the polymer is intrinsically amorphous if X is in the 10 to 90 range (11). For PLA_XGA_Y copolymers, the polymer is intrinsically amorphous when Y is in the 10 to 70 range (for L-LA) or in the 0 to 70 range (for DL-LA) (19). However, one must be careful with these divisions because of the variable extents of transesterification reactions, which tend to randomize the comonomer distribution along the chains. The fate of intrinsically amorphous polymers during degradation appeared more complex depending on chain structures. Two classes can be distinguished. The first class consists of polymers that can never crystallize. The second one groups together polymers that can crystallize during degradation. $PLA_{37.5}GA_{25}$ is a good example of the first class, whereas PLA_{50}, $PLA_{62.5}$, PLA_{75}, $PLA_{87.5}$, $PLA_{75}GA_{25}$, and $PLA_{85}GA_{15}$ belong to the second class. $PLA_{37.5}GA_{25}$ cannot crystallize even after degradation due to the high irregularity of its chain structure. The others are crystallizable because of the presence of isotactic blocks which, once released by degradation, can crystallize. For example, a crys-

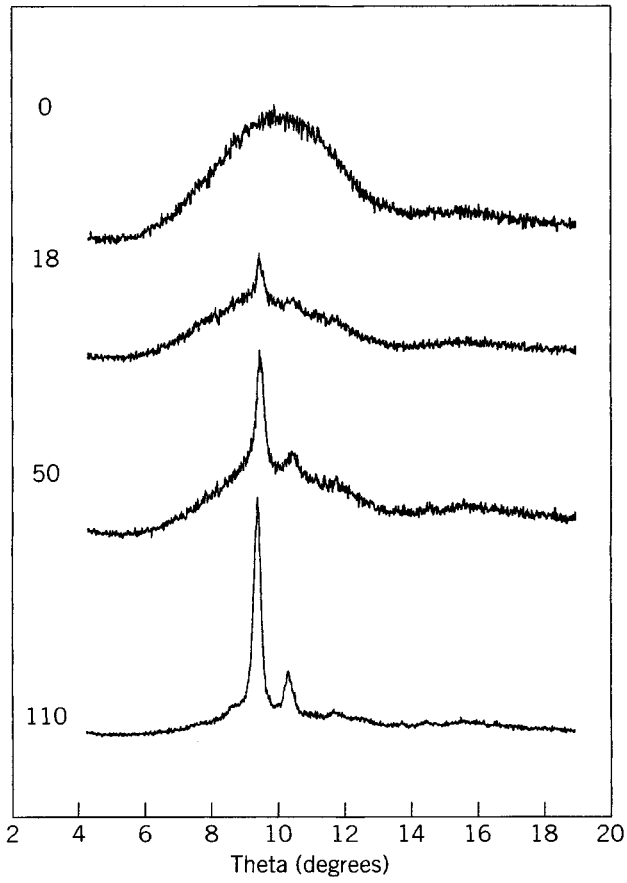


Figure 7. X-ray diffraction spectra of initially amorphous PLA_{100} plates after 0, 18, 50, and 110 weeks in a pH 7.4 phosphate buffer at 37°C. *Source:* From Ref. 149.

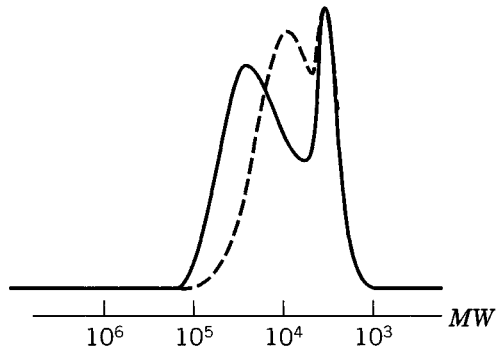


Figure 8. SEC chromatograms of initially amorphous PLA_{100} plates after 70 weeks in a pH 7.4 phosphate buffer at 37°C: ——— (surface), ---- (interior). *Source:* From Ref. 149.

talline oligomeric stereocomplex composed of L-LA and D-LA–rich segments was detected at the end of PLA_{50} degradation (182). The stereoregular segments were initially present within the PLA_{50} matrix, which is known to have a predominantly isotactic structure resulting from the pair-addition mechanism of DL-lactide polymerization (27). $PLA_{62.5}$ leads also to slightly crystalline residues of the stereocomplex type (153). In contrast, PLA_{75} and $PLA_{87.5}$ degradation residues have the same crystalline structure as PLA_{100} (153). Insofar as $PLA_{75}GA_{25}$ and $PLA_{85}GA_{15}$ are concerned, GA units are more hydrophilic than LA ones and, as a consequence, are more inclined to hydrolysis. The preferential degradation of GA units results in L-LA-enriched segments which can crystallize under the degradation conditions, as shown by the appearance of a melting peak on differential scanning calorimetry (DSC) thermograms (Fig. 9). However, the structure of the crystalline residues is slightly different from that of PLA_{100} due to the inclusion of GA units in the crystalline domains (148,150).

A schematic representation is given in Figure 10. The triangle can be divided in two types of zones: C zones are composed of intrinsically crystalline polymers and A zones of intrinsically amorphous polymers. For polymers in C zones, if they are prepared in an amorphous state by quenching, degradation is characterized by crystallization

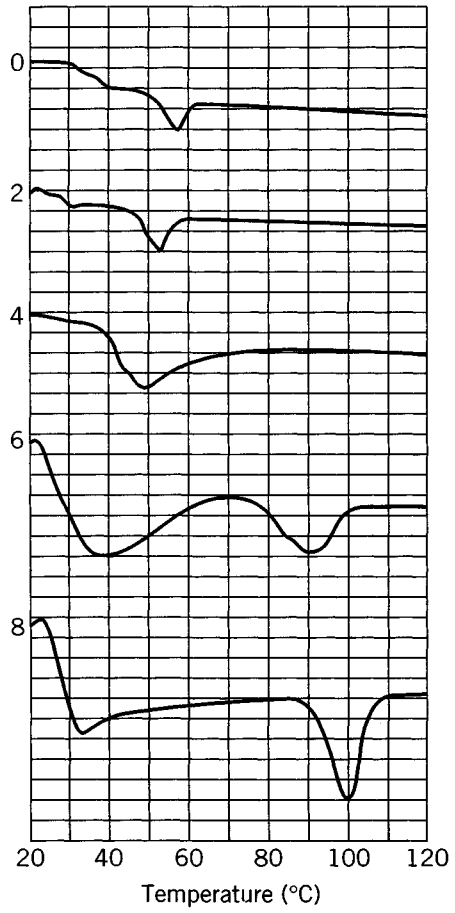


Figure 9. DSC thermograms of $PLA_{75}GA_{25}$ plates after 0, 2, 4, 6, and 8 weeks in vivo degradation. *Source:* From Ref. 151.

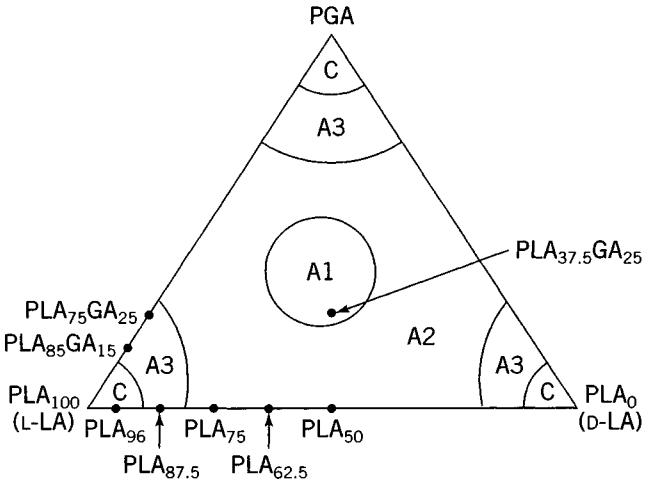


Figure 10. Schematic presentation of the morphological changes of PLAGA polymers with degradation. *Source:* From Ref. 11.

of degradation by-products. If they are prepared in a semicrystalline state by annealing, degradation is characterized by selective degradation of amorphous regions. In both cases, no hollow structures are obtained for large-size devices in spite of the heterogeneous degradation. In the case of amorphous polymers, three subzones can be distinguished: A1, A2, and A3. For A1 polymers, degradation leads to hollow structures that remain amorphous due to the high irregularity of polymer chain structures. For A2 polymers, degradation also leads to hollow structures that partially crystallize, the crystalline structure depending on the initial composition. For A3 polymers, no hollow structures can be obtained, both the surface and interior crystallize. It is noteworthy that degradation of small-size amorphous polymers does not lead to hollow structures, but morphological changes are comparable to large-size ones (183).

All these examples and comments demonstrate that polymer morphology and morphological changes have to be taken into account to control the hydrolytic degradation of PLAGA polymers.

PCL and its copolymers with PLA have also been largely investigated. Pitt et al. observed a steady increase in crystallinity of PCL films from 45% to nearly 80% after 120 weeks' implantation, which was attributed to the crystallization of tie segments after chain cleavage in the amorphous phase. The low glass-transition temperature of PCL ($T_g = -60°C$) facilitated the recrystallization (166). In a detailed study on the microbial and enzymatic degradation of PCL films, Jarrett et al. showed that amorphous material on the top and bottom faces of the crystallites degraded most rapidly, leading to multimodal molar mass distributions (171). Li et al. observed a crystallinity increase during the in vitro degradation of PCL: from initial 47% to 75% after 200 weeks (161). Water absorption was very limited (less than 2%) during the first 63 weeks due to the high crystallinity and hydrophobicity of PCL. Thereafter, water absorption increased more rapidly. It reached 8.1% at 133 weeks and 12.5% at 200 weeks, which can be related

to molar mass decrease and formation of more carboxyl endgroups. On the other hand, weight loss reached 3.4% at 63 weeks, 10.7% at 133 weeks and 14.2% at 200 weeks. Insofar as molar mass changes are concerned, it decreased steadily from initial 58,700 to 7,000 after 200 weeks. After 133 weeks, the molar mass distribution became trimodal due to the selective degradation of amorphous zones and of the crystallite edges, the molar masses of the three peaks being 2,600, 5,200, and 8,800, respectively (Fig. 11). In the case of a Zn metal–initiated $PLA_{60}CL_{40}$ copolymer, the degradation rate was very much enhanced as shown by the increased water absorption and weight loss rates compared with the parent homopolymers PCL and PLA_{100}. Crystallinity increased from initial 14% to 54% at 133 weeks. The crystalline structure was of the PLA_{100} type, showing a phase separation between the two components (161).

From the results presented here, it can be predicted that the morphology of the polymeric matrix should greatly influence the drug release profiles, because for both diffusion and degradation controlled mechanisms, the matrix morphology is a determining factor. Izumikawa et al. investigated PLA_{100}-progesterone microspheres of different morphologies obtained by changing the pressure in the solvent evaporation process (184). Microspheres made of amorphous PLA_{100} were obtained by removing the solvent under reduced pressure. Data showed that the microspheres of crystalline polymeric matrices had rough surfaces with large surface areas and exhibited a rapid drug release. In contrast, the microspheres of amorphous polymeric matrices had smooth surfaces with smaller surface areas and provided a slower drug release. Similarly, Jalil and Nixon investigated the release of phenobarbitone from PLA_{100} microspheres (185). The authors observed that the release profile was highly dependent on the polymer molar mass. The porous nature of the microspheres prepared from high molar mass polymer allowed a very fast release and even the smooth microsphere surface obtained from low molar mass PLA_{100} failed to retain the drug for any extended time. This was attributed to the semicrystallinity of PLA_{100}. Fong et al. evaluated microspheres of thioridazine and ketotifen with a series of PLAGA polymers (186). Drug release was frequently slower with microspheres made from the amorphous PLA_{50} and faster with those from the crystalline PLA_{100}. Recently, Mauduit et al. prepared gentamycin-PLA microparticles by grinding and sieving the solid mass resulting from mixing various amounts of drug and polymer in an acetone solution. The aim was to design a delivery system for local antibiotic therapy administered peroperatively. For PLA_{50} systems, the release profile was biphasic with an initial burst followed by a sustained release lasting for more than two months (97). In contrast, the total load was released within the first 6 hours in the case of PLA_{100} microparticles. In both cases, the drug release profile was correlated to the morphology of the polymeric matrix rather than to its degradability.

Therefore, it can be concluded that amorphous polymers are preferable for sustained drug delivery systems because they usually yield a smooth surface and an uniform structure, which retains the drug for long periods of time. In contrast, semicrystalline polymers generally lead to rough surfaces and porous structures, which are not suitable for sustained delivery of drugs.

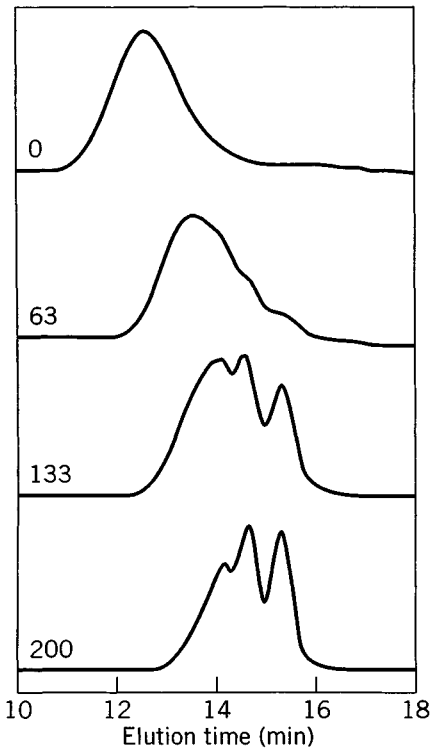


Figure 11. SEC chromatograms of PCL plates after 0, 63, 133, and 200 weeks in a pH 7.4 phosphate buffer at 37°C. *Source:* From Ref. 161.

Chemical Composition and Configurational Structure

It is now well known that the composition of polymer chains (i.e., the contents in L-LA, D-LA, and/or GA units) greatly determines the degradation rate of PLAGA polymers (9–11,24). PLA_X stereocopolymers have variable degradation rates. PLA_{50} degrades the most rapidly, whereas PLA_{100} is the most stable member of the series (24). The copolymerization of LA with GA enhances considerably the degradation rate as compared with the parent homopolymers (26,187–192).

Cutright et al. carried out a systemic in vivo degradation study on a series of PLAGA homo- and copolymers. The degradation rate of these polymers was found to increase as follows: PGA < PLA_{100} < $PLA_{75}GA_{25}$ < $PLA_{50}GA_{50}$ < $PLA_{25}GA_{75}$ (187), showing that degradation rates can be adjusted by varying the proportion of LA to GA. Later, Miller et al. found a slightly different and more logical order: PLA_{100} < PGA < $PLA_{75}GA_{25}$ < $PLA_{25}GA_{75}$ < $PLA_{50}GA_{50}$ (26). The half-life of these polymers decreased from 5 months for PGA to 1 week for $PLA_{50}GA_{50}$ and rapidly increased to 6.1 months for PLA_{100}. Reed and Gilding investigated comparatively the in vitro degradation of PLA_{100}, PGA, and $PLA_{50}GA_{50}$ (188). The authors observed that PGA sutures were totally degraded within

10 to 12 weeks, $PLA_{50}GA_{50}$ discs within 2 to 4 weeks, whereas PLA_{100} discs lost only 10–15% of mass over a period of 16 weeks. Kaetsu et al. developed implantable luteinizing hormone releasing hormone (LHRH) agonist–PLAGA polymer composites and observed that in vivo degradation and release rates could be altered over a wide range by changing molar mass, stereoisomerism, crystallinity, and composition of copolymers (84). PLA_{50} was found to degrade faster than PLA_{100} and, more surprisingly, PLA_{100} degraded faster than PLA_0 (84). Zhu et al. carried out an in vivo degradation study of several PLAGA homo- and copolymers and found that all corresponding threads were completely absorbed by 60 days (189). Ogawa et al. studied the in vivo degradation of $1 \times 10 \times 10$ mm plates made of PLAGA polymers. Both the lag time and the half-life decreased with the increase in GA content (190). Amarpreet and Hubbell prepared a series of 66 terpolymers of DL-lactide, glycolide, and ϵ-caprolactone (191). The half-lives of these polymers were found to vary from a few weeks to several months. Thomasin et al. examined the in vitro degradation of a series of PLA_{50} and PLAGA microspheres (192). With similar molar masses, $PLA_{25}GA_{50}$ degraded faster than $PLA_{37.5}GA_{25}$, PLA_{50} exhibiting the slowest degradation rate.

In the early 80s, Vert et al. pointed out the discrepancies in the literature concerning the degradation rates of various PLAGA polymers and attributed them to the fact that polymeric materials identified by the same name can be very different compounds due to secondary factors related to the origins of the compounds (24). Their analysis led to the conclusion that the time period required for complete resorption of these polymers should be substantially longer than previously supposed. Eitenmüller et al. showed similar trends (193).

A systemic investigation of the degradation characteristics of various large-size PLAGA plates under comparable conditions provided a more consistent pattern. The half-life in terms of mass loss of initially amorphous PLA_{100} was found to be about 110 weeks and that of crystallized PLA_{100} was even longer (149). The introduction of 4% of D-LA units to L-LA chains considerably enhanced the degradation rate since PLA_{96} had a half-life of about 90 weeks (150). PLA_{50} degraded much more rapidly than PLA_{100} and PLA_{96} with a half-life of 10 weeks (146). In the case of the copolymers, $PLA_{37.5}GA_{25}$ had a half-life of 3 weeks only (148). All these data are recalled in Table 4.

Table 4. In Vitro Degradation Rates of PLAGA Polymers

Polymer	$\overline{M}_w$ (E − 3)	$\overline{M}_w/\overline{M}_n$	Half-life (weeks)
PLA_{100}	130.0	1.8	110
PLA_{96}	100.0	1.7	90
$PLA_{87.5}$	190.4	1.9	80
PLA_{75}	48.6	1.6	22
$PLA_{62.5}$	67.6	1.9	23
PLA_{50}	65.0	1.6	10
$PLA_{85}GA_{15}$	112.0	1.8	20
$PLA_{75}GA_{25}$	111.0	1.8	10
$PLA_{37.5}GA_{25}$	51.0	1.6	3

It is noteworthy that the degradation rate of a polymer is closely related to the rate of water absorption or swelling. Intrinsically semicrystalline polymers are generally less inclined to water diffusion and swelling, in contrast to amorphous ones. For example, PLA_{100} and PLA_{96} absorbed respectively 7% and 12% after 10 weeks in phosphate buffer, whereas PLA_{50} absorbed 150% and largely swelled (146,149,150). In the cases of PLAGA copolymers, $PLA_{75}GA_{25}$ absorbed only 3% after 3 weeks, whereas $PLA_{37.5}GA_{25}$ absorbed 23% in the meantime (148). Again, the rate and ratio of water absorption depend on many factors such as initial morphology, chemical composition and configurational structure, molar mass and molar mass distribution, and polymerization conditions.

Attention has scarcely been paid to chemical composition changes of the copolymers in the field of drug delivery. Hutchinson and Furr reported that the LA/GA ratio increased with degradation of PLAGA copolymers as GA blocks degraded preferentially (137). In contrast, Fredericks et al. claimed that there was no preferential attack on either the LA or GA units of Vicryl® polymer chains despite the difference in hydrophilicity (176). Degradation-related composition changes were observed in the case of $PLA_{75}GA_{25}$ and $PLA_{85}GA_{15}$. The L-LA-enriched segments crystallized under in vitro degradation conditions to form crystalline zones of relatively low molar masses (148,150). The crystallization limited in return the preferential degradation of GA units included in crystalline zones, as confirmed recently by Grijmpa et al. (194). In the case of $PLA_{37.5}GA_{25}$, no significant preferential degradation of GA units was observed probably due to the fact that $PLA_{37.5}GA_{25}$ degraded too fast (148).

Copolymers of PLA or PGA with PCL have also been considered. Pitt et al. investigated the in vivo degradation of copolymers of ϵ-caprolactone with DL-lactide in rabbits (82). Copolymers with 11, 23, 47, and 90 mol % DL-lactide degraded much more rapidly than corresponding homopolymers. Song et al. studied the degradation of random and block copolymers of ϵ-caprolactone with DL-lactide and found that the random copolymers degraded faster than the parent homopolymers, block copolymers degrading at intermediate rates (195). Li and Feng investigated the degradation behaviors of ABA, ABC, and ACB triblock copolymers of ϵ-caprolactone (A), DL-lactide (B), and glycolide (C) in water at 37°C and 50°C (196). The order of degradation rates of the different phases was found to be $C > B \gg A$, which permitted various degradation rates by changing copolymer composition. During the degradation process, the crystallinity of the A phase increased. The composition changed too, with an increase in A content and a decrease in B and C. Fukuzaki et al. synthesized a series of low molar mass L-LA-CL copolymers by direct condensation, and studied the in vivo degradation by subcutaneous implantation in the back of rats (22). Pasty copolymers (30–70 mol % CL) degraded faster than solid (0–15 mol % CL) and waxy copolymers (85–100 mol % CL).

The chain structure of the copolymers can be characterized by NMR. In Figure 12, the ^1H NMR spectra of a $PLA_{60}CL_{40}$ copolymer and of the homopolymers PCL and PLA_{100} are shown (161). Comparative analysis of these spectra allowed a complete assignment of all the signals

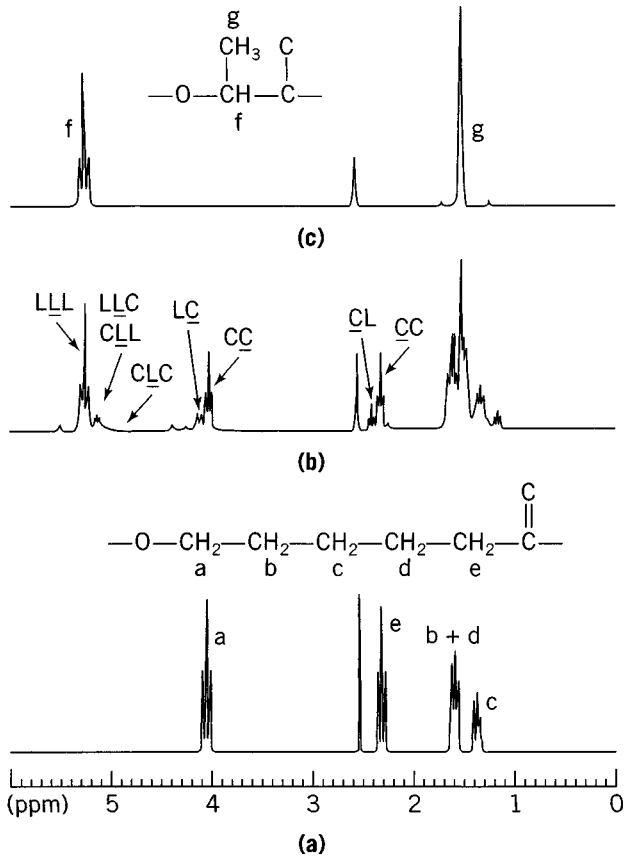


Figure 12. ^{1}H NMR spectra of (**a**) PCL (**b**), $PLA_{60}CL_{40}$, and (**c**) PLA_{100} in DMSO-d_6 solutions. Spectra (**a**) and (**c**) were obtained at 80°C due to their insolubility at 30°C. *Source:* From Ref. 161.

observed for each type of protons. Average sequence lengths $\bar{L}_{PLA}$ and $\bar{L}_{PCL}$ were determined by using the following equations:

$$\bar{L}_{PLA} = ([LLL] + [LLC] + [CLL] + [CLC]) \div \{[CLC] + 1/2([LLC] + [CLL])\} \quad (5)$$

$$\bar{L}_{PCL} = ([CC] + [CL])/[CL] \quad (6)$$

Compositional changes with degradation were also followed by ^{1}H NMR. Appearance of lactic acid and of lactyl end units was detected on the ^{1}H NMR spectrum. On the other hand, the signal of CC dyads progressively diminished as compared to that of LC ones, which was related to the crystallization of lactyl blocks (161).

Espartero et al. carried out a detailed analysis on the ^{1}H and ^{13}C NMR spectra of L- and DL-lactic acid oligomers (197). The use of DMSO-d_6 as a solvent led to a higher spectral resolution as compared to chlorinated solvents. Systematic comparison of oligomer spectra led to the identification of a linearly additive neighboring effect. Assignment of all the ^{13}C NMR chemical shifts belonging to the different constitutive units was realized up to the octamer. Besides, the well-identified positions of the resonances of chain end units in the ^{1}H NMR spectra permitted determination of the absolute average degree of polymerization of oligomers issued from polycondensation. These findings are of great interest for the study of the ultimate degradation stages of PLA and various copolymers (197).

The drug delivery profiles are also dependent on chemical composition and configurational structure. Ogawa et al. studied the in vivo release of leuprolide acetate from microspheres based on PLAGA copolymers. The drug release profile well agreed with that of the polymer degradation (190). Heya et al. investigated the release of thyrotropin-releasing hormone (TRH) from DL-LA/GA copolymer microspheres of rather low molar masses with LA/GA ratio varying from 100/0 to 50/50. The authors found that after the initial burst, the release rate was dominated mainly by the degradation of the copolymer (198). The microspheres prepared with a higher GA content exhibited a faster release rate.

Pitt et al. developed progesterone release systems (films and microspheres) of homo- and copolymers deriving from ϵ-caprolactone, DL-lactide, and glycolide (87). The release from PCL homopolymer and PLACL copolymer was diffusion controlled. This was assigned to the high permeability of PCL to drug molecules. The release from PLA_{50} was very slow when diffusion controlled, in agreement with the low solubility and diffusion coefficients of progesterone in this polymer. The release from PLAGA copolymer matrices was associated with polymer degradation. Fong et al. evaluated various PLA, PLAGA, and PLACL microsphere systems containing thioridazine, ketotifen, or hydrocortisone acetate (186). A rather complex pattern of drug release was observed. The release of drugs from semicrystalline PLA_{100} was more rapid than from amorphous PLA_{100}. This feature can be explained by the presence of channels and pores within the PLA_{100} matrix, as also observed by Mauduit et al. for a gentamycin-releasing system (97). Both types of copolymers, namely PLAGA ($PLA_{90}GA_{10}$, $PLA_{75}GA_{25}$, $PLA_{37.5}GA_{25}$) and PLACL ($PLA_{80}CL_{20}$ and $PLA_{45}CL_{10}$), led to faster release than PLA_{50}. In the case of the copolymers, it was difficult to correlate drug release to specific parameters. The authors suggested that the influence of polymer composition on release rates may be due to a number of polymer properties such as crystallinity, degradation rate, comonomer ratio, permeability, glass transition, and solubility of the drug in the polymer. When the polymer has a slow degradation rate like PLA_{100}, the predominant mode of drug release is theoretically diffusion through the matrix. With fast-degrading polymers like $PLA_{37.5}GA_{25}$, the drug release can occur through diffusion and concomitant release of drug due to the matrix degradation (186). Song et al. investigated long-acting release of Norgestrel (MCN) from PLACL block copolymers (195). The block copolymer showed a double release mechanism: diffusion release due to PCL segment and degradation-caused release due to PLA segment. The effects of these two pathways can be balanced by tailoring the ratio of LA/CL to such an extent that the degradation-caused release could just compensate for the declined amount resulted from diffusion release and a whole zero-order kinetics can be actually achieved.

Molar Mass and Molar Mass Distribution

Molar mass and molar mass distribution are important factors in the polymer degradation and drug release process because of the autocatalytic character of aliphatic polyester hydrolysis. Pitt et al. found that PLA_{50} films with an initial $\overline{M}_n$ of 14,000 were absorbed by week 28, against 60 weeks for those with an initial $\overline{M}_n$ of 49,000 (82). Chawla and Chang investigated the in vivo degradation of four PLA_{50} samples having different high molar masses. At the end of a 48-week implantation period, samples with lower molar mass degraded faster (199). Kaetsu et al. studied the in vivo degradation of four PLA_{50} needle samples with relatively low molar mass (1,100 to 2,200 determined by terminal group titration) (84). In these cases, the higher the initial molar mass, the slower the degradation rate. Ogawa et al. observed that both the lag time and the half-life of PLA_{50} plates increased with molar mass during in vivo degradation (190). Fukuzaki et al. studied the degradation of different PLA_{50} with relatively low molar masses (21). The authors proposed three types of degradation profile according to molar mass, namely parabolic, linear, and S types. The parabolic type observed for $\overline{M}_n$ = 1,500 Da can be explained by the release of the soluble fraction present within the initial oligomers, whereas the S type ($\overline{M}_n$ = 3,500 daltons) reflects a lag time due to higher molar mass.

So far, the effect of molar mass distribution, or polydispersity ($\overline{M}_w/\overline{M}_n$), on PLAGA polymer degradation has been investigated only qualitatively. Nevertheless, the presence of low molar mass species and/or monomers does accelerate the degradation. The elimination of low molar mass and residual monomers is thus very important if one wants a relatively stable polymer. Leeslag et al. showed that the purification of PLA_{100} led to a material more resistant to hydrolytic degradation (179). Nakamura et al. observed an important increase of degradation rate of PLA stereocopolymers in the presence of DL-lactide and glycolide (25). Recently, Mauduit et al. showed that oligomers accelerated the rate of degradation of PLA_{50} films (86).

From these published data, one can conclude that the lower the molar mass, the faster the degradation rate, in agreement with the presence of more carboxylic acid catalyzing groups. Drug release profiles are also affected. In the case of TRH/PLAGA microspheres, Heya et al. observed that the lower the molar mass (in the 6,000–11,000 range), the faster the drug release. Moreover, the initial burst increased with decreasing molar mass (198). Ogawa et al. also observed a more rapid release of drug from lower molar mass PLA or PLAGA matrices (190). Cohen et al. investigated the release of high molar mass, water-soluble proteins from PLAGA microspheres. The authors found that the burst decreased with increasing PLAGA molar mass from 5,000 to 10,000 and 14,000 daltons (142), in agreement with the data of Heya et al. Wada et al. examined low molar mass PLA_{100} and PLA_{50} microspheres containing an anticancer agent (aclacinomycin or ACR) for selective lymphatic delivery. The release rate was reduced as the molar mass was increased from 3,600 to 10,000 for PLA_{100} or from 3,300 to 9,600 for PLA_{50}. Polymers with molar mass higher than 10,000 were regarded as not useful (200,201). Similar observations were made by Juni et al. for the release of local anesthetics from PLA microspheres (202). On the other hand, Bodmeier et al. obtained an acceleration of drug release from PLA_{50} films and microspheres containing low molar mass oligomers (85). In the case of PCL-based drug delivery systems, Huatan et al. found that release of bovine serum albumin (BSA) was slower from high molar mass PCL films than from high-low molar masses PCL blends (88).

Size and Porosity

The size of polymer samples has been recently recognized as an important factor for the degradation of aliphatic polyesters. Kwong et al. observed a rapid disintegration of insulin-containing PLA_{100} pellets 28 days after implantation as compared with microbeads, which remained intact. The faster degradation of pellets was attributed to porosity (90). Ginde and Gupta examined the influence of macroscopic dimensions on the chemical degradation of PGA fibers and pellets (134). The degradation rate was found to be much faster in pellets than in fibers. This feature was assigned to the lack of long range order in pellets. Visscher et al. investigated the effect of particle size on the in vitro and in vivo degradations of three $PLA_{25}GA_{50}$ microsphere samples whose average diameters $\overline{X}$ were respectively less than 45–75 ($\overline{X}$ = 30), 75–106 ($\overline{X}$ = 79) and 106–177 μm ($\overline{X}$ = 130). It was concluded that over the examined size ranges, there were minimal differences in the degradation properties of polymeric matrices and thus of microcapsules (203). Törmälä et al. evaluated the strength retention of self-reinforced PGA rods with different diameters (1.5, 2.0, 3.2, and 4.5 mm) in a phosphate buffer (204). Small rods were found to lose strength more rapidly than large ones. Differences were related to surface area/mass ratios, which controlled water diffusion and thus hydrolysis. Mauduit et al. investigated the degradation of low and high molar mass PLA_{50} particles and films in vitro (97). In contrast to large-size devices, corresponding SEC data remained monomodal during the whole degradation period. Zhu et al. observed the same phenomenon for microspheres of PLA and two PLAGA copolymers (205). Grizzi et al. investigated the influence of size on the degradation of PLA_{50}. Films, powder, and microspheres degraded much less rapidly as compared to large-size specimens (165), showing conclusively that the smaller the polymer size, the slower the degradation rate. This unexpected behavior was well explained by the mechanism of autocatalytic degradation described earlier. In fact, if the size of the polymer matrix is very small, there is no surface-center differentiation. It is of interest to keep in mind that the literature is often misleading in comparing degradation rates of microspheres, fibers, films, pellets, and other massive implants (90,134). Insofar as the drug delivery profiles are concerned, Mauduit et al. observed a faster release of gentamycin from PLA_{50} particles in the size range 0.125–0.25 mm than from larger ones (0.25–0.5 mm and 0.5–1.0 mm). This was assigned to the larger surface area for smaller particles and not to degradation phenomena (97).

The porosity of the polymer matrix is also an important factor. Lam et al. evaluated the in vitro and in vivo deg-

radation of PLA_{100} films. The authors observed a faster degradation of nonporous films as compared with porous ones (206). Smith and Hunneyball prepared 1–10 μm PLA_{50} microspheres by solvent evaporation and microparticles by grinding the glassy solid formed by the cooling of molten PLA, both containing various amounts of prednisolone (207). The microparticles exhibited a more prolonged drug release profile, indicating that the fusion process may have substantial advantages for thermostable drugs requiring long-term release. Eenink et al. developed hollow fibers for the delivery of hormones (tritium labeled–levonorgestrel). The release was found to be dependent on the membrane structure of the hollow fiber wall. A zero-order release was achieved both in vitro and in vivo for as long as 6 months (91).

Drug Load and Drug/Polymer Interactions

Many authors reported that drug release rate increased with increasing the drug load (79,108,198,200,201, 208,209). This can be assigned to the morphology and distribution of drugs within the polymer matrix. With small loads, the release is slow because drug molecules are dissolved or molecularly dispersed within the matrix. In contrast, with high loads, drug crystals can be formed. The initial burst generally leads to channels and pores that facilitate diffusion later on (105,210). Kwong et al. examined the in vitro and in vivo releases of insulin from PLA_{100} microbeads and pellets (90). The microbeads exhibited a burst of 50% during the first hour. In contrast, the pellets showed a relatively small burst (10%) and an almost constant release for more than 48 h. The authors suggested that the release from microbeads consists of a rapid dissolution of surface insulin crystals followed by a pore-release mechanism, whereas the release from the pellets is governed by the pore-release model only. It is of interest to note that the two systems were prepared by different methods, namely solvent casting with total entrapment of insulin for the pellets, and solvent evaporation for the microbeads.

In some systems prepared by solvent evaporation, drug molecules can form a metastable molecular dispersion even for high loads. For example, Benoît et al. detected the absence of crystalline progesterone domains within PLA_{50} matrix with a load of 23 wt % (211). Fitzgerald and Corrigan found that levamisole (14.3 wt %) exists in an amorphous form within $PLA_{25}GA_{50}$ microspheres (89).

Matrix-drug interactions can be critical for both matrix degradation and drug delivery profiles. For acidic drugs, one can expect faster hydrolysis of ester bonds because of acid catalysis. In contrast, in the case of basic drugs, two phenomena can be expected: base catalysis of ester bond cleavage and neutralization of carboxyl endgroups of polymer chains, which minimizes or eliminates the autocatalytic effect. Thus, the degradation can be accelerated or slowed down by a base depending on the relative importance of the two effects.

Maulding et al. reported an acceleration of the degradation of PLA_{50} in the presence of a basic drug, thioridazine, which is a tertiary amine compound. Catalysis was attributed to the nucleophilic nature of the amino group (212,213). Kishida et al. obtained similar results (214). The authors found that the degradation rates of PLA_{100} matrix, which normally hydrolyzes slowly in aqueous media, could be increased by incorporating basic compounds, such as cinnarizine, thioridazine, indenolol, and clonidine, the catalytic effect increasing with the load. The degradation rate depended also on the apparent pK_a of the conjugate acid of each basic compound. The higher the pK_a, the faster the degradation according to the following order: indenorol > clonidine > thioridazine > cinnarizine (214). Cha and Pitt examined the effect of four tertiary amines: methadone, naltrexone, promethazine, and meperidine on the hydrolytic rate of PLA_{100} and of $PLA_{80}GA_{20}$ (215). It was found that the catalytic effect of the amines increases with the load, but its order (meperidine > methadone > promethazine $\gg$ naltrexone) did not correlate with the pK_a nor with $\log(P_{oct})$ (octanol-water partition coefficient) of the amines, in contrast to data reported by Kishida et al. The authors suggested that the steric accessibility of the unsolvated nitrogen might be the determining factor. Moreover, drug release were degradation controlled, faster degradation corresponding to shorter induction time prior to drug release (215). The same authors also examined the case of PLACL copolymer (75–85 mol % L-LA units). In contrast to PLA_{100} and of $PLA_{80}GA_{20}$, Fickian diffusion was responsible for the drug release kinetics (216). Fitzgerald and Corrigan investigated the mechanism governing the release of levamisole from $PLA_{25}GA_{50}$ microspheres and discs (89). Drug release profiles were sigmoidal and fit a degradation-controlled release model. On the other hand, polymer degradation was dramatically accelerated with increasing the load.

Other authors observed a decrease of the degradation rate or of the drug release rate due to interactions between polymer chain ends and drugs. Bodmeier and Chen evaluated degradable PLA pellets prepared by pressing without heat or solvent (79). They detected a lag time in drug release in the case of low molar mass PLA_{50} pellets. This was assigned to interactions between drugs (quinidine sulfate or propranolol hydrochloride) and carboxyl endgroups. Drug-polymer interactions were absent in the case of PLA_{100} pellets. The same authors suspected similar interactions in the case of microspheres and films made of high and low molar masses PLA_{50} blends containing quinidine (85). Mauduit et al. investigated various gentamycin PLA_{50} blends (86,97,217). It was found that the base form of the drug was able to neutralize polymer chain ends on blending in acetone, whereas the sulfate form required an aqueous environment. In the case of gentamycin sulfate–low molar mass PLA_{50} systems, interactions between drug and chain ends stabilized the matrix, the free drug in excess being rapidly released (217). Both phenomena acted against base catalysis.

The effects of sparingly soluble additives were also investigated. Verheyen et al. examined the physicochemical properties of hydroxyapatite-PLA_{100} composites in solution tests (218). Although the authors did not mention it, data showed that the higher the hydroxyapatite content, the slower the decrease of molar mass. Li and Vert investigated the hydrolytic behavior of PLA_{50}-coral blends (219). It was found that coral, which is composed of calcium car-

bonate, significantly slowed down the degradation of PLA_{50} matrix and suppressed the faster internal degradation. Zhang et al. observed a decrease of degradation rate by 1.7 to 3.0 times with incorporation of salts such as $Mg(OH)_2$, $MgCO_3$, $CaCO_3$, and $ZnCO_3$ into $PLA_{25}GA_{50}$ films (220). The stabilizing effect of hydroxyapatite, coral, and other metal salts on the hydrolysis of polymer chains can be assigned to the neutralization of carboxyl end groups by the additives and/or by the degradation medium that penetrated the matrix due to the presence of the polymer-additive interfaces.

Li et al. investigated the mechanism of hydrolytic degradation of PLA_{50} matrix in the presence of a tertiary amine, namely caffeine, in order to elucidate the influence of this basic compound on the hydrolytic cleavage of polyester chains (183). Caffeine was incorporated into PLA_{50} in various contents (0% to 20%) by blending in acetone followed by solvent evaporation. The resulting blends were processed to 1.5-mm-thick plates and 0.3-mm-thick films by compression molding. Degradation was carried out in isoosmolar pH = 7.4 phosphate buffer at 37°C. The effects of caffeine on degradation characteristics were rather complex and largely depended on the load (Fig. 13). For low contents (≤2%), caffeine was molecularly dispersed in matrices and accelerated considerably the degradation with respect to caffeine-free devices. However, the increase of degradation rate was not proportional to the caffeine load due to the combined effects of base–carboxyl endgroup interaction, crystallization, and matrix-controlled or channeling-controlled diffusion of caffeine. In the early stages of degradation, the overall catalytic effect was larger for devices with low caffeine contents than for highly loaded ones where caffeine was in crystallized state and thus less available for basic catalysis. At the later stages, however, the neutralization of carboxyl endgroups became predominant and governed the degradation in the case of highly loaded devices (Fig. 13). From a general viewpoint, plates degraded slightly faster than films.

Therefore, the degradation of PLA polymers in the presence of basic drugs appeared rather complex because of the contribution of a number of parameters (i.e., base catalysis, neutralization of carboxyl endgroups, porosity, dimensions of devices, drug load, and drug morphology). They all contribute to make the drug itself an important and specific factor for the control of both drug release and matrix degradation. None of these factors can be considered separately if one wants to understand the effect of basic drugs on the properties of drug delivery systems.

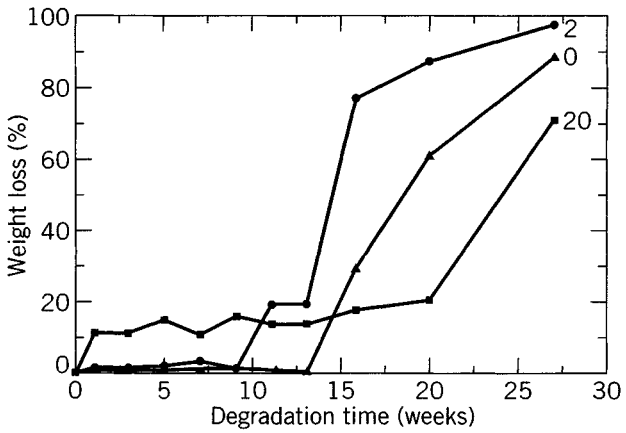


Figure 13. Weight loss of PLA_{50} plates containing 0%, 2%, and 20% of caffeine base with degradation in a pH 7.4 phosphate buffer at 37°C. *Source:* From Ref. 183.

γ Irradiation

Several authors examined the influence of γ irradiation on the degradation of PLAGA biomedical devices. Data are of interest in the field of drug delivery too. Gupta and Deshmukh claimed that irradiation in air or in nitrogen atmosphere can generate chain scission and cross-linking simultaneously (221). Chu et al. considered chain scission as predominant on the basis of the reduction in mechanical properties of Dexon® sutures upon γ irradiation (222). The scission process was speculated to depend on free radical chemistry. In addition, the authors observed formation of surface cracks during the hydrolysis of Dexon® sutures whose number and regularity increased with increasing irradiation dosages. In another study, Chu showed that γ irradiation of Dexon® and Vicryl® fibers resulted in an earlier appearance of pH fall in the degradation medium (177). All these observations are in agreement with a molar mass decrease on irradiation although no molar mass data are available.

Tsai et al. carried out effective sterilization of PLA–mitomycin C microcapsules for parenteral use by ^{60}Co γ irradiation (108). The authors found that the sterilization did not affect microcapsule structure, release rate, and drug stability. However, no molar mass measurements were performed. Spenlehauer et al. found that γ sterilization dramatically decreased the molar masses of PLA_{50}, $PLA_{45}GA_{10}$, and $PLA_{37.5}GA_{25}$ microspheres, and this degradation continued on storage for GA-containing compounds (223). γ sterilization also modified the release pattern of cisplatin-loaded microspheres. Birkinshaw et al. studied γ irradiation of compression-molded PLA_{50} samples in air with doses as high as 10 Mrad (224). Substantial embrittlement occurred at higher dose levels and the irradiated material absorbed water at a slightly slower rate than the unirradiated one. The authors concluded that the primary effect of irradiation on hydrolytic degradation was associated with the initial reduction in molar mass, the degradation mechanism remaining the same. Recently, Volland et al. investigated the influence of γ sterilization on captopril-containing $PLA_{25}GA_{50}$ microspheres (225). The molar mass of the polymer decreased with increasing irradiation dose, but the polydispersity remained unchanged, suggesting a random chain cleavage rather than an unzipping process.

pH and Ionic Strength

Chu examined the effect of pH on the degradation of Dexon® and Vicryl® sutures by using three different buffer solutions with pH = 5.25, 7.44, and 10.06, respectively (226,227). For Vicryl® sutures, maximum retention of tensile properties occurred around pH 7.0. For Dexon® su-

tures, no major difference was observed between physiological and acidic media. In contrast, the alkaline buffer had a dramatic effect on Dexon® degradation (226,227). Makino et al. observed that PLA_{100} degraded rapidly in a strongly alkaline solution or in solutions of high ionic strength. The effects of pH and ionic strength were interpreted in terms of electric potential distribution at the polymer–solution interface. Degradation was also found affected by salt concentration in buffer solutions, suggesting that the cleavage of polymer ester bonds was accelerated by conversion of the acidic degradation products into neutral salts (228).

For Reed and Gilding, pH changes had no effect on the in vitro degradation of PLAGA polymers in citrate-phosphate buffers at pH 5 and pH 7 and boric acid–borax buffer at pH 9. Any sensitivity of PLAGA polymers to pH was actually dominated by combined effects of crystallinity and hydrophobicity, according the authors (188). Kenley et al. studied the in vitro degradation of $PLA_{25}GA_{50}$ cylindrical samples in aqueous buffers with pH varying from 4.5 to 7.4 at 37°C (139). They obtained superimposable total mass and molar mass profiles for all samples, suggesting pH independence for the in vitro hydrolysis. Ginde and Gupta studied the in vitro degradation of PGA pellets and fibers in four different buffer solutions with pH 4.7, 7.0, 9.2, and 10.6, respectively (134). No major difference was found between the slightly acidic and neutral media. However, the two alkaline solutions accelerated considerably the degradation of PGA samples.

Li et al. comparatively investigated the in vitro degradation of large-size PLAGA polymers in three different media: distilled water, iso-osmolar phosphate buffer, and saline (146,148,149). There was no significant difference between the two iso-osmolar media despite the pH fall observed in saline at the later stages of degradation. In contrast, the absence of ionic strength in distilled water promoted water absorption and thus the surface-center differentiation in the early stages (Fig. 14). Furthermore, the phosphate buffer enhanced solubilization of degradation products in the later stages (Fig. 15), the carboxylate form $RCOO^-$ of organic acids being more hydrophilic than the carboxylic form RCOOH (148).

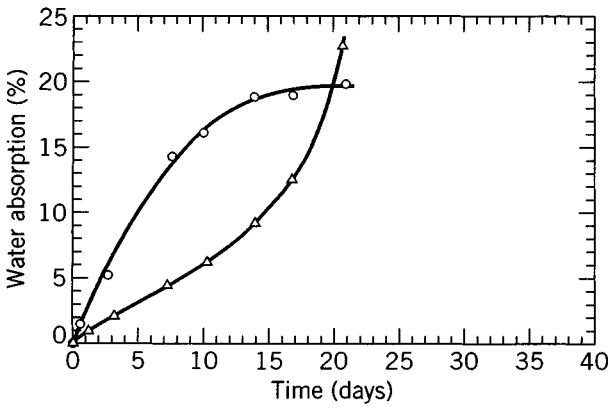


Figure 14. Water absorption profiles of $PLA_{37.5}GA_{25}$ plates with degradation at 37°C in a pH 7.4 phosphate buffer (△) and in water (○). *Source:* From Ref. 148.

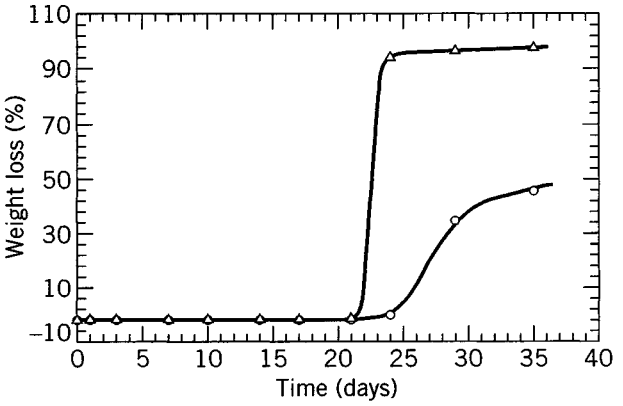


Figure 15. Weight loss of $PLA_{37.5}GA_{25}$ plates with degradation at 37°C in a pH 7.4 phosphate buffer (△) and in water (○). *Source:* From Ref. 148.

Therefore, one can reasonably conclude that alkaline and strong acidic media accelerate polymer degradation. The difference between slightly acidic and physiological media, however, is much less pronounced due to autocatalysis by carboxyl endgroups. The effects of pH and ionic strength on drug release profiles are rarely discussed in the literature. Nevertheless, one can assume that for degradation-controlled release, drug release should be enhanced if degradation is enhanced. In the case of diffusion-controlled release, one should take into account the solubility of the drug in the external medium.

Comparison Between in Vitro and in Vivo Behaviors

Many authors studied comparatively the matrix degradation behaviors in vitro and in vivo. Chegini et al. carried out a comparative SEM study on degradation of Lactomer® ($PLA_{70}GA_{30}$) ligating clips in vivo by implantation in the incision of rabbits and in vitro by incubation in pH 7.3 phosphate-buffered saline (229). Lactomer® clips were found to show a greater change in proportion of breakdown comparing in vivo to in vitro. Törmälä et al. observed a faster loss of mechanical strength of self-reinforced PGA rods and PLA_{100} screws and plates in vivo than in vitro (204,230). This difference in rates of strength loss was assigned to the effect of cellular enzymes or other biological or biochemical factors as well as the mechanical stresses caused to the implants by the rabbits' movements. Albertsson and Karlsson also suggested that the higher in vivo degradation rate resulted probably from the dynamics in in vivo systems (231). Thérin et al. (151) and Spenlehauer et al. (223) also found a faster degradation in vivo than in vitro. Differences were assigned to mechanical stresses due to muscular movements of the rabbits (151), in agreement with data reported by Suuronen et al. (230) and Albertsson and Karlsson (231).

Leeslag et al. investigated the in vivo degradation of high molar PLA_{100} devices used for fixation of mandibular fractures in sheep and dogs or subcutaneously implanted in rats. They also considered the in vitro degradation in

pH = 6.9 phosphate-buffered saline (179). The authors showed that except for dynamically loaded bone plates, there were no significant differences between in vivo and in vitro degradation, thus excluding the additional effect of enzymes. Kenley et al. also found no major difference between $PLA_{25}GA_{50}$ copolymer degradation kinetics in vitro in buffer solutions and in vivo after subcutaneous implantation in rats (139). In contrast, Visscher et al. observed a much faster degradation of $PLA_{25}GA_{50}$ in vitro than in vivo and attributed it to the totally aqueous environment and constant physical movement that the microspheres were subjected to in vitro (203).

Authors also compared the drug release behaviors in vitro and in vivo. Ikada et al. investigated degradation and release behaviors of a dideoxykanamycin B (DKB)–containing composite material prepared from hydroxyapatite and low molar mass PLA_{50} in vitro in pH 8 phosphate buffered saline and in vivo by implantation into the fenestrated tibias of rats (232). Both the amount and the period of retention of DKB were much greater in vivo than in vitro, indicating a faster degradation in vitro. In contrast, Smith and Hunneyball observed a faster release of prednisolone from PLA_{50} microspheres in vivo than in vitro, which was assigned to the faster penetration by biological fluids and/or faster degradation of PLA in vivo (207). On the other hand, Kwong et al. (90), Sanders et al. (138), and Heya et al. (198) obtained a good correlation between in vivo and in vitro drug release profiles.

Therefore, the literature shows that in most cases, drug delivery systems based on PLAGA polymers exhibited comparable in vitro and in vivo matrix degradation and drug release behaviors. Whenever differences are observed, effects of physical factors (temperature, stirring, pH) or physiological ones related to implantation sites (subcutaneous, intramuscular, or in bony tissues) should be considered prior to any reference to enzymatic activities.

CONCLUSION

Degradable aliphatic polyesters, in particular those deriving from lactides, glycolide, and ϵ-caprolactone, have been most widely investigated for applications in the field of sustained drug delivery during the past two decades. Factors that can affect the hydrolytic degradation of polymers and the release profiles of drugs have been gradually identified. This chapter has tried to present the state-of-the-art on the basis of recent advances in this domain. One of the first conclusions is that polymers aimed at making drug delivery systems can bear the same name and be very different for many reasons. Sources of differences can be found at any stage of the history of a drug delivery system: polymer synthesis, device processing, drug-polymer blending, sterilization, release conditions, and implantation sites. Most of these sources are sometimes neglected, ignored, or not taken into account in scientific papers. It is only by considering all of them simultaneously that one can expect success in a real control of the drug delivery profiles from polymeric matrices.

BIBLIOGRAPHY

1. A.S. Hoffman, *ACS Symp. Ser.* **256**, 13–29 (1984).
2. D.V. Rosato, in M. Szycher, ed., *Biocompatible Polymers, Metals and Composites*, Technomic Publishing, Lancaster, Pa., 1983, pp. 1019–1067.
3. U.S. Pat. 2,668,162 (Feb. 2, 1954), E.L. Charles and N.Y. Buffalo (to E.I. DuPont de Nemours).
4. U.S. Pat. 3,297,033 (Jan. 10, 1967), E.E. Schmitt and R.A. Polistina (to Am. Cyanamid Co.).
5. E.J. Frazza and E.E. Schmitt, *J. Biomed. Mater. Res. Symp.* **1**, 43–58 (1971).
6. S. Li and M. Vert, in G. Scott and D. Gilead, eds., *Degradable Polymers: Principles and Applications*, Chapman & Hall, London, 1995, pp. 43–87.
7. S.J. Huang et al., *Am. Chem. Soc. Stab. Degradation Polym.* **17**, 209–214 (1978).
8. R.L. Kronenthal, in R.L. Kronenthal, Z. User, and E. Martin, eds., *Polymers in Medicine and Surgery*, Plenum, New York, 1974, pp. 119–137.
9. S.J. Holland, B.J. Tighe, and P.L. Gould, *J. Controlled Release* **4**, 155–180 (1986).
10. M. Vert, S. Li, G. Spenlehauer, and P. Guérin, *J. Mater. Sci., Mater. Med.* **3**, 432–446 (1992).
11. S. Li, *J. Biomed. Mater. Res., Appl. Biomater.* **48**, 342–353 (1999).
12. R.L. Dunn, in J.O. Hollinger, ed., *Biomedical Applications of Synthetic Biodegradable Polymers*, CRC Press, Boca Raton, Fla., 1995, pp. 17–31.
13. R.H. Müller and K.H. Wallis, *Int. J. Pharm.* **89**, 25–31 (1993).
14. C. Braud and M. Vert, in S.W. Shalaby, A.S. Hoffman, B.D. Ratner, and T.A. Horbett eds., *Polymers as Biomaterials*, Plenum, New York, 1984, pp. 1–16.
15. M. Yokoyama et al., *Makromol. Chem., Rapid Commun.* **8**, 431–435 (1987).
16. S. Gautier, M. Boustta, and M. Vert, *J. Bioact. Compat. Polym.* **12**, 77–98 (1997).
17. H. Ringsdorf, *J. Polym. Sci., Polym. Symp.* **51**, 135–153 (1975).
18. M. Vert, *CRC Crit. Rev. Ther. Drug Carrier Syst.* **2**, 291–327 (1985).
19. A.M. Reed and D.K. Gilding, *Polymer* **20**, 1459–1464 (1979).
20. M. Spinu, C. Jackson, M.Y. Keating, and K.H. Gardner, *J. Macromol. Sci. Pure Appl. Chem.* **A33**, 1497–1530 (1996).
21. H. Fukuzaki, M. Yoshida, M. Asano, and M. Kumakura, *Eur. Polym. J.* **25**, 1019–1026 (1989).
22. H. Fukuzaki, M. Yoshida, M. Asano, and M. Kumakura, *Polymer* **31**, 2006–2014 (1990).
23. N. Wang et al., *Proc. Am. Chem. Soc.* **76**, 373–374 (1997).
24. M. Vert, P. Christel, F. Chabot, and J. Leray, in G.W. Hastings and P. Ducheyne, eds., *Macromolecular Biomaterials*, CRC Press, Boca Raton, Fla., 1984, pp. 119–142.
25. T. Nakamura et al., *J. Biomed. Mater. Res.* **23**, 1115–1130 (1989).
26. R.A. Miller, J.M. Brady, and D.E. Cutright, *J. Biomed. Mater. Res.* **11**, 711–719 (1977).
27. F. Chabot, M. Vert, S. Chapelle, and P. Granger, *Polymer* **24**, 53–60 (1983).
28. K. Hiltunen, J.V. Seppälä, and M. Härkönen, *Macromolecules* **30**, 373–379 (1997).

29. European Pat. 0,443,542 A2 (Feb. 20, 1991), B. Buchholz (to Boehringer Ingelheim International GmbH).
30. S. Bezzi, L. Riccoboni, and C. Sullam, *Mem. R. Accad. Ital. Cl. Sci. Fis. Mat. Nat.* **8**, 201–211 (1937).
31. J. Kleine and H. Kleine, *Makromol. Chem.* **30**, 23–38 (1959).
32. V.F. Jenkins, *Polym. Paint Colour J.* **167**, 626–627 (1977).
33. E.F. Cox, F. Hostettler, and R.R. Kiser, *Macromol. Synth.* **3**, 111–113 (1969).
34. M. Morton and M. Wu, *ACS Symp. Ser.* **286**, 175–182 (1985).
35. R.S. Velishkova, V.D. Toncheva, and I.M. Panayotov, *J. Polym. Sci., Part A* **25**, 3283–3292 (1987).
36. P. Dreyfuss, T. Adaway, and J.P. Kennedy, *Appl. Polym. Symp.* **30**, 183–192 (1977).
37. W.H. Carothers, G.L. Dorough, and F.J. Van Natta, *J. Am. Chem. Soc.* **54**, 761–772 (1932).
38. R.K. Kulkarni, K.C. Pani, C. Neuman, and F. Leonard, *Arch. Surg.* **93**, 839–843 (1966).
39. U.K. Pat. 779,291 (Jan. 28, 1955), J. Kleine.
40. M.C. Tanzi et al., *J. Mater. Sci., Mater. Med.* **5**, 393–396 (1994).
41. G. Schwach, J. Coudane, R. Engel, and M. Vert, *J. Polym. Sci., Part A* **35**, 3431–3440 (1997).
42. E. Lillie and R.C. Schulz, *Makromol. Chem.* **176**, 1901–1906 (1975).
43. K. Chujo et al., *Makromol. Chem.* **100**, 262–266 (1967).
44. H.R. Kricheldorf and A. Serra, *Polym. Bull.* **14**, 497–502 (1985).
45. R. Dunsing and H.R. Kricheldorf, *Polym. Bull.* **14**, 491–496 (1985).
46. H.R. Kricheldorf and I. Kreiser-Saunders, *Makromol. Chem.* **191**, 1057–1066 (1990).
47. Z. Jedlinski and W. Walach, *Makromol. Chem.* **192**, 2051–2057 (1991).
48. L. Sipos, M. Zsuga, and T. Kelen, *Polym. Bull.* **27**, 495–502 (1992).
49. N. Spassky, *Makromol. Chem., Macromol. Symp.* **42/43**, 15–49 (1991).
50. P. Kurcok, J. Penczek, J. Franek, and Z. Jedlinski, *Macromolecules* **25**, 2285–2289 (1992).
51. M. Bero, G. Adamus, J. Kasperczyk, and H. Janeczek, *Polym. Bull.* **31**, 9–14 (1993).
52. Z. Jedlinski et al., *Makromol. Chem.* **194**, 1681–1689 (1993).
53. H.R. Kricheldorf and R. Dunsing, *Makromol. Chem.* **187**, 1611–1625 (1986).
54. H.R. Kricheldorf and I. Kreiser-Saunders, *Makromol. Chem.* **188**, 1861–1873 (1987).
55. H.R. Kricheldorf and I. Kreiser-Saunders, *J. Macromol. Sci., Chem.* **A24**, 1345–1356 (1987).
56. F.E. Kohn, J.G. Van Ommen, and J. Feijen, *Eur. Polym. J.* **19**, 1081–1088 (1983).
57. A.J. Nijenhuis, D.W. Grijmpa, and A.J. Pennings, *Macromolecules* **25**, 6419–6424 (1992).
58. M. Bero, J. Kasperczyk, and Z. Jedlinski, *Makromol. Chem.* **191**, 2287–2296 (1990).
59. A.M. Jonte, R. Dunsing, and H.R. Kricheldorf, *J. Macromol. Sci., Chem.* **A23**, 495–514 (1986).
60. R. Dunsing and H.R. Kricheldorf, *Eur. Polym. J.* **24**, 145–150 (1988).
61. E.J. Goethals, *Makromol. Chem., Macromol. Symp.* **42/43**, 51–68 (1991).
62. M. Bero, J. Kasperczyk, and G. Adamus, *Makromol. Chem.* **194**, 907–912 (1993).
63. H.R. Kricheldorf, J.M. Jonte, and M. Berl, *Makromol. Chem., Suppl.* **12**, 25–38 (1985).
64. X. Zhang, D.A. MacDonald, M.F.A. Goosen, and K.B. Mcauley, *J. Polym. Sci., Part A* **32**, 2965–2970 (1994).
65. U.S. Pat. 5,028,667 (July 2, 1991), S.J. McLain and N.E. Drysdale (to E.I. DuPont de Nemours).
66. A. Le Borgne, V. Vincens, M. Jouglard, and N. Spassky, *Makromol. Chem., Macromol. Symp.* **73**, 37–46 (1993).
67. N. Spassky, M. Wisniewski, C. Pluta, and A. Le Borgne, *Macromol. Chem. Phys.* **197**, 2627–2637 (1996).
68. P. Dubois, C. Jacobs, R. Jérôme, and P. Teyssié, *Macromolecules* **24**, 2266–2270 (1991).
69. H.R. Kricheldorf, I. Kreiser-Saunders, and C. Boettcher, *Polymer* **36**, 1253–1259 (1995).
70. G. Schwach, J. Coudane, R. Engel, and M. Vert, *Polym. Bull.* **37**, 771–776 (1996).
71. G. Schwach, J. Coudane, R. Engel, and M. Vert, *Polym. Int.* **46**, 177–182 (1998).
72. M. Vert, G. Schwach, R. Engel, and J. Coudane, *J. Controlled Release* **53**, 85–92 (1998).
73. R. Arshady, *J. Bioact. Compat. Polym.* **5**, 315–342 (1990).
74. D.A. Wood, *Int. J. Pharm.* **7**, 1–18 (1980).
75. A. Schindler et al., *Contem. Top. Polym. Sci.* **2**, 251–289 (1977).
76. C.G. Pitt, *Drugs Pharm. Sci.* **45**, 71–119 (1990).
77. S.Y. Jeong and S.W. Kim, *Arch. Pharm. Res.* **9**, 63–73 (1986).
78. Y. Ogawa, *J. Biomater. Sci., Polym. Ed.* **8**, 391–409 (1997).
79. R. Bodmeier and H. Chen, *J. Pharm. Sci.* **78**, 819–822 (1989).
80. D.L. Wise, H. Rosenkrantz, J.B. Gregory, and H.J. Esber, *J. Pharm. Pharmacol.* **32**, 399–403 (1980).
81. M.C. Meikle et al., *Biomaterials* **14**, 177–183 (1993).
82. C.G. Pitt et al., *Biomaterials* **2**, 215–220 (1981).
83. M. Yoshida et al., *Polym. J.* **14**, 941–950 (1982).
84. I. Kaetsu et al., *J. Controlled Release* **6**, 249–263 (1987).
85. R. Bodmeier, K.H. Oh, and H. Chen, *Int. J. Pharm.* **51**, 1–8 (1989).
86. J. Mauduit, N. Bukh, and M. Vert, *J. Controlled Release* **25**, 43–49 (1993).
87. C.G. Pitt et al., *J. Pharm. Sci.* **68**, 1534–1538 (1979).
88. H. Huatan, J.H. Collett, D. Attwood, and C. Booth, *Biomaterials* **16**, 1297–1303 (1995).
89. J.F. Fitzgerald and O.I. Corrigan, *J. Controlled Release* **42**, 125–132 (1996).
90. A.K. Kwong et al., *J. Controlled Release* **4**, 47–62 (1986).
91. M.J.D. Eenink et al., *J. Controlled Release* **6**, 225–247 (1987).
92. J.M. Schakenraad et al., *Biomaterials* **9**, 116–120 (1988).
93. J.M. Goodson et al., *J. Periodontol.* **54**, 575–579 (1983).
94. Y. Kinoshita et al., *Biomaterials* **14**, 729–736 (1993).
95. N.H. Shah et al., *J. Controlled Release* **27**, 139–147 (1993).
96. S. Miyamoto and K. Takaoka, *Annal. Chir. Gynaecol.* **82**, 69–76 (1993).
97. J. Mauduit, N. Bukh, and M. Vert, *J. Controlled Release* **23**, 221–230 (1993).
98. T.M.S. Chang, *J. Bioeng.* **1**, 25–32 (1976).
99. R.H. Asch et al., *J. Androl.* **6**, 83–88 (1985).
100. L.M. Sanders et al., *J. Pharm. Sci.* **73**, 1294–1297 (1984).

101. V. Vidmar, S. Pepeljnjak, and I. Jalsenjak, *J. Microencapsul.* **2**, 289–292 (1985).
102. M. Nakano et al., *Int. J. Pharm.* **4**, 291–298 (1980).
103. L.R. Beck, V.Z. Pope, T.R. Tice, and R.M. Gilley, *Adv. Contracept.* **1**, 119–129 (1985).
104. K. Susuki and J.C. Price, *J. Pharm. Sci.* **74**, 21–24 (1985).
105. G. Spenlehauer, M. Verllard, and J.P. Benoit, *J. Pharm. Sci.* **75**, 750–755 (1986).
106. R. Jalil and J.R. Nixon, *J. Microencapsul.* **6**, 473–484 (1989).
107. A. Carrio, G. Schwach, J. Coudane, and M. Vert, *J. Controlled Release* **37**, 113–121 (1995).
108. D.C. Tsai et al., *J. Microencapsul.* **3**, 181–193 (1986).
109. R. Jalil and J.R. Nixon, *J. Microencapsul.* **7**, 375–383 (1990).
110. O. Ike et al., *Biomaterials* **13**, 230–234 (1992).
111. M. Kyo, S.H. Hyon, and Y. Ikada, *J. Controlled Release* **35**, 73–77 (1995).
112. R. Bodmeier and H. Chen, *J. Pharm. Pharmacol.* **40**, 754–757 (1988).
113. S. Takada, Y. Uda, H. Toguchi, and Y. Ogawa, *J. Pharm. Sci. Technol.* **49**, 180–184 (1995).
114. M. Vert et al., in Y. Doi and K. Fukuda, eds., *Biodegradable Plastics and Polymers*, Elsevier, Amsterdam, 1994, pp. 11–23.
115. D.K. Gilding, *Biocompat. Clin. Implant. Mater.* **2**, 209–232 (1981).
116. R.D. Gilbert, V. Stannett, C.G. Pitt, and A. Schindler, in N. Grassie, ed., *Development in Polymer Degradation*, vol. 4, Applied Science Publishers, London, 1982, pp. 259–293.
117. D.F. Williams, *J. Bioeng.* **1**, 279–294 (1977).
118. J.E. Kemnitzer, R. Gross, and S.P. McCarthy, *Macromolecules* **25**, 5227–5234 (1992).
119. A.M. Reed, Ph.D. Thesis, University of Liverpool, 1978.
120. J.B. Herrmann, R.J. Kelly, and G.A. Higgins, *Arch. Surg. (Chicago)* **100**, 486–490 (1970).
121. T.N. Salthouse and B.F. Matlaga, *Surg., Gynecol. Obstet.* **142**, 544–550 (1975).
122. J.M. Schakenraad et al., *J. Biomed. Mater. Res.* **24**, 529–545 (1990).
123. H. Younes et al., *Biomater. Artif. Cells, Artif. Organs* **16**, 705–719 (1988).
124. G.E. Zaikov, *J. Macromol. Sci., Rev. Macromol. Chem. Phys.* **C25**, 551–597 (1985).
125. D.F. Williams, *Eng. Med.* **10**, 5–7 (1981).
126. S.L. Ashley and J.W. McGinity, *Congr. Int. Technol. Pharm.* **5**, 195–204 (1989).
127. M.S. Reeve, S.P. McCarthy, M.J. Downey, and R.A. Gross, *Macromolecules* **27**, 825–831 (1994).
128. R.T. MacDonald, S.P. McCarthy, and R.A. Gross, *Macromolecules* **29**, 7356–7361 (1996).
129. A. Schindler and C.G. Pitt, *Polym. Prepr., Am. Chem. Soc., Div. Polym. Chem.* **23**, 111–112 (1982).
130. C.G. Pitt, R.W. Hendren, A. Schindler, and S.C. Woodward, *J. Controlled Release* **1**, 3–14 (1984).
131. M. Mochizuki et al., *J. Appl. Polym. Sci.* **55**, 289–296 (1995).
132. S.C. Woodward et al., *J. Biomed. Mater. Res.* **19**, 437–444 (1985).
133. P.A. Kramer and T. Burnstein, *Life Sci.* **19**, 515–520 (1976).
134. R.M. Ginde and R.K. Gupta, *J. Appl. Polym. Sci.* **33**, 2411–2429 (1987).
135. M. Singh, A. Singh, and G.P. Talwar, *Pharm. Res.* **8**, 958–961 (1991).
136. Y. Kimura, Y. Matsuzaki, H. Yamane, and T. Kitao, *Polymer* **30**, 1342–1349 (1989).
137. F.G. Hutchinson and B.J.A. Furr, *Biochem. Soc. Trans.* **13**, 520–523 (1985).
138. L.M. Sanders, G.I. McRae, K.M. Vitale, and B.A. Kell, *J. Controlled Release* **2**, 187–195 (1985).
139. R.A. Kenley, M.O. Lee, T.R. Mahoney, II, and L.M. Sanders, *Macromolecules* **20**, 2398–2403 (1987).
140. J.M. Schakenraad et al., *J. Biomed. Mater. Res.* **23**, 1271–1288 (1989).
141. J. Helder, P.J. Dijkstra, and J. Feijen, *J. Biomed. Mater. Res.* **24**, 1005–1020 (1990).
142. S. Cohen et al., *Pharm. Res.* **8**, 713–720 (1991).
143. T. St. Pierre and E. Chiellini, *J. Bioact. Compat. Polym.* **2**, 4–30 (1987).
144. D.H. Lewis, *Drugs Pharm. Sci.* **45**, 1–41 (1990).
145. C.G. Pitt, in M. Vert et al., eds., *Biodegradable Polymers and Plastics*, Royal Society of Chemistry, London, 1992, pp. 7–19.
146. S. Li, H. Garreau, and M. Vert, *J. Mater. Sci., Mater. Med.* **1**, 123–130 (1990).
147. K.R. Huffman and D.J. Casey, *J. Polym. Sci., Polym. Chem. Ed.* **23**, 1939–1954 (1985).
148. S. Li, H. Garreau, and M. Vert, *J. Mater. Sci., Mater. Med.* **1**, 131–139 (1990).
149. S. Li, H. Garreau, and M. Vert, *J. Mater. Sci., Mater. Med.* **1**, 198–206 (1990).
150. M. Vert, S. Li, and H. Garreau, *J. Controlled Release* **16**, 15–26 (1991).
151. M. Thérin et al., *Biomaterials* **13**, 594–600 (1992).
152. M. Vert, S. Li, and H. Garreau, *Clin. Mater.* **10**, 3–8 (1992).
153. S. Li and M. Vert, *Macromolecules* **27**, 3107–3110 (1994).
154. E.A. Schmitt, D.R. Flanagan, and R.J. Linhardt, *Macromolecules* **27**, 743–748 (1994).
155. S.A.M. Ali, P.J. Doherty, and D.F. Williams, *J. Biomed. Mater. Res.* **27**, 1409–1418 (1993).
156. X. Zhang, U.P. Wyss, D. Pichora, and M.F.A. Goosen, *J. Bioact. Compat. Polym.* **9**, 80–100 (1994).
157. H. Pistner et al., *Biomaterials* **14**, 671–677 (1993).
158. H. Pistner et al., *Biomaterials* **15**, 439–450 (1994).
159. H. Pistner, D.R. Bendix, J. Müling, and J. Reuther, *Biomaterials* **14**, 291–298 (1993).
160. T.G. Park, *Biomaterials* **16**, 1123–1130 (1995).
161. S. Li, J.L. Espartero, P. Foch, and M. Vert, *J. Biomater. Sci., Polym. Ed.* **8**, 165–187 (1996).
162. A. Löfgren and A. Albertsson, *J. Appl. Polym. Sci.* **52**, 1327–1338 (1994).
163. A.C. Albertsson and M. Eklund, *J. Appl. Polym. Sci.* **57**, 87–103 (1995).
164. H. Schliephake, D. Klosa, and M. Rahlff, *J. Biomed. Mater. Res.* **27**, 991–998 (1993).
165. I. Grizzi, H. Garreau, S. Li, and M. Vert, *Biomaterials* **16**, 305–311 (1995).
166. C.G. Pitt et al., *J. Appl. Polym. Sci.* **26**, 3779–3787 (1981).
167. M. Vert, in G. Walenkamp, ed., *Biomaterials in Surgery*, G.T. Verlag, Stuttgart, 1998, pp. 97–101.
168. A. Torres, S. Roussos, S.M. Li, and M. Vert, *Appl. Environ. Microbiol.* **62**, 2393–2397 (1996).
169. A. Torres, S. Li, S. Roussos, and M. Vert, *J. Environ. Polym. Degradation* **4**, 213–223 (1996).

Next Page

170. A. Torres, S. Li, S. Roussos, and M. Vert, *J. Appl. Polym. Sci.* **62**, 2295–2302 (1996).
171. P. Jarrett et al., in S.W. Shalaby, A.S. Hoffman, B.D. Ratner, and T.A. Horbett, eds., *Polymers as Biomaterials*, Plenum, New York, 1985, pp. 181–192.
172. F. Lefebvre, C. David, and C. Vander Wauven, *Polym. Degradation Stab.* **45**, 347–353 (1994).
173. S.I. Akahori and Z. Osawa, *Polym. Degradation Stab.* **45**, 261–265 (1994).
174. E.W. Fischer, H.J. Sterzel, and G. Wegner, *Kolloid-Z. Z. Polym.* **251**, 980–990 (1973).
175. B.K. Carter and G.L. Wilkes, in S.W. Shalaby, A.S. Hoffman, B.D. Ratner, and T.A. Horbert, eds., *Polymers as Biomaterials*, Plenum, New York, 1984, pp. 67–92.
176. R.J. Fredericks, A.J. Melveger, and L.J. Dolegiewtz, *J. Polym. Sci., Polym. Phys. Ed.* **22**, 57–66 (1984).
177. C.C. Chu, *Polymer* **26**, 591–594 (1981).
178. C. Chu, *J. Appl. Polym. Sci.* **26**, 1727–1734 (1981).
179. J.W. Leeslag et al., *Biomaterials* **8**, 311–314 (1987).
180. T. Pohjonen and P. Törmälä, in K.-S. Leung, L.-K. Hung, and P.C. Leung, eds., *Biodegradable Implants in Fracture Fixation*, Chinese University of Hong Kong, Hong Kong, 1993, pp. 75–88.
181. R. Gutwald, H. Pistner, J. Reuther, and J. Mühling, *J. Mater. Sci., Mater. Med.* **5**, 485–490 (1994).
182. S. Li and M. Vert, *Polym. Inter.* **33**, 37–41 (1994).
183. S. Li, S. Girod-Holland, and M. Vert, *J. Controlled Release* **40**, 41–53 (1996).
184. S. Izumikawa, S. Yoshioka, Y. Aso, and Y. Takeda, *J. Controlled Release* **15**, 133–140 (1991).
185. R. Jalil and J.R. Nixon, *Proc. 5th Inter. Conf. Pharm. Technol.*, Paris, *1989*, vol. V, pp. 94–103.
186. J.W. Fong, J.P. Nazareno, J.E. Pearson, and H.V. Maulding, *J. Controlled Release* **3**, 119–130 (1986).
187. D.E. Cutright et al., *Oral Surg. Oral Med. Oral Pathol.* **37**, 142–152 (1974).
188. A.M. Reed and D.K. Gilding, *Polymer* **22**, 494–498 (1981).
189. J.M. Zhu, Y.M. Shao, S.Z. Zhang, and W.M. Sui, *J. China Tex. Univ. (Engl. Ed.)* **8**, 57–61 (1991).
190. Y. Ogawa, H. Okada, M. Yamamoto, and T. Shimamoto, *Chem. Pharm. Bull.* **36**, 2576–2581 (1988).
191. S.S. Amarpreet and J.A. Hubbell, *J. Biomed. Mater. Res.* **24**, 1937–1411 (1990).
192. C. Thomasin et al., *J. Controlled Release* **41**, 131–145 (1996).
193. J. Eitenmüller, G. Muhr, K.L. Gerlach, and T. Schmickal, *J. Bioact. Compat. Polym.* **4**, 215–241 (1989).
194. D.W. Grijpma, A.J. Nijenhuis, and A.J. Pennings, *Polymer* **31**, 2201–2206 (1990).
195. C.X. Song, H.F. Sun, and X.D. Feng, *Polym. J.* **19**, 485–491 (1987).
196. Y.X. Li and X.D. Feng, *Makromol. Chem., Macromol. Symp.* **33**, 253–264 (1990).
197. J.L. Espartero et al., *Macromolecules* **29**, 3535–3539 (1996).
198. T. Heya, H. Okada, Y. Ogawa, and H. Toguchi, *Int. J. Pharm.* **72**, 199–205 (1991).
199. A.S. Chawla and T.M.S. Chang, *Biomater., Med. Devices, Artif. Organs* **13**, 153–162 (1985–1986).
200. R. Wada et al., *J. Bioact. Compat. Polym.* **3**, 126–136 (1988).
201. R. Wada, Y. Tabana, S.-H. Hyon, and Y. Ikada, *Bull. Inst. Chem. Res., Kyoto Univ.* **66**, 241–250 (1988).
202. N. Wakiyama, K. Juni, and M. Nakano, *Chem. Pharm. Bull.* **30**, 2621–2628 (1982).
203. G.E. Visscher et al., *J. Biomed. Mater. Res.* **22**, 733–746 (1988).
204. P. Törmälä et al., *Angew. Makromol. Chem.* **185/186**, 293–302 (1991).
205. J.H. Zhu, Z.R. Shen, L.T. Wu, and S.L. Yang, *J. Appl. Polym. Sci.* **43**, 2099–2106 (1991).
206. K.H. Lam et al., *J. Mater. Sci., Mater. Med.* **5**, 181–189 (1994).
207. A. Smith and I.M. Hunneyball, *Int. J. Pharm.* **30**, 215–220 (1986).
208. K. Juni et al., *Chem. Pharm. Bull.* **33**, 311–318 (1985).
209. Z. Ramtoola, O.I. Corrigan, and C.J. Barrett, *J. Microencapsul.* **9**, 415–423 (1992).
210. G. Spenlehauer et al., *J. Controlled Release* **7**, 217–229 (1988).
211. J.P. Benoit, F. Courteille, and C. Thies, *Int. J. Pharm.* **29**, 95–102 (1986).
212. H.V. Maulding et al., *J. Controlled Release* **3**, 103–117 (1986).
213. H.V. Maulding, *J. Controlled Release* **6**, 167–176 (1987).
214. A. Kishida, S. Yoshioka, Y. Takeda, and M. Uchiyama, *Chem. Pharm. Bull.* **37**, 1954–1956 (1989).
215. Y. Cha and C.C. Pitt, *J. Controlled Release* **8**, 259–265 (1989).
216. Y. Cha and C.C. Pitt, *J. Controlled Release* **7**, 69–78 (1988).
217. J. Mauduit, N. Bukh, and M. Vert, *J. Controlled Release* **23**, 209–220 (1993).
218. C.C.P.M. Verheyen et al., *J. Mater. Sci., Mater. Med.* **4**, 58–65 (1993).
219. S. Li and M. Vert, *J. Biomater. Sci., Polym. Ed.* **7**, 817–827 (1996).
220. Y. Zhang, S. Zale, L. Sawyer, and H. Bernstein, *J. Biomed. Mater. Res.* **34**, 531–538 (1997).
221. M.C. Gupta and V.G. Deshmukh, *Polymer* **24**, 827–830 (1983).
222. C.C. Chu, *J. Biomed. Mater. Res.* **16**, 417–430 (1982).
223. G. Spenlehauer, M. Vert, J.P. Benoit, and A. Boddaert, *Biomaterials* **10**, 557–563 (1989).
224. C. Birkinshaw, M. Buggy, G.G. Henn, and E. Jones, *Polym. Degradation Stab.* **38**, 249–253 (1992).
225. C. Volland, M. Wolff, and T. Kissel, *J. Controlled Release* **31**, 293–305 (1992).
226. C.C. Chu, *J. Biomed. Mater. Res.* **15**, 19–27 (1981).
227. C.C. Chu, *J. Biomed. Mater. Res.* **15**, 795–804 (1981).
228. K. Makino, H. Ohshima, and T. Kondo, *J. Microencapsul.* **3**, 203–212 (1986).
229. N. Chegini, D.L. Hay, J.A. von Fraunhofer, and B.J. Masterson, *J. Biomed. Mater. Res.* **22**, 71–79 (1988).
230. R. Suuronen et al., *J. Mater. Sci., Mater. Med.* **3**, 426–431 (1992).
231. A.C. Albertsson and S. Karlsson, in S.A. Barenberg, J.L. Brash, R. Narayan, and A.E. Redpath, eds., *Degradable Materials: Perspectives, Issues and Opportunities*, CRC Press, Boca Raton, Fla., 1990, pp. 263–286.
232. Y. Ikada et al., *J. Controlled Release* **2**, 179–186 (1985).

See also BIODEGRADABLE POLYMERS: POLY(PHOSPHOESTER)S; BIODEGRADABLE POLYMERS: POLYANHYDRIDES; POLY(ORTHO ESTERS).

Previous Page

BLOOD SUBSTITUTES: A REVIEW OF CLINICAL TRIALS

NORA E. CUTCLIFFE
F.J. LOU CARMICHAEL
Hemosol, Inc.
Toronto, Canada
A. GERSON GREENBURG
The Miriam Hospital and Brown University
Providence, Rhode Island

KEY WORDS

Artificial blood
Clinical studies
Clinical trials
Elective surgery
HBOC
Healthy volunteers
Hemoglobin
Oxygen carrier
Oxygen delivery
Oxygen therapeutic
Product characteristics
Red cell substitute
Review
Safety studies
Trauma

OUTLINE

Introduction
Historical Perspective
The Need for Red Cell Substitutes
Purpose, Scope, and Methods
Results
  HBOC Product Characteristics
  HBOC Studies in Healthy Volunteers
  HBOC Studies in Elective Surgery
  HBOC Studies in Traumatic Shock
Discussion
  What We Have Learned
  Future Research Directions
Acknowledgments
Bibliography

INTRODUCTION

For nearly a century the search for a blood substitute has been an ongoing evolutionary process. Indeed, the recognition of the essential nature of blood in ensuring survival preceded the establishment of the very elements that comprise the essential functions of blood. These functions include oxygen delivery, maintenance of vascular volume, provision of clotting factors, delivery and removal of nutrients and waste products, and a communications route for signaling between various organs. It has long been recognized that humans and other mammals are obligate oxygen-dependent organisms. Any decrease in the ability to provide adequate tissue perfusion via efficient oxygen delivery results in harmful metabolic consequences affecting organ function and ultimately survival.

The adverse events associated with transfusion of allogeneic blood have been recognized for some time. In recent years the concern with the transmission of infectious disease has captured the spotlight and driven the search for alternatives to traditional allogeneic transfusion practices. In addition, newer issues concerning the immunologic consequences of the transfusion of blood and blood products with respect to infection and recurrence of malignancy invokes a heightened sense of concern on the part of clinicians (1–3). Newer strategies for the use of red cell transfusion are evolving and the potential for use of a red cell substitute, i.e., an oxygen carrying solution, is deemed both possible and reasonable in many clinical situations (4–6). Several recent reviews have been published, encompassing a variety of blood substitute topics (7–10).

HISTORICAL PERSPECTIVE

There are a variety of approaches that can be used to define a red cell substitute, assuming the primary objective is the delivery of oxygen to tissues. Behind each approach is a unique chemistry and rationale for investigation. It must be recalled that the modern era of hemoglobin-based oxygen carriers (HBOCs) began in the late 1960s (11). Problems with these solutions were considered to be (*1*) altered oxygen delivery due to an increased oxyhemoglobin affinity resulting from the loss of 2,3-diphosphoglycerate (DPG), the allosteric modifier of hemoglobin, when the red cell membrane is removed, and (*2*) a circulating half-life too short to be useful in the then-perceived primary application, trauma resuscitation. To address these issues, chemical modification of stripped or stroma-free hemoglobin to alter these properties was undertaken by many investigators. Many different concepts were explored and many modifiers defined and evaluated (10,12). The details of the modifications are perhaps less critical than the overall concepts as they may apply to the eventual acellular hemoglobin (Hb) solution.

Chemically modified acellular Hb may be stabilized as a 64 kD molecule (cross-linked), stabilized and polymerized or oligomerized, conjugated (molecules added), or stabilized and conjugated. All of these conceptual approaches address the issues of improving oxygen off-loading by decreasing oxyhemoglobin affinity and increasing intravascular persistence by decreasing Hb dimer formation or otherwise preventing its renal excretion. The site of chemical modification may vary (e.g., α-α or the DPG pocket) and the degree of chemical specificity of the modification varies considerably. The agents used to polymerize the stabilized Hb tetramers vary as well. The source of the acellular Hb is another variable accounting for differences in solutions. Indeed, the source of Hb may have an eventual role in clinical utility from a pharmacoeconomic analysis vantage; an assessment of which solution is better may in the long run be determined by the economics of production. Current source material for acellular Hb solutions includes pro-

cessing of outdated human red cells, bovine Hb, and recombinant technologies using *E. coli* as an expression system (10).

THE NEED FOR RED CELL SUBSTITUTES

Fueled by reports of transfusion-related transmission of infectious disease and other adverse consequences, the medical community as well as the general public are increasingly concerned that the transfusion of allogeneic red blood cells (RBCs) and other blood products is risky. Hence, one overriding principle of modern transfusion therapy is transfusion avoidance; unwanted outcomes are avoided if the offending agent is not given (2,13). To this end alternative strategies, including cell salvage, hemodilution, and presurgery deposit have been developed. In addition, application of the ever-increasing knowledge of the relationship of oxygen delivery to outcome in terms of transfusion triggers (14,15) has helped to limit or define the indications for transfusion (2,4,5,10,13,14). In the context of these concerns various investigators have approached the design of clinical Phase II and III trials to address the issue of avoidance of allogeneic transfusion as one significant end point.

Of the many functions of blood, the substitutes, as now perceived, will primarily serve the roles of oxygen delivery and vascular volume expansion. With enhanced knowledge other roles will be identified based on detailed explanations of the physiology related, in large part, to the effects of replacing or enhancing tissue perfusion in a variety of clinical settings. In that sense red cell substitutes will become a delivery system for oxygen, the *essential drug of survival.*

PURPOSE, SCOPE, AND METHODS

This chapter is not intended to be an all-inclusive review of the red cell substitutes. Rather, it is intended to review the current state of the field with respect to published clinical results of present generation Hb-based products. One major goal of this analysis is to place into perspective the various HBOC solutions in current use as well as the models being used for their clinical evaluation. In addition, it is aimed at establishing a framework or reference for ongoing developments in this field. In the absence of published results, clinical trials announced to be *in progress* at the time of submitting this manuscript are not referenced in this review.

Although perfluorocarbon-based red cell substitutes are now well advanced in humans testing (16–18), this literature was not included. For the key results presented in the next section, supportive animal/preclinical studies that have been reported elsewhere (19–23), as well as reports on liposome encapsulated hemoglobins that have not yet entered clinical trials (24), were also excluded. Publications were further narrowed to those reporting results in healthy volunteers and patients undergoing elective surgical and trauma treatment. The reader is referred to other papers for results of HBOC clinical trials in other more novel indications, such as septic shock (25–28), renal dialysis (29), and sickle cell anemia (30,31).

Publications included in this review were compiled mainly through Medline, *Current Contents*, and manual literature searches, with December 1997 as the cutoff date. Material presented at recent North American and European meetings on blood substitutes was also included, where published conference proceedings were available. A small number of nonrefereed publications was also used to supplement primary literature sources. Collectively, these available reports have permitted analysis of the various directions taken by investigators in this field.

RESULTS

The overall approach taken in this section was to describe the products currently in clinical trials insofar as possible from published information (Table 1) and to then describe the various trials in terms of safety and efficacy, two key elements in moving forward to eventual clinical use. Specifically, Tables 2, 3, and 4 correspond to HBOC studies in healthy volunteers, elective surgical indications, and traumatic shock, respectively. In these tables, all product doses are presented in grams Hb. Where mg/kg doses are reported in the literature without total milligram or gram doses, it is assumed that the average patient weighs 70 kg. Results presented in Tables 2, 3, and 4 refer to treated volunteers or patients in comparison with control subjects. These detailed charts are accompanied by an analytical discussion of key results.

HBOC Product Characteristics

It should be noted that direct comparisons of acellular Hb solutions in clinical trials involving acute blood loss, the focus of this chapter, is complicated by the enormous number of variables by which these solutions can be described. For purposes of this work a few have been selected, as presented in Table 1, since they are the logical ones that can be related to clinically useful parameters where the physiologic implications are known. These variables have been detailed elsewhere (10). The fact that there are differences not only in products, but also in models for establishment of safety and efficacy parameters allows a critical comparison of the approaches with reference to known physiology.

HBOC Studies in Healthy Volunteers

Table 2 presents an outline of all Phase I HBOC safety trials conducted in healthy volunteers, as published prior to December 1997. These trials were conducted in North America (U.S. and Canada), and were completed between 1993 and 1995. For each trial, the table specifies the product tested (see also Table 1), the trial location, the number of treated and control subjects, and the dose range of Hb administered. A brief description of protocol design is presented, and key results from each study are summarized. These *initial safety studies* were conducted predominantly in adult males. The majority of these trials were controlled, with the exception of one study (54), in which all subjects were treated with HBOC product. For the remainder of these studies, control articles included crystalloid solutions, human serum albumin, and, in one study (42), autologous blood. Note that several of the publications associated with these studies correspond to subcomponents of larger trials. In addition, some were published in abstract form as initial segments of the studies were completed.

Table 1. HBOC Product Characteristics

Company and product name(s)	Hb source	Chemical modification	Hb (g/dL)	Molecular weight distribution	P_{50} at 37°C (mm Hg)	Viscosity at 37°C (cp)	Colloid osmotic pressure (mm Hg)	Half-life (hs)	MetHb (%)	pH (37°C)
Baxter Healthcare Corp. DCLHb™ (HemAssist™)	Human red cells	Hb is $\alpha\alpha$ cross-linked with bis(3,5-di-bromosalicyl) furmarate (29,32)	9.5–10.5 (29,32, 33,34)	64.5 kD (96–98%) 130 kD (2–3%) (32)	32–33 (32,33, 35,36)	1 (35)	42–44 (32)	2.1–4.3 (25–100 mg/kg) 10.5 (658–1500 mg/kg) (29,33,37)	<5 at release (33,38) 14.6 near expiry (32)	7.3–7.5 (29,32,33)
Biopure Corp. HBOC-201 (Hemopure®)	Bovine red cells	Glutaraldehyde polymerized Hb (39)	13 (39,40, 41,42, 43,44)	68–500 kD (43) Predominantly 130–500 kD (39,44)	34–38 (39, 40,41,42, 43,44)	1.3 (39,40, 43,44)	17 (39,40, 41,43)	8.5 (400 mg/kg) (45) 20–24 (600–800 mg/kg) (39,40,41,42,44)	<15 (39,41,42, 43,44)	7.6–7.9 (39,40,41, 43,44)
Enzon Inc. PEG-Hb	Bovine red cells	Hb is conjugated to polyethylene glycol (PEG) (46)	6 (46)	64 kD species, conjugated to 9–14 PEG molecules (46)	9–16 (46,47)	3.39 (47)	118 (47)	~48 (27,48)	<10 (46)	7.5 (46)
Hemosol Inc. Hemolink™	Human red cells	Hb is $\beta\beta$ cross-linked & polymerized with *o*-raffinose (49)	10 (49)	64 kD (~33%) 126–600 kD (~63%) >600 kD (≤3%) (49)	34 (49)	1 (49)	24 (49)	At 500 mg/kg: 14 (total Hb), 18.4 (oligomeric Hb) 7.4 (cross-linked tetrameric Hb) (49)	<10 (49)	7.5 (49)
Northfield Labs PolyHeme™ (Poly SFH-P)	Human red cells	Pyridoxylated, glutaraldehyde polymerized Hb (50)	8–10 (50,51,52, 53,54,55)	Predominantly polymer, 64 kD (<1%) (50,54,55)	28–30 (50,51,52, 53,54,55)	1.9–2.2[a] (53)	20–25[a] (53,54)	24 (50,55)	<3 (50,52,53, 54,55)	Not available
Somatogen Inc. rHb1.1 (Optro™)	*E. coli* expression system	Genetically fused $\alpha\alpha$ Hb, with mutant β chains (56)	5–8 (56,57,58)	64 kD (100%) (56)	33 (56,58)	0.8 (59)	12 (58)	2.8–12 at plasma [Hb] = 0.5–5 mg/ml (58)	Not available	Not available

[a]For *polymerized pyridoxylated hemoglobin*, not necessarily the polymerized pyridoxylated stroma-free hemoglobin solution used in clinical trials.

Since the vasoactivity of cell-free Hb has been previously reported (23,60), safety studies with HBOCs have focused on product-induced hemodynamic effects. In general however, there is a wide range of reported cardiovascular responses to HBOC products. Some HBOCs have been found to have very little or no vasoactivity in human volunteers (27,54), whereas others have produced a variable dose-dependent increase in blood pressure with a maximum response reached at Hb doses of 0.05 to 0.1 g/kg (33). In studies where blood pressure increased, there was a reciprocal reduction in heart rate that would appear to be a normal physiological response to the rise in blood pressure (33,41,49,58,69). Where studied, cardiac outputs were found to be reduced following the administration of the HBOC in those cases where the blood pressures were elevated. Again, this is most likely an appropriate autonomic nervous system response to increased blood pressure.

With regard to specific product-induced effects, Przybelski et al. (33) studied 24 healthy volunteers receiving DCLHb™ compared to lactated Ringer's (LR) solution in a crossover study design. They reported a dose-related increase in mean arterial pressure (MAP; to a maximum of 20–25% at a the highest dose of 0.1 g/kg) that was mainly the result of increased diastolic pressure. There was a concurrent 16% reduction in heart rate at the 0.1 g/kg (~8.5 g) dose level. Electrocardiogram recordings were found to be normal throughout the study using Holter monitoring or telemetry. Similarly, Viele et al. (58) administered up to 25 g recombinant Hb, rHb1.1, to 34 volunteers and found an increase in MAP of 10–15 mmHg, while heart rate decreased by 15–20 beats per minute. Hughes et al. (62) reported on 9 volunteers receiving up to 28 g of Hemopure® who exhibited a 16% increase in MAP and increased systemic vascular resistance (SVR), along with a reduced heart rate. Cardiac index, as measured by impedance methods, was reduced by 1.3 $L/m/m^2$ at the maximum dose level. Later, Hughes et al. (41) reported on a Phase I trial in 18 subjects also receiving the bovine product (also referred to as HBOC-201), in doses of 16 to 45 g, following phlebotomy of 15% of the estimated blood volume and a 3:1 replacement with LR. In this follow-up Phase Ib study, they also reported an increase in MAP up to 10% above baseline and a 6% decrease in heart rate, with a 15% reduction in cardiac index. More recently, Adamson et al. (49) reported results of a Phase I safety trial in 42 volunteers of which 33 received Hemolink™ in doses ranging from ~2 to 43 g Hb. Following a similar trend as for other HBOC products, a 10–12% increase in MAP was observed, along with a reduction in heart rate.

It is noteworthy that Gould et al. (52,54) briefly reported on a Phase I safety trial in 30 subjects receiving up to 63 g of PolyHeme™ in which only a small (5%) increase in MAP and a 5% reduction in heart rate was seen. Also, in contrast to results described already for other safety trials, no increase in MAP was reported in a Phase I study in which up to ~38 g of Hb conjugated with polyethylene glycol (PEG-Hb) was administered to human volunteers (27).

The range of hemodynamic responses induced by these HBOC products underscores the fact that each product has a different impact on physiological function, likely due to underlying differences in chemical modification. Preclinical studies have suggested that scavenging of nitric oxide (NO), as well as other potential mediators, could play a major role in the vasopressor effects of these agents (23). This hypothesis would suggest that some HBOC products do not interact with NO, although preclinical studies to confirm the presence or absence of NO scavenging activity has not been reported for all products. The significance of vasopressor activity in the clinical setting varies greatly, depending on how these products are used. For example, in trauma and high blood loss surgical procedures, the vasoactivity *may be* of benefit if it does not compromise blood flow to vital end organs. Maintenance of vascular volume is a common benefit of all HBOC products; specific formulations (e.g., with high colloid osmotic pressure) may facilitate resuscitation.

Where reported (33,40,56,62), respiratory function was not adversely affected by the HBOC products. Arterial saturation was found to be maintained, and a good correlation between pulse oximetry and arterial oxygen saturation has been noted (40). Pulmonary function tests were normal where assessed by spirometry and flow volume studies. Both arterial oxygen partial pressures and carbon dioxide partial pressures were unaffected by the HBOCs. In one particularly interesting study (41), the diffusion capacity for carbon monoxide was found to be increased by 20% by HBOC-201. These data support the hypothesis that the cell-free Hb permits a more efficient transfer of gases between the alveolus and the circulation.

Historically, there has been considerable concern with respect to the effects of cell-free Hb on renal function. In this light, it is of interest that no evidence of renal toxicity has been noted in any safety study with current HBOC products. There were no reported adverse effects on serum creatinine or creatinine clearance. Likewise, the tubular cell marker, *N*-acetyl-β-glucosaminidase, was not affected (58). In general, investigators have not found Hb in the urine of the volunteers (41,42,56). These results strongly suggest a lack of HBOC-induced effects on renal function in the test subjects.

Most investigators have reported dose-dependent plasma retention times for the various HBOC products. Although Table 2 shows that relatively low Hb doses were administered in safety studies (e.g., up to 63 g Hb, approximately equivalent to one unit of packed red cells), circulation times may well be longer at higher Hb doses. Although the mechanism of this dose-dependent clearance has not yet been determined, it is likely that different mechanisms are recruited and possibly become saturated as the plasma levels of stabilized cell-free Hb rise. It appears that the tetrameric stabilized products have relatively shorter half-lives, of less than 12 hours, at the doses presented in Table 1 (33,58). In contrast, PEG-Hb at up to 38 g Hb has a half-life of about 48 hours (27). As reported in Phase I safety studies, polymerized HBOCs have intermediate half-lives of ~18–24 hours (39,49,50), again depending on the Hb dose.

There are a number of reports of altered clinical chemistry analytes, although at the doses studied in Phase I HBOC safety trials, none were clinically significant.

Table 2. HBOC Safety Studies in Healthy Volunteers

Product, trial phase, and location	Subjects, [treated + controls], [male (M) + female (F)], age range	Dose range (Hb)	Control	Protocol design	Year of completion	Results	Refs.
DCLHb® Phase I U.S.	n = 24, [of which n = 22 completed crossover], [23 M + 1 F], age 20–49 yrs	~2–8.5 g (25–100 mg/kg)	Lactated Ringer's (LR)	Randomized, controlled, double blind, crossover study: DCLHb® (or LR) was given on day 1; the alternate was given on day 6	1993	*Hemodynamic*. Dose-related increase in mean arterial pressure (MAP), with a greater effect on diastolic blood pressure (DBP) than systolic blood pressure (SBP). No evidence of vasoconstriction. Heart rate (HR) was significantly lower for subjects given 100 mg/kg. Normal electrocardiograms. *Respiratory/oxygenation*. No changes in laser Doppler, pulse oximetry, or toe temperature measurements. *Clinical chemistry*. Dose-related increased in lactate dehydrogenase (LDH)-5 isoenzyme (n = 4, after control; n = 12, after treatment), with no increase in circulating concentrations of total LDH, alanine aminotransferase (ALT), aspartate aminotransferase (AST), alkaline phosphatase (ALP). Total serum creatine kinase (CK) increased at 100 mg/kg; the isoenzyme CK-myocardial band (CK-MB) did not increase. *Pharmacokinetics*. Half-life of 2.5 h at 25 and 50 mg/kg; 3.3 h at 100 mg/kg. *Adverse Events (AEs)*. Mild to moderate abdominal pain (n = 3, after control; n = 6 after treatment). No serious adverse events, no evidence of organ dysfunction or toxicity.	32,33,60,61
Poly SFH-P Phase I U.S.	n = 30 [30 + 0], [? M + ? F], adults	Maximum = 63 g	None used	Uncontrolled study	1993	*Hemodynamics*. No evidence of vasoconstriction. *Clinical Chemistry*. Normal *Hematology*. Normal *Renal effects*. No evidence of renal toxicity. *AEs*. None reported. No gastrointestinal (GI) effect or other adverse events reported.	50,52–54
Hemopure® Phase I U.S.	n = 11 [9 + 2], [11 M], adults	14–28 g	Normal saline	Randomized, controlled, single-blind, single-dose study	1993	*Hemodynamics*. Transient increases in SBP, DBP, MAP, and total peripheral resistance (TPR). Decreased cardiac index (CI) and pulse. *Respiratory/oxygenation*. Respiration and oximetry unchanged. *AEs*. None reported.	62
rHb1.1 Phase I U.S.	n = 93, [76 + 17], [93 M], age unknown[a]	~1–25 g (15–320 mg/kg)	Human serum albumin (HSA)	Design unspecified	1993	*Hemodynamics*. No cardiovascular toxicities. *Respiratory/oxygenation*. No pulmonary toxicities. *Clinical Chemistry*. Hepatic function enzymes normal. *Hematology/coagulation*. Hematological measurements and coagulation parameters normal. *Renal*. No evidence of renal impairment or appreciable renal excretion of rHb1.1. *AEs*. No serious adverse events, but some subjects developed gastrointestinal discomfort, which was managed effectively with pharmacologic intervention.	56

rHb1.1 Phase I U.S.	n = 48 [34 (of which 33 completed the infusion) + 14], [48 M], age 18–35 yrs[a]	~1–25 g (15–320 mg/kg)	HSA	Randomized, controlled, single-blind study	1993	*Hemodynamics*. Non-dose-related increases in MAP, 1 and 2 h after infusion; HR decreased during and for 2 h after infusion. *Clinical chemistry*. No increase in *N*-acetyl-β-glucosaminidase, creatinine clearance increased significantly 1 day after rHb1.1 infusion. Of the 23 subjects who experienced GI effects, 6 had elevated lipase, and 4 of these also had elevated amylase (both effects observed 2–4 h after infusion). *Renal*. No evidence of rHb1.1-mediated nephrotoxicity. *Pharmacokinetics*. Half-life of 2.8 h at plasma concentration of 0.5 mg/mL, and 12 h at 5 mg/mL. *AEs*. GI upset (n = 23/34), fever, chills, headaches, and backache in some subjects.	57,58
rHb1.1 Phase I? U.S.	n = 12[a] [9 + 3], [12 M], age 21–32 yrs[a]	~8–11 g (110–150 mg/kg)	HSA (5%)	Controlled, single-blind study	1994	*AEs*. Increased velocities of peristaltic contractions in 6/9 treated subjects. Increased amplitude and duration of contractile waves in the esophagus. No consistent effect on the resting tone of lower esophageal sphincter (LES), but LES relaxation was inhibited. Spontaneous, simultaneous high-pressure contractions in 8/9 subjects, lower retrosternal chest pain during swallowing in 4 subjects.	63
HBOC-201 Phase Ib U.S.	n = 24, [18 + 6], [12 M + 12 F], age 18–45 yrs[b]	Maximum = 45 g (600–800 mg/kg)	LR	Randomized, controlled, single-blind, single-dose study[c]	1994	*Hematology/coagulation*. Serum iron levels paralleled HBOC-201 concentration, peaking at 8 h (up to 220 μg/dL). Ferritin levels peaked at 48 h (up to 180 ng/mL). Serum erythropoietin increased by 2–6-fold over baseline levels at 24 h. No significant changes in white blood cell or platelet counts, or in prothrombin time (PT) or activated partial thromboplastin time (PTT). *Pharmacokinetics*. Plasma half-life of HBOC-201 was ~20 h. *AEs*. None reported.	39
HBOC-201 Phase Ib U.S.	n = 24, [18 + 6], [12 M + 12 F], age 18–45 yrs[b]	Maximum = 45 g (600–800 mg/kg)	LR	Randomized, controlled, single-blind study[c]	1994	*Respiratory/oxygenation*. Percent oxygen saturation of Hb (Spo_2) can be reliably measured by pulse oximetry or arterial blood gas analysis in the presence of HBOC-201 over the normal range of Spo_2. *Pharmacokinetics*. Plasma half-life of HBOC-201 was ~24 h. *AEs*. None reported.	40,64
HBOC-201 Phase Ib U.S.	n = 41, [18 + 23], [41 M], age 18–45 yrs	16.5–45 g (250–600 mg/kg)	LR	Randomized, controlled, single-blind, dose escalation study[c]	1994	*Hemodynamics*. Small but transient decreases in CI and HR, concomitant with increased BP during the first 8 h after the beginning of infusion. *Respiratory/oxygenation*. Diffusion capacity of oxygen was increased up to 20% above baseline levels in the 38.0 and 45.0 g groups in comparison with controls (~14% below baseline) at 2–4 h after infusion. Other pulmonary function tests and arterial blood gas measurements were unremarkable. Arterial oxygen content and oxygen delivery tended to be greater in active groups than in controls. *Pharmacokinetics*. Elimination of the product was a linear, first-order process, with no renal excretion. Peak plasma	41,44,65

Table 2. HBOC Safety Studies in Healthy Volunteers (*continued*)

Product, trial phase, and location	Subjects, [treated + controls], [male (M) + female (F)], age range	Dose range (Hb)	Control	Protocol design	Year of completion	Results	Refs.
						[Hb] was 1–2 g/dL and plasma half-life approached 20 h at the highest dose. No detectable Hb in the urine. Dosing of HBOC-201 to a target plasma Hb concentration can be achieved using pharmacokinetic principles with measurable effects on oxygen physiology. *AEs*. Minor transient gastrointestinal events such as "gas" were seen in some subjects in both active and control groups, but required no treatment.	
HBOC-201 Phase Ib U.S.	n = 6, [3 + 3], [6 M], age 25–45 yrs	45 g (600 mg/kg)	autologous blood	Randomized, controlled, single-blind, two-way crossover study: on day 1, HBOC-201 or autologous blood was given, with the opposite given on day 8[c]	1994	*Respiratory/oxygenation*. Subjects had similar exercise and diffusion capacity but lower lactate levels (for up to 24 h) during HBOC-201 than during autologous transfusion periods. O_2 use (uptake) and CO_2 production at rest were greater during HBOC-201 than during autologous transfusion periods. Under the study conditions, the physiological effects of 1 g HBOC-201 were similar to 3 g Hb from autologous transfusion. *Pharmacokinetics*. Half-life was ~23 h. No Hb detected in the urine. *AEs*. None reported	42,44,66
Hemolink™ Phase I Canada	n = 42 [33 + 9], [42 M], age 18–40 yrs	~2–43 g (25–600 mg/kg)	LR	Randomized, controlled, double-blind, dose escalation study	1995	*Hemodynamics*. MAP increased to a maximum of 10–12%, but was not clinically significant. HR decreased for up to 24 h postinfusion. *Clinical chemistry*. At the highest dose, clinically insignificant and transient changes in liver enzymes (AST, ALT, gamma-glutamyltransferase [GGTP] and pancreatic enzymes [amylase and lipase] were observed, but did not appear to reflect clinically significant events. *Hematology/coagulation*. No coagulation abnormalities, as determined by platelets counts, PT, and PTT. *Renal*. The product did not impair normal renal function. *Pharmacokinetics*. Plasma half-life for Hemolink™ increased with dose level, ranging from ~1.6 h at a dose of 25 mg/kg to ~15.6 h at 500 mg/kg. There was also a direct relationship between increasing half-life and increasing molecular weight for the various (oligomeric, tetrameric, and non-cross-linked dissociable) Hb fractions of Hemolink™. *AEs*. At the highest dose, subjects had moderate to severe GI discomfort, which transiently interefered with normal everyday activities. Airway function, body temperature, and respiration rate remained unchanged.	49,67
PEG-Hb Phase I U.S.	n = 38, [32 + 6], [38 M], age unknown	~4–38 g (0.83–8.33 ml/kg)	LR	Controlled, unblinded, single infusion study	1995	*Hemodynamics*. No changes in blood pressure. *Renal*. No renal or other organ toxicities. *Pharmacokinetics*. PEG-Hb remains in circulation long enough to be consistent with weekly dosing and current fractionated radiation therapy. *AEs*. Subjects given 5.83 and 8.33 ml/kg experienced transient episodes of GI pain.	48,68,69

[a]The patient population (n = 93) described by Gerber et al. (56) may include the patients enrolled in studies published by Viele et al. (58) and Murray et al. (63).
[b]The patient population described by Hughes et al. (39) may be the same population as that presented in Hughes et al. (40).
[c]In studies reported by Hughes et al. (39–42), 15% of blood volume was withdrawn, and LR was given in a ratio of 3:1 prior to infusion of HBOC-201 or control solution.

Increases in lactate dehydrogenase (LDH) and creatine kinase (CK) above baseline have been reported (33,49), with the cardiac subfractions being negative, suggesting a skeletal muscle source and not a cardiac source for these elevations. In general, analytes measured as markers of liver function fell within normal ranges in all studies. Slightly increased lipase and amylase activity have also been reported (49), in contrast to another study in which serum lipase was elevated to 10 times the upper limit of normal (ULN) and amylase was elevated to 3–4 times the ULN (58). These reported elevations returned to normal levels within 24 to 48 hours, with no clinical evidence of pancreatitis. Detailed iron kinetics were measured in only one safety study (39). Other authors reported no change in the already mentioned clinical chemistry parameters or simply did not comment. It is also noteworthy that, where reported, no antibodies were detected in response to HBOC products at the dose levels administered in safety studies (33,49).

Although there were some striking findings in Phase I safety studies, there were no serious adverse events reported in any of these trials. The most consistent adverse events induced by HBOCs have been gastrointestinal (GI) effects. Most investigators have reported GI symptomatology in awake participants in the Phase I safety studies. The symptoms appear to be dose dependent and include abdominal pain, flatulence, and dysphagia (27,33,41,48, 49,56,58). In an elegant study these effects were shown to be due at least in part to an interruption of normal esophageal motility mechanisms (63). Preclinical studies identified NO scavenging by the hemoglobins as a likely mechanism for adverse GI effects, and these effects appear to be mimicked by the inhibition of NO synthase (70). Interestingly, the recombinant Hb product was also reported to produce fever, chills, headache, and dermatological abnormalities following administration (56). The potential role of residual endotoxin from *E. coli* may be called into question by this finding.

HBOC Studies in Elective Surgery

A large number of abstracts, along with a small number of full text articles, is now available regarding HBOC trials in surgical patients. These publications, which correspond to Phase I, Ib, I/II, II, and III trials with HBOC products, are referenced in Table 3. The areas of surgery that have been studied in these trials were classified here as orthopedic, cardiovascular, and general surgery (i.e., trials in which one or more of the following surgical groups were included: urological, gynecological, hepatic, abdominal, and orthopedic surgery, or where no particular surgical population was specified). Within each of these classifications, trials are organized in chronological order of completion, between 1994 and 1997.

These studies were typically randomized and controlled, with either single or double blinding. Control articles used in these studies varied more widely than for safety trials in volunteers. That is, control solutions included crystalloids (saline and LR), colloids (hydroxyethyl starch), as well as both allogeneic RBCs and autologous blood. Trials involving acute normovolemic hemodilution (ANH) procedures are identified in the column titled "Protocol Details." Dose ranges (up to ~100 g Hb) were generally greater than those administered in the volunteer studies described already. Collectively, these studies in surgical patients addressed both safety and efficacy issues, with key results reported in Table 3. Pharmacoeconomic results (e.g., duration of hospital stay) are also presented, if reported in the published literature.

All studies reported safety with hemodynamic stability and varying degrees of hemodynamic activity. In vascular and cardiac surgery, an increase in MAP and SVR has been observed. A small increase in pulmonary vascular resistance (PVR) has been reported by two groups (34,76), whereas one found no effect on PVR (43). Where reported, cardiac output has been depressed, an appropriate response to increased MAP. In orthopedic and general surgery, hemodynamics were found to be relatively stable following administration of the specific HBOC products used. Due to the variability of the surgical settings and anesthesia, it is not possible to directly compare the hemodynamic effects induced by individual HBOC products.

Global oxygen delivery has been noted to be reduced, commensurate with the reduction in cardiac output (34,43,81,82). Oxygen consumption was depressed or maintained, while the oxygen extraction ratio generally increased. These reported effects may be due in part be due to the right-shifted nature of the products studied (i.e., they have right-shifted oxygen-Hb dissociation curves, associated with P_{50} values higher than that of whole blood). HBOC-induced effects on respiratory function in these trials have not been described in the literature.

Consistent with the safety studies in awake individuals discussed earlier, and consistent with preclinical studies in various animal species (49,88), renal function has not been adversely affected by HBOCs in any of the trials in surgical patients reported to date. However, investigators have reported hemoglobinuria in patients following administration of 75 g DCLHb™, and jaundice has been reported in the same surgical trials (involving cardiac, orthopedic, and abdominal patients) without evidence of hepatic failure (36,85).

Pharmacokinetic data for HBOCs obtained in the surgical setting are similar to the findings in the awake volunteers. Clinical chemistry values generally remain within the normal range or are not significantly different from control patient values (77,81). In some surgical studies, increased serum amylase and/or lipase has been noted (36,72,78,85); consistent with the observations in earlier safety trials, no acute pancreatitis has been reported.

Only a small number of publications have reported on the immunological effects of HBOC administration. One study reported negative DCLHb™ antibody titres up to 6 weeks following administration of a low hemoglobin dose (~3.5 g) in patients undergoing abdominal aortic aneurysm repair (76). Interestingly, patients with hepatic surgery did not have IgE antibodies to HBOC-201 but developed very low levels of IgG to HBOC-201 14 days after administration of ~28 g of the product (45). In a novel, double-dose study design (87), HBOC-201 was administered both intraoperatively and on postoperative day 1 for a total dose of ~100 g Hb. There was no explicit mention

Table 3. HBOC Studies in Elective Surgery

Indication/ patient population	Product, trial phase, and location	Subjects, [treated + control], [M + F], age range	Dose range (Hb)	Protocol details	Completion date	Primary endpoint(s)	Results (safety, efficacy, pharmacoeconomic)	Refs.
				Orthopedic				
Surgery	rHb1.1 Phase I/II U.S.	n = ? [? + ?], [?M + ?F], age unknown	≤25 g	Controlled, single-blinded, dose escalation study. *rHb1.1* or *saline* given perioperatively.	Mid 1994	Safety	*Safety.* *Hemodynamics.* No evidence of hemodynamic impairment. *Renal.* No renal impairment. *Hematology/coagulation.* No evidence of any toxicity or impairment of function. *AEs.* No serious adverse events, and GI symptoms seen in Phase I were not encountered. *Efficacy.* None reported. *Pharmacoeconomic.* None reported.	57
Total hip replacement	DCLHb™ Phase II Europe	n = 80, [? + ?] [?M + ?F], age unknown	~2–18 g (25–200 mg/kg)	Double-blind, controlled, randomized study. *DCLHb™* or *placebo* given preoperatively, prior to anesthesia and surgery.	Early 1995	Safety	*Safety.* *Hemodynamics.* Mean increase in MAP = 8–16 mm Hg. *AEs.* No toxicities reported. *Efficacy.* None reported. *Pharmacoeconomic.* None reported.	35,71
Total hip and knee replacement	rHb1.1 Phase II U.S.	n = 10, [7 + 3], [?M + ?F], age unknown	12.5–50 g	Controlled dose escalation study. 250–800 ml of blood withdrawn and replaced with saline in a ratio of 2:1, then *rHb1.1* or *saline* given preoperatively, prior to anesthetic and surgery. [acute normovolemic hemodilution (ANH) protocol]	Late 1995	Safety	*Safety.* *Hemodynamics.* One patient given 12.5 g experienced an increase in systolic BP 20% above baseline; no other patients demonstrated significant systolic hypertension. No intraoperative myocardial ischemia or infarctions were noted. *Clinical chemistry.* Increased amylase and lipase at 2 h in two patients, but not suggestive of pancreatitis. *AEs.* No treatment-related GI symptomatology was reported by any patient during or postoperatively. No fever or hypersensitivity effects. *Efficacy.* None reported. *Pharmacoeconomic.* None reported.	57,72,73
Surgery	DCLHb™ Phase II? Europe?	n = ?, [12 + ?] [?M + ?F], age unknown	≤75 g	Randomized, controlled study. *DCLHb™* or *allogeneic RBCs* given postoperatively, within 24 h of surgery.	Early 1997	Reduced Allogeneic RBC Transfusion	*Safety.* Well tolerated. *Efficacy.* 33% of patients receiving DCLHb avoided blood transfusion over 7 days. *Pharmacoeconomic.* None reported.	74

Abdominal aortic repair	DCLHb™ Phase II Europe	n = 71, [35 + 36] [?M + ?F], age unknown	3.5–14 g (50–200 mg/kg)	Randomized, controlled, single-blind study. *DCLHb™* or *LR* given preoperatively, after anesthetic, prior to surgery.	Late 1995	Safety	*Safety.* *Hemodynamics.* Maximum increase in MAP ~20 torr. Duration, but not magnitude, of this pressor response is dose dependent. Fewer hypotensive episodes in the perioperative period. CI and oxygen delivery (DO_2) maintained or decreased, oxygen consumption (VO_2) maintained. *Efficacy.* None reported. *Pharmacoeconomic.* None reported.	60,75
Abdominal aortic surgery	HBOC-201 Phase II Europe	n = 13, [7 + 6], [10M + 3F], age 18–70 yrs	~33 g (3 ml/kg @ 13% Hb)	Controlled, randomized, single-dose study. Following anesthesia, 1 liter of blood withdrawn and replaced with LR, then *HBOC-201* or *hydroxyethyl starch (HES)* (6%, mean molecular weight (M_r) = 70,000 (substitution ratio ~ 0.5) given preoperatively, prior to surgery. [ANH protocol]	Mid 1996	Safety	*Safety.* *Hemodynamics.* 30 min after HBOC-201 infusion, MAP, SVR and CI were 149%, 169%, and 75% of preinfusion values, respectively. No change in HR or pulmonary vascular resistance (PVR). *Respiratory/oxygenation* O_2 delivery index (Do_2I) and O_2 consumption index (Vo_2I) 30 min after infusion were 79% and 76% of preinfusion values, respectively, whereas O_2 content in arterial blood (CaO_2) and O_2 extraction ratio (O_2ER) remained unaffected. *Efficacy.* None reported. *Pharmacoeconomic.* No change in intensive are unit (ICU) or postoperative hospital length to stay (LOS); 11 ± 2 days total stay for both groups.	43
Abdominal aortic aneurysm repair	DCLHb™ Phase I/II? U.S.	n = 10, [5 + 5], [?M + ?F], age unknown	~3.5 g (50 mg/kg)	Randomized, controlled study, *DCLHb™* or *Hespan* given postoperatively.	Late 1996	Safety	*Safety.* *Hemodynamics.* DCLHb-treated patients had higher systemic, pulmonary vascular and arterial pressures, as well as higher SVR and PVR. These effects were transient, with no differences between groups at 2 h after administration. *Immunological.* DCLHb antibody titres were negative in all patients at 6 weeks. *AEs.* No patients experienced severe adverse reactions directly attributable to DCLHb. One treated subject suffered a myocardial infarction 36 h after infusion, but it was not deemed attributable to DCLHb. *Efficacy.* None reported. *Pharmacoeconomic.* None reported.	76
After bypass surgery	DCLHb™ Phase III Europe	n = 209 [104 + 105], [?M + ?F], age unknown	75 g	Randomized, controlled study. *DCLHb™* or *allogeneic RBCs* given postoperatively, in the first 24 h postbypass.	Early 1997	Safety and reduced allogeneic RBC transfusion	*Safety.* *Hemodynamics.* Following the first infusion, O_2ER increased significantly (+7%) in the DCLHb group, compared with a 3% fall in the control group. DCLHb increased SVR, most significantly after the first infusion. CK-MB, LDH_1 and troponin I levels were comparable or lower following DCLHb infusion at 1, 3, and 7 days postsurgery. *Mortality.* Comparable for both groups.	34,36,74

Table 3. HBOC Studies in Elective Surgery (*continued*)

Indication/ patient population	Product, trial phase, and location	Subjects, [treated + control], [M + F], age range	Dose range (Hb)	Protocol details	Completion date	Primary endpoint(s)	Results (safety, efficacy, pharmacoeconomic)	Refs.
							AEs. DCLHb-related events (in some patients) included: yellow skin discoloration; hematuria/ hemoglobinuria; hypertension; increases in AST, amylase, and ALT; hyperbilirubinemia; and abnormal hepatic function. *Efficacy*. At 24 h postsurgery, 39% avoided allogeneic RBCs; at 7 days postsurgery (or hospital discharge), 19% avoided allogeneic RBCs. The total number of RBC units given over the 7-day period was similar in both groups. *Pharmacoeconomic*. None reported.	
				General surgery				
Urological (radical prostatectomy)	HBOC-201 Phase I U.S.	n = 20 [12 + 8], [20M + 0F], age unknown[a]	~34–45 g (400–600 mg/kg)	Controlled, single-blind, dose escalation study. *HBOC-201* or *LR* was given postoperatively, on the first postoperative day.	Late 1995	Safety	*Safety*. *Hemodynamics*. A slight increase in mean BP and slight decrease in HR observed. *Clinical chemistry*. No clinically significant changes in liver function (AST, ALT, GGTP, bilirubin). *Renal*. No clinically significant changes in renal function (creatinine). *Hematology/coagulation*. No clinically significant changes in coagulation profile (PT, PTT, platelet count, fibrinogen). *AEs*. No serious AEs or mortality occurred. *Efficacy*. None reported. *Pharmacoeconomic*. No change in hospital LOS.	77
No surgical population specified	rHb1.1 Phase II U.S.	n = 23, [16 + 7], [?M + ?F], age 18–75 years	25–100 g	Controlled, randomized single-blind study. *Optro*™ or *control therapy (allogeneic RBCs or autologous blood)* given to treat blood loss intraoperatively, during surgery.	Late 1995	Safety	*Safety*. *Hemodynamics*. Electrocardiogram (ECG) and HR were stable during transfusion period. No consistent changes in BP were observed. *Oxygenation/pulmonary*. Oxygen saturation was stable. *Clinical chemistry*. No significant changes in serum chemistries, with no evidence of renal function abnormality. Elevated amylase and lipase were observed in some patients, but was not suggestive of acute pancreatitis. *Hematology/coagulation*. No significant changes in hematology, coagulation tests. *AEs*. No drug-related serious adverse events; no signs of GI dysmotility. *Efficacy*. None reported. *Pharmacoeconomic*. None reported.	57,78

Orthopedic, gynecological, and urological	HBOC-201 Phase Ib? U.S.	*n* ~ 54 (3 groups of ~18), [ratio = 2:1], [?M + ?F], age unknown[a]	~28–42 g (400–600 mg/kg)	Randomized, placebo-controlled, single-blind, parallel group studies. *HBOC-201* or *LR* given postoperatively (when Hb < 11 g/dl).	Late 1995	Erythropoietic effects	*Safety.* *Hematology/coagulation.* HBOC-201 accelerated erythropoiesis compared to controls as measured by corrected absolute reticulocyte count (CARC) and hematocrit (Hct), equivalent to endogenous generation of ≥1/2 unit of blood in less than one week. Blood loss and allogeneic and/or autologous transfusion and volume replacement were similar in active and control groups. *Efficacy.* See hematological effects. *Pharmacoeconomic.* None reported.	79
No surgical population specified	HBOC-201 Phase II? U.S.	*n* = 58, [37 + 21], [?M + ?F], age unknown	~42–84 g (600–1200 mg/kg)	Randomized, placebo-controlled, single-blind, dose escalation, study. Following anesthesia and blood loss of ≥500 ml, *HBOC-201* or *LR* was given intraoperatively.	Mid 1996	Hemodynamic effects	*Safety. Hemodynamics.* No significant differences in vital signs (SBP, DBP, HR) when changes from baseline were compared between patients receiving LR or HBOC-201. *Efficacy.* None reported. *Pharmacoeconomic.* None reported.	80
Hepatic (liver resection)	HBOC-201 Phase II Europe	*n* = 12, [6 + 6?], [6M + 6F], avg = 59 yrs	~28 g (400 mg/kg)	Randomized, controlled, single-dose, prospective study. Following anesthesia, 1 L of blood withdrawn and replaced with 1 litre LR, then *HBOC-201* or *HES* (6%, mean MW = 70,000, substitution ratio 0.5) given preoperatively, prior to surgery. [ANH protocol]	Late 1996	Safety	*Safety.* *Hemodynamics.* MAP increased by 18%, and SVR increased by 42%. *Respiratory/oxygenation.* CO, mixed venous oxygen content, and oxygen delivery decreased. Oxygen extraction ratio increased, even in the ICU. *Clinical chemistry.* No changes in amylase. *Hematology/coagulation.* Treated patients developed a more pronounced increase in leukocytes, reticulocytes, and arterial methemoglobin during postoperative days 2–3 compared to controls. No changes in coagulation profiles. *Renal.* No Hb detected in urine. No changes in creatinine. *Pharmacokinetics.* Mean half-life ~8.5 h. *Immunological.* No IgE antibodies to HBOC-201 were observed, but mean concentration of IgG to HBOC-201 increased after day 7 to a maximum of ~10 ng/mL on day 14. *AEs.* No allergic or adverse reactions. *Efficacy.* None reported. *Pharmacoeconomic.* No change in hospital LOS.	45,81–83

Table 3. HBOC Studies in Elective Surgery *(continued)*

Indication/ patient population	Product, trial phase, and location	Subjects, [treated + control], [M + F], age range	Dose range (Hb)	Protocol details	Completion date	Primary endpoint(s)	Results (safety, efficacy, pharmacoeconomic)	Refs.
Orthopedic and abdominal	DCLHb® Phase II? U.S.	n = 36?, [12 + 24]?, [?M + ?F], age unknown[b]	75 g	Randomized, controlled, unblinded, prospective study. Following anesthesia, *DCLHb®* or *allogeneic RBCs* was given intraoperatively, within 12 h after surgery start.	Late 1997	Effects on methemoglobin (MetHb), organ function, coagulation, pharmacokinetics, and allogeneic RBC transfusion	*Safety.* *Hemodynamics.* No cardiac complications. *Clinical chemistry.* No hepatic complications. Amylase was elevated to 3 times the upper limit of normal (ULN) at POD 2, returning to normal by POD 4. *Hematology/coagulation.* Significantly higher metHb levels were observed in the treated group at several time points, but did not affect patient outcome. No adverse effects on hematology or coagulation tests. *Renal.* No renal complications. *Pharmacokinetics.* Harmonic mean half-life was 10.5 h. *AEs.* Transient mild to moderate GI effects, skin discoloration, and hemoglobinuria. *Efficacy.* In combination with autologous predonation, DCLHb may have potential to reduce RBC transfusion and to avoid allogeneic RBCs. *Pharmacoeconomics.* None reported.	37,38,84–86
No surgical population specified	HBOC-201 Phase II? U.S.	n = 33, [19 + 14], [?M + ?F], age unknown	~70–105 g [Intra-op + post-op] (600 + 400 mg/kg to 900 + 600 mg/kg)	Randomized, controlled, single-blind, dose escalation study. Following anesthesia, and blood loss ≥ 500 mL, HBOC-201 or LR was given intraoperatively in OR, followed by a postoperative dose of HBOC-201 or LR, respectively, on postoperative day (POD) 1, at 24 h after the OR dose.	Late 1997	Kinetics and hemodynamic effects	*Safety.* *Hemodynamics.* No significant hemodynamic changes (HR, mean BP) in patients infused during anesthesia and postoperatively. *Pharmacokinetics.* A dose response in plasma Hb levels (<2 g/dL) was observed with both initial and second infusion of HBOC-201; both were safe and well tolerated. *Efficacy.* None reported. *Pharmacoeconomics.* No change in hospital LOS.	87

[a]The general surgical patient population (n ~ 54) described by Hughes et al. (79) may overlap with the urological patient population (n = 20) enrolled in the study published by Monk et al. (77).
[b]It is assumed that the abstracts by Schubert et al. (85,86) and O'Hara et al. (37,38,84) refer to the same patient population (n = 36?). Some results are reported for subsets (n = 12) of this population.

of any immunological change. Although single and double HBOC doses appear to be well tolerated, it remains unclear if repeat administration of HBOCs at any dose will have immunological consequences.

Several HBOC trials have reported no clinically significant changes in hematology tests or coagulation profiles at doses up to 100 g Hb (77,78,81,84) consistent with results from earlier safety studies. In one study, HBOC-201 was shown to accelerate erythropoiesis (compared to LR treatment), as determined by corrected absolute reticulocyte counts and hematocrit measurements (79). These data support the hypothesis that, in addition to their role in boosting oxygen-carrying capacity in the immediate term, HBOC products might be useful in treating patients with various anemias (39,47) by potentially supplementing endogenous iron sources and/or stimulating erythropoiesis, thereby enhancing red cell mass.

In the surgical setting, no serious adverse events have been reported in response to HBOC administration. Moreover, there is an almost complete lack of GI complaints in these patients. The apparent absence of GI effects in the surgical setting may be multifactorial. The degree of postoperative pain may be more marked than the HBOC-induced GI discomfort. The effect may also be blunted by concomitant analgesic administration or the use of other agents. Although GI events do not appear to be of great concern in anesthetized surgical patients, further investigation of relevant mechanisms and clinical outcomes will be required in future studies.

Only two studies have reported on product efficacy in terms of transfusion avoidance. In one small study, the combination of autologous predonation and DCLHb™ was reported to have *the potential* to reduce exposure to allogeneic red cells (86). In a larger Phase III trial, 39% of postbypass patients avoided allogeneic blood in the first 24 hours after surgery; this was reduced to 19% by 7 days postsurgery or hospital discharge (34,36). The total number of red cell units transfused was similar in the control and treatment arms, despite the fact that approximately one-fifth of treated patients avoided blood completely.

Some pharmacoeconomic parameters have also been reported by groups conducting HBOC trials in surgical patients. The most common measure is hospital length of stay (LOS), which has been found to be unchanged in HBOC-treated versus control patients in several groups, including hepatic (45), abdominal aortic (43), urological (77), and general surgery (87). The use of LOS as an appropriate evaluation parameter in these settings can be debated.

HBOC Studies in Traumatic Shock

In comparison with HBOC trials in elective surgery, only a small number of trauma studies have been completed and published (55,91). This situation may be explained by the general belief that it is best to accumulate data in the controlled surgical setting before embarking upon trials in the less controlled trauma arena. Not all HBOC manufacturers have initiated trauma studies, although the majority have expressed an intent to do so.

Table 4 presents the protocol details of published trauma trials, including specific products and trial locations, as well as the number of treated and control subjects, Hb dose ranges, and key results. One of the three published trials was not a controlled study, with all patients receiving the HBOC product, at doses up to 300 g Hb, once the clinical decision to initiate transfusion was made (54,55). In a follow-up, controlled trial in which the same maximum dose was achieved (indeed the highest Hb dose for all clinical trials reported to date), allogeneic red cells were given to patients in the control arm (93). In the third study, in which low doses, up to 20 g Hb, were administered, saline was used as the control solution (91).

Reported hemodynamic parameters showed little if any change. In response to the specific products and dose levels used in these trials, MAP levels were maintained or increased slightly (55,89). Renal function was reported to be normal (55,89). Results of clinical chemistry analyses are presented for only one trial; patients with normal preinfusion values were claimed to exhibit no changes in creatinine, aspartate aminotransferase (AST), alanine aminotransferase (ALT), bilirubin, or amylase levels (55). However, even after excluding patients with abnormal preinfusion values, levels of both AST ($n = 26$) and amylase ($n = 19$) on day 1 were approximately double baseline values, with slight reductions but still elevated levels on day 3. In trauma studies, the trend towards elevated levels of amylase appears consistent with results of other trials in healthy volunteers and elective surgical patients. Further studies will be required to determine the significance and mechanism for these amylase elevations. To date, little if any information has been reported on HBOC-induced effects on immunology, hematology, or coagulation profiles in published trauma studies. One study reported the absence of HBOC-related GI distress (50).

It should be emphasized that at least two different clinical approaches and endpoints have been adopted in the HBOC trauma trials conducted to date. The low-dose trauma trial was primarily conducted as a safety study to support subsequent, larger scale trials in the trauma setting, in which DCLHb™ would be used as a low-volume, pressor, perfusion agent to reduce mortality and morbidity (32,90). In contrast, the high-dose studies have aimed to reduce allogeneic red cell transfusion as the primary endpoint, by using PolyHeme™ as a blood substitute in the traditional sense (55,93).

With regard to efficacy, HBOCs have been shown to reduce both mortality and allogeneic blood exposure, the two key targeted endpoints. In one study protocol, administration of DCLHb™ reduced death and serious adverse events by 25% and 15%, respectively, compared to saline-treated controls, in the first 50 patients who were treated with up to 10 g Hb (91). However, for the entire group of 139 patients, mortality and adverse event rates were not statistically different between treated and control groups (89,90). A larger efficacy trial now underway in DCLHb™-treated trauma patients aims to reduce 28-day mortality by 25% (i.e., from 40% to 30%) (10,90,95). Using different protocol designs, transfusion avoidance has also been demonstrated to some degree in other trauma trials. In an uncontrolled study with PolyHeme™, 59% of patients avoided allogeneic red cell transfusion within the first 24 hours after blood loss, although transfusion requirements during

Table 4. HBOC Studies in Traumatic Shock

Indication/ patient population	Product, trial phase, and location	Subjects, [treated + control], [M + F], age range	Dose range (Hb)	Protocol details	Completion date	Primary endpoint	Results (safety, efficacy, pharmacoeconomic)	Refs.
Hemorrhagic hypovolemic shock (class II–IV) (74% of shock was trauma-related)	DCLHb™ Phase I/II U.S. and Europe	n = 139 [71 + 68], [97M + 42F], 17–91 years	5–20 g (50–200 mL)	Prospective, controlled, randomized, single-blind, dose escalation study. *HemAssist™* or *saline* given perioperatively, within 4 h of shock episode.	Mid 1995	Safety	*Safety*. *Hemodymamics*. 10-g and 20-g doses induced a slight increase in MAP. *Renal*. No increase in renal insufficiency and failure. *AEs*. No increase in rate of complications, adverse events, or overall mortality. No allergic or transfusion reactions. *Efficacy*. None reported *Pharmacoeconomic*. None reported.	89–91
Trauma (blunt and penetrating trauma or non-trauma-related surgery)	Poly SFH-P Phase I/II U.S.	n = 39 [39 + 0], [28M + 11F], 19–83 years	50–300 g	Prospective, uncontrolled, nonrandomized, unblinded study. *PolyHeme™* given pre-, intra- and postoperatively to both awake and anesthetized patients.	Late 1995	Reduced allogeneic RBC transfusion	*Safety*. *Hemodynamics*. No changes in cardiovascular function (including MAP and HR). *Oxygenation/pulmonary*. Utilization of O_2 (extraction ratio) was 27 ± 16% from RBCs vs. 37 ± 13% from Poly SFH-P. *Clinical chemistry*. No changes in creatinine, AST, ALT, bilirubin, or amylase in patients with normal preinfusion values. *Hematology/coagulation*. Plasma Hb concentration after infusion of 300 g of Poly SFH-P was 4.8 ± 0.8 g/dL. Poly SFH-P maintained total Hb despite the marked fall in red cell Hb due to blood loss. *Renal*. No kidney dysfunction. *AEs*. No fever, GI distress, or other significant adverse events related to product infusion. *Efficacy*. 23 patients (59%) avoided allogeneic transfusion in the first 24 h after blood loss. *Pharmacoeconomics*. None reported.	50,53–55,92
Trauma and emergent surgery	PolyHeme™ Phase II U.S.	n = 44 [21 + 23], [33M + 11F], age 19–83 years	≤300 g	Prospective, controlled, randomized study. *PolyHeme™* or *allogeneic RBCs* (un-cross-matched?) given perioperatively.	Late 1996	Reduced allogeneic RBC transfusion	*Safety*. *AEs*. No adverse clinical events attributable to PolyHeme™. *Efficacy*. Treated patients received (an average of) 4.4 units of PolyHeme™ plus 7.8 units of allogeneic RBCs, whereas control patients received 11.3 units allogeneic RBCs, prior to hospital discharge. PolyHeme™ maintained total Hb and O_2 transport despite the marked fall in RBC Hb due to acute blood loss. *Pharmacoeconomic*. None reported.	50,93,94

the entire hospital stay were not disclosed (55). More convincing results from the controlled, follow-up study showed that requirements for allogeneic RBCs were reduced by an average of 3–4 units per patient during the entire hospital stay (94). In these published trauma trials, actual duration of hospital stay, a key pharmacoeconomic parameter, was not reported.

DISCUSSION

What We Have Learned

It is clear from the text and tables herein that the clinical testing of Hb-based red cell substitutes has progressed significantly since the beginning of this decade. At least six HBOC products of various composition (10) have been administered to over 600 subjects in Phase I, II, or III clinical trials, supporting their use in acute blood loss indications. Although many of the cited reports have presented limited data, it appears that, most importantly, these products are safe and well tolerated in the human volunteers and various patient groups evaluated to date.

Earlier concerns regarding the potential for nephrotoxicity and influences on the coagulation mechanism have not been realized. Likewise, pulmonary function does not appear to be affected by HBOCs, nor does the central nervous system. There is no clear data from any reports to date, either written or oral, to validate any concerns in these areas. However, it is also apparent that some adverse events, according to the true definition of the term, have been observed. In awake, healthy volunteers, unexpected GI disturbance and/or esophageal dysfunction have been reported for most of the products tested. Interestingly, the solution of human Hb not containing any 64 kD Hb species is the only product for which these effects have not been reported in either Phase I or II testing (53,55). It is noted that when general anesthesia is a part of the experimental protocol, as it has been with many of the Phase II tests in various patient groups, the GI symptoms are absent or certainly minimized (57,72,78,85). No other significant adverse events or unexpected findings have been reported from the infusions of this diverse group of products that are either universal or systematically recorded.

It has also been observed that there is some degree of vasoactivity associated with the infusion of many of these Hb solutions. Certain investigators consider this a potentially beneficial effect, perceiving an increase in systemic pressure as a good in the resuscitation models. Others view it as potentially harmful, particularly if there is redistribution of flow resulting from the vasoconstriction. The concept that these solutions are more than oxygen carriers is now acknowledged, yet their acceptance as pharmacologically active agents requires further inquiry into the nature of their effects and the potential for harm in both normal and compromised host situations. For example, vasoconstriction is generally believed to be an active physiologic process requiring expenditure of energy and hence consumption of oxygen. If the consumption of additional oxygen is sufficient to affect the total amount of oxygen available for delivery to tissues, then the beneficial net increase in oxygen delivery will be decreased.

With the potential availability of an oxygen carrying cell-free solution we have also learned that the medical community as a whole, and surgery and anesthesia in particular, are willing to alter their existing concepts of transfusion triggers. That is, once a solution with acceptable characteristics is available, the need for alternatives to allogeneic transfusion will change. Indeed, other options will also be exercised in an attempt to minimize exposure to allogeneic blood. The availability of autologous blood through predeposit or intraoperative hemodilution, the latter without compromise of oxygen-carrying capacity, in combination with an HBOC product will likely be a significant factor in altering transfusion decisions in the surgical area. In many of the Phase II (72,81,86) and some of the Phase III (36) protocols, these concepts are now being exercised with the goal of demonstrating transfusion avoidance without an increase in ischemic events, the obvious outcome to be avoided.

Cell-free Hb solutions were once considered to be an ideal replacement for blood or packed RBCs in trauma situations. The brass ring prize was to develop a commercial product for such use. With time, a great deal of knowledge has been acquired in the area of shock resuscitation physiology, making this an even more attractive transfusion alternative. Furthermore, the equivalence of acellular Hb solutions to whole blood has now been demonstrated in various animal and clinical models. These observations are both exciting and encouraging. Specifically, a solution of recombinant Hb (at 5 g/dl) was shown to possess oxygen-carrying capability superior to autologous rat blood, which contains ~8–9 g/dl Hb (57). In a separate study, which evaluated exercise capacity in humans using a bicycle exercise stress test, the physiological effects of 1 unit of HBOC-201 were shown to be equivalent to 3 units of autologous whole blood with respect to exercise function (42,44). The acellular property of these solutions is believed to be a significant factor in enhancing their relative efficaciousness in terms of oxygen delivery.

Future Research Directions

Although a great deal has been learned from these early clinical trials, which have demonstrated safety and to some extent efficacy, there are still gaps in the knowledge that need to be filled to give a richer and more comprehensive picture. Is it necessary to define all of the physiologic nuances before proceeding with new generations of solutions? How will the composition of the new solutions differ in terms of basic characteristics and traits? What new features will be added to address the various problems perceived as the list of indications is expanded? Should these solutions be designed to address reperfusion phenomena along with the free radical interactions? Should they address NO issues along with oxygen delivery concepts? It must be recalled that the generation of NO is also an oxygen-consuming process, such that some of the increased oxygen-carrying capacity will not be used for nutrient tissue perfusion—one initial objective of using these solutions.

At present, little is known of the effects of these products in the presence of certain diseases. This is especially

true of patients with hepatic or renal disease, for the liver and kidney are the primary sites of excretion and metabolism along with the reticuloendothelial system. Physiological effects induced by HBOC products in patients with compromised function in these organs requires further exploration, although there is currently no evidence to suggest additional adverse events will occur.

There is also a need to develop an understanding of the mechanism(s) of HBOC-induced smooth muscle contraction both in the vasculature and the GI tract. Understanding the underlying mechanism will allow agents to be added to existing products to counter these effects, or will permit the design of new Hb solutions to obviate such effects. There are difficulties of course, particularly from a regulatory perspective, when the composition of the solution is altered. The combinatorics of evaluating a product with many biological and physiological effects in animal and clinical models imply an enormous challenge.

It must be noted that most of the solutions presently being evaluated are truly first generation products, relying on some degree of stabilization of the Hb tetramer and then, in some cases, using a polymerization process to enlarge the molecular weight. The former provides an improvement in oxygen delivery and off-loading by decreasing oxyhemoglobin affinity, whereas the latter aids in promoting intravascular persistence, both desirable traits. Whether newer solutions will address these basic issues or add new complexity is not known. Over time, we will need to know the details of models to evaluate the effects of the newer and potentially more complex solutions (24).

On a cautionary note, we will need to understand the pharmacokinetics and the pharmacodynamics of Hb solutions to deal with their complete assessment in the clinical arena. Hence, it will be necessary to understand the details of product metabolism, including the effects of any directly or indirectly derived by-product(s). It is possible that some of the adverse events being observed are not directly induced by HBOC products, but are the effects of molecular species produced by normal metabolic degradation of the hemoglobin material. Due to the magnitude of anticipated clinical doses, these mechanisms could become overloaded or stimulated well beyond normal levels and thereby exert unexpected and untoward up-regulation effects on usually balanced physiological systems. Indeed, since off-label use of HBOCs could open questions as yet unanswered, it will be necessary to develop a better appreciation of these issues before any of the existing solutions reach the market.

As a greater appreciation of oxygen-dependent physiology evolves, as the indications for transfusion are refined, and as alternatives to traditional transfusions continue to be developed, the role of red cell substitutes remains an open question. Certainly, we will need to carefully address the effectiveness of these solutions in reaching universally accepted efficacy endpoints. For now, HBOC products are viewed as part of a continuum of options, to be used in many situations as part of an overall practice pattern where blood conservation and avoidance of allogeneic transfusion are primary objectives. Seen in that light, we have gained enough knowledge now to say they have a bright and useful future, probably well beyond their originally conceived use as resuscitation fluids in the field (5,8,10).

ACKNOWLEDGMENTS

Since submission of this paper, Baxter Healthcare Corporation acquired Somatogen, Inc., in May, 1998. By July, 1998, Baxter halted all clinical trials with HemAssist® (DCLHb®). The company then announced its decision to end the clinical development of this product as of September 16, 1998. At that time, Baxter also stated that it would focus its research and development efforts on second generation products based on recombinant technology, as acquired from Somatogen. Although Baxter halted clinical development of Optro® (rHb1.1) during 1998, it is now developing a new second-generation recombinant hemoglobin product that is targeted for Phase I clinical trials after the year 2000.

BIBLIOGRAPHY

1. A.G. Greenburg, *World J. Surg.* **20**, 1189–1193 (1996).
2. American Society of Anesthesiologists Task Force on Blood Component Therapy (A.G. Greenburg, M.D., Ph.D., member), *Anesthesiology* **84**, 732–747 (1996).
3. H.G. Klein, *Am. J. Surg.* **170**, 21S–26S (1995).
4. A.G. Greenburg, *Am. J. Surg.* **173**, 49–52 (1997).
5. A.G. Greenburg and H.W. Kim, *Artif. Cells, Blood Substitutes Immob. Biotechnol.* **25**(1 and 2), 25–29 (1997).
6. H.W. Kim and A.G. Greenburg, *Int. Symp. Korean Sci. Eng.*, Seoul, Korea, June 24–28, 1996, pp. 1300–1307.
7. N.M. Dietz, M.J. Joyner, and M.A. Warner, *Anesth. Analg.* **82**, 390–405 (1996).
8. R.M. Winslow, *Expert Opin. Invest. Drugs* **5**(11), 1443–1452 (1996).
9. J.E. Ogden and S.L. MacDonald, *Vox Sang.* **69**, 302–308 (1995).
10. A.G. Greenburg, *Adv. Surg.* **31**, 149–165 (1998).
11. G.W. Peskin, K. O'Brien, and S.F. Rabiner, *Surgery* **66**, 185 (1969).
12. A.G. Greenburg, *Crit Care Med.* **14**, 325–351 (1992).
13. R.K. Spence, A.G. Greenburg, and Members of the Blood Management Practice Guidelines Conference, *Am. J. Surg.* **170**(6A), Suppl., 3S–15S (1995).
14. A.G. Greenburg, *Am. J. Surg.* **170**(6A), 44S–48S (1995).
15. J.L. Carson, *Am. J. Surg.* **170**, 32S–36S (1995).
16. S.F. Flaim, in A.S. Rudolph, R. Rabinovici, and G.Z. Feuerstein, *Red Blood Cell Substitutes: Basic Principles and Clinical Applications*, Dekker, New York, 1997, pp. 437–464.
17. P.E. Keipert, *Artif. Cells, Blood Substitutes Immob. Biotechnol.* **23**(3), 381–394 (1995).
18. P.E. Keipert and M.G. Conlan, *Artif. Cells, Blood Substitutes Immob. Biotechnol.* **24**(4), 359 (Abstr.) (1996).
19. T.M.S. Chang and R.P. Geyer, eds., *Blood Substitutes*, Dekker, New York, 1989.
20. T.M.S. Chang, ed., *Blood Substitutes and Oxygen Carriers*, Dekker, New York, 1993.
21. R.M. Winslow, ed., *Hemoglobin-Based Red Cell Substitutes*, John Hopkins University Press, Baltimore, Md., 1992.
22. R.M. Winslow, K.D. Vandegriff, and M. Intaglietta, eds., *Blood Substitutes, Physiological Basis of Efficacy*, Birkhaeuser, Boston, 1995.
23. R.M. Winslow, K.D. Vandegriff, and M. Intaglietta, eds., *Blood Substitutes, New Challenges*, Birkhaeuser, Boston, 1996.

24. R. Rabinovici, W.T. Phillips, G.Z. Feuerstein, and A.S. Rudolph, in A.S. Rudolph, R. Rabinovici, and G.Z. Feuerstein, eds., *Red Blood Cell Substitutes: Basic Principles and Clinical Applications* Dekker, New York, 1997, pp. 263–286.
25. G. Rhea et al., *Crit. Care Med.* **24**(1), Suppl., A39 (Abstr. 3) (1996).
26. G. Reah et al., *Crit. Care Med.* **25**(9), 1480–1488 (1997).
27. P. Bassett, *Drug Market Dev.* **7**(7), 164–168 (1996).
28. R.G. Kilbourn, J. DeAngelo, and J. Bonaventura, in J.-L. Vincent, ed., *Yearbook of Intensive Care and Emergency Medicine*, Springer-Verlag, Berlin, 1997, pp. 230–239.
29. S.K. Swan et al., *Am. J. Kidney Dis.* **26**(6), 918–923 (1995).
30. P. Gonzalez et al., *Blood* **84**(10), Suppl., 413a (Abstr. 1639) (1994).
31. P. Gonzalez et al., *J. Invest. Med.* **45**(5), 258–264 (1997).
32. D.J. Nelson, in A.S. Rudolph, R. Rabinovici, G.Z. Feuerstein, eds., *Red Cell Substitutes: Basic Principles and Clinical Applications*, Dekker, New York, 1997, pp. 353–400.
33. R.J. Przybelski et al., *Crit. Care Med.* **24**(12), 1993–2000 (1996).
34. J.F. Baron et al., *Anesthesiology* **87**(3A), Abstr. A217 (1997).
35. M.A. Garrioch, E.K. Daily, and R.J. Przybelski, *Abstr., Proc. 2nd Congr. Jpn. Soc. Blood Substitutes*, June 29, 1995.
36. J.F. Baron et al., *Poster, Am. Soc. Anesthesiol. Ann. Meet.*, San Diego, Calif., October 18–22, 1997.
37. J.F. O'Hara et al., *Anesthesiology* **87**(3A), Abstr. A344 (1997).
38. J.F. O'Hara et al., *Anesthesiology* **87**(3A), Abstr. A205 (1997).
39. G. Hughes et al., *J. Lab. Clin. Med.* **126**(5), 444–451 (1995).
40. G. Hughes et al., *Ann. Emerg. Med.* **27**(2), 164–169 (1996).
41. G. Hughes et al., *Crit. Care Med.* **24**(5), 756–764 (1996).
42. G. Hughes et al., *Clin. Pharmacol. Ther.* **58**(4), 434–443 (1995).
43. S.M. Kasper et al., *Anesth. Analg.* **83**, 921–927 (1996).
44. W.R. Light et al., in A.S. Rudolph, R. Rabinovici, and G.Z. Feuerstein, eds., *Red Blood Cell Substitutes: Basic Principles and Clinical Applications*, Dekker, New York, 1997, pp. 421–436.
45. T. Standl et al., *Crit. Care* **1** (Suppl. 1), 51 (Abstr. P92) (1997).
46. K.L. Shum et al., *Artif. Cells, Blood Substitutes Immob. Biotechnol.* **24**(6), 655–683 (1996).
47. P. Bassett, *Drug Market Dev.* **8**(6), 126–130 (1997).
48. R. Shorr, *Proc. Int. Bus. Commun., 4th Annu. Blood Substitutes Conf.*, San Diego, Calif., November 21, 1996.
49. J.G. Adamson et al., in A.S. Rudolph, R. Rabinovici, and G.Z. Feuerstein, eds., *Red Blood Cell Substitutes: Basic Principles and Clinical Applications,* Dekker, New York, 1997, pp. 335–352.
50. S.A. Gould, L.R. Sehgal, G.S. Moss, and H.L. Sehgal, in A.S. Rudolph, R. Rabinovici, and G.Z. Feuerstein, eds., *Red Blood Cell Substitutes: Basic Principles and Clinical Applications*, Dekker, New York, 1997, pp. 401–420.
51. S.A. Gould, L.R. Sehgal, H.L. Sehgal, and G.S. Moss, *Proc. 5th Int. Soc. Blood Substitutes Meet.*, San Diego, Calif., March 19, 1993, Abstr. H13.
52. S. Gould et al., *Transfusion* **33**(Suppl.), 60S (Abstr. S231) (1993).
53. S.A. Gould, L.R. Sehgal, H.L. Sehgal, and G.S. Moss, *Transfusion Sci.* **16**(1), 5–17 (1995).
54. S.A. Gould and G.S. Moss, *World J. Surg.* **20**, 1200–1207 (1996).
55. S.A. Gould et al., *J. Trauma, Injury, Infect. Crit. Care* **43**(2), 325–332 (1997).
56. M.J. Gerber, G.L. Stetler, and D. Templeton, in E. Tsuchida, ed., *Artificial Red Cells*, Wiley, New York, 1995, pp. 187–197.
57. J.W. Freytag and D. Templeton, in A.S. Rudolph, R. Rabinovici, and G.Z. Feuerstein, eds., *Red Blood Cell Substitutes: Basic Principles and Clinical Applications*, Dekker, New York, 1997, pp. 325–333.
58. M.K. Viele, R.B. Weiskopf, and D. Fisher, *Anesthesiology* **86**, 848–858 (1997).
59. M.N. Stetter, G.M. Baerlocher, H.J. Meiselman, and W.H. Reinhart, *Transfusion* **37**, 1149–1155 (1997).
60. R.J. Przybelski, E.K. Daily, and M.L. Birnbaum, in R.M. Winslow, K.D. Vandegriff, and M. Intaglietta, eds., *Advances in Blood Substitutes: Industrial Opportunities and Medical Challenges*, Birkhaeuser, Boston, 1997, pp. 71–90.
61. R. Przybelski et al., *Crit. Care Med.* **22**(1), Suppl. (Abstr. A231) (1994).
62. G.S. Hughes and E. Jacobs, *5th Int. Soc. Blood Substitutes Meet.*, San Diego, Calif., March 19, 1993, Abstr. H15.
63. J.A. Murray et al., *Gastroenterology* **109**, 1241–1248 (1995).
64. G. Hughes, E. Jacobs, S. Francom, and J. Riggin, *Crit. Care Med.* 23(1), Suppl. (Abstr.) (1995).
65. G. Hughes et al., *Crit. Care Med.* **23**(1), Suppl. (Abstr.) (1995).
66. G. Hughes et al., *Crit. Care Med.* **23**(1), Suppl. (Abstr.) (1995).
67. D. Wicks, S. Nakao, P. Champagne, and C. Mihas, *Artif. Cells, Blood Substitutes Immob. Technol.* **24**(4), 460 (Abstr.) (1996).
68. R. Shorr, A. Viau, and A. Abuchowski, *Artif. Cells, Blood Substitutes Immob. Biotechnol.* **24**(4), 425 (Abstr.) (1996).
69. J.D. Bristow et al., *Anesthesiology* **31**, 422–428 (1969).
70. L.T. Wong et al., *Artif. Cells, Blood Substitutes Immob. Biotechnol.* **26**, 529–548 (1998).
71. P. Bassett, *Drug Market Dev. Rep.* **907**, 5-86–5-94 (1995).
72. B.J. Leone et al., *Artif. Cells, Blood Substitutes Immob. Biotechnol.* **24**(4), 379 (Abstr.) (1996).
73. K. Berman, *Int. Blood Plasma News*, April 1996, p. 124.
74. M. Lamy, *Proc. Eur. Soc. Anesthesiol. Meet.*, Lausanne, Switzerland, May 5, 1997, Abstr.
75. M. Garrioch et al., *Crit. Care Med.* **24**(1), Suppl., A39 (Abstr. 4) (1996).
76. E.L. Bloomfield et al., *Anesthesiology* **85**(3A), Suppl. (Abstr. A220) (1996).
77. T. Monk, L. Goodnough, G. Hughes, and E. Jacobs, *Anesthesiology* 83(3A) (Abstr. A285) (1995).
78. R. Lessen et al., *Artif. Cells, Blood Substitutes Immob. Biotechnol.* **24**(4), 380 (Abstr.) (1996).
79. G. Hughes, E. Jacobs, S. Francom, and the Hemopure Surgical Study Group, *Crit. Care Med.* **24**(1), Suppl., A36 (Abstr. 2) (1996).
80. J.A. Wahr et al., *Anesthesiology* **85**(3A) (Abstr. A347) (1996).
81. T. Standl, *Acta Haematol.* **98**, Suppl. 1, 123 (Abstr. 484) (1997).
82. T. Standl et al., *Crit. Care* **1**, Suppl. 1, 52–53 (Abstr. P94) (1997).
83. T. Standl et al., *Anesthesiology* **87**(3A) (Abstr. A65) (1997).
84. J.F. O'Hara et al., *Anesthesiology* **87**(3A) (Abstr. A230) (1997).
85. A. Schubert et al., *Anesthesiology* **87**(3A) (Abstr. A220) (1997).
86. A. Schubert et al., *Anesthesiology* **87**(3A) (Abstr. A218) (1997).
87. T.G. Monk et al., *Anesthesiology* **87**(3A) (Abstr. A214) (1997).
88. W. Lieberthal, in A.S. Rudolph, R. Rabinovici, and G.Z. Feuerstein, eds., *Red Blood Cell Substitutes: Basic Principles and Clinical Applications*, Dekker, New York, 1997, pp. 189–217.
89. T. Estep, *Proc. Int. Bus. Commun. 3rd Annu. Blood Substitutes Conf.* Bethesda, Md., October 30, 1995.

90. E.P. Sloan, *Proc. Int. Bus. Commun. 4th Annu. Blood Substitutes Conf.* San Diego, Calif., November 21, 1996.

91. E.P. Sloan et al., *Acad. Emerg. Med.* **2**(5), 365 (Abstr. 078) (1995).

92. S.A. Gould et al., *J. Trauma, Injury, Infect. Crit. Care* **39**(1), 157 (Abstr.) (1995).

93. E.E. Moore, S.A. Gould, D.B. Hoyt, and J.M. Haenel, *Shock* **7**(Suppl.), 145 (Abstr. 576) (1997).

94. K.C. Tang and P.M. Cheng, *Life Sci. Biotechnol. Rep.*, 1–8 (1997).

95. E.P. Sloan, *Proc. Int. Bus. Commun. 5th Annu. Blood Substitutes Conf.*, Cambridge, Mass., November 21, 1997.

CALCIFICATION, DRUG DELIVERY TO PREVENT

NARENDRA R. VYAVAHARE
ROBERT J. LEVY
Children's Hospital of Philadelphia and the University of Pennsylvania
Philadelphia, Pennsylvania

KEY WORDS

Aluminum chloride
Bioprostheses
Bisphosphonates
Bovine pericardium
Calcium phosphates
Ferric chloride
Glutaraldehyde
Heterograft
Polymeric drug delivery
Porcine aortic valve

OUTLINE

Background
- Definitions: Cardiovascular Calcification
- Scope and Importance of the Clinical Problem of Bioprostheses
- Rationale for Controlled Drug Delivery

Treatment Strategies
- Controlled Release Drug Delivery Formulations for Preventing Cusp Calcification
- Formulations for Preventing Aortic Root Calcification
- Limitations of Site Specific Drug Delivery

Future Directions
Conclusions
Bibliography

BACKGROUND

Definitions: Cardiovascular Calcification

Calcification occurs in a wide variety of cardiovascular disease processes including arteriosclerosis, valvular degeneration, endocarditis, and myocardial infarction. Calcification is also associated with implanted medical devices such as bioprosthetic heart valves (BPHV) derived from glutaraldehyde cross-linked porcine aortic valves or bovine pericardium, vascular grafts, and blood pumps (1–3). In particular, calcification is the leading cause of failure of heart valve bioprostheses (4,5). We will focus on BPHV calcification as a model for cardiovascular calcification. Accumulation of crystalline calcium phosphate mineral is most often pathologic calcification in cardiovascular diseases. This pathologic calcification can either be metastatic or dystrophic. The calcification is termed metastatic when it occurs in hypercalcemic hosts with otherwise normal tissues, whereas calcification is termed dystrophic when it occurs in necrotic or damaged tissues in normocalcemic subjects. In contrast to the orderly and regulated pattern of normal skeletal mineralization, dystrophic calcification, although progressive, is haphazard in its localization and poorly regulated. In case of medical implants, the location of mineral nucleation may be intrinsic (i.e., within the boundaries of the tissue or biomaterial involving its original constituents) or extrinsic (i.e., associated with elements or tissue not initially implanted, such as within thrombus, vegetations, or pseudointima). Due to the localized nature of this disease process, site-specific drug delivery systems releasing anticalcification drugs locally would be an ideal approach.

Scope and Importance of the Clinical Problem of Bioprostheses

Thousands of patients undergo heart valve replacement surgeries annually (6). Lifetime anticoagulant therapy is needed for patients with mechanical prostheses. Bioprosthetic heart valves are excellent alternatives when long-term anticoagulation is contraindicated or undesirable, such as in patients with diabetes, women of childbearing age, and individuals in nonindustrialized geographic regions. However, long-term use of BPHV is limited due to cuspal tearing and valvular degeneration related to calcification.

Bioprosthetic heart valve calcification has the following determinants:

- Host factors (e.g., immature subjects calcify bioprosthetic tissue more rapidly than adults)
- Fixation conditions (e.g., glutaraldehyde cross-linking aggravates bioprosthetic calcification) (7)
- Mechanical factors (deposition of calcium phosphates occurs more readily at regions of stress concentrations in bioprosthetic leaflets) (8–10)

Calcific nodules interfere with leaflet function, and calcification has also been shown to occur in the aortic wall region of BPHV, which may compromise the lumen of stentless valve designs (11,12). Animal models for bioprosthetic calcification have been developed and characterized using noncirculatory subdermal implants (rat, rabbit, mouse) and circulatory valve replacements in sheep or calves. These animal models result in pathology comparable to that seen in clinical calcific bioprosthesis failure (13–19). Figure 1 shows the various steps involved in clinical failure of the valves. The treatments that may alter one

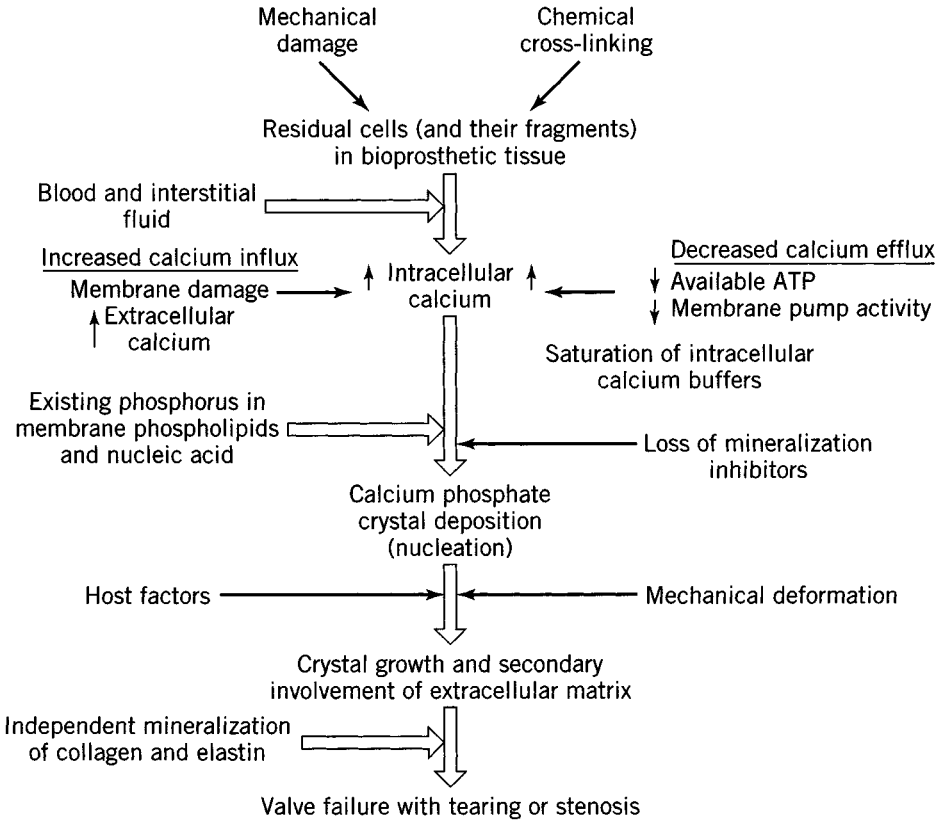


Figure 1. Extended hypothetical model for the calcification of bioprosthetic tissue. This model considers host factors, implant factors, and mechanical damage and relates initial sites of mineral nucleation to increased intracellular calcium in residual cells and cell fragments in bioprosthetic tissue. The ultimate result of calcification is valve failure, with tearing or stenosis. *Source:* Reproduced with permission from Ref. 20.

or more steps are hypothesized to reduce calcification of bioprosthetic valves.

The pathogenesis of BPHV calcification involves an interaction of host and implant factors. Initial calcification has been noted in the devitalized connective tissue cells intrinsic to the bioprosthetic leaflet material. Structural protein calcification, most prominently collagen in leaflets and elastin in aortic wall, then ensues (13). Tissue fixation protocols devitalize cells, thus disrupting their calcium regulation mechanisms. In living cells the intracellular calcium level is approximately 10^{-7} M, whereas extracellular calcium is 10^{-3} M. This 10,000-fold gradient across the plasma membrane is maintained by energy-requiring metabolic pumps, which extrude this ion as well as intracellular buffering mechanisms. In cells modified by glutaraldehyde cross-linking, necrosis, or mechanical injury, the mechanisms for calcium extrusion are no longer functional, thus the calcium influx occurs unimpeded. Plasma membranes and membrane bound organelles such as mitochondria are rich in phospholipids and provide phosphorus for appetite formation (13,14,21). Although calcification has been found to initiate within devitalized cells of glutaraldehyde-fixed BPHVs, extracellular matrix such as collagen (in BPHV cusps) and elastin (in aortic wall) has been shown to independently calcify in animal models (22,23). The role of immunologic factors such as nonspecific inflammation or antigenic-specific immunologic response in mediating calcification is controversial. Valve tissue implanted in congenitally athymic, T-cell deficient (nude) mice calcifies to the same extent as implants in immunologically competent hosts (16).

A growing body of evidence indicates that mineral matrix proteins that function in physiologic calcification of bone and tooth are also associated with pathologic cardiovascular calcification (24–30). Levy et al. have demonstrated the role of exogenous alkaline phosphatase in bioprosthetic mineralization (26). The noncollagenous bone matrix proteins such as osteocalcin and osteopontin have been found to be associated with pathologic calcification of bioprostheses as well as in atherosclerosis (24,25). In particular, bone matrix proteins such as osteopontin, bone acidic glycoprotein (BAG 75) have been shown to be associated with pathologic calcification of BPHV in rat subdermal implants (31). These proteins have been extensively studied in physiologic bone mineralization, although their exact functions are not completely understood. Once their exact role in cardiovascular calcification is understood, site-specific, gene-based therapies for preventing calcification can be envisioned.

Rationale for Controlled Drug Delivery

There are no conventional approaches to prevent cardiovascular calcification. Any systemic use of drugs to prevent this disease process would ultimately have unwanted toxic effects on bone and teeth development and calcium metabolism. This is particularly true for children and young adults where pathologic calcification of BPHV occurs rap-

idly. Bisphosphonates, a class of drugs approved for preventing calcification, represent this type of therapeutic dilemma. Bisphosphonates are poorly absorbed orally and must be given parenterally (32). The affinity of bisphosphonates for bone mineral leads to their accumulation in this organ system with parenteral administration. Osteomalacia and overall diminution in somatic growth are classic side effects of this drug therapy (32). Due to the localized nature of the BPHV calcification, the site-specific delivery of anticalcification agents such as bisphosphonates is ideal. Such site-specific therapy would require less drug, increase its therapeutic effectiveness, and reduce or eliminate its systemic side effects.

TREATMENT STRATEGIES

Two classes of anticalcification agents, namely bisphosphonates and metallic salts such as iron chloride ($FeCl_3$) or aluminum nitrate ($Al(NO_3)_3$), have been studied in animal models in the form of controlled release drug delivery systems (33–45). Thus, drug delivery devices were placed in a close proximity of the heart valve tissue implant and their anticalcification effects were studied. Ethane hydroxybisphosphonate (EHBP) is one of the best known anticalcification agents. It has been approved by the FDA for human use for inhibition of pathologic calcification and for treating hypercalcemia of malignancy (46). The EHBP mechanism is based on a specific interaction with calcium and calcium-phosphate crystal formation and growth. EHBP also inhibits alkaline phosphatase activity (47). Alkaline phosphatase is an important enzyme in physiologic mineralization, and it may also have a role in cardiovascular calcification, because this enzyme has been shown to be present intrinsically in bioprosthetic tissue despite the glutaraldehyde fixation, and it is also adsorbed extrinsically from the host following implantation (48).

The mechanisms of action of Fe^{3+} and Al^{3+} in preventing calcification are incompletely understood but are thought to be due to the retardation of hydroxyapatite crystal growth by a crystal poisoning effect and reduction in the alkaline phosphatase activity (48). Their mechanism of action may also be related to their interactions with phosphorus-rich loci within membranes of devitalized cells and other phosphorus-rich organelles present in BPHV (49); these sites are thought to be the initial donors of phosphorus in the nucleation of calcium phosphate mineral (13,14).

Controlled Release Drug Delivery Formulations for Preventing Cusp Calcification

Table 1 summarizes the different controlled release drug delivery systems studied so far for preventing cardiovascular calcification. The bisphosphonate compounds, in particular EHBP, have been used in the past as anticalcification agents. However, due to their systemic toxicity, conventional drug therapy results in many side effects in bone and calcium metabolism (54). Thus, controlled release delivery systems using polymers were formulated and investigated. The principle of this approach was to maintain the drug levels only at the sites (i.e., valve implants) where it is needed and to prevent systemic side effects through local administration. Thus drug-releasing matrices were implanted in close proximity to BPHV tissue implant. Many studies incorporating EHBP in nondegradable polymers such as ethylene-vinyl acetate (EVA), polydimethylsiloxane (silicone), silastic, and polyurethanes have shown the effectiveness of this strategy in preventing BPHV calcification in a variety of animal models (33–37,39,40,43,44,55,56).

In the rat subdermal model, the controlled release of EHBP from EVA matrices was shown to prevent the calcification of porcine aortic valve cusps for up to 84 days (33,34). In this study, cusps in close proximity to control EVA films without any drug calcified with calcium levels comparable to those observed with clinical failure of heart valves (Fig. 2). The kinetics of drug release from matrices was controlled from hours to years by modifying various parameters such as percent drug loading, incorporation of the less soluble calcium salt of the EHBP, addition of an inert filler such as insulin, and fabrication of membrane coatings (35–37). Based on the rat subdermal studies, the optimal controlled release system with two salts of EHBP, namely sodium and calcium (1,000-fold less soluble than sodium salt) salts equally mixed (1:1) in silastic matrices (30% drug loading), was found to increase the extrapolated duration of EHBP-controlled release to several decades (38). These drug-loaded matrices were then tested for their efficacy in a sheep mitral valve replacement model (39). The matrices were fabricated as rings and were placed around the stent post of the bioprosthesis directly under the sewing cushion as shown in Figure 3. These polymeric implants were shown to be effective in inhibiting calcification in sheep tricuspid valve replacements with porcine aortic bioprostheses (39). However, the same controlled release implants were ineffective in preventing calcification of glutaraldehyde-pretreated bovine pericardium in mitral valve replacements in sheep (150 days) (58) (Table 2). The reasons for this lack of efficacy are not clear, but may be attributed to the fact that mitral valve calcification is more rapidly progressive and drug levels attained by controlled release systems may be insufficient due to washout effects in the circulation. Furthermore, Golomb et al. have prepared chitosan microspheres with encapsulated bisphosphonate (53) and have shown effective inhibition of bioprosthetic tissue calcification by injected microspheres near the BPHV cusp implants in the rat subdermal model.

Metal ion salts such as ferric chloride and aluminum nitrate were studied for their anticalcification efficacy when released from polymer matrices (43,45,50–53). Thus, $FeCl_3$ and $Al(NO_3)_3$ were incorporated into silicon polymer (silastic 6605-41) and polyether urethane (Biomer®) (10 weight% loading) and were implanted in close proximity to glutaraldehyde-fixed bovine pericardium in a rat subdermal model (50). Depending upon their release kinetics both the agents significantly inhibited calcification of bovine pericardium (Table 3). The release of metal ions from Biomer® was rapid with a large initial burst phase (up to 50% within first few hours); thus, less drug was available for prolong action, and the anticalcification effect was only partial. The release of metal ions (Fe^{3+}, Al^{3+}) from silastic polymer, on the other hand, was sustained for the implant

Table 1. Summary of Controlled Release Drug Delivery Systems Studied to Prevent Cardiovascular Calcification

Drug	Matrix/geometry	Tissue	Model	Reference
Na_2EHBP	EVA/hemisphere	Porcine aortic valve	Rat subdermal implant	33,34
Na_2EHBP/Ca_2 EHBP	Silicone-rubber, silastic/slab	Bovine pericardium	Rat subdermal implant	35
EHBP	EVA/hemisphere	Bovine pericardium	Rat subdermal implant	36
Na_2EHBP/Ca_2 EHBP	Polydimethylsiloxane/membrane-coated slabs	Bovine pericardium	Rat subdermal implant	37
Na_2EHBP/Ca_2 EHBP	Polydimethylsiloxane/membrane-coated slab and ring	Bovine pericardium/porcine aortic valve	Rat subdermal implant/sheep tricuspid valve replacement	39
Fe^{3+}/Al^{3+}	Polydimethylsiloxane/slab	Bovine pericardium	Rat subdermal implant	50
Protamine sulfate	Polydimethylsiloxane/slab	Bovine pericardium	Rat subdermal implant	50
Levamisole	Polydimethylsiloxane/slab	Bovine pericardium	Rat subdermal implant	50
Na_2EHBP/Ca_2 EHBP	Polyurethane (mitrathane)/ reservoir	Bovine pericardium	Rat subdermal implant	40
Sodium dodecyl sulfate (SDS)	Polydimethylsiloxane/slab	Porcine aortic valve	Rat subdermal implant	42
EHBP/Fe^{3+} synergism	Polydimethylsiloxane/slab	Bovine pericardium	Rat subdermal implant	43
EHBP/Fe^{3+} synergism	Polydimethylsiloxane/EVA/slab	Rat aortic wall	Rat aortic wall allograft model	44,45
Fe^{3+}	Chitosan/slab	Bovine pericardium/ polyurethane	Rat subdermal implant	51,52
EHBP	Chitosan/microparticles	Bovine pericardium	Rat subdermal implant	53

period (21 days), and thus the anticalcification effect was substantial as compared to controls. Other researchers (51,52) have also shown the release of Fe^{3+} ions from chitosan matrices prevents bovine pericardium calcification and polyurethane calcification in the rat subdermal model.

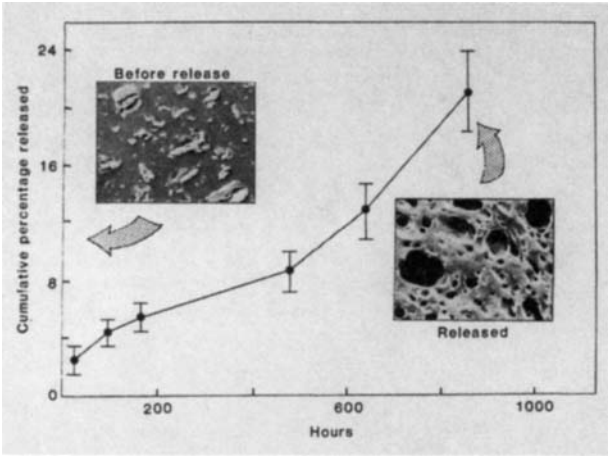
Other agents such as levamisole (alkaline phosphatase inhibitor) or protamine sulfate (tissue charge modifier) when released from polymer matrices near the bovine pericardium implants were ineffective in preventing bovine pericardium calcification in the rat subdermal model (50). In other studies, controlled release of sodium dodecyl sulfate (SDS) near the bovine pericardium implant was also shown to be completely ineffective in preventing bovine pericardium calcification (42). SDS and protamine sulfate were shown by others to be highly effective in preventing BPHV calcification when the BPHV cusps were incubated in these agents in solution prior to implantation (42,59,60). These results suggest that SDS and protamine sulfate may be modifying the bioprosthetic tissue itself in such a way that it makes it resistant to calcification. However, these agents have little role in preventing calcification related to progressive host–implant material interactions.

Formulations for Preventing Aortic Root Calcification

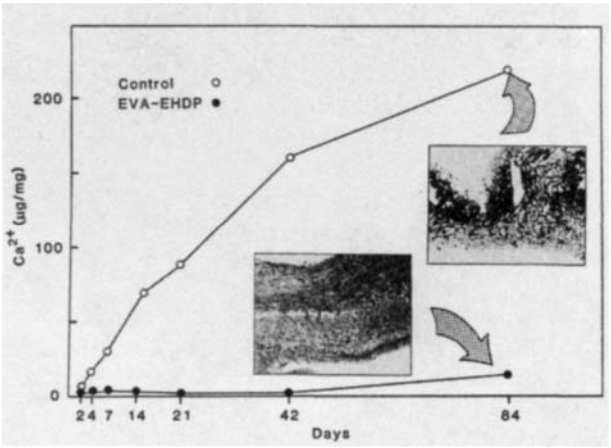
Recent interests in stentless valve bioprostheses have raised concerns about valve failure due to aortic wall calcification, although there are no clinical results as yet to suggest this (11,12,61). It has been observed in the past that the mechanism of aortic wall calcification is different than cusp calcification due to differences in tissue morphology. Many agents that prevent cusp calcification do not prevent aortic wall calcification (61,62). Recently, a microsurgical rat aortic circulatory allograft model has been developed in our laboratory to study the calcification of rat aorta (44). This model was used to study the effect of polymeric (EVA) implant releasing two drugs, EHBP and $FeCl_3$, which act synergistically in preventing aortic wall calcification (45). The results demonstrated that $FeCl_3$ alone was not effective and EHBP releasing from polymer was partially effective, whereas both the drugs released simultaneously from the same implant synergistically inhibited aortic wall calcification (Table 4) (45). No side effects of this drug therapy were found on overall weight gain, serum calcium levels, and bone growth of the animals.

Limitations of Site Specific Drug Delivery

Although the controlled drug delivery systems as described before have shown promising results in preventing BPHV calcification in animal models, a great many difficulties need to be overcome in order to use them in clinical applications. For example, drug release (in effective concentrations) from matrix systems in the circulation may depend upon various factors such as inflammatory response causing capsule formation around the implant, degradation and cracking of implant, osmotic pressures caused by hydrophilic drugs. The matrix type devices (with dispersed drug) have only a limited lifetime and can be depleted of drug before the useful life of a heart valve (usually 15–20 years). Although the feasibility of using reservoir devices (a drug solution within a polymer membrane) has been shown in preventing BPHV calcification in the rat subdermal model, these devices have risks of dose dumping due to breakage of the membrane. The biocompatibility and toxicity of a drug delivery implant itself can become an issue in heart valve replacement surgery. Thus, a better approach could be to incorporate the drug in polymeric microspheres and then inject the microspheres near the im-



(a)



(b)

Figure 2. (**a**) In vitro cumulative percentage EHBP released from an EVA-EHBP matrix (20 weight%). Insets: scanning electron microscopy for drug delivery implants before and after 42 days of release in vitro. (**b**) Inhibition of BPHV calcification by site-specific drug delivery of EHBP from EVA-EHBP matrix (20 weight%) in a rat subdermal implantation model. Insets: light microscopy of BPHV tissue with von kossa staining (calciumphosphate-black) showed extensive intrinsic calcification at 84 days in a control specimen but no visible deposits in the BPHV tissue coimplanted with EVA-EHBP drug delivery matrix. *Source:* Reproduced with permission from Ref. 33.

plant site via catheter. The polymer could then slowly degrade and release the drug near the heart valve implant. Once the dose is completely released, another batch of microspheres could then be injected.

FUTURE DIRECTIONS

Tissue-engineered heart valves are perceived by many as providing a solution to cardiac valve disease and cardiac valve regeneration (63). Tissue-engineered valves have been investigated most extensively by Mayer and his colleagues. This group has designed a polymer scaffold that can be seeded with autologous cells. In a series of sheep studies, they were able to carry out successful pulmonary valve cusp replacements (63). However, a number of major challenges face this approach, including biomechanical and design considerations, matrix biosynthesis following implantation, cell integration with the host, and potential problems with degeneration including calcification as well as primary material failure. Nevertheless, tissue-

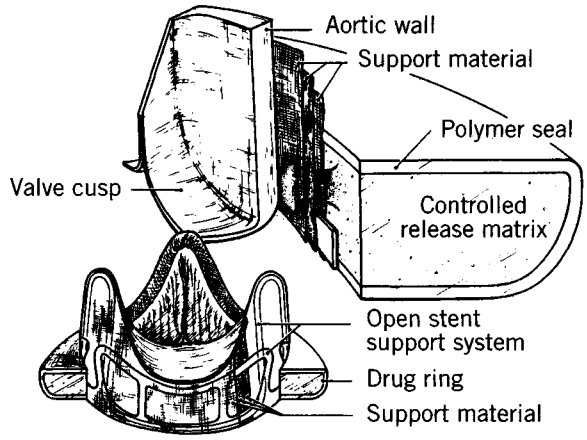


Figure 3. Site-specific delivery of drugs from controlled release matrix positioned at the circumferential support of a porcine aortic bioprosthesis. *Source:* Reproduced with permission from Ref. 57.

Table 2. Inhibition of Calcification by Controlled Release Implants: Sheep Results (150 days)

Position	Type of implant	*n*	Calcium (mg/mg of tissue ± SEM)
Tricuspid	Controlled release-EHBP	5	2.7 ± 1.0
Triscupid	Nondrug-control	6	41.3 ± 14.9
Mitral	Controlled release-EHBP	10	39.9 ± 7.7
Mitral	Nondrug control	10	44.5 ± 7.5

Source: Based partly on Ref. 58.

Table 3. Controlled Release of Metal Ions To Prevent Calcification of Glutaraldehyde Cross-linked Bovine Pericardium in a Rat Subdermal Implant Study (21 Day)

Group	Polymer	*n*	Calcium levels (μg/mg tissue)	Percent calcification
$FeCl_3$	Silastic	10	14.25 ± 2.91	19.26
$FeCl_3$	Biomer	10	44.67 ± 8.04	60.38
$Al(NO_3)_3$	Silastic	10	14.28 ± 5.78	17.87
$Al(NO_3)_3$	Biomer	10	31.04 ± 5.48	38.85
No drug	Silastic	30	52.27 ± 9.35	74.70
No drug	Biomer	20	64.20 ± 10.24	91.16
Control BP	No polymer	40	69.97 ± 10.76	100.0

Source: Based partly on Ref. 50.

Table 4. Anticalfication Efficacy of Controlled Release Implants Releasing EHBP and $FeCl_3$ on 30-Day Rat Allograft Calcification

Group	Calcium (μg/mg of tissue) ± SEM	Phosphorus (μg/mg of tissue) ± SEM
Control (no polymer)	168.68 ± 22.54	104.12 ± 14.44
Control (only polymer)	160.83 ± 8.66	107.22 ± 11.39
CaEHBP release alone	71.87 ± 17.31	65.93 ± 13.22
$FeCl_3$ release alone	151.13 ± 18.54	118.07 ± 11.46
CaEHBP and $FeCl_3$ release together	28.20 ± 7.46	26.60 ± 3.22

Source: Reproduced in part from Ref. 45.

engineered approaches have captured the imagination of the cardiovascular device industry. A number of efforts are underway to improve upon this first generation of tissue-engineered cardiac valve prosthesis. Tissue-engineered cardiac valve prostheses will likely be affected by a number of pathologic processes. In fact, it is predictable that they will be more likely to become diseased than native valves due to the lack of endogenous defense mechanisms. Thus, site-specific controlled release therapy may be relevant for tissue-engineered valves.

Gene-based therapies are becoming a reality both for genetic disease as well as tissue regeneration and local therapeutic purposes. Thus, it is conceivable that controlled release drug delivery for cardiovascular disease and cardiovascular calcification may use gene delivery. In terms of mineralization, antimineralization proteins could be expressed. These might include proteins such as statherin, an anticalcification protein normally found in saliva. Other gene therapy approaches could include antisense oligonucleotide delivery to counteract the local expression of bone-specific proteins that occur in valve calcification, such as bone morphogenic protein or osteopontin (24,25,31). Gene therapy could also take the approach of using genetically modified cells, implanted on diseased cardiac valves, that could resorb calcium deposits.

Synergistic approaches have already been used by our group in our bisphosphonate–ferric chloride studies (45). Synergistic approaches in the future could include combinations of not only pharmaceuticals but gene-based therapies as well as tissue engineering. Ideally, minimally invasive approaches should be the goal for therapy to prevent and reverse cardiovascular calcification. Ultimately this could be a targeted gene delivery through peripheral intravenous administration. Fibroblast growth factor (FGF)–targeted gene therapy has already been demonstrated to be feasible (64), and this represents the first example of peripheral targeting of DNA delivery. At the present time, the most reasonable goal in the near term would be DNA delivery through a site-specific cardiac catheter delivery implant.

CONCLUSIONS

Calcification occurs in variety of cardiovascular diseases and with implanted biomaterials. Although calcification leads to failure of medical devices such as bioprostheses, no current therapy is available to prevent this disease process. Due to localized nature of the calcification, a variety of controlled release systems releasing anticalcification drugs have been investigated successfully in animal models for drugs such as bisphosphonates and metallic ions (Fe^{3+} or Al^{3+}). Matrix and reservoir device configurations have limitations in terms of limited lifetime, maintaining sustained release, degradation, and fear of dose dumping for their clinical applications to prevent calcification. An ideal approach would be a catheter-based delivery implant such as microparticles containing either anticalcification drugs or antisense oligonucleotides to counteract local expression of mineral specific proteins, or gene-based therapies such as DNA delivery and tissue engineering.

BIBLIOGRAPHY

1. F.J. Schoen, *Trans.—Am. Soc. Artif. Intern. Organs* **33**, 8–18 (1987).
2. H.C. Anderson, *Arch. Pathol. Lab. Med.* **107**, 341–348 (1983).
3. A. Milano et al., *Am. J. Cardiol.* **53**, 1066–1070 (1984).
4. F. J. Schoen, R. J. Levy, and H. R. Piehler, *Cardiovasc. Pathol.* **1**, 29–52 (1992).
5. G.L. Grunkemeier, W. R. E. Jamieson, D.C. Miller, and A. Starr, *J. Thorac. Cardiovasc. Surg.* **108**, 709–718 (1994).
6. L.H. Edmunds et al., *Eur. J. Cardiothorac. Surg.* **10**, 812–816 (1996).
7. G. Golomb et al., *Am. J. Pathol.* **127**, 122–130 (1987).
8. H.N. Sabbah, M.S. Hamid, and P.D. Stein, *Ann. Thorac. Surg.* **42**, 93–96 (1986).
9. G.M. Bernacca et al., *J. Biomed. Mater. Res.* **26**, 959–966 (1992).
10. H.E. Jorge et al., *J. Biomed. Mater. Res.* **30**, 411–415 (1996).
11. L.M. Biedrzycki, E. Lerner, R.J. Levy, and F.J. Schoen, *J. Biomed. Mater. Res.* **34**, 411–415 (1997).
12. T.E. David, J. Bos, and H. Rakowski, *J. Heart Valve Dis.* **1**, 244–248 (1992).
13. F.J. Schoen et al., *Lab. Invest.* **52**, 523–532 (1985).
14. F.J. Schoen, J.W. Tsao, and R.J. Levy, *Am. J. Pathol.* **123**, 134–145 (1986).
15. R. Levy et al., *Am. J. Pathol.* **113**, 143–155 (1983).
16. R.J. Levy, F.J. Schoen, and S.L. Howard, *Am. J. Cardiol.* **52**, 629–631 (1983).
17. M. Jones et al., *J. Cardiovasc. Surg.* **4**, 69–73 (1989).
18. M.C. Fishbein et al., *J. Thorac. Cardiovasc. Surg.* **83**, 602–609 (1982).
19. G.R. Barnhart et al., *Circulation* I150–I153 (1982).
20. F.J. Schoen, ed., *Interventional and Surgical Cardiovascular Pathology, Clinical Correlations and Basic Principles*, Saunders, Philadelphia, 1989.
21. F.J. Schoen and R.J. Levy, *Eur. J. Cardiothorac. Surg.* **6**(Suppl. 1), S91–S94 (1992).
22. R.J. Levy et al., *Am. J. Pathol.* **122**, 71–82 (1986).
23. C. Webb, N. Nguyen, F. Schoen, and R. Levy, *Am. J. Pathol.* **141**, 487–496 (1992).
24. L. Fitzpatrick, A. Severson, W. Edwards, and R. Ingram, *J. Clin. Invest.* **94**, 1597–604 (1994).
25. S. Srivatsa et al., *J. Clin. Invest.* **99**, 996–1009 (1997).

Next Page

26. R.J. Levy, C. Gundberg, and C. Scheinman, *Atherosclerosis* **46**, 49–56 (1983).
27. S. Hirota et al., *Am. J. Pathol.* **143**, 1003–1008 (1993).
28. C.M. Giachelli et al., *J. Clin. Invest.* **92**, 1686–1896 (1993).
29. K. Bostrom, et al., *J. Clin. Invest.* **91**, 1800–1809 (1993).
30. C.M. Shanahan, N.R.B. Cary, J.C. Metcalfe, and P.L. Weissberg, *J. Clin. Invest.* **93**, 2393–2402 (1994).
31. T.A. Gura, K.L. Wright, A. Veis, and C.L. Webb, *J. Biomed. Mater. Res.* **35**, 483–495 (1997).
32. R.G.G. Russell and R. Smith, *J. Bone Joint Surg.* **55**, 66–86 (1973).
33. R.J. Levy et al., *Science* **228**, 190–192 (1985).
34. R.J. Levy et al., *Trans. Am. Soc. Artif. Intern. Organs* **31**, 459–463 (1985).
35. G. Golomb et al., *Trans. Am. Soc. Artif. Intern. Organs* **32**, 587–590 (1986).
36. G. Golomb et al., *J. Controlled Release* **4**, 181–194 (1986).
37. G. Golomb et al., *J. Pharm. Sci.* **76**, 271–276 (1987).
38. T.P. Johnston et al., *Trans. Am. Soc. Artif. Intern. Organs* **34**, 835–838 (1988).
39. T.P. Johnston et al., *Int. J. Pharm.* **52**, 139–148 (1989).
40. T.P. Johnston et al., *Int. J. Pharm.* **59**, 95–104 (1990).
41. T.P. Johnston, C.L. Webb, F.J. Schoen, and R.J. Levy, *J. Controlled Release* **25**, 227–240 (1993).
42. D. Hirsch et al., *J. Biomed. Mater. Res.* **27**, 1477–1484 (1993).
43. D. Hirsch et al., *Biomaterials* **14**, 705–711 (1993).
44. R.J. Levy et al., *J. Biomed. Mater. Res.* **29**, 217–226 (1995).
45. N.R. Vyavahare et al., *J. Controlled Release* **34**, 97–108 (1995).
46. H. Fleisch, in G.R. Mundy and T.J. Martin, eds., *Physiology and Pharmacology of Bone*, Springer-Verlag, New York, 1993, pp. 377–418.
47. D. Hirsch, F.J. Schoen, and R.J. Levy, *Biomaterials* **14**, 371–377 (1992).
48. R.J. Levy, F.J. Schoen, W.B. Flowers, and S.T. Staelin, *J. Biomed. Mater. Res.* **25**, 905–935 (1991).
49. C.L. Webb et al., *Am. J. Pathol.* **138**, 971–981 (1991).
50. Y. Pathak, J. Boyd, and R.J. Levy, *Biomaterials* **11**, 718–723 (1990).
51. T. Chandy et al., *Biomaterials* **17**, 577–585 (1996).
52. T. Chandy and C.P. Sharma, *Biomaterials* **17**, 61–66 (1996).
53. S. Patashnik, L. Rabinovich, and G. Golomb, *J. Drug Target*, **4**, 371–380 (1997).
54. R.J. Levy, F.J. Schoen, S.A. Lund, and M.S. Smith, *J. Thorac. Cardiovasc. Surg.* **94**, 551–557 (1987).
55. G. Golomb, M. Levi, G. Van, and M. Joel, *J. Appl. Biomater.* **3**, 23–28 (1992).
56. R.J. Levy, T.P. Johnston, A. Sintov, and G. Golomb, *J. Controlled Release* **11**, 245–254 (1990).
57. E. Bodner and R. Frater, eds., *Replacement Cardiac Valves*, Pergamon, Elmsford, N.Y., 1988.
58. R.J. Levy et al., *J. Controlled Release* **36**, 137–147 (1995).
59. G. Golomb and R.J. Levy, *Trans. Soc. Biomater.* **10**, 179 (1987).
60. M. Jones et al., *Trans. Am. Soc. Artif. Intern. Organs* **34**, 1027–1030 (1988).
61. W. Chen, F. J. Schoen, and R. J. Levy, *Circulation* **90**, 323–329 (1994).
62. M.N. Girardot, M. Torrianni, and J. M. D. Girardot, *Int. J. Artif. Organs* **17**, 76–82 (1994).
63. T. Shinoka et al., *Ann. Thorac. Surg.* **60**(6), Suppl., S513–S516 (1995).
64. B.A. Sosnowski et al., *J. Biol. Chem.* **271**(52), 33647–33653 (1996).

CANCER, DRUG DELIVERY TO TREAT—LOCAL & SYSTEMIC

KATHLEEN J. LEACH
University of Washington
Seattle, Washington

KEY WORDS

Cancer therapy
Chemoembolization
Depot systems
Immunoliposomes
Immunotherapy
Immunotoxins
Implantable pumps
Liposomes
Local delivery
Magnetic targeting
Microspheres
Nanoparticles
Stealth liposomes
Targeted delivery

OUTLINE

Introduction
Local Delivery
  Implantable Pumps or Reservoirs
  Chemoembolization
  Internal Radiation Therapy Using Microspheres
  Locally Implanted Controlled-Release Systems
Systemic Delivery
  Depot Systems
  Targeted Delivery
Cancer Immunotherapy
Summary
Bibliography

INTRODUCTION

In normal cells, growth is carefully regulated through an intricate web of physical and chemical signals. In adults, the rate of cell birth is maintained to be equal to the rate of cell death, whereas in children, slightly higher cell birth rates (or lower cell death rates) are necessary to allow for increases in body size during development. In either case, cell growth is carefully controlled. Cancer is the result of cell growth regulation gone awry. Any cell in the body has the potential to become a cancerous if it receives a series of genetic mutations that result in growth deregulation.

Previous Page

26. R.J. Levy, C. Gundberg, and C. Scheinman, *Atherosclerosis* **46**, 49–56 (1983).
27. S. Hirota et al., *Am. J. Pathol.* **143**, 1003–1008 (1993).
28. C.M. Giachelli et al., *J. Clin. Invest.* **92**, 1686–1896 (1993).
29. K. Bostrom, et al., *J. Clin. Invest.* **91**, 1800–1809 (1993).
30. C.M. Shanahan, N.R.B. Cary, J.C. Metcalfe, and P.L. Weissberg, *J. Clin. Invest.* **93**, 2393–2402 (1994).
31. T.A. Gura, K.L. Wright, A. Veis, and C.L. Webb, *J. Biomed. Mater. Res.* **35**, 483–495 (1997).
32. R.G.G. Russell and R. Smith, *J. Bone Joint Surg.* **55**, 66–86 (1973).
33. R.J. Levy et al., *Science* **228**, 190–192 (1985).
34. R.J. Levy et al., *Trans. Am. Soc. Artif. Intern. Organs* **31**, 459–463 (1985).
35. G. Golomb et al., *Trans. Am. Soc. Artif. Intern. Organs* **32**, 587–590 (1986).
36. G. Golomb et al., *J. Controlled Release* **4**, 181–194 (1986).
37. G. Golomb et al., *J. Pharm. Sci.* **76**, 271–276 (1987).
38. T.P. Johnston et al., *Trans. Am. Soc. Artif. Intern. Organs* **34**, 835–838 (1988).
39. T.P. Johnston et al., *Int. J. Pharm.* **52**, 139–148 (1989).
40. T.P. Johnston et al., *Int. J. Pharm.* **59**, 95–104 (1990).
41. T.P. Johnston, C.L. Webb, F.J. Schoen, and R.J. Levy, *J. Controlled Release* **25**, 227–240 (1993).
42. D. Hirsch et al., *J. Biomed. Mater. Res.* **27**, 1477–1484 (1993).
43. D. Hirsch et al., *Biomaterials* **14**, 705–711 (1993).
44. R.J. Levy et al., *J. Biomed. Mater. Res.* **29**, 217–226 (1995).
45. N.R. Vyavahare et al., *J. Controlled Release* **34**, 97–108 (1995).
46. H. Fleisch, in G.R. Mundy and T.J. Martin, eds., *Physiology and Pharmacology of Bone*, Springer-Verlag, New York, 1993, pp. 377–418.
47. D. Hirsch, F.J. Schoen, and R.J. Levy, *Biomaterials* **14**, 371–377 (1992).
48. R.J. Levy, F.J. Schoen, W.B. Flowers, and S.T. Staelin, *J. Biomed. Mater. Res.* **25**, 905–935 (1991).
49. C.L. Webb et al., *Am. J. Pathol.* **138**, 971–981 (1991).
50. Y. Pathak, J. Boyd, and R.J. Levy, *Biomaterials* **11**, 718–723 (1990).
51. T. Chandy et al., *Biomaterials* **17**, 577–585 (1996).
52. T. Chandy and C.P. Sharma, *Biomaterials* **17**, 61–66 (1996).
53. S. Patashnik, L. Rabinovich, and G. Golomb, *J. Drug Target*, **4**, 371–380 (1997).
54. R.J. Levy, F.J. Schoen, S.A. Lund, and M.S. Smith, *J. Thorac. Cardiovasc. Surg.* **94**, 551–557 (1987).
55. G. Golomb, M. Levi, G. Van, and M. Joel, *J. Appl. Biomater.* **3**, 23–28 (1992).
56. R.J. Levy, T.P. Johnston, A. Sintov, and G. Golomb, *J. Controlled Release* **11**, 245–254 (1990).
57. E. Bodner and R. Frater, eds., *Replacement Cardiac Valves*, Pergamon, Elmsford, N.Y., 1988.
58. R.J. Levy et al., *J. Controlled Release* **36**, 137–147 (1995).
59. G. Golomb and R.J. Levy, *Trans. Soc. Biomater.* **10**, 179 (1987).
60. M. Jones et al., *Trans. Am. Soc. Artif. Intern. Organs* **34**, 1027–1030 (1988).
61. W. Chen, F. J. Schoen, and R. J. Levy, *Circulation* **90**, 323–329 (1994).
62. M.N. Girardot, M. Torrianni, and J. M. D. Girardot, *Int. J. Artif. Organs* **17**, 76–82 (1994).
63. T. Shinoka et al., *Ann. Thorac. Surg.* **60**(6), Suppl., S513–S516 (1995).
64. B.A. Sosnowski et al., *J. Biol. Chem.* **271**(52), 33647–33653 (1996).

CANCER, DRUG DELIVERY TO TREAT—LOCAL & SYSTEMIC

KATHLEEN J. LEACH
University of Washington
Seattle, Washington

KEY WORDS

Cancer therapy
Chemoembolization
Depot systems
Immunoliposomes
Immunotherapy
Immunotoxins
Implantable pumps
Liposomes
Local delivery
Magnetic targeting
Microspheres
Nanoparticles
Stealth liposomes
Targeted delivery

OUTLINE

Introduction
Local Delivery
  Implantable Pumps or Reservoirs
  Chemoembolization
  Internal Radiation Therapy Using Microspheres
  Locally Implanted Controlled-Release Systems
Systemic Delivery
  Depot Systems
  Targeted Delivery
Cancer Immunotherapy
Summary
Bibliography

INTRODUCTION

In normal cells, growth is carefully regulated through an intricate web of physical and chemical signals. In adults, the rate of cell birth is maintained to be equal to the rate of cell death, whereas in children, slightly higher cell birth rates (or lower cell death rates) are necessary to allow for increases in body size during development. In either case, cell growth is carefully controlled. Cancer is the result of cell growth regulation gone awry. Any cell in the body has the potential to become a cancerous if it receives a series of genetic mutations that result in growth deregulation.

These mutations can result from spontaneous replication errors, chemical carcinogens, radiation, or even viral infection. The damage may be lethal to the cell, or it may free the cell from normal checks and balances on growth control, allowing it to proliferate when it should be quiescent. The mutated cell(s) will continue to divide, forming what is called the primary tumor. The tumor may be benign, or it may begin to invade surrounding tissues, breaking through basal lamina that define the natural boundaries of a particular tissue. Invasive tumors are described as malignant. Certain cells from these tumors may also mutate such that they gain the ability to leave the site of the primary tumor, enter the bloodstream, be carried to another tissue or organ, and begin forming a new tumor. These secondary tumors are called metastases and are often the cause of cancer deaths. Throughout the process of tumor development, many tumor cells lose their well-differentiated phenotypes and become more like immature or embryonic cells. They lose many of the unique features of the cell type from which they originated. Because tumor cells come from our own cells, they are very difficult to specifically target without cross-reactivity to other normal cells. As the tumor grows, more mutations occur, making the rapidly dividing cells within each tumor very heterogeneous in their cell surface markings and susceptibilities to various drugs and radiation damage. Tumor cells are also very adept at escaping from the constant patrol of the immune system, which should be able to recognize them as aberrant. For example, tumor cells often shed surface antigens that might identify them as abnormal. It is the combination of all these aspects that makes cancer such a difficult disease to cure and even to treat. In 1998, the American Cancer Society estimated that over half a million Americans are expected to die from cancer. Cancer is the second leading cause of death in the United States, with one in every four deaths attributed to the disease.

Conventional cancer therapies include surgery, chemotherapy, and radiation therapy. Each has its own limitations to providing a complete cure. Surgical resection is limited by the ability to expose and remove the tumor and can only remove those tumors detectable by current imaging techniques. Any cells that are not removed by the surgeon have the ability to proliferate, causing a recurrence. Surgery is also not effective against micrometastases that may have migrated from the site of the primary tumor. The efficacy of surgery is often limited by the surgeon's ability to remove enough healthy tissue at the margins of the tumor to ensure removal of all cancerous cells. Depending on the location of the tumor, this may or may not be feasible. For example, if the tumor is in the brain, the surgeon would probably not be as aggressive in removing healthy tissue at the tumor margins than if it were in the liver, which has regenerative abilities. This increases the risk of leaving behind malignant cells and subsequent tumor recurrence. Often, surgery is used in conjunction with chemotherapy or radiation therapy for improved efficacy. For example, the bulk of the tumor may be removed by surgery, and systemic chemotherapy may be prescribed after surgery if the tumor was found to have metastasized to local lymph nodes. Alternatively, radiation can be used after surgery to kill any parts of the tumor that were impossible to remove without destroying healthy tissue.

Chemotherapy, whether given systemically or by regional perfusion of a particular organ or tissue, is impeded by the lack of specificity of the drugs for cancer cells. Therefore, therapy is often limited by systemic toxicity before truly therapeutic drug levels in the tumor can be achieved. Drug concentrations in the tumor must also be sustained for prolonged periods of time for maximum efficacy so as to catch all the cancer cells during the portion of the cell cycle when they are susceptible to the drug. Chemotherapeutic drugs usually act on rapidly dividing cells, so cells of the intestinal lining and bone marrow can be extensively damaged during treatment. Depending on the health of the patient, toxic drug levels may not be achievable at the site of the tumor, because dosages must often be lowered or therapy halted altogether owing to this nonspecific action on healthy cells. Blood distribution to solid tumors may not be uniform throughout the mass, and therefore some regions of the tumor may not receive therapeutic doses of the drug. Tumor cell heterogeneity may also result in cancer cells that are resistant to a particular chemotherapeutic agent or even to multiple drugs. By treating the patient with a single-drug regimen, cells resistant to that drug are selected for survival; susceptible cells are killed, while the resistant cells are left behind to regrow a tumor composed entirely of resistant cells, making it impossible to effectively treat the tumor with that same drug a second time. By using several drugs in series or in combination, the problem of single-drug resistance can be significantly reduced. Multiple-drug resistance (MDR), where the tumor cells have gained the ability to protect themselves against a range of drugs by upregulating the expression of an efflux pump mechanism (*P*-glycoprotein) that ejects drug molecules from the interior of the cells, is more difficult to circumvent. Even drugs that are chemically dissimilar may be transported out of MDR tumor cells, so switching drugs may not successfully kill the cells. MDR is not as easy to work around than single-drug resistance, but many of the controlled drug delivery systems discussed later in this article have reportedly shown promise in circumventing MDR.

Radiation therapy can be specifically directed to the site of the tumor, but is also limited by the potential for damage to noncancerous tissue. The use of radiation to kill tumor cells is based on the idea that noncancerous cells divide more slowly and have a better chance to repair DNA damage caused by radiation before replicating. The cancer cells hopefully will not be able to make the necessary repairs, and the damage to them will be lethal. Radiation therapy, like surgical resection, is limited by the ability of imaging techniques to identify tumor sites for treatment. If the tumor is too small to be imaged, it will not be identified target for therapy and will be left to grow and possibly metastasize.

None of these traditional therapies, alone or in combination, have achieved complete cures for all cancer types in all patients. Therefore, many researchers have been exploring controlled-release or targeted-delivery options for the treatment of this disease. Although drug delivery systems cannot improve the specificity of the cytotoxic agents,

the delivery vehicle itself can act to target the therapy to the tumor cells to focus the action of a nonspecific drug to the tumor or at least limit its effects to the tissue in closest proximity. Drug delivery systems act by locally concentrating the drugs for sustained periods of time, thereby reducing systemic toxicity.

The field of controlled release has made inroads into many forms of cancer therapy. Drug delivery systems have been proposed in three categories: (*1*) delivery systems that are implanted or injected in or near the tumor to act locally against the neoplasm; (*2*) delivery systems implanted or injected to act simply as a depot for the sustained release of the drug, which acts systemically; and (*3*) delivery systems administered systemically but that contain a targeting mechanism. Table 1 provides examples of controlled-release approaches to cancer therapy discussed in this article. The first type of system can be effective against the primary tumor or against metastases that occur near the primary tumor or are localized to a particular organ. The other two types of drug delivery system allow for the attack of the primary tumor as well as disseminated metastases, with targeted therapy having the ease of systemic administration and the advantage of affecting tumor cells without harming normal tissue. This article discusses examples of each of these types of delivery systems. The topic of immunotherapy for cancer is also covered briefly as it pertains to controlled-release systems. The information provided in this entry is not designed to exhaustively cover all cancer therapies that have been explored or are used clinically but focuses instead on the use of polymers for the sustained release or presence of the therapeutic agent. For reference, Table 2 summarizes the chemical structures, typical dosages, and mechanisms of action for the various chemotherapeutic drugs used in examples throughout this article.

LOCAL DELIVERY

Damage to normal, healthy cells and tissue is usually what limits the aggressiveness of any given cancer therapy. Controlled-release systems implanted or injected at the tumor site can act to reduce systemic toxicity by delivering the drug locally in a sustained manner. This provides high concentrations of the drug at the site of the tumor, with the drug either being degraded before reaching the systemic circulation or diluted in the total blood volume of the patient, thus reducing side effects. The sustained-release aspect of the technology allows the patient more freedom during treatment while maintaining drug levels in the tumor at a constant, therapeutic level for an extended period of time. Conventional intravenous treatments are usually given in bolus form with periods of rest in between or as continuous infusions through percutaneous intravenous catheters. Patients are either restricted by an percutaneous catheter or are given intermittent treatment, which may not provide sustained drug concentrations necessary for maximum efficacy. Local delivery can also bypass physiologic barriers such as the blood–brain barrier, which can limit therapeutic efficacy of drugs delivered systemically. The polymer also acts to protect the drugs, which often have extremely short half-lives in vivo, from degradation until they are released from the device.

Table 1. Examples of Drug-Delivery Systems Used to Treat Cancers

Administration	Action	Examples
Local	Local	Intraarterial infusion, chemoembolization, intratumoral injections, implants of sustained-release systems
Systemic	Systemic	Depot systems such as Zoladex® and Lupron Depot®
Systemic	Tumor cells	Drug–antibody conjugates, drug–polymer conjugates, liposomes, nanoparticles, magnetic localization

The following sections discuss the use of controlled-release systems for the localized treatment of tumors. These include systems implanted or injected in or near the tumor itself or infused into the local blood supply to a tumor or diseased organ. Local drug delivery therapies discussed include the infusion of drugs into the tumor vasculature via implantable pumps, the intratumoral infusion of polymer microspheres that may contain drugs or radioisotopes, or the injection or implantation directly into the tumor of polymer matrices loaded with drugs.

Implantable Pumps or Reservoirs

Infusion systems are one of the simplest drug delivery systems that have been applied to cancer therapy. There are two types: (*1*) controllers, which use gravity as the driving force for fluid delivery; and (*2*) infusion pumps, which use positive pressure to deliver the drug solution. Both types use a drug reservoir that can be exchanged or refilled as needed. For controllers, the height of the reservoir and the resulting pressure head are critical in maintaining the desired level of flow. Infusion pumps are capable of overcoming the back pressure created by arterial infusion catheters, the pumping of viscous liquids, and minor occlusions of the vascular access line by the application of positive pressure, and they can accurately provide low infusion rates. Pumps may be external to the body with the drug administered via a percutaneous catheter, or the pumps may be totally implantable. External pumps are simple devices used extensively to deliver drugs to patients in hospital settings over prolonged periods of time. They may be connected directly to an intravenous (IV) or intraarterial (IA) catheter, or they may access the vascular system via a needle that percutaneously punctures the septum of a surgically implanted port. External pumps free medical personnel from having to slowly and/or repeatedly inject drug solutions using a syringe, but the patient is tethered to the pump during treatments. With an implantable pump, the patient can be freed from the hospital during therapy, a small but important factor in his or her quality of life. Only implantable pumps will be discussed further in this entry, with the focus on those used for the local infusion of drugs into tumor vasculature.

Table 2. List of Chemotherapeutic Agents Used in This Article

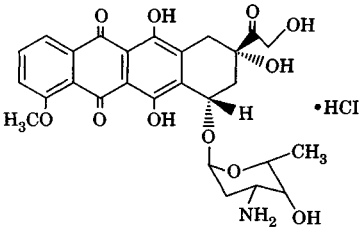
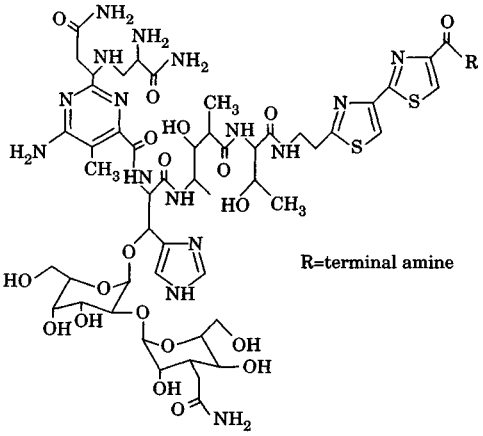
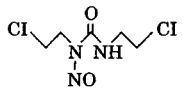
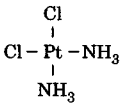
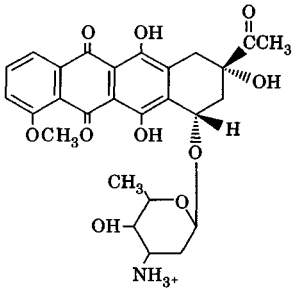
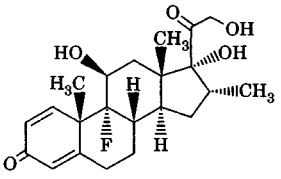
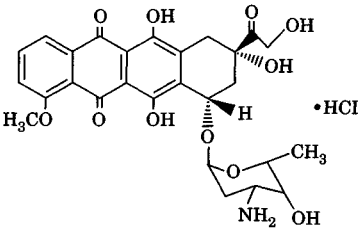
Drug name(s)	Chemical structure	Typical IV dosage	Mechanism of action
Adriamycin (ADR) Doxorubicin (DOX)		60–75 mg/m^2 as bolus or continuous infusion over 2–4 days repeated every 3–4 weeks	DNA intercalation, preribosomal DNA and RNA inhibition, alteration of cell membranes, free radical formation
Bleomycin		10–20 U/m^2 weekly or twice weekly, 15–20 U/m^2/day continuous infusion over 3–7 days	DNA strand scission by free radicals
Carmustine (BCNU)		150–200 mg/m^2 every 6 weeks as a single dose or divided over 2 days	DNA cross-linking, DNA polymerase repair, RNA synthesis inhibition
Cisplatin, cisdiamine-dichloroplatinum (II) (CDDP)		20–40 mg/m^2/day for 35 days every 3–4 weeks; 20–120 mg/m^2 as a single dose every 3–4 weeks	DNA cross-linking, intercalation, DNA precursor inhibition, alteration of cell membranes
Daunorubicin		45 mg/m^2/day for 3 days	DNA intercalation, preribosomal DNA and RNA inhibition, alteration of cell membranes, free radical formation
Dexamethasone		40 mg/day on days 1–4, 9–12, and 17–20, repeated every 4 weeks	Binds to specific proteins in cell, forming a steroid–receptor complex. Binding of this complex with nuclear chromatin alters mRNA and protein synthesis.
Doxorubicin (DOX) Adriamycin (ADR)		60–75 mg/m^2 as bolus or continuous infusion over 2–4 days repeated every 3–4 weeks	DNA intercalation, preribosomal DNA and RNA inhibition, alteration of cell membranes, free radical formation

Table 2. List of Chemotherapeutic Agents Used in This Article *(continued)*

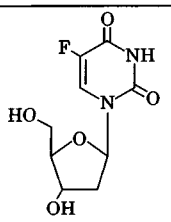
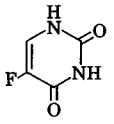
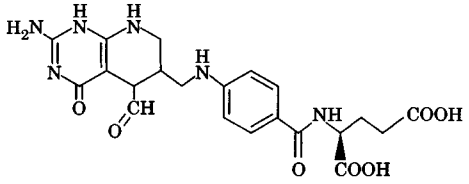
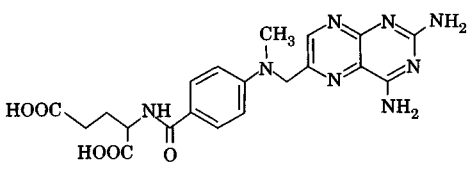
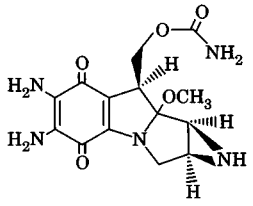
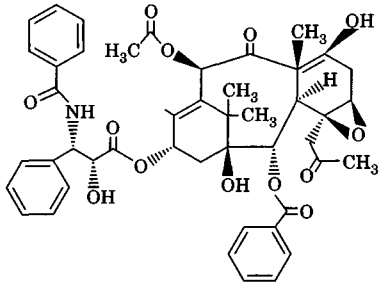
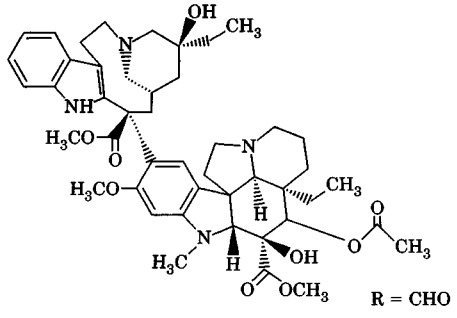
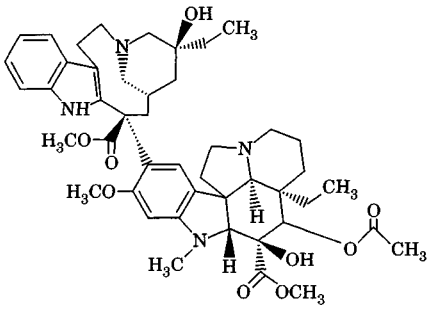
Drug name(s)	Chemical structure	Typical IV dosage	Mechanism of action
5-Floxuridine (FUDR, 5-FUDR)		0.1–0.6 mg/kg/day (intrahepatic) or up to 60 mg/kg/week IV	Inhibition of thymidylate synthesis
5-Fluorouracil (5-FU)		300–450 mg/m^2/day for 5 days (IV); 600–750 mg/m^2 given weekly (IV); 1,000 mg/m^2 for 4–5 days (IV over 24 h)	Inhibition of thymidylate synthase
Leucovorin		10–25 mg/m^2 every 6 h for 6–8 doses	Rescue agent for MTX
Methotrexate (MTX)		20–40 mg/m^2 every 1–2 weeks (solid tumors); 200–500 mg/m^2 every 2–4 weeks for leukemia and lymphoma	DHFR inhibition (stops thymidylate and purine synthesis)
Mitomycin, mitomycin-C (MMC)		10–20 mg/m^2 every 6–8 weeks	DNA cross-linking and depolymerization, free radical formation
Taxol, paclitaxel		135–175 mg/m^2 every 3 weeks	Promotes microtubule assembly and stabilizes tubulin polymers, resulting in formation of nonfunctional microtubules.
Vincristine (VRC)		0.5–1.4 mg/m^2 every 1–4 weeks	Tubulin binding (microtubule assembly inhibition and dissolution of mitotic spindle structure)

Table 2. List of Chemotherapeutic Agents Used in This Article *(continued)*

Drug name(s)	Chemical structure	Typical IV dosage	Mechanism of action
Vinblastine		6–10 mg/m^2 every 2–4 weeks	Tubulin binding (microtubule assembly inhibition and dissolution of mitotic spindle structure)

Source: Data taken from Ref. 117.

Implantable pumps have been shown to result in fewer treatment interruptions and better patient compliance than external pumps (1). Fordy and coworkers compared the use of a totally implantable pump (Infusaid model 400, Infusaid, Inc.) to the use of an implanted port (Infusaport, Infusaid, Inc.) in conjunction with an external pump in 95 patients with liver metastases of colorectal cancer (CRC). The drug was infused into the hepatic artery in all cases. They found a 3-fold lower incidence of treatment interruptions (due to line occlusions, infection, hematoma, etc.) and a 30-fold lower incidence of catheter blockage with the implanted pumps. Implanted pumps showed a lower incidence of line occlusion (0.3% of treatments) compared to 9% for implanted ports. When the IA line becomes occluded, treatment must be temporarily halted to reopen the vascular access. This is often achieved with flushes of heparin or other enzymes, but the flushing is frequently unsuccessful, and the occluded line must be replaced surgically. Because of the reduction in line occlusions with the use of an implanted pump, patients required fewer reoperations, procedures that can be risky in critically ill patients. Implantable pumps were more likely to result in complications due to the surgical implantation of the device (e.g. infection, hematoma, etc.), but overall, implantable pump treatments showed a lower rate of treatment problems (1.7%) than ports (5.7%). Costwise, the price of the implanted pump was 10 times higher than the price of the implanted port option, but the lower incidence of complications has the potential to improve therapy dramatically. The implantable pumps allowed for more extended therapies, which increased the efficacy of the anticancer drugs by ensuring their presence in therapeutic concentrations at critical points in the cell cycle. The Fordy study clearly showed the benefits of implantable pumps over external pumps (1).

In the past decade, two review articles have been published that describe designs of implantable pumps in great detail and discuss a few of their current applications, including the treatment of cancer and cancer-related pain (2,3). The clinical use of implantable pumps has now progressed to the point that most of the current literature does not describe clinical trials to test the efficacy of the pumps but rather the efficacies of various drug combinations, all delivered via these implantable pumps. The remainder of this section describes the features of the implantable pumps that have been approved by the U.S. FDA for the controlled delivery of various chemotherapy drugs and then discusses a few examples in the current literature in which these pumps were used to successfully treat cancer patients. Finally, some of the problems with current pump technology are addressed, with reference to current research being done to improve this type of therapy.

FDA-Approved Devices. Implantable infusion pumps were introduced for continuous drug delivery in 1969. Several implantable pumps have been approved by the FDA, and many more are being tested and used clinically around the world. The Infusaid Models 100, 100, and 550 (Pfizer Infusaid, Inc., Norwood, MA) were FDA approved starting in 1982 for the delivery of various cancer therapeutics, including floxuridine (FUDR), fluorouracil (5-FU), methotrexate sodium (MTX), and cisplatin (CDDP) (2). They have also been approved for the delivery of morphine sulfate for the treatment of pain resulting from incurable cancer. The Infusaid pumps consist of a flexible bellows containing the drug solution that is surrounded by a rigid chamber filled with a charging fluid (usually a volatile chlorofluorocarbon). Vapor pressure from the charging fluid expels the drug solution by compressing the internal drug reservoir. The release of the drug solution is regulated by a capillary flow restrictor or a valve/accumulator combination. The reservoir can be refilled by percutaneous puncture of a needle, which reexpands the reservoir and increases the pressure in the adjacent charging fluid chamber, causing the fluid to recondense. The pump is then ready for its next infusion cycle.

Medtronic, Inc. (Minneapolis, MN) received FDA approval for its SychroMed Infusion System in 1988 for the delivery of CDDP, FUDR, doxorubicin hydrochloride (DOX), and MTX and received FDA approval in 1996 for the intrathecal delivery of morphine sulfate for the treatment of pain (2). The SynchroMed pump delivers a drug solution from a percutaneously refillable reservoir via a peristaltic pump mechanism that is driven by a lithium battery with a life of 1 to 3 years (3). The pump can be programmed with an external computer and a magnetic field telemetry link, allowing for more complex delivery regimens, including those based on circadian rhythms. The

doctor has the option of tailoring the drug dosage, flow rate, and dosage schedule to best fit the needs of the patient, while the patient is able to receive treatments untethered.

Applications to Cancer Therapy. The majority of the literature describing cancer therapy using implantable pumps centers on the treatment of primary and secondary tumors in the liver, especially liver metastases of CRC, with hepatic arterial infusion of chemotherapeutic agents. Only a few examples of the many studies published in the last decade are discussed here. Patt et al. report the results of a study that treated 48 patients with liver metastases of CRC, 19 of whom were treated via Infusaid implantable pumps (4). Therapy consisted of alternating delivery of recombinant human interferon α-2b (6 h) and 5-FU (18 h) into the hepatic artery. This cycle was repeated daily for 5 days, with the cycle repeated every 4–7 weeks thereafter. They found a complete plus partial response rate of 33.3%, but they did not separate the results based on delivery via implantable pumps or external pumps. However, they report that 6 of the patients treated during the trial with implantable pumps elected to continue treatment past the end of the study, whereas none of the patients elected to continue treatments via percutaneous access past the completion of the study. Patient acceptance of the implantable pump was very high.

A 1994 paper by Kemeny et al. presented the results of a study involving 62 patients with liver metastases of CRC treated with hepatic arterial infusion of FUDR, leucovorin (LV), and dexamethasone (DEC) via Infusaid pumps (5). Treatment consisted of a 2-week infusion of FUDR (0.3 mg/kg/day), LV (15 mg/m^2/day), and DEC (20 mg total dose) alternated with a 2-week infusion of saline to keep the delivery catheter patent between treatment periods. Thirty-three of the patients had not previously received systemic chemotherapy for their disease, and this group saw a complete plus partial response rate of 78% (median survival 24.8 months). Patients who had previously received systemic therapy showed a complete plus partial response rate of 52% (median survival 13.5 months). Davidson et al. report that by alternating hepatic arterial infusion of FUDR (0.1 mg/kg/day; given as 7-day continuous infusion) and 5-FU (15 mg/kg; given as a weekly bolus for 3 weeks) by implantable pump, biliary toxicity could also be reduced (6). Out of 57 patients treated for hepatic metastases of CRC, 79% showed a reduction in tumor size or stabilization of disease, with a median survival of 19 months. More than 95% of the patients were free from all or at least irreversible hepatobiliary toxicity, a common side effect of hepatic arterial infusion of drugs.

A second group of cancers often treated by intraarterial infusion of chemotherapeutic agents via implantable pumps is cancers of the head and neck, including squamous cell carcinoma. Baker, Wheeler, and colleagues report the results of 37 patients treated over a 6-year period for advanced cancers of the head and neck using implantable pumps (7,8). The pumps (Infusaid model 400) were equipped with one or two silicone rubber catheters that allowed for singly treating the tumor via one external carotid artery or concurrently treating both sides of the head and neck. Forty-three percent of the 26 patients treated with a combination of cisplatin and FUDR for squamous cell carcinoma showed a partial or complete response to the treatment. The pumps were safe, effective, and had high patient compliance. Median infusion duration was 328 days, with only a small percentage of therapy-limiting complications: infection (5.4%), emboli-to-skin overlying tumor (5.4%), catheter occlusion by drug precipitation (8.1%), and infusion into the brain (21.6%).

Although not directly treating the malignancy itself, implantable pumps have been used extensively for the intrathecal delivery of pain medication for patients with incurable cancer. In 1990, Hassenbusch and colleagues showed great efficacy of pain treatment via the Infusaid model 400 pump to deliver morphine epidurally to patients with inoperable cancer (9). Before implanting the pumps, they used a temporary percutaneous catheter to epidurally deliver the morphine for 2 to 4 days to see if the patients' pain was responsive to morphine. Only those patients whose pain was relieved by the morphine had pumps implanted. Out of the 69 patients admitted to the study, 41 received implantable pumps, and 37 of these patients were evaluable. Mean survival time was 7.1 months, with more than 80% of the patients showing satisfactory pain relief (defined by a 30% decrease in pain analog scale value) at 1, 3, and 6 months. Hoekstra reported the results of a study on the delivery of morphine hydrochloride to 50 patients with terminal cancer via an implantable pump with a intrathecal or epidural catheter (10). They used a Secor® pump system (Cordis S.A., France) that did not provide continuous infusion of the drug but rather was activated by the patient to deliver a bolus dose of the drug when he or she percutaneously pressed two buttons on the pump in the correct sequence. This is a relatively cheap, totally implantable pump option (compared to continuous or programmable pumps) that is patient activated and has the capability of lasting up to 5 years in vivo. Half of the patients in this study achieved a pain-free state using the pumps, with a median implant duration of 3.3 months.

New Directions. Constant delivery of drugs may not always be the most effective or least toxic dosage schedule. A popular modification of traditional chemotherapy regimens is to infuse the drugs in cooperation with the body's natural circadian rhythm. In 1990, Damascelli et al. used a totally implantable, programmable Medtronic Sychromed pump to deliver drugs intravenously to 42 patients with metastatic renal cell carcinoma (11). The patients received 14 days of treatment (FUDR) alternated with 14 days of heparinized saline infusion to maintain catheter patency. Treatment was delivered as follows: 68% of the daily infusion was given between 3 P.M. and 9 P.M., 15% between 9 P.M. and 3 A.M., 2% between 3 A.M. and 9 A.M., and 15% between 9 A.M. and 3 P.M. The starting dose was 0.15 mg/kg/day and was increased by 0.025 mg/kg with each successive cycle. The study was continued for 2 years, with a median implant duration of 210 days. Median survival was 1 year after the start of therapy, with 55% of the patients alive after 1 year. The efficacy of treatment was equivalent to other standard treatments but was associated with a normal quality of life for the patients.

The future holds much for the application of these implantable pumps to cancer therapy, especially with the expanded use of programmable pumps that allow for increasingly complex dosage regimens to be delivered to ambulatory patients. The pumps can be used for local or systemic treatment, depending on the placement of the delivery catheter, and can be used to deliver any drug that can remain stable for the necessary storage times in the pump chamber. Pumps are the most versatile device for drug delivery, as the choice of drug, the infusion rate, and infusion schedule can be easily adapted to personalize the therapy for each individual patient.

Chemoembolization

Other means of enhancing the local cytotoxicity of drugs have also been explored for use as stand-alone, alternative therapies or for use in conjunction with local infusion. Locally induced hypoxia (oxygen deprivation) is one such therapy. Hypoxia is most easily achieved for tumors by ligation or occlusion of the blood vessels that feed the tumor. Historically, ligation was the method of choice, although more recent research has focused on the development of occlusive techniques. Embolization, the use of particulates to effectively shut off blood flow to an organ or tumor so as to cause cell death by hypoxia, is an example of an occlusive technique. In addition to the direct effects of oxygen deprivation on tumor cells, embolization also has several indirect means of enhancing the effects of drugs administered with the emboli. The indirect means include (*1*) increasing the cytotoxic properties of the drugs themselves, (*2*) lowering the total tumor burden on which the drug needs to act, or (*3*) increasing the permeability of the tumor vasculature for better uptake of the drugs. An extension of embolization that uses drug-loaded polymer microspheres to cause local hypoxia in combination with local, sustained-delivery of cytotoxic drugs is called chemoembolization; it is a single-step procedure that does not require persistent percutaneous catheters to deliver the drug and is thus a significant improvement over past treatment strategies. The microspheres function both to induce local hypoxia and to serve as depots for the sustained release of the drug.

Most of the current research on chemoembolization has focused on primary or metastatic liver cancer. The anatomy of the liver is unique because it receives blood from two sources: the hepatic artery and the portal vein. The hepatic artery supplies the liver with fully oxygenated blood, whereas the portal vein drains a portion of gastrointestinal tract and then passes the absorbed nutrients to the liver for detoxification and storage. It was determined in the 1950s that most hepatic tumors derived their supply of oxygen from the hepatic artery and that normal liver tissue was able to survive on portal blood supply alone (12). This separation in blood supply offers a distinct advantage for targeted attack on liver tumors with minimal effects on the healthy liver parenchyma. The bulk of research has thus been focused against primary and secondary hepatic tumors, and cancers of the liver are the focus for the next sections.

Historical Background. Before discussing the use of drug delivery systems in the form of microspheres loaded with a drug as embolizing agents, a brief history describing early research on oxygen deprivation of tumors is informative. As early as 1933, Graham published a paper describing multiple cases of accidental hepatic artery ligation that proved not to be fatal, as once believed, and even resulted in localized necrosis of malignant liver tissue (13). This opened the door for researchers to develop various techniques for clinically stopping blood flow to tumors by permanent or temporary ligation or occlusion of the hepatic artery (14–16). These techniques were used alone or in combination with arterial or local infusion of chemotherapeutic agents for added benefits. In a randomized, controlled study, permanent ligations of the hepatic artery or complete dearterializations of the liver increased survival times in patients with hepatocellular carcinoma (HCC), but the increases were not significant in comparison with the controls who received only palliative treatment (17). It was believed that this lack of therapeutic improvement was due to the rapid formation of collateral circulation, which was shown to come from as many as 26 different sources and had the ability to resupply hypoxic liver tissue with blood in less than 4 days (18). Thus, although the hepatic artery was permanently closed, the hypoxic condition of the tumor was only temporary. Hepatic artery occlusion using the percutaneous infusion of autologous or nondegradable, synthetic materials was less surgically invasive but did not circumvent the problems of collateral vessel formation. Thus, these permanent occlusion methods were not entirely successful in treating hepatic tumors, even in combination with arterial or portal venous infusion of chemotherapeutic drugs (19,20).

Because permanent occlusion resulted in the recruitment of collateral vessels, researchers began to investigate temporarily occlusive techniques that could provide the beneficial hypoxia within the tumor while avoiding the formation of alternative blood supplies. Research on temporary occlusion of the hepatic arterial blood supply in rats showed that if the circulation was halted for less than 4 hours at a time, collateral blood vessels would not form (21). Two generations of temporary occluding devices showed some success by causing localized hypoxia while avoiding collateral vessel formation; however, these treatments still involved surgical implantation and removal of the device (22,23). A nonsurgical alternative to temporary dearterialization is the percutaneous infusion of biodegradable polymer microspheres that could block flow temporarily until their hydrolytic or enzymatic degradation allowed blood flow to resume. By altering the properties of the microspheres, occlusion times could be optimized to allow for maximum tumoricidal effect without the formation of collateral circulation. Cytotoxic drugs could be infused with or loaded into the microspheres for a more effective combination approach. These treatments have been reviewed by Willmott (24) and are discussed in more detail in the following sections.

Embolization Using Blank Microspheres. The use of degradable polymer microspheres for the infarction of tumors has been reviewed extensively in the literature (24–27). The majority of the studies utilized degradable starch microspheres. The biodegradation (28) and patterns of blood

flow (29) after starch microsphere embolization have been well characterized in animals and showed that blood flow to an organ can be halted after arterial administration of the microspheres until the particles had degraded sufficiently to pass through the capillary bed, generally over a period of hours. The effect of starch microsphere embolization alone as a treatment for primary and metastatic liver cancer showed some success in humans, although the results were not significantly better than standard chemotherapies (30).

The combination of starch microsphere embolization with the infusion of drugs was found to be more effective at tumor reduction against both primary (31–34) and secondary (30–37) liver cancer than embolization alone. The microspheres act to retain the drug in the tumor, slowing its release into the systemic circulation. The benefits of the combination therapy have been elucidated by pharmacokinetic studies done in animals showing that tumor uptake of drugs is higher after microsphere embolization (27,38,39).

In addition to the infusion of cytostatic drugs, vasoconstrictors such as angiotensin II have been included in the regimen (40,41) based on research showing that tumor blood vessels are less able to respond to vasoconstrictors than normal blood vessels (42–44). It has been suggested that tumor vessels lack the supportive smooth muscle cells that supply the main forces in the constriction of mature blood vessels. The injection of such vasoconstrictors would cause the blood vessels supplying normal tissue to constrict, reducing the flow of the chemotherapeutic agents to normal tissues whereby the vessels supplying the tumor would remain open, resulting in more selective tumor cell damage. A schematic of this shunting process is shown in Figure 1.

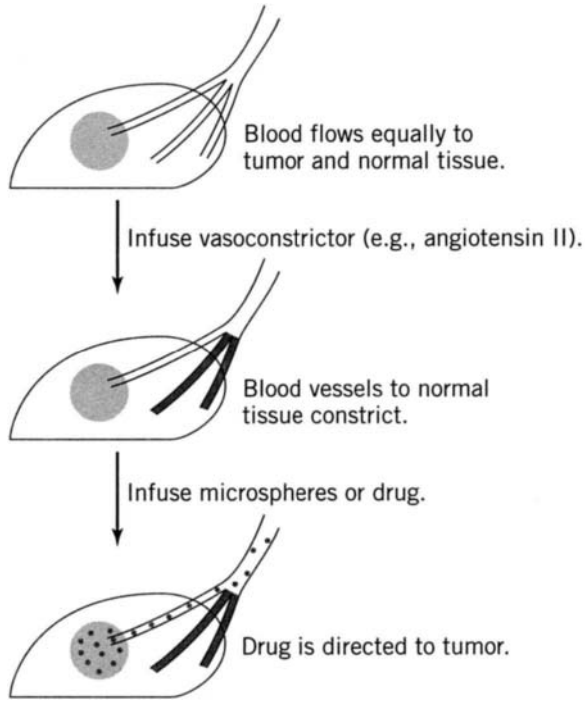


Figure 1. Schematic showing selective constriction of normal vasculature that directs flow of the chemotherapeutic agent (black circles) to the tumor vasculature, which is not able to respond. Shaded region represents tumor.

Drug-Loaded Microspheres. The utility of polymer microspheres is not limited to simply plugging a tumor's arterial blood supply. Microspheres can be loaded with drugs to provide sustained, local delivery of cytotoxic agents in the tumor vasculature. Similarly to blank microsphere embolization in conjunction with locally infused drugs, the hypoxia caused by the embolization increases vascular permeability so more drug can be absorbed by the tumor. In addition, some drugs, such as mitomycin C (MMC), show enhanced cytotoxicity against hypoxic cells (45,46). By loading MMC or other drugs into or onto the microspheres, the effects of local, sustained release of the drug may be synergistic with the effects of localized hypoxia. Researchers have loaded drugs into microspheres made of both nondegradable materials such as polystyrene-*co*-divinyl benzene (ion exchange resin) (47); ethylcellulose (48,49); and degradable materials such as collagen (50), poly(lactic acid) (PLA) or its copolymer, poly(lactide-*co*-glycolide) (PLGA) (51–53), and albumin (54).

Kato et al. published a series of papers in the late 1970s and early 1980s describing work with nondegradable, ethylcellulose microspheres loaded with MMC (48,49,55–57). This pioneering work introduced the term *chemoembolization*, and the microspheres were used to treat many types of cancer in clinical trials in Japan (49). One clinical trial showed significant tumor reduction in 65% of the tumors, pain relief in 80%, and hemostasis in 100% of patients treated with intraarterial infusions of MMC-loaded ethylcellulose microspheres (49). The trial involved 60 patients with a range of primary and secondary carcinomas. Patients were treated with single or multiple infusions. Codde and coworkers loaded nondegradable, ion exchange resin microspheres with doxorubicin and injected them into the hepatic artery of rats with colorectal adenocarcinoma transplanted in their livers (47); they found significantly reduced tumor growth as compared with treatment with free doxorubicin or blank microspheres alone.

As reports were published stating that the effectiveness of permanent occlusion of the vessels is often negated by collateral vessel formation, chemoembolization research switched focus to the development of methods to provide temporary occlusion in combination with the sustained delivery of cytotoxic agents. Degradable polymer microspheres that could be loaded with drugs provided an attractive solution. The majority of research on drug-loaded, degradable microspheres has focused on albumin microspheres, and this topic has been extensively reviewed by Morimoto and Fujimoto (54). The in vitro release characteristics (58) and biodegradation of albumin microspheres in both animals (59) and humans (60) have been studied. In rats, Willmott and colleagues showed that the time for 50% of the microspheres to disappear from the target organ for albumin microspheres with diameters of 10 to 30 μm was 3.6 days in the liver and 2.0 days in the lungs (59). Goldberg et al. showed that in seven patients with colorectal liver metastases, the median biological halftime of

^{131}I-labeled albumin microspheres administered into the liver via the hepatic artery was 2.4 days with a range of 1.5 to 11.7 days (60). Kerr et al. studied the organ distribution and pharmacokinetics of doxorubicin-loaded albumin microspheres after renal artery administration and found that 97% of injected microspheres were retained in the treated kidney and that peak plasma levels in venous blood were significantly lowered from 135 ng/mL when the drug was administered in solution to 16 ng/mL when encapsulated in microspheres (61). Histologically the microspheres were shown to be trapped in small renal arterioles and capillaries. Fujimoto et al. infused MMC-loaded albumin microspheres into 19 patients with inoperable hepatic cancer and found objective tumor responses in 13 out of 19 patients treated with microspheres compared with 6 out of 13 treated by conventional infusion therapy with MMC and 5-FU (62).

These albumin microspheres were hampered by low drug loadings and release profiles characterized by an initial burst before leveling off for sustained release. Cremers et al. describes a method of increasing the amount of drug that can be loaded by combining heparin, a negatively charged mucopolysaccharide, with the albumin (63). Nishioka et al. studied the effects of adding chitin to the albumin microspheres to increase the loading and reduce the burst of cisplatin (64). Although the mechanism is still unclear, the chitin promoted degradation of the microspheres and the release of the cisplatin, increasing the efficacy of embolization therapy.

Degradable polymers other than albumin have also been studied. Daniels et al. loaded collagen microspheres with cisplatin and studied the pharmacokinetics and tissue tolerance in the rat liver and rabbit kidney (50). They found that arterially administered cisplatin-loaded collagen microspheres increased renal platinum concentrations to 250 times the levels in the contralateral, nontreated kidney. Platinum levels in the rat liver were doubled when the drug was delivered from microspheres as compared with when the drug solution was administered systemically (50). Spenlehauer et al. investigated the preparation and in vitro release characteristics of cisplatin-loaded PLA and PLGA microspheres (51,65). In the case of PLA microspheres, they found the optimal cisplatin concentration to be 45% (w/w) and that drug release was proportional to drug loading (51). For both PLA and PLGA, they determined that factors influencing the distribution of drug in or on the surface of the microspheres were more important in controlling the release kinetics from the PLGA microspheres than the degradation rate or molecular weight of the polymer (65). Verrijk et al. also studied cisplatin-loaded PLGA or PLGA-coated albumin microspheres for chemoembolization and found significant cytotoxicity in vitro (52). When the CDDP-loaded PLGA microspheres were administered to the liver via the portal vein, the liver-to-blood platinum ratio was 38 times higher than when free drug was injected by the same route (53).

The progression of the use of local hypoxia as a means to treat tumors from permanent arterial ligation to drug-loaded, degradable microspheres occurred over a period of 60 years. With each new development, the promise and efficacy of such treatments grew. They will always rely on direct access to the tumor blood supply, but advances in percutaneous, imaging-guided catheterizations will make this step as noninvasive as possible. Surgical exposure to blood vessels is no longer a necessary part of organ catheterization. Time will only tell if any of these controlled-release systems will make it into clinical practice as standard cancer therapies for tumors with an isolatable blood supply.

Internal Radiation Therapy Using Microspheres

As an alternative to chemotherapeutic agents, radioactive isotopes such as yttrium-90 (Y-90) have also been loaded into microspheres and infused into the arterial blood supply of a tumor for localized radiation therapy. The microspheres are trapped in the vasculature of the tumor and are able to concentrate the effect of the radioisotopes on the tumor, thus reducing systemic side effects. The first attempts for internal radiotherapy by Grady and coworkers in 1963 used a particulate form of Y-90 injected intravenously for the treatment of lung cancer and injected into the celiac or hepatic artery for liver cancer (66,67). The procedure was deemed simple and nontoxic, and over half of the treated patients showed subjective or objective improvement (67). Y-90 was also adsorbed to ceramic microspheres by Kim et al. (68) and Ariel (69) and delivered intraarterially to humans. The ceramic spheres were shown to be physiologically inert, resisted leaching in body fluids, and were appropriate for the adsorption of any cationic isotope (68). Both researchers saw objective improvement in some of the patients treated by this method, but both agree that more research needs to be done to improve the selective delivery to tumor tissue (68,69).

Y-90 was also bound to ion exchange resin microspheres made from cross-linked poly(styrene-*co*-divinyl benzene) (70–74). Ariel and Padula administered Y-90 adsorbed to resin microspheres into the hepatic artery of 65 patients with symptomatic CRC liver metastases in combination with hepatic arterial infusion of drug (70). They found that 24 patients showed objective improvement and 40 showed subjective improvement. In patients with asymptomatic colorectal metastases in the liver, the average lifespan was increased an average of 28 months by this treatment (71). Gray and colleagues infused angiotensin II prior to infusion of the Y-90 resin microspheres to direct the spheres away from normal liver parenchyma and toward the tumor vasculature (72–74). Angiotensin II constricted only the fully developed, non-tumor-associated vasculature, leaving tumor vasculature open for the infusion of the microspheres (42). They documented an average ratio of tumor radiation dose to normal tissue dose of 6:1 (72) and found that normal liver tissue was tolerant to radiation delivered in this fashion (73). They also reported the regression of liver metastases in 18 of 22 patients treated with this therapy (74).

LOCALLY IMPLANTED CONTROLLED-RELEASE SYSTEMS

Implantable pumps, chemoembolization, and internal radiation therapy provide local treatment of cancer by infusion directly into the blood vessels of the tumor. This direct access to tumor vasculature is not always easy to achieve

and requires skilled medical professionals. Because of this, researchers have devoted much time and resources to developing delivery systems that can be injected or implanted directly into the tumor or left in the cavity created by surgical resection of the tumor. Many of these systems are biodegradable and therefore do not require removal at the end of therapy, unlike implantable pumps, which require a second surgery for device removal. Drug is distributed through the tumor by passive diffusion through the intracellular fluid that bathes the tumor cells. Controlled-release systems placed at the site of the tumor provide sustained delivery of the therapeutic agents in high concentrations locally without systemic side effects. The sustained-delivery property of such systems improves the therapy by providing prolonged exposure to drugs whose effects are generally cell cycle dependent. With delivery to the site of action, the drug is able to work at therapeutic concentrations and is degraded before reaching the circulation or diluted so as to not cause significant systemic side effects. A great deal of research at the preclinical level has been done on the local delivery of chemotherapeutic drugs from polymers, and a few illustrative examples are discussed here. A special section on drug delivery to the brain is included here to show how local delivery can be effective at circumventing anatomic barriers.

Lin et al. encapsulated DOX (ADR) into conical needle devices made of poly(ethylene-*co*-vinyl acetate) (EVAc) or PLA (75). The EVAc needle devices exhibited zero-order release in vitro and showed the greatest in vivo tumoricidal activity in mice bearing subcutaneously transplanted mammary carcinoma. The PLA devices exhibited rapid initial release of the drug in vitro and were not as effective in vivo because therapeutic tumor drug levels could not be sustained. Interestingly, another group found that PLA by itself can inhibit the growth of carcinoma cells in vitro (76). HTB-43 cells, a human hypopharyngeal squamous cell carcinoma cell line, were grown in the presence of extracts from stainless steel, titanium, and PLA that had been incubated in fetal bovine serum at 37°C for 24 hours. The extracts were filtered before addition to the cell cultures, so any inhibition seen would be due to a soluble factor. Cell growth was inhibited by extracts from PLA incubated at a 5% (v/v) concentration in cell culture media but not by extracts of the other materials. Presumably, the growth inhibition was due to products liberated by the hydrolytic degradation of the polymer.

Shikani et al. studied the treatment of nude mice with subcutaneously transplanted human floor-of-mouth squamous cell carcinoma with cisplatin encapsulated in a biodegradable polyanhydride made up of fatty acid dimer and sebacic acid, P(FAD:SA) (77). The polymer wafers contained 7% (w/w) cisplatin and were implanted into the tumors. Mean tumor size 70 days postimplantation for the P(FAD:SA) wafer group was an average 38.1% of the tumor size in the groups that had been treated by intraperitoneal (IP) injection of saline or cisplatin or intratumoral injection of free cisplatin. The mean number of days for the tumor to triple in size was approximately 20 days for the saline-treated controls, 22 days for those treated with blank rods, 24 days for those treated with IP injection of cisplatin solution, and 70 days for those treated with the cisplatin-loaded rods. The sustained release formulation was able to significantly slow the growth rate of the tumor.

Begg et al. encapsulated cisplatin in a rod of a polyether hydrogel and compared its antitumor activity to that of IT or IP injected drug solution (78). The rods were 1.5 mm in diameter and 5 mm in length and contained 2.5–8.0% (w/w) cisplatin. The drug-loaded rods were implanted subcutaneously in the center of RIF1 murine fibrosarcoma grown subcutaneously in mice and resulted in tumor growth rates equivalent to those treated with IT injection of free drug and slower tumor growth rates than IP injection of free drug. However, when combined with radiation therapy where the mice were given 5 days of intermittent radiation, the rod-encapsulated cisplatin was the most effective against tumor growth compared with both IT and IP injection of free drug. The combination of sustained drug release and radiation therapy proved to be beneficial.

Dordunoo et al. have been developing a biodegradable paste containing paclitaxel, an antineoplastic agent from the bark of *Taxus brevifolia* (79). The paste was designed to be spread onto the surface of the pocket left after tumor resection. The paste was made from poly(ϵ-caprolactone) (PCL), a low-melting, biocompatible, and biodegradable polyester that melts at temperatures below 60°C. The paste could therefore be applied to the tumor bed in molten form. Dordunoo and colleagues have evaluated various additives to the system, including gelatin, to modulate the release rate of the paclitaxel in vitro (79). The paste containing 20% (w/w) of gelatin provided the most desirable release rate in vitro and was tested for its antitumor activity in mice that had been subcutaneously inoculated with MDAY-D2 tumor cells. Six days after inoculating the mice with the tumor cells, the tumor site was surgically exposed, and 150 mg of the paste was extruded onto the tumor. As a control, some of the animals received a paste that contained only gelatin (20% w/w) and PCL. After 16 days, the taxol-gelatin-PCL paste–treated animals showed a tumor mass reduction of 63 $\pm$ 27% compared with the untreated controls. Taxol–PCl pastes without the gelatin did not show any antitumor effect, probably due to the low levels of release. The gelatin in the formulation increased the swelling of the paste and accelerated the drug release, allowing for tumoricidal levels of the drug to be achieved at the site of the tumor.

Drug Delivery to the Brain. The brain is a site which notably benefits from local treatment. Some examples of the delivery of chemotherapeutic agents to the brain are discussed here. For more information, see the article CENTRAL NERVOUS SYSTEM, DRUG DELIVERY TO TREAT. The efficacy of systemic chemotherapy against intracranial tumors is limited by the exclusion of chemotherapeutic agents by the blood–brain barrier (BBB). Anatomically, the BBB is the system of brain capillary endothelial cells that do not allow for significant nonspecific transport of molecules from the systemic circulation into the brain tissue. The function of the BBB is to protect the brain from systemic insults, but this mechanism also limits the efficacy of systemically administered drugs for the treatment of brain cancer, as only small fractions of the drug are able to reach the tumor. Local delivery directly into

brain tumors would thus be very beneficial. Henry Brem and coworkers have actively been studying the treatment of recurrent malignant gliomas with 1,3-bis(2-chloroethyl)-1-nitrosourea (BCNU or carmustine) encapsulated in a biodegradable polyanhydride wafer made of poly[1,3-bis(*p*-carboxyphenoxy) propane-*co*-sebacic anhydride] [P(CPP:SA)20:80] (82–85). Malignant gliomas are brain cancers that progress rapidly, and the standard treatment of surgical resection plus external beam irradiation provides only median survival times of less than one year after surgery (80). Slight improvement in the number of long-term survivors resulted from the addition of systemic chemotherapy with BCNU to the therapy, but its use was limited by the systemic toxicity of the drug (80). BCNU also has a half-life in serum of only 15 minutes, further limiting its usefulness when delivered systemically (81). By protecting the drug from degradation and delivering it directly to the tumor site, Brem et al. showed in Phase I–II trials involving 21 patients with recurrent glioma that mean survival time was 48 weeks past reoperation and 94 weeks from the original surgical resection of the tumor after diagnosis (82). Hematology, blood chemistry, and urinalysis tests did not show any systemic effects in any of the patients. This product, called Gliadel® (Rhône-Poulenc Rorer Pharmaceuticals, Inc.) is now FDA approved for use as an adjunct to surgery to prolong survival in patients with glioblastoma multiforme (GBM) for whom surgical resection is also indicated. The disks (1.45 cm diameter and 1 mm thick) are placed into the cavity left behind when the tumor is removed. The usual number of disks per patient is seven to eight. As the polymer degrades hydrolytically into monomers over a period of weeks, the drug is released into the surrounding tissue and fluid. Each disk contains 192.3 mg of P(CPP:SA)20:80 and 7.7 mg of carmustine (BCNU). The chemical structures of the components are shown in Figure 2. After 3 weeks, more than 70% of the polymer has degraded, although monomers have been found at the site of the tumor 2–3 months after implantation (82,83). The CPP monomer is excreted by the kidney, and the SA is metabolized in the liver and expired as carbon dioxide. In a random, double-blind, placebo-controlled clinical trial, 56% of the patients with GBM treated with Gliadel® were still alive 6 months postsurgery, whereas only 36% of the patients treated with the blank wafers (placebo) were alive at that time. Median survival was increased from 20 weeks (placebo group) to 28 weeks with Gliadel® (82). Patients with malignant gliomas other than GBM showed no benefits from this therapy.

While the Gliadel® system was going through clinical trials, Brem's group continued to search for even more effective polymer/drug combinations for the treatment of brain cancers. They published results using a similar delivery system loaded with a different chemotherapeutic agent, 4-hydroperoxycyclophosaphamide (4HC) against rat gliomas (84). In this study, animals with brain tumors treated with 4HC encapsulated in poly(dimer erucic acid-*co*-sebacic acid)1:1, another biodegradable polyanhydride, had a median survival time of 77 days compared with 21 days for animals treated by P(CPP:SA)20:80-encapsulated BCNU. Long-term survival (>80 days) was 40% for 4HC-treated rats versus 30% in the BCNU-treated animals. The 4HC appeared to be more effective than BCNU. In another study, minocycline, a semisynthetic tetracycline that had been shown to inhibit tumor-induced angiogenesis, was encapsulated in an ethylene vinyl acetate copolymer (EVAc) delivery system (85). Antiangiogenic agents have been explored for use in cancer treatment, with the hypothesis that by keeping the tumor from creating new blood vessels, the tumor will not be able to grow. Without the means to provide oxygen and nutrients to new cancer cells, they will die. The sustained-release formulation was tested by itself or in combination with systemic BCNU chemotherapy. Local treatment with minocycline-loaded EVAc extended median survival time by 530% compared with treatment with the blank polymer (85). Systemically administered minocycline did not affect survival time. In combination with systemically administered BCNU, locally released minocycline showed a 93% extension of median survival time compared to BCNU treatment alone and once again, systemic minocycline showed no benefit, even in this combination treatment.

For easier implantation, Boisdron-Celle et al. investigated a microsphere delivery system for the treatment of brain tumors (86). The microspheres were made of poly(lactide-*co*-glycolide)50:50 (PLGA 50:50, Resomer RG506) and were loaded with therapeutic doses of 5-FU. The spheres were small enough to be injected stereotaxically into the brain, and thus the surgeon would not be required to expose the tumor. The microspheres were shown to be biocompatible and degrade within 2 months

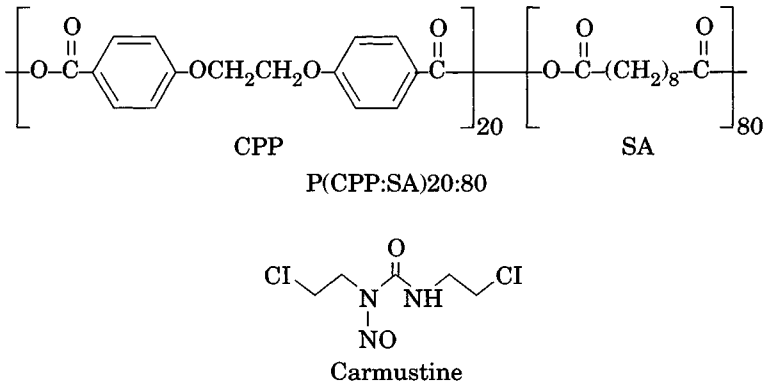


Figure 2. Components of Gliadel® (Rhone-Poulenc Rorer Pharmaceuticals, Inc.). *Source:* From Ref. 92.

in the brain (87). To test the release kinetics and efficacy of this type of delivery system in vivo, Menei et al. (88) stereotactically implanted C6 malignant glioma cells into the brains of rats. One week later, the rats were treated with intratumoral (IT) injection of (*1*) 5-FU solution, (*2*) blank PLGA microspheres, (*3*) fast-releasing 5-FU–loaded microspheres (complete release of drug by 72 hours in vitro), or (*4*) slow-releasing 5-FU–loaded microspheres (complete release by 18 days in vitro). In vivo, the fast-releasing formulation showed entrapped 5-FU crystals until postimplantation day 12; in the slow-releasing formulation, until day 20. Release rates in vivo were slower than in vitro. This disparity in release rates was also reported by Wu et al. (83) for the Gliadel® system described previously. Only the slow-releasing formulation of the 5-FU microspheres showed any impact on the mortality of the animals. Half of the untreated control mice were dead 20 days after the tumor cells were implanted, whereas 50% of the mice treated with the slow-releasing formulation survived past 40 days (88). The mortality in the other two treatment groups (IT injection of 5-FU solution and the fast-releasing formulation) was not statistically different than the untreated controls.

Polymer Implants Used in Developing Experimental Tumor Models. Polymers and controlled-release systems have not just been used to treat cancer but have also been used to develop tumor models in animals. Shors et al. loaded a silicone polymer with benzo(a)pyrene, a known chemical carcinogen, to determine the carcinogenic potential of this chemical when delivered in small doses over an extended period of time (89). They surgically attached the implants to the tracheobronchial mucosa of hamsters and dogs and this resulted in bronchogenic cancers in 93% of the hamsters after 100 days, and squamous metaplasia was regularly found in dogs after 150 days. The authors suggest this technique as a means of producing a model of lung cancer in which neoplasia is induced at selected sites in a well-controlled manner. The models can then be used in the testing of cancer therapies.

Clinicians have known for a long time that certain tumors metastasize preferentially to particular organs. For example, CRC usually metastasizes to the liver. To study what aspects of particular organs or tissue are attractive to various tumor cells, Stackpole et al., devised a method to encapsulate extracts of various organs or defined cocktails of various factors or single agents into polymer devices. These were then implanted subcutaneously and monitored for their ability to attract metastatic cancer cells. In one report, they used polymer implants to influence the location of secondary metastases of B16 melanoma in mice (90). Cellulose disks with a central core of EVAc loaded with various angiogenic agents were implanted subcutaneously in the flank of the mice (90). The implant environment was shown to influence the rate of metastases to the implant site. EVAc loaded with tumor cell mitogenic agents (prepared from a crude extract of mouse lungs) was more efficient at localizing metastases than the implants that released heparin or endothelial cell growth factor.

SYSTEMIC DELIVERY

Although local delivery of agents seems the most logical approach for achieving high concentrations of drug at the tumor site, there is often no easy access to the affected organ or tissue, or the tumor has metastasized and the patient requires systemic therapy. Systemic delivery systems range from simple, sustained-release depot formulations to drug carriers that can target specific organs or tissues. Depot systems are the easiest to develop but do not enhance the specificity of the drug. They simply allow the patient the freedom to receive treatment without the use of a percutaneous intravenous line. Depot systems are able to treat both the primary tumor and metastases equally, but side effects may not be reduced. On the other hand, targeted systems can also be designed to focus their effects on a particular organ, tissue, or even on a particular cell type through the use of antibodies or other targeting moieties. These systems can be designed to have minimal side effects, despite the systemic administration. Examples of targeted systems include nanoparticles, liposomes, and conjugates of drugs with polymers or antibodies. Both depot systems and targeted-delivery systems will be discussed in more detail in the following sections.

Depot Systems

Currently, two controlled-release systems have been approved by the FDA to treat cancer. Both act as depots for the sustained release of anticancer peptides. The first, Zoladex® (Zeneca Pharmaceuticals), contains goserelin acetate, a synthetic decapeptide analogue of luteinizing hormone–releasing hormone (LH–RH) dispersed in a poly(lactide-*co*-glycolide) rod. Zoladex® is indicated for the palliative treatment of advanced prostate cancer and breast cancer. One formulation contains 3.6 mg of goserelin acetate and is designed to last 4 weeks; the second formulation contains 10.8 mg of the peptide and is designed as a 3-month implant. The 4-week rods are 1 mm in diameter, and the 3-month rods are slightly larger, with a diameter of 1.5 mm. The 3-month implant is indicated for prostate cancer patients only. The rods are supplied in a special syringe that is used to implant the delivery system subcutaneously in the upper abdominal wall. In a randomized, prospective clinical trial comparing radiation therapy alone to radiation therapy combined with Zoladex® implants, survival of patients with locally advanced prostate cancer was improved with the addition of Zoladex® to the treatment (91). Both groups of patients received 50 Gy of radiation to the pelvis over 5 weeks and an additional 20 Gy over the following two weeks. Patients in the combined-therapy group received the 4-week implants (Zoladex® 3.6 mg) starting on the first day of radiotherapy and again every 28 days for 3 years. In the combined therapy group, 85% of the patients were disease free at 5 years compared with only 48% of the radiotherapy-only group.

Lupron Depot® (TAP Pharmaceuticals, Inc.) has also been FDA approved for the treatment of prostate cancer. The formulations are supplied as lyophilized microspheres that are resuspended in a diluent for intramuscular injections every 1, 3, or 4 months. The composition of the three

in the brain (87). To test the release kinetics and efficacy of this type of delivery system in vivo, Menei et al. (88) stereotactically implanted C6 malignant glioma cells into the brains of rats. One week later, the rats were treated with intratumoral (IT) injection of (*1*) 5-FU solution, (*2*) blank PLGA microspheres, (*3*) fast-releasing 5-FU–loaded microspheres (complete release of drug by 72 hours in vitro), or (*4*) slow-releasing 5-FU–loaded microspheres (complete release by 18 days in vitro). In vivo, the fast-releasing formulation showed entrapped 5-FU crystals until postimplantation day 12; in the slow-releasing formulation, until day 20. Release rates in vivo were slower than in vitro. This disparity in release rates was also reported by Wu et al. (83) for the Gliadel® system described previously. Only the slow-releasing formulation of the 5-FU microspheres showed any impact on the mortality of the animals. Half of the untreated control mice were dead 20 days after the tumor cells were implanted, whereas 50% of the mice treated with the slow-releasing formulation survived past 40 days (88). The mortality in the other two treatment groups (IT injection of 5-FU solution and the fast-releasing formulation) was not statistically different than the untreated controls.

Polymer Implants Used in Developing Experimental Tumor Models. Polymers and controlled-release systems have not just been used to treat cancer but have also been used to develop tumor models in animals. Shors et al. loaded a silicone polymer with benzo(a)pyrene, a known chemical carcinogen, to determine the carcinogenic potential of this chemical when delivered in small doses over an extended period of time (89). They surgically attached the implants to the tracheobronchial mucosa of hamsters and dogs and this resulted in bronchogenic cancers in 93% of the hamsters after 100 days, and squamous metaplasia was regularly found in dogs after 150 days. The authors suggest this technique as a means of producing a model of lung cancer in which neoplasia is induced at selected sites in a well-controlled manner. The models can then be used in the testing of cancer therapies.

Clinicians have known for a long time that certain tumors metastasize preferentially to particular organs. For example, CRC usually metastasizes to the liver. To study what aspects of particular organs or tissue are attractive to various tumor cells, Stackpole et al., devised a method to encapsulate extracts of various organs or defined cocktails of various factors or single agents into polymer devices. These were then implanted subcutaneously and monitored for their ability to attract metastatic cancer cells. In one report, they used polymer implants to influence the location of secondary metastases of B16 melanoma in mice (90). Cellulose disks with a central core of EVAc loaded with various angiogenic agents were implanted subcutaneously in the flank of the mice (90). The implant environment was shown to influence the rate of metastases to the implant site. EVAc loaded with tumor cell mitogenic agents (prepared from a crude extract of mouse lungs) was more efficient at localizing metastases than the implants that released heparin or endothelial cell growth factor.

SYSTEMIC DELIVERY

Although local delivery of agents seems the most logical approach for achieving high concentrations of drug at the tumor site, there is often no easy access to the affected organ or tissue, or the tumor has metastasized and the patient requires systemic therapy. Systemic delivery systems range from simple, sustained-release depot formulations to drug carriers that can target specific organs or tissues. Depot systems are the easiest to develop but do not enhance the specificity of the drug. They simply allow the patient the freedom to receive treatment without the use of a percutaneous intravenous line. Depot systems are able to treat both the primary tumor and metastases equally, but side effects may not be reduced. On the other hand, targeted systems can also be designed to focus their effects on a particular organ, tissue, or even on a particular cell type through the use of antibodies or other targeting moieties. These systems can be designed to have minimal side effects, despite the systemic administration. Examples of targeted systems include nanoparticles, liposomes, and conjugates of drugs with polymers or antibodies. Both depot systems and targeted-delivery systems will be discussed in more detail in the following sections.

Depot Systems

Currently, two controlled-release systems have been approved by the FDA to treat cancer. Both act as depots for the sustained release of anticancer peptides. The first, Zoladex® (Zeneca Pharmaceuticals), contains goserelin acetate, a synthetic decapeptide analogue of luteinizing hormone–releasing hormone (LH–RH) dispersed in a poly(lactide-*co*-glycolide) rod. Zoladex® is indicated for the palliative treatment of advanced prostate cancer and breast cancer. One formulation contains 3.6 mg of goserelin acetate and is designed to last 4 weeks; the second formulation contains 10.8 mg of the peptide and is designed as a 3-month implant. The 4-week rods are 1 mm in diameter, and the 3-month rods are slightly larger, with a diameter of 1.5 mm. The 3-month implant is indicated for prostate cancer patients only. The rods are supplied in a special syringe that is used to implant the delivery system subcutaneously in the upper abdominal wall. In a randomized, prospective clinical trial comparing radiation therapy alone to radiation therapy combined with Zoladex® implants, survival of patients with locally advanced prostate cancer was improved with the addition of Zoladex® to the treatment (91). Both groups of patients received 50 Gy of radiation to the pelvis over 5 weeks and an additional 20 Gy over the following two weeks. Patients in the combined-therapy group received the 4-week implants (Zoladex® 3.6 mg) starting on the first day of radiotherapy and again every 28 days for 3 years. In the combined therapy group, 85% of the patients were disease free at 5 years compared with only 48% of the radiotherapy-only group.

Lupron Depot® (TAP Pharmaceuticals, Inc.) has also been FDA approved for the treatment of prostate cancer. The formulations are supplied as lyophilized microspheres that are resuspended in a diluent for intramuscular injections every 1, 3, or 4 months. The composition of the three

formulations is summarized in Table 3. Leuprolide acetate is a synthetic nonapeptide of LH–RH. The 1-month formulation is based on a poly(lactide-*co*-glycolide) copolymer, whereas the longer-acting systems use the homopolymer of lactic acid. The 1-month formulation also includes gelatin, which acts to modulate the release rate of the leuprolide acetate. In clinical trials, serum testosterone levels were suppressed to castrate level within 30 days for 95% of the patients (92). During the initial 24 weeks of treatment, 85% of the patients' disease did not progress. These depot formulations appear to be effective against cancer, but they do not necessarily avoid systemic side effects caused by nonspecific activity of the drugs, as can be achieved by the various targeted therapies discussed in the following sections.

Targeted Delivery

As systemic delivery of encapsulated drugs does not circumvent the dangers of nonspecific toxicity, much research has been focused on targeting drugs to the tumor site without the requirement for surgical implantation of the device or exposure of tumor blood vessels. The topic of targeted therapy for cancer has been reviewed by Gupta (93). Targeting can improve the efficacy of cancer therapy by preferential distribution of the drug to the cancer cells or by maximizing the amount of drug that specifically acts against cancer cells. Preferential distribution can still result in adverse effects on normal cells in the vicinity of the tumor cells, whereas drug specificity should affect only the targeted cells. Therapies such as chemoembolization or arterial infusion could be included in the preferential distribution category, but in this article they are discussed under the heading of local therapy due to their specialized administration. The targeted therapies discussed here involve only systems that can be delivered systemically but that focus their effects on specific cells or organs. Targeting has been achieved by (*1*) antibodies conjugated to drugs; (*2*) antibodies conjugated to polymers loaded with drugs; (*3*) liposomes or nanoparticles, with or without conjugation to targeting moieties such as cell receptor ligands or antibodies; and (*4*) the use of external magnets to localize magnetized polymer microspheres. Each of these therapies will be discussed separately in the following sections.

Antibody–Drug Conjugates. More than 15 years of research has gone into the development of antibody–drug conjugates (immunotoxins) for cancer therapy. The hypothesis behind immunotoxin therapy is that the antibody will impart the necessary specificity to the cytotoxic drug (or radionuclide), and the cytotoxic agent will thus affect only the targeted cells. Although many would argue that these conjugates should not be considered controlled-release systems, they do fit the description of controlled drug delivery and therefore will be discussed briefly in this article. For more information on this topic, please consult review articles that have been published during the past decade (94–97). Many immunotoxins are currently being tested in clinical trials and have been shown to have different side effects than the free drug, including hepatotoxicity, reversible vascular leak syndrome, and myalgias (95). Optimal regimens have yet to be determined, but most agree that plasma concentrations of <1 μg/mL will be necessary for therapeutic effect (95). The principle behind immunotoxin therapy has been proven, and now more subtle improvements must be made to enhance their specificity, increase cytotoxicity, and decrease immunogenicity so that the immunotoxins can circulate for longer periods of time to reach their target cells. Attempts are currently being made to use toxins that are less immunogenic, antibodies that are from humans or at least contain a human constant (Fc) region, and the coupling of poly(ethylene glycol) (PEG) to the immunotoxin so as to increase its circulation time (95). Targeting mechanisms other than antibodies have also been explored for targeted delivery of drugs (96). For example, many highly proliferative, malignant cells have high requirements for iron and overexpress the transferrin receptor on their surfaces (96). Transferrin therefore makes a good targeting moiety to direct cytotoxins to such tumor cells. As an alternative to the targeting of antineoplastic drugs to tumor cells, radioisotopes have also been conjugated to antibodies for cancer therapy. Jurcic recently reviewed the literature in the field and included an update on various clinical trials on such conjugates (98). Many different radioisotopes have been used, including β-particle emitters such as iodine-131 and yttrium-90 and α-emitters such as bismuth-212 and astatine-211.

Sherwood et al. reported the development of controlled-release systems for antibodies that could be adapted for the sustained release of immunotoxins (99). These could allow for prolonged immunotoxin therapy without the conventionally required repeated intravenous injections. Sherwood et al. incorporated the antibodies into poly(ethylene-*co*-vinyl acetate) (EVAc) and a biodegradable anhydride copolymer of stearic acid dimer and sebacic acid [P(SAD:SA)]. The release was shown to last for up to 30 days in vitro. The antibodies retained their specific binding after release from the matrices. The next step will be to test whether the systems are capable of releasing antibodies in vivo. To be effective, the antibodies or immunotoxins

Table 3. Summary of Composition of Lupron Depot® Formulations

	7.5 mg (monthly)	3-month 22.5 mg	4-month 30 mg
Leuprolide acetate	7.5 mg	22.5 mg	30 mg
Purified gelatin	1.3 mg	–	–
Poly (DL-lactide-*co*-glycolide)	66.2 mg	–	–
Poly(lactic acid)	–	198.6 mg	264.8 mg
D-Mannitol	13.2 mg	38.9 mg	51.9 mg

Source: From Ref. 92.

would have to either be released directly into the tumor or be absorbed into the bloodstream from the interstitial space after being released from the matrices.

For immunotoxins to be effective as anticancer agents, there are many obstacles to overcome. Some of these obstacles concern the properties and the design of immunotoxin itself, and others pertain to the constraints of the human anatomy and physiology. The problems with the immunotoxin itself, including antigenicity of the components (either the antibody or the toxin) and the ability of the toxin to kill cells, are much easier to study, and much research has gone on toward this end. However, there are other obstacles created by the tumor and the body itself that may be even more critical and even more difficult to overcome. As mentioned in the introduction to this article, tumor cells have an uncanny ability to make themselves blend in with normal cells. They can rapidly change the antigens they present on their surfaces, making it difficult to target an entire population of tumor cells with a single antibody. The cell population within each tumor can also be very heterogeneous with respect to susceptibility to various drugs. Some cells will be susceptible to a particular drug or toxin, and others will be resistant to it. A single drug or toxin may not be effective against all of the cells in the tumor. In this manner, treatment with a single antibody–toxin conjugate will just select for the cells that are not affected by the treatment, and then these cells can proliferate and replace the cells that were killed by the immunotoxin. The final barrier to overcome, and one that is critical for all of the systemically administered, targeted therapies, is the vascular endothelium of the tumor. To be effective, the targeted therapy must be able to exit the bloodstream and penetrate the tumor. This involves passing through the capillary endothelium and basement membrane. In some tumors, the vasculature has been shown to be "leaky," but this has not been proven to be the case for all tumors. And the degree of leakiness might be critical. There will always be a maximum molecular or particulate size that can effectively penetrate the tumor, and the delivery system must always be smaller than that critical size. These problems are difficult ones, and they will come up repeatedly in the discussion of the various types of targeted delivery systems. The targeting moiety must be able to come into contact with its target for the treatment to be effective.

Polymer–Drug Conjugates. See CANCER, DRUG DELIVERY TO TREAT—PRODRUGS.

Liposomes. The main component of liposomes are lipids, which contain two regions: (*1*) a polar, hydrophilic head group (usually a phosphate group) and (*2*) a nonpolar, hydrophobic tail that usually consists of a hydrocarbon chain containing 14–18 carbon atoms. These molecules have an interesting ability to spontaneously self-assemble in water so as to sequester the hydrophobic tail regions from the water. The simplest structure formed by lipids in an aqueous media is a flat bilayer, but this structure is thermodynamically unstable because of the exposed tail groups at the sheet edges. Therefore, the bilayers usually wrap around on themselves, creating vesicles with entrapped water called liposomes. If a drug was included the aqueous phase, it would become entrapped with the water. In addition, liposomes can carry lipid-soluble drugs in the bilayer itself. The applications of liposomes to cancer therapy are discussed in this article; however, information on how to prepare and load the various types of liposomes can be found in LIPOSOMES. The applications of liposomes in fields other than cancer therapy (e.g., gene delivery or vaccines) can be found in those articles.

The placement of liposomes under the rubric of targeted delivery is somewhat controversial because they do not specifically target tumor cells but rather are selectively removed from the circulation by phagocytic cells of the reticuloendothelial system (RES). This makes liposomes good delivery systems for macrophage or tumors of the liver and spleen, but they are not broadly considered targeted systems unless surface modified by the attachment of antibodies to tumor-associated antigens (immunoliposomes) or other targeting molecules. Owing to the rapid removal of liposomes from the circulation by the RES, researchers have focused a great deal of effort into developing techniques to mask them from the immune system. By coating the liposomes so that they are not recognized as foreign by the immune system, circulation times have been increased to greater than 1 day; these liposomes are generally called "stealth liposomes." Standard liposomal formulations as well as the modified liposomes are discussed here.

A vast amount of research has been devoted to the topic of liposomes for cancer therapy. In fact, there are two liposomal formulations of chemotherapeutic agents approved by the FDA to treat AIDS-related Kaposi's sarcoma: Doxil® (Sequus Pharmaceuticals, Inc.) and DaunoXome® (NeXstar Pharmaceuticals, Inc.). Doxil® is doxorubicin hydrochloride encapsulated in STEALTH® liposomes. This product is discussed further under "Stealth Liposomes" in this article. DaunoXome® is an aqueous solution of the citrate salt of daunorubicin (DAU) encapsulated in the aqueous core of lipid vesicles composed of a lipid bilayer of distearoylphosphatidylcholine (DSPC) and cholesterol in a 2:1 molar ratio. The molar ratio of DSPC:cholesterol:DAU is 10:5:1. Figure 3 shows the chemical structures of the components. The liposome helps to protect the drug from chemical and enzymatic degradation, minimizes protein binding, and decreases uptake by normal (non-RES) tissues. The liposomes are 50–80 nm and are believed to penetrate tumor vasculature owing to the increased permeability of tumor blood vessels. Plasma clearance for DaunoXome® is reported as 17.3 ± 6.1 mL/min compared to 236 ± 181 mL/min for the unencapsulated DAU (92). The liposomal formulation is not cleared by the kidneys as rapidly as the free drug. A randomized, controlled clinical study compared treatment of HIV-related Kaposi's sarcoma by DaunoXome® (40 mg/m^2) to a conventional three-drug regimen including DOX (10 mg/m^2), bleomycin (15 U), and vincristine (1 mg) delivered intravenously every 2 weeks (100). Overall response rates (complete plus partial responses) were 25% for DaunoXome® and 28% for the three-drug regimen (a difference that is not statistically significant). Median survival times and median times to progression were also similar for the two therapies. DaunoXone® was thus shown to be safe and effective ther-

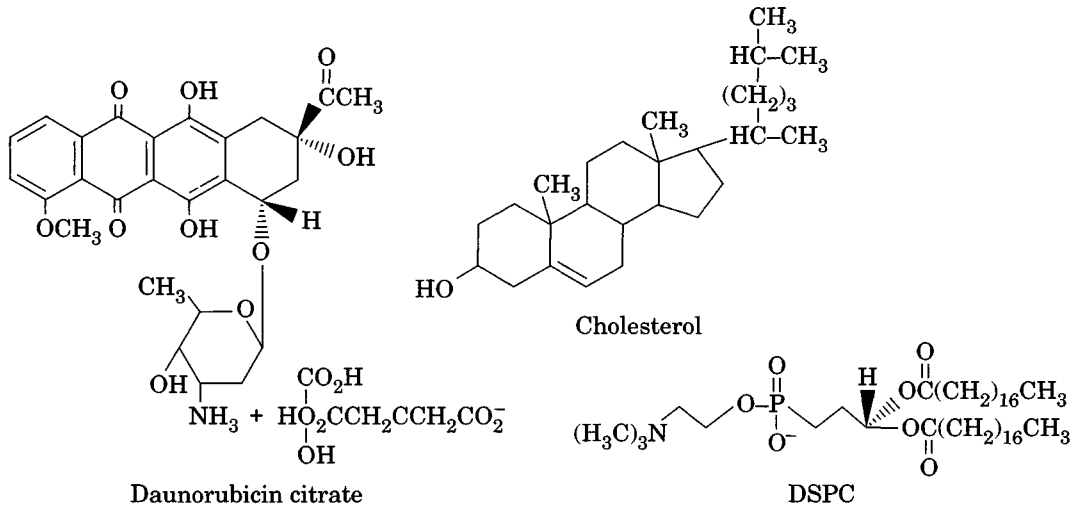


Figure 3. Chemical structures of the three components of DaunoXome®. *Source:* From Ref. 92.

apy for this disease. More importantly, the dose of the drug was able to be reduced with the liposomal encapsulation.

Other cancer drugs have also been investigated in liposomal formulations. Recently, Sharma et al. has reported on the antitumor activity of liposome-encapsulated paclitaxel (101). Paclitaxel has poor aqueous solubility and is currently given as a suspension in Cremophor and ethanol (Taxol®, Bristol-Myers Squibb), additives that cause significant side effects. Sharma and colleagues encapsulated the paclitaxel in two types of liposomes: (*1*) ETL, which contains a single lipid (egg phosphatidylcholine; PC); and (*2*) TTL, which contains a combination of dielaidoyl PC, dimyristoyl PC and 1-stearoyl 2-caproyl PC (molar ratio 1:1:0.9). Both ETL and TTL had drug:lipid molar ratios of 1:33, and both formulations showed a reduction in acute reactions normally seen after IV or IP injection of Taxol®. Mice were able to tolerate an IV dose of 50 mg/kg of the liposomal formulations. An equivalent dose of Taxol® was 100% lethal. At equivalent dosages and schedules, both liposomal formulations delayed tumor growth similar to Taxol® in mice containing subcutaneous xenografts of human ovarian A121 tumors. So although the antitumor efficacy was not improved by liposome encapsulation, the reduction in side effects would certainly be beneficial for the patient.

Mayer and colleagues encapsulated vincristine (VCR) in 120-nm diameter distearoylphosphatidylcholine/cholesterol (55:45 molar ratio) liposomes and investigated the pharmacokinetics, tumor uptake, and antitumor capabilities of this formulation (102). Plasma levels of VCR were found to be at least 100 times greater over the first 24 hours for the liposomal formulation compared to free drug injected intravenously at a dose of 2.0 mg/kg of VCR into mice with L1210 ascites tumors. The area under the tumor VCR concentration-time curve for the first 72 hours after administration (AUC_{72}) was 13 times higher for the liposomal formulation than that for the free drug. In a similar model using a solid tumor (B16/B16 melanoma), the AUC_{72} for the liposomal formulation was 4 times higher than that of the free drug. Drug levels found in noncancerous muscle tissue were similar for both formulations, showing that the liposomal formulations specifically enhanced drug delivery to the tumor, not to all tissues equally.

Liposome-encapsulated DOX has also been shown to overcome MDR. MDR is often associated with high levels of expression of P-glycoprotein, which acts as an ATP-driven pump to transport toxic drugs out of the cell. This mechanism is not drug specific but acts to expel many different drugs. Rahman et al. examined the use of liposomal-encapsulated DOX to overcome MDR in two MDR leukemia cell types: (*1*) HL-60/VCR, which expresses P-glycoprotein; and (*2*) HL-60/ADR, which has no P-glycoprotein (103). HL-60/VCR cells were shown to be 5-fold more sensitive to liposomal DOX than free DOX and accumulated up to 3-fold more drug from the liposomal formulation than from treatment with the free drug. The liposomal formulation had no beneficial effect on the HL-60/ADR cells. This suggested that the liposome specifically interacts with the P-glycoprotein, interfering with its function. Rahman et al. support this hypothesis by showing that blank or drug-loaded liposomes compete with azidopine (a known binding partner of P-glycoprotein) for binding with *P*-glycoprotein. It is not entirely surprising that lipids interfere with this efflux pump mechanism as lipophilic agents, such as cyclosporin A, have previously been shown to interfere with the function of P-glycoprotein, thereby reversing MDR.

Targeted Liposomes. To improve the tumor cell specificity of liposomes, targeting moieties such as antibodies have been conjugated to the surfaces of liposomes. Antibody-targeted liposomes are generally referred to as immunoliposomes. Ohta et al. conjugated the sulfhydryl groups of reduced IgM molecules to maleimide groups on the surface of a liposome (104). The maleimide groups resulted from the incorporation of *N*-(*m*-malemidobenzoyl)dipalmitoylphosphatidylethanolamine (2.5 μmol) with dipalmitoylphosphatidylcholine (25 μmol) and cholesterol (17.5 μmol)

to form the liposomes. DOX was then loaded into the liposomes by the use of a Na^+/K^+ gradient. The liposomes had an average size of 86 nm and each contained approximately 400 molecules of DOX. The immunoliposomes showed specificity in vitro for the cell types corresponding to the antibody, but not all of the formulations retained the cytotoxicity of the free drug. Some antigen–antibody interactions seemed to facilitate the necessary uptake of the drug necessary for the cells to be killed, whereas others resulted in simple binding events without uptake. Preliminary in vivo experiments showed that the liposomes were immediately taken up by the RES. Other researchers have faced the same problem and have worked to include a PEG coating in addition to the antibodies (105–110). Examples of stealth immunoliposomes will be discussed under the heading of stealth liposomes.

Longman et al. developed a creative, two-step approach to targeting liposomes to tumor cells (111). They used the strong binding affinity between streptavidin (SA) and biotin to link the tumor cells to the DOX-loaded liposome in vitro and in vivo. First, they made liposomes of distearoylphosphatidylcholine, cholesterol, and *N*-[4-(*p*-maleimidophenyl)butryl]phosphatidylethanolamine (MPB-PE) (molar ratio 54:45:1). Then they reacted these liposomes with SA, which had been made maleimide reactive by *N*-succinimidyl 3-(2-pyridyldithio) propionic acid (SDDP). This resulted in liposomes covalently coated with SA (SA-liposomes). DOX was then loaded into the liposomes using a pH gradient. The two-step targeting method involves the IV injection of a biotinylated antibody to the tumor cells, followed by the IV injection of the SA-liposomes. The antibody should find the tumor cells and bind to their surface, effectively biotinylating the cell surface, and then when the SA-liposomes are infused, the liposomes will stick to the biotinylated cells. For the in vitro study, P388 cells (murine lymphocytic leukemia cell line) were grown in culture and treated sequentially with the biotinylated antibody to the Thy 1.2 antigen (which is highly expressed on P388 cells) and the SA-liposomes. They demonstrated a 30-fold increase in cell associated lipid and a 20-fold increase in cell-associated DOX using the targeted liposomes as compared with the same two-step procedure using nontargeted liposomes. To test the in vivo tumor cell–binding efficacy of this technique, Longman and colleagues established intraperitoneal (IP) P388 tumors in mice that were injected with the biotinylated antibody, followed 24 hours later by the IP or IV injection of the SA-liposomes or control liposomes. The animals treated with both the biotinylated antibody and the SA liposomes showed statistically significant increases in cell-associated lipid than those controls using nontargeted liposomes. This two-step approach, although it may seem cumbersome at first glance, may allow for the ease of switching the antibody specificity of the treatment without have to reengineer the drug delivery vehicle. Only the various antibodies need be biotinylated for the specific application and used in combination with standard drug-loaded SA-liposomes.

Although antibodies are the most common means of targeting liposomes, other targeting moieties have also been used. To exploit the fact that epithelial cancer cells often overexpress receptors for the vitamin folic acid, Lee and Low incorporated lipids conjugated to folate via a polyethylene glycol spacer (folate-polyethyleneglycol-distearoylphosphatidylethanolamine, or folate-PEG-DSPE) into liposomes of distearoylphosphatidylcholine (DSPC) and cholesterol (112). They studied the in vitro cellular uptake of DOX that had been loaded into these liposomes by KB cells (human nasopharyngeal epidermal carcinoma cell line) and HeLa cells (human cervical carcinoma cell line). For a formulation that included DSPC/cholesterol/folate-PEG-DSPE (molar ratio 56:40:0.1), the cellular uptake by KB cells was increased 45 times over that of nontargeted liposomes containing only the DSPC and cholesterol. Uptake by HeLa cells for the same formulation was 29 times higher for the folate-conjugated liposomes than for the nontargeted liposomes (112). The folate was able to mediate an increase in uptake of the drug because of close association of the liposome with the folic acid receptors on the cells' surfaces. However, this technique still needs to be tested in vivo.

Stealth Liposomes. One of the main problems with standard and even targeted liposomes is their rapid clearance from circulation. Much research has focused on trying to increase circulation times and in vivo stability of liposomes for the delivery of chemotherapeutic agents. The topic has been reviewed by Lasic (113,114). The most common method of sterically stabilizing liposomes is by including a PEG-modified, phosphatidylethanolamine-based lipid into the liposome formulation. This results in liposomes with a "halo" of PEG (PEG-liposomes). Lasic et al. hypothesize that this modification is able to achieve significantly increased circulation times because of the high local concentration of hydrated groups at the surface of the PEG-liposomes that act to sterically inhibit both electrostatic and hydrophobic interactions of blood components (109). Lasic et al. hypothesize that it is the adsorption of blood components such as denatured proteins and opsonins onto the surfaces of liposomes that mark them for clearance by phagocytic cells in the body. Therefore, if these blood components are not able to adsorb or bind to the surface of the liposomes, the liposomes should be able to circulate for extended periods of time, increasing the likelihood that they reach the target.

Regardless of the mechanism of the origin of the extended circulation times, stealth liposomes are used successfully in the clinic. Doxil® (Sequus Pharmaceuticals, Inc.) is a formulation of doxorubicin hydrochloride (DOX-HCl) encapsulated in STEALTH® liposomes that has made it through FDA approval for the treatment of AIDS-related Kaposi's sarcoma. These liposomes are composed of *N*-(carbamoyl-methoxypolyethylene glycol 2000)-1,2-distearoyl-*sn*-glycero-3-phosphoethanolamine sodium salt (MPEG-DSPE), fully hydrogenated soy phosphatidylcholine (HSPC), and cholesterol. The weight ratio of MPEG-DSPE:HSPC:cholesterol in the liposomes is 1:3:1. The chemical structures of the components are shown in Figure 4. In a clinical trial, 53 patients who had experienced disease progression or intolerable toxicities while receiving standard intravenous doxorubicin/bleomycin/vincristine or bleomycin/vincristine treatment were given 20 mg/m^2 Doxil® every three weeks. The liposomal formulation increased the therapeutic effect of the DOX, with 49%

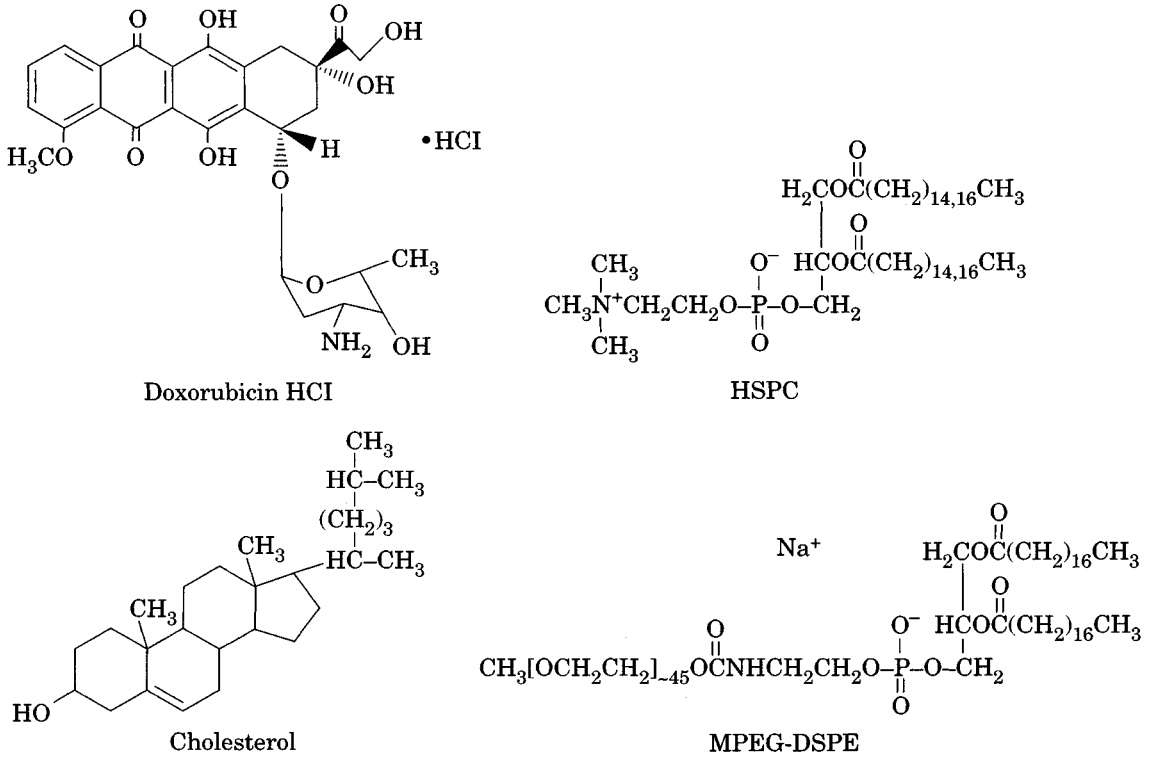


Figure 4. Chemical structures of the three components of Doxil®. *Source:* From Ref. 92.

of the patients experiencing more than one clinical benefit (115). The circulation half-life of the Doxil® formulation is approximately 2 days (116), compared to unencapsulated DOX with a half-life of 18 to 30 h (117).

Allen et al. investigated the in vivo cytotoxicity of VCR encapsulated in stealth liposomes (SL-VCR) against IP and IV tumor models in mice (107). When P388 cells were injected IP, SL-VCR treatment significantly increased mean survival times from 8.5 days (no treatment) or approximately 2 weeks (free VCR) to over 3 weeks. When the P388 cells were injected IV, no effect on mortality was seen for any of the treatments. The experiment was repeated with a different cell line (L1210 leukemia cells), and the liposomal formulation was effective only against tumors that had been started IP. The SL-VCR therapy appears to increase the efficacy only for tumors in the peritoneal cavity. It didn't seem to matter whether the SL-VCR therapy was given IP or IV. As long as the tumor was located in the peritoneal cavity, the SL-VCR therapy was effective in prolonging survival.

As mentioned previously, many researchers have combined the use of stealth liposomes with antibody targeting (105–110). A few examples are discussed here. Emanuel et al. encapsulated DOX in stealth liposomes with surface-linked antibodies (specific to tumor cells or nonspecific controls) and in nontargeted stealth liposomes (108). They showed that DOX accumulation in lung metastases of a polyoma virus-induced fibrosarcoma was higher in animals treated with the tumor-targeted stealth immunoliposomes than the nontargeted liposomes and the nonspecific stealth immunoliposomes. The highest tumor DOX concentrations were achieved through the combination of steric stabilization and antibody targeting. They also showed that the addition of the antibodies to the surface did not effect the circulation time of the stealth liposomes. More recently, Harding et al. stress that the immunogenicity of the antibody can influence the circulation time of the immunoliposomes (110). If the antibody is immunogenic, the body will clear the liposomes quickly, despite the stealth coating. Care must be taken to match the antibody to the model species.

Ahmad et al. reported a study performed on mice injected IV with KLN-205 (murine lung squamous carcinoma) cells (106). A biotinylated monoclonal antibody to the KLN-205 cells (174H.64) was attached via a streptavidin linker to hydrogenated soy phosphatidylcholine (HSPC)/cholesterol/PEG-DSPE (molar ratio 2:1:0.1) liposomes to form the sterically stabilized immunoliposomes. The IV injection of the sterically stabilized immunoliposomes loaded with DOX resulted in 50% of the animals surviving more than 6 months. Animals treated with the untargeted sterically stabilized liposomes showed a mean survival time of approximately 66 days. By combining the benefits of steric stabilization by PEG and the tumor-specific targeting of a monoclonal antibody, the anticancer efficacy of the drug was improved.

Nanoparticles. To improve on the stability of liposomes as controlled-delivery devices for antineoplastic drugs, many researchers turned to polymeric nanoparticles. Nanoparticles are generally defined as particles with diameter less than 1 μm, small enough to be injectable IV.

The drugs may be dissolved in the polymer, entrapped within it, or adsorbed to the surface of the particles. Higher concentrations of hydrophilic drugs can be loaded into nanoparticles as there is no limitation of aqueous solubility as is inherent for loading drugs into liposomes. Leroux et al. have recently reviewed the topic of nanoparticles for the delivery of cancer therapies (118). Nanoparticles are considered targeted delivery systems, as the distribution and pharmacokinetics of anticancer drugs can be modified by encapsulation in polymers. This altered distribution is postulated to lower systemic toxicities and to provide better supply of drug to the tumor, assuming that the tumor location and the drug distribution match. After intravenous administration, hydrophobic nanoparticles are found predominantly in the reticuloendothelial system (RES) (118). The drug levels in the liver and spleen are accordingly very high. It has been hypothesized that intravenously administered nanoparticles can be passively targeted to tumor cells by means of enhanced permeation through tumor neovasculature, although this has not yet been clearly proven (118–120). So although the nanoparticles have enhanced stability and higher drug-loading capabilities than liposomes, they share the same problem of not being able to reach tumor cells efficiently. Similar means of enhancing nanoparticle delivery to tumors have been explored as have been investigated for liposomes, namely antibody targeting (119,121) and PEG coatings (122,123). These two topics are addressed in the following paragraphs.

To study the use of monoclonal antibodies against tumor cell antigens as targeting mechanisms for nanoparticles, Illum et al. coated poly(hexyl 2-cyanoacrylate) nanoparticles with a monoclonal antibody against osteogenic sarcoma cells. Although the antibodies were shown to retain their binding specificity in vitro, they found no enhanced localization of the particles to the tumor in vivo (121). This is probably due to the inability of the nanoparticles to access the tumor cells before they were taken up by the RES.

Recent research on nanoparticles has focused on creating long-circulating, or stealth, nanoparticles. The most common method for reducing RES uptake is by the covalent attachment of PEG to the surface of the particles (122,123). The density of the PEG is critical, and particles that showed highest PEG densities showed increased circulation times (123). It is hoped that such particles could avoid phagocytosis by the RES and could therefore have a better chance at accumulating at the tumor site. Similar results have been shown for the surface adsorption of Poloxamine 908 (124), a block copolymer of poly(ethylene oxide) (PEO) and poly(propylene oxide) (PPO) to hydrophobic polymer nanoparticles. The PPO region of these surface-active polymers adsorbs well to hydrophobic materials and makes the surface hydrophilic with the PEO tails. However, the possibility for desorption in vivo was a concern. In addition, the coating of the nanoparticles with a hydrophilic layer may make it even less likely for the nanoparticles to leave the bloodstream and accumulate in the tumor, so the enhanced circulation time may not be the complete solution.

The overall efficacy of nanoparticles for the delivery of cytotoxic agents has not been adequately proven as yet. Leroux et al. reviewed the in vivo evaluation of drug-loaded nanoparticles (118). A wide range of polymers and drugs have been combined and tested in various animals tumor models. However, despite the large bulk of research, no clear consensus of efficacy was shown. Some formulations showed increased efficacy or decreased systemic toxicities over unencapsulated drug, whereas other formulations showed no benefit. A recent example of a positive result used poly(butylcyanoacrylate) (PBCA) nanoparticles, both uncoated and coated with poloxamine 1508 (125). The drug, mitoxantrone, was loaded in two different ways: adsorbed to the surface after the polymerization of the nanoparticles or incorporated during the polymerization. To test the in vivo cytotoxicity of the four types of nanoparticles, they were administered to separate groups of mice that had received intramuscular inoculations of B16 melanoma cells. Mitoxantrone-loaded liposomes and free drug were included for comparison. Of the four sets of nanoparticles, all but the uncoated/incorporated set showed a statistically significant decrease in tumor volume compared to the liposome formulation and the free mitoxantrone. But for every positive result showing that nanoparticle formulations are effective against tumors in vivo, others show no improvement over the free drug. Thus, room still exists for improvements on nanoparticulate systems for cancer therapy, including better antibody-conjugation techniques so as to maximize specific bindings and decrease undesirable antigenicity of the complex. Combining such antibody-targeted nanoparticles with PEG coatings to prevent RES clearance has the possibility of increasing circulation time and tumor cell specificity, although the problem of extravasation from tumor blood vessels may overwhelm all of these improvements.

Magnetic Localization. Research on targeting polymers to tumors for drug delivery using externally placed magnets has been studied since the early 1960s. Mosso and Rand mixed carbonyl iron microspheres into a silicone polymer that could be cured in vivo using a stannous oxide catalyst (126). The mixture could be infused into the tumor vasculature and held in place with an external magnet until it had cured. A double-lumen catheter was used for the procedure so that angiograms of the blood supply to the tumor could be obtained before and after treatment. The superconducting electromagent was then placed at the animal's flank for kidney infusions or next to the skin for hindlimb infusions. A bolus of 2 to 3 mL of the magnetized silicone/catalyst mixture was infused into the arteries of six dogs. The remaining uninfused silicone was used to measure vulcanization time (approximately 30 minutes). When the uninfused silicone was solidified, the external magnet was removed and the inner catheter was retracted. A second angiography was performed using the remaining guide catheter. The second angiogram confirmed that this technique occluded blood flow to the region. Generally the animals remained healthy, showing some transient ischemia in the region of the occluded vessels. At autopsy, silicone was found to have occluded the arteries, arterial branches, and even the capillary beds. No evidence of retrograde embolization into the aorta was found, and neither was any silicone found at necropsy in the lungs or venous

system. There was some perivascular granulation and fibrosis in tissue surrounding the infarcted vessel, presumably in response to the iron, which may have helped form a direct cohesion between the vessel and the nonadherent silicone rubber.

Research switched focus to methods of temporary occlusion to solve the same problem of collateral blood vessel formation that plagued arterial ligation and other permanent arterial occlusions discussed earlier in this article. Researchers tried both magnetic degradable starch microspheres with covalently bound model drugs and proteins (127) and magnetic degradable albumin microspheres loaded with chemotherapeutic drugs (128–132). Mossbach and Schröder made starch microspheres with diameters less than 10 μm and loaded them with magnetite and covalently bound radio-labeled model proteins and drugs to the surface (127). The microspheres were suspended in NaCl solution and infused IV into one ear of a rabbit through a catheter. An external magnet was placed on the distal portion of the opposite ear ("magnetic ear") in attempts to localize the microspheres. After 10 min, the rabbits were euthanized, and the distal portions of both ears were removed to measure radioactivity from the proteins and drugs bound to the microspheres. Although the majority of the microspheres were retained in the capillary beds of the lungs (80%), the magnetic ear contained 4–8 times the radioactivity of the nonmagnetic ear.

Researchers also studied the use of magnetized albumin microspheres loaded with DOX and their distribution in rats after arterial (128,130,131) or venous (129,131) administration. Widder and Senyei and their colleagues prepared microspheres with an average diameter of 1 μm of human serum albumin (labeled with a small amount of ^{125}I-bovine serum albumin) and loaded with 28.8% (w/w) of Fe_3O_4 particles and 5.8% (w/w) of DOX for infusion into the ventral caudal artery at the base of the tail. The tail was then demarcated into four equal segments approximately 3.5 cm in length. An external magnet was placed over the third segment from the base of the tail to localize the microspheres and was held in place for 30 minutes. Some of the rats were then sacrificed at that time, and the level of radioactivity in each of the four tail segments was measured. The concentration of DOX in each segment was also measured. Results showed that at the highest magnetic field (8,000 oersteds), 37–65% of the infused microspheres remained localized in the third tail segment, with 30–48% being found in the liver. In animals sacrificed 24 h after the removal of the magnet, approximately 50% of the injected microspheres remained localized in segment 3. Histological studies showed that some microspheres had been internalized by endothelial cells and others were trapped between the plasma membranes of adjacent endothelial cells. DOX concentrations in the third tail segment were 100-fold higher than levels achieved after injection of free drug. In a later study, the group showed that arterial administration of magnetic albumin microspheres loaded with DOX resulted in an average of 45% of the microspheres being localized in the third tail segment, when the magnetic field of 8,000 oe was applied for as little as 5 min and as much as 60 min (130).

Morimoto and colleagues developed magnetic albumin microspheres to treat cancer (131,133). The microspheres were made of bovine serum albumin with a small amount of ^{125}I-human serum albumin for detectability, and magnetic fluid (suspension of Fe_3O_4 and colloidal magnetite) cross-linked a heat denaturation process. Microspheres were fractionated by centrifugation, and the <2-μm and 2- 4-μm fractions were saved for use in the in vivo studies. In an animal model to simulate treatment of localized lung cancer, they placed external magnets (3,000 gauss) ventrally and dorsally surrounding the chest cavity of mice and infused 1 mg of the microspheres into the tail vein. The mice were then sacrificed after 10 or 60 min, with the external magnet held in place for the duration of the experiment. Various tissues were isolated for detection of radioactivity to calculate the number of particles trapped in the various tissues. After 10 min, only 10.7% of the administered dose of microspheres 2–4 μm in diameter was found in the lungs without the use of magnets, and magnetic localization doubled this value. After 1 h, 17.0% of the administered dose of the 2- 4-μm spheres was found in the lung without localization, and this was increased to 28.2% with the external magnets. If the magnet was removed after the first 10 min, only 21% of the initial dose was found in the lungs after 1 h. Morimoto et al. also infused microspheres less than 2 μm into the left renal artery with two magnets placed on both sides of the left kidney. Magnetic localization of the microspheres increased 2.5 times over the nonlocalized control to 56.4% of the administered dose after 10 min and remained stable out to 1 h. If the magnet was removed after the first 10 min, only approximately 27% of the administered dose remained localized in the kidney.

Morimoto's group continued their research on the magnetic localization of albumin microspheres, showing the antitumor effect of DOX delivered from such microspheres (129). They administered microspheres (2–4 μm in diameter) containing 6% DOX and 47% magnetite encapsulated in bovine serum albumin into the tail vein of rats with AH 7974 (ascites hepatoma) cell lung tumors. This served as a model for the treatment of lung metastases. An external magnet was placed at the back and breast of the rat at the level of the chest cavity for the first 10 min after administration of the microspheres. The percent of the original microsphere dose localized to the lungs was doubled to 19.7% with the application of the magnet over control animals (no magnet). The levels of DOX in the magnet-localized group increased eightfold over IV injection of free DOX. The antitumor efficacy of this treatment was measured by changes in lung weight (higher weights signify tumor growth). After three treatments with the magnetically localized microspheres containing DOX at 1-week intervals, the average weight of the lungs was 2.4 g compared to 4.3 g for untreated rats and 1.1 g for rats without tumors. The magnetically localized microsphere treatment slowed the growth of the tumor. The antitumor effect was also monitored by animal survival, with median survival of 16.4 days for untreated rats with tumors and 23.6 days for animals with tumors treated by the magnetically localized microspheres containing DOX. Rats treated with

microspheres without localization by external magnets showed a median survival of 17.4 days.

In 1983, Widder et al. reported the selective targeting of magnetic albumin microspheres containing DOX in rats with Yoshida sarcomas (132). In this study, magnetic microspheres were prepared by emulsion polymerization in which the aqueous phase consisted of human serum albumin, DOX, and magnetic iron oxide. Rats were subcutaneously inoculated with Yoshida tumor cells into the lateral aspect of the tail. Tumor size averaged 200 mm^2. Six to eight days after tumor cell inoculation, microspheres suspended in saline containing 0.1% Tween 80 were infused into the ventral caudal artery at a distance of 2 cm proximal to the tumor. A bipolar magnet with a field strength of 5,500 oe was placed with one of its faces in contact with the tumor and held in place for 30 minutes after the administration of the microspheres. Animals were kept for 30 days posttreatment (or until death) and monitored for weight change, tumor size, and metastases. Rats treated with magnetically localized microspheres containing DOX showed an approximately 90% decrease in tumor size, compared with a 120% increase in tumor size for untreated controls and 114% increase for those treated with nonlocalized DOX-loaded microspheres. Intraarterially administered free DOX at equivalent doses showed tumor size increases of 50 to 70%. All of the rats treated with magnetically localized microspheres showed tumor regression, with 75–80% showing total remissions for the DOX-loaded microspheres. All rats in the magnetically localized group survived the full 30 days, and no metastases were found upon autopsy. In the untreated controls, those treated by free DOX, those treated with blank microspheres (magnetically localized but containing no DOX), and those treated with nonlocalized DOX-loaded microspheres, 90–100% of the animals died before the 30-day limit, and no regressions or remissions were seen. Metastases were found in all animals. These dramatic results show the great promise of this form of treatment.

A different family of degradable polyalkylcyanoacrylates has also been developed for preparation of magnetic nanoparticles capable of adsorbing a wide variety of drugs (134). The length of the alkyl chain controls the rate of degradation so that a particular polymer can be chosen to match the specific requirements of an application. Ibrahim et al. made microspheres less than 0.3 μm in diameter and loaded with magnetite by emulsion polymerization of radioactive monomer in the presence of ultrafine magnetic particles. Dactinomycin was adsorbed to the surface of the spheres, and they were administered intravenously into mice. After 10 min the animals were sacrificed, and various tissue samples were homogenized, and their radioactivities was determined. They found that the placement of an external magnet over the kidney increased concentration of the drug in the kidney threefold and decreased liver concentrations of the drug by approximately 30%, showing the ability of the magnetite-loaded microspheres to be localized to a specific organ. Mortality of the animals was not increased with the addition of magnetite to the formulation, showing the magnetic microspheres to be as safe as the polymer itself.

Magnetic localization has also been applied to the area of internal radiotherapy. Häfeli et al. reported the use of poly(lactic acid) (PLA) microspheres with the ionic form of Y-90 loaded into the matrix (135). Magnetite (Fe_3O_4) was also incorporated to make the microspheres magnetically responsive. These microspheres could then be locally infused into a tumor and held there by the magnet or infused IV or into a body cavity and then attracted to a magnet held near the tumor. When the microspheres were injected into the peritoneal cavity with a magnet placed directly over a subcutaneous tumor, 73 $\pm$ 32% of the injected dose of radioactivity was found in the tumor 24 h after the injection of the microspheres. Without the magnet, radioactivity in the tumor was 6 $\pm$ 4%.

The application of magnetically localized cancer therapies in humans has been relatively slow to gain universal popularity because of the need for magnets powerful enough to localize magnetic particles in humans and the controversy surrounding the biologic effects of high-intensity magnetic fields. As these problems are solved, magnetic localization could provide a simpler alternative to the more biological targeting approaches, such as antibody localization, discussed in previous sections. Targeted therapies in general are still actively being investigated, despite all of the problems still left to overcome. The desire for a cancer therapy that does not harm noncancerous tissues is very strong.

CANCER IMMUNOTHERAPY

If the immune system functioned perfectly, neoplastic cells would be destroyed before they had the chance to proliferate and form tumors. However, some cancer cells do manage to slip through the surveillance of the immune system and proliferate uncontrolled. The field of cancer immunotherapy is based on investigating means of enhancing the ability of the immune systems to recognize and kill tumor cells, thereby achieving a cure. It uses the body's own natural immune mechanisms, enhanced by externally administered signals. The immune cells of the body generally rely on soluble signals, such as cytokines and growth factors, to stimulate and direct their activities against abnormal cells. If these signals could be applied artificially in the correct spatial and temporal fashion through controlled release systems, the functioning of the immune system could be enhanced without the use of artificial drug molecules. In a sense, if this sort of therapy were applied prophylactically, it would serve as a cancer vaccine, protecting the patient from ever developing a tumor. Thus, cancer immunotherapy and vaccines are often discussed interchangeably in the literature. The formulation of the therapy would be the same; it is just the time of administration that differs. Immunotherapy is given after cancer has been diagnosed, and vaccines are given before the patient has shown any signs of a tumor.

Various approaches to cancer immunotherapy have been studied. Much of the current research focuses on gene therapy where genes for various cytokines are added to the DNA of tumor cells removed from a patients tumor; then the cells are irradiated such that the cells cannot replicate

and are reinfused into the patient (136,137). Other researchers are directly performing the gene transfer in vivo, which is often a less efficient procedure (138). The premise is that the immune system will see the cancer cell antigens and the immunostimulatory cytokines simultaneously and will be best activated to kill not only these reinfused, transfected cells but also any nontransfected tumor cells that remain in the patient. The downfall of this type of therapy is that it takes a certain amount of time to complete the transfection if done ex vivo, and transfection rates are low when performed in vivo. So other researchers have been developing other means of delivering the cytokines, including liposome and biodegradable and/or bioerodible microspheres.

By far, the most research has been on liposomal formulations of cytokines (139–145). The most common cytokine explored for use in tumor immunotherapy is interleukin 2 (IL-2). IL-2 controls the proliferation and cytotoxicity of natural killer (NK) cells and T lymphocytes and the proliferation of B lymphocytes (146). T lymphocytes play a role in both cellular and humoral immune responses. The cellular immune response acts against cells that appear abnormal in some way (e.g., expressing foreign antigens on their surface), and the humoral response involves antibodies that act by binding to foreign epitopes of proteins, marking them for engulfment and degradation by phagocytic cells. By enhancing the capabilities of both types of immune response, IL-2 is a good candidate for immunotherapy. However, IL-2 has a great number of side effects, including fever, malaise, fluid retention, and hypotension. The dose-limiting toxicity in humans results from vascular leak syndrome and cellular infiltration into the alveoli, which causes pulmonary edema (146). By altering the route and formulation of IL-2, therapies could be made more effective and less toxic.

Liposome-encapsulated IL-2 was shown by Anderson et al. to have improved biodistribution and depot characteristics more than free IL-2 (143). IL-2 was encapsulated in dimyristoylphosphatidylcholine (DMPC) liposomes and administered via various routes: intrathoracic, intraperitoneal (IP), IV, and subcutaneously (SC). Free IL-2 was used as a control. Two hours after IV injection, only about 7% of the free IL-2 dose was still circulating in the blood, 90% having been cleared from the animal. Approximately 37% of the liposomal IL-2 dose was still circulating in the blood after 2 hours, with >70% of the original dose remaining in the animal. The other routes of administration for the liposomal formulation showed similar results. Anderson and colleagues have studied the encapsulation of other cytokines, including IL-1, IL-6, granulocyte and macrophage colony stimulating factor (GM-CSF), and interferon γ (142). More recently, Khanna et al., in conjunction with Anderson, have been conducting research on inhalational therapy using liposomal IL-2 to treat lung cancer (140,145). Initial studies showed that the formulations were relatively stable through the nebulization process and that the liposome aerosols could be distributed evenly through the lungs of anesthetized dogs (145). To test the in vivo efficacy of the formulation against lung cancer, they treated nine dogs with primary or secondary lung tumors with the liposomal IL-2. Two of the dogs had primary lung carcinoma, and the others suffered from lung metastases of various other forms of cancer (140). Three of the animals showed a complete response (regression), and one animal showed stable disease out to 8 months posttreatment.

Liposomal formulations have also been shown to improve the cytotoxicity of IL-1α and tumor necrosis factor α (TNF-α) (139). When these two cytokines were coencapsulated in phosphatidylcholine/phosphatidylserine (molar ratio 7:3) liposomes and administered IV to mice bearing B16F10 melanoma, it was shown that this combination was very effective at increasing survival of the animals. The combination was more effective than the individually encapsulated cytokines. The combination of free drugs at the same dose as that administered in the liposomes induced severe side effects, and therapy was discontinued. The liposomal formulation reduced side effects, thereby increasing the level of drug that can be safely administered for therapy.

Various types of polymeric microspheres have also been developed for the controlled release of cytokines (147–149). Golumbek et al. encapsulated GM-CSF within chondroitan sulfate microspheres and injected them subcutaneously in combination with irradiated tumor cells (149). The tumor cells used were B16/F10 murine melanoma cells, which have been shown to be poorly immunogenic. By themselves, the irradiated cells have not been sufficient to protect mice against subsequent challenges with live tumor cells. However, if these cells were transfected with the gene for GM-CSF prior to use as a vaccine, they were able generate potent systemic immunity against challenge. The simple combination of the GM-CSF-loaded microspheres and the irradiated tumor cells was examined as a replacement for the more complex gene transfer protocol. With no prior vaccination the mice would all die less than 40 days after challenge with live tumor cells. When the vaccine that included irradiated tumor cells plus the GM-CSF microspheres was administered before challenge, 70–80% of the mice were tumor free as long as 90 or 100 days post-challenge. Only 20–40% of the mice vaccinated with the irradiated tumor cells and blank microspheres prior to challenge with live cells were tumor free after 100 days only 20% of those vaccinated with irradiated tumor cells and free GM-CSF were tumor free 90 days post-challenge. The GM-CSF only seemed effective if encapsulated and administered in conjunction with the irradiated tumor cells.

Copolymers of lactic acid and glycolic acid (PLGA) were also investigated as controlled release systems for IL-1α for tumor immunotherapy (148). PLGA 75:25, with a molecular weight of 10,000 g/mol and loaded with IL-1α, was shown to have the most desirable release kinetics in vitro and was then tested in an in vivo tumor model in mice. Mice were inoculated with tumor cells in a foot pad and treated in the same footpad with an injection of the IL-1α microspheres 7 or 12 days after tumor cell inoculation. For controls, blank microspheres or the equivalent dose of soluble IL-1α were given by the same schedule. Untreated animals died after approximately 1 month, as did those treated with the empty microspheres or the soluble cytokine. Only the microsphere-encapsulated IL-1α produced a significant increase in survival, with 60% of the animals

still alive after 43 days. Again, the sustained release of the cytokine was necessary for efficacy of the therapy.

Recently, Egilmez et al. have reported the use of PLA microspheres loaded with IL-2 for cytokine immunotherapy (150). They showed that coinjection of IL-2–loaded PLA microspheres with human squamous cell lung carcinoma cells (2E9) into a subcutaneous site resulted in complete suppression of tumor engraftment in 80% of the SCID mice treated. BSA-loaded microspheres and free IL-2 were not effective when coinjected with the tumor cells. The sustained release of the IL-2 from the PLA microspheres was the key to tumor rejection.

SUMMARY

A large number of different therapies utilizing controlled-delivery technologies have been investigated over the past 60 years. Some of them have made it through the FDA approval process (implantable pumps for local infusion of drugs, Lupron Depot® and Zoladex® for the systemic delivery of peptide drugs, Gliadel® for the local treatment of malignant GBM, and liposomal formulations of doxorubicin and daunorubicin), but most are still at the clinical trial or research level. It is the hope of patients around the world that more of these therapies, including those that target the tumor cells selectively, will make it to the market in the coming years. Many of the therapies discussed in this article have the potential for improving cancer therapy and maybe even for curing additional types of cancers. But until cancer is completely eradicated, research into controlled-delivery applications to cancer therapy will continue.

BIBLIOGRAPHY

1. C. Fordy et al., *Br. J. Cancer* **72**, 1023–1025 (1995).
2. H. Buchwald and T.D. Rohde, *ASAIO Trans. J.* **38**, 772–778 (1992).
3. J.W. Kwan, *Am. J. Hosp. Pharm.* **46**, 320–335 (1989).
4. Y.Z. Patt et al., *J. Clin. Oncol.* **15**, 1432–1438 (1997).
5. N. Kemeny et al., *J. Clin. Oncol.* **12**, 2288–2295 (1994).
6. B.S. Davidson et al., *Am. J. Surg.* **172**, 244–247 (1996).
7. S.R. Baker, R.H. Wheeler, W.D. Ensminger, and J.E. Niederhuber, *Head Neck Surg.* **4**, 118–124 (1981).
8. S.R. Baker, A.A. Forastiere, R. Wheeler, and B. Medvec, *Arch. Otolaryngol. Head Neck Surg.* **113**, 1183–1190 (1987).
9. S.J. Hassenbusch et al., *J. Neurosurg.* **73**, 405–409 (1990).
10. A. Hoekstra, *Int. J. Artif. Organs* **17**, 151–154 (1994).
11. B. Damascelli et al., *Cancer (Philadelphia)* **66**, 237–241 (1990).
12. C. Breedis and G. Young, *Am. J. Pathol.* **30**, 969–985 (1954).
13. R.R. Graham and D. Cannell, *Br. J. Surg.* **20**, 566–579 (1933).
14. S. Bengmark and B. Jeppsson, *Surg. Clin. North Am.* **69**, 411–418 (1989).
15. S. Bengmark and B. Jeppsson, *Surg. Annu.* **20**, 159–177 (1988).
16. B. Ahren and S. Bengmark, *HPB Surg.* **1**, 3–14 (1988).
17. E.C.S. Lai et al., *World J. Surg.* **10**, 501–509 (1986).
18. R.E. Koehler, M. Korobkin, and F. Lewis, *Radiology* **117**, 49–54 (1975).
19. R. Yamada et al., *Radiology* **148**, 397–401 (1983).
20. H. Stridbeck, L.E. Lorelius, and S.R. Reuter, *Invest. Radiol.* **19**, 179–183 (1984).
21. L.-Q. Wang, B.G. Persson, and S. Bengmark, *HPB Surg.* **6**, 105–113 (1992).
22. B. Jeppsson et al., *Eur. Surg. Res.* **11**, 243–253 (1979).
23. B.G. Persson et al., *World J. Surg.* **11**, 672–677 (1987).
24. N. Wilmott, *Cancer Treat. Rev.* **14**, 143–156 (1987).
25. L.H. Blumgart and D.J. Allison, *World J. Surg.* **6**, 32–45 (1982).
26. S. Wallace et al., *Curr. Probl. Cancer* **8**, 1–62 (1984).
27. S. Wallace et al., *Curr. Probl. Cancer* **8**, 1–76 (1984).
28. T. Laakso, P. Edman, and U. Brunk, *J. Pharm. Sci.* **77**, 138–144 (1988).
29. J.O. Forsberg, *Acta Chir. Scand.* **144**, 275–281 (1978).
30. D. Civalleri et al., *Br. J. Surg.* **81**, 1338–1341 (1994).
31. W.D. Ensminger, J.W. Gyves, P. Stetson, and S. Walker-Andrews, *Cancer Res.* **45**, 4464–4467 (1985).
32. J.W. Gyves et al., *Clin. Pharmacol. Ther.* **34**, 259–265 (1983).
33. C.E. Pfeifle, S.B. Howell, and J.J. Bookstein, *Cancer Drug Delivery* **2**, 305–311 (1985).
34. M. Andersson et al., *Acta Oncol.* **28**, 219–222 (1989).
35. T.M. Hunt et al., *Br. J. Surg.* **77**, 779–782 (1990).
36. K.F. Aronsen et al., *Eur. Surg. Res.* **11**, 99–106 (1979).
37. S. Dakhil et al., *Cancer (Philadelphia)* **50**, 631–635 (1982).
38. E.R. Sigurdson, J.A. Ridge, and J.M. Daly, *Arch. Surg. (Chicago)* **121**, 1277–1281 (1986).
39. B. Lindell, K.-F. Aronsen, B. Nosslin, and U. Rothman, *Ann. Surg.* **187**, 95–99 (1978).
40. J.A. Goldberg et al., *Nucl. Med. Commun.* **8**, 1025–1032 (1987).
41. J.A. Goldberg et al., *Br. J. Surg.* **77**, 1238–1240 (1990).
42. M.A. Burton et al., *Cancer Res.* **45**, 5390–5393 (1985).
43. L. Hafstrom, A. Nobin, B. Persson, and K. Sundqvist, *Cancer Res.* **40**, 481–485 (1980).
44. Y. Sasaki et al., 1985, *Cancer* **53**, 311–316 (1985).
45. K.A. Kennedy, S. Rockwell, and A.C. Sartorelli, *Cancer Res.* **40**, 2356–2360 (1980).
46. C.A. Pritsos and A.C. Sartorelli, *Cancer Res.* **46**, 3528–3532 (1986).
47. J.P. Codde et al., *Anticancer Res.* **13**, 539–544 (1993).
48. T. Kato et al., *Cancer (Philadelphia)* **48**, 674–680 (1981).
49. T. Kato et al., *JAMA, J. Am. Med. Assoc.* **245**, 1123–1127 (1981).
50. J.R. Daniels, M. Sternlicht, and A. Daniels, *Cancer Res.* **48**, 2446–2450 (1988).
51. G. Spenlehauer, M. Veillard, and J.-P. Benoit, *J. Pharm. Sci.* **75**, 750–755 (1986).
52. R. Verrijk, I.J.H. Smolders, J.G. McVie, and A.C. Begg, *Cancer Chemother. Pharmacol.* **29**, 117–121 (1991).
53. R. Verrijk, I.J.H. Smolders, N. Bosnie, and A.C. Begg, *Cancer Res.* **52**, 6653–6656 (1992).
54. Y. Morimoto and S. Fujimoto, *Crit. Rev. Ther. Drug Carrier Syst.* **2**, 19–63 (1985).
55. T. Kato, R. Nemoto, and T. Nishimoto, *Tohoku J. Exp. Med.* **127**, 99–100 (1979).
56. T. Kato, R. Nemoto, H. Mori, and I. Kumagai, *Cancer (Philadelphia)* **46**, 14–21 (1980).

57. R. Nemoto et al., *Urology* **17**, 315–319 (1981).
58. S. Fujimoto et al., *Cancer (Philadelphia)* **55**, 522–526 (1985).
59. N. Willmott et al., *J. Pharm. Pharmacol.* **41**, 433–438 (1989).
60. J.A. Goldberg et al., *Nucl. Med. Commun.* **12**, 57–63 (1991).
61. D.J. Kerr et al., *Cancer (Philadelphia)* **62**, 878–883 (1988).
62. S. Fujimoto et al., *Cancer (Philadelphia)* **56**, 2404–2410 (1985).
63. H.F.M. Cremers et al., *J. Controlled Release* **11**, 167–179 (1990).
64. Y. Nishioka et al., *Biol. Chem. Bull.* **16**, 1136–1139 (1993).
65. G. Spenlehauer et al., *J. Controlled Release* **7**, 217–229 (1988).
66. E.D. Grady, W.T. Sale, and L.C. Rollins, *Ann. Surg.* **157**, 97–114 (1963).
67. T.R. Nolan and E.D. Grady, *Am. Surg.* **35**, 181–188 (1969).
68. Y.S. Kim, J.W. LaFave, and L.D. MacLean, *Surgery* **52**, 220–231 (1962).
69. I.M. Ariel, *Ann. Surg.* **162**, 267–278 (1964).
70. I.M. Ariel and G. Padula, *J. Surg. Oncol.* **10**, 327–336 (1978).
71. I.M. Ariel and G. Padula, *J. Surg. Oncol.* **20**, 151–156 (1982).
72. M.A. Burton et al., *Eur. J. Cancer Clin. Oncol.* **25**, 1487–1491 (1989).
73. B.N. Gray et al., *Inter. J. Radiat. Oncol. Biol. Phys.* **18**, 619–623 (1990).
74. B.N. Gray et al., *Austr. N. Z. J. Surg.* **62**, 105–110 (1992).
75. S.Y. Lin et al., *Biomater. Artif. Cells. Artif. Organs* **17**, 189–203 (1989).
76. J.H. Campbell, L. Edsberg, and A.E. Meyer, *J. Oral Maxillofacial Surg.* **52**, 49–51 (1994).
77. A. Shikani, D.W. Eisele, and A. Domb, *Arch. Otolaryngol. Head Neck Surg.* **120**, 1242–1247 (1994).
78. A.C. Begg, M.J.M. Deurloo, W. Kop, and H. Bartelink, *Radiother. Oncol.* **31**, 129–137 (1994).
79. S.K. Dordunoo et al., *J. Controlled Release* **44**, 87–94 (1997).
80. P.I. Kornblith and M. Walker, *J. Neurosurg.* **68**, 1–17 (1988).
81. T.L. Loo, R.L. Dion, R.L. Dixon, and D.P. Rall, *J. Pharm. Sci.* **55**, 492–497 (1966).
82. H. Brem et al., *J. Neurosurg.* **74**, 441–446 (1991).
83. M.P. Wu, J.A. Tamada, H. Brem, and R. Langer, *J. Biomed. Mater. Res.* **28**, 387–395 (1994).
84. K.D. Judy et al., *J. Neurosurg.* **82**, 481–486 (1995).
85. J.D. Weingert, E.P. Sipos, and H. Brem, *J. Neurosurg.* **82**, 635–640 (1995).
86. M. Boisdron-Celle, P. Menei, and J.P. Benoit, *J. Pharm. Pharmacol.* **47**, 108–114 (1995).
87. P. Menei et al., *Biomaterials* **14**, 470–478 (1993).
88. P. Menei et al., *Neurosurgery* **39**, 117–124 (1996).
89. E.C. Shors et al., *Cancer Res.* **40**, 2288–2294 (1980).
90. C.W. Stackpole, E.F. Valle, and A.L. Alterman, *Cancer Res.* **51**, 2444–2450 (1991).
91. M. Bolla et al., *N. Engl. J. Med.* **337**, 295–300 (1997).
92. R. Arky, *Physicians' Desk Reference*, 52nd ed., Medical Economics Company, Montvale, N.J., 1998.
93. P.K. Gupta, *J. Pharm. Sci.* **79**, 949–962 (1990).
94. A.E. Frankel, *Oncology (Huntington)* **7**, 69–78 (1993).
95. M.-A. Ghetie and E.S. Vitetta, *Curr. Opin. Immunol.* **6**, 707–714 (1994).
96. W.A. Hall, *Neurosurg. Clin. North Am.* **7**, 537–545 (1996).
97. C.B. Siegall, *Cancer (Philadelphia)* **74**, 1006–1012 (1994).
98. J.G. Jurcic and D.A. Scheinberg, *Curr. Opin. Immunol.* **6**, 715–721 (1994).
99. J.K. Sherwood, R.B. Dause, and W.M. Saltzman, *Bio/Technology* **10**, 1446–1449 (1992).
100. P.S. Gill et al., *J. Clin. Oncol.* **14**, 2353–2364 (1996).
101. A. Sharma et al., *Int. J. Cancer* **71**, 103–107 (1997).
102. L.D. Mayer et al., *Br. J. Cancer* **71**, 482–488 (1995).
103. A. Rahman et al., *J. Natl. Cancer Inst.* **84**, 1909–1915 (1992).
104. S. Ohta et al., *Anticancer Res.* **13**, 331–336 (1993).
105. T.M. Allen et al., *Biochem. Soc. Trans.* **23**, 1073–1079 (1995).
106. I. Ahmad, M. Longenecker, J. Samuel, and T.M. Allen, *Cancer Res.* **53**, 1484–1488 (1993).
107. T.M. Allen et al., *Int. J. Cancer* **62**, 199–204 (1995).
108. N. Emanuel et al., *Pharm. Res.* **13**, 861–868 (1996).
109. D.D. Lasic et al., *Biochim. Biophys. Acta* **1070**, 187–192 (1991).
110. J.A. Harding et al., *Biochim. Biophys. Acta* **1327**, 282–292 (1997).
111. S.A. Longman et al., *Cancer Chemother. Pharmacol.* **36**, 91–101 (1995).
112. R.J. Lee and P.S. Low, *Biochim. Biophys. Acta* **1233**, 134–144 (1995).
113. D.D. Lasic, *Am. Sci.* **80**, 20–31 (1992).
114. D.D. Lasic, in S. Benita, ed., *Microencapsulation: Methods and Industrial Applications*, Dekker, New York, 1996, pp. 297–328.
115. D.W. Northfelt et al., *J. Clin. Oncol.* **15**, 653–659 (1997).
116. A. Gabizon et al., *Acta Oncol.* **33**, 779–786 (1994).
117. D.S. Fischer, M.T. Knobf, and H.J. Durivage, eds., *The Cancer Chemotherapy Handbook*, 5th ed., Mosby, St. Louis, Mo., 1997.
118. J.-C. Leroux, E. Doelker, and R. Gurney, in S. Benita, ed., *Microencapsulation: Methods and Industrial Applications*, Dekker, New York, 1996, pp. 535–575.
119. S.J. Douglas, S.S. Davis, and L. Illum, *Crit. Rev. Ther. Drug Carrier Syst.* **3**, 233–261 (1987).
120. V. Lenaerts et al., *J. Pharm. Sci.* **73**, 980–982 (1984).
121. L. Illum, P.D. Jones, R.W. Baldwin, and S.S. Davis, *J. Pharmacol. Exp. Ther.* **230**, 733–736 (1984).
122. M.T. Peracchia, C. Vauthier, F. Puisieux, and P. Couvreur, *J. Biomed. Mater. Res.* **34**, 317–326 (1997).
123. S.E. Dunn et al., *Pharm. Res.* **11**, 1016–1022 (1994).
124. L. Illum et al., *Life Sci.* **40**, 367–374 (1987).
125. R. Reszka et al., *J. Pharmacol. Exp. Ther.* **280**, 232–237 (1997).
126. J.A. Mosso and R.W. Rand, *Ann. Surg.* **178**, 663–668 (1973).
127. K. Mosbach and U. Schröder, *FEBS Lett.* **102**, 112–116 (1979).
128. K.J. Widder, A.E. Senyei, and D.G. Scarpelli, *Proc. Soc. Exp. Biol. Med.* **58**, 141–146 (1978).
129. K. Sugibayashi, M. Okamura, and Y. Morimoto, *Biomaterials* **3**, 181–186 (1982).
130. A.E. Senyei, S.D. Reich, C. Gonczy, and K.J. Widder, *J. Pharm. Sci.* **70**, 389–391 (1981).
131. Y. Morimoto, M. Okamura, K. Sugibayashi, and Y. Kato, *J. Pharmacobiodyn.* **4**, 624–631 (1981).
132. K.J. Widder et al., *Eur. J. Cancer Clin. Oncol.* **19**, 135–139 (1983).
133. Y. Morimoto, K. Sugibayashi, M. Okamura, and Y. Kato, *J. Pharmacobiodyn.* **3**, 264–267 (1980).

Next Page

134. A. Ibrahim, P. Couvreur, M. Roland, and P. Speiser, *J. Pharm. Pharmacol.* **35**, 59–61 (1983).
135. U.O. Häfeli et al., *Nucl. Med. Biol.* **22**, 147–155 (1995).
136. G. Dranoff et al., *Proc. Natl. Acad. Sci. U.S.A.* **90**, 3539–3543 (1993).
137. J.W. Simons et al., *Cancer Res.* **57**, 1537–1546 (1997).
138. W.H. Sun et al., *Proc. Natl. Acad. Sci. U.S.A.* **92**, 2889–2893 (1995).
139. M. Saito, D. Fan, and L.B. Lachman, *Clin. Exp. Metastases* **13**, 249–259 (1995).
140. C. Khanna et al., *Cancer (Philadelphia)* **79**, 1409–1421 (1997).
141. S.M. Sugarman and R. Perez-Soler, *Crit. Rev. Oncol./Hematol.* **12**, 231–242 (1992).
142. P.M. Anderson et al., *Cytokine* **6**, 92–101 (1994).
143. P.M. Anderson et al., *J. Immunother.* **12**, 19–31 (1992).
144. E. Kedar et al., *J. Immunother.* **16**, 47–59 (1994).
145. C. Khanna et al., *J. Pharm. Pharmacol.* **49**, 960–971 (1997).
146. P.M. Anderson and M.A. Sorenson, *Clin. Pharmacokinet.* **27**, 19–31 (1994).
147. L.-S. Liu et al., *J. Controlled Release* **43**, 65–74 (1997).
148. L. Chen, R.N. Apte, and S. Cohen, *J. Controlled Release* **43**, 261–272 (1997).
149. P.T. Golumbek et al., *Cancer Res.* **53**, 5841–5844 (1993).
150. N.K. Egilmez et al., *Cancer Immunol. Immunother.* **46**, 21–24 (1998).

See also CANCER, DRUG DELIVERY TO TREAT—PRODRUGS; CENTRAL NERVOUS SYSTEM, DRUG DELIVERY TO TREAT.

CANCER, DRUG DELIVERY TO TREAT—PRODRUGS

ROBERT G.L. SHORR
United Therapeutics
Washington, D.C.

KEY WORDS

Anticancer drugs
Camptothecin
Novel cancer therapeutics
Paclitaxel
Passive targeting
Polyethylene glycol
Polymer conjugates
Tumor accumulation

OUTLINE

Introduction
The Problem
Properties of Tumors and Malignant Cells

The Solution: Tumor Targeting Strategies
Active Targeting
Passive Targeting
Bibliography

INTRODUCTION

Approximately 550,000 deaths, or nearly one-quarter of disease-associated mortality, in America are cancer related. One in four Americans has been projected to experience cancer at some point during his or her life time. Cancer is the number two disease killer of Americans and is the leading cause of death from disease in children ages 1–14. Nearly 90% of cases are solid tumors with metastases distal to the primary tumor site. Cancers causing the most deaths in the United States for both sexes are lung and colorectal, followed by breast and uterine cancer in women and prostate cancer in men. The most frequently diagnosed cancer is cancer of the skin (over 800,000 cases); 40,000 of these are cases of advanced malignant melanoma. Management of metastatic disease remains one of the most challenging aspects of oncology care to date.

The principle treatment modalities for cancer are surgery, radiation therapy, and the use of chemotherapeutic agents. Of these, surgery, if performed at an early enough stage of disease progression, offers the greatest chance for cure. Radiotherapy does not discriminate between normal and healthy tissue and must rely on external methods of targeting radiation beams to the desired location. Collateral damage to healthy organs and tissues can be high and have devastating side effects. Chemotherapeutic agents, although capable of "killing" tumor cells also kill healthy cells, making mop up after radiation treatment or surgery and treatment of metastatic disease a balancing act between aggressive therapy and control of its side effects.

Whereas some progress has been made in the treatment of certain tumor types using chemotherapeutic agents, particularly liquid tumors, nearly half of all patients will fail to respond or relapse to metastatic disease. Despite the appearance of nearly 70 approved chemotherapeutic agents for the treatment of cancer, overall results have been disappointing, particularly for solid tumors (1).

THE PROBLEM

A primary problem in the targeted treatment of cancer is that in most instances the differences between the normal cells of origin and malignant cells are subtle and difficult to quantify and translate to beneficial therapy. Shared properties between normal and tumor cells have confounded the development of tumor-specific agents.

Properties of Tumors and Malignant Cells

Normal tissues may be considered to be those that are continuously renewing their cell populations (bone marrow, intestine), those that proliferate slowly but may regenerate in response to damage (liver, lung), or those that are relatively static (muscle and nerve).

Previous Page

134. A. Ibrahim, P. Couvreur, M. Roland, and P. Speiser, *J. Pharm. Pharmacol.* **35**, 59–61 (1983).
135. U.O. Häfeli et al., *Nucl. Med. Biol.* **22**, 147–155 (1995).
136. G. Dranoff et al., *Proc. Natl. Acad. Sci. U.S.A.* **90**, 3539–3543 (1993).
137. J.W. Simons et al., *Cancer Res.* **57**, 1537–1546 (1997).
138. W.H. Sun et al., *Proc. Natl. Acad. Sci. U.S.A.* **92**, 2889–2893 (1995).
139. M. Saito, D. Fan, and L.B. Lachman, *Clin. Exp. Metastases* **13**, 249–259 (1995).
140. C. Khanna et al., *Cancer (Philadelphia)* **79**, 1409–1421 (1997).
141. S.M. Sugarman and R. Perez-Soler, *Crit. Rev. Oncol./Hematol.* **12**, 231–242 (1992).
142. P.M. Anderson et al., *Cytokine* **6**, 92–101 (1994).
143. P.M. Anderson et al., *J. Immunother.* **12**, 19–31 (1992).
144. E. Kedar et al., *J. Immunother.* **16**, 47–59 (1994).
145. C. Khanna et al., *J. Pharm. Pharmacol.* **49**, 960–971 (1997).
146. P.M. Anderson and M.A. Sorenson, *Clin. Pharmacokinet.* **27**, 19–31 (1994).
147. L.-S. Liu et al., *J. Controlled Release* **43**, 65–74 (1997).
148. L. Chen, R.N. Apte, and S. Cohen, *J. Controlled Release* **43**, 261–272 (1997).
149. P.T. Golumbek et al., *Cancer Res.* **53**, 5841–5844 (1993).
150. N.K. Egilmez et al., *Cancer Immunol. Immunother.* **46**, 21–24 (1998).

See also CANCER, DRUG DELIVERY TO TREAT—PRODRUGS; CENTRAL NERVOUS SYSTEM, DRUG DELIVERY TO TREAT.

CANCER, DRUG DELIVERY TO TREAT—PRODRUGS

ROBERT G.L. SHORR
United Therapeutics
Washington, D.C.

KEY WORDS

Anticancer drugs
Camptothecin
Novel cancer therapeutics
Paclitaxel
Passive targeting
Polyethylene glycol
Polymer conjugates
Tumor accumulation

OUTLINE

Introduction
The Problem
Properties of Tumors and Malignant Cells

The Solution: Tumor Targeting Strategies
Active Targeting
Passive Targeting
Bibliography

INTRODUCTION

Approximately 550,000 deaths, or nearly one-quarter of disease-associated mortality, in America are cancer related. One in four Americans has been projected to experience cancer at some point during his or her life time. Cancer is the number two disease killer of Americans and is the leading cause of death from disease in children ages 1–14. Nearly 90% of cases are solid tumors with metastases distal to the primary tumor site. Cancers causing the most deaths in the United States for both sexes are lung and colorectal, followed by breast and uterine cancer in women and prostate cancer in men. The most frequently diagnosed cancer is cancer of the skin (over 800,000 cases); 40,000 of these are cases of advanced malignant melanoma. Management of metastatic disease remains one of the most challenging aspects of oncology care to date.

The principle treatment modalities for cancer are surgery, radiation therapy, and the use of chemotherapeutic agents. Of these, surgery, if performed at an early enough stage of disease progression, offers the greatest chance for cure. Radiotherapy does not discriminate between normal and healthy tissue and must rely on external methods of targeting radiation beams to the desired location. Collateral damage to healthy organs and tissues can be high and have devastating side effects. Chemotherapeutic agents, although capable of "killing" tumor cells also kill healthy cells, making mop up after radiation treatment or surgery and treatment of metastatic disease a balancing act between aggressive therapy and control of its side effects.

Whereas some progress has been made in the treatment of certain tumor types using chemotherapeutic agents, particularly liquid tumors, nearly half of all patients will fail to respond or relapse to metastatic disease. Despite the appearance of nearly 70 approved chemotherapeutic agents for the treatment of cancer, overall results have been disappointing, particularly for solid tumors (1).

THE PROBLEM

A primary problem in the targeted treatment of cancer is that in most instances the differences between the normal cells of origin and malignant cells are subtle and difficult to quantify and translate to beneficial therapy. Shared properties between normal and tumor cells have confounded the development of tumor-specific agents.

Properties of Tumors and Malignant Cells

Normal tissues may be considered to be those that are continuously renewing their cell populations (bone marrow, intestine), those that proliferate slowly but may regenerate in response to damage (liver, lung), or those that are relatively static (muscle and nerve).

Cancer can be defined as the emergence of cellular clusters that result from continuous production of abnormal cells that invade and destroy normal tissues.

Human tumors often first arise in renewing tissues. The tumor cells are able to divide endlessly, without differentiating into a mature state and without regard to the function of the tissue they are in. As they begin to multiply, angiogenesis factors, growth factors, and cytokines that stimulate the formation of collateral blood vessels and other "support" tissues are released. Some tumors may increase in malignancy with time and shed clonogenic cells that will give rise to metastatic nodules and eventually additional tumor masses. Nowell (2) has suggested that tumor cells are genetically unstable and that a high degree of random mutation during clonal expansion gives rise to lethal or disadvantageous mutations as well as greater autonomy and growth advantages to those cells that will go on to become tumor producers.

According to this model it is not surprising that tumors are heterogeneous in their origins and properties, extending to almost any property measured, including surface markers, karyotype, morphology, metastatic potential, and sensitivity to therapeutic agents (3). Further influencing heterogeneity, even as a tumor expands from a single cell, are differentiation-related diversity, nutritional heterogeneity, and the emergence of new subclones. Differentiation-related diversity may result in the production of different cellular products and membrane markers. Nutritional heterogeneity reflects the immature and often slower-growing vasculature associated with tumors and the appearance of nutritional and oxygen gradients as distance from the vascular tree increases. A dramatic influence on metabolic function and proliferation can be expected across cell layers. In some instances regions of tumor necrosis may emerge. The influence of tumor hypoxia associated with oxygen gradients and radiation therapy outcome is well characterized (see the section "PEG-Hemoglobin"). The development of subclones may be a key underlying mechanism for tumor progression and the emergence of resistance. Subclones with varying degrees of resistance may also contribute to a sense of "trying to hit a moving target" for the oncologist.

Indeed, it is the spread of cancerous cells and the appearance of metastases and resistance that represents a most difficult challenge to the oncologist. The routes and sites of metastases vary with different primary tumors. In general as cancers break through the surface of the organ in which they originated, cells may shed, lodge, and begin to grow on the surface of adjacent organs. Tumor cells may also migrate into the lymphatic system and be carried to the lymph nodes and blood vessels. As malignant cells migrate through the blood stream, many die. Others become trapped in vessels too small to let them pass. GI tract–originating tumor cells may be stopped in the liver or, eventually, lung. Other tumor cells originating in other parts of the body may be stopped first in the microvasculature of the lung. Smaller clusters of tumor cells, present as micrometasteses, may remain relatively dormant and escape detection.

Four stages for cancer progression have been defined with increasing severity of disease and seriousness:

Stage 1. Tumors are small and localized and, depending on location, may be removed surgically.

Stages 2 and 3. Tumors are larger and may have broken through the initial organ to attach to additional surrounding organs and tissues. Lymph node involvement is likely.

Stage 4. Tumors have metastasized to other parts of the body, usually with nodal involvement.

Human tumors vary widely in their properties. They may arise in different parts of the body, vary in retention of normal differentiation patterns or grade, and vary in extent of expansion into surrounding normal tissue and metastases or stage. It is likely that this variability reflects the different or individual initial genetic alterations at the root of the cancer emergence and the cells that ultimately will constitute the tumor mass. The collective biological properties of the tumor cells will determine the overall tumor phenotype. Cancer cells, even when spread throughout the body, are likely to retain at least some physical and biological characteristics of the tissue in which they originated. Tumors arising from endocrine tissue, for example may continue to produce and release hormones. The more de-differentiated a tumor, the more aggressive its growth and ability to generate metastases.

Although the cause of cancer is not completely understood, a combination of hereditary factors, virus or environmental exposures, and lifestyle has been implicated. Linkage between cigarette smoking and lung cancer, for example, is widely accepted. This year more than 140,000 people will be newly diagnosed with lung cancer. Epidemiologists predict that even with smoking cessation programs such numbers are likely to be seen for at least the next three decades.

Recently specific genetic events have been implicated in the emergence of cancer and the control of cell growth. Use of agents to specifically turn off or on these genes has become the focus of intense preclinical and clinical research. It is likely that these agents will find use in conjunction with known cytotoxic agents and newer formulations as part of a "combination" or "cocktail" approach to cancer treatment.

Three major cancer subtypes have been described:

Sarcomas. Arising from connective and supportive tissues (i.e., bone, cartilage, nerve, blood vessels, muscle, and fat)

Carcinomas. Arising from epithelial tissue (i.e., skin, body cavity and organ linings, glandular tissue, breast, and prostate); squamus tumors resemble skin; adenocarcinomas resemble glandular tissue

Leukemias and lymphomas. Arising from blood-cell-forming tissue and involving lymph nodes, spleen, and bone marrow, with overproduction of lymphocytes.

THE SOLUTION: TUMOR TARGETING STRATEGIES

Given the similarities between normal and tumor tissue, the first challenge to the oncologist attempting a tumor

targeting strategy is the localization of tumor sites, both primary and metastatic. In this regard magnetic resonance imaging techniques using metabolic markers, as well as the use of antibodies recognizing tumor-associated antigens and carrying radioisotopes, have been described. Once detected, direct injection of drug into a tumor (if reachable), placement of hydrogels containing drug, or infusion of an antitumor agent into the afferent blood supply feeding a tumor may be considered. This approach to tumor targeting, however, does not take into account the need to target and effectively treat metastatic and micrometastatic disease.

Beyond direct injection into a tumor or otherwise localized "physical delivering" of a therapeutic agent, the ideal tumor targeting strategy is one that allows for highly selective recognition of tumor masses as well as metastatic nodules and miocrometasteses even on systemic administration of drug. Little or no corecognition of normal or related healthy cells and tissue is especially desirable. Because the targeting event may or may not be of therapeutic benefit directly, drugs to be delivered via the targeting agent also need to be carefully considered. For example many drugs will need to be taken up into cells to be effective or further targeted to a specific organelle. For prodrugs that circulate in the blood as inactive or weakly active agents, tumor activation or potentiation of activity is essential.

Active Targeting

Although a complete review is beyond the scope of this article, most tumor targeting efforts have been made using "active" agents with selective affinities for tumor markers. Briefly, potential sites for "active" tumor targeting may be at the cellular level and be structural membrane proteins, receptors, glycoproteins, or lipoproteins associated with malignant cells. They may be associated with supportive tissue such as the vasculature penetrating a tumor mass and stroma. Or they may be directed to necrotic regions of a tumor that expose regions of DNA and chromatin not normally exposed in healthy tissue. The uniqueness of these targets relative to tumor tissue will be a primary driver in the selectivity of any drug to be delivered via this mechanism.

Following are examples of active targeting agents:

Antibodies
Growth factor and hormone receptor ligands (including peptides and small synthetic organic molecules)
Nutrient transporters, vitamins, and virus

There are a number of anticancer agents that might be delivered:

Cytotoxic molecules (small synthetic organic molecules or peptides)
Ribosome-inhibiting proteins and toxins
Antisense nucleotides or genes
Hormones and differentiation promoters
Radioisotopes
Modifiers of resistance
Adjuvants for radiation therapy or conventional chemotherapeutic use

Kabanov and Alakhov (4) have summarized the following requirements for active "magic bullets":

A targeting moiety that is selective for tumor cells independent of their location anywhere in the body, with little or no recognition of normal tissue
An ability to recognize and bind to or be taken up by the targeted cells
An ability carry a "payload" without disintegrating or losing activity or potential activity along the way
An ability to deliver the payload while avoiding nonspecific drug or drug metabolite interactions with nontarget cells
An ability to be cleared from the body rapidly, with preferred accumulation at sites of disease only

Much research has been done concerning targeting moieties that carry a radioisotope for imaging or therapy, but in considering cytotoxic drugs and their analogues for delivery to tumors, the ideal molecule should be "inactive" except upon delivery to the targeted cell. In this regard the concept of a prodrug has emerged; target-site-specific modification can unleash the payload and destroy the tumor cell.

Antibody binding directed against specific antigens is among the most selective interactions known to science. It is not surprising then that in the search for "magic bullets" against cancer, antibodies that specifically recognize tumor-associated antigens have been sought.

The major forms of antibodies that have been used for tumor targeting are the complete intact antibody (typically IgG), or the F(ab′)2, Fab, or Fab′ fragments. Intact antibodies have been described as Y-shaped molecules composed of two identical heavy chains and two identical light chains. Antigen binding sites are at the tips of the Y. The F(ab′)2 fragment can be released from the intact antibody by proteolytic cleavage and contains both antigen-binding tips of the Y. The F(ab′)2 fragment is held together by a disulfide bridge that, on reduction, releases the Fab′ fragments with one binding site per Fab. The molecular weight of an intact IgG is 150,000; that of an F(ab′)2 and Fab are 100,000 and 50,000, respectively. Smaller fragments bind to antigens, often with both lower affinity and avidity.

Use of monoclonal antibodies for the treatment of leukemia and lymphoma has offered considerable success (5,6), but results with solid tumors have been disappointing (7,8). It has been suggested that the main reason for poor efficacy is resistance to uniform tumor penetration by antibody conjugates (7–9). In studies with radiolabeled antibodies only 0.001–0.01% of an administered antibody dose was found to be localized to each gram of solid tumors in humans, with much of it trapped in tumor perivascular space (10,11). Barriers to uniform antibody penetration have been suggested to arise from the endothelial layer and dense fibrous stroma associated with tumors, as well

as the tight packing of tumor cells and the absence of lymphaticdrainage, which contribute to high interstitial pressure and opposition to influx of molecules into the tumor core (12) or nonspecific binding and entrapment (13).

One approach to increase tumor penetration has been to make antibody fragments as small as possible. Much of the rationale for preparation of F(ab')2 and Fab fragments has come from the belief that smaller molecules enter and penetrate tumors more quickly and uniformly than intact antibodies, while being more rapidly cleared from the rest of the body. For imaging and diagnostic application, rapid tumor penetration and body clearance are desirable properties. Still, with the lower affinity and avidity associated with the smaller fragments, biodistribution studies indicate that the larger species are distributed more slowly and are retained for longer periods than the smaller fragments. The suggestion being that, for therapeutic use, higher molecular weights may be more desirable.

In searching for tumor-specific antigens it is necessary to identify targets with the following characteristics:

Ideally, expressed only by tumor cells and similarly by all cells of the tumor

Not shed into the circulation where they can "sponge up" drug directed to the tumor before it reaches the desired tumor mass

Allow for the drug conjugate to be taken up into the cell if required for activity, or to remain associated with the tumor cell surface long enough to be active

In the past much of the screening for tumor specific antigens and antibodies was based upon the immunization of mice and the screening for monoclonals in cultured pools of antibody producing cells. The development of display technology has now allowed for the creation of antigen-binding molecules in vitro (14,15). It is now no longer necessary to immunize animals to raise antibodies. Further, combinatorial approaches coupled with high-throughput screening capabilities can allow for antibody engineering to produce desired affinities, multivalencies, single-chain antibody fragments, and recombinant fusion molecules (16,17). Such engineered proteins can also be humanized by replacing murine framework regions with human framework regions or made entirely human, which eliminates the rejection of murine antibodies characterized as HAMA (human anti–mouse antibody)—a problem associated with early monoclonal antibody trials and products. Three advances have enabled the construction of antibodies and antigen-driven selection in vitro. These are (*1*) the ability to express the antigen-binding domains of the heavy and light chains of antibodies in *Escherichia coli*, either as Fab fragments or as single-chain antigen-binding molecules, (*2*) the large and diverse libraries of Fab and single-chain antigen-binding genes that can be generated by the polymerase chain reaction using heavy- and light-chain genes obtained before or after immunization and harvest of B lymphocytes, and (*3*) the ability to express the antibody fragments on the surface of bacteriophage to facilitate screening and selection.

Numerous tumor antigens have been identified and antibodies or their fragments characterized in animal or human clinical studies. A complete review of this effort is beyond the scope of this work. In general, although a particular marker may be overexpressed by some cells of a tumor, there is often a population that expresses substantially less, or normal healthy cells and tissue that express similar antigens. Thus tumor antigens have appeared to be more tumor selective than tumor specific. In the clinic, or in animal experiments where the tumor antigens are not uniformly available, initial treatment may appear quite promising only to result in the emergence of resistant clones that do not express the targeted antigen. Where the antibody is conjugated to a radioisotope for therapy, this problem is somewhat lessened due to the ability of radiation to penetrate more than one cell layer.

Immunotoxin constructs have been prepared using ribosome-inhibiting proteins and their subunits as chemical conjugates to antibodies or as fusion proteins produced by recombinant means. Ribosome-inhibiting proteins are extremely potent and function by inhibiting protein synthesis. To be effective they must be taken up into cells. Depending on the nature of the antibody–toxin conjugate, processing of the complex may or may not be necessary to release active inhibitor. Binding to normal healthy tissue can contribute to toxicity and side effects.

Despite the fact that a truly specific tumor antigen has not emerged, antibodies continue to be explored for diagnostic and therapeutic uses in cancer in a variety of formats. One interesting approach worthy of mention is the targeting of tumor vasculature with antibody drug and prodrug conjugates so as to cut off the "feeding" of a tumor mass. Attacking the endothelial cells instead of the tumor itself was first proposed by Denekamp (18). Killing of vascular endothelial cells within the tumor was reasoned to be likely to denude the endothelial lining and lead to platelet adhesion, activation of coagulation factors, and sealing off of the vasculature tree via occlusive thrombus formation (19). As each microvessel becomes blocked, tumor cells dependent on that vessel for nutrition and oxygen become unable to survive. It was reasoned that targeting and destruction of only a few relatively accessible endothelial cells should trigger a chain reaction.

Thorpe and Derbyshire (20) have prepared an IgM murine monoclonal antibody, TEC-11, by immunizing BALB/c mice with human umbilical vein endothelial cells in order to test this hypothesis. Hybridoma supernatants were prepared and screened for reactivity against proliferating human umbilical vein endothelial cells, lack of reactivity against quiescent frozen sections, and reactivity against sections of human malignant but not normal tissue. Characterization of TEC-11 indicated that the antibody recognized human endoglin, an essential component of the TGF-β receptor on human endothelial tissue. Endoglin is a dimeric glycoprotein with two 95,000 MW subunits linked by a disulfide bridge (21) that binds TGF-β1 and TGF-β3 with high affinity. Endoglin is expressed on human endothelial cells, fetal syncytiotrophoblast, some macrophage, immature erythroid cells, and dermal endothelium under some conditions of inflammation (22).

Immunotoxins prepared by linking the A-chain of the ribosomal inhibiting protein ricin were tested as conjugates with tumor vasculature targeting antibodies in mice

bearing solid tumors of greater than 1 cm diameter. In these studies, dose-dependent antitumor effects were observed. In following the time course of antitumor activity, the first loss of endothelial cells was observed 2 h post-injection of the antibody–toxin conjugate. By 6 h many blood vessels already showed signs of occlusion, which extended to nearly all vessels by 24 h, followed by physical collapse of the tumor mass. Other tumor-vasculature-selective antibodies have been identified that recognize additional endothelial cell antigens, basement membrane, or tumor stroma and are being explored as immunotoxin conjugates or as conjugates with other cytotoxic agents (23–28).

Although targeting macromolecular drug carrier conjugates to tumor vasculature using antibodies has attracted considerable attention, attacking tumor vasculature formation by blocking angiogenesis is also being explored. Naked antibodies as well as inhibitory molecules and adhesion molecule regulators have shown provocative results in experimental models (29). Targeting stroma using antibodies carrying radioisotope that bind to dead or dying tumor cells at a tumor core have entered phase I clinical trials for the treatment of malignant melanoma. In addition to radioisotope it is believed that such antibodies can be used to target other drugs. This approach has been described as attacking tumors from the inside out (30,31).

Passive Targeting

In contrast to active tumor targeting, observations of hyperpermeability of vasculature and immaturity of the lymph drainage systems of tumor tissue have led to proposals of passive tumor targeting (32–39). It is the nature of the tumor vasculature that is believed to enable such an approach.

Tumor Microvasculature. Tumor microvasculature comprises both vessels from the preexisting organ or tissue in which the tumor has arisen, and new vessels stimulated to grow by the release of angiogenic factors (40,41). Distribution of nutrients as well as drugs through the tumor mass will be influenced by the diameter, length, number, and geometry of the available blood vessels, as well as blood flow (42–45). Jain and others (43–45) have suggested that the nature of the tumor vasculature will vary with location, tumor type, and growth rate. Red blood cell flow velocity may be slower in tumors than in normal tissue (46,47) because of viscous resistance in tumor vessels (48–51).

As tumors grow avascular regions of necrosis, seminecrotoc and stable vascularized regions appear (52). As the tumor expands, additional cell layers are added and a metabolic gradient emerges (53). The precise nature of this gradient and its role in triggering metastases as well as chemotherapeutic responsiveness remains an area of intense investigation (54–56).

Interestingly, in addition to the differences in spatial geometry of tumor vasculature, differences over normal vasculature in both macroscopic and microscopic morphology have been reported (57). These features combine to make distribution of drugs to tumors both heterogeneous and challenging.

Generally vascular permeability and hydraulic conductivity of tumors is higher than for normal tissue (58–63). It has been suggested that molecules with positive charges have a higher permeability (64) and that tumor vascular is more porous than "leaky" (65). It has been hypothesized (66) that pore size and permeability vary not only between tumor types but within an individual tumor as well, in part reflecting the local cytokine environment (67).

In addition to the permeability differences just noted, tumors have been characterized as having high interstitial fluid pressures (32,68–79). Once extravasated molecular movement is likely to be governed by diffusion and convection, tumor pressures play an influential role in molecular entry as well as retention (80–82). Larger tumors may be expected to have reduced transvascular exchange over smaller tumors, and convective transport at a tumor's center might be less than at the tumor's periphery.

It has been suggested that the anatomical features and pressure gradients associated with tumors allow higher molecular weight molecules to accumulate in tumors with considerably longer retention times than expected for normal tissue. It has already been demonstrated that a correlation between molecular size and tumor retention exists (83,84). For "passive" tumor accumulation the "passively targeted" molecule should have the following characteristics:

- Sufficient circulating lifetime so as to allow for sufficient tumor accumulation to achieve desired local concentrations of drug with little or no accumulation in normal tissue
- An ability to be taken up by the targeted cells
- Not lose activity or potential activity while circulating
- An ability to deliver the anticancer activity while avoiding nonspecific drug or drug metabolite interactions with nontarget cells

To achieve the desired molecular weight relative to passive tumor accumulation, use of polymers as a conjugate to lower molecular weight cytotoxic agents has been proposed. These conjugates do not contain or require a tumor-directed binding moiety.

Polymeric Drug Carriers. There has long been the belief that the performance of many small-molecule drugs could be improved by their chemical transformation into polymer conjugates or macromolecular prodrugs. From the polymer perspective, dextran, inulin, polysaccharide B, and a variety of block copolymers have been explored (37,85–101).

Of these, perhaps the most advanced is SMANCS. SMANCS (molecular weight 16,000) is a conjugate of polystyrene-co-maleic acid half-*n*-butylate (SMA) with neocarzinostatin (NCS), developed by Maeda et al. (102,103) (Fig. 1). SMANCS has been approved in Japan for the treatment of primary hepatoma. Hepatic arterial administration has been found to be curative in a number of cases. In patients with little or mild concomitant liver cirrhosis and single-segment-confined tumor, 5-year survival rates are 90%. Overall 5-year survival for all patient

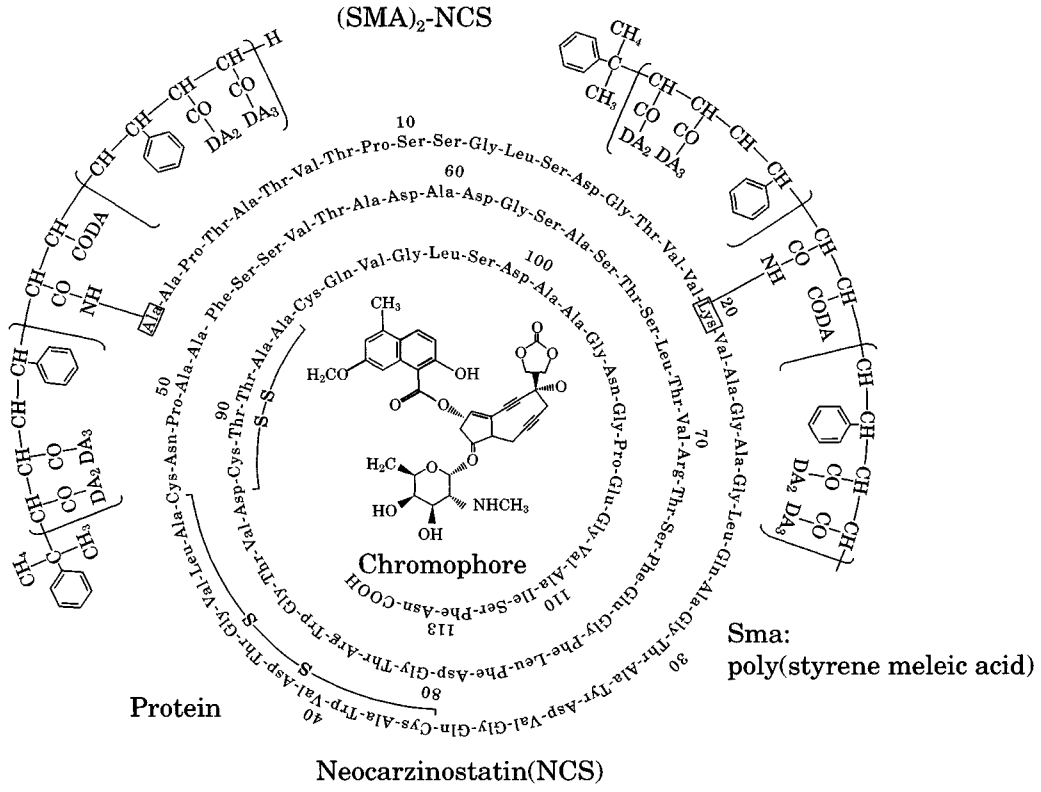


Figure 1. Illustration of the chemical structure of SMANCS.

types is nearly 35%. Additional clinical trials evaluating SMANCS for pleural and ascitic carcinomatosis via the intracavitary route are under way (104).

Little immunosuppression or marrow toxicity with SMANCS has been observed. The active component of SMANCS, neocarzinostatin, is an extremely potent cytotoxic agent effecting DNA cleavage and synthesis. The polymeric portion of SMANCS has been suggested by Maeda to promote tumor accumulation and prolonged tumor retention (105,106). Maeda has described the impact of tumor vasculature and flow on macromolecules as the "enhanced permeability and retention" effect. Lower molecular weight anticancer agents do not show the same degree of accumulation as smaller molecules that can more freely traverse interstitial space. Maeda has suggested that a molecular weight greater than 50,000 is required to begin seeing preferred tumor accumulation.

Other polymeric materials, liposomes, and drug carriers are being actively researched for tumor targeting. Daunorubicin when conjugated to polymers of carboxymethyl dextran, alginic acid, polyglutamate, or carboxymethyl cellulose irreversibly loses its cytotoxic properties. When linked by a hydrolyzable bond however, hydrolysis leads to recovery of the cytotoxic effects (107). Phase I clinical trials of a hydrolyzable dextran conjugate have been initiated (108). Conjugation of doxorubicin to *N*-(2-hydroxypropyl)methylacrylamide (HPMA) via degradable tetrapeptide linkers has also been reported (109). Cleavage of the linker is believed to occur after cellular uptake of the drug-polymer by endocytosis. Phase I clinical trials of this conjugate have also been initiated (110).

Polyethylene Glycol as a Drug Carrier. The use of synthetic or natural polymers as direct chemical conjugates to provide for increased circulating lifetimes of proteins and peptides, as well as protection from different solutes, undesirable degradation, immune responses, and other interactions has been well accepted. Of the different protein polymer conjugates studied, polyethylene glycol (PEG) is the most advanced in terms of clinical usage. Already PEG-conjugated adenosine deaminase for the treatment of adenosine deaminase deficiency–mediated immunodeficiency, and PEG-asparaginase for the treatment of acute lymphoblastic leukemia (111,112) have been approved by the U.S. FDA. Other PEG-conjugated proteins such as PEG-hemoglobin (APEX, Enzon), PEG–interleukin 2 (Chiron), PEG-alpha-interferon (Schering Plough and Hoffman La Roche), and several PEG–colony stimulating factors (Amgen), and enzymes and other proteins (Knoll Pharmaceuticals) are in various stages of preclinical and clinical trial investigations. Examples of PEG activation chemistries used for conjugation to proteins are shown as Figure 2. While major pharmaceutical companies have internal PEG programs, contract CGMP PEGylation services using a variety of activation chemistries and linker groups are also available through Shearwater Polymers, Inc. (Huntsville, Alabama), and Polymasc, Inc. (London, England).

Although the use of higher molecular weight polymers to prolong the circulating life of small-molecule drugs has been proposed in the literature and several cytotoxic agent polymer conjugates have been tested in the clinic, less is known about the performance of such conjugates with PEG.

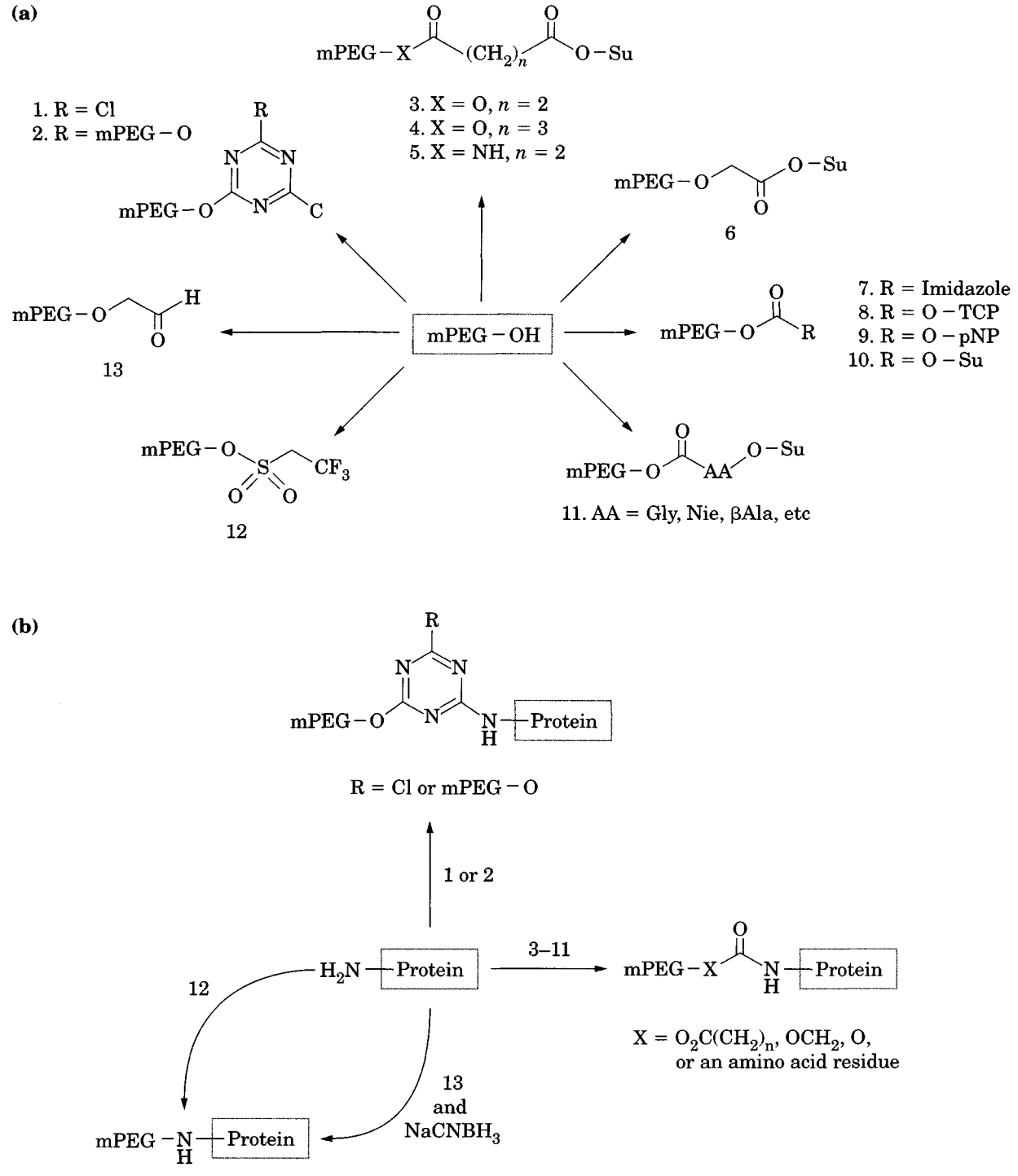


Figure 2. (**a**) Commonly used methods for preparation of mPEG-based modifying reagents. (**b**) Use of mPEG reagents for preparation of conjugates. mPEG represents $CH_3(OCH_2CH_2)n$. Su, succiinmidyl; TCP, trichlorophenyl; pNP, *p*-nitrophenyl; AA, amino acid. *Source:* From Ref. 113.

In general, there are three ways in which PEG might be associated with a drug for conjugation. These are (*1*) nonreversible covalent attachment, (*2*) reversible covalent attachment, (*3*) association or complexation via ionic or hydrophobic interactions. Thus, in some cases the conjugated drug may be attached via a stable linker, with retention of its biological activity, or be linked via degradable bonds so that the long-circulating drug and carrier complex may serve as a depot for slow release. In other cases the polymer itself may be made to be degradable or be composed of degradable smaller fragments to enhance clearance.

The mechanism by which PEG mediates protection and prolongs circulation is not entirely understood, but it is generally agreed that much of the benefit is due to steric hindrance of recognition and uptake events. Thus, at the molecular level, interactions with degrading enzymes or receptors may be reduced, while at the cellular level, capture by the reticuloendothelial system and opsonization may be blocked (114,115).

Torchilin has suggested that an important feature of PEG contributing to the benefits observed is polymer flexibility (free rotation of individual polymer units around interunit linkages). As shown in Figure 3, each PEG chain is capable of creating a "protective" conformational cloud over the point at which it is attached (116). The number of PEGs and their position contribute greatly to the degree of protection and enhanced circulating life. Although it is possible that a covalent nonreversible conjugate might maintain activity, the likelihood of steric interactions and inhibition of small-molecule activity renders the use of reversible PEG conjugates as prodrugs the more likely strategy to succeed.

Already-long-circulating polymeric drug conjugates or macromolecular aggregates have been shown to slowly accumulate in pathological sites, such as tumors with affected vasculature. Long-circulating liposomes stabilized with PEG and containing doxorubicin have been shown to accumulate preferentially in tumors, with enhanced efficacy and decreased toxicity. Ikada et al. (117) have sought to examine the relationship between PEG molecular weight and tumor accumulation. In these studies, bishydroxyl PEGs of 31,000, 50,000, 136,000, 171,000, 215,000, and 277,000 MW were used. For quantitative studies the various PEGs were radiolabeled with ^{125}I. For visualization of accumulation into tumors, the PEGs were bound to the dye RB19.

Mice bearing Meth A fibrosarcoma tumors were prepared by inoculation (0.05 mL) into the back subcutis or right footpad of female CDF mice (age 6 weeks) at 3×10^6 cells per mouse. When tumors had reached 5 mm average diameter (0.3 g) experimental studies were initiated.

Mice with or without tumors received i.v. injections of radiolabeled PEG; at various time intervals aliquots of blood were withdrawn via retroorbital plexus bleed, and radioactivity was measured. Figure 4 shows results obtained for the 31,000, 50,000, 215,000 and 277,000 MW PEGs. A clear correlation between blood retention time and molecular weight was observed. The authors reported no significant difference between tumor-bearing and non-tumor-bearing mice.

To measure tumor accumulation, tumor-bearing and normal mice were injected i.v. with radiolabeled PEGs. Blood samples as well as tissue samples (heart, lung, thymus, liver, spleen, kidney, GI tract, thyroid, and residual carcass) were taken at various time intervals, along with urine and feces. Blood was removed from tissues by washing twice with buffered saline prior to counting for radioactivity. For mice with tumor on their footpad, the foot with the tumor mass and the tumor-free foot were taken, and radioactivity levels were determined. Radioactivity from the normal foot was subtracted from that of the tumor-bearing foot to estimate tumor-selective accumulation.

For mice bearing back subcutis tumors, skins (1.5×1.5 cm^2) with and without tumor mass were taken and counted for radioactivity. Radioactivity levels from non-tumor-bearing skins were subtracted from those of tumor-bearing skins to determine tumor-selective accumulation. Skin and thigh muscle of non-tumor-bearing mice were used as controls.

In some cases tumors of different sizes were utilized to examine the effect of tumor mass on passive accumulation.

As shown in Table 1, body distribution profiles of radiolabeled PEG with different molecular weights following i.v.

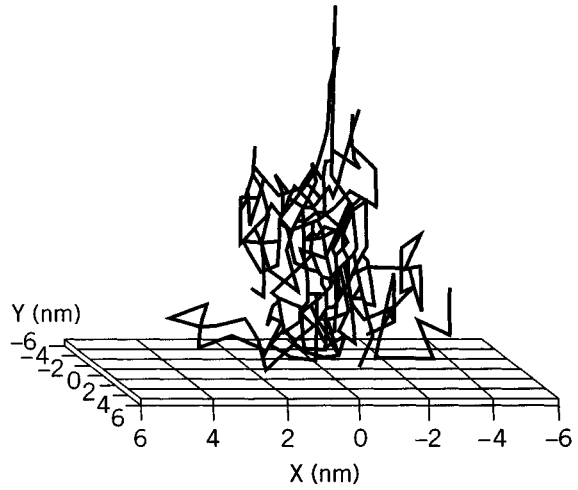


Figure 3. Computer simulation of a "conformational" cloud formation by a surface-attached polymer. Polymer molecule is conditionally assumed to consist of 20 segments, 1 nm each. This simulation was produced by random flight simulation. Unrestricted segment motion was assumed. Space restriction: $Z > 0$. Superposition of 11 random conformations. *Source:* From Ref. 116.

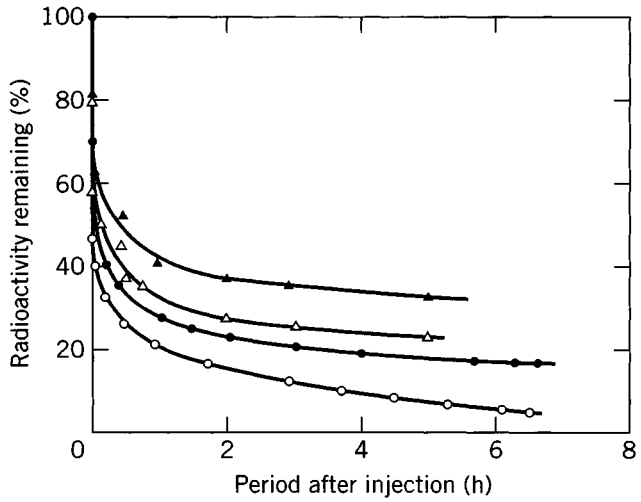


Figure 4. Time course of ^{125}I-labeled PEG concentration in the blood circulation after intravenous injection into mice with a tumor mass at their footpad. Molecular weights of PEG are (○), 31,000; (●), 50,000; (△), 215,000; (▲), 277,000. *Source:* From Ref. 117.

Table 1. Body Distribution of PEG with Different Molecular Weights 3 h after Intravenous Injection into Normal and Tumor Bearing Mice (Footpad)

		Percent radioactivity					
		Normal mouse			Tumor-bearing mouse[a]		
Organ	MW of PEG =	50,000	215,000	277,000	50,000	215,000	277,000
Blood		35.6 ± 2.83	49.0 ± 1.08	52.3 ± 2.41	40.4 ± 5.10	46.2 ± 2.11	54.4 ± 0.70
Heart		0.14 ± 0.05	0.03 ± 0.03	0.02 ± 0.02	0.24 ± 0.03	0.23 ± 0.04	0.24 ± 0.04
Lung		0.15 ± 0.01	0.11 ± 0.10	0.17 ± 0.01	0.69 ± 0.14	0.62 ± 0.10	0.87 ± 0.43
Thymus		0.05 ± 0.01	0.08 ± 0.01	0.08 ± 0.01	0.08 ± 0.01	0.11 ± 0.01	0.08 ± 0.03
Liver		3.50 ± 0.11	6.49 ± 1.54	7.11 ± 1.46	3.78 ± 0.66	4.00 ± 0.69	6.54 ± 0.33
Spleen		0.19 ± 0.03	0.15 ± 0.04	0.27 ± 0.05	0.15 ± 0.02	0.15 ± 0.03	0.28 ± 0.09
Kidney		0.57 ± 0.19	0.64 ± 0.33	0.70 ± 0.00	1.16 ± 0.30	1.32 ± 0.05	1.23 ± 0.26
GI tract		10.82 ± 2.48	15.6 ± 5.22	13.6 ± 2.43	8.29 ± 1.15	6.51 ± 0.55	8.50 ± 0.17
Thyroid gland		0.71 ± 0.24	0.87 ± 0.24	0.23 ± 0.50	0.71 ± 0.20	0.13 ± 0.05	0.42 ± 0.27
Carcass		10.8 ± 9.78	14.7 ± 9.87	8.21 ± 0.90	10.8 ± 1.20	14.5 ± 0.67	14.87 ± 0.36
Excrement		40.1 ± 3.42	36.2 ± 1.22	11.21 ± 2.10	40.2 ± 3.12	28.0 ± 2.20	10.71 ± 0.88
Tumor		—	—	—	0.23 ± 0.03	0.76 ± 0.03	0.53 ± 0.10

[a]Mice were loaded with a tumor mass at the footpad.

injection were not significantly different for tumor-bearing or tumor-free mice. Independent of PEG molecular weight, no specific affinity for any particular organ was found, with the exception that the longer the circulating life, the less accumulation in urine or feces at any given time point.

Figure 5 shows the results observed on examination of tumor accumulation as a function of PEG molecular weight. PEG was accumulated in the tumor tissue to a significantly higher extent than normal tissue, somewhat independently of molecular weight, albeit with the greatest degree of accumulation observed for the 200,000 MW PEG. Similar qualitative results were obtained for both footpad and back subcutis models. Figure 6 shows the time course of accumulation. Clearly, up to 6 h, tumor accumulation increased, followed by a gradual decrease. As shown in Figure 5, the lower molecular weight PEG accumulated to a somewhat lesser degree than the larger polymers.

Light microscopic examination of tumors after i.v. injection of dye-labeled PEGs showed tumor accumulation within the tumor vascularized areas and surrounding tissue, although not in a homogenous manner. Differences as a result of tumor size beyond 0.3 gram were not pronounced because the larger tumors contained significant levels of necrotic tissue, which did not accumulate PEG.

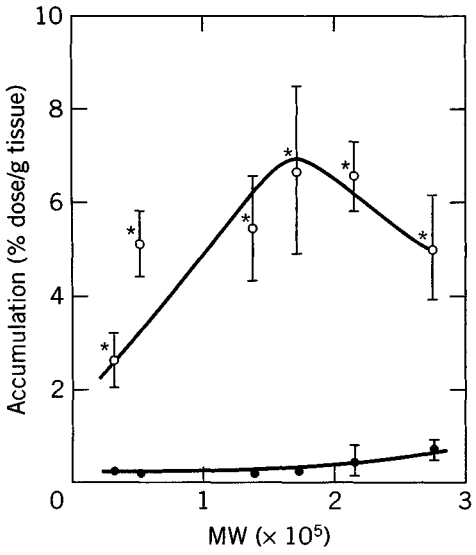


Figure 5. Effect of PEG molecular weight on PEG accumulation at the tumor tissue and the normal muscle after intravenous injection into mice with tumor mass at their footpad (3 h after injection): (○), tumor tissue; (●), normal muscle. $p > 0.05$, significant compared with corresponding accumulation at the normal muscle. *Source:* From Ref. 117.

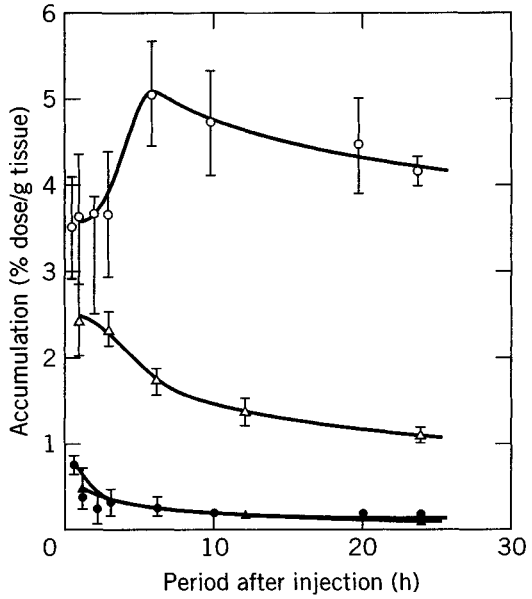


Figure 6. Time course of PEG accumulation at the tumor tissue (open symbols) and the normal muscle (closed symbols) after intravenous injection into mice with a tumor mass at their footpad. Molecular weights of PEG are (○,●), 215,000; (△,▲), 31,000. *Source:* From Ref. 117.

The authors also reported some quantitative differences between the levels and rates of tumor accumulation for the footpad and back subcutis models. The relevance of these differences to predicting outcomes of human disease is not known.

In general the authors concluded that smaller molecular weight PEGs accumulate more rapidly in tumors but are also retained for shorter periods. Higher molecular weight PEGs both accumulate more slowly and are retained for longer periods. A schematic representation of the author's view of the impact of these observations on the design of drug delivery systems is shown in Figure 7.

For those designing prodrugs, where release of active molecules from polymer conjugates occurs via nonselective release chemistries, consideration of the kinetics of accumulation and release are of paramount importance.

PEG-Paclitaxel-2′-Glycinate. Many of the cytotoxic compounds used as cancer chemotherapeutics are poorly soluble in aqueous conditions. In addition to the preferred tumor accumulation properties of PEG already noted, increased solubility of cytotoxic drug conjugates can also be achieved.

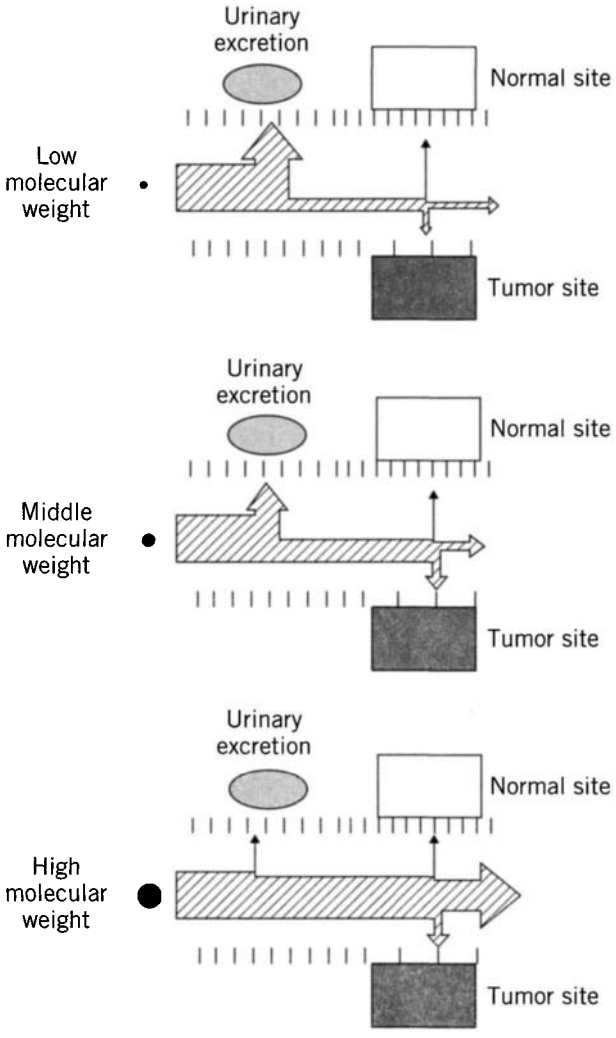


Figure 7. Schematic representation of models for PEG accumulation of low, middle, and higher molecular weights at tumor and normal tissues after intravenous injection. *Source*: From Ref. 117.

Paclitaxel isolated from the bark of the western yew tree (*Taxus brevifolia*) as well as other taxanes isolated from the needle leaves of the same tree have been developed as potent antitumor agents for the treatment of ovarian and breast cancer (118). The antitumor activity of the taxanes stems from their ability to promote tubulin polymerization in rapidly dividing cells such that stable microtubules are produced, cell division is blocked, and cell viability is compromised.

Due to limitations of solubility, taxanes are administered in vehicles containing Cremophor EL, ethanol, or detergents such as Tween 80. Corticosteroids and H_1 and H_2 histamine receptor antagonists may be coprescribed in order to limit allergic reactions to the formulation vehicle (119).

Considerable effort has focused on the development of more soluble analogues of paclitaxel and other taxanes. Non-PEG–amino acid paclitaxel prodrugs have been prepared and described in the literature (120). Although good aqueous solubility was reported (10 mg/mL), an in vitro half-life of <30 min in buffer at pH 7.4, and less than 5 min in human plasma were also observed.

Greenwald et al. (121) have sought to combine the benefits of PEG on drug solubility and long circulation life with enhanced tumor accumulation, by preparing PEG-paclitaxel analogues. In an attempt to maximize safety and efficacy, a prodrug strategy was also utilized. PEG of molecular weight 40,000 was used in these studies. A schematic of the synthesis of PEG-paclitaxel-2′-glycinate is shown in Figure 8.

For cytotoxicity assays and IC_{50} determination or for syngeneic tumor burden studies a P388/0 cell line was used as described in Ref. 122. For solid tumor (human colon adenocarcinoma HT-29, human ovarian adenocarcinoma SKOV-3, and human lung A549) studies, female nu/nu mice (18–24 g) were inoculated subcutaneously at the left flank with 1×10^6 tumor cells. Animals bearing 100-mm^3 tumors were treated as shown in Table 3, and tumor growth inhibition was determined as in Ref. 121. Treatment and control groups were measured when control tumor median volume reached 800–1,100 mm^3.

In vitro cytotoxicity and hydrolysis rates for the 40,000 MW PEG conjugates made are shown in Table 2. The authors report that for the P388/0-inoculated animals, in comparison with paclitaxel controls, an increased life span of 21.8 days was observed for PEG-paclitaxel-2′glycinate, as opposed to 19 days for native paclitaxel. Further, at a total dose of 100 mg/kg many of the animals in the paclitaxel control group died due to drug toxicity, whereas in the PEG-paclitaxel-2′-glycinate group, life spans were increased by 82%, and some animals were cured of tumor burden.

Results of treatment of the different human solid tumor xenografts are shown in Table 3. For all three models the authors report an increase in tumor growth inhibition of 10%.

PEG-Camptothecin. Like paclitaxel, camptothecin is a natural product extracted from trees. In this case *Camptotheca acuminata*. Activity against a number of human

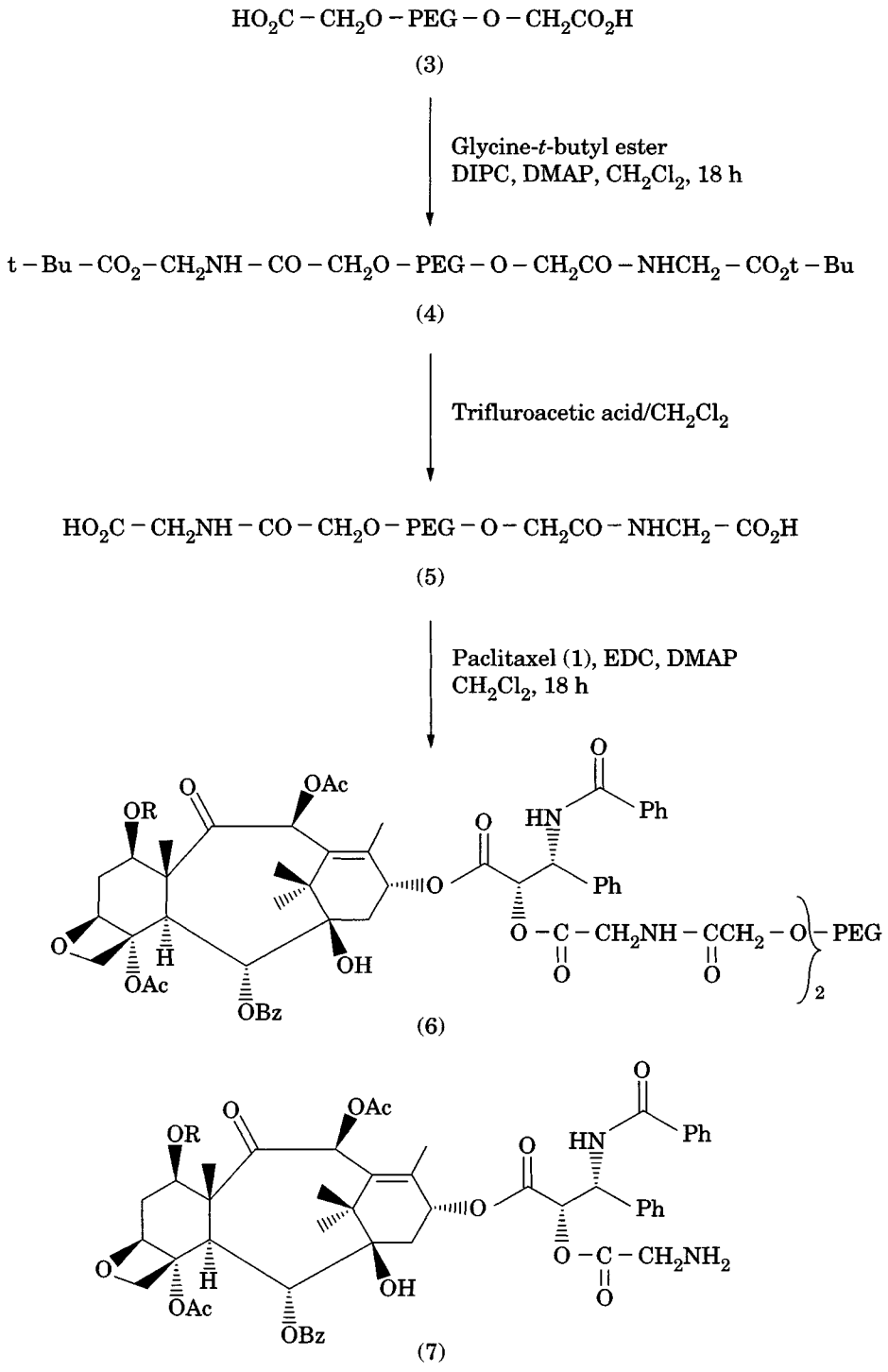


Figure 8. Schematic of PEG-gly-paclitaxel synthesis as described by Pendri et al. (121).

Table 2. In Vivo Cytotoxicity and Rates of Hydrolysis for PEG-40kDa-Conjugated Paclitaxel Derivatives

Compound	Linker	IC50 (nM)[a] P388/0	$t_{1/2}$ (h)[a] PBS (pH 7.4)	$t_{1/2}$ (h)[a] Rat plasma
Paclitaxel (1)	–	6	–	–
PEG-paclitaxel (2)	-O-CO-CH_2-O-PEG	10	5.5	0.4
PEG-gly-paclitaxel (6)	-O-CO-CH_2-NHCO-CH_2OPEG	14	7.0	0.4

Source: From Ref. 121.
[a]All experiments were done in duplicate. Standard deviation of measurements: ± 10%.

Table 3. Antitumor Activity of PEG-Conjugated Gly-Paclitaxel against Subcutaneous Human Tumor Xenografts in Nude Mice

Tumor type	Treatment schedule[a]	Total Dose (mg/kg)[b]	% T/C[c]
HT-29 (colon)	Three cycles of daily × five at intervals of 14 days, i.p.	225	11.3*
A549 (lung)	Daily × 5 for 2 weeks, i.p.	150	9.5*
SKOV3 (ovarian)	2 × week for 4 weeks, i.v.	200	7.4*

Source: From Ref. 121.
[a]Treatments initiated when tumor volumes reached approximately 100 mm^3.
[b]Based on paclitaxel content.
[c]Treatment and control groups were measured when the control group's median tumor volume reached approximately 800–1,100 mm^3.
*$p < 0.01$.

tumor xenograft models has been shown including lung, ovarian, breast, stomach, and pancreatic cancers (122). Also like paclitaxel, camptothecin is poorly soluble in water. Unlike paclitaxel, camptothecin functions as a topoisomerase inhibitor. Topoisomerase is a DNA repair enzyme necessary for cell replication and growth. When inhibited, topoisomerase-induced single-strand breaks cannot be religated, and eventual double-strand DNA breaks occur, triggering apoptosis.

Considerable efforts have focused on the preparation of more soluble analogues as well as prodrug forms of camptothecin. Several prodrug forms are inactive until processed by plasma enzymes or tumor-associated metabolism events. Camptothecin analogues topotecan and ironotecan have been FDA approved for the treatment of some solid tumors.

As described earlier for paclitaxel, Greenwald and coworkers have sought to improve camptothecin performance by conjugation to PEG (C.D. Conover et al., personal communication). Figure 9 illustrates an example of a disubstituted camptothecin conjugated to a 40,000 MW PEG prepared by the authors.

In attempting to prepare PEG conjugates with predictable rates of release, the linkers shown in Table 4 were prepared and characterized. Release kinetic "half-life" ranged from 2 to >24 h for the linkers evaluated. The authors suggest that the ability to predict release, as drug accumulates in tumors, is likely to be more effective than requiring uptake into cells prior to activation of a prodrug by a metabolic event.

Still, as shown in Table 5 in a P388/0 syngeneic-tumor-bearing mouse test, the PEG camptothecins were similar to or slightly less effective than native camptothecin. The authors report the camptothecin-di-20-*O*-ester of PEG40000 glycine as having been selected for further development.

To evaluate accumulation of PEG camptothecin in solid tumor models, female nu/nu mice were inoculated with human colon (HT-29) tumor cells, and the tumors were allowed to grow to 200 mm^3 in size. Mice then received radiolabeled PEG camptothecin or radiolabeled camptothecin. All injections were i.v. via the tail vein. At various time points animals were bled and tissues removed for analysis. Lung, heart, spleen, kidney, muscle, tumor, and blood were collected, weighed, homogenized, and counted for radioactivity. Results were calculated as percent injected dose (%ID) per gram of tissue after correction for blood pool (C.D. Conover et al., personal communication) and are shown in Table 6. Clearly, as predicted by Ikada et al. (117) the PEG-conjugated camptothecin showed a greater degree of tumor accumulation than did its non-PEGylated counterpart.

A treatment comparison of PEG camptothecin to non-PEGylated camptothecin and the camptothecin analogue Topotecan as well as 5-fluorouracil (5-FU) is shown in Figure 10. The authors report that in these studies, at equivalent doses, PEG-camptothecin was more effective in delaying tumor growth than any of the other molecules tested. What is proposed is that the prolonged circulating lifetime of the PEG conjugate allows for a greater degree of tumor accumulation, followed by release of active cytotoxic drug and achievement of higher local concentrations.

PEG-5-Fluorouracil. Nichifor et al. (123) have described polymeric conjugates of 5-FU linked via oligopeptide chains and a glycine ethyl ester bond. PEG, dextran, and poly(5*N*-(2-hydroxyethyl)-L-glutamine polymers were used. Oligopeptide bonds were designed to be sensitive to tumor associated enzymes such as collagenase, cathepsin

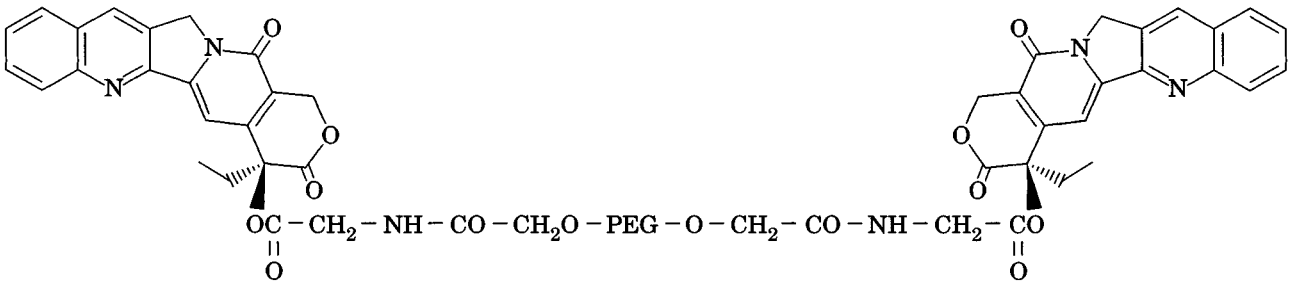


Figure 9. Chemical structure of PEG-camptothecin (camptothecin-di-20-*O*-ester of PEG glycine, 40,000 MW). *Source:* C.D. Conover et al., personal communication.

Table 4. Rates of Hydrolysis and IC-50 Values for Various PEG-Camptothecin Derivatives as Described by Conover et al. (124)

Compound	Linker	IC50 (nM)[a]	$t_{1/2}$ (h)[b] PBS (pH 7.4)	$t_{1/2}$ (h)[b] Rat plasma
1	—	7	—	—
3	-O-CO-CH_2-O-PEG	15	27	2
10	-O-CO-CH_2-O-CH_2-CO-NH-PEG	16	5.5	0.8
11	-O-CO-CH_2-O-CH_2-CO-N(CH_3)-PEG	21	27	3
16	-O-CO-CH_2-O-CO-NH-PEG	7	0.2	ND
17	-O-CO-CH_2-O-CO-N(CH_3)-PEG	18	28	5
24	-O-CO-CH_2-NH-CO-CH_2-O-PEG	12	40	6
25	-O-CO-CH_2-N(CH_3)-CO-CH_2-O-PEG	15	97	10
28	-O-CO-CH_2-NH-PEG	24	12	3
29	-O-CO-CH_2-N(CH_3)-PEG	42	102	>24

Note: ND, not determined.
[a]All experiments were done in duplicate. Standard deviation of measurements: ± 10%.
[b]These results more appropriately represent the half-lives by disappearance of the transport form.

Table 5. Activity of Various PEG-Camptothecin Analogues Measured against P388 Murine Leukemia In Vivo

Test compound	Linker	Total dose[a] (mg/kg)	Mean time to death (days)[b]	% ILS[c]	Survivors on day 40
Control	—	—	13.0	—	0/10
1	—	16	38.0*	192%	7/10
3	-O-CO-CH_2-O-PEG	16	38.0*	192%	9/10
10	-O-CO-CH_2-O-CH_2-CO-NH-PEG	16	17.4*	34%	4/10
11	-O-CO-CH_2-O-CH_2-CO-N(CH_3)-PEG	16	31.6*,**	143%	6/10
17	-O-CO-CH_2-O-CO-N(CH_3)-PEG	16	23.4	80%	0/10
24	-O-CO-CH_2-NH-CO-PEG	16	35.0*	169%	8/10
25	-O-CO-CH_2-N(CH_3)-CO-PEG	16	19.3*,**	48%	0/10
28	-O-CO-CH_2-NH-PEG	16	30.6*	135%	0/10
29	-O-CO-CH_2-N(CH_3)-PEG	16	21.4*,**	65%	0/10

Source: C.D. Conover et al., personal communication.
[a]Equivalent dose of camptothecin, mice dosed days 1–5.
[b]Kaplan–Meier estimates with survivors censored.
[c]Increased life span (ILS) is (T/C − 1) × 100.
*Significant, $p < 0.001$, compared to control (untreated).
**Significant, $p < 0.001$, compared to compound t.
In vivo efficacy study of the water soluble camptothecin derivatives using the P388/0 murine leukemia model. Compound 1 or prodrug derivatives were given daily [intraperitoneal(ip) × 5], 24 h following an injection of P388/0 cells into the abdominal cavity with survival monitored for 40 days.

Table 6. Percent Injected Dose per Gram of PEG-Camptothecin and Camptothecin (CPT) at the Times Shown after Intravenous Injection in Athymic Mice Bearing Human Colon Adenocarcinoma Xenografts

	PEG-β-CPT						CPT					
Specimen	0.8 h	2 h	6 h	24 h	48 h	72 h	0.8 h	2 h	6 h	24 h	48 h	72 h
Tumor	0.47	3.34	3.34	3.70	2.35	1.63	0.33	0.11	0.11	0.10	0.05	0.05
Blood	27.90	19.17	10.91	4.41	1.94	0.73	1.21	0.27	0.08	0.09	0.07	0.07
Liver	1.62	2.02	2.00	2.32	1.89	0.79	4.32	0.54	0.29	0.14	0.07	0.07
Kidney	0.01	0.02	0.04	0.16	0.21	0.22	10.32	0.32	0.10	0.07	0.07	0.03
Spleen	0.01	0.03	0.03	0.07	0.31	0.49	2.73	0.15	0.26	0.14	0.03	0.03
Lung	3.68	2.33	4.00	1.95	0.24	0.33	3.09	0.64	0.19	0.12	0.04	0.05
Heart	2.13	1.87	1.74	1.13	0.88	0.41	1.32	0.17	0.12	0.09	0.09	0.03
Muscle	0.58	1.11	1.50	0.91	0.96	0.44	0.71	0.12	0.09	0.09	0.03	0.03

Source: C.D. Conover et al., personal communication.
Note: Each value is the average from four mice.

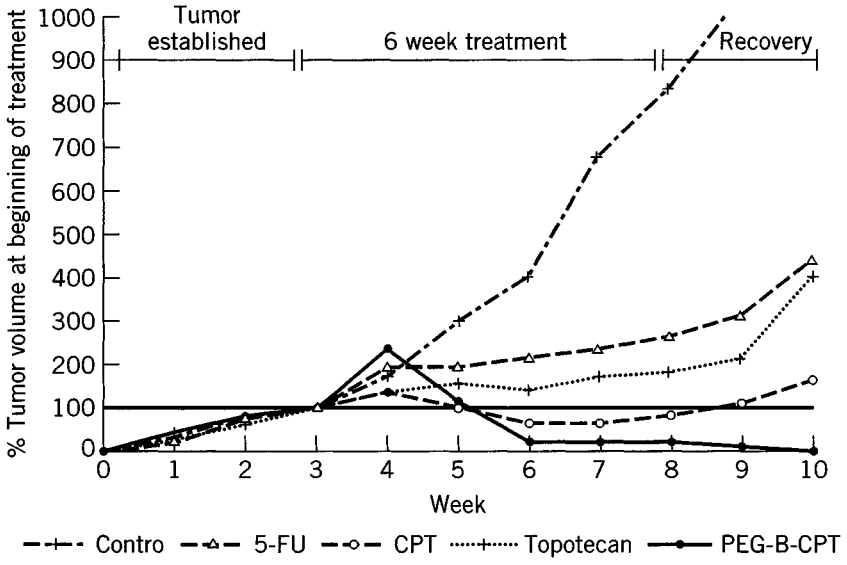


Figure 10. Growth curve of human colon adenocarcinoma (HT-29) tumor xenografts treated with 5-FU, camptothecin, topotecan, or PEG-camptothecin. All compounds were given over a 5-week period, with camptothecin, topotecan, and PEG camptothecin given five times per week (2.5 mg/kg per day) and 5-FU twice per week (80 mg/kg per day). PEG-camptothecin doses were based upon absolute equivalents of camptothecin. *Source:* C.D. Conover et al., personal communication.

B, and cathepsin D. The rationale of the authors was that polymer-promoted accumulated drug would be released under conditions selective for the tumor microenvironment. Preliminary in vitro studies suggest that, of the different polymers tested, rates of release were greatest for the PEG formulations.

PEG-Hemoglobin. Since the 1950s it has been known that as tumors grow, areas of hypoxia appear in direct correlation to distance from the tumor vascular tree. Across these gradients of hypoxia are also metabolic gradients and areas of necrotic tissue and tumor stroma. For many of the more common cytotoxic agents, and certainly for the use of radiation treatments, sufficient tumor oxygenation is a prerequisite for efficacious activity. Indeed, hypoxic tumor cells are known to be substantially more resistant to radiation treatment than their oxygenated counter parts (124,125).

Of the newly diagnosed patients each year in the United States nearly 60% will undergo radiation therapy. Tumor types already implicated or shown to contain substantial hypoxic regions and their approximated incidence are shown in Table 7. The extent of tumor hypoxia varies according to histological type as well as tumor size and stage of disease.

Table 7. Estimated Annual U.S. Incidence of Solid Tumor Types That May Contain Hypoxic and Therefore Radiation-Therapy-Resistant Regions

Tumor type	U.S. incidence
Breast	183,000
Lung	172,000
Colorectal	149,000
Prostate	200,000
Head and neck	51,000
Bladder	51,000
Brain metastases	30,000
Brain	17,000
Cervical, invasive	15,000
Fibrous histiocytoma	8,000

Attempts to sensitize tumors to radiation treatment have included the use of sensitizing molecules that mimic oxygen as well as the use of calcium channel blockers and other molecules or conditions such as hyperthermia designed to increase tumor blood flow, or the ability of hemoglobin to off-load oxygen. Attempts to improve tumor oxygenation directly have included use of hyperbaric oxygen chambers and perfluorochemical (PFC) emulsions. PFCs have been characterized as having a high oxygen carrying capacity in solution. While the initial purpose of PFC development was for the replacement of red blood cells in transfusion medicine, Teicher et al. (126–128) have shown that these agents can be used to deliver oxygen to a variety of hypoxic tumors, with resultant sensitization to radiation treatment.

Although it is clear that PFCs can indeed be used to sensitize tumors in experimental rodent models, clinical development has been hampered by the need for inspiration of 95% oxygen 5% carbon dioxide, as well as a variety of adverse reactions including lower back pain and cytopenia. It is possible that newer formulations of PFC may reemerge for further study.

Hemoglobin solutions, like PFC, have also been explored as replacements for red blood cells in transfusion or trauma medicine. An advantage of these solutions over PFCs is that they do not require inspiration of 95% oxygen 5% carbon dioxide; room air suffices. Side effects with some preparations (Baxter Healthcare), however, have been severe enough to slow clinical progress; with others (Northfield Laboratories, Hemosol, Enzon), esophageal spasm and other GI upsets or mild elevations in blood pressure only have been reported (129).

PEG-hemoglobin has been prepared by the conjugation of activated PEG to the amino groups of hemoglobin. Both APEX Biosciences and Enzon (129) have reported progress in this area. APEX has based its technology upon the use of human purified hemoglobin (hHb), but Enzon has used

purified preparations of bovine hemoglobin (bHb) for its solutions. An advantage of bovine hemoglobin over human is that the bovine hemoglobin tetramer is inherently more stable than the human and does not require covalent cross-linking to prevent dissociation into higher-oxygen-affinity dimers. Both companies use PEG strands of 5,000 molecular weight, although the Enzon product is PEGylated to a greater extent than the APEX product (9–15 PEGs versus 3–6 PEGs, respectively).

In a variety of animal models PEG-bHb has been shown to deliver oxygen in rodents and pigs from which 80–85% of the total blood volume had been replaced with hemoglobin solution. Using a 6 g% solution of PEG-bHb and measuring tissue oxygenation using phosphorescence quenching methods or following physiological markers, full oxygenation of liver, kidney, spleen, muscle, intestine, and brain could be shown, even under extreme conditions of transfusion or trauma (130).

To explore use of PEG-bHb for oxygenation of tumors, human or syngeneic tumors were implanted into rats and allowed to grow, and tumor oxygenation was followed by phosphorescence quenching methods before and after PEG-bHb i.v. administration via tail vein infusion. As shown in Table 8, oxygenation of hypoxic tumors increased 100–300% after administration of 6–15 mL/kg of a 6 g% solution of PEG-bHb (131). The authors reported a time course to maximum oxygenation levels of 2–4 h. It is possible that the delay in maximal oxygenation may reflect tumor accumulation of PEG-bHb and a locally increased concentration of the oxygen carrier.

When rats bearing osteogenic sarcoma tumor implants were treated with 6 mL/kg or 15 mL/kg PEG-bHb (6 g%) and low dose radiation, a greater than 80% complete response rate was observed (131) as compared with lactated Ringer's plus radiation or lactated Ringer's only controls (Fig. 11).

For human colon carcinoma implants, infusion with 15 mL/kg PEG-bHb (6 g%) and treatment with radiation, substantial growth delay was observed over no treatment or radiation treatment only controls. PEG-bHb as a sensitizer to radiation therapy in conjunction with breathing of 100% oxygen is now in phase Ib clinical trials (131). In these studies PEG-bHb is given weekly for up to three infusions, concomitant with daily external radiation. No dose-limiting toxicities have been reported.

In addition to resistance to radiation, hypoxic tumor cells have also been credited with resistance to a number of chemotherapeutic treatments. Teicher et al. (132) have examined the ability of PEG-bHb to reverse tumor-associated hypoxia, with sensitization to a variety of chemotherapeutic agents. It had been demonstrated earlier that use of PFCs could enhance the cytotoxic activity of anticancer alkylating agents such as *cis*-diamminedichloroplatinum(II) (CDDP) (133), carboplatin, cyclophosphamide (134) *N,N',N''* triethylenethiophosphoramide, 1,3-bis(2-chloroethyl)-1-nitrosourea, and L-phenylalanine mustard (135–138).

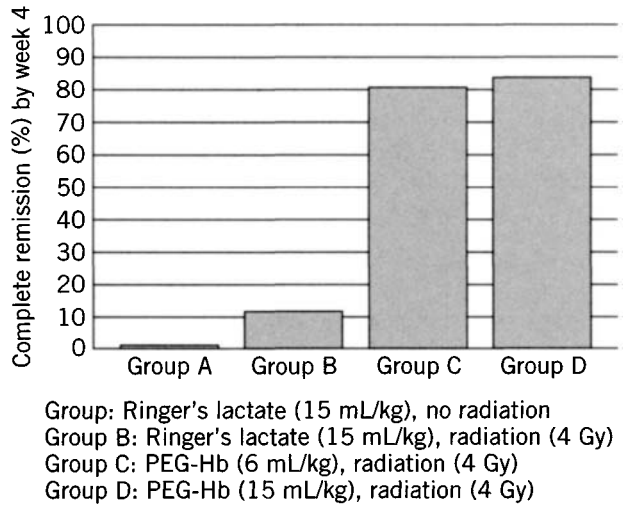


Figure 11. Rats bearing syngeneic osteogenic sarcoma tumors (approximately 1 cm^3) were treated with PEG-bHb, at the doses shown, and a single whole-body dose of radiation (4 Gy). Alternatively rats received lactated Ringer's, at the doses shown, with or without radiation treatment.

In the PEG-bHb studies, rat mammary adenosarcoma 13672 tumors were used. These carcinogen induced tumor cells can metastasize to the lungs and abdominal organs. The tumor is composed of epithelial cells and acini and can grow to 100 mm^3, in size in approximately 2 weeks postimplantation. EMT-6 murine mammary carcinoma cell and tumors (132) were also studied. In both cases 2×10^6 cells were inoculated into the hindlimbs of rats or mice, respectively. To measure tumor oxygenation, a pO_2 histograph (Eppendorf, Inc., Hamburg, Germany) was used. The needle microelectrode was calibrated in aqueous solution saturated with air or 100% nitrogen.

The test animals were anesthetized and placed upon a heating pad, tumor sizes were estimated with calipers, and a small area of the skin covering the tumor mass was removed. A 20-gauge needle was used to perforate the tumor, and the electrode was positioned in the perforation for measurements as described in Ref. 132.

Table 8. Measurement of Tumor Oxygen Tension before and after Administration of 15 mL/kg 6 g% PEG-Hemoglobin

Tumors examined	Pretreatment O_2 tension (mm Hg)	Posttreatment O_2 tension (mm Hg)	% increase
Rat osteogenic sarcoma	3.7 ± 0.2	15.4 ± 0.4	316%
Rat glioma	4.7 ± 0.6	11.2 ± 2.7	138%
Human prostate	5.2 ± 1.3	10.4 ± 1.8	100%
Human ovarian	15.0 ± 1.5	41.2 ± 5.6	175%

Note: Oxygen measurements were by phosphoresence quenching methods 2–4 h after Intravenous Infusion.

To measure tumor growth delay, 2×10^6 EMT-6 cells were inoculated into the hindlimbs of mice. At 100 mm^3 tumor size (7 days postimplantation) cytotoxic therapy was initiated. Cyclophosphamide (150 mg/kg i.p.) or BCNU (15 mg/kg i.p.) on days 7, 9, and 11, 5-FU (30 mg/kg i.p.) and adriamycin (1.75 mg/kg i.p.) were given days 7 through 11. Taxol (24, 36, or 48 mg/kg i.v.) was given days 7 through 11. Animals received drug alone or in conjunction with PEG-bHb (6 g%, 6 mL/kg) and breathed room air, 28%, or 95% oxygen for 6 h after each drug injection. Tumor volumes were monitored and growth delay calculated as time to reach 500 mm^3 relative to untreated controls (132).

To measure tumor cell survival, 13,762 tumor-bearing rats were treated with a single dose of cyclophosphamide (250 mg/kg i.p.), melphalan (20 mg/kg i.p.), taxol (10mg/kg i.v.), or CDDP (8 mg/kg i.p.). EMT-6-bearing mice were treated with cyclophosphamide (100, 300, or 500 mg/kg i.p.), BCNU (50, 100, or 200 mg/kg i.p.), adriamycin (10, 25, or 50 mg/kg i.p.), or taxol (25, 50, or 75 mg/kg i.v.) alone or in conjunction with PEG-bHb (6 g%, 6 mL/kg i.v. just before chemotherapy). Twenty four hours later animals were killed and tumors excised and minced under sterile conditions in a laminar flow hood. A pool of four tumors for each treatment group was washed and treated with collagenase and DNAse prior to filtration and plating for colony-forming assay as described in Ref. 132.

To examine bone marrow toxicity, a pool of femur bone marrow from mice treated as just described was obtained by flushing with a 23-gauge needle. Colony-forming unit assays were carried out as described in Ref. 134.

To examine metastases, animals treated as just described were necropsied on day 20 after tumor implantation, and external metastatic nodules were counted manually and scored as greater than or equal to 3 mm in diameter (132).

As shown in Tables 9 and 10, substantial growth delays were also observed for the combination of PEG-bHb with chemotherapeutic agents over drug alone. For cyclophosphamide a significant decrease in the numbers of lung metastases was also noted. In Figure 12 the authors describe increased tumor cytotoxic effects as having occurred with little or no increase in bone marrow toxicity.

The Case for Polyethylene Glycol. Liposomes stabilized with PEG and containing doxorubicin have gone far in proving the utility of passively targeted anticancer agents. However not all chemotherapeutic anticancer agents lend themselves to fascile formulation in liposomes, stabilized or otherwise.

Although conjugation of cytotoxic agents to SMANCS, HPMA, and other carriers has proceeded to clinical investigation and approvals, little is known about the perfor-

Table 9. Growth Delay of the Murine-6 Mammary Carcinoma and Number of Lung Metastases on Day 20 Produced by Anticancer Chemotherapeutic Alone or in Combination with Administration of PEG-bHb

	Tumor growth delay (days)[a] + PEG-Hb (6 mL/kg)			Number of lung metastases + PEG-Hb (6 mL/kg)		
Treatment group	Alone	Air	95% O_2	Alone	Air	95% O_2
Control			16 ± 3			
Cyclophosphamide (150 mg/kg) days 7, 9, 11	6.2 ± 0.3	7.8 ± 0.5	11.9 ± 0.8	7 ± 3	4 ± 1	2 ± 1
Adriamycin (1.75 mg/kg) days 7–11	4.5 ± 0.3	8.3 ± 0.6	14.9 ± 1.1	13 ± 2	10 ± 1	9 ± 2
5-Fluorouracil (30 mg/kg) days 7, 9, 11	3.1 ± 0.3	7.5 ± 0.5	11.1 ± 0.9	12 ± 2	10 ± 3	9 ± 1
BCNU (15 mg/kg) 5.1 ± 0.3 days 7, 9, 11	6.2 ± 0.4	11.7 ± 0.8	14 ± 2	12 ± 2	9 ± 2	

Source: From Ref. 132.

[a]Mean days ± S.E.M. for treated tumors to reach 500 mm^3 compared with untreated controls. Control tumors reached 500 mm^3 in 124 ± 1.2 days. The anticancer drugs were administered by intraperitoneal injection. PEG-hemoglobin (6 ml/kg) was administered by intravenous injection just prior to each drug injection. 95% oxygen (carbogen) breathing was maintained for 6 h after each drug injection. Each treatment group had five animals, and the experiment was repeated three times, therefore the number of animals per point was 15 (n = 15).

Table 10. Growth Delay of the Murine-6 Mammary Carcinoma and Number of Lung Metastases on Day 20 Produced by Taxol Alone or in Combination with Administration of PEG-bHb

	Tumor growth delay (days)[a] + PEG-Hb (6 ml/kg)				Number of lung metastases + PEG-Hb (6 ml/kg)			
Treatment group	Alone	Air	28% O_2	95% O_2	Alone	Air	28% O_2	95% O_2
Control					16 ± 3			
Taxol (24 mg/kg) days 7–11	2.9 ± 0.3	3.9 ± 0.3	4.4 ± 0.3	6.7 ± 0.5	14 ± 2	10 ± 2	10 ± 2	9.5 ± 2
Taxol (36 mg/kg) days 7–11	4.9 ± 0.4	5.4 ± 0.5	6.1 ± 0.4	6.6 ± 0.5	13 ± 2	10 ± 2	9 ± 2	7.5 ± 2
Taxol (48 mg/kg) days 7–11	5.4 ± 0.5	7.0 ± 0.5	8.0 ± 0.6	9.7 ± 0.6	12 ± 2	8.5 ± 2	6.5 ± 2	4.5 ± 1

Source: From Ref. 132.

[a]Mean days ± S.E.M. for treated tumors to reach 500 mm3 compared with untreated controls. Control tumors reached 500 mm3 in 12.4 ± 1.2 days. The taxol was administered by intravenous injection. PEG-hemoglobin (6 ml/kg) was administered by intravenous injection just prior to each taxol injection. 28% oxygen or 95% oxygen (carbogen) breathing was maintained for 6 h after each drug injection. Each treatment group had five animals and the experiment was repeated three times, therefore the number of animals per point was 15 (n = 15).

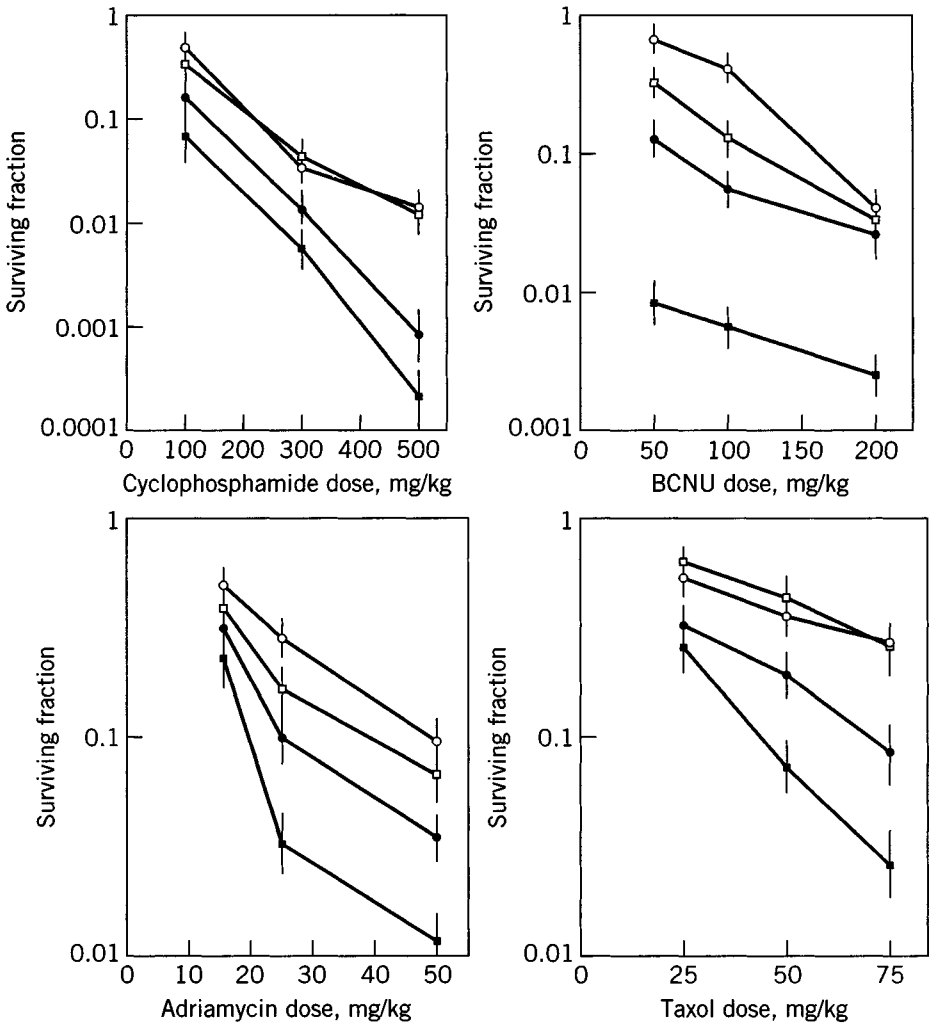


Figure 12. Survival of EMT-6 tumor cells (solid symbols) from tumors treated in vivo, and bone marrow CFU-GM (open symbols) from the same animals after treatment with the drugs and dosages shown alone (○, ●) or with PEG bHb (6 mL/kg, □, ■). Results are the means of three independent determinations, bars are S.E.M.

mance characteristics of small molecules directly linked to PEG, despite considerable experience with proteins.

As described earlier, conjugation to PEG of small-molecule anticancer chemotherapeutics has now been achieved. In addition to promotion of tumor accumulation, as predicted on the basis of molecular weight and tumor flow dynamics, increases in drug solubility have been reported. For compounds such as paclitaxel, increases in solubility are sufficient to abrogate the need for excipients such as Cremophor EL or ethanol.

PEG has been shown to be linkable by covalent reversible bonds and nonreversible covalent bonds to proteins and small-molecule anticancer agents. In some instances demonstration of tumor-selective enzymatic cleavage and release has been proposed and demonstrated. In others less-selective release via blood esterase has been shown.

The further use of PEG for exploration of passive tumor targeting is warranted by the long history of PEG usage as a formulation agent for pharmaceuticals and more than a decade of experience in the clinic with PEG-conjugated proteins for chronic treatment. The facility of PEG chemistry together with available pharmaceutical grade polymer also contributes greatly to the desirability of further exploration of this approach.

BIBLIOGRAPHY

1. T. Beardsley, *Sci. Am.* **270**, 130–138 (1994).
2. P.C. Nowell, *Science* **194**, 23–28 (1976).
3. G.H. Heppner, *Cancer Res.* **44**, 2259–2265 (1984).
4. A.V. Kabanov and V.Y. Alakhov, *J. Controlled Release* **28**, 15–35 (1994).
5. J.N. Lowder et al., *Blood* **69**, 199–210 (1987).
6. E.S. Vitetta et al., *Cancer Res.* **15**, 4052–4058 (1991).
7. H.F. Dvorak, J.A. Nagy, and A.M. Dvorak, *Cancer Cells* **3**, 77–85 (1991).
8. L.T. Baxter and R.K. Jain, *Microvasc. Res.* **41**, 5–23 (1991).
9. F.J. Burrows, Y. Watanabe, and P.E. Thorpe, *Cancer Res.* **52**, 5954–5962 (1992).
10. H. Sands, *Antibody Immunoconjugates Immunoradiopharm.* **1**, 213–226 (1988).
11. A.A. Epenetos et al., *Cancer Res.* **46**, 3183–3191 (1986).
12. R.K. Jain, *Sci. Am.* **271**, 58–65 (1994).
13. M. Juweid et al., *Cancer Res.* **52**, 5144–5153 (1992).
14. C. Marks and J.D. Marks, *N. Engl. J. Med.* **335**, 730–733 (1996).
15. J.D. Marks et al., *J. Mol. Biol.* **222**, 581–597 (1991).

16. X. Cai and A. Garen, *Proc. Natl. Acad. Sci. U.S.A.* **93**, 6280–6285 (1996).
17. R. Schier et al., *J. Mol. Biol.* **255**, 28–43 (1996).
18. J. Denekamp, *Prog. Appl. Microcirc.* **4**, 28–38 (1984).
19. E.A. Jaffe, *Biology of Endothelial Cells*, Martinus Nijhoff, Boston, 1984.
20. P.E. Thorpe and E.J. Derbyshire, *J. Controlled Release* **48**, 277–288 (1997).
21. A. Gougos and M. Latarte, *J. Biol. Chem.* **265**, 8361–8364 (1990).
22. J.R. Westphal et al., *J. Invest. Dermatol.* **100**, 27–34 (1993).
23. A. Gougos and M. Letarte, *J. Immunol.* **141**, 1925–1933 (1988).
24. P.J. O'Connell et al., *Clin. Exp. Immunol.* **90**, 154–159 (1992).
25. H.J. Buhring et al., *Leukemia* **5**, 841–847 (1991).
26. W.J. Reftig et al., *Proc. Natl. Acad. Sci. U.S.A.* **89**, 10832–10836 (1992).
27. J.M. Wang et al., *Int. J. Cancer* **54**, 363–370 (1993).
28. B. Carnemolla et al., *J. Cell Biol.* **108**, 1139–1148 (1989).
29. G. Molema, L.F.M. De Leij, and D.K.F. Meijer, *Pharm. Res.* **14**, 2–10 (1997).
30. A.L. Epstein et al., in V.P. Torchilin, ed., *Handbook of Targeted Delivery of Imaging Agents*, CRC Press, Boca Raton, Fla., 1995, pp. 260–288.
31. L.A. Khawli and A.L. Epstein, *O. J. Nucl. Med.* **41**, 25–35 (1997).
32. R.H. Jain, *Cancer Res.* **47**, 3039–3051 (1987).
33. H.F. Dvorak, J.A. Nagy, J.T. Dvorak, and A.M. Dvorak, *Am. J. Pathol.* **133**, 95–109 (1988).
34. A. Gabizin and D. Papahadjopoulos, *Proc. Natl. Acad. Sci. U.S.A.* **85**, 6949–6953 (1988).
35. D. Liu, A. Mori, and L. Huang, *Biochim. Biophys. Acta* **1104**, 95–101 (1992).
36. H. Maeda and Y. Matsumura, *Crit. Rev. Ther. Drug Carrier Syst.* **6**, 193–210 (1989).
37. L.W. Seymour, *Crit. Rev. Ther. Drug Carrier Syst.* **9**, 135–187 (1992).
38. C. Sung, R.J. Youle, and R.L. Dedrick, *Cancer Res.* **50**, 7382–7392 (1990).
39. K. Uchiyama et al., *Int. J. Pharm.* **121**, 195–203 (1995).
40. J. Folkman, in P.M. Mendelsohn, M.A.P. Howley, and L.A. Liotta, eds., *The Molecular Basis of Cancer*, Saunders, Philadelphia, 1995.
41. R.K. Jain, *Cancer Res.* **48**, 2641–2658 (1988).
42. L.T. Baxter and R.K. Jain, *Microvasc. Res.* **40**, 246–263 (1990).
43. J.W. Baish et al., *Microvasc. Res.* **51**, 327–346 (1996).
44. Y. Gazit et al., *Phys. Rev. Lett.* **75**, 2428–2431 (1995).
45. J.R. Less, T.C. Skalak, E.M. Sevick, and R.K. Jain, *Cancer Res.* **51**, 265–273 (1991).
46. M. Leunig et al., *Cancer Res.* **52**, 6553–6560 (1992).
47. F. Yuan et al., *Cancer Res.* **54**, 4564–4568 (1994).
48. E.M. Sevick and R.K. Jain, *Cancer Res.* **49**, 3506–3512 (1989).
49. P.A. Netti et al., *Microvasc. Res.* **52**, 27–46 (1996).
50. E.M. Sevick and R.K. Jain, *Cancer Res.* **49**, 3513–3519 (1989).
51. E.M. Sevick and R.K. Jain, *Cancer Res.* **51**, 2727–2730 (1991).
52. B. Endrich, H.S. Reinhold, J.F. Gross, and M. Intaglietta, *JNCI, J. Natl. Cancer Inst.* **62**, 387–395 (1979).
53. C.J. Eskey, A.P. Koretsky, M.M. Domach, and R.K. Jain, *Proc. Natl. Acad. Sci. U.S.A.* **90**, 2646–2650 (1993).
54. R.K. Jain, S.A. Shah, and P.L. Finney, *JNCI, J. Natl. Cancer Inst.* **73**, 429–436 (1984).
55. M. Nozue et al., *J. Surg. Oncol.* **63**, 109–114 (1996).
56. K.A. Ward and R.K. Jain, *J. Hyperthermia* **4**, 233–250 (1988).
57. P. Vaupel and R.K. Jain, eds., *Tumor Blood Supply and Metabolic Microenvironment: Characterization and Therapeutic Implications*, Fischer, Stuttgart, 1991.
58. R.K. Jain, *Cancer Metastasis Rev.* **6**, 559–593 (1987).
59. H.F. Dvorak, L.F. Brown, M. Dermar, and A.M. Dvorak, *Am. J. Pathol.* **146**, 1029–1039 (1995).
60. L.E. Gerlowski and R.K. Jain, *Microvasc. Res.* **31**, 288–305 (1986).
61. E.M. Sevik and R.K. Jain, *Cancer Res.* **51**, 1352–1355 (1991).
62. F. Yuan, M. Leunig, D.A. Berk, and R.K. Jain, *Microvasc. Res.* **45**, 269–289 (1993).
63. F. Yuan et al., *Cancer Res.* **54**, 3352–3356 (1994).
64. P.A. Netti et al., *Proc. Natl. Acad. Sci.* **96**, 3137–3142 (1999).
65. S.K. Hobbs et al., *Proc. Natl. Acad. Sci.* **95**, 4607–4612 (1998).
66. W.G. Roberts and G. Palade, *Cancer Res.* **57**, 1207–1211 (1997).
67. F. Yuan et al., *Proc. Natl. Acad. Sci. U.S.A.* **93**, 14675–14770 (1996).
68. E. Arbit, J. Lee, and G. Diresta, in H. Nagai, K. Kamiya, and S. Ishi, eds., *Intracranial Pressure*, Springer-Verlag, Tokyo, 1994, pp. 609–614.
69. Y. Boucher, L.T. Baxter, and R.K. Jain, *Cancer Res.* **50**, 4478–4484 (1990).
70. Y. Boucher and R.K. Jain, *Cancer Res.* **52**, 5110–5114 (1992).
71. Y. Boucher, I. Lee, and R.K. Jain, *Microvasc. Res.* **50**, 175–182 (1995).
72. Y. Boucher et al., *Cancer Res.* **51**, 6691–6694 (1991).
73. Y. Boucher et al., *Br. J. Cancer* **75**, 829–836 (1997).
74. B.D. Curti et al., *Cancer Res.* **53**, 2204–2207 (1993).
75. R. Guttman et al., *Cancer Res.* **52**, 1993–1995 (1992).
76. J.R. Less et al., *Cancer Res.* **52**, 6371–6374 (1992).
77. S.D. Nathanson and L. Nelson, *Ann. Surg. Oncol.* **1**, 333–338 (1994).
78. H.D. Roh et al., *Cancer Res.* **51**, 6695–6698 (1991).
79. C.A. Znati et al., *Cancer Res.* **56**, 964–968 (1996).
80. H.C. Lichtenbeld, F. Yuan, C.C. Michel, and R.K. Jain, *Microcirculation* **3**, 349–357 (1996).
81. L.T. Baxter and R.K. Jain, *Microvasc. Res.* **37**, 77–104 (1989).
82. R.K. Jain and L.T. Baxter, *Cancer Res.* **48**, 7022–7032 (1988).
83. V.P. Torchilin, *Crit. Rev. Ther. Drug Carrier Syst.* **2**, 65–115 (1985).
84. G. Gregoriadis, ed., *Liposome Technology*, vols. 1–3, CRC Press, (Boca Raton, Fla., 1993).
85. T. Fujita et al., *J. Pharmacol. Exp. Ther.* **263**(3), 971–978 (1992).
86. R.A. Srivastava, *Enzyme Microb. Technol.* **13**, 164–170 (1991).
87. J. Suh and B.K. Hwang, *Bioorg. Chem.* **20**, 232–235 (1992).
88. J. Suh, Y. Cho, and G. Kwag, *Bioorg. Chem.* **20**, 236–244 (1992).

89. L. Gros, H. Ringsdorf, and H. Schlupp, *Angew Chem., Int. Ed. Engl.* **20**, 305–325 (1981).
90. J. Kopecek, *Biomaterials* **5**, 19–25 (1984).
91. C.R. Gardner, *Biomaterials* **6**, 153–160 (1985).
92. J. Kopecek and R. Duncan, *J. Controlled Release* **6**, 315–327 (1987).
93. D.R. Friend and S. Pangburn, *Med. Res. Rev.* **1**, 53–106 (1987).
94. J. Drobnik, *J. Adv. Drug Delivery Rev.* **3**, 229–245 (1989).
95. H. Sezaki, Y. Takakura, and M. Hashida, *Med. Res. Rev.* **3**, 247–266 (1989).
96. H. Maeda, *Med. Res. Rev.* **6**, 181–202 (1991).
97. R. Duncan, *Anticancer Drugs* **3**, 175–210 (1992).
98. R. Duncan, *Clin. Pharmacokinet.* **27**, 290–306 (1994).
99. Y. Takakura and M. Hashida, *Crit. Rev. Oncol. /Hematol.* **18**, 207–231 (1995).
100. S.E. Mathews, C.W. Pouten, and M.D. Threadgill, *Adv. Drug Delivery Rev.* **18**, 219–267 (1996).
101. R. Duncan, S. Dimitrijevic, and E.G. Evagorou, *S.T.P. Pharm. Sci.* **6**, 237–263 (1996).
102. H. Maeda, M. Ueda, T. Morinaga, and T. Matsumoto, *J. Med. Chem.* **28**, 455 (1985).
103. H. Maeda, L.W. Seymour, and Y. Miyamato, *Bioconjugate Chem.* **3**, 351–362 (1992).
104. M. Kimura et al., *Anticancer Res.* **13**, 1287–1292 (1993).
105. K. Iwai, H. Maeda, and T. Konno, *Cancer Res.* **44**, 2115–2121 (1984).
106. K. Iwai et al., *Anticancer Res.* **7**, 321–327 (1987).
107. E. Hurwitz, M. Wilchek, and J. Pitha, *J. Appl. Biochem.* **2**, 25–35 (1980).
108. S. Dunhauser-Reidi et al., *Invest. New Drugs* **11**, 187–195 (1993).
109. R. Duncan et al., *J. Makromol. Chem.* **184**, 197–200 (1984).
110. P.A. Vasey et al., *Clin. Cancer Res.* **5**, 83–94 (1999).
111. M.S. Hershfield et al., *N. Engl. J. Med.* **316**, 589–596 (1987).
112. B.L. Asselin et al., *J. Clin. Oncol.* **11**, 1780–1786 (1993).
113. S. Zalipsky, *Adv. Drug Delivery Rev.* **16**, 157–182 (1995).
114. J. Senior et al., *Biochim. Biophys. Acta* **1062**, 77–82 (1991).
115. V.P. Torchillin, *J. Liposome Res.* **6**, 99–116 (1996).
116. V.P. Torchillin and M.I. Papisov, *J. Liposome Res.* **4**, 725–739 (1994).
117. Y. Murakami, Y. Tabata, and Y. Ikada, *Drug Delivery* **4**, 23–31 (1997).
118. M.C. Wani et al., *J. Am. Chem. Soc.* **93**, 2325–2327 (1971).
119. R. Weiss et al., *J. Clin. Oncol.* **8**, 1263–1268 (1990).
120. A.E. Mathew et al., *J. Med. Chem.* **5**, 145–151 (1992).
121. A. Pendri, C.D. Conover, and R. Greenwald, *Anticancer Drug Des.* **13**, 87–395 (1998).
122. B. Giovanella et al., *Cancer Res.* **51**, 3052–3055 (1991).
123. M. Nichifor, E.H. Schacht, and L.W. Seymour, *J. Controlled Release* **39**, 79–92 (1996).
124. P. Vaupel, F. Kallinowski, and P. Okunieff, *Cancer Res.* **49**, 6449–6465 (1989).
125. R.A. Gatenby et al., *Int. J. Radiat. Oncol. Biol. Phys.* **14**, 831–838 (1988).
126. B.A. Teicher, J.M. Crawford, S.A. Holden, and K.N.S. Cathcart, *Cancer Res.* **47**, 5036–5041 (1987).
127. B.A. Teicher et al., *J. Cancer Res. Clin. Oncol.* **120**(10), 593–598 (1994).
128. B.A. Teicher et al., *Cancer J. Sci. Am.* **1**(1), 43–48 (1995).
129. R.G. Shorr, *J. Expert Opin., Int. Bus. Commun. Substitute Conf. Rev.* in press.
130. D. Song et al., *Transfusion* **35**, 552–555 (1995).
131. R. Linberg, C.D. Conover, K.L. Shum, and R.G. Shorr, *In Vivo* **12**, 167–174 (1998).
132. B.A. Teicher et al., *In Vivo* **11**, 301–312 (1997).
133. B.A. Teicher, S.A. Holden, A. Al-Achi, and T.S. Herman, *Cancer Res.* **50**, 3339–3344 (1990).
134. B.A. Teicher and S.A. Holden, *Cancer Treat. Rep.* **71**, 173–177 (1987).
135. B.A. Teicher et al., *Cancer Res.* **49**, 4996–5001 (1989).
136. B.A. Teicher, S.A. Holden, and C.M. Rose, *Cancer Res.* **38**, 285–288 (1986).
137. B.A. Teicher, S.A. Holden, and C.M. Rose, *Int. J. Cancer* **36**, 585–589 (1985).
138. B.A. Teicher, S.A. Holden, and J.L. Jacobs, *Cancer Res.* **47**, 5036–5041 (1987).

See also CANCER, DRUG DELIVERY TO TREAT—LOCAL & SYSTEMIC; CENTRAL NERVOUS SYSTEM, DRUG DELIVERY TO TREAT.

CARDIOVASCULAR DRUG DELIVERY SYSTEMS

BENJAMIN A. HERTZOG
CHRIS THANOS
MARYELLEN SANDOR
Brown University
Providence, Rhode Island

VENKATESH RAMAN
ELAZER R. EDELMAN
Massachusetts Institute of Technology
Cambridge, Massachusetts

KEY WORDS

Angioplasty
Atherosclerosis
Catheter delivery
Channel catheter
Double-balloon catheter
Endoluminal paving
Hydrogel-coated balloon
Intramyocardial delivery
Microparticle delivery
Neointimal hyperplasia
Pericardial delivery
Perivascular delivery
Porous balloon
Restenosis
Vascular stents

OUTLINE

Introduction
Classifications

Previous Page

89. L. Gros, H. Ringsdorf, and H. Schlupp, *Angew Chem., Int. Ed. Engl.* **20**, 305–325 (1981).
90. J. Kopecek, *Biomaterials* **5**, 19–25 (1984).
91. C.R. Gardner, *Biomaterials* **6**, 153–160 (1985).
92. J. Kopecek and R. Duncan, *J. Controlled Release* **6**, 315–327 (1987).
93. D.R. Friend and S. Pangburn, *Med. Res. Rev.* **1**, 53–106 (1987).
94. J. Drobnik, *J. Adv. Drug Delivery Rev.* **3**, 229–245 (1989).
95. H. Sezaki, Y. Takakura, and M. Hashida, *Med. Res. Rev.* **3**, 247–266 (1989).
96. H. Maeda, *Med. Res. Rev.* **6**, 181–202 (1991).
97. R. Duncan, *Anticancer Drugs* **3**, 175–210 (1992).
98. R. Duncan, *Clin. Pharmacokinet.* **27**, 290–306 (1994).
99. Y. Takakura and M. Hashida, *Crit. Rev. Oncol. /Hematol.* **18**, 207–231 (1995).
100. S.E. Mathews, C.W. Pouten, and M.D. Threadgill, *Adv. Drug Delivery Rev.* **18**, 219–267 (1996).
101. R. Duncan, S. Dimitrijevic, and E.G. Evagorou, *S.T.P. Pharm. Sci.* **6**, 237–263 (1996).
102. H. Maeda, M. Ueda, T. Morinaga, and T. Matsumoto, *J. Med. Chem.* **28**, 455 (1985).
103. H. Maeda, L.W. Seymour, and Y. Miyamato, *Bioconjugate Chem.* **3**, 351–362 (1992).
104. M. Kimura et al., *Anticancer Res.* **13**, 1287–1292 (1993).
105. K. Iwai, H. Maeda, and T. Konno, *Cancer Res.* **44**, 2115–2121 (1984).
106. K. Iwai et al., *Anticancer Res.* **7**, 321–327 (1987).
107. E. Hurwitz, M. Wilchek, and J. Pitha, *J. Appl. Biochem.* **2**, 25–35 (1980).
108. S. Dunhauser-Reidi et al., *Invest. New Drugs* **11**, 187–195 (1993).
109. R. Duncan et al., *J. Makromol. Chem.* **184**, 197–200 (1984).
110. P.A. Vasey et al., *Clin. Cancer Res.* **5**, 83–94 (1999).
111. M.S. Hershfield et al., *N. Engl. J. Med.* **316**, 589–596 (1987).
112. B.L. Asselin et al., *J. Clin. Oncol.* **11**, 1780–1786 (1993).
113. S. Zalipsky, *Adv. Drug Delivery Rev.* **16**, 157–182 (1995).
114. J. Senior et al., *Biochim. Biophys. Acta* **1062**, 77–82 (1991).
115. V.P. Torchillin, *J. Liposome Res.* **6**, 99–116 (1996).
116. V.P. Torchillin and M.I. Papisov, *J. Liposome Res.* **4**, 725–739 (1994).
117. Y. Murakami, Y. Tabata, and Y. Ikada, *Drug Delivery* **4**, 23–31 (1997).
118. M.C. Wani et al., *J. Am. Chem. Soc.* **93**, 2325–2327 (1971).
119. R. Weiss et al., *J. Clin. Oncol.* **8**, 1263–1268 (1990).
120. A.E. Mathew et al., *J. Med. Chem.* **5**, 145–151 (1992).
121. A. Pendri, C.D. Conover, and R. Greenwald, *Anticancer Drug Des.* **13**, 87–395 (1998).
122. B. Giovanella et al., *Cancer Res.* **51**, 3052–3055 (1991).
123. M. Nichifor, E.H. Schacht, and L.W. Seymour, *J. Controlled Release* **39**, 79–92 (1996).
124. P. Vaupel, F. Kallinowski, and P. Okunieff, *Cancer Res.* **49**, 6449–6465 (1989).
125. R.A. Gatenby et al., *Int. J. Radiat. Oncol. Biol. Phys.* **14**, 831–838 (1988).
126. B.A. Teicher, J.M. Crawford, S.A. Holden, and K.N.S. Cathcart, *Cancer Res.* **47**, 5036–5041 (1987).
127. B.A. Teicher et al., *J. Cancer Res. Clin. Oncol.* **120**(10), 593–598 (1994).
128. B.A. Teicher et al., *Cancer J. Sci. Am.* **1**(1), 43–48 (1995).
129. R.G. Shorr, *J. Expert Opin., Int. Bus. Commun. Substitute Conf. Rev.* in press.
130. D. Song et al., *Transfusion* **35**, 552–555 (1995).
131. R. Linberg, C.D. Conover, K.L. Shum, and R.G. Shorr, *In Vivo* **12**, 167–174 (1998).
132. B.A. Teicher et al., *In Vivo* **11**, 301–312 (1997).
133. B.A. Teicher, S.A. Holden, A. Al-Achi, and T.S. Herman, *Cancer Res.* **50**, 3339–3344 (1990).
134. B.A. Teicher and S.A. Holden, *Cancer Treat. Rep.* **71**, 173–177 (1987).
135. B.A. Teicher et al., *Cancer Res.* **49**, 4996–5001 (1989).
136. B.A. Teicher, S.A. Holden, and C.M. Rose, *Cancer Res.* **38**, 285–288 (1986).
137. B.A. Teicher, S.A. Holden, and C.M. Rose, *Int. J. Cancer* **36**, 585–589 (1985).
138. B.A. Teicher, S.A. Holden, and J.L. Jacobs, *Cancer Res.* **47**, 5036–5041 (1987).

See also CANCER, DRUG DELIVERY TO TREAT—LOCAL & SYSTEMIC; CENTRAL NERVOUS SYSTEM, DRUG DELIVERY TO TREAT.

CARDIOVASCULAR DRUG DELIVERY SYSTEMS

BENJAMIN A. HERTZOG
CHRIS THANOS
MARYELLEN SANDOR
Brown University
Providence, Rhode Island

VENKATESH RAMAN
ELAZER R. EDELMAN
Massachusetts Institute of Technology
Cambridge, Massachusetts

KEY WORDS

Angioplasty
Atherosclerosis
Catheter delivery
Channel catheter
Double-balloon catheter
Endoluminal paving
Hydrogel-coated balloon
Intramyocardial delivery
Microparticle delivery
Neointimal hyperplasia
Pericardial delivery
Perivascular delivery
Porous balloon
Restenosis
Vascular stents

OUTLINE

Introduction
Classifications

Catheter-Based Systems
The Double-Balloon Catheter
Porous Balloon Catheters
Hydrogel-Coated Balloon Catheters
Other Local Delivery Catheters
Summary
Drug Delivery From Stents
Introduction
Local Drug Delivery: Rationale, Experimental Basis and Biologic Targets
Coated Stents
Conclusion
Delivery From Polymer Devices
Intramyocardial, Pericardial Delivery
Endoluminal Paving
Microparticle Delivery of Drugs to the Cardiovascular System
Bibliography

INTRODUCTION

Because controlled drug delivery can release of precise amounts of drug with determinable and definable release kinetics, there is the potential for its use in both the study and treatment of disease. At the same time, the more the technology of controlled delivery is applied to different fields and indications, the more it is advanced. This symbiotic relationship among technological development, scientific investigation, and therapeutic innovation is evident in the field of cardiovascular medicine. Controlled drug delivery enabled the rigorous evaluation of the biological and physiological processes that govern cardiovascular disease and, in doing so, paved the way for whole new avenues of therapies. This chapter reviews the role of controlled drug delivery systems in the field of cardiovascular medicine.

CLASSIFICATIONS

It is possible to classify drug delivery systems in many ways: on the basis of the drug to be applied, the delivery technology, and the target tissue. Classification of cardiovascular release systems, however, presents some limitations. An attempt to divide release systems based on the class of compounds is virtually impossible as the drugs available are so vast and overlapping in effect, physicochemical properties, and means of synthesis or derivation. Categorization might examine whether drugs are released into the lumen of the blood vessel or heart (endovascular or endocardial delivery), into the wall of the tissue (intravascular or intramyocardial) or external to the tissue (perivascular, epicardial, or pericardial). Alternatively, as the technologies employed span many sites of delivery and can be used for multiple compounds, we chose this means of defining this vast body of work. The chapter starts with a look at catheter delivery systems designed and used to deliver drugs locally. The next section explores the many attempts to use vascular stents as drug delivery systems. The final section discusses the cardiovascular applications of polymer-based drug delivery systems with special attention being paid to two promising therapies, endoluminal paving and microparticle delivery.

CATHETER-BASED SYSTEMS

The technical power and therapeutic success of percutaneous transluminal angioplasty (PTA) often overshadow the dramatic conceptual changes that this procedure has provided. Cardiovascular diseases, particularly atherosclerosis, are processes that involved the entire organism, and systemic therapy was therefore de rigeur. Transluminal angioplasty of isolated vascular segments enabled the focal treatment of such lesions and heralded local therapy that might treat lesions without systemic dosing or toxicity. Angioplasty not only provided direct access to target tissue with the potential for site-specific drug delivery but also the conceptual basis for proceeding locally as well. The need for adjunctive therapy and motivation for pursuing local pharmacologic therapy also was driven by this procedure. From 35 to 50% of all patients undergoing angioplasty suffer some accelerated vascular biological response to the intervention to such an extent as to need to return in 3–6 months for repeat attempt at revascularization. This failure phenomenon, termed *restenosis* (1), remains a major health care problem by virtue of the number of patients involved and because no systemic pharmacologic approach to date has reduced its impact (2).

It has been suggested that one of the main reasons for the failure of systemic drug delivery is that submaximal doses were used in an effort to minimize the unwanted side effects of systemic administration (3). Local and site-specific catheter delivery systems were developed to circumvent these problems. Diverse technologies have been employed represented by devices that include double balloons, porous balloons, hydrogel-coated catheters, injection-needle-studded balloons, and iontophoresis catheters. Although these devices may vary drastically in design and function, they all locally deliver controlled quantities of pharmacological agents to the vessel wall. To date, most local delivery catheters are limited by one or more of a few specific problems, including (*1*) expulsion of contents down arterial side branches, (*2*) arterial wall injury, and (*3*) downstream loss of infused agents (1). Each new generation of local delivery catheters attempts to address some of these faults, although in many cases, the new catheters introduce entirely new limitations of their own.

The Double-Balloon Catheter

One of the first vascular site-specific delivery catheters was the double-balloon catheter (4–8). These double-lumen catheters have two small polyethylene, latex, or poly(ethylene terephthalate) balloons attached to the periphery. One lumen (for balloon inflation) is ported into each of the two balloons, whereas the other serves as the drug infusion channel and is ported to the exterior of the catheter between the two balloons. Typical interballoon spacing is around 1.7 cm for dogs and 1.2 cm for humans (8). The diameter of the balloons is designed so that, when inflated, they expand gently against the endoluminal wall

and form a seal sufficient to prevent blood flow. Typically, the catheter is threaded through the vessel until the desired site is reached. The pressure on the two balloons is slowly increased over several seconds until the vessel is occluded at both the proximal and distal balloons. The blood filling the interballoon space can be drained and replaced with pharmacological agents through the infusion port. In an alternative design the proximal balloon is inflated, the lumen is flushed of blood, and only then is the distal balloon inflated. The drugs in solution between the inflated balloons actually reach the isolated vessel wall segment by direct diffusion or as a result of an applied pressure. Goldman et al. demonstrated that the depth of penetration of an agent is directly related to the distending pressure (8). In their studies, it was found that a distending pressure of 300 mmHg applied for 45 seconds was sufficient to cause horseradish peroxidase (HRP, 40,000 daltons) to penetrate the entire media of a normal dog muscular artery or nearly the entire plaque thickness of mildly and moderately atherosclerotic human coronary arteries. In earlier studies, the same group demonstrated that relatively acute pressure elevations resulted in the entry of labeled albumin (60,000 daltons) into the normal dog aorta. Pressures of 100 mmHg were ineffective, whereas 240 mmHg resulted in increased permeability. The increase in permeability was thought to arise from stretching of the vessel wall, an indirect result of the increased pressure (9). Feasibility studies with HRP (8) have since given way to use of a variety of agents: 14C-labeled fluorouracil (5-FU) to dogs (4), *r*-hirudin and heparin to the carotid arteries of pigs (5), intact endothelial cells to the iliac artery in rabbits (6), and enzymatic plaque dissolving agents to the aortas of rabbits, femoral arteries of dogs, and carotid arteries of humans (7). Other studies have shown that 100 mmHg is sufficient for uptake of DNA plasmids into the arterial wall, and pressures greater than 500 mmHg exhibit a tendency toward additional vascular injury (10).

Although the double-balloon catheter is still used in a number of experimental settings, its use clinically has been limited by problems, including leakage of large volumes of the infused solution through side branches of the vessel. Additionally, the pressure required to form a seal against the inner wall of the vessel, coupled with the long incubation times of this technique (15–30 min), often result in additional vascular injury at the balloon contact sites (8).

Porous Balloon Catheters

The porous balloon catheter attempted to avoid the balloon pressure-induced injury. In its first embodiment Wolinski et al. perforated a poly(ethylene terephthalate) angioplasty balloon with 300 holes of approximately 25 μm in size. The balloon was 2.0 cm in length, and the perforations were cut with a laser in a radial pattern of 6 rows with 50 holes per row. The porous balloon catheter uses the pressure of the perfusing fluid inside the lumen of the balloon to gently expand the balloon against the walls of the vessel. Consequently, the pressure used to distend the balloon also forces the perfusate out of the balloon via the 25 μm perforations and into the wall of the artery. In their first study, Wolinski and Thung demonstrated that HRP and heparin delivered at ~5 atm for 1 min could traverse the entire media of the normal canine artery (11). This device has been used for the delivery of various substances, including angiopeptin, antineoplastic agents such as methotrexate and doxorubicin, antimitotic agents such as colchicine (12), as well as for gene transfer (13,14). The main problem with the porous balloon catheter in its original, and what has now been termed "macroporous" form, is repeatable tissue damage caused by jetting of the high pressure fluids at the balloon pores. Fluid jetting out of the perforations resulted in medial necrosis by 48 hours, even when normal saline was used as the perfusate. When compared to standard angioplasty, simultaneous angioplasty and perfusion of saline resulted in similar lumen dilation as normal angioplasty but greater increase in intimal area at late time points (15).

In response to the limitations of the early porous balloon systems, a second generation of porous balloon catheters was developed, using new surface treatments or nonpressurized openings to deliver materials. Two unique strategies were employed to prevent fluid jetting from these catheters. The microporous balloon catheter consists of an inner porous balloon with an array of 25 μm holes surrounded by a permeable microporous membrane. The catheter described by Lambert et al. used a thin polycarbonate membrane with pores of approximately 0.8 μm in diameter (16). By using a much larger number of smaller pores, microporous catheters can deliver comparable fluid quantities at a given pressure with much lower fluid velocities at each pore. The resistance of this type of balloon to inflation is quite high. Consequently, the high pressure required for inflation causes the infusate to weep from the pores on the surface of the membrane (3).

Other devices were designed with separate inflation and infusion compartments (16–21). These catheters afford simultaneous high pressure angioplasty and low pressure infusion. The *Transport* coronary angioplasty catheter has an inner angioplasty balloon and an outer porous balloon with separate inflation port, which can be used to deliver agents before, during, or after angioplasty with the inner balloon (19). A similar design, often referred to as a *channel catheter*, typically consists of a standard (nonporous) angioplasty balloon covered by a network of perforated channels that can be perfused independently of the main balloon via an additional port (16,17,20,21). The *channeled balloon* catheter consists of 24 exterior channels, each with a single 100 μm drug-infusion pore, and is designed to perform simultaneous high-pressure angioplasty and low-pressure drug infusion. The pores are arranged in a spiral pattern along the entire length of the balloon. Therapeutic agents are infused at low pressure causing them to weep, rather than jetting from the exterior pores. The central lumen can be inflated at high pressure through a separate port, independent of the 24 drug delivery channels (17,20,21). The prototype balloons used in the 1993 study were made from poly(ethylene terephthalate), and they were 20 mm in length with a diameter of 2.75 mm. Drugs including tracer compounds like methylene blue, ^{3}H heparin, and HRP were delivered with variable

efficiency (25–50%) and generally rapid mural washout. Fluorescent and radiolabeled microspheres (15.5 μm Ce^{141}) can also be delivered in this fashion and with excellent vascular penetration (21).

A number of other novel catheters have been designed that use some modification of this technology or porous membranes to deliver pharmacological agents. The Localmed Infusion Sleeve is a multilumen array of perforated channels that can be employed in conjunction with a standard angioplasty balloon (18). The sleeve is loaded onto a standard dilation catheter prior to the procedure. After dilation of the vessel, the infusion sleeve is tracked over the catheter until the perforations are aligned with the balloon and site of injury. The balloon is reinflated, bringing the perforated channels into contact with the arterial wall. A catheter has been developed with a mechanical stent-like device inside the porous balloon (22). The mechanical infrastructure is used to distend and position the balloon against the wall of the vessel while fluids can be infused through the porous balloon at low pressures. This device was used to deliver 10 μm latex microspheres to atherosclerotic rabbit femoral arteries following angioplasty. The new device exhibited a delivery efficiency of 99.9% of the microspheres to the vascular and perivascular region as compared to 85.5% efficiency for a normal porous balloon.

The many experimental evaluations of porous catheter delivery systems have made one thing clear. The biggest challenge with the use of these devices is to minimize damage to the vessel wall while simultaneously producing efficient delivery of pharmacological agents. The damage-delivery relationship must be balanced in such a way that the benefits of local delivery are not overshadowed by the potentially negative consequences of the site specific delivery procedure (12).

Hydrogel-Coated Balloon Catheters

Hydrogel-coated balloon catheters consist of a standard polyethylene balloon coated with a 5–10 μm (dry) layer of cross-linked polyacrylic acid chains. The coating can be made from high molecular weight, medical grade, soluble poly(acrylic acid) polymer covalently bound to the polyethylene balloon (23). The hydrogel coating swells to between 2 and 5 times its original thickness upon exposure to aqueous environments. Water and poly(acrylic acid) form a stable matrix into which any pharmacological or other agents can be dissolved for incorporation (24,25). Intramural delivery of the incorporated pharmacological agents is accomplished when the hydrogel coating comes into contact with the vessel wall upon balloon inflation. Loading of the hydrogel layer with drugs is achieved by one of two methods: either the inflated hydrogel-covered balloon can be immersed in an aqueous solution containing the agents or the balloon surface can be painted with known aliquots of the drug (24,26). Both the surface area of the hydrogel and the thickness of the coating are factors that limit the amount of water and drugs that can be absorbed by the device. Washout of drugs like heparin occurs within seconds from the standard hydrogel-coated balloon device (27,28), and a protective sleeve has been added to cover the hydrogel catheter and enable substantial (almost 75%) retention on the order of minutes (29). In this way 2–5% of the loaded heparin has been delivered to the deep arterial wall during angioplasty (30), with small amounts of intramural heparin detected for over 48 hours (27,28). In addition to passive diffusion, hydrogel compression during balloon inflation results in "pressurized diffusion" of soluble agents from the hydrogel matrix directly into the arterial intimal surface (24). Thus, balloon pressure and the duration of inflation, as well as drug size and concentration, determine depth of penetration (29).

The hydrogel-coated balloon catheter has been used to deliver a vast array of pharmacological and biological agents to the arterial wall, including HRP (29), heparin (27–30), urokinase (26,31), D-phe-L-pro-L-arginyl chloromethyl ketone (PPACK) (23,25), and genes in the form of adenoviral vectors (32). Urokinase-coated balloons successfully reversed abrupt closure and dissolution of intracoronary thrombus in all 11 human patients in one trial (31).

Although the hydrogel balloon permits site-specific intravascular drug delivery to be performed directly during angioplasty with a standard balloon (3), with no additional tissue damage being observed (33), the system is limited by the rapid washout of loaded drugs upon exposure to the bloodstream. This necessitates limited dwell time in situ before deployment, and lack of applicability when large amounts of agent need to be deposited (3).

Other Local Delivery Catheters

A number of other, novel, local and site-specific drug delivery catheters have been developed. A majority of them have been designed to overcome inherent problems in the more traditional balloon or porous balloon devices. One of the primary limitations of balloon-type catheter delivery systems is that the actual drug delivery time must be kept short because the balloon occludes the vessel and blocks distal blood flow. The Dispatch™ catheter (Scimed Life Systems, Maple Grove, MN) is specifically designed to overcome this limitation. The working component of the catheter consists of a POC-6 helical inflation coil that supports an inner urethane sheath. The sheath creates a large-diameter central lumen that maintains distal blood flow while the catheter is in place. In the inflated state, the helical coil and urethane sheath create channels, isolated from the bloodstream, into which a therapeutic fluid can be infused directly against the arterial wall (34–36).

The efficacy of the Dispatch™ catheter was assessed in vivo using ^3H heparin delivered to 12 normal porcine coronary arteries. Following a simulated angioplasty procedure the Dispatch™ catheter was inflated to ~6 atmospheres at the angioplasty site, and ^3H heparin was infused at 0.5 mL/min for either 60 seconds or 15 minutes. The study showed that, for the vessels infused for 15 minutes, 1.3% of the delivered heparin was still present in the arterial wall 5 minutes after the procedure, but that 85% of that heparin was gone 90 minutes after delivery (34). In another study, the Dispatch™ catheter was used to treat 6 human patients with evidence of intracoronary thrombus. Each of the patients successfully received 150,000 units of urokinase over a 30-minute period prior to, or following

conventional angioplasty and/or directional atherectomy. In all 6 patients the local delivery of urokinase using the Dispatch™ catheter resulted in reduction of the stenosis and/or dissolution of the angiographic thrombus. The authors did note that one patient suffered from limited local ischemia resulting from a coronary side branch occlusion due to one of the catheter's coils (35).

The Dispatch™ catheter and hydrogel-coated balloons have been reported to provide a small intramural deposit of heparin and urokinase, respectively (26,34). It is thought that, at least in the case of urokinase, this creates a local reservoir of drug that may diffuse over time throughout the angioplasty site, resulting in a sustained local thrombolytic effect (35,36). In vitro experiments with human plasma have shown that a minimum urokinase concentration of 100 units/mL is required for clot lysis (37). Assuming that the spaces between the coils of the Dispatch™ catheter are filled entirely with the infusion fluid, the local urokinase concentrations is the same as that of the infusion solution. Indeed, 150,000 units of urokinase was delivered over approximately 30 minutes when reservoir solutions of approximately 10,000 units/mL were used (35,36).

Another family of local delivery catheters uses small needles to inject the therapeutic agent. The Infiltrator™ angioplasty balloon catheter is a type of microneedle injection catheter (38). In this particular design, three longitudinal metallic strips with six small injection nipples are mounted on the surface of a conventional balloon catheter. The nipples are connected to a central drug delivery port that is separated from the balloon lumen so that both high-pressure angioplasty and low-pressure drug infusion may be performed. Delivery of 0.4 mL of rhodamine B to porcine coronary arteries via a normal-sized balloon resulted in even distribution of the tracer within the wall of the vessel 10 min after infiltration. Barath et al. reported localized interruption of the internal elastic lamina at the site of nipple penetration and a mild thickening and edema of the media without dissection or separation of the vessel wall layers. The use of this catheter will expand into imaging, diagnosis and research as well as therapeutics. A second needle-injection catheter employs six, 250-μm (31-G) needles positioned symmetrically at the proximal tip of the catheter (39,40). The 5F polyethylene catheter was designed with a central lumen that allows it to be positioned under fluoroscopy using the guidewire from the previous angioplasty procedure. Once in place, the six preshaped needles can be extended laterally into the vessel wall, at which time drug can be injected into the perivascular tissue. It is hoped that the adventitia will act as a local reservoir, with subsequent drug delivery being achieved via diffusion and through the vasa vasorum. Relatively small doses of the fluorescent indicator (~5–7% of the systemically applied dose) resulted in a 500% increase in local tissue concentrations with a notable percentage of the applied marker still present at 14 days (40).

Iontophoresis, a form of electric current–facilitated transport, has been used, through various devices, to enhance the penetration of drugs through skin, directly to myocardium, and into blood vessel walls (12,41–45). A balloon catheter has recently been developed that uses iontophoresis through a semipermeable membrane to drive medications into the wall of a vessel. It has been reported that local tissue concentrations of hirudin were 50 times greater after iontophoretic therapy versus passive diffusion (45). Unfortunately, concentrations of the delivered agent, within the vessel wall, quickly decreased.

Summary

Many of these catheter systems are currently being evaluated in human trials. Exciting preliminary reports have demonstrated reduced poststent restenosis with the transport-catheter delivery of Enoxparin low-molecular heparin. It is intriguing that efficacy requires heparin to be delivered at the time of deployment, not afterwards. Additional research will refine the technology and deployment strategies. Future developments will no doubt expand their potential in the therapeutic and diagnostic realm. The ability, for example, of a catheter to deliver contrast enhancing agents might be employed with sensitive noninvasive imaging modalities. The local delivery of radiotherapeutic sensitizers might further enhance the specificity of brachytherapy.

DRUG DELIVERY FROM STENTS

Introduction

Since its clinical introduction more than a decade ago, endoluminal stenting to relieve obstruction and restore coronary perfusion has become a mainstay in the repertoire of the interventional cardiologist. It was expected in 1998 that more than 500,000 percutaneous interventions involving coronary stents would be performed worldwide that year (46). Several trials have shown the superiority of stenting compared to balloon angioplasty in immediate and intermediate-term results (47,48). This has been largely due to a decrease in the need for repeat target lesion revascularization.

Early experience with stenting was notable for the frequent occurrence of acute and subacute thrombosis: up to 20% in a multicenter European registry from the early 1990s (49). Since then, two factors have contributed to the marked reduction in clinical thrombosis to less than 1%: (*1*) optimization of stent deployment techniques to include high pressure, in-stent angioplasty and (*2*) intensification of adjunct antiplatelet/anticoagulant regimens with the addition of ticlopidine and platelet glycoprotein IIb/IIIa receptor antagonists to conventional aspirin and heparin schedules. Attendant with this reduction in thrombosis has come an increase in hemorrhagic complications as well as an increase in other risks of systemic exposure to these medications, including neutropenia, thrombocytopenia, electrolyte and fluid shifts, and allergic reactions.

The efficacy of coronary stents has also been limited by intermediate-term restenosis from biologic events that primarily include neointimal hyperplasia. Unlike balloon angioplasty, coronary stenting induces more severe and chronic vessel injury that engenders a protracted response (50). Despite increased acute luminal gains compared with balloon angioplasty, however, the exuberant reactive and

reparative responses to stent-induced injury still lead to clinical restenosis in 20–40% of stented arteries (46,47,49,51–54). Although a number of agents have been shown in experimental models of arterial injury to reduce the smooth muscle cell hyperplasia responsible for restenosis (55–58), all of these pharmacologic adjuvants have failed to show any benefit in clinical trials (59–64). Furthermore, weight-adjusted drug dosages in these animal studies were prohibitively high for use in clinical trials (65). Though this dichotomy might imply a lack of relevance of animal models to the pathogenesis of clinical restenosis, it is also likely that suboptimal drug delivery plays a role (66).

Local Drug Delivery: Rationale, Experimental Basis and Biologic Targets

Given the limitations and risks of systemically administered drugs, increasing effort has been devoted to the evaluation of local means of drug delivery to the vasculature. As with the catheter systems, the motivation is the theoretical expectation of maximizing drug concentration and biological effect in local target tissues while maintaining low systemic levels. Achievement of these goals should produce desired therapeutic effects and avoid deleterious side effects. Experimental systems have indeed shown the effectiveness of local delivery. In one early study, rats subject to denuding carotid arterial injury were treated with heparin injected subcutaneously on a periodic basis, delivered continuously by intravenous pump, or released continuously from a drug-embedded matrix (ethylene–vinyl acetate copolymer [EVAc]) placed directly over the injured blood vessel or placed subcutaneously at a distant site (66). Heparin delivered periadventitially by local matrix was as effective as continuous intravenous heparin in reducing neointimal hyperplasia. This inhibition of luminal occlusion was achieved without a measurable increase in the activated partial thromboplastin time, verifying that local delivery can produce therapeutic effects without undesirable systemic effects and that the antiproliferative effects of heparin may well be divorced from the drug's antithrombotic effects. Perivascular release has now been extended to treatment of models of vascular injury using a variety of compounds, including antisense oligonucleotides (67), steroids (68), antimitotics (69), and antithrombotics (70).

In contrast to the acute and limited injury from balloon angioplasty and endothelial denudation, stent placement causes more severe vessel wall damage and a prolonged stimulus for neointimal hyperplasia (71). Cox et al. reported on the failure of intraluminally administered heparin or methotrexate to inhibit neointimal hyperplasia after stent-induced injury (72). To address whether this was a consequence of drug delivery or rather a lack heparin efficacy in stent-related complications, we evaluated several routes of heparin delivery on thrombosis and neointimal hyperplasia in a rabbit model of iliac artery injury (73). Arteries were subject to either balloon denudation alone or denudation followed by stent placement. Heparin was delivered intravenously or to the injured vessel from either the perivascular or endoluminal aspect of the artery. Perivascular administration was again achieved with EVAc matrices. Matrices were synthesized to provide either first-order release kinetics, with most drug released within three days, or release kinetics approaching zero-order, allowing prolonged steady release over two weeks. Heparin ionically bound to the stainless steel stents was rapidly released at the luminal aspect of the artery, with most drug eluted after a few hours. All forms of heparin delivery markedly reduced or eliminated thrombosis in stented arteries, although only prolonged perivascular administration reduced neointimal hyperplasia to the same degree as systemic heparin administration. Early perivascular release resulted in a less dramatic reduction in neointimal hyperplasia, and endoluminal delivery via heparin coating was no different compared to uncoated stents. These results confirmed that local delivery could treat stent-related sequelae in experimental models, but that drug efficacy is related to the site and duration of administration. The differential response of the variety of factors examined underscored the multifaceted nature of the vascular response to injury, suggesting the need to target multiple axes for successful treatment.

Our evolving understanding of the temporal and spatial characteristics of thrombosis and restenosis may help to explain the variability of drug effect with site and duration of delivery. Within the first few days of stent implantation, a marked deposition of fibrin, platelets, and erythrocytes sets the stage for subacute thrombotic occlusion, which typically occurs at 3–10 days after stent placement (74). This process is most pronounced at the stent struts where denudation and vessel injury is more severe. Drugs to inhibit this response may only need to be active at the stent–lumen interface and present for a short period of time. The process of neointimal hyperplasia leading to restenosis, however, appears to follow a different time course. The deep injury imposed by stent struts leads to an early inflammatory reaction involving mononuclear leukocytes adherent to the injured surface. The disappearance of these cells from the lumen by one week after injury coincides with the appearance of tissue-infiltrating macrophages in the nascent neointima. Subsequent smooth muscle migration from the media and proliferation in the neointima lead to vessel restenosis (50). This phase of the vascular response is quite prolonged in experimental models (75), suggesting that local therapy to modulate restenosis will likely require extended release of drug into the deeper vessel layers. Thus, treatment directed at thrombosis and restenosis may need to be targeted to different tissue elements at different points in time, reflecting the underlying pathobiology of these two processes.

Coated Stents

Although perivascular matrices are useful in experimental models, this mode of drug delivery is not available currently for clinical percutaneous coronary interventions. A number of catheter-based systems have been developed for this purpose. Their utility is limited by low delivery efficiency (<1%) (76,77) and rapid drug washout (34). Delivery by catheter of several compounds including heparin (78), methotrexate (72), and colchicine (69) has not been shown to significantly reduce neointimal hyperplasia. Endovas-

cular stents, in addition to providing a mechanical scaffolding, may be more attractive platforms from which to implement local therapy. This can be accomplished by two broad strategies: (*1*) immobilization of drug to the stent surface and (2) continuous release of drug from the stent.

Drug Immobilization. The interaction among bloodborne elements, the injured vessel surface, and the stent itself appear to be of the earliest events in the vascular response to device implantation. It is appealing to attach a drug to the stent capable of favorably modulating this interaction. Heparin, the systemic anticoagulant of choice, would seem to be an ideal candidate. There has been longstanding interest in heparin coating for a variety of catheters and indwelling devices (79). Several studies have evaluated heparin-coated stents in animal models. Chronos et al. showed a marked reduction in platelet attachment to such devices in a baboon arteriovenous shunt ex vivo system, and others demonstrated diminished occlusive thrombosis in rabbit and porcine arterial injury models (80,81). These studies in animal models have focused on acute indices of thrombosis, such as platelet deposition, or surrogate markers, such as animal survival.

Whereas experimental models frequently encounter acute thrombosis within the first 24 hours, clinical subacute thrombosis occurs between 3 and 10 days after stent implantation. To assess the effects of stent surface on thrombus generation within this time frame, our laboratory used histologic evaluation of mural thrombus 3 days after implantation of heparin-coated stents in rabbit iliac arteries (C. Rogers, M. Kjelsberg, P. Seifert, and E. Edelman, unpublished data). Denuded vessels received four types of stents: uncoated stainless steel, steel coated with the inert polymer poly(dichloroparaxylylene), steel with surface-bound heparin (via the binding agent, alkylbenzyldimethylammonium chloride), or steel coated with polymer and heparin. Histologic evaluation at 3 days showed a two-fold reduction in mural thrombus by stent-bound heparin (with or without polymer) compared to uncoated and polymer-coated stents. Yet, this reduction in thrombus deposition was not accompanied by a reduction in inflammatory cell number or in subsequent neointimal hyperplasia. Such data not only predict limited utility in combating the more chronic aspects of the vascular response to injury, but they also shed light on the basic biology of vascular repair. Despite our greatest hopes, the major portion of the thrombotic response appears as an event independent from the inflammation and proliferation that follow.

The sum total of these preclinical experiments was verified in the Benestent-II™ Pilot Study (C. Rogers, M. Kjelsberg, P. Seifert, and E. Edelman, unpublished data), which evaluated the clinical safety and efficacy of heparin-coated stents in conjunction with alterations in adjuvant anticoagulant therapy. A total of 203 patients with stable angina, subdivided into four groups, successfully underwent implantation of heparin-coated stents for treatment of de novo lesions. Three groups received heparin and coumadin with progressively delayed institution of therapy, and the fourth group was treated with aspirin, adding ticlopidine as an adjunct. Although no subacute thrombotic events were observed, study investigators point out the probable multifactorial nature of the favorable outcomes. Although promising, these results await confirmation by larger randomized trials.

Drug Release. Whereas the events culminating in thrombosis take place principally early and at the lumen–vessel boundary, the processes leading to neointimal hyperplasia and restenosis appear to be protracted in duration and occur deeper within the arterial wall. Consequently, continuous and prolonged local drug therapy may be required to inhibit restenosis. This may be accomplished by directly coating the stent with drug or by coating the stent with a drug-eluting polymer matrix. In general, drug release from stent surfaces is rapid and on this basis may have a limited impact on the more prolonged phases of the vascular response to injury. The versatility of polymer matrices as drug reservoirs may expand local stent-based drug release. Although polymer materials have been used in drug delivery for some time, their use as vehicles for percutaneous coronary therapy is in its infancy. Polymeric bioerodible stents have been proposed as both drug reservoir and temporary scaffolding while reparative processes occur in the vascular wall. Despite the theoretical advantage of avoiding permanent placement of a foreign body, stents constructed solely from polymer materials have been limited thus far by significant thrombotic and inflammatory sequelae (82,83). Composite stents offer the mechanical strength of metal combined with the drug-carrying and eluting properties of polymer materials. Lambert et al. showed the feasibility of this type of system, using nitinol stents coated with a polyurethane matrix to locally deliver forskolin to rabbit carotid arteries (84). Most of the drug was released within 24 hours of stent deployment. Another group used a tantalum wire coil stent coated with high molecular weight polymer of poly(L-lactic acid) to deliver dexamethasone to porcine coronary arteries (85). Although this intervention had no effect on neointimal hyperplasia, the study did show sustained release evidenced by detectable serum dexamethasone levels at 28 days and polymer material biocompatibility supported by a lack of difference in tissue response to polymer-coated versus uncoated stents.

Local Pharmacology. Stent-based drug delivery is an appealing but complex potential therapeutic modality, dependent upon device and drug properties. The amount of drug that can be immobilized to or released from a stent is principally determined by the mode of drug attachment and stent configuration. The processes of coating and drug incorporation can modify the biological activity of the compound of interest. All of these issues must be optimized before we can expect a beneficial response from this means of drug delivery.

Coating Process. Specific processes of drug attachment may limit the availability of a drug's active sites or may expose drugs to denaturing or degrading stimuli. Polymer coatings or drug binding agents may themselves alter the activity of the drug, reduce the carrying capacity of the stent or induce a detrimental vascular response independent of the drug. The evolution of heparin coatings serves as a primary example of these phenomena. The early use

of quaternary ammonium compounds to ionically bind heparin was notable for rapid drug leaching from the stent vehicle. Attempts at bonding heparin covalently to stents were initially confounded by loss of anticoagulant activity, presumably due either to masking of the active binding site or undesirable conformational changes that abrogated heparin's effect (79). More recent methods for attachment of heparin at inactive sites or at its end point (83) have maximized retention of biologic activity.

Many of these same factors influence drug delivery with release systems. As discussed earlier, a variety of polymers have been used in composite stents. Issues of biocompatibility may limit the utility of some of these polymers. With poly(glycolic acid), for instance, the resultant inflammatory response may be a function of the total mass of polymer in the stent (86), thereby limiting matrix drug-carrying capacity. In addition, the conditions required for matrix synthesis may alter drug activity, as we learned with the delivery of basic fibroblast growth factor (FGF-2) (87). Although incorporation into and release from EVAc matrices followed desired kinetics, over 99% of the growth factor's biological activity was lost. Basic FGF is intensely sensitive to extreme environmental conditions, and only very specific and gentle matrix production techniques enabled stabilization of the FGF-2 and retention of its effects.

Stent Geometry. The biologic activity of a drug is a function of its dose and distribution within tissue. Stents generally cover less than 10% of targeted vessel wall segments, limiting the surface area available for drug loading and, as a result, the maximum dose of drug available. The amount of drug deposited in distant tissues depends upon the solubility and diffusive properties of the drug as well as the individual design of the device. A careful balance exists between the release of the drug from each strut and the ability of the drug to diffuse through and be distributed within the surrounding tissue. As drug elution is centered at the stent struts a concentration gradient forms with highest drug levels just adjacent to stent struts and lower levels in the region between struts. There can therefore be a gradient of effect within a given tissue over a spectrum of activity ranges from no effect to the desired therapeutic effect to frank toxicity. Struts spaced too far apart leave drug-poor areas, whereas struts too close together may produce areas of overlap. A highly hydrophobic drug such as paclitaxel might be expected to accumulate and persist at potentially toxic levels in close proximity to stent struts.

Drug Pharmacokinetics. Release kinetics from the drug-eluting polymer coatings are determined by a number of factors, including the physicochemical characteristics of the drug and the material properties of the coatings and delivery vehicles. For example, insoluble compounds diffuse slowly from the coated stents into the intercellular milieu. Hydrophilic materials swell as they absorb water, thereby altering material characteristics, and potentially release kinetics as well. Porous polymer materials release drugs far more rapidly than less porous materials, further illustrating the profound influence of polymer-drug properties on drug delivery.

Although polymeric drug delivery systems have been well characterized and sophisticated control of kinetics can achieve almost any pattern of drug release, much less is known about the fate of a drug once it leaves the delivery device. Systemic pharmacokinetics treats an organism as a limited number of homogeneous compartments between which drugs flow with definable rate constants. Target tissues for local drug delivery, however, must be viewed as a continuum with the establishment of a concentration gradient from delivery site to target tissue. Factors influencing local drug levels include the ratio of bound versus soluble drug, volume of distribution, local metabolism and clearance, and specific versus nonspecific binding (12).

Tissue Pharmacokinetics. Recognition of the importance of all of these issues should caution against the assumption that local drug delivery necessarily translates into local drug deposition and a consequent focal therapeutic effect. A biologic or therapeutic agent in this aqueous intercellular milieu remains where released only if it is hydrophobic, largely protein bound, or partitions into the bound or internalized tissue fraction. Paclitaxel, a potent antitumor agent, possesses many of these characteristics. It is a complex natural product with bulky hydrophobic substituents, poor aqueous solubility, extensive protein binding in blood, and an intracellular site of action, where it promotes the abnormal polymerization of microtubules (88). Initial work with this compound and vascular tissue revealed its antiproliferative effect on rat smooth muscle cells in vitro and in vivo. Subsequently, Axel and colleagues locally delivered a single dose of paclitaxel via a microporous balloon system to the injured segment of rabbit carotid arteries and saw an approximate 20% reduction in stenosis in treated versus control animals (89). The efficacy of single dose paclitaxel may be due to its hydrophobicity, intracellular site of action, and its rapid and prolonged biological effect.

The results with paclitaxel-like compounds can be contrasted with the use of heparin. When heparin was rapidly released from stents to rabbit iliac arteries no effect was observed on neointimal hyperplasia (73). Other work from our laboratory showed minimal deposition of radiolabeled-heparin delivered by stents with ionically bound heparin (90). This was thought to arise from the marked solubility of heparin and its consequent absorption and dilution into the bloodstream, resulting in a markedly larger volume of distribution than anticipated for the amount of drug delivered. Computational models give us insight into the basis of experimental results. We have previously described a series of rigorous pharmacokinetic models to simulate vascular heparin deposition (71). When applied to a cross section of artery uniformly loaded with heparin, these models predicted low heparin concentrations in the artery after 1 hour. This supported rapid clearance of heparin and suggested that it and similarly soluble drugs would require continuous release to achieve persistently therapeutic local levels of drug. These types of simulations allow far greater spatial resolution of local forces and events than would be feasible otherwise. For example, delineation of drug partitioning within vessel layers as well as into soluble, bound, or internalized fractions within a section of

tissue would be impossible with current analytical techniques. As valuable as these models are, it is impossible to rigorously define all of the parameters influencing local drug distribution within target tissues.

In addition to these factors, the state of the vessel and nonspecific binding play important roles in drug deposition and effect. We compared vessel wall deposition of basic fibroblast growth factor (FGF-2) in native versus injured rat carotid arteries (91). There was over a two-fold increase in FGF-2 deposition within injured arteries showing intimal hyperplasia versus control arteries, providing evidence that the vessel itself affects local pharmacology. Nonspecific binding, although removing drug from the "active" pool, may also sequester and alter biological efficacy. This phenomenon is most apparent in the interaction of growth factors with extracellular matrix. We looked at the response of cultured endothelial and smooth muscle cells to FGF-2 and transforming growth factor-beta 1 (TGF-β1) administered by bolus, continuous release, or following exposure of the growth factors to extracellular matrix (97). Continuous FGF-2 release was more potent than bolus administration in inducing cellular proliferation. With TGF-β1, however, bolus dosing proved more effective in inhibiting cellular growth. Importantly, both growth factors bound to extracellular matrix, but only FGF-2 was released from the matrix in a controlled fashion that significantly augmented its biological effect.

Endothelial Cell Seeding of Stents. Other attempts at limiting intimal proliferation with implantable devices include seeding of stents with genetically engineered endothelial cells (85,93,94). It has previously been postulated that the presence of endothelial cells alone can reduce the amount of thrombosis and intimal proliferation associated with stenting. Dichek et al. (93) coated stents with fibronectin and grew endothelial cells engineered to express either bacterial β-galactosidase or human tissue-type plasminogen activator. Expression of these proteins was monitored in vitro, and cells remained seeded after balloon expansion. Scott et al. (95) seeded human dermal microvascular endothelial cells with the simian virus 40 large T-antigen gene for 2 weeks in culture. This group was able to seed these cells directly onto the stents without coupling to fibronectin as well as use them in a simulated clinical setting. The same stents were seeded cells, frozen for 4 months and then implanted in vivo. Although they did find that many of the cells dislodged during balloon expansion, they were able to form another monolayer after 3 days in culture. Flugelman et al. (94) applied pulsatile forces to these endothelial cell-seeded stents, and found that substantial amounts of cells on the lateral surfaces of the stent remained intact, with fewer cells remaining on the luminal and abluminal surfaces. Only future technical innovations and experimental validation will determine whether there is promise to this methodology.

Conclusion

The success and prevalence of coronary stenting is limited by early thrombosis and late restenosis. Marked reduction in thrombotic sequelae have been achieved through the use of aggressive antiplatelet and anticoagulant regimens, which, nonetheless, place patients at risk for hemorrhage and other adverse effects. On the other hand, restenosis has not been appreciably affected by a variety of systemic therapeutics. Experimental studies have suggested a pharmacologic rather than biologic failure of these interventions. Local drug delivery is emerging as a technology to circumvent this phenomenon and deliver therapeutic doses of drug to target tissues while avoiding significant systemic exposure and consequent side effects.

Stents may be the ideal vehicles both to provide mechanical stability and to act as reservoirs for pharmacotherapy. Suitable drug candidates may be immobilized to the stent surface or may be released via drug-eluting polymer coatings. The clinical promise of this technology is evident from the Benestent-II™ Pilot Study, which used heparin-coated stents and reported no subacute thrombotic occlusions in a limited number of patients. Local drug therapy involves complex processes that affect delivery to and distribution within tissues. Determinants of drug loading onto stents include stent surface area, polymer and binding agent coating, mode of drug attachment, matrix fabrication, and specifics of matrix design. Once a drug is released, factors including local clearance, bound versus soluble fraction, nonspecific binding, and volume of distribution determine the fate and biologic effect of the agent. Our understanding of local pharmacology continues to evolve through complementary experimental and modeling systems with the goal of providing more rational design of delivery devices and more optimal choice of therapeutic agents.

DELIVERY FROM POLYMER DEVICES

Polymer-based delivery of therapeutic agents has been employed in a wide range of applications from contraceptives to antianginal drugs. Its application to the cardiovascular system has been long investigated. The predictable and prolonged nature of release and the malleability of the technology enables delivery from a number of sites. A polymeric matrix or microsphere, encapsulating or impregnated with drug, first begins to release its agent through the pores and channels inherent in its structure. As the polymer degrades, drug can then also diffuse out between polymer chains. Transdermal adhesive drug patches have been used with antianginals and antihypertensives such as nitroglycerin, clonidine, the beta-blockers timolol and propanolol and, more recently, nitrendipine (96–98). More experimental systems now enable subcutaneous, extravascular, and pericardial administration as well.

The use of these systems has not only provided potential new therapeutic modalities but has also revealed much about the nature of biological disease. EVAc matrices, for example, have been used to release both standard, anticoagulant, and modified, nonanticoagulant heparin (99,100). Release kinetics were tailored to provide rapid first-order, or more prolonged near zero-order, release by alterations in the size, shape, and properties of the drug; geometry of the controlled release device; and application of a coating around the device. The ability of heparin re-

leased in this manner to inhibit smooth muscle cell proliferation and thrombosis was evaluated in three different models of vascular injury: after balloon catheter arterial de-endothelialization, after implantation of an expandable stainless steel stent, and after venous–arterial interposition grafting. In all instances the perivascular release of heparin limited intimal hyperplasia from proliferating smooth muscle cells to an identical extent as heparin systemic infusion and with one-fifth the intravenous dose, and without systemic effect. These results demonstrated that controlled release of a potent smooth muscle cell inhibitor, with profound systemic side effects, could deliver a dose low enough to avoid systemic effects but high enough to provide local protection against vascular disease. More importantly they showed that this accelerated form of vascular disease could be treated locally and paved the way for many other forms of local therapy. Since then a large range of agents have been administered from the perivascular space, including antithrombotics, antimitotics, genes and proteins, antisense oligonucleotides (101–104), growth factors and their antagonists, angiogenesis factors (105).

The work with heparin-binding growth factors is a wonderful example of how local release systems might mimic natural phenomena. Cells in culture respond optimally to the controlled release, rather than bolus administration, of FGF-2, and with good reason. Because this compound lacks a signal sequence, it relies on endogenous forms of controlled release for biological effect. Controlled release may be far more physiologic than bolus release of large doses. When FGF-2 controlled release devices were implanted into the perivascular space of injured rat carotid arteries intimal mass, cell proliferation and perivascular angiogenesis were increased in a dose dependent fashion (106). Thus, the perivascular release of this potent mitogen retained not only its biologic activity but may have reproduced the physiologic means by which the growth factor is released and metabolized in vivo.

Intramyocardial, Pericardial Delivery

Drugs can additionally be released into or around the myocardium. Pacemaker leads have long served as delivery depots. Fibrosis and subsequent conduction block were markedly reduced when leads were coated with porous polyurethane or silicon impregnated with dexamethasone (107). Attempts were also made to release colchicine, hirulog, aspirin, and steroids (108,109). Polymer devices have also been made which can be implanted directly proximal to the ventricular myocardium. Polyurethane devices loaded with antiarrhythmic agents markedly increased the threshold for induction of ventricular tachycardia by rapid ventricular pacing, while intravenous or bolus administration exhibited no effect (110–112).

Drugs can also be delivered directly to the heart via synthetic heart valves. Porcine aortic valve replacements are highly subject to calcification within a span of five years from implantation. Ethanehydroxydiphosphonate and other anticalcification drugs released from polymeric valve ring collars inhibited calcification of valve cuspal implants in rats (113–115).

Drug-loaded polymer delivery devices have proven to be quite successful in their intended capacity as local conveyors of therapeutic agent. These devices have been fabricated in numerous forms from a vast array of polymers and for various indications and sites of application. In addition to the aforementioned polymer devices, two extensively studied methods of polymeric drug delivery include endoluminal paving and microparticle delivery.

Endoluminal Paving

First described in 1988, endoluminal paving is a therapeutic approach to reduce restenosis and loss of patency providing vessel wall strength and support as well as a physical barrier to thrombogenic factors and a possibility for sustained drug release (116). In addition to favorable tissue reaction, endoluminal paving provides a temporary device that is biodegradable, a structural support for damaged tissue, and a method of preventing wall recoil (116). It also presents a barrier between the endoluminal surface and inflammation-inducing elements of the blood (116), is assumed to prevent endoluminal thickening following device degradation (117), and can be a method of physically targeting drugs, an option not available with current systemic drugs (116).

In all, three main types of paving have been developed. The first is solid paving, which involves the use of thin sheets or tubes of a biodegradable polymer. Polymer material surrounds an intraluminally placed thermoforming catheter. The catheter heats the polymer to just above its T_m, and propels the polymer to coat the endoluminal tissue as its balloon is inflated (118). The polymer coating is then allowed to cool to body temperature leaving a solid polymer coating on the endoluminal surface. The second type of endoluminal paving, gel paving, is performed in the same manner as solid paving but uses a polymeric hydrogel or colloidal system instead of a solid polymer film (116). Gel paving is less stable, lasting only days to weeks as the hydrogel biodegrades through bond scission or bioerodes through solvation and physical thinning. Moreover, paving focuses to a far lesser extent on mechanical support and far more on providing a barrier to blood-borne thrombogenic factors and other high molecular weight compounds. The final type of endoluminal paving is liquid paving, which makes use of "flowable" polymeric, macromeric, or prepolymeric solutions. With heating, these solutions adhere and interact with the endoluminal surface.

Whether using the thermal or photothermal procedure for paving, the reaction of the polymer with the underlying tissue is favorable. Vessel media has been shown to remain intact and without further damage following application of polymers as shown by histological cross section (118). When melted, the polymer is capable of molding to the exact shape of the vessel, inclusive of crevices and fissures in the surface, as the polymer binds to the tissue by physical interlocking (117). When the catheter balloon is removed, a smooth surface is left endoluminally despite the previous irregular and thrombogenic surface of the vessel (116). Liquid paving can reportedly interact with the vessel by altering the tissue surface charge, porosity, lubricity, and drug delivery capabilities (116).

Both in vitro and in vivo studies have been described using gel paving technology. Thrombi and platelet deposi-

tion have been reduced in hydrogel-paced segments of isolated perfused rat carotid (119), bovine coronary, and canine carotid arteries. In vivo studies yielded similarly promising results. Patency was determined in a rat carotid arterial crush models (117), a New Zealand White rabbit balloon injury model (120), and in canine carotid arteries (118). Tests still need to be performed to definitively determine paving efficacy and safety.

Microparticle Delivery of Drugs to the Cardiovascular System

Inefficient delivery of drug to tissue, diffusion of drug away from infusion site (76), and injury to tissue caused by infusion pressure (121) all diminish the therapeutic value of catheter-based drug delivery systems. Superior drug vascular deposition might be achieved with polymeric microparticles as delivery vehicles (76). Injected microparticles adhere to and remain with the injected tissue sites far longer than free drug. The particles might become lodged in vasa vasorum as well and from these sites serve as local diffusion depots (122–124). Rates of release can be modulated by modifying the chemical composition or the molecular weight of the polymer (122). Other modifications to microsphere fabrication methods enable it to embody the requirements necessary to function as a successful delivery device. Prerequisites for polymeric drug carriers include a small enough size for infusion through contemporary catheter designs, the capability of carrying a high concentration of drug and releasing that drug in a controlled, sustained manner, and the properties of being both biodegradable and biocompatible (122).

Dexamethasone-encapsulating poly(lactide-*co*-glycolide) spheres, with prolonged release kinetics providing drug for over a month, were infused via porous balloon catheters into balloon denuded rat carotid arteries. Tissue levels of drug were much higher in the locally treated segment of artery than in adjacent segments or in contralateral control arteries, further substantiating the absence of distant drug distribution. Microspheres that persisted in the artery for at least seven days eliminated neointimal formation, but did not produce any significant inflammatory responses. Conversely, the systemic administration of dexamethasone given through intraperitoneal injection did not reduce neointimal growth (122). Radioactive and HRP-laden microspheres were retained for as long as 24 hours and were found mainly in the dissection planes of the artery and the adventitia (125). As studies are carried out for longer timepoints the potential of this therapy will become evident.

BIBLIOGRAPHY

1. R. Wilensky et al., *Trends Cardiovasc. Med.* **3**, 163–170 (1993).
2. R.S. Schwartz, D.R. Holmes, and E.J. Topol, *J. Am. Coll. Cardiol.* **20**, 1284–1293 (1992).
3. R. Riessen and J.M. Isner, *J. Am. Coll. Cardiol.* **25**(5), 1234–1244 (1994).
4. J.H. Anderson, C. Gianturco, and S. Wallace, *Invest. Radiol.* **16**(6), 496–500 (1981).
5. B.J. Meyer et al., *Circulation* **90**(5), 2474–2480 (1994).
6. M.M. Thompson et al., *Eur. J. Vasc. Surg.* **8**(4), 423–434 (1994).
7. T. Kerenyi et al., *Exp. Mol. Pathol.* **49**, 330–338 (1988).
8. B. Goldman, H. Blanke, and H. Wolinsky, *Atherosclerosis* **65**, 215–225 (1987).
9. L.E. Duncan, K. Buck, and A. Lynch, *J. Atheroscler. Res.* **5**, 69–79 (1965).
10. E.G. Nabel et al., *J. Clin. Invest.* **91**, 1822–1829 (1993).
11. H. Wolinski and S.N. Thung, *J. Am. Coll. Cardiol.* **15**, 475–481 (1990).
12. A. Nathan and E.R. Edelman, in E.R. Edelman, ed., *Molecular Interventions and Local Drug Delivery*, Saunders, Philadelphia, 1995, pp. 29–52.
13. M.Y. Flugelman et al., *Circulation* **85**, 1110–1117 (1992).
14. G.D. Chapman et al., *Circ. Res.* **71**, 27–33 (1992).
15. M.L. Stadius, C. Collins, and R. Kernoff, *Am. Heart J.* **126**, 47–56 (1993).
16. C.R. Lambert, J.E. Leone, and S.M. Rowland, *Coronary Artery Dis.* **4**, 469–475 (1993).
17. M.K. Hong et al., *Circulation* **86**(Suppl. 1), I-380 (1992).
18. A.V. Kaplan et al., *J. Am. Coll. Cardiol.* **23**, 187A (1994).
19. D.C. Cumberland et al., *J. Am. Coll. Cardiol.* **23**, 186A (1994).
20. M.K. Hong et al., *Coronary Artery Dis.* **4**, 1023–1027 (1993).
21. M.K. Hong et al., *Catheter. Cardiovasc. Diagn.* **34**(3), 263–271 (1995).
22. R.L. Wilensky et al., *J. Am. Coll. Cardiol.* **21**, 185A (1993).
23. G.L. Nunes et al., *J. Am. Coll. Cardiol.* **23**(7), 1578–1583 (1994).
24. M. Azrin, *Proc. 1st Ann. Int. Symp. Local Cardiovasc. Drug Delivery*, Cambridge, Mass., Sept. 28–29, 1995.
25. G.L. Nunes et al., *Circulation* **86**, I-380 (1992).
26. J.F. Mitchel et al., *Circulation* **90**, 1979–1988 (1994).
27. M.A. Azrin et al., *Circulation* **88**, I-310 (1993).
28. M.A. Azrin et al., *Circulation* **90**, 433–441 (1994).
29. D.B. Fram et al., *J. Am. Coll. Cardiol.* **23**, 1570–1577 (1994).
30. D.B. Fram et al., *J. Am. Coll. Cardiol.* **21**, 118A (1993).
31. J.F. Mitchel et al., *Circulation* **88**, I-660 (1993).
32. P.G. Steg et al., *Circulation* **88**, I-660 (1993).
33. R. Riessen et al., *Hum. Gene Ther.* **4**, 749–758 (1993).
34. D.B. Fram et al., *J. Am. Coll. Cardiol.* **23**(1A–484A), 186A (1994).
35. R.G. McKay et al., *Catheter. Cardiovasc. Diagn.* **33**(2), 181–188 (1994).
36. J.F. Mitchel and R.G. McKay, *Catheter. Cardiovasc. Diagn.* **24**(2), 149–154 (1995).
37. C. Zamarron et al., *Thromb. Haemostasis* **52**, 19–23 (1984).
38. P. Barath and A. Popov, *Proc. 1st Ann. Int. Symp. Local Cardiovasc. Drug Delivery*, Cambridge, Mass., Sept. 28–29, 1995.
39. P. Gonschior et al., *J. Am. Coll. Cardiol.* **23**, 188A (1994).
40. P. Gonschior et al., *Coronary Artery Dis.* **6**(4), 329–334 (1995).
41. R.J. Levy and V. Labhasetwar, *Proc. 1st Ann. Int. Symp. Local Cardiovasc. Drug Delivery*, Cambridge, Mass., Sept. 28–29, 1995.

42. R.S. Schwartz, *Proc. 1st Ann. Int. Symp. Local Cardiovasc. Drug Delivery*, Cambridge, Mass., Sept. 28–29, 1995.
43. I. Soria et al., *Circulation* **88**, I-660 (1993).
44. B. Avitall et al., *Circulation* **85**, 1582–1593 (1992).
45. A. Fernandez-Ortiz et al., *Circulation* **89**(4), 1518–1522 (1994).
46. The Epistent Investigators, *Lancet* **352**, 87–92 (1998).
47. P. Serruys, P. De Jaegere, and F. Kiemeneij, *N. Engl. J. Med.* **331**, 489–495 (1994).
48. D. Fischman, M. Leon, and D. Baim, *N. Engl. J. Med.* **331**, 196–501 (1994).
49. P. Serruys, B. Straus, and K. Beat, *N. Engl. J. Med.* **324**, 13–17 (1991).
50. E. Edelman and C. Rogers, *Am. J. Cardiol.* **81**(7A), 4E–6E (1998).
51. J. Carrozza, R. Kuntz, and M. Levine, *J. Am. Coll. Cardiol.* **20**, 328–337 (1992).
52. M. Levine, B. Leonard, and J. Burke, *J. Am. Coll. Cardiol.* **16**, 332–339 (1990).
53. S. Ellis, M. Savage, and D. Fischman, *Circulation* **86**, 1836–1844 (1992).
54. P. Gordon, C. Gibson, and D. Cohen, *J. Am. Coll. Cardiol.* **21**, 1166–1174 (1993).
55. G. Ferns, M. Reidy, and R. Ross, *Am. J. Pathol.* **137**, 403–413 (1990).
56. M. Liu, G. Roubin, and K. Robinson, *Circulation* **81**, 1089–1093 (1990).
57. D. Muller, E. Topol, and G. Abrams, *Circulation* **82**, III-429 (Abstr.) (1990).
58. D. Handley et al., *Am. J. Pathol.* **124**, 88–93 (1986).
59. E. Hoberg, F. Schwarz, and A. Schomig, *Circulation* **82**, III-428 (1990).
60. K. Lehmann, R. Doria, and J. Feuer, *J. Am. Coll. Cardiol.* **17**, 181A (Abstr.) (1991).
61. H. Whitworth, G. Roubin, and J. Hollman, *J. Am. Coll. Cardiol.* **8**, 1271–1276 (1986).
62. D. Faxon, T. Spiro, and S. Minor, *J. Am. Coll. Cardiol.* **19**, 258A (1992).
63. The Mercator Investigators, *Circulation* **86**, 100–110 (1992).
64. C. Pepine, J. Hirshfeld, and R. Macdonald, *Circulation* **81**, 1753–1761 (1990).
65. A. Lincoff, E. Topol, and S. Ellis, *Circulation* **90**, 2070–2084 (1994).
66. E. Edelman, D. Adams, and M. Karnovsky, *Proc. Natl. Acad. Sci. U.S.A.* **87**, 3773–3777 (1990).
67. M. Simons, E. Edelman, and J. DeKeyser, *Nature (London)* **359**, 67–70 (1992).
68. A. Villa, L. Guzman, and W. Chen, *J. Clin. Invest.* **93**, 1243–1249 (1994).
69. R. Wilensky, I. Gradus-Pizlo, and K. March, *Circulation* **86**, I-52 (1992).
70. D. Muller, G. Golomb, and D. Gordon, *Circulation* **86**, I-381 (Abstr.) (1992).
71. C. Rogers et al., *Circulation* **90**, I-508 (Abstr.) (1994).
72. D. Cox, P. Anderson, and G. Roubin, *Circulation* **78**, II-71 (Abstr.) (1988).
73. C. Rogers, M.J. Karnovsky, and E.R. Edelman, *Circulation* **88**(3), 1215–1221 (1993).
74. J. Garasic, C. Rogers, and E. Edelman, in K. Beyar et al., eds., *Frontiers in Interventional Cardiology*, Martin Dunitz, UK, 1997, pp. 95–100.
75. H. Hanke, J. Kamenz, and S. Hassenstein, *Eur. Heart J.* **16**, 785–793 (1995).
76. R. Wilensky, K. March, and I. Gradus-Pizlo, *Am. Heart J.* **129**, 852–859 (1995).
77. C. Thomas, K. Robinson, and G. Cipolla, *J. Am. Coll. Cardiol.* **23**, 187A (Abstr.) (1994).
78. L. Gimple, R. Owen, and V. Lodge, *Circulation* **82**, III-338 (Abstr.) (1992).
79. A. Lunn, in U. Sigwart, ed., *Endoluminal Stenting* Saunders, Philadelphia, 1996 pp. 80–83.
80. S. Bailey et al., *Circulation* **86**, I-186 (1992).
81. P. Hardhammar, H. van Beusekom, and H. Emanuelsson, *Circulation* **93**, 423–430 (1996).
82. J. Murphy, R. Schwartz, and W. Edwards, *Circulation* **86**, 1596–1604 (1992).
83. The Benestent-II Investigators, *Circulation* **93**, 412–422 (1996).
84. T. Lambert, V. Dev, and R. Eldad, *Circulation* **90**, 1003–1111 (1994).
85. D. Holmes, A. Camrud, and M. Jorgenson, *J. Am. Coll. Cardiol.* **24**, 525–531 (1994).
86. A. Lincoff et al., *J. Am. Coll. Cardiol.* **23**, 18A (Abstr.) (1994).
87. M. Staab, D. Holmes, and R. Schwartz, in S.U, Editor. *Endoluminal Stenting*, Saunders, Philadelphia, 1996, pp. 34–44.
88. E. Edelman and M. Lovich, *Nat. Biotechnol.* **16**, 136–137 (1998).
89. S.J. Sollot, L. Cheng, and R. Pauly, *J. Clin. Invest.* **95**, 1869–1876 (1995).
90. D. Axel, W. Kunert, and C. Goggelmann, *Circulation* **96**, 636–645 (1997).
91. M. Lovich and E. Edelman, *Am. J. Physiol.* **271**, H2014–H2024 (1996).
92. E.R. Edelman, M.A. Nugent, and M.J. Karnovsky, *Proc. Natl. Acad. Sci. U.S.A.* **90**, 1513–1517 (1993).
93. D.A. Dichek et al., *Circulation* **80**, 1347–1353 (1989).
94. M.Y. Flugelman et al., *Circ. Res.* **70**, 348–354 (1992).
95. N. Scott, F. Candal, K. Robinson, and E. Ades, *Am. Heart J.* **129**, 860–865 (1995).
96. L. Ruan et al., *J. Controlled Release* **20**, 231–236 (1992).
97. P.H. Vlasses et al., *J. Cardiovasc. Pharmacol.* **7**(2), 245–250 (1985).
98. T. Nagai et al., *J. Controlled Release* **1**(3), 239–246 (1985).
99. R. Langer and J.B. Murray, *Appl. Biochem. Biotechnol.* **8**, 9–24 (1983).
100. E.R. Edelman et al., *Biomaterials* **12**, 619–626 (1991).
101. E.R. Edelman et al., *Circ. Res.* **76**(2), 176–182 (1995).
102. M.R. Bennett et al., *J. Clin. Invest.* **93**, 820–828 (1994).
103. M. Simons, E.R. Edelman, and R.D. Rosenburg, *J. Clin. Invest.* **93**, 2351–2356 (1994).
104. J. Abe et al., *Biochem. Biophys. Res. Commun.* **198**, 16–24 (1994).
105. F.W. Sellke et al., *Am. J. Physiol.* **267**, H1303–H1311 (1994).
106. E.R. Edelman et al., *J. Clin. Invest.* **89**, 465–471 (1992).
107. D.H. King et al., *Am. Heart J.* **106**, 1438–1440 (1983).

Next Page

108. R.J. Levy et al., in C.G. Gebelein, ed., *Biotechnology and Bioactive Polymers*, Lionfire, Edgewater, Fla., 1994, pp. 259–268.
109. H.G. Mond and K.B. Stokes, *Pace Pacing Clin. Electrophysiol.* **15**, 95–107 (1992).
110. A. Sintov et al., *J. Cardiovasc. Pharmacol.* **16**, 812–817 (1990).
111. R. Siden et al., *J. Cardiovasc. Pharmacol.* **19**, 798–809 (1992).
112. V. Labhasetmar et al., *J. Pharm. Sci.* **83**, 156–164 (1994).
113. R.J. Levy et al., *Science* **228**, 190–192 (1985).
114. G. Golomb et al., *J. Pharm. Sci.* **76**, 271–276 (1987).
115. Y.V. Pathak et al., *Biomaterials* **11**, 718–723 (1990).
116. M.J. Slepian, *Proc. 1st Ann. Int. Symp. Local Cardiovasc. Drug Delivery*, Cambridge, Mass., Sept. 28–29, 1995.
117. J.L. Hill-West et al., *Proc. Natl. Acad. Sci. U.S.A.* **91**, 59–67 (1994).
118. M.J. Slepian, *Cardiol. Clin.* **12**, 715–737 (1994).
119. M.J. Slepian et al., *Circulation* **88**(4), I-319 (1993).
120. M.J. Slepian et al., *Circulation* **4** (P. 2), I-660 (1993).
121. K.A. Robinson et al., *J. Am. Coll. Cardiol.* **21**(2), 118A (1993).
122. L.A. Guzman et al., *Circulation* **94**(6), 1441–1448 (1996).
123. R.L. Wilensky, K.L. March, and D.R. Hathaway, *Am. Heart J.* **122**(4), 1136–1140 (1991).
124. J.J. Rome et al., *Arterioscler. Thromb.* **14**(1), 148–161 (1994).
125. A. Farb, G.C. Carlson, and R. Virami, *Circulation* **88**(Suppl. 1), I-310 (1993).

CARRIER-MEDIATED TRANSPORT, ORAL DRUG DELIVERY

G.J. RUSSELL-JONES
Biotech Australia Pty Ltd.
Roseville, NSW, Australia

KEY WORDS

Cyanocobalamin
Drug delivery
Folate
Invasins
Oral
Peptides
Proteins

OUTLINE

Introduction
Carrier-Mediated Transport Systems
The Intestinal Peptide Transporter
The Bile Acid Transport System
Immunoglobulin Transport
Adhesins, Hemagglutinins, Toxins, and Lectins
Toxins of Bacteria and Plants and Lectins
Receptor-Mediated Endocytosis of Transferrin and the Uptake of Fe
Use of the Vitamin B-12–Mediated Transport System for Uptake of Pharmaceuticals
Characteristics of the Uptake System
Conjugation of Pharmaceuticals to Vitamin B-12
Cell Models of Receptor-Mediated Transport
Oral Delivery of Peptides and Proteins Using the Vitamin B-12 Transport System
Amplification of the Vitamin B-12 Uptake System Using Nanoparticles
Future Directions
The Use of Pathogenic Methods of Invasion for Carrier-Mediated Transport
Carrier-Mediated Transport of Nanoparticles
Conclusions
Bibliography

INTRODUCTION

The intestinal absorption of low-molecular-weight vitamins, sugars, and other nutrients is highly efficient. In contrast, intestinally administered macromolecules are poorly absorbed and have very low oral bioavailability. Prior to absorption, most orally administered substances must first be digested to simple constituent molecules before being absorbed. Thus, oligosaccharides are hydrolyzed to monosaccharides that are in turn absorbed by active transport mechanisms, while dietary proteins are initially degraded by pepsin in the stomach before being further degraded by trypsin, chymotrypsin, and carboxypeptidases in the small intestine to become small peptides, individual amino acids, and dipeptides. Small peptides are hydrolyzed to free amino acids either during or soon after transport. The resultant material that appears in the portal blood is primarily, though not completely, free amino acids (1). Separate uptake mechanisms occur for neutral, basic, and acidic amino acids. Fats are first broken down to long-chain triglycerides in the stomach and upper small intestine and then complexed to and absorbed in association with bile salts. The absorption of fat-soluble vitamins probably occurs as a similar complex. In contrast to the highly efficient absorption of small molecules, the intraduodenal infusion of intact proteins such as ^{3}H-BSA results in only 2% of the dose being transmitted in a macromolecular form to the lymph and blood (2). The absorption of orally administered macromolecules is even lower and ranges between 0.1–2.0% of the administered dose (3). Thus, the absorption of most peptides and proteins following oral administration is so low as to be economically unfeasible.

Despite the generally poor absorption of peptides and proteins, the oral route of delivery of peptide and protein still remains the most desirable method of chronic drug treatment. With the development of an increasing number of peptide and protein pharmaceuticals, a clear need exists for the development of a delivery system other than the current parenteral ones. Thus, molecules such as insulin,

Previous Page

108. R.J. Levy et al., in C.G. Gebelein, ed., *Biotechnology and Bioactive Polymers*, Lionfire, Edgewater, Fla., 1994, pp. 259–268.
109. H.G. Mond and K.B. Stokes, *Pace Pacing Clin. Electrophysiol.* **15**, 95–107 (1992).
110. A. Sintov et al., *J. Cardiovasc. Pharmacol.* **16**, 812–817 (1990).
111. R. Siden et al., *J. Cardiovasc. Pharmacol.* **19**, 798–809 (1992).
112. V. Labhasetmar et al., *J. Pharm. Sci.* **83**, 156–164 (1994).
113. R.J. Levy et al., *Science* **228**, 190–192 (1985).
114. G. Golomb et al., *J. Pharm. Sci.* **76**, 271–276 (1987).
115. Y.V. Pathak et al., *Biomaterials* **11**, 718–723 (1990).
116. M.J. Slepian, *Proc. 1st Ann. Int. Symp. Local Cardiovasc. Drug Delivery*, Cambridge, Mass., Sept. 28–29, 1995.
117. J.L. Hill-West et al., *Proc. Natl. Acad. Sci. U.S.A.* **91**, 59–67 (1994).
118. M.J. Slepian, *Cardiol. Clin.* **12**, 715–737 (1994).
119. M.J. Slepian et al., *Circulation* **88**(4), I-319 (1993).
120. M.J. Slepian et al., *Circulation* **4** (P. 2), I-660 (1993).
121. K.A. Robinson et al., *J. Am. Coll. Cardiol.* **21**(2), 118A (1993).
122. L.A. Guzman et al., *Circulation* **94**(6), 1441–1448 (1996).
123. R.L. Wilensky, K.L. March, and D.R. Hathaway, *Am. Heart J.* **122**(4), 1136–1140 (1991).
124. J.J. Rome et al., *Arterioscler. Thromb.* **14**(1), 148–161 (1994).
125. A. Farb, G.C. Carlson, and R. Virami, *Circulation* **88**(Suppl. 1), I-310 (1993).

CARRIER-MEDIATED TRANSPORT, ORAL DRUG DELIVERY

G.J. RUSSELL-JONES
Biotech Australia Pty Ltd.
Roseville, NSW, Australia

KEY WORDS

Cyanocobalamin
Drug delivery
Folate
Invasins
Oral
Peptides
Proteins

OUTLINE

Introduction
Carrier-Mediated Transport Systems
The Intestinal Peptide Transporter
The Bile Acid Transport System
Immunoglobulin Transport
Adhesins, Hemagglutinins, Toxins, and Lectins
Toxins of Bacteria and Plants and Lectins
Receptor-Mediated Endocytosis of Transferrin and the Uptake of Fe
Use of the Vitamin B-12–Mediated Transport System for Uptake of Pharmaceuticals
Characteristics of the Uptake System
Conjugation of Pharmaceuticals to Vitamin B-12
Cell Models of Receptor-Mediated Transport
Oral Delivery of Peptides and Proteins Using the Vitamin B-12 Transport System
Amplification of the Vitamin B-12 Uptake System Using Nanoparticles
Future Directions
The Use of Pathogenic Methods of Invasion for Carrier-Mediated Transport
Carrier-Mediated Transport of Nanoparticles
Conclusions
Bibliography

INTRODUCTION

The intestinal absorption of low-molecular-weight vitamins, sugars, and other nutrients is highly efficient. In contrast, intestinally administered macromolecules are poorly absorbed and have very low oral bioavailability. Prior to absorption, most orally administered substances must first be digested to simple constituent molecules before being absorbed. Thus, oligosaccharides are hydrolyzed to monosaccharides that are in turn absorbed by active transport mechanisms, while dietary proteins are initially degraded by pepsin in the stomach before being further degraded by trypsin, chymotrypsin, and carboxypeptidases in the small intestine to become small peptides, individual amino acids, and dipeptides. Small peptides are hydrolyzed to free amino acids either during or soon after transport. The resultant material that appears in the portal blood is primarily, though not completely, free amino acids (1). Separate uptake mechanisms occur for neutral, basic, and acidic amino acids. Fats are first broken down to long-chain triglycerides in the stomach and upper small intestine and then complexed to and absorbed in association with bile salts. The absorption of fat-soluble vitamins probably occurs as a similar complex. In contrast to the highly efficient absorption of small molecules, the intraduodenal infusion of intact proteins such as ^{3}H-BSA results in only 2% of the dose being transmitted in a macromolecular form to the lymph and blood (2). The absorption of orally administered macromolecules is even lower and ranges between 0.1–2.0% of the administered dose (3). Thus, the absorption of most peptides and proteins following oral administration is so low as to be economically unfeasible.

Despite the generally poor absorption of peptides and proteins, the oral route of delivery of peptide and protein still remains the most desirable method of chronic drug treatment. With the development of an increasing number of peptide and protein pharmaceuticals, a clear need exists for the development of a delivery system other than the current parenteral ones. Thus, molecules such as insulin,

LH–RH analogs, erythropoietin (EPO), granulocyte colony stimulating factor (G-CSF), thrombopoietin (TPO), heparin, vasopressin, and oxytocin, must still be administered parenterally. Perceived benefits for the development of such alternative delivery systems include increased patient comfort and compliance, ease of administration, reduced medical costs, and increased market. It must be noted, however, that additional costs may arise through the use of alternative carriers such as those described in this article owing to costs associated with the carrier, conjugation and scale up, and so on. The development of such alternative drug delivery systems also has the added benefit of "bringing new life to old drugs," particularly as many drugs come off patent.

In an attempt to overcome the problems of poor bioavailability of peptides and proteins, a number of carrier systems are currently being developed. This article describes the various specific carrier-mediated systems in the intestine that may be harnessed for oral drug delivery. While each of the carrier systems described is vastly different, they share the properties of initial binding to the apical surface of the intestinal epithelial cell (enterocyte), transfer across the cell membrane or entire cell, and release from the basal surface of the intestinal epithelial cell into the circulation.

CARRIER-MEDIATED TRANSPORT SYSTEMS

The Intestinal Peptide Transporter

Evidence from a number of sources has now shown that dipeptides are actively transported from the intestine into the circulation by a specific carrier system that differs from those involved in the transport of individual amino acids (4,5). This carrier system has been termed the intestinal peptide transporter or dipeptide transporter and has been implicated as a normal method of nutrient acquisition (6). This mechanism has been shown to be Na^+ independent (1,7) and to utilize an inward H^+ gradient as its driving force. The intestinal peptide transporter has been shown to be responsible for the transport of aminocephalosporin antibiotics such as cephalexin (7–9). The dipeptide transporter is separate from the brush border peptidases, and at least one report has suggested that a membrane protein of M_r 127,000 is responsible for uptake (10). Several reports point to the possibility that two separate saturable transport systems for dipeptides exist in the small intestine. The Type I system prefers neutral pH and has a low affinity and a high capacity, while the Type II system prefers an acidic pH and has a high affinity and a low capacity. Thus Inui and coworkers (8) found that at neutral pH, cephradine was transported by the Type I system, while at an acidic pH it was transported via the Type II system. It may be possible that a single carrier, rather than two carriers, may exist that changes its conformation and affinity as the pH changes.

Although it was initially thought that the peptide transporter "required" an *N*-terminal nitrogen atom, the studies of Hu and Amidon (11) on the angiotensin converting enzyme inhibitor, Captopril, suggest this not to be the case. Thus, the peptide transporter shows broad substrate specificity (12,13) (Table 1). For optimal interaction with the transporter, dipeptides require a free carboxyl group, as it has been shown that reduction of this group to an alcohol reduces affinity for the transporter, as does cyclization (3). The transporter is stereospecific, showing higher transport of LL-dipeptides. Molecules and dipeptides shown to be transported by these transporters include glycylsarcosine, glycyl-L-proline, L-glutamyl-L-glutamate (8), amino β-lactam antibiotics (14,15), penicillins (amoxicillin, ampicillin, cyclacillin) (12,16), angiotensin-converting enzyme inhibitors (Captopril, Benazepril, Enalapril, Lisinopril, Quinapril) (17), cephalosporins (Cefaclor, Cefadroxil, Cefatrizine, Cefdinir, Cefixime, Ceftibuten) (12,18), and renin inhibitors (3) among others (Table 1). The maximal size of peptide transported via this mechanism appears to be a tripeptide (19), with transport of tetrapeptides occurring to only a limited extent, if at all (12). Intestinal cell models, such as the HT-29 and Caco-2 human carcinoma cell lines, have been shown to express the peptide transporter (12,20).

The identification of the peptide transport process has meant that many orally active molecules such as antibiotics (i.e., penicillins and cephalosporin), which were formerly thought to be taken up by passive diffusion, are in fact absorbed owing to their ability to interact with the normal uptake mechanism for dipeptides and tripeptides. This transport system has the advantage of a high capacity, but is limited to molecules of a small molecular weight (less than 600 Da) and to peptides or molecules having structural homologies with di- and tripeptides. A highly comprehensive treatment of the subject can be found in the review by Walter and co-workers (12).

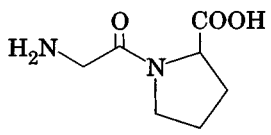
The Bile Acid Transport System

During the normal course of breakdown and absorption of fats, bile acids, synthesized from cholesterol in the liver, are secreted into bile and are then emptied into the small intestine where they aid the digestion and absorption of fats and fat-soluble vitamins. These bile acids are subsequently absorbed from the intestine and gain entry into the liver via the hepatic portal system. Bile salts taken up by hepatocytes may be resecreted into bile. Thus bile acids may circulate 6–10 times per day, representing a total bile acid turnover of 20–30 g bile salts per day in humans (21). The process of bile absorption is remarkably efficient as only 2–5% of bile acids are not absorbed and are excreted in the feces (21). Bile acids that have been recirculated back to the liver cause a feedback inhibition of cholesterol being converted to bile salts by modulating cholesterol-7α-hydrolase activity. The possibility exists, therefore, that it might be possible to lower cholesterol through the interruption of the enterohepatic circulation of bile salts.

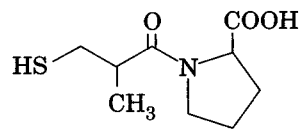
Bile acid absorption from the intestine is a Na^+-dependent process that relies on a specific bile acid transporter located in the ileum. Kramer and coworkers, using photoaffinity labeling, have identified the transporter in rabbits to be a 90–93-kDa protein (22,23), while in rats the putative transporter is a 99-kDa protein (24).

The bile acid transport system in the ileum shows a high degree of substrate specificity such that chenodeoxy-

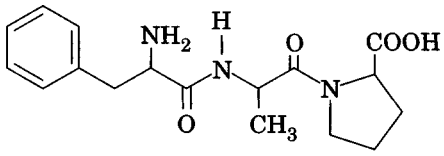
Table 1. Structural Homologies Between Di- and Tripeptides and Some Common Peptide Drugs



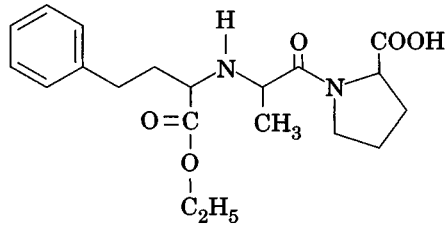
Gly-pro



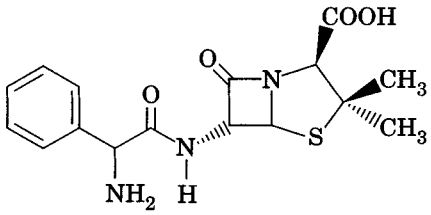
Captopril



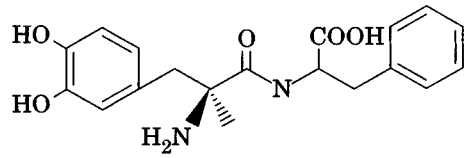
Phe-ala-pro



Enalapril



Ampicillin



D-α-methyldopa-Phe

cholate uptake > deoxycholate > taurolithocholate > tauroursodeoxycholate > cholate ≫ lithocholate (22,23). The specificity for different bile acids for uptake by the small intestine is different than that of hepatic bile acid transport (22,23). Structural studies by Kramer and coworkers have shown that bile acid binding to the transporter depends on the presence of an essential cysteine residue at the binding site of the transporter. Binding is also inhibited following amino modification but not following carboxyl or hydroxyl modification of the transporter (22,23) Tables 2 and 3). Structural recognition of the bile salts by the transporter requires a negative charge on the bile acid molecule, and at least one hydroxyl group at positions 3, 7, or 12 of the steroid is also an essential feature. Similarly, for maximal binding the natural methylbutanoic acid or its taurine or glycine derivatives at position 21 should remain unchanged. Transport is greatly reduced for modified bile acids that contain dianionic, zwitterionic, or uncharged side chains (21,25). Further definition of structural requirements of the transporter may be obtained from studies using the recently cloned bile acid transporter (26).

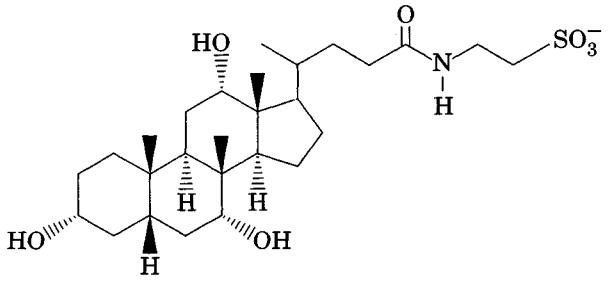
The high uptake capacity of the intestine for bile salts (>20 per day), plus the subsequent targeting of bile salts to the liver, has led many researchers to attempt to use the bile acid transport system to improve intestinal absorption of small, poorly absorbed molecules and to specifically target drugs to the liver (27,28). In studies on model compounds, Kramer and coworkers found that the maximal size of a peptide that could be transported via the bile acid transporter was four amino acids, or around 600 Da (28). Several classes of compounds shown to have an affinity for the bile acid transporter include steroid analogs (ouabain, fusidic acid), cyclic peptides (antamanide), cyclic somatostatin derivatives (octreotide), and renin inhibitors (21,29). Liver-specific targeting with bile salts has been shown for conjugates to chlorambucil, phalloidin, and various oxaprolylpeptides (28).

Successful systemic delivery following oral administration of a bile acid drug conjugate would require the presence of a biodegradable linkage or prodrug approach for the drug to remain in the circulation rather than be delivered to the liver. Although the bile acid transport system appears to offer the possibility of a high-capacity oral uptake system for small peptides, to date the feasibility of this approach for systemic drug delivery remains to be demonstrated.

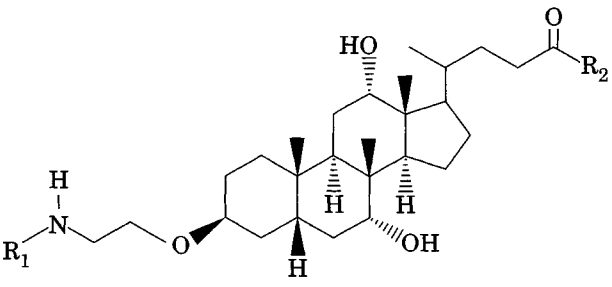
Immunoglobulin Transport

Neonatal IgG Transport. Many neonatal animals have luminal receptors for the transport of IgG. These receptors specifically bind the Fc portion of IgG molecules but do not bind to other immunoglobulin classes; generally located in

Table 2. Structure of Modified Bile Acids for Peptide Conjugation



Bile acid—taurocholate



Peptide-modified bile acid

the proximal intestine, they show interesting binding characteristics in that they bind at pH 6.0 but not at pH 7.4. This makes them ideal for binding to intestinal IgG (pH < 6.5) and release in serosal plasma (pH 7.4) (30). IgG receptors have been shown to be responsible for the accumulation of maternal antibody from milk into the serum of newborn animals in many species, such as the rat (30–34), goat, sheep, pig, horse, cat, dog, and mouse (35,36). Jakoi and coworkers (34) found the IgG receptor to be present in neonatal rats (up to 21 days old) and mice (35,37) but lost following weaning.

During the identification of the IgG transport pathway, molecules such as ferritin have been linked to the IgG molecules to follow uptake and transcytosis. Thus, it would appear possible for large molecules such as ferritin to be carried into the neonate following conjugation to IgG. Similarly, as uptake and transcytosis depends on the Fc region of the IgG molecule, specific IgG antibody could conceivably be used to transport molecules bound to the antigen-binding site of the IgG across the neonatal small intestine into the circulation. Peppard and coworkers (38) have been able to demonstrate the transfer of immune complexes from the lumen of the small intestine of suckling rats to the bloodstream. The levels of transport were lower, however, than would have been expected from normal IgG transport. While little evidence exists for intestinal IgG transport in humans, this particular transport system has potential use in neonatal dogs, goats, sheep, pigs, cats and horses.

The Polymeric Immunoglobulin Receptor. The polymeric immunoglobulin receptor (pIgR) is responsible for the receptor-mediated transport of polymeric IgA and IgM across many types of epithelial surfaces. Transport occurs via binding of the Fc portion of these two molecules to the pIgR on the basal surface of the epithelial cell followed by transport of the molecules from the basolateral to apical surface. In this fashion, material bound to the IgA or IgM may be transported out of the body onto the epithelial surface (39–42). Transport occurs not only across epithelial cells but also via secretion into the bile and has been observed in several cell lines, including MDCK cells (40,41). Transport via this process is unidirectional and rapid, with a half time of less than 30 minutes (33).

Although the IgA has normally been implicated in protection of mucosal surfaces against infection, it also has been postulated that the IgA transport system may have a role in the removal of IgA-containing immune complexes by transport across epithelial surfaces (33). Other studies have shown that during the transport of IgA through the enterocyte, the IgA may also be able to neutralize virions within the cells (43). The possibility exists therefore to utilize this "reverse-transport" process for the removal of toxins, allergens, viruses, and bacteria from the circulation and into the intestine.

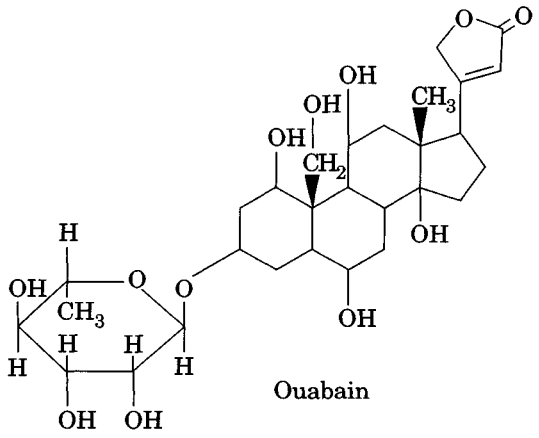
Adhesins, Hemagglutinins, Toxins, and Lectins

A number of structures on the surface of bacteria and viruses are capable of binding specifically to the intestinal epithelium and can in many cases cause internalization of the bacterium or virus within the intestinal epithelial cells. Many plant lectins and toxins also share this property. The binding subunits of these molecules have the potential to be used as both intestinal epithelial targeting molecules for delaying the transit of pharmaceuticals down the intestine and as molecules for eliciting the uptake and transcytosis of the targeting molecule and attached pharmaceutical across the intestinal epithelial cell.

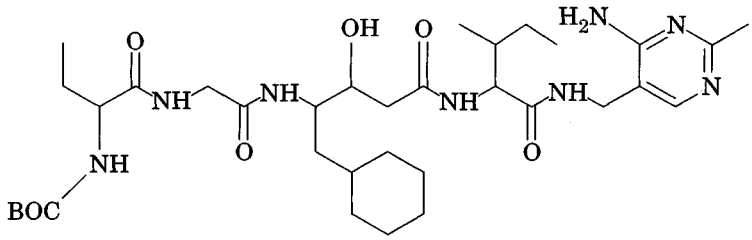
Bacterial Adhesins. The surface of many gram-positive bacteria is often covered with many proteins with potential roles in binding to surfaces and eliciting uptake. These include proteins isolated from various *Streptococcus* species such as the IgA-binding proteins ARP2, ARP4, and bac (44); the IgA-binding protein from Group B streptococci (45); fibrinogen-binding proteins (Mrp4, Sfb, PrtF, FnbA, FnbB, FnBP, FnBp [43]); and the collagen-binding factor (Cna) and clumping factor (ClfA) from *Streptococcus aureus*.

One of the first structures shown to be responsible for adhesion of bacteria to epithelial surfaces is the filamentous surface adhesion or pilus. These adhesins include the K88, K99 (46), F41, and 987P pili found on *Escherichia coli* inhabiting neonatal calves and piglets; the CFA1 and CFAII pili found on *E. coli* strains causing diarrhea in humans; and the *Pseudomonas aeruginosa* PAK pilus (47,48). There is also the type P pili isolated from *E. coli* strains associated with human pyelonephritis (49). Type I and Type 2 fimbriae found on *Aeromonas viscosis* and *Aeromonas naeslundii* (respectively) also have potential roles

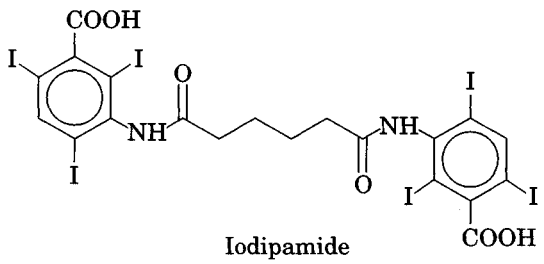
Table 3. Structure of Drugs with an Affinity for the Bile Acid Transporter



Ouabain



Renin Inhibitor



Iodipamide

in adherence and subsequent internalization of these bacteria (44) (Table 4). Similarly, a 36-kDa protein on the surface of *Neisseria gonorrhoeae* has been implicated in the binding of these organisms to surface lactosylceramides on human epithelial cells and may be responsible of uptake of these organisms by the epithelial cells (50).

Internalization by any of the above mechanisms is thought to be microfilament dependent and to be similar to the mechanism of uptake of *Campylobacter jejuni* and *Citrobacter freundii*, which have been shown to be able to initiate microtubule-dependent endocytosis with subsequent uptake into the endothelial endosome (51).

Binding of bacteria to epithelial cells results either in colonization of the epithelial cell surface or internalization of the bacteria within the target cell. While it is not entirely clear why binding sometimes results in internalization, it does depend on the type of cell, the type of cell ligand, and the nature of the interaction (49).

Russell-Jones and coworkers have found that it is possible to use the binding ability of these adhesins to cotransport other molecules into or across the epithelial cells. Thus, when haptens and proteins were covalently linked to 987P and K99 pili and fed to mice, the mice produced a serum antibody response that was significantly higher than that produced when the mice were fed the antigens alone (52) (Table 5).

Bacterial Invasins. Many bacteria possess surface structures apart from pili that have been shown to be responsible for the epithelial invasion of these bacteria. Inter-

Table 4. Specificity of Binding of Various Pili

Pili	Specificity	Species
K99	Gal, GM2	Calves
F41		
Type 1	D-mannose, methyl-α-D-mannopyranoside	Many
P pili – Pap	Galα1 → 4Gal	Human urogenital epithelia
Pseudomonas aeruginosa PAK		Human buccal epithelia
K88ab, ac		Calves, pig
987P		Pig

Source: From Refs. 44–49.

Table 5. Anti-DNP Response to Orally Administered DNP-Carriers

		Immune response			
		Anti-DNP		Anticarrier	
Immunogen	Dose (μg)	Serum IgG	Sec IgA	Serum IgG	Sec IgA
K99	100	<4	<4	1352 ± 128	16.7 ± 2.3
DNP_2K99	500	1176 ± 164	28 ± 14.4	3565 ± 192	88 ± 21
987P	100	<4	<4	1024 ± 89	88 ± 22.4
DNP_{26}987P	500	1024 ± 244	14 ± 3.1	111 ± 34.1	68 ± 19.2
LTB	20	<4	<4	1351 ± 211	12.2 ± 4.4
DNP_2LTB	20	24.3 ± 5.6	<4	445 ± 35	<4
Concanavlin A	20	666 ± 84	<4	nd	
PW mitogen	20	641 ± 119	<4	nd	
Phaseolus vulgaris	20	1378 ± 110	4.8 ± 2.3	nd	
Glycine max	20	1529 ± 65	3.1 ± 6.9	nd	

Note: Each value represents the mean of 5 mice ±1 standard. Animals were fed on day 0 and 14. Serum and intestinal washouts were obtained on day 21 (52).

nalin, a surface protein encoded by the *inlA* gene of *Listeria monocytogenes* is responsible for internalization of *Listeria* within intestinal epithelial cells (53–57). Internalization of *Listeria* is triggered following binding of internalin to E-cadherin on epithelial cells (54,55). A protein with similar function to internalin is found on the surface *Yersinia pseudotuberculosis*; this protein, invasin, is a 986–amino acid protein located in the *Y. pseudotuberculosis* outer membrane (54,58). Expression of this protein on the surface of other gram-negative bacteria such as *E. coli* K-12 enables these cells to efficiently attach to and become internalized by epithelial cells (54,58). Similarly, latex particles coated with internalin are internalized by cultured mammalian cells (49). A second protein from *Y. pseudotuberculosis*, the *ail* gene product, is responsible for binding of these organisms to many eukaryotic cells but only promotes uptake in a few cell types (58).

Viral Hemagglutinins. Many viruses are known to gain access to the intestinal or respiratory epithelium following binding of surface structures on the virus. Normally such an event leads to the virus causing diarrhea in the infected subject. Specific binding proteins have been shown on the surface of rotaviruses (VP7), adenoviruses, and Norwalk virus (59,60). Similarly, surface hemagglutinins have also been implicated in inducing acid-induced fusion of viruses to membranes following initial binding and uptake of influenza virus (61).

Other hemagglutinin molecules exist on the surface of viruses such as rotavirus and aid in the binding, internalization, and transcytosis of these viruses across intestinal epithelial cells (62). Evidence suggests, however, that following binding of some viruses to the endocyte, the surface hemagglutin may be cleaved to yield a fusogenic protein that in turn enables the virus to enter the cell by direct cell membrane penetration rather than by endocytosis (59,63). Such molecules may have some utility in targeting pharmaceuticals to intestinal epithelial cells but may not be suitable for delivery of the pharmaceutical to the circulation as the endocytosed material may not be transcytosed.

Toxins of Bacteria and Plants and Lectins

Apart from the mucosal uptake and transport of adhesins such as pili and viral hemagglutinins, it has also been found that molecules can be covalently linked to the binding subunits of various toxin and plant lectins and to elicit uptake of the linked molecules following oral administration. Toxins of most relevance to initiate receptor-mediated uptake generally consist of an $A–B_n$ subunit structure in which the A subunit is responsible for toxicity while the B subunit functions as the specific binding unit of the toxin. These toxins include the cholera toxin–like molecules such as *E. coli* heat-labile toxin, cholera toxin, *C. jejuni* heat-labile toxin, *Clostridium botulinum* C2 toxin, tetanus

toxin, diphtheria toxin, *Pseudomonas* exotoxin A (64–66), verotoxin, and Shiga toxin (66). All of these toxins share a common property in that they must first bind to and then cross membranes to exert their toxic activity. It is the ability of these toxins to bind to and be internalized by epithelial cells that makes them suitable vehicles for transporting molecules into and across epithelial cells.

A number of plant toxins of the general structure $A–B_n$ are also active orally and as such have the ability to bind to and be internalized by enterocytes. Toxins such as ricin, abrin, viscumin, modeccin, and volkensin all bind to D-galactose and are highly toxic following oral administration to rodents and humans (67) (Table 6); volkensin, for instance, is toxic at doses of as little as 60 ng/kg in rats. Other A–B toxins that could potentially bind to intestinal epithelial cells and cause uptake include botulinum toxin (from *C. botulinum*) (68).

Although there are few examples of oral delivery of pharmaceuticals using toxin-binding subunits or lectins, it has been shown that oral administration of these molecules elicits high titers of serum antibody to both the lectins/toxins and to haptens and proteins covalently linked to them (Table 6), suggesting that these molecules could also be used as vehicles for oral drug delivery. The repeated usefulness of these molecules for oral drug delivery is questionable, as all molecules studied so far are highly immunogenic and hence would elicit an antibody response to the carrier. These antibodies could block the binding of the lectins/toxins. It has also been found that some individuals are highly allergic to some food lectins and may suffer systemic anaphylaxis as a result of ingesting even small quantities of them.

RECEPTOR-MEDIATED ENDOCYTOSIS OF TRANSFERRIN AND THE UPTAKE OF FE

The means by which iron (III) is taken up from the intestine is still a subject of controversy (69,70). Evidence is accumulating, however, to suggest that iron uptake is mediated by lactotransferrin and transferrin. Iron bound to transferrin is internalized by intestinal epithelial cells once the transferrin has been bound by a high-affinity transferrin receptor located in the brush border membrane (71,72). Once inside the cell, the lower pH of the endosomal vesicle (pH 5.5) causes dissociation of iron from the transferrin, thus delivering iron to the cell (73,74). The small size of the iron molecule most likely precludes this molecule from being used as an oral delivery system, although it is possible that molecules could be linked to transferrin and be taken up with it. A disadvantage of this approach would be the possibility of raising autoantibodies to the transferrin molecule itself. In a similar fashion, antibodies to the transferrin receptor could be used to target material to this receptor-mediated uptake system. Use of this strategy has already been demonstrated for overcoming the blood–brain barrier (75).

USE OF THE VITAMIN B-12–MEDIATED TRANSPORT SYSTEM FOR UPTAKE OF PHARMACEUTICALS

Apart from the various uptake pathways described in the previous section, one natural uptake system offers itself as a unique opportunity for use in the oral uptake of pharmaceuticals. In this regard, the vitamin B-12 (VB_{12}) uptake system is unique in that absorption of this vitamin does not occur by facilitated diffusion or active transport but relies upon the receptor-mediated uptake facilitated by a VB_{12}-binding protein, intrinsic factor (IF). During this process, the [VB_{12}:IF] complex binds to an IF receptor located on the epithelium of the small intestine (predominantly in the ileum). Binding of the complex to the receptor triggers internalization of the complex via a yet-to-be-identified subepithelial vacuole (presumably an endosome), whereupon the IF is degraded by cathepsins, and the released VB_{12} binds to intracellular transcobalamin II with subsequent transcytosis of the [VB_{12}:transcobalamin] complex into the circulation. VB_{12} has many advantages as a carrier for oral drug delivery. Its molecular weight is small (1,356 Da), and as such it is poorly immunogenic. It is also relatively inexpensive and can easily be modified to

Table 6. Specificity of Binding and Site of Action of Various Lectins and Toxins

Toxin	Specificity	Site of Action
Diphtheria toxin		Elongation factor EF-2
Pseudomonas aeruginosa exotoxin		Elongation factor EF-2
Cholera toxin	GM1-ganglioside	
Escherichia coli heat-labile toxin	GM1-ganglioside, galactose	
Shigella shigae toxin	*N*-acetyl-D-glucosamine	60S ribosome
	Clostridium-perfringens	
Abrin	Galactose	60S ribosome
Ricin	D-galactose	60S ribosome
Visumin	D-galactose	60S ribosome
Modeccin	D-galactose	60S ribosome
Volkensin	D-galactose	60S ribosome
Botulinum toxin		
Tetanus toxin		

Note: Binding specificity from Refs. 67–68.

provide suitable functional groups for conjugation to peptide or protein pharmaceuticals. The extended period for uptake of VB_{12}, which lasts for 6–8 hours, results in it being a natural sustained-delivery system that is highly suitable for oral peptide/protein delivery (Fig. 1).

Characteristics of the Uptake System

Uptake of VB_{12} from the gut is a relatively slow process that takes place over several hours. After a single feed of $^{57}CoVB_{12}$ serum, $^{57}CoVB_{12}$ levels do not peak for 2–3 h and uptake continues for up to 18 h (76) (Figure 1). For many pharmaceuticals, delivery by such a slow trickle would be an advantage as it leads to a prolonged pharmaceutical window of drug delivery.

The capacity of the VB_{12} uptake system is comparatively low. In humans only 1–2 nmol of VB_{12} is taken up per oral dose (76). However, it is possible to repeat such oral dosing every 20–30 min, which means that the potential daily uptake using one-to-one conjugates of VB_{12} to pharmaceutical is around 50–100 nmol per day. This level of delivery would be sufficient to deliver pharmaceutically relevant doses of peptides such as calcitonin analogues, vasopressin, oxytocin, LH–RH agonists, G-CSF, and EPO.

Conjugation of Pharmaceuticals to Vitamin B-12

For pharmaceuticals to be cotransported across the intestinal epithelial cell layer and into the circulation, they must first be covalently linked to the carrier. In the case of VB_{12}-mediated transport, the VB_{12} must first be modified to provide a suitable functional group for conjugation. This is readily achieved by the acid hydrolysis of one of the propionimide side chains of the corrin ring to form a monocarboxylic acid derivative (76). The isolated monocarboxylic acid derivative can then be conjugated directly to amino groups of proteins or peptides using a suitable carbodiimide (76,77). The direct linkage of VB_{12} to small peptides may in some cases greatly reduce the bioactivity of the conjugated peptide. In such cases it may be necessary to use a spacer between the VB_{12} and the peptide. Suitable spacers include diaminohexane, diaminododecane, adipyl hydrazine, or long-chain spacers formed between amino-

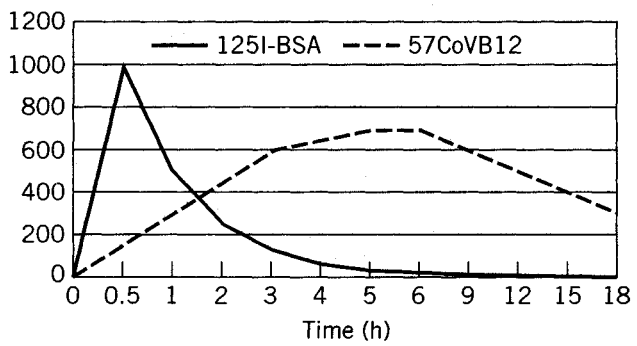


Figure 1. Comparison of uptake of $^{57}CoVB_{12}$ and ^{125}I-BSA. Rats received either $^{57}CoVB_{12}$ or ^{125}I-BSA by oral administration. At various time points the rats were bled and the radioactivity measured in serum.

derivatives of VB_{12} and commercially available cross-linkers such as disuccinimyl suberate (DSS, Pierce), ethylene glycol bis(succinimidyl succinate) (EGS) (76,77). Alternatively, it may be necessary to form a biodegradable bond between the carrier and the drug. Thus Russell-Jones and coworkers (78) found it necessary to link VB_{12} to D-Lys^6-ANTIDE (an LH–RH antagonist) using an iminothiolane derivative of the latter molecule with a succinimidyl 3-(2-pyridyldithio)propionate (SPDP; Pierce) derivative of aminoethyl-eVB_{12} (Table 7). The resultant thiol-cleavable conjugate had a systemic bioactivity similar to that of native ANTIDE. It is also possible to use dithiopyridyl-derivatives of VB_{12} to link directly to free thiols present on the peptide to be joined to VB_{12}. In this fashion it has been shown that forming a thiol-cleavable linkage to a buried thiol in G-CSF is possible (77,79).

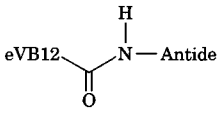
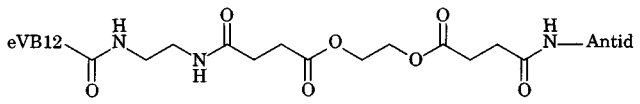
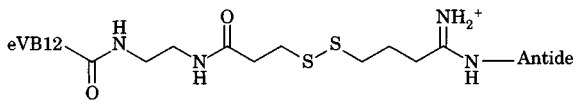
Cell Models of Receptor-Mediated Transport

A number of cell lines exist that polarize upon culture and show receptor-mediated apical-to-basal transport of carrier molecules in an analogous fashion to intestinal epithelial cells. These include two intestinally derived cell lines, the human colon carcinoma cell lines Caco-2 and HT29. Additionally, there are two kidney carcinoma derived lines, the OK cell line, derived from opossum kidney, and the LLCPK1 line, derived from porcine kidney (74,80). These cell lines all exhibit polarized transport when cultured on semipermeable membranes in two-chambered tissue culture wells. The intestinally derived cell lines differ from the kidney cell lines in that they are more heterogeneous and are microviliated, whereas the kidney lines show good homogeneity with little variation from passage to passage.

Vitamin B-12 Transport in Polarized Epithelial Cell Lines. Each of the four cell lines described in the previous section have also been shown to bind, internalize, and transcytose VB_{12} in an IF-dependent fashion. Transport has been shown to be dependent upon polarization of the cells, which occurs when the cells are grown in two-chambered tissue culture wells, with each chamber separated by a permeable filter membrane (81,82). Caco-2 cells have been found to be highly variable in VB_{12} transport with levels of transport ranging from 10–40 fmol/24 h (81,82) to 250 fmol/4 h (80). Caco-2 cells also have been found to transport VB_{12} in an IF-independent fashion, possibly due to the expression of transcobalamin II receptors on their apical surface (83).

Vitamin B-12–Mediated Transport of G-CSF by Caco-2 Cells. Habberfield and coworkers (79) have examined the potential for VB_{12} to act as a carrier to transport EPO and G-CSF across Caco-2 cells grown on semipermeable membranes. When G-CSF was added to the apical chamber of Caco-2 cell cultures, small but detectable levels of G-CSF (14.13 ± 4.4 fmol, or 0.27% of the added dose) were found to cross the monolayer and appear in the basal chamber (Fig. 2). The level of transported material increased dramatically when VB_{12}-G-CSF conjugates were added to the apical chamber. Thus, 398 ± 112, 187 ± 89, and 200 ±

Table 7. Relative Bioactivity of Various Vitamin B-12–ANTIDE Conjugates

Conjugate	Spacer	IC50	Mean LH (ng/ml; ± Std)
Control	–	–	6.4 ± 1.9
ANTIDE	–	4.9 ± 2.8	0.3 ± 0.1
D-Lys^6-ANTIDE	–	2.5 ± 0.5	6.4 ± 1.0
VB_{12}-D-Lys^6-ANTIDE		88 ± 47	6.4 ± 1.0
VB_{12}-EGS-D-Lys^6-ANTIDE		8.9 ± 3.5	8.4 ± 3.0
VB_{12}-SS-D-Lys^6-ANTIDE		11.0 ± 4.0	0.3 ± 0.1

Source: Russell-Jones et al. (76).

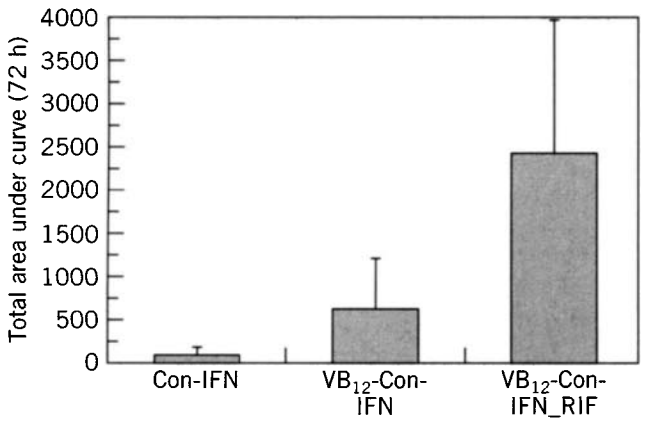


Figure 2. Vitamin B-12–mediated transport of consensus interferon across the rat intestine. Consensus interferon (Con-IFN) was administered to rats by intraduodenal pump infusion, and the quantity of interferon that reached the circulation was assessed. Data represents the area under the curve for 72 h of consensus interferon administered alone, conjugated to VB_{12}, or conjugated to VB_{12} and administered in the presence of rat IP (85).

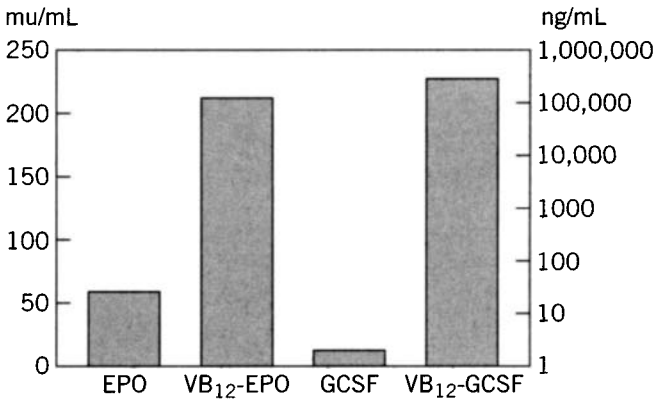


Figure 3. Serum levels of EPO and G-CSF in rats receiving VB_{12}-EPO and VB_{12}-G-CSF intraduodenally. Rats received EPO, VB_{12}-EPO, G-CSF, or VB_{12}-G-CSF by 24-hour intraduodenal pump infusion. The serum levels of EPO (mu/mL) and G-CSF (ng/mL) were calculated by an appropriate ELISA. Data is presented as mu/mL EPO or ng/mL G-CSF.

59 fmol (7.5%, 3.5%, and 3.8%, respectively) of various VB_{12}-G-CSF conjugates were transported in 24 h. The level of transport was dependent on the method of linkage of VB_{12} to G-CSF although it was not proportional to the IF-affinity of the conjugates. Similar results of VB_{12}-mediated transcytosis of EPO, luteinizing hormone–releasing hormone, and interferon have also been shown in Caco-2 cells (76) (Figs. 3 and 4).

Oral Delivery of Peptides and Proteins Using the Vitamin B-12 Transport System

Oral Delivery of LH–RH Analogs. Luteinizing hormone–releasing hormone (LH–RH) is a decapeptide released from the hypothalamus, which stimulates the release of luteinizing hormone (LH) and follicle-stimulating hormone (FSH) from the anterior pituitary. This in turn stimulates ovulation in female animals and spermatogenesis in male animals. Over 1,800 analogs of LH–RH have been synthesized in the past 20 years; some are more potent than LH–RH in stimulating LH and FSH secretion (agonists), while some analogs are able to inhibit the action of LH–RH and are termed antagonists. Russell-Jones and coworkers (77,84) performed ovulation studies in mice using a direct conjugate between eVB_{12} monocarboxylic acid and a D-Lys^6 analogue of LH–RH. D-Lys^6-LH–RH was highly active in stimulating ovulation in pregnant mare serum gonadotropin-primed (PMSG-primed) mice when injected

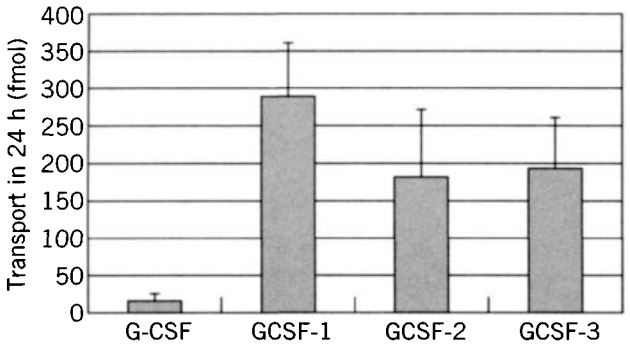


Figure 4. Vitamin B-12–mediated transport of G-CSF by Caco-2 cell cultures. Caco-2 cell cultures were grown on multicell transport chambers. G-CSF or VB_{12}-GCSF conjugates (GCSF-1, GCSF-2, or GCSF-3) were placed in the apical wells, and the quantity of G-CSF reaching the basal chamber after 24 hours was assessed by ELISA (79).

systematically; however, it was much less active when given orally. In contrast, VB_{12}-ε-D-Lys^6-LH–RH was highly active in stimulating ovulation when given either systematically or orally. The oral activity of this conjugate was completely abolished when the VB_{12}-ε-D-Lys^6-LH–RH was given in the presence of excess VB_{12}. In separate studies performed with Dr. J. Sandow (J. Sandow, personal communication, 1992) using VB_{12} linked to D-Lys^6-LH–RH-ethylamide (VB_{12}-D-ε-Lys^6-LH–RH-EA) using various spacers, oral bioavailabilities of between 10 and 45%, depending on the spacer, were obtained in rats. Dr. J. Alsenz and Dr. C. de Schmidt have reported similar oral bioavailabilities for VB_{12}-ε-D-Lys^6-LH–RH-EA conjugates orally administered to rats (J. Alsenz, personal communication, 1996).

Oral Delivery of EPO, G-CSF, and Consensus Interferon via the Vitamin B-12 Transport System. Habberfield and coworkers (79) have recently shown that it is possible to utilize the VB_{12} transport system to promote the intestinal uptake of G-CSF (18,800 Da) and EPO (29,543 Da). In their studies, they implanted miniosmotic pumps into the peritoneal cavity of rats such that their contents drained into the duodenum of the rats. In this way they circumvented the need for multiple feeding of the animals. The pumps were designed to deliver their contents for 24 h and then stop. Rats received either buffer, unconjugated protein, or conjugates of VB_{12} and protein.

Similarly, Habberfield and coworkers (85) found that conjugation of VB_{12} to consensus interferon greatly increased the level of uptake of consensus interferon in rats receiving the VB_{12}-interferon complex duodenally (Fig. 4).

Amplification of the Vitamin B-12 Uptake System Using Nanoparticles

Formulating the pharmaceuticals to be delivered within nanoparticles to which vitamin B_{12} is linked could result in a 1,000- to 10,000-fold increase in the amount of material that could be delivered via the VB_{12} uptake system. This delivery method would also protect the pharmaceutical during the passage down the intestine from enzymes and other degradative processes. Furthermore, incorporating pharmaceuticals within nanoparticles has the added advantage that the peptide or protein to be delivered would not need to be chemically linked to VB_{12} for uptake to occur. This would be particularly beneficial with peptides such as vasopressin, which has not been linked to VB_{12} without loss of functional activity. For effective delivery, such nanoparticulate systems would need to be designed so that they remain intact within the intestine but would release their contents once they reached the circulation.

It has recently been shown that it is possible to initiate intestinal uptake of fluorescent nanoparticles in dogs, pigs, and rats by linking the nanoparticles either to VB_{12}, the binding subunit of the *E. coli* heat-labile toxin (LTB), or Concanavilin A lectin from *Canavalia eusiformis* (ConA). Histological examination of intestinal loops containing injected nanoparticles reveals that they can first be observed bound to the intestinal epithelial layer. Within 1 to 2 hours, the nanoparticles have crossed the epithelial cell layer and can be found below the mucosal cell layer lying in the central lacteal lymph vessel (84). Studies in pigs and dogs have shown that the nanoparticles can then be found in sections of the mesenteric lymph nodes, some 10–20 cm from the intestinal loops.

In separate studies on uptake of nanoparticles into Caco-2 cells, it has been shown that the quantity of uptake of nanoparticles is inversely proportional to size, with 100-nm particles showing 15 to 250-fold higher uptake than larger (500 nm, 1 μm) particles (86).

FUTURE DIRECTIONS

The Use of Pathogenic Methods of Invasion for Carrier-Mediated Transport

The normal method of invasion of epithelial cells by pathogens represents an untapped mechanism by which intestinal uptake of peptide and protein pharmaceuticals may be initiated: Intestinal epithelial cells internalize large nanoparticulate structures such as viruses or bacteria, and in some cases these structures are transported across the cell and into the subepithelial layer of the intestine. Uptake and transport has in many cases been found to depend on the presence of a surface protein on the pathogens that initiated internalization. Further study of these mechanisms and molecules that initiate uptake will inevitably lead to new and exciting methods for oral drug delivery; some of these are Internalin (*L. monocytogenes*). Invasin (*Y. pseudotuberculosis*), and other molecules with similar functional properties from other pathogens. The utility of such systems will ultimately lie in their ability to be used repeatedly without the induction of an immune response to the internalizing molecule.

Carrier-Mediated Transport of Nanoparticles

In an extension to the transport systems described in this article, it should also be possible in the future to use many of the carriers described previously (LTB, toxin-binding subunits, lectins, VB_{12}, etc) to stimulate the uptake of drug-loaded nanoparticles. The carrier molecules would be

covalently linked to the surface of the biodegradable nanoparticles and would be cotransported across the cells during the uptake of the carriers. Nanoparticles used for this purpose would need to be stable in the intestinal environment and to release their contents once they have reached the circulation. While it is possible that many of the carriers described in this review could be used to coat nanoparticles, the low immunogenicity of the VB_{12} molecule may mean that it will ultimately be the delivery system of choice for repeated oral drug delivery.

CONCLUSIONS

The drug delivery specialist would do well to study the mechanisms of pathogenesis of viral and bacterial pathogens, including their method of invasion and transcytosis of cells in a highly specific fashion. It is through such a study that new methods of oral drug delivery will be discovered and developed. Presently, however, the vitamin VB_{12} uptake system shows particular promise in being able to cause the uptake and transport of peptides and proteins linked to the VB_{12} molecule from the intestine into the circulation. In like fashion, the oral uptake of nanoparticles containing entrapped peptide or protein pharmaceuticals may also be possible.

BIBLIOGRAPHY

1. V. Ganapathy and F.H. Leibach, *Am. J. Physiol.* **12**, G153–G160 (1985).
2. A.L. Warshaw, W.A. Walker, and K.J. Isselbacher, *Gastroenterology* **66**, 987–992 (1974).
3. G.M. Pauletti et al., *J. Controlled Release* **41**, 3–17 (1996).
4. D.M. Matthews and S.A. Adibi, *Gastroenterology* **71**, 151–161 (1976).
5. D.M. Matthews, *Physiol. Rev.* **55**, 537–608 (1975).
6. F. Navab and A.M. Asatoor, *Gut* **11**, 373–379 (1970).
7. V. Ganapathy and F.H. Leibach, *Life Sci.* **30**, 2137–2146 (1982).
8. K.I. Inui et al., *J. Pharmacol. Exp. Ther.* **247**, 235–241 (1988).
9. I.J. Hidalgo, F.M. Ryan, G.J. Marks, and P.L. Smith, *Int. J. Pharm.* **98**, 83–92 (1993).
10. W. Kramer et al., *Biochim. Biophys. Acta* **1030**, 41–49 (1990).
11. M. Hu and G.L. Amidon, *J. Pharm. Sci.* **77**, 1007–1011 (1988).
12. E. Walter, T. Kissel, and G.L. Amidon, *Adv. Drug Delivery Rev.* **20**, 33–58 (1996).
13. P.W. Swaan and J.J. Tukker, *J. Pharmacol. Exp. Ther.* **27**, 242–247 (1995).
14. T. Kimura et al., *J. Pharmacobio-Dyn.* **6**, 246–253 (1983).
15. T. Hori et al., *J. Pharm. Pharmacol.* **40**, 646–647 (1988).
16. K. Iseki et al., *J. Pharm. Pharmacol.* **41**, 628–632 (1989).
17. P.W. Swaan, M.C. Stehouwer, and J.J. Tukker, *Biochim. Biophys. Acta* **1236**, 31–38 (1995).
18. W. Kramer, F. Girbig, I. Leipe, and E. Petzoldt, *Biochem. Pharmacol.* **37**, 2447–2435 (1988).
19. S.A. Adibi and Y.S. Kim, in L.R. Johnson, ed., *Physiology of the Gastrointestinal Tract*, Raven Press, New York, 1981, pp. 1073–1096.
20. A.H. Dantzig and L. Bergin, *Biochem. Biophys. Res. Commun.* **155**, 1082–1087 (1988).
21. P.W. Swaan, F.C. Szoka, and S. Øie, *Adv. Drug Delivery Rev.* **20**, 59–82 (1996).
22. W. Kramer et al., *J. Biol. Chem.* **267**, 18598–18604 (1992).
23. W. Kramer et al., *Biochim. Biophys. Acta* **1111**, 93–102 (1992).
24. W. Kramer et al., *J. Biol. Chem.* **268**, 18035–18046 (1993).
25. M. Kågedahl et al., *Pharm. Res.* **14**, 176–180 (1997).
26. W.H. Wong, P. Oelkens, and P.A. Dawson, *J. Biol. Chem.* **270**, 27228–27234 (1995).
27. W. Kramer, G. Burckhardt, F.A. Wilson, and G. Kurz, *J. Biol. Chem.* **258**, 3623–3627 (1983).
28. W. Kramer et al., *J. Biol. Chem.* **269**, 10621–10627 (1994).
29. P.W. Swaan, K.M. Hillgren, F.C. Szoka, and S. Øie, *Bioconjugate Chem.* **8**, 520–525 (1997).
30. R. Rodewald, *J. Cell Biol.* **85**, 18–32 (1980).
31. R. Rodewald, *J. Cell Biol.* **71**, 666–670 (1976).
32. D.R. Abrahamson and R. Rodewald, *J. Cell Biol.* **91**, 270–280 (1981).
33. K.E. Mostov, *Annu. Rev. Immunol.* **12**, 63–84 (1994).
34. E.R. Jakoi, J. Cambier, and S. Saslow, *J. Immunol.* **135**, 3360–3364 (1985).
35. J.P. Kraehenbuhl and M.A. Campiche, *J. Cell Biol.* **42**, 345–365 (1969).
36. D.M. Neville and T.-M. Chang, *Curr. Top. Membr. Transp.* **10**, 65–150 (1978).
37. N. Mackenzie, *Immunol. Today* **5**, 364–366 (1984).
38. J.V. Peppard, L.E. Jackson, J.G. Hall, and D. Robertson, *Immunology* **53**, 385–393 (1984).
39. K.E. Mostov, M. Friedlander, and G. Blobel, *Nature (London)* **308**, 37–43 (1984).
40. R.P. Hirt et al., *Cell (Cambridge, Mass.)* **74**, 245–255 (1993).
41. G. Apodaca, L.A. Katz, and K.E. Mostov, *J. Cell Biol.* **125**, 67–86 (1994).
42. K.E. Mostov, *Cell (Cambridge, Mass.)* **43**, 389–390 (1985).
43. M.B. Mazanec et al., *Proc. Natl. Acad. Sci. U.S.A.* **89**, 6901–6905 (1992).
44. V.A. Fischetti, *ASM News* **62**, 405–410 (1996).
45. G.J. Russell-Jones, E.C. Gotschlich, and M.S. Blake, *J. Exp. Med.* **160**, 1467–1475 (1984).
46. M. Mouricout, J.M. Petit, J.R. Carias, and R. Julien, *Infect. Immun.* **58**, 98–106 (1990).
47. R.T. Irvin et al., *Infect. Immun.* **57**, 3720–3726 (1989).
48. P. Doig et al., *Infect. Immun.* **58**, 124–130 (1990).
49. R.R. Isberg, *Science* **252**, 934–938 (1991).
50. D.K. Paruchuri et al., *Proc. Natl. Acad. Sci. U.S.A.* **87**, 333–337 (1990).
51. T.A. Oelschlaeger, P. Guerry, and D.J. Kopecko, *Proc. Natl. Acad. Sci. U.S.A.* **90**, 6884–6888 (1993).
52. H.J. de Aizpurua and G.J. Russell-Jones, *J. Exp. Med.* **167**, 440–451 (1987).
53. P. Cossart, *J. Cell. Biochem. Suppl.* 18 Part A, 36 (1994).
54. S. Falkow, *Cell (Cambridge, Mass.)* **65**, 1099–1102 (1991).
55. J. Mengaud et al., *Cell (Cambridge, Mass.)* **84**, 923–932 (1996).
56. A. Lingnau et al., *Infect. Immun.* **63**, 3896–3903 (1995).
57. D.A. Drevets, R.T. Sawyer, T.A. Potter, and P.A. Campbell, *Infect. Immun.* **63**, 4268–4276 (1995).
58. R.R. Isberg and S. Falkow, *Nature (Lond.)* **317**, 262–264 (1985).
59. N. Fukuhara, O. Yoshie, S. Kitaoka, and T. Konno, *J. Virol.* **62**, 2209–2218 (1988).
60. R.H. Yolken, *Infect. Dis. Antimicrob. Agents* **6**, 273–291 (1985).
61. S.A. Wharton et al., *J. Biol. Chem.* **263**, 4474–4480 (1988).

Next Page

62. D.J. Keljo and A.K. Smith, *J. Pediatr. Gastroenterol. Nutr.* **7**, 249–256 (1988).
63. K.T. Kaljot, R.D. Shaw, D.H. Rubin, and H.B. Greenberg, *J. Virol.* **62**, 1136–1144 (1988).
64. C. Sears and J.B. Kaper, *Microbiol. Rev.* **60**, 167–215 (1996).
65. A. Waksman et al., *Biochim. Biophys. Acta* **604**, 249–296 (1980).
66. L. Okerman, *Vet. Microbiol.* **14**, 33–46 (1987).
67. F. Stirpe and L. Barbieri, *FEBS Lett.* **195**, 1–8 (1986).
68. R.O. Blaustein, W.J. Germann, A. Finkelstein, and B.R. DasGupta, *FEBS Lett.* **226**, 115–120 (1987).
69. R.J. Simpson et al., *Biochim. Biophys. Acta* **884**, 166–171 (1986).
70. M.E. Conrad, R.T. Parmley, and K. Osterloch, *J. Lab. Clin. Med.* **110**, 418–426 (1987).
71. J. Mazurier, J. Montreuil, and G. Spik, *Biochim. Biophys. Acta* **821**, 453–460 (1985).
72. G. Johnson, P. Jacobs, and L.R. Purves, *J. Clin. Invest.* **71**, 1467–1476 (1983).
73. A. Dautry-Varsat, A. Ciechanover, and H.F. Lodfish, *Proc. Natl. Acad. Sci. U.S.A.* **80**, 2258–2262 (1983).
74. R.D. Klausner et al., *Proc. Natl. Acad. Sci. U.S.A.* **80**, 2263–2266 (1983).
75. R. Cecchelli et al., *Proc. Int. Symp. Controlled Release Bioact. Mater.* **24**, 221–222 (1997).
76. G.J. Russell-Jones, in M.D. Taylor and G.L. Amidon, eds., "Peptide-Based Drug Design: Controlling Transport and Metabolism," American Chemical Society, Washington, D.C., 1995, pp. 181–198.
77. G.J. Russell-Jones, S.W. Westwood, and A.D. Habberfield, *Bioconjugate Chem.* **6**, 459–465 (1996).
78. G.J. Russell-Jones et al., *Bioconjugate Chem.* **6**, 34–42 (1994).
79. A. Habberfield et al., *Int. J. Pharm.* **145**, 1–8 (1996).
80. K.S. Ramanujam, S. Seetharam, M. Ramasamy, and B. Seetharam, *Am. J. Physiol.* **260**, 6416–6422 (1991).
81. D.J. Dix et al., *Gastroenterology* **88**, 1272–1279 (1990).
82. G. Wilson et al., *J. Controlled Release* **11**, 25–40 (1990).
83. S. Bose, S. Seetharam, N.M. Dahm, and B. Seetharam, *J. Biol. Chem.* **272**, 3538–3543 (1997).
84. G.J. Russell-Jones, S.W. Westwood, and A. Habberfield, *Proc. Int. Symp. Controlled Release Bioact. Mater.* **23**, 49–50 (1996).
85. U.S. Pat. 5,574,018 (February 15, 1996), A.D. Habberfield, O.B. Kinstler, and C.G. Pitt.
86. M.P. Desai, V. Labhasetwar, G.L. Amidon, and R.J. Levy, *Pharm. Res.* **13**, 1838–1845 (1996).

See also BIOADHESIVE DRUG DELIVERY SYSTEMS; VACCINE DELIVERY.

CENTRAL NERVOUS SYSTEM, DRUG DELIVERY TO TREAT

MARTIN BURKE
ROBERT LANGER
HENRY BREM
Johns Hopkins University School of Medicine
Baltimore, Maryland

KEY WORDS

BCNU
Blood–brain barrier
Blood–brain barrier disruption
Blood–tumor barrier
Brain tumors
Carrier-mediated drug delivery
Central nervous system
Gene therapy
Immunotherapy
Microspheres
pCPP:SA
Polyanhydride polymers
Prodrugs
Redox chemical delivery system
Vector-mediated drug delivery

OUTLINE

Introduction
Barriers to CNS Drug Delivery
  Blood–Brain Barrier
  Blood–Cerebrospinal Fluid Barrier
  Blood–Tumor Barrier
Strategies for Enhanced CNS Drug Delivery
  Enhancing BBB Permeability by Drug Manipulation
  Disrupting the BBB
  Alternative Routes to CNS Drug Delivery
Interstitial CNS Drug Delivery Using Controlled-Release Polymer Systems
  Development of Polyanhydrides for Controlled Drug Delivery
  Development of Drug-Impregnated Polyanhydride Wafers for the Treatment of Brain Tumors
  Use of Polymer Systems to Facilitate Drug Delivery to the CNS Interstitium from Biological Tissues
Conclusion
Acknowledgments
Disclosure Statement
Bibliography

INTRODUCTION

Billions of dollars in research and development spending aimed at curing human diseases has yielded a vast arsenal of powerful therapeutic agents. However, while many of these drugs demonstrate extraordinary promise in the laboratory, they are often far less successful when applied to patients in clinical trials. In no area of medicine has this recurrent inconsistency been more pronounced, or more tragic, than in the treatment of diseases of the central nervous system (CNS). Despite aggressive research, patients suffering from fatal and/or debilitating CNS diseases, such as brain tumors, HIV encephalopathy, epilepsy, cerebrovascular disease, and neurodegenerative disorders, far

62. D.J. Keljo and A.K. Smith, *J. Pediatr. Gastroenterol. Nutr.* **7**, 249–256 (1988).
63. K.T. Kaljot, R.D. Shaw, D.H. Rubin, and H.B. Greenberg, *J. Virol.* **62**, 1136–1144 (1988).
64. C. Sears and J.B. Kaper, *Microbiol. Rev.* **60**, 167–215 (1996).
65. A. Waksman et al., *Biochim. Biophys. Acta* **604**, 249–296 (1980).
66. L. Okerman, *Vet. Microbiol.* **14**, 33–46 (1987).
67. F. Stirpe and L. Barbieri, *FEBS Lett.* **195**, 1–8 (1986).
68. R.O. Blaustein, W.J. Germann, A. Finkelstein, and B.R. DasGupta, *FEBS Lett.* **226**, 115–120 (1987).
69. R.J. Simpson et al., *Biochim. Biophys. Acta* **884**, 166–171 (1986).
70. M.E. Conrad, R.T. Parmley, and K. Osterloch, *J. Lab. Clin. Med.* **110**, 418–426 (1987).
71. J. Mazurier, J. Montreuil, and G. Spik, *Biochim. Biophys. Acta* **821**, 453–460 (1985).
72. G. Johnson, P. Jacobs, and L.R. Purves, *J. Clin. Invest.* **71**, 1467–1476 (1983).
73. A. Dautry-Varsat, A. Ciechanover, and H.F. Lodfish, *Proc. Natl. Acad. Sci. U.S.A.* **80**, 2258–2262 (1983).
74. R.D. Klausner et al., *Proc. Natl. Acad. Sci. U.S.A.* **80**, 2263–2266 (1983).
75. R. Cecchelli et al., *Proc. Int. Symp. Controlled Release Bioact. Mater.* **24**, 221–222 (1997).
76. G.J. Russell-Jones, in M.D. Taylor and G.L. Amidon, eds., "Peptide-Based Drug Design: Controlling Transport and Metabolism," American Chemical Society, Washington, D.C., 1995, pp. 181–198.
77. G.J. Russell-Jones, S.W. Westwood, and A.D. Habberfield, *Bioconjugate Chem.* **6**, 459–465 (1996).
78. G.J. Russell-Jones et al., *Bioconjugate Chem.* **6**, 34–42 (1994).
79. A. Habberfield et al., *Int. J. Pharm.* **145**, 1–8 (1996).
80. K.S. Ramanujam, S. Seetharam, M. Ramasamy, and B. Seetharam, *Am. J. Physiol.* **260**, 6416–6422 (1991).
81. D.J. Dix et al., *Gastroenterology* **88**, 1272–1279 (1990).
82. G. Wilson et al., *J. Controlled Release* **11**, 25–40 (1990).
83. S. Bose, S. Seetharam, N.M. Dahm, and B. Seetharam, *J. Biol. Chem.* **272**, 3538–3543 (1997).
84. G.J. Russell-Jones, S.W. Westwood, and A. Habberfield, *Proc. Int. Symp. Controlled Release Bioact. Mater.* **23**, 49–50 (1996).
85. U.S. Pat. 5,574,018 (February 15, 1996), A.D. Habberfield, O.B. Kinstler, and C.G. Pitt.
86. M.P. Desai, V. Labhasetwar, G.L. Amidon, and R.J. Levy, *Pharm. Res.* **13**, 1838–1845 (1996).

See also BIOADHESIVE DRUG DELIVERY SYSTEMS; VACCINE DELIVERY.

CENTRAL NERVOUS SYSTEM, DRUG DELIVERY TO TREAT

MARTIN BURKE
ROBERT LANGER
HENRY BREM
Johns Hopkins University School of Medicine
Baltimore, Maryland

KEY WORDS

BCNU
Blood–brain barrier
Blood–brain barrier disruption
Blood–tumor barrier
Brain tumors
Carrier-mediated drug delivery
Central nervous system
Gene therapy
Immunotherapy
Microspheres
pCPP:SA
Polyanhydride polymers
Prodrugs
Redox chemical delivery system
Vector-mediated drug delivery

OUTLINE

Introduction
Barriers to CNS Drug Delivery
  Blood–Brain Barrier
  Blood–Cerebrospinal Fluid Barrier
  Blood–Tumor Barrier
Strategies for Enhanced CNS Drug Delivery
  Enhancing BBB Permeability by Drug Manipulation
  Disrupting the BBB
  Alternative Routes to CNS Drug Delivery
Interstitial CNS Drug Delivery Using Controlled-Release Polymer Systems
  Development of Polyanhydrides for Controlled Drug Delivery
  Development of Drug-Impregnated Polyanhydride Wafers for the Treatment of Brain Tumors
  Use of Polymer Systems to Facilitate Drug Delivery to the CNS Interstitium from Biological Tissues
Conclusion
Acknowledgments
Disclosure Statement
Bibliography

INTRODUCTION

Billions of dollars in research and development spending aimed at curing human diseases has yielded a vast arsenal of powerful therapeutic agents. However, while many of these drugs demonstrate extraordinary promise in the laboratory, they are often far less successful when applied to patients in clinical trials. In no area of medicine has this recurrent inconsistency been more pronounced, or more tragic, than in the treatment of diseases of the central nervous system (CNS). Despite aggressive research, patients suffering from fatal and/or debilitating CNS diseases, such as brain tumors, HIV encephalopathy, epilepsy, cerebrovascular disease, and neurodegenerative disorders, far

outnumber those dying of all types of systemic cancer or heart disease (1).

The clinical failure of many potentially effective therapeutics is often not due to a lack of drug potency but rather to shortcomings in the method by which the drug is delivered. Treating CNS diseases is particularly challenging because a variety of formidable obstacles often impede drug delivery to the brain and spinal cord. In response to the insufficiencies in conventional delivery mechanisms, aggressive research efforts have recently focused on the development of new strategies to more effectively deliver drug molecules to the CNS. This work is crucial to the development of successful treatments for CNS diseases, for the therapeutic potential of any drug can only be realized if the drug reaches its intracranial target. The first half of this article focuses on the specific barriers that inhibit drug delivery to the CNS and various strategies designed to overcome them. The latter half reviews our work and that of other groups involving the use of biocompatible polymer systems to achieve sustained drug delivery directly to the brain interstitium for the treatment of intracranial tumors as well as several nonneoplastic CNS diseases.

BARRIERS TO CNS DRUG DELIVERY

The most conventional methods to deliver drug molecules for the treatment of human illness utilize the cardiovascular system. Typically, drugs are delivered to the cardiovascular system by oral ingestion, intravenous injection or infusion, or injection into tissue such as skin or muscle and subsequently distributed throughout the body. As blood-borne drug molecules pass through capillary networks, they are forced by diffusion and convection from the plasma into the surrounding interstitium where they enter target cells and elicit a desired biological response. This method of drug delivery is often highly effective for the treatment of a broad range of systemic ailments. However, when a pathological condition plagues the CNS, the cardiovascular route of drug delivery is often tragically unsuccessful. A variety of serious CNS diseases are insensitive to systemically delivered drugs, and therefore many neurological patients are often left with few therapeutic options. The failure of systemically delivered drugs to effectively treat many CNS diseases can be rationalized by considering a number of barriers that inhibit drug delivery to the CNS.

Blood–Brain Barrier

When a drug is administered systemically to treat a CNS disease, its delivery is first inhibited by a physiological impediment known as the blood–brain barrier (BBB). An early teleological development, the BBB serves a homeostatic purpose. Through selective permeability to blood-borne molecules, the BBB maintains a constant milieu in the brain parenchyma. This is important for the proper function of neurons, which are highly sensitive to changes in concentrations of both extracellular ions and signaling molecules such as neurotransmitters. However, this same selectivity also limits the penetration of drug molecules into the brain parenchyma. The mechanisms underlying BBB selectivity have therefore been the subject of aggressive research for the past 30 years. Today, the term BBB is often used in a general sense to describe the collection of physiological, metabolic, and biochemical characteristics that distinguish the cerebral capillary endothelium from the endothelium of systemic organ systems.

The first distinguishing physiological characteristic is that cerebral capillary endothelial cells are fused together by pentalaminar tight junctions, named for their five-layered appearance in the electron microscope: the cytoplasmic lipid layer of the first cell, a lucent line, the fused outer lipid layers of the first and second cell, another lucent line, and the cytoplasmic lipid layer of the second cell. This five-layered configuration virtually fuses neighboring endothelial cells in the cerebral microvasculature (2). In contrast, the endothelial cells in systemic capillaries are more loosely joined through a series of focal connections between the two outer lipid layers of adjacent cells. Furthermore, while endothelial cells in most systemic capillaries are fenestrated with gaps and pores that allow for the exchange of ions, large molecules, and even cells between the blood and the surrounding interstitium, these gaps and pores are lacking in the brain endothelium (3–5). As a result, in comparison to the systemic microvasculature, cerebral capillaries are much less permeable to ions and small molecules and are virtually impermeable to most peptides and macromolecules. For example, the electrical resistance, a measurement of resistance to ionic current flow, across most systemic capillary endothelium focal connections is 5–10 Ω cm^2. In contrast, the electrical resistance in the microvasculature of the CNS is typically 1,000 Ω cm^2 or more (6).

Additionally, in comparison to their systemic counterparts, cerebral endothelial cells have a marked deficiency in pinocytic vesicles (2,3). In systemic endothelium, pinocytic vesicles result from the invagination of the cell membrane to engulf an extracellular material (endocytosis). After traversing the cell cytoplasm, the vesicles can fuse with the opposite membrane and release their contents to the surrounding interstitium (exocytosis) (2). This process, known as transcytosis, is important for the extravasation of molecules that are otherwise unable to traverse tightly fused endothelial sheets. The apparent down-regulation of this process in the CNS provides an even greater selectivity to the cerebral capillary endothelium.

Unfortunately, the pentalaminar tight junctions and paucity of pinocytic vesicles that empower the cerebral capillary endothelium to maintain homeostasis in the brain parenchyma also inhibit the intracranial delivery of most drugs via the cardiovascular system. Because the tightly fused endothelial membranes essentially form a continuous layer of lipids, a drug's lipophilicity (defined by the octanol:water partition coefficient) correlates strongly with cerebrovascular permeability (Fig. 1). Because many drugs are functionalized hydrophilic organic compounds, they are unable to traverse the highly hydrophobic lipid barrier and are therefore ineffective in the treatment of CNS diseases.

The selectivity of the cerebral microvasculature is further enhanced by the so-called metabolic blood–brain barrier (MBBB) (7). The presence of a MBBB was first predicted after the discovery that endothelial cells in the

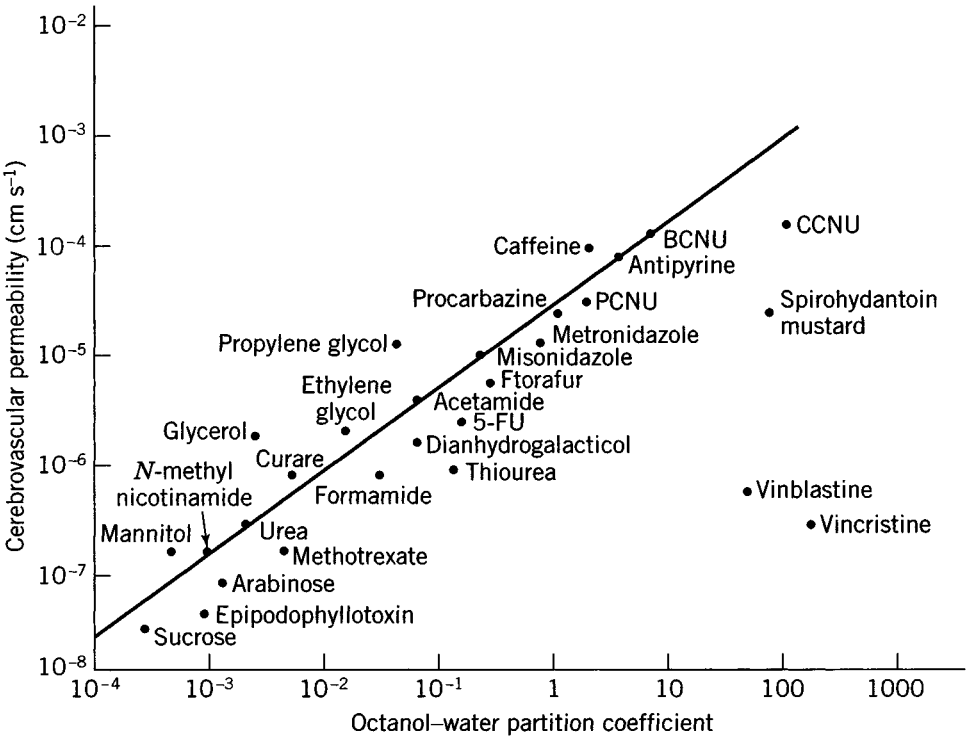


Figure 1. Relationship between the cerebrovascular permeability and the octanol–water partition coefficient of selected chemicals and drugs. Vinblastine and vincristine are clear "outliers," falling well below the line and hence penetrating much less than is expected from their lipophilicity. These drugs are excluded from the brain parenchyma by the active-drug-efflux-transporter protein in the luminal membrane of the cerebral capillary endothelium. *Source:* Reproduced with permission from Ref. 1.

cerebromicrovasculature have four times the mitochondrial content of systemic endothelial cells (2,3). Some molecules that freely enter brain endothelial cells through the luminal membrane undergo rapid metabolic chemical transformations that inhibit them from crossing the antiluminal membrane and reaching the surrounding brain interstitium (7). For example, L-dopa, an amino acid precursor of the neurotransmitters dopamine and norepinephrine, readily traverses the luminal membrane of brain endothelial cells. However, rapid metabolic conversion into dopamine by intracellular enzymes precludes L-dopa from crossing the antiluminal membrane. This metabolic conversion limits the therapeutic potential of exogenous L-dopa for the treatment of neurodegenerative disorders such as Alzheimer's disease.

Finally, the BBB is further reinforced by a high concentration of the *P*-glycoprotein (Pgp) active-drug-efflux-transporter protein in the luminal membrane of the cerebral capillary endothelium (1). This efflux transporter actively removes a broad range of drug molecules from the endothelial cell cytoplasm before they can cross into the brain parenchyma. For example, the octanol:water partition coefficient allows the antineoplastic agents vincristine and vinblastine to readily traverse endothelial membranes (Fig. 1). However, because they are actively pumped from the endothelial cytoplasm into the blood by the Pgp efflux system, these drugs are excluded from the brain parenchyma.

Blood–Cerebrospinal Fluid Barrier

The second barrier that a systemically administered drug encounters before entering the CNS is known as the blood–cerebrospinal fluid barrier (BCB). The ventricles within the brain and the subarachnoid space that surrounds its outer surface are filled with an ultrafiltrate of plasma secreted by the choroid plexus called cerebrospinal fluid (CSF) (2). Because the CSF can exchange molecules with the interstitial fluid of the brain parenchyma, the passage of blood-borne molecules into the CSF is also carefully regulated by the BCB.

Physiologically, the BCB is found in the epithelium of the choroid plexus. The capillary endothelial sheets of the choroid plexus are fused not by pentalaminar fusions but by fenestrated tight junctions and are therefore somewhat more permeable than the capillary networks of the brain. However, these fenestrated capillaries are encased by a sheet of choroid epithelial cells bound by tight junctions, which restricts the rate of extravasation from the choroid capillary networks. This arrangement limits the passage of molecules and cells into the CSF, although, because the choroid endothelial sheets lack pentalaminar fusions, the BCB is somewhat more permeable to ions than the BBB (2).

In addition, the BCB is fortified by an active organic acid transporter system in the choroid plexus capable of driving CSF-borne organic acids into the blood. As a result,

a variety of therapeutic organic acids such as the antibiotic penicillin, the antineoplastic agent methotrexate, and the antiviral agent zidovudine (AZT) are actively removed from the CSF and therefore inhibited from diffusing into the brain parenchyma (1).

Furthermore, substantial inconsistencies often exist between the composition of the CSF and interstitial fluid of the brain parenchyma, suggesting the presence of what is sometimes called the CSF–brain barrier (2,8). This barrier is attributed to the insurmountable diffusion distances required for equilibration between the CSF and the brain interstitial fluid. Therefore, entry into the CSF does not guarantee a drug's penetration into the brain.

Blood–Tumor Barrier

The obstacles to intracranial drug delivery are even more challenging when the target is a CNS tumor. Solid tumors, including those of the brain, support their own growth by stimulating the intratumoral formation of new blood vessels in a process known as angiogenesis (9,10). The resultant intratumoral blood supply delivers oxygen and nutrients to internal neoplastic cells and removes metabolic wastes. Therefore, the cardiovascular system could theoretically be used to deliver drugs to the interstitium of solid tumors. However, research by Jain and others has shown that a variety of obstacles, collectively referred to as the blood–tumor barrier (BTB), often impede this mechanism of drug delivery to solid tumors, especially to solid tumors of the CNS (11–13).

In the CNS, the first of these obstacles is the BBB. The BBB is functional, albeit variably, in the microvasculature of primary and metastatic brain tumors (6,14). Low-grade primary brain tumors and small metastatic foci appear to have a relatively intact BBB, and in larger tumors the functional capacity of the BBB is regionally variable. Toward the center of a solid CNS tumor, the BBB is often severely compromised, but in the tumor periphery, especially at the outermost infiltrative regions of a primary brain tumor, the BBB is often highly functional. Between these two extremes the BBB is variably functional in the tumor microvasculature.

The presence of a BBB in the microvasculature of CNS tumors has clinical consequences. For example, even when primary and secondary systemic tumors respond to chemotherapy delivered via the cardiovascular system, intracranial metastases often continue to grow (6,15). In recent clinical trials for the treatment of systemic malignancies, patients receiving immunotherapy (16) and new chemotherapeutic treatment protocols (17–19) remained disease free systemically while succumbing to CNS metastases. Furthermore, the most effective chemotherapeutic drugs in the treatment of brain tumor patients are those that most efficiently cross the BBB in normal brain capillaries, such as the alkylating agent 1,3-bis-chloroethylnitrosourea (BCNU) (Fig. 1) (20,21).

Even for CNS malignancies in which the BBB is significantly compromised, a variety of physiological barriers common to all solid tumors inhibit drug delivery via the cardiovascular system. First of all, drug delivery to neoplastic cells in a solid tumor is compromised by a heterogeneous distribution of microvasculature throughout the tumor interstitium, which leads to spatially inconsistent drug delivery. Furthermore, as a tumor grows larger, the vascular surface area decreases, leading to a reduction in transvascular exchange of blood-borne molecules. At the same time, the intercapillary distance increases, leading to a greater diffusional requirement for drug delivery to neoplastic cells (11). Moreover, poorly vascularized regions of the tumor receiving insufficient nutrients for growth can house neoplastic cells resting in G_0, rendering them insensitive to cell cycle–dependent antineoplastic agents (6).

Another physiological characteristic of both systemic and CNS solid tumors that restricts drug delivery is an elevation of interstitial pressure inside the tumor (6,11). As the leakiness of the tumor vasculature increases, so does the rate of fluid extravasation leading to a buildup of interstitial fluid. Because the tumor does not possess a sufficient lymphatic system to remove the excess fluid, the intratumoral interstitial pressure increases (12). The net result is a pressure gradient: interstitial pressure is highest at the center of the tumor, while the pressure at the outermost regions approaches that of the surrounding tissue (11). As the elevated interstitial pressure approaches the pressure inside the tumor capillary networks, the rate of extravasation of fluid and macromolecules into the tumor is retarded. Additionally, the high pressure at the tumor's center results in a net flow of fluid from the center into the periphery and the surrounding interstitium, known as peritumoral edema. This continuous fluid flow creates a constant, radially directed convective force diametrically opposed to intratumoral drug penetration (11).

In the CNS, these inherent physiological barriers to solid-tumor drug delivery and the variably intact BBB may work synergistically to restrict the delivery of antineoplastic drugs to malignant cells. For example, the combination of a variably intact BBB and inconsistently dispersed tumor microvasculature can lead to an intratumoral drug distribution that is exceedingly heterogeneous, with some areas left completely unexposed. In the most highly vascularized and therefore potentially accessible peripheral regions of a CNS tumor, the BBB is in fact the most functional and most restricting of transvascular drug exchange. Infiltrative cells at the periphery can also escape into the surrounding interstitium where the BBB is fully functional (20). Furthermore, the high interstitial tumor pressure and associated peritumoral edema leads to increases in hydrostatic pressure in the normal brain parenchyma adjacent to the tumor. As a result, the cerebral microvasculature in these tumor-adjacent regions of normal brain may be even less permeable to drugs than normal brain endothelium, leading to exceptionally low extratumoral interstitial drug concentrations (20). This surrounding region can therefore act as a diffusion sink and further limit intratumoral drug penetration (6).

In conclusion, the delivery of drugs to the CNS via the cardiovascular system is often precluded by a variety of formidable barriers including the BBB, the BCB, and the BTB. In the last 30 years, aggressive research has elucidated the physiological, metabolic, and biochemical mechanisms underlying these barriers. The next section will ex-

plore how this knowledge has been used to rationally design therapeutic strategies for enhanced drug delivery to the CNS.

STRATEGIES FOR ENHANCED CNS DRUG DELIVERY

To circumvent the multitude of barriers inhibiting CNS penetration by potentially therapeutic agents, numerous drug delivery strategies have been developed. These strategies generally fall into one or more of the following three categories: manipulating drugs, disrupting the BBB, and finding alternative routes for drug delivery.

Enhancing BBB Permeability by Drug Manipulation

Lipophilic Analogs. A variety of pharmacological parameters influence a drug's cerebrovascular permeability. Specifically, CNS penetration is favored by low molecular weight, lack of ionization at physiological pH, and lipophilicity (2). Because a drug's lipophilicity correlates so strongly with cerebrovascular permeability (Fig. 1), hydrophobic analogues of small hydrophilic drugs ought to more readily penetrate the BBB. This strategy has been frequently employed by a number of researchers, but the results have often been disappointing.

The best example of such attempts are the series of lipophilic analogues of the nitrosoureas. Nitrosoureas, such as BCNU, elicit antineoplastic activity by alkylating purine and pyrimidine bases in DNA. The modest yet significant clinical success of BCNU against malignant brain tumors has been attributed to the compound's relatively high lipophilicity (log P 1.53) (2). It was therefore hypothesized that further latentiation of BCNU would enhance its antineoplastic activity. To this end, more than 20 BCNU analogs including 1-(2-chloroethyl)-3-cyclohexyl-1-nitrosourea (CCNU, log P 2.83) and methyl-CCNU (log P 3.3) were synthesized.

Quantitative structure activity relationship studies with this series of analogs indicated a surprising result (6). As was later confirmed in clinical trials, these studies demonstrated that the antineoplastic activity of the nitrosourea analogs was inversely proportional to their lipophilicity (2,5). These observations were rationalized as follows. First, the more lipophilic analogs demonstrate diminished alkylating activity and increased dose-limiting toxicity when compared to BCNU. In addition, the more lipophilic analogs are less soluble in the aqueous plasma and bind more readily to plasma proteins, leading to lower concentrations of drug available for diffusion into the CNS. Finally, CCNU and methyl-CCNU are less soluble in the extracellular/intracellular fluid of the brain, limiting their activity against tumor cells. The experience with the nitrosoureas indicates that if a drug is to be efficacious when delivered via the circulatory system for the treatment of a CNS disease, a delicate balance between cerebrovascular permeability and plasma solubility is required. Specifically, the optimal octanol:water partition coefficient is approximately log P 1.5 to 2.5 (22).

A second strategy for increasing the lipophilicity of a hydrophilic therapeutic agent is to surround the hydrophilic molecule with a sphere of lipids in the form of a liposome. Theoretically, encapsulated drugs may diffuse through the walls of the cerebromicrovasculature owing to the high affinity of their lipid coating for the cell membranes of capillary endothelial cells. Once inside the brain, encapsulated drugs may be released into the interstitium and act on target cells. Unfortunately, this strategy has not yet lived up to its theoretical potential. Because liposomes are preferentially taken up by fixed macrophages (3), most enter the reticuloendothelial system of the liver and spleen and never reach the brain (2). Additionally, because of their large size, liposomes that do reach the CNS are unable to traverse the BBB (3).

Prodrugs. Another strategy for drug modification to enhance CNS penetration is the design of prodrugs. A prodrug consists of a drug covalently attached to an unrelated chemical moiety that improves the drug's pharmacokinetic properties. The prodrug itself is not active but becomes active when the attached moiety is cleaved in vivo by enzymatic or hydrolytic processes. To enhance a drug's penetration into the CNS, prodrugs are often designed by attaching chemical moieties that increase the drug's lipophilicity. The best example of this approach is the series of analogs of the pain reliever morphine. As shown in Figure 2, the alkaloid morphine, which possesses two polar hydroxyl groups and a log P value of -1.66, does not readily cross the BBB. Methylation of one hydroxyl group, however, yields the more powerful alkaloid codeine, which has enhanced brain uptake. Further latentiation via acetyla-

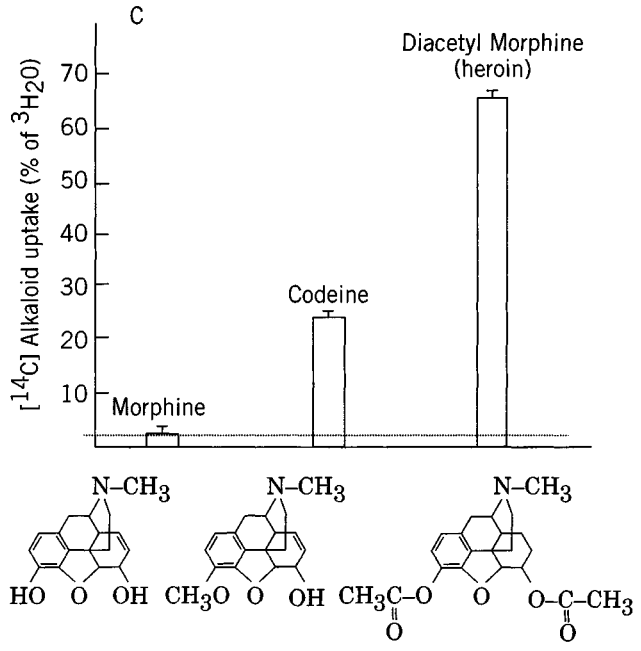


Figure 2. Relationship between BBB penetration of a series of [^{14}C] alkaloids (as a percent of penetration of $^{3}H_2O$) and their chemical structure. Morphine (left) penetrates the BBB poorly because it contains two highly polar hydroxyl groups. Addition of methyl (codeine) and acetyl (heroin) groups increases lipophilicity and fascilitates brain uptake. *Source:* Reproduced with permission from Ref. 1.

tion of both hydroxyl groups yields the hallucinogenic heroin, which demonstrates a dramatic increase in activity over the parent compound. Heroin readily traverses the BBB, and subsequent hydrolytic cleavage of the acetyl groups yields high concentrations of morphine trapped in the brain due to its hydrophilicity (2).

Redox Chemical Delivery Systems. Bodor et al. have developed a creative approach to exploit the permeability characteristics of the BBB to achieve site specific and/or sustained release of drugs to the brain (23–25). The method involves linking a drug to a lipophilic dihydropyridine carrier, creating a complex that, after systemic administration, readily traverses the BBB because of its lipophilicity. Once inside the brain parenchyma, the dihydropyridine moiety is enzymatically oxidized to the ionic pyridinium salt. The acquisition of charge has the dual effect of accelerating the rate of systemic elimination by the kidney and bile and trapping the drug–pyridinium salt complex inside the brain. Subsequent cleavage of the drug from the pyridinium carrier leads to sustained drug delivery in the brain parenchyma (24). This methodology increases intracranial concentrations of a variety of drugs including neurotransmitters, antibiotics, and antineoplastic agents. Recently this methodology has been extended to deliver neuroactive peptides such as enkephalin to the brain. Protecting the peptide–dihydroxypyridine complex with a biolabile lipophilic steroid derivative shields the peptide from enzymatic degradation prior to traversing the BBB (26). This methodology has demonstrated promise in laboratory models, and evaluation of clinical efficacy in neurological patients is awaited with interest.

Carrier-Mediated Drug Delivery. An alternative strategy for enhanced CNS penetration is carrier-mediated drug delivery, which takes advantage of the facilitative transport systems present in the brain endothelium. The cerebrovascular membranes are densely populated with facilitative carrier systems for both glucose and large neutral amino acids (LNAAs). The carrier system for glucose, the primary mechanism whereby the brain receives its only source of energy, is highly specific for monosaccharides, rendering it useless for drug delivery (1). The LNAA carrier system, on the other hand, is capable of transporting numerous endogenous as well as exogenous LNAAs with great structural variety (1,2,6). This characteristic has made exploitation of the LNAA carrier system an attractive strategy for CNS drug delivery.

For example, neurons of the substantia nigra in patients with Parkinson's disease are markedly deficient in the neurotransmitter dopamine (22). Systemic administration of dopamine has no therapeutic benefit because dopamine does not cross the BBB to an appreciable extent (2). The LNAA carrier system has been used to deliver L-3,4-dihydroxyphenalanine (levodopa), an endogenous precursor to dopamine, to the brain. Unlike dopamine, levodopa has a high affinity for the LNAA carrier system. After traversing the antiluminal membrane of the cerebral endothelium, levodopa is decarboxylated to yield dopamine (2). The success of this therapeutic strategy is hindered by the peripheral conversion of levodopa to dopamine leading to systemic toxicity. However, concurrent administration of the carboxylase inhibitor carbidopa ameliorates unwanted side effects and makes the systemic administration of levodopa an effective therapy for Parkinson's disease (2).

The LNAA carrier system could theoretically be exploited to also deliver the antineoplastic agent melphalin, a nitrogen–mustard derivative of phenylalanine, to the brain. However, under physiological conditions, melphalin's affinity for the LNAA carrier protein is lower than that of endogenous LNAAs, and its transport is therefore severely limited (6). A newly synthesized analog of melphalin, D,L-NAM, demonstrates enhanced affinity for the LNAA carrier (27). The addition of hydrophobic side chains seems to allow D,L-NAM to interact more strongly with a hydrophobic binding site in the LNAA carrier protein (1). This strategy may lead to enhanced penetration via the LNAA carrier system.

Receptor/Vector-Mediated Drug Delivery. Other CNS drug delivery strategies focus on manipulating the cerebral endothelial systems for receptor-mediated transcytosis. The BBB possesses several specific transcytosis systems for the extravasation of important nutrients and signaling molecules that cannot diffuse through the cerebromicrovasculature. These include systems for the transport of insulin, transferrin, and insulinlike growth factor. Pardridge et al. propose as a mechanism for intracranial drug delivery the covalent coupling of a therapeutic protein normally excluded from the brain to a protein that is readily transcytosed across the cerebral capillary endothelium (4). For example, the nontransportable protein β-endorphin was linked to the transportable protein-cationized albumin via a disulfide linkage. This "chimeric peptide" was successfully transcytosed into the brain and enzymatically cleaved in the parenchyma by thiol reductase.

This chimeric peptide methodology has been further developed by Friden et al., who proposed the covalent coupling of drug molecules with antibodies to the transferrin receptor (28–30). Based on the observation that cerebral capillary endothelial cells express an abundance of transferrin receptors relative to systemic capillaries (31), it was proposed that the use of antitransferrin receptor monoclonal antibodies may lead to brain-selective targeting of drug molecules. This hypothesis was tested by systemically administering radiolabeled antirat transferrin-receptor antibody OX-26, separating the brain vasculature from the parenchyma via centrifugation through dextran, and quantitating OX-26 content in the two fractions by autoradiography (28). These experiments demonstrated that the OX-26 antibody was indeed transcytosed into the brain parenchyma, reaching peak levels of 0.4–0.5% of the injected dose per gram of brain tissue at 24 hours postadministration. Similar results were obtained when the OX-26 antibody was covalently linked to radiolabeled nerve growth factor (NGF) (28). The systemic delivery of this NGF–OX-26 conjugate also significantly enhanced the survival of cholinergic neurons in a murine model when compared to systemic NGF alone, indicating the therapeutic

potential of this approach in the treatment of Alzheimer's disease.

Pardridge has extended this methodology to achieve the intracranial delivery of polyamide ("peptide") nucleic acids (PNAs) (32). PNAs are a form of antisense oligodeoxynucleotides in which a polyamide backbone is substituted for the phosphate backbone. These molecules possess great therapeutic potential in the treatment of neurological disorders, yet due to their hydrophilicity and large size, they are unable to cross the BBB. Encouraging results have been obtained with a model PNA, antisense to the genome of the human immunodeficiency virus type 1. This PNA can successfully be delivered to the murine brain parenchyma at 0.1% of the initial dose per gram of tissue when covalently coupled to the OX-26 monoclonal antibody.

More recently, this technique has been expanded to successfully deliver drug-loaded immunoliposomes to the brain (33). Immunoliposomes consist of liposomes coated with the inert polymer polyethylene glycol conjugated to the OX-26 antitransferrin-receptor monoclonal antibody. In a recent application, maximum uptake of only 0.03% of the initial dose per gram of brain tissue was achieved for immunoliposomes loaded with the antineoplastic agent daunomycin. However, because a single immunoliposome may carry up to 10,000 drug molecules, this methodology might greatly enhance the capacity of the OX-26 antibody for intracranial drug delivery. Although these techniques hold great promise and warrant further study, the intracranial drug concentrations that may be achieved via the receptor-mediated drug delivery strategy may be limited by saturation of the target receptors and by competitive inhibition from endogenous substrates.

Disrupting the BBB

In spite of recent developments in drug modification for enhanced CNS penetration, the BBB remains a formidable obstacle that compromises the successful treatment of many neurological disorders. The second general class of strategies for enhanced CNS drug delivery involves the systemic administration of drugs in conjunction with transient BBB disruption (BBBD). Theoretically, with the BBB weakened, systemically administered drugs can undergo enhanced extravasation rates in the cerebral endothelium, leading to increased parenchymal drug concentrations. A variety of techniques that transiently disrupt the BBB have been investigated; however, albeit physiologically interesting, many are unacceptably toxic and therefore not clinically useful. These include the infusion of solvents such as dimethyl sulfoxide or ethanol and metals such as aluminum; X-irradiation; and the induction of pathological conditions including hypertension, hypercapnia, hypoxia, or ischemia (3). The mechanisms responsible for BBBD with some of these techniques are not well understood. A somewhat safer technique involves the systemic delivery of the convulsant Metrazol (pentylenetetrazol), which transiently increases the BBB permeability while causing seizures. Concurrent administration of the anticonvulsant pentobarbital blocks seizing while allowing BBBD to persist (26). The BBB can also be compromised by the systemic administration of several antineoplastic agents including VP-16, cisplatin, hydroxyurea, fluorouracil, and etoposide (3). In animal models, the intracarotid administration of etoposide results in a 3-fold increase in cerebrovascular permeability that persists for 4–5 days. This technique yielded a statistically significant increase in the CNS uptake of indium-labeled liposomes in a rat model. However, the potential toxicity associated with long term BBBD is a major concern.

Osmotic BBBD. The most frequently applied clinical technique for achieving BBBD is the intraarterial infusion of a hyperosmolar solution of mannitol (34,35). By infusing the solution directly into an artery that feeds the target area of the brain, it is somewhat possible to achieve localized BBBD and/or drug delivery (36). As the hyperosmolar solution flows through the cerebral capillaries, acute dehydration of endothelial cells results in cell shrinkage, which in turn widens the tight junctions connecting adjacent membranes (36). Subsequent rehydration in the presence of normal plasma leads to complete restoration of the BBB about 4 h following treatment. The hyperosmolar technique of BBBD has been studied extensively in animal models (37–39). These studies demonstrate that osmotic BBBD can be safe and is able to increase concentrations of chemotherapeutic agents in the brain parenchyma 10–90-fold (40). This technique has been applied clinically for more than 15 years, most extensively by Neuwelt et al. (34,35).

The clinical protocol for BBBD in neurooncological patients generally consists of the following. A 25% mannitol solution is infused at 5–10 mL/s for 30 seconds into the carotid or vertebral artery that feeds the area of the brain containing an intracranial tumor. Very soon before or after BBBD, the patient is administered a chemotherapeutic regimen via the circulatory system. In a recent clinical study, Neuwelt et al. examined the efficacy of the coadministration of the antineoplastic agents carboplatin and etoposide in conjunction with BBBD in 34 patients with intracranial tumors (40). In 4 out of 4 patients with primitive neuroectodermal tumors and 2 out of 4 patients with CNS lymphomas, the authors report a complete response (a complete response was defined as "the resolution of enhancing tumor as shown on computed tomograms or magnetic resonance images, no need for steroids, stable or improved neurological function, and negative results on CSF tests.") No response, however, was seen in patients with glioblastoma multiforme, mixed astrocytoma-oligodendroglioma, or metastatic carcinoma.

Unfortunately, the treatment regimen was associated not only with expected reversible myelosuppression but also with unexpected, irreversible high-frequency hearing loss. The latter is believed to be associated with ototoxic effects of carboplatin. It has since been reported that the administration of the chemoprotective agent sodium thiosulfate (which converts carboplatin into a noncytotoxic compound) 1 h after carboplatin administration in conjunction with osmotic BBBD may provide a mechanism to rescue from carboplatin toxicity (41). The authors conclude that this treatment protocol warrants further investigation, especially for the treatment of highly responsive tumors. This study exemplifies both the therapeutic and

toxic potential of BBBD in conjunction with systemic drug administration.

Biochemical BBBD. Recently, new and potentially safer biochemical techniques have been developed to disrupt the BBB. One reason for the unfavorable toxic/therapeutic ratio often observed with hyperosmotic BBBD is that this methodology results in only a 25% increase in the permeability of the tumor microvasculature, in contrast to a 10-fold increase in the permeability of normal brain endothelium (42). Therefore, the normal brain is left vulnerable to potentially neurotoxic chemotherapeutic agents. Black et al. recently developed biochemical techniques to selectively disrupt the intratumoral BBB while minimally altering the normal BBB (42). For example, in animal studies the intracarotid administration of the vasoactive agent leukotriene C4 (LTC4) selectively increases the permeability in brain tumor capillaries while leaving the normal brain unaffected. The selectivity for the tumor microvasculature is attributed to the secretion by endothelial cells in the normal brain of the enzyme γ-glutamyl transpeptidase, which inactivates LTC4. However, because this enzyme requires a glial inductive influence for expression, it is downregulated in tumor endothelial cells, leaving the tumor microvasculature vulnerable to LTC4-mediated BBBD.

Recently, this group has shown that the administration of another potent vasoactive agent, the synthetic bradykinin analogue RMP7, results in even greater selective increase in permeability in brain tumor capillaries. Mechanistic studies suggest that the effects of RMP7 on tumor endothelial cells are mediated by nitric oxide released by the enzyme nitric oxide synthase, which is expressed at higher levels in RG2 rat gliomas than in normal rat brain (43). In efficacy studies with the RG2 model, animals treated with a combination of carboplatin in conjunction with RMP7 exhibited a significantly higher survival rate at 31 days when compared to controls and carboplatin alone. Carboplatin penetration into brain tumors was increased 2.7-fold when the drug was administered in conjunction with RMP7-induced BBBD, with no enhanced uptake into the normal brain parenchyma (44). In a recent clinical study involving nine patients with recurrent malignant glioma, the intracarotid infusion of RMP7 demonstrated a selective increase in the penetration of the radioactive tracer ^{68}GaEDTA into brain tumors without increasing its transport into normal brain (45). Although the efficacy of this strategy has yet to be demonstrated clinically, the results are encouraging and warrant further study.

Alternative Routes to CNS Drug Delivery

Despite advances in rational CNS drug design and BBBD, many potentially efficacious drug molecules still cannot penetrate into the brain parenchyma at therapeutic concentrations. Most of the aforementioned techniques aim to enhance the CNS penetration of drugs delivered via the circulatory system. This method results in delivery of the injected agent throughout the entire body, frequently causing unwanted systemic side effects. Additionally, systemically administered agents must penetrate the BBB to enter the brain, which has proven to be a formidable task. A third class of strategies aimed at enhancing CNS penetration of drug molecules is composed of delivery methodologies that do not rely on the cardiovascular system. These alternative routes for controlled CNS drug delivery obviate the need for drug manipulation to enhance BBB permeability and/or BBBD by circumventing the BBB altogether.

Intraventricular/Intrathecal Route. One strategy for bypassing the BBB that has been studied extensively both in the laboratory and in clinical trials is the intralumbar injection or intraventricular infusion of drugs directly into the CSF. Drugs can be infused intraventricularly using an Ommaya reservoir, a plastic reservoir implanted subcutaneously in the scalp and connected to the ventricles within the brain via an outlet catheter. Drug solutions can be subcutaneously injected into the implanted reservoir and delivered to the ventricles by manual compression of the reservoir through the scalp.

When compared to vascular drug delivery, intra-CSF drug administration theoretically has several advantages. Intra-CSF administration bypasses the BBB and results in immediate high CSF drug concentrations. Because the drug is somewhat contained within the CNS, a smaller dose can be used, potentially minimizing systemic toxicity (6). Furthermore, drugs in the CSF encounter minimized protein binding and decreased enzymatic activity relative to drugs in plasma, leading to longer drug half-life in the CSF (46). Finally, because the CSF freely exchanges molecules with the extracellular fluid of the brain parenchyma, delivering drugs into the CSF could theoretically result in therapeutic CNS drug concentrations.

However, this delivery method has not lived up to its theoretical potential for several reasons. These include a slow rate of drug distribution within the CSF space; increases in intracranial pressure associated with fluid injection or infusion into small ventricular volumes; and a high clinical incidence of hemorrhage, CSF leaks, neurotoxicity, and CNS infections (4). Most importantly, the success of this approach is limited by the CSF-brain barrier, composed of barriers to diffusion into the brain parenchyma. Because the extracellular fluid space of the brain is extremely tortuous, drug diffusion through the brain parenchyma is very slow and inversely proportional to the molecular weight of the drug. For example, 1 h after intraventricular administration, the methotrexate concentration 3.2 mm into the brain has been calculated to be only 1% of that in the CSF. For macromolecules, such as proteins, brain parenchymal concentrations following intra-CSF administration are undetectable (6). For these reasons, intra-CSF chemotherapy in the treatment of intraparenchymal CNS tumors has not proven to be effective. The greatest utility of this delivery methodology has been in cases where high drug concentrations in the CSF and/or the immediately adjacent parenchyma are desired, such as in the treatment of carcinomatous meningitis or for spinal anesthesia/analgesia (46).

Olfactory Pathway. An alternative CNS drug delivery strategy that has received relatively little attention is the intranasal route. Drugs delivered intranasally

Next Page

are transported along olfactory sensory neurons to yield significant concentrations in the CSF and olfactory bulb. In recent studies, intranasal administration of wheat germ agglutinin–horseradish peroxidase resulted in a mean olfactory bulb concentration in the nanomolar range. In theory, this delivery strategy could be effective in the delivery of therapeutic proteins such as brain-derived neurotrophic factor (BDNF) to the olfactory bulb as a treatment for Alzheimer's disease (47). An obvious advantage of this method is that it is noninvasive relative to other strategies. In practice, however, further study is required to determine if therapeutic drug concentrations can be achieved following intranasal delivery.

Interstitial Delivery. The most direct way of circumventing the BBB is to deliver drugs directly to the brain interstitium. By directing agents uniquely to an intracranial target, interstitial drug delivery can theoretically yield high CNS drug concentrations with minimal systemic exposure and toxicity. Furthermore, with this strategy, intracranial drug concentrations can be sustained, which is crucial in the treatment of many neurodegenerative disorders and for the antitumor efficacy of many chemotherapeutic agents.

Injections, Catheters, and Pumps. Several techniques have been developed for delivering drugs directly to the brain interstitium. Until recently, the most widely used method has been the interstitial injection or infusion of drugs using an Ommaya reservoir or implantable pump. The use of this methodology has recently been extensively reviewed by Walter et al. (48) and will only be summarized here. The adaptation of the Ommaya reservoir to achieve interstitial drug delivery simply involves placing the outlet catheter directly in the intracranial target area. This technique has often been applied to neurooncological patients in which the outlet catheter is placed in the resection cavity following surgical debulking of a brain tumor. Chemotherapeutic agents can be periodically injected into the subcutaneous reservoir and then delivered directly to the tumor bed. This technique, however, does not achieve truly continuous drug delivery.

More recently, several implantable pumps have been developed that possess several advantages over the Ommaya reservoir. Like the Ommaya reservoir, these pumps can be implanted subcutaneously and refilled by subcutaneous injection. Unlike the Ommaya reservoir, these pumps are capable of delivering drugs as a constant infusion over an extended period of time. Furthermore, the rate of drug delivery can be varied using external handheld computer control units.

Currently each of the three different pumps available for interstitial CNS drug delivery operates by a distinct mechanism. The Infusaid pump (Infusaid Corp., Norwood, MA) uses the vapor pressure of compressed freon to deliver a drug solution at a constant rate; the MiniMed PIMS system (MiniMed, Sylmor, CA) uses a solenoid pumping mechanism; and the Medtronic SynchroMed system (Medtronic, Minneapolis, MN) delivers drugs via a peristaltic mechanism.

The Ommaya reservoir or infusion pumps have thus far been used in various clinical trials with brain tumor patients to interstitially deliver the chemotherapeutic agents BCNU or its analogs, methotrexate, adriamycin, bleomycin, fluorodeoxyuridine, cisplatin, L-2,4-diaminobutyric acid, interleukin 2 (IL-2), and interferon γ (48). In most of these studies the intratumoral drug concentrations were often high, and the side effects of the therapy were mild. In all of these clinical studies, however, the patient population was small (<30), and the survival benefit was rarely significant. The success of these techniques is limited by catheter clogging or blocking by tissue debris, inadequate drug distribution throughout the tumor, and a high degree of burden to the patient.

Oldfield et al. have suggested that the distribution of large and small drug molecules in the brain could be enhanced using convection to supplement simple diffusion (49). The group proposes maintaining a pressure gradient during interstitial drug infusion to generate bulk fluid convection through the brain interstitium. This technique was employed in mongrel cats to increase the distribution of ^{111}In-labeled transferrin and [^{14}C]sucrose over centimeter distances from the site of infusion. Neuwelt et al. have, however, recently argued that increasing the diffusion gradient by maximizing the concentration of the infused agent results in a higher volume of intraparenchymal drug distribution than is achieved by enhancing fluid convection (50). Further study is warranted to optimize the infusion techniques used in future clinical testing.

Drug Delivery from Biological Tissues. Another strategy to achieve interstitial drug delivery involves releasing drugs from biological tissue. With the dawn of molecular medicine, there has been great interest in using biological tissue as both the source and delivery vehicle for therapeutic proteins. This concept has been the subject of intense research for the past two decades.

The simplest approach to this technique is to implant into the brain a tissue that naturally secretes a desired therapeutic agent. This approach has been most extensively applied to the treatment of Parkinson's disease (22). The debilitating symptoms of Parkinson's disease are largely caused by diminished interstitial dopamine concentrations due to the progressive degeneration of the dopamine-releasing neurons of the substantia nigra. Transplantation of embryonic dopamine-releasing neurons is an attractive therapeutic strategy because these cells demonstrate good post-transplantation survival and growth characteristics in animal models (51). For example, Sladeck et al. have demonstrated that grafting fetal embryonic nerve cell or paraneural tissue to damaged areas of the brain leads to substantial functional recovery in both rodent and primate models of parkinsonism (52). The observed improvements correlated with the duration of graft survival and the extent to which the grafted neurons innervated the host striatum.

When this strategy was first applied clinically, the results were disappointing (53). Transplanted tissue often did not survive owing to a lack of neovascular innervation. Without rapid neovascularization, implanted solid grafts undergo irreparable ischemic injury leading to cell death. Recently, Rogers et al. have demonstrated enhanced vascularization and microvascular permeability in cell-suspension embryonic neural grafts relative to solid

grafts (53), but improvements in clinical results using this technique have not yet been dramatic.

An attractive extension of this method is to use gene therapy to develop optimized biological tissue for interstitial drug delivery. Prior to implantation, cells can be genetically modified to synthesize and release specific therapeutic agents. Laterra et al. have demonstrated the therapeutic potential of this technique in the treatment of brain tumors. Owing to the presence of endothelial mitogens and a high rate of vessel proliferation in CNS tumors, genetically modified endothelial cells might efficiently transplant to brain tumor microvasculature (54). This hypothesis was supported by demonstrating high grafting efficiency of immortalized rat brain endothelial cells genetically engineered to express the β-galactosidase reporter following implantation into experimental gliomas.

The use of nonneuronal cells for therapeutic protein delivery to the CNS has recently been reviewed (55). Thompson et al., for instance, have recently used this technique to develop a novel immunotherapeutic approach for the treatment of CNS tumors (56). Nonreplicating murine melanoma cells genetically engineered to produce the cytokine granulocyte–macrophage colony-stimulating factor (GM-CSF) or interleukin 2 (IL-2) in a paracrine fashion were implanted in the flank and/or the brain of mice challenged with a lethal intracranial injection of wild-type melanoma cells. Systemic GM-CSF administration from cells implanted in the flank in conjunction with intracranial IL-2 delivery demonstrated a synergistic survival benefit.

The survival of foreign tissue grafts may be improved by advancements in techniques for culturing distinct cell types. For example, cultured human tumorigenic neuroblastoma cells synthesize several potentially therapeutic neurotransmitters (57). These cells can be chemically rendered amitotic without depleted neurotransmitter synthesis. Transplantation into the primate brain yielded graft survival for up to 270 days and no evidence of neoplastic growth. Also cografting cells engineered to release neurotrophic factors with cells engineered to release therapeutic proteins may enhance the survival and development of foreign tissue (52).

Ideally it would be possible to perform in vivo genetic engineering to cause specific endogenous brain tissue to express a desired protein, circumventing the ischemic and immunogenic complications encountered with the implantation of foreign tissue grafts. In the last few years there have been numerous attempts to apply this strategy to the treatment of various CNS disorders including Parkinson's disease (58,59), epilepsy (60), Alzheimer's disease (61), and malignant brain tumors (62–64). One technique that has been developed for the treatment of CNS malignancies involves in vivo tumor transduction with the herpes simplex thymidine kinase (*HS-tk*) gene followed by treatment with the antiherpes drug ganciclovir (65). *HS-tk* transduction specifically into replicating glioma cells is achieved in various animal models following intratumoral injections of retroviral vector-producing cells containing the *HS-tk* gene, rendering the transfected tumor cells susceptible to treatment with ganciclovir. Other vector systems used in CNS gene transfer studies include retroviruses, adenoviruses, adeno-associated viruses, encapsulation of plasmid DNA into cationic liposomes, and neural and oligodendrial stem cells. Although this approach holds remarkable therapeutic potential in the treatment of CNS diseases, its efficacy has thus far been hindered by a number of obstacles: restricted delivery of vector systems across the BBB, inefficient transfection of host cells, nonselective expression of the transgene, and deleterious regulation of the transgene by the host CNS (64).

In conclusion, despite significant advancements in interstitial drug delivery to the CNS using injections, catheters, pumps, and biological tissue implants, these techniques have thus far had only modest clinical impact. However, the therapeutic potential of interstitial drug delivery may soon be realized using new advances in polymer technologies to modify the aforementioned techniques. The second half of this chapter will focus on our work and the work of other groups on delivering drugs directly to the brain interstitium using controlled-release polymer systems.

INTERSTITIAL CNS DRUG DELIVERY USING CONTROLLED-RELEASE POLYMER SYSTEMS

Development of Polyanhydrides for Controlled Drug Delivery

Polymeric or lipid-based devices that can deliver drug molecules at defined rates for specific periods of time are now making a tremendous impact in clinical medicine (66,67). For a long time, however, polymers used in medicine were simply adapted from materials originally developed for other applications. For example, the highly flexible material used to construct an artificial heart was borrowed from a woman's girdle. Dialysis tubing was built with sausage casing, and the material used in breast implants was adapted from mattress stuffing. As a result, the scope of polymeric medical devices was limited by the narrow range of physical characteristics found in conventional polymeric materials.

Recognizing the shortcomings in this approach, a program was launched at MIT in 1979 to rationally design polymeric materials specifically for drug delivery applications (68,69). The idea was to first decide what mechanical, chemical, and biological characteristics were required for a particular application and then to design, from first principles, a polymeric material that possessed these properties.

Rational Design of Polyanhydride Polymers. To develop polymeric materials specifically for drug delivery applications, the following characteristics were considered. First, the delivery device should be biodegradable to obviate the need for surgical removal following treatment. Polymeric degradation can occur either by bulk erosion throughout the polymeric matrix (like a sugar cube) or by surface erosion, whereby the matrix dissolves layer by layer (like a bar of soap). Bulk erosion, the mechanism by which polyester-based suture materials erode, is not desirable for drug delivery applications because it can lead to drug dumping and potential toxicity. Surface erosion of a ho-

mogeneous polymer/drug formulation, however, would lead to constant, zero-order release of the entrapped drug, as long as the surface area of the device remained fairly constant over time. One geometry that would achieve this constancy is a long flat slab as shown in Figure 3. Polymeric degradation in vivo can be achieved by either enzymatic or hydrolytic mechanisms. Although enzyme levels can vary from patient to patient as well as both regionally and temporally within the same patient, excess water is ubiquitous. Therefore, we decided that drug release profiles would be more consistent if the polymer degraded via hydrolytic degradation.

The challenge was then to find a combination of monomers and bonds that would yield a polymeric material that would erode from its surface via hydrolytic degradation. We predicted that hydrophobic monomers would minimize the penetration of water into the delivery device and allow only the bonds at the surface to be cleaved. The exclusion of water inside the device would also protect unstable drugs from hydrolytic degradation. Toxicologists at MIT believed that the hydrophobic monomers carboxyalkanoic acid and sebacic acid would be nontoxic and nonmutagenic. This strategy would only work, however, if the bonds linking the hydrophobic monomers were highly labile in the presence of water. After considering the stability of various polymeric linkages, we predicted that anhydride bonds would demonstrate the appropriate instability to promote surface erosion. A variety of polyanhydride polymers and copolymers were therefore synthesized by then graduate students or postdoctoral fellows Rosen and Linhardt; initial studies demonstrated that, indeed, these new materials displayed surface eroding properties (70). MIT postdoctoral fellow Leong subsequently showed that altering the ratio of monomers in several copolymer systems achieved variable degradation rates (71). For example, altering the monomer ratio in the copolymer system composed of sebacic acid (SA) and the more hydrophobic 1,3-bis-*para*-carboxyphenoxypropane (pCPP) results in degradation rates ranging from a few days to up to 5 years. (Fig. 4). When this new class of polymers was then applied to drug delivery, zero-order or near-zero-order release was achieved with many drug/polymer formulations (Fig. 5).

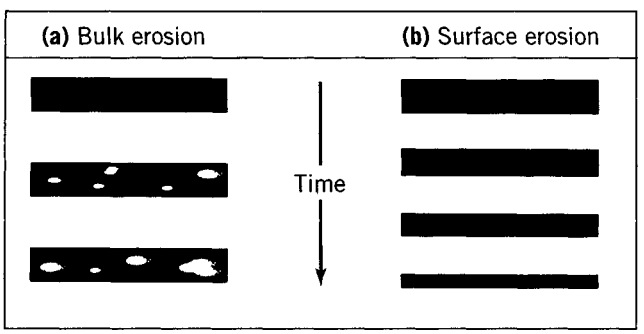


Figure 3. Polymers designed for drug delivery applications may degrade by (**a**) bulk erosion or (**b**) surface erosion. Surface erosion is generally preferred when constant drug release is desired. *Source:* Reproduced with permission from Ref. 67.

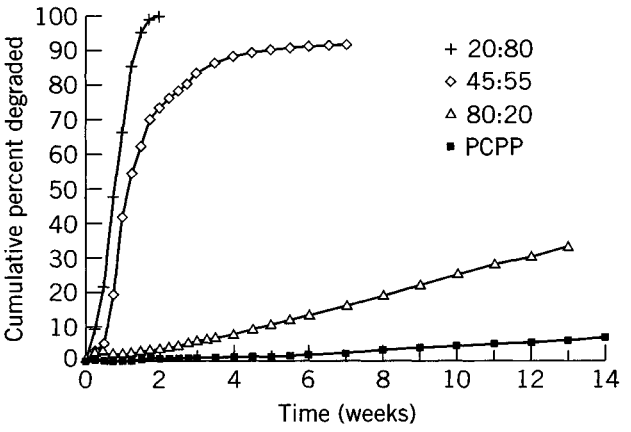


Figure 4. Rate of polyanhydride degradation versus time. pCPP and SA copolymers were formulated into 1.4-cm-diameter disks 1 mm thick by compression molding and placed into a 0.1 M pH 7.4 phosphate buffer solution at 37°C. The cumulative percentage of the polymer that was degraded was measured by absorption at 250 nm. *Source:* Reproduced with permission from Ref. 69.

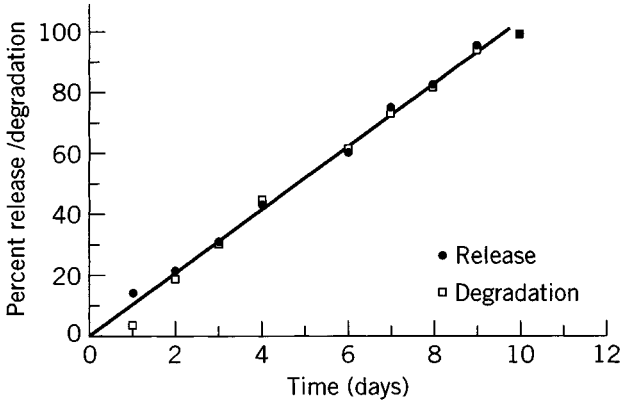


Figure 5. Release of *p*-nitroaniline and the degradation of poly-(carboxyphenoxyacetic acid) (P-CPA) versus time. Disks (1.4 cm in diameter and 1 mm thick) of PCPA were prepared containing 5% (w/w) *p*-nitroaniline by compression molding and degraded in 0.1 M pH 7.4 phosphate buffer at 37°C. The cumulative release of *p*-nitroaniline and degradation of PCPA were measured by absorbance at 380 and 235 nm, respectively. *Source:* Reproduced with permission from Ref. 69.

Synthesis of Polyanhydrides. Because the first polyanhydrides had low molecular weights (under 20,000 Da), they were brittle and not strong enough to be formed into practical drug delivery devices. However, Domb has developed several methods for synthesizing polyanhydrides with molecular weights up to 250,000 Da (72), including several solution methods such as catalyzed dehydrative coupling, dehydrochlorination, and one-step polymerization using phosgene- or diphosgene-coupling agents. The most successful synthesis, however, was achieved via polycondensation of melted monomers.

The optimized polycondensation synthesis scheme for the copolymer system composed of SA and pCPP in a 20:80 molar ratio is shown in Figure 6 (72). Highly purified SA

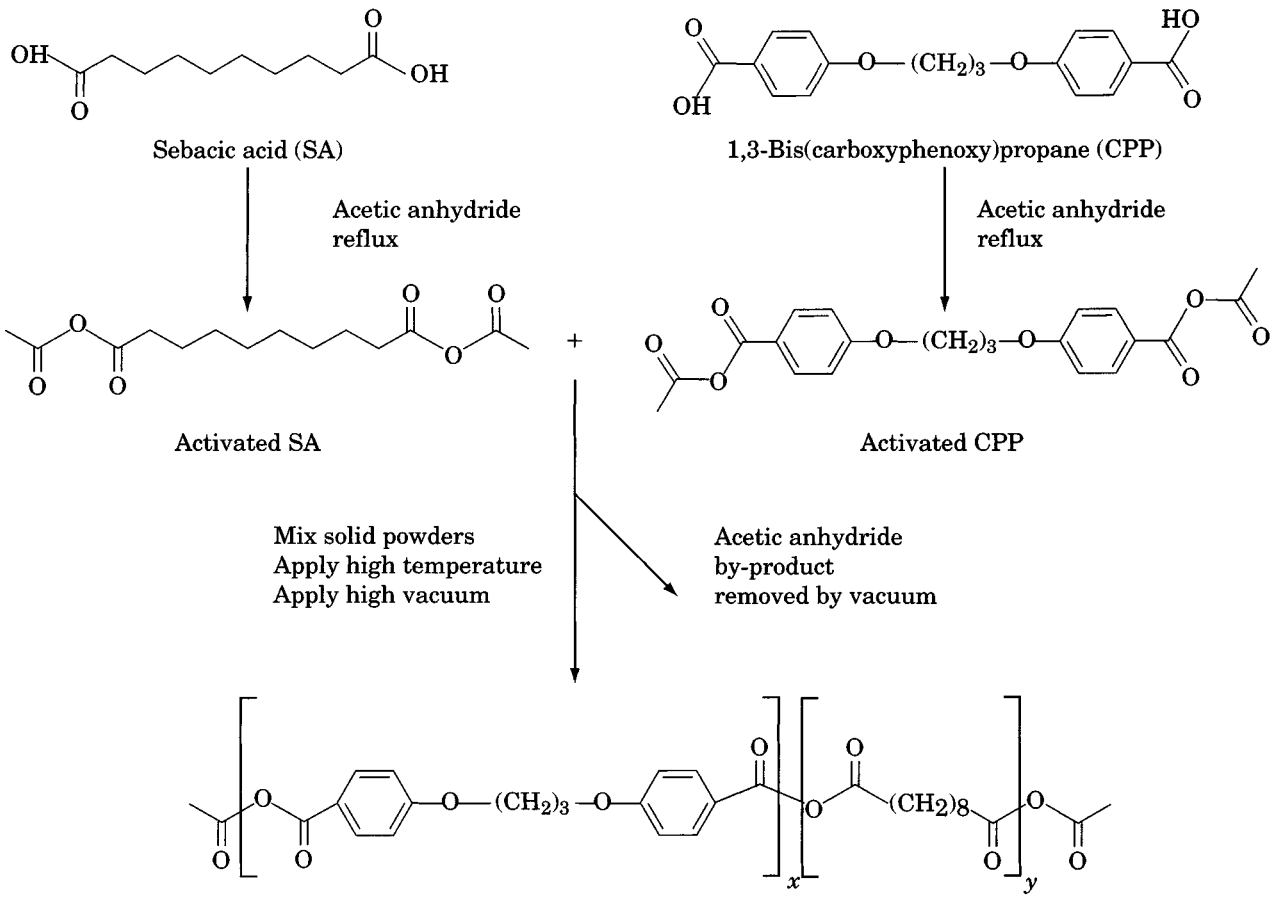


Figure 6. Synthesis scheme of pCPP:SA polyanhydrides by melt polycondensation. *Source:* Reproduced with permission from Ref. 67.

and pCPP monomers are first activated via reflux in acetic anhydride, leading to acylation of the terminal carboxylic acid functionalities. These activated monomers are then mixed together as solids in desired proportions and heated. As the monomers begin to melt, they start to react, forming a pCPP:SA copolymer with acetic anhydride as the byproduct. As the reaction begins, the system is purged with nitrogen or argon, followed by the application of high vacuum, which leads to the removal of the volatile acetic anhydride. Without acylation in the first step, the byproduct of polymerization would be water, which is less volatile when acetic anhydride and could cause polymeric degradation. Because this synthetic technique does not require potentially toxic catalysts, the product is pure, high-molecular-weight polyanhydride polymer suitable for formulation into practical drug delivery devices.

Techniques for Drug Incorporation. Various methods have been developed for incorporating drugs into biodegradable polymers for controlled drug delivery applications. The trituration method involves physically mixing the polymer and drug in fine powder form (73). This method is universally applicable because it requires only that drugs may be formed into small particles. However, this method can result in inhomogeneous drug distribution leading to inconsistent drug release profiles. Also, release of loosely bound drug particles on the polymer surface can lead to a "burst effect," a disproportionately large burst of drug being delivered at the beginning of the release period. Another approach, the cosolution method, involves codissolving solvent and drug in an organic solvent and then evaporating the solvent in vacuo. This method tends to yield homogeneous drug/polymer formulations leading to highly reproducible release profiles. However, this method requires that the drug be soluble and stable in organic solvents such as methylene chloride or chloroform. Furthermore, solvent evaporation leaves pores and channels within the polymer matrix through which the drug can diffuse. A high rate of drug diffusion leads to release profiles that are non–zero order. A third method, the mix/melt method, involves heating the polymer above its melting point and then physically mixing the drug into the viscous polymer liquid (68). Cooling this mixture yields a dense and homogeneous polymer/drug matrix with minimal pores and channels for drug diffusion and highly reproducible release kinetics. Heating the polymer, however [about 80°C is required for pCPP:SA (20:80)], can potentially lead to interaction of the drug with the polymer and/or heat deactivation of temperature-sensitive drugs. The advantages and disadvantages of these drug-incorporating

techniques must be considered for each individual polymer/drug formulation.

Techniques to Fabricate Drug/Polymer Formulations into Drug Delivery Devices. After a drug has been incorporated into a polyanhydride polymer matrix, a variety of techniques fabricate the drug/polymer formulation into a size and shape suitable for drug delivery (71). One such technique is compression molding: The drug/polymer formulation is ground or spray-dried into a fine powder, placed into a piston-type mold, and then compressed with a vice or hydraulic press into a flat slab or wafer. This method is applicable to a wide variety of polymer formulations. The melt-molding technique involves melting the drug/polymer formulation and molding the gel into a desired geometry. Another method, known as the solvent-casting method, involves pouring an organic solution containing polymer and drug into a flat, open mold chilled over dry ice. Slowly the solvent evaporates to yield a thin, flat film containing polymer and drug intimately mixed.

Various methods also exist for preparing drug-loaded polyanhydride microspheres that can be incorporated into a suspension and injected into tissue (74). In the hot-melt microencapsulation method, polymers and drug are cosuspended in a silicone or olive oil and the mixture is heated to 5°C above the polymer melting point with continuous stirring. When the solution is cooled, the polymer is solidified into microspheres while entrapping the drug within. Another method for preparing microspheres is the spray-drying microencapsulation technique. In this method, polymer and drug are codissolved in an organic solvent, and the solution is sprayed through an atomizer into a drying chamber where the drug-loaded microspheres are immediately dried by an upward flow of nitrogen. Drugs that are heat sensitive can be incorporated into polyanhydride microspheres via the solvent-removal microencapsulation method (75). In this method the polymer and drug are codissolved in a volatile organic solvent. This solution is then suspended in an organic oil that is immiscible with the organic solvent. A surfactant such as Span 85 is added, and the mixture is continuously stirred. Petroleum ether is then introduced, causing the condensation of polymer into the shape of microspheres with drug trapped inside.

With these various techniques, almost any drug, from small anticancer agents to large therapeutic macromolecules such as proteins, can be released in a controlled fashion from a biodegradable polymer matrix.

Development of Drug-Impregnated Polyanhydride Wafers for the Treatment of Brain Tumors

In 1984, the Department of Neurosurgery at Johns Hopkins University and the Department of Chemical Engineering at MIT joined forces to apply this new drug delivery technology to the treatment of brain tumors. Despite substantial advances in imaging and surgical techniques, the prognosis for patients diagnosed with glioblastoma multiforme, the most malignant and deadly form of brain cancer, remains dismal. Survival is still measured in months, and rarely do these patient survive for more than 2 years. Because most malignant gliomas demonstrate a marked propensity for local recurrence rather than metastasizing to other areas of the brain or to the peripheral organs, we predicted that directing intense therapy at the site of the initial tumor would result in powerful control of postsurgical tumor growth. We believed that drug delivery directly to the brain interstitium using polyanhydride wafers would circumvent the BBB and release unprecedented levels of drug directly to an intracranial target in a sustained fashion for extended periods of time.

Preclinical Studies. With the lack of mutagenicity and carcinogenicity of the pCPP:SA polymers already established at MIT, we carried out a series of preclinical experiments in collaboration with Colvin et al. to determine the safety and efficacy of drug-loaded intracranial polymer implants. The alkylating agent BCNU was chosen for our initial studies because of its established antineoplastic activity against malignant gliomas. These preclinical studies investigated the biocompatibility of the pCPP:SA (20:80) polymer in the brain, the in vivo drug release profile of BCNU-loaded wafers, and the safety and efficacy of BCNU-loaded wafers in a murine model of malignant glioma.

The biocompatibility of the pCPP:SA (20:80) polymer was first tested by implanting placebo wafers in the corneas of rabbits. This assay has proven to be a highly sensitive system for determining the inflammatory effect of implanted agents (76). Over the course of a 6-week implantation period, the pCPP:SA (20:80) polymer implant did not cause neovascularization, corneal edema, or the infiltration of white blood cells (77). The biocompatibility of pCPP:SA polymers was then tested in the CNS of Fischer 344 rats and compared with that of other well-tolerated neurosurgical biomaterials: oxidized regenerated cellulose (Surgicel®) and absorbable gelatin sponge (Gelfoam®) (78). Rats underwent bilateral frontal-lobe implantation of pCPP:SA (20:80), Surgicel®, and Gelfoam® and were closely monitored for inflammatory responses upon serial sacrifice over a 5-week period. The pCPP:SA polymers elicited a minimal, transient, localized inflammatory response comparable to the well-tolerated clinical implants. The local response to pCPP:SA (20:80) wafers subsided as the polymer device degraded. Similar studies were performed in the rabbit brain which again demonstrated no differences from the inflammatory response elicited by pCPP:SA polymer and Gelfoam® implants (79).

To initially assess the therapeutic potential of intracranial drug delivery from a locally implanted polymer, the drug release profile was determined for intracranial implants of ethylene-vinyl acetate copolymer (EVAc) wafers impregnated with BCNU in Fischer 344 rats (80). EVAc was chosen as a delivery device because the in vitro and in vivo release kinetics of this nonbiodegradable polymer system are well established. The EVAc polymer used in these studies was obtained from the Du Pont Company (Wilmington, DE) and contained 40% vinyl acetate by weight. The polymer was first washed copiously with ethyl alcohol to remove inflammatory impurities. To prepare the BCNU-loaded EVAc polymers, drug and polymer (3:7 BCNU-to-EVAc w/w ratio) were codissolved in methylene chloride, and the solution was poured into cylindrical glass molds

at −70°C. Solvent evaporation yielded cylindrical polymers homogeneously loaded with 30% BCNU that were transferred to glass plates at −30°C and allowed to dry for 7 days. The drug-loaded EVAc cylinders were then cut into 10-mg disks, exposed to ultraviolet radiation for 1–2 hours, and implanted into the rat brain (81). Using a Bratton-Marshall assay to quantify BCNU concentrations in brain homogenates, the controlled release of BCNU in the implant hemisphere was observed for the entire 9 days of the study. Drug levels peaked at 49.6 μg/g brain tissue. Much lower levels of BCNU were measured in the contralateral hemisphere and systemic circulation and only for 1 day.

Similar results were obtained with various ^{3}H-BCNU-loaded pCPP:SA (20:80) wafers implanted intracranially in New Zealand White rabbits (82). Drug-loaded polymers prepared by either the trituration or solution method were studied. Autoradiographic analysis of coronal sections bisecting the polymer implant was used to assess both the local drug concentrations as a function of distance from the polymer and the percent of the brain exposed to drug. In this study the results were compared to local injection of ^{3}H-BCNU. At days 3 and 7, BCNU concentrations of 6 mM were observed up to 10 mm from the polymer implant. In contrast, direct injection of ^{3}H-BCNU resulted in almost no detectable levels of drug in the brain on day 3. The percent of brain exposed as a result of polymeric drug delivery was determined at days 3, 7, and 10 to be 50%, 15%, and <10%, respectively. Both the average drug concentration and percent of brain exposed increased with greater ^{3}H-BCNU loading doses. The results obtained with the polymers prepared by solution and by trituration were not significantly different.

The ability of BCNU-loaded polymers to control the growth of established solid tumors was first evaluated in a flank model in Fischer 344 rats (83). BCNU-loaded EVAc wafers implanted adjacent to an established 9L gliosarcoma tumor resulted in a delay in tumor growth (defined as the time required for tumor volume to increase by 1 log) of +16.3 days compared to controls ($p < 0.05$). In contrast, BCNU delivered systemically via intraperitoneal (IP) injections and BCNU delivered systemically from a contralateral EVAc implant resulted in significantly smaller growth delays of +11.2 days and +9.3 days, respectively. The efficacy of BCNU-loaded EVAc wafers in the treatment of an established intracranial tumor was then evaluated. Sixty Fischer 344 rats underwent a craniectomy followed by placement of a 1-mm^3 9L gliosarcoma implant in the cerebral cortex of the left parietal lobe. On the fourth day after tumor implantation, animals were randomized into one of four treatment groups receiving: (*1*) empty EVAc polymers implanted at the tumor site, (*2*) systemic BCNU (14 mg/kg) via a single IP injection, (*3*) interstitial delivery of BCNU (14 mg/kg) via EVAc, and (*4*) interstitial delivery of BCNU (14 mg/kg) via pCPP:SA (20:80) wafers. As shown in Figure 7, the systemic delivery of BCNU resulted in only a 2.4-fold increase in mean survival compared to controls, while the same drug dose delivered by EVAc and pCPP:SA (20:80) polymers resulted in significantly greater 7.3- and 5.4-fold increases, respectively ($p < 0.05$). Even more encouraging was that although there was a 100% mortality rate for the control animals and the animals receiving IP

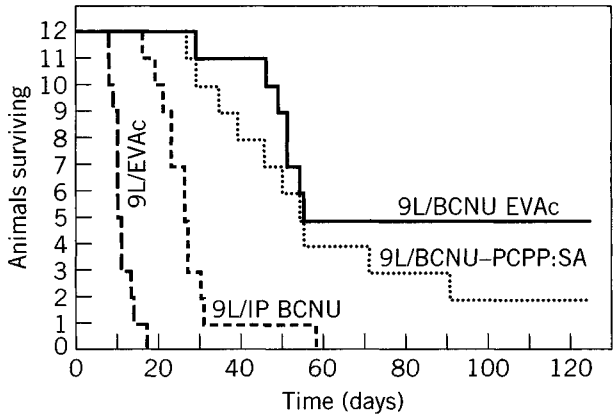


Figure 7. Survival curves of 9L glioma rats bearing intracranial tumors treated with BCNU either systemically (9L/IP BCNU) or polymerically delivered intracranially (9L/BCNU EVAc and 9L/BCNU–pCPP:SA). *Source:* Reproduced with permission from Ref. 83.

BCNU, the animals treated interstitially with drug-loaded EVAc and pCPP:SA (20:80) wafers had 42% and 17% long-term survival, respectively, to the scheduled date of sacrifice (125 days posttumor implantation). Pathological evaluation revealed no viable tumor in any of these long-term survivors, apparently indicating that the animals were cured.

The therapeutic benefit of interstitial delivery of BCNU from biodegradable pCPP:SA (20:80) polymer wafers was also compared with the intratumoral injection of the same dose of BCNU (84). In this study, Fischer 344 rats received intracranial implants of 9L gliosarcoma and were subsequently treated on day 5. The median survival for the animals receiving BCNU via polymer implants was extended 271% over controls, compared with only 36% for the same amount of BCNU injected intratumorally. These results demonstrate the advantages of sustained polymeric drug delivery over direct interstitial injection.

In preparation for clinical trials, the biocompatibility of pCPP:SA (20:80) wafers impregnated with BCNU was then evaluated in the primate brain (85). Eighteen *Macaca fasicularis* monkeys underwent a frontal lobectomy and received the following implants: (*1*) no treatment, (*2*) empty pCPP:SA (20:80) polymer wafers, (*3*) pCPP:SA (20:80) polymers impregnated with BCNU, and (*4*) empty pCPP:SA (20:80) polymer in one hemisphere and a BCNU-loaded polymer in the opposite hemisphere. The last group received concurrent external beam radiation therapy (XRT). Animals were closely monitored over a period of 80 days and showed no signs of neurological deficits. Extensive analysis of serially collected blood samples showed no signs of toxicity normally associated with systemic delivery of BCNU. Serial computerized tomography (CT) and magnetic resonance imaging (MRI) scans revealed a radioopaque mass and minimal edema surrounding the site of polymer implantation. Detailed histological examination following serial sacrifice indicated a mild, localized, transient inflammatory reaction consistent with that observed in the rat and rabbit studies. Monkeys receiving concur-

rent radiation therapy demonstrated no further deleterious effects attributable to the polymers with or without BCNU.

From these experiments, we concluded that the intracranial implantation of BCNU-impregnated pCPP:SA (20:80) polymer wafers is safe in the brains of rats, rabbits, and primates. Furthermore, this intracranial drug delivery strategy is capable of delivering active drug in a sustained fashion directly to the site of an intracranial tumor, and the potential benefits of concurrent XRT are not lost. In animal glioma models, significant prolongation of survival and encouraging cure rates were consistently observed. Owing to the success of these preclinical studies, clinical trials to evaluate the efficacy of this therapy in human patients with malignant glioma were initiated.

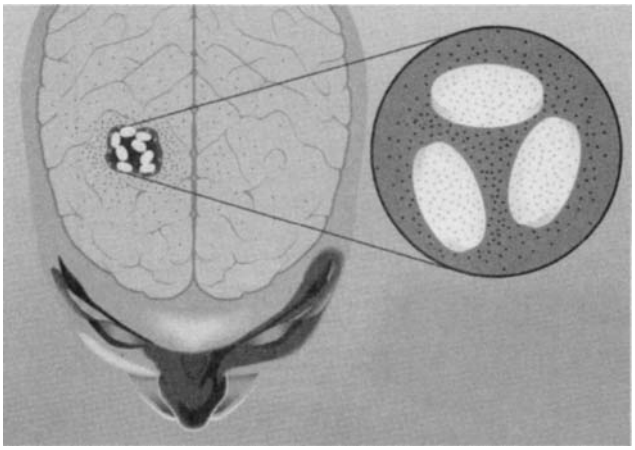


Figure 8. Up to eight polymer implants line a tumor resection cavity, where the loaded drug is gradually released as the implants dissolve. The inset shows conceptually how drug molecules diffuse away from these implants. *Source:* Reproduced with permission from Ref. 66.

Clinical Studies. The safety of implanting BCNU-loaded pCPP:SA (20:80) polymer wafers into the brains of neurooncology patients was first assessed in a Phase I–II clinical trial that began in 1987 (86). Twenty-one patients were enrolled at five institutions in the United States. The admission criteria included indication for reoperation for recurrent malignant glioma, a unilateral single focus of tumor in the cerebral cortex with an enhancing volume of at least 1.5 cm^3 on CT scans, and a Karnofsky Performance Scale (KPS) score of at least 60 (indicating that the patient is able to function independently). All patients had previously undergone XRT, had no significant hepatic or renal disease, and were not suffering from any other life-threatening illness.

Polymer wafers loaded with various doses of BCNU (1.93%, 3.85%, and 6.35% w/w) were prepared as follows. Clinical-grade pCPP:SA polymer was prepared by melt polycondensation of pCPP and SA monomers in a 20:80 molar ratio. Polymer and BCNU were codissolved in methylene chloride and spray-dried into microspheres. The drug-loaded microspheres were then compression-molded into cylindrical wafers measuring 1.4 cm in diameter and 1.0 mm thick (about the size of a dime).

In each patient, after maximum debulking of the recurrent tumor, the resection cavity was lined with up to eight BCNU-loaded polymer wafers (Figs. 8 and 9). The placement of the polymer wafers added approximately 3 minutes to the total time of surgery. For the first 7 weeks following polymer implantation, patients were closely monitored for signs of local and systemic toxicity by regular neurological examination, serial CT scans or magnetic resonance (MR) images, KPS score determination, hematologic and blood chemistry analysis, and urinalysis.

The treatment was well tolerated at all three dosing levels. CT scans and MR images revealed no direct toxicity in the brain attributable to the BCNU polymer implants. (Fig. 10). Furthermore, no patient experienced the significant reduction in blood cell counts normally associated with the systemic administration of BCNU. The overall median survival time following polymer implantation was 46 weeks, and 8 of the 21 patients (38%) survived more than 1 year. It was therefore concluded that the local delivery of BCNU from pCPP:SA (20:80) polyanhydride polymer wafers was safe in human patients and that further clinical investigation was indicated to assess the efficacy of this new treatment modality.

A prospective, randomized, placebo-controlled study was carried out to evaluate whether pCPP:SA (20:80) polymer wafers impregnated with BCNU (3.85% w/w) could reduce the 6-month mortality in patients with recurrent malignant glioma (87). Two hundred and twenty-two patients were enrolled at 27 medical centers in the United States and Canada. The admission criteria were similar to those used for the Phase I–II study. All patients entered had failed conventional therapies and were at the end stages of their fatal disease.

At the time of reoperation, the tumor resection cavity was lined with up to eight polymer wafers with or without 3.85% BCNU. When the code was broken 6 months after the last patient was entered, 110 patients had received the BCNU-loaded implants, and 112 had received the placebo. The 6-month survival rate for patients receiving BCNU-loaded polymer implants was 60% compared with 47% for patients receiving placebo wafers ($p = 0.061$). For the subset of patients with glioblastoma multiforme, the 6-month survival for the patients receiving BCNU loaded wafers was 50% greater than in those treated with placebo (64% vs. 44%, $p = 0.020$). The overall survival curve after adjustment by the proportional hazards regression model is shown in Figure 11. The median survival was 31 weeks in patients receiving drug-loaded wafers and 23 weeks for the placebo group ($p = 0.006$, after accounting for the effects of prognostic factors). Again, no clinically important deleterious effects were attributable to the polymer implants. Based on these results, it was concluded that local delivery of BCNU from pCPP:SA polymer wafers is a safe and effective treatment for recurrent malignant glioma. On September 24, 1996, the U.S. Food and Drug Administration (FDA) approved the 3.85% BCNU wafers for the treatment of recurrent malignant glioma, making this the first new treatment for brain tumors to be approved by the FDA in 23 years. These polymer wafers are now manufactured by

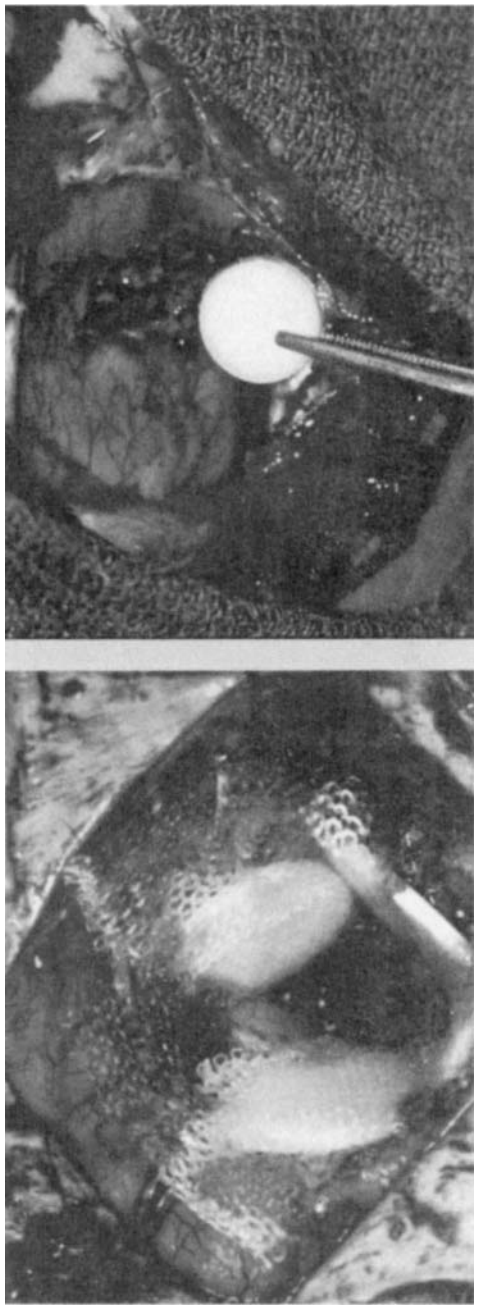


Figure 9. The surgical implantation of BCNU-loaded polyanhydride wafers within a tumor resection cavity. Placement of polymer wafers requires about 3 additional minutes of operation time. *Source:* Reproduced with permission from Ref. 66.

Guilford Pharmaceuticals in Baltimore, Maryland, under the name Gliadel® and are distributed by Rhone Poleunc Rorer worldwide except for Sweden, Norway, Denmark, and Finland, where it is distributed by Orion, Inc.

Based on the success of the 3.85% BCNU-loaded pCPP:SA wafers in the treatment of recurrent malignant glioma, we hypothesized that an even greater therapeutic benefit could be achieved using the BCNU polymer as a part of the initial treatment. To this end, a Phase I–II study was carried out to evaluate the safety of BCNU polymer implantation in conjunction with XRT for the treatment of newly diagnosed malignant glioma (88). Twenty-two patients at three hospitals in the United States received up to eight 3.85% BCNU-loaded wafers and a standard course of postoperative XRT. Again, no systemic or local toxicity was attributable to the BCNU-loaded polymer. Neurotoxicity was equivalent to that typically associated with craniotomy and XRT. The patient population was older than in the two previous clinical studies (mean age = 60), which is typically a negative predictor of outcome. Nonetheless, the median postoperative survival was 42 weeks, and 4 patients survived more than 18 months. It was therefore concluded that implantation of 3.85% BCNU-loaded polymer wafers in conjunction with XRT is safe as the initial treatment for malignant glioma.

The first Phase III clinical trial evaluating the efficacy of 3.85% BCNU-loaded polymers in patients with newly diagnosed malignant glioma was carried out in Finland and Norway by Valtonen et al. (89). Thirty-two patients were enrolled in a prospective, randomized, placebo-controlled study in which 16 patients received 3.85% BCNU-loaded wafers and 16 patients received placebo wafers following the initial surgical resection of a malignant glioma. As shown in Figure 12, median survival for the treatment group was 58 weeks compared with 40 weeks for the placebo group. ($p = 0.001$). Ten of the 16 patients (63%) in the treatment group survived for 1 year after polymer implantation, while only 3 of 16 patients (19%) in the placebo group were still alive ($p = 0.029$). When the patients with glioblastoma were considered separately, median survival was 53 weeks for patients receiving BCNU and only 40 weeks for those receiving placebo ($p = 0.0083$). Two years after treatment 31% of the patients that received Gliadel were alive versus just 6% in the placebo group, and at 3 years 25% of the treatment group were still alive compared to 6% of those receiving placebo. Another clinical trial involving a greater number of patients is being carried out by the European Association of Neurosurgeons to further evaluate the efficacy of Gliadel® wafers implanted at the time of initial surgical resection in patients with glioblastoma multiforme.

Together, these clinical trials, summarized in Table 1, demonstrate that 3.85% BCNU-loaded pCPP:SA polymer wafers are safe and effective in the treatment of newly diagnosed as well as recurrent malignant glioma. This treatment provides an effective means for circumventing the BBB, resulting in sustained, high concentrations of drug in the region of an intracranial tumor. Furthermore, the systemic toxicities usually associated with chemotherapy are avoided, and the potential benefits of adjuvant XRT are still present.

Future Clinical Studies with BCNU-Loaded Wafers. We believe that the clinical success of the Gliadel® wafer serves as proof of principle and that the polymer wafer–mediated intracranial drug delivery strategy opens the door for a dramatic expansion in the armamentarium available for the treatment of brain tumors. Eight clinical trials have already begun, and many more are planned

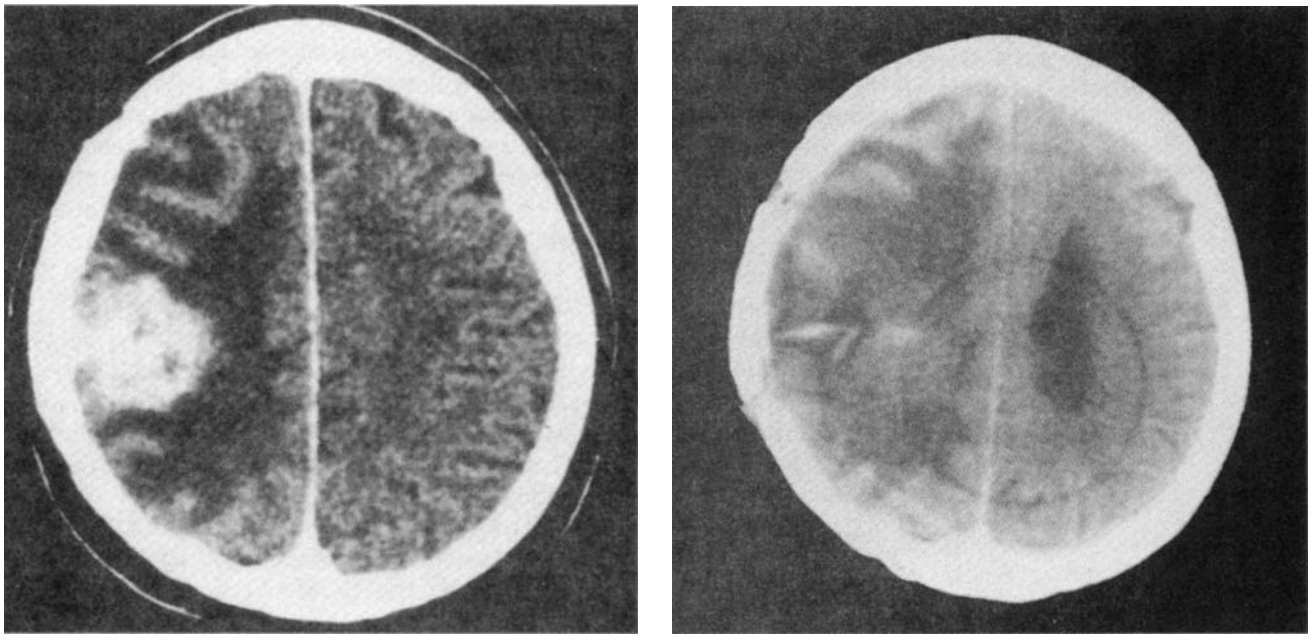


Figure 10. Computerized tomography (CT) scans show a recurrent malignant brain tumor preoperatively (left panel) and BCNU-loaded polymer wafers postoperatively (right panel). As the wafers dissolve and release the drug, they gradually disappear from the scans. *Source:* Reproduced with permission from Ref. 66.

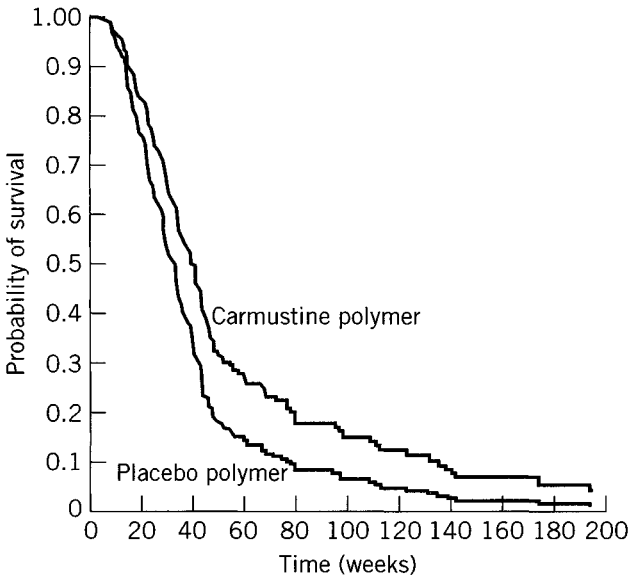


Figure 11. Overall survival for patients receiving implantation of carmustine (BCNU)-loaded polymers or placebo controls at the time of operation for a recurrent brain tumor after adjustment for prognostic factors. The curves illustrate the treatment effect expected if all patients were about age 48, white, had performance status >70, underwent >75% resection, had local irradiation, had not previously been exposed to nitrosoureas, and had glioblastomas pathologically classified as active. *Source:* Reproduced with permission from Ref. 87.

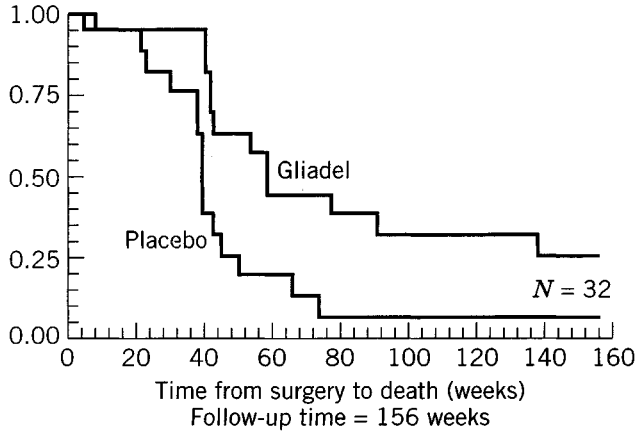


Figure 12. Kaplan-Meirer survival curves for patients receiving implantation of BCNU-loaded polymers (Gliadel®) or placebo controls at the time of initial operation for Grade III or Grade IV tumors. All patients with Grade III tumors were included in the group receiving Gliadel®. *Source:* Reproduced with permission from Ref. 89.

that aim to improve upon the demonstrated survival benefit of Gliadel®.

Recent laboratory investigations have shown that it may be possible to improve upon the efficacy of the 3.85% BCNU-loaded Gliadel® wafers simply by increasing the loading dose of BCNU (90). In the murine 9L glioma model, BCNU dose escalation from 3.8% to 32% polymer by weight revealed a dose-response relationship (hazard ratio 0.8354 for each mg/kg increase, $p < 0.001$) (Fig. 13). The best bal-

Table 1. Clinical Studies with BCNU-Loaded pCPP:SA (20:80) Polymer Wafers at the Time of Publication

Title of clinical study	Principal investigator/ Funding source	Pts.	Participating institutions	Dates of study	Refs.
Interstitial chemotherapy with drug polymer implants for the treatment of recurrent gliomas. (Phase I–II—safety)	Henry Brem, M.D. Department of Neurological Surgery, Johns Hopkins Hospital, Baltimore, MD, USA/Nova Pharmaceutical Corporation, Baltimore, MD, USA	21	Johns Hopkins Hospital, Baltimore, MD; University of AL, Birmingham, AI; Northwestern University, Evanston, IL; University of CA, Los Angeles, CA; Duke University, Durham, NC	9/87–3/90	86
Placebo-controlled trial of safety and efficacy of intraoperative controlled delivery by biodegradable polymers of chemotherapy for recurrent gliomas. (Phase III—efficacy)	Henry Brem, M.D./ Guilford Pharmaceuticals Inc., Baltimore, MD, USA; Scios-Nova Corporation, Mountain View, CA, USA; NCDDG of the NCI of the NIH, USA	222	27 medical centers in the USA and Canada	3/89–9/93	87
The safety of interstitial chemotherapy with BCNU-loaded polymer followed by radiation therapy in the treatment of newly diagnosed malignant gliomas. (Phase 1—safety)	Henry Brem, M.D./ Guilford Pharmaceuticals Inc., Baltimore, MD, USA; Scios-Nova Corporation, Mountain View, CA, USA; NCDDG of the NCI of the NIH, USA	22	Johns Hopkins Hospital, Baltimore, MD; Charlotte Memorial Hospital, Charlotte, NC; Columbia Presbyterian Medical Center New York, NY	7/90–9/94	88
Compassionate Use Study	N/A	40	Johns Hopkins Hospital, Baltimore, MD		N/A
Treatment IND	Guilford Pharmaceuticals	380	170 medical centers in the USA		N/A
Interstitial chemotherapy with BCNU-loaded polymers for initial treatment of high-grade gliomas: a randomized double-blind study (Phase III—efficacy)	Simo Valtonen, M.D. Turku University Central Hospital, Turku, Finland/ Orion Pharma (UT, PT), Espoo, Finland	32	Turku University Central Hospital, Turku, Finland; Helsinki University Central Hospital, Helsinki, Finland; Tampere University Hospital, Tampere, Finland; University Hospital of Trondheim, Trondheim, Norway	3/92–3/95	89

Note: Abbreviations: NCDDG, National Cooperative Drug Discovery Group; NCI of the NIH, National Cancer Institute of the National Institutes of Health, Bethesda, MD, USA.

ance between toxicity and antitumor efficacy, achieved with the 20% BCNU-loaded polymer wafers, resulted in a 75% long-term survival rate. Furthermore, 20% BCNU-loaded wafers are well tolerated in the non-human primate brain (90,91). Based on these preclinical findings, Olivi is leading an NIH-funded, open-label dose escalation clinical trial at 11 medical centers in the United States to evaluate the safety of Gliadel® wafers containing between 6.5% and 20% BCNU in patients with recurrent malignant glioma. A Phase III trial will subsequently evaluate the efficacy of the highest-tolerated BCNU loading dose.

Gliadel® may possess therapeutic potential in secondary CNS tumors as well. In addition to primary CNS tumors, many neurooncology patients present with systemic tumors that have metastasized to the brain (92). In fact, the majority of newly diagnosed intracranial tumors are the result of metastases from primary tumors outside the CNS. As the therapeutic options for patients with systemic malignancies are rapidly improving, fatalities due to CNS metastases are increasing. This is because many drugs with proven efficacy against the systemic aspects of these diseases do not sufficiently cross the BBB. At present the mainstays for the treatment of intracranial metastases are surgery in combination with XRT and/or systemic chemotherapy. Ewend proposed that in the treatment of intracranial metastases, local delivery of chemotherapy from polyanhydride wafers in combination with XRT might demonstrate enhanced efficacy over standard therapies. This hypothesis has been tested in a new series of murine models of the most common forms of intracranial metastases including melanoma, renal cell carcinoma, colon adenocarcinoma, lung carcinoma (15), and breast carcinoma (93). Treatment with BCNU-loaded wafers in combination with XRT was effective in prolonging median survival in all five metastatic tumor models. In most cases, the combination of XRT with local chemotherapy was more efficacious than either treatment alone. For example, the results achieved in the intracranial model of metastatic melanoma are presented in Figure 14. Based on these preclinical studies, a Phase II clinical trial has been initiated to evaluate the therapeutic potential of surgical resection

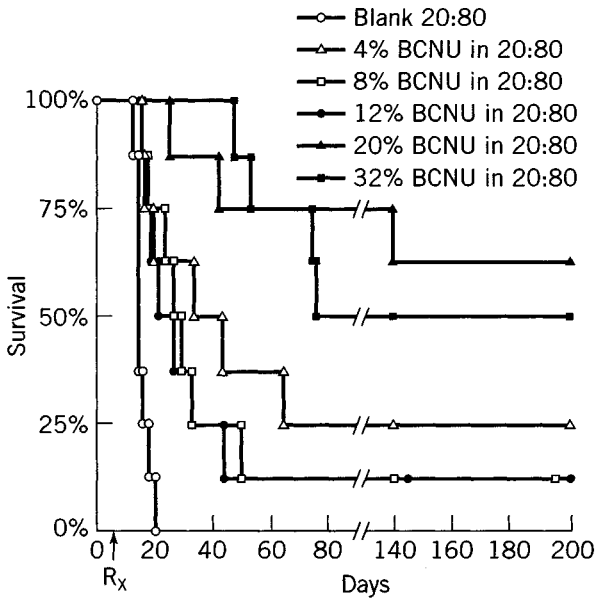


Figure 13. Survival curves for rats bearing 9L gliosarcomas treated 5 days after tumor implantation with pCPP:SA (20:80) polymers containing escalating doses of BCNU compared with control animals treated with empty polymers ($n=8$ for each group). *Source:* Reproduced with permission from Ref. 90.

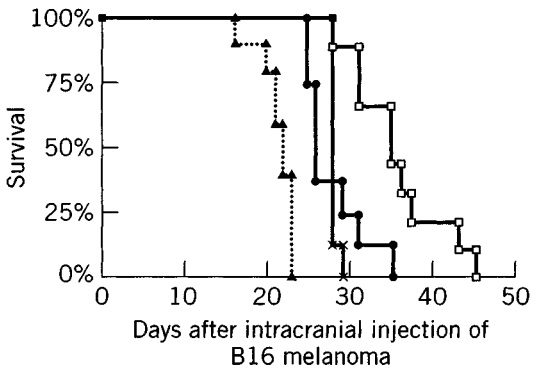


Figure 14. The efficacy of BCNU, delivered locally by biodegradable polymer, in treating a murine model of solitary intracranial metastases of B16 malignant melanoma. The treatment groups include blank polymer control (closed triangle), 20% loaded BCNU polymer implant (closed circle), radiation therapy with 300 cGy per day for 3 days (×), and 10% loaded BCNU polymer implant followed by radiation therapy with 300 cGy per day for 3 days (open square). The combination therapy was superior to either BCNU alone or XRT alone ($p<0.006$). *Source:* Reproduced with permission from Ref. 15.

in combination with Gliadel® and XRT in patients with operable CNS metastases from systemic malignancies.

Two additional clinical studies are underway to evaluate the therapeutic potential of Gliadel® in the treatment of recurrent supratentorial glial tumors. The first is a Phase I study of Gliadel® in children and adolescents, and the other is a Phase II study in adults. Another set of studies has been initiated that combines the local delivery of BCNU with an additional anticancer agent delivered systemically. In one study, a Phase I trial, patients with glioblastoma multiforme or anaplastic astrocytoma are receiving intracranial implantation of Gliadel® wafers in conjunction with serially escalated systemic doses of carboplatin. In another study, patients with glioblastoma multiforme are receiving Gliadel® and XRT in conjunction with oral administration of the cytodifferentiating agent 13-*cis*-retinoic acid.

Another approach to improve the efficacy of Gliadel® in the treatment of brain tumors is to inhibit the neoplastic cellular resistance mechanisms to BCNU therapy. The cytotoxicity of BCNU against tumor cells depends on initial DNA alkylation at the O^6-position of guanine bases (94). The primary cellular chemotherapeutic resistance mechanism against BCNU therapy is the dealkylation reaction carried out by the enzyme alkylguanine-DNA alkyl transferase (AGAT). AGAT removes O^6-guanine adducts stoichiometrically, a reaction that renders this cytoprotective enzyme irreversibly inactive, making de novo protein synthesis the only means by which AGAT activity can be restored. Pegg et al. have shown that AGAT depletion with exogenous substrates such as O^6-benzyl guanine (O^6BG) enhances the sensitivity of various animal and human tumor cell lines to treatment with alkylating agents such as BCNU (94–97). Because many human gliomas express high levels of AGAT, O^6BG could potentiate the efficacy of Gliadel® in the treatment of human brain tumors. To test this hypothesis, a Phase I clinical trial is being initiated in which patients with recurrent malignant gliomas will receive Gliadel® wafers in combination with escalating doses of intravenous O^6BG.

Thirteen other clinical trials are also scheduled to begin soon. These studies include combining local BCNU with systemic chemotherapy, permanent I-125 seeds, other drug-resistance modulatory agents, various XRT protocols, and the use of Gliadel® in the treatment of nonglial tumors of the CNS. The current and planned clinical studies are summarized in Table 2.

Laboratory Investigations with a Variety of Biodegradable Intracranial Controlled Drug Release Systems. BCNU-loaded wafers possess great therapeutic potential in the treatment of brain tumors. However, many anticancer agents are substantially more potent than BCNU against neoplastic cells in vitro. Because many of these agents do not significantly cross the BBB, their therapeutic potential in the treatment of brain tumors remains unrealized. Finding ways to deliver a wide variety of anticancer agents to the brain is crucial: Malignant gliomas are noted for their cellular pleomorphism and associated potential for acquired resistance to a single chemotherapeutic agent, and multiple drug regimens are often required to eradicate all the malignant cells in a CNS tumor. To this end, we have investigated the potential efficacy of a wide variety of drug/polymer formulations in the treatment of brain tumors.

pCPP:SA Polymers. As described above, the benefits of the pCPP:SA wafers for the intracranial delivery of drugs include circumvention of the BBB, controlled drug release by surface erosion, and the protection of hydrolytically and/or metabolically unstable drugs. Because of these fa-

Table 2. Future Clinical Applications of BCNU-Loaded Polyanhydride Wafers in the Treatment of Brain Tumors

Clinical trials currently underway	Clinical trials with letter of intent approved
Dose escalation study to evaluate the safety of Gliadel wafers containing between 6.5 and 20% BCNU in patients with recurrent malignant glioma	Phase I Gliadel and escalating doses of intravenous O^6-benzyl guanine trial in patients with recurrent malignant glioma
Phase II trial of surgery with Gliadel wafers and radiation in patients with operable CNS metastases from systemic cancer	Use of Gliadel with concomitant radiotherapy and IV BCNU in the treatment of patients with newly diagnosed glioblastoma multiforme
Phase III clinical trial to further evaluate the efficacy of 3.85% BCNU wafers implanted at the time of initial surgical resection in patients with glioblastoma multiforme	Phase I treatment of adults with recurrent supratentorial low-grade gliomas with Gliadel wafers
Phase I study of Gliadel in children and adolescents with recurrent supratentorial glial tumors	Phase II Gliadel, carboplatin, and XRT in newly diagnosed glioblastoma multiforme either as de novo or recurrent from low-grade gliomas
Phase II treatment of adults with recurrent supratentorial low-grade gliomas with Gliadel wafers	Phase I treatment of adults with recurrent supratentorial high-grade glioma with Gliadel wafers plus Irinotecan (CPT-11)
Phase I trial of Gliadel and carboplatin as initial treatment in patients with glioblastoma multiforme or anaplastic astrocytoma	Phase I/II pilot study using concurrent multimodality treatment for patients with relapsed glioblastoma multiforme using permanent I-125 seeds and Gliadel wafers
Use of Gliadel and 13-cis-retinoic acid in patients with primary glioblastoma multiforme	Use of Gliadel and permanent low-activity I-125 radioactive seeds for the treatment of recurrent malignant astrocytomas
	Drug resistance modulation with 6MP combined with Gliadel for the treatment of recurrent malignant gliomas; a Phase I study
	Use of Gliadel, fractionated radiation therapy, and stereotactic radiosurgery in patients with newly diagnosed malignant glioma
	Clinical and radiographic evaluation of patients receiving Gliadel wafers and stereotactic radiosurgery boost with the Gamma Knife in the initial treatment of malignant gliomas
	Phase I/II study of Gliadel wafer placement and intensity of modulated radiation therapy using the Peacock system for patients undergoing gross total resection for glioblastoma multiforme
	Phase I/II study of Gliadel, Gamma Knife radiosurgery, and postoperative fractionated radiation therapy in the treatment of patients with newly diagnosed high-grade malignant gliomas
	Phase II study of Gliadel wafers followed by RSR13 plus radiotherapy for the treatment of newly diagnosed malignant glioma
	Use of Gliadel in the management of aggressive pituitary adenomas and craniopharyngiomas

vorable properties and the ease with which polymer/drug formulations can be prepared under mild conditions, the possibilities for intracranial drug release from pCPP:SA wafers are vast. We have studied several potentially therapeutic pCPP:SA/drug formulations in an attempt to improve upon the success of the BCNU-loaded wafers in the treatment of CNS tumors.

Taxol, an antitumor alkaloid, elicits antineoplastic activity by promoting tubulin polymerization and has demonstrated efficacy in clinical trials for ovarian and breast carcinoma, as well as for melanoma. Recently, Walter and Cahan have reported a quantitative analysis of brain tumor cell sensitivity to taxol in vitro (98). In this study, taxol demonstrated potent, exposure-time-dependent antitumor activity against human and murine malignant glioma. However, because taxol does not cross the BBB to an appreciable extent, its efficacy against intracranial tumors following systemic administration is severely limited. It was hypothesized that the therapeutic potential of taxol could be realized if the drug were delivered locally from biodegradable polymers.

This hypothesis was tested in the murine 9L gliosarcoma model (99). On the fifth day after intracranial tumor implantation in Fischer 344 rats, three separate groups were implanted with pCPP:SA (20:80) wafers loaded with 20%, 30%, and 40% taxol (w/w). A fourth group received placebo polymers. As shown in Figure 15, median survival was extended for all three taxol loadings ($p < 0.02$). In vivo studies were carried out to quantitatively assess the release of ^{3}H-labeled taxol in the rat brain. It was found that polymeric delivery of taxol resulted in widely distributed intracranial drug concentrations. Similar in vitro and in vivo studies have recently been performed by Sampath with taxotere, a synthetic derivative of taxol. Intracranial controlled release of taxotere is also able to extend survival in the 9L glioma model (100). These studies demonstrate that pCPP:SA wafers loaded with taxol or taxotere may be efficacious in the treatment of gliomas in humans.

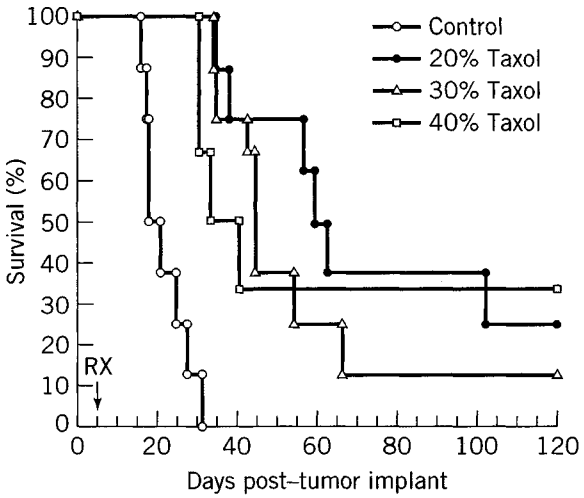


Figure 15. Survival curves for rats receiving an intracranial 9L gliosarcoma tumor implant on Day 0 followed by treatment on Day 5 with an intratumoral 10 mg pCPP:SA (20:80) polymer implant loaded with 20, 30, or 40% taxol by weight. Control animals received a 10-mg PCPP:SA (20:80) implant with no loaded drug. *Source:* Reproduced with permission from Ref. 99.

Camptothecin is an inhibitor of the DNA-replicating enzyme topoisomerase 1. This naturally occurring alkaloid was first isolated from the tree *Camptotheca acuminata* in China by Monroe Wall in 1966. Although this compound demonstrated extraordinary promise as a potentially new antineoplastic agent in preclinical studies, the clinical trials were abruptly derailed due to unexpected toxicity and low antineoplastic activity. Mary Wolpert of the National Cancer Institute proposed that the local delivery of camptothecin into the brain may achieve efficacious concentrations in brain tumors without systemic side effects. This hypothesis has been tested by Weingart and others in our laboratories (101,102).

In a series of in vitro studies, camptothecin demonstrated potent antineoploastic activity against several rat and human glioma cell lines. The therapeutic potential of camptothecin-loaded pCPP:SA (20:80) wafers was then tested in Fischer 344 rats. Sustained delivery of ^{3}H-camptothecin from pCPP:SA wafers at tumoricidal concentrations was demonstrated for over 21 days. In rats challenged with an intracranial implant of 9L gliosarcoma, systemic administration of camptothecin did not extend survival compared to controls. However, local delivery via pCPP:SA wafers (50% camptothecin w/w) resulted in significant prolongation of survival ($p < 0.05$), and 40–79% of the animals were apparently cured.

More recently, Sampath and others have examined the in vitro cytotoxicity of twenty new analogs of camptothecin, synthesized by Monroe Wall's laboratory, against murine and human glioma cell lines (103). They concluded that several 10,11-methylene dioxy analogs of camptothecin are significantly more potent than the parent compound. The local delivery of these camptothecin analogs from pCPP:SA wafers holds great promise for future development in intracranial tumor models and clinical trials.

Adriamycin is an anthracycline antitumor antibiotic frequently used in the treatment of systemic malignancies. This compound intercalates with the DNA of dividing cells resulting in strand scission and double-stranded cross breaks (48). Although adriamycin demonstrates cytotoxicity against malignant gliomas in vitro, the drug is hydrophilic and therefore only minimally crosses the BBB, and when delivered systematically at high dosing regimens, it causes unacceptable cardiac toxicity. Therefore, adriamycin is a promising candidate for intracranial polymeric drug delivery.

Polymer-based drug delivery of adriamycin was first developed by Lin et al. using EVAc needles (104). In our laboratories Watts, Carter, et al. have investigated the intracranial delivery of adriamycin from pCPP:SA wafers for the treatment of malignant glioma (105,106). Initial in vitro studies of the release kinetics of adriamycin from pCPP:SA (20:80) wafers prepared by the solution method showed a large burst effect. This was attributed to the high solubility of this highly hydrophilic compound in aqueous media, which enhances the rate of drug diffusion from the polymer matrix. When adriamycin-loaded pCPP:SA wafers were prepared alternatively by the mix/melt method, it was found that the burst effect was minimized and more zero-order release was achieved in vitro. Polymers prepared by the mix/melt method normally have a denser polymer matrix than polymers prepared by the solution or trituration methods (68): A denser matrix slows the rate of drug diffusion through the polymer wafer. In Fischer 344 rats, adriamycin-loaded wafers prepared by the mix/melt method were also better tolerated and therefore more efficacious than those prepared by the solution method in vivo. In the 9L glioma model, rats receiving 3% and 5% adriamycin-loaded pCPP:SA wafers prepared by mix/melt method demonstrated a median survival of 29 and 45 days, respectively, compared to 19 days for untreated controls. Therefore, sustained delivery of adriamycin from pCPP:SA wafers prepared by the mix/melt method may provide another alternative for the treatment of malignant glioma.

Recently, the endogenous seco-steroid hormone, 1,25-dihydroxyvitamin D_3 (1,25 D_3) has demonstrated potent antiproliferative activity against a variety of systemic malignancies in vitro and in vivo. Although the mechanism by which 1,25 D_3 exerts antiproliferative activity is controversial, it is believed to involve the upregulation via the classic steroid receptor–mediated pathway of cell cycle control proteins that inhibit tumor cells from leaving G_1 and entering the phase of DNA synthesis (107). 1,25 D_3 also possesses potent antiangiogenic activity (108). The success of 1,25 D_3 in the treatment of cancer is limited, however, because the drug causes toxic hypercalcemia at supraphysiological systemic concentrations. The use of 1,25 D_3 against intracranial neoplasms is even more hindered by the drug's limited penetration of the BBB following systemic administration. Posner's group at Johns Hopkins University has designed and synthesized new analogs of 1,25 D_3 that demonstrate maintained or enhanced antiproliferative activity in vitro and dramatically minimized calcemic activity in vivo (109). Burke et al. have proposed that combining the polymer-wafer intracranial

delivery method with the anticalcemic analogs may make it possible to achieve efficacious intracranial concentrations of 1,25 D_3 analogs for the treatment of intracranial tumors.

In a series of in vitro proliferation assays, several 1,25 D_3 analogs demonstrated potent antiproliferative activity against a variety of murine tumor cell lines frequently metastatic to the brain, including B16 malignant melanoma, EMT6 breast cell carcinoma, and RENCA renal cell carcinoma (110). Using quantitative high-performance liquid chromatography, in vitro release kinetics studies were carried out that demonstrated that these pH-sensitive 1,25 D_3 analogs can be successfully loaded and released from pCPP:SA (20:80) wafers with maintained structural integrity (111). These studies suggest that 1,25 D_3 analog–loaded pCPP:SA wafers may possess therapeutic potential in the treatment of intracranial metastases. In vivo studies to test this hypothesis are underway.

In the absence of an intratumoral blood supply, the three-dimensional growth of solid tumors is controlled by the limits of diffusion that restrict the transport of nutrients and waste products (112). Typically, avascular tumors cannot grow beyond about 4 mm^3, a size at which tumors are often asymptomatic and have little metastatic potential (104). To support exponential growth, solid tumors stimulate the process of intratumoral angiogenesis, the proliferation and migration of endothelial cells that bring about the formation of new blood vessels. Folkman first suggested that inhibiting the process of tumor angiogenesis may be a powerful strategy for controlling the growth of solid tumors (113).

Because malignant gliomas are among the most vascular of all solid tumors, we have investigated the application of this strategy to the treatment of primary brain tumors. Many inhibitors of angiogenesis have been discovered, most of which are not directly cytotoxic to tumor endothelial cells. Therefore sustained delivery, such as from pCPP:SA polymer wafers, appears to be crucial for the efficacy of these biological response modifiers. In our laboratories the well-known antiangiogenic agent cortisone acetate, as well as two novel angiogenic inhibitors, squalamine and minocycline, have demonstrated the ability to restrict the growth of 9L glioma in the rat flank (114–116). For example, the intratumoral implantation of pCPP:SA (50:50) wafers loaded with cortisone acetate resulted in a 2.3-fold reduction in the tumor growth rate (107).

The controlled release of the antibiotic minocycline for the inhibition of brain tumor angiogenesis has been studied extensively in our laboratory. The antiangiogenic potential of minocycline was first predicted and demonstrated in 1991 by Tamargo, Bok, and Brem using the rabbit cornea angiogenesis assay (114). We then showed that EVAc polymers loaded with 50% minocycline (w/w) could significantly inhibit the growth of 9L glioma in the rat flank when compared to blank polymer alone; subsequently, we investigated the ability of locally delivered minocycline to extend survival in the 9L glioma model with or without the concurrent intraperitoneal administration of BCNU to determine whether the retardation of tumor cell growth by angiogenesis inhibition could potentiate the efficacy of chemotherapy (117). Although the local delivery of minocycline begun at the time of tumor implantation resulted in a 530% increase in median survival, no prolongation was seen when minocycline-loaded polymers were implanted on postchallenge day 5. However, treatment on postchallenge day 5 with intracranial minocycline-loaded polymer implants and concurrent intraperitoneal administration of BCNU resulted in a 93% increase in median survival over intraperitoneal BCNU alone. Systemic delivery of minocycline with intraperitoneal BCNU was not more effective than BCNU alone. These studies suggest that the local delivery of antiangiogenic agents such as minocycline can work synergistically with standard chemotherapy to control intracranial tumor growth.

To enhance the efficacy of XRT in the treatment of cancer, patients are often administered radiosensitizing agents prior to tumor irradiation. A radiosensitizing agent does not possess antineoplastic activity when administered alone but can greatly potentiate the efficacy of XRT by making tumor cells more sensitive to DNA damage. For example, the halogenated pyrimidines, such as 5-iodo-2′-deoxyuridine (IUdR) are readily incorporated into the replicating DNA of many human tumor cell lines, including malignant glioma. When malignant glioma cells are exposed to IUdR prior to irradiation, higher killing ratios are observed compared with treatment with radiation alone (118). However, because of rapid blood clearance and marrow suppression toxicity after systemic administration, the therapeutic potential of halogenated pyrimidines for the radiosensitization of human malignant gliomas has remained unrealized. Williams has proposed that the local delivery of IUdR and other halo-pyrimidines from biodegradable polymers implanted at the time of surgery could overcome the obstacles associated with systemic delivery and effect the radiosensitization of malignant glioma.

In a recent study, the controlled release of IUdR from pCPP:SA (20:80) wafers was characterized in vitro and in U251 human glioma xenografts grown in the flank of nude mice (118). Radiosensitization was then demonstrated in U251 tumors receiving IUdR from pCPP:SA (20:80) polymer implants. While minimal yet significant growth delay was observed for xenografts treated with placebo wafers and XRT ($p = 0.046$), extended growth delay and even tumor regression were observed when tumors were irradiated 5 days after the intratumoral implantation of pCPP:SA wafers loaded with 50% IUdR (w/w). This strategy holds promise for the radiosensitization of human gliomas and other tumors.

Saltzman has recently carried out more elaborate intracranial drug release studies in the rat, rabbit, and primate brain and used the data to develop mathematical models of intracranial drug delivery from biodegradable polymer wafers (91,119). A recent study determined the in vivo release profiles of BCNU, taxol, and the alkylating agent 4-hydroperoxycyclophosphamide (4-HC) from pCPP:SA (20:80) wafers implanted intracranially in adult *M. fasicularis* monkeys (91). Significant drug concentrations (0.4 μM for BCNU, 0.6 μM for taxol, and 3 μM for 4-HC) were measured up to ~5 cm from the polymer implant even 30 days after implantation.

With a mathematical model, this collection of data was used to evaluate the pharmacokinetics of polymerically delivered drugs in the brain. This model predicts that the fate of a drug delivered to the brain interstitium from a biodegradable polymer wafer depends on (*1*) rates of drug transport via diffusion and fluid convection; (*2*) rates of elimination from the brain via degradation, metabolism, and permeation through capillary networks; and (*3*) rates of local binding and internalization. A more detailed visual representation of this model is shown in Figure 16. These models are able to predict the intracranial drug concentrations that result from BCNU-loaded pCPP:SA (20:80) wafers as well as other drug–polymer combinations, paving the way for the rational design of drugs specifically for intracranial polymeric delivery.

FAD:SA Polymers. Since their introduction in the late 1970s, the polyanhydrides have found increasing use as vehicles for controlled delivery of many drugs, peptides, and proteins (69). Because various general synthetic techniques have been developed, the possibilities for altering both the monomers used as well as their respective ratios are vast. It is therefore possible to rationally design anhydride copolymers with desirable properties for the delivery of specific classes of drug molecules. pCPP:SA polymer wafers have demonstrated near zero-order in vivo controlled-release profiles with a wide range of drugs. It has been observed, however, that some drugs, especially highly hydrophilic compounds, undergo an initial burst of drug release. Furthermore, some water penetration does occur into pCPP:SA wafers (120), making very hydrolytically unstable drugs vulnerable to degradation. To improve upon these shortcomings, a new biodegradable anhydride copolymer of fatty acid dimer (FAD) and sebacic acid (SA) was designed by Domb (121). FAD, a dimer derived from a naturally occurring oleic acid, is more hydrophobic than CPP. The FAD:SA copolymer was therefore predicted to provide more zero-order release of highly hydrophobic drugs and even greater protection of hydrolytically unstable compounds.

The FAD:SA copolymer is synthesized by mixing acylated FAD and SA monomers in various ratios and polymerizing the solid mixture by melt polycondensation at 180°C under vacuum. Polymerizing the FAD and SA monomer in a 1:1 ratio yields a copolymer with a melting point of 60–70°C and molecular weights up to 110,000 Da. Drug-loaded FAD:SA (50:50) polymer wafers are typically prepared by the mix/melt technique.

The tests of biocompatibility of the FAD:SA (50:50) polyanhydride polymer in the brain of Fischer 344 rats mirrored the tests used to establish the intracranial biocompatibility of pCPP:SA polymers (122). As before, the systemic and local reaction to FAD:SA polymer implants was compared to that of the clinically used Surgicel® and Gelfoam® implants. Rats receiving FAD:SA wafers demonstrated no neurological deficits or behavioral modifications, and the transient, minimal, local reaction in the area of the brain surrounding the implant was similar to that observed for the pCPP:SA wafers. It was therefore concluded that this novel polyanhydride polymer was as biocompatible as the pCPP:SA polymer in the rat brain.

The chemotherapeutic agent cyclophosphamide has been widely used for the treatment of systemic malignancies. Cyclophosphamide itself has no antineoplastic activity, but after systemic administration this compound is rapidly metabolized by the hepatic p450 microsomal enzyme system into active metabolites including 4-HC and

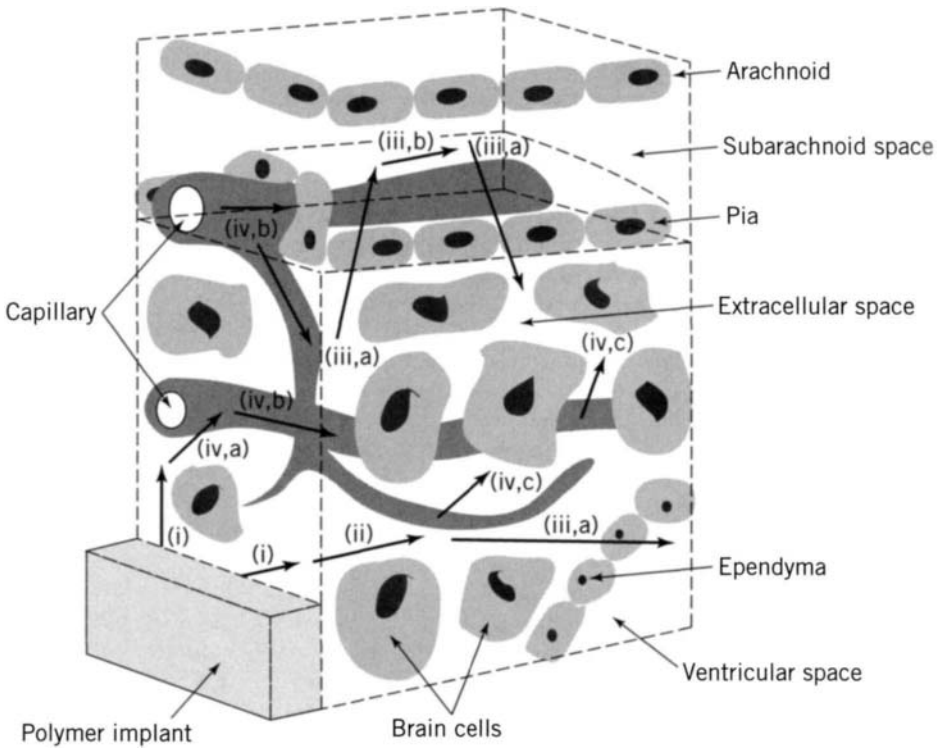


Figure 16. Fate of drug released from the polymer pellet to the brain. After drug molecules are released from the polymer matrix, they enter the extracellular space of the brain; they can be transported by diffusion due to drug concentration gradients (**i**); convection due to fluid pressure gradients (**ii**); drug migration into ventricular space via pial or ependymal surfaces (**iii,a**), circulation in the subarachnoid or ventricular spaces (**iii,b**), and subsequent diffusion back into the brain interstitium (**iii,c**); and permeation through the endothelium (**iv,a**), circulation in the cerebral blood vessels (**iv,b**), and reentry by permeation back into the brain interstitium (**iv,c**). *Source:* Reproduced with permission from Ref. 91.

phosphoramide mustard, both of which possess potent DNA-alkylating activity. These metabolites are, however, very hydrophilic and toxic at high systemic concentrations, so their efficacy in the systemic treatment of brain tumors is limited. It was proposed that the local delivery of the active metabolite 4-HC to the brain via biodegradable polymers may be a powerful treatment for malignant glioma.

Local delivery of 4-HC from biodegradable polymers was particularly challenging because the metabolite is not only very hydrophilic but extremely hydrolytically unstable as well. It was predicted that the highly hydrophobic FAD:SA polymer wafer would be able to deliver 4-HC for an extended period of time and protect the entrapped drug from hydrolytic degradation. The in vivo release kinetics of 20% 4-HC–impregnated FAD:SA (50:50) wafers prepared by the mix/melt method were studied in the brains of Fischer 344 rats by Buahin et al. (123). The 7-hydroxyquinoline assay to quantitate 4-HC levels in blood and brain tissue showed a biphasic release profile. An early burst of drug was followed by a period of slower release and a second larger peak between days 5–20. These results may be due to the coating of the polymer with oily fatty acid dimer degradation products. The levels of 4-HC in the blood were consistently lower than those measured in the brain.

The efficacy of 4-HC–loaded FAD:SA (50:50) wafers was then evaluated in the rat 9L gliosarcoma model and compared to the efficacy of an intratumoral injection of the highest tolerated dose of 4-HC (85). While the median survival of rats receiving a 2-mg intratumoral injection of 4-HC on postchallenge day 5 was extended by 36%, a 121% extension was observed in rats receiving the same amount of 4-HC released in a sustained fashion from FAD:SA (50:50) wafers. The FAD:SA polymer matrix seems to be able to protect the hydrolytically unstable 4-HC–alkylating agent and release the compound in a sustained fashion to effectively treat experimental brain tumors.

Another class of compounds that demonstrates promising antitumor activity in vitro against brain tumors is the platinum-based family of cisplatin derivatives. The platinum drugs elicit antineoplastic activity by binding to DNA, leading to interstrand cross-links. Like 4-HC, however, cisplatin and its analogs are highly water soluble and therefore only minimally cross the BBB. The efficacy of these agents delivered systemically for the treatment of intracranial tumors is limited by severe dose-dependent hematopoetic and gastrointestinal toxicity. The parent compound, cisplatin, is also highly neurotoxic and can lead to nephrotoxicity, emesis, ototoxicity, and peripheral neuropathy (124). The synthetic analog carboplatin is significantly less neurotoxic than cisplatin and retains antineoplastic activity in vitro (124). Olivi et al. have therefore investigated the toxicity and efficacy of carboplatin delivered intracranially from both FAD:SA and pCPP:SA polymer wafers (125). The in vitro drug release profiles of 5% carboplatin-loaded (w/w) FAD:SA (20:80) and pCPP:SA (20:80) wafers prepared by the mix/melt method were evaluated in buffered saline using flameless atomic absorption spectrophotometry. Carboplatin was released faster from the less hydrophobic pCPP:SA (20:80) wafers than from the polymers composed of the same ratio of FAD:SA (Fig. 17). By day 7 all of the drug had been released from the pCPP:SA wafers, and only 65% of the drug was released from the FAD:SA wafers during this period.

The efficacy of the two carboplatin–polymer formulations was then evaluated in the F98 rat gliosarcoma model. Both polymer formulations with 5% carboplatin loading extended median survival more than 3-fold over controls ($p < 0.004$). This was significantly better than the best systemic dose of carboplatin. These results suggest that carboplatin delivered from FAD:SA or pCPP:SA wafers may be efficacious against intracranial tumors in humans.

The extent of penetration into the brain parenchyma and therefore the therapeutic potential of antitumor agents delivered interstitially from biodegradable polymers depends on the rate of drug elimination from brain tissue (83,112). Hence, Saltzman has proposed that minimizing the tissue elimination rates of antineoplastic agents delivered from polymers will enhance their efficacy in the treatment of brain tumors (126). To test this hypothesis, the antineoplastic agent methotrexate (MTX), an antimetabolite, was covalently coupled to M_r 70,000 dextran via a short-lived ester bond ($t_{1/2} \approx 3$ days in buffered saline) and a longer-lived amide bond ($t_{1/2} > 20$ days in buffered saline). A novel three-dimensional tissuelike matrix resembling a human brain tumor was developed by suspending H80 human glioma cells in agarose entrapment medium within a hollow fiber. The relative penetration distances for MTX and the two MTX–dextran conjugates was then evaluated by diffusing the drugs into the tumor cell matrix for 10 days and determining the extent of penetrating cytotoxic activity. Whereas the cytotoxicity of MTX and the MTX-ester-dextran conjugate penetrated about 10 mm, the cytotoxicity penetration of the MTX-amide-dextran conjugate was >20 mm. This enhanced penetration correlated with the enhanced stability of the MTX-amide-dextran linkage.

MTX and the MTX-amide-dextran conjugate were then loaded into FAD:SA (50:50) wafers, and the efficacy of these polymer formulations was evaluated in the 9L glioma model. Treatment with the two formulations

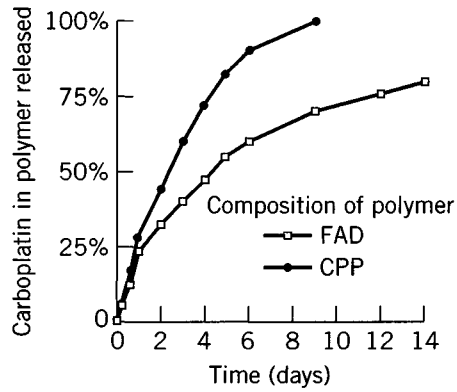


Figure 17. Drug release kinetics in vitro from two separate anhydride polymer formulations: pCPP:SA (CPP) and a more hydrophobic fatty acid dimer–sebacic acid copolymer (FAD). Each polymer weighed 10 mg and was loaded with 5% carboplatin by weight. *Source:* Reproduced with permission from Ref. 125.

yielded modest but significant increases in survival, and the MTX-amide-dextran conjugate seemed to shift the dose-response curve to a lower dosage. These studies support the proposal that conjugation of a polymerically delivered chemotherapeutic agent to a water-soluble macromolecule increases drug penetration into the brain by increasing the period of drug retention in brain tissue. This strategy may enhance the intracranial penetration distances of a wide variety of chemotherapeutic agents, potentiating their efficacy in the treatment of brain tumors.

Polymer Microspheres for the Intracranial Delivery of Proteins. The delivery of proteins from a polymeric matrix was first demonstrated in 1976 (127). Since that time, advancements in rational polymer design have made it possible to deliver a wide range of therapeutic proteins with retained tertiary structural integrity and catalytic activity (128). Hanes et al. have recently developed IL-2–loaded biodegradable polymer microspheres for local cytokine delivery to improve the immunotherapeutic approach to brain tumor treatment (129). In theory, polymeric cytokine delivery has several advantages over delivery from transduced cells, including obviating the need for transfecting cytokine genes, producing longer periods of cytokine release in vivo, and yielding more reproducible cytokine release profiles and total cytokine dose. Additionally, Sampath has recently shown that local cytokine therapy acts synergistically with local chemotherapy in a murine brain tumor model (130). As a strategy to treat CNS tumors, polymeric delivery may one day greatly enhance the efficacy of immunotherapy in the treatment of human brain tumors.

In conclusion, the capacity of the biodegradable polymer delivery methodology to deliver drugs directly to the brain interstitium is vast. Many of the polymer/drug formulations tested in our laboratories (summarized in Table 3) demonstrate greater therapeutic potential than the clinically approved 3.85% BCNU-loaded wafers in the murine 9L glioma model. It is our hope that these and other polymer drug combinations will soon be studied in clinical trials and lead to substantial improvements in the prognosis for patients diagnosed with malignant brain tumors. A proposed algorithm for incorporating polymer-mediated local delivery of bioactive agents into an overall regimen for the care of neurooncological patients is presented in Figure 18.

Nonneoplastic Diseases of the CNS. The strategy of controlled drug delivery to the brain interstitium with polymeric matrices has been applied experimentally to a variety of nonneoplastic diseases of the CNS as well. For example, Aebischer et al. have demonstrated that local delivery of NGF from EVAc rods can prevent the loss of choline acetyl transferase (ChAT) expression in basal forebrain neurons following a fimbria-fornix lesion, indicating the therapeutic potential of this strategy in the treatment of Alzheimer's disease (131). Ebner et al. then showed that NGF could be released into the brain for more than 4 weeks following injection of drug-loaded biodegradable polymer microspheres (132). Theoretically, NGF-releasing microspheres could be useful not only in Alzheimer's therapy but in prolonging graft survival and augmenting nerve regeneration as well.

Freese et al. at MIT have reported the controlled release of dopamine from a polymer brain implant as a potential novel therapy for patients with Parkinson's disease (133). Near-zero-order release for more than 60 days was

Table 3. Preclinical Studies with Various Polymer/Drug Formulations for the Treatment of Brain Tumors

Polymer/Drug formulation[a]	Mechanism of drug's antineoplastic activity	Extension in Median Survival in 9L Glioma Model[b]	Refs.
pCPP:SA (20:80)/3.8% BCNU	DNA alkylation	127%	90
pCPP:SA (20:80)/20% BCNU	DNA alkylation	>1,200%	90
pCPP:SA (20:80)/20% taxol	Inhibition of microtubule depolymerization	215%	99
pCPP:SA (20:80)/50% camptothecin	Inhibition of the DNA-replicating enzyme topoisomerase 1	306%	101,102
pCPP:SA (20:80)/5% adriamycin	Intercalation with DNA leading to strand scission and double-stranded cross-breaks	137%	105,106
pCPP:SA (20:80)/5% carboplatin	Binding to DNA leading to interstrand cross-links	Not yet tested in 9L model	125
pCPP:SA (20:80)/1,25 D_3 analogs	Upregulation of cell-cycle control proteins and inhibition of angiogenesies	Not yet tested in 9L model	109,110
EVAc/50% minocycline	Inhibition of tumor angiogenesis	331% (in combination with IP BCNU)	114,117
pCPP:SA (20:80)/IUdR	Radiosensitization via incorporation into replicating DNA	Not yet tested in 9L model	118
FAD:SA (50:50)/20% 4-hydroperoxycyclophosphamide	DNA alkylation	121%	123
FAD:SA (20:80)/5% carboplatin	Binding to DNA leading to interstrand cross-links	Not yet tested in 9L model	125
FAD:SA (50:50)/1% methotrexate-dextran conjugates	Antimetabolite	140%	126
Polymer microspheres/cytokine IL-2	Promotion of antitumoral immune response	Not yet tested in 9L model	129

[a]The indicated drug loading dose, percent polymer by weight, represents the dose that yields the best efficacy/toxicity ratio in the murine brain; this does not apply to 4% BCNU.

[b]In the 9L glioma model, Fischer 344 rats are challenged on day 0 with an intracranial injection or implantation of 9L gliosarcoma cells. On day 5 animals are treated with polymer wafers loaded with the indicated amounts of drug (weight/weight). Extension in median survival expresses the difference in median survival between the treatment group and control animals receiving tumor challenge but no drug; ($p < 0.05$).

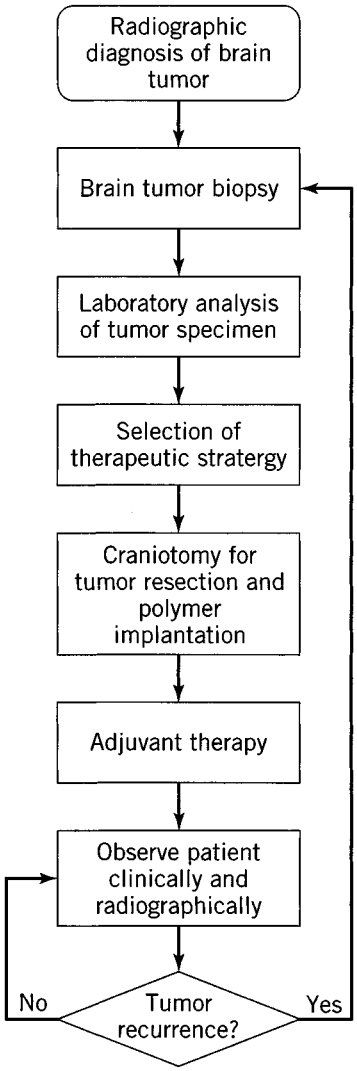


Figure 18. Proposed future clinical approach to management of patients with malignant brain tumors. *Source:* Reproduced with permission from Ref. 66.

achieved by coating a dopamine-loaded EVAc polymer matrix with an impermeable layer of EVAc and creating a single cavity for diffusional drug release in the impermeable layer.

Tamargo and others at Johns Hopkins University have also shown that intratumoral implantation of EVAc wafers loaded with the corticosteroid dexamethasone can effectively treat peritumoral brain edema with minimal systemic drug exposure (134,135). This finding is important because systemic administration of corticosteroids, the most common clinical approach to treating edema, is sometimes associated with serious systemic side effects.

Use of Polymer Systems to Facilitate Drug Delivery to the CNS Interstitium from Biological Tissues

Several distinct approaches use polymer technology to enhance the survival and therapeutic potential of biological tissue implants as vehicles for drug delivery. One approach involves incorporating biologically active moieties into the backbone of biodegradable polymers and using these polymers to form highly porous scaffolds for cell transplantation (136,137). Synthetic polymers can be rationally designed so that the polymer scaffold guides cell organization and growth while allowing the diffusion of nutrients to the transplanted cells. For example, vascularization of the implant could theoretically be artificially induced by the slow release of angiogenic factors from the polymer matrix or the incorporation of capillary growth, promoting amino acid sequences such as the arginine-lysine-aspartic acid (RGD) sequence into the polymeric backbone (138). Furthermore, with recent advancements in cell culture techniques, large populations of cells genetically engineered to express desired proteins could be formed in vitro using a small sample of a patient's own cells, thus circumventing immunogenic complications (139). At MIT, we have demonstrated the feasibility of this technique in the engineering of liver, bone, tendon, skin, ureter, intestine, and cartilage (136). This technique could theoretically also be applied to the CNS to enhance the survival of tissue grafts designed to release therapeutic proteins.

An alternative strategy has been pursued by Aebischer et al. that involves the immunoisolation of transplanted tissue via encapsulation in a permselective polymeric membrane. In this approach, transplanted cells are kept selectively separated from the host tissue by a polymeric membrane with defined pore size that permits the passage of nutrients and neurotransmitters but is impermeable to cells, complement, antibodies, and viruses (140). This technique has been applied to deliver PC12 cells, a dopamine-secreting cell line derived from a rat pheochromocytoma, to the striatum of guinea pigs (141). The use of neoplastic cells is possible because the polymer capsule prevents tumor formation by physically sequestering the transplanted tissue. The therapeutic potential of this strategy was evaluated in the 6-hydroxydopamine unilaterally lesioned rat model of Parkinson's disease. Significant behavioral recovery was observed from 1 to 4 weeks following implantation of PC12 cell-loaded microcapsules as compared with empty microcapsules. Cell encapsulation technology holds promise as a strategy for long-term delivery of neurotransmitters to the brain (142).

CONCLUSION

The treatment of CNS diseases is particularly challenging because the delivery of drug molecules to the brain is often precluded by a variety of physiological, metabolic, and biochemical obstacles that collectively comprise the BBB, BTB, and BCB. Two general strategies, drug modification and BBBD, have been employed to enhance the BBB penetration of drug molecules delivered via the cardiovascular route. Aided by an increased understanding of BBB and tumor physiology, significant progress has been made in these techniques. A third general strategy encompasses alternative routes to CNS drug delivery that attempt to circumvent the BBB altogether. The effectiveness of one of these routes, drug delivery directly to the brain interstitium, has recently been markedly enhanced through the rational design of polymer-based drug delivery systems.

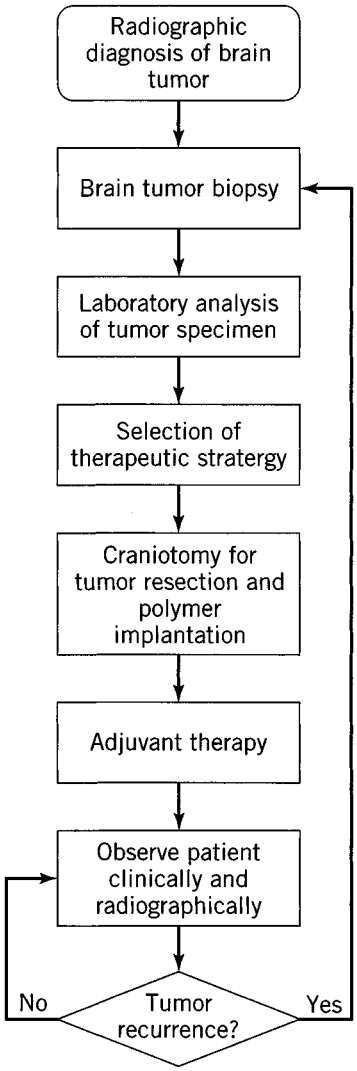


Figure 18. Proposed future clinical approach to management of patients with malignant brain tumors. *Source:* Reproduced with permission from Ref. 66.

achieved by coating a dopamine-loaded EVAc polymer matrix with an impermeable layer of EVAc and creating a single cavity for diffusional drug release in the impermeable layer.

Tamargo and others at Johns Hopkins University have also shown that intratumoral implantation of EVAc wafers loaded with the corticosteroid dexamethasone can effectively treat peritumoral brain edema with minimal systemic drug exposure (134,135). This finding is important because systemic administration of corticosteroids, the most common clinical approach to treating edema, is sometimes associated with serious systemic side effects.

Use of Polymer Systems to Facilitate Drug Delivery to the CNS Interstitium from Biological Tissues

Several distinct approaches use polymer technology to enhance the survival and therapeutic potential of biological tissue implants as vehicles for drug delivery. One approach involves incorporating biologically active moieties into the backbone of biodegradable polymers and using these polymers to form highly porous scaffolds for cell transplantation (136,137). Synthetic polymers can be rationally designed so that the polymer scaffold guides cell organization and growth while allowing the diffusion of nutrients to the transplanted cells. For example, vascularization of the implant could theoretically be artificially induced by the slow release of angiogenic factors from the polymer matrix or the incorporation of capillary growth, promoting amino acid sequences such as the arginine-lysine-aspartic acid (RGD) sequence into the polymeric backbone (138). Furthermore, with recent advancements in cell culture techniques, large populations of cells genetically engineered to express desired proteins could be formed in vitro using a small sample of a patient's own cells, thus circumventing immunogenic complications (139). At MIT, we have demonstrated the feasibility of this technique in the engineering of liver, bone, tendon, skin, ureter, intestine, and cartilage (136). This technique could theoretically also be applied to the CNS to enhance the survival of tissue grafts designed to release therapeutic proteins.

An alternative strategy has been pursued by Aebischer et al. that involves the immunoisolation of transplanted tissue via encapsulation in a permselective polymeric membrane. In this approach, transplanted cells are kept selectively separated from the host tissue by a polymeric membrane with defined pore size that permits the passage of nutrients and neurotransmitters but is impermeable to cells, complement, antibodies, and viruses (140). This technique has been applied to deliver PC12 cells, a dopamine-secreting cell line derived from a rat pheochromocytoma, to the striatum of guinea pigs (141). The use of neoplastic cells is possible because the polymer capsule prevents tumor formation by physically sequestering the transplanted tissue. The therapeutic potential of this strategy was evaluated in the 6-hydroxydopamine unilaterally lesioned rat model of Parkinson's disease. Significant behavioral recovery was observed from 1 to 4 weeks following implantation of PC12 cell-loaded microcapsules as compared with empty microcapsules. Cell encapsulation technology holds promise as a strategy for long-term delivery of neurotransmitters to the brain (142).

CONCLUSION

The treatment of CNS diseases is particularly challenging because the delivery of drug molecules to the brain is often precluded by a variety of physiological, metabolic, and biochemical obstacles that collectively comprise the BBB, BTB, and BCB. Two general strategies, drug modification and BBBD, have been employed to enhance the BBB penetration of drug molecules delivered via the cardiovascular route. Aided by an increased understanding of BBB and tumor physiology, significant progress has been made in these techniques. A third general strategy encompasses alternative routes to CNS drug delivery that attempt to circumvent the BBB altogether. The effectiveness of one of these routes, drug delivery directly to the brain interstitium, has recently been markedly enhanced through the rational design of polymer-based drug delivery systems.

The present outlook for patients suffering from many types of CNS diseases remains poor, but recent developments in drug delivery techniques warrant reasonable hope that the formidable barriers shielding the CNS may ultimately be overcome. Substantial progress will only come about, however, if continued vigorous research efforts to develop more therapeutic and less toxic drug molecules are paralleled by the aggressive pursuit of more effective mechanisms for delivering those drugs to their CNS targets.

ACKNOWLEDGMENTS

The authors thank Eileen Bohan, Betty Collevecchio, and Betty Tyler for their generous research assistance as well as Ann Finkbeiner and Sarvenaz Zand for their thoughtful review of this manuscript. This work was supported by NIH Grant U01-CA52857.

DISCLOSURE STATEMENT

Dr. Brem and Dr. Langer are consultants to Guilford Pharmaceuticals, Inc., and Dr. Brem is a consultant to Rhone-Poulenc Rorer. Guilford has provided a gift for research in Dr. Brem's laboratory. The Johns Hopkins University, Dr. Brem, and Dr. Langer own Guilford stock, the sale of which is subject to certain restrictions under University policy. The terms of this arrangement are being managed by the University in accordance with its conflict-of-interest policies.

BIBLIOGRAPHY

1. N.J. Abbot and I.A. Romero, *Mol. Med. Today* March, pp. 106–113 (1996).
2. W.M. Pardridge, *Annu. Rev. Pharmacol. Toxicol.* **28**, 25–39 (1988).
3. R.J. Tamargo and H. Brem, *Neurosurg. Q.* **2**(4), 259–279 (1992).
4. W.M. Scheld, *Rev. Infect. Dis.* **2**(7), 1669–1690 (1989).
5. H. Brem et al., *Polymeric Site-specific Pharmacotherapy*, John Wiley and Sons, New York, 1994, pp. 117–139.
6. N.H. Grieg, *Cancer Treat. Rev.* **14**, 1–28 (1987).
7. G.W. Goldstein and A.L. Betz, *Sci. Am.* **255**, 74–83 (1986).
8. P.H. Hutson, G.S. Sarna, B.D. Kantamaneni, and G. Curzon, *J. Neurochem.* **44**, 1266–1273 (1985).
9. E.P. Sipos, R.J. Tamargo, J.D. Weingart, and H. Brem, *Ann. N.Y. Acad. Sci.* **732**, 263–272 (1994).
10. A.K. Sills, E.P. Sipos, J. Laterra, and H. Brem, *Adv. Neuro-Oncol.* **2**, 81–96 (1997).
11. R.K. Jain, *J. Natl. Cancer Inst.* **81**(8), 570–576 (1989).
12. R.K. Jain, *Sci. Am.* **271**(1), 58–65 (1994).
13. R.K. Jain, *Sci.* **271**, 1079–1080 (1996).
14. F. Yuan et al., *Cancer Res.* **54**, 4564–4568 (1991).
15. M.G. Ewend et al., *Cancer Res.* **56**, 5217–5223 (1996).
16. O. Merimsky, M. Inbar, B. Gerarg, and S. Chaitchik, *Melanoma Res.* **2**, 401–406 (1992).
17. M. Mastrangelo, R. Bellet, and D. Berd, *PPO Updates* **5**, 1–11 (1991).
18. A. Abner, *Chest* **103**(Suppl.), 445S–448S (1993).
19. A. Gerl et al., *Clin. Exp. Metastasis* **12**, 226–230 (1994).
20. V.A. Levin, C.S. Patlak, and H.D. Landahl, *J. Pharmacokinet. Biopharm.* **8**(3), 257–296 (1980).
21. V.A. Levin and P.M. Kabra, *Cancer Chemother. Rep.* **58**, 787–792 (1974).
22. Y. Madrid, L.F. Langer, H. Brem, and R. Langer, *Adv. Pharmacol.* **22**, 299–324 (1991).
23. N. Bodor and P. Buchwald, *Pharmacol. Ther.* **76**(1–3), 1–27 (1997).
24. N. Bodor, H.H. Farag, and M.E. Brewster, *Science* **214**(18), 1370–1372 (1981).
25. F.A. Omar, H.H. Farag, and N. Bodor, *J. Drug Target.* **2**(4), 309–316 (1994).
26. N. Bodor et al., *Science* **257**, 1698–1700 (1992).
27. Y. Takada et al., *Cancer Res.* **52**, 2191–2196 (1992).
28. P.M. Friden, *Neurosurgery* **35**(2), 294–298 (1994).
29. P.M. Friden et al., *Proc. Natl. Acad. Sci. U.S.A.* **88**, 4771–4775 (1991).
30. P.M. Friden et al., *Science* **259**, 373–377 (1993).
31. W.A. Jeffries et al., *Nature (London)* **312**(8); 162–163 (1984).
32. W.M. Pardridge, R.J. Boado, and Y.S. Kang, *Proc. Natl. Acad. Sci. U.S.A.* **92**, 5592–5596 (1995).
33. J. Huwyler, D. Wu, and W.M. Pardridge, *Proc. Natl. Acad. Sci. U.S.A.* **93**, 14164–14169 (1996).
34. R.A. Kroll and E.A. Neuwelt, *Neurosurgery* **42**(5), 1083–1099 (1998).
35. R.A. Kroll et al., *Neurosurgery* **43**(4), 879–886 (1998).
36. D.E. Bullard, S.H. Bigner, and D.D. Bigner, *Cancer Res.* **45**, 5240–5245 (1985).
37. E.A. Neuwelt et al., *Ann. Intern. Med.* **94**(1), 449–454 (1981).
38. E.A. Neuwelt et al., *Cancer Res.* **45**, 2827–2833 (1995).
39. M. Ohata et al., *Cancer Res.* **45**, 1092–1096 (1995).
40. E.A. Neuwelt et al., *Neurosurgery* **37**(1), 17–28 (1995).
41. E.A. Neuwelt et al., *Cancer Res.* **56**, 706–709 (1996).
42. T. Inamura, T. Nomura, R.T. Bartus, and K.L. Black, *J. Neurosurg.* **81**, 752–758 (1994).
43. S. Nakano, K. Matsukado, and K.L. Black, *Cancer Res.* **56**, 4027–4031 (1996).
44. K. Matsukado et al., *Neurosurgery* **39**(1), 125–134 (1996).
45. K.L. Black et al., *J. Neurosurg.* **86**, 603–609 (1997).
46. R.E. Harbaugh, R.L. Saunders, and R.F. Reedert, *Neurosurgery* **23**(6), 693–698 (1988).
47. R.G. Thorne, C.R. Emory, T.A. Ala, and W.H. Frey, *Brain Res.* **692**, 278–282 (1995).
48. K.A. Walter et al., *Neurosurgery* **37**(6), 1129–1145 (1995).
49. E.H. Oldfield et al., *Proc. Natl. Acad. Sci. U.S.A.* **91**, 2076–2080 (1994).
50. E.A. Neuwelt et al., *Neurosurgery* **38**(4), 746–754 (1996).
51. J. Sladek and D. Gash, *J. Neurosurg.* **68**, 337–351 (1988).
52. D.M. Yurek and J.R. Sladek, *Annu. Rev. Neurosci.* **13**, 415–440 (1990).
53. K. Leigh, K. Elisevich, and K.A. Rogers, *J. Neurosurg.* **81**, 272–283 (1994).
54. B. Lai et al., *Proc. Natl. Acad. Sci. U.S.A.* **91**, 9695–9699 (1994).
55. E.Y. Snyder et al., *Neurobiol. Dis.* **4**, 69–102 (1997).
56. R.C. Thompson et al., *J. Immunother.* **19**(6), 405–413 (1997).
57. D.M. Gash et al., *Science* **233**, 1420–1421 (1986).
58. P. Horellou and J. Mallet, *Mol. Neurobiol.* **15**(2), 241–256 (1997).
59. P. Horellou, O. Sabate, M.H. Buc-Caron, and J. Mallet, *Exp. Neurol.* **144**(1), 131–138 (1997).

60. W.M. O'Conner et al., *Exp. Neurol.* **148**(1), 167–178 (1997).
61. M.H. Tuszynski et al., *Gene Ther.* **3**(4), 305–314 (1996).
62. B.L. Maria and T. Friedman, *Semin. Pediatr. Neurol.* **4**(4), 333–339 (1997).
63. S. Benedetti et al., *Hum. Gene Ther.* **8**(11), 1345–1253 (1997).
64. B.V. Zlokovic and M.L. Apuzzo, *Neurosurgery* **40**(4), 805–812 (1997).
65. C. Raffel et al., *Hum. Gene Ther.* **5**, 863–890 (1994).
66. H. Brem and R. Langer, *Sci. Med.* **3**(4), 1–11 (1996).
67. J. Hanes and M. Burke, *Hosp. Pharm. Rep.*, December, pp. 1–11 (1997).
68. J. Tamada and R. Langer, *J. Biomater. Sci., Polym. Ed.* **3**(4), 315–353 (1992).
69. M. Chasin et al., in M. Chasin and R. Langer, eds., *Biodegradable Polymers as Drug Delivery Systems*, Dekker, New York, 1990, pp. 43–69.
70. K.W. Leong, V. Simonte, and R. Langer, *Macromolecules* **20**, 705–712 (1987).
71. K.W. Leong, B.C. Brott, and R. Langer, *J. Biomed. Mater. Res.* **19**, 941–955 (1985).
72. A.J. Domb and R. Langer, *J. Polym. Sci.* **25**, 3373–3386 (1987).
73. M. Chasin, D. Lewis, and R. Langer, *BioPharm. Manuf.* **1**, 33–46 (1988).
74. E. Mathiowitz and R. Langer, *J. Controlled Release* **5**, 13–22 (1987).
75. E. Mathiowitz et al., *J. Appl. Polym. Sci.* **35**, 755–774 (1988).
76. R. Langer, H. Brem, and D. Tapper, *J. Biomed. Mater. Res.* **15**, 267–277 (1981).
77. K.W. Leong, P. D'Amore, M. Marletta, and R. Langer, *J. Biomed. Mater. Res.* **20**, 51–64 (1986).
78. R.J. Tamargo et al., *J. Biomed. Mater. Res.* **23**, 253–266 (1989).
79. H. Brem et al., *Sel. Cancer Ther.* **5**, 55–65 (1989).
80. M.B. Yang, R.J. Tamargo, and H. Brem, *Cancer Res.* **49**, 5103–5107 (1989).
81. R.J. Tamargo, R. Langer, and H. Brem, *Methods Neurosci.* **21**, 135–149 (1994).
82. S.A. Grossman et al., *J. Neurosurg.* **76**, 640–647 (1992).
83. R.J. Tamargo et al., *Cancer Res.* **53**, 329–333 (1993).
84. K.G. Buahin and H. Brem, *J. Neuro-Oncol.* **26**, 103–110 (1995).
85. H. Brem et al., *J. Neurosurg.* **68**, 334 (1988).
86. H. Brem et al., *J. Neurosurg.* **74**, 441–446 (1991).
87. H. Brem et al., *Lancet* **345**, 1008–1012 (1995).
88. H. Brem et al., *J. Neuro-Oncol.* **26**, 111–123 (1995).
89. S. Valtonen et al., *Neurosurgery* **41**(1), 44–49 (1997).
90. E.P. Sipos et al., *Cancer Chemother. Pharmacol.* **39**, 383–389 (1997).
91. L.K. Fung et al., *Cancer Res.* **58**, 672–684 (1998).
92. J.H. Galicich, N. Sunderesan, and H.T. Thaler, *J. Neurosurg.* **53**, 63–67 (1980).
93. M.G. Ewend et al., *Am. Assoc. Neurol. Surg.*, Denver, Colo. 1997, Abstract.
94. S.R. Wedge and E.S. Newlands, *Br. J. Cancer* **73**, 1049–1052 (1996).
95. A.E. Pegg, *Cancer Res.* **50**, 6119–6129 (1990).
96. M.E. Dolan et al., *Cancer Res.* **51**, 3367–3372 (1991).
97. S.C. Schold et al., *Cancer Res.* **56**, 2076–2081 (1996).
98. M.A. Cahan, K.A. Walter, M.O. Colvin, and H. Brem, *Cancer Chemother. Pharmacol.* **33**, 441–444 (1994).
99. K.A. Walter et al., *Cancer Res.* **54**, 2207–2212 (1994).
100. P. Sampath et al., *Am. Assoc. Neurol. Surg.*, Denver, Colo. 1997, Abstract.
101. J.D. Weingart et al., *Int. J. Cancer* **62**, 605–609 (1995).
102. J.D. Weingart, B. Tyler, O.M. Colvin, and H. Brem, *3rd Drug Discovery Dev. Symp.* 1993, Abstract.
103. P. Sampath et al., *Soc. Neuro-Oncol.*, Charlottesville, Va., 1997, Abstract.
104. S.Y. Lin et al., *Biomater., Artif. Cells, Artif. Organs* **17**, 189–203 (1989).
105. V.L. Perry et al., *Cong. Neurol. Surg.*, 1998, Abstract.
106. M. Watts et al., *Am. Assoc. Neurol. Surg.*, Denver, Colo., 1997, Abstract.
107. D. Feldman, F.H. Glorieux, and J.W. Pike, *Vitamin D*, Academic Press, San Diego, Calif., 1997.
108. T. Oikawa et al., *Eur. J. Pharmacol.* **178**, 247–250 (1990).
109. G.H. Posner et al., *J. Med. Chem.* **41**(16), 3008–3014 (1998).
110. M. Burke et al., *Proc. 10th Workshop Vitam. D*, Strasbourg, France, May 24–29, 1997.
111. M. Burke et al., *5th Ann. Brown Univ. Symp. Vitam. D*, Providence, R.I. September 7–9, 1997, Abstract.
112. J. Folkman, *N. Engl. J. Med.* **333**, 1757–1763 (1995).
113. J. Folkman, *N. Engl. J. Med.* **285**, 1182–1186 (1971).
114. R.J. Tamargo, R.A. Bok, and H. Brem, *Cancer Res.* **51**, 672–675 (1991).
115. R.J. Tamargo, K.W. Leong, and H. Brem, *Neuro-Oncol.* **9**, 131–138 (1990).
116. A.K. Sills et al., *Cancer Res.* **58**(13), 2784–2792 (1998).
117. J.D. Weingart, E.P. Sipos, and H. Brem, *J. Neurosurg.* **82**, 635–640 (1995).
118. J.A. Williams et al., *J. Neuro-Oncol.* **32**, 181–192 (1997).
119. W.M. Saltzman et al., *Pharm. Res.* **13**(5), 671–682 (1996).
120. W. Dang et al., *J. Controlled Release* **42**, 83–92 (1996).
121. A. Domb et al., *Polym. Prep.* **32**(2), 219–220 (1991).
122. H. Brem et al., *J. Controlled Release* **19**, 325–330 (1992).
123. K.G. Buahin et al., *Polym. Adv. Technol.* **3**, 311–316 (1992).
124. A. Olivi et al., *Cancer Chemother. Pharmacol.* **31**, 449–454 (1993).
125. A. Olivi et al., *Cancer Chemother. Pharmacol.* **39**, 90–96 (1996).
126. W. Dang, O.M. Colvin, H. Brem, and W.M. Saltzman, *Cancer Res.* **54**, 1729–1735 (1994).
127. R. Langer and J. Folkman, *Nature (London)* **263**, 797–800 (1976).
128. R. Langer, *Nature (London)* **392**, 5–10 (1998).
129. J. Hanes et al., *Conf. Formul. Drug Delivery II*, La Jolla, Calif., October 5–8, 1997.
130. P. Sampath et al., *Congr. Neurol. Surg.*, New Orleans, La, September 27–October 2, 1997.
131. D. Hoffman, L. Wahlberg, and P. Aebischer, *Exp. Neurol.* **110**, 39–44 (1990).
132. P.J. Camarata et al., *Neurosurgery* **30**, 313–319 (1992).
133. A. Freese et al., *Exp. Neurol.* **103**, 234–238 (1989).
134. R.J. Tamargo et al., *J. Neurosurg.* **74**, 956–961 (1991).
135. C.S. Reinhard et al., *J. Controlled Release* **16**, 331–340 (1991).
136. R. Langer and J.P. Vacanti, *Science* **260**, 920–926 (1993).
137. L.G. Cima et al., *J. Biomech. Eng.* **113**, 143–151 (1991).

Next Page

138. D.A. Barrera, E. Zylstra, P.T. Lansbury, and R. Langer, *J. Am. Chem. Soc.* **115**, 11010–11011 (1993).
139. R. Langer, *Ann. Biomed. Eng.* **23**, 101–111 (1995).
140. P. Aebischer, S.R. Winn, and P.M. Galletti, *Brain Res.* **448**, 364–368 (1988).
141. S.R. Winn et al., *Exp. Neurol.* **113**, 322–329 (1991).
142. P. Aebischer et al., *J. Biomech. Eng.* **113**, 178–183 (1991).

CHARACTERIZATION OF DELIVERY SYSTEMS, DIFFERENTIAL SCANNING CALORIMETRY

PIERRE SOUILLAC
J. HOWARD RYTTING
University of Kansas
Lawrence, Kansas

KEY WORDS

Differential scanning calorimetry (DSC)
Differential thermal analysis (DTA)
Drug purity
Heat conduction calorimetry
Isoperibol calorimetry
Polymorphism
Pseudopolymorphism
Thermogravimetric analysis (TGA)

OUTLINE

Introduction
DTA and DSC
  DTA
  DSC
  Practical Aspects
  Pharmaceutical Applications
Modulated Differential Scanning Calorimetry
Heat Conduction Calorimetry
Thermogravimetry
Isoperibol Calorimetry
Conclusions
Bibliography

INTRODUCTION

Among the most useful and underused tools available to pharmaceutical scientists, in both research and development, are the various types of calorimeters. A large variety of calorimeters are currently available for the collection of information necessary for the preformulation and formulation of drugs: differential thermal analysis (DTA), differential scanning calorimetry (DSC), modulated differential scanning calorimetry (MDSC), thermogravimetric analysis (TGA), isoperibol calorimetry, and heat conduction calorimetry.

DSC has been one of the most widely used calorimetric techniques for the determination of various thermal parameters, which allow a better understanding of drug characteristics and provide a basis for drug formulation. DTA, often regarded as a more qualitative technique, is still widely used. Recently, the development of a novel application of DSC, MDSC, which uses a modulated (sinusoidal) heating rate, has permitted the resolution of overlapping thermal phenomena as well as the detection of higher order phase transitions such as glass transitions (T_g).

Often, other thermal analysis techniques are used concomitantly with DSC for the determination of parameters necessary for the formulation of drugs. TGA is widely used for the determination and characterization of pseudopolymorphs (hydrates and solvates). Heat conduction calorimeters (or microcalorimeters) are used to evaluate changes in heat due to chemical or physical reactions as well as to determine the rates of chemical reactions including degradation. Isoperibol calorimetry is used to measure various types of enthalpies (i.e., enthalpies of solution, mixing, hydration, or binding) as well as to determine the thermodynamics of binding.

DTA AND DSC

Upon undergoing a physical change (i.e., phase transition or crystallization) or during a chemical reaction, a material usually absorbs or evolves heat. The principle of these two techniques is based on the differential detection of energy changes between the sample undergoing a thermal event (at a given temperature) and a reference (inert) when both are subjected to the same heating program. DTA is a technique in which the difference in temperature between the sample and a reference is recorded versus temperature, whereas DSC is a technique in which the difference in heat flow between the sample and a reference is recorded versus temperature.

DTA

DTA has been widely used and is considered the simplest of the differential techniques. Typically, a DTA apparatus is composed of a sample holder which itself is comprised of two cells. One cell contains the sample and the other one an inert reference material (Fig. 1). Reference materials should not undergo thermal events in the temperature range of interest and should not react with either the thermocouples or the cells. Alumina and silica are generally used as reference materials (1). The sample holder is centered inside a furnace equipped with a temperature controller. Thermocouples can be either placed inside the sample and the reference (block type measuring system) or inserted in each cell (heat flux).

With the first type of apparatus design, the thermocouples are very sensitive to the nature of the material used. This particular design makes the method quite sensitive and allows for rapid detection of the thermal event associated with the sample (2). The signal is dependent on the

Previous Page

138. D.A. Barrera, E. Zylstra, P.T. Lansbury, and R. Langer, *J. Am. Chem. Soc.* **115**, 11010–11011 (1993).
139. R. Langer, *Ann. Biomed. Eng.* **23**, 101–111 (1995).
140. P. Aebischer, S.R. Winn, and P.M. Galletti, *Brain Res.* **448**, 364–368 (1988).
141. S.R. Winn et al., *Exp. Neurol.* **113**, 322–329 (1991).
142. P. Aebischer et al., *J. Biomech. Eng.* **113**, 178–183 (1991).

CHARACTERIZATION OF DELIVERY SYSTEMS, DIFFERENTIAL SCANNING CALORIMETRY

PIERRE SOUILLAC
J. HOWARD RYTTING
University of Kansas
Lawrence, Kansas

KEY WORDS

Differential scanning calorimetry (DSC)
Differential thermal analysis (DTA)
Drug purity
Heat conduction calorimetry
Isoperibol calorimetry
Polymorphism
Pseudopolymorphism
Thermogravimetric analysis (TGA)

OUTLINE

Introduction
DTA and DSC
  DTA
  DSC
  Practical Aspects
  Pharmaceutical Applications
Modulated Differential Scanning Calorimetry
Heat Conduction Calorimetry
Thermogravimetry
Isoperibol Calorimetry
Conclusions
Bibliography

INTRODUCTION

Among the most useful and underused tools available to pharmaceutical scientists, in both research and development, are the various types of calorimeters. A large variety of calorimeters are currently available for the collection of information necessary for the preformulation and formulation of drugs: differential thermal analysis (DTA), differential scanning calorimetry (DSC), modulated differential scanning calorimetry (MDSC), thermogravimetric analysis (TGA), isoperibol calorimetry, and heat conduction calorimetry.

DSC has been one of the most widely used calorimetric techniques for the determination of various thermal parameters, which allow a better understanding of drug characteristics and provide a basis for drug formulation. DTA, often regarded as a more qualitative technique, is still widely used. Recently, the development of a novel application of DSC, MDSC, which uses a modulated (sinusoidal) heating rate, has permitted the resolution of overlapping thermal phenomena as well as the detection of higher order phase transitions such as glass transitions (T_g).

Often, other thermal analysis techniques are used concomitantly with DSC for the determination of parameters necessary for the formulation of drugs. TGA is widely used for the determination and characterization of pseudopolymorphs (hydrates and solvates). Heat conduction calorimeters (or microcalorimeters) are used to evaluate changes in heat due to chemical or physical reactions as well as to determine the rates of chemical reactions including degradation. Isoperibol calorimetry is used to measure various types of enthalpies (i.e., enthalpies of solution, mixing, hydration, or binding) as well as to determine the thermodynamics of binding.

DTA AND DSC

Upon undergoing a physical change (i.e., phase transition or crystallization) or during a chemical reaction, a material usually absorbs or evolves heat. The principle of these two techniques is based on the differential detection of energy changes between the sample undergoing a thermal event (at a given temperature) and a reference (inert) when both are subjected to the same heating program. DTA is a technique in which the difference in temperature between the sample and a reference is recorded versus temperature, whereas DSC is a technique in which the difference in heat flow between the sample and a reference is recorded versus temperature.

DTA

DTA has been widely used and is considered the simplest of the differential techniques. Typically, a DTA apparatus is composed of a sample holder which itself is comprised of two cells. One cell contains the sample and the other one an inert reference material (Fig. 1). Reference materials should not undergo thermal events in the temperature range of interest and should not react with either the thermocouples or the cells. Alumina and silica are generally used as reference materials (1). The sample holder is centered inside a furnace equipped with a temperature controller. Thermocouples can be either placed inside the sample and the reference (block type measuring system) or inserted in each cell (heat flux).

With the first type of apparatus design, the thermocouples are very sensitive to the nature of the material used. This particular design makes the method quite sensitive and allows for rapid detection of the thermal event associated with the sample (2). The signal is dependent on the

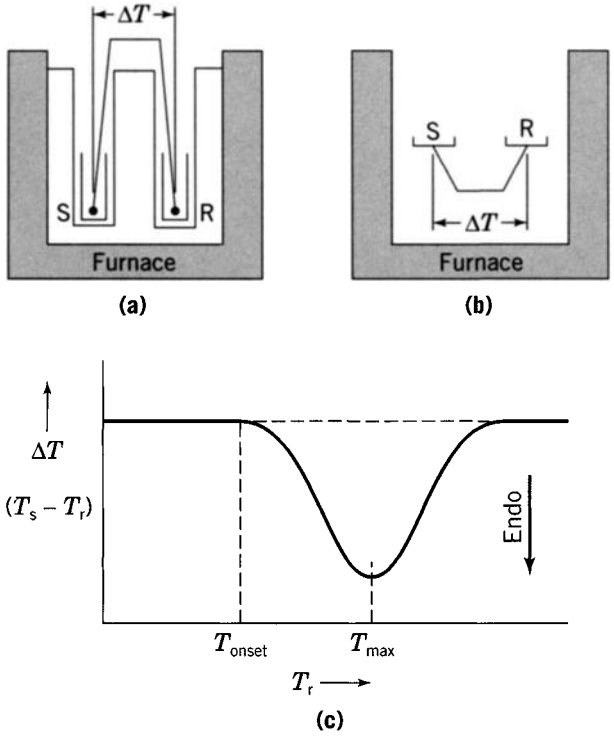


Figure 1. DTA apparatus. (**a**) Classical apparatus; (b) heat flux apparatus; (c) typical DTA curve. (S: sample, R: reference). *Source:* From Ref. 1.

difference in heat capacities between the sample and the reference, the heating rate, and the thermal resistance of the system.

$$\Delta T = R(dT/dt)(C_s - C_r) \quad (1)$$

where ΔT is the differential temperature between the sample and the reference, C_s and C_r are the heat capacities of the samples and the reference, respectively, and R is the thermal resistance. The thermal resistance is not only affected by the characteristics of the instrument but also by the properties of the sample and the reference (1).

With the second type of DTA apparatus the thermocouples are not inside the sample but attached beneath the cells. A slower response between the thermal event associated with the sample and its detection is observed. On the other hand, the response is less affected by the properties of the sample (1). In this case, the thermal resistance is only dependent on the characteristics of the instrument.

Independent of the apparatus design, both sample and reference are subjected to the same heating program. When the sample does not undergo a thermal event, the differential temperature is equal to zero. During a phase transition of the sample, an energy change will occur and the temperature of the sample will be different from the temperature of the reference (which does not undergo phase transition). The temperature differential is amplified, recorded, and plotted versus temperature. The minimum temperature differential that can be detected is about 0.01°C (3).

However, despite its simplicity and design, DTA has been progressively replaced by the more quantitative technique, DSC.

DSC

DSC has provided qualitative information as well as quantitative determinations of physicochemical parameters of drugs. Differential scanning calorimeters measure the heat capacity (C_p) of the system as a function of temperature. Following the change in heat capacity of the sample as a function of temperature allows for the detection of phase transitions of various orders. DSC has been used in a variety of pharmaceutical applications: the characterization of solid crystals (polymorphism) (4–8); the study of phase changes (9); the evaluation of drug-excipient interactions (10,11); the study of thermal denaturation of biopolymers (12–16); and the influence of penetration enhancers on the lipid bilayer structure (17,18). The measurement of heat capacity is based on the differential monitoring of temperature or heat supplied (depending on the type of instrument) between a sample and a reference. The sample and the reference are submitted to the same preset temperature program in which temperature increases linearly at a predetermined rate. The thermal events associated with the samples are monitored versus temperature.

Two types of differential scanning calorimeters have been used to perform thermal analyses relevant to pharmaceutical science: heat flux DSC and power compensation DSC (19). A differential measurement of the heat flow is performed in both cases. This differential heat flow is deduced from either monitoring the difference in temperature between the sample and a reference (heat flux DSC) or monitoring the difference in the input of heating power necessary to maintain the sample and a reference at the same temperature (power compensation DSC). Most modern instruments allow for a wide range of scanning temperatures (from −170°C to 700°C) as well as for a wide range of heating rates (from 0.1°C/min to 200°C/min). However, the heating rates used for thermal analysis of most pharmaceutical compounds are typically between 5°C/min to 20°C/min. The choice of heating rate should be based on the characteristics of the particular compound (or system) of interest and the thermal parameters that are to be determined. Indeed, high scanning rates allow for relatively high heat flow sensitivity but low resolution, whereas low scanning rates permit high resolution but lower heat flow sensitivity. High scanning rates are often necessary for the determination of glass-transition temperatures. The increase in heat capacity of the system due to an increase in molecular mobility at the glass-transition temperature is relatively small and large heating rates are needed for its detection. On the other hand, for a system in which two different thermal phenomena are occurring in the same temperature range, a low heating rate is recommended to obtain a better resolution of the two thermal events. Unfortunately, a balance between resolution and sensitivity is often necessary.

Types of Differential Scanning Calorimeters. ***Heat Flux DSC.*** Two types of heat flux DSCs are encountered: the

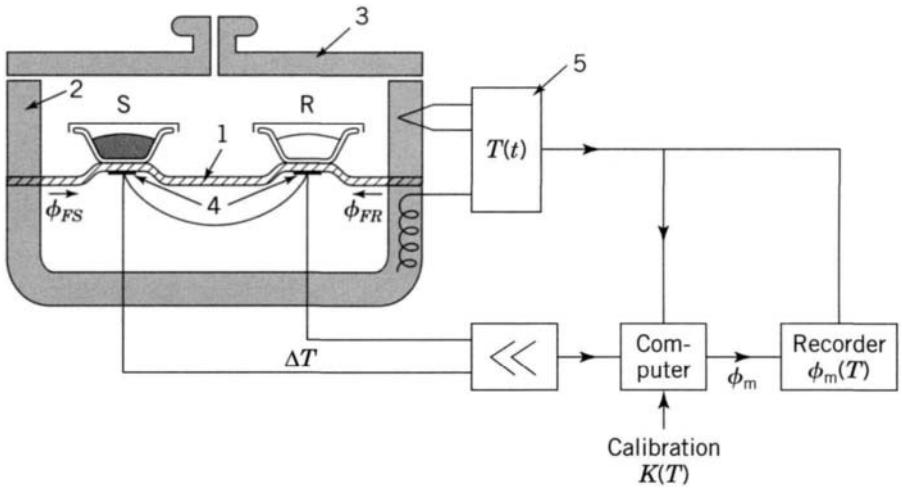


Figure 2. Heat flux DSC with disk-type measuring system. (1) Disk; (2) furnace; (3) lid; (4) differential thermocouples; (5) programmer and controller. (R: reference; S: sample; ϕ_{FS}: heat flow rate from the furnace to the sample; ϕ_{FR}: heat flow rate from the furnace to the reference; ϕ_m: measured heat flow rate; K: calibration factor) *Source:* From Ref. 2.

disc type and the cylinder type. The disc type calorimeter is the most commonly used (Fig. 2). A sample and a reference are symmetrically placed on the same furnace (thermoelectric disc). Energy input is transferred to the sample and reference through the sample holder (or cell) and the sample pan. The temperature probes are placed within the disc and the temperature differential is detected as a voltage (2). Differential heat flow to the sample and reference is monitored as a function of temperature.

Power Compensation DSC. With power compensation DSCs, the sample and reference are placed on two different furnaces (Fig. 3). Both furnaces contain a temperature probe and a heating resistor. The same temperature is maintained at all times between the sample and the reference. The difference in the amount of heat supplied to both furnaces in order to maintain the temperature differential between the sample and the reference at zero is monitored and can be directly correlated to thermal events occurring to the sample (2).

This difference is followed as a function of temperature. When the sample does not undergo any thermal event, the same amount of heat is supplied to both furnaces; a horizontal baseline should be observed assuming that the change in heat capacity of the sample as a function of temperature is negligible. When the sample undergoes a thermal event, the differential temperature starts to deviate from zero. A decrease or increase in the amount of electrical energy supplied to the reference will reestablish the temperature differential to zero. This heating power differential is monitored and after amplification a significant deviation from the horizontal baseline is observed.

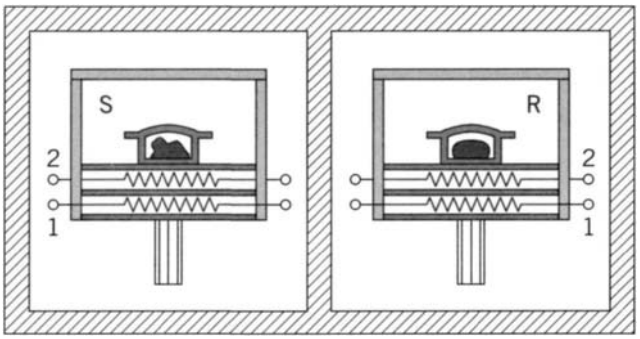


Figure 3. Power compensation DSC. (1) Heating wire; (2) resistance thermometer. (S: sample; R: reference) *Source:* From Ref. 2.

Practical Aspects

Sample Preparation. The amount of material necessary for these types of measurement are generally in the milligram range. The use of small amounts of sample presents the advantage of a better thermal gradient within the sample as well as the consumption of less material. The sample is generally placed in disposable a pan. Different types of sample pans (e.g., composition, geometry) are available. The reference usually consists of an empty pan of the same type as the pan containing the sample. Aluminum pans are the most common type. A lid can be crimped on the pans to avoid contamination of the DSC cell holder and to provide a better thermal gradient throughout the sample. When a sample is heated, depending on the size of the sample, a thermal gradient will exist within the sample. The thermal gradient throughout the sample can be reduced by reducing its size to a minimum or by compacting the sample with a lid. Hermetically sealed sample pans are necessary for volatile compounds or when liquid to gas transitions are studied. However, the pressure resistance of the pans should be carefully taken into account before designing any experiment. Gold or platinum sample pans can be used (*1*) for compounds reacting with aluminum or (*2*) when high temperatures are needed (above 600°C) (20). Gold also has the advantage over aluminum that it has a better thermal conductivity. However, due to the difference in cost between gold and aluminum, aluminum pans are most commonly used.

Determination of thermal parameters at temperatures below room temperature are sometimes necessary. With the increased use of lyophilized protein formulations, the determination of the glass-transition temperatures of frozen solutions (T'_g) for diverse additives is often useful for the development of the lyophilization cycle (21,22). The cooling system depends on the temperature range of inter-

est. For the lowest temperatures (−170°C), liquid nitrogen is used. To avoid any moisture condensation that could interfere with the measurement, a purge gas system is required for measurements below room temperature. Dry nitrogen, argon, or helium are the recommended gases. The instrumental baseline can be affected by the flow rate of the purge gas, and therefore the flow rate should remain as stable as possible in the range of 20 to 50 mL/min (3). Nitrogen purge is also highly recommended at temperatures above room temperature when the sample of interest is prone to oxidative degradation pathways.

Calibration. Because the response of a calorimeter differs depending on the choice of several instrumental parameters, calibration of the instrument is necessary prior to analysis of a sample. Moreover, the transfer of heat between the furnace and the sample pans is not instantaneous. Even under ideal sample preparation conditions, there will be a difference between the temperature of the furnace and the temperature of the sample at any time during the temperature scan. The temperature lag between the furnace temperature and the sample (and reference) temperatures should be reproducible and should not depend on the type of sample analyzed. Usually, the thermal lag increases as the heating rate increases. To minimize the thermal lag problem, the calibration should be performed under the same conditions as those of the experiments; heating rate, type of sample pans, purge gas flow, and sample size should be identical during the calibration and the subsequent experimental measurements. The calibration of differential scanning calorimeters relies on chemical standards of high purity (metals or organic compounds). Calibration is performed for both the temperature scale and the amplitude of the signal obtained (baseline and thermal event). The material used for calibration should ideally (*1*) be pure, (*2*) have a thermal behavior that is perfectly described and reproducible, (*3*) be characterized by the presence of a thermal event in the same temperature range as the temperature range of interest, and (*4*) not react with the sample pans (2). Calibration can be performed using only one calibrant when the temperature range of interest is narrow, or with several calibrants for a large temperature range. In the case of a one-point calibration, indium is the most commonly used calibrant with a melting temperature at 156.6°C and an enthalpy of fusion equal to 28.7 J/g. For the newest instruments, the calorimetric response over the entire temperature range can be assumed constant and a multipoint calibration is usually not necessary. However, when a multipoint calibration is desired or when the temperature range of interest is far from the indium melting temperature, other substances may be used. Water can be used to calibrate calorimeters around 0°C. For high temperature ranges, fusion of tin, lead, or zinc can be used (2). The melting temperature (and the enthalpies of fusion) for tin, lead, and zinc are, respectively, 231.9°C (14.24 $cal.g^{-1}$), 327.4°C (5.55 $cal.g^{-1}$), and 419.5°C (26.6 $cal.g^{-1}$) (23). The melting temperature of organic compounds such as cyclopentane (−93.43°C), 1,2-dichloroethane (−32°C), decane (−30°C), phenyl ether (30°C), *o*-terphenyl (58°C), or biphenyl (69.3°C) can also be used for calibration purposes.

Detection of Thermal Events. Different types of thermal events can be detected by DSC: (*1*) endothermic events (i.e., melting, dehydration), (*2*) exothermic events (i.e., crystallization, denaturation of proteins), or (*3*) changes in heat capacity (i.e., glass-transition temperature). Heat capacity is plotted versus temperature when dynamic measurements are performed. These types of plots are called thermoanalytical curves or thermograms (Fig. 4). Different software (depending on the calorimeter manufacturer) is used for the extraction of numerical data from the curves obtained.

Phase transitions of a substance (i.e., melting or crystallization) are detected over a range of temperatures and not at a single temperature, thus making the determination of a single transition temperature difficult. Different temperatures have been used to describe a phase transition (Fig. 5). In the case of a melting endotherm, the temperature at the apex of the peak is denoted T_m. The onset temperature (T_0) corresponds to the temperature at which the signal first deviates from the baseline. The extrapolated onset temperature (T_e) corresponds to the tempera-

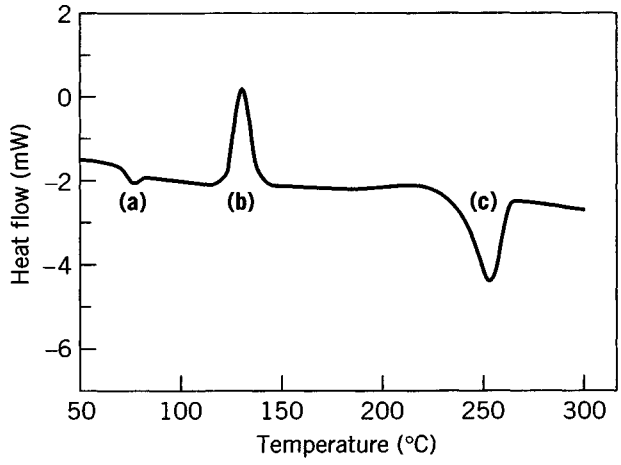


Figure 4. Typical DSC thermoanalytical curve. (**a**) Glass transition with associated enthalpic relaxation; (**b**) cold crystallization exotherm; (**c**) melting endotherm. *Source:* From Ref. 20.

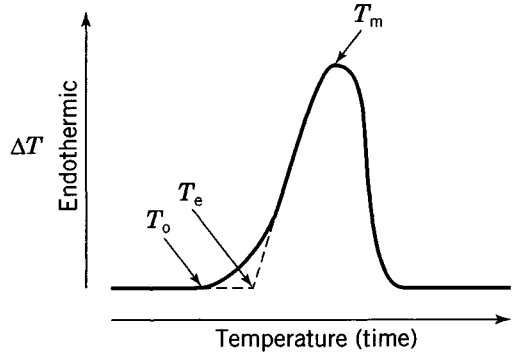


Figure 5. Typical endotherm. T_0: onset temperature; T_e: extrapolated onset temperature; T_m: peak temperature. *Source:* From Ref. 19.

ture at the intersection of the tangent to the maximum slope of the peak with the extrapolated linear base line. The extrapolated onset temperature is usually used as the melting temperature unless otherwise stated.

The same characteristic temperatures are used in the case of a crystallization exotherm. However, the temperature of the apex of the peak is usually denoted T_c.

Small sample size, homogeneous particle size, and good thermal contact between the sample pan and the calorimeter improve the quality of the data obtained. The quality of the data obtained is affected by the heating rate; the maximum temperature of the peak increases and the peak broadens as the scanning rate increases when the data are plotted versus temperature (Fig. 6).

The quality of the data obtained is also affected by the purity of the substance analyzed. The maximum temperature of the melting endotherm decreases and the melting endotherm broadens as the purity of the sample decreases. The change in shape of the melting endotherm due to a decrease in the purity of the sample provides the basis for sample purity determination by DSC and is discussed in a separate section.

The melting (or freezing) temperature of a substance should be determined by studying the phase transition from the solid state to the liquid state (increasing temperature program) rather than by studying the phase transition from the liquid state to the solid state (decreasing temperature program). Indeed, upon cooling a liquid can stay liquid below its freezing temperature to form a supercooled liquid. This phenomenon is frequent and causes a significant underestimation of the melting temperature (freezing temperature). Studying the transition temperature upon cooling and heating the sample should give relatively accurate results in the absence of supercooling phenomenon.

Determination of glass-transition temperatures (T_g) is slightly different due to the fact that glass transitions are not first-order phase transitions (such as melting or crystallization). The enthalpy change during higher order phase transition is equal to zero. A peak is not generally observed; instead, a change in heat capacity values causes a drift in the baseline. The extrapolated onset temperature (T_f) and the temperature obtained at half the height of the baseline shift (T_{mid}) have been used to define the glass-transition temperature (19) (Fig. 7). Due to the dramatic effect of the thermal history of the sample on the glass-transition determination for polymers, a cycle at high scanning rate (20°C/min) should be performed on the samples prior to analysis. This preliminary cycle would erase the thermal history of the sample (3).

Not only the temperature but also the enthalpies of transition can be estimated for the first-order transitions. If the sample weight is known and if the calorimeter has been correctly calibrated with a calibrant having a known enthalpy of transition (generally heat of fusion), the enthalpies of transition can be determined from the thermoanalytical curves. The heat absorbed by (endothermic events) or released from (exothermic events) the sample during a phase transition can be obtained from the area under the curve of the transition.

Very often a change in the baseline values before and after the phase transition peak are observed. This phenomenon occurs because the heat capacity of a substance in a given phase is generally slightly different from the heat capacity of the same substance in a different phase. Consequently, the true estimation of the baseline during the phase transition, necessary for the determination of the area under the curve, can be difficult (19). Different mathematical techniques of integration are used for the estimation of the enthalpy values (20,24) (Fig. 8).

When hermetically sealed pans are used (constant volume instead of constant pressure), internal energy of transition should be used rather than enthalpy of transition.

Pharmaceutical Applications

Drug Purity. DSC can be used to determine the purity of pharmaceutical drug substances. The method is based on the melting point depression measurement of an impure material (25). The presence of an impurity in a sample depresses the melting temperature of the main component and broadens the melting endotherm (Fig. 9).

The Van't Hoff equation gives the melting point depression as a function of the mole fraction of the impurity:

$$T_0 - T_m = \frac{RT_0^2\chi_2}{\Delta H_0} \qquad (2)$$

where $T_0 - T_m$ is the melting point depression, R is the gas constant in cal/mol.K, T_0 is the melting temperature

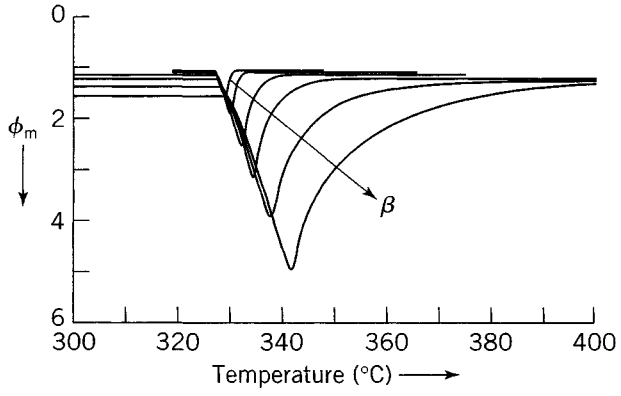


Figure 6. Measured curves showing the peak temperature maximum changing with the heating rate β. *Source:* From Ref. 2.

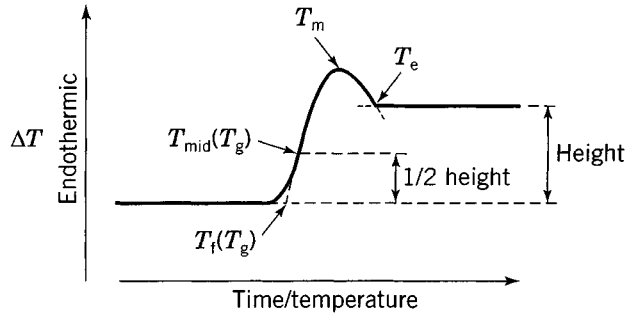


Figure 7. Typical transitions of a glass-forming material. T_f: extrapolated onset temperature; T_{mid}: glass-transition temperature. *Source:* From Ref. 19.

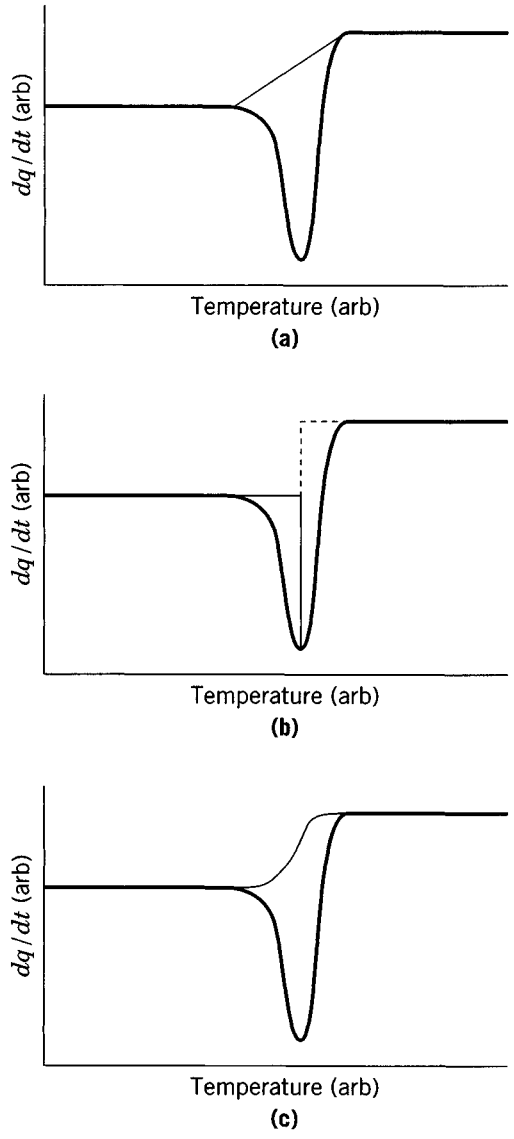


Figure 8. Methods of determining peak area by the construction of different baselines. (**a**) Tangential; (**b**) stepped; (**c**) sigmoidal. *Source:* From Ref. 20.

of the pure component in Kelvin, T_m is the melting temperature of the impure material, χ_2 is the mole fraction of the impurity, and ΔH_0 is the enthalpy of fusion of the pure component in cal/mol.

Several assumptions and limitations apply to the calculation of the fraction of impurity present in the sample (27,28). It is assumed that the impurity forms an ideal solution with the main component and that no chemical reaction takes place in the molten state between the impurity and the main component. The melting temperature and the enthalpy of fusion of the pure compound of interest have to be known. The fraction of molten sample at any temperature, F, and the sample temperature at equilibrium, T_S, are given by the following equations:

$$F = (T_0 - T_m)/(T_0 - T_S) \quad (3)$$

$$T_S = T_0 - RT_0^2\chi_2(1/F)/\Delta H_0 \quad (4)$$

When T_S is plotted versus $1/F$, a straight line with a slope of $RT_0^2\,\chi_2/\Delta H_0$ is obtained and the mole fraction of the impurity can be calculated. Figure 10 gives an example of such a plot for an impure sample of testosterone.

This method should be used only if the amount of impurity is less than about 2% (i.e., dilute solution) (19). Indeed, a significant deviation from linearity of the plots T_S versus $1/F$ is observed for samples containing high levels of impurity.

Polymorphism and Pseudopolymorphism. Polymorphism is defined as the tendency for a compound to exist in the solid state with different crystal structures (or polymorphs). Despite their chemical identity, polymorphs generally have different physical characteristics (i.e., melting point, heat of fusion, solubility, X-ray pattern, density, hygroscopicity, dissolution rate, infrared spectrum). Pseudopolymorphs are defined as crystals containing solvent molecules. They can be further differentiated as hydrates when water is the solvent incorporated in the crystal pattern or solvates when other types of solvents (i.e., acetonitrile, methanol, or chloroform) are incorporated. By using various solvents, temperatures, and rates of crystal-

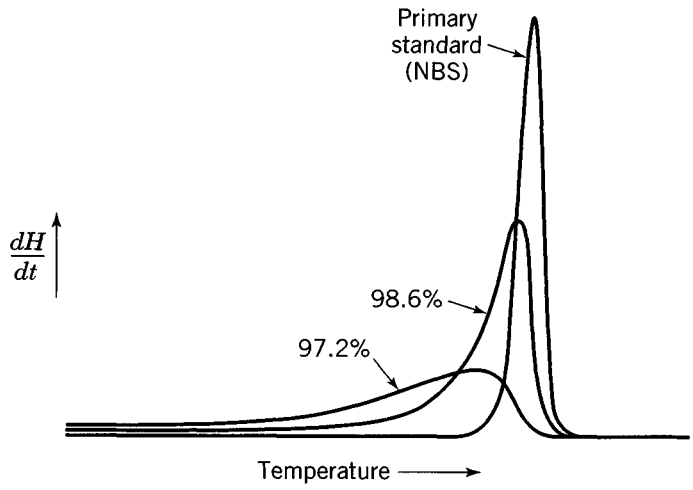


Figure 9. Effect of purity on melting endotherm of benzoic acid. *Source:* From Ref. 26.

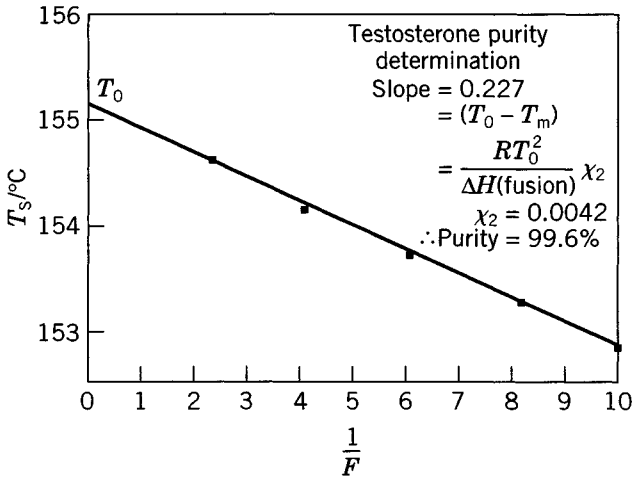


Figure 10. Graphical evaluation of testosterone purity. *Source:* From Ref. 26.

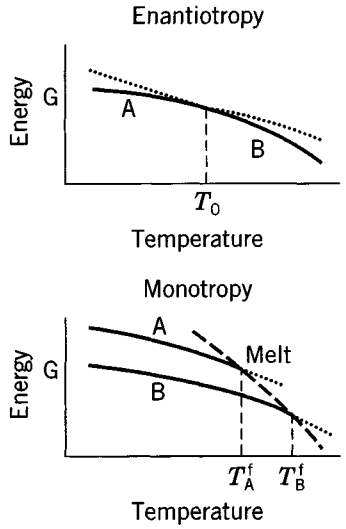


Figure 11. Relationship between Gibbs energy G and temperature for two modifications in the case of enantiotropy and monotropy. *Source:* From Ref. 5.

lization, different polymorphs may be obtained. Because different polymorphic forms of the same drug exhibit significant differences in their physical characteristics, therapeutic activity from one form to another may be different. Studying the polymorphism of a drug and the relative stability of the different polymorphs is a critical part of preformulation development.

Polymorphism of drugs has been extensively studied using DSC and other techniques. Numerous reviews have been published on the subject (5,29,30). Studies of the physical stability of polymorphic forms have led to the definition of two different types of polymorphic behavior, enantiotropy and monotropy; the difference is based on the reversibility of the transformation from one form to the other one (4,31). Enantiotropy is defined as the reversible change from one polymorphic form to another (31). Polymorphic changes can occur below the melting point of either polymorph and thus the stability of the different forms is dependent on temperature (4). At temperatures below the transition temperature, the form with the lower melting point is the most stable form, whereas the form with the highest melting temperature is the most stable at temperatures above the transition temperature (32). Monotropy, on the other hand, is defined as an irreversible transition from a metastable form to a stable form. The higher melting form is the most stable throughout the temperature range (31) (Fig. 11).

Differentiation between monotropy and enantiotropy is important for understanding the relative stability of different polymorphic forms of a given compound and can be achieved by DSC experiments (Fig. 12).

Other techniques (calorimetric or not) are useful in the differentiation process between monotropy and enantiotropy. Thermogravimetric analysis and thermomicroscopy are very often used and give complementary information necessary for a complete understanding of the polymorphic system. Determination of the transition temperature is also crucial and can be done by solubility studies based on the fact that at the transition temperature both forms have the same solubility (33). Heat of solution data give valuable insight to polymorphic transitions.

Amorphous Compounds: Glass-Transition Temperature. Amorphous solids are often defined as supercooled liquids. Their molecules are not arranged in an orderly fashion but in a random manner, giving pharmaceutically interesting physicochemical characteristics to these types of solids. Dissolution rates and consequently bioavailability can be tremendously improved upon formation of an amorphous solid rather than the crystalline form of the same drug. This improvement is critical for many poorly soluble drugs. Amorphous pharmaceutical solids can be produced by several means: supercooling of the melt, vapor condensation, precipitation from solution, lyophilization, or milling of crystals (34). Unfortunately, due to their high internal energy, most of the metastable amorphous solids have a tendency to crystallize during manufacturing and storage. Knowledge of the (*1*) rate of crystallization, (*2*) glass-transition temperature (T_g), and (*3*) influence of temperature and humidity on the physical stability of amorphous solids is of importance in preformulation studies. The glass-transition temperature corresponds to the temperature where the characteristics of the solid change from the rubbery state (above T_g and below T_m) to the glassy state (below T_g) (Fig. 13).

Molecular motion of amorphous solids is highly temperature dependent. At temperatures well below the glass-transition temperature, the molecules of an amorphous solid are kinetically frozen, whereas their motion significantly increases as the temperature gets closer to the T_g or even above the T_g. Due to the thermodynamic instability of amorphous solids as compared to the crystalline state, spontaneous crystallization is always possible as soon as molecular mobility is above the threshold of nucleation. Molecular mobility, even at temperatures below T_g, is usually high enough to allow for nucleation and thus crystal-

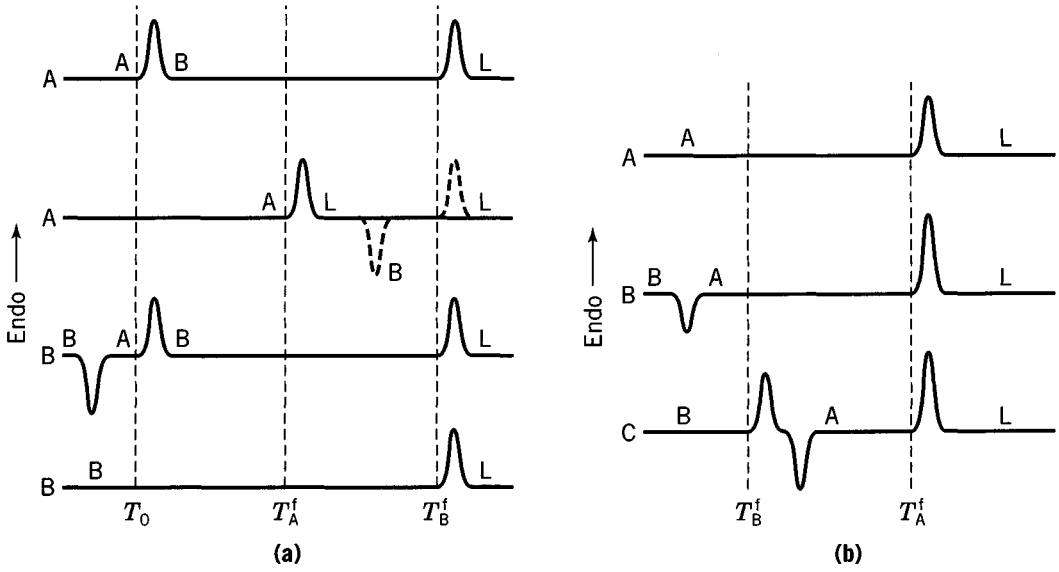


Figure 12. DSC curves for (**a**) enantiotropic and (**b**) monotropic polymorphism. *Source:* From Ref. 5.

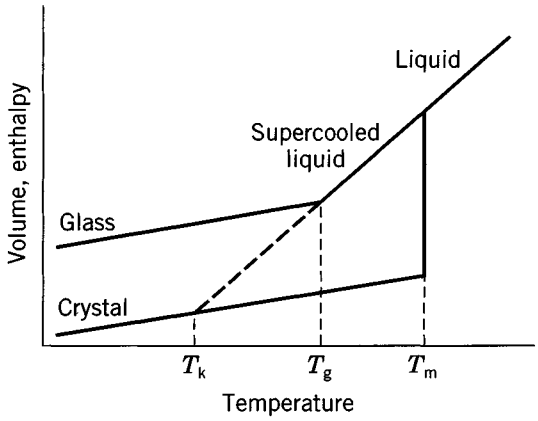


Figure 13. Schematic depiction of the variation of enthalpy (or volume) with temperature. *Source:* From Ref. 34.

lization (35). The determination of the glass-transition temperature of an amorphous solid is of primary importance for the formulation and prediction of stability of pharmaceutical solids. The determination of T_g is possible by DSC because a solid above T_g has a higher C_p than a solid below T_g (36). The strength or fragility of amorphous systems is indicated by the amplitude of the change in C_p (36). The molecular mobility of strong glasses (i.e., proteins) is not temperature dependent near T_g. Strong glasses are characterized by small changes in heat capacity at T_g. On the other hand, fragile glasses are more sensitive to thermal excitation and are characterized by a larger change in heat capacity at T_g.

However, the change in heat capacity is often very small and thus difficult to detect with classical DSC. The presence of moisture in the sample is critical, because water can act as a plasticizer and thus reduce the T_g of the system (37,38). The glass-transition temperature is also very sensitive to the history of the sample and the heating and cooling rate used for its determination (39). The study of amorphous systems is also possible by the detection of crystallization, upon heating of the sample, as an exothermic peak. The extent of the amorphous character of a sample can be estimated by the value of the enthalpy of crystallization. Comparing the crystallization enthalpy value of a given sample to the enthalpy value of a purely amorphous sample of the same drug, as defined by an independent method (i.e., X-ray diffraction), gives the amorphous content of the sample (40,41).

Due to the recent interest in development of protein formulations in the pharmaceutical field and the search for "ideal" protectants during the lyophilization process, the glass-transition temperature of frozen amorphous solutions (T_g') is often determined using DSC. Determining the T_g' of frozen solutions is critical to optimize the freeze-drying cycle. Indeed, T_g' represents the maximum allowable operating temperature during primary drying. If the product temperature exceeds the glass-transition temperature, the product could collapse due to the significant increase of the viscosity of the sample (42–44).

Micro-DSC: Protein Applications. Due to recent improvement of the sensitivity of differential scanning calorimeters, the study of thermal transitions in biological systems has been tremendously expanded. DSC is now routinely used to help predict the stability of proteins in liquid formulations. By determining the effect of formulation parameters (i.e., pH, salt concentration), as well as the effect of additives on the melting temperature of proteins, DSC has become a necessary analytical tool. DSC has also been used to study protein–ligand interactions (45–47). The complexity in interpreting the data obtained with macromolecules resides in the fact that it is difficult to separate

the interactions specific to the protein from the solvent interactions (46).

To manifest their biological activity, proteins must be folded in a specific configuration. Covalent and noncovalent intramolecular bonds keep the protein in the folded state. The stability of the native state in aqueous solution is determined by amino acid sequence, temperature, pH, salt concentration, and presence of ligands (48). Due to their polymeric composition, proteins can be subject to physical denaturation without chemical degradation. Upon heating, covalent and noncovalent forces are disrupted and unfolding of the protein follows. Thermal denaturation of the protein can be classified either as reversible or irreversible depending on whether the protein returns to the native conformation upon cooling. In differential scanning experiments, complete reversibility of the unfolding process is often tested by reheating the same sample after cooling; both curves should be superimposable. In the case of a reversible denaturation, only two populations of conformations of the protein are present in solution: the native (N) and the unfolded (U) populations.

$$N \overset{K}{\leftrightarrow} U \tag{5}$$

In the case of an irreversible denaturation, the reversibly unfolded population present in solution undergoes further reactions (i.e., aggregation, precipitation, or disulfide cross-linking) to form an irreversibly denatured population (I).

$$N \overset{K}{\leftrightarrow} U \overset{k}{\rightarrow} I \tag{6}$$

For reversible denaturation, a two-state model can be used to represent the experimental phenomenon observed by DSC for most small monomeric proteins. The melting temperature (T_m) is the temperature at which 50% of the protein is in one of the native conformations and 50% is in one the unfolded conformations (49). Reversible denaturation of proteins can be represented by the following equilibrium expression:

$$K = \frac{[U]}{[N]} \tag{7}$$

where $[U]$ is the concentration of unfolded form, $[N]$ is the concentration of native form, and K is the equilibrium constant for the unfolding process (15). Equations 8 and 9 are used to interpret DSC data when the unfolding process is under thermodynamic control (no kinetic limitations):

$$\left(\frac{d \ln K}{dT}\right)_P = \frac{\Delta H_{VH}}{RT^2} \tag{8}$$

$$\Delta H_{VH} = ART^2 \frac{C_{ex,1/2}}{\Delta h_{cal}} \tag{9}$$

where T is the absolute temperature at which the process is half completed, ΔH_{VH} is the Van't Hoff enthalpy, R is the gas constant, Δh_{cal} is the calorimetric specific enthalpy, A is a constant with a value of 4.0 (two-state model), and $C_{ex,1/2}$ is the excess specific heat at T (50) (Fig. 14).

Moreover, the calorimetric specific enthalpy (Δh_{cal}) is related to the calorimetric enthalpy (ΔH_{cal}) by the following equation:

$$\Delta H_{cal} = \Delta h_{cal} M \tag{10}$$

where M is the molecular weight of the protein. For a strict two-state process, $\Delta H_{HV} = \Delta H_{cal}$. The presence of intermediates during the unfolding process can be suspected when $\Delta H_{HV} < \Delta H_{cal}$. On the other hand, when $\Delta H_{HV} > \Delta H_{cal}$, the presence of intermolecular cooperation (subunits) can be suspected.

For irreversible denaturation, the analysis of the DSC data is still possible but should take into account the kinetics of formation of the irreversibly formed protein states (51–53).

Due to weakness of the forces involved in the folding process, highly sensitive differential scanning calorimeters are used in order to permit the accurate detection of the thermal phenomena of interest (i.e., denaturation or unfolding). These types of instruments are called high sensitive differential scanning calorimeters (HSDSC) or micro differential scanning calorimeters (micro-DSC). Most of the instruments commercially available are designed for these specific types of applications and thus have a limited temperature range (−20°C to 130°C), as well as a limited scanning rate range (0.01°C/min to 2.5°C/min). In most of these calorimeters, the reference and cell holder are placed in an adiabatic shield. The volume of the sample holders are usually larger (ca. 1 mL) than in conventional DSC. Due to the fact that the cells are fixed in place, cleaning of the cells between samples can be problematic. Indeed, upon unfolding and especially if the sample precipitates, proteins have a tendency to adsorb to the wall of the cells. Thorough cleaning, using various acidic and/or organic solutions, followed by extensive rinsing, should be performed. To assess the efficiency of the cleaning procedure, a baseline check using the same buffer solution in both the reference and sample cells should be performed prior to

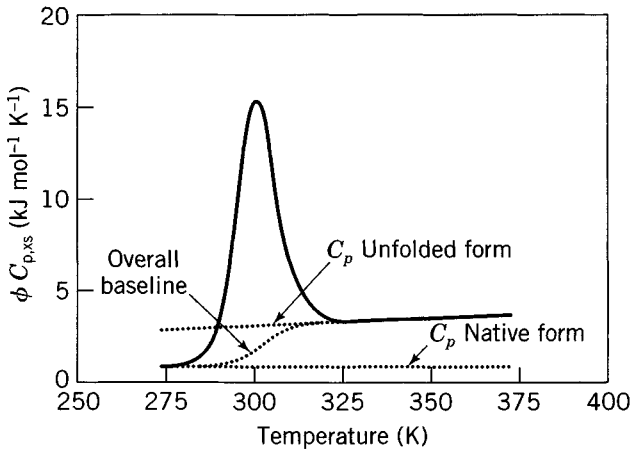


Figure 14. Typical melting thermogram for protein. *Source:* From Ref. 15.

any other experiments. In a typical experiment, the reference cell usually contains the placebo formulation (every component of the formulation but the macromolecule). The scope of applications for HSDSC is not limited to proteins (54–58). Numerous studies involving lipids and biological membranes (59,60) or polynucleotides (61) have been published.

MODULATED DIFFERENTIAL SCANNING CALORIMETRY

As mentioned in the introduction, a novel extension of classical DSC was developed a few years ago. Its application to pharmaceutical science led to new insights on the determination of complex thermal parameters in multicomponent formulations. With classical DSC, depending on the scanning rate, either resolution or heat flow sensitivity are emphasized, but at the expense of one another. MDSC is a technique that allows for simultaneous resolution of overlapping thermal phenomena and provides good sensitivity for the detection of small thermal events. Indeed, by applying a modulated temperature program, low underlying heating rates are associated with a large instantaneous heating rate due to a large modulation amplitude (20). This novel approach permits the deconvolution of thermal phenomena into two different signals, reversible and irreversible. The reversibility of any thermal event is defined within the time scale of the temperature modulation. MDSC can be easily achieved using both types of instruments: power compensation and heat flux DSC (62). Two different instrument designs are commercially available: a Modulated DSC™ (TA instrument) pioneered by Reading (62), and a Dynamic DSC™ (Perkin-Elmer instrument) developed by Schawe (63,64). With the MDSC™ model, a sinusoidal ripple is overlaid on the standard linear temperature ramp (62), whereas with the DDSC™ model, the temperature program is composed of repeating units consisting of an isotherm followed by an isotherm or a heat segment followed by a cool segment (65).

With the TA instrument, a small sinusoidal term is added to the linear temperature program so the temperature can be separated into (*1*) a modulated temperature component and (*2*) an underlying linear component. The sinusoidal temperature profile can be described by the following equation (62):

$$Temp = T_0 + bt + B \sin(\omega t) \qquad (11)$$

where T_0 is the starting temperature, b is the underlying heating rate, and B and ω are the amplitude and the frequency of the sinusoidal function, respectively. The total heat flow out of the sample can be expressed as:

$$dQ/dt = C_p(b + B\omega \cos(\omega t)) + f'(t, T) + C \sin(\omega t) \qquad (12)$$

where Q is the amount of heat absorbed by the sample, $f'(t, T)$ is the average underlying kinetic component of the calorimetric response, C is the amplitude of the kinetic response to the sine wave modulation, and $(b + B\omega \cos(\omega t))$ corresponds to dT/dt (linear temperature program). The heat flow can be separated into (*1*) a heating rate–dependent heat flow that is influenced by heat capacity, and (*2*) an absolute temperature–dependent heat flow (or kinetic) which is influenced by the temperature at a given time. These two types of heat flow can be separated due to their different responses to the sinusoidal temperature program and the underlying temperature ramp. Indeed, the heat capacity contribution is present at all times (reversible and irreversible processes) whereas the kinetic contribution is predominant during irreversible processes. Discrete Fourier transform is used to separate both types of heat flow. The reversing heat flow component is calculated, and the nonreversing heat flow component is obtained by subtracting the reversing heat flow component from the total heat flow (20) (Fig. 15). The determination of heat capacity values is possible through the reversing component of the response, whereas the determination of enthalpies of crystallization, relaxation, and evaporation is possible through the nonreversing component of the response. Depending on the frequency and amplitude chosen for the temperature program, glass-transition temperature and melting are phenomena that can appear in either components (reversing and nonreversing) (66).

To avoid supercooling of the sample heating rate, frequency of modulation, and amplitude of modulation should be chosen in a such way that the overall heating rate is at all times positive. Moreover, the frequency of the sine function should be chosen such that at least six modulations are completed over any single thermal event, so that the frequency is not too slow in comparison to the rate at which the sample undergoes a thermal transition (62).

With the Perkin-Elmer instrument, the temperature program is composed of repeating units. The repeating units can either be composed of (*1*) an isotherm segment followed by a scan segment (Iso-Scan mode) or (*2*) a heat segment followed by a cool segment (Heat-Cool mode). The Iso-Scan mode should be used for the determination of thermal events in which supercooling of the sample could be detrimental to the quality of data obtained (enthalpy of crystallization). On the other hand, the Heat-Cool mode should be used for the determination of reversible thermal

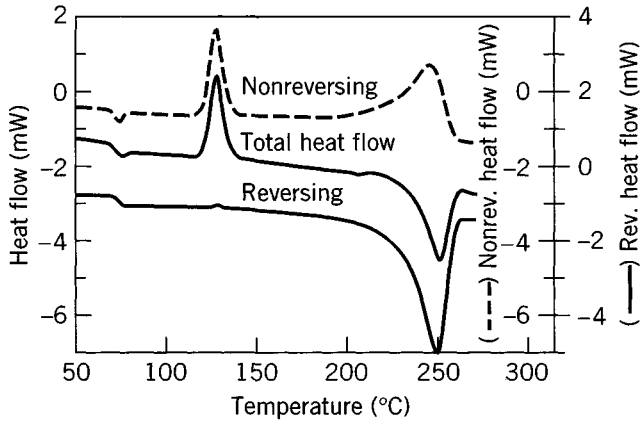


Figure 15. Thermograms of PET showing the total, reversing, and nonreversing heat flow signals. *Source:* From Ref. 20.

events (i.e., glass-transition temperature) that have to be separated from overlapping nonreversible events (i.e., enthalpy of relaxation). After correcting for the phase lag of time-dependent processes, the data analysis software separates the storage-specific heat (storage C_p) from the loss-specific heat (loss C_p). The storage-specific heat characterizes the molecular motion of the sample, whereas the loss-specific heat characterizes the dissipative properties of the sample (65) (Fig. 16).

MDSC is used in polymer sciences to determine glass-transition temperatures. Accurate determination of T_g is achieved because the specific heat change (reversible thermal event) is separated from the enthalpy of relaxation (nonreversible thermal event). The change in heat capacity appears sigmoidal in shape (due to the absence of interference from relaxation phenomena) and is independent of the thermal history of the sample (66–70).

HEAT CONDUCTION CALORIMETRY

Heat conduction calorimetry has been used in a wide range of applications including the stability of drugs in the solid state, the study of water adsorption by solids, the study of protein–ligand interactions, and various biological reactions (71–88). Heat conduction calorimeters are isothermal microcalorimeters and thus allow for the detection of reactions at ambient temperature rather than requiring that a reaction be studied at high temperatures (as is the case with DSC). Most of the microcalorimeters are of the twin design and are comprised of a reaction cell and a reference cell. The reference cell is usually filled with an inert material with preferably the same characteristics as the sample with regards to heat capacity and heat conductance. The sample cells can be of different designs depending on the type of experiment. For batch-type experiments, static cells are usually used. For very slow processes, such as biological processes, sealed ampoules are usually used. For titration experiments, a specific type of cell has to be used to allow for stirring and injection of one of the reactants (89). The heat generated or absorbed by the reaction taking place in the sample cell is usually detected by a thermopile placed between the cell and a heat sink. The heat sink (thermostated water bath or a metal block) allows for thermal equilibrium. After an equilibration period, the temperatures of the heat sink and the sample cells are the same. As the reaction inside the cell takes place, heat will be conducted from the cell to the heat sink (for reactions evolving heat) or from the heat sink to the sample cell (for reactions absorbing heat). Because no reaction is taking place in the reference cell, a differential heat flow measurement is performed (90–92). However, because the heat generated by many of the processes studied by heat flux calorimeters is small, very sensitive detectors have to be used. The detection limit of the most sensitive calorimeters is in the nanowatt range. The working temperature of the thermostat ranges from $-40°C$ to $200°C$ with a precision of $\pm 0.0001°C$. One of the disadvantages of heat conduction calorimeters is their large time constant. For multistep titration experiments, several hours might be needed to complete the experiment. However, a dynamic correction method can be used to shorten the experiment time (93,94). Calibration is usually performed by the use of electrical heaters. Electrical calibration is accurate but may not be representative of the reaction taking place during a biological or chemical reaction. Chemical calibration can be performed to better mimic the reaction taking place inside the cell. Different types of chemical calibration can be used depending on the type of reaction vessel (95). When the calorimeter is used below room temperature, dry nitrogen is flushed through the system to avoid condensation.

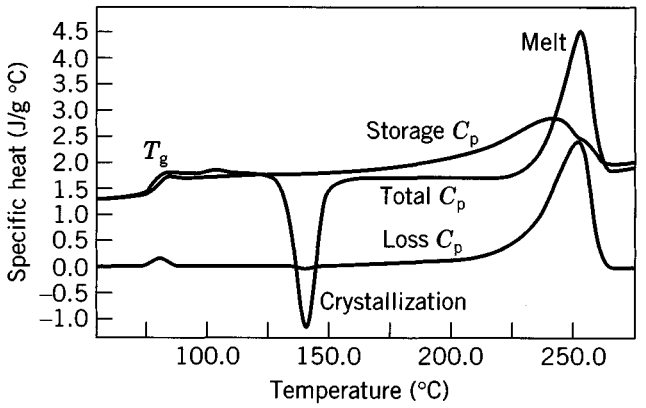


Figure 16. Thermograms of PET showing the storage, loss, and total specific heat curves. *Source:* From Ref. 65.

Among the various applications of heat conduction calorimetry, the study of drug degradation has been one the most interesting to pharmaceutical science. Kinetics of drug decomposition are usually estimated by following the rate of disappearance of the parent compound or the rate of appearance of decomposition products. However, for compounds relatively stable at room temperature, accurate determination of the rate of decomposition can be difficult due to insufficient amounts of degradants in the sample. The study of the rates of decomposition of drugs at elevated temperatures and the extrapolation of the rates at lower temperatures are possible using the Arrhenius relationship based on the following assumptions: (*1*) the mechanism of drug degradation is independent of temperature and (*2*) the energy of activation used in the Arrhenius equation is also independent of temperature (25). To assess the validity of these two assumptions, stability data at room temperature are usually necessary. However, the formation of sufficient amounts of degradation products (above their detection limits) might be a very slow process at room temperature. Moreover, no data are obtained characterizing the early stages of drug degradation due to insufficient amounts of degradants present in the sample (72,73). On the other hand, due to the production or consumption of heat associated with most chemical reactions, heat conduction calorimetry can be used to follow the rate of heat change in the sample as a function of time at a given temperature. Kinetics of chemical reactions can be subsequently deduced. By performing measurements at different temperatures, the activation energy can be determined.

THERMOGRAVIMETRY

TGA has been used in pharmaceutical research and development primarily to characterize pseudopolymorphism of drugs and to detect the presence of residual solvent in drug substances (i.e., from crystallization) or excipients. Decomposition of drugs can also be followed if a mass change accompanies drug degradation. Thermogravimetric analysis is a thermal technique in which the weight of a sample is monitored as a function of temperature. An electronic microbalance, which is thermally isolated from the furnace (to avoid interference), is used. Only the sample holder is surrounded by the furnace (Fig. 17). Most commercially available balances are null point balances; the sample is maintained in the same zone of the furnace as the mass of the sample changes. The balance is zeroed at its null position and deviations from this position are detected and monitored as a function of temperature (96). Electronic or optical methods are used to detect the deviation of the balance from its null position as the mass of the sample changes. Electronic detection uses the change in the capacity of a condenser, whereas optical detection uses the interception of a light beam to sense the change of the balance from its null position (97). Usually the restoring mechanism to the null position is electromagnetic. The furnace, which is usually a resistive heater, can be one of several different designs. The furnace can be inside, part of, or external to the housing (1). Because heating and weighing of the sample have to occur simultaneously, the sample cannot be in direct contact with the furnace. Thus, problems of heat transfer may arise (96). Temperature gradients can occur not only between the furnace and the sample but also within the sample. The latter can be improved by using a small sample size (generally in the order of a few milligrams). To avoid interference from the moisture content of air, the sample chamber should be purged using a dry inert gas such as nitrogen or helium at a flow rate of 15 to 25 mL/min (3).

Most current instruments permit a wide range of heating rates (from 0.1°C/min to 1,000°C/min). The most sensitive thermogravimetric analyzers are capable of detecting mass changes on the order of 0.1 μg.

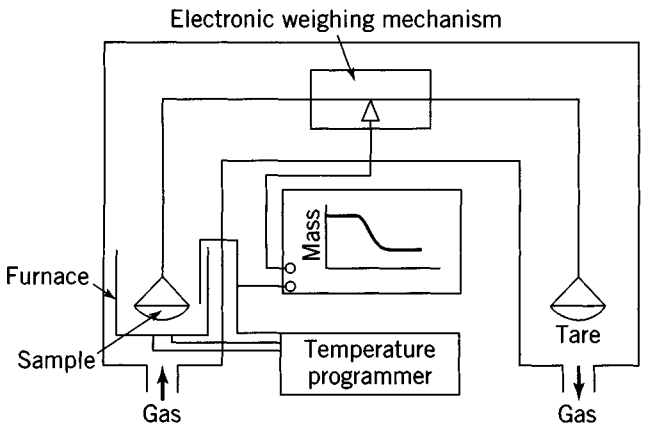


Figure 17. Thermobalance. *Source:* From Ref. 1.

The thermogravimetric data can be presented by plotting the (*1*) mass change of the sample (%) versus temperature or (*2*) rate of mass change of the sample versus temperature (differential thermogravimetry [DTG]) (Fig. 18).

A rapid initial mass loss is usually characteristic of a desorption phenomenon, whereas a mass loss after a flat portion is more characteristic of decomposition of the sample (i.e., dehydration). Depending on the stoichiometry of the reaction and on the presence of intermediates, decomposition can occur in one or several stages (1). On the other hand, a gain in mass is characteristic of a reaction of the sample with its surroundings (i.e., oxidation). Interpreting the data obtained by thermogravimetric analysis can be difficult; comparison of the data obtained with DSC and TGA for the same sample facilitates the data analysis (Fig. 19).

ISOPERIBOL CALORIMETRY

Isoperibol calorimetry is used in a wide range of pharmaceutical applications in which solid–liquid or liquid–liquid interactions can be studied. Typical applications include measurements of solubility, heat and rate of dissolution, polymorphism, ligand interactions and binding, metal ion chelation and analysis as well as equilibrium and rate constants. The temperature of a reaction vessel is monitored as a function of time during mixing of two reactants. The instrument is comprised of (*1*) a reaction vessel (usually silvered inside and outside) containing the solvent, (*2*) a thermistor used as the temperature measuring device, (*3*) an electrical heater for calibrating and warming the solvent, (*4*) a stirrer allowing for continuous mixing, (*5*) a batch assembly or titration device containing the second

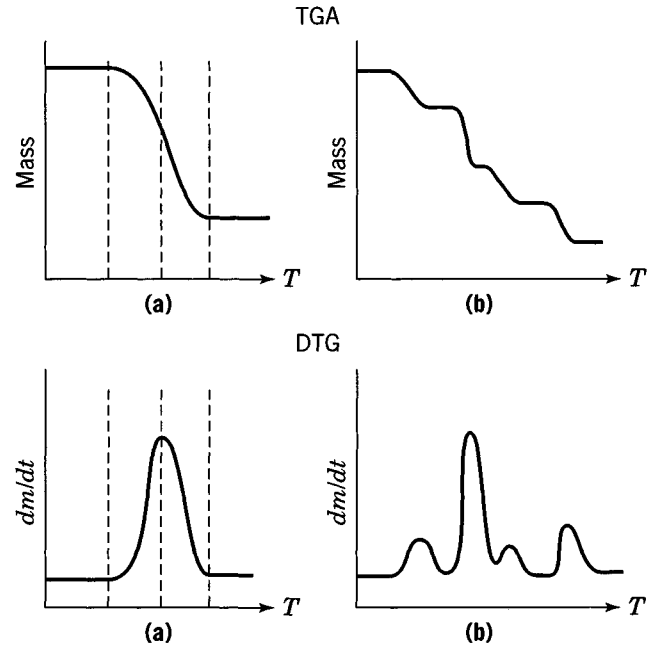


Figure 18. Comparison of TGA and DTG curves. *Source:* From Ref. 1.

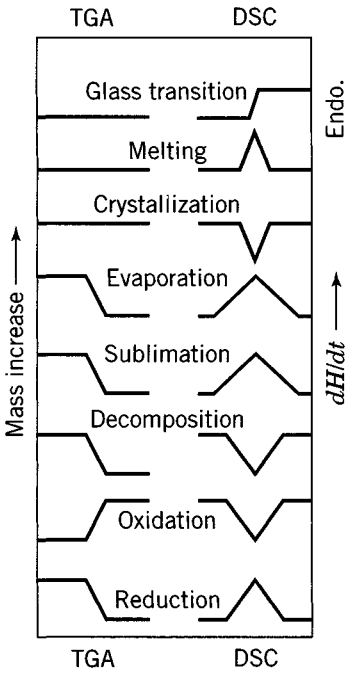


Figure 19. Comparison of the schematic TGA and DSC curves recorded for a variety of physicochemical processes. *Source:* From Ref. 3.

component (liquid or solid), and (*6*) a thermostated water bath acting as the constant surroundings (98) (Fig. 20).

The word *isoperibol* is used to describe that during the reaction phase the temperature of the surroundings stays constant (98,99). As the temperature inside the reaction vessel changes due to the reaction, heat exchange between the reaction vessel and the surroundings occurs. A correction factor must be applied to account for this heat exchange (98,100).

Because the value of the energy equivalent is necessary for the calculation of the heat of reaction taking place in the reaction vessel, determination of the energy equivalent of the system is performed before and/or after experiments. The energy equivalent value is obtained by electrical calibration. After submersion of the reaction vessel into the water bath and an initial equilibration period, a known current is passed through the heater for a known period of time. The increase in temperature of the solvent contained in the reaction vessel is recorded and corrected for heat leak with the surroundings. Subsequently, the energy equivalent of the system can be calculated using the following equation:

$$E_q = \frac{IVt}{\Delta T_1} \tag{13}$$

where E_q is the energy equivalent of the system, T is the current, V is the voltage, t is the period of time during which the heater was on, and ΔT_1 is the corrected increase in temperature.

After calculating the energy equivalent of the system, the heater is turned on to bring the temperature of the solvent to the same temperature as the water bath (surroundings). When the temperature differential between the reaction vessel and the surroundings is equal to zero, the heater is turned off and the experimental reaction procedure can be started.

The temperature inside the reaction vessel is recorded before the reaction occurs to give the slope of the initial (prereaction or lead) phase. Usually a slight positive slope is obtained due to heating from the stirring system. The reaction (mixing between the two reactants) is initiated, and the change in temperature due to the interaction between the two reactants is recorded. The temperature of the reaction vessel is recorded after the reaction period to give the slope of the final (postreaction or trail) phase. By extrapolating the slopes from the initial and final phases and after correcting for heat exchange with the surroundings, the corrected change in temperature due to the reaction is calculated. Knowing the energy equivalent of the system and the corrected change in temperature due to the reaction, the enthalpy of reaction can be determined using the following equation:

$$\Delta H_{reaction} = E_q \times \Delta T_2 \tag{14}$$

where $\Delta H_{reaction}$ is the enthalpy of reaction, E_q is the energy equivalent of the system, and ΔT_2 is the corrected temperature change.

There are two different ways of initiating the reaction: the batch mode (or breaking ampoule mode) and the continuous titration mode. With the batch mode, the temperature of the reaction vessel is followed as a function of time. One reactant is sealed in a glass ampoule or contained in a stainless steel device, with glass seals; the device is secured in the reaction vessel containing the solvent (second reactant). At the beginning of the reaction phase, the ampoule or the two end pieces of glass are broken, releasing the sample into the reaction vessel and allowing for mixing of the sample with the solvent. The sample contained inside the glass ampoule or the stainless steel device can be a solid or a liquid. Batch solution calorimetry has been used to determine the enthalpy of solution, mixing, or hydration of numerous pharmaceutical compounds (76,101–104). Batch solution calorimetry has also been used to characterize polymorphism of drugs. Different values of enthalpy of solution are usually obtained for different polymorphic forms of a compound in a particular solvent. Enthalpy values for one given polymorphic form are usually different from one solvent to another. However, the difference in enthalpy values from one polymorphic form to another should be independent of the solvent (92). Batch solution calorimetry has also been used to determine the degree of crystallinity of a sample by comparison of the values obtained for a pure amorphous sample and a pure crystalline sample of the same compound (105). The enthalpy of solution for the pure crystalline sample corresponds to the most endothermic (or least exothermic) value, whereas the enthalpy of solution for the pure amorphous sample will be the most exothermic (or least endothermic) value. Partially crystalline samples are characterized by an enthalpy of solution between these two extreme values. A linear relationship between the en-

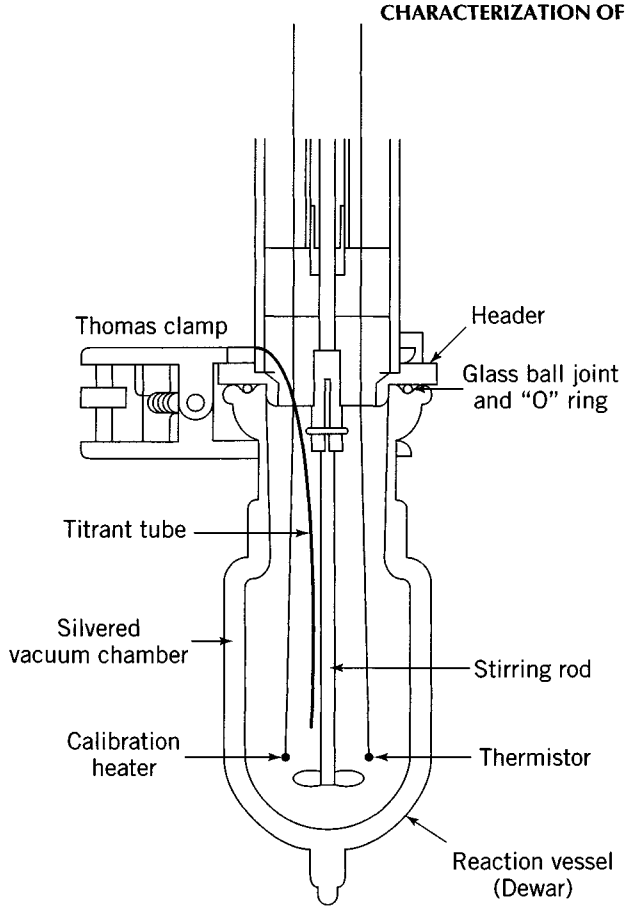


Figure 20. Isoperibol calorimeter reaction vessel. *Source:* Courtesy of Hart Scientific.

thalpy of solution and the degree of crystallinity is expected if (*1*) no reactions occur between the solvent and the sample and (*2*) the dissolution processes of the amorphous and crystalline samples are fast enough in the particular solvent to allow precise measurements.

With the titration mode, the temperature of the reaction vessel is followed as a function of the amount of titrant added. One of the reactants (titrant), placed in a thermostated motor-driven syringe, is added to the reaction vessel containing the other component through a continuous injection at a constant rate. The titration mode has been used to investigate the interactions between two components in solution (i.e., titration, complexation) (106–108). Equilibrium constants and enthalpy and entropy changes can be calculated using this method (109–111). Equilibrium constants can be obtained with precision only if they are relatively small ($\log K < 4$) and if the enthalpy of reaction is large so that changes in temperature can be accurately observed. The free energy and entropy of binding can be calculated from the binding constant and the measured enthalpy change.

CONCLUSIONS

Thermal analysis is successfully used in preformulation and formulation of pharmaceuticals and is part of the necessary battery of tests for the development of new drug entities. Classical DSC is routinely used. However, (*1*) the accuracy and the ease with which thermal events such as T_g are detectable and (*2*) the possibility of resolving overlapped complex thermal events using MDSC increases the interest for this new technique. Microcalorimetry techniques (isothermal microcalorimeters, micro-DSC, and isoperibol calorimeters) are not yet routinely used but are increasingly of interest in pharmaceutical science because of the valuable information they provide.

BIBLIOGRAPHY

1. M.E. Brown, *Introduction to Thermal Analysis: Techniques and Applications*, Chapman & Hall, London, 1988.
2. G.W.H. Höhne, W. Hemminger, and H.J. Flammersheim, *Differential Scanning Calorimetry: An Introduction for Practitioners*, Springer-Verlag, Berlin, 1996.
3. T. Hatakeyama and F.X. Quinn, *Thermal Analysis: Fundamentals and Applications to Polymer Science*, Wiley, New York, 1994.
4. R.J. Behme, D. Brooke, R.F. Farney, and T.T. Kensler, *J. Pharm. Sci.* **74**(10), 1041–1046 (1985).
5. D. Giron, *Thermochim. Acta* **248**, 1–59 (1995).
6. R.K. Khankari, D. Law, and D.J.W. Grant, *Int. J. Pharm.* **82**, 117–127 (1992).
7. M.M.J. Lowes, M.R. Caira, A.P. Lotter, and J.G. Van Der Watt, *J. Pharm. Sci.* **76**(9), 744–752 (1987).
8. N.T. Nguyen, S. Ghosh, L.A. Gatlin, and D.J.W. Grant, *J. Pharm. Sci.* **83**(8), 1116–1123 (1994).
9. I. Hatta, H. Ichikawa, and M. Todoki, *Thermochim. Acta* **267**, 83–94 (1995).
10. F. Balestrieri et al., *Thermochim. Acta* **285**, 337–345 (1996).
11. S. Venkataram, M. Khohlokwane, and S.H. Wallis, *Drug Dev. Ind. Pharm.* **21**(7), 847–855 (1995).
12. J.F. Brandts, C.Q. Hu, and L.N. Lin, *Biochemistry* **28**, 8588–8596 (1989).
13. J.F. Brandts and L.N. Lin, *Biochemistry* **29**, 6927–6940 (1990).
14. G. Barone et al., *Pure Appl. Chem.* **67**, 1867–1872 (1995).
15. B. Chowdhry and S. Leharne, *J. Chem. Educ.* **74**(2), 236–241 (1997).
16. J. Lu and K.B. Hall, *Biophys. Chem.* **64**, 111–119 (1997).
17. H. Tanojo, J.A. Bowstra, H.E. Junginger, and H.E. Boddé, *Pharm. Res.* **11**(11), 1610–1616 (1994).
18. A. Martini, M. Crivellente, and R. De Ponti, *Eur. J. Pharma. Biopharm.* **42**(1), 67–73 (1996).
19. J.L. Ford and P. Timmins, *Pharmaceutical Thermal Analysis: Techniques and Applications*, Ellis Horwood Ser. Pharm. Technol. Wiley, New York, 1989.
20. N.J. Coleman and D.Q.M. Craig, *Int. J. Pharm.* **135**, 13–29 (1996).
21. F. Franks, *Cryo-Letters* **11**, 93–110 (1990).
22. L.M. Her and S.L. Nail, *Pharm. Res.* **11**(1), 54–59 (1994).
23. O. Kubaschewski and E.L. Evans, *Metallurgical Thermochemistry*, 4th ed., Pergamon, Oxford, 1958.
24. R.N. Goldberg and E.J. Prosen, *Thermochim. Acta* **6**, 1–11 (1973).

25. S. Lindenbaum, in J. Swarbrick and J. Boylan, eds., *Encyclopedia of Pharmaceutical Technology*, vol. 2, Dekker, New York, 1989, pp. 233–250.
26. J.L. McNaughton and C.T. Mortimer, *International Review of Science: Physical Chemistry Series 2*, Vol. 10, Butterworths, London, 1975, pp. 1–44.
27. E.E. Marti, *Thermochim. Acta* **5**(2), 173–220 (1972).
28. A.A. Van Dooren and B.W. Muller, *Int. J. Pharm.* **20**, 217–233 (1984).
29. L. Borka and J.K. Haleblian, *Acta Pharm. Jugosl.* **40**(1–2), 71–94 (1990).
30. C. Rodriguez and D.E. Bugay, *J. Pharm. Sci.* **86**, 263–266 (1997).
31. M. Kuhnert-Brandstatter, *Thermomicroscopy in the Analysis of Pharmaceuticals*, Pergamon, New York, 1971.
32. A.G. Mitchell, *J. Pharm. Pharmacol.* **37**, 601–604 (1985).
33. W.I. Higuchi, P.K. Lau, T. Higuchi, and J.W. Shell, *J. Pharm. Sci.* **52**, 150–153 (1963).
34. B.C. Hancock and G. Zografi, *J. Pharm. Sci.* **86**(1), 1–12 (1997).
35. M. Yoshioka, B.C. Hancock, and G. Zografi, *J. Pharm. Sci.* **83**(12), 1700–1705 (1994).
36. C.A. Angell, *Science* **267**, 1924–1933 (1995).
37. J.T. Carstensen and K.V. Scoik, *Pharm. Res.* **7**(12), 1278–1281 (1990).
38. B.C. Hancock and G. Zografi, *Pharm. Res.* **11**(4), 471–477 (1994).
39. C.T. Moynihan, A.J. Easteal, J. Wilder, and J. Tucker, *J. Phys. Chem.* **78**(26), 2673–2677 (1974).
40. M.L. Shively and S. Myers, *Pharm. Res.* **10**, 1071–1075 (1993).
41. Y. Roos and M. Karel, *J. Food Sci.* **57**(3), 775–777 (1992).
42. S.L. Nail and L.A. Gatlin, in K.E. Avis, H.A. Lieberman, and L. Lachman, eds., *Pharmaceutical Dosage Forms: Parenteral Medications*, vol. 2, Dekker, New York, 1993, pp. 163–233.
43. M.J. Pikal and S. Shah, *Int. J. Pharm.* **62**, 165–186 (1990).
44. L.M. Her and S.L. Nail, *Pharm. Res.* **11**(1), 54–59 (1994).
45. J.F. Brandts and L.N. Lin, *Biochemistry* **29**, 6927–6940 (1990).
46. P.R. Connelly, *Curr. Opin. Biotechnol.* **5**, 381–388 (1994).
47. G. Barone et al., *Pure Appl. Chem.* **67**(11), 1867–1872 (1995).
48. B.A. Shirley, in T.J. Ahern and M.C. Manning, eds., *Stability of Protein Pharmaceuticals. Part A: Chemical and Physical Pathways of Protein Degradation*, Plenum, New York, 1992. Chapter 6.
49. D.B. Volkin and C.R. Middaugh, in T.J. Ahern and M.C. Manning, eds., *Stability of Protein Pharmaceuticals. Part A: Chemical and Physical Pathways of Protein Degradation*, Plenum, New York, 1992, Chapter 8.
50. B.Z. Chowdhry and S. Cole, *Trends Biotechnol.* **167**, 11–18 (1989).
51. J.M. Sánchez-Ruiz, J.L. López-Lacomba, M. Cortijo, and P.L. Mateo, *Biochemistry* **27**, 1648–1652 (1988).
52. E. Freire, W.W. van Osdol, O.L. Mayorga, and J.M. Ruiz, *Annu. Rev. Biophys. Biophys. Chem.* **19**, 159–188 (1990).
53. M.L. Galisteo et al., *Thermochim. Acta* **199**, 147–157 (1992).
54. P.L. Privalov, *Adv. Protein Chem.* **33**, 167–241 (1979).
55. P.L. Privalov, *Adv. Protein Chem.* **35**, 1–104 (1982).
56. G. Castronuovo, *Thermochim. Acta* **193**, 363–390 (1991).
57. A. Cooper and C.M. Johnson, *Methods Mol. Biol.* **22**, 109–124 (1994).
58. A. Cooper and C.M. Johnson, *Methods Mol. Biol.* **22**, 125–136 (1994).
59. A. Blume, *Thermochim. Acta* **193**(12), 299–347 (1991).
60. R.M. Epand and R.F. Epand, *Biophys. J.* **66**(5), 1450–1456 (1994).
61. K.J. Breslauer, E. Freire, and M. Straume, *Methods Enzymol.* **211**, 533–567 (1992).
62. M. Reading, A. Luget, and R. Wilson, *Thermochim. Acta* **238**, 295–307 (1994).
63. J.E.K. Schawe, *Thermochim. Acta* **261**(9), 183–194 (1995).
64. J.E.K. Schawe, *Thermochim. Acta* **260**(8), 1–16 (1995).
65. M.P. DiVito, R.B. Cassel, M. Margulies, and S. Goodkowsky, *Am. Lab.* **27**(12), 28–34 (1995).
66. P.S. Gill, R. Sauerbrunn, and M. Reading, *J. Therm. Anal.* **40**, 931–939 (1993).
67. D.J. Hourston, M. Song, H.M. Pollock, and A. Hammiche, *J. Therm. Anal.* **49**, 209–218 (1997).
68. A. Boller, C. Schick, and B. Wunderlich, *Thermochim. Acta* **266**, 97–11 (1995).
69. C. Tomasi, P. Mustarelli, N.A. Hawkins, and V. Hill, *Thermochim. Acta* **278**, 9–18 (1996).
70. J.M.E. Sarciaux and M.J. Hageman, *J. Pharm. Sci.* **86**(3), 365–371 (1997).
71. L.D. Hansen et al., *Pharm. Res.* **6**(1), 20–27 (1989).
72. L.D. Hansen, D.L. Eatough, and E.A. Lewis, *Can. J. Chem.* **68**, 2111–2114 (1990).
73. L.D. Hansen, *Pharm. Technol.* **20**, 64–74 (1996).
74. M.J. Pikal and K.H. Dellerman, *Int. J. Pharm.* **50**, 233–252 (1989).
75. R. Oliyai and S. Lindenbaum, *Int. J. Pharm.* **73**, 33–36 (1991).
76. K.C. Thompson, J.P. Draper, M.J. Kaufman, and G.S. Brenner, *Pharm. Res.* **11**(9), 1362–1365 (1994).
77. G. Buckton, P. Darcy, and A.J. Mackellar, *Int. J. Pharm.* **117**, 253–256 (1995).
78. Y. Aso, S. Yoshioka, T. Otsuka, and S. Kojima, *Chem. Pharm. Bull.* **43**(2), 300–303 (1995).
79. T. Sebhatu, M. Angberg, and C. Ahlneck, *Int. J. Pharm.* **104**, 135–144 (1994).
80. L.E. Briggner, G. Buckton, K. Bystrom, and P. Darcy, *Int. J. Pharm.* **105**, 125–135 (1994).
81. G. Buckton, P. Darcy, D. Greenleaf, and P. Holbrook, *Int. J. Pharm.* **116**, 113–118 (1995).
82. M. Angberg, C. Nystrom, and S. Castensson, *Acta Pharm. Suec.* **25**, 307–320 (1988).
83. M. Angberg, C. Nystrom, and S. Castensson, *Int. J. Pharm.* **61**, 67–77 (1990).
84. L.D. Hansen, J.W. Crawford, D.R. Keiser, and R.W. Wood, *Int. J. Pharm.* **135**, 31–42 (1996).
85. M. Pudipeddi, T.D. Sokoloski, S.P. Duddu, and J.T. Carstensen, *J. Pharm. Sci.* **85**(4), 381–386 (1995).
86. A. Chen and I. Wadsö, *J. Biochem. Biophys. Methods* **6**, 307–316 (1982).
87. I. Wadsö, *Thermochim. Acta* **267**, 45–59 (1995).
88. M.G. Nordmark et al., *J. Biochem. Biophys. Methods* **10**, 187–202 (1984).
89. I. Wadsö, *Chem. Soc. Rev.* **26**(2), 79–86 (1997).
90. I. Wadsö, *Thermochim. Acta* **294**, 1–11 (1997).
91. G. Buckton and A.E. Beezer, *Int. J. Pharm.* **72**, 181–191 (1991).

92. M.J. Koenigbauer, *Pharm. Res.* **11**(6), 777–783 (1994).
93. M. Bastòs, S. Hägg, P. Lönnbro, and I. Wadsö, *J. Biochem. Biophys. Methods* **23**, 255–258 (1991).
94. P. Bäckman et al., *J. Biochem. Biophys. Methods* **28**, 85–100 (1994).
95. L.E. Briggner and I. Wadsö, *J. Biochem. Biophys. Methods* **22**, 101–118 (1991).
96. W. Hemminger and G. Höhne, *Calorimetry: Fundamentals and Practice*, Verlag Chemie, Weinheim, 1984.
97. E.L. Charsley and S.B. Warrington, *Thermal Analysis: Techniques and Applications*, Royal Chemistry Society, London, 1992.
98. K.N. Marsh and P.A.G. O'Hare, *Solution Calorimetry, Experimental Thermodynamics*, vol. 4, Blackwell, Oxford, 1994.
99. L.D. Hansen and D.J. Eatough, *Thermochim. Acta* **70**, 257–268 (1983).
100. K. Grime, *Analytical Solution Calorimetry*, Wiley, New York, 1985.
101. M.J. Pikal, A.L. Lukes, J.E. Lang, and K. Gaines, *J. Pharm. Sci.* **67**, 767–773 (1978).
102. D.J.W. Grant and P. York, *Int. J. Pharm.* **28**, 103–112 (1986).
103. D. Gao and J.H. Rytting, *Int. J. Pharm.* **151**, 183–192 (1997).
104. S. Lindenbaum and S.E. McGraw, *Pharm. Manuf.* **2**, 26–30 (1985).
105. J.K. Guillory and D.M. Erb, *Pharm. Manuf.* **9**, 29–33 (1985).
106. R.M. Izatt, E.H. Redd, and J.J. Christensen, *Thermochim. Acta* **64**, 355–372 (1983).
107. P.R. Connelly, R. Varadarajan, J.M. Sturtevant, and F.M. Richards, *Biochemistry* **29**, 6108–6114 (1990).
108. W. Tong, J.L. Lach, T. Chin, and J.K. Guillory, *Pharm. Res.* **8**(7), 951–957 (1991).
109. J.J. Christensen, J. Ruckman, D.J. Eatough, and R.M. Izatt, *Thermochim. Acta* **3**, 203–218 (1972).
110. D.J. Eatough, J.J. Christensen, and R.M. Izatt, *Thermochim. Acta* **3**, 219–232 (1972).
111. D.J. Eatough, R.M. Izatt, and J.J. Christensen, *Thermochim. Acta* **3**, 233–246 (1972).

CHARACTERIZATION OF DELIVERY SYSTEMS, GEL PERMEATION CHROMATOGRAPHY

CAMILLA A. SANTOS
Brown University
Providence, Rhode Island

KEY WORDS

Cross-linked gels
Molecular weight
Polymer characterization
Polystyrenedivinylbenzene
Size exclusion chromatography

Gel permeation chromatography (GPC) is a form of size-exclusion chromatography used to separate molecules according to their size in solution and is a key element of polymer characterization in today's environment. It is used to quickly determine the molecular weight distribution of polymers, yielding information on the macromolecular nature of the polymer being studied. GPC has been in use since the late 1950s, when water-soluble polymers were separated according to size using cross-linked dextran gels, and commercial use of GPC began in the 1960s when rigid gels were developed for use with organic solvents (1). In GPC, molecular weight averages are determined by effecting size separation of a low concentration of polymer in organic solvent as the dilute polymer solution passes through a column packed with microporous gel. Size exclusion can also be effected in an aqueous mobile phase, and this is typically termed gel filtration chromatography. This article will concern itself with GPC, the size-exclusion chromatography utilizing an organic mobile phase.

The GPC system is composed of a solvent delivery system capable of delivering a constant volume of solvent, an injection port for injection of a small amount of a dilute polymer solution without disturbance of solvent flow, a column or series of columns packed with microporous gel, a detector, and a data system to automatically process data. The columns of a GPC system are typically packed with cross-linked polystyrenedivinylbenzene gel of a particle size range of 5–10 μm and a pore size range of 0.5–10^5 nm (2). Originally, column length was on the order of 4 feet, and the polystyrenedivinylbenzene gel particle size was approximately 40 μm or larger (1). Owing to improvements in the gels being used, column length is now typically 30–60 cm with a diameter of 7.5 cm (2). Columns can also be packed with other cross-linked polymers or porous glasses and silica, which are typically used in aqueous phase systems (1,3). Within each particle are numerous pores. As the dilute polymer solution passes through the column, it is separated by size because the low-molecular-weight chains of the polymer are able to migrate into and out of the gel particle pores, and the larger chains are forced to flow relatively unhindered through the interstices in the column, their larger size prohibiting diffusion into the pores of the gel particles. Thus, large molecular weights of a dilute polymer solution elute first, and smaller-molecular-weight chains elute much later. A mixed range of pore sizes in the packed column gel allows effective separation of a molecular weight distribution of $<100 - 4 \times 10^7$ (2).

The system should have the capability of operating at both ambient and high temperatures and must contain a device that can maintain a constant temperature along the length of the columns. The capability of operating at elevated temperatures is a function primarily of the packed gel. Effective size-exclusion separation can be achieved in shorter times at elevated temperatures as diffusion rates increase with increasing temperatures. Current GPC systems achieve separations on the order of minutes, making this characterization technique very popular. Typically, the

Next Page

organic solvents used in GPC system were nonpolar, but advances in the stability of the cross-linked gels allow some systems to now operate with more polar solvents.

There are many types of detectors used in GPC systems. The detector must be capable of continuous monitoring of solute elution and can be either a bulk property or solute property detector. Bulk property detectors measure a change in the bulk property of the eluting solvent, such as the refractive index of the solvent, which will change with the presence of a solute. Solute property detectors detect changes in the physical property of the solvent (occurring when solute is present), such as the ultraviolet absorption of the solvent. The limiting factor in any detector is the signal-to-noise ratio, and this must be considered when detecting minor concentrations of sample (this is not usually a problem in GPC as adequate sample mass is normally available) (3). Examples of common detectors are the refractive index detector, the ultraviolet detector, the viscometric detector, and the low-angle light-scattering detector.

The detector monitors the concentration of the eluting polymer. The molecular weight distribution is calculated by measuring the elution volume or peak retention volume, V_R. This is a function of the ability of the polymer in solution to diffuse into the pores of the gel. The retention volume is the volume of solution eluted as measured from the beginning of the injection into the column to the peak of the fraction of the particular molecular weight eluted as determined by the chromatogram. High-molecular-weight solutes will elute at a low V_R, and low-molecular-weight solutes will elute at a high V_R. V_R is related to the interstitial volume, V_O, the internal pore volume, V_i, and the equivalent liquid volume of the gel, V_S, by the equation

$$V_R = V_O + kV_i + k_{LC}V_S$$

where k is the coefficient of distribution, indicating the ease of the polymer solution to move into the pores. If $k = 0$, then the polymer cannot enter the pores of the gel at all, and if $k = 1$, then the polymer can freely enter the pores. Typically, k_{LC}, which is the ratio of the volume of solute in the stationary phase (within the gel) to the volume in the mobile phase, is negligible and the equation reduces to

$$V_R = V_O + kV_i$$

V_O and V_i are constant for a given column. Thus, V_R is dependent on solute molecular weight and as such, a calibration curve can be generated using solutes of known monodisperse molecular weights. The molecular weight is related to the elution time and is plotted as a log (base 10) function against elution time (otherwise known as retention volume). This plot is typically linear over the range of molecular weights of the standards (1–3). From this calibration plot, the molecular weight of an unknown sample can be calculated in terms of weight average molecular weight (M_w), number average molecular weight (M_n), and the z-average molecular weight (M_z).

The limitation of the GPC system is the need for calibration with known molecular weight standards. Ideally, the standards should contain numerous monodisperse polymer chains of known molecular weight of the same polymer being tested. However, this is not usually the case. Polystyrene is the typical monodisperse polymer used to calibrate the GPC system, and there is some element of error introduced when other polymers are compared to the polystyrene standards. The system separates polymer chains by their effective size and does not account for branching of the polymer or for polymer–solvent interactions, both of which may affect the polymer size in solution. A detailed explanation of the calibration involved in GPC systems is beyond the scope of this article, and the reader is kindly referred to the texts listed in the reference section.

A survey of the current literature finds GPC used in many situations. For instance, the manner in which a polymer degrades can be described by GPC by evaluating samples throughout the degradation timeframe (4). Another use is to determine if a loaded agent (either a pharmaceutical drug or an excipient intended to enhance controlled release of a substance) has any effect of the degradation of a polymer, either increasing the speed of degradation or retarding it (5). Stability of a polymer in various storage conditions can be determined using GPC, yielding crucial information concerning shelf life. These are just a few uses of gel permeation chromatography, a method which has grown over the past 40 years to become one of the main tools utilized in polymer characterization.

BIBLIOGRAPHY

1. A.R. Cooper, in L.S. Bark and N.S. Allen eds., *Analysis of Polymer Systems*, Applied Science Publishers, London, 1982, pp. 243–301.
2. D. Campbell and J.R. White, *Polymer Characterization: Physical Techniques*, Chapman & Hall, London, 1989.
3. J. Sherma et al., *CRC Handbook of Chromatography*, vol. II, CRC Press, Boca Raton, Fla., 1994.
4. C.A. Santos et al., *J. Controlled Release*, in press.
5. W.L. Webber, F. Lago, C. Thanos, and E. Mathiowitz, *J. Biomed. Mater. Res.* **41**, 18–29 (1998).

CHARACTERIZATION OF DELIVERY SYSTEMS, MAGNETIC RESONANCE TECHNIQUES

PAUL A. BURKE
Amgen, Inc.
Thousand Oaks, California

KEY WORDS

Biodegradable polymers
Drug delivery
EPR
Hydrogels
Magnetic resonance

Previous Page

organic solvents used in GPC system were nonpolar, but advances in the stability of the cross-linked gels allow some systems to now operate with more polar solvents.

There are many types of detectors used in GPC systems. The detector must be capable of continuous monitoring of solute elution and can be either a bulk property or solute property detector. Bulk property detectors measure a change in the bulk property of the eluting solvent, such as the refractive index of the solvent, which will change with the presence of a solute. Solute property detectors detect changes in the physical property of the solvent (occurring when solute is present), such as the ultraviolet absorption of the solvent. The limiting factor in any detector is the signal-to-noise ratio, and this must be considered when detecting minor concentrations of sample (this is not usually a problem in GPC as adequate sample mass is normally available) (3). Examples of common detectors are the refractive index detector, the ultraviolet detector, the viscometric detector, and the low-angle light-scattering detector.

The detector monitors the concentration of the eluting polymer. The molecular weight distribution is calculated by measuring the elution volume or peak retention volume, V_R. This is a function of the ability of the polymer in solution to diffuse into the pores of the gel. The retention volume is the volume of solution eluted as measured from the beginning of the injection into the column to the peak of the fraction of the particular molecular weight eluted as determined by the chromatogram. High-molecular-weight solutes will elute at a low V_R, and low-molecular-weight solutes will elute at a high V_R. V_R is related to the interstitial volume, V_O, the internal pore volume, V_i, and the equivalent liquid volume of the gel, V_S, by the equation

$$V_R = V_O + kV_i + k_{LC}V_S$$

where k is the coefficient of distribution, indicating the ease of the polymer solution to move into the pores. If $k = 0$, then the polymer cannot enter the pores of the gel at all, and if $k = 1$, then the polymer can freely enter the pores. Typically, k_{LC}, which is the ratio of the volume of solute in the stationary phase (within the gel) to the volume in the mobile phase, is negligible and the equation reduces to

$$V_R = V_O + kV_i$$

V_O and V_i are constant for a given column. Thus, V_R is dependent on solute molecular weight and as such, a calibration curve can be generated using solutes of known monodisperse molecular weights. The molecular weight is related to the elution time and is plotted as a log (base 10) function against elution time (otherwise known as retention volume). This plot is typically linear over the range of molecular weights of the standards (1–3). From this calibration plot, the molecular weight of an unknown sample can be calculated in terms of weight average molecular weight (M_w), number average molecular weight (M_n), and the z-average molecular weight (M_z).

The limitation of the GPC system is the need for calibration with known molecular weight standards. Ideally, the standards should contain numerous monodisperse polymer chains of known molecular weight of the same polymer being tested. However, this is not usually the case. Polystyrene is the typical monodisperse polymer used to calibrate the GPC system, and there is some element of error introduced when other polymers are compared to the polystyrene standards. The system separates polymer chains by their effective size and does not account for branching of the polymer or for polymer–solvent interactions, both of which may affect the polymer size in solution. A detailed explanation of the calibration involved in GPC systems is beyond the scope of this article, and the reader is kindly referred to the texts listed in the reference section.

A survey of the current literature finds GPC used in many situations. For instance, the manner in which a polymer degrades can be described by GPC by evaluating samples throughout the degradation timeframe (4). Another use is to determine if a loaded agent (either a pharmaceutical drug or an excipient intended to enhance controlled release of a substance) has any effect of the degradation of a polymer, either increasing the speed of degradation or retarding it (5). Stability of a polymer in various storage conditions can be determined using GPC, yielding crucial information concerning shelf life. These are just a few uses of gel permeation chromatography, a method which has grown over the past 40 years to become one of the main tools utilized in polymer characterization.

BIBLIOGRAPHY

1. A.R. Cooper, in L.S. Bark and N.S. Allen eds., *Analysis of Polymer Systems*, Applied Science Publishers, London, 1982, pp. 243–301.
2. D. Campbell and J.R. White, *Polymer Characterization: Physical Techniques*, Chapman & Hall, London, 1989.
3. J. Sherma et al., *CRC Handbook of Chromatography*, vol. II, CRC Press, Boca Raton, Fla., 1994.
4. C.A. Santos et al., *J. Controlled Release*, in press.
5. W.L. Webber, F. Lago, C. Thanos, and E. Mathiowitz, *J. Biomed. Mater. Res.* **41**, 18–29 (1998).

CHARACTERIZATION OF DELIVERY SYSTEMS, MAGNETIC RESONANCE TECHNIQUES

PAUL A. BURKE
Amgen, Inc.
Thousand Oaks, California

KEY WORDS

Biodegradable polymers
Drug delivery
EPR
Hydrogels
Magnetic resonance

Microspheres
MRI
NMR

OUTLINE

Introduction
Principles and Spectroscopic Methods
  Solution NMR
  Solid-State NMR
  Electron Paramagnetic Resonance
  Magnetic Resonance Imaging
Applications
  Distribution of Water and of Active Agent
  Internal Environment During Polymer Erosion
  Rates of Drug Release and Polymer Erosion in Vivo
  Diffusion, Gelation, and Pore Size Distribution
  Interfaces and Colloidal Suspensions
Summary
Bibliography

INTRODUCTION

Controlled release drug delivery systems are often characterized by heterogeneity of phase, consisting of a matrix and a drug that is in either solid or solution form or in transition between these states. This attribute complicates characterization of interior structure and microenvironment. Hydrogels, various implants, microspheres, and controlled release tablets represent quintessential controlled release technologies, and yet the internal features of many such systems are poorly understood. Invasive techniques, or indirect measures (such as the observed rate of drug release or the condition of drug following release), have substituted for direct observation. The unevenness of commercial success in the field has heightened the need to differentiate what works from what does not; as a result the use of sophisticated, noninvasive methods such as those based on magnetic resonance has grown. In some cases depot systems can be characterized in vivo, in real time. Detailed information regarding the internal microenvironments of a variety of matrix systems has resulted.

PRINCIPLES AND SPECTROSCOPIC METHODS

Magnetic resonance refers to the absorption of electromagnetic radiation of a frequency corresponding to the energy difference between a multiplicity of states created by the application of a strong magnetic field. Experimental methods exploiting this phenomenon include solution and solid-state NMR spectroscopy, electron paramagnetic resonance spectroscopy (EPR), and magnetic resonance imaging (MRI). The semiclassical vector model of nuclear magnetization is a good starting point for understanding time domain (as opposed to frequency domain) methods, which predominate. Fortunately some excellent introductory texts make this subject accessible to anyone with a background in classical mechanics and elementary electromagnetic theory (1–3). Although the present discussion assumes familiarity with these concepts, the uninitiated will likely appreciate the potential of magnetic resonance methods. Specific techniques relevant to drug delivery system characterization are highlighted; most of these are practicable with commercial instrumentation. For a comprehensive overview of NMR methods (including imaging), the reader is referred to the Encyclopedia of NMR (4).

Solution NMR

The most rudimentary solution NMR methods result in a one-dimensional spectrum of spin 1/2 nuclei such as ^{1}H, ^{13}C, ^{31}P, ^{15}N, or ^{19}F (1). Solution NMR can be used to determine pH by means of the Henderson-Hasselbalch equation. Given an acid with known pK_a, a chemical shift that is sensitive to protonation state can be used to determine directly the ratio of protonated and unprotonated species in a sample. This concept is illustrated in Figure 1 (5). The same principle applies in EPR, where hyperfine splittings are sensitive to protonation state. This experiment relies on the sensitivity of magnetic resonance methods to processes that are fast or slow relative to the angular frequency difference ($\Delta\omega$) between the species involved (1). Loosely speaking, $\Delta\omega$ is referred to as the time scale of the experiment and is on the order of milliseconds for most solution NMR experiments. Proton transfer, being comparatively rapid, results in a time-averaged chemical shift, weighted according to the relative proportion of protonated and unprotonated species. Under conditions of slow ex-

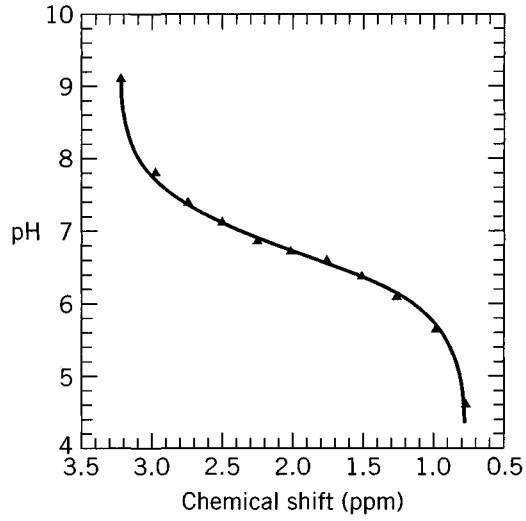


Figure 1. Solution NMR titration curve for inorganic phosphate solutions prepared with various ratios of monobasic and dibasic forms (155 mM ionic strength). Symbols depict the correspondence between experimentally determined chemical shifts and the measured pH. Also shown is the theoretical standard curve calculated using the following parameters: $pK_a = 6.75$; $\delta(HPO_4^{2-}) = 3.23$ ppm; $\delta(H_2PO_4^{-}) = 0.75$ ppm.

change, individual peaks are observed for each species; peak intensities are proportional to the population of each state. Examples of slow exchange include that between the cytosol and surrounding medium of living cells, and exchange within solids (6,7).

Diffusion in solutions can be measured using pulse field gradient (PFG) NMR, a variant of a spin-echo pulse sequence used to measure spin-spin relaxation times (T_2) (8). A transient magnetic field gradient pulse is applied to mark the positions of the nuclei of interest. Subsequently, a time interval is introduced during which diffusion is allowed to occur. The spins are refocused by reapplication of the original gradient pulse, and the attenuation in the echo amplitude related mathematically to the diffusion constant. PFG NMR is appropriate to the measurement of diffusion processes that are fast relative to T_2, such as water diffusion within hydrogels (9,10).

Solution NMR methods are of limited applicability to systems of heterogeneous phase. If the analyte lacks isotropic molecular motion, broad resonances will result. In the worst case the signal is not detectable. This is due to incomplete averaging of chemical shift anisotropy, dipole-dipole interactions, and (for nuclei of spin >1/2) quadrupolar interactions (7,11). Phase heterogeneity in a sample can be problematic even if the analyte is itself fully dissolved. In w/o emulsions where the magnetic susceptibilities of the dispersed and continuous phases differ, local magnetic field gradients result, giving broad lines and altering relaxation rates (12). Magnetic interactions between water and polymer protons in a hydrogel result in cross-relaxation, invalidating the conventional mathematical formalism used to interpret echo amplitude attenuation in PFG NMR (10).

Solid-State NMR

In high-resolution, solid-state NMR, experimental techniques, as opposed to isotropic molecular motion, average spin interactions. Isotropic chemical shifts of dilute spin 1/2 nuclei are recovered by magic angle spinning (MAS), where the sample rotates about an axis which is at a fixed angle (the magic angle) with respect to the external magnetic field. Dipolar coupling to protons is removed by spin locking. When applied to ^{13}C, which has a natural abundance of 1%, labeling is often unnecessary. For other nuclei, incorporation of spin 1/2 isotopes by synthetic means is an option; this can become a costly and time-consuming affair. An alternative is to use commercially available compounds as reporter groups (for example, ^{13}C or ^{15}N labeled amino acids (13)). Another limitation of solid-state NMR methods is poor sensitivity. Even with isotopic enrichment acquisitions can require hours or even days.

Rotational-echo double resonance (REDOR) is one of several solid-state NMR techniques used to determine internuclear distances (up to 5 Å) of heteroatoms, for example, ^{13}C and ^{15}N (14). The measurement is based on the distance-dependent heteronuclear dipolar coupling constant. Precise mathematical analysis requires that a given labeled site interacts with no more than one heteroatom; otherwise, an average dipolar coupling is obtained (13). Related techniques enable determination of homonuclear interatomic distances.

Solid-state deuterium NMR can elucidate molecular motions in solids using a quadrupole echo pulse sequence (15). The spectrum is dominated by the quadrupole interaction of the spin 1 nucleus and is sensitive to motions over a wide time scale range, from milliseconds to microseconds. Pharmaceutical applications of solid-state NMR techniques have been reviewed recently (16).

Electron Paramagnetic Resonance

EPR differs from NMR in that the spins involved are those of unpaired electrons (17). EPR can detect free radicals in, for example, gamma-irradiated samples (18,19). Most analytes, however, lack unpaired electrons, and exogenous reporter groups such as paramagnetic metal ions or free radicals are required. Stable nitroxide spin labels can be introduced through chemical modification (20). EPR spectra, typically presented as the first derivative of the absorption profile, are sensitive to molecular motion on the microsecond time scale; the rate of label motion is determined by analysis of the line shape. This time frame is extended to the millisecond range using saturation transfer EPR (ST-EPR) (21). Other details, such as the reporter group protonation state or the polarity of its microenvironment, can be elucidated from the hyperfine splittings. The application of EPR to pharmaceutics has been reviewed by Mader et al. (22).

Magnetic Resonance Imaging

In MRI, an image is constructed from the spatial distribution, and different relaxation times, of spins within a sample (23). As a medical diagnostic, MRI detects water proton spins, exploiting the variable water contents of body tissues and fluids. Paramagnet spins likewise can be used to construct images. One limitation of MRI as it relates to drug delivery systems is resolution. Even with advanced instrumentation the resolution limit is 20–50 μm, adequate for macroscopic observations but insufficient to illuminate microscopic architecture.

APPLICATIONS

Distribution of Water and of Active Agent

Water environments in hydrogel systems have been characterized with magnetic resonance techniques. Roorda et al. measured the relaxation times of ^{17}O labeled water in poly(hydroxyethyl methacrylate) (PHEMA) hydrogels (24). Advantages of ^{17}O include negligible natural abundance signals and absence of exchange with matrix oxygens. The rotational mobility of hydrogel water was reduced compared to pure water, and the degree of mobility restriction correlated with the hydrogel polymer content. Relaxation curves were fit with a single exponential decay, showing that the hydrogel contained a single water population on the millisecond time scale. This result contrasted with that obtained using invasive techniques.

Pitt et al. used nitroxide spin labels and spin probes to characterize the molecular environments of hydrogels and hydrophobic polyester matrices (25–27). The existence of distinct bulk water and lipophilic polymer phases within

hydrogels was tested. A spin-labeled amino ligand—the lipophilicity of which depends on protonation state—was bound to the gel surface and the ligand molecular motions examined. Single-component EPR spectra were observed over a wide pH range, indicating a single, homogeneous water environment within the gel. Similar results were obtained in an investigation of PHEMA using spin-labeled solutes. In contrast, composite spectra were observed in several polyester-containing polymer-polymer blends, indicating phase separation.

Schmitt et al. used solid-state ^{2}H NMR to characterize the water environments in pellets of poly(lactide-*co*-glycolide) (PLGA) copolymers as a function of lactide content, in order to provide a mechanistic explanation for the known decrease of hydrolysis rate with increasing lactide content (28). Using a quadrupole echo pulse sequence, the authors quantitated bound and free water populations in the hydrated pellets. Although the *total* water content was comparable for all lactide:glycolide ratios studied, the water distribution was not. With increasing lactide content, the fraction of bound water decreased. It was thus concluded that bound, but not free, water is reactive in the hydrolysis reaction.

Greenley et al. used REDOR to characterize the distribution of ^{13}C- and ^{15}N-labeled amino acids imbibed in cross-linked polyacrylic acid matrices (13). Since the resulting sample contains a distribution of carbon-nitrogen internuclear distances, an ensemble average dipolar interaction was observed. A significant dipolar interaction was present even at very low concentrations of imbibed compounds, indicating cluster formation. The amino acid clusters appeared to increase in size with increasing drug concentration in the matrix.

Goldenberg et al. used chemical shift analysis to characterize active agent distribution within micellar delivery systems (29). The chemical shift of a given nucleus is largely determined by the shielding influences of its substituent groups and atoms, but also can vary with the physical properties of the medium. Based on chemical shift analysis of both surfactant and active agents, some of the extremely water-insoluble agents studied were found to form clusters within the nonionic micelles, as opposed to being dispersed within either the hydrocarbon core or the surrounding poly(oxyethylene) mantle.

Tobyn et al. used EPR to study interactions between a polysaccharide matrix and incorporated nitroxide spin labels in an oral dosage form (30). Wet granulation, in contrast to dry mixing, was found to be effective for dispersing the crystalline spin labels.

Internal Environment During Polymer Erosion

The internal environment of PLGA microspheres was characterized using solution ^{31}P NMR (5). Microspheres were suspended in sheep serum (pH ~ 8), which contains endogenous inorganic phosphate at a concentration of a few millimolar. In the settled microsphere suspension two phosphate peaks were obtained, demonstrating the presence of a solution environment within the microspheres, with slow chemical exchange between internal phosphate and that in the surrounding medium, as well as a difference in pH between the two phosphate pools (Fig. 2). The ^{31}P spectrum was monitored through day 45. The calculated internal pH changed modestly during this time frame, stabilizing at pH 6.4 (Fig. 3). The slight acidity of the interior is presumably due to the carboxylic acid degradation products of the polyester. That a more acidic value was not obtained suggests that the exterior medium effectively neutralized at least some of the acid generated on polymer hydrolysis; this scenario is consistent with the high porosity (by scanning electron microscopy) of the microspheres used in this study.

EPR has been used to measure pH in both w/o emulsions and polymer matrices, using spin probes sensitive to a wide pH range. Kroll et al. (31) monitored aqueous phase pH as a function of time and of temperature in w/o oint-

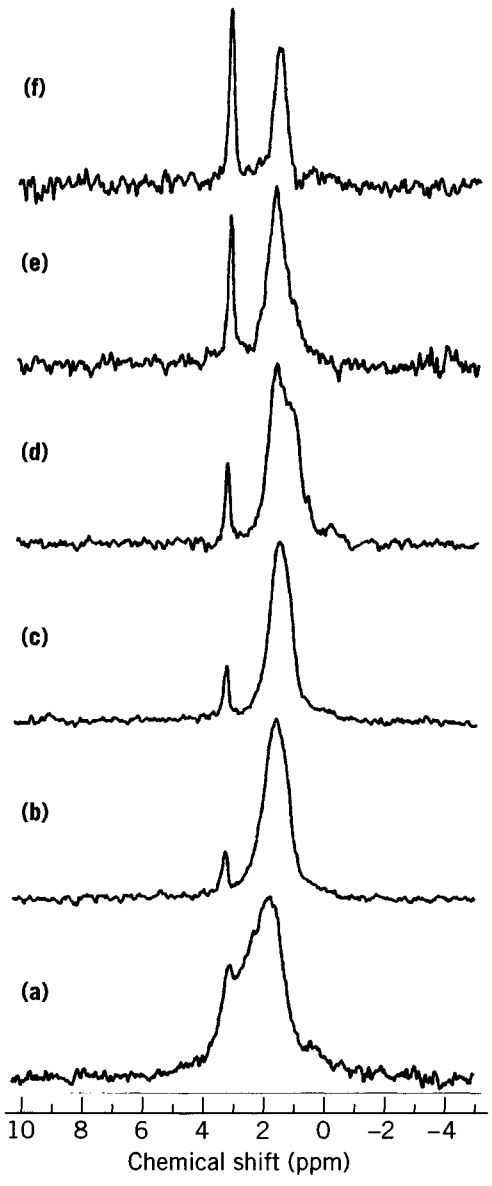


Figure 2. ^{31}P NMR spectra of PLGA microspheres in sheep serum at (**a**) 3 hours; (**b**) 2 days; (**c**) 6 days; (**d**) 14 days; (**e**) 30 days; (**f**) 45 days.

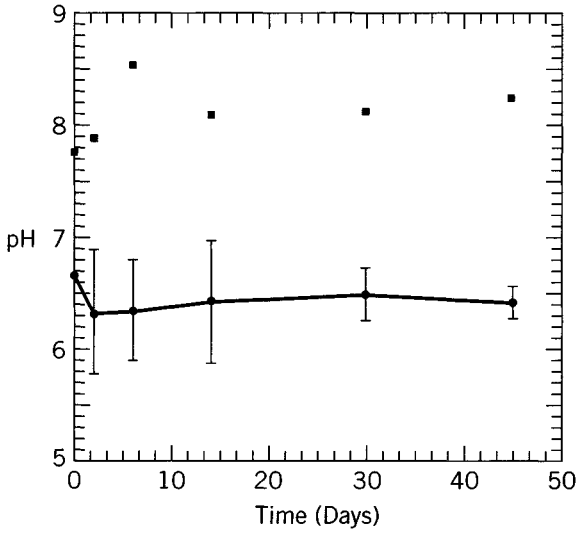


Figure 3. PLGA microsphere interior pH as a function of time, determined from the spectra in Figure 2. ●, pH of microsphere interior; ■, pH of suspension medium.

ments containing acetylsalicylic acid and benzocaine. Low-frequency (≤1 GHz) EPR has been used for in vivo characterization of the pH inside PLGA implants (32). Low frequency enables detection to depths of 1 cm or more using surface coils. Six nitroxide spin probes, with pK_a values ranging from 1.0 to 7.2, were incorporated into monolithic PLGA matrices that were implanted subcutaneously in mice. While a dearth of endogenous paramagnets simplifies interpretation, precision in the pH determination was limited by an inability to resolve spectral components arising from spin probes of varying mobility (and possibly in regions of differing pH). It was concluded that the pH dropped from 4 to 2 over a three-week period.

The pH inside polyanhydride discs was monitored in vitro, with spatial resolution of roughly 20 μm, using two-dimensional (spectral-spatial) EPR imaging (33). The pH was monitored in a cross section of the 2-mm-thick wafer over a 7-day period. The outer disc layers exhibited an acidic environment (pH 4.7) after 2 days. The solvent penetration front proceeded with zero-order kinetics at a rate of 0.3 mm day^{-1}, with outer layers gradually reaching the pH of the outer medium (buffered with phosphate to pH 7.4), and the interior showing pH > 5.0. After 7 days, the pH gradient disappeared, and the pH throughout the disc matched that of the surrounding medium. This constituted the first direct observation of pH gradients within biodegradable polymers.

Rates of Drug Release and Polymer Erosion in Vivo

Low-frequency EPR was coupled with MRI in studies of drug release and matrix erosion in vitro and in vivo (34,35). PLGA and polyanhydride implants were studied. In order to obtain spatial information, sandwich implants were fabricated with outer layers containing ^{14}N-nitroxide and an inner layer containing ^{15}N-nitroxide (34). (The splitting observed is determined by the nitrogen nuclear spin, and therefore different for the layers.) The rate of nitroxide release was assessed by following the ratio of the two nitroxides remaining at the site. A zero-order decrease in the relative ^{14}N component (corresponding to the outer tablet layers) was observed. In vivo MRI studies indicated a surface erosion front mechanism, both in vitro and in vivo. Differences between in vitro and in vivo rates of both spin probe release and polymer erosion were noted, however (34,35). Surprisingly, a decrease in the spin probe mobility during the course of polyanhydride erosion was observed. This was assumed to derive from coprecipitation of soluble monomer (liberated during polymer erosion) with the encapsulated probe. Rates of bioerosion of polylactide bone screws in humans have been followed by MRI (36,37).

Diffusion, Gelation, and Pore Size Distribution

Magnetic resonance imaging has been used to characterize diffusion, determine pore size distribution, and monitor gelation in hydrogels. Imaging imparts spatial resolution (in one or more dimensions) to diffusion analysis, and can be useful in the study of diffusion times longer than those accessible by PFG NMR. Null point MRI has been used to map Fickian diffusion of paramagnetic ions and spin probes through hydrogels and other heterogeneous media, via the effect of the paramagnet on water proton T_1s (38,39). The technique has been extended to two dimensions using fast inversion recovery (40), and has been combined with magnetization transfer in the characterization of alginate gelation in the absence of a paramagnetic tracer (41). Pore size distribution within calcium alginate gels has been determined from water proton T_2 maps, exploiting an inverse relationship between T_2 and alginate concentration (42,43). The temperature dependence of the diffusion constant of the tracer compound trifluoroacetamide was determined in a thermoresponsive poly(*N*-isopropylacrylamide) hydrogel using one-dimensional ^{19}F MRI (44). Fyfe et al. investigated the hydration of hydroxymethylcellulose tablets, following concentrations and mobilities of both water and the polymer as functions of time and distance through a combination of techniques (45). Susceptibility to error introduced by entrapped gas bubbles within the tablet matrix was reported (46). NMR imaging was recently applied to compression-coated tablets in order to characterize the drug release mechanism (47).

Magnetic resonance methods have been used to characterize intracranial and transdermal drug transport. The delivery of paramagnetic contrast markers to the rabbit parenchyma by an osmotic pump was followed by MRI, and the results used to refine a theoretical model of local drug delivery to the brain. The model was used to predict distribution profiles of drugs delivered by implanted polymeric systems (48). Kinsey et al. used MRI to characterize water mobility in skin samples in vitro, with the aim of applying the results to transdermal drug delivery via passive diffusion or by electroporation (49). Under the highest resolution conditions studied, major anatomical structures such as sebaceous glands and hair follicles were well resolved.

Interfaces and Colloidal Suspensions

Emulsions can exhibit sustained release effects and play a role in some microencapsulation processes (50). Emulsifi-

cation of surface active drugs such as proteins can cause denaturation. Nevertheless, little is known about the physical environment under these conditions. For example, the ultimate fate of the surface denatured layer is not known. Stabilization of proteins toward double emulsion methods has been empirical (51). Recently, emulsions have been characterized by solution NMR methods. Lonnqvist et al. characterized double (w/o/w) emulsions by PFG NMR (12), which was used to determine droplet size distributions, and to distinguish oil-only from drug-containing droplets. Inner and outer water populations were distinguished and the average lifetime of an inner aqueous droplet determined. Ter Beek et al. used ^{13}C and ^{31}P solution NMR to characterize β-casein at an oil-water interface (52). They relied on the dependence of ^{13}C chemical shift on protein secondary structure to conclude that the mobile portions of the surface-adsorbed protein derived from random coil, as opposed to α-helical, portions of the protein. ^{31}P signals from β-casein's five phosphoserine residues served as probes of motion in the molecule's highly charged N-terminal region, comparing surface-adsorbed versus solution (primarily micellar) β-casein. Finally, solution ^{31}P NMR has been used to illuminate the structure of amphotericin B containing liposomes (53), as well as the fusogenic properties of cationic liposome-DNA complexes (54). The restricted molecular motions at interfaces make these systems amenable to solid-state NMR methods, which have been applied to lipid bilayers (15,55) and to protein-lipid interactions in emulsions (56).

SUMMARY

Controlled release delivery systems are highly complex dosage forms. The past few years have witnessed the increased use of magnetic resonance techniques in the characterization of these systems. Although the body of literature to date is limited, early applications have demonstrated the power of magnetic resonance to address critical questions in the field, and to challenge dogmas based on invasive or indirect measurements. Despite the requirements of specialized instrumentation and training, such noninvasive analytical techniques will likely prove indispensable in the development of well-characterized, high quality drug delivery systems suitable for commercialization.

BIBLIOGRAPHY

1. F.A. Bovey, *Nuclear Magnetic Resonance Spectroscopy*, 2nd ed., Academic Press, San Diego, Calif., 1988.
2. A.E. Derome, *Modern NMR Techniques for Chemistry Research*, Pergamon, Oxford, 1987.
3. T.C. Farrar and E.D. Becker, *Pulse and Fourier Transform NMR. Introduction to Theory and Methods*, Academic Press, New York, 1971.
4. D.M. Grant and R.K. Harris, *Encyclopedia of NMR*, Wiley, New York, 1996.
5. P.A. Burke, *Proc. Int. Symp. Control Relat. Bioact. Mater.* **23**, 133–134 (1996).
6. G. Navon, S. Ogawa, R.G. Shulman, and T. Yamane, *Proc. Natl. Acad. Sci. U.S.A.* **74**, 888–891 (1977).
7. C.A. Fyfe, *Solid State NMR for Chemists*, CFC Press, Guelph, Ontario, 1983.
8. P. Stilbs, *Prog. NMR Spectrosc.* **19**, 1–45 (1987).
9. W.R. Korsmeyer, E. von Meerwall, and N.A. Peppas, *J. Polym. Sci. Polym. Phys. Ed.* **24**, 409 (1986).
10. L.J. Peschier et al., *Biomaterials* **14**, 945–952 (1993).
11. C.S. Yannoni, *Acc. Chem. Res.* **15**, 201–208 (1982).
12. I. Lonnqvist, B. Hakansson, B. Balinov, and O. Soderman, *J. Colloid Interface Sci.* **192**, 66–73 (1997).
13. R. Greenley, H.S. Zia, J. Garbow, and R.L. Rodgers, *ACS Symp. Ser.* **469**, 213–236 (1991).
14. J.M. Griffiths and R.G. Griffin, *Anal. Chim. Acta* **283**, 1081–1101 (1993).
15. R.G. Griffin et al., in G.J. Long and F. Grandjean, eds., *The Time Domain in Surface and Structural Dynamics*, Kluwer Academic Publishers, Amsterdam, 1988, pp. 81–105.
16. D.E. Bugay, *Pharm. Res.* **10**, 317–327 (1993).
17. J.A. Weil, J.R. Bolton, and J.E. Wertz, *Electron Paramagnetic Resonance: Elementary Theory and Practical Applications*, Wiley, New York, 1994.
18. K. Mader, A. Domb, and A. Swartz, *Appl. Radiat. Isot.* **47**, 1169–1674 (1996).
19. L. Martini, J.H. Collett, and D. Attwood, *J. Pharm. Pharmacol.* **49**, 601–605 (1997).
20. L.J. Berliner, *Spin Labeling: Theory and Applications*, Plenum, New York, 1989.
21. J.S. Hyde, *Methods Enzymol.* **49**, 480–511 (1978).
22. K. Mader, H.M. Swartz, R. Stosser, and H.H. Borchert, *Pharmazie* **49**, 97–101 (1994).
23. D.D. Stark, *Magnetic Resonance Imaging*, Mosby, St. Louis, Mo., 1992.
24. W.E. Roorda, J. de Bleyser, H.E. Junginger, and J.C. Leyte, *Biomaterials* **11**, 17–23 (1990).
25. C.G. Pitt, X.C. Song, R. Sik, and C.F. Chignell, *Biomaterials* **12**, 715–721 (1991).
26. C.G. Pitt, J. Wang, C.F. Chignell, and R. Sik, *J. Polym. Sci. Part B: Polym. Phys.* **30**, 1029–1071 (1992).
27. C.G. Pitt et al., *Macromolecules* **26**, 2159–2164 (1993).
28. E.A. Schmitt, D.R. Flanagan, and R.J. Linhardt, *Macromolecules* **27**, 743–748 (1994).
29. M.S. Goldenberg, L.A. Bruno, and E.L. Rennwantz, *J. Colloid Interface Sci.* **158**, 351–363 (1993).
30. M.J. Tobyn, J. Maher, C.L. Challinor, and J.N. Staniforth, (1996) *J. Controlled Release* **40**, 147–155 (1996).
31. C. Kroll, K. Mader, R. Strober, and H.H. Borchert, *Eur. J. Pharm. Sci.* **3**, 21–26 (1995).
32. K. Mader, B. Gallez, K.J. Liu, and H.M. Swartz, *Biomaterials* **17**, 457–461 (1996).
33. K. Mader et al., *Polymer* **38**, 4785–4794 (1997).
34. K. Mader et al., *J. Pharm. Sci.* **86**, 126–134 (1997).
35. K. Mader et al., *Pharm. Res.* **14**, 820–826 (1997).
36. H. Pihlajamaki, J. Kinnunen, and O. Bostman, *Biomaterials* **18**, 1311–1315 (1997).
37. H.K. Pihlajamaki, P.T. Karjalainen, H.J. Aronen, and O.M. Bostman, *J. Orthop. Trauma* **11**, 559–564 (1997).
38. A.E. Fischer and L.D. Hall, *Magn. Reson. Imaging* **14**, 779–783 (1996).
39. B.J. Balcom, A.E. Fischer, T.A. Carpenter, and L.D. Hall, *J. Am. Chem. Soc.* **115**, 3300–3305 (1993).

Next Page

40. A.E. Fischer et al., *J. Phys. D* **28**, 384–397 (1995).
41. J.J. Tessier, T.A. Carpenter, and L.D. Hall, *J. Magn. Reson. Ser. A* **113**, 232–234 (1995).
42. K. Potter, T.A. Carpenter, and L.D. Hall, *Carbohyd. Res.* **246**, 43–49 (1993).
43. K. Potter, T.A. Carpenter, and L.D. Hall, *Magn. Reson. Imaging* **12**, 309–311 (1994).
44. R. Dinarvand, B. Wood, and A. D'Emanuele, *Pharm. Res.* **12**, 1376–1379 (1995).
45. C.A. Fyfe and A.I. Blazek, *Macromolecules* **30**, 6230–6237 (1997).
46. C.A. Fyfe and A.I. Blazek, *J. Controlled Release* **52**, 221–225 (1998).
47. B.J. Fahie et al., *J. Controlled Release* **51**, 179–184 (1998).
48. S. Kalyanasundaram, V.D. Calhoun, and K.W. Leong, *Am. J. Physiol. (Regul. Integr. Comp. Physiol.)* **42**, R1810–R1821 (1997).
49. S.T. Kinsey, T.S. Moerland, L. McFadden, and B.R. Locke, *Magn. Reson. Imaging* **15**, 939–947 (1997).
50. S.D. Putney and P.A. Burke, *Nat. Biotechnol.* **16**, 153–157 (1998).
51. J.L. Cleland and A.J.S. Jones, *Pharm. Res.* **13**, 1464–1475 (1996).
52. L.C. Ter Beek et al., *Biophys. J.* **70**, 2396–2402 (1996).
53. A.S. Janoff et al., *Proc. Nat. Acad. Sci. U.S.A.* **85**, 6122–6126 (1988).
54. K.W. Mok and P.R. Cullis, *Biophys. J.* **73**, 2534–2545 (1997).
55. R.G. Griffin, *Methods Enzymol.* **72**, 108–174 (1981).
56. J.A.G. Areas et al., *Magn. Reson. Chem.* **35**, S119–S124 (1997).

CHARACTERIZATION OF DELIVERY SYSTEMS, MICROSCOPY

JULES S. JACOB
Brown University
Providence, Rhode Island

KEY WORDS

Drug delivery
Imaging
LM
Microstructure
SEM
TEM

OUTLINE

Introduction
Optical Microscopy
  Imaging Modes
  Sample Preparation
Transmission Electron Microscopy
  Sample Preparation for TEM
  Localization of Enzymes, Proteins, and DNA
  Negative Staining
  Replica Techniques and Freeze-Fracture/Freeze-Etch
Scanning Electron Microscopy
  Sample Preparation
  Imaging of Drug Delivery Systems
Summary
Bibliography

INTRODUCTION

The characterization of drug delivery systems using optical and electron optical methods provides important information about size, microstructure, surface topography and texture, porosity and physical state, and distribution of drug in the final product. All of these factors contribute to the performance and drug release characteristics of the delivery system and can offer insight into troubleshooting manufacturing problems as well as suggest ways for improving delivery.

The topics to be covered include optical or light microscopy (LM), transmission electron microscopy (TEM), and scanning electron microscopy (SEM). The advantages and disadvantages of each type of microscopy as well as preparation methods for drug delivery systems are discussed.

In practice, as characterization methods for drug delivery systems, LM, TEM, and SEM are used in an integrated approach. Preliminary information from LM is used to screen the sample and set initial processing parameters for electron microscopic examination. TEM is best suited for high-resolution analysis of the matrix of delivery systems, whereas SEM is applicable to surface topography and limited views of the interior (Table 1). However, the information derived from each method is continually checked against observations derived from the other methods to ensure validity of interpretation and to guard against introduction of artifacts inherent to sample preparation.

OPTICAL MICROSCOPY

The light microscope is often used as a screening tool in the characterization of drug delivery systems. The stan-

Table 1. Suitability of Imaging Techniques for Characterization of Drug Delivery Systems

Characterization	LM	TEM	SEM
Size	Yes	Yes	Yes
Size distribution	Yes	Yes	Yes
Macrostructure (0.1–10 mm)	Yes	Yes	Yes
Mesostructure (1–100 microns)	Yes	Yes	Yes
Microstructure (1–1,000 nm)	No	Yes	Yes
Internal morphology	Yes	Yes	Yes
External morphology	No	Replica only	Yes
Surface topography	No	Replica only	No
Porosity	No	Yes	Yes
Internal drug distribution	Yes	Yes	Yes
Surface drug distribution	No	No	Yes

Previous Page

40. A.E. Fischer et al., *J. Phys. D* **28**, 384–397 (1995).
41. J.J. Tessier, T.A. Carpenter, and L.D. Hall, *J. Magn. Reson. Ser. A* **113**, 232–234 (1995).
42. K. Potter, T.A. Carpenter, and L.D. Hall, *Carbohyd. Res.* **246**, 43–49 (1993).
43. K. Potter, T.A. Carpenter, and L.D. Hall, *Magn. Reson. Imaging* **12**, 309–311 (1994).
44. R. Dinarvand, B. Wood, and A. D'Emanuele, *Pharm. Res.* **12**, 1376–1379 (1995).
45. C.A. Fyfe and A.I. Blazek, *Macromolecules* **30**, 6230–6237 (1997).
46. C.A. Fyfe and A.I. Blazek, *J. Controlled Release* **52**, 221–225 (1998).
47. B.J. Fahie et al., *J. Controlled Release* **51**, 179–184 (1998).
48. S. Kalyanasundaram, V.D. Calhoun, and K.W. Leong, *Am. J. Physiol. (Regul. Integr. Comp. Physiol.)* **42**, R1810–R1821 (1997).
49. S.T. Kinsey, T.S. Moerland, L. McFadden, and B.R. Locke, *Magn. Reson. Imaging* **15**, 939–947 (1997).
50. S.D. Putney and P.A. Burke, *Nat. Biotechnol.* **16**, 153–157 (1998).
51. J.L. Cleland and A.J.S. Jones, *Pharm. Res.* **13**, 1464–1475 (1996).
52. L.C. Ter Beek et al., *Biophys. J.* **70**, 2396–2402 (1996).
53. A.S. Janoff et al., *Proc. Nat. Acad. Sci. U.S.A.* **85**, 6122–6126 (1988).
54. K.W. Mok and P.R. Cullis, *Biophys. J.* **73**, 2534–2545 (1997).
55. R.G. Griffin, *Methods Enzymol.* **72**, 108–174 (1981).
56. J.A.G. Areas et al., *Magn. Reson. Chem.* **35**, S119–S124 (1997).

CHARACTERIZATION OF DELIVERY SYSTEMS, MICROSCOPY

JULES S. JACOB
Brown University
Providence, Rhode Island

KEY WORDS

Drug delivery
Imaging
LM
Microstructure
SEM
TEM

OUTLINE

Introduction
Optical Microscopy
  Imaging Modes
  Sample Preparation
Transmission Electron Microscopy
  Sample Preparation for TEM
  Localization of Enzymes, Proteins, and DNA
  Negative Staining
  Replica Techniques and Freeze-Fracture/Freeze-Etch
Scanning Electron Microscopy
  Sample Preparation
  Imaging of Drug Delivery Systems
Summary
Bibliography

INTRODUCTION

The characterization of drug delivery systems using optical and electron optical methods provides important information about size, microstructure, surface topography and texture, porosity and physical state, and distribution of drug in the final product. All of these factors contribute to the performance and drug release characteristics of the delivery system and can offer insight into troubleshooting manufacturing problems as well as suggest ways for improving delivery.

The topics to be covered include optical or light microscopy (LM), transmission electron microscopy (TEM), and scanning electron microscopy (SEM). The advantages and disadvantages of each type of microscopy as well as preparation methods for drug delivery systems are discussed.

In practice, as characterization methods for drug delivery systems, LM, TEM, and SEM are used in an integrated approach. Preliminary information from LM is used to screen the sample and set initial processing parameters for electron microscopic examination. TEM is best suited for high-resolution analysis of the matrix of delivery systems, whereas SEM is applicable to surface topography and limited views of the interior (Table 1). However, the information derived from each method is continually checked against observations derived from the other methods to ensure validity of interpretation and to guard against introduction of artifacts inherent to sample preparation.

OPTICAL MICROSCOPY

The light microscope is often used as a screening tool in the characterization of drug delivery systems. The stan-

Table 1. Suitability of Imaging Techniques for Characterization of Drug Delivery Systems

Characterization	LM	TEM	SEM
Size	Yes	Yes	Yes
Size distribution	Yes	Yes	Yes
Macrostructure (0.1–10 mm)	Yes	Yes	Yes
Mesostructure (1–100 microns)	Yes	Yes	Yes
Microstructure (1–1,000 nm)	No	Yes	Yes
Internal morphology	Yes	Yes	Yes
External morphology	No	Replica only	Yes
Surface topography	No	Replica only	No
Porosity	No	Yes	Yes
Internal drug distribution	Yes	Yes	Yes
Surface drug distribution	No	No	Yes

dard upright light microscope is capable of resolving structures that are 0.2 μm or larger as restricted by the wavelength of light. The components of a light microscope include a light source, condenser lenses to focus light on the specimen, a stage to move the specimen, objective lenses to focus and enlarge the transmitted light image, and eyepiece lenses to provide additional enlargement for viewing (Fig. 1). Most modern research microscopes are "compound" or equipped with multiple objective lenses, ranging from 0.5 to 100 enlargements in power and used mounted on a turret to provide a range of magnifications. At higher magnification, 40X and 63X and 100X, most objective optics are designed to be used with optically corrected immersion oil to reduce image degradation resulting from diffraction. With intermediate, objective, and eyepiece lenses summed together, the range of magnification spans from 3X to 1,500X. The images can be viewed directly, recorded photographically with a camera attachment, or digitally with a video camera attachment. Digital processing and image analysis of captured video microscope images has been widely used to characterize drug delivery systems in terms of size, porosity, and distribution.

Imaging Modes

Bright field imaging, using differences in optical density and color of light transmitted through a sample, is the routine mode for viewing samples with a conventional light microscope. However, small particulates in solution can best be visualized using dark-field optics to increase specimen contrast by reversing background and sample optical densities. Another means of increasing contrast is to use a phase contrast condenser and matched lenses to increase sample edge contrast by introducing a phase shift between transmitted and scattered light passing through the specimen. Hoffman modulation optics can be used to produce nearly three-dimensional images of light microscopic samples, using a special polarizer condenser to change amplitude rather than phase of scattered light transmitted through the sample, and a slit to regulate the level of illumination.

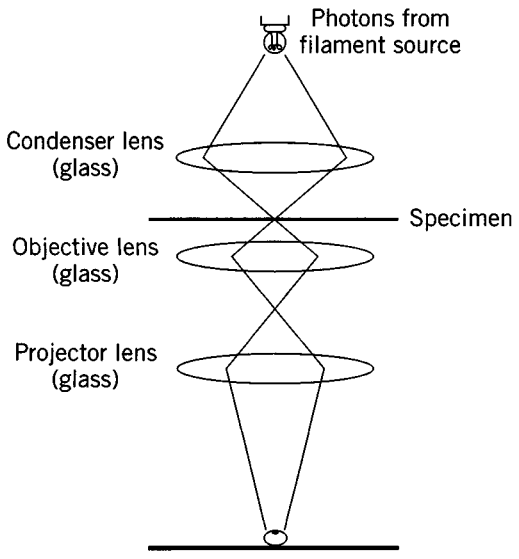


Figure 1. Simplified arrangement of optics in the upright light microscope.

Polarized light microscopy is of great utility for analyzing the crystalline state of polymers comprising most drug delivery devices. When two polarizers are 'crossed' so that planes of transmitted light are perpendicular in orientation to each other, crystalline specimens appears birefringent against a totally dark background. Changes in crystallinity resulting from fabrication can be easily determined by direct observation.

Confocal light microscopes are specialized instruments, used to "optically section" specimens as thick as 1 mm by controlling the plane of focus of objective lenses with computer-regulated, stepper motors. Laser light sources are used to provide more powerful illumination to penetrate thicker samples. The laser can be used to excite fluorescent dyes, such as fluorescein isothiocyanate and rhodamine to name a few, and the emission from the fluorophores can be used to localize "labeled" molecules encapsulated in devices. Using image analysis software, it is possible to 'reconstruct' the optical slices and rebuild the sample in three dimensions, observing contour images of the slices for more information.

Sample Preparation

Samples for light microscopy that can be observed directly include particulates dispersed in solution, small, dry particulates including microspheres, emulsions, fluids, thin films (either pressed, melted, or solvent-cast). Specimens thicker than 40–50 μm are normally sectioned to produce thinner specimens. Cryostat sectioning of samples, quickly frozen in liquid freon or liquid nitrogen can be used to rapidly produce 5–20-μm-thick sections suitable for observation. Samples may also be infiltrated with epoxy or acrylate-based embedding media (such as LR white and glycolmethacrylate [GMA]), cured and sectioned using glass knives to produce higher quality sections in the 1–10-μm thickness range. This procedure will be discussed in greater detail in the "Sample Preparation for TEM."

Staining. The contrast of specimens can often be improved using a variety of stains that have different chemical specificities. Many biological stains can be used to stain polymers and achieve contrast effects. Stains used for the characterization of drug delivery systems are divided into three basis categories. Acid stains are negatively charged stains containing hydroxyl, carboxyl, or sulphonic groups, such as eosin y, and will bind to positively charged polymers. Basic stains are positively charged molecules, such as toluidine blue, methylene blue, and Alcian blue, and bind to negatively charged polymers. Solvent stains or lysochromes are generally un-ionized, lipophilic substances, such as Sudan black, and oil red O, which partition by solubility into hydrophobic substances and stain them (Table 2).

Additionally, immunochemical and enzymatic techniques may be used on cryostat sections to localize bio-

Table 2. Application of LM and TEM Stains for Characterization of Drug Delivery Systems

Stain	Imaging	Affinity	Application
Eosin Y	LM	Anionic dye with affinity to cationic moieties	Staining of positively-charged polymers
Alcian blue	LM	Cationic dye with affinity to anionic moieties	Staining of negatively-based polymers
Methylene blue	LM	Cationic dye with affinity to anionic moieties	Staining of negatively-charged polymers
Toluidine blue	LM	Cationic dye with affinity to anionic moieties	cationic dye with affinity to anionic moieties
Methyl green-pyronin	LM	Nucleic acids	Localization of encapsulated nucleic acids
Sudan black	LM	Lipid	Hydrophobic polymer stain
Oil red O	LM	Lipid	Hydrophobic polymer stain
Uranyl acetate	TEM	Phosphate/amino moieties	Negative/positive stain
Lead citrate	TEM	Negatively charged moieties	Positive stain
Ammonium molybdate	TEM	Cationic molecule with affinity to anionic moieties	Negative stain
Phosphotungstic acid	TEM	Anionic molecule with affinity to cationic moities	Negative stain Positive stain—polyamides and olypropylene
Osmium tetroxide	TEM	Unsaturated hydrocarbons, double bonds	Positive stain
Iodine	LM/TEM	Polyamides/polyvinylalcohol	Positive stain
Silver sulfide	LM/TEM	Cationic attraction to surface anions	Positive stain

logical encapsulants. Sections are incubated with specific antibodies to the target molecule and reacted with secondary antibodies labeled with markers such as horseradish peroxidase (HRP; brown, insoluble, enzyme reaction product), alkaline phosphatase (AP; red or blue, insoluble enzyme reaction product), phycoerythrin (pink-colored, fluorescent), fluorescein isothiocyanate (green-fluorescent), and rhodamine (red-fluorescent). Other labeling schemes used at the light microscopic level include protein A–gold with silver enhancement and biotin-labeled antibodies, primary or secondary antibodies reacted with avidin-marker enzyme conjugate (either HRP or AP labels). The localization of biomolecules and enzymes will be discussed in greater depth in "Sample Preparation for TEM."

TRANSMISSION ELECTRON MICROSCOPY

TEM extends the level of observation provided by the light microscope by orders of magnitude. Generally speaking, modern TEM is capable of resolving structures with dimensions smaller than 0.2 nm and provides magnification in the ranging from less than 500-fold to millionfold. Instead of focusing light rays with glass lenses, as in LM, TEM focuses electrons emitted by a heated filament to provides images restricted only by the wavelength of electrons or 0.003 nm.

The design of the TEM has many striking similarities to the optics employed in light microscopes (Fig. 2). Both systems use condenser lenses to focus incident electrons or light rays onto the sample and objective lenses to focus the electrons or light rays that interact and pass through the sample. However in the case of TEM the lenses are powerful electromagnets capable of bending the path of electrons. Electromagnets are also used to accelerate electrons as they are emitted from the filament source so that they have sufficient energy to penetrate the specimen. Typically energies in the range of 60 to 100 kV are used for this purpose. Even using powerful lenses and high accelerating voltages, the TEM must operate under high vacuum, generally less than 10^{-4} mmHg, to prevent collisions of electrons with air molecules and resultant loss in resolution.

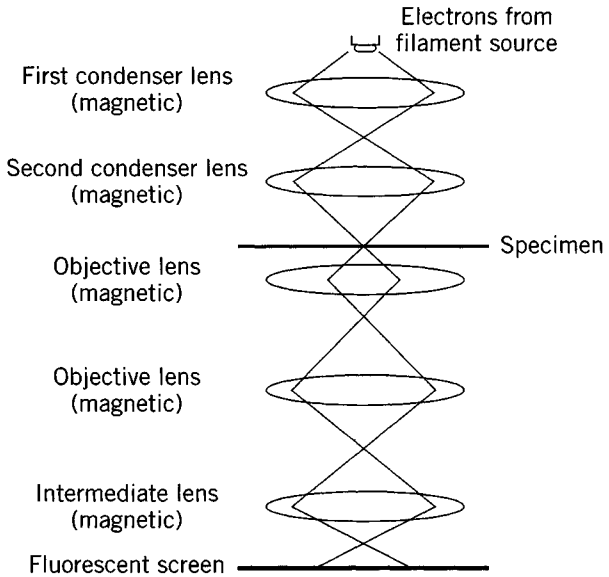


Figure 2. Simplified arrangement of optics in the transmission electron microscope.

The TEM has two sets of apertures or micron-sized holes laser-drilled into metal foil: condenser and objective. Condenser apertures serve to limit the diameter of the electron beam that reaches the specimen, thereby controlling to some extent beam damage. The incident electron beam strikes and interacts with atoms of the sample, particularly heavy metal stain atoms. Those electrons that emerge from the sample consequently have different energies resulting from their atomic interactions. The differences in energy result in differences in sample contrast. The contrast of the sample electrons may further be controlled by inserting different objective apertures. Smaller objective apertures tend to improve contrast by removing peripherally deflected electrons from the signal beam. Objective lenses focus the electron beam and projector lenses, like the eyepiece lenses of light microscopes, enlarge the focused image so that it can be observed. The final image

is viewed through binoculars focused upon a phosphor-loaded screen inside the microscope chamber and may be photographically recorded by exposing sheet or roll film mounted in an automatic camera system situated in vacuo beneath the viewing screen.

Sample Preparation for TEM

The requirement for high vacuum in all electron microscopy systems imposes important restrictions on the preparation of samples, namely that the samples be dehydrated to remove water, which would hinder the effectiveness of the vacuum system. In the case of biological electron microscopy, an important requirement is that the material be prepared so that it resembles the living state, with the introduction of as little artifact as possible. However, for the purpose of analyzing controlled release systems, it is vital that the sample be prepared with minimal losses of therapeutic agents or disruption of device morphology and material matrix. Borrowing from biological TEM, the following steps are necessary for most aspects of thin section TEM: (*1*) fixation or preservation of the sample to prevent disruption and extraction during subsequent manipulations; (*2*) dehydration; (*3*) infiltration with embedding material; (*4*) curing of the infiltrated sample; (*5*) sectioning and collection of the cured sample; and finally (*6*) staining of the sectioned material for observation.

Fixation. As with biological TEM, two types of fixing agents are popularly used: aldehydes and heavy metal tetroxides. In many instances both agents are used sequentially (1). Glutaraldehyde and formaldehyde are capable of cross-linking proteins and other agents containing free terminal amino groups. Additionally, glutaraldehyde has some limited reactivity with nucleic acids, carbohydrates, and lipids. For protein and peptide drugs encapsulated in polymer matrices, aldehydes quickly penetrate most systems (especially hydrogel-based devices) immobilizing the proteins by cross-linking within the device matrix, thus preventing extraction during subsequent steps. Fixation is generally complete within one to three hours and can be greatly shortened for systems measuring less than 1 mm, yet in many instances samples may be stored in fixative for years with minimal artifactual change. Aldehyde fixation is sufficiently gentle that many enzymes retain at least partial activity following fixation and suffer only minimal changes in antigenicity when reduced levels of fixatives are employed. This characteristic provides researchers with a powerful tool, since lightly fixed, controlled delivery systems can be processed, sectioned, and used to localize encapsulated enzymes after substrate addition, providing that the resulting reaction products are water-insoluble. Additionally, antibody histochemistry can be used to localize nearly any target material, assuming that a suitable primary antibody is available.

Osmium or, less commonly, ruthenium tetroxides are generally used as secondary fixatives, following aldehyde fixation, yet can be used as primary fixatives in protein-free systems. Tetroxides react with unsaturated double bonds commonly found in lipids and many polymers, cross-linking adjacent reactive moieties. The fixing agents also have some reactivity with proteins. Additionally, the heavy metal constituents of the fixative, either osmium, rubidium, or ruthenium are electron dense and serve as powerful contrast enhancing agents or TEM stains, which can be used to enhance polymer morphology. The fixatives have mordant properties that increase the binding of other stains, notably lead-based stains. Ruthenium tetroxide, particularly, has found favor among polymer chemists, owing to its heightened reactivity with ether, alcohol, amine, and aromatic functional moieties compared to osmium tetroxide. The ruthenium form is believed to enhance contrast in surface, crystalline regions of polymers relative to bulk, amorphous domains.

Aldehyde and tetroxide fixation are often used in a complementary fashion to offset the deficiencies of a single fixative (2,3). Unfortunately, artifacts are associated with the simultaneous use of the two types of fixatives. Since aldehyde fixatives offer greater penetrating power than the tetroxides, they are normally employed first, followed by a secondary fixation in tetroxide. A commonly used two-step protocol uses 3–4% (w/v) paraformaldehyde and 1–2% (v/v) glutaraldehyde in physiological buffer (PBS) for 2–5 h at 4°C with continuous agitation, followed by washing in PBS to remove unreacted aldehyde and a secondary fixation in 0.5–2% (w/v) osmium tetroxide in PBS for 2–4 h. For purposes of enzyme or antibody localization the secondary fixation is generally eliminated because of the harsher denaturing activity of tetroxides on proteins and most agents, and the concentrations of formaldehyde and glutaraldehyde are generally reduced to 1% and 0.5%, respectively.

The fact that these fixatives are aqueous-based imposes important limitations on their use for controlled delivery systems. Because many of the agents to be localized are water soluble, it is often necessary to quantitate losses of the agents during processing, especially during fixation, and determine if the final product is an accurate estimate of the original. As an alternative to aqueous fixation, in special cases nonaqueous and vapor-phase fixation may be employed. Osmium tetroxide has excellent solubility in many organic solvents as well as water and may be reacted with the sample, providing the organic solution is a nonsolvent for the delivery system. Lipid-free hexane, as an example, can be used as a solvent for osmium tetroxide and used to fix poly(lactide) polymer (PLA) and poly(lactide-*co*-glycolide) (PLGA) systems, since hexane is a nonsolvent for PLA and PLGA. Alternately, because of the high vapor pressures of both aldehydes and tetroxides, it is possible to fix very thin samples in a closed system containing vapors of the fixatives for prolonged periods of time at 4°C or for progressively shorter periods of time at higher temperatures (4). Vapor-phase fixation is inefficient, often unsatisfactory, and is most often used as a last alternative in difficult circumstances where the encapsulated agent is quickly extracted after brief immersion in fixative solution.

Dehydration. After fixation, the sample is sufficiently stable that water may be removed without disrupting morphology. Again, borrowing from biological TEM, nondestructive dehydration may be accomplished by three means: (*1*) treatment with dehydrating solvents; (*2*) criti-

cal point drying; or (*3*) lyophilization. Air-drying and heating have generally been avoided for TEM processing because of sample collapse associated with these techniques. Sample collapse is an artifact associated with the collapse of hollow structures to flat morphologies attributed to interfacial tensions during drying. In biological TEM, only the first treatment, employing dehydrating solvents, is used. Critical point drying and lyophilization are used for sample preparation during SEM. However, in the absence of biological tissue, as is the case with controlled delivery systems, all three methods may be employed (Table 3).

Dehydration with fluids is normally accomplished using graded series of either alcohols or acetones ranging from 30 to 100% (v/v) solvent in steps of 10%, starting from the lowest dehydrant concentration to pure dehydrant. It is important that the dehydrating fluid not be a solvent for the delivery system and that losses of encapsulated material during dehydration be minimal, as determined by assay of the dehydrant fluids (Table 4).

Critical point drying is normally performed after exchange with volatile solvents such as alcohol. The samples are sealed in a cooled, dehydrant-filled vessel, and the dehydrant is replaced with a transitional agent, such as carbon dioxide or Freon. The sample is then heated under pressure to the critical point for the transitional agent where the density of the vapor phase and liquid phase are the same. Critical point drying achieves specimen drying without sample collapse because the specimen is always immersed in a dense vapor phase and interfacial tensions resulting from the liquid phase are eliminated.

Lyophilization removes water without using dehydrant solutions and therefore eliminates an important source of encapsulant losses. Samples are quickly frozen in liquid nitrogen, dry ice, or Freon to eliminate damaging ice crystal formation. Water is removed via sublimation under reduced pressure as the sample slowly thaws. Lyophilized samples often suffer from a small degree of sample collapse, as compared to critical point-dried samples, but are clearly superior to air-dried or heated samples. It is often possible to prepare some samples without fixation, freeze, and lyophilize them directly and examine them by SEM. Portions of the sample can be infiltrated, sectioned, and observed by TEM, providing that the encapsulant and sample matrix are sufficiently stable during processing.

Embedment and Infiltration. Embedment is necessary for TEM preparation to provide solid support throughout the sample for purposes of sectioning. The media commonly used are either epoxy- or acrylate-based liquids having sufficiently low viscosity to be able to permeate the sample completely and then harden by polymerization after either chemical, thermal, or photochemical initiation (Table 5). Historically, the epoxy embedding media such as Epon 812 (now replaced by Embed 812), araldite, and mixtures of the two have been most widely used. Samples are typically infiltrated or soaked in the dehydrant-diluted epoxy resin solution for up to 48 h because of the relatively high viscosity of the media, followed by a supplemental treatment with full-strength epoxy. Unwieldy infiltration schedules prompted the search for lower viscosity epoxies, such as Spurr's media, which allowed times to be reduced by half. Epoxy-embedded samples are hardened by heat curing at 60–70°C and produce extremely hard blocks that may be cut, sawed, or machined, section easily, and have excellent stability under an electron beam (Table 6).

Acrylate-based embedding media are more hydrophilic than epoxies and offer important advantages for both general and specialized usages (Table 6). Commonly used ac-

Table 3. Suitability of Dehydration Methods for Imaging Techniques

Dehydration	LM	TEM	SEM
Graded ethanol series (30, 50, 70, 80, 90, 95, 100% v/v)	Yes	Yes	Yes
Graded acetone series (30, 50, 70, 80, 90, 95, 100% v/v)	Yes	Yes	Yes
Air-drying	Yes	No	Yes
Lyophylization	Rarely	Rarely	Yes
Critical point drying	Rarely	Rarely	Yes
Fluorocarbon sublimation (Peldri)	No	No	Yes
Hexamethyldisilizane	No	No	Yes

Table 4. Suitability of Dehydration Media and Methods for Polymer Delivery Systems

Dehydration	Hydrogel	Celluloses	PLGA	PLA	PCL	Polyanhydride	Protein	EV Ac
Ethanol/water	Excellent	Excellent	Good	Good	Good	Good	Good	Good
Acetone/water	Excellent	Excellent	Poor	Poor	Poor	Poor	Excellent	Poor
2,2-Dimethoxypropane	Excellent	Excellent	Poor	Poor	Poor	Poor	Good	Poor
Peldri II	Excellent	Excellent	Poor	Poor	Poor	Poor	Excellent	Fair
Critical point drying	Excellent	Excellent	Good	Good	Good	Good	Excellent	Good
Lyophylization	Excellent	Excellent	Excellent	Excellent	Excellent	Excellent	Excellent	Excellent
Hexamethyldisilizane	Excellent	Excellent	Poor	Fair	Poor	Poor	Excellent	Poor
Air-drying	Poor	Poor	Good	Good	Good	Good	Poor	Good
Air-drying/60°C heat	Poor	Poor	Fair	Fair	Poor	Poor	Poor	Poor

Note: PLGA, poly(lactide-*co*-glycoglide) 50:50; PLA, poly(lactide); PCL, poly(caprylactone); EVAc, ethylene-*co*-vinyl acetate.

Table 5. Suitability of Embedment Media for Imaging Techniques

Embedment media	LM	Immunochemistry	Enzyme histochemistry	TEM	SEM
PEG/PVA	Good	Excellent	Excellent	No	Yes
GMA	Excellent	Good (with etching)	Good (with etching)	No	Yes (without infiltration)
Epon/araldite	Excellent	Poor (with etching)	Poor (with etching)	Yes	No
Spurr's low viscosity	Excellent	Fair (with etching)	Fair (with etching)	Yes	No
LR white/LR gold	Excellent	Good (LM/TEM)	Good (LM/TEM)	Yes	Yes (without infiltration)
Lowicryl	Excellent	Good (LM/TEM)	Good (LM/TEM)	Yes	Yes (without infiltration)

Table 6. Chemical Properties of Embedment Media

Embedment media	Low temperature	Hydrophilicity	Viscosity	UV cure	Heat cure	Chemical cure
PEG/PVA	−40 to −20°C	Yes	High	No	No	No
GMA	No	Yes	Low	No	No	Yes
Epon/araldite	No	No	High	No	70°C	No
Spurr's low viscosity	No	No	Medium	No	70°C	No
LR white/LR gold	−20 to 4°C	Yes	Low	Yes	60°C	Yes
Lowicryl	−40 to 4°C	Yes	Low	Yes	60°C	Yes

rylates, such as Lowicryl, LR white, and LR gold have extremely low viscosities, indeed much lower than epoxies, and can be used to infiltrate samples without dehydrant dilution, reducing the likelihood of solvent extraction. Acrylate monomers have superior infiltrative properties and often plasticize and fatigue brittle thermoplastics. They have been used with success in infiltrating difficult samples (Table 7). Samples can be infiltrated, for periods of 24 hours to years, and even cured at −20 to 4°C using blue-light photoinitiation. Since low-temperature treatment preserves the antigenicity and enzyme activity of protein encapsulants, it is not surprising that the acrylates have been widely used for enzyme and antibody localization studies at the TEM level. Histochemical experiments are facilitated by the hydrophilic properties of the hardened blocks, which are much more permeable to aqueous stains and solutions than epoxies (5). For general use, acrylate monomers may be cured by heating at 60°C or else exothermic catalysis with benzoyl peroxide. Acrylate-embedded samples produce hard blocks, softer than epoxies, that section easily and offer moderate electron-beam stability. Two shortcomings of acrylates and LR white in particular are the requirement to exclude oxygen from the sample during curing, necessitating the use of closed embedding capsules, and the inability of acrylates to infiltrate hard materials, causing samples to drop-out during sectioning.

Sectioning. Embedded sample blocks are first trimmed with razor blades to form a trapezoid with dimensions not exceeding 2–3 mm on a side. Semithin sections, ranging from 0.5 to 1 μm, are produced using glass knives mounted on an ultramicrotome. Once a suitable area has been identified by light microscopy, the block face may be reduced in size to 1–2 mm on a side, and from that point on sectioning is typically continued with a diamond knife. Sections, ranging in thickness from 70 to 90 nm, with interference colors of silver and gold, respectively, are produced as a floating ribbon on the surface of a liquid-filled trough or "boat" attached to the knife. Most commonly, the boat fluid is water; however, to reduce extraction of water-soluble encapsulants during sectioning, other fluids may be substituted. The sections are collected on copper grids, dried with filter paper, and may be examined directly or else stained with electron dense materials to improve contrast. In the case of fragile sections embedded in acrylate media, support-film-coated grids, composed of thin films of formvar or parlodian polymers are often used to improve the stability of the sections under the electron beam. Additionally, support films or else thin section-support film sandwiches on grids may be coated with a thin deposition of evaporated, electron-transparent carbon metal to improve thermal conductivity.

A specialized form of thin sectioning, performed with frozen samples is cryoultramicrotomy. Tissue is quickly

Table 7. Suitability of Embedment Media for Infiltration of Polymer Delivery Systems

Embedment media	Hydrogel	Celluloses	PLGA	PLA	PCL	Polyanhydride	Protein	EV Ac
PEG/PVA	Excellent	Excellent	Fair	Fair	Fair	Fair	Good	Fair
GMA	Excellent	Excellent	Good	Good	Good	Good	Excellent	Poor
Epon/araldite	Excellent	Excellent	Poor	Poor	Poor	Poor	Good	Poor
Spurr's low viscosity	Excellent	Excellent	Good	Good	Fair	Fair	Good	Poor
LR white/LR gold	Excellent	Excellent	Excellent	Excellent	Good	Good	Excellent	Poor
Lowicryl	Excellent	Excellent	Excellent	Excellent	Excellent	Excellent	Excellent	Fair

Note: PLGA, poly(lactide-*co*-glycoglide) 50:50; PLA, poly(lactide); PCL, poly(caprylactone); EV Ac, ethylene-*co*-vinyl acetate.

frozen by rapid contact with a liquid nitrogen-chilled copper block and sectioned using an ultramicrotome capable of maintaining temperatures at less than −70°C during sectioning. Sectioning is normally performed on dry glass knives and sections are transferred to formvar-coated copper grids for TEM observation. This technique is not commonly used because of the technical proficiency required to obtain acceptable results; however, the method is unsurpassed for localizing bioactive agents at the TEM level, using histochemical methods, without danger of chemical denaturation from fixation and dehydration.

Staining. Most commonly used TEM stains are uranyl acetate and lead citrate used singly or in a two-step procedure (see Table 2). Lead and uranium both have high atomic numbers and are extremely electron dense. The heavy metal atoms interact with the incident electron beam to produce highly contrasted images. The citrate and acetate salts are most commonly used because of their relative resistance to precipitation compared with other chemical forms of the stains. Staining is normally performed in carbon dioxide–deprived environments to prevent formation of insoluble, heavy metal-carbonate precipitates, called cookies and needles.

Staining may be performed either on thin sections collected on grids or else en bloc on the sample before dehydration. In the first case, sample grids are floated on the surface of droplets of particle-free, filtered stain for periods of 10–60 min, followed by washing in distilled water. Typically, staining with uranyl acetate is performed first followed by staining in lead citrate. Alternately, immediately following fixation, samples may be immersed in solutions of 0.5–2% (w/v) uranyl acetate for periods of 2–5 h at 4°C. En bloc samples are then dehydrated, infiltrated, and embedded using normal protocols.

Vapor phase staining with osmium tetroxide vapors can be used to increase the contrast of samples embedded in acrylate mediums. Sections on sample grids are sealed in a closed vessel containing osmium tetroxide solution in a smaller open vessel or else as crystals and incubated at room temperature for periods of up to 6 h. This procedure will also preserve unfixed samples in addition to improving specimen contrast.

Additionally, material scientists have employed a number of stains to contrast polymeric materials (see Table 2). Mercuric trifluoracetate has been used to contrast polystyrene and polybutadiene, either singly or as block copolymers (6). Iodine has been used to stain polyamides and poly(vinyl alcohols) (PVA) (7,8). Silver sulfide was used to increase contrast of microporous structures in polymers including cellulose, polyesters, acrylics, and PVA (9,10). Phosphotungstic acid has been used to contrast polyamides and polypropylene (11,12).

Localization of Enzymes, Proteins, and DNA

Histochemistry may be used to localize biomolecules encapsulated in drug delivery devices using samples lightly fixed in 1% (w/v) formaldehyde and 0.5% (v/v) glutaraldehyde for periods of 1–2 h at 4°C. A suitable primary antibody, either monoclonal (reactive with a single specific epitope) or polyclonal (reactive with multiple specific epitopes) must first be obtained or developed within an animal such as a sheep, goat, horse, rabbit, or pig and established to be specific to the target molecule and not cross-reactive with other agents in the sample. The procedure may be performed either on thin sections on grids of samples embedded in LR white or Lowicryl or else using thin slices of the unembedded, fixed sample, which may then be processed for TEM (13). Chemical etching of epoxy-based embedding media, such as Spurr's and Epon/araldite, as well as acrylate-based media such as GMA, has been used to enable limited histochemistry (14). Samples are first incubated with blocking agents, such as serum albumin, gelatin, or glycine to reduce nonspecific binding of primary antibodies to free, reactive aldehyde groups.

Antibody staining may be done in two ways: either directly with the primary antibody or indirectly with a second agent directed against the primary antibody. In the first case, the primary antibody is chemically conjugated to an electron dense marker such as ferritin or colloidal gold to facilitate visualization at the TEM level. Typically, the primary antibody is used in a diluted form to increase specificity (1:100–1:500 for polyclonal antibodies versus 1:250–1:2,000 for monoclonal antibodies, as determined experimentally) and reacted with the blocked sample for periods of 1–24 h at room temperature. The sample is then washed and examined using TEM.

The second scenario, indirect labeling, has greater specificity and more general applicability. An untagged primary antibody is used, followed by secondary incubation with either a tagged secondary antibody directed against both the host animal and antibody class (IgG, IgM, etc.) for the primary antibody. The secondary antibody is normally available commercially and may be tagged with colloidal gold or ferritin markers. The second reaction is normally carried out at dilutions of 1:100–1:250 for periods of 1–3 h at room temperature. Alternately, protein A- or protein G-colloidal gold complexes may be used in place of the secondary antibody. Protein A and protein G are cell wall proteins isolated from staphylococcal and streptococcal bacteria, respectively, with specificity against the Fc portion of IgG molecules from most common laboratory animals.

Enzyme localization at the TEM level may be carried out for a number of enzymes producing an insoluble end product, including acetylcholinesterase (15), galactosidase, alkaline phosphatase (16), acid phosphatase (17), adenyl cyclase (18), arylsulfastase (19), ATPases (20), catalase (21), cytochrome oxidase (22), cytosine monophosphastase, esterases (23), glucose-6-phosphatase (24), nictotine adenine dinucleotide phosphatase (25), 5′-nucleotidase (26), peroxidase (27), and thiamine pyrophosphatase (28), to name a few. Typically, thin sections of lightly fixed samples, either embedded in acrylate medium or reacted as thin slices and then postembedded are reacted with excess substrate at optimal pH for the enzyme and with all necessary cofactors supplemented in the reaction buffer. Trapping agents, often insoluble metal salts or other enzymes such as peroxidase, are often employed to produce an electron dense, insoluble end product that may be visualized by TEM.

It is important to note that appropriate controls for all localization schemes should be employed at all times. In the case of immunochemical methods, nonspecific or nonimmune serum from the same animal species should be used as control for the primary antibody and in the case of enzyme methods, controls should include samples without added substrate or trapping agents. In all instances, LM should be used to confirm and target the extent and location of the reactions before carrying the analysis to the TEM level.

Negative Staining

This method of visualization does not involve sectioning of embedded material and is best carried out on either fixed or unfixed material that is sufficiently thin to be be penetrated by the incident electron beam (~10 and 200 nm), although it can be used to crudely visualize and size larger particles such as bacteria, cells, and polystyrene latex particles (1–5 μm). Unlike positive staining, where the specimen reacts or binds heavy metal stains, the sample particles in negative stain are very often unstained and are instead embedded in a droplet of dried stain, resulting in negative contrast images. An important artifact is that images of hollow spherical objects are often collapsed because of interfacial tensions during drying. Commonly used negative stains are 1% (w/v) solutions of uranyl acetate, phosphotungstic acid, or ammonium molybdate. Plastic films, made from formvar or parlodian, on copper grids are used as supports for the particles. Specimens are applied to the grids in one of two ways: either mixed directly with the stain or else applied in a stepwise manner with the particles in suspension introduced onto the grid, followed by a droplet of stain. The method is simple and may be used to visualize a variety of biological entities such as large proteins, nucleic acids, viruses, ribosomes, and bacteria. Negative staining has also been useful in the structural analysis of liposomes for drug delivery (Fig. 3) and oily emulsions.

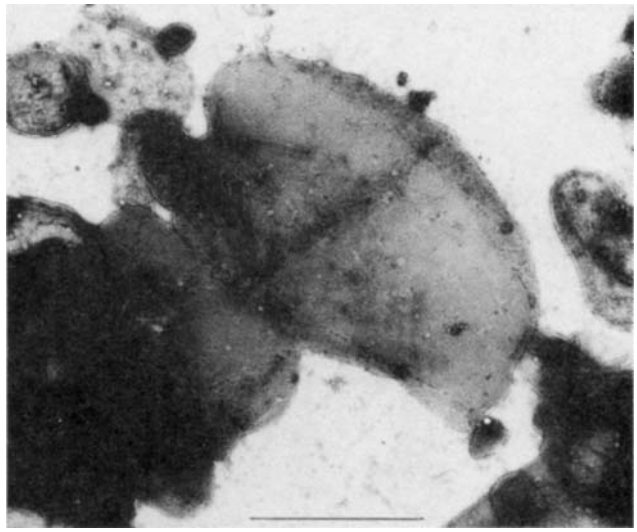


Figure 3. Negative stain TEM of liposomes. Phosphatidyl choline, unilamellar liposomes were prepared by vortex treatment and bath sonication of 10 mg/mL dispersion of the lipid in 50 mM phosphate buffer. A 10-microliter droplet of the suspension was placed on a carbon-formvar-coated grid. After 1 min the droplet was removed by wicking with filter paper and replaced with a microdroplet of 1% uranyl acetate (w/v) in distilled water for 30 sec. The stain was removed, and the grid was air-dried for 1 min and examined directly in the TEM at 80 kV. The vesicles appear collapsed after drying down with stain. This phenomenon is an accepted artifact of the negative staining. Bar = 1 μm.

Replica Techniques and Freeze-Fracture/Freeze-Etch

The use of metal shadowing techniques to prepare faithful replicas of surfaces is used extensively in materials sciences and can be used to collect high-resolution topographic details of drug delivery devices with resolutions of 3–4 nm. Replicas are prepared using a vacuum evaporator capable of routinely achieving vacuums of from 10^{-4} to 10^{-7} mmHg. Typically, the sample is fixed, applied to a clean surface such as freshly cleaved mica or a glass substrate, and placed under high vacuum. The most commonly used replica technique is the one-stage, fixed-angle replica: an electron dense platinum coating is evaporated onto the sample surface at an angle of 45°, followed by a second protective coating of electron-transparent carbon metal, applied at an angle of 80–90°, to conduct surface charge during TEM examination. The sample is removed from the instrument and the replica is displaced from the sample by floating at the interface of a chromic acid or bleach solution. Treatment with acid and bleach is used to destroy the sample and subsequent washing with water removes residue from the replica. The replica can then be mounted on a copper grid and examined directly by TEM. By measuring the length of the shadow (area where metal deposition was occluded by sample interference) cast by samples, it is possible to determine the height of the sample using the angle of platinum deposition and a simple geometric relationship.

A variation of this method is rotary shadowing, in which case the sample is mounted onto a motor-driven stage in the evaporator and rotated at 10–50 rpm while platinum is evaporated at an angle of ~25°. The replica produced using this technique yields exquisite detail of all areas of the specimen because no shadow is created, as is the case with static evaporation.

A less commonly used form of replication is the two-stage negative replica. This method provides a lower resolution image than the one-stage replica, but has the advantage of not destroying the sample. Bulk samples are coated with several layers of 1% (w/v) collodion plastic in solvent. After drying, the plastic replica is stripped from the sample and a negative, platinum–carbon replica is prepared of the plastic replica, as already described. The plastic replica can be separated from the metal replica by dissolution in solvent.

Smaller samples (<10 μm in diameter) may be spray- or air-dried from a liquid suspension onto plastic-coated grids and simply shadowed with metal to reveal hidden surface detail without destroying the underlying sample with strong agents. Shadowing in this manner has many similarities to negative staining and can be used to render surface topography of nanoparticles and microspheres.

Finally, a variation of the replica technique widely used for evaluating liposomes and emulsions is freeze-fracture (Fig. 4a). Samples are frozen by immersion in liquid Freon on copper or gold supports and introduced into a refrigerated vacuum evaporator capable of cooling to −170°C. Vacuums of 10^{-4} mmHg are achieved, the sample is warmed to −110°C and the sample is fractured by cutting with a liquid nitrogen–cooled razor blade mounted to a microtome inside the vacuum unit. The fractured surface is replicated using either single-sided or rotary platinum–carbon evaporation and the sample is separated from the replica by thawing in bleach or chromic acid. The replica is then washed with water and examined by TEM. The freeze-fracture replica can yield morphological information about the interior compartments of closed vesicles.

A variation of the freeze-fracture technique uses etching or sublimation of frozen water to reveal not only fracture planes, but also interior and exterior surfaces as well (Fig. 4b). Freeze-etching is performed immediately following fracture, for periods of 1–5 min at −100°C instead of −110°C.

SCANNING ELECTRON MICROSCOPY

SEM is an important supplement to LM and TEM. SEM is probably the most commonly used method for characterizing drug delivery systems, owing in large part to simplicity of sample preparation and ease of operation. The three-dimensional information derived from the micrographs offers important information about macro- (0.1–10 mm), meso- (1–100 μm) and microstructure (10–1,000 nm), often within the same micrograph! SEM has been used to determine particle size distribution, surface topography, and texture and to examine the morphology of fractured or sectioned surfaces.

The modern SEM has a resolution of ~3 nm (Fig. 5) and provides magnifications ranging from less than 30-fold to 300,000-fold. Electrons emitted by a excitation of a lanthanum hexaboride crystal or heated filament are accelerated at voltages of 1–30 kV and focused onto the sample surface as a tight incident beam (Fig. 6). The 3–5 nm beam is translated about the probe area in a raster pattern. A variety of electrons and electromagnetic radiation with different energies are ejected from the sample surface in response to the incident electron beam. Secondary electrons having relatively low energy ranges of 0–50 eV are the result of inelastic scattering from atoms located near the surface of the sample. These electrons can be collected with a detector and used to produce three-dimensional images of the sample surface. Nearly all scanning electron micrographs are produced using secondary electrons. Backscat-

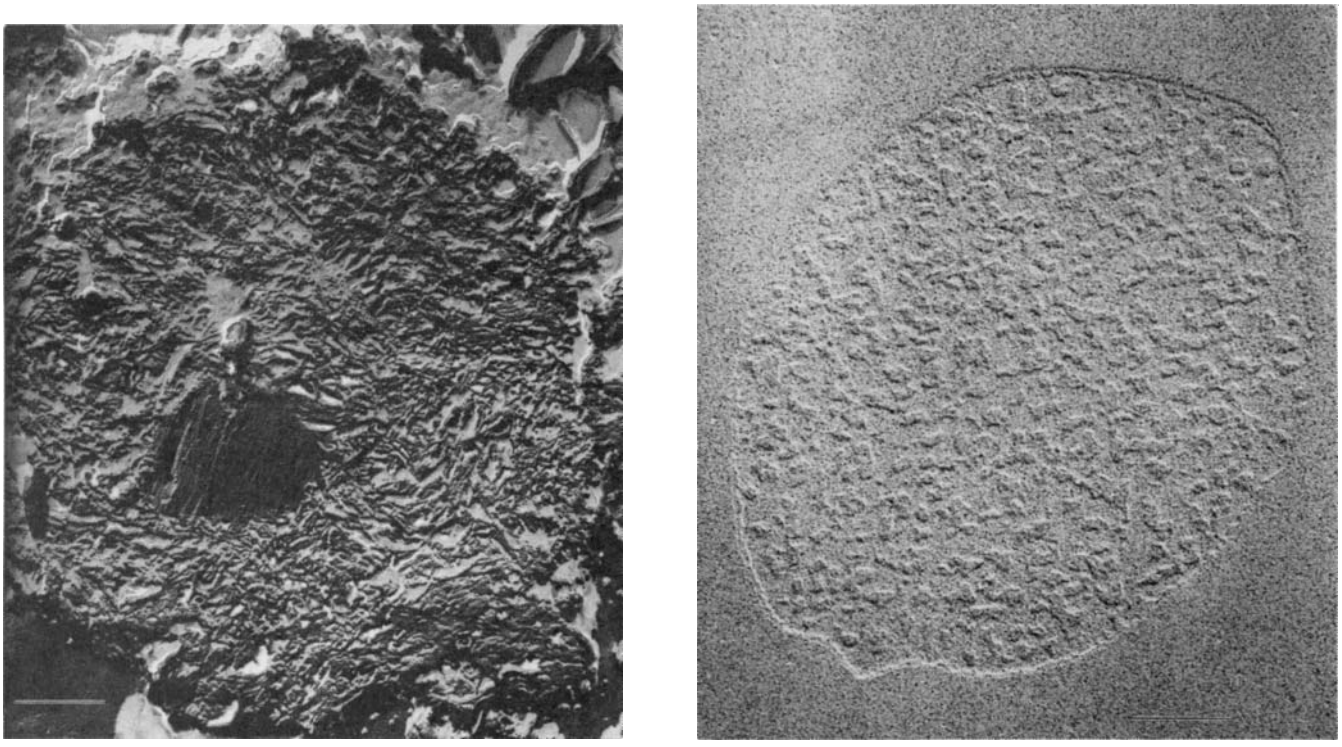


Figure 4. Freeze-fracture and freeze-fracture/etch of PLA microspheres prepared by solvent removal. (**a**) A single microsphere that has been frozen in chilled Freon 22, fractured at −110°C, and replicated with platinum and carbon evaporation while at high vacuum (10^{-4} mmHg) in a Balzer BAF-400 instrument. This image shows a fracture plane in the polymer matrix and shows uniform crystallinity. (**b**) A similar microsphere that has been etched by sublimation of ice to water vapor at a slightly higher temperature (−100°C). The extreme crystallinity of the surface of the fracture plane is evident. Bar = 0.1 μm.

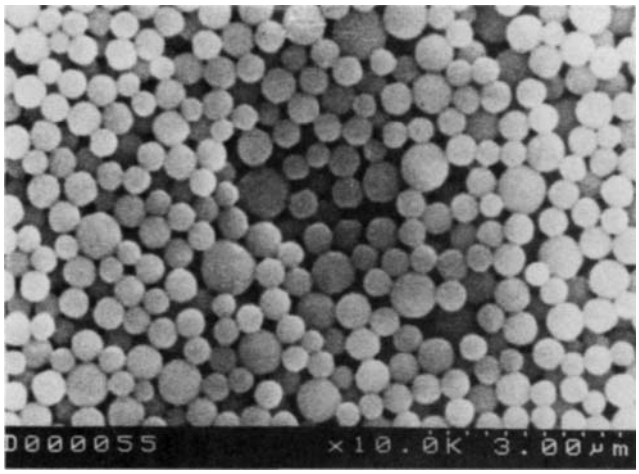


Figure 5. SEM of microspheres prepared by phase inversion nanoencapsulation (PIN). PLGA 50:50 microspheres range in size from 200 to 500 nm and have a high degree of monodispersity and smooth surface texture.

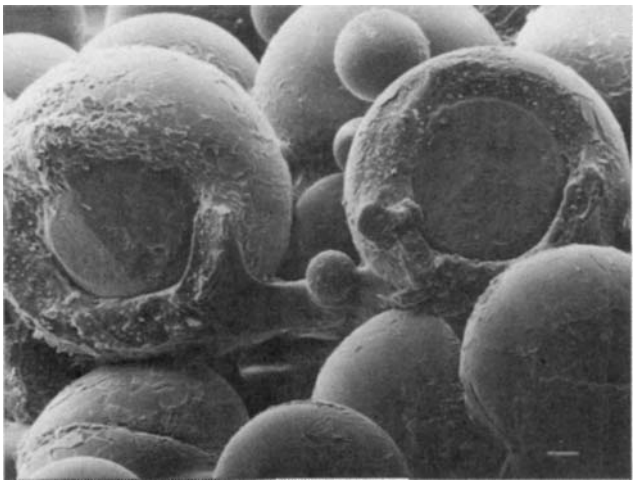


Figure 7. Three-dimensionality of SEM images. Double-walled microspheres composed of ethylene-*co*-vinyl acetate (EVA) in the inner layer and PLA in the outer layer. Two of the spheres were sectioned with a razor blade to reveal the inner cores. Bar = 50 μm.

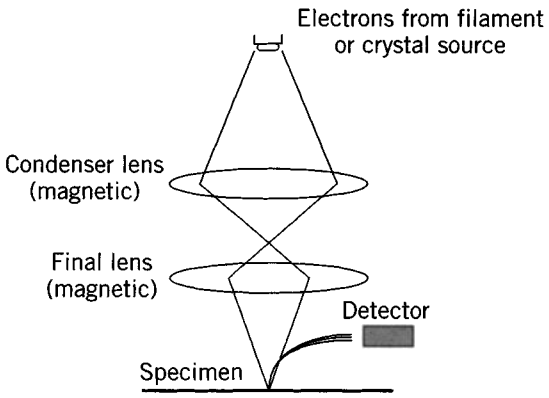


Figure 6. Simplified arrangement of optics in the scanning electron microscope.

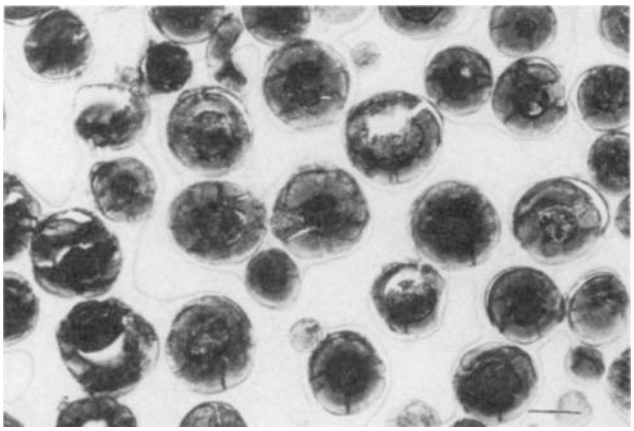
tered electrons having higher energy ranges than secondary electrons are the result of elastic scattering with atoms located deeper beneath the surface. Backscattered electron images can be useful in distinguishing materials having large differences in atomic number and have been useful in gold-labeling experiments. Additionally, X-rays generated by sample interaction with the probe beam may be collected and used to evaluate the elemental composition of the sample.

The various signals collected by secondary, backscattered, and X-ray detectors at each point on the probed surface are processed, amplified, and displayed as a real-time, video image on a monitor. The images may be printed on photographic film or stored and printed digitally.

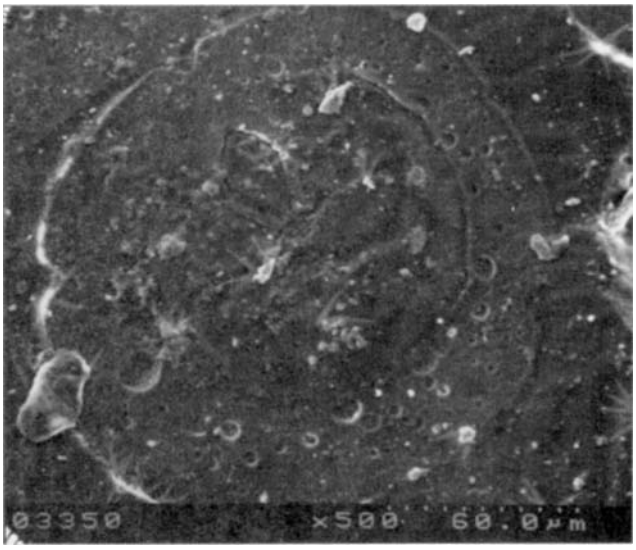
The SEM is most commonly used for generating three-dimensional surface relief images derived from secondary electrons (Fig. 7). The mechanism evoked to explain this phenomenon has been dubbed the edge effect. Simply put, secondary electrons from depressions or cavities on the sample surface are trapped within the surface topography resulting in diminished emission from these features, whereas the converse situation is true for elevations or peaks on the sample surface where electron emission is enhanced.

A great advantage of SEM over other techniques is the tremendous versatility of the method. Samples ranging in size from nanometers, such as viruses and small microspheres, to centimeter-scale bulk samples, such as vascular grafts or osmotic pumps, may be analyzed, even on the same sample holder. Although the working resolution of the instrument is less than TEM, the ease of sample preparation and simplicity of use more than compensate for resolution limitations. The large sample chamber and goniometer accommodate extremely large samples compared to TEM and provide for nearly unlimited points of viewing, owing to translational, tilting, and rotary movements.

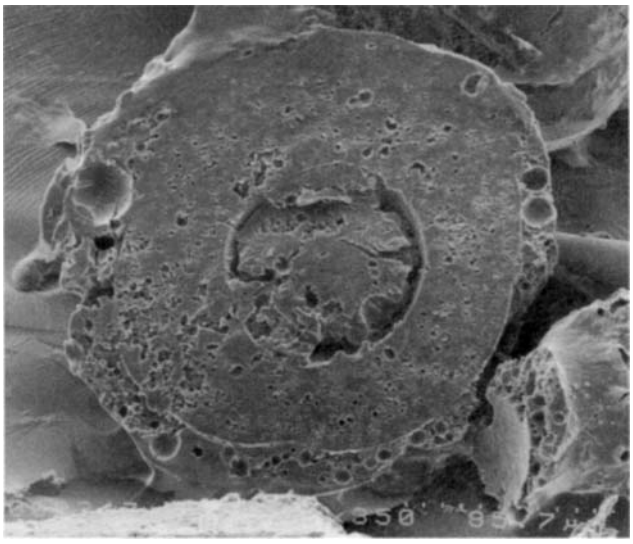
The SEM has a few disadvantages compared to LM and TEM. SEM is used primarily to observe surface topography and texture. SEM does not see through a sample, although it is possible to view inside a sample by examining fractured or sectioned specimens. SEM does not distinguish colors as does LM. The analysis of stained samples or polarized light can often be used to identify polymeric materials. Also, it is difficult to distinguish differences in materials. Identification of materials must be confirmed by comparison to pure reference samples fabricated using identical conditions and processed for SEM using the same protocols as the sample. Another disadvantage is that labeling techniques using immunochemicals or enzymes are limited to the use of electron-dense markers, such as gold or lead, and samples must be visualized using backscattered electron imaging. Additionally, the use of thermoplastic polymers or polymeric materials with low glass-transition temperatures for fabrication of drug delivery systems imposes limitations on the use of SEM. These materials require special precautions to avoid sample distortion, resulting from thermal changes during observation.



(a)



(b)



(c)

Figure 8. Analysis of double-walled microspheres using LM and SEM. (**a**) Double-walled microspheres made of polystyrene (inner layer) and PLA (outer layer) loaded with particles of ferric oxide (central core). Samples were embedded in GMA and sectioned with glass knives. LM indicates that nearly all the spheres are double-walled and shows the uniformity of loading. Bar = 100 μm. Courtesy of Benjamin Hertzog. (**b**) and (**c**) double-walled microspheres composed of polyanhydride and PLA. (**b**) A microsphere that was poorly embedded in GMA and sectioned with glass knives. The sections were mounted on stubs using carbon-impregnated, adhesive tape, coated, and examined by SEM. (**c**) A microsphere that was sectioned with a razor blade and prepared for SEM. SEM analysis shows the porosity of the inner layers and localization of the drug. For more information about double-walled microspheres refer to Ref. 29.

It is often necessary to use low accelerating voltages (less than 10 kV) to avoid excess heating, and heavy metal coating protocols must be optimized to reduce thermal artifacts. Finally, as in TEM, samples must in most cases be dehydrated because of the high vacuum requirement of most electron microscopes.

It is worth noting that a specialized version of the SEM, the environmental SEM, is commercially available and is applicable for the observation of hydrated, unfixed samples, although at lower resolutions than conventional high-vacuum SEM systems. This instrument functions by maintaining a differential vacuum; that is, a high vacuum environment is maintained near the electron gun while a lower vacuum environment is used for the sample chamber. Future developments will probably bring this specialized instrument

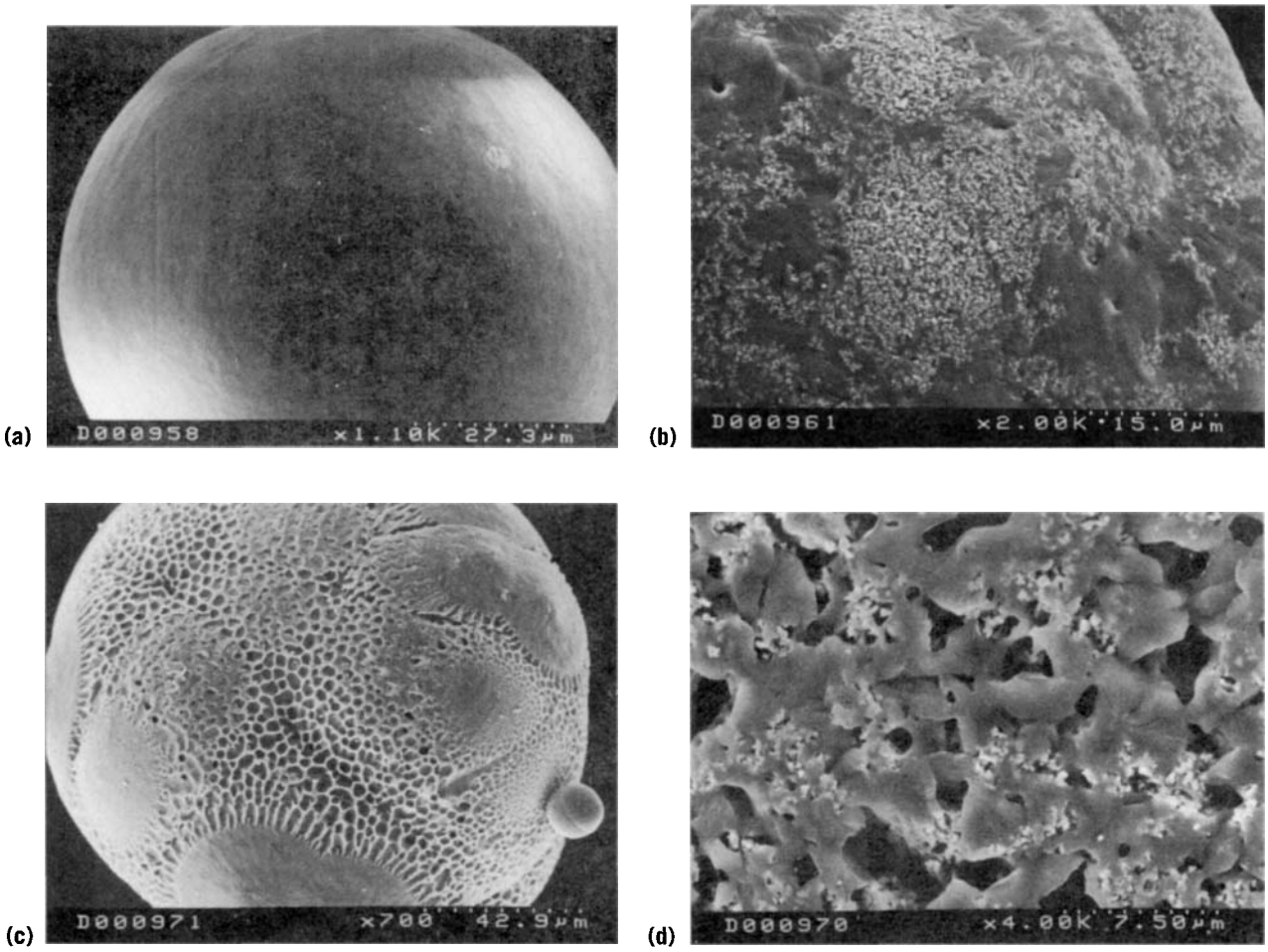


Figure 9. SEM analysis of topography and encapsulant distribution in solvent evaporation spheres. Poly(caprylactone) (PCL) (**a–b**) and PLA spheres (**c–d**) were prepared by dispersing a 20% (w/v) polymer solution in methylene chloride into a bath of 1% poly(vinyl alcohol) (w/v). The microspheres were stirred until they had hardened and were collected by filtration. Microspheres were prepared with and without 300 nm ferric oxide particle by including the particles in the polymer solution. (**a**) The smooth surface morphology of the unloaded microspheres. (**b**) The clustered distribution of iron oxide particle on the surface of the PCL spheres. (**c**) The extreme porosity and uneven distribution of pores on unloaded PLA spheres. (**d**) Higher magnification of the surface shows that the metal particles are associated with crystalline regions (spherulites).

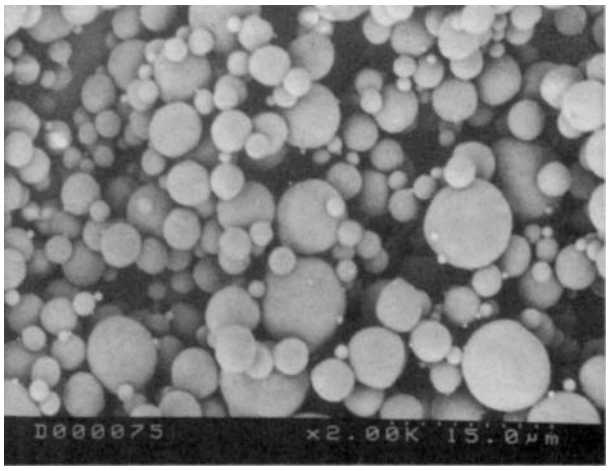
into more widespread use for analysis of controlled release systems.

Sample Preparation

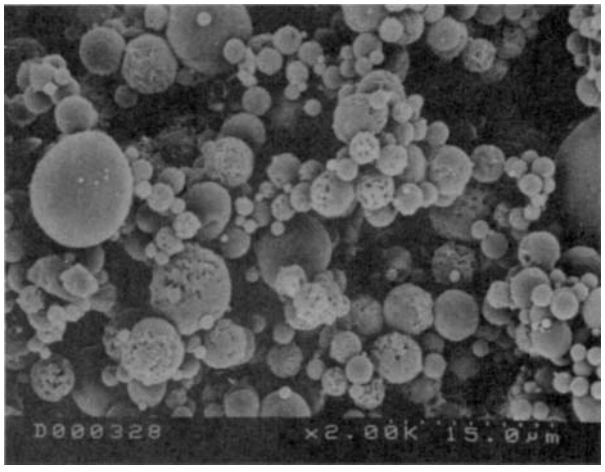
Fixation. Fixation is generally not necessary, except where biological encapsulants are involved, such as biomolecules and cells, in which cases the general fixation procedures described for TEM are directly applicable. For biomolecules, these steps are only required when solvents are used for dehydrating the sample, not when lyophilization is used for dehydration.

Oftentimes, a postosmication step is employed to heighten contrast and increase the secondary electron signal derived from the sample. This treatment involves soaking the sample in thiocarbohydrazide, which binds to osmium tetroxide already on the sample and binds additional osmium tetroxide when the sample receives a second, supplemental osmium fixation. This additional coating of heavy metal greatly amplifies the number of secondary electrons emitted from the sample by providing additional atomic targets for the primary probe beam.

Sectioning. Although SEM is primarily used for analysis of surface topography, it is possible to look at interior surfaces by simply sectioning the bulk sample with a razor blade (Figs. 7, 8). This procedure suffers from artifacts introduced by compressing the sample downwards during cutting and is especially troublesome for soft samples. Cryosectioning obviates many of these concerns. Samples are quickly frozen by immersion in liquid Freon or liquid nitrogen and fractured by sectioning on a liquid nitrogen–chilled metal surface with a chilled razor blade. Samples

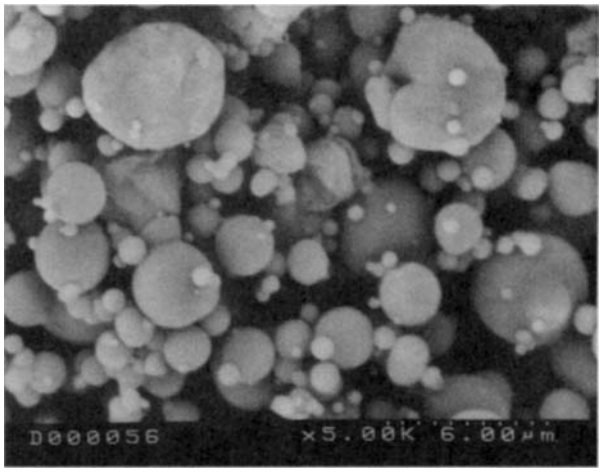


(a)

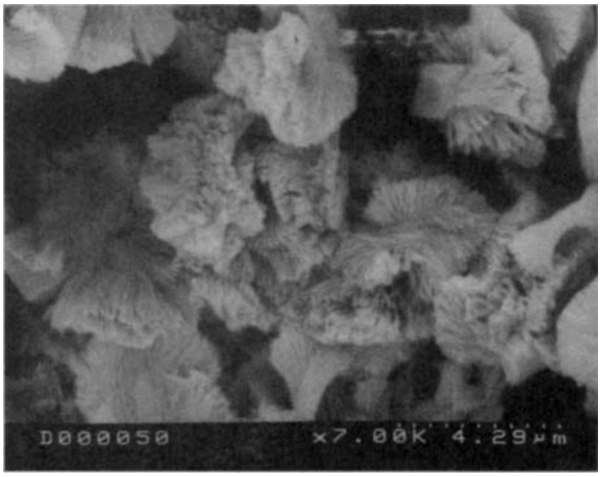


(b)

Figure 10. SEM of spray-dried microspheres. A 3% (w/v) solution of PLGA 50:50 in methylene chloride was spray-dried with a 1.0 mm atomizer nozzle at 50 psi atomizer pressure using a flow rate of 30 mL/min at 40°C. (**a**) Unloaded microspheres ranging in size from 0.1 to 15 μm with smooth surface morphology. (**b**) Microspheres loaded with 10% antibiotic (w/w) as encapsulant. The drug-loaded spheres have the same size range but extremely rough, porous surface texture.



(a)



(b)

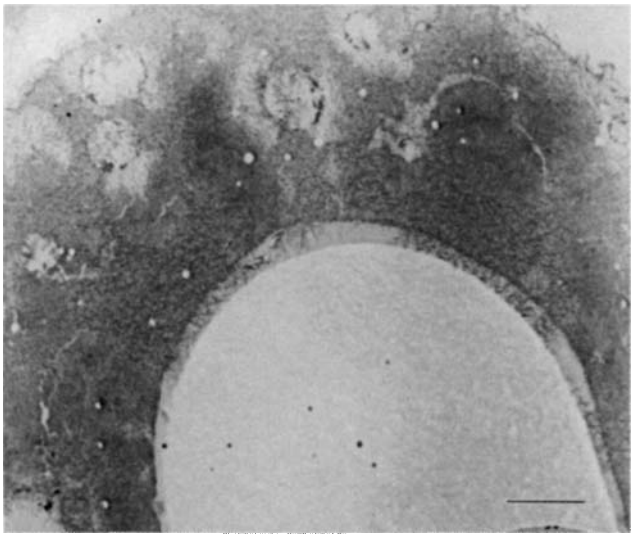
Figure 11. (**a**) SEM of PLA microspheres prepared using PIN. The spheres are discrete, range in size from 0.1 to 6 μm and have smooth surface texture. (**b**) PLA particles prepared under similar solvent/nonsolvent conditions using the organic phase separation process. These particles range in size from 2 to 5 μm and have extremely coarse surface texture. The particles are individual spherulites of PLA. For detail of PIN, see Ref. 30, and for details of organic phase separation see Ref. 31. Bar = 1 μm.

as small as 300 μm in diameter may be sectioned using the razor blade technique.

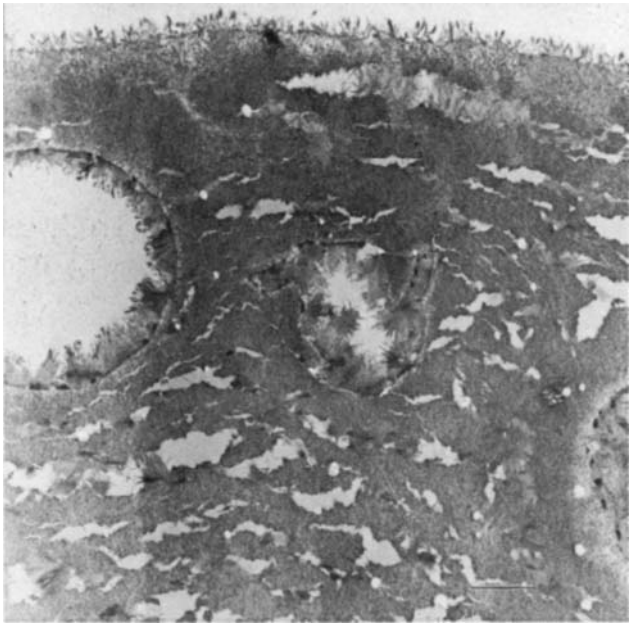
Smaller samples may be prepared by cryostat sectioning of PVA-PEG embedded, frozen samples. Sections, between 10 and 50 μm in thickness, can be collected on a glass slide, dehydrated by either air-drying or freezing and lyophilization, and the entire slide mounted for observation by SEM. Alternately, smaller samples may be quickly embedded, without infiltration in acrylate-based embedding media such as LR white or GMA, sectioned with a glass knife and microtomed to produce 1–10-μm-thick sections mounted on glass slides for SEM analysis (see Fig. 8).

Dehydration. As with all electron microscopes (excluding the environmental SEM), high vacuum is a requirement for image formation, and samples must be thoroughly desiccated before entering the vacuum chamber. As mentioned previously (in the discussion of dehydration of TEM samples, care must be taken to avoid collapse. Samples are best prepared by critical point drying, lyophilization, or else by using solvent substitution with hexamethyldisilizane. Fluorocarbon solvents, such as Peldri II (a proprietary product of Ted Pella Co., California, now discontinued), that slowly sublimate from the solid state at room temperature have been widely used in the past. This latter procedure requires graded ethanol dehydration before solvent exchange, as does critical point drying.

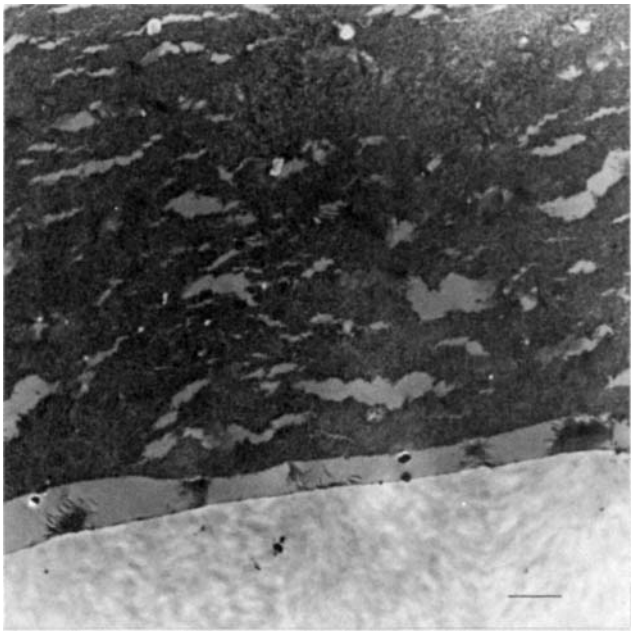
Mounting. The dried sample is normally attached to an aluminum sample holder or stub using silver- or carbon-



(a)



(b)



(c)

Figure 12. TEM of double-walled microspheres. (**a**) A survey cross section of PLA-polystyrene microspheres. Three distinct zones are identified: the outer PLA zone, an intermediate zone, and an inner core of polystyrene. Bar = 10 μm. (**b**) Details of the outer PLA zone and surface. The crystallinity of the polymer is obvious from observation of the inclusions and surface. Bar = 3 μm. (**c**) Details of the PLA-polystyrene zones and interfacial region. Bar = 3 μm. The polystyrene core at the bottom appears nearly featureless, which is consistent with the amorphous nature of the polymer. The microspheres were infiltrated with LR white and cured at 40°C for 4 days to minimize thermal changes to the polymer. Thin sections were stained with uranyl acetate to contrast the PLA layer.

based conductive cements that are commercially available for this purpose. A variety of double-sided adhesive tapes and tabs, impregnated with carbon, are often more convenient for smaller samples such as microspheres, which might become totally immersed in a layer of liquid cement.

A vexing artifact, commonly called charging, arises when SEM samples are poorly attached to the underlying substrate or contain residual moisture or a combination of both. Charging results from accumulation of electrons within the sample, imparted by irradiation from the incident electron beam. The excess electron load would normally be dissipated by conduction to the sample holder. Objects that are charging often appear to glow brightly on the viewing screen compared to objects that are optimally prepared. The artifact can often be eliminated by repeating the dehydration step with new sample or else by remounting and recoating the same sample.

Coating. Thin coatings (20–30 nm) of electron-dense metals, typically gold, palladium, platinum, or combinations, are applied to the mounted sample using either sputter-coating or thermal vacuum evaporation. The coatings serve two purposes: (*1*) to heighten sample signal by providing additional heavy metal atoms for interaction with the incident electron beam and (*2*) to conduct accumulated sample charge and heat to the sample holder.

Sputter-coating is most commonly used for SEM coating for reasons of simplicity and nondestructiveness. The mounted sample is placed in a vacuum chamber, the chamber is evacuated using a rotary pump, and an inert carrier gas, typically argon, is introduced to produce a partial vacuum of approximately 10^{-2} mmHg. The argon atmosphere is ionized by electrodes located near a metal foil, or target, composed of gold or gold–palladium metal. The interaction of ionized argon atoms with the metal foil causes heavy metal atoms to be ejected from the foil, covering the underlying sample with a finely dispersed, particulate coating. The process is complete within minutes and produces relatively little heating damage compared to thermal vacuum evaporation. Thermal vacuum evaporation is more commonly used for deposition of platinum and carbon coatings, as previously described in "Replica Techniques and Freeze Fracture."

Imaging of Drug Delivery Systems

SEM is most often used to characterize drug delivery systems based on surface morphology, texture, and size. The examination of the surface of polymeric drug delivery systems can provide important information about the porosity and microstructure of the device (Figs. 5, 9–11). Increased porosity translates into rapid release of drug. The size and distribution of surface pores can be evaluated by direct measurement using the image scale marker or interpolation from micrographs using the magnification factor to calculate dimensions of objects (Fig. 9).

The distribution and morphology of drug on the surface and encapsulated in the matrix (fractured and sectioned samples) can also be directly observed (see Fig. 9). It is important to first examine pure samples of drug and excipients, prepared in exactly the same form used for encapsulation but with minimal SEM preparation (no exposure to solvents). These reference samples should be compared to drug samples that have been carried though the same SEM processing protocol as the delivery devices. Artifactual changes in morphology of encapsulant resulting from processing, notably, aggregation, coalescence, or dissolution should be investigated and distinguished from real changes resulting from manufacture. This information is best used in conjunction with data from size exclusion, high performance chromatography (SEC-HPLC) analysis of drugs extracted or released from delivery systems. SEC-HPLC describes the aggregation state of drug following encapsulation and SEM depicts the morphology of the drug particles in the system.

Examination of cross or tangential sections can similarly provide information about the uniformity of drug distribution throughout the delivery system (Figs. 7, 8b, 8c).

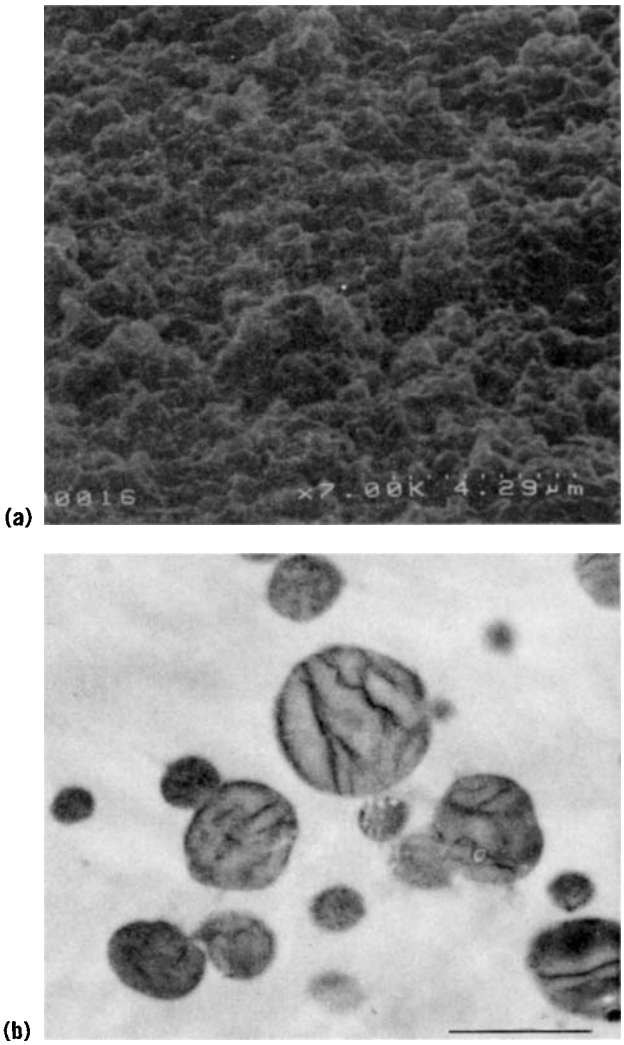


Figure 13. SEM and TEM of PLA microspheres prepared by solvent removal. (**a**) Microspheres dried on a glass coverslip and observed from a 75° tilt angle. (**b**) The same microspheres were prepared for thin-section TEM. The crystallinity of the inner core is revealed in the micrographs. Bar = 1 μm.

Table 8. Suitability of TEM Techniques for Characterization of Drug Delivery Systems

TEM technique	Imaging	Application to drug delivery systems
Thin-section	Interior morphology	Drug distribution, polymer morphology
Immunochemistry	Interior morphology	Drug distribution
Enzyme histochemistry	Interior morphology	Drug distribution
Negative stain	Exterior morphology	Small particles (<1 μm) liposomes, nanoparticles, lataxes
Freeze-fracture	Internal morphology	Drug distribution, polymer morphology (especially liposomes)
Freeze-etch	Internal morphology/internal and external surfaces	Drug distribution, polymer morphology (especially liposomes)
Replica	Exterior morphology	Small particles (<1 μm) liposomes, nanoparticles, latexes

Pores on the surface of the delivery vehicles can often be traced to the interior matrix and the interconnectivity of surface and interior voids can be estimated. As an example, the distribution of drug particles near porous microstructures can offer important information about drug release (Fig. 9d).

The morphology of the polymer matrix can be evaluated and differences between crystalline and amorphous regions and their locations in the delivery system can be discriminated and mapped. Crystalline regions can be identified by the presence of spherulites (Figs. 9d, 11b). This is important because release of drug from crystalline regions is slower than from amorphous domains. Therefore domains of crystalline and amorphous polymer contribute to a mixed release profile: the sum of slow- and fast-releasing polymer matrices in a single system. Changes in polymer morphology during manufacturing and storage can be monitored by SEM and used in concert with information about polymer molecular weight, from gel permeation chromatography and crystallinity, from differential scanning calorimetry, to provide a full profile of the polymer component of the delivery system.

SUMMARY

In conclusion, LM, TEM, and SEM provide complementary morphological information about drug delivery systems and should be used in an integrated approach for purposes of characterization (Table 1, Figs. 4, 7, 8, 12, and 13). LM can be used to provide macro- and microstructural information about drug delivery systems, including size and morphology. Stains can be used to localize encapsulants and preferentially stain polymers based on ionic and lipophilic properties (see Table 2). TEM provides micro- and nanostructural data and extends the optical range of LM to the atomic level (Table 8). TEM analysis yields information about polymer morphology in the matrix of the delivery systems and the localization of encapsulant in the matrix (Figs. 12 and 13b). Using more advanced replica techniques, it is possible to examine the surface of delivery systems and observe the morphology of vesicles and nanoparticles (see Table 8).

Finally, SEM completes the characterization by providing a three-dimensional depiction of macro-, meso-, and nanostructure on exterior and interior (cut) surfaces of drug delivery systems. SEM provides a convenient means of studying porosity and interconnectivity of pores. Most importantly, the distribution of encapsulant in the polymer matrix and the interaction of drug with surrounding polymer can be analyzed, as well as crystallinity differences in the polymer matrix itself. The abundance of information derived from SEM analysis can be further supplemented by LM and TEM data, as well as information from other physical characterization methods such as differential scanning calorimetry, Fourier transform infrared, gel permeation chromatography, and high-performance liquid chromatography to gain a fuller understanding of the mechanisms underlying controlled release in drug delivery systems.

BIBLIOGRAPHY

1. A.B. Maunsbach, *J. Ultastruct. Res.* **15**, 242–282 (1966).
2. M.A. Hayat, *Fixation for Electron Microscopy*, Academic Press, New York, 1981, p. 207.
3. A.M. Glauert, *Fixation, Dehydration and Embedding of Biological Specimens*, Elsevier, Amsterdam, 1975.
4. L.C. Sawyer and D.T. Grubb, *Polymer Microscopy*, Chapman & Hall, New York, 1987, p. 97.
5. P. Gerrits, R. Horobin, and D. Wright, *J. Microsc. (Oxford)* **160**, 279–290 (1990).
6. S.Y. Hobbs, V.H. Watkins, and R.R. Russell, *J. Polym. Phys. Ed.* **18**, 393–395 (1980).
7. K. Hess and H. Kiessig, *Naturwissenschaften* **31**, 171 (1943).
8. K. Hess and H. Mahl, *Naturwissenschaften* **41**, 86 (1954).
9. M. Sotton, *C.R. Hebd. Seances Acad. Sci.* **270B**, 1261 (1971).
10. W. Fredericks and K. Bosch, *Histochemistry* **100**, 297–302 (1993).
11. B.J. Spit, *Proc. 5th Int. Congr. Electron Microsc.*, Philadelphia, August 29–September 5, 1962, vol. 1, p. BB7.
12. C.W. Hock, *J. Polym. Sci. Part A2* **5**, 471–478 (1967).
13. W. Kuhlmann and P. Peschke, *Histochemistry* **75**, 151–161 (1982).
14. J. Litwin and K. Beier, *Histochemistry* **88**, 193–196 (1988).
15. R.M. Friedenberg and A.M. Seligman, *J. Histochem. Cytochem.* **20**, 771–792 (1972).
16. J. Hugson and M. Borgers, *J. Histochem. Cytochem.* **14**, 429–431 (1966).
17. A.L. Frank and A.K. Christensen, *J. Cell Biol.* **36**, 1 (1968).
18. L. Cutler, G. Rodan, and M.B. Feinstein, *Biochim. Biophys. Acta* **542**, 357–371 (1978).
19. J. Kawano and E. Akiwa, *J. Histochem. Chytochem.* **35**, 523–530 (1987).
20. S.A. Ernst, *J. Histochem. Cytochem.* **20**, 23–38 (1981).
21. A.B. Novikoff and R.J. Goldfischer, *J. Histochem. Cytochem.* **17**, 675–680 (1969).

Next Page

22. A.M. Seligman et al., *J. Cell Biol.* **38**, 1–14 (1968).
23. R.A. Monahan, H.F. Dvorak, and A.M. Dvorak, *Blood* **58**, 1089–1099 (1981).
24. L.W. Tice and R.J. Barnett, *J. Histochem. Cytochem.* **9**, 635–636 (1961).
25. C.E. Smith, *J. Histochem. Cytochem.* **28**, 689–699 (1980).
26. G.W. Kreutzberg and S.T. Hussain, *Neuroscience* **11**, 857–866 (1984).
27. R.C. Graham and M.J. Karnovsky, *J. Histochem. Cytochem.* **14**, 291–302 (1966).
28. A.B. Novikoff and S. Goldfischer, *Proc. Natl. Acad. Sci. U.S.A.* **47**, 802 (1961).
29. K. Pekarek, J. Jacob, and E. Mathiowitz, *Nature (London)* **367**, 258–260 (1994).
30. E. Mathiowitz et al., *Nature (London)* **386**, 410–414 (1997).
31. U.S. Pat. 4,919,929 (April 24, 1990), L.R. Beck (to Stolle Research and Development Corp.).

CHARACTERIZATION OF DELIVERY SYSTEMS, PARTICLE SIZING TECHNIQUES

K.L. WARD
M.A. TRACY
Alkermes, Inc.
Cambridge, Massachusetts

KEY WORDS

Coulter principle
Electrical sensing zone
Electron microscopy
Image analysis
Laser diffraction
Light scattering
Optical microscopy
Particle sizing
Photon correlation spectroscopy
Quasielastic light scattering
Sieving
Static light scattering
Total intensity light scattering

OUTLINE

Introduction
Sieving Methods
Microscopy Methods
Electrical Sensing Zone (Coulter Principle) Method
  Dispersion of Samples
Laser Light Scattering Methods
  Static Light Scattering
  Laser Diffraction
  Dynamic Light Scattering
Comparing Results From Different Particle Sizing Methods
Bibliography

INTRODUCTION

Particle size is an important variable in drug delivery systems, affecting such parameters as rates of dissolution, rates of release, injectability, and dose delivery. Table 1 gives examples of the broad size ranges of particulate systems encountered. Unfortunately, no single method is capable of covering this large range of sizes. As a result, a wide variety of methods have been developed to measure particle size, using quite different physical principles. Because it is not possible to fully describe all of the methods in the space allotted here, we have focused this discussion on four of the techniques most widely used by drug delivery scientists, covering the millimeter to nanometer size range (sieving) microscopy (electron and optical), electrical sensing zone (Coulter principle), and laser light scattering methods. For a more comprehensive review of particle size analysis, including methods such as sedimentation that are not discussed here, see the work by Allen (1). Figure 1 gives the size ranges that can be measured by each of the techniques. Because each method has its strengths and limitations, the objective of this chapter is to provide the reader with an understanding of the physical principles and practical differences between these techniques which, it is hoped, will help in selecting the most appropriate method for the job. Within this work, examples are given which demonstrate how these methods can be applied to drug delivery systems.

SIEVING METHODS

Sieving is one of the oldest methods of particle size determination. It involves passing sample through different sized meshes and determining the fraction captured by each mesh. This can be achieved with the powder in the dry or wet state. Sieving is most suitable for large particles (>75 μm), and it is often the pharmaceutical method of choice for sizing coarse powders, e.g., for nasal drug delivery (2). There is a U.S. Pharmacopeia (USP) method for accurately determining a particle size distribution by analytical sieving (3). There are limitations to this method, though, including a large sample requirement (>25 g) and difficulty in sieving cohesive and oily powders (3).

MICROSCOPY METHODS

Examination of particles by microscopy is an absolute method for measuring particles, as it allows direct obser-

Table 1. Particle Dimension Estimates in Drug Delivery and Pharmaceutical Systems

Particle Size (μm)	Examples
0.001–0.5	Proteins, polymers, oligonucleotides, DNA, micelles, microemulsions, colloidal suspensions
0.5–10	Suspensions, fine emulsions, micronized drugs
10–50	Coarse emulsions, flocculated suspensions
50–150	Fine powders
150–1,000	Coarse powders
1,000–3,400	Granules

22. A.M. Seligman et al., *J. Cell Biol.* **38**, 1–14 (1968).
23. R.A. Monahan, H.F. Dvorak, and A.M. Dvorak, *Blood* **58**, 1089–1099 (1981).
24. L.W. Tice and R.J. Barnett, *J. Histochem. Cytochem.* **9**, 635–636 (1961).
25. C.E. Smith, *J. Histochem. Cytochem.* **28**, 689–699 (1980).
26. G.W. Kreutzberg and S.T. Hussain, *Neuroscience* **11**, 857–866 (1984).
27. R.C. Graham and M.J. Karnovsky, *J. Histochem. Cytochem.* **14**, 291–302 (1966).
28. A.B. Novikoff and S. Goldfischer, *Proc. Natl. Acad. Sci. U.S.A.* **47**, 802 (1961).
29. K. Pekarek, J. Jacob, and E. Mathiowitz, *Nature (London)* **367**, 258–260 (1994).
30. E. Mathiowitz et al., *Nature (London)* **386**, 410–414 (1997).
31. U.S. Pat. 4,919,929 (April 24, 1990), L.R. Beck (to Stolle Research and Development Corp.).

CHARACTERIZATION OF DELIVERY SYSTEMS, PARTICLE SIZING TECHNIQUES

K.L. WARD
M.A. TRACY
Alkermes, Inc.
Cambridge, Massachusetts

KEY WORDS

Coulter principle
Electrical sensing zone
Electron microscopy
Image analysis
Laser diffraction
Light scattering
Optical microscopy
Particle sizing
Photon correlation spectroscopy
Quasielastic light scattering
Sieving
Static light scattering
Total intensity light scattering

OUTLINE

Introduction
Sieving Methods
Microscopy Methods
Electrical Sensing Zone (Coulter Principle) Method
  Dispersion of Samples
Laser Light Scattering Methods
  Static Light Scattering
  Laser Diffraction
  Dynamic Light Scattering
Comparing Results From Different Particle Sizing Methods
Bibliography

INTRODUCTION

Particle size is an important variable in drug delivery systems, affecting such parameters as rates of dissolution, rates of release, injectability, and dose delivery. Table 1 gives examples of the broad size ranges of particulate systems encountered. Unfortunately, no single method is capable of covering this large range of sizes. As a result, a wide variety of methods have been developed to measure particle size, using quite different physical principles. Because it is not possible to fully describe all of the methods in the space allotted here, we have focused this discussion on four of the techniques most widely used by drug delivery scientists, covering the millimeter to nanometer size range (sieving) microscopy (electron and optical), electrical sensing zone (Coulter principle), and laser light scattering methods. For a more comprehensive review of particle size analysis, including methods such as sedimentation that are not discussed here, see the work by Allen (1). Figure 1 gives the size ranges that can be measured by each of the techniques. Because each method has its strengths and limitations, the objective of this chapter is to provide the reader with an understanding of the physical principles and practical differences between these techniques which, it is hoped, will help in selecting the most appropriate method for the job. Within this work, examples are given which demonstrate how these methods can be applied to drug delivery systems.

SIEVING METHODS

Sieving is one of the oldest methods of particle size determination. It involves passing sample through different sized meshes and determining the fraction captured by each mesh. This can be achieved with the powder in the dry or wet state. Sieving is most suitable for large particles (>75 μm), and it is often the pharmaceutical method of choice for sizing coarse powders, e.g., for nasal drug delivery (2). There is a U.S. Pharmacopeia (USP) method for accurately determining a particle size distribution by analytical sieving (3). There are limitations to this method, though, including a large sample requirement (>25 g) and difficulty in sieving cohesive and oily powders (3).

MICROSCOPY METHODS

Examination of particles by microscopy is an absolute method for measuring particles, as it allows direct obser-

Table 1. Particle Dimension Estimates in Drug Delivery and Pharmaceutical Systems

Particle Size (μm)	Examples
0.001–0.5	Proteins, polymers, oligonucleotides, DNA, micelles, microemulsions, colloidal suspensions
0.5–10	Suspensions, fine emulsions, micronized drugs
10–50	Coarse emulsions, flocculated suspensions
50–150	Fine powders
150–1,000	Coarse powders
1,000–3,400	Granules

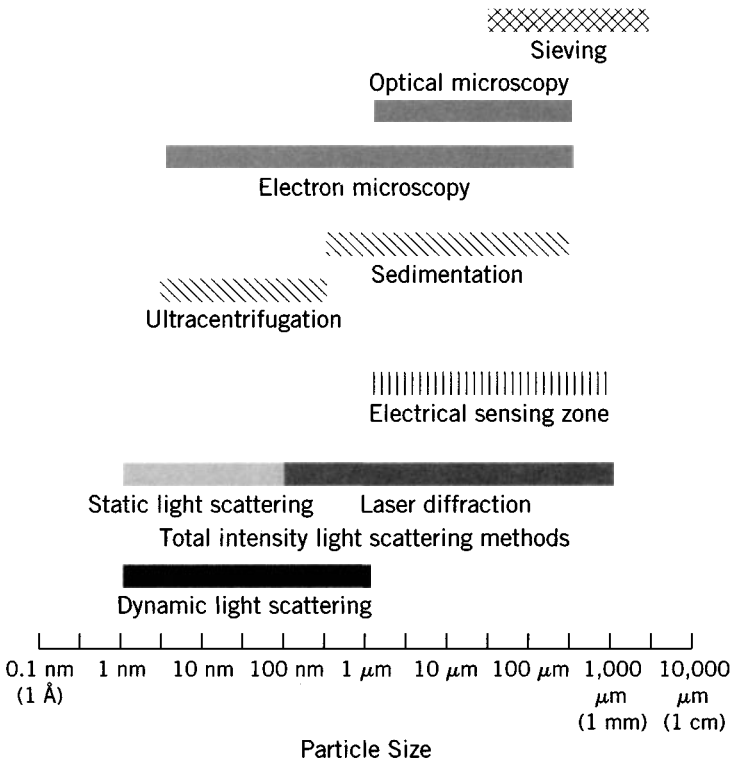


Figure 1. Approximate size ranges for methods used for particle size analysis.

vation of both the size and morphology of individual particles. Although it can be time consuming, microscopy is often used to validate the results of other sizing methods. Optical microscopy is most often used for particles between 3 and 150 μm. Larger than 150 μm, a magnifying glass is sufficient and sieving is the preferred method of particle size analysis. A lower limit of 3 μm is recommended due to gross overestimation of particle diameters close to the wavelength of light. Diffraction halos can result in oversizing a 1 μm particle by 15%, and even greater errors are introduced at smaller sizes (1). Another limitation of optical microscopy is the small depth of focus, which means that for wide-size distributions, only some particles in a particular field of view will be visible at any one time. For these reasons, it is recommended that particles from 20 nm to 3 μm be examined by scanning electron microscopy (SEM) (4), which can also be used to study larger (up to 1 mm) particles (5).

When viewed in an optical microscope, most particles appear as two-dimensional silhouettes, for which there are three major statistically acceptable measures of size:

- *Martin's diameter* is the length of a line which bisects the image of a particle into two equal areas. It can be measured in any direction relative to the particle's orientation, but a fixed direction must be used throughout the sample.
- *Feret's diameter* is the distance between parallel tangents on opposite sides of the particle. The orientation of the tangents is the same for the entire sample.
- The *projected area diameter*, i.e., the diameter of a circle having the same projected area as the particle, is preferred over other measures such as Martin's or Feret's diameter since two dimensions are included as opposed to one.

Particle sizes as measured by microscopy tend to be greater than those measured by other methods because the third dimension, perpendicular to the viewing plane, is the smallest for nonspherical particles in stable orientations. A globe and circle eyepiece graticule, calibrated against a stage micrometer, is typically used to estimate projected areas. In manual techniques, untrained operators tend to overestimate the areas of irregular silhouettes, whereas experienced operators are able to compensate for this tendency (6). This somewhat subjective determination, however, leads to some degree of operator bias. Use of commercially available automatic image analyzers can eliminate these biases, as well as speed up the process and remove errors due to the slowness and tedium of manual methods. Image analyzers also make shape analysis more practical. Automatic systems, on the other hand, are less able to distinguish artifacts, such as abutting particles, without some intervention by a human operator. They are also unable to adjust focus within a field of view, making them less useful for samples with a wide distribution of sizes. Several excellent reviews have been written on the application of automatic image analysis (1,7).

Particle size analysis by microscopy is best suited to determining a size distribution by number. Statistical accuracy is determined by the number of particles counted, although time limitations make it impractical to examine every particle on a slide. A general rule is that counting 625 or more particles yields a standard error of 2% or less

(1). Extreme care should be taken if such a number distribution is to be converted to a weight or volume distribution. A single 50-μm particle in a weight distribution, for example, accounts for as much mass as 1,000 5-μm particles, and so miscounting the largest particles can drastically affect the overall results. Counting at least 25 particles in the largest size category helps to limit such errors but usually increases the time of analysis, as more of the sample must be examined to achieve this standard. Detailed procedures for determining particle size distributions by microscopy and reporting particle size data are described in the U.S. Pharmacopeia (8) and in the Pharmacopeial Forum (9), respectively.

ELECTRICAL SENSING ZONE (COULTER PRINCIPLE) METHOD

The electrical sensing zone method, also known as the Coulter technique, was presented in 1956 as an automatic method for counting and sizing blood cells (10) and was soon applied to many kinds of particulate materials (11,12). The apparatus consists of two electrodes immersed in an electrolyte solution, separated by the wall of a glass tube with a single small orifice connecting the fluid inside the tube to the solution surrounding it. Particles suspended in the outer fluid are pulled through the orifice by applying vacuum to the fluid inside the tube. Electrical current flowing between the electrodes can only pass through the narrow orifice, and a particle that passes through the orifice, displacing a volume of electrolyte, momentarily increases the impedance of the circuit. The resulting change in resistance (ΔR) is related to the volume (V) of a spherical particle by the following equation:

$$\Delta R = (16\rho_f V/\pi^2 D^4)F \qquad (1)$$

where ρ_f is the resistivity of the fluid, D is the diameter of the orifice, and F is a function that incorporates certain correction factors, including a shape factor. In other words, ΔR is proportional to the particle volume, modified by the function F. Empirically, this function has little effect for particles much smaller than the orifice, and causes divergence from linearity in a predictable fashion as the particle size approaches the aperture diameter. Modern instruments are capable of reliably sizing particles between 2% and 60% of the orifice diameter, e.g., 2–60 μm for a 100-μm-diameter aperture. Aperture diameters from 30 to 2000 μm give the apparatus an overall range of 0.6 μm to 1,200 μm, but only a portion of this range can be measured with a given aperture. Consequently, a difficult two-tube technique is required for complete analysis of any sample with a broad-size distribution.

An electrical sensing zone instrument can count and size thousands of particles in a few seconds, and semiskilled operators can use it with reproducible results. Up to 256 size channels in a relatively narrow range leads to very high resolution, although with some increase in noise levels. The large number of particles analyzed, often many tens of thousands, greatly improves the statistical accuracy of a number-based distribution, and also improves the accuracy when the data are converted to a volume distribution. Care must be taken to control the concentration of suspended particles, though, because of the problem of coincidence. This is the passage of two particles through the orifice at roughly the same time, possibly detected as a single larger peak, which leads to oversizing when it becomes significant at higher concentrations. At low concentrations, the Coulter method is used for counting particulate contaminants in parenteral fluids. This application is described extensively in the British Pharmacopeia (13), and is also described in detail elsewhere (14). Other applications include the study of drug delivery systems such as liposomes (15), albumin microparticles (16), and microspheres for sustained release of proteins (17). A general method for all applications is described in British Standard 3406 (18).

Dispersion of Samples

Whenever a powder is suspended in a liquid for purposes of particle size analysis, whatever the method, accurate results will only be obtained if the sample is properly dispersed. Usually, this is accomplished by the addition of a surfactant and possibly low power sonication. With the Coulter method, an additional factor is the requirement of an electrolyte solution. Some electrolytes, especially in nonaqueous media, can cause a sample to aggregate, thereby increasing the measured particle size. An example of a pharmaceutical with an electrolyte sensitivity is lyophilized particles of recombinant human growth hormone (rhGH), a water-soluble protein that has to be suspended in an organic solvent for particle size analysis. Lithium chloride or zinc chloride dissolved in acetone cause some agglomeration of the protein powder, although in the latter case the size distribution appears stable over time. When magnesium perchlorate is dissolved in 80/10/10 (% v/v) acetone/methanol/dimethyl sulfoxide, however, the measured particle size is smaller, as shown in Figure 2. Analysis on a laser diffraction instrument confirms that particles are larger in the presence of zinc chloride, relative to neat acetone or the magnesium perchlorate solution.

LASER LIGHT SCATTERING METHODS

Instruments that use light scattering principles for particle size analysis have become popular because they allow

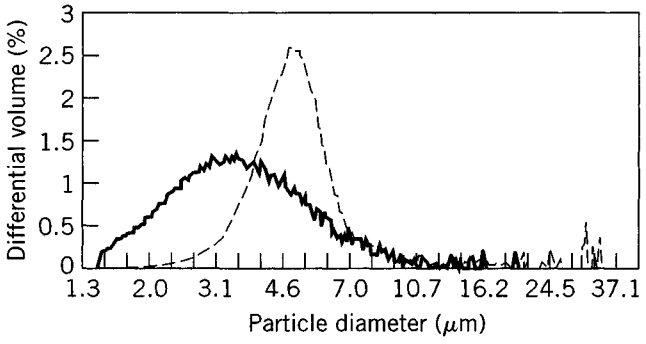


Figure 2. Size distribution of rHGH particles suspended in organic solvents with two different electrolytes. The solid line represents the data with magnesium perchlorate and the dotted line the data with zinc chloride.

quick and absolute determination of particle size, i.e., without the need for calibration. Although all of these approaches use a laser to measure particle size, there are really three major light scattering methods, each based on different principles. The first two techniques, static light scattering (SLS) and laser diffraction, are sometimes referred to as total intensity light scattering (TILS) methods and use time-averaged measurements of scattered light flux, whereas dynamic light scattering (DLS) instruments measure fluctuations in the intensity of scattered light and relate them to size-dependent parameters such as diffusion coefficients. Figure 1 shows the optimum particle size ranges for each method. SLS instruments are most often used for determining the molecular weights of macromolecules. Broad particle size distributions of 0.1–1000 μm can easily be measured with instruments based on laser diffraction principles. And for fine particulates from 2 nm up to about 2 μm, DLS is the method of choice. All these methods require dilute concentrations where interactions between particles and secondary scattering are minimized, although this must be balanced against the requirement for enough sample to obtain a sufficient signal-to-noise ratio. The discussion that follows briefly describes the theory behind each of these techniques and few practical issues. This does not represent the full extent of light scattering methods, though, that also can be used to obtain information on particle interactions, macromolecular solution dynamics, molecular relaxation, and phase changes.

Static Light Scattering

The basic principles of light scattering are presented here to provide a basis for understanding how particle size information is obtained from light scattering methods. For more detailed theoretical discussion, see the work by van de Hulst (19). When incident light hits a particle, the particle acts as an oscillating dipole emitting scattered light in all directions. For homogeneous small particles, such as single macromolecules, the scattering particles act as point dipole oscillators. The scattering intensity for N ($= \rho N_A/M$) particles per unit volume is then described by the Rayleigh equation:

$$I = N(8\pi^4(1 + \cos^2\theta)\alpha^2)\, I_o/r^2\lambda^4 \qquad (2)$$

where r is distance from the particle, λ is wavelength of incident light, α is particle polarizability, I_0 is intensity of incident light (unpolarized), θ is scattering angle, ρ is density of the particles, M is molecular weight of the particles, N_A is Avogadro's number. Some of the underlying assumptions of this model are that the particles are dilute and therefore not interacting with each other and do not absorb light (19).

Another assumption of Rayleigh scattering is that interference effects are absent. It has been shown that this is a valid assumption only for molecules or particles with overall dimensions $<\lambda/20$ (19). This limit decreases as the particle refractive index approaches the refractive index of the medium (20). A larger molecule no longer acts as a point dipole oscillator but as a collection of many of them. Light scattered from different points within the molecule results in destructive interference. The Rayleigh-Gans-Debye theory corrects the Rayleigh equation 2 for intramolecular interference effects, and the resulting equation is most commonly written as in equation 3 (20).

$$(Kc/R_\Theta) = [1/M_w + 2Bc][1 + (16\pi^2/3\lambda^2)(r_g^2 \sin^2(\theta/2))] \qquad (3)$$

where K is $2\pi^2[n(dn/dc)]^2/\lambda^4 N_A$ (for unpolarized light), $R_\Theta = Ir^2/I_0(1 + \cos^2\theta)$, c is the particle concentration, n is the refractive index of the solvent, M_w is the weight average molecular weight of the particle, B is the thermodynamic second virial coefficient, and r_g is the radius of gyration of the particle. This equation provides the basis for measuring size-related parameters, namely molecular weight and radius of gyration, which are commonly used to characterize polymers in solution, including those used in many drug delivery devices. Measuring molecular weights by light scattering is described in the USP (21). A method of extrapolating data from equation 3 to the limits $c = \theta = 0$, $\theta = 0$, and $c = 0$ to determine M_w, r_g, and B, respectively, in a single plot is called a Zimm plot and is described in detail by several authors (20,22). Several manufacturers make SLS instruments for the measurement of molecular weights, where the scattered light intensity is measured at multiple angles and equation 3 is applied in the limit as $\theta = 0$. This technique is sometimes called multiple angle laser light scattering (MALLS). SLS measured at single or multiple angles is even more powerful when used in conjunction with size exclusion chromatography (SEC) as a postcolumn detection method, as it allows absolute determination of polymer molecular weights without need for calibration (23–25).

Laser Diffraction

If particles are sufficiently large compared to the wavelength of light, the particles diffract light in predictable patterns, according to the laws of geometrical optics (Fraunhofer diffraction). Large particles scatter more radiation but mostly at low angles, whereas smaller particles produce fainter, more complicated scattering patterns that extend to higher angles. In analogy to Young's single slit experiment, light diffracted from a large particle of diameter d (>1 μm) produces an intensity pattern at a large distance from the particle with mimima at angles given by the equation below, where m is any integer.

$$d \sin\theta = (m + 1/2)\lambda \qquad (4)$$

Thus, in principle, the particle size can be determined from the diffraction pattern. For some particles, though, such as transparent and submicron particles, the Fraunhofer approximation begins to break down. In such cases, an alternative is the Mie theory, which rigorously describes the scattering pattern for spheres of any size. This theory is quite complex, but with the help of modern computers, most laser diffraction instruments offer sizing results based on both Fraunhofer diffraction and Mie theory. In the case of Mie theory, a close estimate of the particle's refractive index is required to accurately compute particle size.

Instruments that use laser diffraction for particle size analysis are commercially available from a number of manufacturers. The chief attraction of these instruments is their ability to quickly and easily measure size distributions over a broad range, on average between 0.1 and 1000 μm, with the range subdivided into about 100 size intervals. Many instruments use information from additional detectors or polarization ratios to extend this range up to 2,000 μm or down to 0.04 μm (1). Some models are available with modules for sizing dry powders as well as liquid suspensions. The equipment typically consists of a transparent sample cell through which a fluid suspension is recirculated, or through which a dry powder is blown. A laser beam is directed through the cell, and one or more Fourier lenses on the other side focus the scattered radiation on an array of solid-state detectors, from low angles up to at least 40°. Using optical models based on Fraunhofer or Mie theory, the overlapping patterns of scattered light are deconvoluted in an iterative fashion to generate a volume-weighted size distribution (1). This method has been applied to a number of drug delivery systems, including powder aerosols for pulmonary delivery (26), and microspheres for sustained drug delivery (27,28).

Laser diffraction instruments in general provide very reproducible results, but the distributions obtained from different manufacturers' instruments can vary significantly, especially in the lower size range (1). One reason for these discrepancies is that the complete solution for the diffraction pattern using Mie theory is available only for spheres. For partially transmitting or nonspherical particles, converting the scattered light flux into a size distribution is less straightforward. Each manufacturer uses its own proprietary algorithms, leading to different results from different instruments (1). Nonspherical shapes can affect the distribution in other ways as well. One advantage of laser diffraction as compared with other techniques is that all orientations of a suspended particle can be presented to the laser beam, which prevents oversizing due to neglect of one dimension. Unfortunately, it may also produce a broader distribution, or a multimodal size distribution in the case of extremely anisotropic shapes such as rods or flakes (29). In such cases, combining this technique with microscopy may help to determine whether particle shape is affecting the appearance of the size distribution.

Dynamic Light Scattering

For the techniques already discussed, particle size-related information is derived from time-averaged measurements of the intensity of scattered light at various angles. In contrast, DLS, also known as photon correlation spectroscopy (PCS) or quasielastic light scattering (QELS) involves measuring the variation in the scattered light intensity over time. Physically, the instantaneous scattered intensity can be thought of as the superposition of waves scattered from individual scattering centers subject to Brownian motion. As the scattering molecules or particles move toward or away from the detector, minute shifts in the frequency of the scattered light are introduced that generate beat frequencies proportional to the magnitude of the shift (30). As particle size decreases, particles exhibit increasingly rapid motions, resulting in greater Doppler shifts and higher frequency fluctuations. These variations in the scattered light intensity can be related mathematically to size-dependent molecular transport properties such as diffusion coefficients. The theories describing that relationship are quite complex and beyond the scope of this discussion, but a thorough explanation may be found in the work of Berne and Pecora (31). Particle size for noninteracting spheres is related to the diffusion constant (D) through the Stokes-Einstein equation:

$$D = kT/6\pi\eta R \tag{5}$$

where η is the solution viscosity, R is the hydrodynamic radius of the particle, k is Boltzmann's constant, and T is the absolute temperature.

Manufacturers of DLS instruments claim an applicable size range from about 0.002 to 2 μm, although the technique is most reliable below about 0.5 μm (32). Measuring particles larger than 1 μm is complicated by their tendency to sediment, as well as inter- and intramolecular scattering effects. The apparatus for determination of particle size by DLS typically involves shining a polarized laser beam through a dilute suspension of the sample, and measuring scattered radiation at one or more angles from the incident light. An autocorrelator stores scattered light intensities at different times and calculates a correlation function that decays exponentially with time. For small, monodisperse particles undergoing Brownian motion

$$C(t) \propto (\exp(-qDt)) \tag{6}$$

where $C(t)$ is the value of the correlation function at time t, q is the wave vector $= 4\pi n/\lambda \sin(\theta/2)$, n is the solvent's refractive index, and D is the diffusion constant. For multicomponent or polydisperse systems, the correlation function can be fit to a weighted sum of exponentials which can be deconvolved using computer programs such as CONTIN. From the components generated in this way, a size distribution can be determined, although multimodal distributions cannot always be resolved (1). A rule of thumb for spherical particles is that two modes differing by at least a factor of two in their mean diameter can be distinguished by CONTIN analysis. Results are usually given in terms of an average particle size and a polydispersity index. This method is particularly suitable for sizing drug delivery systems such as liposomes (33), microemulsions (34,35), and nanoparticles (36–39). DLS has also been used to examine the kinetics of aggregation for macromolecules such as insulin (40).

COMPARING RESULTS FROM DIFFERENT PARTICLE SIZING METHODS

It is important to realize that each method of particle size analysis may produce a somewhat different result. These differences do not necessarily imply that one technique is more accurate than another, only that distinct principles are involved that measure particle size in different ways. For example, in the electrical sensing zone method the

signal is proportional to the displacement volume of a particle. Porous particles, into which electrolyte solution can penetrate, appear smaller by this method than by a light scattering method, in which the diffraction pattern is dependent on the envelope volume of the particle. A number of studies have found that extremely nonspherical shapes also appear larger when measured by laser diffraction as compared with the Coulter method (41,42). The greatest differences between the techniques, about 40%, were observed for rods and plates, whereas the results for less extreme shapes differed by less than 10%. It has been suggested that the ratio of mean values obtained by these two methods could be used to predict shape, provided the particles are nonporous (42). In selecting a method for particle size analysis, one should consider not just whether a method may oversize some particles, but also the characteristics requirements of the material to be analyzed. For some applications, reproducibility and ease of use may be more important than absolute size determination.

BIBLIOGRAPHY

1. T. Allen, *Particle Size Measurement*, 5th ed., Chapman & Hall, London, 1997.
2. A.D. Ascentiis et al., *Pharm. Res.* **13**, 734–738 (1996).
3. *Pharmacopeial Forum* **22**, 3240–3244 (1996).
4. *Scanning Electron Microscopy*, U.S. Pharmacopeia 25, U.S. Pharmacopeial Convention, Inc., Rockville, Md., 1995, pp. 1954–1957.
5. R. Falk et al., *J. Controlled Release* **44**, 77–85 (1997).
6. I.F. Nathan, M.I. Barnet, and T.D. Turner, *Powder Technol.* **5**, 105–110 (1972).
7. T.A. Barber, in J.Z. Knapp, T.A. Barber, and A. Lieberman, eds., *Liquid- and Surface-Borne Particle Measurement Handbook*, Dekker, New York, 1996, pp. 61–112.
8. *Optical Microscopy*, U.S. Pharmacopeia 25, U.S. Pharmacopeial Convention, Inc., Rockville, Md., 1995, pp. 2715–2717.
9. *Pharmacopeial Forum* **19**, 4640–4642 (1993).
10. W.H. Coulter, *Proc. Natl. Electron. Conf.* **12**, 1034 (1956).
11. H.E. Kubitschek, *Nature (London)* **182**, 234–235 (1958).
12. R.W. Lines and W.M. Wood, *Ceramics* **16**, 27–30 (1965).
13. *British Pharmacopoeia*, Vol. 11, HMSO, London, 1993, pp. A163.
14. R.W. Lines, in J.Z. Knapp, T.A. Barber, and A. Lieberman, eds., *Liquid- and Surface-Borne Particle Measurement Handbook*, Dekker, New York, 1996, pp. 113–154.
15. H. Talsma and D.J.A. Crommelin, *Pharm. Technol. Int.* **5**, 37 (1993).
16. I. Vural, H.S. Kas, A.A. Hincal, and G. Cave, *J. Encapsulation* **7**, 511 (1990).
17. O.L. Johnson et al., *Pharm. Res.* **14**(6), 730–735 (1997).
18. *British Standard 3406: Part 5*, British Standards Institution, London, 1983.
19. H.C. van de Hulst, *Light Scattering by Small Particles*, Dover, New York, 1981.
20. P.C. Hiemenz, *Polymer Chemistry: The Basic Concepts*, Dekker, New York, 1984.
21. *Spectrophotometry and Light Scattering*, U.S. Pharmacopeia 25, U.S. Pharmacopeial Convention, Rockville, Md., 1995, pp. 1830–1835.
22. M.B. Huglin, ed., *Light Scattering from Polymer Solutions*, Academic Press, New York, 1972.
23. P.J. Wyatt, C. Jackson, and G.K. Wyatt, *Am. Lab.* May-June (1988).
24. L. Jeng et al., *J. Appl. Polym. Sci.* **48**, 1359–1374 (1993).
25. U. Dayal and S.K. Mehta, *J. Liq. Chromatogr.* **17**(2), 303–316 (1994).
26. H.-K. Chan et al., *Pharm. Res.* **14**(4), 431–437 (1997).
27. A. Matsumoto et al., *J. Controlled Release* **48**(1), 19–27 (1997).
28. M.-K. Yeh, S.S. Davis, and A.G.A. Coombes, *Pharm. Res.* **13**(11), 1693–1698 (1996).
29. N. Gabas, N. Hiquily, and C. Lagueric, *Part. Part. Syst. Charact.* **11**(2), 121–126 (1994).
30. B.B. Weiner, in J.Z. Knapp, T.A. Barber, and A. Lieberman, eds., *Liquid- and Surface-Borne Particle Measurement Handbook*, Dekker, New York, 1996, pp. 155–171.
31. B.J. Berne and R. Pecora, *Dynamic Light Scattering*, Wiley, New York, 1976.
32. N. de Jaeger et al., *Part. Part. Syst. Charact.* **8**(9), 179–186 (1991).
33. E.C.A. van Winden, W. Zhang, and D.J.A. Crommelin, *Pharm. Res.* **14**(9), 1151–1160 (1997).
34. M.R. Lance, C. Washington, and S.S. Davis, *Pharm. Res.* **13**(7), 1008–1014 (1996).
35. F. Liu, J. Yang, L. Huang, and D. Liu, *Pharm. Res.* **13**(11), 1642–1646 (1996).
36. J.-Y. Cherng et al., *Pharm. Res.* **13**(7), 1038–1042 (1996).
37. H. Heiati, N.C. Phillips, and R. Tawashi, *Pharm. Res.* **13**(9), 1406–1410 (1996).
38. R.H. Müller, S. Maassen, C. Schwarz, and W. Mehnert, *J. Controlled Release* **47**(3), 261–269 (1997).
39. M.T. Peracchia et al., *J. Controlled Release* **46**(3), 223–231 (1997).
40. M. Dathe et al., *Int. J. Pep. Protein Res.* **36**, 344–349 (1990).
41. J.A. Davies and D.L. Collins, *Part. Part. Syst. Charact.* **5**, 116–121 (1988).
42. A.T. Palmer, P.J. Logiudice, and J. Cowley, *Am. Lab.* November (1994).

CHARACTERIZATION OF DELIVERY SYSTEMS, SPECTROSCOPY

GREGORY T. FIELDSON
ALZA Corporation
Palo Alto, California

KEY WORDS

ATR spectroscopy
Characterization
Chemometrics
Infrared spectroscopy
Quantitative analysis

OUTLINE

- Introduction
- Infrared Spectroscopy
  - Physical Phenomena
  - Information
  - Ranges
- Techniques
  - Transmission Spectroscopy
  - Attenuated Total Reflectance Spectroscopy
  - Microscopy
- Analysis of Infrared Spectra
  - Qualitative Analysis
  - Quantitative Analysis
- Applications
  - Research
  - Development
  - Manufacturing
- Bibliography

INTRODUCTION

Infrared spectroscopy is a measurement of the absorption of light by molecular vibrations. The vibrational portion of the electromagnetic spectrum is in the infrared region, with wavelengths ranging from 2.5 to 25 μm.

Infrared spectra record the presence of most asymmetric covalent bonds, and the technique has long been used as a means of identifying chemical structure. As with other related spectroscopic techniques, such as ultraviolet (UV) and visible light spectroscopy, the degree of light absorption is related to concentration. Therefore, infrared spectroscopy is a simple technique for identifying chemicals and measuring concentration in both simple and complex systems.

As an analytical tool, infrared spectroscopy has broad applications throughout drug delivery research as well as product development and manufacture. As a basic research tool, it is used to investigate biological systems, characterize materials, and conduct clinical studies. In product development process, it is a tool for refining formulations and processes. In manufacturing, it is an on-line monitoring tool for process control and a quality assurance tool for testing long-term stability.

INFRARED SPECTROSCOPY

Infrared spectra are a comparison of infrared light reaching a detector in the presence and absence of a sample. The reference, or background, spectrum and sample spectrum may be collected simultaneously along parallel pathways, as in a dual-beam spectrometer, or may be collected sequentially, with samples and references alternately placed in the light path as in a single-beam spectrometer. The ratio of the sample signal to the reference signal forms the infrared absorption spectrum.

Physical Phenomena

The energy of vibrational transitions in covalently bonded molecules corresponds to the frequencies of infrared light. For incident light to couple with a molecular vibration and be absorbed, certain selection rules must be met (1). The most important criterion for infrared spectroscopy is that the vibration results in an oscillating dipole. Therefore, asymmetric covalent bonds (for example, the carbon–oxygen bond in ethers) will absorb infrared light, whereas symmetric covalent bonds (for example, the carbon–carbon bond in ethane) will not absorb infrared light.

A variety of vibrational modes exist within a molecule. Common modes include bond stretching and bending, bond-pair scissoring, wagging, rocking, and twisting. Detailed information about the various vibrational modes in infrared spectroscopy can be found in the basic references (2–7).

Information

The infrared spectrum is typically plotted as a graph of the fraction of light absorbed by the sample through the range of light frequencies. The frequency of each absorbance peak is the result of a particular molecular vibration. The collection of absorbance peaks for a molecule, the infrared spectrum, reflects the overall covalent bond structure.

The magnitude of the absorbance peaks is directly proportional to the number of molecules in the infrared path. When calibration standards are available, the concentration of a sample can be accurately determined.

Ranges

The frequency of infrared light is usually reported in reciprocal centimeters (cm^{-1}) and is called the wavenumber. The standard vibrational infrared wavenumber range is 4,000–400 cm^{-1}, which corresponds to a wavelength range of 2.5– 25 μm.

Peak heights are recorded as either a percent transmittance or an absorbance; these units are explained in "Quantitative Analysis." In general, infrared spectrometers are capable of measuring concentration in solids or liquids with an accuracy of about 0.1 vol %. The lower detection limit is dependent on the absorption characteristics of each particular chemical.

TECHNIQUES

A variety of techniques have been developed for measuring infrared spectra. The most important techniques for drug delivery research and development are described in the following sections, with a basic description of the technique and their utility and limitations.

Transmission Spectroscopy

Transmission spectroscopy is the simplest infrared technique and the standard method for most infrared work. In this technique, a comparison is made between light transmitted through a sample cell and a blank or reference cell.

Sample cells useful for many different applications may be easily obtained (8).

Transmission spectroscopy is capable of handling most types of samples. Aside from the ability to transmit light through the sample, the key requirement is that the path length within the sample is such that the incident light is neither excessively nor minimally absorbed. Accomplishing this may require extensive sample preparation as well as some prior assumptions about the infrared absorption of the sample. The analysis of transmission spectra is simple and uncomplicated, with extensive free and commercial sample libraries available as references (9–14).

One important limitation of transmission spectroscopy is the difficulty in recording spectra of wet samples. Water is an extremely strong infrared absorber, so obtaining usable spectra of compounds in aqueous solutions can be impossible. The requirement of a direct transmission path through the sample can preclude the use of transmission spectroscopy for studying some types of drug delivery systems. Lastly, the appearance of optical interference fringes in samples with poorly matched refractive indices (to the surrounding air or crystal cell faces) can make quantitative comparison of spectra uncertain.

Attenuated Total Reflectance Spectroscopy

Attenuated total reflectance (ATR) spectroscopy, or internal reflectance spectroscopy (IRS), is a valuable extension of the basic infrared sampling technique because it greatly expands the range of samples available for testing, minimizes the sample preparation in many instances, and introduces new experimental possibilities (15,16). ATR infrared spectroscopy is based on physical phenomena that occur during the internal reflection of light in a dense material. The infrared spectrum of a sample is obtained by placing it in contact with a crystal within which infrared light is being reflected.

There are two important differences between this technique and transmission IR spectroscopy. First, the spatial region that is measured is determined by optical parameters, not by the dimensions of the sample. This region can be related to an equivalent thickness in transmission spectroscopy and ranges from 0.25 to 10 μm, depending on materials and infrared frequency (17,18). Second, the spectra is measured in a region adjacent to the ATR crystal, and infrared light is not transmitted through the sample. As the sampled region is dependent on wavelength, ATR spectra may not be compared directly with transmission spectra. It is possible to transform the spectra into an approximately equivalent transmission spectrum, but it is preferable to avoid such comparisons when possible because of distortions that occur in ATR spectra, particularly in the case of overlapping absorbance peaks (19). It is better practice to prepare ATR reference spectra for use with ATR samples.

The short path length of ATR spectroscopy allows for the testing of aqueous systems as the absorbance of water in this short equivalent path length is not overwhelming. The near-surface sampling of ATR spectroscopy makes sampling of multilayered and opaque materials possible. The combination of transmission and ATR spectroscopy can also be used to identify differences between surface and bulk concentrations (20–22). Even more usefully, this surface orientation has been exploited to measure the transport rate of molecules through polymeric materials and biological samples (23–26).

From a practical perspective, sample preparation for ATR spectroscopy is often much simpler than transmission spectroscopy, primarily because sample thickness does not need to be controlled. Sample throughput can also be improved because, unlike many transmission methods, it is possible to change ATR samples without affecting the purged environment of the sample compartment. Another important benefit is that in vivo measurements can be made with ease.

The primary disadvantage of ATR spectroscopy is the restricted frequency range, which results from the ATR sample crystal that is used. Another disadvantage is reduced signal quality because of optical losses throughout the infrared path in the ATR apparatus. More subtly, extrapolating the near-surface measurement (as obtained in ATR spectroscopy) to bulk properties can lead to errors, as a surprising number of mixtures will contain surface-to-bulk concentration anisotropy. Also, fewer reference libraries of spectra collected by ATR spectroscopy exist for use in sample identification.

Microscopy

Both transmission and ATR infrared spectroscopy may be used in conjunction with an infrared microscope. These accessories are extremely useful in isolating and identifying small particles in a sample. Additionally, by scanning the microscope over the surface of a sample, a two-dimensional map of sample composition can be made. Microscopic infrared spectroscopy may be applied to samples as small as 10 μm in diameter.

ANALYSIS OF INFRARED SPECTRA

Qualitative Analysis

The simplest analysis of an infrared spectrum is a qualitative assessment of the absorbance peaks heights and locations. The presence of particular absorbance peaks may be used to decipher the chemical structures within the sample. More typically, a spectrum is compared with a reference library to identify an unknown compound. In a similar manner, the purity of a material may be assessed by noting the appearance of additional peaks that are not present in a high-purity reference.

Spectra obtained from different solutions of the same compound or different phases of a crystalline compound can also provide important qualitative information. Intramolecular interactions, especially hydrogen-bonding, are evident in shifts of the frequency location of related infrared peaks. As a result, the spectrum of a compound dissolved in hydrogen bonding or nonpolar solvents will display distinct differences. In solids, different crystal forms of single compound may be distinguished by their infrared spectrum.

Quantitative Analysis

The root of applied, quantitative spectroscopy is the basic relationship between the absorption of electromagnetic waves and the amount of the absorbing chemical in the infrared path. In transmission spectroscopy, at low absorbance, this relationship is expressed by the Beer-Lambert law

$$dI = \alpha I dz = -\epsilon C I dz \quad (1)$$

where I is the light intensity at position z, α is the absorption coefficient, ϵ is the molar extinction coefficient, and C is the molar concentration of the absorbing group. This expression is strictly valid in the limit as $\alpha \rightarrow 0$ but is generally applicable unless the absorption coefficient, α, is quite large. Integration of equation 1 through a sample of thickness L gives the usual expression for percent transmittance

$$T = \frac{I}{I_0} 100 = \exp\left(\int_0^L \epsilon C dz\right) \times 100 \quad (2)$$

where T is the percent transmittance, I is the intensity of the transmitted light, and I_0 is the intensity of the incident light. The transmittance is often converted into absorbance, A, by

$$A \equiv -ln\left(\frac{I}{I_0}\right) = \int_0^L \epsilon C dz \quad (3)$$

When C is constant throughout the sample, equation 3 reduces to

$$A = \epsilon C L \quad (4)$$

As the link between light absorption and the molar concentration of an absorbing group, equation 4 is the basis for quantitative infrared spectroscopy. The value of the molar extinction coefficient is usually determined experimentally (27).

APPLICATIONS

Infrared spectroscopy is applied to drug delivery research, development, and commercial product manufacture in a tremendous variety of ways. The applications range from fundamental research into protein–membrane interactions to on-line process monitoring in commercial production. The common thread that unites all of the applications is the need to investigate changes in covalent or intramolecular interactions in a nondisrupting manner.

Research

Basic Lipid Research. One area of infrared-based research that has broad implications in many aspects of drug delivery is the study of lipid bilayers. Infrared spectroscopy is capable of revealing small changes in the orientation of a lipid bilayer without perturbing the sample (28–30). As a result, infrared spectroscopy has been used in numerous studies. The effect of composition, temperature, and pressure on phase transitions has been closely studied, typically using a combination of infrared spectroscopy and differential scanning calorimetry (DSC) or nuclear magnetic resonance (NMR) spectroscopy (31–36). The resulting information may be used directly as a guide in the development of liposomal formulations (37–40). Understanding of lipid behavior also has a general impact on other drug delivery technologies, such as transdermal delivery and drug targeting (41–43).

Materials and Formulations for Drug Delivery. Materials and formulations for drug delivery systems are frequently developed using infrared spectroscopy. In controlled release formulations the relationship of raw materials and processing to dissolution rates and release rates may successfully be measured with infrared spectroscopy (44–47). For implant drug delivery devices, the interaction between biological proteins and materials is measurable, as well as the impact of altering these materials (for example, heparinization of an implant surface) (48–50). Strategies for preparing conformationally stable protein formulations for intravenous injections and implant devices are frequently based upon infrared spectroscopic results (51–54).

Biological Structure and Composition. Infrared tools developed for studying lipids can be extended to biological lipid membranes as well (55). Fundamental research into the perturbation of cell membranes by various proteins is conducted using infrared spectroscopy (56–59); cell membranes have been reconstructed on ATR cells for accurate measurements of protein–membrane interactions and liposome–membrane interactions (28,60).

Because the stratum corneum is commonly accepted as the primary barrier of the skin and these bilayers are quite amenable to infrared sampling, many researchers have used infrared spectroscopy to study the stratum corneum lipids (61). These studies have examined the normal structure of the stratum corneum (62–67) and the impact of hydration (68–72), chemical permeation enhancers, mechanical disruption, and electrical disruption upon the barrier (73–82).

It especially worth noting that infrared spectroscopy has been used repeatedly as a noninvasive, clinical tool for studying topical and transdermal formulations. These studies have investigated the accumulation of penetrant in the skin, the extraction of lipids from the skin, and the perturbation of the skin lipids when subjected to various treatments (65,68,70,71,80,83–85).

Correlative Methods. The infrared absorption spectrum of a chemical inherently contains a detailed description of the covalent structure and both intermolecular and intramolecular secondary interactions. As a result, infrared spectroscopy should be a successful tool for developing quantitative structure analysis relationships (QSARs), linking a simple, inexpensively measured property to a higher-level effect.

Outside of drug delivery, infrared spectroscopy was successfully applied to the prediction of polymer membranes' permeability (86,87). Drawing upon this methodology, a

proprietary model, using infrared spectrum, is used to predict the effectiveness of chemical permeation enhancers for transdermal drug delivery. The resulting neural network models, based upon infrared spectral inputs, are the most accurate models developed to date (W. van Osdol, personal communication, 1998).

Development

Composition. Infrared spectroscopy is a primary tool for compositional analysis of mixture components that are present in concentrations greater than 0.1 vol %. Although sample preparation or calibrations may sometimes represent a challenge, this application is routine.

Stability. In conjunction with composition analysis, infrared spectroscopy is also a rapid test of the gross chemical stability of any formulation, component, or material that can be sampled. The creation or disruption of covalent chemical bonds results in changes in the infrared absorption. Detection of significant changes (>0.1 vol %) by infrared spectroscopy may be used as an inexpensive screen that triggers the deployment of more elaborate techniques (such as liquid or gas chromatography and mass spectroscopy) to identify the precise nature of a stability problem (88,89).

Manufacturing

Quality Control. Infrared spectra are routinely used as an acceptance criterion for receiving materials in the manufacturing environment. Gross errors, such as mislabeled materials, are almost instantly detected. Other changes in the infrared spectrum, when compared to a reference standard, can be used to detect minor errors, such as an incorrect mixture composition, excessive degradation, or significant impurities (90–93).

Quality Assurance. Infrared spectroscopy has been developed as an on-line tool for process control. Sampling methods exist for almost every type of process operation, and when accurate, rapid composition monitoring and control is desired, infrared spectroscopy can be applied (94–96).

Infrared spectroscopy may also play a role in product testing. Finished products may be compared to reference standards to assess compliance with composition specifications. Additionally, infrared spectroscopy may be used to monitor the long-term stability of product, detecting changes that result from both chemical and morphologic changes to the product (97).

Defect Analysis. A common application of infrared spectroscopy is the analysis of failed product or materials. An example is analysis of particles that appear in a finished drug delivery system. The use of infrared microscopy, combined with searches of infrared spectral libraries, will rapidly identify the nature of the contaminant (98). Other forensic applications can result from complex problems that are not as readily solved. Unexpected crystalline material in a product may be rapidly identified by infrared spectroscopy, but discovering the root cause of the crystals may require extensive investigation and elimination of the problem may entail significant process changes (99,100).

BIBLIOGRAPHY

1. J.I. Steinfeld, *Molecules and Radiation*, 2nd ed., MIT Press, Cambridge, Mass., 1985.
2. N.B. Colthup, *Introduction to Infrared and Raman Spectroscopy*, 3rd ed., Academic Press, Boston, 1990.
3. S. Johnston, *Fourier Transform Infrared*, Ellis Horwood, New York, 1991.
4. D.L. Pavia, G.M. Lampman, and G.S. Kriz, Jr., *Introduction to Spectroscopy: A Guide for Students of Organic Chemistry*, Saunders College Publishing, Orlando, Fla., 1979.
5. B.C. Smith, *Fundamentals of Fourier Transform Infrared Spectroscopy*, CRC Press, Boca Raton, Fla., 1996.
6. B. Stuart, *Modern Infrared Spectroscopy*, Wiley, Chichester, England, 1996.
7. B. Schrader, ed., *Infrared and Raman Spectroscopy*, Wiley-VCH, Weinheim, 1995.
8. P.B. Coleman, ed., *Practical Sampling Techniques for Infrared Analysis*, CRC Press, Boca Raton, Fla., 1993.
9. G. Socrates, *Infrared Characteristic Group Frequencies*, 2nd ed., Wiley, Chichester, England, 1994.
10. *Bio-Rad Sadtler IR Database*, Bio-Rad Laboratories, Philadelphia (software).
11. *Nicolet Aldrich FT-IR Libraries*, Nicolet Corporation, Madison, Wis. (software).
12. *GRAMS / 32 Search*, Galactic Industries Corporation, Salem, N.H. (software).
13. D. Lin-Vien et al., eds., *Handbook of Infrared and Raman Characteristic Frequencies of Organic Molecules*, Academic Press, Boston, 1991.
14. C.J. Pouchert, ed., *The Aldrich Library of FT-Ir Spectra*, 2nd ed., Aldrich Chemical Company, Milwaukee, Wis., 1985.
15. N.J. Harrick, *J. Opt. Soc. Am.* **55**(7), 851–857 (1965).
16. F.M. Mirabella, Jr., ed., *Internal Reflection Spectroscopy: Theory and Applications*, Dekker, New York, 1993.
17. K. Ohta and R. Iwamoto, *Anal. Chem.* **57**, 2491–2499 (1985).
18. K. Ohta and R. Iwamoto, *Appl. Spectrosc.* **39**(3), 418–425 (1985).
19. J.B. Huang and M.W. Urban, *Appl. Spectrosc.* **46**(6), 1014–1019 (1992).
20. M. Yanagimachi, M. Toriumi, and H. Masuhara, *Appl. Spectrosc.* **46**(5), 832–840 (1992).
21. K.J. Kuhn, B. Hahn, V. Percec, and M.W. Urban, *Appl. Spectrosc.* **41**(5), 843–847 (1987).
22. K.S. Kalasinsky, G.R. Lightsey, P.H. Short, and J.R. Durig, *App. Spectrosc.* **44**(3) 404–407 (1990).
23. G.T. Fieldson and T.A. Barbari, *AIChE J.* **41**(4), 795–804 (1995).
24. G.T. Fieldson and T.A. Barbari, *Polymer* **34**(6), 1146–1153 (1993).
25. H.M. Reinl, A. Hartinger, P. Dettmar, and T.M. Bayerl, *J. Invest. Dermatol.* **105**, 291–295 (1995).
26. J.E. Harrison et al., *Pharm. Res.* **13**(4), 542–546 (1996).
27. American Society for Tasting Materials, *Standard Practices for General Techniques of Infrared Quantitative Analysis*, ASTM, Philadelphia, 1992.
28. U.P. Fringeli, *Chimia* **46**, 200–214 (1992).

29. D.G. Cameron, H.L. Casal, and H.H. Mantsch, *J. Biochem. Biophys. Methods* **1**, 21–36 (1979).
30. D.C. Lee and D. Chapman, *Biosci. Rep.* **6**(3), 235–256 (1986).
31. R.N.A.H. Lewis, R.N. McElhaney, M.A. Monck, and P.R. Cullis, *Biophys. J.* **67**, 197–207 (1994).
32. I. Cornut, B. Desbat, J.M. Turlet, and J. Dufourcq, *Biophys. J.* **70**, 305–312 (1996).
33. H.H. Mantsch, A. Martin, and D.G. Cameron, *Biochemistry* **20**, 3138–3145 (1981).
34. D.G. Cameron, H.L. Casal, and H.H. Mantsch, *Biochemistry* **19**, 3665–3672 (1980).
35. R.G. Snyder, G.L. Liang, H.L. Strauss, and R. Mendelsohn, *Biophys. J.* **71** 3186–3198 (1996).
36. M.P. Sanchez-Migallon, F.J. Aranda, and J.C. Gomez-Fernandez, *Biochim. Biophys. Acta* **1281**(1), 23–30 (1996).
37. J.H. Crowe, S.B. Leslie, and L.M. Crowe, *Cryobiology* **31**(4), 355–366 (1994).
38. K. Ozaki and M. Hayashi, *Int. J. Pharm.* **160**(2), 219–227 (1998).
39. Y. Setiawan, T. Rise, and D.E. Moore, *Pharm. Res.* **11**(5), 723–728 (1994).
40. P.L. Chong and P.T. Wong, *Biochim. Biophys. Acta* **1149**(2), 260–266 (1993).
41. Y. Takeuchi et al., *Chem. Pharm. Bull.* **40**(2), 484–487 (1992).
42. S. Zellmer et al., *Chem. Phys. Lipids* **94**(1), 97–108 (1998).
43. S. Zellmer, W. Pfeil, and J. Lasch, *Biochim. Biophys. Acta* **1237**, 176–182 (1995).
44. R. Ek et al., *Int. J. Pharm.* **125**, 257–264 (1995).
45. K.J. Pekarek et al., *J. Controlled Release* **40**(3), 169–178 (1996).
46. M.R. Kreitz, J.A. Domm, and E. Mathiowitz, *Biomaterials* **18**(24), 1645–1651 (1997).
47. S. Yamamura and J.A. Rogers, *Int. J. Pharm.* **130**(1), 65–73 (1996).
48. R. Barbucci and A. Magnani, *Biomaterials* **15**(12), 955–962 (1994).
49. R.W. Sarver, Jr. and W.C. Krueger, *Anal. Biochem.* **212**, 519–525 (1993).
50. G. Khang, H.B. Lee, and J.B. Park, *Bio-Med. Mater. Eng.* **5**(4), 245–258 (1995).
51. M.M. Tan, S.A. Corley, and C.L. Stevenson, *Pharm. Res.* **15**(9), 1442–1448 (1998).
52. J.M. Hadden, D. Chapman and D.C. Lee, *Biochim. Biophys. Acta* **1248**(2), 115–122 (1995).
53. M.J. Pikal and D.R. Rigsbee, *Pharm. Res.* **15**(2), 362–363 (1998).
54. M.J. Pikal and D.R. Rigsbee, *Pharm. Res.* **14**(10), 1379–1397 (1997).
55. H.H. Mantsch and D. Chapman, eds., *Infrared Spectroscopy of Biomolecules*, Wiley-Liss, New York, 1996.
56. J.H. Crowe, L.M. Crowe, and D. Chapman, *Arch. Biochem. Biophys.* **232**(1), 400–407 (1984).
57. E. Goormaghtigh et al., *Biochemistry* **32**, 6104–6110 (1993).
58. L.K. Tamm and S.A. Tatulian, *Biochemistry* **32**, 7720–7726 (1993).
59. H.L. Casal, D.G. Cameron, I.C.P. Smith, and H.H. Mantsch, *Biochemistry* **19**(3), 444–451 (1980).
60. H.M. Reinl and T.M. Bayerl, *Biochim. Biophys. Acta* **1151**, 127–136 (1993).
61. S. Nanda, S. Anand, and A. Nanda, *Indian J. Pharm. Sci.* **60**(4), 185–188 (1998).
62. N.A. Puttnam, *J. Soc. Cosmet. Chem.* **23**, 209–226 (1972).
63. K. Knutson et al., *J. Controlled Release* **2**, 67–87 (1985).
64. C.L. Gay et al., *J. Invest. Dermatol.* **103**(2), 233–239 (1994).
65. D. Bommannan, R.O. Potts, and R.H. Guy, *J. Invest. Dermatol.* **95**(4), 403–408 (1990).
66. B. Ongpipattanakul, M.L. Francoeur, and R.O. Potts, *Biochim. Biophys. Acta* **1190**, 115–122 (1994).
67. R.O. Potts and M.L. Francoeur, *Semin. Dermatol.* **11**(2), 129–138 (1992).
68. P.A.D. Edwardson, M. Walker, and C. Breheny, *Int. J. Pharma.* **91**, 51–57 (1993).
69. V.H.W. Mak, R.O. Potts, and R.H. Guy, *Pharm. Res.* **8**(8), 1064–1065 (1991).
70. M. Gloor, G. Hirsch, and U. Willebrandt, *Arch. Dermatol. Res.* **271**, 305–313 (1981).
71. R.O. Potts, D.B. Guzek, R.R. Harris, and J.E. McKie, *Arch. Dermatol. Res.* **277**, 489–495 (1985).
72. A. Alonso, N.C. Meirelles, V.E. Yushmanov, and M. Tabak, *J. Invest. Dermatol.* **106**, 1058–1063 (1886).
73. B. Ongpipattanakul, R.R. Burnette, R.O. Potts, and M.L. Francoeur, *Pharm. Res.* **8**(3), 350–354 (1991).
74. S.L. Krill, K. Knutson, and W.I. Higuchi, *J. Controlled Release* **25**, 31–42 (1993).
75. Y. Takeuchi et al., *Chem. Pharm. Bull.* **40**(7), 1887–1892 (1992).
76. R.P. Oertel, *Biopolymers* **16**, 2329–2345 (1977).
77. T. Kurihara-Bergstrom, K. Knutson, L.J. DeNoble, and C.Y. Goates, *Pharm. Res.* **7**(7), 762–766 (1990).
78. A.N.C. Anigbogu, A.C. Williams, B.W. Barry, and H.G.M. Edwards, *Int. J. Pharm.* **125**, 265–282 (1995).
79. K. Yoneto et al., *J. Pharm. Sci.* **85**(5), 511–517 (1996).
80. A. Naik, L.A.R.M. Pechtold, R.O. Potts, and R.H. Guy, *J. Controlled Release* **37**, 299–306 (1995).
81. S.-Y. Lin, K.-J. Duan, and T.-C. Lin, *Spectrochim. Acta, Part A* **52A**, 1671–1678 (1996).
82. M.J. Clancy, J. Corish, and O.I. Corrigan, *Int. J. Pharm.* **105**, 47–56 (1994).
83. D. Bommannan, R.O. Potts, and R.H. Guy, *J. Controlled Release* **16**, 299–304 (1991).
84. S. Thysman, D. Van Neste, and M. Préat, *Skin Pharmacol.* **8**, 229–236 (1995).
85. F. Pirot et al., *Proc. Natl. Acad. Sci. U.S.A.* **94**, 1562–1567 (1997).
86. M. Wessling et al., *J. Membr. Sci.* **86**(1–2), 193–198 (1994).
87. A. Bos, Doctoral Dissertation, University of Twente, Enschede, The Netherlands, 1993.
88. B.J. Tyler and B.D. Ratner, *J. Biomater. Sci. Polym. Ed.* **6**(4), 359–373 (1994).
89. M.C. Tanzi et al., *J. Biomed. Mater. Res.* **36**(4), 550–559 (1997).
90. J.P. Coates. *The Industrial Applications of Infrared Internal Reflectance Spectroscopy*, Dekker, New York, 1993, p. 374.
91. C. Wojciechowski et al., *Food Chem.* **63**(1), 133–140 (1998).
92. H. Peters, E. Unger, and F. Moll, *Pharmazie* **50**(1), 43–48 (1995).
93. Z. Bouhsain, S. Garrigues, and M. de la Guardia, *Analyst* **121**(12), 1935–1938 (1996).
94. Z. Bouhsain, S. Garrigues, and M. de la Guardia, *Analyst* **122**(5), 441–445 (1997).
95. L. Rintoul et al., *Analyst* **123**(4), 571–577 (1998).

96. E.D.S. Kerslake and C.G. Wilson, *Adv. Drug Delivery Rev.* **21**(3), 205–213 (1996).
97. Y. Wu et al., *J. Appl. Polym. Sci.* **46**, 201–211 (1992).
98. T. Gál and P. Tuth, *Can. J. Appl. Spectrosc.* **37**(2), 55–57 (1992).
99. H. Zhu et al., *J. Pharm. Sci.* **86**(12), 1439–1447 (1997).
100. J.E. Charbonneau, *Scanning* **20**(4), 311–317 (1998).

CHARACTERIZATION OF DELIVERY SYSTEMS, SURFACE ANALYSIS AND CONTROLLED RELEASE SYSTEMS

BUDDY D. RATNER
CONNIE KWOK
University of Washington Engineered Biomaterials (UWEB)
Seattle, Washington

KEY WORDS

Bioadhesion
Biocompatibility
Biodegradable polymers
Contact angle
Contamination
Deposition
Diffusion barriers
ESCA method
Infrared spectroscopy
Microsphere
Polymer colloids
Polymer matrix
Scanning probe microscopes
Secondary ion mass spectrometry (SIMS)
Surface analysis

OUTLINE

Introduction
- Diffusion Barriers
- Biocompatibility
- Surface Erosion
- Drug Concentration Profiles in the Surface Region
- Adhesion
- Bioadhesion
- Contamination
- General Analysis

A Historical Consideration
A Short Overview of Methods
- ESCA
- Contact-Angle Methods
- SIMS
- The Scanning Probe Microscopies
- Surface Infrared Methods

Some Examples from the Literature
- Surface Tools for Studying Site-Specific, Microsphere Delivery Systems (ESCA, SIMS)
- Surface Tools to Study the Surface Erosion of Biodegradable Polymers (ESCA, SIMS, AFM)
- Measuring Drug Concentration Profiles (ESCA, SSIMS, SIM Imaging, TOF-SIMS, AFM)
- Use of Surface Analytical Tools in Controlled-Release-System Bioadhesion Studies
- Surface Tools to Study Diffusion Barriers (ESCA)

Concluding Remarks
Acknowledgments
Bibliography

INTRODUCTION

The study of controlled-release and drug-release devices has been dominated by considerations of the bulk or average properties of materials or devices. Concentrations of drugs within a matrix, porosity, diffusion barriers, and erosion are important bulk matter concepts that are central to controlled release. Yet the outermost surface atoms of these systems play a central role in their performance. This article justifies surface studies for controlled-release systems, examines surface methods in a historical context, and then focuses on a few relevant examples.

Surface analysis is a term loosely used to describe the measurement of the outermost chemistry and structure of a material, with "outermost" ranging from 2 Å (an atomic surface monolayer) to a 10-μm region at the surface. There is no precise definition of surface in terms of depth into a material. Rather, *surface* can be operationally defined as the relevant, outermost zone that explains the performance of a material or device. Each of the major surface analysis tools probes to a different depth into a material. A few common methods and their penetration depths are summarized in Table 1. The specific reason why the surface region is important for controlled release is illustrated in Figure 1. Let us briefly examine each of the points highlighted in the figure.

Diffusion Barriers

Diffusion barriers and protective layers are widely used in drug-release systems. These surface coatings can provide zero-order release, extended-release, or protection from environmental agonists such as stomach acids. Typically, these coatings are thin. Their nature can be explored using surface analysis methods, and new barrier layers can be developed and optimized. An example of the use of surface methods to develop controlled-release barriers is presented in the last section of this article.

Biocompatibility

The word *biocompatibility* has been, to date, only loosely defined. However, it is clear that once toxicology issues (i.e., those associated with leachable substances toxic to cells) are addressed, biocompatibility is strongly influenced by surface properties. Because long-term controlled-release devices are rapidly encapsulated in a collagenous sheath after implantation and because the thickness of this sheath can be variable, achieving precise controlled release can be problematic. Contemporary implanted controlled-release devices address this by conservative en-

96. E.D.S. Kerslake and C.G. Wilson, *Adv. Drug Delivery Rev.* **21**(3), 205–213 (1996).
97. Y. Wu et al., *J. Appl. Polym. Sci.* **46**, 201–211 (1992).
98. T. Gál and P. Tuth, *Can. J. Appl. Spectrosc.* **37**(2), 55–57 (1992).
99. H. Zhu et al., *J. Pharm. Sci.* **86**(12), 1439–1447 (1997).
100. J.E. Charbonneau, *Scanning* **20**(4), 311–317 (1998).

CHARACTERIZATION OF DELIVERY SYSTEMS, SURFACE ANALYSIS AND CONTROLLED RELEASE SYSTEMS

BUDDY D. RATNER
CONNIE KWOK
University of Washington Engineered Biomaterials (UWEB)
Seattle, Washington

KEY WORDS

Bioadhesion
Biocompatibility
Biodegradable polymers
Contact angle
Contamination
Deposition
Diffusion barriers
ESCA method
Infrared spectroscopy
Microsphere
Polymer colloids
Polymer matrix
Scanning probe microscopes
Secondary ion mass spectrometry (SIMS)
Surface analysis

OUTLINE

Introduction
- Diffusion Barriers
- Biocompatibility
- Surface Erosion
- Drug Concentration Profiles in the Surface Region
- Adhesion
- Bioadhesion
- Contamination
- General Analysis

A Historical Consideration
A Short Overview of Methods
- ESCA
- Contact-Angle Methods
- SIMS
- The Scanning Probe Microscopies
- Surface Infrared Methods

Some Examples from the Literature
- Surface Tools for Studying Site-Specific, Microsphere Delivery Systems (ESCA, SIMS)
- Surface Tools to Study the Surface Erosion of Biodegradable Polymers (ESCA, SIMS, AFM)
- Measuring Drug Concentration Profiles (ESCA, SSIMS, SIM Imaging, TOF-SIMS, AFM)
- Use of Surface Analytical Tools in Controlled-Release-System Bioadhesion Studies
- Surface Tools to Study Diffusion Barriers (ESCA)

Concluding Remarks
Acknowledgments
Bibliography

INTRODUCTION

The study of controlled-release and drug-release devices has been dominated by considerations of the bulk or average properties of materials or devices. Concentrations of drugs within a matrix, porosity, diffusion barriers, and erosion are important bulk matter concepts that are central to controlled release. Yet the outermost surface atoms of these systems play a central role in their performance. This article justifies surface studies for controlled-release systems, examines surface methods in a historical context, and then focuses on a few relevant examples.

Surface analysis is a term loosely used to describe the measurement of the outermost chemistry and structure of a material, with "outermost" ranging from 2 Å (an atomic surface monolayer) to a 10-μm region at the surface. There is no precise definition of surface in terms of depth into a material. Rather, *surface* can be operationally defined as the relevant, outermost zone that explains the performance of a material or device. Each of the major surface analysis tools probes to a different depth into a material. A few common methods and their penetration depths are summarized in Table 1. The specific reason why the surface region is important for controlled release is illustrated in Figure 1. Let us briefly examine each of the points highlighted in the figure.

Diffusion Barriers

Diffusion barriers and protective layers are widely used in drug-release systems. These surface coatings can provide zero-order release, extended-release, or protection from environmental agonists such as stomach acids. Typically, these coatings are thin. Their nature can be explored using surface analysis methods, and new barrier layers can be developed and optimized. An example of the use of surface methods to develop controlled-release barriers is presented in the last section of this article.

Biocompatibility

The word *biocompatibility* has been, to date, only loosely defined. However, it is clear that once toxicology issues (i.e., those associated with leachable substances toxic to cells) are addressed, biocompatibility is strongly influenced by surface properties. Because long-term controlled-release devices are rapidly encapsulated in a collagenous sheath after implantation and because the thickness of this sheath can be variable, achieving precise controlled release can be problematic. Contemporary implanted controlled-release devices address this by conservative en-

Table 1. Methods to Characterize the Surfaces of Controlled-Release Systems

Method	Principle	Depth analyzed	Spatial resolution	Analytical sensitivity	Cost
Contact angles	The wetting of liquid drops on surface is used to estimate the surface energy.	3–20 Å	1 mm	Low or high depending on the chemistry	$
ESCA	X rays stimulate the emission of electrons of characteristic energy.	10–250 Å	10–150 μm	0.1 atom %	$$$
Auger electron Spectroscopy[a]	A focused electron beam causes the emission of Auger electrons.	50–100 Å	100 Å	0.1 atom %	$$$
SIMS	Ion bombardment leads to the emission of surface secondary ions.	10 Å–1 μ[b]	100 Å	Very high	$$$
FTIR-ATR	IR radiation is adsorbed in exciting molecular vibrations.	1–5 μm	10 μm	1 mol %	$$
AFM	Measurement of the force of interaction between a sharp tip and a surface	10 Å	50 Å	Single molecules	$$
SEM	Secondary electron emission caused by a focused electron beam is measured and spatially imaged.	5 Å	40 Å (typically)	High but hot quantitative	$$

Note: $—up to $5000
$$—$5000–$100,000
$$$—>$100,000
[a]Auger electron spectroscopy is damaging to organic materials and best used for inorganics.
[b]Static SIMS ≈ 10 Å; dynamic SIMS to 1 μm.

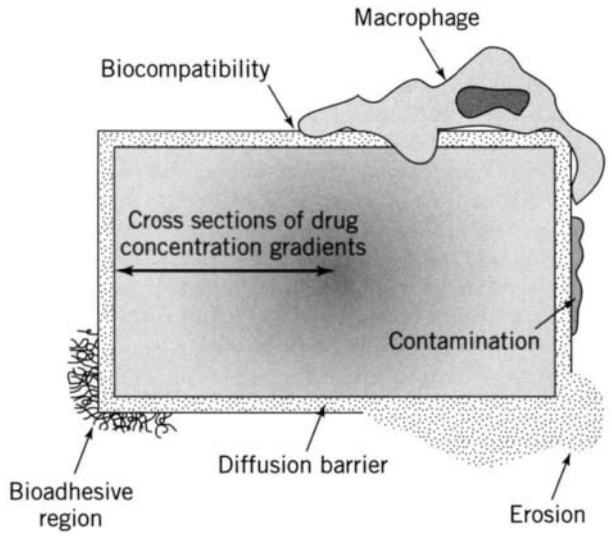


Figure 1. Applications for surface analysis in controlled release.

gineering so that even for the thickest expected capsule, drug concentrations in the efficacious range will diffuse to the body. Still, it is clear that control (or elimination) of the foreign body capsule would be desirable, and modern approaches to designing surfaces for implantation address this point (1,2). To design precision surfaces to control the healing, precision surface analysis is required.

Surface Erosion

Some drug-release systems function through surface erosion. The kinetics of this process, the chemistry of the surface reactions occurring, and the morphological changes taking place at the surface can be probed with surface analytical methods.

Drug Concentration Profiles in the Surface Region

Surface analysis methods can be used to measure drug concentrations in a surface zone, concentration gradients, and surface blooming of drugs. Also, using cross-sectional slices, drug profiles within a device can be directly measured. Thus, surface analysis can be used for studying release mechanisms and for quality control purposes.

Adhesion

Many controlled-release systems are multilayer or multicomponent devices. Because adhesion is largely a surface phenomenon, the adhesion of one layer to another and the integrity of joints holding together components of a device can be assessed with surface analysis tools.

Bioadhesion

The development of successful controlled-release strategies for mucosal sites requires that devices adhere to these slippery, hydrated surfaces. Such bioadhesion is often attributed to noncovalent chemical interactions (H-bonding), specific covalent bond formation, or interdiffusion of one polymeric species into another. The molecular size scale of these interactions is appropriate for study using surface analytical methods, and the analytical complexity associated with the interactions makes surface analysis methods particularly valuable.

Contamination

Surfaces are readily contaminated. Two explanations for this are the intrinsic driving forces for all surfaces to reduce their free energy and the obvious accessibility (exposure) of a surface to the external world. An unintentional contamination layer (hydrocarbon, silicones, plasticizer, etc.) can influence the performance of a carefully engineered controlled-release device. The ability of surface

analysis methods to detect and identify surface contaminant layers can help explain changes in performance and pinpoint the origin of surface contamination. The quantitative nature of surface analytical methods can be used to develop strategies for removal of surface contaminants and to establish quality control standards (e.g., minimum acceptable levels) for unavoidable contaminants.

General Analysis

Although surface analysis methods exhibit their greatest strengths in their ability to measure the surface zone, they are also valuable general analytical tools. They can be used to identify unknowns and to perform quantitative analysis, often in situ and with little sample preparation (3).

A HISTORICAL CONSIDERATION

The justification for the use of surface analysis methods to study controlled-release systems has been presented in the preceding section. It is useful to briefly review the history of these methods and then consider the principles behind them.

The appreciation of the importance and uniqueness of surfaces has been slow to arrive in the scientific community. This is, in part, because much of the instrumentation needed to study surfaces was perfected only with the last 30 years. Although contact angles and wettability considerations have been used to directly or indirectly investigate surfaces since antiquity, techniques such as electron spectroscopy for chemical analysis (ESCA) have much more contemporary origins.

The quantitative use of contact angles of liquid drops on solid surfaces to explain surface properties can trace its origins to the work of Thomas Young and others in the early nineteenth century. However, contact-angle measurement as a routine surface analysis tool is attributed to the work of Zisman at the Naval Research Laboratories starting in the 1940s (4). Zisman explored the relationships between contact angles, composition, and the thermodynamic parameter, surface free energy. This led to his development of the concept of critical surface tension, an approximation to the surface free energy.

The ESCA method (also called X-ray photoelectron spectroscopy [XPS]) is based on the photoelectric effect, first explained by Einstein in 1905. In 1925, an experimental demonstration was made of this method, but this was closer to a heroic physics demonstration than a practical analytical method. In the 1960s and 1970s, Professor Kai Seigbahn developed the ESCA technique and the instrumentation as we know it today (5,6). He defined its use in surface analysis and coined the ESCA acronym.

The principle of another surface analysis method widely used for inorganic surface, Auger electron spectroscopy (AES), is based on the cloud chamber observations of Pierre Auger in the 1920s. Auger electrons, given off from materials under bombardment with energetic surfaces, are different from photoemitted electrons measured in ESCA in that their energies are independent of the energy of the impinging energy source. Because an electron source, rather than an X-ray source, can be used to excite the emission and because electron sources are easier to design than X-ray sources, Auger instrumentation made more rapid strides than ESCA instrumentation. Still, at the end of the twentieth century, ESCA is used much more widely than AES (except in the semiconductor industry) because of its enhanced information content and lower sample damage.

Secondary-ion mass spectrometry (SIMS) developed in the 1950s and 1960s as a method to depth-profile materials. However, the pioneering work of Benninghoven revealed the potential of SIMS used in the static mode. Static SIMS permitted analysis of the outermost surface zone and offered rich molecular information about organic surfaces (7).

Surface analysis applied to biomedical problems evolved from the work of early visionaries and pioneers who appreciated both the unique nature of the surface zone and the relationship between the surface structure and biological response (8–11). The advent of modern ultrahigh-vacuum-surface analysis methods, spurred by the growth of the semiconductor industry and petrochemical catalysis, greatly advanced the ability to accurately study surfaces so that surface structures might be considered in the context of biological interactions (12,13). More recently, synchrotron methods, the scanning probe microscopies, and modern optical techniques have made impressive strides in permitting the study of the surface structure of biomedically important materials (14–16). Of special note is the ability of many of these methods to study the solid–water interface.

A SHORT OVERVIEW OF METHODS

The principles behind a number of the commonly used surface analysis methods are illustrated in Figure 2. Characteristics and specifications for these methods are summarized in Table 1. A few comments on those surface methods especially applicable to drug-release systems follows. It is important to appreciate that although each of the methods can provide reliable information on surfaces, combinations of these methods allow the construction of a more complete picture of surface structure.

ESCA

ESCA is probably the single most useful technique for studying the surfaces of devices and materials of technological importance. Many good review articles and books on this method are available (17–21). The instrumentation is well developed and is almost user-friendly. Sample preparation is generally simple—just insert the sample into the analysis vacuum chamber and commence the acquisition of data. Metals, polymers, ceramics, particulates, thin films, fabrics, and intact devices can all be readily examined. The information content, including all elements present, atomic stoichiometry, molecular detail, and depth-profile data in the outermost ~80 Å, is exceptionally high. Modern instruments offer good analytical sensitivity (approximately 0.1 atom %), good spatial resolution (approximately 25 $m\mu^2$), low sample damage, and good spectroscopic resolution. Finally, novel methods have been evolved to enhance the information content of ESCA. For example,

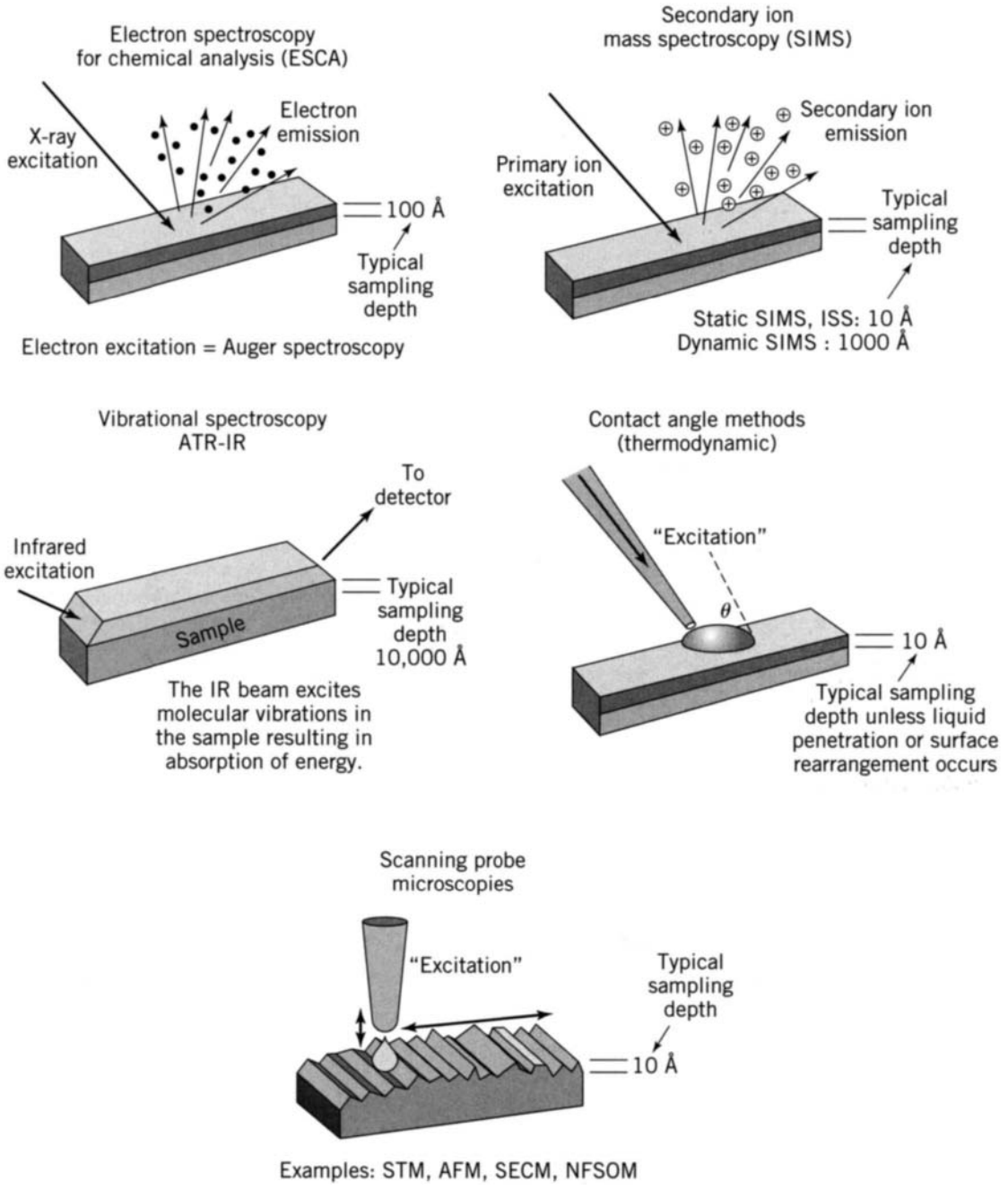


Figure 2. The principles of five surface analysis methods.

hydrated frozen samples can be studied to look at the polymer–aqueous interface (22). Also, chemical derivatization methods can enhance the accuracy of surface group identification and quantification (23).

Contact-Angle Methods

Contact-angle methods to probe surface properties are highly surface sensitive, low cost, readily performed in most laboratories, and reasonably easy to understand. In the simplest configuration, a small drop of a pure liquid of known surface tension is placed on the solid surface to be measured. The angle of a tangent to the drop profile originating from the point of contact of drop and surface is measured, typically with a magnifying scope and protractor scale. The angle through the fluid phase is, by convention, the value reported. Analyses offering higher precision can be performed with a Wilhelmy plate apparatus. The measured force of insertion or removal of a flat plate of the material of interest through an air–liquid interface is measured and can be used to compute the contact angle between plate and liquid (24). Other techniques include underwater contact-angle measures with drops of an insoluble hydrocarbon or air and measurements of the an-

gle of drop flow on a tilting stage. The relative simplicity of these methods must be tempered by a consideration of their limitations. The angles measured are influenced by operator experience, purity of the measurement liquid, penetration of the liquid into the substrate, sample roughness, drop size, surface swelling, and a number of other variables. Also, information about surface chemistry is inferred rather than directly measured. Still, with care, useful information can be obtained. Application of acid–base concepts to contact-angle measurements by Fowkes has significantly advanced specific information content obtainable from these methods (25). Useful review articles are available on contact-angle methodology (24–26).

SIMS

In recent years, SIMS analysis of surfaces has approached ESCA in general utility and interpretability. In SIMS, the surface is bombarded with an energetic primary-ion beam, and the masses of charged atomic and molecular fragments sputtered into the vacuum region are measured. SIMS is performed in one of two modes. Dynamic SIMS, with a high primary-ion flux, gives elemental compositional information and provides composition as a function of depth over a range of roughly 100 to 10,000 Å. Because of high sample damage, dynamic SIMS is rarely useful for organic materials. In static SIMS (SSIMS), an extremely low primary-ion dose is played over the surface. This results in the erosion of less than 10% of the surface monolayer. The consequence is that only the outermost zone of a sample (approximately 10 Å deep) is probed, and complex molecular information can be read from the mass spectral output (7). In recent years, time-of-flight (TOF) mass analyzers for SIMS have revolutionized analytical sensitivity (detection down to 10^{10} molecules or less), mass accuracy (often masses can be expressed to four significant figures after the decimal point), and spatial resolution (elemental analysis can be performed in regions as small as 0.1 μm in diameter along with compositional mapping) (27). The downsides of the static SIMS method are expensive instrumentation (>500,000), the need for highly trained operators for quality data acquisition, the ability to probe only the outermost layer, and complex spectral interpretation. Still, if both ESCA and static SIMS can be performed, a detailed understanding of the surface chemistry and structure will be accessible.

The Scanning Probe Microscopies

The scanning probe microscopies (SPMs) are the latest tools in the armamentarium of methods available to the surface analyst (16). An atomic or molecularly sharp tip is passed over a surface using extremely precise piezoelectric controllers, and the electrical or mechanical interaction of the tip with the surface is measured. The output is plotted as tip response per spatial location. SPM methods include the scanning tunneling microscope (STM), which is primarily applicable to electrically conducting samples, and the atomic force microscope (AFM), useful for conductors and insulators. AFM is most applicable to the types of samples likely to be encountered in controlled-release systems and is the focus here. AFM can produce maps of surface topography with a height (z) resolution of 1 Å and an x,y spatial resolution of typically 50 Å. The sensitivity and accuracy in the z-plane permits surface textures to be observed with unprecedented accuracy and sensitivity compared with, for example, a scanning electron microscope (SEM). The microscope can be operated in air, underwater, or in vacuum, offering much flexibility for exploring real-world systems. Finally, it can be used in a number of specialized modes to enhance information content. The lateral force microscopy (LFM) mode permits surface friction to be measured at the nm scale. The tapping mode is useful for softer samples that could be readily damaged or moved by tip forces. The AFM can be used as a nanointendometer to measure hardness or modulus in nano-scale regions (16). Derivatization of the tip permits chemical imaging to be performed (28). Other variations of the SPM method include the scanning electrochemical microscope (SECM) for electrical information about surfaces in ionic media and the near-field optical scanning microscope (NFOSM) for optical information with spatial resolutions well below the defraction limit of light.

Surface Infrared Methods

The infrared (IR) spectroscopy methods, part of a class of techniques referred to as vibrational spectroscopies, have a long history in surface analysis (29). IR spectroscopy is well understood and information rich. However, special methods must be applied to make it surface sensitive. Although vibration spectroscopy methods can measure surface zones as thin as 10 Å, the most generally useful of the techniques for drug-release systems, attenuated total reflectance (ATR) IR, probes 1–5 μm into a material (30). In ATR, the sample or device of interest is pressed against a trapezoidal crystal of high refractive index (often germanium), and an IR beam is passed through the crystal, allowing a portion of the IR beam extending beyond the face of the crystal to be absorbed by the sample. Hence, an IR absorption spectrum can be measured. ATR accessories are readily obtained for most laboratory IR spectrometers. Thus, if the high probe depth of this method is not a limitation for the specific question being asked, ATR remains a good method for surface analysis of materials and devices.

SOME EXAMPLES FROM THE LITERATURE

Although the application of surface analysis methods to controlled release is relatively new, there are a surprisingly large number of published examples to cite on this subject. These examples will be organized into the following categories:

- Use of surface tools in site-specific delivery systems (ESCA, SIMS)
- Use of surface tools in biodegradable polymers and the study of surface erosion (ESCA, SIMS, AFM)
- Use of surface tools in establishing drug concentration profiles (ESCA, SSIMS, SIM imaging, TOF-SIMS, AFM)

- Use of surface tools in bioadhesion studies involving controlled-release systems (ESCA, AFM, FTIR-ATR)
- Use of surface tools to study a diffusion barrier (ESCA)

Surface Tools for Studying Site-Specific, Microsphere Delivery Systems (ESCA, SIMS)

Polymer colloids have been shown to be useful in site-specific drug delivery systems, especially for pulmonary administration or intravenous drug delivery. However, one major drawback is their significant uptake by macrophages (phagocytosis) in the lung or liver/spleen (the reticuloendothelial system, RES), thereby reducing the delivery efficacy of the device. Davies et al. (31,32) have proposed that by copolymerizing poly(ethylene oxide) (PEO) of M_r 2,000 with polystyrene, they were able to reduce the opsonization and engulfment of the particles by macrophages. Using both ESCA and SIMS, they reported that this observation might be due to the enrichment of ether carbon (C-O) on the particle surface. C-O surface density increased dramatically as the amount of the PEO in the polymerization mixture increased, and this increased C-O surface coverage correlated with decreased macrophage uptake and increased particle circulation time in the blood (33). Evora et al. (34) reported similar studies with 1,2-dipalmitoylphosphatidylcholine (DPPC), a natural surfactant in the lung, on the surface of microspheres during pulmonary drug delivery. ESCA indicates that DPPC dominated the surface chemistry, and its presence on the aerosol surface lowered the phagocytosis of the particles by alveolar macrophages. Both examples demonstrated the use of surface analytical tools, specifically ESCA and SIMS, to chemically characterize the surfaces and use the information obtained to understand biological responses.

Surface Tools to Study the Surface Erosion of Biodegradable Polymers (ESCA, SIMS, AFM)

Biodegradable polymers have always been of interest for the controlled release of drugs, because the release device need not be removed after all of the drug has been delivered. However, the polymers must possess predictable erosion kinetics with mechanical and surface characteristics suitable for drug delivery systems. Mechanistically, biodegradable polymers resorb either by bulk or surface erosion. In this section, we focus on applying surface analysis techniques to study the kinetics of surface erosion. Specifically, the relationship between polymer erosion and drug release is examined. Shakesheff et al. (35,36) demonstrated the use of in situ AFM to visualize the dynamic surface morphology changes that result from the surface biodegradation of a poly(ortho ester) sample containing protein. This technique allowed the degradation process occurring at the polymer/water interface to be visualized directly at the nanometer lateral (x and y) and vertical (z) scale on surfaces within a hydrolyzing (aqueous) medium. In the study, they noticed that the presence of bovine serum albumin (BSA) particles (a model drug) in the polymer film yielded a rougher surface morphology in comparison to a BSA-free film. A time-course study over 90 min on the degradable polymer was conducted, and the vivid AFM images corresponding to each time point were presented. Using image analysis methods, the relative changes of volume of protein particles and polymer matrix over the time course of the experiment were calculated. Later, the researchers, using the same in situ AFM technique along with ESCA and SSIMS, examined more intensively the surface degradation mechanisms of various polymer blends of poly(sebacic anhydride) (PSA) and poly(D,L-lactic acid) (PLA) (37). The blends are normally immiscible. However, when the molecular weight of the PLA is less than 3,000 Da, the polymer blends showed limited miscibility. Using this intrinsic characteristic of the two polymers, both miscible (PLA, 2,000 Da) and immiscible (50,000 Da) blends of polymer with various PLA loading were prepared. In both cases, ESCA and SIMS suggested preferential concentration of PLA on the surface. Because PSA tends to form semicrystalline materials while PLA leads to an amorphous polymer, various amounts of each of the components on the surface, in additional to their different degradation rates (2–4 weeks for PSA versus 12–16 weeks for PLA), could dramatically influence the release characteristics. In situ AFM showed that as the PLA in the immiscible blend is increased from 30 to 50%, an inversion in the phase morphology occurs with PLA morphology changing from isolated granules in a network of PSA to a network of PLA separating PSA areas. When PLA reaches 70% in the blend, surface enrichment of PLA even produced a permeation barrier that retards penetration of the hydrolyzing solution into the polymer matrix. Thus, the surface becomes resistant to degradation even after 3 h of exposure to the solution, in comparison with 30% PLA where degradation was observed shortly after exposure of 5 min. At this 70% PLA blend composition, the *surface* dominance of PLA is the limiting factor in the degradation process of the polymer. In these examples, combining surface chemical information from ESCA and SIMS with surface morphology information from AFM, it is possible to characterize the complex surfaces of these polymer blends and record the effect of the surface organization on degradation. This offers important insights in designing biodegradable drug delivery devices.

Measuring Drug Concentration Profiles (ESCA, SSIMS, SIM Imaging, TOF-SIMS, AFM)

As early as 1985, ESCA was used to determine drug distributions within polymer matrices in controlled-release systems (38–40). The drug concentration profile is important in understanding and designing systems with desired and predictable release characteristics. Carli and Garbassi (39,40) reported that with the use of ESCA, they could understand the distribution of drug molecules loaded in a polymer matrix, that is, whether the drug molecules are in excess on the surface or homogeneously distributed throughout the matrix. By using unique label atoms in the drug (Cl for griseofulvin) and the polymer (N for crospovidone), they proposed that the use of Cl/N ratio could identify the drug location. Cl/N values higher than the theoretical ones suggest a drug excess in the surface, whereas lower Cl/N values indicate drug entrapment in the inner

core of the polymer matrix. With these criteria, they related the drug profiles to various loading techniques and the release kinetics observed. In most cases, they observed preferential location of the drug on the device surface.

Starting in the late 1980s, Davies et al. (41–43) began to apply SSIMS and SIMS imaging to controlled-release systems. SSIMS analysis offers high surface molecular specificity and is complementary to the chemical quantification provided by ESCA. Using SSIMS, this group observed molecular fingerprints of a drug molecule, indomethacin, in polymer beads (42), focusing on the intense signals of the 139 D and 359 D mass spectral peaks on the outermost surface of the beads. However, for the older SIMS instrument used, quantification and the detection limit for high-molecular-weight fragments posed major obstacles in applying SSIMS to peptide-containing reservoirs. To overcome these limitations, John et al. (44) applied TOF-SIMS to analyze a peptide/polymer drug delivery system. TOF-SIMS permits molecular weights to at least 10,000 Da to be measured. Furthermore, using SIMS and TOF-SIMS imaging analysis, the surface molecular ions on the polymer matrices can be chemically mapped. Specifically, John et al. used TOF-SIMS and its imaging techniques to look at the distribution of the drug molecules along the surfaces of cross sections (of thickness between 100 and 200 μm) prepared from different polymer formulations. Previous studies could determine only if the drug was concentrated on the surface or entrapped in the bulk. With TOF-SIMS imaging, the drug molecular distribution in each layer through a polymer matrix can be examined. Belu and Bryan (45) also demonstrated that they were able to chemically image cross-sectional layers of a drug capsule simultaneously and identified precisely the distribution of drug and coating materials. They even argue that one can easily gain insightful information on competitor's samples using the in situ TOF-SIMS analysis. zur Mühlen et al. (46) also applied AFM to image the drug distribution on the surface of lipid nanoparticles and attempted to relate the images to release characteristics. Similar to the study of Davies et al. (37) described earlier, zur Mühlen et al. examined the surface after elution studies. The authors concluded that the fast initial release was by the outer noncrystalline layers of the particles, while the subsequent sustained release was associated with the inner crystalline particle layers.

Use of Surface Analytical Tools in Controlled-Release-System Bioadhesion Studies

Controlled-release systems made from bioadhesive polymers prolong the residence time of devices on a biological surface before being eliminated by the body and allow more time for drug molecules to penetrate into the tissue. Bioadhesive systems are especially important when dealing with mucous and highly hydrated tissues in dentistry, orthopedics, and ophthalmology. Peppas and Buri (47) offer an extensive review of bioadhesive polymers on soft tissues in the context of drug delivery, and they describe various surface analytical techniques. Recently, Westwood et al. (48) applied both ESCA and AFM to determine the chemical as well as topological nature of an ophthalmic drug delivery system (Occumer). They concluded that both techniques provide direct evidence for the complexion behavior of drug and polymer (anionic/cationic) as well as information on the surface topology and chemical coverage of Occumer.

In addition to the commonly used ESCA and SIMS surface techniques, Fourier transform infrared attenuated total reflection spectroscopy (FTIR-ATR) is emerging as a complementary tool for drug delivery design (49). It is used mostly in transdermal delivery applications. Jabbari et al. (50) reported the use of ATR in studying the penetration of poly(acrylic acid) (PAA), an important mucoadhesive for controlled-release applications, into a mucin layer. ATR spectra showed that swelling of the PAA allowed chain penetration at the polymer/mucin interface over a 12-min interval, and the extent of the chain interpenetration determined the bioadhesiveness. Mak et al. (51) have examined the potential use of ATR in vivo to study percutaneous penetration enhancement using 4-cyanophenol (CP) as the model penetrant across a human subjects' stratum corneum, the skin's outermost barrier, in the presence and absence of a penetration enhancer (oleic acid). Using the distinct IR peaks of CP, the authors were able to conclude that CP permeated faster when codelivered with oleic acid and examined penetration time. This study demonstrates the potential use of ATR as a noninvasive, in situ technique in studying transdermal delivery in vivo.

Surface Tools to Study Diffusion Barriers (ESCA)

Diffusion barriers on controlled-release systems have been proposed to achieve zero-order release kinetics as well as to extend the efficacy of drug release devices. Kwok et al. (52,53) focused on applying the radio frequency–glow discharge plasma deposition technique (RF-GDPD) to coat an ultrathin, rate-limiting barrier (~100 Å) on an antibiotic-containing polyurethane polymer. In the study, ESCA was used as a surface analytical tool to relate the RF–plasma operating conditions to the release characteristics observed.

The plasma operating conditions determine the degree of structural alteration and cross-linking for the thin plasma-deposited film (PDF), which, in turn, affects the release rate of antibiotics through this layer. In principle, higher cross-linking density (measured indirectly by the C/O ratio) and thicker films will give slower release rates. Usually, higher deposition power yields higher cross-linking PDF, while longer deposition time gives thicker PDFs. Kwok et al. (unpublished data) reported that the optimal plasma conditions to attain such a PDF was first to argon-etch and pretreat the matrices with an 80 W *n*-butyl methacryate (BMA) plasma for 1 min, followed by immediate BMA plasma deposition at 40 W and 150 mT for 20 min. Pretreatment was used to increase the adhesion between the PDF and the matrix, thereby preventing coating delamination. An ESCA study to develop this pretreatment protocol is described elsewhere (Kwok et al., unpublished data). Briefly, by using the specified plasma deposition protocols, the authors eliminated the initial burst effect, significantly reduced the release rates, and closely approached the zero-order release. The release rates were at the N_{kill} (minimum required kill rate for *Pseudomonas aeruginosa*) for at least 5 days, compared to 1 day for uncoated matrices.

Figure 3 depicts a cross-plot of average release rates and C/O ratios versus deposition powers. Deposition powers higher than 40 W resulted in CASING (cross-linking by activated species of inert gases), which eroded the surface antibiotic, cross-linked the polyurethane surface and made it a barrier for the release of antibiotics yet not as effective a barrier as a deposited overlayer (54). This was also observed in ESCA by the presence of nitrogen (an element found only in the polyurethane matrix but not in BMA deposition) and unusual high C/O ratios at higher powers (50 and 60 W). Thus, the highest deposition power did not necessarily result in the lowest release rate—there was an optimum at 40 W in this case. Figure 4 is a cross-plot of average release rates and C/O ratios versus deposition times. An increased C/O ratio of 6.4 to 8.2 was observed as the deposition time increased from 5 to 15 min, in comparison with an uncoated polyurethane that had a C/O ratio of 4.3. Beyond 15-min deposition times, the C/O ratio is unchanged; therefore, the thickness of the film had exceeded the sampling depth of ESCA (~100 Å), and ESCA no longer detected the oxygen in the underlying polyurethane. From the 15-min deposition time onward, the spectra obtained described the chemical composition of only the uppermost PDFs, and the C/O ratio remained constant. This is also reflected in the measurements of the release rates, which were consistent when the PDFs were made at deposition times longer than 15 min. This study demonstrated the use of ESCA as a routine check tool to relate the surface chemistry of PDF and the plasma operating parameters. The information was used to optimize the plasma conditions so that the desired diffusional barrier could be obtained. The bactericidal efficacy of the released antibiotics was evaluated and showed that the released antibiotics were biologically active in preventing the bacteria from adhering to the polyurethane, thereby decreasing the chances of biofilm-related infection (55,56).

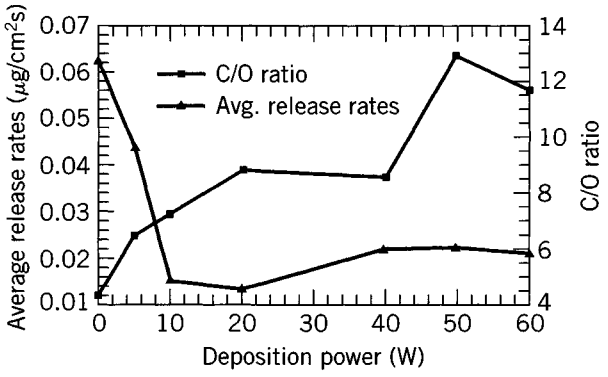


Figure 3. Correlation of release rates with C/O ratios and deposition powers. The system was at a pressure of 150 mT, and deposition time were 15 min throughout. *Note:* 0 W means uncoated polyurethane films.

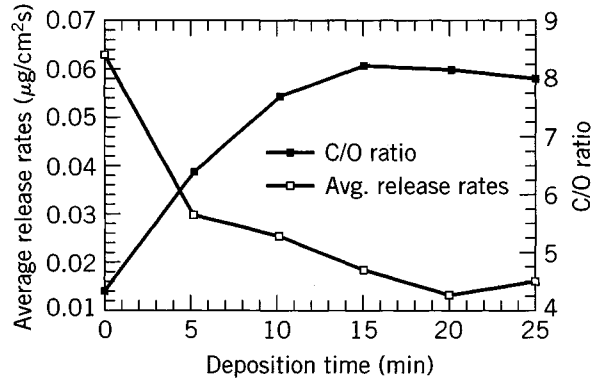


Figure 4. Correlation of release rates with C/O ratios and deposition times. The system was at a pressure of 150 mT, and deposition powers were at 40 W throughout. *Note:* 0 min means uncoated polyurethane films.

CONCLUDING REMARKS

Possibilities for surface analysis to contribute to the development and understanding of bulk controlled-release devices have been highlighted in this article. Advances will be made as researchers begin to focus on the importance of surfaces and the contributions that surface analysis can make to these systems. Challenges include the problems in working with highly hydrated (swollen) systems, with systems immersed in aqueous environments and with systems that are delivering agents as the analysis is being performed ("moving targets").

ACKNOWLEDGMENTS

The support of National Science Foundation (NSF) grant BES-9410429, National Institute of Health (NIH) grant RR01296 (NESAC/BIO), and NSF Engineering Research Center EEC-9529161 (University of Washington Engineered Biomaterials (UWEB) for some of the studies reported herein and during the writing of this article is appreciated.

BIBLIOGRAPHY

1. B.D. Ratner, *J. Mol. Rec.* **9**, 617–625 (1997).
2. B.D. Ratner, *J. Biomed. Mater. Res.* **27**, 837–850 (1993).
3. B.J. Tyler, B.D. Ratner, D.G. Castner, and D. Briggs, *J. Biomed. Mater. Res.* **26**(3), 273–289 (1992).
4. W.A. Zisman, *Adv. Chem. Ser.* **43** (1964).
5. K. Seigbahn, *J. Electron. Spectrosc. Relat. Phenom.* **36**(2), 113–129 (1985).
6. K. Seigbahn, *Science* **217**, 111–121 (1982).
7. A. Benninghoven, *J. Vac. Sci. Technol., A* **3**, 451–460 (1985).
8. J.D. Andrade, *Med. Instrum.* **7**(2), 110–120 (1973).
9. R.E. Baier, *Bull. N.Y. Acad. Med.* **48**(2), 257–272 (1972).
10. E. Nyilas, E.L. Kupski, P. Burnett, and R.M. Haag, *J. Biomed. Mater. Res.* **4**, 369–432 (1970).
11. D.J. Lyman, J.L. Brash, and K.G. Klein, in R.J. Hegyeli, ed., *Proceedings of the Artificial Heart Program Conference*, 1969, pp. 113–121.
12. C.B. Duke, *J. Vac. Sci. Technol. A* **2**(2), 39–143 (1984).
13. G.A. Somorjai, *MRS Bull.* **23**(5), 11–29 (1998).
14. Y.R. Shen, *Nature (London)* **337**, 519–525 (1989).
15. D.G. Castner et al., *Langmuir* **9**, 537–542 (1993).

16. B.D. Ratner and V. Tsukruk, eds., *Scanning Probe Microscopy of Polymers*, ACS Symp. Ser. vol. 694, American Chemical Society, Washington, D.C., 1998.
17. D. Briggs and M.P. Seah, eds., *Practical Surface Analysis*, Wiley, Chichester, U.K., 1983.
18. B.D. Ratner and B.J. McElroy, in R.M. Gendreau, ed., *Spectroscopy in the Biomedical Sciences*, CRC Press, Boca Raton, Fla., 1986, pp. 107–140.
19. B.D. Ratner and D.G. Castner, in J.C. Vickerman, ed., *Surface Analysis: The Principal Techniques*, 1st ed., Wiley, Chichester, U.K., 1997, pp. 43–98.
20. J.J. Pireaux et al., *J. Electron. Spectrosc. Relat. Phenom.* **52**, 423–445 (1990).
21. G. Beamson and D. Briggs, *High Resolution XPS of Organic Polymers: The Scienta ESCA 300 Database*, 1st ed., Wiley, Chichester, U.K., 1992.
22. K.B. Lewis and B.D. Ratner, *J. Colloid Interface Sci.* **159**, 77–85 (1993).
23. A. Chilkoti and B.D. Ratner, in L. Sabbatini and P.G. Zambonin, eds., *Surface Characterization of Advanced Polymers*, VCH Publishers, Weinheim, 1993, pp. 221–256.
24. D.E. Gregonis et al., in R.B. Seymour and G.A. Stahl, eds., *Macromolecular Solutions*, Pergamon, New York, 1982, pp. 120–133.
25. F.M. Fowkes, in J.D. Andrade, ed., *Surface and Interfacial Aspects of Biomedical Polymers*, vol. 1, Plenum, New York, 1985, pp. 337–372.
26. E. Sacher, in B.D. Ratner, ed., *Surface Characterization of Biomaterials*, Elsevier, Amsterdam, 1988, pp. 53–64.
27. A. Benninghoven, *Angew. Chem., Int. Ed. Engl.* **33**, 1023–1043 (1994).
28. T. Boland and B.D. Ratner, *Proc. Natl. Acad. Sci. U.S.A.* **92**(12), 5297–5301 (1995).
29. J.T. Yates, Jr. and T.E. Madey, eds., *Vibrational Spectroscopy of Molecules on Surfaces*, Plenum, New York, 1987.
30. N.J. Harrick, *Internal Reflection Spectroscopy*, Interscience, New York, 1967.
31. M.C. Davies et al., *Polym. Prep. Am. Chem. Soc., Div. Polym. Chem.* **34**(2), 72–73 (1993).
32. A. Brindley, S.S. Davis, M.C. Davies, and J.F. Watts, *J. Colloid Interface Sci.* **171**(1), 150–161 (1995).
33. S.E. Dunn et al., *Pharm. Res.* **11**(7), 1016–1022 (1994).
34. C. Evora et al., *J. Controlled Release* **51**, 143–152 (1998).
35. K.M. Shakesheff et al., *Polym. Prepr., Am. Chem. Soc., Div. Polym. Chem.* **36**(1), 71–72 (1995).
36. K.M. Shakesheff et al., *Langmuir* **11**(7), 2547–2553 (1995).
37. M.C. Davies et al., *Macromolecules* **29**, 2205–2212 (1996).
38. F. Carli et al., *Polym. Sci. Technol.* **34**, 397–407 (1986).
39. F. Carli and F. Garbassi, *J. Pharm. Sci.* **74**(9), 963–967 (1985).
40. F. Garbassi and F. Carli, *SIA, Surf. Interface Anal.* **8**, 229–233 (1986).
41. M.C. Davies, A. Brown, J.M. Newton, and S.R. Chapman, *SIA, Surf. Interface Anal.* **11**(12), 591–595 (1988).
42. M.C. Davies and A. Brown, *ACS Symp. Ser.* **348**, 101–112 (1987).
43. M.C. Davies, M.A. Khan, A. Brown, and P. Humphrey. in A. Benninghoven, A.M. Huber, and H.W. Werner, eds., *Secondary Ion Mass Spectrometry VI*, Wiley, Chicheser, U.K., 1988, p. 667.
44. C.M. John, R.W. Odom, A. Annapragada, and M.Y. Fu Lu, *Anal. Chem.* **67**(21), 3871–3878 (1995).
45. A.M. Belu and S.R. Bryan, *Proc. Surf. Biomater. Meet.*, 1998.
46. A. zur Mühlen, E. zur Mühlen, and W. Mehnert, *Pharm. Res.* **13**(9), 1411–1416 (1996).
47. N.A. Peppas and P.A. Buri, *J. Controlled Release* **2**, 257–275 (1985).
48. A.D. Westwood, D.J. Leder, and D.H. Donabedian, *ACS Polym. Mater. Sci. Eng.* **76**, 130–131 (1997).
49. U.P. Fringeli, *Chimia* **46**(5), 200–214 (1992).
50. E. Jabbari, N. Wisniewski, and N.A. Peppas, *J. Controlled Release* **26**(2), 99–108 (1993).
51. V.H.W. Mak, R.O. Potts, and R.H. Guy, *Pharm. Res.* **7**(8), 835–841 (1990).
52. C. Kwok et al., in *Proceedings of 23rd International Symposium on Controlled Release of Bioactive Materials*, Controlled Release Society, Deerfield, Ill., 1996, pp. 230–231.
53. C.S.K. Kwok, B.D. Ratner, and T.A. Horbett. *Polym. Prepr. Am. Chem. Soc., Div. Polym. Chem.* **38**(1), 1077–1078 (1997).
54. F.Y. Chang, M. Shen, and A.T. Bell, *J. Appl. Polym. Sci.* **17**, 2915–2918 (1973).
55. C. Kwok et al., in *Fifth World Biomaterials Congress Program and Transaction*, Society of Biomaterials, University of Toronto Press, Toronto, Canada, 1996, p. 605.
56. J.D. Bryers et al., in *24th Annual Meeting for Society of Biomaterials*, Society for Biomaterials, Minneapolis, Minn., 1998, p. 347.

CHARACTERIZATION OF DELIVERY SYSTEMS, XPS, SIMS AND AFM ANALYSIS

M.C. DAVIES
K.M. SHAKESHEFF
C.J. ROBERTS
S.J.B. TENDLER
University of Nottingham
Nottingham, United Kingdom
N. PATEL
Molecular Profiles Ltd.
Nottingham, United Kingdom
S. BRYAN
Physical Electronics Ltd.
Eden Prairie, Minnesota

KEY WORDS

Chemical imaging
Controlled drug delivery
Secondary ion mass spectrometry
Surfaces
TOF-SIMS

OUTLINE

Introduction
SIMS Process and Instrumentation

General Comments on SIMS Spectra of Pharmaceutical Materials
Small Organic Molecules
Polymeric Materials
Biomolecules and Cells
Application of TOF-SIMS to the Analysis of Pharmaceutical Delivery Systems
Controlled Release Dosage Forms
Contaminants
Nano- and Micro-Particle Delivery Systems
Biodegradable Polymeric Systems
Concluding Remarks
Bibliography

INTRODUCTION

Surface chemistry plays a major role in the formation, stability, performance, and biointeractions of many pharmaceutical delivery systems. Surface coatings are widely used to protect the bulk drug carrier whether it be at the macroscopic level with micron-thick polymer film coatings or at the monolayer scale where polymer brush monolayers allow stealth liposomes and nanoparticles to avoid recognition by the reticuloendothelial system (1). Surface chemistry can promote selective interactions, as in the case of bioadhesive delivery systems that exploit the interaction between the hydrated polymer interface and the mucosal linings of the gastrointestinal tract.

Knowledge of the surface properties of delivery systems gives an important insight into both the development of conventional and novel delivery systems and also into their function and operation. Exactly which surface feature is important in the performance of delivery systems may be initially difficult to define (2). Surface topography, chemistry, hydration, charge, and bioactivity may all play an important role. In the chapter CHARACTERIZATION OF DELIVERY SYSTEMS, SURFACE ANALYSIS AND CONTROLLED RELEASE SYSTEMS the application of X-ray photoelectron spectroscopy (XPS or ESCA) was reviewed and the ability to obtain quantitative elemental and chemical state information was highlighted. Here, we describe the powerful complementary role of secondary ion mass spectrometry (SIMS) in defining the *molecular* chemical structure of interfaces.

SIMS PROCESS AND INSTRUMENTATION

In the SIMS experiment, a surface is bombarded with stream of ions or atoms within an ultrahigh vacuum environment. This bombardment causes the emission or sputtering of electrons, neutral and charged species from the interface. The positive and negative ions of varying mass are collected and analysed within a mass spectrometer. Figure 1 illustrates a simple schematic of the process. The data are presented as a mass spectrum that may be interpreted using conventional mass spectrometry rules. A number of reviews (3–7) and reference databases (8,9) are available to aid the novice and the experienced operator alike in spectral interpretation. In certain acquisition modes, it is possible to produce chemical maps of surfaces

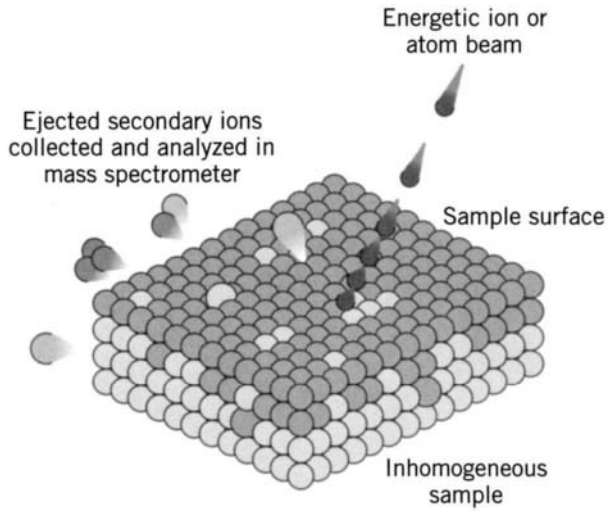


Figure 1. Schematic of the SIMS process.

by selecting a specific ion within the spectrum. An excellent detailed overview on the current state of the art of SIMS instrumentation and the physics of the SIMS process has been presented by Briggs recently (10) and, therefore, only relevant summary details are described here.

Current SIMS instruments have time-of-flight (TOF) mass spectrometers that are capable of routine high mass resolution in excess of m/M >3000, mass ranges from m/z 0 to 10,000 and spatial imaging resolutions at the submicron level. For most applications in this field, a mass spectrum may be acquired in one of two ways:

1. Where there is not a great need to define differences in chemical heterogeneity across the surface, a defocused beam can be used to obtain the spectrum.
2. Where the identification of different components, regions, or features across the surface is a key aim of the analysis, the primary ion or atom beam can be rastered over a predefined area and an entire mass spectrum acquired at each pixel point. The overall mass spectrum from that area is the summation of all the spectra acquired at all pixel points. This mode of data acquisition may be used to undertake retrospective image analysis (11) (Fig. 2). Ions in the summed spectrum that are known to be diagnostic for different chemical species or regions can be selected and an image formed from their intensity at each pixel. In addition, a region of interest from the resultant image, e.g., a coating film, may be selected and a mass spectrum formed from the summation of spectra from all the pixels in the defined region. This is a very powerful form of retrospective microanalysis of surfaces.

GENERAL COMMENTS ON SIMS SPECTRA OF PHARMACEUTICAL MATERIALS

There is a growing SIMS literature on inorganic and polymeric compounds employed in many fields of materials sci-

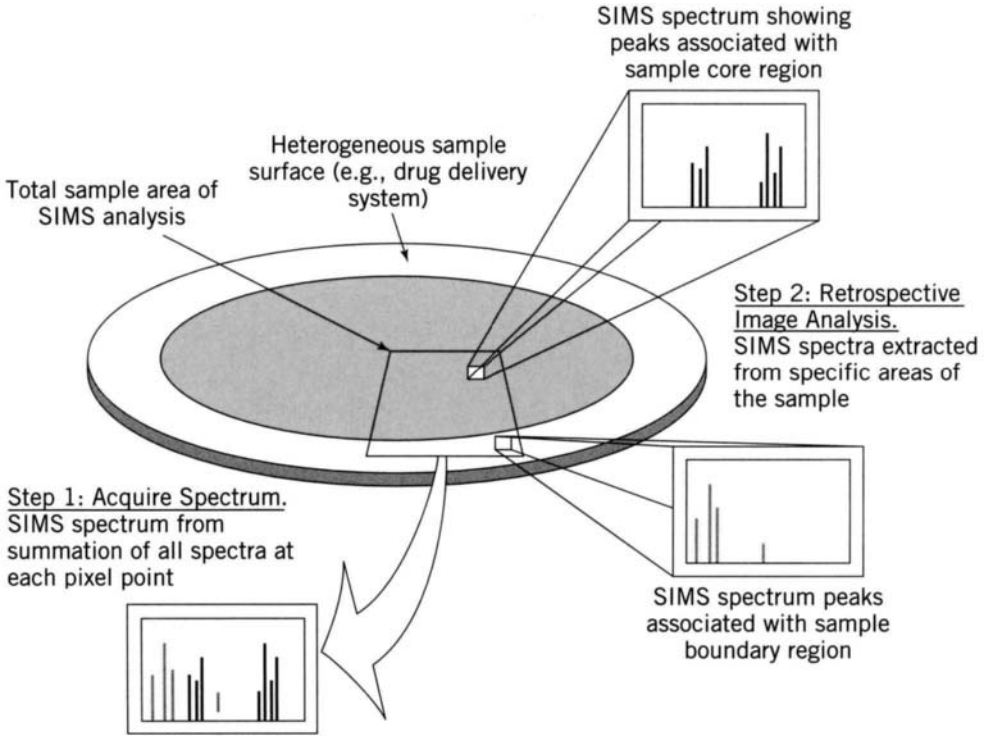


Figure 2. Schematic of the TOF-SIMS analysis of heterogenous surfaces. Retrospective data analysis is used to derive data from different regions of the sample.

ence. Although some activity has been within the drug delivery area, the majority of work within the medical sciences to date has focused on the SIMS analysis of biomaterials, which is reviewed elsewhere (2,5,6,12). In this chapter, we provide an overview of the general features of SIMS spectra of typical materials employed in drug delivery systems. A number of application areas are then discussed in more detail in the latter half of this article.

Small Organic Molecules

Conventional mass spectrometry is widely used in the elucidation of the molecular structure of organic molecules (13). The same principles may be employed to detect the presence of low molecular weight molecules (typically m/z <1000) within surfaces of delivery systems. Many drug molecules form quasimolecular ions $(M + H)^+$ or $(M - H)^-$ with a distinctive fragmentation pattern, which may be readily interpreted using mass spectrometry rules. For example, the presence of theophylline within the surface of cellulose spheroid beads was detected using SIMS where the molecular ions $(M + H)^+$ and $(M - H)^-$ ions and associated fragments were readily observed within both the negative and positive ion mass spectrum, respectively (14). Such an approach can be employed to detect the presence of many other types of pharmaceutical materials within dosage forms such as excipients and additives (5,15), e.g., plasticizers, inorganic fillers, pigments, surfactants and, to be discussed later, contaminants.

Polymeric Materials

A diverse range of polymers are currently employed in conventional and advanced drug delivery. Over the last 15 years, a rich literature has been compiled on the SIMS analysis of polymers (see Ref. 7 for most recent overview of area). The systematic examination of different classes of materials, including homologous series of some of the more technologically important ones, has made a significant contribution to our understanding of SIMS polymer data. From this work it has emerged that the SIMS spectra of polymers are dominated by ions that arise from cleavage of polymer chain that reflects the monomer structure (i.e., $(M+/-H)^{+/-}$, where M is monomer molecular weight) and any pendent or substituent side groups. This is illustrated in the negative ion SIMS spectrum in Figure 3 for the biodegradable polymer polylactic acid (PLA). Here, the major anions arise from $(nM - H)^-$ and $(nM + O - H)^-$ for n = 1–2 at m/z 71 and 143, and 87 and 159, respectively. Similar fragmentation patterns have been observed for many other classes of biomedical polymers that are used in drug delivery and biomaterials (2,5).

For copolymer systems, it is possible to detect ions that arise from all the monomers present. For example, ions diagnostic of both glycolide (GA) and lactide (LA) acids are present in the SIMS spectrum of the poly(lactide-*co*-glycolide) copolymer (PLGA) (16,17). From an analysis of the relative intensity of the diagnostic peaks, one can estimate the surface contribution of each component of the copolymer. Such data is not quantitative, because the surface environment, i.e., the so-called matrix effects (18), influence the intensity of the ions in the SIMS data. However, numerous examples exist in the literature that have shown that such an approach can be employed to derive relationships that reflect the surface chemistry in a quantitative manner (10).

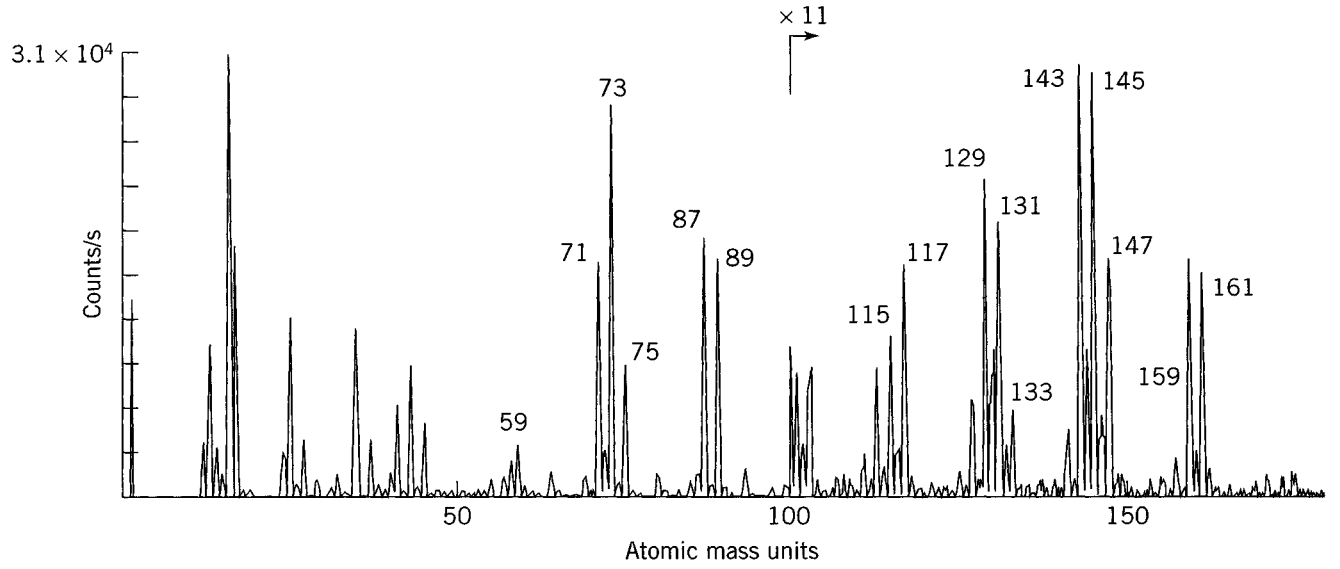


Figure 3. Negative ion SIMS spectrum of a PLGA film.

It is possible to deduce some important structural information from such semiquantitative analyses. One can detect ions in the SIMS spectra that arise from the sequence (i.e., dimers, trimers, etc.) of the copolymer chain. A number of groups have employed statistical analyses of the intensities of these ions to determine the level of random versus block nature of a copolymer, properties that may affect material performance. Such an approach has been employed on copolymers of polyalkyl methacrylates (19) and also for the biodegradable polymer PLGA (17). An examination of ion intensities has allowed the detection of the presence and level of polymer endgroups necessary for the stability of colloidal nanoparticle systems (20). Other surface properties such as polymer tacticity (21), cross-linking, and molecular weight as either oligomers (22) or as polymer brush (23) have been addressed using SIMS.

Biomolecules and Cells

The molecular characterization of biomolecules is better suited to other powerful forms of mass spectrometry such as MALDI (24,25) due to the limited mass range of TOF-SIMS (m/z <10,000). However, the technique does have some value in the detection of biomolecules adsorbed or grafted to interfaces. Chemometrics has been used to study the low molecular weight regions (m/z 0–200) of TOF-SIMS spectra of protein films to identify diagnostic peaks and clusters for different protein molecules (26). Further studies suggest that the technique is sensitive to protein orientation and/or conformation at surfaces (27). SIMS imaging has revealed coexisting phases in lipid monolayers (28). The ability to detect surface-immobilized peptides (29) and oligonucleotides (30) suggests a considerable future potential in the use of TOF-SIMS analysis in identifying and estimating the surface density of targeting biomolecules grafted at the interface of advanced delivery systems.

Given a rich literature in the high-resolution elemental imaging of cells using SIMS (31), there has been relatively little activity in the pharmaceutical sector. Very recently, Winograd and his group (32) have demonstrated that it possible to get *molecular* TOF-SIMS images across a cell treated with a number of dopants, including the drug cocaine.

APPLICATION OF TOF-SIMS TO THE ANALYSIS OF PHARMACEUTICAL DELIVERY SYSTEMS

Controlled Release Dosage Forms

Over the last 10 years a number of reports have demonstrated the detection of drugs (5–14) including peptides (33) in drug delivery systems surfaces using SIMS. Current instrumentation allows not only the chemical identification of surface species but also their spatial location within an interface. This ability may be exploited in the characterization of multicomponent formulations, a good example of which is shown in Figure 4. A polymer-coated bead (circa 1 mm) has been sectioned in half and the exposed cross-sectional surface has been analyzed by TOF-SIMS. The positive ion spectrum in Figure 4a is dominated by the signals of the drug, metoprolol at m/z 72 and 116 and the protonated molecular ions, MH^+ at m/z 268. It is possible to generate chemical images from such surfaces by identification of ions that are diagnostic of the drug, any excipients present, and the polymer coating. The MH^+ image in Figure 4b shows that the drug is well distributed throughout the bead with the exception of the central region. This area is dominated by Si^+ cations arising from a silica core. The polymer film is clearly distinguished by the ethyl substituent on the polymer chain from the ethylcellulose coating. Using the retrospective image analysis (11) already described, it is possible to generate SIMS

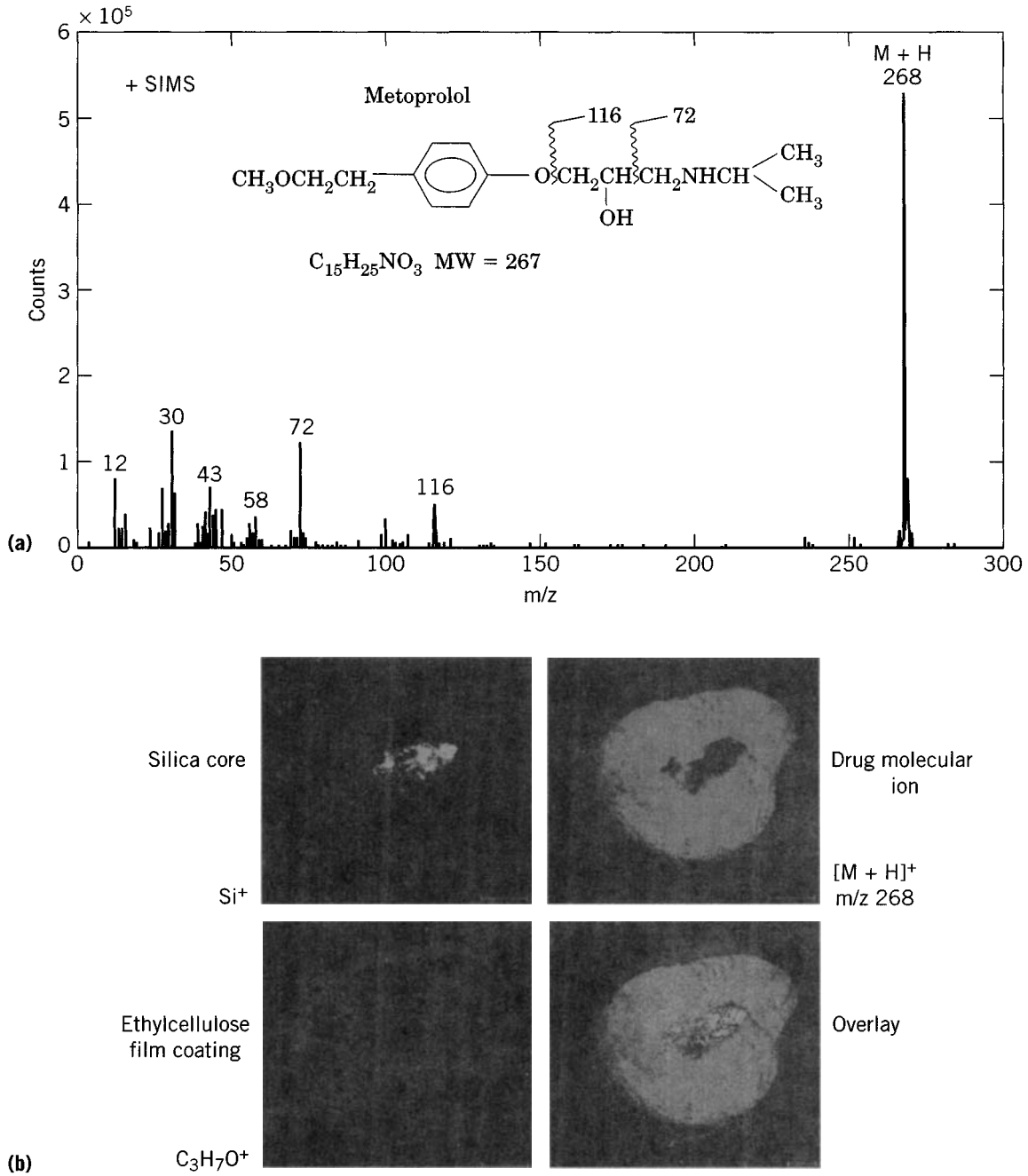


Figure 4. TOF-SIMS analysis of sectioned bead: (**a**) SIMS spectrum of drug; (**b**) SIMS images of drug, core, and coating. *Source:* The authors are grateful to Scott Bryan of Physical Electronics for kindly allowing the use of this figure.

spectra solely from each of the silica core, main drug-laden body of the bead, and the outer film coating regions. These spectra may be compared to standard control spectra of the materials. Such capability plays a powerful role not only in the characterization of the integrity of delivery systems but also in the use of SIMS in investigations within the patent protection field.

Contaminants

One of the most significant areas for the routine exploitation of SIMS surface analysis in mainstream material science is in the detection and identification of surface contaminants. The presence of contaminants such as residual catalysts, mold-releasing agents and surfactants may also indeed feature within the interface of biomaterials and

drug delivery systems. Ratner and co-workers have used XPS and SIMS to show that the surfaces of two different batches of a commercially available biomedical polymer Biomer were not composed of pure polyurethane but also contained a phenol antioxidant, Irganox 245, in one case and a di-isopropyl-amino-ethyl-methacrylate in the other (34). A common surface contaminant of SIMS polymer spectra is poly(dimethylsiloxane), a mold lubricant (3,4). SIMS has also been used to detect and monitor the efficiency of various techniques for the removal of residual surfactants such as sodium lauryl sulfate (35) and poly(vinyl alcohol) (PVA) (36) from the surface of biodegradable polyhydroxybutyrate and PLGA nanoparticles, respectively.

Nano- and Micro-Particle Delivery Systems

There has been considerable interest in the application of colloidal formulations in drug delivery. SIMS (and XPS) are powerful tools for the characterization of the surface chemistry of nanoparticles and microcapsules. The surface enrichment of both polymer endgroups responsible for colloid stability (20), and one or more of the components of a copolymer colloid formulation have been detected by SIMS (37,38). The technique has also provided a detailed analysis of the interfacial chemistry of colloids with surface-grafted poly(ethylene oxide) (PEO) chains intended as model systems for site-specific drug delivery (39). The detection of ions diagnostic of the PEO within the SIMS spectra and their increase in relative intensity with rising PEO bulk levels provided clear evidence of the surface enrichment of PEO polymer brush. The analysis of sugars coupled to model colloid surfaces (40) suggests SIMS may also have considerable potential for the analysis of targeting molecules on colloid surfaces.

Biodegradable Polymeric Systems

SIMS and XPS have been used to characterize the surface chemistry of homopolymers and copolymers of most biodegradable polymeric systems including the polyesters, poly(ortho esters), polyanhydrides, polyorganophosphazines, poly(β-malic acids) and some of natural origin such as gelatin and modified hyaluronic acids, which are reviewed elsewhere (41). In most cases there was no evidence of phase separation and/or preferential orientation of one or more component within the copolymer films and the surface chemistry mirrored the bulk. Such a situation may not arise where polymer blends are used to develop materials with novel and controllable biodegradation kinetics as was shown for a multitechnique study of films formed from blends of PLA and poly(sebacic anhydride) (PSA) (42). Diagnostic ions of both polymers were observed in the SIMS spectra and an analysis of the relative intensities of each set of ions revealed that there was a surface excess of PLA in all of the blend compositions. To date, limited work has been done on the SIMS analysis of the surface degradation of biodegradable polymers. Leadley et al. successfully exploited the molecular specificity of SIMS to confirm the mechanism of hydrolysis of some poly(ortho ester) polymers (43) and the high mass range of ToF-SIMS has been employed to detect the presence of low molecular weight oligomers formed by the hydrolytic cleavage of surface chains (J.R. Gardella, personal communication).

CONCLUDING REMARKS

There is rich potential for the exploitation of SIMS in the surface characterization of pharmaceutical delivery systems. The most fruitful information will arise when the technique is employed in tandem with other surface and biophysical techniques as part of a comprehensive strategy for the analysis of the surfaces of drug delivery devices. Such an approach cannot only aid our understanding of the physicochemical properties of such systems but also makes a valuable contribution to our understanding of their function and biological interactions.

BIBLIOGRAPHY

1. L. Illum and S.S. Davis, *Life Sci.* **40**(16), 1553–1560 (1987).
2. M.C. Davies, C.J. Roberts, S.J.B. Tendler, and P.M. Williams, in J Braybrook, ed., *Biocompatibility: Assessment of Materials and Devices for Medical Applications*, 1997, pp. 64–100.
3. D. Briggs, *SIA, Surf. Interface Anal.* **9**, 391–404 (1986).
4. D. Briggs, *Br. Polym. J.* **21**, 3–15 (1989).
5. M.C. Davies and R.A.P. Lynn, *Crit. Rev. Biocompat.* **5**(4), 297–341 (1990).
6. M.C. Davies, in W.J. Feast, H.S. Munro, and R.W. Richards, eds.; *Polymer Surfaces and Interfaces II*, Wiley, New York, 1993, pp. 203–225.
7. D. Briggs, *Surface Analysis of Polymers by XPS and Static SIMS*, Cambridge University Press, Cambridge, U.K., 1998, pp. 119–184.
8. D. Briggs, A. Brown, and J.C. Vickerman, *Handbook of Static Secondary Ion Mass Spectrometry*, Wiley, London, 1989.
9. Static SIMS Library, *Surface Spectra*, Static SIMS Library, Manchester, U.K., 1998.
10. D. Briggs, *Surface Analysis of Polymers by XPS and Static SIMS*, Cambridge University Press, Cambridge, U.K., 1998, pp. 88–118.
11. S. Reichlmaier, S.R. Bryan, and D. Briggs, *J. Vac. Sci. Technol., A* **13**, 1217–1223 (1995).
12. B.D. Ratner, *SIA, Surf. Interface Anal.* **23**, 521–528 (1995).
13. F.W. McLafferty and F. Turecek, *Interpretation of Mass Spectrometry*, 4th ed., University Science Books, Mill Valley, Calif.
14. M.C. Davies et al., *SIA, Surf. Interfac. Anal.* **14**, 115–120 (1989).
15. M.C. Davies and A. Brown, *ACS Symp. Ser.* **348** (1987).
16. M.C. Davies, M.A. Khan, A. Brown, and P. Humphrey, in A. Benninghoven, A.M. Huber, and H.W. Werner, eds., *Secondary Ion Mass Spectrometry VI*, Wiley, Chichester, U.K., 1988.
17. A.G. Shard, C. Volland, M.C. Davies, and T. Kissel, *Macromolecules* **29**(2), 748–754 (1996).
18. P. Williams, *Annu. Rev. Mater. Sci.* **15**, 517–548 (1985).
19. D. Briggs and B.D. Ratner, *Polym. Commun.* **29**, 6–8 (1988).
20. M.C. Davies et al., *J. Colloid Interfac. Sci.* **156**, 229–239 (1993).
21. X.V. Eynde, L.T. Weng, and P. Betrand, *SIA, Surf. Interface Anal.* **25**(1), 41–45 (1997).
22. I.V. Bletsos, D.M. Hercules, D. Griefendorf, and A. Benninghoven, *Anal. Chem.* **57**, 2384–2388 (1985).

23. D. Briggs and M.C. Davies, *SIA, Surf. Interface Anal.* **25**(9), 725–733 (1997).
24. K.J. Wu and R.W. Odom, *Anal. Chem.* **68**, 456–461 (1998).
25. C. Fenselau, *Anal. Chem.* **69**, A661–A665 (1997).
26. D.S. Mantus, B.D. Ratner, B.A. Carlson, and J.F. Moulder, *Anal. Chem.* **65**(10), 1431–1438 (1993).
27. J.B. Lhoest, E. Detrait, P. VandenBosch de Aguilar, and P. Betrand, *J. Biomed. Mater. Res.* **41**(1), 95–103 (1998).
28. K. Leufgen et al., *Prog. Biophys. Mol. Biol.* **65** (S1), PC435.
29. C. Drouot et al., *Tetrahedron Lett.* **38**(14), 2455–2458 (1997).
30. J.S. Patrick, R.G. Cooks, and S.J. Pachuta, *Biol. Mass. Spectrom.* **23**(11), 653–659 (1994).
31. C. Chassard-Bouchaud, *Conf. Ser. Inst. Phys.*, 793–798 (1990).
32. T.L. Colliver et al., *Anal. Chem.* **69**(13), 2225–2231 (1997).
33. C.M. John et al., *Anal. Chem.* **67**(21), 3871–3878 (1995).
34. B.J. Tyler, B.D. Ratner, D.G. Castner, and D. Briggs, *J. Biomed. Mater. Res.* **26**, 273–289 (1992).
35. F. Koosha, R.H. Muller, S.S. Davis, and M.C. Davies, *J. Controlled Release* **94** 149–157 (1989).
36. P.D. Scholes et al., *J. Controlled Release*, in press.
37. M.C. Davies et al., *Langmuir* **12**, 3866–3875 (1996).
38. M.C. Davies et al., *Langmuir* **10**, 1399–1409 (1994).
39. A. Brindley, S.S. Davis, M.C. Davies, and J.F. Watts, *J. Colloid Interfac. Sci.* **171**, 150–161 (1995).
40. M.C. Davies et al., *Langmuir* **9**(7), 1637–1645 (1993).
41. A.G. Shard et al., in A.J. Domb, J. Kost, and D.M. Wiseman, eds., *Handbook of Bioerodable Polymers*, Gordon & Breach, Amsterdam, 1997, pp. 417–450.
42. K.M. Shakesheff et al., *Macromolecules* **29**(6), 2205–2212 (1996).
43. S.R. Leadley et al., *Biomaterials* **19**, 1353–1360 (1998).

CHARACTERIZATION OF DELIVERY SYSTEMS, X-RAY POWDER DIFFRACTOMETRY

SUNEEL K. RASTOGI
RAJ SURYANARAYANAN
University of Minnesota
Minneapolis, Minnesota

KEY WORDS

Amorphous
Crystalline
Crystallinity
Drug delivery system
Hydrate
Interaction
Internal standard
Phase identification
Phase transformation
Polymorph
Processing
Quantitative analysis
Solid dispersion
Storage
X-ray powder diffractometry

OUTLINE

Introduction
Phase Identification
  Raw Materials
  Dosage Forms
  Limitations of XRD
Determination of Crystallinity
  Use of Internal Standard
  Use of Peak Intensity
  Other Methods
Quantitative Analysis
  Theory
  The Direct Method
  The Internal Standard Method
  Choice of Internal Standard
  Preformulation
  Dosage Forms
  Sources of Error in Quantitative XRD
Phase Transitions Induced during Processing or Storage
  Special Instrumentation
  Interactions between Solids
Characterization of Drug Delivery Systems
  Physical State of the Active Ingredient
  Solid Dispersions
  Influence of Drug Load
  Drug–Cyclodextrin Complexes
  Degree of Crystallinity
  Limitations of XRD in the Characterization of Drug Delivery Systems
Other Applications
Summary
Bibliography

INTRODUCTION

Discovered in 1895 by the German physicist Roentgen, X-rays are electromagnetic radiation, and their wavelength can range between 10^{-2} and 10^{2} Å. When X-rays pass through matter, they interact with the electrons and are scattered in all directions. Crystalline substances are characterized by long-range periodicity of the constituent molecules (or atoms). Because the interplaner distances are similar in magnitude to the wavelength of X-rays, their interaction results in diffraction. This was hypothesized and proven by Max von Laue in 1912. The condition under which diffraction occurs is described by the Bragg equation (1,2):

$$n\lambda = 2d \sin\theta \quad (1)$$

where d = the distance between the successive planes of a crystal, n = order of reflection (an integer), λ = the wave-

23. D. Briggs and M.C. Davies, *SIA, Surf. Interface Anal.* **25**(9), 725–733 (1997).
24. K.J. Wu and R.W. Odom, *Anal. Chem.* **68**, 456–461 (1998).
25. C. Fenselau, *Anal. Chem.* **69**, A661–A665 (1997).
26. D.S. Mantus, B.D. Ratner, B.A. Carlson, and J.F. Moulder, *Anal. Chem.* **65**(10), 1431–1438 (1993).
27. J.B. Lhoest, E. Detrait, P. VandenBosch de Aguilar, and P. Betrand, *J. Biomed. Mater. Res.* **41**(1), 95–103 (1998).
28. K. Leufgen et al., *Prog. Biophys. Mol. Biol.* **65** (S1), PC435.
29. C. Drouot et al., *Tetrahedron Lett.* **38**(14), 2455–2458 (1997).
30. J.S. Patrick, R.G. Cooks, and S.J. Pachuta, *Biol. Mass. Spectrom.* **23**(11), 653–659 (1994).
31. C. Chassard-Bouchaud, *Conf. Ser. Inst. Phys.*, 793–798 (1990).
32. T.L. Colliver et al., *Anal. Chem.* **69**(13), 2225–2231 (1997).
33. C.M. John et al., *Anal. Chem.* **67**(21), 3871–3878 (1995).
34. B.J. Tyler, B.D. Ratner, D.G. Castner, and D. Briggs, *J. Biomed. Mater. Res.* **26**, 273–289 (1992).
35. F. Koosha, R.H. Muller, S.S. Davis, and M.C. Davies, *J. Controlled Release* **94** 149–157 (1989).
36. P.D. Scholes et al., *J. Controlled Release*, in press.
37. M.C. Davies et al., *Langmuir* **12**, 3866–3875 (1996).
38. M.C. Davies et al., *Langmuir* **10**, 1399–1409 (1994).
39. A. Brindley, S.S. Davis, M.C. Davies, and J.F. Watts, *J. Colloid Interfac. Sci.* **171**, 150–161 (1995).
40. M.C. Davies et al., *Langmuir* **9**(7), 1637–1645 (1993).
41. A.G. Shard et al., in A.J. Domb, J. Kost, and D.M. Wiseman, eds., *Handbook of Bioerodable Polymers*, Gordon & Breach, Amsterdam, 1997, pp. 417–450.
42. K.M. Shakesheff et al., *Macromolecules* **29**(6), 2205–2212 (1996).
43. S.R. Leadley et al., *Biomaterials* **19**, 1353–1360 (1998).

CHARACTERIZATION OF DELIVERY SYSTEMS, X-RAY POWDER DIFFRACTOMETRY

SUNEEL K. RASTOGI
RAJ SURYANARAYANAN
University of Minnesota
Minneapolis, Minnesota

KEY WORDS

Amorphous
Crystalline
Crystallinity
Drug delivery system
Hydrate
Interaction
Internal standard
Phase identification
Phase transformation
Polymorph
Processing
Quantitative analysis
Solid dispersion
Storage
X-ray powder diffractometry

OUTLINE

Introduction
Phase Identification
  Raw Materials
  Dosage Forms
  Limitations of XRD
Determination of Crystallinity
  Use of Internal Standard
  Use of Peak Intensity
  Other Methods
Quantitative Analysis
  Theory
  The Direct Method
  The Internal Standard Method
  Choice of Internal Standard
  Preformulation
  Dosage Forms
  Sources of Error in Quantitative XRD
Phase Transitions Induced during Processing or Storage
  Special Instrumentation
  Interactions between Solids
Characterization of Drug Delivery Systems
  Physical State of the Active Ingredient
  Solid Dispersions
  Influence of Drug Load
  Drug–Cyclodextrin Complexes
  Degree of Crystallinity
  Limitations of XRD in the Characterization of Drug Delivery Systems
Other Applications
Summary
Bibliography

INTRODUCTION

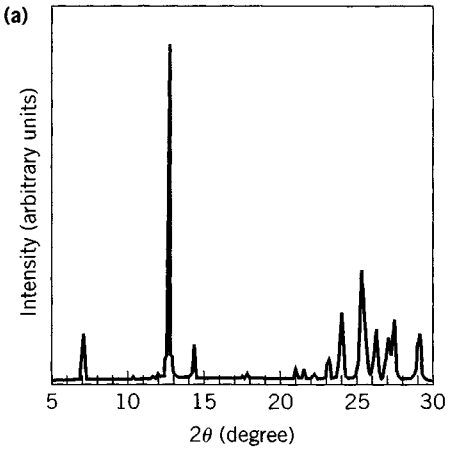
Discovered in 1895 by the German physicist Roentgen, X-rays are electromagnetic radiation, and their wavelength can range between 10^{-2} and 10^{2} Å. When X-rays pass through matter, they interact with the electrons and are scattered in all directions. Crystalline substances are characterized by long-range periodicity of the constituent molecules (or atoms). Because the interplaner distances are similar in magnitude to the wavelength of X-rays, their interaction results in diffraction. This was hypothesized and proven by Max von Laue in 1912. The condition under which diffraction occurs is described by the Bragg equation (1,2):

$$n\lambda = 2d \sin\theta \quad (1)$$

where d = the distance between the successive planes of a crystal, n = order of reflection (an integer), λ = the wave-

length of the X-rays, and θ = the angle that the incident beam of X-rays make with the sample.

The technique of X-ray powder diffractometry (XRD) was devised independently by Debye and Scherrer (1916) in Germany (3) and Hull (1917) in the United States (4). X-ray diffraction data show peak intensity as a function of diffraction angle (θ) and can be presented in several ways (Fig. 1). Crystalline materials exhibit characteristic XRD patterns in which the positions and relative intensities of peaks are well defined and reproducible. The technique is usually nondestructive and is suited for analysis of pharmaceuticals both in pure state as well as in finished dosage forms. In recent years, the U.S. Food and Drug Administration (FDA) has realized the potential utility of XRD as a fingerprinting tool for characterization of pharmaceuticals (6). A brief description of the principles and applications of XRD is provided in the U.S. Pharmacopeia (7). In 1995, Byrn et al. developed some strategic approaches to regulatory issues involving solid pharmaceuticals in the form of flow charts/decision tree (8). From one such flow chart (Fig. 2), it is evident that XRD can be utilized for identifying and characterizing polymorphs. If multiple polymorphic forms exist, their quantitation can also be performed by XRD.



(b)

2θ (degree)	d-spacings (A)	Relative intensity (%)
7.11	12.4	13
12.6	7.02	100
14.25	6.21	10
17.67	5.02	1
20.88	4.25	2
21.45	4.14	2
22.11	4.02	2
23.19	3.83	6
23.85	3.73	16
23.94	3.71	20
25.29	3.52	33
25.38	3.51	32
26.19	3.40	15
27.03	3.30	12
27.39	3.25	18
29.04	3.04	15

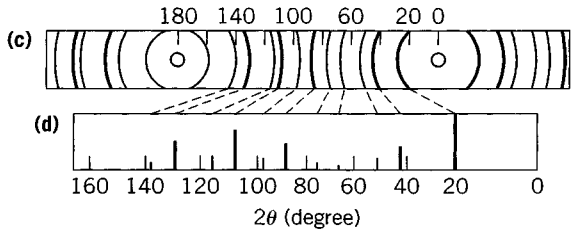


Figure 1. Different ways of presentation of X-ray powder diffraction data. (**a**) Diffraction pattern recorded experimentally (raw data), (**b**) tabular form of the experimentally obtained data, (**c**) Debye–Scherrer diffraction pattern, and (**d**) reduced diffraction pattern. (**a**), (**b**), and (**d**) are obtained by using a powder diffractometer with Bragg-Brentano geometry, whereas (**c**) is obtained using a Debye–Scherrer camera. *Source:* (**c**) and (**d**) are reproduced with permission of the copyright owner, John Wiley & Sons, Inc., from Ref. 5.

PHASE IDENTIFICATION

XRD finds widespread application for the identification of crystalline solid phases. The diffraction pattern of every crystalline form of a compound is unique, which is the basis of its identification. The FDA requires proper control of the solid form of the drug in the formulation (6,8–10).

Phase identification is based on a comparison of the experimental data with standard powder patterns published in a database known as the *Powder Diffraction File* (PDF). This database was first introduced by Hanawalt et al. (11) in 1938 and has been issued annually since 1950. It is currently administered and distributed by the International Centre for Diffraction Data (ICDD). The database contains a collection of single-phase XRD patterns where the *d*-spacings (in Å) and relative intensities are tabulated. Each powder pattern is assigned a quality mark, the details of which can be found in the ICDD literature. This process of phase identification has been revolutionized by the introduction of compact disks for storage of standard data and faster search/match software algorithms for accessing and searching databases (12).

Raw Materials

XRD is widely used for the identification and characterization (polymorphic forms, state of solvation, degree of crystallinity) of solid phases (13–15). The solid state of several forms of acemetacin were characterized by thermomicroscopy, differential scanning calorimetry (DSC), thermogravimetry, infrared spectroscopy (IRS), XRD, and pycnometry (13). Six crystalline forms of the drug were identified, of which five were anhydrates and one was a monohydrate. An amorphous phase was also identified. Each crystalline phase was characterized by a unique XRD pattern (Fig. 3). Similarly, the XRD patterns of seven crystalline phases (three anhydrate forms, two monohydrate forms, a quarter-hydrate and a methanol hemisolvate) of dehydroepiandrosterone revealed clear differences (14). XRD can also be used to identify and differentiate the different solid phases of pharmaceutical excipients. For example, the different polymorphs of mannitol exhibited differences in their diffraction patterns (15). These studies demonstrate the utility of XRD for the rapid identification of the various solid forms of pharmaceutical compounds.

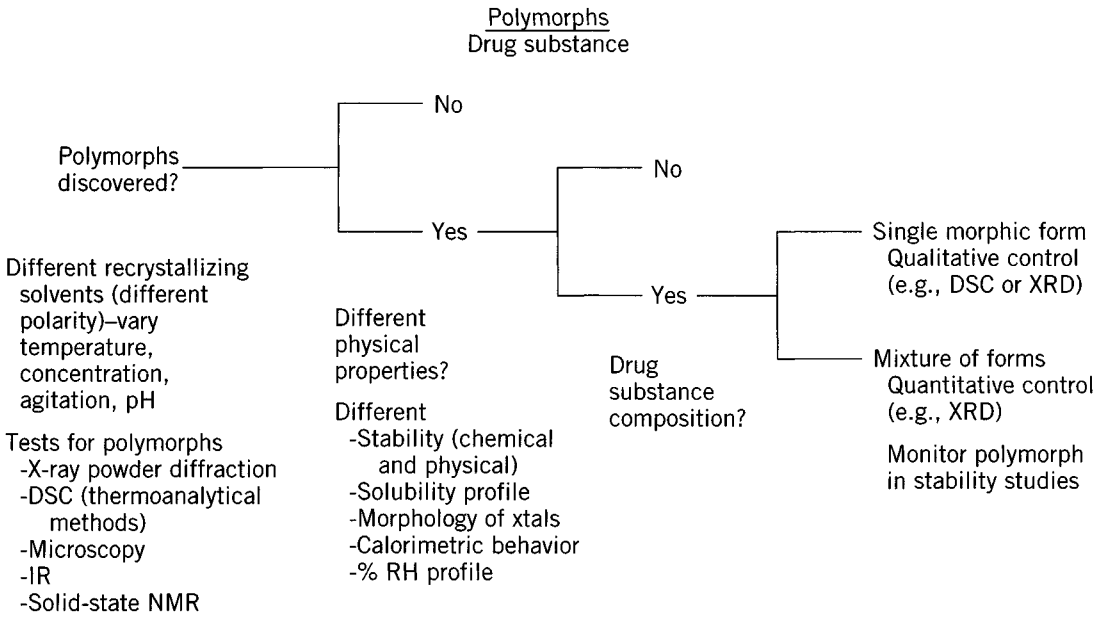


Figure 2. Flow chart/decision tree describing a logical sequence for collecting data for the identification and characterization of polymorphs. *Source:* Reproduced with permission of the copyright owner, Plenum Publishing Corporation, from Ref. 8.

Dosage Forms

Solid dosage forms are usually multicomponent systems and contain one or more excipients in addition to the active ingredient. In such cases, each phase produces its XRD pattern independently of the others. Thus, simultaneous identification of multiple ingredients in a dosage form is possible (16). The technique may permit the detection of crystalline impurities. The method is nondestructive, and active ingredients in dosage forms can be analyzed with minimal or no sample preparation. However, in some formulations, the diffraction peaks of the ingredients overlap to such an extent that unambiguous identification of one or more ingredients may become difficult, if not impossible. Phadnis et al. (16) have described a pattern-subtraction technique that permitted selective subtraction of the XRD pattern of constituents of a formulation from the overall XRD pattern. The same approach was also used to improve the sensitivity of the technique. Chlordiazepoxide hydrochloride is available as an injectable and as oral (tablet and capsule) formulations. Because this is a low-dose drug, the content per tablet or capsule ranges between 5 and 25 mg. The drug is crystalline and has a characteristic XRD pattern (Fig. 4a). In physical mixtures of drug and microcrystalline cellulose, the presence of chlordiazepoxide hydrochloride was not readily discernable (Fig. 4b) because the drug constituted only 5% w/w of the mixture. However, using the pattern-subtraction technique, it was possible to subtract the XRD pattern of microcrystalline cellulose from that of the mixture. Identification of the drug was possible because the subtracted pattern (Fig. 4d) clearly revealed the peaks due to chlordiazepoxide hydrochloride. It should be pointed out here that conventional pharmacopeial identification techniques such as high-performance liquid chromatography (HPLC) require extraction of the active ingredient from the formulation, resulting in loss of valuable information about the solid state of the drug.

Limitations of XRD

This technique can only be used if the analyte is crystalline. Noncrystalline (amorphous) materials produce diffraction patterns with one or more broad diffuse maxima. Because the technique is not very sensitive, crystalline impurities in low concentrations may be undetected. Other potential problems in the analyses of organic solids have been discussed comprehensively and elegantly by Jenkins (17).

DETERMINATION OF CRYSTALLINITY

Solids are classified as either crystalline or noncrystalline (amorphous). Although the crystalline state is characterized by an ordered lattice, the amorphous state is characterized by the lack of long-range periodicity of the constituent molecules or atoms. The crystalline and amorphous states represent the two extremes of lattice order and intermediate states are possible. The term *degree of crystallinity* is useful in attempts to quantify these intermediate states of lattice order. During pharmaceutical processing, a drug is subject to a number of stresses such as milling and compression, which can cause a decrease in lattice order (18,19). Many properties, including chemical stability, water uptake and loss, and dissolution rate, depend on the degree of crystallinity of the drug.

Several XRD methods are available for the determination of degree of crystallinity. Ruland described a rigorous

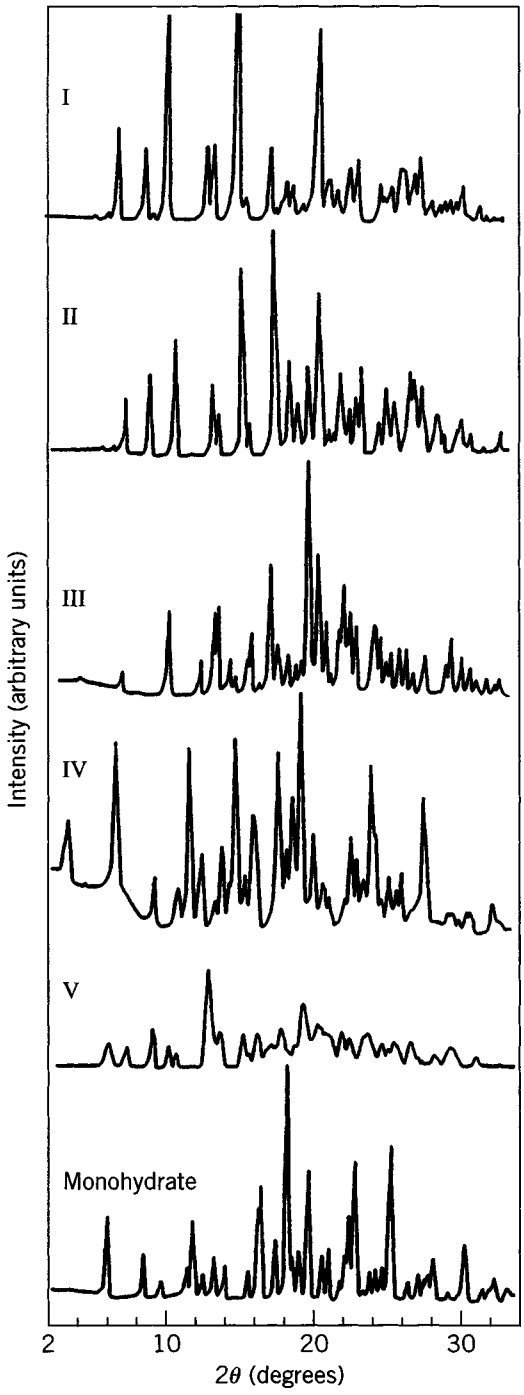


Figure 3. XRD patterns of different solid forms of acemetacin. I to V are different polymorphs of the anhydrate. *Source:* Reproduced with permission of the copyright owner, Govi-Verlag Pharmazeutischer Verlag GmbH, from Ref. 13.

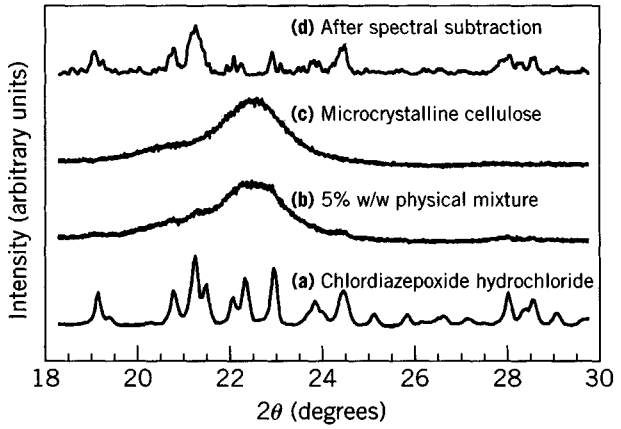


Figure 4. (**a**) The XRD pattern of chlordiazepoxide hydrochloride powder, (**b**) the XRD pattern of a powder mixture of chlordiazepoxide hydrochloride (5% w/w) and microcrystalline cellulose (95% w/w), (**c**) the XRD pattern of microcrystalline cellulose powder, **d**) the residual pattern after proportional subtraction of the microcrystalline cellulose XRD pattern from that of the physical mixture (**b**). The full scale in (**d**) is different from that of the other three XRD patterns. *Source:* Reproduced with permission of the copyright owner, Elsevier Science B. V., from Ref. 16.

method of determination of crystallinity (20). The method is based on Hosemann's paracrystal theory and takes into account all forms of lattice imperfections, including those produced by paracrystalline disorder. The applicability of this method to pharmaceutical systems has been demonstrated. (21,22). However, because the method requires extensive and time-consuming calculations, it has rarely been applied to evaluate the crystallinity of pharmaceuticals.

A simpler yet reliable method was developed by Hermans and Weidinger (23). This method is based on three assumptions: (*1*) the XRD pattern can be divided to demarcate between crystalline intensity (I_c) and amorphous intensity (I_a), (*2*) the experimentally measured crystalline intensity is directly proportional to the crystalline weight fraction (x_c) in the sample, and (*3*) the experimentally measured amorphous intensity (background intensity) is proportional to the amorphous weight fraction (x_a) in the sample. Thus,

$$x_c = pI_c \tag{2}$$

$$x_a = qI_a \tag{3}$$

where p and q are proportionality constants. If x is the sum of the crystalline and amorphous weight fractions, then it can be shown that

$$I_a = \frac{x}{q} - \frac{p}{q} I_c \tag{4}$$

Samples of varying degrees of crystallinity can be prepared and analyzed to obtain the values of I_c and I_a. Based on equation 4, a plot of I_a versus I_c must be a straight line with a slope of p/q. The degree of crystallinity (x_{cr}) is related to XRD intensities I_c and I_a through the relation

$$x_{cr} = \frac{x_c}{x_c + x_a} \times 100 = \frac{I_c}{I_c + I_a \dfrac{q}{p}} \times 100 \tag{5}$$

For a given unknown sample, the value of x_{cr} can be obtained by substituting the experimentally obtained val-

ues of I_c and I_a into equation 5. Black and Lovering (24), simplified equation 5 to

$$x_{cr} = \frac{I_c}{I_c + I_a} \times 100 \quad (6)$$

and determined the degree of crystallinity of several compounds including digoxin. In order to determine the degree of crystallinity using equations 5 and 6, it is necessary to separate the crystalline (I_c) and amorphous (I_a) intensities. This is at best arbitrary and based on subjective judgment, making it a potentially serious source of error.

Use of Internal Standard

The use of an internal standard will assist in minimizing some of the errors in the measurement of intensities. Saleki-Gerhardt et al. used this approach to assess the percent disorder (percent disorder = 100 − x_{cr}) of sucrose (25). Sucrose samples were prepared with percent disorder ranging from 0 to 100 to which a constant proportion of lithium fluoride (internal standard) was added. The integrated intensities of a peak unique to sucrose and lithium fluoride were determined. A linear standard curve was obtained when the intensity ratio (intensity of sucrose peak/intensity of lithium fluoride peak) was plotted as a function of percent disorder.

Use of Peak Intensity

It is possible to use the peak height (instead of integrated intensity) as a measure of diffraction line intensity, provided the variations in disorder and particle size do not significantly influence the shape of the XRD peaks. Imaizumi et al. (26) used this method for the evaluation of degree of crystallinity of several samples of indomethacin, again using lithium fluoride as an internal standard.

Other Methods

Ryan described a method to calculate the relative degree of crystallinity (RDC) of imipenem in a lyophilized product containing imipenem and amorphous cilastatin sodium (27). The full width at half the maximum intensity (FWHM) of the diffraction lines can be used to rank-order samples of varying degrees of crystallinity (28). Assuming that there are no particle size effects, an increase in crystallinity will result in an increase in peak height and a decrease in FWHM.

In spite of the popularity of XRD for crystallinity evaluation, the technique lacks precision and is subject to artifacts. It is also unsuitable for the detection and quantitation of small changes in lattice order. Pikal et al. performed XRD and solution calorimetry of spray-dried and freeze-dried cehphalothin sodium (29). The differences in crystallinity between these could be evaluated by solution calorimetry but not by XRD. For the quantitation of small levels of disorder in highly crystalline samples, water sorption (25) and microcalorimetry (30) appear to be the techniques of choice. Recently, using FT-Raman spectroscopy, it was possible to detect down to either 1% amorphous or 1% crystalline content (31). This technique can therefore be used to quantify small levels of disorder in highly crystalline samples and also small levels of order in highly disordered samples.

QUANTITATIVE ANALYSIS

Theory

Alexander and Klug derived the theoretical basis for quantitative analysis by XRD (32). When a beam of X-ray passes through any homogenous substance, the fractional decrease in the intensity, I, is proportional to the distance traversed, x. Thus,

$$-\frac{dI}{I} = \mu dx \quad (7)$$

where μ is a proportionality constant known as the *linear attenuation coefficient*. The value of μ depends on the density of the substance and the wavelength of the X-rays. The *mass attenuation coefficient*, μ^*, obtained by dividing μ by the density of the substance, is a constant independent of the physical state. The mass attenuation coefficient of a substance is the weighted average of the mass attenuation coefficients of that substance's constituent elements. Thus,

$$\mu^* = \sum_{k=1}^{n} w_k \mu_k^* \quad (8)$$

where, $w_1, w_2, \ldots, w_n$ are the weight fractions of elements 1, 2, . . . , n in the substance and $\mu_1^*, \mu_2^*, \ldots, \mu_n^*$ are their respective mass attenuation coefficients.

A solid mixture containing several components can be regarded as being composed of only two components—the analyte (component 1) and the sum of the other components (the matrix, subscripted as M). The relationship between the intensity of diffraction peak i of the unknown component (I_{il}) and its weight fraction (x_1) in the mixture is described by the equation:

$$I_{il} = \frac{Kx_1}{\rho_1(x_1(\mu_1^* - \mu_M^*) + \mu_M^*)} \quad (9)$$

where K is a constant, ρ_1 is the density of component 1, and μ_1^* and μ_M^* are the mass attenuation coefficients of components 1 and the matrix, respectively.

The Direct Method

The direct method is applicable to two component mixtures where $\mu_1^* \neq \mu_M^*$. Such cases are frequently encountered in pharmaceutical systems where a solid drug might be contaminated by pseudopolymorphs or decomposition products. It is necessary to determine the intensity of peak i of a sample consisting of only the analyte [$(I_{il})_0$]. Equation 9 is modified so that the relative intensity of the XRD peak of component 1 [expressed as $I_{il}/(I_{il})_0$] is given by

$$\frac{I_{i1}}{(I_{i1})_0} = \frac{x_1\mu_1^*}{x_1(\mu_1^* - \mu_M^*) + \mu_M^*} \quad (10)$$

As mentioned previously, it is possible to calculate the mass attenuation coefficients of the analyte and the matrix based on their chemical compositions. It is then possible to calculate the relative intensity $[I_{il}/(I_{il})_0]$ as a function of the weight fraction of the analyte in the mixture and thus generate a theoretical standard curve. This eliminates the need for the preparation of experimental standard curves.

A simpler case of quantitative analysis arises when $\mu_1^* = \mu_M^*$. This occurs when the analyte and the matrix have the same molecular formula. Two examples are polymorphic mixtures and enantiomer–racemic compound mixture. In such cases, equation 10 reduces to

$$\frac{I_{il}}{(I_{il})_0} = x_1 \tag{11}$$

A plot of the relative intensity as a function of the analyte weight fraction will be linear.

The Internal Standard Method

In this method, an internal standard is added, and its weight fraction in the mixtures is maintained constant in all the samples. The integrated intensities of line 1 of the analyte (I_1) and line s of the internal standard (I_s) are determined. The relationship between the intensity ratio and the analyte weight fraction (x_1) in the mixture is expressed as

$$x_1 = k\frac{I_1}{I_s} \tag{12}$$

Thus, the intensity ratio is linearly related to the analyte weight fraction in the mixture.

Choice of Internal Standard

Shell (33) suggested that an ideal internal standard should have high crystal symmetry so that its XRD pattern consists of strong but few peaks. It must be chemically stable and should not interact with the system ingredients. The high-intensity lines of the analyte and the internal standard should not overlap with one another but should be close to each other. To facilitate the preparation of a homogeneous mixture, the density of the internal standard should not be very different than those of the system ingredients. Corundum(α-Al_2O_3), silicon, lithium fluoride, and zinc oxide have been used as internal standards. Among organic compounds, adamantane has several of the properties desired in an internal standard. However, it has not found widespread use in quantitative XRD.

Besides the methods mentioned above, several others have been described in the literature. These include (*1*) the method of standard additions, (*2*) the reference intensity ratio (RIR) method, and (*3*) Reitveld analysis. These methods are described in standard texts (34,35) but have found little use in analyses of pharmaceuticals.

The application of XRD for the quantitative analyses of pharmaceutical systems was pioneered by Shell (33). Early quantitative XRD studies were based on the heights of XRD peaks (36,37). It is well known that variations in particle size and microstrain can affect the peak heights. However, the integrated peak intensities are much less affected by these factors. Thus, for quantitative XRD, it is desirable to measure the integrated intensities (2).

Preformulation

The direct method described above has been successfully used to determine the weight fractions of anhydrous carbamazepine ($C_{15}H_{12}N_2O$) and carbamazepine dihydrate ($C_{15}H_{12}N_2O \cdot 2H_2O$) in their mixtures (38). Based on the mass attenuation coefficients of carbamazepine anhydrate and dihydrate, the intensity ratios $(I_{il}/(I_{il})_0)$ were calculated as a function of the sample composition (Fig. 5). These were in good agreement with the experimentally obtained values of $I_{il}/(I_{il})_0$. The relative amounts of α- and β-carbamazepine in a mixture have also been quantified using this method (39). The internal standard method has been used for the simultaneous quantification of the $S(+)$-enantiomer and the racemic compound of ibuprofen (40).

Dosage Forms

XRD has been used for quantification of active ingredients in intact formulations. As early as 1964, Papariello et al. determined the glutethimide content in intact tablets by XRD (41). However, the authors were somewhat limited by the fact that computer-based data collection and analysis was not possible at that time. Using the direct method (equation 10), the carbamazepine content in intact, multicomponent tablet formulations was determined (42). Though the experimentally observed intensity ratios were in good agreement with the theoretical intensity ratios, the

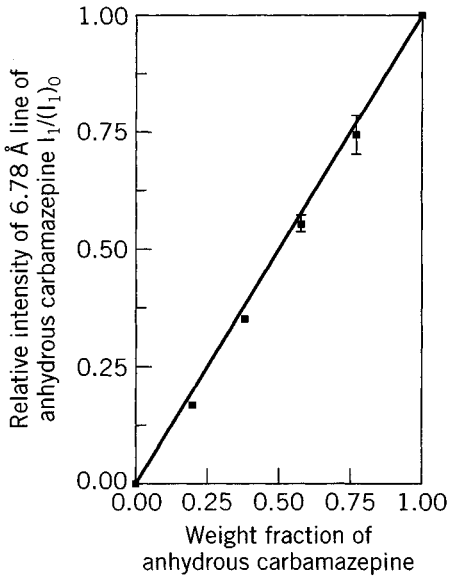


Figure 5. The relative intensity of the 6.78-Å line of anhydrous carbamazepine as a function of its weight fraction in a binary mixture of anhydrous carbamazepine and carbamazepine dihydrate. The line is based on theoretical values, while the data points are experimental measurements. Error bars represent standard deviations. *Source:* Reproduced with permission of the copyright owner, Plenum Publishing Corporation, from Ref. 38.

relative error in the determination of carbamazepine content was high (± 10%). When the tablets were crushed and the powder sample was analyzed after the addition of an internal standard, the precision and accuracy improved substantially (43). The experimentally determined weight fraction of carbamazepine in the tablets ranged between 98.7 and 102% of the true weight fraction, and the highest coefficient of variation value was 2.2%. The relative error in the determination of carbamazepine content was reduced to ±4%.

Kuroda and coworkers used the technique for the quantitative analysis of active components in a variety of formulations including ointments (44), vaginal tablets (45), oral suspension (46), plasters (47) and rectal suppositories (48). Both the direct as well as the internal standard method were used, and the active ingredient was quantified even at concentrations down to 0.05% w/w. There was a good agreement of the results obtained by XRD and by chemical analysis.

Sources of Error in Quantitative XRD

There are numerous sources of error in quantitative XRD. These are discussed comprehensively in the literature (1,49).

PHASE TRANSITIONS INDUCED DURING PROCESSING OR STORAGE

The active ingredient as well as the excipients in a dosage form can undergo a variety of physical transformations during processing or storage. These include polymorphic transformations, alterations in the degree of crystallinity, and changes in the state and degree of hydration. Such processing- and storage-induced phase transformations can profoundly influence the performance of the dosage form (50). XRD has been used to identify crystalline reactants, products, and intermediates (if any). The technique has been used to monitor phase transitions both qualitatively and quantitatively. An added advantage of the technique is that it provides quantitative information about the degree of crystallinity.

The transition of anhydrous carbamazepine to carbamazepine dihydrate in aqueous suspensions was observed to follow first-order kinetics (51). The dehydration of 6-mercaptopurine monohydrate was studied both in the presence and absence of 6-thioxanthine (52). Whereas pure 6-mercaptopurine monohydrate converted directly to polymorphic form II of the anhydrate, in the presence of 6-thioxanthine it converted to a different anhydrate (form III) through an intermediate. The effect of processing operations such as grinding and compression on the crystallinity of an experimental drug, TAT-59, was monitored by XRD (53). An increase in compression pressure or grinding time caused a decrease in drug crystallinity. This was accompanied by a decrease in the stability of TAT-59.

Special Instrumentation

Recent advances in instrumentation and data analysis software have greatly facilitated the study of pharmaceutical systems. Variable-temperature powder diffractometry (VTXRD) is a technique whereby XRD patterns are obtained while the sample is subjected to controlled temperature program. During such studies, it is also possible to control the environment and maintain the sample under the desired relative humidity (54,55). Conventionally, thermoanalytical techniques such as DSC or themogravimetric analysis (TGA) have been used for the investigation of reactions in solid drugs. These techniques have several drawbacks. They do not unambiguously identify crystalline phases and provide little or no information about the degree of crystallinity. Because intermediate phases (if any) may not be readily identified, these techniques are not necessarily useful for discerning the reaction mechanism. These drawbacks can be overcome by using VTXRD, which provides an excellent compliment to thermoanalytical techniques. Because the crystalline intermediates can be easily identified, the technique provides critical information about the reaction mechanism. For example, VTXRD was used to investigate the dehydration of theophylline monohydrate (Fig. 6). Dehydration of the monohydrate resulted in the formation of anhydrous theophylline (50). However, the VTXRD study revealed that theophylline monohydrate dehydrated to a metastable anhydrous phase that then transformed to the stable anhydrate. Fawcett et al. (56) have built an instrument that allows simultaneous XRD and DSC studies on the same sample. Another unique feature of the instrument is that the gaseous reaction product can be subjected to mass spectrometric analysis (57).

By attaching a low-temperature stage to an XRD, characterization of solutes in frozen aqueous solutions has been accomplished (58). Sodium nafcillin does not crystallize when its aqueous solution is frozen. However, when the sample is annealed at −4°C, the solute gradually crystallizes. Using XRD, it was possible to monitor the amount of sodium nafcillin crystallizing as a function of the annealing time. Recently, the low-temperature stage of an XRD was modified so that the sample chamber could be evacuated using a vacuum pump. As a result, it was possible to carry out the entire freeze-drying process in situ in the sample chamber of the XRD (59).

Interactions between Solids

In a powder mixture, the powder pattern of each crystalline phase is produced independently of the other constituents. This makes it feasible to study solid–solid interactions such as those between the drug and excipients in a formulation. If there is no interaction, then the diffraction pattern of a solid mixture will be the summation of diffraction patterns of individual constituents. If the interaction between the constituents results in the formation of crystalline product, then this will be characterized by the appearance of new peaks in the powder pattern. However, if the interaction results in amorphous products, this will be evident from the broad halos in the XRD pattern. Thus, irrespective of the nature of product phase, XRD is capable of revealing solid–solid interactions. Position-sensitive detectors (PSD) allow very rapid data collection and are particularly useful for investigating fast reactions. The com-

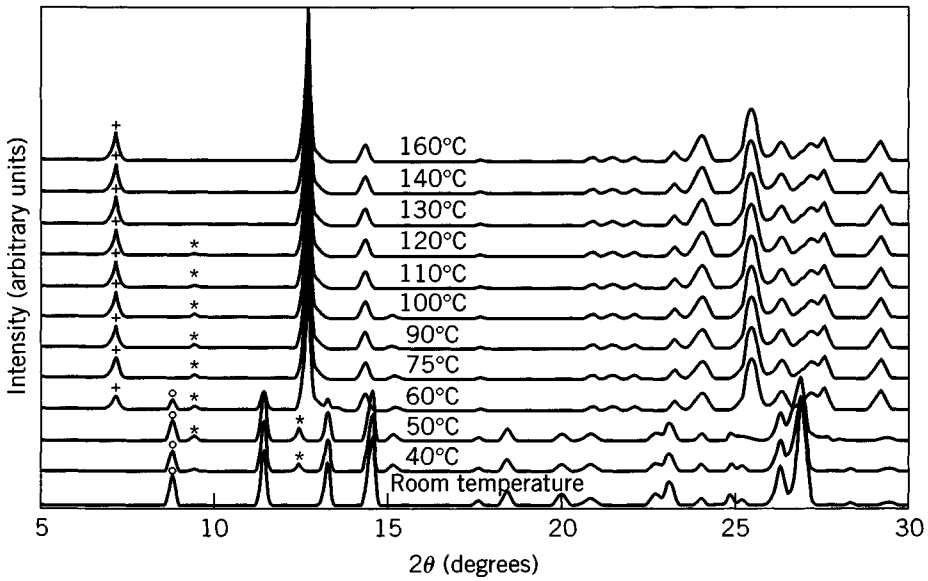


Figure 6. VTXRD of theophylline monohydrate. XRD patterns were taken at all the temperatures indicated in the figure. The *, +, and o marks indicate peaks unique to metastable anhydrous theophylline, stable anhydrous theophylline, and theophylline monohydrate, respectively. *Source:* Reproduced with permission of the copyright owner, American Chemical Society and American Pharmaceutical Association, from Ref. 50.

ponents of a formulation can undergo a variety of interactions resulting in formation of various dispersion systems such as glass dispersions, solid solutions, eutectic mixtures, and inclusion complexes. XRD is useful for characterizing such interactions.

CHARACTERIZATION OF DRUG DELIVERY SYSTEMS

The principles and procedures discussed so far can be extended for the characterization of complex drug delivery systems. In sustained- and controlled-release formulations, the release of the active ingredient is controlled through the use of excipients that are often polymeric in nature. XRD has been used for the characterization of a wide variety of formulations, including microspheres (60–62), hydrogel matrices (63), solid lipospheres (64), microcapsules (62), solid-dispersion polymer films (65,66), solid-dispersion granules (67), waxy matrix tablets (68), and nanoparticles (69,70).

Physical State of the Active Ingredient

There are a variety of polymer-based delivery systems. Hydrogels are polymeric materials that can take up and retain water within their structure. This ability, combined with their biocompatibility, makes them useful for drug delivery applications. The physical state of the drug in such delivery systems depends on the solubility of the drug in the matrix. The drug could either be completely dissolved in the matrix, or a fraction of the incorporated drug could be dissolved, and the rest could be dispersed in the matrix. To model the kinetics of drug release from these dosage forms, it is necessary to know the physical state of the drug in the matrix. XRD has been used to determine the physical state of salicylic acid in a hydrogel topical formulation (63). Formulations were prepared with high salicylic acid concentrations so that a fraction of the incorporated salicylic acid was undissolved. A fixed weight of each formulation was subjected to XRD, and the integrated intensities of two peaks of salicylic acid were determined. The intensity of each of these peaks was linearly related to the weight percent of salicylic acid in the formulations. The intercept on the x-axis was the solubility of salicylic acid in the matrix. The results obtained by XRD were confirmed by scanning electron microscopic studies. Many transdermal dosage forms are monolithic systems where the active ingredient is incorporated in a rate-controlling polymeric matrix. The XRD method described here can find application in the characterization of the physical state of the drug in such systems.

Solid Dispersions

XRD has been used to differentiate between various types of solid-dispersion systems (71,72) such as solid solutions (73), glass dispersions (74), binary eutectics (74), solid-surface dispersions (75,76), physical mixtures (66), and amorphous precipitates of drug in the crystalline carrier. The identification of the polymorphic form of drug in solid-dispersion systems is readily possible (60,64). XRD can also been used to generate the phase diagram of binary solid systems. In the case of oxezapam (77) and ketoprofen (78), an increase in dissolution rate was brought about by rendering the drugs amorphous. XRD has been used for the quantification of crystalline frusemide in solid dispersions with polyvinylpyrrolidone (79).

XRD has been used to monitor solid-state phase transformations and decomposition reactions of crystalline ingredients in solid delivery systems. Marini et al. described the time-dependent phase changes in β-cyclodextrin when stored under dry nitrogen at room temperature (80). The technique can be used to detect phase transformations during processing (81) and storage (61,75,82) of solid-dispersion systems.

Influence of Drug Load

Lee et al. prepared transdermal formulations of estradiol by dispersing the drug in a polymeric matrix and heating

to temperatures ranging from 110 to 165°C (83). After complete dissolution of estradiol, the system was cooled, which resulted in crystallization of the drug. Interestingly, XRD patterns of the final product revealed that the solid state of the crystallized drug was dependent on the concentration of drug in the polymer. Whereas estradiol hemihydrate crystallized at low drug concentrations, high concentrations favored the formation of a new solid form (so far unreported and termed "form X"). Flux measurements revealed that the release rate of form X was significantly higher than that of the hemihydrate.

Drug–Cyclodextrin Complexes

Many drugs form complexes with cyclodextrins, and the XRD pattern of these solid complexes is usually markedly different from that of pure drug or pure cyclodextrin (84,85). However, in some cases, complexation results in an amorphous product (86). XRD was used to determine the degree of crystallinity of indomethacin complexed with β-cyclodextrin (87). The colyophilization of naproxen and β-cyclodextrin resulted in the formation of an amorphous solid with increased solubility (88). In this case, it was not possible to ascertain whether increased solubility was a result of molecular encapsulation of drug inside the cyclodextrin cavity or due to formation of an amorphous solid dispersion. It was concluded that complementary techniques such as IR spectroscopy should be used to develop a more complete understanding of the system. Similarly, the solid complexes of tretinoin with β-cyclodextrin and dimethyl β-cyclodextrin were amorphous to X-rays (89). The formation of an inclusion complex was proven by NMR spectroscopy and DSC.

Degree of Crystallinity

The degree of crystallinity of the active ingredient can have a significant influence on the performance of a dosage form. Interestingly, the crystallinity of the excipients in a formulation can also influence product performance. XRD has been useful in explaining the alterations in the release rate of drugs from different delivery systems due to changes in crystallinity of both the drug and the excipients. Izumikawa et al. have demonstrated that the drug release rate from progesterone-loaded poly(L-lactide) microspheres was closely correlated with the crystallinity of the polymer matrix (90). Chan et al. investigated the dispersion properties of dry powder aerosols for inhalation delivery of recombinant human deoxyribonuclease (rhDNase) (91). Powder blends of rhDNase with varying amounts of carrier material (NaCl) were prepared, and the crystallinity of these blends was determined using XRD. The study revealed that the crystallinity of the powder blends increased linearly with increase in NaCl content (Fig. 7). This increase in crystallinity caused a decrease in the cohesive force between particles, leading to a proportional increase in the respirable fraction (i.e., % wt. of particles <7 μm in the aerosol). Thus, XRD can be used to select the weight fraction of NaCl that provides the optimum formulation performance. These results were supported by scanning electron microscopic studies.

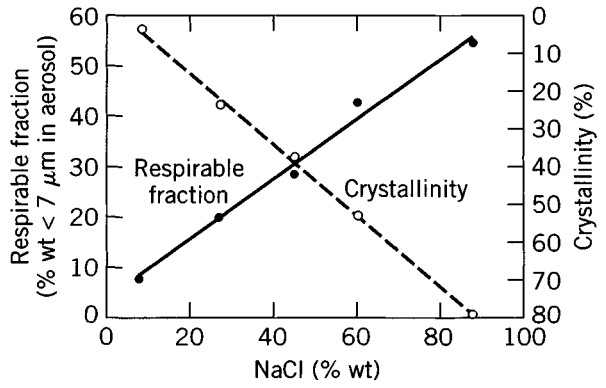


Figure 7. The relationship between sodium chloride content, the percent crystallinity, and the dispersing properties (expressed here as "respirable fraction") of rhDNase powders. Pure rhDNase powder is amorphous. *Source:* Reproduced with permission of the copyright owner, Plenum Publishing Corporation, from Ref. 91.

Limitations of XRD in the Characterization of Drug Delivery Systems

The major limitation of XRD technique is its very limited utility in the characterization of amorphous systems. This is because amorphous materials exhibit one or more broad diffuse maxima. For example, XRD revealed the formation of an X-ray amorphous solid dispersion between crystalline ibuprofen and PVP (92). However, the exact nature of interaction between the drug and polyvinylpyrrolidone (PVP) could only be determined using infrared spectroscopy and thermal analysis. In drug–PVP solid dispersions, increasing the amount of PVP in the system resulted in a decrease in the intensity of the XRD peaks of the drug (93,94). This has often been interpreted as being due to a decrease in drug crystallinity. However the decrease in peak intensity may have resulted from partial dissolution of drug in PVP. Thus, XRD alone is often insufficient for the characterization of multicomponent delivery systems.

OTHER APPLICATIONS

There are several other potential applications of XRD, though these find use only infrequently. These include (*1*) evaluation of preferred orientation in powders and compacts (95,96), (*2*) determination of crystal structure (97,98), (*3*) determination of crystallite size and local lattice distortion (microstrain) (99), and (*4*) determination of density of crystalline substances.

SUMMARY

The importance of solid-state characterization of drugs and delivery systems is increasingly recognized by the pharmaceutical community. Because XRD provides direct and unequivocal information about the lattice structure of a crystalline solid, it is a valuable technique for solid-state characterization studies. XRD is an excellent complement to other techniques such as DSC, TGA, solid-state NMR spectroscopy, and microscopy. Recent advances in instru-

mentation and computerized data analysis have improved the capability of both qualitative and quantitative XRD. XRD can be used to develop a mechanistic understanding of the phase changes that occur during pharmaceutical processing and storage. The technique finds application in several stages of the design and development of delivery systems, including preformulation, formulation, during manufacture (in process control), and in the evaluation of the finished product (quality control).

BIBLIOGRAPHY

1. H.P. Klug and L. Alexander, *X-ray Diffraction Procedures for Polycrystalline and Amorphous Materials*, 2nd ed., Wiley, New York, 1974, pp. 120–174.
2. B.D. Cullity, *Elements of X-ray Diffraction*, 2nd ed., Addison-Wesley, Reading, Mass., 1978, pp. 3–31, 81–106.
3. P. Debye and P. Scherrer, *Phys. Z.* **17**, 277–283 (1916).
4. A.W. Hull, *J. Am. Chem. Soc.* **41**, 1168–1175 (1917).
5. R. Jenkins, *X-Ray Fluorescence Spectroscopy*, Wiley, New York, 1988, p. 39.
6. T. Layloff, *Pharm. Tech.* **15**, 146–148 (1991).
7. *The United States Pharmacopeia*, 23rd rev., U.S. Pharmacopeial Convention, Rockville, Md., 1994, pp. 265–267, 1843–1844, 2216.
8. S. Byrn et al., *Pharm. Res.* **12**, 945–954 (1995).
9. *Preliminary Draft Guidance for Industry: CMC Content and Format of INDs for Phases 2 and 3 Studies of Drugs, Including Specified Therapeutic Biotechnology-Derived Produces*, Food and Drug Administration, Washington, D.C., 1997.
10. Food and Drug Administration, *Fed. Regist.* **62**, 62889–62890 (1997).
11. J.D. Hanawalt, H.W. Rinn, and L.K. Frevel, *Ind. Eng. Chem., Anal Ed.* **10**, 457–512 (1938).
12. J.I. Langford and D. Louer, *Rep. Prog. Phys.* **59**, 131–234 (1996).
13. A. Burger and A. Lettenbichler, *Pharmazie* **48**, 262–272 (1993).
14. L. Chang, M.R. Caira, and J.K. Guillory, *J. Pharm. Sci.* **84**, 1169–1179 (1995).
15. B. Debord et al., *Drug Dev. Ind. Pharm.* **13**, 1533–1546 (1987).
16. N.V. Phadnis, R.K. Cavatur, and R. Suryanarayanan, *J. Pharm. Biomed. Anal.* **15**, 929–943 (1997).
17. R. Jenkins, *Adv. X-Ray Anal.* **35**, 653–660 (1992).
18. Y. Takahashi, K. Nakashima, H. Nakagawa, and I. Sugimoto, *Chem. Pharm. Bull.* **32**, 4963–4970 (1984).
19. N. Kaneniwa, K. Imagawa, and M. Otsuka, *Chem. Pharm. Bull.* **33**, 802–809 (1985).
20. W. Ruland, *Acta Crystallogr.* **14**, 1180–1185 (1961).
21. Y. Nakai, E. Fukuoka, S. Nakajima, and M. Morita, *Chem. Pharm. Bull.* **30**, 1811–1818 (1982).
22. M. Morita and S. Hirota, *Chem. Pharm. Bull.* **30**, 3288–3296 (1982).
23. P.H. Hermans and A. Weidinger, *J. Appl. Phys.* **19**, 491–506 (1948).
24. D.B. Black and E.G. Lovering, *J. Pharm. Pharmacol.* **29**, 684–687 (1977).
25. A. Saleki-Gerhardt, C. Ahlneck, and G. Zografi, *Int. J. Pharm.* **101**, 237–247 (1994).
26. H. Imaizumi, N. Nambu, and T. Nagai, *Chem. Pharm. Bull.* **28**, 2565–2569 (1977).
27. J.A. Ryan, *J. Pharm. Sci.* **75**, 805–807 (1986).
28. R. Suryanaranan and S. Venkatesh, *Pharm. Res.* **7**, S-104 (1990).
29. M.J. Pikal, A.L. Lukes, J.E. Lang, and K. Gaines, *J. Pharm. Sci.* **67**, 767–773 (1978).
30. T. Sebhatu, M. Angberg, and C. Ahlneck, *Int. J. Pharm.* **104**, 135–144 (1994).
31. L.S. Taylor and G. Zografi, *Pharm. Res.* **15**, 755–761 (1998).
32. L. Alexander and H.P. Klug, *Anal. Chem.* **20**, 886–889 (1948).
33. J.W. Shell, *J. Pharm. Sci.* **52**, 24–39 (1963).
34. R. Jenkins and R.L. Snyder, *Introduction to X-ray Powder Diffractometry*, Wiley, New York, 1996, pp. 355–387.
35. R.L. Snyder and D.L. Bish, in D.L. Bish and J.E. Post, eds., *Modern Powder Diffraction*, Mineralogical Society of America, Washington, D.C., 1989, pp. 101–144.
36. C.L. Christ, R.B. Barnes, and E.F. Williams, *Anal. Chem.* **20**, 789–795 (1948).
37. A.J. Aguiar, J. Krc, Jr., A.W. Kinkel, and J.C. Samyn, *J. Pharm. Sci.* **56**, 847–853 (1967).
38. R. Suryanarayanan, *Pharm. Res.* **6**, 1017–1024 (1989).
39. R. Suryanarayanan, *Powder Diffr.* **5**, 155–159 (1990).
40. N.V. Phadnis and R. Suryanarayanan, *Pharm. Res.* **14**, 1176–1180 (1997).
41. G.J. Papariello, H. Letterman, and R.E. Huettemann, *J. Pharm. Sci.* **53**, 663–667 (1964).
42. R. Suryanarayanan and C.S. Herman, *Int. J. Pharm.* **77**, 287–295 (1991).
43. R. Suryanarayanan, *Adv. X-Ray Anal.* **34**, 417–427 (1991).
44. K. Kuroda and G. Hashizume, *Yakugaku Zasshi* **87**, 148–158 (1967).
45. K. Kuroda, G. Hashizume, and K. Fukuda, *Yakugaku Zasshi* **87**, 1175–1183 (1967).
46. K. Kuroda, G. Hashizume, and K. Fukuda, *J. Pharm. Sci.* **57**, 250–254 (1968).
47. K. Kuroda, G. Hashizume, and F. Kume, *Chem. Pharm. Bull.* **17**, 818–821 (1969).
48. K. Kuroda and G. Hashizume, *Chem. Pharm. Bull.* **20**, 2059–2062 (1972).
49. R. Suryanarayanan, in H.G. Brittain, ed., *Physical Characterization of Pharmaceutical Solids*, Dekker, New York, 1995, pp. 187–221.
50. N.V. Phadnis and R. Suryanarayanan, *J. Pharm. Sci.* **86**, 1256–1263 (1997).
51. W.W.L. Young and R. Suryanarayanan, *J. Pharm. Sci.* **80**, 496–500 (1991).
52. H. Nakamachi et al., *Chem. Pharm. Bull.* **29**, 2956–2965 (1981).
53. Y. Matsunaga, N. Bando, H. Yuasa, and Y. Kanaya, *Chem. Pharm. Bull.* **44**, 1931–1934 (1996).
54. H. Hashizume et al., *Powder Diffr.* **11**, 288–289 (1996).
55. S.K. Rastogi, M. Zakrzewski, and R. Suryanarayanan, *47th Annu. Denver X-Ray Conf.*, Colorado Springs, August 3–7, 1998.
56. T.G. Fawcett et al., *Adv. X-Ray Anal.* **29**, 323–332 (1986).
57. T. Fawcett, *Chemtech (Heidelberg)* **17**, 564–569 (1987).
58. R.K. Cavatur and R. Suryanarayanan, *Pharm. Res.* **15**, 194–199 (1998).
59. R.K. Cavatur and R. Suryanarayanan, *47th Annu. Denver X-Ray Conf.*, Colorado Springs, August 3–7, 1998.
60. V. Rosilio et al., *J. Biomed. Mater. Res.* **25**, 667–682 (1991).
61. Y. Aso, S. Yoshioka, and T. Terao, *Int. J. Pharm.* **93**, 153–159 (1993).

Next Page

62. A.K. Dash, *J. Microencapsul.* **14**, 101–112 (1997).
63. R. Suryanarayanan, S. Venkatesh, L. Hodgin, and P. Hanson, *Int. J. Pharm.* **78**, 77–83 (1992).
64. D. Aquilano, R. Cavalli, and M.R. Gasco, *Thermochim. Acta* **230**, 29–37 (1993).
65. Y. Kohda et al., *Int. J. Pharm.* **158**, 147–155 (1997).
66. K. Danzo, F. Higuchi, and A. Otsuka, *Chem. Pharm. Bull.* **43**, 1759–1763 (1995).
67. K. Goracinova et al., *Drug Dev. Ind. Pharm.* **22**, 255–262 (1996).
68. M. Otsuka and Y. Matsuda, *J. Pharm. Sci.* **83**, 956–961 (1994).
69. J. Kreuter, *Int. J. Pharm.* **14**, 43–58 (1983).
70. R. Cavalli, D. Aquilano, M.E. Carlotti, and M.R. Gasco, *Eur. J. Pharm. Biopharm.* **41**, 329–333 (1995).
71. G.P. Bettinetti, *Boll. Chim. Farm.* **128**, 149–162 (1989).
72. W.L. Chiou and S. Reigelman, *J. Pharm. Sci.* **60**, 1281–1302 (1971).
73. H.H. El-Shattawy, D.O. Kildsig, and G.E. Peck, *Drug Dev. Ind. Pharm.* **10**, 1–17 (1984).
74. A. Hoelgaard and N. Moller, *Arch. Pharm. Chemi, Sci. Ed.* **3**, 34–47 (1975).
75. T. Ishizaka, H. Honda, and M. Koishi, *J. Pharm. Pharmacol.* **45**, 770–774 (1993).
76. I. Sugimoto et al., *Chem. Pharm. Bull.* **30**, 4479–4488 (1982).
77. R. Jachowicz and E. Nurnberg, *Int. J. Pharm.* **159**, 149–158 (1997).
78. K. Takayama, N. Nambu, and T. Nagai, *Chem. Pharm. Bull.* **30**, 3013–3016 (1982).
79. C. Doherty, P. York, and R. Davidson, *J. Pharm. Pharmacol.* **37**, 57P (1985).
80. A. Marini et al., *Solid State Ionics* **63–65**, 358–362 (1993).
81. H. Lin, Y. Huang, L. Hsu, and Y. Tsai, *Int. J. Pharm.* **112**, 165–171 (1994).
82. J.D. Ntawukulilyayo, S. Bouckaert, and J.P. Remon, *Int. J. Pharm.* **93**, 209–214 (1993).
83. S.M. Lee et al., in N.A. Peppas, D.J. Mooney, A.G. Mikos, and L. Brannon-Peppas, eds., *Proceedings of the Topical Conference on Biomaterials, Carriers for Drug Delivery, and Scaffolds for Tissue Engineering*, American Institute of Chemical Engineers, New York, 1997, pp. 196–198.
84. F. Giordano et al., *Farmaco, Ed. Prat.* **43**, 345–355 (1988).
85. D. Watanabe et al., *Chem. Pharm. Bull.* **44**, 833–836 (1996).
86. P. Mura, G. Bettinetti, F. Melani, and A. Manderioli, *Eur. J. Pharm. Sci.* **3**, 347–355 (1995).
87. R. Casella, D.A. Williams, and S.S. Jambhekar, *Int. J. Pharm.* **165**, 15–22 (1998).
88. G.P. Bettinetti et al., *Farmaco* **44**, 195–213 (1989).
89. P. Montassier, D. Duchene, and M. Poelman, *Int. J. Pharm.* **153**, 199–209 (1997).
90. S. Izumikawa, S. Yoshioka, Y. Aso, and Y. Takeda, *J. Controlled Release* **15**, 133–140 (1991).
91. H. Chan et al., *Pharm. Res.* **14**, 431–437 (1997).
92. N.M. Najib, M.A. El-Hinnawi, and M.S. Suleiman, *Int. J. Pharm.* **45**, 139–144 (1988).
93. G.P. Bettinetti et al., *Farmaco, Ed. Prat.* **43**, 331–343 (1988).
94. A.S. Kearney, D.L. Gabriel, S.C. Mehta, and G.W. Radebaugh, *Int. J. Pharm.* **104**, 169–174 (1994).
95. E. Fukuoka, M. Makita, and S. Yamamura, *Chem. Pharm. Bull.* **39**, 3313–3317 (1991).
96. E. Fukuoka, M. Makita, and S. Yamamura, *Chem. Pharm. Bull.* **41**, 595–598 (1993).
97. R.J. Cernik et al., *J. Appl. Crystallogr.* **24**, 222–226 (1991).
98. M. Tremayne et al., *J. Solid State Chem.* **100**, 191–196 (1992).
99. E. Fukuoka, K. Terada, M. Makita, and S. Yamamura, *Chem. Pharm. Bull.* **41**, 1636–1639 (1993).

CHEMICAL APPROACHES TO DRUG DELIVERY

NICHOLAS BODOR
University of Florida
Gainesville, Florida

JAMES J. KAMINSKI
Schering-Plough Research Institute
Kenilworth, New Jersey

KEY WORDS

Blood-brain barrier
Brain targeting
Chemical delivery systems
Eye targeting
Metabolism
Molecular packaging
Peptide delivery
Soft anticholinergics
Soft drugs
Soft steroids

OUTLINE

Introduction
SD Design
  Soft Analogue Approach
  Inactive Metabolite Approach
Chemical Delivery Systems (CDSs)
  Enzymatic Physical-Chemical–Based CDSs
  Site-Specific, Enzyme-Activated CDSs
  Receptor-Based CDSs
Conclusions
Bibliography

INTRODUCTION

The search for novel chemical entities which may become effective therapeutic agents for the treatment of various diseases traditionally involves identifying a lead compound of well-defined structure that exhibits the desired biological activity in a relevant assay. In most cases, the primary test considered relevant is a mechanism-based in vitro assay rather than an in vivo animal model. The in vitro assay may involve inhibition of a specific enzyme or may involve antagonism of a particular receptor thought to be involved in the pathogenesis of the disease.

The source of the lead compound could be from a corporate collection of compounds, from third-party databases of chemical entities and natural products offered for sale,

Previous Page

62. A.K. Dash, *J. Microencapsul.* **14**, 101–112 (1997).
63. R. Suryanarayanan, S. Venkatesh, L. Hodgin, and P. Hanson, *Int. J. Pharm.* **78**, 77–83 (1992).
64. D. Aquilano, R. Cavalli, and M.R. Gasco, *Thermochim. Acta* **230**, 29–37 (1993).
65. Y. Kohda et al., *Int. J. Pharm.* **158**, 147–155 (1997).
66. K. Danzo, F. Higuchi, and A. Otsuka, *Chem. Pharm. Bull.* **43**, 1759–1763 (1995).
67. K. Goracinova et al., *Drug Dev. Ind. Pharm.* **22**, 255–262 (1996).
68. M. Otsuka and Y. Matsuda, *J. Pharm. Sci.* **83**, 956–961 (1994).
69. J. Kreuter, *Int. J. Pharm.* **14**, 43–58 (1983).
70. R. Cavalli, D. Aquilano, M.E. Carlotti, and M.R. Gasco, *Eur. J. Pharm. Biopharm.* **41**, 329–333 (1995).
71. G.P. Bettinetti, *Boll. Chim. Farm.* **128**, 149–162 (1989).
72. W.L. Chiou and S. Reigelman, *J. Pharm. Sci.* **60**, 1281–1302 (1971).
73. H.H. El-Shattawy, D.O. Kildsig, and G.E. Peck, *Drug Dev. Ind. Pharm.* **10**, 1–17 (1984).
74. A. Hoelgaard and N. Moller, *Arch. Pharm. Chemi, Sci. Ed.* **3**, 34–47 (1975).
75. T. Ishizaka, H. Honda, and M. Koishi, *J. Pharm. Pharmacol.* **45**, 770–774 (1993).
76. I. Sugimoto et al., *Chem. Pharm. Bull.* **30**, 4479–4488 (1982).
77. R. Jachowicz and E. Nurnberg, *Int. J. Pharm.* **159**, 149–158 (1997).
78. K. Takayama, N. Nambu, and T. Nagai, *Chem. Pharm. Bull.* **30**, 3013–3016 (1982).
79. C. Doherty, P. York, and R. Davidson, *J. Pharm. Pharmacol.* **37**, 57P (1985).
80. A. Marini et al., *Solid State Ionics* **63–65**, 358–362 (1993).
81. H. Lin, Y. Huang, L. Hsu, and Y. Tsai, *Int. J. Pharm.* **112**, 165–171 (1994).
82. J.D. Ntawukulilyayo, S. Bouckaert, and J.P. Remon, *Int. J. Pharm.* **93**, 209–214 (1993).
83. S.M. Lee et al., in N.A. Peppas, D.J. Mooney, A.G. Mikos, and L. Brannon-Peppas, eds., *Proceedings of the Topical Conference on Biomaterials, Carriers for Drug Delivery, and Scaffolds for Tissue Engineering*, American Institute of Chemical Engineers, New York, 1997, pp. 196–198.
84. F. Giordano et al., *Farmaco, Ed. Prat.* **43**, 345–355 (1988).
85. D. Watanabe et al., *Chem. Pharm. Bull.* **44**, 833–836 (1996).
86. P. Mura, G. Bettinetti, F. Melani, and A. Manderioli, *Eur. J. Pharm. Sci.* **3**, 347–355 (1995).
87. R. Casella, D.A. Williams, and S.S. Jambhekar, *Int. J. Pharm.* **165**, 15–22 (1998).
88. G.P. Bettinetti et al., *Farmaco* **44**, 195–213 (1989).
89. P. Montassier, D. Duchene, and M. Poelman, *Int. J. Pharm.* **153**, 199–209 (1997).
90. S. Izumikawa, S. Yoshioka, Y. Aso, and Y. Takeda, *J. Controlled Release* **15**, 133–140 (1991).
91. H. Chan et al., *Pharm. Res.* **14**, 431–437 (1997).
92. N.M. Najib, M.A. El-Hinnawi, and M.S. Suleiman, *Int. J. Pharm.* **45**, 139–144 (1988).
93. G.P. Bettinetti et al., *Farmaco, Ed. Prat.* **43**, 331–343 (1988).
94. A.S. Kearney, D.L. Gabriel, S.C. Mehta, and G.W. Radebaugh, *Int. J. Pharm.* **104**, 169–174 (1994).
95. E. Fukuoka, M. Makita, and S. Yamamura, *Chem. Pharm. Bull.* **39**, 3313–3317 (1991).
96. E. Fukuoka, M. Makita, and S. Yamamura, *Chem. Pharm. Bull.* **41**, 595–598 (1993).
97. R.J. Cernik et al., *J. Appl. Crystallogr.* **24**, 222–226 (1991).
98. M. Tremayne et al., *J. Solid State Chem.* **100**, 191–196 (1992).
99. E. Fukuoka, K. Terada, M. Makita, and S. Yamamura, *Chem. Pharm. Bull.* **41**, 1636–1639 (1993).

CHEMICAL APPROACHES TO DRUG DELIVERY

NICHOLAS BODOR
University of Florida
Gainesville, Florida

JAMES J. KAMINSKI
Schering-Plough Research Institute
Kenilworth, New Jersey

KEY WORDS

Blood-brain barrier
Brain targeting
Chemical delivery systems
Eye targeting
Metabolism
Molecular packaging
Peptide delivery
Soft anticholinergics
Soft drugs
Soft steroids

OUTLINE

Introduction
SD Design
  Soft Analogue Approach
  Inactive Metabolite Approach
Chemical Delivery Systems (CDSs)
  Enzymatic Physical-Chemical–Based CDSs
  Site-Specific, Enzyme-Activated CDSs
  Receptor-Based CDSs
Conclusions
Bibliography

INTRODUCTION

The search for novel chemical entities which may become effective therapeutic agents for the treatment of various diseases traditionally involves identifying a lead compound of well-defined structure that exhibits the desired biological activity in a relevant assay. In most cases, the primary test considered relevant is a mechanism-based in vitro assay rather than an in vivo animal model. The in vitro assay may involve inhibition of a specific enzyme or may involve antagonism of a particular receptor thought to be involved in the pathogenesis of the disease.

The source of the lead compound could be from a corporate collection of compounds, from third-party databases of chemical entities and natural products offered for sale,

or from libraries of compounds prepared using the techniques of combinatorial chemistry. In any case, the screening of these compound collections using random, focused or high-throughput screening technologies could identify a lead compound of interest.

Once identified, the structure of the lead compound is systematically, and in some cases randomly, modified to learn as much as possible about the relationship that may exist between its structure and the observed biological activity. This empirically derived knowledge, if it exists, is then used to design other novel compounds that might exhibit even greater biological activity.

In some instances, the structure of the enzyme (protein) or receptor of interest, in the presence of the lead structure or one of its analogues (ligand), might be known from an X-ray crystal structure of the ligand–protein complex. In these cases, structure-based design methods can be invoked to propose compounds that could exhibit maximum biological activity by optimizing the intermolecular interactions occurring between the ligand and specific amino acids in the active site of the enzyme, or at the receptor.

Despite all these attempts to introduce rationale and logic into the drug discovery paradigm, the structural (chemical) modifications made to the lead compound in order to optimize biological activity rarely consider their effect on determining the physicochemical and metabolic characteristics of the candidate selected. As a result, very few compounds with maximal or optimal biological activity have become clinically useful drugs. The main, and most frequent, reason for this being the toxicity observed in the development of these compounds. As this situation occurs so frequently, we have to recognize that the main objective of the drug discovery (design) process should not be to optimize the activity (potency) of the drug, but rather to optimize its therapeutic index (i.e., to optimize the ratio between the toxic and therapeutic doses of the drug). Ideally, drugs should have rather large therapeutic indices, indicating a significant and safe separation between these two important dose levels. However, most of the time, undesired and toxic side effects of novel biologically active compounds run parallel with the desired activity. Thus, even if more potent drugs are obtained, their therapeutic index remains essentially unchanged.

Side effects are usually related to the intrinsic receptor affinity responsible for the desired biological activity. Therefore, it is possible that changes in the pharmacokinetic and pharmacodynamic properties of a drug can parallel biological activity changes. Furthermore, when introduced into the body, drugs can be extensively metabolized. Most drugs generate multiple metabolites whose chemical structures are closely related to each other. These metabolic products can exhibit an enhanced or different biological activity, or they can exhibit their own toxicity.

Data accumulated on metabolic activation, toxification, and/or detoxification of biologically active compounds demonstrate the necessity to include metabolic considerations as an integral part of the drug discovery (design) process. Rather than determining the metabolic profile of only the candidate selected for preclinical evaluation, structure–activity relationship studies should be conducted concomitantly with structure–metabolism (toxicity) relationship studies throughout the drug discovery (design) process. This combination of structure–activity, structure–metabolism and structure–toxicity relationship studies is the principal tenet of the retrometabolic drug design concept, a cycle which includes soft drug design (SD) and chemical delivery system (CDS) design (Fig. 1) as distinct from prodrug design. Chemical approaches for drug delivery using prodrug strategies have been extensively reviewed recently (1–3) and the reader is directed to these comprehensive references.

Retrometabolic drug design approaches include two distinct methods to improve the therapeutic index of a drug and form the subject matter of this article. One is the general concept of CDSs. A CDS is defined as a biologically inert molecule that requires several steps in its conversion to the active drug, and that enhances drug delivery to a particular organ or site. SD design strategies represent the alternate method in the retrometabolic drug design cycle. Although both approaches involve chemical modifications to obtain an improved therapeutic index and both require enzymatic reactions to fulfill drug targeting, there is not much in common between the principles of SD design and those of CDS-based retrometabolic drug design. Whereas the CDS is inactive by definition and sequential enzymatic reactions provide the differential distribution and drug activation, SDs are active isosteric/isoelectronic analogues of the lead drug that are deactivated in a predictable and controllable manner after achieving their therapeutic role. In the extreme case for a CDS, enzymatic processes produce the drug at the site and nowhere else in the body, whereas in the SD case, the drug is present at the site and absent in the rest of the body due to enzymatic activity at those sites.

SD DESIGN

A SD by definition is a biologically active species. However, in general, the SD behaves very differently from the drug itself, and this behavior is by design. The SD undergoes a predicted and controlled singular transformation to a nontoxic and inactive metabolite, or in some cases, is degraded to more than one nontoxic and inactive metabolite. The

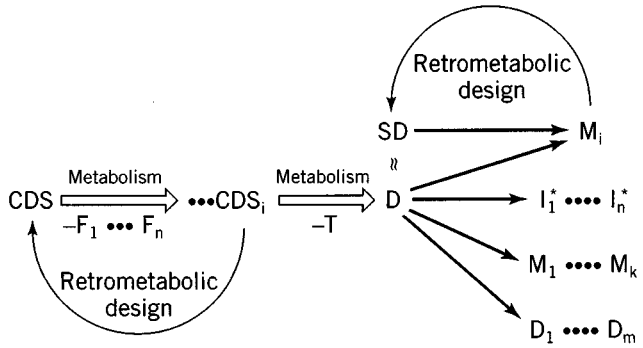


Figure 1. The retrometabolic drug design cycle. CDS: chemical delivery system; SD: soft drug; CDS_i: CDS metabolites; D: lead drug; M_i: inactive metabolites; I_n^*: reactive intermediates; M_n: other metabolites; D_n: analogue metabolites; F_n: modifier functions; T: targetor moiety.

main point is that by design, the SD simplifies the transformation, distribution, and activity profile that most drugs exhibit. SD design aims to produce biological activity of a specific, desired kind and then predicted processes deactivate or metabolize the SD in one step to an inactive species. When applied at the desired site of action, be it topical or internal, the SD elicits the desired biological effect locally, but as soon as it is distributed from the site, it is susceptible to deactivation, thereby preventing any undesirable (toxic) side effect, which would be otherwise characteristic for this class of drug.

The SD concept was introduced in 1980, and since then five distinct SD classes have been identified:

1. *Soft analogues*. These SDs are close structural analogues of known active drugs but have a specific metabolically sensitive site built into their structure that provides a one-step controllable detoxification.
2. *SDs based on the inactive metabolite approach*. An inactive metabolite of a lead drug is chemically modified to provide an isosteric–isoelectronic analogue of the lead drug that exhibits the desired biological activity. The biologically active analogue is metabolically converted to the inactive metabolite in one step.
3. *Controlled release SDs*. Controlled release endogenous agents are derivatives of natural hormones or neurotransmitters (natural SDs) for which a local or site-specific delivery is developed.
4. *Activated SDs*. These compounds are not analogues of known drugs but are derived from nontoxic chemical compounds activated by introduction of a specific pharmacophore whose presence in the molecule is responsible for eliciting the desired biological activity.
5. *SDs based on the active metabolite*. A metabolite that significantly retains the activity of the parent drug can be chemically transformed to a potent drug, but undergoes a one-step deactivation process, as it is already at its highest oxidation state.

Examples of each of these classes of SDs are described in the literature. However, the most useful and successful strategies for designing safe and selective drugs have been the *inactive metabolite* and *soft analogue* approaches.

Soft Analogue Approach

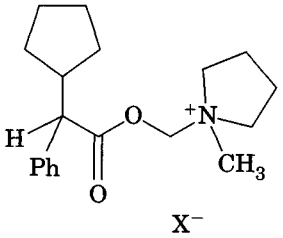
Research on soft analogues began after the discovery of "soft quaternary salts", **1** (Fig. 2). These compounds undergo a facile hydrolysis via a short-lived intermediate to form an aldehyde, an amine, and a carboxylic acid upon deactivation. Structures exemplified by **1** were first used for the improved delivery of drugs containing tertiary amines such as pilocarpine (4) and erythromycin (5). The term "soft" in the context of these quaternary salts was adopted to reflect their relative ease to biodegrade as compared with conventional "hard" quaternary salts that generally require multiple oxidative steps to be metabolized.

The simplest example of a useful SD is provided by the isosteric analogue **2** of cetylpyridinium chloride **3** (Fig. 3), a well-known hard quaternary antimicrobial agent that generally requires several oxidative steps to lose its surface active antimicrobial properties. The structure of **2** and **3** are very similar in that both side chains are essentially 16 atoms in length. Accordingly, their physical properties, as measured by their respective critical micelle concentration values, are also very similar (6). Whereas both compounds exhibit comparable antimicrobial activity against a wide variety of microorganisms, **2** undergoes facile hydrolytic cleavage leading to its deactivation. Because of this facile degradation, **2** is approximately 40 times less toxic than **3** (i.e., the median oral lethal dose for **2** and **3**, determined using white Swiss mice, was 4,110 mg/kg and 108 mg/kg, respectively).

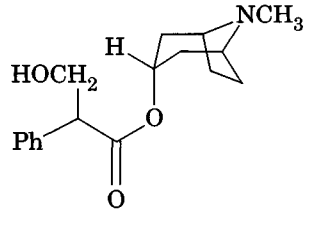
Other examples for the design of soft analogues based on soft quaternary salts were provided by the soft anticholinergic agents (7) and the soft cholinesterase inhibitors (8).

The soft anticholinergic agents were designed to exhibit high local, but practically no systemic, anticholinergic activity. It is well-established that anticholinergic agents exhibit many useful clinical effects. For example, the local antisecretory activity of these compounds was long thought to be beneficial for inhibiting eccrine sweating (perspiration). Indeed, a number of anticholinergic agents such as atropine, scopolamine, or their quaternary ammonium salts inhibit perspiration. However, these compounds are also responsible for producing the many side effects observed (e.g., dry mouth, urinary retention, drowsiness, and mydriasis). Therefore, these compounds are not useful as antiperspirants, but their soft analogues may provide a viable alternative.

Although the structural differences between hard and soft anticholinergics agents of this type are relatively small, they are nonetheless profound (Fig. 4). Classical quaternary ammonium anticholinergics, **4** and **5**, have two or three carbon atoms separating the quaternary head from the ester function. For many years, the dogma was that this separation was critical for effective receptor binding. The corresponding soft analogue **6** would contain just one carbon atom separating the quaternary head from the ester function allowing facile hydrolytic deactivation. Several compounds of type **6** were synthesized and evaluated; many were found to be at least as potent as atropine (7). The example compound in the following diagram, **7**, is equipotent with atropine in a number of in vitro and in vivo anticholinergic tests, but it is extremely short acting following intravenous administration due to its facile hydrolytic deactivation. When applied topically to humans, **7** exhibited high local antisecretory activity with no observation of systemic toxicity.



7



Atropine

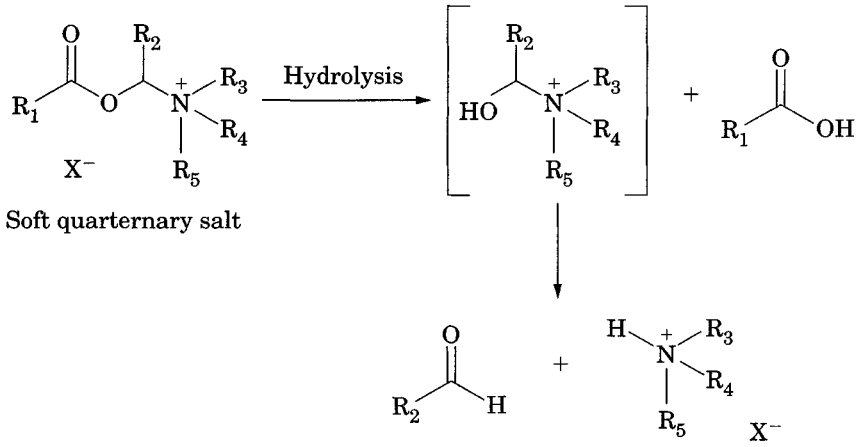


Figure 2. Hydrolytic deactivation of soft quaternary salts, **1**.

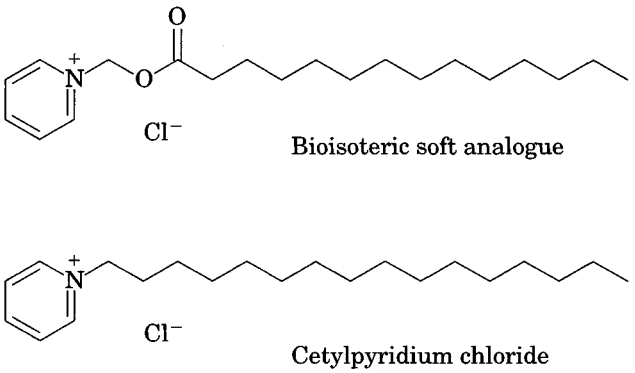


Figure 3. Bioisosteric soft analogue, **2**, of cetylpyridinium chloride, **3**.

These examples clearly illustrate the application of replacing neighboring methylene groups with an ester or "reverse ester" function resulting in a bioisosteric soft analogue. The method as described is in fact general and not restricted to quaternary salts. Some of the basic isosteric and isoelectronic design concepts of SD design are integrated as part of the inactive metabolite approach.

Inactive Metabolite Approach

This is one of the most promising and versatile methods for developing new and safer drugs. The main objective is to include the metabolism of the active species into the design process. The following strategies can be used in developing new drugs based on the inactive metabolite approach:

- The design process starts with a known inactive metabolite of a drug as the lead compound.
- Novel structures are designed from the inactive metabolite; these structures are isosteric and/or isoelectronic with the drug from which the lead inactive metabolite was derived.
- New structures are designed so that their metabolism produces the starting inactive metabolite in one step without any other metabolic processes occurring (predicted metabolism).
- The specific binding and transport properties and metabolic rates of the SD can be controlled by molecular manipulation in the activation stage of the process (controlled metabolism).

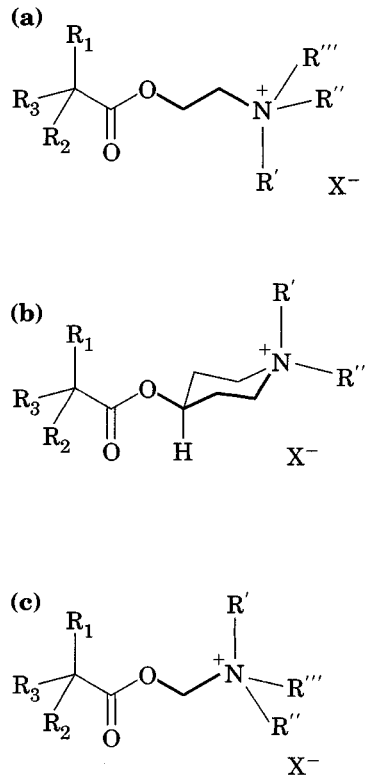


Figure 4. Traditional quaternary ammonium anticholinergic agents, **4** and **5**, and a soft anticholinergic analogue, **6**.

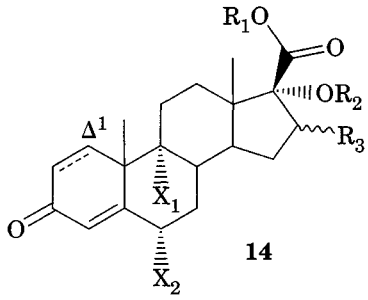
With respect to these considerations, two points are worthy of elaboration. The inactive metabolite selected does not have to be isolated and identified. In addition, there are two classes of SDs based on inactive metab-

olites. In one class, the inactive metabolite formed involves the pharmacophore; in the other class, it does not. Enzymatic modifications affect only the portions of the molecule that are not directly responsible for eliciting activity. Understandably for the second class, there is more freedom to modify inactive metabolites in the activation stage.

Many examples of potential drugs designed using this approach are available, which include several dermatological and ophthalmic products under development, but the principles can be illustrated with some general examples. One of the few instances in which these principles have been accidentally used for the design of nonpharmaceutical products is the pesticide dichlorodiphenyltrichloromethane (DDT), **8**, along with its analogues and metabolites (Fig. 5) (9). In 1939, DDT was discovered as a powerful insecticide. During World War II, it was also demonstrated that DDT could also be used to treat typhus and malaria. DDT undergoes several in vivo oxidative dehydrohalogenations and oxidations to produce the inactive metabolite **9**. This inactive acidic metabolite is of low toxicity and can be excreted as a water-soluble species. Therefore, it is an ideal lead compound for the inactive metabolite approach.

It was found that ethyl 4,4′-dichlorobenzilate, **10**, is highly active as a pesticide, but is less carcinogenic than DDT or dicofol (kelthane, **11**). The ethyl ester moiety apparently functions similarly to the trichloromethyl group in DDT imparting pesticidal activity to **10** however, **10** is considerably less toxic than **8** because metabolism of the labile ethyl ester generates the corresponding nontoxic carboxylic acid, **9**, the inactive metabolic of Figure 5.

Another good example of the inactive metabolite approach is provided by the antiinflammatory corticosteroids known to have multiple adverse effects that often limit their usefulness. Corticosteroids undergo a variety of oxidative and reductive metabolic conversions that lead to the formation of numerous steroidal metabolites. A major metabolic route of hydrocortisone, **12**, is oxidation of the dihydroxyacetone side chain, which ultimately leads to the formation of cortienic acid (Fig. 6). Cortienic acid **13** is a major metabolite excreted in human urine and lacks corticosteroid activity, and therefore, is an ideal lead candidate for the inactive metabolite approach (10–12). The design process can directly involve the important pharmacophoric features found in the 17-α and 17-β side chains. Suitable isosteric/isoelectronic substitution of the α-hydroxy and β-carboxy substituents with esters or other functional groups should restore the original corticosteroid activity without imparting the potential to produce adverse effects. Modification of the 17-β carboxyl function, in addition to changes in the 17-α position and retention of the customary activity enhancing structural modifications (e.g., introduction of Δ^1, fluorination at 6-α and/or 9-α, methyl introduction at 16-α or 16-β) lead to a host of active analogues exemplified by the general structure of soft steroids, **14**. Critical functions for activity are clearly the haloester in the 17-β position and the novel carbonate (13) and ether (14) substitutions in the 17-α positions, which provided the best activity.



14

R_1 = alkyl, haloalkyl

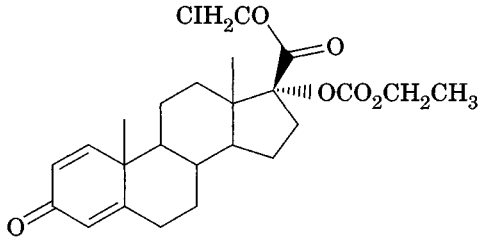
R_2 = alkyl, alkoxyalkyl, COOalkyl

R_3 = H, α- or β-CH_3

X_1, X_2 = H, F

Δ^1 = double bond (absent or present)

One of these compounds derived from prednisolone, lotoprednol etabonate, **15**, was selected for clinical development. Based on receptor binding studies, **15** is approximately fivefold more potent than dexamethasone and was successfully developed as a unique ophthalmic antiinflammatory and antiallergic agent. The compound is highly active pharmacologically, but lacks the intraocular pressure (IOP)–elevating side effect characteristic of the other steroids in use. The FDA has recently approved **15** for marketing in the United States.



15, loteprednol etabonate

An example in which SDs based on the inactive metabolite approach can be obtained by introducing the hydrolytically sensitive function at a position remote to the pharmacophore is the case of soft β-blockers. In this case, there is more freedom to choose the structural modification; consequently, transport and the rate of metabolism can be controlled more easily. The β-amino alcohol is the main pharmacophore in β-adrenergic antagonists. The β-blockers metoprolol, **16**, and atenolol, **17**, undergo metabolism involving the β-amino alcohol pharmacophore, but they are also metabolized to a significant extent at the *para* position of the phenol ring producing the corresponding inactive phenylacetic acid derivative, **18**. Esterification of this phenylacetic acid lead to the soft β-blockers, which exhibited different transport, rate of cleavage, and metabolic properties (15,16).

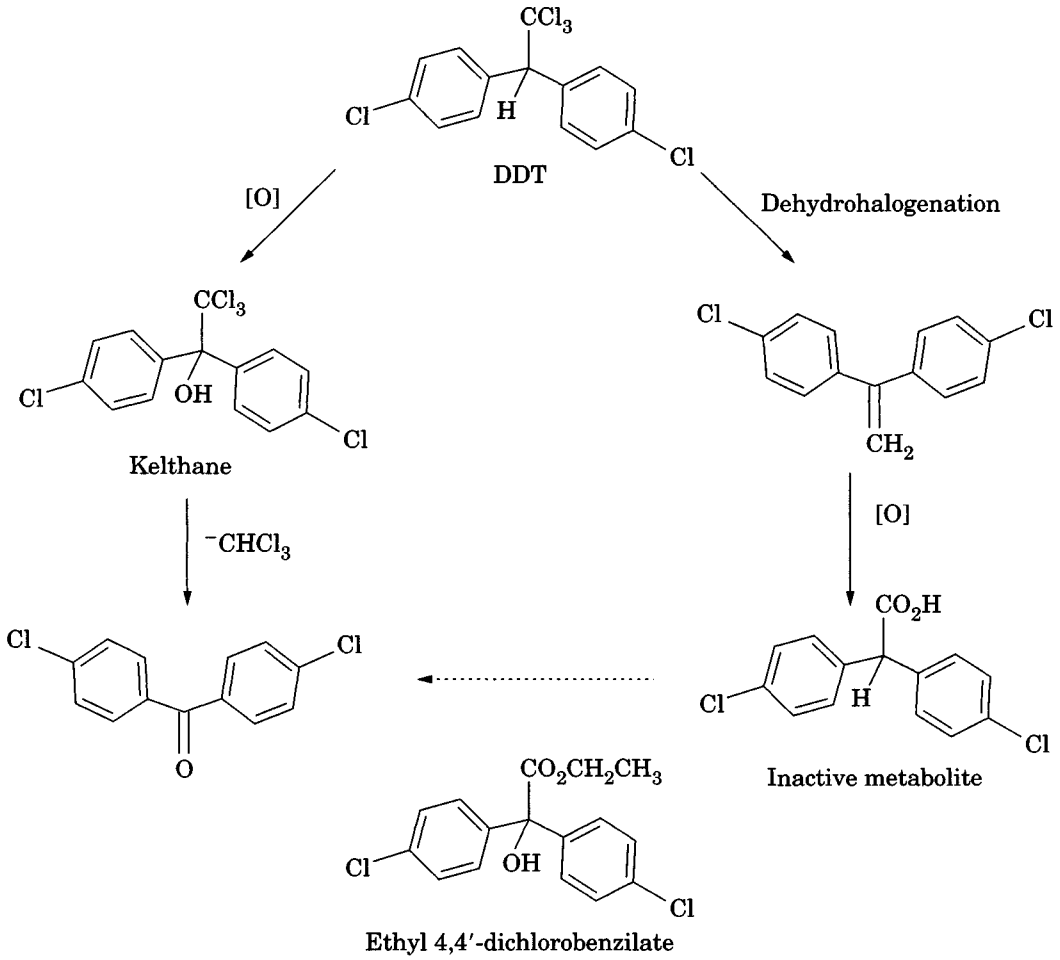
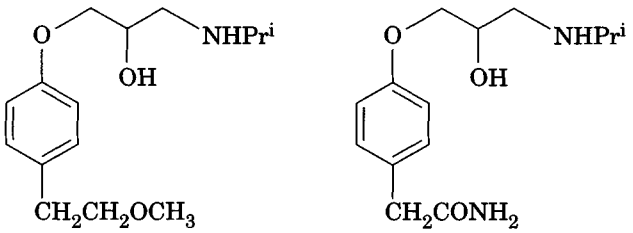
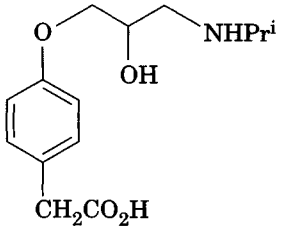


Figure 5. Metabolism of DDT.



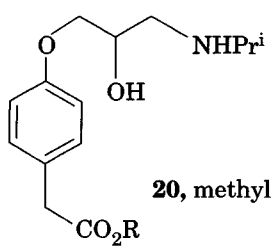
16, metoprolol

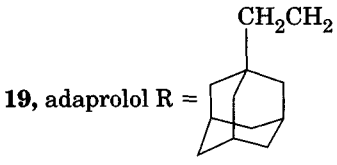
17, atenolol



18, inactive phenylacetic acid derivative

If for the desired pharmacological activity, membrane transport (lipophilicity) and relative stability are important, the R group of the ester moiety should be relatively lipophilic and stable. Among the various soft β-blockers the adamantane ethyl derivative, adaprolol, **19**, is being developed as a topical antiglaucoma agent with prolonged and significant reduction of IOP and rapid hydrolysis in human blood. Thus, it produces a significant separation between local activity and undesired systemic cardiovascular/pulmonary activity. On the other hand, if short systemic action is the objective, then R groups that make the ester moiety susceptible to rapid hydrolysis should be used. Methyl thiomethyl and related esters, **20**, were recently discovered as ultra short acting β-blockers (17).

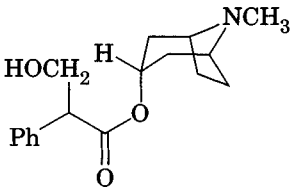




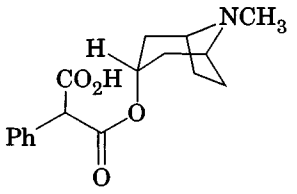
19, adaprolol R =

20, methyl thiomelhylester R = CH_2SCH_3

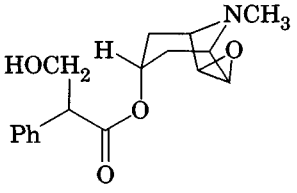
Finally, the flexibility and potential of SD design is clearly illustrated by the possibility of developing two distinct classes of soft anticholinergic agents. Whereas soft anticholinergics, exemplified by **6**, have been described previously (see Fig. 4c), soft anticholinergic agents based on the inactive metabolite approach have more recently been disclosed (18–22). Here the lead is atropine or the closely related scopolamine. The benzylic hydroxymethyl function in atropine can be oxidized to the corresponding carboxylic acid, a hypothetical inactive metabolite, **21**. Esterification of the carboxyl group in **21** yields the inactive metabolite–based soft anticholinergics, **22**.



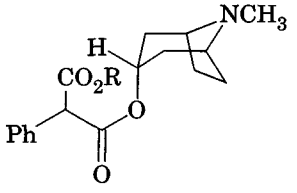
Atropine



21, inactive metabolite



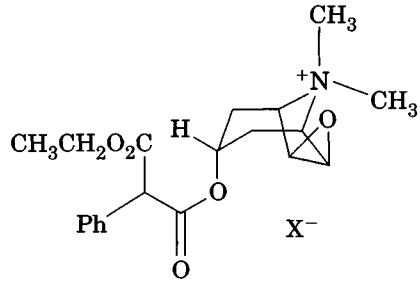
Scopolamine



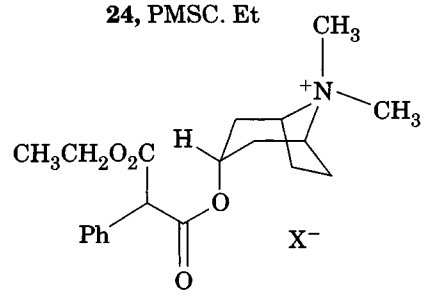
22, R = alkyl
23, R = CH_2CH_3

Soft anticholinergics of this type exhibited good intrinsic activity, with antispasmodic pA_2 values of up to 7.85 relative to 8.29 for atropine. However, systemic in vivo activities were much shorter compared to the "hard" atropine. Accordingly, when equipotent mydriatic concentrations of atropine and tematropium, **25**, the corresponding methyl quaternary salt of the ethyl ester **23** were compared, the same maximal mydriasis was obtained, but the area under the mydriasis versus time curve for **25** was only 11–19% of that for atropine (23,24). This observation is consistent with the facile hydrolytic deactivation of the SD. Similarly, the cardiovascular activity of **25** exhibited ultrashort duration. The effect of **25** on the heart rate and its ability to antagonize the cholinergic cardiac depressant action induced by acetylcholine injection, or by electrical vagus stimulation, was determined in comparison to atropine. It was found that a dose of 1 mg/kg of atropine could completely abolish the bradycardia induced by acetylcholine injection or electrical vagus stimulation for more than two hours following intravenous injection. On the other hand, similar doses of **25** exerted muscarinic activity for only 1–3 minutes following intravenous injection. Even a ten-fold increase of **25** to 10 mg/kg did not lead to any significant prolongation or duration of anticholinergic activity.

Further improvement was obtained by using the corresponding ethyl ester soft analogue of methscopolamine, **24**, which proved significantly more potent than the similar soft analogue, **25** (19).



24, PMSC. Et



25, Tematropium (PMTR. Et)

Meanwhile, the SD **24** was shorter acting than even tropicamide, and consistent with the SD approach, the untreated eye did not exhibit mydriasis as compared to administration of methscopolamine, which did. All of these results provide further support for the ultrashort duration of action, and for the potential of use of these agents as safe topical muscarinic drugs. Their ultrashort systemic activity provides the basis for their successful SD-based targeting.

CHEMICAL DELIVERY SYSTEMS (CDSS)

CDSs refer to inactive chemical derivatives of a drug where one or more chemical modifications were carried out on the drug by design. The moieties attached to the drug in these modifications are monomolecular units generally comparable in size to the drug. Importantly, these modifications provide a site-specific, or site-enhanced delivery of the drug. Generation of the drug requires multistep enzymatic and/or chemical transformations.

During the chemical manipulations, two types of bioremovable moieties are introduced to convert the drug into an inactive precursor form: a targetor (T) responsible for targeting, site-specificity and imparting "lock-in" character, and modifier functions (F_1, F_2, . . . , F_n) that serve to protect certain functionality, alter lipophilicity, or modulate other molecular properties to prevent premature, undesirable metabolic conversions. Targeting is achieved by design. The CDS undergoes sequential metabolic conversions that remove the modifier functions and finally after fulfilling its site- or organ-targeting role, the targetor moiety is removed. The CDS concept evolved from strategies used to design prodrugs but is very different and significantly more complex. Within the present formalism, prodrugs contain one or more modifier functions (F) for pro-

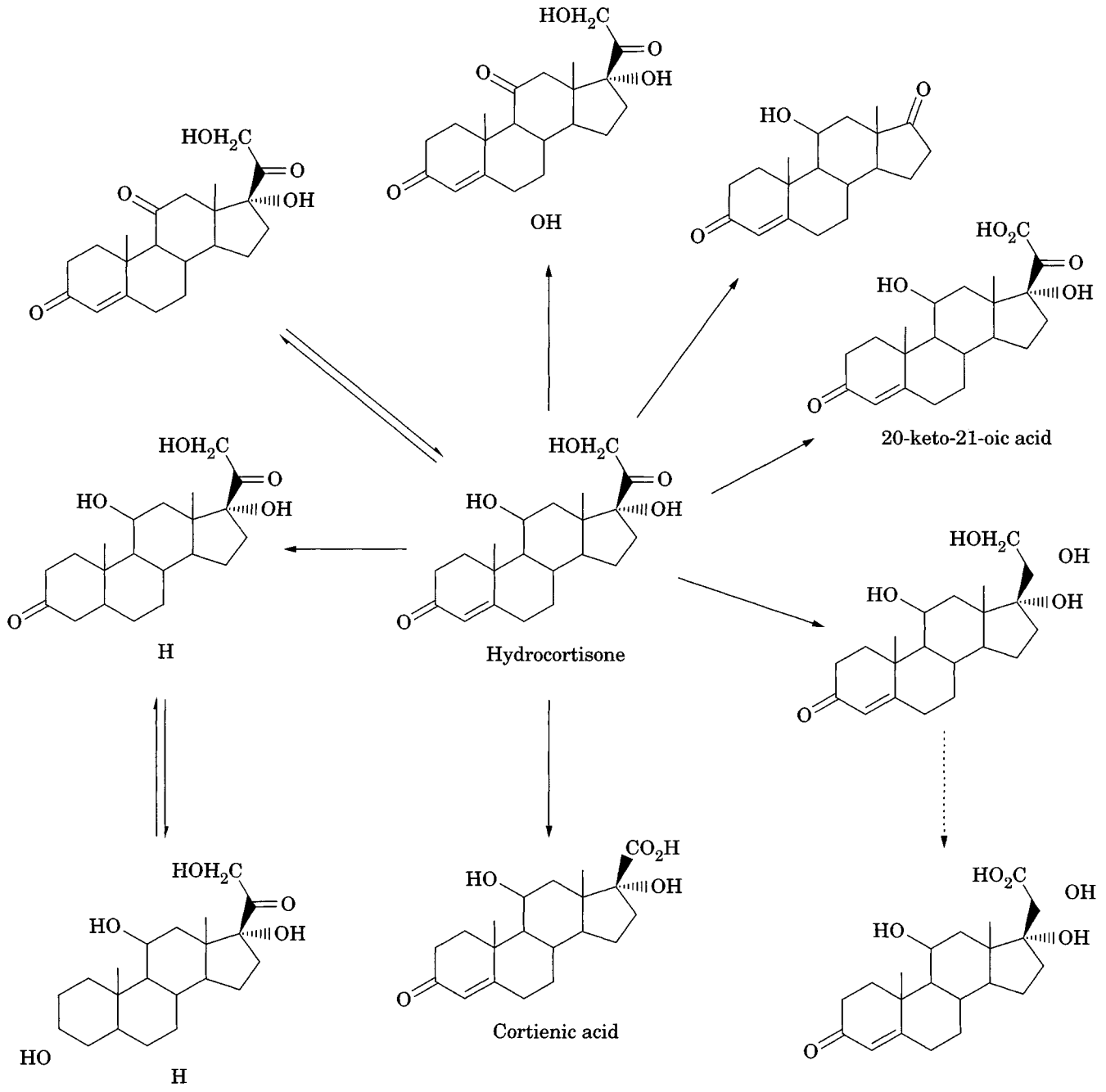


Figure 6. Metabolism of hydrocortisone, **12**.

tected or enhanced overall delivery, but they do not contain any targetor function (T). In general, prodrugs do not achieve significant drug targeting, which is the major way to improve the therapeutic index of a drug. It is important to reiterate that the CDS, and all its intermediary metabolic products leading to the active drug, are biologically inactive and do not produce any undesirable side effects. Chemical delivery systems will only be activated to the desired drug by a designed metabolic conversion at the site of action, and no other metabolism should occur.

With a chemical delivery system, targeting is achieved by design, capitalizing on specific enzymes found primarily, exclusively, or exhibiting higher levels of activity at the site of action, or by exploiting site-specific trafficking properties at the site of action (e.g., the blood-brain barrier). The strategically [BBB] predicted, multienzymatic transformations result in the differential distribution of the drug.

Chemical delivery systems have been divided into the following classes:

1. *Enzymatic physical-chemical–based CDS.* These chemical delivery systems exploit site-specific trafficking properties by sequential metabolic conver-

sions at the site of action, which result in modified transport properties.

2. *Site-specific enzyme activated CDS.* These chemical delivery systems exploit specific enzymes found primarily, exclusively, or exhibiting higher levels of activity at the site of action.
3. *Receptor-based CDS.* These chemical delivery systems capitalize on the transient and reversible nature of the drug binding to its receptor to enhance selectivity and activity.

Enzymatic Physical-Chemical–Based CDSs

In this approach, the drug is chemically modified to introduce the protective functions (F_n) and the targetor moiety (T). Upon administration, the resulting CDS is distributed throughout the body. Predictable enzymatic reactions convert the original CDS by removing some of the protective functions and by modifying the targetor moiety, leading to a precursor form that is still active but has significantly different physicochemical properties. Although these intermediates are continuously eliminated from the rest of the body, efflux–influx processes at the targeted site are not the same due to the presence of a specific membrane or other distributional barriers. These processes ultimately allow release of the active drug in a specific concentration at the site of action.

For example, the BBB can be regarded as a biological membrane that is permeable to most lipophilic compounds but not to hydrophilic molecules. In most cases, the transport criteria apply to both sides of the barrier. Thus, if a lipophilic CDS that can enter the brain is converted there to a hydrophilic molecule, one can assume that it is "locked-in" and is no longer be able to come out. The same conversion taking place in the rest of the body actually accelerates peripheral elimination and further contributes to brain targeting. In principle, many targetor moieties are possible for a general system of this type, but the one developed some years ago that proved most useful was based on the 1,4-dihydrotrigonelline ↔ trigonelline system (Fig. 7) (25–27). Here the targetor of this redox system is the lipophilic 1,4-dihydro form, which is converted in vivo to the highly hydrophilic quaternary form. Because this system is closely related to the ubiquitous NAD^+ ↔ NADH coenzyme system, this conversion occurs very easily everywhere in the body. The resulting charged species is locked into the brain but is easily eliminated from the body due to the acquired positive charge. After a relatively short time, a sustained, brain-specific release of the active drug is achieved.

Examples of the use of this system for a wide variety of drug classes have been described: various steroid hormones (28,29), antiinfective agents (30,31), antivirals (32,33), anticancer agents (34), antiretroviral agents (35–38) neurotrophomodulator catechol derivatives (39,40), and many others.

Most recently, successful brain deliveries of enkephalin (41,42) and thyrotropin-releasing hormone (TRH) analogues using a combination of approaches including the redox targetor system were reported (43). Delivery of such peptides through the BBB is an even more complex problem because endogenous enzymes recognize and rapidly degrade most naturally occurring neuropeptides (44). In the applied "molecular packaging" strategy (45), the peptide unit in the delivery system appears as a perturbation on a bulky molecule which is dominated by lipophilic modifying groups that direct BBB penetration and prevent recognition by peptidases. A brain-targeted packaged peptide delivery system contains the following major components: the redox targetor (T); a spacer function (S) consisting of specific amino acids selected to ensure timely removal of the charged targetor (T) and spacer (S) from the peptide; the peptide itself; and a bulky lipophilic moiety (L) attached through an ester bond, or occasionally through a C-terminal adjuster (A), at the carboxy terminus to impart lipid solubility and to disguise the peptide nature of the molecule. To achieve delivery using such a complex system, it is imperative that the designated enzymatic reactions occur in a specific sequence. Upon delivery, the first step must be oxidation of the targetor (T) to assure the "lock-in" character. This step is followed by removal of the lipophilic function (L) to form a direct precursor of the peptide

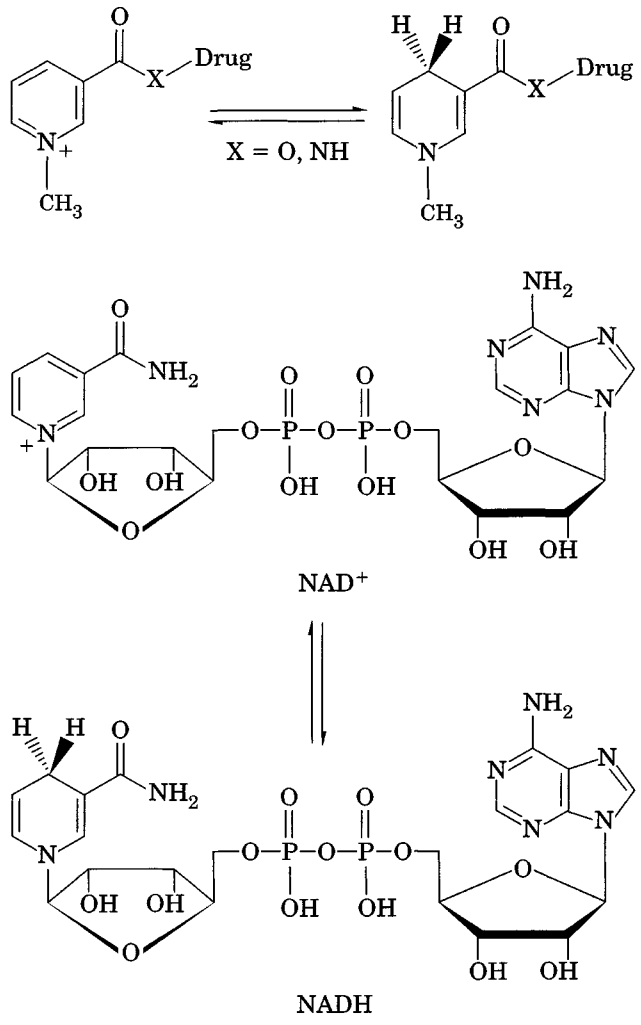


Figure 7. The pyridinium ↔ 1,4-dihydropyridine redox and NAD^+ ↔ NADH coenzyme systems.

that is still attached to the targetor. Subsequent cleavage of the targetor–spacer moiety (T–S) finally produces the active peptide.

Delivery of a TRH analogue, **26**, to the central nervous system using this approach is summarized in Figure 8. In this case, a precursor sequence (Gln-Leu-Pro-Gly) is in fact delivered, necessitating two additional steps. One where the C-terminal adjuster glycine (Gly) is cleaved by peptidyl glycine α-amidating monooxygenase to form the terminal prolinamide, and one where the N-terminal pyroglutamyl is formed from glutamine by glutaminyl cyclase. To improve and to optimize this delivery strategy, an efficient synthetic route for the peptide chemical delivery system was established, and the role of the spacer (S) and lipophilic (L) functions were investigated recently for Tyr-D-Ala-Gly-Phe-D-Leu (DADLE), an analogue of leucine enkephalin that binds to opioid receptors (42). Intravenous injection of several chemical delivery systems synthesized by a segment-coupling method produced a significant and long-lasting response in rats monitored by tail-flick latency measurements. Compared to the delivered peptide (DADLE), the packaged peptide and the intermediates formed during the sequential metabolism had weak affinity to opioid receptors. The antinociceptive effect was naloxone reversible and methylnaloxonium irreversible, suggesting that central opiate receptors must be solely responsible for mediating the induced analgesia. These observations support the hypothesis that the peptide chemical delivery system successfully delivered, retained and released the peptide in the brain. Changing the spacer (S)

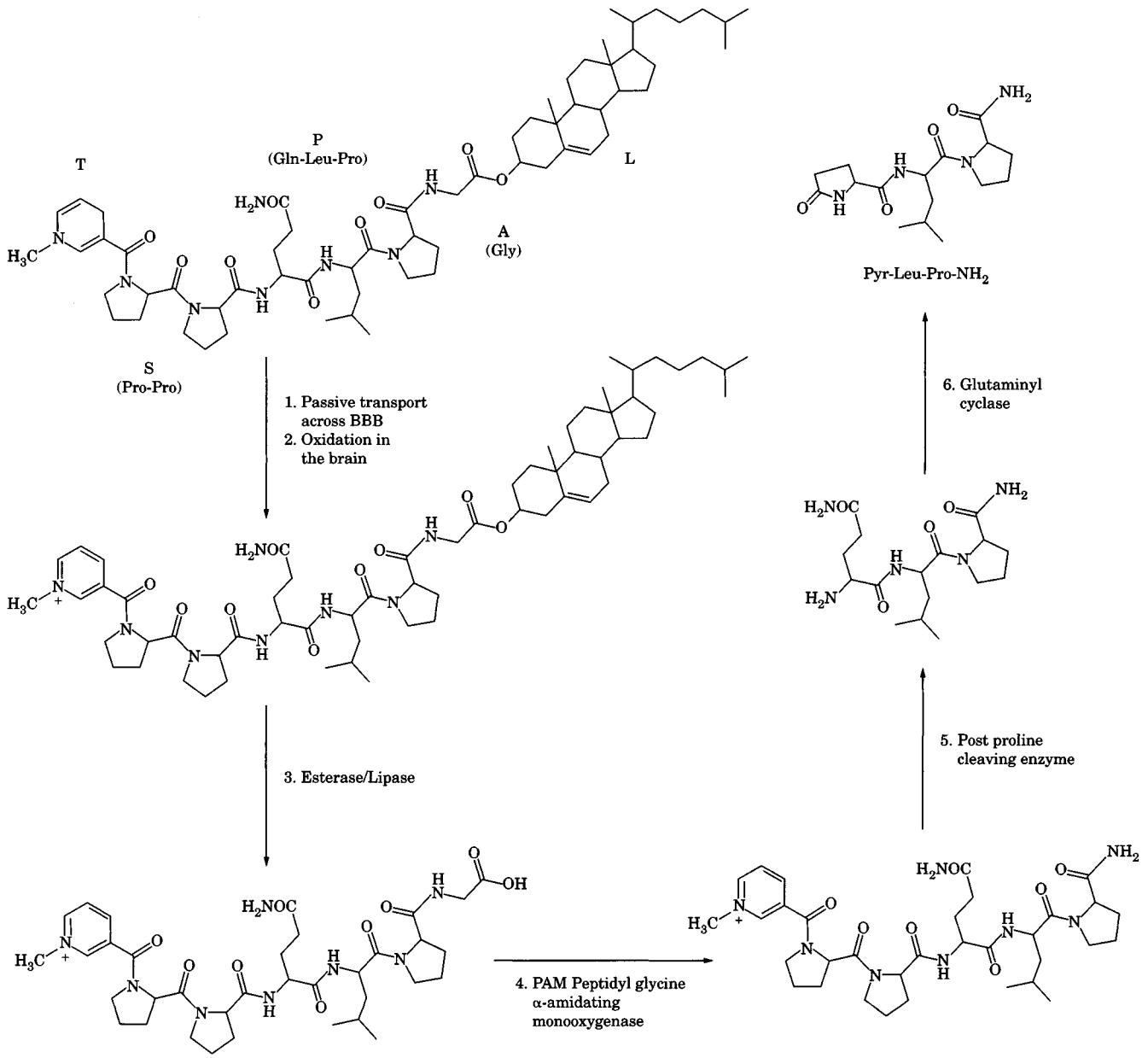


Figure 8. CDS for brain targeting of a TRH analogue.

and lipophilic (L) components can greatly influence the efficacy. The bulkier cholesterol group exhibited a greater efficacy than the smaller 1-adamantane ethyl group, but the most important factor which modulated DADLE release and pharmacologic activity was the identity of the spacer (S) function. Proline as the spacer produced more potent analgesia compared to alanine. Selection of the optimum spacer proved also important for the efficacy of the TRH chemical delivery system as measured by the decrease in barbiturate-induced sleeping time in mice following intravenous injection. At equimolar doses the TRH analogue exhibited only a marginal decrease, whereas the chemical delivery system with L-Ala as the spacer produced a 30% reduction, and the one with L-Ala–L-Ala as the spacer produced a decrease greater than 50% (45).

Site-Specific, Enzyme-Activated CDSs

This second type of CDS is based on enzymatic conversions of a CDS that take place only at the site of action as a result of the differential distribution of certain enzymes within the body. If some specific enzymes are present only around the designated site of action, their use in a strategically designed system can lead to high site specificity. The drug is chemically modified to introduce the targetor (T) moiety and the necessary protective function(s). Following administration, the resulting chemical delivery system is distributed throughout the body. Although it is continuously eliminated from the rest of the body without producing any pharmacologic effects, predictable enzymatic reactions convert the original CDS to the active drug only at the targeted site where the necessary enzymes are found primarily, exclusively, or at a higher level of activity.

Certainly, the system depends upon the existence of such enzymes. The basis of the retrometabolic design that resulted in a successful site- and stereospecific delivery of IOP-reducing β-adrenergic blocking agents to the eye is a general metabolic process that applies to all lipophilic ketone precursors of β-amino alcohols (46–51). Recognizing that lipophilic esters of adrenolone are effectively reduced within the eye to epinephrine, whereas oral administration does not result in epinephrine formation (52), the ketone function was identified as the targetor that can be reduced to produce the β-amino alcohol pharmacophore necessary for action. Since the approach could be extended to other β-agonists (53), the possibility arose to produce ophthalmically useful β-adrenergic antagonists within the eye from the corresponding ketones. However, ketones of the phenol ether type β-blockers are not good precursors to produce the β-amino alcohols because they decompose to their corresponding phenols in solution. To stabilize them, they were converted to oximes, which require a facile enzymatic hydrolysis to the bioreducible ketone. Although the oximes are much more stable relative to their corresponding ketones, their aqueous stability does not provide an acceptable shelf-life. However, significant stabilization can be obtained using the corresponding methoximes. A variety of oxime and methoxime analogues have been synthesized and studied (46–51). They were all shown to undergo the predicted specific activation within, and only within, the eye. Highest concentrations of the active β-agonists were observed in the iris-ciliary body. When applied topically in rabbits, both the oximes and the methoximes exhibited significantly higher IOP-reducing activities than there corresponding alcohols. On the other hand, topical or intravenous administration did not produce any cardiovascular effects in normal rabbits, rats, and dogs, nor after inducing tachycardia. Following intravenous administration, the oxime disappeared rapidly from the blood, and at no time could the corresponding alcohol be detected (52). This observation suggests that the required enzymatic hydrolysis–reductive activation sequence that occurs in the eye does not take place in the systemic circulation.

To summarize, in these chemical delivery systems, a β-aminooxime or β-methoxime function replaces the corresponding β-amino alcohol pharmacophore in the original molecules (Fig. 9). This oxime derivative is enzymatically hydrolyzed within the eye by enzymes located in the iris-ciliary body, and subsequently, reductive enzymes stereospecifically produce only the S-(-) stereoisomer of the β-blocker (18).

Receptor-Based CDSs

This last class of CDS is based on formation of a reversible covalent bond between the delivered entity and some part of the targeted receptor site. The targetor moiety in these CDSs is expected to undergo a modification that allows transient anchoring of the active agent. This class of CDS has been developed to a lesser extent than the previous ones.

The possibility of a receptor-based CDS for naloxone, **31**, a pure opioid antagonist, was explored. The presence of an essential sulfhydryl group near the binding site in opioid receptors was long suspected because agonist binding capacity is destroyed by sulfhydryl scavenging agents such as *N*-ethylmaleimide (54). Recent mutagenesis and other studies began to elucidate the mechanism for this inhibition of binding at opioid receptors (55,56). There is evidence that Leu-enkephalin, or even morphine analogues, containing sulfhydryl groups can form mixed disulfide linkages with opioid receptors (57). Chlornaltrexamine, an irreversible alkylating affinity label on the opiate receptor, can maintain its antagonist effect for 2–3 days, suggesting that covalent binding can increase the duration of action at these receptors. A more reversible spirothiazolidine system was investigated (Fig. 10). Spirothiazolidine derivatives were selected because they should be subject to biological cleavage of the imine formed after spontaneous cleavage of the carbon-to-sulfur bond (58), and they have been investigated previously in CDSs for the controlled release of endogenous agents such as hydrocortisone or progesterone (59,60). As modifications at the 6-position are possible without the loss of activity, the spirothiazolidine ring was attached at this site. Opening of the thiazolidine ring allows oxidative anchoring of the delivered agent to sulfhydryl groups nearby via disulfide bridging. Blocking of the receptor is reversible, because endogenous sulfhydryl compounds can presumably regenerate the sulfhydryl group at the receptor. If a favorable conformation can be attained, greater affinity at the opioid

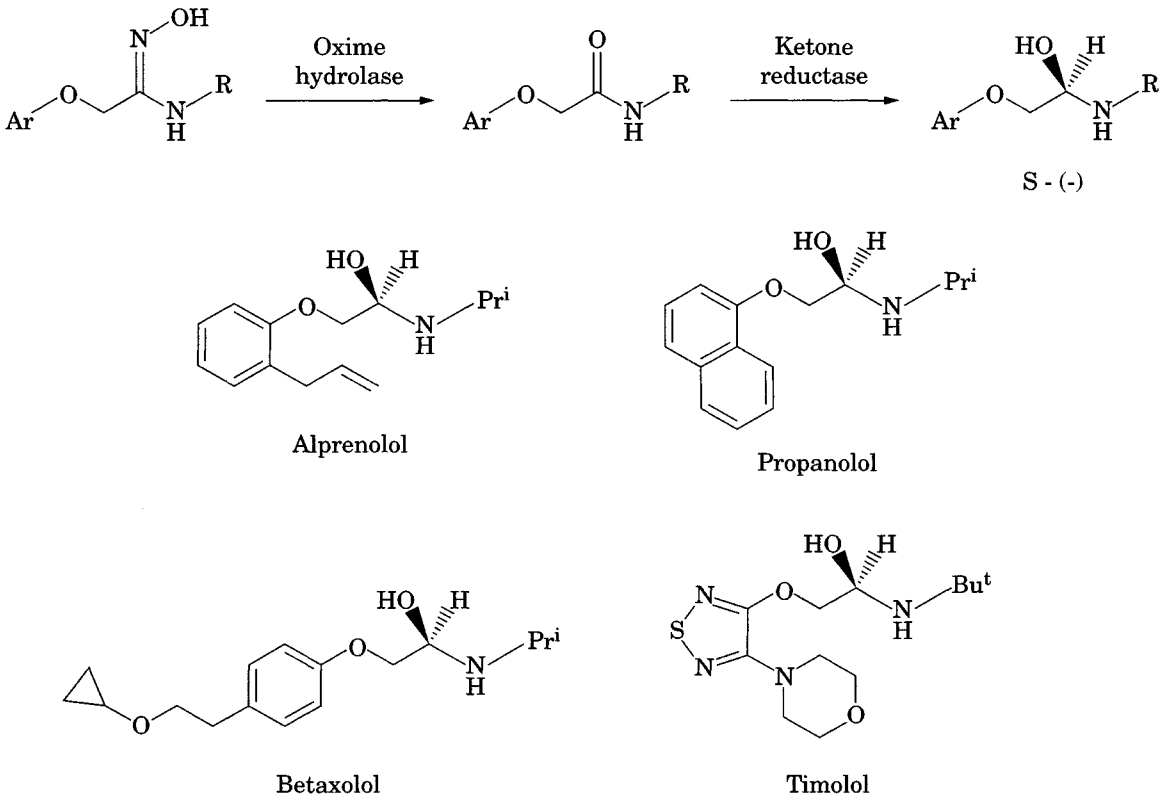


Figure 9. Site- and stereospecific delivery of β-adrenergic antagonists to the eye.

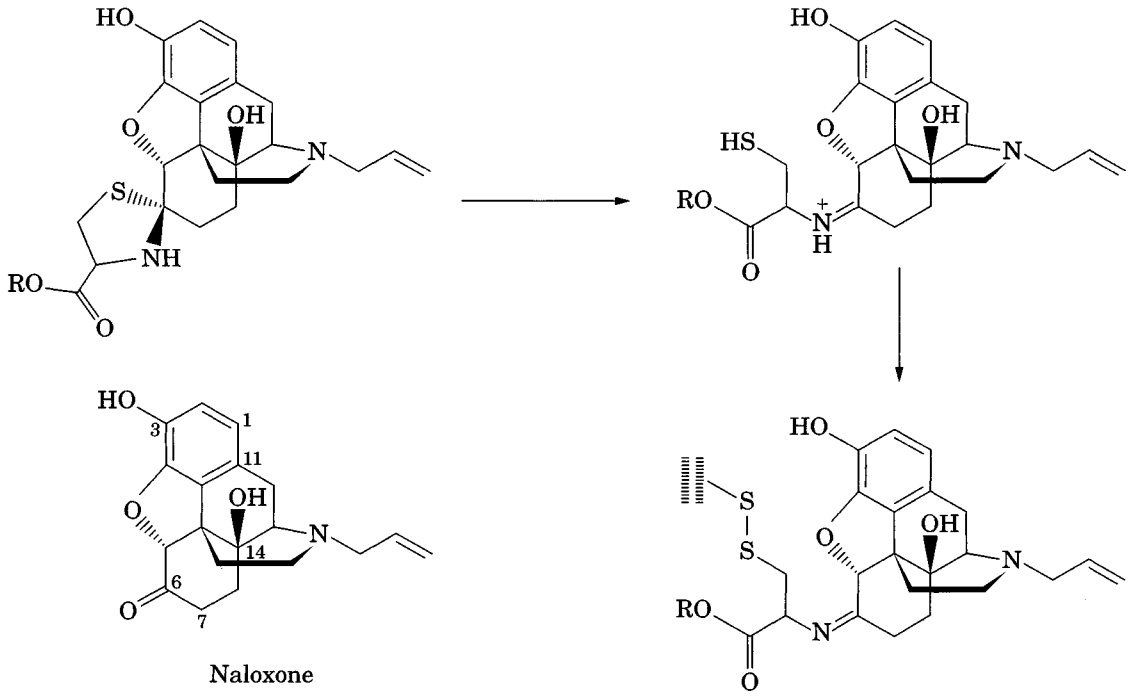


Figure 10. Spirothiazolidine CDS of naloxone, **31**.

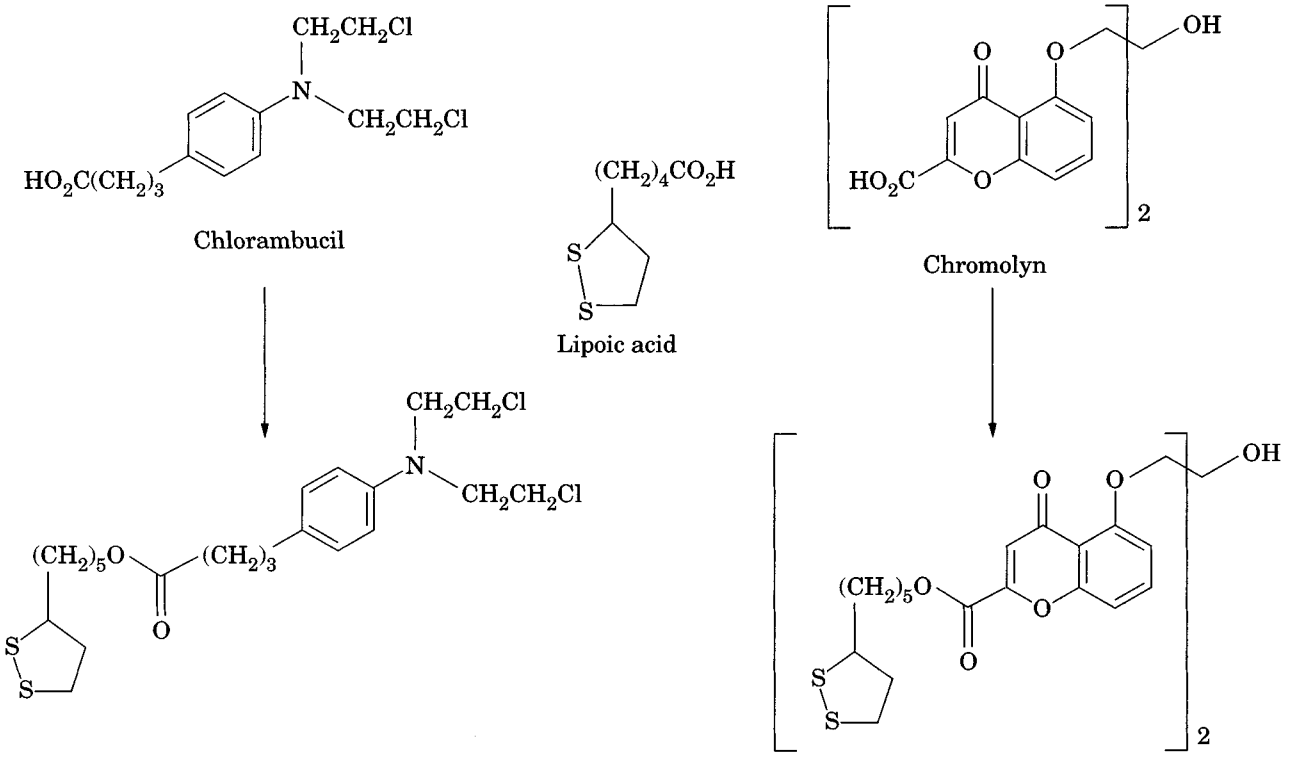


Figure 11. Lipoic acid–based CDS for lung targeting.

receptor can be expected. Indeed, naloxone-6-spirothiazolidine exhibits an increased affinity at opioid receptors. The increase is especially significant at the κ-receptors known to be involved in sedative analgesia. The intrinsic activity for guinea pig ileum of the naloxone chemical delivery system also demonstrated a 25-fold increase compared to naloxone itself.

Because several other G-protein–coupled receptors (e.g., TRH, D_1 and D_2 dopamine, vasopressin, follicle-stimulating hormone, and cannabinoid receptors) are also sensitive to sulfhydryl reagents (56), there is considerable potential for this class of CDS if modification of the corresponding ligands at appropriate sites can be performed. In addition, as earlier evaluations of spirothiazolidine-based systems indicated an enhanced deposition to the lung, the possibility to use similar mechanisms in developing other lung tissue targeting chemical delivery systems presented itself. Because of its potential to form disulfide bonds, lipoic acid, **32**, a nontoxic coenzyme for acyl transfer and redox reactions, was investigated as a targetor for selective delivery to lung tissue (61). The corresponding chemical delivery systems for chlorambucil, **33**, an antineoplastic agent, and chromolyn, **34**, a bischromone used in antiasthmatic prophylaxis, were synthesized via an ester linkage (Fig. 1). In vitro kinetic and in vivo pharmacokinetic studies demonstrated that the respective CDSs were sufficiently stable in buffer and biological media, hydrolyzed rapidly into the respective active parent drugs, and, relative to the underivatized parent compounds, significantly enhanced delivery and retention of the active drug in lung tissue.

CONCLUSIONS

Several novel metabolic-based drug design approaches have been described. The particular advantage of these approaches is to enhance drug targeting to the site of action. Retrometabolic approaches include two major classes: CDSs and SDs. They are opposite in terms of how each approach achieves their drug targeting role, but they have in common the basic concept of designed metabolism to control drug action and targeting. For CDSs, the molecule is designed to be inactive and to undergo strategic enzymatic activation in order to release the active agent only at the site of action. Delivery of this kind was successfully made to the brain, to the eye, and to other organs such as the lung. On the other hand, SDs are intrinsically potent new chemical entities that are strategically deactivated after they achieve their therapeutic role. These two approaches are general in nature and can be applied essentially to all drug classes.

BIBLIOGRAPHY

1. J.J. Kaminski and N. Bodor, in C.R. Clark and W.H. Moos, eds., *Drug Discovery Technologies*, Ellis Horwood, Chichester, U.K., 1990, pp. 65–91.
2. C.G. Wermuth, J.C. Gaignault, and C. Marchandeau, in C.G. Wermuth, ed., *The Practice of Medicinal Chemistry*, Academic Press, London, 1996, pp. 672–696.

3. C.G. Wermuth, in C.G. Wermuth, ed., *The Practice of Medicinal Chemistry*, Academic Press, London, 1996, pp. 697–715.
4. U.S. Pat. 4,061,722 (December 6, 1977), N. Bodor (to INTER$_x$ Research Corp.).
5. U.S. Pat. 4,264,765 (April 28, 1981), N. Bodor and L. Freiberg (to Abbott Laboratories).
6. N. Bodor, J.J. Kaminski, and S. Selk, *J. Med. Chem.* **23**, 469–474 (1980).
7. N. Bodor et al., *J. Med. Chem.* **23**, 474–480 (1980).
8. Jpn. Pat. 21201 (February 10, 1983), N. Bodor and Y. Oshiro.
9. M.B. Abou-Donia and D.B. Menzel, *Biochem. Pharmacol.* **17**, 2143–2161 (1968).
10. N. Bodor, in H.P. Tipnis, ed., *Advances in Drug Delivery Systems*, MSR Foundation, Bombay, 1985, pp. 111–127.
11. N. Bodor, in E. Christophers, A.M. Kligman, E. Schopf, and R.B. Stoughton, eds., *Topical Corticosteroid Therapy: A Novel Approach to Safer Drugs*, Raven Press, New York, 1988, pp. 13–25.
12. N. Bodor, *Curr. Probl. Dermatol.* **21**, 11–19 (1993).
13. P. Druzgala, G. Hochaus, and N. Bodor, *J. Steroid Biochem.* **38**, 149–154 (1991).
14. P. Druzgala and N. Bodor, *Steroids* **56**, 490–494 (1991).
15. N. Bodor et al., *Pharm. Res.* **3**, 120–125 (1984).
16. N. Bodor, A. El-Koussi, M. Kano, and M. Khalifa, *J. Med. Chem.* **31**, 1651–1656 (1988).
17. H. Yang, W.M. Wu, and N. Bodor, *Pharm. Res.* **12**, 329–336 (1995).
18. N. Bodor and L. Prokai, *Pharm. Res.* **7**, 723–725 (1990).
19. G.N. Kumar, R.H. Hammer, and N. Bodor, *Drug Des. Discovery* **10**, 11–21 (1993).
20. G.N. Kumar, R.H. Hammer, and N. Bodor, *Drug Des. Discovery* **10**, 1–9 (1993).
21. G.N. Kumar, R.H. Hammer, and N. Bodor, *Bioorg. Med. Chem.* **1**, 327–332 (1993).
22. G.N. Kumar, R.H. Hammer, W.M. Wu, and N. Bodor, (1993) *Curr. Eye Res.* **12**, 501–506 (1993).
23. R. Hammer et al., *Novel Soft Anticholinergic Agents. Drug Des. Delivery* **2**, 207–219 (1988).
24. R. Hammer, W.M. Wu, J.S. Sastry, and N. Bodor, *Curr. Eye Res.* **10**, 565–570 (1991).
25. N. Bodor, H. Farag, and M.E. Brewster, *Science* **214**, 1370–1372 (1981).
26. N. Bodor and M.E. Brewster, *Pharmacol. Ther.* **19**, 337–386 (1983).
27. N. Bodor and H. Farag, *J. Med. Chem.* **26**, 313–318 (1983).
28. N. Bodor and J.J. Kaminski, *Annu. Rep. Med. Chem.* **22**, 303–313 (1987).
29. M.E. Brewster, K.S. Estes, and N. Bodor, *J. Med. Chem.* **31**, 244–249 (1988).
30. E. Pop, W.M. Wu, and N. Bodor, *J. Med. Chem.* **32**, 1789–1795 (1989).
31. E. Pop, W.M. Wu, E. Shek, and N. Bodor, *J. Med. Chem.* **32**, 1774–1781 (1989).
32. K. Rand et al., *J. Med. Virol.* **20**, 1–8 (1986).
33. M.E. Brewster and N. Bodor, *Adv. Drug Delivery Rev.* **14**, 177–197 (1994).
34. K. Raghavan, E. Shek, and N. Bodor, *Anticancer Drug Des.* **2**, 25–36 (1987).
35. P.T. Torrence et al., *FEBS Lett.* **234**, 135–140 (1988).
36. S. Gogu, S.K. Aggarwal, S.R.S. Rangan, and K.C. Agrawal, *Biochem. Biophys. Res. Commun.* **160**, 656–661 (1989).
37. E. Palomino, D. Kessel, and J.P. Horowitz, *J. Med. Chem.* **32**, 622–625 (1989).
38. R. Little et al., *Biopharm. Sci.* **1**, 1–18 (1990).
39. A. Kourounakis, N. Bodor, and J. Simpkins, *Int. J. Pharm.* **141**, 239–250 (1996).
40. A. Kourounakis, N. Bodor, and J. Simpkins, *J. Pharm. Pharmacol.* **49**, 1–9 (1997).
41. N. Bodor and M.J. Huang, *J. Pharm. Sci.* **81**, 954–960 (1992).
42. K. Prokai-Tatrai, L. Prokai, and N. Bodor, *J. Med. Chem.* **39**, 4775–4782 (1996).
43. L. Prokai, X.D. Ouyang, W.M. Wu, and N. Bodor, *J. Am. Chem. Soc.* **116**, 2643–2644 (1994).
44. J. Brownlees and C.H. Williams, (1993) *J. Neurochem.* **60**, 793–803 (1993).
45. N. Bodor and L. Prokai, in M. Taylor and G. Amidon, eds., *Peptide-Based Drug Design: Controlling Transport and Metabolism*, American Chemical Society, Washington, D.C., 1995, pp. 317–337.
46. A. El-Koussi and N. Bodor, *Int. J. Pharm.* **53**, 189–194 (1989).
47. N. Bodor, H. van der Goot, G. Domany, L. Pallos, and H. Timmerman, eds., *Trends in Medicinal Chemistry*, Elsevier, Amsterdam, 1989, pp. 145–164.
48. N. Bodor, *Adv. Drug Delivery Rev.* **16**, 21–38 (1995).
49. L. Prokai, W.M. Wu, G. Somogyi, and N. Bodor, *J. Med. Chem.* **38**, 2018–2020 (1994).
50. N. Bodor et al., *J. Ocul. Pharmacol. Ther.* **13**, 389–403 (1997).
51. H. Farag et al., *Drug Des. Discovery* **15**, 117–130 (1997).
52. N. Bodor, A. El-Koussi, M. Kano, and T. Nakamuro, *J. Med. Chem.* **31**, 100–106 (1988).
53. I.K. Reddy and N. Bodor, *J. Pharm. Sci.* **83**, 450–453 (1994).
54. J.R. Smith and E.J. Simon, *Proc. Natl. Acad. Sci. U.S.A.* **77**, 281–284 (1980).
55. B.D. Joseph, and J.M. Bidlak, *Eur. J. Pharmacol.* **267**, 1–6 (1996).
56. M. Shahrestanifar, W.W. Wang, and R.D. Howells, *J. Biol. Chem.* **271**, 5505–5512 (1996).
57. K. Kanematsu et al., *Chem. Pharm. Bull.* **38**, 1438–1440 (1990).
58. W.M. Schubert and Y. Motoyama, *J. Am. Chem. Soc.* **87**, 5507–5508 (1965).
59. N. Bodor et al., *Int. J. Pharm.* **10**, 307–321 (1982).
60. N. Bodor and K.B. Sloan, *J. Pharm. Sci.* **71**, 514–520 (1982).
61. M. Saah et al., *J. Pharm. Sci.* **85**, 496–504 (1996).

See also CANCER, DRUG DELIVERY TO TREAT—PRODRUGS; PENDENT DRUGS, RELEASE FROM POLYMERS.

Next Page

COATINGS

C.T. RHODES
PharmaCon, Inc.
West Kingston, Rhode Island
S.C. PORTER
Colorcon
West Point, Pennsylvania

KEY WORDS

Cellulosic
Compaction coating
Controlled release
Drug master file
Enteric coatings
Excipient
Fluidized bed coating
Food and Drug Administration
Melt coating
Microsphere
Noncellulosic
Pan coating
Plasticizer
Polymer
Product validation

OUTLINE

Fundamental Requirements
  Regulatory Concerns
  Sources of Information on Coating Materials and Processes
  Mechanisms by Which Coatings Can Effect Controlled Release
Manufacturing Methods for the Application of Coating Materials for Controlled Release
  Pan Coating
  Fluidized-Bed Coating
  Compression Coating
  Melt Coating
  Development of New Controlled Release Coating Products
Trends in the Formulation and Manufacture of Coated, Controlled-Release Products
  Rigorous Evaluation of Data by FDA Before Marketing Approval Is Granted
  Optimization, Validation, and Product Evaluation for Coating Formulation and Processing
  Enteric-Coated, Controlled Release Products
  Coated Pharmaceuticals for Colonic Delivery
  Developments in Materials and Processing
Materials Used in Controlled-Release Products
  Enteric Coatings: Cellulosic
  Enteric Coatings: Noncellulosic
  Nonenteric Coatings: Cellulosic
  Nonenteric Coatings: Noncellulosic
  Plasticizers
Bibliography

The coating of pharmaceutical products goes back many years. For example, Shakespeare refers to gilding (gold coating) pills. Certainly, even as recently as the 1950, pharmacists in England and the United States were, for example, trained to coat pills with silver or gold leaf or shellac. To what extent such drug delivery systems provided controlled release is a matter of conjecture. Probably the first reliable coating products were enteric-coated tablets designed to protect acid labile drugs from degradation in the relatively low pH conditions of the stomach. However, even here there is reason to doubt the efficacy of many of the enteric-coated products that were marketed as recently as the 1960s.

It is probably true that coated pharmaceuticals that can be relied on to provide controlled release are less than 50 years of age. The development of such products has depended, to a very considerable extent, on the availability of chemically modified coatings (especially cellulose derivatives), which are supplied to the pharmaceutical industry as materials of reliable quality. Also, the improvements in coating equipment technology, especially the invention of the Wurster film coating device, has been essential to the improvement in coating technology.

This article is focused on coatings and the method by which coatings can be applied to manufacture controlled release products. It will be appreciated that coatings are sometimes applied to pharmaceutical products for reasons separate from a desire to modify drug release. For example, coatings are applied to some tablets, e.g., ibuprofen, which have an unpleasant taste or to improve shelf life stability, e.g., conjugated estrogens. The thrust of this chapter is controlled release, although in some instances coatings designed for control of drug release may also confer other benefits, such as improving ease of swallowing tablets by geriatric patients. Thus in this chapter, sugar coating, which is not normally used primarily as a method of control of drug release, receives only minimal attention.

The essential elements of a coated pharmaceutical product is that a core (consisting of drug, or drug plus excipients) is encased by a layer, or layers, of materials that regulate the rate at which drug is released into the surrounding medium. The primary coating materials, usually polymeric, often require the addition of other excipients such as plasticizers, pore formers, or antiaggregation agents for the product to be conveniently manufactured or for the coating to perform in the desired fashion. It is therefore appropriate to give attention to some of these types of excipients. The demarcation between a coated and a matrix-type pharmaceutical, controlled release product is not always clear. Thus, as Tice and Tabibi have pointed out (1), a microcapsule has its drug:

Previous Page

COATINGS

C.T. RHODES
PharmaCon, Inc.
West Kingston, Rhode Island
S.C. PORTER
Colorcon
West Point, Pennsylvania

KEY WORDS

Cellulosic
Compaction coating
Controlled release
Drug master file
Enteric coatings
Excipient
Fluidized bed coating
Food and Drug Administration
Melt coating
Microsphere
Noncellulosic
Pan coating
Plasticizer
Polymer
Product validation

OUTLINE

Fundamental Requirements
  Regulatory Concerns
  Sources of Information on Coating Materials and Processes
  Mechanisms by Which Coatings Can Effect Controlled Release
Manufacturing Methods for the Application of Coating Materials for Controlled Release
  Pan Coating
  Fluidized-Bed Coating
  Compression Coating
  Melt Coating
  Development of New Controlled Release Coating Products
Trends in the Formulation and Manufacture of Coated, Controlled-Release Products
  Rigorous Evaluation of Data by FDA Before Marketing Approval Is Granted
  Optimization, Validation, and Product Evaluation for Coating Formulation and Processing
  Enteric-Coated, Controlled Release Products
  Coated Pharmaceuticals for Colonic Delivery
  Developments in Materials and Processing
Materials Used in Controlled-Release Products
  Enteric Coatings: Cellulosic
  Enteric Coatings: Noncellulosic
  Nonenteric Coatings: Cellulosic
  Nonenteric Coatings: Noncellulosic
  Plasticizers
Bibliography

The coating of pharmaceutical products goes back many years. For example, Shakespeare refers to gilding (gold coating) pills. Certainly, even as recently as the 1950, pharmacists in England and the United States were, for example, trained to coat pills with silver or gold leaf or shellac. To what extent such drug delivery systems provided controlled release is a matter of conjecture. Probably the first reliable coating products were enteric-coated tablets designed to protect acid labile drugs from degradation in the relatively low pH conditions of the stomach. However, even here there is reason to doubt the efficacy of many of the enteric-coated products that were marketed as recently as the 1960s.

It is probably true that coated pharmaceuticals that can be relied on to provide controlled release are less than 50 years of age. The development of such products has depended, to a very considerable extent, on the availability of chemically modified coatings (especially cellulose derivatives), which are supplied to the pharmaceutical industry as materials of reliable quality. Also, the improvements in coating equipment technology, especially the invention of the Wurster film coating device, has been essential to the improvement in coating technology.

This article is focused on coatings and the method by which coatings can be applied to manufacture controlled release products. It will be appreciated that coatings are sometimes applied to pharmaceutical products for reasons separate from a desire to modify drug release. For example, coatings are applied to some tablets, e.g., ibuprofen, which have an unpleasant taste or to improve shelf life stability, e.g., conjugated estrogens. The thrust of this chapter is controlled release, although in some instances coatings designed for control of drug release may also confer other benefits, such as improving ease of swallowing tablets by geriatric patients. Thus in this chapter, sugar coating, which is not normally used primarily as a method of control of drug release, receives only minimal attention.

The essential elements of a coated pharmaceutical product is that a core (consisting of drug, or drug plus excipients) is encased by a layer, or layers, of materials that regulate the rate at which drug is released into the surrounding medium. The primary coating materials, usually polymeric, often require the addition of other excipients such as plasticizers, pore formers, or antiaggregation agents for the product to be conveniently manufactured or for the coating to perform in the desired fashion. It is therefore appropriate to give attention to some of these types of excipients. The demarcation between a coated and a matrix-type pharmaceutical, controlled release product is not always clear. Thus, as Tice and Tabibi have pointed out (1), a microcapsule has its drug:

> . . . centrally located within the particle where it is encased within a unique polymer membrane. . . . Whereas a microsphere has its drug dispersed throughout the particle; that is the internal structure of a matrix of drug and polymer excipient.

Obviously, therefore, some of the materials used as coatings to control drug release may also be used for a similar function in matrix-type products, and are discussed elsewhere in this encyclopedia. It is also true that some excipients may be used in coated pharmaceuticals for one purpose and be used in other pharmaceuticals to fulfill a different function. Thus, magnesium stearate, most commonly used in pharmaceutical technology as a tablet lubricant, has been used to prevent agglomeration of coated microparticles (2).

FUNDAMENTAL REQUIREMENTS

There are three preeminent requirements for any coating intended for use in controlling the rate of release of drug from a commercially available product:

1. The coating must control the release pattern of the drug such that the release profile, zero-order, first-order pulsatile, or other is within acceptable limits so as to comply with the pharmacokinetic and/or pharmacodynamic requirements of the particular drug product.
2. All components of the coating must be acceptable to the relevant regulatory agencies for the route of administration and species for which the product is intended.
3. The coating materials must be commercially available at a reasonable price, reproducibly meeting functionally relevant standards so that process validation can clearly demonstrate that the manufacturing process is fully under control and that the product is likely to show an acceptably low level of batch-to-batch variation.

The first of these three desiderata is considered in other parts of this encyclopedia, and thus will not be discussed in this chapter. It is, however, essential before considering specific coating components to give some attention to regulatory concerns.

Regulatory Concerns

There are many polymeric materials that research workers have identified as having potential for control of drug release. Unfortunately, relatively few have been approved for use in either human or veterinary pharmaceutical products. It would be most imprudent for any controlled release project involving the use of a coating to be initiated without some attention being given to the regulatory status of the components being considered, if it is hoped that ultimately a product can be marketed. It would be attractive if a simple list of "acceptable" components could be provided to readers of this encyclopedia. However, there are several reasons that prevent the preparation of such a list. The processes of globalization and harmonization are far from being complete. Although significant progress is being made, there are still important differences in the regulatory requirements of the United States, the European Union, and Japan (3–5). Thus, what may be acceptable in one jurisdiction is not necessarily acceptable in another.

Even within one jurisdiction, different levels of acceptance may apply to an excipient intended for the oral or intramuscular route or for use in humans or feed animals. Also, of course, the approval of a coating component depends on the quality and quantity of minor constituents. Thus, approval may well be source specific. In the United States, the mechanism of Drug Master Files provides a most useful mode, whereby the manufacture of an excipient can establish, with the U.S. FDA, a detailed record of test data pertaining to its own marketed product. Upon authorization by the sponsor of the Drug Master File, FDA personnel can access the file when considering a marketing submission document (NDA, PLA, etc.) that involves use of the excipient. Information from excipient suppliers as to the current regulatory acceptability of one of their products for administration to humans or animal species by a specified routes of administration can be most useful.

In the recent past, there was considerable gloom in the pharmaceutical industry about the possibilities of obtaining regulatory approval for new excipients. The formation of the International Pharmaceutical Excipient Council (IPEC) has raised hopes that in the future this process will be less difficult than previously (6). (Call 201-628-3231 for information on IPEC.)

At the time marketing permission is requested from a regulatory agency such as the FDA, the sponsor is required to demonstrate that the manufacturing process is fully validated (7). Validation of process can only be successful if there are reliable, functionally relevant standards for the raw materials so that batch-to-batch variability of such raw materials is low. This requirement can often create problems for excipients of natural origin that commonly show considerable batch, seasonal, and source variability. Thus, unless a new coated, controlled release product is being developed for a nutraceutical for sale through health food stores that insist on all components being "natural," any group considering a new product is probably well advised to avoid the use of natural products, such as shellac. Although shellac is still used quite substantially in coated products, it is very difficult to obtain reliable, quality material. Substantial batch-to-batch variability of shellac has been the source of difficulties with the FDA because of a lack of sufficiently precise control over drug release.

Sources of Information on Coating Materials and Processes

It is hoped that this chapter provides a useful coverage of the fundamentals of both coating materials and processes. However, since this field is so vast, and also because it is in a state of flux, those readers interested in details on a particular coating material or piece of coating equipment may find it useful to supplement this chapter with information derived from other sources.

For general coverage of the selection of formulation and processing factors in the development of a coated, con-

trolled release products, the discussions presented by Rudnic and Kotke (8) and Schwartz and O'Connor (9) are recommended.

It is generally recognized that national pharmacopoeias (e.g., USP, BP, PF, JP) have done an excellent job in setting standards for drug substances. Unfortunately, until quite recently, comparatively little attention had been given by national or professional bodies to developing chemical, physical, or biological standards for excipients, including materials used in coatings; thus, USP/NF does not have monographs on all the commonly used coating excipients. Although this failing is now recognized, there is still no official compendium that might be used by those seeking standards for pharmaceutical excipients. However, the *Handbook of Pharmaceutical Excipients* (10) has attained quasiofficial status in this regard. Although this book is not perfect (some feel that there is an uneven level of treatment in the different monographs, and others feel that additional substances should be included), this text is often used by those seeking standards for excipients.

Another book likely to find increasing use by those looking for specifications for excipients is that written by Ash and Ash (11), which provides a global survey of more than 6,000 products, which can be accessed by trade name, chemistry, function, and manufacturer. However, for those who become directly concerned with developing a controlled release coated product, there is much to be said for consulting the manufacturers' literature. Although there is considerable variation in the content and detail of such material, much is comprehensive, detailed, and objective. Reputable manufacturers of excipients, which derive a substantial portion of their income from the pharmaceutical industry, have an obvious interest in disseminating reliable information about their products.

Additional sources of specialized information are consultants or the services of contract houses that provide formulation and processing development assistance. The Coating Place in Verona, Wisconsin, is one such organization. Those interested in locating such contract houses may find the Drug Information Association's *Pharmaceutical Contract Support Organizations Register* of value (12).

For those who are interested in becoming current with the most recent research developments in controlled release coating technology, perusal (manual or computer-assisted) of abstracting journals such as *Current Contents* and the primary literature in research journals is, of course, essential. Among those journals that are particularly likely to publish research or review papers in this area are the *Journal of Controlled Release, International Journal of Pharmaceutics, Drug Development and Industrial Pharmacy, Pharmaceutical Research, Journal of Microencapsulation, Journal of Pharmacy and Pharmacology*, and *Journal of Pharmaceutical Sciences*.

Mechanisms by Which Coatings Can Effect Controlled Release

Elsewhere in this book, detailed consideration is given to the mathematical definition of various release profiles and how such profiles can be obtained. This brief summary of mechanisms by which coatings and the components therein can function to control release is only intended so that the properties of the components described in later sections of this chapter can be related to the overall objective for which the product is designed.

Although there is considerable semantic confusion concerning the various terms (sustained, extended, modified) applied to controlled release products, the present authors follow Berner and Dinh (13) who state that a controlled-release product "involves control of either the time course or location of drug delivery." The simplest mechanism by which a coating can control temporal aspects of drug release is to apply layers of a single material that can erode, melt, or become permeable at body temperature and thus allow release of drug. By a judicious selection of blends of pellets with varying thicknesses of coating, it may be possible to construct a dissolution profile of the form required for a particular drug. A number of waxes and similar materials are used for controlled release products that function in this manner, and some of these products have been successfully marketed for many years. Recently, considerable interest has been directed to the use of hot-melt coating methods, some of which incorporate modified, fluidized-bed coaters, to the manufacture of such formulations (14).

Enzymes present in the gastrointestinal tract, or elsewhere, have considerable potential for exploitation as agents to stimulate the breakdown of the coating of a controlled release product, and thus release the drug at an appropriate time after ingestion or at a particular location in the tract. For example, there is evidence that short, linear chains of amylose are resistant to enzymatic attack in the small intestine (15), but can be degraded by colonic microflora. There is thus considerable interest in coating drug delivery systems with a mixture of an appropriate form of amylose and other coating materials, such as ethylcellulose so that the resultant drug delivery system is capable of releasing drug in the colon. The coatings described by Milojevic and associates (16) may prove to be precursors of coatings that will eventually be commercialized. Also, the possible use of coatings containing azopolymers that are impermeable in the stomach but are converted to amides in the colon by bacteria, such conversion resulting in coating collapse, also may have potential (17).

The variation in pH that occurs as an orally administered drug delivery system moves down the gastrointestinal tract and has been very widely used as the trigger to cause the release of drug in enteric-coated drug delivery systems. Polymers, often esters of phthalic acid, used as enteric coatings commonly possess pendent carboxylic acid groups that are un-ionized in the relatively low pH of the stomach (normally about 1.5 to 4.5), but which ionize and thus repel one another, causing coating disruption as the pH rises when the delivery system enters the small intestine.

Diffusion of water from the exterior of the product across the coating, followed subsequently by diffusion in the reverse direction of dissolved drug, is very commonly the major mechanism by which coated products achieve control of drug release. In the least complicated limit case, the rate of release of drug might be regarded as a simple function of the diffusion coefficient of water or the solvated

drug in the polymer, which is regarded as invariant in properties. In reality, such simple conditions rarely exist in commercially available products. Coatings often contain several components in addition to the primary component polymeric species, which provides the backbone of the coating. Some of the secondary coating components may be deliberately added in order to modify the permeability of the primary polymer by providing channels or pores within the coating (18,19). Other materials, such as plasticizers, although they are added for entirely different reasons, can, in some instances, significantly modify drug release rates (20). Also, it must be kept in mind that changes in processing variables, such as inlet temperature in a fluidized-bed coater, which may be required during the scale-up from laboratory to pilot scale to manufacturing scale, may result in significant changes to dissolution profiles. Thus, it is wise not to rigidly define release rate profiles for coated, controlled release products at an early stage of the research and development process.

It should also be kept in mind that the various theoretical models that have been advanced to rationalize the release of drug from coated, controlled release products are often quite insufficient to reliably and precisely predict in vivo dissolution rates. Although we may find it intellectually convenient to classify coatings in terms of their purported mechanism of control, the reality probably is that in many formulations the actual behavior of the product in the patient is a hybrid of several models with surface erosion, enzymatic degradation, pH-induced changes, swelling of coating components, etc., all playing roles in the control of drug release. Finally, one must be careful not to fall into the error of assuming that in vitro dissolution tests (even those performed using the flow-thru cell) are necessarily always predictive of pharmacokinetic or pharmacodynamic parameters (21).

The osmotic pump approach to the design of coated, controlled release drug products is one of the most exciting developments that has occurred in controlled release coating technology, and the background of this concept is described elsewhere in this encyclopedia.

Multilamellar coating products in which there are clear differences in composition of two or more sequentially applied coats are available and can offer special advantages. For example, Shah and his associates teach in their patent (22) the use of a core-containing drug that is coated with an erodible polymer coating which, in turn, is surrounded by an enteric-release type coating. In example 1 of their patent, Shah and his co-workers describe compaction coating of granules by an erodible coating comprising hydroxypropylmethylcellulose, microcrystalline cellulose, and polyvinyl pyrrolidone. These coated granules were then enteric coated by a spray method with a mixture of hydroxypropylmethylcellulose phthate and acetylated monoglyceride. The outer coating protects the drug until the small intestine is reached. The inner coating (proximal to the core) is of such a thickness and composition that the drug is released in the colon. Multilamellate coatings in which each coating has a different function to perform offer the potential of developing very sophisticated, controlled release coating system.

If a coating is prepared around a drug delivery system in which the outermost layer contains a bioadhesive material, then the control of the locus at which drug release occurs becomes possible. A number of materials, including hydroxypropylcellulose, polyacrylic acid, and sodium carboxymethycelluse have been examined for this application (23,24). Bioadhesive coatings have potential for topical buccal, periodontal, gastric, intestinal, ophthalmic, and vaginal delivery (25–28).

MANUFACTURING METHODS FOR THE APPLICATION OF COATING MATERIALS FOR CONTROLLED RELEASE

Although considerable ingenuity has been applied to developing manufacturing methods which might be used for the application of coating materials for control release products, the four basic approaches are (*1*) pan coating using solvent evaporation, (*2*) fluidized-bed coating using solvent evaporation, (*3*) compaction coating, and (*4*) melt coating.

For those coating methods that involve the use of a solvent system (i.e., methods 1 and 2), it is convenient to define whether the solvent is aqueous or organic since the selection of solvent not only has regulatory implications (e.g., EPA), but also affects the nature or type of materials used in the coating formulation.

It is possible that other coating methods, such as various types of coacervation, may come to be of greater commercial importance for controlled release, coated products in the future.

Pan Coating

The oldest form of pharmaceutical coating—sugar coating—was an art rather than a science. The basis of the process was, in effect, to use giant saucepans, which were continually agitated, as the cook supervised the addition of coating fluid and the subsequent solvent evaporation. Film coating (using cellulosic-type materials for controlled release) naturally evolved from practices and equipment that had been used in sugar coating of tablets.

Conventional coating pans were top-open-ended truncated spheroids mounted on a power unit, which allowed the pan to be rotated at an angle of about 45° to the horizontal at a speed of between 20 and 50 rpm. Both ingress of coating fluid and the egress of solvent vapors was via the top of the pan.

The basic conventional pan design has been substantially improved by a number of modifications which have inter alia improved air flow, throughput, and coating uniformity. Different shaped pans, cylinders, hexagons, and pear shapes can offer advantages. Improvement of air flow patterns have been made by using side-vented cylindrical pans and perforated pans. In the Hi-Coater (Vector) and Acela-Cata (Thomas), airflow is through the tablet bed and then out of the perforated walls of the pan. The Glatt coater allows airflow with or against the direction in which coating spray is being applied.

In the old days of manual sugar coating, the coating fluid was ladled into the pan. With modern film coating, the coating is sprayed into the tablet bed, often with the

assistance of an air jet. Specialized sword and plough spray devices are available. Modern pan coating certainly represents a great improvement over traditional methods, but there are many in the industry who believe that for the most reproducible, controlled release coatings showing minimal defects and tablet-to-tablet variability fluidized-bed methods are, for many formulations, probably to be preferred.

Fluidized-Bed Coating

The fundamental principle behind fluidized-bed coating in general and the Wurster technique in particular is to suspend tablets in an upward moving column of warm air during the coating process. This minimizes tablet abrasion and unevenness of film distribution caused by tablet-to-tablet contact. The basic Wurster fluidized-bed coating chamber is essentially cylindrical in shape with the axis of the cylinder in the vertical plane and the top of the chamber having a convex exterior. Drying air is forced into the base of the cylinder with the coating materials being sprayed by an atomizer into the center of the base of the cylinder. An open-ended, inner cylinder acts as a partition guiding the air flow and the drug delivery units to be coated up the center of the unit across the inside of the roof and then down the outer space of the cylinder to the base of the unit where the spraying and drying cycle recommences. Each time a unit of product reaches the bottom of the coating chamber, it receives an additional dose of coating material. The solvent is removed when the unit rises up the center of the chamber and descends down the periphery. The coating is therefore built up in a series of incremental steps and thus, from a processing point of view, although not in terms of composition or function, the coating is multilayered. This cyclic process of spraying, drying, spraying, and drying can allow optimum conditions for gradual deposition of a coating of uniform thickness and structure. Batches of product from about 0.5 to 500 kg can be coated, and particles as small as 50 μm up to conventional tablets can be coated on this type of equipment. The original Wurster design has, in recent years, been significantly improved by, for example, introducing improved spray-nozzle design (Wurster HS) and improved airflow (Swirl Accelerator). There are various types of fluidized-bed coating equipment now commercially available (tangential spray, top spray, etc.). Different operators have their own preferences and, of course, the individual requirements of each controlled release coating formulation must be considered as well as equipment availability. Probably for controlled release coating products with aqueous coatings, bottom or tangential spray equipment is likely to be preferred. A detailed, comprehensive and authoritative review of Wurster and other fluidized-bed coating technologies has been published by Christensen and Bertelsen (29).

Compression Coating

It is possible to compress a coating around a preformed (relatively soft) core by using a special tablet press (e.g., Drycota by Manesty or Precoter by Killian). The process basically consists of compression of the core to give a relatively soft compact, which is then fed into a die of a tablet press that already has received half of the coating material. The core is centered within the die, the remainder of the coating material added, and the product then compressed (9). Compaction coating of tablets is not as common as perhaps some of us expected when the equipment was introduced. Perhaps there is still a need for coating mixtures of improved compressibility and flow. Certainly the very high production rates that can be obtained on a tablet press make this coating approach very attractive.

Melt Coating

For those controlled release coating materials that have a relatively low melting point and have acceptable thermostability, melt coating is possible. Materials applied in this manner include polyglycolyzed glycerides, hydrogenated vegetable oils, glyceride, ethylene glycol polymers, Carnauba wax, and synthetic wax. Top spraying, fluidized-bed coaters are probably the most commonly used type of equipment for this purpose, and operating temperatures as high as 200–250°C have been employed. Jozwiakowski, Jones, and Franz (30), and Jones and Percel (31) reviewed the processes.

Development of New Controlled Release Coating Products

If a new, controlled release coating product is developed, it is quite likely that it uses a synthetic polymer applied to the core as an aqueous dispersion, rather than a material of natural origin dissolved in an organic solvent. There are certainly advantages in terms of process validation, and likely response from regulatory agencies from the use of aqueous-based coatings of synthetic polymers. However, even with these systems, scale-up from laboratory to pilot scale to manufacturing scale may well require modification to either formulation or processing variables. Even though such changes may seem to be inconsequentially minor, it is still possible that they may cause significant changes to the release profile. Similarly, changes in formulation or processing variables that may occur during clinical trials can modify the behavior of the product (32). In a marketing approval document submitted to a regulatory agency, it may be necessary to justify reliance on clinical trials results that derive from formulations which are not entirely identical. Also, regulatory agencies require data demonstrating that the manufacturing process is validated (8). The FDA, for example, normally require data on at least three production-scale batches before marketing approval is given. It must be kept in mind that a formulation and process that may yield coated products commendably free of coating defects when prepared at the laboratory scale may at a later point in the development process exhibit coating defects such as those described by Rowe (33). Rudnic and Kottke (9, p. 379) have presented a useful table to use in diagnosing coating problems.

TRENDS IN THE FORMULATION AND MANUFACTURE OF COATED, CONTROLLED-RELEASE PRODUCTS

The trends of major importance in the current development of the formulation and manufacture of coated, con-

trolled release dosage forms may be divided into two categories. Firstly, there are trends common to the manufacture of all types of drug delivery systems and, secondly, there are trends specific to this type of product. In the first class we include:

1. More rigorous evaluation of data by the FDA before marketing approval is granted
2. Increasing interest and regulatory concern about validation and optimization

In the second group we include:

1. Greater knowledge of, and control over, enteric-coated drug delivery systems
2. Lively interest in coated products for colonic drug delivery
3. Improvements in both materials and equipment used in controlled release, coated products

Rigorous Evaluation of Data by FDA Before Marketing Approval Is Granted

The so-called Generic Drugs scandal (34) was a major factor in causing the FDA to become increasingly rigorous in its perusal of requests to market new pharmaceutical products. The introduction of the Application Integrity Policy, designed to discover or discourage fraud, has undoubtedly had significant effects on the research and development process in many companies. The requirement that the FDA District Office conducts a Preapproval Inspection before a new product can be marketed has caused some dramatic changes in both the pharmaceutical industry per se and also in contract houses that perform services to our industry in research, development, manufacturing, or product evaluation.

Optimization, Validation, and Product Evaluation for Coating Formulation and Processing

During the past decade or so, a number of most useful reports have been published describing various approaches to optimizing the selection of formulation and processing variables for coatings. Johansson, Ringberg, and Nicklasson (35) described the use of sequential, reduced factorial studies on the fluidized bed coating process for organic solvent–dissolved ethylcellulose. Voight and Wunsch (36) reported an optimization study for the coating of granules by spray-coating. Optimization of a Wurster-type spray-drying process, including different thicknesses of film, was reported by Bianchini and Vecchio (37). Losa and co-workers (38), Bodmeier and Paratakul (39), and Parikh and associates (40) have also described studies relevant to optimization of coated pharmaceuticals. The paper by Parikh and associates is of special interest to those wishing to optimize and validate the aqueous spray-coating process. Farivar and co-workers (41) conducted a factorial design-type optimization study of ethycellulose-coated microcapsules, which included the evaluation of dissolution as a response parameter. Hsieh and associates (42) have reported a novel approach to coating controlled release products in which the coating is incomplete, i.e., the drug delivery system has an open, uncoated face. Theoretical and experimental work indicated the potential of this approach. Brook and co-workers (43) have reported a separate study of the utility of partial coating in attaining controlled release. Optimization of this approach is possible. The Li team (44) have reported interesting studies of the rational development of a diltiazem, controlled release product in which a two-step layering process using a Wurster column is used.

Although there is often overlap between optimization and validation, and some workers tend to use the terms almost interchangeably, it is probably useful to maintain a distinction between their meanings. Optimization relates to studies of the influence of formulation and processing variables on the properties of a drug delivery system. Such studies often involve the application of empirical mathematical models to defining the interrelationship of such variables. Validation has taken on a special regulatory meaning and is now generally used to refer to the process whereby the sponsor of an NDA, ADA, or some other marketing approval document tries to convince a regulatory authority, such as the FDA, that the formulation and process are under control, that batch-to-batch variability is at an acceptably low level, and that the process is sufficiently robust so that minor perturbation of any one formulation or processing variable do not have a catastrophic effect on the product. Obviously, therefore, the validation of the coating segment of the manufacturing process normally involves evaluation of such basic parameters as coating temperature, coating times, equipment loading, and coating composition, together with such other values as may be important for an individual product. Before commencing a process validation study for a coating process, it can be helpful to examine published reports of other workers. However, some caution is advisable. Studies that might have been deemed acceptable by regulatory agency A in 1990 will not necessarily be regarded as acceptable by regulatory agency B in 2000.

Dietrich and Brausse (45) reported a validation study in which the effects of spray-drying temperature, air velocity, and relative humidity on release rates of a controlled release, coated product was explored. The starting point for any current validation study should be the definition of all functionally relevant attributes of the raw materials. Depending on the individual excipient, USP/NF, *Handbook of Pharmaceutical Excipients*, or the manufacturer's data may well provide most, if not all, of what is needed in this respect. However, depending on the nature and function of the excipient, it also may be prudent for the manufacturer of the drug delivery system to consider the use of additional test methods for excipients, intermediates, or final product. Such test methods may not only be useful during process validation, but may also be of value in routine testing of marketed product or during troubleshooting. For test data to be submitted to the FDA it is, of course, essential that the data be derived by objective test methods applied in accordance with an acceptable standard operating procedure. Thus, manual flexing of a cast polymer film between the two hands of an experienced polymer technologist, although perhaps of use in troubleshooting a

plasticization problem, is not likely to be regarded as a test of pivotal value for documentation submitted to the FDA.

Microscopic examination of films, either cast or in situ on the drug delivery system, can provide useful data on the fine structure of the coating, which may well be related to function. For example, Hasirci and colleagues (46) used optical and scanning electron microscopy to demonstrate the pore structure of a hydrophobic tablet coat. Evaluation of pharmaceutical polymer films using a confocal laser scanning microscope (47) may well become of increasing importance. Gopferich, Alsonso, and Langer (48) have published a most useful paper in which a variety of techniques—polarized light microscopy, electron microscopy, specialized chemical analysis, and elemental analysis—were employed to characterize coating structure. Pourkavoos and Peck (49) have characterized coated tablets using thermogravimetric analysis, differential scanning calorimetry, and mercury intrusion porisimetry.

Zhou and co-workers (50) have described an approach for determining tablet coating distribution from the weight distribution of uncoated and coated tablets. The authors indicate the potential value of the method in scale-up and validation studies.

Fukumori and associates (51) have published a most interesting paper in which a computer simulation of agglomeration in a Wurster coating process is described. Results were compared with experimentally generated data. Voigt and Wunsch (52) have reported the use of equipment for evaluating drug release from film-coated pellets. Wu, Jean, and Chen (53) have used scanning electron microscopy in their investigation of the relationship between coating structure and dissolution rate. Murthy and Ghebre-Sellasie (54) have investigated dissolution stability of coated pharmaceuticals. Pathak and Dorle (55) have examined dissolution of coated microcapsules; their results indicate that the release mechanism does not follow a simple process. Lee and Liao (56) have presented an interesting theoretical study on the effect of coating deformation on dissolution. Dissolution studies of a coated theophylline product have been reported by Lavasanifar and co-workers (57).

Malamataris and Pilpel (58) have studied compaction properties of coated products using the Heckal and the Cooper and Eaton equations to assist in the interpretation of the data. Since there is an increasing interest in the use of drug delivery systems that consist of controlled release, coated microcapsules incorporated into compressed tablets (that can, if desired, also be coated), there is substantial value in examining compaction behavior of coated products. The combination of a multiparticulate drug delivery and a compressed tablet yields a hybrid product that can have the advantages of the reliable controlled delivery of coated microcapsules and the convenience, stability, and patient acceptability of compressed tablets (59). Although not a large amount of experimental data pertains directly to the resistance of polymer-coated microcapsules to coating fracture during the process of tablet compaction, it seems likely that the following factors are of importance in delineating the extent of such fracture:

1. Shape, size, and other characteristics of the particles to be coated
2. Composition and thickness of the polymer coating applied to the particles
3. Nature of the tablet matrix and the ratio of coated particles to total tablet weight
4. Compression force applied when the tablet is produced

Chang and Rudnic (60) have shown that not all controlled release coatings applied to cubic KCl crystals are equally resistant to compaction fracture.

Enteric-Coated, Controlled Release Products

During the past decade or so there have been significant advances in the reliability of enteric coatings and their sensitivity to the pH at which drug is released. Agyilrath and Banker (61) indicated the various factors that influence the dissolution of enteric coatings:

1. The pK_a of the polymer
2. Total free carboxylic and content of the polymer
3. Nature of the core material
4. Ionic strength of the dissolution fluid
5. Coating thickness
6. Presence or absence of plasticizers and other nonenteric components in the coating layer

Porter and Ridgeway (62) used X-ray crystallography in an investigation of two enteric coating polymers, cellulose acetate phthalate and polyvinyl acetate phthalate, which were found to be essentially amorphous in nature. Lin and Kawashima (63) reported on the development of an enteric-coated formulation using cellulose acetate phthalate. Malfertheiner and co-workers (64) have described clinical evaluation of some enteric-coated aspirin products. The topic of how effective enteric-coated aspirin is in preventing blood loss caused by ulceration of the gastrointestinal tract is still a topic of lively interest. Ebel and associates (65) have applied an empirical mass transfer model for enteric coat dissolution that uses in vivo dissolution data to characterize the pH-dependent solubility properties of the polymer film and estimation of a mass transfer coefficient. The authors presented data comparing predicted and experimentally determined mass transfer coefficients. Taniguchi and associates (66) have described enteric coating of an enzyme. Lin and co-workers (67) have reported the enteric coating of a vaccine using cellulose acetate phthalate as coating material. Kiriyama and colleagues (68) have reported on the bioavailability of a tripeptide protease inhibitor, enteric-coated by hydroxypropyl methylcellulose phthalate. Duodenal absorption appears satisfactory. Arica and co-workers (69) have described successful enteric coating and evaluation of diclofenac sodium.

Coated Pharmaceuticals for Colonic Delivery

The controlled release of drugs in the colon has, in recent years, become a topic of great interest to many pharma-

ceutical scientists. This interest derives primarily from two causes. Firstly, there is a desire to develop therapies allowing specific delivery of drugs to the colon for the treatment of such conditions as ulcerative colitis. Secondly, the exciting possibility of using the colon as a portal entry for polypeptides and small proteins into the vascular system has stimulated many research groups to work in this field. (There are, of course, many matrix-type approaches also being examined for colonic drug delivery.) In earlier sections of this chapter, some references to coated drug delivery systems designed for drug release in the colon have been given (15–17,22). The references given hereafter are samples of some of the many varied strategies being employed for coated products for colonic drug delivery.

Van-den-Mooter and co-workers (70,71) have published two papers dealing with the use of copolymers of 2-hydroxyethylmethacrylate (HEMA) and methylmethacrylate (MMA), and terpolymers of HEMA, MMA, and methacrylic acid were synthesized in the presence of an azobenzene derivative for use as coatings for pharmaceutical products designed for colonic drug delivery. In vivo testing of the coating was reported. Ashford and Fell (72) have published a useful review of oral delivery of drugs to the colon. Niwa and co-workers (73) have described an ethylcellulose capsule that only ruptures and allows the drug within to be released when a swellable polymer, such as low-substituted hydroxypropyl cellulose, has expanded so much as to destroy capsule integrity. The lag time during which the pressure within the capsule is developing is such that the drug is released in the colon. The release time of the drug was mainly dependent on the thickness of the capsule. Wakerly and associates (74) have investigated the use of film coatings consisting of ethylcellulose and pectin for colonic drug delivery. In vitro dissolution studies in a flow-thru cell indicate the potential of this approach. Gardener and co-workers (75) have reported on the use of a pig model for studying colonic drug delivery systems.

Developments in Materials and Processing

Published studies, from both academia and industry, clearly indicate that much energy and skill is being devoted to improving existing coating materials and processing methods as well as exploring the potential of new materials and coating techniques. Fukimore and co-workers (76) described the potential of aqueous coats of ethylacrylate methymethacrylate 2-hydroxyethyl methacrylate copolymer. Park, Cohen, and Langer (77) have presented a most interesting report describing the use of aqueous coatings of an adsorptive water-soluble polymer polyethyleneimine for control of protein release. Bhagat and associates (78) have described a novel coating process leading to the formation of a uniform defect-free coating. This coating process, termed diffusion controlled interfacial complexation, involves a chemical reaction as part of the coating process. The technique can be applied to tablets that may be characterized by zero-order release. Ramade (79) has presented a review on the role of polymers in drug delivery that contains some useful data for any worker considering testing polymers for inclusion in drug delivery systems. Bianchini and Vecchio (80) have described the coating of dose units prepared by extrusion-spheronization. Pourkavoos and Peck (81) reported on the mechanism and extent of sorption of water following aqueous film coating. Ashton and co-workers (27) have described the design and evaluation of a coated drug delivery device intended for implantation in the eye. Deasy (82) has described, in a helpful review article, some recent advances in the design and evaluation of coated products.

Coating of pharmaceuticals as a method of assuring reproducible controlled release has come of age. The uncertainties about reliability of the natural-origin raw materials used for coating has been replaced by quiet confidence in the standardization of the synthetic materials now commonly used. The difficulties encountered during the conversion from organic solvents to water have been resolved, and prospects for future developments are good.

What factors should be taken into account when a pharmaceutical research and development group selects a formulation and processing strategy for a controlled release product? More specifically, what are the advantages of coated, vis-à-vis noncoated, products? It is not possible to give a precise answer to this question of general applicability. Obviously, the physicochemical, pharmacokinetic, and pharmacoeconomic attributes of the drug substance, together with such factors as the formulation group's experience in previous controlled release projects, the availability of equipment, and patents may all play legitimate roles in this type of decision. It would certainly be unreasonable to claim that coated, controlled release approaches should always be selected in preference to noncoated methods. However, there are certain strong advantages of coating procedures that do merit careful consideration:

1. The supply of a variety of reliable-quality excipients, which are acceptable to regulatory agencies
2. A successful track record of products being taken from research and development through pilot-scale to large-scale manufacturing with, in many cases, surprisingly few problems
3. Manufacturing methods that normally do not require the fabrication of any new manufacturing equipment but rely on well-tested manufacturing methods, which in many instances, are readily validated
4. The availability of a remarkably flexible range of formulation and processing variables, which can be used to custom build controlled release profiles for a plethora of purposes

MATERIALS USED IN CONTROLLED-RELEASE PRODUCTS

The following section presents data on some of the more common materials used in pharmaceutical, controlled release coatings. This list is not represented as a comprehensive statement of all materials which have ever been proposed for use in such products. Generally, the materials outlined in Table 1 and described in more detail in this section are used for one or more of three main functions: (*1*) provisions of the backbone structure of the coating, (*2*) facilitation or control over transport of drug across the

Table 1. Materials Listed as Components in Controlled Release Coating

Enteric coatings

A. *Cellulosic*
   1. Cellulose acetate phthalate (CAP)[a]
   2. Hydroxypropylmethylcellulose phthalate (HPMCP)[a]
B. *Noncellulosic*
   1. Methacrylic acid polymers[a,b]
   2. Polyvinylacetate phthalate (PVAP)
   3. Shellac[a]

Nonenteric coatings

A. *Cellulosic*
   1. Ethylcellulose (EC)[a]
   2. Hydroxyethylcellulose (HEC)[a]
   3. Hydroxypropylmethylcellulose (HPMC)[a]
   4. Methylcellulose (MC)[a]
   5. Sodium caroboxymethylcellulose (NaCMC)[a]
B. *Noncellulosic*
   1. Carnauba wax[a]
   2. Castor oil[a]
   3. Cetyl alcohol[a]
   4. Ethylene vinyl acetate copolymer
   5. Hydrogenated vegetable oils[a]
   6. Polyvinyl alcohol[a]
   7. Silicon-based polymers

Plasticizers

1. Benzyl benzoate[a]
2. Chlorobutanol[a]
3. Dibutyl sebacate[a]
4. Diethyl phthalate[a]
5. Glycerol[a]
6. Polyethylene glycol[a]
7. Sorbitol[a]
8. Triacetin[a]
9. Triethyl citrate[a]

[a]Monograph in USP23/NF18.
[b]Also used as nonenteric coatings.

membrane, or (*3*) plasticization of the coating. Coatings may well contain other components, such as colors or antioxidants, but specific attention is not given to components the primary function of which is not covered by one of these three categories. The functions of the first two classes is self-evident; however, it is appropriate to define what is meant by a plasticizer, since this term is sometimes used as a catchall to cover any excipient other than the primary coating material regardless of what function the excipient is expected to fulfill in the coating. A plasticizer, in terms of its functional definition, is an excipient, usually a low molecular weight organic solvent, added to coating material to assist in the processing by rendering the film more flexible. It is believed that such materials act by lowering the polymer glass-transition temperature. Plasticizers must be compatible, in terms of solubility parameter, with the polymer to which they are added to make it more flexible. Thus, plasticizers are not general purpose but must be chosen from materials that have been shown to be useful for a particular polymer.

Examination of the substances listed in this section indicates that a substantial number of the materials are cellulose derivatives. The review of chemically modified cellulose by Kumar and Banker (83) provides most useful background data in this area. Also, for more detailed information on polymers used in controlled drug delivery, the book edited by Tarcha (84) is likely to be of value. Also, for those excipients listed in the USP/NF, it is appropriate to check standards given in this official compendium. The materials described here are presented in a sequence which relates to function and alphabetical order. The list of suppliers for the various materials is not necessarily exhaustive.

Enteric Coatings: Cellulosic

Cellulose Acetate Phthalate (CAP). CAP is a cellulose ester referred to as cellacephate in BP and as Cellulosi acetas phthalus in Ph. Eur. It is soluble at pH values above about 6.0, and thus will tend to release drug toward the distal end of the small intestine. CAP is soluble in acetone and ethyl acetate. Plasticizers, such as triacetin or castor oil, are usually incorporated into this polymer. CAP is approved for oral use in the U.S. and European Union. It has been reported that CAP may be incompatible with ferrous sulfate, ferrous chloride, silver nitrate, and other inorganic salts. Also, since CAP has free carboxylic acid incompatibilities with acid-sensitive drugs (e.g., omeprazole) are possible. Application from aqueous dispersion may be possible (85). Suppliers include Eastman Kodak and FMC.

Hydroxypropylmethylcellulose Phalate (HPMCP). HPMCP is a monophthalic ester of hydroxypropylcellulose. The NF specifies two grades viz 200731 and 220824. BP refers to HPMCP as hypromelluse phthalate and Ph. Eur. as methylhydroxypropylcellusoi phthalus. It normally releases drug in the proximal part of the small intestine. Shin-Etsu (86) markets three grades that vary in molecular weight (higher values generally yield tougher films) and in the pH at which drug release normally occurs (from about 5.0 to 5.5). Plasticizers, such as castor oil, diacetin, diethyl and dibutylphthalate and polyethylene glycols, are commonly used with this polymer. Aqueous coating is possible (87). HPMCP is approved for oral use in the European Union, U.S., and Japan. Possible incompatibilities include strong oxidizing agents. Also, inclusion of more than about 10% titanium dioxide as a color may adversely affects physical stability or gastric resistance of the film coat. This material is also made by Eastman.

Enteric Coatings: Noncellulosic

Methacrylic Acid Polymer and Other Polymeric Methacrylates. There are three grades specified in NF18 of these materials, often referred to as polymeric methacrylates or Eudragit®. (Polyacrylates in NF18 are listed under ammonio methacrylate copolymer and methacrylic acid copolymer.) Eudragit E, which is soluble below pH 5.0, is used as a nonenteric coating. Eudragit L100-55 is used as an enteric coating for drug release at a pH of above 5.5, NE 30 D is used as a permeable, controlled release coating, RL 30 D is used in controlled release coatings where a high

permeability film is required. The manufacturer of Eudragit has published a guide to the use and properties of the whole range of Eudragits (88). Aqueous enteric coating is possible with Eudragit. By blending different grades of Eudragit, the formulator may be able to control release pH from about 5.5 to 7.0, and also the permeability of the film at constant pH (89). Lehman has presented authoritative reviews of polymethacrylate coating systems (90). Ghebre-Sellasie and co-workers (91) have reviewed the use of aqueous dispersions of Eudragits for controlled release. Eudragits have been used in topical, oral, parenteral, ophthalmic, and other types of pharmaceutical products.

Polyvinylacetate Phthalate (PVAP). PVAP is a reaction product of phthalic anhydrode and partially hydrolyzed polyvinyl acetate. As an enteric film coating it releases drug at pH values above about 5.0 so that absorption may occur throughout the small intestine. It is approved for oral use in the European Union and the U.S. Trade names include Opaseal®, pHthalvin®, and Sureteric®. The Colorcon literature (92) provides quite specific advice on processing conditions using, for example, an Acela-Cota. Porter (93) has described aqueous film coating using PVAP.

Shellac. Shellac is obtained from a gummy exudation produced by female insects. *Laccifer lacca Kerr*. Commercially, it is available in several grades (bleached, orange, white, etc.). Although its precise composition is both unknown and variable, its main component is a resin. The quality of this material shows significant variation, both with respect to source and storage time. The pH at which drug is released is about 7.0, which may well be somewhat too high for most enteric-coated products. Unless there is some specific requirement that an enteric coating shall be "natural," this material is *not* recommended for anyone developing a new product. Depending on the grade, it is acceptable for oral use in the European Union, U.S., and Japan. Suppliers include Classic Flavors, H.E. Daniel, Ikeda, and Ruger.

Nonenteric Coatings: Cellulosic

Ethylcellulose (EC). EC is a cellulose ether derivative with three hydroxy groups available for substitution. It is sometimes referred to as cellulose ethyl ether. Grades with differing degrees of substitution and/or molecular weight are available commercially. This polymer is virtually insoluble in water, but is freely soluble in organic solvents. Higher viscosity grades (e.g., Ethocel® 100) tend to produce tougher films. The permeability of ethylcellulose films can be increased by adding materials such as hydroxypropyl cellulose, polyethylene glycol, etc. (94,95). Plasticizers used with ethylcellulose include dibutyl phthalate, diethyl phthalate, dimethylphthalate, benzyl benzoate, cetyl alcohol, castor oil, and corn oil. Oxidative degradation can be reduced by adding stabilizers such as octyl phenol or butylated hydroxyphenal. An ultraviolet light absorber, such as 2,4,dihydroxybenzophenone (at about 0.7%) has also been used as a stabilizer. Aqueous dispersion such as Aquacoat® (FMC) and Surelease® (Colorcon) are available. The Surelease literature (96) contains a number of cookbook-type recipes. Ethylcellulose is accepted for oral use in many parts of the world. Suppliers include Colorcon, FMC, Dow, and Hercules.

Hydroxyethylcellulose (HEC). HEC, Ph. Eur. hydroxyethylcellulosum, is cellulose 2-hydroxyethyl ether. This water-soluble polymer, available under such trade names as Cellosize® and Natrosol®, is available in several grades (97) and is approved for oral use in the European Union, U.S., and elsewhere. Suppliers include Allchem, Amerchol, Aqualon, Sumisho, and Union Carbide.

Hydroxypropyl Methylcellulose (HPMC). HPMC (hypromelose, BP, hydroxypropylcellulosum, Ph. Eur.) is cellulose 2-hydroxypropyl methyl ether. HPMC is an excellent water-soluble film former, low viscosity grades, e.g., Methocel® HG (Dow), are commonly used in controlled release, coated pharmaceuticals. It is approved for oral and topical use in the European Union, U.S., and Japan. *The Handbook of Pharmaceutical Excipients* (10) reports that it may be incompatible with oxidizing agents, metallic salts, and ionic organics (98). Suppliers include Aldrich, Dow, Aqualon, Cortaulds, and Hercules.

Methylcellulose (MC). MC (methylcellulosum, Ph. Eur.) is cellulose methyl ether. It is soluble in water and organic solvents and used in a number of controlled release, coated products (99). It is approved (at varying levels) in the European Union, U.S., and Japan for use in oral, topical, buccal, vaginal, and parenteral pharmaceutical use. This material can be obtained from Dow.

Sodium Carboxymethylcellulose (NaCMC). NaCMC (carboxymethylcellulose sodium, USP/NF; carmelose sodium, BP; carboxylmethylcellulosum natricum, Ph. Eur.) is the sodium salt of cellulose carboxycellose ether. NaCMC is soluble in water and polar organic solvents (100). A number of different grades are commercially available with different degrees of substitution and viscosity. NaCMC is approved in the European Union, U.S., and Japan for dental, oral, topical, and parenteral use. Suppliers include Hercules and Cortaulds.

Nonenteric Coatings: Noncellulosic

Carnauba Wax. This material, sometimes referred to as Brazil Wax or Sera Carnauba, is a gummy exudate obtained from the Brazilian wax palm. It is photlabile. It has been accepted (for different purposes) for inclusion in foods and/or oral pharmaceuticals in the European Union, U.S., and Japan. Suppliers include Spectrum, Ruger, Aldrich, and Penta. Sterotex® is a trade name.

Castor Oil. There is an NF monograph (hydrogenated castor oil) for this material in which it is defined as mainly consisting of the triglyceride of hydrosteric acid. It has been used in topical and oral pharmaceutical products in the European Union, U.S., and Japan.

Cetyl Alcohol. The NF monograph defines cetyl alcohol as containing not less than 90.0% of cetyl alcohol with the

remainder consisting of related alcohols. It is referred to as alcohol cetylicus in Ph. Eur. *The Handbook of Pharmaceutical Excipients* (10) states that cetyl alcohol is incompatible with oxidizing agents and also suggests that it may cause allergic reactions. Cetyl alcohol has been used in topical and oral pharmaceutical products in the European Union, U.S., and Japan. Suppliers include Aldrich, Proctor and Gamble, Ruger, and Spectrum. This material is marketed under a number of trade names, including Dyhdag®, Lanette®, and Nacol®.

Ethylene Vinylacetate Copolymer. This material, sometimes referred to as EVA copolymer, is used as a coating material in transdermal products in the U.S. Suppliers include Allied Signal, Bayer, and Focus.

Hydrogenated Vegetable Oils. Oils derived from cottonseed, palm, and soybean are covered by this title. Trade names include Lubritab®, Sofisan®, and Sterotex®.

Polyvinyl Alcohol. This material is commercially available in at least three different viscosity grades. It is used in the U.S. in ophthalmologic, parenteral, topical, and oral products.

Silicon-Based Polymers. These relatively new materials for use in controlled release coatings are presently attracting considerable attention. They can be applied as a coating from aqueous dispersions (101).

Plasticizers

Benzyl Benzoate. Benzyl benzoate, which has been accepted for oral use in both the U.S. and U.K., has been used as a plasticizer for several cellulosic-type films. Suppliers include Ruger, Aldrich, and Spectrum.

Chlorobutanol. Chlorobutanol has many uses in pharmaceutical technology, including that of plasticizing some cellulose esters and ethers. It has been widely used in topical, oral, and parenteral pharmaceutical products throughout the world. Suppliers include R. W. Greef, Aldrich, and Ruger.

Dibutyl Sebacate. This plasticizer is used in a number of oral products. Suppliers include Union Carbide and Unitex.

Diethy Phthalate. This material has been used as a plasticizer (in the range of 10 to 30%). It is included in oral products in the U.K. and U.S. Suppliers include Allchem, Daihachi Chem., Eastman, Aldrich, and Spectrum.

Glycerol (Glycerin). This multipurpose excipient has been used as a plasticizer. It is used in many types of pharmaceutical products throughout the world. Suppliers include Ruger, Asland, Croda, Compton and Knowles, Proctor and Gamble, and Ellis and Everard.

Polyethylene Glycol. Polyethylene glycol (also known as Macrogol) is commercially available in a variety of molecular weight ranges. It is widely used in many parts of the world in parenteral, topical, and oral pharmaceutical products. Suppliers include BASF, Dow, duPont, Texaco, and Union Carbide.

Sorbitol. Sorbitol has many pharmaceutical uses including that of plasticization. It is available in many different grades and is included in many oral pharmaceutical products used in many parts of the world. Suppliers include Aldrich, ICI, Penta, Ruger, and Spectrum.

Triacetin. This plasticizer has been included in oral pharmaceuticals in both the U.K. and U.S. Suppliers include Aldrich, Eastman, and Ruger.

Triethyl Citrate. This plasticizer has been used in oral pharmaceuticals, including coated products prepared using aqueous coating methods. Suppliers include Aldrich, Penta, H.E. Daniels, and Sharon. Hydagen® is a trade name for this material.

BIBLIOGRAPHY

This chapter was previously published in *Drug Development and Industrial Pharmacy*, Volume 24, Issue 12, by Marcel Dekker, Inc. (November 11, 1998). Reprinted with permission.

1. T.R. Tice and S.E. Tabibi, in A. Kydonieus, ed., *Treatise on Controlled Drug Delivery*, Dekker, New York, 1991, p. 320.
2. U.S. Pat. 4,863,743 (September, 1989), D. Hsiao and T. Chou (to Key Pharmaceuticals, Inc., Kenilworth, N. J.).
3. A.C. Cartright and B.R. Matthews, eds., *International Pharmaceutical Product Registration*, Ellis Horwood, New York, 1994.
4. G.E. Peck, in G.S. Banker and C.T. Rhodes, eds., *Modern Pharmaceutics*, 3rd ed., Dekker, New York, 1995, Chapter 19.
5. B.A. Matthews, in G.S. Banker and C.T. Rhodes, eds., *Modern Pharmaceutics*, 3rd ed., Dekker, New York, 1995, Chapter 20.
6. A. Merrill, *Pharm. Technol.*, December, pp. 34–40 (1995).
7. I.R. Berry and R.A. Nash, *Pharmaceutical Process Validation*, 2nd ed., Dekker, New York, 1994.
8. E.M. Rudnic and M.K. Kottke, in G.S. Banker and C.T. Rhodes, eds., *Modern Pharmaceutics*, 3rd ed., Dekker, New York, 1995.
9. J.R. Schwartz and R.E. O'Connor, in G.S. Banker and C.T. Rhodes, eds., *Modern Pharmaceutics*, 3rd ed., Dekker, New York, 1995.
10. *Handbook of Pharmaceutical Excipients*, 2nd ed., Royal Pharmaceutical Society of Great Britain, London, and the American Pharmaceutical Association, Washington, D.C., 1994.
11. M. Ash and I. Ash, *Handbook of Pharmaceutical Additives*, Gower, Aldershot, England, 1995.
12. *Pharmaceutical Contract Support Organizations Register*, Drug Information Association, Washington, D.C., 1996.
13. B. Berner and S. Dinh, in A. Kydonieus, ed., *Treatise on Controlled Drug Delivery*, Dekker, New York, 1991, p. 2.
14. A.S. Achanta, P.S. Adusmili, K.W. James, and C.T. Rhodes, *Drug Dev. Ind. Pharm.* **23**, 441–450 (1997).

15. R.L. Botham et al., in G.O. Phillips, P.A. Williams, and D.J. Wedlock, eds., *Gums and Stabilizers for the Food Industry*, Oxford University Press, London, 1994, pp. 187–195.
16. S. Milojevic et al., *J. Controlled Release* **38**, 75–84, 85–94 (1996).
17. M. Saffran et al., *Science* **233**, 1081 (1986).
18. M. Donbrow and D.Y. Samuelov, *J. Pharm. Pharmacol.* **32**, 461–470 (1979).
19. U.S. Pat. 4,587,118 (May 6, 1986), C.M. Hsiao (to Key Pharmaceutical, Inc., Miami, Fla.).
20. T.A. Wheatley and C.R. Steuernagel, in J.W. McGinity, ed., *Aqueous Polymeric coatings for Pharmaceutical Dosage Forms*, 2nd ed., Dekker, New York, 1997, p. 50.
21. *USP 23 / NF18*, U.S. Pharmacopoeial Convention, Inc., Rockville, Md., 1994, pp. 1793–1799.
22. U.S. Pat. 5,482,718 9 (January 9, 1996), N.H. Shah, W.P. Kearney, and A. Railkar (to Hoffman-LaRoche, Inc., Nutley, N.J.).
23. V. Lenaerts and R. Gurny, *Bioadhesive Drug Delivery Systems*, CRC Press, Boca Raton, Fla., 1990.
24. H.R. Chueh, H. Zia, and C.T. Rhodes, *Drug Dev. Ind. Pharm.* **21**, 1725–1748 (1995).
25. A. Joglekar, C.T. Rhodes, and M. Danish, *Drug. Dev. Ind. Pharm.* **17**, 2103–2153 (1991).
26. N.A. Pappas and J.J. Sahlin, *Biomaterials* **17**, 1553–1561 (1996).
27. P. Ashton et al., *J. Ocul. Pharmacol.* **10**, 691–701 (1994).
28. J.G. Needleman, *Br. Dent. J.* **170**, 405–408 (1991).
29. F.N. Christensen and P. Bertelsen, *Drug. Dev. Ind. Pharm.* **23**, 451–463 (1997).
30. M.J. Jozwiakowski, D.M. Jones, and R.M. Franz, *Pharm. Res.* **7**, 1119–1135 (1990).
31. D.M. Jones and P.J. Percel, in I. Ghebre-Sellasic, ed., *Multiparticulate Oral Drug Delivery*, Dekker, New York, 1994, pp. 113–142.
32. D.C. Monkhouse and C.T. Rhodes, eds., *Drug Products for Clinical Trials*, Dekker, New York, 1997.
33. R.C. Rowe, in J.W. McGinity, ed., *Aqueous Polymeric Coatings for Pharmaceutical Dosage Forms*, 2nd ed., Dekker, New York, 1997, Chapter 12.
34. M.R. Hamrel, *Clin. Res. Drug Regul. Affairs* **14**, 139–154 (1997).
35. M.E. Johansson, A. Ringberg, and M. Nicklasson, *J. Microencapsul.* **4**, 217–222 (1987).
36. R. Voigt and G. Wunsch, *Pharmazie* **40**, 772–776 (1985).
37. R. Bianchini and C. Vecchio, *Boll. Chim. Farm.* **128**, 373–379 (1989).
38. C. Losa et al., *Pharm. Res.* **10**, 80–87 (1993).
39. R. Bodmeier and O. Paratakul, *Pharm. Res.* **11**, 882–888 (1994).
40. N.H. Parikh, S.C. Porter, and B.D. Rohera, *Pharm. Res.* **10**, 535–534 (1993).
41. M. Farivar, H.S. Kas, L. Omer, and A.A. Hineal, *J. Microencapsul.* **10**, 309–317 (1993).
42. D.S. Hsieh, W.D. Rhine, and R. Langer, *J. Pharm. Sci.* **72**, 17–22 (1983).
43. I.M. Brook, C.W. Douglas, and R. vanNoort, *Biomaterials* **7**, 292–296 (1986).
44. S.P. Li et al., *Pharm. Res.* **12**, 1338–1342 (1995).
45. R. Dietrich and R. Brausse, *Arzneimi. Forsch.* **38A**, 1210–1219 (1988).
46. V.M. Hasirci and I.L. Kamel, *Biomaterials* **9**, 42–48 (1988).
47. K. Carlsson et al., *Opt. Lett.* **10**, 53–55 (1985).
48. A. Gopferich, M.J. Alsonso, and R. Langer, *Pharm. Res.* **11**, 1568–1574 (1994).
49. N. Pourkavoos and G.E. Peck, *Pharm. Res.* **10**, 1212–1218 (1993).
50. J. Zhou, T. Williams, H. Swopes, and T. Hale, *Pharm. Res.* **13**, 381–386 (1996).
51. Y. Fukimora et al., *Chem. Pharm. Bull.* **40**, 2159–2163 (1992).
52. R. Voigt and G. Wunsch, *Pharmazie* **41**, 114–117 (1986).
53. J.C. Wu, W.J. Jean, and H. Chen, *J. Microencapsul.* **11**, 507–518 (1994).
54. K.S. Murthy and I. Ghebre-Sellassie, *J. Pharm. Sci.* **82**, 113–126 (1993).
55. Y.V. Pathak and A.K. Dorle, *J. Microencapsul.* **7**, 185–190 (1990).
56. D.J. Lee and Y.C. Liao, *J. Pharm. Sci.* **84**, 1366–1373 (1995).
57. A. Lavanisifar et al., *J. Microencapsul.* **14**, 91–100 (1997).
58. S. Malamataris and N. Pilpel, *J. Pharm. Pharmacol.* **35**, 1–6 (1983).
59. M.K. Kottke, G. Stetsko, S.E. Rosenbaum, and C.T. Rhodes, *J. Geriatr. Drug Ther.* **5**, 77–92 (1990).
60. R.K. Chang and E.M. Rudnic, *Int. J. Pharm.* **70**, 261–270 (1991).
61. G.A. Agyilrath and G.S. Banker, in P.J. Tarcha, ed., *Polymers for Controlled Drug Delivery*, CRC Press, Boca Raton, Fla., 1991, p. 37.
62. S.C. Porter and K. Ridgeway, *J. Pharm. Pharmacol.* **35**, 341–344 (1983).
63. S.Y. Lin and Y. Kawashima, *Pharm. Res.* **4**, 70–74 (1987).
64. P. Malfertheiner, A. Stanescu, W. Rogatti, and H. Ditschuneit, *J. Clin. Gastroenterol.* **10**, 269–272 (1988).
65. J.P. Ebel, M. Jay, and R.M. Beihn, *Pharm. Res.* **10**, 233–238 (1993).
66. M. Taniguchi, S. Tanahashi, and M. Fujii, *Appl. Microbiol. Technol.* **33**, 629–632 (1990).
67. S.Y. Lin, Y.L. Tzan, C.J. Lee, and C.N. Weng, *J. Microencapsul.* **8**, 317–325 (1991).
68. A. Kiriyama et al., *Biopharm. Drug Dispos.* **17**, 125–134 (1996).
69. B. Arica et al., *J. Microencapsul.* **13**, 699 (1996).
70. G. Van-den-Mooter, C. Samyn, and R. Kinget, *Pharm. Res.* **11**, 1737–1741 (1994).
71. G. Van-den-Mooter, C. Samyn, and R. Kinget, *Pharm. Res.* **12**, 244–247 (1995).
72. M. Ashford and J.T. Fell, *J. Drug Target.* **2**, 241–257 (1994).
73. K. Niwa, T. Takaya, T. Morimoto, and K. Takada, *J. Drug Target.* **3**, 83–89 (1995).
74. Z. Wakerly, J.T. Fell, D. Atwood, and D. Parkins, *Pharm. Res.* **13**, 1210–1212 (1996).
75. N. Gardener et al., *J. Pharm. Pharmacol.* **48**, 688–693 (1996).
76. Y. Fukimore et al., *Chem. Pharm. Bull.* **36**, 3070–3078 (1988).
77. T.G. Park, S. Cohen, and R. Langer, *Pharm. Res.* **9**, 37–39 (1992).
78. H.R. Bhagat, R.W. Mendes, E. Mathiowitz, and H.N. Bhargava, *Pharm. Res.* **8**, 576–583 (1991).
79. V.V. Ramade, *J. Clin. Pharmacol.* **30**, 10–23 (1990).

80. R. Bianchini and C. Vecchio, *Farmaco* **44**, 645–654 (1989).
81. N. Pourkavoos and G.E. Peck, *Pharm. Res.* **10**, 1363–1371 (1993).
82. P.B. Deasy, *J. Microencapsul.* **11**, 487–505 (1994).
83. V. Kumar and G.S. Banker, *Drug Dev. Ind. Pharm.* **19**, 1–32 (1993).
84. P.J. Tarcha, ed., *Polymers for Controlled Drug Delivery*, CRC Press, Boca Raton, Fla., 1991.
85. A.M. Ortega, Ph.D. Thesis, Purdue University, West Lafayette, Ind., 1977.
86. Shin-Etsu Chemical Company, Ltd., technical literature on HPMCP, 1993.
87. N.A. Muhammad, W. Boisvert, M.R. Harris, and J. Weiss, *Drug Dev. Ind. Pharm.* **18**, 1787–1797 (1992).
88. Eudragit literature, Rohm. Pharm. GmBh, 1990.
89. K.O.R. Lehman, *Drug Dev. Ind. Pharm.* **12**, 265–287 (1986).
90. K.O.R. Lehman, in J.W. McGinity, ed., *Aqueous Polymeric Coating for Pharmaceutical Dosage Forms*, 2nd ed., Dekker, New York, 1997, Chapter 4.
91. I. Ghebre-Sellasi, in J.W. McGinity, ed., *Aqueous Polymeric Coatings for Pharmaceutical Dosage Forms*, 2nd ed., Dekker, New York, 1997, Chapter 7.
92. Sureteric®, Colorcon, West Point, Pa., 1995.
93. S.C. Porter, in J.W. McGinity, ed., *Aqueous Polymeric Coatings for Pharmaceutical Dosage Forms*, 2nd ed., Dekker, New York, 1997, Chapter 9.
94. *Ethocel*, Dow Chemical Company, 1993.
95. *Ethocel Bibliography*, Dow Chemical Company, 1993.
96. Surelease technical literature, Colorcon, West Point, Pa., 1990.
97. B. Kovacs and G. Merenyi, *Drug Dev. Ind. Pharm.* **16**, 2302–2333 (1990).
98. G. Banker and G. Peck, *Drug Dev. Ind. Pharm.* **7**, 693–716 (1981).
99. N.M. Sanghavi, P.R. Kamath, and D.S. Amin, *Drug Dev. Ind. Pharm.* **16**, 1843–1848 (1990).
100. G. Banker et al., *Drug Dev. Ind. Pharm.* **8**, 41–51 (1982).
101. L.C. Li and G.E. Peck in J.W. McGinity, ed., *Aqueous Polymeric Coatings for Pharmaceutical Dosage Forms*, 2nd ed., Dekker, New York, 1997, Chapter 14.

See also MICROENCAPSULATION; MICROENCAPSULATION FOR GENE DELIVERY.

DIAGNOSTIC USE OF MICROSPHERES

MARGARET A. WHEATLEY
PADMA NARAYAN
Drexel University
Philadelphia, Pennsylvania

KEY WORDS

Biodegradable
Contrast agent
Diagnostic imaging
Imaging
Liposome
Magnetic resonance imaging
Microbubble
Microcapsule
Microparticle
Microsphere
Radiopaque
Therapeutic
Ultrasound

OUTLINE

X-Ray Contrast Agents
- Physical Principles
- Early CA for X-Ray Imaging
- Main Areas of Use of Microencapsulated X-Ray Agents
- Microcapsule Types Developed for X-Ray CA
- Contrast Imaging with Therapeutic Modalities

MRI Contrast Agents
- Physical Principles
- Early CA for MR Imaging
- Main Areas of Use for MRI CA
- Microcapsule Types Developed as CA for MRI
- Contrast Imaging with Therapeutic Modalities

Ultrasound CA
- Physical Properties
- Early CA for Ultrasound Imaging
- Main Areas of Use of CA in Ultrasound Imaging
- Microcapsule Types Developed as CA for Ultrasound
- Contrast Imaging with Therapeutic Modalities

Conclusion
Bibliography

In 1896 a physicist, Hascheck, and a physician, Lindenthanl, working together, injected a "heavy mixture" into the hand veins of a cadaver for X-ray analysis during autopsy (1). Although not involving microcapsules at this early stage, it was the beginning of what has become a large and rapidly developing enterprise to produce contrast agents (CA) that can be safely injected into a patient to assist the physician in diagnosis, by improving the quality of information obtained during noninvasive diagnostic procedures. The search for diagnostic CA has spread from X-ray to other imaging modalities, principally to magnetic resonance imaging (MRI) and ultrasound (2). Microencapsulated agents have been developed using a wide variety of methods, from liposomal entrapment (3) to use of biodegradable polymers (4). In addition, microencapsulated agents have been used in such areas as targeted imaging (5), biodistribution studies (6), therapy involving embolization (7), and combinations of these, such as concomitant drug delivery and imaging (8).

Microencapsulation of imaging agents offers many advantages that parallel those found with encapsulated drugs. Advantages of encapsulated imaging agents include increased stability, prolonged in vivo half-life, reduction of possible adverse side effects, concentration of the agent resulting in lower required doses, ease of administration, and the possibility of agent targeting. The next generation of contrast agents is expected to facilitate areas such as highly specific targeting and functional imaging.

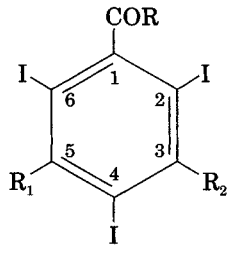
Each imaging modality has certain requirements to obtain good contrast, for example X-ray CA need to be radiopaque, whereas ultrasound CA need to produce a large impedance mismatch between themselves and the suspending fluid (usually blood). General requirements that encompass all agents include lack of toxicity, stability during imaging, ease of elimination from the body and most importantly, being amenable to intravenous injection, requiring the agent to be small enough to pass the pulmonary bed (preferably less than 6 μm diameter).

X-RAY CONTRAST AGENTS

Physical Principles

Contrast in X-ray imaging is produced by use of a radiopaque material that strongly absorbs incident radiation. At imaging energies, the absorption is due to electron density. Electron density relates to the number of electrons per atom multiplied by the number of atoms per volume, or approximately the density of the material. The most effective agents contain a heavy element such as the barium in barium sulfate ($BaSO_4$). $BaSO_4$ was one of the first agents to be used, and is still in use today, predominantly for gastrointestinal (GI) imaging. The most commonly used heavy element is iodine, generally covalently bound to an organic moiety such as in diatrizoate, which has three iodines on a benzene ring (Table 1.).

Table 1. Main Structures of Typical Monomeric Iodinated X-Ray CA

Basic monomer structure	Group	Structure/significance	
	I	Radiopaque marker	
	–COR	Ionic	Nonionic
		$R = Kat^+; Na^+; Meg^+$	$R = -N(R)_2$ amine carrying hydroxyl groups
		Affects osmolarity, solubility	
	$-R_{1/2}$	R-OC-HN-	R-OC-N- R
		Influences elimination and toxicity	

Early CA for X-Ray Imaging

Intravascular agents became available with the development of liquid iodinated media. There was a steady progression from insoluble oils such as Lipiodol, a halogenated poppy seed oil (9) to water-soluble ionic media such as meglumine (Meg^+) diatrizoate, also known as Renografin®. The early 1980s saw rapid and significant changes. The agents at the time were ionic monomers, which had high osmolarity, with an in-solution iodine to particle ratio of 3:2. The first change involved the development of ionic dimers such as ioxalgic acid (Hexabrix), which in-solution has an iodine to particle ratio of 6:2 and therefore a lower osmolarity for an equivalent iodine dose. The next improvement came with the development of nonionic agents (monomers such as Iohexol known as Omnipaque and dimers such as Iodixanol or Acupaque). The monomer and dimers showed a large reduction in both osmolarity and in the associated side effects together with even higher iodine to particle ratios. Improved toxicological characteristics are associated with key alterations in structure and properties, namely: the absence of acid groups ($-COO^-$), low osmolarity, symmetry of the molecule and a high number of $-OH$ groups. However, as the molecular size increases there is a concomitant increase in solution viscosity. Because of the high viscosity of many nonionic contrast agents, they are usually warmed to body temperature before intravascular injection. These more recent aqueous iodinated CA have been reviewed (10,11). Table 1 summarizes the main structures of monomeric iodinated agents, Table 2 summarizes the main structures of dimeric iodinated agents, and Table 3 reviews the salient properties of each.

Main Areas of Use of Microencapsulated X-Ray Agents

Microencapsulation of X-ray CA has advantages over use of unencapsulated agents, primarily in the area of targeting to the liver and embolization:

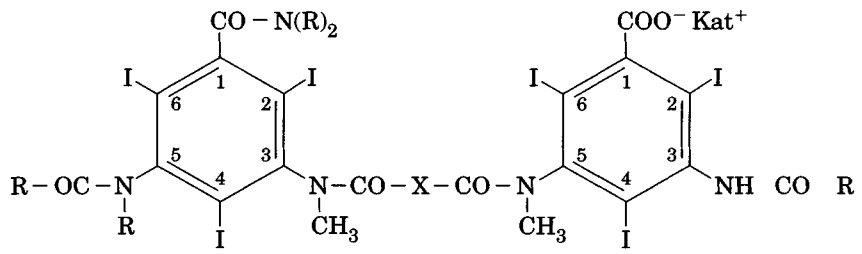
1. Computed tomography (CT) scans of the liver are currently one of the most important techniques for examination of metastatic lesions. Without the use of contrast, greater than 10% of focal hepatic lesions can go undetected (12). The use of iodinated CA such as meglumine diatrizoate, iothalamate, and metrizoate also does not, however, significantly improve attenuation differences between parenchyma and lesions, because the agent distributes uniformly throughout the vasculature and the interstitial spaces of the tissue (12). In addition, the agents are rapidly cleared from the liver, with optimal conditions for image acquisition occurring only within 2–3 minutes after injection, giving insufficient time for an entire liver scan. Particulates such as microencapsulated CA, however, are usually taken up by the reticuloendothelial system (RES) and with time become concentrated in the liver and spleen. Since few tumor cells have an RES, they are not enhanced by CA and appear as areas of decreased density (13–15). Microencapsulation concentrates the agent in the liver, and dramatically increases the residence time.
2. An additional area in which microencapsulated X-ray CA have been widely investigated is for the therapeutic use of transient or permanent embolization. Embolization is used for treatment of hemorrhages and hemoptysis, arteriovenous malformations, and malignant neoplasmas, and has been reviewed by Benoit and Puisieux (16). Puisieux holds a patent describing the use of cellulose embolization gel (17). Usually postoperative follow-up is conducted by angiography, but if the embolus possesses X-ray contrast properties, angiography can be avoided and the embolus itself can be followed (18–21).

Microcapsule Types Developed for X-Ray CA

Hydrogels. The use of poly(2-hydroxyethyl methacrylate) (PHEMA) microspheres to which a radiopaque marker was chemically attached was suggested by Horak

Table 2. Main Structures of Typical Dimeric Iodinated X-Ray CA

Basic dimer structure



Group	Structure/significance
X	$-CH_2$; $-CH_2-O-CH_2-$
R[a]	D,L, Threitol: $HOCH_2-CHNH-CHOH-CH_2OH$

[a]Ionic or nonionic depends on acid group substitution of both benzene rings

Table 3. Properties of Iodinated CA of 300 mgI_2/mL at 37°C

Class of CA	I_2:particle ratio	Typical osmolarity mOsmols/kg water	Viscosity (cps)
Ionic monomer	3:2	1,500–2,000	2.4–5.0
Ionic dimer	6:2	690	6.0
Nonionic monomer	3:1	580	4.6–5.7
Plasma	—	300	1.2
Nonionic dimer	6:1	272	9.0

et al. for preparation of contrast-containing embolic material (19). Using 3-acetylamino-2,4,6-triiodobenzoic acid attached to the reactive hydroxyl functions, they prepared microcapsules with greater than 40 wt % iodine content. However, the resulting capsules were hard, brittle, and nonswelling. Jayakrishman et al. attempted to circumvent these disadvantages by preparing highly porous microcapsules using suspension polymerization of 2-hydroxy-ethyl methacrylate in the presence of polymeric diluents such as poly(methyl methacrylate) (PMMA) and poly(tetraethyl glycol) (18). The radiopaque markers iothalamic and iopanoic acid were esterified to the free hydroxyl groups, yielding greater than 30 wt % bound iodine. The same group has prepared similar PMMA capsules by alkaline hydrolysis of ethylene glycol dimethacrylate cross-linked PMMA, which were then impregnated with $BaSO_4$ by precipitation using barium chloride and sodium sulfate solution. More than 70 wt % $BaSO_4$ was incorporated into the capsules, which demonstrated good contrast properties. A loading of 40–50 wt % was reported in PHEMA microspheres with a size range of 90 to 1500 μm, produced by a solvent evaporation method. Porosity was imparted to the microspheres by incorporation of the porogen sodium chloride (NaCl), and the $BaSO_4$ was trapped inside by cross-linking the capsule surface using γ-irradiation or homomethylene diisocyanate in *n*-heptane.

Polysaccharides. Starch microcapsules have been studied for many years as potential drug delivery and embolytic devices, and their synthesis has been extensively characterized (22). Rongved and co-workers describe the synthesis of the succinic acid derivatives of iohexol and iodixanol (monomeric and dimeric nonionic CA) bound to starch particles through an amino acid–ester bond (23). They used the method of Leegwater to prepare the starch particles from potato starch (24). Glycine derivatives had a shorter (4.5 h) half-life than alanine derivatives (8.6 h) in human blood serum, indicating that they would be superior CA for imaging of the liver. Mir et al. caused hepatic embolism by injecting starch microcapsules into the renal artery followed by injection of Renografin-60 in dog (25). They also noted a negative effect on the degradation rate of the starch capsules. Epenetos and co-workers used starch in a similar way to cause hepatic embolism, but this was to promote enhanced uptake of ^{131}I, which had been labeled with monoclonal antibodies to carcinoembryonic antigen (26). The iodine was used not only as the curative agent but also for imaging to monitor tumor uptake. Clinical improvement and a drop in circulating carcinoembryonic antigen was noted.

Another example of use of polysaccharide microspheres for embolization in conjunction with contrast material is

presented by Dion et al. (27) with the use of dextran microspheres (Sephadex G-25, 40–150 μm, Sephadex G-50, 100–300 μm, Pharmacia Laboratories) suspended in 10 mL of equal parts of saline and contrast material. The resulting mixture was isogravitational, which facilitated injection, and the microspheres reached more distally, producing more complete occlusion. Ethyl cellulose microspheres containing 20% $BaSO_4$ (5–301 μm) were used by Yang and others (28) as long-term peripheral emboli for percutaneous maxillofacial arterial embolization in dog. At 2 and 6 months the microspheres were neither degraded nor resorbed and the occluded peripheral arterioles were not recannulized. Absence of focal necrosis of the bones and soft tissue indicates that these microspheres have the potential for maxillofacial artery embolization without significant cosmetic problems.

Polyesters, Polyamines, Ethyl Ester, Polyanhydrides, and Polyurethane. Biodegradable poly(DL-lactide) microcapsules (0.5–3 μm) containing either ethyliopanoate or ethyldiatrizolate have been evaluated for detection of liver metastases using CT (4). High liver uptake was reported, and capsules were actively taken up by the Kupffer cells. The same group has also investigated the use of poly(benzyl L-glutamate) microcapsules (PBLG), which possess available side chains for modification with functional groups (5). Maximum uptake of the capsules in the liver was 15–60 minutes postinjection, and contrast effect lasted up to 2 hours. PBLG-estrone conjugates of the same capsules displayed potential in estrogen receptor targeted therapy. The liver was also the target of a study involving microcapsules prepared from iodipamide ethyl ester (6,29). Using rats, they showed that the agent was actively accumulated in the liver and contrast remained high for over 2 hours, then gradually cleared in approximately 2 days. Leander et al. used the VX2 carcinoma model in rabbit to show the efficacy of a biodegradable particulate of (1'-Ethyloxycarbonyloxy)-ethyl-5-acetylamino-3-(*N*-methyl-acetylamino)-2,4,6-triiodo-benzenecarboxylate, based on a prodrug ester design of metrizoic acid, which accumulates rapidly in the liver (30). Some 40% of small tumors (2–4 mm) were detected, compared with 27% for iohexol and 15% for controls. Mathiowitz et al. have investigated radiopaque ($BaSO_4$) microcapsules prepared from alginate and polyanhydrides for nonhepatic use in a study of GI transit of capsules (31). The method allowed the investigators to pinpoint regions of the GI tract where high concentrations of capsules adhered. Nonbiodegradable capsules such as those made from polyurethane have been used to prepare microcapsules of 150–1500 μm for embolization, which contained tantalum as an imaging agent (32). The high atomic number of tantalum renders it considerably more radiopaque than either barium or iodine, and it is well tolerated by the body. The capsule surfaces were modified with methacrylic acid in order to increase hydrophilicity and improve ease of passage through microcatheters. The lack of biodegradability makes the embolism more permanent.

Liposomes. Liposomes, bilayered vesicles composed of phospholipids entrapping an aqueous space, have been extensively investigated for drug delivery. Being nontoxic, easily injected, and readily taken up by the RES, they are also a natural choice for development as CA, especially to target organs such as the liver (33,34). The group of Seltzer has studied the use of multilamella vesicles containing diatrizoate (13,35,36). The vesicles were 1.4–2 μm in size and contained 55.5 mg of iodine per mL. Maximum spleen enhancement in rat was 6 times that for unencapsulated agent. Marked liver and spleen opacification was measured 60–90 minutes after injection. In another study from the same laboratory, the liver, bile ducts, gallbladder, spleen, and GI tract were enhanced with use of entrapped Iosefamate, which is excreted through the hepatobiliary system when it is released from the liposomes (37). Later, Seltzer's group showed that the phospholipid composition (phosphatidylcholine/cholesterol/stearylamine [PC/C/S] compared with distearoyl phosphatidylcholine/sphingomyelin [DSPC/SM]) but not the nature of the entrapped iodinated species (ionic[^{125}I] diazotriate or nonionic labeled iotrol) could influence the in vivo biodistribution and the in vitro permeabilities of the liposomes in the presence of serum (38). The leakage of ^{125}I activity was 2 to 3 times greater from PC/C/S liposomes and after injection into rat, the clearance half times for ^{125}I activity from the liver, spleen, and whole body were 4.4, 4.5, and 2.8 hours, respectively. For DSPC/SM the clearance was significantly slower, at 24.0, 18.4, and 17.2 hours, respectively. Other groups have used multilamella vesicles (MLV) (39) with similar results as well as large unilamella vesicles which have a higher entrapment capacity (40,41). An alternative approach employed liposomes made with labeled lipids. The use of brominated lipids (42) and iodocholesterol (43) has demonstrated poor opacification, but ethiodol was more successful (43).

Chylomicron Remnant-Like Polyiodinated Triglycerides. Weichert and his group at Michigan have reported on a particulate contrast agent which exploits the natural lipid transport system to specifically target the liver (44–48). The approach involves synthesis of a polyiodinated triglyceride (ITG) which is then assembled into the core of a synthetic chylomicron remnant by processing in a microfluidizer. The resulting microemulsion (ITG-LE) has a mean diameter of between 200 and 300 nm. Cholesterol was found to produce smaller, more stable emulsions, and inclusion of α-tocopherol helped protect the phospholipids that were present. The ITG-LE is metabolized in the hepatic parenchyma and eliminated through the bile. This allows thorough examination of the hepatobiliary system using standard or spiral CT. In a rabbit/VX2 carcinoma model, at CT enhanced with triglyceride (especially when combined with iohexol), sensitivity values and liver to lesion attenuation differences were greater with lower iodine doses than with iohexol or at CT during arterial portography.

Ethyl Ester Derivatives of Diatrizoic Acid. Another nanometer scale particle of 200–400 nm has been developed for blood-pool and liver imaging. It consists of ethyl ester derivatives of diatrizoic acid which are milled in the presence of different surfactants (49). The balance between

blood-pool and liver-spleen enhancement could be controlled by modifying the surfactant used. Complete elimination of the agent was within a week of administration. All formulations produced superior enhancement of the blood-pool and liver-spleen compared with iohexol, and persisted for at least 30 minutes after injection. These nanoparticles have also been used to advantage for passive targeting of the lymphatic system, with demonstration of intranodal architecture (50–52). In a 1995 study, Wisner et al. examined the anatomic and temporal distribution of lymph node opacification after subcutaneous, submucosal, or intestinal injection of this agent for indirect lymphography of subdiaphragmatic lymph nodes in normal dogs (53). CT examinations revealed excellent opacification and visibility of lymph nodes after contrast administration. Advantages include visualization of some internal architectural detail because of the nonuniform distribution in larger nodes. The mechanism is not known, but is presumed to involve particle uptake by lymph node macrophages.

Contrast Imaging with Therapeutic Modalities

Many innovations in particulate CA development have their routes in techniques developed for drug delivery. It is an attractive concept that a therapeutic agent could be injected at the same time as administration of the CA, and even that the mechanisms involved in imaging could facilitate and/or enhance drug or even gene delivery at a particular site. One example of concurrent CT imaging and treatment, the practice of chemoembolization (CE) using radiopaque microspheres, has already been mentioned for treatment of hemorrhage (16,17). Radiopaque emulsion of iodized oil (lipiodol) have also been described in the literature for this purpose. Rougier and co-workers report Phase I–II French trials for treatment of primary metastatic liver carcinomas with CE performed during hyperselective arteriography using gelfoam and hyperfluid lipiodol with interarterial adriamycin (54). Two Japanese groups reported favorable results, one using transcatheter hepatic subsegmental arterial chemoembolization (TAE) with iodized oil (Lipiodol-TAE) for small hepatocellular carcinomas (55), and the second using selective arterial infusion of styrene maleic acid neocarzinostatin/lipiodol for renal cell carcinoma (56). In both cases tumor growth was inhibited, and the treatment was followed closely with the contrast-enhanced imaging. However, other studies show that not all drug–CA combinations in chemoembolization are beneficial. Dehmer et al. showed that ipohexol impaired the action of fibrinolysis by streptokinase, urokinase, and by recombinant tissue-type plasminogen activator (57).

Investigators at Massachusetts General Hospital and Harvard Medical School have been exploiting the unique characteristics of micellar carriers for therapeutic and diagnostic agents (58,59). They synthesized amphiphilic AB-type block copolymers of methoxy poly(ethylene glycol) (MPES) (12 kDa) and poly[ϵ,*N*-(triiodobenzoyl)]-L-lysine which formed ~80 nm micelles in water, with a 44% iodine content. Rabbit studies showed that IV injection (250 mg iodine/kg) gave significant enhancement of blood-pool, liver and spleen, and a prolonged half-life of about 24 h. Biodistribution and CT-imaging studies in rats have been described (60). Significant and sustained enhancement of blood-pool (aorta and heart), liver and spleen were observed for a period of at least 3 hours. Figure 1 shows CT images demonstrating the effects of iodine-containing polymeric micelles in rat.

MRI CONTRAST AGENTS

Physical Principles

The nuclei of certain atoms can act like minute magnets and become lined up when placed in a magnetic field. MRI measures the energy required to change the alignment of the nuclei in a magnetic field. An external field is applied across a part of the body to align the magnetic nuclei in the longitudinal direction, and a radio wave is broadcast into the tissue in the transverse direction, which induces some of the magnets to tilt over, usually by either 90° or 180° depending on the duration of the pulse (61). The radio wave is turned off and after some time the nuclei retransmit the signal at the same frequency as it was received, as they return to their equilibrium orientation. The time required for the net tissue magnetization vectors to return to equilibrium conditions in the external magnetic field after a 180° resonant frequency pulse is known as the T_1 or longitudinal relaxation time. T_1 is also known as the spin lattice relaxation time since during the relaxation process relaxation energy in the form of heat is lost through molecular collisions to the surrounding tissue (lattice). A second parameter T_2, the transverse or spin-spin relaxation time, is a measure of a dephasing phenomenon taking place between the protons as they precess about the transverse plane. It is somewhat analogous to the tone that one would hear if a number of tuning forks, all with a note close to but slightly different from each other, were struck simultaneously. There would be an initial loud tone, followed by a waxing and waning muted tone that was rapidly damped due to the destructive interference of the different wave forms. Following a 90° resonant frequency pulse the protons precess together in the x–y plane. If all the protons had exactly the same resonant frequency they would produce a strong signal proportional to the number of nuclei. Small differences in resonant frequency, however, result in a rapid dephasing of the signal with a time constant T_2. T_2 is a measure of how long the substance maintains the transverse magnetization, which is perpendicular to the external field (61). T_2^* is an effective time constant governing decay in an inhomogeneous external field, and it is smaller than T_2.

In MRI the majority of the signals arise from protons of cellular water and lipids. Natural contrast is a direct result of inherent differences in the various microenvironments of the constituent protons. CA can alter this contrast by affecting any of three parameters, T_1, T_2 and ρ, the nuclear spin density. The majority of CA for MRI change T_1 and T_2, although the spin density has been shown to be changed by injection of furosemide, olive oil, or clomiphene (62).

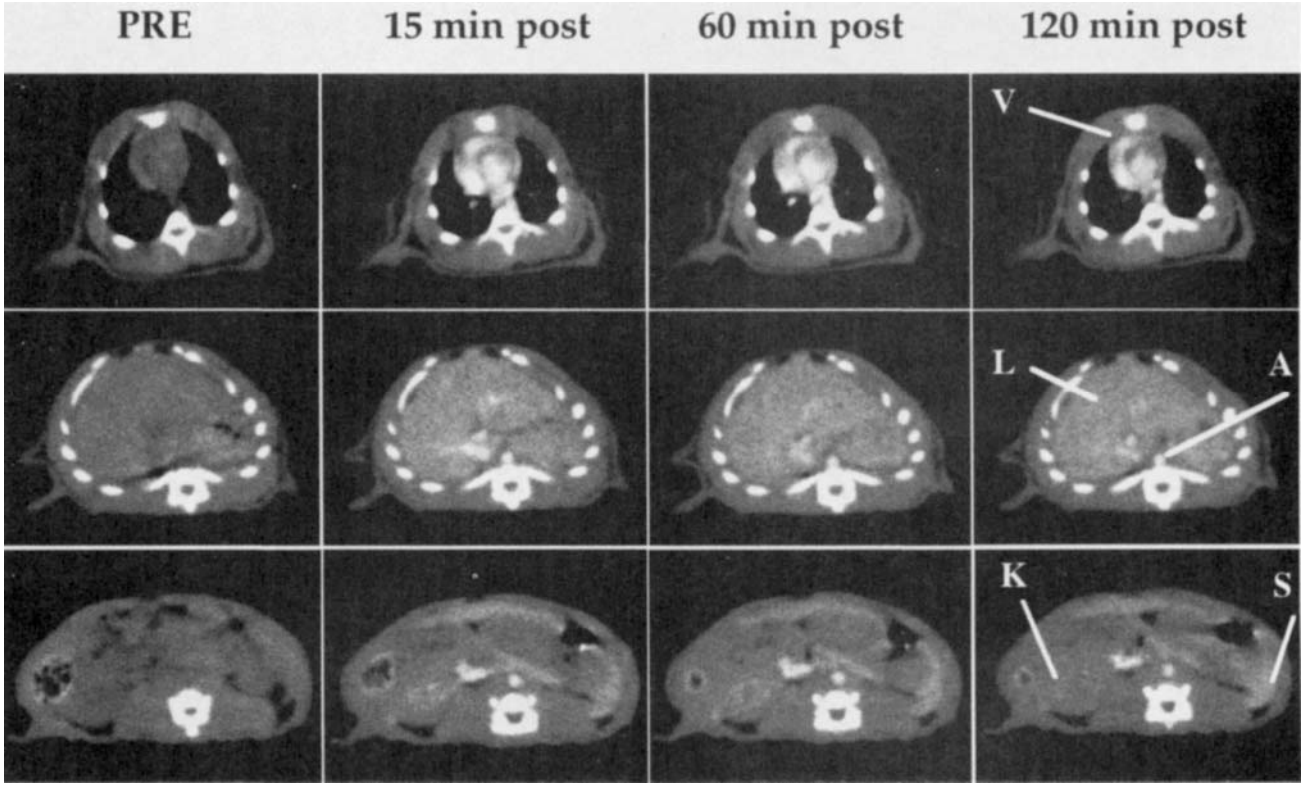


Figure 1. CT images demonstrating effects of iodine-containing polymeric micelles in various rat organs (V, ventricle; L, liver; A, aorta; K, kidney; S, spleen) at different postinjection times. MPEG-iodomicelles were injected into the rat tail vein at a dose of 170 mg I/kg. *Source:* From Ref. 60 with permission of the publishers.

There are three types of CA for MRI: paramagnetic, superparamagnetic, and ferromagnetic. Addition of small amounts of paramagnetic material to the microenvironment of the proton brings about a contrast effect. Paramagnetics affect both T_1 and T_2. At the low concentrations usually used in imaging the T_1 shortening effect predominates and the change in tissue is best seen on T_1-weighted images. The magnetic fields induced in paramagnetics by the external field are additive to that of the applied field and the increased signal intensity is known as positive enhancement. Paramagnetics also produce local magnetic inhomogeneities and thus shorten T_2 relaxation times as well. At high concentrations such as would be found in the urine, the T_2 shortening predominates and T_2-weighted images are preferred. Certain metals, including manganese(II), iron(III), and gadolinium(III), and stable free radicals such as nitroxides and melanin contain unpaired electrons which impart strong paramagnetic properties. Paramagnetic ions have magnetic dipoles 1,000 times that of protons, and the predominant mechanism of proton relaxation is through dipole–dipole interaction with the surrounding spin lattice (62). Appropriately fluctuating local magnetic fields generated in the magnetic spin lattice by random rotational and translational motions promote relaxation. Unpaired electrons can greatly influence relaxation times because the magnetic moment of an electron is 657 times larger than the magnetic moment of a proton. The increase in relaxation rate is proportional to the concentration of the paramagnetic agent and to the square of the magnetic moment and inversely proportional to the sixth power of the distance between the paramagnetic center and the proton to which it is bound (11). The formula for relaxation rate is given by Gadian and Bydder (63):

$$1/T_{1,\text{obs}} = 1/T_{1,\text{o}} + 1/T_{1,\text{p}} \qquad (1)$$

where $T_{1,\text{obs}}$ is observed relaxation time, $T_{1,\text{o}}$ is intrinsic relaxation time, and $T_{1,\text{p}}$ is the contribution the CA makes to the relaxation rate.

Early CA for MR Imaging

First-row transition metals with partially filled 3d electron shells and lanthanide metal ions with partially filled 4f electron shells are possible paramagnetic ions. Mn(II), Cr(III), and Fe(III) have 5, 3, and 5 unpaired 3d electrons, respectively; however, Gd(III) of the lanthanides with 7 unpaired electrons has been found to be most effective. Because of its toxicity, gadolinium has to be chelated to, for example, diethyltriamine pentaacetic acid (DTPA), making Gd DTPA. The first clinically approved agent in the U.S. was gadopentetate dimeglumine (Magnevist®; Berlex Laboratories, Cedar Knolls, NJ), approved in 1988. The agent

moves from the blood vessels to the tissue by diffusion, except in the brain and spinal cord. The plasma half-life is 90 minutes, and it is excreted intact by glomerular filtration (64). The structure is shown in Figure 2. The chelating agent on its own is also toxic, because of its high affinity for cations.

Development of paramagnetic MRI contrast agents has followed a similar pattern to that for X-ray agents, with a search for less ionic chelating moieties. Some examples include Gd DTPA-BMA (Omniscan; Salutar, Sunnyvale, CA) and Mn-DPDP (Salutar, Sunnyvale, CA), Gd-DOTA meglumine (Gadoterate; Guerbet Laboratories, Aulnay-sous Bois, France), Gd-BOPTA (Bracco, Milan, Italy), EOB-DTPA (Schering, Berlin, Germany), and HP-DO3A (Gadoteridol; Squibb Diagnostics, Princeton, NJ). The more lipophilic agents are excreted by both the kidney and liver.

Ferromagnetic materials consist of a crystalline array of many paramagnetic elements that behave in synchrony when placed in an external magnetic field. A subset of these are superparamagnetic particles that lack magnetic memory. Ferrites and magnetites (Fe_3O_4) belong to this class. The array of paramagnetic elements produces a localized disturbance in magnetic field homogeneity, which affects the proton relaxation, causing a rapid dephasing of the spins. Superparamagnetic and ferromagnetic agents reduce T_2 relaxation much more than T_1 relaxation, which can be a disadvantage because it causes a decrease in signal intensity on spin-echo images (65). Although T_2 is reduced, their main reduction is in T_2^*, hence the effects are best observed on gradient echo sequences where T_2^* effects are retained. Dysprosium and its chelates have a similar effect. Ferromagnetics are referred to as negative enhancers because they cause a local blackening of the image in T_2-weighted and gradient-echo pulse sequences. Both superparamagnetic and ferromagnetic agents are in the form of particulates and are therefore not suitable for neuroradiological uses. Superparamagnetic agents have a smaller particle size; however, if ferromagnetics are reduced in size to below 10 nm they lose their permanent magnetic characteristics and become superparamagnetic. It is ferro- and superparamagnetic particles that have been the subject of the majority of microencapsulation research in MRI.

The state of the art in MRI contrast has been reviewed (66–68). Specific areas of contrast use have been reviewed for blood-pool imaging (69), metastases to the liver (70), myocardial perfusion (71), cerebral perfusion (72), pediatric neuroimaging (11), and the brain (73).

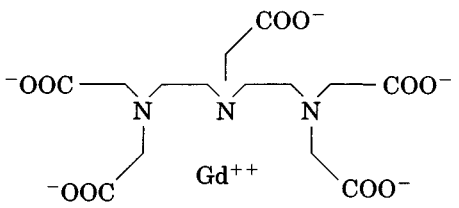


Figure 2. The structure of Gd DTPA.

Main Areas of Use for MRI CA

Brasch (66) defines seven main areas of use for MRI CA. Many parallel areas of use for CT agents and current research are ever expanding the applicability of CA in MRI. The main areas of all contrast use in MRI are briefly reviewed here.

1. Extracellular agents (small molecular weight agents such as Magnevist described previously) comprise the gadolinium-based agents and are used primarily to define extracellular fluid spaces and defects in the blood-brain barrier on T_1-weighted images (66,72). After intravenous injection, the agents diffuse from the blood vessels into the surrounding extravascular spaces. Encapsulation of these agents can increase the blood-pool and total residence time and alter the biodistribution.
2. Blood-pool and capillary-integrity markers rely on high (>20,000 daltons) molecular weight agents (69) which escape only slowly from the vascular compartments. Approaches to macromolecular contrast media (MMCM) include ex vivo labeling of blood cells or plasma components or use of modified agents in the form of macromolecules (albumin-$(Gd\text{-}DTPA)_{30}$, dextran-$(Gd\text{-}DTPA)_{15}$, polylysine-$(Gd\text{-}DTPA)_{30}$), colloids, and liposomes. They have been used to define tissue ischemia and/or the adequacy of reperfusion procedures in the heart, lungs, kidney, and brain. One advantage of these agents is that they can be synthesized with a high number of reporter groups (i.e., the paramagnetic agent such as Gd).
3. MRI is used in the heart to assess myocardial perfusion (71). This is not possible without the use of CA. Newly developed ultrafast imaging sequences are expected to greatly assist in this measurement.
4. In the same way as in CT, there is extensive research into developing CA for the liver (70). Agents can be directed either to the hepatocytes or the RES. Certain paramagnetic complexes of Fe(III) and Gd(III) have been shown to be taken up by hepatocytes through a nonspecific anion transporter and subsequently secreted in the bile (74). Other agents with hepatobiliary excretion include Gd-BOPTA, Gd-EOB-DTPA and Mn-DPDP. Superparamagnetic iron oxide particles coated with asialoglycoprotein (ASG) have also been specifically targeted to normal hepatocytes (75). Particles that are targeted to the RES include paramagnetic liposomes (76) and dextran-coated superparamagnetic iron oxide particles (77). Enhancement is achieved in less than an hour with iron oxide particles and lasts for more than a day. This advance has reduced the size threshold for detection from a 10 mm lesion down to 3 mm. Some concerns do, however, exist about reports of hypotension at high CA doses.
5. Again, by the same mechanisms as with CT agents, very small particles can travel to the lymph and act as CA. One route is via subcutaneous injection (78); the more usual route is intravenous injection (79). Weissleder (79) used ultrasmall superparamagnetic

iron oxide particles (USIPO) with a mean diameter of 11 nm. Phagocytic uptake in the normal nodes results in low signal intensity in T_2-weighted MRI, compared to high intensity in nodal metastases.

6. Tumor-specific and antigen-specific enhancement is also under investigation. Studies report on the attachment to monocrystalline iron oxide nanoparticles (2.9 nm) of antimyosin Fab fragment directed against infarcted myocardium and human polyclonal immunoglobulin G directed against abscesses, and of monoclonal anti-Burkitt lymphoma antibody attached to Gd-DTPA (66). An interesting targeted molecule has been investigated which uses the observation that phosphate-containing compounds accumulate in bone and soft-tissue calcifications (80). In this study, gadopentetate dimeglumine modified with 1-hydroxy-3 aminopropane-1,1-diphosphonate was used to image infarcted myocardium with a high degree of success.
7. Finally, agents are being developed for use in the GI tract. Positive enhancers have been administered both orally and rectally in the presence of mannitol to increase the osmolarity and minimize dilution by intestinal contents, for example Gd-DTPA (81). An inexpensive agent consisting of ferric ammonium citrate (Geritol) has also been suggest for oral and rectal administration (66,82). In other studies negative enhancers have been used in the bowel and including $BaSO_4$ (83), kaolin (84) and perfluorooctylbromide (Imagent®; Alliance Pharmaceuticals, San Diego, CA) (85). Iron oxide particles and crystalline iron oxide on an organic polymer matrix have also been studied (86). An oral agent consisting of 3.5-μm-size sulphonated-divinylbenzene copolymer coated with superparamagnetic iron oxide has been developed by Nycomed and reported on by Van Beers and his group (87). They reported significantly improved delineation of lesions, small bowel and paraaortic regions post contrast. An agent consisting of 2–5 μm magnetic albumin microspheres (MAM) has been shown to be orally stable over 24 hours in rabbits and dogs (88). Possessing a larger magnetic moment than paramagnetic agents, the transverse relaxation rate (R2) can be as much as 40 times the longitudinal rate (R1). MAM cause marked signal loss in the stomach and small bowel on both T_1- and T_2-weighted pulse sequences. They are promoted as reducing motion artifact throughout the GI tract. Undoubtedly the best tasting oral CA that has been proposed recently is blueberry juice, which is high in Mn(II) and acts as a positive CA on T_1-weighted images and negative CA on T_2-weighted images (89).

Microcapsule Types Developed as CA for MRI

Macromolecular Contrast Media. MMCM inhibit diffusion of the imaging species and slow renal filtration, greatly reducing the stringent requirement for timing of image acquisition and permitting imaging of multiple body regions without need for further dosing (90). The majority of the agents being investigated involve chemical linking of chelated imagers such as Gd-DTPA to either exogenous macromolecules such as poly-L-lysine, and dextran, or endogenous blood components such as red blood cells or human serum albumin. The resulting complexes have very high dosing efficiency due to the multiplicity of imaging moieties per molecule (>60). In addition, the combination with a macromolecule slows the molecular rotation so that it more closely resembles that of water.

Poly-L-lysine is an attractive candidate for MMCM because of the large number of ϵ-lysine residues available for substitution with either agent or a targeting moiety. Low molecular weight polymers (e.g., PL-Gd-$DTPA_{40}$) are not satisfactory because of rapid clearance (91). Higher molecular weight agents have longer circulation times, but also demonstrate renal accumulation, which could limit their use (92). PL-DTPA has been investigated for cardiac (93–95), pulmonary (96–99), and renal (100,101) use. Grandin et al. (101) compared the imaging characteristics of Magnevist with the Schering poly-L-lysine conjugate using T_1-weighted spin-echo images in the rat hepatic tumor model. Peak intensity of the MMCM was reached at 3 minutes and remained high at 60 hours, whereas at 3 minutes tumor-to-liver contrast of the Magnevist was insignificant and baseline was already achieved by 60 hours. The same group conducted a similar study to investigate reperfused ischemia of the rat intestine (102). They reported that contrast between reperfused and normal intestine was higher on PL-DTPA-enhanced images than on unenhanced or Gd-DTPA-enhanced T_1 and T_2-weighted images. Because previous studies showed that no enhancement was evident during total vascular occlusion, they suggest this as a potential method of detecting reperfused ischemia of the intestine.

Weissleder et al. (103) studied the uptake of partially derivatized Gd-DTPA by the adrenal glands, based on the theory that positive charge is essential for adrenal uptake. The highest uptake was in the liver, followed by the adrenal glands and the spleen. At two hours the adrenal uptake of the partially derivatized agent was 3.4 times higher than the fully derivatized one. The same group has synthesized and evaluated the long-circulating copolymer, methoxy poly(ethylene) glycol-succinyl-(*N*-ϵ-poly(L-lysyl) DTPA) (MPEG-PL-DTPA) (52,104–106). The agent was found to be nontoxic, and although it binds fewer Gd per molecule compared with PL-Gd-DTPA with the same degree of polymerization, this is partially compensated for by an increase in atomic relaxivity, (R_1 = 12 (mmol s 1)$^{-1}$ for PL-Gd-DTPA and R_1 = 18 (mmol s 1)$^{-1}$ for MPEG5-PL-Gd-DTPA at 20 MHz, 37°C. High-quality, high-resolution images were obtained in rabbit and rat using a combination of three-dimensional time of flight angiographic technique and MPEG-PL-Gd-DTPA injection. Postinjection images clearly show blood vessels that were absent in precontrast images (69). Equally significant results were obtained in pulmonary magnetic resonance angiography and imaging of tumor neovascularity. The copolymer has also been used for passive targeting to solid tumors (106). A group at Cal Tech has even used poly-L-lysine with bound DNA and Gd-DTPA to develop a particle that delivers both the transfecting gene and an MRI CA to enable the monitoring of DNA for gene therapy in real time (107). PL-Gd-

DTPA has also been conjugated with antihuman antibodies to demonstrate increased signal intensity from experimental human tumors implanted in nude mice (108). Finally poly(glutamic acid, lysine, tyrosine) (PEKY) has also been used to coat superparamagnetic particles followed by attachment of carcinoembryonic antigen (final radius ~50 nm) for tumor-specific targeting (109).

Some groups have chosen dextran linked to Gd-DTPA to increase the CA molecular weight and prolong its residence time in the blood (110,111). Blustajn and co-workers investigated carboxymethyldextran-Gd-DTPA (Guerbet, Aulnay, France) to measure liver blood volume with T_1-weighted spin-echo sequences (112). They reported remarkable stability of signal enhancement over time, allowing the summation of a large number of measurements. However, not all reports involve chemical linkage of the high molecular weight polymer to the chelate. Simple mixing of dextrose or poly(ethylene glycol) 3350 or 8000 has been shown to improve the relaxivity of Gd-DTPA and Gd-HP-DO3A, and this improvement followed a geometric function of concentration (113).

Albumin-labeled Gd-DTPA CA have been reported with long half-lives (3.6 h) in rats, and have been found to be more potent than the corresponding individual chelates (114–117). However their usefulness is limited due to concerns over cardiovascular toxicity, immunogenicity, and retention of Gd for long periods of time in the liver and bone (118). More recently a related agent, MS-325 (Epix Medical, Inc, Cambridge, MA) has been described in preclinical evaluations in rabbits and nonhuman primates (119). MS-325 consists of a diphenylcyclohexyl group attached to Gd chelated by a phosphodiester linkage which binds reversibly to serum albumin. A 5 to 10 times higher reduction in monomolecular tumbling of the chelate upon binding compare to Gd-DTPA is reported. The reversible binding results in a small volume of distribution, increased plasma half-life, and reduced extravasation while preserving efficient excretion due to the reversible nature of the binding.

Starch Microspheres. Starch has been used to microencapsulate superparamagnetic oxide particles (SPIO) and USPIO, usually for passive targeting to macrophages (120–123). Nycomed (Oslo, Norway) has been active in this area. Magnetic starch microspheres (MSM), with a mean size of 0.3–0.4 μm have been shown to be well suited as T_2 CA at 0.5T and 1.5T using conventional spin-echo and fast turbo spin-echo (120). The same MSM were used by Kreft to differentiate diffuse and focal splenic disease (121). One hour after injection of 20 μm/kg, lymphomatous spleen showed significantly ($P < 0.001$) reduced enhancement relative to normal splenic tissue. Diffuse lymphoma (signal-to-noise ratio, SNR: 10.3 ± 1.7) could easily be differentiated from control animals (SNR: 5.5 ± 0.6) on T_2-weighted images. Rongved and co-workers used Gd-DTPA-loaded starch particles cross-linked with epichlorohydrin and found the in vitro spin-lattice relaxivities were 40–260% higher than that for Gd-DTPA (122). The relaxivity increased with decreasing Gd content. The in vitro degradation rate of the particles decreased with decreasing Gd content, with half-lives of from 24 h with 12.2 wt % Gd(III) to 0.67 h with 1.1 wt %. The exact mechanism was not clear. In in vitro studies, MSM have been shown to accumulate in macrophages were they were localized to the lysosomes (123). The accumulation was highly competed by regular microspheres, suggesting a receptor-mediated mechanism. In contrast to unencapsulated SPIO, the MSM were found to be nontoxic to the cells. Colet et al. (124) expanded on this work using perfused rat liver to show that binding to Kupffer cells is caused by membrane lectins.

Dextran-Coated SPIO. Dextran-coated SPIO have been widely studied, especially for targeted CA. Many patents have appeared such as that assigned to Advanced Magnetics, Inc. (125), and monocrystalline iron oxide from Weissleder (126). A French group at Pouliquen's laboratory has used dextran-coated SPIO encapsulated in isobutyl cyanoacrylate to target the liver and spleen, where they report a sevenfold decrease of T_2 relaxivity rate and a halving of the R_2/R_1 ratios (127). Weissleder's group at Massachusetts General have studied the effect of particle surface on the biodistribution and have synthesized targeted CA including agents to pancreatic receptors (128–130). Dextran-coated SPIO with diameters of 4.4–6 nm were modified with poly-L-lysine (PL), and in some cases the PL was then succinilated. They found that negatively charged and neutral particles had the longest circulation times. Linking cholecystokinin to 430 nm spheres by a noncovalent method resulted in a 50% drop in blood half-life to 20 minutes, and shortened in vitro T_2 relaxation times (129). Pancreatic T_2 relaxation times decreased in a dose-dependent fashion as demonstrated by ex vivo imaging. Similar dextran-coated SPIO were demonstrated to be taken up by receptor-mediated endocytosis when opsonized with albumin (130). In angiography, their dextran-coated monocrystalline iron oxide (MION-46) nanoparticles resulted in a three to fourfold increase of aortic SNR and markedly improved the quality of images of the vasculature of the lungs, abdomen, and extremities (131). This was attributed to the long plasma half-life (180 minutes in rats). Long-circulating iron oxide particles for MRI have been reviewed (132). The particles are particularly useful for lymph node imaging, as seen in Figure 3 which shows



Figure 3. SPGR images of the pelvis before (left) and 24 h after (right) intravenous administration of long-circulating iron oxide particles in a patient with primary prostate cancer. The lymph node metastasis (white arrow) is of much higher signal than the contralateral normal lymph node (black arrow). *Source:* Courtesy of Dr. R. Weissleder.

the spoiled grass (SPGR) images of the pelvis before and after MION injection. The same MION agent has recently also been described for use in in vivo cell trafficking studies (133). One advantage of the use of MION lies in the fact that the cells internalize the label, leaving the cell surface receptors free for adhesion. Roughly 5×10^6 particles were taken up per lymphocyte, and they were retained for at last 3 days. Labeling did not affect viability or biodistribution. Detection threshold was determined to be 2.5×10^6 cells/30 μL sampling volume. Lymphocyte in the spleen resulted in MRI signal intensity changes that were readily detectable by MRI.

Other groups have developed dextran-coated SPIO linked to antibodies directed against leukocyte common antigen (CD45) by biotin-streptavidin binding to successfully target brain tumors (134). A recent report of the use of dextran-coated USPIO (AMI-227 Combidex; Advanced Magnetics Inc., Cambridge, MA; also known as ferumoxtran) in humans describes improved myocardial/blood-pool contrast with a trend toward contract-to-noise ratio improvement in the short axis and significant improvement in the long axis cine by an average of 128% (135).

Actively Targeted Microspheres. In a 1992 review of drug targeting in MRI, Weissleder et al. conclude that "target selectivity and receptor and/or antigen specificity is the most important issue if functional MRI is to establish itself in the next decade" (136). Although the review includes passive targeting, they list carriers including antibodies, proteins and polysaccharides, cells and liposomes, and targets ranging from colorectal tumor, heart (myosin), liver (ASG receptor), autonomic nervous system, peripheral nervous system (axonal transport), inflammatory cells, receptors (fucose, manose, ASG), inflammation, lymph nodes, cell traffic, and liver and spleen. Many actively targeted imaging microspheres have been described elsewhere in the literature (101,104–108,130,134). In addition, magnetite nanoparticles with a PEKY coating (see also Ref. 109) have been developed which have then been crosslinked with the homobifunctional regent ethleneglycol bis(succinimidylsuccinate) followed by coupling to carcinoembryonic antigen (137). Poly(ethylene glycol) was used to prolong the particle circulation time as were mucin, albumin, *N*-acetyl neuraminic acid, glucuronic acid, or glycophorin. The ability of these protective agents to prevent rapid elimination rates was disappointing, although the relaxivity was very good, between 300 and 500 mM^{-1} sec^{-1}. Work on an ASG receptor–targeted agent consisting of arabinogalactan-coated USPIO made by coating BMS 180550, (developed by Advanced Magnetics, Inc., Cambridge, MA) and obtained here from Bristol-Myers-Squibb, has been described by Leveille-Webster and co-workers (138). The particles were targeted specifically to hepatocytes, as opposed to Kupffer cells, which are the usual target in the liver. The goal was to develop an agent that could be used to monitor the regenerative responses after acute liver injury. A similar ASG-USPIO was reported by Reimer and co-workers in a comparative study of three agents, the hepatocyte targeting agent, a USPIO targeted to the lymph and bone marrow, and an RES-directed iron oxide agent (139). They showed that signal intensity changes, which reflect local change on relaxivity, were not affected by intracellular redistribution such as clustering.

The nanomolar, or high affinity, folate receptor is expressed or up-regulated on tumors of epithelial origin including ovarian, endometrial, and breast cancers. This fact has been exploited by Wiener and co-workers who developed Gd complexes of folate-conjugates dendrimer-conjugates (140). They showed that cells accumulate the conjugate in a receptor-specific manner. Although no imaging studies were reported, the approach looks promising for tumor targeting of MRI CA.

An abscess-specific CA has been investigated which involves the labeling of neutrophils with SPIO particles (141). The particles had to be coated with polystyrene (Estapoe® M1-0.07/60, 0.8 μm; Rhone-Poulenc, Combevoie, France) to prevent strong, irreversible cell aggregation. The coated particles became engulfed by the neutrophils and permanently sealed inside of them. After 48 hours postinjection, T_2-weighted images of an artificially induced abscess in rabbit muscle produced dark contrast around a characteristically bright center of the inflammation. However, care had to be taken to balance the number of ingested particles needed for adequate imaging with a noted decrease in chemotactic potential upon uptake of the particles.

Metaloporphyrins have been evaluated as positive MRI CA for a variety of tumors including human carcinoma, lymphoma, and fibrosarcoma (142–144). Tumor enhancement was evident in all cases. The long-circulating copolymer MPEG-PL-DPTA has also been investigated as a carrier for diagnostic and therapeutic drug delivery to tumors in vivo (106). The copolymer was labeled with both Gd and ^{111}In. The adducts were succinilated to test the theory that a hydrophilic polymer may be able to overcome diffusion barriers in a solid tumor which are thought to be caused by interstitial polysaccharides which impede motion across tumor interstitium (145). The copolymer accumulates in solid tumors at the level of 1.5–2% injected dose/g of tumor in 24 h. The polycarboxylated copolymer was also associate with *cis*-diamminedichloroplatinum(II) by coincubation, and the resulting drug–copolymer complex showed a cytotoxic effect in mouse F9 teratocarcinoma, and induced reversal in tumor growth after intravenous administration. In vitro the release profile in the presence of blood components showed a burst effect over the first 23 minutes (20% release) followed by a slow, essentially linear release with a half-life of 79 h. Despite a fourfold reduction in activity as an inhibitor of F9 proliferation in cell culture, the adduct was remarkably successful in vivo, with all animals surviving 6 consecutive treatments with a resulting reduction of tumor volume to an average of 90% of pretreatment values. Two of the eight animals showed complete tumor regression. The pronounced toxic side effects observed in control animals treated with uncomplexed drug were notably absent in the treated population.

Pislaru reported on the use of bis-Gd-mesoporphyrin to evaluate the possibility of noninvasive measurement of infarct size after thrombolysis in a dog using the Cu-coil technique (146). The agent demonstrates a high affinity for necrotic tissue. In the animal model, strong enhancement (150–280%) was observed on T_1 weighted images, which

closely correlated with postmortem triphenyltetrazolium chloride staining results.

Finally, reports have appeared in the literature that propose both CT and MRI imaging of antibody-labeled iron oxide particles and physical movement of these microcapsules in response to a magnetic field gradient (147). The antibody is cross-linked to silicone-coated iron oxide to give particles similar to BioMag™ (148). In rats, the injected particles could be transported through the cerebrospinal fluid and localized to the medial aspect of one or other cerebral hemisphere using an external magnet.

Liposomes. A paramagnetic species in free solution can directly relax only adjacent water protons. It follows that use of liposomes can only be effective with entrapped CA if protons can pass across the membrane or if the membrane is sufficiently leaky. This is usually achieved by use of small unilamella liposomes (SUV) with a small internal volume compared with the surface area, which facilitates water exchange (149). Theoretical expressions have been derived that allow calculation of water permeabilities of liposomes for use in CA preparation (150). Variations of liposome size and permeability have been shown to influence changes in relaxation rate in bulk water (151,152). In rats, liposomal Gd-DTPA caused significant improvement in contrast between liver and tumor, on T_1-weighted MR images, and smaller 70 nm liposomal Gd-DTPA caused the greatest contrast enhancement (153). This reflects the larger surface-area-to-volume ratio of smaller vesicles. Alternatively, the imaging moiety can be incorporated into the bilayer, so that that it is exposed on the outer surface, which is in contact with the aqueous environment (149). In either case, whether the agent is entrapped or exposed on the surface, liposomes act as blood-pool agents to increase the circulation time of the agent and to target it to the liver and spleen. Specific target molecules can also be attached to the liposome bilayer to create an immunoliposome, adding a further degree of sophistication to the agent.

Karlik and coworkers prepared SUV from phosphatidylcholine and dipalmitoyl phosphatidylethanolamine-DTPA, chelating either Gd(III) or the spin label, nitroxide free radical (154). In vivo in rats, the spin label significantly highlighted liver and spleen compared with noncontrast liposomes, and the enhancement increased with time. However, the Gd-containing liposomes were far more effective. The spin label had a short tissue half-life, compared with the Gd-liposomes which had a 24 h half-life in liver. The results are similar to those reported by Kabalka and by Schwendener, both using a sterylamine DTPA-Gd chelate (155,156). Unger claims the highest relaxivity for SUV prepared with Mn(II) complexes of DTPA, which were derivatized with hydroxylated acyl chains (149). They reported R_1 and R_2 values of over 20 $mM^{-1}\ sec^{-1}$, some five times higher than Gd-DTPA.

Polymerizable paramagnetic liposomes have been proposed by Storrs et al. which have derivatized gadopentetate dimeglumine as the hydrophilic head group and diacetylene groups in the hydrophobic acyl chains which cross-link when irradiated with ultraviolet light (157). About 2–5% of the head groups are left uncoordinated with Gd(III) to ensure that there is no free ion present. The liposomes were well tolerated by rats, and images showed an increase in the T_1-weighted signal intensity which persisted through the 90-minute experiment (20% in the liver and 34% in the kidney at one-sixth the clinical dose of Gd(III)).

Finally, liposomes that are sensitive to pressure have been suggested for use in cardiovascular MRI (158). They consist of gas-filled liposomes between 4 and 9 μm in size. Various gases have been investigated including nitrogen, argon, air, xenon, neon, pefluoropentane, and sulfur hexafluoride. Assuming ideal gas behavior, it can be shown that magnetic field perturbation is inversely proportional to the pressure. Pressure changes could cause the transverse relaxation of the surrounding medium to change. This does not take into account effects of any membrane around the bubble. The $1/T_2$ for gas-filled liposomes decreased linearly with pressure, but the effect was different for different gases. Oxygen (or air) had the greatest effect on T_2 relaxation, which was attributed to either bubble stability or the inherent paramagnetic properties of oxygen. Although the effects are far smaller than those noted in ultrasound, these gas-filled bubbles are considered to be a first step in developing pressure-sensitive MRI agents.

Microcapsules for Fluorine MRI. The use of ^{19}F in MRI allows for contrast-only imaging since there is no background signal from the tissue. Fluorine is highly sensitive and the CA, usually perfluorocarbons (PFC), are low in toxicity. Different mixtures of PFC with melting points around 37°C can be used for temperature mapping due to the absence of signal in the solid phase. Further, because oxygen is highly soluble in PFC, and because dissolution is accompanied by a decrease in T_1, fluorine MRI has been used to measure the partial pressure of oxygen, an area that has been reviewed by Clark (159). Most imaging agents are fluorocarbon emulsions such as perfluorotributylamine. Sotak suggested the use of perfluoro-2,2,2′,2′-tetramethyl-4,4′-bis(1,3-dioxalane) (PTBD) to overcome some of the problems of earlier agents such as multiple chemical shifts and short T_2 (160). Despite the superior properties of PTBD, PFC emulsions can not be targeted away from the RES, and only contain 10–40% (w/v) of active fluorocarbon. This means that multiple doses are often required, and the SNR is frequently insufficient to measure oxygen pressure.

Webb and co-workers have reported the development of sonochemically produced protein microspheres to overcome these problems and to allow for the flexibility of surface modification to redirect the biodistribution of the agent (161). The bovine serum albumin spheres have a mean diameter of 2.5 μm, are filled with liquid perfluorooctane, and are similar to the air-filled microspheres used in ultrasound known as Albunex®. They are produced by high power ultrasound irradiation at the interface of an aqueous protein solution and a nonpolar liquid. They target the RES and give high SNR (up to 300% compared with commercially available emulsions), and do not induce an immune response. High encapsulation efficiencies result in a sixfold increase in the volume of PFC per dose.

An area where microencapsulation has produced superior agents to unencapsulated examples is in temperature mapping. Well-defined mixtures of PFC with appropriate melting points can be encapsulated for temperature mapping and the surface properties of the capsules can be modified. When modified with PEG 2000, the microspheres were retained in the circulation 30 times longer than the unmodified capsules (circulation half-lives of 70 and 2.5 minutes, respectively). These capsules represent a class of fluorine imaging agents that can give good quality fluorine images in a reasonable data acquisition time, with high SNR.

Contrast Imaging with Therapeutic Modalities

As was the case with CT CA, the possibility of concomitant imaging and therapy is an attractive possibility. A recent review dealing with macromolecular systems for chemotherapy specifically concentrated on this concept for MRI (162). Although acknowledging the current drawbacks of limited tissue penetration and relatively slow rates of internalization by endocytosis, the authors pointed out that the field is yet in its infancy, and much is yet to be learned about how macromolecular prodrug chemistry affects their biological properties. Torchilin and co-workers describe the use of micelles for both drug delivery and imaging for CT, MRI, and γ-scintigraphy (58,59). Agent was prepared from amphiphilic AB-type copolymers to produce micelles in which poly(ethylene glycol) groups surround and protect a hydrophobic core that contains the drug and/or imaging agent. The entrapped species dictates the imaging modality for example, iodine for CT, Gd-DTPA-PE for MRI, and ^{111}In-DTPA-SA for scintigraphy. The important feature of Gd-DTPA-PE is its amphiphilic nature, which facilitates incorporation into a micelle. Excellent MRIs can be obtained with these agents (58). An interesting feature of these agents is the ability to gently massage the 20 nm particles from the subcutaneous injection site in the rabbit hind paw, down the lymphatic pathway, to the thoracic duct. In the case of γ-scintigraphy, the investigators used direct massage of the popliteal node to "squeeze" the ^{111}In-labeled micelles to the systemic circulation. In MRI, axilliary lymph nodes became visible only 4 minutes after administration of Gd-containing micelles.

Reports are starting to appear in the literature addressing issues in imaging and gene/DNA transfer. As mentioned earlier, Meade and co-workers at the California Institute of Technology report on the elegant use of MRI as a method of noninvasive monitoring of gene transfer (107). They synthesized a new class of agents and demonstrated in vitro the ability of these agents to transfect genes into cells while enhancing the MRI contrast of the targeted cells. The strategy involved preparation of multimodal particles composed of DNA (luciferase plasmid) condensed with poly-D-lysine (PDL) conjugates with Gd-DTPA-PDL, and poly-L-lysine (PL) conjugates with transferin-PL. Approximately 1,500 Gd ions were taken up per cell. Significantly, higher gene expression (over twofold) was observed compared with particles without MRI contrast. A possible explanation could lie in the higher degree of neutralization of the PL backbone when Gd-DTPA-PDL was present. Nantz et al. have reported imaging a DNA transfection event using a Gd-chelated liposomal CA formulated with the cationic transfection lipid DOTAP, complexed with the reported gene encoding for luciferase (163).

Again in an attempt to use MRI as a noninvasive tool for monitoring in vivo events, drug release from an implanted hydrogel has been followed by depicting the three-dimensional structure of the implanted biodegradable drug delivery matrix with time (164). Release was from bis-hydroxysuccinimide ester of poly(ethylene glycol)disuccinate cross-liked with albumin, to which gentamicin and Gd-DTPA were covalently attached in stoichiometric quantities. Impressive three-dimensional reconstructions and MRI images of the implant (Fig. 4) are shown, and a correlation coefficient of 0.965 for concentration of released gentamicin and hydrogel volume are reported. The degradation of the hydrogels was followed by serial MRI. Complete resorbtion was judged to take 4 weeks, and the half-life of a 1-mL "button" containing 18 mg of gentamicin was approximately 7 days (Fig. 5).

Bacterial glycopeptides have been used for penetration of the blood-brain barrier with enhancement of drug delivery and imaging (165). In rabbit, Gd-DTPA, which is normally excluded from the brain parenchyma, showed enhancement 4 hours after administration of 1 μg of pneumococal cell wall and became prominent, particularly in the region of the occipital cortex, 5 hours after challenge.

Finally, in an interesting combination of MRI and ultrasound, the use of target-specific delivery of macromolecular agents with MR-guided focused ultrasound has been reported (166). In this study MRIs of a Gd-labeled liposome were used to select a target region in rabbit muscle for application of pulsed-focused ultrasound to deliver biotin-labeled liposomes. Tissue changes observed in T_2-

Color Figure

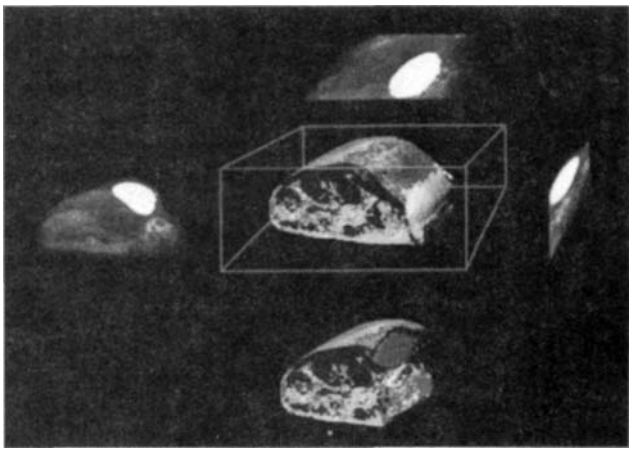


Figure 4. MRI of gentamicin-hydrogel. A gentamicin-hydrogel was implanted into a paraspinal abscess in a rat. Sixty individual MRI slices (individual slice thickness of 700 μm to render a slab of 4.2 cm) through the midabdominal of a rat were acquired and are displayed as axial (left), coronal (top), and sagittal (right) images or as colorized 3D reconstructions in which hydrogel is segmented in green (see color plate). The calculated gel volume by MRI (0.94 mL) corresponds to 16.292 mg of gentamicin. *Source:* From Ref. 164, courtesy of Dr. R. Weissleder and the publishers.

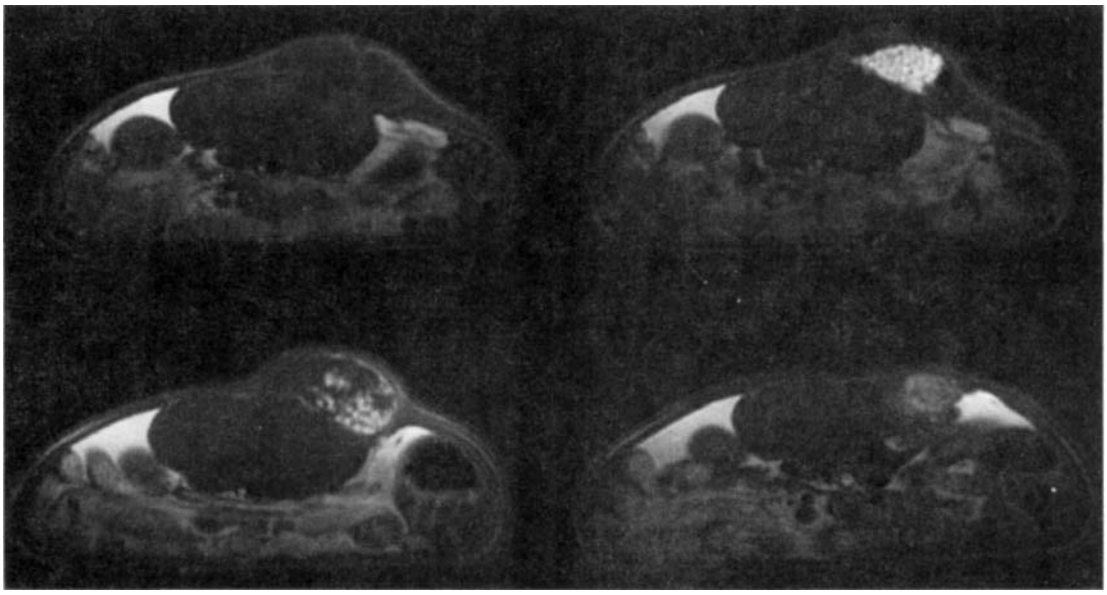


Figure 5. Degradation of gentamicin-hydrogel. MRI of an implanted hydrogel is shown. The brightness of the hydrogel is due to the paramagnetic Gd label that makes it better distinguishable from muscle signal intensity. Time point: precontrast (top left), postcontrast (top right), 5 days (bottom left), and 18 days (bottom right). *Source:* From Ref. 164, courtesy of Dr. R. Weissleder.

weighted images and the accumulation of Gd-liposomes in the regions treated with pulsed-focused ultrasound were a function of the total energy deposition, the duty cycle, and the power of the focused ultrasound pulse. The changes seemed reversible in the case of low-energy deposition.

ULTRASOUND CA

Physical Properties

An ultrasound CA must modify one or more of the acoustic properties of tissue which determine the ultrasound imaging process (167). Essentially there must be an acoustic impedance mismatch between the CA and the suspending fluid, usually blood. Acoustic impedance is the product of the density of the medium and the speed of sound in that medium. The most important properties that are affected are backscatter cross section (σ), attenuation, and acoustic propagation velocity, although the latter is less frequently used. The backscatter cross section is related to the received ultrasound intensity I_s, the incident intensity I_i, and the distance R between the transducer that emits the radiation and a single small scatterer (168):

$$I_S = \frac{I_i \sigma}{4\pi R^2} \tag{2}$$

For multiple scatterers this value is multiplied by the number of scatterers. The relationship assumes that the scatter is much smaller than the wavelength. This is usually the case because the size of the agent is in the order of 1–6 μm, much smaller than the wavelength of the acoustic field (at 3 MHz the wavelength in water is 0.5 mm). The scattering cross section σ (m^2) can be described by the Born approximation (169):

$$\sigma = \frac{4\pi}{9} k^4 r^6 \left[\left(\frac{\kappa_S - \kappa}{\kappa} \right)^2 + \frac{1}{3} \left(\frac{3(\rho_S - \rho)}{2\rho_S + \rho} \right)^2 \right] \tag{3}$$

where k is wave number $= 2\pi/\lambda (m^{-1})$; λ is wavelength (m); κ_s is compressibility of the scattering particle; κ is compressibility of the medium; ρ_s is density of the scattering particle (kg/m^3); ρ is density of the medium (kg/m^3). This can be expressed as

$$\sigma = A \left[B^2 + \frac{1}{3} C^2 \right] \tag{4}$$

where A is amplitude term; B is compressibility term; and C is density term.

The objective in developing an ultrasound CA is to maximize the scattering cross section. It is nonlinearly related to the geometric cross section. It can be seen from the amplitude term in equations 3 and 4 that the cross section is related to the sixth power of the radius and the fourth power of the frequency. For a given radius, the higher the applied frequency, the greater the cross section, and for a given frequency, the larger the radius the higher is the cross section. We know, however, that particles that are to cross the pulmonary capillary bed must have diameters less that about 6 μm if they are to avoid being trapped, so there is an upper limit on size.

The compressibility term and the density term of equation 3 demonstrate that the physical properties of the scatterer compared with those of the medium are paramount. Of the two terms the compressibility difference is domi-

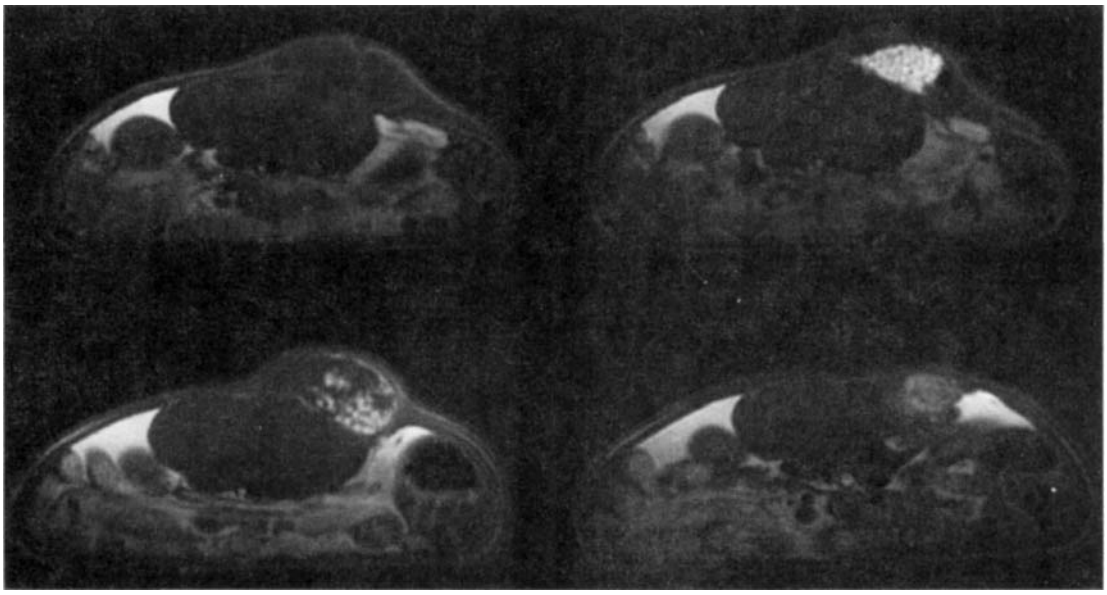


Figure 5. Degradation of gentamicin-hydrogel. MRI of an implanted hydrogel is shown. The brightness of the hydrogel is due to the paramagnetic Gd label that makes it better distinguishable from muscle signal intensity. Time point: precontrast (top left), postcontrast (top right), 5 days (bottom left), and 18 days (bottom right). *Source:* From Ref. 164, courtesy of Dr. R. Weissleder.

weighted images and the accumulation of Gd-liposomes in the regions treated with pulsed-focused ultrasound were a function of the total energy deposition, the duty cycle, and the power of the focused ultrasound pulse. The changes seemed reversible in the case of low-energy deposition.

ULTRASOUND CA

Physical Properties

An ultrasound CA must modify one or more of the acoustic properties of tissue which determine the ultrasound imaging process (167). Essentially there must be an acoustic impedance mismatch between the CA and the suspending fluid, usually blood. Acoustic impedance is the product of the density of the medium and the speed of sound in that medium. The most important properties that are affected are backscatter cross section (σ), attenuation, and acoustic propagation velocity, although the latter is less frequently used. The backscatter cross section is related to the received ultrasound intensity I_s, the incident intensity I_i, and the distance R between the transducer that emits the radiation and a single small scatterer (168):

$$I_S = \frac{I_i \sigma}{4\pi R^2} \tag{2}$$

For multiple scatterers this value is multiplied by the number of scatterers. The relationship assumes that the scatter is much smaller than the wavelength. This is usually the case because the size of the agent is in the order of 1–6 μm, much smaller than the wavelength of the acoustic field (at 3 MHz the wavelength in water is 0.5 mm). The scattering cross section σ (m^2) can be described by the Born approximation (169):

$$\sigma = \frac{4\pi}{9} k^4 r^6 \left[\left(\frac{\kappa_S - \kappa}{\kappa} \right)^2 + \frac{1}{3} \left(\frac{3(\rho_S - \rho)}{2\rho_S + \rho} \right)^2 \right] \tag{3}$$

where k is wave number $= 2\pi/\lambda (m^{-1})$; λ is wavelength (m); κ_s is compressibility of the scattering particle; κ is compressibility of the medium; ρ_s is density of the scattering particle (kg/m^3); ρ is density of the medium (kg/m^3). This can be expressed as

$$\sigma = A \left[B^2 + \frac{1}{3} C^2 \right] \tag{4}$$

where A is amplitude term; B is compressibility term; and C is density term.

The objective in developing an ultrasound CA is to maximize the scattering cross section. It is nonlinearly related to the geometric cross section. It can be seen from the amplitude term in equations 3 and 4 that the cross section is related to the sixth power of the radius and the fourth power of the frequency. For a given radius, the higher the applied frequency, the greater the cross section, and for a given frequency, the larger the radius the higher is the cross section. We know, however, that particles that are to cross the pulmonary capillary bed must have diameters less that about 6 μm if they are to avoid being trapped, so there is an upper limit on size.

The compressibility term and the density term of equation 3 demonstrate that the physical properties of the scatterer compared with those of the medium are paramount. Of the two terms the compressibility difference is domi-

nant. For example, the compressibility of air and water are 2.3×10^{-4} cm^2/dyne, and 4.6×10^{-11} cm^2/dyne respectively. In comparison, the compressibility of a rigid substance such as nickel, is 5.0×10^{-13} cm^2/dyne. Using a radius of 5 μm, and a frequency of 5 MHz (the medical imaging range is 3–10 MHz), the scattering cross section of a liquid, solid, and gas can be calculated as approximately 0 m^2, 6.65×10^{-15} m^2, and 0.38 m^2, respectively.

Gas bubbles have an added advantage when being considered as ultrasound CA because they can act as harmonic oscillators and resonate when insonated at their resonant frequency. Resonance increases the backscatter cross section by three orders of magnitude (168). An approximate relationship between resonant frequency f(s^{-1}) and particle radius r(m), which ignores surface tension, thermal effects, and effects due to viscous damping by the surrounding medium, is given by equation 5 (170):

$$f_r = \frac{1}{2\pi r}\sqrt{\frac{3\gamma P}{\rho}} \tag{5}$$

where P is pressure (N/m^2); γ is C_p/C_v (heat capacity ratio equals 1.4 for an adiabatic process in air); and ρ is density of medium (kg/m^3). Using values for air and ambient pressure we obtain a relationship for resonant frequency f_o in kHz for a diameter d in μm as:

$$f_o = \frac{6500}{d} \tag{6}$$

which indicates that the resonant frequency falls right in the medical imaging frequency range (171). Expressions have also been derived which account for the damping of the resonance frequency caused by the encapsulation of the bubble which is used to increase bubble stability (172,173).

An interesting property of an oscillating bubble has recently gained increasing attention as a possible new imaging technique (174,175). At slightly higher intensities of the sound field the oscillations of the bubbles are driven to a point where the alternate expansions and contractions of the bubble's size are not equal. This nonlinear response gives rise to the generation of harmonics of the insonating frequency which are emitted by the bubbles. Harmonic images are created by transmitting at the fundamental and receiving at the second harmonic, twice the fundamental frequency. Since the tissues and vessel walls are not oscillating in this fashion, this allows for contrast-specific imaging. Machines are currently available that can use this imaging technique in a clinical setting. Even though the harmonic signals are considerably weaker than the fundamental, the signal-to-clutter ratio enhancement is over 1,000 (176).

As already derived, the best medium for ultrasound CA is a gas in the form of very small bubbles with diameters less than 10 μm, preferably less than 6 μm. When considering the approach to be taken in developing these microbubbles, it is important to review some of the physics describing the stability of gas bubbles of this size in a liquid. The expression for the pressure difference ΔP between the outside and inside of a bubble of radius r in a liquid with surface tension γ is give by the Laplace equation:

$$\Delta P = \frac{2\gamma}{r} \tag{7}$$

It is derived by noting that at equilibrium the tendency for the surface area to decrease due to the sum of the external pressure and the surface tension, is balanced by the rise of internal pressure which would result from this area decrease. If we consider a 0.1 mm radius bubble in champagne, the pressure difference would be $2(7.4 \times 10^{-2}$ $Nm^{-1})$ $(1.0 \times 10^{-4}$ m) which is 1.5 kPa. Unfortunately, such bubbles are too large for CA use! The pressure inside a more suitable 10-μm bubble would be 15 kPa, enough to rapidly collapse any bubble that is not well stabilized. In fact free bubbles of this size have extremely short half-lives. Epstein and Plesset derived a relationship (equation 8) for the shrinkage (or enlargement) of bubbles in a still liquid, which took into account the diffusion coefficient of the gas and the gas solubility in the suspending medium (177):

$$\frac{\delta r}{\delta t} = \frac{-Dy}{r}\left[\frac{1 - \frac{C_i}{C_S} + \frac{2\gamma}{rP_h}}{1 + \frac{4\gamma}{3rP_h}}\right]\left(1 + \frac{r}{\sqrt{\pi Dt}}\right) \tag{8}$$

where r is radius of bubble (m); D = diffusion coefficient (m^2/s); C_i/C_s = ratio of dissolved gas concentration C_i to saturated concentration C_s; γ = surface tension (N/m); P_h = hydrostatic pressure (N/m^2); t = time (s); $y = (RTC_0)/P_hM$; M = gas molecular weight; R = gas constant; T = absolute temperature.

Using this equation, de Jong (178) calculates the lifetime of a free air bubble in water saturated with air to be 5×10^3 seconds for a 100-μm bubble and only 6.0 seconds for a 10-μm bubble. Because it takes 2 s for an injected bubble to travel to the right side of the heart and 10–27 s to travel to an end organ, free air bubbles are clearly inadequate. Gases with lower solubility and higher molecular weights have much greater persistence. Recently encapsulated gases such as PFC and sulfur hexafluoride (SF_6) have gained preeminence for use as ultrasound CA.

Before discussing the evolution of CA from their beginning in 1968 (179), it is important to briefly review the different modes used in ultrasound imaging. The transducer emits the ultrasound in short pulses and also receives the reflected signal, or echo. The simplest instrument is an A-mode scanner, which depicts the amplitude of the received echo against time. M-mode, or sometimes TM (time motion) scanning depicts the movement of tissue with time, and is most often used in cardiac imaging. The time it takes for a transmitted disturbance to return to the transducer depends on the depth of the reflector, and, if the reflector is moving, this depth changes with time. The M-mode display depicts this change of depth with time and is very useful in analyzing dynamics of heart valves. It is composed of a rastor of A-mode lines. The most familiar ultrasound scan is the B-mode, which gives a two-dimensional image through the tissue, for example, an image of a fetus in the womb. The ultrasound beam is scanned through the tissue either mechanically or, more

usually, by electronic beam steering using a multielement transducer. The time of arrival of the echoes indicates the depth from which the beam was reflected, and signals are displayed as spots with a brightness proportional to their intensity (known as gray scale). Tissue movement can be seen as the beam is periodically swept through the region if the image is updated at a sufficiently high rate. These scans are known as real-time images. In addition to B-mode, Doppler ultrasound is also an area where CA are having an impact. The usual scatterers in blood are the red blood corpuscles, and these are, of course, moving with the flow of blood. The frequency of echoes reflected from these, and any other moving species (for example CA), have an altered frequency, depending on their velocity and direction relative to the transducer. This is the familiar Doppler effect, noticed by trainspotters as they stand by the side of the rails and hear a train whistle shift in pitch as the train approaches and then passes them. The cyclical variation of blood velocities in arteries (and veins) can be monitored as the heart beats, and in fact can be heard because the frequency is shifted into the audible range. Duplex scanners are available in which both the B-mode image and Doppler image are displayed simultaneously one beside the other. A further refinement, known as color flow mapping (CDI), superimposes a color-coded Doppler signal onto a real-time B-mode image. The color coding can indicate both direction and speed of flow, and regions of abnormal flow can be detected. (Usually red indicates motion toward and blue indicates motion away from the transducer, with gradation of color depending on velocity.) A new modality that is gaining interest because of CA is color amplitude imaging (CAI, also known as power Doppler). In CAI the density as opposed to the velocity of moving scatters is displayed. This is achieved because the amplitude, and thus the power and intensity of the echo, depends on the number of particles. In fact the Doppler frequency shift is not used so the signal is not dependent on direction. Finally, as already mentioned, harmonic imaging is now being developed in which the nonlinear properties of oscillating bubbles are being used to gain contrast-specific images with high SNR, free from clutter of surrounding tissue (180,181). The tissue is interrogated at the fundamental frequency and the signal is received at the second harmonic (twice the fundamental).

Early CA for Ultrasound Imaging

The first ultrasonic detection of bubbles in the blood was in 1963 during investigation of microbubbles formed during decompression sickness (182). However, it was not until Gramiak noticed a cloud of echoes during injection of indocyanine green into the left heart in 1968 that the possibility of their use for ultrasound contrast was considered (179). The realization that the signal originated from microbubbles created by cavitation at the catheter tip upon injection was followed by development of the first-generation agents consisting of hand-agitated solutions of compounds such as indocyanine green, saline, Renografin, 5% dextrose, and even the patient's own blood (183–185). The bubbles that were produced were extremely short lived and too large to avoid clearance by the lung. Later, Lang reported production of microbubbles bubbles in Renografin by sonication (186). The early work on CA has been reviewed (187).

Main Areas of Use of CA in Ultrasound Imaging

Ultrasound has many advantages over other imaging modalities, primarily in the areas of safety, low cost, convenience, and the possibility of real-time imaging. However, without contrast ultrasound is limited in the detection of small tumors and in Doppler evaluation of low-velocity blood flow either in small, deep vessels, or in areas of low flow due to pathology. The initial emphasis for CA development was in echocardiography, and it remains an active area of interest today. Since the initial investigations, the use of contrast has spread to all areas and modes of ultrasound imaging with the possible exception of fetal monitoring. The main areas are reviewed here.

Cardiac and Blood Vessel Imaging. de Jong defines the main areas as (178):

- Identification of cardiac structures (e.g., endothelial boarder)
- Detection of intracardiac shunts
- Visualization of blood flow in M-mode
- Detection of valvular regurgitation
- Analysis of complex congenital heart disease (e.g., arterial and ventricular septal defects, transpositions)
- Cardiac output determination by indicator dilution curves, left ventricular ejection fraction
- Perfusion studies
- Patency

Fan and co-workers have reported on in vitro studies comparing the commercially available Albunex and Echovist® with sonicated indocyanine green, Renografin-60, normal saline, and mannitol for potential CDI echocardiography (188). The commercial preparations were clearly superior. Reviews have appeared for cardiac use of Albunex (189), and the use of the gas-filled, lipid-coated preparation MRX-115 (now DMP-115 or Definity) for myocardial perfusion (190). Contrast has been investigated to alleviate problems of attenuation due to overlying tissue such as the skull, for example in transcranial Doppler (191). Using Levovist®, Bauer reports visualization of the circle of Willis in 100% of patients as opposed to only 80% in the absence of contrast. Levovist® has also been used by Sitzer to study renal arterial stenosis using contrast and CDI (192). They report a maximum enhancement of 21 dB after 15 s, and a clinically useful increase that lasted three minutes. Langholz reports that leg veins have been successfully imaged with Levovist after injection into the dorsal foot vein (193).

Liver Imaging. As with X-ray and MRI, liver imaging is an area in which strong interest in contrast enhancement of ultrasound images exists. Ultrasonography is the initial modality of choice for liver scans in clinical practice, for the reasons already given. Use of contrast adds greatly to

these investigations (53,194). Kudo and co-workers report on sonographic angiography in which 5–20 mL of a vigorously agitated mixture of carbon dioxide, heparinized normal saline, and the patients own blood were injected through a catheter placed within the hepatic artery. Hepatocellular carcinomas could be distinguished from focal nodular hyperplastic nodules by distinguishing the hypervascular pattern. Adenomatous hyperplasia, hemangiomas, and metastases displayed yet another hypervascular pattern (195). The same technique was used to identify tumors of less than 1 cm in diameter, which had been missed by other methods (196). Finally, a new polymeric agent, Sonovist®, is reported, which is taken up by the Kupffer cells and upon ultrasonic radiation is stimulated to resonate and collapse, producing a strong Doppler signal (197). This signal is absent in tumors that lack an RES.

Oncology. In addition to hepatic imaging, CA are used in many other areas of oncology, including central nervous system tumors (198), prostate (199), and breast (200). Cosgrove has performed extensive studies into identifying key features of tumor vasculature to aid in predicting prognostic outcome (201). Doppler has been used to attempt to predict the metastatic propensity of tumors (202). A quite dramatic demonstration of the enhanced power of CA Doppler was demonstrated by the same team who identified connections between adjacent vessels in breast tumors that were not seen in benign tumors and which presumably represented arterio-arterial shunts (203). Identification or absence of these shunts has been used to change the diagnosis of breast lumps, and those with shunts were confirmed to be malignant upon biopsy, whereas those without were found to be benign (204).

Gynecology. Ultrasound CA have been used in gynecological examination for both sonohysterography (transvaginal examination of the endometrium) and sonohysterosalpingography (investigation of tubular patency) (205). Both hyper- and hypoechoic agents are becoming widely used.

GI Tract. Ultrasonic investigation of the GI tract is severely hampered by the natural presence of gas, which acts as a reflector. A cellulose-based agent for oral administration has been developed by ImaRx Pharmaceutical Corp. and licensed by Bracco Diagnostics (Princeton, NJ). The cellulose serves to disperse and displace gas bubbles, allowing good GI imaging (206,207).

Microcapsule Types Developed as CA for Ultrasound

Whereas nearly all CA for ultrasound use microbubbles as the reflective agent, not all can be considered as true microcapsules. One of the earliest examples, Echovist (Schering, Germany), consists of a saccharide crystal base from which microbubbles are liberated upon dissolution in saline, just prior to injection. Other agents, for example, the phase-shift agent EchoGen® (Sonus, CA), consist of a liquid emulsion that essentially boils at body temperature. All of these agents can be described under the heading of "microcapsule" for consistency, however, micro*bubble* would perhaps be a more suitable title. The last 10 years have seen a flurry of activity in the ultrasound contrast area, with many new companies and agents appearing on the scene. Table 4 is presented to orient the reader as to the compositions and current names of some of the recent agents.

Several reviews have appeared describing recent ultrasound CA (167,176,178,194,208–211).

Gelatin, Collagen, and Alginate. In one of the earliest reports of capsules for ultrasound contrast, 80 μm gelatin-encapsulated nitrogen bubbles were reported to produce rim enhancement in VX2 carcinomas in rabbit, which lasted for several minutes (212). The large diameter required arterial injection of the agent close to the tumor area to avoid loss of the agent by entrapment in capillaries. The following year solid collagen microspheres of 3-μm diameter were prepared by an emulsion technique in which warm collagen was dispersed in cottonseed oil followed by cooling. However, in vitro testing in dog indicated that the strong enhancement in liver was due to microcapsule aggregation (213). We have reported on two methods for producing alginate-encapsulated gas bubbles using ionotropic gelation with calcium ions. In one case we designed a dual-barrel injection method in which gas was injected into the nascent alginate capsules as they emerged from the spray nozzle, and in the other a pregassed sodium alginate solution was fed to a single-barrel spray nozzle (214). Both methods produced echogenic gas-filled capsules, but in the first method the size was around 100–150 μm and in the second 30–40 μm.

Galactose Particles. Another early experimental agent, Echovist (Schering, Germany), consisted of crystalline galactose particles that contained numerous sites to entrap gas (215). The gas was released as bubbles with a mean diameter of 3 μm (but a size range up to 15 μm) when the particles were dissolved in a saturated galactose solution. Despite giving good right heart opacification, this agent was replaced by a similar agent, Levovist, with improved stability and narrower size range (90% $<$ 8 μm), which passes the lungs and can be used to image the left heart (216). Levovist differs from Echovist not only in the way that the galactose particles are produced but also because it contains 0.1% palmitic acid, which stabilizes the bubbles. The bubbles are released by addition of sterile water. Levovist has undergone extensive animal and human testing, is approved in Germany, and is awaiting approval in the United States. Although no grayscale (B-mode) tissue enhancement is reported, woodchuck hepatic tumors and large and small vessel enhancement has been seen in color and spectral Doppler, and enhanced echogenicity was demonstrated for ophthalmic and retinal vessels (217,218). Multicenter European trials report the agent to be well tolerated, and Phase II clinical trials in the U.S. have shown significant improvement in vessel enhancement (219). Breast tumors have shown distinct enhancement with agent on color-coded Doppler and the signals have been reported to allow reliable demonstration of vascularization characteristics (200). The same study suggested

Table 4. Examples of Agents Currently of Interest

Investigatory Name (Company)	Current Name	Composition/Gas
SHU 454 (Schering)	Echovist®	Galactose/air
SHU 508 (Schering)	Levovist®	Galactose/fatty acid–stabilized PFC (German approved)
Albunex® (MBI)	Albunex®	Sonicated HSA/Air (FDA approved)
FS069 (MBI)	Optison®	HSA/PFC
Quantison (Andaris)	Quantison®	HSA/spray-dried
PESDA (U. Nebraska)	PESDA	HSA/dextrose/PFC
AF0150 (Alliance)	Imagent®	Surfactant/PFC
QW3600 (Sonus)	Echogen®	PFC emulsion
MRX-115 (ImaRx)	Aerosomes®	Phospholipid/PFC
Now DMP 115 or Definity® (DuPont Merck)		
BR1(Bracco)	Sonovue®	PEG4000/phospholipids/SF_6
IDE particles (Univ. of Rochester)	Bubbicles	Iodapamide ethyl ester/air
SH U 563A (Schering)	Sonovist®	Polybutyl-2-cyanoacrylate/PFC
SonoRx (Bracco)	SonoRx®	Semithicone-coated cellulose (GI applications)
ST68,ST44 (Drexel Univ.)	ST68,ST44	Surfactants/PFC

that arrival, retention, and washout studies could give information about the growth dynamics of the tumor. Recently Levovist has been demonstrated to act as an active sound source during disintegration (stimulated acoustic emission or SAE) in myocardial contrast echocardiography (220). An advantage is that Doppler signals can be received even from stationary bubbles or ones with very low flow velocities. Myocardial contrast (MC) was studied in 36 patients using harmonic power Doppler investigations. Delineation of MC from contrast signals of the cavities was possible, whereas signal intensities in the cavities, even at the endocardial border, were at least 20 times higher than those of MC. In other studies in Europe, Levovist has been used as a continuous infusion for quantitative assessment using color power Doppler (221). Relative microbubble numbers could be accurately quantified in vivo, opening the door to the application of formal quantitative enhanced ultrasound in patients.

Protein Microcapsules. Another agent that was on the scene early is Albunex (MBI, California), which is the first agent to be approved by the FDA. Albunex® consists of air-filled albumin spheres with a mean diameter of 3–5 μm, produced by sonicating a 5% solution of human serum albumin. The usual concentration is 3–5 $\times$ 10^8 microspheres/mL of sterile, isotonic buffer at pH 6.4–7.4. The wall thickness is estimated to be around 15 nm. Its refrigerated shelf life is around 1 year (190). The half-life after injection is around 1 minute, and after 3 minutes more than 80% of the contrasts is found in the liver. Goldberg has demonstrated that Albunex can produce dramatic Doppler signal enhancement in both normal and tumor vessels in woodchuck with a naturally occurring hepatocellular carcinoma (222). Doppler signal enhancement recorded via a cuff transducer around the celiac artery gave an optimal signal gain of approximately 10 dB. Albunex has been proven effective for enhancing left ventricular endocardial definition in Phase III multicenter clinical trials (223). It has also been used to measure cardiac output (190), in dobutamine (a vasodilator) stress echocardiography (224), fallopian tube patency (225), vesicoureteral reflux (a common pediatric urinary tract abnormality), and detection of thrombus (226). In the thrombus study, the Albunex appeared to adhere to the thrombi. One of the chief disadvantages of Albunex is its short half-life, and Vandenberg conducted a study that indicated that Albunex is acoustically labile to acoustic pulse pressures greater than 0.33 MPa (227).

A second generation agent, Optison® (originally FS069), has been developed, which has greater in vivo half-life than Albunex (190). As mentioned previously, one of the factors in the stability of gas bubbles is the solubility of the entrapped gas in the blood (see equation 8). In Optison, the relatively soluble, low molecular weight components of air are replaced by perfluoropropane, an insoluble, relatively high molecular weight polyfluorinated hydrocarbon. The capsules are taken up by the RES in a similar fashion to Albunex, and the PFC is expired from the lungs after it is released when the protein coat is metabolized. In addition to left heart opacification, Optison has shown promise in use in myocardial perfusion and harmonic imaging (228,229).

Quantison® (Andaris Ltd., Nottingham, UK) also has a shell composed of human serum albumin (recombinant), but these capsules are produced by spray-drying and are thought to have a 200-nm shell. They are considerably more resistant to pressure than Albunex (178).

Porter in Nebraska has used a sonicated mixture of 1 part dextrose and 5 parts human serum albumin to stabilize perfluoropropane in an agent called PESDA, which has a particle size of 4.7 μm and a concentration of 6.0 $\times$ 10^9/ml (230). Porter has also encouraged the use of so-called transient response, or intermittent imaging, to improve the amount of MC observed from gaseous agents (231). The technique, which uses ultrasound in an interrupted mode such as 1 frame per cardiac cycle as opposed to the usual frame rate of 30 frames per second or greater, causes less overall acoustic destruction of the bubbles. Also, if this is combined with a high acoustic output, it may induce an emission from the microbubble when it is destroyed during the less frequent insonation, similar to the SAE noted previously with Levovist. In vitro this SAE was

measured with a 20-MHz probe transducer positioned confocally with a 1-MHz cavitation transducer (232). The average internal cavitation activity thus measured was higher for a pulse repetition frequency (PRF) of 10 Hz compared with one of 100 Hz, and both decreased with time. At PRF of 1,000 Hz and 5,000 Hz, the overall cavitation activity was higher than at either 10 or 100 Hz and did not decrease with time, indicating sustained bubble reseeding. The same effect was demonstrated in vivo in dog with intravenous injection of agent (233). The heart was simultaneously imaged with a 1.7-MHz harmonic transducer using a peak negative pressure (PNP) of 0.3–0.9 MPa and frame rates of 43–10 Hz, and one frame rate every one (1:1) to three (1:3) cardiac cycles. Cavitational activity increased as frame rate decreased, and higher PNP increased intramyocardial contrast. PESDA has been used in a human trial (92 patients) to detect coronary artery disease(CAD) (234). A perfusion defect was observed with myocardial contrast echography at rest or after stress that strongly correlated with the presence of CAD.

Stabilized PFC Emulsions. Perfluorooctyl bromide is radiopaque due to the terminal bromine. When a phospholipid-stabilized emulsion with particle size 0.1–0.4 μm, is administered intravenously, it can act as both an X-ray and ultrasound CA (235,236). The chief mechanism of ultrasound enhancement is from the compressibility difference between the emulsion droplets and blood. Use of these agents caused several side effects, and emphasis has now switched to a phospholipid-stabilized gaseous agent, known as Imagent US (237). Imagent is a powder consisting of buffer salts and phospholipid shells encapsulating perfluorohexane gas and nitrogen. Sterile water is added to suspend the capsules prior to injection. The agent has been shown to opacify the left ventricle, enhance the myocardium, and visualize regions of infarct in rabbit (238). Imagent has also been shown to enhance the placenta in rats (239). Recent second harmonic studies appear to show linear branching and discrete punctuated densities within the myocardium consistent with intramyocardial coronary vessels (240).

A different type of PFC emulsion is described by Correas and co-workers at Sonus Corporation, who describe a so-called 'phase shift' CA (241). The agent, Echogen, exists at room temperature as a liquid emulsion of the isomers dodecafluoro-*n*-pentane and dodecafluoroisopentane, with a mean diameter of about 0.3 μm. Upon injection, it vaporizes at body temperature. After rapid diffusion of dissolved gases from the blood into the PFC microbubbles the diameter is thought to increase to between 2 and 5 μm. The gas is exhaled through the lungs. The agent has been shown to exhibit parenchymal enhancement and tumor visualization (242). Vascular enhancement lasted 2 to 3 minutes, and liver and kidney enhancement was observed for up to 20 minutes. A maximum enhancement of 18.7 dB for a 0.6 mL/kg dose was reported. Detection of flow characteristics have been demonstrated to be markedly enhanced on spectral Doppler, color flow Doppler and CAI (243). Echogen is currently undergoing clinical trials. A clinical trial of perflenapent (2% dodecafluoropentane emulsion; Echogen Sonus Pharmaceuticals, Bothell, WA) has recently been described (244). Contrast enhancement was observed in 94% of patients, compared with 8% of placebo group, and lasted between 5 and 15.4 minutes. It was concluded that perflenapent emulsion is a safe and effective CA for ultrasound of the liver, kidneys, and vasculature.

Liposomes and Phospholipid-Stabilized Gas Bubbles. Unger and co-workers have described a dipalmitoylphosphatidyl choline liposome–containing gases such as nitrogen, oxygen, xenon, and PFC (originally Aerosomes®, now DMP-115 or Definity) (3,190). They have shown that the stability in the blood is very dependent on the solubility of the entrapped gas and the relative saturation of the blood. For example, air- or nitrogen-containing liposomes give far less contrast in the left heart in dogs ventilated on 100% oxygen, compared with those on atmospheric oxygen, whereas PFC-containing liposomes showed no such sensitivity (245). This result was attributed to the greater solubility of oxygen compared with nitrogen. Oxygen is thought to diffuse across the Aerosomes wall to exchange with nitrogen and hasten bubble loss. The agent can be prepared in an extruder, dried under vacuum, and filled with the gas of choice (246). Commercial preparation currently involves agitation using a mechanical shaking device to agitate sealed vials with the appropriate head space of gas (247). The resulting vesicles are around 2.5 μm in diameter. Acoustic measurements gave maximal attenuation at around 2 MHz, indicating that the bubbles were around 3 μm in diameter. The lipid-coated microbubbles have been used in a Phase II clinical study involving patients with acute myocardial infarction. The material (DMP-115 now Definity) was injected as an intravenous bolus. Images were obtained with second harmonic mode using commercially available ultrasound equipment, and the data were recorded on SVHS videotape and later analyzed off-line with software from Dr. Sanjiv Kaul's laboratory. The images were obtained at end systole of every heart cycle. Figure 6a is a composite of three images obtained at baseline in the two chamber view. Figure 6b is a composite of three images obtained after injection of the contrast and after attenuation was no longer present, in the same view. Figure 6c is the myocardial portion of Figure 6a subtracted from the myocardial portion of Figure 6b and the remainder subjected to a "heated object" lookup table. That is, white represents the most intense contrast and black would represent no contrast. Red therefore would be some limited amount of contrast. Figure 6d is a sestimibi scan of the same patient in the view analogous to the ultrasound image. The sestimibi and ultrasound contrast images (Figure 6c and 6d) demonstrate decreased myocardial perfusion in the anterior-apical regions of the left ventricle. The images were obtained from a 36-year-old male patient who had an acute anterior myocardial infarction 3 days prior to the ultrasound and sestimibi studies.

An agent identified as BY963 and described as being phospholipid-stabilized microbubbles has been reported for use in transcranial Doppler. The lipid in this case is a saturated stearic acid containing phospholipid of "plant origin," and the size of the resulting microbubbles is 3.9 μm (248,249).

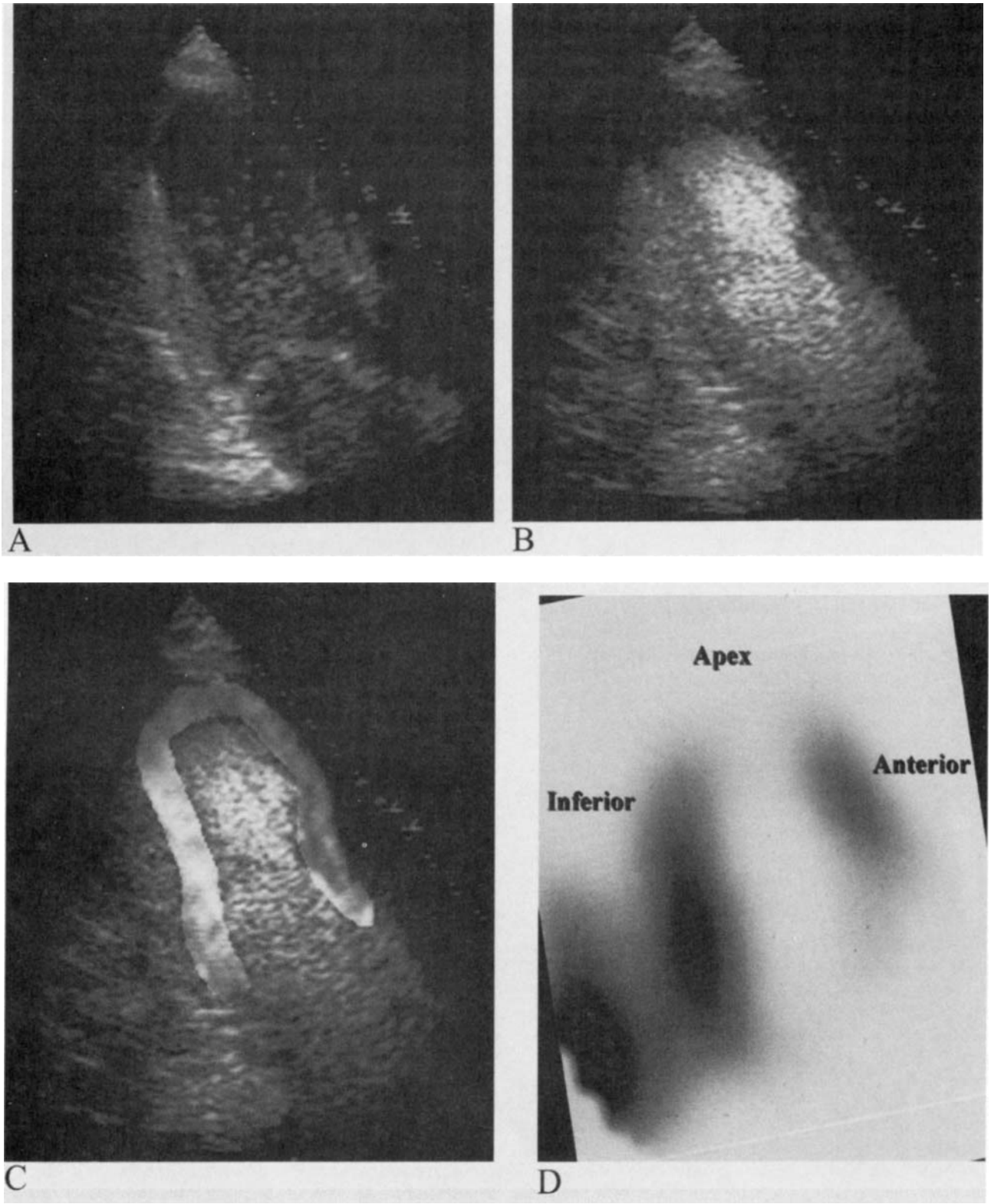


Figure 6. Images from a 36-year-old male patient with anterior wall myocardial infarction 3 days prior to the myocardial ultrasound study. (**A**) Three aligned unenhanced images of the left ventricle in the 2-chamber long axis view. (**B**) Three aligned DMP 115–enhanced images of the left ventricle in the 2-chamber long axis view. (**C**) Digital subtracted color enhancement of the left ventricle in the 2-chamber long axis view enhanced with DMP 115. (**D**) ^{99m}Tc sestimibi image of the heart of the patient. See color plate. *Source:* Courtesy of Dr. Unger, Imarex Pharmaceutical.

Color Figure

Lipid-coated microbubbles have been described for detection of brain tumors, neurosonography, and internalization in tumors by D'Arrigo and co-workers (250–253). The proprietary lipid mixture contains mostly glycerides and cholesterol esters, and the capsules are 99% <4.5 μm in size.

Bracco Research in Switzerland has reported on an agent, Sonovue® (was BR1), consisting of SF_6 stabilized with a lyophilized coat of poly(ethylene glycol) (PEG) 4000 and the phospholipids distearoylphosphatidylcholine and dipalmitoylphosphatidylglycerol (254). Reconstitution of the freeze-dried agent in 5 mL of sterile water yields a milky suspension of 2×10^8 bubbles/mL with a mean diameter of 2.5 μm with 90% < 8 μm. The agent was found to be highly echogenic in vitro over the range 1–10 MHz and to opacify the left heart. In a study in dogs, the agent was tested for its ability to detect myocardial perfusion defects as a result of coronary occlusion and myocardial reperfusion after thrombosis and intravenous administration of CA (255). Contrast echo detected myocardial perfusion defects in all the injections performed during coronary occlusion and detected myocardial perfusion with a sensitivity of 50% versus microspheres, and the extent showed a good correlation with microspheres (r = 0.73).

Iodipamide Ethyl Ester "Nano-Sponges." A group at Rochester University has taken a novel approach to the concept of bubble stabilization by developing porous particles, 1–2 μm in diameter, primarily for hepatic imaging (256). Initially the microspheres were relatively smooth amorphous spheres of iodipamide ethyl ester (IDE) prepared by precipitation of IDE in dimethylsulfoxide/ethanol by addition of an aqueous solution of poly(vinyl pyrrolidone). After intravenous injection they were taken up by the Kupffer cells and accumulated in the liver within 10 to 20 minutes (257). The rather low enhancement (~3 dB) has been improved by modifying the particle surface to give many crevices for stabilization of minute gas bubbles (258). These modified microspheres have been named Bubbicles. The iodine in the IDE allows for dual ultrasound and X-ray imaging.

Porous Inorganic Particles. A similar concept to a nanosponge (and to Ecovist described in "Galactose Particles") is reported by Glajch and co-workers in a patent that describes the preparation of porous inorganic particles for use as ultrasound CA (259). The inorganic particles, for example alkali salts of carbonates or phosphates, are prepared in such a way as to make them highly porous, and the pores trap the gas of choice. Once inside the body, the particles dissolve within one to two hours, depending on fabrication conditions. Unlike Bubbicles, these particles would be less likely to be retained in the liver for extended periods of time, and the slow dissolution rate renders them more long lived than Echogen.

***n*-Butyl-2-cyanoacrylate.** A different polymeric particle has been developed at Schering (SH U 563, or Sonovist), which consists of *n*-butyl-2-cyanoacrylate shells with a mean size of 1 μm and a thickness of about 100 nm (260). The thin shell allows the capsule to resonate when stimulated by ultrasound and to produce a strong harmonic signal (261). When the capsules break they emit a broadband frequency spectrum, which can be used in SAE. They are prepared by emulsion polymerization of the monomer and water in a surfactant-stabilized gas–water system. In vivo they strongly enhance spectral and color Doppler and B-mode, whereas in the vascular phase, and once taken up by the liver, allow dramatic demarcation of VX2 tumors (261).

Poly(*t*-butyloxycarbonylmethyl glutamate). Polymeric microballoons with a shell composed of the biodegradable polymer poly(*t*-butyloxycarbonylmethyl glutamate) have been described for use as CA (262–264). The mean size is around 3 μm, with 99% <8 μm. The microballoons are prepared by interfacial polymer deposition. An in vitro backscatter coefficient of 7.5 MHz was measured, and liver parenchyma was enhanced in rats after intravenous injection of 7.8×10^9 microballoons/kg. Enhancement reached a maximum 2 minutes after injection and lasted 1 to 2 hours (264).

Cellulose Compounds as GI CA. Initial investigations by Lund and co-workers, using simethicone and methylcellulose to diminish the gas artifact encountered during abdominal imaging, have led to the development of a GI CA, SonoRx® (Bracco Diagnostics, Princeton, NJ) (265,266). The agent consists of 22 μm cellulose particles with a 0.25% simethicone coating in a suspension containing an antifoaming agent (sodium lauryl sulfate), flavoring, and coloring. Clinical trials involved comparison of scans before and within 15 minutes of consuming agent or placebo. Improvement of imaging of cases with upper abdominal pathologies was dramatic (208). A combination of SonoRx and an intravenous agent has been suggested for detection of pancreatic tumors.

Poly(DL-lactide-*co*-glycolide) Microcapsules. In our laboratory we are developing a biodegradable polymeric agent with a shell composed of poly(DL-lactide-*co*-glycolide) (PLGA) (P. Narayan and M.A. Wheatley, unpublished data, 1998). The capsules, which can be made from any polymer amenable to microcapsule formation, are prepared by encapsulating a solid, volatilizable core, which is removed by lyophilization after the capsules are hardened. The evacuated capsules are filled with the gas of choice (usually PFC or SF_6) by venting the lyophilization chamber with the appropriate gas. Depending on the method of encapsulation we have achieved populations with a mean diameter of 6.7 μm (coacervation) or 4.9 μm (solvent evaporation). Figure 7 shows scanning electron micrographs of (*1*) whole capsules and (*2*) sectioned capsules made by coacervation. When 0.2 mL/kg of PLGA microcapsules containing decafluorobutane (concentration of approximately 5×10^8 microcapsule/mL) was injected through a shunt in the jugular vein of rabbit, they produced noticeable enhancement on CDI (Fig. 8). Studies are ongoing.

Surfactant-Stabilized Microbubbles. We have also developed a surfactant-stabilized microbubble, which has a far more flexible shell than the polymer-encapsulated agent.

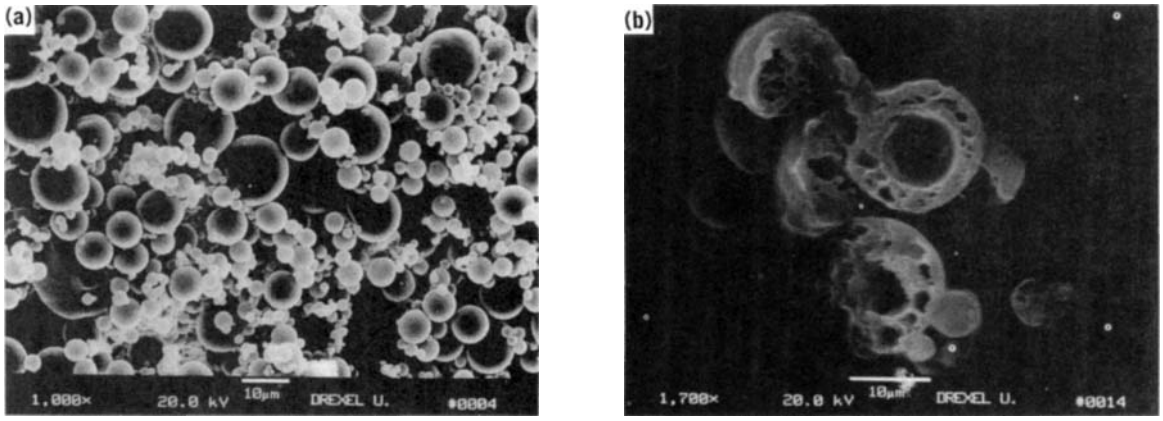
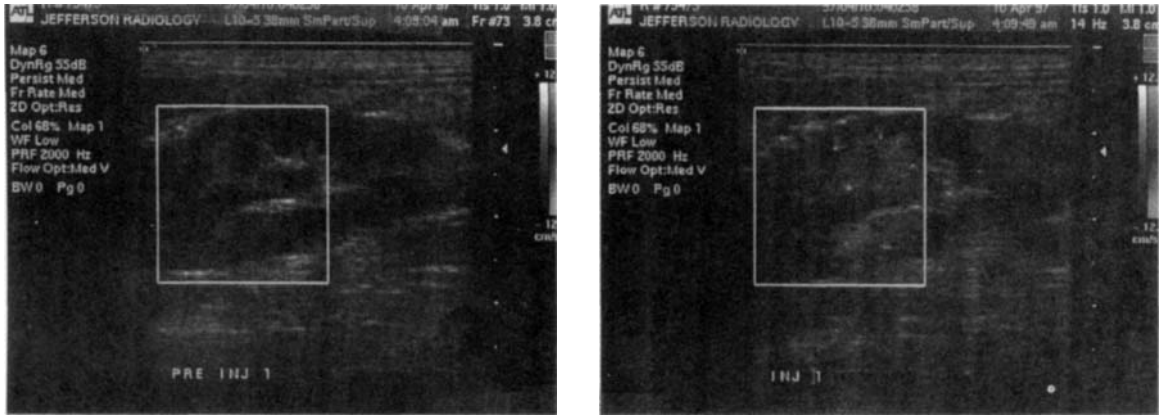


Figure 7. Scanning electron micrographs of hollow PLGA microcapsules prepared by a coacervation method. (**a**) Surface view of whole capsules; (**b**) Cross section of capsules. Bar = 10 μm.



(a) (b)

Figure 8. Color Doppler image of right kidney (see color plate). (**a**) preinjection and (**b**) postinjection of 0.2 mL/kg of PLGA-decafluorobutane capsules. *Source:* Images obtained in collaboration with F. Forsberg and B.B. Goldberg at Thomas Jefferson University Hospital and funded in part by grants number NIH HL52901 and NIH CA52823.

Color Figure

It is composed of two nonionic surfactants; for example ST68 contains Span 60 and Tween 80, whereas ST44 contains Span 40 and Tween 40 (267). The agent is produced by sonication of a phosphate-buffered saline solution of the two surfactants (268). The resulting microbubbles have a mean diameter of roughly 3.8 μm and a concentration of 7 $\times$ 10^8 microbubbles/mL. The agent can be made with a variety of entrapped gases, for example air, PFC, and SF_6, by purging the surfactant mixture with the gas of choice prior to and during sonication. The exact size distribution is dependent on the gas used and the preparation technique, but in all cases 95% of the bubbles are less than 10 μm in diameter. In vitro a pulsatile flow system was used to acquire digitized RF A-lines (269). For the air-filled agent backscatter changes nonlinearly with dose; the maximum was 13.1 dB $\pm$ 1.0 dB for a dose of 0.30 μm/mL of suspending fluid. Attenuation reached approximately 11 dB/cm for dosages above 0.27 μl/mL and for frequencies between 2.5 and 6.0 MHz. In vivo, intravenous injections of ST68 were given to rabbits at doses from 0.01 to 0.23 mL/kg. A clear increase in flow signal was observed for 1 to 2 minutes. An in vivo dose response curve was calculated from audio Doppler signals obtained with a 10 MHz cuff transducer placed around the distal aorta. Maximum enhancement was 18.3 dB $\pm$ 3.13 dB for a 0.13 mL/kg dose (269). In color Doppler and CAI all agents produced remarkable enhancement, but PFC-filled agents gave the most dramatic and long lasting effect (up to 15 minutes). Figure 9 compares (*1*) the preinjection Doppler image (*2*) with the image after injection of 0.1 mL/kg of ST68-containing PFC. Injections were through the catheterized jugular vein. In addition to the Doppler enhancement, parenchymal enhancement can be observed in the B-mode. Even more dramatic enhancement was obtained with a similar dose but using CAI as shown in Figure 10.

Recently we have investigated the use of the agent for harmonic imaging. Again the PFC-filled agent gave the best results, but the SF_6 was a close second. Figure 11 shows the poorly defined harmonic color Doppler image of a New Zealand white rabbit kidney (*1*) before contrast, and

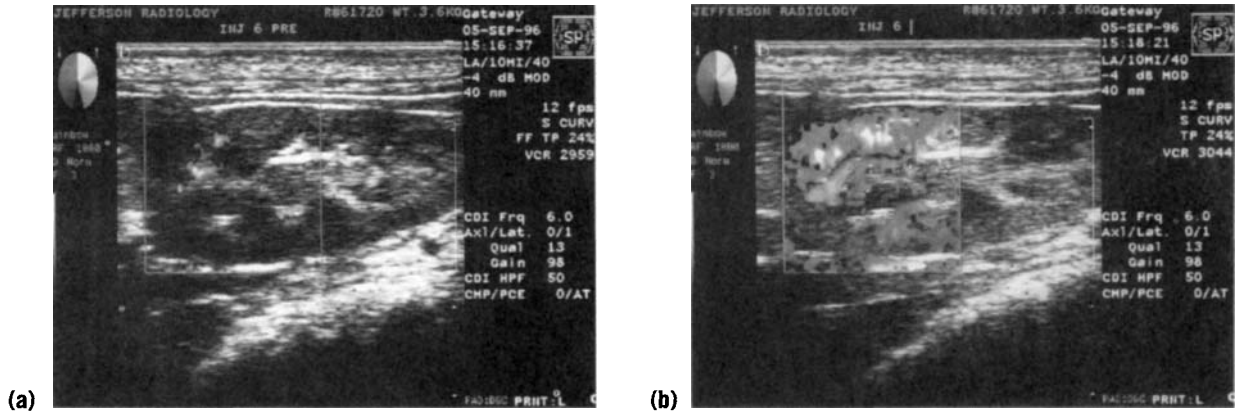


Figure 9. Color Doppler image of right kidney (see color plate). (**a**) Preinjection and (**b**) postinjection of 0.1 mL/kg of ST68-containing PFC. The color reaches the kidney capsule, and marked parenchymal enhancement is seen on the B-mode (outside the color box). *Source:* Images obtained in collaboration with F. Forsberg, and B.B. Goldberg at Thomas Jefferson University Hospital and funded in part by grants number NIH HL52901 and NIH CA52823.

Color Figure

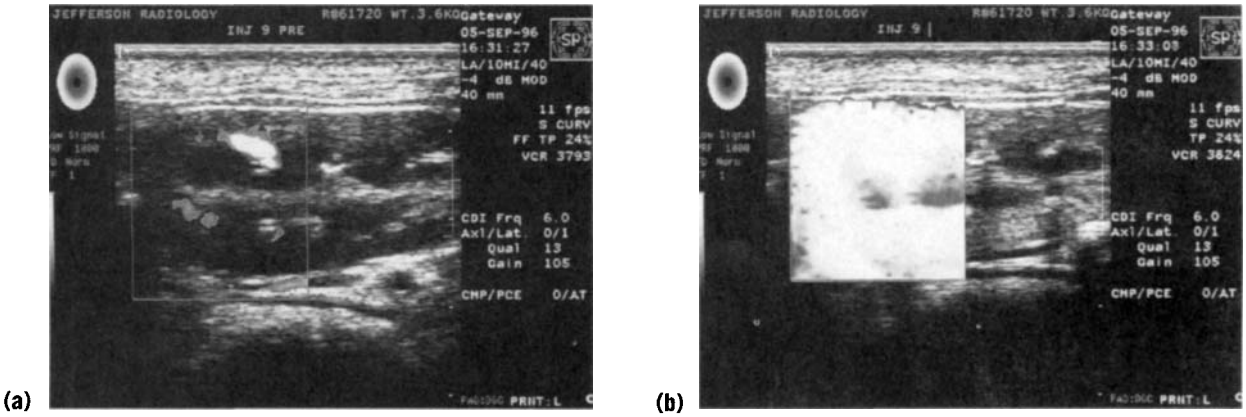


Figure 10. CAI of right kidney (see color plate). (**a**) Preinjection and (**b**) postinjection of 0.1 mL/kg of ST68-containing PFC. Color blooming and flash artifact subsided after a few passes. Enhancement lasted 15 minutes. *Source:* Images obtained in collaboration with F. Forsberg and B.B. Goldberg at Thomas Jefferson University Hospital and funded in part by grants number NIH HL52901 and NIH CA52823.

Color Figure

(2) the strong color and greatly enhanced B-mode image after intravenous contrast, using ST44-PFC. After contrast the kidney is clearly outlined, and shadowing can be observed in the lower edge of the kidney due to the high reflectance of the ultrasound wave by the agent closer to the transducer. Enhancement lasted from 10 to 15 minutes depending on the surfactant mixture that was used. The results are again more dramatic in color amplitude mode, as shown in Figure 12. These results are extremely encouraging, and are the subject of ongoing research.

Actively Targeted Ultrasound CA. Developments in ultrasound CA have followed those in MRI, with development of agents which contain a targeting moiety specific for a site at a given pathology. Active targeting to a thrombus is being pursued by several groups. One such agent is being developed at Imarex (Tucson, Arizona). The agent, MRX-408 consists of an Aerosome-bearing ligands (RGD analogues) specific to the GPIIBIIIA receptor of activated platelets in thrombus (270–273). Compared with injections of the nontargeted Aerosomes MRX-113 or MRX-115, significant increases in intensity of ultrasound postcontrast with MRX-408 were shown using videodensitometry. Thrombus was created in dog by advancing a guidewire-binding thrombin-coated thread into various vessels, including the aortobifemoral system, inferior vena cava, and left auricular appendage.

Others are exploiting the strong binding between avidin and biotin in a targeting method reminiscent of site-specific drug delivery (274,275). The thrombus was first pretargeted with a biotin–antibody conjugate (biotin–antifibrin monoclonal antibody), followed by injection of excess avidin. This resulted in a clot labeled with avidin via an antibody–biotin bridge. Biotinylated, lipid-coated, PFC

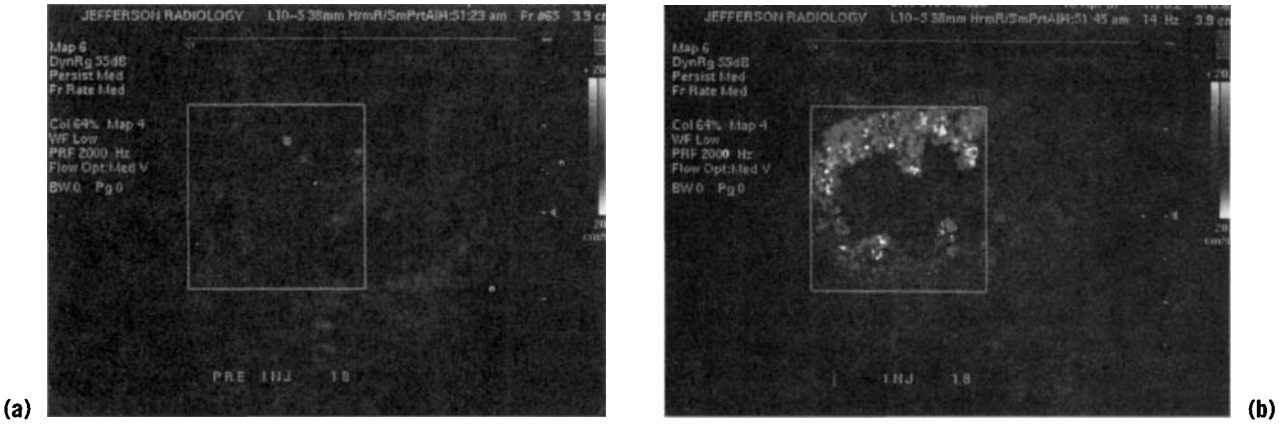


Figure 11. Color Doppler harmonic image of right kidney (see color plate). (**a**) Preinjection and (**b**) postinjection of 0.1 mL/kg of ST44-containing PFC. With a mechanical index of 0.6 the precontrast image is poorly defined. Strong color and B-mode enhancement are obtained with contrast. *Source:* Images obtained in collaboration with F. Forsberg and B.B. Goldberg at Thomas Jefferson University Hospital and funded in part by grants number NIH HL52901 and NIH CA52823.

Color Figure

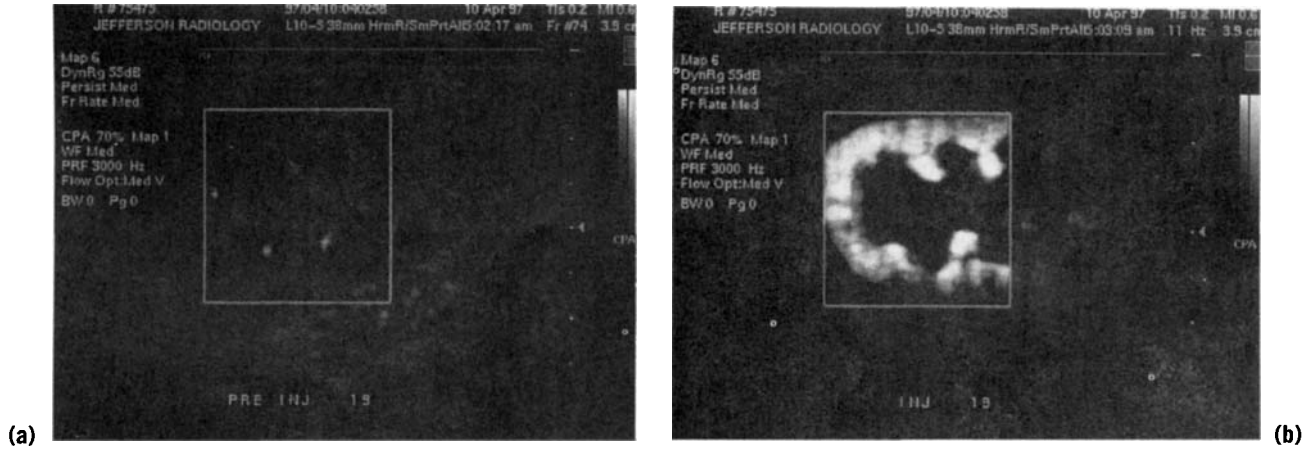


Figure 12. Color amplitude harmonic image of right kidney (see color plate). (**a**) Preinjection and (**b**) postinjection of 0.1 mL/kg of ST68-containing PFC. The dark vertical lines in the lower kidney indicate strong shadowing. *Source:* Images obtained in collaboration with F. Forsberg and B.B. Goldberg at Thomas Jefferson University Hospital and funded in part by grants number NIH HL52901 and NIH CA52823.

Color Figure

emulsion was then administered, which bound to the avidin exposed on the thrombus surface. They demonstrated that in dog, thrombi exposed to antifibrin-targeted contrast exhibited significantly increased echogenicity ($P < .05$). The great advantage of this method is that a single biotinylated agent could be used in a variety of targeting situations. The initial treatment with a unique biotin–antibody conjugate defines the target site by the choice of antibody. The same biotinylated agent targets any site once the avidin in the follow-up injection has bound to the specific biotin–antibody conjugate at the site.

Antibody is also used in an agent targeted to atherosclerosis as well as thrombi (276). The CA was again a liposome-based agent composed of phosphatidylcholine, 4-(*p*-maleimidophenyl)butyrylphosphatidyl ethanolamine, phosphatidylglycerol, and cholesterol. Antibody was conjugated via the amine group on the phosphatidyl ethanolamine (PE) using 3-(2-pyridyldithiolpropionic acid) *N*-hydroxysuccinimide ester. Electron microscopy revealed attachment of the agent to in vitro thrombi, and attachment was demonstrated ex vivo by ultrasound imaging of postmortem samples from standard Yucatan miniswine model of induced atherosclerosis.

Ultrasound Contrast Imaging with Therapeutic Modalities

The therapeutic applications of ultrasound have primarily used the potential of ultrasound to induce cell damage, both lethal cell lysis induced by ultrasonic cavitation (277) and transient permeabilization of cell membranes (278). Cavitation can be either unstable (also called transient) or stable. Transient cavitation is described as the generation,

growth, and disruption of microbubbles. Bubble disruption produces a very high local pressure change and extremely high, transient temperatures. Stable cavitation gives rise to oscillation of the microbubbles, which itself is accompanied by large shock waves that produce microstreaming of liquids. Catheter delivery of ultrasound has been demonstrated to dissolve clots (279,280) and transcutaneous ultrasound has been reported to enhance the effect of thrombolytic agents (281). It is a logical extension to investigate the effect of the presence of CA on these and similar effects, because the microbubbles can act as cavitation nuclei. Tachibana and Tachibana demonstrated in vitro that Albunex could accelerate the fibrinolytic effect of urokinase in the presence of 170 kHz ultrasound (282). Porter has shown, again in vitro, that PESDA can enhance clot disruption (283). Finally, Siegel and co-workers have demonstrated both in vitro and in vivo in rabbit that the phase shift agent Echogen (dodecafluoropentane emulsion) significantly enhances the clot disrupting effect of low frequency ultrasound (284).

In the area of drug and gene delivery, ultrasound has not lagged behind progress already described for MRI. The Unger group has been in the forefront, with initial investigations into the successful use of microbubbles to increase the rate of heating during ultrasound hyperthermia as early as 1992 (285). They followed this with the use of gas-filled liposomes (286), and in both cases found that the microbubbles were destroyed. This gave the idea of incorporation of drug into the lipid bilayer of the agent, and the use of ultrasound to first release the drug and then facilitate its delivery (287). Using 1 MHz continuous wave ultrasound, they have demonstrated an increased rate of expression from liposomal agents in vitro in cell culture (288,289). Gene expression was assessed 48 hours after transfection with cationic liposomes complexed to the gene for chloramphenicol acetyltransferase. Interestingly, ultrasound given before during or after addition of the gene to the cells increased the rate of gene expression. However, perhaps the most significant observation came when they used fluorinated gas precursors in the liposomes and achieved even higher gene expression. Miller and coworkers have demonstrated the use of Albunex in cultured Chinese hamster ovary cells exposed to 2.25 MHz ultrasound to produce cavitation nuclei to facilitate transient permeabilization (sonoporation) at spattila peak pressure amplitudes as low as 0.1 MPa (290). Above this pressure considerable lysis was observed, increasing rapidly above the cavitation threshold of 0.4 MPa, as determined by H_2O_2 production test. In DNA transfection tests, Luciferase production reached a maximum of 0.33 ng per 10^6 cells at 0.8 MPa exposure.

CONCLUSION

The use of CA has greatly enhanced the diagnostic potential of the major noninvasive imaging techniques, whether they are an inexpensive agent such blueberry juice, used with the most expensive imaging technology of MRI (89), or highly sophisticated agents such as those enabling gene transfection to be followed by MRI (107). Microencapsulation adds further dimensions to these agents. Indeed in some case, such as gaseous ultrasound CA, microencapsulation affords the imaging moiety enough stability to pass the lung to be used in the left heart and other areas of the body. Examples of the advantages of microencapsulation in CA can be chosen for all modalities. In many cases microencapsulation decreases inherent toxicity of the agent, as seen with microencapsulated SPIO (123), and frequently the natural biodistribution of the unencapsulated agent is altered. Using much of the experience acquired in drug delivery research, targeting by passive and active targeting can be directed to numerous sites: for example, tumors (201), lymph (79), blood clots (226), and even different cell types in the liver (75,76). In addition, microencapsulation has reduced the threshold for detection of hepatic lesions and continues to do as the field advances. The future will see many more advances as microencapsulated agents are developed that will demonstrate even more exquisitely specific targeting, and that will differentiate normal from abnormal physiological activity in the developing field of functional imaging.

BIBLIOGRAPHY

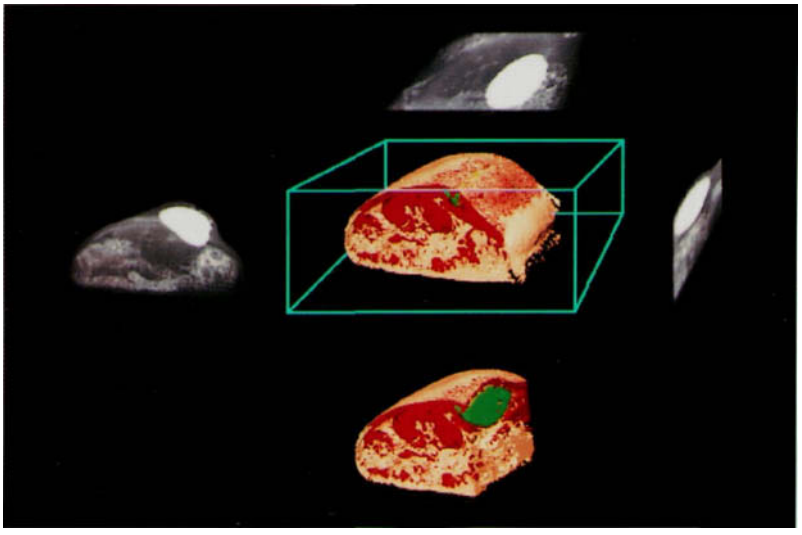
1. E.R.N. Grigg, *The Trail of the Invisible Light: From X-Strahlen to Radio(bio)logy and Therapeutics*, Sec. 76, vol. 1, Pergamon, Oxford, 1993.
2. D.D. Shaw, *Invest. Radiol.* **28**(3), S138–S139 (1993).
3. E.C. Unger et al., *Radiology* **185**, 453–456 (1992).
4. D.J. Yang et al., *ACS Symp. Ser.: Polymeric* **520**, 371–381 (1993).
5. D.J. Yang et al., *J. Pharm. Sci.* **83**(3), 328–331 (1994).
6. M.R. Violante, K. Mare, and H.W. Fischer, *Invest. Radiol.* **16**, 40–45 (1981).
7. O. Laccourreye et al., *Invest. Radiol.* **28**, 150–154 (1993).
8. H. Taniguchi, T. Takahashi, T. Yamaguchi, and K. Sawai, *Cancer (Philadelphia)* **64**, 2001–2006 (1989).
9. S. Batnitzky, in R. Miller and J. Skucas, eds., *Radiographic Contrast Agents*, University Park Press, Baltimore, Md., 1977, pp. 429–469.
10. G. Marshall, *Radiogr. Today* **61**(694), 9–11 (1995).
11. S. Chuang, *Am. J. Neuroradiol.* **13**, 785–791 (1992).
12. M.E. Bernardino, in Z. Parver, ed., *Contrast Media: Biological Effects and Clinical Applications*, CRC Press, Cleveland, Ohio, 1987, pp. 25–39.
13. S.E. Seltzer et al., *Invest. Radiol.* **19**, 142–151 (1984).
14. M.R. Violante and H.W. Fischer, in Z. Parver, ed., *Contrast Media: Biological Effects and Clinical Applications*, CRC Press, Cleveland, Ohio, 1987, pp. 89–103.
15. M.S. Sands, M.R. Violante, and G. Gadenolt, *Invest. Radiol.* **22**, 408–416 (1987).
16. J.B. Benoit and F. Puisieux, in P. Guiot and P. Couvreur, eds., *Polymeric Nanoparticles and Microspheres*, CRC Press, Boca Raton, Fla., 1986, pp. 137–174.
17. Fr. Demande 2,548,902 (January 18, 1985), P. Trampont, P. Madoule, B. Bonnemain, and F. Puissieu (to Guerbet).
18. A. Jayakrishnan, B.-C. Thanoo, K. Rathinam, and M. Mohanty, *J. Biomed. Mater. Res.* **24**, 993–1004 (1990).
19. D. Horak et al., *Biomaterials* **8**, 142–145 (1987).

20. B.-C. Thanoo and A. Jayakrishnan, *J. Microencapsul.* **66**(2), 233–244 (1989).
21. B.-C. Thanoo and A. Jayakrishnan, *Biomaterials* **11**, 477–481 (1990).
22. B. Lindberg, K. Lote, and H. Teder, in S.S. Davis, L. Illum, J.G. McVie, and E. Tomlinson, eds., *Microspheres and Drug Therapy*, Elsevier, Amsterdam, 1984, pp. 153–188, 189–203.
23. P. Rongved, J. Klaveness, and P. Strande, *Carbohydr. Res.* **297**, 325–331 (1997).
24. D.C. Leegwater and J.B. Luten, *Staerke* **23**, 430–432 (1971).
25. S. Mir et al., *Invest. Radiol.* **120**, 119–122 (1984).
26. A.A. Epenetos et al., *Nucl. Med. Commun.* **8**, 1047–1058 (1987).
27. J.E. Dion et al., *Radiology* **160**, 717–721 (1986).
28. J.-Y. Yang et al., *Invest. Radiol.* **30**(6), 354–358 (1995).
29. M.R. Violante and P.B. Dean, *Radiology* **134**, 237–239 (1980).
30. P. Leander et al., *Invest. Radiol,* **28**, 513–519 (1993).
31. D.E. Chickering, J.S. Jacob, and E. Mathiowitz, *Proc. Int. Symp. Controlled Relat. Bioact. Mater.* **20**, 244–245 (1993).
32. B.-C. Thanoo, M.C. Sunny, and A. Jayakrishnan, *Biomaterials* **12**, 526–529 (1991).
33. O.A. Rozenberg, K.P. Hanson, and E.A. Zherbin, *Radiology* **149**(3), 877–878 (1983).
34. G.L. Kendrasiak, G.D. Frey, and R.C. Heim, *Invest. Radiol.* **20**, 995–1002 (1985).
35. A. Havron, S.E. Seltzer, M.A. Davis, and P.M. Shulkin, *Radiology* **149**, 507–511 (1981).
36. S.E. Seltzer, *Radiology* **171**, 19–21 (1989).
37. S.E. Seltzer et al., *AJR, Am. J. Roentgenol*, **43**(3), 575–579 (1984).
38. M. Zalutsky, A. Noska, and S.A. Seltzer, *Invest. Radiol.* **22**(2) 141–147 (1987).
39. E.A. Zherbin et al., *Vestn. Akad. Med. Nauk SSSR* **4**, 84–89 (1982).
40. P.J. Ryan, M.A. Davis, and D. Melchior, *Biochim. Biophys. Acta* **756**(1), 106–110 (1983).
41. P.J. Ryan et al., *Radiology* **152**, 759–762 (1984).
42. V.J. Caride et al., *Invest. Radiol.* **17**, 381–385 (1982).
43. G.L. Jendrasiak, G.D. Frey, and R.C. Heim, *Invest. Radiol.* **20**, 995–1002 (1985).
44. J.P. Weichert et al., *Invest. Radiol.* **28**, S284–S285 (1994).
45. M.A. Longino, D.A. Bakan, J.P. Weichert, and R.E. Cousell, *J. Pharm. Res.* **13**(6) 875–879 (1996).
46. D.A. Bakan et al., *Hepatology* **24**(4) Pt.2,481A (1996).
47. D.A. Bakan, M.A. Longino, J.P. Weichert, and R.E. Cousell, *J. Pharm. Sci.* **85**(9), 908–914 (1996).
48. F.T. Lee et al., *Radiology* **203**, 465–470 (1997).
49. D.L. Rubin et al., *Invest. Radiol.* **29**(Suppl. 2), S280–S283 (1994).
50. G.L. Wolf and G.S. Gazelle, *Invest. Radiol.* **28**(Suppl. 4), S2–S4 (1993).
51. G.L. Wolf, *Radiology* **185**, 115 (1992).
52. G.L. Wolf et al., *Acad. Radiol.* **1**(4), 352–357 (1994).
53. E. Wisner et al., *Acad. Radiol.* **2**, 405–412 (1995).
54. P. Rougier et al., *Proc. 12th Annu. Meet. Eur. Soc. Med. Oncol., Cancer Immunother.* Nice, France, November 28–30 1986.
55. R. Murakami et al., *Acta Radiol.* **35** (Fasc. 6), 576–580 (1994).
56. Y. Tsushinma et al., *Cardiovasc Intervent. Radiol.* **16**(3) 189–192 (1993).
57. G.J. Dehmer et al., *J. Am. Coll. Cardiol.* **25**(5), 1069–1075 (1995).
58. V.P. Torchilin and V.S. Trubetskoy, *Polym. Prepr.* **38**(1), 545–546 (1997).
59. V.P. Torchilin et al., *Acad. Radiol.* **3**, 232–238 (1996).
60. V.P. Torchilin, M.D. Frank-Kamentsky, and G.L. Wolf, *Acad. Radiol.* **6**, 61–65 (1999).
61. S.W. Young, *Magnetic Resonance Imaging: Basic Principles*, Raven Press, New York, 1988, p. 24.
62. R.C. Brasch, M.D. Ogan, and B.L. Engelstad, in Z. Parvez, R. Moncada, and M. Sovak, eds., *Contrast Media: Biological Effects and Clinical Applications*, vol. III, CRC Press, Boca Raton, Fla., 1987, pp. 131–143.
63. D.G. Gadian and G.M. Bydder, *Contrast Agents Magnet. Reson. Imaging, Proc. Int. Workshop,* San Diego, Calif., January 1986, pp. 14–18.
64. H.J. Weinmann, R.C. Brasch, W.R. Press, and G.E. Wesbey, *AJR, Am. J. Roentgenol.* **142**, 619–624 (1984).
65. G.L. Wolf, *Contrast Media Magn. Reson. Imaging, Proc. Workshop*, Berlin, February 1–3, 1990, pp. 15–17.
66. R.C. Brasch, *Radiology* **183**, 1–11 (1992).
67. G. Marshall, *Radiogr. Today* **61** (697) 9–12 (1995).
68. G. Marshall, *Radiogr. Today* **61** (698), 9–10 (1995).
69. A. Bogdanov, Jr., R. Weissleder, and T.J. Brady, *Adv. Drug Delivery Rev.* **16**, 335–348 (1995).
70. A.-E. Mahfouz, B. Hamm, and D. Mathieu, *Eur. Radiol.* **6**, 607–614 (1996).
71. J. Crnac, M.C. Schmidt, P. Theissen, and U. Sechtem, *Herz* **22**, 16–28 (1997).
72. E.C. Unger, K. Ugurbil, and R.E. Latchaw, *J. Magn. Reson. Imaging* **4**, 235–242 (1994).
73. W. Bradley, Jr., W.T.C. Yuh, and G.M. Bydder, *J. Magn. Reson. Imaging* **3**, 199–218 (1993).
74. R.B. Lauffer et al., *Magn. Reson. Med.* **4**, 582–590 (1987).
75. P. Reimer et al., *Radiology* **177**, 729–734 (1990).
76. E.C. Unger, P. MacDougall, P. Cullis, and C. Tilcock, *Magn. Reson. Imaging* **7**, 417–423 (1989).
77. D.D. Stark et al., *Radiology* **168**, 297–301 (1988).
78. R. Weissleder et al., *Radiology* **171**(3), 835–839 (1989).
79. R. Weissleder et al., *Radiology* **175**, 494–498 (1989).
80. I. Adzamli, D. Johnson, and M. Blau, *Invest. Radiol.* **29**, 243–248 (1991).
81. S. Kaminsky et al., *Radiol. Diagn.* **30**, 541–548 (1989).
82. P. Ang et al., *Radiology* **172**(P), 51 (1989).
83. R. Tart, et al., *Radiology* **172**(P), 517 (1989).
84. J.J. Linskey and R.G. Bryant, *Magn. Reson. Med.* **8**, 285–292 (1988).
85. R. Mattrey, *AJR, Am. J. Roentgenol.* **152**, 247–252 (1989).
86. P.F. Park et al., *Radiology* **164**, 37–41 (1987).
87. B. Van Beers et al., *Eur. J. Radiol.* **14**, 252–257 (1992).
88. D. Widder, R.R. Edelman, W.L. Grief, and L. Monda, *AJR, Am. J. Roentgenol.* **149**(4), 839–843 (1987).
89. K. Hiraishi et al., *Radiology* **194**, 119–123 (1994).
90. R.C. Brasch, *Magn. Reson. Med.* **22**, 282–287 (1991).
91. G. Schumann-Crampion et al., *Invest. Radiol.* **26**, 969–974 (1991).
92. V.S. Vexler, O. Clement, H. Schmitt-Willich, and R.C. Brasch, *J. Magn. Reson. Imaging* **4**, 381–388 (1994).

93. M. Saeed et al., *Radiology* **180**, 153–160 (1991).
94. V.S. Vexler et al., *Invest. Radiol.* **27**, 935–942 (1992).
95. Y. Berthezene et al., *Radiology* **181**, 773–777 (1991).
96. Y. Berthezene et al., *Invest. Radiol.* **27**, 346–351 (1992).
97. Y. Berthezene et al., *Radiology* **183**, 667–672 (1992).
98. Y. Berthezene et al., *Radiology* **185**, 97–103 (1992).
99. J.C. Bock, U. Pison, P. Kaufman, and R. Felix, *J. Magn. Reson. Imaging* **4**, 473–476 (1992).
100. V.S. Vexler et al., *J. Magn. Reson. Imaging* **2**, 311–319 (1992).
101. C. Grandin et al., *Invest. Radiol.* **30**(10), 572–582 (1995).
102. I. Mottet, et al., *Magn. Reson. Med.* **35**, 131–135 (1996).
103. R. Weissleder et al., *J. Magn. Reson. Imaging* **3**(1), 93–97 (1993).
104. A.A. Bogdanov, Jr. et al., *Radiology* **187**, 701–706 (1993).
105. H.W. Frank, R. Weissleder, A.A. Bogdanov, Jr., and T.J. Brady, *AJR, Am. J. Roentgenol.* **162**, 1041–1046 (1994).
106. A.A. Bogdanov, Jr. et al., *J. Drug Target.* **4**(5), 321–330 (1997).
107. J.F. Kayyem, R.M. Kumar, S.E. Fraser, and T.J. Meade, *Chem. Biol.* **2**, 615–620 (1995).
108. S. Gohr-Rosenthal, H. Schmitt-Willich, W. Ebert, and J. Conrad, *Invest. Radiol.* **28**, 789–795 (1993).
109. L.X. Tiefenauer, G. Kuhne, and R.Y. Andres, *Bioconjugate Chem.* **4**, 347–352 (1993).
110. W.A. Gibby, J. Billings, J. Hall, and T.W. Ovitt, *Invest. Radiol.* **25**, 164–172 (1990).
111. S.C. Wang et al., *Radiology* **175**(2), 483–488 (1990).
112. J. Blustajn et al., *Magn. Reson. Imaging* **15**(4), 415–421 (1997).
113. C. Tilcock et al., *J. Magn. Reson. Imaging* **1**, 463–467 (1991).
114. R.B. Lauffer and T.J. Brady, *Magn. Reson. Imaging* **3**, 11–16 (1985).
115. U. Schmiedl et al., *Radiology* **163**, 205–219 (1987).
116. U. Schmiedl, R.C. Brasch, M. Ogan, and M.E. Moseley, *Acta Radiol., Suppl.* **374**, 99–102 (1990).
117. H.C. Schwickert et al., *Acad. Radiol.* **2**, 851–958 (1995).
118. A.B. Baxter, S. Melnikoff, D.P. States, and R.C. Brasch, *Invest. Radiol.* **26**, 1035–1040 (1991).
119. D.J. Parmelee, R.C. Walovitch, H.S. Oullet, and R.B. Lauffer, *Invest. Radiol.* **32**(12), 741–747 (1997).
120. B. Kreft et al., *J. Magn. Reson. Imaging* **6**(2), 378–383 (1996).
121. B. Kreft et al., *J. Magn. Reson. Imaging* **4**(3), 373–379 (1994).
122. P. Rongved, B. Lindberg, and J. Klaveness, *Carbohydr. Res.* **214**, 325–330 (1991).
123. A. Fahlvik, P. Artursson, and P. Edman, *Int. J. Pharm.* **65**, 249–259 (1990).
124. J.-M. Colet, Y. Van Haverbeke, and R.N. Muller, *Invest. Radiol.* **29**(Suppl. 2), S223–S225 (1994).
125. U.S. Pat. 5,314,679 (May 24, 1994), J.M. Lewis et al. (to Advanced Magnetics Inc.).
126. U.S. Pat. 5,492,814 (February 29, 1996), R. Weissleder (to The General Hospital Corporation).
127. D. Pouliquen et al., *Magn. Reson. Imaging* **7**, 619–627 (1989).
128. M.I. Papisov et al., *J. Magn. Reson. Mater.* **122**, 383–386 (1993).
129. P. Reimer et al., *Radiology* **193**, 527–531 (1994).
130. E. Schulze et al., *Invest. Radiol.* **30**(10), 604–610 (1995).
131. H. Frank, R. Weissleder, and T. Brady, *AJR, Am. J. Roentgenol.* **162**, 209–213 (1993).
132. R. Weissleder, A. Bogdanov, E.A. Neuwelt, and M. Papisov, *Adv. Drug Delivery Rev.* **16**, 321–334 (1995).
133. U. Schoepf et al., *BioTechniques* **24**, 642–651 (1998).
134. K.G. Go et al., *Eur. J. Radiol.* **16**, 171–175 (1993).
135. A.E. Stillman, N. Wilke, and M. Jerosch-Herold, *J. Magn. Reson. Imaging* **7**, 765–767 (1997).
136. R. Weissleder, A. Bogdanov, and M.I. Papisov, *Magn. Reson. Q.* **8**(1), 55–63 (1992).
137. L.X. Tiefenauer, G. Tschirky, G. Kuhne, and R.Y. Andres, *Magn. Reson. Imaging* **14**(4), 391–402 (1996).
138. C. Leveille-Webster, J. Rogers, and I.M. Arais, *Hepatology* **23**, 1631–1641 (1996).
139. P. Reimer et al., *J. Magn. Reson. Imaging* **2**, 177–181 (1992).
140. E. Weiner, S. Konda, A. Shadron, M. Brechbiel, and O. Gansow, *Invest. Radiol.* **32**(12), 748–754 (1997).
141. F.M. Krieg, R.Y. Andres, and K.H. Winterhalter, *Magn. Reson. Imaging* **13**(3), 393–400 (1995).
142. J.A. Nelson, U. Schimedl, and E.G. Shankland, *Invest. Radiol.* **25**, S71–S73 (1990).
143. M.D. Ogan, D. Revel, and R.C. Brasch. *Invest. Radiol.* **22**, 822–828 (1987).
144. D.A. Place et al., *Invest. Radiol.* **25**, S69–S70 (1990).
145. R. Jain, *Cancer Metastasis Rev.* **9**, 253–266 (1990).
146. S. Pislaru et al., *Eur. Heart J.* **18**, 572 (1997).
147. H.H. Engelhard and D.A. Petruska, *Cancer Biochem. Biophys.* **13**, 1–12 (1992).
148. V.E. Groman et al., *BioTechniques* **3**, 156–160 (1985).
149. E.C. Unger, D.K. Shen, G. Wu, and T. Fritz, *Magn. Reson. Med.* **22**, 304–308 (1991).
150. D. Barsky, B. Putz, K. Schulten, and R.L. Magin, *Magn. Reson. Med.* **24**, 1–13 (1992).
151. G. Bacic, M.R. Niesman, R.L. Magin, and H.M. Swartz, *Magn. Reson. Med.* **13**, 44–61 (1990).
152. C. Tilcock, E. Unger, P. Cullis, and P. MacDougall, *Radiology* **171**, 77–80 (1989).
153. E. Unger et al., *Radiology* **171**, 81–85 (1989).
154. S. Karlik, E. Florio, and C.W.M. Grant, *Magn. Reson. Med.* **19**, 56–66 (1991).
155. G.W. Kabalka et al., *Magn. Reson. Med.* **8**, 89–95 (1988).
156. R. Schwendener et al., *Invest. Radiol.* **25**(8), 922–932 (1990).
157. R. Storrs et al., *J. Magn. Reson. Imaging* **5**, 719–724 (1995).
158. A.L. Alexander et al., *J. Magn. Reson. Imaging* **35**, 801–806 (1996).
159. L.C. Clark, J.L. Ackerman, and S.R. Thomas, *Adv. Exp. Med. Biol.* **180**, 835–845 (1984).
160. C.H. Sotak et al., *Magn. Reson. Med.* **29**, 188–195 (1993).
161. A.G. Webb et al., *J. Magn. Reson. Imaging* **6**(4), 675–683 (1996).
162. S.E. Mathews, C.W. Poulton, and M.D. Threadgill, *Adv. Drug Delivery Rev.* **18**, 219–267 (1996).
163. E.R. Wisner et al., *J. Med. Chem.* **40**, 3992–3996 (1997).
164. R. Weissleder et al., *Antimicrob. Agents Chemother.* **39**(4), 839–845 (1995).
165. B. Spellerberg et al., *J. Exp. Med.* **182**, 1037–1044 (1995).
166. M.D. Bednarski, J.W. Lee, M.R. Callstrom, and K.C.P. Li, *Radiology* **204**, 263–268 (1997).
167. P.N. Burns, *Radiol. Med.* **87**, 71–82 (1994).
168. J. Ophir and K.J. Parker, *Ultrasound Med. Biol.* **15**, 319–333 (1989).

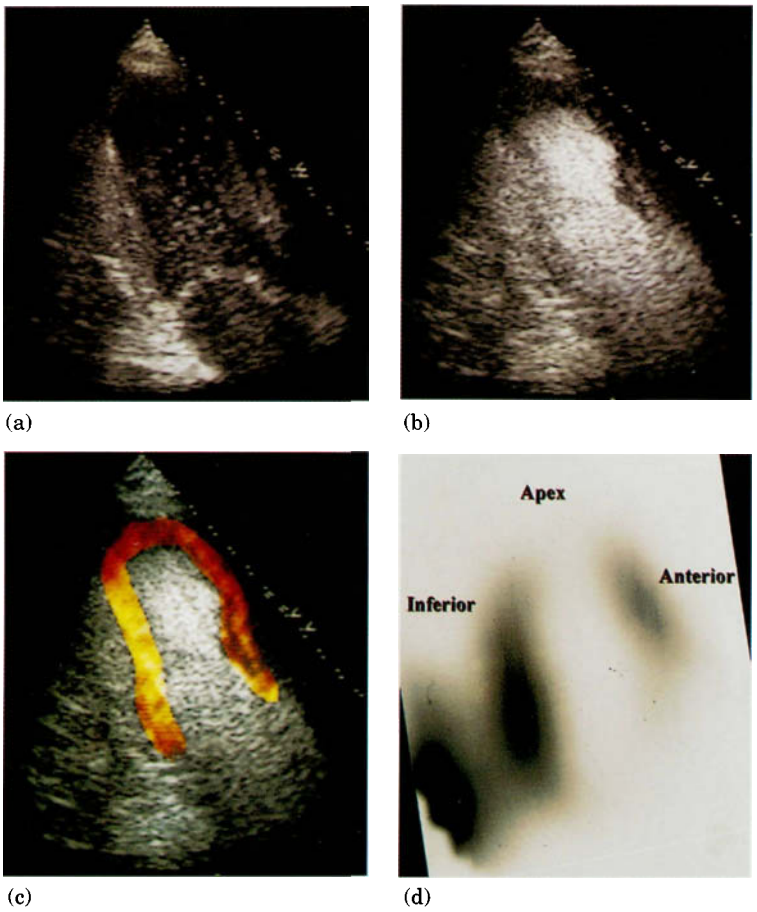
169. P.M. Morse and K.V. Ingard, *Theoretical Acoustics*, McGraw-Hill, New York, 1968.
170. A.L. Anderson and L.D. Hampton, *J. Acoust. Soc. Am.* **67**, 1865–1889 (1980).
171. E.G. Tickner and N.S. Rasnor, *Adv. Bioeng.*, pp. 101–103 (1978).
172. N. de Jong, L. Hoff, T. Skotland, and N. Bom, *Ultrasonics* **30**, 95–103 (1992).
173. C.C. Church, *J. Acoust. Soc. Am.* **97**(30), 1510–1521 (1995).
174. B.A. Schrope and V.L. Newhouse, *Ultrasound Med. Biol.* **19**, 567–570 (1993).
175. P.N. Burns, J.E. Powers, and T. Fritzsch, *Radiology* **182**, 142 (Abstr.) (1992).
176. B.B. Goldberg, J.-B. Liu, and F. Forsberg, *Ultrasound Med. Biol.* **20**, 319–333 (1994).
177. P.S. Epstein and K.J. Plesset, *J. Chem. Phys.* **18**, 1505–1509 (1950).
178. N. de Jong, *IEEE Eng. Med. Biol.* 72–82 (1996).
179. R. Gramiak and P.M. Shah, *Invest. Radiol.* **3**, 356–366 (1968).
180. P. Burns, *Clin. Radiol.* **51**(Suppl. 1), 50–55 (1996).
181. F. Forsberg et al., *Int. J. Imaging Syst. Technol.* **8**, 69–81 (1997).
182. R.S. McKay, *Proc. 2nd Symp. Underwater Physiol.*, National Academy of Sciences, Research Council Number 11181, 41 (1963).
183. H. Feigenbaum et al., *Circulation* **41**(4), 615–621 (1970).
184. M.C. Ziskin, A. Bonakdapour, D.P. Weinstein, and P.R. Lynch, *Invest. Radiol.* **7**, 500–505 (1972).
185. S.B. Feinstein et al., *J. Am. Coll. Cardiol.* **3**, 14–20 (1984).
186. R.M. Lang et al., *J. Am. Coll. Cardiol.* **8**, 232–235 (1986).
187. R.S. Meltzer and J. Roelandt, eds., *Contrast Echocardiography*, Martinus Nijhoff, Dordrecht, The Hague, The Netherlands, 1982.
188. P. Fan et al., *Ultrasound Med. Biol.* **19**, 45–57 (1993).
189. A. Killam and H.C. Dittrich, in B.B. Goldberg, ed., *Ultrasound Contrast Agents*, Martin Dunitz Ltd., London, 1997, pp. 43–55.
190. E. Unger et al., in B.B. Goldberg, ed., *Ultrasound Contrast Agents*, Martin Dunitz Ltd., London, 1997, pp. 57–74.
191. F. Bauer, C.M. Allen, and C. Missouris, *Adv. Echo-Contrast* **4**, 56 (Abstr. 50) (1995).
192. M. Stizer, *Adv. Echo-Contrast* **4**, 55 (Abstr. 55) (1995).
193. J. Langholz, *Adv. Echo-Contrast* **4**, 56 (Abstr. 51) (1995).
194. E. Leen and C.S. McArdle, *Clin. Radiol.* **51**(Suppl. 1), 35–39 (1996).
195. M. Kudo et al., *AJR, Am. J. Roentgenol.* **158**(1), 65–74 (1992).
196. M. Kudo et al., *Radiology* **182**(1), 155–160 (1992).
197. T. Fritzsch, D. Heidmann, and M. Reinhardt, in B.B. Goldberg, ed., *Ultrasound Contrast Agents*, Martin Dunitz Ltd., London, 1997, pp. 169–192.
198. U. Bogdahn et al., *Radiology* **192**, 141–148 (1994).
199. D.O. Cosgrove, *Proc. 4th Int. Symp. Recent Adv. Urol. Cancer*, Paris, 1995, p. 13.
200. V.F. Duda, G. Rode, and R. Schlief, *Ultrasound Obstet. Gynecol.* **3**, 191–194 (1993).
201. D. Cosgrove, *Adv. Echo-Contrast* **3**(38), 45 (1994).
202. R.P. Kedar et al., *Radiology* **181**(P), 202 (1991).
203. R.P. Kedar et al., *Radiology* **198**, 679–686 (1996).
204. D.O. Cosgrove and M.J.K. Blomley, in B.B. Goldberg, ed., *Ultrasound Contrast Agents*, Martin Dunitz Ltd., London, 1997, pp. 159–168.
205. A. Fleischer, A.K. Parson, and J.A. Cullinan, in B.B. Goldberg, ed., *Ultrasound Contrast Agents*, Martin Dunitz Ltd., London, 1997, pp. 137–148.
206. A.S. Lev-Toaff, D.A. Merton, J. Dumsha, and B.B. Goldberg, *Radiology* **185**, 783–788 (1992).
207. A.S. Lev-Toaff and B.B. Goldberg, in B.B. Goldberg, ed., *Ultrasound Contrast Agents*, Martin Dunitz Ltd., London, 1997, pp. 121–135.
208. B.B. Goldberg, ed., *Ultrasound Contrast Agents*, Martin Dunitz Ltd., London, 1997.
209. D. Cosgrove, *Clin. Radiol.* **51**(Suppl. 1), 1–4 (1996).
210. L. Needleman and F. Forsberg, *Ultrasound Q.* **13**, 121–138 (1996).
211. G. Marshall, *Radiogr. Today* **61**(696), 9–10 (1995).
212. B.A. Carroll et al., *Invest. Radiol.* **3**, 260–266 (1980).
213. J. Ophir, A. Gobuty, R.E. McWhirt, and N.F. Maklad, *Ultrason. Imaging* **2**, 67–77 (1980).
214. M.A. Wheatley, B. Schrope, and P. Shen, *Biomaterials* **11**(9), 713–717 (1990).
215. H. Becher and R. Schlief, *Am. J. Cardiol.* **64**, 374–377 (1989).
216. T. Fritzsch et al., *Invest. Radiol.* **25**, S160–S161 (1990).
217. B.B. Goldberg et al., *J. Ultrasound Med.* **14**, S7 (1995).
218. B.B. Goldberg et al., *Radiology* **177**, 713–717 (1990).
219. R. Schlief, *Proc. 1st Symp. Contrast Agents Diagn. Ultrasound, Leading Edge Diagn. Ultrasound*, Atlantic City, N.J., May 9, 1995, pp. 25–26.
220. H. Becher et al., *J. Am. Coll. Cardiol.* **31**(2), Suppl. A, Abstr. 907-1, p. 400A (1998).
221. M.J. Blomley et al., *Radiology* **205**(P), 418 (1997).
222. B. Goldberg et al., *Radiology* **177**(3), 713–717 (1990).
223. L.J. Crouse et al., *J. Am. Coll. Cardiol.* **22**(5), 1494–1500 (1993).
224. G. Galanti et al., *J. Am. Soc. Echocardiogr.* **6**, 272–278 (1993).
225. J.H. Wible, Jr. et al., *Invest. Radiol.* **29**, S145–S148 (1994).
226. L. Needlemann, T.L. Nack, and R.I. Goldberg, *Radiology* **185**(P), 143 (1992).
227. B.F. Vandenberg and H.E. Melton, *J. Am. Soc. Echocardiogr.* **6**, 582–589 (1994).
228. H.C. Dittrich et al., *J. Am. Soc. Echocardiogr.* **7**, S16 (1994).
229. F. Forsberg et al., *J. Ultrasound Med.* **15**, 853–860 (1996).
230. T.R. Porter, A. Kricsfeld, and K. Kilzer, *J. Am. Coll. Cardiol.* **26**, 33–40 (1995).
231. T.R. Porter, *Proc. 3rd Ann. Symp. Contrast Agents Diagn. Ultrasound, Leading Edge Diagn. Ultrasound*, Atlantic City, NJ, May 13, 1997, pp. 45–46.
232. T. Porter et al., *Circulation* **94**(Suppl.), I-319, (Abstr. 1858) (1996).
233. T. Porter, S. Li, and C. Everbach, *J. Am. Coll. Cardiol.* **31**(2), Suppl. A, Abstr. 907-3, p. 400A (1998).
234. A. Morares et al., *J. Am. Coll. Cardiol.* **31**(2), (Suppl. A), Abstr. 907-4, p. 400A (1998).
235. R.F. Mattrey et al., *Radiology* **163**, 339–343 (1987).
236. S.F. Flaim, D.R. Hazard, J. Hogan, and R.M. Peters, *Invest. Radiol.* **26**, S122–S124 (1991).
237. R. Mattrey and T.J. Pelura, in B.B. Goldberg, ed., *Ultrasound Contrast Agents*, Martin Dunitz Ltd., London, 1997, pp. 83–99.

238. R. Satterfield et al., *Invest. Radiol.* **4**, 325–331 (1993).
239. R.F. Mattrey et al., *Acad. Radiol.* **3**, S320–S321 (1996).
240. S.L. Mulvagh et al., *J. Am. Coll. Cardiol.* **25**, 288A (1995).
241. J.-M. Correas, D. Kessler, D. Worah, and S. Quay, in B.B. Goldberg, ed., *Ultrasound Contrast Agents*, Martin Dunitz Ltd., London, 1997, pp. 100–120.
242. F. Forsberg et al., *Int. J. Ultrasound Med.* **14**, 949–957 (1995).
243. C.R. Pugh, P.H. Arger, and C.M. Sehgal, *J. Ultrasound Med.* **15**, 843–852 (1996).
244. M.L. Robbin and A.J. Eisenfeld, *Radiology* **207**, 717–722 (1998).
245. T. Barrette et al., *Abstr., Proc. Symp. Am. Inst. Ultrasound Med.*, San Francisco, March 26–29, 1995.
246. U.S. Pat. 5,580,575 (December 3, 1995), E. Unger et al. (to ImaRx Pharmaceutical Corp., Tucson, Ariz.).
247. U.S. Pat. 5,656,211 (August 12, 1997), E. Unger, T. McCreer, D. Yellowhair, and T. Barrette (to Imarx Pharmaceutical Corp., Tucson, Ariz.).
248. M. Kaps et al., *Stroke* **5**, 1006–1008 (1997).
249. P. Sollender, K.D. Beller, and R. Linder, *Acad. Radiol.* **3**(Suppl. 2), 194–197 (1996).
250. J.S. D'Arrigo, R.H. Simon, and S.-Y. Ho, *J. Neuroimaging* **1**, 134–139 (1991).
251. R.H. Simon et al., *Ultrasound Med. Biol.* **19**(2), 123–125 (1993).
252. R.H. Simon et al., *Invest. Radiol.* **25**, 1300–1304 (1990).
253. E. Barbarese, S.-Y. Ho, J.S. D'Arrigo, and R.H. Simon, *J. Neuro-Oncol.* **26**, 25–34 (1995).
254. M. Schneider et al., *Invest. Radiol.* **30**(8), 451–457 (1995).
255. D. Rovai et al., *J. Am. Soc. Echocardiogr.* **11**(2), 169–180 (1998).
256. D.P. Phillips et al., in B.B. Goldberg, ed., *Ultrasound Contrast Agents*, Martin Dunitz Ltd., London, 1997, pp. 149–158.
257. K.J. Parker, T.A. Tuthill, R.M. Verner, and M.R. Violante, *Ultrasound Med. Biol.* **13**(9), 555–566 (1987).
258. K.J. Parker et al., *Invest. Radiol.* **21**, 1135–1139 (1990).
259. U.S. Pat. 5,147,631 (September 15, 1992), J.L. Glajch, G.L. Loomis, and W. Mahler (to Du Pont Merck Pharmaceutical).
260. J.R. Harris, F. Depoix, and K. Urich, *Micron* **26**(2), 103–111 (1995).
261. T. Fritzsch, D. Heldmann, and M. Reinhardt, in B.B. Goldberg, ed., *Ultrasound Contrast Agents*, Martin Dunitz Ltd., London, 1997, pp. 169–176.
262. M. Schneider et al., *Invest. Radiol.* **26**, S190–S191 (1991).
263. M. Schneider et al., *Invest. Radiol.* **27**, 134–139 (1992).
264. M. Schneider, A. Broillet, P. Bussat, and R. Ventrone, *Invest. Radiol.* **29**, S149–S151 (1994).
265. P.J. Lund et al., *Radiology* **185**, 783–788 (1992).
266. M.G. Harisinghani et al., *Clin. Radiol.* **52**, 224–226 (1997).
267. U.S. Pat. 5,352,436 (October 4, 1994) M.A. Wheatley, S. Peng, S. Singhal, and B.B. Goldberg, (to Drexel University).
268. M.A. Wheatley and S. Singhal, *React. Polym.* **25**, 157–166 (1995).
269. F. Forsberg et al., *Ultrasound Med. Biol.* **23**(8), 1201–1208 (1997).
270. T.P. McCreary et al., *Circulation*, **96** (Suppl. 8), I-213 (1997).
271. M. Takeuchi et al., *J. Am. Coll. Cardiol.* **31**(2), Suppl. A, Abstr. 907–2, p. 400A (1998).
272. M. Takeuchi et al., *J. Am. Coll. Cardiol.* **31**(2), Suppl. A, Abstr. 803–6, p. 57A (1998).
273. W.H. Wright et al., *Radiology* **205**(P), 418 (1997).
274. G.M. Lanza et al., *Circulation* **94**(12), 3334–3340 (1996).
275. G.M. Lanza et al., *Circulation* **94** (Suppl.), I-319, (Abstr. 1860), (1996).
276. S.A. Demos et al., *J. Pharm. Sci.* **86**(2), 167–171 (1997).
277. M.W. Miller, D.L. Miller, and A.A. Brayman, *Ultrasound Med. Biol.* **22**, 1131–1154 (1996).
278. M. Frechheimer et al., *Proc. Natl. Acad. Sci. U.S.A.* **84**, 8463–8467 (1987).
279. W. Steffen et al., *J. Am. Coll. Cardiol.* **24**, 1571–1579 (1994).
280. C.W. Hamm et al., *Lancet* **343**, 605–606 (1994).
281. A. Blinc, C.W. Francis, J.L. Trudnowski, and E.L. Carstensen, *Blood* **81**, 2636–2643 (1993).
282. K. Tachibana and S. Tachibana, *Circulation* **92**(5), 1148–1150 (1995).
283. T.R. Porter et al., *Am. Heart J.* **132**, 964–968 (1996).
284. T. Noshihiko et al., *J. Am. Coll. Cardiol.* **30**(2), 561–568 (1997).
285. U.S. Pat. 5,149,319 (September 22, 1992), E. Unger.
286. U.S. Pat. 5,209,720 (May 11, 1993), E. Unger.
287. U.S. Pat. 5,580,575 (December 3 1996), E. Unger et al. (to Imarx Pharmaceutical Corp., Tucson, Ariz.).
288. E.C. Unger, *2nd Thoraxcent. Eur. Symp. Ultrasound Contrast Imaging*, Rotterdam, The Netherlands, January 23–24, 1997.
289. R. Sweitzer, T. McCreary, and E. Unger, *Ultrasound Contrast Medium Res. Radiol.*, San Diego, Calif., February 7–9, 1977.
290. S. Bao, B.D. Thrall, and D. Miller, *Ultrasound Med. Biol.* **23**(6), 953–959 (1997).



Back

Figure 4. MRI of gentamicin-hydrogel. A gentamicin-hydrogel was implanted into a paraspinal abscess in a rat. Sixty individual MRI slices (individual slice thickness of 700 μm to render a slab of 4.2 cm) through the midabdominal of a rat were acquired and are displayed as axial (left), coronal (top), and sagittal (right) images or as colorized 3D reconstruction in which hydrogel is segmented in green. The calculated gel volume by MRI (0.94 mL) corresponds to 16.292 mg of gentamicin. *Source:* From Ref. 164, courtesy of Dr. R. Weissleder.

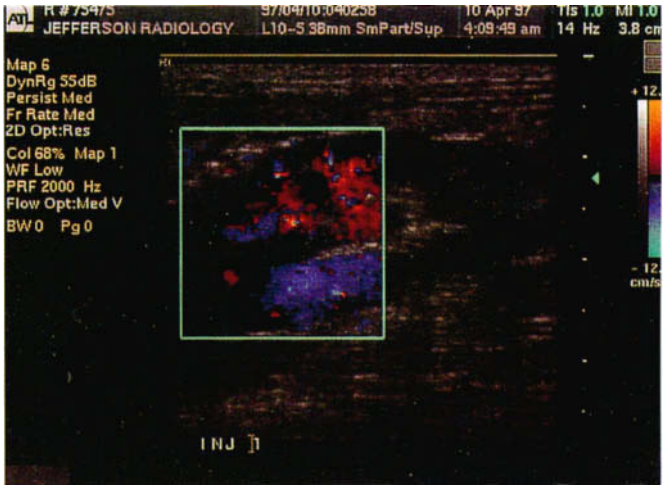


Back

Figure 6. Images from a 36-year-old male patient with anterior wall myocardial infarction three days prior to the myocardial ultrasound study. **(a)** Three aligned unenhanced images of the left ventricle in the 2-chamber long axis view. **(b)** Three aligned DMP 115-enhanced images of the left ventricle in the 2-chamber long axis view. **(c)** Digital subtracted color enhancement of the left ventricle in the 2-chamber long axis view enhanced with DMP 115. **(d)** ^{99m}Tc sestimibi image of the heart of the patient. *Source:* Courtesy of Dr. Unger, Imarex Pharmaceutical.



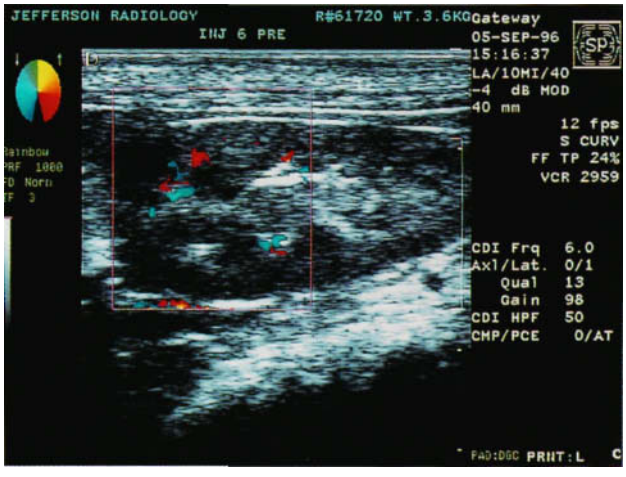
(a)



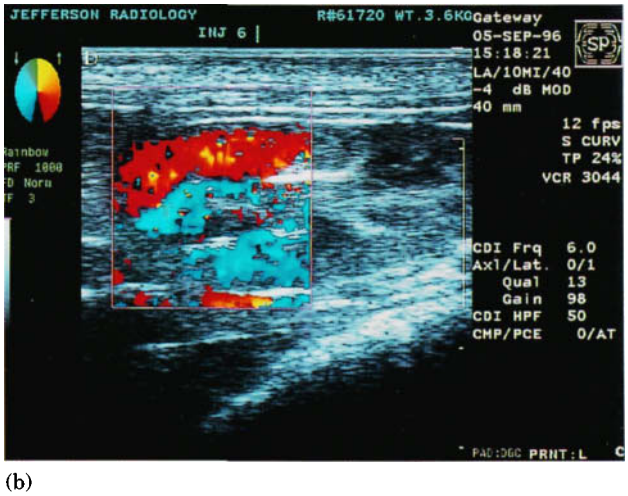
(b)

Figure 8. Color Doppler image of the right kidney. **(a)** Preinjection and **(b)** postinjection of 0.2 mL/kg of PLGA-decafluorobutane capsules. *Source:* Images obtained in collaboration with F. Forsberg and B.B. Goldberg at Thomas Jefferson University Hospital and funded in part by grants number NIH HL52901 and NIH CA52823.

Back



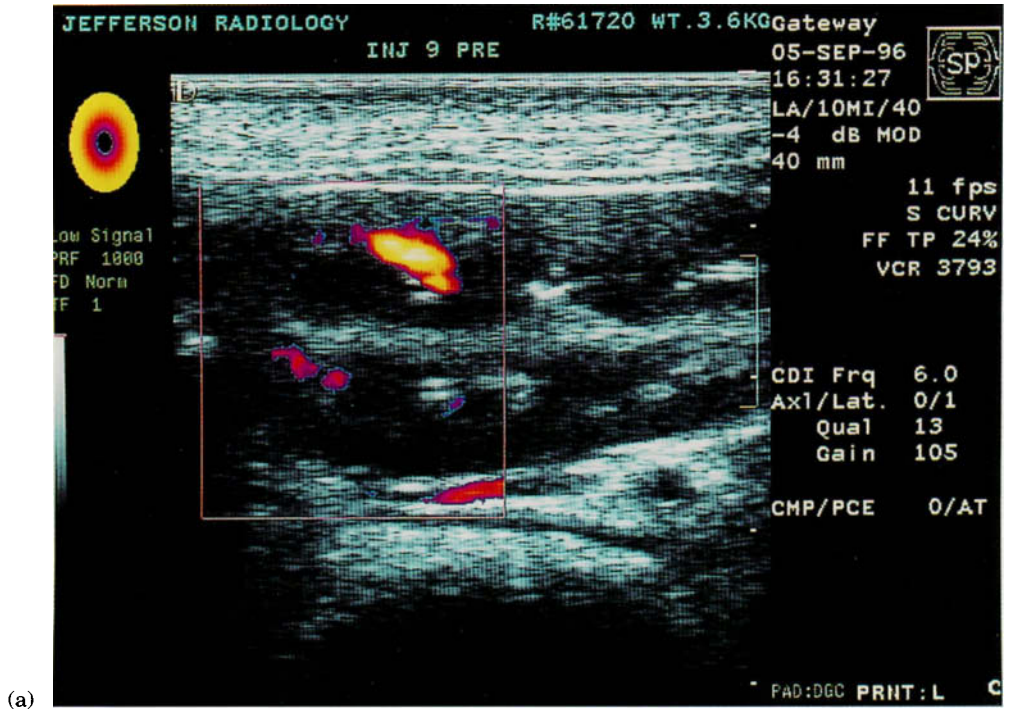
(a)



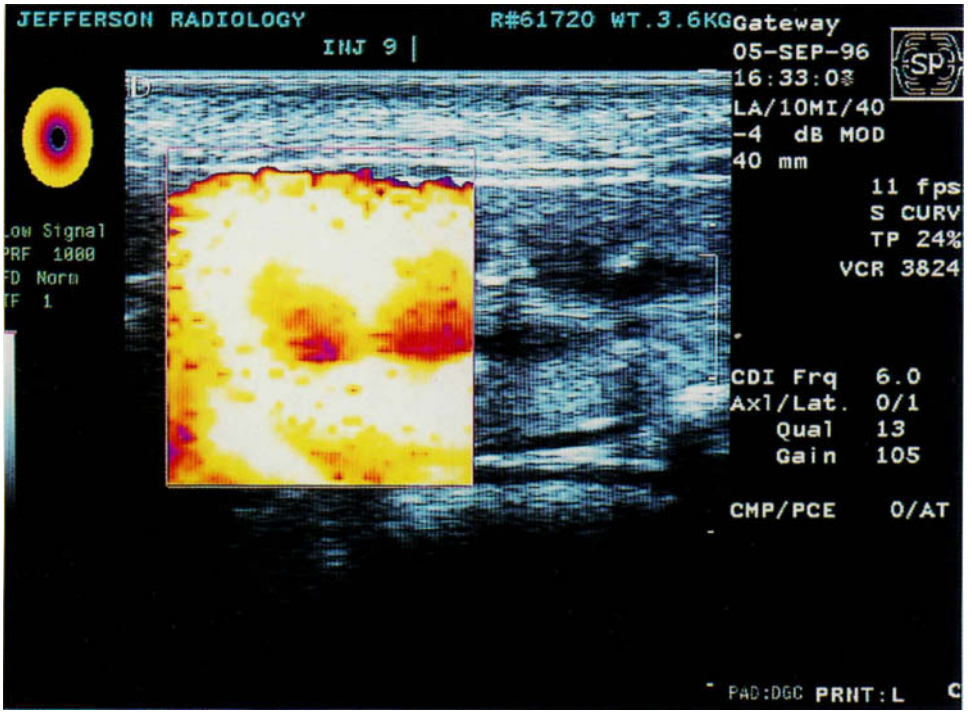
(b)

Back

Figure 9. Color Doppler image of the right kidney. **(a)** Preinjection and **(b)** postinjection of 0.1 mL/kg of ST68-containing PFC. The color reaches the kidney capsule, and marked parenchymal enhancement is seen on the B-mode (outside the color box). *Source:* Images obtained in collaboration with F. Forsberg and B.B. Goldberg at Thomas Jefferson University Hospital and funded in part by grants number NIH HL52901 and NIH CA52823.



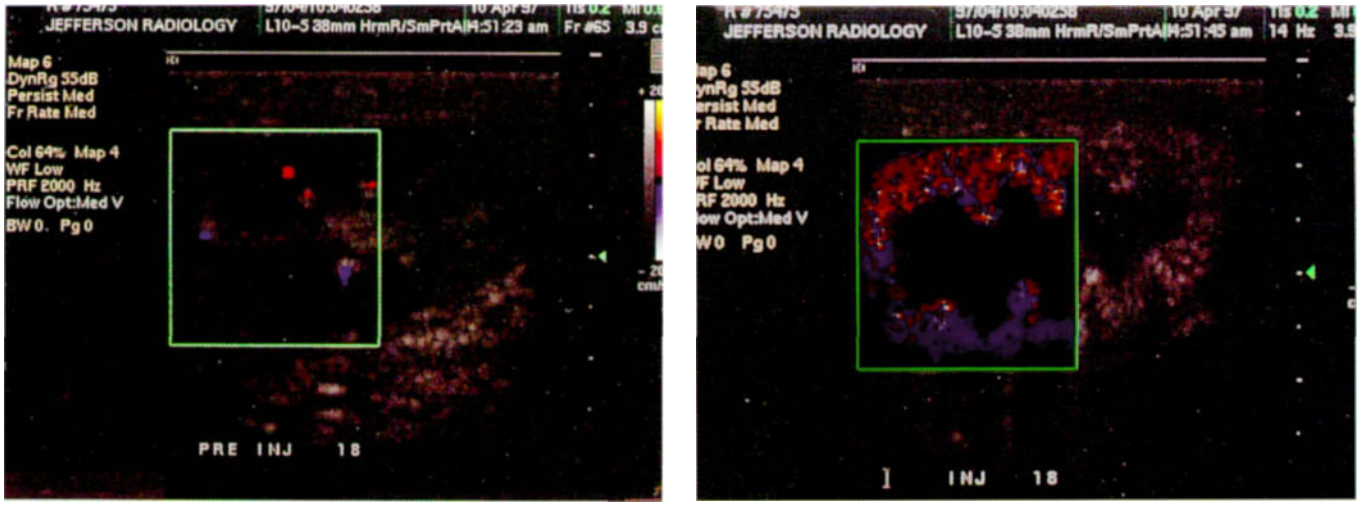
(a)



(b)

Figure 10. CAI of right kidney. **(a)** Preinjection and **(b)** postinjection of 0.1 mL/kg of ST68-containing PFC. Color blooming and flash artifact subsided after a few passes. Enhancement lasted 15 minutes. *Source:* Images obtained in collaboration with F. Forsberg and B.B. Goldberg at Thomas Jefferson University Hospital and funded in part by grants number NIH HL52901 and NIH CA52823.

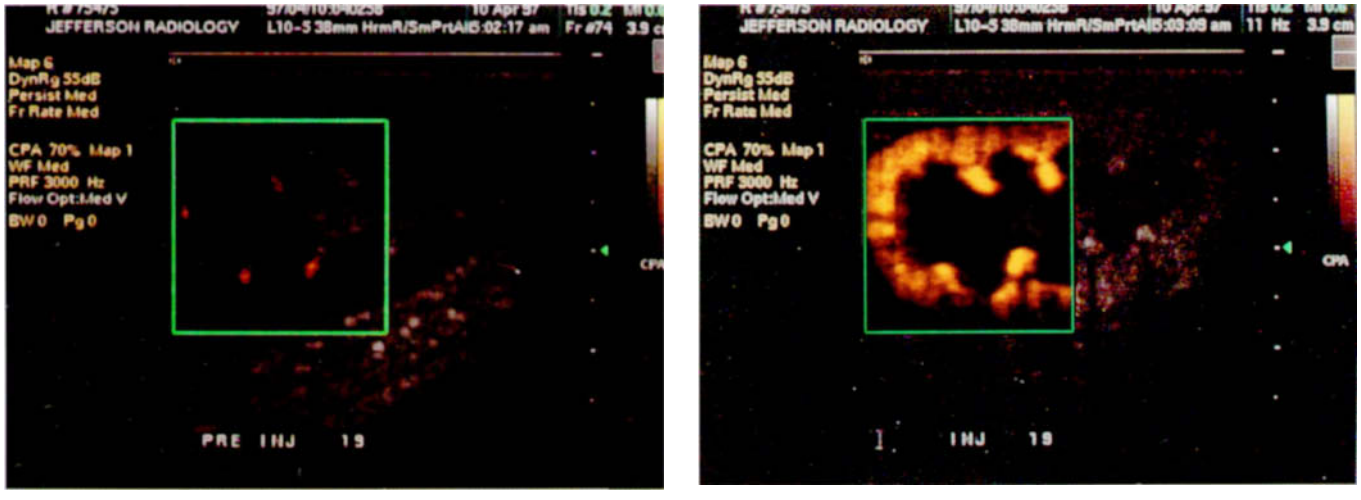
Back



(a) (b)

Back

Figure 11. Color Doppler harmonic image of the right kidney. **(a)** Preinjection and **(b)** postinjection of 0.1 mL/kg of ST44-containing PFC. With a medical index of 0.6 the precontrast image is poorly defined. Strong color and B-mode enhancement are obtained with contrast. *Source:* Images obtained in collaboration with F. Forsberg and B.B. Goldberg at Thomas Jefferson University Hospital and funded in part by grants number NIH HL52901 and NIH CA52823.



(a) (b)

Back

Figure 12. Color amplitude harmonic image of the right kidney. **(a)** Preinjection and **(b)** postinjection of 0.1 mL/kg of ST68-containing PFC. The dark vertical lines in the lower kidney indicate strong shadowing. *Source:* Images obtained in collaboration with F. Forsberg and B.B. Goldberg at Thomas Jefferson University Hospital and funded in part by grants number NIH HL52901 and NIH CA52823.

ECONOMIC ASPECTS OF CONTROLLED DRUG DELIVERY

MARK SPEERS
CLARISSA BONNANO
Health Advances, Inc.
Wellesley, Massachusetts

KEY WORDS

Commercialize
Competitors
Economics
Markets
Pricing
Prioritize
Strategy
Transactions
Unmet needs
Value

OUTLINE

Overview
Sources of Economic Value
- Value of Patent Extension
- Value of Compliance Improvement
- Value of Improved Therapeutic Efficacy
- Value in Reduced Manufacturing Costs
- Value of Market Share Expansion

Prioritizing Reformulation Candidates
- Developing a Starting List of Drug Candidates
- Examining the Technology
- Assessing the Therapeutic or Administrative Unmet Needs
- Performing a Competitive Screen
- Sizing the Market

The Future
- Some Aspects of the Industry Will Not Change
- Other Aspects Will Undoubtedly Change

OVERVIEW

Many drugs are launched with less than ideal delivery characteristics—either in the route of administration, the frequency of administration, and/or the incidence of side effects. Pharmaceutical companies have traditionally focused on developing novel compounds with documented safety and efficacy in treating a disease. To a large extent, these companies have relied upon the monopoly position their patent positions afford. These companies have known that most patients and clinicians tolerate inconvenience and side effects to benefit from the therapeutic benefits.

A separate industry has arisen that focuses on the improvement of drug delivery systems. Drug delivery systems are technologies that aid or enable the administration of therapeutic compounds. These systems include devices, such as inhalers or transdermal patches, as well as formulation technologies. Since R.P. Scherer and KV Pharmaceuticals were founded in the pre–World War II era, more than 100 companies have become actively involved in developing drug delivery systems, and the industry is growing at a considerable pace. According to the investment bank Dillon Read & Company, the drug delivery market will grow from $11.5 billion, or 12% of the total pharmaceutical market in 1996, to $35 billion, or 20% of the total pharmaceutical market in 2005.

Pharmaceutical companies have traditionally partnered with drug delivery companies to codevelop second-generation proprietary products. For example, Alza has developed several sustained-release cardiovascular products, arguably the most successful drug delivery products introduced to date, with the pharmaceutical firms Bayer AG and Pfizer. Drug companies need to use a range of technologies to reformulate their products, as each drug represents different technical challenges and different unmet clinical needs. Drug delivery companies, therefore, apply their technologies across a range of clinical segments. Although they are founded as focused niche players (e.g., depot injectables of small molecules, inhaled forms of peptides), a few of the older, established drug delivery companies have diversified their technology platforms so as to expand their commercial applicability.

Drug delivery deals with pharmaceutical companies are announced daily. Although the specific terms of these transactions are seldom disclosed, the headline deal values appear, initially, to be inconsistent and random. Table 1 lists some recent transactions. In our experience, however, the deals generally make sense when considered in a market context.

The terms of the relationship between pharmaceutical and drug delivery companies are ultimately determined by the value that the reformulation creates in the marketplace. The sources of value in reformulation include extending patent life, compliance improvement, improved therapeutic efficacy, reduced manufacturing costs and market share expansion. In today's managed care environment, with restricted pricing power for the pharmaceutical firms and managed care organizations' use of drug formularies, drug reformulations only command premium prices when they actually deliver value on these dimensions.

SOURCES OF ECONOMIC VALUE

Value of Patent Extension

Generic drugs have assumed a prominent role in the pharmaceutical industry. The modern generics industry only

Table 1. Drug Delivery Transactions

Date	Drug delivery company	Pharmaceutical company	Therapeutic(s)	Transaction value ($ millions)
3/96	Inhale	Baxter	Heparin, Factor VIII analogs	80, 20 in equity
8/96	Sano	Bristol-Myers Squibb	BuSpar	40
1/97	OSI	Hoechst Marion Russel	EPO	30
2/97	Emisphere	Eli Lilly	Insulin, growth hormone	60
7/97	Unigene	Warner Lambert	Calcitonin	54.5, 3 in equity
9/97	Aradigm	SmithKline Beecham	Morphine sulfate	40, 5 in equity
9/97	Alkermes	Alza	RMP-7 bradykinin	60, 50% royalties
12/97	TheraTech	Proctor & Gamble	Estradiol/testosterone	35

Source: Ref. 1.

began in 1984 with the passage of the Drug Price Competition and Patent Term Restoration Act. However, the pace and level of generic substitution has increased dramatically as the generics companies gained legitimacy and as managed care rewarded the practice.

Because patents guarantee market exclusivity and artificially high premiums, patent expiration translates into rapidly declining sales for brand-name pharmaceuticals. Generic versions of drugs are typically introduced at 20–25% of the branded drugs' prices. The branded drug's market erodes rapidly and loses 60–80% of the total days of therapy within 6 months—the influence of managed care and mandatory substitution laws. Figure 1 demonstrates a typical branded drug's precipitous loss of market share. For example, after Tagamet went off-patent in May of 1994, SmithKline Beecham retained only 34% of the sales of cimetidine in 1995.

Reformulating a branded drug may create an improved version that is preferred by clinicians and patients over the less expensive generic versions of the original branded product. Patents on the reformulated product allow the company to effectively extend the patent life of the drug. This strategy can dramatically affect the branded drug's market share (Fig. 2). In this scenario, one year before patent expiration, the company with the branded product launches a reformulation that quickly preserves market share. Generic versions capture only a small portion of the market, until the patent expires on the reformulated product. When Hoechst Marion Roussel reformulated Cardizem to Cardizem CD, a once-daily version of the drug, the company retained 86% of sales of diltiazem after patent expiration, a marked contrast to the market evolution for Tagamet.

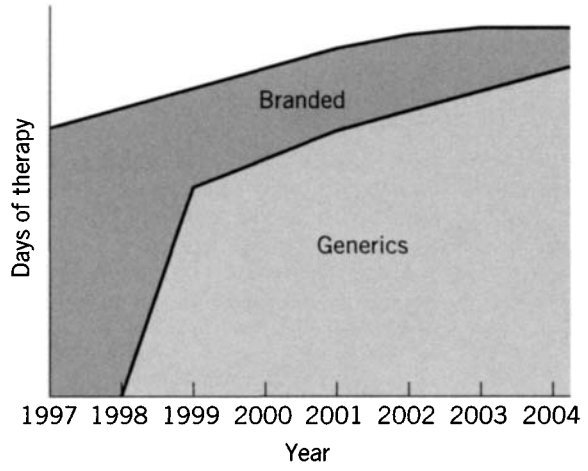


Figure 1. Generic penetration without reformulation.

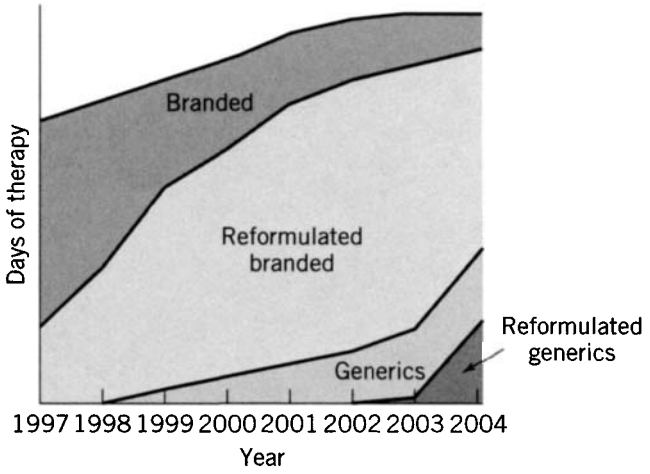


Figure 2. Generic penetration with reformulation.

Generic drugs are expected to represent an increasing percentage of the pharmaceutical market. One of the trends driving growth of this industry is the large number of upcoming patent expirations on blockbuster products. Table 2 lists the drugs among the top 100 best-selling drugs in the U.S. that will be going off-patent between 1998 and 2005. Figure 3 summarizes the value of these drugs to several major pharmaceutical firms. An important strategic move for these companies is to reformulate these branded drugs with drug delivery technologies. Likewise, generic companies are targeting these drugs as their opportunity to develop premium-priced products. Finally, well-capitalized drug delivery companies are targeting some of these generics as their first candidates to develop products for their own account.

Value of Compliance Improvement

One of the most significant impediments to keeping patients healthy and curing disease is noncompliance with prescribed medication regimens. Noncompliance explains

Table 2. Major Drugs Going Off-Patent 1998–2005

Patent expiration	Drug	Manufacturer	Indication	1997 Worldwide sales ($ millions)
1998	Atrovent (ipratropium bromide)	Boehringer Ingelheim	Asthma	691.7
	Omnipaque (iohexol)	Nycomed Amersham	Contrast enhancement	393.0
1999	Beclovent (beclomethasone dipropionate)	Glaxo Wellcome	Asthma	542.8
	Versed (midazolam)	Hoffmann-LaRoche	Depression	431.3
	Fortaz (ceftazidime)	Glaxo Wellcome	Infections	426.4
	Nizoral (ketoconazole)	Johnson & Johnson	Fungal infections	364.0
2000	Vasotec (enalapril)	Merck	Hypertension	2,510.0
	Pepcid (famotidine)	Merck	Ulcers	1,180.0
	Rocephin (ceftriaxone sodium)	Hoffmann-LaRoche	Infections	1,011.4
	Humulin (insulin)	Eli Lilly	Diabetes	939.0
	Procardia XL (nifedipine)	Pfizer	Hypertension	822.0
	Ceftin (cefuroxime axetil)	Glaxo Wellcome	Infections	649.4
	Glucophage (metformin)	Bristol-Myers Squibb	Diabetes	579.0
	Sporanox (itraconazole)	Johnson & Johnson	Fungal infections	537.0
	BuSpar (buspirone)	Bristol-Myers Squibb	Anxiety	443.0
2001	Losec (omeprazole)	Astra AB	Ulcers	2,815.8
	Prozac (fluoxetine)	Eli Lilly	Depression	2,559.0
	Prilosec (omeprazole)	Astra Merck	Ulcers	2,240.0
	Mevacor (lovastatin)	Merck	Cholesterol reduction	1,100.0
	Zestril (lisinopril)	Zeneca	Hypertension	1,035.0
	Prinivil (lisinopril)	Merck	Hypertension	585.0
	Accutane (isotretinoin)	Hoffmann-LaRoche	Acne	451.3
	Ambien (zolpidem tartrate)	Searle	Insomnia	396.0
	Accupril (quinapril)	Warner-Lambert	Hypertension	378.0
2002	Augmentin (amoxicillin)	SmithKline Beecham	Infections	1,517.0
	Mevalotin (pravastatin)	Sankyo	Cholesterol reduction	1,406.7
	Pulmicort Turbuhaler (budesonide)	Astra AB	Asthma	643.9
	Intron A (α-2B interferon)	Schering-Plough	Cancer and viral infections	598.0
	Axid (nizatidine)	Eli Lilly	Ulcers	526.5
	Nolvadex (tamoxifen)	Zeneca	Breast cancer	501.1
	Relafen (nabumetone)	SmithKline Beecham	Arthritis	489.0
2003	Biaxin (clarithromycin)	Abbott	Infections	1,300.0
	Cardura (doxazosin)	Pfizer	Benign prostatic hypertrophy	626.0
	Flovent (fluticasone propionate)	Glaxo Wellcome	Asthma	516.6
	Lotensin (benazepril hydrochloride)	Novartis	Hypertension	456.1
2004	Cipro (ciprofloxacin)	Bayer	Infections	1,441.1
	Procrit (epoetin alfa)	Johnson & Johnson	Red blood cell enhancement	1,169.0
	Taxol (paclitaxel)	Bristol-Myers Squibb	Ovarian cancer	941.0
	Diflucan (fluconazole)	Pfizer	Fungal infections	881.0
	Ortho-Novum	Johnson & Johnson	Contraception	658.0
	(norethindrone/mestranol)	SmithKline Beecham	Hepatitis B	584.0
	Engerix-B (hepatitis B vaccine)	Rhone-Poulenc Rorer	Deep vein thrombosis	462.2
	Lovenox (enoxaparin sodium)	Bristol-Myers Squibb	Ovarian cancer	437.0
	Paraplatin (carboplatin)			
2005	Zocor (simvastatin)	Merck	Cholesterol reduction	3,575.0
	Zoloft (sertraline)	Pfizer	Depression	1,507.0
	Paxil (paroxetine)	SmithKline Beecham	Depression	1,474.0
	Pravachol (pravastatin)	Bristol-Myers Squibb	Cholesterol reduction	1,437.0
	Zithromax (azithromycin)	Pfizer	Infections	821.0
	Prevacid (lansoprazole)	TAP Pharmaceuticals	Ulcers	730.0
	Lamisil (terbinafine)	Novartis	Fungal infections	628.4
	Zofran (ondansetron)	Glaxo Wellcome	Nausea and vomiting	619.9
	Zoladex (goserelin)	Zeneca	Breast cancer	569.9
	Retrovir (zidovudine)	Glaxo Wellcome	HIV infection	470.7

Source: Ref. 2.

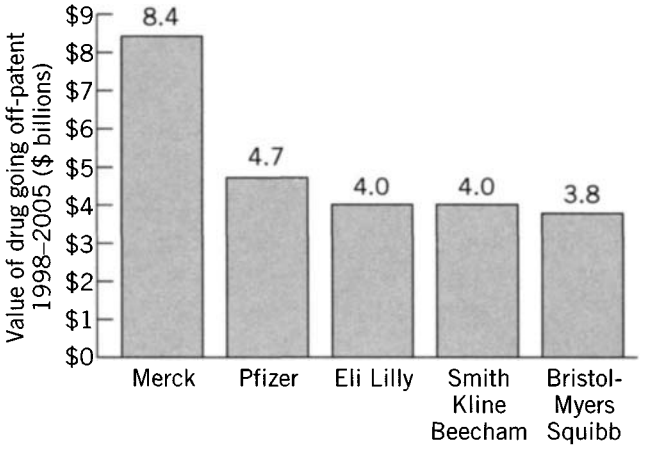


Figure 3. Market pressures to discover new drugs or reformulate old drugs. Value based on worldwide revenues.

why therapies often demonstrate greater efficacy in closely monitored clinical trials than in routine medical practice. Although compliance with prescribed regimens is not a significant issue in the closely supervised hospital setting, it is one of the most important issues for outpatients. With the average length of stay in hospitals decreasing and patients being released in a less stable state, compliance is becoming an even more significant issue. According to the Washington-based Center for the Advancement of Health, noncompliance is estimated to cost the U.S. health care system at least $100 billion annually in direct and indirect costs, significantly exceeding the $30 billion cost of prescriptions themselves.

Regardless of any therapy's potential benefits, adherence to the prescribed regimen—the correct timing, dosage, method of delivery, physical status—determines the drug's ultimate success. Clinicians often have to make predictions about expected patient compliance in deciding which drug to prescribe, if any. Clinicians may choose a suboptimal drug for fear that compliance on the more appropriate therapy will be low.

Many factors influence patient compliance, including the nature of the disease and disease symptoms, cognitive or functional ability, and financial resources. Some important factors influencing compliance, the frequency and mode of administration and the extent of drug-related side effects, can be modified through drug reformulation.

Frequency and Mode of Administration. Clinicians have learned that to achieve high patient compliance, in the absence of serious noncompliance penalties, drug regimens must be convenient and uncomplicated. Inconvenient (injectables) or complex (many dosages per day) regimens lead to poor compliance.

The oral formulation is the most preferred mode of administration as it is the easiest form for patients to tolerate. In terms of the frequency of administration, less is more. Drugs that must be taken only once per day are ideal, because they gain the highest compliance. Compliance has been shown to drop off sharply for drugs that have to be taken more than three times per day, thus drugs with more frequent dosing schedules are generally considered unacceptable for therapies that must be taken chronically. Figure 4 illustrates how clinicians rank the main alternative modes and frequencies of administration.

A sustained release oral reformulation that allows for once per day dosing is the preferred form of drug delivery. Aerosol formulations have not been as convenient as oral because they have often required frequent (3 or more times per day) dosing. In addition, the effectiveness of aerosol formulations has been hampered by the inconsistency of inhalers, which results in inadequate or varying levels of drug absorption. Nasal delivery has also lacked consistency in dosage absorbed due to backflow of drug after administration and variations in nasal architecture and volume of mucus between patients. Transdermal systems, although usually providing dosing from three to seven days, are perceived by patients as less attractive because patches can result in skin irritation and may not adhere to the skin efficiently. Depot injections offer significant improvement over frequent injections or intravenous infusions.

There are exceptions to Figure 4. For example, some patients whose compliance on daily oral medications is poor may even prefer depot injections. Contraceptives are a good example. Yet in general, patient safety may be compromised because the drug cannot be discontinued quickly. In addition, rarely will patients self-administer injectable drugs, adding to the inconvenience and cost of the therapy because patients may have to use home care or visit the doctor's office for their medication.

The most successful drug delivery formulations have been, as would be expected, oral sustained release reformulations. Currently, Bayer AG's Adalat CC product for hypertension leads the oral sustained-release market. Reformulated in 1993 from a 3–4/day to 1/day, Adalat CC has climbed to sales of $1.1 billion worldwide in 1997. Another highly successful reformulation has been TAP Pharmaceuticals' Lupron Depot for prostate cancer and endometriosis. Reformulated from a daily injection in 1989 to a once per month injection, Lupron Depot has climbed to worldwide sales of $990 million in 1997.

Extent and Nature of Side Effects. Side effects are common with many drugs and eliminating them can significantly increase the value of the therapy. For example, amphotericin B is the most powerful antifungal available, but its use is limited by a severe nephrotoxic side effect profile. Up to 40% of the patients who require amphotericin do not receive the full therapeutic course as a result of the risk of kidney failure. The clinical value of reducing the severity of this side effect is huge, and three companies (NeXstar, the Liposome Company, and Sequus) have developed liposomal formulations that protect the kidney while maintaining equivalent efficacy to the generic formulation. The improved formulations command a price premium of 10 times the generic and after less than 2 years on the market they have increased dollar sales of amphotericin 14-fold.

Side effects may be caused by the action of the drug's active ingredient and therefore are unavoidable. However,

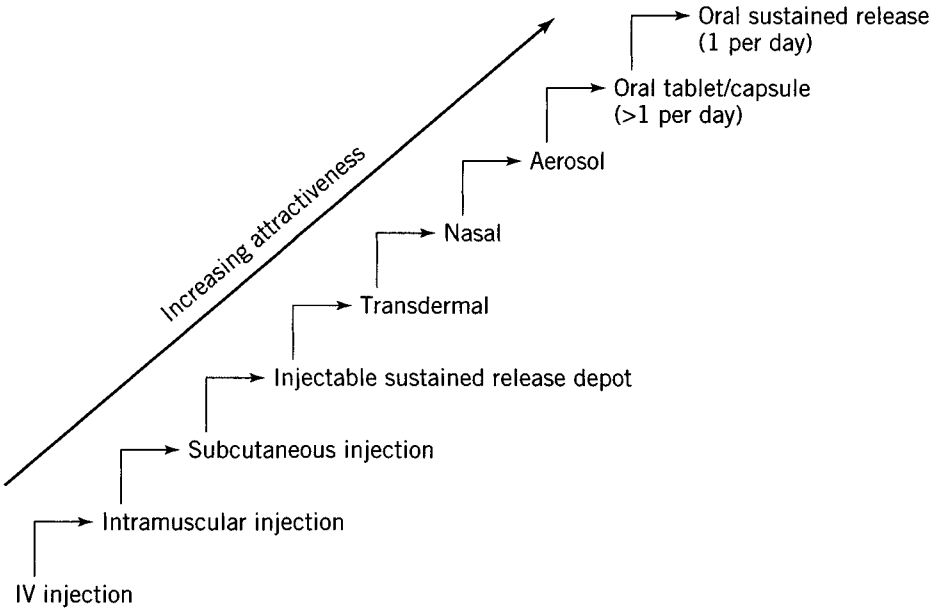


Figure 4. Hierarchy of reformulation.

drug delivery technologies can reduce or eliminate side effects such as nephrotoxicity and improve compliance.

Value of Improved Therapeutic Efficacy

Drug delivery technologies can improve medical outcomes not only by affecting compliance but also by improving therapeutic efficacy. Improvements in bioavailability may help drugs work more effectively, as can technologies that allow the release of the drug at specific times. For example, Covera HS, an Alza reformulation of hypertensive drug initially launched by Searle in 1996, is designed to deliver peak concentrations when blood pressure and heart rate are at their highest. In the field of diabetes, a number of companies are working on technologies to help diabetics maintain stable, close to normal physiologic levels of insulin, because closely titrated patients have been shown to incur fewer long-term complications from the disease than those with widely fluctuating levels.

Value in Reduced Manufacturing Costs

One method of increasing profitability on a drug is decreasing manufacturing costs. Often orally formulated drugs with poor bioavailability must be administered in high doses, because only a small percentage of the active ingredient is absorbed by the body. Drug reformulations that improve the bioavailability of the drug require less active ingredient to produce an equivalent therapeutic effect, thereby reducing manufacturing costs.

Although the manufacturing cost of a small molecule is low, active ingredients such as proteins and peptides are very expensive. Maximizing the bioavailability of these types of agents will be rewarded in the market.

Value of Market Share Expansion

Due to the size and delicate structure of peptides and proteins, these molecules have traditionally been delivered via injection. Although this format is rarely desirable, injections may be acceptable for some indications. Some indications require periodic physician visits or admission to the hospital, during which injection therapy does not significantly increase cost or inconvenience to the patient.

However, patients will simply not tolerate injections for many chronic conditions. More patient-friendly formats would therefore allow pharmaceutical firms to apply their drugs to a much broader patient population. In addition, it would expand the range of chemical compounds that may be considered as drugs.

Although much of the value in drug delivery currently lies in the reformulations of small molecules, the potential market for reformulating biotech drugs is considerable. The vast majority of these drugs remain in development, and many are appropriate for chronic diseases. Most of these drugs, however, will never reach their potential as therapeutics until they are reformulated into formats that are more acceptable to patients.

The oral delivery of large molecules constitutes the biggest opportunity within the drug delivery industry. The challenges lie in protecting these molecules from inactivation by peptidases in the gastrointestinal tract while gaining absorption from the intestine to the bloodstream. Because the oral route has been considered a longer-term option, companies have also been investigating transdermal, parenteral depot, and transmucosal delivery systems.

PRIORITIZING REFORMULATION CANDIDATES

One of the most critical components of a drug or drug delivery company's strategy is the choice of which compounds to reformulate. This process should include the following explicit steps: developing a starting list of drug candidates, examining the delivery technology, assessing the therapeutic or administrative unmet needs, performing a competitive screen, and sizing the market (Fig. 5).

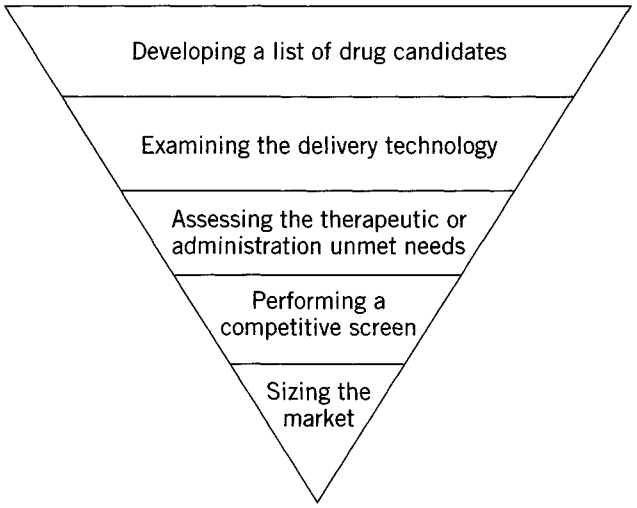


Figure 5. Prioritizing reformulation candidates.

Developing a Starting List of Drug Candidates

Because there is considerable value in extending the patent life of a compound, drug companies often focus on their blockbuster drugs that are coming off-patent. The beginning to that list is Table 2. The pharmaceutical industry's "graveyard" is another source of drug candidates that have clinical potential but have failed in clinical trials due to side effects or administrative problems. There may be even more value in resurrecting these drugs that have consumed costly drug discovery dollars but would not gain regulatory approval and/or market acceptance without reformulation.

Drug delivery companies are often faced with the choice of reformulating an existing product or collaborating with a drug company to reformulate a product that is not yet FDA-approved. The latter choice obviously bears far more risk because the drug is unproven. In addition, reformulating an existing product is particularly appropriate for delivery technologies that have never been reviewed by the U.S. FDA. Thus, the main variable under consideration when the FDA examines the product is the delivery technology. The review process is considerably shorter than if the FDA has to scrutinize the efficacy of a new drug as well. After the FDA is comfortable with the safety of the delivery system, the company might consider reformulating novel compounds. Another important consideration for drug delivery companies is whether the compound is easily sourced. For instance, amoxicillin is certainly easier to come by than paclitaxel.

Examining the Technology

Each delivery technology has different technical constraints, and companies must evaluate the drugs under consideration against these constraints. For example, many technologies have a maximum payload or molecular weight that can be delivered. Other systems will work more effectively with water-soluble or water-insoluble compounds or with compounds that can withstand a wide range in temperature.

Some drugs and indications present technical challenges as well. Insulin has a narrow therapeutic index; the dose absorbed by the body must be accurate, or hypoglycemic events may occur. This does not allow significant variability in absorption between doses or patients. For some depot formulations, an irretrievable format must be acceptable to clinicians. Drugs that are reformulated from injectable drugs to oral drugs inevitably demonstrate different pharmacodynamic and pharmacokinetic profiles. Some biologics cannot tolerate harsh manufacturing (e.g., encapsulation) techniques.

As more drug delivery technologies compete for a limited number of drug reformulations, it is critical that the drug delivery company honestly assesses its strengths and weaknesses. This screen should dramatically reduce the relevant list of drugs for further screening.

Assessing the Therapeutic or Administrative Unmet Needs

A drug reformulation must satisfy an unmet need to succeed in the marketplace. For the set of reformulation candidates that have been selected, clinicians can help identify therapeutic or administrative unmet needs. Their input can assist companies in determining what type of reformulation technology would be appropriate.

The cardiovascular and respiratory categories are currently the two biggest therapeutic segments of the drug delivery industry. Reformulations in these areas have generally met administrative unmet needs. In the cardiovascular segment, many drugs have been reformulated into sustained-release products, which increase compliance for the asymptomatic conditions of hypertension and high cholesterol. In the asthma segment, many of the reformulations have used new inhaler systems, exploiting the ease of use of these technologies.

Therapeutic reformulations have generally offered improvements on the side effect profile of drugs. Many nonsteroidal antiinflammatory drugs have been reformulated with delayed release technologies that reduce gastric irritation. Kos' new Niaspan product is a reformulation of the cholesterol product niacin. Long hailed by clinicians as an effective therapy for cholesterol and triglyceride management, niacin is difficult for patients to tolerate because of the side effect of flushing and administration multiple times per day. Niaspan improves upon this product by creating a 1/day controlled-release product to be taken at night. Niaspan also reduces the liver toxicity and flushing side effect associated with niacin. Although patients may still experience some flushing, administration of the controlled release product at night minimizes the discomfort of this side effect.

Performing a Competitive Screen

Another important step in selecting reformulation candidates is evaluating potential competitive advances. Drug reformulations of compounds going off-patent are prime candidates for significant competitive activity. In addition, many successful drugs are part of successful drug classes. Reformulations of drugs within the same class present a significant competitive threat as well.

In order to perform a comprehensive competitive screen, companies must also analyze drugs in the pipeline and other novel therapies. No matter how successful a reformulation is, it will not meet with commercial success if a therapy in a competitor's pipeline will soon cure or dramatically alter the treatment of a disease. Even experimental surgical remedies should be viewed as competitive with a drug reformulation, if the procedure is expected to change treatment and gain widespread acceptance.

Sizing the Market

In order to negotiate a successful deal between pharmaceutical and drug delivery companies, both sides need to understand the market potential of the product. The components of market size are the relevant patient population, the price of the therapy, and penetration and market share estimates.

Estimates of most patient populations are readily available in clinical literature. However, the relevant "subset" of the patient population is a more difficult estimate. For example, depending upon the drug candidate, the subset may be defined as those patients with concomitant diabetes, or those patients seen as outpatients, or those patients insured by indemnity insurers. These subset estimates require clinician interviews, secondary research of the literature, and/or mining providers' databases and patient records.

The price of therapy, which includes the price per day and days of therapy required, can initially be estimated using analogs from the product class. With the scrutiny of managed care, few reformulations command a price premium unless they offer extraordinary improvements over existing products. The increasingly common pricing strategy for many companies is to lower the price to gain market share.

Market share estimates should reflect the degree of competition in the category and the marketing partner's previous success in this category. In addition, the pace of penetration is influenced by the degree of fragmentation of the market, indicating how easily physicians can be targeted through a marketing campaign.

Another important benchmark in preparing for negotiations is to identify analogous deals that have been conducted on similar products. Example deals can not only help in determining the value of a technology, but can also suggest creative deal structures.

THE FUTURE

Some Aspects of the Industry Will Not Change

We anticipate that the drug delivery industry will continue to constitute its own segment of the pharmaceutical industry. Vertical integration of pharmaceutical companies into drug delivery will not be economically viable as each pharmaceutical company's drug portfolio requires a wide variety of drug delivery technologies. In addition, pharmaceutical companies would be reluctant to partner with the drug delivery subsidiaries of their archrivals.

Although there are undoubtedly complementary drug delivery technologies that will be required to solve specific reformulation challenges, we believe that the boutique nature of the drug delivery industry will continue for the foreseeable future. The pharmaceutical companies will remain open to funding much of the necessary research, and drug delivery companies will remain open to collaborating as necessary.

Other Aspects Will Undoubtedly Change

We expect a large shift in the mix of drugs that are being reformulated. Historically, the vast majority of reformulations have occurred just before a branded drug was to lose its patent. The branded pharmaceutical companies developed these products.

In the near term, we expect to see generic drug companies and drug delivery companies competing to reformulate generic drugs and, effectively, introduce improved drugs. These reformulation opportunities only exist because drug delivery technologies were not harnessed before the branded products' patent expirations.

The sophistication of drug delivery technologies is advancing rapidly and companies' success rates are growing. As a result, in the longer term, pharmaceutical companies will proactively elect to reformulate drugs well before they reach their patent maturities. As a recent example, Pfizer announced that it was teaming with R.P. Scherer to reformulate a faster-acting form of its blockbuster Viagra less than 4 weeks after it launched the drug. In fact, as drug delivery matures as a science, pharmaceutical companies will involve the technologies in their initial formulations.

BIBLIOGRAPHY

1. R. Longman, *Windhover's In Vivo* **15**, 49–60 (1997).
2. *MedAdNews* **17**, 94 (1998).

FABRICATION OF CONTROLLED-DELIVERY DEVICES

JAMES P. ENGLISH
Absorbable Polymer Technologies
Pelham, Alabama
WENBIN DANG
ZHONG ZHAO
Guilford Pharmaceuticals
Baltimore, Maryland

KEY WORDS

Capsule filling
Drug delivery
Drug–polymer conjugates
Encapsulation
Extrusion
Fabrication
Fluid-bed coating
Injection molding
Manufacturing processes
Polymer
Solvent evaporation
Tablet coating
Tableting
Transdermal patches

OUTLINE

Applications
- Human Pharmaceuticals
- Veterinary Pharmaceuticals
- Agricultural Products
- Cosmetics

Regulatory Considerations
Manufacturing Processes
- Polymeric Materials
- Manufacturing of Polymeric Controlled-Delivery Products by Melt Processing
- Solvent Processing of Polymeric Controlled Delivery Products
- Tableting and Tablet Coating
- Capsule Filling
- Transdermal and Iontophoretic Devices
- Drug–Polymer Conjugates
- Combination Processes

Bibliography

Manufacturing or fabrication of controlled delivery devices can be defined as "the processing of a bioactive agent into a finished product such that the finished product exhibits controlled delivery of the bioactive agent to a host site." Controlled delivery can be continuous delivery, extended delivery, delayed delivery, pulsatile delivery, or triggered delivery. Using this definition, the bioactive agents may be human or veterinary pharmaceuticals, cosmetic agents, or biocidal agents including pesticides, herbicides, fungicides, and parasiticides. The materials used to sequester and subsequently deliver the bioactive agent are typically polymeric; however, other materials such as waxes and fats are also used. Several physicochemical factors controlling the delivery of a bioactive agent to the host:

- Local pH of the host site
- Hydrophilic or hydrophobic nature of the active agent
- Solubility of the active in the local environment
- Solubility of the active in the delivery matrix
- Permeability of the delivery matrix to water
- Permeability of the delivery matrix to the active agent
- Biostability of the delivery matrix

APPLICATIONS

Because of the significant advantages of controlled delivery, which include enhanced efficaciousness, reduced toxicity, and improved product stability, the list of products using controlled delivery continues to grow, particularly in cost-neutral or cost-advantageous situations. There are some cases where controlled delivery is actually an enabling technology for a product. For example, the active agent is unstable or is highly toxic without the controlled delivery device. The most active areas for development, marketing, production, and sales of controlled delivery products are human pharmaceuticals, veterinary pharmaceuticals, cosmetics, and agricultural products.

Human Pharmaceuticals

Oral Drug Delivery. Oral drug delivery is considered to be the holy grail of drug delivery because convenience results in high patient compliance. In the area of human pharmaceuticals, controlled drug delivery had its beginnings in simple wax coatings, which prolonged the delivery of drugs taken orally. Combining many very small encapsulated drug pellets having variations in the solubility and thickness of the coating in a gelatin capsule resulted in the first extended-release cold formulation. Several enteric polymers have been developed which are insoluble in a low pH environment, but swell or dissolve in a high pH environment. Coating a drug with an enteric polymer protects the drug through the low pH of the stomach while allowing it to be released later in the higher pH environment of the intestines (1). Many drugs that are otherwise suitable for oral delivery have a very bad taste, e.g., acetaminophen.

Therefore, coating the drug to mask the taste is often necessary. Taste-masking is sometimes an added benefit obtained in coating oral drugs for other controlled release reasons.

Although oral drug delivery is very desirable, there are many problems encountered in oral delivery that severely restrict the number of drugs that can be delivered orally. The chemical environment of the gastrointestinal tract is very severe. The pH varies from a low of 0.9–1.5 in the stomach to a high of 8.1–9.3 in the intestine. A variety of adverse chemical entities, ranging from salts to digestive enzymes, are present at varying concentrations throughout the gastrointestinal tract (2). And, these chemical entities may react with or otherwise denature many drugs. Therefore, most product development activities in oral drug delivery are focused on protecting a particular drug in the gastrointestinal tract until it reaches its site of most active absorption and prolonging its residence at that site while the drug is being delivered. Very elaborate products have been developed combining features such as enteric coating, particle size, and bioadhesion for delivery of actives to targeted areas of the gastrointestinal tract, particularly the small intestine. An aspirin product has been developed and recently approved for use in some countries that is specifically designed for prophylaxis of cardiovascular disease (3).

Transdermal Drug Delivery. Again, because convenience results in high patient compliance, transdermal drug delivery is another highly desirable means of controlled drug delivery. In transdermal drug delivery, the drug delivery device can be a reservoir-type or a matrix-type device. In a reservoir-type device, the device has an impermeable backing film on the outer side, followed by a reservoir containing the drug, then a semipermeable, rate-controlling membrane, followed by an adhesive layer for attachment to the skin, and a final protective, removable inner film (4). Alternatively, for a matrix-type device, the drug can be dispersed in a polymeric matrix, laminated to the backing film and coated with an adhesive layer, followed by a protective, removable inner film. Some devices actually have the drug combined directly with the adhesive (5). The matrix serves as the drug reservoir, and in combination with the skin itself, the rate-controlling portion of the device, thus eliminating the rate-controlling membrane and simplifying the manufacturing of the product.

The skin is designed as a protective membrane for the body and is composed of several complex layers. The most impermeable of these layers is the stratum corneum (the outermost layer of the epidermis). It is difficult to effectively penetrate this barrier; skin penetration is highly dependent on the particular drug. Therefore, as with oral drug delivery, there are limitations to the number of drugs that can be effectively delivered transdermally. Several penetration enhancers, such as oleic acid, oleic acid esters, and poly(ethylene glycol) (PEG) have been discovered and are often added to transdermal formulations as an aid in crossing this barrier (6). Another drawback to transdermal delivery is that it typically takes several hours for a drug to reach a systemic equilibrium. Products containing drugs such as nicotine, glyceryl trinitrate, scopolamine, fentanyl, flurbiprofen, and several steroidal hormones are being marketed (7–10). Several others are under development.

Parenteral Delivery. Perhaps the most complex of the controlled drug delivery systems are the human parenteral systems. Biodegradable microsphere and implantable-rod systems which deliver peptides for treatment of prostate cancer have been developed and approved in several countries. Implantable osmotic pumps are used in laboratory animals to conveniently evaluate the controlled delivery of active agents under a variety of conditions. Implantable silicone rods have also been developed and marketed for delivery of steroidal hormones (11–16).

Dental. A biodegradable, in situ–forming implant containing doxycycline has been approved in the U.S. for treatment of periodontal disease. The polymer and drug are both dispersed in a water-soluble solvent. When injected into the periodontal pocket, the mixture sets by extraction of the solvent. The implant then delivers its payload and subsequently biodegrades (17,18). Nondegradable fibers containing tetracycline are also used to treat periodontal disease. The fibers are placed in the periodontal pocket where they release tetracycline. The fibers are removed by the dentist once their payload is spent (19). Fluoride salts are routinely added to dental composites, pulp liners, pit and fissure sealants, and bases to aid in recalcification following dental restoration.

Veterinary Pharmaceuticals

Veterinary pharmaceuticals are replete with controlled delivery products. Products marketed include parasiticides, pesticides, fungicides, vaccines, nutritional supplements, growth hormones, and fertility and estrus regulators. Types of delivery include rumen-bolus delivery, parenteral delivery, and topical delivery. Rumen-bolus delivery is used primarily for delivery of nutritional supplements and parasiticides to ruminant animals. Rumen boluses are designed to be heavy and typically have a complex geometry to prevent their regurgitation. Parenteral delivery is the favored route for delivery of growth hormones, some parasiticides, and antibiotics. Microspheres and implants (pellets and rods) are typical forms. Topical delivery is used primarily for pesticides and ectoparsiticides. Molded or extruded ear tags and collars are the primary forms used (20–25).

Agricultural Products

The typical agricultural applications of controlled delivery technology are encapsulated fertilizers, pesticides, and herbicides. For agricultural products, cost effectiveness is a major consideration; therefore, process and coating-material selection are limited to the simple and inexpensive. Spray-coating is very common. Interfacial polymerization processes are sometimes used where the coating forms as the product is being sprayed on the host at the time of use thus eliminating isolation of the microcapsules. Some pheromone products are also available for trapping or confusing certain insects (26).

Cosmetics

Numerous controlled delivery cosmetic products are marketed ranging from encapsulated fragrances to topical insect repellants. The most common controlled delivery cosmetics are skin-cream preparations made with liposomes containing various moisturizers and antioxidant vitamins such as vitamin C and E. Liposomes are small bilayer lipid vesicles formed by phospholipids and similar amphipathic lipids. They were originally thought to be an almost perfect drug delivery system for targeted delivery, but because of numerous problems with bioavailability and formulation stability, they have not yet found widespread use in human pharmaceuticals. However, they are being successfully used in a variety of cosmetic formulations. Methods have recently been developed to improve liposome stability by lyophilization, and liposomes continue to be tested for controlled delivery of a wide variety of pharmaceuticals.

Liposomes are formed when the lipid comes in contact with water. The lipids rearrange into concentric bilayers around aqueous inner compartment(s). Actives can be entrapped in the aqueous or the bilayer regions of the liposomes. Liposomes range in size from nanometers to micrometers and can have one (unilamellar) to many (multilamellar) lipid bilayers. Liposomes with fewer numbers of bilayers have more encapsulated volume to lipid volume and are more permeable. The liposome formation process can be simple, where thin, dry lipid films are simply hydrated, or more complex emulsification processes. Because laboratory processes are not always representative of large-scale processes, product development can often be difficult and costly. High-pressure microfluidization is one useful technology for manufacturing liposomes. Here, high pressure streams are caused to collide at high velocities in microchannels inside an interaction chamber resulting in high shear, impact, and cavitation forces and resulting in uniform, fine-particle emulsions (27–32).

REGULATORY CONSIDERATIONS

Most controlled delivery devices will fall under some kind of regulatory agency control and/or monitoring depending on the active agent. Human and veterinary pharmaceuticals are regulated by the U.S. FDA and by similar agencies in foreign countries. Pesticides, herbicides, and fungicides are regulated by the U.S. Environmental Protection Agency (EPA) or its equivalent in foreign countries. In the following descriptions of manufacturing processes for controlled delivery of bioactive agents, the reader is likely to be subject to such governmental regulations in manufacturing products of this type.

MANUFACTURING PROCESSES

There are numerous processes used in manufacturing pharmaceutical controlled drug delivery devices. In the United States, the manufacturing of controlled delivery devices for drug substances is subject to the regulations set forth in Parts 210–226 of the Code of Federal Regulations. These regulations contain the minimum current good manufacturing practice for methods to be used in, and the facilities and controls to be used for, the manufacturing, processing, packaging, or holding of a drug. These regulations assure that the drug meets the FDA requirements for safety, identity, and strength, and that the drug meets the quality and purity characteristics that it is represented to possess. Failure to comply with the regulations renders a drug to be adulterated; and such drugs, as well as the person who is responsible for the failure to comply, are subject to regulatory action (33). Similar regulations exist in other countries.

Polymeric Materials

Because most controlled delivery devices use polymeric materials to sequester and subsequently deliver an active agent, most controlled delivery manufacturing processes involve the processing of polymeric materials.

A polymer is a material where many smaller molecules are joined together to form a much larger molecule, a macromolecule, often having a molecular weight in the millions. The smaller molecules joined together to form the polymer are called monomers, and the process of joining them together to form the polymer is called polymerization.

Polymer Structure and Molecular Weight. The molecular weight of a polymer is quite different from the molecular weight of a small-molecule organic compound. Polymers are polydisperse species that are heterogeneous in molecular weight. A polymer is actually made up of many molecules of differing size. For polymers, the term *molecular weight* means an average molecular weight. And, the average molecular weight and the degree of polydispersity, or molecular weight distribution (MWD), are both required to completely characterize its molecular weight. Analytical techniques are available to accurately determine the number-average molecular weight (Mn), the weight-average molecular weight (Mw), and the polydispersity (MWD) of a polymer. Mn, determined by measurement of colligative properties, is defined as

$$\mathrm{Mn} = \Sigma N_x \mathrm{M}_x \tag{1}$$

Where N_x is the mole fraction of molecules of size M_x. Mw, determined by light-scattering measurements, is defined as:

$$\mathrm{Mw} = \Sigma \mathrm{w}_x \mathrm{M}_x \tag{2}$$

Where w_x is the weight fraction of molecules whose molecular weight is M_x. The polydispersity or MWD is defined as:

$$\mathrm{MWD} = \mathrm{Mw}/\mathrm{Mn} \tag{3}$$

Although this value may be determined by measuring the actual values of Mw and Mn, more often it is determined by a process known as size exclusion chromatography (SEC), or gel permeation chromatography (GPC). SEC and GPC are two names for the same analytical process. SEC

or GPC is an analytical process whereby a solution of the polymer is passed through a column containing micrometer-sized particles having angstrom-sized pores on their surfaces. The smaller molecules of the polymer are retained on the column longer than the larger molecules and a fractionation of the polymer molecules occurs. The mobile phase is then continually analyzed by various methods, usually refractive index or ultraviolet absorption, to quantify the fraction of the polymer sample as it is eluted from the column. The molecular weight is determined by comparison of the elution time of the polymer fractions to the elution time of known molecular-weight standards. These standards are usually narrow-molecular-weight-range polystyrene. The retention times of several (5–10) polymer standards are determined to obtain a molecular-weight-calibration curve. This method provides a Mw and Mn relative to the standards, and the MWD of the polymer sample.

There are several important factors to consider in selecting or developing a polymer for controlled delivery:

- Biocompatibility and toxicology
- Regulatory acceptance or concerns
- Degradation rate and degradation products and their biocompatibility and toxicology, if biodegradable
- Cost
- Chemical, physical, and mechanical properties
- Suitable solvents
- Processing requirements
- Compatibility limits of the active agent with the polymer
- Required sterilization methods
- Thermal transition temperatures

The relative importance of these factors varies depending on the particular application. For example, if the product contains a thermally sensitive active agent, a polymer requiring thermal processing might not be acceptable.

In developing polymers for use in controlled delivery, manufacturers carefully consider each of the aforementioned factors. The polymers' suitability for particular applications is determined, and the polymer is marketed based on its advantages. The manufacturing requirements for the polymer vary depending on the intended applications and applicable regulations. Manufacturers seek market advantages based on their polymer's suitability for an intended application, its quality, consistency, and cost, most of which depend on their particular manufacturing process. Patented or proprietary processes are often used.

Polymer Classification. There are several different ways of classifying polymers. The most common are addition and condensation polymers, referring to composition or structure of the polymer, and step and chain polymers, referring to the polymerization reaction mechanization. Polymers may be organic (containing carbon in the main chain), semi-inorganic (containing no carbon in the main chain, but containing carbon in side groups or chains), or inorganic (containing no carbon at all). Organic and semi-inorganic polymers are used extensively in controlled drug delivery; however, there are no completely inorganic polymers that have found utility. Numerous types of organic polymers are used for controlled drug delivery, but only one class of semi-inorganic polymer, the polysiloxanes or silicone elastomers, has found extensive use.

Polymer molecules may be linear (with all the monomer units linked together continuously), branched (where part of the monomer units have linked together to form side branches extending from the main polymer chain with various degrees of subordinate branching), or cross-linked (where the main polymer chains are covalently interconnected at various points). Extensively cross-linked polymers essentially form a three-dimensional matrix where the polymer becomes one extremely large molecule. A high degree of cross-linking results in insoluble, intractable materials. Polymers may be thermosetting (set irreversibly when heated, usually because of cross-links forming between the polymer chains) or thermoplastic (soften when heated but return to their original condition on cooling). Thermoplastic polymers are by far the most often used for controlled drug delivery. Polymers may also be flexible (having moderate to high elongations when stressed with little reversibility in strain), rigid (having very low elongations when stressed with essentially no reversibility in strain), or elastomeric (having high elongations when stressed with a high reversibility in strain). Polymers may be amorphous or semicrystalline. In typical use polymers are never completely crystalline because they are polydisperse. Even highly crystalline polymers always have some amorphous zones, and thus have a glass-transition temperature (T_g) in addition to their crystalline-melting temperature (T_m). The T_g is a temperature region below which a significant reduction in segmental and translational molecular mobility occurs resulting in solidification of the polymer.

Elastomeric polymers typically have highly flexible, kinked chains with a low degree of secondary interchain attractive forces and a low degree of cross-linking. When a stress is applied, the chains unkink to the point of restriction by the cross-links and rekink when the stress is removed. Fracture or permanent deformation occurs at strains beyond the point of significant resistance. "Thermoplastic elastomers" are materials where the polymer chains form regions having a high degree of secondary bonding or undergo partial crystallization, when stretched, forming pseudo cross-links (noncovalent). These pseudo cross-links provide resistance to straining similar to covalent cross-links, but because of the absence of covalent crosslinks, these materials remain thermoplastic and can be melt processed. Elastomeric polymers are typically above their T_g at use temperatures. Flexible polymers are usually semicrystalline with low to moderate crystallinity at their use temperatures. The T_g of flexible polymers vary, but are usually $<100°C$. Rigid polymers, on the other hand, are usually amorphous, have a high T_g, have very rigid polymer chains, are extensively cross-linked, or possess various combinations of these characteristics at their use temperatures (34).

Polymers useful in controlled drug delivery may be further characterized as biodegradable or nonbiodegradable,

depending on whether or not the polymer is degraded in a biological environment. Both types are used extensively. Some water-soluble polymers such as PEG and poly(vinyl pyrollidone) are absorbed and excreted by a biological host without degradation of the polymer. Such polymers are said to be bioabsorbable to distinguish them from biodegradable polymers. Synthetic biodegradable polymers that have found use in drug delivery are polylactide (PLA), poly(lactide-*co*-glycolide) (PLGA), poly(caprolactone) and polyanhydrides. Some synthetic bioabsorbable polymers that have found use in drug delivery are poly(vinyl pyrollidone) and PEG (35). Silicone elastomers, polyurethanes, poly(vinyl chloride) (PVC), and numerous other nondegradable, nonabsorbable polymers are also used.

Manufacturing of Polymeric Controlled-Delivery Products by Melt Processing

Polymer Rheology. Manufacturing of polymer-based, controlled delivery products by melt processing involves heating the polymer to a point where melt flow can occur. Depending on the molecular structure of the polymer, this point may be well above its melting point. However, at a sufficiently high temperature, the polymer is soft enough for flow to occur. Viscous flow can be modeled by a dashpot where a piston is displaced against the resistance of an oil (a Newtonian fluid) having an absolute or dynamic viscosity of η. When a shear force is applied to the fluid medium, the fluid continues to deform and the shear stress τ is proportional to the shear strain rate $d\gamma/dt$:

$$\tau = \eta(d\gamma/dt) \tag{4}$$

On cooling, a polymer may solidify either by crystallization or by passing through its glass-transition temperature, T_g. The route of solidification is determined by the molecular structure of the polymer. Crystal formation is favored by linear, unbranched polymer structures. Crystal formation is also assisted by the presence of polar groups in the chain. Branching, and stereoirregularity in general, disrupt chain packing and crystallinity. Thus, highly stereoirregular polymers are typically amorphous.

At some temperature well below the T_g, molecular motion becomes sufficiently slow enough that the behavior of the polymer can be modeled by a spring. When a tensile stress σ is applied, the tensile strain e_t is proportional to a constant E, called Young's modulus:

$$e_t = \sigma/E \tag{5}$$

From some point below T_g to some point above T_m, thermoplastic polymers exhibit what is known as viscoelastic behavior where the polymer exhibits both viscous flow and elastic properties in response to an applied stress. Therefore, the total strain is the sum of the elastic or instantaneous strain and the viscous (time-dependent and strain-rate-sensitive) strain components. The strain in response to an applied stress in this region is given by:

$$\epsilon_{total} = \sigma/E + \sigma t/K \tag{6}$$

where E and K are both constants. The viscous and viscoelastic behavior of the polymer are both very important in fabrication of polymeric devices by melt processing. Viscoelastic behavior changes with temperature leading to time-temperature equivalence particularly at very low strain rates. Thus, an increase in temperature is equivalent to a decrease in strain rate. Viscous flow is highly strain-rate-sensitive and becomes increasingly important as the temperature continually increases above T_g. When the material is stretched at a temperature above T_g, the molecules flow and align. The material in this aligned region becomes stronger, allowing more molecular flow to occur in the less aligned regions. Ultimately, this alignment gives the polymer directional properties with increased strength in the direction of alignment. This characteristic, known as orientation, is very important in the processing of fibers and films. Polymers with less symmetrical or irregular structures, polymers with compatible fluid additives or contaminants, or polymers with lower molecular weight species present, have a greater tendency for viscous flow. Some polymers are purposely formulated with plasticizers, which are essentially high boiling solvents for the polymer, that provide interchain lubricity, effectively lowering the T_g. Plasticized PVC is used in pesticidal collars and ear tags (36–38).

Scale-up of a manufacturing process to prepare a polymer for controlled delivery applications is somewhat different than for most commodity applications. For most commodity applications, the specifications of the final polymer are far less stringent than for polymers used in controlled delivery with far fewer regulatory requirements. And often there are numerous final products that can be made from a particular grade of such a polymer. Thus, the market size for a particular type and grade of a polymer used to make commodity products is typically very large. Here, cost is normally a key factor. On the other hand, final controlled delivery products are usually high value-add and their performance in the intended application usually requires very exacting specifications. Therefore, the specifications of all raw materials, including any polymers used to manufacture these products, are also very exacting. Also, the market for a controlled release product is typically a relatively small niche market requiring much smaller volumes of raw materials. Thus, for many controlled release applications the polymers used are custom made in relatively small size lots. A production lot of such polymers is therefore often very small by comparison and may range in size from <1 kg to 25 kg, especially for biodegradable controlled drug delivery products for human use. Production quantities of such polymers are therefore usually prepared in small-scale stirred batch reactors ranging in size from 1 to 50 gallons in a clean-room environment with close adherence to applicable regulatory guidelines. There are, however, some polymers used for human drug delivery that are prepared in relatively large quantities. Examples are the cellulose ethers and esters that are prepared in large-scale batch reactors. Typical batch sizes are 1,000–2000 kg. These polymers are used in enteric-coated oral formulations and currently represent one of the largest volume polymeric raw materials used in human controlled drug delivery.

Extrusion and Injection Molding. Extrusion is a process used for melting, blending, and forming a polymeric ma-

terial into a desired finished product. Postforming operations such as orientation, pressing, or final molding may also be coupled with extrusion. Rod, tubing, film, channels, and filaments are examples of shapes that can be continuously extruded. Coatings and coextruded shapes (two different polymers extruded through a die and combined into the final product shape) of all of the above can also be produced. Extruders are also used for compounding and pelletizing materials to be later molded by various processes.

An extruder consists of a heated barrel having one or more rotating extrusion screws through it. The single screw variety is the most common. The screw turns and the material moves forward through the extruder in a fashion similar to the action of a progressive-cavity pump. The barrel is often vented to remove volatiles (residual monomers, solvents, moisture, and entrapped air), thus preventing defects in the finished product. A screen pack and breaker plate (support for the screen) for filtering the material are located at the barrel exit. The pressure is measured and controlled at the exit by a feedback control loop to the screw-rotation-speed controller. Heated dies are attached to the end of the extruder to form the polymeric material into the desired shape. A melt-metering pump usually precedes the forming die to provide precise flow control.

Extruders are sized by barrel diameter and can be as small as one-half inch to as large as about 8 inches; although, for most controlled delivery applications the smaller size machines will most likely be used. The length of the flighted portion of the screw to the inside diameter of the barrel determines the available surface area of the barrel and the average residence time of the material. The barrel and screw are designed of materials suitable for the temperature, pressure, and chemical aggressiveness of the material being extruded. Typical process pressures are <35 mPa; however, pressures up to 70 mPa are not uncommon. The materials used are usually surface-hardened, high-strength alloys. They are sometimes chromeplated for added corrosion resistance. Barrel liners of highly corrosion-resistant materials are also available.

Extruders are usually heated by external electrical heater bands controlled in various zones over the length of the barrel. Heating is controlled through a feedback controller loop which actuates an electrical contacter to activate the heating elements. Because of the high shear forces involved in extrusion, heat can begin to build once the materials begin to be extruded, and it often becomes necessary to cool the extruder. Extruders are typically cooled by passing a heat transfer fluid through internal cores or jackets in the barrel, or cooling coils surrounding the barrel. Cooling is controlled through a feedback controller loop which actuates a valve to the circulating heat-transfer-fluid system.

The geometry of the screw can vary considerably depending on the material and the final product desired. The screw can have a constant pitch or "lead" or variations in screw pitch or lead beginning larger at the feed throat (point of introduction of material) and getting progressively smaller as the material progresses through and exits the barrel. The later is usually used when an intense mixing action is desirable. However, each application typically has its own requirements. The major or outer diameter of the screw is as close as possible to the barrel diameter to prohibit material from passing over the screw flights. The minor or "root" diameter of the screw will typically vary in the first screw type already described, having a smaller minor or root diameter at the feed throat and getting progressively larger and becoming constant as the later portion of the barrel (metering section) is approached. This provides a deep "channel" on material entry to accommodate incoming unmelted and uncompressed material and floods the entry zone with material to prevent starving of the extruder. Most screws are also bored, at least in the feed section, to provide entry of heat-transfer fluids for cooling.

The screen pack is located at the exit of the barrel and consists of several screens of different mesh size to filter rough contaminants from the melt. The finest mesh screen is located in the middle of progressively coarser mesh screens. The ones preceding it are for progressively finer filtering of the melt, and the ones after it are for support. The breaker plate is a thick metal plate with numerous large (~1/8-inch diameter) holes located past the screen pack and before the melt-metering pump and the forming die; it serves to support the screen pack and equilibrate the melt pressure to the pump. The metering pump is a positive displacement pump, which is controlled separately from the extruder screw to provide precise flow to the forming die (39–42).

Injection molding is probably the most widespread molding technique for quickly and easily forming a polymer melt into a finished product. In this process, the mold is split to allow part removal. It is kept closed during injection by an appropriate clamping force. The mold is filled by forcing a precompounded (containing all additives), molten polymer formulation into the mold. The injection-molding machine may be a simple piston (ram) injector design, or a more complex reciprocating-screw design. Either type consists of a feed hopper attached to a heated cylindrical barrel with an injection nozzle attached to the end of the barrel. The reciprocating screw or ram are typically capable of applying 70–140 mPa of pressure to the melt during the injection cycle. This is the operation sequence of the reciprocating-screw machine:

1. With the reciprocating screw forward, unmelted material is fed from the hopper.
2. The material is then plasticated and forced to the front of the barrel by the rotating screw, which simultaneously moves backward against a hydraulic cylinder (reciprocates) as the front of the barrel fills.
3. The mold clamp is released, the mold opens, and the part, formed on the previous cycle, is ejected.
4. The mold closes and the clamp pressure is reapplied.
5. The screw moves forward, as a ram, injecting the melt into the mold, and remains forward to begin the next cycle.

The mold temperature is kept warm but held at a suitable solidification temperature for the material being injected. Too cold a mold can lead to material freezing before the

mold is filled. Materials used to construct injection molding equipment are similar to those used to build extruders. The molds must also be constructed of rugged materials to avoid both the erosive and corrosive forces of material flow. The major advantages to injection molding are speed and the ability to simultaneously form multiple complex geometric parts. These are the disadvantages:

- The high temperature and shear require the polymers and actives to be very stable.
- The process wastes materials in runners and sprues.
- The mold and equipment costs are high.
- Mold erosion occurs from material flow.
- Runners and sprues are difficult to clean from the final products.
- The directional flow patterns, inherent in the process, can leave residual internal stresses in the part.

Some examples of controlled delivery products produced by extrusion and injection molding are antibiotic periodontal fibers and insecticidal collars and ear tags (43,44). Extrusion and injection molding processes are very efficient and available equipment is capable of producing several pounds to several hundred pounds of final product per hour.

Compression Molding. Compression molding is usually used to process thermosetting polymers and is a simple and economical process. However, it can also be used to process thermoplastic materials where it is advantageous in producing the product and provided that appropriate molding conditions are used. In compression molding, the material to be molded is placed in the preheated mold in the form of a loose powder or prill. An excess of several percent is usually added to the mold to ensure complete filling. The mold is closed and sufficient pressure (several mPa) is applied to force the material into the mold cavity. The pressure is dependent on the flow characteristics of the molding material and the complexity of the part being molded. Excess material is forced out of the mold as flash or through a vent. For thermosetting materials the pressure is maintained long enough for the part to cure. The molds are generally heated and cooled by passing a heat transfer fluid through internal cores; however, internal or external electrical heating elements can also be used if precautions are taken to avoid hot spots. The advantages of compression molding are several:

- Waste is low because no runners or sprues are used.
- The final parts are easier to clean because no runners or sprues are used.
- Mold erosion from material flow is minimized.
- Residual internal stresses are low because of the short, multidirectional flow patterns of the material.
- The mold and equipment costs are low.
- Low process temperatures can be used.

There are some disadvantages to compression molding:

- It is not suitable for intricate parts because the flow is minimal.
- Because of polymer viscoelasticity, thermoplastic parts are difficult to mold without distortion.
- It is best suited for fairly thin (≤1/4-inch) products.

Solvent Processing of Polymeric Controlled Delivery Products

Solvent Casting of Films. Solvent casting has been an established process for the preparation of polymeric films for decades. The polymer and soluble or dispersable additives are first dissolved and dispersed in a suitable solvent. The solution is then cast onto a continuous, release-coated belt or web-supported film and passed through an oven to drive off the solvent. The solvent is usually reclaimed. The dried film is continuously removed from the belt and wound as it passes from the oven. Care must be taken in design of the process line to ensure that it is particularly suited to the product being manufactured. Consideration should be given to the flow characteristics of the casting solution, the evaporation rate of the solvent, and the changing flow characteristics of the polymer solution throughout the drying process to ensure a uniform film. The thermal stability of the polymer and any additives or active agents must also be considered. Solvent casting of films containing active agents for controlled delivery can be advantageous to melt processing if the active is thermodynamically unstable. However, because of the high initial process investment and the inherent difficulty in process control, solvent casting should only be considered for manufacturing controlled drug delivery devices when absolutely necessary. Solvent casting of films is often used as a part of the overall manufacturing process in manufacturing transdermal patch products.

In Situ–Forming Implant Depots. The first in situ–forming implant depot formulation to be approved for delivery of a drug in humans is ATRIDOX™. The product is designed for controlled delivery of an antibiotic for treatment of periodontal disease. It is supplied as an injectable liquid. When injected into the periodontal cavity, the formulation sets forming a drug-delivery depot that delivers the antibiotic doxycycline to the cavity. ATRIDOX is based on the ATRIGEL® drug-delivery technology developed by Atrix Laboratories, Inc. The technology consists of a biodegradable polymer, a bioactive agent, excipients, and additives dissolved in a water-soluble, bioabsorbable, and biocompatible solvent. The formulations may be liquids, pastes, or putties; however, the liquid injectable is the preferred form for most applications (17,18). Products based on the ATRIGEL technology are typically made using a high-intensity mixer to dissolve the polymer and dissolve or disperse the active agent and any excipients.

Another company, Matrix Pharmaceutical, Inc., has developed a proprietary biodegradable gel matrix consisting of purified bovine collagen for the targeted, intralesional delivery of chemotherapeutic agents (45,46). The system is prepared by dispersing chemotherapeutic agents in an aqueous solution of a protein such as purified bovine collagen. The chief advantage of this system is that the bovine

collagen gel allows one to optimize the retention and release of the drug at a targeted injection site, thus minimizing systemic toxicity. The therapeutic effect of the delivery is further enhanced by the inclusion of a vasoconstrictor such as epinephrine. The tumor or other diseased tissues are exposed to high concentrations of the drugs for prolonged periods of time because of the site-specific and sustained release of the drug. In one study, cisplatin either in a single solution (CDDP suspension) or within the Matrix gel (cisplatin/epinephrine gel) are injected into a mouse tumor (100 mm^3). The free cisplatin was cleared from the site within 1 h, whereas the gel retained the drug between 24 to 72 h (47).

One product based on this concept, AccuSite (fluorouracil/epinephrine) Injectibel Gel for the treatment of recurrent genital warts has been approved in seven European countries and has completed Phase III studies in the United States (48). Here the gel matrix is a viscous, aqueous gel consisting of fluorouracil (30 mg/mL) and epinephrine (90.1 mg/mL) and other inactive buffering and osmotic excipients, within a purified bovine collagen matrix gel. This technology is covered by several U.S. and European patents (49–52).

Another Matrix product, IntraDose Injectable Gel, has advanced into a second level of Phase II clinical trials in the U.S. for treatment of inoperable liver cancer. The product consists of a dispersion of cisplatin and epinephrine in a purified bovine collagen matrix.

The protein gel matrix is a simple yet effective delivery system that permits direct delivery of chemotherapeutic agents to a tumor and provides a high local concentration of drug while minimizing systemic toxicity. The major disadvantage of the system is that it cannot provide long-term release of the drug (usually less than 1–3 days) because the drug can easily diffuse out of the gel matrix.

Encapsulation. Encapsulation, especially microencapsulation (particles ranging in size from a few to several hundred micrometers), is a process whereby particles of an active agent are surface coated to provide changes in the physicochemical properties of the active agent. There are many different processing techniques used depending on the desired properties of the final product, the properties of the agent being coated, and the properties of the coating material. The term microsphere is often used synonymously with microcapsule; however, a distinction should be made between the two terms as they are used in controlled delivery, because the final products produced and their release characteristics are quite different. Microcapsules are essentially discontinuous microspheres where the active core material is completely covered with a nonactive surface coating. The coating thickness may be varied depending on the characteristics desired in the final product. The surface coating of a microcapsule sequesters the active and serves as a protectant and/or a sustained release, rate-controlling membrane. The release mechanism of the active agent is usually mediated by diffusion of the active agent through the coating. On the other hand, microspheres are micrometer-sized homogeneous, monolithic spheres containing the active agent dispersed in a nonactive matrix material. The matrix material is often biodegradable. And in this case, the release mechanism of the active agent is usually mediated by degradation of the matrix. Although the final products are quite different, some of the processes used to prepare microspheres and microcapsules are very similar.

Some of the more common processes used to form microspheres and microcapsules are as follows:

- Spray-drying
- Fluid-bed coating
- Phase separation
- Solvent evaporation
- Solvent extraction
- Cryogenic solvent extraction

Several proprietary processes also exist.

Spray-Drying. Spray-drying is a process that transforms the feed material from a fluid state into a dried particulate form by spraying the feed into a hot drying medium. It is a one-step, continuous, particle-drying process. The feed material can be in the form of a solution, suspension, emulsion, or paste. The resulting product can be powdered, granular, or agglomerated particles, depending upon the physical and chemical properties of the feed material, the drier design, and its operation. Spray-drying is used in all major industries where particle drying is required, ranging from food and pharmaceutical manufacturing to chemical industries such as mineral ores and clays (53).

Spray-drying involves atomization of the feed into a drying medium, resulting in the evaporation of the solvent and the formation of dried particles. Atomization is a process that breaks up the bulk liquid into millions of individual spray droplets. The energy necessary for this process is supplied by centrifugal force (rotatory atomizer), pressure (pressure nozzle), kinetic (two-fluid nozzle), or sonic vibration (ultrasonic nozzle). The selection of the atomizer type depends on the nature of the feed and the desired characteristics of the final product. For all atomizer types, increasing the amount of energy available for atomization results in smaller droplet sizes. If the atomization energy is held constant and the feed rate is increased, larger particles result. Atomization also depends upon the fluid properties of the feed material, where higher viscosity and surface tension result in larger droplet sizes at the same atomization energy.

In most cases, air is used as the spray-drying medium; however, dry nitrogen can be used for moisture-sensitive compounds. Contact with the spray-drying medium causes evaporation of the solvent (water or organic solvent) from the droplet surfaces. The evaporation is rapid due to the vast surface area of the droplets in the spray. The manner in which the spray contacts the drying medium is an important design factor. It influences droplet behavior; and therefore, has a great effect on the properties of the dried product. Contact with the spray-drying medium is determined by the position of the atomizer in relation to the drying air inlet. Co-current flow (the product and air pass through the dryer in the same direction), counter-current flow (the spray and air enter the dryer at the opposite di-

rection), and mixed flow driers are available. The selection of the appropriate design is based on the required particle size, the required dried particle form and the temperature to which the dried particle can be subjected. For example, if a fine-particle product (mean size 20–120 μm) is required, but a low product temperature must be maintained at all times during the drying operation, a co-current, rotatory-atomizer spray-drier is selected (53).

Product separation from the drying air follows completion of the drying stage. Primary separation of the dried product takes place at the base of the drying chamber. Small fractions can be recovered in separation equipment such as a cyclone.

Spray-drying is a useful method for the processing of pharmaceuticals since it offers a means for obtaining powders with predetermined properties, such as particle size and shape. In addition a number of formulation processes can be accomplished in one step in a spray-drier; these include encapsulation, complex formation, and even polymerization (54). Spray-drying (55) and spray-congealing (56) processes can be used for preparing microparticles for controlled release applications. In the spray-congealing process, no solvent is used. The feed, which consists of the coating and core materials, is fed to the atomizer in the molten state. Microparticles form when the droplets meet cool air in the drying chamber and congeal.

Oil-soluble vitamins, such as A and D, have been microencapsulated by spray-drying an emulsion of the oil in a gum arabic or gelatin solution. Spray-drying has also been used in the preparation of polymer-coated microcapsules for the purposes of taste masking (57).

Biodegradable microparticles have also been prepared by spray-drying. PLA and PLGA microspheres have been prepared from solutions or suspensions of a number of drugs dissolved or dispersed in methylene chloride (58,59). Microcapsules of progesterone and PLA were formed with diameters of less than 5 μm. Crystallization of the drug occurred in the aqueous phase when microspheres were prepared by a solvent evaporation method, but spray-drying avoided this problem. The main difficulty encountered in preparing spray-dried microcapsules is the formation of polymer fibers as a result of inadequate forces to disperse the feed liquid into droplets; the successful atomization into droplets is dependent on both the type of polymer used and the viscosity of the spray solution (60).

Spray-drying is also used as one of the steps in the multistep manufacturing process for GLIADEL®. GLIADEL, a product of Guilford Pharmaceuticals, Inc., is a biodegradable implant containing the anticancer agent BCNU. It is approved in the U.S. and several other countries for the treatment of malignant glioma. After the tumor has been removed from the patient's brain, up to 8 wafers are implanted into the cavity created by the removal of tumor mass. The drug BCNU is slowly released from the polymer matrix as the polymer degrades. BCNU is incorporated into the biodegradable polyanhydride matrix at 3.85% loading by spray-drying. Microspheres with a size ranging from 1 to 20 μm are obtained (61). The microspheres are subsequently compressed into small wafers to prepare the final dosage form. The spray-drying method is especially useful in this application since the drug BCNU is both heat- and moisture-sensitive.

The feasibility of encapsulating proteins into polymers has also been demonstrated. Bovine serum albumin (BSA) was incorporated into poly(DL-lactide)(DL-PLA) microspheres by a spray-drying method. Successful incorporation of the protein depends on the selection of an appropriate solvent system. Dichloromethane, ethyl acetate, and nitromethane proved to be the most suitable solvents for the DL-PLA/BSA system (62).

Spray-polycondensation is another method that can be used in the preparation of microcapsules. In this technique, polymer formation from reactive monomers, encapsulation, and product separation from the vehicle are all accomplished in a one-stage process. The feed consists of a dispersion of the core material and monomers, or precondensates of relatively low molecular weight, in addition to other film-forming agents and the catalyst. This technique was used to produce microcapsules that developed slow release properties after curing (55).

Spray-drying has proven to be a useful technique in producing controlled release products. The main advantage of this process is that it is convenient, fast, and allows the use of mild conditions. However, considerable loss of material can occur during spray-drying from adhesion of the particles to the inside wall of the spray-drier and agglomeration of the microparticles if improper process conditions are used. In order for the spray-drying process to be successful, appropriate selection of the spray-drying equipment and optimization of the spray-drying conditions are essential.

Fluid-Bed Coating. Fluid-bed coating is a process whereby particulates are suspended in a column of heated air or inert gas while a solution or emulsion of a polymer or other film-forming coating material is applied to the particles through spray nozzles. High-quality microcapsule products are economically produced by this process. Typical products are taste-masked drugs, enteric-coated drugs, and sustained-release drugs (63,64).

Fluid-bed coating is a complex process consisting of three major operations: fluidization, atomization, and drying. The coating chamber has a high volume of flow to suspend, agitate, and dry the coated particles. The spraying nozzles can be located at various positions in the coating chamber providing top, bottom, and side or tangential spraying of the particles. Bottom spraying, or Würster coating as it is often called, is the most common technique used for encapsulation particles as small as 30–40 μm (65). A detailed review article on this process was provided by Christensen and Bertelsen (66). The Würster technique is a circulating fluid-bed specifically designed for small particle coating. It consists of a container with one or more Würster partition inserts, typically one partion for lab-scale equipment and three for production-scale equipment. The product load ranges from a few kilograms for laboratory scale equipment (e.g., Glatt, GPCG 3 and STREA-1, Niro) to a few hundred kilograms for production-scale equipment (e.g., Glatt, GPCG 200). The coating process consists of three phases: the start-up phase, the coating phase, and the drying phase. The start-up phase consists of an optional preheating of the equipment and the sub-

strate to either shorten the heating period, prevent overwetting of the substrate during the initial coating application, or both. In the coating phase, several processes take place simultaneously: atomization of the coating solution or suspension, transport of the film droplets to the substrate, adhesion of the droplets to the substrate, and film formation onto the substrate. The properties of the substrate such as particle density, size, and tackiness are very important in determining the coating process parameters during this phase. The coated product is finally dried to prevent adherence of the individual particles and remove residual solvents. High-quality microcapsule products are economically produced by this process. Typical products are taste-masked drugs, enteric-coated drugs, and sustained-release drugs (63–66).

Phase Separation. The phase separation process, or coacervation process as it is sometimes called, involves:

- Preparing an organic solution of a water-insoluble, matrix material (usually polymeric)
- Addition of an aqueous solution of the active agent or dispersion of particulates of an active agent to the organic solution with vigorous agitation
- Introduction of a coacervating agent or event for the matrix material to the matrix solution/active agent emulsion or dispersion
- Depending on the means of coacervation, the coacervated matrix solution/active agent emulsion or dispersion is then added to an appropriate hardening agent to extract the excess matrix solvent
- collecting, washing, and drying of the final product

Coacervation may be brought about by various means. It can be induced by:

- A change in the temperature of the system
- A change in the pH of the system
- A change in electrolyte balance
- Addition of nonsolvents
- Addition of other materials which are incompatible with the polymer solution

The term coacervation used in this context is borrowed from the description of an equilibrium state of colloidal systems. In the phase separation process for encapsulation the term refers to a state of partial precipitation of the matrix phase by the coacervation agent. The matrix material at this point is still solvent rich, and not completely precipitated, and thus maintains a high degree of flow necessary for good film- and particle-forming properties. Several of the coacervation methods described here are being successfully used to prepare a variety of products from peptide microcapsules to encapsulated electrolytes (67–72).

Solvent Evaporation. The emulsification-solvent-evaporation technique for preparation of microspheres was described by Beck et al. for the delivery of contraceptive steroids (73). It is the most widely used manufacturing technique for biodegradable microspheres. The microsphere formation process consists of three stages:

1. Droplet formation
2. Droplet stabilization
3. Microsphere hardening

First, a dispersed phase containing the polymer is emulsified in an immiscible continuous phase containing a stabilizing agent. The second phase involves the diffusion of the solvent from the emulsion droplet into the continuous phase and its subsequent evaporation. Simultaneous inward diffusion of the nonsolvent into the droplet causes polymer precipitation, microsphere formation, and hardening. Depending on the nature of the two phases, the process may be termed oil-in-water (o/w) or water-in-oil (w/o) method. The solvent evaporation process requires the use of a surfactant to stabilize the dispersed-phase droplets formed during emulsification and inhibit coalescence. Surfactants are amphipathic in nature and therefore align themselves at the droplet surface, thereby promoting stability by lowering the free energy at the interface between the two phases. Furthermore, the creation of a charge or steric barrier at the droplet surface confers resistance to coalescencing and microsphere flocculation. Surfactants employed in the o/w process tend to be hydrophilic in nature and by far poly(vinyl alcohol) is the most widely used. The emulsification systems used for microparticle production have included both low- and high-speed mechanical stirring, sonication, and microfluidization. The particle size and size distribution can be controlled by the emulsification speed and mixing vessel design. Following emulsification, the removal of remanent solvent and complete microsphere hardening is usually accomplished by gentle agitation of the suspension. After evaporation of the solvent, the final stage of the emulsification-solvent-evaporation process is the isolation of microspheres from the dispersed phase containing surfactant. This has generally been achieved by centrifugation and filtration, and it is usually followed by a further cleaning process in which the particles are washed several times with distilled water. The microspheres are finally dried using lyophilization or fluid-bed drying.

Solvent Extraction. Solvent extraction is similar in nature to o/w solvent evaporation process except that following emulsification the preformed microspheres are poured into a large volume of nonsolvent to extract the remaining organic solvent, thus causing rapid hardening of the particles.

Microencapsulation by either the solvent evaporation or the solvent extraction process is normally achieved by first emulsifying or dispersing a drug-containing polymer solution in an immiscible solvent by stirring, agitation, or some other vigorous mixing technique followed by extraction or evaporation of the polymer solvent. This process is difficult to scale-up for several reasons. The key limiting factor in reducing overall process time is the time required to form a uniform emulsion. Increased batch sizes in large tanks require a longer time to form the emulsion, resulting in longer overall production times. Longer exposure times of the active agent to the process solvents can lead to the degradation or deactivation of the active agent. Furthermore, as the emulsion tank size increases, stir speeds and

viscosity within the larger tank have to be empirically optimized by the trial and error at each stage of the scale-up. Control of the particle size can become less reliable as batch size is increased because it is difficult to maintain the same shear while still providing uniform mixing in larger vessels. Herbert et al. (74) and Ramstack et al. (75) described a process that potentially overcomes this problem. This process uses a static mixer instead of a dynamic mixer to prepare the emulsion. In this process, a first phase comprising the active agent and the polymer and a second phase comprising the dispersing medium are pumped through a static mixer into a quench medium where the polymer solvent is either extracted or evaporated to form microparticles containing the active agent. The key advantage of this process is that accurate and reliable scaling from laboratory to commercial batch sizes can be achieved while obtaining a narrow and well-defined particle size distribution. One other significant advantage is that the process can be made continuous.

Cryogenic Solvent Extraction. A cryogenic solvent extraction process was developed (76) for preparing microspheres. This process proves to be especially useful in encapsulation of biologicals such as proteins and peptides. In this process, a solution of the polymer and the active agent to be encapsulated are atomized into a liquified gas (e.g., liquid nitrogen, liquid argon). The atomized particles freeze when they contact the liquified gas (liquid nitrogen), forming frozen spheres. These frozen spheres then sink to the surface of a frozen nonsolvent below the liquified gas. The liquid gas is evaporated and spheres begin to sink into the nonsolvent as the nonsolvent thaws. The solvent in the spheres is extracted into the nonsolvent to form microspheres containing the agent to be encapsulated. In this process, it is important that the polymer/active agent freeze immediately upon contacting the cold liquid, and then be slowly thawed while the polymer solvent is extracted from the microspheres. The thawing rate is dependent on the choice of solvents and nonsolvents. It is important to select a solvent for the polymer having a higher melting point than the nonsolvent for the polymer so that the nonsolvent melts first, allowing the frozen microspheres to sink without agglomerating into the nonsolvent where they later thaw. The solvent and nonsolvent for the polymer must also be miscible to allow extraction of the solvent from the microspheres. The microspheres are collected by filtration and lyophilized.

Tableting and Tablet Coating

Tableting is perhaps the simplest, most common, and most economical method of processing an active agent into a drug-delivery product. Tableting is typically reserved for oral dosage forms of an active agent; however, there are some tableted or compressed wafer, controlled release implant depots produced, such as the GLIADEL wafer discussed earlier. The tableting process involves feeding a metered amount (usually from ~0.5 to 5 g) of a "granulation" (large particle blend) of an active agent to the dies of a tableting press where the granules are compressed into a tablet of the desired shape. Some manufacturers use intricate shapes for product identification. The premixed granulation contains the active and various excipients to modify the flow, compaction, die release, and dissolution characteristics of the tablet. Granulation is accomplished wet (using solvent) or dry (using no solvent) by high-intensity mixers or fluidized-bed granulators. Although single-cavity presses can be used for specialized applications and testing, high-speed rotary presses capable of producing thousands of tablets per minute are typical. The pressures used in tablet compression are quite high, ranging from ~50 to 500 mPa; therefore, the dies used in tableting are typically made with high-strength, surface-hardened alloys.

Tableting has become much more sophisticated as the demand for controlled release, oral drug delivery has grown. Technology now exists that produce bilayer tablets providing two different release rates for a drug. The technology uses different polymeric excipients in the tablet providing both immediate and sustained release. Various over-the-counter analgesics use this technology. Tablets composed of compacted microencapsulated beads have also been developed to provide both sustained release and protection from the irritating effects of certain drugs such as non-steroidal anti-inflammatory drugs. The drug is microencapsulated in a separate process, such as the fluidized-bed process, and then incorporated into the tableting formulation. Effervescent tablets are also produced to provide chewable and fast-dissolving tablets for patients who have difficulty swallowing. The drug is again typically incorporated into the effervescent tablet formulation as microencapsulated beads.

Many tableted products are also subsequently coated to provide controlled release products. Coating usually takes place in a pan coater, which is a rotating drum, similar to a clothes drier, which tumbles the tablets in front of a spray nozzle for application of the coating. The coating is dried by a continuous flow of process air. The process air is often heated and solvent reclamation is used for organic-solvent-based coatings. The batch sizes for pan coating can vary between ~100 and 2,000 kg. Small laboratory models are also available. Various wax and enteric coatings are applied in this manner. For very small tablets, fluidized-bed coating may also be used.

Capsule Filling

By far the most versatile of all dosage forms is the gelatin capsule. Gelatin capsules can be filled with powders, small pellets or small tablets, liquids, or semisolids, as well as some combinations of these forms. The capsule also provides efficient taste-masking. The drug product is released by dissolution of the gelatin in the stomach. Gelatin capsules can be prepared from hard or soft gelatin; however, hard-gelatin capsules are more versatile for controlled drug delivery.

Hard-gelatin capsules are available in several different sizes, and high-speed filling machinery, capable of filling ~1,500 capsules per minute, is available. The machines typically consist of a drug hopper, a capsule hopper, a dose-metering device, a dose chamber, a filling or tamping pin, a capsule tray, and a finished-capsule collection bin. The capsules are automatically opened, filled, and closed dur-

ing the manufacturing process. Technologies have been developed whereby controlled release beads and minitablets are used to fill a gelatin capsule for convenient administration of an oral, controlled release dosage form. Examples of such products are the sustained release cold medications, where sustained release antihistamines, antitussives, and analgesics are first preformulated into extended release microcapsules or microspheres and then placed inside a gelatin capsule. Another example is enteric-coated lipase minitablets that are placed in a gelatin capsule for more effective protection and dosing of these enzymes (77).

Transdermal and Iontophoretic Devices

Transdermal patches have proven to be an effective means of delivering drugs. Because of the different physicochemical characteristics of individual drugs, each drug typically has a particular delivery formulation and optimal type of transdermal delivery device. The drug is typically sequestered in a device that has an impermeable backing film on the outer side, followed by a reservoir or matrix containing the drug, then a semipermeable, rate-controlling membrane, and an adhesive inner layer for attachment to the skin (4). Preferably, the device can be a monolithic, matrix-type design with the drug dissolved or dispersed in a polymeric matrix, which is then applied directly to the impermeable membrane, and is finally coated with a pressure-sensitive adhesive (5). The active agent diffuses through the polymeric matrix, through the adhesive layer to the skin and, in combination with the skin itself, serves as the rate-controlling portion of the device. In a simpler variant of the matrix-type device, the drug is dispersed directly in the adhesive. This matrix-type device eliminates the rate-controlling membrane and simplifies the manufacturing of the product. In practice, the drug–polymer matrix is usually formed from a solution or melt blend of the polymer and drug, or a solution or melt of the polymer with the drug dispersed in it. The polymer–drug melt blend or solution is then coated onto the impermeable base film.

The impermeable base film is usually a multipolymer film composite or metalized film. Material combinations such as polyethylene/poly(ethylene terephthalate), poly(vinylidene chloride)/poly(ethylene terephthalate) laminates, or polyethylene/metalized poly(ethylene terephthalate) are typically used for the backing film. For a monolithic device, the matrix polymer is selected from a variety of flexible or elastomeric thermoplastic polymers suitable for sequestration and diffusion of the active agent and any penetration enhancers. If the matrix backing film is to be coated by solution casting of the matrix film, the matrix polymer should be soluble in a low-boiling organic solvent. Thermoplastic poly(ether urethane)s and several other polymers are used as matrix materials. Melt blending and extrusion coating is preferable if the drug is thermally stable. After the monolithic drug–polymer matrix is applied to the backing film, a drug-permeable adhesive for adhering the patch to the skin, and a final protective film laminate that is impermeable to the active ingredients are applied. The final protective film usually has a release coating of Teflon® or silicone to permit easy removal at the time of use. The adhesive is a low-irritating, pressure-sensitive type such as a pressure-sensitive acrylic or silicone adhesive. The final laminate is die cut to the appropriate size for the desired release profile of the drug, and the product is packaged in protective foil-lined pouches. Various proprietary versions of conventional continuous film-coating and laminating equipment are used. In a typical process, the drug–polymer matrix material is applied to the backing film by continuous direct extrusion or solvent casting onto the film which is supported on a continuous web. In the case of solvent casting, the composite is passed through an oven to remove the solvent. All the problems associated with solution casting of films, discussed earlier, apply. An adhesive film layer and protective release film are finally applied by transfer coating to the backing-film–drug-matrix laminate. Transfer coating is a process whereby two materials are laminated by passage through a pair of rollers where a low-pressure nip is applied.

Reservoir-type devices are much more complicated to manufacture. For a typical reservoir device, a drug-impermeable, protective-release film is first coated with a pressure-sensitive adhesive. The adhesive-coated protective film can then be laminated to semipermeable, rate-controlling membrane by a transfer-coating process. Reservoirs of the premixed drug formulation are then applied to the membrane side of the product-build laminate. A suitable heat- or pressure-sealable, drug-impermeable backing film is then applied and sealed at the periphery of the reservoir. The final laminate is then die cut to form the final patch. From a manufacturing standpoint, the monolithic- or matrix-type device is preferable whenever the appropriate sequestration and delivery profile for the drug can be met (78–82).

Iontophoresis is a process used to enhance the skin permeation of certain ionized drugs. Here the driving force to skin penetration of the drug is an applied electric potential. The current generator is typically a low-voltage source of direct current with a low current flow of less than one milliampere per square centimeter of skin surface area. The two electrodes are placed in contact with the skin through electrolyte-containing hydrogels or foams. The anode and cathode are typically placed within a few centimeters of each other. The anode, or positive electrode, serves as the drug reservoir; and when the voltage potential is applied, ionized species of drug are transported across the skin membrane (83). Pilocarpine is delivered in this manner in an approved test method for cystic fibrosis. Here the administered pilocarpine serves to cause local sweating which is then collected and tested for chloride-ion content. The presence of abnormally high chloride ion in body fluids is a strong indicator for the disease.

Drug–Polymer Conjugates

Extensive research and development efforts have concentrated on the alteration of drug properties through drug–polymer conjugation. Efforts have primarily been focused on enhancing the solubility and bioavailability of the drug, or on targeted delivery of the drug by creating sites for natural recognition. The most investigated and successful

class of polymers that have been used for drug–polymer conjugation to date are the PEGs.

PEG is a linear or branched neutral polyether with the following structure:

$$HO\text{-}(CH_2CH_2O)_n\text{-}CH_2CH_2OH \quad (7)$$

Despite its apparent simple structure, PEG has been used in a variety of bioanalytical and biomedical applications (84–89). The versatility of PEG stems mainly from the fact that it is nontoxic (approved by FDA for internal consumption), soluble in both water and most organic solvents, and available in a wide range of molecular weights. In addition, PEG can be readily linked covalently to other molecules through its terminal primary hydroxyl groups. This particular area of PEG's applications is commonly known as PEGylation. In general, covalent attachment of PEG to other molecules:

- Enhances their solubility
- Alters their pharmicokinetics by prolonging plasma circulation half-life
- Reduces their clearance rate through the kidneys
- Renders proteins nonimmunogenic

The use of PEG to alter the properties of drugs began with the early observations by Davis and Abuchowski that the covalent attachment of PEG to proteins resulted in protein–polymer conjugates that were biologically active, nonimmunogenic, and had prolonged plasma circulation half-lives (90). Subsequent researchers in this area have established that molecules (mostly proteins such as enzymes) retain most of their bioactivity after the PEGylation process, indicating that covalent attachment of PEG does not interfere with the active sites of these molecules (91,92). A molecular-weight range for PEG between 2,000 and 20,000 daltons is commonly used in the modification of proteins and peptides. Monofunctional PEGs, such as the ones end-capped by a methyl group (mPEGs) are preferred for the modification of proteins to eliminate unwanted cross-linking that accompanies the use of difunctional PEGs (93–95).

Methods of Forming a Covalent Linkage Between PEG and Proteins. PEG can be derivatized and covalently linked to various functional groups of a protein such as the amino and carboxylic acid groups. However, the preferred route of PEGylation is through the amino groups. The derivitization process begins with an activation step wherein the terminal hydroxyl group of PEG is replaced by a nucleophile which subsequently reacts with the amino groups of a protein.

One commonly used reagent is trichloro-*s*-triazine (cyanuric chloride). This is the reagent originally used by Davis and coworkers (90) and has recently been improved to ensure reproducibility and complete conversion of mPEG to the intermediate (96). The hydroxyl group of PEG displaces one chloride attached to the triazine ring and the remaining two chlorides are used for reaction with the amino groups of a protein. This simple reaction provides an effective one-step activation of PEG; however, it is not optimal in that cyanuric chloride released from the reaction is toxic. And, because of its nonselective reactivity toward other functional groups such as cysteinyl and tyrosyl groups other, less desirable, derivatives can be formed (97). It is not surprising that substantial loss of protein activity have been observed after such modification (98,99).

Another popular way to activate PEG is through a PEG-succinimidyl succinate intermediate (SS-PEG) (100,101). The intermediate is normally prepared first by succinylation of the hydroxyl end group of PEG followed by coupling with *N*-hydroxy succinimide (NHS) in the presence of dicyclohexylcarbodiimide. This derivative can react rapidly with proteins under mild conditions (near neutral pH, room temperature), and leads to modified proteins with high bioactivity (100). However, the PEG-succinate aliphatic ester linkage is susceptible to hydrolysis in an aqueous environment leading to a gradual dissociation of PEG from the protein (94).

The hydrolytic stability of the linkage between PEG and a protein can be enhanced by using a urethane linkage instead of an ester linkage. Such coupling can be achieved through a one-step process using carbonyldiimidazole (102), but such PEG derivatives have only mild reactivity with proteins and the modification process usually takes a long time. However, the resulting modified proteins, retain high bioactivity (103,104). Similar activations can also be accomplished in a single step using the chloroformate of 4-nitrophenol and 2,4,5-trichlorophenol (105). The major drawback of these processes is that 4-nitrophenol and 2,4,5-trichlorophenol in the reaction are toxic and hydrophobic and may be retained by the protein.

An activation process developed more recently uses succinimidyl carbonate as the intermediate (106). In this process PEG is first treated with phosgene to generate a chloroformate of PEG which subsequently reacts with NHS. The by-product, NHS, generated during the protein coupling step is not toxic and can be easily separated. However, caution must be exercised in the coupling process because of the use of phosgene.

Other less common derivatives of PEG that are reactive with amino groups have been reported in the literature with varying degrees of success. Some examples are PEG-carboxymethyl azide (107), PEG-tosylate (108,109), and PEG-imidoester (110). Currently the most frequently used PEG derivatives for amino coupling are the NHS active esters such as SS-PEG, succinimidyl carbonate, and succinimidyl propionate (111).

PEG derivatives that are reactive with other amino acid residues of a protein, such as arginine residues, can be achieved by phenylglyoxal (112), cysteine residues by maleimide containing reagents (91,97), and carboxylic acids by amino PEG (113–115).

Examples of PEGylated Proteins and Peptides. Covalent attachment of PEG has been applied to a large number of proteins and peptides with varying degrees of success. For instance, PEG-adenosine deaminase has been approved by the FDA as a replacement therapy for patients with severe combined immunodeficiency disease who are not suitable candidates for bone marrow transplantation. PEGylated

recombinant interleukin-2 (rIL-2) has been tested in randomized human clinical trials (116–118). Covalent attachment of PEG enhances solubility, increases circulatory half-life, and eliminates the possibility of potential aggregates of rIL-2, which may elicit an immune response. Other PEG-modified proteins that have been investigated include brain-derived neurotrophic factor (119,120), interleukin-15 (121), interleukin-6 (122), tumor necrosis factor-alpha III (123), human megakaryocyte growth and development factor (124), human granulocyte colony stimulating factor (125), and recombinant human interferon-gamma (126). As more and more proteins become available one can expect to see an increasing number of proteins and peptides conjugated with PEG for various bioanalytical and biomedical applications. Covalent coupling of PEG to proteins and peptides represents an efficient way of improving the physicochemical properties of the proteins such as the reduced immunogenicity, improved plasma pharmacokinetics, increased resistance to proteolysis, and reduced renal excretion rate. The intensive research in the area during the past two decades has led to many exciting developments as evidenced by the increasing number of efficient and specific reagents for PEGylation, as well as more and more protein and peptide drugs being successfully PEGylated and advancing into human clinical trials. With the increasing number of recombinant proteins made available by genetic engineering and the increasing need to extend the patent protection of existing proteins and peptides, one can expect to see more and more applications of PEGylation.

Currently, most commercial PEGylation processes are batch processes of less than 1 kg, where the larger-scale synthetic procedures are merely the smaller-scale procedures proportionally enlarged to the larger batch size. This method of scale-up can result in problems in that suitable PEGylating agents need to be individually selected depending on the properties of the protein being used and on the particular functional group or groups on the protein to be PEGylated. The reaction conditions need to be optimized so that an even mixing between the PEGylating agent and the protein is achieved to ensure a uniform degree of PEGylation of all the protein molecules. Excessive PEGylation can adversely affect the binding sites of the particular protein, leading to a loss of bioactivity. Precise control of reaction temperature is also important in achieving successful PEGylation while retaining the bioactivity of the protein. Also, because the binding affinity varies among functionalized PEGylating agents, the final purification procedure must be carefully tailored to ensure complete removal of any unreacted agents. Dialysis is the purification method routinely used in small-scale PEGylation processes, whereas ultra-high-speed membrane centrifugation is the standard method used in larger scale processes. If required, further purification of the PEGylated protein can be achieved by passing the product through ion exchange columns. One can expect to see newer and better analytical methods for PEGylated proteins and more commercially available functionalized PEGs in the future.

Combination Processes

A controlled release dosage form may need to be prepared using a combination of processes. One example is the GLIADEL wafer described earlier. The production of GLIADEL involves both a spray-drying and a compression molding process. Spray-drying is used in the incorporation of BCNU into polymer matrix. The polymer—poly(carboxyphenoxypropane: sebacic acid)—is first dissolved in methylene chloride. After the polymer is completely dissolved, an appropriate amount of BCNU is added to the polymer solution. The drug–polymer solution is then fed into a spray-drier to form microspheres of the drug–polymer mixture. The feed rate, inlet air temperature, and vacuum are carefully controlled during the spray-drying process to ensure uniformity and lot-to-lot consistency. To produce the final GLIADEL wafer, approximately 200 mg of the spray-dried microsphere powder is weighed into a punch and die assembly and compressed into wafers using a press. The wafer is approximately 14 mm in diameter and 1 mm thick. The wafers are then inspected, packaged, and sterilized by irradiation.

Several tableted and gelatin-capsule oral dosage forms are also prepared using combined processes. In a typical combination process for a tableted oral dosage form, the active is first encapsulated in a fluidized-bed or spray-drying process. The microspheres or microcapsules thus formed are subsequently tableted. The tablets may also be coated for added protection in the stomach or to obtain the final release profile desired.

BIBLIOGRAPHY

1. *Enteric Polymer Literature*, EFC-205C, Eastman Chemical Company, Kingsport, Tenn., 1998.
2. L.C. Junqueira, J. Carneiro, and R.O. Kelley, *Basic Histology*, 6th ed., Appleton & Lange, Norwalk, Conn., 1989.
3. U.S. Pat. 5,603,957 (February 18, 1997), O. Burquiere et al. (to Flamel Technologies, France).
4. U.S. Pat. 5,008,110 (April 16, 1991), A.G. Benecke et al. (to The Procter & Gamble Company.).
5. U.S. Pat. 5,676,969 (October 14, 1997), J. Wick et al. (to Bertek, Inc.).
6. U.S. Pat. 5,227,169 (July 13, 1993), S. Heiber et al. (to TheraTech, Inc.).
7. U.S. Pat. 5,023,084 (June 11, 1991), Y.W. Chien et al. (to Rutgers, The State University of New Jersey).
8. U.S. Pat. 5,126,144 (June 30, 1992), H. Jaeger et al. (to LTS Lohmann Therapie-Systems GmbH & Co. KG.).
9. U.S. Pat. 4,839,174 (June 13, 1989), R.W. Baker et al. (to Pharmetrix Corp.).
10. U.S. Pat. 5,364,630 (November 15, 1994), J.L. Osborne (to ALZA Corporation).
11. T.R. Tice and D.R. Cowsar, *Pharm. Tech.*, 26–34 (1994).
12. U.S. Pat. 4,320,758 (March 23, 1982), J.B. Eckenhoff et al. (to ALZA Corporation).
13. U.S. Pat. 5,023,088 (June 11, 1991), P.S.L. Wong et al. (to ALZA Corporation).
14. A.B. Berenson and C.M. Wiemann, *Am. J. Obstet. Gynecol.* **172** (4), Pt. 1, 1128–1135; discussion: pp. 1135–1137 (1995).
15. A.M. Kaunitz, *Int. J. Fertil. Menopausal Stud.* **41**(2), 69–76 (1996).
16. U.S. Pat. 5,660,848 (August 26, 1997), A.J. Moo-Young (to The Population Council, Center for Biomedical Research).

17. *Annual Report*, Atrix Laboratories, Inc., Fort Collins, Colo., 1996.
18. U.S. Pat. 4,938,763 (July 3, 1990), R.L. Dunn, D.R. Cowsar, J.P. English, and D.P. Vanderbilt (to Southern Research Institute).
19. J.M. Litch et al., *J. Periodont. Res.* **31**(8), 540–544 (1996).
20. U.S. Pat. 5,733,566 (March 31, 1998), D.H. Lewis (to Alkermes Controlled Therapeutics Inc.).
21. U.S. Pat. 4,166,107 (August 28, 1979), J.A. Miller et al. (to The United States of America as represented by the Secretary of Agriculture).
22. U.S. Pat. 5,018,481 (May 28, 1991), W.B. Rose (to Mobay Corp.).
23. U.S. Pat. 4,195,075 (March 25, 1980), W.V. Miller (to Shell Oil Co.).
24. U.S. Pat. 4,150,109 (April 17, 1979), P.R. Dick et al.
25. U.S. Pat. 4,879,117 (November 7, 1989), M.A. Rombi.
26. C. Thies, *Today's Chemist at Work*, November, 40–43 (1994).
27. U.S. Pat. 5,614,215 (March 25, 1997), A. Ribier et al. (to L'Oreal).
28. U.S. Pat. 4,217,344 (August 12, 1980), G. Vanlerberghe et al. (to L'Oreal).
29. U.S. Pat. 4,241,046 (December 23, 1980), D.P. Papahadjopoulos.
30. U.S. Pat. 5,077,056 (December 31, 1991), M.B. Bally et al. (to The Liposome Company, Inc.).
31. U.S. Pat. 4,235,871 (November 25, 1980), D.P. Papahajopoulos et al.
32. U.S. Pat. 5,616,334 (April 1, 1997), A.S. Janoff et al. (to The Liposome Company, Inc.).
33. *Code of Federal Regulations*, Title 21, Food and Drug Administration, Washington D.C., September 29, 1978, Pt. 210–211.
34. G. Odian, *Principles of Polymerization*, McGraw-Hill, New York, 1970.
35. A. Domb, J. Kost, and D. Wiseman, eds., *Handbook of Biodegradable Polymers*, Harwood Academic Publishers; Overseas Publishers Association, Amsterdam, 1997.
36. J.D. Ferry, *Viscoelastic Properties of Polymers*, 2nd ed. Wiley, New York, 1970.
37. J.E.A. John and W.L. Haberman, *Introduction to Fluid Mechanics*, 2nd ed., Prentice-Hall, Englewood Cliffs, N.J., 1980.
38. G.M. Barrow, *Physical Chemistry*, 2nd ed. McGraw-Hill, New York, 1966.
39. G. Schenkel, *Plastics Extrusion Technology and Theory*, American Elsevier, New York, 1966.
40. J.A. Schey, *Introduction to Manufacturing Processes*, McGraw-Hill, New York, 1977.
41. S. Gross, *Modern Plastics Encyclopedia*, McGraw-Hill, New York, 1970.
42. D.F. Mielcarek, *Chem. Eng. Process*, June, 59–67 (1987).
43. I.I. Rubin, *Injection Molding Theory and Practice*, Wiley, New York, 1972.
44. N.M. Bikales, ed., *Encyclopedia of Polymer Science and Technology*, Vol. 9, Wiley-Interscience, New York, 1968.
45. E. Luck and D. Brown, *Proc. Vet. Cancer Soc.*, Purdue University, Lafayette, Ind., May 6–8, 1985, pp. 22–23.
46. N. Yu, F. Conley, E. Luck, and D. Brown, *NCI Monogr.* **6** (1988).
47. Matrix Pharmaceutical, Inc., web page, available at: *www.matx.com*
48. J.M. Swinehart et al., *Arch Dermatol.* **133**, 67–73 (1997).
49. U.S. Pat. 4,978,332 (December 18, 1990), E. Luck (to Matrix Pharmaceutical).
50. U.S. Pat. 4,619,913 (October 28, 1986), E. Luck and D. Brown (to Matrix Pharmaceutical).
51. U.S. Pat. 5,290,552 (March 1, 1994), D. Sierra, E. Luck, and D. Brown (to Matrix Pharmaceutical).
52. U.S. Pat. 5,750,146 (May 12, 1998), R. Jones and M. Li (to Matrix Pharmaceutical).
53. K. Masters, *Spray-drying Handbook*, Wiley, New York, 1984.
54. J. Broadhead, S.K. Edmond Rouan, and C.T. Rhodes, *Drug Dev. Ind. Pharm.* **18**(11 and 12), 1169–1206 (1992).
55. C. Voellmy, P. Speiser, and M. Soliva, *J. Pharm. Sci.* **66**(5), 631–634 (1977).
56. P.B. Deasy, *Microencapsulation and Related Drug Processes*, Dekker, New York, 1984, pp. 181–193.
57. F. Nielson, *Manuf. Chem.*, 38–41 (1982).
58. R. Bodmeier and H.J. Chen, *Pharm. Pharmacol.* **40**, 754–757 (1988).
59. D.L. Wise, G.J. McCormick, and G.P. Willet, *Life Sci.* **19**, 867–874 (1976).
60. F. Pavanetto, I. Genta, P. Giunchedi, and B. Conti, *J. Microencapsul.* **10**(4), 487–497 (1993).
61. W. Dang, T. Daviau, and H. Brem, *Pharm. Res.* **19**, 683–691 (1996).
62. B. Gander, E. Wehrli, R. Alder, and P. Merkle, *J. Microencapsul.* **12**(1), 83–97 (1995).
63. U.S. Pat. 5,552,152 (September 3, 1996), R.W. Shen (to The Upjohn Company).
64. U.S. Pat. 5,498,447 (March 12, 1996), H. Nishii (to Sumatomo Pharmaceuticals Co., Ltd.).
65. Y. Fukomori et al., *Chem. Pharm. Bull.* **36**, 1491–1501 (1988).
66. F.N. Christensen and P. Bertelsen, *Drug Dev. Ind. Pharm.* **23**(5), 451–463 (1997).
67. C. Migliaresi, L. Nicolais, P. Ginisti, and E. Chiellin, *Polymers in Medicine III*, Elsevier, Amsterdam, 1987.
68. U.S. Pat. 5,000,886 (March 19, 1991), J.R. Lawter et al. (to American Cyanamid Company).
69. U.S. Pat. 4,673,595 (June 16, 1987), P. Orsolini et al. (to Debiopharm, S.A.).
70. U.S. Pat. 4,166,800 (September 4, 1979), J.W. Fong (to Sandoz, Inc.).
71. U.S. Pat. 5,503,851 (April 2, 1996), R. Mank et al. (to Ferring Arzneimittel GmbH.).
72. M.A. Tracy, *Biotechnol Prog.* **14**(1), 108–115 (1998).
73. L.R. Beck et al., *Fertil. Steril.* **31**, 545–551 (1979).
74. U.S. Pat. 5,654,008, P.F. Herbert and A.M. Hazrati (to Alkermes, Inc.).
75. U.S. Pat. 5,650,173, J.M. Ramstack, P.F. Herbert, J. Strobel, and T.J. Atkins (to Alkermes, Inc.).
76. U.S. Pat. 5,019,400 (May 28, 1991), W. Gombotz et al. (to Enzytech, Inc.).
77. *Product Literature*, Scandipharm, Inc., Hoover, Ala., 1998.
78. U.S. Pat. 5,679,373 (October 21, 1997), J. Wick et al. (to Bertek, Inc.).
79. U.S. Pat. 5,006,342 (April 9, 1991), G.W. Cleary et al. (to Cygnus Corp.).
80. U.S. Pat. 4,710,191 (December 1, 1987), A. Kwiatek et al. (to Jonergin, Inc.).
81. U.S. Pat. 5,662,925 (September 2, 1997), C.D. Ebert et al. (to TheraTech, Inc.).

Next Page

82. G.A. Van Buskirk et al. *Pharm Res.* **14**(7), 848–852 (1997).
83. U.S. Pat. 5,445,607 (August 29, 1995), S. Venkateshwaran et al. (to TheraTech, Inc.).
84. J.M. Harris, ed., *Biotechnical and Biomedical Applications*, Plenum, New York, 1992.
85. C. Delgado, G.E. Francis, and D. Fisher, *Ther. Drug Carrier Syst.* **9**(3–4), 249–304 (1992).
86. H.F. Gaertner and R.E. Offord, *Bioconjugate Chem.* **7**(1), 38–44 (1996).
87. N.L. Burnham, *Am. J. Hosp. Pharm.* **51**(2), 210–218 (1994).
88. S. Tsunoda, Y. Tsutsumi, and T. Mayumi, *Nippon Rinsho* **56**(3), 573–578 (1998).
89. G.E. Francis et al., *J. Drug Target.* **3**(5), 321–340 (1996).
90. A. Abuchowski, T. van Es, N.C. Palczuk, and F.F. Davis, *J. Biol. Chem.* **252**(11), 3578–3581 (1997).
91. J. Glass et al., *Biopolymer* **18**, 383–393 (1979).
92. K. Ulbrich, J. Strohalm, and J. Kopeck, *Makromol. Chem.* **187**, 1131 (1986).
93. A. Abuchowski and F. Davis, in J. Holcenbery and J.P. Roberts, eds., *Enzymes as Drugs*, Wiley, New York, 1981, p. 367–383.
94. S. Dreborg and E. Akerblom, *Crit. Rev. Ther. Drug Carrier Syst.* **6**, 315–365 (1990).
95. J. Harris, *J. Macromol. Sci., Rev. Macromol. Chem. Phys.* **C25**, 325 (1985).
96. S. Schafer and J. Harris, *J. Polym. Sci., Part A: Polym. Chem.* **24**, 375–378 (1986).
97. M. Atassi, ed., *Immunochemistry of Proteins*, vol. 1, Plenum, New York, 1977, p. 1.
98. S. Davis, A. Abuchowski, Y.K. Park, and F.F. Davis, *Clin. Exp. Immunol.* **46**(3), 649–652 (1981).
99. K.J. Wieder, N.C. Palczuk, T. van Es, and F.F. Davis, *J. Biol. Chem.* **254**(24), 12579–12587 (1979).
100. A. Abuchowski et al., *Cancer Biochem. Biophys.* **7**(2), 175–186 (1984).
101. U.S. Pat. 4,101,380 (July 18, 1978), M. Rubinstein (to Research Products Rehovot, Ltd.).
102. L. Tondelli, M. Laus, A. Angeloni, and P. Ferruti, *J. Controlled Release* **1**, 251 (1985).
103. H. Berger, Jr. and S.V. Pizzo, *Blood* **71**(6), 1641–1647 (1998).
104. K. Yoshinaga and J. Harris, *J. Bioact. Compat. Polym.* **4**, 17–24 (1989).
105. F. Veronese, R. Largajolli, C. Boccu, and O. Schiavon, *Appl. Biochem. Biotechnol.* **11**, 141 (1985).
106. S. Zalipsky, R. Seltzer, and S. Menon-Rudolph, *Biotechnol. Appl. Biochem.* **15**(1), 100–114 (1992).
107. U.S. Pat. 4,179,337 (December 18, 1979), F. Davis, T. van Es, and N. Palczak.
108. F. Kawai, *CRC Crit. Rev. Biotechnol.* **6**, 273 (1987).
109. G. Royer and G. Ananthramaiah, *J. Am. Chem. Soc.* **101**, 3394 (1979).
110. Eur. Pat. Appl. 0,236,987 (September 16, 1987), H. Ueno and M. Fujino (to Takeda Chemicals, Ltd.).
111. Shearwater Polymers, URL: *www.swpolymers.com*.
112. Eur. Pat. Appl. 0,340,741 (November 8, 1989), A. Sano et al. (to Sumitano Pharmaceuticals Co., Ltd.).
113. S. Romani et al., eds., *Chemistry of Peptides and Proteins*, Vol. 2, de Gruyter, Berlin, 1984, p. 29.
114. A. Pollak and G. Whiteside, *J. Am. Chem. Soc.* **98**, 289–291 (1976).
115. M. Kimura, U. Matsumura, Y. Miyauchi, and H. Maeda, *Proc. Soc. Exp. Biol. Med.* **188**, 364 (1988).
116. A. Carr et al., *Int Conf AIDS* **7–12**(11), 2–23 (Abstr. No. We.B.292) (1996).
117. N. Katre, *J. Immunol.* **144**(1), 209–213 (1990).
118. R.J. Goodson and N.V. Katre, *Bio Technology* **8**(4);343–346 (1990).
119. W.M. Pardridge, D. Wu, and T. Sakane, *Pharm. Res.* **15**(4);576–582 (1998).
120. T. Sakane and W.M. Pardridge, *Pharm. Res.* **14**(8);1085–1091 (1997).
121. D.K. Pettit et al., *J. Biol. Chem.* **272**(4);2312–2318 (1997).
122. Y. Tsutsumi et al., Thromb. Haemostasis **77**(1);168–173 (1997).
123. Y. Tsutsumi et al., *J. Pharmacol. Exp. Ther.* **278**(3);1006–1011 (1996).
124. L.A. Harker et al., *Blood* **88**(2);511–521 (1996).
125. K.E. Jensen-Pippo et al., *Pharm. Res.* **13**(1);102–107 (1996).
126. Y. Kita et al., *Drug Des Delivery* **6**(3), 157–167 (1990).

See also COATINGS; MICROENCAPSULATION.

FERTILITY CONTROL

CAMILLA A. SANTOS
Brown University
Providence, Rhode Island

KEY WORDS

Biodegradable
Contraception
Depo-Provera
EVA
Hormones
Hydrogels
Implants
Injectable
IUD
Microspheres
Norplant
PLA
Silicone
Transdermal
Vaginal rings

OUTLINE

Background and History
Contraceptive Devices
  Female Contraceptives
  Male Contraceptives
Abortifacients
Summary
Bibliography

82. G.A. Van Buskirk et al. *Pharm Res.* **14**(7), 848–852 (1997).
83. U.S. Pat. 5,445,607 (August 29, 1995), S. Venkateshwaran et al. (to TheraTech, Inc.).
84. J.M. Harris, ed., *Biotechnical and Biomedical Applications*, Plenum, New York, 1992.
85. C. Delgado, G.E. Francis, and D. Fisher, *Ther. Drug Carrier Syst.* **9**(3–4), 249–304 (1992).
86. H.F. Gaertner and R.E. Offord, *Bioconjugate Chem.* **7**(1), 38–44 (1996).
87. N.L. Burnham, *Am. J. Hosp. Pharm.* **51**(2), 210–218 (1994).
88. S. Tsunoda, Y. Tsutsumi, and T. Mayumi, *Nippon Rinsho* **56**(3), 573–578 (1998).
89. G.E. Francis et al., *J. Drug Target.* **3**(5), 321–340 (1996).
90. A. Abuchowski, T. van Es, N.C. Palczuk, and F.F. Davis, *J. Biol. Chem.* **252**(11), 3578–3581 (1997).
91. J. Glass et al., *Biopolymer* **18**, 383–393 (1979).
92. K. Ulbrich, J. Strohalm, and J. Kopeck, *Makromol. Chem.* **187**, 1131 (1986).
93. A. Abuchowski and F. Davis, in J. Holcenbery and J.P. Roberts, eds., *Enzymes as Drugs*, Wiley, New York, 1981, p. 367–383.
94. S. Dreborg and E. Akerblom, *Crit. Rev. Ther. Drug Carrier Syst.* **6**, 315–365 (1990).
95. J. Harris, *J. Macromol. Sci., Rev. Macromol. Chem. Phys.* **C25**, 325 (1985).
96. S. Schafer and J. Harris, *J. Polym. Sci., Part A: Polym. Chem.* **24**, 375–378 (1986).
97. M. Atassi, ed., *Immunochemistry of Proteins*, vol. 1, Plenum, New York, 1977, p. 1.
98. S. Davis, A. Abuchowski, Y.K. Park, and F.F. Davis, *Clin. Exp. Immunol.* **46**(3), 649–652 (1981).
99. K.J. Wieder, N.C. Palczuk, T. van Es, and F.F. Davis, *J. Biol. Chem.* **254**(24), 12579–12587 (1979).
100. A. Abuchowski et al., *Cancer Biochem. Biophys.* **7**(2), 175–186 (1984).
101. U.S. Pat. 4,101,380 (July 18, 1978), M. Rubinstein (to Research Products Rehovot, Ltd.).
102. L. Tondelli, M. Laus, A. Angeloni, and P. Ferruti, *J. Controlled Release* **1**, 251 (1985).
103. H. Berger, Jr. and S.V. Pizzo, *Blood* **71**(6), 1641–1647 (1998).
104. K. Yoshinaga and J. Harris, *J. Bioact. Compat. Polym.* **4**, 17–24 (1989).
105. F. Veronese, R. Largajolli, C. Boccu, and O. Schiavon, *Appl. Biochem. Biotechnol.* **11**, 141 (1985).
106. S. Zalipsky, R. Seltzer, and S. Menon-Rudolph, *Biotechnol. Appl. Biochem.* **15**(1), 100–114 (1992).
107. U.S. Pat. 4,179,337 (December 18, 1979), F. Davis, T. van Es, and N. Palczak.
108. F. Kawai, *CRC Crit. Rev. Biotechnol.* **6**, 273 (1987).
109. G. Royer and G. Ananthramaiah, *J. Am. Chem. Soc.* **101**, 3394 (1979).
110. Eur. Pat. Appl. 0,236,987 (September 16, 1987), H. Ueno and M. Fujino (to Takeda Chemicals, Ltd.).
111. Shearwater Polymers, URL: *www.swpolymers.com*.
112. Eur. Pat. Appl. 0,340,741 (November 8, 1989), A. Sano et al. (to Sumitano Pharmaceuticals Co., Ltd.).
113. S. Romani et al., eds., *Chemistry of Peptides and Proteins*, Vol. 2, de Gruyter, Berlin, 1984, p. 29.
114. A. Pollak and G. Whiteside, *J. Am. Chem. Soc.* **98**, 289–291 (1976).
115. M. Kimura, U. Matsumura, Y. Miyauchi, and H. Maeda, *Proc. Soc. Exp. Biol. Med.* **188**, 364 (1988).
116. A. Carr et al., *Int Conf AIDS* **7–12**(11), 2–23 (Abstr. No. We.B.292) (1996).
117. N. Katre, *J. Immunol.* **144**(1), 209–213 (1990).
118. R.J. Goodson and N.V. Katre, *Bio Technology* **8**(4);343–346 (1990).
119. W.M. Pardridge, D. Wu, and T. Sakane, *Pharm. Res.* **15**(4);576–582 (1998).
120. T. Sakane and W.M. Pardridge, *Pharm. Res.* **14**(8);1085–1091 (1997).
121. D.K. Pettit et al., *J. Biol. Chem.* **272**(4);2312–2318 (1997).
122. Y. Tsutsumi et al., Thromb. Haemostasis **77**(1);168–173 (1997).
123. Y. Tsutsumi et al., *J. Pharmacol. Exp. Ther.* **278**(3);1006–1011 (1996).
124. L.A. Harker et al., *Blood* **88**(2);511–521 (1996).
125. K.E. Jensen-Pippo et al., *Pharm. Res.* **13**(1);102–107 (1996).
126. Y. Kita et al., *Drug Des Delivery* **6**(3), 157–167 (1990).

See also COATINGS; MICROENCAPSULATION.

FERTILITY CONTROL

CAMILLA A. SANTOS
Brown University
Providence, Rhode Island

KEY WORDS

Biodegradable
Contraception
Depo-Provera
EVA
Hormones
Hydrogels
Implants
Injectable
IUD
Microspheres
Norplant
PLA
Silicone
Transdermal
Vaginal rings

OUTLINE

Background and History
Contraceptive Devices
  Female Contraceptives
  Male Contraceptives
Abortifacients
Summary
Bibliography

BACKGROUND AND HISTORY

Many countries have experienced a population growth during this century. The societal and economic impacts of an increased population are enormous. There is concern that the world will not be able to meet the increasing needs of feeding and supporting an ever-growing population. Controlling the population growth through education and improved contraceptive devices available to all is perhaps the main driving force behind today's contraceptive research. Research in the field of fertility control promotes the use of a contraceptive agent or device that requires minimal medical intervention and provides safe, reliable contraception for an extended time. Providing contraceptive technology to third world countries, which have an immediate need for population control at a low cost with minimal medical intervention, is the goal behind research in this field.

The main objective of many fertility control devices is to achieve contraception by inhibiting ovulation. This can be accomplished with the administration of progesterone, which inhibits the preovulatory surge of luteinizing hormone (1). Additionally, many progesterones cause cervical mucus thickening and a thinning of the endometrial lining, reducing capacity of the endometrium to support implantation. Common side effects of excessive hormone dosage include irregular bleeding patterns, weight gain, breast tenderness, and acne. Contraceptive devices being developed today need to optimize hormone delivery and minimize side effects, while maintaining beneficial contraceptive effects. Another issue to consider is whether to deliver natural hormones or synthetic steroids. Natural hormones are synthesized from blood cholesterol, transported in the blood bound to albumin and specific binding globulins, and are rapidly degraded by the liver (1). Natural hormones are advantageous because their effect on the body is known, but their main disadvantages are the requirement for production from a pure source, their rapid degradation in the body, and the fact that they are difficult to deliver orally. The development of synthetic hormones has overcome these primary disadvantages of natural hormone therapies and has greatly improved contraceptive systems. Synthetic hormones avoid hepatic degradation and can thus be administered in much lower quantities, decreasing the numerous side effects normally encountered with natural hormones. Advancements in different types of systems for delivering hormones (both synthetic and natural) greatly aid in reducing unwanted side effects, as have improvements in the development of synthetic steroids themselves. The aim of this article is to acquaint the reader with the different types of fertility control devices commercially available today, as well as those in the preclinical and research stages. Developments in synthetic steroids have allowed the subsequent development of many of the contraceptive systems to be discussed. It should be noted that this article emphasizes the vehicle of delivery rather than the variety of steroid delivered.

A brief pharmacological analysis of the estrogens and progestins used in contraceptive devices is presented in Goodman and Gilman's *The Pharmacological Basis of Therapeutics* and is helpful toward understanding the action of many fertility control devices (2). One of the most potent naturally occurring estrogens is 17β-estradiol, as well as estrone and estriol. The most common synthetic estrogen is ethinyl estradiol. All of the estrogens are 18-carbon steroids, which contain a phenolic A ring necessary for binding to estrogen receptors. The estrogens are produced in the ovaries and placenta, and in the adipose tissue of postmenopausal women and men. Estrogens are readily absorbed through the skin, mucus membranes, and gastrointestinal tract and passively diffuse through cell membranes to reach nuclear estrogen receptors. The steroids are rapidly degraded by the liver and therefore have limited oral effectiveness. Synthetic estrogens have been modified to obtain slow hepatic degradation. Estrogens are not considered contraceptives except when administered in high doses; they are usually coadministered with progestins to maintain the endometrium and prevent irregular bleeding. The synthetic estrones are 17α-ethinyltestosterone (ethisterone), 17α-ethinyl-19-nortestosterone (norethindrone, norethisterone), and esters of 17α-hydroxyprogesterone. The potent contraceptive steroids are the progestins. The progestins diffuse freely across cell membranes and depend on a Δ^4-3-one A ring structure in an inverted 1β,2α-conformation to bind to nuclear receptors, but this structure also binds to receptors for glucocorticoids, androgens, and mineralocorticoids. Progesterone is secreted by the ovaries in the luteal phase of the menstrual cycle and also in the testis, adrenal cortex, and placenta. Progesterone therapy extends the luteal phase of the cycle and mimics endometrial changes similar to early pregnancy. Secretion or administration of progesterone leads to the development of a secretory endometrium, and the abrupt decline in progesterone leads to menstruation. Continuous administration of progestins disrupts the cycle and leads to endometrial and ovarian atrophy. Low doses of the steroid can alter the endometrium and cervical mucus, inhibiting implantation but not affecting ovulation. Like the estrogens, the progestins are metabolized in the liver and excreted in the urine.

Synthetic steroids for oral contraception were not tested on a large scale until the early 1950s. After the development and testing of the numerous synthetic steroids, many contraceptive devices were designed. The main intent of many of these devices was to stem the fast-growing world population, and emphasis was placed on long-term contraceptive action with minimal medical intervention. The main forces behind research initiatives in this area were, and still remain, the World Health Organization (WHO), the Population Council, and pharmaceutical companies. By 1953, the injectable depot medoxyprogesterone acetate (Depo-Provera®) had been developed for use in cancer treatment and underwent clinical trials by the end of the decade (Table 1). Depo-Provera was tested as a contraceptive agent in several countries in the 1960s and marketed in the 1960s in Europe and Asia. During this same time frame another contraceptive device, vaginal rings made of silicone releasing progestins, began to be investigated. Norplant® clinical trials began in the early 1970s, as did clinical trials of the vaginal rings and the Copper T 380A intrauterine device (IUD). By 1973, research advanced to include biodegradable systems such as Capronor®, a

Table 1. History of Fertility Control Development

	1950s
early	Beginning development of oral contraceptives
1953	Depo-Provera developed for cancer treatment
1957	Noristerat two-month injectable developed
1958	Clinical trials with Depo-Provera as a cancer treatment begins
	1960s
1963	First clinical trials with Depo-Provera as contraceptive, a three-month injectable suspension of microcrystalline steroid
1968	Cylofem (one-month injectable) research initiated
	Research begins on vaginal rings made of silicone-rubber-releasing progestins
	1970s
1972	Norplant preliminary trials in humans, testing continued throughout the 1970s
	Clinical trials begin with Copper T 380A IUD
1973	In vitro research with Capronor
	Progestasert IUD developed
1974	Mesigyna developed (one month injectable)
1976	Implanon developed
	Progestasert IUD marketed in the U.S. by Alza Pharmaceuticals
	Copper T 200 approved by U.S. FDA
1978	Work begins with hydrogels releasing progesterone (hydroxyethyl methacrylate)
	IPCS trials begin
	Vaginal Contraceptive Film (VCF) marketed in Europe
1979	Preliminary trials with vaginal rings made of Silastic-releasing progestins for 90 days
	Research begins with vaginal rings releasing spermicide, continued in the 1990s
	Poly(l-actic acid) (PLA) microspheres containing NET (norethisterone), trials in baboons
	1980s
1981	Development of vaginal rings releasing progestins and estrogen for one month
	Human trials with PLA microspheres releasing NET
1982	Capronor trials in humans
	Injectable norethisterone enanthate (NET-EN)
1983	Norplant-2, in vitro research
	Depo-Provera marketed in Finland as a contraceptive
1984	Clinical studies began with Cyclofem
	Clinical studies began with NET release from poly(dl-lactide-*co*-glycolide) (PLGA) (3–6 mos application)
	Phase III trials with vaginal rings releasing progestin (LNG)
	Biodegradable pellets fused with cholesterol and releasing NET developed
	FDA approves Copper T 380A IUD
1985	Norplant clinical trials in the United States
1986	Polyethylene oxide-based hydrogel strips releasing methyl ester developed for early abortion (24 h)
	Norplant-2 humantesting began
	VCF available in the U.S.
1988	Ethylene–vinyl acetate (EVA) strips releasing MSGB developed to prevent fertilization
	ParaGard380/Copper T 380A IUD marketed in the U.S.
1989	Transdermal delivery of LNG from an osmotic pump with an EVA membrane tested in rabbits
	Phase II clinical trials with PLGA microspheres releasing NET
	1990s
1990	FDA approval of Norplant
1991	Research continues on vaginal rings releasing LNG and rings releasing spermicide (silicone-covered EVA, releasing for 30 days)
	Chitosan matrix for steroid release tested in vitro
1992	Depo-Provera approved by FDA
	LNG ROD device approved for use in Finland
1993	FDA extends effective duration of Copper T 380A to 10 years
1996	Implantable 2-rod system (LNG ROD) approved by FDA

poly(ϵ-caprolactone) polymer encasing the synthetic progestin levonorgestrel (LNG). Biodegradable injectable systems were developed, specifically the forerunners of the poly(lactide-*co*-glycolide) and steroid microspheres that are still in the testing stages today. The 1970s also saw the development and production of IUDs designed to deliver steroids over the course of one year, such as the Progestasert® device. In the 1980s, injectables with an estrogen as well as a progestin were tested clinically, mainly Cyclofem®. The vaginal rings were still being researched, as were several injectable formulations. Optimization of the type of synthetic steroid and the exact amount of release were the main goals of many of the new systems. Transdermal delivery of steroids was also investigated. In the 1990s, the U.S. FDA approved two contraceptive methods, Norplant and Depo-Provera, and research continued on the many other forms of contraceptive devices, including new systems designed for male contraception.

Although Depo-Provera and other depot injections of pure steroid are not considered controlled release per se, they have been included in this section because they are among the few commercially available long-term contraceptives. There are many formulations of crystalline steroid injection currently in the testing phases, but these have not been mentioned in this article as the release profiles are first order and depend only on the solubility of the crystalline steroid involved, not on controlled release from a polymeric delivery vehicle.

In addition to the numerous contraceptive devices both on the market and in the design stages, investigators are creating devices used to induce abortion. Recent developments in controlled release have allowed the design of devices to release abortifacients over 24 hours, with the hope of reducing the side effects of potent drugs currently administered in a bolus form.

The aim of this article is to familiarize the reader with the different types of controlled release systems designed for fertility control purposes on the market and in the research stages. Basic mechanisms of release are discussed, and examples of each type of device are provided wherever possible.

CONTRACEPTIVE DEVICES

Female Contraceptives

Marketed Products. There are several marketed contraception products that rely on constant release of steroid to achieve their goal. Such products include Norplant, Depo-Provera, and the Progestasert IUD.

Norplant. Norplant is a constant, low dose, progestin-only contraceptive device that was developed by the Population Council and first marketed by Leiras Pharmaceuticals, Turku, Finland, in 1983. Today it is used worldwide by more than 3 million women (3). In the U.S. the device is marketed by Wyeth-Ayerst Laboratories, Philadelphia, PA. The original Norplant consists of six capsules of crystalline LNG encapsulated in Silastic®. The capsules are implanted in the inner region of the upper arm, with the use of a 10-gauge trocar, and are designed for 5 years of contraceptive efficacy. Each rod contains 36 mg of the synthetic progestin LNG, with a total daily release rate from the six capsules of 70 μg/day initially, dropping to 30 μg/day after a few months with a slow decline over five years of action. Release from the capsules has been reported to continue for ten years, but the high level of contraceptive efficacy is maintained for only the first five years (4). Efficacy of the device is dependent upon its steroid release to achieve 0.25 ng/mL serum concentration of LNG, which is sufficient to inhibit pregnancy (3). The capsules are 34-mm long and have an outer diameter of 2.41 mm. The inner diameter of the Silastic tubing is 1.57 mm. The core of the device is 30 mm in length and consists solely of crystalline levonorgestrel (5–8). The main advantages of the Norplant system are its ease of use, five-year duration of action, reversibility at any time by simple removal of the capsules, and its low dose of daily steroid when compared with oral contraceptives. Its main disadvantages are the need for surgical implantation and removal and irregular bleeding patterns (9,10).

In terms of a polymer delivery vehicle, Norplant is a membrane limited device in which the release is governed by diffusion. The membrane-limiting barrier of Norplant is made of the common medical elastomer, Silastic. Silastic is the commercial term for poly(dimethylsiloxane) (PDMS) manufactured and patented by Dow Corning. It is a silicone elastomer, which is a lightly cross-linked macromolecular network that will burn upon the application of high heating. It has a glass-transition temperature of −123°C, is an amorphous polymeric material, is flexible at room temperatures, and has low mechanical strength. In general, silicone has the physical capability to be stretched reversibly between temperatures of −75°C and 240°C. The ultimate tensile strength of silicone polymers can reach 110 kg/cm^2 (the ultimate tensile strength is the strength required to rupture in tension), and the ultimate elongation can reach 700%. Silicones are also resistant to compression and return to their original dimensions upon the removal of any compressive forces. Silicone elastomer is a blend of silicone gum (uncross-linked), filler, and a catalyst that induces cross-linking. Once reacted, these ingredients yield PDMS. It is a nonporous, hydrophobic material, impermeable to ions. Water diffuses easily into the matrix. A filler is normally added for strength and consists of silica particles of approximately 30-μm diameter, composing 15–20% of the volume. Strength is increased by decreasing the freedom of the polymer chains as they form around the silica filler particles. In addition to increasing the tensile strength, the filler increases the tear strength and abrasion resistance. The silica particles are porous, being composed of diatomaceous earth and have a negative effect on diffusion of active agents (i.e., steroids) due to adsorption between the filler and these solid materials (11).

PDMS has a backbone of silicone and oxygen. The Si-O bond is very strong and resistant to hydrolytic attack. Silicone polymers are also resistant to aqueous systems (i.e., acids, bases, salts) such as those found in the body. They have a high permeability to organic solvents and can be sterilized by gas ethylene oxide. For these reasons, PDMS is very biocompatible and is used in a variety of medical applications. Silastic is known to be one of the most easily diffused polymers and lipophilic compounds, such as pro-

gesterone, are soluble in it and diffuse at a high rate through a solid matrix of Silastic 382 (7,12).

There are two types of diffusion-controlled polymeric release systems, reservoir and matrix. It is also possible to have a combination of both types in one system. Reservoir systems, such as Norplant, ideally have zero-order release, where the drug is released independent of time, and the kinetics of the release are controlled by the design of the device. The system depends on surface area, concentration difference, diffusion coefficient, partition coefficient, and thickness of the device. Flux in a reservoir system is described by the equation

$$\text{flux} = -D\Delta C_m/\Delta x \quad (1)$$

where D is the diffusion coefficient of the drug, ΔC_m is the concentration difference, and Δx is the diffusion distance (thickness). The crystalline steroid in Norplant is rather large and has a low solubility in water, causing it to aggregate as water diffuses into the capsule over time. The aggregation of steroid crystals acts to decrease the release rate, necessitating the implantation of six capsules to maintain adequate drug delivery over five years (6,7,13–15).

The Norplant system was approved by the FDA in 1990 and has a reported pregnancy rates of 0.7 per 100 over the course of 4 years (16) and 1.5 per 100 (over 5 years), significantly below the pregnancy rates for users of nonmedicated IUDs (6,17). Continuation rates for Norplant users are high, at 76–90% at the end of the first year as compared with 50–75% for IUD and oral contraceptive users (3). Main reasons for discontinuation are common problems associated with progestin-only contraceptive methods, mainly abnormal bleeding. After removal of the implant, fertility is 90% at 2 years (16). A fibrotic capsule commonly forms around the Norplant implants but it does not hinder release of the steroid as diffusion of the steroid through the membrane is the limiting factor and not the solubility of the drug in the body (15).

Other Implantable Capsules. Contraceptive systems comprised of only two capsules constitute the second generation of the Norplant system. The Norplant-2 system was designed as an improvement over the original Norplant system, which consists of six capsules implanted under the skin of the upper arm (7). The second-generation device, Norplant-2, consists of two capsules implanted in a similar fashion in the same location. The two capsules of Norplant-2 are solid 1:1 weight ratio of micronized crystalline LNG and PDMS without filler, encapsulated within an ultrathin Silastic tube. Norplant-2 covered capsules are 44 mm in length and 24 mm in diameter, with each rod containing 70 mg of steroid. The release of steroid from Norplant-2 is much more efficient than the release from Norplant mainly because the steroid is micronized and in constant contact with the polymer matrix, increasing its diffusional capability. In the Norplant system, the steroid is crystalline and rather large, so as water enters the capsule over time the steroid aggregates due to its low solubility in water. This clumping tends to decrease its release from within the capsule. Norplant-2 release is membrane controlled, much like the six capsules of Norplant (6,7,13–15).

Norplant-2 was delayed in clinical trials due to procurement problems, as production was ceased for the Silastic elastomer used as the inner core for Norplant-2 (3,10). However, because initial testing of Norplant-2 was promising, the Population Council sought to continue development with a similar device. The system was redesigned with another elastomer as the inner matrix, a copolymer of dimethylsiloxane and methylvinylsiloxane (18). This copolymer is cured in a physical mixture with the steroid LNG. The total content of steroid in the two-rod system is 150 mg. This system is known as the LNG ROD implant and is approved for use in Finland and China. It is marketed in Finland by Leiras Pharmaceuticals, Turku. The two-rod system was also approved by the FDA in 1996 (19). Testing done to date has shown the LNG ROD system to be comparable to Norplant-2. Three-year studies of LNG ROD implants in 398 women showed no pregnancies. Serum concentrations of LNG are above 300 pg/mL for the first year, dropping well below this during the third year. The lowest serum level detected was 151 pg/mL, and the device still achieved its contraceptive efficacy at this low dose (18). The main advantages of LNG ROD over Norplant are the reduced number of capsules needed to achieve contraceptive efficacy. Additionally, the LNG RODs are more rigid than those in the original Norplant system, allowing easier implantation and retrieval of the system (3). Advantages of both systems are convenience, long-term action, high effectiveness, voluntary reversibility, and low dose of steroid. The disadvantages of the original Norplant system also apply to the LNG ROD system, mainly the need for surgical implantation and removal, and bleeding irregularities (5,9,10). In three years of use, there were no differences in menstrual irregularity or efficacy of the two-rod system as compared to the six-rod system, but the two-rod system was easier to insert and remove (16). In both systems, the average steroid serum level is affected by duration of use and by weight of the patient (18). The LNG ROD system is approved by the FDA for 3 years of use, even thought it remains effective for 5 years.

Depo-Provera. Depo-Provera is an intramuscular injection of 150 mg of microcrystalline depot medroxyprogesterone acetate (DMPA), which is administered in an aqueous solution. It has a much higher serum concentration of MPA than the LNG levels with Norplant, as shown in Figure 1 (3,20). The steroid is absorbed into the bloodstream over the course of several months. Another injection is given at 3 months. It is the most common injectable contraceptive system and was FDA approved in 1992 (21). Depo-Provera is currently marketed by the Pharmacia and Upjohn Company in the United States as well as in many other countries. An identical formulation is also marketed by Organon under the brand name Megestron (21,22). The mode of contraceptive action is the same as that of any progestin; its contraceptive effect lies primarily in its capacity to inhibit ovulation, as well as in its ability to cause cervical mucus thickening and reduce endometrial capacity to support implantation (21,23).

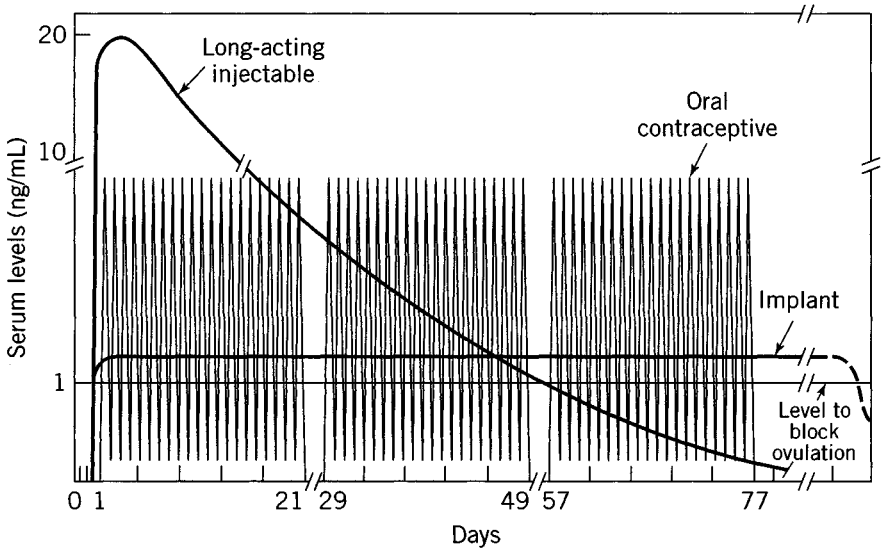


Figure 1. Release profiles of hormone levels in blood serum for three different types of contraceptive devices: daily oral contraceptives, Norplant implants and Depo-Provera 3-month injectable. *Source:* From Ref. 20.

The release profile of Depo-Provera is first-order, and serum levels of the drug are seen as one large bolus which drops off continuously over the time course of action. The high initial serum level peaks occur within the first three weeks postinjection and are most likely due to rapid absorption of loose particulates of drug (21). Advantages of the Depo-Provera system are its ease of administration (single injection every three months), high user compliance, high effectiveness, length of action, and reversibility. Side effects are the same as those common for progestin-only contraceptive series, mainly irregular bleeding patterns and weight gain. An additional disadvantage of the system is its irretrievability after injection (22,23).

Recent analysis has shown the pharmacokinetics of DMPA are affected by particle size, and recipient's diet, body mass, and fat distribution (9). The WHO is sponsoring a pharmacokinetic and pharmacodynamic study to determine the effects of three compositions of particle size, 3–10, 10–20, and 20–40 μm, to determine the effect of particle size of DMPA on pregnancy rate.

Cyclofem. An attempt to offer an alternative to Depo-Provera resulted in Cyclofem (formerly known as Cycloprovera), marketed by the Pharmacia and Upjohn Company, and HRP 102, manufactured by Schering AG. Cyclofem is a one-month injectable similar to Depo-Provera and is available for use in several countries but has not yet been FDA approved in the United States (9,22,24). In both Cyclofem and HRP 102, the steroid is in microcrystalline form and contains an estrogen compound to simulate more natural hormone levels and reduce the irregular bleeding side effects common to most progestogen-only systems (Depo-Provera is a crystalline progestin-only formulation) (22,25). Cyclofem contains 25 mg DMPA and 5 mg estradiol cypionate, and HRP 102 contains 50 mg norethindrone enanthate (NET-EN) and 5 mg estradiol valerate (25). There are several one- or two-month injectables currently marketed outside the United States under varying brand names, such as Mesigyna, Doryxus, and Cyclo Geston (22). Each of these systems employs the same method of drug delivery as Depo-Provera, namely a slow uptake of the crystalline steroid injection due to the low solubility of the steroid in the aqueous environment of the body. The systems are composed of a variety of synthetic progestins each with an estrogen component. Release from the one- and two-month injectable systems is typically similar to Depo-Provera, an initial burst that gradually declines.

Another variation on Depo-Provera is the injectable Noristerat. Noristerat is a two-month injectable composed solely of the synthetic progestin NET-EN and is manufactured by Schering AG. It is a crystalline steroid, and its use is approved for use in over 40 countries (10).

Intrauterine Devices. There are several marketed IUDs that employ release of a substance to achieve their contraceptive efficacy. The initial IUDs relied on the slow release of copper to inhibit pregnancy, and later devices employed the use of steroids delivered directly to the uterus to prevent conception. IUDs are typically designed in the shape of a T, with drug release normally occurring from the stem portion of the device.

There are several designs of copper-releasing IUDs, and the most common is the Copper T IUD, which releases copper through corrosion over the course of 12 years. The copper particles act to cause a sterile inflammation of the endometrial lining, thus prohibiting contraception. In the many copper-releasing IUDs, the copper wire thickness varies from 0.2 to 0.4 mm with a surface area of exposed copper that varies correspondingly from 200 to 380 mm^2. The corrosion is time dependent and exhibits a linear release pattern, with release directly proportional to the surface area of exposed copper. An exposed area of 375 mm^2 releases 37.5 μg/day of copper and an exposed area of 250 mm^2 releases 25 μg/day (26). Examples of copper-releasing IUDs include the Copper T 380A developed by the Population Council, the polyethylene Nova-T (Cu T Ag 200) developed by Leiras and Outokumpo Oy, Finland, and the polyethylene Multiload developed by Multilan, Switzerland, which is available in several sizes to accommodate different body types (26).

The current version of the Copper T IUD is the ParaGard® T 380A intrauterine copper contraceptive, and has 380 mm^2 of exposed copper wire surface area. It is marketed in the U.S. by Ortho-McNeil Pharmaceutical (27). The IUD is comprised of a polyethylene T, with 176 mg of copper wire on the stem of the device and an additional 66.5 mg of copper wire on the arms. The IUD has a monofilament polyethylene thread attached at the tip of the T to aid in retrieval. In 1994, the FDA approved this device for 10 years of contraceptive use. Its original design was intended for a shorter time frame but recent clinical analysis has shown its contraceptive effect to extend to 10 years. The copper-releasing Copper T 380 Ag IUD manufactured by Leiras is similar to the Copper T 380A, but differs in that the copper wire has a silver core. The silver wire acts to slow the rate of corrosion and fragmentation of the copper. Ortho Pharmaceuticals of Canada markets Gyne T 380 Slimline, a device similar to the original Copper T device. It differs in its structural design; the side arms of the Slimline IUD are designed to fit into the inserter tube more easily for easier administration (19).

There are several marketed IUDs releasing steroid available today. All of the progestin-releasing IUDs produce a local sterile inflammation in the endometrial cavity much like other IUDs. However, the steroid-releasing IUDs do not rely on endometrial inflammation to achieve contraception but instead depend on the effect of the steroid delivered. The only one manufactured in the U.S. is the Progestasert IUD, illustrated in Figure 2 (28). Progestasert releases progesterone and has been marketed in the U.S. since 1976. It was the first contraceptive device to use the natural hormone progesterone, and is currently the only IUD marketed in the U.S. that delivers a steroid (28). The device has solid poly(ethylene vinyl acetate) (EVA) side arms and a hollow core. The microcrystalline progesterone steroid is suspended in the core in medical grade silicone oil along with barium sulfate (for radiopaque properties). The drug reservoir is encased by the EVA (9% w/w vinyl acetate) copolymer membrane. The EVA membrane is 0.25 mm thick and has a surface area of 2 cm^2. Release is governed by diffusion through this rate-limiting membrane. Progestasert is loaded with 38 mg of progesterone and releases at a rate of 65 μg/day over the course of 1 year (28). Release begins at 70 μg/day and decreases over the course of 1 year to 55 μg/day, at which point 60% of the loaded drug has been released (26). The device was originally designed for use as a 1-year contraceptive agent, but testing has shown the same level of efficacy for 18 months. The pregnancy rate at this time is reported as 1.8/100 for parous women and 2.5/100 for nulliparous women (28), whereas the pregnancy rate at 2 years of use is dramatically higher at 7.4/100 (29). Progestasert does not achieve its contraceptive effect by inhibiting ovulation, but instead prevents implantation in the endometrium by suppressing the normal cyclic changes of the endometrium lining as well as thickening cervical mucus (20,29). Progesterone released from the IUD is completely metabolized in the uterine wall and does not reach systemic circulation (29). Ovulation is not inhibited with the Progestasert device. The advantages of Progestasert over other nonsteroidal IUDs is its increased effectiveness, decrease in menstrual blood loss, and decreased dysmenorrhea. Disadvantages include its need to be replaced on a yearly basis, intermenstrual bleeding and spotting, and the possibility of increased ectopic pregnancies (24,29,30).

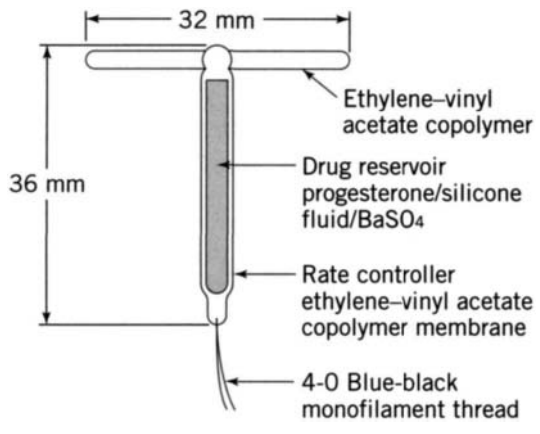


Figure 2. Progestasert IUD. *Source:* ALZA Pharmaceuticals, from Ref. 28.

Other medicated IUDs use the more potent synthetic steroids to achieve contraception. The LNG Nova-T IUD has a polyethylene stem and side arms. The stem is covered by a matrix consisting of Silastic and LNG (2:1 weight ratio) covered with a nonmedicated Silastic membrane. It is designed to release LNG at a rate of 20 μg/day for 5 years. Early designs of this system had a stem outer diameter of 2.5 mm, which consisted of a thinned vertical stem of polyethylene (0.9-mm diameter) encased in the drug-loaded matrix and covered with Silastic tubing (0.41-mm thick) (31). In vivo release rates show an initial release of 24 μg/day, decreasing to 16 μg/day at the end of 2 years. By the end of the fifth year, 60% of the loaded drug is released (26). The synthetic steroid is released into the uterus much like the progesterone released by Progestasert, but avoids complete degradation and is systemically absorbed. The hormone acts to suppress the endometrium as well as inhibit ovulation (26).

Vaginal Contraceptive Film®. The Vaginal Contraceptive Film (VCF®) is a small, thin, semitransparent square composed of 28% nonoxynol 9 in a base of poly(vinyl alcohol) and glycerin. It is a 2-inch by 2-inch square film that is 50 μm thick (32). VCF is the same device as C-Film, marketed in Great Britain since the mid-1970s. VCF contains a total of 70 mg of nonoxynol-9, delivering an average of 56–73 mg of drug (33). Nonoxynol-9 is a nonionic detergent that acts as a spermicide by creating a chemical barrier to spermatozoa in the vagina and disrupting the lipid membrane of the sperm (34). VCF is intended to be placed in the vagina against the cervix and dissolves into a gel upon contact with the vagina, in the time course of 15 minutes to 1 hour. The film and its contents are completely washed away by vaginal and cervical mucus discharge (35). It has a 96% efficacy rate and is an effective spermicide for up to 1 hour, although preliminary studies indicate that a large enough dose to inhibit spermatozoa (0.100 mg/mL) remains in the vagina for up to 4 hours (34). VCF has been available in

the United States since 1986 and is marketed by Apothecus Pharmaceutical Corporation (36).

Precommercial and Preclinical Products. There are many types of contraceptive devices in the design and preclinical stages. Development of new synthetic steroids has led to development of optimal systems, and current regulations require extensive testing of these systems prior to clinical use. This section describes the current formulations still in the research phase.

Vaginal Rings. Development of contraceptive vaginal rings (CVRs) began in the late 1960s and early 1970s. Both the Population Council and the WHO have promoted research of this promising device. Although there are several designs of vaginal rings, the main features are essentially the same. The rings are donut-shaped with an outer diameter of 50–58 mm. They release either a progestin or a combination of progestin and estrogen. The progestin-only rings typically are designed to remain in place for the entire duration of action (normally 3 months), whereas the combined progestin–estrogen delivery system is removed every fourth week to simulate menstrual bleeding. When compared with oral tablets, vaginal rings deliver a lower dosage of hormones to achieve the same contraceptive effect. The rings are simple to self-administer and remove, produce little or no local irritation, provide a near zero-order sustained release of steroid, and the treatment can be ceased at any time to provide a reversible contraceptive effect. The rings are held in place by the vaginal muscles, and it is not necessary to fit the CVR to each user or to position the CVR in a certain place in the vagina. The rings can be removed for 3 hours without decreasing the efficacy of the device (9,37,38).

The mechanism of release is very similar among the many CVR designs. Steroids delivered vaginally are absorbed across the vaginal epithelium directly into the systemic bloodstream without any metabolic alteration in the digestive tract, in specific, within the liver. The release kinetics of the vaginal rings optimize the efficacy of the steroid while minimizing its required loading, aspects that benefit the user by decreasing common side effects of hormone therapy. Vaginal rings are an optimal delivery system for natural progesterone, which is a safe contraceptive for lactating women because it is not harmful to infants but cannot be administered orally because it is metabolized too quickly (39,40). The main disadvantage of the vaginal ring containing progestin only is irregular bleeding; vaginal rings with a combined estrogen and progestin result in better bleeding patterns.

The vaginal rings are made of Silastic and loaded with a steroid. Several different designs releasing both natural progesterone and several varieties of synthetic progestins with or without an estrogen component have been designed (Table 2). The intent of the many designs is to optimize the type of steroid and its daily dosage in a form that minimizes the side effects while still maintaining the contraceptive efficacy of the system. The main mechanism of drug release is diffusion. Diffusion depends on concentration gradients, where one element diffuses from an area of high concentration to an area of low concentration. Silastic is known to be one of the most easily diffused polymers, and lipophilic compounds, such as progesterone, are soluble in and diffuse at a high rate through a solid matrix of Silastic 382 (7,12). There are two types of diffusion controlled polymeric release systems, reservoir and matrix. It is also possible to have a combination of both types in one system, such as in some designs for the vaginal rings.

The best tolerated vaginal rings in clinical studies have an outer diameter of 50–58 mm and a thickness of 7–9.5 mm (41). There are four types of CVR that have been developed to date. The initial design consisted of a homogenous matrix of drug-loaded elastomer. The solid matrix of drug-loaded polymer was not encased within a rate-limiting membrane. Steroid diffused both through the polymer matrix and through pores left by released drug. There was a high burst effect with this design and a rapid decline in release due to depletion of the drug from the outer regions of the matrix, and subsequent testing was abandoned (38,42). Another design is the band design, in which a band of drug-loaded collagen is placed in a groove on the outer surface of a solid ring of polysiloxane (38). The two main types of ring design that have shown reliable and effective release rates over the course of 3 to 6 months are the core and shell designs. In the core design, a 3.5 mm homogenous core of drug-loaded PDMS is covered with a 5 mm layer of nonmedicated polysiloxane (38,42). The shell ring, depicted in Figure 3, is a design in which an inner layer of solid elastomer provides support, the middle layer is a matrix of polymer and drug, and the outer layer is a thin rate-limiting membrane of Silastic (38,40,42,43).

In the core ring, the matrix is in the form of an inner core of polymer loaded with steroid, and the reservoir boundary is an outer layer of pure polymer, generally Silastic. The outermost layer of progesterone in the matrix core diffuses away and leaves pores or channels for the remaining progestin to diffuse out. Because each molecule must still diffuse out of the unloaded outer layer of pure Silastic, the outer membrane maintains constant release rates. It was determined that the core ring device releases drug according to the diffusion model, which can be described by the equation

$$Q = KCDt/h \qquad (2)$$

where Q is the amount of drug released, t is the time, K is the partition coefficient of drug between the polymeric device and surrounding fluid, D is the diffusion coefficient of the drug in the polymer, and h is the thickness of the hydrodynamic diffusion layer (12). After several weeks, the rings deviate from their expected release profile. This is due to a depletion zone that is created as the outermost layer of steroid in the matrix is diffused away, increasing the diffusion distance for the remaining steroid (12). The release of progesterone from core-loaded vaginal rings made of Silastic 382 show an inverse dependence on diffusion distance. This is characteristic of membrane-controlled drug delivery. Release rates can be varied with parameter changes of the inner core to yield high, medium, or low loading depending on the core diameter (12). The natural progesterone is more soluble in Silastic than its synthetic counterpart LNG, and tends to diffuse faster through the membrane than through the inner core, which

Table 2. Designs of Contraceptive Vaginal Rings

Design type	Progestin (or spermicide)	Estrogen	Length of use	Outer layer	Middle layer	Inner layer	Developer/ Manufacturer	Refs.
Homogenous	Progesterone 20 mg/day	None	90 days	PDMS and 22.5% w/w steroid	None	None	WHO/Dow Corning, Population Council	(12,40,42)
Core	LNG 20–25 μg/day	None	90 days	PDMS	None	5 mg LNG and PDMS	WHO	(26,38)
Core	Progesterone 15 mg/day	None	—	PDMS	None	PDMS with 20% w/w progesterone	—	(16,42)
Core	Progesterone 5 mg/day	None	90 days	Thin Silastic	None	Silastic with 25% w/ w steroid	WHO/Dow Corning	(12,40)
Core	3-ketodesogestrel 75 or 150 μg/day	Ethinylestradiol 15 μ/day	120 days	Silastic	None	Silastic and drug	Organon	(24,32)
Core	ST-1435 60 mg loaded	Ethinylestradiol 120 mg loaded		Silastic	None	Silastic and drug	—	(26,38)
Shell	Medroxyprogesterone acetate 100 mg	None	3–6 mos	PDMS	PDMS and drug	PDMS	—	(38)
Shell	Norgestrel 50 or 100 mg	None	3–6 mos	PDMS	PDMS and drug	PDMS	—	(38)
Shell	Norethindrone 100 or 200 mg	None	3–6 mos	PDMS	PDMS and drug	PDMS	—	(38)
Shell	Norethindrone 850 μ/day	Estradiol 200 μ/day	3 mos	PDMS	PDMS and drug	PDMS	—	(38)
Shell (suspended)	LNG 230–290 μ/day	Estradiol 150–180 μ/day		PDMS tubing	PDMS, LNG (30–77 mg), estradiol (20–66 mg)	PDMS	Population Council	(26,38,42)
Shell	LNG 25 μ/day	None	90 days	Thin Silopren® membrane	Drug-loaded Silopren matrix	Silopren support structure	Schering AG	(40)
—	NET acetate 600 μg or 1 mg/day	Ethinylestradiol 20–65 μg/day		—	—	—	—	(38)
Core	Nonoxynol-9	None	30 days	Silastic	None	EVAc and drug	—	(45)
Homogenous	RS-37367 spermicide 48 μg/cm/h	None	8 days	PDMS and 1.37% w/w drug	None	None	—	(46)

Note: Table cells containing a dash indicate that data for this feature was not specified.

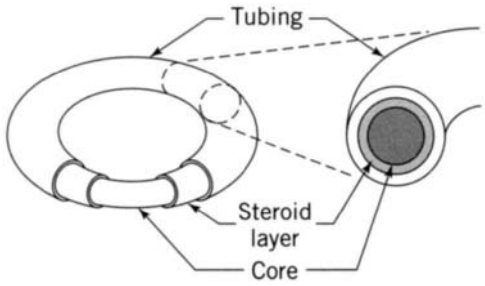


Figure 3. Cross section of the shell design contraceptive vaginal ring. *Source:* From Ref. 43.

accounts for the decreased release rate over time (42). After insertion, peak plasma levels of LNG from a core CVR design were detected within 1–8 hours, reaching 200% of their constant-release level. Release then becomes fairly constant after the initial burst but decreases by 23% to 26% over the course of 90 days (26). The factors governing release are the dissolution of the drug within the drug-loaded layer, diffusion of the drug through the rate-limiting Silastic membrane, and dissolution of the steroid within the body fluids.

Core ring designs are also being evaluated by Olsson and Odlind for the release of 3-keto desogestrel and ethinylestradiol in clinical trials (44). The core ring for delivery of two steroids is designed a bit differently; the ring is made of two Silastic tubes connected by glass stoppers. The outer diameter of the ring is 6 cm and the cross-sectional diameter is 4.9 mm. This type of CVR was developed by Organon International (Oss, The Netherlands). The rings have a daily release rate of 150 μg 3-keto desogestrel and 15 μg ethinylestradiol. The rings maintain their contraceptive efficacy for three consecutive cycles of 21 days each, with a removal period of 7 days in between cycles. Upon removal, the rings should be rinsed in water and stored in a dry location. Preliminary trials with these two-compartment rings indicate their usefulness as a contraceptive device, but also demonstrate that not all women find the CVR a comfortable means of birth control as there was some discomfort associated with use of the rings as well as some irregular bleeding patterns.

The shell rings are the most successful CVR design (38). The steroid is kept close to the rate-limiting outer Silastic membrane, acting to decrease the diffusion distance from within the matrix to the membrane. The release in these systems is governed by the outer layer of pure polymer, and release is more constant than the core ring design due to the near constant diffusion distance within the drug-loaded matrix. If the outer membrane is doubled in thickness, the release is decreased by one-half, indicating that the outer shell is the rate-limiting membrane (42). The shell CVR device provides a fairly constant diffusion distance due to the narrow inner drug-loaded polymer matrix, which is surrounded by a nonmedicated polymer membrane. The outer membrane is the rate-limiting device, and a thin enclosed ring of drug-loaded polymer provides a near-constant diffusion distance to the outer limiting membrane. These two aspects work together to provide the shell device with fairly constant release kinetics.

The manufacture of the early shell rings was a three-step injection molding process done by hand. With the increase in promising clinical trials, a new technique has emerged that produces uniform shell rings with decreased cost. In the new manufacturing process, a rod of Silastic is coated with a drug-polymer layer. After this first layer has cured, an additional layer of pure polymer is applied. The rod is then cut into sections and formed into a ring with a band of polymer to secure it (42).

Vaginal rings have also been explored for use in delivering spermicides. Vaginal rings of ethylene–vinyl acetate copolymer (EVAc) loaded with 33% of the spermicide nonoxynol-9 and covered with Silastic have been shown to release the agent over 30 days (45). This device can be used intermittently or continuously for a total of 30 days. Additionally, vaginal rings are being investigated as a delivery vehicle for the spermicide RS-37367, tested in macaque monkeys (46). This spermicide is more potent than nonoxynol-9, and has been shown in primates to be effective even when the ring is removed immediately prior to coitus. The RS-37367-containing vaginal rings are 2.3 cm in outer diameter, 1.5 cm in inner diameter, and approximately 0.4 cm in cross section. They are a homogenous matrix of 1.37% w/w drug with Silastic, formed by the injection molding technique described earlier. The devices were tested for up to 8 days in vivo.

There was some initial concern about infection with use of the CVR as it is a foreign device that is removed from and replaced into a body cavity. In 2-year studies, there was no increased incidence of vaginal infection with use of the CVRs, although there was a noted increase in vaginal secretions (38). No cervical changes were noted over this time course either.

The CVR appears to be a very promising delivery vehicle for contraceptive steroids. It is easy to use, requires minimal supervision, maintains constant serum levels of steroid, and there is minimal user requirement (once-a-month insertion). Further testing is needed, however, to optimize drug loading and provide additional safety data.

Implantable Devices. A single implanted rod of nonbiodegradable EVAc similar to Norplant is being developed by Organon to deliver ST-1435, which is 3-keto desogestrel, the main metabolite of desogestrel. The device is called Implanon® (47). One 4-cm rod releases approximately 25 μg/day of steroid for 2 years (3,16,24,48). Due to the potency of the progestin used in this system, less drug than LNG is needed to achieve contraceptive efficacy (minimum serum concentrations of 0.09 mg/dL), and the system has reportedly fewer side effects than systems using LNG (3). Implanon consists of a drug-loaded EVAc matrix core surrounded by a rate-limiting EVAc membrane, with final dimensions of 40 mm in length and 2 mm in diameter. Testing with this contraceptive device has been performed in beagle dogs, and clinical studies have been performed in women. Implanon is manufactured in a coaxial-melt-extrusion process. The steroid is in micronized form, and 68.3 mg of steroid are contained in each rod.

The Nestorone® implant is a single-rod implant, much like the Norplant implants. It is a 4-cm-long device, 2.5 mm in diameter, that contains a core matrix of Nestorone progestin, which is a potent 19-norprogesterone derivative

(ST-1435) that is inactive when delivered orally and Silastic in a 2:1 weight ratio. Much like Norplant and Implanon, Nestorone is a constant, slow release device, and was designed to improve the insertion and removal problems encountered with Norplant (3,4,49,50). Nestorone contains 78 mg of synthetic steroid and is implanted in the ventral aspect of the upper left arm. Nestorone is advantageous because it is a potent steroid that inhibits ovulation but is not effective when delivered via the oral route. Thus, it is safe contraceptive agent for lactating women, as the steroid does not affect breastfeeding infants. The Population Council is developing this device, designed for 2 years of contraceptive efficacy. The device consists of a core of polymer-steroid, covered in a rate-limiting cellulose membrane, then encased within Silastic tubing. The ends of the rod are sealed with Silastic tape. Phase II clinical testing has demonstrated the effective release to be 45–50 μg/day (4).

Another single-rod implant under development is called Uniplant (3,4). This rod contains 38 mg of the progestin nomegestrol acetate, and preliminary clinical trials demonstrate a daily release rate of 75 μg/day. The single capsule is 3.5 cm long and is designed for 1 year of contraceptive efficacy.

Other types of devices still in the clinical development stages are the biodegradable systems. With biodegradable systems, a concern is the amount of time the degraded device remains in the body after release of drug is complete. The longer a device remains in situ after drug delivery, the greater the potential for tissue injury (51). The most common mechanisms of drug delivery through implantable devices is diffusion, biodegradation due to hydrolysis of chemical bonds within the polymer chain or backbone, or a combination of both. The implantable biodegradable systems consist of polyesters, poly(ortho esters) and poly(acyrlic acids). By-products of degradation from these polymers are nontoxic and induce little to no adverse reaction at their location within the body. An additional requirement of biodegradable contraceptive systems is the need to retain structural integrity throughout the length of time of drug delivery in case removal is necessary (3).

Capronor is a system using poly(ϵ-caprolactone) (PCL), which is of the polyester class, and was reported to be clinical testing (9) but no current data could be found regarding present development of this device. The biodegradable polymer is semicrystalline and rigid, and is able to withstand gamma irradiation for sterilization purposes. It is permeable to lipophilic steroids, such as LNG. The contraceptive device consists of a hollow capsule of PCL, which encases about 16 mg of LNG and 61 mg of ethyl oleate as a suspending vehicle. Capronor is 2.4 mm in diameter and 2.5–4 cm in length depending on the amount of drug to be encapsulated (12 or 21.6 mg LNG), with heat-sealed ends (8,26). Release rates of this device are about 45 μg/day, and release is governed by diffusion as the polymer degradation rate is relatively slow (18–24 months) (9). This release is approximately 10 times faster than release of LNG from the Silastic Norplant system (3,8,52). The device is intended to be placed subcutaneously in the ischial area for drug release up to one year (20,53,54). The ester bonds of PCL undergo hydrolytic degradation, which occurs throughout the bulk of the material and is independent of geometry. PCL degrades first to ϵ-hydroxycaproic acid, and then to H_2O and CO_2. The contraceptive is a reservoir-type device in which the drug is encased within a polymer wall. The wall must be thick enough to limit the release of the drug and prevent the smaller drug particles from diffusing out of the device rapidly, leaving the larger particles behind. With a wall of appropriate thickness, the device can approximate zero-order release. Release is modulated with excipients placed in the crystalline steroid region (3,8). The suspending medium for the drug acts to keep the drug in constant contact with the capsule wall, allowing for dissolution of the drug through the wall. The polymer wall degrades slowly via hydrolysis, and there is a long induction period between the time the ester linkages are cleaved and the molecular weight of the material drops off. This allows the polymer wall sufficient time to act as the limiting membrane for diffusion of the drug (53). Studies of the degradation of an implanted device show the half-life for molecular weight to be 10.6 months, as determined by intrinsic viscosity in toluene. The crystallinity over this time frame increased from 46.8 to 60.0%, which is indicative of the structural integrity of the system. Clinical studies of steroid release from Capronor were done on two systems, one comprised of a single 2.5-cm device and the other of a 4.0-cm device. In the trials with the 4.0-cm device, 80% of menstrual cycles showed suppressed ovulation, whereas all cycles with the 2.5-cm device were ovulatory. Thus, the 4.0-cm device is the optimal contraceptive system. It delivers an average of 33 μg/day over the course of one year, with release decreasing with time (3,8). One of the disadvantages of the Capronor system is the possible rupture of the device once it is implanted. Breakage of the PCL membrane would allow the remaining load of steroid to be released as a bolus (55).

Another type of bioerodible system investigated in the 1980s (no data could be found regarding current studies) is the poly(ortho ester) rod device in which the hydrolysis rates are pH dependent (56–58). The cross-linked poly(ortho ester) matrix is formed at room temperature in a reaction that is nearly instantaneous. The cylindrical devices tested in vitro and in vivo in rabbit models are in the form of molded capsules of 2.4 mm in diameter and 20 mm in length, where the drug is suspended within a polymer matrix. In vitro release rates averaged 20 μg/day, whereas the in vivo release was significantly higher at 33 μg/day. The release of LNG is governed in part by surface erosion of the device, but mainly by solubility of the steroid. The polymer hydrolyzes faster than the drug is solubilized, creating a foamed drug layer around the implant, a layer that also contains relatively insoluble degradation products. The in vitro release appears lower due to the aqueous environment used as the sink, whereas the in vivo release is higher due in part to lipophilic carriers within the body that act to solubilize the drug and the degradation products more quickly. As the osmotic pressure and polymer erosion increase, the matrix is weakened and eventually ruptures, leaving an open cell. The open cells gradually increase the surface area and drug release is accelerated. Slightly acidic salts with low water solubility are incorporated into the matrix to control the swelling. Another way

in which the swelling is controlled is by incorporating an acidic monomer in the polymerization process. The fact that the polymer erodes faster than the drug is solubilized obviates the need for this device; a pellet of solid steroid would achieve similar release. Therefore, the poly(ortho ester) devices are still in the developmental stages.

Rice-sized norethindrone pellets fused with cholesterol are another biodegradable contraceptive system (24,26). The ellipsoidal pellets are composed of 85–90% steroid and 10–15% cholesterol, with each pellet containing about 35 mg of drug. Two to four pellets are implanted subdermally in the upper arm. Release is dependent upon surface area of the pellets, with reported release rates of 110 or 210 μ grams per day, to provide contraceptive efficacy for up to 12 months. Release is dependent solely upon solubility of the steroid in this type of device. It is possible to remove the pellets before they biodegrade, but there is a time limit within which removal can be accomplished. The pellets degrade completely within 24 months. Primary results show the four-pellet system to be most effective, but studies are still underway to determine the number of pellets needed, their size, and the cholesterol–hormone ratio (3).

Hollow fibers made of poly(L-lactic acid) (PLA) have been investigated in rabbits for release of LNG (59). The hollow fibers are manufactured with dry-wet phase inversion spinning technology and form the rate-limiting barrier for a solution of micronized steroid in castor oil. The polymer is extruded through a spinneret into a nonsolvent bath to form a porous membrane. Porosity of the fiber (and thus steroid permeability through the membrane) is greatly affected by the parameters of the solvent-nonsolvent system and process conditions (26). The steroid solution is loaded into the hollow fiber in a series of steps. First, the ends of the hollow fiber are heat sealed with Silastic. The steroid solution is then injected into the fiber through the Silastic end, and finally, the device is heat-sealed at the desired length and the silicone ends are discarded. The PLA hollow fiber is a reservoir device and provides a zero-order release of LNG. Release of steroid is governed by the dimensions of the hollow fiber (length, thickness, porosity, etc.), with the ideal release falling between 0.1 and 10 μg/cm/day for 210 days. PLA provides a useful vehicle for steroid delivery. It is biodegradable but has a low rate of degradation and also has a low permeability for steroids. These factors act to make the hollow fiber device ideal for long-term administration of low doses of steroid and obviate the need for surgical removal. The devices can be administered in a simple injection and have the advantage over other injectable contraceptives in that they can be removed if desired. The dimensions of the device are a maximum length of 3 cm and maximum diameter of 1.5 mm. Experimental data showed release in rabbits at an average of 2 μg/cm/day. The hollow fibers can be sterilized with γ radiation.

PLA has also been investigated for use in a contraceptive delivery device composed of a block copolymer of PLA and PCL. Release from the block copolymer of PCL:PLA is controlled more easily than release from the random copolymer system (55). Ye and Chien (55) describe several devices made from the block copolymer of PCL:PLA. One system is a disc laminate system and the other is a cylinder system for subdermal implantation. Both systems release a combination of LNG and estradiol (E_2). The copolymer in each system is prepared by sequence polymerization in dry toluene at 90°C in the presence of an AL/Zn bimetallic alkoxide catalyst. Release studies of the disc and cylinder systems were conducted in vitro in Valia-Chen permeation cells.

Initially there were two disc systems, one made by solvent casting and another made by compression molding. The solvent cast system exhibited faster release than the compression-molded system due to the channels formed when the solvent evaporated. Additionally, release was also different on each side of the solvent cast film, with release from the side in contact with air slower than release from the side of the film in contact with the casting surface. For these reasons, the solvent cast film system was abandoned. The disc system made by compression molding consisted of combining two matrix systems. The outer matrix system was in contact with the release medium and consisted of the block copolymer loaded with LNG, whereas the inner matrix was loaded with ethinyl estradiol (E_2). The intent of this design was to slow the release of E_2 from the combined system, as E_2 has faster release kinetics than LNG. The investigators found release of LNG from the outer disc to be matrix diffusion controlled, linear with Q vs. $t^{1/2}$. The inner matrix release was found to be quite different, controlled instead by a membrane barrier and linear with Q vs. t. The barrier membrane for release of E_2 from the inner matrix is the outer matrix of block copolymer loaded with LNG. Release from both components of the disc system was found to increase with PCL content of the block copolymer. As the weight fraction of PCL was increased from 0.6 to 0.9, release of LNG increased from 2.7 to 37.5 $\mu g/cm^2/h^{1/2}$ and release of E_2 increased from 9.3 to 32.9 $\mu g/cm^2/h$ per unit thickness of the device. The increase in release with an increasing PCL content is attributed to an overall increase in free volume of the system. Matrix thickness was also investigated for its effect on release, and it was found to affect only release of E_2 from the inner matrix. LNG release was not affected. E_2 release decreased as the outer membrane thickness increased, and the permeation rate was found to be inversely proportional in a linear manner with the outer membrane thickness. An increase in loading of LNG in the outer matrix increased release of LNG but did not affect release of E_2 from the inner matrix (55).

The second type of PCL:PLA block copolymer system investigated by Ye and Chien was a cylinder of the block copolymer. PCL:PLA loaded with both LNG and E_2 was extruded through Teflon tubing (inner diameter 1.6 mm). The device was cut to 0.5 cm in length and coated by dipping into a polymer solution containing 20% LNG (w/w). Various copolymer ratios and drug loadings were evaluated, and all exhibited the typical burst effect with steady release thereafter. A system made with a single coat of LNG-polymer exhibited zero-order release, whereas systems made with additional coats had decreased release rates. LNG release was found to be dependent upon the core loading, the number of external coats, and the loading of each coat, as well as the thickness of the outer coats.

Release of E_2 from the core was dependent upon the core loading and the thickness of the outer coating layers (55).

In both systems described by Ye and Chien, release of LNG and E_2 can be controlled by modulating the parameters of the system, allowing an optimal drug delivery device to be developed for the purpose of contraception. Further research is needed, however, to identify the optimal design and determine in vivo release rates of both LNG and E_2.

Injectable Devices. The advantages of an injectable contraceptive microsphere delivery system are the ease of administration via single injection, biodegradation of the polymer device, low release of steroid with minimal loading, and long duration of release. The disadvantages of any microsphere delivery system are its relative irretrievability after administration (9,60). Microspheres made of poly(DL-lactide-*co*-glycolide) (PLGA) 85:15 exhibit zero-order release over a 3-month period (61–63). The norethindrone–PLGA microspheres are manufactured in a solvent evaporation process. Clinical trials with PLGA spheres loaded with 47% norethindrone (a synthetic progestin) have been conducted in the attempt to optimize the dosage. A release of 100 mg/day appears adequate. The injection is administered with a 21-gauge needle. Serum levels of the progestin are 2 ng/mL, about 15–30 times lower than serum levels for Depo-Provera. The system approximates zero-order, with steadier release of the drug at a concentration low enough to minimize side effects while still maintaining efficacy.

The PLGA-steroid microspheres are a matrix device from which release occurs in two phases. The first phase of release is through diffusion. This occurs for about 2 months, with an initial burst and gradual decline in the amount of drug released. At the end of 2 months, the PLGA spheres begin to degrade, and the drug release gradually increases and peaks as trapped drug particles are made available for diffusion. At the 3-month mark there is very little drug left to maintain adequacy as a contraceptive (26,62).

The principle of norethindrone release from PLGA spheres can also be applied to the release of other steroids, such as norgestimate, another synthetic progestin (64). This system, which was evaluated by Hahn et al. in the 1980s (no current data could be found), has a 20–70 weight % loading, depending on need. These solvent-evaporation particles appear as a "free flowing powder" and encapsulation efficiency is 81.8–91.2%. As the spheres release drug via diffusion, the rate of release can be controlled by geometry as well as crystallinity and molecular weight of the polymer. Generally, a more crystalline polymer releases drug more slowly (due to a decrease in diffusion of the drug through the polymer matrix and increased degradation time of the polymer). A higher molecular weight polymer also tends to decrease the release rate. However, smaller spheres increase the release rate due to the increased surface area available for diffusion of drug. There is also a membrane thickness effect, where higher loading increases the release rate due to smaller effective membrane thickness, reducing the area over which diffusion must take place. In vivo testing on the PLGA–norgestimate microspheres, as well as PLA–steroid microspheres, has been conducted in rats and baboons to determine the optimal loading and dosage necessary for contraceptive efficacy.

PLGA is also the delivery vehicle of choice for administration of natural progesterone in microsphere form. The PLGA-progesterone system was developed by Biotek, Inc., in conjunction with CONRAD. The microspheres released progesterone over a 90-day period in vitro and was further tested in vivo in 77 rabbits. However, the FDA is questioning the use of solvents in the manufacturing process for the PLGA microsphere formulation, and thus testing has been suspended (65).

Sterility is also important in any injectable system. PLGA microspheres can be sterilized via γ irradiation, although this does cause a slight increase in the release rate. Storage is also a major concern for marketability, and the PLGA systems can be stored for up to 12 months in a cool, dry location.

PLGA has also been used as the delivery vehicle for luteinizing hormone-releasing hormone (LH-RH) analog (66,67). The LH-RH analog is a profertility agent when administered in pulsatile manner, but has a contraceptive effect when administered continuously. LH-RH has poor oral bioavailability, so the PLGA system greatly increases its potential as a contraceptive agent. The LH-RH analog is hydrophilic, as opposed to the lipophilic nature of the other steroids commonly used for contraception, and has a rather low diffusivity through PDMS, thus the choice of PLGA as the delivery vehicle (67). Spheres of PLGA and LH-RH analog have shown continuous release for over 40 days in rats. Disks made of the same materials have shown continuous release longer than the microspheres. PLGA was chosen over PLA due to its faster degradation rate of 6 months versus 12 months (66). It is not desired for the spheres to remain in the body much longer than the 3-month release time.

Another contraceptive system, designed by Nuwayser et al., employs PLA to coat steroids (68). The polymer-coated steroid systems are manufactured via air-suspension coating. The thickness of the polymer wall can be adjusted so as to control the diffusion of the drug and hence control the release characteristics of the system. The coated devices are similar to reservoir devices, and release is controlled by geometry, membrane permeability to the drug, and the thermodynamics of the encapsulated steroid. Increasing the thickness of the polymer wall decreases the release rate, and decreasing the capsule size while maintaining the same wall thickness also decreases the release rate. In order to administer these spheres via injection with a 15–22 gauge needle, the particle size must be kept below 500 μm. With the air suspension coating, the wall thickness can easily be controlled as the coating is applied incrementally. The devices under investigation have a high core-to-polymer ratio (on the order of 90:10). Using a high molecular weight PLA also ensures that the drug is released through diffusion before the polymer begins to degrade. The air-suspension-coated devices were tested in rabbits using an intramuscular injection as the route of administration. The release was mainly zero-order with a slight initial burst, and constant release of 2 μg/day/mg spheres continued for over 200 days.

One disadvantage with the PLGA microspheres is their rapid degradation when compared with other polymers, such as PCL. Research has been conducted into developing a zero-order release system that is composed of microspheres made of PLA-PLGA-PCL block copolymers (60,69). The copolymer microspheres are manufactured via solvent evaporation, and zero-order release is obtained with a balance of the ratio of PCL to PLA or PLGA. It was found that microspheres made of 60–65% PCL blocks exhibit zero-order release for approximately 5 months. The release of steroid (LNG) from the PCL blocks is controlled by diffusion because the PCL polymer degrades slowly. Steroid release from the PLA-PLGA block is controlled by erosion due to the faster degradation of these polymers. Thus, the combined system produces a long-acting device in which the release is balanced between the quick zero-order release from PLA-PLGA and the first-order release from PCL, yielding a constant release of drug for an extended length of time.

Another type of injectable contraceptive system uses a natural hydrogel. In vitro work using chitosan as the delivery vehicle began in 1991 (70). Chitosan is a polysaccharide that is hydrophilic, bioabsorbable, and nontoxic. Bioabsorption is due to lysosomal enzymes digesting the partially acetylated chitin derivatives of the chitosan polymer. The chitosan systems investigated are in the form of beads and films. The films are prepared by mixing the steroid and polymer in a solvent and evaporating the solvent, whereas the beads were prepared by a solvent removal technique using compressed air. Chitosan is a good vehicle for release of drugs because it is biocompatible, easy to control, and hydrophilic. The chitosan films showed first-order release due to the large surface area over which swelling occurs rapidly and uniformly. The beads showed zero-order release due to the swelling front, which begins at the outer core and gradually advances to the center of the bead as the pores open up. The drug is released as the matrix swells.

Transdermal Devices. Transdermal delivery is useful when a small amount of drug is needed to accomplish the desired medical purpose. This type of system is beneficial for steroid delivery because the drugs are very potent at low dosages. The main obstacle in steroid delivery is the low permeability of the skin to many compounds. Factors to be considered in transdermal delivery are drug and formulation stability, irritability of the skin, storage properties of the device, and cosmetic appearance (71). Transdermal delivery of steroids is currently being used in estrogen replacement therapy (10,72). In order to use this system for contraceptive purposes, the release rate of drug must be carefully optimized. Transdermal systems are reservoir-type devices that deliver drugs via diffusion. Release is controlled by the membrane through which the drug permeates, the diffusional resistance of the skin, and the thermodynamic activity of the drug (which affects its interaction with the delivery device) (71). Permeation enhancers are often incorporated within the reservoir to alter the drug's thermodynamic activity or the skin permeability.

One type of patch designed for contraceptive use is 4.91 cm^2, made with an impermeable backing of clear polyester film coated with heat-sealable polyethylene, and is being investigated by Friend et al. (72). The reservoir of the device is filled with 6.4 mg of LNG suspended in a hydroxypropyl cellulose and ethyl acetate/ethanol mixture. The membrane of the device is EVAc, adhering to the skin via a silicone-based adhesive. An optimal delivery of 30–35 μg/day of LNG is desired. For the steroid to penetrate the somewhat impermeable barrier of skin, a penetration enhancer must be incorporated into the design of the system. The penetration enhancer that functions most efficiently with a transdermal patch comprised of an EVA membrane is a mixture of ethyl acetate and ethanol. The devices are designed to be worn for 24 hours, and in vivo tests in rabbits indicate that this system may be suitable for contraceptive use in humans. Other transdermal patches are being developed for weekly use, where the user wears three medicated patches over the course of three consecutive weeks and a placebo patch during the fourth week to simulate menstruation through withdrawal bleeding (71).

Experiments delivering a combination of progestin and estrogen transdermally have also been conducted (73). Delivery of LNG and estradiol through a transdermal delivery system with an EVA membrane and ethanol as the permeation enhancer provide promising results. Experiments were performed in vitro on rat and human cadaver skin. It was found that release of steroids was controlled by a variety of factors, namely the composition of the reservoir formulation, the weight fraction of vinyl acetate in the EVA membrane, the membrane thickness, and the loading of steroid. It was also determined that the limiting factor in this system is the polymeric membrane and not the skin.

Intrauterine Devices. Intrauterine devices that release progestins are currently being used in the United States, such as Progestasert. Other IUDs were developed for 3-year use, such as the Intrauterine Progesterone Contraceptive System (IPCS) developed by Alza Corporation. The main difference between the Progestasert and the IPCS is the increased drug loading in the IPCS, which holds 52 mg of progesterone instead of 38 mg. The IPCS is 36 mm long, 32 mm wide, with an 8 mm insertion width. The device is a reservoir-type system, with EVAc encasing a solution of progesterone in silicone oil. The stem holds the drug, while the cross arms are solid copolymer (30). Trials with the IPCS were discontinued due to an increased pregnancy rate at 20–22 months, fully a year before its designed contraceptive efficacy was reached (20). Additionally, there is the Alza UTS system in which drug is released from the side arms as well as from the stem (74).

Another delivery vehicle being investigated is a fibrous system, in which fibers are loaded with steroid and wrapped around IUDs or vaginal rings (75). The fibers can be either biodegradable PLA, PLGA, or PCL, or nonbiodegradable polyethylene and polypropylene. It is possible to have a monolithic device in which the polymer and drug are mixed before spinning the fibers, or a coaxial fiber where the drug is the core of the device and is encased in a polymer sheath. Testing to date has been successful. The fibers are easily manufactured and stored and can be used in a variety of applications.

Another device similar to the IUD is an intracervical device (ICD) that contains a synthetic progesterone (either

LNG or Nestorone) (20,76). It was initially thought that an ICD would be more beneficial than an IUD because placement of the device in the cervix would decrease the basic problems of IUDs associated with intrauterine muscular contractility. The ICD is designed to release 10–25 μg of the progesterone daily over 5 years. The steroid is contained within a Silastic rod affixed to the vertical arm of a frame similar to the Nova-T IUD. In human testing, however, the ICD showed unsatisfactory release of the steroid through the Silastic carrier and an increase in expulsion rate over traditional IUDs.

Hydrogels are being investigated for their role in vaginal spermicide delivery. The spermicide nonoxynol-9 and ethylendiaminetetraacetic acid (EDTA) are loaded into a gel matrix composed of Carbopol 934P (77). Initial testing demonstrated a synergistic effect between EDTA and Carbopol in increasing the potency of nonoxynol-9, thus requiring lower dosage levels. Carbopol 934P is a high molecular weight poly(acrylic acid) polymer produced by B.F. Goodrich (78). It is made by cross-linking acrylic acid with allyl sucrose and polymerizing in benzene. The gel network is highly cross-linked and is typically in the form of a resin. Carbopol has a glass-transition temperature of 105°C when dry, but the glass-transition temperature drops dramatically when water is introduced to the system. Cross-linked networks swell to 1000 times their original volume in pH > 6, and Carbopol 934P is a flexible gel when hydrated. When the polymer is dry, drug is entrapped in the "glassy core." As the water penetrates the external surface of the polymer–drug matrix, the Carbopol polymer forms a gelatinous layer and drug becomes entrapped in the hydrogel domain. Carbopol is unique in that it forms "discrete microgels" of the polymer, and water forms tiny channels between the microgels as the system is hydrated. The water eventually forces the microgels to separate due to osmotic pressure, and the microgel–drug complex is sloughed off. Release of drug continues from within the stable gel layer of the microgel complex. Drug release from Carbopol is affected by the solubility of the drug, the rate of hydration of the polymer network, the degree of cross-linking and swelling of the matrix, as well as ionic interactions between the polymer and the drug. Polymer swelling is affected by the pH of the local environment, which affects drug release as well. Highly soluble drugs typically exhibit Fickian release and the release profile is dependent mainly upon the solubility and diffusion kinetics of the drug. The Carbopol matrix is the limiting membrane in the delivery of poorly soluble drugs, and release is typically near zero-order.

Contraceptive Films. Allendale Labs, Inc., is developing a vaginal contraceptive film much like VCF (marketed by Apothecus Pharmaceutical Corp) (33). The films differ in the composition of the polymeric carrier; VCF contains 70 mg of nonoxynol-9 in a base of poly(vinyl alcohol), whereas the Allendale-N9 film contains 100 or 130 mg nonoxynol-9 in a hydroxypropylmethylcellulose matrix. It is thought that the Allendale-N9 film will be less irritable to the mucosal tissues of the vagina, as well as enhance the stability of the device in warm, humid climates of third world countries. In Phase I clinical trials both Allendale-N9 films inhibited the action of sperm in the vagina, and there were no significant differences detected between VCF and the Allendale-N9 films. Further testing is needed to determine the efficacy of each film.

Another device that is undergoing testing is comprised of EVAc film (40% vinyl acetate by weight) loaded with 65% 2′-carbomethoxyphenyl 4-guanidinobenzoate (MSGB) (79). The EVAc-MSGB film is a nonbiodegradable and nonswellable matrix system that is highly flexible and can be molded into several different forms. MSGB is released from the system through diffusion through interconnecting pores. Its design is for in utero release, as MSGB is a sperm acrosin inhibitor. MSGB is advantageous to hormonal contraceptive systems as it does not interfere with the normal hormonal regulation of the endometrium. It is designed for an application of 1 to 2 years, but no test results on humans have been published.

Male Contraceptives

Very few male contraceptives are available today. However, research is progressing to allow men a wider choice of contraceptive systems. One such system involves delivery of testosterone through an implanted device. In this system, crystalline testosterone is fused into a pellet formation and six 200-mg pellets are implanted in the abdominal wall (80). The pellets are biodegradable and the release of drug suppresses sperm output for about 6 months. The release kinetics have been shown to approach zero-order. Another system that could possibly act as a contraceptive agent in males is the injectable LH-RH-containing PLGA spheres mentioned previously (67). Developments are being made for an injectable system much like Depo-Provera, in which testosterone enanthate would be administered along with DMPA (81). Sundaram et al. report on the use of a synthetic testosterone, 7α-methyl-19-nortestosterone (MENT) for use in subdermal contraceptive implants in men (82). MENT is more potent than testosterone, maintains normal muscle mass, and does not hyperstimulate the prostate because it does not undergo 5α-reduction in the prostate. In conjunction with an LH-RH analogue, this potent steroid could be used in a system designed for 1 year of contraceptive use.

A further development in male contraceptives is the navel administration of testosterone via a transdermal device (83). The device is designed to administer testosterone for one month or longer, and initial testing shows a zero-order release both in vitro and in vivo testing on rhesus monkeys. The system is a disk-shaped bandage-type device that contains microspheres of hormone suspended in liquid and immobilized in a cross-linked polymer. (Further description of the liquid or polymer were not available.) In vitro release rates were 40.25 μg/cm^2/day and in vivo release rates were 27.66 μg/cm^2/day. The decreased in vivo release rate is most likely due to the additional barrier of skin.

Cylindrical capsules of PLGA have also been investigated for their use in delivering buserelin acetate (84). Buserelin is a gonadotropin-releasing hormone (GnRH) agonist (D-Ser(Bu^t)^6-GnRH-(1-9)nonapeptide-ethylamide). GnRH, previously known as LH-RH, is one of the hypothalamic peptides and promotes pituitary secretion of follicle stimulating hormone (FSH) and luteinizing hormone (LH).

FSH induces spermatogenesis and LH causes the testicular Leydig cells to produce testosterone. A GnRH agonist will inhibit FSH and LH secretion from the pituitary, thus decreasing testosterone secretion and suppressing spermatogenesis. The PLGA capsules are 10 mm in length and contain 3.3 mg of buserelin acetate. The devices can be sterilized by γ-irradiation and are intended to be implanted subcutaneously in the abdominal wall lateral to the rectus abdominis muscle. Preliminary testing of the device as a contraceptive has been inconclusive as the delivery of GnRH agonists must be carefully combined with the administration of androgens so as to inhibit only spermatogenesis and avoid adversely affecting other androgen-supported functions in the body.

ABORTIFACIENTS

In the past, prostaglandin analogs have commonly been used as abortion-inducing agents. However, there are many side effects of prostaglandin use, especially to the gastrointestinal tract; vomiting and diarrhea are very common. To avoid the side effects, 24-hour delivery systems for the prostaglandin were developed. One such device is a polyethylene-oxide based hydrogel strip into which 3 mg of drug have been loaded (85). The strip measures 1.3 $\times$ 10 $\times$ 30 mm, and releases an average of 53% of the drug over 24 hours. The hydrogel is cross-linked with aliphatic difunctional isocyanate and an aliphatic triol. It swells to three times its dry volume and releases the drug through diffusion at zero-order. It has been demonstrated to be 85% effective, yet some of the side effects still persist. Another abortifacient device is a reservoir-type system (86). The device consists of three layers, a drug-loaded membrane surrounded by an outer rate-controlling membrane on one side and a drug-impermeable membrane on the other. The system is mounted on a holder and delivers from 50 to 100 μg/hour depending on loading. The device is 1.5 cm in diameter and 3.7 cm in length.

SUMMARY

There are many types of contraceptive agents both in use and being developed today. This article was limited to discussing the contraceptive devices involving controlled release and does not touch upon systems involving vaccines or pure polymer systems without drug release (such as a plug of silicon placed in the vas deferens for male contraception). There is quite a variety of controlled release systems, and as research progresses more and more of these systems will become available to the general public. Additionally, advances in the types of synthetic steroids used in contraceptive devices act to minimize the numerous side effects of current systems and will greatly improve the efficacy and acceptability of future devices.

BIBLIOGRAPHY

1. A.C. Guyton, *Textbook of Medical Physiology*, Saunders, Philadelphia, 1991.
2. F. Murad and J.A. Kuret, in A.G. Gilman, T.W. Rall, A.S. Nies, and P. Taylor, eds., *Goodman and Gilman's The Pharmacological Basis of Therapeutics*, 8th ed., Pergamon, New York, 1990, Chapter 58.
3. P.D. Darney, *Am. J. Obstet. Gynecol.* **170**, 1536–1543 (1994).
4. O. Peralta, S. Diaz, and H. Croxatto, *J. Steroid Biochem. Mol. Biol.* **53**, 223–226 (1995).
5. S. Koetsawang, S. Varakamin, S. Satayapan, and N. Dusitsin, in G.I. Zatuchni, A. Goldsmith, J.D. Shelton, and J.J. Sciarra, eds., *Long-Acting Contraceptive Delivery Systems*, Harper & Row, Philadelphia, 1984, pp. 459–470.
6. I. Sivin, in S.S. Ratnam, E.S. Teoh, and S.M. Lim, eds., *Contraception*, The Parthenon Publishing Group, Park Ridge, N.J., 1986, pp. 121–126.
7. S. Segal, *Am. J. Obstet. Gynecol.* **157**, 1090–1092 (1987).
8. P.D. Darney et al., *Fertil. Steril.* **58**, 137–143 (1992).
9. H.L. Gabelnick and P.E. Hall, *J. Controlled Release* **6**, 387–394 (1987).
10. L. Mastroianni, Jr., P.J. Donaldson, and T.T. Kane, eds., *The Current Status of Contraceptive Research*, National Academy Press, Washington, D.C., 1990, pp. 30–40.
11. M.R. Brunstedt, in D.F. Williams, ed., *Materials Science and Technology: A Comprehensive Treatment*, VCH Publishers, Mannheim, Germany, 1992, Chapter 11.
12. S.A. Matlin, A. Belenguer, and P.E. Hall, *Contraception* **45**, 329–341 (1992).
13. S. Kuldip, O.A.C. Viegas, and S.S. Ratnam, *Contraception* **45**, 453–461 (1992).
14. S. Koetsawang et al., in S.S. Ratnam, E.S. Teoh, and S.M. Lim, eds., *Contraception*, The Parthenon Publishing Group, Park Ridge, N.J., 1986, pp. 133–142.
15. D.N. Robertson, in G.I. Zatuchni, A. Goldsmith, J.D. Shelton, and J.J. Sciarra, eds., *Long-Acting Contraceptive Delivery Systems*, Harper & Row, Philadelphia, 1984.
16. J. Newton, *British Medical Bulletin* **49**, 40–61 (1993).
17. I. Sivin, in G.I. Zatuchni, A. Goldsmith, J.D. Shelton, and J.J. Sciarra, eds., *Long-Acting Contraceptive Delivery Systems*, Harper & Row, Philadelphia, 1984, pp. 488–500.
18. I. Sivin et al., *Contraception* **55**, 81–85 (1997).
19. *Reproductive Health Product Development*, available at: *http://www.popcouncil.org/*, 1997, updated October 7, 1998, accessed October 14, 1998.
20. L. Liskin and W.F. Quillin, *Popul. Rep. Ser. K* **2** (XI), K19–K47 (1983).
21. *Depo-Provera*, available at: *http:www.depo-provera.com*, 1997, accessed October 14, 1998.
22. R. Lande, *Popul. Rep. Ser. K* **5**, 1–5 (1995).
23. H. Nash, *Contraception* **12**, 377–393 (1975).
24. L. Liskin, R. Blackburn, and R. Ghani, *Popul. Rep. Ser. K* **3** (XV), K57–K84 (1987).
25. P.E. Hall, in G.I. Zatuchni, A. Goldsmith, J.D. Shelton, and J.J. Sciarra, eds., *Long-Acting Contraceptive Delivery Systems*, Harper & Row, Philadelphia, 1984, pp. 515–522.
26. A.P. Sam, *J. Controlled Release* **22**, 35–46 (1992).
27. *PARAGARD T 380A Intrauterine Copper Contraceptive*, available at: *http://ortho-mcneil.com/*, 1998, updated October 12, 1998, accessed October 14, 1998.
28. ALZA Pharmaceuticals, *Progestasert Intrauterine Contraceptive System: Clinical Evidence*, Palo Alto, Calif., 1994.
29. R. Aznar and J. Giner, in G.I. Zatuchni, A. Goldsmith, J.D. Shelton, and J.J. Sciarra, eds., *Long-Acting Contraceptive Delivery Systems*, Harper & Row, Philadelphia, 1984, pp. 613–620.

30. D.A. Edelman, L.P. Cole, R. Apelo, and P. Lavin, in G.I. Zatuchni, A. Goldsmith, J.D. Shelton, and J.J. Sciarra, eds., *Long-Acting Contraceptive Delivery Systems*, Harper & Row, Philadelphia, 1984, pp. 621–627.
31. S. El-Mahgoub, *Contraception* **22**, 271–286 (1980).
32. A.S. Lichtman, V. Davajan, and D. Tucker, *Contraception* **8**, 291–297 (1973).
33. C.K. Mauck et al., *Contraception* **56**, 97–102 (1997).
34. C.K. Mauck et al., *Contraception* **56**, 103–110 (1997).
35. Apothecus Pharmaceutical Corporation, *VCF Vaginal Contraceptive Film: A Compendium of Medical and Technical Data*, Oyster Bay, New York, 1995.
36. *Apothecus Pharmaceutical Corporation VCF Vaginal Contraceptive Film*, available at: *http://www.apothecus.com/*, accessed October 14, 1998.
37. E. Diczfalusy and B.M. Landgren, in G.I. Zatuchni, A. Goldsmith, J.D. Shelton, and J.J. Sciarra, eds., *Long-Acting Contraceptive Delivery Systems*, Harper & Row, Philadelphia, 1984, pp. 213–227.
38. D.R. Mishell, Jr., *Ann. Med.* **25**, 191–197 (1993).
39. S. Diaz et al., *Contraception* **32**, 603–621 (1985).
40. B.M. Landgren, P.E. Hall, and S.Z. Cekan, *Contraception* **45**, 343–349 (1992).
41. S. Roy and D.R. Mishell, Jr., in G.I. Zatuchni, A. Goldsmith, J.D. Shelton, and J.J. Sciarra, eds., *Long-Acting Contraceptive Delivery Systems*, Harper & Row, Philadelphia, 1984, pp. 581–594.
42. T.M. Jackanicz, in G.I. Zatuchni, A. Goldsmith, J.D. Shelton, and J.J. Sciarra, eds., *Long-Acting Contraceptive Delivery Systems*, Harper & Row, Philadelphia, 1984, pp. 201–212.
43. D.R. Mishell, Jr., et al., *Am. J. Obstet. Gynecol.* **130**, 55–62 (1978).
44. S.-E. Olsson and V. Odlind, *Contraception* **42**, 563–572 (1990).
45. W.M. Saltzman and L.B. Tena, *Contraception* **43**, 497–505 (1991).
46. B.H. Vickery, J.C. Goodpasture, and L.Y.W. Lin, in G.I. Zatuchni, A. Goldsmith, J.D. Shelton, and J.J. Sciarra, eds., *Long-Acting Contraceptive Delivery Systems*, Harper & Row, Philadelphia, 1984, pp. 228–240.
47. *A Tradition in Reproductive Medicine*, available at: *http://www.organon.com/*, 1998, updated accessed October 14, 1998.
48. J.A.A. Geelen et al., *Contraception* **47**, 215–226 (1993).
49. M. Laurikka-Routti and M. Haukkamaa, *Fertil. Steril.* **58**, 1142–1147 (1992).
50. S. Diaz et al., *Contraception* **51**, 33–38 (1995).
51. L.R. Beck et al., in G.I. Zatuchni, A. Goldsmith, J.D. Shelton, and J.J. Sciarra, eds., *Long-Acting Contraceptive Delivery Systems*, Harper & Row, Philadelphia, 1984, pp. 406–417.
52. G.I. Dhall, U. Krishna, and R. Sivaram, *Contraception* **44**, 409–417 (1991).
53. C.G. Pitt and A. Schindler, in G.I. Zatuchni, A. Goldsmith, J.D. Shelton, and J.J. Sciarra, eds., *Long-Acting Contraceptive Delivery Systems*, Harper & Row, Philadelphia, 1984, pp. 48–63.
54. S.J. Ory et al., *Am. J. Obstet. Gynecol.* **145**, 600–605 (1983).
55. W.-P. Ye and Y.W. Chien *J. Controlled Release* **41**, 259–269 (1996).
56. J. Heller, D.W.H. Penhale, B.K. Fritzinger, and S.Y. Ng, in G.I. Zatuchni, A. Goldsmith, J.D. Shelton, and J.J. Sciarra, eds., *Long-Acting Contraceptive Delivery Systems*, Harper & Row, Philadelphia, 1984, pp. 113–128.
57. J. Heller, B.K. Fritzinger, S.Y. Ng, and D.W.H. Penhale, *J. Controlled Release* **1**, 225–232 (1985).
58. J. Heller, B.K. Fritzinger, S.Y. Ng, and D.W.H. Penhale, *J. Controlled Release* **1**, 233–238 (1985).
59. M.J.D. Eenink and J. Feijen *J. Controlled Release* **6**, 225–247 (1987).
60. Z. Gu et al., *J. Controlled Release* **22**, 3–14 (1992).
61. G.S. Grubb et al., *Fertil. Steril.* **51**, 803–810 (1989).
62. L.R. Beck et al., *Am. J. Obstet. Gynecol.* **147**, 815–821 (1983).
63. L.R. Beck et al., *Am. J. Obstet. Gynecol.* **135**, 419–426 (1979).
64. D.W. Hahn et al., in G.I. Zatuchni, A. Goldsmith, J.D. Shelton, and J.J. Sciarra, eds., *Long-Acting Contraceptive Delivery Systems*, Harper & Row, Philadelphia, 1984, pp. 96–112.
65. *Systemic Hormonal Methods for Women*, available at: *http://www.reproline.jhu.edu/*, 1997, updated August 20, 1997, accessed October 16, 1998.
66. J.S. Kent, L.M. Sanders, T.R. Tice, and D.H. Lewis, in G.I. Zatuchni, A. Goldsmith, J.D. Shelton, and J.J. Sciarra, eds., *Long-Acting Contraceptive Delivery Systems*, Harper & Row, Philadelphia, 1984, pp. 169–179.
67. B.H. Vickery et al., in G.I. Zatuchni, A. Goldsmith, J.D. Shelton, and J.J. Sciarra, eds., *Long-Acting Contraceptive Delivery Systems*, Harper & Row, Philadelphia, 1984, pp. 180–189.
68. E.S. Nuwayser et al., in G.I. Zatuchni, A. Goldsmith, J.D. Shelton, and J.J. Sciarra, eds., *Long-Acting Contraceptive Delivery Systems*, Harper & Row, Philadelphia, 1984, pp. 64–76.
69. Y.-X. Li and X.-D. Feng, *Makromol. Chem., Macromol. Symp.* **33**, 253–264 (1990).
70. T. Chandy and C.P. Sharma, *Biomater. Artif. Cells, Immobil. Biotechnol.* **19**, 745–760 (1991).
71. V.V. Ranade and M.A. Hollinger, *Drug Delivery Systems*, CRC Press, Boca Raton, Fla. 1996.
72. D.R. Friend, P. Catz, and S. Phillips, *Contraception* **40**, 73–80 (1989).
73. G. Chen, D. Kim, and Y. Chien, *J. Controlled Release* **34**, 129–143 (1995).
74. T.G. McCarthy, E.L. Cheng, A. Loganath, and S.S. Ratnam, in S.S. Ratnam, E.S. Teoh, and S.M. Lim, eds., *Contraception*, The Parthenon Publishing Group, Park Ridge, N.J., 1986, pp. 95–98.
75. D.R. Cowsar and R.L. Dunn, in G.I. Zatuchni, A. Goldsmith, J.D. Shelton, and J.J. Sciarra, eds., *Long-Acting Contraceptive Delivery Systems*, Harper & Row, Philadelphia, 1984, pp. 145–163.
76. P. Lahteenmaki et al., in G.I. Zatuchni, A. Goldsmith, J.D. Shelton, and J.J. Sciarra, eds., *Long-Acting Contraceptive Delivery Systems*, Harper & Row, Philadelphia, 1984, pp. 595–600.
77. C.-H. Lee, R. Bagdon, and Y.W. Chien, *J. Pharm. Sci.* **85**, 91–95 (1996).
78. *CARBOPOL: The Proven Polymers in Pharmaceuticals. Controlled Release Tablets and Capsules*, B.F. Goodrich, Cleveland, Ohio, 1994, Bull. 17.
79. J.W. Burns, A.T. Fazleabas, I.F. Miller, and L.J.D. Zaneveld, *Contraception* **38**, 349–364 (1988).
80. D.J. Handelsman, A.J. Conway, and L.M. Boylan, *J. Clin. Endocrinol. Metab.* **75**, 1326–1332 (1992).
81. G.M.H. Waites, *Br. Med. Bull.* **49**, 210–221 (1993).
82. K. Sundaram, N. Kumar, and C.W. Bardin, *Ann. Med.* **25**, 199–205 (1993).
83. Y.W. Chien, *J. Pharm. Sci.* **73**, 1064–1067 (1984).

Next Page

84. H.M. Behre, D. Nashan, W. Hubert, and E. Nieschlag, *J. Clin. Endocrinol. Metab.* **74**, 84–90 (1992).
85. I.T. Cameron and D.T. Baird, *Contraception* **33**, 121–125 (1986).
86. M. Bygdeman et al., *Contraception* **27**, 141–151 (1983).

FOOD AND DRUG ADMINISTRATION REQUIREMENTS FOR CONTROLLED RELEASE PRODUCTS

HENRY J. MALINOWSKI
PATRICK J. MARROUM
U.S. Food and Drug Administration
Rockville, Maryland

KEY WORDS

Area under the curve (AUC)
Bioavailability
Bioequivalence
Controlled release
Delayed release
Dissolution
Extended release
In vitro in vivo correlation (IVIVC)
Modified release
Peak plasma concentration (C_{max})
Pharmacokinetics

OUTLINE

Introduction
Types of Controlled-Release Products
Definitions
Laws, Regulations and Guidances for Controlled-Release Products
  Need for Clinical Studies
  Bioavailability Study Requirements for Controlled Release Products
  Controlled-Release New Drug Applications
Information to Characterize the Drug Entity
  Physicochemical Characterization
  Pharmacokinetic Characterization
Information to Characterize the Dosage Form
  Physicochemical Characterization
  Bioavailability/Bioequivalence Studies
  Dissolution Testing for Controlled-Release Drug Products
  Setting Dissolution Specifications
Bibliography

INTRODUCTION

Controlled-release pharmaceutical dosage forms may offer one or more advantages over conventional (immediate release) dosage forms of the same drug, including a reduced dosing frequency, a decreased incidence and/or intensity of adverse effects, a greater selectivity of pharmacologic activity, and a reduction in drug plasma fluctuation resulting in a more constant or prolonged therapeutic effect. In some cases, controlled-release products may be therapeutically advantageous primarily for certain subpopulations of patients. For example, a controlled-release drug product may allow a child to attend school without drug administration during the school day. In other instances, controlled-release products may have no significant advantages or may actually be less effective or more hazardous than conventional dosage forms of the same drug. Therefore, not all drugs are good candidates for formulation as controlled-release drug products (1). For example, some drugs are more effective if fluctuation in plasma concentrations occur. For such drugs, tolerance to drug effect may develop with the constant levels seen with controlled-release drug products. Ordinarily, oral controlled-release dosage forms result in a longer recommended dosing interval for the controlled-release dosage form, usually twice as long, compared with the dosing interval for the immediate release dosage form. Also, a controlled-release drug product may be warranted if significant clinical advantages for the controlled-release dosage form can be demonstrated, for example, decreased side effects resulting from a lower peak plasma concentration with the controlled-release dosage form relative to the immediate-release dosage form.

TYPES OF CONTROLLED-RELEASE PRODUCTS

The most common type of controlled-release products are oral dosage forms. These products normally provide for a 12- or 24-h dosing interval. Dosing intervals for oral controlled-release products beyond once-a-day dosing are limited by physiologic characteristics of the human gastrointestinal tract. Gastrointestinal transit time, which normally averages 24 h but can vary from a few hours to several days, prevents oral controlled-release products with a dosing interval beyond 24 h. Other types of controlled-release products include transdermal patches that are applied to the skin for periods of 1 day to perhaps 1 week. In addition, controlled-release implants are dosage forms that are implanted below the skin surface and have been developed for continuous therapy for as long as 5 years.

DEFINITIONS

Before beginning a discussion of the regulatory requirements of controlled-release products, it is useful to understand several commonly used definitions for these types of products:

Controlled-release dosage forms. A class of pharmaceuticals or other biologically active products from which a drug is released from the delivery system in a planned, predictable, and slower-than-normal manner (2).

Modified-release dosage form. This refers, in general, to a dosage form for which the drug-release characteristics of time course and/or location are chosen to accomplish

84. H.M. Behre, D. Nashan, W. Hubert, and E. Nieschlag, *J. Clin. Endocrinol. Metab.* **74**, 84–90 (1992).
85. I.T. Cameron and D.T. Baird, *Contraception* **33**, 121–125 (1986).
86. M. Bygdeman et al., *Contraception* **27**, 141–151 (1983).

FOOD AND DRUG ADMINISTRATION REQUIREMENTS FOR CONTROLLED RELEASE PRODUCTS

HENRY J. MALINOWSKI
PATRICK J. MARROUM
U.S. Food and Drug Administration
Rockville, Maryland

KEY WORDS

Area under the curve (AUC)
Bioavailability
Bioequivalence
Controlled release
Delayed release
Dissolution
Extended release
In vitro in vivo correlation (IVIVC)
Modified release
Peak plasma concentration (C_{max})
Pharmacokinetics

OUTLINE

Introduction
Types of Controlled-Release Products
Definitions
Laws, Regulations and Guidances for Controlled-Release Products
  Need for Clinical Studies
  Bioavailability Study Requirements for Controlled Release Products
  Controlled-Release New Drug Applications
Information to Characterize the Drug Entity
  Physicochemical Characterization
  Pharmacokinetic Characterization
Information to Characterize the Dosage Form
  Physicochemical Characterization
  Bioavailability/Bioequivalence Studies
  Dissolution Testing for Controlled-Release Drug Products
  Setting Dissolution Specifications
Bibliography

INTRODUCTION

Controlled-release pharmaceutical dosage forms may offer one or more advantages over conventional (immediate release) dosage forms of the same drug, including a reduced dosing frequency, a decreased incidence and/or intensity of adverse effects, a greater selectivity of pharmacologic activity, and a reduction in drug plasma fluctuation resulting in a more constant or prolonged therapeutic effect. In some cases, controlled-release products may be therapeutically advantageous primarily for certain subpopulations of patients. For example, a controlled-release drug product may allow a child to attend school without drug administration during the school day. In other instances, controlled-release products may have no significant advantages or may actually be less effective or more hazardous than conventional dosage forms of the same drug. Therefore, not all drugs are good candidates for formulation as controlled-release drug products (1). For example, some drugs are more effective if fluctuation in plasma concentrations occur. For such drugs, tolerance to drug effect may develop with the constant levels seen with controlled-release drug products. Ordinarily, oral controlled-release dosage forms result in a longer recommended dosing interval for the controlled-release dosage form, usually twice as long, compared with the dosing interval for the immediate release dosage form. Also, a controlled-release drug product may be warranted if significant clinical advantages for the controlled-release dosage form can be demonstrated, for example, decreased side effects resulting from a lower peak plasma concentration with the controlled-release dosage form relative to the immediate-release dosage form.

TYPES OF CONTROLLED-RELEASE PRODUCTS

The most common type of controlled-release products are oral dosage forms. These products normally provide for a 12- or 24-h dosing interval. Dosing intervals for oral controlled-release products beyond once-a-day dosing are limited by physiologic characteristics of the human gastrointestinal tract. Gastrointestinal transit time, which normally averages 24 h but can vary from a few hours to several days, prevents oral controlled-release products with a dosing interval beyond 24 h. Other types of controlled-release products include transdermal patches that are applied to the skin for periods of 1 day to perhaps 1 week. In addition, controlled-release implants are dosage forms that are implanted below the skin surface and have been developed for continuous therapy for as long as 5 years.

DEFINITIONS

Before beginning a discussion of the regulatory requirements of controlled-release products, it is useful to understand several commonly used definitions for these types of products:

Controlled-release dosage forms. A class of pharmaceuticals or other biologically active products from which a drug is released from the delivery system in a planned, predictable, and slower-than-normal manner (2).

Modified-release dosage form. This refers, in general, to a dosage form for which the drug-release characteristics of time course and/or location are chosen to accomplish

therapeutic or convenience objectives not offered by conventional dosage forms (2).

Extended-release dosage form. This is a specific type of modified-release dosage form that allows at least a two-fold reduction in dosage frequency as compared to that drug presented as an immediate- (conventional-) release dosage form (2).

Delayed-release dosage form. This is a specific type of modified-release dosage form that releases a drug at a time other than promptly after administration. An example is enteric-coated tablets (2).

The requirements discussed in this article cover all types of controlled-release dosage forms. The primary focus will be on oral controlled-release drug products, which are most common. Requirements for other types of controlled-release drug products, such as transdermal patches or implants, are similar to those described in this article.

LAWS, REGULATIONS AND GUIDANCES FOR CONTROLLED-RELEASE PRODUCTS

Need for Clinical Studies

Premarketing evaluation of a controlled-release product should include consideration of the possible development of tolerance to the drug, the occurrence of sensitivity reactions or local tissue damage due to dosage-form-dependent persistence or localization of the drug, the clinical implications of dose dumping or of an unexpected decrease in bioavailability by physiological or physicochemical mechanisms, and a quantitative alteration in the metabolic fate of the drug related to nonlinear or site-specific disposition.

Specific claims for all therapeutic advantages of a controlled-release product over the conventional dosage forms should be based on adequate clinical studies, the results of which should be available to health professionals upon request. Where no therapeutic advantage is claimed, the need for clinical studies may be lessened.

An important consideration for the development of controlled-release products as original new drugs is the quantity of evidence needed in particular circumstances to establish substantial proof of effectiveness. The usual practice for all new molecular entities is to accept as proof two or more clinical studies that conclusively define the safety and efficacy of the drug. Within the U.S. Food and Drug Administration (FDA) Modernization Act of 1998 are described situations in which alternative approaches regarding the quantity of evidence to support effectiveness may be possible (3). These include (*1*) situations in which effectiveness of a new use may be extrapolated entirely from existing efficacy studies; (*2*) situations in which a single adequate and well-controlled study of a specific new use can be supported by information from other related adequate and well-controlled studies, such as studies in other phases of a disease; in closely related diseases; or other conditions of use (different dose, duration of use, regimen), of different dosage forms, or of different endpoints; and (*3*) situations in which a single multicenter study, without supporting information from other adequate and well-controlled studies, may provide evidence that a use is effective. In each of these situations, it is assumed that any studies relied on to support effectiveness meet the requirements for adequate and well-controlled studies in 21 CFR 314.126 (4). It should also be appreciated that reliance on a single study of a given use, whether alone or with substantiation from related trial data, leaves little room for study imperfections or contradictory (nonsupportive) information. In all cases, it is presumed that the single study has been appropriately designed; that the possibility of bias due to baseline imbalance, unblinding, post hoc changes in analysis, or other factors is judged to be minimal; and that the results reflect a clear prior hypothesis documented in the protocol. Moreover, a single favorable study among several similar attempts that failed to support a finding of effectiveness would not constitute persuasive support for a product use unless there were a strong argument for discounting the outcomes in the studies that failed to show effectiveness (e.g., if the study was obviously inadequately powered or there was a lack of assay sensitivity as demonstrated in a three-arm study by failure of the study to show efficacy of a known active agent).

Whether to rely on a single study to support an effectiveness determination is not often an issue in contemporary drug development. In most drug development situations, the need to find an appropriate dose, to study patients of greater and lesser complexity or severity of disease, to compare the drug with other therapy, to study an adequate number of patients for safety purposes, and to otherwise know what needs to be known about a drug before it is marketed will result in more than one adequate and well-controlled study upon which to base an effectiveness determination.

In certain cases, effectiveness of a new controlled-release drug product may be demonstrated without additional adequate and well-controlled clinical efficacy trials. Ordinarily, this will be because other types of data provide a way to apply the known effectiveness to a new population or a different dose, regimen, or dosage form. Controlled-release dosage forms may be approved on the basis of pharmacokinetic data linking the new dosage form to a previously studied immediate-release dosage form. Because the pharmacokinetic patterns of modified- and immediate-release dosage forms are not identical, it is generally important to have some understanding of the relationship of blood concentration to response, including an understanding of the time course of that relationship, to extrapolate the immediate-release data to the modified-release dosage form (3).

Bioavailability Study Requirements for Controlled Release Products

The bioavailability requirements for controlled-release products are covered in the U.S. Code of Federal Regulations under 21 CFR 320.25(f) (5). The aims of these requirements are to determine that the following conditions are met:

- The drug product meets the controlled-release claims made for it.
- The bioavailability profile established for the drug product rules out the occurrence of clinically significant dose dumping. This is usually achieved by the conduct of a food effect study whereby the drug is administered with and without a high-fat breakfast.
- The drug product's steady-state performance is equivalent to a currently marketed noncontrolled- or controlled-release drug product that contains the same active drug ingredient or therapeutic moiety and that is subject to an approved full new drug application.
- The drug product's formulation provides consistent pharmacokinetic performance between individual dosage units.

The reference material for such a bioavailability study shall be chosen to permit an appropriate scientific evaluation of the controlled-release claims made for the drug product. The reference material is normally one of the following:

- A solution or suspension of the active drug ingredient or therapeutic moiety
- A currently marketed immediate-release drug product containing the same active drug ingredient or therapeutic moiety and administered according to the dosage recommendations in the labeling of immediate-release drug product
- A currently marketed controlled-release drug product subject to an approved full new drug application containing the same active drug ingredient or therapeutic moiety and administered according to the dosage recommendations in the labeling proposed for the controlled-release drug product

Guidelines for the evaluation of controlled-release pharmaceutical dosage forms provide assistance to those designing, conducting, and evaluating studies. However, a drug may possess inherent properties that require considerations specific to that drug and its dosage form that may override the generalities of these guidelines. Guidances related to the evaluation of controlled-release drug products as well as many other types of guidances are available on the Internet at the Center for Drug Evaluation and Research Web site (*http://www.fda.gov/cder/*).

Controlled-Release New Drug Applications

As mentioned earlier, a fundamental question in evaluating a controlled-release product is whether formal clinical studies of the dosage form's safety and efficacy are needed or whether only a pharmacokinetic evaluation will provide adequate evidence for approval. A rational answer to this question must be based on evaluation of the pharmacokinetic properties and plasma concentration/effect relationship of the drug. Where there is a well-defined predictive relationship between the plasma concentrations of the drug and the clinical response (regarding both safety and efficacy), it may be possible to rely on plasma concentration data alone as a basis for the approval of the controlled-release product. In the following situations, it is expected that clinical data be submitted for the approval of the controlled-release New Drug Application (NDA):

- When the controlled-release product involves a drug that is an unapproved new molecular entity, because there is no approved reference product to which a bioequivalence claim could be made
- When the rate of input has an effect on the drug's efficacy and toxicity profile
- When a claim of therapeutic advantage is intended for the controlled-release product
- When there are safety concerns with regards to irreversible toxicity
- Where there are uncertainties concerning the relationship between plasma concentration and therapeutic and adverse effects or in the absence of a well-defined relationship between plasma concentrations and either therapeutic or adverse clinical response
- Where there is evidence of functional (i.e., pharmacodynamic) tolerance
- Where peak-to-trough differences of the immediate-release form are very large

In all of these instances except for the first, a 505(b)(2) NDA could be submitted for approval to the FDA. The regulations for such application are covered under 21 CFR 314.54. These regulations state that any person seeking approval of a drug product that represents a modification of a listed drug, for example, a new indication or a new dosage form, and for which investigations other than bioavailability or bioequivalence studies are essential to the approval of the changes may submit a 505(b)(2) application. However, such an application may not be submitted under this section of the regulations for a drug product whose only difference from the reference-listed drug is that the extent of absorption or rate of absorption is less than that of the reference-listed drug or if the rate of absorption is unintentionally less than that of the reference-listed drug (6).

INFORMATION TO CHARACTERIZE THE DRUG ENTITY

Physicochemical Characterization

Although the required physicochemical information to characterize the drug entity in a controlled-release dosage form should generally be no different from that for the drug entity in an immediate-release dosage form, additional physicochemical information related to solubility, dissolution, stability, and other release-controlling variables of the drug under conditions that may mimic the extremes of the physiologic environment experienced by the dosage form is necessary (7).

Pharmacokinetic Characterization

Absorption. It is necessary to characterize the relative bioavailability and the fractional absorption profile versus

time for the drug entity in the controlled-dosage form to evaluate the input profile of the controlled-release dosage form. This can be achieved by using deconvolution techniques that allow one to determine the fraction of drug absorbed versus time. Two commonly used techniques are the Wagner–Nelson method, which is used for drugs exhibiting one-compartment pharmacokinetics, and the Loo–Riegelman method, for drugs with two-compartment pharmacokinetic characteristics. The fractional absorption input profile can serve to assess the drug-release claims for that formulation. Further drug-release-rate and release-rate constants can be determined from the fractional absorption data. Moreover, this information, together with the disposition characteristics for the drug entity, can be used to characterize and predict changes in the bioavailability of the drug entity when input is modified for the controlled-release dosage forms. For example, the drug may exhibit saturable first-pass hepatic metabolism, which could result in decreased systemic availability when the input rate is decreased.

Although it may not be a regulatory requirement in designing a controlled-release dosage form, it may be useful to determine the absorption characteristics of the drug entity in various segments of the gastrointestinal tract (particularly the colon for dosage forms that may release drug in the color) (8).

Disposition. The information required to characterize the disposition processes for the drug entity in a controlled-release dosage form should include those generally determined for the drug entity in an immediate-release dosage form. This may include the following:

- Disposition parameters—clearance, volume of distribution, half-life, mean residence time, or model dependent or noncompartmental parameters
- Linearity or characterization of nonlinearity over the dose and/or concentration range that could possibly be encountered
- Accumulation of drug in the blood following multiple doses
- Ratio of parent drug to metabolites if different from immediate-release products

The following information is usually not included in a controlled-release NDA but is known from the development of the molecular entity as an immediate-release formulation:

- Metabolic profile and excretory organ dependence with special attention to active metabolites and active enantiomers of racemic mixtures
- Enterohepatic circulation
- Protein-binding parameters and dialyzeability
- Effect of age, gender, race, and relevant disease states on drug disposition from the controlled-release drug product.
- Plasma/blood ratio

In addition, in cases where the drug can be given in the morning or at bed time or where there is evidence that the clinical response varies significantly as a function of the time of the day, it is recommended that circadian variability in the drug's disposition parameters and pharmacodynamics be characterized to determine whether changes in the rate of drug input with time have an impact on safety and efficacy.

INFORMATION TO CHARACTERIZE THE DOSAGE FORM

Physicochemical Characterization

Similar characterization of the physicochemical properties of the dosage form should be undertaken as for the drug entity. Dissolution profiles from pH 1 to pH 7.4 should be obtained, with particular attention to the effect of the formulation changes on dissolution characteristics. A determination of whether the release of the drug from the formulation is dependent on the dissolution conditions such as pH, rotation speed, and type of apparatus and medium. Characterization of formulations that are highly insoluble in purely aqueous systems may require the addition of small amounts of surfactant to mimic in vivo conditions, where bile salts act as surfactants, more closely.

Bioavailability/Bioequivalence Studies

The type of bioavailability studies that need to be carried out depends upon how much is known about the drug, its clinical pharmacokinetics and biopharmaceutics, and whether bioequivalence studies are intended to be the sole basis for product approval. Several dosage strengths of the controlled-release dosage form should normally be developed to allow flexibility for clinicians to titrate the patient over the recommended therapeutic dose range of the marketed immediate-release dosage form. Scoring of the tablet is sometimes possible in the case where it does not affect the controlled-release mechanism of the formulation.

Each strength of the controlled-release product should be included in a single-dose crossover that involves a reference treatment that can consist of an approved formulation whether immediate or controlled-release, a solution or a suspension. In certain cases for substitution claims, the bioequivalence of the different strengths should be assessed. Also, a multiple-dose, steady-state study using the highest dose of the controlled-release dosage form versus a reference product is required for NDA approval (9,10). Comparison of such parameters such as AUC, C_{max}, T_{max}, and fluctuation index as well as C_{min} at steady state should be made between the controlled-release product and the reference product. If the drug exhibits nonlinear characteristics in its absorption or disposition, then a steady-state study would also be required for the lowest and highest strength.

In the case of a controlled-release dosage form, where the dosage strengths differ from each other only in the amount of identical beaded material contained, a single-dose and a multiple-dose steady-state study at the highest dosage strength will be sufficient for NDA/Abbreviated New Drug Application (ANDA) approval as long as supported by dissolution data. The types of studies needed can be categorized in the following sections.

Case I: Controlled-Release Oral Dosage Form of a Marketed Immediate-Release Drug for which Clinical Studies Have Been Conducted. The following studies would be needed for most controlled-release dosage forms. If approval is to be sought without clinical trials, it is recommended that there be preconsultation with the regulatory authorities to ensure that an adequate database exists for such approval.

Single-Dose Crossover Study. A single-dose crossover study would include the following treatments: the controlled-release dosage form administered under fasting conditions, an immediate-release dosage form administered under fasting conditions, and the controlled-release dosage form administered immediately after completion of a high-fat meal typically consisting of the following: two eggs fried in butter, two strips of bacon, two slices of toast with butter, 4 oz of hash brown potatoes, and 8 oz of whole milk (11). Alternatively, other meals with 1,000-calorie content, with 50% of the calories derived from fat, could be used. The dosage form should be administered immediately following the completion of the breakfast or meal. Absence of food effect will be concluded when the 90% confidence interval for the ratio of means (population geometric means based on log transformed data) of fed and fasted treatments fall within 80–125% for AUC and 70–143% for C_{max} (11). If there are no significant differences seen in the rate (C_{max}) or extent of bioavailability of the controlled-release product in this food effect study, then no further food effect studies are necessary. If significant differences in bioavailability are found, it would be useful to define the cause of the food effect on the controlled-release dosage form as well as the effect of time between meal and drug administration on the food–drug effect.

The purposes of this study are to assess bioavailability, rule out dose dumping, determine whether there is any need for labeling specifications regarding special conditions for administration with respect to meals, and provide information concerning the pattern of absorption of the controlled-release dosage form (12). The drug input function should be defined for controlled-release dosage forms by an appropriate method, for example, the Wagner–Nelson, Loo–Riegelman, or other deconvolution methods. This will aid in assessing the release-rate characteristics of the controlled-release product as well as in the development of an appropriate in vitro dissolution test. For dosage forms that exhibit high intrasubject variability, replicate design studies, in which subjects receive each treatment twice, are suggested.

An illustration of the importance of the study of the effect of food on the bioavailability of a drug from a controlled-release formulation is the case of nisoldipine (13). Nisoldipine is formulated as a once-a-day controlled-release formulation of a dihydropyridine calcium channel blocker that is approved in the United States for the treatment of hypertension.

During the course of development, a food effect study was conducted that revealed that a high-fat breakfast had a profound effect on the bioavailability of nisoldipine from this formulation. As can be seen from Figure 1, food increased the peak plasma concentration (C_{max}) from 2.75 to 7.5 ng/mL, an increase of 2.75-fold, while the area under

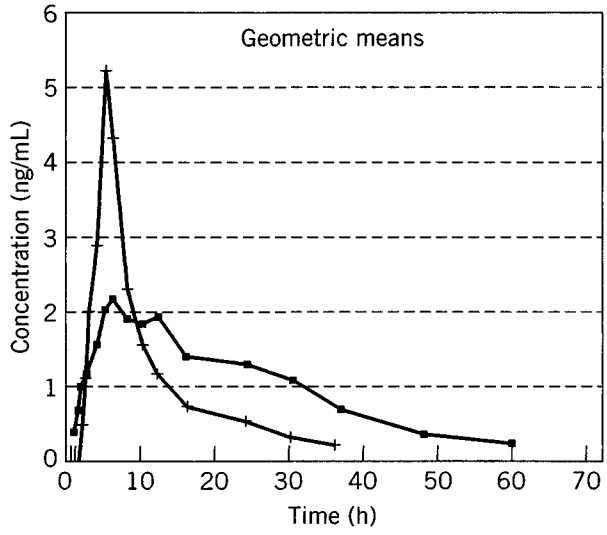


Figure 1. Nisoldipine plasma concentration time profile with and without the administration of a high-fat breakfast.

the curve (AUC) decreased from 70.4 to 53 ng × h/mL. These results raised a question related to the safety and efficacy of this controlled-release formulation when taken with food.

However, an E_{max} pharmacokinetic pharmacodynamic (PK/PD) model established the relationship between nisoldipine plasma concentrations and the reduction in blood pressure. This model was constructed using data from a study in which 23 patients with essential hypertension were given, on an escalating basis, 30, 60, 90, and 120 mg of nisoldipine as could be tolerated by the patients. The EC_{50} was estimated to be 3.54 ng/mL, and the E_{max}, expressed as the maximum drop in diastolic pressure, was 23.9 mm of Hg (14). The PK/PD model enabled the assessment of the clinical impact of the rapid increase in the rate of bioavailability of nisoldipine from this controlled-release formulation when taken with food. Because the relationship between dose and blood pressure lowering was log linear (the dose of drug would have to be increased greatly to observe an effect on the blood pressure) and the maximal drop in diastolic blood pressure would not be expected to pose any harmful hemodynamic effect to the patient and, with some additional experience in the fed state available from the clinical trials, the effect of food on the bioavailability of nisoldipine was not deemed to pose any safety concerns to the patients. However, in the labeling of this drug, it was recommended that Sular® be administered on an empty stomach for optimal efficacy (15).

Multiple-Dose, Steady-State Studies. When data exist for the immediate-release product establishing linear pharmacokinetics, a steady-state study with the controlled-release product at one dose level (at the high end of the dosage range) using an immediate-release formulation as a control should be conducted. At least three consecutive trough concentrations (C_{min}) taken at the same time of the day should be taken to ascertain that the subjects are at steady state. Concentrations over at least one dosage interval of the controlled-release product should be mea-

sured in each leg of the crossover study. In cases where the controlled-release dosage interval is not 24 h, it may be preferable to measure concentrations over an entire day in each leg for purposes of assessing diurnal variation.

Where it exists, consideration must be given to the "therapeutic window." of the drug. The occupancy time, which is defined as the percentage of time over a dosage interval where the concentration lies within the therapeutic window, should be determined.

Appropriate concentration measurements should include unchanged drug and major active metabolites. For racemic drugs, consideration should be given to specific measurement of the active enantiomers. However, approval of the controlled-release product is based on the results of the clinical trials. The pharmacokinetic data is used to establish the pharmacokinetic and bioavailability characteristics of the controlled-release formulation.

If the controlled-release product is aimed at a specific subpopulation, for example, children, it should be tested in that subpopulation. A controlled-release dosage form does not necessarily have to be administered at the same total daily dose as for the immediate-release reference. For example, if first-pass metabolism was greater for the controlled-release dosage form, the total daily dose may be more than the total daily dose of the immediate release product. Also, transdermal patches may contain a reservoir of drug that will not be absorbed during the time of use of the patch. The goal of differences in treatment dosage is to achieve equal exposure.

Steady-state studies in selected patient population groups and/or drug interaction studies may also be necessary, depending upon the therapeutic use of the drug and the type of individuals for which the controlled-release product will be recommended. In such studies, it may be advisable to carry out more than one interval measurement per patient to assess variability with both the controlled-release and the immediate-release dosage forms.

Example of an NDA with Clinical Data. This NDA for a once-a-day diltiazem formulation is a typical example of an NDA application with clinical data. The clinical data consisted of two clinical trials. The first study was a multicenter placebo-controlled randomized-dose-ranging study in which 198 patients participated. This clinical trial combined a dose-escalation arm with 180 to 540 mg doses and a fixed-dose parallel arm involving doses of 90 to 360 mg. In the fixed-dose arm, those patients randomized to 90 or 180 mg remained on these doses throughout the study. Those randomized to 360 mg received 180 mg for the first 2 weeks before receiving the 360-mg dose. The second clinical study was also a randomized double-placebo-controlled-dose escalation study, with doses from 120 to 540 mg in 56 patients with mild to moderate hypertension.

Figure 2 shows the changes in blood pressure among the different doses compared with the placebo (16). The biopharmaceutics and clinical pharmacology portion of the NDA consisted of six studies, including (17)

- A single-dose relative bioavailability study comparing the controlled-release product to an approved immediate-release diltiazem

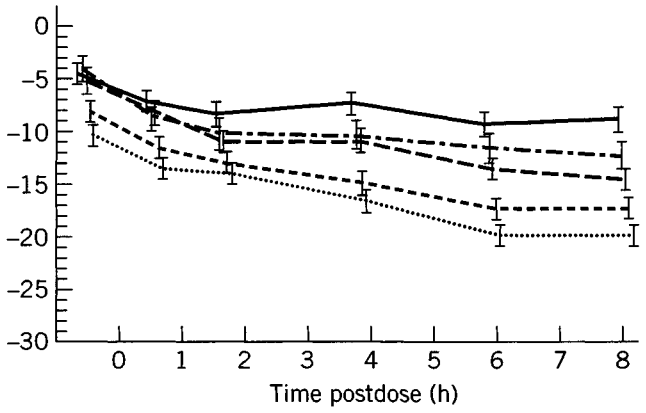


Figure 2. Change in supine diastolic blood pressure from baseline predose levels (mm Hg) compared with placebo across all dose levels.

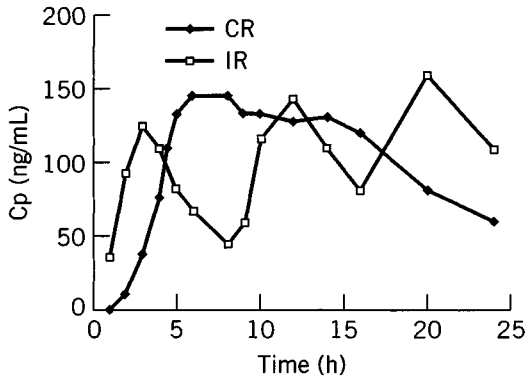


Figure 3. Comparative single-dose plasma concentration time profile of diltiazem from a once-a-day controlled-release (CR) formulation and three doses of the immediate-release (IR) formulation.

- A multiple-dose relative bioavailability study comparing the controlled-release product to an approved immediate-release diltiazem
- A food effect study

Figure 3 shows the comparative plasma concentration time profile for this controlled release formulation relative to the approved immediate release formulation. These three studies, along with the clinical data, fulfilled the regulatory requirements for this NDA.

It is to be noted that the trough level at the end of the dosing interval for the controlled-release product was lower than that of the immediate release formulation as can be seen in Figure 4. However, because the efficacy of the controlled-release product was established in the two clinical trials, the lower trough levels were of no clinical concern.

The sponsor also conducted the following:

- A dose proportionality study, because diltiazem is known to undergo saturable first-pass metabolism, and thus the degree of nonlinearity in pharmacokinetics needed to be characterized for the controlled-release product.

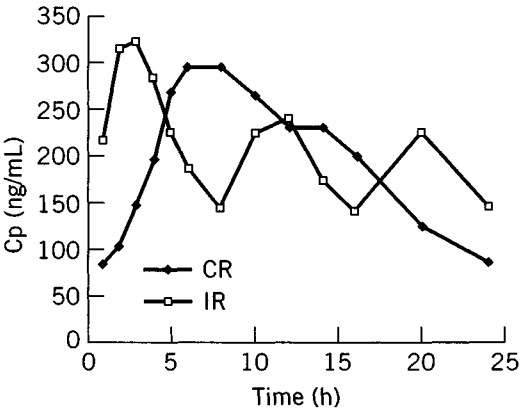


Figure 4. Comparative steady-state plasma concentration time profile of diltiazem from a once-a-day controlled-release formulation and three doses of the immediate-release formulation given during a 24-h dosing interval.

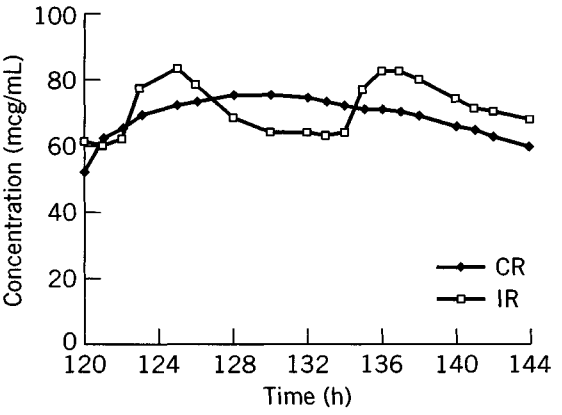


Figure 5. Example of a controlled-release product with steady-state C_{min} values at the end of the dosing interval lower than those for the corresponding immediate-release product.

- A bioequivalence study comparing this once-a-day product with the two other once-a-day diltiazem products that are already approved for marketing. This study was undertaken for marketing purposes by the sponsor of the NDA and was not required from the regulatory point of view.
- An in vivo/in vitro correlation study that would enable the sponsor to obtain in vivo bioavailability waivers and possibly wider dissolution specifications. Such a study is highly desirable in an NDA but is not a requirement.

Case II: Controlled-Release NDA with No Clinical Studies or PK/PD Information. It may be possible to obtain approval of an NDA for a controlled-release drug product based on bioequivalence data alone. In this situation, there is an absolute need to establish bioequivalence conclusively. To allow marketing of a controlled-release drug product in the absence of clinical data or PK/PD information for the controlled-release product requires that all parameters related to bioequivalence be shown to meet the equivalence criteria under steady-state conditions. These parameters include C_{max}, AUC, and C_{min} (absolute lowest concentration over an interval).

Similar C_{max} comparisons for the test and reference products relate to establishing comparable safety and efficacy. Safety relates to the fact that the controlled-release product should not have C_{max} or C_{min} values significantly higher than the immediate-release product, whereas efficacy could relate to the controlled-release product not having a C_{max} or C_{min} significantly lower than the immediate-release product. AUC could relate to both safety and efficacy, and the controlled- and immediate-release products should show comparable AUCs during a dosing interval at steady state. In addition, C_{min} values should be comparable related to efficacy at the end of the dosing interval for the controlled-release product. Lower C_{min} values for the controlled-release product would raise issues in this regard, and this is illustrated in Figure 5. The lower values of C_{min} for this controlled-release product, which was the subject of an NDA that contained no clinical data, caused concerns regarding its approvability. To allow the marketing of this controlled-release product without prior testing in patients to establish efficacy was considered to be unacceptable.

Case III: Oral Controlled-Release Dosage Form of a Marketed Immediate-Release Drug for Which Extensive Pharmacodynamic/Pharmacokinetic Data Exist. The same bioavailability/bioequivalence requirements as discussed in Case I apply to the controlled-release dosage form of a marketed immediate-release drug for which extensive PK/PD data exist. In certain cases the PK/PD information can serve in lieu of clinical trials to establish the safety and efficacy profile of the controlled-release drug product.

Case IV: Nonoral Controlled-Release Dosage Form of a Marketed Immediate-Release Drug for Which Extensive Pharmacodynamic/Pharmacokinetic Data Exist. The bioavailability studies described earlier (except for the food effect study) would be appropriate for the evaluation of a controlled-release formulation designed for nonoral route of administration. If an altered biotransformation pattern of active metabolites is observed, the need for clinical data becomes more apparent. One or more clinical efficacy studies would be required. In addition to bioavailability studies, special studies should be concerned with specific risk factors, for example, irritation and/or sensitization at the site of application or injection.

Case V: Generic Equivalent of an Approved Controlled-Release Product. The Drug Price Competition and Patent Term Restoration Act amendments of 1984 to the Food, Drug and Cosmetic Act of 1938 gave the FDA statutory authority to accept and approve for marketing ANDAs for generic substitutes of pioneer products, including those approved after 1962. To gain approval according to the law, ANDAs for a generic controlled-release drug product must, among other things, be both pharmaceutically equivalent

and bioequivalent to the innovator controlled-release product, which is termed the *reference-listed drug product* as identified in FDA's *Approved Drug Products with Therapeutic Equivalence Ratings* (the "Orange Book").

Pharmaceutical Equivalence. As defined in the Orange Book, to be pharmaceutically equivalent, the generic and pioneer formulations must (*1*) contain the same active ingredient, (*2*) contain the same strength of the active ingredient in the same dosage form, (*3*) be intended for the same route of administration, and (*4*) be labeled for the same conditions of use. The FDA does not require that the generic and reference-listed controlled-release products contain the same excipients or that the mechanism by which the release of the active drug substance from the formulation be the same (18). For substitution purposes, the two products have to be pharmaceutical equivalents.

Bioequivalence Requirements. The same bioequivalence requirements apply to the establishment of the equivalence of the formulation used in efficacy trials if it is different from the formulation intended for marketing and generic controlled-release product approval. For development of a generic equivalent of an approved controlled-release product, the new generic formulation must be comparable with respect to rate and extent of bioavailability (usually using AUC, C_{max}, C_{min}, and the degree of fluctuation as criteria) in a crossover steady-state study compared to the reference controlled-release product.

In 1993, the Division of Bioequivalence of the Office of Generic Drugs issued a Guidance entitled "Oral Extended (Controlled) Release Dosage Form In Vivo Bioequivalence and In Vitro Dissolution Testing," which outlines the required studies for the approval of a controlled-release product (19). The following is a summary of the required studies as outlined in the 1993 guidance.

Single-Dose Fasting Two-Way Crossover Bioequivalence Study. The objective of this study is to compare the rate (as measured by C_{max}) and extent of absorption (as measured by AUC) of a generic formulation with that of a reference-listed formulation when administered in equal labeled doses. The FDA-designated reference product is identified by the symbol + in the Orange Book.

Design. The study design is a single-dose, two-treatment, two-period, two-sequence crossover with an adequate washout period between the two phases of the study. An equal number of subjects should be randomly assigned to the two possible dosing sequences. An institutional review board should approve the proposed protocol for the study prior to its initiation.

Selection of Subjects. The applicant should enroll a number of subjects sufficient to ensure adequate statistical results. It is recommended that a minimum of 24 subjects be used in this study. More subjects may be required for a drug that exhibits high intrasubject variability in metrics of rate and extent of absorption. Subjects should be healthy volunteers, 18 to 50 years of age, and within 10% of ideal body weight for height and build. Written, informed consent must be obtained from all subjects before their acceptance into the study.

Procedure. Following an overnight fast of at least 10 hours, subjects should be administered a single dose of the test or reference product with 240 mL water. They should continue fasting for 4 h after administration of the test or reference treatment.

Blood Sampling. In addition to the predose (0 h) sample, venous blood samples should be collected postdose so that there are at least four sampling time points on the ascending part and six or more on the descending part of the concentration-time curve. The biological matrix (plasma, serum, or whole blood) should be immediately frozen after collection and, as appropriate, centrifugation and kept frozen until assayed.

Analysis of Blood Samples. The active moieties should be assayed using a suitable analytical method validated with regard to specificity, accuracy, precision (both within and between days), limit of quantitation, linearity, and recovery. Stability of the samples under frozen conditions, at room temperature, and during freeze–thaw cycles, if appropriate, should be determined. If the analytical method is a chromatographic method, chromatograms of unknown samples, including all associated standard curve and quality control chromatograms, should be submitted for one-fifth of subjects, chosen at random (20).

Pharmacokinetic Analysis of Data. Calculation of area under the plasma concentration-time curve to the last quantifiable concentration (AUC 0—t) and to infinity. Calculation of C_{max} and T_{max} should be performed according to standard techniques.

Statistical Analysis of Pharmacokinetic Data. The log-transformed AUC and C_{max} data should be analyzed statistically using analysis of variance. These two parameters for the test product should be shown to be within 80–125% of the reference product using the 90% confidence interval (21–23).

Clinical Report and Adverse Reactions. Subject medical histories, physical examination reports, and all incidents of adverse reactions to the study formulations should be reported.

Multiple-Dose, Steady-State, Two-Way Crossover Bioequivalence Study. The objective of this study is to document that the steady-state rate and extent of absorption of the test controlled-release product is equivalent to the rate and extent of absorption of the reference-listed drug containing the same amount of the active ingredient in the same dosage form.

Design. The study design is a multiple-dose, two-treatment, two-period, two-sequence crossover with adequate washout period between the two phases of the study. An equal number of subjects should be randomly assigned to the two possible dosing sequences. Before initiation of the multiple-dose steady-state study, an institutional review board should approve the study protocol. Moreover, the steady-state study should be done after the completion of the single-dose study.

Selection of Subjects. Same as for the single-dose study.

Procedures. Controlled-release products that are administered once a day should be dosed following an overnight fast of at least 10 h; subjects should continue fasting for 4 h postdose. For controlled-release products that are dosed every 12 h, the morning dose should be given following an overnight fast of about 10 h, and subjects should continue fasting for 4 h postdose; the evening dose should be administered after a fast of at least 2 h, and subjects

should continue fasting for 2 h postdose. Each dose should be administered with 240 mL water.

Blood Sampling. At least three trough concentrations (C_0) on three consecutive days should be determined to ascertain that the subjects are at steady state prior to measurement of rate and extent of absorption after a single-dose administration in a dosing interval at steady state. For controlled-release drug products administered more often than every 24 h, assessment of trough levels just prior to two consecutive doses is not recommended because a difference in the consecutive trough values may occur due to circadian rhythm irrespective of whether or not steady state has been attained. Adequate blood samples should be collected at appropriate times during a dosing interval at steady state to permit estimation of the total area under the concentration-time curve, peak concentration (C_{max}), the absolute lowest plasma concentration (C_{min}), and time to peak concentration (T_{max}).

Pharmacokinetic Data. The following pharmacokinetic data are to be reported for the evaluation of bioequivalence of the generic controlled-release product to the reference-listed product:

- Individual and mean blood drug concentration levels.
- Individual and mean trough levels (C_0) as well as the lowest plasma concentration (C_{min}).
- Individual and mean peak level (C_{max}).
- Calculation of individual and mean steady-state AUC.
- Individual and mean percent fluctuation; fluctuation for the test product should be evaluated for comparability with that for the reference product.
- Individual and mean time to peak concentration (T_{max})

Statistical Analysis of Pharmacokinetic Data. Same as for the single-dose study.

Clinical Report and Adverse Reactions. Same as for the single-dose study.

For controlled-release capsule formulation marketed in multiple strengths, a single-dose bioequivalence study under fasting conditions is required only for the highest strength, provided that the compositions of the lower strengths are proportional to that of the highest strength and that all strengths contain identical beads or pellets. Single-dose bioequivalence studies may be waived for the lower strengths on the basis of acceptable dissolution profiles. Multiple-dose steady-state and single-dose food/fasting studies are to be conducted on the highest strength of the capsule formulation. For controlled-release products that are not beaded and are not compositionally proportional, the single-dose bioequivalence study is required for each strength, and the multiple-dose bioequivalence study is required only to the highest strength. This requirement can also be waived in the presence of an in vivo/in vitro correlation whose predictability has been established. For this waiver to be granted the following conditions have to be met:

- The lower strengths must be compositionally proportional or qualitatively the same
- The lower strengths must have the same release mechanism
- The lower strengths must have similar in vitro dissolution profiles
- The lower strengths must be manufactured using the same type of equipment and the same process, and at the same site as other strengths that have bioavailability data

In addition one of the following situations should exist:

- Bioequivalence has been established for all strengths of the reference-listed product.
- Dose proportionality has been established for the reference-listed product, and all reference product strengths are compositionally proportional or qualitatively the same; they must have the same release mechanism, and the in vitro dissolution profiles for all strengths must be similar.
- Bioequivalence has been established between the generic product and the reference-listed product at the highest and lowest strengths; for the reference-listed product, all strengths are compositionally proportional or qualitatively the same and have the same release mechanism, and the in vitro dissolution profiles are similar.

The criterion for granting such waivers is that the difference in predicted means of C_{max} and AUC is no more than 10% based on dissolution profiles of the highest-strength and the lower-strength product.

Single-Dose, Food/Fasting Study. The objective of this study is to document that the rate and extent of absorption of the generic controlled-release product is equivalent to the rate and extent of absorption of the reference-listed drug when both products are administered immediately after a high-fat meal and to assess the effect of a high-fat meal on the bioavailability of the generic controlled-release product.

Statistical Analysis. Absence of food effect will be concluded when the 90% confidence interval for the ratio of means (population geometric means based on log-transformed data) of fed and fasted treatments fall within 80–125% for AUC and 70–143% for C_{max}.

Case VI: Controlled Release Dosage Form as a New Molecular Entity. Independent of whether a controlled-release dosage form is evaluated by clinical studies, this dosage form should be characterized as described previously; that is, per dose proportionality, food effects, absorption characteristics (rate, pattern, and extent), and fluctuation. Moreover, the additional requirements for an immediate-release new molecular entity will also be applicable to controlled-release applications.

Retention of Samples. The clinical laboratory conducting any in vivo study should retain an appropriately identified reserve sample of the test and reference products for a period of 5 years. Each reserve sample should consist of at least 200 dosage units. For more information on retention

of bioequivalence samples, please refer to 21 CFR 320.63.V (24).

Dissolution Testing for Controlled-Release Drug Products

In vitro dissolution testing is important for (*1*) providing process control and quality assurance, (*2*) determining stable release characteristics of the product over time, and (*3*) facilitating certain regulatory determinations (e.g., absence of effect of minor formulation changes or of change in manufacturing site on performance). In certain cases, especially for oral controlled-release formulations, the dissolution test, related to an in vivo/in vitro correlation (IVIVC), can serve not only as a quality control for the manufacturing process but also as an indicator of how the formulation will perform in vivo. A main objective of developing and evaluating an IVIVC is to establish the dissolution test as a surrogate for human bioequivalence studies.

An IVIVC describes a meaningful relationship between in vitro dissolution and expected in vivo bioavailability results. The availability of an IVIVC provides for excellent control of product quality, particularly for marketed batches of a drug product, that will not be tested in humans. The concept of IVIVC, particularly for oral controlled-release drug products, has been studied considerably over the years. Several workshops and publications have provided useful information regarding IVIVCs.

The *Report of the Workshop on CR Dosage Forms: Issues and Controversies* (1987) indicated that the state of science and technology at that time did not permit consistently meaningful IVIVC for oral controlled-release dosage forms and encouraged IVIVC as a future objective. Dissolution testing was considered useful only for process control, stability, minor formulation changes, and manufacturing site changes (7).

A U.S. Pharmacopeial Convention (USP) Pharmacopeial Forum stimuli article in 1988 established the classification of IVIVC into levels A, B, and C. In addition, USP Chapter 1088 describes techniques appropriate for level A, B, and C correlations and methods for establishing dissolution specifications (25).

A level A correlation is usually estimated by a two-stage procedure: deconvolution followed by comparison of the fraction of drug absorbed with the fraction of drug dissolved. A correlation of this type (shown in Figure 6) is generally linear and represents a point-to-point relationship between in vitro dissolution and the in vivo input rate (e.g., the in vivo dissolution of the drug from the dosage form). In a linear correlation, the in vitro dissolution and in vivo input curves may be directly superimposable or may be made to be superimposable by the use of a scaling factor. Nonlinear correlations, although uncommon, may also be appropriate (26).

A level B correlation uses the principles of statistical moment analysis. The mean in vitro dissolution time is compared either to the mean residence time or to the mean in vivo dissolution time. A level B correlation does not uniquely reflect the actual in vivo plasma level curve because a number of different in vivo curves will produce similar mean residence time values. An example of such a correlation is shown in Figure 7.

A level C correlation establishes a single-point relationship between a dissolution and a pharmacokinetic parameter. A level C correlation does not reflect the complete shape of the plasma concentration-time curve, which is important to the definition of the performance of oral controlled-release products. A multiple level C correlation relates one or several pharmacokinetic parameters of interest to the amount of drug dissolved at several time points of the dissolution profile. This is illustrated in Figure 8, where the relationship between the maximum plasma concentrations and percent dissolved at several time points is given (27).

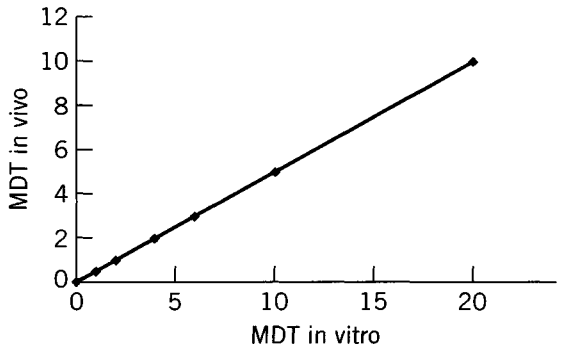


Figure 7. Level B correlation.

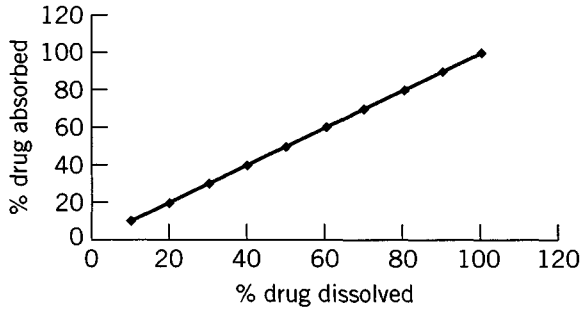


Figure 6. Level A correlation.

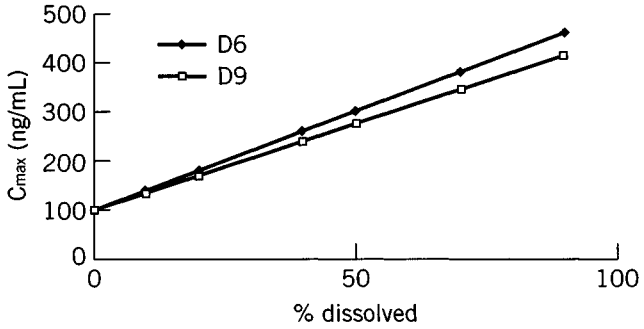


Figure 8. Multiple level C correlation.

The report entitled *In Vitro / In Vivo Testing and Correlation for Oral Controlled / Modified Release Dosage Forms* (8) concludes that although science and technology may not always permit meaningful IVIVC, the development of an IVIVC is an important objective on a product-by-product basis. Procedures for development, evaluation, and application of an IVIVC are described. Validation of dissolution specifications by a bioequivalence study involving two batches of product with dissolution profiles at the upper and lower dissolution specifications is suggested.

Further information related to IVIVCs was developed in a USP/American Association of Pharmaceutical Scientists/FDA-sponsored workshop that resulted in a report entitled *Workshop II Report: Scale-up of Oral Extended Release Dosage Forms* (20). This report identified the objectives of an IVIVC to be the use of dissolution as a surrogate for bioequivalence testing as well as an aid in setting dissolution specifications. The report concluded that dissolution may be used as a sensitive, reliable, and reproducible surrogate for bioequivalence testing. The report gave support to the concepts of USP Chapter 1088 and further found that an IVIVC may be useful for changes other than minor changes in formulation, equipment, process, manufacturing site, and batch size (28,29).

An FDA Guidance for Industry, "Extended Release Solid Oral Dosage Forms: Development, Evaluation and Application of In Vitro/In Vivo Correlations," provides recommendations for establishing useful IVIVCs (30). Human data should be utilized for regulatory consideration of an IVIVC. Bioavailability studies for IVIVC development should be performed with enough subjects to adequately characterize the performance of the drug product under study. Although crossover studies are preferred, parallel studies or cross-study analyses may be acceptable. The reference product in developing an IVIVC may be an intravenous solution, an aqueous oral solution, or an immediate-release product. IVIVCs are usually developed in the fasted state. When a drug is not tolerated in the fasted state, studies may be conducted in the fed state. Any in vitro dissolution method may be used to obtain the dissolution characteristics of the oral controlled-release dosage form, but the same system should be used for all formulations tested. The most commonly used dissolution apparatus is USP apparatus (basket) or II (paddle), used at compendially recognized rotation speeds (e.g., 100 rpm for the basket and 50–75 rpm for the paddle). In other cases, the dissolution properties of some oral controlled-release formulations may be determined with USP apparatus III (reciprocating cylinder) or IV (flow through cell). An aqueous medium, preferably not exceeding pH 6.8, is recommended as the initial medium for development of an IVIVC. For poorly soluble drugs, addition of surfactant may be appropriate. In general, nonaqueous and hydroalcoholic systems are discouraged unless all attempts with aqueous media are unsuccessful. The dissolution profiles of at least 12 individual dosage units from each lot should be determined. A suitable distribution of sampling points should be selected to define the profiles adequately (31–33).

IVIVCs are established in two stages. First, the relationship between dissolution characteristics and bioavailability characteristics needs to be determined. Second, the reliability of this relationship must be tested. The first stage may be thought of as developing an IVIVC, whereas the second stage may involve evaluation of predictability. The most commonly seen process for developing a level A IVIVC is to (*1*) develop formulations with different release rates, such as slow, medium, fast, or a single-release rate if dissolution is condition independent; (*2*) obtain in vitro dissolution profiles and in vivo plasma concentration profiles for these formulations; and (*3*) estimate the in vivo absorption or dissolution time course using an appropriate deconvolution technique for each formulation and subject [e.g., Wagner–Nelson, numerical deconvolution (34)]. These three steps establish the IVIVC model. Alternative approaches to developing level A IVIVCs are possible. The IVIVC relationship should be demonstrated consistently with two or more formulations with different release rates to result in corresponding differences in absorption profiles. Exceptions to this approach (i.e., use of only one formulation) may be considered for formulations for which in vitro dissolution is independent of the dissolution test conditions (e.g., medium, agitation, pH).

The in vitro dissolution methodology should adequately discriminate among formulations. Dissolution testing can be carried out during the formulation screening stage using several methods. Once a discriminating system is developed, dissolution conditions should be the same for all formulations tested in the bioavailability study for development of the correlation and should be fixed before further steps toward correlation evaluation are undertaken. During the early stages of correlation development, dissolution conditions may be altered to attempt to develop a one-to-one correlation between the in vitro dissolution profile and the in vivo dissolution profile.

Time scaling may be used as long as the time-scaling factor is the same for all formulations (35). An IVIVC that has been developed should be evaluated to demonstrate that predictability of in vivo performance of a drug product from its in vitro dissolution characteristics is maintained over a range of in vitro dissolution release rates and manufacturing changes. Because the objective of developing an IVIVC is to establish a predictive mathematical model describing the relationship between an in vitro property and a relevant in vivo response, a logical evaluation approach focuses on the estimation of predictive performance or, conversely, prediction error. Depending on the intended application of an IVIVC and the therapeutic index of the drug, evaluation of prediction error internally and/or externally may be appropriate. Evaluation of internal predictability is based on the initial data used to develop the IVIVC model. Evaluation of external predictability is based on additional test data sets that may reduce the number of bioequivalence studies performed during the initial approval process as well as with certain scale-up and postapproval changes. However, for the applications outlined in the following sections, the adequacy of the in vitro dissolution method to act as a surrogate for in vivo testing should be shown through an IVIVC for which predictability has been established (36). The criterion for granting in vivo bioavailability/bioequivalence waivers with an IVIVC is that the predicted C_{max} and AUC from

the in vitro dissolution data for the test and reference formulation should not differ by more than 20%. This is illustrated in Figure 9.

Waivers of bioequivalency studies are possible without an IVIVC for small changes in oral controlled-release drug products. For formulations consisting of beads in capsules, with the only difference between strengths being the number of beads, approval of lower strengths without an IVIVC is possible, provided bioavailability data are available for the highest strength and the dissolution profiles in several media are the same across strengths. Where the FDA Guidance for Industry Scale Up and Post-Approval Changes for Modified Release oral dosage forms (SUPAC-MR) *Modified Release Solid Oral Dosage Forms; Scale-Up and Postapproval Changes: Chemistry, Manufacturing, and Controls, In Vitro Dissolution Testing, and In Vivo Bioequivalence Documentation* (37) recommends a biostudy, biowaivers for the same changes made on lower strengths are possible without an IVIVC if (*1*) all strengths are compositionally proportional or qualitatively the same, (*2*) in vitro dissolution profiles of all strengths are similar, (*3*) all strengths have the same release mechanism, (*4*) bioequivalence has been demonstrated at the highest strength (comparing changed and unchanged drug product), and (*5*) dose proportionality has been demonstrated for this oral controlled-release drug product. In the last circumstance, documentation of dose proportionality may not be necessary if bioequivalence has been demonstrated on the highest and lowest strengths of the drug product, comparing changed and unchanged drug product for both strengths as recommended in SUPAC-MR.

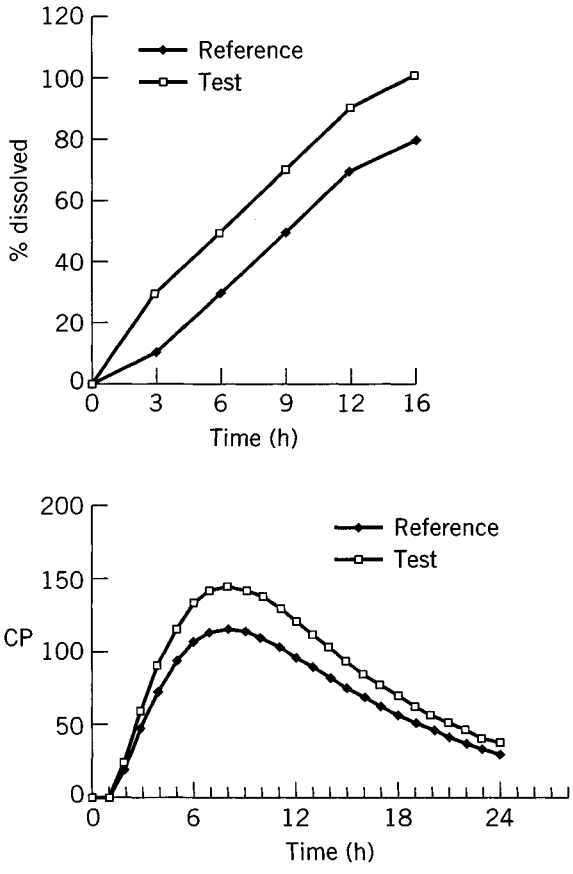


Figure 9. Criterion for granting an in vivo bioavailability waiver based on predicted C_{max} and AUC from in vitro dissolution data using IVIVC.

If an IVIVC has been established, waivers for more significant changes are possible. A biowaiver will likely be granted for an oral controlled-release drug product using an IVIVC for (*1*) level 3 process changes as defined in SUPAC-MR, (*2*) complete removal of or replacement of nonrelease-controlling excipients as defined in SUPAC-MR, and (*3*) level 3 changes in the release-controlling excipients as defined in SUPAC-MR.

If an IVIVC is developed with the highest strength, waivers for changes made on the highest strength and any lower strengths may be granted if these strengths are compositionally proportional or qualitatively the same, the in vitro dissolution profiles of all the strengths are similar, and all strengths have the same release mechanism.

This biowaiver is applicable to strengths lower than the highest strength, within the dosing range that has been established to be safe and effective, provided that the new strengths are compositionally proportional or qualitatively the same, have the same release mechanism, have similar in vitro dissolution profiles, and are manufactured using the same type of equipment and the same process at the same site as other strengths that have bioavailability data available.

Certain changes almost always necessitate in vivo bioavailability testing and in some cases might necessitate clinical trials, even in the presence of an IVIVC. These include the approval of a new formulation of an approved oral controlled-release drug product when the new formulation has a different release mechanism, approval of a dosage strength higher or lower than the doses that have been shown to be safe and effective in clinical trials, approval of another sponsor's oral controlled-release product even with the same release-controlling mechanism, and approval of a formulation change involving a non-release-controlling excipient in the drug product that may significantly affect drug absorption (38).

Setting Dissolution Specifications

In vitro dissolution specifications should generally be based on the performance of the clinical/bioavailability lots. These specifications may sometimes be widened within the range allowed in the guidance so that scale-up lots, as well as stability lots, meet the specifications associated with the clinical/bioavailability lots. This approach is based on the use of the in vitro dissolution test as a quality control test without any in vivo significance, even though in certain cases (e.g., oral controlled-release formulations), the rate-limiting step in the absorption of the drug is the dissolution of the drug from the formulation. An IVIVC adds in vivo relevance to in vitro dissolution specifications, beyond batch-to-batch quality control. In this approach, the in vitro dissolution test becomes a meaningful predictor of in vivo performance of the formulation, and dissolution specifications may be used to minimize the possibility of releasing lots that would exhibit different in vivo performance.

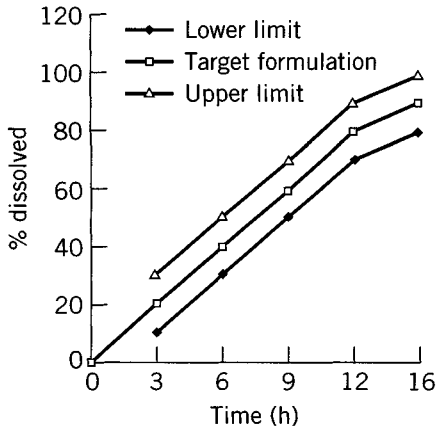


Figure 10. Upper and lower dissolution specifications in a case where no IVIVC exists.

A minimum of three time points is recommended to set the specifications. These time points should cover the early, middle, and late stages of the dissolution profile. The last time point should be the time point where at least 80% of drug has dissolved. If the maximum amount dissolved is less than 80%, the last time point should be the time when the plateau of the dissolution profile has been reached.

Specifications should be established based on average dissolution data for each lot under study, equivalent to USP stage 2 testing. Specifications that allow lots to pass at stage 1 of testing may result in lots with less than optimal in vivo performance passing these specifications at USP stage 2 or stage 3.

Setting Dissolution Specifications without an IVIVC. The recommended range at any dissolution time point specification is ± 10% deviation of the labeled claim from the mean dissolution profile obtained from the clinical/bioavailability lots as shown in Figure 10. In certain cases, reasonable deviations from the ± 10% range can be accepted provided that the range at any time point does not exceed 25%. Specifications greater than 25% may be acceptable based on evidence that lots (side batches) with mean dissolution profiles that are allowed by the upper and lower limit of the specifications are bioequivalent.

Setting Dissolution Specifications Where an IVIVC Has Been Established. Optimally, specifications should be established such that all lots that have dissolution profiles within the upper and lower limits of the specifications are bioequivalent. Less optimally but still possible, lots exhibiting dissolution profiles at the upper and lower dissolution limits should be bioequivalent to the clinical/bioavailability lots or to an appropriate reference standard. In the case where an IVIVC whose predictability has been established, dissolution specifications should be set in such a way that the average predicted C_{max} and AUC that correspond to the lower and upper limit of the dissolution specifications should differ by no more than 20% from each other.

Importance of Proper Dissolution Conditions. Dissolution testing of controlled-release products is a very important test that can show a relationship to the expected bioavailability for the lots of controlled-release product being tested. However, the dissolution conditions during the test are very important and if not properly chosen can give results that are not predictive of the actual in bioavailability.

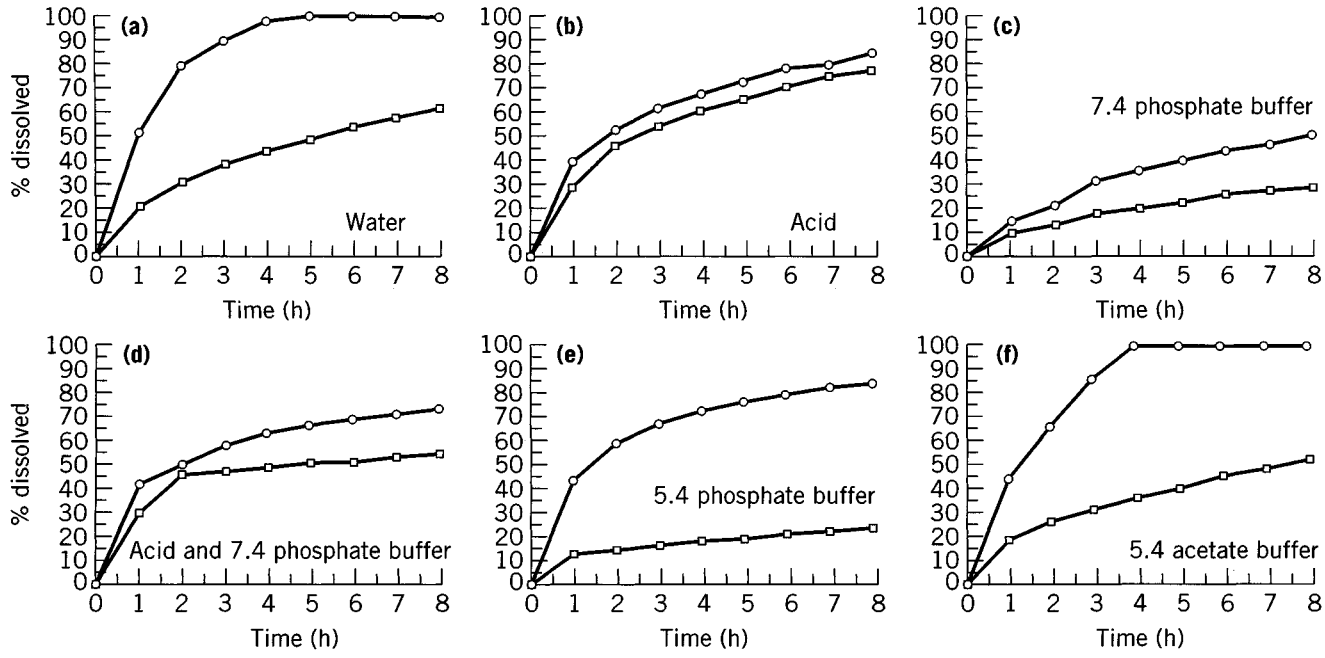


Figure 11. Quinidine gluconate dissolution profiles in several different media.

In Figure 11, dissolution profiles for two products tested under varying dissolution conditions are shown. Condition (b), which is dissolution testing in acid, shows similar dissolution profiles for the two products. If these two products were comparable in bioavailability, these conditions might be appropriate for testing these products; however, looking at other dissolution conditions, for example, in water, as can be seen in Figure 11(a) the data show significant differences in the dissolution profiles for these two products. If the products have different bioavailability characteristics, testing in, for example, water, might be more appropriate. For these two products it was established that the unapproved product had only approximately 40% of bioavailability of the reference product. Therefore, dissolution conditions shown in Figures 11(c)–(f) that distinguish between these two products—that is, conditions that show differing dissolution profiles—would be appropriate, whereas dissolution conditions that do not distinguish these two products would be inappropriate. In this particular example, the product with poor bioavailability was marketed without FDA approval. It is possible that only dissolution testing in acid was utilized by the manufacturer to show comparability between the two products. As it turns out, this was a very risky choice. The unapproved product, which was marketed, had very poor bioavailability that could not be determined by dissolution testing in acid. Only by conducting the bioequivalence study prior to marketing, establishing bioequivalence, then determining appropriate dissolution conditions, can bioequivalence between two controlled-release products be ensured (39).

BIBLIOGRAPHY

1. A.T. Florence and P.U. Jani, *Drug Saf.* **10**(3), 233–266 (1994).
2. P.J. Marroum, *5th Int. Symp. Drug Dev.*, East Brunswick, N.J., May 15–17, 1997.
3. *Guidance for Providing Clinical Evidence of Effectiveness for Human Drug and Biological Products*, Center for Drug Evaluation and Research, Food and Drug Administration, Washington, D.C., 1998.
4. *Code of Federal Regulations*, Title 21, Food and Drug Administration, Washington, D.C., 21 CFR 314.126, 1998.
5. *Code of Federal Regulations*, Title 21, Food and Drug Administration, Washington, D.C., 21 CFR 320.25(f), 1998.
6. *Code of Federal Regulations*, Title 21, Food and Drug Administration, Washington, D.C., 21 CFR 314.54, 1998.
7. J.P. Skelly et al., *Pharm. Res.* **7**, 975–982 (1990).
8. J.P. Skelly et al., *Pharm. Res.* **4**, 75–77 (1987).
9. J.P. Skelly, *Division Guidelines for the Evaluation of Controlled Release Drug Products*, Center for Drug Evaluation and Research, Food and Drug Administration, Washington, D.C., 1984.
10. J.P. Skelly and W.H. Barr. in J.R. Robinson and V.H.L. Lee, eds., *Controlled Drug Delivery: Fundamentals and Application*, Dekker, New York, 1987, pp. 293–333.
11. *Draft Guidance on the Food-Effect Bioavailability and Bioequivalence Studies*, Center for Drug Evaluation and Research, Food and Drug Administration, Washington, D.C., 1997.
12. A. Karim, in A. Yacobi, and E. Holperin-Wolega, eds., *Oral Sustained Release Formulations, Design and Evaluation*, Pergamon, New York, 1987, pp. 293–333.
13. P.J. Marroum, *Nisoldipine Coat Core Clinical Pharmacology and Biopharmaceutics*, Center for Drug Evaluation and Research, Food and Drug Administration, Washington, D.C., 1994.
14. H.G. Schaefer et al., *Eur. J. Clin. Pharm.* **51**, 473–480 (1997).
15. S.T. Chen, *Nisoldipine C.C.*, Secondary Clinical Review, Division of Cardiorenal Drug Products, Center for Drug Evaluation and Research, Food and Drug Administration, Washington, D.C., 1994.
16. R. Kimball, *Medical Review of Viazem*, Division of Cardiorenal Drug Products, Center for Drug Evaluation and Research, Food and Drug Administration, Washington, D.C., 1994.
17. P.J. Marroum, *Core Clinical Pharmacology and Biopharmaceutics*, Center for Drug Evaluation and Research, Food and Drug Administration, Washington, D.C., 1994.
18. *Approved Drug Products with Therapeutic Equivalence Evaluations*, 18th ed., Center for Drug Evaluation and Research, Food and Drug Administration, Washington, D.C., 1998, pp. vii–xxi.
19. *Guidance for Oral Extended (Controlled) Release Dosage Forms: In Vivo Bioequivalence and In Vitro Dissolution Testing*, Office of Generic Drugs, Center for Drug Evaluation and Research, Food and Drug Administration, Washington, D.C., 1993.
20. V.P. Shah et al., *Pharm. Res.* **9**(4), 588–592 (1992).
21. *Guidance for Statistical Procedures for Bioequivalence Studies Using a Standard Two Treatment Crossover Design*, Office of Generic Drugs, Center for Drug Evaluation and Research, Food and Drug Administration, Washington, D.C., 1992.
22. D.J. Schuirman, *Drug Inf. J.* **24**, 315–323 (1990).
23. D.J. Schiurman, *J. Biopharm. Pharmacokinet.* **15**, 657–680 (1987).
24. *Code of Federal Regulations*, Title 21, Food and Drug Administration, Washington, D.C., 21 CFR 320.63(v), 1998.
25. *The United States Pharmacopeia 23*, U.S. Pharmacopeial Convention, Rockville, Md., 1995, Chapter 1088, pp. 1924–1929.
26. H. Malinowski, in G. Amidon, J.R. Robinson, and R.L. Williams, eds., *Scientific Foundations for Regulating Drug Product Quality*, AAPS Press, Alexandria, Va., 1997, pp. 259–273.
27. P. Marroum, *Development of In Vivo In Vitro Correlations*, SUPAC-MR/IVIVC Guidance FDA Training Program Manual, Center for Drug Evaluation and Research, Food and Drug Administration, Washington, D.C., 1997, pp. 62–76.
28. J.P. Skelly et al., *Eur. J. Pharm. Biopharm.* **39**, 162–167 (1993).
29. H. Malinowski and J.D. Henderson, in P. Welling and F.L.S. Tse, eds., *Pharmacokinetics Regulatory-Industrial-Academic Perspectives*, 2nd ed., Dekker, New York, 1995, pp. 452–477.
30. H. Malinowski et al., *Dissolut. Technol.* **4**(4), 23–32 (1997).
31. M. Siewert, *Eur. J. Drug Metab. Pharmacokinet.* **18**(1), 7–18 (1993).
32. J.P. Skelly and G.F. Shiu, *Eur. J. Drug Metab. Pharmacokinet.* **18**(1), 121–129 (1993).
33. H.H. Blume, I. McGilvery, and K.K. Midha, *Eur. J. Pharm. Sci.* **3**, 113–124 (1995).
34. J. Wagner, in J. Wagner, ed., *Pharmacokinetics for the Pharmaceutical Scientist*, Technomic Publishing, Lancaster, Pa., 1993, pp. 159–205.

35. D. Brockmeier, D. Voegele, and H.M. Hattingberg, *Drug Res.* **33**(1), 598–601 (1983).

36. P.J. Marroum, in G. Amidon, J.R. Robinson, and R.L. Williams, eds., *Scientific Foundations for Regulating Drug Product Quality*, AAPS Press, Alexandria, Va., 1997, pp. 305–319.

37. *Guidance for Modified Release Solid Oral Dosage Forms; Scale-Up and Post Approval Changes: Chemistry, Manufacturing, and Controls: In Vitro Dissolution Testing and In Vivo Bioequivalence Documentation*, Center for Drug Evaluation and Research, Food and Drug Administration, Washington, D.C., 1997.

38. H. Malinowski, *Ba, BE and Pharmacokinetics Studies*, FIP Bio-International 96, Business Center for Academic Societies of Japan, Tokyo, 1996.

39. V.K. Prasad et al., *Int. J. Pharm.* **13**, 1–8 (1982).

HYDROGELS

ANTHONY M. LOWMAN
Drexel University
Philadelphia, Pennsylvania
NICHOLAS A. PEPPAS
Purdue University
West Lafayette, Indiana

KEY WORDS

Cross-linking
Diffusion
Erosion
Modeling
Permeability
Pore size
Responsive hydrogels
Swelling

OUTLINE

Structure and Properties of Hydrogels
- Equilibrium Swelling Theories
- Rubber Elasticity Theory
- Network Pore Size Calculation

Diffusion in Hydrogels
- Macroscopic Analysis
- Effects of Network Morphology
- Experimental Determination of Diffusion Coefficients

Classifications
- Diffusion-Controlled Release Systems
- Swelling-Controlled Release Systems
- Chemically Controlled Release Systems
- Environmentally Responsive Systems

Applications
- Neutral Hydrogels
- pH-Sensitive Hydrogels
- Temperature-Sensitive Hydrogels
- pH- and Temperature-Sensitive Hydrogels
- Complexing Hydrogels
- Glucose-Sensitive Systems
- Oral Insulin Delivery Systems
- Other Promising Applications

Bibliography

Hydrogels are three-dimensional, water-swollen structures composed of mainly hydrophilic homopolymers or copolymers (1). They are rendered insoluble due to the presence of chemical or physical cross-links. The physical cross-links can be entanglements, crystallites, or weak associations such as van der Waals forces or hydrogen bonds. The cross-links provide the network structure and physical integrity.

Hydrogels are classified in a number of ways (1,2). They can be neutral or ionic based on the nature of the side groups. They can also be classified based on the network morphology as amorphous, semicrystalline, hydrogen-bonded structures, supermolecular structures, and hydrocolloidal aggregates. Additionally, in terms of their network structures, hydrogels can be classified as macroporous, microporous, or nonporous (1–3).

Since the development of poly(2-hydroxethyl methacrylate) gels in the early 1960s, hydrogels have been considered for use in a wide range of biomedical and pharmaceutical applications, mainly due to their high water content and rubbery nature. Because of these properties, hydrogel materials resemble natural living tissue more than any other class of synthetic biomaterials (1,4). Furthermore, the high water content allows these materials to exhibit excellent biocompatibility. Some applications of hydrogels include contact lenses, biosensors, sutures, dental materials, and controlled drug delivery (1,4–8). Park and Park (9) present a very useful commentary in relation to the biocompatibility of implantable hydrogel-based delivery systems.

The use of hydrogel-based controlled release systems that can swell in the presence of a biological fluid has been studied for over 30 years. A goal of many researchers is to develop hydrogel devices to provide time-independent, sustained release of bioactive agents (8). Researchers have attempted to achieve these goals by manipulation of the polymer composition and the device geometry. Hydrogel devices have been proposed for delivery by almost all of the conventional routes.

Two of the most important characteristics in evaluating the ability of a polymeric gel to function in a particular controlled release application are the network permeability and the swelling behavior. The permeability and swelling behavior of hydrogels are strongly dependent on the chemical nature of the polymer(s) composing the gel as well as the structure and morphology of the network. As a result, there are different mechanisms that control the release of drugs from hydrogel-based delivery devices. Such systems are classified by their drug release mechanism as diffusional-controlled release systems, swelling-controlled release systems, chemically controlled release systems, and environmentally responsive systems (2).

Hydrogels may exhibit swelling behavior dependent on the external environment. Thus, in the last 30 years there has been a major interest in the development and analysis of environmentally or physiologically responsive hydrogels (10). These hydrogels show drastic changes in their swell-

ing ratio due to changes in their external pH, temperature, ionic strength, nature of the swelling agent, and electromagnetic radiation. Some advantages to environmentally or physiologically responsive hydrogels are relevant in drug delivery applications. In an exceptional new review in the field, am Ende and Mikos (11) offer a thorough physicochemical and mathematical interpretation of the conditions of diffusional release of various bioactive agents in hydrogels and other polymeric carriers, with emphasis on the conditions of stability of peptides and proteins during delivery.

An additional advantage of hydrogels, which has received considerable attention recently, is that they may provide desirable protection of drugs, peptides, and especially proteins from the potentially harsh environment in the vicinity of the release site (12). In particular, such carriers may be able to function as carriers for the oral delivery of sensitive proteins or peptides (13). Finally, hydrogels may be excellent candidates as biorecognizable biomaterials (14). As such, they can be used as targetable carriers of bioactive agents, as bioadhesive systems or as conjugates with desirable biological properties.

In this article, we present an overview of the structure and properties of hydrogels, the diffusional behavior of hydrogels, and the mechanisms for release from polymeric controlled release systems. Additionally, we review important contributions in this area with specific emphasis on new synthetic methods that promise to provide imaginative solutions of drug delivery problems.

STRUCTURE AND PROPERTIES OF HYDROGELS

In order to evaluate the feasibility of using a particular hydrogel as a drug delivery device, it is important to know the structure and properties of the polymer network. The structure of an idealized hydrogel is shown in Figure 1. The most important parameters that define the structure and properties of swollen hydrogels are the polymer volume fraction in the swollen state, $\upsilon_{2,s}$, effective molecular weight of the polymer chain between cross-linking points, $\overline{M}_c$, and network mesh or pore size, ξ (15).

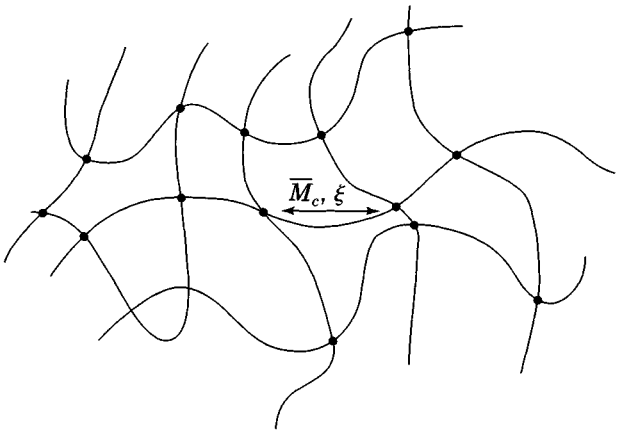


Figure 1. Schematic representation of the cross-linked structure of a hydrogel. $\overline{M}_c$ is the molecular weight of the polymer chains between cross-links (●) and ξ is the network mesh size.

The polymer fraction of the polymer in the swollen gel is a measure of the amount of fluid that a hydrogel can incorporate into its structure.

$$\upsilon_{2,s} = \frac{\text{volume of polymer}}{\text{volume of swollen gel}} = \frac{V_p}{V_{\text{gel}}} = 1/Q \qquad (1)$$

This parameter can be determined using equilibrium swelling experiments (16). The molecular weight between cross-links is the average molecular weight of the polymer chains between junction points, both chemical and physical. This parameter provides a measure of the degree of cross-linking in the gel. This value is related to the degree of cross-linking in the gel (X) as:

$$X = \frac{M_o}{2M_c} \qquad (2)$$

Here, M_o is the molecular weight of the repeating units making up the polymer chains.

The network mesh size represents the distance between consecutive cross-linking points and provides a measure of the porosity of the network. These parameters, which are not independent, can be determined theoretically or through a variety of experimental techniques.

Equilibrium Swelling Theories

Neutral Hydrogels. Flory and Rehner (17) developed the initial depiction of the swelling of cross-linked polymer gels using a Gaussian distribution of the polymer chains. They developed a model to describe the equilibrium degree of cross-linked polymers that postulated that the degree to which a polymer network swelled was governed by the elastic retractive forces of the polymer chains and the thermodynamic compatibility of the polymer and the solvent molecules. In terms of the free energy of the system, the total free energy change upon swelling is written as:

$$\Delta G = \Delta G_{\text{elastic}} + \Delta G_{\text{mix}} \qquad (3)$$

Here, $\Delta G_{\text{elastic}}$ is the contribution due to the elastic retractive forces and $\Delta G_{\text{elastic}}$ represents the thermodynamic compatibility of the polymer and the swelling agent.

Upon differentiation of equation 3 with respect to the number of solvent molecules in the system (at constant T and P), an expression can be derived for the chemical potential change ($\Delta\mu$) in the solvent in terms of the contributions due to swelling.

$$\mu_1 - \mu_{1,0} = (\Delta\mu)_{\text{elastic}} + (\Delta\mu)_{\text{mix}} \qquad (4)$$

Here, μ_1 is the chemical potential of the swelling agent within the gel and $\mu_{1,0}$ is the chemical potential of the pure fluid. At equilibrium, the chemical potential of the swelling agent inside and outside of the gel must be equal, therefore the elastic and mixing contributions to the chemical potential balance one another at equilibrium.

The chemical potential change upon mixing can be determined from the heat of mixing and the entropy of mixing. Using appropriate thermodynamic relationships, the chemical potential of mixing can be expressed as:

$$(\Delta\mu)_{\text{mix}} = RT(ln(1 - v_{2,s}) + \chi_1 v_{2,s}^2) \quad (5)$$

where χ_1 is the polymer solvent interaction parameter defined by Flory (17,18).

The elastic contribution to the chemical potential is determined from the statistical theory of rubber elasticity (18). The elastic free-energy is dependent on the number of polymer chains in the network, v_e, and the linear expansion factor, α. For gels that were crosslinked in the absence of a solvent, the elastic contribution to the chemical potential is written as:

$$(\Delta\mu)_{\text{elastic}} = RT\left(\frac{V_1}{v\bar{M}_c}\right)\left(1 - \frac{2\bar{M}_c}{\bar{M}_n}\right)\left(v_{2,s}^{1/3} - \frac{v_{2,s}}{2}\right) \quad (6)$$

where v is the specific volume of the polymer, V_1 is the molar volume of the swelling agent, and $\bar{M}_n$ is the molecular weight of linear polymer chains prepared using the same conditions in the absence of a cross-linking agent. By combining equations 5 and 6, the swelling behavior of neutral hydrogels cross-linked in the absence of a solvent can be described by the following equation.

$$\frac{1}{\bar{M}_c} = \frac{2}{\bar{M}_n} - \frac{(v/V_1)[ln(1 - v_{2,s}) + v_{2,s} + \chi_1 v_{2,s}^2]}{\left(v_{2,s}^{1/3} - \frac{v_{2,s}}{2}\right)} \quad (7)$$

In many cases, it is desirable to prepare hydrogels in the presence of a solvent. If the polymers were cross-linked in the presence of a solvent, the elastic contributions must account for the volume fraction density of the chains during cross-linking. Peppas and Merrill (19) modified the original Flory-Rehner to account for the changes in the elastic contributions to swelling. For polymer gels cross-linked in the presence of a solvent, the elastic contribution to the chemical potential is:

$$(\Delta\mu)_{\text{elastic}} = RT\left(\frac{V_1}{v\bar{M}_c}\right)\left(1 - \frac{2\bar{M}_c}{\bar{M}_n}\right)v_{2,r}\left(\left(\frac{v_{2,s}}{v_{2,r}}\right)^{1/3} - \frac{v_{2,s}}{2v_{2,r}}\right) \quad (8)$$

Here, $v_{2,r}$ is the volume fraction of the polymer in the relaxed state. The relaxed state of the polymer is defined as the state of the polymer immediately after cross-linking of the polymer but prior to swelling or deswelling. For the case of gels prepared by cross-linking in the presence of a solvent, the equation for the swelling of the polymer gel can be obtained by combining equations 5 and 8 as the mixing contributions for both cases are the same. The swelling of hydrogels cross-linked in the presence of a solvent can then be written as:

$$\frac{1}{\bar{M}_c} = \frac{2}{\bar{M}_n} - \frac{(v/V_1)[ln(1 - v_{2,s}) + v_{2,s} + \chi_1 v_{2,s}^2]}{v_{2,r}((v_{2,s}/v_{2,r})^{1/3} - (v_{2,s}/2v_{2,r}))} \quad (9)$$

By performing swelling experiments to determine $v_{2,r}$, the molecular weight between cross-links can be calculated for a particular gel using this equation (16).

Ionic Hydrogels. Ionic hydrogels contain pendent groups that are either cationic or anionic in nature. For anionic gels, the side groups of the gel are unionized below the pK_a and the swelling of the gel is governed by thermodynamic compatibility of the polymer and the swelling agent. However, above the pK_a of the network, the pendent groups are ionized and the gels swell to a large degree due to the development of a large osmotic swelling force due to the presence of the ions. In cationic gels, the pendent groups are unionized above the pK_b of the network. When the gel is placed in fluid of pH less than this value, the basic groups are ionized and the gels swell to a large degree (Figure 2). The pH-dependent swelling behavior of ionic gels, which is completely reversible in nature, is depicted in Figure 3.

The theoretical description of the swelling of ionic hydrogels is much more complex than that of neutral hydrogels. Aside from the elastic and mixing contributions to swelling, the swelling of an ionic hydrogel is affected by the degree of ionization in the gel, ionization equilibrium between the gel and the swelling agent, and the nature of the counterions in the fluid. As the ionic content of a hydrogel is increased, in response to an environmental stimulus, increased repulsive forces develop and the network becomes more hydrophilic. The result is a more highly swollen network. Because of Donnan equilibrium, the

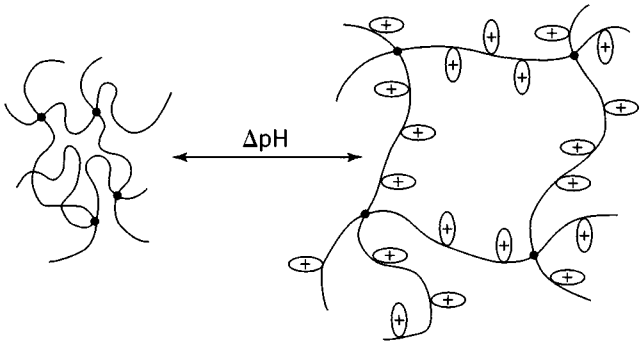


Figure 2. Expansion (swelling) of a cationic hydrogel due to ionization of pendent groups, at specific pH values.

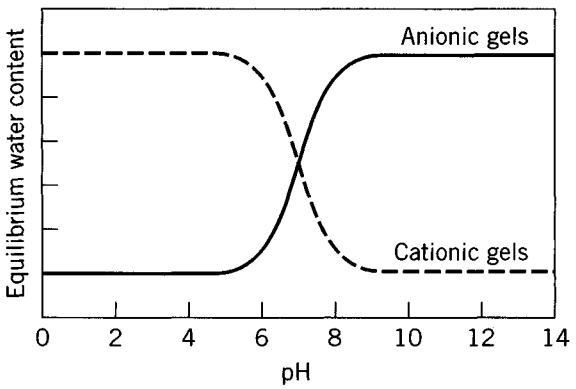


Figure 3. Equilibrium degree of swelling of anionic and cationic hydrogels as a function of the swelling solution pH.

chemical potential of the ions inside the gel must be equal to the chemical potential of the ions in the solvent outside of the gel (20). An ionization equilibrium is established in the form of a double layer of fixed charges on the pendent groups and counterions in the gel. Finally, the nature of counterions in the solvent affects the swelling of the gel. As the valence of the counterions increase, they are more strongly attracted to the gel and reduce the concentration of ions needed in the gel to satisfy Donnan equilibrium conditions.

The swelling behavior of polyelectrolyte gels was initially described as being a result of a balance between the elastic energy of the network and the osmotic pressure developed as a result of the ions (20–27). In electrolytic solutions, the osmotic pressure is associated with the development of a Donnan equilibrium. This pressure term is also affected by the fixed charges developed on the pendant chains. The elastic term is described by the Flory expression derived from assumptions of Gaussian chain distributions.

Models for the swelling of ionic hydrogels were developed by equating the three major contributions to the swelling of the networks. These contributions are due to mixing of the polymer and solvent, network elasticity, and ionic contributions. The general equation is given as

$$\Delta G = \Delta G_{\text{mix}} + \Delta G_{\text{el}} + \Delta G_{\text{ion}} \tag{10}$$

In terms of the chemical potential, the difference between the chemical potential of the swelling agent in the gel and outside of the gel is:

$$\mu_1 - \mu_{1,0} = (\Delta\mu)_{\text{elastic}} + (\Delta\mu)_{\text{mix}} + (\Delta\mu)_{\text{ion}} \tag{11}$$

For weakly charged polyelectrolytes, the elastic contribution and mixing contributions do not differ from the case of nonionic gels. However, for highly ionizable materials there are significant ionization effects and $\Delta\mu_{ion}$ is important. At equilibrium, the elastic, mixing, and ionic contributions must sum to 0.

The ionic contribution to the chemical potential is strongly dependent on the ionic strength and the nature of the ions. Brannon-Peppas and Peppas (26,27) and Ricka and Tanaka (20) both developed expressions to describe the ionic contributions to the swelling of polyelectrolytes. Assuming that the polymer networks under conditions of swelling behave similarly to dilute polymer solutions, the activity coefficients can be approximated as 1 and activities can be replaced with concentrations. Under these conditions, the ionic contribution to the chemical potential is described by the following:

$$(\Delta\mu)_{\text{ion}} = RTV_1\Delta c_{\text{tot}} \tag{12}$$

Here, Δc_{tot} is the difference in the total concentration of mobile ions within the gel. The difference in the concentration of mobile ions is due to the fact that the charged polymer requires the same number of counterions to remain in the gel to achieve electroneutrality. The difference in the total ion concentration could then be calculated from the equilibrium condition for the salt.

Brannon-Peppas and Peppas (26,27) developed expressions for the ionic contributions to the swelling of polyelectrolytes for anionic and cationic materials. The ionic contribution for anionic network is:

$$(\Delta\mu)_{\text{ion}} = \frac{RTV_1}{4I}\left(\frac{v_{2,s}^2}{v}\right)\left(\frac{K_a}{10^{-pH} + K_a}\right)^2 \tag{13}$$

For the cationic network, the ionic contribution is:

$$(\Delta\mu)_{\text{ion}} = \frac{RTV_1}{4I}\left(\frac{v_{2,s}^2}{v}\right)\left(\frac{K_b}{10^{pH-14} + K_a}\right)^2 \tag{14}$$

In these expressions, I is the ionic strength, K_a and K_b are the dissociation constants for the acid and base, respectively. It is significant to note that this expression has related the ionic contribution to the chemical potential to characteristics about the polymer/swelling agent that can readily determinable (e.g., pH, K_a, and K_b).

For the case of anionic polymer gels that were cross-linked in the presence of a solvent, the equilibrium swelling can be described by:

$$\frac{V_1}{4I}\left(\frac{v_{2,s}^2}{v}\right)\left(\frac{K_a}{10^{-pH} + K_a}\right)^2 = (ln(1 - v_{2,s}) + v_{2,s} + \chi_1 v_{2,s}^2) + \left(\frac{V_1}{v\overline{M}_c}\right)\left(1 - \frac{2\overline{M}_c}{\overline{M}_n}\right)v_{2,r} \cdot \left(\left(\frac{v_{2,s}}{v_{2,r}}\right)^{1/3} - \frac{v_{2,s}}{2v_{2,r}}\right) \tag{15}$$

For the cationic hydrogels prepared in the presence of a solvent, the equilibrium swelling is described by the following expression:

$$\frac{V_1}{4I}\left(\frac{v_{2,s}^2}{v}\right)\left(\frac{K_b}{10^{pH-14} + K_a}\right)^2 = (ln(1 - v_{2,s}) + v_{2,s} + \chi_1 v_{2,s}^2) + \left(\frac{V_1}{v\overline{M}_c}\right)\left(1 - \frac{2\overline{M}_c}{\overline{M}_n}\right)v_{2,r} \left(\left(\frac{v_{2,s}}{v_{2,r}}\right)^{1/3} - \frac{v_{2,s}}{2v_{2,r}}\right) \tag{16}$$

For the case of ionic hydrogels, the molecular weight between cross-links can be calculated by performing swelling experiments and applying equations 15 (anionic gels) or 16 (cationic gels).

Rubber Elasticity Theory

Hydrogels are similar to natural rubbers in that they have the ability to respond to applied stresses in a nearly instantaneously and almost irreversible manner (18,28). These polymer networks have the ability to deform readily under low stresses. Also, following small deformations (less than 20%) most gels can fully recover from the deformation in a rapid fashion. Under these conditions, the behavior of the gels can be approximated to be elastic. This property can be exploited to calculate the cross-linking density or molecular weight between cross-links for a particular gel.

The elastic behavior of cross-linked polymers has been analyzed using classical thermodynamics, statistical thermodynamics, and phenomenological models. Based on classical thermodynamics, the equation of state for rubbers can be expressed as (18,28):

$$f = \left(\frac{\partial U}{\partial L}\right)_{T,V} + T\left(\frac{\partial f}{\partial T}\right)_{L,V} \tag{17}$$

where f is the retractive force of the elastic polymer in response to an applied load, U is the internal energy and L is the length of the sample. For an ideal elastomer, $(\partial U/\partial L)_{T,V}$ is zero as deformation of the sample does not result in changes in the internal energy as the bonds are not stretched.

The connection between the classical and statistical thermodynamics can be made after applying the following Maxwell equation:

$$\left(\frac{\partial S}{\partial L}\right)_{T,V} = -\left(\frac{\partial f}{\partial T}\right)_{L,V} \tag{18}$$

By combining equations 17 and 18, the retractive force of an ideal elastomer can be written as:

$$f = -T\left(\frac{\partial S}{\partial L}\right)_{T,V} = -kT\left(\frac{\partial\, ln\Omega(r,\, T)}{\partial r}\right)_{T,V} \tag{19}$$

Here, r is the end-to-end distance of the polymer chain and Ω is the probability that a polymer chain of length r will have a specific conformation at a given temperature (T).

Upon evaluation of this equation for a system of n chains, the change in the Helmholtz free energy upon elastic deformation can be written as:

$$(\Delta A)_{elastic} = \frac{3nKT}{\bar{r}_f^2}\int_{\bar{r}_f}^{\bar{r}} r dr \tag{20}$$

Assuming that elastic deformation is not accompanied by a volume change, integration yields the classical equation for rubber elasticity.

$$\frac{f}{a} = \tau = \frac{\rho RT}{\overline{M}_c}\frac{\bar{r}_o^2}{\bar{r}_f^2}\left(\alpha - \frac{1}{\alpha^2}\right) \tag{21}$$

Here, a is the cross-sectional area, τ is the stress, ρ is the density of the polymer, α is the elongation ratio and $\bar{r}_o^2/\bar{r}_f^2$ is the front factor. The front factor is the ratio of the end-to-end distance of polymer chains in a real network and dilute chains in solution. Typically, this factor can be assumed less than or equal to one.

The previous expression was derived assuming an ideal network without any defects. In the ideal networks, all of the chains would participate equally to the elastic stress. However, in real networks, defects exist such as entanglements or dangling chain ends. After correcting for the case of real networks and assuming a front factor of one, the equation of state for rubber elasticity becomes:

$$\tau = \frac{\rho RT}{\overline{M}_c}\left(1 - \frac{2\overline{M}_c}{\overline{M}_n}\right)\left(\alpha - \frac{1}{\alpha^2}\right) \tag{22}$$

A similar analysis can be applied to swollen hydrogels where the polymer volume fraction in the network is less than unity. For the case of swollen gels, the number of cross-links per unit volume is different than for the case of unswollen polymer networks. The equation of state for real, swollen polymer gels can be expressed as:

$$\tau = \frac{\rho RT}{\overline{M}_c}\left(1 - \frac{2\overline{M}_c}{\overline{M}_n}\right)\left(\alpha - \frac{1}{\alpha^2}\right)\upsilon_{2,s}^{1/3} \tag{23}$$

This equation holds for networks cross-linked in the absence of any diluents. For the case of a swollen network cross-linked in the presence of a solvent, the equation of state can be written as (29):

$$\tau = \frac{\rho RT}{\overline{M}_c}\left(1 - \frac{2\overline{M}_c}{\overline{M}_n}\right)\left(\alpha - \frac{1}{\alpha^2}\right)\left(\frac{\upsilon_{2,s}}{\upsilon_{2,r}}\right)^{1/3} \tag{24}$$

For elongation of a polymer network along a single axis, the stress is inversely proportional to the molecular weight between cross-links in the polymer network. From mechanical analysis under short deformations, important structural information about the polymer networks can be obtained (30–32).

Network Pore Size Calculation

One of the most important parameters in controlling the rate release of a drug from a hydrogel is the network pore size, ξ. The pore size can be determined theoretically or using a number of experimental techniques. A direct technique for measuring this parameter is quasielastic laser-light scattering (33) or electron microscopy. Some indirect experimental techniques for determination of the hydrogel pore size include mercury porosimetry (34,35), rubber elasticity measurements (30), or equilibrium swelling experiments (16,36). However, the indirect experiments allow for calculation of the porous volume (mercury porosimetry) or the molecular weight between cross-links (rubber elasticity analysis or swelling experiments).

Based on values for the cross-linking density or molecular weight between cross-links, the network pore size can be determined by calculating end-to-end distance of the swollen polymer chains between cross-linking points (16,18,36).

$$\xi = \alpha(\bar{r}_o^2)^{1/2} \tag{25}$$

In this expression, α is the elongation of the polymer chains in any direction and $(\bar{r}_o^2)^{1/2}$ is the unperturbed end-to-end distance of the polymer chains between cross-linking points. Assuming isotropic swelling of the gels, the elongation is related to the swollen polymer volume fraction.

$$\alpha = \upsilon_{2,s}^{-1/3} \tag{26}$$

The unperturbed chain distance is calculated through the Flory characteristic ratio, C_n.

$$(\bar{r}_o^2)^{1/2} = l(C_n N)^{1/2} \tag{27}$$

Here, l is the length of the bond along the backbone chain (1.54 Å for vinyl polymers). The number of links per chain, N, is related to the cross-link density as:

$$N = \frac{2\overline{M}_c}{M_o} \tag{28}$$

Here, M_o is the molecular weight of the monomeric repeating units. Upon combination of these equations, the pore size of a swollen polymeric network can be calculated using the following equation:

$$\xi = \left(\frac{2C_n\overline{M}_c}{M_o}\right)^{1/2} l v_{2,s}^{-1/3} \tag{29}$$

DIFFUSION IN HYDROGELS

The release of drugs and other solutes from hydrogels results from combination of classical diffusion in the polymer network and mass transfer limitations (2). To optimize a hydrogel system for a particular application, the fundamental mechanism of solute transport in the membranes must be understood completely. In this section, we focus on the mechanism of drug diffusion in hydrogels as well as the importance of network morphology in controlling the transport of drugs in hydrogels.

Macroscopic Analysis

The transport or release of a drug through a polymeric controlled release device can be described by classical Fickian diffusion theory (2,37). This theory assumes that the governing factor for drug transport in the gels is ordinary diffusion. Drug delivery devices can be designed so that other mechanisms control the release rate such as gel swelling or polymer erosion.

For the case of one-dimensional transport, Fick's law can be expressed as (38):

$$J_i = -D_{ip}\frac{dC_i}{dX} \tag{30}$$

Here, J_i is the molar flux of the drug (mol/cm^2 s), C_i is the concentration of drug and D_{ip} is the diffusion coefficient of the drug in the polymer. For the case of a steady-state diffusion process, i.e., constant molar flux, and constant diffusion coefficient, equation 30 can be integrated to give the following expression:

$$J_i = K\frac{D_{ip}\Delta C_i}{\delta} \tag{31}$$

Here, δ is the thickness of the hydrogel and K is the partition coefficient, defined as

$$K = \frac{\text{drug concentration in gel}}{\text{drug concentration in solution}} \tag{32}$$

For many drug delivery devices, the release rate will be time dependent. For non–steady-state diffusion problems, Fick's second law is used to analyze the release behavior. Fick's second law is written as:

$$\frac{\partial C_i}{\partial t} = \frac{\partial}{\partial X}\left(D_{ip}\frac{\partial C_i}{\partial X}\right) \tag{33}$$

This form of the equation is for one-dimensional transport with nonmoving boundaries. Equation 33 can be evaluated for the case of constant diffusion coefficients and concentration-dependent diffusion coefficients.

Constant Diffusion Coefficients. Equation 33 can be solved by application of the appropriate boundary conditions. Most commonly, perfect-sink conditions are assumed. Under these conditions, the following boundary and initial conditions are applicable (Fig. 4):

$$t = 0, \quad X < \pm\frac{\delta}{2}, \quad C_i = C_o \tag{34a}$$

$$t > 0, \quad X = 0, \quad \frac{\partial C_i}{\partial X} = 0 \tag{34b}$$

$$t > 0, \quad X = \pm\frac{\delta}{2}, \quad C_i = C_s \tag{34c}$$

Here, C_o is the initial drug concentration inside the gel and C_s is the equilibrium bulk concentration. Upon application of the boundary conditions, Fick's second law for planar geometries can be integrated and the solution can be written in terms of the amount of drug released at a given time, M_t, normalized to the amount released at infinite times, M_∞ (38).

$$\frac{M_t}{M_\infty} = 1 - \sum_{n=0}^{\infty}\frac{8}{(2n+1)^2\pi^2}\,exp\left[\frac{-D_{ip}(2n+1)^2\pi^2 t}{\delta^2}\right] \tag{35}$$

Alternatively, the solution to equation 33 can be written in terms of the integrated complimentary error function, *ierfcx* (39).

$$\frac{M_t}{M_\infty} = 4\left(\frac{D_{ip}t}{\delta}\right)^{1/2}\left[\frac{1}{\pi^{1/2}} + 2\sum_{n=0}^{\infty}(-1)^n ierfc\,\frac{n\delta}{2(D_{ip}t)^{1/2}}\right] \tag{36}$$

At short times, equation 36 can be approximated as:

$$\frac{M_t}{M_\infty} = 4\left(\frac{D_{ip}t}{\pi\delta}\right)^{1/2} \tag{37}$$

Concentration-Dependent Diffusion Coefficients. In most systems, the drug diffusion coefficient is dependent on the

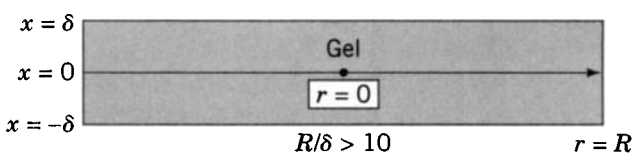


Figure 4. Depiction of the slab geometry used for one-dimensional analysis of Fick's second law.

drug concentration as well as the concentration of the swelling agent. In order to analyze the diffusive behavior of drug delivery systems when this is the case, one must choose an appropriate relationship between the diffusion coefficient and the drug concentration. Based on free-volume theory, Fujita (40) proposed the following relationship between the diffusion coefficient and the drug concentration in the gel.

$$D_{ip} = D_{iw}\, exp[-\beta(C_i - C_o)] \tag{38}$$

Here, D_{iw} is the diffusion coefficient in the pure solution, β is a constant dependent on the system, and C_o is the concentration of drug in solution. Additionally, a similar equation was written to relate the diffusion coefficient to the concentration of the swelling agent and the drug in the gel.

$$D_{ip} = D_{iw}\, exp[-\beta(C_s - C_i)] \tag{39}$$

Here, C_s is the swelling agent concentration.

Effects of Network Morphology

The structure and morphology of a polymer network significantly affects the ability of a drug to diffuse through a hydrogel. For all types of release systems, the diffusion coefficient (or effective diffusion coefficient) of solutes in the polymer is dependent on a number of factors such as the structure and pore size of the network, the polymer composition, the water content, and the nature and size of the solute. Perhaps the most important parameter in evaluating a particular device for a specific application is the ratio of the hydrodynamic radius of the drug, d_h, to the network pore size, ξ (Figure 5). Accordingly, hydrogels for controlled release applications are classified according to their pore size (3). The transport properties of drugs in each type of gel vary according to the structure and morphology of the network.

Macroporous Hydrogels. Macroporous hydrogels have large pores, usually between 0.1 and 1 μm. Typically, the pores of these gels are much larger than the diffusing species. In the case of these membranes, the pores are sufficiently large so that the solute diffusion coefficient can be described as the diffusion coefficient of the drug in the water-filled pores. The process of solute transport is hindered by the presence of the macromolecular mesh. The solute diffusion coefficient can be characterized in terms of the diffusion coefficient of the solute in the pure solvent (D_{iw}) as well as the network porosity (ϵ) and tortuosity (τ). Additionally, the manner in which the solute partitions itself within the pore structure of the network affects the diffusion of the drug. This phenomenon is described in terms of the partition coefficient, K_p. These parameters can be incorporated to describe the transport of the drug in the membranes in terms of an effective diffusion coefficient (D_{eff}).

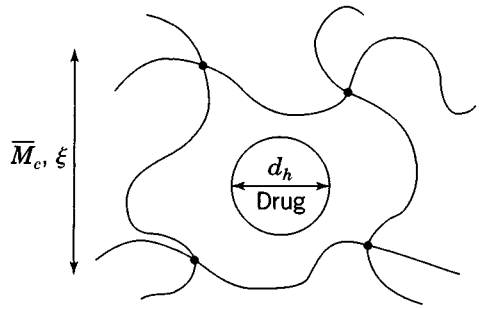


Figure 5. The effects of molecular size (r_s) on the diffusion of a solute in a network of pore size ξ.

$$D_{eff} = D_{iw}\frac{K_p\epsilon}{\tau} \tag{40}$$

Microporous Hydrogels. These membranes have pore sizes between 100 and 1000 Å. In these gels, the pores are water filled and drug transport occurs due to a combination of molecular diffusion and convection in the water-filled pores. In these gels, significant partitioning of the solute within the pore walls may occur for systems in which the drug and polymer are thermodynamically compatible. The effective diffusion coefficient can be expressed in a form similar to that for macroporous membranes.

Transport in microporous membranes is different from macroporous membranes because the pore size begins to approach the size of the diffusing solutes. Numerous researchers have attempted to describe transport for the case of the solute pore size being approximately equal to the network pore size. The rate of the diffusion coefficient in the membrane and pure solvent can be related to the ratio of the solute and pore radius.

$$\frac{D_{ip}}{D_{iw}} = (1 - \lambda^2)(1 - 2.104\lambda + 2.09\lambda^3 - 0.95\lambda^5) \tag{41}$$

In this expression, the diffusion coefficient in the membrane, D_{ip}, is related to λ, the ratio of the solute radius (r_s) to the pore radius (r_p).

$$\lambda = \frac{r_s}{r_p} \tag{42}$$

This theory was initially proposed by H. Faxen in 1923; however, other researchers have provided more recent corrections to this theory (41–43). An excellent review of all of these diffusional theories has been provided by Deen (44).

Nonporous Hydrogels. Nonporous gels have molecular sized pores equal to the macromolecular correlation length, ξ (between 10 and 100 Å). Gels of this type are typically formed by the chemical or physical cross-linking of the polymer chains. In these gels, the polymer chains are densely packed and serve to severely limit solute transport. Additionally, the cross-links serve as barriers to diffusion. This distance between the physical obstructions is known as the mesh size. Transport of solutes in these membranes occurs only by diffusion.

The macromolecular mesh of nonporous membranes is not comparable to the pore structure microporous gels.

Therefore, the theories developed for the microporous membranes are nonapplicable to nonporous gels. The diffusional theories developed for nonporous membranes are based on the concept of free-volume. The free-volume is the area within the gel not occupied by the polymer chains (45). Diffusion of solutes in nonporous membranes will occur within this free volume.

The first theory describing transport in nonporous gels was presented by Yasuda et al. (46). This theory relates the normalized diffusion coefficient, the ratio of the diffusion coefficient of the solute in the membrane ($D_{2,13}$) to the diffusion coefficient of the solute in the pure solvent ($D_{2,1}$), to degree of hydration of the membrane, H (g water/g swollen gel). The subscripts 1, 2, and 3 represent the solvent or water, solute, and the polymer. The normalized diffusion coefficient can be written as

$$\frac{D_{2,13}}{D_{2,1}} = \varphi(q_s)exp\left[-B\left(\frac{q_s}{V_{f,1}}\right)\left(\frac{1}{H} - 1\right)\right] \quad (43)$$

where $V_{f,1}$ is the free-volume occupied by the water, φ is a sieving factor which provides a limiting mesh size below which solutes of cross-sectional area q_s cannot pass, and B is a parameter characteristic of the polymer. Based on this theory, a permeability coefficient for the drug in the swollen membrane, $P_{2,13}$ is given by

$$P_{2,13} = \frac{D_{2,13}K}{\delta} \quad (44)$$

Yasuda and Lamaze (47) confirmed this theory experimentally using urea, creatinin and secobarbital.

Peppas and Reinhart (48) also developed a theoretical model to describe solute transport in highly swollen, nonporous hydrogels. In this description, the diffusional jump lengths of the solute were assumed the same in the gel and the pure solvent. Additionally, the free-volume of the hydrogel was taken to be the same as the free-volume of the pure solvent. Using this approach, the normalized diffusion coefficient can be described in terms of the degree of swelling and the molecular weight of the polymer chains as

$$\frac{D_{2,13}}{D_{2,1}} = k_1\left(\frac{\overline{M}_c - \overline{M}_c^*}{\overline{M}_n - \overline{M}_c^*}\right)exp\left(-\frac{k_2 r_s^2}{Q - 1}\right) \quad (45)$$

where k_1 and k_2 are parameters based on the polymer structure, Q is the degree of swelling (g swollen polymer/g dry polymer), r_s is the solute radius, $\overline{M}_c$ is the molecular weight of the polymer chains between cross-links, $\overline{M}_n$ is the molecular weight of linear polymer chains prepared using the same conditions in the absence of a crosslinking agent and $\overline{M}_c^*$ is the critical molecular weight between cross-links below which a solute of size r_s could not diffuse. In this depiction, the term $(\overline{M}_c - \overline{M}_c^*/\overline{M}_n - \overline{M}_c^*)$ is comparable to the sieving factor (φ) presented by Yasuda. These researchers experimentally verified the dependence of the diffusion coefficient on the solute size and cross-linking density (49). Recently, the group of Prausnitz has studied the size exclusion effects in highly swollen networks (50).

Peppas and Moynihan (51) developed a theory for the case of moderately or poorly swollen, nonporous networks. In this case, the diffusional jump length of the solute in the membrane ($\lambda_{2,13}$) does not equal the diffusional jump length of the solute in the pure solvent ($\lambda_{2,13}$) and the free-volume of the gel does not equal the free-volume of the pure solvent. In this model, the normalized diffusion coefficient is written as

$$\frac{D_{2,13}}{D_{2,1}} = f(v_{2,s}^{-3/4})exp[k_3(\overline{M}_c - \overline{M}_n) - \pi r_s^2 l_s \Phi(V)] \quad (46)$$

where $f(v_{2,s}^{-3/4})$ is a parameter representing the characteristic size of the diffusional area, k_3 is a structural parameter and l_s is the length of the solute. The free-volume contributions, $\Phi(V)$, are expressed as

$$\Phi(V) = \frac{V_1 - V_3}{(Q - 1)V_1^2 + V_1 V_3} \quad (47)$$

where V_1 and V_3 are the free-volumes of the polymer and the pure solvent.

Harland and Peppas (52) developed a theory for diffusion in a semicrystalline polymer. In this type of gel, the diffusion occurs only in the pores between the impermeable crystalline regions. The diffusion coefficient of the solute in the crystalline phase (D_c) can be expressed in terms of the diffusion coefficient in the amorphous phase (D_a) as

$$D_c = \frac{D_a(1 - v_c)}{\tau} \quad (48)$$

where τ is the tortuosity and v_c is the volume fraction of the crystalline region.

For the case of semicrystalline hydrogels, the crystallites present the greatest obstacle to diffusion. Therefore, the diffusion coefficient for the gel in the swollen membrane is assumed to be equal to the diffusion coefficient of the solute in the crystalline regions. For the case of moderately or poorly swollen networks, the normalized diffusion coefficient can be written as

$$\frac{D_{2,13}}{D_{2,1}} = \frac{(1 - v_c)}{\tau} f(v_{2,s}^{-3/4})exp[k_3(\overline{M}_c - \overline{M}_n) - \pi r_s^2 l_s \Phi(V)] \quad (49)$$

For highly swollen networks, the normalized diffusion coefficient can be expressed as

$$\frac{D_{2,13}}{D_{2,1}} = \frac{(1 - v_c)}{\tau}\left(\frac{\overline{M}_c - \overline{M}_c^*}{\overline{M}_n - \overline{M}_c^*}\right)exp\left(-\frac{\pi r_s^2 l v_a}{V_w v_s}\right) \quad (50)$$

where v_a is the volume fraction of the amorphous region, v_s is the volume fraction of the solvent and V_w is the volume fraction of the water.

Experimental Determination of Diffusion Coefficients

Membrane Permeability Experiments. The membrane permeation method is used to study the diffusion coeffi-

cients of solutes through thin membranes. The drug permeates through an equilibrium-swollen membrane from a reservoir containing a high concentration of drug (donor cell) to a reservoir containing a lower concentration (receptor).

In these experiments, the drug concentration should be monitored over time in the receptor cell. The solute permeability, P, can be determined from the following expression.

$$ln\left(\frac{2C_o}{C_t} - 1\right) = \frac{2A}{Vl} Pt \tag{51}$$

In this expression, C_o is the donor cell concentration (initially), C_t is the time-dependent receptor cell concentration, A is the cross-sectional area of the membrane, V is the volume of the cells and l is the membrane thickness. A plot of $(Vl/A)ln(2C_o/C_t - 1)$ versus time yields a straight line of slope P if the gel remains at equilibrium.

The diffusion coefficient is related to the partition coefficient by equation 44. The partition coefficient can be determined experimentally through equilibrium partitioning studies. In this type of experiment, hydrogels are swollen to equilibrium in drug solutions of concentration C_o. Once equilibrium has been reached, the partition coefficient is calculated as

$$K = -\frac{C_{m,eq}}{C_{s,eq}} \tag{52}$$

where $C_{m,eq}$ is the equilibrium concentration of drug in the membrane and $C_{s,eq}$ is the equilibrium concentration of the drug in the solution.

Controlled Release Experiments. Another relatively easy technique for determination of diffusion coefficients is to measure the release of drug release from thin hydrogels (aspect ratio >10). In release experiments, the membranes containing the dispersed drug are placed in drug-free solutions and the concentration of the drug in the solutions is monitored over time. It is recommended that nearly perfect sink conditions be maintained throughout the experiment.

The diffusion coefficient can be found by fitting the release data to equation 37. This equation is valid for the initial 60% of the total amount released. This technique is most accurate for systems in which diffusion is the dominant mechanism for drug release. In order to determine whether a particular device is diffusion controlled, the early time release data can be fit to the following empirical relationship proposed by Ritger and Peppas (39).

$$\frac{M_t}{M_\infty} = kt^n \tag{53}$$

The constants, k and n, are characteristics of the drug–polymer system. The diffusional exponent, n, is dependent on the geometry of the device as well as the physical mechanism for release. For classical Fickian diffusion, Ritger and Peppas (39) determined that value for the diffusional exponent was 0.5 for slab geometries, 0.45 for cylindrical devices, and 0.43 for spherical devices.

By determining the diffusional exponent, n, one can gain information about the physical mechanism controlling drug release from a particular device. Based on the diffusional exponent (53), the drug transport in a slab geometry is classified as Fickian diffusion ($n = 0.5$), Case II transport ($n = 1$), non-Fickian or anomalous transport ($0.5 < n < 1$) and Super Case II transport (Table 1). Representative release curves for each case are shown in Figure 6. For systems exhibiting Case II transport, the dominant mechanism for drug transport is due to polymer relaxation as the gels swells. These types of devices, known as swelling-controlled release systems, are described in more detail later. Anomalous transport occurs due to a coupling of Fickian diffusion and polymer relaxation.

Berens and Hofenberg (54) proposed the following model to describe the release behavior of dynamically swelling hydrogels.

$$\frac{M_t}{M_\infty} = k_1 t + k_2 t^{1/2} \tag{54}$$

This expression describes the release rates in terms of relaxation-controlled transport process, $k_1 t$, and the diffusion-controlled process, $k_2 t^{1/2}$.

Other Techniques. There are several other methods for experimental determination of diffusion coefficients in polymeric systems. These techniques involve more complex instrumentation techniques that cannot be described in depth in this work. These techniques include NMR spec-

Table 1. Drug Transport Mechanisms in Hydrogel Slabs

Diffusional exponent, n	Type of transport	Time dependence
0.5	Fickian diffusion	$t^{1/2}$
$0.5 < n < 1$	Anomolous transport	t^{n-1}
1	Case II transport	Time independent
$n > 1$	Super Case II transport	t^{n-1}

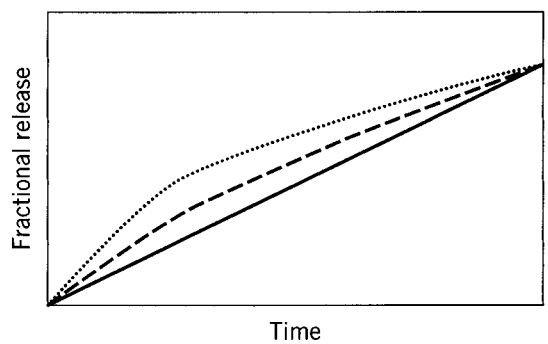


Figure 6. Comparison of the release behavior of systems exhibiting (···) classical Fickian diffusion behavior, (— —) anamolous release behavior, and (——) zero-order release or Case II transport.

Next Page

troscopy (55), scanning electron microscopy (56), Fourier transform infrared spectroscopy (57), and quasielastic laser-light scattering (33).

CLASSIFICATIONS

Because of their nature, hydrogels can be used in many different types of controlled release systems. These systems are classified according to the mechanism controlling the release of the drug from the device. Hydrogel-based drug delivery systems are classified as diffusion-controlled systems, swelling-controlled systems, chemically controlled systems, and environmentally responsive systems (2). In this section, the mechanism of drug release in each type of system is described.

Diffusion-Controlled Release Systems

Diffusion is the most common mechanism controlling release in hydrogel-based drug delivery system. There are two major types of diffusion-controlled systems; reservoir devices and membrane devices. Drug release from each type of system occurs by diffusion through the macromolecular mesh or through the water-filled pores.

Reservoir Systems. Reservoir systems consist of a polymeric membrane surrounding a core containing the drug (Fig. 7). Typically, reservoir devices are capsules, cylinders, slabs, or spheres. The rate-limiting step for drug release is diffusion through the outer membrane of the device. For a device with a membrane thickness of δ, the molar flux of drug leaving the device is described by equation 31.

To maintain a constant release rate or flux of drug from the reservoir, the concentration difference must remain constant. This can be achieved by designing a device with excess solid drug in the core. Under these conditions, the internal solution in the core remains saturated. This type of device is an extremely useful device as it allows for time-independent or zero-order release.

The major drawback of this type of drug delivery system is the potential for catastrophic failure of the device. In the event that the outer membrane ruptures, the entire content of the device are delivered nearly instantaneously. When preparing these devices, care must be taken to ensure that the device does not contain pinholes or other defects that may lead to rupture.

Matrix Systems. In matrix devices, the drug is dispersed throughout the three-dimensional structure of the hydrogel (Fig. 8). Release occurs due to diffusion of the drug throughout the macromolecular mesh or water-filled pores. The fractional release from a one-dimensional device can be modeled using equation 33. In these systems, the release rate is proportional to time to the one-half power. This is significant in that it is impossible to obtain time independent or zero-order release in this type of system with simple geometries.

Drug can be incorporated into the gels by equilibrium partitioning, where the gel is swollen to equilibrium in concentrated drug solution, or during the polymerization reaction. Equilibrium partitioning is the favorable loading method for drug–polymer systems with large partition coefficients or for sensitive macromolecular drugs such as peptides or proteins that could be degraded during the polymerization.

Swelling-Controlled Release Systems

In swelling-controlled release systems, the drug is dispersed within a glassy polymer. Upon contact with biological fluid, the polymer begins to swell. No drug diffusion occurs through the polymer phase. As the penetrant enters the glassy polymer, the glass transition temperature of the polymer is lowered allowing for relaxations of the macromolecular chains. The drug is able to diffuse out of the swollen, rubbery area of the polymers. This type of system is characterized by two moving fronts: the front separating the swollen (rubbery) portion and the glassy regions which moves with velocity, v, and the polymer–fluid interface (Fig. 9). The rate of drug release is controlled by the velocity and position of the front dividing the glassy and rubbery portions of the polymer.

For true swelling-controlled release systems, the diffusional exponent, n, is 1. This type of transport is known as Case II transport and results in zero-order release kinetics. However, in some cases, drug release occurs due to a combination of macromolecular relaxations and Fickian diffusion. In this case, the diffusional exponent is between 0.5 and 1. This type of transport is known as anomalous or non-Fickian transport. A complete mathematical treatment of this type of release behavior has been provided in two excellent reviews (37,53).

Chemically Controlled Release Systems

There are two major types of chemically controlled release systems: erodible drug delivery systems and pendent chain systems (58,59). In erodible systems, drug release occurs due to degradation or dissolution of the hydrogel. In pendent chain systems, the drug is affixed to the polymer back-

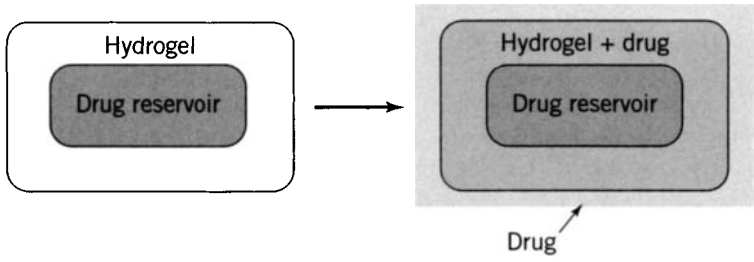


Figure 7. Schematic depiction of drug-release from a hydrogel-based reservoir delivery system.

Previous Page

troscopy (55), scanning electron microscopy (56), Fourier transform infrared spectroscopy (57), and quasielastic laser-light scattering (33).

CLASSIFICATIONS

Because of their nature, hydrogels can be used in many different types of controlled release systems. These systems are classified according to the mechanism controlling the release of the drug from the device. Hydrogel-based drug delivery systems are classified as diffusion-controlled systems, swelling-controlled systems, chemically controlled systems, and environmentally responsive systems (2). In this section, the mechanism of drug release in each type of system is described.

Diffusion-Controlled Release Systems

Diffusion is the most common mechanism controlling release in hydrogel-based drug delivery system. There are two major types of diffusion-controlled systems; reservoir devices and membrane devices. Drug release from each type of system occurs by diffusion through the macromolecular mesh or through the water-filled pores.

Reservoir Systems. Reservoir systems consist of a polymeric membrane surrounding a core containing the drug (Fig. 7). Typically, reservoir devices are capsules, cylinders, slabs, or spheres. The rate-limiting step for drug release is diffusion through the outer membrane of the device. For a device with a membrane thickness of δ, the molar flux of drug leaving the device is described by equation 31.

To maintain a constant release rate or flux of drug from the reservoir, the concentration difference must remain constant. This can be achieved by designing a device with excess solid drug in the core. Under these conditions, the internal solution in the core remains saturated. This type of device is an extremely useful device as it allows for time-independent or zero-order release.

The major drawback of this type of drug delivery system is the potential for catastrophic failure of the device. In the event that the outer membrane ruptures, the entire content of the device are delivered nearly instantaneously. When preparing these devices, care must be taken to ensure that the device does not contain pinholes or other defects that may lead to rupture.

Matrix Systems. In matrix devices, the drug is dispersed throughout the three-dimensional structure of the hydrogel (Fig. 8). Release occurs due to diffusion of the drug throughout the macromolecular mesh or water-filled pores. The fractional release from a one-dimensional device can be modeled using equation 33. In these systems, the release rate is proportional to time to the one-half power. This is significant in that it is impossible to obtain time independent or zero-order release in this type of system with simple geometries.

Drug can be incorporated into the gels by equilibrium partitioning, where the gel is swollen to equilibrium in concentrated drug solution, or during the polymerization reaction. Equilibrium partitioning is the favorable loading method for drug–polymer systems with large partition coefficients or for sensitive macromolecular drugs such as peptides or proteins that could be degraded during the polymerization.

Swelling-Controlled Release Systems

In swelling-controlled release systems, the drug is dispersed within a glassy polymer. Upon contact with biological fluid, the polymer begins to swell. No drug diffusion occurs through the polymer phase. As the penetrant enters the glassy polymer, the glass transition temperature of the polymer is lowered allowing for relaxations of the macromolecular chains. The drug is able to diffuse out of the swollen, rubbery area of the polymers. This type of system is characterized by two moving fronts: the front separating the swollen (rubbery) portion and the glassy regions which moves with velocity, v, and the polymer–fluid interface (Fig. 9). The rate of drug release is controlled by the velocity and position of the front dividing the glassy and rubbery portions of the polymer.

For true swelling-controlled release systems, the diffusional exponent, n, is 1. This type of transport is known as Case II transport and results in zero-order release kinetics. However, in some cases, drug release occurs due to a combination of macromolecular relaxations and Fickian diffusion. In this case, the diffusional exponent is between 0.5 and 1. This type of transport is known as anomalous or non-Fickian transport. A complete mathematical treatment of this type of release behavior has been provided in two excellent reviews (37,53).

Chemically Controlled Release Systems

There are two major types of chemically controlled release systems: erodible drug delivery systems and pendent chain systems (58,59). In erodible systems, drug release occurs due to degradation or dissolution of the hydrogel. In pendent chain systems, the drug is affixed to the polymer back-

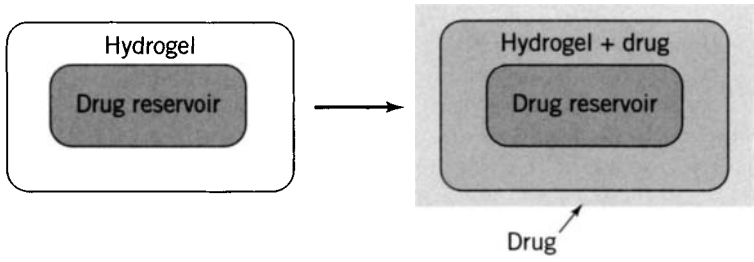


Figure 7. Schematic depiction of drug-release from a hydrogel-based reservoir delivery system.

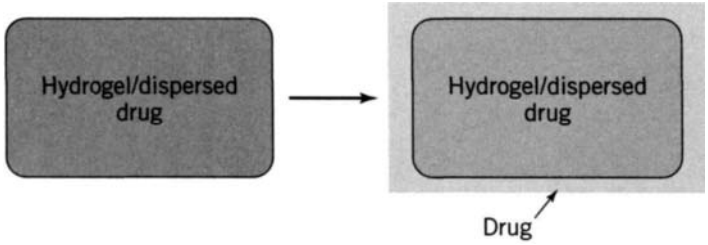


Figure 8. Schematic depiction of drug-release from a hydrogel-based matrix delivery system.

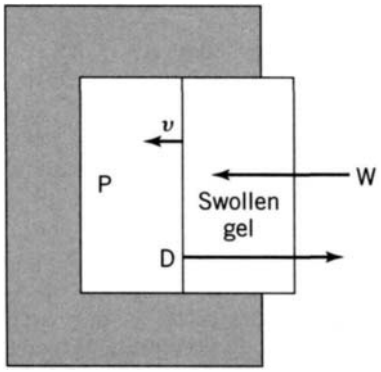


Figure 9. Schematic representation of the behavior of a one-dimensional swelling controlled release system. The water (W) penetrates the glassy polymer (P) to form a gel. The drug (D) is released through the swollen layer.

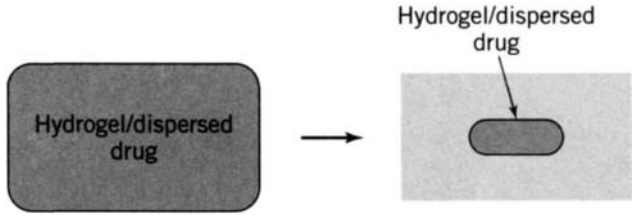


Figure 10. Schematic diagram of drug release from a hydrogel-based erodible delivery system.

bone through degradable linkages. As these linkages degrade, the drug is released.

Erodible Drug Delivery Systems. Erodible drug delivery systems, also known as degradable or absorbable release systems, can be either matrix or reservoir delivery systems. In reservoir devices, an erodible membrane surrounds the drug core. If the membrane erodes significantly after the drug release is complete, the dominant mechanism for release would be diffusion. Predictable, zero-order release could be obtained with these systems. In some cases, the erosion of the membrane occurs simultaneously with drug release. As the membrane thickness decreased due to erosion, the drug delivery rate would also change. Finally, in some erodible reservoir devices, the drug diffusion in the outer membrane does not occur. Under these conditions, drug release does not occur until the outer membrane erodes completely. In this type of device, the entire contents are released in a single, rapid burst. These types of systems have been investigated for use as enteric coatings.

For erodible matrix devices, the drug is dispersed within the three-dimensional structure of the hydrogel. Drug release is controlled by drug diffusion through the gel or erosion of the polymer. In true erosion-controlled devices, the rate of drug diffusion is significantly slower than the rate of polymer erosion, and the drug is released as the polymer erodes (Fig. 10).

In erodible system, there are three major mechanisms for erosion of the polymer. The first mechanism for erosion is the degradation of the cross-links. This degradation can occur by hydrolysis of water-labile linkages, enzymatic degradation of the junctions, or dissolution of physical cross-links such as entanglements or crystallites in semicrystalline polymers. The second mechanism for erosion is solubilization of insoluble or hydrophobic polymers. This could occur as a result of hydrolysis, ionization, or protonation of pendent groups along the polymer chains. The final mechanism of erosion is the degradation of backbone bonds to produce small molecular weight molecules. Typically, the degradation products are water soluble. This type of erosion can occur by hydrolysis of water-labile backbone linkages or by enzymatic degradation of backbone linkages. The most commonly studied erodible polymer systems are poly(lactic acid) (PLA), poly(glycolic acid) (PGA), and copolymers of PLA and PGA.

Pendent Chain Systems. Pendent chain systems consist of linear homo- or copolymers with the drug attached to the backbone chains. The drug is released from the polymer by hydrolysis or enzymatic degradation of the linkages (Fig. 11). Zero-order release can be obtained with these systems, provided that the cleavage of the drug is the rate-controlling mechanism.

Environmentally Responsive Systems

Hydrogels may exhibit swelling behavior dependent on the external environment. Over the last 30 years there has been a significant interest in the development and analysis of environmentally or physiologically responsive hydrogels (10). Environmentally responsive materials show drastic changes in their swelling ratio due to changes in their external pH, temperature, ionic strength, nature and composition of the swelling agent, enzymatic or chemical reaction, and electrical or magnetic stimulus (60). In most responsive networks, a critical point exists at which this transition occurs.

Responsive hydrogels are unique in that there are many different mechanisms for drug release and many different

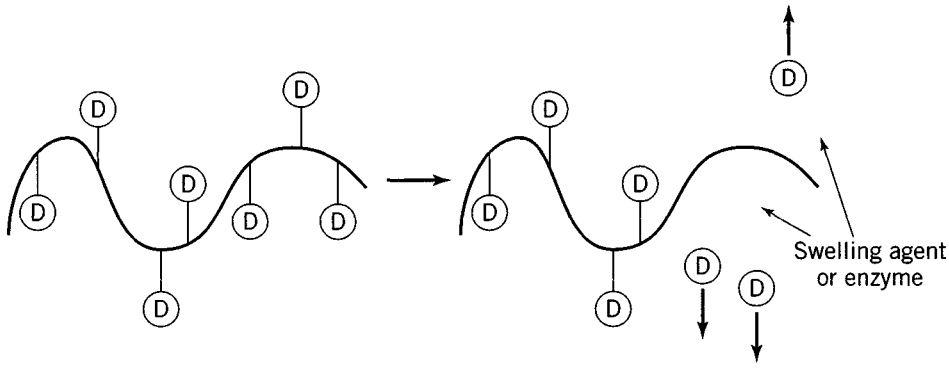


Figure 11. Schematic diagram of the release of drug from a pendent chain system due to scission of the bonds connecting the drug to the polymer backbone.

types of release systems based on these materials. For instance, in most cases drug release occurs when the gel is highly swollen or swelling and is typically controlled by gel swelling, drug diffusion, or a coupling of swelling and diffusion. However, in a few instances, drug release occurs during gel syneresis by a squeezing mechanism. Also, drug release can occur due to erosion of the polymer caused by environmentally responsive swelling.

Another interesting characteristic about many responsive gels is that the mechanism causing the network structural changes can be entirely reversible in nature. This behavior is depicted in Figure 12 for a pH- or temperature-responsive gel. The ability of these materials to exhibit rapid changes in their swelling behavior and pore structure in response to changes in environmental conditions lends these materials favorable characteristics as carriers for bioactive agents, including peptides and proteins. This type of behavior may allow these materials to serve as self-regulated, pulsatile drug delivery systems. This type of behavior is shown in Figure 13 for pH- or temperature-responsive gels. Initially, the gel is in an environment in which no swelling occurs. As a result, very little drug release occurs. However, when the environment changes and the gel swells, rapid drug release occurs (either by Fickian diffusion, anomalous transport, or Case II transport). When the gel collapses as the environment changes, the release can be turned off again. This can be repeated over numerous cycles. Such systems could be of extreme importance in the treatment of chronic diseases such as diabetes. Peppas (60) and Siegel (61) have presented detailed analyses of this type of behavior.

pH-Sensitive Hydrogels. One of the most widely studied types of physiologically responsive hydrogels is pH-responsive hydrogels. These hydrogels are swollen from ionic networks. These ionic networks contain either acidic or basic pendent groups. In aqueous media of appropriate pH and ionic strength, the pendant groups can ionize developing fixed charges on the gel as shown in Figure 2 for an ionic gel. The swelling behavior of these materials has been analyzed in a previous section.

There are many advantages to using ionic materials over neutral networks. All ionic materials exhibit a pH and ionic strength sensitivity. The swelling forces developed in these systems are increased over the nonionic materials. This increase in swelling force is due to the localization of fixed charges on the pendent groups. As a result, the mesh size of the polymeric networks can change significantly with small pH changes. In these materials, the drug diffusion coefficients and release rates vary greatly with environmental pH.

Temperature-Sensitive Hydrogels. Another class of environmentally sensitive materials that are being targeted for use in drug delivery applications is thermally sensitive polymers. This type of hydrogel exhibits temperature-sensitive swelling behavior due to a change in the polymer–swelling agent compatibility over the temperature range of interest. Temperature-sensitive polymers typically exhibit a lower critical solution temperature (LCST), below which the polymer is soluble. Above this temperature, the polymers are typically hydrophobic and do not swell significantly in water (62). However, below the LCST, the cross-linked gel swell to significantly higher degrees because of the increased compatibility with water. For polymers that exhibit this sort of swelling behavior, the rate of drug release would be dependent on the temperature. The highest release rates would occur when the temperature of the environment is below the LCST of the gel.

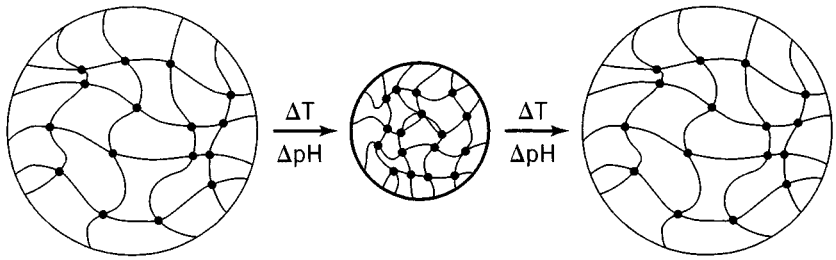


Figure 12. Swollen temperature- and pH-sensitive hydrogels may exhibit an abrupt change from the expanded (left) to the collapsed (syneresed) state (center) and then back to the expanded state (right) as temperature and pH change.

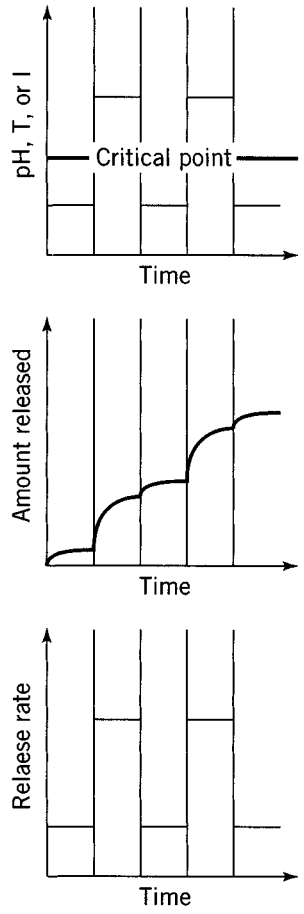


Figure 13. Cyclic change of pH, T, or ionic strength (I) leads to abrupt changes in the drug release rates at certain time intervals in some environmentally responsive polymers.

Complexing Hydrogels. Some hydrogels may exhibit environmental sensitivity due to the formation of polymer complexes. Polymer complexes are insoluble, macromolecular structures formed by the noncovalent association of polymers with the affinity for one another. The complexes form due to association of repeating units on different chains (interpolymer complexes) or on separate regions of the same chain (intrapolymer complexes). Polymer complexes are classified by the nature of the association as stereocomplexes, polyelectrolyte complexes, and hydrogen-bonded complexes (63). The stability of the associations is dependent on such factors as the nature of the swelling agent, temperature, type of dissolution medium, pH and ionic strength, network composition and structure, and length of the interacting polymer chains.

In this type of gel, complex formation results in the formation of physical cross-links in the gel. As the degree of effective cross-linking is increased, the network mesh size and degree of swelling is significantly reduced. As a result, the rate of drug release in these gels decreases dramatically upon the formation of interpolymer complexes.

Materials Sensitive to Chemical or Enzymatic Reaction. More recently, researchers have proposed controlled release devices that can respond to specific chemicals or enzymes in the body (64,65). Under normal conditions, the structure of the hydrogel would be sufficient to prevent drug release from occurring. However, in the presence of specific substances, chemical or enzymatic reactions could occur that may hydrolyze specific groups of the polymer chain resulting in an increased pore structure and rate of drug release from the gel. If degradation of the gel occurs, the systems cannot be fully reversible.

In some instances, enzymes can be incorporated into the structure of the hydrogel. In the presence of specific chemicals, the enzyme could trigger a reaction which would change the microenvironment of the hydrogel. Changes in the local microenvironment (such as pH or temperature) could lead to gel swelling or collapse. In these situations, the release rates would be altered significantly. This type of system could be completely reversible in nature.

Magnetically Responsive Systems. Magnetically responsive systems consist of polymers or copolymers containing magnetic microbeads (66). These systems can be prepared from most polymers; however, the most commonly used copolymer for these systems is the hydrophobic polymer, poly(ethylene-*co*-vinyl acetate) (PEVAc). Such systems are not typically classified as hydrogels because they do not swell to any appreciable degree. The drug release mechanism from a typical magnetic system is shown in Figure 14. The three-dimensional structure of these systems is such that no drug release can occur when no magnetic field is applied. However, when a magnetic field is applied, the microbeads pulsate allowing for the formation of micropores. Additionally, the pulsation of the beads "squeezes" the drug out of the gel through these pores. When the field is removed, drug release is halted rapidly. Such systems have been targeted for use as pulsatile drug delivery vehicles and have shown to exhibit extremely reproducible behavior.

APPLICATIONS

Neutral Hydrogels

A major goal in drug delivery is to develop systems that deliver drugs at a constant rate over an extended period. This can be achieved by using release systems in which gel swelling is the controlling mechanism for drug release. Researchers have also attempted to develop constant-release systems by alteration of device geometry and polymer composition. One of the first researchers to use hydrogels for swelling-controlled release was Good (67). In this work, glassy poly(2-hydroxyethyl methacrylate) (PHEMA) containing tripelennamine hydrochloride was swollen in water. The release rate of the solute was non-Fickian, but zero-order release was not obtained. The first such system in which zero-order release was observed was developed by Hopfenberg and Hsu (68). In these systems, cross-linked polystyrene was used to release red dyes into hexane. Other polymers that have been used extensively in controlled release systems include poly(vinyl alcohol) (PVA), poly(*N*-vinyl-2-pyrollidone) (PNVP), poly(ethylene glycol) (PEG), poly(ethylene oxide) (PEO), and PEVAc or

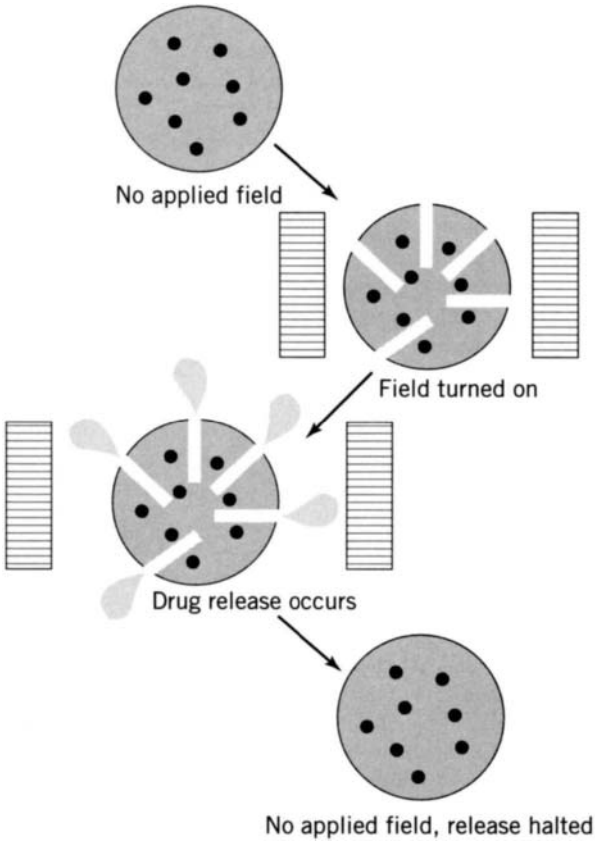


Figure 14. Schematic representation of drug release from a magnetically controlled system. Initially, when the field is off, no drug release occurs. When the field is turned on, the oscillations of the beads creates macropores (●) through which drug release occurs. Drug release is halted when the field is switched off.

copolymers thereof. In this section, we discuss applications of some of these materials.

Poly(2-hydroxyethyl methacrylate). PHEMA has been the most widely used polymer in drug delivery applications. It is an extremely hydrophilic polymer and is highly stable. The permeability of these membranes is easily controlled based on the degree of cross-linking used. Researchers have studied the swelling behavior, morphology, and diffusional behavior of PHEMA gels and copolymers thereof. The release of a wide range of drugs from these gels has also been studied. For example, Anderson et al. (69) studied the release behavior of hydrocortisone from PHEMA gels. The release behavior was non-Fickian, but true zero-order release was not achieved with these gels. Another significant study was performed by Sefton and Nishimura (70). They investigated the diffusional behavior of insulin in PHEMA-based hydrogels. Song et al. (71) developed one of the first pharmaceutically relevant zero-order release systems. They used a reservoir device consisting of a cross-linked PHEMA cylinder encapsulating a solution of silicon oil and progesterone. Zero-order release was obtained with these devices for up to 10 days. Lee (72,73) was able to use PHEMA to achieve zero-order release for short periods of time. In his work, oxprenolol was released from highly cross-linked PHEMA gels at constant rates for up to 3 hours.

The group of Peppas contributed greatly to the understanding of the underlying phenomena of macromolecular relaxations in swelling-controlled release systems. In particular, they studied hydrogels prepared from PHEMA and hydrophobic poly(methyl methacrylate) (PMMA). Franson and Peppas (74) prepared cross-linked copolymer gels of PHEMA-*co*-MAA of varying compositions. Theophylline release was studied and it was found that near zero-order release could be achieved using copolymers containing 90% PHEMA. Further studies by Davidson and Peppas (75) studied the effects of hydrophobicity and cross-link density on the release kinetics and diffusional properties of PHEMA-*co*-MMA membranes. Additionally, Korsmeyer and Peppas (76) examined the behavior of copolymer gels consisting of PHEMA and hydrophilic PNVP (PHEMA-*co*-NVP). In this work, zero-order release of theophylline was observed for up to 5 hours.

Poly(vinyl alcohol). Another hydrophilic polymer that has received attention is PVA. This material holds tremendous promise as a biological drug delivery device because it is nontoxic, hydrophilic, and exhibits good mucoadhesive properties (77). In one of the first applications of this material, Langer and Folkman (78) investigated the use of copolymers of PHEMA (Hydron®) and PVA as delivery vehicles for polypeptide drugs.

Two methods exist for the preparation of PVA gels. In the first method, linear PVA chains are cross-linked using glyoxal, gluteraldehyde, or borate. In the second method, pioneered by Peppas (79), semicrystalline gels were prepared by exposing aqueous solutions of PVA to repeated freezing and thawing. The freezing and thawing induced crystal formation in the materials and allowed for the formation of a network structure crosslinked with the quasipermanent crystallites. The latter method is the preferred method for preparation as it allows for the formation of an "ultrapure" network without the use of toxic cross-linking agents.

Korsmeyer and Peppas (80) prepared PVA gels by cross-linking with borate. They studied the swelling behavior and mechanical properties of these gels. In this work, the release rate of theophylline was dependent on the degree of cross-linking. Future studies by Moriomoto et al. (81) examined the release behavior of a wide range of drugs. In this work, they were able to release indomethacin, glucose, insulin, heparin, and albumin from chemically cross-linked PVA gels.

Since the development of the semicrystalline PVA gels by Peppas, significant work has been done in characterizing of these systems. Peppas and Hansen (82) studied the kinetics of crystal formation during the freezing and thawing process. Subsequent work by Urushizaki et al. (83) evaluated the effects of the number of freezing and thawing cycles on the networks properties. The gels became more rigid with increasing number of cycles. Peppas and Stauffer (84) have also investigated the effects of crystallization conditions such as freezing temperature, number

of cycles, and freezing time on the structure and properties of the PVA networks.

Studies on the uses of PVA prepared by the freezing and thawing technique as controlled release devices have recently been reported. Peppas and Scott (85) and Ficek and Peppas (86) used PVA gels for the release of bovine serum albumin. In the work of Peppas and Scott, drug release occurred by classical Fickian diffusion. Ficek and Peppas (86) developed a method to prepare novel PVA microparticles containing bovine serum albumin by a freezing and thawing technique. In this work, they were able to release bovine serum albumin using these microparticles.

Other researchers have investigated the use of PVA gels as mucoadhesive delivery devices. The Tsutsumi et al. reported novel buccal delivery systems for ergotamine tartrate (87). Peppas and Mongia (88) have also considered PVA for mucoadhesive drug delivery applications. In this work, they investigated the mucoadhesive behavior of PVA gels prepared by the freezing and thawing technique. Additionally, they studied the release behavior of theophylline and oxprenolol from these materials. Additionally, the group of Peppas reported on the release behavior of ketanserin (89) and metronidazole (90) from these systems.

New phase erosion controlled release systems based on the semicrystalline phase have been reported by Mallapragada and Peppas (90,91). These systems exhibited an unusual molecular control of the drug or protein delivery by a simple dissolution of the carrier. Hydrophilic carriers pass through a process of chain unfolding from the semicrystalline phase to the amorphous one, eventually leading to complete chain disentanglement. It has been shown that PVA and PEG are the best systems for such release behavior, and that such devices have the potential to be used for a wide range of drug delivery applications release. A detailed mathematical analysis has been developed to analyze such swellable systems (91–93).

Poly(ethylene oxide) and Poly(ethylene glycol). Hydrogels of PEO and PEG have received significant attention in the last few years in biological drug delivery applications, especially because of their associated stealth characteristics and their protein resistance (94). Three major preparation techniques exist for the preparation of crosslinked PEG networks: (*1*) chemical crosslinking between PEG chains, (*2*) radiation cross-linking of PEG chains, and (*3*) chemical reaction of mono- and difunctional PEGs.

Some of the first chemically cross-linked PEG networks were prepared by McNeill and Graham (95). The crosslinked linear PEG chains used diisocyanates. These gels were used as reservoir devices for the controlled delivery of smaller molecular weight drugs. More recently, McNeill and Graham (96) have investigated the release behavior of small molecular weight solutes from PEG cross-linked with 1,2,6 hexanetriol. The release of proxyphylline from PEG spheres, slabs, and cylinders was studied. For each of the matrix devices, they observed non-Fickian release kinetics. Bromberg (97) also studied the release of chemically cross-linked PEG networks. In this work, PEG networks were cross-linked using tris(6-isocyanatohexyl)-isocyanurate. The kinetics of insulin release from PEG gels obeyed non-Fickian release kinetics.

The advantage of using radiation cross-linked PEO networks is that no toxic cross-linking agents are required. However, it is difficult to control the network structure of these materials. Stringer and Peppas (98) have recently prepared PEO hydrogels by radiation cross-linking. In this work, they analyzed the network structure in detail. Additionally, they investigated the diffusional behavior of smaller molecular weight drugs, such as theophylline, in these gels. Kofinas et al. (99) have prepared PEO hydrogels by a similar technique. In this work, they studied the diffusional behavior of two macromolecules, cytochrome C and hemoglobin, in these gels. They noted an interesting, yet previously unreported dependence between the crosslink density and protein diffusion coefficient and the initial molecular weight of the linear PEGs.

Peppas and coworkers (100–104) have presented exciting new methods for the preparation of PEG gels with controllable structures. In this work, highly cross-linked and tethered PEG gels were prepared from PEG dimethacrylates and monomethacrylates. The diffusional behavior of diltiazem and theophylline in these networks was studied. The technique presented in this work is promising for the development of a new class of functionalized PEG-containing gels that may be of use in a wide variety of drug delivery applications.

pH-Sensitive Hydrogels

Hydrogels that have the ability to respond to pH changes have been studied extensively over the years. These gels typically contain side ionizable side groups such as carboxylic acids or amine groups (105,106). The most commonly studied ionic polymers include polyacrylamide (PAAm), poly(acrylic acid) (PAA), poly(methacrylic acid) (PMAA), poly(diethylaminoethyl methacrylate) (PDEAEMA), and poly(dimethylaminoethyl methacrylate) (PDMAEMA).

Cationic copolymers based on PDEAEMA and PDMAEMA have been studied by the groups of Peppas and Siegel. The group of Siegel has focused on the swelling and transport behavior of hydrophobic cationic gels. Siegel and Firestone (107,108) studied the swelling behavior of hydrophobic hydrogels of PDMAEMA and PMMA. Such systems were collapsed in solutions of pH greater than 6.6. However, in solutions of pH less than 6.6, such systems swelled due to protonation of the tertiary amine groups. The release of caffeine from these gels was studied (109). No caffeine was released in basic solutions; however, in neutral or slightly acidic solutions steady release of caffeine was observed for 10 days. More recently, Cornejo-Bravo and Siegel (110) have investigated the swelling behavior of hydrophobic copolymers of PDEAEMA and PMMA. Additionally, Siegel (111) has presented an excellent model of the dynamic behavior of ionic gels.

The groups of Peppas has studied the swelling behavior of more hydrophilic, cationic copolymers of P(DEAEMA-*co*-HEMA) and P(DMAEMA-*co*-HEMA) (112,113). These gels swelled in solutions of pH less than 7 and were in the collapsed state in basic solutions. These materials swelled to a greater degree than those prepared by Siegel. These materials were used to modulate the release behavior of protein and peptide drugs (114). Schwarte and Peppas (115)

studied the swelling behavior of copolymers of PDEAEMA grafted with PEG. The permeability of dextrans of molecular weight 4,400 and 9,400 was studied. The membrane permeabilities in the swollen membranes (pH = 4.6) were two orders of magnitude greater than permeabilities of the collapsed membranes.

Anionic copolymers have received significant attention as well. The swelling and release characteristics of anionic copolymers of PMAA and PHEMA P(HEMA-*co*-MAA) have been investigated. In acidic media, the gels did not swell significantly; however, in neutral or basic media, the gels swelled to a high degree due to ionization of the pendent acid group (116,117). Brannon-Peppas and Peppas have also studied the oscillatory swelling behavior of these gels (118). Copolymer gels were transferred between acidic and basic solutions at specified time intervals. In acidic solutions, the polymer swelled due to the ionization of the pendent groups. In basic solutions, rapid gel syneresis occurred. Brannon-Peppas and Peppas (119) modeled the time-dependent swelling response to pH changes using a Boltzman superposition-based model. The pH-dependent release behavior of theophylline and proxyphylline from these anionic gels was also studied (120,121). Khare and Peppas (122) studied the pH-modulated release behavior of oxprenolol and theophylline from copolymers of P(HEMA-*co*-MAA) and P(HEMA-*co*-AA). In neutral or basic media, the drug release occurred rapidly by a non-Fickian mechanism. The release rate was slowed significantly in acidic media. In another study, am Ende and Peppas (123) examined the transport of ionic drugs of varying molecular weight in P(HEMA-*co*-AA). They compared experimental results to a free-volume–based theory and found that deviations occurred due to interactions between the ionized backbone chains and pendent acid groups. The swelling and release behavior of interpenetrating polymer networks of PVA and PAA was also investigated (124,125). These materials also exhibit strong pH-responsive swelling behavior. The permeability of these membranes was strongly dependent on the environmental pH and the size and ionic nature of the solute. Recent new studies have used ATR-FTIR spectroscopy to characterize the interactions between polyelectrolytes and solutes (125,126).

Heller et al. (127) studied the behavior of another type of pH-responsive hydrogel. In this work, they evaluated the pH-dependent release of insulin from degradable poly(ortho esters). Other researchers have used chitosan (CS) membranes for drug delivery applications. These materials exhibited pH-dependent swelling behavior due to gelation of CS upon contact with anions (128). Interpenetrating networks of CS and PEO have been proposed as drug delivery devices due to their pH-dependent swelling behavior (129,130). More recently, Calvo et al. (131) prepared novel CS-PEO microspheres. These systems were to provide a continuous release of entrapped bovine serum albumin for 1 week. In another study, methotrexate, an anticancer drug, was encapsulated in microspheres of pH-sensitive CS and alginate (132). Zero-order release of the drug was observed from the microspheres in pH = 1.2 buffer for greater than 1 week. The Kikuchi et al. (133) studied pH-responsive calcium-alginate gel beads. In such systems, modulated release of dextran was achieved by varying the pH and ionic strength of the environmental solution. Such systems may be promising for use in protein and peptide delivery applications.

Temperature-Sensitive Hydrogels

Some of the earliest work with temperature-sensitive hydrogels was done by the group of Tanaka (134). They synthesized with cross-linked poly(*N*-isopropylacrylamide) (PNIPAAm) and determined that the LCST of the PNIPAAm gels was 34.3°C. Below this temperature, significant gel swelling occurred. The transition about this point was reversible. They discovered that the transition temperature was raised by copolymerizing PNIPAAm with small amounts of ionic monomers. Beltran et al. (135) also worked with PNIPAAM gels containing ionic comonomers. They observed results similar to those achieved by Tanaka.

The earliest investigators studying PNIPAAm gels discovered that the response time of the materials in response to temperature changes was rather slow. Future studies focused on developing newer materials that had the ability to collapse and expand in a more rapid fashion. Dong and Hoffman (136) prepared heterogeneous gels containing PNIPAAm that collapsed at significantly faster rates than homopolymers of PNIPAAm. Kabra and Gehrke (137) developed new method to prepare PNIPAAm gels that resulted in significant increases in the swelling kinetics of the gels. They prepared gels below the LCST to produce a permanent phase-separated microstructure in the gels. These gels expanded at rates 120 faster and collapsed at rates 3,000 times faster than homogeneous PNIPAAm gels. The group of Okano (138,139) developed an ingenious method to prepare comb-type graft hydrogels of PNIPAAm. The main chain of the cross-linked PNIPAAm contained small molecular weight grafts of PNIPAAm. Under conditions of gel collapse (above the LCST), hydrophobic regions were developed in the pores of the gel resulting in a rapid collapse. These materials had the ability to collapse from a fully swollen conformation in less than 20 minutes, whereas comparable gels that did not contain graft chains required up to a month to fully collapse. Such systems show major promise for rapid and abrupt or oscillatory release of drugs, peptides, or proteins.

Thermoresponsive polymers may be particularly useful in a wide variety of drug delivery applications (62,140). Okano et al. (141) studied the temperature-dependent permeability of PNIPAAm gels. They were able to use these gels as "on-off" delivery devices in response to temperature fluctuations. This type of behavior was useful for controlling the release of insulin (142) and heparin (114). These gels were also used as "squeezing" systems (143). More recently, conjugates of PNIPAAm with trypsin have been developed (144). Such systems could be extremely targeted delivery of enzymes. Another promising application of these systems was explored by the Vernon et al. (145). In this work, islets of Langerhans were entrapped by thermal gelation of PNIPAAm for use as a rechargeable artificial pancreas.

pH- and Temperature-Sensitive Hydrogels

Over the last 10 years, researchers have developed a novel class of hydrogels that exhibit both pH- and temperature-

sensitive swelling behavior. These materials may prove to be extremely useful in enzymatic or protein drug delivery applications. Hydrogels were prepared from PNIPAAm and PAA that exhibited dual sensitivities (146,147). These gels were able to respond rapidly to both temperature and pH changes. The Kim et al. investigated the use of such systems for carriers for insulin (148) and calcitonin (149). In general, these hydrogels only exhibited strong temperature-sensitive swelling behavior with large amounts of PNIPAAm in the gel. Cationic pH- and temperature-sensitive gels were prepared using polyamines and PNIPAAm (150). These systems were evaluated for local delivery of heparin.

Chen and Hoffman prepared new graft copolymers of PAA and PNIPAAm that responded more rapidly to external stimulus than previously studied materials (151). These materials exhibited increased temperature sensitivity due to the presence of the PNIPAAm grafts. Such systems were evaluated for use in prolonged mucosal delivery of bioactive agents, specifically peptide drugs (152).

Brazel and Peppas (153) studied the pH- and temperature-responsive swelling behavior of gels containing PNIPAAm and PMAA. These materials were used to modulate the release behavior of streptokinase and heparin in response to pH and temperature changes (154). Baker and Siegel (155) used similar hydrogels to modulate the glucose permeability. However, only large amounts of PNIPAAm were needed to observe large temperature sensitivities. The group of Peppas developed novel pH- and temperature-sensitive terpolymers of PHEMA, PMAA, and PNIPAAm (156). These systems were prepared to contain PNIPAAm-rich blocks, and as a result, these materials were able to exhibit strong temperature sensitivity with only 10% PNIPAAm in the gel. Using these materials, they were effectively able to modulate the release kinetics of streptokinase (157).

Complexing Hydrogels

Another promising class of hydrogels that exhibit responsive behavior is complexing hydrogels. Osada studied complex formation in PMAA hydrogels (158). In acidic media, the PMAA membranes collapsed in the presence of linear PEG chains due to the formation of interpolymer complexes between the PMAA and PEG. The gels swelled when placed in neutral or basic media. The permeability of these membranes was strongly dependent on the environmental pH and PEG concentration (159). Similar results were observed with hydrogels of PAA and linear PEG (160). Interpenetrating polymer networks of PVA and PAA that exhibit pH- and weak temperature-sensitive behavior due to complexation between the polymers were prepared and the release behavior of indomethacin was studied (161,162).

The group of Peppas has developed a class graft copolymer gels of PMAA grafted with PEG, P(MAA-*g*-EG) (163–170; A.M. Lowman and N.A. Peppas, unpublished data). These gels exhibited pH-dependent swelling behavior due to the presence of acidic pendent groups and the formation of interpolymer complexes between the ether groups on the graft chains and protonated pendent groups. In these covalently cross-linked, complexing P(MAA-*g*-EG) hydrogels, complexation resulted in the formation of temporary physical cross-links due to hydrogen bonding between the PEG grafts and the PMAA pendent groups. The physical cross-links were reversible in nature and dependent on the pH and ionic strength of the environment. As a result, complexing hydrogels exhibit drastic changes in their mesh size over small changes of pH as shown in Figure 15. One particularly promising application for these systems is the oral delivery of protein and peptide drugs (170). As shown in Figure 16, these copolymers severely limited the release of insulin in acidic environments such as those found in the stomach. However, in conditions similar to those found in the intestines, insulin release occurred rapidly.

Glucose-Sensitive Systems

Major developments have been reported in the use of environmentally responsive hydrogels as glucose-sensitive systems that could serve as self-regulated delivery devices for the treatment of diabetes. Typically, these systems have have been prepared by incorporating glucose oxidase into the hydrogel structure during the polymerization. In the presence of glucose, the glucose oxidase catalyzed the reaction between water and glucose to form gluconic acid. The gluconic acid lowered the pH of the microenvironment of the gel.

The first such systems developed by Kost et al. (171) consisted of glucose oxidase immobilized in hydrogels based on PHEMA and PDMAEMA. These systems exhibited glucose-sensitive swelling behavior. In the presence of glucose, gluconic acid was formed resulting in a decrease in the local pH. As a result, the cationic-based hydrogels swelled to larger degrees in the presence of glucose due to the production of gluconic acid. The glucose-responsive swelling behavior allowed for control over insulin permeation in these membranes by adjusting the environmental glucose concentrations (172,173). The kinetics of gel swelling and insulin release from cationic, glucose-sensitive hydrogels was also studied (174).

Glucose responsive systems were proposed that were based on anionic hydrogels (175,176). Ito et al. (175) prepared systems of porous cellulose membranes containing an insulin reservoir. The pores of these devices were grafted with PAA chains functionalized with glucose oxidase. In the presence of glucose, the decrease in environmental pH caused the PAA chains to collapse, opening the pores and allowing for insulin release. More recently, glucose-sensitive complexation gels of P(MAA-*g*-EG) were developed by the group of Peppas (176). In these gels, as the pH decreased in response to elevated glucose concentrations, interpolymer complexes formed resulting in rapid gel syneresis. The rapid collapse resulted in insulin release due to a "squeezing" phenomenon.

Other glucose responsive systems have been developed that take advantage of the formation of complexes between glucose molecules and polymeric pendent groups. Lee and Park (177) prepared erodible hydrogels containing allyl glucose and poly(vinyl pyrrolidone). These systems were cross-linked by the noncovalent associations between concanavalin-A (Con-A) and the glucose pendent groups.

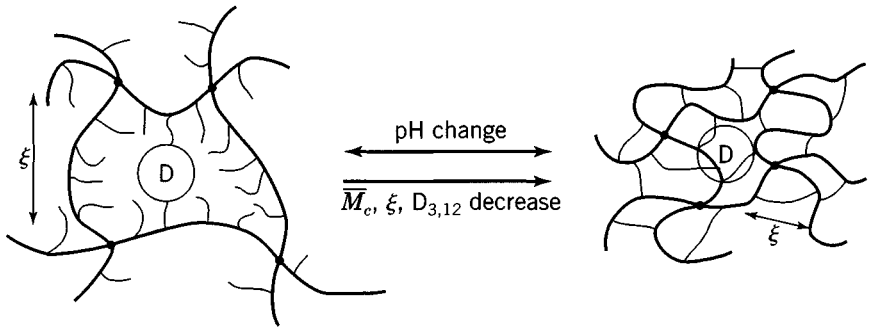


Figure 15. The effect of interpolymer complexation on the correlation length, ζ, and the effective molecular weight between cross-links, $\overline{M}_c$, in P(MAA-*g*-EG) graft copolymer networks with permanent, chemical cross-links (●).

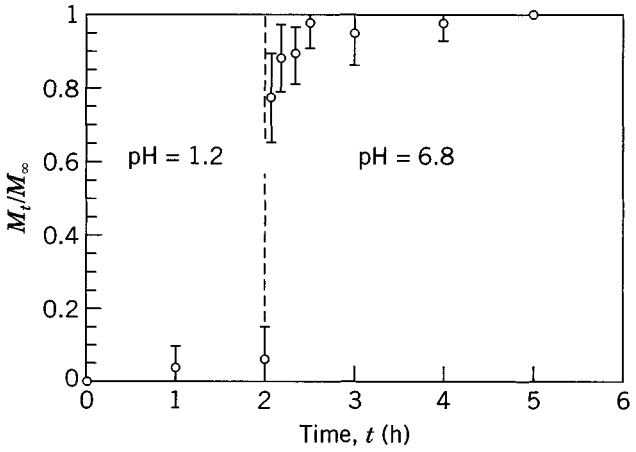


Figure 16. Controlled release of insulin in vitro from P(MAA-*g*-EG) microparticles simulated gastric fluid (pH = 1.2) for the first two hours and phosphate-buffered saline solutions (pH = 6.8) for the remaining three hours at 37°C (170).

In the presence of free glucose, the Con-A was bound to the free glucose, and the gels dissolved due to disruption of the physical cross-links. Newer materials developed by the group of Okano exhibited glucose responsive swelling behavior and insulin release (178–180). These gels were based on phenylboronic acid (PBA) and acrylamides. Another class of glucose-sensitive gels was prepared containing PBA, PNIPAAm, and PVA (181). These gels were designed to allow for the release of insulin at physiological pH and temperature.

Oral Insulin Delivery Systems

One of the major objectives of researchers working in the controlled release field is to design an effective, oral insulin delivery system. However, this is a difficult task due to the degradation of the drug in the upper gastrointestinal (GI) system barrier and the slow transport of insulin across the lining of the colon into the bloodstream (182–184). Numerous attempts have been made by researchers to use hydrogels as carriers for oral delivery of insulin in order to protect the drug in the stomach and release it into more favorable regions of the GI tract.

Touitou and Rubinstein (185) designed a reservoir system consisting of insulin encapsulated by a polyacrylate gel. The coating was designed to dissolve only in the colon. In this work, weak hypoglycemic effects were observed only with very high insulin doses and the addition of absorption enhancers. Saffran (186) developed a biodegradable hydrogel containing insulin. The device consisted of insulin dispersed in a terpolymer of styrene and PHEMA cross-linked with a difunctional azo-containing compound. The azo bond was cleaved by microflora present in the colon, and the polymer degraded, allowing for release of insulin into the colon. In this work, a hypoglycemic effect was obtained only with addition of absorption enhancers and protease inhibitors. However, the hypoglycemic effect obtained was not affected by the initial dosing.

Morishita et al. (187) administered insulin contained within Eudragit 100 gels. In these systems, the pH-responsive Eudragit® degraded in the upper small intestine, allowing for insulin release. They observed strong hypoglycemic effects in healthy and diabetic rats after the addition of absorption enhancers. Platé et al. (188) developed a hydrogel system containing immobilized insulin and protease inhibitors that was effective in lowering the blood glucose levels in rabbits. More recently, Mathiowitz et al. (189) have developed insulin containing poly(anhydride) microspheres. These materials adhered to the walls of the small intestine and released insulin based on degradation of the polymeric carrier. They observed a 30% decrease in the blood glucose levels of healthy rats. Lowman et al. (190) have developed a bioadhesive, complexation hydrogel system for oral delivery of insulin. This delivery system consisted of insulin-containing microparticles of crosslinked copolymers of P(MAA-*g*-EG). The P(MAA-*g*-EG) were more effective in delivering biologically active insulin than traditional enteric coating-type carriers because of the presence of the PEG grafts. The addition of PEG to the gels was critical because the PEG chains participate in the macromolecular complexes, function as a peptide stabilizer, and enhance the mucoadhesive characteristics of the gels. In this work, strong dose-dependent hypoglycemic effects were observed in healthy and diabetic rats following oral administration of these gels.

Other Promising Applications

Promising new methods for the delivery of chemotherapeutic agents using hydrogels have been recently reported. Novel bioreconizable sugar-containing copolymers have been investigated for the use in targeted delivery of anticancer drugs (191–193). Peterson et al. have used poly(*N*-

2-hydroxypropyl methacrylamide) carriers for the treatment of ovarian cancer (193).

In the last few years there have been new creative methods of preparation of novel hydrophilic polymers and hydrogels that may represent the future in drug delivery applications. The focus in these studies has been the development of polymeric structures with precise molecular architectures. Stupp et al. (194) synthesized self-assembled triblock copolymer, nanostructures that may have very promising applications in controlled drug delivery. Novel biodegradable polymers, such as polyrotaxanes, have been developed that have particularly exciting molecular assemblies for drug delivery (195). Dendrimers and star polymers (196) are exciting new materials because of the large number of functional groups available in a very small volume. Such systems could have tremendous promise in drug-targeting applications. Merrill (197) has offered an exceptional review of PEO star polymers and applications of such systems in the biomedical and pharmaceutical fields. Griffith and Lopina (198) have prepared gels of controlled structure and large biological functionality by irradiation of PEO star polymers. The new structures discussed in this section could have particularly promising delivery applications when combined with emerging new technologies such as molecular imprinting (199,200).

A number of investigators have concentrated on the development of environmentally responsive gels that exhibit biodegradability. This can be achieved by a number of synthetic methods. Kopecek and associates (201) have developed biodegradable hydrogels by incorporating azo compounds. Bae and associates (202) have synthesized very promising biodegradable carriers by preparing 8-arm, star-shaped, block copolymers containing PLA and PEO. Another potentially useful biodegradable system is a photo-cross-linked polymer based on poly(L-lactic acid-*co*-L-aspartic acid) (203), which could be prepared in situ for delivery of antiinflammatory drugs following surgery.

BIBLIOGRAPHY

1. N.A. Peppas, *Hydrogels in Medicine*, CRS Press, Boca Raton, Fla., 1986.
2. R. Langer and N.A. Peppas, *J. Mater. Sci.: Rev. Macromol. Chem. Phys.* **C23**(1), 61–126 (1983).
3. N.A. Peppas and D.L. Meadows, *J. Membr. Sci.* **16**, 361–377 (1983).
4. B.D. Ratner and A.S. Hoffman, in J.D. Andrade, ed., *Hydrogels for Medical and Related Applications*, American Chemical Society, Washington, D.C., 1976, pp. 1–36.
5. K. Park, *Controlled Release: Challenges and Strategies*, American Chemical Society, Washington, D.C., 1997.
6. N.A. Peppas, *Curr. Opin. Colloids Int. Sci.* **2**, 531–537 (1997).
7. N.A. Peppas and R. Langer, *Science* **263**, 1715–1720 (1994).
8. R. Baker, *Controlled Release of Biologically Active Agents*, Wiley, New York, 1987.
9. H. Park and K. Park, *Pharm. Res.* **13**, 1770–1776 (1996).
10. N.A. Peppas, *J. Bioact. Compat. Polym.* **6**, 241–246 (1991).
11. M.T. am Ende and A.G. Mikos, in L.M. Sanders and R.W. Hendren, eds., *Protein Delivery: Physical Systems*, Plenum, Tokyo, 1997, pp. 139–165.
12. V.H.L. Lee, M. Hashida, and Y. Mizushima, *Trends and Future Perspectives in Peptide and Protein Drug Delivery*, Harwood Academic Publishers, Chur, Switzerland, 1995.
13. J.A. Fix, *Pharm. Res.* **13**, 1760–1764 (1996).
14. J. Kopecek, P. Kopecková, and V. Omelyanenko, in N. Ogata, S.W. Kim, J. Feijen, and T. Okano, eds., *Biomedical and Drug Delivery Systems*, Springer, Tokyo, 1996, pp. 91–95.
15. N.A. Peppas and A.G. Mikos, in N.A. Peppas, ed., *Hydrogels in Medicine and Pharmacy*, vol. 1, CRC Press, Boca Raton, Fla., 1986, pp. 1–25.
16. N.A. Peppas and B.D. Barr-Howell, in N.A. Peppas, ed., *Hydrogels in Medicine and Pharmacy*, vol. 1, CRC Press, Boca Raton, Fla., 1986, pp. 27–55.
17. P.J. Flory and J. Rehner, *J. Chem. Phys.* **11**, 521–526 (1943).
18. P.J. Flory, *Principles of Polymer Chemistry*, Cornell University Press, Ithaca, N.Y., 1953.
19. N.A. Peppas and E.W. Merrill, *J. Polym. Sci., Polym. Chem. Ed.*, **14**, 441–457 (1976).
20. J. Ricka and T. Tanaka, *Macromolecules* **17**, 2916–2921 (1984).
21. A. Katchalsky, *Experientia* **5**, 319–320 (1949).
22. T. Tanaka, *Polymer* **20**, 1404–1412 (1979).
23. M. Rubinstein, R.H. Colby, A.V. Dobrynin, and J.F. Joanny, *Macromolecules* **29**, 398–426 (1996).
24. U.P. Schroder and W. Opperman, in J.P. Cohen-Addad, ed., *The Physical Properties of Polymeric Gels*, Wiley, New York, 1996, pp. 19–38.
25. R. Skouri, F. Schoesseler, J.P. Munch, and S.J. Candau, *Macromolecules* **28**, 197–210 (1995).
26. L. Brannon-Peppas and N.A. Peppas, *Chem. Eng. Sci.* **46**, 715–722 (1991).
27. L. Brannon-Peppas and N.A. Peppas, in L. Brannon-Peppas and R.S. Harland, eds., *Absorbent Polymer Technology*, Elsevier, Amsterdam, 1990, pp. 67–75.
28. R.G. Treloar, *The Physics of Rubber Elasticity*, 2nd ed., Oxford University Press, Oxford, 1958.
29. N.A. Peppas and E.W. Merrill, *J. Appl. Polym. Sci.* **21**, 1763–1770 (1977).
30. A.M. Lowman and N.A. Peppas, *Macromolecules* **30**, 4959–4965 (1997).
31. K.S. Anseth, C.N. Bowman, and L. Brannon-Peppas, *Biomaterials* **17**, 1647–1657 (1996).
32. J.E. Mark, *Adv. Polym Sci.* **44**, 1–26 (1982).
33. R.S. Stock and W.H. Ray, *J. Polym. Sci., Polym. Phys. Ed.* **23**, 1393–1447 (1985).
34. D.N. Winslow, in E. Matijevic and R.J. Good, eds., *Surface and Colloid Science*, Plenum, New York, 1984, pp. 259–282.
35. A.G. Mikos et al., *J. Biomed. Mater. Res.* **27**, 183–189 (1993).
36. T. Canal and N.A. Peppas, *J. Biomed. Mater. Res.* **23**, 1183–1193 (1989).
37. B. Narasimhan and N.A. Peppas, in K. Park, ed., *Controlled Drug Delivery*, American Chemical Society, Washington, D.C., 1997, pp. 529–557.
38. J. Crank, *The Mathematics of Diffusion*, Oxford University Press, Oxford, 1956.
39. P.L. Ritger and N.A. Peppas, *J. Controlled Release* **5**, 23–26 (1987).
40. H. Fujita, *Fortschr. Hochpolym.-Forsch.* **3**, 1–14 (1961).
41. F.G. Smith, III and W.M. Deen, *J. Colloid Interface Sci.* **78**, 444–465 (1980).

42. D.M. Malone and J.L. Quinn, *Chem. Eng. Sci.* **33**, 1429–1440 (1978).
43. J.L. Anderson and J.A. Quinn, *Biophys. J.* **14**, 130–150 (1974).
44. W.M. Deen, *AIChE J.* **33**, 1409–1425 (1987).
45. J.D. Ferry, *Viscoelastic Properties of Polymers*, Wiley, New York, 1980.
46. H. Yasuda et al., *Makromol. Chem.* **126**, 177–186 (1969).
47. H. Yasuda and C.E. Lamaze, *J. Macromol. Sci., Phys.* **B5**, 111–134 (1971).
48. N.A. Peppas and C.T. Reinhart, *J. Membr. Sci.* **15**, 275–287 (1983).
49. C.T. Reinhart and N.A. Peppas, *J. Membr. Sci.* **18**, 227–239 (1984).
50. A.P. Sassi, H.W. Blanch, and J.M. Prausnitz, *J. Appl. Polym. Sci.* **59**, 1337–1346 (1996).
51. N.A. Peppas and H.J. Moynihan, *J. Appl. Polym. Sci.* **30**, 2589–2606 (1985).
52. R.S. Harland and N.A. Peppas, *Colloid Polym. Sci.* **267**, 218–225 (1989).
53. N.A. Peppas and R.W. Korsmeyer, in N.A. Peppas, ed., *Hydrogels in Medicine and Pharmacy*, vol. 3, CRC Press, Boca Raton, Fla., 1987, pp. 103–135.
54. A.R. Berens and H.B. Hofenberg, *Polymer* **19**, 490–496 (1978).
55. P. Stilbs, *Prog. NMR Spectrosc.* **19**, 1–45 (1987).
56. F.P. Price, P.T. Gilmore, E.L. Thomas, and R.L. Laurence, *J. Polym. Sci., Polym. Symp.* **63**, 33–44 (1978).
57. J.J. Sahlin and N.A. Peppas, *J. Biomater. Sci., Polym. Ed.* **8**, 421–436 (1997).
58. J. Heller and R.W. Baker, in R.W. Baker, ed., *Controlled Release of Bioactive Materials*, Academic Press, New York, 1980, pp. 1–37.
59. J. Heller, in J.M. Anderson and S.W. Kim, eds., *Advances in Drug Delivery Systems*, Plenum, New York, 1984, pp. 101–154.
60. N.A. Peppas, in R. Gurny, H.E. Juninger, and N.A. Peppas, eds., *Pulsatile Drug Delivery*, Wiss. Verlagsgese., Stuttgart, 1993, pp. 41–56.
61. R.A. Siegel, in K. Park, ed., *Controlled Drug Delivery*, American Chemical Society, Washington, D.C., 1997, pp. 1–27.
62. S.W. Kim, in N. Ogata, S.W. Kim, J. Feijen, and T. Okano, eds., *Advanced Biomaterials in Biomedical Engineering and Drug Delivery Systems*, Springer, Tokyo, 1996, pp. 125–133.
63. E.A. Bekturov and L.A. Bimendina, *Adv. Polym. Sci.* **43**, 100–147 (1981).
64. J. Heller, in J. Kost, ed., *Pulsed and Self-Regulated Drug Delivery Systems*, CRC Press, Boca Raton, Fla., 1990, pp. 93–122.
65. R. Langer, *Science* **249**, 1527–1533 (1990).
66. E.R. Edelman, J. Kost, H. Bobech, and R. Langer, *J. Biomed. Mater. Res.* **19**, 67–74 (1985).
67. W.R. Good, in R. Kostelnik, ed., *Polymeric Delivery Systems*, Gordon & Breach, New York, 1976, pp. 139–155.
68. H.B. Hopfenberg and K.C. Hsu, *Polym. Eng. Sci.* **18**, 1186 (1978).
69. J.M. Anderson et al., in J.D. Andrade, ed., *Hydrogels for Medical and Related Applications*, American Chemical Society, Washington, D.C., 1976, pp. 167–178.
70. M. Sefton and E. Nishimura, *J. Pharm. Sci.* **69**, 208–213 (1980).
71. S.Z. Song, J.R. Cardinal, S.H. Kim, and S.W. Kim, *J. Pharm. Sci.* **67**, 1352 (1981).
72. P.I. Lee, *Polymer* **25**, 973 (1984).
73. P.I. Lee, *J. Controlled Release* **73**, 1344 (1986).
74. N.M. Franson and N.A. Peppas, *J. Appl. Polym. Sci.* **28**, 1299 (1983).
75. G.W.R. Davidson and N.A. Peppas, *J. Controlled Release* **3**, 243 (1986).
76. R.W. Korsmeyer and N.A. Peppas, *J. Controlled Release* **89**, 1–9 (1984).
77. N.A. Peppas, in N.A. Peppas, ed., *Hydrogels in Medicine and Pharmacy*, vol. 2, CRC Press, Boca Raton, Fla., 1987, pp. 1–48.
78. R. Langer and J. Folkman, *Nature (London)* **263**, 970–974 (1976).
79. N.A. Peppas, *Makromol. Chem.* **176**, 3433–3440 (1975).
80. R. Korsmeyer and N.A. Peppas, *J. Membr. Sci.* **9**, 211–227 (1981).
81. K. Morimoto et al., *Pharm. Res.* **6**, 338–344 (1989).
82. N.A. Peppas and P.J. Hansen, *J. Appl. Polym. Sci.* **27**, 4787–4797 (1982).
83. F. Urushizaki, H. Yamaguchi, K. Nakamura, and S. Numajiri, *Int. J. Pharm.* **58**, 135–142 (1990).
84. N.A. Peppas and R.S. Stauffer, *J. Controlled Release* **16**, 305–310 (1991).
85. N.A. Peppas and J.E. Scott, *J. Controlled Release* **18**, 95–100 (1992).
86. B.J. Ficek and N.A. Peppas, *J. Controlled Release* **27**, 259–264 (1993).
87. K. Tsutsumi et al., *S.T.P. Pharm. Sci.* **4**, 230–236 (1994).
88. N.A. Peppas and N.K. Mongia, *Eur. J. Pharm. Biopharm.* **43**, 51–58 (1997).
89. N.K. Mongia, K.S. Anseth, and N.A. Peppas, *J. Biomater. Sci., Polym. Ed.* **7**, 1055–1064 (1996).
90. S.K. Mallapragada and N.A. Peppas, *J. Controlled Release* **45**, 87–94 (1997).
91. S.K. Mallapragada and N.A. Peppas, *AIChE J.* **43**, 870–876 (1997).
92. N.A. Peppas and P. Colombo, *J. Controlled Release* **45**, 35–40 (1997).
93. B. Narasimhan and N.A. Peppas, *J. Pharm. Sci.* **86**, 297–304 (1997).
94. N.B. Graham, in J.M. Harris, ed., *Poly(Ethylene Glycol) Chemistry, Biotechnical and Biomedical Applications*, Plenum, New York, 1992, pp. 263–281.
95. M.E. McNeill and N.B. Graham, *J. Controlled Release* **1**, 99–107 (1984).
96. M.E. McNeill and N.B. Graham, *J. Biomater. Sci., Polym. Ed.* **7**, 937–951 (1996).
97. L. Bromberg, *J. Appl. Polym. Sci.* **59**, 459–466 (1996).
98. J.L. Stringer and N.A. Peppas, *J. Controlled Release* **42**, 195–202 (1996).
99. P. Kofinas, V. Athanassiou, and E.W. Merrill, *Biomaterials* **17**, 1547–1550 (1996).
100. A.M. Lowman, T.D. Dziubla, and N.A. Peppas, *Polym. Prepri.* **38**, 622–623 (1997).
101. K.B. Keys, F.M. Andreopoulos, and N.A. Peppas, *Macromolecules* **31**, 8149–8156 (1998).
102. N.A. Peppas, *J. Biomater. Sci., Polym. Ed.* **9**, 535–542 (1998).
103. L.M. Schwarte and N.A. Peppas, *Polymer* **39**, 6057–6066 (1998).

104. H. Ichikawa and N.A. Peppas, *Polym. Prepri.* **40**, 363–364 (1999).
105. A.B. Scranton, B. Rangarajan, and J. Klier, *Adv. Polym. Sci.* **120**, 1–54 (1995).
106. W. Oppermann, in R.S. Harland and R.K. Prud'homme, eds., *Polyelectrolyte Gels: Properties, Preparation, and Applications*, American Chemical Society, Washington, D.C., 1992, pp. 159–170.
107. R.A. Siegel and B.A. Firestone, *Macromolecules* **21**, 3254–3259 (1988).
108. B.A. Firestone and R.A. Siegel, *Polym. Commun.* **29**, 204–208 (1988).
109. R.A. Siegel, M. Falamarzian, B.A. Firestone, and B.C. Moxley, *J. Controlled Release* **8**, 179–182 (1988).
110. J.M. Cornejo-Bravo and R.A. Siegel, *Biomaterials* **17**, 1187–1193 (1996).
111. R.A. Siegel, in J. Kost, ed., *Pulsed and Self-Regulated Drug Delivery*, CRC Press, Boca Raton, Fla., 1990, pp. 129–155.
112. D. Hariharan and N.A. Peppas, *Polymer* **37**, 149–161 (1996).
113. N.A. Peppas and D. Hariharan, *Bull. Gattefosse Rep.* **84**, 29–36 (1991).
114. A. Gutowska, Y.H. Bae, J. Feijen, and S.W. Kim, *J. Controlled Release* **22**, 95–104 (1992).
115. L.M. Schwarte and N.A. Peppas, *Polym. Prepr.* **38**(2), 596–597 (1997).
116. L. Brannon-Peppas and N.A. Peppas, *Biomaterials* **11**, 635–640 (1990).
117. J.H. Kou, G.L. Almidon, and P.I. Lee, *Pharm. Res.* **5**, 592–597 (1988).
118. L. Brannon-Peppas and N.A. Peppas, *Int. J. Pharm.* **70**, 53–57 (1991).
119. L. Brannon-Peppas and N.A. Peppas, *J. Controlled Release* **16**, 319–330 (1991).
120. R. Bettini, P. Colombo, and N.A. Peppas, *J. Controlled Release* **37**, 105–111 (1995).
121. L. Brannon-Peppas and N.A. Peppas, *J. Controlled Release* **8**, 267–274 (1989).
122. A.R. Khare and N.A. Peppas, *J. Biomater. Sci., Polym. Ed.* **4**(3), 275–289 (1993).
123. M.T. am Ende and N.A. Peppas, *J. Controlled Release* **48**, 47–56 (1997).
124. L.F. Gudeman and N.A. Peppas, *J. Membr. Sci.* **107**, 239–248 (1995).
125. N.A. Peppas and S.L. Wright, *Macromolecules* **29**, 8798–8804 (1996).
126. M.T. am Ende and N.A. Peppas, *Pharm. Res.* **12**, 2030–2035 (1995).
127. J. Heller, A.C. Chang, G. Rodd, and G.M. Grodsky, *J. Controlled Release* **11**, 193–201 (1990).
128. R. Bodmeier and O. Paeratakul, *J. Pharm. Sci.* **78**, 964–969 (1989).
129. S. Shiraishi, T. Imai, and M. Otagiri, *J. Controlled Release* **25**, 217–223 (1993).
130. K. Yao et al., *J. Appl. Polym. Sci.* **48**, 343–348 (1993).
131. P. Calvo, C. Remuñán-López, J.L. Vila-Jato, and M.J. Alonso, *J. Appl. Polym. Sci.* **63**, 125–132 (1997).
132. R. Narayani and K. Panduranga Rao, *J. Appl. Polym. Sci.* **58**, 1761–1769 (1995).
133. A. Kikuchi et al., *J. Controlled Release* **47**, 21–29 (1997).
134. S. Hirotsu, Y. Hirokawa, and T. Tanaka, *J. Chem. Phys.* **87**, 1392–1395 (1987).
135. S. Beltran et al., *Macromolecules* **24**, 549–551 (1991).
136. L.C. Dong and A.S. Hoffman, *J. Controlled Release* **13**, 21–31 (1990).
137. B.G. Kabra and S.H. Gehrke, *Polym. Commun.* **32**, 322–323 (1991).
138. R. Yoshida et al., *Nature (London)* **374**, 240–242 (1995).
139. Y. Kaneko et al., *Macromol. Symp.* **109**, 41–53 (1996).
140. A.S. Hoffman, *J. Controlled Release* **6**, 297–305 (1987).
141. T. Okano, Y.H. Bae, H. Jacobs, and S.W. Kim, *J. Controlled Release* **11**, 255–265 (1990).
142. Y.H. Bae, T. Okano, and S.W. Kim, *J. Controlled Release* **9**, 271–276 (1989).
143. R. Yoshida et al., *J. Controlled Release* **32**, 97–102 (1994).
144. M. Matsukata et al., *Bioconjugate Chem.* **7**, 96–101 (1996).
145. B. Vernon, A. Gutowska, S.W. Kim, and Y.H. Bae, *Macromol. Symp.* **109**, 155–167 (1996).
146. L.C. Dong, Q. Yan, and A.S. Hoffman, *J. Controlled Release* **19**, 171–178 (1992).
147. H. Feil, Y.H. Bae, and S.W. Kim, *Macromolecules* **25**, 5528–5530 (1992).
148. Y.H. Kim, Y.H. Bae, and S.W. Kim, *J. Controlled Release* **28**, 143–152 (1994).
149. A. Serres, M. Baudyš, and S.W. Kim, *Pharm. Res.* **13**(2), 196–201 (1996).
150. Y. Nabeshima et al., in N. Ogata, S.W. Kim, J. Feijen, and T. Okano, eds., *Advanced Biomaterials in Biomedical Engineering and Drug Delivery Systems*, Springer, Tokyo, 1996, pp. 315–316.
151. G.H. Chen and A.S. Hoffman, *Nature (London)* **373**, 49–52 (1995).
152. A.S. Hoffman et al., in N. Ogata, S.W. Kim, J. Feijen, and T. Okano, eds., *Advanced Biomaterials in Biomedical Engineering and Drug Delivery Systems*, Springer, Tokyo, 1996, pp. 62–66.
153. C.S. Brazel and N.A. Peppas, *Macromolecules* **28**, 8016–8020 (1995).
154. C.S. Brazel and N.A. Peppas, *J. Controlled Release* **39**, 57–64 (1996).
155. J.P. Baker and R.A. Siegel, *Macromol. Rapid Commun.* **17**, 409–415 (1996).
156. S.K. Vakkalanka and N.A. Peppas, *Polym. Bull.* **36**, 221–225 (1996).
157. S.K. Vakkalanka, C.S. Brazel, and N.A. Peppas, *J. Biomater. Sci. Polym. Ed.* **8**, 119–129 (1996).
158. Y. Osada, *J. Polym. Sci., Polym. Lett. Ed.* **18**, 281–286 (1980).
159. Y. Osada, K. Honda, and M. Ohta, *J. Membr. Sci.* **27**, 339–347 (1986).
160. S. Nishi and T. Kotaka, *Macromolecules* **19**, 978–984 (1986).
161. J. Byun, Y.M. Lee, and C.S. Cho, *J. Appl. Polym. Sci.* **61**, 697–702 (1996).
162. H.S. Shin, S.Y. Kim, and Y.M. Lee, *J. Appl. Polym. Sci.* **65**, 685–693 (1997).
163. J. Klier, A.B. Scranton, and N.A. Peppas, *Macromolecules* **23**, 4944–4949 (1990).
164. N.A. Peppas and J. Klier, *J. Controlled Release* **16**, 203–214 (1991).
165. C.L. Bell and N.A. Peppas, *J. Biomater. Sci., Polym. Ed.* **7**, 671–683 (1996).
166. C.L. Bell and N.A. Peppas, *Biomaterials* **17**, 1203–1218 (1996).

167. C.L. Bell and N.A. Peppas, *J. Controlled Release* **39**, 201–207 (1997).
168. C.L. Bell and N.A. Peppas, *Adv. Polym. Sci.* **122**, 125–175 (1995).
169. N.A. Peppas and A.M. Lowman, in S. Frøkjaer, L. Christup, and P. Krogsgaard-Larsen, eds., *Peptide and Protein Delivery*, Alfred Benzon Symposium, Munksgaard, Copenhagen, 1998, pp. 206–216.
170. A.M. Lowman, N.A. Peppas, M. Morishita, and T. Nagai, in I. McCullough and S. Shalaby, eds., *Tailored Polymeric Materials for Controlled Delivery Systems*, American Chemical Society, Washington, D.C., 1998, pp. 156–164.
171. J. Kost, T.A. Horbett, B.D. Ratner, and M. Singh, *J. Biomed. Mater. Res.* **19**, 1177–1133 (1984).
172. K. Ishihara, M. Kobayashi, and I. Shinohara, *Polym. J.* **16**, 625–631 (1984).
173. G. Albin, T.A. Horbett, and B.D. Ratner, *J. Controlled Release* **2**, 153–164 (1985).
174. M. Goldraich and J. Kost, *Clin. Mater.* **13**, 135–142 (1993).
175. Y. Ito, M. Casolaro, K. Kono, and Y. Imanishi, *J. Controlled Release* **10**, 195–203 (1989).
176. C.M. Hassan, F.J. Doyle, and N.A. Peppas, *Macromolecules* **30**, 6166–6173 (1997).
177. S.J. Lee and K. Park, *Polym. Prepr.* **35**(2), 391–392 (1994).
178. D. Shiino et al., *J. Controlled Release* **37**, 269–276 (1995).
179. D. Shiino et al., *J. Biomater. Sci. Polym. Ed.* **7**(8), 697–705 (1996).
180. T. Aoki et al., *Polym. J.* **28**(4), 371–374 (1996).
181. Hisamitsu, K. Kataoka, T. Okano, and Y. Sakurai, *Pharm. Res.* **14**(3), 289–293 (1997).
182. M. Saffran, B. Pansky, G.C. Budd, and F.E. Williams, *J. Controlled Release* **46**, 89–98 (1997).
183. V.H.L. Lee, S. Dodd-Kashi, G.M. Grass, and W. Rubas, in V.H.L. Lee, ed., *Protein and Peptide Drug Delivery*, Dekker, New York, 1991, pp. 691–740.
184. M. Saffran, in D.R. Friend, ed., *Oral Colon-Specific Drug Delivery*, CRC Press, Boca Raton, Fla., 1992, pp. 115–142.
185. E. Touitou and A. Rubinstein, *Int. J. Pharm.* **30**, 93–99 (1986).
186. M. Saffran et al., *Science* **233**, 1081–1084 (1986).
187. I. Morishita et al., *Int. J. Pharm.* **78**, 9–16 (1992).
188. N.A. Platé et al., *Vysokomol. Soedin.* **36**, 1876–1879 (1994).
189. E. Mathiowitz et al., *Nature (London)* **386**, 410–414 (1997).
190. M. Morishita et al., Yakuzaigaku **57**, 96–97 (1997).
191. R.C. Rathi, P. Kopecková, and J. Kopecek, *Macromol. Chem. Phys.* **198**, 1–16 (1997).
192. D.A. Putnam, J.G. Shiah, and J. Kopecek, *Biochem. Pharmacol.* **52**, 957–962 (1996).
193. C.M. Peterson et al., *Cancer Res.* **56**, 3980–3985 (1996).
194. S.I. Stupp et al., *Science* **276**, 384–389 (1997).
195. T. Ooya and N. Yui, *J. Biomater. Sci., Polym. Ed.* **8**, 437–445 (1997).
196. P.R. Dvornik and D.A. Tomalia, *Curr. Opin. Colloid Interface Sci.* **1**, 221–235 (1996).
197. E.W. Merrill, *J. Biomater. Sci., Polym. Ed.* **5**, 1–11 (1993).
198. L. Griffith and S.T. Lopina, *Macromolecules* **28**, 6787–6794 (1995).
199. K. Mosbach and O. Ramström, *Bio / Technology* **14**, 163–170 (1996).
200. S.H. Cheong et al., *Macromolecules* **30**, 1317–1322 (1997).
201. H. Ghandehari, P. Kopecková, P.Y. Yeh, and J. Kopecek, *Macromol. Chem. Phys.* **197**, 965–980 (1996).
202. Y.K. Choi, S.W. Kim, and Y.H. Bae, *Polym. Prepr.* **37**, 109–110 (1996).
203. J. Elisseeff, K. Anseth, R. Langer, and J.S. Hrkach, *Macromolecules* **30**, 2182–2184 (1996).

IMMUNOISOLATED CELL THERAPY

MICHAEL J. LYSAGHT
Brown University
Providence, Rhode Island
PATRICK AEBISCHER
University of Lausanne Medical School
Lausanne, Switzerland

KEY WORDS

Artificial liver
Artificial pancreas
Bioartificial xenograft
Encapsulation
Gene therapy
Macrocapsule
Membrane
Matrix
Microcapsule

OUTLINE

Introduction
Biomaterials and Cells for Immunoisolation
  Membranes
  Matrix
  Cells
  Implant Design
Therapeutic Applications of Immunoisolation
  Alleviation of Chronic Pain
  Support of the Failing Liver
  Parkinson's Disease
  Delivery of Gene Therapy
  The Artificial Pancreas
Concluding Perspectives
Acknowledgments
Additional Reading

INTRODUCTION

In the late twentieth century, biomedical engineers and clinicians have increasingly adopted what may be termed the fundamental tenet of substitutive medicine: it is frequently the wiser choice to simply replace a failing organ than to struggle with attempts at repair and restoration. Such replacement can sometimes be accomplished with organ transplantation but more frequently relies upon man-made devices such as hemodialyzers, blood oxygenators, mechanical heart valves, pacemakers, and artificial hips or knees.

Transplanted organs more closely replicate natural function but are constrained in supply and require pharmacological immunosuppression. *Artificial organs* can be manufactured in large quantities and require no immunosupression but rarely offer the full functional capability of their natural counterparts. In the early seventies Dr. William Chick, who passed away in 1998, proposed a third approach to organ replacement: biohybrid organs, which combined living tissue and biomaterials into a single therapeutic device. Chick's primary interest was in the development of an artificial pancreas in which living cells were separated from the host by a selective membrane barrier. A satisfactory artificial pancreas still remains an elusive target, but immunoisolation, as this approach is now called, has provided the enabling technology for the development of a diverse collection of novel medical therapeutics. It has become a promising route to the delivery of gene therapy, and it offers the largest successful clinical experience thus far with the xenotransplantation of living animal-derived tissue into human hosts.

The concept of immunoisolation is illustrated in Figure 1. Living cells are ensconced in a supporting matrix and surrounded by a semipermeable membrane, which supports the transport of small molecules (oxygen, nutrients, and electrolytes) while restricting the passage of large molecules (immunoglobulins) and cells. The membrane is a mechanical analogue of pharmacological immunosupression. Both thwart the normally lethal response of a host immune system to foreign living tissue, albeit by different mechanisms. One important difference is that immunoisolatory membranes can often protect transplanted xenogeneic grafts (i.e., those originating in a different species than the recipient) whereas presently available immunosupressive drugs cannot. Table 1 lists some of the more important classes of membranes, matrices, and cells used in immunoisolation over the past two decades. As the therapy developed, membranes and matrices have steadily evolved, but the types and classes of cells have changed dramatically. These advances in exploitation of cell and molecular biology have transformed immunoisolation from a specialized approach to a bioartificial pancreas to a multifaceted technology of potential utility whenever long-term site-specific protein delivery is required.

BIOMATERIALS AND CELLS FOR IMMUNOISOLATION

Membranes

Membranes are simply thin barriers capable of providing selective transport between adjacent phases. Synthetic biocompatible membranes are widely used in today's hemodialyzers, blood oxygenators, and plasma filters. With over 100 million hemodialyzers produced each year, the technology of medical-grade membranes has become highly advanced. The membranes most often used for immunoisolation are open-cell foams cast in the form of thin capillaries or "hollow fibers." These structures are made from thermoplastics such as polysulfone or acrylic copolymers. Fiber diameter is typically 500 to 1000 μm and a wall

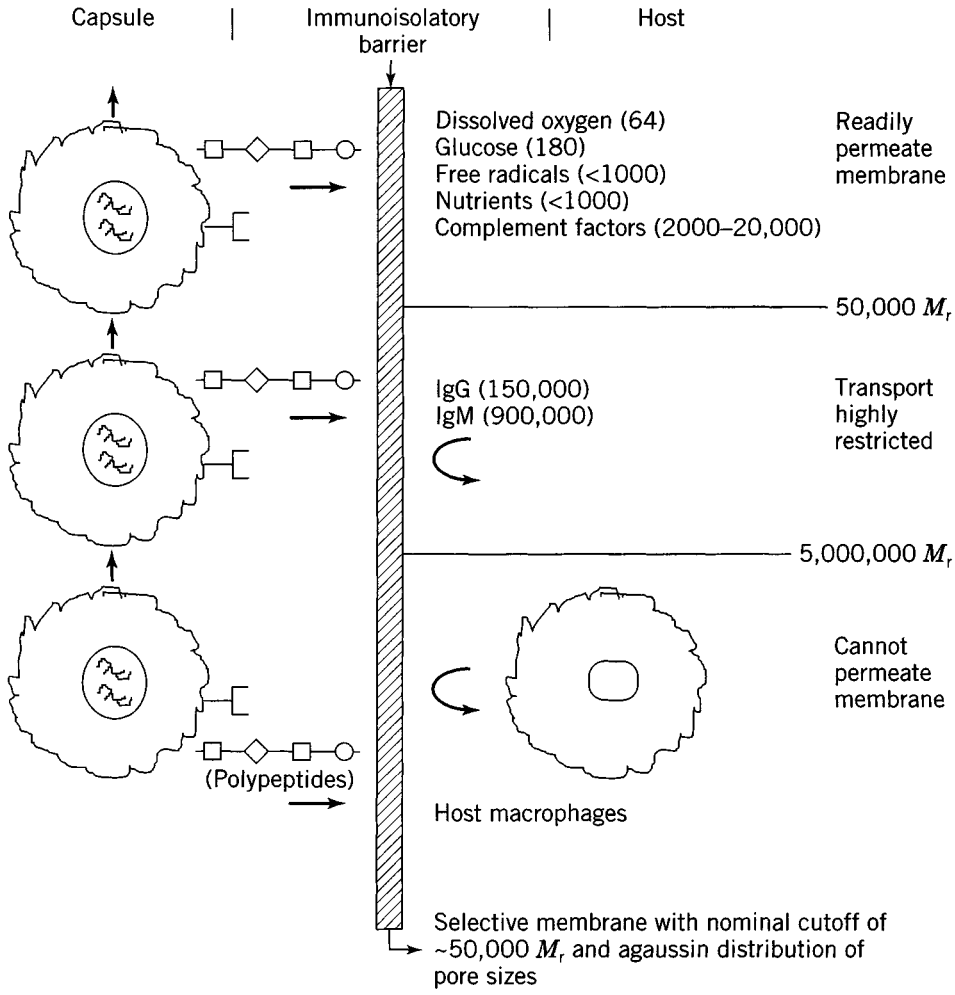


Figure 1. Immunoisolated cell therapy relies upon a membrane to separate foreign secretory cells from a host. Molecules secreted by the cells, usually proteins, can pass through the membrane if they are smaller than 50,000 M_r. In similar fashion, oxygen glucose and molecules such as insulin can diffuse from the host to the cells. However, the membrane blocks the passage of host cells and restricts transport of host immunoglobulins. Membranes allow passage of complement factors and free radicals that appear to be generated primarily when an implant containing xenogeneic cells is directly implanted into host tissue.

thickness of about 15% of the diameter. In recent years, the physical strength of membranes for immunoisolation has been increased by adding metallic or polymeric supports. The composite structures are several thousand times as strong as hemodialysis membranes with comparable dimensions. Some investigators prefer to use a different kind of membrane prepared by the interfacial polymerization of weak polyelectrolytes. Typically, cells are suspended in a droplet containing an aqueous solution of alginate. Alginate is a naturally occurring polymer derived from seaweed, which contains a slight positive charge. The droplet is then bathed in a solution containing polylysine, a synthetic, negatively charged polypeptide. The two polymers react and the resultant film encapsulates the cell in a droplet with a diameter of about 500 μm. A third approach, still in development, applies a conformal coating of photopolymerizable acrylic film on the surface of cells or clusters of cells.

Membranes formulated to allow permeation of molecules as large as proteins while preventing passage of cells are termed microporous. Membranes capable of discriminating between small and large molecules are called semipermeable. As a general rule, microporous membranes are used with allogeneic cells and semipermeable membranes with xenogeneic membranes. It is important to recognize that molecularly separative membranes contain a distribution of pore sizes and function as relative, rather than absolute, barriers to the transport of higher molecular species. A membrane with a nominal molecular weight cutoff of 50,000 daltons rejects well over 99% of IgG (60,000 daltons) or IgM (950,000 daltons) in a challenge solution but still permits passage of a very small fraction of the presenting immunoglobulins.

Matrix

Cells in a capsule are usually supported on a matrix. First-generation matrices were prepared from gelled versions of the same polymers used to coat tissue culture dishes: alginate, agarose, or collagen. Such matrices were weak with a jellylike morphology. More recently, matrices have been prepared not as gels but as scaffolds or macroreticulated foams made from plastic resins, which are sometimes coated with water-soluble polymers. These highly tailored materials are more stable and lead to mechanically stronger implants than earlier gels.

Cells

The first generation of cell technology for immunoisolation involved primary cells, which had been harvested from a

Table 1. Elements of an Immunoisolatory Implant

	Cells
Primary	Islets, hepatocytes, adrenal chromaffin cells
Dividing	Cell lines, such as PC-12 cells which secrete dopamine
Engineered	Cell lines which have received the gene for proteins like factor VIII or EPO
Tailored	Engineered cells which also contain complement restriction factors, antiapoptotic genes, and which may be conditionally immortalized to reduce immunogenicity.
	Matrices
Hydrogels	Natural polymers such as alginate or collagen
Scaffolds	Urethane foams
	Membranes
Hemodialysis membranes	Polysulfone, PAN-VC with cutoff around 50,000 daltons
Weak polyelectrolysis	Films of polylysine and alginate
Conformal	Adherent surface coating
Microporous	Freely permeable to proteins (allograft only)
Reinforced	Membranes cast on a reinforcing structure

donor, isolated, and purified. Since transplant-quality human cells, like human organs, are exceedingly scarce, investigators turned to porcine or bovine sources. Tissue was usually broken down into single-cell suspensions. For the pancreas, cells were maintained as islets, clusterlike organoids containing several thousand insulin-producing β cells. Primary cells were true transplants; the graft originated in a living donor. The second class of cells to be developed for encapsulation was dividing cells from immortalized cell lines. Here, grafted cells originated in tissue culture flasks or in bioreactors. For example, the well-established PC-12 cell line was used to form capsules that secreted dopamine for the treatment of experimental Parkinson's disease. Of course, dividing cells did not continue to multiply indefinitely inside a capsule. Rather they reached a numerically stable population set by the carrying capacity of the capsule. Dividing cell lines vastly simplified the procurement of uniform stable populations of cells and fit in well with cell-banking techniques in widespread use in the biopharmaceutical industry. But only a few cell lines producing therapeutically useful products were available. So the next step was to engineer dividing cells so by adding the genes necessary to produce a desired protein. Engineered cells could be selected for high output (upwards of 1,000 ng/24h-million cells) and could be engineered to produce virtually any protein whose gene was available. More recently, genetic engineering has been employed for a different purpose: cells are being fine-tuned at the molecular level for their future life inside an immunoisolatory capsule. Using strategies borrowed from whole organ xenotransplantation, restriction factors have been added to the surface of grafts reducing their susceptibility to host complement. And antiapoptotic genes have been incorporated into the cell genome to enhance both performance and survival under the low-oxygen and nutrient-scarce environment that awaits cells after encapsulation. Investigators are also attempting to develop cell lines with a simple chemical switch capable of turning on and off proliferation to allow large-scale expansion of a cell line, which would not subsequently divide, inside a capsule.

Implant Design

A wide variety of designs has been advanced to combine cell, matrix, and membrane into a device suitable for implantation. Designs vary widely but in all cases the maximum distance of a grafted cell from host is 200 to 500 μm. Cells further away from their ultimate source of nutrients and electrolytes simply fail to thrive. Several additional considerations apply to the selection of device design. Small beads or "microcapsules" have the optimal ratio of surface area to volume and require no redesign when scaling from small animal models to larger species. But once implanted they cannot be retrieved, and microcapsules do not conform readily to conventional medical-device or pharmaceutical quality assurance protocols. Larger implants or "macrocapsules" contain the entire therapeutic dose in a single device. These may be in the form of a sandwich of flat sheet membranes sealed at the periphery or a capillary sealed at the ends. These devices have the look and the feel of medical grade implants. They can be tested for membrane and seal integrity and some designs can be even be filled, or refilled, after implantation. All can be retrieved, and this feature facilitates the regulatory approval process. However, these designs are limited in the number of cells which can be contained in a practical design to around 5 million for a capillary device and around 100 million for a flat sheet device. Moreover, species scaling is complex. Consider the fact that a typical human weighs about 3,000 times more than a laboratory mouse, and it is problematic to make an implantable device 3,000 times larger, especially while not exceeding a thickness limitation of 500–1,000 μm. Flow-through designs, whether implantable or extracorporeal, draw heavily upon the technology already employed in available membrane devices such as hemodialyzers, blood oxygenators, and plasma filters. They have very large capacity and can hold several grams of foreign tissue if desired. Some designs incorporate a second set of fibers to provide oxygen to the mass of cells. Flow-through devices are well suited for use in extracorporeal circuits. But current flow-through implants are far more invasive than passive diffusion designs and require both surgical breaches of the host vasculature and lifelong, low-level anticoagulation.

THERAPEUTIC APPLICATIONS OF IMMUNOISOLATION

Serious preclinical and clinical evaluation of immunoisolation began early in the 1990s. Funding availability, investigative resourcefulness, and simple happenstance

have all contributed the relative rates of progress of the different applications, but the pacing item has usually been the type of cell required. Pain control and liver support both use primary cells; they have little else in common but both have moved into advanced clinical trials. In contrast, applications involving engineered cells and the delivery of gene therapy continue to offer enormous promise but remain earlier in their development. Engineered cells releasing ciliary derived neurotrophic factor (CNTF) have been studied in small-scale clinical trials for neurodegenerative diseases such as amyotrophic lateral sclerosis (ALS) and Huntington disease, but most gene therapy applications are still at the preclinical stage of development. And despite its formative role in the field, a clinically useful bioartificial pancreas remains an unfulfilled goal.

Alleviation of Chronic Pain

The implant used for chronic pain comprises a short length of hollow fiber is filled with chromaffin cells harvested from calf adrenal glands. Adrenal chromaffin cells, so called because of their affinity for certain dyes, secrete the body's natural analgesics. These natural biochemicals are known to moderate pain by a variety of mechanisms including a partial blockage of the presynaptic release of the neurotransmitters required to send pain impulses from one neuron to the next. Prior to human evaluation, encapsulated chromaffin cell implants were shown to be highly effective in animal models of both acute and chronic pain. Device design and implant technique, which is analogous to a spinal tap, were finalized in sheep. The spinal column was chosen as the implant site because it provides an ideal anatomical location to intercept nerve impulses travelling from the peripheral to the central nervous system. The site is immunopriviliged and further allows the implant to be bathed in cerebrospinal fluid. The safety of the implant and its ability to maintain cell viability and secretory function has been confirmed in detailed animal models, a preliminary clinical investigation, and a Phase I clinical trial. The more than 100 patients in these series represent the most extensive clinical experience to date with cross-species transplantation of living tissue. The effectiveness of this therapy is now being evaluated in pivotal clinical trial to evaluate efficacy in a randomized, placebo-controlled, double-blind, multicenter trial. An empty implant was used as the placebo. Results of this trial are expected around the year 2000.

Support of the Failing Liver

The liver is among the most biochemically complex organ of the human body and one of the few with a capacity for self-regeneration. Serious liver failure is a discouraging prognosis with the option of transplantation numerically limited to the fortunate few. The bioartificial liver is intended to maintain critical liver failure patients until a transplantable organ becomes available. The approach is simple in concept and more governed by the dictates of surgical pragmatism than the principles of pharmacological elegance. Hepatocytes are harvested from a porcine source and placed in the extraluminal chamber of a membrane exchange device designed along the principles of a hollow fiber hemodialyzer. Blood flows on one side of the membrane, the cells are on the other. In contrast to the pain implant, which contains a few milligrams of cells and is expected to last function months or years, the liver device contains between 20 and 200 g of purified hepatocytes, which are used for a very short period of 6 to 24 hours. Here, the mission of the membrane barrier is to prevent cell–cell contact while allowing protein traffic; hence, open microporous membranes are favored. Donor hepatocytes are believed to help clear substances normally removed by the liver and may even be active in synthesis. The procedure has been evaluated clinically in a Phase I trial involving just under 40 patients with diagnosed terminal liver failure. The device functioned as expected with no untoward safety problems; this has cleared the way for a larger multicenter randomized trial, which began with U.S. FDA approval late in 1998. Clinical response in the Phase I trial were very impressive indeed. However, the path to liver support systems is littered with a history of interventions that raised hopes in initial evaluation only to confound early enthusiasm in larger-scale application. The results of the Phase III trial, which will be conducted at several centers in the United States and Europe, are expected in 2002. Although the study design and stated goal is bridging patients to transplant, investigators will look carefully for signs of liver regeneration; the ultimate goal of liver support is recovery of liver function without transplantation.

The question naturally arises whether it is reasonable and prudent to obtain living components of implants and other biological devices from bovine (chromaffin cells) and porcine (hepatocytes) sources. FDA regulations for good manufacturing procedures (cGMPs) are scrupulously observed in cell harvesting to assure purity, identity, and freedom from foreign microorganisms. Concern about endogenous retroviruses from porcine sources or other adventitious zoonotic agents is another matter. No infectious pathogens have been identified in extensive testing and monitoring to date. An intact membrane would provide a formidable barrier for viral or retroviral transmission from graft to host. The clinical course of all patients is being closely monitored. Investigators are neither cavalier or complacent and recognize that experience in xenogeneic cell therapy may well shape the equally as important area of whole organ xenotransplantation.

Parkinson's Disease

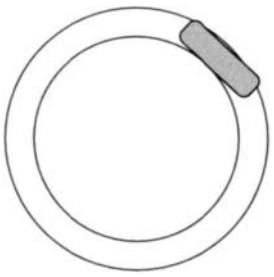
Parkinson's disease results from a deficiency of dopamine in the striatal region of the brain. Studies conducted in the early nineties used encapsulated PC-12 cell implants as a local source of dopamine in animal models of this condition. Although a naturally occurring mutant, PC-12 cells displayed most of the features of engineered cell lines including capacity for unlimited division and high constitutive release of a therapeutically useful product. Despite generally successful and widely published results in rodents and primates, the approach was never evaluated clinically. Numerous other avenues to treating Parkinson's disease are being investigated, including stem cell therapy, use of encapsulation to deliver growth factors to regenerate

the brain's own dopamine producing circuitry, and human fetal transplantation.

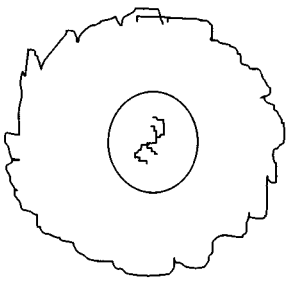
Delivery of Gene Therapy

Experience with PC-12 cells persuaded workers in the field of both the feasibility and practical benefits of dividing cell lines for encapsulation. Molecular biologists set about with characteristic enthusiasm to create multiple families of implantable cell lines producing medically useful proteins. In the broader sense, and as illustrated in Figure 2, this strategy amounted to use of immunoisolation as a pathway for delivery of gene therapy. Genes of interest were isolated and inserted into a carrier cell line using the conventional techniques of molecular biology. Cells were expanded, standardized, encapsulated, and implanted. The gene product was thereafter produced in situ. Because cells producing the gene were enclosed in a membrane capsule, investigators could reverse the experiment and remove the gene should this prove necessary or desirable. Some investigators preferred human-derived cell lines because allogeneic grafts do not normally secrete antigenic proteins and are thus easier to immunoisolate. Others advocated xenogeneic cell lines because they would be immediately destroyed in the event of escape from the capsule. Both approaches have merit and it is too early to tell which will prevail. A middle ground is also a possibility: xenogeneic cells can be humanized with complement restriction factors and other immune down-regulators. Alternatively, a variety of markers could be added to human cell lines to aid with their identification and destruction by the host immune system outside the capsule.

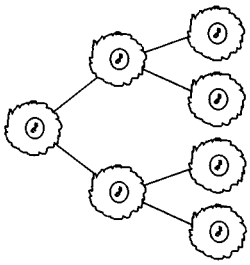
The first successful marriages of gene therapy and immunoisolation were reported in 1992 with cells transfected with the genes for neurotrophic factors and of lyosomal enzymes. Since that time a score of different protocols have been described in the literature (Table 2), and the number is likely to proliferate. In the first reported clinical trial, 6 patients diagnosed with ALS received implants containing a rodent cell line producing CNTF. Numerous preclinical studies and clinical trials not involving encapsulation had suggested that CNTF might be able to retard the deterioration of neurons that characterizes ALS and causes the eventual loss of peripheral motor activity. The device and implant protocol were very similar to that used for chronic pain; only the cells differed significantly from previous experience. In this trial, implanted cells survived and continued to release CNTF over the life of the experiment. The concentration of CNTF in monthly samples of spinal fluid averaged around 500 pg/mL. Progression of the disease was not markedly reduced relative to standard care although a much larger and longer trial would be needed to draw any firm conclusions about efficacy. Nevertheless, the intervention demonstrated production and delivery of the desired gene product at clinically useful concentrations and time frames. In this context the trial was at least as successful as the vast majority of clinical studies based upon ex vivo gene therapy. A second protocol has been initiated in Huntington patients, delivering the same product but this time with capsules implanted into the ventricles rather than into the cerebrospinal fluid. No results are yet available. Several additional applications are being evaluated in small and large animal models, as summarized in Table 2.



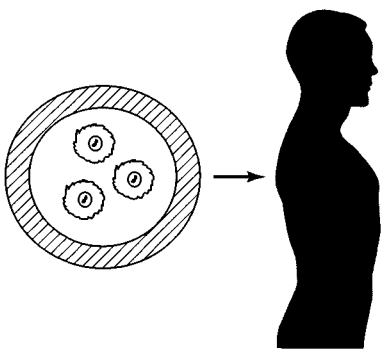
(a) Gene is added to viral vector.



(b) Vector implants gene into nucleus of carrier cells.



(c) Transfected cells are selected and proliferated.



(d) Cells are encapsulated and implanted in host.

Figure 2. Encapsulation has been used as a method of delivering gene therapy. (**a**,**b**) Conventional molecular biological techniques are employed to add a gene coding for a therapeutic protein to a dividing cell line. (**c**) Modified cells are grown divided and grown up in vitro. (**d**) A population of the modified cells are then encapsulated and implanted in a host. This approach has been successfully applied in animal models for delivery of erythropoietin, factor IX, several neurotrophic factors, and other proteins implicated in monogenetic diseases. It has also been used clinically to deliver the neurotrophic factor CNTF to patients with amyotrophic lateral sclerosis and Huntington disease.

Table 2. Encapsulation for Delivery of Gene Therapy

Target disease	Gene	Cell type	Status
ALS	*CNTF*	Hamster-BHK	Clinical, Phase I
Huntington	*CNTF*	Hamster-BHK	Clinical, Phase I
Hemophilia A	Factor VII	Murine	Preclinical, Rodent
Dwarfism	HGH	Murine myoblasts	Preclinical, Rodent
Anemia	EPO	Murine	Preclinical, Rodent
Type II diabetes	Glucagon-like peptide I	Murine	Preclinical, Rodent
Parkinson's	GDNF	Murine	Preclinical, Primate
Cancer	Cytochrome P450 2B1	Murine	Preclinical, Rodent

With its technical feasibility validated by the ALS trial, gene therapy is viewed by many as the most compelling application of immunoisolation. One practical problem is that biopharmaceutical firms owning rights to genes have usually invested massively in production facilities. Even a modest GMP level facility that produces a pharmaceutical product based upon recombinant protein costs upwards of $200 million. Such firms are understandably restrained in their enthusiasm for approaches that would render such facilities redundant. At the same time, the biotech start-ups with the technology for immunoisolation rarely have the resources to develop or acquire proprietary genes. For this reason commercial interest in encapsulation has tended to focus on therapeutic targets, such as the central nervous system, which remain beyond the reach of traditional drug development. Also favored are applications where cells release products in response to physiologic stimuli (e.g., the bioartificial pancreas) or metabolize circulating blood components (e.g., the bioartificial liver). Encapsulation may not fulfill its clinical promise of in situ drug delivery until the first round of gene products come off-patent.

The Artificial Pancreas

The bioartificial liver and cell therapy for chronic pain are in Phase III clinical trials. Immunoisolated gene therapy has reached the clinic and is fecund with promise. What then of the bioartificial pancreas? The path from first inspiration to clinical success takes many strange twists, and this is well illustrated by the history of the bioartificial pancreas. Successful demonstration of the reversal of induced diabetes in rodents in the mid-seventies by immunoisolated cells was the original defining moments in the origin of tissue engineering. By now similar results have been routinely obtained in dozens of laboratories around the world. In fact, so compelling is the treatment of induced diabetes in rodents that no fewer than five original reports on this subject have appeared in *Science* magazine. But attempts to obtain similar results in larger animals, canines and primates, have generally proven disappointing. There is simply no widely accepted set of large animal experiments demonstrating long-term satisfactory reversal of diabetes and normalization of glucose kinetics. Even marginal results in larger animals have often required supplementary use of immunosuppression or some level of injected insulin.

Much of the complexity with the bioartificial pancreas comes down to the fact that about 700,000 islets, containing about 2 billion β cells, would be required for transplantation. (This is two orders of magnitude more cells than have been successfully encapsulated in clinical implants to date.) Harvesting so many cells is one problem and housing them in a practical implant is another. Most successful rodent studies involve transplantation of about 500 rat islets to a mouse recipient. The 500 islets are usually handpicked from a partially digested rat pancreas. It is simply not practical to handpick the 700,000 islets required for a human graft, so investigators use semiautomated cell harvesting devices. Techniques for mass isolation have never reached the stage of consistently producing healthy batches of large islets given the natural variability in tissue sources and digestive enzymes. Furthermore, an islet is a not just a cluster of cells but a mini-organoid that enjoys its own vascular supply to distribute oxygen and nutrients to all of its constituent cells. In contrast, implants rely upon diffusion to provide adequate oxygenation and nutrition. The diffusion approach is manageable in small devices but very challenging in implants of the size required to house upwards of 10^9 cells. Perhaps the most satisfactory results to date have been achieved with flow-through designs but these are highly invasive and their use would be justified only in the most threatening of patient circumstances. Yet another complexity is the dose of soluble antigens released by the large quantity of cells needed to replace pancreatic function. The issue exists with all implants but is far more formidable when grams rather than milligrams of tissue are implanted. Over the past two decades, these and other difficulties have frustrated the efforts of several brilliant and dedicated investigative teams to reproduce in large hosts the tantalizing results obtained early on in rodents.

Fortunately, the resourcefulness of molecular biology has opened a second path to the bioartificial pancreas. At least three groups have set about to develop glucose-response, insulin-secreting cell lines. Because of the mass of tissue involved, cell lines of human origin, or at least highly humanized animal cells, seem preferred. Cells must not lose integrity of function over 25–50 passages. To make device size manageable, these cells should produce insulin at least on the order of 1 ng/10^6 cells-24 hours. They cannot be overly sensitive to hypoxia or other insults encountered by encapsulated cells. At the same time, such cells cannot threaten the patient should they escape the immunoisolatory implant. Ten years ago, development of such a cell line would have been considered a quixotic undertaking. Today, emboldened by increasing knowledge of glucose

regulation in the normal β cells and the emerging portfolio of antiapoptotic molecular technology, many investigators believe it to be within reach. We expect to see impressive large-animal results with manmade β cell lines within the next five years and hopefully, this time, a more rapid progression to clinical success.

CONCLUDING PERSPECTIVES

In 1955, the term *artificial organ* provoked skepticism, incredulity, and even hostility. Twenty years later in 1975 both transplantation and organ replacement were medically accepted and rapidly growing. Today, two score years later, multiple manifestations of high technology substitutive medicine accounts for about 7% of the total global health care enterprise. In like fashion, we fully expect over the next two decades that tissue engineering, including immunoisolated cell therapy, will emerge from its investigative origins and play a fulcral role in twenty-first-century medicine.

ACKNOWLEDGMENTS

Ms. Jacqueline Sutherland assisted the author with the preparation of the manuscript for this article.

ADDITIONAL READING

P. Aebischer et al., *Nat. Med.* **2**, 1041 (1996).
P. Aebischer and M.I. Lysaght, *Xeno* **3**, 43–48 (1995).
P. Aebischer et al., *Exp. Neurol.* **126**, 151–158 (1994).
J. Brauker et al., *Transplant Proc.* **24**, 2924 (1992).
J. Brauker et al., *Hum. Gene Ther.* **9**, 879–888 (1998).
E. Buscher et al., *Anesthsiology* **85**, 1005–1012 (1996).
S.C. Chen et al., *Ann. NY Acad. Sci.* **831**, 350–360 (1997).
C.K. Colton, *Trends Biotechnol.* **14**, 158–162 (1996).
K.E. Dionne, B.M. Cain, and R.H. Li, *Biomaterials* **17**, 257–266 (1996).
N. Deglon et al., *Hum. Gene Ther.* **7**, 2135–2146 (1996).
C. Ezzell, *J. NIH Res.* **7**, 47–51 (1995).
P.E. Lacy et al., *Science* **254**, 1782–1784 (1991).
R. Lanza and W. Chick, *Ann. NY Acad. Sci.* **831**, 323–331 (1997).
P.J. Morris, *Trends Biotechnol.* **14**, 163–167 (1996).
C. Rinsch et al., *Hum. Gene Ther.* **8**, 1881–1889 (1997).
M.E. Sugamori and M.V. Sefton, *Trans. Am. Soc. Artif. Intern. Organs* **35**, 791–799 (1989).
S.J. Sullivan et al., *Science* **252**, 718–721 (1991).
B.A. Zielinski and P. Aebischer, *Biomat.* **15**, 1049–1056 (1994).

IN VITRO–IN VIVO CORRELATION

STEPHEN S. HWANG
SUNEEL K. GUPTA
ALZA Corporation
Palo Alto, California

KEY WORDS

Bioavailability
Compartmental analysis
Correlation
Deconvolution
Dissolution
Extended-release product
GI absorption
In vitro evaluation
In vivo evaluation
Linear system analysis
Manufacturing control
Oral dosage forms
Pharmacokinetics

OUTLINE

Introduction
USP Definition of Correlation
In Vivo Evaluation
  Pharmacokinetic Study Design
  Mechanistic Considerations
  Theory
  Numerical Algorithm
  Deviation from Ideal
In Vitro Evaluation
Correlation between the In Vivo and the In Vivo Profiles
Examples
Application of In Vitro/In Vivo Correlations
  Dissolution/Release Rate Specifications
  Manufacturing Control
  Process Change Assurance
Conclusions
Bibliography

INTRODUCTION

Pharmaceutical companies rely heavily on the in vitro dissolution or release test to develop extended-release products and to ensure their performance in vivo. In 1971, Wagner (1) had already stated that "future research in dissolution rates should be directed mainly towards establishing correlations of the in vitro data with in vivo data." A strong correlation between the in vitro and the in vivo results means that the in vitro test results can predict the in vivo performance accurately and therefore indicates the test's usefulness as a tool for development and production control. To reach a valid correlation, one has to have valid methods to yield meaningful measurements, both in vitro and in vivo. It is also important that the scientific community reach a consensus about what it means by in vitro/in vivo correlation. The completion of these criteria was marked by the publication of "Stimuli" by the U.S. Pharmacopoeial Convention's (USP's) subcommittee on Biopharmaceutics in *Pharmacopeial Forum* in 1988 (2) and the workshop on in vitro and in vivo testing and correlation for oral controlled/modified-release dosage forms in De-

cember 1988 cosponsored by the American Association of Pharmaceutical Scientists, the U.S. Food and Drug Administration (FDA), the Federation Internationale Pharmaceutique, and the USP. The outcome of this workshop is documented in the workshop report (3).

This article discusses the accepted definition of correlation, the available methods for evaluating in vivo data, the commonly used in vitro testing methods, the currently accepted methods of establishing the correlation, and the possible applications of such a correlation. This article also includes many of the published works on the correlation of the in vivo and the in vitro results. The examples include the correlation between the in vivo human data and the in vitro data, the in vivo dog data and the in vitro data, and the human data and the dog data.

USP DEFINITION OF CORRELATION

The USP (4) defines three levels of in vitro and in vivo correlation: level A, level B, and level C. Level A is the highest category of correlation. It represents a point-to-point relationship between in vitro dissolution and in vivo input rate of the drug from the dosage form. Level B correlation examines the relationship between the mean in vitro dissolution time and the mean in vivo residence time or mean in vivo dissolution time. Like level A, level B utilizes all the in vitro and in vivo data but is not considered to be a point-to-point correlation because many different plasma drug concentration curves can give identical mean residence time values. Level C correlation examines the relationship between one dissolution time point (e.g., $t_{50\%}$) and one in vivo pharmacokinetic parameter (e.g., AUC, C_{max}, T_{max}). It represents a single-point correlation. It does not reflect the complete shape of the plasma drug concentration curve, the critical factor that defines the performance of modified-release products.

IN VIVO EVALUATION

Pharmacokinetic Study Design

To define the in vivo release profile of an extended-release product, one must include all necessary treatments in the study. Before discussing these treatments in the pivotal study, one should understand the drug kinetics over the dose and concentration range of interest, the mode of dosing (fed versus fasted), the time of dosing, the effect of body posture (5) or the influence of exercise (6), and many other details. It is beyond the scope of this article to enumerate what factors could affect the drug kinetics. In the simplest case when the drug kinetics is linear, time invariant, and not affected by any usual physiological activities or food, then the study needs minimally to include two treatments: the extended-release product and a reference product. Based on the concept of gastrointestinal (GI) bioavailability (7), the reference is ideally an oral solution. This reference can be modified without compromising the stated objective by using an oral suspension or an immediate-release dosage form, such as a tablet or a capsule. The basic idea is to have the reference readily available in the GI tract for absorption. For in vitro/in vivo correlation, one could use an intravenous dose as the reference as well. This reference defines the drug disposition function and hence a clear absorption profile. However, this absorption profile differs from the in vitro release profile by a bioavailability factor. Administered as a bolus, the reference gives a direct observation of the characteristic function. From a purely theoretical point of view, the reference product can be administered with any known input function (e.g., constant infusion). In such a case, the characteristic function is not directly observed but derived.

In most cases, not everything is known about the drug kinetics. In such cases, one should be conservative in the study design to guard against many aforementioned experimental factors that may affect the drug kinetics. Instead of a single administration of the reference at any dose, one would use the actual therapeutic dose/regimen of the immediate-release product that the extended-release product is trying to match. For example, a 240-mg pseudoephedrine extended-release product designed for once-daily administration can be compared to four 60-mg doses of an oral solution given at 6-h intervals (8). This approach gives a useful direct pharmacokinetic comparison between the extended-release product and a product given at a therapeutically effective regimen. It guards against any complications such as nonlinear kinetics, food effects, and diurnal effects, which can invalidate a simulation based on the data from the simpler design. This design can be further expanded to study both the extended-release product and the immediate-release product at several dose levels to account fully for possible dose dependence in the kinetics. As usual, the study is limited by the number of blood samples that can be withdrawn from healthy volunteers. This limitation unavoidably results in realistic compromises in study design and objectives. The overall goals can be reached only through many studies that individually address a piece of the puzzle.

Traditional Crossover Design. Intersubject variability in pharmacokinetic parameters is typically much larger than intrasubject variability. Therefore, it is more efficient to use a crossover study design to discover the subtle differences between formulations. In a typical randomized two-way crossover study, half the subjects receive extended-release product followed by the reference product; the other half receive these two treatments in the reverse order.

Stable Isotope-Labeled Drug As Reference. Although the intrasubject variability in pharmacokinetic parameters is small when compared with the intersubject variability, it may still be large and demand a large sample size, and it makes the results of a small pilot study unreliable. Intrasubject variability can be reduced by giving both treatments concurrently as long as the analytical method can differentiate between the two different drug sources. This differentiation can be accomplished by labeling both sources of drug with different isotopes or labeling one source of drug with an isotope. For example, the reversible metabolism of sulindac has been investigated using different radioactive isotopes to label sulfoxide and sulfide (9).

The use of stable isotope-labeled drug has been reviewed by Browne (10) and is an excellent approach to increase the reliability of the results when the basic assumptions are met. A middle-of-the-road approach is to give two treatments sufficiently apart such that the carryover drug from the first treatment can be properly modeled from the data (11).

Scintigraphic Monitoring. Scintigraphic monitoring technology has blossomed over the past 10 years. Today, a trace amount of lanthanides can be placed into a commercial formulation. These metals, when neutron activated, become radioactive, providing the means for following the dosage form in vivo. During earlier studies, researchers used this method to account for the bioavailability variations potentially caused by the dosage's short transit time (12). As we begin to realize that both the rate and the extent of drug absorption could be site dependent, the appropriate derivation of the in vivo release profile becomes almost impossible without the location information.

Mechanistic Considerations

After ingestion, the drug must be released from the dosage form and then dissolved. For some dosages, the release and dissolution can occur in one step rather than by two separate processes. The dissolved drug is simultaneously being degraded, emptied from any location, and absorbed through the GI membrane. The degradation, either chemically or microbially, can differ significantly from stomach to large intestine. The absorbed drug will then pass through the liver before appearing in the systemic circulation. The drug could be metabolized by the GI membrane and the liver, a process that is collectively known as first-pass metabolism because it happens before the drug's appearance in the systemic circulation. First-pass metabolism occurs for all drugs that undergo liver metabolism. The first-pass extraction ratio, E, accounts for part of the bioavailability loss. When the first-pass metabolism follows linear kinetics, then the extent of first-pass metabolism should remain unchanged regardless of the release rate from the dosage form. The impact of a nonlinear first-pass process is much more complex and has been discussed elsewhere (13).

Theory

This section defines the mathematics in the derivation of the in vivo release profile of an extended-release product from the pharmacokinetic data generated from a study as mentioned earlier. The methods generally derive from compartment models or linear system properties. Mathematically, the two approaches yield the same answer. The linear-system–based deconvolution method makes fewer assumptions about the system, giving a more robust derived answer; the compartment approach gives a conceptual picture of the process and allows scientists to derive the necessary equations with the comfort of a physical process instead of mathematical abstraction.

History. It is not surprising, given the long history of applying compartmental analysis techniques in endocrinology, that the early development of pharmacokinetics is mostly, if not completely, based upon the compartment analysis. In 1963, Wagner and Nelson (14) published their method of deriving the absorption profile from pharmacokinetic data for a drug with a one-compartment disposition model. When applied to an oral data set alone, the method implies that the function describing the entire plasma drug concentration profile can be described by the convolution of two functions: a staircase-step function for the absorption process and a single-exponential disposition function. The method also requires that the absorption is completed before the last plasma drug sample in order to have a clean elimination phase. Loo and Riegelman (15) reported a mathematical equation to calculate the amount of drug absorbed when the drug disposition follows a two-compartment model. The application of a linear-system–based deconvolution approach to the pharmacokinetic data seems to have originated with the publication by Benet and Chiang (16). However, the publication lacks an explicit mathematical expression and numerical algorithm. The application of a linear-system approach to pharmacokinetics was broadly addressed by Cutler (17) in 1978. That same year, the linear-system–based deconvolution methods were reported by Vaughan and Dennis (18) and Cutler (19) using staircase function and polynomials as input functions.

Compartment Models. The cumulative amount of drug absorbed at any time t, $A_a(t)$, is the sum of the amount present in the body and the cumulative amount eliminated. The cumulative amount eliminated from the body is:

$$Cl \int_0^t C(\tau)d\tau$$

where Cl is the body clearance for the drug and C is the plasma or serum drug concentration. The clearance always derives from the dose, D_{iv}, and the area under the curve, AUC_{iv}, after a dose of the drug is given intravenously. The equation defining the amount of drug present in the body at time t is disposition-model dependent. For a one-compartment disposition model, the amount of drug present in the body at time t equals $C(t)\ V$, where V is the distribution volume for the drug. Therefore, the cumulative amount of drug absorbed at any time t, $A_a(t)$, can be calculated from the following equation:

$$A_a(t) = VC(t) + Cl \int_0^t C(\tau)d\tau$$

If the drug-disposition model includes a peripheral compartment, compartment 2, then the equation defining the total amount of drug present in the body needs to include the amount of drug present in compartment 2. According to Wagner (20), the amount of drug in compartment 2 is given as $k_{12}e^{-k_{21}t}\int_0^t C(\tau)e^{k_{21}\tau}d\tau$. Thus, the cumulative amount of drug absorbed at any time t for a drug following a two-compartment disposition model is defined by the following equation:

$$A_a(t) = VC(t) + Cl\int_0^t C(\tau)d\tau + k_{12}e^{-k_{21}t}\int_0^t C(\tau)e^{k_{21}\tau}d\tau$$

The amount of drug absorbed is not a direct measurement of the in vivo performance of a dosage form. A theoretical purist would insist that the more appropriate measurement for the correlation to an in vitro release/dissolution measurement should be the corresponding in vivo measurement, such as the in vivo release/dissolution rate. This theoretical concern can be addressed by incorporating an absorption phase in the in vitro measurement to reflect the in vivo absorption process. The difference between the cumulative amount of drug released/dissolved, $A_r(t)$, and the cumulative amount absorbed is simply the amount of drug present in the GI tract (21), $G(t)$. When the GI absorption process is governed by a first-order process with a rate constant, k_a, and a bioavailability factor, F, then the amount of drug present in the GI tract is mathematically defined by the absorption rate.

$$G(t) = \frac{dA/dt}{Fk_a}$$

In this scenario, the cumulative amount of drug released/dissolved from an extended-release product is expressed as

$$A_r(t) = \frac{V}{k_aF}\left[\frac{dC}{dt} + (k + k_a)C + k_ak\int_0^t C(\tau)d\tau\right]$$

for a drug following the one-compartment disposition model, and

$$A_r(t) = \frac{V}{k_aF}\left[\frac{dC}{dt} + (k_{12} + k_{10} + k_a)C + k_{10}k_a\int_0^t C(\tau)d\tau + (k_a - k_{21})k_{12}e^{-k_{21}t}\int_0^t C(\tau)e^{k_{21}\tau}d\tau\right]$$

for a drug following the two-compartment disposition model.

Linear System. In a linear-system approach, one considers the body as a system that yields responses based on the input. One of the necessary and sufficient conditions for a linear system is a response proportional to the input. When the input function is an impulse that is equivalent to a bolus dose, the response of the system is a characteristic function, C*. For any input function, $in(\tau)$, the resulting plasma drug concentration, $C(t)$, is given as

$$C(t) = \int_0^t in(\tau)C^*(t - \tau)d\tau$$

The convolution integral is a simple multiplicative relationship in the Laplace domain, (i.e., $c(s) = in(s)c^*(s)$ where $c(s) = L\{C(t)\}$, and so on) and the derivation of the input function is a straightforward division, $in(s) = c(s)/c^*(s)$. When the impulse input is given intravenously, the characteristic function defines the disposition process, and the input function describes the input to the site where the impulse dose is given. This input to the impulse-administering site is commonly understood as the amount absorbed, although it is not an exact measurement of absorption across the GI-tract membrane unless the impulse input is given at the absorption site of interest (e.g., the portal vein). Although the mathematics are deceptively simple, numerical assumptions are necessary to make the convolution equation useful. Here we follow the work of Vaughan and Dennis to illustrate the application of the deconvolution method to pharmacokinetic data. First, assume that the input is a staircase function (i.e., it consists of a finite set of rectangular pulses of intensity, I_i, from time t_{i-1} to t_i, with $t_0 = 0$ and t_i corresponding to the plasma drug sampling time). The input function can be explicitly given as follows:

$$I_1 = \frac{C(t_1)}{\int_0^{t_1} C^*(\tau)d\tau}$$

$$I_2 = \frac{C(t_2) - I_1\int_{t_1}^{t_2} C^*(\tau)d\tau}{\int_0^{t_2-t_1} C^*(\tau)d\tau}$$

$$\vdots$$

$$I_n = \frac{C(t_n) - \sum_j I_j\int_{t_j}^{t_n} C^*(\tau)d\tau}{\int_0^{t_n-t_{n-1}} C^*(\tau)d\tau}$$

This approach uses all the data from the impulse input without imposing a model and simply assumes the input as constant between sampling intervals. It is simple and easy to understand. Unfortunately, the inaccuracy of the deconvolution output tends to be larger than desirable because this method accepts every data point as exact and passes all noise to the derived input function.

For drugs undergoing reversible metabolism, the input can be a combination of the drug and its metabolite(s). Mathematically, the input is a vector, and the deconvolution process discussed above has to be expanded into an n-dimensional problem. This case has been reported elsewhere (22).

Linear-System Basis in Compartment Model–Derived Equations. Any linear compartment model meets the definition of a linear system. Therefore, it should not be surprising that any equation that derives from linear-system properties alone should also be applicable to any linear compartment model. However, the reverse is not true because the equations may have been based on assumptions specific to the particular compartment model. A compartment-model–based absorption equation may be invalid if one doubts whether the compartment model truly describes the drug disposition regardless of how closely the model can describe the data. A good example is the presence of three two-compartment models to describe the same plasma drug-disposition profile (23). A more general discussion of the model identification issues is found in

other references (24). Interesting points related to the influence of the sampling site and lung metabolism on the derived pharmacokinetic parameters have also come up. Therefore, it is important to understand the deconvolution from the linear system perspective and determine how much of the derived information is independent of the model selection.

Any linear compartment model is a linear system with a multiexponential characteristic function

$$\sum_{i=1}^{n} A_i e^{-k_i t}$$

When the impulse dose is given intravenously, the multiexponential function is continuously declining and

$$\sum_{i=1}^{n} A_i > 0$$

The input function was derived by Veng-Pedersen (25). Wagner made the comparison between this approach and the compartment-model-derived absorption equations in 1983 (20). Specifically, the Laplace transformation of a monoexponential function, $a_1 e^{-k_1 t}$, is $a_1/(s + k_1)$, and the Laplace transformation of a biexponential function, $a_1 e^{-k_1 t} + a_2 e^{-k_2 t}$, is $a_1/(s + k_1) + a_2/(s + k_2)$. In the Laplace domain, the input function for a monoexponential characteristic function can be solved:

$$in(s) = \frac{c(s)}{a_1/(s + k_1)}$$

The solution for the cumulative input function is

$$A_a(t) = \frac{1}{a_1}\left[C(t) + k_1 \int_0^t C(\tau)d\tau\right]$$

When a one-compartment disposition model is imposed, then $1/a_1$ becomes the distribution volume of the compartment. However, one can derive this equation without imposing the compartment model. Similarly, the input function for a biexponential system can be derived:

$$in(s) = \frac{c(s)}{a_1/(s + k_1) + a_2/(s + k_2)}$$

$$\frac{in(s)}{s} = \frac{c(s)}{a_1 + a_2}\left(1 + \frac{\lambda_1\lambda_2}{Rs} + \left(\lambda_1 + \lambda_2 - R - \frac{\lambda_1\lambda_2}{R}\right)\frac{1}{s + R}\right)$$

where $R = a_1\lambda_2 + a_2\lambda_1/a_1 + a_2$.

The explicit cumulative-amount-absorbed equation can be solved by imposing inverse Laplace transformations on the previous equation:

$$A_a(t) = \frac{1}{a_1 + a_2}\left[C(t) + \frac{\lambda_1\lambda_2}{R}\int_0^t C(\tau)d\tau + \left(\lambda_1 + \lambda_2 - R - \frac{\lambda_1\lambda_2}{R}\right)Re^{-Rt}\int_0^t C(\tau)e^{R\tau}d\tau\right]$$

For the two-compartment model with elimination from the central compartment (1) only, the rate constants for the intercompartmental processes are commonly known as the following:

$$k_{21} = \frac{a_1\lambda_2 + a_2\lambda_1}{a_1 + a_2}$$

$$k_{10} = \frac{\lambda_1\lambda_2}{k_{21}}$$

$$k_{12} = \lambda_1 + \lambda_2 - k_{21} - k_{10}$$

Thus, the equation for calculating the amount absorbed based on a biexponential characteristic function is identical to that derived from a two-compartment model. Therefore, the equation is valid even when the particular disposition model is not consistent with the actual situation such as elimination from the peripheral compartment.

Numerical Algorithm

As mentioned previously, one way to approximate the input is to assume it is a staircase function. A polynomial function has been proposed by Cutler to approximate the input. Veng-Pedersen reported the use of a spline function (26) and a polyexponential function (27) to approximate the input function. One alternate approach is to assume the input function to be the solution of an mth-order ordinary differential equation (28), which is mathematically equivalent to a polyexponential function (29–32). The presence of physically impossible negative input caused by the data noise has been addressed by using a B-spline function (33) or a Fritsch-Butland nondecreasing cubic function to approximate the cumulative input function (34).

Deviation from Ideal

Despite the mathematical simplicity and beauty, the real world is full of complications that, in some cases, invalidate the mathematics. Here are some of the complexities.

In Vivo Dissolution. It has been stated that one should use a readily available dosage as the reference to define the characteristic function, which is relatively simple for drugs with reasonable solubilities—that is, the therapeutic dose can be dissolved in a reasonable amount of water. When the drug is not so soluble, the situation becomes much more complicated. One must choose among a suspension, a nonaqueous solution, and an immediate-release dosage form, such as a tablet or a capsule. Each choice has its drawbacks. The most difficult issue is the uncertainty related to the in vivo dissolution for each choice.

Absorption/Metabolism at Different GI Regions. Studies have used various techniques, such as intubation and high frequency (HF) capsules, to investigate the extent of absorption of drugs introduced directly to the colon. For colonically introduced glibenclamide (35), acetaminophen (36), ondansetron (37), and nifedipine (38), the extent of absorption appears to be similar to that administered orally and supports the assumption of a uniform absorption process throughout the GI tract. Contrary to these uniform-absorption examples, the colonically introduced

gepirone (39) has a higher bioavailability than an oral solution, and numerous drugs introduced into the lower GI tract have been reported to have a lower bioavailability than an oral solution—for example, ciprofloxacin (40), cimetidine, furosemide, hydrochlorothiazide (41), danazo (42), benazepril (43), isosorbide-5-mononitrate (44), amoxicillin (45), and sumatriptan (46). It seems prudent to investigate the absorption of the drug solution introduced into the lower GI tract experimentally. The usefulness of such information is demonstrated by an example—namely, the diminished bioavailability of an extended-release amoxicillin product that was published (47) after the publication of the amoxicillin intubation results. It is clear from these examples that useful information can be gained through independent experiment and that a simulation that takes account of location-dependent absorption, such as a model of n absorption sites (48), will be more realistic than the uniform absorption assumption. The diminished absorption of metoprolol in the lower GI tract has been demonstrated by comparing the plasma drug concentration profiles after the intragastric infusion and an oral administration of an OROS® metoprolol tablet (49). The presystemic metabolism of a drug could be site dependent as well. Researchers have measured selegiline and its metabolites—*N*-desmethylselegiline, L-methamphetamine, and L-amphetamine—in the plasma samples collected after giving selegiline to eight healthy young males by the oral route and direct infusion to the duodenum, jejunum, and terminal ileum through a nasoenteric tube (50). The plasma selegiline concentration profile was the highest after oral dosing and the lowest after dosing to the terminal ileum. The plasma *N*-desmethylselegiline concentration profiles followed a pattern similar to that of selegiline; plasma *L*-methamphetamine and *L*-amphetamine concentration profiles were essentially the same regardless of the site of administration. This example clearly demonstrates the complexity of the problem.

IN VITRO EVALUATION

Many methods exist for testing a dosage form for release/dissolution rate; more scientists are relying on the compendial methods. Typically, one uses USP apparatus 1, the basket method, and apparatus 2, the paddle method. The release/dissolution medium is typically aqueous, with surfactant if required. According to FDA guidance (51), the basket is run at 100 rpm, and the paddle is evaluated at 50 and 75 rpm. The dissolution medium (900 mL) of pH 1–1.5, 4–4.5, 6–6.5, and 7–7.5 is maintained at 37°C. The use of compendial equipment facilitates the across-laboratory comparison. However, this fact should not discourage scientists from exploring other methods to find a better-correlated test. Devane and Butler (52) gave a few examples of establishing in vitro/in vivo correlation where the adoption of initial dissolution method relies on the biopharmaceutical classification of the drug (53). The effect of food on the drug release from an extended-release product is a concern for the formulation scientists not just because of the regulatory agencies' requirement but also because of the realistic expectation that many patients may take the product with food. It is therefore of interest that one can evaluate the food effect in vitro. One study investigated the in vitro dissolution behavior of four theophylline extended-release products utilizing the rotating-dialysis-cell method (54). The effects of pH, oil, and enzymes on the dissolution profiles were studied. The in vitro observations of the oil effect were related to the in vivo food effect reported in the literature, and the authors concluded that the rotating dialysis cell can be a useful tool in studying factors that may be responsible for dissolution-related food effects on the absorption of controlled-release products.

CORRELATION BETWEEN THE IN VIVO AND THE IN VIVO PROFILES

In many examples, the correlation is established between the cumulative profiles. This practice may reflect

1. The way we measure the drug release/dissolution
2. The way Wagner and Nelson derived their equation
3. The fact that the cumulative profile is inherently stabler than the rate profile

A statistical concern exists with this approach: The observations at each time point are not truly independent. It is clear that the cumulative amount dissolved at time t_i equals the cumulative amount dissolved at time t_{i-1} plus the amount dissolved between t_{i-1} and t_i. Therefore, the first observation is used n times in the linear regression. It is statistically cleaner to use the incremental data rather than the cumulative data. Liu et al. (55) have demonstrated that the correlation of any two sets of cumulative fractions is inherently high. Even using randomly generated x–y pairs, the average correlation coefficient was 0.935. Therefore, a χ-square test using the incremental fraction data has been proposed to evaluate the correlation. It is more appropriate to show the correlation between the in vivo and the in vitro rates rather than the cumulative amounts.

In an example (56) of metoprolol tartrate extended-release tablet formulation, the authors evaluated several correlations' ability to predict the in vivo performance. This is an important criterion in selecting an in vitro method to control the in vivo performance of the extended-release product.

EXAMPLES

The examples are collected to show how the correlation between the in vitro and the in vivo data is done in actual practice. The first group are examples using human in vivo data. The second group are examples using dog pharmacokinetic data. The third group are examples trying to correlate the human and the dog pharmacokinetic data.

The interest in correlation between the in vitro and the in vivo performance is not limited to the extended-release product. Actually, it seemed to have started with the work by Levy and Hollister (57) with the immediate-release as-

pirin tablet. In the case of immediate-release product, the correlation is theoretically more difficult because it is more difficult to separate the dissolution and the absorption processes when both are rapid.

Two commercial cinnarizine capsules have been studied in a group of 12 healthy male volunteers (58). The formulations have similar in vitro dissolution rates as measured by amount dissolved at 30 min at pH 1 and at pH 6 but very different dissolution rates at pH between 1 and 6. These two capsules had no distinguishable AUC and C_{max} values in the subgroup of volunteers with high gastric acidity, whereas in the low-gastric-acidity group, they had statistically different AUC and C_{max} values with a twofold difference in mean. This finding clearly demonstrated the importance of measuring the dissolution rate over a wide range of pH and understanding the important physiology parameters. In a study of five sugar-coated metronidazole tablets in 10 healthy male volunteers (59), there was no significant correlation between the in vitro dissolution parameters and the pharmacokinetic parameters. The authors stated that "although the in vivo findings seem to agree well with the dissolution rate/pH relationship, the relative values and the ranking between the tablets tested did not agree with those of dissolution rates." Therefore, the correlation between the in vitro and the in vivo performance seems to be more drug specific and difficult to generalize.

The relationship between in vitro and in vivo drug release from OROS® oxprenolol systems have been examined by analyzing the plasma drug concentration data from two pharmacokinetic studies (60). An intravenous dose was used as the reference in the first study, and an oral bolus was used as the reference in the second study. The in vivo release drug-release rate was derived using a numerical deconvolution technique (61). The in vivo drug release from the product in most volunteers followed the same pattern as measured in vitro; only after 6–8 h was the decline in the in vivo release rate somewhat greater than expected. The same product was also investigated by Bradbrook et al. (62). The percentage of dose remained to be absorbed as derived from the Loo-Riegelman method was almost identical to the percentage of dose remained to be released over the first few hours. The difference between the in vivo and the in vitro measurements seemed to increase with time but disappeared at the end of sampling period.

Two extended-release formulations of etodolac have been studied (63). In the pilot pharmacokinetic study, these two formulations were studied in 14 healthy male volunteers with an oral solution of equal dose. The in vitro dissolution data were used to simulate the expected plasma drug concentration for each formulation. There appeared to be a good agreement between the simulation and the observed plasma drug concentrations. The simulation was further carried out for formulations of other strengths used in a steady-state study. The in vivo performance was accurately predicted by the in vitro dissolution data.

Four cellulosic polymer-based matrix tablet formulations of chlorpheniramine maleate were studied in 24 healthy male volunteers (64). The amount of drug absorbed at various times was calculated according to the Wagner-Nelson method. The dosages were also evaluated in vitro using USP apparatus 2 (50 rpm) and 1,000 mL of water. The plot of the amount released versus amount absorbed indicated a strong linear relationship for each formulation. The lines were approximately parallel with a different positive x-intercept for each formulation. After correcting for a lag time according to Levy and Hollister (57), a one-to-one correlation was established.

Three extended-release formulations of bromocriptine have been evaluated against an immediate-release capsule under fasting condition in a group of 14 healthy male volunteers (65). All extended-release formulations were based on a swelling hydrocolloid principle and contained hydroxypropylmethylcellulose (HPMC), microcrystalline cellulose, and cetyl palmitate but had quite different in vitro release profiles. The in vitro dissolution rate was measured in 500 mL of 0.1 HCl using USP apparatus 2 at 50 rpm. The dissolution profiles for all three extended-release formulations were essentially overlapping each other after normalizing to each formulation's mean dissolution time. For the three extended-release formulations, the in vitro and in vivo data are qualitatively in agreement with the bioavailability decreases with the prolonged in vitro release. However, this relationship breaks down when one considers the fastest dissolving extended-release formulation has a 123% bioavailability relative to the even faster-dissolving immediate-release capsule reference. Thus, this in vitro test seems to have only limited value in predicting the formulations' in vivo performance.

Six extended-release formulations of diltiazem HCl have been evaluated in 12 healthy volunteers (66). These included three multiple-unit dosage forms and one matrix tablet and two commercially available nondisintegrating tablets. The in vitro dissolution test used USP apparatus 2 and a distilled water medium with pH progression. The work demonstrated a linear relationship between the cumulative percentage released and the cumulative percentage absorbed for all three experimental multiple-unit dosages. There was also a statistically significant correlation between the pharmacokinetic parameter, mean residence time, and the in vitro dissolution parameter, mean dissolution time for all formulations studied.

Two theophylline extended-release formulations were compared with a solution under fasting condition in 12 healthy male volunteers (67). Both formulations consisted of the same spherical pellets but with different amounts of ethylcellulose/methylcellulose coating. Both formulations were demonstrated to have pH independent in vitro dissolution rates. The in vitro dissolution data were scaled using the Levy and Hollister technique to achieve a one-to-one correlation for each formulation. It is not clear from the publication whether one correlation equation can be established for both formulations. If the correlation is formulation specific, then it is of very little value for guiding further formulation work.

Five HPMC based extended-release formulations of diclofenac sodium have been evaluated in six healthy male volunteers (68). The release rate was controlled by the viscosity grade of the polymer and the amount of the polymer used. The authors reported a significant correlation between AUC, C_{max}, and the time for 50 or 80% drug to be released in vitro.

A marketed extended-release pseudoephedrine capsule and an experimental extended-release formulation of pseudoephedrine have been studied in six healthy volunteers (69). There was an evident linear relationship in the plot of cumulative fraction dissolved versus fraction absorbed. An extended-release OROS® formulation of pseudoephedrine HCl has been evaluated both in vitro and in 27 healthy male volunteers (8). The in vivo absorption profile was in good agreement with the in vitro release profile. There is a strong one-to-one relationship between the drug release rate and the absorption rate. Four cellulosic polymer-based matrix tablet formulations of pseudoephedrine sulfate were evaluated in 20 healthy male volunteers (70). The formulations were also evaluated in vitro using USP apparatus 2 at 50 rpm and 1,000 mL 0.1 N HCl. The results were essentially the same as what was observed for chlorpheniramine formulations, and a one-to-one correlation was established after correcting for the lag time and the difference in the first-order dissolution rate constant and the first-order absorption rate constant. The OROS nifedipine product, PROCARDIA XL, has been dosed to four mongrel dogs (71). The amount of drug released in the dog is in good agreement with the amount released in vitro.

A HPMC formulation of oxprenolol HCl has been evaluated in vitro and in five healthy mongrel dogs (72). A straight-line relationship was evident between the cumulative percent absorbed in vivo and the cumulative percent released in vitro. These results were somewhat disturbing because the more than twofold difference in the total AUC value reported between the conventional and the extended release formulations given at equivalent dose.

A series of seven 2-hydroxypropylcellulose (HPC)–based extended-release nifedipine formulations and one fast-release formulation were evaluated in gastric-acidity–controlled beagle dogs (73). The authors plotted the pharmacokinetic parameters, the absolute retarding parameter, mean residence time, and area under the plasma drug concentration curve against the mean in vitro dissolution time for each formulation. Although there is not a mathematical equation to describe the relationship, there are enough data points for interpolation. This approach clearly demonstrated the benefit of a well-designed experiment.

Three extended-release salbutamol products, Volmax®, and two HPMC-based matrix tablet formulations have been studied both in vitro and in vivo (74). An intravenous dose of salbutamol and an oral immediate-release product, Ventolin®, were also included in the in vivo study as the reference. The in vivo study used five mongrel dogs, and the in vitro study used USP apparatus 1 at 100 rpm and 500 mL of water as dissolution medium. The in vivo percentage of drug absorbed was calculated by numerical deconvolution using the KINBES® computer program. The in vitro dissolution profiles were generally faster than the corresponding in vivo absorption profiles for the three oral products; a good agreement between in vivo and in vitro results was evident for one of the HPMC formulations. In general, a higher amount dissolved in vitro than in vivo. This difference is at least partially due to the less than 100% bioavailability for oral salbutamol in dogs. A good linear relationship seems to exist between the amount absorbed in vivo and the amount dissolved in vitro, with a positive intercept on the axis for the amount dissolved. Both the incomplete bioavailability and the relatively slow absorption process ($t_{1/2}$ = 2 h) for the immediate-release oral product suggested that a better correlation might be achieved with the deconvoluted in vivo dissolution rate using the oral immediate-release product as the reference instead of the intravenous dose. Two ethylcellulose microsphere formulations of zidovudine were compared with zidovudine powder in four beagle dogs (75). The plasma drug concentration data were fitted to a first-order absorption/first-order elimination model. The observed in vitro release data were compared with the in vivo release profile generated from the best-fit absorption rate constant that, despite its name, actually reflected the drug-release process rather than the rapid-absorption process. Among three dissolution media, one was recommended on the basis of the agreement between the in vitro and in vivo results.

Two HPMC (Methocel® K4M) matrix tablets of zileuton were compared to an oral solution in nine beagle dogs using a single-dose design (76). The oral solution and immediate-release product plasma drug concentration profiles were fitted to polyexponential functions, and the matrix tablets' plasma drug concentration profiles were fitted to a smoothing cubic-spline function and then deconvoluted using the PCDON® software. The in vitro dissolution testing used USP apparatus 1 (100 rpm), 2 (100 rpm), and 3 (25 oscillations per min); and the dissolution medium was 10 mM sodium doecyl sulfate solution (900, 900, and 200 mL, respectively). The linear relationship was good between the in vitro and the in vivo data though the slope was approximately 2, indicating a much faster in vivo release rate. Despite the lack of a one-to-one correlation, a third HPMC (Methocel® K100LV) matrix tablet formulation was selected on the basis of the in vitro results and evaluated against an immediate-release tablet in eight beagle dogs using a multiple-dose design. The in vivo performance of the third formulation was consistent with that predicted from the in vitro dissolution data. Thus, the in vitro test method was a useful tool for selecting formulations despite the fact that it did not have a one-to-one correlation to the in vivo results.

Four theophylline extended-release formulations were evaluated in eight male beagle dogs under fasting condition (77). These formulations include theophylline/microcrystalline cellulose (Avicel® RC-581) beads, theophylline/microcrystalline cellulose (Avicel® PH-101) beads, Avicel® PH-101 beads coated with Surelease/HPMC, and a HPC/lactose/magnesium stearate matrix tablet. An intravenous dose of 80 mg theophylline, an oral theophylline solution, and an oral dose of theophylline syrup were included as references. The ratio of percentage cumulative released in vivo versus in vitro over time was evaluated as an indicator of the correlation. The in vivo release profiles for all four formulations are similar to the in vitro release profile in a pH 7.2 medium.

The GI physiology is quite different between dog and human. One notable difficulty is the relatively short GI transit time in dogs [reported to be between 6 and 12 h for four beagle dogs (78)]. The average gastric pH under fast-

ing condition was 1.8 ($n = 4$) for beagle dogs and 1.1 ($n = 10$) for human ($P < .05$); the average gastric-emptying time was 100 min for dogs and 60 min for human ($P > .05$). It was also reported that the average intestinal pH for dogs was higher and more variable than that for humans (79). The importance of such a difference is not exactly clear and is most likely to be drug and formulation specific. In a study of four griseofulvin tablet formulations, the ultramicrosize tablet showed a lower bioavailability in humans (80) but was the most bioavailable formulation in beagle dogs (81). On the other hand, the microsized formulations showed similar in vivo results to those in humans. Four brands of uncoated diazepam tablets have been studied in humans (82) and in beagle dogs (83). The correlation between the in vivo pharmacokinetic parameters (T_{max}, AUC, and the plasma metabolite concentration at 0.25 and 0.5 h) and the in vitro dissolution parameters (T_{30}, T_{50}, and T_{70}, where T_x is the time for X% of drug dissolved) were evaluated. Both the rate and the extent of the absorption in beagle dogs appeared to be correlated to the in vitro dissolution rate at pH 4.6 but not to the dissolution rate at pH 1.2. No statistically significant correlation existed in pharmacokinetic parameters between beagle dogs and humans. A consistent rank order was evident only between the serum drug concentration at 1 h in humans and the plasma drug concentration at 0.25 h in dogs; the rank order of other pharmacokinetic parameters was quite different between humans and dogs. In the study of fulfenamic acid (84) capsules, no significant correlation was evident between the dog and human results and the dissolution results, mainly because of the similar in vivo performance of all the products studied. Five tablet formulations of nalidixic acid have been studied in humans and beagle dogs (85). The rank order of tablets according to C_{max} was exactly the same between humans and beagles. The area under the plasma drug concentration curve also showed the same rank order between humans and beagles except for one formulation with a poor disintegrating ability. The bioavailability of five brands of sugar-coated metronidazole tablets has been evaluated in humans, as discussed earlier, and in beagle dogs (86). The in vitro dissolution rate of these five tablets showed a wide range of pH dependence. The gastric acidity was measured for each volunteer and each dog. The relative values of C_{max} and AUC_{0-24} ranked similarly between corresponding gastric acidity groups of beagle dogs and humans, and a statistically significant correlation was evident between AUC_{0-24} for beagle dogs and humans having low gastric acidity. It is also interesting to note that the tablet with a pH-independent dissolution rate had almost identical plasma drug concentration profiles between the low- and the high-gastric-acidity groups; the four formulations with pH-dependent dissolution rates had disparate plasma drug concentration profiles between the high-gastric-acidity and the low-gastric-acidity groups of dogs. Two commercial cinnarizine capsules, representing the extreme dissolution test results from 32 commercial capsules, were evaluated in 12 healthy beagle dogs (87). The gastric pH was quite variable from treatment to treatment and the between-dog variability in bioavailability cannot be statistically attributed to the gastric pH factor despite the statistically significant gastric pH effect on the bioavailability found in humans (88).

The food effect on the pharmacokinetics of two theophylline extended-release products has been evaluated in four male beagle dogs (89). The overall trends in relative bioavailability of these two products with and without food appeared to be similar to those reported in humans. A study of the food effect on a commercial theophylline extended-release product, Theo-24, in Hormel-Hanford miniswine (90) failed to reproduce the food effect observed in humans. Three extended-release theophylline matrix tablet formulations were evaluated with two commercial theophylline products in five mongrel dogs and six healthy male volunteers (91). Four formulations showed extended-release performance in both humans and dogs; one formulation showed incomplete absorption in both humans and dogs. For both human and dog data, the cumulative percent of dose absorbed appeared to be linearly related to the cumulative percent of dose released with a slope value close to one (92). Three extended-release theophylline capsule formulations with different in vitro dissolution rates were evaluated under fasting condition in 30 healthy male volunteers and six female beagle dogs (93). Although the agreement is not quantitative, the in vivo rate and the extent of absorption in both humans and dogs are in the same rank order as the in vitro dissolution rate. Qualitatively, the food exerted the same effect on the absorption profile for both humans and dogs. Four novel extended-release formulations of valproic acid have been studied in six healthy volunteers (94) and in five dogs (95,96). An apparent linear relationship existed between each formulation's absorption half-life for the human and that for the dogs (97). However, the relationship is not one-to-one implying that one cannot apply the dog absorption data directly to man and one needs to study a few formulations in both human and dog in order to establish the useful relationship. In addition, three extended-release formulations with diminished bioavailability in dogs were equally bioavailable as the immediate-release product in humans. For valproic acid, a wrong decision apparently could have been made if the formulation selection had been based on the dog pharmacokinetic data.

APPLICATION OF IN VITRO/IN VIVO CORRELATIONS

The ultimate objective of in vitro dissolution/release rate testing is to ensure the product's in vivo performance. In too many cases, the correlation between the in vitro and the in vivo performance has not been explicitly established. Even in these cases, the dissolution tests are still performed because it is unthinkable to release a lot of product without the dissolution test. Because we have established the in vivo meaning of an in vitro dissolution test, it is important for us to apply the correlation and rely on the in vitro results to make decisions that we used to make on the basis of the pharmacokinetic data. The resulted savings in the resources must be good for all, although the extent of benefit may be quite different for each societal subgroup. The following are just some possible applications of the in vitro/in vivo correlations assuming a level A correlation.

Dissolution/Release Rate Specifications

Without a correlation, the specifications of an in vitro test can be established only empirically. This approach is data driven but is valid only if all the batches have been extensively evaluated in clinical trials; furthermore, it probably can detect only relatively large differences between different batches. It is therefore more precise to set up the specification using the correlation to evaluate the in vivo consequences of the range. Clearly, the pharmacokinetic consequences alone are not sufficient to set up the specification. The pharmacodynamic knowledge is the key to making the specification clinically meaningful. In the absence of the information, some scientists may be willing to rely on the empirical bioequivalence range of ±20% as the first guidance. In the case of a one-to-one correlation, this automatically translates into a dissolution rate range of ±20%. If the empirically derived dissolution range is much wider than ±20%, then the companies invariably believe that the products have been punished by the presence of a one-to-one correlation. It is important for the regulatory agencies to recognize the scientific progress the industry has made in establishing the in vivo meaning of an in vitro test and reward the effort. Even though the batches may not be bioequivalent to each other, a product is still better controlled by an in vitro test with meaningful in vivo predictability than one without.

Manufacturing Control

The extended-release products are distinguished through their input rate to the absorption site. Therefore, the rate of the drug release from these products is an important feature and should be carefully controlled and evaluated. The in vitro dissolution/release test is meaningful only when the test results are correlated to the products' in vivo performance.

Process Change Assurance

The manufacturing processes of approved products are regulated by the regulatory agencies. The manufacturers are required to demonstrate that any kind of change, even an engineering improvement, does not cause changes in the finished product's in vivo performance. Consequently, many changes have to be supported by a bioequivalence study. With the availability of an in vitro test with a one-to-one correlation to the product's in vivo performance, a bioequivalence study should no longer be necessary. The dissolution/release tests measure only the rate process and cannot ensure the product performance for an excipient change. In such cases, the scientists and the regulatory agencies may consider a pilot pharmacokinetic study as an assurance that the new excipient does not inadvertently affect the absorption.

CONCLUSIONS

The methods for derivation of the in vivo release and absorption profile have been well established. There are many methods for measuring the drug products' in vitro release/dissolution rate. The scientific community has reached the consensus to define what we mean by in vitro/in vivo correlation. Therefore, all the necessary tools are available to make the in vitro dissolution test have in vivo meaning.

BIBLIOGRAPHY

1. J.G. Wagner, *Biopharmaceutics and Relevant Pharmacokinetics*, Drug Intelligence Publications, Hamilton, Ill., 1971, p. 114.
2. U.S. Pharmacopoeia Subcommittee on Biopharmaceutics, *Pharmacopeial Forum*, pp. 4160–4161 (1988).
3. J.P. Skelly et al., *Pharm. Res.* **7**, 975–982 (1990).
4. *The United States Pharmacopeia 23*, U.S. Pharmacopeial Convention, Rockville, Md., 1995, pp. 1924–1929.
5. M.S. Roberts and M.J. Denton, *Eur. J. Clin. Pharmacol.* **18**, 175–183 (1980).
6. M.A. van Baak, *Clin. Pharmacokinet.* **19**, 32–43 (1990).
7. W.R. Gillespie and P. Veng-Pedersen, *Biopharm. Drug Dispos.* **6**, 351–355 (1985).
8. S.S. Hwang et al., *J. Clin. Pharm.* **35**, 259–267 (1995).
9. D.E. Duggan, K.F. Hooke, and S.S. Hwang, *Drug Metab. Dispos.* **8**, 241–246 (1980).
10. T.R. Browne, *Clin. Pharmacokinet.* **18**, 423–433 (1990).
11. M.O. Karlsson and U. Bredberg, *Pharm. Res.* **6**, 817–821 (1989).
12. L.C. Feely and S.S. Davis, *Pharm. Res.* **6**, 274–278 (1989).
13. J.G. Wagner, in A. Yacobi and E. Halperin-Walega, eds., *Oral Sustained Release Formulations: Design and Evaluation*, Pergamon, New York, 1988, pp. 95–124.
14. J.G. Wagner and E.J. Nelson, *J. Pharm. Sci.* **52**, 610–611 (1963).
15. J.C.K. Loo and S. Riegelman, *J. Pharm. Sci.* **57**, 918–928 (1968).
16. L.Z. Benet and C.W.N. Chiang, *13th Nat. Meet. APhA Acad. Pharm. Sci.*, November 5–9, 1972, Abstr. 2, p. 169.
17. D.J. Cutler, *J. Pharmacokinet. Biopharm.* **6**, 265–282 (1978).
18. D.P. Vaughan and M. Dennis, *J. Pharm. Sci.* **67**, 663–665 (1978).
19. D.J. Cutler, *J. Pharmacokinet. Biopharm.* **6**, 243–263 (1978).
20. J.G. Wagner, *J. Pharm. Sci.* **72**, 838–842 (1983).
21. S.S. Hwang, W. Bayne, and F. Theeuwes, *J. Pharm. Sci.* **82**, 1145–1150 (1993).
22. S. Hwang and M. Knowles, *J. Pharm. Sci.* **83**, 629–631 (1994).
23. J.G. Wagner, *J. Pharmacokinet. Biopharm.* **3**, 457–478 (1975).
24. K.R. Godfrey, R.P. Jones, and R.F. Brown, *J. Pharmacokinet. Biopharm.* **8**, 633–648 (1980).
25. P. Veng-Pedersen, *J. Pharm. Sci.* **69**, 298–304 (1980).
26. P. Veng-Pedersen, *J. Pharm. Sci.* **69**, 305–311 (1980).
27. P. Veng-Pedersen, *J. Pharmacokinet. Biopharm.* **8**, 463–481 (1980).
28. S. Vajda, K.R. Godfrey, and P. Valko, *J. Pharmacokinet. Biopharm.* **16**, 85–107 (1988).
29. D. Verotta, *J. Pharmacokinet. Biopharm.* **18**, 483–489 (1990).
30. S. Vajda, K.R. Godfrey, and P. Valko, *J. Pharmacokinet. Biopharm.* **18**, 489–491 (1990).
31. P. Veng-Pedersen, *J. Pharmacokinet. Biopharm.* **18**, 491–495 (1990).
32. D. Verotta, *J. Pharmacokinet. Biopharm.* **18**, 495–499 (1990).

Next Page

33. D. Verotta, *J. Pharmacokinet. Biopharm.* **21**, 609–636 (1993).
34. Z. Yu, S.S. Hwang, and S.K. Gupta, *Biopharm. Drug Dispos.* **18**, 475–488 (1997).
35. D. Brockmeier, H.-G. Grigoleit, and H. Leonhardt, *Eur. J. Clin. Pharmacol.* **29**, 193–197 (1985).
36. T. Gramatte and K. Richter, *Br. J. Clin Pharmacol.* **37**, 608–611 (1993).
37. P-H. Hsyu et al., *Pharm. Res.* **11**, 156–159 (1994).
38. H. Bode et al., *Eur. J. Clin. Pharmacol.* **50**, 195–201 (1996).
39. L.K. Tay et al., *J. Clin. Pharmacol.* **32**, 827–832 (1992).
40. S. Harder, U. Fuhr, D. Beermann, and A.H. Staib, *Br. J. Clin. Pharmacol.* **30**, 35–39 (1990).
41. S.A. Riley et al., *Aliment. Pharmacol. Ther.* **6**, 710–706 (1992).
42. W.N. Charman et al., *J. Clin. Pharmacol.* **33**, 1207–1213 (1993).
43. K.H. Chan et al., *Pharm. Res.* **11**, 432–437 (1994).
44. W.G. Kramer, *J. Clin. Pharmacol.* **34**, 1218–1221 (1994).
45. W.H. Barr et al., *Clin. Pharmacol. Ther.* **56**, 279–285 (1994).
46. P.E. Warner et al., *Pharm. Res.* **12**, 138–143 (1995).
47. J. Gottfries et al., *Scand. J. Gastroenterol.* **31**, 49–53 (1996).
48. Y. Plusquellec and G. Houin, *Arzneim. Forsch. /Drug Res.* **44**(I), 679–682 (1994).
49. S.J. Warrington et al., *Br. J. Clin. Pharmacol.* **19**, 19S–224S (1985).
50. J.S. Barrett et al., *Pharm. Res.* **13**, 1535–1540 (1996).
51. Food and Drug Administration, *Guidance Oral Extended Release Dosage Forms: In Vivo Bioequivalence and In Vitro Dissolution Testing*, FDA, Washington, D.C.
52. J. Devane and J. Butler, *Pharm. Tech.* **21**(9), 146–159 (1997).
53. G.L. Amidon, H. Lennernäs, V.P. Shah, and J.R. Crison, *Pharm. Res.* **12**, 413–420 (1995).
54. S.K. El-Arini, G.K. Shiu, and J.P. Skelly, *Pharm. Res.* **7**, 1134–1140 (1990).
55. F-Y. Liu, N.C. Sambol, R.P. Giannini, and C.Y. Liu, *Pharm. Res.* **13**, 1501–1506 (1996).
56. N.D. Eddington et al., *Pharm. Res.* **15**, 466–473 (1998).
57. G. Levy and L. Hollister, *J. Pharm. Sci.* **53**, 1446–1452 (1964).
58. H. Ogata et al., *Int. J. Pharm.* **29**, 113–120 (1986).
59. H. Ogata et al., *Int. J. Pharm.* **23**, 277–288 (1985).
60. F. Langenbucher and J. Mysicka, *Br. J. Clin. Pharmacol.* **19**, 151S–162S (1985).
61. F. Langenbucher, *Pharm. Ind.* **44**, 1166–1172 (1982).
62. I.D. Bradbrook et al., *Br. J. Clin. Pharmacol.* **19**, 163S–169S (1985).
63. M. Dey et al., *Int. J. Pharm.* **49**, 121–128 (1989).
64. P. Mojaverian et al., *Pharm. Res.* **9**, 450–456 (1992).
65. J. Drewe and P. Guitard, *J. Pharm. Sci.* **82**, 132–137 (1993).
66. C. Caramella et al., *Biopharm. Drug Dispos.* **14**, 143–160 (1993).
67. K.-H. Yuen, A.A. Desmukh, and J.M. Newton, *Pharm. Res.* **10**, 588–592 (1993).
68. C.-H. Liu et al., *J. Pharm. Pharmacol.* **47**, 360–364 (1995).
69. V. Pade, J. Aluri, L. Manning, and S. Stavchansky, *Biopharm. Drug Dispos.* **16**, 381–391 (1995).
70. P. Mojaverian et al., *J. Pharm. Biomed. Analy.* **15**, 439–445 (1997).
71. D.R. Swanson, B.L. Barclay, P.S.L. Wong, and F. Theeuwes, *Am. J. Med.* **83**(Suppl. 6B), 3–9 (1987).
72. K.P. Devi et al., *Pharm. Res.* **6**, 313–317 (1989).
73. Z. Wang, F. Hirayama, and K. Uekama, *J. Pharm. Pharmacol.* **46**, 505–507 (1994).
74. R.M. Hernandes et al., *Int. J. Pharm.* **139**, 45–52 (1996).
75. K. Abu-Izze, L. Tambrallo, and D.R. Lu, *J. Pharm. Sci.* **86**, 554–559 (1997).
76. Y. Qiu, H. Cheskin, J. Briskin, and K. Engh, *J. Controlled Release* **45**, 249–256 (1997).
77. Z. Yu, J.B. Schwartz, and E.T. Sugita, *Biopharm. Drug Dispos.* **17**, 259–272 (1996).
78. W.A. Cressman and D. Sumner, *J. Pharm. Sci.* **60**, 132–134 (1971).
79. C.Y. Lui et al., *J. Pharm. Sci.* **75**, 271–274 (1986).
80. N. Aoyagi et al., *J. Pharm. Sci.* **71**, 1165–1169 (1982).
81. N. Aoyagi et al., *J. Pharm. Sci.* **71**, 1169–1172 (1982).
82. H. Ogata et al., *Int. J. Clin. Pharmacol. Ther. Toxicol.* **20**, 159–165 (1982).
83. H. Ogata et al., *Int. J. Clin. Pharmacol. Ther. Toxicol.* **20**, 576–581 (1982).
84. N. Kaniwa et al., *Int. J. Clin. Pharmacol. Ther. Toxicol.* **21**, 576–581 (1983).
85. H. Ogata et al., *Int. J. Clin Pharmacol. Ther. Toxicol.* **22**, 240–245 (1984).
86. H. Ogata et al., *Int. J. Pharm.* **23**, 289–298 (1985).
87. H. Ogata et al., *Int. J. Pharm.* **29**, 121–126 (1986).
88. H. Ogata et al., *Int. J. Pharm.* **29**, 113–120 (1986).
89. G.K. Shiu et al., *Pharm. Res.* **6**, 1039–1042 (1989).
90. G.K. Shiu et al., *Pharm. Res.* **5**, 48–52 (1988).
91. Z. Hussein, M. Bialer, M. Friedman, and I. Raz, *Int. J. Pharm.* **37**, 97–102 (1987).
92. Z. Hussein and M. Friedman, *Pharm. Res.* **7**, 1167–1171 (1990).
93. C.S. Cook et al., *Int. J. Pharm.* **60**, 125–132 (1990).
94. M. Bialer et al., *Biopharm. Drug Dispos.* **6**, 401–411 (1985).
95. M. Bialer, M. Friedman, and J. Dubrovsky, *Biopharm. Drug Dispos.* **5**, 1–10 (1984).
96. M. Bialer, M. Friedman, and J. Dubrovsky, *Int. J. Pharm.* **20**, 53–63 (1984).
97. M. Bialer, M. Friedman, and J. Dubrovsky, *Biopharm. Drug Dispos.* **7**, 495–500 (1986).

INFECTIOUS DISEASE, DRUG DELIVERY TO TREAT

SHIGEFUMI MAESAKI
MOHAMMAD ASHLAF HOSSAIN
SHIGERU KOHNO
Nagasaki University School of Medicine
Nagasaki, Japan

KEY WORDS

Antibiotics
Antifungal agents
Antimicrobial agents
Antimycobacterial agents
Antiparasitic agents
Antiviral agents

Previous Page

33. D. Verotta, *J. Pharmacokinet. Biopharm.* **21**, 609–636 (1993).
34. Z. Yu, S.S. Hwang, and S.K. Gupta, *Biopharm. Drug Dispos.* **18**, 475–488 (1997).
35. D. Brockmeier, H.-G. Grigoleit, and H. Leonhardt, *Eur. J. Clin. Pharmacol.* **29**, 193–197 (1985).
36. T. Gramatte and K. Richter, *Br. J. Clin Pharmacol.* **37**, 608–611 (1993).
37. P-H. Hsyu et al., *Pharm. Res.* **11**, 156–159 (1994).
38. H. Bode et al., *Eur. J. Clin. Pharmacol.* **50**, 195–201 (1996).
39. L.K. Tay et al., *J. Clin. Pharmacol.* **32**, 827–832 (1992).
40. S. Harder, U. Fuhr, D. Beermann, and A.H. Staib, *Br. J. Clin. Pharmacol.* **30**, 35–39 (1990).
41. S.A. Riley et al., *Aliment. Pharmacol. Ther.* **6**, 710–706 (1992).
42. W.N. Charman et al., *J. Clin. Pharmacol.* **33**, 1207–1213 (1993).
43. K.H. Chan et al., *Pharm. Res.* **11**, 432–437 (1994).
44. W.G. Kramer, *J. Clin. Pharmacol.* **34**, 1218–1221 (1994).
45. W.H. Barr et al., *Clin. Pharmacol. Ther.* **56**, 279–285 (1994).
46. P.E. Warner et al., *Pharm. Res.* **12**, 138–143 (1995).
47. J. Gottfries et al., *Scand. J. Gastroenterol.* **31**, 49–53 (1996).
48. Y. Plusquellec and G. Houin, *Arzneim. Forsch. /Drug Res.* **44**(I), 679–682 (1994).
49. S.J. Warrington et al., *Br. J. Clin. Pharmacol.* **19**, 19S–224S (1985).
50. J.S. Barrett et al., *Pharm. Res.* **13**, 1535–1540 (1996).
51. Food and Drug Administration, *Guidance Oral Extended Release Dosage Forms: In Vivo Bioequivalence and In Vitro Dissolution Testing*, FDA, Washington, D.C.
52. J. Devane and J. Butler, *Pharm. Tech.* **21**(9), 146–159 (1997).
53. G.L. Amidon, H. Lennernäs, V.P. Shah, and J.R. Crison, *Pharm. Res.* **12**, 413–420 (1995).
54. S.K. El-Arini, G.K. Shiu, and J.P. Skelly, *Pharm. Res.* **7**, 1134–1140 (1990).
55. F-Y. Liu, N.C. Sambol, R.P. Giannini, and C.Y. Liu, *Pharm. Res.* **13**, 1501–1506 (1996).
56. N.D. Eddington et al., *Pharm. Res.* **15**, 466–473 (1998).
57. G. Levy and L. Hollister, *J. Pharm. Sci.* **53**, 1446–1452 (1964).
58. H. Ogata et al., *Int. J. Pharm.* **29**, 113–120 (1986).
59. H. Ogata et al., *Int. J. Pharm.* **23**, 277–288 (1985).
60. F. Langenbucher and J. Mysicka, *Br. J. Clin. Pharmacol.* **19**, 151S–162S (1985).
61. F. Langenbucher, *Pharm. Ind.* **44**, 1166–1172 (1982).
62. I.D. Bradbrook et al., *Br. J. Clin. Pharmacol.* **19**, 163S–169S (1985).
63. M. Dey et al., *Int. J. Pharm.* **49**, 121–128 (1989).
64. P. Mojaverian et al., *Pharm. Res.* **9**, 450–456 (1992).
65. J. Drewe and P. Guitard, *J. Pharm. Sci.* **82**, 132–137 (1993).
66. C. Caramella et al., *Biopharm. Drug Dispos.* **14**, 143–160 (1993).
67. K.-H. Yuen, A.A. Desmukh, and J.M. Newton, *Pharm. Res.* **10**, 588–592 (1993).
68. C.-H. Liu et al., *J. Pharm. Pharmacol.* **47**, 360–364 (1995).
69. V. Pade, J. Aluri, L. Manning, and S. Stavchansky, *Biopharm. Drug Dispos.* **16**, 381–391 (1995).
70. P. Mojaverian et al., *J. Pharm. Biomed. Analy.* **15**, 439–445 (1997).
71. D.R. Swanson, B.L. Barclay, P.S.L. Wong, and F. Theeuwes, *Am. J. Med.* **83**(Suppl. 6B), 3–9 (1987).
72. K.P. Devi et al., *Pharm. Res.* **6**, 313–317 (1989).
73. Z. Wang, F. Hirayama, and K. Uekama, *J. Pharm. Pharmacol.* **46**, 505–507 (1994).
74. R.M. Hernandes et al., *Int. J. Pharm.* **139**, 45–52 (1996).
75. K. Abu-Izze, L. Tambrallo, and D.R. Lu, *J. Pharm. Sci.* **86**, 554–559 (1997).
76. Y. Qiu, H. Cheskin, J. Briskin, and K. Engh, *J. Controlled Release* **45**, 249–256 (1997).
77. Z. Yu, J.B. Schwartz, and E.T. Sugita, *Biopharm. Drug Dispos.* **17**, 259–272 (1996).
78. W.A. Cressman and D. Sumner, *J. Pharm. Sci.* **60**, 132–134 (1971).
79. C.Y. Lui et al., *J. Pharm. Sci.* **75**, 271–274 (1986).
80. N. Aoyagi et al., *J. Pharm. Sci.* **71**, 1165–1169 (1982).
81. N. Aoyagi et al., *J. Pharm. Sci.* **71**, 1169–1172 (1982).
82. H. Ogata et al., *Int. J. Clin. Pharmacol. Ther. Toxicol.* **20**, 159–165 (1982).
83. H. Ogata et al., *Int. J. Clin. Pharmacol. Ther. Toxicol.* **20**, 576–581 (1982).
84. N. Kaniwa et al., *Int. J. Clin. Pharmacol. Ther. Toxicol.* **21**, 576–581 (1983).
85. H. Ogata et al., *Int. J. Clin Pharmacol. Ther. Toxicol.* **22**, 240–245 (1984).
86. H. Ogata et al., *Int. J. Pharm.* **23**, 289–298 (1985).
87. H. Ogata et al., *Int. J. Pharm.* **29**, 121–126 (1986).
88. H. Ogata et al., *Int. J. Pharm.* **29**, 113–120 (1986).
89. G.K. Shiu et al., *Pharm. Res.* **6**, 1039–1042 (1989).
90. G.K. Shiu et al., *Pharm. Res.* **5**, 48–52 (1988).
91. Z. Hussein, M. Bialer, M. Friedman, and I. Raz, *Int. J. Pharm.* **37**, 97–102 (1987).
92. Z. Hussein and M. Friedman, *Pharm. Res.* **7**, 1167–1171 (1990).
93. C.S. Cook et al., *Int. J. Pharm.* **60**, 125–132 (1990).
94. M. Bialer et al., *Biopharm. Drug Dispos.* **6**, 401–411 (1985).
95. M. Bialer, M. Friedman, and J. Dubrovsky, *Biopharm. Drug Dispos.* **5**, 1–10 (1984).
96. M. Bialer, M. Friedman, and J. Dubrovsky, *Int. J. Pharm.* **20**, 53–63 (1984).
97. M. Bialer, M. Friedman, and J. Dubrovsky, *Biopharm. Drug Dispos.* **7**, 495–500 (1986).

INFECTIOUS DISEASE, DRUG DELIVERY TO TREAT

SHIGEFUMI MAESAKI
MOHAMMAD ASHLAF HOSSAIN
SHIGERU KOHNO
Nagasaki University School of Medicine
Nagasaki, Japan

KEY WORDS

Antibiotics
Antifungal agents
Antimicrobial agents
Antimycobacterial agents
Antiparasitic agents
Antiviral agents

Cytozoic microorganisms
Drug delivery
Infectious disease
β-Lactamase
Lipid formulations of AmB
Liposome
MIC
Systemic fungal infections
Therapeutic index

OUTLINE

Introduction
Liposomal Antimicrobial Agents against the Cytozoic Microorganisms *Salmonella typhimurium, Listeria monocytogenes*, and *Chlamydia trachomatis*
Liposomal Antimicrobial (Piperacillin or Tobramycin) Agents against Bacteria
Liposome-Encapsulated Antimycobacterial Agents
Liposome-Encapsulated Antifungal Agents
Liposome-Encapsulated Antiviral Agents
Liposome-Encapsulated Antiparasitic Agents
Bibliography

INTRODUCTION

Infectious diseases are caused by pathogenic organisms that enter the host, continue multiplying, and cause damage to the host tissue in many ways, resulting in symptoms and signs that may range from trivial to life threatening in nature depending on various host, agent, and environmental factors that facilitate growth and transmission. Many antiinfectious drugs have been developed since 1910, when Paul Ehrlich discovered salvarsan, and 1929, when Alexander Fleming discovered penicillin. Various antimicrobial drugs are available for the treatment of infectious diseases. β-Lactam antibiotics, such as penicillin and cephalosporin, are most commonly used because of their wide antimicrobial spectrum, increased selective toxicity, and potency. Third-generation cephems have wider spectra and more potent antimicrobial activities than second-generation cephems. These are still less active against methicillin-resistant *Staphylococcus aureus* (MRSA) and *Pseudomonas aeruginosa*.

Antimicrobial agents are the substances produced by some living organisms or prepared synthetically from naturally occurring substances that act on other living microorganisms and cause cell death or growth inhibition, resulting in inactivation of the pathogen and recovery from the disease. Thus, they are either microbiocidal or microbiostatic in action. The antimicrobial agents obtained from living organisms or semisynthetically prepared from naturally occurring substances are known as antibiotics. The principle of antimicrobial chemotherapy is based on the administration of the most strongly antimicrobial agents against the causative microorganisms. An ideal drug for treating infectious disease needs to be administered at a concentration above the minimum inhibitory concentration (MIC) of the microorganisms. Moreover, it is necessary for the drug to be safe and have minimum adverse effects. In the past few decades, many kinds of antimicrobial agents with broad efficacy against various kinds of microorganisms have been developed. Because antibiotic treatment of severe infections is not always successful, intensification of the treatment is needed. Targeting antibiotics to infected tissues or cells by encapsulation in liposomes is under investigation and may be of importance in the treatment of infections that prove refractory to conventional forms of antibiotic therapy. For these reasons, drug delivery systems can be utilized to enhance the efficacy of antimicrobial agents against infectious disease.

Liposomes are microvesicles composed of continuous bilayers of phospholipids surrounding an aqueous phase. Phospholipid, a component of the cell membrane, is amphipathic, consisting of hydrophilic heads and hydrophobic tails. Liposomes have been extensively used to deliver antibiotics, antifungal agents, and antiviral compounds for the treatment of infections in animal models. Three rationales have been invoked to justify the use of liposomes as carriers of antiinfectious agents: (*1*) passive targeting of compounds to the mononuclear phagocytic system (MPS) for enhanced effects at this site; (*2*) targeted drug delivery; and (*3*) site-avoidance delivery, wherein the rate of transfer of drug to the toxic site is reduced but not the drug-transfer rate to the active site. All strategies result in an increase in the therapeutic index of the drug; however, to obtain optimal drug therapy, the characteristics for a particular drug for site-specific delivery differ from those of site-avoidance delivery.

Future developments that will permit a larger variety of agents to be delivered in liposomes include the development of fusogenic liposomes and of liposomes that avoid the reticuloendothelial system. By modifying the lipid composition of the liposomes, it is possible to manipulate their intracellular degradation and thereby the intracellular release and therapeutic availability of the antibiotic. Efficacy of liposome-encapsulated antibiotics in the treatment of infectious diseases outside the mononuclear phagocyte system may be realized by manipulation of the liposome composition. Evidence for this is found in the treatment of systemic fungal infections, in which liposomes appear to be very effective as a carrier of amphotericin B (AmB). The most advanced application of liposome-based therapy is in this field, and clinical studies with liposome-encapsulated AmB have been in progress for several years.

Advanced liposomal therapeutic action has been attained by liposome surface modification, initially with specific glycolipids and subsequently with surface-grafted polyethelenglycol (PEG), reducing in vivo rapid recognition and uptake, and resulting in prolonged blood circulation and providing selective localization in pathological sites. The result is improved efficacy of encapsulated agents. The surface PEG may produce a barrier, as described for colloids. Reduced in vivo uptake may result from inhibition of plasma–protein adsorption, or opsonization, by the coating. Several physical studies support this mechanism, including those involving electrophoretic mobility. The dependence of blood circulation and tissue distribution on

PEG molecular weight correlates with ζ-potential estimates of PEG-coating thickness. Effects on tissue distribution are reported for liver and spleen, the major phagocytic organs. The biological properties of these liposomes depend on the surface polymer rather than the lipid bilayer, yielding important advantages for lipid-mediated control of drug interaction and release without affecting the biodistribution.

The recent developments of the drug delivery systems and their application in treating different types of infectious diseases are described in the following paragraphs.

LIPOSOMAL ANTIMICROBIAL AGENTS AGAINST THE CYTOZOIC MICROORGANISMS *SALMONELLA TYPHIMURIUM, LISTERIA MONOCYTOGENES*

Phagocytosis plays an important role in limiting invasion by pathogens. Several microorganisms can withstand the host cellular events after phagocytosis; thus, they can survive and multiply intracellularly. They are known as cytozoic microorganisms. The commonly believed mechanism is the altered production or inactivation of reactive oxygen metabolytes induced by the toxins or other substances from the pathogen. Intracellular infections involving the MPS (parasitic, fungal, bacterial, and viral infections), an improved therapeutic index and reduced toxicity resulting from encapsulation of the antibiotics in liposomes in animal models have been demonstrated. By manipulating the liposomal composition, rates of uptake and intracellular degradation can be influenced, and thereby the rates at which liposome-encapsulated agents are released and become available to exert their therapeutic action are also influenced. With respect to the targeting of macrophage modulators at the MPS by means of liposomes for maximal stimulation of the nonspecific antimicrobial resistance, experimental evidence is now available of the potential usefulness of liposomes as carriers of these agents. This approach may also be of importance for the potentiation of treatment of severe infections.

There are three varieties of drug transportation into cells: passive transport, active transport, and phagocytosis. Macrolides are actively transported into the polymorphonuclear leukocytes via the nucleoside transport system or glycolytic pathway. Aminoglycosides are not the choice for intracytoplasmic infections such as salmonellosis. However, liposome-encapsulated cephalothin or streptomycin was effective in intraphagcytic killing of *S. typhimurium* and experimental salmonellosis. Desiderio and Campbell used multilamellar liposomes, composed of phosphatidylcholoine, cholesterol, and phosohatidylserine, that entrapped an aqueous solution of cephalothin for in vitro experiments (1). Resident murine macrophages interiorized the liposome–antibiotics complex, and this event resulted in relatively high intracellular concentration of cephalothin. Treatment of infected macrophages with liposome-encapsulated cephalothin enhanced the intracellular killing of *S. typhimurium* compared with that of macrophages treated with free cephalothin. Tadakuma et al. reported its superior efficacy against experimental salmonellosis in mice; liposomal streptomycin was selectively delivered to the spleen and liver with concentrations in these organs about 100 times higher than those in mice receiving the free drugs (2).

Listeriosis is a severe disseminated infection in immunocompromized patients. Liposome-encapsulated ampicillin demonstrated efficacy for the treatment of murine disseminated listeriosis (3). All mice treated with liposome-encapsulated ampicillin survived. The in vitro susceptibility of *C. trachomatis* to liposome-encapsulated tetracycline was compared with that of free tetracycline. A chlamydia-infected mouse fibroblast monolayer was continuously exposed to varying concentrations of antibiotics. The MIC for anionic, cationic, and neutral liposomes containing tetracycline was approximately 2, 10, and 20 times smaller than that of free tetracycline (4).

Liposomal aminoglycosides showed excellent efficacy compared with free aminoglycosides or empty liposome. This therapeutic strategy should be developed for clinical application. Although the human defense mechanism against microbial infection is very complicated, biological response modifiers (BRMs) such as vaccination or cytokine therapy have been investigated. One of the most useful and protective vaccines for prevention of tuberculosis is the *Mycobacterium vaccae* vaccine, developed by Stanford et al. (5). As for the cytokines, interleukin 2, granulocyte macrophage-colony–stimulating factor, and tumor necrosis factor have very strong antimicrobial activity. Interferon alone, however, has weak efficacy and should be combined with other effective cytokines. These BRMs constitute an excellent strategy for antimicrobial chemotherapy.

LIPOSOMAL ANTIMICROBIAL (PIPERACILLIN OR TOBRAMYCIN) AGENTS AGAINST BACTERIA

Penicillin proved to be miraculous in its action against gram-positive and gram-negative bacteria, diminishing their roles as nosocomial pathogens, and this resulted in its promiscuous use in the following years. Subsequently, semisynthetic penicillins, such as methicillin, ampicillin, amoxycillin, and then cephalosporins, were developed. Unfortunately, several bacteria capable of producing β-lactamase (and thus resistant to penicillin) were isolated. Penicillinase-producing organisms such as *S. aureus* have caused the virtual elimination of penicillin from therapy against this organism. *S. aureus* has become resistant to methicillin and is known as a very refractile organism that causes opportunistic infections. Piperacillin itself is known to be inactive against β-lactamase–producing *S. aureus*. However, Nacucchio et al. reported the enhanced antibacterial activity of liposome-encapsulated piperacillin against *S. aureus* (6). The results, expressed as the percentage of bacterial growth inhibition at 50% MIC of piperacillin, demonstrated that growth inhibition was the highest when piperacillin was liposome encapsulated. Even adsorption of piperacillin to liposomes rendered significant enhancement of the antistreptococcal capacity when compared with the effect of piperacillin alone. Exogenous β-lactamase hydrolyzed piperacillin and eradicated its antistreptococcal activity. Encapsulation of piperacillin within liposomes conferred a high degree of

protection against hydrolysis. The enhanced antibacterial activity of liposome-encapsulated piperacillin was probably due to protection of the drug from hydrolysis by staphylococcal β-lactamase or stearic hindrance to the action of the β-lactamase by the lipid surface of liposomes.

Lower-respiratory-tract infections consisting of *P. aeruginosa* occur almost exclusively in patients with compromised local respiratory or systemic host defense mechanisms. Exposure to the hospital environment, particularly given in an intensive care setting, use of respiratory inhalation equipment, and prior antibiotic therapy, increases the likelihood of such infections. Lower-respiratory-tract colonization with mucoid strains of *P. aeruginosa* is a function of age in patients with cystic fibrosis. *P. aeruginosa* clearly plays a critical role in the progressive lung lesions and resulting disability observed in most patients with this disease. Under certain conditions *P. aeruginosa* produces a polysaccharide capsule, referred to as the *glycocalyx*. This material appears to form a matrix around the bacterium, anchoring it to its environment and protecting it from phagocytic cells and antibiotics.

Liposome-encapsulated anti-*Pseudomonas* agents were first developed in 1990 by Kotsifaki (7). The growth inhibition of four *P. aeruginosa* strains by liposome-trapped penicillin G indicated an association of its efficacy with the nature of the *O*-antigenic polymeric side chain. For instance, the P28-800 and PCF-95 strains, characterized by a rough polysaccharide chain, were the most susceptible, whereas strain P28-0, possessing an intact lipopolysaccharide, resisted the activity of the entrapped drug. Among the rough strains, P642, a β-lactamase producer, was not affected by the encapsulated drug. Lagace reported that ticarcillin- and tobramycin-resistant strains of *P. aeruginosa* were shown to have a markedly increased sensitivity to antibiotics enclosed in liposomes (8). The liposome-enclosed antibiotic was as effective against the β-lactamase–producing strain as against the non-β-lactamase–producing strain. The in vitro activities of encapsulated and free tobramycin were evaluated against *P. aeruginosa* by Poyner (9). The effects of free and liposome-encapsulated tobramycin on siderophore production by *P. aeruginosa* were examined and involved using MIC and sub-MIC quantities of tobramycin. Compared with free tobramycin, siderophore production was more effectively retarded in the presence of sub-MIC quantities of liposomal tobramycin, particularly at 0.5 MIC. Siderophore production was particularly reduced in the presence of positively charged phosphatidylcholine liposomes. Beaulac studied the efficacy of fluid liposome-encapsulated tobramycin against *P. aeruginosa* in an animal model of chronic pulmonary infection (10). Chronic infection in the lungs was established by intratracheal administration of a mucoid variant of *P. aeruginosa* prepared in agar beads, and antibiotic treatments were given intratracheally. Animals treated with encapsulated tobramycin in fluid liposomes had a number of colony-forming units (CFUs) less than the minimal CFUs of lungs for animals treated with encapsulated tobramycin in rigid liposomes, free antibiotic, or liposomes without tobramycin. Tobramycin measured in the lungs at 16 after the last treatment following the administration of encapsulated antibiotic was still active. Low levels of tobramycin were detected in the kidneys after the administration of encapsulated antibiotic, while a higher concentration was detected in the kidneys following the administration of free antibiotic. These results suggest that local administration of fluid liposomes with encapsulated tobramycin may offer advantages over free antibiotics, including sustained concentration of the antibiotic, minimal systemic absorption, reduced toxicity, and increased efficacy, and that it could greatly improve the management of chronic pulmonary infection in cystic fibrosis patients.

LIPOSOME-ENCAPSULATED ANTIMYCOBACTERIAL AGENTS

Mycobacteriosis, or mycobacterial infections, are caused by various species of the genus *Mycobacterium*. The most commonly encountered diseases are tuberculosis, caused by *Mycobacterium tuberculosis*, mycobacterial infections other than tuberculosis (MOTT), and leprosy, caused by *Mycobacterium leprae*. Antimycobacterial agents are those aimed at elimination or inactivation of infections caused by mycobacteria. The active drugs are expected to act on the agent within the cells or a caseous lesion. In recent years, the resurgence of multidrug-resistant (MDR) tuberculosis and the increased prevalence of atypical mycobacteriosis have been observed in immunocompromised patients, including those with AIDS or organ transplantation, and occasionally in immunocompetent patients as well. In the recent past, Rifampin-resistant strains have been on the increase. Strains of *Mycobacterium avium-intracellulare* complex (MAC) are common environmental organisms of low virulence. MACs have been frequently identified as the pathogen causing atypical mycobacteriosis in people with poor immune status. The disease differs in severity but is often debilitating and can be fatal. In addition to infections of the lung, fever, lymphadenopathy, weight loss, and so on, the disease may cause remote symptoms such as arthritis and osteomyelitis as a result of dissemination. A considerable number of patients with MAC infection do not respond to the conventional antimycobacterial agents. Thus, the quests for novel antimycobacterial drugs and modification of their cytotoxic potency by encapsulation in liposomes have been considered worthwhile.

Perhaps the most important recent advance in the field of infections due to MACs is the identification and development of more effective agents for the treatment and prevention of disseminated disease. These agents include clarithromycin, azithromycin, rifabutin and other rifamycins, ethambutol, clofazimine, fluoroquinolones, amikacin, and liposome-encapsulated gentamicin. Most clinicians currently use multidrug therapy to maximize efficacy and to minimize the emergence of resistance. Prospective clinical trials of multidrug regimens suggest that MAC colony counts in blood decline during therapy, usually accompanied by alleviation of clinical symptoms. The small size and short duration of these trials have not permitted an evaluation of survival or quality of life. Because the contribution of any single agent to multidrug trials is difficult to

assess, short-term trials of monotherapy have been conducted recently; clarithromycin, azithromycin, ethambutol, and liposome-encapsulated gentamicin have proved most active.

The earliest report of a successful treatment for mycobacterial infection involved the use of liposome-encapsulated streptomycin. Vladimirsky reported that intravenously injecting mice infected with *M. tuberculosis* H37 RV with liposome-encapsulated streptomycin led to the amount of mycobacteria decreasing significantly in the spleen but not in the lungs, as compared with an injection of a buffered solution of streptomycin (12). Several kinds of aminoglycosides encapsulated in liposomes were investigated for therapeutic efficacy against MAC infection. Duzgunes studied the therapeutic effects of free and liposome-encapsulated amikacin on MAC infection by using the beige-mouse model of the disease (13). The results showed reduction of the CFU counts in the spleen and kidneys treated with liposome-encapsulated amikacin compared with those of both untreated controls and free-drug-treated mice (14). Liposomal kanamycin injections led to a greater reduction in the degree of gross pulmonary lesions and the growth of the organisms in the visceral organs (lungs, liver, spleen, and kidneys) of MAC-infected mice than did either free kanamycin alone or free kanamycin mixed with empty liposomal vesicles (15). Nightingale reported that a liposome-encapsulated gentamicin was given intravenously twice weekly for 4 weeks to AIDS patients with MAC bacteremia, with MAC colony counts in blood subsequently falling by 75% or more in all treated groups (16).

Other antimycobacterial agents were encapsulated in liposomes and investigated for their efficacy against MAC. Saito estimated the in vitro efficacy of liposome-entrapped rifampin against MAC infection induced in mice. Intraperitoneal injections of liposome-entrapped rifampin led to a greater reduction in bacterial growth in the lungs and spleen of infected mice than did free rifampin alone. However, liposome-entrapped rifampin given to mice via the intramuscular or subcutaneous route failed to show such an increased therapeutic efficacy. It was concluded that entrapment of rifampin in liposomal vesicles increased incorporation of the drug into host peritoneal macrophages and the activity of the agent against MAC phagocytosed into the macrophages (17). Majumdar investigated the therapeutic efficacies of liposome-encapsulated ciprofloxacin against growth of the MAC inside human peripheral blood monocyte/macrophages. Liposome-encapsulated ciprofloxacin was at least 50 times more effective against the intracellular bacteria than was the free drug: At a concentration of 0.1 μg/mL, liposome-encapsulated ciprofloxacin had greater antimycobacterial activity than the free drug at 5 μg/mL (18). The therapeutic efficacies of liposome-encapsulated ciprofloxacin and clarithromycin against MAC in a model of intramacrophage infection were evaluated by Onyeji. Liposome entrapment of clarithromycin significantly enhanced the activities of the drugs when compared with the antimycobacterial effects of equivalent concentrations of the free drugs, and liposome-encapsulated clarithromycin plus ethambutol was more effective in organism eradication than each agent used singly (19). Mehta reported therapeutic efficacy of liposome encapsulation of clofazimine in the beige-mouse model of disseminated MAC infection. An equivalent dose of liposome-encapsulated clofazimine was more effective in eliminating the bacteria from the various organs studied, particularly from the liver. Moreover, because of the reduced toxicity of liposomal encapsulation of clofazimine, higher doses could be administered, resulting in a significant reduction in the numbers of CFU in the liver, spleen, and kidneys (20,21). In recent study, Deol investigated the therapeutic efficacies of isoniazid and rifampin encapsulated in lung-specific stealth liposomes against *M. tuberculosis* infection induced in mice. The efficacies of isoniazid and rifampin encapsulated in lung-specific stealth liposomes were higher than those of free drugs against tuberculosis, as evaluated on the basis of CFUs detected, organomegaly, and histopathology. Furthermore, liposomal drugs had marginal hepatotoxicities as determined from the levels of total bilirubin and hepatic enzymes in serum (22).

Aminoglycosides have been used for the treatment of mycobacterial infection (Fig. 1). Liposome-encapsulated amikacin showed significantly greater inhibitory activity against the survival of MAC inside mouse peritoneal macrophages than free drug (23). Liposome-encapsulated gentamicin significantly reduced the number of organisms in the spleen and liver of the infected beige mice, but it did not sterilize these organs (24). Liposome-encapsulated kanamycin was injected into mice infected with MAC once every week for up to 8 weeks, which led to a greater reduction in the degree of gross pulmonary lesions and in the growth of the organisms in the lung, liver, spleen, and kid-

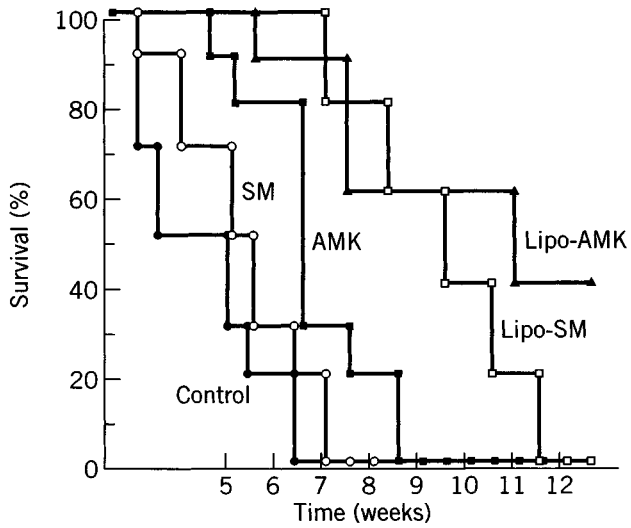


Figure 1. Survival rate over time in liposomal streptomycin and amikacin treatment for systemic *M. tuberculosis* infection in mice. *M. tuberculosis* (H37 Rv) (2×10^6 CFU/ml) was injected intravenously to BALB/c mice (5 weeks old, male). Treatment was started 24 h after infection. Streptomycin (SM), amikacin (AMK), liposomal amikacin (Lipo-AMK), and liposomal streptomycin (Lipo-SM) were injected intravenously on days 3, 5, 7, and 9. *Source:* Based on data from Ref. 11.

neys (15). The effect of liposome-encapsulated streptomycin against MAC infection in beige mice regarding the liposome was studied (25). At four weeks, liposome-encapsulated streptomycin reduced the colony-forming units in the liver and spleen to about the same extent as a 50- to 100-fold higher dose of free drug. These observations suggest that liposomes were taken up by the infected macrophages of the liver and spleen and that the encapsulated streptomycin was delivered to the intracellular compartments containing mycobacteria. The effects of unilamellar and multilamellar liposomes were similar in this model. This suggests that similar quantities of streptomycin may have been delivered to the intracellular sites of infection, although higher tissue levels were achieved with multilamellar liposomes. It is likely that not all of the streptomycin in multilamellar vesicles was released into the phagosome internalizing the liposome.

LIPOSOME-ENCAPSULATED ANTIFUNGAL AGENTS

Fungi are eukaryotic organisms that grow in a filamentous or yeastlike form or both. Fungi pathogenic to humans occur worldwide, some of which are common in defined geographic areas; in general, they can be divided into two basic groups, yeasts and molds. They are recognized as a significant and frequent cause of morbidity and mortality. Fungi may cause varying degrees of illnesses, starting from superficial to life-threatening, deep-seated mycosis. They are found to cause serious opportunistic infections in immunocompromised patients with, for example, leukemia, AIDS, and bone marrow transplants and in those treated for a long time with antineoplastic or immunosuppressive agents in particular. Frequent use of broad-spectrum antibacterial agents, intravenous catheters, and immunosuppressive therapies that are aimed at improving support to prolong survival, especially in critically ill patients, predisposes one to fungal infections.

Systemic fungal infections may arbitrarily be divided into two broad categories: endemic diseases such as blastomycosis, coccidioidomyosis, and histoplasmosis and opportunistic diseases such as aspergillosis, cryptococcosis, and candidosis, which occur almost exclusively in patient with impaired host defenses. Antifungal therapy is implemented according to several factors, such as the causative agent, the progression or invasion of the disease, and so on. Antifungal therapy may have to be administered empirically in febrile neutropenic patients who do not respond to treatment with an antibacterial drug (26).

Although newer pathogenic fungi causing deep-seated mycosis have emerged, antifungal agents have not substantially increased in number. There are few classes of agents that, in turn, have few mechanisms of action and limited response rates. The major groups of antifungal agents in clinical use are polyene antibiotics, azole derivatives, allylamine–thiocarbamates, morpholines, and miscellaneous compounds such as 5-fluorocytosin and griseofulvin. The polyenes and azoles are most widely used. Amphotericin B (AmB), nystatin and, natamycin are the polyene antifungal agents used for treatment of human diseases, with AmB being the only parenteral preparation with a broad range of antifungal activity. Over the past several years, increased efforts in both basic and clinical antifungal pharmacology have resulted in a number of entirely new reengineered or reconsidered compounds, that are at various stages of preclinical and early clinical development (27–29).

AmB is used to treat severe fungal infections. Its usefulness is compromised by a high incidence of adverse reactions, including fever, chills, nausea, vomiting, headache, and renal dysfunction with associated anemia, hypokalemia, and hypomagnesemia. Infrequently anaphylactic shock, thrombocytopenia, acute liver failure, flushing, vertigo, generalized seizures, and dose-related cardiac arrest or ventricular fibrillation have been reported. In children, overdose of AmB may cause cardiac arrhythmias and death. The damaging action of AmB to cells originates from its binding to sterols incorporated in cellular membranes (ergosterol in the case of fungal cells and cholesterol in mammalian cells); greater avidity for ergosterol-containing membranes than for cholesterol-containing membranes favors the clinical usefulness (30). Infusion-related side effects such as fever, rigors, and chills are common but not so alarming that AmB therapy should be discontinued, as would be recommended in the event of renal dysfunction. Renal insufficiency in association with azotemia, renal tubular acidosis, and impaired urinary concentrating ability resulting in electrolyte imbalance may be severe enough to lead to dose reduction or premature discontinuation of the drug (31).

Three ways have been suggested by which the therapeutic index of AmB might be improved: increasing the selectivity of drug-induced damage to fungal, as opposed to mammalian cells; decreasing toxicity to host cells bearing low-density lipoproteins (LDL) receptors; and decreasing toxicity for cells of the immune system. The lipid formulations of AmB are prepared with either phospholipids or detergents, and the resultant associations fall into two categories, liposomes and mixed micelles. Because only unbound AmB is active against cells, the damaging action of an AmB formulation depends on the ability of AmB to dissociate from complexes. At least three factors that can modify the distribution of AmB in vivo and affect the efficacy are suggested: its ability to bind to selected molecules found in plasma, its ability to bind to tissues and organs, and the ability of vesicles of differing sizes to traverse the epithelium. The lipid-based formulations are clearly less toxic, even at considerably higher doses; their pharmacokinetic properties and effectiveness differ in long-term assays because of different physicochemical characteristics (32). Adverse reactions to intravenous AmB are to some extent dependent on its mode of delivery. One potential problem with some of the new lipid formulations is their high manufacturing cost.

Three types of lipid-based formulations of AmB incorporated into liposomes, sheets, or discs are under intensive clinical investigation. The lipid-based formulations differ in size, structure, shape, lipid composition, and molar AmB content. Their physicochemical differences determine their thermodynamic stability, the distribution of AmB between the lipid formulation and lipoproteins, and their tissue distribution, levels in blood, uptake by macrophages, and pen-

etration to the site of infection. Despite all these differences, they are all less toxic than AmB to mammalian cells, animals, and humans.

Many of the newer lipid formulations including AmB–lipid complex (ABLC, Abelcet), AmB colloidal dispersion (ABCD, Amphocil), and liposomal AmB (L-AmB, AmBisome) have been found to be relatively less toxic in animals and in vitro studies as well, but lowered toxicity in vitro does not always predict lower toxicity in vivo. These formulations are described in Table 1. At equivalent concentrations of AmB, deoxycolate AmB (D-AmB) has been found more effective in fungal infections than the lipid-based formulations. The small amount of free AmB that dissociates from the complexes impairs their antifungal effectiveness.

Liposomes are biocompatible, biodegradable, microvesicular systems for drug delivery owing to their amenability to controlled release and site-directed delivery. The recent development of lipid formulations with longer half-lives opens new therapeutic avenues in treating infections, including those in non-MPS tissues. The passive targeting of liposomes to the sites of infection is of great value with respect to clinical application. Liposomal entrapment can exchange the pharmacokinetics and hence reduce the toxicity of AmB. Liposomal AmB is AmB incorporated into lipid bilayer; AmBisome is a formulation of AmB in unilamellar liposomes.

Studies with mice showed that liposome encapsulation of AmB reduced its toxicity and allowed higher doses to be administered, thus increasing the therapeutic efficacy of the compound in animal models of systemic mycosis, including candidiasis (33). The priorities of liposomes differ depending on the composition of the lipids constituting the membrane. AmBisome's lack of effect on immune system cells at high concentrations may explain the decrease in toxic phenomena observed in vivo when this form of the drug is tested. The decrease in toxicity might then allow for the demonstration of the more positive effects of AmB on the immune system. Macrophages may function as a reservoir of AmB for intracellular and extracellular antimicrobial action.

The lipophilic AmB is located within the lipid layers of the liposome. Because the affinity of AmB to ergosterol in the fungus membrane is the highest among the antifungal agents, and its affinity to the lipid carrier and cholesterol in human cell membranes is the lowest, a selective transfer of AmB from the lipid carrier to its target, the fungus membrane, can be expected. The result is a great reduction in toxicity, which allows the administration of much higher doses of AmB. Although the antifungal activity of most lipid formulations is reduced to some extent, the use of much higher dosages might lead to an increased therapeutic index compared with conventional AmB. AmBisome, Amphocil, and ABLC share the advantage of low nephrotoxicity (34).

One trial involved sequestration of AmB from some host tissues while delivering the drug to the rethiculoendotherial cells where various intracellular pathogens, including *Cryptococcus neoformans*, reside. Mice were challenged intraperitoneally, intratracheally, or intracerebrally, and the course of infection in untreated control mice was compared with that of mice given D-AmB or L-AmB. Over six times more AmB in L-AmB than D-AmB could be delivered in mice without any acute toxicity. In murine pulmonary cryptococcosis, L-AmB–treated mice survived significantly longer than control mice; thus, L-AmB was found to be effective against pulmonary cryptococcosis. AmB from liposomes is readily available to the cryptococci. L-AmB may permit efficient delivery of much larger doses than are feasible with D-AmB. However, it is possible that the adjuvancy of either the AmB or the liposomes activates macrophages to kill more cryptococci and thus prolongs survival. Intracranially challenged mice treated with L-AmB had significantly reduced cell counts in brain and spleen; thus, it was suggested that effective intracranial concentrations of AmB were delivered in the liposomes and that liposomes may offer a way to protect at least some organs against the toxic effects of AmB (35).

In a controlled, randomized trial, a short antifungal prophylaxis course of AmBisome was found to reduce the incidence of proven invasive fungal infections significantly during the first month following liver transplantation surgery. AmBisome was well tolerated, although backache, thrombocytopenia, and renal function impairment were reported in a few patients (36). Aerosolized liposomal AmB deposited aerosolized form may be advantageous. This would provide delivery of the AmB to the lung tissue, but the drug would probably also get into systemic circulation. Because liposomal AmB is rapidly cleared by the reticuloendothelial system (RES), administration of higher doses is often required to obtain sufficient levels of drug in lung lead to side effects, in a murine model of pulmonary and systemic cryptococcosis, aerosolized liposomal AmB could be delivered to target and was found effective (37).

Table 1. Characteristics of Some Lipid Formulation of AmB

Lipid formulation	Composition	Shape	Size
AmB–lipid complex (ABLC)	Dimyristoyl phosphatidylcholine Dimyristoyl phosphatidyl glycerol	Sheets	1.6–11 μm
AmBisome	Hydrogenated phosphatidylcholine Cholesterol Distearoyl phosphatidylglycerol	Unilamellar Vesicles	0.06 μm
AmB colloidal dispersion (ABCD)	Cholesteryl sulfate	Discs	0.12 μm
Lipid nanosphere AmB	Soybean oil Egg lecithin Maltose	Vesicles	25–50 nm

Micelles are colloid particles formed by an aggregation of detergent molecules. Special drug career systems and dosage forms, such as nanoparticles and liposomes, hold the promise of overcoming the pharmacokinetic limitations. Nanoparticles are stable, solid colloidal particles of various sizes that consist of macromolecular material. Nanoparticles represent an interesting carrier system for specific enrichment in macrophage-containing organs like the liver and the spleen. Injectable nanoparticle carriers have important potential applications, as in site-specific drug delivery. Conventional carriers are generally eliminated by the RES. Although in deep mycoses, efforts to lower the toxicity of AmBisome, Abelcet, and Amphocil showed comparable efficacies, studies on the efficacies of NS-718, AmB encapsulated in lipid nanospheres are in progress in Japan. Lipid nanospheres are composed of equal amounts of egg lecithin and soybean oil. The carrier potentials of lipid nanosphere are characterized by lower uptake by the RES and good distribution to the sites of inflammation (38).

NS-718 was found to more effective than D-AmB or L-AmB against clinical isolates of *Candida albicans* and *Aspergillus fumigatus*. NS-718 was well tolerated and improved survival markedly at equivalent doses in treating pulmonary aspergillosis in rats. Increased activity was also supported by pharmacokinetic study (Fig. 2) (39). In another study, NS-718 was found to have better in vitro efficacy against clinical isolates of *C. neoformans* than other AmB formulations; it was well tolerated, and its efficacy was much higher than that of D-AmB or L-AmB in treating pulmonary cryptococcosis in mice (40) (Fig. 3).

The development of immunoliposomes is an important step in the pursuit for an effective cellular targeting system. Upon binding to the specific cellular receptor via an antibody–antigen link, the immunoliposomes cluster into the coated pits and are subsequently internalized into cellular vacuoles. The immunoliposomes are then processed through the endosome–lysosome system. Trials of their in vitro and in vivo antifungal activity, toxicity, and efficacy against systemic candidiasis in murine models showed prolonged circulation, reduced toxicity, and improved efficacy by PEG conjugated to L-AmB (41). In murine models of invasive pulmonary aspergillosis, PEG- and 34A monoclonal antibodies conjugated to L-AmB were found to have higher efficacy than those of L-AmB and PEG conjugated to L-AmB (Fig. 4). Conjugation of PEG could reduce uptake by the RES and prolong circulation time, and conjugation of 34A-monoclonal antibody to L-AmB could deliver the drug to the target tissue, that is, the endothelia of mouse pulmonary capillaries. Thus, it was suggested that functional liposomes encapsulating AmB could have great potential against refractory fungal infections because

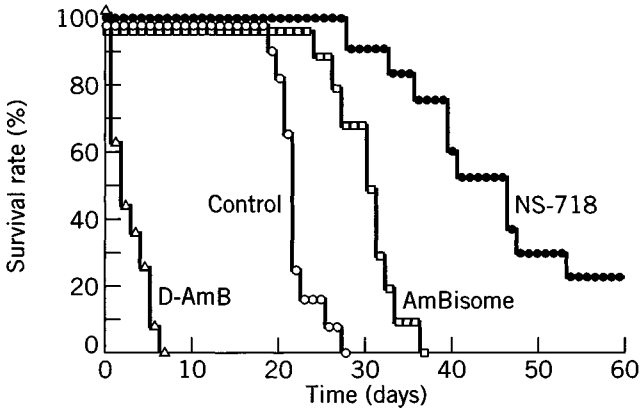


Figure 3. Survival rate over time of mice with pulmonary cryptococcosis, treated with NS-718. NS-718 (2mg/kg), AmB sodium deoxycholate (D-AmB) (2mg/kg), and AmBisome (2mg/kg) were injected intravenously once a day for 5 days after infection. *Source:* Based on data from Ref. 40.

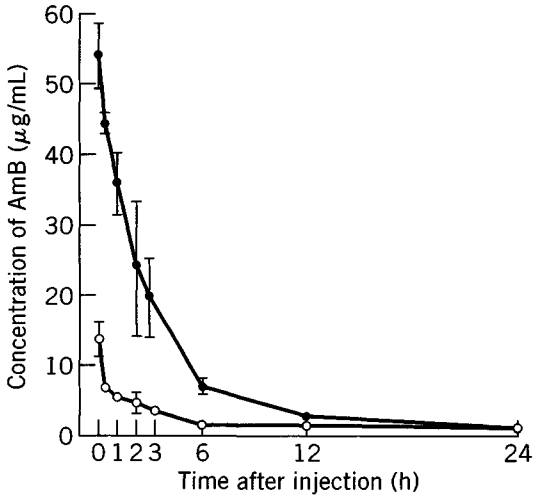


Figure 2. The concentrations of AmB in plasma after a single administration of 3mg/kg NS-718 and AmB sodium deoxycholate (D-AmB) in rats with invasive pulmonary aspergillosis. *Source:* Based on data from Ref. 43.

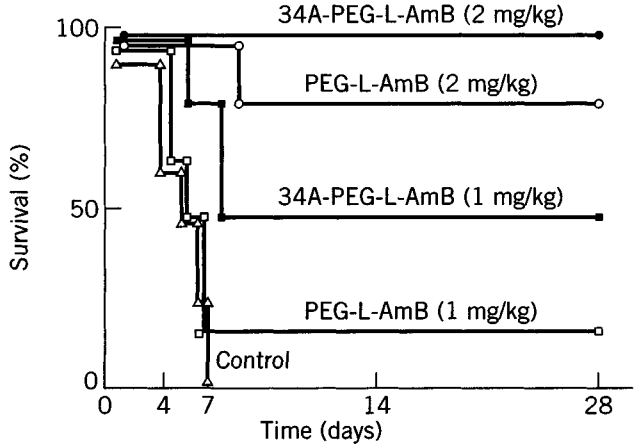


Figure 4. Effects of an immunoliposome, 34A-polyethylene glycol-liposomal-AmB (34A-PEG-L-AmB), on the survival rate over time in mice experimentally infected with invasive pulmonary aspergillosis. Liposomal AmB was injected intravenously in once a day for 5 days after infection. *Source:* Based on data from Ref. 43.

extended-circulation immunoliposomes are well tolerated and show comparable efficacy to other AmB formulations in murine invasive pulmonary aspergillosis (42,43).

ABLC is a formulation of lipid aggregates of dimyristoyl phosphatidylcholine (DMPC) and dimyristoyl phosphatidylglycerol (DMPG), and it has an unusual ribbonlike lipid structure that may attenuate the toxicity of AmB (44). Biological characteristics of ABLC were investigated in murine model of a variety of systemic mycoses such as candidiasis, aspergillosis, cryptococcosis, and histoplasmosis; ABLC was effective against all model infections studied, though comparable or a little lower in efficacies than D-AmB, but improved therapeutic index was noted. LD_{50} of ABLC was more than 40 mg/kg compared to that of D-AmB, 3 mg/kg. Putatively, AmB is released gradually only in the infection site, most likely because yeast lipase disrupted the drug lipid interaction. Therefore, ABLC can be given at much higher doses, and therapeutic benefits can be achieved (45). In vitro antifungal activity and in vivo efficacy and acute toxicity in murine model of candidiasis were studied; ABLC was well tolerated and was found as effective as AmB (46).

In a multicenter (although not well-established) study, ABLC was found to have apparently better clinical and microbiological activity in patients with AIDS-associated cryptococcal meningitis and was significantly better tolerated than a standardized regimen of AmB but was not free from toxicities (47). Internalization of low-density-protein (LDL)-bound AmB into cells may result in toxicity, which may be minimized by a career like ABLC. In a patient with disseminated zygomycosis including renal lesions, the combined use of ABLC and granulocyte-colony-stimulating factor was successful; the patient's condition remained stable, and no relapse occurred after 1 year of follow-up (48).

AmB colloidal dispersion (ABCD) consists of a cholesteryl sulfate complex of AmB and is a disklike stable complex of the constituents in a 1:1 molar ratio. There is no free drug in this type of arrangement and low lipoprotein binding in serum or other milieu, suggesting that the drug moiety lipid-binding sites are minimally exposed and the preparation is in lyophilized form. In animal models, the half-life of ABCD is longer than that of D-AmB, which suggests that once lipid binding of ABCD occurs, dissociation occurs much slowly. AmB in ABCD reaches the antifungal target, but activity is variable. ABCD has been found effective in different animal models of systemic mycosis including coccidioidomycosis, candidiasis, and aspergillosis, and much higher doses could be administered safely (49). Efficacy and safety of ABCD was compared with that of a D-AmB suspension in a murine model of disseminated cryptococcosis, and improved therapeutic index was suggested (50). In a murine model of systemic cryptococcosis, the efficacies of commercially available lipid-based formulations and D-AmB were evaluated. The lipid-based formulations showed efficacy in prolongation of survival. ABCD and L-AmB showed equivalent potencies and were superior to ABLC; ABCD was better in clearing infections other than in the brain (51). Measurement of plasma concentration of AmB for 4 weeks after a single intravenous infusion of ABCD administered to healthy volunteers indicated that the pharmacokinetics of AmB following infusions do not differ significantly from those of D-AmB. Acute side effects reported were similar to those of D-AmB and were dose dependent. But no clinically significant changes in biochemical parameters in renal or liver function tests were noticed (52).

Four patients with cryptococcal meningitis were assessed clinically and were treated with ABCD, and it was suggested that despite having undetectable levels in the cerebrospinal fluid (CSF), ABCD is an efficacious alternative form of therapy for cryptococcal meningitis for patients intolerant to D-AmB (53). In an open-label multicenter study in hospitalized patients with invasive fungal infections and impaired renal function, ABCD was found to be effective and well tolerated in immunocompromised patients with invasive fungal infections and was safe for those with underlying renal impairment (54). In another multicenter study, ABCD was administered in patients with invasive mycoses, and clinical response and adverse effects were evaluated. The conditions of patients were also monitored by biochemical parameters, blood counts, routine urinalysis, culture, microscopy, radiography, and serologic findings. ABCD was found active and less nephrotoxic than AmB, particularly in patients nonresponsive or intolerant to D-AmB. It was also suggested that the colloidal particles of ABCD remain intact after intravenous injection and are rapidly cleared by hepatic reticuloendothelial cells, resulting in low intrarenal concentrations of AmB, which appeared to be the cause of reduction of nephrotoxicity (55). There are some noncommercially developed lipid-based formulations, such as multilamellar liposomal AmB, small unilamellar liposomal AmB, and AmB-intralipid.

Nystatin, another polyene derivative antibiotic, is to some extent similar to AmB in action, but parenteral administration being toxic, it should be used as a topical preparation. Incorporation of nystatin into multilamellar liposome was found to retain the in vitro antifungal activity and protected human erythrocytes from toxicity (56). Liposomal formulation of nystatin was well tolerated and improved survival at equivalent doses as compared to free nystatin; it showed markedly increased activity at higher doses in treating systemic candidiasis in mice. Clinical trials are under way to evaluate its efficacy and rational application (57). Fluconazole, a bis-triazole antifungal agent encapsulated in a biodegradable scleral implant, was studied in vitro and also in pigmented rabbits. Periodic measurement of released fluconazole and effects on ocular tissue by ophthalmoscopy, histology, and electrophysiological studies were done. Concentration of fluconazole in rabbit vitreous remained within 99% of MIC for *C. albicans* for 3 weeks, and no toxicity was noticed. Thus, usefulness of biodegradable, polymeric scleral implants containing fluconazole was suggested (58).

LIPOSOME-ENCAPSULATED ANTIVIRAL AGENTS

Viruses are very small, "filterable" submicroscopic organisms, characterized by only a core of DNA or RNA in their genomes; they are surrounded by a protein coat and can

replicate only in living cells. In some of the well-known viral infections, viral receptors are detected on host cells, which has been proposed to be important in causing disease. Many viral infections are self-limiting in nature and produce low-grade illness for short periods; others may cause prolonged suffering and at times life-threatening infections. Antiviral agents are aimed at suppression of viral replication; many of the currently available antiviral agents have therapeutic and prophylactic effects. However, viral containment or elimination is extremely difficult in individuals with impaired immune status.

In a murine model of respiratory Influenza A virus infection, improved therapeutic and prophylactic efficacies of the antiviral antibody were noted when liposomes were used as carriers for it. Thus, it was suggested that liposomes facilitated specific delivery and that targeting the antibodies to the infection site could enhance the in vivo protective efficacies of the antibody (59). In experimental Influenza A virus infection in mice, intranasal administration of 5,7,4′-trihydroxy-8-methoxyflavone solution in hydroxypropyl cellulose showed significant inhibition of virus proliferation in both nasal and bronchoalveolar cavities, which suggested potential for drug delivery by hydroxypropyl cellulose (60).

Human serum albumin (HSA) and negatively charged *cis*-aconitic anhydride–reacted HSA were found to covalently couple to liposome. After conjugation with polyethyleneglycol prolonged activity and dual attack on human immunodeficiency virus type 1 (HIV-1) life cycle in vitro and in vivo as a result of an effective drug delivery system it was suggested that the attachment of an anti-CD4 monoclonal antibody to the outer surface of liposomes resulted in their interaction with both monocytes and lymphocytes (61). Thus, it was suggested that immunoliposome targeting to CD4+ cells in human blood might provide a means of targeting antiviral agents in cells at risk of HIV infection (62). Nanoparticles prepared by emulsion polymerization from polyhexylcyanoacrylate were loaded with nucleoside analog zalcitabine or the HIV protease inhibitor saquinavir and then tested for antiviral activity in primary human monocytes/macrophage cells in vitro, showing comparable results to those of free drugs. The delivery of antiviral agents to the monocyte phagocytic system was enhanced by nanoparticulate formation of saquinavir and could also overcome pharmacokinetic problems; thus, improved activities of the drugs by enhancing cellular uptake and in HIV target cells and tissues were suggested (63).

A single intravitreal injection of liposome-encapsulated (*S*)-1-(3-hydroxy-2-phosphonylmethoxypropyl) cytosine (cidofovir) in a rabbit model of focal nonlethal *Herpes simplex* virus (HSV) type 1 viral retinitis was found to have remarkably protective and prolonged antiviral effect. The slow rate of release of cidofovir was considered responsible for the long-term effect (64). Intravitreal injection of acyclovir diphosphate dimystoylglycerol in a rabbit model of focal nonlethal HSV type 1 viral retinitis resulted in reduction of severity of infection and rapid clearing of vitreous and optical media as compared to the effects of gancyclovir, acyclovir, and buffer. The drug delivery system modified the antiviral effects and the duration of activity as well, and treatment for cytomegalovirus retinitis and other retinal diseases was suggested (65).

LIPOSOME-ENCAPSULATED ANTIPARASITIC AGENTS

Parasites are living organisms that grow, feed, and are sheltered on or in different organisms while contributing nothing to the survival of the host. Parasitic diseases comprise a large portion of health problems in underdeveloped or developing countries in tropical and subtropical areas. In developed countries, parasitic diseases occur infrequently, though contamination of water supplies, improperly cooked meat, or worldwide travel are important factors to consider. Some parasitic infections have been found in association with impaired immune status, such as results from AIDS.

The use of drug delivery systems in parasitic diseases other than lipid formulations of AmB in leishmaniasis are not well known and lag behind use against other infectious diseases. In experimental leishmaniasis, pentamidine isethionate and its methoxy derivative, encapsulated in mannose-grafted liposomes, showed improved therapeutic effects over pentamidine isethionate, though the methoxy derivative was less toxic. Sugar-grafted liposomes were suggested to have better carrier potential than liposomes or free drug (66). Colloidal carrier potential and the targeted and controlled delivery of albendazole encapsulated in polyhexylcyanoacrylate nanoparticle was evaluated in vitro and also in murine models of hepatic alveolar echinococcosis. Cytotoxicity study showed no toxicity for peritoneal macrophages but reduced viability of the parasites. In vivo, no acute toxicity of albendazole-loaded nanoparticles was observed, and the injectable form showed equivalent parasitostatic effect (67).

BIBLIOGRAPHY

1. J.V. Desiderio and S.D. Campbell, *J. Infect. Dis.* **148**, 563–570 (1983).
2. T. Tadakuma et al., *Antimicrob. Agents Chemother.* **28**, 28–32 (1985).
3. E. Fattal et al., *Antimicrob. Agents Chemother.* **35**, 770–772 (1991).
4. H. Al-Awadhi, G.V. Stoke, and M. Reich, *J. Antimicrob. Chemother.* **30**, 303–311 (1992).
5. J.M. Grange et al., *Lancet* **3**, 1350–1352 (1995).
6. M.C. Nacucchio, M.J. Gatti Bellora, D.O. Sordelli, and M. D'Aquino, *J. Microencapsul.* **5**, 303–309 (1988).
7. H. Kotsifaki et al., *J. Chemother.* **2**, 82–86 (1990).
8. J. Lagace, M. Dubreuil, and S. Montplaisir, *J. Microencapsul.* **8**, 53–61 (1991).
9. E.A. Poyner, H.O. Alpar, and M.R. Brown, *J. Antimicrob. Chemother.* **34**, 43–52 (1994).
10. C. Beaulac et al., *Antimicrob. Agents Chemother.* **40**, 665–669 (1996).
11. H. Koga et al., *Tuberculosis* **69**, 55–60 (1993).
12. M.A. Vladimirsky and G.A. Ladigina, *Biomed. Pharmacother.* **36**, 8–9 (1982).
13. N. Duzgunes et al., *Antimicrob. Agents Chemother.* **40**, 2618–2621 (1996).

Next Page

14. N. Duzgunes et al., *Antimicrob. Agents Chemother.* **32**, 1404–1411 (1988).
15. H. Tomioka, H. Saito, K. Sato, and T. Yoneyama, *Am. Rev. Respir. Dis.* **43**, 1421–1428 (1991).
16. S.D. Nightingale et al., *Antimicrob. Agents Chemother.* **37**, 1869–1872 (1993).
17. H. Saito and H. Tomioka, *Antimicrob. Agents Chemother.* **33**, 429–433 (1989).
18. S. Majumdar et al., *Antimicrob. Agents Chemother.* **36**, 2808–2815 (1992).
19. C.O. Onyeji, C.H. Nightingale, D.P. Nicolau, and R. Quintiliani, *Antimicrob. Agents Chemother.* **38**, 523–527 (1994).
20. R.T. Mehta et al., *Antimicrob. Agents Chemother.* **37**, 2584–2587 (1993).
21. R.T. Mehta, *Antimicrob. Agents Chemother.* **40**, 1893–1902 (1996).
22. P. Deol, G.K. Khuller, and K. Joshi, *Antimicrob. Agents Chemother.* **41**, 1211–1214 (1997).
23. L. Kesavalu et al., *Tubercle* **71**, 215–218 (1990).
24. S.P. Klemens, M.H. Cynamon, C.E. Swenson, and R.S. Ginsberg, *Antimicrob. Agents Chemother.* **34**, 967–970 (1990).
25. N. Duzgunes et al., *J. Infect. Dis.* **164**, 143–151 (1991).
26. G. Medoff et al., *Clin. Infect. Dis.* **15**(S1), S274–S281 (1992).
27. N.H. Georgopapadakou and T.J. Walsh, *Antimicrob. Agents Chemother.* **40**, 279–291 (1996).
28. R.J. Hay, *J. Am. Acad. Dermatol.* **31**, S82–S85 (1994).
29. A.H. Groll and T.J. Walsh, *Curr. Opin. Infect. Dis.* **10**, 449–458 (1997).
30. J.D. Cleary et al., *Ann. Pharmacother.* **27**, 715–719 (1993).
31. J.W. Hiemenz and T.J. Walsh, *Clin. Infect. Dis.* **22**(S2), S133–S144 (1996).
32. J. Brajtburg and J. Bolard, *Clin. Microbiol. Rev.* **9**, 512–531 (1996).
33. G. Lopez-Berestein et al., *J. Infect. Dis.* **147**, 939–945 (1983).
34. S. de Marie, *Leukemia* **10**(S2), S93–S96 (1996).
35. J.R. Graybill et al., *J. Infect. Dis.* **145**, 748–752 (1982).
36. J. Tollemar et al., *Transplantation* **59**, 45–50 (1995).
37. B.E. Gilbert, P.R. Wyde, and S.Z. Wilson, *Antimicrob. Agents Chemother.* **36**, 1466–1471 (1992).
38. J. Seki et al., *J. Controlled Release* **28**, 352–353 (1994).
39. T. Otsubo et al., *Antimicrob. Agents Chemother.* **43**, 471–475 (1999).
40. M.A. Hossain et al., *Antimicrob. Agents Chemother.* **42**, 1722–1725 (1998).
41. E.W.M. van Etten, M.T. ten Kate, L.E.T. Stearne, and I.A.J.M. Bakker-Woudenberg, *Antimicrob. Agents Chemother.* **39**, 1954–1958 (1995).
42. S. Kohno et al., *Adv. Drug Delivery Rev.* **24**, 325–329 (1997).
43. T. Otsubo et al., *Antimicrob. Agents Chemother.* **42**, 40–44 (1998).
44. A.S. Janoff et al., *Proc. Natl. Acad. Sci. U.S.A.* **85**, 6122–6126 (1988).
45. J.M. Clark et al., *Antimicrob. Agents Chemother.* **35**, 615–621 (1991).
46. K. Mitsutake et al., *Mycopathologia* **128**, 13–17 (1994).
47. P.K. Sharkey et al., *Clin. Infect. Dis.* **22**, 315–321 (1996).
48. C.E. Gonzalez, D.R. Couriel, and T.J. Walsh, *Clin. Infect. Dis.* **24**, 192–196 (1997).
49. D.A. Stevens, *J. Infect.* **28**(S1), S45–S49 (1994).
50. J.S. Hostetler, K.V. Clemons, L.H. Hanson, and D.A. Stevens, *Antimicrob. Agents Chemother.* **36**, 2656–2660 (1992).
51. K.V. Clemons and D.A. Stevens, *Antimicrob. Agents Chemother.* **42**, 899–902 (1998).
52. S.W. Sanders et al., *Antimicrob. Agents Chemother.* **35**, 1029–1034 (1991).
53. G. Valero and J.R. Graybill, *Antimicrob. Agents Chemother.* **39**, 2588–2590 (1995).
54. E.J. Anaissie et al., *Antimicrob. Agents Chemother.* **42**, 606–611 (1998).
55. A. Oppenheim, R. Herbrecht, and S. Kusne, *Clin. Infect. Dis.* **21**, 1145–1153 (1995).
56. R.T. Mehta et al., *Antimicrob. Agents Chemother.* **31**, 1897–1900 (1987).
57. R.T. Mehta et al., *Antimicrob. Agents Chemother.* **31**, 1891–1903 (1987).
58. H. Miyamoto et al., *Curr. Eye Res.* **16**, 939–935 (1997).
59. J.P. Wong, L.L. Stadnyk, and E.G. Saravolac, *Immunology* **81**, 280–284 (1994).
60. T. Nagai et al., *Biol. Pharm. Bull.* **20**, 1082–1085 (1997).
61. J.A.A.M. Kamps et al., *Biochim. Biophys. Acta* **1278**, 183–190 (1996).
62. N.C. Philips and C. Tsuoukas, *Cancer Detect. Prev.* **14**, 383–390 (1990).
63. R. Bender et al., *Antimicrob. Agents Chemother.* **40**, 1467–1471 (1996).
64. D. Kuppermann et al., *J. Infect. Dis.* **173**, 18–23 (1996).
65. I. Taskintuna et al., *Retina* **17**(1), 57–64 (1997).
66. G. Banerjee et al., *J. Antimicrob. Chemother.* **38**(1), 145–150 (1996).
67. J.M. Rodrigues, Jr. et al., *Int. J. Parasitol.* **25**, 1437–1441 (1995).

INTELLIGENT DRUG DELIVERY SYSTEMS

JOSEPH KOST
Ben-Gurion University
Beer-Sheva, Israel

KEY WORDS

Antibody interaction
Chelation
Electrically modulated systems
Glucose-responsive systems
Inflammation-sensitive systems
Intelligent polymers
Magnetically modulated systems
Modulated systems
Morphine-triggered delivery
pH sensitive systems
Photo-responsive systems
Responsive systems
Smart polymers
Temperature-sensitive systems
Ultrasonically modulated systems
Urea responsive systems

Previous Page

14. N. Duzgunes et al., *Antimicrob. Agents Chemother.* **32**, 1404–1411 (1988).
15. H. Tomioka, H. Saito, K. Sato, and T. Yoneyama, *Am. Rev. Respir. Dis.* **43**, 1421–1428 (1991).
16. S.D. Nightingale et al., *Antimicrob. Agents Chemother.* **37**, 1869–1872 (1993).
17. H. Saito and H. Tomioka, *Antimicrob. Agents Chemother.* **33**, 429–433 (1989).
18. S. Majumdar et al., *Antimicrob. Agents Chemother.* **36**, 2808–2815 (1992).
19. C.O. Onyeji, C.H. Nightingale, D.P. Nicolau, and R. Quintiliani, *Antimicrob. Agents Chemother.* **38**, 523–527 (1994).
20. R.T. Mehta et al., *Antimicrob. Agents Chemother.* **37**, 2584–2587 (1993).
21. R.T. Mehta, *Antimicrob. Agents Chemother.* **40**, 1893–1902 (1996).
22. P. Deol, G.K. Khuller, and K. Joshi, *Antimicrob. Agents Chemother.* **41**, 1211–1214 (1997).
23. L. Kesavalu et al., *Tubercle* **71**, 215–218 (1990).
24. S.P. Klemens, M.H. Cynamon, C.E. Swenson, and R.S. Ginsberg, *Antimicrob. Agents Chemother.* **34**, 967–970 (1990).
25. N. Duzgunes et al., *J. Infect. Dis.* **164**, 143–151 (1991).
26. G. Medoff et al., *Clin. Infect. Dis.* **15**(S1), S274–S281 (1992).
27. N.H. Georgopapadakou and T.J. Walsh, *Antimicrob. Agents Chemother.* **40**, 279–291 (1996).
28. R.J. Hay, *J. Am. Acad. Dermatol.* **31**, S82–S85 (1994).
29. A.H. Groll and T.J. Walsh, *Curr. Opin. Infect. Dis.* **10**, 449–458 (1997).
30. J.D. Cleary et al., *Ann. Pharmacother.* **27**, 715–719 (1993).
31. J.W. Hiemenz and T.J. Walsh, *Clin. Infect. Dis.* **22**(S2), S133–S144 (1996).
32. J. Brajtburg and J. Bolard, *Clin. Microbiol. Rev.* **9**, 512–531 (1996).
33. G. Lopez-Berestein et al., *J. Infect. Dis.* **147**, 939–945 (1983).
34. S. de Marie, *Leukemia* **10**(S2), S93–S96 (1996).
35. J.R. Graybill et al., *J. Infect. Dis.* **145**, 748–752 (1982).
36. J. Tollemar et al., *Transplantation* **59**, 45–50 (1995).
37. B.E. Gilbert, P.R. Wyde, and S.Z. Wilson, *Antimicrob. Agents Chemother.* **36**, 1466–1471 (1992).
38. J. Seki et al., *J. Controlled Release* **28**, 352–353 (1994).
39. T. Otsubo et al., *Antimicrob. Agents Chemother.* **43**, 471–475 (1999).
40. M.A. Hossain et al., *Antimicrob. Agents Chemother.* **42**, 1722–1725 (1998).
41. E.W.M. van Etten, M.T. ten Kate, L.E.T. Stearne, and I.A.J.M. Bakker-Woudenberg, *Antimicrob. Agents Chemother.* **39**, 1954–1958 (1995).
42. S. Kohno et al., *Adv. Drug Delivery Rev.* **24**, 325–329 (1997).
43. T. Otsubo et al., *Antimicrob. Agents Chemother.* **42**, 40–44 (1998).
44. A.S. Janoff et al., *Proc. Natl. Acad. Sci. U.S.A.* **85**, 6122–6126 (1988).
45. J.M. Clark et al., *Antimicrob. Agents Chemother.* **35**, 615–621 (1991).
46. K. Mitsutake et al., *Mycopathologia* **128**, 13–17 (1994).
47. P.K. Sharkey et al., *Clin. Infect. Dis.* **22**, 315–321 (1996).
48. C.E. Gonzalez, D.R. Couriel, and T.J. Walsh, *Clin. Infect. Dis.* **24**, 192–196 (1997).
49. D.A. Stevens, *J. Infect.* **28**(S1), S45–S49 (1994).
50. J.S. Hostetler, K.V. Clemons, L.H. Hanson, and D.A. Stevens, *Antimicrob. Agents Chemother.* **36**, 2656–2660 (1992).
51. K.V. Clemons and D.A. Stevens, *Antimicrob. Agents Chemother.* **42**, 899–902 (1998).
52. S.W. Sanders et al., *Antimicrob. Agents Chemother.* **35**, 1029–1034 (1991).
53. G. Valero and J.R. Graybill, *Antimicrob. Agents Chemother.* **39**, 2588–2590 (1995).
54. E.J. Anaissie et al., *Antimicrob. Agents Chemother.* **42**, 606–611 (1998).
55. A. Oppenheim, R. Herbrecht, and S. Kusne, *Clin. Infect. Dis.* **21**, 1145–1153 (1995).
56. R.T. Mehta et al., *Antimicrob. Agents Chemother.* **31**, 1897–1900 (1987).
57. R.T. Mehta et al., *Antimicrob. Agents Chemother.* **31**, 1891–1903 (1987).
58. H. Miyamoto et al., *Curr. Eye Res.* **16**, 939–935 (1997).
59. J.P. Wong, L.L. Stadnyk, and E.G. Saravolac, *Immunology* **81**, 280–284 (1994).
60. T. Nagai et al., *Biol. Pharm. Bull.* **20**, 1082–1085 (1997).
61. J.A.A.M. Kamps et al., *Biochim. Biophys. Acta* **1278**, 183–190 (1996).
62. N.C. Philips and C. Tsuoukas, *Cancer Detect. Prev.* **14**, 383–390 (1990).
63. R. Bender et al., *Antimicrob. Agents Chemother.* **40**, 1467–1471 (1996).
64. D. Kuppermann et al., *J. Infect. Dis.* **173**, 18–23 (1996).
65. I. Taskintuna et al., *Retina* **17**(1), 57–64 (1997).
66. G. Banerjee et al., *J. Antimicrob. Chemother.* **38**(1), 145–150 (1996).
67. J.M. Rodrigues, Jr. et al., *Int. J. Parasitol.* **25**, 1437–1441 (1995).

INTELLIGENT DRUG DELIVERY SYSTEMS

JOSEPH KOST
Ben-Gurion University
Beer-Sheva, Israel

KEY WORDS

Antibody interaction
Chelation
Electrically modulated systems
Glucose-responsive systems
Inflammation-sensitive systems
Intelligent polymers
Magnetically modulated systems
Modulated systems
Morphine-triggered delivery
pH sensitive systems
Photo-responsive systems
Responsive systems
Smart polymers
Temperature-sensitive systems
Ultrasonically modulated systems
Urea responsive systems

OUTLINE

- Pulsatile Systems
  - Magnetically Modulated Systems
  - Ultrasonically Modulated Systems
  - Electrically Regulated Systems
  - Photoresponsive Systems
- Responsive Systems
  - Temperature-Sensitive Systems
  - Systems Sensitive to pH
  - Inflammation-Responsive Systems
  - Glucose and Other Saccharide-Sensitive Polymers
- Systems Utilizing Enzymes
  - Urea Responsive Delivery
  - Glucose-Responsive Insulin Delivery
  - Morphine-Triggered Naltrexone Delivery Systems
- Systems Utilizing Antibody Interactions
- Systems Utilizing Chelation
- Concluding Remarks
- Bibliography

The ideal drug delivery system should provide therapeutics in response to physiological requirements, having the capacity to "sense" changes and alter the drug-release process accordingly. The basic approach that drug concentration–effect relationships are significantly invariant as a function of time in humans has led to the development of constant-rate drug delivery systems (1). Nevertheless, there are a number of clinical situations where such an approach may not be sufficient. These include the delivery of insulin for patients with diabetes mellitus, antiarrhythmics for patients with heart rhythm disorders, gastric acid inhibitors for ulcer control, and nitrates for patients with angina pectoris as well as selective β-blockade, birth control, general hormone replacement, immunization, and cancer chemotherapy. Recent studies in the field of chronopharmacology indicate that the onset of certain diseases exhibits strong circadian temporal dependency. Thus, drug delivery patterns can be further optimized by pulsed or self-regulated delivery, adjusted to the staging of biological rhythms (2).

Modulated drug delivery systems are devices that are implanted or injected into the body and are capable of releasing drugs in response to external stimuli such as magnetic fields, heat, ultrasound, pH, or concentration of a specific molecule. These "intelligent" delivery systems can be classified as open- or closed-loop systems. Open-loop control systems are those in which information about the controlled variable is not automatically used to adjust the system inputs to compensate for the change in the process variables, whereas in closed-loop control systems, the controlled variable is detected, and as a result the system output is adjusted accordingly. In the controlled drug delivery field, open-loop systems are known as *pulsatile* or *externally regulated*, and the closed-loop systems as *self-regulated*. The externally controlled devices apply external triggers for pulsatile delivery such as magnetic, ultrasonic, thermal, electric, and electromagnetic irradiation, whereas in the self-regulated devices, the release rate is controlled by feedback information without any external intervention. The self-regulated systems utilize several approaches as rate-control mechanisms: pH-sensitive polymers, enzyme–substrate reactions, pH-sensitive drug solubility, competitive binding, antibody interactions, and metal concentration–dependent hydrolysis.

This article outlines the fundamental principles of both pulsatile and self-regulated systems for drug delivery.

PULSATILE SYSTEMS

Magnetically Modulated Systems

An early approach to pulsatile delivery involved incorporating magnetic beads in elastic polymers. When an oscillating magnetic field was applied, more drug was released (Fig. 1). Studies demonstrated that insulin and other molecules could be continuously released by embedding the hormone in a carrier such as ethylene-vinyl acetate copolymer (EVAc) (3). In vitro studies were then conducted characterizing the critical parameters affecting release rates (4). This information was utilized to design subcutaneous implants of EVAc–insulin, which decreased the glucose levels of diabetic rats for 105 days (5). The next step in designing a delivery system for use in diabetes was to develop a system that would be capable of releasing insulin at a higher rate upon demand. In vitro studies were conducted showing that EVAc–protein matrices containing magnetic beads exhibit enhanced release rates when placed in an oscillating external magnetic field (6–8). In vivo studies (9) showed that when polymeric matrices containing insulin and magnetic beads were implanted in diabetic rats, glucose levels could be repeatedly decreased on demand by application of an oscillating magnetic field.

The systems consists of drug powder dispersed within a polymeric matrix together with magnetic beads. One method of formulating this system is to add approximately 50% of the drug–polymer mixture to a glass mold that has been cooled to $-80°C$ using dry ice. The magnetic particles are added, followed by the remaining drug–polymer mixture (7). In addition to the experimental polymer matrices containing both magnets and insulin, controls, including polymer matrices that contained a magnet but no insulin and that contained insulin but no magnet, were made.

When a polymer matrix containing insulin and a magnet was implanted into a diabetic rat (9), the blood glucose

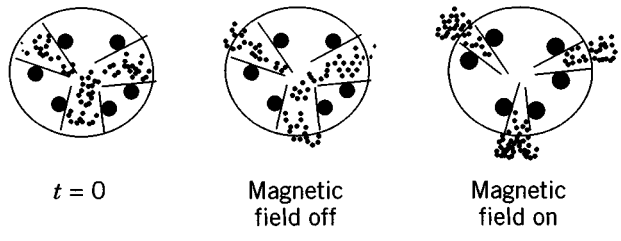


Figure 1. Schematic presentation of a magnetic-triggered controlled-release system. Large dots are magnetic beads; small dots represent drug (1).

level fell from over 400 mg % to nearly 200 mg %. In the absence of the magnetic field, the blood glucose level remained near this value over the 51-day implantation period. However, every time the magnetic field was applied, the blood glucose level decreased. The average decrease for the three rats in the experimental group, which were triggered a total of 26 times, was 29.4%. The difference in glucose changes between the experimental group and the controls (14 rats, 97 triggers) was highly significant. These results were confirmed by an insulin radioimmunoassay (RIA).

The factors that are critical in controlling the release rates in these systems can be characterized by two main groups: (*1*) magnetic field characteristics and (*2*) mechanical properties of the polymer matrix. It was found that the extent of release enhancement increases as the magnetic field amplitude rises. When the frequency of the applied field was increased from 5 to 11 Hz, the release rate of bovine serum albumin (BSA) from EVAc copolymer matrices rose in a linear fashion (7). Saslavski et al. (10) investigated the effect of magnetic field frequency and repeated field application on insulin release from alginate matrices and found that with repeated applications, inverse effects can occur: High frequencies gave a significant release enhancement for the second magnetic field application, after which the enhancement level decreased owing to faster depletion at these frequencies.

The mechanical properties of the polymeric matrix also affect the extent of magnetic enhancement (6). For example, the modulus of elasticity of the EVAc copolymer can be easily altered by changing the vinyl acetate content of the copolymer. The release-rate enhancement induced by the magnetic field increase as the modulus of elasticity of EVAc decreases. A similar phenomenon was observed for the cross-linked alginate matrices: higher release-rate enhancement for less rigid matrices. Edelman et al. (11) also showed that enhanced release rates observed in response to an electromagnetic field (50 G, 60 Hz) applied for 4 min were independent of the duration of the interval between repeated pulses.

Ultrasonically Modulated Systems

Kost et al. (12) suggested the feasibility of ultrasonic-controlled polymeric delivery systems in which release rates of substances can be repeatedly modulated at will from a position external to the delivery system. Both bioerodible and nonerodible polymers were used as drug carrier matrices. The bioerodible polymers evaluated were polyglycolide, polylactide, poly(bis(*p*-carboxyphenoxy) alkane anhydrides and their copolymers with sebacic acid. The releasing agents were *p*-nitroaniline, *p*-aminohippurate, bovine serum albumin, and insulin.

Enhanced polymer erosion and drug release were observed when the bioerodible samples were exposed to ultrasound. The systems response to the ultrasonic triggering was rapid (within 2 min) and reversible. The enhanced release was also observed in nonerodible systems exposed to ultrasound where the release is diffusion dependent. Release rates of zinc bovine insulin from EVAc matrices were 15 times higher when exposed to ultrasound compared with the unexposed periods. It has also been demonstrated that the extent of enhancement can be regulated by the intensity, frequency, or duty cycle of the ultrasound (12).

To assess the effect of ultrasonic energy on the integrity of the releasing molecules, insulin samples were evaluated by high-pressure liquid chromatography (HPLC). No significant difference was detected between insulin samples exposed to ultrasound and unexposed samples, suggesting that the ultrasound is not degrading the releasing molecules (12).

In vivo studies have suggested the feasibility of ultrasound-mediated drug release enhancement (12). Implants composed of polyanhydride polymers loaded with 10% para-aminohippuric acid (PAH) were implanted subcutaneously in the back of catheterized rats. When exposed to ultrasound, a significant increase in the PAH concentration in urine was detected (400%) (Fig. 2). The Rats' skin histopathology of the ultrasound-treated area after an exposure of 1 h at 5 W/cm^2 did not reveal any differences between treated and untreated skin.

It was proposed (12) that cavitation and acoustic streaming are responsible for this augmented degradation and release. In experiments conducted in a degassed buffer, where cavitation was minimized, the observed enhancement in degradation and release rates was much smaller. It was also considered that several other parameters (temperature and mixing effects) might be responsible for the augmented release due to ultrasound. However, experiments were conducted that suggested that these parameters were not significant. A temperature rise of only 2.5°C was recorded in the samples during the triggering

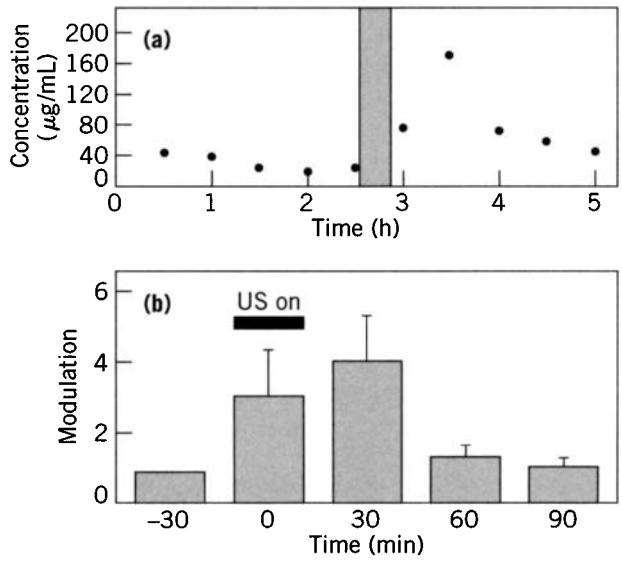


Figure 2. (**a**) Para-amino hippuric acid (PAH) concentration in the urine of Sprague-Dawley rats as a function of time before, during, and after a 20-min exposure to ultrasound (shaded area). (**b**) Modulation versus time expressed as a mean and standard deviation of four experimental rats. (Modulation was defined as the ratio of PAH concentration during and after the ultrasound [US] exposure to the mean of the PAH concentration before the exposure) (12).

period. A separate release experiment done at 40°C instead of 37°C showed that the rate increase was below 20%. To evaluate the ultrasound effect on the diffusion boundary layer, release experiments were performed under vigorous shaking. The increase of the release rates due to shaking were always below 20%. Therefore, it was concluded that the effect of the ultrasound on the augmented release cannot be due to mixing or temperature only.

Similar phenomena were observed by Miyazaki et al. (13) who evaluated the effect of ultrasound (1 MHz) on the release rates of insulin from ethylene-vinyl alcohol copolymer matrices and reservoir-type drug delivery systems. When diabetic rats receiving implants containing insulin were exposed to ultrasound (1 W/cm^2 for 30 min), a sharp drop in blood glucose levels was observed after the irradiation, indicating a rapid rate of release of insulin in the implanted site. The authors speculate that the ultrasound caused increased temperature in the delivery system, which may facilitate diffusion.

Over the past 40 years, numerous clinical reports have been published concerning phonophoresis (14). The technique involves placing the topical preparation on the skin over the area to be treated and massaging the area with an ultrasound probe. In the last decade, with the development of transdermal delivery as an important means of systemic drug administration, researchers investigated the possible application of ultrasound into transdermal delivery systems. Kost et al. (14–16) studied in rats and guinea pigs the effect of therapeutic ultrasound (1 MHz) on skin permeability of D-mannitol, a highly polar sugar alcohol; insulin, a high-molecular-weight polysaccharide; and physostigmine, a lipophilic anticholinesterase drug. Ultrasound nearly completely eliminated the lag time usually associated with transdermal delivery of drugs. Three to five minutes of ultrasound irradiation (1.5 W/cm^2 continuous wave or 3 W/cm^2 pulsed wave) increased the transdermal permeation of inulin and mannitol in rats by 5–20-fold within 1–2 h following ultrasound application. Ultrasound treatment also significantly increased the inhibition of cholinesterase during the first hour after application in both physostigmine-treated rats and guinea pigs.

Miyazaki et al. (17) performed similar studies evaluating the effect of ultrasound (1 MHz) on indomethacin permeation in rats. Pronounced effect of ultrasound on transdermal absorption for all three ranges of intensities (0.25, 0.5, and 0.75 W/cm^2) was observed. Bommannan et al. (18) examined the effects of ultrasound on the transdermal permeation of lanthanum nitrate, an electron-dense tracer. The results demonstrate that exposure of the skin to ultrasound can induce considerable and rapid tracer transport through an intercellular route. Prolonged exposure of the skin to high-frequency ultrasound (20 min, 16 MHz), however, resulted in structural alterations of epidermal morphology. Tachibana and Tachibana (19–21) have reported use of low-frequency ultrasound (48 KHz) to enhance transdermal transport of lidocaine and insulin across hairless mice skin. Low-frequency ultrasound has also been used by Mitragotri et al. (22,23) to enhance transport of various low-molecular-weight drugs including salicylic acid and corticosterone as well as high-molecular-weight proteins including insulin, γ-interferon, and erythropoeitin across human skin in vitro and in vivo.

Mitragotri et al. (24) also evaluated the role played by various ultrasound-related phenomena, including cavitation, thermal effects, generation of convective velocities, and mechanical effects. The authors' experimental findings suggest that among all the ultrasound-related phenomena evaluated, cavitation plays the dominant role in sonophoresis using therapeutic ultrasound (frequency, 1–3 MHz; intensity, 0–2 W/cm^2). Confocal microscopy results indicate that cavitation occurs in the keratinocytes of the stratum corneum upon ultrasound exposure. The authors hypothesized that oscillations of the cavitation bubbles induce disorder in the stratum corneum lipid bilayers, thereby enhancing transdermal transport. The theoretical model developed to describe the effect of ultrasound on transdermal transport predicts that the sonophoretic enhancement depends most directly on the passive permeant diffusion coefficient in water and not on the permeant diffusion coefficient through the skin.

Electrically Regulated Systems

Electrically controlled systems provide drug release by the action of an applied electric field on a rate-limiting membrane and/or directly on the solute, thus controlling its transport across the membrane. The electrophoretic migration of a charged macrosolute within a hydrated membrane results from the combined response to the electrical forces on the solute and its associated counterions in the adjacent electrolyte solution (25). Grimshaw et al. (26) reported four different mechanisms for the transport of proteins and neutral solutes across hydrogel membranes (*1*) electrically and chemically induced swelling of a membrane to alter the effective pore size and permeability, (*2*) electrophoretic augmentation of solute flux within a membrane, (*3*) electrosmotic augmentation of solute flux within a membrane, and (*4*) electrostatic partitioning of charged solutes into charged membranes.

Electrically controlled membrane permeability has also been of interest in the field of electrically controlled or enhanced transdermal drug delivery (e.g., iontophoresis, electroporation) (27,28).

Kwon et al. (29) studied the effect of electric current on solute release from cross-linked poly(2-acrylamido-2-methylpropane sulfonic acid-*co*-*n*-butylmethacrylate). Edrophonium chloride, a positively charged solute, was released in an on–off pattern from a matrix (monolithic) device with electric field. The mechanism was explained as an ion exchange between positive solute and hydroxonium ion, followed by fast release of the charged solute from the hydrogel. The fast release was attributed to the electrostatic force, squeezing effect, and the electroosmosis of the gel. However, the release of neutral solute was controlled by diffusion effected by swelling and deswelling of the gel.

Anionic gels as vehicles for electrically modulated drug delivery were studied by Hsu and Block (30). Agarose and combination of agarose with anionic polymers (polyacrylic acid, xanthan gum) were evaluated. The authors conclude the use of carbomer (polyacrylic acid) in conjunction with agarose enables the formulator to achieve zero-order re-

lease with electrical application. Increased anisotropicity of a gel system due to the application of electrical current could alter the effectiveness of a drug delivery system.

D'Emanuele and Staniforth (31) proposed a drug delivery device that consists of a polymer reservoir with a pair of electrodes placed across the rate-limiting membrane. By altering the magnitude of the electric field between the electrodes, the authors proposed to modulate the drug release rates in a controlled and predictable manner. A linear relationship was found between current and propanolol hydrochloride permeability through poly(2-hydroxyethyl methacrylate) (PHEMA) membranes cross-linked with ethylene glycol dimethacrylate (1% v/v). Buffer ionic strength and drug reservoir concentration as well as electrode polarity were found to have significant effects on drug permeability (32).

Labhasetwar et al. (33) propose similar approach for a cardiac drug delivery modulation. The authors studied a cardiac drug implant in dogs that is capable of electric current modulation. Cation-exchange membrane was used as an electrically sensitive rate-limiting barrier on the cardiac-contacting surface of the implant. The cardiac implant demonstrated in vitro drug-release rates that were responsive to current modulation. In vivo results in dogs have confirmed that electrical modulation resulted in regional coronary enhancement of the drug levels with current responsive increase in drug concentration.

A different approach for electrochemical-controlled release is based on polymers that bind and release bioactive compounds in response to an electric signal (34). The polymer has two redox states, only one of which is suitable for ion binding. Drug ions are bound in one redox state and released from the other. The attached electrodes serve to switch the redox states, and the amount of current passed can control the amount of ions released.

Photoresponsive Systems

Photoresponsive gels change their physical or chemical properties reversibly upon photoradiation. A photoresponsive polymer consists of a photoreceptor, usually a photochromic chromophore, and a functional part. The optical signal is captured by the photochromic molecules, and then the isomerization of the chromophores in the photoreceptor converts it to a chemical signal. Photoinduced phase transition of gels was reported by Mamada et al. (35). Copolymer gels of *N*-isopropylacrylamide and a photosensitive molecule, bis(4-dimethylamino)phenyl)(4-vinylphenyl)methyl leucocyanide, showed a discontinuous volume-phase transition upon ultraviolet irradiation, caused by osmotic pressure of cyanide ions created by the ultraviolet irradiation. Suzuki and Tanaka (36) reported on phase transition in polymer gels induced by visible light, where the transition mechanism is due only to the direct heating of the network polymer by light. Yui et al. (37) proposed photoresponsive degradation of heterogeneous hydrogels comprising cross-linked hyaluronic acid and lipid microspheres for temporal drug delivery. A visible light–induced degradation of cross-linked hyaluronic acid gels by photochemical oxidation using methylene blue as a photosensitizer. (The hyaluronic acid gels were also proposed by the authors to be inflammation responsive [38].)

RESPONSIVE SYSTEMS

Polymers that alter their characteristics in response to changes in their environment have been of great recent interest. Several research groups have been developing drug delivery systems based on these responsive polymers that more closely resemble the normal physiological process. In these devices, drug delivery is regulated by means of an interaction with the surrounding environment (feedback information) without any external intervention. The most commonly studied polymers having environmental sensitivity are either pH or temperature sensitive (Fig. 3).

Temperature-Sensitive Systems

Temperature-sensitive polymers can be classified into two groups based on the origin of the thermosensitivity in aqueous media. The first is based on polymer–water interactions, especially specific hydrophobic/hydrophilic balancing effects and the configuration of side groups. The other is based on polymer–polymer interactions in addition to polymer–water interactions. When polymer networks swell in a solvent, there is usually a negligible or small positive enthalpy of mixing or dilution. Although a positive enthalpy change opposes the process, the large gain in the entropy drives it. In aqueous polymer solutions, the opposite is often observed. This unusual behavior is associated with a phenomenon of polymer-phase separation as the temperature is raised to a critical value, known as the lower critical solution temperature (LCST). *N*-alkyl acrylamide homopolymers and their copolymers, including acidic or basic comonomers show this LCST (39,40). Polymers characterized by LCST usually shrink, as the temperature is increased through the LCST. Lowering the temperature below LCST results in the swelling of the polymer. Bioactive agents such as drugs, enzymes, and antibodies may be immobilized on or within the temperature-sensitive polymers. Responsive drug-release patterns regulated by temperature changes have been recently demonstrated by several groups (39,41–52).

Systems Sensitive to pH

The pH range of fluids in various segments of the gastrointestinal tract may provide environmental stimuli for responsive drug release. Studies by several research groups (53–65) have been performed on polymers containing weakly acidic or basic groups in the polymeric backbone. The charge density of the polymers depends on pH and

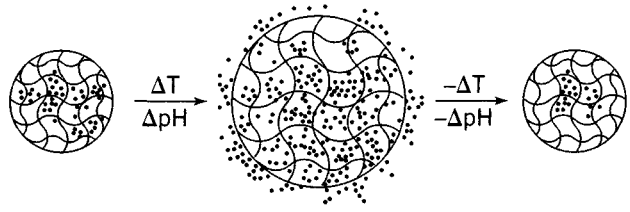


Figure 3. Schematic presentation of pH- or temperature-controlled drug delivery systems. Small dots represent drugs; lines represent polymer chains (1). (Δ can be positive or negative.)

ionic composition of the outer solution (the solution into which the polymer is exposed). Altering the pH of the solution will cause swelling or deswelling of the polymer. Thus, drug release from devices made from these polymers will display release rates that are pH dependent. Polyacidic polymers will be unswollen at low pH, because the acidic groups will be protonated and hence unionized. With increasing pH, polyacid polymers will swell. The opposite holds for polybasic polymers, because the ionization of the basic groups will increase with decreasing pH. Siegel et al. (66) found the swelling properties of the polybasic gels are influenced also by buffer composition (concentration and pK_a). A practical consequence proposed is that these gels may not reliably mediate pH-sensitive swelling-controlled release in oral applications, because the levels of buffer acids in the stomach (where swelling and release are expected to occur) generally cannot be controlled. However, the gels may be useful as mediators of pH-triggered release when precise rate control is of secondary importance.

Annaka and Tanaka (54) reported that more than two phases (swollen and collapsed) can be found in gels consisting of copolymers of randomly distributed positively and negatively charged groups. In these gels, polymer segments interact with each other through attractive or repulsive electrostatic interactions and through hydrogen bonding. The combination of these forces seems to result in the existence of several phases, each characterized by a distinct degree of swelling, with abrupt jumps between them. The existence of these phases presumably reflects the ability of macromolecular systems to adopt different stable conformations in response to changes in environmental conditions. For copolymer gels prepared from acrylic acid (the anionic constituent) and methacryl-amidopropyl-trimethyl ammonium chloride (460 mmol/240 mmol), the largest number of phases was seven. A similar approach was proposed by Bell and Peppas (64); membranes made from grafted poly(methacrylic acid-*g*-ethylene glycol) copolymer showed pH sensitivity due to complex formation and dissociation. Uncomplexed equilibrium swelling ratios were 40 to 90 times higher than those of complexed states and varied according to copolymer composition and polyethylene glycol graft length.

Giannos et al. (67) proposed temporally controlled drug delivery systems, coupling pH oscillators with membrane-diffusion properties. By changing the pH of a solution relative to the pK_a, a drug may be rendered charged or uncharged. Because only the uncharged form of a drug can permeate across lipophilic membranes, a temporally modulated delivery profile may be obtained with a pH oscillator in the donor solution.

Heller and Trescony (68) were the first to propose the use of pH-sensitive bioerodible polymers. In their approach, described in the section on systems utilizing enzymes, an enzyme–substrate reaction produces a pH change that is used to modulate the erosion of a pH-sensitive polymer containing a dispersed therapeutic agent.

Bioerodible hydrogels containing azoaromatic moieties were synthesized by Ghandehari et al. (69). Hydrogels with lower cross-linking density underwent a surface erosion process and degraded at a faster rate. Hydrogels with higher cross-linking densities degraded at a slower rate by a process where the degradation front moved inward to the center of the polymer.

Recently recombinant DNA methods were used to create artificial proteins that undergo reversible gelation in response to changes in pH or temperature (70). The proteins consist of terminal leucine zipper domains flanking a central, flexible, water-soluble polyelectrolyte segment. Formation of coiled-coil aggregates of the terminal domains in near-neutral aqueous solutions triggers formation of a three-dimensional polymer network, with the polyelectrolyte segment retaining solvent and preventing precipitation of the chain. Dissociation of the coiled-coil aggregates through elevation of pH or temperature causes dissolution of the gel and a return to the viscous behavior that is characteristic of polymer solution. The authors suggest these hydrogels have potential in bioengineering applications requiring encapsulation or controlled release of molecules and cellular species.

Inflammation-Responsive Systems

Yui et al. (38) proposed an inflammation-responsive drug delivery system based on biodegradable hydrogels of cross-linked hyaluronic acid. Hyaluronic acid is specifically degraded by hydroxyl radicals, which are produced by phagocytic cells such as leukocytes and macrophages, locally at inflammatory sites. In their approach, drug-loaded lipid microspheres were dispersed into degradable matrices of cross-linked hyaluronic acid.

Glucose and Other Saccharide-Sensitive Polymers

The basic principle of competitive binding and its application to controlled drug delivery was first presented by Brownlee and Cerami (71), who suggested the preparation of glycosylated insulins, which are complementary to the major combining site of carbohydrate-binding proteins such as Concavalin A (Con A). Con A is immobilized on sepharose beads. The glycosylated insulin, which is biologically active, is displaced from the Con A by glucose in response to, and proportional to, the amount of glucose present, which competes for the same binding sites. Kim et al. (72–79) found that the release rate of insulin also depends on the binding affinity of an insulin derivative to the Con A and can be influenced by the choice of saccharide group in glycosylated insulin. By encapsulating the glycosylated insulin-bound Con A with a suitable polymer that is permeable to both glucose and insulin, the glucose influx and insulin efflux would be controlled by the encapsulation membrane (Fig. 4).

It was found (73) that the glycosylated insulins are more stable against aggregation than commercial insulin and are also biologically active. The functionality of the intraperitoneally implanted device was tested in pancreatectomized dogs by an intravenous glucose tolerance test (IVGTT). The effect of an administered 500 mg/kg dextrose bolus on blood glucose level was compared with normal and pancreatectomized dogs without an implant. Figure 5 shows the results of this study (78). In addition, the blood glucose profile for a period of 2 days demonstrated that a diabetic dog, implanted with the self-regulating insulin

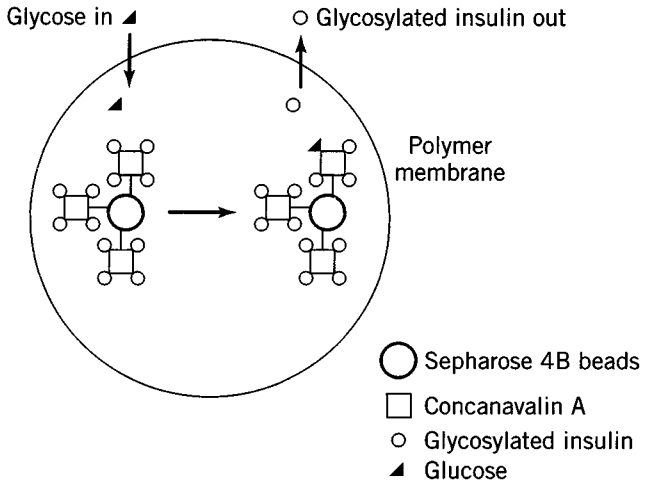


Figure 4. Schematic presentation of a self-regulated insulin delivery system based on competitive binding (79).

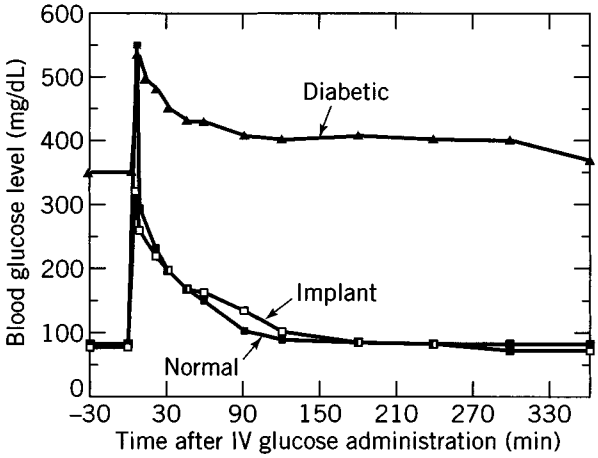


Figure 5. Peripheral blood glucose profiles of dogs administered bolus dextrose (500 mg/kg) during an intravenous glucose tolerance test. Blood glucose levels at $t = -30$ min show the overnight fasting level 30 min prior to bolus injection of dextrose (79).

delivery system, was capable of maintaining acceptable glucose levels (50–180 mg/dL) for the majority of the experiment (40 h) (75–77). Makino et al. (72) proposed a modification based on hydrophilic nylon microcapsules containing Con A and succinil-amidophenyl-glucopyranoside insulin.

Kokufata et al. (80) reported on a gel system that swells and shrinks in response to specific saccharides. The gel consists of a covalently cross-linked polymer network of *N*-isopropylacrylamide in which the lectin, Con A, is immobilized. Con A displays selective binding affinities for certain saccharides. For example, when the saccharide dextran sulphate is added to the gel, it swells to a volume up to 5 times greater. Replacing dextran sulphate with nonionic saccharide α-methyl-D-mannopyranoside brings about collapse of the gel back to almost its native volume. The process is reversible and repeatable.

Taylor et al. (81) proposed similar approach for the delivery of insulin. The self-regulating delivery device, responsive to glucose, has been shown to operate in vitro. The device comprises an reservoir of insulin and a gel membrane that determines the delivery rates of insulin. The gel consists of a synthetic polysucrose and a lectin, Con A. The mechanism is one of displacement of the branched polysaccharide from the lectin receptors by incoming glucose. The gel loses its high viscosity as a result but reforms on removal of glucose, thus providing the rate-controlling barrier for the diffusion of insulin or any other antihyperglycemic drugs.

A similar approach was also presented by Park et al. (82–84), who synthesized glucose-sensitive membranes based on the interaction between polymer-bound glucose and Con A.

Kitano et al. (85) proposed a glucose-sensitive insulin-release system based on a sol–gel transition. A phenylboronic acid (PBA) moiety was incorporated in poly(*N*-vinyl-2-pyrrolidone) by the radical copolymerization of *N*-vinyl-2-pyrrolidone with *m*-acrylamidophenylboronic acid (poly [NVP-*co*-PBA]). Insulin was incorporated into a polymer gel formed by a complex of poly(vinyl alcohol) with poly(NVP-*co*-PBA) (Fig. 6). PBA can form reversible covalent complexes with molecules having diol units, such as

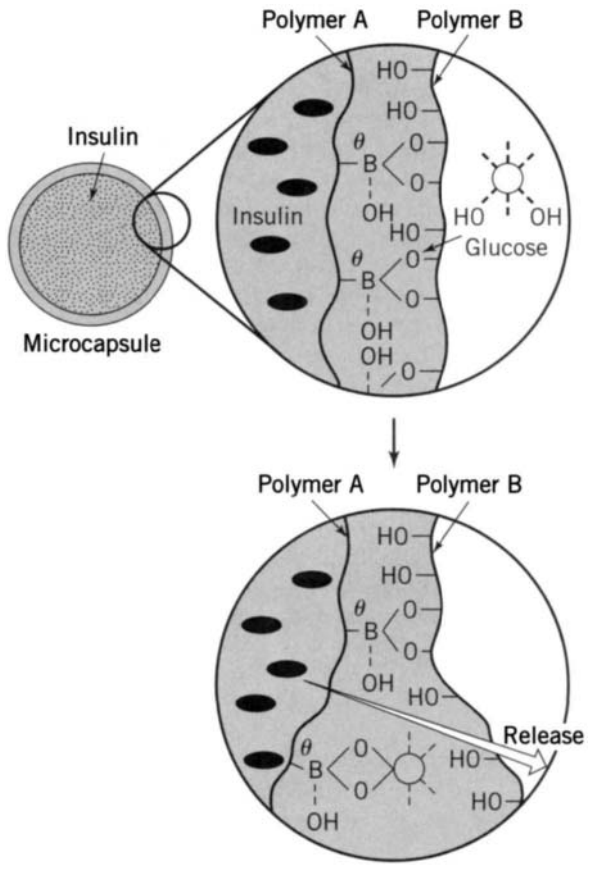


Figure 6. Schematic presentation of glucose-sensitive insulin-release system using PVA–poly(NVP-*co*-PBA) complex system (85).

glucose or PVA. With the addition of glucose, PVA in the PVA–boronate complex is replaced by glucose. This leads to a transformation of the system from gel to sol state, which facilitates the release of insulin from the polymeric complex. The same group (86) modified the approach suggesting glucose-responsive gels based on the complexation between polymers having PBA groups and PVA. The introduction of an amino group into PBA polymers was effective for increasing the complexation ability and the glucose responsivity at physiological pH.

SYSTEMS UTILIZING ENZYMES

In this approach, the mechanism is based on an enzymatic reaction. One possible approach studied is an enzyme reaction that results in a pH change and a polymer system that can respond to that change.

Urea Responsive Delivery

Heller and Trescony (68) were the first to attempt using immobilized enzymes to alter local pH and thus cause changes in polymer erosion rates. The proposed system is based on the conversion of urea to NH_4HCO_3 and NH_4OH by the action of urease. As this reaction causes a pH increase, a polymer that is subjected to increased erosion at high pH is required.

The authors suggested a partially esterified copolymer of methyl vinyl ether and maleic anhydride (Scheme 1). This polymer displays release rates that are pH dependent. The polymer dissolves by ionization of the carboxylic acid group (87).

A schematic presentation of the experimental device is shown in Figure 7. The pH-sensitive polymer shown in Scheme 1 containing dispersed hydrocortisone is surrounded with urease immobilized in a hydrogel prepared by cross-linking a mixture of urease and bovine serum albumin with glutaraldehyde. When urea diffuses into the hydrogel, its interaction with the enzyme leads to a pH increase, therefore enhancing erosion of the pH-sensitive polymer with concomitant changes in the release of hydrocortisone.

Figure 8 shows release of hydrocortisone from the described device. Although the device has no therapeutic relevance, it established the feasibility of creating self-responsive delivery system.

Ishihara et al. (89,90) suggested a nonerodible system based on a similar idea. The system is comprised of a pH-sensitive membrane prepared by copolymerizing 4-carboxyacrylanilide with methacrylate, sandwiched within a membrane containing urease immobilized in free radically crosslinked *N,N*-methylenebisacrylamide. The permeation of a model substance (1,4-bis(2-hydroxyethoxy) benzene varied with the urea concentration in the external solution.

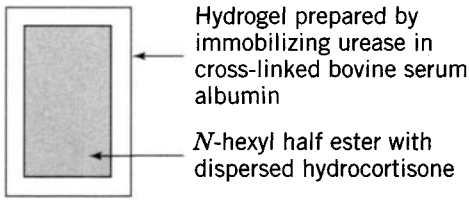


Figure 7. Schematic presentation of urea-sensitive drug delivery system (88).

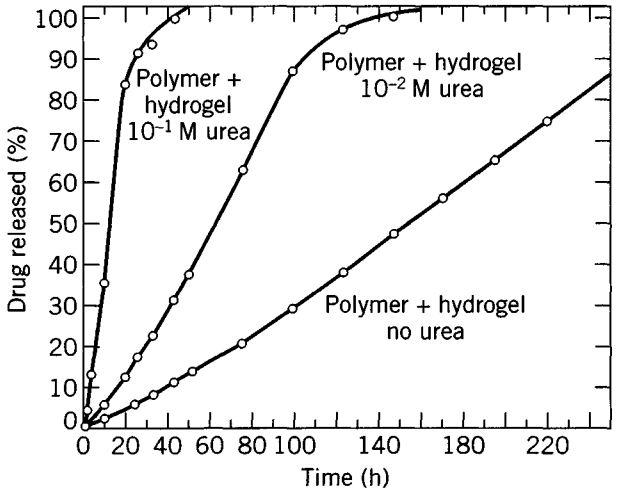
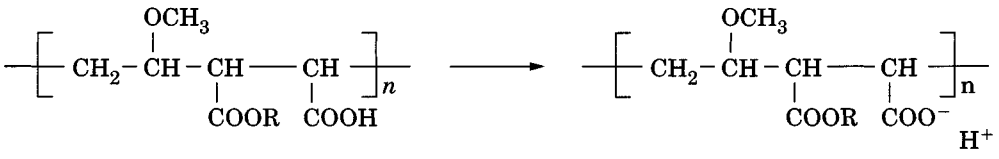


Figure 8. Hydrocortisone release from the *N*-hexyl ester of methylvinylether and maleic anhydride disks coated with immobilized urease in the presence and absence of external urea, 35°C, pH 6.25, hydrocortisone loading 10 wt % (68).

Glucose-Responsive Insulin Delivery

Glucose-responsive delivery systems utilizing enzymes are based on the enzymatic reaction of glucose oxidase with glucose shown in Scheme 2. Several approaches have been devised.



Insoluble Soluble

Scheme 1. Solubilization of a partially esterified copolymer of methyl vinyl ether and maleic anhydride by ionization of pendent carboxylic acid functions (87).

$$\text{Glucose} + O_2 \xrightarrow[\text{oxidase}]{\text{Glucose}} \text{Gluconic acid} + H_2O_2$$

Scheme 2. Glucose oxidase catalyzes the conversion of glucose to gluconic acid and hydrogen peroxide.

Systems based on pH-sensitive polymers consist of immobilized glucose oxidase in a pH-responsive hydrogel, enclosing a saturated insulin solution or incorporated with insulin (91–99). As glucose diffuses into the hydrogel, glucose oxidase catalyzes its conversion to gluconic acid, thereby lowering the pH in the microenvironment of the hydrogel and causing swelling (Fig. 9). Because insulin should permeate the swelled hydrogel more rapidly, faster delivery of insulin in the presence of glucose is anticipated. As the glucose concentration decreases in response to the released insulin, the hydrogel should contract and decrease the rate of insulin delivery.

Horbett and coworkers (91–98) immobilized glucose oxidase in a cross-linked hydrogel made from *N,N*-dimethylaminoethyl methacrylate (DMA), hydroxyethyl methacrylate (HEMA), and tetraethylene glycol dimethacrylate (TEGDMA). Membranes were prepared at −70°C by radiation polymerization, previously shown to retain the enzymatic activity (100). To obtain sufficient insulin permeability through the gels, porous HEMA/DMA gels were prepared by polymerization under conditions that induce a separation into two phases during polymerization: one phase rich in polymer and the other rich in solvent plus unreacted monomer. When gelation occurs after the phase separation, the areas where the solvent/monomer phase existed become fixed in place as pores in the polymer matrix. The authors used a dilute monomer solution to obtain porous gel, typically 1–10 μm in diameter (92).

The rate of insulin permeation through the membranes was measured in the absence of glucose in a standard transport cell; then glucose was added to one side of the cell to a concentration of 400 mg/dL while the permeation measurement was continued. The results indicated that the insulin transport rate is enhanced significantly by the addition of glucose. The average permeability after addition of 400 mg/dL glucose was 2.4 to 5.5 times higher than before glucose was added. When insulin permeabilities through the porous gels were measured in a flowing system in which permeabilities were measured with fluid flowing continuously past one side of the membrane, no effect of glucose concentration on insulin permeabilities could be detected. The authors propose that inappropriate design of the membranes used in the experiments is the explanation for their lack of response to glucose concentration (91).

A mathematical model describing these glucose-responsive hydrogels demonstrates two important points (91,92). (*1*) Progressive response to glucose concentration over a range of glucose concentrations can be achieved only with a sufficiently low glucose oxidase loading; otherwise, depletion of oxygen causes the system to become insensitive to glucose; and (*2*) a significant pH decrease in the membrane, with resultant swelling, can be achieved only if the amine concentration is sufficiently low that pH changes are not prevented by the buffering of the amines.

Although the great advantage of reservoir systems is the ease with which they can be designed to produce constant release-rate kinetics, their main disadvantage are leaks, which are dangerous because all the incorporated

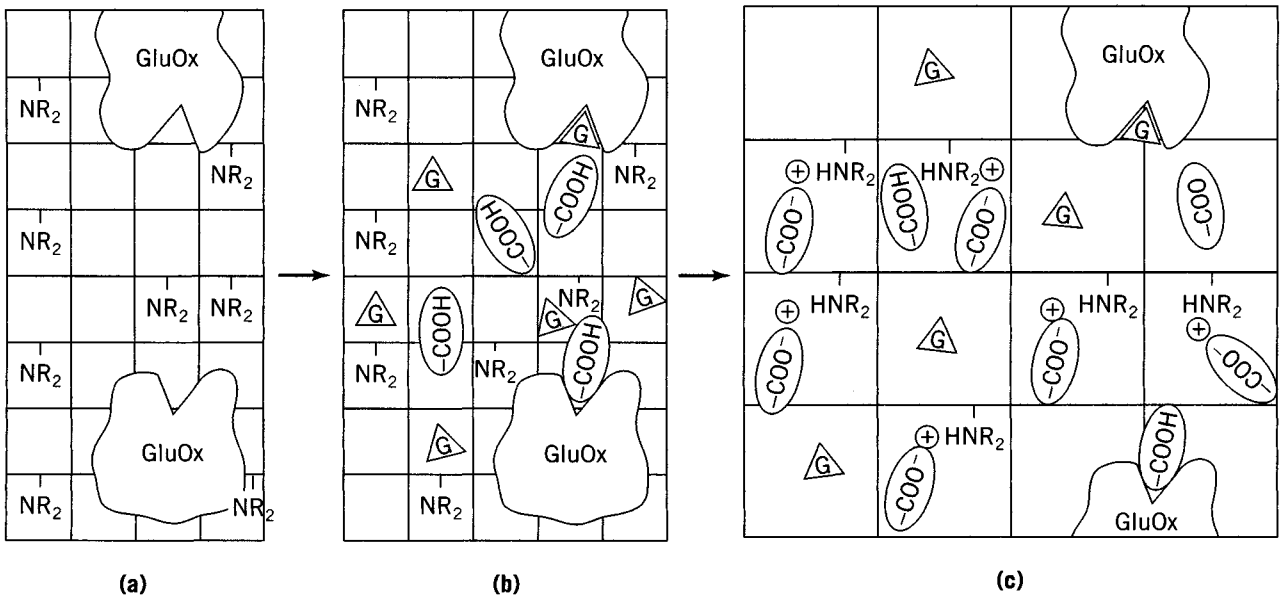


Figure 9. Mechanism of action of glucose-sensitive polymeric hydrogel. (**a**) In the absence of glucose, at physiologic pH, few of the amine groups are protonated. (**b**) In the presence of glucose, the glucose oxidase produces gluconic acid that can (**c**) protonate the amine groups. The fixed positive charge on the polymeric network led to electrostatic repulsion and membrane swelling and therefore enhanced insulin release (98).

drug could be rapidly released. In attempt to overcome this problem, Goldraich and Kost (99) proposed to incorporate the drug (insulin) and the enzyme (glucose oxidase) into the pH-responsive polymeric matrices.

Ishihara et al. (89,90,101–104) investigated two approaches for glucose-responsive insulin delivery systems; one approach is similar to that investigated by Horbett et al. (97). The polymers were prepared from 2-hydroxyethyl acrylate (HEA)-DMA and 4-trimethylsilystyrene (TMS) by radical polymerization of the corresponding monomers in dimethylformamide (DMF). The mole fractions of HEA, DMA, and TMS in the copolymer were 0.6, 0.2, and 0.2, respectively. Membranes were prepared by solvent casting. Capsules containing insulin and glucose oxidase were prepared by an interfacial precipitation method using gelatin as an emulsion stabilizer. The average diameter of the polymer capsules obtained was 1.5 mm (101,104). The water content of HEA–DMA–TMS copolymer membranes increased with a decrease in the pH of the medium. An especially drastic change was observed in the pH range of 6.3 to 6.15. The permeation of insulin through the copolymer membrane increased in response to pH decreases. The permeation rate of insulin at pH 6.1 was greater than that at pH 6.4 by about 42 times. The permeation of insulin through the copolymer membranes was very low in buffer solution without glucose. Addition of 0.2 M glucose to the upstream compartment induced an increase in the permeation rate of insulin. When glucose was removed, the permeation rates of insulin gradually returned to their original levels (101) (Fig. 10).

A similar approach for glucose-responsive insulin release based on hydrogels of poly(diethyl aminoethyl methacrylate-*g*-ethylene glycol) containing glucose oxidase and catalase was also proposed by Podual et al. (105).

The other approach proposed by Ishihara et al. (103) is based on an immobilized glucose oxidase membrane and a redox polymer having a nicotinamide moiety. The device consists of two membranes. One membrane, with the immobilized glucose oxidase, acts as a sensor for glucose and forms hydrogen peroxide by an enzymatic reaction; the other membrane is a redox polymer having a nicotinamide moiety that controls the permeation of insulin by an oxidation reaction with the formed hydrogen peroxide. The oxidation of the nicotinamide group increases hydrophilicity and therefore should enhance the permeability to water-soluble molecules such as insulin. The results showed relatively small increases in insulin permeability.

Iwata et al. (106,107) pretreated porous poly(vinylidene fluoride) membranes (average pore size of 0.22 μm) by air plasma, and subsequently acrylamide was graft-polymerized on the treated surface. The polyacrylamide was then hydrolyzed to poly(acrylic acid). In the pH range of 5 to 7, grafted poly(acrylic acid) chains are solvated and dissolved but cannot diffuse into the solution phase because they are grafted to the porous membrane. Thus, they effectively close the membrane pores. In the pH range of 1 to 5, the chains collapse and the permeability increases. To achieve the sensitivity of the system toward glucose, glucose oxidase was immobilized onto a poly(2-hydroxyethyl methacrylate) gel.

Ito et al. (108) adopted the approach proposed by Iwata et al. (107) using a porous cellulose membrane with surface-grafted poly(acrylic acid) as a pH-sensitive membrane. By immobilization of glucose oxidase onto the poly(acrylic acid)-grafted cellulose membrane, it became responsive to glucose concentrations (Fig. 11). Figure 12 shows the change in permeability of insulin through poly(acrylic acid)-grafted cellulose membranes following the addition of 0.2 M glucose to the buffered solution. The permeation coefficient after glucose addition was about 1.7 times that before the addition of glucose. The authors suggest to improve the proposed system (sensitivity of insulin

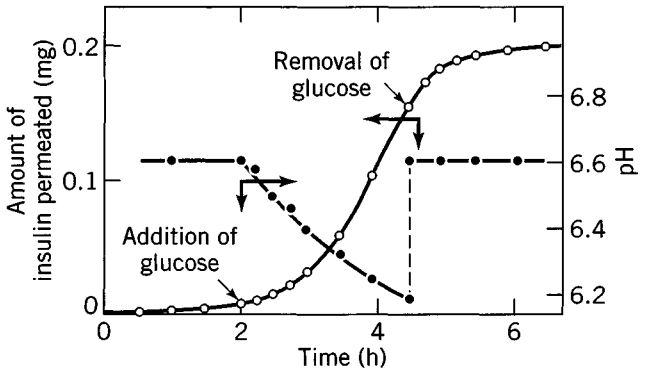


Figure 10. Effect of the addition and removal of glucose on insulin permeation through the HEA–DEA–TMS copolymer membrane and on the pH of the feed-side solution at 30°C. (HEA is 2-hydroxyethyl acrylate; DEA is *N,N*-diethylaminoethyl methacrylate; and TMS is 4-trimethylsilystyrenel; [●] pH; [○] insulin permeated [104]).

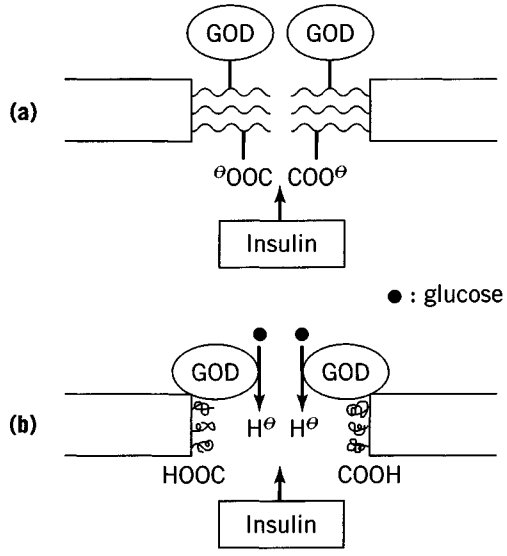


Figure 11. Principle of the controlled-release system of insulin. (**a**) In the absence of glucose, the chains of poly(acrylic acid) grafts are rodlike, lowering the porosity of the membrane and suppressing insulin permeation. (**b**) In the presence of glucose, gluconic acid (COOH) produced by glucose oxidase (GOD) protonates the poly(acrylic acid), making the graft chains coillike and opening the pores to enhance insulin permeation (108).

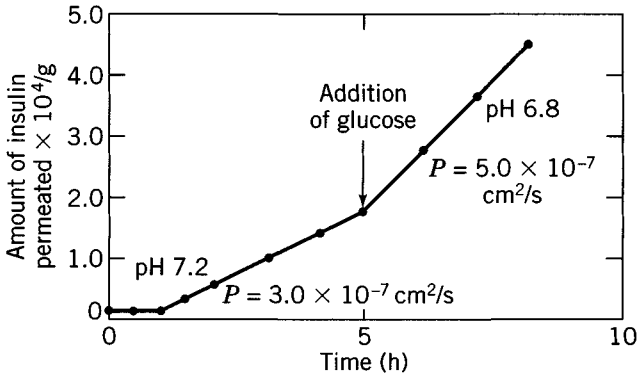


Figure 12. Permeation of insulin through poly(acrylic acid)-grafted membrane in 0.1 M tris-HCl–buffered solution. The concentration of added glucose is 0.2 M (108).

permeability to glucose concentrations) by modification of the graft chain: density, length, and size or density of pores.

Siegel and Firestone (109,110) proposed an implantable "mechanochemical" pump that functions by converting changes in blood glucose activity into a mechanical force, generated by the swelling polymer that pumps insulin out of the device.

More recently Siegel (111) proposed self-regulating oscillatory drug delivery based on a polymeric membrane whose permeability to the substrate of an enzyme-catalyzed reaction is inhibited by the product of that reaction. This negative feedback system can, under certain conditions, lead to oscillations in membrane permeability and in the levels of substrate and product in the device. Any one of these oscillating variables can then be used to drive a cyclic delivery process. Figure 13 illustrates a possible scheme for such drug delivery systems. The device consists of a chamber containing the drug to be delivered (D), plus an enzyme. The chamber is partially bounded by a membrane that controls solute influx and efflux. The substrate (S) for the enzyme is present externally at constant concentration and diffuses through the membrane into the chamber and is converted by the enzyme to a product (P). The product in turn diffuses out of the membrane. However, the product concentration in the chamber inhibitorily affects the permeabilities of the membrane to the substrate. That is, increasing product concentration causes decreasing flux of substrate into the device. Siegel propose several means to control drug delivery based on the presented scheme. Drug solubility could be affected by substrate or product concentration, which will be seen to oscillate. Alternatively, the permeability of the membrane to drug can oscillate with time along with the substrate permeability.

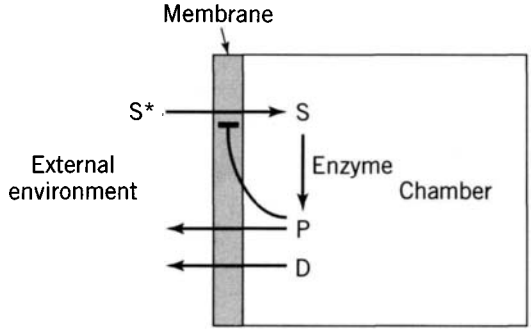
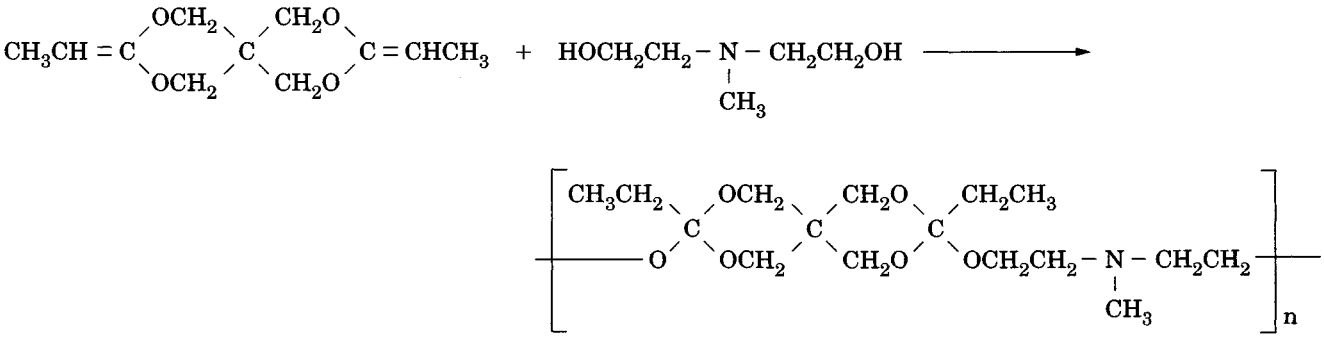


Figure 13. General scheme for proposed drug delivery oscillator (111).

Heller et al. (88,112,113) suggested a system in which insulin is immobilized in a pH-sensitive bioerodible polymer prepared from 3,9 bis (ethylidene 2,4,8,10-tetraoxaspirol(5,5)undecane and *N*-methyldiethanolamine (Scheme 3), which is surrounded by a hydrogel containing immobilized glucose oxidase. When glucose diffuses into the hydrogel and is oxidized to gluconic acid, the resultant lowered pH triggers enhanced polymer degradation and release of insulin from the polymer in proportion to the concentration of glucose. The response of the pH-sensitive polymers containing insulin to pH pulses was rapid. Insulin was rapidly released when the pH decreased from 7.4 to 5.0. Insulin release was shut off when the pH increased (Fig. 14). The amount of insulin released showed dependents on the pH change. However, when the in vitro studies were repeated in physiologic buffer, response of the device was only minimal. The authors found the synthesized amine containing polymer (Scheme 3) undergoes general acid catalysis where the catalyzing species is not hydronium ion but rather the specific buffer molecules used. Therefore, further development of this system will require the development of a bioerodible polymer that not only has adequate pH sensitivity but also undergoes specific ion catalysis.

Glucose-dependent insulin release was proposed by Langer and coworkers (114–116) based on the fact that insulin solubility is pH dependent. Insulin was incorporated into EVAc matrices in solid form. Thus, the release was governed by its dissolution and diffusion rates. Glucose oxidase was immobilized to sepharose beads that were incorporated along with insulin into EVAc matrices. When glucose entered the matrix, the produced gluconic acid caused a rise in insulin solubility and consequently enhanced release. To establish this mechanism in the physiological pH of 7.4, the insulin was modified by three additional lysine groups so that the resultant isoelectric point was 7.4. In vitro and in vivo studies demonstrated the response of the system to changes in glucose concentration. In the in vivo experiments, a catheter was inserted into the left jugular vein, and polymer matrices containing insulin and immobilized enzyme were implanted subcutaneously in the lower back of diabetic rats. Serum insulin concentrations were measured for different insulin matrix implants. A 2 M glucose solution was infused, 15 min into the experiments, through the catheter. Rats that received trilysine insulin/glucose oxidase matrices showed a 180% rise in serum insulin concentration that peaked at 45 min into the experiment. Control rats that received matrices containing no insulin or insulin but no glucose oxidase or diabetic rats without implants showed no change in serum insulin.



Scheme 3. Preparation of poly(orthoester)s containing tertiary amine groups in polymer backbone (122).

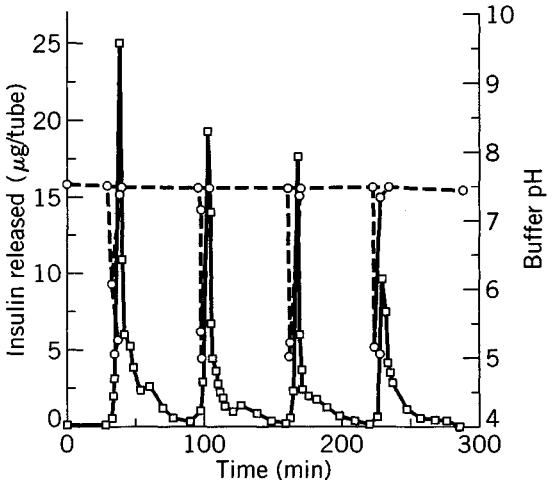


Figure 14. Release of insulin from a linear polymer prepared from 3,9-bis(ethylidene)-2,48,10-tetraoxaspiro [5,5] undecane and *N*-methyldiethanolamine as a function of external pH variations between pH 7.4 and 5.0 at 37°C: disks, 3 × 0.55 mm; insulin loading, 10 wt %; nonrecycling media was continuously perfused at a flow rate of 2 mL/min; total efflux was collected at 1–10 min intervals; (○) buffer pH; (□) insulin release (122).

Morphine-Triggered Naltrexone Delivery Systems

Heller and coworkers (88,112,117–122) have been developing a naltrexone drug delivery system that would be passive until drug release is initiated by the appearance of morphine external to the device. Naltrexone is a long-acting opiate antagonist that blocks opiate-induced euphoria, and thus the intended use of this device is in the treatment of heroin addiction. Activation is based on the reversible inactivation of enzymes achieved by the covalent attachment of hapten close to the active site of the enzyme–hapten conjugate with the hapten antibody. Because the antibodies are large molecules, access of the substrate to the enzyme's active site is sterically inhibited, thus effectively rendering the enzyme inactive. Triggering of drug release is initiated by the appearance of morphine (hapten) in the tissue and dissociation of the enzyme–heptan–antibody complex rendering the enzyme active. This approach is being developed by incorporating the naltrexone in an bioerodible polymer (Fig. 15). This polymer matrix is then covered by a lipid layer that prevents water entry into the polymer matrix and therefore prevents its degradation and the release of naltroxane. The system is placed in a dialysis bag. The bag contains lipaze (enzyme) that is covalently attached to morphine and reversibly inactivated by antimorphine complexation. Thus, when morphine is present in the tissues surrounding the device, morphine diffuses into the dialysis bag and displaces the lipase–morphine conjugate from the antibody, allowing the now-activated enzyme to degrade the protective lipid layer, which in turn permits the polymeric core degradation and release into the body of the narcotic antagonist, naltrexone.

A key component of this morphine-responsive device is the ability to reversibly and completely inactivate an enzyme and to be able to rapidly disassociate the complex with concentrations as low as 10^{-8} to 10^{-9} M. To achieve this sensitivity, lipase was conjugated with several morphine analogs and complexed with affinity chromatography–purified polyclonal antimorphine antibodies. In vivo studies (118) suggest that the concentration of morphine in a device implanted in a typical heroin-addicted patient is estimated to be about 10^{-7} to 10^{-8} M. Recent studies have shown that reaching such sensitivity is possible (88).

SYSTEMS UTILIZING ANTIBODY INTERACTIONS

Pitt et al. (123) proposed utilizing hapten–antibody interactions to suppress enzymatic degradation and permeabil-

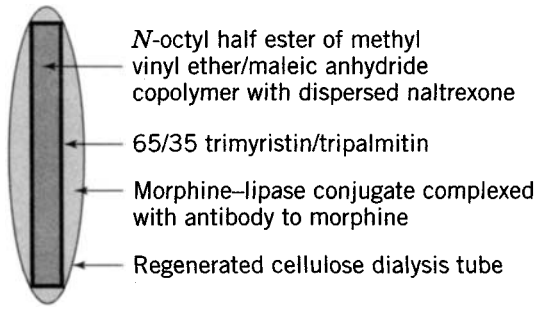


Figure 15. Schematic representation of triggered naltrexone delivery device (88).

ity of polymeric reservoirs or matrix drug delivery systems. The delivery device consists of naltrexone contained in a polymeric reservoir or dispersed in a polymeric matrix configuration. The device is coated by covalently grafting morphine to the surface. Exposure of the grafted surface to antibodies to morphine results in coating of the surface by the antibodies, a process that can be reversed by exposure to exogenous morphine. The presence of the antibodies on the surface or in the pores of the delivery device will block or impede the permeability of naltrexone in a reservoir configuration or enzyme-catalyzed surface degradation and concomitant release of the drug from a matrix device. A similar approach was proposed for responsive release of a contraceptive agent. The β-subunit of human chorionic gonadotropin (HCG) is grafted to the surface of the polymer, which is then exposed to antibodies to β-HCG. The appearance of HCG in the circulatory system (indicative of pregnancy) will cause release of a contraceptive drug. (HCG competes for the polymer-bound antibodies to HCG and initiates release of the contraceptive drug.)

Pitt et al. (123,124) also proposed a hypothetical reversible antibody system for controlled release of ethinyl estradiol (EE). EE stimulates biosynthesis of sex-hormone-binding globulin (SHBG). High serum levels of EE stimulate the production of SHBG, which increases the concentration of SHBG bound to the polymer surface and reduces the EE release rate. When the EE serum level falls, the SHBG level falls, as does binding of the SHBG to the polymer surface, producing an automatic increase in the EE release rate.

The polymers evaluated by Pitt and coworkers for covalent attachment of haptens were poly(ethylene vinyl acetate) copolymers for reservoir devices and hydroxylated polyester urethanes where the release is enzymatic degradation dependent. The polymers were prepared from ϵ-caprolactone and δ-valerolactone, lightly cross-linked with 1,6-hexanediisocyanate. The residual hydroxyl groups of the elastomer were shown to be suitable sites for hapten derivatization by treatment with chloroacetic anhydride. Biodegradability studies of the cross-linked polymers were conducted by implanting films subdermally in rabbits and measuring weight loss and dimensional changes with time. No weight loss was observed after 4 weeks of implantation. This results were in contrast with the immediate and rapid surface erosion of polymers prepared from ϵ-caprolactone and δ-valerolactone cross-linked with bis-2-2-(ϵ-caprolactone-4-yl)propane in which weight loss was detected within 2 weeks and increased thereafter in an approximately linear fashion (125).

SYSTEMS UTILIZING CHELATION

Self-regulated delivery of drugs that function by chelation was also suggested (126). These include certain antibiotics and drugs for the treatment of arthritis as well as chelators used for the treatment of metal poisoning. The concept is based on the ability of metals to accelerate the hydrolysis of carboxylate or phosphate esters and amides by several orders of magnitude. Attachment of the chelator to a polymer chain by a covalent ester or amide link serves to prevent its premature loss by excretion and reduces its toxicity. In the presence of the specific ion, a complexing with the bound chelating agent will take place, followed by metal-accelerated hydrolysis and subsequent elimination of the chelated metal. Measurement of the rates of hydrolysis of polyvinyl alcohol coupled with quinaldic acid chelator (PVA-QA) in the presence of CO(II), Zn(II), Cu(II), and Ni(II) confirmed that it is possible to retain the susceptibility of the esters to metal-promoted hydrolysis in a polymer environment.

CONCLUDING REMARKS

During the last three decades, polymeric-controlled drug delivery has become an important area of research and development. In this short time, a number of systems displaying constant or decreasing release rates have progressed from the laboratory to the clinic and clinical products. Although these polymeric-controlled delivery systems are advantageous compared to the conventional methods of drug administration, they are insensitive to the changing metabolic state. To more closely control the physiological requirements of the specific drugs, responsive mechanisms must be provided. The approaches discussed represent attempts conducted over the past two decades to achieve pulsatile release. It should be pointed out that these drug delivery systems are still in the developmental stage, and much research will have to be conducted for such systems to become practical clinical alternatives. Critical considerations are the biocompatibility and toxicology of these multicomponent polymer-based systems, the response times of these systems to stimuli, the ability to provide practical levels of the desired drug, and addressing necessary formulation issues in dosage or design (e.g., shelf life, sterilization, and reproducibility). A key issue in the practical utilization of the pulsatile, externally triggered systems (i.e., those that are magnetic, ultrasound, electrically regulated, and photoresponsive) will be the design of small portable trigger units that the patient can easily use. Ideally, such systems could be worn by the patient, as in a wristwatch-like system, and could be either preprogrammed to go on and off at specific times or turned on by the patient when needed. A critical issue in the development of responsive, self-regulated systems such as those containing enzymes or antibodies is the stability and/or potential leakage and possible immunogenicity of these bioactive agents. The successful development of responsive polymer delivery systems will be a significant challenge. Nevertheless, the considerable pharmacological benefit these systems could potentially provide—particularly given ongoing research in biotechnology, pharmacology, and medicine, which may provide new insights on the desirability and requirements for pulsatile release—should make this an important and fruitful area for future research.

BIBLIOGRAPHY

1. R. Langer, *Nature (London)* **392**, 5–10 (1998).
2. J. Kost and R. Langer, *Adv. Drug Delivery Rev.* **6**, 19–50 (1991).

3. H. Creque, R. Langer, and J. Folkman, *Diabetes* **29**, 37–40 (1980).
4. L. Brown, L. Siemer, C. Munoz, and R. Langer, *Diabetes* **35**, 684–691 (1986).
5. L. Brown et al., *Diabetes* **35**, 692–697 (1986).
6. J. Kost, R. Noecker, E. Kunica, and R. Langer, *J. Biomed. Mater. Res.* **19**, 935–940 (1985).
7. E. Edelman, J. Kost, H. Bobeck, and R. Langer, *J. Biomed. Mater. Res.* **19**, 67–83 (1985).
8. D. Hsieh, R. Langer, and J. Folkman, *Proc. Natl. Acad. Sci. U.S.A.* **78**, 1863–1867 (1981).
9. J. Kost, J. Wolfrum, and R. Langer, *J. Biomed. Mater. Res.* **21**, 1367–1373 (1987).
10. O. Saslavski, P. Couvrer, and N. Peppas, in J. Heller et al., eds., *Controlled Release of Bioactive Materials*, Controlled Release Society, Basel, 1988, pp. 26–27.
11. E. Edelman, L. Brown, J. Taylor, and R. Langer, *J. Biomed. Mater. Res.* **21**, 339–353 (1987).
12. J. Kost, K. Leong, and R. Langer, *Proc. Natl. Acad. Sci. U.S.A.* **86**, 7663–7666 (1989).
13. S. Miyazaki, C. Yokouchi, and M. Takada, *J. Pharm. Pharmacol.* **40**, 716–717 (1988).
14. J. Kost, in B. Berner and S. Dinh, eds., *Electronically-Controlled Drug Delivery*, CRC Press, Boca Raton, Fla., 1998, pp. 215–228.
15. J. Kost and R. Sanger, in V. Shah and H. Maibach, eds., *Cutaneous Bioavailability, Bioequivalence and Penetration*, Plenum Press, 1994, pp. 91–104.
16. D. Levy, J. Kost, Y. Meshulam, and R. Langer, *J. Clin. Invest.* **83**, 2074–2078 (1989).
17. S. Miyazaki, O. Mizuoka, and M. Takada, *J. Pharm. Pharmacol.* **43**, 115–116 (1990).
18. D. Bommannan et al., *Pharm. Res.* **9**, 1043–1047 (1992).
19. K. Tachibana, *Pharm. Res.* **9**, 952–954 (1992).
20. K. Tachibana and S. Tachibana, *Anesthesiology* **78**, 1091–1096 (1993).
21. K. Tachibana and S. Tachibana, *J. Pharm. Pharmacol.* **43**, 270–271 (1991).
22. S. Mitragotri, D. Blankschtein, and R. Langer, *Pharm. Res.* **13**, 411–420 (1996).
23. S. Mitragotri, D. Blankschtein, and R. Langer, *Science* **269**, 850–853 (1995).
24. S. Mitragotri, D. Edwards, D. Blankschtein, and R. Langer, *J. Pharm. Sci.* **84**, 697–706 (1995).
25. A.J. Grodzinsky and P.E. Grimshaw, in J. Kost, ed., *Pulsed and Self-Regulated Drug Delivery*, CRC Press, Boca Raton, Fla., 1990, pp. 47–64.
26. P.E. Grimshaw, A.J. Grodzinsky, M.L. Yarmush, and D.M. Yarmush, *Chem. Eng. Sci.* **104**, 827–840 (1989).
27. M. Prausnitz, R. Bose, R. Langer, and J. Weaver, *Proc. Natl. Acad. Sci. U.S.A.* **90**, 10504–10508 (1993).
28. D. Rolf, *Pharm. Technol.* **12**, 130–140 (1988).
29. I.C. Kwon, Y.H. Bae, T. Okano, and S.W. Kim, *J. Controlled Release* **17**, 149–156 (1991).
30. C. Hsu and L. Block, *Pharm. Res.* **13**, 1865–1870 (1996).
31. A. D'Emanuele and J.N. Staniforth, *Pharm. Res.* **8**, 913–918 (1991).
32. A. D'Emanuele and J.N. Staniforth, *Pharm. Res.* **9**, 215–219 (1992).
33. V. Labhasetwar, T. Underwood, S. Schwendemann, and R. Levy, *Proc. Natl. Acad. Sci. U.S.A.* **92**, 2612–2616 (1995).
34. L.L. Miller, G.A. Smith, A. Chang, and Q. Zhou, *J. Controlled Release* **6**, 293–296 (1987).
35. A. Mamada, T. Tanaka, D. Kugwatchkakun, and M. Irie, *Macromolecules* **23**, 1517–1519 (1990).
36. A. Suzuki and T. Tanaka, *Nature (London)* **346**, 345–347 (1990).
37. N. Yui, T. Okano, and Y. Sakurai, *J. Controlled Release* **26**, 141–145 (1993).
38. N. Yui, T. Okano, and Y. Sakurai, *J. Controlled Release* **22**, 105–116 (1992).
39. A.S. Hoffman, *J. Controlled Release* **6**, 297–305 (1987).
40. T. Tanaka, in H.F. Mark and J.I. Kroschwitz, eds., *Encyclopedia of Polymer Science and Technology*, vol. 7, Wiley, New York, 1985, pp. 514–531.
41. T. Ueda, K. Ishihara, and N. Nakabayashi, *Macromol. Chem., Rapid Commun.* **11**, 345 (1990).
42. D.W. Urry et al., *Proc. Natl. Acad. Sci. U.S.A.* **85**, 3407–3411 (1988).
43. M. Yoshida et al., *Drug Des. Delivery* **7**, 159–174 (1991).
44. M. Palasis and H. Gehrke, *J. Controlled Release* **18**, 1–12 (1992).
45. T. Okano, Y.H. Bae, and S.W. Kim, in J. Kost, ed., *Pulsed and Self-Regulated Drug Delivery*, CRC Press, Boca Raton, Fla., 1990, pp. 17–46.
46. Y. Okahata, H. Noguchi, and T. Seki, *Macromolecules* **19**, 493–494 (1986).
47. H. Katano et al., *J. Controlled Release* **16**, 215–228 (1991).
48. S. Vakalanka, C. Brazel, and N. Peppas, *J. Biomater. Sci., Polym. Ed.* **8**, 119–129 (1996).
49. A. Serres, M. Baudys, and S. Kim, *Pharm. Res.* **13**, 196–201 (1996).
50. N. Ogata, *J. Controlled Release* **48**, 149–155 (1997).
51. J.E. Chung et al., *J. Controlled Release* **53**, 119–130 (1998).
52. M. Baundys, A. Serres, C. Ramkisoon, and S.W. Kim, *J. Controlled Release* **48**, 304–305 (1997).
53. L. Brannon-Peppas and N.A. Peppas, *J. Controlled Release* **8**, 267–274 (1989).
54. M. Annaka and T. Tanaka, *Nature (London)* **355**, 430–432 (1992).
55. B.A. Firestone and R.A. Siegel, *Polym. Commun.* **29**, 204–208 (1988).
56. L.-C. Dong and A.S. Hoffman, *Proc. Int. Symp. Controlled Release Bioact. Mater.* **17**, 325–326 (1990).
57. J.H. Kou, D. Fleisher, and G. Amidon, *J. Controlled Release* **12**, 241–250 (1990).
58. M. Pradny and J. Kopecek, *Makromol. Chem.* **191**, 1887–1897 (1990).
59. R.A. Siegel, M. Falmarzian, B.A. Firestone, and B.C. Moxley, *J. Controlled Release* **8**, 179–182 (1988).
60. K. Kono, F. Tabata, and T. Takagishi, *J. Membr. Sci.* **76**, 233–243 (1993).
61. D. Hariharan and N.A. Peppas, *J. Controlled Release* **23**, 123–136 (1993).
62. R.A. Siegel and B.A. Firestone, *Macromolecules* **21**, 3254–3259 (1988).
63. H. Allcock and A. Ambrosio, *Biomaterials* **17**, 2295–2302 (1996).

64. C. Bell and N. Peppas, *Biomaterials* **17**, 1201–1218 (1996).
65. K. Jarvinen et al., *Pharm. Res.* **15**, 802–805 (1998).
66. R.A. Siegel, I. Johannes, A. Hunt, and B.A. Firestone, *Pharm. Res.* **9**, 76–81 (1992).
67. S. Giannos, S. Dinh, and B. Berner, *J. Pharm. Sci.* **84**, 539–543 (1995).
68. J. Heller and P.V. Trescony, *J. Pharm. Sci.* **68**, 919–921 (1979).
69. H. Ghandehari, P. Kopeckova, and J. Kopecek, *Biomaterials* **18**, 861–872 (1997).
70. W. Petka et al., *Science* **281**, 389–392 (1998).
71. M. Brownlee and A. Cerami, *Science* **26**, 1190–1191 (1979).
72. K. Makino, E.J. Mack, T. Okano, and S.W. Kim, *J. Controlled Release* **12**, 235–239 (1990).
73. S. Sato, S.Y. Jeong, J.C. McRea, and S.W. Kim, *J. Controlled Release*, 67–77 (1984).
74. S. Sato, S.Y. Jeong, J.C. McRea, and S.W. Kim, *Pure Appl. Chem.* **56**, 1323–1328 (1984).
75. L. Seminoff et al., *Proc. Int. Symp. Controlled Release Bioact. Mater.* **15**, 161–161 (1988).
76. L. Seminoff and S.W. Kim, in J. Kost, ed., *Pulsed and Self-Regulated Drug Delivery*, CRC Press, Boca Raton, Fla., 1990.
77. S.W. Kim, et al., *J. Controlled Release* **11**, 193–201 (1990).
78. S.Y. Jeong, S.W. Kim, D. Holemberg, and J.C. McRea, *J. Controlled Release* **2**, 143–152 (1985).
79. S.Y. Jeong, S.W. Kim, M.J.D. Eenink, and J. Feijen, *J. Controlled Release* **1**, 57–66 (1984).
80. E. Kokufata, Y.-Q. Zhang, and T. Tanaka, *Nature (London)* **351**, 302–304 (1991).
81. M. Taylor, S. Tanna, P. Taylor, and G. Adams, *J. Drug Target* **3**, 209–216 (1995).
82. A. Obaidat and K. Park, *Biomaterials* **11**, 801–806 (1997).
83. A. Obaidat and K. Park, *Pharm. Res.* **13**, 998–995 (1996).
84. S. Lee and K. Park, *J. Mol. Recognition* **9**, 549–557 (1996).
85. S. Kitano et al., *J. Controlled Release* **19**, 161–170 (1992).
86. I. Hisamitsu, K. Kataoka, T. Okano, and Y. Sakurai, *Pharm. Res.* **14**, 289–293 (1997).
87. J. Heller, R. Baker, R. Gale, and J. Rodin, *J. Appl. Polym. Sci.* **2**, 1991–2009 (1978).
88. J. Heller, in K. Park, ed., *Controlled Drug Delivery: Challenges and Strategies*, American Chemical Society, Washington, D.C., 1997, pp. 127–146.
89. K. Ishihara, N. Muramoto, H. Fuji, and I. Shinohara, *J. Polym. Sci., Polym. Chem. Ed.* **23**, 2841–2850 (1985).
90. K. Ishihara, N. Muramoto, H. Fuji, and I. Shinohara, *J. Polym. Sci., Polym. Lett. Ed.* **23**, 531–535 (1985).
91. G. Albin, T. Horbett, and B. Ratner, in J. Kost, ed., *Pulsed and Self-Regulated Drug Delivery*, CRC Press, Boca Raton, Fla., 1990, pp. 159–185.
92. G. Albin, T.A. Horbett, S.R. Miller, and N.L. Ricker, *J. Controlled Release* **6**, 267–291 (1987).
93. G. Albin, T.A. Horbett, and B.D. Ratner, *J. Controlled Release* **3**, 153–164 (1985).
94. L.A. Klumb and T.A. Horbett, *J. Controlled Release* **18**, 59–80 (1992).
95. L.A. Klumb and T.A. Horbett, *J. Controlled Release* **27**, 95–114 (1993).
96. J. Kost, T.A. Horbett, B.D. Ratner, and M. Singh, *J. Biomed. Mater. Res.* **19**, 1117–1133 (1985).
97. T. Horbett, J. Kost, and B. Ratner, *Am. Chem. Soc., Div. Polym. Chem.* **24**, 34–35 (1983).
98. T. Horbett, J. Kost, and B. Ratner, in S. Shalaby, A. Hoffman, T. Horbett, and B. Ratner, eds., *Polymers as Biomaterials*, Plenum, New York, 1984, pp. 193–207.
99. M. Goldraich and J. Kost, *Clin. Mater.* **13**, 135–142 (1993).
100. I. Kaetsu, M. Kumakura, and M. Yoshida, *Biotechnol. Bioeng.* **21**, 847–861 (1979).
101. K. Ishihara, *Proc. Int. Symp. Controlled Release Bioact. Mater.* **15**, 168–169 (1988).
102. K. Ishihara, M. Kobayashi, and I. Shonohara, *Macromol. Chem., Rapid Commun.* **4**, 327–331 (1983).
103. K. Ishihara, M. Kobayashi, N. Ishimaru, and I. Shinohara, *Polym. J.* **16**, 625–631 (1984).
104. K. Ishihara and K. Matsui, *J. Polym. Sci. Polym. Lett. Ed.* **24**, 413–417 (1986).
105. K. Podual, N. Peppas, and F. Doyle, *Proc. Int. Symp. Controlled Release Bioact. Mater.* **25**, 135–136 (1998).
106. H. Iwata and T. Matsuda, *J. Membr. Sci.* **38**, 185–199 (1988).
107. H. Iwata et al., *Proc. Int. Symp. Controlled Release Bioact. Mater.* **15**, 170–171 (1988).
108. Y. Ito, M. Casolaro, K. Kono, and Y. Imanishi, *J. Controlled Release* **10**, 195–203 (1989).
109. R. Siegel, in J. Kost, ed., *Pulsed and Self-Regulated Drug Delivery*, CRC Press, Boca Raton, Fla., 1990, pp. 129–157.
110. R.A. Siegel and B.A. Firestone, *J. Controlled Release* **11**, 181–192 (1990).
111. R. Siegel, in K. Park, ed., *Controlled Release: Challenges and Strategies*, American Chemical Society, Washington, D.C., 1997.
112. J. Heller, R.V. Sparer, and G.M. Zenter, in M. Chasin and R. Langer, eds., *Biodegradable Polymers as Drug Delivery Systems*, Dekker, New York, 1990, pp. 121–161.
113. J. Heller, *Adv. Drug Delivery Rev.* **10**, 163–204 (1993).
114. L. Brown, F. Ghodsian, and R. Langer, *Proc. Int. Symp. Controlled Release Bioact. Mater.* **15**, 116–167 (1988).
115. L. Brown, E. Edelman, F. Fishel-Ghodsian, and R. Langer, *J. Pharm. Sci.* **85**, 1341–1345 (1996).
116. F. Fischel-Ghodsian et al., *Proc. Natl. Acad. Sci. U.S.A.* **85**, 2403–2406 (1988).
117. K. Roskos, V. Tefft, and J. Heller, *J. Clin. Mater.* **13**, 109–119 (1993).
118. K.V. Roskos, B.K. Fritzinger, J.A. Tefft, and J. Heller, *Biomaterials* **16**, 1235–1239 (1995).
119. K.V. Roskos, J.A. Tefft, B.K. Fritzinger, and J. Heller, *J. Controlled Release* **19**, 145–160 (1992).
120. J.A. Tefft, K.V. Roskos, and J. Heller, *J. Biomed. Mater. Res.* **26**, 713–724 (1992).
121. G.R. Nakayama, K.V. Roskos, B.K. Fritzinger, and J. Heller, *J. Biomed. Mater. Res.* **29**, 1389–1396 (1995).
122. J. Heller, A.C. Chang, G. Rodd, and G.M. Grodsky, *J. Controlled Release* **13**, 295–304 (1990).
123. C.G. Pitt et al., *J. Controlled Release* **2**, 363–374 (1985).
124. C.G. Pitt, *Pharm. Int.*, 88–91 (1986).
125. C.G. Pitt, R.W. Hendren, and A. Schindler, *J. Controlled Release* **1**, 3–14 (1985).
126. C.G. Pitt et al., in J. Kost, ed., *Pulsed and Self-Regulated Drug Delivery*, CRC Press, Boca Raton, Fla., 1985, pp. 117–127.

LIPOSOMES

CHRISTOPHER J. KIRBY
Cortecs Research Laboratory
London, United Kingdom
GREGORY GREGORIADIS
University of London School of Pharmacy
London, United Kingdom

KEY WORDS

Anticancer drugs
Antimicrobial agents
Cationic liposomes
Controlled release
Drug delivery
Drug targeting
Endocytosis
Gene delivery
Gene vaccines
Immunological adjuvants
Lamellae
Lipid polymorphism
Liposomes
Microencapsulation
Phospholipids
Steric stabilization
Tumor extravasation

OUTLINE

Introduction
Molecular Aspects of Liposome Formation
  Self Assembly of Lipids
  Lipid Polymorphism
  Aqueous Dispersions of Lamellar Phase Lipid: Liposomes
Liposomes As Drug Delivery Systems
  The Drug Delivery Concept
  Incorporation of Solutes
  Morphology and Nomenclature of Liposomes
Preparation of Liposomes in the Laboratory
  Oligo- and Multilamellar Vesicles
  Small Unilamellar Vesicles
  Large Unilamellar Vesicles
Scale-Up and Industrial Manufacture of Liposomes
  Lipid Intermixing and Hydration
  Entrapment
  Sizing
  Other Issues
Characterization
  Overall Structure of Liposomes
  Liposomal Stability
Fate of Liposomes in Vivo and its Control
  Retention of Drugs by Liposomes
  Vesicle Clearance Rates: The Role of Lipid Composition
Tailoring of Liposomes
  Long-Circulating Liposomes
  Targeted Liposomes
  Polymerized Liposomes
  pH- and Temperature-Sensitive Liposomes
  Cationic Liposomes
Applications for Liposomes
  Cancer
  Antimicrobial Agents
  Gene Therapy
  Liposomes as Immunological Adjuvants
  Genetic Immunization
  Other Applications
Bibliography

INTRODUCTION

The evolution of the science and technology of liposomes as a drug carrier has passed through a number of distinct phases. Lamellar structures in lipid–water systems had previously been studied as models of biomembranes and interpreted in terms of dynamic properties, solute sequestration, and release characteristics (1). The latter prompted the development of the liposome drug carrier concept (2), and in 1970 animals were, for the first time, injected with liposomes containing a variety of potentially therapeutic agents (3–6). This has now culminated in several injectable liposome-based drug formulations licensed for clinical use (5).

It has often been asked why it has taken so much time and effort to bring a liposomal drug onto the market. On the surface, this appears to be a legitimate question. However, the issue here is not the development of a new drug (which itself can take many years) but rather, the development of a whole approach (i.e., the use of a delivery system) to improve the efficacy of a great number of existing drugs. The liposome was adopted as a promising delivery system because its organized structure could accommodate drugs, depending on their solubility characteristics, in both the aqueous and lipid phases. In retrospect, it is not surprising that following initial work in vivo with liposomes containing therapeutic agents, several potential problems became apparent. First, although it was encouraging to note that entrapped enzymes, proteins, and lipid-

soluble agents by and large acquired the pharmacokinetics of the carrier, water-soluble drugs of low molecular weight leaked extensively into the circulating blood. Secondly, there was rapid and quantitative interception of liposomes and their contents by the cells of the reticuloendothelial system (RES) through endocytosis, an event that appeared to limit the use of the system to, at best, the treatment of intralysosomal diseases or metal storage conditions. Equally disconcerting were the low levels of drug entrapment, vesicle size heterogeneity, and poor reproducibility and instability of formulations. Yet interest in liposomes, especially among academic workers, spread rapidly. We attribute this to the remarkable structural versatility of the system, which enables the design of countless liposome versions to satisfy particular needs in terms of both technology and optimal function in vivo.

In the ensuing years, great strides (5) were made toward understanding the way in which liposomes interact with the biological milieu at the molecular and cellular level. As a result, ways were found to improve liposomal stability in biological fluids so that drugs would not leak significantly, vesicle presence in the circulation would be extended, and targeting to alternative sites would be made possible. At the same time, important advances in liposome technology provided indications that many of the difficulties with entrapment and stability during storage could be overcome. Indeed, optimism generated by such progress led to the foundation of at least three liposome-based companies in the early 1980s, forcefully encouraging ideas and enthusiasm into the path of the realities of industrial research and development, and leading eventually to useful products. However, the contribution that liposome research has made (and will make) to targeted drug delivery is not just the happy prospect of additional liposome-based drugs. Of greater importance is the wealth of information that has become available on the ways that the body interacts with drug carriers and the harnessing of such information to circumvent anatomical and physiological barriers to optimal performance of the carrier. This cannot but prove instrumental in our efforts to ensure that old and new drugs act effectively.

MOLECULAR ASPECTS OF LIPOSOME FORMATION

Self Assembly of Lipids

Liposomes are microscopic aggregates of highly ordered lipid molecules which are normally dispersed in a hydrophilic solvent, typically water. This description applies to various types of microparticles, but the distinguishing feature of liposomes is that their lipid components are in a lamellar arrangement. When any molecule is dispersed in a solvent, its fate is dependent on the polarity of the molecule, which reflects the distribution of the electron clouds surrounding it. Polar molecules tend to dissolve in polar solvents such as water, whereas nonpolar ones are generally hydrophobic and only dissolve in nonpolar organic solvents. However, it is common to have both polar and nonpolar residues on the same molecule, in which case it is described as amphiphilic and its solvent dispersion characteristics are more complicated. Transient structuring of the hydrogen bonds between water molecules allows very small amounts of amphiphile to dissolve in the free form, but at more appreciable concentrations, the hydrophobic residues must be masked from the polar environment. This is achieved by reorientation of the amphiphile molecules into ordered structures in which the hydrophobic regions are brought into proximity with each other while the polar groups are juxtaposed between them and the water continuum. How this is accomplished depends on the way in which adjacent amphiphile molecules are able to align with each other, and this is in turn dependent on their spatial geometry (1).

When the cross-sectional areas of the polar and nonpolar regions are approximately equal, the molecule is effectively cylindrical in shape and adjacent cylinders then align in a parallel arrangement to form a two-dimensional monolayer, with the polar head groups forming one surface of this monolayer and the fatty acid acyl chains the other. (Fig. 1). Two of these monolayers are organized back-to-back to form a bilayered sheet or lamella in which the hydrophobic regions are sandwiched between the polar groups and segregated from the bulk water. Such an arrangement is typical of naturally occurring phospholipids such as the phosphatidylcholines (lecithins), which form the major component of cell membranes.

On the other hand, if there is a significant difference between the cross-sectional areas of the polar and nonpolar regions, the amphiphile molecules approximate to the shape of a wedge rather than a cylinder and are unable to align in a planar arrangement (7). These differences may be due to steric factors such as head group size, or variation in the number of fatty acyl chains, or to electrostatic effects arising from attractive or repulsive forces between adjacent head groups. In these situations, the aligning amphiphiles are forced to form curved structures, the most common of which include hexagonal phases (cylinders) and micelles (ranging from spheres to elongated rods). Depending on which end of the molecule is widest, each of these structures adopts a normal or reverse (inside out) configuration. Thus, if the polar head group is broader than the nonpolar region, curvature will be "positive," with the polar group forming the outer surface of the curve (e.g., micelles [L_1 phase] and normal hexagonal [H_I] phase). Conversely, if the nonpolar tail is broader than the head group, curvature will be "negative," with the fatty acyl chains forming the outer surface (reverse micelles [L_2] or reverse hexagonal [H_{II}] phase). Another important nonbilayer phase is the cubic phase, alternative forms of which can resemble close-packed micelles or bicontinuous structures. It is quite normal to accommodate non-bilayer-forming amphiphiles into lipid bilayers by including amphiphiles of opposite shape tendency to compensate. Thus mixtures of wedges, inverse wedges, and cylinders can be formulated which still favors a planar arrangement.

Lipid Polymorphism

This capability of amphiphiles to form a variety of structures and phases is known as polymorphism, and is of the utmost importance in normal biological processes such as cell trafficking, digestion, absorption, and fusion. An im-

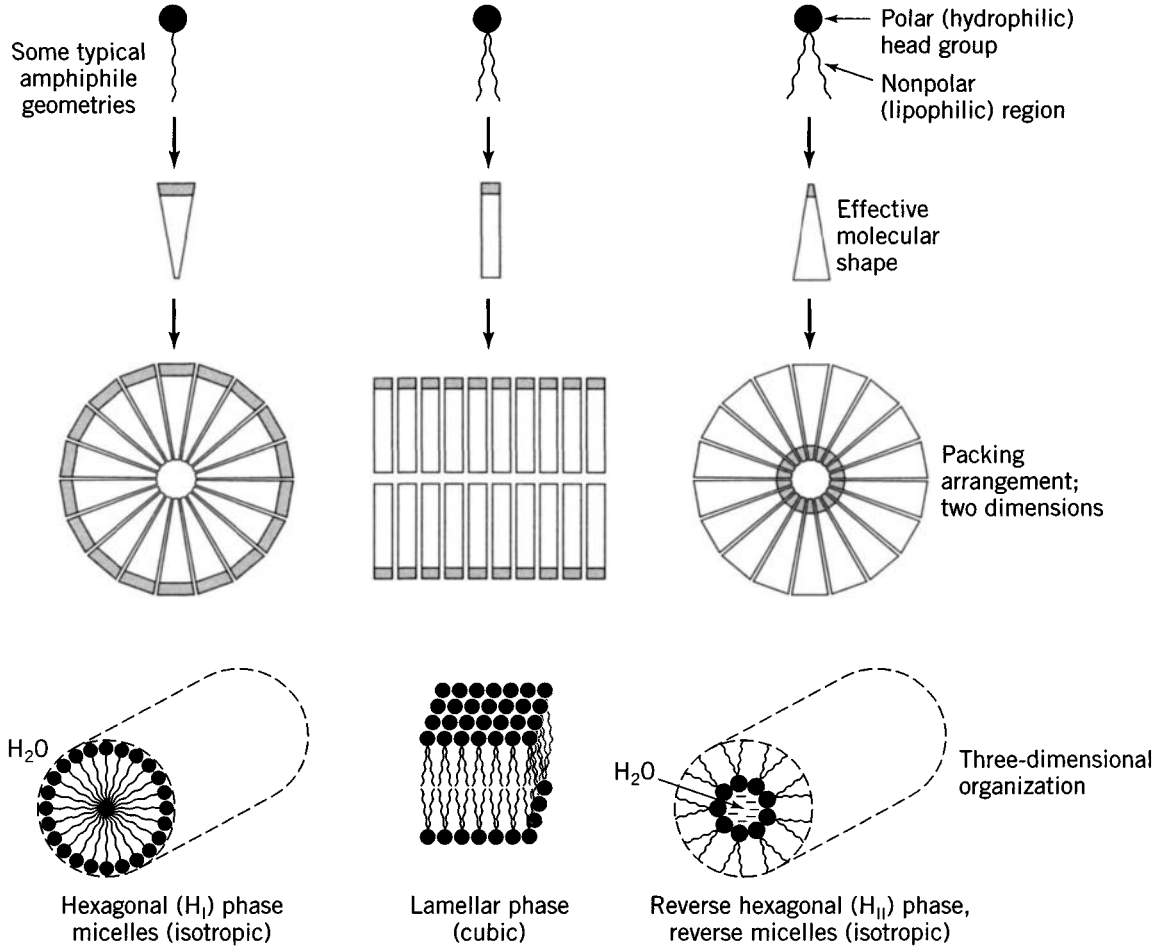


Figure 1. Dependence of phase behavior on the molecular geometries of the individual amphiphile molecules. *Source:* Adapted from Ref. 7, with permission.

portant aspect is that different phases can interconvert, either by inward or outward migration of particular amphiphiles, or by individual amphiphiles changing their shape. For example, increased temperature can increase the dynamic motion of the hydrocarbon chains, effectively broadening the nonpolar region. Changes in pH can affect ionization of polar head groups and so alter their diameter, as can changes in their level of hydration. Thus, bilayer to nonbilayer transitions can take place, resulting in loss of membrane barrier function or increased fusogenicity. These transitions can be exploited to design lipid-based carrier systems with predetermined release properties which are triggered by changes in their microenvironment or in the local ambient conditions.

Aqueous Dispersions of Lamellar Phase Lipid: Liposomes

Normal micelles, which show only short-range order, form spontaneously when the appropriate amphiphiles are added to water and dilute freely in excess water. For liquid crystalline phases, which also exhibit *long-range* order, the situation is different. Cubic and normal hexagonal phases do not disperse spontaneously, but procedures have been developed by which they can be converted into a colloidal form without loss of short-range order, producing "cubosomes" and "hexasomes," respectively. When lamellar phase lipid is diluted with excess aqueous phase, areas of lamellae are able to detach from the bulk lipid and round off to form sealed spherical liposomes (Fig. 2), thereby ensuring that hydrophobic chains at the bilayer "edges" are not exposed to the aqueous phase. In practice, detachment of lamellae from uncharged bilayer lipid is extremely slow unless the mixture is agitated, in which case all of the lipid eventually becomes dispersed in the form of liposomes. Such structures were first described in the early 1960s (1) and within a short time led to intense activity by a large number of research groups throughout the world.

LIPOSOMES AS DRUG DELIVERY SYSTEMS

The Drug Delivery Concept

The common structural features shared by liposome bilayers and biological membranes led to their widespread early use as membrane models for investigating the structural and functional relationships of natural cell membranes and their components. For example, integral membrane

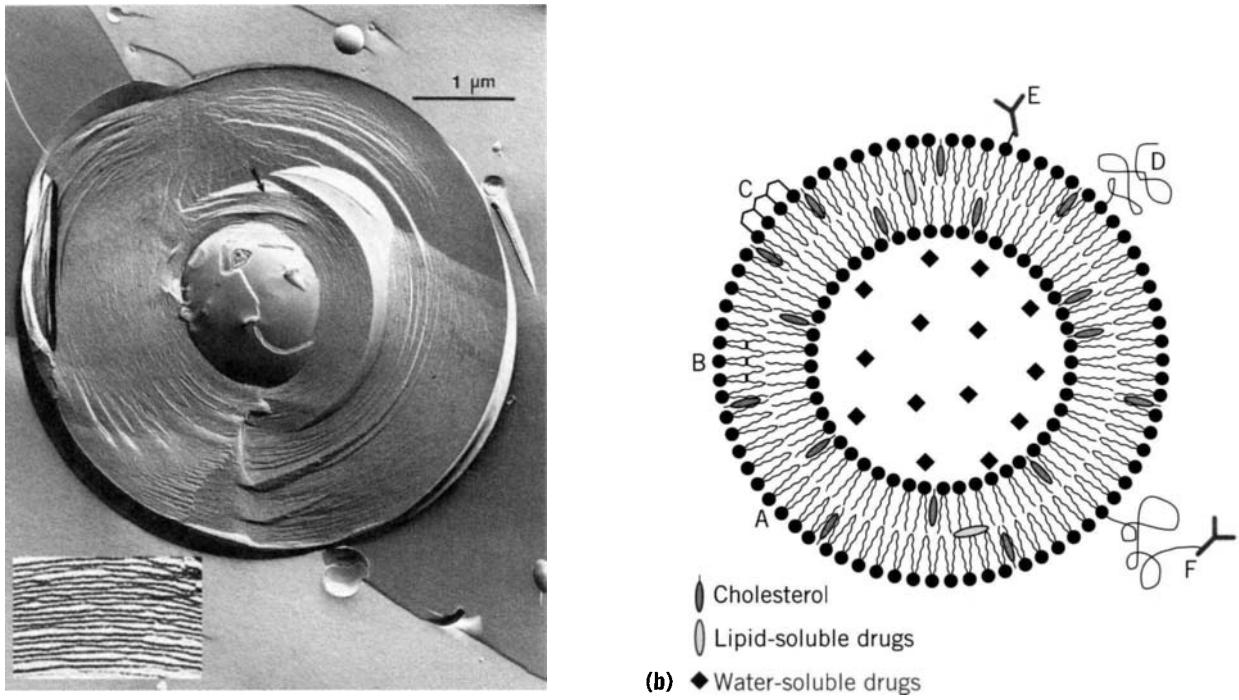


Figure 2. (**a**) Freeze-fracture electron micrograph of a multilamellar liposome prepared in water. The inset shows the area indicated by the arrow, magnified a further 6.7 times, to show the detail of the lamellae. *Source:* Micrograph courtesy of Mr. B. E. Brooker. (**b**) A diagrammatic representation of a unilamellar liposome showing the molecular structure of the lipid bilayer. The diagram also shows some of the modifications that can be made in order to tailor liposomes for specific applications, as discussed later in this article. Thus, A, B, and C are amphiphiles polymerized at the terminal and central regions of the fatty acyl chain, and at the polar head group, respectively. D denotes a poly(ethylene glycol) (PEG) modified phospholipid for preparing sterically stabilized liposomes, whereas E and F indicate ligand (antibody)-targeted amphiphiles with the targeting moiety attached to the head group and to the terminal region of a PEG chain, respectively.

proteins could be reconstituted into lipid bilayers to allow characterization in their natural state or to study their vectorial transport properties. However, their potential use as carriers for drugs, cosmetics, and many other types of active agent has excited a much greater volume of interest and led to their eventual commercialization (5). Such applications are dependent on the fact that liposomes are sealed structures, so that water-soluble substances dissolved in the internal aqueous phase are entrapped and isolated from the external environment. Many nonpolar compounds, as well as other amphiphiles, can also be included. For example, smaller alkanes partition into the central hydrocarbon region of the bilayer, whereas larger ones and amphiphilic molecules align themselves between and in parallel with the phospholipid chains. Insoluble substances such as colloidal metal particles have also been incorporated. Once inside, labile substances are protected from external conditions that might otherwise lead to their degradation. The liposomes themselves can be constructed with widely different physical structures, lipid composition, and surface properties, thus enabling a great deal of control over the fate of their contents. For these reasons, they have been explored very widely as delivery vehicles, particularly of drugs and other biologically active materials (5,8). The basic aspects of the drug delivery concept are briefly summarized as follows.

- *Protection*. Both the active material and the host are protected by virtue of the membrane barrier function and the possibility of coencapsulation of protective agents.
- *Sustained release*. Such release is dependent on the ability to vary the permeability characteristics of the membrane by control of bilayer composition and lamellarity.
- *Controlled release*. Drug release is enabled by exploiting lipid phase transitions in response to external triggers such as changes in temperature or pH.
- *Targeted delivery*. Such delivery can be achieved by relying on natural attributes such as liposome size and surface charge to effect passive delivery to body organs or by incorporating antibodies or other ligands to aid delivery to specific cell types. At the same time, drugs can be directed away from vulnerable or unintended targets.
- *Internalization*. This occurs by encouraging cellular uptake via endocytosis or fusion mechanisms; for example, to deliver genetic materials into cells.

Examples of these control mechanisms are discussed later in this text.

Because the basic unit of liposome structure, the lipid bilayer, is itself formed spontaneously, this makes incorporation of additional levels of sophistication much more straightforward, thereby enabling the tailoring of liposomes for many different situations and applications. Their tremendous versatility, ease of construction, and similarity to natural membranes has given them many advantages over other systems that have been developed for use in drug delivery.

Incorporation of Solutes

The amount of solute incorporated into the liposomes is defined both in terms of the encapsulation efficiency, which is the percentage of the starting material that becomes encapsulated, and the encapsulation capacity, which is the amount incorporated per unit amount of bilayer lipid. When material becomes encapsulated during liposome manufacture it is said to be passively entrapped, whereas if it is incorporated at a subsequent stage, it is described as actively loaded, or alternatively remotely loaded to indicate that incorporation has taken place at a site other than where manufacture took place. As already indicated, both hydrophilic and lipophilic materials may be incorporated, the former in the internal aqueous spaces and the latter within the lipid bilayer. The usual method of incorporating lipophilic substances is to dissolve them together with the amphiphile(s) in an organic solvent and then to remove the solvent so that the different bilayer components are left behind in a homogeneous, molecularly dispersed form. If an appropriate amount of the substance is added, then encapsulation efficiencies of 100% normally are achieved. However, the encapsulation *capacity* is likely to be much lower, and if added at greater than 5 mol % of the total lipid, it may well have adverse effects on the normal bilayer properties. On the other hand, water-soluble materials are able to partition between the internal and external water phases of the liposome, and encapsulation efficiencies generally are much lower than 100%, and dependent on the nature of the solute, the liposome components and the preparation method employed. These variables are discussed in the forthcoming sections.

Morphology and Nomenclature of Liposomes

Lamellar-forming lipids, like other amphiphiles, normally exist in a densely packed crystalline form when in the dry state. Below a certain characteristic temperature, the nonpolar hydrocarbon chains are fully extended and rigid, but above this temperature thermal excitation is increased and the chains enter a more disordered, liquid-like state. If water is added to the lipid above this *transition temperature* (T_c), the polar head groups at the surface of the exposed amphiphile become hydrated and start to reorganize into the lamellar form. The water diffuses through this surface bilayer causing the underlying lipid to undergo a similar rearrangement, and the process is repeated until all of the lipid is organized into a series of parallel lamellae, each separated from the next by a layer of water. Once this liquid crystalline phase is fully swollen and in equilibrium with excess water, mild agitation allows portions of close-packed, multilamellar lipid to break away (1). The resulting large spherical liposomes, each consisting of numerous concentric bilayers in close apposition, alternating with layers of water, are known as multilamellar vesicles (MLV). These are heterogeneous in size, varying from a few hundreds of nanometers in diameter to around ten μm, in the latter case representing some hundreds of lamellae thick.

The main advantage of MLV is that they are simple to make and have a relatively rugged construction. However, because the interior is largely occupied by the internal lamellae, the volume available for solute incorporation is very limited, and under normal condition only a small percentage of the available material is taken up. Their large size range is generally considered to be a drawback for many medical applications requiring parenteral administration, because it leads to rapid clearance from the bloodstream by the cells of the RES. On the other hand, this effect has been exploited for passive targeting of substances to the fixed macrophages of the liver and spleen; e.g., for delivery of antimicrobial agents to microorganisms which are otherwise refractive to treatment because of their localization within these cells (9), chelating agents to remove accumulated metal ions (10), and exogenous enzymes to treat inherited enzyme deficiency conditions such as Gaucher's disease (5).

If the lipid contains a component of negatively charged amphiphile, then at low ionic strengths of the hydration media, the interlamellar distance is increased substantially due to charge-charge repulsive forces between adjacent lamellae. When the lipid is allowed to hydrate undisturbed followed by gentle swirling, individual lamellae are able to detach to form large unilamellar vesicles (LUV) (11). In practice, it is generally more convenient to use one of a variety of methods developed specifically for manufacturing this type of liposome. LUV vary in size from around 100 nm up to tens of micrometers in diameter, and because the interior is not occupied by internal lamellae, there is ample space for incorporation of "drug." This also means that any cells taking up LUV are less subject to lipid overload. However, the absence of additional lamellae means that they are more fragile than MLV and have increased permeability to small solutes.

The lower limit of liposome size is fixed by the maximum curvature that the lipid bilayer is able to achieve, around 21 nm in the case of unsaturated, natural phospholipids such as egg and soy lecithin. These single-layered liposomes are known as small unilamellar vesicles (SUV), and the upper limit of size is designated as 100 nm. Because of their small size, clearance from the systemic circulation is significantly reduced, so they remain circulating for longer and thus have a better chance of exerting the desired therapeutic effect in tissues other than those of the RES. However, the small size also decrees that they have a much lower capacity for drug entrapment, typically less than 1% of the material available.

SUV, together with MLV and LUV are the three major morphological categories of liposomes, and these may be subdivided further. For example, several types of MLV are known. Oligolamellar (or paucilamellar) vesicles have in-

termediate lamellarity between LUV and MLV, and their formation is favoured under certain conditions. Multivesicular liposomes (MVL) can also be prepared, in which several separate compartments are present within a single MLV (12). On the other hand, stable plurilamellar vesicles (SPLV) have a similar appearance to classical MLV under the microscope, but have different physical and biological properties owing to the fact that the latter appear to be in a state of osmotic compression (13). LUV and SUV are often subdivided according to their size. It is also common to classify liposomes according to the various manufacturing procedures, as described in the following section.

PREPARATION OF LIPOSOMES IN THE LABORATORY

Early developments in liposome methodology were aimed particularly at achieving good solute entrapment (8). The move toward commercialization has placed increasing emphasis on such needs as stability, scale-up, reproducibility, and process validation (8). Numerous methods have been developed to meet widely different requirements. These can be broadly divided into two categories, those involving physical modification of existing bilayers and those involving generation of new bilayers by removal of a lipid solubilizing agent. The various methods available are discussed here from the perspective of the different structural types of liposome that they produce. Due to lack of space, this article can offer no more than a brief qualitative description of the more widely known procedures. For more in-depth details, the reader is referred to the various reviews, original papers, and manuals that are available (8,14,15).

Oligo- and Multilamellar Vesicles

Physical Methods. ***Simple "Hand-Shaken" MLV.*** MLV may be prepared from single-source natural or synthetic lipids, by suspending the latter (1), preferably in a finely divided form, in an aqueous solution maintained at a temperature greater than the T_c of the lipid. For unsaturated phospholipids such as egg and soy phosphatidylcholine (PC), which have T_c values below 0°C, this is conveniently done at room temperature. Stirring or swirling considerably speeds up lipid hydration and liposome formation, and the possibility of lipid oxidation can be minimized by working in an inert atmosphere of nitrogen or argon. As the liposomes form, a small proportion of the solution and its associated solute becomes entrapped within the interlamellar spaces. Uptake may continue over several hours, though in practice two hours of gentle stirring is normally adequate to achieve near-maximal incorporation. At the end of this period, the loaded liposomes can be separated from nonencapsulated solute using a process such as centrifugation or dialysis.

It is often desirable to prepare liposomes from mixtures of amphiphile, for example to improve their stability or to impart functional properties such as charge. In this case it is essential that the different lipids be thoroughly mixed at the molecular level. This has traditionally been achieved in the laboratory by codissolving them in a common solvent such as a 2:1 (v/v) mixture of chloroform and methanol and then removing the solvent. If done using a rotary evaporator, the lipid can be deposited as a thin film, which aids solvent removal and subsequent dispersion of the lipid. Hydration, separation, and harvesting can then be carried out as already described.

A major drawback of conventional MLV is their low efficiency for incorporation of water-soluble solutes, which is partly due to the fact that much of the volume is occupied by the internal lamellae. Thus, in neutral liposomes, only a few percent of the starting material may become entrapped. The encapsulation efficiency can be increased in several ways. Inclusion of a charged amphiphile, such as phosphatidyl glycerol or phosphatidic acid at a molar ratio of 10–20%, causes electrostatic repulsion between adjacent bilayers, leading to increased interlamellar separation, thus allowing more solute to be accommodated. However, if the solute itself is charged, entrapment may be increased or decreased depending on the relative sign, and may lead to solute association with the external surface. Freeze-drying of the lipid from solution in an organic solvent tends to form an expanded foam with an increased surface area, which increases the amount of aqueous phase that can be incorporated (16). A solvent with a high freezing point such as tertiary butanol should be used, so that it becomes deposited in the condenser rather than dissolving in the pump oil. Drying of the lipid onto an inert support, whether water-insoluble such as glass beads, or water-soluble such as sorbitol, also increases lipid surface area and may increase the level of solute entrapment.

It has been found that solute concentration in the interior of hand-shaken MLV is less that that in the external aqueous phase (13). This is because, as the phospholipid is hydrating, water passes across the semipermeable lamellae more rapidly than does the solute, and so the liposomes are correspondingly depleted. This can be alleviated by subjecting the suspension to cycles of freezing and thawing, which causes transient defects in the lamellae through which solute redistribution can take place.

Dehydration/Rehydration Vesicles (DRV). The DRV method was designed to achieve high levels of entrapment, particularly of sensitive biological molecules such as proteins and nucleic acids, using simple, mild conditions (17,18). The conventional MLV method described at the beginning of this section satisfies the latter two criteria, but since the multilayers form and seal off with the vast majority of the lipid never having come into contact with the solute, encapsulation efficiencies are extremely low. The intention of the DRV method is to maximize exposure of solute to the lipid before its final lamellar configuration has been fixed, so that the liposomes ultimately form around the solute. This is achieved by first preparing MLV in distilled water and then converting these to SUV using established procedures (to be described later), so that the phospholipid achieves the highest possible level of dispersion within an aqueous phase. Lipid packing constraints resulting from the high curvature of SUV mean that up to 70% of the total phospholipid will be present in the outer leaflet of the lamella. Thus when SUV are mixed with a solution of the material to be entrapped (again in distilled water), the majority of the amphiphile is directly exposed to the solute. At this stage the water is removed, most pref-

erably by freeze-drying, to produce an intimate mixture of the dry components. The original vesicles are now in a metastable state, with the phospholipid head groups in close proximity and oriented toward the active component (Fig. 3). A small, defined amount of water is added (17–19), initiating fusion of the vesicles surrounding the active, and formation of larger liposomes, which now encapsulate a large proportion of the solute. The amount of water added at this stage is critical to achieving the optimal level of entrapment, a point that has been missed by some workers. Following the hydration step, the liposomes are diluted with an isotonic buffer such as phosphate-buffered saline (17), and washed to remove nonencapsulated material using a process such as centrifugation or dialysis. At the rehydration stage, there is an increase in the overall solute concentration (e.g., 10-fold) because of the reduced amount of water added (e.g., 10 times less than the original amount). Subsequent dilution with isotonic buffer produces a large osmotic gradient between the internal and external phases, which leads to a redistribution of solute, both within the forming liposome and with the external aqueous phase. This may be aided by increased permeability to solute as a result of bilayer stretching caused by hyperosmotic inflation. At this stage, liposome formation is completed and equilibration achieved.

A wide variety of active materials have been incorporated into DRV, ranging from small ionic compounds and cyclodextrin–drug complexes to proteins and DNA (17–21). Encapsulation efficiencies are high, typically 40–50% under the standardized conditions described, and these levels can be increased substantially by using additional lipid. For solutes that are used in small amounts, much higher proportions can be encapsulated, e.g., values greater than 70% are normally achieved for DNA. Retention of encapsulated carboxyfluorescein dye during incubation with mouse plasma at 37°C was found to be substantially higher than for SUV or reverse phase evaporation vesicles (REV). DRV may be oligo- or multilamellar depending on the conditions used to prepare them. Thus, when ascorbic acid was encapsulated at an initial concentration of 23 mM, freeze-fracture microscopy showed a normal multilamellar appearance. However, when a concentration of 115 mM was used, followed by equilibration in isotonic buffer, many were oligolamellar, with regions of multilayer alternating with broad expanses of aqueous phase (20) (Fig. 4). Liposomes retained 40% of the original solute, which in view of the high concentration at the rehydration stage (more than 1 M), represents a particularly high loading of ascorbic acid. This is presumably due to the increased internal aqueous volume available for solute entrapment. Increas-

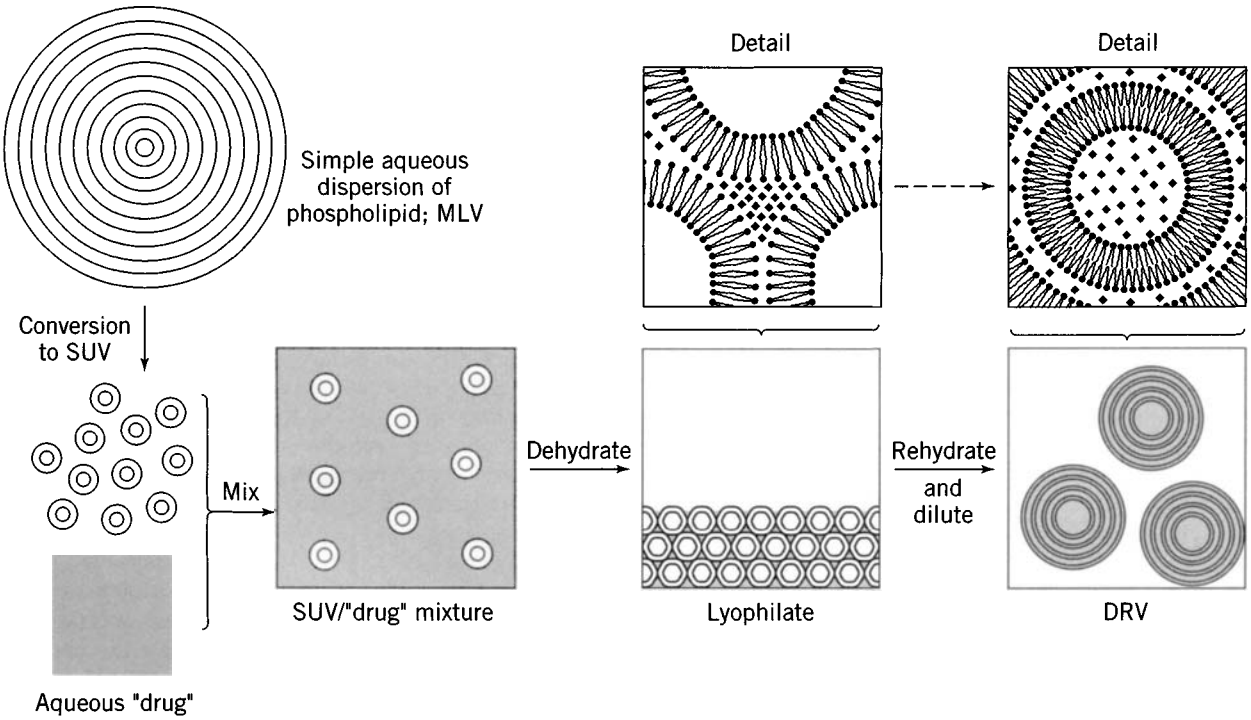


Figure 3. Manufacture of liposomes by the dehydration-rehydration method. A more detailed description of the individual steps is given in the text. The diagram is purely descriptive and no attempt has been made to draw any of the vesicles and other components to scale. During the freezing process, some deformation of the SUV is likely to occur as a result of osmotic shrinkage, caused by increasing external solute concentration arising from progressive formation of ice crystals. Further destabilization of the bilayer during dehydration facilitates rearrangement/fusion to form DRV during the subsequent rehydration step. The relative alignment of the individual drug and phospholipid molecules in the lyophilate (detail) is essentially similar to that in the final product.

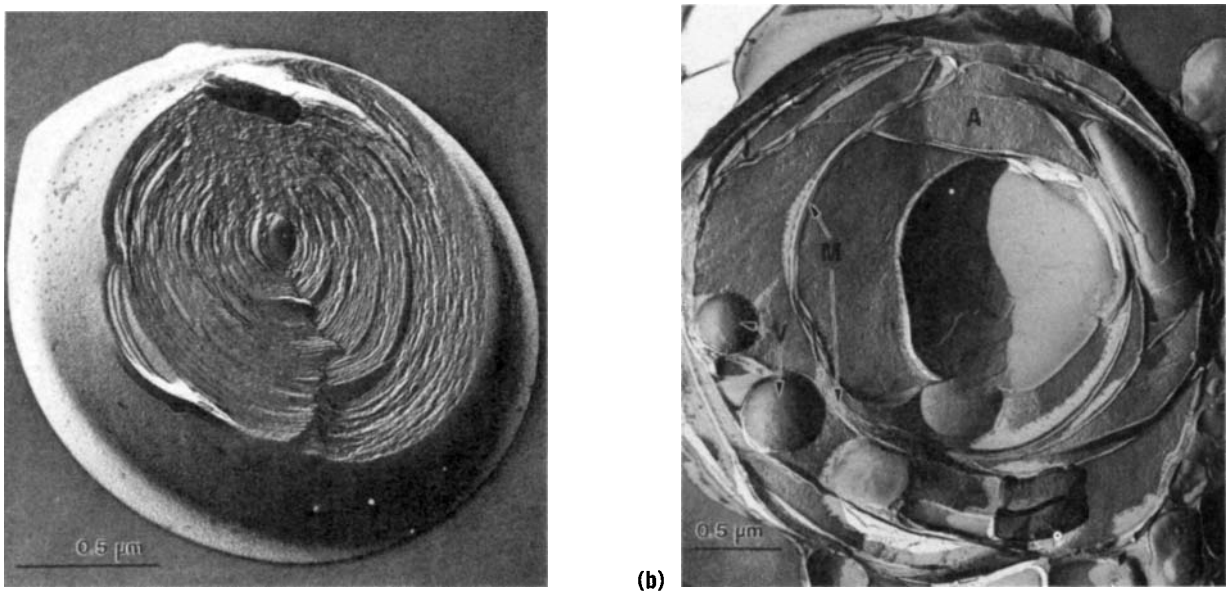


Figure 4. Freeze-fracture electron micrographs of liposomes containing ascorbic acid. DRV prepared in the presence of (**a**) 23 mM and (**b**) 115 mM ascorbic acid. M, regions of multilamellar lipid; V, internal vesicular structure; A, aqueous spaces containing ascorbic acid. *Source:* Courtesy of Mr. B. E. Brooker (see Ref. 20).

ing levels of entrapment at increased solute concentration have also been seen with sodium and potassium chloride, and it may be possible to harness controlled osmotic inflation to achieve still higher loading of other coencapsulated solutes such as macromolecules. These liposomes contained a number of internal vesicular structures, perhaps related to a heterogeneous solute distribution during the dehydration stage, and the particularly high osmotic gradient during rehydration.

The DRV procedure remains one of the most efficient methods for direct loading of drugs into liposomes. Unlike other high entrapment methods, it avoids the use of potentially damaging conditions such as sonication and the use of organic solvents or detergents, which might cause damage to sensitive biological materials. Its simplicity means that scale-up is relatively straightforward.

Resizing of Liposomes. For some applications, the large size and size heterogeneity of multilamellar liposomes is a disadvantage. Both parameters can be reduced by various physical processes that, when used to their full capability, result in the formation of unilamellar liposomes, and so are described more fully in the relevant section. Many of these procedures can be used under less extreme conditions to reduce size, lamellarity, and polydispersity while maintaining the essential oligo- or multilamellar nature of the liposomes. Such processes inevitably lead to reduced entrapment due to redistribution of solute molecules between the liposomes and the external aqueous phase, though losses can be reduced if processing is carried out in the presence of the mother liquor. Bath sonication, microfluidisation and membrane extrusion have been widely used in this respect. Of these, microfluidization (22) and membrane extrusion (C.J. Kirby, unpublished results) have been used to reduce the size range of DRV while still retaining substantial proportions of the encapsulated solutes.

Removal of Lipid-Solubilizing Agents. In practice, the only commonly used agents during preparation of MLV are organic solvents (Fig. 5).

Simple Hydration of Solvent-Solubilized Lipids. Single- or mixed-source amphiphiles dissolved in organic solvents can be hydrated in solution without prior solvent removal. If the solvent is water-miscible such as ethanol or propylene glycol, it can be removed at the end of the procedure (e.g., by dialysis or filtration) or else allowed to remain. The *ethanol injection* procedure discussed later (23) was originally developed for producing SUV, but when the lipid is dissolved at increased concentration and added to the aqueous phase by simple admixture, the resulting liposomes are largely multilamellar. These might then be used to produce feedstock for further processing into other types of liposomes such as DRV. Alternatively, water-immiscible solvents such as ether, chloroform, or methylene chloride may be employed, removing them during processing by evaporation. As with hand-shaken MLV, solute encapsulation is generally very poor. More complex variations of this approach, designed to give improved encapsulation efficiencies, are be discussed later.

Stable Plurilamellar Vesicles. This is a variant of the REV method, which had been developed previously for preparing LUV. As with the DRV procedure, it aimed to increase the level of encapsulation of drugs in MLV by including them before the final lamellar configuration had been fixed. An aqueous phase containing the drug is emulsified together with excess of an ethereal solution of lipids, using bath sonication to form an oil-in-water type emulsion, while evaporating the solvent under a stream of ni-

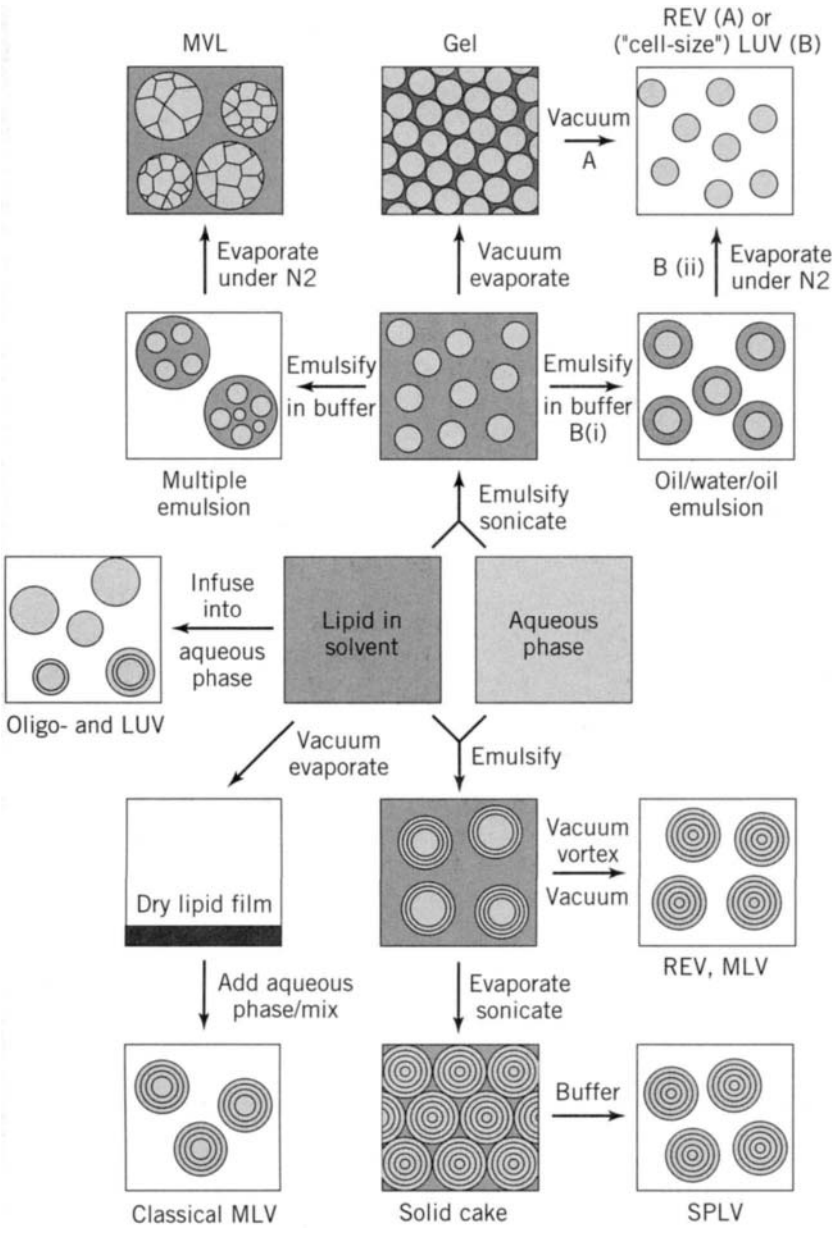


Figure 5. Solvent evaporation processes for liposome preparation. This scheme shows a considerably simplified summary of the different methodologies that are dependent on solvent evaporation, i.e., entailing the use of volatile solvents. No attempt is made at drawing to scale and various steps have been omitted. For convenience, steps A and B (i) and (ii) are shown as producing a similar product, whereas the "cell-sized" LUV derived from B (i) and (ii) may be considerably larger than the REV from step A. In addition, different processes require different solvents, but no such distinctions are made here.

trogen. The resulting cake is then suspended in buffer and washed. The important differences from the parent method are that the amount of lipid is proportionately higher and sonication is used throughout. Whereas the continuous water phase of REV is derived from the original disperse phase of the emulsion, in SPLV it is added later. It has been suggested that toward the end of the process, the aqueous cores collapse and are occupied by lamellae, with the solute load becoming distributed throughout the interlamellar spaces. Maximum levels of entrapment were reported to be 37%, but in terms of the amount of drug incorporated per unit amount of lipid, that level is about 10 times less than the typical value for DRV. In comparison with conventional MLV, SPLV were found to have improved physical stability and biological efficacy. This was claimed to be related to the fact that, unlike MLV, they are not solute-depleted and are in a state of osmotic equilibrium with the surrounding media. The main drawbacks of the SPLV procedure are the need to use volatile organic solvents and sonication, both of which are serious obstacles to potential scale-up and incorporation of sensitive materials such as proteins.

Multilamellar Reverse Phase Evaporation Vesicles (MLV-REV). This is another derivation of the REV method, again differing from the latter in that more lipid and less water are used in order to encourage the formation of multilamellar liposomes (24). The main difference from the SPLV method is that the solvent is removed under vacuum in two stages, and the aqueous continuous phase for the liposomes is derived from the disperse phase of the emulsion (as with the parent REV method). The initial phase of evaporation leads to formation of a gel consisting of aque-

ous cores surrounded by multilayers of lipid. The gel is removed from the vacuum, vortexed, and then reevacuated. During the final stage, phase inversion occurs, wherein a proportion of the cores release their aqueous content, and this is used to form a continuous phase for the newly formed liposomes. Up to 91% of the solute was encapsulated within these MLV-REV, but again from the point of view of mass loading, this is only 50% of that which is typically achieved with DRV. As with the SPLV approach, a major drawback is the need for volatile organic solvents and the implications for safety and scale-up potential.

Multivesicular Liposomes. This approach involves the use of multiple, water-in-oil-in-water type emulsions (12). These are created by first dispersing the aqueous drug solution into a chloroform–ether organic phase containing dissolved amphiphile, thus forming a fine water-in-oil type emulsion, and then dispersing this in turn into a second aqueous phase to form the multiple emulsion. Compositions and conditions are chosen such that each droplet of organic disperse phase contains multiple droplets of the initial aqueous solution. The solvents are removed under a stream of nitrogen, wherein the amphiphile is deposited around the internal aqueous, drug-containing microdroplets, which end up as separate aqueous compartments within a single liposome. Therefore, these are actually multicompartment vesicles in which adjacent, nonconcentric compartments are separated by a single, common unilamellar boundary. The method can achieve very high encapsulation efficiencies of up to 89%, but requires specialized lipids and rather complex conditions. Again, limitations are imposed by the need to use volatile organic solvents, but it is noteworthy that the method has been successfully scaled-up for commercial use.

Small Unilamellar Vesicles

Most of the commonly used methods for preparing SUV involve size-reduction of preexisting bilayers using procedures that have already been referred to in the previous section. The earliest, and probably still the most widely used approach at the bench scale, is by ultrasonic irradiation (25). SUV can be formed rapidly and conveniently by high-power probe sonication but are vulnerable to oxidative damage of unsaturated lipids. This can be reduced by maintaining them in an inert atmosphere during processing and by using a cooling bath to dissipate the large amounts of heat produced. Ideally the equipment should be fitted with an electronic controller to allow the sonic energy to be delivered in short pulses interspersed with longer cooling intervals (for example, 1 s sonication and 3–4 s cooling). Small particles of titanium shed from the probe are removed at the end of the process by centrifugation. A more gentle approach is to use bath sonication, where it is easier to control temperature and to maintain an inert atmosphere, and metal contamination is avoided. Unfortunately, processing time is substantially longer than when a probe sonicator is used.

Many of the literature reports describing preparation of SUV by probe sonication entail the lipid being processed at relatively low concentration. Interestingly, we have noted that when lipid concentration is increased progressively, up to a maximum of around 250 mg/mL, there is a substantial reduction in the time required to form clear SUV using probe sonication (C.J. Kirby, unpublished results, 1992). By this means, gram quantities can be processed in a relatively short time. This suggests that there is less chance of damage to the lipid when working at higher concentrations, a surprising observation because one would instinctively expect the opposite to be true. The reason may be that the high lipid concentration results in an increased likelihood of bilayer fragments being able to reanneal after high power sonication to form SUV. Whatever the reason, the phenomenon allows a certain level of increased throughput in what is otherwise a convenient but notoriously difficult procedure to scale up.

Alternative ways of preparing SUV by sizing make use of high pressure homogenization or extrusion. High-pressure homogenization devices include the French Pressure Cell (26), the Microfluidiser™ (27), and the Gaulin homogenizers (28). The latter two can have particularly high throughputs and employ high shear and cavitation effects to ultimately convert MLV to SUV. The Gaulin range can be used to forcibly hydrate a suspension of dry lipid and convert this to SUV in a single-step process. More impressively, differential scanning calorimetry (DSC) studies indicated that separate amphiphiles could be combined at the molecular level to form SUV having a homogeneous lipid distribution without the involvement of organic solvents (28). To our knowledge, no other mechanical procedure has been reported to be able to achieve this.

High-pressure extrusion involves forcing multilamellar liposomes at high pressure through membranes having "straight-through," defined size pores (29). The liposomes have to deform to pass through the small pores, as a result of which lamellar fragments break away and reseal to form small vesicles of similar diameter to that of the pore. Polycarbonate membranes are manufactured with pore diameters ranging from 8 μm down to 0.03 μm, and ceramic or stainless steel membranes are also available. Repeated cycling through small-diameter pores at temperatures greater than the T_c of the lipid produces a homogeneous population of SUV. A particular advantage of the method is that the disruptive effects of sonication are avoided.

Rapid injection of an ethanolic solution of lipid into an aqueous solution produces a dispersion of vesicles of 30 to 110 nm in diameter depending on the concentration of lipid used (23). Compared with sonicated SUV, these have a relatively heterogeneous size range and have added disadvantages in that a dilute suspension of liposomes is formed, the method is restricted to using ethanol-soluble lipids, and the ethanol may need to be removed afterwards. However, a modification of this method, used to incorporate a lipid-soluble antifungal drug into liposomes, has been successfully scaled up to a batch size of hundreds of kilograms and regulatory approval obtained (30).

Dispersions of the acidic phospholipids, phosphatidic acid, or phosphatidylglycerol, either alone or mixed with other phospholipids, can be induced to form unilamellar liposomes simply by transiently increasing the pH. SUV can be favored by adjusting the experimental conditions (31). However, despite its apparent simplicity, the method

is very restrictive in terms of the lipid compositions that can be used and the conditions of preparation. The vesicles tend to be of a heterogeneous size range, which is influenced by factors such as the nature of the other lipids present, ionic strength, cholesterol content, and the rate and extent of titration.

Large Unilamellar Vesicles

LUV occupy the size range following on from SUV, but unlike the smaller SUV are not subject to lipid packing constraints. Their single bilayer membrane makes them well suited as model membrane systems whereas the large internal aqueous volume:lipid mass ratio means that the efficiency of drug encapsulation for both small and large molecules can be maximized. As with the liposome types already discussed, methods for preparing LUV fall into two categories, the first involving generation of new bilayers by removal of a lipid solubilizing agent, whereas the second involves physical modification of preformed bilayers. For LUV preparation, the solubilizing agents include detergents and chaotropic ions as well as organic solvents.

Removal of Detergents and Chaotropic Agents. For procedures involving detergent removal (32), the lipid is initially dissolved by an aqueous solution of the detergent to form mixed lipid–detergent micelles, and the detergent is then removed by a diffusion-based process such as dialysis, diafiltration, or gel chromatography. The method produces almost exclusively uni- or oligolamellar vesicles ranging in diameter from SUV size up to several micrometers depending on the conditions used. Ionic detergents, such as cholate and deoxycholate or nonionic detergents such as Triton × 100 and octylglucoside, have been used. Detergent removal methods have been especially useful for functional reconstitution of membrane proteins. Many of these proteins retain their activity better in the presence of the nonionic species but these often have a relatively low critical micellar concentration making them difficult to remove by the aforementioned procedures. Use of hydrophobic adsorbent beads has proved particularly useful in these cases. The principle of detergent removal was applied in the first commercially available apparatus for laboratory production of liposomes, the Lipoprep™, which relied on a fast flow dialysis cell to remove detergent (33). The approach has the considerable advantage of allowing close control of the final size of the liposomes, which have a homogeneous size range. Disadvantages are that encapsulation efficiency is low compared with most other methods of LUV preparation, and detergent removal by ordinary dialysis techniques is a time-consuming process that can take several days to reduce residual detergent to a negligible level. Even traces of detergent can have pronounced effects on liposome permeability and can greatly increase the transmembrane movement of phospholipids. Detergents may also have deleterious effects on the material being encapsulated. Giant liposomes have been prepared by solubilizing phospholipids in a micellar form, in solutions of chaotropic ions such as trichloroacetate, and then removing the latter by dialysis or dilution (34). The liposomes, which are uni- or oligolamellar have diameters in the region of 10–20 μm.

Removal of Organic Solvents. Solvent vaporization liposomes tend to be of a larger size range than those prepared by detergent removal. Three distinct types of process have been described, each involving addition of a solution of lipid in organic solvent, to an aqueous solution of the material to be encapsulated (see Fig. 5).

Solvent Infusion. Solvent such as diethyl ether, petroleum ether, ethylmethyl ether, or dichlorofluoromethane-containing dissolved lipid(s), is infused slowly into the aqueous phase, which is maintained at a temperature above the boiling point of the solvent so that bubbles are formed (35). The lipid is deposited as a multilayer around the vapor–water interphase, and as the solvent evaporates off, uni- and oligolamellar liposomes remain in solution. High encapsulation efficiencies (up to 46%) were reported when high concentrations of lipid (15 mM final concentration) were used, and most of the vesicles were in the size range 0.1–0.4 μm. The major disadvantage is the need for exposure of the active to organic solvents, with the possibility of damage to labile materials such as proteins.

Reverse Phase Evaporation. Modifications of this method aimed at preparing MLV have already been described (36). Those approaches proceed via the formation of a water-in-oil (diethyl ether) emulsion containing excess lipid. In the parent case, the amount of amphiphile used is greatly reduced such that, when all of the solvent has been removed (by rotary evaporation), there is just enough lipid to form a monolayer around each of the microdroplets of aqueous phase. At this stage emulsion inversion takes place. This involves collapse of a proportion of these inverted micelles so that their aqueous contents now form the new continuous phase, while their lipid components go to form an outer leaflet around the remaining structures, thus converting them from inverted micelles to a vesicular form. In the absence of cholesterol, these uni- and oligolamellar vesicles have diameters in the range of 0.05–0.5 μm, while with 50 mol % cholesterol, mean diameters are about 0.5 μm. High encapsulation efficiencies of up 65% can be achieved using hydrophilic solutes. Particular drawbacks of the method include the need to work with volatile organic solvents and to expose potentially labile solutes (e.g., proteins) to these, and the need to use sonication to form a stable emulsion.

Double Emulsion Evaporation. A variant of this procedure has already been described for the preparation of MVL (12). In fact, the original method (37) was used to prepare cell-sized liposomes of average diameter about 9 μm. There are again formed by preparing a multiple, water-in-oil-in-water type emulsion followed by solvent evaporation as described for MVL. However, the conditions differ in terms of lipid concentration, solvent composition, and duration of shaking, such that each droplet of organic phase contains only a single microdroplet of drug solution, and the final product is an aqueous suspension of LUV. Although only a small proportion (about 30%) of the lipid present actually becomes incorporated into liposomes, the captured volume is very high at around 52 liters per mole of lipid used. The main disadvantages are that the procedure is quite complex and that specialized lipid mixtures are required. As in the two preceding methods, the pres-

ence of organic solvents may prohibit its use for encapsulation of labile materials.

Physical Modification of Existing Bilayers. Extrusion procedures have already been referred to in the context of downsizing of MLV and ultimately of forming SUV. If MLV are repeatedly extruded under moderate pressure (<500 lb/in^2) through membranes containing straight-through, defined size pores, smallish LUV are formed, with diameters between 60 and 100 nm, depending on the pore size. These have trapped volumes of up to 3 μL/μmol lipid. Where appropriate, drugs can be actively loaded after liposome formation via transmembrane gradients. Alternatively, solute incorporation can be facilitated by prior intermixing with the lipid using freeze-thaw cycles or by using the DRV procedure. This may be particularly useful for entrapping macromolecules.

Exposure of sonicated phospholipid mixtures to alternate cycles of freezing and thawing followed by a brief sonication results in fusion of the SUV and can be used to prepare large, mainly unilamellar liposomes with a relatively large trapping capacity (38). This method was based on a procedure that had previously been used for reconstitution of membrane proteins and is mild in that it avoids the use of detergents and organic solvents, and the period of sonication is quite brief. Disadvantages are that sugars, divalent cations, and high concentrations of ions and proteins all inhibit the membrane fusion process, and the liposomes are heterogeneous in size.

Another procedure employing fusion to produce LUV makes use of electrostatic effects. SUV composed of negatively charged phospholipids are mixed with calcium ions which cause the vesicle to aggregate and then fuse (39). This results in the formation of "cochleate cylinders," which are rolled-up portions of lipid bilayer. Chelation of calcium by adding ethylene diamine tetraacetic acid (EDTA) results in conversion of the cochleates to large uni- and oligolamellar vesicles having a relatively large encapsulation capacity. The main limitation is that the method is only applicable to negatively charged lipids.

SCALE-UP AND INDUSTRIAL MANUFACTURE OF LIPOSOMES

As in many areas of technology, the transition from an optimized research laboratory process to liposome manufacture at the production level is likely to be a daunting prospect, particularly because commercialization of liposome-based products is a relatively recent occurrence. In this context it is reassuring that many of the procedures discussed already have been successfully scaled up, and some are in commercial production. The preparation method chosen at the research phase is likely to have depended on the nature of the material being encapsulated and on the liposome type perceived to be optimal for its intended application. The latter is defined by parameters such as liposome size, lamellarity, permeability, fluidity, hydrophilicity, and other surface properties. Some methodologies are certainly more amenable to scale-up than others, and hopefully some thought will have been given at that stage toward potential future requirements. The subject has been reviewed by various authors (40–42) and so is dealt with only briefly here.

When discussing the implications of scale-up, it is convenient to break down liposome manufacture into the different components of the process which are directly affected. The most important of these are the achievement of a molecular dispersion of different lipid species, hydration of the amphiphiles (wherein actual formation of the liposomes takes place), solute entrapment, and sizing. The first two are interdependent and so are discussed together.

Lipid Intermixing and Hydration

Liposomes are often composed of lipid mixtures (e.g., to increase stability and to provide functionality) and organic solvents are commonly used to enable different lipids to be combined as a homogeneous molecular dispersion. Volatile solvents such as chloroform, methylene chloride, and diethylether have been widely used in this respect because they have high solubilizing capacity for lipids and are easy to remove by evaporation. On the other hand, for large-scale use they are difficult to work with and rigorous safety measures must be in place to guard against fire and toxicity hazards. Moreover, stringent regulations govern the levels of any trace residues that may be present in pharmaceutical products. Some of the methodologies that use them tend to be complex and so pose additional problems for large-scale production. However, volatile solvents have additional roles such as promoting lipid hydration via thin film formation and, in the case of the emulsion methods, in helping to configure liposome structure. In this context it is noteworthy that the MVL method (12), which involves the preparation of multiple, chloroform-containing emulsions, has been used for commercial scale production of Depotfoam™, which has been proposed as a sustained release depot system for localized injection via various routes. In this case however, the liposomal product has a unique configuration which has not been achieved using other methodologies, and as a general rule it is advisable to avoid large-scale use of procedures based on volatile solvents where a similar product can be prepared by other means.

Intermixing of lipid components is also achieved using water-miscible solvents with relatively low volatility such as ethanol, methanol, and propylene glycol, and these are easier to work with than volatile solvents. They also enable rapid hydration of the dissolved amphiphiles. An ethanol-based procedure has been applied for large-scale commercial production of a lipid-soluble antifungal drug econazole into liposomes, enabling 450-kg batch sizes to be produced (30). Ethanol is a pharmaceutically acceptable solvent and, in this case, was left in place at the end of the procedure, helping to maintain the sterility of the formulation. However in other situations its presence may be undesirable, necessitating its removal from the final product. Another disadvantage is the limited capacity of these solvents to dissolve certain liposome components such as certain other phospholipids and cholesterol, thus increasing the amount of solvent which has to be added. If necessary, removal can often be achieved using procedures such evaporation or di-

alysis and, in the case of larger liposomes, by centrifugation or ultrafiltration. Evaporation of smaller amounts of methanol or ethanol can be carried out rapidly and conveniently using a freeze-drier, but a cold trap of liquid nitrogen is needed to prevent contamination of the pump oil. A good compromise is to use a high boiling point solvent such as tertiary butanol which is readily deposited in the freeze-drier condenser.

Detergent removal methods have also been scaled up to produce larger volumes of liposomes, particularly containing bilayer-associated drugs. A range of lipophilic cytostatic drugs were incorporated in volumes of 0.1 to 5 liters for use in clinical trials (43), achieving incorporation efficiencies ranging from 85 to 100% compared with only 1.6% for a hydrophilic drug. Further scale-up to batches exceeding 10 liters was carried out using a topical steroid β-methasone (44), and a production unit capable of producing batches of between 100 and 200 L was reported. In this case, the methodology was chosen in order to produce monodisperse liposomes of defined size distribution. In all cases the initial association between lipid and drug was achieved by dissolution in organic solvents followed by evaporation to form a thin film, and where mixed lipid components are required, the same procedure would have to be followed. Apart from the likelihood of small amounts of residual detergent remaining in the product, a further drawback of this method for large-scale use is the relatively long time periods involved.

Entrapment

For successful commercial usage of liposomes it is vital that sufficient material can be incorporated for the intended application and that it is retained by the vesicles until their subsequent use. This is particularly important for pharmaceutical applications where a shelf life of two years is often required. Both aspects are readily achievable for bilayer-associated substances but are much more of a problem for water-soluble ones and largely dictated by the properties of the latter. If low encapsulation efficiencies are acceptable, then it may be sufficient to use one of the mechanical procedures already described. On the other hand, various approaches have been used to increase the level of encapsulation and retention of hydrophilic substances. Interaction with the bilayers can be increased by including lipids of opposite charge, by preparing lipophilic derivatives (45), or in certain cases, by incorporating lipophilic chelating agents for the solute into the bilayer (46). Otherwise, manufacturing procedures that enable high encapsulation efficiencies can be used. If it is deemed appropriate to use volatile organic solvents, REV, or one of its derivative methods might be considered feasible. An alternative possibility is to use the DRV method, if necessary using extrusion or microfluidization to reduce the size of the resulting liposomes. This method has added advantages in that sensitive biological molecules can be incorporated with high efficiency, and also the lyophilized intermediate can, in theory, be stored indefinitely before being reconstituted as and when needed. This second point could help to alleviate the problems of leakage of smaller molecules during long-term storage.

Another approach to achieving high encapsulation efficiencies while eliminating the consequences of leakage during storage is to use the active loading principle (47,48) by means of which a drug can be remotely loaded into liposomes at the time it is needed, for example at the patients' bedside. This approach is dependent on the fact that small charged molecules have a very low ability to diffuse across lipid membranes, whereas if their charge is neutralized, many become lipophilic and able to cross much more readily. By passively incorporating ionizable substances into liposomes, and then adjusting the external pH, transmembrane pH or concentration gradients can be established and used to load certain drugs into the liposome. For example, a weakly basic drug such as doxorubicin added to liposomes with a relatively high external pH becomes deprotonated and thence lipophilic, enabling it to partition across the membrane. Once inside, it becomes protonated due to the low internal pH, preventing its exit and enabling more of the uncharged drug to enter. Other approaches can result in precipitation of the loaded drug by interaction with encapsulated cations, thus promoting further drug entry.

Sizing

The suitability of high-pressure homogenization systems for scale-up of the sizing stage has already been discussed. In particular, the claimed ability of the Gaulin Micron range to be able to convert highly concentrated particulate suspensions of lipids directly to SUV by forced hydration, to achieve homogeneous lipid intermixing, and to be operated continuously (28) suggests that it is well fitted for effective scale-up of the earlier stages. The possibility of enabling incorporation of proteins and peptides with good retention of activity is also worthy of further investigation. One reported drawback is that the cavitational effects can result in mechanical erosion and contamination of the product with metal particles, but these could presumably be removed using appropriate filters. Also, because SUV are formed, the entrapped volumes are rather low. The Microfluidiser has also been widely used for preparing large volumes of small vesicles and has proved useful for producing empty SUV for scaling up of the DRV procedure.

Sizing by extrusion through polycarbonate membranes can be conveniently carried out in the laboratory using small, compact apparatus, resulting in liposomes with well-defined size characteristics (49). In earlier studies, the technique was limited due to clogging of the membrane resulting in reduced throughput, but it has now been successfully scaled up to enable processing of multiliter volumes. Initial improvements were achieved in batch mode by increasing the surface area of the membranes and using stirring to prevent clogging (43). More recently a continuous flow device was introduced which employed higher pressures and achieved flow rates of up to 500 mL/min. High lipid concentrations of up to 400 mg/mL could be processed, and no signs of membrane clogging were seen after using a range of lipid compositions (50).

Other Issues

The major drive to develop liposomes has come from the pharmaceutical industry, and so particular emphasis has

been placed on factors such as sterility, apyrogenicity, stability, and reproducibility. Sterility is normally achieved either by ultrafiltration of the final product through 0.2 μm filters in the case of smaller oligo- and unilamellar liposomes, or by carrying out the whole manufacturing process in a sterile environment. Both approaches have been successful for a range of liposome-based products and so should pose no problems with forthcoming ones. Other approaches have been discussed (51). The adoption of good quality control procedures and the use of high-quality raw materials from approved suppliers should help to minimize problems of poor stability and pyrogenicity. If a solvent solubilization step is present, dissolved lipids can be ultrafiltered to remove pyrogenic substances. Antioxidants can be included to minimize oxidative degradation, particularly where unsaturated lipids are used. In some cases it might be feasible to freeze-dry the product in order to improve stability during storage, but this is generally most appropriate in the case of bilayer-soluble drugs.

CHARACTERIZATION

There are numerous methods for the characterization of liposomes, depending on the aspect of the system under investigation (52). Such aspects include those that are related to the overall structure of liposomes, for instance vesicle size, lamellarity (i.e., number of bilayers), surface potential, and morphology. Others relate to the stability of liposomes in terms of either changes in vesicle size and other general characteristics on storage, or ability of vesicles to retain entrapped drugs in a given medium (e.g., buffer, biological fluids). Finally, it is often necessary to determine the extent, if any, of component modification during the production of liposomes or storage, especially in the case of unsaturated phospholipids that can be easily peroxidised or degraded.

Overall Structure of Liposomes

Vesicle size can be determined either by hydrodynamic methods (53) (e.g., gel exclusion chromatography using Sepharose 4B or 2B, Sephacryl S500, and S1000) or by photon correlation spectroscopy (54–56) using instrumentation that is appropriate for the size range of the vesicles. Values are expressed as z average mean in nanometers or micrometers. A polydispersity index provides information on the range of vesicle size distribution. Size measurements can also be made in a z sizer which, in addition, also determines the z-potential (zP) of vesicles. zP values range from negative to positive and reflect the surface charge of the vesicles. The latter is particularly useful in formulations where the drug incorporated in liposomes is charged and thus able to modify the overall surface charge. The lamellarity of liposomes is determined by small-angle X-ray scattering (57,58) which can reveal whether bilayers are arranged nonconcentrically (multivesicular structures).

Morphological observations of liposomes can be carried out by light microscopy (53) and electron microscopy (EM) (58) under a variety of conditions. For instance, bright field and phase contrast microscopy are used extensively, especially in conjunction with fluorescent dyes. However, light microscopy is only suitable for large (e.g., LUV and MLV) and giant liposomes (53). With transmission electron microscopy, liposome samples in suspension are firstly negatively stained (e.g., with OsO_4, UO^{2+}) and then directly examined (58). The technique can reveal unilamellar, oligolamellar, or multilamellar structures. Alternatively, a three-dimensional image of liposomes is obtained by freeze-fracture electron microscopy (FFEM) where samples of liposome suspensions are quickly frozen, fractured at very low temperature (e.g., -150°C) and immediately replicated by appropriate means (59). Replicas are then examined by EM. In some cases, to facilitate identification of liposomes (e.g., in tissues where local structures can be mistaken for liposomes) these are labelled with gold particles which can be either entrapped within the vesicles or attached onto the vesicle surface using immunogold labeling (58). This, however, requires the presence of a protein on the liposomal surface. In cryoelectron microscopy a thin aqueous film on a specimen grid is formed by dipping the grid in and withdrawing it from the liposomal suspension (58). The film is rapidly vitrified, cooled to its melting point, and then examined by EM. As with FFEM, confirmation of vesicle images with entrapped gold particles or immunogold labeling is often necessary when biological samples are examined.

Other methods for the characterization of liposomes include spectroscopy, which can be used to measure the turbidity of a liposomal suspension (52). Sets of calibration curves are then employed to devise semiquantitative estimates of vesicle size or concentration. On the other hand, the structure and dynamics of the acyl chains of liposomal phospholipids can be determined by infrared or Raman spectroscopy, and the hydration of phospholipid polar heads (and their interaction with counterions) by Fourier transformation methods (60). Liposomal parameters such a liquid-crystalline transition temperature (T_c), or diffusion constants within bilayers can be measured by NMR and electron paramagnetic resonance (EPR) (60). In addition, electron resonance techniques can provide information on vesicle size and number of lamellae (60), and EPR spin labeling coupled with the addition of paramagnetic ions is a particularly useful method for the estimation of vesicle internal volumes. Finally, thermodynamic methods are useful in the study of T_c energetics (DSC), or liposome dissolution heat (isothermal calorimetry) (60).

Liposomal Stability

Changes in the structural characteristics of liposomes on storage can be monitored by one or more of the techniques already mentioned. These techniques, however, cannot detect subtle structural changes (e.g., vesicle porosity) that lead to the leakage of drugs entrapped in the aqueous phase of liposomes. Drug retention by liposomes on storage or in the presence of a biological fluid can be determined by a variety of techniques (60,61).

It is always appropriate that in designing the lipid composition of liposomes for the entrapment of a drug within their aqueous phase, the stability of the bilayers within a given milieu is monitored. A typical example is the effect of blood components on the ability of a liposomal formu-

Next Page

lation to retain entrapped solutes (61). To that end, one of the easiest and most effective methods is the use of calcein or carboxyfluorescein as marker solutes. Calcein and carboxyfluorescen self-quench at high concentrations (e.g., above 0.05 M) but acquire a green fluorescent colour on excessive dilution. Suspended liposomes containing quenched dye appear as brown or orange. However, destabilization of the vesicles leads to the leakage of some of the dye and its excessive dilution into the medium. Measurement of the resulting fluorescence by spectrofluorimetry reveals the extent of leakage. For liposomal formulations containing drugs, drug leakage on storage or in the biological milieu can be monitored by techniques that separate entrapped from leaked drug. This can be achieved by ultracentrifugation, dialysis, molecular size chromatography, or ion exchange chromatography.

FATE OF LIPOSOMES IN VIVO AND ITS CONTROL

Following work in the early 1970s (2–6,62–67) with drug-containing MLV, several basic aspects of their behavior in vivo became apparent. For instance, rate of clearance of vesicles from the blood of intravenously injected rats was rapid, dose-dependent, and biphasic. It was subsequently observed that neutral MLV (68) and SUV (69) exhibit a slower rate of clearance than negatively and (more recently) positively charged MLV, and that SUV had a longer residence time than MLV (69). Another observation was that small, water-soluble drugs (e.g., 5-fluorouracil and penicillin G) leaked considerably from circulating MLV (6). In view of what we know today, this is hardly surprising as the MLV used contained little cholesterol. On the other hand, larger entrapped solutes such as albumin and amyloglycosidase did not appear to leak (3,4,68). Finally and perhaps more importantly, liposomes with entrapped materials were shown to end up in the fixed macrophages of the RES, mainly in the liver and spleen, through the lysosomotropic pathway (4,66,67). Within lysosomes, vesicles were seen (67) to lose their organized structure (presumably through the action of phospholipases) and to release their contents. Depending on their molecular size and ability to withstand the hostile milieu of the organelles, drugs could then act either locally (e.g., hydrolysis of stored sucrose by liposomal fructofuranosidase) (62) or, after diffusion through the lysosomal membrane, in other cell compartments (e.g., inhibition of DNA-directed RNA synthesis by liposomal actinomycin D in partially hepatectomized rats) (66). Such understanding of liposomal fate and behaviour led to a number of proposed applications, including the treatment of certain inherited metabolic disorders (4,62,70), intracellular infections (6,9), cancer (6,71), gene therapy (4), and because of antigen-presenting cell involvement in vesicle uptake in vivo, immunopotentiation and vaccine delivery (72).

The demonstration in the early 1970s that liposomes coated with cell-specific ligands (e.g., antibodies and asialoglycoproteins), can interact with, and be internalized by, alternative (other than macrophages) cells expressing appropriate receptors, both in vitro (73) and in vivo (73,74) culminated in the concept (73) of vesicle targeting and to novel avenues of liposome research and potential use. Perhaps more encouraging were indications that even ligand-free liposomes could enhance the delivery of drugs to solid tumors in vivo (74). It was soon realized (63), however, that success in this area would require not only quantitative retention of entrapped drugs by the vesicles (also needed for "passive" targeting to fixed macrophages), but also a sufficient time period for circulating (targeted, ligand-bearing) vesicles to encounter and associate with the target. Because vesicle behavior in vivo, resulting from a given structural feature of the system, must be closely related to the particular environment in which that system exists, knowledge of the influence of the biological milieu on both drug leakage and vesicle clearance rates appeared essential.

Retention of Drugs by Liposomes

Initial indications as to why liposomes might become permeable to entrapped drugs, or destabilized in the presence of blood, thereby allowing drugs to leak out, came from the finding (75,76) that plasma high density lipoproteins (HDL) remove phospholipid molecules from the vesicle bilayer. It appeared logical to assume (77) that prevention of such HDL action, for instance by increasing the packing of the lipid components in the bilayer, would enable the vesicles to remain intact. Experiments to test this assumption were thus carried out, initially using MLV (77) and later with SUV (78). In both cases, additional cholesterol (e.g., a phospholipid: cholesterol molar ratio of 1:1) increased the bilayer stability in the presence of blood components (77–80) with very little loss of phospholipid or of an entrapped water-soluble marker, either in vitro (78) or after intravenous (78,79), intraperitoneal (78), or subcutaneous (81) injection. A role for HDL in the destabilization of liposomes was further substantiated by (*1*) the demonstration (82) that cholesterol-free SUV exposed to blood plasma from lipoprotein-deficient mice or a patient with congenital lecithin-cholesterol acyltransferase deficiency (characterized by low HDL levels) were more stable than when incubated with plasma from normal mice or humans; (*2*) the identification (82) of HDL as the only lipoprotein, among a number of lipoprotein species added to lipoprotein-deficient plasma, that could restore vesicle-destabilizing activity.

It was thus of interest to see whether reduction of vesicle leakage to solutes by cholesterol-induced bilayer packing could also be achieved with bilayers made rigid by substituting egg PC with high-melting phospholipids. As anticipated (77,80), SUV or MLV made of hydrogenated lecithin, distearyl phosphatidylcholine (DSPC) or sphingomyelin (SM) were less permeable to entrapped solutes in the presence of blood plasma, with bilayer stability becoming even greater when additional cholesterol was present (81–86). Thus, liposomes composed of equimolar DSPC and cholesterol were able to completely retain their marker solute (carboxyfluorescein) content, even after 48 hours of exposure to plasma at 37°C (84).

Vesicle Clearance Rates: The Role of Lipid Composition

In the course of work on liposomal stability it was observed (83) that solute retention by cholesterol-rich SUV, al-

lation to retain entrapped solutes (61). To that end, one of the easiest and most effective methods is the use of calcein or carboxyfluorescein as marker solutes. Calcein and carboxyfluorescen self-quench at high concentrations (e.g., above 0.05 M) but acquire a green fluorescent colour on excessive dilution. Suspended liposomes containing quenched dye appear as brown or orange. However, destabilization of the vesicles leads to the leakage of some of the dye and its excessive dilution into the medium. Measurement of the resulting fluorescence by spectrofluorimetry reveals the extent of leakage. For liposomal formulations containing drugs, drug leakage on storage or in the biological milieu can be monitored by techniques that separate entrapped from leaked drug. This can be achieved by ultracentrifugation, dialysis, molecular size chromatography, or ion exchange chromatography.

FATE OF LIPOSOMES IN VIVO AND ITS CONTROL

Following work in the early 1970s (2–6,62–67) with drug-containing MLV, several basic aspects of their behavior in vivo became apparent. For instance, rate of clearance of vesicles from the blood of intravenously injected rats was rapid, dose-dependent, and biphasic. It was subsequently observed that neutral MLV (68) and SUV (69) exhibit a slower rate of clearance than negatively and (more recently) positively charged MLV, and that SUV had a longer residence time than MLV (69). Another observation was that small, water-soluble drugs (e.g., 5-fluorouracil and penicillin G) leaked considerably from circulating MLV (6). In view of what we know today, this is hardly surprising as the MLV used contained little cholesterol. On the other hand, larger entrapped solutes such as albumin and amyloglycosidase did not appear to leak (3,4,68). Finally and perhaps more importantly, liposomes with entrapped materials were shown to end up in the fixed macrophages of the RES, mainly in the liver and spleen, through the lysosomotropic pathway (4,66,67). Within lysosomes, vesicles were seen (67) to lose their organized structure (presumably through the action of phospholipases) and to release their contents. Depending on their molecular size and ability to withstand the hostile milieu of the organelles, drugs could then act either locally (e.g., hydrolysis of stored sucrose by liposomal fructofuranosidase) (62) or, after diffusion through the lysosomal membrane, in other cell compartments (e.g., inhibition of DNA-directed RNA synthesis by liposomal actinomycin D in partially hepatectomized rats) (66). Such understanding of liposomal fate and behaviour led to a number of proposed applications, including the treatment of certain inherited metabolic disorders (4,62,70), intracellular infections (6,9), cancer (6,71), gene therapy (4), and because of antigen-presenting cell involvement in vesicle uptake in vivo, immunopotentiation and vaccine delivery (72).

The demonstration in the early 1970s that liposomes coated with cell-specific ligands (e.g., antibodies and asialoglycoproteins), can interact with, and be internalized by, alternative (other than macrophages) cells expressing appropriate receptors, both in vitro (73) and in vivo (73,74) culminated in the concept (73) of vesicle targeting and to novel avenues of liposome research and potential use. Perhaps more encouraging were indications that even ligand-free liposomes could enhance the delivery of drugs to solid tumors in vivo (74). It was soon realized (63), however, that success in this area would require not only quantitative retention of entrapped drugs by the vesicles (also needed for "passive" targeting to fixed macrophages), but also a sufficient time period for circulating (targeted, ligand-bearing) vesicles to encounter and associate with the target. Because vesicle behavior in vivo, resulting from a given structural feature of the system, must be closely related to the particular environment in which that system exists, knowledge of the influence of the biological milieu on both drug leakage and vesicle clearance rates appeared essential.

Retention of Drugs by Liposomes

Initial indications as to why liposomes might become permeable to entrapped drugs, or destabilized in the presence of blood, thereby allowing drugs to leak out, came from the finding (75,76) that plasma high density lipoproteins (HDL) remove phospholipid molecules from the vesicle bilayer. It appeared logical to assume (77) that prevention of such HDL action, for instance by increasing the packing of the lipid components in the bilayer, would enable the vesicles to remain intact. Experiments to test this assumption were thus carried out, initially using MLV (77) and later with SUV (78). In both cases, additional cholesterol (e.g., a phospholipid: cholesterol molar ratio of 1:1) increased the bilayer stability in the presence of blood components (77–80) with very little loss of phospholipid or of an entrapped water-soluble marker, either in vitro (78) or after intravenous (78,79), intraperitoneal (78), or subcutaneous (81) injection. A role for HDL in the destabilization of liposomes was further substantiated by (*1*) the demonstration (82) that cholesterol-free SUV exposed to blood plasma from lipoprotein-deficient mice or a patient with congenital lecithin-cholesterol acyltransferase deficiency (characterized by low HDL levels) were more stable than when incubated with plasma from normal mice or humans; (*2*) the identification (82) of HDL as the only lipoprotein, among a number of lipoprotein species added to lipoprotein-deficient plasma, that could restore vesicle-destabilizing activity.

It was thus of interest to see whether reduction of vesicle leakage to solutes by cholesterol-induced bilayer packing could also be achieved with bilayers made rigid by substituting egg PC with high-melting phospholipids. As anticipated (77,80), SUV or MLV made of hydrogenated lecithin, distearyl phosphatidylcholine (DSPC) or sphingomyelin (SM) were less permeable to entrapped solutes in the presence of blood plasma, with bilayer stability becoming even greater when additional cholesterol was present (81–86). Thus, liposomes composed of equimolar DSPC and cholesterol were able to completely retain their marker solute (carboxyfluorescein) content, even after 48 hours of exposure to plasma at 37°C (84).

Vesicle Clearance Rates: The Role of Lipid Composition

In the course of work on liposomal stability it was observed (83) that solute retention by cholesterol-rich SUV, al-

though always high during relatively short (e.g., up to 2 h) periods of exposure to blood plasma, was significantly reduced when some formulations (e.g., those made of PC) were incubated for longer periods, whereas with others (e.g., SM) remained unchanged. It turned out (84) that this phenomenon correlated with the residence time in the blood circulation of the corresponding vesicles, i.e., the greater the vesicle stability, the longer the half-life (Figs. 6, 7; Table 1). However, this relationship between stability and clearance observed for neutral SUV (of size up to about 80 nm diameter) did not apply to very stable negatively charged SUV (85) or, more importantly (because of the higher drug load they can accommodate), to larger neutral vesicles (85). In the latter case, clearance rates were found to increase progressively with increasing size, even though bilayer stability remained high for prolonged periods during incubation with plasma (85). It thus appeared that vesicle size and surface charge both override the state of bilayer stability in determining vesicle clearance from the circulation.

On the basis of such findings, a tentative hypothesis was put forward (87) to unify observations concerning the role of liposomal phospholipids and cholesterol in promoting bilayer stability in vitro and (for neutral vesicles) circulatory half-life in vivo. Figure 8 proposes that, for liposomes that survive attack and complete disintegration by HDL, destabilization of the bilayer facilitates the adsorption onto, or insertion into it, of plasma proteins (opsonins) thought to be responsible (88) for the presentation of vesicles and other particles in a form recognizable by macrophages. The hypothesis predicts that the lower the destabilization of the bilayer, the fewer or smaller the "gaps" on

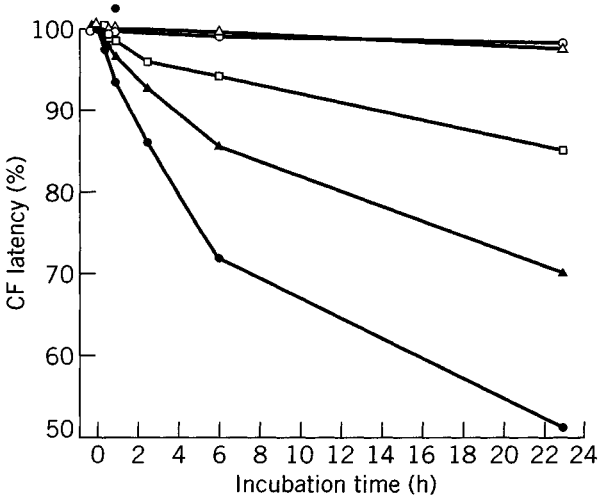


Figure 6. The effect of phospholipid composition of liposomes on their permeability in plasma. In a typical experiment shown here, small unilamellar liposomes containing quenched carboxyfluorescein (CF) and composed of SM (○), 77% SM, 23% egg phosphatidylcholine (PC) (△), 47% SM, 53% PC (□), 23% SM, 77% PC (▲) and PC (●) were incubated in the presence of mouse plasma at 37°C. All liposomal preparations contained cholesterol, equimolar to the total phospholipid. CF latency values (indicative of liposomal stability) at time intervals are % of total CF present *Source:* From Ref. 84, with permission.

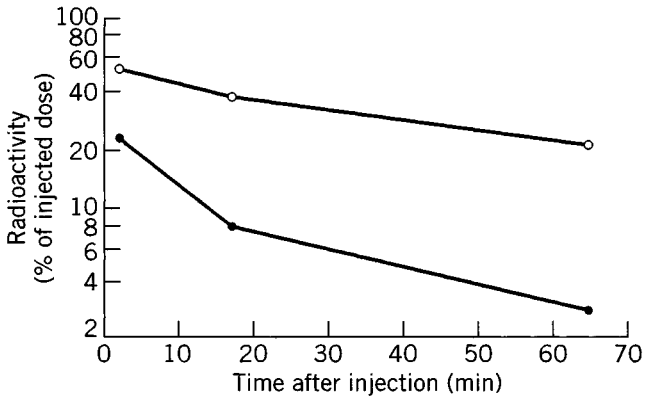


Figure 7. Entrapped drug clearance after intravenous injection of mice with vincristine-containing liposomes. Cholesterol-free (●) and cholesterol-rich (○) egg PC liposomes containing [^{3}H]vincristine were injected intravenously into mice. Animals were bled at time intervals and plasma samples chromatographed on Ultrogel AcA 34 columns. Radioactivity eluting in the fractions corresponding to the liposomal peak was then estimated and expressed as % (mean) of the total radioactivity injected per total mouse plasma. *Source:* From Ref. 98, with permission.

Table 1. Half-Lives of Liposomes After Intravenous Injection

	Half-life in vivo (h)	
Liposomes	Quenched CF	[s1^{4}C]SM
SM	11.0	10.0
77% SM, 23% PC	11.0	10.7
47% SM, 53% PC	7.0	7.0
23% SM, 77% PC	4.5	3.6
PC	2.1	2.3

Note: Liposomes as described in Fig. 6 containing CF and ^{14}C-labeled SM were injected intravenously into mice. Animals were bled at time intervals and plasma samples assayed for latent (quenched) CF and ^{14}C radioactivity. Half-lives were estimated from the linear clearance patterns plotted on a logarithmic scale.
Source: From Ref. 84, with permission.

it (and the lower the leakage of solutes) and, therefore, the smaller the amount of opsonins capable of associating with the vesicles. Thus, vesicles with decreasing amounts of opsonin on their surface would be expected to exhibit a proportionally reduced uptake by the RES. However, the scheme in Figure 8, although probably valid in general terms, is too simple to reflect real events. Indeed, since 1976 a number of workers have shown that a variety of plasma components (including α_2-macroglobulin (89), blood coagulation factors (90), components of the complement cascade (91), C reactive protein (92), and fibronectins (93) can, depending on their lipid composition and surface properties, bind to liposomes. More recent work (94) has revealed that liposomes interact (or fail to interact) with tissue-specific opsonins that are capable of facilitating or inhibiting (dysopsonins) uptake of vesicles with differing lipid compositions by the macrophages of the liver, spleen, or bone marrow. The ways by which the bilayer surface in its varying states of fluidity or destabilization encourages

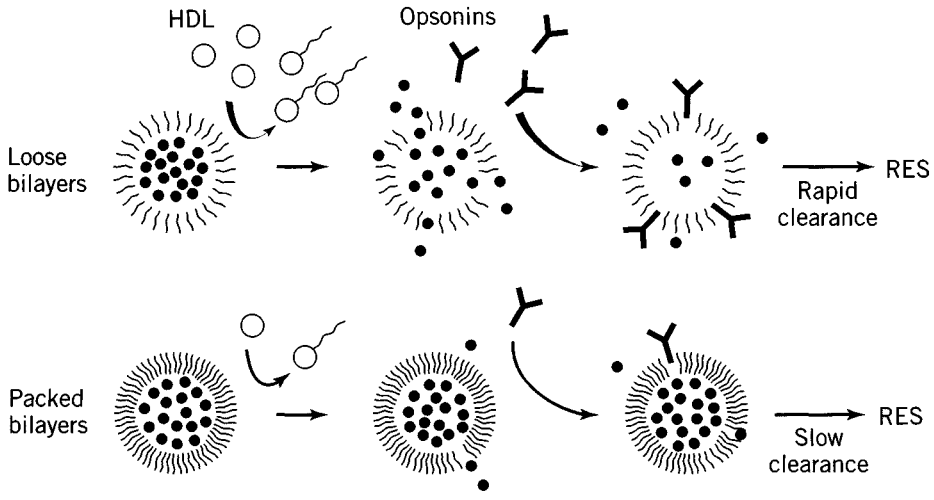


Figure 8. Correlation between stability of liposomes and clearance from blood circulation. In proposed scheme, extent of bilayer porosity and leakage of solutes in blood is dependent on the facility with which HDL remove phospholipid molecules from the bilayer. Loose bilayers are attacked by HDL more effectively than packed bilayers. The greater the gaps after HDL attack, the more extensive the opsonin adsorption on vesicles and uptake by the RES.

or discourages interaction with specific opsonins is not clear at present. Nonetheless, the failure (94) of a liver-specific opsonin to enhance uptake of liposomes rich in cholesterol or composed of "high melting" phospholipids by Kupffer cells is compatible with the sequence of events in Figure 8.

TAILORING OF LIPOSOMES

The properties of the basic liposome types and procedures for preparing them have been outlined in the previous section, illustrating the enormous diversity of structure and compositions that can be achieved. The versatility of the system means that additional refinements can be added and the scope broadened so that existing applications are optimized and new ones can be developed. The aspects of further development that have made the greatest impact are discussed here.

Long-Circulating Liposomes

For many years, a major obstacle to the use of liposomes for drug delivery via the parenteral route was the rapid clearance from the blood circulation by the RES before they had had the chance to exert their intended effect. Clearance is slower in the case of SUV, particularly when their composition is based on mixtures of SM (83) or DSPC (84) together with cholesterol, where increased lipid packing makes the bilayer more rigid and less likely to be opsonized by blood proteins (see Fig. 8). In these cases, the rate of clearance is also dose-dependent in that a larger amount of lipid saturates the sites of uptake in the mononuclear phagocytes. It was subsequently found that liposome clearance could also be substantially reduced in a manner which was less dependent on size or dose by inclusion of monosialoganglioside (GM_1) or hydrogenated phosphatidylinositol (HPI) in the bilayer lipid (95). This is related to the more hydrophilic nature of the head groups of these amphiphiles, which made it easier for the resultant vesicles to evade detection by the RES, and led to their being termed Stealth™ liposomes. It was later found that the same effects could be achieved by incorporating PEG groups at the liposome surface (95,96), usually by including a PEG-substituted phosphatidylethanolamine (PE) as a bilayer component. The liposomes so formed are often described as sterically stabilized, and are now used more widely than those based on GM_1 or HPI since the lipids are less expensive (and more clinically acceptable than GM_1). Moreover, the clearance pattern was less governed by lipid content, enabling greater flexibility in terms of the bilayer composition of the liposomes.

The reduced rate of clearance of liposomes (as a result of the choice of lipid composition or PEGylation) has important implications for the application of liposomes in drug delivery. One such application is to use the liposomes as circulating drug reservoirs, e.g., to give improved pharmacokinetic control of phase-specific cytostatic agents (97,98) and/or to increase the stability of vulnerable substances in the blood. This is achieved by a combination of increased control over the rate of drug release from the carrier and of the rate of clearance of the carrier from the bloodstream. Such effects are made increasingly possible by being able to prolong the circulation time of the liposomes while (in the case of PEGylated vesicles) being less reliant on liposome size and lipid composition. Prolonged circulation time also gives increased opportunity for liposomes to interact with non-RES target sites in the body, both by passive and by ligand-mediated targeting. These examples are discussed in greater detail later in this article, particularly under the heading of "Cancer."

Targeted Liposomes

One of the major tenets of the drug delivery concept is control of the physiological distribution of the administered carrier in the body, so that the effects of the associated drug are focused at the intended site of action and its therapeutic index is maximized. This aspect has been avidly explored throughout most of the period since liposomes were first proposed as drug delivery vehicles almost three decades ago (3,4). Some progress was gained by harnessing the structural variability of normal, unmodified liposomes to achieve so-called *passive* targeting. Thus the larger size

range of MLV, which predisposes them to removal from the RES, has been exploited to deliver various therapeutic agents to these cells, e.g., to replace genetically deficient enzymes (70) and to target antimicrobial agents to intracellular pathogens (9). By the same token, the small-size of SUV makes them more able to extravasate from leaky vasculature (95). However, passive targeting is limited in its scope, and tremendous effort has been directed toward the development of more universal levels of control by associating molecules with recognition properties with the liposome surface. The essential requirements (95) of this *active* targeting approach are summarized as follows:

- Characteristics of the target cell population must be identified which are qualitatively and/or quantitatively different from other cells that might be encountered by the delivery vehicle, and which are appropriate as recognition features for a targeting mechanism. Typical examples are antigenic determinants, including various types of membrane receptor, which are unique or overexpressed (by virtue of the aggressive growth rate of the cell).
- It must be possible to generate targeting ligands that are able to interact with some degree of exclusivity with these epitopes. Examples include antibodies (either intact or as active fragments), other proteins and peptides, lipoproteins, glycoproteins, and growth factors. Specific examples will be given later.
- The ligand must be capable of being attached stably and accessibly to the drug carrier so that interaction with the target epitope brings the liposome into close proximity with the cell surface.
- The liposome–ligand construct must be stable within the biological milieu and present for sufficient time to maximize the chances of it interacting with the target cell population.
- Binding should increase the chances of the drug reaching the cell interior, for example, by receptor-mediated endocytosis or membrane fusion events or by local diffusion across the cell membrane. Also, once internalized, the drug must retain its stability (e.g., against damage from lysosomal processing) and be available to exert its intended action.

Ligand Coupling Strategies. The general strategy of this approach is exemplified by the developments achieved with antibodies and what are now known as immunoliposomes. The earliest report of antibody-mediated liposome targeting appeared 24 years ago (73). In that first report, liposomes containing a radiolabeled antitumor drug, bleomycin, were associated with a series of polyclonal antibodies and then incubated with a range of cells against which the various antibodies had been raised. In all cases, radioactivity was higher in those cells incubated with the corresponding antibody than in the same cells incubated with the other, nonspecific antibodies, thus confirming an in vitro targeting effect. In the same study, asialofetuin, which is known to bind to galactose receptors on the liver parenchymal cells, was associated with doubly labeled liposomes and then administered to rats, some of which had first been injected with free asialofetuin. The latter group of animals showed reduced association of the two radiolabels with the liver, thereby providing the first evidence of targeting of liposomes in vivo. A little later (74), in vivo targeting of liposomes was also demonstrated by the use of tumor-specific antibodies.

Many different coupling strategies have been used to associate the targeting ligands and the liposomes. The aforementioned study used a relatively crude approach whereby the two components were sonicated together, presumably enabling hydrophobic portions of the proteins to insert into the perturbed bilayers, and a similar approach by another group confirmed the targeting ability of the resulting vesicles (99). Others have used targeting moieties loosely bound to the liposome surface. Thus a hapten-specific antibody was used to bring about interaction between liposomes and cells, both of which were coated with the hapten (100), whereas in a separate study, liposomes opsonized with antibody were targeted to tumor cells resulting in their internalization by receptor-mediated endocytosis (101). The majority of the subsequent studies have used chemical coupling methods to link a targeting moiety to an amphiphilic molecule inserted into the liposome bilayer. Early approaches included immunoglobulin G (IgG) cross-linked to liposomal PE using glutaraldehyde (102), or to aldehyde groups formed by periodate-oxidation of liposomal glycosphingolipids (103). Another early method which became very popular involved covalent coupling of fatty acid chains directly to IgG using cross-linking agents, and then incorporation of the resultant molecules into liposomes by detergent dialysis (104). However, by far the most widely used approach to date involves the use of heterobifunctional cross-linking reagents for introducing thiol-based linkages between the lipid anchor and the ligand, thereby minimizing the chances of formation of homopolymers.

In the original method, thiol-reactive derivatives were prepared, both of the antibody (via free amino groups) and the PE anchor; the latter was incorporated into liposomes, and then free thiol groups were formed by reduction. Interaction of the two species resulted in coupling of the immunoglobulin molecule to the liposome surface via a thiol linkage (86,105). An alternative approach is to use the thiol groups generated when a $F(ab')_2$ fragment of IgG is reduced to form two Fab′ fragments (106). A particular drawback with the thiol linkage is its limited stability in blood, and an important improvement was to replace this with the much more stable thiol–ether linkage (107). This is achieved by using maleimido-based thiol reagents to derivatize either the lipid anchor or the ligand so that subsequent interaction produces a stable thiol–ether bond. The same approach can of course also use Fab′ fragments as already discussed (106). Over the years, many modifications and improvements have been made to this technique and are now widely used in many different targeting applications.

An alternative to the strategy of coupling the ligand directly to the liposome surface has been to make use of the high affinity avidin–biotin interaction (108). Avidin and streptavidin are glycoproteins with molecular weights of 67 and 60 kDa, respectively, either of which can tightly

bind four molecules of low molecular weight biotin, and the components can be configured in different ways to achieve ligand binding. Biotinylation of the bilayer anchoring molecule and the ligand can be readily achieved via free amino groups and then bridged together by addition of (strept)avidin to form a tightly bound complex. Alternatively, (strept)avidin can be covalently bound to the bilayer using one of the aforementioned procedures and then complexed to a biotinylated ligand. Either approach provides a flexible way of enabling the separate components to be prepared and stored in advance and then put together on a "mix and match" basis as required.

Progress in the development of ligand-based liposome targeting has been held up by numerous obstacles that can affect various stages of the targeting process. During construction of the carrier, the ligand may be damaged or lose activity as a result of the conjugation process. Formation of IgG fragments may result in reduced affinity. On the other hand, binding of intact antibody has been observed to result in rapid clearance of the construct, probably as a result of the affinity of the Fc portion of the antibody for the Fc receptors in the liver. Moreover, chronic use of antibody-coated liposomes may lead to immune responses against the (foreign) proteins. This can be approached by preparing chimeric or else wholly humanized antibodies. Once in the bloodstream, exposure to blood components may lead to cleavage of the ligand from the carrier or else to drug leakage. On the other hand, if the liposome is too stable, it might not release its contents once its destination has been reached. Early attempts to combine the immunoliposome and Stealth approaches were problematic because the PEG chains obstructed access of antibody to the liposome surface during the conjugation procedure and to the cell surface epitope during the targeting procedure. This was eventually resolved both by using an avidin–biotin approach similar to that already described, or by conjugating the antibody to the terminal region of the PEG moiety.

At the level of the target cell, it has proved difficult to identify truly tumor-specific markers, in addition to which there may be considerable surface heterogeneity between different cells in a given tumor cell population. Moreover, it was demonstrated quite early that the simple fact of a carrier binding to its target epitope does not in any way guarantee its internalization (109), and other mechanisms for drug entry into the cell (e.g., passive diffusion or fusion) may well be ineffective. Different antibodies may themselves vary in their ability to be internalized. Reliance on overexpression of ubiquitous antigens known to internalize (e.g., transferrin, folate, and low density lipoproteins) is still accompanied by nonspecific binding to normal cells expressing these receptors. However, despite the gloomy picture that this may present, sound progress has been made such that positive results are now being achieved in vivo. These is discussed in more detail in the section "Applications for Liposomes".

Polymerized Liposomes

The concept of liposome polymerization has been around for about 20 years but may still be some way from becoming a viable proposition. For a recent review, see Bonte et al. (110). The basic premise is that polymerizable amphiphiles can be used to form lipid vesicles and then made to polymerize using conventional triggers. The ideal outcome is a liposome of high but controllable stability with fluid, liquid crystalline properties. A variety of polymerizable phospholipids have been synthesised, with the reactive groups in different regions of the molecule as shown in Table 2. Thus, the polymer backbone can be in the head group region, through the midchain hydrocarbon region, or through the end of the hydrocarbon chains.

Polymerized liposomes are very stable in the presence of blood components and have been widely studied as potential drug delivery vehicles, where they have been seen as a possible solution to the instability of natural phospholipid liposomes. Their use in this respect would require that they be only partially polymerized to permit eventual drug release when required. To achieve this goal, windows of normal or trigger-responsive lipids would need to be included. In fact, by using mixtures of normal and polymerizable lipids, different domains can be formed, the size and distribution of which are dependent on the preparation conditions. This was well demonstrated in a study using a mixture of polymerizable octadecadienoyl phosphatidylcholine and nonpolymerizable dipalmitoyl phosphatidylcholine, where treatment of the resultant liposomes with solvents removed the normal lipids to leave "skeletonized" porous liposomes which could be observed by scanning electron microscopy. However, various technical hurdles must be overcome before polymerized liposomes are ready for use as drug delivery vehicles, and concerns remain about the possibility of toxic residues. Inert fragments of polymer backbone are known to accumulate in the body and biodegradable amphiphiles have been proposed as a way of overcoming this. Of the limited in vivo studies that have been carried out, one showed rapid clearance of methacrylate-derived liposomes from the blood of injected mice, by the liver and spleen.

A related potential application is the use of polymerized liposomes as an artificial blood substitute for transporting hemoglobin or synthetic oxygen carriers around the body. For example, synthetic hemoglobin embedded by copolymerization into the bilayer of imadazole dienoylphospholipid liposomes formed oxygen carriers which were stable for several months and were similar to human blood in terms of their oxygen-carrying capacity and binding affinity. Polymerized liposomes have also been used for studying membrane dynamics during various processes of cell biology. These include molecular recognition phenomena such as occur between membrane receptors and lectins, between cells and the extracellular matrix, and between phospholipase and other enzymes with the lipid bilayer. In addition, they have provided valuable information regarding the localized membrane changes that occur during processes such as endo- and exocytosis and membrane budding.

pH- and Temperature-Sensitive Liposomes

These modifications were developed in order to increase the selectivity of drug action in the body via controlled re-

Table 2. Reactive Groups for Liposome Polymerization

Functional group	Link region	Polymerization method
Methacrylic	Head group, acyl chain	Chemical or UV
Thiol–disulphide bonds	Head group, acyl chain (end)	Chemical or UV
Dienoate	Acyl chain	Chemical or UV
Vinyl	Acyl chain	UV
Diacetylinic	Acyl chain	UV, γ radiation

lease from the carrier. The former originated from attempts to design liposomes that would become leaky and release their contents in the low pH environment surrounding anoxic tumor cells (111), but it was subsequently realized that the same strategy could be used to exploit the changes occurring during endosomal acidification (112). The approach is dependent on the use of an amphiphile that under physiological conditions does not normally exist in a lamellar phase, but can be induced to do so in the presence of a second titratable amphiphile that conditionally stabilizes the bilayer in a *pH dependent* manner. The nonlamellar amphiphile used in virtually all cases to date has been PE. Except under conditions of high pH and low ionic strength, or at temperatures well below its transition temperature, unsaturated PE preferentially adopts the inverted hexagonal (H_{II}) phase, which as discussed at the beginning of this article, has considerable fusogenic character. Several different stabilizing amphiphiles have been used, the most common being oleic acid and cholesterol hemisuccinate. Under neutral or mildly alkaline conditions, each of these will be deprotonated and hence negatively charged. When present with PE under these conditions, the latter is unable to form the H_{II} phase and favors a lamellar phase whereupon liposomes can be formed. If, however, the pH is subsequently reduced, the titratable amphiphile becomes protonated and the loss of charge results in a transition to the H_{II} phase, thus destabilizing the liposome structure.

When conventional liposomes are taken up by receptor-mediated endocytosis, the endosomal pH is sequentially reduced to reach 5.0 or lower at the lysosome stage, where the combined effects of low pH and enzymic action generally result in degradation of the liposome and its contents. If, on the other hand, pH-sensitive liposomes are used, the nonbilayer transitions take place between the early and late endosomal stages, resulting in destabilization of the endosome and delivery of its contents into the cytoplasm. Such effects are particularly important in gene delivery (see the following section) and are referred to again in the section "Applications for Liposomes." A major drawback in the exploitation of pH-sensitive liposomes is their poor stability in vivo, such that larger ones based on dioleoyl phosphatidyl ethanoldiamine (DOPE) and oleic acid leaked most of their contents in the presence of plasma at 37°C, and were rapidly cleared by the RES. This was found to be due to loss of oleic acid to plasma components. To approach this problem, a double chain amphiphile, 1,2-dipalmitoyl *sn*-3-succinylglycerol, was synthesized and used to prepare liposomes which were found to remain stable and to retain their pH sensitivity after prolonged plasma incubation (113). Immunoliposomes of this composition were able to deliver their contents into the cytoplasm of L929 cell cultures.

The concept of temperature-sensitive liposomes was also developed with the aim of selective drug delivery to tumors. In this case, the liposomes are prepared using phospholipid mixtures which have transition temperatures a few degrees higher than body temperature (114). It is known that liposomes show increased permeability at temperatures in the vicinity of the transition temperature, due to formation of defects in the bilayer. By injecting drugs containing cytotoxic drugs into the systemic circulation and then applying localized heat externally to the target area, e.g., to the vicinity of a tumor, the liposomes can be induced to release their payload of drug in that region.

Cationic Liposomes

This term has become synonymous with gene transfection. In fact it is somewhat confusing because although the starting material is liposomal, electrostatic interaction with DNA leads to extensive loss of the original morphology. In early studies, encapsulation was assumed to be a prerequisite for successful transfection but this idea had to be revised when it was found that lipid–DNA complexes formed by simple mixing of DNA, and cationic SUV were much more effective (115). The basis of the approach is that positive charge in the form of cationic lipid is used to neutralize the considerably extended, polyanionic nucleic acid chain to form a highly compact microstructure, which has become known as a lipoplex. Each of these particles carries a small net positive charge, which enables it to approach and interact with the negatively charged cell membranes and perhaps ultimately gain entry by receptor-mediated endocytosis (Fig. 9). There is still conjecture concerning the fine structure of the lipoplex. Examination by FFEM typically shows a heterogeneous mixture that includes the presence of aggregated spherical structures together with elongated fibrils (116) forming what has been described as the "spaghetti-meatball" appearance. The spherical units are believed to comprise condensed DNA associated with cationic lamellar lipid, whereas the fibrils appear to be strands of DNA surrounded by lipid bilayer in tubular form. It has proved difficult to confirm any structure–transfection activity relationship in the various morphological variations that have been observed.

A large and diverse range of cationic lipid transfection agents have been synthesized, not only to improve the efficiency of transfection, but also to increase biodegradability, decrease toxicity, and increase stability during storage

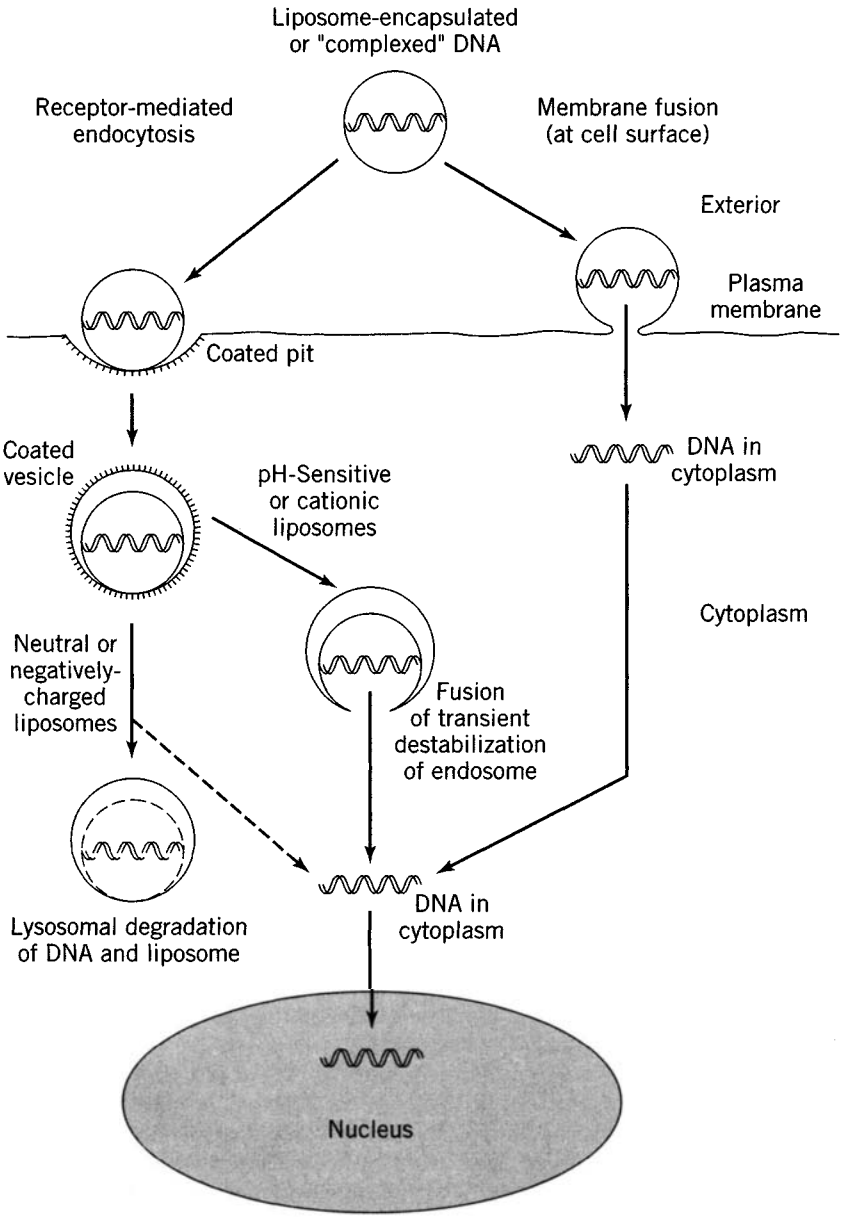


Figure 9. Proposed modes of cellular uptake of liposome-associated nucleic acid. The membrane fusion pathway remains putative. *Source:* From Ref. 118, with permission.

and in the presence of blood components. These have been the subject of recent reviews (117,118) and are not discussed in any detail here. The standard was set by dioleoyloxypropyl-trimethylammonium chloride (DOTMA) in 1989 (115) and was rapidly followed by many others. Cationic lipids vary widely with respect to their polar head group, hydrophobic tail, and the interlinking region of the molecule. All are dependent on amine-containing head groups for their positive charge, and in the majority the lipophilic region consists of two fatty acyl chains as in conventional phospholipids. Of the others, a few have used single acyl chains, but better results have been achieved using the cholesterol backbone, as in 3β*N*-(*N*′,*N*′-dimethylaminoethane)-carbamoyl) cholesterol (DC-Chol) (119), which formed the basis of the first cationic liposome system to be tested in human trials. The great majority have been used together with a neutral helper lipid which has usually been DOPE, though in some cases cholesterol has also been useful in this respect. The function of the helper lipid is thought to be due to its propensity to form the fusogenic hexagonal (H_{II}) phase and hence to promote endosomal disruption and release into the cell cytoplasm (see previous section). In the case of cationic amphiphiles based on the cholesterol moiety, DOPE is also required for these to form liposomes, whereas the double chain species form liposomes on their own.

Cationic amphiphiles with monovalent head groups have a limited capacity to condense DNA, but this can be increased by substitution for a multivalent group such as one based on spermine, to form lipopolyamines (120) such as dioctadecyl-amidoglycyl-spermine and dipalmitylphosphatidylethanolamidospermine. The greater charge density means that the resultant structures are smaller and more compact, and therefore better able to bind to the

coated pits and be taken up by endocytosis. In addition their greater buffering capacity can give increased protection against low intralysosomal pH. In a related approach, protamines, which are natural polyamine components of sperm, have been included together with DC-Chol/DOPE, providing effective transfection of Chinese hamster ovary (CHO) cells (121). These natural cationic peptides may also have nuclear localization signals that might help them to gain entry into the nucleus. A similar system using 1,2-dioleoyloxy-3-(trimethylammonium) propane (DOTAP) liposomes together with protamine was injected intravenously into mice, showing expression of the luciferase gene in all organs, particularly in the lung (122).

APPLICATIONS FOR LIPOSOMES

Cancer

This application has been widely reviewed in recent publications (5,95,123–126). Possibilities for using liposomes for the treatment of cancer have been approached from several different directions. Chemotherapeutic agents, including conventional low molecular weight cytotoxic drugs as well as peptides and proteins, have been administered in undirected and in ligand-targeted liposomes. Cytokines and other immunomodulators have been encapsulated in MLV and used to activate macrophages and make them tumoricidal. Genetic material, including DNA, antisense molecules, and ribosomes, has been presented in liposomes to bring about different antitumor effects. Many of these approaches have given promising results and two formulations based on cytotoxic anthracyclines are now in commercial use.

A variety of cytotoxic drugs have been administered in liposomes via various routes to a range of animal tumor models (95,123–126). Much of this work has focused on the anthracyclines. Although for certain cytotoxic drugs encapsulation into liposomes was found to cause increased toxicity, early studies indicated that for others, including the anthracyclines, toxicity was reduced. This appears to be due to the fact that rapid uptake and sequestration of liposomes by the macrophages of the RES reduces the peak plasma levels of the drug and their associated toxicity, particularly to the myocardium. The macrophage-associated drug is ultimately released back into the circulation to produce an effect akin to continuous infusion. However, although the therapeutic benefits of conventional infusion are well known, the significance of such an effect in the context of liposomal delivery remains controversial, and certainly in some cases reduced toxicity is accompanied by reduced efficacy.

One effect that is clearly beneficial is the fact that many rapidly growing tumors have poorly formed, leaky vasculature through which liposomes of appropriate diameter can pass, and because of ineffective lymphatic drainage, will then accumulate. The longer the liposomes are able to circulate in the blood, the greater the level of accumulation. This effect is the basis of three different liposomal anthracycline products (Table 3) which have given successful results in clinical trials, two of which are on the market. Of these, TLC® D-99 (The Liposome Company), which is still in Phase III, comprises doxorubicin actively loaded into egg PC–cholesterol liposomes of around 150 nm in diameter using a pH gradient (5,126). Comparative studies of dogs treated with TLC D-99 or with the same amount of free drug showed retention and occasionally increased antitumor activity in the former group, without the histological evidence of myocardial toxicity that was seen with the free drug. Several Phase III trials are ongoing in U.S. and Europe to evaluate TLC D-99 alone and in combination therapy in metastatic breast cancer.

Daunosome® (NeXstar, Inc.) consists of daunorubicin incorporated by a remote loading technique into 40–50 nm-diameter SUV composed of DSPC and cholesterol and is supplied as a ready to use aqueous liposome suspension (5,127) (see Table 3). This composition forms a particularly rigid bilayer which inhibits opsonization by the plasma lipoproteins, and this together with their small size results in an extended circulation time of 24 hours in the blood. It is also claimed that a substantial portion of the extravasated liposomes are taken up intact by the tumor, where they then release their contents over a prolonged period of time to produce sustained drug action within the tumor. The product has so far been approved for first-line therapy of AIDS-related Kaposi's sarcoma in the U.S. and other countries. Promising results against a variety of other tumors have led to Phase II clinical trials, which are currently underway to look at its utility for treating lymphoma, leukemia, and myeloma, as well as solid tumors in breast, ovary, and brain (127).

The third product, Doxil® (Sequus Pharmaceuticals) (see Table 3) is based on doxorubicin, which is again incorporated by active loading, this time into sterically stabilized liposomes comprising hydrogenated soy PC, PEG-DSPE (distearyl phosphatidylethanolamine) and cholesterol, and having an approximate diameter of 85 nm (5,95,128). The drug is in the form of a gel-like precipitate which enables high concentrations to be encapsulated and retained within the liposomes. The slightly increased size compared with DaunoXome (and hence increased loading), is achieved by virtue of the fact that sterically stabilized liposomes are less size dependent with respect to their clearance rate. Thus, circulation times of 15 to 30 hours in rodents and dogs and 40 to 60 hours in humans can be achieved with consequently increased accumulation in the vicinity of the tumor. The steric stabilization also results in decreased contact with other tissues such as the myocardium while circulating in the blood, with the drug remaining sequestered inside the liposomes during this time. Once localized in the tumor tissue, various mechanisms have been proposed to account for liposome breakdown and drug release, including low pH, the action of lipases and other released enzymes, and the consequences of engulfment by tumor-resident macrophages. Once released, doxorubicin is sufficiently lipid soluble to diffuse into the tumor cells, leading to their destruction (128). Doxil was the first liposomal drug approved by the FDA and has been on the market for treatment of AIDS-related Kaposi's sarcoma since 1995. It has also shown very promising results in a range of solid tumors including ovarian and breast carcinoma for which advanced clinical trials are underway (128). Sequus Pharmaceuticals is also developing cisplatin

Table 3. Liposome-Based Products Developed or Under Development (UD)

Product	Drug	Target disease
	Aronex Pharmaceuticals, The Woodlands, TX	
Liposomal nystatin (trademark not yet given; intravenous) (UD)	Nystatin	Systemic fungal infections
Liposomal tretinoin (trademark not yet given; intravenous) (UD)	All-trans retinoic acid	Leukemia
Liposomal annamycin (trademark not yet given; intravenous) (UD)	Annamycin	Kaposi's sarcoma Retractory breast cancer
	IGI, Vineland Laboratories, Vineland, NJ	
Newcastle disease vaccine (intramuscular) (Novasomes)	Newcastle disease virus (killed)	Newcastle disease (chicken)
Avian Rheovirus vaccine (intramuscular) (Novasomes)	Avian rheovirus (killed)	For vaccination of breeder chickens; for passive protection of chicks against rheovirus infection
	NeXstar Pharmaceuticals (formerly Vestar), Boulder, CO	
AmBisome (intravenous)	Amphotericin B	Systemic fungal infections; visceral leishmaniasis
DaunoXome (intravenous)	Daunorubicin	First line treatment for advanced Kaposi's sarcoma. Breast cancer and other solid tumors
MiKasome (intravenous) (UD)	Amikacin	Serious bacterial infections
VincaXome (intravenous) (UD)	Vincristine	Solid tumors
	Novavax, Rockville, MD	
E. coli 0157:H7 vaccine (oral) (Novasomes) (UD)	*E. coli* 0157:H7 (killed)	*E. coli* 0157 infection
Shigella flexneri 2A vaccine (oral) (UD)	S. flexneri 2A (killed)	S. flexneri 2A infection
	SEQUUS Pharmaceuticals (formerly Liposome Technology), Menlo Park, CA	
Doxil (intravenous)	Doxorubicin	Kaposi's sarcoma. Refractory ovarian, recurrent breast, prostate and primary liver cancers
Amphotec™ (intravenous)	Amphotericin B	Systemic fungal infections
	The Liposome Company, Princeton, NJ	
D99 (intravenous) (UD)	Doxorubicin	Metastatic breast cancer
ABELCET™ (intravenous) (Ribbons)	Amphotericin B	Systemic fungal infections
C53 (intravenous) (UD)	Prostaglandin E_1	Systemic inflammatory diseases
	Swiss Serum and Vaccine Institute, Berne, Switzerland	
Epaxal-Berna vaccine (intramuscular) (IRIV[a] liposomes)	Inactivated hepatitis A virions (HAV) (antigen; RG-SB strain)	Hepatitis A
Trivalent influenza vaccine (intramuscular) (UD)	Hemagglutinin and neuraminidase from H_1N_1, H_3N_2, and B strains according to recommendations by WHO	Influenza
HAV/HB_s-IRIV combined[b] vaccine (intramuscular) (UD)	HAV, genetically engineered hepatitis B antigens (HBs)	Hepatitis A and B
Diphtheria/tetanus/hepatitis A combined vaccine (intramuscular) (UD)	Diphtheria and α and β tetanus toxoids; inactivated HAV virions	Diphtheria, tetanus, hepatitis A
Hepatitis A and B/diphtheria/tetanus/influenza supercombined vaccine[a] (intramuscular) (UD)	Inactivated HAV virons, HB_s, diphtheria, and α and β tetanus toxoids, hemagglutinin and neuraminidase from influenza strains as in trivalent influenza vaccine	Hepatitis A and B, diphtheria, tetanus, and influenza

[a]IRIV, immunopotentiating reconstituted influenza virosomes.
[b]Combined vaccines denote the presence of up to three antigens in the formulation.
[c]Supercombined vaccines denote the presence of more than three antigens.

in sterically stabilized liposomes, which may be effective in combination therapy with Doxil. Other companies are incorporating different cytotoxic drugs into liposomes, some of which are currently in Phase II clinical trials (5).

The beneficial effects of steric stabilization of liposomes using PEG are not completely clear cut. The accumulation efficiencies of long circulating (by virtue of their rigid bilayers) liposomes by a series of mouse tumors were investigated in the absence and presence of a surface coating of PEG. By comparing the area under the curve (AUC) for plasma drug levels with that of the tumor, it appeared that PEGylation actually reduced the proportion of drug that accumulated in the tumor (129). This occurred despite the fact that the sterically stabilized liposomes circulated for longer in the blood than did the corresponding conventional ones. Steric stabilization also tends to mediate against uptake of liposomes by the tumor cells in the same way that it prevents interaction with other cells. Given these facts, the conflict between the need to design liposomes which fully retain their drug content while circulating in the blood and the need to make this drug available to tumor cells after extravasation remains a difficult issue (129). Its resolution may ultimately depend on controlled release strategies such as the use of pH-sensitive liposomes that respond to reduced pH within the tumor microenvironment or of the combination of temperature-sensitive liposomes and localized hypothermia. Exciting possibilities have also been raised by the recent development of liposomes that can be made highly fusogenic by loss of PEG groups, which potentially enable them to fuse with adjacent cells (130).

The use of ligand-mediated targeting to increase the specificity of drug transfer to tumor cells is still at an early stage, but since the emergence of long-circulating liposomes, promising results in vivo are starting to appear. Early studies (131) reported substantial therapeutic effects when PEG-stabilized or GM_1-stabilized immunoliposomes, containing doxorubicin and a lipophilic prodrug, respectively, were used to treat newly established lung cancers in mice. In the former case, attempts to treat more advanced tumors were unsuccessful. Effective treatment involving receptor-mediated internalization was also achieved using immunoliposomes targeted against malignant cells within the vasculature (132). More recently a comprehensive series of studies has been carried out (133) using sterically stabilized, doxorubicin-containing liposomes targeted against cancers overexpressing the HER2/neu proto-oncogene. HER2 is an internalizing receptor, highly expressed in a wide range of tumors where it plays an important role in aggressive growth and so is unlikely to be down-regulated. It also has other important advantages as a target in that it is a readily accessible cell surface protein with infrequent expression in a limited range of normal cells. A highly reactive antibody is available which has been fully humanized to reduce the chances of immunogenicity, and in these studies was generally conjugated as the Fab′ fragment to the terminal region of liposome-grafted PEG chains. After in vitro optimization, the system was tested against subcutaneous xenografts of different tumors showing various levels of HER2 expression. Interestingly, similar levels of gross uptake were seen in tumors with high and very low expression levels, whereas the antitumor effect was substantially higher in the former (134). This correlated with electron microscopic evidence using colloidal gold-labeled liposomes that in nontargeted systems (low HER2 expression or antibody-free liposomes), the label was concentrated in tumor-resident macrophages and in intercellular spaces, whereas in positively targeted systems it was present both between and *within* the tumor cells (133). This latter distribution presumably accounted for the superior antitumor effects of the targeted systems, whereas the observed gross similarities in tumor distribution using targeted and nontargeted systems agrees with earlier indications that extravasation is the rate-determining step (133).

A completely different strategy for anticancer therapy is to use liposomes to deliver activating factors, such as cytokines to macrophages, so that they become tumoricidal (135). Because the total number of available macrophages in the body is limited, the major indication is for the treatment of metastatic disease after surgical removal of the primary tumor. Activated macrophages ignore normal cells but selectively kill tumor cells, regardless of the numerous levels of biological heterogeneity that normally make metastases so difficult to treat. A widely used method of activation is to expose the macrophages to muramyl dipeptide (MDP), the minimal structural unit of Mycobacterium cell wall. By incorporating lipid soluble derivatives of MDP into MLV enriched with phosphatidylserine, these are preferentially taken up after intravenous injection by macrophages residing in the lung, which is one of the major sites of metastatic disease. Promising studies in mice were followed by successful treatment of dogs after surgical removal of osteosarcoma (135). The approach has progressed through Phase I and Phase II trials, where it was evaluated in combination with chemotherapy and is currently in Phase III for newly diagnosed osteosarcoma patients, where it is hoped that the treatment will destroy residual tumor cells that were not eliminated by chemotherapy. Adults and children have been treated with minimal side effects, and an added attraction is that activation of alveolar macrophages can be achieved by oral administration of liposomal MDP.

Antimicrobial Agents

Liposomes have been widely investigated as delivery systems for treatment of bacterial, fungal, viral, and parasitic diseases, and the topic has been reviewed in recent publications (5,135–137). Therapeutic benefits can be brought about in various different ways. The use of liposomes for passive delivery of immunomodulators to macrophages has been discussed already with respect to cancer treatment, but this approach can also be used to bring about nonspecific resistance to infections in general (135). Thus a wide range of infectious diseases have been shown to respond to treatment by macrophages activated by MDP or cytokines such as interferon γ (IFN-γ) associated with liposomes. Phagocytosed microorganisms often take up residence and multiply in the host cells, making them refractory to treatment by antimicrobial agents due to poor penetration or reduced intracellular activity of the drug.

However, this same phagocytic activity can be used to passively deliver particulate drug carriers such as liposomes to the interior of the cell while at the same time masking the toxicity of the drug to the host. Early studies (9) involved treatment of protozoal Leishmania infections using liposome-encapsulated antimonial drugs and produced substantial increases in therapeutic index due both to improved delivery and reduced toxicity. Similar effects have subsequently been shown in a wide range of bacterial, viral, and fungal infections (123,127).

In recent years there has been a dramatic increase in the incidence of potentially fatal, systemic fungal infections, particularly in patients who are immunocompromised as a result of treatment for diseases such as cancer, diabetes, and AIDS; as a result of organ transplantation; or due to various other factors. Amphotericin B is the drug of choice for treating such infections because its spectrum of activity is much larger than any other clinically acceptable drug (137). It is a lipophilic drug whose mode of action is to interact with ergosterol in plant and fungal membranes (the equivalent of cholesterol in mammalian cells), thereby causing membrane disruption and cell death. The drug does interact with cholesterol but to a lesser extent, and this partial specificity can be amplified by administering it in a particulate form so that it is taken up by the macrophages, which may themselves be hosts to the fungi but can also carry the drug to other sites of infection. Appropriate dosage forms can also reduce the rate of clearance from the bloodstream, enabling increased chance of extravasation through leaky vasculature due to inflammation of diseased tissue. While complexed within these formulations, amphotericin B is unavailable to interact with cell membranes in the body. Thus incorporation into liposomes and other lipidic complexes resulted in substantial reductions in toxicity compared with free drug or with the established formulation Fungizone™ (a deoxycholate-containing micellar dispersion), enabling doses up to five times larger than the latter to be given (127). Three such lipid formulations are now available (see Table 3). AmBisome™ (NeXstar Pharmaceuticals, Inc.) (5,127) is the only truly liposomal form, consisting of SUV composed of hydrogenated soy PC, distearoyl phosphatidylglycerol and cholesterol, stored as a lyophilized powder. Molecules of drug are believed to align in parallel to form cylindrical structures, two of which fit end to end to form a bilayer-spanning pore across which ions and other solutes can pass. These pores can be inserted into the fungal cell membrane, allowing rapid loss of cell contents. In vitro studies have shown binding of AmBisome liposomes to fungal cells, followed by liposome disintegration and subsequent cell disruption (127).

Amphotec™ (Sequus Pharmaceuticals) (5,138) is a non-liposomal form of amphotericin B. Instead it is a stable, disk-shaped complex of drug together with cholesterol sulphate, 115 nm in diameter and 4 nm thick. As with the previous formulation, it is stored in a lyophilized form and reconstituted for use. Comparative studies have indicated that its efficacy is approximately similar to that of AmBisome (138). The third formulation, known as ABELCET™ (The Liposome Company), is also not a true liposome, but is an interdigitated complex of lipid and drug, the lipid components comprising dimyristoyl phophatidylcholine and dimyristoyl phosphatidylglycerol (5,126). Numerous studies at the research level have looked at the use of liposomal drugs to treat bacterial and viral infections and again the main focus has been on intracellular pathogens, particularly in immunocompromised patients. These have included targeting of the HIV virus itself, and of *Mycobacterium* species such as *M. avium*, which causes serious opportunistic infections in AIDS sufferers, and *M. tuberculosis*, which reflects the recent resurgence of multidrug resistant forms of TB. The MiKasome™ system (NeXstar) where the antibiotic amikacin is encapsulated in SUV composed of HSPC, DSPG and cholesterol is currently in Phase I clinical trials (127). Genetic approaches to cancer treatment are discussed in the following section.

Gene Therapy

Liposome-based gene transfection systems have been promoted as a means of achieving the transfection efficacy of viral constructs without the associated risks. The earliest attempts at liposome-based gene transfer in vivo involved conventional entrapment in negatively charged vesicles, and transfection efficiencies were accordingly low. A plasmid containing the preproinsulin gene was injected intravenously into rats, a transient hypoglycaemic response was noted, and increased levels of insulin were detected in the blood, liver, and spleen (139). Improvements arose when increased insights into the mechanisms of uptake prompted the development of pH-sensitive liposomes (111), which could exploit the cellular endocytic mechanisms, and these were rapidly followed by the concept of cationic lipid delivery systems. However, the reactivity of cationic liposomes within the blood, and their rapid removal by the RES (after opsonization) (88), has meant that their application in vivo has generally been limited to localized delivery by various routes. For example, plasmids complexed with Lipofectin™ (DOTMA/DOPE) were injected into specific areas of the brain of Xenopus embryos to study gene function in the developing embryo, whereas expression in mammals was achieved in later studies after injection into mouse brain (140).

DNA–liposome complexes have been used to stimulate immunogenic responses against malignant tumors in vivo. Initial studies carried out in mice (141) involved direct injection into the tumor of the genes for foreign major histocompatibility complex proteins associated with DC-Chol cationic liposomes. The treatment resulted in complete tumor regression in many of the animals, and tumors remote from the injection site and not expressing the transfected gene product also underwent rejection. Based on these positive results, a human clinical trial was carried out whereby the human *HLA-B7* gene in the same type of complex was injected into cutaneous tumors in human melanoma patients (142). Antigen expression, with generation of cytotoxic *T*-lymphocytes specific for *HLA-B7* was seen in the tumors of all 5 patients, and in 1 case, complete regression of the primary tumor occurred.

Site-specific delivery within the vasculature was demonstrated by using a double balloon catheter to isolate a

segment of artery, then injecting into this segment a plasmid associated with either DOTMA/DOPE liposomes or a retroviral vector. Transfection was confirmed histochemically and shown to be limited to the treated segment (143). Such selective transfection in vivo might be applicable for treatment of diseases such as atherosclerosis or cancer. A similar approach involving the use of antisense oligonucleotides was carried out for treatment of neointimal hyperplasia, which frequently occurs after balloon angioplasty, with neointima formation being completely inhibited for 2 weeks after treatment.

The lung is an ideal target for in vivo gene therapy because it is a discrete compartment that is directly accessible via the respiratory airways. Though it has been successfully targeted both by the intravenous and intratracheal routes, the latter is undoubtedly the most convenient, and expression of different reporter genes was readily demonstrated, initially by instillation of DOTMA/DOPE-gene complexes, and subsequently using aerosols. A major impetus for these model studies has been the need for a treatment for cystic fibrosis, which is one of the most common lethal hereditary diseases. After initial studies in mice, a placebo-controlled, human clinical trial was carried out using a cystic fibrosis transmembrane conductance regulator (CFTR) plasmid complexed with DC-Chol/DOPE in the form of an aerosol, administered intranasally to CF patients (144). This resulted in a partial restoration of 20% of normal CFTR activity persisting for up to 7 days, and with no evidence of adverse clinical or histological effects. It was concluded that such a result might be an acceptable clinical outcome, though the duration of effect would need to be extended. Similar studies carried out recently, using DOTAP and DC-Chol liposomes, have shown similar clinical results.

Despite the significant progress so far, there is still a long way to go before the ideal vector becomes a reality. Some headway has been made in improving stability within the bloodstream, and Stealth technology might eventually enable ligand-conjugated complexes to be delivered to specific cell types within the body (130). The rate-limiting step of gene transfer from the cell cytoplasm to the nucleus needs to be solved in order to obtain substantially increased expression levels. Other major goals include the achievement of long-term expression and the ability to regulate transcription of newly introduced genes to permit external control over their expression. Mechanisms for achieving these goals are being developed in the field of viral genetics and may eventually be applied in the liposome field.

Liposomes as Immunological Adjuvants

Immunization against microbial infections and cancer is an attractive alternative to chemotherapy. However, vaccines consisting of attenuated organisms, although efficacious in producing diverse and persistent immune responses by mimicking natural infections usually without the disease, can be potentially unsafe. On the other hand, the extracellular localization of killed virus vaccines and their subsequent phagocytosis by professional antigen presenting cells (APC) or antigen-specific B cells, lead to MHC-II class restricted presentation and to T helper cell and humoral immunity but not to significant cytotoxic T cell (CTL) responses. Moreover, subunit vaccines produced from biological fluids may not be entirely free of infectious agents (145).

New-generation vaccines that are based on recombinantly made subunit and synthetic peptide antigens are usually nonimmunogenic and the need for immunopotentiation is well recognized (146). Although a great variety of structurally unrelated agents (immunological adjuvants) are capable of inducing immune responses to vaccine antigens, most of them are toxic (146). Surprisingly, for over 70 years the only immunological adjuvant licenced for use in humans was, until recently, aluminium salts or hydroxide (alum) (146). Alum, however, is far from ideal, fails to induce cell-mediated immunity and is often unsuitable for a variety of antigens. Twenty years after the discovery of the immunological adjuvant properties of liposomes (72) and a multitude of related animal immunization studies carried out in between (147,148), liposomes as adjuvants have come of age, with the first liposome-based vaccine (Epaxal-Berna; against hepatitis A) (5,149) licensed for use in humans (see Table 3). Epaxal-Berna is based on virosomes produced from the influenza virus (IRIV; immunopotentiating reconstituted influenza virosomes) (149). Vaccines based on novasomes (nonphospholipid biodegradable paucilamellar vesicles formed from single chain amphiphiles with or without other lipids) have also been licensed for the immunization of fowl against Newcastle virus disease and avian rheovirus (5). Other novasome-based (oral) vaccines against bacterial infections are under development (see Table 3) (5).

The way in which liposomes induce immune responses to antigens associated with them is not clear but has been attributed to a depot (slow antigen release) mechanism and the ability of vesicles and antigen content to migrate to regional lymph nodes after local injection (or, when given orally to be endocytozed by M cells which then provide antigen to the lymphoid cells in the Peyer's patches). In the case of liposomes, further improvement of adjuvanticity has been achieved by the use of coadjuvants such as lipopolysaccharide, positively charged lipids, and interleukin-2, and also by ligand-mediated targeting to antigen-presenting cells (147).

The approach adopted for the IRIV vaccines is of particular interest as it has been claimed (149) to combine several components that are known to contribute to immunostimulation and are, at the same time, harmless (e.g., egg PC). Thus, PE serves as a binding site for the hepatitis A virions (HAV). HAV attachment to host cells occurs by binding to the PE regions of their membrane, an appropriate feature of PE for Epaxal-Berna. It is also known to directly stimulate (in the form of liposomes) B cells and to generate antibodies without T-cell help. The inclusion of the influenza virus envelope phospholipids contributes to vesicle stability. Moreover, a key role is played by the haemagglutinin (HA) component: HA (the major antigen of the influenza virus) through its HA_1 epitope containing sialic acid, is expected to mediate IRIV binding to its receptors on macrophages and other antigen-presenting cells and subsequent receptor-mediated endocytosis, thus initiating

a successful immune response. On the other hand, the HA_2 subunit of HA causes fusion of viral and endosomal membranes. The essential feature of IRIVs is that, in addition to the antigen they carry, they are also endowed with the fusion-inducing HA component that, presumably, mediates rapid release of the antigen into the target cell membranes. This proposed (149) mechanism for IRIV adjuvanticity is thought to account for the results obtained with the hepatitis A vaccine and the promising outlook of the trivalent influenza and "combined" or "supercombined" vaccines.

Genetic Immunization

A novel and exciting concept (150) developed recently, namely de novo production of the required vaccine antigen by the host's cells in vivo, promises to revolutionize vaccination, especially where vaccines are either ineffective or unavailable. The concept entails the direct injection of antigen-encoding plasmid DNA which, following its uptake by cells, finds its way to the nucleus where it transfects the cells episomally. Antigen so produced is recognized by the host as foreign and is then subjected to pathways similar to those undergone by the antigens of internalized viruses (but without their disadvantages) leading to protective humoral and cell-mediated immunity.

It was initially observed (151) that intramuscular injection of DNA vaccines leads to such types of immunity as CTL response. This was surprising because antigen presentation requires the function of professional APCs. However, myocytes which were shown to take up the plasmid, albeit only to a small extent and with only a fraction of cells participating in the uptake, are not professional APCs. Although myocytes carry MHC class I molecules and can present endogenously produced viral peptides to the $CD8^+$ cells to induce CTLs, they do so inefficiently as they lack vital costimulatory molecules such as the B7-1 molecule (151). It has thus been difficult to accept that antigen presentation leading to a CTL response occurs via myocytes. Instead, it was reported that CTL responses are, at least in part, the result of transfer of antigenic material between the muscle cells and professional APC. It is also likely that plasmid secreted by the myocytes or as such is taken up directly by APC (including dendritic cells) infiltrating the injection site. Moreover, the extent of DNA degradation by extracellular deoxyribonucleases is unknown but, depending on the time of its residence interstitially, degradation could be considerable. It follows that approaches to protect DNA from the extracellular biological milieu, introduce it into cells more efficiently, or target it to immunologically relevant cells, should contribute to optimal DNA vaccine design (152). One such approach is the use of liposomes.

The interaction of cationic SUV with DNA to form a condensed lipoplex has been discussed in an earlier section ("Cationic Liposomes"). The pathway to transfection is thought to commence with the binding of the positively charged complex to the negatively charged cell membranes followed by endocytosis. This leads to destabilization of the endosomal membrane whereupon, through lateral diffusion of anionic lipids from the cytoplasm-facing endosomal monolayer, DNA is thought to be displaced from the complex and released into the cytosol (153). Intravenous application of the complexes has met with only modest success. Contributing causes include the formation of large aggregates between complexes and anionic plasma proteins leading to the neutralization of the cationic charge and rapid removal of the aggregates by the RES, and hence to reduction or even abolition of transfection activity. So far, results from a few reported studies on genetic immunization with SUV–plasmid DNA complexes have been rather disappointing in that immune responses were either similar to or modestly higher than those achieved with naked DNA (154). Therefore, conventional liposome entrapment procedures may offer an alternative approach.

Liposome-Entrapped DNA. It was recently proposed (155,156) that, as APC are a preferred alternative to muscle cells as targets for DNA vaccine uptake and expression, liposomes would be a suitable means of delivery of entrapped DNA to such cells. Locally injected liposomes are known (147) to be taken up avidly by APC, either after these have infiltrated into the site of injection or else within the lymphatics, and this event has been implicated in their immunoadjuvant activity. Liposomes would also protect their DNA content from deoxyribonuclease attack (152). Because of the structural versatility of the system, its tranfection efficiency could be further improved by the judicious choice of vesicle surface charge, size and lipid composition, or by the coentrapment of cytokine genes and other adjuvants (e.g., immunostimulatory sequences), together with the plasmid vaccine (152).

It has been shown that a variety of plasmid DNAs can be quantitatively entrapped into the aqueous phase of multilamellar liposomes by the mild dehydration-rehydration procedure. Incorporation values were, as expected, higher (57–90% of the amount used; about 10–500 μg) when a cationic lipid was present in the bilayers (152). The possibility that DNA was not entrapped within the bilayers of cationic liposomes but was rather complexed with their surface was examined by gel electrophoresis of cationic liposomes entrapping the DNA and of similar liposomes complexed with externally added DNA, in the presence of sodium dodecylsulphate (SDS). Whereas most of the complexed DNA was dissociated from the vesicles, presumably because of its displacement by the anionic SDS, there was very little dissociation of the entrapped DNA (157).

Plasmid-containing liposomes were tested in immunization experiments (155) using a plasmid (pRc/CMV HBS) encoding the S region of the hepatitis B surface antigen (HBsAg; subtype ayw). Figure 10 illustrates how mice (Balb/c) injected repeatedly by the intramuscular route with 5 or 10 μg plasmid entrapped in cationic liposomes elicited, at all times tested, much greater (up to 100-fold) antibody (IgG_1) responses against the encoded antigen than animals immunized with the naked DNA. This was also true for IFN-γ and interleukin 4 (IL-4) levels in the spleens of immunized mice (155). In a more recent study, the role of the route of injection of the pRc/CMV HBS plasmid was examined for both humoral and cell-mediated immunity, using Balb/c mice and an outbred strain (T.O.) of the same species. Results (152) comparing responses for

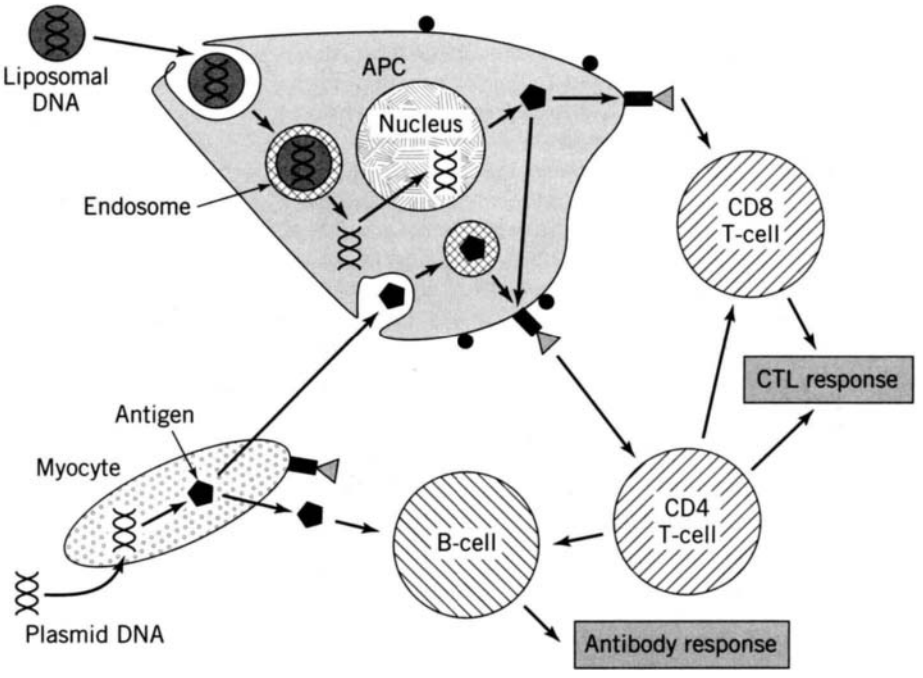


Figure 10. Schematic representation of proposed mechanisms of DNA immunization. Naked plasmid DNA is taken up by a small number of myocytes after intramuscular injection which are then transfected episomally. The produced antigen is released from the cells to interact with APC and thus induce immunity. In contrast, liposomal plasmid DNA interacts with APC directly. The way by which naked DNA enters the muscle cells to localize in the nucleus is unknown at present. For a proposed intracellular pathway of the liposomal DNA, see text. *Source:* Scheme designed by Dr. Yvonne Perrie, Centre for Drug Delivery Research.

liposome-entrapped and naked DNA indicate greater antibody (IgG_1) responses for the former not only by the intramuscular route but also after subcutaneous and intravenous injection. Interestingly, there was not much difference in the titers between the two strains, suggesting that immunization with liposomal pRc/CMV HBS is not MHC restricted. A similar pattern of results was obtained with IFN-γ and IL-4 in the spleen (152). The ability of liposomes to mediate immune responses to entrapped, plasmid encoded antigens has recently been demonstrated with another plasmid encoding the *Mycobacterium leprae* heat shock protein 65 (158).

The way by which liposomal plasmid promotes immunity to the encoded antigen is not likely to involve muscle cells. Although cationic liposomes could in theory bind to the negatively charged myocytes and be taken up by them, protein in the interstitial fluid would neutralize the liposomal surface and thus be expected to interfere with such binding (152). Moreover, vesicle size (about 800 nm average diameter) would render access to the cells difficult if not impossible. It is more likely then that cationic liposomes are endocytosed by APC (see Fig. 10), possibly including dendritic cells. As discussed earlier, it appears that the key ingredient of the DNA liposomal formulations in enhancing immune responses is the cationic lipid. It is conceivable that some of the endocytosed DNA escapes the endocytic vacuoles prior to their fusion with lysosomes to enter the cytosol for eventual episomal transfection and presentation of the encoded antigen. It is perhaps at this stage of intracellular trafficking of DNA, spanning its putative escape from endosomes and access to their nucleus, that the cationic lipid (possibly together within the fusogenic phosphatidylethanolamine component), plays a significant but yet unravelled role (152). However, the question still remains as to why liposome-entrapped DNA is more efficient in inducing immunity to the encoded antigen than complexed DNA.

Other Applications

Various other applications for liposomes have been explored or actively pursued but due to lack of space have not been discussed earlier. Among these, their use as carriers for radioisotopes or contrast agents for use in diagnostic imaging has received considerable attention over many years (159–161). A range of different imaging modalities have been used, the major ones being gamma scintigraphy (γ S), computed tomography (CT), and magnetic resonance (MR), the basis behind all of these being to measure a signal difference between the target (e.g., a tumor) and the surrounding tissues. Carriers such as liposomes are used to amplify the signal differential, i.e., to apply contrast, with the contrast agents used for γ S, CT, and MR being γ-emitting radionuclides, radiopaque materials, and paramagnetic metal ions, respectively. Imaging can be approached either by applying the contrast to the target or to the background, and the best results to date using liposomal systems have used the second approach, based on the fact that tumor cells generally have reduced phagocytic function compared with surrounding tissues. Thus the latter has an increased inclination to accumulate particle (liposome)-associated contrast and tumors register as holes within this background. Caution must be exercised due to the fact that areas of inflammation will also give a positive signal, and in fact good results have been obtained for imaging of arthritic areas. Because liposomes have a natural tendency to be cleared by the RES, they have been widely used for imaging hepatosplenic tumors and metastases and may be the systems of choice for CT and MR imaging in that application (159). However for γ S, they

are not significantly better than conventional colloidal systems, and their main promise is for imaging of non-RES tumors. Application of long-circulating, sterically stabilized liposomes may broaden the scope for tumor imaging due to their increased ability to extravasate from the tumor vasculature, and further developments in targeting will give additional potential. They are also useful for imaging the blood-pool, in order to detect vascular abnormalities such as atherosclerotic lesions, thrombi, tumors, and intravascular shunts (159). Another imaging technique that is giving promising results is ultrasound.

The first, large-scale commercial application for liposomes was in the field of cosmetics, and that industry remains by far the most prolific user, with over 200 different liposome-based products (161). These include a multitude of product types, ranging from humectants and tanning agents to hair restorers and antiaging products. Active components may be in the aqueous phase, including moisturizers, vitamins, plant extracts, and hydrolyzed proteins, or in the membrane bilayer, including lecithin itself, α-tocopherol, retinoids, and carotenoids. In general, intact liposomes do not penetrate beyond the outermost layers of the stratum corneum, though some of their constituents may reach more deeply, by mechanisms which are as yet unclear. Notable exceptions are *transfersomes*, which seem to allow enhanced penetration and have been shown to permit entry of encapsulated peptide drugs into the systemic circulation (162).

It has been suggested that the various aspects of the drug delivery approach, in other words, increased stability of the encapsulant, passive (and active) targeting to different phases, and delayed and/or controlled release, can be used to enhance the activity of functional food ingredients in complex foods (163,164). For example, food enzymes could be used in a more selective and efficient manner, antioxidant vitamins could be used more effectively and various synthetic food additives (e.g., antimicrobial agents) could be replaced by safer naturally occurring ingredients (e.g., nisin or egg white lysozyme). As an illustration, hard cheeses, which can take over a year to ripen, can be produced in a fraction of the normal time using liposome-encapsulated enzymes, with retention of their normal properties and without the damaging consequences of the alternative approaches (165). This could potentially lead to considerable savings in terms of the costs of prolonged, controlled temperature storage and various other risk factors. Unfortunately, raw material and process costs currently outweigh these savings. In addition to the applications already discussed, many others have been developed and undoubtedly many more will emerge in the future. Experience to date suggests that some at least will have a major impact.

BIBLIOGRAPHY

1. A.D. Bangham, M.M. Standish, and J.C. Watkins, *J. Mol. Biol.* **13**, 238–252 (1965).
2. G. Gregoriadis, P.D. Leathwood, and B.E. Ryman, *FEBS Lett.* **14**, 95–99 (1971).
3. G. Gregoriadis and B.E. Ryman, *Eur. J. Biochem.* **24**, 485–491 (1972).
4. G. Gregoriadis and B.E. Ryman, *Biochem. J.* **129**, 123–133 (1972).
5. G. Gregoriadis, *Trends Biotechnol.* **13**, 527–537 (1995).
6. G. Gregoriadis, *FEBS Lett.* **36**, 292–296 (1973).
7. J.N. Israelachvili, D.J. Mitchell, and B.W. Ninham, *Biochim. Biophys. Acta* **470**, 185–201 (1977).
8. G. Gregoriadis, ed. *Liposome Technology*, Vols. I, II, III, CRC Press, Boca Raton, Fla., 1984 (1st ed.), 1993 (2nd ed.).
9. C.R. Alving et al., *Proc. Natl. Acad. Sci. U.S.A.* **75**, 2959–2963 (1978).
10. Y.E. Rahman, in G. Gregoriadis, ed., *Liposomes as Drug Carriers*, Wiley, Winchester, 1988, pp. 485–495.
11. J.P. Reeves and R.M. Dowben, *J. Cell Physiol.* **73**, 49–60 (1969).
12. S. Kim et al., *Biochim. Biophys. Acta* **728**, 338–348 (1983).
13. S.M. Gruner, R.P. Lenk, A.S. Janoff, and M.J. Ostro, *Biochemistry* **24**, 2833–2843 (1985).
14. M.C. Woodle and D. Papahadjopoulos, *Methods Enzymol.*, **171**, 193–217 (1989).
15. R.R.C. New, *Liposomes, a Practical Approach*, Oxford IRL Press, New York, 1990.
16. U.S. Pat. 4,311,712 (Jan. 19, 1982), J.R. Evans, F.J.T. Fildes and J.E. Oliver (to Imperial Chemical Industries, Ltd.).
17. C.J. Kirby and G. Gregoriadis, *Bio/Technology* **2**, 979–984 (1984).
18. C.J. Kirby and G. Gregoriadis, in G. Gregoriadis, ed., *Liposome Technology*, 2nd ed., vol. 1, CRC Press, Boca Raton, Fla., 1984, pp. 19–27.
19. G. Gregoriadis et al., in J.E. Celis, ed., *Cell Biology: A Laboratory Handbook*, 2nd ed., vol. 4, Academic Press, Orlando, Fla., 1998, pp. 131–140.
20. C.J. Kirby et al., *Int. J. Food Sci. Technol.*, **26**, 437–449 (1991).
21. B. McCormack and G. Gregoriadis, *Biochim. Biophys. Acta* **1291**, 237–244 (1996).
22. G. Gregoriadis, H. da Silva, and A.T. Florence, *Int. J. Pharm.* **65**, 235–242 (1990).
23. S. Batzi and E.D. Korn, *Biochim. Biophys. Acta* **298**, 1015–1019 (1973).
24. C. Pidgeon, A.H. Hunt, and K. Dittrich, *Pharm. Res.* **3**, 23–34 (1986).
25. C.H. Huang, *Biochemistry* **8**, 344–352 (1969).
26. R.L. Hamilton et al., *J. Lipid Res.* **21**, 981–992 (1980).
27. E. Mayhew et al., *Biochim. Biophys. Acta* **775**, 169–174 (1984).
28. M.M. Brandl, D. Bachmann, M. Drechsler, and K.H. Bauer, in G. Gregoriadis, ed., *Liposome Technology*, 2nd ed., vol. 1, CRC Press, Boca Raton, Fla., 1992, pp. 49–65.
29. F. Olson et al., *Biochim. Biophys. Acta* **601**, 559–571 (1980).
30. R.W. Kriftner, in O. Braun-Falco, H.C. Korting, and H.I. Maibach, eds., *Liposome Dermatics*, Springer-Verlag, Berlin, 1992, pp. 91–100.
31. H. Hauser and N. Gains, *Proc. Natl. Acad. Sci. U.S.A.* **79**, 1683–1687 (1982).
32. Y. Kagawa and E. Racker, *J. Biol. Chem.* **246**, 5477–5487 (1971).
33. H.G. Weder and O. Zumbuehl, in G. Gregoriadis, ed., *Liposome Technology*, 1st ed., vol. 1, CRC Press, Boca Raton, Fla., 1983, pp. 79–107.
34. N. Oku and R.C. MacDonald, *Biochemistry* **22**, 855–863 (1983).

35. D.W. Deamer and A.D. Bangham, *Biochim. Biophys. Acta* **443**, 629–634 (1976).
36. F. Szoka and D. Papahadjopoulos, *Proc. Natl. Acad. Sci. U.S.A.* **75**, 4194 (1978).
37. S. Kim and G.M. Martin, *Biochim. Biophys. Acta* **646**, 1–9 (1981).
38. U. Pick, *Arch. Biochem. Biophys.* **212**, 186–194 (1981).
39. D. Papahadjopoulos, W.J. Vail, K. Jacobson, and G. Poste, *Biochim. Biophys. Acta* **394**, 483–491 (1975).
40. F.W. Martin, in P. Tyle, ed., *Specialized Drug Delivery Systems, Manufacturing and Production Technology*, Dekker, New York, 1990, pp. 267–316.
41. S. Amselem, A. Gabizon, and Y. Barenholz, in G. Gregoriadis ed., *Liposome Technology*, 2nd ed., vol. 1, CRC Press, Boca Raton, Fla., 1992, pp. 501–525.
42. E.C.A. van Winden, N.Z. Zuidam, and D.J.A. Crommelin, in D.D. Lasic and D. Papahadjopoulos, eds., *Medical Applications of Liposomes*, Elsevier, Amsterdam, 1998, pp. 567–604.
43. R.A. Schwendener, in G. Gregoriadis, ed., *Liposome Technology*, 2nd ed., vol. 1, CRC Press, Boca Raton, Fla., 1992, pp. 487–500.
44. H.G. Weder, in O. Braun-Falco, H.C. Korting, and H.I. Maibach, eds., *Liposome Dermatics*, Springer-Verlag, Berlin, 1992, pp. 101–109.
45. P. Van Hoogevest and P. Fankhauser, in G. Lopez-Berestein and I.J. Fidler, eds., *Liposomes in the Therapy of Infectious Diseases and Cancer*, Liss, New York, 1989, pp. 453–466.
46. European Pat. EP 198765-A (April 3, 1986), A. Rahman (to Georgetown University).
47. D.W. Deamer, R.C. Prince, and A.R. Crofts, *Biochim. Biophys. Acta* **274**, 323–335 (1972).
48. T.D. Madden et al., *Chem. Phys. Lipids* **53**, 37–46 (1990).
49. M.J. Hope, M.B. Bally, G. Webb, and P.R. Cullis, *Biochim. Biophys. Acta* **812**, 55–65 (1985).
50. T. Schneider, A. Sachse, G. Rossling, and M. Brandl, *Drug Dev. Ind. Pharm.* **20**, 2787–2807 (1994).
51. N.J. Zuidam, H. Talsma, and D.J.A. Crommelin, in Y. Barenholz and D.D. Lasic, eds., *Handbook of Non-medical Applications of Liposomes*, vol. 3, CRC Press, Boca Raton, Fla., 1995, pp. 71–80.
52. Y. Barenholz and S. Anselem, in G. Gregoriadis, ed., *Liposome Technology*, 2nd ed., vol. 1, CRC Press, Boca Raton, Fla., 1993, pp. 527–616.
53. D. Lichtenberg and Y. Barenholz, *Methods Biochem. Anal.*, **33**, 337–462 (1988).
54. H. Ruf, Y. Georgolis, and E. Grell, *Methods Enzymol.* **172**, 364–390 (1989).
55. S.W. Provencher, *Macromol. Chem.* **180**, 201–207 (1979).
56. Coulter ®Counter—*Medical and Biological Bibliography*, Coulter Electronics Ltd., Luton, England, 1990.
57. J. Boustra, G.S. Gooris, J.A. Van der Spek, and W. Bras, *Invest. Dermatol.* **97**, 1005–1012 (1991).
58. N. Skalko et al., *Biochim. Biophys. Acta* **1370**, 151–160 (1998).
59. G. Gregoriadis, N. Garcon, H. da Silva, and S. Sternberg, *Biochim. Biophys. Acta* **1147**, 185–193 (1993).
60. D.D. Lasic, *Liposomes: From Physics to Applications*, Elsevier, Amsterdam, 1973.
61. J. Senior and G. Gregoriadis, in G. Gregoriadis, ed., *Liposome Technology*, 1st ed., vol. 3, CRC Press, Boca Raton, Fla., 1984, pp. 262–282.
62. G. Gregoriadis and R. Buckland, *Nature (London)*, **244**, 170–172 (1973).
63. G. Gregoriadis, *N. Engl. J. Med.* **295**, 704–710, 765–770 (1976).
64. D. Papahadjopoulos, ed., *Liposomes and Their Uses in Biology and Medicine*, vol. 308, N.Y. Acad. Sci., New York, 1978.
65. G. Gregoriadis, ed., *Liposomes as Drug Carriers: Recent Trends and Progress*, Wiley, Chichester, U.K., 1988.
66. C.D.V. Black and G. Gregoriadis, *Biochem. Soc. Trans.* **2**, 869–871 (1974).
67. A.W. Segal et al., *Br. J. Exp. Pathol.* **55**, 320–327 (1974).
68. G. Gregoriadis and D. Neerunjun, *Eur. J. Biochem.* **47**, 179–185 (1974).
69. R.L. Juliano and B. Stamp, *Biochem. Biophys. Res. Commun.* **63**, 651–658 (1975).
70. P.E. Belchetz, I.P. Braidman, J.C.W. Crawley, and G. Gregoriadis, *Lancet* **2**, 116–117 (1977).
71. G. Gregoriadis and D. Neerunjun, *Res. Commun. Chem. Pathol.* **10**, 351–362 (1975).
72. A.C. Allison and G. Gregoriadis, *Nature (London)* **252**, 252 (1974).
73. G. Gregoriadis and D. Neerunjun, *Biochem. Biophys. Res. Commun.* **65**, 537–544 (1975).
74. D. Neerunjun, G. Gregoriadis, and R. Hunt, *Life Sci.* **21**, 357–370 (1977).
75. L. Krupp, A.V. Chobanian, and J.P. Brecher, *Biochem. Soc. Trans.* **17**, 590 (1989).
76. G. Scherphof, G. Roerdink, M. Waite, and J. Parks, *Biochim. Biophys. Acta* **542**, 296–307 (1978).
77. G. Gregoriadis and C. Davis, *Biochem. Biophys. Res. Commun.* **89**, 1287–1293 (1979).
78. C.J. Kirby, J. Clarke, and G. Gregoriadis, *Biochem. J.* **186**, 591–598 (1980).
79. C.J. Kirby and G. Gregoriadis, *Life Sci.* **27**, 2223–2230 (1980).
80. C.J. Kirby, J. Clarke, and G. Gregoriadis, *FEBS. Lett.* **111**, 324–328 (1980).
81. A. Tumer, C.J. Kirby, J. Senior, and G. Gregoriadis, *Biochim. Biophys. Acta* **760**, 119–125 (1983).
82. J. Senior, G. Gregoriadis, and K. Mitropoulos, *Biochim. Biophys. Acta* **760**, 111–118 (1983).
83. G. Gregoriadis and J. Senior, *FEBS Lett.* **119**, 43–46 (1980).
84. J. Senior and G. Gregoriadis, *FEBS Lett.* **145**, 109–114 (1982).
85. J. Senior, J.C.W. Crawley, and G. Gregoriadis, *Biochim. Biophys. Acta* **839**, 1–8 (1985).
86. B. Wolff and G. Gregoriadis, *Biochim. Biophys. Acta* **802**, 259–273 (1984).
87. G. Gregoriadis, *News Physiol. Sci.* **4**, 146–151 (1989).
88. D. Absolom, *Methods Enzymol.* **132**, 281–318 (1986).
89. C.D.V. Black and G. Gregoriadis, *Biochem. Soc. Trans.* **4**, 253–256 (1976).
90. F. Bonte and R. Juliano, *Chem. Phys. Lipids* **40**, 359 (1986).
91. H.C. Loughrey, M.B. Bally, L.W. Reinish, and P.R. Cullis, *Thromb. Haemostasis* **64**, 172–176 (1990).
92. R.L. Richards, H. Gewurtz, J. Siegel, and C.R. Alving, *J. Immunol.* **112**, 1185–1189 (1979).
93. J.D. Rossi and B.A. Wallace, *J. Biol. Chem.* **258**, 3327–3331 (1983).

94. S.M. Moghimi and H.M. Patel, in G. Gregoriadis, ed., *Liposome Technology*, 2nd ed., vol. 3, CRC Press, Boca Raton, Fla., 1993, pp. 44–58.
95. G. Gregoriadis and B. McCormack, eds., *Targeting of Drugs: Strategies for Stealth Therapeutic Systems*, Plenum, New York, 1998.
96. A.L. Klibanov, K. Maruyama, V.P. Torchilin, and L. Huang, *FEBS Lett.* **268**, 235–237 (1990).
97. R. Juliano and B. Stamp, *Biochem. Pharmacol.* **27**, 21–27 (1978).
98. C.J. Kirby and G. Gregoriadis, *Biochem. Pharmacol.* **32**, 609–615 (1983).
99. L. Huang and S.J. Kennel, *Biochemistry* **18**, 1702–1707 (1979).
100. J.N. Weinstein et al., *Science* **195**, 489–491 (1977).
101. L.D. Leserman, J.N. Weinstein, R. Blumenthal, and W.D. Terry, *Proc. Natl. Acad. Sci. U.S.A.* **77**, 4089–4093 (1980).
102. V.P. Torchilin, B.A. Khaw, V.N. Smirnov, and E. Haber, *Biochem. Biophys. Res. Commun.* **89**, 114–119 (1979).
103. T.D. Heath, R.T. Fraley, and D. Papahadjopoulos, *Science* **210**, 539–541 (1980).
104. A. Huang, L. Huang, and S.J. Kennel, *J. Biol. Chem.* **255**, 8015–8018 (1980).
105. L.D. Leserman, J. Barbet, F. Kourilsky, and J.N. Weinstein, *Nature (London)* **288**, 602–604 (1980).
106. F.J. Martin, W.L. Hubbell, and D. Papahadjopoulos, *Biochemistry* **20**, 4229–4438 (1981).
107. F.J. Martin and D. Papahadjopoulos, *J. Biol. Chem.* **257**, 286–288 (1982).
108. H.C. Loughrey, M.B. Bally, and P.R. Cullis, *Biochim. Biophys. Acta* **901**, 157–160 (1987).
109. J.N. Weinstein, R. Blumenthal, S.O. Sharrow, and P.A. Henkart, *Biochim. Biophys. Acta* **509**, 272–288 (1978).
110. F. Bonte, in F. Puisieux, P. Couvreur, J. Delattre, and J.-P. Devissaguet, eds., *Liposomes, New Systems and New Trends in Their Applications*, Editions de Santé, Paris, 1995, pp. 75–97.
111. M.B. Yatvin, W. Kreutz, B.A. Horwitz, and M. Shinitzky, *Science* **210**, 1253–1254 (1980).
112. R.M. Straubinger, K. Hong, D.S. Friend, and D. Papahadjopoulos, *Cell (Cambridge, Mass.)* **32**, 1069–1079 (1983).
113. D. Collins, D. Litzinger, and L. Huang, *Biochim. Biophys. Acta* **1025**, 234–242 (1990).
114. J.N. Weinstein, R.L. Magin, R.L. Cysyk, and D.S. Zaharko, *Cancer Res.* **40**, 1388–1395 (1980).
115. P.L. Felgner and G.M. Ringold, *Nature (London)* **337**, 387–388 (1989).
116. B. Sternberg, F.L. Sorgi, and L. Huang, *FEBS Lett.* **356**, 361–366 (1994).
117. S. Bhattacharya and L. Huang, in D.D. Lasic and D. Papahadjopoulos, eds., *Medical Applications of Liposomes*, Elsevier, Amsterdam, 1998, pp. 371–394.
118. C.J. Kirby, in R.A. Meyers, ed., *Encyclopaedia of Molecular Biology and Molecular Medicine*, VCH, Weinheim, 1996, pp. 415–425.
119. X. Gao and L. Huang, *Biochem. Biophys. Res. Commun.* **179**, 280–285 (1991).
120. J.P. Behr, *Tetrahedron Lett.* **27**, 5861–5864 (1986).
121. F.L. Sorgi, S. Bhattacharya, and L. Huang, *Gene Ther.* **4**, 961–968 (1997).
122. S. Li and L. Huang, *Gene Ther.* **4**, 891–900 (1997).
123. A.A. Gabizon, in F. Puisieux, P. Couvreur, J. Delattre, and J.-P. Devissaguet, eds., *Liposomes, New Systems and New Trends in their Applications*, Editions de Santé, Paris, 1995, pp. 507–522.
124. D.D. Lasic and F. Martin, eds., *Stealth Liposomes*, CRC Press, Boca Raton, Fla., 1995.
125. D.D. Lasic and D. Papahadjopoulos, eds., *Medical Applications of Liposomes*, Elsevier, Amsterdam, 1998.
126. C.E. Swenson, J. Freitag, and A.S. Janoff, in D.D. Lasic and D. Papahadjopoulos, eds., *Medical Applications of Liposomes*, Elsevier, Amsterdam, 1998, pp. 689–702.
127. P.G. Schmidt, J.P. Adler-Moore, E.A. Forssen, and R. Profitt, in D.D. Lasic and D. Papahadjopoulos, eds., *Medical Applications of Liposomes*, Elsevier, Amsterdam, 1998, pp. 703–732.
128. F.J. Martin, in D.D. Lasic and D. Papahadjopoulos, eds., *Medical Applications of Liposomes*, Elsevier, Amsterdam, 1998, pp. 635–688.
129. L.D. Mayer, P.R. Cullis, and M.B. Bally, in D.D. Lasic and D. Papahadjopoulos, eds., *Medical Applications of Liposomes*, Elsevier, Amsterdam, 1998, pp. 231–258.
130. D. Kirpotin et al., *FEBS Lett.* **388**, 115–118 (1996).
131. T.M. Allen, C.B. Hansen, and D.D. Stuart, in D.D. Lasic and D. Papahadjopoulos, eds., *Medical Applications of Liposomes*, Elsevier, Amsterdam, 1998, pp. 297–323.
132. T.M. Allen, I. Ahmad, D.E. Lopes de Menezes, and E.H. Moase, *Biochem. Soc. Trans.* **23**, 1073–1079 (1995).
133. D.B. Kirpotin et al., in D.D. Lasic and D. Papahadjopoulos, eds., *Medical Applications of Liposomes*, Elsevier, Amsterdam, 1998, pp. 325–345.
134. J.W. Park et al., *Cancer Lett.*, pp. 153–160 (1997).
135. L.L. Worth, I.J. Fidler, and E.S. Kleinermann, in D.D. Lasic and D. Papahadjopoulos, eds., *Medical Applications of Liposomes*, Elsevier, Amsterdam, 1998, pp. 47–60.
136. I.A.J.M. Bakker-Woudenberg, in F. Puisieux, P. Couvreur, J. Delattre, and J-P. Devissaguet, eds., *Liposomes, New Systems and New Trends in their Applications*, Editions de Santé, Paris, 1995, pp. 371–396
137. K.M. Wassan and G. Lopez-Berestein, in D.D. Lasic and D. Papahadjopoulos, eds., *Medical Applications of Liposomes*, Elsevier, Amsterdam, 1998, pp. 181–188.
138. P.K. Working, in D.D. Lasic and D. Papahadjopoulos, eds., *Medical Applications of Liposomes*, Elsevier, Amsterdam, 1998, pp. 605–624.
139. C. Nicolau et al., *Proc. Natl. Acad. Sci. U.S.A.* **80**, 1068–1072 (1983).
140. C.E. Holt, N. Garlick, and E. Cornel, *Neuron* **4**, 203–207 (1990).
141. G.E. Plautz et al., *Proc. Natl. Acad. Sci. U.S.A.* **90**, 4645 (1993).
142. G.J. Nabel et al., *Proc. Natl. Acad. Sci. U.S.A.* **90**, 11307–11311 (1993).
143. E. Nabel, G. Plautz, and G. Nabel, *Science* **249**, 285–1288 (1990).
144. N.J. Caplen et al., *Nat. Med.* **1**(1), 39–46 (1995).
145. G. Gregoriadis, B. McCormack, and A.C. Allison, eds., *New Generation Vaccines: The Role of Basic Immunology*, Plenum, New York, 1993.
146. R. Bomford, in R. Spier and B. Griffiths, eds., *Animal Cell Biotechnology*, vol. 2, Academic Press, London, p. 235.
147. G. Gregoriadis, *Immunol. Today* **11**, 89–97 (1990).
148. C.R. Alving, *J. Immunol. Methods* **140**, 1–13 (1991).

149. R. Gluck, in M.F. Powell and M.J. Newman, eds., *Vaccine Design: The Subunit and Adjuvant Approach*, Plenum, New York, p. 325.

150. M. Chattergoon, J. Boyer, and D.B. Weiner, *FASEB J.* **11**, 754–763 (1997).

151. H.L. Davis, R.G. Whalen, and B.A. Demeneix, *Hum. Gene Ther.* **4**, 151–159 (1993).

152. G. Gregoriadis, *Pharm. Res.* **15**, 661–670 (1998).

153. F.C. Szoka, Y. Xu, and O. Zelpati, *J. Liposome Res.* **6**, 567–587 (1996).

154. M. Sedegah, R. Hedstrom, P. Hobart, and and S.L. Hoffman, *Proc. Natl. Acad. Sci. U.S.A.* **91**, 9866 (1984).

155. G. Gregoriadis, R. Saffie, and B. De Souza, *FEBS. Lett.* **402**, 107–110 (1997).

156. G. Gregoriadis, B. McCormack, Y. Perrie, and R. Saffie, in D.D. Lasic and D. Papahadjopoulos, eds., *Medical Applications of Liposomes*, Elsevier, Amsterdam, 1998, pp. 61–73.

157. Y. Perrie and G. Gregoriadis, *J. Pharm. Pharmacol.* **50**, 155 (1998).

158. G. Gregoriadis and B. McCormack, *J. Liposome Res.* **8**, 48 (1998).

159. C. Tilcock, in J.R. Phillipot and F. Schuber, eds., *Liposomes as Tools in Basic Research and Industry*, CRC Press, Boca Raton, Fla., 1995, pp. 225–240.

160. V. Torchilin, in D.D. Lasic and D. Papahadjopoulos, eds., *Medical Applications of Liposomes*, Elsevier, Amsterdam, 1998, pp. 515–543.

161. D. Lasic, in D.D. Lasic, ed., *Liposomes, from Physics to Applications*, Elsevier, Amsterdam, 1993, pp. 477–488.

162. G. Cevc and G. Blume, *Biochim. Biophys. Acta* **1104**, 226–232 (1992).

163. C.J. Kirby, *Chem. Br.* **26**, 847–850 (1990).

164. C.J. Kirby, in G. Gregoriadis, *Liposome Technology*, 2nd ed., vol. 2, CRC Press, Boca Raton, Fla., 1993, pp. 216–231.

165. C.J. Kirby, B.E. Brooker, and B.A. Law, *Int. J. Food Sci. Technol.* **22**, 355–363 (1987).

MICROENCAPSULATION

EDITH MATHIOWITZ
MARK R. KREITZ
Brown University
Providence, Rhode Island
LISA BRANNON-PEPPAS
Biogel Technology
Indianapolis, Indiana

KEY WORDS

Characterization
Coacervation
Emulsion
Formulation
Gelation
Hot melt
Interfacial polymerization
Membrane
Microcapsule
Microencapsulation
Microsphere
Phase separation
Polymer
Solvent evaporation
Solvent removal
Spray-drying

OUTLINE

Introduction
Background
  Classification of Microencapsulation Techniques
  Classification of Microspheres and Microcapsules
  Classification of Polymeric Membranes
  Release Characteristics of Microspheres and Microcapsules
  Emulsion Formation
  Evaluation of Emulsions
  Phase Properties of Emulsion: Hydrophilic-Lipophile Balance
  Polymer Characterization
  Phase Separation of Polymers
  Interfacial Phenomenon
Solvent Evaporation
Complex Coacervation: Gelatin and Gum Arabic
Organic Phase Separation: Coacervation
Interfacial Polymerization
  Interfacial Coacervation
  Thermal Denaturation
  Gelation: Alginate
  Gelation Agarose
  Hot Melt Microencapsulation
  Solvent Removal
  Spray-Drying
  One-Step Formation of Double-Walled Microspheres
  Novel Encapsulation Techniques
  Applications of Microencapsulation
    Encapsulation in the Food, Consumer Products, and Cosmetics Industries
    Applications of Encapsulation for Agricultural Products
    Applications and Opportunities for Encapsulation to Enhance Human Health
Bibliography

INTRODUCTION

Microencapsulation is one of the most intriguing fields in the area of drug delivery systems. It is an interdisciplinary field that requires knowledge of the field of pure polymer science, familiarity with emulsion technology (1), and an in-depth understanding of drug and protein stabilization (2). In the early 1970s this area was considered more of an art than a science because most of the research was developed in pharmaceutical companies and very little information was discussed in scientific meetings. Today, the topic of microencapsulation is extensively studied inside major pharmaceutical companies and universities as well as research institutes. Some journals are now solely dedicated to the area of microencapsulation (e.g., *Journal of Microencapsulation*). Although scientists at the beginning of the 1970s were primarily concerned with the encapsulation of dyes to produce carbonless paper, scientists today have mastered the technology to such a level that cells as well as delicate proteins and genes can be encapsulated. Because two entries in this encyclopedia are dedicated to liposomes and nanoparticles, they are not going to be discussed in this article. In addition, traditional methods such as coating are discussed in a separate article related to coatings. This article is divided into three main sections. In the first section we discuss general aspects of polymer topics related to microencapsulation. Then we describe in more detail the main methods of preparing microcapsules and microspheres, and we end with a general summary of the different fields of application of microencapsulation.

BACKGROUND

Classification of Microencapsulation Techniques

Microencapsulation is a technology devoted to entrapping solids, liquids, or gases inside one or more polymeric coat-

ings (3–43). Two major classes of encapsulation methods have evolved, chemical and physical. The first class of encapsulation involves polymerization during the process of preparing the microcapsules. Examples of this class are usually known by the name of interfacial polymerization or in situ polymerization (44–49). The second type involves the controlled precipitation of a polymeric solution wherein physical changes usually occur. Several books examine the different processes of microencapsulation, and readers are strongly recommended to consult them (2,5,19,30,39, 42,49–58). Perhaps one of the best courses on the fabrication of microcapsules is given at the University of Washington by Dr. Thies.

There are a huge and increasing number of encapsulation processes. In addition, many new patents evolve solely on the basis of novel ways to produce microspheres. Thus, many scientists try to develop a systemic nomenclature for encapsulation classification. In Table 1 we classified the different types of methods according to published literature. It is sometimes difficult to classify encapsulation methods because specific techniques can be hybrids of two or more methods or can use different mechanisms simultaneously. Also, many names have changed throughout the years (e.g., solvent evaporation has been called water drying and double emulsion), and this can create confusion.

Interfacial polymerization involves the condensation of two monomers at the interface of the organic and aqueous phases. Polyamide capsules are a great example of this system and are discussed later in this article (44–48).

Complex coacervation was the process used to make the microcapsules in the first successful encapsulated product, carbonless copy paper (11,14,22,27,29,32,59–66). Complex coacervation encapsulation processes use the interaction of two oppositely charged polyelectrolytes in water to form a polymer-rich coating solution called a coacervate (68). This solution (or coacervate) engulfs the liquid or solid being encapsulated, thereby forming an embryo capsule. Cooling the system causes the coacervate (or coating solution) to gel via network formation. Gelatin is a primary component of most complex coacervation systems.

Coacervation uses the common phenomenon of polymer–polymer incompatibility to form microcapsules. The polymer that is to become the capsule wall material is dissolved in a solvent and to this solution a second polymer (called the phase inducer) is introduced. Because the two polymers are incompatible, two polymer-rich phases form. If drug particles are then introduced, one phase, rich in the desired coating polymer, engulfs the drug being encapsulated thereby forming embryo capsules. In principle, the range of polymers that can be used in this process is essentially infinite. In practice, the number of polymers that have been used successfully is relatively small, for reasons that will be discussed later.

The precipitation and/or gelation processes listed in Table 1 cover many techniques. One example is the precipitation of water-soluble polymers such as gelatin with water-miscible solvents such as isopropanol. Other examples include the precipitation of ethyl cellulose from cyclohexane by cooling, the gelation of sodium alginate with aqueous calcium salt solutions (41,68–74), and the thermally induced precipitation of proteins to form microspheres. In all cases, the objective is to precipitate a preformed polymer around the core (sometimes a multiparticulate core) to cause encapsulation.

Salting-out also listed in Table 1, involves the addition of salt to an aqueous polymer solution ultimately causing the polymer to phase separate from solution. One potential problem with this process is the possibility of incorporating a relatively high concentration of salt in the final capsule wall, as these salts may have an adverse effect on capsule release behavior.

Solvent evaporation (18,36,75–80) is the most popular way to accomplish encapsulation. A core material and capsule wall material are briefly dissolved in a water-immiscible, volatile organic solvent and the resulting solution is emulsified in an aqueous solution. The solvent is allowed to evaporate, thereby producing solid microcapsules or microparticles. Another version involves forming a double emulsion where an aqueous core material solution is emulsified in a polymer–volatile organic solvent solution. The resulting emulsion is emulsified in water giving a double emulsion. Evaporation of the volatile solvent yields a solid microcapsule with an aqueous core. Much of the effort on encapsulation in the pharmaceutical field has concentrated on using biodegradable polymers. A recent review by Brannon-Peppas (43) describes some of these advances with both microparticles and nanoparticles.

Hot melt encapsulation was developed to avoid the use of solvents throughout the process (81). Solvent removal (82,83) was developed as a modification of the solvent evaporation technique, using organic solvents as the extracting medium. In spray-drying, the evaporation of the

Table 1. Classification of Microencapsulation Methods

Process	Coating material	Suspended medium
Interfacial polymerization	Water-soluble and insoluble monomers	Aqueous/organic solvent
Complex coacervation	Water-soluble polyelectrolyte	Water
Coacervation	Hydrophobic polymers	Organic solvent
Thermal denaturation	Proteins	Organic
Salting-out	Water-soluble polymer	Water
Solvent evaporation	Hydrophilic or hydrophobic polymers	Organic or water
Hot melt	Hydrophilic or hydrophobic polymers	Aqueous/organic solvent
Solvent removal	Hydrophilic or hydrophobic polymers	Organic solvents
Spray-drying	Hydrophilic or hydrophobic polymers	Air, nitrogen
Phase separation	Hydrophilic or hydrophobic polymers	Aqueous/organic

solvent is achieved in a special, temperature-controlled cyclone. And finally, phase separation is a new method in which a one-step precipitation of two polymers or more produces double-walled microspheres (84).

When someone is faced with the challenge of encapsulating a substance, the first question should be, "What is the final application of the product?" As examples, if the final target is pesticide encapsulation, one must first choose polymers that are stable and nonerodible, or if one is to encapsulate therapeutic drugs such as proteins, the choice of polymers becomes more restricted to bioerodible ones. Once the polymer system is chosen, the next step is to select an appropriate encapsulation method. This can undertaken by either reviewing the relevant literature or developing new methods of encapsulation. Once the correct method of encapsulation has been determined the next step is to prepare the microcapsules, ensuring reproducibility, high encapsulation efficiency, and preservation of the activity of the encapsulated substance. This is achieved by thorough characterization, both before and after microsphere fabrication. It is an integral component, necessary for replication and optimization, and is discussed later in this article.

Classification of Microspheres and Microcapsules

Two general structures exist: microcapsules and microspheres. A microcapsule is a system that contains a well-defined core and a well-defined envelope: the core can be solid, liquid, or gas; the envelope is made of a continuous, porous or nonporous, polymeric phase. Figure 1a shows the different microcapsule configurations; the drug can be dispersed inside the microcapsule as solid particulates with regular or irregular shapes. Other forms may consist of a pure or dissolved solution, suspension, emulsion, or a combination of suspension and emulsion. Specific applications sometimes require modifications, e.g., when proteins are encapsulated they may contain stabilizers as well as the active ingredient (2). Also, the core can be something other than a chemical meant for release. An interesting application is the encapsulation of gases for the use of ultrasonic imaging (85–87). Alternatively, a microsphere is a structure made of a continuous phase of one or more miscible polymers in which particulate drug is dispersed, at either the macroscopic (particulates) or molecular (dissolution) level (Fig. 1b). However, the difference between the two systems is the nature of the microsphere matrix, in which no well-defined wall or envelope exists. Different methods of encapsulation result, in most cases, in either a microcapsule or a microsphere. For example, interfacial polymerization almost always produces a microcapsule, whereas solvent evaporation may result in a microsphere or a microcapsule, depending on the amount of loading. Yet, one can use solvent evaporation twice to create a sphere within a sphere, or as we discuss later, novel methods have been designed to use solvent evaporation to create in one step a double-walled microsphere, which is essentially a microcapsule (84).

Classification of Polymeric Membranes

Polymeric films and membranes can be classified in various ways. One such classification is based on porosity, with the following categories:

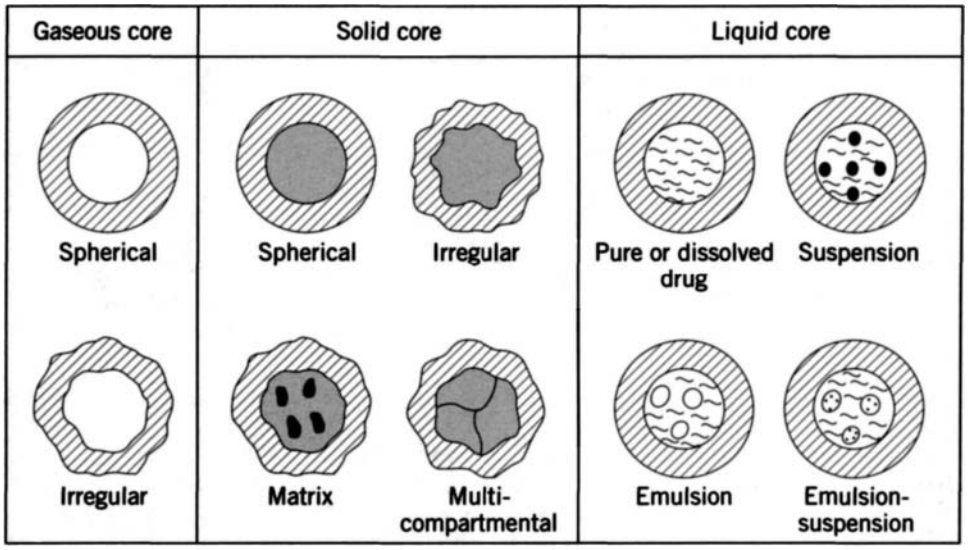
1. Macroporous membranes, which have large pores (0.1–1 μm)
2. Microporous membranes, in which the pores are appreciably smaller (100–500 Å)
3. Nonporous (gel, solution-diffusion) membranes. In the last category the "pores" are of the order of molecular dimensions. They are formed by entanglement and/or cross-linking of the molecular chains and mesh size refers to the space between these chains.

Release Characteristics of Microspheres and Microcapsules

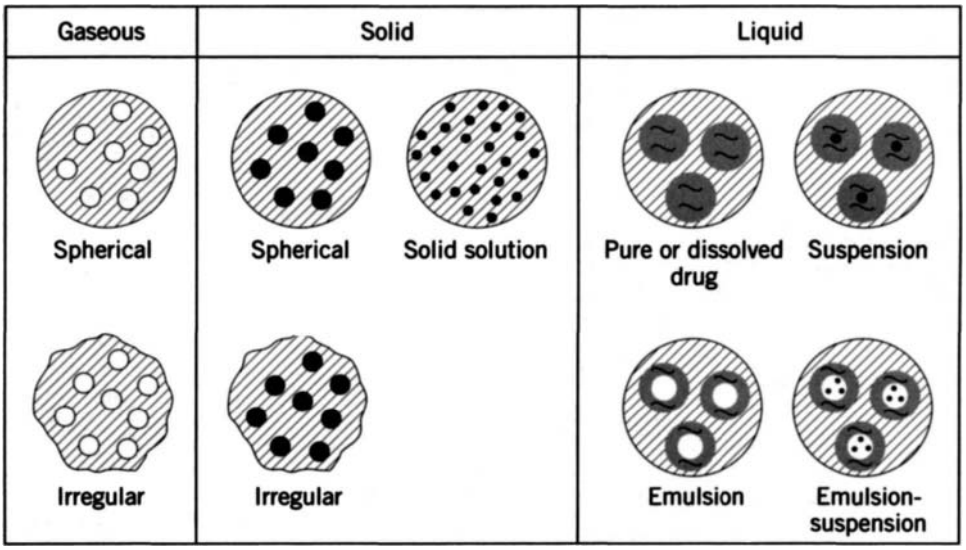
Release of core material from a nonerodible microcapsule can occur in several ways. Figure 2 contains four theoretical curves (A, B, C, and D) that describe four types of release behavior. All curves are plotted as percent drug released versus time. The mathematical descriptions of these release processes have been given (88–90).

Curve A represents the release behavior of a perfect, nonerodible, spherical microcapsule which releases the encapsulated material by steady-state diffusion through a coating of uniform thickness. The rate of release remains constant as long as the internal and external concentrations of core material and the concentration gradient through the membrane are constant. If a finite time is needed to establish the initial, constant concentration gradient in the capsule wall membrane then there is a time lag in core material release. Curve A in Figure 2 displays a system with no time lag. If some of the encapsulated material migrates through the microcapsule membrane during storage, a burst effect occurs, as represented by Curve B. If the microcapsule acts as an inert matrix particle in which core material is dispersed (a microsphere), the Higuchi model is valid up to 60% release (91). In this case, a plot of percent drug released versus square-root time is linear, as shown by Curve C in Figure 2. First-order release is represented by Curve D. The curve is linear if log percent core material left in the capsule is plotted versus time.

Actual capsule release data have been plotted for all of the described ways and analyzed in terms of the appropriate model. Good agreement between actual results and assorted model release curves may exist for some portion of the release curve, but significant deviations occur often, either during initial states of release or after most of the core material carried by a capsule sample has been released. Many capsule samples experience an unusually rapid rate of release when first immersed in an in vitro release medium, i.e., they have a large burst effect. First-order release plots tend to fit a broader range of capsule release data than other plots. It is relevant to note that proper adjustment of the release constant in the first-order release equation can make a first-order release curve approximate, within a few percent, the release curve calculated from the Higuchi equation up to 60% release. If microcapsule release data are linear with square root of time and also fit a first-order release plot, the expression most accurately describing the release behavior can be determined by plotting the total amount of drug released (Q′)



(a)



(b)

Figure 1. Various configurations of (**a**) microcapsules and (**b**) microspheres.

and 1/Q′ versus release rate. For the first-order release, Q′ is directly proportional to release rate whereas for square root of time release, 1/Q′ is directly proportional to release rate.

The desire to fit capsule release data to various models is worthwhile. However, it must be recognized that the actual release kinetics of microcapsules and microspheres can vary greatly from those developed to describe release from macroscopic controlled release delivery devices. Microcapsules are small particles and even small doses contain many microcapsules. The release behavior of a microcapsule formulation is the sum of the release of a population of microcapsules (38,39). This population consists of individual microcapsules that differ from each other in the quality of their walls. Some capsule walls are more permeable than others because of irregularities, which may appear as pits or craters under a scanning electron microscope. Dappert and Thies (38,39,47) discussed the release behavior of microcapsule populations. One capsule population considered contained microcapsules that individually released their contents at a constant rate, but the individual release rate constants fit a log-normal distribution. For such a capsule population, the predicted release curve will approximate first-order release kinetics.

All microcapsule release behaviors reported in the literature represent microcapsule populations and not individual microcapsules. Therefore, the successful replication of microcapsule preparations and confirmation of reproducible release rates is an optimal result. The Lupron Depo™, a product already in the marketplace, demonstrates that these milestones can be achieved. In the following section, we discuss the specific releases as relevant to the specific encapsulation methods.

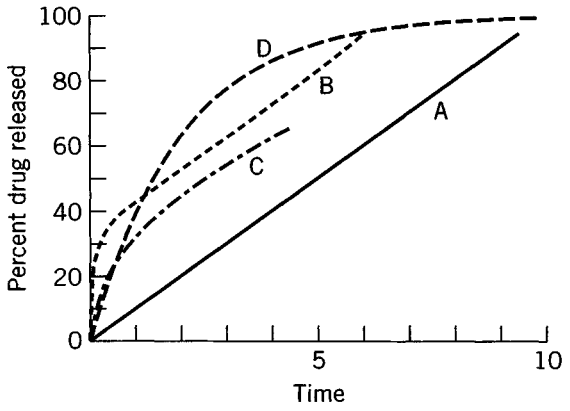


Figure 2. Theoretical release curves expected for different types of nonerodible delivery systems. A, Membrane reservoir-type free of lag time and burst effects; B, same as A, with burst effects; C, matrix or monolithic sphere with square root time-release; D, system with first-order release.

Emulsion Formation

The first step in almost any encapsulation technique (described in Table 1) involves the formation of an emulsion, usually of a polymeric solution inside a continuous phase (1). Similarly, in order to disperse the drug inside this polymeric solution (assuming a nonsoluble drug), emulsions must be created. Thus, an understanding of the properties of emulsions is extremely important. The emulsion formation determines the resulting particle size in the final process of encapsulation. An emulsion is achieved by applying mechanical energy which deforms the interface between the two phases to such an extent that droplets form. These droplets are typically large and are subsequently disrupted or broken up into smaller ones. The ability to disrupt the larger droplets is a critical step in emulsification and in encapsulation where an emulsion is prepared. When considering dyes as the main encapsulate, the problems involved at this stage can be minor because most dyes are quite stable. However, drugs (e.g., labile proteins) or cells may be destroyed by the application of mechanical shear and, if necessary, preventive measures should be taken to stabilize these, even at this stage of the process.

A suitable surfactant is needed to produce a stable emulsion, a result achieved by lowering the surface tension (γ, usually from 40 to 5 mN/m^{-1}). For pharmaceutical applications surfactants must acceptable for therapeutic use (92).

Many devices have been designed to produce emulsions. Depending on the desired particle size, a range of devices from simple overhead stirrers or impellers to more sophisticated devices such as homogenizers, ultrasonic power generators, or ball and roller mills are available. The following is a list of techniques and equipment used to form emulsions. Also, an excellent reference is Chapter 2 in Becher (1).

1. *Shaking.* Shaking is self-evident but in many encapsulation techniques countertop shakers or agitators are used.
2. *Pipe flow: laminar and turbulent.* Pipe flow may include constriction on the flow baffles on which the liquid can infringe to increase the velocity gradient or turbulence.
3. *Injection.* The dispersed phase is injected into a continuous phase as a cylindrical jet, where it is broken up into fairly large droplets.
4. *Stirring: simple stirrer, rotor-stator, scraper, and vibrator.* Many types of stirring exist, e.g., for pumps revolution rates up to 300/s. Rotor-stator machines exist in great variety and are described under the name of homogenizers. In the laboratory the name "Ultra Turrax" is often used.
5. *Colloid mill.* This is a rotor-stator device as well, with the exception of having a very narrow slit (e.g., 0.1 mm) and is designed to achieve very high (simple) shear up to $10^7 s^{-1}$.
6. *Ball and roller mills.* These are more suited for disruption of solid particles or very viscous emulsion droplets.
7. *High-pressure homogenizer.* In the homogenizer the liquid is brought under a high pressure p_h (e.g., 10 to 40 MPa) by a positive pump and is forced through a narrow (e.g., 0.1 mm) valve slit; owing to the pressure, the valve opens against a spring. The potential energy is converted into kinetic energy as the liquid obtains a high velocity u ($p_h = _u^2/2$; u is, e.g., 200 m s^{-1}). The kinetic energy is dissipated into heat during passage through the valve. This takes a very short time (0.1 ms); so energy density is very high (up to 10^{12} Wm^{-3}).
8. *Ultrasonic: vibrating knife and magneto-striction.* Ultrasonic waves can be generated in many ways. A common one is the "liquid whistle" or Pohlmann generator. The liquid stream impinges on a knife or blade, which is then brought to vibrate at high frequency (6–40 kHz); the liquid is forced through a narrow slit at speeds over 50 m s^{-1}, which requires a pressure of some 1 MPa or more. Magneto-striction devices often work at a frequency of 20 kHz.
9. *Aerosol to liquid: mechanical and electrical.* One may atomize the dispersed phase in air and let the droplets be taken up by the continuous phase.
10. *Foaming or boiling.* Some oils spread over a water–gas interface. If air is beaten in or the water boiled, the thinly spread oil layer is disrupted, and very small droplets may result. This may happen as an additional mechanism during various stirring operations. Also by steam injection, droplets can be disrupted to very small ones, though at high cost of steam.

Some of the methods are exclusively used in laboratories such as shaking, vibrator stirring, magneto-striction ultrasonic systems, and aerosol to liquid systems. For large-scale production of emulsions, rotor-stator stirring, colloidal mills, and high-pressure homogenizers are most often used, with some newer processes also using ultrasonic techniques.

Evaluation of Emulsions

Three types of characteristics are critical in evaluating an emulsion procedure, each with its own methods of evaluation (1). They can easily be adapted to encapsulation techniques such as solvent evaporation or interfacial polymerization. The parameters that should be studied are:

1. *Emulsion capacity.* The maximum amount of dispersed phase that can be emulsified under specific conditions without causing aggregation.
2. *Emulsion stability.* The amount of phase separation taking place, mostly by the sedimentation rate, which is estimated either under by gravity or by centrifugation. The governing theory is that sedimentation rate depends on droplet size. This relation, however, may not be so simple because sedimentation rate depends on fluctuation of the droplets and their apparent viscosity at very low velocity gradients of the continuous phase. This condition may also be affected by the variables studied, leading to misinterpretation. In microcapsules this first step is important because once the emulsion is stabilized the next step of hardening the capsules follows.
3. *Droplet size.* This may be some kind of average or full distribution. Sometimes the number of drops is determined, or some characteristic, depending on the drop size, such as turbidity under specific conditions. Droplet size distribution may change after emulsification. This can be due to coalescence but it also may be due to isothermal distillation, unless the dispersed phase is completely insoluble in the continuous one. Again, the initial size of the emulsion may differ from the final size of the microspheres or microcapsules.

Determination of droplet size distribution as function of the process and product variables is by far the best method to study emulsification, particularly in microencapsulation where the process does not stop at the point of making the emulsion, but continues to the further steps of formation of hard particles. Particle comparison between the original size of the emulsion and the final size of the microsphere is beneficial.

Phase Properties of Emulsion: Hydrophilic-Lipophile Balance

One of the important parameters in studying emulsions is the selection of a surfactant which satisfactorily emulsifies the different phases. For this, the hydrophilic-liphophile balance (HLB) is a useful index. The concept of HLB in its early stage was qualitative; however, schemes designed to put this concept on a quantitative basis have been advanced and a new method, which takes into consideration the temperature and the kind of oil used, has been introduced. Around 1950 Griffin [see also Schick (93)] found that it was possible to define the polarity for nonionic agents in terms of an empirical quantity which he called the HLB. This is represented by an arbitrary scale, in which the least hydrophilic materials have low HLB numbers and increasing HLB corresponds to increasingly hydrophilic character. Broadly, these HLB numbers can be used to characterize the applicability of particular surfactant. In a given homologous series of surfactants there is a range in which the HLB is optimal for a particular application. Table 2 lists the HLB ranges suitable for various applications.

In many cases the HLB number may be calculated from composition data. For example, for fatty acid esters of many polyhydric alcohols,

$$HLB = 20\left(1 - \frac{S}{A}\right) \tag{1}$$

where S is the saponification number of the ester and A is the acid number of the fatty acid. In another example, for glyceryl monostearate, $S = 161$ and $A = 198$; hence, its HLB is 3.8.

For some fatty acid esters it is not practical to obtain good saponification-number data, e.g., esters of tall oil and rosin, beeswax, and lanolin fatty acids. However, for these, the HLB may be calculated from the relation

$$HLB = \frac{E + P}{5} \tag{2}$$

where E is the weight percent of oxyethylene content and P is the weight percent of polyol content.

For materials where only ethylene oxide is used to produce the hydrophilic moiety, e.g., fatty-alcohol ethylene oxide adducts, this equation reduces to

$$HLB = E/5 \tag{3}$$

where E has the same meaning as above.

The use of weight percent in these equations is quite significant, because a better dependence of micellar properties on chain length is found when this quantity is used rather than the ethylene oxide mole ratio.

Davies devised a method for calculating HLB numbers for surfactants directly from their formulae using empirically derived group numbers. Thus, a group number is assigned to various component groups in emulsifiers, e.g., CH_3-CH_2-COO-, -CH_2CH_2O, etc., and the HLB is then calculated from the following relation (94):

$$HLB = 7 + \Sigma(\text{hydrophilic group numbers}) - \Sigma(\text{lipophilic group numbers}) \tag{4}$$

For a number of cases, Davies (94) has shown that the HLB numbers calculated from the previous equation and

Table 2. HLB Ranges and Applications

Range	Application
3–6	W/O emulsifier
7–9	Wetting agent
8–15	O/W emulsifier
13–15	Detergent
15–18	Solubilizer

Source: From Ref. 93.

those experimentally determined are in satisfactory agreement. However, this equation contains the implicit assumption that all ethylene oxide groups make the same hydrophilic contribution, which is manifestly incorrect (94), and the equation fails with increasing poly(oxyethylene) content.

Additional techniques can be used to determine HLB. These include water titration, algebraic addition of contribution from various groups making up the chemical structure from spreading, and by measurements of such properties as dielectric constant, and behavior as a substrate in gas-liquid chromatography [see Schick (95), pp. 607–613].

A rough estimate of HLB can frequently be made on the basis of water solubility or dispersibility. Table 3 shows the ranges of HLB numbers indicated by various types of dispersibility. An up-to-date listing of HLB numbers for a large range of emulsifying agents (including a few ionic species) is given in Schick (95).

A valuable attribute of the HLB scale is that the HLB of mixtures of surfactants can be calculated (to a good first approximation, at least) by algebraic addition. For example, a blend containing 4 parts of Span® 20 and 6 parts of Tween® 60 would have an effective HLB of:

$$0.4 \times 8.6 + 0.6 \times 14.9 = 12.3 \qquad (5)$$

It has recently been shown that this algebraic additivity is not strictly obeyed, but the deviation is usually sufficiently small so that the system is insensitive to the discrepancy. In a few cases, the requirements may be more stringent, but this merely requires final adjustment of the composition of the emulsifier.

As a corollary to the previous discussion, each nonaqueous phase to be emulsified has a *required* HLB, which is of course different depending on whether water or oil is to be the continuous phase. The required HLB for a particular oil is usually determined by preparing emulsions over a range of HLB values (obtained, for example, by blending Span® and Tween® emulsifiers in various proportions) and observing the HLB at which maximum stability occurs. A list of required HLB values for a variety of oil phases is given in Table 4.

Using a particular emulsifier pair, the HLB corresponding to maximum stability may result, however, in an emulsion insufficiently stable for the purpose desired. In this case, it may be necessary to examine the effect of the *chemical type* of the emulsifying agent, i.e., substituting an oleate for a stearate, or an ether-type nonionic for an ester.

Table 3. HLB by Dispersibility

	HLB range
No dispersibility in water	1–4
Poor dispersion	3–6
Milky dispersion after vigorous agitation	6–8
Stable milky dispersion	8–10
Translucent to clear dispersion	10–13
Clear solution	13+

Source: From Ref. 94.

Table 4. HLB Values Required to Emulsify Various 0:1 Phases

Oil phase	W/O emulsion	O/W emulsion
Acetophenone		14
Acid, dimer		14
Acid, lauric		16
Acid, linoleic		16
Acid, oleic		17
Acid, ricinoleic		16
Acid, stearic		17
Alcohol, cetyl		15
Alcohol, decyl		14
Alcohol, lauryl		14
Alcohol, tridecyl		14
Benzene		15
Carbon tetrachloride		16
Castor oil		14
Chlorinated paraffin		8
Kerosene		14
Lanolin, anhydrous	8	12
Oils		
Mineral, aromatic	4	12
Mineral, paraffinic	4	10
Mineral spirits		14
Petrolatum	4	7–8
Pine oil		16
Waxes		
Beeswax	5	9
Candelilla		14–15
Carnuba		12
Microcrystalline		10
Paraffin	4	10

Source: From Ref. 93.

In each case, however, the required HLB is equal to (or nearly equal to) the required HLB determined in the initial experiment.

Geiger et al. (96) studied the behavior of a W/O/W multiple emulsion formulation as potential controlled delivery system. The authors were interested in understanding the release due to a swelling-breakdown phenomenon. The breakdown was caused by the water flow from the external aqueous phase to the internal aqueous phase. Various experimental analyses, such as granulometry, rheology, and conductimetry, as well as a micropipette aspiration method, were used to study the stability of W/O/W emulsions. The predominant role of the lipophilic surfactant during the swelling phase was confirmed. Two different mechanisms were proposed and both imply that the migration of the lipophilic surfactant from one interface to another takes place successively. The lipophilic surfactant could diffuse from the first to the second interface, thus rigidifying the membrane, or from the oily phase to the first interface, resulting in delayed coalescence of the aqueous droplets during swelling. Thus, the more lipophilic the surfactant, the more the oil globule capacity increases and the more the release is delayed.

Polymer Characterization

A broad range of polymers can be used to form microcapsules. However the list of polymers approved for used in

oral and/or parenteral drug formulations is limited. This list includes proteins, polysaccharides, cellulose derivatives, synthetic polyesters developed as synthetic suture materials, polyanhydrides, and polyphosphazene. Characterization data for candidate polymer wall materials can play an important role in the development of a successful and reproducible encapsulation procedure. Thus, considerable attention should be paid to obtaining meaningful characterization data for polymer samples being used to form microcapsules. All the physical properties allow better fit of individual polymers to the correct encapsulation techniques. For example, it is not recommended to use polyanhydrides in solvent evaporation because the polymer may degrade during the process of encapsulation. Once the microcapsules are made, a new series of characterizations are required because morphological changes occur during encapsulation.

Phase Separation of Polymers

A wide range of polymer phase separation can be used to encapsulate materials: interfacial coacervation, binary polymer/solvent systems, polymer/solvent/nonsolvent systems, polymer/polymer/solvent systems, complex coacervation, and salting-out.

All these processes provide a way to surround each discrete internal phase droplet or particle of drug with homogeneous and reliably concentrated polymeric layers which can be later solidified in some manner to form a stable capsule. Thus, the next section addresses the general concepts of phase separation relevant to microencapsulation.

Interfacial Coacervation. The first example of a suitable phase separation process is the case of polymer adsorption, which Chang (49) has used to prepare small capsules. In this process, polymer dissolved in an organic phase migrates to the water–organic liquid interface where it precipitates spontaneously from solution to form a membrane. Chang calls this interfacial coacervation. Phase separation occurs spontaneously. An example of this process is the emulsification of an aqueous protein solution in diethyl ether using an oil-soluble nonionic surfactant. Span® 85, sorbitan trioleate, is preferred because it does not denature the protein. Chang used collodian nitrocellulose as the wall structure.

The emulsification process gives microcapsules that can be separated from much of the ether suspending medium and resuspended in *n*-butyl benzoate. *n*-Butybenzoate was selected because it is a poor solvent for collodian, a water-immiscible solvent, and a solvent with a density of 1.0. The suspension is left uncovered in order to allow evaporation of ether.

Chang often uses collodian (i.e., nitrocellulose) as the wall material, but stresses that microcapsules (or membranes) also can be formed in interfacial coacervation or precipitation of other polymers using different solvents (e.g., polystyrene in benzene). The success of this procedure depends on having a sufficiently high initial protein concentration in the aqueous phase. Microencapsulation usually is not possible with a very dilute solution of protein. Nothing more was noted about the mechanism whereby the protein (and probably the emulsifying agent in the system) influences the oil/water interfacial tension ($\gamma_{o/w}$) or how changes in $\gamma_{o/w}$ influences precipitation of the oil phases' polymer.

Phase Separation in Binary Polymer/Solvent Systems. The most conventional phase equilibria involving nonionic polymers dissolved in organic solvents have been discussed extensively by Flory (97). Flory's book focused on systems where all phases formed are completely liquid in nature and several systems of this nature play a key role in microencapsulation. The simplest case is of a binary system containing polymer and solvent. Figure 3 is a phase diagram of this system. Temperature changes alone are used to induce phase separation. Assuming a monodisperse polymer, phase separation is characterized by formation of two distinct phases, one rich in polymer and the other containing little polymer. Under equilibrium conditions, chemical potentials of the solvent (μ_1) and polymer (μ_2) in Phase I equals that in Phase II (i.e., $\mu_1^{I} = \mu_1^{II}$; $\mu_2^{I} = \mu_2^{II}$). Furthermore, at some critical temperature (T_c), incipient phase separation will take place:

$$\left(\frac{\partial^2 \mu_1}{\partial v_2^2}\right)_{T,P} = 0; \left(\frac{\partial \mu_1}{\partial v_2}\right)_{T,P} = 0 \tag{6}$$

and from these relations it can be shown that:

$$v_{2C} = \frac{1}{1 + \sqrt{X}}; \; X_{1C} = \frac{1}{2} + \frac{1}{\sqrt{X}} \tag{7}$$

where v_2 = volume fraction of polymer, v_{2C} = critical volume fraction of polymer, X = number of segments in a given polymer molecule, and X_{1C} = critical value of polymer–solvent interaction free energy. For this simplest case, theoretical binodials can be calculated and compared with experimental values. Such binodials have some important features. First, v_{2C} is predicted to be small, and this is confirmed by experimentation. In addition, at temperatures well below T_c, the dilute phase may retain an unappreciable amount of solute (especially true at higher

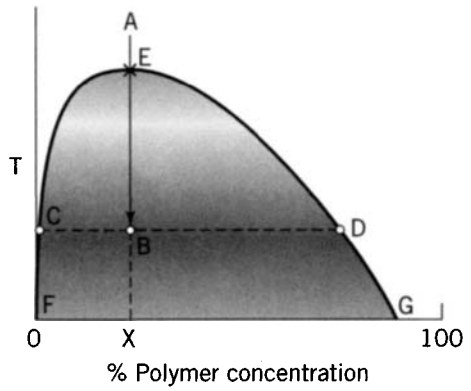


Figure 3. Phase separation in a two-phase system (polymer/solvent) induced by temperature.

M_w values). However, even the so-called concentrated phase contains a large amount of solvent which means that the system is still liquid in nature and thus could flow and engulf the core.

Thus, lowering the temperature (T) of a polymer–solvent mixture at constant v_2 and M_w often is a simple method of inducing phase separation and thereby obtaining a "polymer-rich" phase which can form a capsule wall. This could, in principle, be accomplished at constant T and v_2 by increasing M_w (i.e., continuing polymerization of the polymer). Alternately, at constant T and M_w, v_2 could be varied. Of course, if encapsulation is to occur, the polymer-rich phase must engulf at the internal phase. That is, formation of a concentrated polymer-rich phase having a low total volume does not necessarily mean adsorption and encapsulation occurs. Adsorption of this polymer-rich phase is a prerequisite for wall deposition (see next section) and may not be achieved in many cases.

Phase Separation in Polymer/Solvent/Nonsolvent Systems. A second method to produce phase separation involves addition of nonsolvent to a polymer–solvent system (Fig. 4). In such a case one moves from a two- to a three-component system (polymer/solvent/nonsolvent), thereby grossly complicating theoretical calculations. Nevertheless, it still is true that at equilibrium, chemical potentials of each component must be equal in the two phases:

$$\mu_1^{I} = \mu_1^{II}; \mu_2^{I} = \mu_2^{II}; = \mu_3^{II} \qquad (8)$$

where subscripts 1, 2, and 3 refer to nonsolvent, solvent, and polymer, respectively. If it is assumed:

$$V_1 = V_2; X_{23} = 0; X_{12} = X_{13} = 1.5 \qquad (9)$$

(V_1 = molar volume solvent; V_2 = molar volume nonsolvent; X_{23} = polymer–solvent interaction free energy; X_{12} = solvent–nonsolvent interaction free energy; and X_{13} = polymer–nonsolvent interaction free energy), a special case which can be solved is obtained and theoretical binodials can be calculated. Binodials calculated in this manner have critical points which occur at low polymer concentrations. This concentration decreases as M_w increases. As the binodial merges with the solvent–nonsolvent axis, at point D in Figure 4, the polymer concentration in the dilute phase becomes negligible (i.e., approaches zero) if the nonsolvent just slightly exceeds that required at the critical point. Thus, a two-phase system is formed with one phase relatively rich in polymer and the other containing relatively little polymer and mostly solvent. Provided the polymer molecules in the polymer-rich phase adsorb at the internal phase–solution interface, encapsulation occurs. A possible problem with systems of this type is that the nonsolvent could be of such a nature that it is preferentially absorbed by the internal phase and thereby prevents encapsulation even though phase separation occurs. An additional important point is that a mixed solvent system usually cannot be treated like a single solvent system. Generally speaking, the nonsolvent–solvent ratios differ markedly for the two phases in equilibrium whose compositions are indicated by the ends of the tie line. Only if $\mu_{12} \cong \mu_{23}$ will the solvent compositions in each phase be similar (they are equal if $\mu_{13} = \mu_{23}$). A large difference between μ_{13} and μ_{23} favors absorption of the better solvent in the polymer-rich phase and this undoubtedly contributes to serious aggregation problems when efforts are made to prepare microcapsules by encapsulation processes involving polymer solvent–nonsolvent mixtures.

Phase Separation in Polymer/Polymer/Solvent System. A third type of phase separation occurs in systems containing mixtures of two chemically different polymers, as seen in Figure 5. In such cases, formation of true polymer-in-polymer solutions is rarely observed. This is particularly true for polymer mixtures free of solvent. In the presence of solvent, two phases are generally formed under all but dilute solution conditions. The inability of two polymers to mix has led to the general rule of polymer–polymer incompatibility. This incompatibility has proved to be a problem in many cases where homogeneous mixtures of two poly-

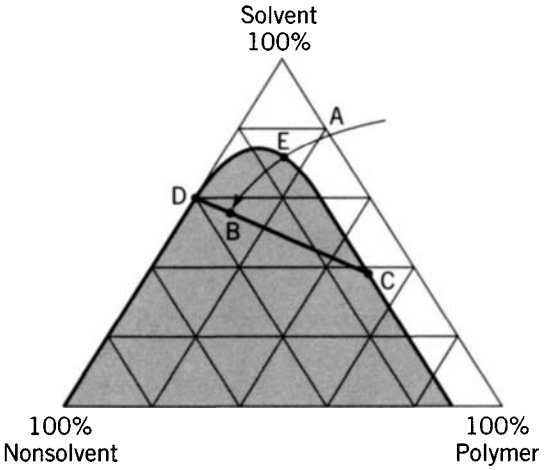


Figure 4. Phase separation diagram for a polymer/solvent/nonsolvent system.

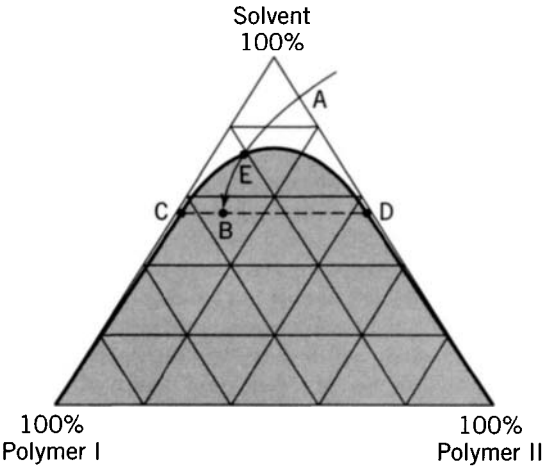


Figure 5. Phase separation diagram for a polymer/polymer/solvent system.

mers are desired (e.g., polymer blends, cases of plasticization), but it is a very important phenomena for use as an encapsulation technique; particularly, our group has used it to make double-walled microspheres in one step (84).

Polymer–polymer incompatibility is a widely encountered phenomenon because the free energy change occurring when the two polymers are mixed is generally >0. The free energy of mixing (ΔG_m) can be described by:

$$\Delta G_m = \Delta H_m - T\Delta S_m \quad (10)$$

For two polymers: ΔS_m is small.

ΔH_m generally is >0 (i.e., endothermic mixing). ΔS_m is so small that even if the heat of mixing (per segment) is just greater than zero, polymer–polymer incompatibility would occur. Thus, the widespread nature of incompatibility is attributable to the small contribution of the ΔS_m term and the tendency for polymer–polymer mixing processes to be endothermic in nature (i.e., $\Delta H_m > 0$).

It was originally predicted that polymer–polymer incompatibility is not influenced by the solvent used. That is, polymer pairs incompatible in one solvent are incompatible in all solvents. This often has been found to be the case, provided that the same molecular weight of polymer is used, but exceptions do exist. Theoretical phase diagrams developed for specific monodisperse model systems also revealed that polymer/polymer/solvent phase separations are characterized by formation of two phases, each of which contains essentially only one of the two polymers involved. Figure 5 is a phase diagram of such a system. The higher the M_w, the sharper the separation of the two polymers. These features have been confirmed experimentally by numerous workers and by our group. The actual phase separation process is influenced by such factors as solvent, temperature, nature of the two polymers involved, and their initial concentrations and the molecular weights. Complete separation of two polymers is not always achieved by polymer–polymer incompatibility. In most cases of encapsulation by phase separation, the low molecular weight polymers commonly used to induce phase separation become entrapped in the microcapsule wall, thereby affecting properties of the wall. Our experience with polymers such as polylactide and polystyrene with M_w in the range of 20,000 to 50,000 always showed complete solubility of 15% W/W, where used with polymer ratios of 1:1.

The importance of polymer–polymer phase separation in encapsulation is its capability to consistently form a distinct, relatively concentrated polymer phase which, if the polymer is adsorbed by the internal drug phase, readily wraps it completely thereby forming a capsule.

These methods are theoretically applicable to encapsulation of both water-soluble and water-insoluble substances. However, when water-insoluble solids or liquids must be encapsulated, an additional useful form of polymer phase separation phenomena is encountered, complex coacervation.

Complex Coacervation. Complex coacervation is the spontaneous liquid–liquid phase separation that frequently occurs when solutions of oppositely charged polyelectrolytes are mixed in the same solvent (usually water). It is encountered in biological systems and differs fundamentally from the polymer–polymer incompatibility mentioned earlier in that one phase contains most of the two polymers whereas the second phase is a dilute polymer solution. Figure 6, a phase diagram for the gelatin–gum arabic–water complex coacervation system, illustrates this point. Polymer–polymer incompatibility yields two phases with each containing predominately one of the two polymers.

Significantly, complex coacervation is truly a complex phenomenon. Polyelectrolytes useful for coacervation come in all shapes and forms with varying numbers and types of charged sites distributed along the polymer chains. The polyelectrolytes may have charged sites that are fully ionized at all pH values (e.g., SO_3) or sites where the group is weakly ionized (e.g., COOH), and the degree of ionization varies strongly with pH. Both positively and negatively charged sites can be on the same molecule (polyampholytes). Furthermore, many useful polyelectrolytes are natural gums, biopolymers, etc., and they often (usually) have complex structures which are not fully resolved. These factors grossly complicate matters, especially when rigorous analyses of such processes are desired.

The best known example of complex coacervation is the gelatin-gum arabic (GGA) system studied by Bungenberg de Jong and co-workers (57). Additional studies by Veis (98) have shown that the interaction of two gelatins of differing ionic points (pI = 5.0 and pI = 9.0) also provides an example of complex coacervation. Each polymer pair (under proper pH conditions) interacts to form a complex which appears as a concentrated, separated phase (i.e., coacervate). Temperatures of 40°C are used in order to obtain the so-called coacervate in a liquid state. These complexes are not the precipitated complexes formed by interacting oppositely charged polyelectrolytes of high charge density. For proper encapsulation, it is preferred to have liquid coacervates which can flow around or completely wrap the internal phase particles or droplets. Of course, the coacervate must wet the internal phase (i.e., be adsorbed by it) if it is to form the capsule wall. As mentioned before, a key

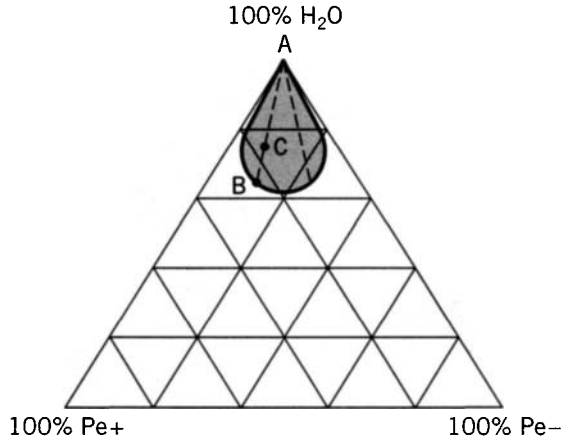


Figure 6. Phase separation diagram for a polyelectrolyte system.

feature of complex coacervation is that the supernatant or equilibrium liquid formed is a dilute polymer solution, whereas the coacervate is a polymer-rich phase (11–15% solids) containing both polymers.

Two factors which affect complex coacervation are pH and neutral salt ions. Because the ionic charge on gelatin and gum arabic varies with pH, coacervation of these species is sensitive to pH. Bungenberg de Jong (67) found that coacervation of alkali-precursor gelatin (pI = 4.8) and gum arabic occurred only between pH 2.0 and 4.8. At pHs outside this range no coacervate formed due to an imbalance in electrostatic charges. Neutral salt ions decrease the coacervation tendency of two polymers. This is attributed to the ability of such ions to screen the charged sites on the polyions involved and thereby reduce their mutual attraction. For example, Bungenberg de Jong (67) reported that 0.02M $CaCl_2$ or 0.035M KCl completely reverses coacervation of gelatin and gum arabic at 40°C. Suppression by salts is stronger the higher the valence of the added ion. Coacervation tendencies of gelatin and gum arabic also decrease with increasing initial concentrations of these polyions. Such self-suppression of coacervation has been attributed to an increase in ionic strength of the system due to increased diffusible microion concentration. Veis (98) reports that the volume of coacervate and fraction of gelatin in the coacervate decreases uniformly with increasing concentration of gelatin for coacervate systems consisting of two isoionic gelatins. The process of coacervation was first treated theoretically by Overbeek and Voorn (99) and later by Veis (98).

Interfacial Phenomenon

Adsorption of polymers on the core phase is a key step in encapsulation processes based on polymer phase separation phenomena. Thus we discuss were the surface free energy (γ, dynes/cm or ergs/cm^2) effects that occur in such processes.

Consider a case in which a droplet of liquid core material (representing the active drug) is engulfed by a liquid phase rich in polymer (i.e., the coacervate phase). Figure 7 is a schematic diagram of the process. Phase 1 is the drop of core material being engulfed, Phase 3 is the coacervate phase that is engulfing the core material, and Phase 2 is the continuous (or supernatant) phase in which Phases 1 and 3 are dispersed. If Phase 1 is designated such that $\gamma_{12} > \gamma_{23}$, the free energy change (ΔG_3) that occurs when Phase 3 spreads over Phase 1 is:

$$\begin{aligned} \Delta G_3 &= G_{\text{after}} - G_{\text{before}} \\ \Delta G3 &= \gamma_{13} + \gamma_{32} - \gamma_{12} \end{aligned} \tag{11}$$

Because the spreading coefficient S_3 is defined as $-\Delta G_3$:

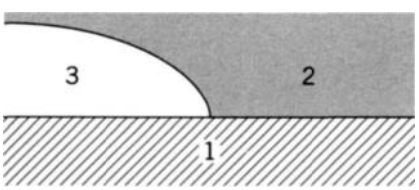


Figure 7. Schematic presentation of a three-phase system.

$$S_3 = -\Delta G_3 = \gamma_{12} - (\gamma_{12} + \gamma_{32}) \tag{12}$$

Because the core material, coacervate, and supernatant form a three-phase system, the spreading of Phase 1 over Phase 2 and the spreading of Phase 2 over Phase 1 must also be considered. The surface free energy change that occurs on spreading of Phase 1 over Phase 2 is given by:

$$\begin{aligned} \Delta G_1 &= G_{\text{after}} - G_{\text{before}} = \gamma_{12} + \gamma_{13} - \gamma_{23} \\ S_1 &= -\Delta_1 = \gamma_{23} - (\gamma_{12} + \gamma_{13}) \end{aligned} \tag{13}$$

The surface free energy change that occurs on spreading, of Phase 2 over Phase 1 is given by:

$$\begin{aligned} \Delta G_2 &= G_{\text{after}} - G_{\text{before}} = \gamma_{12} + \gamma_{23} - \gamma_{13} \\ S_2 &= -\Delta G_2 = \gamma_{13} - (\gamma_{12} + \gamma_{23}) \end{aligned} \tag{14}$$

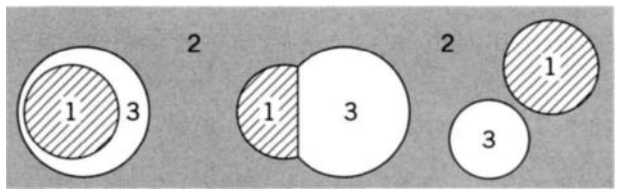
Therefore, three spreading coefficients (S_1, S_2, and S_3) describe the equilibrium state of a three-phase system. The three S values can have three sets of values (100):

$$\begin{aligned} S_1 < 0,\ S_2 < 0,\ S_3 > 0;\ S_1 < 0,\ S_2 < 0,\ S_3 \\ < 0;\ S_1 < 0,\ S_2 > 0,\ S_3 < 0 \end{aligned} \tag{15}$$

Figure 8 shows the equilibrium configurations that results for each of the above three sets of S values. Of greatest significance to capsule-makers is that complete engulfing of core material by the coacervate occurs only when $S_1 < 0$, $S_2 < 0$, $S_3 > 0$, that is, one must have:

$$\begin{aligned} S_1 < 0 &= \gamma_{23} - (\gamma_{12} - \gamma_{13}) \\ S_2 < 0 &= \gamma_{13} - (\gamma_{12} + \gamma_{23}) \\ S_3 > 0 &= \gamma_{12} - (\gamma_{13} + \gamma_{32}) \end{aligned} \tag{16}$$

In encapsulation systems involving polymer phase separation (coacervation), γ_{23} usually is >0.2 dyne/cm. Because γ_{23} is so small, it is reasonable to assume that $\gamma_{23} \approx 0$. If this is done, and $\gamma_{12} > \gamma_{13}$, S_3 is > 0, S_1 is <0, and S_2 is <0. Thus, microcapsules form spontaneously. This is an assumption, and this may be part of the reason why methods such as coacervation may fail to produce microspheres.



(a) Complete engulfing	(b) Partial engulfing	(c) No engulfing
$S_1 < 0$	$S_1 < 0$	$S_1 < 0$
$S_2 < 0$	$S_2 < 0$	$S_2 > 0$
$S_3 > 0$	$S_3 < 0$	$S_3 < 0$

Figure 8. Schematic diagram showing the spreading coefficient, S, necessary for (**a**) complete engulfing of an internal phase (1) by a coacervate phase (3) in a continuous phase (2); (**b**) partial engulfing; (**c**) no engulfing.

Next Page

But the new method to make double-walled microspheres are more useful.

SOLVENT EVAPORATION

One of the oldest and most widely used methods of microsphere preparation is the solvent evaporation technique (18,36,75–80,101). This method yields drug-loaded polymer particles that could be called microspheres when drug loading is low or microcapsules when the drug loading is high.

The solvent evaporation encapsulation process, depicted in Figure 9, is a way of precipitating small polymer particles from an oil-in-water emulsion. The polymer is dissolved in a volatile organic solvent that is immiscible with water. Methylene chloride is a preferred solvent because of its high volatility (boiling point [bp] 41°C) and its capacity for dissolving a broad range of polymers. Table 5 lists a number of solvents that can be used and, it should be noted that, many solvents suitable for this process have a finite degree of water solubility, even though they are normally classified as water-insoluble solvents. Mixed solvents can also be used. The mixtures used so far tend to contain a water-immiscible solvent (e.g., CH_2CI_2) and a water-miscible solvent (e.g., acetone). The water-immiscible solvent is the predominant component of the mixture.

Once the desired coating polymer is dissolved in the organic solvent, the drug to be encapsulated is added to this solution. The drug agent may be a solid (crystalline or amorphous) or a nonvolatile liquid. The added drug may completely dissolve in the polymer solution or it may be completely insoluble and simply form a dispersion, suspension, or suspension-emulsion. In the latter case, the solid particles must be micronized so that their mean diameter is much less than the desired mean microsphere size. This is true for any encapsulation technique, and generally, a particle size/microsphere size ratio of 1:10 or less is preferred. The solubility of the drug in the organic solvent is also a major factor in determining the morphology of microspheres produced by the solvent evaporation process and the final state of the polymer itself (crystalline or amorphous).

The drug/polymer/solvent mixture (i.e., the oil phase) is emulsified in water to form an oil-in-water emulsion. The size of the oil phase droplets obtained is determined by how rapidly the system is agitated when the oil phase is added to the aqueous phase, and determines the size of the microspheres produced. Emulsification is carried out in a blender if small microspheres are desired (<20 μm) or with a suspended agitator for larger microspheres. In order to aid emulsification, a surfactant is normally dissolved in the water phase before the oil-in-water emulsion is formed. A good example is partially hydrolyzed (88%) poly(vinyl alcohol) (PVA).

Once the desired oil phase droplet size and emulsion stability have been obtained the system is stirred at a constant rate and the solvent evaporates. This is the basis of the name, because most of the solvent disappears by evaporation. Evaporation can occur in an open system at reduced pressure and range of evaporation temperatures can be used. Once solvent evaporation appears to be complete, the capsules are separated from the suspending medium by filtration, washed, and dried. The maximum drying temperature must remain below the glass-transition temperature of the polymer encapsulant or the microspheres fuse together. Although most of the process depends on evaporation, some of the solvent may diffuse into the aqueous solution and then evaporate. The amount that diffuses into the aqueous solution directly depends on the solubility of the organic solvent in water.

The solvent evaporation process is conceptually simple, but a large number of process variables exist which can profoundly affect the nature of the product obtained. Table 6 lists a number of such variables. How each of these variables influences a given system must be determined experimentally, although some general trends are known. For example, semicrystalline polymers often give porous structures with spherulites on the surface of the microspheres. Uniform, pore-free spheres are most readily obtained with amorphous polymers. If a polymer is not soluble in a single solvent, mixed solvents can be used (e.g., CH_2Cl_2/ethanol or CH_2Cl_2/acetone mixtures).

One requirement of the solvent evaporation process is that the active agent (i.e., drug) partition favorably into the oil phase. This partitioning is favored by using active

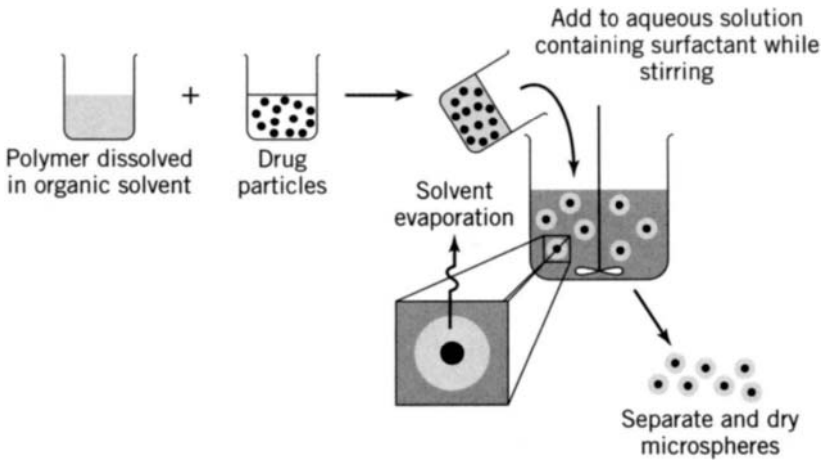


Figure 9. Microencapsulation by solvent evaporation. Note that the dark dots represent drug particles; however when the drug is water-soluble, an additional step is required to prepare a water-in-oil emulsion, which is later encapsulated as shown here.

Previous Page

But the new method to make double-walled microspheres are more useful.

SOLVENT EVAPORATION

One of the oldest and most widely used methods of microsphere preparation is the solvent evaporation technique (18,36,75–80,101). This method yields drug-loaded polymer particles that could be called microspheres when drug loading is low or microcapsules when the drug loading is high.

The solvent evaporation encapsulation process, depicted in Figure 9, is a way of precipitating small polymer particles from an oil-in-water emulsion. The polymer is dissolved in a volatile organic solvent that is immiscible with water. Methylene chloride is a preferred solvent because of its high volatility (boiling point [bp] 41°C) and its capacity for dissolving a broad range of polymers. Table 5 lists a number of solvents that can be used and, it should be noted that, many solvents suitable for this process have a finite degree of water solubility, even though they are normally classified as water-insoluble solvents. Mixed solvents can also be used. The mixtures used so far tend to contain a water-immiscible solvent (e.g., CH_2CI_2) and a water-miscible solvent (e.g., acetone). The water-immiscible solvent is the predominant component of the mixture.

Once the desired coating polymer is dissolved in the organic solvent, the drug to be encapsulated is added to this solution. The drug agent may be a solid (crystalline or amorphous) or a nonvolatile liquid. The added drug may completely dissolve in the polymer solution or it may be completely insoluble and simply form a dispersion, suspension, or suspension-emulsion. In the latter case, the solid particles must be micronized so that their mean diameter is much less than the desired mean microsphere size. This is true for any encapsulation technique, and generally, a particle size/microsphere size ratio of 1:10 or less is preferred. The solubility of the drug in the organic solvent is also a major factor in determining the morphology of microspheres produced by the solvent evaporation process and the final state of the polymer itself (crystalline or amorphous).

The drug/polymer/solvent mixture (i.e., the oil phase) is emulsified in water to form an oil-in-water emulsion. The size of the oil phase droplets obtained is determined by how rapidly the system is agitated when the oil phase is added to the aqueous phase, and determines the size of the microspheres produced. Emulsification is carried out in a blender if small microspheres are desired (<20 μm) or with a suspended agitator for larger microspheres. In order to aid emulsification, a surfactant is normally dissolved in the water phase before the oil-in-water emulsion is formed. A good example is partially hydrolyzed (88%) poly(vinyl alcohol) (PVA).

Once the desired oil phase droplet size and emulsion stability have been obtained the system is stirred at a constant rate and the solvent evaporates. This is the basis of the name, because most of the solvent disappears by evaporation. Evaporation can occur in an open system at reduced pressure and range of evaporation temperatures can be used. Once solvent evaporation appears to be complete, the capsules are separated from the suspending medium by filtration, washed, and dried. The maximum drying temperature must remain below the glass-transition temperature of the polymer encapsulant or the microspheres fuse together. Although most of the process depends on evaporation, some of the solvent may diffuse into the aqueous solution and then evaporate. The amount that diffuses into the aqueous solution directly depends on the solubility of the organic solvent in water.

The solvent evaporation process is conceptually simple, but a large number of process variables exist which can profoundly affect the nature of the product obtained. Table 6 lists a number of such variables. How each of these variables influences a given system must be determined experimentally, although some general trends are known. For example, semicrystalline polymers often give porous structures with spherulites on the surface of the microspheres. Uniform, pore-free spheres are most readily obtained with amorphous polymers. If a polymer is not soluble in a single solvent, mixed solvents can be used (e.g., CH_2Cl_2/ethanol or CH_2Cl_2/acetone mixtures).

One requirement of the solvent evaporation process is that the active agent (i.e., drug) partition favorably into the oil phase. This partitioning is favored by using active

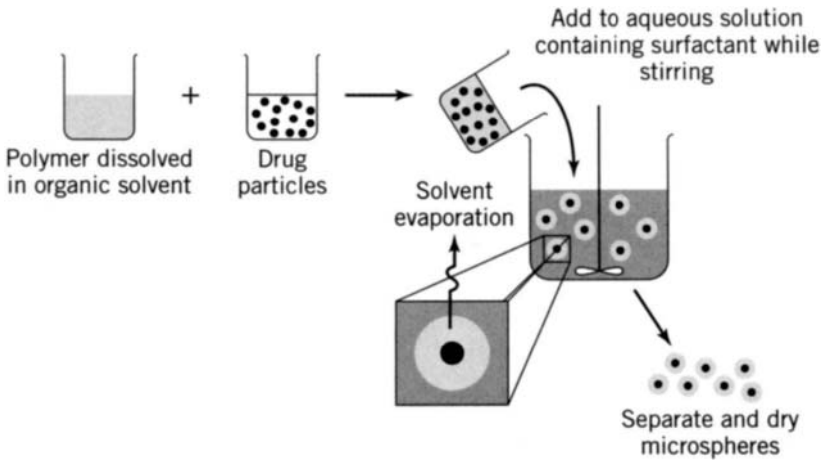


Figure 9. Microencapsulation by solvent evaporation. Note that the dark dots represent drug particles; however when the drug is water-soluble, an additional step is required to prepare a water-in-oil emulsion, which is later encapsulated as shown here.

Table 5. Properties of Some Organic Solvents

Solvent	bp (°C)	fp (°C)	solubility in H_2O g/100 g solvent
Methylene chloride	41	−96.7	2
Chloroform	61.2	−63.5	0.82
Ethyl acetate	77.1	−82.4	8.5 (15°C)

Table 6. Parameters Affecting Solvent Evaporation

1. Polymer molecular weight and concentration
2. Polymer crystallization
3. Type of drug and method of incorporation (solid, liquid, suspension).
4. Organic solvent used
5. Type of surfactant in aqueous phase
6. Organic solvent/aqueous phase cation
7. Evaporation temperature
8. Rating of stirring

agents that are insoluble or sparsely soluble in water. Such agents may be insoluble in the organic solvent. In the latter case, the microspheres contain a dispersion of crystals embedded in a polymer matrix. The crystals should be the same ones dispersed initially in the polymer–solvent solution, assuming that there is no partial solubilization and/or recrystallization. If the active agent dissolves completely in the organic solvent phase, it may or may not form crystalline domains in the polymer matrix that makes up the microsphere. For example, microspheres with low active agent payloads (e.g., <20 wt %) have no crystalline domains as determined by differential thermal analysis. At higher payloads, crystallinity appears.

Preventing migration of active agent into the aqueous phase from the solvent phase is often a problem. Crystalline active agents completely soluble in the solvent phase tend to form free crystals in the aqueous phase or on the surface of the microspheres. This effect can be minimized by removing from the system the emulsifier located in the aqueous phase before solvent evaporation is complete. When the emulsifier is left in the system until evaporation is complete, it favors free crystal formation. Thus, by stopping agitation midway through the evaporation process, one can remove the emulsifier by a series of washing and decantation steps. Agitation (and evaporation) is then continued in the presence of emulsifier-free water until solvent loss is complete. This either eliminates or drastically reduces the amount of free crystals formed.

Mathiowitz et al. (55) used this method, with the following modifications, to prepare polyanhydride microspheres. (Please note that this is not a preferred method for polyanhydrides.) Poly(carboxyphenoxypropane-*co*-sebacic-acid) (poly(CPP-SA) 50:50) was dissolved in methylene chloride. Two different polymer concentrations were used (0.05 and 0.20 g/mL). The solution was loaded with drug and suspended in 200 mL of vigorously stirred distilled water containing 1% (w/v) PVA. After 4 hours of mixing, the microspheres were washed with water and dried overnight in a lyophilizer.

Figure 10a is a scanning electron micrograph (SEM) of the external surface of a poly(CPP-SA) 50:50 polymer microsphere containing 5% (W/W) insulin. For this particular formulation the initial polymer concentration was 0.05 g/mL of methylene chloride. The microspheres are spherical in shape and contain some pores on the surface; a cross-sectional view of the microsphere reveals a very porous internal structure (Fig. 10b), which is typical of this particular process. Porosity can be varied by changing the rate of solvent evaporation (via the temperature or stirring rate) as well as the concentration of the initial polymer solution. When the previously described fabrication was repeated with an initial polymer concentration of 0.20 g/mL, polymer in methylene chloride, the resulting microspheres showed a marked drop in porosity (Fig. 10c).

Besides resulting in high microsphere porosity, solvent evaporation also accelerates polymer degradation during the first stages of preparation due to the presence of the water phase. For these reasons, polyanhydride solvent evaporation is not recommended. Other fabrication methods were developed to make slower releasing and longer acting polyanhydride microspheres (see "Hot Melt Microencapsulation" and "Solvent Removal").

The biological activity of insulin released from microspheres was determined in vivo by monitoring daily blood and urine glucose levels in polymer-implanted diabetic female Sprague-Dawley rats. Diabetes was previously induced with a tail vein injection of 65 mg/kg of streptozotocin in pH 4.5, 0.1 M citrate buffer, the optimal dose for inducing diabetes in these rats. When serum glucose levels reached a minimum of 400 mg/dL the rats were considered diabetic and were treated with the insulin-loaded polyanhydride microspheres. Daily urine glucose outputs were estimated with Chemstrips UG. Blood was drawn daily from the tail vein and serum glucose levels were read on a Glucose Analyzer.

Dry microspheres were implanted subcutaneously through a small (1 cm) surgical incision in the skin of the dorsum of the rat and the skin was closed with monofilament nylon sutures. Where indicated, certain microspheres were injected in an aqueous suspension in 0.1 M pH 7.4 phosphate buffer through a 22-gauge needle. Three groups were studied; healthy rats, diabetic control rats, and diabetic rats that were implanted with the drug-loaded spheres. When insulin-loaded (10%), solvent evaporation microspheres were implanted in diabetic rats, the blood glucose level was lowered precipitously for one day, with the majority of the rats dying due to insulin overdose. The porous structure of the spheres presumably allowed water to enter the sphere quickly and led to complete insulin release in a short period of time, which may explain the extremely fast and generally fatal hypoglycemia that was observed. Figure 10d depicts insulin-loaded microspheres that were found in the rat tissue after one day of implantation (note the porous structure of the microsphere). Better results were obtained with microspheres made by hot-melt and solvent removal (see "Hot Melt Microencapsulation" and "Solvent Removal").

Polyester microspheres made by solvent evaporation were reported on extensively in the last 10 years, and the most successful microsphere product that is being used in

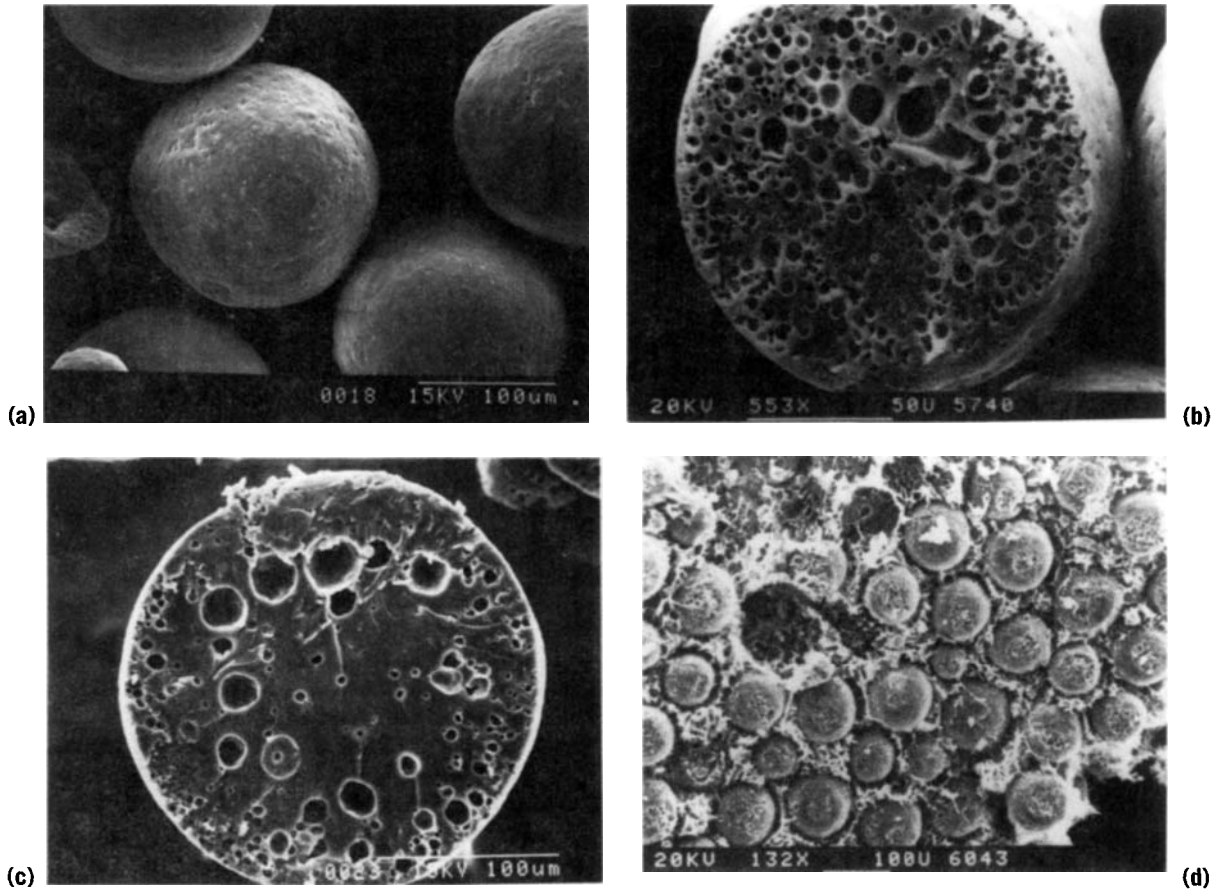


Figure 10. SEM of (**a**) external surface of polyanhydride microsphere made by solvent evaporation; (**b**) cross section of a polyanhydride microsphere made with low polymer concentration; (**c**) cross section of a polyanhydride microsphere made with high concentration; (**d**) insulin-loaded polyanhydride microspheres after two days of subcutaneous implantation in rats.

humans today is the Lupron Depo™. To understand the development of the Lupron Depo™ it may be interesting to follow some of the procedures described by Okada (102). In the double emulsion technique used, first the drug is dissolved in an aqueous solution. The patent describes how the pH can be adjusted by adding materials such as carbonic acid, acetic acid, oxalic acid, citric acid, tartaric acid, succinic acid, phosphoric acid, sodium or potassium salts, hydrochloric acid, or sodium hydroxide. In addition, agents such as albumin, gelatin, citric acid, ethylenediamine sodium tetraacetate, dextrin, and sodium hydrosulfite could be added as a stabilizer for the water soluble drug. The inner aqueous layer may also contain a preservative such as *p*-oxybenzoic acid esters (e.g., methylparaben, propylparaben, etc.), benzyl alcohol, chlorobutanol, or thimerosal (102).

Once the inner aqueous layer is prepared it is poured into a polymer solution (oil layer) and the mixture is emulsified to give a water-in-oil emulsion (102). The emulsification can be effected by the conventional dispersion techniques, e.g., intermittent shaking, mixing via an impeller, turbine mixer or the like, colloid mill operation, mechanical homogenization, ultrasonication, etc. (102).

When the viscosity of the inner aqueous layer in such a water-in-oil emulsion is greater than about 5,000 centipoises, or preferably greater than 10,000 centipoises from the beginning, the emulsion is immediately subjected to conditions that change the viscosity (102). Increasing the viscosity can be achieved by either heating or cooling. If gum acacia is used, adding metal ions such as iron or copper ion for carboxymethylcellulose, or calcium or magnesium ion for sodium pectinate, are useful (102).

If heating is used, then the procedure must be carried out in a closed vessel to avoid evaporation of the solvent contained in the oil layer. When proteins are used, the temperature used can be from 40 to 120°C for as little as 5 minutes to about 8 hours. This treatment thickens or solidifies the inner aqueous layer (102).

Cooling the emulsion to a low temperature is accomplished at temperatures of −5 to 35°C which are maintained with stirring for 1 minute to 6 hours. In the case of agar whose gelation point is about 40°C, the emulsification is conducted under heating, at about 50 to 80°C, and then caused to gel at the aforementioned temperature. For all types of inner aqueous layers, freezing may be effected by cooling to about −60 to 0°C, but the temperature should not be below the solidification point of the oil layer (102).

This step seems to reduce the amount of drug lost to the aqueous solution. Using gelatin as an example of a drug-retaining substance: a water-in-oil emulsion of predetermined particle size is first prepared and then cooled to about 0–10°C for 5 to 30 minutes with constant stirring, whereby the inner aqueous layer is caused to gel into a semisolid consistency. When agar is used as the drug-retaining substance, the desired semisolid consistency can be obtained by using a lower concentration than in the case of gelatin and the same procedure as that for gelatin. When albumin is employed, solidification is effected with a condensing agent such as glutaraldehyde (102). For large proteins this step is not recommended.

An attempt at developing leuprolide acetate-loaded, injectable microcapsules capable of one-month, zero-order rate delivery was reported by Ogawa et al. (103). A large amount of leuprolide acetate, a hydrophilic drug, was entrapped in poly(lactic acid) (PLA) and poly(lactide-*co*-glycolide) (PLGA) microcapsules prepared by an in-water drying method using a (W/O/W) emulsion. Under the conditions used, it was possible for the drug to be completely entrapped by the microcapsules at a loading of 10 to 20% (W/W). However, the release profiles of the drug in vitro fell short of controlled release for one month.

Leuprolide acetate is a highly potent analog of luteinizing hormone-releasing hormone (LHRH). Okada et al. (105) succeeded in preparing one-month release, injectable microcapsules of leuprolide acetate using poly(DL-lactide-*co*-glycolide) to treat an endocrine-dependent prostate cancer. A single injection of the microcapsules (100 μg/kg/day as leuprolide acetate) suppressed luteinizing hormone (LH), follicle-stimulating hormone (FSH), and estradiol for more than 4 weeks and caused a dramatic regression of growth in the Jones experimental endometriosis model in female rats. These results encouraged scientists to develop a one-month release, parenteral preparation of leuprolide acetate, subsequently used in the therapy of endometriosis in human beings (104).

The drug release profiles of the microcapsules after subcutaneous (s.c.) and intramuscular (i.m.) injection into rats was determined by following the amount of the analog remaining at the incised injection site. The release profiles after s.c. and i.m. injection were almost identical; they provided a pseudo zero-order release for 4 weeks, after a small initial burst. The regression line of the amount remaining, calculated by a least-squares regression analysis, revealed that the rate of release of leuprolide acetate was 2.8% of the dose/day, the initial burst was 17.8%. The correlation coefficient was 0.99. The serum levels of leuprolide acetate in rats after the PLGA microcapsules were injected s.c. showed that the initial burst of the analog was followed by a plateau level for 4 weeks. Administration of the microcapsules to normal female rats resulted in a transient rise and subsequent drastic decrease of serum LH and FSH levels. The decreased serum levels reached minima 2 to 3 weeks after the injection, and were maintained for another 1 to 2 weeks. The estradiol levels reached a minimum 3 weeks after the injection and remained there for another week. Thereafter, the levels of FSH and estradiol recovered gradually and rebounded slightly by 6 or 8 weeks of treatment. In contrast, the suppressed serum levels of LH persisted for 6 weeks. Daily cytological examination of vaginal smears indicated that the estrous cycle had stopped at diestrus in all rats 3 days after the microcapsules were injected, and remained at this stage for 6 weeks. The normal estrous cycle was recovered 8 weeks after the treatment began.

Expected depression in LH, FSH, and estradiol serum levels occurred at doses of more than 100 μg/kg/day. Serum LH levels were decreased already by a dose of 1 to 10 μg/kg/day; the levels were equivalent to those in diestrus rats. At a dose of 100 mg/kg/day, the serum FSH levels were also depressed, and significantly reduced serum levels of estradiol were produced by all doses between 1 to 250 μg/kg/day; the levels at a dose of over 100 μg/kg/day were close to that produced by ovarioectomy.

The infinite area under serum level-time curve in female rats after leuprolide acetate was injected s.c. as a saline solution (100 μg/kg) was 118.8 ng · h/mL, as described previously. The total body clearance (Cl_{tot}) is calculated by:

$$Cl_{tot} = \text{Dose/AUC} = 100 \times 10^3/118.8 = 841.8 \text{ mL/h/kg} \quad (17)$$

The release rate (k) of leuprolide from the microcapsules (TAP-6M), calculated in a similar manner in TAP-3M, was 3.1% of the dose/day, which is equal to:

$$k = 900 \times 10^3\ 0.031/0.305 \times 24 = 3811 \text{ ng/h/kg} \quad (18)$$

where the average body weight during 4 weeks of treatment was 305 g. If the analog is infused at a constant rate (k), the serum drug levels at a steady state (C_{ss}) is given by equation 19.

$$C_{ss} = k/Cl_{tot} = 4.53 \text{ ng/mL} \quad (19)$$

The serum levels estimated using body weight during 4 weeks of treatment as described before are 5.55 ng/mL (body weight, 249 g) to 3.98 ng/mL (body weight, 347 g). The experimental values agreed well with these calculated serum levels at a steady state. The microcapsules eliminated the time lag of the initial drug release and produced a more constant and lasting serum level of the analog throughout the 4 weeks of treatment than did an implantable depot formulation of D-Ser(tBu)-AzaGly LHRH and microcapsules of nafarelin or decapeptyl (104).

Okada et al. (105) worked on developing a more interesting system of Leuprorelin for 3-month delivery. The pharmacological effects of Leuprorelin 3-month depot microspheres were investigated in rats and dogs. After s.c. and i.m. injection, the microspheres provided similar linear drug release and sustained serum drug levels for 3 months. Persistent suppression of serum LH, FSH (in rats) and testosterone (in rats and dogs) for over 16 weeks was achieved when the microspheres were given at a dose of 100 (rat) and 25.6 (dog) μg/kg/day. These hormone release responses, upon periodic challenge tests, revealed that for a single injection of the microspheres over 3 months the strongest suppression was achieved at a dose of 100 μg/kg/

day. This 3-month depot formulation is expected to be more convenient than the 1-month depot with improved patient compliance and therapeutic effects. To obtain a 3-month release injection of leuprolide acetate, microspheres, were prepared with poly(DL-lactide-*co*-/glycolide) (DL-PLGA) or PLA using an in-water drying method, after which drug release was evaluated. The content of water-soluble oligomers in the polymers was found to strongly affect the initial burst, and reducing the content to less than 0.1% was necessary to keep the first-day release below 10%. Drug loading of more than 15% also increased the initial drug release; the acceptable maximum loading was 12%. Elevation of the glass-transition temperature of the microspheres was observed with an increase in drug loading. This suggests formation of a rigid structure, possibly with arrangement of the polymer around the drug cores such as in a micelle. This structure provides a hydrophobic barrier against diffusion of the hydrophilic peptide, resulting in high trapping efficiency and long-term sustained release dependent on polymer erosion. The microspheres prepared with PLA of 12,000 to 18,000 M_w provided linear sustained release and persistent serum levels of the drug in rats for over 3 months (106).

In order to prepare the long-release systems, the microspheres of Leuprorelin were made without the gelatin in the inner drug solution. Briefly, in the case of 12% drug-loaded PLA microspheres, 550 mg of drug dissolved in 1 mL of distilled water (W_1) and 4 g of PLA dissolved in 7.5 mL of CH_2Cl_2 were combined and agitated vigorously with a homogenizer to form a W/O emulsion. This emulsion was poured into 1 L of a 0.25% PVA solution (w_2) under stirring. This $W_1/O/W_2$ emulsion was stirred gently for 3 hours to evaporate the organic solvent, producing microspheres. The microspheres were sieved with a 74-μm screen to remove large particles and then centrifuged at 1,000 rpm for 5 minutes. The resulting microspheres were washed with water and lyophilized. PLGA 75:25 (M_w 9,000–23,000), PLGA 90:10 (M_w 9,200–22,900) and PLA (M_w 4,700–162,100) were used. To determine the effects of drug loading on drug release, microspheres containing 9, 12, 15, and 18% drug were prepared using PLA (M_w 18,200). The volume of the inner water phase and organic solvent and temperature of the W/O emulsion and outer water layer were varied with the kind of polymer and percent drug loading to maintain appropriate viscosity and obtain spherical and similar size microspheres (107).

The results of screening biodegradable polymers, PLA and PLGA, for the 3-month depot formulation indicated that microspheres prepared using PLA with a molecular weight of 12,000 to 18,000 gave linear sustained drug release for over 13 weeks. A similar sustained release pattern was confirmed by serum drug level assays following s.c. injection of these microspheres. The microspheres prepared using PLA (M_w 15,000), containing less than 0.1% water-soluble oligomers and loaded with 12% drug, may be the most desirable formulation for the 3-month depot injection (106).

Analyses of microparticle size and morphology during degradation by Brannon-Peppas et al. (107,108) have shown that the method of incorporating β-estradiol into PLGA microparticles has an effect on drug delivery that may be followed by changes of the microstructure of the particles over time. Nondestructive observation of microparticles during their full degradation has verified the coupling of drug release during early periods of degradation where small changes in the particle structure may be observed. However, it has also been shown that these particles retain their structural integrity and shape for many months in vitro after all drug delivery has been completed.

Schugens et al. (109) studied two semicrystalline poly(L-lactides) with different molecular weights as coating polymers in microencapsulation by the W/O/W double emulsion-evaporation technique. The scientists have shown that crystallizable chains have clearly a deleterious effect on the encapsulation efficiency of indigocarmine and on the internal morphology of microparticles. Moreover, a substantial increase in the molecular weight of poly(L-lactide) (from 60 to 840 kDa) requires dilution of the polymer solution to prevent exceedingly high viscosity and leads to less stable primary emulsions and more porous solid microspheres. Microparticles of semicrystalline poly(L-lactide) have proved unsuitable for the sustained drug release. When poly(DL-lactide) (M_n 50 kDa), was used, more efficient microencapsulation was obtained. This was true particularly when the primary emulsion was stabilized with gelation.

Using a predictive mathematical model from Li et al. (110) several important extrinsic process variables were developed to simulate process dynamics of microsphere formation. These included the composition profile in the dispersed phase, the solvent concentration profile in the continuous phase, and the solvent removal profile in the dispersed phase. This was one of the attempts to move closer to understanding microencapsulation in detail. By superimposing the composition profile in the dispersed phase with the phase transition boundary, the progression of phase transition in microsphere formation was evaluated. The authors found that a low dispersed phase/continuous phase ratio, high continuous phase-addition rate, high temperature, high heating rate, and high initial polymer concentration in the dispersed phase contributed to enhanced solvent removal. The higher solvent removal led to a heterogeneous composition distribution in the dispersed phase and the early crossover of the gelation point (viscous boundary) of the peripheral region which initiates the onset of solidification in this region. These phenomena resulted in an increasing pore size, lower surface area, denser periphery, higher residual solvent, and slower drug release. In addition, the progress toward the glassy boundary may also play a major role in the ultimate solvent residual. Slow solvent removal gave rise to a homogenous distribution of the components in the dispersed phase due to the delay of hardening. The extrinsic manageable parameters could be varied during microsphere formation to obtain the desired rate of solvent removal as well as the desired microsphere properties. The mathematical model was used to simulate such conditions to facilitate the experimental design for the desired microsphere properties.

Poly(L-lactic acid-*co*-L-lysine(Z)) (PLLA) with different Lys(Z) contents was synthesized by Sn(II) salt-catalyzed ring-opening copolymerization of 3(*s*)-benzyloxycarbonylaminobutyl-6(*S*)-methylmorpholine-2,5-dione with lac-

tide. Microcapsules of the copolymers were prepared by solvent evaporation from W/O/W emulsion, and fluorescein isothiocyanate (FITC) dextran release from the microcapsules was investigated. The FITC-dextran release was dependent on the composition and molecular weight of the copolymers. The release from the microcapsules containing Lys(Z) of 6.5 mol% was slowest among the present microcapsules, which is due to smooth surface and very small microcapsules included in a large microcapsule. On the other hand, the release from microcapsules containing Lys(Z) of 31 or 50 mol% became faster after several days of incubation. Gel permeation chromatography measurement of the microcapsules revealed that the copolymers were degraded during the incubation. Cracks and pores were formed on the microcapsule wall. PLLA microcapsules having comparable molecular weight to the copolymers showed neither release acceleration nor degradation in short-time incubation. Therefore, the introduction of Lys(Z) units made PLLA susceptible to degradation to result in delayed acceleration of release (111).

PLA microspheres containing soluble dyes as water-soluble model compounds were prepared using the W/O/W solvent evaporation method. The authors reported that addition of electrolytes such as NaCl or $CaCl_2$ into the external aqueous phase significantly improved brilliant blue (BB) entrapment efficiency compared to the case of no additives (75). NaCl was the most effective for obtaining high entrapment efficiency (80–90% of theoretical BB content). The average diameter of the obtained microspheres was in the region of 10–20 μm in all cases. PLA microspheres containing 5 and 10% (W/W) BB exhibited the so-called burst release. The release rate decreased with decrease in the internal aqueous droplet volume in the preparation process. In particular, with PLA microspheres containing 5% (W/W) BB, those prepared with the smallest internal droplet volume (63 μL), the initial burst release was reduced significantly and 50% (W/W) of the loaded BB remained in the microspheres for 7 days.

Reza and Whateley (112) developed sustained local release systems for iodinated iodo-2′-deoxyuridine (IudR) from biodegradable polymeric microspheres to facilitate the controlled delivery of IudR to brain tumors. The selective uptake of IUdR into the cell nucleus results in cell disruption over the short range of the low energy Auger electrons. The biodegradable microspheres can be precisely implanted in the brain by stereotactic techniques and the IUdR within the microspheres is protected from degradation and thus a sustained source of radiolabeled IUdR is available in the vicinity of the residual tumor cells. PLGA 85:15 microspheres containing cold IUdR and the Auger-electron emitter ^{125}I, as ^{125}IudR were prepared using the O/W, O/O, and W/O/W emulsion-solvent evaporation methods. The W/O/W emulsion method was most effective in achieving good drug loading with the use of bovine plasma in the internal water phase. The use of 20% acetone in the methylene chloride and the presence of Span® 40 in the organic phase improved the drug encapsulation efficiency. Electrolytes (NaCl and IudR) in the external aqueous phase also improved drug loading.

Okumo et al. examined the effects of size, charge, and conformation on the release of peptides from microspheres of DL-PLGA 50:50. These microspheres were prepared using a double emulsion technique and were characterized for size, morphology, and peptide release kinetics. The volume of water used as the internal phase has a significant effect on the release of the linear hexapeptide Ac-Trp-Ala-Gly-Gly-Asp-Ala-NH_2. For example, when no water was added, the release appears to be erosion-controlled. In contrast, when 150, 500, or 1000 μL of water are added, the release shifts to a diffusion-controlled mechanism. Changing the size, charge, and conformational flexibility of the model peptides had no significant effect on their release kinetics. The authors suggest that release kinetics that were observed for the neutral capped amino acid and the positively charged cyclic hexapeptide are due to unique specific interactions between these compounds and DL-PLGA (113).

A new preparation method for multireservoir-type microspheres was investigated on the basis of the phase separation of PLA and PLGA. Matsumoto et al. (114) have found that distinctive phase separation occurred when the total polymer concentration exceeded a critical level. The critical polymer concentration inducing this phase separation was independent of the PLA/PLGA ratio but highly dependent on the lactide/glycolide ratio, solvent, and molecular weight of PLGA. When various amino acid powders were added to the resultant two-phase polymeric solution, each powder seemed to be distributed either to the PLGA-rich phase or to the PLA-rich phase depending on its solubility parameter. When used, cisplatin powder also was completely distributed in the PLGA-rich phase. Using these findings, the preparation of the multireservoir-type microspheres of cisplatin was tried. The PLGA-PLA biphasic polymeric solution dispersing the drug powder was emulsified, and then solidified by the solvent evaporation method. Microscopic observation proved that the obtained microspheres have the unique "polymer alloys" structure, and the drug was distributed in the internal phase (PLGA-rich phase). The encapsulation efficiency was almost 100% at 10% loading. The in vitro dissolution study revealed that the release of cisplatin lasted 45 days without initial burst.

The distribution of a drug substance between two phases is represented as follows:

$$\frac{[X_a]}{[X_b]} = V_s \frac{(\delta_s - \delta_b)^2 - (\delta_a - \delta_s)^2}{2.3RT} \qquad (20)$$

where $[X_a]$ and $[X_b]$ are concentrations of drug substance s in a phase and b phase, respectively; δ_a, δ_b, and δ_s are solubility parameters of a phase, b phase, and substance s, respectively; V_s is the molecular volume of substance s; R is the gas constant; and T is absolute temperature. This equation means that the distribution of substance s varies depending on the solubility parameters of a phase and b phase. In the present situation, however, because substance s always exists as a solid state, V_s is considerably large so that the distribution of substance s favors one side (114).

To examine the applicability of equation 20 to predict the distribution of drug substance in the PLA-PLGA biphasic polymeric solution, 5 amino acids with different solubility parameters were selected as model compounds. If

PLGA and PLA separated completely, solubility parameters of the PLGA phase ($\delta_{PLGA/p}$) and PLA phase ($\delta_{PLA/p}$) were calculated by the following equations:

$$\delta_{PLGA/p} = \delta_{PLGA} + (1 - a)\delta_{solv}$$
$$\delta_{PLA/p} = b\delta_{PLA} + (1 - b)\delta_{solv} \quad (21)$$

where a and b are volume fractions of PLGA and PLA, respectively, δ_{PLGA}, δ_{PLA}, δ_{solv} are solubility parameters of PLGA (11.00), PLA (10.69), and solvent (114).

The authors showed that the distribution of drugs was dependent on the solubility parameter difference; that is, in the case of a positive value, drugs had a tendency to be distributed on the PLGA phase; in the case of a negative value, drugs had a tendency to be distributed on the PLA phase; and when the value was close to zero, drugs had a tendency to be distributed on the interface between PLGA and PLA phase.

An additional drug that was evaluated by Matsumoto et al. was cisplatin, known to be one of the most effective anticancer drugs in chemotherapy. However, due to various side effects (e.g., renal disturbances, nausea, vomiting), a lot of care has been taken in its clinical use. To minimize the side effects and to increase the therapeutic effects, it must be possible to restrict the blood level of the drug to the therapeutic level for a long period of time (114).

Cisplatin was predicted to be distributed in the PLGA phase from its solubility parameter (~12.2). This was proven by the fact that the drug was incorporated in the PLGA-rich phase when cisplatin powder was added to the PLGA-PLA biphasic polymeric solution. The distribution of the drug was highly dependent on the mixing ratio of polymers. When the PLGA/PLA ratio was given as 20:80 or 33:67, cisplatin was partitioned to the inner phase (PLGA-rich phase). On the other hand, when the PLGA ratio increased up to 67 or 80%, due to accompanying the phase inversion, the drug powder was distributed in the continuous phase (114).

Cleland et al. described how the administration of a subunit vaccine (e.g., gp120) for acquired immunodeficiency syndrome (AIDS) can be facilitated by a single shot vaccine that mimics repeated immunizations. To achieve this type of vaccine, they developed PLGA microspheres that provide a pulsatile release of gp120. Studies of a water-in-oil-in-water microencapsulation process with either methylene chloride or ethyl acetate as the polymer solvent revealed that the encapsulation efficiency was greatly enhanced by increasing the kinematic viscosity of the polymer phase via a reduction in temperature (~0°C) and an increase in polymer concentration. Excess methylene chloride (1.5% v/v) in the second emulsion reduced the encapsulation efficiency, whereas excess ethyl acetate (9% v/v) in the second emulsion was necessary for microsphere formation. The optimization of process variables allowed for complete encapsulation of the gp120 (100% efficiency). Drying of the microspheres had a significant impact on the initial emulsion, the density of the inner emulsion water droplets in the microspheres was reduced requiring significant polymer erosion to occur prior to protein release. The protein was released under physiological conditions in two discrete phases: an initial burst released over the first day and after several weeks or months a second burst of protein was released. The second burst of protein was dependent upon the PLGA inherent viscosity and lactide:glycolide ratio (bulk erosion). The initial gp120 released under physiological conditions as well as the gp120 extracted from the microspheres maintained their native conformation, as measured by a variety of physicochemical methods. Thus, PLGA or PLA microsphere formulations were developed to provide a second burst of gp120 to mimic immunizations at 1, 2, 3, or 6 months. A single administration vaccine for gp120 may then include two or more microsphere formulations resuspended with soluble gp120 (primary immunization) to provide three immunizations or more over the course of one year (115).

Sah (117) developed a process in which ethyl acetate was used to prepare DL-PLGA microspheres. They first emulsified a polymer/ethyl acetate solution with a 1% aqueous PVA solution (W_1) to make an oil-in-water (O/W_1) emulsion. The $O:W_1$ phase ratio was carefully chosen so as to saturate the W_1 by a small proportion of the dispersed solvent and to form successfully embryonic microspheres without generating polymer precipitates. The effects of the $O:W_1$ phase ratio on the morphology and size of microspheres were interpreted in terms of the solvent miscibility with water, as well as the influence of the W_1 volume on breakup of the dispersed phase. The extraction rate of ethyl acetate from the nascent microspheres was then adjusted by making use of both its miscibility with water and its volatility at atmospheric pressure. Variation of these parameters made it possible to fabricate hollow or matrix-type microspheres with different size distributions. It was also found that the tendency of microspheres to aggregate on drying was related to the extent of microsphere hydration and the residual ethyl acetate in wet microspheres, which probably decreased the glass transition of the polymer.

The use of methylene chloride may impose a problem in obtaining product approval by regulatory agencies. As evidenced by Lupron Depot, a small amount of methylene chloride remaining in a microsphere product is acceptable by the U.S. FDA, but only if the product's therapeutic benefits clearly outweigh a safety concern over the residual solvent. However, when faced with a microsphere product to be marketed as preventive medicament, such as a vaccine, the regulatory agency may raise a concern over the possible risk that the residual solvent triggers: methylene chloride is a suspected carcinogen and mutagen. In recognition of this issue, a number of investigations have sought safer solvents (Table 7). Among those found, ethyl acetate is considered one of the most preferable solvents (116).

Thompson et al. (117) developed biodegradable controlled release microspheres containing rismorelin porcine, a potent analog of growth hormone-releasing hormone (GHRH), using DL-PLGA in a modified solvent evaporation technique. Rismorelin porcine microspheres were prepared with a modified solvent evaporation technique to reduce water leeching of the peptide. A typical batch of microspheres is 2 g, consisting of polymer and drug. Ten percent weight/weight rismorelin porcine-containing microspheres were fabricated by dissolving 1.8 g of PLGA in 50 mL of methylene chloride. To this polymer

Table 7. News Solvent for Solvent Evaporation Process

Solvent	Preparation method
Acetone	A salting-out procedure using an electrolyte-saturated continuous phase
Ethyl acetate	Rapid freezing of a polymeric phase in a liquefied gas, followed by solvent extraction
Ethyl formate	In situ solidification of polymeric materials due
N-methyl-2-pyrrolidone dimethyl sulfoxide	To dissipation of solvents to external aqueous media
Methylethyl ketone	A solvent extraction technique making use of partial water-miscibility of the solvent
Phthalic acid diethyl ether	Freeze-drying of the polymeric solution by ball milling to produce randomly shaped particles

solution, 200 mg of micronized rismorelin porcine was added, forming a suspension of drug in the polymer solution. The viscosity of this polymer solution/drug suspension was intentionally kept low to aid in the formation of small, spherical microspheres. The suspension was sonicated at room temperature for approximately 1 minute to disperse the micronized rismorelin porcine particles. The polymer solution/drug suspension was emulsified with stirring into 250 mL phosphate-buffered saline (PBS) containing 0.4 w/v % AIRVOL™ PVA as an emulsifier to form an oil-in-water emulsion. Rismorelin porcine is insoluble in PBS and other salt-containing solutions. The partitioning of drug into the aqueous phase did not occur under these conditions. Stirring at 300 rev/min was continued at room temperature for approximately 16 hours to allow complete solubilization and evaporation of methylene chloride. The resulting rismorelin porcine microspheres were recovered using vacuum filtration, washed with PBS, dried under vacuum in a desiccator, and sieved to size using 60 mesh and 120 mesh U.S. Standard sieves (250 μm and 125 μm, respectively). Rismorelin porcine PLA/PGA microspheres with different loading values (5%, 10%, and 25%) were prepared by varying the ratio of drug to polymer in the suspension solution (117). Release rates of rismorelin porcine were characterized in vitro by use of a cell perfusion system and evaluated in vivo in pigs. Rismorelin porcine is 4-methylhippuroyl (1) porcine GHRH (2-76)-OH, which is a potent analog of a natural porcine GHRH. The biological efficacy of the rismorelin porcine microspheres was determined in swine by urinary urea nitrogen depression as well as by serum blood urea nitrogen. The physical site of injection of microspheres did not influence release profile in swine. In vivo release of rismorelin porcine from microspheres ceased after 9 to 12 days in all studies.

Diaz et al. (118) studied DL-PLGA microspheres of ^{125}I-bovine calcitonin prepared by the double emulsion technique (including Tween® 80 in the water phase and Span® 60 in the oil phase of the first emulsion) in vitro and in vivo. The release of ^{125}I-bovine calcitonin was determined in vitro at 37°C in isotonic phosphate buffer (pH 7.4). ^{125}I-bovine calcitonin microspheres (5 mg) were administered under the skin on the back of Wistar rats and the radioactivity at the injection site was subsequently measured over a 6-week period. The in vivo and in vitro ^{125}I-bovine calcitonin profiles were affected by the surfactant agents, but in vivo release was much faster than in vitro. Following injection in rats, microspheres made with Tween® 80 and Span® 60 to give a HLB value of 6 and 8 in the first emulsion, released 20 and 14% of the radioactivity within the first 24 hours, but only 1.3 and 1.2%/day at later times (up to 6 weeks), respectively. Under these conditions, they take 8 and 10 weeks, respectively, to release the total amount of calcitonin.

FITC-labeled bovine serum albumin has been entrapped in sub-5 μm particles of DL-PLGA using a W/O/W solvent evaporation technique. The concentration of PVA stabilizer in the external continuous phase was found to affect not only the particle size, size distribution, and protein content, but also the release characteristic and internal structure of the microparticles. The importance of primary emulsification was underlined by the finding that the protein content of microparticles with a mean size of 1 mm could be increased from about 1% W/W to around 12% W/W by increasing the amount of protein added to the primary emulsion and the homogenization time in this stage. Under conditions of low stabilizer concentration, multinucleate particles were formed by polymer precipitation and envelopment of the droplets of the primary W/O emulsion. In this case surface protein loading was on the order of 30% W/W. Under conditions of high PVA stabilizer concentration, disruption of the primary emulsion occurred, resulting in submicrometer particles which were characterized by a high surface protein loading on the order of 70% W/W. A mechanism for protein microencapsulation was presented which is heavily influenced by the shear stresses induced during the process of secondary emulsification (119).

Effects of additives on the drug release kinetics from biodegradable matrices is an important determinant in designing a drug delivery system. Song et al. (120) studied the influence of an array of additives on the drug release from double-layered PLGA matrices. Various additives such as L-tartaric acid dimethyl ester, Pluronic® F127 (F127); 2-hydroxypropyl derivative of β-cyclodextrin (HPB), methyl derivative of β-cyclodextrin and Beeswax (Wax), differing in molecular size, hydrophilicity, and steric configuration were selected for this study. An antiproliferative 2-aminochrome, U-86983 (U-86, Pharmacia and Upjohn), was used as a model agent for local delivery for the inhibition of restenosis. The in vitro release of U-86 from PLGA matrices without additive showed typical biphasic release kinetics, i.e., a slow diffusion release (Phase I) followed by a fast erosion-mediated release (Phase II). Water-soluble additives in the PLGA matrices changed the biphasic release pattern to a near monophasic profile by increasing the release rate of the Phase I. Increasing the ratio of additives to PLGA in matrices causes a significant increase in the U-86 release rates. The high molecular weight, water-soluble additive, F127, resulted in a matrix showing perfect zero-order release kinetics. The water-soluble cyclodextrin derivative, HPB, gave the highest release rate among all the matrices formulated. A hydropho-

bic additive, Beeswax, however showed biphasic release kinetics comparable to PLGA control matrices, but delayed the onset of the Phase II by 4 days. The morphological evaluation of matrices by SEM suggests that the water-soluble additives are leachable and thus generate a highly porous structure in the matrices. The matrix pore configuration (e.g., interconnected or closed) created with different additives determined the mechanism of drug release kinetics from the various matrix formulations.

Jager-Lezer et al. (121) examined the release kinetics of a water-soluble drug from two different W/O/W multiple emulsions prepared with two lipophilic surfactants at different concentrations. The study of the kinetics under both iso-osmotic and hypo-osmotic conditions allowed the author to distinguish between two possible release mechanisms, swelling-breakdown or facilitated diffusion. The results obtained indicate that water-soluble drug release occurs by a mechanism of swelling followed by a breakdown of the oil globules, in which the lipophilic surfactant is a decisive factor. It appears that the globule's swelling capacity is considerably increased when the lipophilic surfactant concentration increases, and the more the oil globule swells, the less the water-soluble drug releases. It seems that the stability could be improved by increasing the lipophilic surfactant concentration which could strengthen the interfacial film. In contrast, an excess of hydrophilic surfactant destabilized the emulsion.

Laugel et al. (122) studied the efficiency of suitable tracer incorporation in the aqueous inner phase for multiple emulsion studies. The use of dihydralazine as tracer allowed the evaluation of both the yield of preparation and the stability of eight multiple emulsions. In these, concentrations of several components were optimized, e.g., oil, lipophilic and hydrophilic emulsifiers, coemulsion and viscosity increasing agents. From entrapment data and droplet breakdown curves calculated from the dihydralazine chromatographic data, one emulsion was selected to study the release of some encapsulated moisturizing solutes such as urea, chitosan, and poly(ethylene glyco). Dihydralazine proved of value to discriminate between the two mechanisms responsible for the solute release, i.e., the breakdown of the multiple droplets and the diffusion of the solute through the oil layer. Diffusion curves were obtained from the levels of moisturizing substance in the outer aqueous phase, corrected by the amounts liberated by the droplet breakdown, calculated through dihydralazine levels. The lipophilicity of the solutes measured under conditions similar to those partitioning in the emulsions correlated with the diffusional route of solute transfer. Thus, the partition coefficient was an efficient parameter to predict the importance and the rate of the diffusion.

A mathematical model was developed by Li et al. (123) for the formation of PLGA microspheres loaded with a peptide using solvent extraction/evaporation methods. Intrinsic variables, such as solvent–polymer interaction parameters, and extrinsic variables, such as dispersed phase/continuous phase ratio, temperature and dispersed phase composition, were evaluated. A mathematical model based on mass transfer was developed by incorporating these variables and, by superimposing with the state of phase transition, the model was used to predict the microsphere properties. The mass transfer in the dispersed phase was based on diffusion theory and was a function of the driving force of chemical potential gradient and transport parameters. The solvent removal process involved solvent diffusion out of the dispersed phase followed by evaporation at the continuous phase–air interface, a process which can be facilitated by forced convective flow. Mathematically, the process can be expressed by coupling the equations for mass transfer in the dispersed phase and first order evaporation from the continuous phase. Two phase transitions, the viscous and glassy boundaries, were used to represent the phase transitions in the polymer solution. The phase transition can be superimposed on the composition profile in the dispersed phase; the solidification of microsphere can be evaluated from such a treatment (123).

Izumikawa et al. (124) studied the physiochemical properties of progesterone-loaded poly(L-lactide) microspheres prepared by the solvent evaporation method. The solvent evaporation process was found to govern the physical characteristics of microspheres. Solvent removal at atmospheric pressure yielded microspheres of crystalline polymer matrices, whereas faster solvent removal under a reduced pressure gave microspheres of amorphous polymer matrices. The crystallinity of the polymer matrices was closely correlated with the morphology and physical properties of microspheres, and affected the drug release rate. The microspheres of crystalline polymer matrices had rough surfaces with large surface areas, and exhibited a rapid drug release, whereas the amorphous microspheres provided a slower drug release. The results of X-ray powder diffraction, differential scanning calorimetry (DSC), and Fourier-transform infrared (FTIR) spectroscopy suggested that progesterone formed a molecular dispersion in the amorphous polymer matrices.

COMPLEX COACERVATION: GELATIN AND GUM ARABIC

When oppositely charges polyelectrolytes with a relatively low charge density are mixed at an appropriate temperature, pH, and concentration, a liquid polyelectrolyte complex called a complex coacervate is formed (11,22,32,80) The first commercial microencapsulation process used complex coacervates formed by acid precursor gelatin and gum arabic. Figure 11 is a schematic diagram of this encapsulation process.

The first step is to form a solution of gelatin (≈11 wt %) in 45–55°C water and gum arabic (11 wt %) in 45–55°C water. Distilled or deionized water must be used to avoid problems with solution. In most cases, high bloom strength (250–300 bloom) acid precursor gelatins were used, although lower bloom strength gelatins (150–225 bloom) can also be used. Bloom strength is a measure of how strong a gelatin sample forms and is indirectly related to gelatin molecular weight. High bloom strength gelatins tend to produce high molecular weight gelations and low bloom strength gelations tend to produce low molecular weight gelations, though there is not a direct correlation between bloom strength and molecular weight.

Once the gelatin and gum arabic solutions are prepared, the drug being encapsulated is emulsified or dispersed in

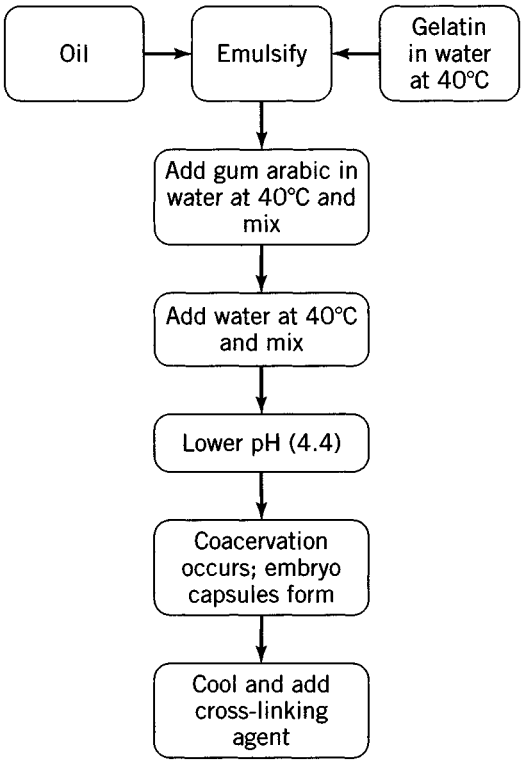


Figure 11. Microencapsulation by complex coacervation.

the 45–55°C gelatin solution. The drug is kept at the same temperature as the gelatin solution when the emulsion is made. The emulsion when formed should be above 45°C. Once the drug/gelatin emulsion or dispersion is formed, it is diluted by addition of a known volume of 45–55°C distilled (or deionized) water and 11 wt % gum arabic solution (45–55°C). The pH of the resulting mixture is adjusted to 3.8–4.4 by addition of acetic acid. The concentration of the acetic acid used can range from 10% (v/v) to glacial.

After the pH is adjusted, the system is allowed to cool slowly to room temperature. The system is stirred gently throughout this cooling period. Once room temperature is reached, the encapsulation mixture is cooled below 10°C and at this point, glutaraldehyde is added to cross-link the polymers. The pH of the system can then be raised to 9–10 with aqueous sodium hydroxide. The system is finally allowed to increase slowly to room temperature and the glutaraldehyde reaction proceeds for at least several hours (an overnight reaction is usually most convenient).

Slow cooling from 45 to 55°C to room temperature is essential to the success of the GGA encapsulation process. During this cooling process, the liquid coacervate slowly deposits around the core agent thereby forming embryo microcapsules. If the system is cooled too quickly, much of the GGA coacervate does not deposit around the active agent, but remains as discrete coacervate drops. (Such drops are called free coacervate and contain no active agent). Free coacervate is very undesirable, because coating material located in free coacervate drops is coating material not deposited around the active agent being encapsulated.

Rabiskova and Valaskova (32) encapsulated drugs that are often applied as solutions in plant oils. The encapsulation of the oils in the complex coacervate microcapsules can be improved by the addition of surfactants. Rabiskova used soybean, olive, and peanut oils as the representatives of plant oils. Using complex coacervation of gelatin and acacia they have found that when the surfactants with HLB values from 1.8 to 6.7 were used, the amount of encapsulated oil was high (65–85%). A significant decrease of the oil content in the microcapsules was found when Tween® 61 (HLB = 9.6) had been added to the mixture. No oil was found inside the microcapsules from the coacervate emulsion mixture containing Tween® 81 (HLB = 10) and Tween® 80 (HLB = 15), respectively.

ORGANIC PHASE SEPARATION: COACERVATION

Two chemically different polymers dissolved in a common solvent are usually incompatible. Thus, such a mixture separates into two phases. One phase is rich in one polymer, whereas the second phase is rich in the second polymer. As long as the phase containing the desired coating polymer preferentially wets or adsorbs on the surface of the core phase or drug, then embryo microcapsules spontaneously form which can be isolated and dried.

Figure 12 is a schematic diagram of a typical encapsulation process based on polymer–polymer incompatibility (58,125). The polymer that is to serve as the capsule wall

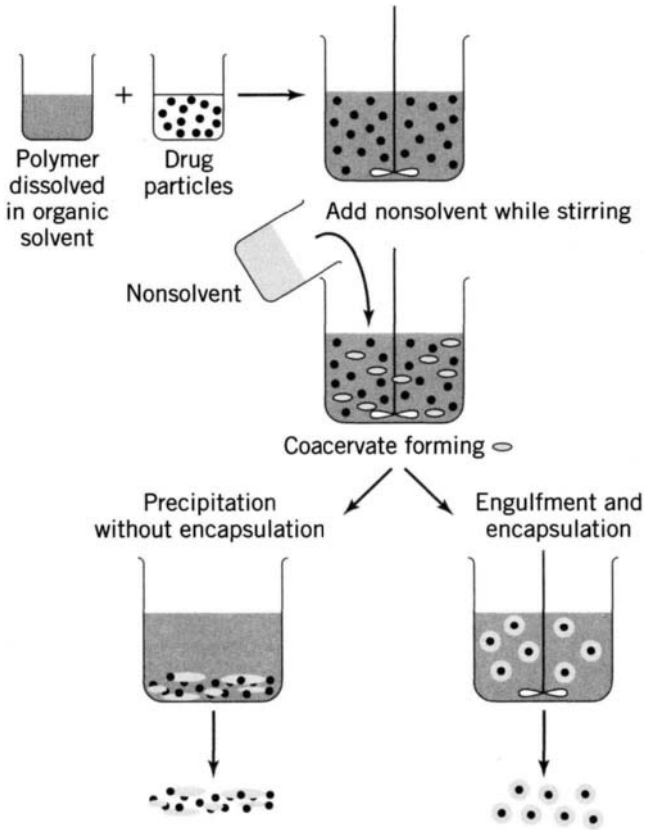


Figure 12. Microencapsulation by coacervation.

material is dissolved in an organic solvent. The material to be encapsulated is then added to this solution and an emulsion or dispersion is formed. To this emulsion a second polymer, or nonsolvent, that is incompatible with the capsule wall material is added. In Figure 12 it is nonsolvent but it could be cottonseed oil, silicone oil, low molecular weight polybutadiene, or any of a number of other materials. This second polymeric material is called the phase inducer and causes the coating material to phase separate. As long as the coating phase adsorbs on the core material, embryo capsules are formed. The system is then cooled and the embryo capsule walls are chemically cross-linked. Chemical cross-linking makes it possible to isolate the capsules as a free-flowing powder.

One of the polymers used to form the capsule wall could be Elvax® 40, a Dupont ethylene vinyl acetate copolymer that contains 40 wt % vinyl acetate. Fifty percent of the vinyl acetate units are hydrolyzed to form vinyl alcohol units. The latter are the units which react and could form a cross-linked or network polymer.

Many researchers have used triangular phase diagrams to describe microencapsulation by coacervation (60,126–129). Madan used phase diagrams to illustrate the coacervate region for several gelatin coacervation processes. He showed that the coacervation inducer could alter the area of coacervate formation on the phase diagram. Benita and Donbrow (60) used a phase diagram to describe the effect of polyisobutylene concentration on the coacervation of ethylcellulose microcapsules. They indicated that a minimum concentration was necessary for the formation of coacervate droplets while a relatively high polyisobutylene concentration prevented phase separation. Phase diagrams have also been used to describe the effect of polyisobutylene on the formation of Eudragit RS microcapsules. Namely, the two liquid phase regions which occurred prior to wall formation may be described, as well as changes in the phase diagrams that were related to occurrences in the microencapsulation process. Phase diagrams have been used to show how various surfactants affected the microencapsulation regions of cellulose acetate phthalate and of cellulose acetate trimellitate (129). Phase diagrams also have been used to describe coacervation as affected by coating polymer concentration, solvent amount, nonsolvent amount, and additives; however, they have not been used to identify potential solvent systems for microcapsule formation or to predict release rates from the microcapsules.

Membrane technology has shown that solubility parameters can be used to select solvents for membrane preparation. Klein and Smith (130) used Hansen's parameters for polarity and hydrogen bonding to form two-dimensional plots for ethylcellulose and cellulose acetate. These plots were then used to predict solvent systems for the formation of asymmetric membranes. Using Hansen's polarity parameters and hydrogen bonding parameters, Chawla and Chang (131) plotted the solubility of cellulose acetate. Several membranes were formed and shown to behave in a predictable fashion based on the solubility parameter of the solvent system. Shen and Cabasso (132) used Hansen's parameters to investigate their solvent systems and a phase diagram to describe how their ethylcellulose membranes were formed. This discussion suggests that potentially useful solvent systems for microcapsule membrane formation could also be chosen using solubility parameters.

Robinson (133) has suggested the use of the solubility parameter, the polymer–solvent interaction parameter and the polymer–solvent interaction parameter for the identification of potentially useful solvents for microcapsule preparation. He determined the solubility of ethylcellulose and plotted the solvent fractional polarity on a two-dimensional map versus the solubility parameter of the system that should be near the limit of the ethylcellulose solubility region for coacervation to occur. Robinson, however, did not report the preparation of microcapsules based on his findings.

Solubility parameters may provide a predictive method by which solvent systems can be chosen for the formation of microcapsules. As shown by the work in membrane technology, it may be possible to predict general structural characteristics of the microcapsule coat, thereby allowing the microcapsules to be formed with desired release rates.

Moldenhauer and Nairn (25) employed a coacervation method using an ethylcellulose and ion-exchange resin–drug complex to show that solubility parameters of the microencapsulation system can be correlated with morphological characteristics and release rates. Microcapsules prepared using solvent mixtures, which had a solubility parameter in the area of a two-dimensional solubility parameter map, usually exhibited similar release rates and morphological characteristics. The ability of polyisobutylene to promote mononucleated microcapsules decreased as the dispersive solubility parameter decreased. Three of the microencapsulation solvent systems were also analyzed using phase diagrams. It was found that the solubility parameter map provided predictive methods of solvents selection for microencapsulation, whereas the phase diagram provided information about the solvent and nonsolvent, with which the phase diagram are formed.

The phase separation of PLGA solutions in methylene chloride induced by the addition of a silicone oil in order to promote protein microencapsulation was studied by Nihant et al. (29). Because the process is very fast, the system was out of equilibrium at all times studied. The effect of the main processing parameters on the microencapsulation process has been analyzed and has highlighted that the kinetics of the main encapsulation steps have a great effect on the characteristics of the final microspheres. These results have been discussed on the basis of a physicochemical study of coacervation.

Ethylcellulose microcapsules containing theophylline were prepared by Sa et al. (134) by the phase separation coacervation process. To induce phase separation a nonsolvent and a variable amount of polyisobutylene were used. Results indicated that the overall release was governed by a diffusion controlled process. No statistical difference was evident between the different sized microcapsules with respect to their drug content, wall thickness, and in vitro drug dissolution profiles. Polyisobutylene was, however, found to influence the release profiles of drug to a great extent. An increase in polyisobutylene concentration retarded the release of theophylline from the micro-

Next Page

capsules due to the formation of small and spheroidal coacervate droplets in larger volumes, which resulted in the formation of more evenly coated microcapsules. Although the release of theophylline from the microcapsules was found to fit both the first-order and diffusion-controlled release processes, differential rate treatment indicated that the overall release was governed by diffusion controlled process (134).

In a different study Bachtsi and Kiparissides (59) developed oil-containing PVA microcapsules that were prepared by the simple coacervation method followed by the chemical cross-linking of the coacervated PVA membrane with glutaraldehyde. The effect of various parameters such as the microcapsule size, the degree of cross-linking of the coacervated polymer membrane, the amount of the desolvating agent, the surfactant concentration, and the ionic strength of the aqueous release medium on the release rate of the oil from the microcapsules into a model surfactant solution was experimentally investigated. It was shown that the oil release rate exhibited first-order kinetics. The permeability coefficient of the santosol oil the PVA coacervated/cross-linked membrane was found to vary from 10^{-4} to 10^{-6} cm/s and was strongly dependent on both the environmental conditions of the release medium and the physical and morphological characteristics of the microcapsules (59).

INTERFACIAL POLYMERIZATION

When two reactive monomers are dissolved in immiscible solvents (e.g., water and an alkane), the monomers diffuse to the oil–water interface where they react to form a polymeric membrane. This phenomenon has been used to form a range of microcapsules. Figure 13 is a schematic diagram of microencapsulation using an interfacial polymerization reaction. The interfacial reaction occurs rapidly and is

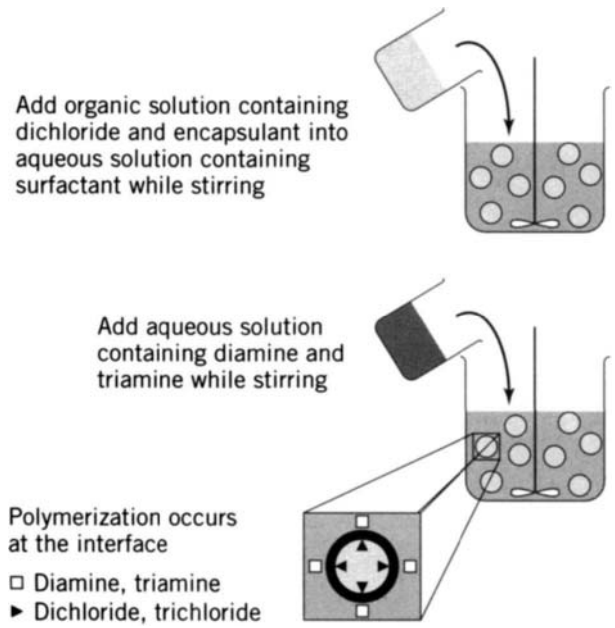


Figure 13. Microencapsulation by interfacial polymerization.

therefore considered a rapid means of preparing microcapsules. It was, however, found to be incorrect for some systems and long reaction times were needed to get strong microcapsules. The preferred acid chloride has relatively long carbon chains between the acid chloride groups, because such acid chloride hydrolyzes slowly at an oil–water interface. The acid chlorides are always added to the oil phase, whereas the amines are always added to the water phase. Isocyanates can be used rather than (or as a partial substitute for) acid chlorides (135). A base could be added to the aqueous phase to neutralize the HCl byproduct formed by reaction of an acid chloride with an amine.

The yield and quality of the membrane of the microcapsules obtained by interfacial polymerization may be controlled by a number of factors, some of which have been listed by Morgan (136). Specifically, in microencapsulation systems the chemical natures of the chloride and amine components and of the solvent, and the conditions under which the polycondensation reaction is performed, determines the nature and molecular weight of the polymer as well as its degree of cross-linking and crystallinity, and whether or not the membrane is porous. Experimental parameters likely to be of importance are the concentrations of the monomers, the temperature, the rate of mixing, and the reaction time. Cohen and Mathiowitz (44) determined the effect of the chemical nature of the monomer components; all reaction parameters were kept constant except for the monomer concentrations and reaction time. During these studies it became clear that the properties of the membrane vary after the initial formation of the microcapsules. There was much evidence that after the formation of the "premembrane" the polymerization proceeds via diffusion of the amine through the membrane where it reacts with the chloride at the inner face of the microcapsule wall. The effective amine concentration at the reaction site is then very much less than in the bulk aqueous solution (44).

Microcapsules were fabricated by preparing an aqueous solution of water and PVA as a surfactant (Fig. 13), and in some cases silane was added as a coupling agent (137). To this solution an organic solution containing the dichloride was added while stirring. After the correct emulsion size was obtained an aqueous solution of diamine was added. The polycondensation reaction which ensued was allowed to continue for different lengths of time. In several cases the silane was added to the chloride suspension prior to the addition of the amine solution. In this way there was an initial formation of a premembrane, resulting from the reaction between the chloride and the amine groups of the silane. After this step the amine was added, in solution, which underwent polycondensation with the chloride. The length of time for the reaction varied with the type of monomer. (For each system the disappearance of the dichloride monomer was followed by thin-layer chromatography.) The time required for the concentration of acid chloride to decrease by 0.5% is called the maturation time. After maturation the microcapsules were separated by decantation, repeatedly washed with distilled water, and dried by rapid washing with acetone (44,137).

Table 8 lists the amine and chloride components used, and Table 9 summarizes the compositions of the monomer mixtures employed. In different attempts the amine/

capsules due to the formation of small and spheroidal coacervate droplets in larger volumes, which resulted in the formation of more evenly coated microcapsules. Although the release of theophylline from the microcapsules was found to fit both the first-order and diffusion-controlled release processes, differential rate treatment indicated that the overall release was governed by diffusion controlled process (134).

In a different study Bachtsi and Kiparissides (59) developed oil-containing PVA microcapsules that were prepared by the simple coacervation method followed by the chemical cross-linking of the coacervated PVA membrane with glutaraldehyde. The effect of various parameters such as the microcapsule size, the degree of cross-linking of the coacervated polymer membrane, the amount of the desolvating agent, the surfactant concentration, and the ionic strength of the aqueous release medium on the release rate of the oil from the microcapsules into a model surfactant solution was experimentally investigated. It was shown that the oil release rate exhibited first-order kinetics. The permeability coefficient of the santosol oil the PVA coacervated/cross-linked membrane was found to vary from 10^{-4} to 10^{-6} cm/s and was strongly dependent on both the environmental conditions of the release medium and the physical and morphological characteristics of the microcapsules (59).

INTERFACIAL POLYMERIZATION

When two reactive monomers are dissolved in immiscible solvents (e.g., water and an alkane), the monomers diffuse to the oil–water interface where they react to form a polymeric membrane. This phenomenon has been used to form a range of microcapsules. Figure 13 is a schematic diagram of microencapsulation using an interfacial polymerization reaction. The interfacial reaction occurs rapidly and is

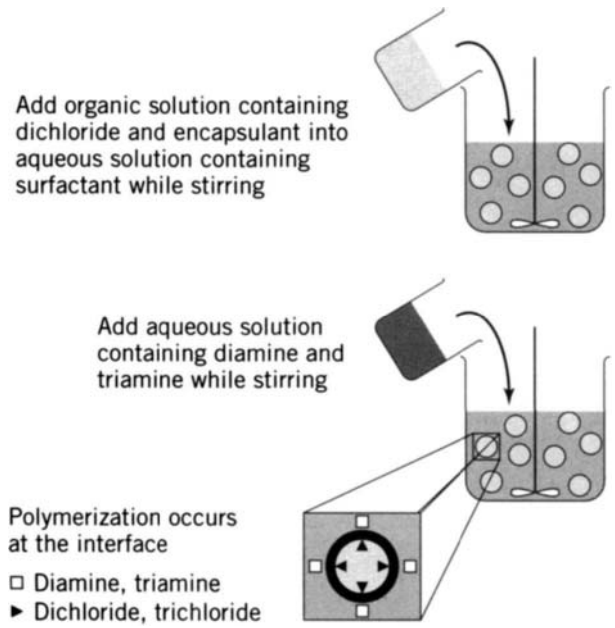


Figure 13. Microencapsulation by interfacial polymerization.

therefore considered a rapid means of preparing microcapsules. It was, however, found to be incorrect for some systems and long reaction times were needed to get strong microcapsules. The preferred acid chloride has relatively long carbon chains between the acid chloride groups, because such acid chloride hydrolyzes slowly at an oil–water interface. The acid chlorides are always added to the oil phase, whereas the amines are always added to the water phase. Isocyanates can be used rather than (or as a partial substitute for) acid chlorides (135). A base could be added to the aqueous phase to neutralize the HCl byproduct formed by reaction of an acid chloride with an amine.

The yield and quality of the membrane of the microcapsules obtained by interfacial polymerization may be controlled by a number of factors, some of which have been listed by Morgan (136). Specifically, in microencapsulation systems the chemical natures of the chloride and amine components and of the solvent, and the conditions under which the polycondensation reaction is performed, determines the nature and molecular weight of the polymer as well as its degree of cross-linking and crystallinity, and whether or not the membrane is porous. Experimental parameters likely to be of importance are the concentrations of the monomers, the temperature, the rate of mixing, and the reaction time. Cohen and Mathiowitz (44) determined the effect of the chemical nature of the monomer components; all reaction parameters were kept constant except for the monomer concentrations and reaction time. During these studies it became clear that the properties of the membrane vary after the initial formation of the microcapsules. There was much evidence that after the formation of the "premembrane" the polymerization proceeds via diffusion of the amine through the membrane where it reacts with the chloride at the inner face of the microcapsule wall. The effective amine concentration at the reaction site is then very much less than in the bulk aqueous solution (44).

Microcapsules were fabricated by preparing an aqueous solution of water and PVA as a surfactant (Fig. 13), and in some cases silane was added as a coupling agent (137). To this solution an organic solution containing the dichloride was added while stirring. After the correct emulsion size was obtained an aqueous solution of diamine was added. The polycondensation reaction which ensued was allowed to continue for different lengths of time. In several cases the silane was added to the chloride suspension prior to the addition of the amine solution. In this way there was an initial formation of a premembrane, resulting from the reaction between the chloride and the amine groups of the silane. After this step the amine was added, in solution, which underwent polycondensation with the chloride. The length of time for the reaction varied with the type of monomer. (For each system the disappearance of the dichloride monomer was followed by thin-layer chromatography.) The time required for the concentration of acid chloride to decrease by 0.5% is called the maturation time. After maturation the microcapsules were separated by decantation, repeatedly washed with distilled water, and dried by rapid washing with acetone (44,137).

Table 8 lists the amine and chloride components used, and Table 9 summarizes the compositions of the monomer mixtures employed. In different attempts the amine/

Table 8. Monomers Used for Preparation of Polyamide Microcapsules

Amine monomers	
Ethylene diamine (EDA)	$NH_2(CH_2)_2NH_2$
Diethylene triamine (DETA)	$NH_2(CH_2)_2NH(CH_2)_2NH_2$
Mixtures of the above two amines	
Hexamethylene diamine (HMDA)	$NH_2(CH_2)_6NH_2$
Hexamethylene diamine/diethylene triamine mixtures	
Triethylene tetramine (TETRA)	$NH_2CH_2CH_2(NHCH_2CH_2)_2NH_2$
Tetraethylene pentamine (TEPTA)	$(NH_2CH_2CH_2NHCH_2CH_2)_2NH$
Bis-hexamethylene triamene (BHMT)	$NH_2(CH2)_6NH(CH_2)NH_2$
BHMT in HMDA mixture	
Chloride monomers	
Terephthaloyl dichloride (Tr)	$1,4\text{-}C_6H_4(COCl)_2$
Trimesoyl chloride (Tm)	$1,3,5\text{-}C_6H_3(COCl)_3$

Table 9. Compositions of Monomer Mixtures Used for Preparation of Microcapsules

Name of batch	Amine:chloride (re. eq.)	Triamine:diamine (rel. eq.)
(EDA,Tr)	30	—
(DETA,Tr)	30	—
(HMDA,Tr)	30	—
(EDA + DETA,Tr)b	30	4:1
(HMDA + DETA,Tr)b	30	4:1
(HMDA + DETA,Tr)b	30	4:1
(EDA, Tm)	30	—
(HMDA, Tm)	30	—

chloride ratio was kept constant (30:1 or 15:1, in equivalent units) in order to avoid effects due to the diminishing monomer concentrations. For cases where the amine:chloride ratio was 30:1, the concentrations were 5.62 and 0.197 mole eq/L, respectively. Because these concentrations were constant, the main variable parameter was the character of the monomer. Note that from the list in Table 8 one could select monomers which are bifunctional or monomers which are of functionality three or higher. The polymer from two bifunctional monomers was linear and when one or both monomers had a functionality of three or higher, the resulting polymer was cross-linked (44).

It can be seen from Table 9 that Cohen and Mathiowitz (44) used an amine:chloride ratio of 15 or 30:1. This is near the upper limit of, or greater than, the ratio used by Morgan. These authors suggested that for amines with partition coefficients of between 14 and 180, amine:chloride ratios of 3 to 17:1 are optimal for obtaining high molecular weight polymers. They measured the partition coefficients for some amines and found values of 22 for HMDA and 27 for DETA, whereas that of EDA must be very high because of its low solubility in the organic phase. Thus the ratios are much higher than those required by Morgan's rule (44).

Reaction time in microcapsule preparation is extremely important in determining the time at which that capsules have attained their maximum impermeability. Consider microcapsules from (EDA,Tr), for, example; these are observed to form very rapidly (44). However, microcapsules separated from the reaction vessel after very short periods proved to be extremely fragile and collapsed even during the drying process. Further, analysis of the Tr content (of the core material; microcapsules were removed from the reaction vessel after various times) showed that an appreciable period is required for complete consumption of this monomer. When EDA was replaced by an amine monomer of higher molecular weight and functionality, it was found that the time required for full maturation was appreciably longer. For example, the approximate maturation times determined were (EDA,Tr) 5 min, (HMDA,Tr) 10 min, (DETA,Tr) 180 min, and (TEPTA,Tr) 240 min (44).

Thermal gravimetric analysis (TGA) is a often-used technique for characterizing polymer thermal stability, but Mathiowitz and Cohen have introduced this technique to determine the mechanical strength of microcapsules and also to study the maturation of the microcapsules immediately after preparation. This method is particularly useful because it enables examination of the individual microencapsulation and thus provides information about the reproducibility of the rate of release amongst a population of microcapsules. This in turn helped us to develop a mathematical model for photochemical rupture (47).

The effect of the reaction time on the thermal behavior of microcapsules from DETA is illustrated in Figure 14. The "immature" capsules released their contents at low temperatures, whereas the mature ones are stable until they reach a sharp rupture temperature. This may be due to more rapid diffusion of the core contents through thinner walls of immature capsules.

The time required for maturation was determined by the diffusion of the amine from the bulk aqueous solution through the membrane to the organic phase. The rate of this diffusion, which is low when compared with the reaction rate of the monomers in solution, is determined by the permeability of the membrane. The permeability, in turn, depends on factors such as the molecular weight of the polymer and the extent of its cross-linking. The growth of the membrane, which accompanies maturation, can be

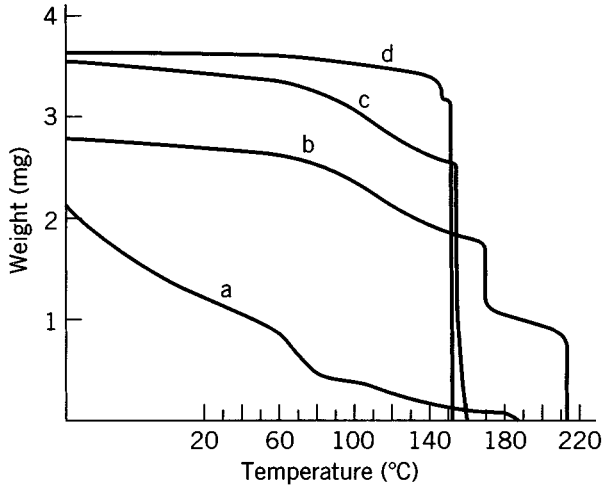


Figure 14. Effect of reaction time on thermal behavior of (DETA,Tr)S microcapsules as measured by TGA: (a) 1, (b) 4, (c) 10, (d) 100 minutes after starting the polymerization reaction. *Source:* With permission from Ref. 45.

seen clearly in electron micrographs (data not shown). After 1 minute the internal side had a smooth internal surface. After 4 minutes, small spheres of polymer were found to be formed on this surface and subsequently grow and cover the whole inner face of the membrane. The results suggest that, throughout the formation of the membranes of linear polymers, the diffusion rate of amine is constant. For the cross-linked polymers, however, there appear to be channels though which diffusion is more rapid. These channels could be voids or could contain a high proportion of polymer which is not cross-linked (44).

An indication of the stability of the membranes to heat can be obtained from TGA measurements. The membranes were prepared either by direct interfacial polymerization or by rupturing microcapsules and were carefully dried before use. In this way it was found that (EDA,Tr), (DETA + EDA,Tr) and (DETA,Tr) all begin to lose weight at 220–230°C, whereas (HDMA,Tr) does so only above 300°C.

Dry membranes were investigated also by DSC. The DSC curve for (DETA,Tr) shows no structure; at about 230°C, where weight loss starts, there was a slight change of slope and as the temperature rises, there was a continuously increasing heat loss. There is no sign of melting up to 450°C. This type of behavior is typical of cross-linked polymers. Visually, one observed that the material chars on heating. By contrast, the DSC curve for (EDA,Tr) shows a melting temperature at 450°C and the glass temperature at 225°C. (EDA + DETA,Tr) membranes also show an endotherm at 70°C, but no melting was observed. Repeated measurements suggest that $T_g \cong 260$°C. Above this temperature the polymer starts to decompose.

FTIR spectra can be very helpful in providing information on the bonding state of polyamides. What prominent features may we expect in these spectra? If there are any residual NH_2 groups present which have not reacted during the polymerization, one expects to see the absorptions corresponding to the stretching modes of NH_2. In both primary amines and primary amides these modes are known to give an intense doublet around 3,450 and 3,225 cm^{-1}. The N-H stretch of secondary amines and amides gives a single strong absorption band near 3,335 cm^{-1}. Amide vibrational spectra are characterized by two intense bands, called amide I and amide II. The first of these is largely due to C = O stretching and is found at 1,665–1,640 cm^{-1}. The amide II band, at about 1,540 cm^{-1}, is due to a coupling of vibrations of C-N and of N-H, when the H is *trans* to the C =.

The FTIR results indicate that during the polycondensation reaction the doublet structure associated with the $-NH_2$ of the amine monomer (Figs. 15a,b,c) disappears and is replaced by an intense singlet (compare Figure 15a with 15d,f, and 15b with 15e,f). In many cases this latter band has a shoulder on the high frequency side. This structured band is undoubtedly the N-H stretch of the secondary amines and amides. It has been found also in other polyamides, and the main peak and shoulder have been assigned to a superposition of "free" and hydrogen-bonded N-H.

On this basis it was concluded that little or no unreacted NH_2 was present in the polymer. However, because of the breadth of the N-H adsorption, it was not possible to conclude that there was none present.

The X-ray powder diffraction patterns of a number of dried membrane materials were recorded for membranes of the (EDA + DETA,Tr) series. There were differences in crystallinity, with (EDA,Tr) > (EDA + DETA,Tr) > (DETA,Tr), and with the last membrane being essentially amorphous. Also, membranes of (HMDA + DETA,Tr) are of higher crystallinity than (DETA,Tr) ones (44). Thus, addition of one of the bifunctional amines EDA of HMDA to the trifunctional DETA in the preparation of the microcapsules leads to membranes of higher crystallinity than those membranes we have shown to be appreciably cross-linked. Morphological studies of microcapsules by SEM and transmission electron microscopy (TEM) were done on each sample. The external and internal faces and a cross section of the membrane wall was evaluated. Preparation for TEM required embedding the samples and cutting by microtome, the latter being difficult because of the fragility of the materials. Most membranes were stained with uranyl acetate which attaches to free amino groups and increases the resolution. Figure 16 capsules of (DETA,Tr) are seen from the external side (some capsules full, some ruptured). The structure is homogeneous and "closed." In fact, most of the membranes we studied looked similar at the external face, but there were differences in the internal faces. The internal faces and membrane cross-sectioning (Fig. 16) of (DETA,Tr) also show quite closed structures. The internal face is hilly, suggesting that the interfacial polymerization takes place in the organic phase. TEM studies (Fig. 16f) of the cross section provide a similar picture, with the polymer density apparently lower in the hills than in the other regions of the membranes. The thickness of the membrane of the (DETA,Tr) microcapsules was 2 μm, as measured by SEM.

Microcapsules of (EDA,Tr) appear nonporous under the optical and scanning electron microscopes. However, SEM

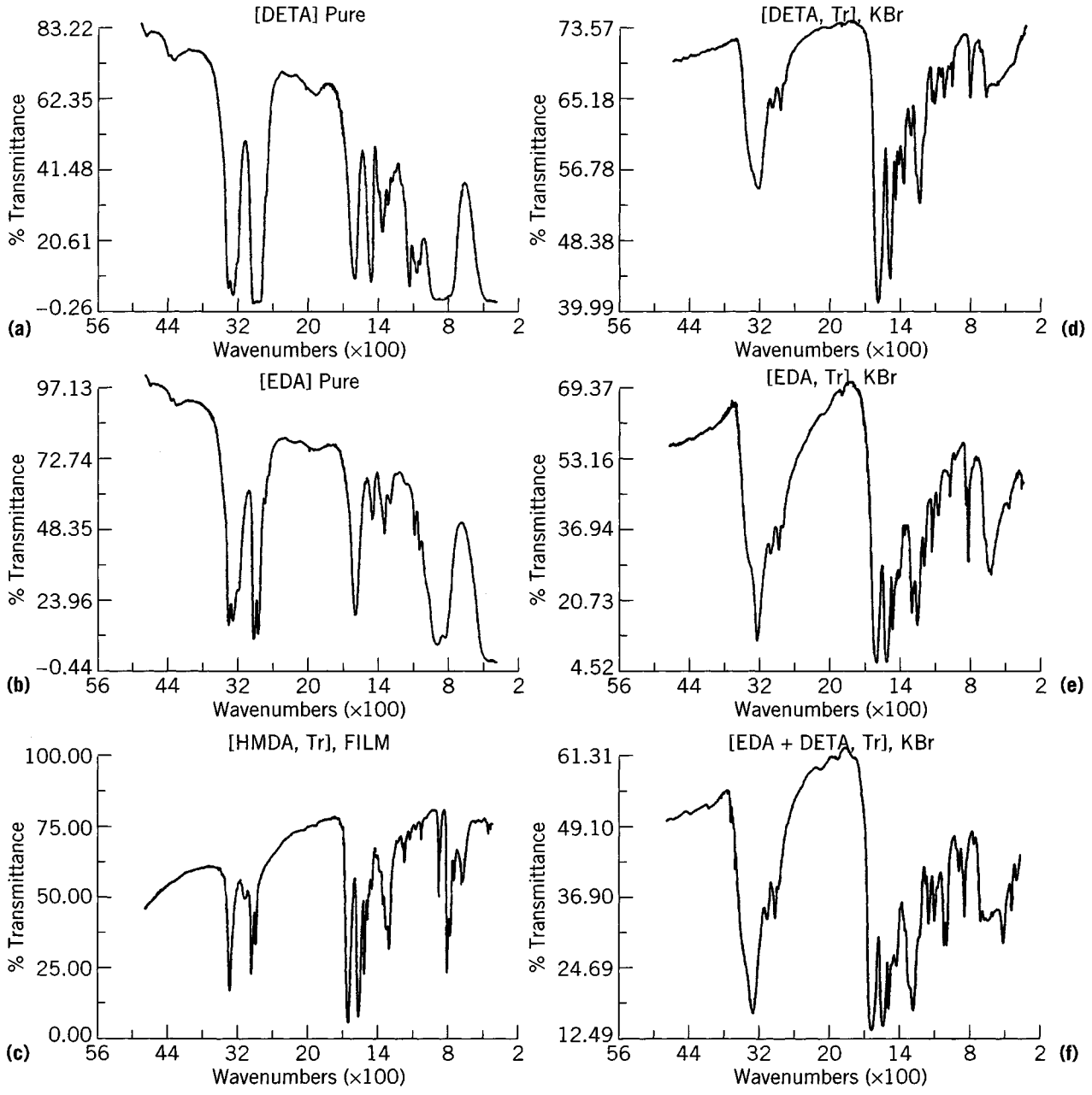


Figure 15. FTIR spectra of some amines and Tr membranes.

examination of the internal face and cross section of the membranes reveal a very porous structure (Fig. 17a,b). This membrane is clearly of the "skinned" type: one side has a closed structure, but the membrane is full of voids. This is shown also in the TEM pictures of the cross section (Fig. 17e). Note that the long axes of the pores lie parallel to the faces of the membrane. These pores are less than 1 μm in diameter, which classifies the membrane as microporous.

Figures 17c and 17d, show the internal face and cross section of such membranes with a double relative concentration of Tr. Here the number of pores is fewer and the internal face more homogeneous, but the structure is still porous.

In Figure 18a we see the internal face of capsule from (EDA + DETA(1:1.5),Tr). The structure is less porous than is (EDA,Tr), as was confirmed by the cross section (not shown). This membrane after silanation is shown in Figure 18b and its cross section in Figure 18e. Such treatment appears to decrease the porosity. An increase of the proportion of triamine further decreases the porosity, as shown for the internal face and cross section of a membrane from (EDA + DETA(1:4),Tr) in Figures 18a,b. In this case the wall thickness was 2.5 μm. In additional papers the use of those microspheres as swelling-controlled, diffusion-controlled, and photochemically controlled delivery systems were studied separately (46–48).

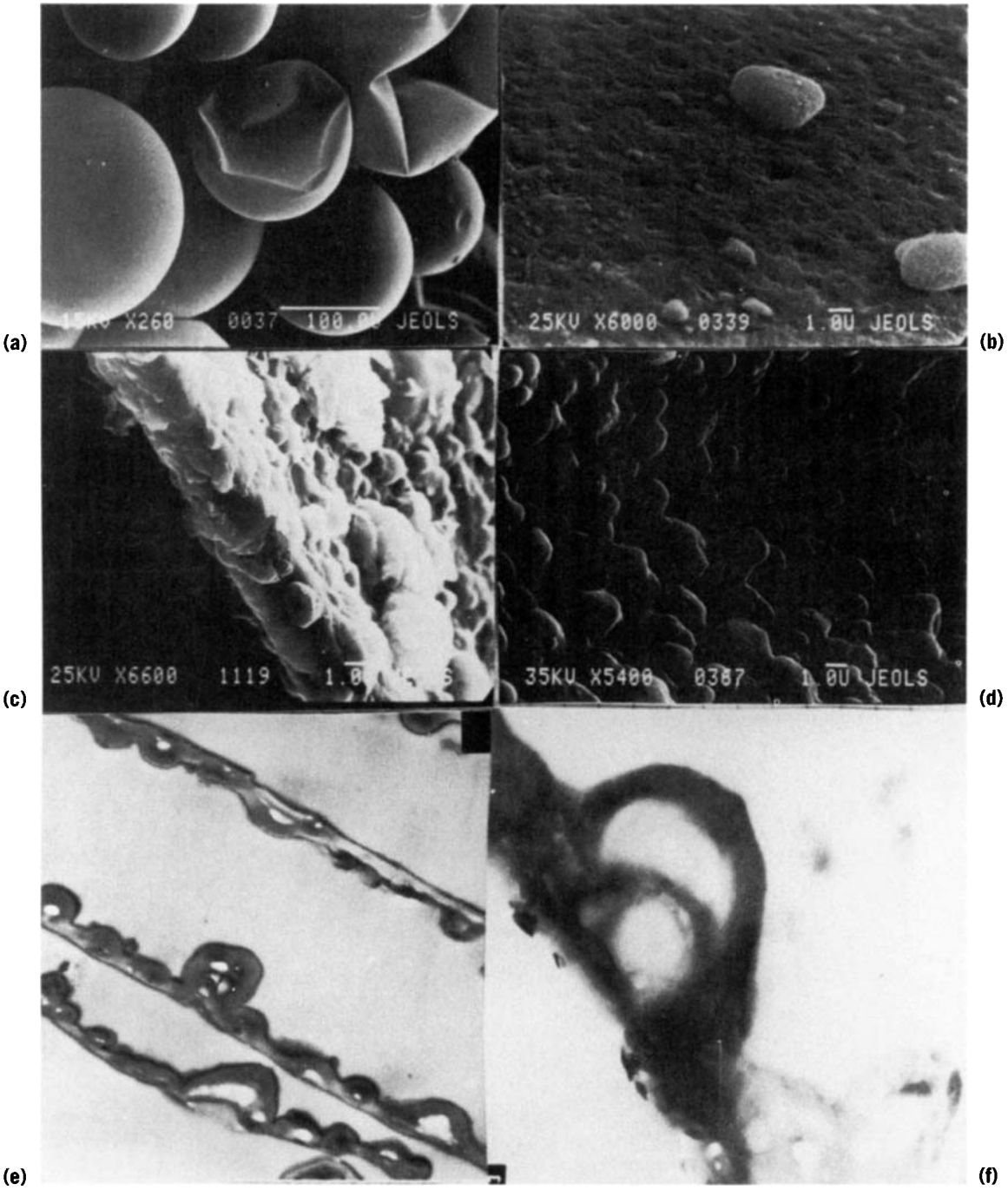


Figure 16. (DETA,Tr) MC: (**a**) SEM of external face; (**b**) SEM of external face; (**c**) SEM of cross section of membrane; (**d**) SEM of internal face; (**e**) TEM of cross section stained with uranyl acetate, ×10,000 (**f**) TEM of cross section, unstained, ×20,000. *Source:* With permission from Ref. 44.

Interfacial Coacervation

The first example of a phase separation process is an extreme case of polymer adsorption used to prepare small capsules (49). In this process Chang dissolved a polymer in the organic phase, and this polymer migrated to the water–organic liquid interface where it precipitated spontaneously from solution to form a membrane. This process is called interfacial coacervation (135). Phase separation in this case is not induced by addition of a nonsolvent, change in temperature, or the presence of incompatible polymers, instead occurring spontaneously at the interface. A good example of this process is the emulsification of an aqueous protein solution in diethyl ether using a nonionic surfactant that is soluble in oil. Sorbitan trioleate (Span® 85) is a good surfactant. The emulsification process gives microcapsules that can easily be separated from the

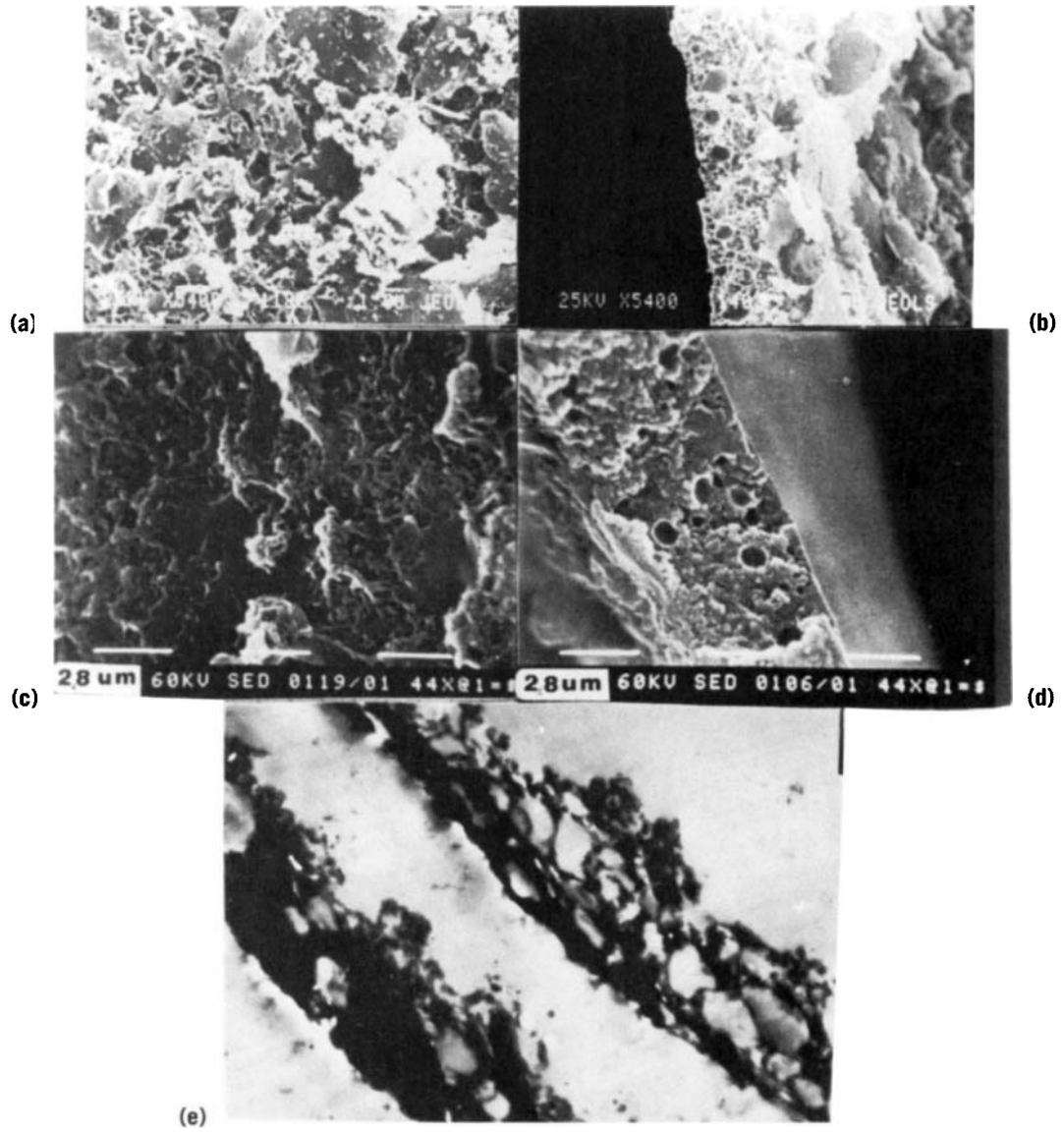


Figure 17. (EDA,Tr) MC: (**a**) SEM of internal face; (**b**) SEM of cross section of same membrane; (**c**) SEM of internal face of (EDA,Tr)x MC; (**d**) SEM of cross section of same membrane; (**e**) TEM of (EDA,Tr) MC shown in (**b**), ×10,000. *Source:* With permission from Ref. 44.

ether suspending medium and resuspended in *n*-butyl benzoate. Chang often used collodian (nitrocellulose) as a wall material, but emphasized that microcapsules can also be formed by interfacial coacervation or precipitation of other polymers using other solvents.

THERMAL DENATURATION

A number of water-soluble proteins are sensitive to heat and can denature when heated. The denaturation process causes the protein chain to unfold and become chemically cross-linked. This insolubilizes the protein and creates a convenient method of forming protein microspheres. Figure 19 is a schematic flow diagram of a process for forming protein microspheres. A relatively concentrated aqueous protein solution (e.g., 20 wt %) is emulsified in an aliquot of oil at room temperature. This emulsion is then poured into an excess of agitated hot oil (120–200°C), which denatures the protein while simultaneously driving off the water. The product is a solid protein microsphere which can be isolated from the oil by a series of settling and decantation steps. The higher the temperature of the hot oil bath, the more thoroughly the microspheres are cross-linked. Proteins suitable for this process include serum albumin and egg albumin.

Jameela et al. (138) produced chitosan microspheres in the following manner. A 4% solution of chitosan in 5% acetic acid containing 2% sodium chloride was prepared. Six grams of this viscous solution was weighed, mixed with progesterone (20% by weight of chitosan) and dispersed in a mixture of 35 mL of liquid paraffin and 25 mL of petro-

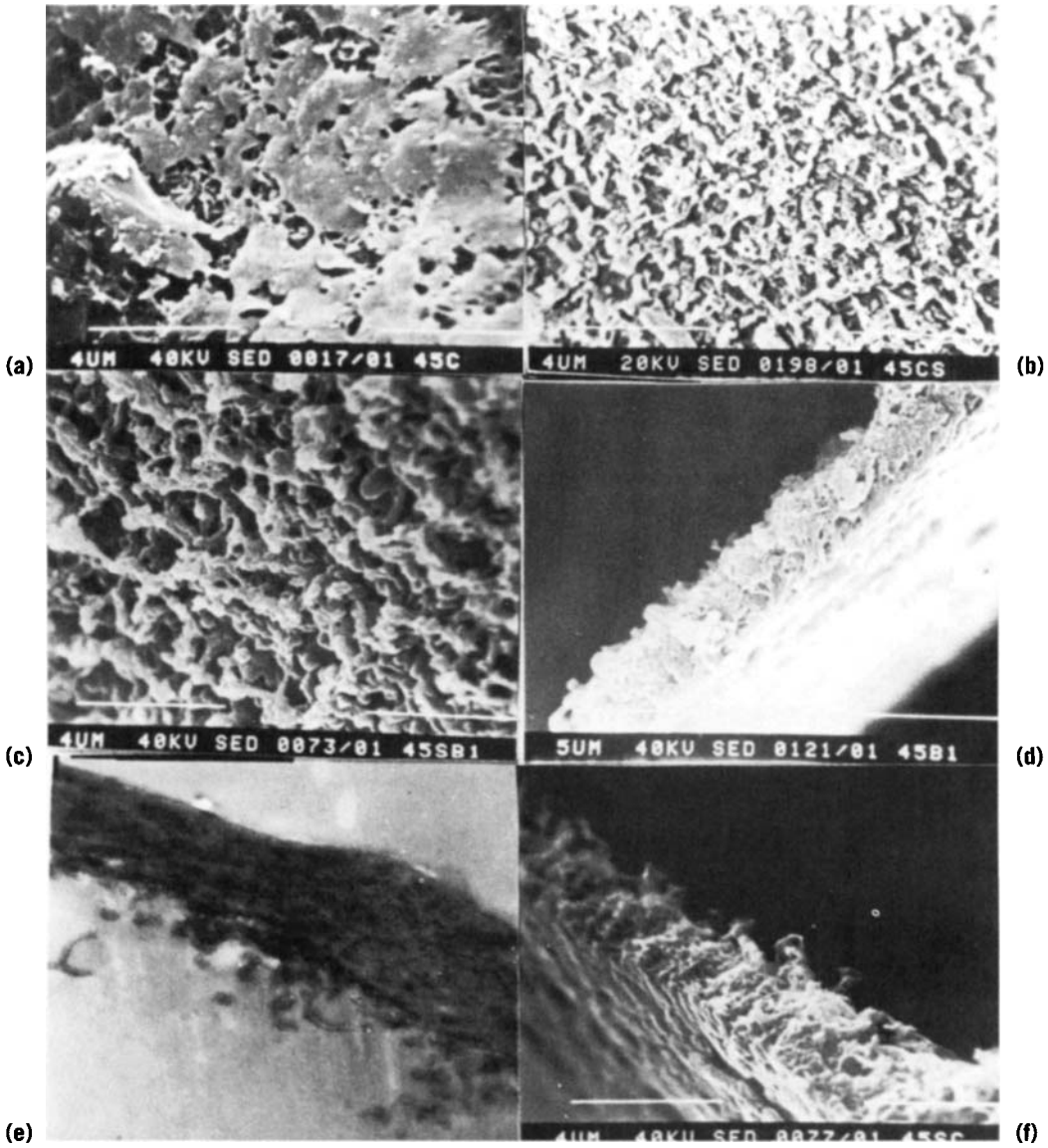


Figure 18. (EDA + DETA,Tr) MC: (**a**) SEM of internal face of (EDA + DETA,Tr)c MC; (**b**) SEM of internal face of (EDA + DETA,Tr)cS MC; (**c**) SEM of internal face of (EDA + DETA,Tr)bS MC; (**d**) SEM of cross section of same MC; (**e**) TEM of same MC shown in (**b**), ×10,000; (**f**) SEM of cross section of MC shown in (**b**). *Source:* With permission from Ref. 44.

leum ether containing 0.85 g of sorbitan sesquioleate, in a 100-mL round-bottomed flask at room temperature (27°C). The dispersion was stirred at 2,000 rpm for 5 min, and then 10 mL of glutaraldehyde-saturated toluene was introduced into the flask and the stirring continued. Microspheres were prepared using different amounts of glutaraldehyde saturated toluene for cross-linking. Highly cross-linked microspheres were prepared by adding 1 mL aqueous glutaraldehyde at the end of 30 min, in addition to 10 mL of glutaraldehyde-saturated toluene which was introduced initially. The cross-linking reaction was allowed to proceed for a total of 1.5 hours. The hardened microspheres were then separated by centrifugation, washed four times with petroleum ether, once with acetone, once with a 5% solution of sodium metabisulphite, three times with water, centrifuged, vacuum-dried at room temperature and stored in a desiccator. Progesterone content in the microspheres was measured by extracting 5 mg of powdered microspheres with three 5 mL portions of ethanol, filtering the solution through a 0.45 μm filter and assaying spectrophotometrically at 247 nm. Particle size analysis of the microspheres was done using standard test sieves. Particles that passed through one sieve, but retained on the other were collected and weighed in an analytical balance, and the percent weight distribution was plotted against size (138).

The extent of drug release had a remarkable dependence on the cross-linking density of the microspheres, the highly cross-linked spheres releasing only around 35% of the incorporated steroid in 40 days compared to 70% from

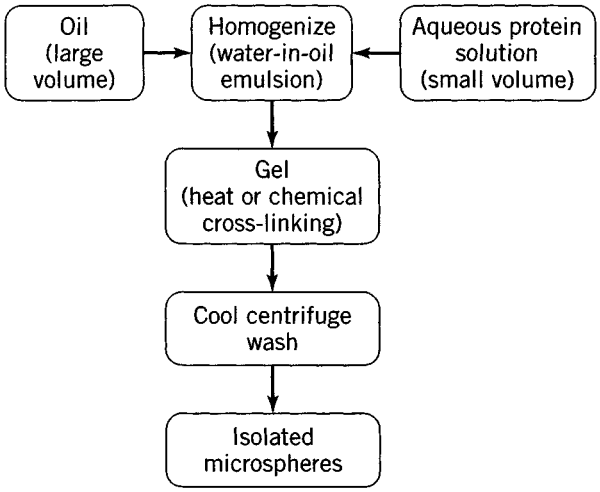


Figure 19. Thermal denaturation process.

spheres lightly cross-linked. Determination of the in vivo bioavailability of the steroid from microsphere formulation by intramuscular injection in rabbits showed that a plasma concentration of 1 to 2 ng/mL was maintained up to 5 months without a high "burst effect." Data obtained suggest that the cross-linked chitosan microspheres would be an interesting system for long term delivery of steroids (139).

Modena et al. (139) investigated hyaluronidase injectable microparticles. The goal of these researchers was to obtain a sustained release preparation of hyaluronidase or to use the enzyme as drug carrier. Microspheres were prepared by emulsification of the protein and were cross-linked either by thermal or chemical means. Results show that hyaluronidase microspheres with good morphological characteristics can be obtained by this preparation method.

Heelan and Corrigan (140) used whey protein (WPI) microspheres containing hydrochlorothiazide, eosin, blue violet, and sodium salicylate. The release of these compounds from WPI microspheres occurred rapidly, with at least 70% of the incorporated material released for all systems within the first 20 minutes. Release of microsphere contents was essentially complete within one hour. The degree of glutaraldehyde cross-linking was found to have no effect on the release profile, for durations of cross-linking up to 24 hours. Out of a range of release equations examined, the experimental release data was best described by a biexponential equation, and this agrees with the work of others for the release of drugs from albumin microspheres. Swelling of the microsphere systems was examined as this may contribute to the rapid release of drug from these systems.

Akbuga and Bergisadi prepared cross-linked chitosan microspheres containing 5-fluorouracil (5-FU). Variables included drug and chitosan concentrations, the cross-linking process, the type of oil, stirring rate, and additives. Initial 5-FU concentration, the type and concentration of chitosan, the viscosity of oil phase and glutaraldehyde concentration affected drug release for chitosan microspheres. 5-FU release from cross-linked chitosan microspheres is characterized by an initial rapid release of drug. Addition of substances such as alginic acid, chitin, agar, sodium caprylate, and stearic acid changed the release properties of 5-FU microspheres.

Monodisperse albumin micropheres were prepared by Muramatsu and Nakauchi (142) Uniform-sized emulsion droplets were successfully obtained by passing an albumin solution through the membrane and into kerosene at appropriate, applied pressures. After heating the emulsion monodisperse albumin microspheres were prepared. The heat-denaturing process itself did not affect the monodispersity once uniform emulsion droplets had been prepared. The shape and size of the albumin microspheres were strongly dependent on the concentration of the albumin solution and the heat denaturing temperature. Lower albumin concentrations produced nonspherical particles and higher denaturing temperatures made the particles smaller. Incorporated riboflavin released quite rapidly from the albumin microspheres, and increases in both albumin concentration and denaturing temperature caused the drug release to be sustained, presumably because a rigid and dense matrix was formed within the albumin microspheres.

Chitosan microspheres containing phenobarbitone were successfully prepared by glutaraldehyde cross-linking of an aqueous acetic acid dispersion of chitosan in light liquid paraffin containing sorbitan mono-oleate as a stabilizing agent. Uniform and spherical microspheres, with a loading efficiency up to 57.2%, could be fabricated, depending on the conditions. The main parameters which affected the preparation and performance of the microspheres were the molecular weight and concentration of chitosan as well as the concentration of the stabilizing agent. The incorporation of citric acid into the microspheres was found to increase the formation of a water-soluble gel when the microspheres come in contact with the dissolution medium, increasing the rate of drug release. The particle size was shifted toward smaller diameters with increased concentration of chitosan (1% w/v) and chitosan with low molecular weight. Rapid initial release (20–30% of the incorporated drug) was exhibited in all the prepared microspheres followed by slow release of the remaining drug. The release rate of the drug from the microspheres of high molecular weight chitosan was slow in comparison with that prepared from medium and low molecular weight chitosan. High concentrations of sorbitan mono-oleate increased the rate of the drug release (143). Lim and Wan (63) prepared chitosan microspheres by preparing a W/O emulsion comprising a mixture of light and heavy liquid paraffins containing sodium dioctyl sulphosuccinate as the oil phase and a chitosan solution as the aqueous phase. Pentasodium trypolyphosphate was included as a counterion. The chitosan microspheres obtained showed a high degree of aggregation. This was markedly reduced by the incorporation of magnesium stearate in the dispersed phase. The resultant microspheres were discrete and spherical with smooth surfaces. Additionally, with an increasing magnesium stearate content, larger-sized microspheres were produced. The DSC analysis data suggested that the magnesium stearate was converted to stearic acid during the

preparation process. Chitosan microspheres containing propranolol hydrochloride were similarly prepared, but their surface was convoluted and their shape was not well defined. Unlike the microspheres without drug, the size of the drug-loaded microspheres decreased with increasing magnesium stearate content. The release of propranolol hydrochloride from the microspheres was fast, irrespective of the content of magnesium stearate. Drug encapsulation efficiency was enhanced when a greater amount of magnesium stearate was used (63).

GELATION: ALGINATE

One of the most important and useful properties of alginates is the ability to form gels by reaction with calcium salts (Fig. 20). These gels, which resemble a solid in retaining their shape and resisting stress, consist of almost 100% water (normally 99.0–99.5% water and 0.5–1.0% alginate). A gel, in classical colloid terminology, is defined as a system which owes its characteristic properties to a cross-linked network of polymer chains which form at the gel point. A considerable amount of research has been carried out in recent years to elucidate the nature of the cross-links and determine the structure of alginate gels.

It had been suggested that the cross-links were caused either by simple ionic bridging of two carboxyl groups on adjacent polymer chains via calcium ions or by chelation of single calcium ions by hydroxyl and carboxyl groups on each of a pair of polymer chains. Although these bonds may play a role in the gelation mechanism, they are not sufficiently energetically favorable to account for the gelation of alginate. It has been shown on the basis of fiber diffraction data and model-building calculations that the shape of both polymannuronic acid segments and the polyguluronic acid segments of alginic acid is ribbon-like and extended, and that these extended ribbons can stack together in sheets. On the basis of these data and the properties of gels, it has been suggested that the cooperative association of either polymannuronic acid segments or polyguluronic acid segments is involved in the formation of the cross-linked network of polymer chains.

Lim et al. developed a method of enclosing viable cells, tissues, and other labile biological substances within a semipermeable membrane. Preliminary in vitro studies of several types of microencapsulated cells and tissues (red blood cells, sperm cells, hepatoma cells, hepatocytes, pancreatic endocrine tissues, and islets) were described by Lim (19). Essentially, the process involves suspending the living cells or tissues in sodium alginate solution.

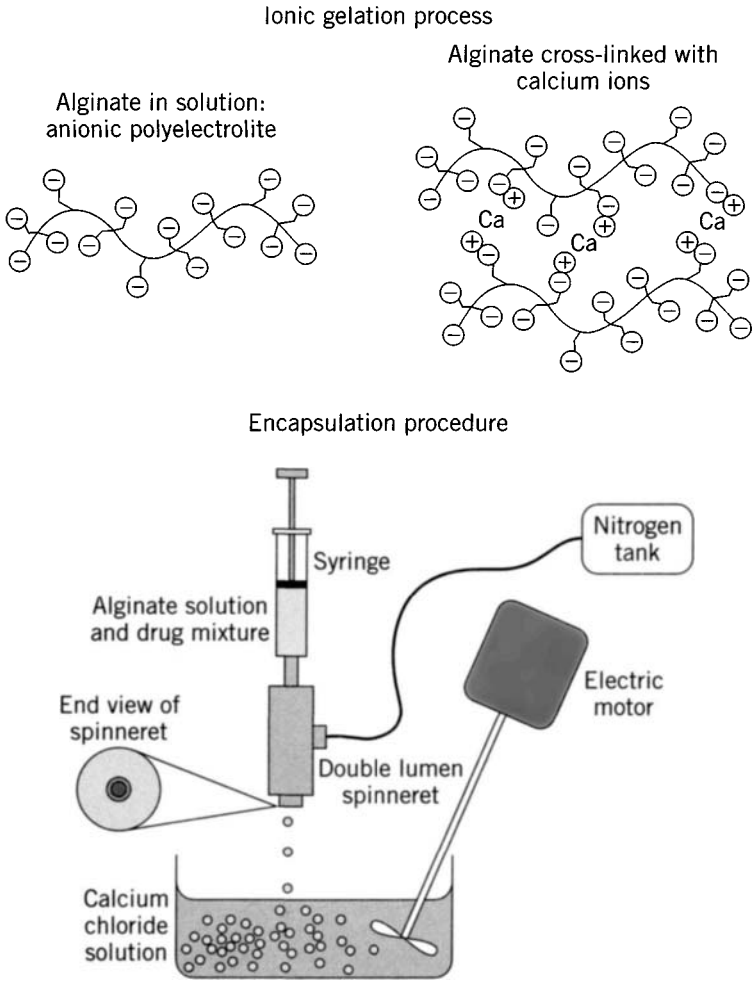


Figure 20. Sodium alginate gelation process.

The cell or tissue suspension is extruded through a microdroplet-forming device producing microdroplets which fall into a $CaCl_2$ solution and form gelled microbeads with the cells or tissues entrapped (Fig. 20). These cell-containing, gel microbeads are next treated with a solution of polylysine which displaces the surface layer of calcium ions and forms a permanent polysalt shell or membrane. Finally, the interior calcium alginate gel is "liquefied," either to stay in or to come out (depending on molecular weight and size of the starting alginate) of the capsule with a calcium sequestrant such as buffered citrate solution (19).

Diclofenac sodium is an ideal candidate for incorporation in a controlled release device to diminish its adverse effects after oral administration. Gohel et al. prepared microspheres by using sodium alginate as a polymer and $CaCl_2$ as a cross-linking agent. In this investigation, 3 full factorial design was used to investigate the joint influence of three variables: the stirring speed (X_1), concentration of $CaCl_2$ (X_2), and percent of heavy liquid paraffin in a blend of heavy and light liquid paraffin in the dispersion medium (X_3) on the time required for 80% drug dissolution (t_{80}). Potential variables such as concentration of sodium alginate and drug:sodium alginate ratio were kept constant. A statistical model with significant interaction terms is derived to predict t_{80}. The results of multiple linear regression analysis and F-statistics revealed that, for obtaining controlled drug release, the microspheres should be prepared using relatively lower stirring speed, higher interactions were found to be statistically significant in nature. A response plot was presented to show the effects of X_1, X_2, and X_3 on t_{80}. The drug was released by diffusion of anomalous type. A model was validated for accurate prediction of drug release profile (70,71).

Stable membranes were formed around alginate beads using a transacylation reaction between polysaccharidic esters, namely propylene glycol alginate (PGA) or pectin, and various proteins (human serum albumin [HSA], ovalbumin, bovine hemoglobin, lactoserum proteins). In a standard procedure, two reagents formed by dropwise addition into a calcium solution. Then the transacylation reaction was started by alkalization of the bead suspension. A membrane was formed around the beads made of a protein directly bound to a polysaccharide through amide linkages. The thickness of the membranes and the lysis time in trypsin were increased by raising the amount of NaOH used in the transacylation step. In a modified procedure, coated beads were obtained, incorporating PGA in the initial Na-alginate solution, and HSA in the transacylation bath. Activated charcoal was encapsulated in HSA-PGA beads, giving particles with adsorption properties toward creatinine. Assays were performed using PGA associated with alkaline phosphate as the membrane-forming protein. Stable beads were obtained having a relative activity of 39.3% as compared with free enzyme (73).

Lee et al. (72) developed a sustained release formulation which delivers melatonin (MT). MT is a pineal hormone of clinical value because of its short half-life, for those who have disordered circadian rhythm. The purpose of the study was to prepare MT-loaded microspheres by the emulsion melting/cooling method using stearyl alcohol (SA) and also dual-walled chitosan and sodium alginate beads, and to evaluate the release characteristics in simulated gastric and intestinal fluid. The MT-loaded microspheres were spherical, ranging in diameter from about 250 to 750 μm. When poly(ethylene glycol) 4000 (PEG) as a water-soluble additive, or aluminum tristearate (AT) as a water-insoluble additive, was incorporated, the surface roughness was further reduced resulting in a smooth matrix structure. The dual-walled chitosan and sodium alginate beads entrapping small MT-loaded microspheres were not spherical in structure. As the additive incorporated into SA microspheres increased, the drug content decreased. The release profiles of the MT-loaded microspheres were independent of pH. When the melted SA solution was cooled rapidly (in 10 minutes) to 25°C, the drug content increased but the release rate of MT-loaded microspheres decreased. The release rate of drug decreased as the amount of SA increased but an increase of agitation speed and amount of AT and PEG resulted in increased release rates. The release rate of drug from dual-walled chitosan beads increased slightly, but was retarded in the case of dual-walled alginate beads, when compared with MT-loaded microspheres. The emulsion melting/cooling method used to prepared MT-loaded microspheres using SA is simple and inexpensive, and may provide an alternative for the preparation of an oral sustained release dosage form of MT without using harmful organic solvents. The dual-walled chitosan and sodium alginate beads may also provide a convenient way to control the release of drugs (72).

Calcium alginate microspheres were prepared by an emulsification process (68). The effects of two copolymers, namely poly(vinylpyrrolidone) (PVP) and ethylcellulose, on the properties of the microspheres were studied. Microspheres prepared with and without PVP exhibited a better flow property but the drug content was lower and the drug release rate higher. The method of incorporating PVP was found to significantly affect the size distribution and drug content of the microspheres. Ethylcellulose produced marked aggregation of the microspheres which also showed a lower drug content, but a slower drug release. The retardation in drug release was attributed to the formation of aggregated microspheres with a less permeable matrix. The addition of triethylcitrate, which is a water-soluble plasticizer, was found to increase the rate of drug release, whereas the use of a higher viscosity grade of ethylcellulose produced the opposite effect. Ethylcellulose improved the flowability of the microspheres to a greater extent than PVP (68).

Porous microspheres were formed by the gelation of two polysaccharides, a polyanionic sodium alginate and a polycationic chitosan, followed by lyophilization which creates the porous structure (74). Porous microspheres were also formed by gelation of sodium alginate with $CaCl_2$ and gelation of sodium alginate with polylysine. FITC-BSA was incorporated into the microspheres by mixing the protein with the polysaccharide solution prior to gelation. Interleukin-2 (IL-2) was incorporated into the preformed microspheres by diffusion from an external aqueous solution of IL-2. Sustained release of the proteins from porous

alginate/chitosan microspheres is of longer duration than from alginate/$CaCl_2$, or from alginate/polylysine microspheres. Activity of the released IL-2 was investigated by determining the induction of cytotoxic T lymphocytes (CTL) when incubated with tumor cells and lymphocytes. It was found that the IL-2 remained active in the alginate/chitosan microspheres because the released IL-2 triggered induction of CTL more efficiently than free IL-2. Tumor-killing specific activity of CTL was the same whether induced by the sustained released IL-2 or by the addition of free IL-2 (74).

Microspheres of theophylline were prepared by ionotropic gelation method. The objective of this study was to investigate the influence of variables such as stirring speed, concentration of $CaCl_2$, and composition of the dispersion medium on the characteristics of the microspheres. A 3^3 randomized full factorial design was used to study the effect of the selected variables on the time for 90% drug dissolution (t_{90}). A linear model with interactive terms was generated using the multiple linear regression approach. F-statistics were carried out to evolve the reduced model. Significant interactions were not detected between the selected variables and good agreement was observed between the predicted and experimental checkpoint. The microspheres were evaluated during in vivo studies in dogs and the pharmacokinetic parameters were estimated by performing nonlinear regression analysis. The Wagner-Nelson method was adopted to compute the percentage drug absorbed. A good correlation was observed between the in vitro and in vivo results (70).

Chitosan microspheres were prepared by Berthold et al. (144) by a novel precipitation process using sodium sulfate as a precipitant. Low, medium, and high molecular weight chitosan was chosen for the formulation of microspheres. The extent of precipitation was controlled by the concentration of sodium sulfate and monitored by turbidity measurement. The amount of sodium sulfate required for the preparation of the microspheres depended on the molecular weight of chitosan. The particle size was determined by photon correlation spectroscopy and centrifugal sedimentation. The morphological characteristics were examined using SEM. The surface charge was measured by microelectrophoresis. After preparation the loading property with various antiinflammatory drugs was investigated using spectrophotometry. The influence of surface adsorption on the drug modification was controlled by DSC. Drug liberation was tested in vitro using side-by-side diffusion cells with dialysis membrane made of cellulose acetate. The highest loading (up to 30.5% relative to the polymer mass) was achieved with prednisolone sodium phosphate. The adsorbed drug was present in an amorphous form. The drug release from the microspheres was dependent on the drug/polymer ratio (144).

GELATION AGAROSE

Agarose is a water-soluble, nonionic polysaccharide that self-associates in water to form a gel (145). Thus, it can be used to fabricate spherical gel particles in which an active agent is entrapped. Figure 21 contains a flow diagram of

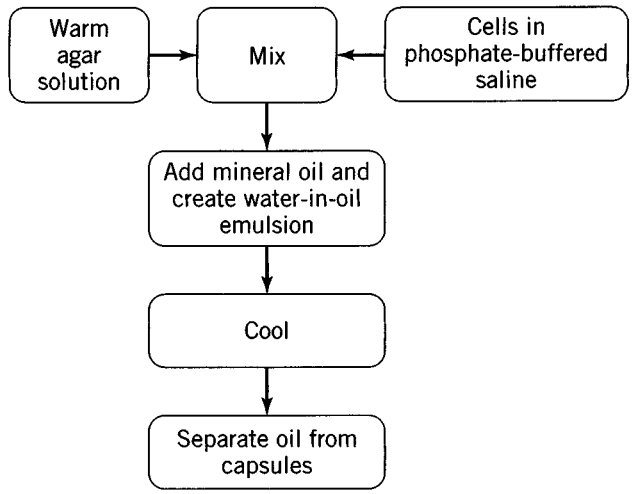


Figure 21. Microencapsulation by gelation using agarose.

recently developed fabrication procedure. The first step in the process consists of forming a molecularly dispersed solution of agarose in water. This requires heating an agarose-water mixture above 70°C, which is the melting point of agarose gels. The resulting solution is cooled to 40°C at which point the core material solidifies, thereby setting up the agarose gel structure and converting the aqueous droplets to spherical gel particles. The mineral oil is separated away from the gel particles by decantation and washing.

This procedure uses the large difference in gelation and melting temperatures of agarose. Agarose samples that gel at low temperatures (15–20°C) exist, but these gels, once formed, do not melt until 70°C. Thus, agarose can be completely dissolved in water at an elevated temperature, and then the solution obtained can be cooled to a reasonable temperature (i.e., above 25°C) without gelation occurring. At temperatures of 25–40°C, heat-sensitive core materials (e.g., live cells) can be added to the agarose solution. The agarose gel structure is then formed by cooling the mixture to 5–10°C. Significantly, the obtained gel particle has a matrix structure and is not a microcapsule with a continuous membrane surrounding a continuous core.

HOT MELT MICROENCAPSULATION

Hot melt is a process developed in the 1970s for photographic applications. In this process the melted polymer is mixed with drug, which can be encapsulated as solid or liquid particles. The mixture is then suspended in a immiscible solvent that is heated 5°C above the melting point of the polymer and stirred continuously using an overhead stirrer and a four blade impeller. Once the emulsion is stabilized (Fig. 22), it is cooled until the core material has solidified. The solvents used in this process could be silicon and olive oil. The low solubility of various drugs in these organic solvents makes them effective. It is recommended to sieve the drug, but in general, drug particle size is less than 50 μm. Using drugs with small particles sizes was

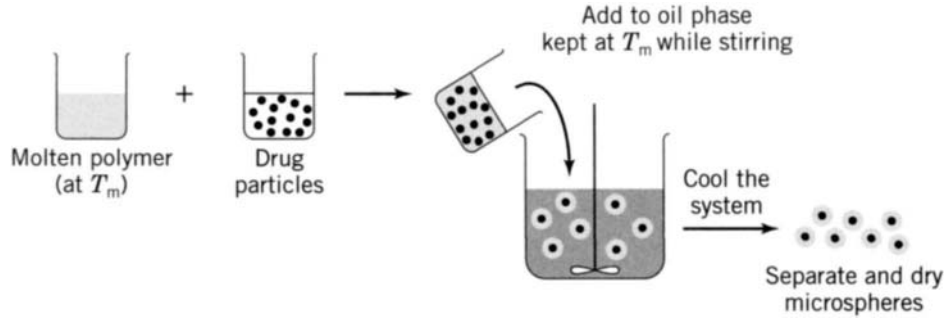


Figure 22. Microencapsulation by hot melt. Note that the dark dots represent drug particles; however, when the drug is water-soluble, an additional step may be required to prepare a water-in-oil emulsion, which is later encapsulated as shown here.

found to improve the drug distribution within microspheres. After cooling, the microspheres are washed by decantation with petroleum ether to give a free-flowing powder. Then they are sieved, dried, and stored in a freezer (when biodegradable polymers are used). Size distribution can be controlled by the stirring rate and the yield of encapsulation is 70–90%. This microencapsulation procedure is reproducible with respect to yield and size distribution, but the disadvantage of this approach is the moderate temperatures to which the drug must be exposed.

One way to overcome this problem is to synthesize polymers with lower melting points. This can be achieved by changes in the backbone of the polymer (i.e., in polyanhydrides), or using polymers that have a low melting point. When more stable drugs are involved the temperature, as well as the type of the polymer used, may be more versatile. Mathiowitz and Langer used this method to prepare polyanhydride microspheres (81). Surface morphology of the polyanhydride microspheres was studied via stereo microscopy and SEM and was performed immediately after preparation and after different periods of degradation. Both external and internal faces were examined. The microspheres were mounted on metal stubs, cut with a blade, and sputter-coated with gold-palladium. SEM of the poly(CPP-SA) are shown in Figure 23a. Microspheres are spherical, and the external surfaces appear smooth and crenellated. The crenellated surface is a typical result of this method. It is possible that the external surface is loaded with spherulites which formed during the slow cooling. No traces of drug or dye are found on the outer surfaces and cross sections reveal a dense internal structure, as seen in Figure 23b. Morphological studies made after 24 hours of in vitro degradation show that only the surface of the microsphere was attacked. The surface possessed small cracks and an irregular structure, whereas the internal face remains intact the same microspheres (Fig. 23c). A well-defined degrading zone, characterized by a spherical shape appeared and moved progressively from the surface towards the center of the microsphere. The erosion zone is composed of monomers (macromolecules). Figure 24d shows the same microspheres after 20 days of in vitro degradation. The microspheres show a weak structure (composed of monomers) which collapses easily (again these are insoluble monomers). The weight of this material is 5–10% of the initial weight; after 4 weeks the microspheres completely disintegrate. Figure 23e,f demonstrate a case where the drug loading of the microsphere was too high (70%) resulting in high amounts of drug on the surface of the microsphere.

A good correlation was achieved when comparing weight loss of degrading samples with the production of the degradation products (81,83). These observations suggest that these microspheres display surface erosion. Incorporating hydrophilic molecules such as acid orange (M_W 364) at high loadings (30%) changes the degradation rate of the polymer. Release experiments were conducted in 10–50 mL of 0.1M, pH 7.4 phosphate buffer at 37°C in small columns. The release of acid orange was almost complete in 200 min and the degradation of the polymer lags behind the dye (81). Actually the release kinetics are affected more by the water uptake of the dye than by the degradation process. The influence of loading on the release profile was more pronounced when the loading is about 2%. Here release was controlled by polymer erosion. Except for the small burst effect at the beginning, the dye and polymer were released simultaneously. At higher loadings, the dye was released much faster than the polymer eroded. At high loadings of hydrophilic drugs, the release rate is not controlled by polymer erosion. Instead the polymer degradation is faster than that of a pure microsphere, and the drug is released faster than polymer dissolves. The reason for this is that the polymer starts to degrade from inside as well. The hot melt fabrication technique produces spheres with density independent of size. The study was confined to low loadings, that is, 2–5%, and the particles of the drug were mostly of small size (less than 50 μm) and for acid orange the size was less than 50 μm. The results demonstrate that the smaller the microspheres, the faster the release rate. It should be noted, however, that as the size of the microspheres approaches that of the incorporated drug particles, dissolution- or diffusion-controlled release may also occur due to particles touching the surface of the microspheres. Such a phenomenon may be occurring in the smallest microspheres. Incorporating insulin in microspheres changes the (release) degradation profile (81,83). In this case, drug release corresponds closely to polymer degradation. One explanation is the fact that zinc insulin has a low solubility in water (0.22 mg/dL) so that diffusional escape and osmotic swelling are diminished, which helps to achieve erosion-controlled release. Alternatively, it is possible that the small size of the insulin particles entrapped in the microspheres enabled good dispersion inside the polymer. The release of insulin in bioactive form was evident from the in vivo experiments. A possible mech-

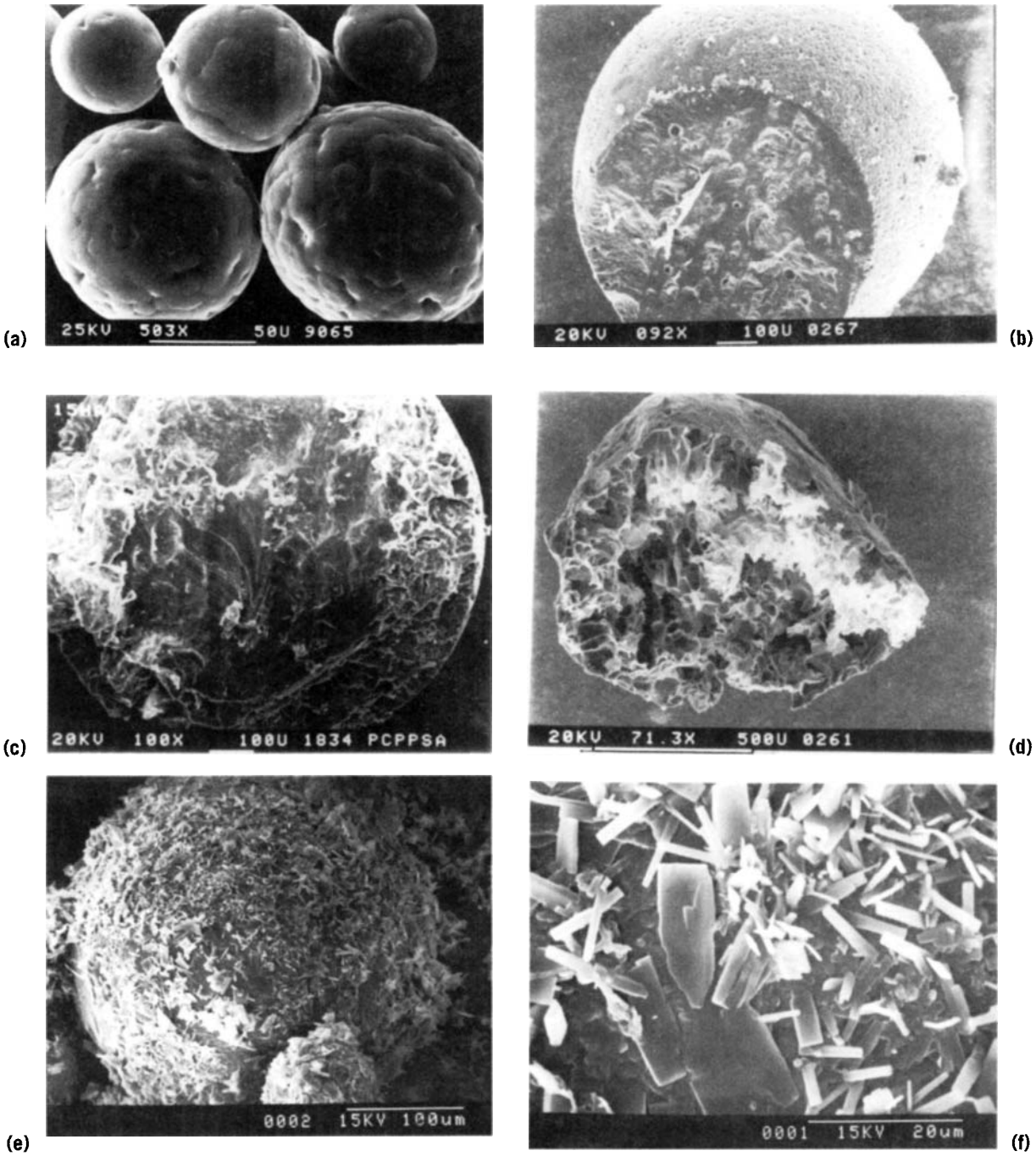


Figure 23. SEM of polyanhydride microspheres (**a**) external surface; (**b**) cross section; (**c**) cross section after 24 hours in buffer; (**d**) cross section after 20 days in buffer; (**e**) microsphere with 70% loading of salicilic acid; (**f**) higher magnification of same capsule.

anism describing these observations is that the release from polyanhydride microspheres loaded this low levels of drug involved two main steps. When microspheres are immersed in a buffer solution, the degradation process starts. A particle of drug, which is very close to the surface, dissolves and is released. As the degrading zone, which is composed of monomers, advances toward the center, all the hydrophilic drugs are released. Fewer hydrophilic drugs, however, may be entrapped in the polymer, until the polymer completely dissolves. The latter phenomenon was observed for insulin.

The effect of in vivo performance of Zn/insulin-loaded (15% W/W) poly(CPP-SA) 20:80 microcapsules prepared by hot melt microencapsulation and implanted in diabetic rats, was sustained normoglycemia for up to 4 days (81) with no deaths due to insulin overdose. This stands in

Next Page

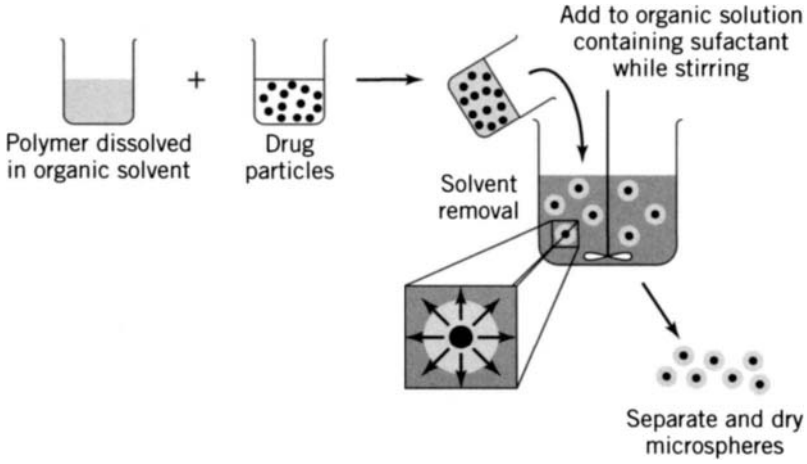


Figure 24. Microencapsulation by solvent removal.

sharp contrast to the microspheres made by solvent evaporation which caused short-lived, often fatal hypoglycemia (see "Solvent Evaporation").

SOLVENT REMOVAL

This method is a modification of organic phase precipitation (15) which, in specific situations, offers significant advantages. The fabrication occurs at room temperature and totally in organic solvents, an important consideration because for hydrolytically labile polymers such as polyanhydrides the avoidance of aqueous solutions is particularly important. Mathiowitz et al. (82,146) used this method to develop an improved technique of encapsulating insulin. In this example the polymer was dissolved in methylene chloride, the desired amount of drug was added and then the mixture was suspended in silicone oil containing Span® 85 and methylene chloride. After pouring the polymer solution into the silicone oil, petroleum ether was added and the mixture was stirred until the methylene chloride was extracted into the oil solution and sufficient microcapsule hardening was achieved. The resulting microspheres were isolated by filtration, washed with petroleum ether and dried overnight under vacuum (Fig. 24). The size of microspheres was always smaller than 300 μm. The best correlation between the expected and achieved loadings (82,83) was obtained with the hydrophilic substances myoglobin, acid orange, and insulin. This is understandable because the microencapsulation occurred in an organic solvent, preventing the loss of drug by diffusion.

The difference between solvent removal and organic phase separation is evident when comparing Figure 24 and Figure 12. In solvent removal the polymeric solution is introduced into the continuous phase, an emulsion is formed first and then the organic solvent is extracted to the continuous phase. In organic phase separation the polymer is dissolved in the continuous phase, a phase inducer is introduced, a coacervate is formed and, finally, encapsulation of drug occurs.

SEM of microspheres made from polymer without drug are shown in Figure 25. The amorphous, poly(CPP-SA) 50:50 microspheres are spherical with smooth and dense surfaces (Fig. 25a and 25b), whereas the crystalline poly(SA) (poly[sebacic acid]) microspheres display a very rough morphology containing fractures extending throughout the entire structure (Fig. 25c). The microspheres of poly(CPP-SA) 20:80 (Fig. 25d) and poly(CPP-SA) 50:50 exhibited a less porous internal structure (82,83), but the external dense layer was always present. A cross section of the poly(carboxyphenoxyhexane-*co*-sebacic acid) 50:50 microspheres reveals a very porous structure surrounded by a dense layer near the surface (Fig. 25d). When microspheres containing drugs were prepared, no change was observed in the external surface, for drug loadings up to 16.5%. Above that level, some crystals appeared on the surface (83).

The dense external structure and the porous core are typical of most of the microspheres produced by this method, especially the less crystalline polymers. A closer inspection of the physical events occurring during microsphere formation may help in understanding their performance. A schematic representation of the process is described in Figure 24 and a description of the process taking place is proposed. The polymer solution is introduced into the oil phase followed by rapid diffusion of the methylene chloride into the oil phase. The concentration of the polymer near the wall is high, which explains why precipitation of the outer shell occurs first (82,83), leaving high concentrations of polymer dissolved in methylene chloride inside the core. This organic solvent can be later removed by addition of a nonsolvent or by applying high vacuum. The process of microencapsulation is presumably diffusion controlled—at least during the first stages where the difference in concentration of methylene chloride between the two phases (silicone and polymer solution) is significant. After precipitation begins, the process becomes more complicated. It involves diffusion of methylene chloride, both in the polymer solution and in the already precipitated polymer. The first precipitation occurs in the external area of the forming sphere, and this layer slows subsequent diffusion of methylene chloride into the oil phase. This dense external structure and porous internal core are presumably obtained because during precipitation of the microspheres the external surface precipitates first, thus making it difficult for the microsphere to shrink. The re-

Previous Page

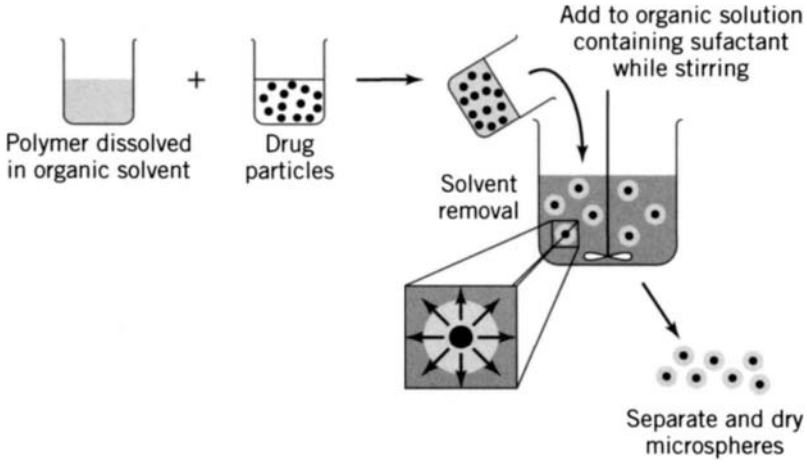


Figure 24. Microencapsulation by solvent removal.

sharp contrast to the microspheres made by solvent evaporation which caused short-lived, often fatal hypoglycemia (see "Solvent Evaporation").

SOLVENT REMOVAL

This method is a modification of organic phase precipitation (15) which, in specific situations, offers significant advantages. The fabrication occurs at room temperature and totally in organic solvents, an important consideration because for hydrolytically labile polymers such as polyanhydrides the avoidance of aqueous solutions is particularly important. Mathiowitz et al. (82,146) used this method to develop an improved technique of encapsulating insulin. In this example the polymer was dissolved in methylene chloride, the desired amount of drug was added and then the mixture was suspended in silicone oil containing Span® 85 and methylene chloride. After pouring the polymer solution into the silicone oil, petroleum ether was added and the mixture was stirred until the methylene chloride was extracted into the oil solution and sufficient microcapsule hardening was achieved. The resulting microspheres were isolated by filtration, washed with petroleum ether and dried overnight under vacuum (Fig. 24). The size of microspheres was always smaller than 300 μm. The best correlation between the expected and achieved loadings (82,83) was obtained with the hydrophilic substances myoglobin, acid orange, and insulin. This is understandable because the microencapsulation occurred in an organic solvent, preventing the loss of drug by diffusion.

The difference between solvent removal and organic phase separation is evident when comparing Figure 24 and Figure 12. In solvent removal the polymeric solution is introduced into the continuous phase, an emulsion is formed first and then the organic solvent is extracted to the continuous phase. In organic phase separation the polymer is dissolved in the continuous phase, a phase inducer is introduced, a coacervate is formed and, finally, encapsulation of drug occurs.

SEM of microspheres made from polymer without drug are shown in Figure 25. The amorphous, poly(CPP-SA) 50:50 microspheres are spherical with smooth and dense surfaces (Fig. 25a and 25b), whereas the crystalline poly(SA) (poly[sebacic acid]) microspheres display a very rough morphology containing fractures extending throughout the entire structure (Fig. 25c). The microspheres of poly(CPP-SA) 20:80 (Fig. 25d) and poly(CPP-SA) 50:50 exhibited a less porous internal structure (82,83), but the external dense layer was always present. A cross section of the poly(carboxyphenoxyhexane-*co*-sebacic acid) 50:50 microspheres reveals a very porous structure surrounded by a dense layer near the surface (Fig. 25d). When microspheres containing drugs were prepared, no change was observed in the external surface, for drug loadings up to 16.5%. Above that level, some crystals appeared on the surface (83).

The dense external structure and the porous core are typical of most of the microspheres produced by this method, especially the less crystalline polymers. A closer inspection of the physical events occurring during microsphere formation may help in understanding their performance. A schematic representation of the process is described in Figure 24 and a description of the process taking place is proposed. The polymer solution is introduced into the oil phase followed by rapid diffusion of the methylene chloride into the oil phase. The concentration of the polymer near the wall is high, which explains why precipitation of the outer shell occurs first (82,83), leaving high concentrations of polymer dissolved in methylene chloride inside the core. This organic solvent can be later removed by addition of a nonsolvent or by applying high vacuum. The process of microencapsulation is presumably diffusion controlled—at least during the first stages where the difference in concentration of methylene chloride between the two phases (silicone and polymer solution) is significant. After precipitation begins, the process becomes more complicated. It involves diffusion of methylene chloride, both in the polymer solution and in the already precipitated polymer. The first precipitation occurs in the external area of the forming sphere, and this layer slows subsequent diffusion of methylene chloride into the oil phase. This dense external structure and porous internal core are presumably obtained because during precipitation of the microspheres the external surface precipitates first, thus making it difficult for the microsphere to shrink. The re-

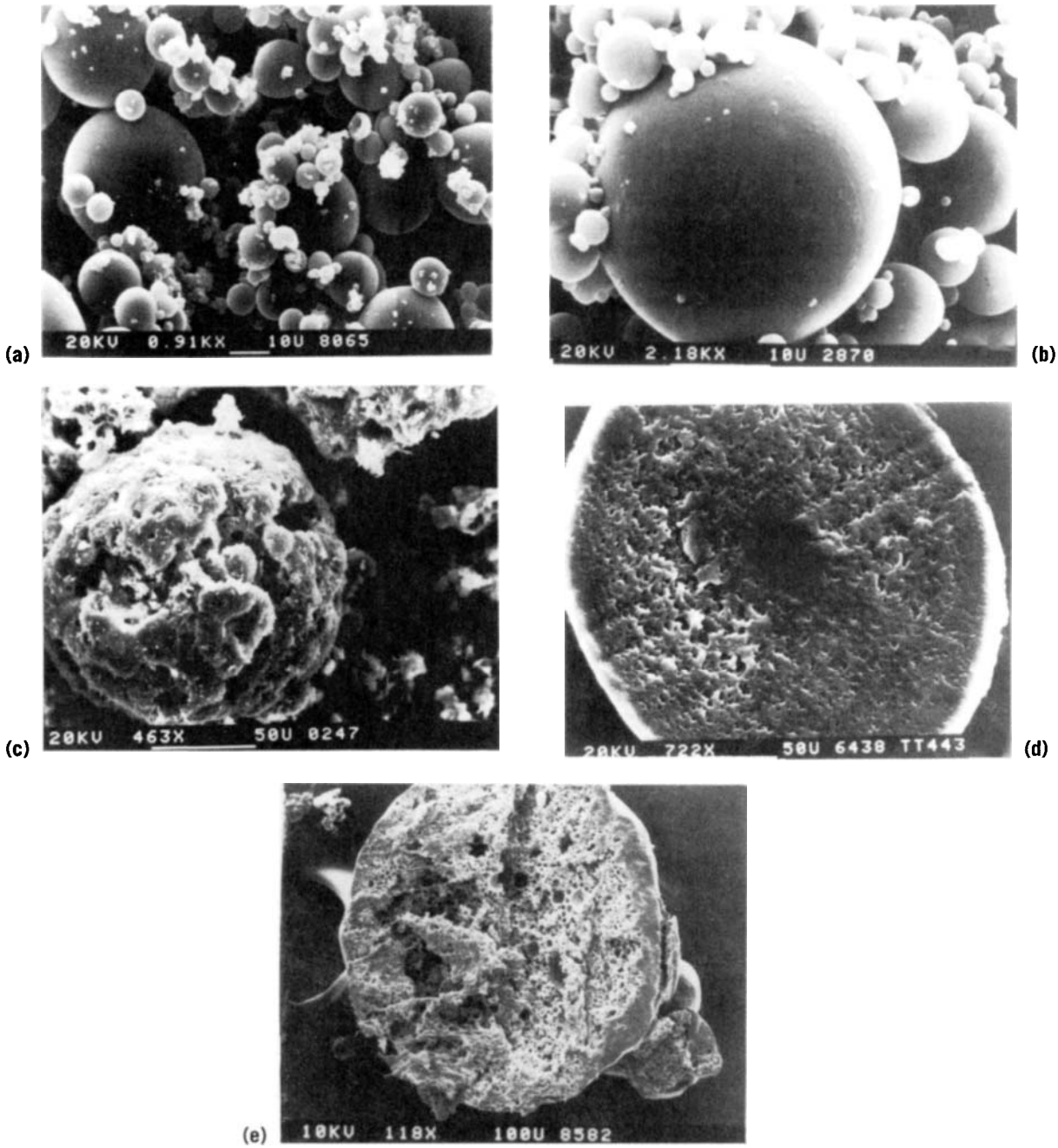


Figure 25. Morphology of microspheres made by solvent removal: (**a**) external surface of poly(CPP-SA) 50:50 microspheres; (**b**) higher magnification of (**a**); (**c**) external surface of poly(SA); (**d**) cross section of poly(CPP-SA) 20:80; (**e**) cross section of poly(CPH-SA) 50:50 microsphere.

mainder of the solvent then diffuses out of the microsphere leaving a porous structure.

In the more crystalline poly(SA) microspheres, there was no formation of a dense external layer, but a quick precipitation of the entire polymer emulsion led to a very porous structure. In other cases in the literature (84,146). The rate of precipitation may also be a key to understanding the type of microspheres which were obtained. The rough surface of the poly(SA) microspheres may be due to the faster precipitation of poly(SA) compared with poly(CPP-SA) 50:50. Thus precipitation occurred in the poly(SA) microspheres before a stable emulsion could form. In contrast, in slower precipitating systems—poly(CPP-SA) 50:50, for example—there is first the formation of an emulsion and then precipitation. This "two-step" process during microencapsulation can be further controlled using different surface-active compounds to stabilize the emulsion. It should be noted that all experiments were done with the same organic solvents, because different solvents may lead to different external morphologies.

DSC and X-ray analysis of the polymers, dyes, and drug-loaded microspheres were performed in order to characterize the physical state of the polymers and dyes after microencapsulation (82,146). In cases where the drug formed a dispersion in the first stage of microencapsulation, we would expect that, at the end of the process, crystalline drug particles would be dispersed in the polymer matrix. In such a system DSC would display two endotherms, each relating to the melting point of either drug or polymer. In cases where the drug is dissolved in the organic polymeric solution, solvent removal causes the drug to either dissolve in the polymer or crystallize out and form a dispersion. In the latter case DSC would again display two endotherms. In the former case, where the drug forms a solution inside the polymer, no separate event relating to the melting of the drug would occur. However, some changes in the melting of the polymer might occur, provided the concentration of the drug in the polymer phase is high enough to cause changes exceeding the sensitivity of DSC. Mathiowitz thus monitored melting points of the dyes and polymer before and after encapsulation. A sharp endotherm was observed for free acid orange, *p*-nitroaniline and methyl red (119.4, 149.8, 181.2°C, respectively) corresponding to the melting phase transitions. The "blank" microspheres displayed a sharp endotherm at 78°C corresponding to the melting of the crystalline regions of the polymer (83).

In loaded microspheres (up to 16% loading), no melt corresponding to the acid orange appeared around 121°C (83). These facts may imply that the dye forms a solution inside the polymer (at loadings lower than 23%). However, the absence of the thermal event at low loadings does not always indicate that this is the case. In order to verify this point X-ray diffraction was used and indicates that acid orange was dispersed as crystals in the microspheres (data not shown) (82,146).

X-ray diffraction analysis of methyl red–loaded microspheres indicated no crystalline diffraction related to the dye, nor did the DSC show any endotherm related to the melting of the dye. However, the melting point of the polymer had slightly decrease compared to blank microspheres. X-ray diffraction displayed the typical diffraction pattern of pure poly(SA), but the crystallinity decreased from 55% to about 40% (82,146). However, the change in the melting point and the decrease in crystallinity suggested that the drug may be soluble in the polymer. It is quite possible that the dye, being soluble in the amorphous state, hindered the crystallization of the polymer and thus decreased the degree of crystallinity.

Similar experiments were performed with poly(CPP-SA) 50:50 microspheres loaded with the same substances. Both DSC and X-ray diffraction confirmed that acid orange was dispersed as crystals in the polymer, whereas the hydrophobic dyes formed solutions inside the polymer (82,146).

Blank poly(CPP-SA) 50:50 microspheres prepared by solvent removal were implanted subcutaneously in rats. The spheres were smaller than 300 μm and were injected as an aqueous suspension. After 10 days of implantation several spherical microsphere remnants were found among the remains of degraded microspheres in tissue samples taken from the implantation site. These remnants were composed of the same polymer degradation products as seen in the nonintact remnants (as judged by infrared spectroscopy) and eventually disappeared from the implantation area. Although the appearance of external remnants might, at first glance, appear to contradict other evidence supporting surface erosion, the SEM analysis of microspheres already presented suggests a possible explanation based on polymer density. Cross sections of microspheres during release show an outer zone in which degradation has already occurred but the degradation products have not yet disappeared. In addition, cross-sectional views of undegraded microspheres formed by both solvent removal and hot melt microencapsulation show a dense external surface and a less dense inner core (82,83,146). It is quite plausible that during degradation the external surface erodes completely, leaving behind a dense but permeable layer of degradation products that must dissolve and diffuse away. Meanwhile, erosion continues into the core, where the degraded material is less dense and is able to more easily dissolve and diffuse out. The fact that the remnants disappear after a longer time in vivo is further evidence that solubilization of the degradation products may be the controlling step in the disappearance of the microspheres, but not in the release of the drug.

Histological studies of both samples revealed a moderate acute inflammatory response that peaked at day 3. Histological examination of tissue removed at day 40 from the implantation site revealed a layer of amorphous fibril material within the subcutaneous tissue, a remnant of the implanted polymer. There was no evidence of tissue reaction to this material within the subepidermis.

An in vivo study with insulin-loaded microspheres prepared by solvent removal demonstrated more successful serum and urine glucose control than previously seen with microspheres made by solvent evaporation. Five diabetic rats were implanted with 200 mg of insulin-loaded (10%) microspheres. The results demonstrate near-zero urine glucose levels and serum glucose control. A similar experiment with 200 mg of 5% (W/W) loaded microspheres decreased urine glucose effectively for 3 days and resulted in only 1 day of normoglycemia, whereas 100 mg of 10% (W/W) loaded microspheres showed 3 days of lowered urine glucose and 2 days of serum glucose control. For comparison, urine and blood glucose levels for both diabetic control and healthy control rats (5 rats in each group) were measured. As expected, glucose was never found in the urine of healthy rats and the untreated diabetic rats showed no significant lowering of blood or urine glucose levels (82).

Atkins et al. (144) prepared spherical, monolithic, poly(DL-lactide-*co*-glycolide) (PLGA) 50:50 and PLGA 75:25 microspheres with a honeycomb-like internal architecture, composed of and containing a range of vancomycin loadings. Microspheres were prepared using W/O emulsification, except that Span® 40 was used as the continuous oil phase surfactant. In a typical fabrication the organic polymer phase was prepared by the ultrasonication (100 W bath) of 1 g of either 75:25 or 50:50 PLGA together with either 1, 0.333, or 0.1 g vancomycin in 30 mL acetonitrile

at 35°C for 15 minutes, providing theoretical percentage loadings of 50, 16.7, and 5% vancomycin, respectively. This organic phase was maintained at 55°C in a water bath. The continuous oil phase consisted of 125 g light mineral oil containing 2% (W/W) Span® 40 maintained at 55°C. The organic polymer phase was slowly added to the continuous phase and emulsified at 55°C using a high shear head at 3,000 rpm for 30 minutes. Droplet formation was monitored by light microscopy and the final emulsion was stirred at 440 rpm with a three-blade impeller in an off-center position for a further 60 minutes at 55°C to facilitate solvent evaporation. The emulsion was cooled to just above 35°C to prevent the precipitation of Span® 40, and left for 1 hour to allow the microspheres to harden. The microspheres were separated by vacuum filtration using solvent resistant polypropylene-backed PTFE filters (1 μm pore size) and washed with excess petroleum ether at 55°C to remove the Span® 40. The resultant microspheres were air-dried and weighed to determine percentage yield. The free-flowing preparation of grey/white microspheres were stored desiccated, under vacuum at room temperature (147). In a way, this method is a combination of solvent evaporation and solvent removal, because some of the solvent is removed by the organic phase and some is evaporated by the applied heat.

Porous salmon calcitonin-loaded PLGA microspheres (size range 35–140 mm) of varying matrix characteristics were prepared by an aqueous emulsification process using either a temperature gradient (Tmp) or dilution (Dil) of the continuous phase. The Tmp technique resulted in microspheres with a hollow internal core and a porous wall. The core size and thickness of the porous wall were dependent on the temperature gradient used. A rapid ramp in temperature from 15 to 40°C resulted in a large core and a thin wall, whereas a gradual temperature rise resulted in a smaller core. The Dil technique produced microspheres with a uniform, honeycomb-like pore structure without a core where pore size was dependent on the dilution volume used. The specific surface area was higher and bulk density lower for microspheres prepared by the Tmp technique, whereas there was no significant difference in the peptide load (3.2–4.5%) between both techniques. A rapid removal of CH_2Cl_2 was observed in the case of the Tmp technique while the Dil technique facilitated a slower and gradual CH_2Cl_2 removal. Residual CH_2Cl_2 was approximately <10–20 ppm for microspheres prepared by the Tmp technique, whereas the levels were 20–130 ppm for microspheres produced by the Dil technique. Higher retention of methanol (~15–20%) was observed in the droplet formation stage with the Tmp technique, subsequent removal of which affected the core size. In the Dil technique, very low levels of methanol (<2%) were retained in the droplets soon after dispersion resulting in a uniform porous structure without core. Slower removal of methanol from the microspheres was partly responsible for the core formation (148).

The use of supercritical solvents as an extraction method to prepare microspheres is an interesting approach. The aerosol solvent extraction system (ASES) uses a supercritical gas as nonsolvent for an organic solution of drug and polymer in order to form microparticles by a flocculation process. Due to the miscibility of organic solvent and supercritical gas phase, microparticles with residual organic solvents below 30 ppm are formed. This principle was tested to encapsulate model drugs such as hyoscine butylbromide, indomethacin, piroxicam and thymopentin. As a carrier, the polymer poly(L-lactide) was used. The resulting microparticles were investigated with regard to particle formation, morphology, particle size, size distribution, and drug loading. The lower the polarity of incorporated drug, the greater the extraction, which reduced the drug loading of the microparticles. The extraction capacity of the gas phase depends on temperature and pressure which determines density and polarity of the gas. The obtained results show that the production conditions have to be optimized for each drug/polymer combination. Totally nonpolar drugs are completely extracted together with the organic solvent; however, polar drugs (especially peptides and proteins) are easy to incorporate with the ASES process (149).

Poly(L-lactide) microspheres containing a low molecular weight pharmaceutical agent were prepared using the precipitation with a compressed antisolvent (PCA) process with supercritical carbon dioxide as the antisolvent. Gentamycin, naloxone, and naltrexone were solubilized in methylene chloride using hydrophobic ion pairing (HIP) to stoichiometrically replace polar counter ions with an anionic detergent, aerosol OT (AOT, sodium bis-2-ethylhexyl sulfosuccinate). Through HIP complexation, solubilities in excess of 1 mg/mL were attainable in methylene chloride, allowing levels of direct incorporation that are not possible with other PCA approaches. The drug/polymer particles were spherical in shape and between 0.2 and 1.0 μm in diameter, as determined by SEM. Drug incorporation efficiencies were determined and in vitro release profiles measured. At 37°C, the release of the ion-paired drugs into phosphate-buffered saline displays minimal burst effects and exhibits release kinetics that are approximately linear with the square root of time, indicating matrix diffusion control of drug release. For gentamycin, linear release from the poly(L-lactide) microspheres was observed for more than 7 weeks, even at a drug loading of near 25% (W/W). Naltrexone exhibits similar release characteristics, although more drug was found on the surface of the microspheres. Conversely, rifampin, which was not ion-paired, was poorly encapsulated (150).

SPRAY-DRYING

Spray-drying is a method for preparing microspheres that is reproducible, rapid, and easy to scale up. Mathiowitz et al. (151) used this fabrication technique to examine its influence on crystallinity (by X-ray and DSC), external morphology (by SEM) and release kinetics of polyanhydrides. Model drugs, including the dyes, acid orange 8 and methyl red, and the protein, bovine somatotropin (STH), were examined with a variety of polyanhydride homo- and copolymers.

The following polymers were studied poly(sebacic anhydride) (PSA), copolymers of 1,3 bis-(carboxyphenoxypropane) (CPP) and sebacic acid (SA) having molar ratios of 20:80 and 50:50, copolymers of 1,6 bis-(carboxyphenoxy

hexane) (CPH) and sebacic acid (SA) having a molar ratio of 50:50, copolymers of fumaric acid (FA) and sebacic acid (SA) having a molar ratio of 20:80, and poly(valeric anhydride) (PCPV).

In order to create a delivery system using spray-drying it is essential to dissolve the polymer in a volatile liquid. Polyanhydrides degrade in aqueous solutions, and therefore it is preferable to process them in organic solvents. With volatile solvents such as methylene chloride it possible to encapsulate various heat-sensitive drugs, including proteins, at low temperature. For this particular study only polymer that was soluble in methylene chloride was used. The polymer is first dissolved in methylene chloride, and the drug can be either dissolved (e.g., methyl red) or suspended as particles (e.g., acid orange 8 and STH). Because the spray-dryer nozzle was 0.5 mm in diameter, it was important to obtain very small particles of the insoluble drug. Particle size reduction, via spray-drying a dilute, aqueous, acid orange solution, resulted in raisin-shaped particles, 1 to 5 μm in size. These particles were subsequently suspended in the polymer solution and sprayed-dried as already described. STH (the pure drug) had a narrow size distribution (1 to 2 mm). Methyl red was soluble in the organic solvent and was sprayed dried as a solution. Throughout this work, the conditions of spraying were kept identical: the same organic solvent and the same polymer concentration were used. This fact allowed us to correlate the morphology of a series of polymers, spray-dried under the same conditions. In general, it was possible to spray dry the crystalline polymers PSA, P(CPP-SA) 20:80, P(FA-SA) 20:80, and P(FA-SA) 50:50. However, each polymer displayed a different morphology as judged by SEM. When using more hydrophobic polymers—P(CPP-SA) 50:50, P(CPH-SA) 50:50, and PCPV—some aggregation occurred during spraying. This could have been a result of the more viscous solutions of these polymers as well as their low glass transition.

SEM of black microspheres made of PSA are shown in Figure 26a. The microspheres are spherical in shape with few aggregates and display a rough external structure. Some of the polymer precipitated as long rods, which could be a result of fast precipitation that is typical of the PSA polymer. Microspheres made of P(CPP-SA) 20:80 polymers exhibited a crenellated external surface (Figure 26b) and sizes ranging from 1 to 5 μm. The same external surface appeared when acid orange-loaded (3%) P(CPP-SA) microspheres were examined. When methyl red was encapsulated, the external surfaces of the individual microspheres were spherical in shape with few pores on the surfaces. In this particular preparation some of the spheres accumulated in the spray-dryer trap.

The STH-loaded P(CPP-SA) 20:80 microspheres were spherical with smooth external surfaces, but with a few pores on the surface of some of the capsules. In this case, the drug was supplied as fine particles, 1 to 2 μm in size. It is possible that some of the spheres were single particles of drug encapsulated by a continuous polymer membrane. P(FA-SA) 20:80 was the next crystalline polymer that was studied. In this case, the microspheres were spherical and smaller than 10 μm (Figure 26c). High magnification reveals a highly porous structure. This porous structure was typical of all spray dried fumaric polymers—both blank and loaded microspheres.

The external surfaces of the amorphous P(CPP-SA) 50:50 and P(CPH-SA) 50:50 microspheres were smooth and dense. However, the microspheres tended to fuse before the final drying. The same phenomenon was observed with PCPV microspheres (Figure 26d). This aggregation can be prevented by lowering the concentration of the polymer solution. However, the glass transitions of these polymers are very low, and this may have been the main reason for the high degree of fusion during spray-drying (151).

DSC and X-ray analyses of the spray-dried polymers loaded with dyes and drugs were performed in order to characterize the physical state of the polymers after microencapsulation. By monitoring the melting points of the dyes and the polymer before and after encapsulation it was possible to determine when a solution or phase separated system was obtained. A sharp endotherm was observed for free acid orange and methyl red (119.4 and 181.2°C, respectively) corresponding to the melting phase transitions. The "blank" spray-dried PSA microspheres displayed a sharp endotherm at 81°C, corresponding to the melting of the crystalline regions of the polymer. The crystallinity of the PSA microspheres was lower than the crystallinity of the original polymer (decrease of 7.6 cal/g). However, the crystallinity was not completely destroyed, and the typical powder diffraction of the PSA units was still retained. After acid orange is incorporated, the crystallinity of the polymer remains almost unchanged. To further study the behavior of the spray-dried microspheres, the P(CPP-SA) 20:80 microspheres were analyzed by DSC. A dramatic decrease was seen in the melting point of the blank microspheres (58.5°C) compared with the pure polymer (72°C). The melting was broad, and the numbers reported represent the peak maxima. This was true for microspheres loaded with acid orange (56.6°C), methyl red (56.2°C), and STH (58°C). The decrease in melting point could be a result of residual solvent (up to 5% by weight) in the microspheres, which acts as a diluent. There was also a pronounced decrease in the heat of fusion, which directly reflects a decrease in crystallinity. X-ray diffractions of two different loadings of acid orange in P(CPP-SA) 20:80 microspheres are shown in Figure 27. The four well-defined diffraction patterns, which correspond to the P(CPP-SA) 20:80 (152) are hardly seen and are replaced by broad bands, indicating a profound decrease in the degree of crystallinity. The blank microspheres seemed to be less crystalline than the loaded spheres, as judged by X-ray diffraction (Fig. 28). A comparison of blank P(CPP-SA) 20:80 microspheres to microspheres loaded with acid orange, as well as methyl red, is shown in Figure 28. As mentioned previously, the polymer still retains some crystallinity, but the fine structures of the crystalline areas are gone. The lower degree of crystallinity is more pronounced in the methyl red sample and is also supported by the lower heat of fusion (83,151). Previous publications, describing different encapsulation systems, indicated that methyl red may form solutions with polyanhydrides, resulting in a lower degree of crystallinity (83).

P(FA-SA) 20:80 behaved differently. The melting point, as well as the heat of fusion, was lowered for both loaded

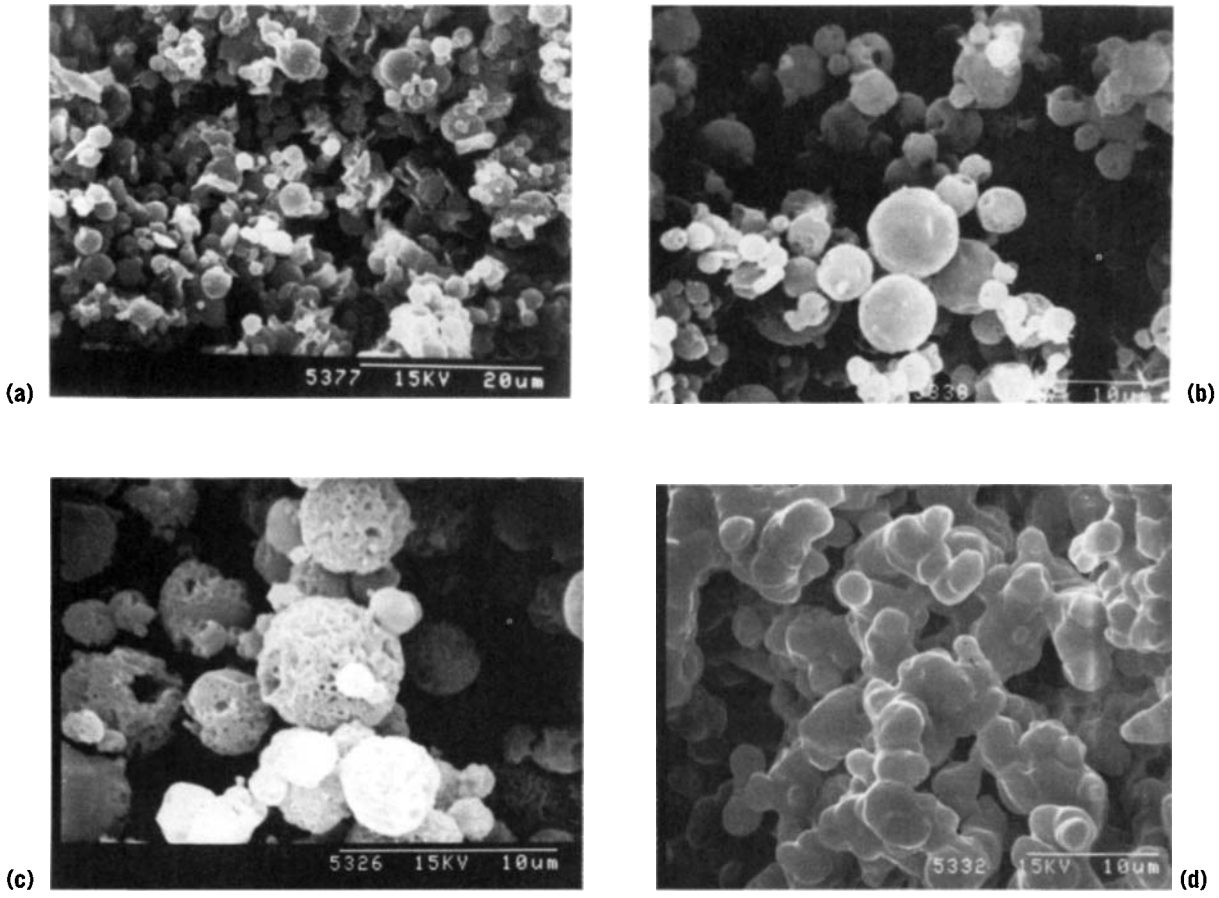


Figure 26. SEM of spray-dried microspheres: (**a**) blank poly(SA): (**b**) blank poly(CPP-SA) 20:80; (**c**) blank poly(FA-SA) 20:80; and (**d**) PCPV microspheres.

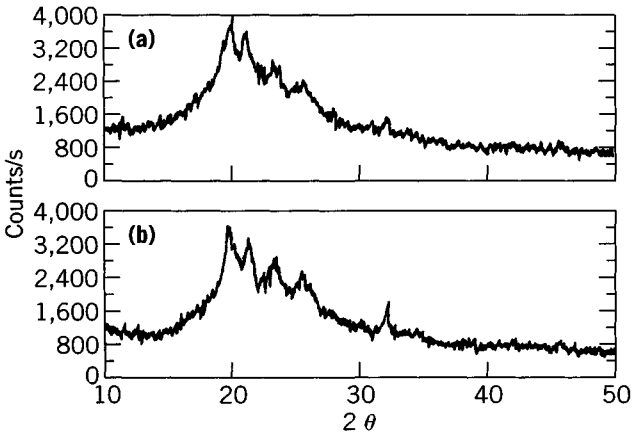


Figure 27. X-ray diffraction of P(CPP-SA) 20:80 spray-dried microspheres (**a**) loaded with 3% acid orange and (**b**) loaded with 10% acid orange. *Source:* With permission from Ref. 151.

and unloaded microspheres. However, the fine structure of the P(FA-SA) 20:80 polymer was retained (Fig. 29). This indicates that the polymers crystallized during the spray-drying process.

It was evident from the X-ray powder diffraction, as well as from thermal studies, that the polymers tend to lose their degree of crystallinity during spray-drying. This phenomenon is known in spray-drying of both polymers as well as small molecules (152,153). The fast drying process provides very short times for the polymer to precipitate, resulting in a more amorphous structure. Addition of drugs, especially those soluble in the organic solvents, further decreases the degree of crystallinity.

The release of acid orange from P(CPP-SA) 20:80 occurred over a period of 15 hours, and the polymer degraded completely over 24 hours. Similar release rates were observed in P(FA-SA) 20:80 microspheres, where polymer degradation was more closely correlated to release rates. In this case, both the porous structure and the good solubility of the degradation products resulted in a better correlation between the release and degradation products. Release of STH (Fig. 30) lasted over 24 hours and resulted in the release of about 90% of the drug. The short release rates (24 hours) that were obtained are expected. First, the degradation time of P(CPP-SA) 20:80 polymer is very fast (81). In addition, the size of the microspheres is very small (1–5 mm). This type of delivery system may find applications in cases where fast release is needed, for example, in oral delivery systems.

The release of the incorporated material can occur via two independent processes. The first is diffusion of the drug through fluid-filled pores formed by the dissolution of

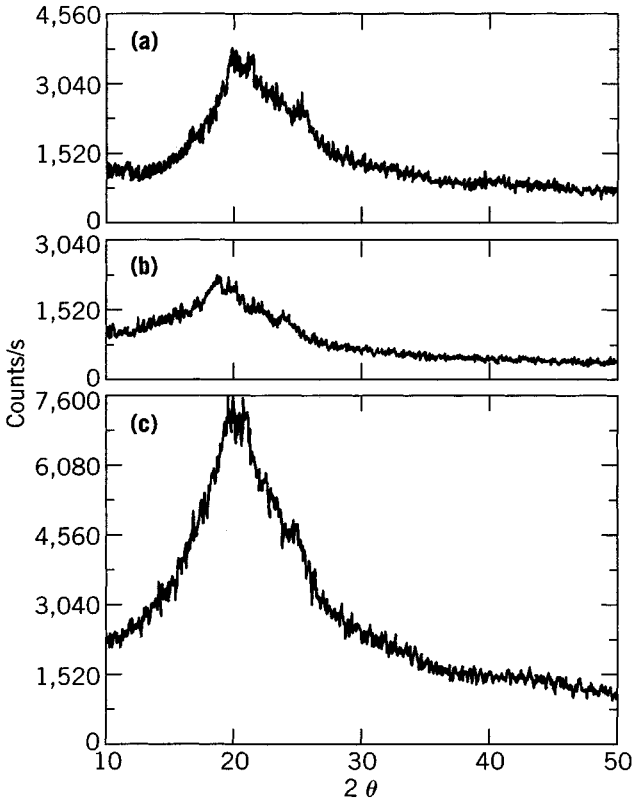


Figure 28. X-ray diffraction of P(CPP-SA) 20:80 spray-dried microspheres: (**a**) blank; (**b**) loaded with methyl red; and (**c**) loaded with acid orange. *Source:* With permission from Ref. 151.

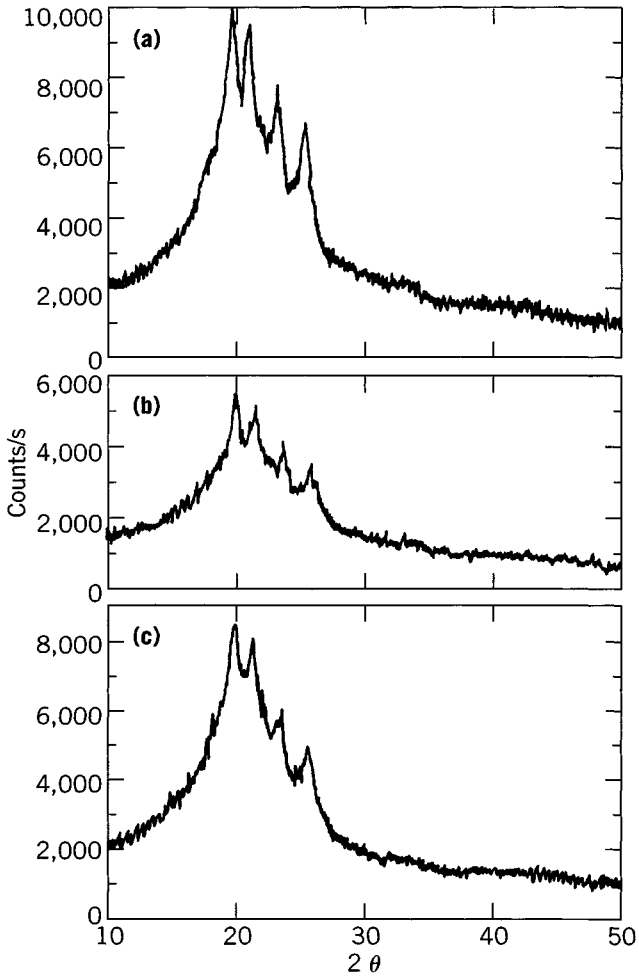


Figure 29. X-ray diffraction of P(FA-SA) 20:80 spray-dried microspheres: (**a**) blank; (**b**) loaded with acid orange; and (**c**) loaded with methyl red. *Source:* With permission from Ref. 151.

the incorporated drug particles; the second is via erosion of the polymer matrix as the anhydride bonds are hydrolyzed. The total release of drug is the sum of these two release rates.

For most of the polymer types used, the erosion of the polymer is less than 15% over the first four hours. During this time period, cumulative drug release is in the range of 60–70%. Thus, to compare the effect of different polymers and drug loadings, the release over this early time period was modeled as a diffusion process, since the release due to erosion is low. The following mass balance applies for the drug within the microspheres:

$$\frac{\partial C}{\partial t} = D_e \nabla^2 C \tag{21}$$

where C is the concentration of the drug in the particle, t is the time, D_e is the effective diffusion of the drug in the polymer matrix, and ∇^2 is the Laplacian.

The first equation can be integrated, and the cumulative fraction of the drug released as a function of time can be computed as follows:

$$\frac{M_t}{M_\infty} = -\frac{6}{\pi^2} \sum_{n=1}^{\infty} \frac{1}{n^2} \exp\left(-n^2 \pi^2 D_e \frac{t}{r_0^2}\right) \tag{22}$$

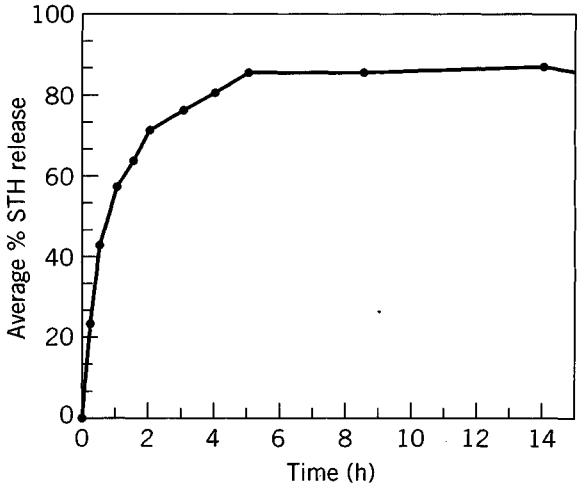


Figure 30. STH released from P(CPP-A) 20:80 microspheres. *Source:* With permission from Ref. 151.

where

$$\frac{M_t}{M_\infty} \tag{23}$$

is the cumulative fraction released, and r_0 is the sphere radius.

The effective diffusion coefficient is governed by the fabrication parameters, such as the quantity of drug loaded, the size of the drug particles loaded, the crystallinity of the polymer, and the porosity of the system. The release curves are fitted to the second equation using a least squares fitting method and an estimate of the effective diffusion coefficient (D_e) is obtained. Knowing the diffusion coefficient of the drug in saline D_s, a retardation factor can be calculated as follows: $R = D_s/D_e$.

The degree of retardation provides information as to whether the drug or dye was successfully encapsulated. Diffusion coefficients were calculated for the 20:80 polymer for both acid orange and STH. The diffusion coefficients in saline for acid orange and STH (D_s) were estimated as 1×10^{-5} cm2/s and 1×10^{-6} cm^2/s, respectively. The estimated effective diffusion coefficients and the net retardation factors are summarized in Table 10.

The microspheres produced have approximately the same diameter as the drug particles that were incorporated. Thus, it is likely that only a single drug particle is contained within each microsphere. The retardation factors for acid orange and STH are on the same order of magnitude, despite the large difference in molecular weight. This supports the notion that the individual drug particles are completely entrapped within the polymers as the initial release is not a function of the characteristic properties of the drug.

Kreitz (154) studied the degradation of spray-dried PLGA microspheres for a period of up to three months using FTIR and SEM. Briefly, 10 g of PLGA 50:50 (35,000 M_w) were dissolved in methylene chloride, producing a 5% (w/v) polymer solution. This solution was spray-dried at 40°C, and the resultant microspheres were lyophilized. Fifty milligrams of the microspheres and 1 mL of buffer were added to separate microcentrifuge tubes for each time point (1 and 3 days and 1, 2, 3, 4, 6, 8, 10, 12, 16, and 20 weeks), and were placed in a 37°C water bath. At the specified time points the buffer was removed from a tube, the polymer was washed with distilled water and then lyophilized. SEM and FTIR were performed on each of the degradation samples and on preliminary (nondegraded) samples.

In the SEMs (Fig. 31) the degradation of the microspheres over three weeks is shown. In Figure 31a (day zero), the spheres are seen as 0.5–5 μm-diameter distinct particles with porous, crenellated surfaces. After only 1 day in 37°C buffer (Fig. 31b) the microspheres have lost their original surface features. They now appear smooth and have started to coalesce, indicating a drop in the glass-transition temperature due to degradation. At 3 days (Fig. 31c) the coalescence has proceeded but the original morphology remains discernible. At 7 days (Fig. 31d) the continuing degradation induces agglomeration from individual spheres, and at 2 weeks (Fig. 31e) the polymer appears as an amorphous mass, the original morphology now gone. The samples at 3 weeks (Fig. 31f) and subsequent time points were viscous liquids, having undergone extensive degradation.

Table 10. Diffusion Coefficients D_s, (Salin), D_e (Polymer), and Retardation Factors for P(CPP SA) 20:80 Microspheres

Drug	D_s cm^2/s	D_e cm^2/h	R
Acid orange	1.0×10^{-5}	6.3×10^{-9}	5.7×10^{6}
STH	1.0×10^{-6}	8.0×10^{-10}	4.5×10^{6}

The FTIR spectra of the microspheres' degradation over 12 weeks are shown in Figure 32, from 2,000 cm^{-1} to 600 cm^{-1}. The most apparent changes in the progression are seen in the peak at 1,760 cm^{-1}, which represents the carbonyl bond of the polyester, and in the peak triplet around 1,400 cm^{-1}, which represents the bonds between the lactide-lactide (L-L, 1,456 cm^{-1}), glycolide-glycolide (G-G, 1,425 cm^{-1}), and lactide-glycolide (L-G, 1,398 cm^{-1}) mer units of the polymer. The spectra remain fairly constant over the first week of degradation. At 2 weeks the carbonyl peak is broader, possibly due to the transition of some crystalline regions to amorphous regions. The peak triplet at 2 weeks shows no distinct change. At 3 weeks the L-L (left) peak in the triplet appears to have receded slightly relative to the G-G and L-G peaks, suggesting greater degradation of this bond relative to the other two types of ester bonds present in this polymer. Also, the carbonyl peak is slightly broader than that of 2 weeks indicating further crystalline-to-amorphous transition. At 4 weeks the carbonyl peak appears sharper and all three peaks of the triplet have decreased relative to the peak of the carbonyl bond. The carbonyl peak's sharpness may be the result of the amorphous regions' partial degradation and dissolution, leaving behind the more crystalline regions. The reduction in the triplet peak at this stage indicates a general progression of the polymer degradation via hydrolysis of the ester bonds. At 6 weeks the carbonyl peak appears unchanged from that of 4 weeks while the triplet peaks have decreased extensively. The peaks of the G-G and L-G bonds have decreased to a greater extent than that of the L-L peak. At 8 weeks the carbonyl peak's sharpness indicates continued degradation and dissolution of oligomers from the polymer. The G-G peak is the only one of the triplet which remains, a finding that continues to the last measurement at 12 weeks. This may be due to the degradation resistance of oligomer blocks consisting mostly of glycolide mers.

In the present Luck et al. studies the influence of the polymer composition and the production method of microspheres on the in vitro plasma protein adsorption were investigated using two-dimensional electrophoresis. Microparticles were prepared from poly(L-lactide) (L-PLA), (PLGA), and ABA triblock copolymers containing hydrophilic poly(oxyethylene) (B-block) domains connected to hydrophobic polyesters (A-blocks). Two different microencapsulation methods were employed, namely the W/O/W emulsion solvent evaporation method and the spray-drying technique. It could be demonstrated that the polymer composition and, especially, the encapsulation technique, influenced the interactions with plasma proteins

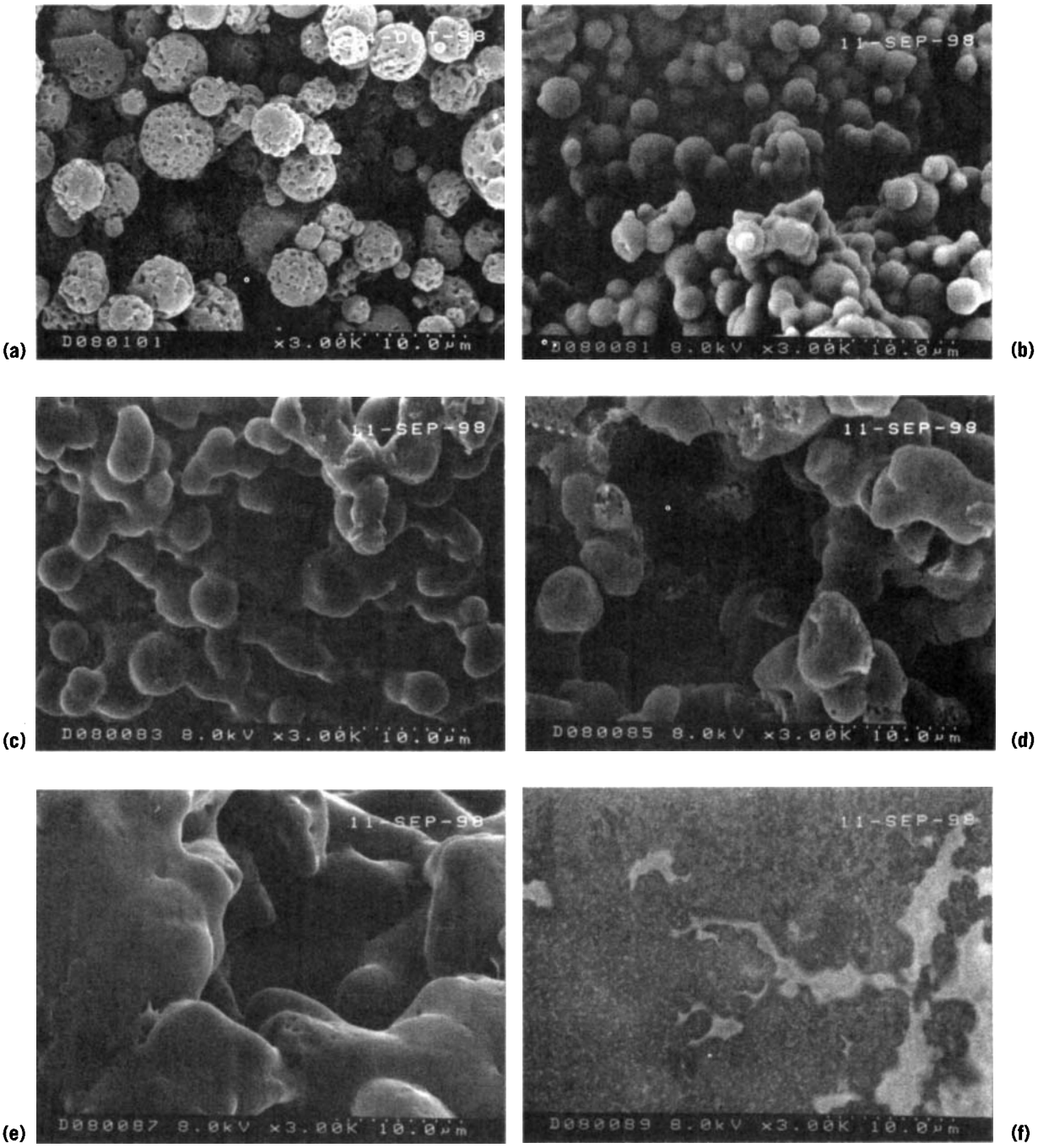


Figure 31. SEM series showing the procession of PLGA microsphere degradation at (**a**) time zero, (**b**) 1 day, (**c**) 3 days, (**d**) 2 weeks, and (**f**) 3 weeks.

significantly. For example, the percentages of several apolipoproteins in the plasma protein adsorption patterns of spray-dried PLGA and L-PLA particles were distinctly higher when compared with the adsorption patterns of the particles produced by the W/O/W technique. Some adsorbed proteins were found to be characteristic or even specific for particles produced by the same method or consisting of identical polymers. PVA used as stabilizer in the W/O/W technique may decisively influence the surface properties relevant for protein adsorption. The plasma protein adsorption on particles composed of ABA copolymers was drastically reduced when compared to microspheres made from pure polyesters. The adsorption patterns of ABA particles were dominated by albumin. The plasma protein adsorption patterns detected on the different microspheres are likely to affect their in vivo performance as parenteral drug delivery systems (155). It is known that the hydrophobicity of a surface can influence protein adsorption, i.e.,

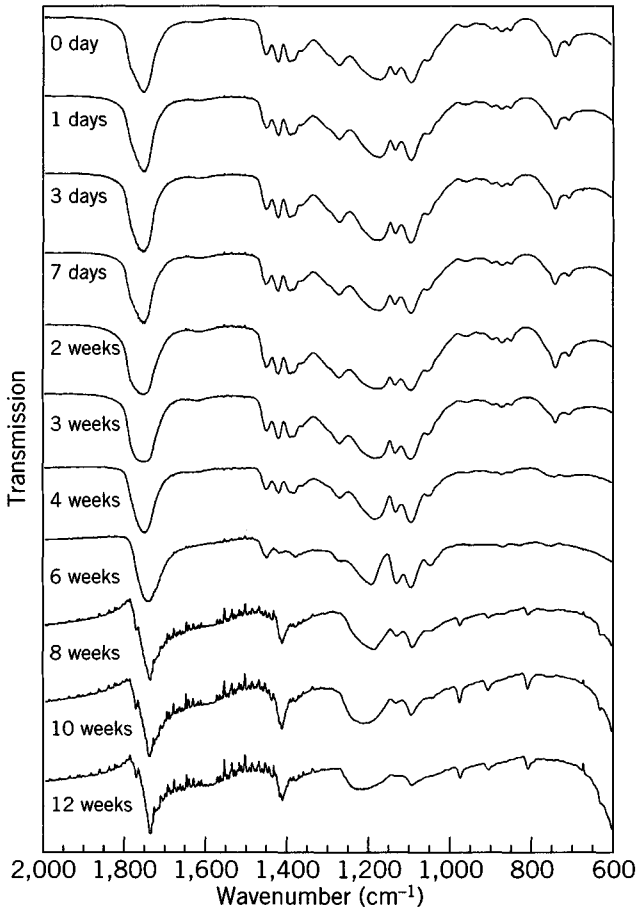


Figure 32. FTIR degradation studies on the same microspheres as shown in Figure 31.

hydrophobic surfaces favor protein adsorption. Therefore, the hydrophobicity of films made of the polymers used for the microparticle formation was characterized using contact angle measurements. The measurement of contact angles gave the following rank order of hydrophobicities as a function of contact angles: L-PLA>PLGA>ABAI>ABAII (155). The most striking difference between the two particle types was the strong adsorption of the apolipoproteins on the spray-dried particles (155).

Three methods were used, namely spray-drying, W/O/W solvent evaporation and ASES, for the preparation of microparticles having the same size range, to study the influence of the preparation method on polymer degradation in vitro (phosphate-buffered saline, 37°C, one month). The following five polymers of the biodegradable PLA and PLGA groups were selected to prepare blank and drug-loaded microparticles: L-PLA (M_w 81,200); DL-PLGA 75:25 (M_w 64,300); DL-PLGA 50:50 (M_w 52,600); DL-PLGA 50:50 (M_w 14,500); and DL-PLGA 50:50 (M_w 3,400). Tetracosactide was selected as the model peptide. When microparticles were prepared by solvent evaporation, the mean diameter and, more markedly, the drug encapsulation efficiency decreased with decreasing molecular weight and an increasing proportion of glycolic acid in the polymer. In contrast, no direct influence of the polymer nature on these parameters was observed in spray-dried microparticles. Polymer degradation was heterogeneous in L-PLA and DL-PLGA 75:25 microparticle and was not influenced by the presence of the drug at a nominal loading of 1% (W/W), when prepared by the three methods (note that with ASES, only L-PLA could be used for microencapsulation). In batches made of DL-PLGA 50:50 (M_w 52,600), the degradation rate decreased slightly with increased drug loading. Only for the case of DL-PLGA 50:50 (M_w 14,500) was the polymer degradation rate for spray-dried microparticles higher than that of microparticles prepared by the W/O/W solvent evaporation method. Generally, the degradation rates of the different microparticles followed the expected order: L-PLA < DL-PLGA 75:50 < DL-PLGA 50:50 (M_w 52,600) < DL-PLGA 50:50 (a mixture of M_w 52,600 and M_w 3,400). Polymer degradation was homogenous in DL-PLGA 50:50 microparticles. Decreasing the molecular weight of DL-PLGA 50:50 from 52,600 to 14,500 did not result in accelerate polymer degradation (156).

ONE-STEP FORMATION OF DOUBLE-WALLED MICROSPHERES

With the increasing complexity of therapeutic regimens, drug delivery systems may become more sophisticated. There are many approaches to achieving long-term release of pharmacologic agents using microspheres, but this technology is not without problems. One drawback to this sort of system is the initial "burst" effect caused by the rapid release of the drug particles trapped on the surface during manufacturing. One solution to this problem that was developed was to prepare multilayered microspheres consisting of concentric spheres of polymer. Traditional methods to form such delivery systems (e.g., pan- or dip-coating and air suspension coating) require multiple steps, which decreases process yield (157–159). First, the core would be formed, and then each of the coating layers was added in separate steps. More recently, Mathiowitz et al. have developed a method to manufacture multilayered microspheres in a single step (84,101,160–162). This process combines the natural tendency of polymers to phase separate as solution concentration increases with the microencapsulation process of solvent evaporation. Moreover, it is a one-step process for creating double-layered microspheres and has advantages over other methods for coating microspheres. In the dip-coating process, the coating is usually nonuniform in both coverage and thickness (Fig. 33). Also, each coating adds an additional step to the manufacturing process, increasing quality control problems at each stage, and further decreasing the yield. Coating processes involving fluidized beds have produced microspheres with a uniform coating, but fluidized beds are difficult to design for particle sizes of less than 100 μm.

The one-step process described here combines the phenomenon of phase separation with emulsion theory and can be used to produce spheres of diameters less than 20 μm and up to 1,000 μm. The basic difference between this process and organic phase separation or coacervation is that two polymers are used to cause the phase separation and that both are used in high concentration. Thus the

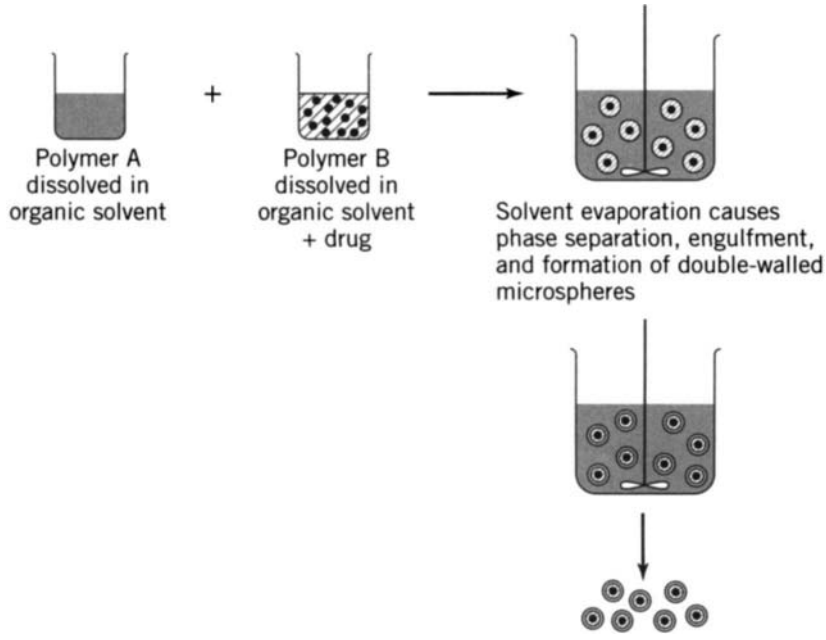


Figure 33. Formation of one-step double-walled microspheres.

final product, unlike coacervation, is the formation of two layers each containing two separate polymers.

The section entitled "Interfacial Phenomenon" and Figure 8 describe the tendency of a liquid to spontaneously spread across a solid or liquid surface in terms of the surface and interfacial tensions of the components. It can be modified to represent a system in which two dissimilar phases are dispersed within a third by substituting the appropriate interfacial tensions for the surface tensions in Harkin's equation (163):

$$\lambda_{AB} = \gamma_{BS} - \gamma_{AS} - \gamma_{AB} \qquad (24)$$

where γ_{AS} and γ_{BS} are the interfacial tensions of the solvent and polymer A or B, respectively, and γ_{AB} is the interfacial tension between polymers A and B. For positive values of λ_{AB}, polymer A spontaneously spreads on polymer B. The actual configuration of the two dissimilar phases (A and B) depends on the values of the three possible spreading coefficients and can be described as complete engulfing, partial engulfing, and nonengulfing (see Fig. 8).

Combination of the emulsion theory described here with the phenomenon of phase separation provides a novel approach for preparing double-walled polymer microspheres. By introducing a two-polymer solution into a continuous phase, a stable emulsion is created in which phase separation occurs within each drop. The phase separation can be engineered such that one polymer engulfs the others, forming double-walled microspheres in a single step. Each of the configurations shown in Figure 8 can be visualized using SEM (Fig. 33). Figure 34a shows a cross section of a double-walled sphere of polyanhydride and PLA exhibiting phase separation and complete engulfment. Figure 34b shows a nonengulfing, chaotic structure formed from PLA and polystyrene when precipitation occurred after phase separation but before engulfment. And Figure 34c shows a high-magnification SEM photo of the wall material in Figure 34a indicating that some of the core phase is entrapped in the wall.

The microspheres were formed by first preparing separate solutions (10–20% w/v) of the two polymers in a volatile organic solvent (see Fig. 33). The drug or protein was added to the appropriate polymer solution at this stage and dispersed evenly. Then the two polymer solutions were mixed and dripped into a stirred bath of 0.5% PVA in water. As the solvent evaporated, the polymer solution concentration increased to the point where they were no longer mutually soluble and began to separate. If allowed enough time before hardening, the two phases configured themselves according to the modified Harkin's equation. There was only one thermodynamic equilibrium configuration of polymer A spreading on polymer B, but the extent of spreading was determined by the rate of polymer precipitation, as controlled by the rate of solvent evaporation. Therefore, two scenarios to produce double-walled microspheres were possible and achieved by balancing the thermodynamic and kinetic factors. In the first, polymers for which Harkin's equation predicts complete engulfment were given sufficient time during the evaporation process for the polymers to reach thermodynamic equilibrium. In this case, complete engulfment was the most stable thermodynamically, and the kinetic factors were minimized by slowing the rate of polymer precipitation. In the second scenario, the completely engulfed configuration was a transient intermediate in the progression from a non–phase separated system toward equilibrium, and the precipitation rate was manipulated such that the polymers were trapped in this configuration, thus allowing the formation of double-walled microspheres when not predicted by the modified Harkin's equation. Once the microspheres had hardened, they were filtered, washed with water, and freeze-dried in preparation for storage and further characterization by optical microscopy with or without cross-polarized light, SEM, TEM, FTIR spectroscopy and DSC.

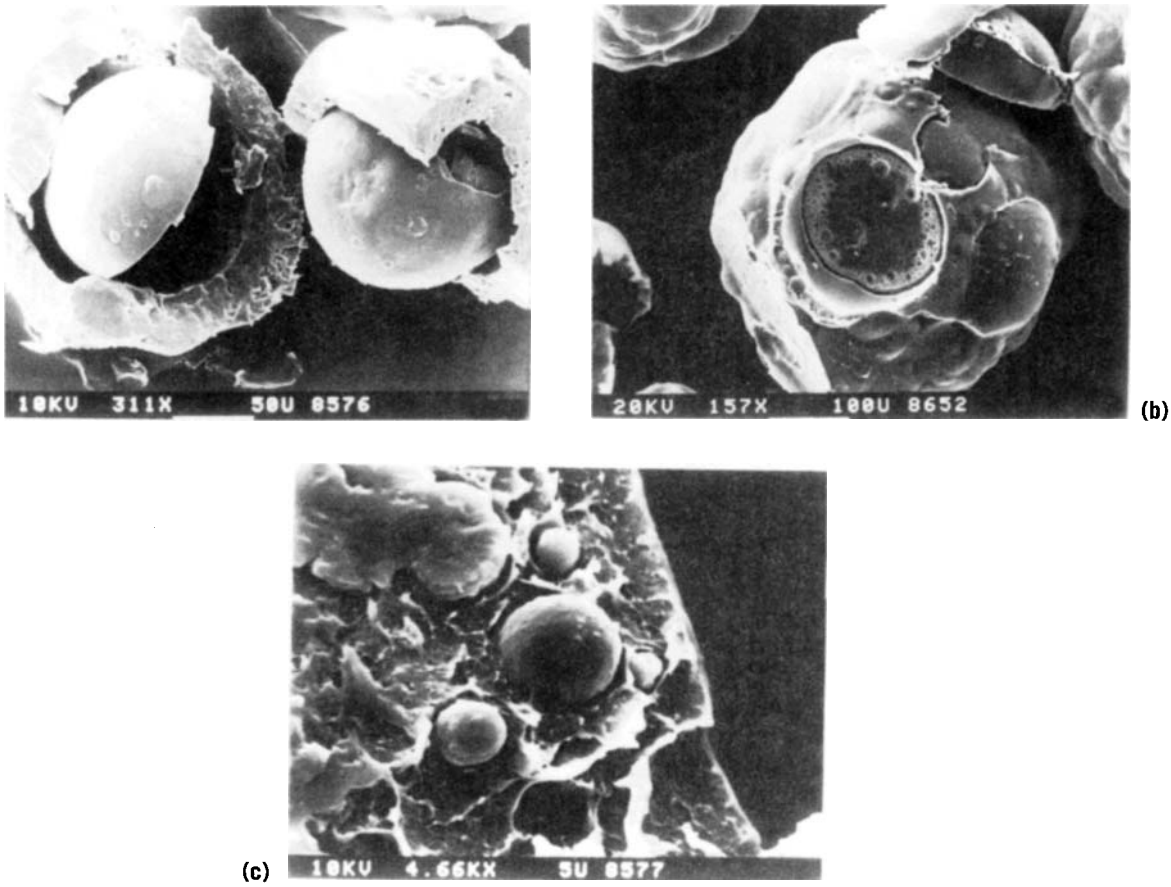


Figure 34. SEM of (**a**) double-walled microsphere; (**b**) multiphase microspheres; (**c**) higher magnification of the external layer in (**a**).

Optical microscopy proved to be a useful tool to study the microspheres as they were hardening. Cross-polarized light allowed the different polymers to be identified as they crystallized, and fluorescently labeled proteins aided in determining in which layer the protein has been trapped (84,101,162).

In a series of two papers (160,161) a more detailed description of the degradation of double-walled microspheres with a core of poly(CPP-SA) 20:80 and a coat of PLLA is given. The first paper presents the in vitro degradation, whereas the second paper discusses the in vivo degradation of these double-walled microspheres implanted subcutaneously and intramuscularly in rats. The second paper also correlates the degradation of the microspheres in the two environments, a critical step in the development of polymeric delivery systems for drugs or therapeutic proteins. Single polymer (SW) microspheres of PLLA, also made by solvent evaporation, were included in the study for comparison.

The general trends observed for double-walled microspheres of an inner core of poly(CPP-SA) 20:80 and outer layer of PLLA was that the inner core degraded first, becoming more granular in appearance as the polyanhydride broke down into short chain oligomers and then finally monomers. These monomers were insoluble in chloroform and were therefore not detectable by GPC or FTIR spectroscopy. DSC (Fig. 35) and SEM analyses of intact microspheres clearly showed their presence out to 6 months after being introduced to the buffer solution (161). The GPC data shows that the SW PLLA microspheres degraded significantly over the 6 months of in vitro degradation, despite the minimal morphologic changes seen by SEM. The PLLA of the double-walled microspheres degraded slightly faster than did the PLLA in the SW microspheres. At the early time points, the molecular weights of the two polymers could be calculated separately, showing that the poly(CPP-SA) 20:80 initially maintained a polymeric molecular weight, but after 2 weeks was no longer detectable.

FTIR also showed the disappearance of the anhydride bonds over the first two weeks of degradation (Fig. 36). DSC confirmed this, showing a decrease in size of the melting transition for the poly(CPP-SA) 20:80 polymer with the emergence of an intermediate peak due to the oligomers and monomers of the degraded polyanhydride. The SW PLLA microspheres remained dense and smooth in appearance throughout the study, and the FTIR spectra remained constant. The melting temperature of the PLLA decreased over the 6-month study due to the drop in molecular weight, which was confirmed by GPC.

Selected samples of the SW microspheres implanted subcutaneously were analyzed by SEM, and the micrographs are shown in Figure 37. After 1 week, the implant

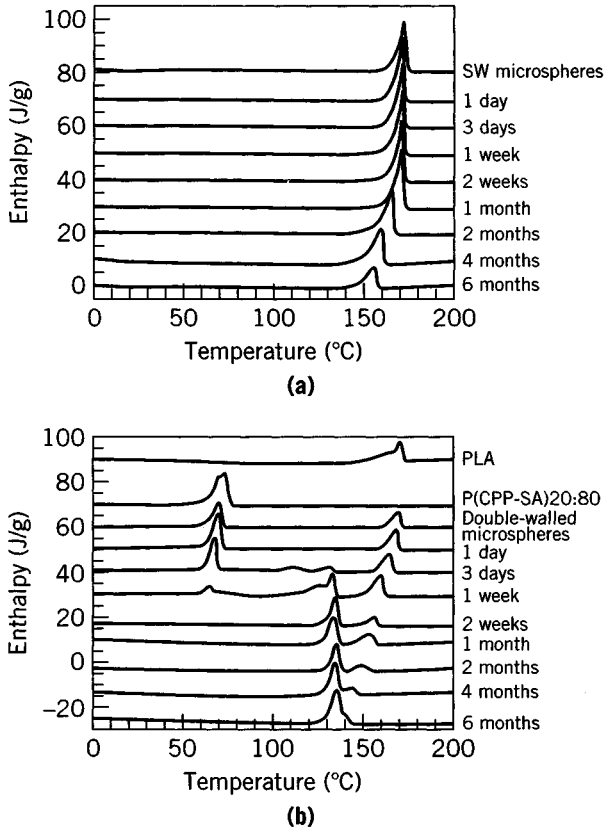


Figure 35. DSC thermogram of microspheres degraded in vitro. (**a**) SW PLLA and (**b**) Double-walled PLLA and poly(CPP-SA) 20:80. *Source:* With permission from Ref. 160.

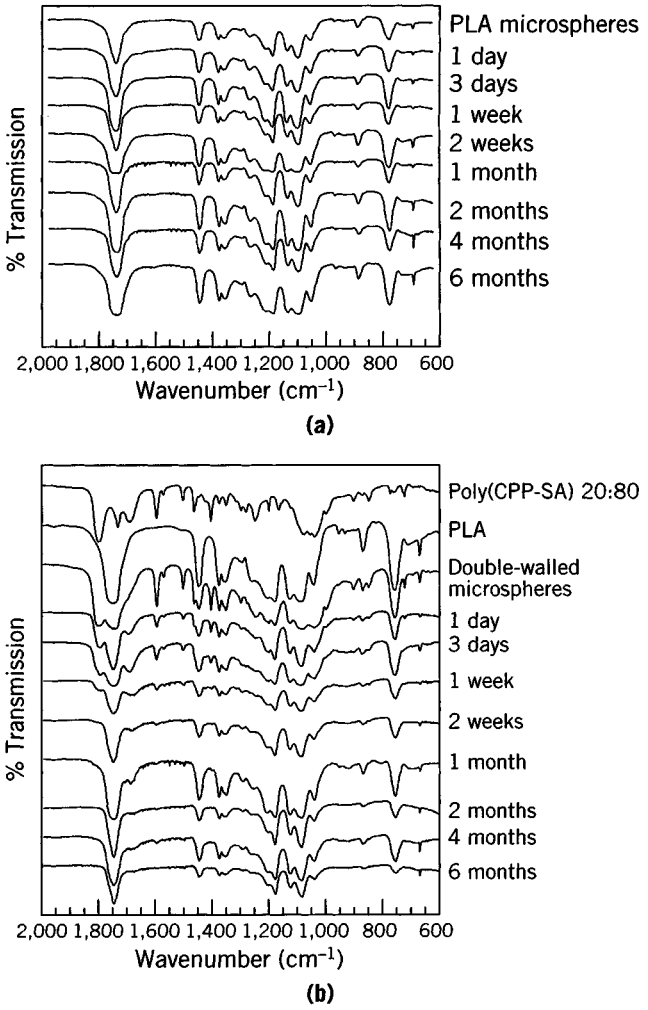


Figure 36. Transmission FTIR spectra of microspheres before and after in vitro degradation: (**a**) SW PLLA microspheres and (**b**) double-walled PLLA and poly(CPP-SA) 20:80. *Source:* With permission from Ref. 160.

site was slightly inflamed and the implant was filled with some excess fluid, resulting in a gap in the center of the implant seen after cross-sectioning (Fig. 37). This inflammation had cleared after 2 weeks. Even out to 6 months of degradation in vivo, the PLLA still appeared very dense. SW PLLA microspheres implanted intramuscularly degraded similarly to those implanted subcutaneously (data not shown).

Selected SEM micrographs of double-walled microspheres implanted subcutaneously are shown in Figure 38. Figure 38a shows the subcutaneous implant site after 1 week, revealing the empty center that was filled with fluid upon explantation. Higher magnification of the spheres after 1 week showed the degradation of the polyanhydride core (Fig. 38b). A higher magnification of the interface shows the differences in the rates of degradation of the two polymers (Fig. 38c). The PLLA coating was still relatively intact. After 1 and 6 months of degradation, the inner core continued to degrade and disappear, shrinking in size (Figures 38d, 38e, and 38f).

The degradation of the microspheres showed the same trends in vitro as in vivo. Microscopy showed no differences in the pattern or kinetics of the degradation. Physical characterization showed more differences between the degradation in vitro and in vivo, but the separate extraction step required for the in vivo sampling may have skewed these results. The M_w of the microspheres degraded in vitro decreased faster than did the M_w of those degraded in vivo. In both cases and at all time points, the M_w of the double-walled microspheres was lower than that of the SW microspheres. FTIR spectroscopy and DSC analyses of the double-walled microspheres degraded in vivo identified PLLA as the only polymer present in the extracted sample at all time points. No differences were seen by these two methods between the samples degraded in vitro and in vivo.

Degradable, multilayered microspheres such as those described in this article could serve as complex delivery vehicles for therapeutic agents. The applications for such microspheres within the field of drug delivery are numerous, and a well-characterized degradation profile, both in vitro and in vivo, will aid in the development of a clinically useful delivery system.

Next Page

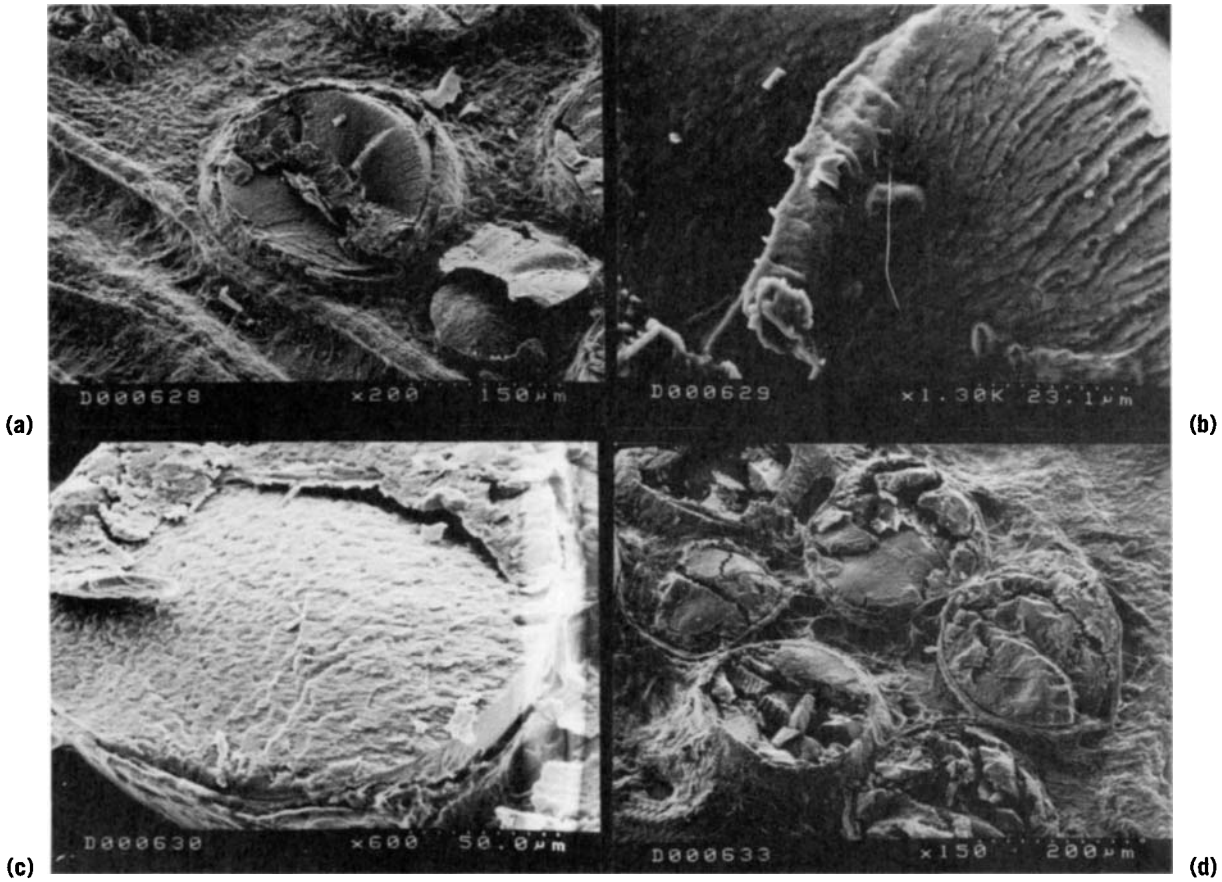


Figure 37. SEM of SW PLLA microspheres degraded at subcutaneous sites in vivo. (**a**) After 1 week, (**b**) higher magnification of interface after 1 week of degradation. (**c**) after 1 month, and (**d**) 6 months of degradation. *Source:* With permission from Ref. 161.

NOVEL ENCAPSULATION TECHNIQUES

One of the most interesting methods is being used for scale-up preparation of the injectable Prolease microsphere product, manufactured by Alkermes. The process is based on solvent extraction in nonaqueous solutions and, in addition, it is produced under cryogenic conditions. These two facts ensure high encapsulation efficiency of the drug while maintaining its integrity. A good review on the process, as well as approaches to scale it up, have been discussed by Tracy (164).

Mathiowitz et al. group has recently develop a new method to produce microspheres and nanospheres in the range of 0.2 to 30 μm, called the PIN (phase inversion microencapsulation) method (165). This process is based on the spontaneous formation of microspheres in an environment of a nonsolvent. Here the challenge is in developing oral delivery systems for proteins and genes, and the PIN system has been used to successfully deliver small molecules, insulin, and plasmid DNA by the oral route. The method is very gentle and thus the activities of very sensitive bioactive molecules and proteins such as IL-2 are not destroyed (166; N.K. Egilmez et al., unpublished data). Encapsulation of IL-2, PEG-modified IL-2 (PEG/IL-2), and interleukin-12 (IL-12) using the PIN technique resulted in release of bioactive cytokines for up to one month in vitro (Y.S. Jong et al., unpublished data). The in vivo bioactivity of IL-2 released from PIN microspheres was demonstrated in a human tumor xenograft/SCID mouse model (166). Subcutaneous coinjection of IL-2 microspheres and tumor cells resulted in complete suppression of tumor engraftment in 80% of the animals. More recently, IL-12 releasing PIN microspheres were shown to be similarly effective in a mouse head and neck tumor model (M.A. Kuriakose et al., unpublished data) indicating the versatility of the PIN technique for functional encapsulation and release of different proteins.

APPLICATIONS OF MICROENCAPSULATION

With the vast array of encapsulation techniques currently available, nearly any active agent can be successfully incorporated into a microparticulate formulation. The limiting factors in applying these processes are imagination and, ultimately, cost. Encapsulation is a fairly standard practice in both the food, consumer product, and cosmetics industries. Flavors have been encapsulated since the 1930s, vitamins since the 1940s, and ink for carbonless paper since 1956 (167). The main purpose behind encap-

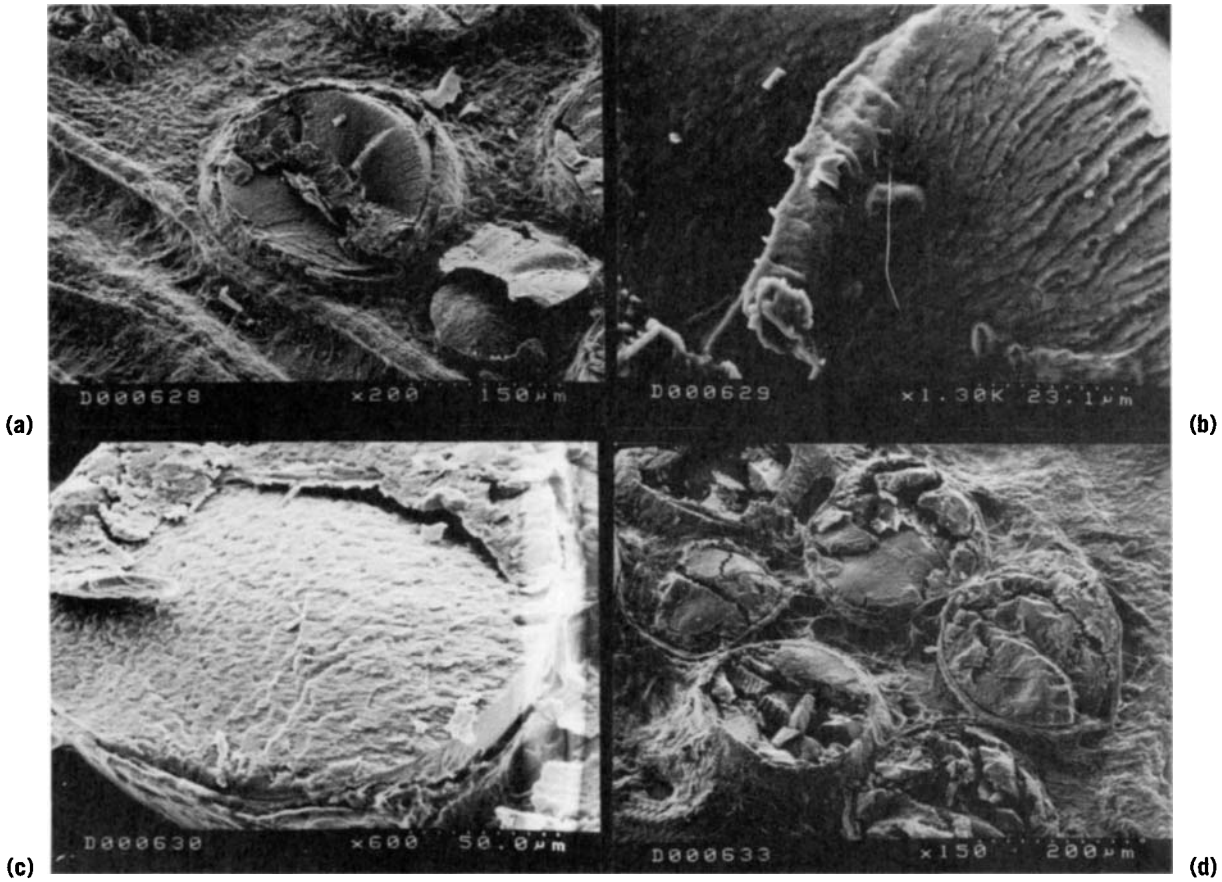


Figure 37. SEM of SW PLLA microspheres degraded at subcutaneous sites in vivo. (**a**) After 1 week, (**b**) higher magnification of interface after 1 week of degradation. (**c**) after 1 month, and (**d**) 6 months of degradation. *Source:* With permission from Ref. 161.

NOVEL ENCAPSULATION TECHNIQUES

One of the most interesting methods is being used for scale-up preparation of the injectable Prolease microsphere product, manufactured by Alkermes. The process is based on solvent extraction in nonaqueous solutions and, in addition, it is produced under cryogenic conditions. These two facts ensure high encapsulation efficiency of the drug while maintaining its integrity. A good review on the process, as well as approaches to scale it up, have been discussed by Tracy (164).

Mathiowitz et al. group has recently develop a new method to produce microspheres and nanospheres in the range of 0.2 to 30 μm, called the PIN (phase inversion microencapsulation) method (165). This process is based on the spontaneous formation of microspheres in an environment of a nonsolvent. Here the challenge is in developing oral delivery systems for proteins and genes, and the PIN system has been used to successfully deliver small molecules, insulin, and plasmid DNA by the oral route. The method is very gentle and thus the activities of very sensitive bioactive molecules and proteins such as IL-2 are not destroyed (166; N.K. Egilmez et al., unpublished data). Encapsulation of IL-2, PEG-modified IL-2 (PEG/IL-2), and interleukin-12 (IL-12) using the PIN technique resulted in release of bioactive cytokines for up to one month in vitro (Y.S. Jong et al., unpublished data). The in vivo bioactivity of IL-2 released from PIN microspheres was demonstrated in a human tumor xenograft/SCID mouse model (166). Subcutaneous coinjection of IL-2 microspheres and tumor cells resulted in complete suppression of tumor engraftment in 80% of the animals. More recently, IL-12 releasing PIN microspheres were shown to be similarly effective in a mouse head and neck tumor model (M.A. Kuriakose et al., unpublished data) indicating the versatility of the PIN technique for functional encapsulation and release of different proteins.

APPLICATIONS OF MICROENCAPSULATION

With the vast array of encapsulation techniques currently available, nearly any active agent can be successfully incorporated into a microparticulate formulation. The limiting factors in applying these processes are imagination and, ultimately, cost. Encapsulation is a fairly standard practice in both the food, consumer product, and cosmetics industries. Flavors have been encapsulated since the 1930s, vitamins since the 1940s, and ink for carbonless paper since 1956 (167). The main purpose behind encap-

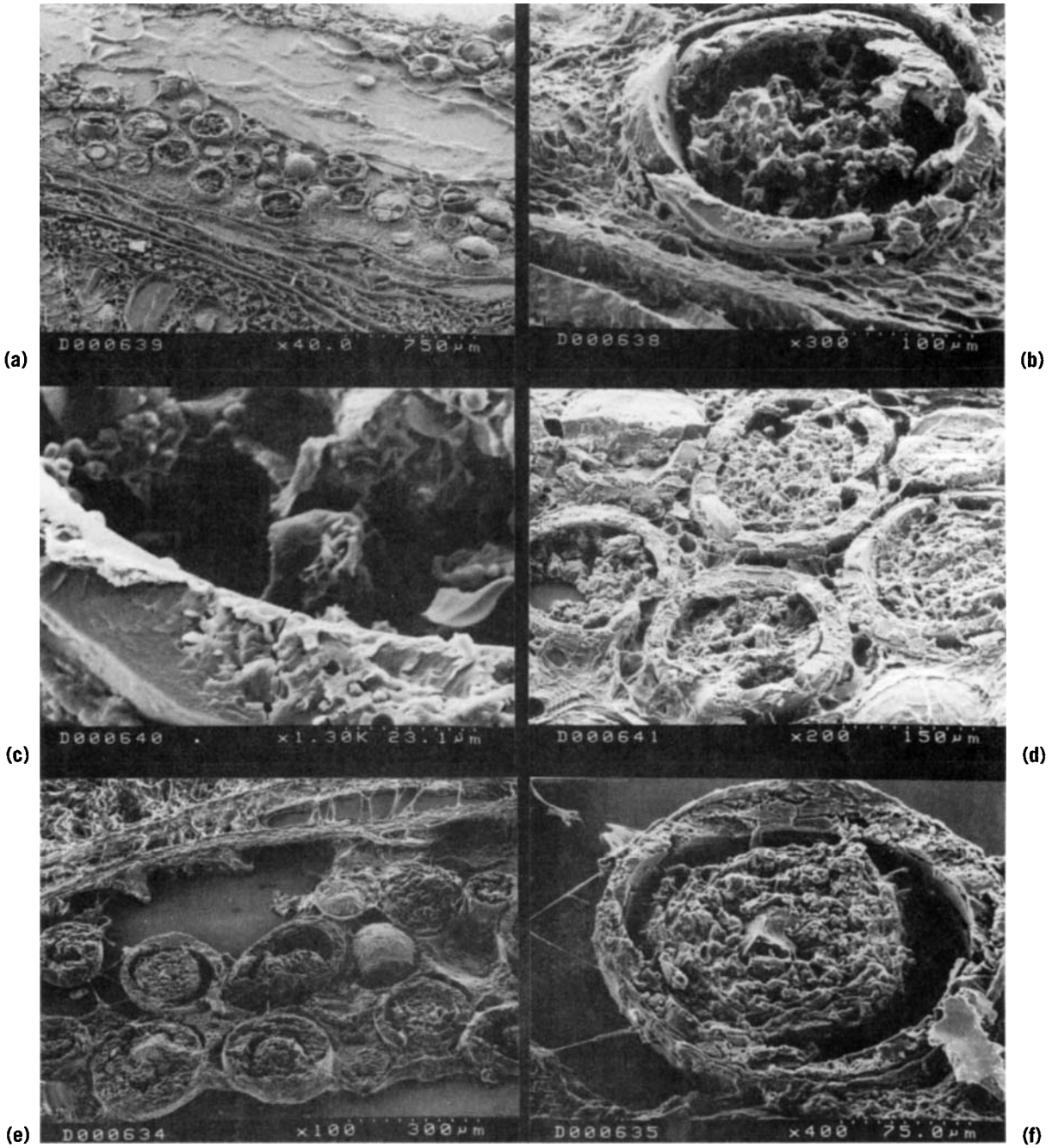


Figure 38. SEM of double-walled microspheres degraded subcutaneously in vivo. (**a**) After 1 week, showing gap in center of implant due to inflammation, (**b**) after 1 week, (**c**) higher magnification after 1 week of degradation, (**d**) after 1 month, (**e**) after 6 months, and (**f**) after 6 months of degradation. *Source:* With permission from Ref. 161.

sulating these materials was often for their protection and enhanced stability, as in foods and vitamins. The release of the active agent was triggered by drastic environmental changes in going from a dry to a wet environment or by physical trauma to the capsules in grinding or chewing. Encapsulated ink for carbonless paper is actually a triggered release device, where the trigger is the physical force that ruptures the capsule and releases the ink.

Encapsulation in the Food, Consumer Products, and Cosmetics Industries

For most products in the foods and consumer products industries, encapsulation must be accomplished on a very large scale and cannot add a significant cost to the product either in materials, processing, or labor. Even with these limiting factors, the majority of these products currently

on the market have at least one component encapsulated. The most common techniques for encapsulating materials are spray-drying, extrusion, molecular inclusion, and coacervation (167). Of these, spray-drying and coacervation are true microencapsulation processes which have been discussed earlier in this article.

Spray-drying is often used to convert an oil or other liquid into a solid for easier handling and increased shelf life. This stability is dependent upon the wall materials used as well as the microcapsule porosity and the presence of any trace prooxidants or antioxidants. In general, spray-drying may be accomplished at a low cost and appropriate equipment is readily available. The resulting particles can be small and a variety of edible, soluble, and degradable wall materials may be used. Coacervation will usually give larger particles (20 μm and larger) and can also be made at a fairly low cost. A high loading can be achieved if the material to be encapsulated and the wall material are immiscible. Both liquids and solids have been encapsulated using coacervation with wall materials such as wax, protein, fat, carbohydrate, and gelatin.

Many of the same polymers used for pharmaceutical and medical applications are also used for cosmetic formulations, including polysaccharides, polypeptides, acrylates, and methacrylates (168). Most encapsulated ingredients in cosmetics products are in the nanoparticle size range. These nanoparticles usually contain cosmetic hydrophilic components which are designed to modulate the release in and onto the skin (169). Nanocapsules for cosmetic applications usually contain a lipophilic active substance which should be protected from the environment by encapsulation and release the active agent slowly over time. One of the key components in Lacome's Primordial is nanoencapsulated vitamin E.

Applications of Encapsulation for Agricultural Products

Encapsulated products with controlled release behavior can have significant advantages in the use of pesticides (59). Along with the traditional advantage of more constant release over extended periods of time, encapsulated pesticides can also show reduced mammalian toxicity, reduction of evaporative losses, and reduction in flammability of liquids. Most encapsulated pesticide materials are produced by interfacial polymerization or phase separation. The most widely used shell materials for interfacial polymerization are polyamides polyurea and polyurethane. For a variety of formulations, including Penncap M (encapsulated diazinon by Pennwalt), Penncaptrin (encapsulated permethrin by Pennwalt), Antifly (encapsulated pyrethrins by Kedem Chemicals), and Empire (encapsulated chlorpyriphos by Dow), the toxicity of the encapsulated material is no more than one-tenth that of the unencapsulated material with a longer efficacy and without a reduction in activity. The greatest advantage of the phase separation technique of encapsulation is the tremendous range of natural polymers, synthetic elastomers, and other synthetic polymers which may be used as the particle wall material. Markus has compiled a table of 46 different polymers that have been used in phase separation encapsulation and also provides examples of processes to encapsulate biological pesticides (59).

Applications and Opportunities for Encapsulation to Enhance Human Health

Although most of the current applications that have been realized using encapsulation are undoubtedly useful, they do not directly address the field of human health insofar as life-threatening conditions are concerned. Encapsulation has been used for decades for vitamins and other drugs, but only one product is currently on the market which uses microencapsulation to deliver a life-saving drug over 4 weeks. This is the Lupron Depot®, from Tap Pharmaceuticals, which contains leuprolide acetate, a LHRH agonist, gelatin, PLGA, and D-mannitol (135). This therapy results in inhibition of the growth of certain hormone dependent tumors.

Many of the formulations mentioned earlier in this article are being studied to treat the wide range of diseases and conditions which would respond well to controlled drug delivery. Other possible medical uses of encapsulation include artificial red blood cells, treatment of acute poisoning and kidney failure using encapsulated adsorbents and immunoadsorbents, encapsulation of living cells as well as encapsulation of enzymes for treatment of phenylketonuria, histidenemia, and other conditions (170). It is the hope of all working in this field that the Lupron Depot® is only a beginning and that medical science can embrace the opportunities that encapsulation can provide with the same enthusiasm that the consumer products and cosmetics fields have already shown.

BIBLIOGRAPHY

1. P. Becher, *Encyclopedia of Emulsion Technology*, Dekker, New York, 1983.
2. S. Cohen and H. Bernstein, *Microparticulate Systems for the Delivery of Proteins and Vaccines*, Marcel Dekker, New York, 1996.
3. C. Amiet-Charpentier, P. Gadille, B. Digat, and J.P. Benoit, *J. Microencapsul.* **15**, 639–659 (1998).
4. M.R. Baichwal and I.A. Abraham, *Indian J. Pharm. Sci.* **42**, 48–51 (1980).
5. J.A. Bakan and J.A. Anderson, in L. Lachman, H.A. Lieberman, and J.L. Kanig, eds., *Theory and Practice of Industrial Pharmacy*, Lea & Febiger, Philadelphia, 1976.
6. R.L. Broughton, F.V. Lamberti, and M.V. Sefton, *Proc. Int. Symp. Controlled Release Bioact. Mater.* **9**, 124 (1982).
7. R. Cadorniga, J.L. Lastres, and P. Frutos, *Boll. Chim. Farm.* **118**, 380 (1979).
8. P.B. Deasy, M.R. Brophy, B. Ecanow, and M.M. Joy, *J. Pharm. Pharmacol.* **32**, 15–20 (1980).
9. A.V. Deshpande and A.P. Njikam, *Indian J. Pharm.* **39**, 76 (1977).
10. D.L. Gardner and D.J. Fink, in E.S.E. Hafez and W.A.A. van Os, eds., *Biodegradable and Delivery Systems for Contraception*, MTP Press, Lancaster, England, 1980, Chapter 3.
11. A.A. Kassem and A.A. El-Sayed, *Bull. Fac. Pharm. Cairo Univ.* **12**, 77 (1975).
12. P.M. John, H. Minatoya, and F.J. Rosenberg, *J. Pharm. Sci.* **68**, 475 (1979).
13. A.P. Jarvis, Jr. and T.A. Gardina, *BioTechniques* **1**, 22 (1983).

14. L. Genc, M. Demirel, E. Guler, and N. Hegazy, *J. Microencapsul.* **15**, 45–53 (1998).
15. S.V. Lamberti, M.A. Wheatley, R.A. Evangelista, and M.V. Sefton, *Polym. Prepr.* **24**, 75 (1983).
16. T. Kato, R. Nemoto, H. Mori, and I. Kumagai, *Cancer (Philadelphia)* **46**, 14 (1980).
17. F. Lim, *J. Pharm. Sci.* **70**, 351 (1981).
18. M.L. Lorenzo-Lamosa, C. Remunan-Lopez, and M.J.A. Vila-Jato, *J. Controlled Release* **52**, 109–118 (1998).
19. F. Lim, *Biomedical Applications of Microencapsulation*, CRC Press, Boca Raton, Fla., 1984.
20. J. Lukaszczyk and P. Urbas, *J. Microencapsul.* **15**, 609–620 (1998).
21. L.A. Luzzi, *J. Pharm. Sci.* **56**, 634 (1967).
22. P.L. Madan, L.A. Luzzi, and J.C. Price, *J. Pharm. Sci.* **61**, 1586 (1972).
23. P.L. Madan, in T. Kondo, ed., *Microencapsulation: New Techniques and Applications*, Techno, Inc., Tokyo, 1979.
24. J.W. MiGinity, A.B. Combs, and A.N. Martin, *J. Pharm. Sci.* **64**, 889 (1975).
25. M.G. Moldenhauer and J.G. Nairn, *J. Controlled Release* **22**, 205–218 (1992).
26. S. Motycka and J.G. Nairn, *J. Pharm. Sci.* **68**, 211 (1979).
27. B.S. Nath, *Indian J. Pharm.* **35**, 26 (1973).
28. B.S. Nath, K. Satyanarayana, and K.N. Bao, *Indian J. Pharm.* **35**, 131 (1973).
29. N. Nihant, C. Grandfils, R. Jerome, and P. Teyssie, *J. Controlled Release* **35**, 117–125 (1995).
30. J.R. Nixon, ed., *Microencapsulation*, Dekker, New York, 1976.
31. J.R. Nixon, *J. Pharm. Sci.* **70**, 376 (1981).
32. M. Rabiskova and J. Valaskova, *J. Microencapsul.* **15**, 747–751 (1998).
33. D.A. Wood, T.L. Whateley, and A.T. Florence, *Int. J. Pharmacol.* **8**, 35 (1981).
34. G. Weiss et al., *J. Microencapsul.* **15**, 335–346 (1998).
35. A. Watanabe and T. Hayashi, in J.R. Nixon, ed., *Microencapsulation*, Dekker, New York, 1976, Chapter 2.
36. D. Vanichtanunkul, P. Vayumhasuwan, and U. Nimmannit, *J. Microencapsul.* **15**, 753–759 (1998).
37. M.I. Ugwoke and R. Kinget, *J. Microencapsul.* **15**, 273–281 (1998).
38. T. Dappert and C. Thies, *J. Membr. Sci.* **4**, 99 (1978).
39. C. Thies, *Polym.—Plast. Technol. Eng.* **5** (1975).
40. Y. Takeda, N. Nambu, and T. Nagai, *Chem. Pharm. Bull.* **29**, 264 (1981).
41. N.N. Salib, M.A. El-Menshawy, and A.A. Ismail, *Pharm. Ind.* **40**, 1230 (1978).
42. S.J. Risch and G.A. Reineccius, *Flavor Encapsulation*, American Chemical Society, Washington, D.C., 1988.
43. L. Brannon-Peppas, *Int. J. Pharm.* **116**, 1–9 (1995).
44. E. Mathiowitz and M.D. Cohen, *J. Membr. Sci.* **40**, 1–26 (1989).
45. E. Mathiowitz and M.D. Cohen, *J. Membr. Sci.* **40**, 27–41 (1989).
46. E. Mathiowitz and M.D. Cohen, *J. Membr. Sci.* **40**, 55–65 (1989).
47. E. Mathiowitz and M.D. Cohen, *J. Membr. Sci.* **40**, 67–86 (1989).
48. E. Mathiowitz and M.D. Cohen, *J. Membr. Sci.* **40**, 43–54 (1989).
49. T.M.S. Chang, *Artificial Cells*, Thomas, Springfield, Ill., 1972.
50. T. Kondo, in E. Matijevic, ed., *Surface and Colloid Science*, Plenum, New York, 1978, pp. 1–41.
51. A.F. Kydonieus, *Controlled Release Technologies: Methods, Theory, and Applications*, CRC Press, Boca Raton, Fla., 1980.
52. A. Kondo, *Microcapsule Processing and Technology*, Dekker, New York, 1979.
53. P.I. Lee and W.R. Good, *Controlled-Release Technology: Pharmaceutical Applications*, American Chemical Society, Washington, D.C., 1987.
54. A. Rolland, *Pharmaceutical Particulate Carriers: Therapeutic Applications*, Dekker, New York, 1993.
55. E. Mathiowitz and R. Langer, in M. Donbrow, ed., *Microcapsules and Nanoparticles in Medicine and Pharmacy*, CRC Press, Boca Raton, Fla., 1993, pp. 99–123.
56. S.S. Davis, L. Illum, J.G. McVie, and E. Tomlinson, *Microspheres and Drug Therapy*, Elsevier, New York, 1984.
57. G.R. Somerville and J.T. Goodwin, in A.F. Kydonieus, ed., *Controlled Release Technologies: Methods, Theory, and Applications*, CRS Press, Boca Raton, Fla., 1980, Chapter 8.
58. A. Markus, in S. Benita, ed., *Microencapsulation: Methods and Industrial Applications*, Dekker, New York, 1996, pp. 73–91.
59. A.R. Bachtsi and C. Kiparissides, *J. Controlled Release* **38**, 49–58 (1996).
60. S. Benita and M. Donbrow, *J. Colloid Interface Sci.* **77**, 102 (1980).
61. A.A. Kassem, A.A. Badawy, and A.A. El-Sayed, *Bull. Fac. Pharm. Cairo Univ.* **14**, 115 (1975).
62. S.A.H. Khalil, J.R. Nixon, and J.E. Carless, *J. Pharm. Pharmacoly* **20**, 215 (1968).
63. L.Y. Lim and S.C. Wan, *J. Microencapsul.* **15**, 319–333 (1998).
64. J.R. Nixon, S.A.H. Khalil, and J.E. Carless, *J. Pharm. Pharmacol.* **20**, 348 (1968).
65. R.E. Phares and G.J. Sperandio, *J. Pharm. Sci.* **53**, 515–518 (1964).
66. H. Takenaka, Y. Kawashima, and S.Y. Lin, *J. Pharm. Sci.* **69**, 513 (1980).
67. H.G. Bungenberg de Jong, in H.R. Kruyt, ed., *Colloid Science*, Elsevier, New York, 1949, Chapters 8 and 10.
68. L.W. Chan and P.W.S. Heng, *J. Microencapsul.* **15**, 409–420 (1998).
69. N.-H. Cho et al., *J. Controlled Release* **53**, 215–224 (1998).
70. M.C. Gohel et al., *J. Controlled Release* **45**, 265–271 (1997).
71. M.C. Gohel and A.F. Amin, *J. Controlled Release* **51**, 115–122 (1998).
72. B.-J. Lee, J.S. Choe, and C.-K. Kim, *J. Microencapsul.* **15**, 775–787 (1998).
73. M.C. Levy and F. Edwards-Levy, *J. Microencapsul.* **13**, 169–183 (1996).
74. L.-S. Liu et al., *J. Controlled Release* **43**, 65–74 (1996).
75. T. Uchida, K. Yoshida, and S. Goto, *J. Microencapsul.* **13**, 219–228 (1996).
76. E. Leo et al., *J. Microencapsul.* **15**, 421–430 (1998).
77. Z.G. Gao, K.H. Oh, and C.-K. Kim, *J. Microencapsul.* **15**, 75–83 (1998).
78. Y.-H. Cheng, L. Illum, and S.S. Davis, *J. Controlled Release* **55**, 203–212 (1998).

79. M.J. Blanco-Prieto et al., *J. Controlled Release* **43**, 81–87 (1997).
80. P. Benelli et al., *J. Microencapsul.* **15**, 431–443 (1998).
81. E. Mathiowitz and R. Langer, *J. Controlled Release* **5**, 13–22 (1987).
82. E. Mathiowitz et al., *J. Appl. Polym. Sci.* **35**, 755–774 (1988).
83. E. Mathiowitz, D. Kline, and R. Langer, *Scanning Microsc.* **4**, 329–340 (1990).
84. K. Pekarek, J. Jacob, and E. Mathiowitz, *Nature (London)* **367**, 258–260 (1994).
85. U.S. Pat. 5,611,344 (March 18, 1997), H. Benrstein, J. Straub, H. Brush, and R. Wing, (to Acusphere).
86. U.S. Pat. 5,853,698 (December 29, 1998), J. Straub, E. Mathiowitz, H. Bernstein, and H. Brush (to Acusphere).
87. U.S. Pat. 5,837,221 (July 29, 1996), H. Bernstein, J. Straub, H. Brush, and C. Church, (to Acusphere).
88. R.W. Baker and H.K. Lousdale, in A.C. Tanguary and R.E. Lacey, eds., *Controlled Release of Biologically Active Agents*, Plenum Press, New York, 1974, p. 15.
89. Y.W. Chien, in J.R. Robinson, ed., *Sustained and Controlled Release Drug Delivery Systems*, Dekker, New York, 1978, Chapter 4.
90. D.R. Paul in D.R. Paul and F.W. Harris, eds., *Controlled Release Polymeric Formulations*, American Chemical Society, Washington, D.C., 1976, Chapter 1.
91. T. Higuchi, *J. Pharm. Sci.* **52**, 1145 (1963).
92. A. Wade and P.J. Weller, *Hand Book of Pharmaceutical Excipients*, Pharmaceutical Press, London, 1994.
93. M.J. Schick, *Nonionic Surfactants: Physical Chemistry*, Dekker, New York, 1987.
94. J.T. Davies, *Proc. 2nd Int. Congr. Surf. Act.*, London, 1957, vol. 1, p. 426.
95. M.J. Schick, *Nonionic Surfactants*, Dekker, New York, 1989.
96. S. Geiger et al., *J. Controlled Release* **52**, 99–107 (1998).
97. P.J. Flory, *Principles of Polymer Chemistry*, Cornell University Press, Ithaca, N.Y., 1953.
98. A. Veis, *Biological Polyelectrolyles*, Dekker, New York, 1970.
99. J.Th.G. Overbeek and M.J. Voorn, *J. Cell. Comp. Physiol.* **49**, 7–26 (1957).
100. S. Torza and S.J. Mason, *J. Colloid Interface Sci.* **33**, 67–83 (1970).
101. K.J. Pekarek et al., *J. Controlled Release* **40**, 169–178 (1996).
102. H. Okada, Y. Ogawa, and T. Yashiki, *Prolonged Release Microcapsule and Its Production*, Tokyo, Takeda Chemical Industries, 1987, pp. 1–20.
103. Y. Ogawa et al., *Chem. Pharm. Bull.* **3**, 1095–1103 (1988).
104. H. Okada, T. Heya, Y. Ogawa, and T. Shimamoto, *J. Pharmacol. Exp. Ther.* **244**, 744–750 (1988).
105. H. Okada, Y. Doken, Y. Ogawa, and H. Toguchi, *Pharm. Res.* **11**, 1199–1203 (1994).
106. H. Okada, Y. Doken, Y. Ogawa, and H. Toguchi, *Pharm. Res.* **11**, 1143–1147 (1994).
107. D.T. Birnbaum et al., *Proc. Top. Conf. Biomater. Carriers Drug Delivery Scaffolds Tissue Eng.*, November 17–19, 1997, pp. 138–140.
108. D.T. Birnbaum, J.D. Kosmala, and L. Brannon-Peppas, *Polym. Prepr.* **38**, 600–601 (1997).
109. C. Schugens et al., *J. Controlled Release* **32**, 161–176 (1994).
110. W.I. Li, K.W. Anderson, R.C. Mehta, and P.P. DeLuca, *J. Controlled Release* **37**, 199–214 (1995).
111. T. Kidchob, S. Kimura, and Y. Imanishi, *J. Controlled Release* **54**, 283–292 (1998).
112. M.S. Reza and T.L. Whateley, *J. Microencapsul.* **15**, 789–801 (1998).
113. F.W. Okumu, J.L. Cleland, and R.T. Borchardt, *J. Controlled Release* **49**, 133–140 (1997).
114. A. Matsumoto et al., *J. Controlled Release* **48**, 19–27 (1997).
115. J.L. Cleland et al., *J. Controlled Release* **47**, 135–150 (1997).
116. H. Sah, *J. Controlled Release* **47**, 233–245 (1997).
117. W.W. Thompson, D.B. Anderson, and M.L. Heiman, *J. Controlled Release* **43**, 9–22 (1997).
118. R.V. Diaz et al., *J. Controlled Release* **43**, 59–64 (1997).
119. H. Rafati et al., *J. Controlled Release* **43**, 89–102 (1997).
120. C.X. Song, V. Labhasetwar, and R.J. Levy, *J. Controlled Release* **45**, 177–192 (1997).
121. N. Jager-Lezer et al., *J. Controlled Release* **45**, 1–13 (1997).
122. C. Laugel et al., *J. Controlled Release* **38**, 59–67 (1996).
123. W.-I. Li, K.W. Anderson, and P.P. DeLuca, *J. Controlled Release* **37**, 187–198 (1995).
124. S. Izumikawa, S. Yoshioka, Y. Aso, and Y. Takeda, *J. Controlled Release* **15**, 133–140 (1991).
125. U.S. Pat. 3,674,704 (July 4, 1972), R.G. Bayless, C.P. Shank, R. Botham, and D.W. Werkmeister.
126. P.L. Madan, *Drug. Dev. Ind. Pharm.* **4**, 95–116 (1978).
127. M. Donbrow, A. Hoffman, and S. Benita, *J. Microencapsul.* **7**, 1–15 (1990).
128. J.W. Beyger and J.G. Nairn, *J. Pharm. Sci.* **75**, 573–578 (1986).
129. S.P. Sanghvi and J.G. Nairn, *J. Pharm. Sci.* **80**, 394–398 (1991).
130. E. Klein and J.K. Smith, *Ind. Eng. Chem. Prod. Res. Dev.* **11**, 207–210 (1972).
131. A.S. Chawla and T.M.S. Chang, *J. Appl. Polym. Sci.* **19**, 1723–1730 (1975).
132. T.C. Shen and I. Cabasso, in R.B. Seymour, ed., *Macromolecular Solutions: Solvent-Property Relationships in Polymers*, Pergamon Press, New York, pp. 108–117.
133. D.H. Robinson, *Drug. Dev. Ind. Pharm.* **15**, 2597–2620 (1989).
134. B. Sa, A.K. Bandyopadhyay, and B.K. Gupta, *J. Microencapsul.* **13**, 207–218 (1996).
135. T.L. Whateley, in S. Benita, ed., *Microencapsulation: Methods and Industrial Applications*, Dekker, New York, 1996, pp. 349–375.
136. P.W. Morgan, *Condensation Polymers by Interfacial and Solution Methods*, Interscience, New York, 1965.
137. E. Mathiowitz, A. Raziel, M.D. Cohen, and E. Fischer, *J. Appl. Polym. Sci.* **26**, 809–822 (1981).
138. S.R. Jameela, T.V. Kumary, A.V. Lal, and A. Jayakrishnan, *J. Controlled Release* **52**, 17–24 (1998).
139. T. Modena et al., *J. Microencapsul.* **15**, 85–92 (1998).
140. B.A. Heelan and O.I. Corrigan, *J. Microencapsul.* **15**, 93–105 (1998).
141. J. Akbuga and N. Bergisadi, *J. Microencapsul.* **13**, 161–168 (1996).
142. N. Muramatsu and K. Nakauchi, *J. Microencapsul.* **15**, 715–723 (1998).
143. A.A. Al-Helw, A.A. Al-Angary, G.M. Mahrous, and M.M. Al-Dardari, *J. Microencapsul.* **15**, 373–382 (1998).
144. A. Berthold, K. Cremer, and J. Kreuter, *J. Controlled Release* **39**, 17–25 (1996).
145. K. Nilsson et al., *Nature (London)* **302**, 629 (1983).

146. E. Mathiowitz, P. Dor, C. Amato, and R. Langer, *Polymer* **35**, 547, 755 (1990).

147. T.W. Atkins, S.J. Peacock, and D.J. Yates, *J. Microencapsul.* **15**, 31–44 (1998).

148. R. Jeyanthi, B.C. Thanoo, R.C. Metha, and P.P. DeLuca, *J. Controlled Release* **38**, 235–244 (1996).

149. J. Bleich and B.W. Muller, *J. Microencapsul.* **13**, 131–139 (1996).

150. R. Falk et al., *J. Controlled Release* **44**, 77–85 (1997).

151. E. Mathiowitz et al., *J. Appl. Polym. Sci.* **45**, 125–134 (1992).

152. E. Mathiowitz, E. Ron, G. Mathiowitz, and R. Langer, *Macromolecules* **23**, 3212–3218 (1990).

153. E. Ron et al., *Macromolecules* **24**, 2278–2282 (1991).

154. M.R. Kreitz, Ph.D. Thesis, Brown University, Providence, R.I., 1999.

155. M. Luck et al., *J. Controlled Release* **55**, 107–120 (1998).

156. C. Witschi and E. Doelker, *J. Controlled Release* **51**, 327–341 (1998).

157. G.O. Fanger and J.E. Vandergaer, *Proc. 166th Annu. Meet. Am. Chem. Soc.*, Chicago, 1973.

158. E.S. Nuwayser et al., in G.I. Zatuchni, A. Goldsmith, J.D. Shelton and J.J. Sciarra, eds., *Long-Acting Contraceptive Delivery Systems*, Harper & Row, Philadelphia, 1984, pp. 64–76.

159. E.L. Parrot, *Pharmaceutical Technology*, Burgess, Minneapolis, Minn., 1970.

160. K. Leach-Pekarek, S. Takahashi, and E. Mathiowitz, *Biomaterials* **19**, 1981–1988 (1998).

161. J. Leach-Pekarek and E. Mathiowitz, *Biomaterials* **19**, 1973–1980 (1998).

162. K. Pekarek, J. Jacob, and E. Mathiowitz, *Adv. Mater.* **6**, 684–687 (1994).

163. W.D. Harkin, *The Physical Chemistry of Surface Films*, Reinhold, New York, 1952.

164. M. Tracy, *Biotechnol. Prog.* **14**, 108–115 (1998).

165. E. Mathiowitz et al., *Nature (London)* **386**, 410–416 (1997).

166. N.K. Egilmez et al., *Cancer Immunol. Immunother.* **46**, 21–24 (1998).

167. L. Brannon-Peppas, in M. El-Nakaly, D.M. Piatt, and B.A. Charpentier, eds., *Polymeric Delivery Systems, Properties and Applications*, American Chemical Society, Washington, D.C., 1993, pp. 42–52.

168. C.G. Gebelein, T.C. Cheng, and V.C. Yang, in C.G. Gebelein, T.C. Cheng, and V.C. Yang, eds., *Cosmetic and Pharmaceutical Applications of Polymers*, Plenum, New York, 1991, pp. 1–7.

169. S. Benita, M.-C. Martini, and M. Seiller, in S. Benita, ed., *Microencapsulation: Methods and Industrial Applications*, Dekker, New York, 1996, pp. 587–631.

170. *Physicians' Desk Reference*, Medical Economics Data Production Company, Montvale, N.J.; 1994, pp. 2385–2388.

See also COATINGS; LIPOSOMES; MICROENCAPSULATION FOR GENE DELIVERY; NANOPARTICLES.

Next Page

MICROENCAPSULATION FOR GENE DELIVERY

ERIC KAI HUANG
YONG SHIK JONG
Brown University
Providence, Rhode Island

KEY WORDS

DNA vaccination
Gene therapy
Microencapsulation
Nonviral
Plasmid DNA
Polymer
Vector

OUTLINE

Introduction
Background
  DNA Vaccination
  Microencapsulation for DNA Vaccination
Fabrication Techniques
  Physiochemical Properties of Plasmid DNA
  Manipulation of Plasmid DNA
  Encapsulation Techniques for Plasmid DNA
In Vivo Applications
  Microsphere Uptake and Gene Delivery
  Microsphere-Based Oral DNA Vaccination
  Microsphere-Based Parental DNA Vaccination
Conclusion
Bibliography

INTRODUCTION

Since Watson and Crick's determination of DNA structure, advances in molecular biology and recombinant DNA technologies have had an enormous impact on biological sciences. DNA-based diagnostics and recombinant pharmaceuticals have emerged as important additions to medical research and treatment methods. Gene therapy, however, has yet to provide similar tangible benefits. Nonetheless, it is often heralded as a panacea, the ultimate application of recombinant DNA research.

Gene therapy is based on the premise that a disease is the failed expression of a gene or expression of a defective one, which can be treated by the transfer of genes into specific cells of patients rather than through conventional pharmaceutical means. Gene transfer can be used to restore and/or supplement defective functions or interfere with the expression of aberrant genes. Currently, there are three categories of gene therapy (1). The ex vivo approach involves the removal of patient cells from the body, the transduction of these cells using an appropriate vector, and the subsequent return of the genetically altered cells to the

146. E. Mathiowitz, P. Dor, C. Amato, and R. Langer, *Polymer* **35**, 547, 755 (1990).

147. T.W. Atkins, S.J. Peacock, and D.J. Yates, *J. Microencapsul.* **15**, 31–44 (1998).

148. R. Jeyanthi, B.C. Thanoo, R.C. Metha, and P.P. DeLuca, *J. Controlled Release* **38**, 235–244 (1996).

149. J. Bleich and B.W. Muller, *J. Microencapsul.* **13**, 131–139 (1996).

150. R. Falk et al., *J. Controlled Release* **44**, 77–85 (1997).

151. E. Mathiowitz et al., *J. Appl. Polym. Sci.* **45**, 125–134 (1992).

152. E. Mathiowitz, E. Ron, G. Mathiowitz, and R. Langer, *Macromolecules* **23**, 3212–3218 (1990).

153. E. Ron et al., *Macromolecules* **24**, 2278–2282 (1991).

154. M.R. Kreitz, Ph.D. Thesis, Brown University, Providence, R.I., 1999.

155. M. Luck et al., *J. Controlled Release* **55**, 107–120 (1998).

156. C. Witschi and E. Doelker, *J. Controlled Release* **51**, 327–341 (1998).

157. G.O. Fanger and J.E. Vandergaer, *Proc. 166th Annu. Meet. Am. Chem. Soc.*, Chicago, 1973.

158. E.S. Nuwayser et al., in G.I. Zatuchni, A. Goldsmith, J.D. Shelton and J.J. Sciarra, eds., *Long-Acting Contraceptive Delivery Systems*, Harper & Row, Philadelphia, 1984, pp. 64–76.

159. E.L. Parrot, *Pharmaceutical Technology*, Burgess, Minneapolis, Minn., 1970.

160. K. Leach-Pekarek, S. Takahashi, and E. Mathiowitz, *Biomaterials* **19**, 1981–1988 (1998).

161. J. Leach-Pekarek and E. Mathiowitz, *Biomaterials* **19**, 1973–1980 (1998).

162. K. Pekarek, J. Jacob, and E. Mathiowitz, *Adv. Mater.* **6**, 684–687 (1994).

163. W.D. Harkin, *The Physical Chemistry of Surface Films*, Reinhold, New York, 1952.

164. M. Tracy, *Biotechnol. Prog.* **14**, 108–115 (1998).

165. E. Mathiowitz et al., *Nature (London)* **386**, 410–416 (1997).

166. N.K. Egilmez et al., *Cancer Immunol. Immunother.* **46**, 21–24 (1998).

167. L. Brannon-Peppas, in M. El-Nakaly, D.M. Piatt, and B.A. Charpentier, eds., *Polymeric Delivery Systems, Properties and Applications*, American Chemical Society, Washington, D.C., 1993, pp. 42–52.

168. C.G. Gebelein, T.C. Cheng, and V.C. Yang, in C.G. Gebelein, T.C. Cheng, and V.C. Yang, eds., *Cosmetic and Pharmaceutical Applications of Polymers*, Plenum, New York, 1991, pp. 1–7.

169. S. Benita, M.-C. Martini, and M. Seiller, in S. Benita, ed., *Microencapsulation: Methods and Industrial Applications*, Dekker, New York, 1996, pp. 587–631.

170. *Physicians' Desk Reference*, Medical Economics Data Production Company, Montvale, N.J.; 1994, pp. 2385–2388.

See also COATINGS; LIPOSOMES; MICROENCAPSULATION FOR GENE DELIVERY; NANOPARTICLES.

Previous Page

MICROENCAPSULATION FOR GENE DELIVERY

ERIC KAI HUANG
YONG SHIK JONG
Brown University
Providence, Rhode Island

KEY WORDS

DNA vaccination
Gene therapy
Microencapsulation
Nonviral
Plasmid DNA
Polymer
Vector

OUTLINE

Introduction
Background
  DNA Vaccination
  Microencapsulation for DNA Vaccination
Fabrication Techniques
  Physiochemical Properties of Plasmid DNA
  Manipulation of Plasmid DNA
  Encapsulation Techniques for Plasmid DNA
In Vivo Applications
  Microsphere Uptake and Gene Delivery
  Microsphere-Based Oral DNA Vaccination
  Microsphere-Based Parental DNA Vaccination
Conclusion
Bibliography

INTRODUCTION

Since Watson and Crick's determination of DNA structure, advances in molecular biology and recombinant DNA technologies have had an enormous impact on biological sciences. DNA-based diagnostics and recombinant pharmaceuticals have emerged as important additions to medical research and treatment methods. Gene therapy, however, has yet to provide similar tangible benefits. Nonetheless, it is often heralded as a panacea, the ultimate application of recombinant DNA research.

Gene therapy is based on the premise that a disease is the failed expression of a gene or expression of a defective one, which can be treated by the transfer of genes into specific cells of patients rather than through conventional pharmaceutical means. Gene transfer can be used to restore and/or supplement defective functions or interfere with the expression of aberrant genes. Currently, there are three categories of gene therapy (1). The ex vivo approach involves the removal of patient cells from the body, the transduction of these cells using an appropriate vector, and the subsequent return of the genetically altered cells to the

patient. The in situ approach involves injecting the vector directly into the affected tissues. Finally, the in vivo approach uses the bloodstream to transport the vector to the affected tissues and/or cells.

Clinical success has been limited to genetic diseases caused by a single gene defect such as adenosine deaminase deficiency (2). However, advances in molecular biology are rapidly leading to the identification of defective genes and an increased understanding of the regulation of gene expression. Gene transfer constitutes the sine qua non of gene therapy. In fact, the application of human gene therapy is limited more by the lack of effective delivery methods for gene transfer. The December 1995 Report and Recommendations issued by NIH states that "Given the central role of vectors for delivering genes to somatic cells for therapeutic purposes, the Panel endorses *vigorous* and *expanded* research aimed at developing improved vectors" [our emphasis]. Thus, the development of both viral and nonviral gene transfer methods has come to the forefront of gene therapy research.

Viral-vector-mediated gene transfer makes use of the evolutionary advances by viruses to deliver genetic information into the cells they infect (3). Viral vectors are commonly recombinant animal viruses that contain exogenous information in their genome. They are usually replication-defective to prevent the occurrence of a pathological condition. There are four main types of viral vectors currently used in clinical trials: retrovirus, adenovirus, adeno-associated virus, and herpes-simplex virus (4). The advantages and disadvantages of each are described in Table 1. Generally viral vectors are more efficient than nonviral vectors, but do not have much in the way of capacity to deliver large expression cassettes (5). There is also the possibility of recombination into a replication-competent virus. However, viruses remain the most resourceful in entering cells and will probably be included in the next generation of hybrid vectors containing viral components expressly for this purpose. The basic scheme for viral transduction is as follows. An expression cassette is inserted into a replication-defective viral vector. This virus is inserted into a packaging cell, which produces all the necessary viral proteins necessary to package the virus. Target cells are then infected with these vectors (either in vitro or in vivo), thus allowing the viruses to transmit the genetic information. What happens to the information then depends on the type of virus as well as the type of target cell.

Nonviral vectors rely on chemical or physical means to facilitate cellular uptake and intracellular transport of plasmid DNA without viral packaging (6). These vectors including liposomes, gene gun, ligand-mediated polylysine complexes, direct injection, and others. Table 2 summarizes the main nonviral vector approaches employed for gene therapy. These vectors contain plasmid DNA; circular double stranded DNA which exists extrachromosomally in bacteria. Nonviral vectors are considered to be more safe than viral vectors (no risk of infection or tumor formation), have no limit to the expression cassette size carried, and are easier to manufacture and purify (1). Their main drawbacks are low transfer efficiency and transient gene expression (7). With the exception of the gene gun, where adsorbed DNA can be shot directly into nucleus, nonviral vectors have generally been designed to enhance endosomal escape, cytoplasmic transport, and/or nuclear uptake of plasmid DNA. Strategies include inclusion of ligands for specific targeting, adenoviral attachment for endosomal escape, and other numerous modifications (8,9). However, it should be noted that some tissues have the intrinsic ability to internalize and express exogenous plasmid DNA. For example, in muscle tissue, the use of viral or chemical nonviral vectors to enhance gene transfer has been shown to be less efficient than injecting purified, plasmid DNA alone (10).

The goal of this article is not to present a review of all available viral and nonviral vectors. An excellent review by Nakanishi provides a comprehensive discussion of the various vector systems, both viral and nonviral, as well as their applications in human gene therapy (11). This article focuses on one specific emerging technology, vectors based on thermoplastic microencapsulation of plasmid DNA. A variety of polymers have been used for DNA delivery, including liposomes (DOTMA/DOPE), hydrogels (chitosan, alginate, poly[vinylpyrrolidone]), dendrimers (polyamidoamine), and water-soluble polymers (polylysine), which provides for either DNA condensation, charge neutralization, or binding/complexation (6,12–14). Some of these sys-

Table 1. Viral Vectors Used for Gene Therapy

Viral vector system	Advantages	Disadvantages
Retrovirus	Stable, long-term expression	Requires mitogenic cells for infection
	Can infect wide range of cell types	Small expression cassette (~9 kb)
		Possibility of insertional mutagenesis
		Difficult to concentrate/purify
Adenovirus	Can infect nondividing cells	Strongly immunogenic
	Capable of high expression levels	Small expression cassette (~7.5 kb)
	Easy to concentrate/purify	Significant risk of recombination into replication-competent
Adeno-associated virus	Can infect nondividing cells	Very small expression cassette (~5 kb)
	Does not cause any known human pathologies	Requires coinfection with helper virus
	Site-specific integration	System still not well characterized
Herpes-simplex virus	Ability to establish lifelong latent infections	Wild type virus is cytotoxic
	High titre stocks	Reactivation of wild-type virus is possible
	Large expression cassette capacity	High prevalence of seropositivity in general population

Table 2. Nonviral Vectors Used for Gene Therapy

Nonviral vector system	Advantages	Disadvantages
Cationic lipids and liposomes	Simple procedure Large expression cassette capacity Low immunogenicity/toxicity	Low transfection efficiency Transient expression Unstable complex formation Nonspecific targeting
Ligand-mediated polylysine complex	Specific targeting possible Low toxicity	Weak gene expression Low transfection efficiency May be immunogenic
Direct injection of DNA	No carrier molecules needed Minimum contaminants Low immunogenicity	Cannot be applied to cultured cells Low efficiency Transient expression Mechanism of entry not well-understood

tems are described in other articles. The particular vectors described in this article focus on the use of water-insoluble, thermoplastic, biodegradable polymers to encapsulate plasmid DNA. These polymers differ in that they do not interact with DNA (chemically or electrostatically) and serve simply to physically entrap DNA uniformly within a matrix structure. Once hydrated, plasmid DNA is released from the matrices in its "naked" form, via diffusion (through preexisting pores), which is enhanced by the actual hydrolytic degradation of the matrix itself (Fig. 1). The use of these types of systems has not been limited to plasmid DNA; whole viruses and oligonucleotides have also been successfully encapsulated within these polymer matrices for a number of different applications (15,16). However, the focus of this review is the use of these encapsulation systems specifically for applications in DNA vaccination.

BACKGROUND

DNA Vaccination

DNA vaccination can be defined as the induction of an immune response to antigen expression by cells in situ, following direct gene transfer of the antigen encoding DNA. Mechanistically, DNA vaccination is somewhat analogous to the use of live attenuated viral vaccines, as both result in intracellular production of antigenic proteins. However, it is inherently a subunit vaccine and the immune response is directed toward specific components instead of the whole virus. First, the antigen expressing plasmid DNA is administered into the host animal, most commonly via direct injection of the plasmid DNA in a buffer. Second, transfected cells begin expression of the antigen, which in some cases is actively secreted. Third, the host animal develops a specific immune response against the expressed antigen. Interest in DNA vaccination stems primarily from its ability to induce both cytotoxic T cell and antibody responses, with low DNA doses, for long periods of time (17,18). Antigens are produced de novo in its native form and thus compared to administration purified recombinant antigens, result in efficient presentation of both Class I and Class II major histocompatibility complex (MHC) (19). Moreover, DNA vaccination protocols require significantly less (up to 1,000-fold less) protein compared to the protein doses required for the more classical subunit vaccine approaches (20). Although there are some potential risks (tolerance, autoimmunity, integration), experimental studies to date indicate they are unlikely and the primary disadvantage appears to be the fact that DNA vaccination is limited to protein antigens.

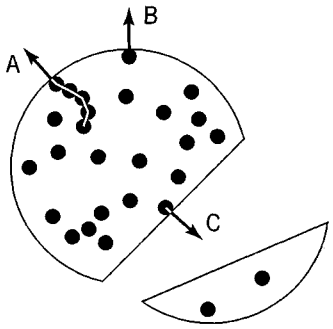


Figure 1. Macromolecule release from degrading matrix-type controlled release microsphere. (A) Diffusion of molecules from within the polymer matrix following the formation of interconnecting pores. (B) Diffusion of surface localized molecules. (C) Diffusion of molecules from within the polymer matrix following degradation of encapsulating polymer material.

Much of the work with DNA vaccination has focused on the use of direct injection of plasmid DNA. Direct injection of plasmid DNA was first demonstrated as a viable gene transfer technique in 1990 (21). This form of gene transfer uses purified bacterial DNA constructs without any additional chemical or biological agents, often referred to as naked DNA. Although transfection efficiencies are generally low, this technique has been used successfully in a number of different animal models. Subsequently, it was shown that direct gene transfer with plasmid DNA could provoke an immune response against the encoded protein antigen (19,22) heralding this revolutionary new approach to vaccine development. A number of excellent reviews have been written regarding DNA vaccination. Interested readers should access "The DNA Vaccine Web" by Robert Whalen (http://www.genweb.com/Dnavax/dnavax.html), which provides a comprehensive overview of DNA vaccination, including an extensive bibliography of related research and review articles.

Researchers have devised a number of strategies to improve the efficacy of DNA vaccination. The first involves

the selection of the plasmid construct. In addition to the promoter, enhancer, and intron sequences, inclusion of palindromic single-stranded immunostimulatory sequences, specifically the unmethylated cytosine motif adjacent to a guanine residue (CpG) can dramatically upregulate the immune response (23). The same study demonstrated that the location of these sequences within the plasmid construct is important as well. It appears that these sequences increase the immune response through increased proliferation and cytokine release of B and T lymphocytes. The second is the selection of the inoculation site. Direct injection of plasmid DNA is most effective in muscle tissue both in terms of transfection efficiency and transgene expression. However, it has been demonstrated that other tissue such as the epidermis, which is much less permissive to direct injection vectors, can provide for more efficient vaccination (24,25). This apparent dichotomy has been attributed to the fact that the epidermis contains a rich population of specialized "professional" antigen presenting cells (APCs), that are absent in normal muscle tissue. In fact, it is thought that immune responses generated following intramuscular injection of DNA may be due primarily to APCs migrating into the injection site (26,27). It is important to note that the increased vaccine efficacy does not necessarily imply transfection of APCs themselves as it has been shown that transfected muscle cells can transfer antigens to APCs to trigger an immune response (28). The third strategy lies in the selection of the vector system. A number of vectors have been developed to increase transfection efficiency and provide alternative innoculation sites where naked plasmid DNA is ineffective (e.g., the oral route). The inoculation site is especially important as the type of immune response generated is modulated in part by the site of antigen exposure and lymphoid tissue targeted (29). Specialized vectors have been developed for intradermal, intranasal, intraperitoneal, and oral plasmid DNA delivery through the use of liposomes, gene guns, microbes, and cochleates (30) to increase the versatility of DNA vaccination protocols.

Microencapsulation for DNA Vaccination

The primary rationale for thermoplastic microencapsulation of plasmid DNA for DNA vaccination is based on the exploitation of two biological phenomenon, gastrointestinal (GI) tissue uptake and microsphere phagocytosis.

Although the extent of uptake remains somewhat controversial, particle uptake along the GI tract is an established biological phenomenon (31,32). It is thought that the uptake phenomenon is primarily due to a size effect; particles smaller than 10 μm in diameter can cross the GI barrier (33). The study of GI uptake of particles has focused on the possibility of targeting gut-associated lymphoid tissue or Peyer's patches known to be important in mounting the mucosal immune response (34,35). As delivery of purified unencapsulated antigens alone to this mucosal site is difficult, a major focus of GI uptake has been the development of effective oral vaccines. Thus, delivery systems have been designed to protect labile antigens from degradation within the harsh environment of the GI tract and to transport them across the "M" cell barrier for presentation to cells of the immune system (B cell follicular regions, interfollicular T cell zones, and APCs). Antigens derived from the simian immunodeficiency virus, influenza, staphylococcal enterotoxin, and others have been delivered orally via microsphere systems to generate both systemic and localized mucosal immunity (36).

Uptake can occur via paracellular as well as transcellular routes (37) and thus does not necessarily imply cellular internalization. In contrast, phagocytosis is defined as direct cellular internalization, a process primarily exhibited by antigen processing cells of the immune system such as macrophages and neutrophils. A form of endocytosis, phagocytosis refers specifically to internalization of soluble and insoluble macromolecules greater than 250 nm in size. The phagocytic capabilities of APCs are astounding, as it has been estimated that macrophages phagocytose 10^{11} senescent red blood cells on a daily basis. The intrinsic ability of APCs for phagocytosis of microspheres combined with their immunoregulatory function provides a potential passive targeting mechanism for efficient delivery therapeutic molecules to the immune system (38–40).

Advanced controlled release systems provides an alternative approach to the standard oral, intravenous, or intramuscular delivery of pharmaceutical agents. Controlled release systems have traditionally been designed to deliver drugs in a localized, prolonged manner through a sustained depot effect (41,42). These systems can be designed to locally administer drugs to any site in the body. Furthermore, in the case of labile drugs, they can provide protection from rapid in vivo degradation and more efficient dosing. Microencapsulation constitutes one approach for fabrication of matrix-based polymer controlled release systems in microsphere geometry. Microencapsulation of drugs within polymer materials can allow for control of the release rate and duration of delivery to enhance the pharmacokinetics of drugs compared with traditional dosage forms. A detailed review of microencapsulation and drug delivery is reviewed elsewhere in this encyclopedia.

Given that plasmid DNA degrades rapidly in vivo, on the order of minutes (43,44), controlled release systems designed for DNA delivery and gene transfer offer similar advantages. Most importantly for DNA vaccine applications, fabrication of these systems into small microsphere form offers the added possibility of targeting specific tissue; in the case of oral administration, the Peyer's patch, and for parental injections, the APCs. Conceptually, DNA would be released extracellulary within the Peyer's patch or the parental injection site upon administration. Internalization of DNA released from microspheres by adjacent cells is not thought to be facilitated and is assumed to follow the same pathway as direct injection of naked plasmid DNA. In the case where cells have successfully phagocytosed microspheres, DNA would be released intracellularly and serve to facilitate translocation of encapsulated DNA across the cellular membrane, the first barrier for naked plasmid DNA. It should be noted that although there are numerous reports of cytoplasmic internalization, there are no reports regarding nuclear internalization of microspheres. The two pathways are not mutually exclusive, as plasmid DNA release in these systems occurs immediately

following hydration and is not specifically triggered to occur upon cytoplasmic entry.

FABRICATION TECHNIQUES

Physiochemical Properties of Plasmid DNA

Plasmid DNA exhibits a number of distinct physiochemical characteristics which present a number of challenges distinct from peptide or protein encapsulation (45). Plasmid DNA is an extremely large, negatively charged macromolecule with molecular weights in the millions of daltons; at least an order of magnitude higher than proteins. Moreover, plasmid DNA can exist in three different conformations (supercoiled, open circular, and linear), each with different hydrodynamic characteristics. Gene transfer is most effective with the supercoiled form (46,47) and thus delivery systems must optimize the encapsulation and release of this particular fraction. Although plasmids appear stable in organic solvents and are thermally stable (on the order of years), they are extremely sensitive to physical manipulation such as sonication, a processing step crucial for most microencapsulation techniques (48). In addition, aqueous DNA solutions are extremely viscous at relatively low concentrations, providing challenges for both loading and dispersion during the fabrication stage.

Manipulation of Plasmid DNA

Generally, fabrication steps involve (*1*) dispersion of plasmid DNA within the polymer solution, (*2*) formation of desired geometry, and (*3*) removal of solvent. The primary difficulty in encapsulation of DNA through traditional microencapsulation techniques is dispersion of DNA within the polymer matrix. Lyophilized solutions of DNA form macroaggregates, resembling a ball of cotton, which cannot be milled or otherwise physically micronized without shearing DNA strands. Although DNA can be spray-dried into particles (49), most techniques disperse DNA in solution to form an emulsion of DNA droplets dispersed in a continuous polymer–solvent phase. Once dispersed, techniques generally follow traditional "double emulsion" microencapsulation protocols designed for peptides and proteins. Formation of the initial emulsion has been achieved via vigorous vortex, homogenization, or sonication. A homogenous emulsion is critical for minimizing microsphere size distribution as well as reducing variability in drug loading (50). However, the principal limitation of this process stems from the physical sensitivity of DNA, which requires that both the duration and magnitude of agitation must be minimized (51). Thus an optimal emulsion, in terms of decreasing droplet size, is difficult to achieve. Although Adami et al. have reported that condensation of plasmid DNA with a peptide allowed for sonication at 100 W for up to 60 seconds, uncondensed, naked plasmid DNA was fragmented in less than 15 seconds (52).

Encapsulation Techniques for Plasmid DNA

A number of fabrication techniques have been used for encapsulation of plasmid DNA for various therapeutic applications (Table 3). However, only two techniques, solvent evaporation and phase inversion nanoencapsulation, have been used to fabricate microsphere formulations for DNA vaccination.

Table 3. Fabrication Techniques for Plasmid DNA Encapsulation

Technique	Reference	Polymer
Solvent evaporation	53,54	PLGA
	40	PLGA
	55	PLGA
	56	PLGA
Phase inversion nanoencapsulation	37	P(FA:SA)
Heat extrusion	57	EVAc
Solvent cast coating	58	Proprietary
	59	PLGA

Solvent evaporation is one of the most common techniques used to produce matrix-type delivery systems in microsphere geometry (53,60). Briefly, the polymer is dissolved in an organic solvent is emulsified with the drug of choice in an aqueous solution to produce a dispersed phase of drug/water within a continuous phase of polymer/solvent. The emulsion is subsequently dripped into a stirred aqueous bath for removal of solvent. Due to the limited miscibility between the organic solvents used and the aqueous bath, solvent is gradually removed from the polymer matrix via evaporation over a period of hours.

Jones et al. first reported encapsulation of plasmid DNA in poly(lactide-*co*-glycolide) (PLGA) microspheres using solvent evaporation (53,54). Microspheres were reported as 1~2 μm in diameter with an encapsulation efficiency of 25%. The in vitro bioactivity of released plasmid DNA was determined to be 25% compared to unencapsulated plasmid controls using bacterial transformation assays and luciferase expression in tissue culture transfection assays. A second group reported using solvent evaporation for encapsulation of plasmid DNA in PLGA-based microspheres (40,51). The volume percent analysis of microsphere size indicated 85% of the microspheres were between 1.1 μm and 10 μm in diameter with a theoretical loading of 0.45% (w/w). In vitro coincubation of microspheres containing a luciferase reporter plasmid DNA with a macrophage cell (P388D1) resulted in engulfment and luciferase expression at 24 hours postengulfment, confirming release and bioactivity of the encapsulated plasmid DNA. The conformation of plasmids released from microspheres, as reported by both groups, showed that there was a partial conversion from supercoiled DNA to open circular DNA, which Hedley et al. attributed to the fabrications conditions during solvent evaporation.

Phase inversion nanoencapsulation (PIN) is a recently developed microencapsulation technique which has been used to encapsulated small drugs, proteins, and genes (37). In this method, nanosized microspheres are fabricated by the spontaneous phase inversion of dilute polymer solutions, which are then quickly dispersed into an excess of nonsolvent for the polymer. This method differs from existing methods of encapsulation in that no stirring or agitation of the nonsolvent bath is required. Most traditional microencapsulation techniques required the formation of

a polymeric emulsion using stirrers, sonicators, air-jet, etc., and the final size of the particles is determined by the rate of stirring. In the PIN technique, as solvent leaves the polymer solution and enters the bulk nonsolvent phase, polymer instantaneously precipitates into the form of microspheres in what appears to be a self-assembling system.

A reporter plasmid DNA encapsulated into poly(fumaric acid-*co*-sebacic acid) (P(FA:SA), 20:80, Mw 2k) microspheres (0.1 ~ 5.0 μm) via the PIN technique was reported by Mathiowitz et al. (37). Extraction analysis of microspheres following encapsulation showed a DNA loading of 0.1% (w/w) which retained a large fraction of the supercoiled form following fabrication (Fig. 2). Furthermore, in vitro release studies indicated that plasmid DNA was released from PIN microspheres in supercoiled and open circular conformation up to a period of 4 days.

IN VIVO APPLICATIONS

Microsphere Uptake and Gene Delivery

The feasibility of using microsphere uptake to deliver genes into the Peyer's patch for functional gene transfer was first demonstrated by Mathiowitz et al. (37). Using PIN, a reporter plasmid was encapsulated in microspheres composed of P(FA:SA). P(FA:SA) is an extremely bioadhesive polyanhydride that degrades rapidly via hydrolytic degradation (61). The authors selected P(FA:SA) upon the theory that increased bioadhesion can promote particle uptake in the gastrointestinal tract. In vivo light and transmission electron microscopy studies of GI tissue sections, following oral feeding of P(FA:SA) microspheres, indicated traversal of microspheres across both the mucosal epithelium and the follicle-associated epithelium covering the lymphatic elements of Peyer's patches (37).

Analysis of small intestinal tissue, five days after a single dose (50 mg microspheres encapsulating 50 μg pCMV/βgal) to rats, revealed functional expression of the encapsulated reporter gene product β-galactosidase. Whole tissue X-gal histological staining of the Peyer's patch areas revealed transfection of cells primarily in the serosal surface of Peyer's patch area. Control animals receiving a much higher dose (500 μg) of unencapsulated plasmid DNA did not show any expression in the Peyer's patch. Analysis of frozen cross sections showed that the majority of transfected cells were located in the muscularis mucosae and the adventitia below the Peyer's patches. The general localization of transfected cells was consistent with previous observations using fluorescently tagged microspheres, which suggests that the serosal tissue layer acts as a sieve to trap appropriately sized microspheres that have passed through the mucosal barrier (62).

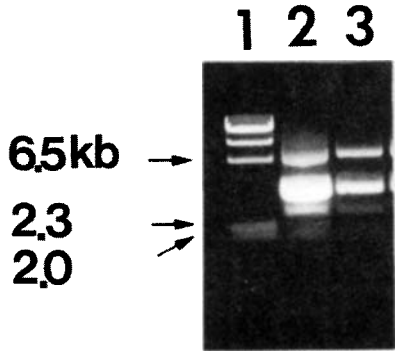


Figure 2. Agarose gel electrophoresis analysis of encapsulated pCMV/βgal plasmid DNA. (1) λ *Hind* III; (2) unencapsulated stock pCMV/βgal; (3) pCMV/βgal extracted from microspheres.

Microsphere-Based Oral DNA Vaccination

The efficacy of inducing an immune response, following oral administration of microspheres containing the antigen encoding plasmid DNA, was demonstrated by Jones et al. (53,54). Solvent evaporation was used to encapsulate luciferase reporter plasmid DNA in PLGA microspheres (~2 μm) and a 50 μg DNA dose fed to mice. Although neither luciferase expression nor PLGA uptake was evaluated, induction of luciferase specific serum IgA, IgG, and IgM responses were evident from 3 to 9 weeks following a single dose indicating successful gene transfer. A dose response study of 1, 5, 20, and 50 μg doses suggested increased titres with increasing dose. Interestingly, even the 1 μg dose was sufficient to induce the humoral response. Moreover, analysis of fecal extracts showed significant levels of IgA antibodies, which was detectable up to 16 weeks, illustrating that the oral route is effective in inducing mucosal as well as systemic immune responses.

In addition to oral administration (O), these same studies reported comparative data regarding delivery of encapsulated plasmid DNA via intramuscular (IM) and intraperitoneal (IP) injections. Analysis of serum IgG titres following a single dose (IP, IM, O) of 50 μg of encapsulated plasmid DNA indicated that the IP route provoked the strongest IgG response at both 3 and 6 weeks following administration. IP injections of unencapsulated small hepatitis B surface antigen plasmid DNA alone does not induce a cellular and humoral immune response (63) indicating improved transfection with microencapsulation at this site. In contrast, animals given the encapsulated plasmid DNA via O administration showed the highest levels of fecal IgA levels, reflecting the importance of the delivery site in modulating the immune response. In both IP and O administration, animals receiving the encapsulated plasmid DNA showed enhanced serum IgG levels compared to the unencapsulated naked DNA controls. Somewhat surprisingly, animals receiving naked unencapsulated plasmid DNA orally also developed specific IgG titres, albeit at lower levels. Although other reports indicated that direct oral administration of plasmid DNA was ineffective (64), this observation suggests the intriguing possibility that plasmid DNA may have some ability to bypass the enzymatic and mucosal barrier of the GI tract.

Microsphere-Based Parental DNA Vaccination

A parental DNA vaccine application based on microsphere phagocytosis has been reported by Hedley et al. (40). In an effort to target APCs in a parental inoculation site, a microsphere system was evaluated to enhance vaccination efficacy. The authors hypothesized that successful delivery

of a single antigen expressing DNA construct could be more efficient than direct delivery of the synthetic antigen, as it has been shown previously that an APC expressing a peptide gene construct results in over 10,000 Class I MHC associated peptide molecules (65).

Using solvent evaporation, plasmid DNA was encapsulated in PLGA microspheres. Subsequently, plasmid DNA (VSV N_{52-59}) encoding for a peptide derived from the vesicular stomatitis virus (VSV), was encapsulated in PLGA microspheres (1.1~10 μm). Both intraperitoneal and subcutaneous immunization of mice with encapsulated VSV N_{52-59} plasmid DNA produced significant cytotoxic T lymphocyte (CTL) responses, which were more pronounced when compared with a subcutaneous injection of purified VSV N_{52-59} peptide alone. Moreover, comparison of intraperitoneal or subcutaneous injections of 2~5 μg VSV N_{52-59} plasmid DNA generated stronger CTL responses compared with an intramuscular injection of a much larger 200 μg of unencapsulated VSV N_{52-59} plasmid DNA. The increased immune response was attributed to decreased degradation of the administered plasmid DNA dose as well as increased uptake of plasmid DNA, via microsphere phagocytosis, by APCs.

CONCLUSION

At the time of this review, there are over 270 approved human gene transfer protocols approved by the Office of Recombinant DNA Activities (see website at http://www.nih.gov/od/orda/protocol.htm). Currently, the three major targets are infectious disease, monogenic disease, and cancer. Due to the diverse nature of these categories, there is most likely no "perfect" vector. The most effective vectors will need to be tailored to the disease. Application of gene therapy to target vaccine development has recently provided an alternative approach to vaccination. DNA vaccination is an entirely new area of research which will require specialized vector systems for optimal therapeutic efficacy. While still in the very early stages, with further development, microencapsulation techniques may find a niche for specific applications in DNA vaccination.

BIBLIOGRAPHY

1. W.F. Anderson, *Nature (London)* **392**(Suppl.), 25–30 (1998).
2. R.M. Blaese et al., *Science* **270**, 475–480 (1995).
3. W.H. Gunzburg and B. Salmons, *Mol. Med. Today* **1**(9), 410–417 (1995).
4. P.D. Robbins, H. Tahara, and S.C. Ghivizzani, *Trends Biotechnol.* **16**(1), 35–40 (1998).
5. P.C. Watt, M.P. Sawicki, and E.J. Passaro, *Am. J. Surg.* **165**(3), 350–354 (1993).
6. F.D. Ledley, *Hum. Gene Ther.* **6**, 1129–1144 (1995).
7. G. Romano, P.P. Claudio, H.E. Kaiser, and A. Giordano, *In Vivo* **12**(1), 59–67 (1998).
8. F.L. Cosset and S.J. Russell, *Gene Ther.* **3**(11), 946–956 (1996).
9. P. Yeh and M. Perricaudet, *FASEB J.* **11**(8), 615–623 (1997).
10. H.L. Davis et al., *Hum. Gene Ther.* **4**, 733–740 (1993).
11. M. Nakanishi, *Crit. Rev. Ther. Drug Carrier Syst.* **12**(4), 263–310 (1995).
12. R. Riessen et al., *Hum. Gene Ther.* **4**(6), 749–758 (1993).
13. K. Anwer et al., *Hum. Gene Ther.* **9**(5), 659–670 (1998).
14. R.J. Mumper, J. Wang, J.M. Claspell, and A.P. Rolland, *Proc. Int. Symp. Controlled Release Bioact. Mater.* **22**, 178–179 (1995).
15. S. Akhtar and K.J. Lewis, *J. Cell. Biochem.* **17E**(Suppl.), 205 (1993).
16. E.R. Edelman, M. Simons, M.G. Sirois, and R.D. Rosenberg, *Circ. Res.* **76**(2), 176–182 (1995).
17. J.B. Ulmer, J.J. Donnelly, and M.A. Liu, *Curr. Opin. Invest. Drugs* **2**(9), 983–989 (1993).
18. J.B. Ulmer et al., *Vaccine* **12**(16), 1541–1544 (1994).
19. J.B. Ulmer et al., *Science* **259**, 1745–1749 (1993).
20. S. Lu et al., *Virology* **209**, 147–154 (1995).
21. J.A. Wolff et al., *Science* **247**, 1465–1468 (1990).
22. D.C. Tang, M. Devit, and S.A. Johnston, *Nature (London)* **356**, 152–154 (1992).
23. Y. Sato et al., *Science* **273**, 352–354 (1996).
24. E.F. Fynan et al., *Proc. Nat. Acad. Sci. U.S.A.* **90**, 11478–11482 (1993).
25. I. Nakano et al., *J. Virol.* **71**, 7101–7109 (1997).
26. R.E. Spier, *Vaccine* **14**, 1285–1288 (1996).
27. M. Corr, D.J. Lee, D.A. Carson, and H. Tighe, *J. Exp. Med.* **184**, 1555–1560 (1996).
28. T.M. Fu et al., *Mol. Med.* **3**(6), 362–371 (1997).
29. N.F. Pierce and J.B. Kaper, *J. Immunol.* **124**, 307–311 (1980).
30. G. Gregoriadis, *Pharm. Res.* **15**(5), 661–670 (1988).
31. E. Sanders and C.T. Ashworth, *Exp. Cell Res.* **22**, 137–145 (1961).
32. A.T. Florence, *Pharm. Res.* **41**(12), 809–812 (1997).
33. J.H. Eldridge et al., *Adv. Exp. Med. Biol.* **251**, 191–202 (1989).
34. M.E. LeFevre and D.D. Joel, *Life Sci.* **21**(10), 1403–1408 (1977).
35. A. Florence and P.U. Jani, *Drug Saf.* **10**, 233–266 (1994).
36. N. Santiago, S. Haas, and R.A. Baughman, in M.F. Powell and M.J. Newman, eds., *Vaccine Design: The Subunit and Adjuvant Approach*, Plenum, New York, 1995, pp. 413–438.
37. E. Mathiowitz et al., *Nature (London)* **386**, 411–414 (1997).
38. Y. Tabata and Y. Ikada, *Adv. Polym. Sci.* **94**, 107–141 (1990).
39. C. Scheicher, M. Mehlig, H.P. Dienes, and K. Reske, *Eur. J. Immunol.* **25**, 1566–1572 (1995).
40. M.L. Hedley, J. Curley, and R. Urban, *Nat. Med.* **4**(3), 365–368 (1998).
41. R. Langer, *Science* **249**, 1527–1533 (1990).
42. R. Langer, *Nature (London)* **392**(Suppl.), 5–10 (1998).
43. M. Manthorpe et al., *Hum. Gene Ther.* **4**, 419–431 (1993).
44. D. Lew et al., *Hum. Gene Ther.* **6**, 553–564 (1995).
45. C.R. Middaugh, R.K. Evans, D.L. Montgomery, and D.R. Casimiro, *J. Pharm. Sci.* **87**(2), 130–146 (1998).
46. A.H. Wyllie and A.J. Strain, *Biochem. J.* **218**, 475–482 (1984).
47. J.A. Wolff et al., *Hum. Mol. Genet.* **1**(6), 363–369 (1992).
48. H.I. Elsner and E.B. Lindblad, *DNA* **8**, 679–701 (1989).
49. D.J. Freeman and R.W. Niven, *Pharm. Res.* **13**(2), 202–209 (1996).
50. R. Krishnamurthy and J.A. Lumpkin, *BioPharm*, January, pp. 32–36 (1998).
51. U.S. Pat. 5,783,567 (July 21, 1998). M.L. Hedley, J.M. Curley, and R.S. Langer (to Pangaea Pharmaceuticals, Inc.).
52. R.C. Adami et al., *J. Pharm. Sci.* **87**(6), 678–683 (1998).

Next Page

53. D.H. Jones et al., *Vaccine* **15**(8), 814–817 (1997).
54. D.H. Jones, J.C.S. Clegg, and G.H. Farrar, *Dev. Biol. Stand.* **92**, 149–155 (1998).
55. D. Wang, D. Robinson, G. Kwon, and J. Samuel, *Keystone Symp. Mol. Cell. Biol.*, Keystone, Colo., January 19–25, 1998.
56. H. Cohen et al., *Proc. Int. Symp. Controlled Release Bioact. Mater.* **25**, 374–375 (1998).
57. Y.S. Jong et al., *J. Controlled Release* **47**, 123–134 (1997).
58. V. Labhasetwar et al., *J. Pharm. Sci.* **87**(11), 1347–1350 (1998).
59. V. Labhasetwar et al., *Proc. Int. Symp. Controlled Release Bioact. Mater.* **25**, 372–373 (1998).
60. L.R. Beck et al., *Fertil. Steril.* **31**(5), 545–551 (1979).
61. D.E. Chickering and E. Mathiowitz, *J. Controlled Release* **34**, 251–261 (1995).
62. P.U. Jani, G.W. Halbert, J. Langridge, and A.T. Florence, *J. Pharm. Pharmacol.* **42**, 821–826 (1990).
63. W. Bohm, T. Mertens, R. Schirmbeck, and J. Reimann, *Vaccine* **16**, 949–954 (1998).
64. E. Manickan, K.L. Karem, and B.T. Rouse, *Crit. Rev. Immunol.* **17**, 139–154 (1997).
65. L.C. Anton, J.W. Yewdell, and J.R. Bennink, *J. Immunol.* **158**, 2535–2542 (1997).

ADDITIONAL READING

M.T. Aguado, *Vaccine* **11**, 596–597 (1993).
T. Alexakis et al., *Appl. Biochem. Biotechnol.* **50**, 93–106 (1995).
J. Cohen, R.A. Siegel, and R. Langer, *J. Pharm. Sci.* **73**(8), 1034–1037 (1984).
S. Cohen, M.J. Alonso, and R. Langer, *Int. J. Technol. Assess. Health Care* **10**, 121–130 (1994).
J. Fang et al., *Proc. Nat. Acad. Sci. U.S.A.* **93**, 5753–5758 (1996).
M. Kanke et al., *Parenter. Sci. Technol.* **42**, 157–165 (1988).
T.J. Smith, *BioPharm*, April, pp. 54–55 (1994).

See also LIPOSOMES; POLYMERIC SYSTEMS FOR GENE DELIVERY, CHITOSAN AND PINC SYSTEMS.

MUCOSAL DRUG DELIVERY, BUCCAL

WENDY WEBBER
Brown University
Providence, Rhode Island

KEY WORDS

Biodegradable
Buccal mucosa
Epithelium
Local delivery
Peptides
Periodontal disease
PLGA
Sublingual delivery
Sublingual mucosa
Systemic circulation

OUTLINE

The Structure of the Oral Mucosae
Delivery to the Systemic Circulation
  Via Buccal Mucosa
  Applications in Buccal Delivery
  Via Sublingual Mucosa
  Applications in Sublingual Delivery
Local Delivery to the Mouth
  Applications in Local Delivery
Bibliography

Although often thought of under the umbrella term of buccal delivery, drug delivery via the membranes of the oral cavity is traditionally divided into three categories: (*1*) buccal delivery, which infers drug administration through the lining of the cheek to the systemic circulation; (*2*) sublingual, the administration of drug via membranes of the floor of the mouth or the underside of the tongue to the systemic circulation; and (*3*) local delivery to the mouth, which involves treatment of conditions within the oral cavity by administration to the affected mucosal tissues. These sites for delivery differ in both structure and composition, as well as in degree of permeability and, therefore, also vary in their ability to retain a delivery device for a desired length of time. The following article provides a chronologically oriented overview of the various methods and technologies that exist or have been attempted in the utilization of the oral mucosae for applications in buccal delivery, sublingual delivery and local drug delivery to the mouth. Table 1 summarizes some of the specific drugs delivered to the oral mucosa.

THE STRUCTURE OF THE ORAL MUCOSAE

In general terms, the oral mucosae is made up of an outermost layer of stratified squamous epithelium, which is covered with mucus and consists of a stratum distendum, stratum filamentosum, stratum suprabasale, and a stratum basale. Below this lies a basal lamina, the lamina propria, and the submucosa (Fig. 1). The epithelium serves as the mechanical barrier that protects underlying tissues, whereas the lamina propria acts as a mechanical support and also carries the blood vessels and nerves. Some regions of the oral mucosa are keratinized, whereas others are not (Fig. 2). The nonkeratinized regions, such as buccal mucosa, are more permeable than the keratinized regions. This is due, to some extent, to the composition of intercellular lipids comprising the particular region. Whereas keratinized regions contain predominantly neutral lipids (ceramides), nonkeratinized areas are composed of a glycosyl ceramide that appears to be derived from membrane-coating granules that differ morphologically from the lamellate membrane-coating granules of keratinized tissue.

Previous Page

53. D.H. Jones et al., *Vaccine* **15**(8), 814–817 (1997).
54. D.H. Jones, J.C.S. Clegg, and G.H. Farrar, *Dev. Biol. Stand.* **92**, 149–155 (1998).
55. D. Wang, D. Robinson, G. Kwon, and J. Samuel, *Keystone Symp. Mol. Cell. Biol.*, Keystone, Colo., January 19–25, 1998.
56. H. Cohen et al., *Proc. Int. Symp. Controlled Release Bioact. Mater.* **25**, 374–375 (1998).
57. Y.S. Jong et al., *J. Controlled Release* **47**, 123–134 (1997).
58. V. Labhasetwar et al., *J. Pharm. Sci.* **87**(11), 1347–1350 (1998).
59. V. Labhasetwar et al., *Proc. Int. Symp. Controlled Release Bioact. Mater.* **25**, 372–373 (1998).
60. L.R. Beck et al., *Fertil. Steril.* **31**(5), 545–551 (1979).
61. D.E. Chickering and E. Mathiowitz, *J. Controlled Release* **34**, 251–261 (1995).
62. P.U. Jani, G.W. Halbert, J. Langridge, and A.T. Florence, *J. Pharm. Pharmacol.* **42**, 821–826 (1990).
63. W. Bohm, T. Mertens, R. Schirmbeck, and J. Reimann, *Vaccine* **16**, 949–954 (1998).
64. E. Manickan, K.L. Karem, and B.T. Rouse, *Crit. Rev. Immunol.* **17**, 139–154 (1997).
65. L.C. Anton, J.W. Yewdell, and J.R. Bennink, *J. Immunol.* **158**, 2535–2542 (1997).

ADDITIONAL READING

M.T. Aguado, *Vaccine* **11**, 596–597 (1993).
T. Alexakis et al., *Appl. Biochem. Biotechnol.* **50**, 93–106 (1995).
J. Cohen, R.A. Siegel, and R. Langer, *J. Pharm. Sci.* **73**(8), 1034–1037 (1984).
S. Cohen, M.J. Alonso, and R. Langer, *Int. J. Technol. Assess. Health Care* **10**, 121–130 (1994).
J. Fang et al., *Proc. Nat. Acad. Sci. U.S.A.* **93**, 5753–5758 (1996).
M. Kanke et al., *Parenter. Sci. Technol.* **42**, 157–165 (1988).
T.J. Smith, *BioPharm*, April, pp. 54–55 (1994).

See also LIPOSOMES; POLYMERIC SYSTEMS FOR GENE DELIVERY, CHITOSAN AND PINC SYSTEMS.

MUCOSAL DRUG DELIVERY, BUCCAL

WENDY WEBBER
Brown University
Providence, Rhode Island

KEY WORDS

Biodegradable
Buccal mucosa
Epithelium
Local delivery
Peptides
Periodontal disease
PLGA
Sublingual delivery
Sublingual mucosa
Systemic circulation

OUTLINE

The Structure of the Oral Mucosae
Delivery to the Systemic Circulation
  Via Buccal Mucosa
  Applications in Buccal Delivery
  Via Sublingual Mucosa
  Applications in Sublingual Delivery
Local Delivery to the Mouth
  Applications in Local Delivery
Bibliography

Although often thought of under the umbrella term of buccal delivery, drug delivery via the membranes of the oral cavity is traditionally divided into three categories: (*1*) buccal delivery, which infers drug administration through the lining of the cheek to the systemic circulation; (*2*) sublingual, the administration of drug via membranes of the floor of the mouth or the underside of the tongue to the systemic circulation; and (*3*) local delivery to the mouth, which involves treatment of conditions within the oral cavity by administration to the affected mucosal tissues. These sites for delivery differ in both structure and composition, as well as in degree of permeability and, therefore, also vary in their ability to retain a delivery device for a desired length of time. The following article provides a chronologically oriented overview of the various methods and technologies that exist or have been attempted in the utilization of the oral mucosae for applications in buccal delivery, sublingual delivery and local drug delivery to the mouth. Table 1 summarizes some of the specific drugs delivered to the oral mucosa.

THE STRUCTURE OF THE ORAL MUCOSAE

In general terms, the oral mucosae is made up of an outermost layer of stratified squamous epithelium, which is covered with mucus and consists of a stratum distendum, stratum filamentosum, stratum suprabasale, and a stratum basale. Below this lies a basal lamina, the lamina propria, and the submucosa (Fig. 1). The epithelium serves as the mechanical barrier that protects underlying tissues, whereas the lamina propria acts as a mechanical support and also carries the blood vessels and nerves. Some regions of the oral mucosa are keratinized, whereas others are not (Fig. 2). The nonkeratinized regions, such as buccal mucosa, are more permeable than the keratinized regions. This is due, to some extent, to the composition of intercellular lipids comprising the particular region. Whereas keratinized regions contain predominantly neutral lipids (ceramides), nonkeratinized areas are composed of a glycosyl ceramide that appears to be derived from membrane-coating granules that differ morphologically from the lamellate membrane-coating granules of keratinized tissue.

Table 1. Drugs Delivered via Oral Mucosae

Type of delivery	Drug	Reference	Year
Systemic, Buccal	Verapamil	Davis and Johnson (1)	1979
	Insulin	Ishida et al. (2)	1981
		Nagai (3)	1985
	Glyceryl trinitrate	Davis et al. (4)	1983
	Ketobemidone	Hansen et al. (5)	1991
	Diclofenac sodium	Cassidy et al. (6)	1993
	Buprenorphine	Guo (7)	1994
		McQuinn et al. (8)	1995
	Diltiazem	Ahuja et al. (9)	1995
	LHRH	Lee and Chien (10)	1995
	Testosterone	Kim et al. (11)	1995
	Nitroglycerin	Iga and Ogawa (12)	1996
	Progesterone	Voorspoels et al. (3)	1997
	Peptides	Veillard et al. (14)	1987
		Merkle et al. (15)	1986
		Harris and Robinson (16)	1990
Sublingual	Nitrates	Field (17)	1858
		Riseman et al. (18)	1958
		Pimlott and Addy (19)	1985
		Thadani and Lipicky (20)	1994
		Abrams (21)	1995
	Lidocaine	Bergman et al. (22)	1968
	Buprenorphine	Edge et al. (23)	1979
		Brewster et al. (24)	1981
	Temazepam	Russell et al. (25)	1988
Local	Lidocaine	Nagai and Konishi (26)	1987
	Prostaglandin	Nagai and Konishi (26)	1987
	Fluoride	Bottenberg et al. (27)	1991
	Miconazole nitrate	Reading et al. (28)	1981
		Bouckaert et al. (29)	1992
	Nystatin	Encarnacion and Chin (30)	1994
	Hydrocortisone	Fabregas and Garcia (31)	1995
	Chlorhexidine	Soh et al. (32)	1982
		Coventry and Newman (33)	1982
		Soskolne et al. (34)	1983
		Addy et al. (35)	1988
		Steinberg et al. (36)	1990
	Tetracycline	Goodson et al. (37)	1983
		Addy et al. (35)	1988
		Tonetti et al. (38)	1990
		Heijl et al. (39)	1991
		Baker et al. (40)	1988
		Minabe et al. (41)	1989
		Heller et al. (42)	1989
		Deasy et al. (43)	1989
		Eckles et al. (44)	1990
		Roskos et al. (45)	1995
		Maze et al. (46)	1995
		Webber et al. (unpublished data)	1997
	Metronidazole	Loesche et al. (47)	1987
		Addy et al. (36)	1988
	Doxycycline	Larsen (48)	1990
	Growth factors	Lynch et al. (49)	1991
	BMPs	Wozney (50)	1995
		Sigurdsson et al. (51)	1995

In general, it appears that the patterns of epithelial differentiation observed in the oral mucosa vary to produce a surface layer that sufficiently meets the demands placed upon that particular tissue (54,55). Furthermore, in dealing with drug delivery, the amount of a certain drug absorbed through the buccal mucosa are determined by many factors, including the pKa of the base, the rate of partition of the unionized form of the drug, the lipid–water partition coefficient of that particular drug, and lastly, on the pH of the solution (56).

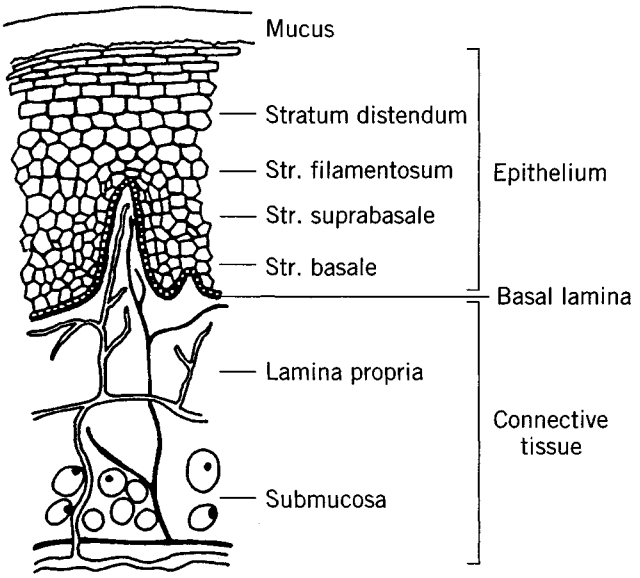


Figure 1. Schematic cross section through the oral mucosa showing the epithelium, basal lamina, and connective tissue. *Source:* From Ref. 52.

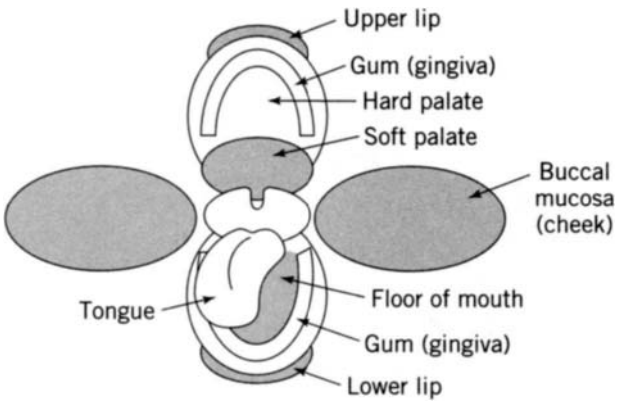


Figure 2. Schematic representation of the "open" oral cavity, showing keratinized (white) and nonkeratinized (shaded) regions of the mouth. *Source:* From Ref. 53.

DELIVERY TO THE SYSTEMIC CIRCULATION

Via Buccal Mucosa

Administration of a drug via the buccal mucosa (the lining of the cheek) to the systemic circulation is defined as buccal delivery. Though the buccal mucosa is significantly less permeable than the sublingual mucosa and usually not able to provide rapid drug absorption or good bioavailabilities, it is more permeable than skin and also boasts other advantages over alternative delivery routes. The fact that the buccal mucosa is less permeable than the sublingual makes it a more desirable site for sustained release delivery. The oral mucosa itself provides a protective covering for the underlying tissues, acting as a physical barrier against toxins and microorganisms. Patient compliance is high with buccal delivery due to the accessibility of the cheek lining and lack of invasive measures. In the case of an adverse reaction, administration of drug can be stopped at any time by device removal. Most importantly, however, drugs administered via the buccal mucosa directly enter the systemic circulation, thereby avoiding enzymatic degradation in the gastrointestinal tract as well as first-pass metabolism in the liver. Furthermore, peptides and proteins are not only susceptible to the acidic environment of the stomach, but they are generally high in molecular weight and are hydrophilic in nature, and therefore cannot permeate the intestinal mucosa as easily as they can the buccal tissues. For these reasons, buccal delivery is being researched with increasing intensity as a route of administration for the increasing number of peptide drugs currently on the market.

Applications in Buccal Delivery

Due to the buccal mucosae being more permeable than the skin, as well as the other advantages already mentioned, the buccal mucosae have been increasingly used as a route of drug delivery. Evidence of a biexponential absorption curve suggests that the buccal membrane can also act as a storage area for certain drugs before they are passed into the bloodstream. In studies by Davis and Johnston in 1979, in which occurrence of the antianginal agent verapamil in biological fluids and tissues was assayed fluorometrically, the buccal absorption of verapamil was found to occur in a biphasic manner (1). Despite this fact, interest in the buccal mucosa as a route for delivery led Ishida et al. in 1981 (2) to attempt to develop an oral dosage form that would solve the problem of insulin administration via injection. The system was a core of cacao butter, insulin, and additive surrounded by a layer of hydroxypropyl cellulose-H and Carbopol-934 (a polyacrylic acid) that adhered to the oral mucosa of beagle dogs for up to 6 hours. Furthermore, a decrease of blood sugar levels was maintained at over 70% for 3 hours. The amount of insulin absorbed in this manner, however, was found to be only 0.5% of the amount absorbed when given as an intramuscular insulin injection (2).

Release of glyceryl trinitrate from modified hydroxypropylmethylcellulose (Synchron) matrix tablets via the buccal route was accomplished in 1983 by Davis and his colleagues. The matrix tablets look like conventional tablets, but contain a drug that is entrapped in a slowly eroding, nondisintegrating Synchron and lactose base. The Synchron formulation showed sustained release of a model drug in excess of 3 hours, whereas normally dissolving tablets had completed release within 20 minutes (4).

Nagai et al. published a good deal of research in the 1980s, a portion of which was concerning oral mucosal adhesive tablets for the administration of insulin. They used a combination of hydroxypropylcellulose and Carbopol to prepare tablets that would turn into a gel-like substance in the swollen state. This gel would adhere firmly to the oral mucosa for extended periods of time, releasing the insulin in a controlled manner (26). The bioavailability was about 0.5% of that observed in intramuscular administration in dogs, but has recently been improved to 0.75% by

using Witepsol® as the core base in place of cocoa butter (57). The adhesive tablets were then developed into a system releasing triamcinolone acetonide ointment to treat aphthous stomatitis. The product, Aftach®, is a small, thin, double-layered tablet and is now commercially available (3). The upper layer consists of lactose and serves as a supporting layer; the triamcinolone acetonide is dispersed in the lower lydroxypropylcellulose and Carbopol 934 adhesive layer (57).

Ketobemidone is a powerful narcotic analgesic that is traditionally administered perorally or rectally and, therefore, has a low and variable bioavailability. In 1991, Hansen et al. began studies in which they synthesized various carboxylic acid and carbonate esters of ketobemidone. The goal was to improve the bioavailability of the drug by using the buccal approach. However, due to the limited lipophilicity of the compound, the drug did not permeate the oral mucosa. To improve penetration of the drug across the oral mucosa, Hansen and her colleagues developed more lipophilic prodrugs of ketobemidone, which are converted back to the active parent drug during or after absorption across the mucosa (5). The esters synthesized were, in fact, found to have increased lipophilicity over the parent drug and are potentially more capable of crossing the buccal mucosal barrier.

Buccal delivery of the nonsteroidal antiinflammatory drug diclofenac sodium (Voltaren) from a hydrogel disk was studied in humans by Cassidy et al. (6). The 1-cm^2 hydrogel disks were formulated with 80 wt% hydroxyethyl methacrylate and 20 wt% hydrophobic difunctional macromolecular cross-linker. A 50 wt % solution of diclofenac sodium in 85.5% (v/v) methanol:water was loaded into the dry disks over a period of 48 hours. Patients had the hydrogel device affixed to their buccal mucosa for 4 hours, and blood samples were taken at regular intervals for diclofenac sodium quantification. Results were compared with intravenous infusion of the drug into the same patients for 4 hours at 3 mg/hour. The study demonstrated that diclofenac was readily transported across the buccal mucosa, with a steady-state flux of 2.1 mg/cm^2-hr. (6).

Carbopol 934, polyisobutylene (PIB), and polyisoprene (PIP) formed by a two-roll milling process and loaded with buprenorphine was formulated for controlled drug delivery by researchers at 3M Pharmaceuticals. Guo noted that the surface properties of the buccal patches were dependent upon the Carbopol 934 content as well as the existing polymeric ratio. Polymer patches with higher Carbopol content, or higher PIB:PIP ratios, had higher water uptake capacity, which led to increased swelling and more buprenorphine release (7). The analgesic buprenorphine was delivered safely and effectively over a 12-hour period to the upper gum or lip from these thin, noneroding, ethylcellulose-backed, mucoadhesive polymeric disks. However, this period only accounted for release of 15% of the drug load, which indicates that an extended application time could result in prolonged buprenorphine release. Evaluation of the 3M Transmucosal Drug Delivery System was discussed by Benes et al. in the June 1995 3M Delivery newsletter. Results demonstrated that the 3M system, named CYDOT™, is also comfortable and acceptable to the wearer of the device (58). Pharmacologically relevant serum concentrations of buprenorphine were attained using these devices and sustained for 12–24 hours in humans in 1995 (8). Greater drug delivery was achieved from patches applied to the gum rather than the lip, most likely because of the superior mucoadhesion present at this site.

In 1995, it was reported by Ahuja et al. that diltiazem, a calcium channel blocker commonly used in the treatment of cardiovascular disorders, could be formulated into polymeric buccal tablets that achieved up to an 86% in vitro release of the diltiazem obtained from a dissolution study after 4 hours. The multilayered tablets were comprised of a cap layer of Carbopol 934 combined with either hydroxypropyl cellulose, hydroxypropylmethyl cellulose, or poly(vinyl pyrrolidone) compressed using a die punch set around an already compressed core of drug. In vitro release data was compiled using bovine cheek pouch membrane in a Franz diffusion cell (9).

Lee and Chien developed a method of controlling transmucosal delivery of luteinizing hormone-releasing hormone (LHRH) from a bilayer system composed of a fast-releasing layer containing a polypyrrolidone (PVP (K-30)) and a sustained-release layer formulated from Carbopol 934 and PVP (K-90). The delivery device also contains an enhancer, sodium cholate, which promotes the transmucosal permeation of LHRH and a stabilizer, cetylpyridinium chloride, which stabilizes LHRH from degradation by the oral microflora. Simulation of the system in vivo involves adhering the film to the alveolar mucosa, with the other side facing the buccal mucosa in a specially designed device holder. Results demonstrated a burst release of LHRH from the fast-release layer, thereby providing a rapid delivery of the hormone, and a prolonged release of LHRH from the sustained-release layer. Therefore, varying the formulation of the device can result in modulation in the rate of LHRH transmucosal permeation (10).

Buccal delivery of testosterone was achieved in 1995 by Kim et al. The buccal matrix was comprised primarily of a blend of water-soluble polymers that melt near body temperature. Testosterone (T) was dispersed in the polymer matrix. When introduced into the buccal cavity, the polymer matrix melts and disperses within 5 minutes, exposing mucosal tissues to the testosterone. A single 10-mg transbuccal dose of the testosterone was found to induce a prompt rise in testosterone levels in the serum as well as dihydrotestosterone (DHT) concentrations. Furthermore, the method of administration was associated with a more normal DHT:T ratio than other preparations. The serum testosterone levels remained elevated above baseline for 24 hours. Therefore, transbuccal delivery of testosterone seems promising due to its simplicity, acceptability, reversibility, lack of toxicity, and protection from hepatic first-pass metabolism (11).

Two types of sustained release buccal dosage forms were prepared by Iga and Ogawa for nitroglycerin and isosorbide dinitrate (12). One device is a slowly disintegrating plain tablet, whereas the other is a slowly disintegrating polyethylene film-covered tablet, which has a single hole on the top surface through which disintegration and drug release can occur. The plain tablets disintegrated in 3–6 hours, whereas the film-covered tablets resulted in an almost constant plasma drug level for both drugs for over 10

hours until the tablet was removed. The tablets achieved almost complete bioavailabilities for both nitroglycerin and isosorbide dinitrate, which is in contrast to the near negligible bioavailabilities achieved when delivering these drugs orally, indicating that this type of sustained release buccal dosage form could be of importance in increasing the bioavailabilities of rapidly eliminating drugs and prolonging their absorption times (12).

The buccal delivery possibilities of progesterone were investigated in 1997 by Voorspoels et al. using a slow release degradable bioadhesive tablet in dogs. The bioadhesive tablet consisted of micronized progesterone, drum-dried waxy maize starch, Carbopol 974P, and sodium stearylfumarate compressed into a tablet. The tablet was placed above the right upper canine in the oral cavity. Delivery of progesterone involves release of the drug from the bioadhesive tablet, which is erosion controlled, followed by dissolution of the progesterone into the saliva, and finally, absorption of the drug into the buccal mucosa. The mean residence time of the drug was measured as well as the absolute bioavailability. Results indicated that buccal delivery may be useful, as mean residence time was dramatically improved by the administration of a bioadhesive tablet compared with intravenous formulations (13).

Applications in Peptides. Due to the emergence of peptides as a major class of future drugs, the buccal epithelium is being closely scrutinized as a possible route of peptide delivery. Initial studies of peptide absorption and permeability through the buccal mucosa were performed by Veillard et al., and preliminary results showed that although a higher drug dosage was administered via the buccal route than intravenously, corresponding plasma levels were much lower from buccal delivery than by direct intravenous injection (14). Therefore, penetration enhancers may be needed to achieve the desired activity when using the buccal route for peptide delivery.

Further studies on peptide delivery by Merkle and his colleagues in 1986 closely followed those by Veillard. Hydroxyethylcellulose patches containing the tripeptide protirelin and backed with an impermeable laminate were designed as buccal patches (15). Protirelin has a molecular weight of 362 and was readily absorbed across the buccal mucosa, as shown by increases in pituitary thyrotropin and prolactin levels, whereas calcitonin with a molecular weight of 3,500 could not permeate the buccal mucosa at all. However, after 30 minutes of contact with the mucosa between 48% and 72% of the protirelin was still found in the patches, indicating that a large portion of the drug was unable to be absorbed within this short contact time. This was most likely due to the high viscosity of the polymer, as much more drug was released when a lower viscosity polymer was used.

Via Sublingual Mucosa

Sublingual delivery traditionally involves systemic administration of drug via membranes of the floor of the mouth or the ventral surfaces of the tongue. The sublingual mucosa is relatively permeable due to the thin membrane and large veins, allows rapid absorption and acceptable bioavailabilities of many drugs, and is a convenient and easily accessible location. Furthermore, the sublingual mucosa is a smooth surface, not furred like the top of the tongue, and is free of mucus and undigested food, unlike the stomach.

Applications in Sublingual Delivery

The history of sublingual delivery dates back to 1858 when A. G. Field first realized that nitroglycerin dropped on the tongue was readily absorbed through the membranes (17). But it was not until a century later that Riseman et al. noted that many nitrates are highly effective in treating patients with angina pectoris when administered from either hypodermic injection, inunction, buccally or sublingually. Of the six nitrates tested to treat angina pectoris, including nitroglycerin, erythrol tetranitrate, pentaerythritol tetranitrate, mannitol hexanitrate, triethenolamine trinitrate, and sodium nitrate, the erythrol tetranitrate administered buccally or sublingually had the greatest prophylactic impact (18). However, it appears that the prolonged duration of action of the tablets may be due to their prolonged duration of tablet dissolution, directly leading to a prolonged period of absorption into the bloodstream. Therefore, another study by the group was undertaken to determine if, in fact, the prolonged dissolution time was essential for the prolonged therapeutic effect, as well as to assess the effect of varying the dosage of the erythrol tetranitrate. Results showed that the erythrol tetranitrate is absorbed more rapidly and uniformly from the sublingual route than from the buccal pouch. However, the prolonged beneficial effects of erythrol tetranitrate are not dependent upon prolonged absorption. The effects are long lasting even following sublingual administration of erythrol tetranitrate with rapid dissolution time (59).

Research in 1985 by Pimlott and Addy measured the absorption of isosorbide dinitrate (ISDN) into the systemic circulation after application of tablets to the buccal, palatal, and sublingual mucosal sites. For the buccal and sublingual sites, maximum plasma levels of ISDN were achieved at 5 minutes, after which levels fall gradually. Concentrations of ISDN were about 1.2 ng/mL after 30 minutes from either the sublingual or buccal route. On the other hand, plasma levels of ISDN were undetectable at all times from the palatal mucosa (19).

Another study involving oral nitrate treatment for patients with angina pectoris was completed by Thadani and Lipicky in 1994. It is currently accepted that intermittent use of short-acting oral nitrates used to terminate an attack of angina as well as provide prophylaxis for anticipated activity, and intermittent use of long-acting oral nitrates to provide prophylaxis for anticipated activity are both valid and successful therapies. However, tolerance presents a problem in limiting multiple dosing regimens of most oral long-acting nitrates and continual prophylaxis has not yet been achieved by any long-acting oral nitrate. Here, nitroglycerin spray and sublingual tablets of isosorbide dinitrate were used to successfully relieve an established attack of angina, and infrequent use of such substances is not associated with the development of tolerance (20).

Studies evaluating the use of sublingual buprenorphine in patients following surgery and comparing its effects

with intramuscularly administered morphine were done by Edge et al. in 1979. Each patient received either a tablet of 0.4 mg buprenorphine and an injection of 5% dextrose in 1 mL, or a dummy tablet and an injection of 10 mg morphine in 1 mL. A pain "score" was obtained from the patients by means of a visual linear analog. Results indicated a slower onset of action by the buprenorphine, but a much longer duration than the morphine (23).

Temazepam is one of the shorter acting membranes of the 1,4 benzodiazepine group of drugs that is commonly prescribed for short-term therapy for adult insomnia. The pharmacokinetics of a new 10 mg sublingual temazepam tablet were compared with the currently marketed 10 mg oral gelatin capsule by Russell et al. in 1988 (25). Evidence shows the sublingual formulation to have a 98.4% bioavailability relative to the oral capsule, and the mean maximum plasma concentrations were similar. Therefore, it seems that the sublingual tablet is an acceptable alternative to the currently used oral capsule.

Although most sublingual delivery is accomplished via mouthwashes, oral sprays, or topical gels, controlled release tablets are currently being investigated as the most promising future technology for delivery drug sublingually.

LOCAL DELIVERY TO THE MOUTH

The classification of local delivery to the mouth includes any system that is applied to the oral mucous membranes in order to treat conditions of the mouth such as periodontal disease, gingivitis, oral candidiasis, and other chronic lesions or topical fungal infections. Traditional methods of delivery to the diseased site have involved chewing gums, mouthwashes, ointments, and gels. However, these methods share a common disadvantage in that they all have relatively short residence times and, therefore, fail to maintain therapeutic concentrations long enough to affect the bacterial population. Furthermore, drug is lost in the saliva (i.e., with swallowing), and patients on these treatments often have low patient compliance due to the need for frequent drug application. Current technology, however, is attempting to prolong residence time and increase patient compliance by using sustained release drug delivery systems.

Applications in Local Delivery

One of the earlier controlled release products to go through clinical trials was the Orabase system by Kutscher et al. composed of a finely ground pectin, gelatin, and carboxymethyl cellulose in a polyethylene–mineral oil gel base. This vehicle, in which therapeutics could be incorporated, has the ability to adhere to the site of application without causing any deleterious effects on the underlying tissue. Results varied with duration of maintenance ranging anywhere between 15 and 152 minutes, depending on the site in the oral cavity to which the device was adhered (60).

A device by Nagai et al. similar to that described earlier to deliver insulin systematically was also fabricated of hydroxypropyl cellulose and Carbopol, yet loaded with lidocaine for the local treatment of toothache. Unfortunately, lidocaine was not absorbed and remained in the dosage form for up to 6 hours. Nagai and Konishi, known for their work in the buccal delivery field, also formulated an adhesive gingival plaster that is loaded with prostaglandin $F_{2\text{-}\alpha}$ for the facilitation of tooth movement in the orthodontic process (26). A minimum of 70% of the drug load was released within the first 6 hours. In vivo studies in monkeys showed that application of the plaster to the gingiva did, in fact, accelerate tooth movement and, therefore, decrease movement time.

Bottenberg and his colleagues researched the possibility of using various bioadhesive polymers as fluoride-containing, slow-release tablets for oral use, specifically in the war against dental caries. Modified starch, poly(acrylic acid) (PAA), poly(ethylene glycol) (PEG) and sodium carboxymethylcellulose were the bioadhesive polymers investigated. A modified maize starch tablet containing 5% (w/w) PAA and PEG with a 300,000-dalton molecular weight proved to be the most successful formulation. Two formulations were then tested in vivo, including a drum-dried waxy maize and a PEG. Tablets were placed on the attached gingiva in the upper canine region, held for 30 seconds, and then moistened with the tongue. After insertion of the tablets, saliva samples were taken at regular intervals. In vivo, fluoride levels between 150 and 1,000 μg/mL were maintained for up to 8 hours, which is significantly longer than levels obtained with the administration of 4 times the amount of fluoride in a fluoride toothpaste. A patent for the application of modified starch as a bioadhesive slow-release drug carrier was applied for in 1991 (27).

A miconazole-loaded oral gel was tested in a study by Reading et al. for its efficacy against erythema, plaques, and perlèche in children with oral candidiasis. After one week, the gel boasted a 100% clinical cure rate for both plaques and perlèche. It showed a 97% cure rate for erythema (28). Buccal gels loaded with miconazole nitrate are also used for the treatment of topical fungal infections such as oral candidiasis. These gels are traditionally applied several times a day. Immediately following each application, the salivary miconazole nitrate concentration is at its maximum and then is rapidly cleared from the oral cavity. In an effort to prolong residence time of the drug, Bouckaert et al. formulated a bioadhesive tablet of modified starch and 5% PAA. Although a drug amount sixfold lower than that existing in the gel was released from the tablet, the salivary miconazole nitrate concentrations produced by the tablet were higher than by the gel and remained at a therapeutic level for over 10 hours. In vivo, a mean adhesion time of the tablet to the mucosa was in excess of 9.5 hours. The polymer tablets eventually eroded completely, and none had to be removed due to irritation to the mucosa. Furthermore, erosion seems to play an important role in the drug release rate from these systems. Although further investigation is required, variability in drug level appears to be due to tablet erosion by soft tissue movements and the individual movement patterns occurring within the mouth (29).

Mucosal Oral Therapeutic System (MOTS) is a controlled nystatin-releasing osmotic system based on an osmotic technique for delivering highly water-soluble or insoluble drugs that was developed by Encarnacion and Chin

at the Alza Corporation in California (31). Nystatin is an antibiotic that exerts both a fungistatic and fungicidal effect for the treatment of oral candidiasis. Salivary concentrations of nystatin produced by the MOTS exceeded those produced by a nystatin pastille for all time points beyond 30 minutes. Release continued for at least 2 hours. The higher sustained concentration produced by the MOTS would hopefully decrease the duration of therapy and thereby increase patient compliance.

Buccoadhesive matrix tablets have also been used for delivery of hydrocortisone hemisuccinate in the treatment of aphthous stomatitis and other gingival ulcers. The polymers used included hydroxypropylcellulose, hydroxypropylmethycellulose, polycarbophil, and modified maize starch. The maize starch formulation, which proved to have the optimal gingival tolerance, was found to deliver hydrocortisone in vitro for up to 24 hours, dissolve, and eventually result in the complete erosion of the tablet (31).

Local Delivery to Treat Dental Disease. Much of the local delivery research is geared toward the treatment of periodontal disease and gingivitis. Periodontal disease is a disease of the supporting structures of the teeth, namely the periodontal ligament, cementum, alveolar bone, and the tissue components of the gingiva (see Fig. 1). Abundant evidence implicates the microorganisms in the dental plaque as the primary causative agent of various forms of periodontal disease. In fact, there exists a strong correlation between the presence and amount of plaque and calculus on the teeth and the severity of disease. When microflora are allowed to build up in the moist, warm, anaerobic, ecologically ideal environment of the sulcus, the bacteria proliferate and produce an excess of enzymes and toxins that diffuse through the gum epithelium and cause inflammation. This condition, known as gingivitis, leads to an increase in polymorphonuclear neutrophil (PMN) migration into the sulcus. The PMNs destroy bacteria but also release enzymes, such as collagenase, that cause the breakdown of collagen. The sulcus deepens, forming a periodontal pocket into which plaque can migrate. Plaque then colonize the cementum, causing it to break down. Macrophages invade to fight the infection, releasing interleukin I, a substance inducing osteoclast stimulation, which in turn leads to bone resorption. Alveolar bone resorption hallmarks the breakdown of the structural support system and leads to eventual tooth loss (61).

A healthy periodontal situation appears to be associated with a primarily facultative gram-positive organism located almost entirely supragingivally on the tooth's surface. Normally, the host's defense mechanisms, including saliva, crevicular fluid, and PMNs, provide the necessary protection to the dentogingival area. The constant contact between saliva and the oral mucosa serves as a flushing action, ridding the mouth of excess bacteria. Saliva also contains substances that not only interfere with bacterial adhesion and growth, but actually phagocytose the bacteria. The crevicular fluid is formed in the gingival connective tissue as a result of extraction from the microcirculation, then unidirectionally flushes through the tissues and junctional epithelium into the gingival crevice. The flushing action serves to minimize bacterial colonization of the crevice and increases in relation to the level of inflammation in the gingival tissues. The crevicular fluid also contains protective components such as complement proteins, antibodies, and nonspecific opsonins. Many bacteria harbored in the gingival crevice turn on the host's immune response, activating the complement cascade (61). PMNs are also thought to play an integral role in the protection of the gingival tissues from bacteria. When plaque builds up in the gingival sulcus, the PMNs provide a barrier by preventing direct contact between the bacteria and the epithelial cells. PMNs in the gingival sulcus proceed to phagocytose the bacteria, in an effort to save the tissues from bacterial attack (62). Therefore, the onset of gingivitis and periodontal disease occurs when the bacterial composition of the mouth is imbalanced and plaque growth is allowed to flourish. Due to the fact that the primary cause of these dental diseases is bacterial overgrowth, antibiotics are frequently used in their treatment. Common local microbial therapies evaluated include chlorhexidine, tetracycline, and metronidazole.

A study in 1982 by Soh et al. investigated the effect of direct application of chlorhexidine to periodontal pockets (32). After 28 days it was found that chlorhexidine treatment had significantly reduced periodontal inflammation, whereas further deterioration had occurred in the placebo cases.

In an effort to prolong residence time of chlorhexidine in the periodontal pocket, Coventry and Newman in 1982 attempted the slow release of 20% chlorhexidine gluconate from Cuprophan (cellulose-based) hollow fiber dialysis tubing inserted in the periodontal pocket. The tubing had been loaded with the drug solution via capillary action, heat sealed, and then cut to a length suitable for the periodontal pocket. The devices were retrieved after only one week, at which time significant reduction in disease manifestations were noted (33).

In 1983, Soskolne et al. examined release kinetics of chlorhexidine from two formulations of sustained release devices, including a faster-releasing ethyl cellulose system or a slower-releasing ethyl cellulose–PEG system. Data confirmed the kinetics of chlorhexidine release in vivo to be diffusion controlled, as expressed by the Higuchi model. The effects of the drug on the bacterial flora within the periodontal pockets was also noted. Data shows release of up to 80% of the chlorhexidine within 3 days from the fast release devices, whereas the slow release devices had a release of about 50% of the drug after 6 days. The microbial floral content was examined in 16 pockets from 6 patients. All chlorhexidine-treated pockets had a decreased relative amount of motile rods and spirochetes, as well as a corresponding increase in nonmotile organisms in comparison with the placebo-treated pockets and to the flora present prior to chlorhexidine treatment (34).

A partially cross-linked soluble Byco protein, obtained from Croda Colloids in England, was used for the sustained release of chlorhexidine in 1990. Steinberg et al. found that the release kinetics of the degradable films were affected by the chlorhexidine loading, the cross-link density of the polymer, and the particular chlorhexidine salt

used (36). Highly cross-linked films exhibited antibacterial activity for over 24 days, whereas low cross-linked films maintained therapeutic levels for only 10 days. This was an improvement over earlier versions, such as the degradable films made of hydroxypropylcellulose in 1988. All of the drug from these films was released within 24 hours (63).

In 1990, Larsen prepared some acrylic strips as described by Addy et al. (35) to examine release of doxycycline in vitro from three other bioabsorbable materials to compare with release from the acrylic strips. The bioabsorbable materials used were a hemostatic gauze made of oxidized regenerated cellulose, a collagen wound dressing, and a fibrin sealant. Results indicated that only the hemostatic gauze and the fibrin sealant may be capable of prolonged doxycycline release in vivo due to the rapid dissolution of the other devices or low levels of concentration and residual activity remaining in these devices after only a few days (48).

Controlled release of another antibiotic, tetracycline, was attempted by Goodson et al. in 1983 from monolithic fibers of various polymeric compositions for use in periodontal therapy. Fibers made of polyethylene, polypropylene, polycaprolactone, polyurethane, and cellulose acetate released 100% of their drug load within the first 24 hours. Ethylene vinyl acetate fibers, however, achieved sustained release of tetracycline for up to 9 days (37). The monolithic fibers were prepared by the melt extrusion process, in which 25% tetracycline and 75% ethylene vinyl acetate was heated to 214°C and extruded as a 0.5 mm fiber. Goodson and his colleagues continued the research to find, in 1985, that these monolithic fibers released 57% of the drug into the periodontal pocket within the first 9 days. Furthermore, immediately following treatment, the total bacterial counts (spirochetes, motile rods, and nonmotile rods) were significantly reduced in the periodontal pockets (64). This research went one step further when the team declared the release of drug into the periodontal pocket from these fibers to be zero-order. This can be explained by the structure of the device. The fiber delivery system is composed of a polymeric matrix loaded with tetracycline hydrochloride powder. After extrusion, some of the tetracycline crystallites end up on the fiber surface. Upon device insertion into the periodontal pocket, the crystallites dissolve, forming pores on the surface. In turn, these pores allow solvation of deeper particles, resulting in zero-order drug delivery (38). This contrasts with the nonlinear release pattern of the fiber observed previously in vitro by Goodson et al. (37). In addition, fiber therapy alone was determined to be more effective than scaling alone, based on the degree of elimination of causative bacteria, amount of reduction in total viable counts, degree of elimination of bleeding on probing, and the amount of reduction in gingival index. It was, however, shown that combining scaling and fiber therapy is the most effective treatment (39).

In vitro studies by Baker et al. in 1988 used tetracycline-loaded biodegradable microparticles prepared by solvent evaporation with between 5 and 30 wt% of drug and suspended in a carrier gel to accomplish release of up to 3 days. The prepared formulation was injected into the periodontal pocket via syringe and needle. Such in vitro results typically correspond to about 10 or more days of release in vivo considering the low rate of crevicular fluid exchange within the periodontal pocket (40). Although nonbiodegradable polymers tried in this microparticle formulation included polysulfone, polystyrene, and polycarbonate, the biodegradable polymer of choice was a lactic acid–glycolic acid copolymer that tends to degrade in 4–12 weeks in an aqueous environment. Patents were obtained by Baker in both 1988 and 1990 (patent numbers 4,780,320 and 4,919,939, respectively) for these formulations of drug-containing microparticles suspended in a fluid carrier medium for the treatment of periodontal disease. The poly(lactide-*co*-glycolide) (PLGA) system was found to deliver tetracycline for a period of 25 hours, although the authors estimate this to be the equivalent of up to 10 to 20 days of release in vivo (65,66).

Investigators Minabe et al. in 1989 administered cross-linked processed collagenic film preparations loaded with tetracycline to the periodontal pocket to halt excessive growth of periodontopathogenic bacteria. They found that they could control the amount of drug release somewhat by adjusting the original drug loading and the time of the cross-link process. It was also found that an amount of drug exceeding the therapeutic dose was present in the gingival crevicular fluid of the periodontal pocket for up to 10 days postinsertion (41).

An intracrevicular application of 40% tetracycline HCl in a white petrolatum carrier gel was compared to scaling and root planing by Eckles et al. (44) in the treatment of periodontitis. Results indicated that biologically effective tetracycline was released from the gel into the gingival crevicular fluid for at least 3 days. Posttreatment analysis indicated that reduced probing pocket depths and bleeding on probing relative to baseline measurements remained for 8–12 weeks. Reduced percentages of spirochetes and motile rods, as well as the increase in cocci that accompanies this phenomenon, lasted for 2–8 weeks (44). However, similar effects seen in scaled and root-planed sites lasted longer and, therefore, led to the conclusion that the subgingival application of tetracycline cannot replace conventional treatment methods, but only supplement them.

A new type of poly(ortho ester) was prepared by Heller et al. in 1989 by the condensation of a triol and an alkyl ortho ester. This reaction produces a viscous paste at room temperature, despite molecular weights in excess of 50,000 daltons. This is beneficial for mixing in therapeutic agents without using solvents, as well as for application into the periodontal pocket. Furthermore, such materials may be useful in drug delivery because rates of release can be altered by adding small amounts of basic or acidic excipients to the polymer (42). For example, the system was loaded with tetracycline and injected into periodontal pockets using a blunt needle. Complete release occurred within 24 hours. However, when 0.5 wt% of the basic excipient $Mg(OH)_2$ was incorporated into the polymer, release was extended to about 10 days (45). This was based on the knowledge that poly(ortho esters) contain a pH-sensitive linkage in their backbone. Therefore, hydrolysis of the polymer chain can be sped up by the addition of acidic excipients to the environment, or retarded by the incorporation of basic excipients.

Deasy et al. delivered tetracycline hydrochloride or metronidazole from degradable polyhydroxybutyric acid strips for the treatment of periodontal disease. The system components were physically mixed using a mortar and pestle, then aliquots of the mixture were compressed under 106 kg cm^{-2} of force into strips 0.5 mm in thickness. In vitro studies were performed in simulated gingival fluid and revealed that increasing the loading of tetracycline resulted in increased drug release, whereas at a constant drug loading of 25%, metronidazole was released much faster. In vivo, the strips loaded with tetracycline produced the greatest results. The strips were inserted into periodontal pockets at 4-day intervals for 16 days, reducing the plaque index, gingival index, and pocket depths significantly when compared with untreated controls. The microflora of the treated pockets was altered favorably, increasing the proportion of cocci and decreasing the numbers of gram-negative rods, fusiforms, and spirochetes. Unfortunately, the clinical improvements resulting from the treatment were not maintained upon the conclusion of the treatment (43).

In 1995, Maze et al. achieved 10-day controlled release of tetracycline hydrochloride from biodegradable PLGA film strips in periodontitis patients. Films were prepared by film casting a dispersion of the antibiotic in a 85:15 solution of the polymer dissolved in methylene chloride. All films were γ-irradiated and secured in the periodontal pockets via a suture/cement technique. Results indicated that film-treated pockets caused significant probe depth reduction for 26 weeks, a clinical attachment level gain for 12 weeks, lower percentages of spirochetes for 4 weeks, decreased levels of motile rods for 8 weeks, and a corresponding increase in cocci levels for 4 weeks. Furthermore, when compared with scaling and root planing, the films appear to have an enhanced antibacterial effect (46).

Webber et al., in 1997, successfully modulated the release of tetracycline from degradable PLGA films to achieve release over a 30-day period. The incorporation of soluble salt excipients in the polymer films changed the release kinetics of the system dramatically. The classical triphasic PLGA release curve involving the initial release due to diffusion of the drug, a lag phase, and then the second release due to degradation of the polymer is no longer apparent. Instead, the salt-loaded systems achieve continuous release of drug for 30 days. Figure 3 depicts the release curves for the five experimental systems. All of the films were fabricated via the solvent casting technique using 1 g of PLGA polymer (Boehringer Ingelheim, Resomer RG503, lot #223808, M_r = 34,000) dissolved in 1 mL of methylene chloride (Fisher Scientific) per film. The films contained either 0% (control films), 1%, 5%, or 25% loadings (w/w) of sodium chloride that was predissolved in 200 μL of distilled water and sonicated into the polymer solution. One system contained a blend of 75% PLGA (Boehringer Ingelheim, Resomer RG503, lot #223808, M_r = 34,000) and 25% PLGA (Polysciences, lot #85761, M_r = 5,000) as well as 25% NaCl. All systems also contained a 5% loading (w/w) of tetracycline HCl also predissolved in 100 μL of distilled water and sonicated into the polymer solution.

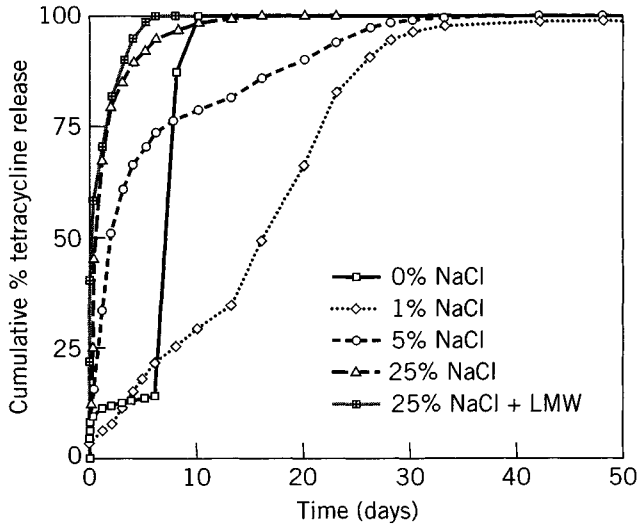


Figure 3. Comparison of tetracycline release from PLGA solvent cast films loaded with different amount of NaCl. *Source:* W. Webber, unpublished data.

This approach to modulating release of therapeutics from the PLGA matrix was unique in that the degradation of the polymer was not altered during the process of modulation. Figures 4 and 5 show degradation trends as monitored by gel permeation chromatography readings of molecular weight and differential scanning calorimetry measurements of glass-transition temperatures, respectively. In both cases, the salt-loaded films degrade at the same rate as the control (or 0% NaCl) film. Therefore, mod-

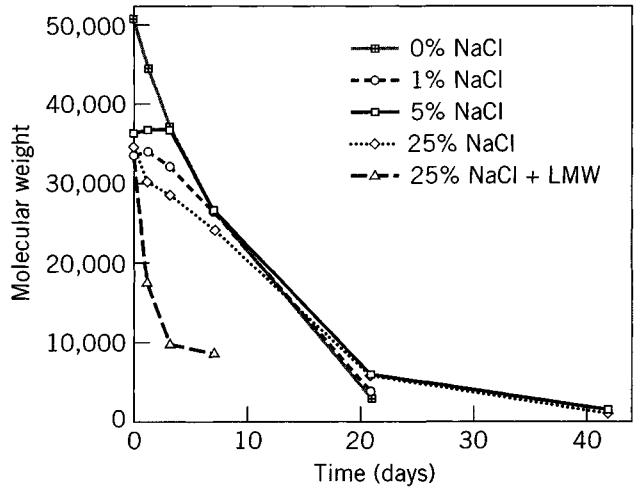


Figure 4. A measure of molecular weight of the various PLGA systems over time as measured by gel permeation chromatography. The similar decreasing trend in the control and salt-loaded systems shows that the salt is not speeding up the degradation process. The last system containing some low molecular weight polymer, however, does decrease in molecular weight faster than the other systems. In this case, the low molecular weight excipient is acting as a plasticizer and speeding up the polymer degradation. *Source:* W. Webber, unpublished data.

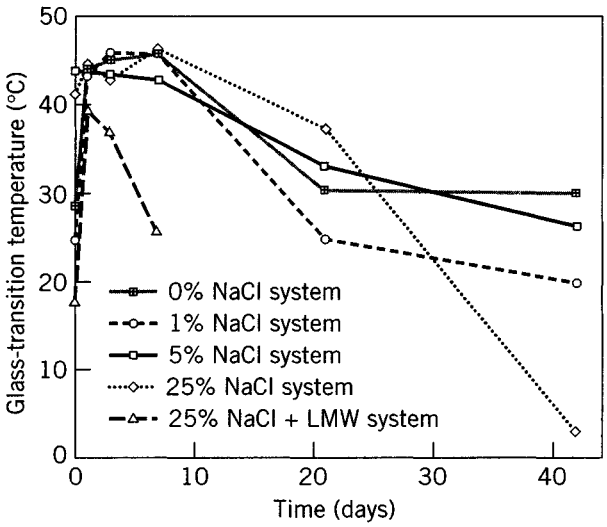


Figure 5. A measure of glass-transition temperature of the various PLGA systems over time as measured by differential scanning calorimetry. Again, the similar decreasing trend in the control and salt-loaded systems shows that the salt is not speeding up the degradation process. The last system containing some low molecular weight polymer, however, does decrease in molecular weight faster than the other systems. These results correlate well with the molecular weight data seen in Figure 4. *Source:* W. Webber et al., unpublished data.

ulation of tetracycline release is most likely caused by pore formation occurring where the salt particles are located. Further experimentation has shown that the systems are swelling and the water is being trapped within the polymer matrix, causing the tetracycline to be released at a constant rate for an extended period of time (W. Webber et al., unpublished data).

Studies by Loesche et al. in 1987 evaluated ethylcellulose films containing 20% metronidazole for their ability to reduce the proportionate levels of spirochetes in periodontal pockets. Though the films were brittle and unable to remain fixed within the pocket, they did succeed in reducing levels of plaque and spirochetes. It was also found that the use of films over a one-week period in conjunction with scaling and root planing had more of an impact clinically than the use of scaling and root planing alone (47).

Release of three antimicrobials, including chlorhexidine, tetracycline, and metronidazole, occurred from acrylic resin vehicles in which the drugs were polymerized into the acrylic strips and placed into periodontal pockets. Strips were changed on a weekly basis over a period of 14 weeks (35). All drug treatments produced immediate improvements based on reduced bleeding, reduced crevicular fluid flow, increased percentage of cocci, and decreased total motiles in comparison with the control groups. The study showed that sole use of antimicrobial drugs could achieve results similar to those reached by conventional mechanical debridement techniques, but the combination of root planing followed by metronidazole strip treatment appeared to be the most effective.

Polypeptide growth factors are an important class of potent biologic mediators which have recently been found to significantly enhance regeneration of both hard and soft tissue components of the periodontium. Studies by Lynch et al. demonstrate the effectiveness of short-term application of a combination of platelet-derived growth factor B (PDGF-B) and insulin-like growth factor one (IGF-1) on periodontal attachment apparatus formation during the early phases of postsurgical wound healing (67). Following conventional periodontal surgery in 13 beagle dogs, a methylcellulose gel containing a combination of 3 μg of recombinant PDGF-B and IGF-1 was applied. More than 96% of the protein was cleared by 96 hours, and none of it could be detected at 2 weeks postapplication. However, histological analyses at 2 and 5 weeks revealed 5 to 10-fold increases in new bone and cementum in the treated sites compared with the control sites (49).

Bone morphogenetic proteins (BMPs) represent a unique family of proteins that induce new bone formation at the site of implantation without affecting the growth rate of preexisting bone. Studies show that recombinant human BMP-2 (rhBMP-2) induces ectopic bone formation in vivo and can cause mesenchymal precursor cells to differentiate into cartilage- and bone-forming cells in vitro (50). RhBMP-2 has been tried and proven to repair bony defects in animal models of bone loss due to periodontal disease. Sigurdsson et al. suggest that implantation of a rhBMP-2 containing device not only regenerates original alveolar bone height, but also additional periodontal attachment apparatus. In Sigurdsson's research, defects were treated with polypropylene-reinforced expanded poly(tetrafluoro ethylene) membranes. The membranes are supposed to maintain the necessary space required for successful reconstruction of periodontal architecture. Histologically, the membrane-treated defects showed significant alveolar bone and cementum regeneration as well as some periodontal ligament fibers forming between the new bone and cementum. Supraalveolar defects treated with rhBMP-2 revealed bone and cementum regeneration to average 95% and 40% of the defect height, respectively, whereas control defects achieved only 20% and 10%, respectively. Therefore, the space provision membranes offer a significant, natural potential for bone and cementum regeneration, whereas the rhBMP-2 filler offers an unlimited regeneration potential for alveolar bone and a noteworthy regeneration potential for cementum (51).

Due to its high permeability, natural protective barrier against toxins and microorganisms, and high patient treatment compliance, the oral mucosal tissues have been the site of delivery for a variety of drugs in numerous therapies. Controlled release from polymeric systems allows for increased device residence time and therefore achieves longer delivery of drug. Although more immediate delivery of substances is possible through the sublingual mucosa, buccal mucosa is permeable to larger molecular weight species such as peptides and proteins and has the potential for achieving sustained delivery for up to many weeks.

BIBLIOGRAPHY

1. B.J. Davis and A. Johnston, *Br. J. Clin. Pharmacol.* **7**, 434–435 (1979).

2. M. Ishida, Y. Machida, N. Nambu, and T. Nagai, *Chem. Pharm. Bull.* **29**, 810–816 (1981).
3. T. Nagai, *J. Controlled Release* **2**, 121–134 (1985).
4. S.S. Davis et al., *Adv. Pharmacother.* **1**, 17–25 (1983).
5. L.B. Hansen, L.L. Christrup, and H. Bundgaard, *Acta Pharm. Nord.* **3**, 77–82 (1991).
6. J. Cassidy et al., *Pharm. Res.* **10**, 126–129 (1993).
7. J.-H. Guo, *J. Pharm. Pharmacol.* **46**, 647–650 (1994).
8. R.L. McQuinn et al., *J. Controlled Release* **34**(3BR273), 243–250 (1995).
9. A. Ahuja, M. Dogra, and S.P. Agarwal, *Indian J. Pharm. Sci.* **57**, 26–30 (1995).
10. Y. Lee and Y.W. Chien, *J. Controlled Release* **37**, 251–261 (1995).
11. S. Kim, W. Snipes, G.D. Hodgen, and F. Anderson, *Contraception* **52**, 313–316 (1995).
12. K. Iga and Y. Ogawa, *Proc. Int. Symp. Controlled Release Bioact. Mater.* **23**, 155–156 (1996).
13. J. Voorspoels, F. Comhaire, W.D. Sy, and J.P. Remon, *Proc. Int. Symp. Controlled Release Bioact. Mater.* **24**, 185–186 (1997).
14. M. Veillard, M. Longer, T.W. Martens, and J.R. Robinson, *J. Controlled Release* **6**, 123–131 (1987).
15. H.P. Merkle, R. Anders, J. Sandow, and W. Schurr, *Delivery Syst. Pept. Drugs*, 159–175 (1986).
16. D. Harris and J.R. Robinson, *Biomaterials* **11**, 652–658 (1990).
17. A.G. Field, *Med. Times Gaz.* **16**, 291 (1858).
18. J.E.F. Riseman, G.E. Altman, and S. Koretsky, *Circulation* **17**, 22–39 (1958 January).
19. S.J. Pimlott and M. Addy, *Oral Surg., Oral Med. Oral Pathol.* **59**, 145–148 (1985).
20. U. Thadani and R.J. Lipicky, *Cardiovas. Drugs Ther.* **8**, 611–623 (1994).
21. J. Abrams, *Arch. Intern. Med.* **155**, 357–364 (1995).
22. S. Bergman, I.A. Siegel, and S. Ciancio, *J. Dent. Res.* **47**, 1184 (1968).
23. W.G. Edge, G.M. Cooper, and M. Morgan, *Anaesthesia* **34**, 463–467 (1979).
24. D. Brewster, M.J. Humphrey, and M.A. McLeavy, *J. Pharm. Pharmacol.* **33**, 500–506 (1981).
25. W.J. Russell, N.R. Badcock, D.B. Frewin, and L.N. Sansom, *Eur. J. Clin. Pharmacol.* **35**, 437–439 (1988).
26. T. Nagai and R. Konishi, *J. Controlled Release* **6**, 353–360 (1987).
27. P. Bottenberg et al., *J. Pharm. Pharmacol.* **43**, 457–464 (1991).
28. J.H. Reading, P.D. Clifford, R.W. Coles, and N. Rajagopolan, *Curr. Ther. Res.* **30**, 605–610 (1981).
29. S. Bouckaert et al. *Eur. J. Clin. Pharmacol* **43**, 137–140 (1992).
30. M. Encarnacion and I. Chin, *Eur. J. Clin. Pharmacol.* **46**, 533–535 (1994).
31. J.L. Fabregas and N. Garcia, *Drug Dev. Ind. Pharm.* **21**, 1689–1696 (1995).
32. L.L. Soh, H.N. Newman, and J.D. Strahan, *J. Clin. Periodontol.* **9**, 66–74 (1982).
33. J. Coventry and H.N. Newman, *J. Clin. Periodontol.* **9**, 129–133 (1982).
34. A. Soskolne, G. Golomb, M. Friedman, and M. Sela, *J. Periodontal Res.* **18**, 330–336 (1983).
35. M. Addy et al., *J. Periodontol.* **59**, 557–564 (1988).
36. D. Steinberg, M. Friedman, A. Soskolne, and M.N. Sela, *J. Periodontol.* **61**, 393–398 (1990).
37. J.M. Goodson et al., *J. Periodontol.* **54**, 575–579 (1983).
38. M. Tonetti, M.A. Cugini, and J.M. Goodson, *J. Periodontal Res.* **25**, 243–249 (1990).
39. L. Heijl et al., *J. Clin. Periodontol.* **18**, 111–116 (1991).
40. R.W. Baker, E.A. Krisko, and F. Kochinke, *Proc. Int. Symp. Controlled Release Bioact. Mater.* **15**, 238a–238b (1988).
41. M. Minabe et al., *J. Periodontol.* **60**, 113–117 (1989).
42. J. Heller, S.Y. Ng, B.K. Fritzinger, and K.V. Roskos, *Biomaterials* **11**, 235–237 (1989).
43. P.B. Deasy, A.E.M. Collins, D.J. MacCarthy, and R.J. Russell, *J. Pharm. Pharmacol.* **41**, 694–699 (1989).
44. T.A. Eckles et al., *J. Clin. Periodontol.* **17**, 454–462 (1990).
45. K.V. Roskos et al., *Biomaterials* **16**, 313–317 (1995).
46. G.I. Maze et al., *J. Clin. Periodontol.* **22**, 860–867 (1995).
47. W.J. Loesche et al., *J. Periodontal Res.* **22**, 224–226 (1987).
48. T. Larsen, *J. Periodontol.* **61**, 30–34 (1990).
49. S.E. Lynch et al., *J. Periodontol.* **62**, 458–467 (1991).
50. J.M. Wozney, *J. Periodontol.* **66**, 506–510 (1995).
51. T.J. Sigurdsson, D.N. Tatakis, M.B. Lee, and U.M.E. Wikesjo, *J. Periodontol.* **66**, 511–521 (1995).
52. M.E. deVries, *Dev. Drug Delivery* (1991).
53. M.E. deVries, Ph.D. Thesis, University of Leiden, Leiden, The Netherlands, 1991.
54. P.W. Wertz and C.A. Squier, *Crit. Rev. Ther. Drug Carrier Syst.* **8**, 237–269 (1991).
55. N. Chidambaram and A.K. Srivatsava, *Drug Dev. Ind. Pharm.* **21**, 1009–1036 (1995).
56. A.H. Beckett and E.J. Triggs, *J. Pharm. Pharmacol.* **19** (Suppl.), 31s–41s (1967).
57. T. Nagai and Y. Machida, *Pharm. Int.* **6**, 196–200 (1985).
58. L. Benes et al., *7th Int. Symp. Recent Adv. Drug Delivery Syst.*, Salt Lake City, Utah, 1995.
59. G.E. Altman, J.E.F. Riseman, and S. Koretsky, *Am. J. Med. Sci.* **240**, 100–110 (1960).
60. A.H. Kutscher et al., *Oral Surg. Oral Med. Oral Pathol.* **12**, 1080–1089 (1959).
61. R.A. Seymour and P.A. Heasman, *Drugs, Diseases an the Periodontium*, Oxford University Press, New York, 1992.
62. S.S. Socransky, *J. Periodontol.* **48**, 497–504 (1977).
63. T. Noguchi, M. Fukuda, and I. Ishikawa, *Adv. Den. Res.* **2**, 401–404 (1988).
64. J.M. Goodson, S. Offenbacher, D.H. Farr, and P.E. Hogan, *J. Periodontol.* **56**, 265–272 (1985).
65. U.S. Pat. 4,780,320 (October 25, 1988).
66. U.S. Pat. 4,919,939 (April 24, 1990).
67. S.E. Lynch et al., *J. Clin. Periodontol.* **16**, 545–548 (1989).

See also BIOADHESIVE DRUG DELIVERY SYSTEMS; MUCOSAL DRUG DELIVERY, INTRAVITREAL; MUCOSAL DRUG DELIVERY, NASAL; MUCOSAL DRUG DELIVERY, OCULAR; MUCOSAL DRUG DELIVERY, VAGINAL DRUG DELIVERY AND TREATMENT MODALITIES.

Next Page

MUCOSAL DRUG DELIVERY, INTRAVITREAL

SUZANNE EINMAHL
ARATI A. DESHPANDE
CYRUS TABATABAY
ROBERT GURNY
University of Geneva
Geneva, Switzerland

KEY WORDS

Biodegradable polymers
CMV retinitis
Endophthalmitis
Intraocular disease
Intravitreal
Iontophoresis
Liposomes
Microspheres
Nonbiodegradable polymers
Ocular drug delivery
Prodrugs
Proliferative vitreoretinopathy
Sustained release

OUTLINE

Introduction
Vitreoretinal Diseases
  Proliferative Vitreoretinopathy
  Cytomegalovirus Retinitis
  Endophthalmitis
  Posterior Uveitis
Drug Delivery Systems
  Biodegradable Polymers
  Nonbiodegradable Polymers
  Nanoparticles, Microspheres and Liposomes
  Iontophoresis
  Prodrugs and Codrugs
Conclusion
Acknowledgments
Bibliography

INTRODUCTION

Drug delivery to the posterior segment is a major challenge in ophthalmology. Treatment of vitreoretinal diseases has so far been limited to conventional forms of drug administration, that is, topical instillation, subconjunctival injection, or systemic (oral and parenteral) administration. Unfortunately, owing to the anatomical and physiological barriers that exist, in most cases these routes have not proved to be efficient for treating vitreoretinal disorders because the intravitreal or retinal levels of drugs achieved were too low.

The topical route of drug delivery severely limits the access of most drugs to the vitreoretinal tissues. In general, approximately 1% or less of an applied dose is absorbed across the cornea and reaches the anterior segment tissues, and only a tiny fraction of this absorbed dose will then move to the posterior segment of the eye (1). This is due to the existence of protective mechanisms in the eye that are essential for its normal visual function; those include solution drainage, lacrimation, diversion of exogenous substances into the systemic circulation via the conjunctiva, and the structure of the cornea itself, which is relatively impermeable to most drugs (1).

Subconjunctival injections represent an attempt to increase intraocular drug levels while minimizing the frequency of dosing. However, with this technique, higher drug concentrations are generally achieved in the anterior chamber rather than in the posterior segment tissues. Drug delivery to the eye after systemic administration depends on the ocular vascular circulation for transport to the targeted area. The inner two-thirds of the retina are perfused by the central retinal artery. The capillary walls are quite permeable to many substances (1). However, for most drugs, the concentrations achieved in the vitreous humor are much lower than the corresponding serum concentrations unless the eye is inflamed. In this latter case, drug concentrations in the posterior segment can reach as high as 10% of the serum drug levels. The blood–retinal barrier (BRB) plays a major role in restricting drug coming from the choriocapillaries and entering the vitreoretinal compartment as well as restricting drug elimination from this space. This barrier is characterized by the *zonulae occludentes* between the contiguous cells of the retinal vessels and the retinal pigmented epithelium, which prevent the flow of substances by the paracellular pathway, thereby diverting them to a highly selective transcellular route. The ability of a drug to penetrate the BRB is related to its lipid solubility. Furthermore, some substances are transported out of the vitreous body by an active transport system that is inhibited by probenecid, a situation similar to that in the kidney tubular epithelial cells (2). Circumstances that may alter the BRB, inducing its breakdown, include posttraumatic inflammation; viral, bacterial, or fungal infection; and iatrogenic causes such as vitrectomy (3).

Because of these constraints in delivering drugs to their site of action in the vitreoretinal tissues in such a way as to achieve therapeutic levels, it appears then that the only way to attain therapeutic concentrations is by intravitreal injection (4). The vitreous humor is a hydrophilic gel containing 99% water and 1% organic substances such as collagen and hyaluronic acid through which drugs diffuse freely as they would in water (5). After injection into the vitreous body, drugs may be eliminated by diffusion into the aqueous humor of the posterior chamber with subsequent removal by the normal egress of fluid from the anterior chamber. This pathway is limited by the small surface available for diffusion. Drugs eliminated by this route generally have half-lives in the range of 20 to 30 h (6). The other possible elimination pathway from the vitreous is through the retina via penetration of the BRB: this is the so-called posterior route. Drugs eliminated by this way typically exhibit half-lives in the range of 5 to 10 h (6).

Previous Page

MUCOSAL DRUG DELIVERY, INTRAVITREAL

SUZANNE EINMAHL
ARATI A. DESHPANDE
CYRUS TABATABAY
ROBERT GURNY
University of Geneva
Geneva, Switzerland

KEY WORDS

Biodegradable polymers
CMV retinitis
Endophthalmitis
Intraocular disease
Intravitreal
Iontophoresis
Liposomes
Microspheres
Nonbiodegradable polymers
Ocular drug delivery
Prodrugs
Proliferative vitreoretinopathy
Sustained release

OUTLINE

Introduction
Vitreoretinal Diseases
  Proliferative Vitreoretinopathy
  Cytomegalovirus Retinitis
  Endophthalmitis
  Posterior Uveitis
Drug Delivery Systems
  Biodegradable Polymers
  Nonbiodegradable Polymers
  Nanoparticles, Microspheres and Liposomes
  Iontophoresis
  Prodrugs and Codrugs
Conclusion
Acknowledgments
Bibliography

INTRODUCTION

Drug delivery to the posterior segment is a major challenge in ophthalmology. Treatment of vitreoretinal diseases has so far been limited to conventional forms of drug administration, that is, topical instillation, subconjunctival injection, or systemic (oral and parenteral) administration. Unfortunately, owing to the anatomical and physiological barriers that exist, in most cases these routes have not proved to be efficient for treating vitreoretinal disorders because the intravitreal or retinal levels of drugs achieved were too low.

The topical route of drug delivery severely limits the access of most drugs to the vitreoretinal tissues. In general, approximately 1% or less of an applied dose is absorbed across the cornea and reaches the anterior segment tissues, and only a tiny fraction of this absorbed dose will then move to the posterior segment of the eye (1). This is due to the existence of protective mechanisms in the eye that are essential for its normal visual function; those include solution drainage, lacrimation, diversion of exogenous substances into the systemic circulation via the conjunctiva, and the structure of the cornea itself, which is relatively impermeable to most drugs (1).

Subconjunctival injections represent an attempt to increase intraocular drug levels while minimizing the frequency of dosing. However, with this technique, higher drug concentrations are generally achieved in the anterior chamber rather than in the posterior segment tissues. Drug delivery to the eye after systemic administration depends on the ocular vascular circulation for transport to the targeted area. The inner two-thirds of the retina are perfused by the central retinal artery. The capillary walls are quite permeable to many substances (1). However, for most drugs, the concentrations achieved in the vitreous humor are much lower than the corresponding serum concentrations unless the eye is inflamed. In this latter case, drug concentrations in the posterior segment can reach as high as 10% of the serum drug levels. The blood–retinal barrier (BRB) plays a major role in restricting drug coming from the choriocapillaries and entering the vitreoretinal compartment as well as restricting drug elimination from this space. This barrier is characterized by the *zonulae occludentes* between the contiguous cells of the retinal vessels and the retinal pigmented epithelium, which prevent the flow of substances by the paracellular pathway, thereby diverting them to a highly selective transcellular route. The ability of a drug to penetrate the BRB is related to its lipid solubility. Furthermore, some substances are transported out of the vitreous body by an active transport system that is inhibited by probenecid, a situation similar to that in the kidney tubular epithelial cells (2). Circumstances that may alter the BRB, inducing its breakdown, include posttraumatic inflammation; viral, bacterial, or fungal infection; and iatrogenic causes such as vitrectomy (3).

Because of these constraints in delivering drugs to their site of action in the vitreoretinal tissues in such a way as to achieve therapeutic levels, it appears then that the only way to attain therapeutic concentrations is by intravitreal injection (4). The vitreous humor is a hydrophilic gel containing 99% water and 1% organic substances such as collagen and hyaluronic acid through which drugs diffuse freely as they would in water (5). After injection into the vitreous body, drugs may be eliminated by diffusion into the aqueous humor of the posterior chamber with subsequent removal by the normal egress of fluid from the anterior chamber. This pathway is limited by the small surface available for diffusion. Drugs eliminated by this route generally have half-lives in the range of 20 to 30 h (6). The other possible elimination pathway from the vitreous is through the retina via penetration of the BRB: this is the so-called posterior route. Drugs eliminated by this way typically exhibit half-lives in the range of 5 to 10 h (6).

Lipophilic drugs are eliminated more rapidly for the same reason: They pass into the vitreoretinal compartment more readily after systemic administration. The elimination of an intravitreally administered drug is influenced by infection and inflammation. Infection tends to accelerate the rate of clearance, whereas the effect of inflammation on vitreous pharmacokinetics is drug dependent. In general, the half-life of nontransported drugs, such as aminoglycosides, is reduced in the presence of ocular inflammation, whereas the half-life of carbenicillin, an actively transported drug, is slightly increased. Intravitreal dosage route was initially reserved primarily for the treatment of endophthalmitis; nowadays this route is also occasionally used for the treatment of diseases such as proliferative vitreoretinopathy (PVR), viral retinitis, and uveitis. Intravitreal injection allows high intraocular drug levels to be reached rapidly, thus resolving the problems of conventional application. Unfortunately, successful treatment of most vitreoretinal diseases requires multiple injections to maintain therapeutically effective drug concentrations in the vitreous for a desired period of time. Additionally, even if repeated drug injections into an already compromised eye improve the ocular condition, this strategy can cause several complications, such as increased risk of ocular infection, intraocular hemorrhage, retinal detachment, and cataract. Moreover, the initial peak level of drug achieved immediately after a bolus intravitreal injection may result in toxicity to the retina and other ocular tissues.

Because of the rapid clearance of drugs from the eye and the variable toxicity encountered in previous studies, researchers have thus been encouraged to develop new systems of drug delivery to the posterior segment that would sustain a therapeutic level of the drug over an extended period of time. Thus, the "peak and valley" effects could be minimized, and drug concentrations could be maintained at an effective therapeutic level for a prolonged period of time. Several delivery systems with a slow-release feature have been developed, including polymeric matrices (biodegradable or not), colloidal systems (liposomes and microspheres), and other delivery systems such as iontophoresis or the prodrug approach.

This article first provides an overview of the vitreoretinal disorders amenable to intraocular drug therapy such as PVR, viral retinitis, endophthalmitis, and uveitis and then discusses the various systems of sustained drug delivery for treatment of these diseases.

VITREORETINAL DISEASES

Proliferative Vitreoretinopathy

Among the severe and blinding diseases of the posterior segment of the eye, many are pathophysiologically characterized by a proliferation of one or more cell types and are therefore referred to as proliferative disorders.

PVR is a pathologic condition occurring as a complication of retinal detachment in 5–10% of the cases (7) in which benign cells proliferate in the vitreous cavity, resulting in the formation of membranes on both surfaces of the detached retina. It is the most common cause of failure following retinal reattachment surgery (8). There are some risk factors that increase susceptibility to the development of PVR: repeated procedures (such as failure of previous surgery), damaged retinal surface (retinal folds or holes), treatment modality (vitrectomy, cryotherapy), and preoperative vitreous hemorrhage (9).

First described in 1939, PVR was formerly known as "massive vitreous retraction," "massive preretinal retraction," and "massive periretinal proliferation." In 1983, the Retina Society introduced the new terminology to reflect the pathologic changes in the vitreous and the retina (7). They also established a standardized classification to determine the different stages of the disease so as to compare and evaluate methods of treatment and clinical results. This classification has since been revised many times (10).

The pathogenesis (11) of PVR is related to the loss of integrity of the vitreoretinal structures. The first important step of the disease process is the disruption of the BRB, allowing serum components to penetrate into the vitreous cavity (12). Serum, a stimulus to migration, exerts chemotaxis to retinal pigmented epithelial (RPE) cells, glial cells, and Müller cells, which migrate into the vitreous cavity through retinal holes. Fibronectin and platelet-derived growth factors promote cellular adhesion to the vitreous collagen and fibroblast proliferation, leading to membrane formation. The presence of contractile elements in these epiretinal membranes, mainly composed of myofibroblasts, provokes cell contraction, which can distort or redetach the retina. The epiretinal membranes formed are stabilized by the collagen of the extracellular matrix. An inflammatory response is often provoked, as evidenced by the presence of various white blood cells such as macrophages and lymphocytes (13). Even though the mechanism that triggers certain cells or cell types to proliferate is still obscure, many attempts have been made to find a pharmacological cure for the disease.

The development of suitable treatments for PVR has been assisted by experimental animal models, produced by intravitreal injection of autologous (14) or heterologous fibroblasts (15) or by the injection of macrophages, which mimics the development of PVR from its initial stage onwards (16).

The pharmacological treatment of PVR consists in the inhibiting progression of the disease at various stages (Table 1). PVR parallels the wound-healing process and follows a course that can be divided into three phases: inflammation, cellular proliferation, and regeneration (Fig. 1) (26). The time course of PVR development is important in the selection of particular drugs. In the initial stage, that is, the inflammatory phase, long-effect steroids are more suitable. In the proliferative phase, antiproliferative drugs can be used. Because inflammatory factors may still continue to act in this stage, better control may be achieved if the antiproliferative drugs are combined with steroids.

Drugs such as corticosteroids and nonsteroidal antiinflammatory agents (NSAIs) prevent the breakdown of the blood–retinal barrier (17). As they act early in the disease process, they are particularly effective in reducing the incidence of PVR in experimental models (26). Corticosteroids were the first drugs investigated to treat PVR (27). Their major mechanism of action is the reduction of the inflammatory response in the eye, thereby moderating the

Table 1. The Mechanism of Action of Drugs for the Treatment of PVR

Pathogenesis	Pharmacologic therapy
Breakdown of the blood–retinal barrier	Steroids and nonsteroidal antiinflammatory agents (17)
Cell migration	Colchicine (18), taxol (19)
Cell attachment	Synthetic tetrapeptide (20), heparin (21)
Cell proliferation	Fluoropyrimidines, daunorubicin, taxol, colchicine, and other antineoplastic drugs (19)
Cell contraction	Fluorouridine (22), colchicine, taxol, cytochalasin B (19)
Synthesis of extracellular matrix	D-penicillamine (23), *cis*-hydroxyproline (24), β-aminopropionitrile (25), 5-fluorouracil (26)

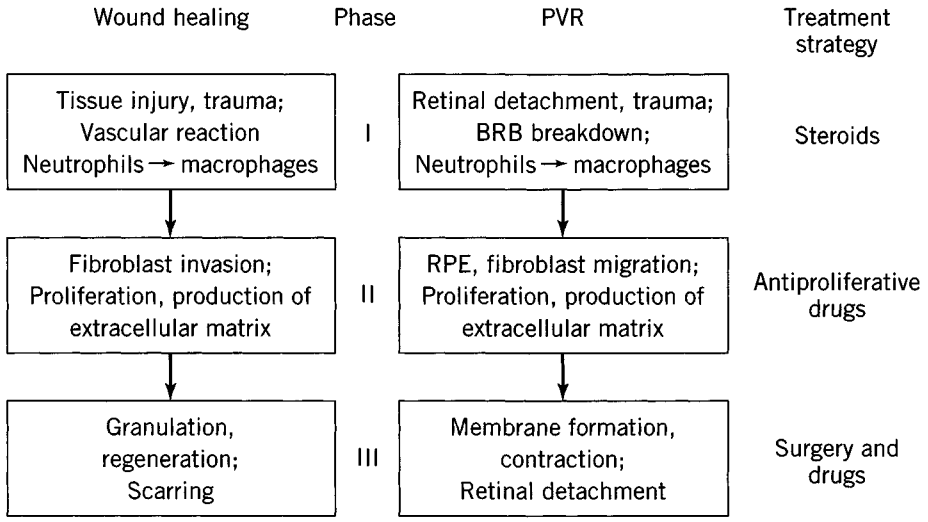


Figure 1. Parallels in the evolution of PVR and wound healing: treatment strategy. I, inflammatory phase; II, proliferative phase; III, regeneration (contraction and consequence); BRB, blood–retinal barrier; RPE, retinal pigment epithelium. *Source:* Adapted from Ref. 16.

breakdown of the BRB; however, it is known that at low doses corticosteroids stimulate cell proliferation, whereas at supraphysiologic doses they have an inhibiting effect. This bimodal behavior has been demonstrated in vitro (28). Intravitreal dexamethasone (27) and triamcinolone acetonide (29) have been investigated in experimental models of PVR in rabbits and found efficient in reducing the frequency of retinal detachment. Chandler (30) administered triamcinolone acetonide 24 h preceding the injection of fibroblasts in rabbit eyes and found better results when the eyes were pretreated, which suggests that the inhibition of the inflammatory process is a main part of the management of PVR.

A wide variety of intravitreal antiproliferative drugs have been used experimentally for the treatment of intraocular proliferative conditions. They have all been shown to be effective, particularly against RPE cells and fibroblasts, both in vitro (28) and in animal studies. Antiproliferative drugs act on the various stages of cell growth, that is, the growth phase (G1), the synthesis of DNA (S), the postsynthetic phase (G2), and the mitosis (M) (31). Among the antimetabolites, fluoropyrimidines have been the first and the most extensively studied. 5-Fluorouracil (5-FU), a synthetic pyrimidine analog, affects the S phase of the cell cycle. It is a substrate for the thymidilate synthetase enzyme and inhibits thymidine formation for DNA synthesis. It may also incorporate into RNA and inhibit replication, transcription, and cell division (32); it also inhibits ribosomal synthesis of intracellular procollagen (26). 5-FU has been found effective in reducing the incidence of PVR in experimental models (33,34). A single 1-mg intravitreal injection of 5-FU in rabbit eye can reduce the rate of tractional retinal detachment in experimental PVR without causing any noticeable retinal toxicity (35). Unfortunately, 5-FU has limited clinical application owing to its short intravitreal half-life: Therapeutic levels are maintained in the vitreous for only 12–24 h (36), yet the PVR process is active for a longer time. Multiple intravitreal injections are necessary to obtain a significant effect, as demonstrated by Stern et al. (37). 5-Fluorouridine, another member of the fluoropyrimidines family, is more potent than 5-FU in inhibiting fibroblast proliferation in vitro (38). This is due to its additional anticontractile effect.

Daunomycin (also called daunorubicin) (39), aclacinomycin A (40), and adriamycin (41) are anthracycline antibiotics with complex biological effects on DNA binding, free radical formation, membrane binding, and metal ion chelation (42). Their mechanism of action is independent of the cell cycle. Daunomycin has been shown to be one of the most effective intraocular antiproliferative agent for the treatment of experimental PVR (43,44). It is very potent but also more toxic than 5-fluorouracil; its safety margin is very small (45).

Taxol is a substance isolated from the plant *Taxus brevifolia* and has antitumor activity in several experimental systems. In contrast to other plant products such as colchicine, taxol acts as a promoter rather than an inhibitor of microtubule assembly. It prevents fibroblast migration and replication by stabilizing microtubules and blocking the cell in the G2 and M phases. In an experimentally in-

duced PVR, taxol effectively controlled the development of retinal detachment after an intravitreal injection as little as 0.5 μg (46).

Colchicine, an alkaloid from the *Colchicum autumnale* plant, interferes with microtubule metabolism and blocks the cell in the mitotic phase of its growth cycle. It inhibits in vitro fibroblast migration and proliferation at very low concentrations (18). Oral colchicine has been studied in rabbits and found effective in the prevention of PVR (47); on the other hand, intravitreal colchicine seems to be quite toxic to the retina (48).

Retinoids are products derived from vitamin A that have an antiproliferative effect on RPE cells and inhibit their migration (49). Several studies have been made with retinoic acid, a very lipophilic substance that is the most potent member of this family of compounds. At concentrations up to 10 μg/mL in silicone oil (50,51), retinoic acid did not cause any retinal toxicity and prevented PVR in experimental models.

The general problem with antiproliferative drugs is their narrow therapeutic interval: Retinal toxicity is all too common when these compounds are administered intravitreally (52,53).

Cytomegalovirus Retinitis

Cytomegalovirus (CMV) retinitis is an opportunistic infection frequently seen in patients with AIDS and other forms of immune suppression. CMV retinitis is the most common opportunistic ocular infection in patients with AIDS, occurring in 15–40% of patients (54). Often bilateral, it is part of a systemic CMV infection. It may be the first manifestation of AIDS in 1.8% of cases (55). If untreated, this disease can progressively lead to blindness.

Ganciclovir (formerly known as DHPG and BW-759U) was the first antiviral agent that showed activity against CMV in patients with AIDS. It is a nucleoside analog of acyclovir, with 10 to 100 times greater activity against CMV (56,57). Ganciclovir has been determined to act as a virustatic agent, rather than completely eliminating the virus and its recurrence from the retina. This is the reason why CMV retinitis is so hard to eradicate. Intravenous treatment with ganciclovir has been widely studied and determined useful in the management of CMV retinitis by delaying or reducing vision loss in AIDS patients (58,59), and the current recommended treatment strategy is an induction therapy with high doses of intravenous ganciclovir followed by a maintenance regimen with lower doses (60). This produces clinical regression of the retinitis in nearly all patients, but recurrence frequently occurs when patients are on maintenance therapy (61). On the other hand, it may prevent development of the virus in the other eye if it is not already infected (62). However, ganciclovir has a small margin of safety, and severe complications such as neutropenia, fever, anorexia, thrombocytopenia, progressive neuropathy, diarrhea, psychosis, and phlebitis occur following parenteral administration (58,63). The treatment must then be stopped after a certain period of time for these intolerant patients. The limited systemic use of these drugs in intolerant patients owing to severe side effects has lead to the evaluation of intravitreal injection. In a study by Pulido et al., 400 μg of intravitreally injected ganciclovir was determined to be nontoxic (64), so this dosage has been used clinically to treat CMV retinitis (65). Unfortunately, maintenance of sufficient intravitreal levels of ganciclovir requires repeated injections, at least twice weekly until healing occurs and then once per week until relapse (66).

Another drug used in the treatment of CMV retinitis is foscarnet. It acts by inhibiting viral DNA and RNA polymerases. One of its major side effects is reversible nephrotoxicity and anemia, but it has no harmful effect on the bone marrow (67). Therefore, synergistic or additive effects have been proved in vitro when a combination of ganciclovir and foscarnet was used; one could thus use lower doses of both drugs and then reduce their side effects (68). On the other hand, foscarnet is an alternative to ganciclovir if resistant strains of CMV develop (69). Intravitreal foscarnet has also been investigated (70) and was found to be active against CMV without retinal toxicity. The combined intravitreal injection of ganciclovir and foscarnet can also be particularly useful when the infection is clinically resistant to either intravitreal drug alone (71).

Zidovudine, formerly known as azidothymidine or AZT, a drug effective against HIV but not CMV, showed some beneficial effects in some cases (72). It is believed to act by diminishing HIV enhancement of CMV infection or by improving the general immune status. Unfortunately, both AZT and ganciclovir are toxic to the bone marrow.

A new drug, cidofovir, also known as HPMPC, has been recently evaluated in treating CMV retinitis. It is a nucleotide analog with a higher potency and a longer duration of action than ganciclovir or foscarnet (73,74). Intravitreal cidofovir is an effective treatment at concentrations as low as 20 μg, but it is associated with side effects such as uveitis and iritis (75).

Other viral retinitis types include acute retinal necrosis syndrome (ARN), which is a necrotizing retinitis with retinal vasculitis and vitritis that occurs in both healthy and immunocompromised individuals; it frequently renders the affected eye legally blind. Several lines of evidence suggest that this is a viral infection, probably mediated by varicella–zoster virus (VZV) (76) or herpes simplex virus (HSV) (77). The current recommended treatment involves intravenous acyclovir or vidarabine (78) and topical and oral steroids.

Endophthalmitis

Endophthalmitis is an inflammatory response to the invasion of the internal structures of the eye by replicating microorganisms: bacteria (in 90% of cases) (79), fungi, or parasites (79). This disease is most often a complication of ocular surgical procedures such as cataract extraction, corneal transplantation, glaucoma filtering surgery, or retinal detachment surgery. Another cause is a penetrating ocular trauma, which can occur in up to 20–30% of cases. The vitreous body and the retina are generally involved, and depending on the virulence of the infectious agent, this disease can lead to retinal necrosis and blindness within a very short period of time. The different species of microorganisms identified in bacterial endophthalmitis are

Staphylococcus aureus, Pseudomonas aeruginosa, Proteus, and coliform species, with increasing incidence of *Staphylococcus epidermidis* (80). An anaerobic species, *Bacillus*, is associated with penetrating ocular trauma, most often in rural areas (81). All these microorganisms cause exogenous endophthalmitis; the agents invade the eye from outside, for example, during ophthalmic surgery or penetrating injury. Sometimes, however, endophthalmitis can be endogenous, or blood borne. Endogenous endophthalmitis is most often mycotic, caused by *Candida albicans*. The frequency of endogenous infections, though three times less frequent than exogenous infections, is now increasing in both immunocompromised patients and patients under prolonged treatment with antibiotics, corticosteroids, or antimetabolites (82).

The symptoms of acute endophthalmitis are ocular pain and decreased visual acuity, with edematous lids, conjunctival hyperemia and chemosis, and corneal edema. On the other hand, patients with chronic endophthalmitis (caused by organisms of low virulence) do not present many clinical signs other than photophobia.

An early diagnosis and the beginning of an optimal therapy are both important to increase the chance of getting rid of the microorganisms and enhancing the visual prognosis. At this stage, the intravitreal injection of an antibiotic and eventually vitrectomy plays a very important role, not only in removing the infectious microorganisms, their associated toxins, and the inflammatory components, but also in capturing the infecting organism(s) for a microbiological identification (83) and proper antibiotic selection.

Before the use of intravitreal injections of antibiotics, the treatment of endophthalmitis had poor results (84). Indeed, the eye is an organ extremely susceptible to inflammation; it has poor defense mechanisms, and most antibiotics penetrate very poorly into the ocular cavity. There are actually two crucial parameters to note when treating such a disease: the drug must achieve sufficient levels in the vitreous, above the ID_{50}, and it must do so over a prolonged period of time. That is why topical, systemic, and subconjunctival administration of antibiotics failed to adequately treat endophthalmitis. In a series of experiments over the past 20 years, Peyman and coworkers as well as D'Amico et al. attempted to determine the toxic levels of various antibiotics by clinical, histological, and electroretinographic examination; to measure the clearance of nontoxic doses from the intraocular fluids after intravitreal injection; and to compare the effectiveness of intravitreal injection with systemic or subconjunctival administration in treating experimentally induced endophthalmitis (Table 2).

Experimental endophthalmitis was produced by injecting various organisms into the animal eye, with or without vitrectomy. Those studies in rabbits or monkeys showed that intravitreal administration of antibiotics is the most effective way of achieving high and immediate intravitreal drug levels without retinal toxicity (108,109).

Current therapeutic strategy for presumed endophthalmitis includes the intravitreal injection of a single or, more frequently, a combination of broad-spectrum antibiotics (110). These antibiotics are used at the highest possible nontoxic dose. Besides antibiotics, intravitreal corticosteroids such as dexamethasone play an important role in the management of bacterial endophthalmitis because of their beneficial effect in reducing the inflammation that accompanies the infection. Adjunctive treatment of endophthalmitis is the systemic administration of another antibiotic, especially in the case of endogenous endophthalmitis, to provide extraocular coverage and to maintain some intravitreal levels, with steroids used to reduce the inflammatory response.

Therapy for fungal endophthalmitis is similar to that for bacterial endophthalmitis except that antifungals, rather than antibacterials, are administered. The recommended therapeutic strategy is the direct intravitreal administration of amphotericin B. If the treatment fails, miconazole may be used (1). Systemic antifungal treatment is also employed.

Posterior Uveitis

Posterior uveitis, whether it is endogenous and chronic or associated with systemic diseases such as Behçet's disease, is a pathology characterized by vitreal inflammation and retinal vasculitis. In the majority of patients, the etiologic agent is not known. It has been postulated that in many cases uveitis may be autoimmune in origin. Uveitis usually has a low response to treatments with steroids or cytotoxic drugs, and it may require long-term chronic treatment. If untreated, the outcome is generally severe, eventually leading to progressive blindness.

The immunomodulating drug cyclosporin was investigated and found effective in treating experimental autoimmune uveitis (111) and acute inflammation unresponsive to usual treatment (112). Cyclosporin A is a cyclic polypeptide composed of 11 amino acids that effectively inhibits the development of experimentally induced uveitis (113). It acts by inhibiting the synthesis of interleukin 2 by the T helper lymphocytes (114). Cyclosporin A has been shown in several human clinical trials to be effective in treating chronic uveitis, especially that associated with Behçet's disease (115). Unfortunately, its systemic administration causes severe complications, such as renal toxicity, hypertension, and immunosuppression, which limit its use. Topical administration, on the other hand, resulted in nondetectable levels of the drug in all the intraocular structures because of its poor ocular bioavailability (116). To avoid these toxic effects and to achieve sufficient levels in the vitreous, cyclosporin was injected intravitreally and prevented experimental autoimmune uveitis (117). Grisolano and Peyman found no toxic effects in rabbits treated with 100 μg of intravitreal cyclosporin (118).

An adjunct to immunosuppressive treatment for noninfectious inflammation of the posterior segment is the use of corticosteroids. They are frequently employed to reduce intraocular inflammation and are currently the mainstay in the treatment of uveitis. Local steroid injections are preferred so as to avoid the side effects associated with systemic steroid administration. It is possible that a combination of drugs, attacking different targets in the immune response system, might work synergistically and thus would allow effective treatment with lower doses and presumably fewer side effects.

Next Page

Table 2. Management of Endophthalmitis: Peak Concentrations and Half-Lifes of Various Drugs in the Vitreous Following Intravitreal Injection

Class of drugs	Dose (mg)	Concentration (μg/mL)	Half-life (h)	Ref.
		Penicillins		
Ampicillin	5	900	6	85
Carbenicillin	1	270	10	86
Methicillin	2	632–2,000	3–5	87
Oxacillin	0.5	200	6	88
Penicillin G	2,000 U	500–1,000	3	89
		Cephalosporins		
Cefazolin	1	330	7	86
Cefotetan	1	670	7.5	90
Ceftazidime	0.2	91.9	7.4	91
Ceftriaxone	2	1,345	12	92
Cephalotin	2	380–550	—	93
Moxolactam	2	130	20	94
		Aminoglycosides		
Amikacin	0.25	110	24	95
Gentamicin	0.1	18	33	86
Gentamicin	0.1	100	32	96
Kanamycin	0.5	330	18	97
Netilmicin	0.25	167	24	98
Tobramycin	0.5	383	16	99
		Miscellaneous		
Aztreonam	0.1	62	7.5	100
Chloramphenicol	2	60	10	101
Ciprofloxacin	0.1	80	2.2	102
Clindamycin	1	235	7–8	103
Erythromycin	0.5	250	10	104
Lincomycin	1.5	900	10	105
Vancomycin	1	786	38.5	106
		Corticosteroids		
Dexamethasone	0.4	267	3	107

Source: Adapted from Ref. 6.

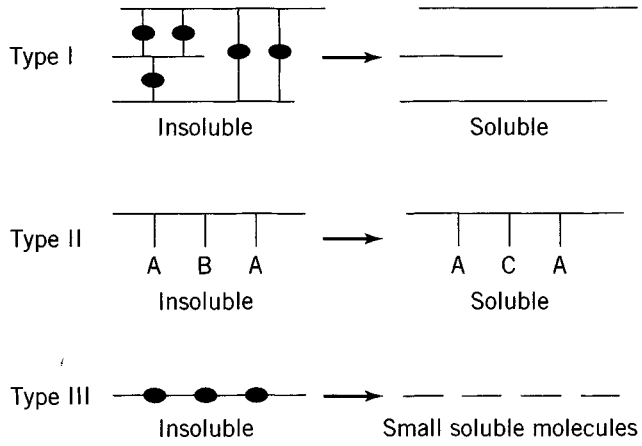


Figure 2. Schematic representation of three different breakdown mechanisms. ●, hydrolitically unstable bonds; A, hydrophobic substituent; B → C, hydrolysis, ionization, protonation. *Source:* Adapted from Ref. 119.

DRUG DELIVERY SYSTEMS

Biodegradable Polymers

Systems that control and prolong the action of therapeutic agents have grown in importance during the recent years with the development of biodegradable polymers. They are particularly important in the case of implants, because their use eliminates the step of removing the implant after the drug has been released, which, in some applications, can represent a significant advantage over other systems.

Biodegradable polymers gradually dissolve by hydrolytic or enzymatic cleavage of the polymeric structure or by simple dissolution. Heller (119) defined three mechanisms of polymer erosion (Fig. 2). Mechanism I concerns polymers that are made water insoluble by their hydrolytically unstable cross-links. These polymers, such as cross-linked gelatin, collagen, or poly(vinyl alcohol), provide highly hydrophilic matrices. Thus, substances with low molecular weight and high water solubility diffuse rapidly through the polymeric network independently of the rate of erosion of the matrix. These polymers are mainly used for the release of sparingly water-soluble drugs and for macromolecules such as enzymes and antigens (120).

Mechanism II includes polymers that are initially water insoluble and are solubilized by hydrolysis, ionization, or protonation of a pendent group yet lack backbone cleavage. This mechanism has the feature of not causing any significant change in the molecular weight of the polymer. These polymers, such as poly(vinyl methyl ether/maleic anhydride), cannot therefore be used for implants because of the difficulty of their elimination.

Mechanism III refers to hydrophobic polymers that are converted to small soluble molecules by backbone cleavage. As long as these breakdown products are not toxic, these polymers, for example, polyanhydrides, polycaprolactones, poly(ortho ester)s, poly(lactic acid)s (PLA), poly(glycolic acid)s (PGA), and their copolymers, are suitable as implantable carriers for the administration of drugs to any organ. They offer a wide range of applications in the ophthalmic field, whether applied on the surface of the eye or as intraocular implants.

The breakdown of polymers does not necessarily proceed through one mechanism only, and erosion occurs by a combination of these mechanisms (Table 3).

Poly(vinyl alcohol). Poly(vinyl alcohol) (PVA) is used in ophthalmology as a viscosifier for collyria and also as an intravitreal drug delivery carrier. PVA is synthesized by the polymerization of vinyl acetate to poly(vinyl acetate), which is then hydrolyzed to PVA. Its solubility in water will depend on the extent of hydrolysis and the degree of polymerization (122).

In a recent study, Hainsworth et al. evaluated various methods of sustained delivery to achieve therapeutic levels of ciprofloxacin (123). He compared in vitro two devices made either of PVA or of the bioerodible PLA. He found that the release of ciprofloxacin from the PVA matrix was very fast; over 90% of the drug was released within the

Table 2. Management of Endophthalmitis: Peak Concentrations and Half-Lifes of Various Drugs in the Vitreous Following Intravitreal Injection

Class of drugs	Dose (mg)	Concentration (μg/mL)	Half-life (h)	Ref.
		Penicillins		
Ampicillin	5	900	6	85
Carbenicillin	1	270	10	86
Methicillin	2	632–2,000	3–5	87
Oxacillin	0.5	200	6	88
Penicillin G	2,000 U	500–1,000	3	89
		Cephalosporins		
Cefazolin	1	330	7	86
Cefotetan	1	670	7.5	90
Ceftazidime	0.2	91.9	7.4	91
Ceftriaxone	2	1,345	12	92
Cephalotin	2	380–550	—	93
Moxolactam	2	130	20	94
		Aminoglycosides		
Amikacin	0.25	110	24	95
Gentamicin	0.1	18	33	86
Gentamicin	0.1	100	32	96
Kanamycin	0.5	330	18	97
Netilmicin	0.25	167	24	98
Tobramycin	0.5	383	16	99
		Miscellaneous		
Aztreonam	0.1	62	7.5	100
Chloramphenicol	2	60	10	101
Ciprofloxacin	0.1	80	2.2	102
Clindamycin	1	235	7–8	103
Erythromycin	0.5	250	10	104
Lincomycin	1.5	900	10	105
Vancomycin	1	786	38.5	106
		Corticosteroids		
Dexamethasone	0.4	267	3	107

Source: Adapted from Ref. 6.

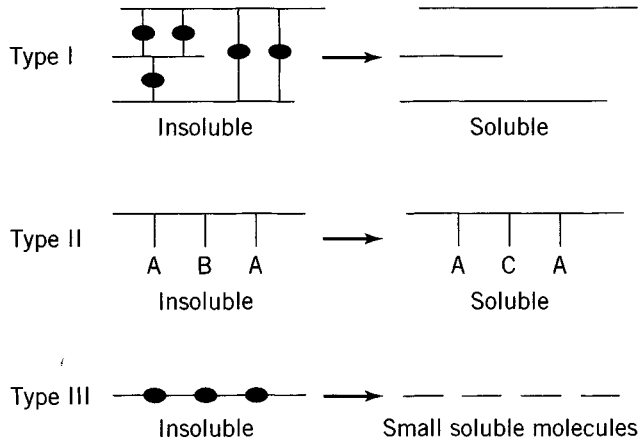


Figure 2. Schematic representation of three different breakdown mechanisms. ●, hydrolitically unstable bonds; A, hydrophobic substituent; B → C, hydrolysis, ionization, protonation. *Source:* Adapted from Ref. 119.

DRUG DELIVERY SYSTEMS

Biodegradable Polymers

Systems that control and prolong the action of therapeutic agents have grown in importance during the recent years with the development of biodegradable polymers. They are particularly important in the case of implants, because their use eliminates the step of removing the implant after the drug has been released, which, in some applications, can represent a significant advantage over other systems.

Biodegradable polymers gradually dissolve by hydrolytic or enzymatic cleavage of the polymeric structure or by simple dissolution. Heller (119) defined three mechanisms of polymer erosion (Fig. 2). Mechanism I concerns polymers that are made water insoluble by their hydrolytically unstable cross-links. These polymers, such as cross-linked gelatin, collagen, or poly(vinyl alcohol), provide highly hydrophilic matrices. Thus, substances with low molecular weight and high water solubility diffuse rapidly through the polymeric network independently of the rate of erosion of the matrix. These polymers are mainly used for the release of sparingly water-soluble drugs and for macromolecules such as enzymes and antigens (120).

Mechanism II includes polymers that are initially water insoluble and are solubilized by hydrolysis, ionization, or protonation of a pendent group yet lack backbone cleavage. This mechanism has the feature of not causing any significant change in the molecular weight of the polymer. These polymers, such as poly(vinyl methyl ether/maleic anhydride), cannot therefore be used for implants because of the difficulty of their elimination.

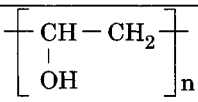
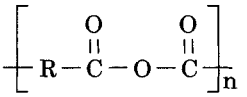
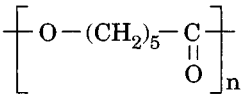
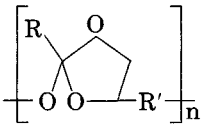
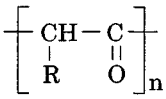
Mechanism III refers to hydrophobic polymers that are converted to small soluble molecules by backbone cleavage. As long as these breakdown products are not toxic, these polymers, for example, polyanhydrides, polycaprolactones, poly(ortho ester)s, poly(lactic acid)s (PLA), poly(glycolic acid)s (PGA), and their copolymers, are suitable as implantable carriers for the administration of drugs to any organ. They offer a wide range of applications in the ophthalmic field, whether applied on the surface of the eye or as intraocular implants.

The breakdown of polymers does not necessarily proceed through one mechanism only, and erosion occurs by a combination of these mechanisms (Table 3).

Poly(vinyl alcohol). Poly(vinyl alcohol) (PVA) is used in ophthalmology as a viscosifier for collyria and also as an intravitreal drug delivery carrier. PVA is synthesized by the polymerization of vinyl acetate to poly(vinyl acetate), which is then hydrolyzed to PVA. Its solubility in water will depend on the extent of hydrolysis and the degree of polymerization (122).

In a recent study, Hainsworth et al. evaluated various methods of sustained delivery to achieve therapeutic levels of ciprofloxacin (123). He compared in vitro two devices made either of PVA or of the bioerodible PLA. He found that the release of ciprofloxacin from the PVA matrix was very fast; over 90% of the drug was released within the

Table 3. Classification of Biodegradable Polymers Following the Heller Terms

Polymer	Mechanism of erosion	Chemical structure
Poly(vinyl alcohol)	Type I	
Gelatin	Type I	Mixture of purified protein fractions obtained by hydrolysis of animal collagen
Collagen	Types I and III	Protein extracted from animal tissues such as skin, sinews, and bones
Polyanhydrides	Type III	
Polycaprolactone and its copolymers	Type III	
Poly(ortho ester)s	Type III	
Poly(lactic acid)s, poly(glycolic acid)s, and their copolymers	Type III	

Source: Ref. 121.

first 24 h, and this release showed a square-root dependence of time, whereas release from PLA matrices followed a similar but slightly slower pattern.

On the other hand, as an intravitreal administration, PVA is most frequently coupled with ethylene vinyl acetate (EVA) in nonbiodegradable implants. These devices will be discussed later in this article.

PLA, Poly(glycolic acid), and Their Copolymers. Initially, poly(α-hydroxy acid)s were developed as synthetic, bioresorbable sutures in the 1960s. As a result of their good histocompatibility (124), this family of polyesters now includes the most-investigated biodegradable polymeric carriers for drug delivery systems. The principal polymers of this class are homo- and copolymers derived from lactic and glycolic acids: PLA, PGA, and its copolymers (PLGA).

Poly(α-hydroxy acids) are generally synthesized by a condensation reaction at high temperatures. The ring-opening polymerization of cyclic glycolic and lactic acid diesters is an efficient method to produce high-molecular-weight polymers. The simple step-growth polymerization method leads only to low-molecular-weight polymers with poor mechanical properties (125). The presence of an asymmetric carbon in lactic acid makes it possible to obtain levorotatory (L), dextrorotatory (D), or racemic (D,L) forms of the corresponding polymer, which can have different physicochemical properties.

The mechanism of degradation of these polyesters is a homogeneous erosion of the core. The polymeric chains are first cleaved by hydrolysis and then by an enzymatic chain scission process, thereby releasing acidic monomers that are rapidly eliminated by a physiological pathway. PGA is far too sensitive to hydrolysis to be considered useful as a carrier for sustained drug delivery (126). PLA degrades more slowly than PLGA; it also shows less initial burst of the drug than PLGA.

Drug delivery from PLGA matrices appears to follow biphasic kinetics (127). A mechanism to explain this profile would include a delayed increase in the permeability of PLGA arising from different factors, such as a reduction of the glass-transition temperature (T_g), an increase in the degree of hydration of the polymer, or a delayed onset of polymer weight loss by a bulk process (127). Kunou et al. studied the in vitro release pattern of plugs made with different types of PLA and PLGA and containing various percentages of ganciclovir as a model drug (128). The in vitro release of ganciclovir was shown to follow a triphasic process: (*1*) initial burst, (*2*) diffusional stage, and (*3*) final burst due to swelling and disintegration of the polymeric matrix (Fig. 3). The initial burst is certainly due to the rapid release of the drug located on the surface and in the water channels of the polymeric matrix. During the second phase, the drug is slowly released, controlled by the degradation rate of the polymer. In general, the release rate decreases with increasing molecular weight of PLA and PLGA and lactide content of PLGA. On the other hand, an increase in ganciclovir loading results in a higher release rate (128). During this second phase, a significant weight loss is observed. However, drug release from the implant is more rapid than the polymer weight loss. This observation suggests that the drug can diffuse through channels in the polymeric matrix during biodegradation but that the weight of the polymer does not change until a moment in hydrolysis when oligomers are produced by a random chain-scission mechanism, small enough to be soluble in

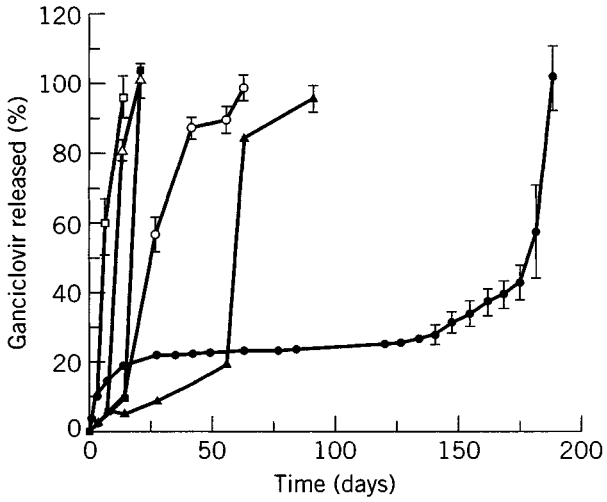


Figure 3. Effects of the molecular weight and lactic acid/glycolic acid ratio of PLA (PLGA) on in vitro release from scleral implants loaded with 10% ganciclovir. ○, PLA-20,000; ●, PLA-130,000; △, PLGA (75/25)-20,000; ▲, PLGA (75/25)-121,000; □, PLG(50/50)-20,000; ■, PLGA(50/50)-95,000. *Source:* Reproduced from Ref. 128 with permission.

water. The third phase of release occurs when the polymeric bulk swells and disintegrates.

The degradation rate can be varied by many factors in addition to the composition and configuration of the polymer or copolymer used, its porosity, and also the physicochemical properties of the incorporated drug.

The in vivo applications of poly(α-hydroxy acids) in the field of ophthalmology are mainly as topical and intraocular drug delivery systems, and as implants as well as microspheres. Besides microspheres, which will be discussed later in this article, implantable biodegradable polymeric matrices have been developed as new drug delivery systems in the vitreous. These implants are generally in the form of small cylinders that can be implanted in the eye by means of a syringe with a conventional needle (19- or 20-gauge) (129). Table 4 summarizes the different studies using these polyesters.

Rubsamen et al. (129) investigated PLGA-based rods containing 5-FU to treat experimental PVR in rabbit eyes. The devices can deliver therapeutic levels of 5-FU for almost 3 weeks and reduce the incidence of tractional retinal detachment. No adverse mechanical or toxic effects were apparent during the time of the study. However, because these devices were not fixed in the vitreous cavity, they might move and come into contact with the retina. Consequently, a stable localization of the device in the vitreous base through a suture fixation or an alternative mode of fixation at the site of implantation might be desirable.

In 1994, Hashizoe and coworkers designed a new device that is implanted at the *pars plana* and releases drugs directly into the vitreous (134). These scleral plugs, made of PLGA (40 kDa), were charged with 1% doxorubicin. The scleral plug gradually released doxorubicin in a concentration maintained within the therapeutic level for 1 month without any notable toxicity to the retina. In another study, Hashizoe et al. (131) demonstrated that the implantation of a scleral plug composed of PLA (20 kDa) and 1% doxorubicin effectively inhibited intravitreal proliferation of fibroblasts and could be a very effective way to treat PVR. Compared to the release of doxorubicin from the PLGA scleral plug (134), the authors observed that the PLA plugs have a longer period of drug release and showed less initial burst. Kunou and coworkers (128) investigated the use of scleral plugs to release ganciclovir for the treatment of CMV retinitis. The concentration of ganciclovir was maintained within the therapeutic range for over 3 months in the vitreous and for over 5 months in the retina and the choroid. A modulated release could be obtained with the scleral implant by varying the ratio and composition of the polymers, the molecular weight, and the drug concentration. Hashizoe et al. (137) further investigated the retinal toxicity of these plugs containing ganciclovir. At 3 months after implantation, only slight inflammatory changes occurred around the plug; the authors concluded that the biocompatibility of the device might be clinically acceptable. One of the advantages of scleral plugs is that the device becomes swollen during hydrolysis and seals the sclerotomy from inside. Fixation on the sclera is easy and requires no sutures. The same observations were made when other drugs were incorporated into the scleral plug, such as fluconazole (136), adriamycin (133), or betamethasone (135).

Table 4. Use of PLA–PLGA Implants for Intravitreal Administration

Polymer	Drug	Implant form	Animal model	Duration (weeks)	Year	Author (et al.)	Ref.
PLA	Fluorescein-Na	Implant	Rabbit	4	1994	Kimura	130
PLA	Ciprofloxacin	Disc	Rabbit	4	1996	Hainsworth	123
PLA	Doxorubicin	Scleral plug	Rabbit	>4	1995	Hashizoe	131
PLA, PLGA	Ganciclovir	Scleral plug	Rabbit	>20	1995	Kunou	128
PLGA	5-Fluorouracil	Cylinder	Rabbit	3	1994	Rubsamen	129
PLGA	5-Fluorouridine, dexamethasone	Cylinder	Pig	several	1996	Foster	132
PLGA	Adriamycin	Scleral plug	Rabbit	>4	1993	Hashizoe	133
PLGA	Doxorubicin	Scleral plug	Rabbit	>4	1994	Hashizoe	134
PLGA	Betamethasone	Scleral plug	Rabbit	>4	1996	Kunou	135
PLGA	Fluconazole	Scleral plug	Rabbit	3	1997	Miyamoto	136
PLGA	Ganciclovir	Scleral plug	Rabbit	12	1997	Hashizoe	137

On the other hand, it would be interesting to develop an injectable liquid-polymer drug delivery system that would solidify in the vitreous cavity and might overcome some disadvantages of the current solid implants. Indeed, the problem with polyesters is their very high melting point, above 170°C (138). Davis et al. reasoned that a family of injectable poly(α-hydroxy acid)s would provide an important therapeutic alternative to implants that require surgical procedures (139). They formulated a polymer system called Meltamer composed of block copolymers that are solid at 37°C but melt at various temperatures above 42°C and resolidify at body temperature. In vivo screening in rabbit eyes demonstrated that the heated polymer can be easily and safely injected into various ocular sites. The biocompatibility was excellent for more than 5 weeks, and the polymer completely degraded after that period of time (140).

Polycaprolactones. Other polymers from the polyesters family have been evaluated as long-term drug delivery systems. Poly-ϵ-caprolactone (PCL) was used in 1973 as a subdermal delivery system for contraceptive steroids under the trademark Capronor (141).

PCL is synthesized by a ring-opening polymerization of the monomer ϵ-caprolactone. It is semicrystalline, rather hydrophobic compared to poly(α-hydroxy acid)s, and has a high molecular weight. However, because of the great interest for low-molecular-weight polymers due to their controllable degradation profile and their low melting point, low-molecular-weight (LMW) polycaprolactones were prepared by means of hydrolytic degradation of high-molecular-weight (HMW) commercial PCL (142). Polymers of molecular weight from 4,000 to 10,000 were obtained without any structural changes. Comparison of the in vitro release rate of 5-FU as a model drug showed that the LMW PCL matrices exhibited more uniform drug release than the HMW devices. In a further study (143), Chin et al. mixed HMW and LMW PCL in different proportions, incorporated ganciclovir inside, and observed that the in vitro release rate of ganciclovir increased with the proportion of LMW. In general, these experiments demonstrated first-order kinetic release from matrices of PCL.

As with PLA and PLGA, PCL hydrolyzes by random chain scission through hydrolytic cleavage of ester groups to ϵ-hydroxycaproic acid, leading to a continual decrease of the molecular weight without any significant loss of weight. Enzyme catalysis is excluded in this first phase, because the diffusion of such HMW substances is impossible in the polymer bulk. When the molecular weight reaches about 5,000, the cleavage of the chain is catalyzed by enzymes and accompanied by a loss of weight resulting from the diffusion of small polymeric fragments from the matrix, which subsequently fragments and undergoes phagocytosis (141).

Concerning the application of PCL in the ophthalmologic field, many investigations have been made concerning the use of topical instillation of colloidal PCL-nanoparticles for the administration of β-blocking agents or indomethacin.

Intraocular application of polycaprolactone-based delivery systems has been investigated by Borhani et al. (144,145). They mixed HMW and LMW polycaprolactones in different proportions with 5-FU, and the pellets obtained showed, as expected, a faster release rate when the proportion of LMW polycaprolactone increased (144). In an in vivo study in rabbits (145) with 5-FU (10% or 20%) and HMW PCL, Borhani et al. demonstrated that these devices permit a slow release of 5-FU and thus increase the efficacy by providing a constant concentration of drug during the active period of PVR. An inflammatory cell reaction was found in the sclera near the implant site; however, in a study of biocompatibility and toxicity of PCL, no implant-related inflammation was observed (145).

Peyman and associates (146) have developed a PCL-based biodegradable porous implant for sustained and constant drug delivery. Nontoxic water-soluble inorganic salts such as NaCl or KCl were used as pore-forming agents and incorporated into PCL by a melting process. Biodegradable porous reservoir devices were prepared and loaded with different substances, for example, 5-FU, ganciclovir, foscarnet, and the dye carboxyfluorescein. During the in vitro release of the drug, the inorganic salts dissolved in water, leaving pores in the PCL devices. As the percentage of inorganic salt increases, a higher density of pores was observed in the devices. The porous reservoir devices provided a constant release of the drugs, depending on the pore size of the polymer. A concentration gradient across the wall of the polymer was created that forced the flow of the drug from the inner reservoir system to the surrounding aqueous medium. The release pattern followed zero-order kinetics without any initial burst, and the release lasted more than 6 months (Fig. 4) (146). This PCL reservoir device can be produced with various ratios of HMW polymer, allowing the device to degrade very slowly and therefore dissolving only after all the drug is released.

Polyanhydrides. Polyanhydrides were first investigated in the 1930s as substitutes for polyesters in textile applications, but because of their hydrolytic instability, the idea was soon abandoned, and attention turned to their use as

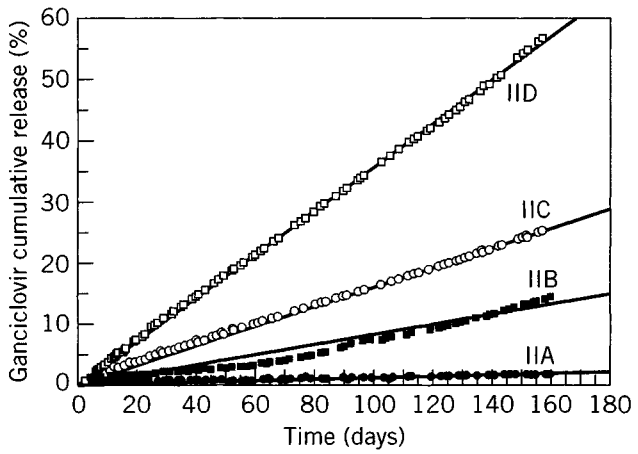


Figure 4. Cumulative release of ganciclovir over time from porous reservoir. IIA, 0% of porogen; IIB, 20% of porogen; IIC, 30% of porogen; IID, 40% of porogen. *Source:* Reproduced from Ref. 146 with permission.

biomaterials. Their very rapid hydrolysis is due to the lability of the anhydride links. The rate of hydrolysis of the polymeric chains on their surface is much faster than the penetration of water into the core of the matrix; this so-called heterogeneous surface erosion enables a zero-order kinetic profile and a good control over the rate and the duration of the release (147).

The most frequently investigated ocular matrix carrier consists of 1,3-bis(carboxyphenoxy) propane (PCPP) and its copolymers with sebacic acid (SA), a more hydrophilic monomer. Previous studies also described carriers with other 1,3-bis(carboxyphenoxy) alkanes with SA (148). Pure PCPP has an extremely long life (over 3 years) (147,149), whereas after copolymerization with 80% of SA, this is reduced to a few days. The ratio of the two monomers plays an important role in the rate of hydrolysis of the resulting polymer: When the proportion of SA increases, the hydrophobicity of the polymer decreases, resulting in a faster rate of hydrolysis of the polymeric chains at the surface. It should also be noted that polyanhydrides are pH-sensitive; they undergo faster breakdown at high pH and are more stable in acidic media.

Because of their surface erosion and excellent biocompatibility (149), polyanhydrides have been particularly useful for the controlled delivery of antimetabolites for the postsurgical treatment of glaucoma (121).

In a recent study (150), Lewis et al. reported the use of polyanhydride as an intravitreal bioerodible vehicle for 5-FU in the treatment of proliferative vitreoretinopathy. PCPP-SA loaded with 20% of 5-FU was compressed into a T-shaped device and sutured to a sclerotomy. Sustained release of 5-FU decreased the short- and long-term rate of retinal detachment in experimental PVR in rabbits. Alonso and coworkers described (151) the use of 1,3-bis(carboxyphenoxy) butane and SA to study the intraocular biocompatibility and in vitro kinetics of gentamicin. The implants were well tolerated in the vitreous body of rabbit eyes, and continuous levels of gentamicin were released in vitro.

Poly(ortho ester)s. The predominant mode of drug release from the previously mentioned hydrophilic systems such as PLA and PLGA is diffusion, with poor correlation between the rate of polymer erosion and the rate of drug release. For this reason, the development of new polymers that contain pH-labile linkages in their backbone has been proposed. Under certain conditions, the hydrolysis of such hydrophobic polymers can be confined predominantly to the outer surface. The resultant heterogeneous surface erosion allows excellent control of the release kinetics. Poly(ortho ester)s (POEs), as well as the previously described polyanhydrides, are polymers whose main characteristic is a release of the drug by surface erosion, following zero-order kinetics.

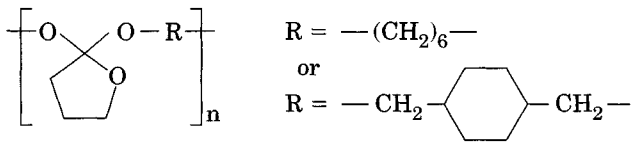
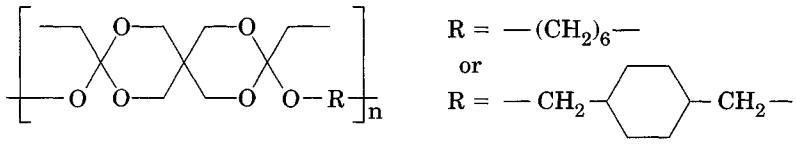
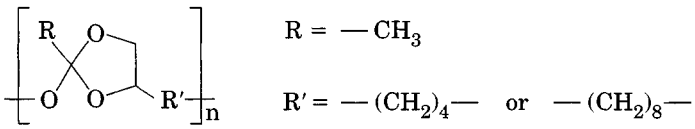
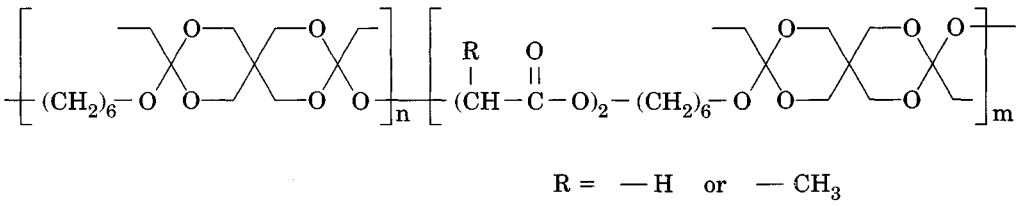
Since the late 1970s, four generations of POEs have been synthesized to produce bioerodible carriers for drug delivery (Table 5). The first was synthesized at ALZA Corp. in California; it was a hydrophobic solid polymer whose hydrolysis was catalyzed in acidic media (actually by the acidic coproducts released by the breakdown of the polymer). Various potential applications were described by Choi and Heller in their patents, but none concerned ophthalmic use (152).

The second generation of POEs was also a solid. The backbones of these polymers contain acid-labile linkages that are stable in alkaline media, hydrolyze slowly in pH 7.4 phosphate buffer, and degrade at increasing rates as the acidity of the medium increases. To produce drug delivery devices with lifetimes ranging from hours to months, studies were carried out by different investigators who incorporated acidic or basic excipients into hot-molded samples to modify erosion rates (152).

Recently, a new polymer has been described (153) and characterized by Merkli and coworkers (152). This viscous ointmentlike material allows the incorporation of drugs by simple mixing into the polymer at room temperature without the use of a solvent. This characteristic is of considerable interest with respect to peptide and protein delivery as well as for other thermolabile drugs. This third generation of POEs can be injected using a syringe with an appropriate hypodermic needle without any other surgical intervention, which is a significant advantage when compared with solid bioerodible devices that must be placed either with a trocar or through a surgical procedure. It is the only POE up to now that has been used in ophthalmic formulations. It has been investigated as an injectable bioerodible polymeric implant for controlled subconjunctival release of antimetabolites such as 5-FU and mitomycin C after glaucoma filtration surgery (154). The release of drugs from this semisolid POE occurs via a combined erosion and diffusion mechanism. For a LMW POE, the degradation rate is relatively fast, and the diffusion component is almost absent. On the other hand, for an HMW POE, the degradation rate of the polymer is slower, so the effect of drug diffusion through the flexible polymeric chains is more noticeable. The semisolid POE exhibits Newtonian behavior (152), and its viscosity is related to polymeric chain rigidity. In semisolid POE with low viscosity, high-chain flexibility facilitates hydrolysis. The first step of the reaction is the rapid hydrolysis of the labile orthoester bonds. This initial reaction is followed by a slower hydrolysis that produces a carboxylic acid and a triol. For more viscous polymers, where the chains are less flexible, water penetration is severely hindered, and the rate of initial hydrolysis is slowed. Consequently, to obtain drug release over an extended period of time, it is necessary to synthesize HMW polymers, but the major concern with these POEs is their very high viscosity, which makes their injection through a hypodermic needle very difficult.

A number of parameters have been shown to be important in controlling the release rate of drugs incorporated in POEs (155). Among these are the hydrophilicity of the drug, the particle size, and the amount incorporated. The influence of acidic excipients added to the system is directly proportional to their concentration, solubility, and pK_a. The use of highly water-soluble acids characterized by a low pK_a value leads to a fast polymer degradation where the drug is released principally by polymer erosion. For POEs stabilized with a basic excipient such as magnesium hydroxide, the release of the therapeutic agent is principally determined by diffusion and can be controlled by the amount of base incorporated into the polymer. The

Table 5. Chemical Structures of the Four Generations of Poly(ortho ester)s

Generation	Chemical structure
First	
Second	
Third	
Fourth	

concomitant release of 5-FU and dexamethasone has been investigated by Zignani and coworkers (unpublished data). The addition of dexamethasone phosphate, a hydrophobic steroidal antiinflammatory agent, to the highly hydrophilic and basic POE prolongs the release of the hydrophilic antimetabolite 5-FU while minimizing inflammation due to the polymer (Fig. 5). This system is promising for a subconjunctival application following glaucoma filtration surgery or intravitreally for the management of PVR.

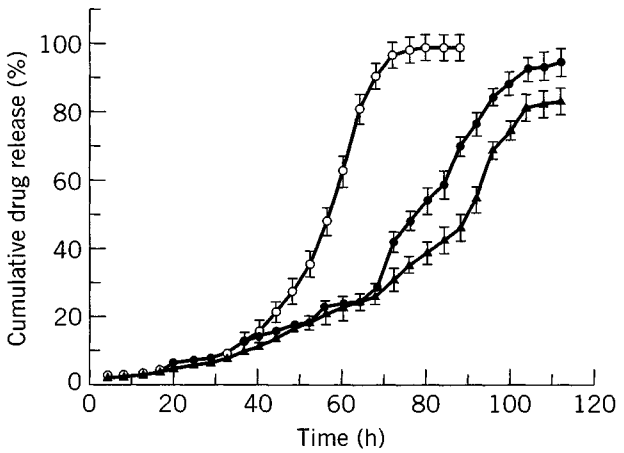


Figure 5. Cumulative in vitro release of 5-fluorouracil (1%) and dexamethasone sodium phosphate (1%) from POE in PBS at 37°C. ○, 5-FU (1%); ●, 5-FU (1%) in the presence of dexamethasone phosphate (1%); ▲, dexamethasone phosphate (1%) in the presence of 5-FU (1%). *Source:* Zignani et al., unpublished data.

The biotolerance of the semisolid biodegradable POE was investigated subcutaneously and with the cage-implant system (156); the biocompatibility appeared to be acceptable. The subconjunctival biocompatibility was studied by Bernatchez et al. (157). The acute inflammation resolved rapidly, and no chronic inflammation developed. After further purification of the polymer and using an aseptic preparation method, Zignani (158–160) further improved the biocompatibility of the polymer. After extensive testing, the same authors reported that the initial monomers and intermediate degradation products induced only a slight to moderate inflammatory reaction and no chronic response. As a matter of fact, aseptic preparation is up to now the only way to obtain sterile preparations because it has been shown that irradiation procedures produce degradation of the polymer and induce free radical formation (161–163).

A new family of POE, a self-catalyzed polymer, has been developed by Ng et al. (164). These POEs are similar to the second generation in that they contain short dimer segments of α-hydroxy acids in their backbone. Because POEs are susceptible to acid-catalyzed degradation, polymer hydrolysis can be controlled by the amount of incorporated α-hydroxy acids, and no acidic excipient has to be added (165). Concerning the in vitro drug release (166), it was found that the acidic 5-FU was released much faster than the weakly basic mitomycin C. These polymers appear to be very promising candidates for ophthalmic applications.

Nonbiodegradable Polymers

Ethylene Vinyl Acetate. The EVA copolymers are a family of materials with a number of promising advantages.

EVA, a thermoplastic lipophilic polymer, is mainly used as a membrane in reservoir systems and is quite permeable to certain lipophilic substances such as pilocarpine but is sufficiently hydrophobic to be relatively impermeable to hydrophilic drugs as well as water. The intrauterine progesterone contraceptive system Progestasert® (167) and the pilocarpine ocular insert Ocusert® produced by ALZA Corporation in Palo Alto, California (168), are examples of commercially introduced sustained-release systems based on EVA. In both cases, EVA is the constituent of a membrane that controls the rate of release of the drug, keeping it almost constant over several days.

In 1992, Ashton and coworkers developed an implantable sustained-release device to treat chronic disorders of the eye (169). This device consists of a central core of drug entirely coated in PVA, a permeable polymer. The surface area available for release, and consequently the release rate, is, then controlled by additional layers of EVA, which is impermeable to the drugs used, and PVA (Fig. 6). Water diffuses into the device and dissolves part of the pellet, forming a saturated drug solution. The drug then diffuses from the device, and as long as the solution inside the device is saturated, the release rate is constant. This is a so-called reservoir system (170). This device has been implanted intravitreally in animal and human eyes (Fig. 7) for the treatment of various vitreoretinal disorders (Table 6). As it is nondegradable, this system is almost devoid of any intraocular inflammatory response. However, it has to

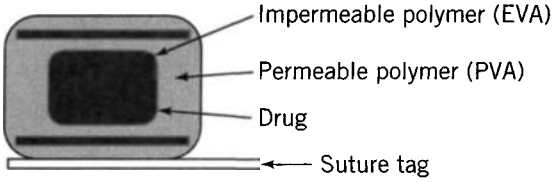


Figure 6. Diagram of the implantable sustained-release device. *Source:* Reproduced from Ref. 170 with permission.



Figure 7. Position of the device in the eye. *Source:* Reproduced from Ref. 170 with permission.

be removed or replaced to prevent any risk of fibrous encapsulation.

The first device was developed by Smith et al. in 1992 to treat CMV retinitis with ganciclovir (170). We have seen before that the treatment of CMV retinitis requires repeated intravitreal injections of ganciclovir to maintain therapeutic levels in the eye and to prevent relapse. Because of the severe complications associated with these frequent injections and the short intravitreal half-time of ganciclovir, this drug is a good candidate for a local sustained-release delivery system. Pellets of ganciclovir were thus prepared as described earlier and implanted intravitreally into rabbit eyes. Sustained levels of ganciclovir could be maintained in the vitreous of rabbits for more than 80 days after implantation of the polymeric device, and both the device and the resulting chronic low concentrations of ganciclovir appeared to be well tolerated (170). Ashton et al. compared the pharmacokinetics data of a ganciclovir implant in healthy rabbit eyes and in diseased human eyes. The rabbit eye was found to be a good model for studying the intravitreal pharmacokinetics of ganciclovir, suggesting a common elimination mechanism (178). Sanborn et al. (171) implanted devices releasing ganciclovir at a steady rate over approximately 4–5 months in patients with AIDS-associated CMV retinitis and found that the progression of the disease was first halted out and subsequently reversed, with all patients eventually being free of retinitis.

In 1993, Anand and associates reported the cumulative experience with this device: 30 eyes from 22 patients received the intraocular device and were followed up for a median of 125 days (172). Conventional intravenous therapy had failed in these patients; however, 5 patients had no history of intravenous therapy. The authors reported initial stabilization of the disease in 90% of eyes, with a mean time to disease progression of 133 days. In 1994, a new implant was developed, characterized by a slower release rate and a longer life span (8 months). In a randomized controlled clinical trial conduced by Martin et al. (173), this implant was found to be effective with a median time to progression of retinitis of 226 days, compared with 15 days for untreated patients. The devices were well tolerated intraocularly and did not experience significant biodegradation. Furthermore, Anand et al. (179) as well as Charles and Steiner (180) reported the histopathologic and electron microscopic features of some of the human eyes treated with the device and were encouraged by the relative lack of toxicity of the ganciclovir-containing intraocular devices and the fact that they are effective in sustaining clinical nonprogression of CMV retinitis. This ganciclovir device was approved by the U.S. Food and Drug Administration (FDA) in 1996 and is commercially available under the name Vitrasert™ (Chiron Vision Corporation), each implant containing a minimum of 4.5 mg of ganciclovir and being designed to release the drug over a 5- to 8-month period of time.

The life span of the device is an important factor influencing the therapeutic outcome and the potential costs and risks of repeated implantation procedures. In many reported cases, progression of disease in patients with intraocular devices has been attributed to depletion of drug

Table 6. Use of the EVA–PVA Devices for Intravitreal Administration

Drug	Model	Duration (weeks)	Year	Author (et al.)	Ref.
		CMV retinitis			
Ganciclovir	Rabbit	>11	1992	Smith	170
Ganciclovir	Human	20–25	1992	Sanborn	171
Ganciclovir	Human	19	1993	Anand	172
Ganciclovir	Human	33	1994	Martin	173
		Uveitis			
Cyclosporin	Rabbit	10 years	1996	Pearson	174
Cyclosporin, dexamethasone	Rabbit	>10	1996	Enyedi	175
Dexamethasone	Rabbit	>18	1995	Cheng	176
Dexamethasone	Rabbit	>18	1996	Hainsworth	177

from the device. When the device becomes depleted, it then has to be replaced. Morley and associates (181) described their initial surgical experience in replacing ganciclovir implants in patients with AIDS-associated CMV retinitis. Most patients retained good vision after ganciclovir implant replacement; however, the implants were occasionally difficult to extract because they were fibrosed into the scleral wound. Furthermore, in four of nine eyes that received a second implant, a retinal detachment developed. The purpose of a very recent study by Chen and Ashton (182) was to investigate various factors affecting in vitro release rate and to develop an implantable intraocular device providing sustained release of ganciclovir over 2 years. Pellets of ganciclovir were coated in a solution of PVA and then partially coated in films of the impermeable EVA, leaving a diffusion pore to allow release. The assembly was coated in PVA and heat treated. A slower release rate was obtained by decreasing the size of these pores and by increasing the heating temperature during the manufacturing process. On the other hand, increasing the percentage amount of PVA added to the pellet enhanced the release, while coating the device one more time, even in 5% PVA solution, significantly slowed down the release. Finally, a release rate of approximately 1.5 μg/h was achieved. Thus, these devices have a theoretical life span of over 600 days (183).

Treatment of posterior chronic uveitis with these EVA–PVA devices was also investigated. Cyclosporin devices were prepared by Pearson et al. (174). No significant decrease of cyclosporin level in the core of the device could be measured after intravitreal implantation in rabbit eyes during the 6 months of the study. Data suggest that owing to the high potency of cyclosporin and the very slow release rate of the device, these implants would provide sustained intravitreal levels of the drug for about 10 years (174). A second series of devices was prepared containing cyclosporin and dexamethasone (175). These two drugs might be beneficial in diseases such as uveitis and also proliferative vitreoretinopathy. Based on the fact that cyclosporin and corticosteroids reduce inflammation by different mechanisms, a device containing both drugs in combination would be more effective than a device containing either agent alone. These devices maintained therapeutic levels of both cyclosporin and dexamethasone in the vitreous over 10 weeks, and the presence of dexamethasone did not seem to change the release characteristics for cyclosporin (175). In an experimental model of PVR, the device containing both drugs lessened the severity of the disease and delayed the onset of neovascularization, but addition of cyclosporin to a device containing dexamethasone did not enhance efficacy (184). Devices were also prepared, containing dexamethasone alone for the treatment of PVR (177) and uveitis (176). Dexamethasone was released continuously for 3–4 months at an effective concentration in both cases. Furthermore, the devices were well tolerated, with no indication of toxicity or inflammation.

Polysulfone. Polysulfone is a water-impermeable polymer. A polysulfone capillary fiber (PCF) has been investigated as a slow-release delivery system. It is an anisotropic ultrafiltration fiber mainly developed for cell culture purposes by Amicon Corporation. PCF has the following important features: (*1*) it has deep macrovoids in its outer membrane, which increases the surface area for drug diffusion and release; (*2*) it seems to be permeable to lipophilic as well as hydrophilic compounds; (*3*) the PCF–drug device can be readily sterilized; (*4*) the device prevents dispersion of drug formulations, such as liposomes or microspheres, in the vitreous, and (*5*) most importantly, the bioactivity of the drug is unchanged by utilizing the PCF device because the fabrication process does not require chemical reaction, heat, or solvent exposure. The obvious disadvantage of this device is the need for surgical removal of the drug-depleted device because it is not a biodegradable system.

Rahimy and coworkers found that the PCF system is capable of maintaining a relatively constant intravitreal level of the hydrophilic dye carboxyfluorescein (CF) for up to 45 days (185). The in vitro CF release profile appears to be biphasic: The device releases about 50% of its CF content during the first 10 days; from day 10 to day 30, it exhibits slower release with approximately zero-order kinetics. From this standpoint, the PCF device can be classified as a reservoir diffusion-controlled system. Dye diffusion through the PCF membrane is mainly driven by the concentration gradient between the PCF core and the incubation medium. The transport of dye molecules across the PCF membrane remains constant if the core is main-

tained in a saturated state, such as a solid or suspension form. However, such a state is difficult to maintain in this case because the drug used is highly water soluble. As a result, it can be expected that during the second phase of the release, the rate would decrease as the concentration in the core drops below the saturation value. Intravitreal implantation of this device into rabbit eyes showed sustained-release kinetics. The in vivo time-course study showed CF levels for up to 45 days in the vitreous cavity. Furthermore, both clinical and histopathological data demonstrated that the PCF device is well tolerated by rabbit eyes (185).

Promising results have been obtained with daunomycin-charged PCF, as studied by Rahimy and coworkers, for the treatment of PVR (186). This device was implanted intravitreally in rabbit eyes, and the results demonstrated that the device could prolong the release of daunomycin at a therapeutic concentration in the vitreous for at least 21 days. At the doses of daunomycin used, the device prevented tractional retinal detachment in an experimental model of PVR and was well tolerated without causing toxicity to ocular tissues.

Silicone. Silicone oil is a highly hydrophobic polymer of dimethylsiloxane showing transparency, good tolerance, and properties similar to the vitreous humor concerning the refractive index and the viscoelasticity. These characteristics have led to its use in vitreoretinal surgery; silicone oil is most frequently used as an intraocular tamponade after vitrectomy (187). It can serve as a long-term tamponade, preventing recurrent retinal detachment. However, owing to many complications such as emulsification, keratopathy, increased intraocular pressure, and cataract formation, its use is restricted to specific applications like repair of retinal detachment with proliferative vitreoretinopathy (188).

Most of the antiproliferative drugs are water soluble and thus cannot be used with silicone oil. However, lipophilic drugs, such as carmustine (also known as BCNU), can be dissolved in silicone oil, which in turn acts as a depot material and releases the drug gradually into the vitreous cavity, thus prolonging its activity (189). High doses of BCNU can be loaded in the oil without increasing its toxicity, because the effective dose gradually released to the tissues is much smaller. However, silicone oil does not dissolve and does not have sustained-release properties itself.

Another antiproliferative lipophilic drug used in association with silicone oil is retinoic acid. Araiz (50) concluded that retinoic acid given in a single intravitreal administration in solution with silicone oil produces a significant and lasting reduction in cellular proliferation in an experimental model of PVR.

Nanoparticles, Microspheres and Liposomes

Nanoparticles and Microspheres. Microparticles and nanoparticles are colloidal drug carriers in the micron and submicron size range. These systems were first developed to resolve solubility problems of poorly soluble drugs as well as for long acting injectable formulations and improved drug targeting. These carriers have been evaluated as ophthalmic drug delivery vehicles over the past 15 years. An important potential use for these systems was to improve the classical aqueous eye drop formulations, which have several disadvantages such as a rapid elimination of the drugs from the precorneal site. Consequently, colloidal suspensions were designed to combine ophthalmic sustained action with the ease of application of eye-drop solutions (190).

Nanospheres have a diameter between 10 and 1,000 nm and are monolithic particles made of a porous or solid polymeric matrix, whereas nanocapsules consist of a solid or liquid drug reservoir surrounded by a polymeric membrane. Nanoparticles are usually prepared by the emulsion polymerization method, with synthetic polymers such as polyalkylcyanoacrylates (PACA), polyacrylamides, and polymethylmethacrylates. PACA has certain advantages over the two others polymers; it is biodegradable and has no adverse toxic profile (191).

Concerning the ophthalmic potential applications of nanoparticles, they are mainly used as a topical treatment for glaucoma, inflammation, or external infections of the eye because they are administered as drops and provide sustained action. However, only a few studies have been conducted concerning the intravitreal application of nanoparticles. El-Samaligy and coworkers (192) described the intravitreal injection of acyclovir and ganciclovir nanoparticles made of biodegradable polymers, such as bovine serum albumin (BSA), polyethylcyanoacrylate (PECA), and chitosan. All of these polymers exhibited interesting characteristics during in vitro evaluation (drug-loading capacity, particle size, homogeneity of nanosphere formation, and drug release). PECA was chosen for in vivo studies in rabbits because it demonstrated the best drug loading and the smallest particle size. Therapeutic levels of ganciclovir were detected in the vitreous for up to 10 days following injection of the nanospheres. Lens opacification and vitreous turbidity appeared after the PECA–nanospheres injection, most certainly due to the drug formulation, a colloidal opaque dispersion.

Microparticles have a particle size above 1 μm and comprise microspheres and microcapsules. Microspheres are polymeric drug combinations in which the drug is homogeneously dispersed in the polymer matrix. The polymers used for the preparation of microspheres are mainly based on PLA and PLGA. These bioerodible systems present the advantage that the microspheres degrade after delivering the drug; they do not have to be removed. Following administration of the suspension in the eye, the particles remain at the delivery site and the drug is released from the polymeric matrix through diffusion, polymer degradation, erosion, or a combination of these processes.

So far, it seems difficult for biodegradable polymer microspheres to encapsulate hydrophilic drugs and obtain satisfactory release profiles without burst effects (193,194). When using the conventional method of preparation of the microspheres, microcrystals of the hydrophilic substance may form in the matrix with a nonhomogeneous distribution. These microcrystals create pores in the microspheres, which in return increase the surface area of

the matrix and by this means induce a faster degradation and release of the drug by diffusion. The near-linear release of drugs has been correlated with a corresponding linear decrease of molecular weight of the polymer and to the fast progression in pore formation. Diffusion of the drug from the deeper layers of the microspheres to the surface might partially explain the faster release from the lower-molecular-weight polymers. For hydrophobic drugs, the most important mechanism of release seems to be the degradation of the polymer matrix.

The factors affecting biodegradation are therefore the following: (*1*) LMW polymers and copolymers with a medium to high content of glycolide have faster degradation time (with 50:50 PLGA having the shortest half-life), (*2*) smaller-size microspheres show faster degradation, (*3*) the presence of drug may affect degradation time, and (*4*) vitrectomized eyes show faster clearance times compared to normal eyes (195).

Besides topical ophthalmic applications, which have been widely studied (191), some authors have investigated microspheres for subconjunctival (194,196,197) as well as intravitreal injections to provide sustained release of drugs (Table 7). In 1991, Khoobehi et al. (193) investigated the intravitreal injection of microspheres as a sustained-delivery system. Microspheres were made of different combinations of PLA and PLGA and contained fluorescein as a drug model. After intravitreal injection in the rabbit eye, high concentrations of the dye were detected within 24 h; they gradually decreased after 5 days, and lower concentrations were still measurable for 16 days. The in vitro and in vivo release rates from PLGA microspheres were faster than from PLA (193).

Moritera and associates (198) entrapped 5-FU in PLA and PLGA microspheres and injected it intravitreally in rabbits. The drug was released over a period up to 7 days, and the release profile was accelerated by using lower-molecular-weight polymers or copolymers. The microspheres were observed as a white mass in the vitreous cavity and were completely cleared out, on average after 48 days. Administration of microspheres had no adverse effects on the ocular tissues, even though the degradation products of PLA and PLGA are acidic. Moritera also injected PLA microspheres with adriamycin in rabbits (199). This drug, 50 times more potent than 5-FU, was released at a continuous rate for over 14 days, was effective in preventing the rate of retinal detachment after 4 weeks in an experimental model of PVR, and showed no toxicity to the retina even at a relatively high dose. Peyman and associates (200) demonstrated the efficacy of microspheres in increasing the half-life of encapsulated antimetabolites when injected intravitreally in primate eyes. Both cytosine arabinoside (ara-C) and 5-FU were entrapped in PLGA microspheres. ara-C and 5-FU released from microspheres were still detectable in the eye 11 days after injection, and the clearance kinetics were similar for both drugs. The release patterns for all these hydrophilic drugs showed an initial burst. On the other hand, Giordano et al. (201) entrapped retinoic acid, a highly hydrophobic drug, in PLGA microspheres and obtained a constant release of the drug. This system could provide therapeutic levels of retinoic acid for 40 days (Fig. 8) and avoids the use of silicone oil as a reservoir; neither does it require surgery to implant or remove the drug delivery system. Veloso and coworkers (202) recently reported the use of PLGA microspheres loaded with ganciclovir for the treatment of experimental CMV retinitis in rabbits. Using a new preparation technique, the authors obtained a very high loading of the drug, and the microspheres released ganciclovir within the therapeutic range for at least 42 days. The progression of the retinitis decreased after 3 days. Neither retinal toxicity nor adverse tissue reaction were observed after 8 weeks. Acyclovir was also investigated as a candidate for microsphere incorporation for chronic treatment of herpes simplex infections or acute retinal necrosis syndrome (140). In vitro release of acyclovir was slower when higher-molecular-weight PLA, higher-lactide-content PLGA, and larger microspheres were used. After intravitreal injection in rabbit eyes, acyclovir levels were sustained for 14 days after microsphere injection, whereas no more acyclovir was detected 3 days after administration of raw drug (140).

A biocompatibility study was conducted by Giordano and coworkers (195); following intravitreal injection of empty microspheres of relatively low molecular weight PLGA, a mild, localized, nonprogressive foreign-body reaction was observed. The choroid and retina were normal, and no clinical inflammatory signs were observed 4 days postoperatively and thereafter.

Liposomes. Liposomes were first investigated in the 1960s as a membrane model. They have been studied for many years since as a potential drug delivery system. Liposomes are microscopic vesicles composed of membrane-like lipid bilayers surrounding aqueous compartments. These lipid layers are composed of natural phospholipids such as egg lecithin or synthetic phospholipids, for example, dipalmitoylphosphatidylcholine. Cholesterol is usually

Table 7. Intravitreal Injection of Microspheres

Polymer	Drug	Animal model	Duration (days)	Year	Author (et al.)	Ref.
PLGA/PLGA	Fluorescein Na	Rabbit	16	1991	Khoobehi	193
PLA/PLGA	5-FU	Rabbit	7	1991	Moritera	198
PLA	Adriamycin	Rabbit	14	1992	Moritera	199
PLGA	5-FU, ara-C	Monkey	11	1992	Peyman	200
PLGA	Retinoic acid	Rabbit	40	1993	Giordano	201
PLA/PLGA	Acyclovir	Rabbit	14	1997	Conti	140
PLGA	Ganciclovir	Rabbit	42	1997	Veloso	202
PLGA	Fluconazole	Rabbit	21	1992	Kimura	203

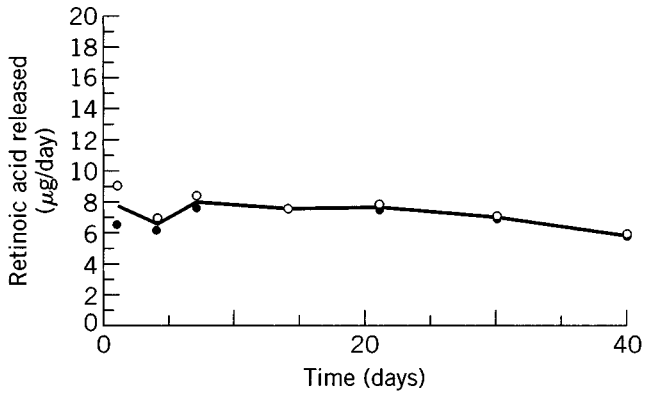


Figure 8. In vitro release rate of retinoic acid. Solid and open circles represent two different sets of experiments. The line represents the average of two measurements. *Source:* Reproduced from Ref. 201 with permission.

included in the formulation to stabilize the liposomal membrane and to minimize leaching out of the encapsulated water soluble drug. Substances such as α-tocopherol are added to decrease liposome permeability (204).

Liposomes may be classified as multi- or unilamellar depending on the number of concentric, alternating layers of phospholipids and aqueous spaces. Small unilamellar vesicles (SUV) have a diameter less than 100 nm. LUV refers to large unilamellar vesicles; and MLV, to multilamellar vesicles.

The rate of drug release from liposomes will depend upon the quality of the liposomes as well as the property of the drugs and the state of the eye. The drugs escape either by leakage through the membranes of intact liposomes or by diffusion from degraded or destabilized liposomes. Barza et al. (204) examined the effect of the size and composition of liposomes on their pharmacokinetic disposition following intravitreal injection. LUV liposomes have a longer retention time in the eye than SUVs. Concerning the components of liposomes, cholesterol stabilizes liposomal membranes, so in this case the rate of drug release is determined by the clearance of the liposome itself, whereas for non-cholesterol-containing vesicles, it is determined by the rate of leakage of the drug from the liposome. The physicochemical properties of the encapsulated drug determine its rate of release. Hydrophilic drugs are captured in the aqueous phase of liposomes, whereas lipophilic drugs, such as amphotericin B, are usually bound to the lipid bilayer or dissolved in the lipid phase. Such drugs will thus not leach out as readily as hydrophilic compounds to the external water phase. The state of the eye is also a major factor; liposomes showed a higher clearance rate in infected eyes, maybe due to an enhanced rate of diffusion of the liposome, an increased rate of flow from the vitreous to the anterior chamber, an augmented uptake by fixed or mobile phagocytes, or a breakdown of the blood–retinal barriers.

The pharmacokinetics of liposomally encapsulated drugs is not yet fully understood. Following intravitreal injection of liposomes, several processes begin simultaneously; intact as well as degraded liposomes clear from the vitreous body, the vesicles leak their contents in the vitreous humor, and these contents are eliminated. The mode of elimination of liposomes themselves from the vitreous remains unclear. The liposomes may egress by diffusion via the anterior route, or they may be removed by phagocytosis, for example, by pigmented epithelial cells or by degradation in situ as well as by other mechanisms or a combination of these processes (204). The state of the blood–retinal barrier and the structural integrity of the vitreous body may markedly affect the pharmacokinetic behavior of intravitreal liposomes. The liposomes are more rapidly cleared in vitrectomized eyes (205), and the breakdown of the blood–retinal barrier induced by inflammation allows the liposomes to egress and the drug to leak more easily from the vitreous.

Liposomes have been administered by practically every conceivable route. Some degree of success has been achieved for the topical and parenteral routes; a prolongation of plasma half-lives with liposome-encapsulated drugs has been reported. The development of liposomes for ocular drug delivery has been studied for various approaches of administration. Topical instillation is the most convenient and frequently used means of administration for ophthalmic therapy (206). Liposome encapsulation enhances the corneal penetration of topically applied drugs. It provides a convenient way to retard their release from a relatively inert depot without changing the intrinsic characteristics of the agents and to increase the duration of therapeutic levels. Some investigators have also experimented with the subconjunctival and intravitreal injection of liposomally entrapped drugs. Others have attempted to target ocular tissues by a systemic route of administration (207) (Table 8).

Antibiotics for the treatment of endophthalmitis were the first drugs to be encapsulated into liposomes and injected intravitreally in rabbit eyes. As early as 1986, Fishman and associates (208) incorporated gentamicin in MLV. The authors observed a lower peak value of gentamicin in the vitreous, which would presumably result in a decrease of toxic effects on the intraocular structures. However, enhanced toxicity from liposome-entrapped drugs arising from longer exposure may still be possible. Nevertheless, the release profile was significantly improved, and liposome encapsulation was thought very promising for sustained intravitreal drug administration. Another antibiotic, clindamycin, was studied by Fiscella (209) and Rao (210). The clearance of encapsulated clindamycin was 10 hours, compared to 3 hours for nonencapsulated clindamycin. Furthermore, this treatment was successful and efficacious in treating an experimental model of *S. aureus* endophthalmitis. Tobramycin, an antibiotic with marked inhibitory action against many gentamicin-resistant strains of bacteria, such as *P. aeruginosa*, was encapsulated in liposomes by Kim and Kim (211) and allowed to reduce the initial burst of the drug so as to prolong its action in the vitreous (Fig. 9) and to prevent any retinal toxicity. Zeng and associates (212) prepared liposomes with amikacin, a more effective antibiotic than gentamicin. The duration of therapeutic concentrations was generally prolonged. They observed that liposomes were more rapidly

Table 8. Applications of Liposomes for Intravitreal Administration

Drug	Type	Animal model	Duration (days)	Year	Author (et al.)	Ref.
			Endophthalmitis			
Gentamicin	MLV	Rabbit	8	1986	Fishman	208
Clindamycin	MLV	Rabbit	2	1987	Fiscella	209
Clindamycin	LUV	Rabbit	N.A.	1989	Rao	210
Tobramycin	MLV	Rabbit	18	1990	Kim	211
Amikacin	MLV	Rabbit	9	1993	Zeng	212
Amphotericin B	SUV	Rabbit	35	1985	Tremblay	213
Amphotericin B	SUV	Monkey	N.A.	1985	Barza	214
Amphotericin B	LUV	Rabbit	N.A.	1989	Liu	215
			CMV retinitis			
Trifluorothymidine	LUV	Rabbit	28	1987	Liu	216
Ganciclovir	LUV	Rabbit	28	1987	Peyman	217
Ganciclovir	MLV	Rabbit	14	1992	Díaz-Llopis	218
Ganciclovir	LUV	Human	24	1994	Akula	219
Ganciclovir	LUV	Rabbit	60	1996	Le Bourlais	220
2′ nor-cyclic GMP	MLV	Rabbit	N.A.	1993	Shakiba	221
Foscarnet	LUV	Rabbit	3	1997	Grümbel	222
Cidofovir	MLV	Rabbit	240	1995	Besen	223
Cidofovir	MLV	Rabbit	120	1996	Kuppermann	224
			Uveitis			
Cyclosporin	LUV	Rabbit	16	1988	Alghadyan	225
			PVR			
5-fluorouracil	LUV	Rabbit	N.A.	1988	Joondeph	226
ara-C, FUMP	MLV	Rabbit	14	1991	Assil	227
FUMP	MLV	Rabbit	N.A.	1994	Gariano	228
5-fluorouridine	MLV	Rabbit	N.A.	1997	García-Arumí	229
Cytarabine	LUV	Rabbit	N.A.	1989	Liu	230
Fluoroorotate	+ + +	Rabbit	N.A.	1989	Heath	231
Daunomycin	LUV	Rabbit	14	1993	Hui	16

Notes: N.A., nonavailable; LUV, large unilamellar vesicles; MLV, multilamellar vesicles; SUV, small unilamellar vesicles; + + +, various types of vesicles.

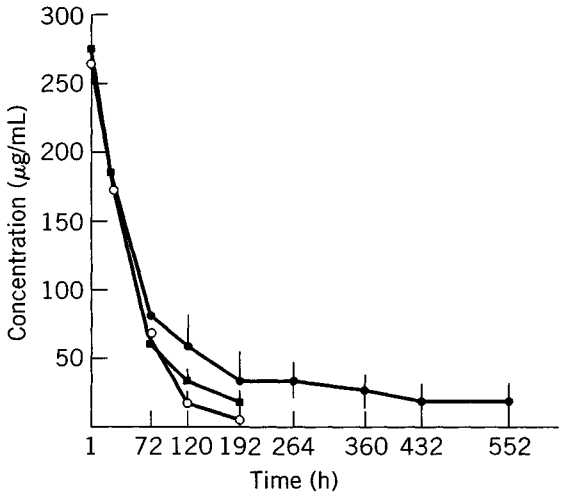
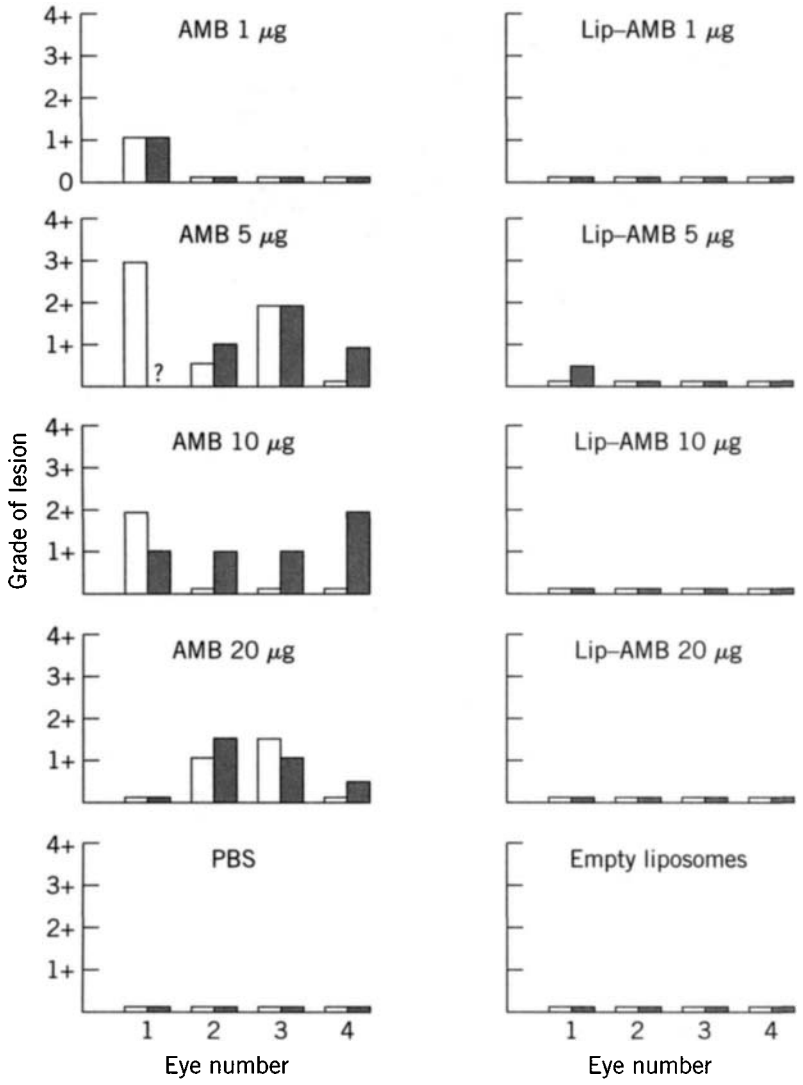


Figure 9. Tobramycin concentrations in the vitreous following intravitreal injection of liposome-encapsulated tobramycin (LET), tobramycin in PBS (TS), and tobramycin in empty liposome (TEL) in rabbits. ●, LET; ○, TS; ■, TEL. *Source:* Reproduced from Ref. 211 with permission.

cleared in vitrectomized eyes and in severely infected eyes. This is probably due to damage of the blood–retinal barrier and therefore an enhanced elimination of the drug. They concluded, however, that in severe endophthalmitis the intravitreal injection of liposomes alone could not suppress the inflammation.

Amphotericin B is a hydrophobic drug that showed different behavior from the other antibiotics described above. In a study in 1986 by Tremblay and coworkers (213), it was shown that liposome encapsulation of amphotericin B noticeably reduced its toxicity in rabbit eyes (Fig. 10) but without enhancing the therapeutic levels compared to nonencapsulated amphotericin B. The toxicity of this drug was also reduced in primate eyes (214). Indeed, unlike water-soluble molecules, which are trapped in the aqueous phase of the liposomes, amphotericin B is presumably intercalated in the liposomal bilayers. Because amphotericin B binds to sterols, this protective effect of the liposomes may result from competition for drug binding between cholesterol in the liposome and in the host's cellular membranes, reducing the acute interaction between amphotericin B and the sterol receptors. Liu and coworkers (215) further investigated the efficacy of liposomally bound amphotericin B for the treatment of experimental fungal en-



Extent of vitreal band formation and retinal damage observed ophthalmoscopically 5 weeks after injection of commercial amphotericin B (AMB) or liposomal amphotericin B (lip–AMP) in the indicated dosage in pigmented rabbits. Each bar is the result in one eye using the following score system:

Grade	Vitreal bands	Retinal damage
0	None	None
1+	Minimal	Silvery sheen or atrophy of the retina occupying 0.5–1 whole field visible at one time
2+	Moderate	Retinal sheen or atrophy of the retina occupying >1 field visible at one time
3+	Severe	More extensive than above (no such lesions actually found)

Control eyes receive phosphate-buffer saline (PBS) or empty (drug-free) liposomes.

Figure 10. Gross toxicity of intravitreal amphotericin B. □, vitreal bond formation; ■, retinal damage. *Source:* Reproduced from Ref. 213 with permission.

dophthalmitis in rabbit eyes. Liposomal amphotericin B eradicated the infection in only 40% of the eyes treated, whereas the same dosage of free drug eradicated 100% of the infection. This reduction of efficacy might be due to the membrane-stabilizing effect of cholesterol and, consequently, the reduced availability of the drug against infective organisms or to competition between liposomal membrane cholesterol and fungal ergosterol. As a result, it appears that intravitreal liposomal preparations are not ideal for treating acute clinical conditions, such as endophthalmitis, that require initially high doses of antibiotics. Liposomes may, however, be advantageous for chronic dis-

orders for which a persistent low concentration of drug is necessary. In this latter case, liposomal preparations not only avoid the initial toxicity of the drug but also reduce the need for repeated intravitreal injections.

A disease such as CMV retinitis requires frequent intravitreal injections and long-term treatment. In 1987, the first antiviral compound, trifluorothymidine, was tested for liposomal encapsulation. Liu et al. (216) found that a substantial amount of drug remained in the vitreous 28 days after intravitreal injection, an effective concentration against most HSV types and CMV. Ganciclovir, the highly efficacious antiviral drug, has been extensively studied. Peyman et al. were the first to encapsulate it into LUV (217). The injection of liposome-entrapped ganciclovir appeared as a whitish suspension located in the inferior part of the vitreous body. This haze disappeared after 4 weeks, a period of time during which the total concentration of ganciclovir was within the therapeutic range to treat different viral strains. Díaz-Llopis et al. (218) further compared liposomal ganciclovir to a free ganciclovir solution. Liposomally encapsulated ganciclovir increased the time period required for reinjection in the treatment of CMV retinitis. The results reported are comparable to those of Peyman (217), but Díaz-Llopis used a simplified production procedure. The first clinical study performed in human eyes was undertaken by Akula et al. (219) in 1994. Intravitreal injection of liposomal ganciclovir formed a whitish suspension located in the inferior part of the vitreous cavity that gradually disappeared over 2 weeks and allowed the retention of ganciclovir for up to 24 days. Finally, Le Bourlais and coworkers (220) managed to obtain sustained release from liposomal ganciclovir for up to 60 days without toxic effects on the retina. A cyclic phosphate derivative of ganciclovir, 2′-nor-cyclic GMP, anionic in nature at neutral pH, proved an ideal candidate for encapsulation into MLV (221). This drug is as potent as ganciclovir and has a long-lasting antiviral effect, thus requiring less frequent dosing. The liposomal incorporation of 2′-nor-cyclic GMP allowed the half-life to be prolonged up to 1,000 h, more than 75 times that of ganciclovir, without any toxic signs. Finally, cidofovir was recently investigated by Besen (223) and Kuppermann (224). This compound has a different mechanism of action from ganciclovir and foscarnet; it might be beneficial for viral strains resistant to usual therapy. Cidofovir is 10 times more potent and more selective than ganciclovir and requires only short exposure time for antiviral action. Being polar and water soluble, it is highly suitable for liposomal encapsulation. Liposomal cidofovir was present in the vitreous 90 days after injection at a concentration 10 times above the ID_{50} of CMV. The efficacy of a single injection of this liposomal formulation of cidofovir may thus prevent reactivation of retinitis for more than 8 months. Kuppermann and coworkers used a lower, more appropriate dose of cidofovir (224). This system possessed a potent antiviral effect lasting up to 4 months.

PVR is a clinical condition that requires a sustained delivery of antiproliferative drugs, thus prolonging the duration of the therapeutic effect while minimizing the toxic side effects of a high initial dose. Liposome-encapsulated 5-FU was investigated by Joondeph et al. (226). This formulation allowed higher intraocular levels of 5-FU over a prolonged period after injection of a dose that, when given in the free form, is indeed toxic to the retina. Antimetabolites such as ara-C and 5-fluorouridine-5′-monophosphate (FUMP) were encapsulated by Assil and coworkers (227) and investigated for the treatment of experimental PVR in rabbits. The half-lives of both drugs were significantly prolonged. ara-C was found to be less effective than FUMP in reducing tractional retinal detachment, probably because of its lower potency (227). Liposomal FUMP was found very efficacious by increasing exposure time of fibroblasts to the drug from 1 to 72 hours, resulting in a 20-fold increase in efficacy. FUMP was further investigated by Gariano and coworkers (228) to evaluate its retinal toxicity when entrapped in MLV. It was found nontoxic at doses sufficient to inhibit PVR. García-Arumí and coworkers (229) encapsulated 5-fluorouridine in collagen-coated liposomes, knowing that this protein is the most important constituent of the extracellular matrix of epiretinal membranes in PVR and that cells involved in this process have specific receptors for collagen. This coating may increase the affinity of the target cells for the surface of liposomes. In an electron microscopy study, these authors confirmed that intravitreally injected liposomes bind extensively to the internal limiting lamina of the retina without entering the retina, thus potentially decreasing retinal toxicity. Liposomal ara-C has also been shown to be nontoxic to the retina when encapsulated into liposomes (230). Heath et al. selected a so-called liposome-dependent drug, fluoroorotate, a compound that seems not to enter cells unless bound to liposomes (231). Heath demonstrated the in vitro antiproliferative and anticontractile effects of fluoroorotate, properties that are essential for the treatment of PVR. The liposome drug complex was delivered to epiretinal membranes within the rabbit eye while minimizing toxicity to underlying tissues such as the retina. A single injection of liposomal fluoroorotate effectively inhibited retinal detachment in an experimental model of PVR (231). Finally, in a study by Hui et al. (16), daunomycin was encapsulated into liposomes and investigated in an experimental model of PVR. A prolonged half-life and minimized toxicity were reported following the encapsulation process.

Another approach of delivering local concentrations of a drug while lessening toxic effects at other sites is to administer liposomally encapsulated drugs by a systemic route. Various strategies have been attempted to target the released contents of liposomes. One approach has been to formulate liposomes that release their contents in response to hyperthermia (heat of 40–42°C). These liposomes are called "temperature-sensitive" and have been studied since 1984; Khoobehi et al. (232) delivered carboxyfluorescein and ara-C from temperature-sensitive liposomes, using a noninvasive microwave generator as an external trigger. Liposomes prepared from synthetic phospholipids rapidly released their contents at a phase-transition temperature of 41°C; however, in the presence of serum, the transition temperature decreased to approximately 40°C. The amounts of dye and drug released were different owing to the different physicochemical characteristics of both substances. Khoobehi et al. (233) further investigated the release of drugs from temperature-sensitive liposomes, ara-C, and 5-fluorouridine. A microwave-generated hyper-

thermia was applied to the rabbit eye, and the intravitreal release of the drugs was measured. The amounts were all higher in the heated eyes. The application of heat did not cause any damage to the ocular tissues. Ogura and coworkers (234) managed to deliver a model substance, carboxyfluorescein, to selective areas of the retina. As penetration of the drug into the retinal tissue is significantly restricted by intercellular tight junctions between vascular endothelial cells, retinal pigmented epithelial cells, and photoreceptors that form the blood–retinal barrier, the authors induced a breakdown of this barrier by laser pulses. The drug encapsulated in temperature-sensitive liposomes, situated in the lumen of the vessels, could then penetrate into the retina through areas where the barrier was disrupted. Liposomal encapsulation prevented any retinal toxicity compared with injection of the free drug. No evidence of retinal injury after laser exposure was found.

In summary, data generated in the last two decades clearly demonstrate that liposomes have great potential as novel drug delivery systems. The following advantages can be mentioned (207). First of all, liposomes can incorporate both hydrophilic and lipophilic compounds; therefore, even water-insoluble constituents can be administered in a liquid dosage form in which the therapeutic agent is dissolved. Composed of lipids similar to those present in biological membranes, liposomes are expected to be biocompatible and biodegradable. Liposomes can provide slow or controlled release and consequently prolonged action of encapsulated drugs. As long as the drug is incorporated within the liposomes, it cannot be metabolized. The rate of drug release can be influenced by selecting appropriate lipid components of the liposomal membrane, such as cholesterol or hydrogenated phospholipids. Finally, there is considerably reduced retinal toxicity of intravitreally injected drugs when they are encapsulated within liposomes.

Drug delivery using liposomes may be useful for the treatment of posterior segment diseases; however, there are also inherent problems encountered with these methods. One of the major problems limiting the widespread use of liposomes is both chemical and physical stability. Chemical instability may be due to hydrolysis or oxidation of the lipid components; physical instability may be caused by drug leakage from the vesicles and/or aggregation or fusion of the vesicles into larger particles. All these processes influence the bioavailability of encapsulated drugs. Some of these stability problems can be overcome by lyophilization; if the finished product is preserved in a relatively more stable dry state, its shelf life is longer. Sterilization is often difficult because most methods are unsuitable for liposomal products; phospholipids are thermolabile and sensitive to sterilization procedures involving the use of heat, radiation, and/or chemical sterilizing agents. The method available for sterilization of liposomes is filtration through 0.22-μm membranes; however, filtration is not suitable for LUV and does not remove viruses or pyrogens (207). Finally, intravitreally administered liposomes tend to spread diffusely within the vitreous cavity and cause cloudiness, interfering with the patient's visual acuity and the ability of the ophthalmologist to examine the fundus until complete biodegradation of the formulation has occurred (217,235).

Iontophoresis

Iontophoresis, from the Greek *ionto*, ion, and *phoresis*, to bear, is a process that allows increased penetration of ionized molecules across or into tissues by application of a low electric current (mA) (236). The drug is applied with an electrode carrying the same charge as the drug, while the ground electrode, which is of the opposite charge, is placed elsewhere on the body to complete the electric circuit (236) (Fig. 11).

The factors governing the penetration of drugs by iontophoresis have been studied by Hughes and Maurice (238); the penetration of a drug is proportional to the current and to the duration of its application, whereas the concentration of the drug solution does not seem to be an important factor (239). Other factors are the design of the electrode and the physicochemical properties of the drug, such as its charge (it should be ionized at a physiological pH and soluble in water) and its size (the drug should have a relatively small molecular size, <600 Da [24]).

Two types of iontophoresis are performed in the eye, namely, transcorneal and transscleral iontophoresis (237). Although transcorneal iontophoresis is capable of producing high and sustained levels of drug in the cornea and the aqueous humor, thus allowing the treatment of anterior segment diseases, only meager concentrations are achieved in the vitreous humor. This is due to the iris–lens diaphragm, which limits the penetration of the drug into the vitreous cavity. Incidentally, significant drug concentration levels were achieved in aphakic eyes, as reported by Fishman and colleagues (241). To circumvent the iris–lens barrier, transscleral iontophoresis is applied through the pars plana rather than the cornea. Because it is as effective in phakic as in aphakic eyes, it provides therapeutic vitreous drug levels to treat posterior segment disorders. Transscleral iontophoresis may thus replace or supplement intravitreal injections. This procedure has gained interest as a local drug delivery system for sub-

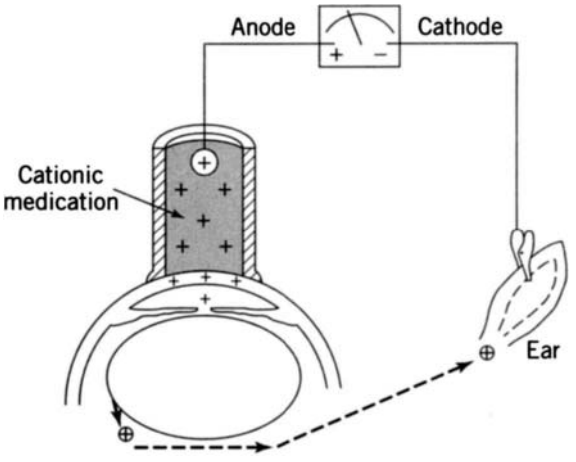


Figure 11. Ocular iontophoresis in the rabbit. *Source:* Reproduced from Ref. 237 with permission.

stances that are not amenable to topical delivery and require repeated administration over an extended period of time, such as antibiotics, antifungal, antiviral, antimetabolite, and steroid drugs (242) (Table 9).

The first application of transscleral iontophoresis was carried out by von Sallman as early as 1943; atropine and scopolamine were introduced in the vitreous humor by using an electrode circling the sclera (243). Since that time, iontophoretic delivery of antibiotics has been successful in providing vitreal therapeutic levels of drugs. Burstein et al. (243) administered gentamicin to rabbit eyes by means of transscleral iontophoresis. After the application of current for 3 minutes, a depot of gentamicin was introduced into the vitreous humor, which allowed therapeutic levels to be maintained in the adjoining ocular tissues for more than 24 h. Grossman and coworkers (245) compared transcorneal and transscleral iontophoresis of gentamicin to each other and with respect to subconjunctival injection. The highest intravitreal levels were achieved by transscleral iontophoresis, 53.4 μg/mL after 16 h, whereas the peak level achieved through transcorneal iontophoresis was 0.5 μg/mL after 30 min, and through subconjunctival injection, 2.6 μg/mL after 30 min. The vitreal levels remained within the therapeutic range for 24 h. Barza et al. (239) delivered iontophoretically three antibiotics, cefazolin, ticarcillin, and gentamicin, to rabbit eyes. Three hours after application of a current for 10 min over the *pars plana*, mean vitreal concentration of the antibiotics reached 94 to 207 μg/mL. Drug penetration showed a correlation with the current intensity and the duration of iontophoresis but not with the concentration of the drug solution. The procedure caused focal damage to the retina, for example, hemorrhagic necrosis, edema, and infiltration by polymorphonuclear cells, but the authors supposed that such an amount of injury is no greater than that caused by an intravitreal injection or surgical implantation of a sustained-release drug delivery device. Transscleral iontophoresis of gentamicin was also found effective in monkeys (244). Vitreal levels achieved were similar to those obtained in rabbit eyes with a lower current (239). The procedure was well tolerated, and the small burns produced by the electric current were over the *pars plana*, an area of the eye not critical for vision. The authors concluded that transscleral iontophoresis could be applied in humans with topical anesthesia only. Vancomycin is an antibiotic compound bearing two positive charges and having a relatively high molecular weight of 1,448 Da. It is very effective against gram-positive bacteria and *Bacillus* species. After application of 3.5 mA for 10 min, vitreal levels of vancomycin were well above the minimal therapeutic concentration of 5 μg/mL 8 h after treatment (240). Ciprofloxacin, a zwitterionic molecule, was investigated by Yoshizumi et al. (246). After transscleral iontophoresis, higher vitreal concentrations were achieved when the negatively charged form of ciprofloxacin was used rather than the positively charged form. However, aqueous levels were higher than vitreous levels, which were under the MIC_{90} of several organisms commonly causing endophthalmitis.

Grossman and Lee (247) attempted to deliver ketoconazole, an antifungal agent, to the vitreous of rabbits by transscleral iontophoresis. The water solubility of this drug is relatively low. The peak concentration achieved in the vitreous was not sufficient for therapeutic fungicidal activity. Transscleral iontophoresis is consequently not an effective means to deliver this antifungal drug for the treatment of endogenous endophthalmitis.

Lam and coworkers (248) performed transscleral iontophoresis of dexamethasone sodium phosphate into rabbit eyes and obtained high and long-lasting therapeutic

Table 9. Ocular Iontophoretic Drug Delivery

Drugs	Current (mA)	Duration (min)	Peak level (μg/mL)	Animal model	Year	Author (et al.)	Ref.
			Endophthalmitis				
Gentamicin	2.0	3	20.0	Rabbit	1985	Burstein	243
Gentamicin	1.5	10.0	28.0	Monkey	1987	Barza	244
Gentamicin	2.0	10.0	53.4	Rabbit	1990	Grossman	245
Gentamicin	2.0	10.0	207.0	Rabbit	1986	Barza	239
Cefazolin	2.0	10.0	119.0	Rabbit	1986	Barza	239
Ticarcillin	2.0	10.0	94.0	Rabbit	1986	Barza	239
Vancomycin	3.5	10.0	13.4	Rabbit	1988	Choi	240
Ciprofloxacin	5.0	15.0	0.2	Rabbit	1991	Yoshizumi	246
Ketoconazole	4.0–6.0	15.0	0.1	Rabbit	1989	Grossman	247
			Uveitis				
Dexamethasone	1.6	25.0	139.3	Rabbit	1989	Lam	248
Dexamethasone	0.4	4.0	N.A.	Rat	1997	Behar-Cohen	249
			CMV retinitis				
Ganciclovir	1.0	15.0	74.0	Rabbit	1994	Lam	250
Foscarnet	1.0	10.0	200.0	Rabbit	1993	Sarraf	251
Foscarnet	1.0	10.0	203.0 μM[a]	Rabbit	1996	Yoshizumi	252

Notes: N.A., nonavailable.
[a]Given as a supplementation of intravenous foscarnet.

concentrations of this antiinflammatory drug, maybe owing to pools of dexamethasone that would have accumulated in the different ocular tissues. In an experimental model of uveitis, Behar-Cohen et al. (249) investigated iontophoresis of dexamethasone by applying the electrode on both sclera and cornea of rat eyes. This procedure allowed the reduction of inflammation in both anterior and posterior segments of the eye as efficiently as systemic corticotherapy without any clinical or histological damages to the eyes.

Transscleral iontophoresis of antiviral agents such as ganciclovir could be useful for the treatment of CMV retinitis. Lam et al. (250) showed that a single iontophoretic application of ganciclovir over the *pars plana* may deliver a therapeutic dose of this drug into the vitreous, resulting in significant levels even 3 days after its administration. Foscarnet was also successfully delivered by transscleral iontophoresis (251). The peak concentration achieved 4 h after the administration of the current was below the concentration reported to cause retinal toxicity, and therapeutic levels could be maintained up to 60 h after iontophoresis.

The advantages of iontophoresis include the minimization of systemic exposure to the drug; the delivery of high concentrations of the drug directly to the targeted site; a minimal discomfort for the patient, only under topical anesthesia; and improved consistency in the penetration of the drug (238). It is a noninvasive procedure that may replace or supplement intravenous therapy or intravitreal injection of drugs (252).

Nevertheless, iontophoresis is not a harmless procedure. Transscleral iontophoresis might be associated with damage to the retina and the choroid, as described by Maurice (253). He observed destruction of most of the layers of the retina, with an engorgement of the choroid. Barza et al. (240,245) noticed hemorrhagic necrosis; edema; inflammatory infiltration of the retina, the choroid, and the ciliary body; and retinal burns. Lam and coworkers (254) presented a detailed description of the pathologic features occurring after transscleral iontophoresis. The pathologic changes varied with the duration of application. In contrast to the extensive retinal changes caused by 2 to 25 min of transscleral iontophoresis, a short application period ($\leq$1 min) did not result in histopathologic changes. Although the mechanism of retinal damage caused by transscleral iontophoresis is not known, it is suspected to be produced by heat or by the directly applied electrical current. On the other hand, during iontophoresis, electrolysis takes place in the electrode chamber, and the pH of the solution is sharply raised (or decreased, depending on the polarity of the electrode). Hence, negatively charged hydroxide ions may be driven into the vitreous and accumulate in the vicinity of the area undergoing iontophoresis toward the end of the procedure, causing chemical burns.

Prodrugs and Codrugs

The term *prodrug* was first introduced in 1958 by Albert (255) to describe an inactive compound, formed by linking a drug to an inert chemical, namely, the promoiety, by a covalent bond that could be broken in vivo by any mechanism, spontaneously or enzymatically, to yield the active drug substance. Furthermore, the prodrug should possess better delivery properties than the parent drug molecule (256). The use of prodrugs for ocular delivery has been reviewed by Lee and Li (257). Prodrugs are mainly used topically to increase corneal drug absorption to enhance efficacy, reduce the incidence of systemic side effects by lowering the required dose, and prolong the duration of action and thereby improve patient compliance. In the case of intravitreal delivery, the main advantage of prodrugs is that they prolong the action of drugs that are rapidly cleared out from the vitreous when administered in a conventional dosage form.

Steffansen and coworkers (258) developed a drug delivery system of 5-FU prodrugs suspended in silicone oil to maintain therapeutic intravitreal levels of 5-FU over several days for the treatment of PVR. They synthesized several lipophilic *N*-alkoxycarbonyl derivatives of 5-FU, with alkyl chain lengths ranging from 6 to 18 carbon units. All prodrugs hydrolyzed quantitatively to the parent 5-FU in aqueous buffer. Hydrolysis was accelerated in the presence of plasma or rabbit vitreous, which exhibited an enzymatic contribution, but in all cases the reaction followed first-order kinetics. The release rate of 5-FU depended on the alkyl chain length; the more lipophilic the prodrug, the more sustained the release rate.

Taskintuna and associates (259) investigated a lipid prodrug, acyclovir diphosphate dimyristoylglycerol (ACVDP-DMG). ACVDP-DMG represents the combination of acyclovir with cytidine diphosphate diacylglycerol (Fig. 12), a naturally occurring phospholipid, and it is very active against HSV and CMV. ACVDP-DMG is the prototype of a class of liposome prodrugs that the authors term *prosomes*. This compound makes up part of a liposome wall together with naturally occurring phospholipids, as opposed to conventional liposomes in which the drug is placed inside the liposomes. This prosome was found superior to both ganciclovir and acyclovir in a rabbit model of HSV retinitis. The ACVDP-DMG seemed to be specifically absorbed by the retina following intravitreal injection in rabbits, because the liposome walls seemed to fuse with the retinal cell membranes, allowing incorporation and progressive release of the drug into the retinal cells. This system did not seem to cause any toxic effects to the retina or the lens. In a pharmacokinetic study (260), liposomal ACVDP-DMG provided therapeutic levels of acyclovir for 18 days.

The use of a conjugate drug, a so-called codrug, is a novel approach that allows sustained release of two drug entities. These two drugs become relatively insoluble when covalently linked, and hydrolysis of the chemical bond allows both drugs to be released slowly in equimolar quantities. The codrug has a distinct advantage over the use of either drug alone because it incorporates the properties of both parent compounds while allowing a sustained delivery over an extended period of time. Consequently, a controlled release is achieved without recourse to more traditional polymeric drug delivery systems, some of which have been shown to induce a mild, localized foreign-body reaction with glial proliferation and inflammation.

A study by Berger and coworkers (261) was designed to evaluate the efficacy of two codrugs in preventing the de-

Next Page

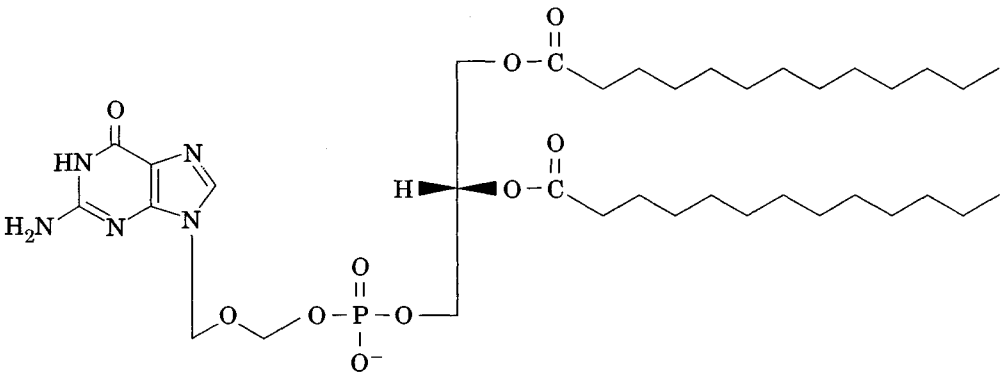


Figure 12. Structure of acyclovir diphosphate dimyristoylglycerol. *Source:* Ref. 261.

velopment of PVR in a rabbit model. The codrugs are composed of an antimetabolite, 5-FU, covalently linked to a corticosteroid, dexamethasone (DEX) or triamcinolone acetonide (TA), by a carbonate bond (Fig. 13). After synthesis of the codrugs by chemical reaction, the authors prepared pellets by direct compression of the DEX–5-FU powdered codrug and a suspension of the TA–5-FU codrug. The DEX–5-FU pellet released the drugs over 1 week in vitro. Using an experimental model of PVR in rabbits, the authors implanted the pellet intravitreally and observed a reduction of the incidence of retinal detachment from 70 to 20% until day 13, after which by day 20 the retinal detachment was up to 40%. The TA–5-FU codrug in suspension is more hydrophobic and provided considerably longer sustained release in vitro than the more soluble DEX–5-FU codrug. The TA–5-FU suspension reduced the incidence of retinal detachment from 89 to 30% from day 14 until day 28. Corelease occurs in two steps. The first step, codrug dissolution, is determined by the solubility of the compound and is the rate-determining step. The second step, codrug hydrolysis, occurs rapidly. This may explain why the more hydrophobic drug was the more effective in inhibiting experimental PVR.

In another investigation by Guo (262), an intravitreal device composed of the prodrug acyclovir–flurbiprofen was developed for the treatment of acute retinal necrosis (ARN), a disease that is accompanied by severe vasculitis. Treatment of inflammation can cause difficulty as steroids may induce a flare of viral activity. In AIDS-associated ARN, patients frequently respond poorly to systemic acyclovir, necessitating intravitreal injections. However, the damaged blood–retinal barrier enhances the clearance of acyclovir, requiring more frequent drug administration. A system capable of maintaining sustained therapeutic levels of acyclovir and flurbiprofen would thus be a real advantage. Pellets of codrug released both parent drugs in vitro following a zero-order kinetics. The release rate increased in the presence of proteins and enzymes. Bearing in mind that inflammation can elevate ocular protein concentrations by a factor of 10, this would result in accelerated drug release from this codrug system. The codrug delivery system may therefore form the basis of a disease-regulated delivery system, increasing release rate to match the severity of the condition and then decreasing to preserve the life span of the device (262).

CONCLUSION

In the past, most intraocular diseases, including sight-threatening endophthalmitis, devastating CMV retinitis, proliferative vitreoretinopathy, and uveitis, were treated by systemic and subconjunctival administration of drugs. These routes of treatment led, in the majority of cases, to the loss of the eye owing to the poor penetration of the various drugs into the vitreous cavity. This can be explained by the tight junctional complexes that interconnect cells of the retinal pigment epithelium and also tightly bind together the endothelial cells forming the walls of the retinal capillaries. These surfaces form the so-called blood–retinal barrier and prohibit passage of substances across the cells. In diseases such as endophthalmitis, the inflammation breaks down this barrier, but at this stage of the disease the retina has already been irreversibly damaged. The means of bypassing physiological and anatomical barriers and achieving high vitreous concentrations is through intravitreal administration. The use of intraocular drugs had formerly been restricted to the treatment of endophthalmitis. Nowadays, it is also considered for disorders that have been described in this article such as CMV retinitis, proliferative vitreoretinopathy, and uveitis. All these clinical conditions require frequent and repeated intravitreal injections of drugs, which may cause severe complications such as retinal detachment, vitreous hemorrhage, or intraocular infections. That is why sustained delivery systems have been developed recently to prolong the therapeutic levels of these drugs in the vitreous and thus diminish the frequency of the injections. This article has reviewed some of these systems (Table 10).

Biodegradable polymers have an advantage over other controlled-release systems in obviating the need to surgically remove the drug-depleted device. Potentially, biodegradable matrix systems also enjoy a number of other advantages in terms of simplicity in design and predictability of release if the latter is controlled solely by the erosion of the matrix. In many cases, however, the release occurs also by diffusion through the matrix, making the process more difficult to control—particularly if the matrix is hydrophilic and thereby absorbs water, promoting degradation in the interior of the matrix. To maximize control over the release process, it is desirable to have a polymeric system

Previous Page

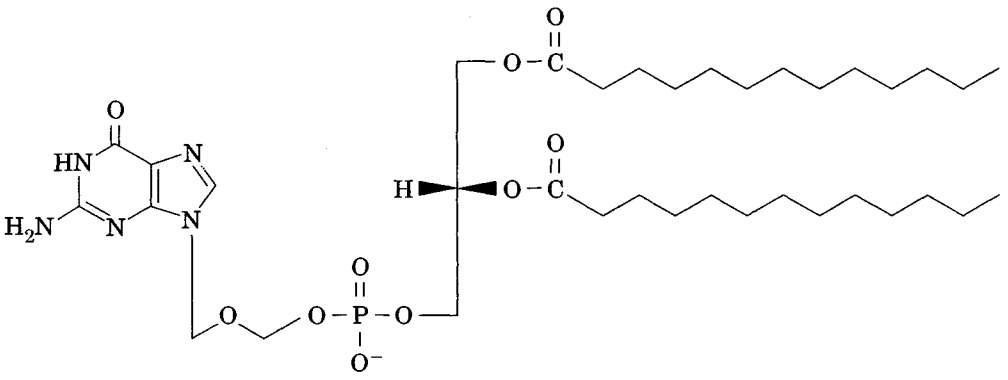


Figure 12. Structure of acyclovir diphosphate dimyristoylglycerol. *Source:* Ref. 261.

velopment of PVR in a rabbit model. The codrugs are composed of an antimetabolite, 5-FU, covalently linked to a corticosteroid, dexamethasone (DEX) or triamcinolone acetonide (TA), by a carbonate bond (Fig. 13). After synthesis of the codrugs by chemical reaction, the authors prepared pellets by direct compression of the DEX–5-FU powdered codrug and a suspension of the TA–5-FU codrug. The DEX–5-FU pellet released the drugs over 1 week in vitro. Using an experimental model of PVR in rabbits, the authors implanted the pellet intravitreally and observed a reduction of the incidence of retinal detachment from 70 to 20% until day 13, after which by day 20 the retinal detachment was up to 40%. The TA–5-FU codrug in suspension is more hydrophobic and provided considerably longer sustained release in vitro than the more soluble DEX–5-FU codrug. The TA–5-FU suspension reduced the incidence of retinal detachment from 89 to 30% from day 14 until day 28. Corelease occurs in two steps. The first step, codrug dissolution, is determined by the solubility of the compound and is the rate-determining step. The second step, codrug hydrolysis, occurs rapidly. This may explain why the more hydrophobic drug was the more effective in inhibiting experimental PVR.

In another investigation by Guo (262), an intravitreal device composed of the prodrug acyclovir–flurbiprofen was developed for the treatment of acute retinal necrosis (ARN), a disease that is accompanied by severe vasculitis. Treatment of inflammation can cause difficulty as steroids may induce a flare of viral activity. In AIDS-associated ARN, patients frequently respond poorly to systemic acyclovir, necessitating intravitreal injections. However, the damaged blood–retinal barrier enhances the clearance of acyclovir, requiring more frequent drug administration. A system capable of maintaining sustained therapeutic levels of acyclovir and flurbiprofen would thus be a real advantage. Pellets of codrug released both parent drugs in vitro following a zero-order kinetics. The release rate increased in the presence of proteins and enzymes. Bearing in mind that inflammation can elevate ocular protein concentrations by a factor of 10, this would result in accelerated drug release from this codrug system. The codrug delivery system may therefore form the basis of a disease-regulated delivery system, increasing release rate to match the severity of the condition and then decreasing to preserve the life span of the device (262).

CONCLUSION

In the past, most intraocular diseases, including sight-threatening endophthalmitis, devastating CMV retinitis, proliferative vitreoretinopathy, and uveitis, were treated by systemic and subconjunctival administration of drugs. These routes of treatment led, in the majority of cases, to the loss of the eye owing to the poor penetration of the various drugs into the vitreous cavity. This can be explained by the tight junctional complexes that interconnect cells of the retinal pigment epithelium and also tightly bind together the endothelial cells forming the walls of the retinal capillaries. These surfaces form the so-called blood–retinal barrier and prohibit passage of substances across the cells. In diseases such as endophthalmitis, the inflammation breaks down this barrier, but at this stage of the disease the retina has already been irreversibly damaged. The means of bypassing physiological and anatomical barriers and achieving high vitreous concentrations is through intravitreal administration. The use of intraocular drugs had formerly been restricted to the treatment of endophthalmitis. Nowadays, it is also considered for disorders that have been described in this article such as CMV retinitis, proliferative vitreoretinopathy, and uveitis. All these clinical conditions require frequent and repeated intravitreal injections of drugs, which may cause severe complications such as retinal detachment, vitreous hemorrhage, or intraocular infections. That is why sustained delivery systems have been developed recently to prolong the therapeutic levels of these drugs in the vitreous and thus diminish the frequency of the injections. This article has reviewed some of these systems (Table 10).

Biodegradable polymers have an advantage over other controlled-release systems in obviating the need to surgically remove the drug-depleted device. Potentially, biodegradable matrix systems also enjoy a number of other advantages in terms of simplicity in design and predictability of release if the latter is controlled solely by the erosion of the matrix. In many cases, however, the release occurs also by diffusion through the matrix, making the process more difficult to control—particularly if the matrix is hydrophilic and thereby absorbs water, promoting degradation in the interior of the matrix. To maximize control over the release process, it is desirable to have a polymeric system

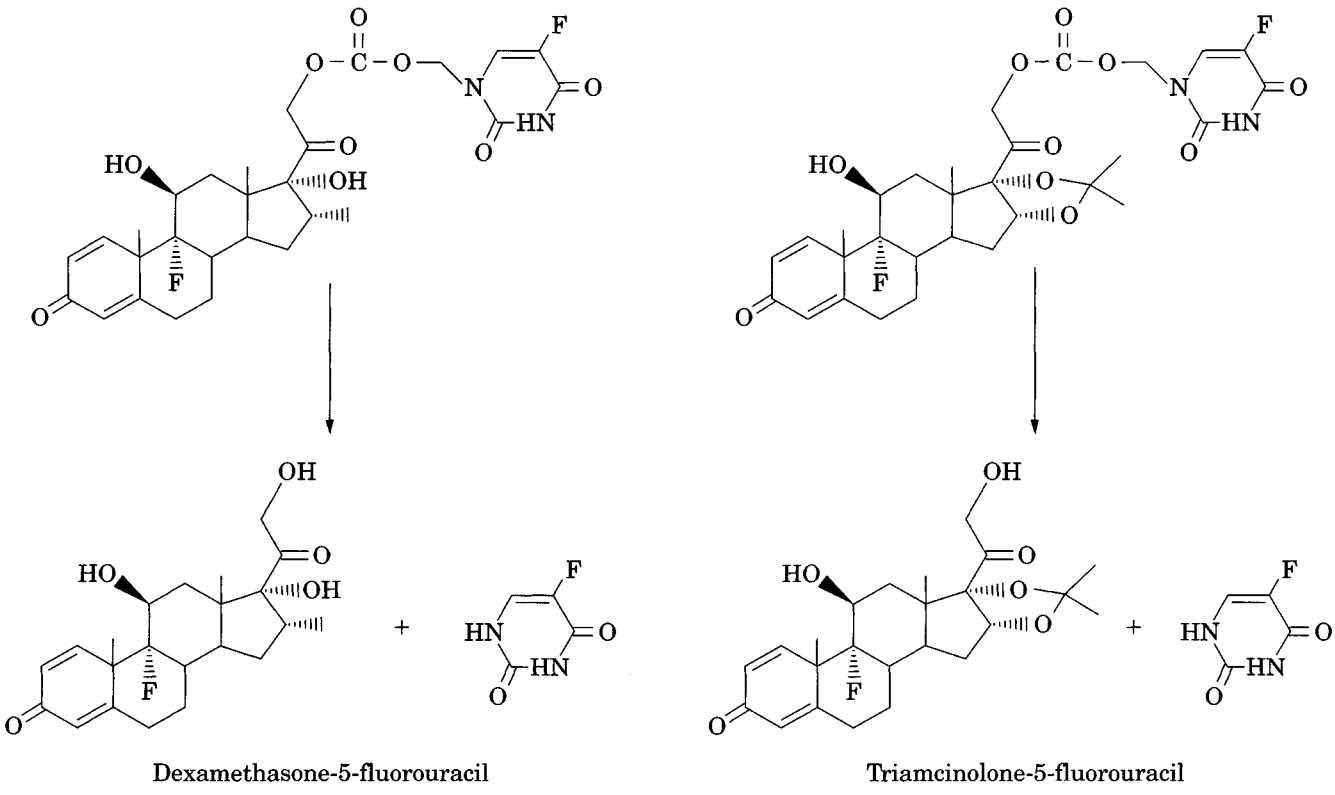


Figure 13. Chemical structures of dexamethasone–5-fluorouracil and triamcinolone–5-fluorouracil codrugs and hydrolysis to the parent drugs. *Source:* Ref. 261.

that degrades only from the surface and delays the permeation of drug molecules. Achieving such a heterogeneous degradation requires the rate of hydrolytic degradation on the surface to be much faster than the rate of water penetration into the bulk. The ideal polymer would have a hydrophobic backbone but with a water-labile linkage. Many classes of polymers have been designed with these considerations in mind. Among them, polyanhydrides and POEs erode from surface. Taking advantage of the pH dependence of the rate of ortho ester cleavage, preferential hydrolysis at the surface is obtained by either addition of basic substances to suppress degradation in the bulk or incorporation of acidic catalysts to promote degradation on the surface.

Devices that are not biodegradable such as the EVA–PVA implants are of clinical utility for chronic, sight-threatening diseases such as CMV retinitis and uveitis. These conditions are likely to require long-term drug therapy; therefore, any device may need to be replaced once depleted of drug. On the other hand, in diseases such as PVR, which requires relatively short-term therapy (weeks or months), a biodegradable system is clearly more desirable.

Microspheres and liposomes have been shown to increase the efficacy, reduce the toxicity, prolong the activity, and provide site-specific delivery for many drugs when administered to the eye. However, liposomes tend to have a short shelf life and to migrate within the eye (possibly to unwanted locations) following intraocular injection. Furthermore, the intravitreal injection of a liposome preparation always disturbs the patient's vision. Microspheres are more stable, their production is reproducible, and the release rate is controllable; but the injection of microspheres in the vitreous is always followed by an impairment of the visual acuity.

Transscleral iontophoresis has proved to be fast and painless and in most cases results in the delivery of a high and long-lasting vitreal concentration of the drug. However, several authors have noticed damage to the retina such as burns and disorganization of the retinal cell layers. These lesions are probably as harmful as those created by an intravitreal injection or surgical implantation of a sustained-release drug delivery device.

The prodrug or codrug approach, on the other hand, is a good method of providing sustained release of one or more drugs. The main advantage of this system is the absence of any polymeric material that might cause problems of biocompatibility.

The ideal drug release system should then fulfill the following criteria: (*1*) the systems should provide a sustained therapeutic concentration of drug in a reliable and predictable way over an adequate period to obtain the desired clinical response: inhibition of the inflammation or prevention of proliferation and contraction of epiretinal membranes in the case of proliferative vitreoretinopathy; (*2*) the concentration of drug should be relatively uniform over the administration period, with no early or late excessive release of the drug; (*3*) the device should be easily

Table 10. Advantages and Drawbacks of the Drug Delivery Systems Described in this Article

Pros	Cons
Biodegradable polymeric systems	
No need to be removed	Possible toxicity of breakdown products
No impairment of the clarity of ocular media	Rapid degradation
For *short-term* therapy (weeks to months)	Often sterilization problems
Controllable release rates	
Eventually injectable through a needle	
Nonbiodegradable polymeric systems	
No degradation products	To be removed after depletion
No impairment of the clarity of ocular media	Risk of encapsulation
For *long-term* therapy (months to years)	
Controllable release rates	
Nanoparticles, microspheres	
Injectable through needle	Vitreal haze after injection
Long shelf life	Initial burst effect
Good control over release	
Liposomes	
Good biocompatibility	Vitreal haze after injection
Reduction of drug toxicity	Short shelf life
Injectable through needle	Difficult to sterilize
Iontophoresis	
Noninvasive	For ionized drug
	Damages to the eye (burns)
Prodrugs and codrugs	
Concomitant equimolar release of both drugs from the codrug	No tailored release from the codrug
No need for polymeric carrier material	
Good tolerance	

implantable or injectable but must remain stable and nonmigratory within the eye; (*4*) the device should be totally biodegradable to avoid the need for explantation at a later date; (*5*) the device should have a long shelf life, should be easily handled by surgeons and operating room personnel, and should be easily sterilized; and (*6*) there should be no toxic effect from sustained exposure to the drug or degradation products of the device.

None of the sustained-delivery systems introduced to date fulfill all these criteria. Yet all of the exciting approaches described in this article may lead to the improvement of vision in patients with severe posterior segment diseases.

ACKNOWLEDGMENTS

This work was supported by Swiss National Science Foundation grants #32.46795.96 and #32.35925.92

BIBLIOGRAPHY

1. V.H.L. Lee, K.J. Prince, D.A. Frambach, and B. Martini, in S.J. Ryan, ed., *Retina*, Mosby, St. Louis, Mo., 1989, pp. 483–498.
2. J.G. Cunha-Vaz and D.M. Maurice, *J. Physiol. (London)* **191**, 467–486 (1967).
3. D.M. Maurice and S. Mishima, in M.L. Sears, ed., *Pharmacology of the Eye*, Springer-Verlag, Berlin, 1984, pp. 19–116.
4. G.A. Peyman and R. Herbst, *Arch. Ophthalmol. (Chicago)* **91**, 416–418 (1974).
5. D.M. Maurice, *J. Physiol. (London)* **137**, 110–125 (1957).
6. T.S. Lesar and R.G. Fiscella, *Drug Intell. Clin. Pharm.* **19**, 642–654 (1985).
7. The Retina Society Terminology Committee, *Ophthalmology* **90**, 121–125 (1983).
8. W.F. Rachal and T.C. Burton, *Arch. Ophthalmol. (Chicago)* **97**, 480–483 (1979).
9. M. Cowley et al., *Arch. Ophthalmol. (Chicago)* **107**, 1147–1151 (1989).
10. C. Claes, H.M. Freeman, and F.I. Tolentino, in H.M. Freeman and F.I. Tolentino, eds., *Proliferative Vitreoretinopathy (PVR)*, Springer-Verlag, New York, 1988, pp. 3–11.
11. P.A. Campochiaro, *Arch. Ophthalmol. (Chicago)* **115**, 237–241 (1997).
12. P.A. Campochiaro, J.A. Bryan, B.P. Conway, and E.H. Jaccoma, *Arch. Ophthalmol. (Chicago)* **104**, 1685–1687 (1986).
13. D.G. Charteris, P. Hiscott, I. Grierson, and S.L. Lightman, *Ophthalmology* **99**, 1364–1367 (1992).

14. D.B. Chandler, F.A. Quansah, T. Hida, and R. Machemer, *Graefe's Arch. Clin. Exp. Ophthalmol.* **224**, 86–91 (1986).
15. A. Ophir, M.S. Blumenkranz, and A.J. Claflin, *Am. J. Ophthalmol.* **94**, 450–457 (1982).
16. Y.N. Hui et al., *Graefe's Arch. Clin. Exp. Ophthalmol.* **231**, 109–114 (1993).
17. J.H. Stahl, D.B. Miller, B.P. Conway, and P.A. Campochiaro, *Graefe's Arch. Clin. Exp. Ophthalmol.* **225**, 418–420 (1987).
18. M. Lemor, S. de Bustros, and B.M. Glaser, *Arch. Ophthalmol. (Chicago)* **104**, 1223–1225 (1986).
19. C. Verdoorn et al., *Arch. Ophthalmol. (Chicago)* **104**, 1216–1219 (1986).
20. R.L. Avery and B.M. Glaser, *Arch. Ophthalmol. (Chicago)* **104**, 1220–1222 (1986).
21. M. Gonvers, *Am. J. Ophthalmol.* **100**, 239–245 (1985).
22. M.K. Hartzer et al., *Exp. Eye Res.* **48**, 321–328 (1989).
23. L.J.B. McGuigan et al., *Invest. Ophthalmol. Visual Sci.* **29**, 112–118 (1988).
24. N.D. Radtke, A.D. Weinsieder, and R.J. Ballou, *Graefe's Arch. Clin. Exp. Ophthalmol.* **224**, 230–233 (1986).
25. A.R. Irvine, H.W. Flynn, D. Miller, and S.C. Pflugfelder, *Arch. Ophthalmol. (Chicago)* **110**, 1450–1454 (1992).
26. M.S. Blumenkranz and M.K. Hartzer, in S.J. Ryan, ed., *Retina*, Mosby, St. Louis, Mo., 1989, pp. 401–411.
27. Y. Tano, G. Sugita, G. Abrams, and R. Machemer, *Am. J. Ophthalmol.* **89**, 131–136 (1980).
28. M.S. Blumenkranz, A.J. Claflin, and A.S. Hajek, *Arch. Ophthalmol. (Chicago)* **102**, 598–604 (1984).
29. Y. Tano, D.B. Chandler, and R. Machemer, *Am. J. Ophthalmol.* **90**, 810–816 (1980).
30. D.B. Chandler et al., *Graefe's Arch. Clin. Exp. Ophthalmol.* **225**, 259–265 (1987).
31. A. Barrada et al., *Ophthalmic Surg.* **14**, 845–847 (1983).
32. J.A. Leon et al., *Invest. Ophthalmol. Visual Sci.* **31**, 1709–1716 (1990).
33. A. Ophir, *Ophthalmic Res.* **23**, 128–132 (1991).
34. M.S. Blumenkranz, A. Ophir, A.J. Claflin, and A.S. Hajek, *Am. J. Ophthalmol.* **94**, 458–467 (1982).
35. M.S. Blumenkranz, E. Hernandez, A. Ophir, and E.W.D. Norton, *Ophthalmology* **91**, 122–130 (1984).
36. G. Jarus, M.S. Blumenkranz, E. Hernandez, and N. Sossi, *Ophthalmology* **92**, 91–96 (1985).
37. W.H. Stern et al., *Am. J. Ophthalmol.* **96**, 33–42 (1983).
38. M.S. Blumenkranz, M.K. Hartzer, and A.S. Hajek, *Arch. Ophthalmol. (Chicago)* **105**, 396–399 (1987).
39. P. Wiedemann et al., *Graefe's Arch. Clin. Exp. Ophthalmol.* **220**, 233–235 (1983).
40. U.H. Steinhorst et al., *Invest. Ophthalmol. Visual Sci.* **34**, 1753–1760 (1993).
41. M.A. Sunalp, P. Wiedemann, N. Sorgente, and S.J. Ryan, *Exp. Eye Res.* **41**, 105–115 (1985).
42. P. Wiedemann, K. Lemmen, R. Schmiedl, and K. Heimann, *Am. J. Ophthalmol.* **104**, 10–14 (1987).
43. J.A. Khawly, P. Saloupis, D.L. Hatchell, and R. Machemer, *Graefe's Arch. Clin. Exp. Ophthalmol.* **229**, 464–467 (1991).
44. M. Kirmani et al., *Retina* **3**, 269–272 (1983).
45. M. Santana et al., *Graefe's Arch. Clin. Exp. Ophthalmol.* **221**, 210–213 (1984).
46. F.M. van Bockxmeer, C.E. Martin, D.E. Thompson, and I.J. Constable, *Invest. Ophthalmol. Visual Sci.* **26**, 1140–1147 (1985).
47. M. Lemor, J.H. Yeo, and B.M. Glaser, *Arch. Ophthalmol. (Chicago)* **104**, 1226–1229 (1986).
48. C. Davidson, W.R. Green, and V.G. Wong, *Invest. Ophthalmol. Visual Sci.* **24**, 301–311 (1983).
49. A.A. Deshpande, C. Tabatabay, and R. Gurny, *J. Controlled Release* **48**, 115–129 (1997).
50. J.J. Araiz et al., *Invest. Ophthalmol. Visual Sci.* **34**, 522–530 (1993).
51. M. Nakagawa et al., *Invest. Ophthalmol. Visual Sci.* **36**, 2388–2395 (1995).
52. G.A. Peyman et al., *Ophthalmic Surg.* **15**, 844–846 (1984).
53. G.A. Peyman et al., *Ophthalmic Surg.* **15**, 411–413 (1984).
54. D.E. Henderley, W.R. Freeman, D.M. Causey, and N.A. Rao, *Ophthalmology* **94**, 425–434 (1987).
55. R.F. Sison et al., *Am. J. Ophthalmol.* **112**, 243–249 (1991).
56. J.A. Schulman et al., *Jpn. J. Ophthalmol.* **30**, 116–124 (1986).
57. J.A. Schulman et al., *Ophthalmic Surg.* **17**, 429–432 (1986).
58. G.N. Holland et al., *Ophthalmology* **94**, 815–823 (1987).
59. D.A. Jabs, C. Newman, S. de Bustros, and B.F. Polk, *Ophthalmology* **94**, 824–830 (1987).
60. H.L. Hennis, A.A. Scott, and D.J. Apple, *Surv. Ophthalmol.* **34**, 193–203 (1989).
61. D.A. Jabs, C. Enger, and J.G. Bartlett, *Arch. Ophthalmol. (Chicago)* **107**, 75–80 (1989).
62. G.N. Holland et al., *Arch. Ophthalmol. (Chicago)* **107**, 1759–1766 (1989).
63. D.J. D'Amico et al., *Arch. Ophthalmol. (Chicago)* **104**, 1788–1793 (1986).
64. J.S. Pulido, G.A. Peyman, T. Lesar, and J. Vernot, *Arch. Ophthalmol. (Chicago)* **103**, 840–841 (1985).
65. M.H. Heinemann, *Arch. Ophthalmol. (Chicago)* **107**, 1767–1772 (1989).
66. I. Cochereau-Massin et al., *Ophthalmology* **98**, 1348–1355 (1991).
67. P. Lehoang et al., *Ophthalmology* **96**, 865–874 (1989).
68. M.A. Jacobson and J.J. O'Donnell, *J. AIDS* **4**, S11–S15 (1991).
69. W.L. Drew et al., *J. Infect. Dis.* **163**, 716–719 (1991).
70. M. Diaz-Llopis et al., *Am. J. Ophthalmol.* **114**, 742–747 (1992).
71. P. Berthe et al., *Invest. Ophthalmol. Visual Sci.* **35**, 1038–1045 (1994).
72. D.R. Guyer et al., *Arch. Ophthalmol. (Chicago)* **107**, 868–874 (1989).
73. L.S. Kirsch et al., *Ophthalmology* **102**, 533–543 (1995).
74. D.A. Jabs, *Arch. Ophthalmol. (Chicago)* **115**, 785–786 (1997).
75. E. Chavez de la Paz et al., *Ophthalmology* **104**, 539–544 (1997).
76. T.P. Margolis et al., *Am. J. Ophthalmol.* **112**, 119–131 (1991).
77. J.H. Yeo et al., *Ophthalmology* **93**, 1418–1422 (1986).
78. D.A. Jabs et al., *Retina* **7**, 9–13 (1987).
79. T.A. Meredith, in S.J. Ryan, ed., *Retina*, Mosby, St. Louis, Mo., 1989, pp. 183–188.
80. C.A. Puliafito, A.S. Baker, J. Haaf, and C.S. Foster, *Ophthalmology* **89**, 921–929 (1982).
81. H.C. Boldt et al., *Ophthalmology* **96**, 1722–1726 (1989).
82. A. Tarkkanen, V. Tommila, O. Valle, and I. Raivio, *Br. J. Ophthalmol.* **51**, 188–192 (1967).

83. R.K. Forster, R.L. Abbott, and H. Gelender, *Ophthalmology* **87**, 313–319 (1980).
84. M. Neveu and A.J. Elliott, *Am. J. Ophthalmol.* **48**, 358–373 (1959).
85. G.A. Peyman, D. Sanders, and M. Goldberg, *Advances in Uveal Surgery, Vitreous Surgery, Treatment of Endophthalmitis*, Appleton-Century-Crofts, New York, 1975.
86. M. Barza, A. Kane, and J.L. Baum, *Invest. Ophthalmol. Visual Sci.* **24**, 1602–1606 (1983).
87. M.J. Daily, G.A. Peyman, and G. Fishman, *Am. J. Ophthalmol.* **76**, 343–350 (1973).
88. R.T. Kasbeer and G.A. Peyman, *Graefe's Arch. Clin. Exp. Ophthalmol.* **196**, 279–287 (1975).
89. J.P. Duguid et al., *Br. J. Ophthalmol.* **31**, 193–211 (1947).
90. W. Philipp et al., *Graefe's Arch. Clin. Exp. Ophthalmol.* **228**, 475–480 (1990).
91. K. Mochizuki et al., *Ophthalmic Res.* **24**, 150–154 (1992).
92. R.K. Shockley et al., *Arch. Ophthalmol. (Chicago)* **102**, 1236–1238 (1984).
93. J.J. Rutgard, R.A. Berkowitz, and G.A. Peyman, *Ann. Ophthalmol.* **10**, 293–298 (1978).
94. N.H. Leeds, G.A. Peyman, and B. House, *Ophthalmic Surg.* **13**, 653–656 (1982).
95. P. Nelsen, G.A. Peyman, and T.O. Bennett, *Am. J. Ophthalmol.* **78**, 82–89 (1974).
96. L.M. Cobo and R.K. Forster, *Am. J. Ophthalmol.* **92**, 59–62 (1981).
97. G.A. Peyman, D.R. May, E.S. Ericson, and D. Apple, *Arch. Ophthalmol. (Chicago)* **92**, 42–47 (1974).
98. H. Sloane, G.A. Peyman, M. Raichand, and S. West, *Can. J. Ophthalmol.* **16**, 22–26 (1981).
99. T.O. Bennett and G.A. Peyman, *Graefe's Arch. Clin. Exp. Ophthalmol.* **191**, 93–107 (1974).
100. M. Barza and M. McCue, *Antimicrob. Agents Chemother.* **24**, 468–473 (1983).
101. J. Koziol and G.A. Peyman, *Can. J. Ophthalmol.* **9**, 316–321 (1974).
102. P.A. Pearson, D.P. Hainsworth, and P. Ashton, *Retina* **13**, 326–330 (1993).
103. J.T. Paque and G.A. Peyman, *Ophthalmic Surg.* **5**, 34–39 (1974).
104. H. Meisels and G.A. Peyman, *Ann. Ophthalmol.* **8**, 939–943 (1976).
105. A.G. Schenk and G.A. Peyman, *Graefe's Arch. Clin. Exp. Ophthalmol.* **190**, 281–292 (1974).
106. M.A. Smith et al., *Ophthalmology* **93**, 1328–1335 (1986).
107. R.O. Graham and G.A. Peyman, *Arch. Ophthalmol. (Chicago)* **92**, 149–154 (1974).
108. G.A. Peyman, in I.K. Reddy, ed., *Ocular Therapeutics and Drug Delivery. A Multi-disciplinary Approach*, Technomic Publishing, Basel, 1996, pp. 265–282.
109. J.A. Schulman and G.A. Peyman, in A.K. Mitra, ed., *Ophthalmic Drug Delivery Systems*, Dekker, New York, 1993, pp. 383–425.
110. G.A. Peyman and S.S. Bassili, *Ophthalmic Surg.* **26**, 294–303 (1995).
111. R.B. Nussenblatt et al., *Arch. Ophthalmol. (Chicago)* **100**, 1146–1149 (1982).
112. R.B. Nussenblatt, A.G. Palestine, and C.C. Chan, *Am. J. Ophthalmol.* **96**, 275–282 (1983).
113. G. Striph, B. Doft, B. Rabin, and B. Johnson, *Arch. Ophthalmol. (Chicago)* **104**, 114–117 (1986).
114. R.B. Nussenblatt and A.G. Palestine, *Surv. Ophthalmol.* **31**, 159–169 (1986).
115. R.B. Nussenblatt et al., *Am. J. Ophthalmol.* **115**, 583–591 (1993).
116. D. BenEzra, G. Maftzir, C. de Courten, and P. Timonen, *Br. J. Ophthalmol.* **74**, 350–352 (1990).
117. R.B. Nussenblatt et al., *Arch. Ophthalmol. (Chicago)* **103**, 1559–1562 (1985).
118. J. Grisolano and G.A. Peyman, *Ophthalmic Surg.* **17**, 155–156 (1986).
119. J. Heller, *Biomaterials* **1**, 51–57 (1980).
120. A.A. Deshpande, J. Heller, and R. Gurny, *Crit. Rev. Ther. Drug Carr. Sys.* **15**, 381–420 (1998).
121. A. Merkli, C. Tabatabay, and R. Gurny, *Eur. J. Pharm. Biophys.* **16**, 51–283 (1995).
122. N.A. Peppas, in N.A. Peppas, ed., *Hydrogels in Medicine and Pharmacy*, CRC Press, Boca Raton, Fla., 1987, pp. 1–48.
123. D.P. Hainsworth et al., *J. Ocul. Pharmacol.* **12**, 183–191 (1996).
124. H. Kobayashi, K. Shiraki, and Y. Ikada, *J. Biomed. Mater. Res.* **26**, 1463–1476 (1992).
125. M. Vert, P. Christel, F. Chabot, and J. Leray, in G.W. Hastings and P. Ducheyne, eds., *Macromolecular Biomaterials*, CRC Press, Boca Raton, Fla., 1984, pp. 119–142.
126. M.B. Sintzel, S.B. Bernatchez, C. Tabatabay, and R. Gurny, *Eur. J. Pharm. Biophys.* **42**, 358–374 (1996).
127. S.S. Shah, Y. Cha, and C.G. Pitt, *J. Controlled Release* **18**, 261–270 (1992).
128. N. Kunou et al., *J. Controlled Release* **37**, 143–150 (1995).
129. P.E. Rubsamen et al., *Arch. Ophthalmol. (Chicago)* **112**, 407–413 (1994).
130. H. Kimura et al., *Invest. Ophthalmol. Visual Sci.* **35**, 2815–2819 (1994).
131. M. Hashizoe et al., *Curr. Eye Res.* **14**, 473–477 (1995).
132. R.E. Foster et al., *Invest. Ophthalmol. Visual Sci.* **37**, (Abstr.) S196 (1996).
133. M. Hashizoe et al., *Invest. Ophthalmol. Visual Sci.* **34**, (Abstr.) 1489 (1993).
134. M. Hashizoe et al., *Arch. Ophthalmol. (Chicago)* **112**, 1380–1384 (1994).
135. N. Kunou et al., *Invest. Ophthalmol. Visual Sci.* **37**, (Abstr.) S41 (1996).
136. H. Miyamoto et al., *Curr. Eye Res.* **16**, 930–935 (1997).
137. M. Hashizoe et al., *Curr. Eye Res.* **16**, 633–639 (1997).
138. R. Gurny et al., *Eur. J. Hosp. Pharm.* **3**, 15–19 (1993).
139. P. Davis, K. Kiss, J.M. Parel, and S.W. Cousins, *Invest. Ophthalmol. Visual Sci.* **33**, (Abstr.) 727 (1992).
140. B. Conti et al., *Eur. J. Pharm. Sci.* **5**, 287–293 (1997).
141. C.G. Pitt and A. Schindler, in G.I. Zatuchni, A. Goldsmith, J.D. Shelton, and J.J. Sciarra, eds., *Long-acting Contraceptive Delivery Systems*, Harper & Row, Philadelphia, 1984, pp. 48–63.
142. D. Yang, M.H. Rahimy, and G.A. Peyman, *Invest. Ophthalmol. Visual Sci.* **34**, (Abstr.) 1493 (1993).
143. S. Chin, M.H. Rahimy, and G.A. Peyman, *Invest. Ophthalmol. Visual Sci.* **34**, (Abstr.) 1490 (1993).
144. H. Borhani, M.H. Rahimy, and G.A. Peyman, *Invest. Ophthalmol. Visual Sci.* **34**, (Abstr.) 1488 (1993).
145. H. Borhani, G.A. Peyman, M.H. Rahimy, and H. Thompson, *Int. Ophthalmol.* **19**, 43–49 (1995).

146. G.A. Peyman et al., *Ophthalmic Surg. Lasers* **27**, 384–391 (1996).
147. K.W. Leong, B.C. Brott, and R. Langer, *J. Biomed. Mater. Res.* **19**, 941–955 (1985).
148. D.A. Lee et al., *Ophthalmology* **94**, 1523–1530 (1987).
149. K.W. Leong, P. D'Amore, M. Marletta, and R. Langer, *J. Biomed. Mater. Res.* **20**, 51–64 (1986).
150. H. Lewis, S. Schwartz, D. Lee, and K. Leong, *Invest. Ophthalmol. Visual Sci.* **32**, (Abstr.) 1047 (1991).
151. J.I. Alonso et al., *Invest. Ophthalmol. Visual Sci.* **32**, (Abstr.) 1293 (1991).
152. A. Merkli, J. Heller, C. Tabatabay, and R. Gurny, *J. Biomater. Sci., Polym. Ed.* **4**, 505–516 (1993).
153. J. Heller, S.Y. Ng, B.K. Fritzinger, and K.V. Roskos, *Biomaterials* **11**, 235–237 (1990).
154. A. Merkli, J. Heller, C. Tabatabay, and R. Gurny, *J. Controlled Release* **29**, 105–112 (1994).
155. A. Merkli, J. Heller, C. Tabatabay, and R. Gurny, *J. Controlled Release* **33**, 415–421 (1995).
156. S.B. Bernatchez et al., *J. Biomed. Mater. Res.* **27**, 677–681 (1993).
157. S.B. Bernatchez et al., *J. Biomed. Mater. Res.* **28**, 1037–1046 (1994).
158. M. Zignani et al., *J. Controlled Rel.* **48**, 115–129 (1997).
159. M. Zignani et al., *J. Biomed. Mater. Res.* **39**, 277–285 (1998).
160. M. Zignani, T. Le Minh, C. Tabatabay, and R. Gurny, *Proceed. Int. Symp. Control. Rel. Bioact. Mater.* **24**, 907–908 (1997).
161. A. Merkli, J. Heller, C. Tabatabay, and R. Gurny, *Pharm. Res.* **11**, 1485–1491 (1994).
162. M.B. Stinzel, A. Merkli, C. Tabatabay, and R. Gurny, *Drug Dev. Ind. Pharm.* **23**, 857–878 (1997).
163. M.B. Stinzel et al., *Int. J. Pharm.* **175**, 165–176 (1998).
164. S.Y. Ng, T. Vandamme, M.S. Taylor, and J. Heller, *Macromolecules* **30**, 770–772 (1997).
165. M.B. Stinzel et al., *Biomater.* **19**, 791–800 (1998).
166. M.B. Stinzel et al., *J. Controlled Release* **55**, 213–218 (1998).
167. B.B. Pharriss et al., *J. Reprod. Med.* **17**, 91–97 (1976).
168. R.L. Friederich, *Ann. Ophthalmol.* **6**, 1279–1274 (1974).
169. P. Ashton et al., *J. Ocul. Pharmacol.* **10**, 691–701 (1994).
170. T.J. Smith et al., *Arch. Ophthalmol. (Chicago)* **110**, 255–258 (1992).
171. G.E. Sanborn et al., *Arch. Ophthalmol. (Chicago)* **110**, 188–195 (1992).
172. R. Anand et al., *Arch. Ophthalmol. (Chicago)* **111**, 223–227 (1993).
173. D.F. Martin et al., *Arch. Ophthalmol. (Chicago)* **112**, 1531–1539 (1994).
174. P.A. Pearson et al., *Arch. Ophthalmol. (Chicago)* **114**, 311–317 (1996).
175. L.B. Enyedi, P.A. Pearson, P. Ashton, and G.J. Jaffe, *Curr. Eye Res.* **15**, 549–557 (1996).
176. C.K. Cheng et al., *Invest. Ophthalmol. Visual Sci.* **36**, 442–453 (1995).
177. D.P. Hainsworth, P.A. Pearson, J.D. Conklin, and P. Ashton, *J. Ocul. Pharmacol.* **12**, 57–63 (1996).
178. P. Ashton et al., *J. Ocul. Pharmacol.* **8**, 343–347 (1992).
179. R. Anand, R.L. Font, R.H. Fish, and S.D. Nightingale, *Ophthalmology* **100**, 1032–1039 (1993).
180. N.C. Charles and G.C. Steiner, *Ophthalmology* **103**, 416–421 (1996).
181. M.G. Morley, J.S. Duker, P. Ashton, and M.R. Robinson, *Ophthalmology* **102**, 388–392 (1995).
182. J. Chen and P. Ashton, *Proc. Int. Symp. Controlled Release Bioact. Mater.* **24**, 619–620 (1997).
183. J. Chen et al., *Invest. Ophthalmol. Visual Sci.* **37**, S41 (1996).
184. P.A. Pearson, L.B. Enyedi, G.J. Jaffe, and P. Ashton, *Invest. Ophthalmol. Visual Sci.* **35**, (Abstr.) 1923 (1994).
185. M.H. Rahimy et al., *J. Drug Target.* **2**, 289–298 (1994).
186. M.H. Rahimy et al., *J. Ocul. Pharmacol.* **10**, 561–570 (1994).
187. P.A. Cibis, B. Becker, E. Okun, and S. Canaan, *Arch. Ophthalmol. (Chicago)* **68**, 590–599 (1962).
188. Q.H. Nguyen et al., *Opthalmology* **99**, 1520–1526 (1992).
189. M.H. Arroyo et al., *Retina* **13**, 13, 245–250 (1993).
190. A. Zimmer and J. Kreuter, *Adv. Drug Delivery Rev.* **16**, 61–73 (1995).
191. A. Joshi, *J. Ocul. Pharmacol.* **10**, 29–45 (1994).
192. M.S. El-Samaligy et al., *Drug Delivery* **3**, 93–97 (1996).
193. B. Khoobehi, M.O. Stradtmann, G.A. Peyman, and O.M. Aly, *Ophthalmic Surg.* **22**, 175–180 (1991).
194. B. Khoobehi, M.O. Stradtmann, G.A. Peyman, and O.M. Aly, *Ophthalmic Surg.* **21**, 840–844 (1990).
195. G.G. Giordano, P. Chevez-Barrios, M.F. Refojo, and C.A. Garcia, *Curr. Eye Res.* **14**, 761–768 (1995).
196. H. Kimura et al., *Invest. Ophthalmol. Visual Sci.* **33**, 3436–3441 (1992).
197. C.A. Harper et al., *Int. Ophthalmol.* **17**, 337–340 (1993).
198. T. Moritera et al., *Invest. Ophthalmol. Visual Sci.* **32**, 1785–1790 (1991).
199. T. Moritera et al., *Invest. Ophthalmol. Visual Sci.* **33**, 3125–3130 (1992).
200. G.A. Peyman, M. Conway, B. Khoobehi, and K. Soike, *Int. Ophthalmol.* **16**, 109–113 (1992).
201. G.G. Giordano, M.F. Refojo, and M.H. Arroyo, *Invest. Ophthalmol. Visual Sci.* **34**, 2743–2751 (1993).
202. A.A.S. Veloso, Q. Zhu, R. Herrero-Vanrell, and M.F. Refojo, *Invest. Ophthalmol. Visual Sci.* **38**, 665–675 (1997).
203. H. Kimura et al., *Invest. Ophthalmol. Visual Sci.* **33**, (Abstr.) 1013 (1992).
204. M. Barza, M. Stuart, and F. Szoka, *Invest. Ophthalmol. Visual Sci.* **28**, 893–900 (1987).
205. W.H. Stern et al., *Invest. Ophthalmol. Visual Sci.* **28**, 907–911 (1987).
206. V.H.L. Lee, P.T. Urrea, R.E. Smith, and D.J. Schanzlin, *Surv. Ophthalmol.* **29**, 335–348 (1985).
207. D. Meisner and M. Mezei, *Adv. Drug Delivery Rev.* **16**, 75–93 (1995).
208. P.H. Fishman, G.A. Peyman, and T. Lesar, *Invest. Ophthalmol. Visual Sci.* **27**, 1103–1106 (1986).
209. R.G. Fiscella, G.A. Peyman, and P.H. Fishman, *Can. J. Ophthalmol.* **22**, 307–309 (1987).
210. V.S. Rao, G.A. Peyman, B. Khoobehi, and S. Vangipuram, *Int. Ophthalmol.* **13**, 181–185 (1989).
211. E.K. Kim and H.B. Kim, *Yonsei Med. J.* **31**, 308–314 (1990).
212. S. Zeng et al., *Ophthalmology* **100**, 1640–1644 (1993).
213. C. Tremblay et al., *Invest. Ophthalmol. Visual Sci.* **26**, 711–718 (1985).
214. M. Barza et al., *Am. J. Ophthalmol.* **100**, 259–263 (1985).
215. K.R. Liu, G.A. Peyman, and B. Khoobehi, *Invest. Ophthalmol. Visual Sci.* **30**, 1527–1534 (1989).

Next Page

216. K.R. Liu et al., *Ophthalmology* **94**, 1155–1159 (1987).
217. G.A. Peyman et al., *Retina* **7**, 227–229 (1987).
218. M. Diaz-Llopis et al., *Doc. Ophthalmol.* **82**, 297–305 (1992).
219. S.K. Akula et al., *Br. J. Ophthalmol.* **78**, 677–680 (1994).
220. C. Le Bourlais et al., *J. Microencapsul.* **13**, 473–480 (1996).
221. S. Shakiba et al., *Invest. Ophthalmol. Visual Sci.* **34**, 2903–2910 (1993).
222. H.O.C. Gümbel et al., *2nd Int. Symp. Exp. Clin. Ocul. Pharmacol. Pharm.* Munich, Germany, September 11–14, 1997, p. 16.
223. G. Besen et al., *Arch. Ophthalmol. (Chicago)* **113**, 661–668 (1995).
224. B.D. Kuppermann et al., *J. Infect. Dis.* **173**, 18–23 (1996).
225. A.A. Alghadyan et al., *Int. Ophthalmol.* **12**, 109–112 (1988).
226. B.C. Joondeph, B. Khoobehi, G.A. Peyman, and B.Y. Yue, *Ophthalmic Surg.* **19**, 252–256 (1988).
227. K.K. Assil et al., *Invest. Ophthalmol. Visual Sci.* **32**, 2891–2897 (1991).
228. R.F. Gariano et al., *Retina* **14**, 75–80 (1994).
229. J. Garcia-Arumi et al., *Ophthalmologica* **211**, 344–350 (1997).
230. K.R. Liu et al., *Ophthalmic Surg.* **20**, 358–361 (1989).
231. T.D. Heath, N.G. Lopez, G.P. Lewis, and W.H. Stern, *Invest. Ophthalmol. Visual Sci.* **28**, 1365–1372 (1987).
232. B. Khoobehi et al., *Ophthalmology* **95**, 950–955 (1988).
233. B. Khoobehi, G.A. Peyman, M.R. Niesman, and M. Oncel, *Jpn. J. Ophthalmol.* **33**, 405–412 (1989).
234. Y. Ogura et al., *Invest. Ophthalmol. Visual Sci.* **32**, 2351–2356 (1991).
235. G.A. Peyman et al., *Int. Ophthalmol.* **12**, 175–182 (1988).
236. D. Sarraf and D.A. Lee, *J. Ocul. Pharmacol.* **10**, 69–81 (1994).
237. J.M. Hill, R.J. O'Callaghan, and J.A. Hobden, in A.K. Mitra, ed., *Ophthalmic Drug Delivery Systems*, Dekker, New York, 1993, pp. 331–354.
238. L. Hughes and D.M. Maurice, *Arch. Ophthalmol. (Chicago)* **102**, 1825–1829 (1984).
239. M. Barza, C. Peckman, and J. Baum, *Ophthalmology* **93**, 133–139 (1986).
240. T.B. Choi and D.A. Lee, *J. Ocul. Pharmacol.* **4**, 153–164 (1988).
241. P.H. Fishman et al., *Invest. Ophthalmol. Visual Sci.* **25**, 343–345 (1984).
242. V. Baeyens et al., *Adv. Drug Deliv. Rev.* **28**, 335–361 (1997).
243. N.L. Burstein, I.H. Leopold, and D.B. Bernacchi, *J. Ocul. Pharmacol.* **1**, 363–368 (1985).
244. M. Barza, C. Peckman, and J. Baum, *Invest. Ophthalmol. Visual Sci.* **28**, 1033–1036 (1987).
245. R.E. Grossman, D.F. Chu, and D.A. Lee, *Invest. Ophthalmol. Visual Sci.* **31**, 909–916 (1990).
246. M.O. Yoshizumi et al., *J. Ocul. Pharmacol.* **7**, 163–167 (1991).
247. R. Grossman and D.A. Lee, *Ophthalmology* **96**, 724–729 (1989).
248. T.T. Lam, D.P. Edward, X.A. Zhu, and M.O.M. Tso, *Arch. Ophthalmol. (Chicago)* **107**, 1368–1371 (1989).
249. F.F. Behar-Cohen et al., *Exp. Eye Res.* **65**, 533–545 (1997).
250. T.T. Lam et al., *J. Ocul. Pharmacol.* **10**, 571–575 (1994).
251. D. Sarraf et al., *Am. J. Ophthalmol.* **115**, 748–754 (1993).
252. M.O. Yoshizumi et al., *Am. J. Ophthalmol.* **122**, 86–90 (1996).
253. D.M. Maurice, *Ophthalmology* **93**, 128–131 (1986).
254. T.T. Lam, J. Fu, and M.O.M. Tso, *Graefe's Arch. Clin. Exp. Ophthalmol.* **223**, 389–394 (1991).
255. A. Albert, *Nature* **182**, 421–423 (1958).
256. L.L. Christrup, J. Moss, and B. Steffansen, in J. Swarbrick and J.C. Boylan, eds., *Encyclopedia of Pharmaceutical Technology*, Dekker, New York, 1996, pp. 39–70.
257. V.H.L. Lee and V.H.K. Li, *Adv. Drug Delivery Rev.* **3**, 1–38 (1989).
258. B. Steffansen, P. Ashton, and A. Buur, *Int. J. Pharm.* **132**, 243–250 (1996).
259. I. Taskintuna et al., *Retina* **17**, 57–64 (1997).
260. S. Shakiba et al., *Antimicrob. Agents Chem.* **39**, 1383–1385 (1995).
261. A.S. Berger et al., *Invest. Ophthalmol. Visual Sci.* **37**, 2318–2325 (1996).
262. H. Guo et al., *Invest. Ophthalmol. Visual Sci.* **35**, 1907 (1994).

See also BIOADHESIVE DRUG DELIVERY SYSTEMS; MUCOSAL DRUG DELIVERY, BUCCAL; MUCOSAL DRUG DELIVERY, NASAL; MUCOSAL DRUG DELIVERY, OCULAR; MUCOSAL DRUG DELIVERY, VAGINAL DRUG DELIVERY AND TREATMENT MODALITIES.

MUCOSAL DRUG DELIVERY, NASAL

PAOLO COLOMBO
University of Parma
Parma, Italy

KEY WORDS

Butorphanol
Calcitonin
Desmopressin
Drug delivery
Enhancer
Inhalation
Insufflator
Insulin
Nasal route
Particle size
Powder
Spray
Sumatriptan

OUTLINE

Introduction
Nasal Delivery: Historical and Behavioral Use
Anatomy and Physiology of the Nose
Toxicological Considerations
Dosage Forms and Materials
Metering and Insufflators
Qualitative and Quantitative Aspects of Nasal Dose Delivery

216. K.R. Liu et al., *Ophthalmology* **94**, 1155–1159 (1987).
217. G.A. Peyman et al., *Retina* **7**, 227–229 (1987).
218. M. Diaz-Llopis et al., *Doc. Ophthalmol.* **82**, 297–305 (1992).
219. S.K. Akula et al., *Br. J. Ophthalmol.* **78**, 677–680 (1994).
220. C. Le Bourlais et al., *J. Microencapsul.* **13**, 473–480 (1996).
221. S. Shakiba et al., *Invest. Ophthalmol. Visual Sci.* **34**, 2903–2910 (1993).
222. H.O.C. Gümbel et al., *2nd Int. Symp. Exp. Clin. Ocul. Pharmacol. Pharm.* Munich, Germany, September 11–14, 1997, p. 16.
223. G. Besen et al., *Arch. Ophthalmol. (Chicago)* **113**, 661–668 (1995).
224. B.D. Kuppermann et al., *J. Infect. Dis.* **173**, 18–23 (1996).
225. A.A. Alghadyan et al., *Int. Ophthalmol.* **12**, 109–112 (1988).
226. B.C. Joondeph, B. Khoobehi, G.A. Peyman, and B.Y. Yue, *Ophthalmic Surg.* **19**, 252–256 (1988).
227. K.K. Assil et al., *Invest. Ophthalmol. Visual Sci.* **32**, 2891–2897 (1991).
228. R.F. Gariano et al., *Retina* **14**, 75–80 (1994).
229. J. Garcia-Arumi et al., *Ophthalmologica* **211**, 344–350 (1997).
230. K.R. Liu et al., *Ophthalmic Surg.* **20**, 358–361 (1989).
231. T.D. Heath, N.G. Lopez, G.P. Lewis, and W.H. Stern, *Invest. Ophthalmol. Visual Sci.* **28**, 1365–1372 (1987).
232. B. Khoobehi et al., *Ophthalmology* **95**, 950–955 (1988).
233. B. Khoobehi, G.A. Peyman, M.R. Niesman, and M. Oncel, *Jpn. J. Ophthalmol.* **33**, 405–412 (1989).
234. Y. Ogura et al., *Invest. Ophthalmol. Visual Sci.* **32**, 2351–2356 (1991).
235. G.A. Peyman et al., *Int. Ophthalmol.* **12**, 175–182 (1988).
236. D. Sarraf and D.A. Lee, *J. Ocul. Pharmacol.* **10**, 69–81 (1994).
237. J.M. Hill, R.J. O'Callaghan, and J.A. Hobden, in A.K. Mitra, ed., *Ophthalmic Drug Delivery Systems*, Dekker, New York, 1993, pp. 331–354.
238. L. Hughes and D.M. Maurice, *Arch. Ophthalmol. (Chicago)* **102**, 1825–1829 (1984).
239. M. Barza, C. Peckman, and J. Baum, *Ophthalmology* **93**, 133–139 (1986).
240. T.B. Choi and D.A. Lee, *J. Ocul. Pharmacol.* **4**, 153–164 (1988).
241. P.H. Fishman et al., *Invest. Ophthalmol. Visual Sci.* **25**, 343–345 (1984).
242. V. Baeyens et al., *Adv. Drug Deliv. Rev.* **28**, 335–361 (1997).
243. N.L. Burstein, I.H. Leopold, and D.B. Bernacchi, *J. Ocul. Pharmacol.* **1**, 363–368 (1985).
244. M. Barza, C. Peckman, and J. Baum, *Invest. Ophthalmol. Visual Sci.* **28**, 1033–1036 (1987).
245. R.E. Grossman, D.F. Chu, and D.A. Lee, *Invest. Ophthalmol. Visual Sci.* **31**, 909–916 (1990).
246. M.O. Yoshizumi et al., *J. Ocul. Pharmacol.* **7**, 163–167 (1991).
247. R. Grossman and D.A. Lee, *Ophthalmology* **96**, 724–729 (1989).
248. T.T. Lam, D.P. Edward, X.A. Zhu, and M.O.M. Tso, *Arch. Ophthalmol. (Chicago)* **107**, 1368–1371 (1989).
249. F.F. Behar-Cohen et al., *Exp. Eye Res.* **65**, 533–545 (1997).
250. T.T. Lam et al., *J. Ocul. Pharmacol.* **10**, 571–575 (1994).
251. D. Sarraf et al., *Am. J. Ophthalmol.* **115**, 748–754 (1993).
252. M.O. Yoshizumi et al., *Am. J. Ophthalmol.* **122**, 86–90 (1996).
253. D.M. Maurice, *Ophthalmology* **93**, 128–131 (1986).
254. T.T. Lam, J. Fu, and M.O.M. Tso, *Graefe's Arch. Clin. Exp. Ophthalmol.* **223**, 389–394 (1991).
255. A. Albert, *Nature* **182**, 421–423 (1958).
256. L.L. Christrup, J. Moss, and B. Steffansen, in J. Swarbrick and J.C. Boylan, eds., *Encyclopedia of Pharmaceutical Technology*, Dekker, New York, 1996, pp. 39–70.
257. V.H.L. Lee and V.H.K. Li, *Adv. Drug Delivery Rev.* **3**, 1–38 (1989).
258. B. Steffansen, P. Ashton, and A. Buur, *Int. J. Pharm.* **132**, 243–250 (1996).
259. I. Taskintuna et al., *Retina* **17**, 57–64 (1997).
260. S. Shakiba et al., *Antimicrob. Agents Chem.* **39**, 1383–1385 (1995).
261. A.S. Berger et al., *Invest. Ophthalmol. Visual Sci.* **37**, 2318–2325 (1996).
262. H. Guo et al., *Invest. Ophthalmol. Visual Sci.* **35**, 1907 (1994).

See also BIOADHESIVE DRUG DELIVERY SYSTEMS; MUCOSAL DRUG DELIVERY, BUCCAL; MUCOSAL DRUG DELIVERY, NASAL; MUCOSAL DRUG DELIVERY, OCULAR; MUCOSAL DRUG DELIVERY, VAGINAL DRUG DELIVERY AND TREATMENT MODALITIES.

MUCOSAL DRUG DELIVERY, NASAL

PAOLO COLOMBO
University of Parma
Parma, Italy

KEY WORDS

Butorphanol
Calcitonin
Desmopressin
Drug delivery
Enhancer
Inhalation
Insufflator
Insulin
Nasal route
Particle size
Powder
Spray
Sumatriptan

OUTLINE

Introduction
Nasal Delivery: Historical and Behavioral Use
Anatomy and Physiology of the Nose
Toxicological Considerations
Dosage Forms and Materials
Metering and Insufflators
Qualitative and Quantitative Aspects of Nasal Dose Delivery

Penetration Enhancers and Bioadhesion
Drugs Developed for Nasal Administration
Butorphanol
Calcitonin
Dihydroergotamine
Sumatriptan
Desmopressin
Cromolyn Sodium
Steroid Drugs
The Insulin Case and Future Developments: Vaccines and Brain Targeting Through the Nose
Acknowledgments
Bibliography

INTRODUCTION

This article intends to update the state of the art of nasal drug delivery from a pharmaceutical and technological point of view. Many important contributions can be found in literature on the subject, focusing on different aspects of interest to researchers, such as the Proctor edited book (1), the edited and directly contributed books of Chien (2,3), and the reviews of Illum (4), Wilson (5), Edman (6), Merkus (7), Gizurarson (8), Duchene (9), Harris (10), Buri (11), and Alpar (12).

A Nasal Drug Delivery Focus Group, organized in an American Association of Pharmaceutical Scientists section (13), has also been constituted as well as an Open Forum for free exchange and information in all R and D areas ranging from the formulation to the marketing of nasal preparations.

NASAL DELIVERY: HISTORICAL AND BEHAVIORAL USE

New materials and new technologies have stimulated pharmaceutical researchers to identify and use alternatives to the classical oral and injectable routes. One of the routes currently being studied is the nasal way, even though the physiological evolution of the nose followed the olfactive and respiratory necessity to provide humid, warmed, and filtered air for the lungs. In fact, nasal mucosa evolved in order to have a wide surface, large blood supply, and efficient filtering system. Because the mucosa is often affected by various diseases that alter its functionality, the first nasal drug delivery system was for restoring normal nasal conditions. Man discovered the possibility of using nasal mucosa for absorbing substances giving systemic effects. Unfortunately, the most convincing examples of systemic effects obtained by administering active principles inside the nose were those which misused the nose, such as the behavioral habit of sniffing cocaine or tobacco. An instructive behavioral employment of the nose for drug absorption, usually in order to have hallucinations or more general mental effects, is the religious rite of the Amazonian population of Yanomamo to assume *epenà*, that, is a powdered mixture of different plant parts like *Mimosa acacioides*, *Piptadenia peregrina*, and others not identified (14). The interest of this rite for pharmaceutical researchers is linked to the administration devices the natives use in order to deposit the powdered drug in the nose (Fig. 1). The devices consist of an insufflator having the form of a long linear pipe activated by an assistant or, alternatively, a Y-shaped curved tube which allows for self-administration. These "medical devices" focalize the typical aspect of nasal delivery that is the need for a nebulizer or an insufflator for depositing solid or liquid formulations into the nose.

All these uses, or misuses, of the nose for systemic drug delivery have provided a lot of important information as to the employment of the nasal route for therapeutically drug delivery. The effects, and in particular, the toxicity manifested by the mucosa in response to drug deposition are of paramount importance for setting the therapeutical delivery of drugs in terms of safety and efficacy. From these experiences it is worthwhile underlining some aspects that are particularly useful for the design of therapy and dosage form for the nose. The rapid onset of the effect is linked to high mucosa permeability and indicates using the nose for therapies requiring prompt response. Then, the maniacal use of the nose because of the effects involving the brain opens the possibility of directly reaching the brain after deposition on the olfactory mucosa. Finally, the fact that drugs are successfully administered in powder form increases the formulation possibilities for designing the appropriate dosage form.

ANATOMY AND PHYSIOLOGY OF THE NOSE

The nose is characterized by two nasal cavities, separated by a septum and divided into three main regions: vestibule (nostril), atrium (or preturbinate region), and turbinate region (15). The last region is composed of an olfactory upper part and of two respiratory medium and lower parts that join together in the rhinopharynx. The turbinate region is characterized by cornets and meati, gaps situated between cornets and the nasal external part. The nostrils are the entry of the nasal cavity.

The nose presents sensitive, vegetative, and sensorial nervous conduction. The trigeminal nerves respond to al-

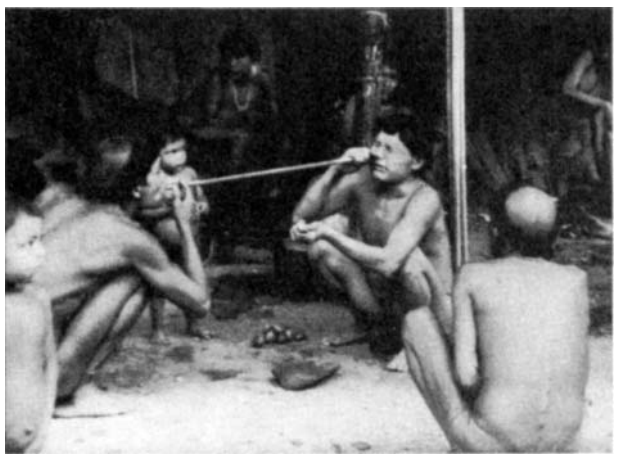


Figure 1. Yanomano Indian tribe using the insufflator pipe for *epenà* nasal administration.

lergic stimulus causing sneezing; the vegetative system provides secretory and vasomobility functions, and particular elements of the olfactory mucosa control the activity of sensorial nerves.

Nasal cavities are covered by respiratory mucosa that, within the nostrils, is characterized by a stratified, squamous and keratinized epithelium, with hairs, called vibrissae. Beyond the limen nasi, the epithelium loses its keratin cover and becomes the respiratory mucosa with pluristratified cylindrical epithelium. It is provided with vibratile cilia and other mucus secreting cells. Goblet cells and submucosa glands produce a high amount of mucus, which is the protective barrier against external agents. The continuous film of mucus is structured in two layers: the lower one is smooth with low viscosity, the upper one is more viscous and elastic and moves following the cilia movements.

The nose, which has an extensive vascular network, has two main functions: the sense of smell given by the olfactory mucosa and the inspired air conditioning by purification, heating, and moisture regulation. The greatest particles are removed by the vibrissae of the vestibule. Other particles are removed by the anatomic structures of the nasal cavities. The combined action of the cilia and mucus layer is called mucociliary clearance, an important defense mechanism against inhaled dust, allergens, and microorganisms. The coordinated beating of the cilia results in the movement of the upper mucus layer towards the nasopharynx, where it is swallowed. Finally, there is an air flow control because the respiratory air volumes are monitored by the cornets, which alternatively change their volume, giving a variable resistance to the breathed air.

TOXICOLOGICAL CONSIDERATIONS

The poor nasal bioavailability of many substances (in particular, peptide and protein drugs) can be substantially improved by the use of absorption enhancers. The acceptability of these enhancers is not only dependent on their promoting effect but also on their safety profile for systemic and local adverse effects (16–21). Nasal drug formulations must not alter the histology and physiology of the nose in the sense that the mucosa must retain its functionality as a barrier toward external substances and microorganisms. In any case, damage induced must be reversible. The histological toxicity refers to the alteration of mucosa, including membrane protein removal, cell loss, excessive mucus discharge, ciliotoxicity, and disturbance of the normal enzymatic balance (22,23). In addition, the dosage form and its components should not interfere with the mucociliary clearance.

Various methods have been used to test the toxicity of drugs and additives on the nasal mucosa and the mucociliary system. Traditionally, histopathological examination of a prefixed membrane specimen by light and scanning electron microscopy is regarded as the indicator of cytotoxicity. These methods suffer from inspector subjectivity and the impossibility of highlighting subtle changes in nasal mucosa and do not provide the nasal sensitivity tolerance measurement in response to a particular formulation. Therefore, in order to determine minute changes occurring in the mucosal tissue due to exposure to formulations, a biochemical approach has been developed (24). The extent of the release of total proteins, although not very specific as to the type of damage, provides a general indication about the extent of irritation.

The release of enzymes lactate dehydrogenase (LDH) and 5′nucleotidase (5′-ND), directly indicate the extent of damage suffered by the mucosa. Membrane-bound 5′-ND release in the nasal perfusate gives an indication of the level of membrane perturbation, whereas the cytosolic enzyme LDH indicates cell leaching and/or lysis (25).

Mucociliary transport and clearance interferences can be measured in vivo (26,27) or in vitro (28). Determination of ciliary beat frequency in vitro has been carried out on explants of ciliated mucosa from human adenoid tissue (29), from the trachea of different animal species (30,31), or from chicken embryo trachea (32). The frog palate preparation as an ex vivo model for the mucociliary transport velocity study has also been proposed for the indication of topical tolerability of different substances (33). Effects on the ciliary beat frequency detected in vitro may be more pronounced than the influence in vivo. In vitro experiments directly expose ciliated epithelia to test solution, whereas in vivo the cilia are protected by mucus (34). Therefore, in vitro ciliary beat frequency tests should be used as indicators for potential damage to nasal epithelium, rather than proof of such damage occurring in the in vivo situation. One of the best known in vivo tests is the saccharin transit time, i.e., the time required for the subject to taste a saccharin particle placed on the inferior turbinate of the naris (35). However, the most powerful method used for measuring the deposition and clearance of drugs in the nasal cavity remains scintigraphy.

DOSAGE FORMS AND MATERIALS

Nasal dosage forms consist of preparations containing dispersed or dissolved drugs, filled in a container designed to be squeezed or spray activated (36). The aim of delivery is to deposit the formula on the mucosa and coat the available surface, in particular the respiratory part, which is the major absorption site for drugs. Other therapeutic situations must require a localized accumulation of the product in certain districts of the nasal cavity. This can be achieved through an appropriate design of the insufflator and of the formulation to produce a fine dispersion of droplets or particles capable of sticking to the mucosa (37). This avoids the coalescence of the mist with a backflow of product and limits a fast transport to the pharynx by mucociliary clearance. Therefore, dispersion pattern and bioadhesion are the two key factors to be considered during the development phase of the formulation.

At present, the application of the product by spraying is very elegant and accepted. Therefore, the objective of formulation design is to obtain an aerosol useful for inspiration and deposition in the upper airways. In the past, drops were often instilled in the nose, but the advancement of insufflator technology has made this form obsolete and limited to pediatric use or to patients less able to perform

the insufflative maneuvers. Liquid preparations are common dosage forms for nasal delivery. Because the nasal epithelium is essentially a lipophilic transport barrier, transnasal transport is related to the nasal mucosa tissue–water partition coefficient, suggesting also an important role of the stereochemical conformation during membrane transport (38). Therefore, aspects such as formula pH, ionic strength, surface active agents, viscosity, and drug concentration have to be considered in order to facilitate the transport (39). However, from a technological point of view, the liquid preparations present problems linked to formula stability, low drug concentration at the absorption site, and short residence time in nasal cavity.

These drawbacks accelerated the development of nasal powders as alternative nasal dosage forms with improved chemicophysical and microbiological stability. Furthermore, drug dissolution on nasal mucosa provides elevated drug concentration at the deposition site, giving rise to a high flux of active ingredient. In many cases the superiority of nasal powder compared with nasal liquid was demonstrated, in particular with peptidic drugs (40–42). Administration of powders requires a nasal insufflator for dose emission and deposition of particles in the nose. It has been assessed that the site and pattern of inhalatory powder deposition in the respiratory tract are affected by the aerodynamic properties of the powder (43). Moreover, the formalities of dose delivery control the deposition mechanisms, i.e., inertial impacting, sedimentation, and diffusion. It could be postulated that efficient nasal delivery of powder from a spraying device requires impacting with adhesion and/or sedimentation of particles on nasal mucosa; therefore, powder properties such as particle size, shape, surface, density, and flow must be optimized to activate the proper mechanism for therapeutic treatment. The number of drugs directly administrable to the nose in powder form is limited because of unsuitable characteristics such as large particle size, low solubility, poor absorption, and irritability. These limits can be overcome through the use of a suitable solid excipient as carrier. Such a carrier must be compatible, hydrophilic, soluble, and of an aerodynamic particle size favorable to nasal deposition. The most common material used are sugars, β-cyclodextrin, cyclodextrin derivatives, phospholipids, starches, cellulose derivatives, poly(vinylpyrrolidone) and others. Swellable polymers proved very useful as nasal carriers, because the swelling phenomenon was added as a transport enhancing effect. Particle size is the main parameter affecting nasal drug delivery. It was found that powders around 100 μm in size are efficiently delivered in terms of amount and type of delivery, when an insufflator device using a gelatin capsule as reservoir was used (44). In the particle size range between 150 and 50 μm there was an evident change in the insufflation behavior: for size over 150 μm, the spray pattern suggested more favorable conditions for impacting the nasal mucosa; below 50 μm, a more uniform deposition by sedimentation is expected, but the possibility of particle respirability can increase as well. Other formulations used for nasal delivery involve nasal gels; one example is vitamin B_{12} gel, which provides a superior bioavailability compared with oral delivery (45). A scopolamine gel is expected to be filed soon for approval (46).

METERING AND INSUFFLATORS

Devices for nasal delivery differ according to the formulation to be dispensed. Liquid solutions are delivered using metered atomizing pumps, metered-dose pressurized nasal inhalers, rhinal tubes for variable volume delivery, and plastic spray or squeeze bottles (47). Pumps and squeeze bottles operate by mechanical actuation to sample a liquid volume from a reservoir and to produce a mist cloud having the shape of an inverse cone or of a sagittal plume. The use of these devices is usually extensively explained in the product leaflets, and the intervention of a pharmacist for assembling the nasal spray device is often requested.

Quantity dispensed and reproducibility are the major points to be assessed. Pumps, both mechanically or gas actuated, are very precise and accurate in delivery, provided that they are primed according to the indications of the producer. The delivery rate is very fast because emission is usually completed in less that one second. The size of droplets produced with these devices prevents the entrance of the preparation into the lung, and their size and velocity provide an impacting on the nasal mucosa with a distributed deposition. The multidose preparations require preservatives in the solution that can alter the mucosa. Metered unidose insufflator devices are the technological solution to avoiding preservative use. An example of these is reproduced in Figure 2. However, considering that there are two nostrils and that deposition carried out in both nostrils doubles absorption, bidose devices have been developed and marketed both by the Pfeiffer (48) and Valois (49) companies.

Powder delivery requires different types of insufflators, which can be mechanically or respiratory actuated. The user requests are for a small-sized portable device, with high spraying performance and visible feedback, moisture protected and easy to handle. The mechanically designed devices consist of a rubbery bulb connected through the dose reservoir to a nasal adapter (Fig. 3). The squeezing of the rubbery bulb provides a stream of air capable of emitting the appropriately loaded powder in the insufflator. The insufflators designed to be used by breathing through

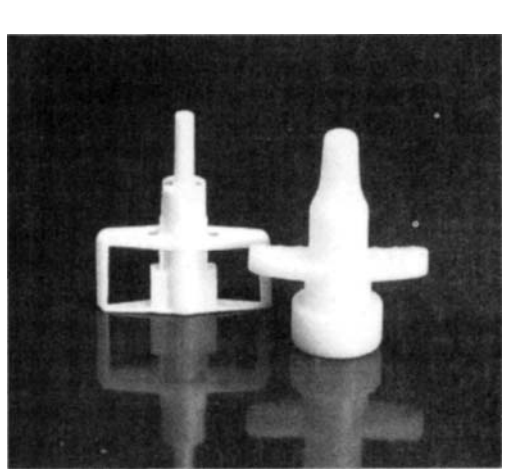


Figure 2. Monospray systems for nasal administration of monodose of liquid formulation (Valois Pharm, France).

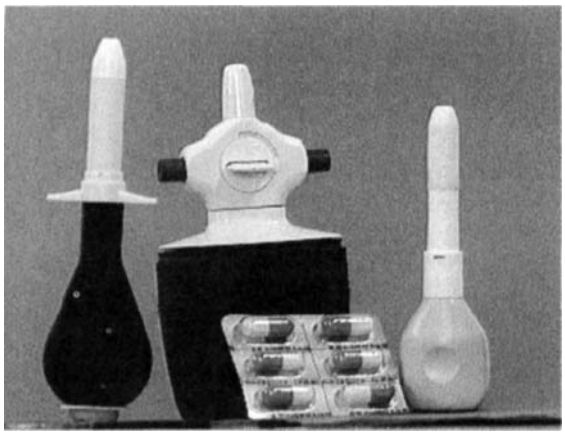


Figure 3. Different insufflators for nasal administration of powdered formulations. From left to right: Rinoflatore® (Fisons, Rome, Italy), Miat Nasal Insufflator® (Miat, Milan, Italy), Puvlizer® (Teijin, Tokyo, Japan).

the nose are a nose adapted version of the dry powder inhalers, designed for lung delivery. With both types of devices, the drug unidose is loaded in a gelatin capsule that is pierced just before activation. Because the capsule is located between the air jet producer and the nose adapter, the air stream that flows through creates a turbulence inside the capsule, capable of aerosolizing and emitting the amount of powder contained. This phenomenon, called "dancing cloud" by the Hovione company (50), causes a complete, gradual, and efficient emission of the powder content of the motionless capsule. The devices loaded with gelatin capsule can deliver different amounts of powder without adversely affecting their behavior (51).

QUALITATIVE AND QUANTITATIVE ASPECTS OF NASAL DOSE DELIVERY

Nasal delivery of a drug requires metering of the dose and its emission by means of a device capable of producing an aerosol suitable for deposition on nasal mucosa. The words *cloud, plume*, or *puff* are used indifferently for indicating the nasal aerosol. The goal of puff production is to appropriately deposit the drug according to the pathology to be treated, which could be for localized or systemic effects. For example, a disease such as rhinitis requires a deposition on the total area of the mucosa, whereas a targeting to the brain would require localized deposition at the roof of the nose. Other therapeutic possibilities require the adaptation of the puff for deposition at different sites.

In any case, nasal delivery of drug involves both qualitative and quantitative aspects of drug delivered. The qualitative aspect refers to the aerodynamic behavior of the cloud produced and is described by the spray pattern and the cloud geometry, whereas the quantitative aspect is linked to the dose of drug sprayed per puff. The qualitative aspect is assessed by photographic technique in order to obtain the sequence of dose emission from the pump or insufflator and to collect information on spray pattern and geometry. Plume shape, height, area, density, particle size, and velocity are the parameters involved in the spray pattern and geometry determination.

In the case of liquid preparations, the qualitative aspect is primarily dependent on the device used for insufflation. The spray geometry in the case of pump metered-dose insufflators or squeeze plastic bottles is totally different. It is not surprising to find that different geometry can result in different bioavailability of the drug. This is probable not only when comparing two different types of nasal insufflators but also in the case of the same type manufactured by different producers. As an example, Figure 4 shows two mists of the same liquid formulation produced using two similar pumps manufactured by different producers. The two preparations were not bioequivalent, because delivery with one pump gave a bioavailability 30% lower than the reference (C. Vecchio and R. Bettini, University of Parma, Department of Pharmacy, personal communication, 1998). Registrative health authorities require for droplet size distribution determination using two different methods, such as laser scattering and cascade impactor. In addition, the spray pattern and plume geometry must be compared for bioequivalence studies.

In the case of nasal powder, the powder cloud, which looks like a plume emerging from a chimney, grows in dimension during emission, with a maximum height and width depending on the characteristics of the product sprayed and the device used. The cloud aspect is mainly dependent on the formulation's characteristics and, particularly, on the fundamental (size and shape) and derived (packing and flow) properties of the powder (44). Using a rubbery bulb insufflator, the clouds originating from small particle size powder are fluffy and homogeneous in density, whereas the clouds obtained from large particle size powders are characterized by visible individual particle trajectories (Fig. 5). The rate of particle delivery decreased with decreasing size, whereas the time needed to completely emit the dose through the nose adapter of the insufflator increased with decreasing size. For nasal impacting, the powder cloud should remain as compact as possible to

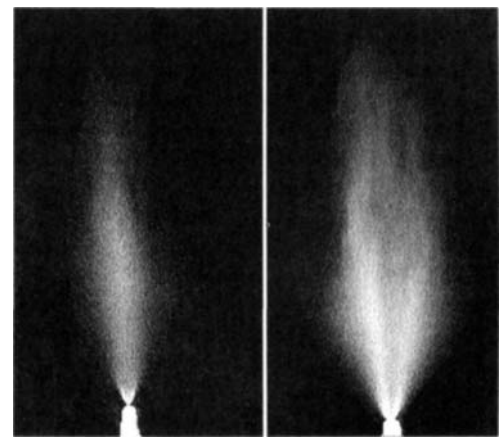


Figure 4. Nasal puffs obtained by spraying the same desmopressin nasal solution through two different metered-dose pumps. Puff (**a**) provided a superior bioavailability compared with puff (**b**). The amounts emitted were not significantly different.

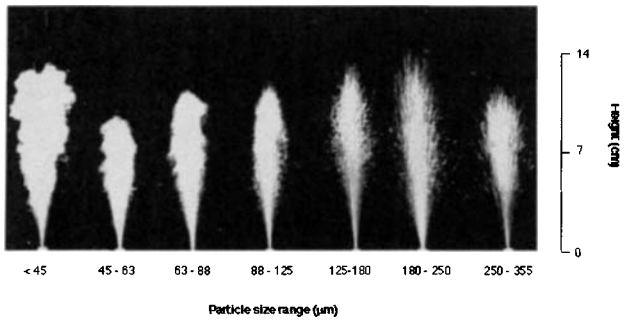


Figure 5. Influence of nasal powder particle size on the puff appearance (Miat Nasal Insufflator).

achieve an efficient shot of powder to the nasal mucosa, whereas for sedimentation a larger cloud would be preferred. The measurement of the expansion area of the axial section of the clouds during emission evaluates the packing of the cloud: as the particle size decreased below 100 μm, the area of the puff increased (44). Serum progesterone levels following nasal administration in rabbits of two powder mixtures containing co-ground progesterone-β-cyclodextrin or co-lyophilized progesterone and β-cyclodextrin showed rapid increase (52). Progesterone co-grounded powder exhibited a significantly higher extent of bioavailability, without a significant difference in rate compared with the co-lyophilized powder. The progesterone-β-CD co-ground powder was ejected by the insufflator at higher speed and as a compact cloud.

The quantitative aspect of nasal delivery is different according to the physical state of the preparation, i.e., liquid or solid, and it is largely dependent on the type of device used for spraying. In the case of liquid preparations, there are obviously different delivery behaviors according to the device used. Metered pumps are designed for delivering a very precise and accurate amount of nasal solution. The alternative, the squeeze bottle, suffers from a strong dependence on the energy used in squeezing the bottle in order to emit the dose. Therefore, the device affects the accuracy of delivery. As an example, a solution of xylometazoline was delivered in different amounts from squeeze bottle by different patients. Figure 6 shows the behavior of successive sprays performed by male or female patients: it is evident that the males exert more strength in spraying than females, because they sprayed out more product per shot. The same solution charged in a metered pump device is less dependent on the varying strength of the patient, as Figure 6 shows as well. Finally, metered pumps are regularly used in prescription preparations, and the squeeze bottle is the choice for over-the-counter preparations.

The quantitative aspect of a nasal solution filled in multidose reservoir is first tested by the labeled number of sprays that must be available using the preparation completely. It is also required that the number of priming operations to be performed before the device is ready for use should be declared. After this preliminary characteristic, the content uniformity per spray is a regulatory requisite. This must be checked from dose to dose, from container to container, and from batch to batch, considering

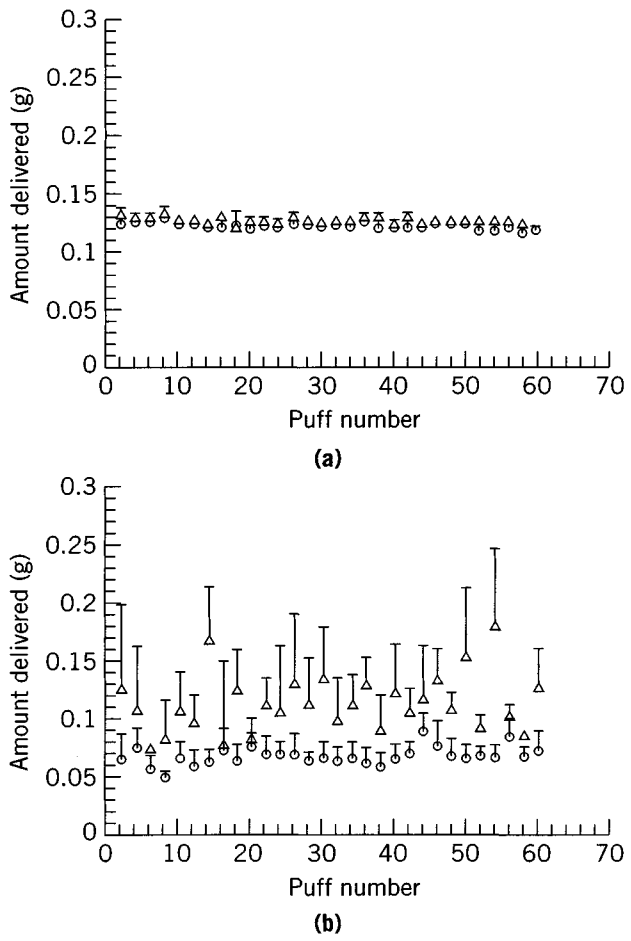


Figure 6. Differences between women (○) and men (△) in delivering the same xylometazoline nasal solution from (**a**) metered-dose pump and (**b**) squeeze bottle.

that the accepted variability is established between 85 and 115% of the labeled dose.

Nasal inhalation powders are delivered using insufflators that generally work on a unidose basis. The drug is dosed in a hard gelatin capsule and the capsule is loaded and pierced in the insufflator. The production of the puff is done by squeezing the rubbery bubble that produces the air stream necessary for nebulizing the powder. The dimension of the rubbery bubble determines the amount of the emitted powder and the complete delivery of the dose from the capsule. This aspect is strictly dependent on the properties of the formulation inside the capsule. Successive generations of powder insufflators were proposed with the aim of allowing depositing the dose in the two nostrils. This quantitative problem was solved by using insufflators that have a small bubble, so determining the need to squeeze the bubble many times to completely emit the amount loaded into the capsule, alternating the nostril involved in the insufflation. The amount of dose emitted by this sequence of insufflation is reported in Figure 7, where it can be appreciated that the successive squeezing allow sharing the amount deposited in the two nostrils and the delivery depends on particle size of powder.

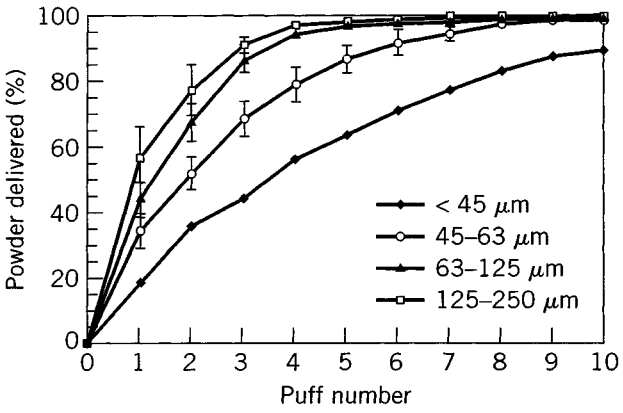


Figure 7. Cumulative percentage of nasal powder delivered from Puvlizer nasal insuffiator as a function of the puff number (powder loaded; 25 mg).

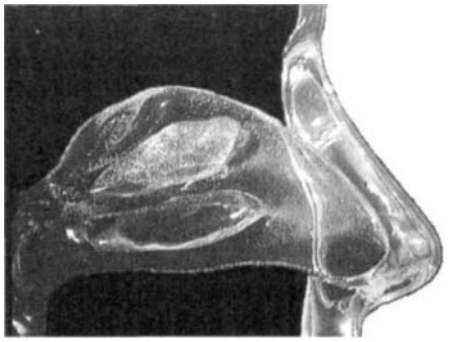


Figure 8. Powder deposition in the left section of the artificial nasal cavity showing a large coating of atrium and superior cornet.

Deposition of emitted dose in the nasal cavity was studied using various techniques both in vivo and in vitro. Scintigraphic techniques are the most powerful for determining the site of dose deposition and were used to show the influence of dosage form and device. One of the first papers published on the subject compared in vivo the sites of deposition and the patterns of clearance following intranasal administration of nasal spray and nasal drops. It was found that spray was deposited anteriorly in the nasal cavity, with little dose reaching the turbinates, whereas drops dispersed the drug throughout the length of the cavity. A substantial difference was also observed in terms of clearance, evidentiating that the spray was cleared more slowly (53).

Technological tests of pattern deposition have been suggested by health authorities and consist of spraying the product against a flat surface, such as a Kieselgel sheet, to highlight the printing of the droplets sprayed by the pump. This test is requested as quality control and must be effected using the same device at two distances from the sheet, in order to have a printing of the distribution of droplets at different levels of cloud. In vitro studies were also done using a cast of the human nose. A significant difference was observed among the deposition of liquid solution applied by a drop bottle, a squeeze bottle, a metered pump, and a pressurized inhaler. This study also provided indications on the method of delivery, because it was observed that in the case of pressurized aerosols, a double delivery in each nostril effected in different directions provided better distribution of the product (54).

Few data are available concerning the deposition of powder in the nose (55). The requisite particle size for nasal deposition has been stated as less than 10 μm (1). An unpublished work correlated the deposition pattern in a silicone cast of the human nose with the particle size of the powder sprayed. It was found that atrium deposition was predominant independently of particle size (Fig. 8). Other authors have investigated the use of a glass model of the nasal cavity, without the turbinate presence, to estimate nasal deposition (56, 57). Recently, using a silicone model including the turbinate structure, good nasal deposition was obtained despite the fact that the particle size measured with aerodynamic methods was less than optimal. The model with turbinates gave higher deposition in the nasal cavity, as well as reducing the fraction penetrating the nose (58).

PENETRATION ENHANCERS AND BIOADHESION

A drug given by the nasal route is absorbed very quickly, entering the bloodstream similarly to an injection. Therefore, the nasal route must be primarily considered for rapid effect. However, this effect is also transient, because the efficient clearance mechanisms of the nose rapidly activate as well, so limiting the absorption time. Therefore, employing nasal delivery for prolonged release requires the development of particular strategies in order to keep the substance on the mucosa for a long time without altering the functionality of the nose.

Mucociliary clearance is the most significant physiological factor that affects nasal drug absorption, because it determines the time a drug remains at the absorption site. Some pathophysiological conditions, such as rhinitis, the common cold, hay fever, sinusitis, asthma, and nasal polyposis, may affect the retention of drugs in the nasal cavity. Environmental factors such as humidity, temperature, airborne toxins and chemicals, and many pharmaceutical excipients may also affect the clearance (59, 60). In order to achieve high absorption with only minimal effects on the mucociliary mechanism, the absorption process must be rapid, preferably within the first 15 minutes after administration (61). If the rate of clearance could be slightly decreased or halted in a reversible manner, then such retardation would be useful in increasing the contact time between the active drug and nasal mucosa, thereby increasing bioavailability.

Nasal mucosa allows effective absorption of a variety of lipophilic drugs and hydrophilic drugs, such as peptides and proteins (62). The major difficulty in administering those drugs intranasally is their low nasal bioavailability due to enzymatic degradation, mucociliary clearance, and poor mucosal membrane permeability. The attempts made to overcome these problems include coadministration of absorption enhancers and/or mucoadhesive substances.

The influence of the enhancers on the absorption of the drug across the nasal membrane is related to a direct effect on the drug and/or to an influence on the mucosa. For some drugs the solubilizing or stabilizing effect is of major importance. With regard to mucosa, enhancers may act by alterating the properties of the mucus layer, by opening the tight junctions between epithelial cells, increasing membrane fluidity, creating disorders in the phospholipid of membrane, and facilitating the leaking of proteins and lipids from the membrane. The improvement of peptide and protein absorption is probably due to one or a combination of these mechanisms.

The most evaluated compounds as enhancers are surfactants (laureth-9), bile salts (glyco-taurocholate, deoxycholate), chelators (EDTA, citric acid), fatty acid salts (oleic, caprylic, capric, and lauric), phospholipids (L-α-lysophosphatidylcholine [DDPC], didecanoyl-PC), fusidates (sodium taurodihydrofusidate, STDHF), glycyrrhetinic acid derivatives (carbenoxolone, glycyrrhizinate), cyclodextrins (α-, β-, γ-cyclodextrins), hydroxypropyl-β-cyclodextrin and dimethyl-β-cyclodextrin (DMβCD), randomly methylated β-cyclodextrin (RAMEB), chitosan, and particulate carriers (microcrystalline cellulose, starch microspheres, and liposomes).

Nasal absorption enhancers differ substantially in efficacy and safety. Bile salts, surfactants, Ca^{2+} chelators and STDHF have been assumed to increase nasal drug transport, but they have shown morphological damage and severe inhibition of nasal ciliary movement. In vivo laureth-9 and sodium deoxycholate are associated with nasal irritation, and STDHF leads to painful stinging and lacrimation (1). Calcium chelators penetrate into the cells where they interact with intracellular Ca^{2+}, causing severe damage or even cell death. Therefore, research has been focusing on new classes of promoters of nasal drug absorption. Controlled studies in humans using medium-chain phospholipid DDPC as insulin enhancer have shown that nasal mucosal physiology was unaffected after intranasal administration, but that insulin bioavailability was low, despite intranasal doses about 20 times higher than subcutaneous doses (63). Cyclodextrins (CDs) are cyclic oligosaccharides showing a polar outer surface and an apolar interior cavity able to include lipophilic guest molecules. CDs can enhance lipophilic drug absorption by solubilization and protection against physicochemical and enzymatic degradation. Thus, CDs are also able to enhance hydrophilic drug absorption by the extraction of specific lipids from biological membranes, leading to an increase in membrane permeability and fluidity. The extent of protection and absorption enhancement seems to depend strongly on the nature of the drug used as well as on the CD used. For example, in vivo studies in rats have demonstrated that the addition of 5% α-CD to a nasal preparation of insulin resulted in an absolute bioavailability of approximately 30%; on the contrary, β- and γ-CDs did not affect insulin absorption. However, DMβCD gave rise to a large increase in insulin absorption, with a bioavailability of 100%. In contrast to the result obtained in rats, experiments in rabbits and human volunteers showed no absorption-enhancing effect of CDs for insulin, with a bioavailability of approximately 3–5% (64). Studies in rabbits have concluded that α-CD is able to increase nasal absorption of human growth hormone (hGH). In fact, it has been seen that the presence of 30% α-CD in a powder formulation of hGH raises the nasal bioavailability from 8% to 23–25% (65). RAMEB enhanced dihydroergotamine (DHE) nasal absorption when administered by liquid and powder formulations including CD (RAMEB:DHE ratio 10:1), showing a bioavailability of 50% and 56%, respectively (66).

New compounds recently studied, chitosans are biodegradable high weight cationic polysaccharides. Their mechanism of transport enhancement is a combination of bioadhesion and transient opening of the tight junctions in the membrane. The cell-binding activity of chitosans is related to electrostatic interactions between cell surfaces charged negatively and the cationic polyelectrolyte structure. Chitosans have no arresting effect on the mucociliary clearance, and they do not cause significant changes in nasal mucosa histology. Medium molecular weight chitosans are able to enhance the nasal absorption in animals and human volunteers of polypeptides and other polar drugs, such as insulin, salmon calcitonin, and morphine metabolites (67). Because rapid mucociliary clearance decreases the time of drug contact with the absorbing regions of nasal mucosa, the use of compounds having bioadhesion properties has been revealed as very efficient in overcoming this problem. It has been shown that formulations including bioadhesive materials are retained in the nasal cavity with half-life clearance of 3 h or longer, compared with 15–20 minutes for usual formulations (68). Mucoadhesives are synthetic or natural polymers that interact with the mucus layer. Recently, bioadhesive microspheres based on materials such as starch, albumin and Sephadex, with particle sizes of 40–60 μm, have been developed. Starch microspheres are able to increase considerably the nasal absorption of insulin in rats and sheep, and of hGH and salmon calcitonin in sheep (69,70). The absorption enhancement by starch microspheres is not only related to their mucoadhesive properties but also to their capability of opening tight junctions by the dehydration of mucosal cells. The use of degradable starch microspheres as a nasal delivery system for hGH resulted in an increase of plasma peak height from 1.0 to 9 ng/mL and of area under the curve (AUC) from 28 to 892 ng min/mL, with a relative bioavailability of 2.7%.

Other bioadhesive polymeric systems have also been used in nasal peptide drug delivery (71). Microcrystalline cellulose was suggested to provide prolonged residence time due to its insolubility (41). Recent studies concluded that the absorption-enhancing effect of particulate carriers correlates directly with their Ca^{2+} binding capacity. In fact, the opening of the tight junctions may also be explained by a local decrease in Ca^{2+} concentration (72). There are many ongoing investigations to improve nasal bioavailability by a combination of microcrystalline cellulose (MCC) with permeation enhancers (sodium taurocholate [ST], ammonium glycyrrhizinate [AG], and glycyrrhetinic acid [GA]). Insulin absolute bioavailability from a 1.5% w/v suspension resulted in 1.96%. The presence of ST, AG, and GA in the MCC suspension provided bioavailabilities of 8.36, 7.83, and 2.15%, respectively. Thus, the combination of a bioadhesive polymer and permeation

relatively nontoxic enhancers can be of promising potential for developing a nasal spray formulation for peptide drugs (73).

Finally, liposomes are attracting considerable interest for drug delivery to nasal mucosa. In fact, they are known to sustain the release of the entrapped drugs and to decrease the mucociliary clearance of the drugs due to their surface viscosity. Their action on nasal mucosa is related to the incorporation of phospholipids in the membrane, opening "new pores" in the paracellular tight junction (74). Proliposomes, i.e., a free-flowing powder immediately forming a liposomal dispersion on adding water, have also been manufactured for nasal delivery with the intention of sustaining the delivery of propanolol through nasal mucosa (75).

DRUGS DEVELOPED FOR NASAL ADMINISTRATION

Nasal preparations for local effect have been available over-the-counter for a long time. Recently the nose was considered for delivering drugs with systemic effects, and appropriate products were marketed. The products described here, delivered under prescription, are examples of systemic effect nasal preparations and include also some relevant products for topical effect. Oxytocin and nafarelin nasal sprays have not been reviewed.

Butorphanol

Butorphanol is a potent synthetic mixed agonist-antagonist opioid analgesic. Butorphanol is well absorbed orally, but due to extensive first-pass metabolism, oral bioavailability is very low. Alternative nonparenteral routes of administration, such as transnasal, sublingual, and buccal have been developed. The biopharmaceutical evaluation of the transnasal formulation discovered significant advantages over sublingual and buccal formulations (76). Butorphanol administered intranasally showed linear pharmacokinetics for doses ranging from 1 to 4 mg; the bioavailability and the maximum concentration were higher than those found after administering the drug via sublingual and buccal routes. Because both sublingual and buccal dosage forms are physically placed in the mouth, some portion of the dose is swallowed, absorbed orally, and subject to first-pass metabolism. In contrast, little butorphanol can escape from the sinus cavity after nasal administration, so that the majority of the dose is absorbed through the desired route. Therefore, butorphanol intranasal administration is a useful tool for the treatment of moderate to severe pain. The most frequently reported adverse effects with butorphanol administered nasally were congestion and insomnia.

Butorphanol for nasal administration is marketed as Stadol NS Nasal Spray (Bristol Myers Squibb Co.) (77). It is an aqueous solution of butorphanol tartrate for nasal administration as a metered spray. Each bottle contains 2.5 mL of a 10 mg/mL solution of butorphanol tartrate with sodium chloride, citric acid, and benzethonium chloride in purified water, with pH 5.0. Stadol NS is used in postoperative analgesia, mainly in the treatment of migraine pain. Onset of analgesia, which is within a few minutes for intravenous administration and within 10–15 minutes for intramuscular injection, is within 15 minutes for the nasal spray doses. Peak analgesic activity occurs within 30–60 minutes following intravenous and intramuscular administration and within 1–2 hours following nasal spray administration. Compared with the injectable form, Stadol NS has a longer duration of action (4–5 hours). Mean peak blood levels of about 1 ng/mL occur at 30–60 minutes after 1 mg dose administered nasally. The absolute bioavailability of Stadol NS is 60–70% and does not change in patients with allergic rhinitis. The fraction of Stadol NS absorbed is unaffected by the concomitant administration of a nasal vasoconstrictor, but the rate of absorption is decreased. Therefore, a slower onset can be anticipated if Stadol NS is administered concomitantly with or immediately following a nasal vasoconstrictor.

The patient should be instructed on the proper use of Stadol NS. The pump reservoir must be fully primed prior to initial dose. After priming, each metered spray delivers an average of 1.0 mg of butorphanol tartrate, and the 2.5 mL bottle delivers an average of 14–15 doses of Stadol NS. If not used for 48 hours or longer, the unit must be reprimed.

Calcitonin

Calcitonin is a 32 amino acid polypeptide hormone secreted by the parafollicular cells of thyroid glands. It provides the right bone growth by regulating Ca^{2+} turnover in cells. Nowadays it can be successfully employed in the treatment of osteoporosis and in Paget's desease, characterized by abnormal bone formation. The synthetic salmon calcitonin is currently formulated in several ways. Oral administration is contraindicated because the hormone is subjected to digestive degradation. Injectable calcitonin has been available on the market since 1984. Because of injection inconvenience to patients, intranasal administrations seemed to be more attractive. Many studies have been carried out to demonstrate the efficiency of nasal delivery, and the benefits have been compared with the parenteral route. The drug has been delivered as snuff, drops, and nebulized sprays. In late 1995 a new nasal spray was approved by the U.S. FDA.

Data obtained in experiments comparing the nasal with subcutaneous administrations have shown an equivalence, because both preparations were capable of alleviating pain and reducing bone disorder in the population of osteoporotic patients (78). Nasal calcitonin delivery is safe, preventative, and may increase bone mass of the lumbar spine. Fracture efficacy data are not yet available, although preliminary results are promising. Nasal calcitonin may be an analgesic to bone and of benefit in glucocorticoid-induced osteoporosis (79). The dose of nasal calcitonin for the treatment of established osteoporosis is 200 international units daily.

Although compliance problems are bypassed, by nasal administration low bioavailability increases the amount of dose administered. Results regarding the bioavailability of calcitonin nasal spray (Miacalcin®, Sandoz) have shown a great variability. Miacalcin is rapidly absorbed by nasal mucosa, and the plasma concentration peak appears after

31–39 minutes, which is twice as long as the 16–25 minutes found for the parenteral route. In volunteers approximately 3% of nasal dose, compared with intramuscular injection, is available (data ranged between 0.3 and 30.6%) (80). Adverse effects, which include nausea, rhinitis, and nasal discomfort, are generally mild and transient and always less common than others related to parenteral formulations. The nasal spray has been reported as having no serious adverse reactions associated with high doses. An increase in the bioavailability may be obtained using enhancers and proteolitic enzyme inhibitors (81), which improve the transport of the hormone through the nasal epithelium.

The delivery device is basically a pump system, which must be primed before the first use. The pump is activated once a faint spray is emitted, and it does not need to be reactivated before each successive use.

Dihydroergotamine

DHE is an ergot alkaloid used for the treatment of orthostatic hypotension and mainly for the prophylactic therapy of migraine. DHE was mainly available in parenteral dosage forms. The oral route is not suitable due to very low bioavailability (1%) caused by incomplete absorption and, particularly, to a high first-pass effect by the liver. However, alternative routes of administration that result in plasma levels comparable to the intramuscular route have been investigated (82). It has been demonstrated that intranasal administration provides a feasible delivery of DHE into systemic circulation. In fact, pharmacokinetic studies performed on humans show that DHE administered intranasally presents rapid absorption with a bioavailability, relative to intramuscular injection, of approximately 38%. A linear kinetics in the dosage range of 1 to 4 mg was observed (83). Another important pharmacokinetic result, concerning the reliability of this route of administration of DHE for the treatment of migraine, was that the vasomotor phenomena which could affect the nasal mucosa during a migraine attack, rhinitis, or the simultaneous administration of a local vasoconstrictor, had little or no influence on the bioavailability of DHE administered intranasally.

The first nasal solution consisted of an ampoule with DHE methanesulfonate salt at 4 mg/mL, and caffeine as enhancer. The ampoule had to be placed into a nebulizer when the migraine attack occurred, and after it was opened, it had to be used within 24 hours due to limited pharmaceutical and microbiological stability. Furthermore, the low concentration of DHE required large volumes to be sprayed into the nostrils, causing a spillage of solution from the nose. To overcome these drawbacks and to improve the nasal formulation, a pharmaceutically more stable nasal spray of higher concentration of DHE, able to administer a intranasal dose in a much smaller spray volume, was developed. Recently, the nasal spray (Migranal, Novarti's) was approved by the FDA (84). In two recent clinical trials of nasal spray, patients experienced headache relief as early as 30 minutes after treatment. Up to 60% of patients had responded within 2 hours, and up to 70% within 4 hours, following a single 2 mg treatment.

An interesting work in rabbits was carried out comparing two different formulations, liquid and lyophilized powder, containing a concentration of DHE of 10 mg/mL and RAMEB (66). It was assessed that the amount of RAMEB in liquid sprays did not affect the bioavailability of DHE. Nevertheless, by adding RAMEB to liquid, DHE solubility was increased. This allowed for more concentrated formulations and made possible administering higher doses in one puff, avoiding the spillage of liquid from the nasal cavity. Furthermore, the presence of RAMEB also increased the stability of the drug. Different results have been obtained from powdered formulations in which the DHE absorption was dependent of the amount of β-cyclodextrin and of the powder volume. The addition of CD seemed to improve absorption by enabling a rapid dissolution in the mucus layer of the DHE powder sprayed into the nostril.

Sumatriptan

Sumatriptan is a serotonin receptor agonist used in the treatment of migraine and cluster headache. It is available in a subcutaneous injection form or as tablets for oral dosage, but recently also as a nasal spray. The rationale of the nasal form is that the subcutaneous form is difficult to be self-administered for several patients, the oral route provides low bioavailability (14%), and administration during nausea or vomiting due to migraine may be unpleasant. The nasal spray is generally well tolerated; the most frequently reported events are transient disturbance of taste and nausea or vomiting.

The nasal formulation (Imigran, Glaxo Wellcome) is a solution of sumatriptan hemisulphate (10 mg/250 μL), buffered at pH 5.5, considering this pH within the normal range of nasal secretions. The solution is hypertonic. A high concentration is required for administering the dose in a small volume, suitable for spraying into the nostrils. Because of the low solubility of sumatriptan succinate used in the subcutaneous form, the hemisulphate salt has been preferred for the nasal form. Sumatriptan is a basic compound (pK_a 9.63), so it is almost completely ionized at pH 5.5. The good absorption at this pH supports the hypothesis of a paracellular mechanism driving the absorption (85).

The bioavailability and the rate of absorption are intermediate between the values observed after subcutaneous and oral administration. The times to peak plasma concentrations are 12 min for a 6 mg subcutaneous dose, 2 h after a 100 mg oral dose, and 1 h for a 20 mg intranasal dose. Following the latter route, sometimes a secondary peak was observed after 1.5–2 h. It is likely that part of the dose runs out of the back of the throat and is swallowed with the saliva, becoming a second oral dose. After 2 h from a 20 mg dose, more than 50% of the patients reported headache relief. A second administration at this time is effective in two-thirds of the nonresponders (86).

Desmopressin

Desmopressin, the synthetic analogue of the naturally occurring antidiuretic hormone, vasopressin, has for many years been the drug of choice in the treatment of diabetes

insipidus. Traditionally, it has been delivered by the intranasal route using the rhinyle catheter method, and was one of the first examples of a peptide that could be given systematically by the nasal route. Desmopressin solution was administered intranasally as a spray, using a metered-dose pump, or as drops, using a rhinyle catheter. Plasma levels showed that desmopressin was absorbed to a greater extent after administration of the spray, with a two- to three-fold increase in the relative bioavailability compared with the drops. Moreover, the use of an intranasal spray device can deposit well-controlled doses within the nasal cavity, which remain there sufficiently long to provide a clear enhancement in absorption and bioavailability (26).

DDAVP® Nasal Spray (desmopressin acetate) or DDAVP® Rhinal Tube (Rhône-Poulenc Rorer Pharmaceutical, Inc.) are available as aqueous solution for intranasal use (87). Each milliliter contains desmopressin acetate 0.1 mg, chlorbutanol, and sodium chloride. Intranasal DDAVP provides a prompt onset of antidiuretic action with a long duration after each administration. Its antidiuretic effect is about one-tenth that obtained with an equivalent dose administered by injection.

Cromolyn Sodium

Cromolyn sodium is indicated for the prevention and treatment of the symptoms of allergic rhinitis, because it inhibits the degranulation of sensitized mast cells and the release of histamine. The available product is a nasal solution (Nasalcrom® Nasal Solution, FISONS Pharmaceuticals) (88). Each milliliter of Nasalcrom contains 40 mg cromolyn sodium in purified water with benzalkonium chloride to preserve and EDTA to stabilize the solution.

Cromolyn sodium is poorly absorbed from the gastrointestinal tract. After instillation of Nasalcrom, less than 7% of the total dose administered is absorbed and is rapidly excreted unchanged in the bile and urine. The remainder of the dose is either expelled from the nose or swallowed and excreted via the alimentary tract.

Another nasal dosage form of cromolyn available on the market is formulated as nasal powder (Lomudal®, Fison Italchimici). It is presented as capsules containing 20 mg powder cromolyn sodium. The nasal powder administration requires the use of a special insufflator called Rinoflatore (see Fig. 3).

Steroid Drugs

Oral biavailability of steroid drugs is extremely low due to extensive elimination by hepatic first-pass metabolism. Nasal absorption of steroids, including progesterone, estradiol, and testosterone, has resulted in systemic bioavailability comparable with intravenous administration in rats and rhesus monkeys. For example, progesterone oral systemic bioavailability was approximately 7.9%, which is significantly less than the bioavailability achieved by nasal route (72–82%). The results demonstrate that nasal delivery can result in as much as a 10-fold reduction in the hepatogastrointestinal first-pass elimination of progesterone (89).

Other steroid drugs (i.e., glucocorticoids), such as budesonide, dexamethasone, flunisolide, fluticasone propionate, triamcinolone acetonide, and beclomethasone dipropionate are administered in the nasal cavity to obtain a local effect. Budesonide is an antiinflammatory glucocorticosteroid marketed as Rhinocort® Nasal Inhaler (Astra) (90). It is a metered-dose pressurized aerosol unit containing a suspension of micronized budesonide, indicated for the management of symptoms of seasonal or perennial allergic rhinitis in adults and children. A 3-week clinical study with placebo in seasonal rhinitis, comparing Rhinocort and orally ingested budesonide in 98 patients with allergic rhinitis due to birch pollen, demonstrated that the therapeutic effect of budesonide can be attributed to its topical effects. Only about 20% of an intranasal dose from the Rhinocort inhaler reached the systemic circulation. Biopsies of the nasal mucosa of 50 adult patients after 12 months of treatment and of 10 patients after 3–5 years of therapy showed no histopathological evidence of adverse effects. Rhinocort Nasal Inhaler is supplied in a 7 g canister containing 200 metered doses, provided with a metering valve and nasal adapter, together with patient's instructions for use. Each activation delivers approximately 32 μg of micronized budesonide to the patient.

Beclomethasone diproprionate (BDP) is another antiinflammatory steroid. Beconase® AQ Nasal Spray (Glaxo Wellcome, Inc.) or Vancenase® AQ nasal spray (Schering Plough Corp.) is a metered-dose, manual pump spray unit containing a suspension of BDP in an aqueous medium containing microcrystalline cellulose, carboxymethylcellulose sodium, dextrose, benzalkonium chloride, polysorbate 80, and phenylethyl alcohol (91). After initial priming (3–4 activations) each activation of the pump delivers from the nasal adapter 100 mg of suspension containing 42 μg of BDP. Beconase AQ Nasal Spray is indicated for the relief of the symptoms of seasonal or perennial allergic and nonallergic (vasomotor) rhinitis. The mechanism of the aerosolized drug's action in the nose is unknown. When given by nasal inhalation, the drug is deposited primarily in the nasal passages. Only about 20–25% of the dose is absorbed. A portion of the drug is swallowed. Biopsies of nasal mucosa obtained during clinical studies showed no histopathologic changes. Rino Clenil® (Chiesi Farmaceutici) is another metered-dose pressurized aerosol containing BDP 0.01 g, sorbitan trioleate, and propellant.

THE INSULIN CASE AND FUTURE DEVELOPMENTS: VACCINES AND BRAIN TARGETING THROUGH THE NOSE

Intranasal administration of drugs is likely to gain further importance in time. A large number of experiments on nasal drug delivery have used insulin as a model drug. The high interest in this drug itself makes it a suitable molecule to check the efficacy of nasal formulation. Despite the fact that insulin nasal delivery is not yet a reality, a very important challenge in the field of nasal drug delivery is the total or partial substitution of insulin daily injections with an intranasal therapy for diabetes mellitus. Up to now, several trials with different intranasal formulations have resulted in low and variable bioavailability and in uncertainty about long-term safety. Therefore, an intra-

nasal therapy is not likely to be available in the near future (63). Moreover, considerations exist as to whether the oral form of insulin would be more convenient. The reasons are based on the fact that the intestinal administration of insulin showed that the drug is absorbed via the liver. This is the same as insulin produced by the pancreas and is different from the injected or inhaled insulin that goes directly into the circulation. Obviously, an ideal diabetes mellitus therapy should be capable of simulating the profile of normal insulin secretion (92,93). As mentioned earlier, high and predictable bioavailability and long-term safety are the main conditions for an intranasal formulation to be introduced into therapeutic practice. At present, neither a liquid nor a solid dosage form can assure both. We refer to the review of Merkus et al. (64) for a deeper evaluation of the mechanisms by which the adjuvants improve absorption of insulin.

New results are expected in the fields of vaccination and brain targeting (94). The first effective immunizations by this route were demonstrated in the late 1920s. Immune reactions develop in two different ways depending on the site of the first contact with the antigen. If the antigen directly enters the bloodstream, B-lymphocytes are primed to express specific antibodies and to release them into systemic circulation. If otherwise the infective agent (or the exogenous substance) is contacted by a mucosal surface, a different mechanism is activated. The antigen is picked up by specific M-cells of the epithelium and presented to T- and B-lymphocytes located in follicles forming the so-called mucosal associated lymphoid tissue (MALT). Thereafter, the primed lymphocytes migrate from the original MALT (e.g., the nasal associated lymphoid tissue) to the regional lymph nodes; here they get into further differentiation and then reach, by means of the systemic circulation, all the other mucosal surfaces, where both humoral and cellular immunity is provided. Vaccination by parenteral injection provides effective systemic immunity, but also implies high costs, low patient compliance, and several side effects. Some of these disadvantages could be avoided by immunization via mucosal surfaces. Future vaccination must be inexpensive, easy to distribute and administer. These are exactly the possibilities offered by intranasal vaccination. For the time being, no intranasal vaccine has yet been licensed. However, a wealth of studies have been undertaken in this direction. In particular, intranasal vaccines against the influenza virus have been found to be highly effective in several experiments in humans. Very interesting results have been obtained in the research for a vaccine against human immunodeficiency virus (HIV). In experiments on mice, intranasal immunization was superior to vaginal, gastric, or rectal immunization for the induction of systemic and mucosal anti-HIV antibody responses (95). Other investigations have been devoted to herpes virus, *Helicobacter pylori, Streptococcus pneumoniae*.

Finally, the nasal mucosa is also a very suitable site for the administration of peptides and small proteins to the brain that do not diffuse through the blood-brain barrier. An interesting summary on this subject has been reported by Sakane et al. (96). Many studies have demonstrated the presence of a particular transport mechanism from the olfactory mucosa to the brain, exploiting an easier access to the cerebrospinal fluid (CSF). The nerves coming from the olfactory bulb spread out in bundles close to the cribriform plate (the part of the ethmoid bone constituting the roof of the anterior cranial fossa). The bundles cross this bony wall and enter the nasal cavity, ending in many small protrusions of the mucosal surface. Each nervous bundle is surrounded by supporting cells and by a space containing CSF; this space is probably an extension of the subarachnoid space, and its presence provides a reliable explanation of the high rate of absorption from the olfactory region to the CSF.

As demonstrated by Gizurarson et al. (97), after instillation to the olfactory region of the nasal cavity, a significantly higher concentration of insulin reaches the brain as compared to subcutaneous administration. The relative bioavailability (intraolfactory versus subcutaneous) was 370%, with high differences between the administration techniques used. Based on these results, peptides and small proteins are the most interesting molecules for drug delivery to the brain exploiting intranasal administration.

ACKNOWLEDGMENTS

This article has been made possible thanks to the collaborative work of the young researchers active in nasal delivery studies at the Pharmaceutical Department of the University of Parma: Daniela Cocconi, Elena Pasini, Angela Armanni, Stefano Cagnani, Monica Sala, and Stefano Bonfante. Professor Dimitri Rekkas of the University of Athens must to be thanked as well for his helpful suggestions.

BIBLIOGRAPHY

1. D.F. Proctor and I. Anderson, *The Nose: Upper Airway Physiology and the Atmospheric Environment*, Elsevier, Amsterdam, 1982.
2. Y.W. Chien, *Transnasal Systemic Medications*, Elsevier, Amsterdam, 1985.
3. Y.W. Chien, K.S.E. Su, and S.F. Chang, *Nasal Systemic Drug Delivery*, Dekker, New York, 1989.
4. L. Illum, *S.T.P. Pharmacol.* **3**(7), 594–598 (1987).
5. C.G. Wilson and N. Washington, in M.H. Rubinstein, ed., *Physiological Pharmaceutics Biological Barriers to Drug Absorption*, Ellis Horwood, Chichester, 1989, pp. 139–154.
6. P. Edman and E. Bjork, *Adv. Drug Delivery Rev.* **8**, 165–177 (1992).
7. J.C. Verhoef and F.V.H.M. Merkus, in A.G. de Boer, ed., *Drug Absorption Enhancement*, Harwood Academic Publishers, Chur, Switzerland, 1994, pp. 119–154.
8. S. Gizurarson, *Adv. Drug Delivery Rev.* **11**, 329–347 (1993).
9. D. Duchene and G. Ponchel, *Drug Dev. Ind. Pharm.*, **19**(1 and 2), 101–122 (1993).
10. A.S. Harris, *J. Drug Target.* **1**, 101–116 (1993).
11. P. Buri and A.L. Cornaz, *Eur. J. Pharm. Biopharm.* **40**(5), 261–270 (1994).
12. A.J. Almeida and H.O. Alpar, *J. Drug Target.* **3**, 455–467 (1996).
13. American Association of Pharmaceutical Scientists, available at: *http://www.aaps.org*
14. E. Biocca, *Viaggi tra gli Indi: Alto Rio Negro—Alto Orinoco: Appunti di un Biologo*, Consiglio Nazionale delle Ricerche, Roma, Italy, 1965, vol. 2, pp. 235–239.

15. N. Mygind and R. Dahl, *Adv. Drug Delivery Rev.* **29**, 3–12 (1998).
16. V.H.L. Lee, A. Yamamoto, and U.B. Kompella, *Crit. Rev. Ther. Drug Carrier Syst.* **8**, 91–192 (1991).
17. K. Overgaard et al., *J. Clin. Endocrinol. Metab.* **72**, 344–349 (1991).
18. L. Illum and S.S. Davis, *Clin. Pharmacokinet.* **23**, 30–41 (1992).
19. F.W.H.M. Merkus et al., *J. Controlled Release* **24**, 201–208 (1993).
20. H. Critchley, S.S. Davis, F. Farraj, and L. Illum, *J. Pharm. Pharmacol.* **46**, 651–656 (1994).
21. N.G.M. Schipper, J.C. Verhoef, S.G. Romeijn, and F.W.H.M. Merkus, *Calcif. Tissue Int.* **56**, 280–282 (1995).
22. S.G. Chandler, L. Illum, and N.W. Thomas, *Int. J. Pharm.* **76**, 61–70 (1991).
23. S.G. Chandler, N.W. Thomas, and L. Illum, *Pharm. Res.* **11**, 1623–1630 (1994).
24. Z. Shao and A.K. Mitra, *Pharm. Res.* **9**, 1184–1189 (1992).
25. Z. Shao, R. Krishnamoorthy, and A.K. Mitra, *Pharm. Res.* **9**, 1152–1163 (1992).
26. A.S. Harris, I.M. Nilsson, Z.G. Wagner, and U. Alkner, *J. Pharm. Sci.* **75**, 1085–1088 (1986).
27. H.J.M. van de Donk, A.G.M. van den Heuvel, J. Zuidema, and F.W.H.M. Merkus, *Rhinology* **20**, 127–137 (1982).
28. S. Gizurarson, C. Marriot, G.P. Martin, and E. Bechgaard, *Int. J. Pharm.* **65**, 243–247 (1990).
29. W.A.J.J. Hermens, P.M. Hooymans, J.C. Verhoef, and F.W.H.M. Merkus, *Pharm. Res.* **7**, 144–146 (1990).
30. L. Jian and A.L.W. Po, *Int. J. Pharm.* **95**, 101–104 (1993).
31. A.R. Khan, B. Bengtsson, and S. Lindberg, *Eur. J. Pharmacol.* **130**, 91–96 (1986).
32. H.J.M. van de Donk, I.D. Muller Plantema, J. Zuidema, and F.W.H.M. Merkus, *Rhinology* **18**, 119–133 (1980).
33. P.C. Braga, G. Piatti, M. Dal Sasso, and A. Bernini, *J. Pharm. Pharmacol.* **44**, 938–940 (1992).
34. E. Marttin, N.J.M. Skipper, J.C. Verhoef, and F.W.H.M. Merkus, *Adv. Drug Delivery Rev.* **29**, 13–38 (1998).
35. I. Andersen et al., *Am. Rev. Respir. Dis.* **110**, 301–305 (1974).
36. C.R. Behl et al., *Adv. Drug Delivery Rev.* **29**, 89–116 (1998).
37. C.R. Behl et al., *Adv. Drug Delivery Rev.* **29**, 117–133 (1998).
38. D.C. Corbo, J.C. Liu, and Y.W. Chien, *J. Pharm. Sci.* **79**, 202–206 (1990).
39. A.A. Hussain, *Adv. Drug Delivery Rev.* **29**, 39–49 (1998).
40. N.G.M. Schipper, S.G. Romeijn, J.C. Verhoef, and F.W.H.M. Merkus, *Pharm. Res.* **5**, 682–686 (1993).
41. T. Nagai et al., *J. Controlled Release* **1**, 15–22 (1984).
42. D. Provasi et al., *Proc. Int. Symp. Controlled Release Bioact. Mater.* **19**, 421–424 (1992).
43. M.T. Vidgren, A. Karkkainen, P. Karjalainen, and J. Nuutinen, *Int. J. Pharm.* **42**, 216–221 (1988).
44. A. De Ascentiis et al., *Pharm. Res.* **13**, 734–738 (1996).
45. *Physicians' Desk Reference,* Medical Economics Data Production Company, Montvale, N.J., 1996, p. 1792.
46. *SCRIP* **2300**, 23 (1998).
47. H. Kublik and M.T. Vidgren, *Adv. Drug Delivery Rev.* **29**, 157–177 (1998).
48. Pfeiffer, Compiser system 101573,1611.
49. Valois Pharm., available at *http://www.cosmeticindex.com/ci/val/index.html*
50. Hovione, available at: *http://www.hovione.com/hovione.htm*
51. A. De Ascentiis, Ph.D. Thesis, University of Parma, Department of Pharmacy, 1994.
52. D. Provasi et al., *Eur. J. Pharm. Biopharm.* **40**, 223–227 (1994).
53. J.G. Hardy, S.W. Lee, and C.G. Wilson, *J. Pharm. Pharmacol.* **37**, 294–296 (1985).
54. N. Mygind and S. Vesterhauge, *Rhinology* **11**, 79–88 (1978).
55. I. Gonda, *Adv. Drug Delivery Rev.* **29**, 179–184 (1998).
56. G.W. Halloworth and J.M. Padfield, *J. Allergy Clin. Immunol.* **77**(2), 348–353 (1996).
57. K.D. Ostrander et al., *Pharm. Tech.*, 98–106 (September, 1995).
58. S. Leung, D. Velasquez, and D. Schultz, *Pharm. Res.* **14**(11), Suppl. (November 1997).
59. W.A. Lee, R.E. Ennis, and L.C. Foster, *Proc. Int. Symp. Controlled Release Bioact. Mater.* **15**, 77 (1988).
60. W.A.J.J. Hermens and F.W.H.M. Merkus, *Pharm. Res.* **4**, 445–449 (1987).
61. S. Gizurarson, S.N. Rasmussen, and F. Larsen, *J. Pharm. Sci.* **80**, 505–506 (1991).
62. A.E. Pontiroli, *Adv. Drug Delivery Rev.* **29**, 81–87 (1998).
63. F.W.H.M. Merkus, N.G.M. Schipper, and J.C. Verhoef, *J. Controlled Release* **41**, 69–75 (1996).
64. F.W.H.M. Merkus, J.C. Verhoef, S.G. Romeijn, and N.G.M. Schipper, *Pharm. Res.* **8**, 588–592 (1991).
65. C. Vermehren, H.S. Hansen, and M.K. Thomsen, *Int. J. Pharm.* **128**, 239–250 (1996).
66. E. Martin, S.G. Romeijn, J.C. Verhoef, and F.W.H.M. Merkus, *J. Pharm Sci.* **86**, 802–807 (1997).
67. L. Illum, N.F. Farraj, and S.S. Davis, *Pharm. Res.* **11**, 1186–1189 (1994).
68. L. Illum, N. Farraj, H. Critchley, and S.S. Davis, *Int. J. Pharm.* **46**, 261–265 (1988).
69. E. Björk and P. Edman, *Int. J. Pharm.* **47**, 233–238 (1988).
70. L. Illum et al., *Int. J. Pharm.* **63**, 207–211 (1990).
71. L. Pereswetoff-Morath, *Adv. Drug Delivery Rev.* **29**, 185–194 (1998).
72. C.R. Oechslein, G. Fricker, and T. Kissel, *Int. J. Pharm.* **139**, 25–32 (1996).
73. P. Dondeti, H. Zia, and T.E. Needham, *Int. J. Pharm.* **122**, 91–105 (1995).
74. L. Illum, *3rd Ann. Meet. Nasal Drug Delivery Focus Group, Am. Assoc. Pharm. Sci.*, Boston, November 5, 1997.
75. B. Ahn, S. Kim, and C. Shim, *J. Controlled Release* **34**, 203–210 (1995).
76. W.C. Shyu et al., *Biopharm. Drug Dispos.* **14**, 371–379 (1993).
77. *Physicians' Desk Reference*, Medical Economics Data Production Company, Montvale, N.J., 1996, pp. 775–778.
78. B. Combe, C. Cohen, and F. Aubin, *Calcif. Tissue Int.* **61**, 10–15 (1997).
79. S. Silverman, *Am. J. Med. Sci.* **313**(1), 13–16 (1997).
80. *Physicians' Desk Reference*, Medical Economics Data Production Company, Montvale, N.J., 1996, pp. 2275–2276.
81. K. Morimoto and M. Kakemi, *Int. J. Pharm.* **113**, 1–8 (1995).
82. D.T.-W. Lau et al., *Pharm. Res.* **11**(11), 1530–1534 (1994).
83. H. Humbert, M.D. Cabiac, C. Dubray, and D. Lavene, *Clin. Pharm. Ther.* September, pp. 265–275, (1996).
84. *SCRIP* **2294** (December 19), 21 (1997).

Next Page

85. A. Barrow et al., *Biopharm. Drug Dispos.* **18**(5), 443–458 (1997).
86. P. Fowler et al., *Cephalgia* **15**(Suppl. 14), 238 (1995).
87. *Physicians' Desk Reference*, Medical Economics Data Production Company, Montvale, N.J., 1996, pp. 2017–2018.
88. *Physicians' Desk Reference*, Medical Economics Data Production Company, Montvale, N.J., 1996, pp. 994–995.
89. D.C. Corbo, Y.C. Huang, and Y.W. Chien, *Int. J. Pharm.* **46**, 133–140 (1988).
90. *Physicians' Desk Reference*, Medical Economics Data Production Company, Montvale, N.J., 1996, pp. 556–558.
91. *Physicians' Desk Reference*, Medical Economics Data Production Company, Montvale, N.J., 1996, pp. 1076–1078.
92. J.A. Galloway and R.E. Chance, *Horm. Metab. Res.* **26**, 591–598 (1994).
93. J. Hilsted et al., *Diabetologia* **38**, 680–684 (1995).
94. A.J. Almeida and H.O. Alpar, *J. Drug Target.* **3**, 455–467 (1996).
95. H.F. Staats, S.P. Montgomery, and T.J. Palker, *AIDS Res. Hum. Retroviruses* **13**(11), 945–952 (1997).
96. T. Sakane, S. Yamashita, T. Nadai, and H. Sezaki, *S.T.P. Pharmacol. Sci.* **7**(1), 98–106 (1997).
97. S. Gizurarson, T. Thorvaldsson, P. Sigurdsson, and E. Gunnarsson, *Int. J. Pharm.* **140**, 77–83 (1996).

See also BIOADHESIVE DRUG DELIVERY SYSTEMS; MUCOSAL DRUG DELIVERY, BUCCAL; MUCOSAL DRUG DELIVERY, INTRAVITREAL; MUCOSAL DRUG DELIVERY, OCULAR; MUCOSAL DRUG DELIVERY, VAGINAL DRUG DELIVERY AND TREATMENT MODALITIES.

MUCOSAL DRUG DELIVERY, OCULAR

O. FELT
V. BAEYENS
M. ZIGNANI
P. BURI
R. GURNY
University of Geneva
Geneva, Switzerland

KEY WORDS

Bioadhesion
Eyedrops
Hydrogels
Inserts
Liposomes
Microparticles
Nanoparticles
Ocular delivery systems
Ocular pharmacokinetics
Pseudo-latexes
Residence time
Thermosetting gels
Tolerance

OUTLINE

Introduction
Hydrogels
  Definition and Classification
  Preformed Hydrogels
  In Situ Forming Gels
Dispersed systems
  Liposomes
  Microparticles and Nanoparticles
Inserts
  Definition
  Soluble Inserts
  Insoluble Inserts
  Bioerodible Inserts
Conclusion
Bibliography

INTRODUCTION

Historically, the use of topical devices for eye treatment is mentioned in Assyrian medical texts. Vegetable drugs (e.g., caraway, cassia, onions) were commonly prescribed and were applied as powders, ointments, or washes mixed with water, milk, wine, or oil (1). As an example, it was suggested to treat purulent conjunctivitis with "a local application of tanner's verdigris on vellum with copper dust, arsenic and yellow sulphide of arsenic mixed in curd" (1).

Actually, topical delivery of eyedrops into the lower cul-de-sac is the most common method for the administration of therapeutic agents in the treatment of ocular diseases and in diagnostics. However, one of the major problems encountered with solutions is the rapid and extensive elimination of drugs from the precorneal lachrymal fluid by solution drainage, lachrymation, and nonproductive absorption by the conjunctiva or the nasal mucosa, which may cause undesirable side effects (2,3) (Fig. 1). It must be noted that this high drainage rate is due to the tendency of the eye to maintain its residence volume at 7–10 μL permanently, whereas volumes topically instilled range from 20 to 50 μL. In fact it has been demonstrated in vivo that 90% of the dose was cleared within 2 min for an instilled volume of 50 μL and, within 4 min for an instilled volume of 10 μL (4). Consequently, the ocular residence time of conventional solutions is limited to a few minutes, and the overall absorption of a topically applied drug is

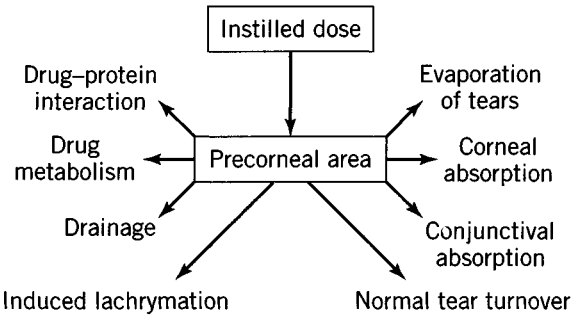


Figure 1. Drug elimination pathways from the precorneal area.

Previous Page

85. A. Barrow et al., *Biopharm. Drug Dispos.* **18**(5), 443–458 (1997).
86. P. Fowler et al., *Cephalgia* **15**(Suppl. 14), 238 (1995).
87. *Physicians' Desk Reference*, Medical Economics Data Production Company, Montvale, N.J., 1996, pp. 2017–2018.
88. *Physicians' Desk Reference*, Medical Economics Data Production Company, Montvale, N.J., 1996, pp. 994–995.
89. D.C. Corbo, Y.C. Huang, and Y.W. Chien, *Int. J. Pharm.* **46**, 133–140 (1988).
90. *Physicians' Desk Reference*, Medical Economics Data Production Company, Montvale, N.J., 1996, pp. 556–558.
91. *Physicians' Desk Reference*, Medical Economics Data Production Company, Montvale, N.J., 1996, pp. 1076–1078.
92. J.A. Galloway and R.E. Chance, *Horm. Metab. Res.* **26**, 591–598 (1994).
93. J. Hilsted et al., *Diabetologia* **38**, 680–684 (1995).
94. A.J. Almeida and H.O. Alpar, *J. Drug Target.* **3**, 455–467 (1996).
95. H.F. Staats, S.P. Montgomery, and T.J. Palker, *AIDS Res. Hum. Retroviruses* **13**(11), 945–952 (1997).
96. T. Sakane, S. Yamashita, T. Nadai, and H. Sezaki, *S.T.P. Pharmacol. Sci.* **7**(1), 98–106 (1997).
97. S. Gizurarson, T. Thorvaldsson, P. Sigurdsson, and E. Gunnarsson, *Int. J. Pharm.* **140**, 77–83 (1996).

See also BIOADHESIVE DRUG DELIVERY SYSTEMS; MUCOSAL DRUG DELIVERY, BUCCAL; MUCOSAL DRUG DELIVERY, INTRAVITREAL; MUCOSAL DRUG DELIVERY, OCULAR; MUCOSAL DRUG DELIVERY, VAGINAL DRUG DELIVERY AND TREATMENT MODALITIES.

MUCOSAL DRUG DELIVERY, OCULAR

O. FELT
V. BAEYENS
M. ZIGNANI
P. BURI
R. GURNY
University of Geneva
Geneva, Switzerland

KEY WORDS

Bioadhesion
Eyedrops
Hydrogels
Inserts
Liposomes
Microparticles
Nanoparticles
Ocular delivery systems
Ocular pharmacokinetics
Pseudo-latexes
Residence time
Thermosetting gels
Tolerance

OUTLINE

Introduction
Hydrogels
  Definition and Classification
  Preformed Hydrogels
  In Situ Forming Gels
Dispersed systems
  Liposomes
  Microparticles and Nanoparticles
Inserts
  Definition
  Soluble Inserts
  Insoluble Inserts
  Bioerodible Inserts
Conclusion
Bibliography

INTRODUCTION

Historically, the use of topical devices for eye treatment is mentioned in Assyrian medical texts. Vegetable drugs (e.g., caraway, cassia, onions) were commonly prescribed and were applied as powders, ointments, or washes mixed with water, milk, wine, or oil (1). As an example, it was suggested to treat purulent conjunctivitis with "a local application of tanner's verdigris on vellum with copper dust, arsenic and yellow sulphide of arsenic mixed in curd" (1).

Actually, topical delivery of eyedrops into the lower cul-de-sac is the most common method for the administration of therapeutic agents in the treatment of ocular diseases and in diagnostics. However, one of the major problems encountered with solutions is the rapid and extensive elimination of drugs from the precorneal lachrymal fluid by solution drainage, lachrymation, and nonproductive absorption by the conjunctiva or the nasal mucosa, which may cause undesirable side effects (2,3) (Fig. 1). It must be noted that this high drainage rate is due to the tendency of the eye to maintain its residence volume at 7–10 μL permanently, whereas volumes topically instilled range from 20 to 50 μL. In fact it has been demonstrated in vivo that 90% of the dose was cleared within 2 min for an instilled volume of 50 μL and, within 4 min for an instilled volume of 10 μL (4). Consequently, the ocular residence time of conventional solutions is limited to a few minutes, and the overall absorption of a topically applied drug is

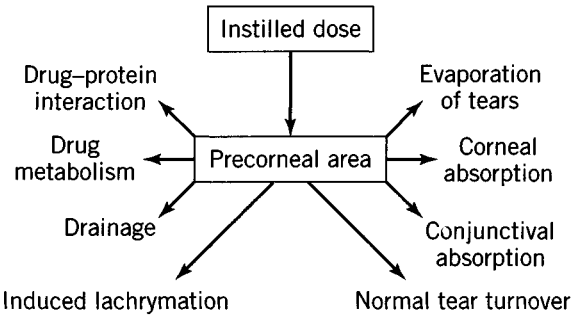


Figure 1. Drug elimination pathways from the precorneal area.

limited to 1–10% (5,6). Drug uptake occurs as a massive pulse entry, followed by a rapid decline, which means a short initial period of overdosing, followed by a long period of underdosing (7).

Initial attempts to overcome the poor bioavailability of topically instilled drugs typically involved the use of ointments based on mixtures of white petrolatum and mineral oils (8,9) and suspensions (10,11). Ointments ensure superior drug bioavailability by increasing the contact time with the eye, minimizing the dilution by tears, and resisting nasolachrymal drainage. Because these vehicles have the major disadvantage of providing blurred vision, they are nowadays mainly used for either nighttime administration or for treatment on the outside and edges of the eyelids (12). Use of suspensions as ophthalmic delivery systems relies on the assumption that particles may persist in the conjunctival sac. The efficiency of suspensions has shown high variability, which occurred as a result of inadequate dosing, probably mainly due to the lack of patient's compliance in adequately shaking the suspension before administration (13). These disadvantages have led to other approaches being investigated. One of the common methods to optimize prolonged precorneal residence time is to use hydrogels (14,15), liposomes (16), micro- and nanocarrier systems (16–19), and inserts (20,21). In comparison with traditional formulations, these systems have the following advantages:

- Increased contact time
- Prolonged drug release
- Reduction of systemic side effects
- Reduction of the number of applications
- Better patient compliance

A rapid overview of the most common diseases, e.g., ocular inflammations, glaucoma, and dry eye syndrome, treated with the ophthalmic dosage forms reviewed in this article is briefly provided here. Ocular inflammations are triggered by trauma, viral or bacterial infections, immunorelated phenomena, or corneal ulceration. Depending on the etiologic agent, the treatment of ocular inflammations consists of a topical steroidal therapy (dexamethasone) in combination with nonsteroidal antiinflammatory drugs (diclofenac), immunosuppressive agents (azathioprine), antimicrobial agents (tobramycin), and mydriatic-cycloplegic drugs (pilocarpine) (22).

Glaucoma results from the impairment of the aqueous humor flow and is characterized by an elevation of the intraocular pressure, progressive optic neuropathy, visual impairment, and eventually blindness (22). The most frequent drug therapy is based on the use of parasympathomimetics (pilocarpine), with or without adrenergic agonists (epinephrine) or β-blockers, including timolol, betaxolol, carteolol, and metipranolol.

Dry eye syndrome and keratoconjunctivitis sicca (KCS) are ocular surface pathologies concerned with reduction and unstability of the precorneal tear film. KCS is associated with local symptoms such as irritation, photophobia, foreign body sensation, and burning (23). The treatment of this disease relies on the use of artificial tear formulations able to fulfill the physicochemical role of normal tear including lowering the surface tension of the tear film, forming a hydrophilic layer compatible with adsorbed mucin, and enhancing the tear volume when necessary (23).

The aim of the following article is to describe the various polymeric systems used to achieve prolonged contact time of drugs with the cornea and increase their bioavailability. Advantages and shortcomings of the different systems reviewed are discussed as well as their characteristics and their in vivo applications.

HYDROGELS

Definition and Classification

The most common way to improve drug retention on the corneal surface is undoubtedly by using polymers to increase solution viscosity. Previous studies on rabbits by Robinson et al. (24,25) established that the rate of drainage from the eye of an instilled solution is markedly reduced as the viscosity of the solution is increased. More recently, the approach to improve precorneal retention is based on the use of mucoadhesive polymers. The principle for use of bioadhesive vehicles relies on their ability to interact with the mucin coating layer present at the eye surface (26).

Kim et al. (27) define hydrogels as polymers endowed with the ability to swell in water or aqueous solvents and induce a liquid–gel transition. However, in ophthalmology the limit between actual hydrogels and highly viscosified solutions is not clearly established. According to Plazonnet et al. (28), aqueous gels are at the upper limit of viscous preparations, and they are formed when high molecular weight polymers or high polymer concentrations are incorporated in the formulations.

Currently, two groups of hydrogels are distinguished, namely preformed and in situ forming gels (Fig. 2). Preformed hydrogels can be defined as simple viscous solutions which do not undergo any modifications after administration. In situ forming gels are formulations, applied as

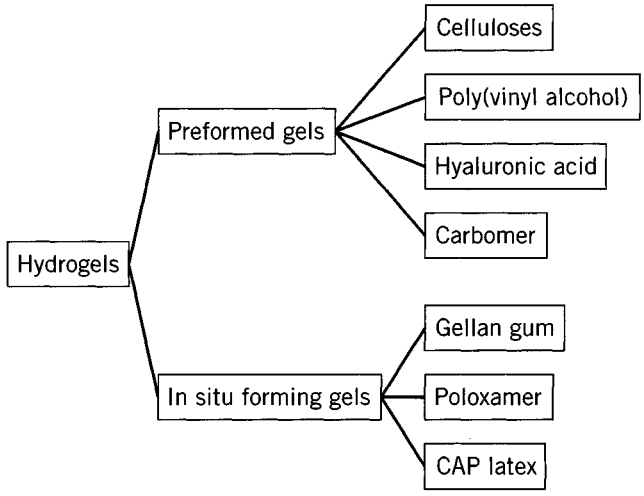


Figure 2. Classification of ophthalmic hydrogels. *Source:* Adapted from Ref. 29.

solutions, sols, or suspensions, that undergo gellation after instillation due to physic-chemical changes inherent to the eye (29).

The polymers chosen to prepare ophthalmic hydrogels should meet some specific rheological characteristics. It is generally well accepted that the instillation of a formulation should influence tear behavior as little as possible (6). Because tears have a pseudoplastic behavior, pseudoplastic vehicles would be more suitable as Newtonian formulations, which have a constant viscosity independent of the shear rate, whereas pseudoplastic solutions exhibit decreased viscosity with increasing shear rate, thereby offering lowered viscosity during blinking and stability of the tear film during fixation. The importance of the rheological properties of topical semisolid preparations regarding ocular tolerance and thus, good efficacy, has been reviewed by Zignani et al. (30).

Preformed Hydrogels

Preformed hydrogels for topical administration in the eye can be based on natural, synthetic, or semisynthetic polymers. Some characteristics of the more commonly used polymers are listed in Table 1.

Cellulose Derivatives. Because pure cellulose is not water soluble due to its relatively high crystallinity, cellulosic derivatives have been used for a long time as viscosifiers in collyria. Methylcellulose (MC) was first introduced in ophthalmic formulations in the 1940s as a mean of decreasing their fluidity (31). Some years later, Mueller and Deardorff (32) showed in man that solutions of homatropine hydrobromide exhibited enhanced cycloplegic and mydriatic activity in the presence of MC. Further promising results were obtained in 1962 by Haas and Merrill (33), who reported a lowered intraocular pressure in man after administration of pilocarpine incorporated in an MC vehicle. Since then, cellulosic polymers have been extensively studied as vehicle for ocular drug delivery. Currently, a large number of commercial formulations contain cellulosic viscosifiers, including Adsorbotear® (Alcon, Fort Worth, Texas) and Tears Naturale (Alcon, Fort Worth, Texas).

The cellulosic derivatives most commonly used in ophthalmology are:

- Methylcellulose (MC)
- Hydroxyethylcellulose (HEC)
- Hydroxypropycellulose (HPC)
- Hydroxypropylmethylcellulose (HPMC)
- Sodium carboxymethylcellulose (CMC Na)

The boundary between viscous solutions and gels for cellulosic derivatives is particularly difficult to define, because data regarding the hydrocolloid concentration or the viscosity of the final formulation are not always available. Therefore, some studies listed in Table 2 deal more with viscous solutions than with actual hydrogels.

Comparing the performance of three different cellulosic derivatives, namely HEC, HPC, and HPMC, Ludwig et al. (41) reported that HEC solutions were the most effective in reducing the elimination rate of sodium fluorescein from the cornea, probably due to a better tolerance. In fact, HEC was rated as the most comfortable by the volunteers, whereas HPC and HPMC gave rise to complaints of irritation and blurred vision. Several studies have clearly demonstrated the efficacy of cellulosic polymers in increasing ocular availability of numerous drugs when compared with simple saline solutions by decreasing the drainage rate from the eye (25,40,44). For example, Chrai and Robinson (25), using MC as the viscosity-inducing polymer, found a 10-fold decrease in the drainage rate constant for a 100-fold change in viscosity. However, they reported that increasing the viscosity above 15–20 cps, which appeared as the optimum viscosity, did not lead to a proportional improvement.

Subsequent advances in the polymers field with respect to ocular drug delivery have led to the use of poly(vinyl alcohol) (PVA); sodium hyaluronate, and carbomer, which often give better results (35,38,44,47) than celluloses.

Poly(vinyl alcohol). PVA is a synthetic polymer commercially obtained by polymerization of vinylacetate to poly(vinyl acetate) and subsequent hydrolysis to PVA (49).

Table 1. Characteristics of Polymers Used To Prepare Preformed Hydrogels for Ophthalmic Applications

Polymer	Origin	Characteristics
Cellulosic derivatives	Semisynthetic	Good tolerance Optical clarity Newtonian behavior Similar refractive index as the cornea
Poly(vinyl alcohol)	Synthetic	Newtonian behavior Wetting agent
Sodium hyaluronate	Skin, connective tissues, muscles, tendon, vitreous body, aqueous humor	Biocompatible Mucoadhesive Pseudoplastic behavior Viscoelastic behavior
Carbomer	Synthetic	Good tolerance Bioadhesion Possibility to be neutralized by the active compound in its basic form

Table 2. Preformed Hydrogels Containing Cellulosic Derivatives for Ophthalmic Administration

Polymer	Concentration (%)	Therapeutic agent	Refs.
MC	N.A.	Pilocarpine nitrate	25
MC	N.A.	Pilocarpine hydrochloride	34
MC	1.0	None	35
MC	0.6	Antazoline hydrochloride Pilocarpine hydrochloride	36
HEC	1.1–3.4	Sodium fluorescein	37
HEC	12.0	Pilocarpine	38
HEC	1.1	Sodium fluorescein	39
HEC	0.325; 0.50	Pilocarpine nitrate	40
HEC	1.1; 1.7	Sodium fluorescein	41
HEC	0.2–0.50	L-653,328	42
HEC	2.0	Naphazoline atenolol	43
HPC	5.5	Pilocarpine	38
HPC_{LMw}	4.5	Tropicamide	44
HPC_{MMw}	1.40	Tropicamide	44
HPC	1.8; 3.4	Sodium fluorescein	41
HPC	0.35; 1.8	Sodium fluorescein	39
HPC_{LMw}	5.0	Pilocarpine nitrate	45
HPC_{MMw}	1.2	Pilocarpine nitrate	45
HPMC	0.36; 0.60	Sodium fluorescein	39
HPMC	0.36; 0.64	Sodium fluorescein	41
HPMC	0.5	None	46
CMC Na	4.0	Pilocarpine	47
CMC Na	4.0	Acetazolamide	48
CMC Na	1.63	Tropicamide	44
EHEC	5.0	Pilocarpine	38

Note: MC, methylcellulose; HEC, hydroxyethylcellulose; HPC, hydroxypropylcellulose; HPC_{LMw}, low molecular weight hydroxypropylcellulose; HPC_{MMw}, medium molecular weight hydroxypropylcellulose; HPMC, hydroxypropylmethylcellulose; CMC Na, sodium carboxymethylcellulose; EHEC, ethylhydroxyethylcellulose.

PVA was introduced in the early 1960s (50) and has been reported to have corneal contact time superior to MC when tested on rabbits. Conflicting results were obtained by Linn and Jones (51), who found that PVA exhibited a significantly shorter elimination time than another cellulosic derivative, namely HPMC (Fig. 3). Numerous authors (46,52,53) reported quite similar results in favor of 0.5% MC over 1.4% of PVA in rabbits or humans. These last findings seemed more reasonable than those of Krishna and Brow (50) because 0.5% MC solutions exhibit significantly greater viscosity compared with 1.4% solutions based on PVA. Patton and Robinson (24) highlighted those presuming contradictory results. By testing solutions based on MC and PVA, the authors concluded that two vehicles exhibiting or at least approximating to Newtonian behavior in the same viscosity range could not have significantly different effects on ocular drug bioavailability. Moreover, they established that an optimal viscosity range (12–15 cps) also existed for PVA as demonstrated for MC (25).

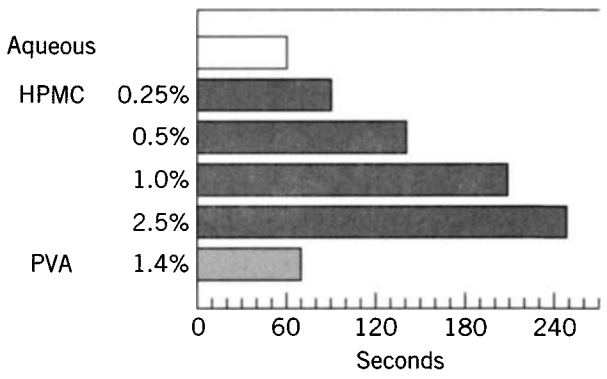


Figure 3. Lachrymal excretion time of various vehicles. Average of 20 separate instillations of each vehicle. *Source:* Adapted from Ref. 51 with permission.

Since then, numerous studies have been conducted, mostly comparing celluloses with PVA in an effort to determine the ideal ophthalmic vehicle. Some drugs tested in formulations containing PVA as well as the subsequent observations are listed in Table 3.

Lachrymal drainage evaluations of PVA formulations by γ scintigraphy (35,54) have demonstrated a significant delay of the drainage in man and rabbits, when compared with a saline solution. Hardberger et al. (35) have reported that the average $T_{1/2}$ for saline was markedly shorter (4.2 minutes) than for 1.4% PVA solutions (24 minutes).

Some commercial products, particularly for the treatment of dry eye, are based on PVA, including HypoTears® (IOLAB Corp., Claremont, California) and Liquifilm® (Allergan, Irvine, California).

Sodium Hyaluronate. The sodium salt of hyaluronic acid (SH) is a high molecular weight biological polymer composed of repeating disaccharide units of glucuronic acid and *N*-acetylglucosamine, a specific ultrapure fraction being patented as Healon® (Kabi Pharmacia, Sweden) by Balazs (57) in 1979. Its use as a vehicle in ocular drug delivery has been extensively reviewed by Bernatchez et al. (58). The efficacy of SH to increase precorneal residence time of ophthalmic formulations in humans has been investigated by several authors using different methods summarized in Table 4.

γ scintigraphic data of Snibson et al. (60) pointed out a very interesting phenomenon. They demonstrated that the residence times of 0.2% and 0.3% SH solutions on the cornea were significantly longer for patients having dry eye syndrome than in healthy subjects. The rationale for such a result was that the alteration of tear mucin in dry eyes might have modified the interaction of SH with the ocular surface.

An extended residence time is one of the factors used to select artificial tears for the therapy of KCS. At present, the therapeutic schedule in the treatment of dry eye implies frequent instillations, which lead to two major shortcomings: patient discomfort and side effects due to preservatives used in multiple dosage forms such as benzalkonium chloride, well known for their potential toxicity to the corneal epithelium. Because SH can protect against damages caused by benzalkonium chloride (62), it has been frequently proposed as a vehicle of choice in tear substitutes (61,63–65) and all the studies reported improvement of several symptoms associated with KCS, such as blurred vision, pain, photophobia, with this kind of

Table 3. Ophthalmic Formulations Based on PVA

PVA (%)	Drug	Species[a]	Effects[b]	Reference
0.0–10.0	Pilocarpine nitrate	R	1–3%: optimum concentrations range 10%: probably obstruction of the lachrymal duct	24
1.4	Tracer ^{99m}Tc	R/H	Diminution of the drainage rate	35
1.2	Pilocarpine nitrate	R/H	Improvement of the miotic response	45
3.0–6.5	Tracer ^{99m}Tc	R/H	Significant corneal retention within the first 20–50 s	54
1.4–4.2	Fluorescein	H	1.4–4.2%: Diminution of tear constant elimination 4.2%: discomfort, blurred vision	55
6.0	Pilocarpine	R	Improved precorneal retention Improved bioavailability	56

[a]H; human; R; rabbit.
[b]Comparative conclusions are made toward saline solutions.

Table 4. Effect of SH on the Precorneal Residence Time of Topical Solutions

Tracer	n^a	HA concentration (%)	Half-life (s)	Refs.
Fluorescein	4	0	96	37
		0.10	144	
		0.19	138	
		0.25	>240	
^{99m}Tc	7	0	96	59
		0.125	168[b]	
		0.250	>1200	
^{99m}Tc	6	0	36	60
		0.2	279[b]	
		0.3	437[b]	
	12 KCS[c]	0	40	
		0.2	468	
		0.3	909	
^{99m}Tc	6 KCS[c]	0.2	321	61

[a]Number of healthy individuals unless mentioned otherwise
[b]Not significantly different from the control.
[c]Keratoconjunctivitis sicca.
Source: Adapted from Ref. 58.

treatment. A further advantage of SH in this application is its pseudoplastic behavior.

The ability of SH to prolong drug release by increasing precorneal drug residence time has been studied (mostly in animals) for several ophthalmic compounds such as pilocarpine (66–71) or, more recently, gentamicin (72). Residence time of gentamicin in humans was found to be 2.23-fold superior when instilled in 0.25% SH formulations than in an isotonic phosphate buffer solution, and drug bioavailability was significantly improved for at least 10 minutes.

Carbomer. Cross-linked poly(acrylic acid) of high molecular weight, commercially available as Carbopol® (B.F. Goodrich Chemical Company, Cleveland, Ohio), is widely used in ophthalmology to enhance precorneal retention to the eye.

Preparation of Carbopol hydrogels is simply based on the dispersion of the polymer in water at room temperature, followed by a neutralization process with agents such as sodium hydroxide, triethanolamine, or directly with active basic compounds. The maximal viscosity is obtained at neutral pH.

Carbopol offers the advantage of exhibiting excellent mucoadhesive properties when compared with others polymers (e.g., cellulose derivatives, PVA and SH). The mechanisms involved in the mucoadhesion ability of Carbopol have been investigated previously (73,74). Four mechanisms of interaction between mucin and poly(acrylic acid) have been described (73,74):

- Electrostatic interaction
- Hydrogen bonding
- Hydrophobic interaction
- Interdiffusion

These mechanisms can be explained by the similar features of the mucus network and the cross-linked poly(acrylic acid):

- Macromolecular expanded network
- Negative charges
- Significant hydratation in aqueous media
- Significant number of carboxyl groups

The efficacy of Carbopol in enhancing precorneal residence time has been extensively studied by incorporating tracers such as sodium fluorescein (75) or active compounds such as pilocarpine or prednisolone (47,76–78). Some in vivo studies on rabbits or humans are reported in Table 5.

Comparing different types of poly(acrylic acid) (Carbopol 940, 934, 941, and 910), Unlü et al. (81) concluded that Carbopol 940 showed superior appearance and clarity. The results reported in these studies showed the superiority of poly(acrylic acid) as a sustained release agent over reference solutions (77,82) or over some hydrogels (47,56,79). However, the majority of authors avoided tolerance evaluations. Only Ludwig et al. (75) noted some differences in acceptability of Carbopol formulations (0.1 and 0.2%) from one patient to another; some volunteers complained of blurred vision. This result was confirmed by a clinical trial in human by Amin et al. (83), who observed a slight irritation after administration of Carbopol 940 gel, whereas the Draize test on rabbits showed no ocular irritation.

Table 5. Preformed Ophthalmic Hydrogels Based on Carbopol

Carbopol type	Concentration (%)	Drug	Reference
Carbopol 934	N.A.	Prednisolone sodium phosphate	77
Carbopol 940		Prednisolone acetate	
Carbopol 940	1.0–6.0	Pilocarpine	47
Carbopol 941			
Carbopol 940	1.0–4.0	Flurbiprofen	79
Carbopol 940	0.3	Tropicamide	80
Carbopol 934	0.49	Pilocarpine nitrate	56

A large number of commercial ophthalmic preparations contain Carbopol, including tear substitutes such as Lacrigel® (Europhta, Monaco), Lacrinorm® (Chauvin, Montpellier, France) or formulations containing active compounds such as Iduviran® (Chauvin, Montpellier, France) and Pilopine® (Alcon, Fort Worth, Texas).

Other natural or synthetic polymers have also been evaluated as potential vehicles to prolong the residence time of drugs at the surface of the eye but are currently being further investigated. Therefore, they are not extensively discussed in this article but are principally mentioned here for reference: chondroitin sulfate (63,67), xanthan gum (40,83,84), poly(vinylpyrrolidone) (44,85,86), and chitosan (87). Briefly, xanthan gum and chitosan are both polysaccharides of natural origin, being respectively obtained by an aerobic fermentation of a carbohydrate with *Xanthomonas campestris* and by deacetylation of chitin. An important difference between the two polymers is the anionic character of xanthan gum, whereas chitosan exhibits positive charges. Xanthan gum has been proposed as a material for artificial tears preparations (83) as well as vehicle for drug delivery (40,84). The possible advantage of chitosan over xanthan gum lies in the presence of positive charges at physiological pH on the sugar backbone of chitosan, which are supposed to interact with the negative charges of the mucus, thereby confering a bioadhesive property to this polysaccharide. Therefore, chitosan has attracted attention for topical ophthalmic applications, for example to enhance tobramycin delivery to the eye (87). γ scintigraphic evaluations have shown that the presence of chitosan was efficient to prolong precorneal residence time of formulations based on this polysaccharide, when compared with a commercial solution (87).

In Situ Forming Gels

The use of preformed hydrogels still has drawbacks that can limit their interest for ophthalmic drug delivery or as tear substitutes. They do not allow accurate and reproducible administration of quantities of drugs and, after administration, they often produce blurred vision, crusting of eyelids, and lachrymation. A new approach is to try to combine advantages of both solutions and gels, such as accuracy and facility of administration of the former and prolonged residence time of the latter. Thus, in situ hydrogels can be instilled as eyedrops and undergo an immediate gelation when in contact with the eye. The liquid to semisolid phase change can be triggered by:

- Increased temperature
- Increased pH
- Ionic strength of the tear film

Thermoreversible Hydrogels. These hydrogels are liquid at room temperature (20–25°C) and undergo gelation when in contact with body fluids (35–37°C), due to an increase in temperature.

Different thermal setting gels have been described in the literature, including for example acrylic acid copolymers (84,88) and *N*-isopropylacrylamide derivatives (89,90). However, specific requirements inherent to ophthalmic administration such as tolerance have limited the choice of such polymers.

Poloxamers, commercially available as Pluronic® (BASF-Wyandotte, USA), are the most commonly used thermal setting polymers in ophthalmology. They are formed by a central hydrophobic part (polyoxypropylene) surrounded by hydrophilic part (ethylene oxide). Depending on the ratio and the distribution along the chain of the hydrophobic and hydrophilic subunits, several molecular weights are available, leading to different gelation properties. Pluronic F-127, which gives colorless and transparent gels, is the most commonly used polymer in pharmaceutical technology. Briefly, hydrogels based on Pluronic are commonly prepared (91,92) by solubilization of the polymer in cold water (5–10°C) followed by gelation upon warming to ambient temperature.

Three principal mechanisms have been proposed to explain the liquid–gel phase transition after an increase in temperature, including the gradual desolvation of the polymer, increased micellar aggregation, and the increased entanglement of the polymeric network (93–95). Furthermore, Miller and Drabik (93) have suggested that intramolecular hydrogen bonds might promote gelation. The importance of the entanglement process in the gelation phenomenon of poloxamers has been confirmed by Gilbert et al. (96), who used a fluorescent probe technique to evaluate the hydration and diffusion processes in Pluronic F-127 solutions. A schematic representation of the gelation process, proposed by Waring and Harris (95) is shown in Fig. 4. The mucomimetic property of poloxamers is supposed to be due to their hydrophobic and hydrophilic sequences simulating mucin action by adsorption of the aqueous layer of tears on the hydrophobic epithelium (Fig. 5). Owing to their protective and mucomimetic action, poloxamers have also been evaluated for the treatment of dry eye (95,97). For example, Flow Base® (95), containing 18% of poloxamer 407, sodium chloride, and potassium chloride

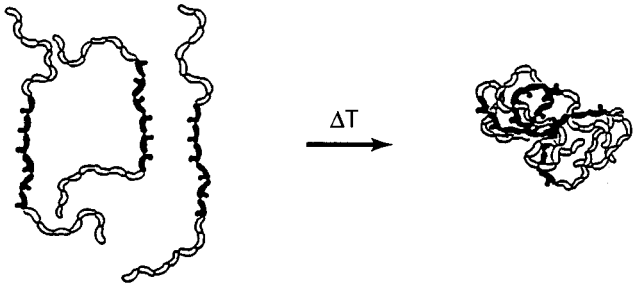


Figure 4. Liquid–gel transition of formulations based on poloxamers. *Source:* From Ref. 95 with permission.

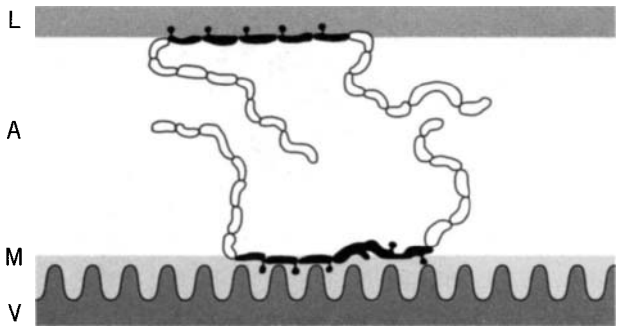


Figure 5. Model of the supposed action of poloxamers as tear substitutes. L, lipophilic phase; A, aqueous phase; M, mucus; V, villosities. *Source:* From Ref. 95 with permission.

has been shown to possess clinically advantageous properties as a tear substitute. The major drawback of this product is the formation of solid residues on the eyelids after instillation of 50 μL of solution, this problem being overcome by instillation of smaller volumes.

Poloxamers have also been widely investigated as ocular drug delivery systems. Miller and Donovan (98) reported enhanced activity of pilocarpine in poloxamers 407 gels when compared with a simple solution, whereas Dumortier et al. (99) have shown that a thermoreversible gel does not improve the kinetic profile of morphine over a reference solution. It must be noted that in both investigations the same polymer was used but not at the same concentrations (25% (98) and 20% (99), respectively), which might explain the discrepancies of the results.

Studying the influence of some parameters on the release rate of solutes from Pluronic F-127 hydrogels in vitro, Gilbert et al. (100) pointed out that increasing polymer concentration decreased the release rate of the drug, whereas increasing drug lipophilicity decreased the release rate. A recent γ scintigraphic study (101) on a semi-interpenetrating network based on poloxamer and poly(acrylic acid), Smart Hydrogel™, has been shown to remain significantly longer at the surface of the eye than a reference solution ($t_{50\%}$ about 25-fold higher).

Some applications of thermoreversible hydrogels in ophthalmology refer to the use of other polymers, the poloxamines, which are copolymers of poly(ethylene oxide) and poly(propylene oxide) obtained from a precursor, commercialized as Tetronic® (102).

Despite all the promising results obtained with thermoreversible gels, there remains an important drawback associated with the use of these hydrogels; the risk of gelling before administration by an increase in the ambient temperature during packaging or storage.

Pseudolatexes: pH-Induced Gelation. El-Aasser (103) defined pseudolatexes as artificial latexes prepared by the dispersion of a preexisting polymer in an aqueous medium. In situ gelling pseudolatexes for ophthalmic use can be described as aqueous colloidal dispersions of polymer, which become viscous gels after instillation in the conjunctival cul-de-sac due to modification of the pH (104).

Pseudolatexes are obtained by dispersion of an organic solution of a preformed polymer in an aqueous medium, leading to an O/W emulsion. Solvents from the internal phase are then evaporated to obtain a fluid dispersion of polymeric particles with a size generally smaller than 1 μm (104). Two principal methods are commonly used to prepare ophthalmic pseudolatexes, the solvent evaporation process (105–107) and the salting out process (106,108,109). Both methods allow the production of a lyophilized and easily redispersible powder. Thus, pseudolatexes have the advantage of ensuring the physical stability of the latex as well as the stability of active compounds such as pilocarpine, which is sensitive to aqueous media. In addition, such systems represent an interesting technological alternative that avoids the use of organic solvents, which can cause problems such as toxicity and pollution. Bioactive materials can be added into these systems at various times of the preparation: in the aqueous or in the organic phases during preparation or by adsorption on the final latex (105).

Ibrahim has listed (104) some prerequisites necessary for an optimal formulation of ophthalmic pseudolatex:

- Solubility of the polymer selected in organic solvents as well as insolubility in water
- Existence on the macromolecule of ionizable groups, which can react with the electrolytes of the lachrymal fluid
- Use of a high molecular weight polymer
- Rapid coagulation process after instillation to avoid precorneal drainage of the instilled formulation before the phenomenon of gelation appears
- Compatibility of the different components of the colloidal dispersion with precorneal tissues

First preliminary investigations of pH-sensitive nanoparticulate systems (latex) for ophthalmic administration began in the early 1980s (110) and have been extensively studied by Boye (19). He proposed the preparation of latexes containing pilocarpine with cellulose acetate phthalate (CAP). The choice of this polymer was determined by the compatibility of the polymer with the active compound, the ability of the CAP latex to be a free-running solution at pH 4.2 and a gel at 7.2, and finally, the latex stability at relatively low pH which is a prerequisite to ensuring the stability of pilocarpine.

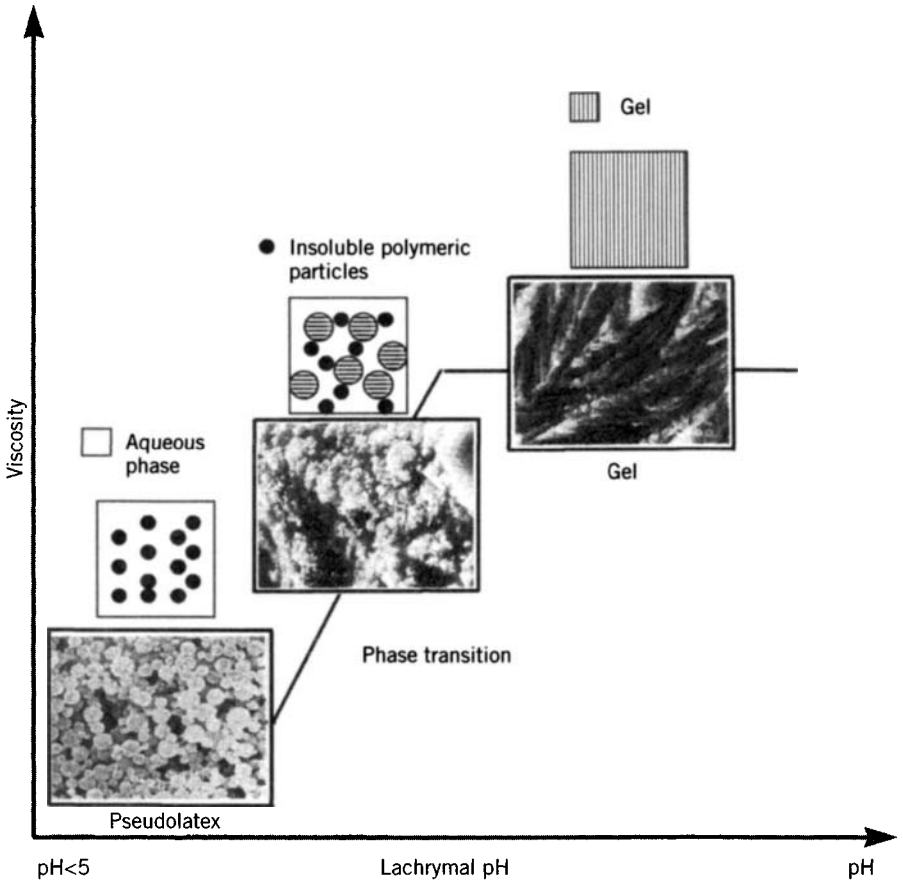


Figure 6. Transformation of the colloidal dispersion in gel. *Source:* From Ref. 111 with permission.

The principle of the sol–gel transition of the polymer CAP is shown schematically in Fig. 6. The gelation capacity of CAP latexes has been visualized in vitro by scanning electron microscopy and in vivo in rabbits by incorporating methylene blue in the ophthalmic formulations (106).

The efficacy of a preparation based on a pseudolatex has been evaluated by measuring pharmacological responses (19,105) and precorneal residence time by γ scintigraphy (19,111). This technique has clearly demonstrated the superiority of CAP latex over a solution to prolong the corneal residence time of pilocarpine, as shown in Fig. 7.

Finally, it is important to note that irritation tests (19) on rabbits including examination of the cornea, the iris and the conjunctiva have demonstrated that the investigated pseudolatexes did not induce visible irritation. However, a sensation of discomfort seems to be unavoidable after the coagulation of the solution in the conjunctival cul-de-sac as is the case for any semisolid preparation.

Ionically Induced Gelation: Gellan Gum. Gellan gum is an anionic exocellular polysaccharide produced by the bacterium *Pseudomonas elodea*, having the characteristic property of cation-induced gelation (112,113). The acetylated form is commercially available as Gelrite® (Kelco Division of Merck and Co, USA). The sol–gel transition process is induced by the presence of monovalent or divalent ions such as Na^+ and Ca^{2+}. Some other parameters influence the phase transition, e.g., the concentration of polysaccharide, the temperature of the preparation, and the nature and the concentration of cations. Kang et al. (114) have determined that divalent ions such as magnesium or calcium were superior to monovalent cations in promoting the gelation of the polysaccharide (Fig. 8). However the concentration of sodium in tears (2.6 g/L) is quite sufficient to induce the gelation (115). Because the presence of lach-

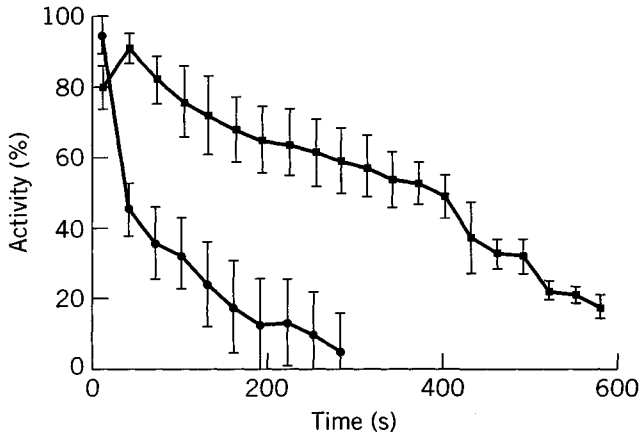


Figure 7. Corneal residence time of the pH-triggered 2% pilocarpine hydrochloride preparation (■), compared to a 2% solution (●). *Source:* From Ref. 111 with permission.

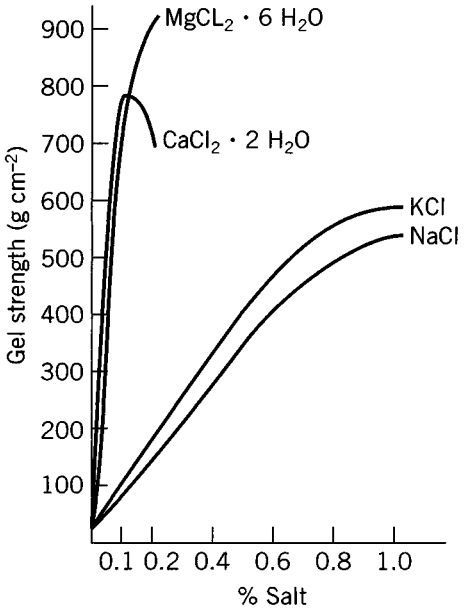


Figure 8. Effects of cations on gel strength of deacetylated gellan gum. *Source:* From Ref. 114 with permission.

rymal fluid is required to induce gel formation, accidental gelation during storage does not occur as with thermoreversible gels. The gelling mechanism is based on a modification of the conformation of the polysaccharide. It corresponds to the formation of double-helical junction zones in the presence of cations, followed by aggregation of the double-helical segments, leading to a three-dimensional network (116).

Corneal contact time of formulations based on gellan gum has been investigated using two main methods, which are fluorometry (117,118) and γ scintigraphy (40,119). Both techniques have demonstrated improved residence times with Gelrite when compared with saline or various commercial solutions. Gelrite has also provided corneal residence times superior to those of other hydrogel preparations based on polymers such as cellulosic derivatives or xanthan gum (Fig. 9) (40). A γ scintigraphic study by Greaves et al. (119) analyzing three formulations has pointed out the defectiveness of the gel in rabbits. In the case of humans, Gelrite showed longer contact time with the cornea than HEC, whereas a contradictory observation was noted in rabbits (119). This result is explained by the lower basal turnover and the slower blink rate in rabbits compared with man.

Efficacy of gellan gum has been also evaluated by measuring pharmacokinetic parameters (115) and pharmacological response (40,120). Rozier et al. (115) found an increased ocular bioavailability of timolol maleate when incorporated in Gelrite formulations versus the commercial Timoptic® solution. This result was confirmed by Vogel et al. (120), who observed a twofold decrease of the intraocular pressure of patients after administration of Gelrite-containing timolol.

Sanzgiri et al. (14) proposed a mechanism of drug release in vitro from gellan matrices of methylprednisolone (MP). The data suggested that MP release was influenced by the dissolution of the drug, its diffusion from the matrix, and possibly by erosion of the matrix; the combination of the three processes resulting in overall diffusion-controlled release kinetics as shown by the release index of the drug.

Exceptional rheological properties of gellan gum such as thixotropy, pseudoplasticity, and thermoplasticity (116) are further advantages for its use in ophthalmology: the fluidity of the solution can be increased simply by shaking or slightly warming the preparation.

Recently two other natural polymers believed to be able to form in situ gels by interacting with the lachrymal fluid have been evaluated as potential adjuvants in ophthalmic formulations (121,122). Carrageenans, a group of water-soluble sulphated galactans extracted from red seaweed, showed similar features to gellan gum regarding their rheological behavior, gelling properties (114), and tolerance. This suggested that they could be interesting polymers for prolonging the residence time of topical ocular formulations (121). Some alginates, rich in guluronic acid residues, have been demonstrated to exhibit reversible liquid–gel transition after administration and to be efficient in reducing intraocular pressure when carrying pilocarpine (122).

DISPERSED SYSTEMS

Liposomes

Liposomes are microscopic vesicles composed of alternating aqueous compartments and lipid bilayers (mainly

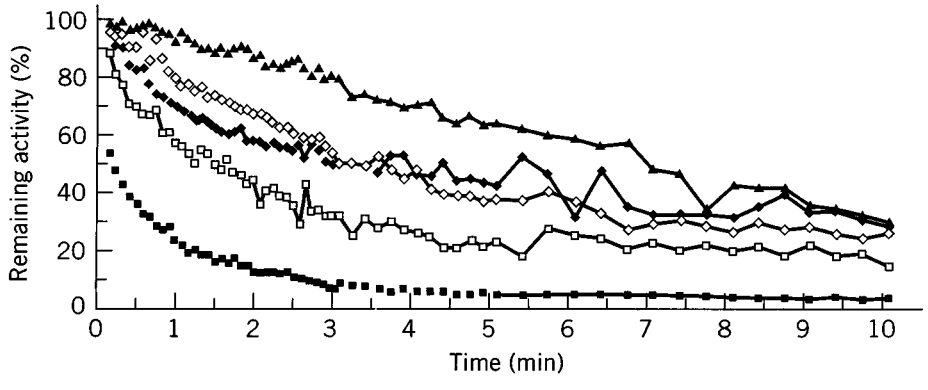


Figure 9. Precorneal drainage of ^{99m}Tc-DTPA incorporated in various formulations containing pilocarpine nitrate 2%. (■) Reference solution (n = 13), (□) HEC 0.325% (n = 9), (◆) HEC 0.5% (n = 8), (◇) xanthan gum 0.3% (n = 9), (▲) Gelrite 0.6% (n = 9). *Source:* From Ref. 40 with permission.

phospholipids and cholesterol). Liposomes are classified in three categories according to their size and the number of bilayers: (*1*) small unilamellar vesicles (SUV), (*2*) large unilamellar vesicles (LUV), and (*3*) multilamellar vesicles (MLV). Depending on their composition liposomes can have a positive, negative, or neutral surface charge.

The efficacy of liposomes in ophthalmic therapy depends on several parameters, including (*1*) the drug encapsulation efficiency, (*2*) the size and the charge of the vesicles, (*3*) the distribution of the drug in the liposomes, (*4*) the stability of the liposomes after instillation, (*5*) the residence time of the liposomes in the conjunctival sac, and finally, (*6*) the affinity of the liposomes for the cornea (123). Of these, a major factor affecting ocular drug bioavailability is the unstability of liposomes to the proteins in the conjunctival sac. Tall et al. (124) reported that proteins exert a destabilizing effect on the integrity of liposomes. However, Stratford et al. (125) have studied in vitro the effect of tears proteins on the release of epinephrine and inulin from liposomes. They reported only a slight increase of drug concentration in the release medium containing the simulating composition tears (126) when compared with a simple phosphate buffer solution.

The use of liposomes as ocular delivery systems was first reported by Smolin et al. (127) and Schaeffer and Krohn (128). Animal studies by Smolin et al. (127) demonstrated that entrapping idoxuridine in liposomes was more effective than the free drug in the treatment of acute and chronic herpetic keratitis. Studying the corneal uptake of penicillin G and indoxole with different types of liposomes, Schaeffer and Krohn (128) reported that corneal uptake of drugs was largely increased with positively charged liposomes. This suggests that the interaction between the cornea and liposomes is probably based on an electrostatic interaction, owing to the negatively charged epithelium at physiological pH. This in vitro study determined that the degree of association of liposomes with the corneal surface is decreasing as follows: $MLVs^+ > SUVs^+ > MLVs^- > SUVs^- > MLVs = SUVs$. Fitzgerald et al. (129) similarly reported that positively charged egg lecithin MLVs were retained markedly longer in the precorneal region than neutral or negative MLVs. However, γ scintigraphy experiments have demonstrated that vesicle retention occurred mainly in the inner canthus as well as in other extraocular regions, but not on the corneal surface where significant absorption takes place (129).

Various investigations concerning different liposome–ophthalmic drug combinations are reported in Table 6. The various studies concerning the use of liposomes in ophthalmic field have been also extensively reviewed by Lee et al. (123) and Mezei and Meisner (130,131).

Contradictory results were obtained from the studies listed in Table 6, suggesting high entrapment efficacy of lipophilic drugs in liposomes compared with hydrophilic compounds. Singh and Mezei (141) have tested triamcinolone acetonide and dihydrostreptomycin sulfate as lipophile and hydrophile model drugs, respectively. Concentrations of triamcinolone acetonide in different ocular tissues were markedly increased with liposomes, compared with a control suspension. On the other hand, the hydrophilic drug dihydrostreptomycin sulfate showed reduced ocular concentrations when associated with liposomes. Meisner et al. (135) also reported that atropine salt was less promising than free base to achieve a long-acting drug delivery. Schaeffer and Krohn (128) obtained a 10-fold enhancement of the corneal penetration of the hydrophilic penicillin G entrapped in liposomes over polysorbate 80 solutions. This can be explained, in part, by the amphiphilic behavior of penicillin G, which is not completely internalized in the aqueous phase but intercalates into liposomal membranes by insertion of its hydrophobic moiety.

More recently, the use of polymer-coated liposomes, which are expected to achieve superior precorneal retention time when compared with uncoated vesicles, has been investigated. Surprisingly, both cationic and anionic mucoadhesive polymers, namely chitosan (137) and Carbopol (142), failed to improve the corneal retention (137) or the drug bioavailability (142).

The ocular irritability of neutral and positive liposomes has been assessed by Draize test, histological examination, and rabbits blinking test (143,144). The two former methods indicated that irritation induced by each type of liposome might be considered as negligible, whereas the blinking method of Tanaka et al. (144) confirmed the safety of neutral liposomes but demonstrated that positive liposomes may cause pain or discomfort.

The use of liposomes in ocular drug delivery is still at an experimental stage and no liposomal ocular commercial products are available. This is due to a number of remaining limitations to their routinal use. Several shortcomings are inherent to liposomes such as their short shelf life, their limited drug loading capacity, as well as sterilization difficulties, because most of the methods can cause irreversible damage to the liposomes (123,131). Furthermore, the improvement of liposomes as drug carrier systems in ophthalmology requires a good understanding of the mechanisms involved in their interaction with the cornea. For instance, endocytosis is considered by most investigators as the dominant mechanism of interaction between liposomes and cells over fusion, adsorption, or lipid exchange processes (145). However, the cornea has been shown to exhibit only slight phagocytic activity (146), and endocytosis is probably not the main mechanism of interaction of the vesicles with corneal cells. Therefore, adsorption or lipid exchange is believed to be the major mechanism of interaction between the liposomes and the corneal cells (147).

Microparticles and Nanoparticles

Microparticles and nanoparticles are colloidal drug carriers in the micrometer and submicrometer range, which have been evaluated for ophthalmic drug delivery purposes over the past 15 years (148). Micro- or nanoparticles are divided in two groups, micro- or nanospheres and micro- or nanocapsules. Microspheres are monolithic particles possessing a porous or solid polymer matrix, whereas microcapsules consist of a polymeric membrane surrounding a solid or a liquid drug reservoir (148). Practically, the term nanoparticles is applied to nanospheres and nanocapsules because it is often difficult to determine if they are real capsules or matrix-type particles.

Table 6. Ocular Liposomal Formulations for Topical Application

Drug	Liposomal characteristics: Type	Liposomal characteristics: Size	Subject	Parameter(s) examined	Refs.
Acetylcholinesterase	MLV, MLV$^-$, MLV$^+$	0.2–4.0 μm	Rabbit	Prophylactic antimiotic efficacy	133
Acyclovir	SUV	N.A.	Mouse cornea	Binding ability Antiviral efficacy	134
Atropine base and sulfate	MLV, MLV$^-$, MLV$^+$	0.4–4.2 μ 0.4–4.2 μm 0.4–4.2 μm	Rabbit	Mydriasis	135
Dexamethasone and esters derivatives	MLV	1 μm	Rabbit cornea	Corneal steroid absorption	136
Dihydrostreptomycin sulfate	MLV, LUV, LUV$^+$ SUV, SUV$^+$	N.A.	Rabbit	Ocular drug disposition	137
Epinephrine	MLV	1.5 μm	Rabbit	Ocular drug concentration	125,138
Idoxuridine	MLV	0.2 μm	Rabbit	Antiviral efficacy	139
	N.A.	N.A.	Rabbit	Corneal penetration of ^{125}I-labeled drug	
Indoxole	MLV, MLV$^-$, MLV$^+$	N.A.	Rabbit cornea	Drug corneal interaction and penetration	128
	SUV, SUV$^-$, SUV$^+$		Rat		
Inulin	MLV	1.5 μm	Rabbit	Ocular drug concentration	125,138
Penicillin G	MLV, MLV$^-$, MLV$^+$	N.A.	Rabbit cornea	Drug corneal interaction and penetration	128
	SUV, SUV$^-$, SUV$^+$		Rat		
Pilocarpine base and hydrochloride	MLV, MLV$^-$, MLV$^+$	0.1–0.2 μm	Rabbit	Miosis, intra ocular pressure	140
Triamcinolone acetonide	MLV	5.0 μm	Rabbit	Ocular drug concentration	141
Tropicamide	MLV	0.3–1.2 μm	Rabbit	Precorneal clearance and bioavailability	142

Source: Adapted from Refs. 123 and 132.

The application of such systems in the ophthalmic field has been extensively reviewed by Kreuter and colleagues (148–150). Upon topical instillation of a particulate suspension in the cul-de-sac, the drug is slowly released in the lachrymal pool by dissolution and mixing, diffusion, or mechanical disintegration or erosion of the polymeric matrix (149). The upper size limit for microparticles for ophthalmic administration is about 5–10 μm. The ophthalmic administration of particles of higher size can result in an itching sensation and can induce lachrymation, with the possible consequence of reducing drug bioavailability.

The manufacturing methods used to produce micro- and nanoparticulate carriers are numerous, such as interfacial polymerization (151,152), desolvatation (153,154), or aggregation by pH adjustment and heat treatment (155). Nanoparticles for ophthalmic drug delivery have been mainly produced by emulsion polymerization and are based on several synthetic or natural biocompatible polymers, as shown in Table 7. The active compound can be dissolved, trapped, encapsulated, adsorbed or linked to these colloidal systems (148). The various fabrication processes have been extensively reviewed in specialized books or reviews (156–158) and in the chapter NANOPARTICLES of this encyclopedia.

As shown in Table 7, the principal materials used so far to prepare colloidal systems for ophthalmic drug delivery have been synthetic biodegradable polymers belonging to the group of poly(alkyl cyanoacrylate). These polymers can be degraded following two concomitant metabolization pathways, which are the erosion of the polymer backbone leading to the formation of formaldehyde (187) or the cleavage of the ester inducing the formation of a water-soluble polymer backbone and the corresponding alcohol (188). In vivo, the presence of enzymes favors the second pathway, which is quite convenient because it reduces the production of the toxic formaldehyde under physiological conditions. The nontoxicity of nanoparticles based on some polymers has been demonstrated in vivo, i.e., poly(isobutyl cyanoacrylate) and poly(hexyl cyanoacrylate) were found to be well tolerated after topical application in rabbits (148) and empty poly(butyl cyanoacrylate) nanoparticles in saline did not induce adverse effect in humans (189).

Drug release from poly(alkyl) cyanoacrylate nanoparticles can occur by different isolated or concomitant mechanisms (29):

- Degradation of the polymer (rate depending on the length of the alkyl chain)
- Desorption of the active compound adsorbed from the surface of the nanoparticles
- Diffusion through the polymeric matrix

Precorneal elimination and penetration of particles in the cornea have been evaluated using various labeling methods with radioactive tracers such as ^{141}Ce (190), ^{99m}Tc (183), ^{14}C (191,192), ^{111}In (193), or ^{3}H (165), or with fluorescent probes (194–196). Initial attempts to evaluate res-

Next Page

Table 7. Micro- and Nanoparticles as Drug Delivery Systems for Topical Ocular Application

Drug	Polymer	Refs.
Acyclovir	Chitosan	159
Amikacin	Poly(butyl cyanoacrylate)	160
Betaxolol	Poly(ϵ-caprolactone)	161
	Poly(isobutyl cyanoacrylate)	161,162
	Poly(lactide-*co*-glycolide)	161
Carteolol	Poly(ϵ-caprolactone)	163
Chloramphenicol	Poly(lactic acid)	164
Hydrocortisone	Albumin	165
Indomethacin	Poly(ϵ-caprolactone)	166
	Poly(ϵ-caprolactone) coated with chitosan	167,168
	Poly(ϵ-caprolactone) coated with poly(L-lysine)	167,168
Metipranolol	Poly(ϵ-caprolactone)	17
Pilocarpine	Albumin	169–172
	Gelatin	169
	Poly(butyl cyanoacrylate)	18,173–177
	Poly(hexyl cyanoacrylate)	174,177
	Poly(lactic acid)	178
	Poly(methyl methacrylate-*c*-acrylic acid)	11,179–181
	Poly(methyl methacrylate)	174
	Polyamide	182
	Polyphthalamide	183
Progesterone	Poly(hexyl cyanoacrylate)	184
	Poly(butyl cyanoacrylate)	185
Timolol	Poly(alkyl cyanoacrylate)	186

Source: Adapted from Ref. 147.

idence time were made in the early 1980s by Sieg and Triplett (190), who labeled polystyrene microspheres of 3 μm and 25 μm diameter with ^{141}Ce. They found that precorneal elimination of smaller particles was dependent on the volume instilled, unlikely for the 25 μm diameter particles. The washout phase was greatly enhanced after administration of 50 μL of 3 μm particles instead of 25 μL. Hence, this indicated that there was a lower limit for particle-size retention in the eye, in addition to the well-recognized upper size limit for preventing the onset of irritation. The study of Wood et al. (191), evaluating the disposition of poly(hexyl cyanoacrylate) nanoparticles, showed that colloidal particles were rapidly removed from the precorneal area in a similar way to aqueous solutions but were better retained, which was attributed to mucin binding or buoyancy of the nanoparticles.

Diepold et al. (192) and Zimmer et al. (165) have reported that the residence time of nanoparticles was significantly higher in inflamed ocular tissues than in healthy eyes. The increased retention of nanoparticles is probably due to some peculiar physiological modifications accompanying the inflammatory process. One can cite as possible causes an increased cell permeability (165), a secretion in the precorneal area of substances (e.g., albumin, fibrin) that can bind with nanoparticles, and a partial blockade of the nasolachrymal duct due to the swollen conjunctival tissue (192). These studies suggest that colloidal carriers could considerably improve the therapeutic index of some antiinflammatory, antibacterial, or antiviral drugs (150).

Calvo et al. (196), using confocal laser scanning microscopy, have observed ex vivo and in vivo that poly(ϵ-caprolactone) (PCL) nanocapsules penetrated the corneal epithelial cells by an endocytic mechanism. Furthermore, PCL nanocapsules (196) exhibited a selectivity for the cornea versus the conjunctiva, which means that such systems could reduce systemic absorption. This result was in accord with the in vivo data of Losa et al. (17), who found reduced cardiovascular side effects of metipranolol when incorporated in PCL nanocapsules.

Most applications of drug-loaded ophthalmic delivery systems involve glaucoma therapy, using either cholinergic agonists like pilocarpine (11,18,169,174,181) or β-blockers such as betaxolol (161–163) or carteolol (163). Zimmer et al. (171), evaluating miotic response and intraocular pressure (IOP) of rabbits after administration of pilocarpine-loaded microspheres and nanospheres based on albumin, reported a great improvement of the bioavailability of the drug, when compared with a reference solution. These particles increased the ocular bioavailability by 50–90% when considering the miotic response and by 50–70% when considering the IOP-lowering effect. Furthermore, the authors have shown that this result could be improved by coadministering these particles with bioadhesive polymers such as hyaluronic acid, mucin, sodium carboxymethylcellulose, or poly(acrylic acid) (172).

INSERTS

Definition

This section is devoted to solid devices delivering drugs to the anterior segment of the eye that are denoted by the general name *insert*, originating from the Latin *inserere*, to introduce. Historically, the first solid medication precursors of the present insoluble inserts were described in the nineteenth century. They consisted of squares of dry filter paper, previously impregnated with drug solutions (e.g., atropine sulfate, pilocarpine hydrochloride) (197); small sections were cut and applied under the eyelid. *Lamellae*, the precursors of the present soluble inserts, consisted of glycerinated gelatin containing different ophthalmic drugs (197). However, the use of lamellae ended when more stringent requirements for sterility of ophthalmic preparations were enforced. Nowadays, ophthalmic inserts are again provoking great interest, as evidenced by the increasing number of publications in the field in recent years. Table 8 gives an overview of the different drugs applied with inserts.

The uses of ocular inserts have been extensively reviewed by Bawa (198), Saettone (197), Saettone and Salminen (199), Khan and Durrani (200), and Shell (201,202). Gurtler and Gurny (203) have reviewed ophthalmic inserts in the patent literature, and Baeyens et al. (22) have described inserts as ocular drug delivery devices in veterinary medicine.

Ophthalmic inserts are defined as preparations with a solid or semisolid consistency, the size and shape of which are especially designed for ophthalmic application (i.e., rods or shields) (203). These inserts are placed in the lower fornix and, less frequently, in the upper fornix or on the

Previous Page

Table 7. Micro- and Nanoparticles as Drug Delivery Systems for Topical Ocular Application

Drug	Polymer	Refs.
Acyclovir	Chitosan	159
Amikacin	Poly(butyl cyanoacrylate)	160
Betaxolol	Poly(ϵ-caprolactone)	161
	Poly(isobutyl cyanoacrylate)	161,162
	Poly(lactide-*co*-glycolide)	161
Carteolol	Poly(ϵ-caprolactone)	163
Chloramphenicol	Poly(lactic acid)	164
Hydrocortisone	Albumin	165
Indomethacin	Poly(ϵ-caprolactone)	166
	Poly(ϵ-caprolactone) coated with chitosan	167,168
	Poly(ϵ-caprolactone) coated with poly(L-lysine)	167,168
Metipranolol	Poly(ϵ-caprolactone)	17
Pilocarpine	Albumin	169–172
	Gelatin	169
	Poly(butyl cyanoacrylate)	18,173–177
	Poly(hexyl cyanoacrylate)	174,177
	Poly(lactic acid)	178
	Poly(methyl methacrylate-*c*-acrylic acid)	11,179–181
	Poly(methyl methacrylate)	174
	Polyamide	182
	Polyphthalamide	183
Progesterone	Poly(hexyl cyanoacrylate)	184
	Poly(butyl cyanoacrylate)	185
Timolol	Poly(alkyl cyanoacrylate)	186

Source: Adapted from Ref. 147.

idence time were made in the early 1980s by Sieg and Triplett (190), who labeled polystyrene microspheres of 3 μm and 25 μm diameter with ^{141}Ce. They found that precorneal elimination of smaller particles was dependent on the volume instilled, unlikely for the 25 μm diameter particles. The washout phase was greatly enhanced after administration of 50 μL of 3 μm particles instead of 25 μL. Hence, this indicated that there was a lower limit for particle-size retention in the eye, in addition to the well-recognized upper size limit for preventing the onset of irritation. The study of Wood et al. (191), evaluating the disposition of poly(hexyl cyanoacrylate) nanoparticles, showed that colloidal particles were rapidly removed from the precorneal area in a similar way to aqueous solutions but were better retained, which was attributed to mucin binding or buoyancy of the nanoparticles.

Diepold et al. (192) and Zimmer et al. (165) have reported that the residence time of nanoparticles was significantly higher in inflamed ocular tissues than in healthy eyes. The increased retention of nanoparticles is probably due to some peculiar physiological modifications accompanying the inflammatory process. One can cite as possible causes an increased cell permeability (165), a secretion in the precorneal area of substances (e.g., albumin, fibrin) that can bind with nanoparticles, and a partial blockade of the nasolachrymal duct due to the swollen conjunctival tissue (192). These studies suggest that colloidal carriers could considerably improve the therapeutic index of some antiinflammatory, antibacterial, or antiviral drugs (150).

Calvo et al. (196), using confocal laser scanning microscopy, have observed ex vivo and in vivo that poly(ϵ-caprolactone) (PCL) nanocapsules penetrated the corneal epithelial cells by an endocytic mechanism. Furthermore, PCL nanocapsules (196) exhibited a selectivity for the cornea versus the conjunctiva, which means that such systems could reduce systemic absorption. This result was in accord with the in vivo data of Losa et al. (17), who found reduced cardiovascular side effects of metipranolol when incorporated in PCL nanocapsules.

Most applications of drug-loaded ophthalmic delivery systems involve glaucoma therapy, using either cholinergic agonists like pilocarpine (11,18,169,174,181) or β-blockers such as betaxolol (161–163) or carteolol (163). Zimmer et al. (171), evaluating miotic response and intraocular pressure (IOP) of rabbits after administration of pilocarpine-loaded microspheres and nanospheres based on albumin, reported a great improvement of the bioavailability of the drug, when compared with a reference solution. These particles increased the ocular bioavailability by 50–90% when considering the miotic response and by 50–70% when considering the IOP-lowering effect. Furthermore, the authors have shown that this result could be improved by coadministering these particles with bioadhesive polymers such as hyaluronic acid, mucin, sodium carboxymethylcellulose, or poly(acrylic acid) (172).

INSERTS

Definition

This section is devoted to solid devices delivering drugs to the anterior segment of the eye that are denoted by the general name *insert*, originating from the Latin *inserere*, to introduce. Historically, the first solid medication precursors of the present insoluble inserts were described in the nineteenth century. They consisted of squares of dry filter paper, previously impregnated with drug solutions (e.g., atropine sulfate, pilocarpine hydrochloride) (197); small sections were cut and applied under the eyelid. *Lamellae*, the precursors of the present soluble inserts, consisted of glycerinated gelatin containing different ophthalmic drugs (197). However, the use of lamellae ended when more stringent requirements for sterility of ophthalmic preparations were enforced. Nowadays, ophthalmic inserts are again provoking great interest, as evidenced by the increasing number of publications in the field in recent years. Table 8 gives an overview of the different drugs applied with inserts.

The uses of ocular inserts have been extensively reviewed by Bawa (198), Saettone (197), Saettone and Salminen (199), Khan and Durrani (200), and Shell (201,202). Gurtler and Gurny (203) have reviewed ophthalmic inserts in the patent literature, and Baeyens et al. (22) have described inserts as ocular drug delivery devices in veterinary medicine.

Ophthalmic inserts are defined as preparations with a solid or semisolid consistency, the size and shape of which are especially designed for ophthalmic application (i.e., rods or shields) (203). These inserts are placed in the lower fornix and, less frequently, in the upper fornix or on the

cornea. They are usually composed of a polymeric vehicle containing the drug and are mainly used for topical therapy.

Further advantages of inserts over other drug delivery systems discussed already are (22):

- accurate dosing
- absence of preservatives
- increased shelf live, due to the absence of water

However, they have one significant disadvantage, their solid consistency, which means that they are perceived by patients as a foreign body in the eye (199). Besides the initial discomfort, other potential disadvantages arising from their solid state are possible movement around the eye, occasional inadvertent loss during sleep or while rubbing the eyes, interference with vision, and difficult placement (and removal for insoluble types) (199). Most of the ongoing research is therefore dedicated to improving ocular retention and to ensure an easy placement by the patient, while reducing the foreign body sensation in the eye. Ophthalmic inserts are generally classified according to their solubility behavior and their possible bioerodibility (203) (Fig. 10).

Soluble Inserts

Soluble inserts are the most frequently investigated class of ophthalmic inserts (see Table 8). Their main advantage relies on their complete solubility compared with their insoluble counterparts, so that they do not need to be removed from the eye after deposition. They are usually divided into two categories according to their polymer composition. The first type is based on natural polymers whereas the second is derived from synthetic or semisynthetic polymers.

Natural Polymers. Natural polymers include collagen, which was the first ophthalmic insert excipient described in the literature. Inserts containing collagen were first developed by Fyodorov (198,240) as corneal bandages following surgical operations and eye disease. Later, collagen shields as drug carriers were suggested by Bloomfield et al. (223). As described for contact lenses, the therapeutic agents are generally absorbed by soaking the collagen shield in a solution containing the drug and, once placed in the eye, the drug is gradually released from the interstices between the collagen molecules, as the collagen dissolves. Accordingly, the residence time of drugs (241) such as antibacterials (222,242), antiinflammatory agents (234,236), antivirals (239,243), or combination drugs (230) was increased when compared with traditional eye drops (see Table 8). However, as observed for contact lenses, most drugs are released quite rapidly by a diffusion process, whereas dissolution requires a much longer time. The corneal shields, currently available for clinical use, do not contain drugs but are designed as disposable therapeutic corneal bandages (199). For example, Bio-Cor® (developed by Bausch and Lomb, Clearwater, Florida) is made of porcine scleral collagen, whereas Medilens® (developed by Chiron Ophthalmics, Irvine, California) and ProShield® (developed by Alcon Surgical, Forth Worth, Texas) are prepared from bovine corium tissue (243–245).

The main advantages of collagen shields over contact lenses is their solubility and that they do not need to be removed. However, collagen may cause an inflammatory response in the ocular tissues. Also, if shields are not used in association with antibacterials, a secondary infection may occur (239). Nowadays, these devices have the further disadvantage of not being well accepted by the authorities, because of possible prion-based infection.

Synthetic and Semisynthetic Polymers. Ophthalmic inserts containing synthetic, i.e., poly(vinyl alcohol) (205, 233), and semisynthetic, i.e., cellulose based (204,205,208, 209,216,225,233), polymers are frequently described in the literature (see Table 8). This stems in part from their advantage of being based in products well adapted for ophthalmic use and their ease of manufacture by conventional methods, including extrusion (225), compression (204), and compression molding (246). Drug release from such systems is generally characterized by two phases (203,247). The first corresponds to the penetration of tear fluid into the insert, which induces a rapid diffusion of the drug and forms a gel layer around the core of the insert. This external gelification induces the second phase corresponding to a decreased release rate, again controlled by diffusion. The major problems of these soluble inserts are the rapid penetration of the lachrymal fluid into the device, the blurred vision caused by the solubilization of insert components, and the glassy constitution of the insert increasing the risk of expulsion. Ethylcellulose, a hydrophobic polymer, can be used to decrease insert deformation and therefore prevent blurred vision (225,228,233). Regarding the risk of expulsion, several authors (217,218,225,228) have incorporated carbomer, which is at low concentrations a strong, but well-tolerated bioadhesive polymer. Recently, Baeyens et al. (226,228) and Gurtler et al. (225,248) have used CAP in combination with gentamicin sulfate to decrease drug solubility. Prolonged release of the drug above the minimal inhibitory concentration (MIC) was obtained for more than 50 h, whereas gentamicin incorporated without CAP was released for less than 24 h. Subsequently, a new insert providing release of gentamicin and dexamethasone at different rates was developed. The prolonged release of gentamicin—an antibacterial agent—is combined with the immediate release of dexamethasone—an antiinflammatory agent—against structural damage that can be caused by the infection (Fig. 11). The release rate can also be decreased by using Eudragit as an insert coating agent (204,205,216). This polymer is normally used for enteric coating, and Saettone et al. (204) have observed in rabbits that Eudragit-coated inserts containing pilocarpine induced a miotic effect of longer duration, compared with the corresponding uncoated products.

Lacrisert® is a soluble insert that was successfully commercialized by Merck Sharp and Dohme in 1981 (198). The device weighs 5 mg, measures 1.27 mm in diameter with a length of 3.5 mm, and is composed of HPC and is useful in the treatment of dry eye syndrome. The device is placed in the lower fornix where it slowly dissolves over 6–8 h to stabilize and thicken the tear film (249).

Table 8. Currently Available Inserts for Ocular Drug Delivery

Drugs	Type of insert	Carrier	Assays	Refs.
		Antiglaucoma		
Pilocarpine	Soluble	HPC/D-lactose/glyceryl palmito-stearate/Eudragit® RS	in vitro release in vivo miotic response	204
Pilocarpine	Soluble	PVA/XG/HPMC/HA/GB/Eudragit RS 30 D	in vitro release in vivo miotic response	205,206
Pilocarpine	PVP		in vitro release in vivo miotic response	207
Pilocarpine	Soluble	Alginate; MC	in vitro release in vivo miotic response in vivo release	208
Pilocarpine	Soluble	HPC; PVM/MA	in vitro release in vivo release	209
Pilocarpine	Soluble	HA; HAE	in vitro mucoadhesion in vivo retention in vivo miotic response	68
Pilocarpine	Bioerodible	PVMMA	in vitro release in vivo release	209
Pilocarpine	Bioerodible	Gelatin	in vitro release in vivo miotic response	210
Pilocarpine	Insoluble (diffusion)	Ethylene vinyl acetate, alginate	in vivo release	211
Pilocarpine	Insoluble (contact lens)	HEMM/EGDM	in vivo miotic response	212
Pilocarpine	Insoluble (contact lens)	MOPTSS/TEGDM/CHM/MA/MM	in vitro release	213,214
Pilocarpine/epinephrine	Insoluble (osmotic)	Ethylene vinyl acetate	in vitro release	215
Timolol	Soluble	HPC/Eudragit RS	in vitro release	216
Timolol	Soluble/bioerodible	HPC; PVA; PVMMA; PVA/Carbopol 940	in vitro release in vivo release	217
Timolol and prodrugs of timolol	Soluble/bioerodible	PVA; HPC; PVMMA; PVA/Carbopol 940	in vitro release in vivo release	218
Tilisolol	Soluble	HPM	in vitro release in vivo release	219

		Antibacterial		
Chloramphenicol	Soluble	PVA	in vivo release	206
Erythromycin	Soluble	Copolymers of *N*-vinylpyrrolidone	in vitro release in vivo release	220,221
Gentamicin	Soluble	Collagen	in vitro release in vivo release	222
Gentamicin	Soluble	Collagen	in vivo release	223
Gentamicin	Soluble	Collagen	in vitro release in vivo retention and release	224
Gentamicin	Soluble	HPC/EC/Carbopol 934P	in vivo release	225,226
Gentamicin	Bioerodible	Gelatin	in vitro release	227
Gentamicin and dexamethasone	Soluble	HPC/EC/Carbopol 934P	in vivo release	228,229
Gentamicin and dexamethasone	Soluble	Collagen	in vitro release in vivo release	230
Tobramycin	Soluble	Collagen	in vitro release in vivo treatment	231
Tobramycin	Soluble	Collagen	in vivo efficacy	
Tetracycline or chloramphenicol	Insoluble (contact lens)	PMM	in vitro release in vivo efficacy	232
		Antiinflammatory		
Dexamethasone	Soluble	PVA; HPC; EC; CAP; Eudragit	in vivo release	233
Dexamethasone	Soluble	Collagen	in vivo release	234
Dexamethasone	Bioerodible	Gelatin	in vivo release	233
Prednisolone	Insoluble (contact lens)	HEM/*n*-vinyl 2-pyrrolidone	in vitro release in vivo release	235
Prednisolone acetate	Soluble	Collagen	in vivo release	236
Hydrocortisone	Insoluble (osmotic)	Ethylene vinyl acetate	in vitro release	237
		Antiviral		
Idoxuridine	Bioerodible	Polypeptide	in vivo treatment	238
Trifluorothymidine	Soluble	Collagen	in vivo release	239

CAP, cellulose acetate phthalate; CHM, cyclohexane methacrylate; EC, ethylcellulose; EGDM, ethylene glycol dimethacrylate; GB, glyceryl behenate; HA, hyaluronic acid; HAE, ethyl ester hyaluronic acid; HEM, 2-hydroxyethylmetacrylate; HEMM, hydroxyethyl methyl metacrylate; HPC, hydroxypropylcellulose; HPM, hydroxypropyl methacrylate; HPMC, hydroxypropylmethylcellulose; MA, methacrylic acid; MC, methylcellulose; MM, methyl methacrylate; MOPTSS, metacryloxypropyl tris(trimethylsiloxy) silane; PAA, polyacrylic acid; PMM; poly(methyl methacrylate); PVA, poly(vinyl alcohol); PVM/MA, poly(methyl vinyl ether/maleic acid); PVMMA, n-butyl half ester of poly(methyl vinyl ether/maleic anhydride); PVP, poly(vinyl pyrrolidone); TEGDM, triethylene glycol dimethacrylate; XG, xanthan gum.

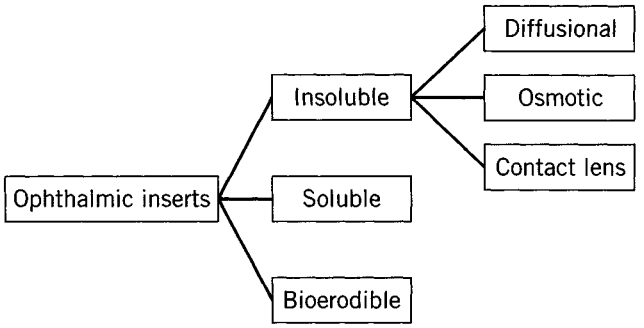


Figure 10. Classification of ophthalmic inserts. *Source:* Adapted from Ref. 203.

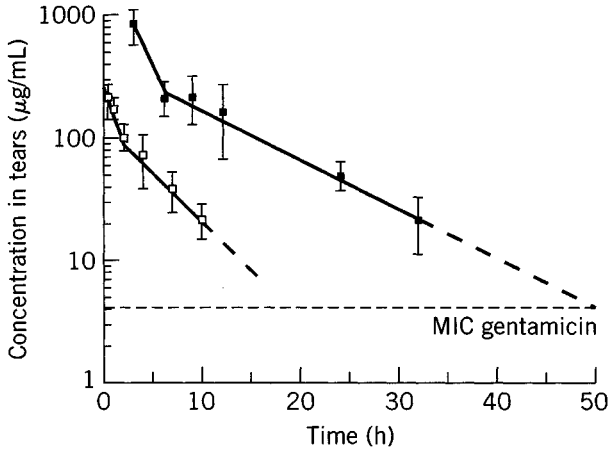


Figure 11. Combined release of gentamicin sulfate (■) and dexamethasone phosphate (□) at different release rates from a single insert containing 5.0 mg of gentamicin sulfate (25.0% w/w) and 1.0 mg of dexamethasone phosphate (5.0% w/w) (tested in rabbit, mean ± S.E.M., $n = 6$). *Source:* Adapted from Ref. 228.

New Ophthalmic Delivery System (NODS®), originally patented by Smith & Nephew Pharmaceuticals, Ltd., in 1985, consists of a medicated flag (4 mm × 6 mm, thickness 20 μm, weight 0.5 g) that is attached to a paper-covered handle by means of a short (0.7 mm) and thin (3–4 μm) membrane (Fig. 12) (206). All components (flag, membrane, and handle) are made of the same grade water-soluble poly(vinyl alcohol). For use, the flag is touched onto the surface of the lower conjunctival sac. The membrane dissolves, rapidly releasing the flag, which swells and dissolves in the lachrymal fluid, delivering the drug. When evaluated in humans, NODS produced an increase in bioavailability for pilocarpine and chloramphenicol with respect to standard eyedrop formulations (206).

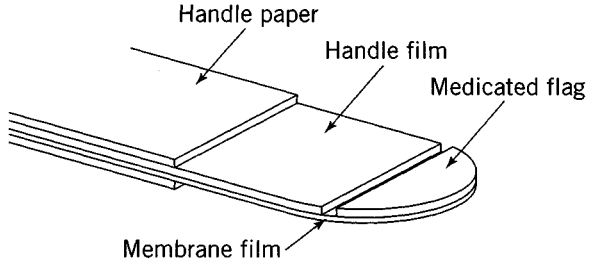


Figure 12. Schematic representation of the NODS system. *Source:* Adapted from Ref. 198.

Insoluble Inserts

Insoluble inserts can be classified into three categories (203): diffusional and osmotic systems, and hydrophilic contact lenses. Each class of insert shows a different drug release profile. Diffusional and osmotic systems contain a reservoir that is in contact with the inner surface of the drug rate controller to which its supplies the drug. The reservoir contains, respectively, a liquid, a gel, a colloid, a semisolid, a solid matrix, or a carrier containing drug. Carriers are made of hydrophobic, hydrophilic, organic, natural, or synthetic polymers. The third category, contact lenses, is a particular group of insoluble ophthalmic devices. However, the main disadvantage of these devices is their insolubility, because they need to be removed from the eye after treatment.

Diffusional Inserts. Diffusional inserts consist of a central reservoir of drug enclosed in specially designed semipermeable or microporous membranes allowing the drug to diffuse from the reservoir at a precisely determined rate. Drug release from such a system is controlled by the lachrymal fluid permeating through the membrane until a sufficient internal pressure is reached to drive the drug out of the reservoir. These diffusional systems prevent a continuous decrease in release rate by the use of a barrier membrane of fixed thickness, resulting in a zero-order release pattern.

Ocusert® (developed by Alza Corporation, Palo Alto, California) is undoubtedly the most commonly described insoluble insert in the literature (199,202,211,250–256) (Fig. 13). This flat, flexible, elliptical device consists of a pilocarpine reservoir with alginic acid, a mixture surrounded on both sides by a membrane of ethylene-vinyl acetate copolymer. The device is encircled by a retaining ring impregnated with titanium dioxide. The dimensions of the elliptical device are: major axis, 13.4 mm; minor axis, 5.7 mm; thickness, 0.3 mm. Two types of Ocusert are available for humans: the Pilo-20® and Pilo-40®, providing two different release rates for pilocarpine (20 μg/h and 40 μg/h, respectively) over a period of seven days (211).

Osmotic Inserts. The osmotic inserts are mostly described in the patent literature, and in vivo tests are rarely reported (203). They are generally made up of a central core surrounded by a peripheral component. The central part can consist of a single reservoir or two distinct compartments (Fig. 14). The single reservoir contains the drug, with or without an additional osmotic solute dispersed through a polymeric matrix, so that the drug is surrounded by the polymer as discrete small deposits. If the central part is made up of two compartments, the drug and the osmotic solute are placed in separate chambers, the drug

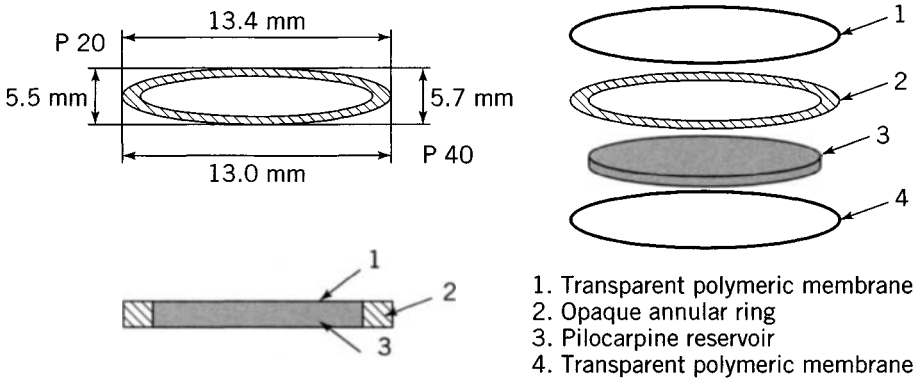


Figure 13. Schematic representation of the Ocusert system. *Source:* Adapted from Ref. 198.

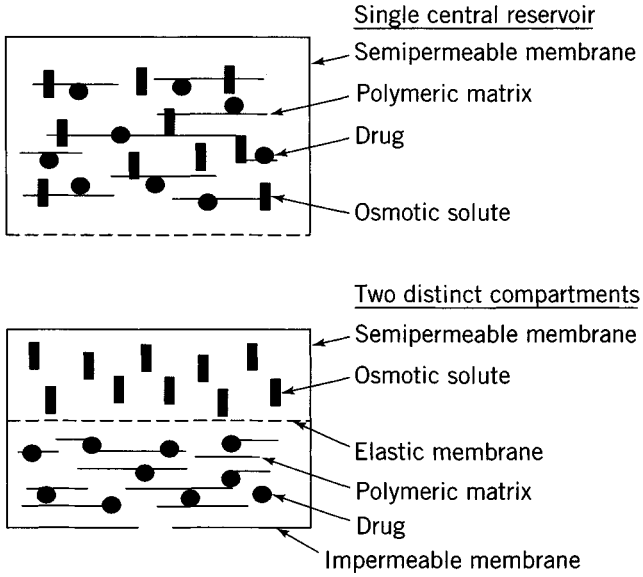


Figure 14. Schematic representation of the two types of osmotic inserts.

reservoir being surrounded by an elastic impermeable membrane, and the osmotic solute reservoir by a semipermeable membrane. The peripheral part of these osmotic inserts comprises in all cases a covering film made of an insoluble semipermeable polymer.

The majority of patents deal with systems having a unique central reservoir (215,237). The release of drug from these inserts can occur via two distinct release mechanisms: an osmotic and a diffusional release (203). When the insert is placed in the ocular environment, this starts the osmotic release, meaning tear fluid diffuses to the peripheral deposits through the semipermeable polymeric membrane, wets them, and induces their dissolution. The solubilized deposits generate a hydrostatic pressure against the polymer matrix triggering its rupture in the form of pores releasing the drug. This osmotic part of the release is characterized by a zero-order release profile. Ideally, the drug is continuously released from the osmotic insert by the increasing formation of apertures in the device forming a lattice of composition dispensing paths in the polymer on all sides of the inserts. In fact, these paths are interconnected, forming tortuous microchannels of irregular shapes and size causing a second drug release corresponding to a diffusional nonconstant release.

The release of drug from systems having a central reservoir subdivided into two compartments (257,258) starts as soon as the device is placed in the eye. Tears diffuse into the osmotic compartment, inducing osmotic pressure that stretches the elastic membrane and contracts the compartment containing the drug, so that the active compound is forced through the single drug release aperture. Thus, these systems are characterized by two distinct compartments and a single aperture having a very small diameter.

Contact Lenses. The initial use of contact lenses was for vision correction. The use of contact lenses has been extended as potential drug delivery devices by presoaking them in drug solutions. The main advantage of this system is the possibility of correcting vision and releasing drug simultaneously. Contact lenses are composed of a hydrophilic or hydrophobic polymer that swells by absorbing water. The swelling, caused by the osmotic pressure of the polymer segments, is opposed by the elastic retroactive forces arising along the chains as cross-links are stretched until a final swelling (equilibrium) is reached.

Refojo (259) has proposed a subdivision in five groups of contact lenses, namely rigid, semirigid, elastomeric, soft hydrophilic, and biopolymeric. Rigid contact lenses have the disadvantage of being composed of polymers (e.g., PMMA) hardly permeable to moisture and oxygen. Moreover, these systems are not suitable for prolonged delivery of drug to the eye and their rigidity makes them very uncomfortable to wear. The permeability problem was resolved using gas permeable polymers such as cellulose acetate butyrate. However, the discomfort associated with the foreign object and long adaptation period remain the shortcomings of rigid contact lenses. For this reason, soft hydrophilic contact lenses were developed for prolonged release of drugs such as pilocarpine (212), chloramphenicol and tetracycline (232), and prednisolone sodium phosphate (235) (see Table 8). The most commonly used polymer in the composition of these types of lenses is HEMM copolymerized with PVP or EGDM. PVP is used for increasing water of hydration, whereas EGDM is used to decrease the water of hydration.

Shell and Baker (247) have shown that drug release from presoaked contact lenses was extremely rapid, with

Table 9. Advantages and Shortcomings of Some Topical Ocular Drug Delivery Systems

Drug delivery system	Advantages	Shortcomings
Hydrogels	Reduction of the number of applications	Slight blurred vision
	Good compliance	No true sustained release effect
	Better tolerance than ointments	
Liposomes	Accurate dosing	Insufficient stability
	Improved bioavailability for lipophilic drugs	Short shelf life
		Limited drug loaded capacity
Micro- or nanoparticles	Accurate dosing	Too slight improvement for heavy processes of fabrication
	Slight increased ocular bioavailability	
Inserts	Accurate dosing	Difficulty of placement
	Absence of preservatives	Foreign body sensation
	Increased shelf life, due to the absence of water	

an in vivo residence time in general not longer than 24 h (200). In addition, preservatives, such as benzalkonium chloride, cannot be avoided and they have greater affinity with the hydrophilic contact lens material than for the aqueous drug solution (198). Bawa has described other approaches to decrease drug release rate from contact lenses. These include the introduction of the drug into the monomer mixture followed by polymerization of the monomers in the presence of the drug. This procedure removes the need for preservatives and consequent eye sensitization, because the drug is added in the matrix as a solid (213,214). However, the main problem associated with all contact lenses is their high cost of manufacture, and the difficulty of incorporating a precise amount of drug into the matrix. Disposable contact lenses have been commercially available for many years already, and the continued progress made in polymer chemistry should facilitate the development of this type of inserts.

Bioerodible Inserts

These inserts are formed by bioerodible polymers, i.e., materials that undergo hydrolysis of chemical bonds and hence dissolution (cross-linked gelatin derivatives, polyester derivatives) (209,211,233,238,260). The great advantage of these inserts is the possibility of modulating their erosion rate by modifying their final structure during synthesis, and by addition of anionic or cationic surfactants. However, erodible systems can have significantly variable erosion rates based on individual patient physiology and lachrymation patterns, whereas degradation products and residual solvents used during the polymer preparation can cause inflammatory reaction.

In conclusion, the majority of therapeutic agents can be delivered using inserts which are a promising alternative administration route, because of their various advantages compared with classical dosage forms. However, only few of these compounds have been commercialized. This can be attributed to the reluctance of ophthalmologists and patients to replace the traditional ophthalmic solutions as well as the cost and the need to train both the prescribers and the patients to place the inserts correctly in the eyes.

In the future, the use of ophthalmic inserts will certainly increase because of the development of new polymers, the emergence of new drugs having short biological half-lives or systemic side effects, and the need to improve the efficacy of ophthalmic treatments by ensuring an effective drug concentration in the eye for several days.

CONCLUSION

Although the various systems described in this article have been generally demonstrated to be successful approaches for prolonged ocular therapy, they all fall short of the ideal for a variety of reasons (Table 9). For example, the use of hydrogels remains associated with possible blurring vision, liposomes are often insufficiently stable after sterilization, and inserts are subject to a lack of patient compliance, due to their difficulty of placement in the eye (particularly for the elderly) and the sensation in the eye of foreign body. For these reasons, new polymers are currently under investigation to improve such systems and new approaches are being developed. Some authors have proposed the incorporation of lectins (261) or cyclodextrins (262,263) in ophthalmic formulations, or the use of codrugs (264) and prodrugs. Lectins have shown to bind to corneal and conjunctival surfaces as well as to the constituents of the tear film. Therefore, they are currently being investigated in the formulation of drug carrier complexes, where they could anchor the dosage form to the epithelial surfaces. The principle of using cyclodextrins in ophthalmic formulations relies on their ability to solubilize water-insoluble drugs and on capacity to reduce local drug irritation in the eye, which could, in turn, result in an improved bioavailability.

BIBLIOGRAPHY

1. S. Duke-Elder, in S. Duke-Elder, ed., *System of Ophthalmology*, Henry Kimpton, London, 1962, pp. 461–479.
2. V.H.L. Lee and J.R. Robinson, *J. Pharm. Sci.* **68**, 673–684 (1979).
3. L. Salminen, *J. Ocul. Pharmacol.* **6**, 243–249 (1990).
4. S.S. Chrai and J.R. Robinson, *J. Pharm. Sci.* **62**, 1112–1121 (1973).
5. V.H.L. Lee, *Pharm. Int.* **6**, 135–138 (1985).
6. M. Van Ooteghem, in P. Edman, ed., *Biopharmaceutics of Ocular Drug Delivery*, CRC Press, Boca Raton, Fla., 1993, pp. 27–42.
7. V. Baeyens and R. Gurny, *Pharm. Acta Helv.* **72**, 191–202 (1997).

8. M.F. Saettone, B. Giannaccini, F. Barattini, and N. Tellini, *Pharm. Acta Helv.* **2**, 3–11 (1982).
9. J.L. Greaves, C.G. Wilson, and A.T. Birmingham, *Br. J. Clin. Pharmacol.* **35**, 188–192 (1993).
10. R.N. Weinreb et al., *Am. J. Ophthalmol.* **110**, 189–192 (1990).
11. Z. Mazor, U. Ticho, U. Rehany, and L. Rose, *Br. J. Ophthalmol.* **63**, 58–51 (1979).
12. N.K. Gangrade, N.B. Gaddipati, M.G. Ganesan, and I.K. Reddy, in I.K. Reddy, ed., *Ocular Therapeutics and Drug Delivery*, Technomic Publishing, Lancaster, Pa., 1996, pp. 377–403.
13. O. Olejnik, in A.K. Mitra, ed., *Ophthalmic Drug Delivery Systems*, Dekker, New York, 1993, pp. 177–197.
14. Y.D. Sanzgiri et al., *J. Controlled Release* **26**, 195–201 (1993).
15. S. Kumar, B.O. Haglund, and K.J. Himmelstein, *J. Ocul. Pharmacol.* **10**(1), 47–56 (1994).
16. D.M. Maurice, *Int. Ophthalmol. Clin.* **33**, 81–91 (1993).
17. C. Losa et al., *J. Ocul. Pharmacol.* **8**, 191–198 (1992).
18. R. Diepold et al., *Graefe's Arch. Clin. Exp. Ophthalmol.* **227**, 188–193 (1989).
19. T. Boye, Ph.D Thesis, No. 2176, University of Geneva, School of Pharmacy, Geneva, Switzerland (1986).
20. S.R. Nadkarni and S.H. Yalokowsky, *Pharm. Res.* **10**, 109–112 (1993).
21. J.L. Greaves et al., *Br. J. Clin. Pharmacol.* **33**, 603–609 (1992).
22. V. Baeyens et al., *Adv. Drug Delivery Rev.* **28**, 335–361 (1997).
23. S.P. Kulkarni et al., *Drug Dev. Ind. Pharm.* **23**, 465–471 (1997).
24. T.F. Patton and J.R. Robinson, *J. Pharm. Sci.* **64**, 1312–1316 (1975).
25. S.S. Chrai and J.R. Robinson, *J. Pharm. Sci.* **63**, 1218–1222 (1974).
26. R. Krishnamoorthy and A.K. Mitra, in A.K. Mitra, ed., *Ophthalmic Drug Delivery Systems*, Dekker, New York, 1993, pp. 199–221.
27. S.W. Kim, Y.H. Bae, and T. Okano, *Pharm. Res.* **9**, 283–290 (1992).
28. B. Plazonnet et al., in M.F. Saettone, M. Bucci, and P. Speiser, eds., *Ophthalmic Drug Delivery; Biopharmaceutical, Technological and Clinical Aspects*, Liviana Press/ Springer-Verlag, Padova and Berlin, 1987, pp. 117–139.
29. P. Buri and F. Gurtler, in P. Buri et al., eds., *Les préparations ophthalmiques*, Lavoisier, Paris, 1995, pp. 127–215.
30. M. Zignani, C. Tabatabay, and R. Gurny, *Adv. Drug Delivery Rev.* **16**, 51–60 (1995).
31. K.C. Swan, *Arch. Ophthalmol. (Chicago)* **33**, 378–380 (1945).
32. W.H. Mueller and D.L. Deardorff, *Am. J. Pharm. Assoc.* **45**, 334–341 (1956).
33. J.S. Haas and D.C. Merrill, *Am. J. Ophthalmol.* **54**, 21–25 (1962).
34. S.P. Loucas and H.M. Haddad, *Metab. Ophthalmol.* **1**, 27–34 (1997).
35. R. Hardberger, C. Hanna, and C.M. Boyd, *Arch. Ophthalmol. (Chicago)* **93**, 42–45 (1975).
36. C. Melis-Decerf and M. Van Ooteghem, *J. Pharm. Pharmacol.* **31**, 12–15 (1979).
37. A. Ludwig and M. Van Ooteghem, *J. Pharm. Belg.* **44**, 391–397 (1989).
38. R.D. Schoenwald, R.L. Ward, L.M. DeSantis, and R.E. Roehrs, *J. Pharm. Sci.* **67**, 1280–1283 (1978).
39. A. Ludwig and M. Van Ooteghem, *S. T. P. Pharmacol. Sci.* **2**, 81–87 (1992).
40. G. Meseguer et al., *Int. J. Pharm.* **95**, 229–234 (1993).
41. A. Ludwig, N.J. Van Haeringen, V.M.W. Bodelier, and M. Van Ooteghem, *Int. Ophthalmol.* **16**, 23–26 (1992).
42. J. Grove, M. Durr, M. Quint, and B. Plazonnet, *Int. J. Pharm.* **66**, 23–28 (1990).
43. M. Dittgen, S. Oestereich, and D. Eckhardt, *S. T. P. Pharmacol. Sci.* **2**, 93–97 (1992).
44. M.F. Saettone et al., *Int. J. Pharm.* **20**, 187–202 (1984).
45. M.F. Saettone et al., *J. Pharm. Pharmacol.* **34**, 464–466 (1982).
46. J.H. Trueblood, R.M. Rossomondo, W.H. Carlton, and L.A. Wilson, *Arch. Ophthalmol. (Chicago)* **93**, 127–130 (1975).
47. S.G. Deshpande and S. Shirokolar, *J. Pharm. Pharmacol.* **41**, 197–200 (1989).
48. S.S. Tous and K. Abd-El Nasser, *S. T. P. Pharmacol. Sci.* **2**, 125–131 (1992).
49. N.A. Peppas, in N.A. Peppas, ed., *Hydrogels in Medicine and Pharmacy*, CRC Press, Boca Raton, Fla., 1987, pp. 1–37.
50. N. Krishna and F. Brow, *Am. J. Ophthalmol.* **57**, 99–106 (1964).
51. M.L. Linn and L.T. Jones, *Am. J. Ophthalmol.* **65**, 76–78 (1973).
52. F.C. Bach et al., *Am. J. Ophthalmol.* **68**, 659–662 (1970).
53. S.R. Waltman and T.C. Patrowicz, *Invest. Ophthalmol. Visual Sci.* **9**, 966–973 (1970).
54. I. Zaki, P. Fitzgerald, J.G. Hardy, and C.G. Wilson, *J. Pharm. Pharmacol.* **38**, 463–466 (1986).
55. A. Ludwig and M. Van Ooteghem, *Drug Dev. Ind. Pharm.* **14**, 2267–2284 (1988).
56. N.M. Davies, S.J. Farr, J. Hadgraft, and I.W. Kellaway, *Pharm. Res.* **8**, 1039–1043 (1991).
57. U.S. Pat. 4,141,973 (1979), E.A. Balazs.
58. S.F. Bernatchez, O. Camber, C. Tabatabay, and R. Gurny, in P. Edman, ed., *Biopharmaceutics of Ocular Drug Delivery*, CRC Press, Boca Raton, Fla., 1993, pp. 105–120.
59. R. Gurny et al., *Graefe's Arch. Clin. Exp. Ophthalmol.* **228**, 510–518 (1991).
60. G.R. Snibson et al., *Eye* **5**, 594–602 (1990).
61. G.R. Snibson et al., *Cornea* **11**, 288–293 (1992).
62. Y.S. Wysenbeek, N. Loya, and I. Ben Sira, *Invest. Ophthalmol. Visual Sci.* **29**, 194–199 (1988).
63. M.B. Limberg, C. McCaa, G.E. Kissling, and H.E. Kaufman, *Am. J. Ophthalmol.* **103**, 194–197 (1987).
64. C. Tabatabay, *J. Fr. Ophthalmol.* **8**, 513 (1985).
65. J.G. Orsoni et al., *Ophthalmologie* **2**, 355–357 (1988).
66. O. Camber, P. Edman, and R. Gurny, *Curr. Eye Res.* **6**, 779–784 (1987).
67. M.F. Saettone, D. Monti, M.T. Torracca, and P. Chetoni, *J. Ocul. Pharmacol.* **10**(1), 83–92 (1994).
68. M.F. Saettone et al., *Int. J. Pharm.* **51**, 203–212 (1989).
69. M.F. Saettone et al., *Int. J. Pharm.* **72**, 131–139 (1991).
70. R. Gurny et al., *J. Controlled Release* **6**, 367–373 (1987).
71. O. Camber and P. Edman, *Curr. Eye Res.* **8**, 563–567 (1989).
72. S.F. Bernatchez, C. Tabatabay, and R. Gurny, *Graefe's Arch. Clin. Exp. Ophthalmol.* **231**, 157–171 (1993).
73. S.S. Leung and J.R. Robinson, *J. Controlled Release* **5**, 223–231 (1988).
74. H. Park and J.R. Robinson, *Pharm. Res.* **4**, 457–464 (1987).
75. A. Ludwig, N. Unlü, and M. Van Ooteghem, *Int. J. Pharm.* **61**, 15–25 (1990).

76. R.C. Allen et al., *Am. J. Ophthalmol.* **97**, 723–729 (1984).
77. R.D. Schoenwald and J.J. Boltralik, *Invest. Ophthalmol. Visual Sci.* **18**, 61–66 (1979).
78. M.F. Saettone, B. Giannaccini, A. Guiducci, and P. Savigni, *Int. J. Pharm.* **31**, 261–270 (1986).
79. S. Mengi and S.G. Deshpande, *S. T. P. Pharmacol. Sci.* **2**, 118–124 (1992).
80. M.F. Saettone, B. Giannaccini, P. Savigni, and A. Wirth, *J. Pharm. Pharmacol.* **32**, 519–521 (1980).
81. N. Unlü, M. Van Ooteghem, and A.A. Hincal, *Pharm. Acta Helv.* **67**, 5–10 (1992).
82. N. von der Ohe, M. Stark, H. Mayer, and H. Brewitt, *Graefe's Arch. Clin. Exp. Ophthalmol.* **234**, 452–456 (1996).
83. P.D. Amin, C.P. Bhogte, and M.A. Deshpande, *Drug Dev. Ind. Pharm.* **22**, 735–739 (1996).
84. M. Albasini and A. Ludwig, *Farmaco* **50**, 633–642 (1995).
85. M.F. Saettone, in A.A. Hincal, H.S. Kasand, and M. Sumnu, eds., *New Approaches to Controlled Drug Delivery*, Editions de Santé, Paris, 1991, pp. 192–200.
86. A.H. Abd-El-Gawad, E.M. Ramadan, and U.A. Seleman, *Pharm. Ind.* **54**, 977–980 (1992).
87. O. Felt, P. Buri, and R. Gurny, *2nd Int. Symp. Exp. Clin. Ocul. Pharmacol. Pharm.*, 1997, p. 22.
88. A.S. Hoffman, A. Afrassiabi, and L.C. Dong, *J. Controlled Release* **4**, 213–222 (1986).
89. A.S. Hoffman, *J. Controlled Release* **6**, 297–305 (1987).
90. T.G. Park and A.S. Hoffman, *Proc. Int. Symp. Controlled Release Bioact. Mater.* **17**, 112–113 (1990).
91. I.R. Schmolka, *J. Biomed. Mater. Res.* **6**, 571–582 (1972).
92. *Technical Data on Pluronic® Polyol Gels*, Publ. No. 0-513, I.C. BASF Wyandotte Corp., Wyandotte, Mich., 1979.
93. S.C. Miller and B.R. Drabik, *Int. J. Pharm.* **18**, 269–276 (1984).
94. M. Vadnere, G. Amidon, S. Lindebaum, and J.L. Haslam, *Int. J. Pharm.* **22**, 207–218 (1984).
95. G.O. Waring and R.R. Harris, in I.H. Leopold and R.P. Burns, eds., *Symposium on Ocular Therapy*, Wiley, New York, 1979, pp. 127–140.
96. J.C. Gilbert, C. Washington, M.C. Davies, and J. Hadgraft, *Int. J. Pharm.* **40**, 93–99 (1987).
97. M.A. Lemp, *Int. Ophthalmol. Clin.* **13**, 221–223 (1973).
98. S.C. Miller and M.D. Donovan, *Int. J. Pharm.* **12**, 147–152 (1982).
99. G. Dumortier et al., *S. T. P. Pharmacol. Sci.* **2**(1), 111–117 (1992).
100. J.C. Gilbert, J. Hadgraft, A. Bye, and L.G. Brookes, *Int. J. Pharm.* **32**, 223–228 (1986).
101. P. Gilchrist et al., *137th Br. Pharm. Conf.*, Scarborough, September 15–19, 1997.
102. C. Koller and P. Buri, *S. T. P. Pharmacol. Sci.* **3**, 115–124 (1987).
103. M.S. El-Aasser, *Adv. Emulsion Polymer. Latex Technol., 10 Annu. Short Course,* Lehigh University, Bethlehem, Pa., 1979, pp. 1–13.
104. H. Ibrahim, Ph.D Thesis, No. 2369, University of Geneva, School of Pharmacy, Geneva, Switzerland (1989).
105. R. Gurny, T. Boye, H. Ibrahim, and P. Buri, *Proc. Int. Symp. Controlled Release Bioact. Mater.* **12**, 300–301 (1985).
106. H. Ibrahim, R. Gurny, C. Bindschaedler, and P. Buri, *5th Congr. Int. Technol. Pharm.*, APGI, Paris, 1989, pp. 70–76.
107. H. Ibrahim et al., *Int. J. Pharm.* **77**, 211–219 (1991).
108. H. Ibrahim et al., *4th Eur. Congr. Biopharm. Pharmacokinet.*, April 17–19, 1990.
109. H. Ibrahim et al., *Int. J. Pharm.* **87**, 239–246 (1992).
110. R. Gurny, *Pharm. Acta Helv.* **56**, 130–132 (1981).
111. R. Gurny, H. Ibrahim, and P. Buri, in P. Edman, ed., *Biopharmaceutics of Ocular Drug Delivery*, CRC Press, Boca Raton, Fla., 1993, pp. 81–90.
112. P. Jansson and B. Lindberg, *Carbohydr. Res.* **124**, 135–139 (1983).
113. M.A. O'Neill, R.R. Selvendran, and V.J. Morris, *Carbohydr. Res.* **124**, 123–133 (1983).
114. K.S. Kang et al., *Appl. Environ. Microbiol.* **43**, 1086–1091 (1982).
115. A. Rozier, J. Grove, C. Mazuel, and B. Plazonnet, *Proc. Int. Symp. Controlled Release Bioact. Mater.* **16**, 109–110 (1989).
116. P.B. Deasy and J. Quigley, *Int. J. Pharm.* **73**, 117–123 (1991).
117. Aust. Pat. 63189/86 (September 26, 1986), C. Mazuel and M. Friteyre (to Merck Sharp and Dohme Chibret).
118. D.M. Maurice and S.P. Srinivas, *J. Pharm. Sci.* **81**, 615–619 (1992).
119. J.L. Greaves et al., *Curr. Eye Res.* **9**, 415–420 (1990).
120. R. Vogel et al., *Invest. Ophthalmol. Visual Sci.* **31**, 404 (1990).
121. E. Verschueren, L. Van Santvliet, and A. Ludwig, *S. T. P. Pharmacol. Sci.* **6**, 203–210 (1996).
122. S. Cohen, E. Lobel, A. Trevgoda, and Y. Peled, *J. Controlled Release* **44**, 201–208 (1997).
123. V.H.L. Lee, P.T. Urrea, R.E. Smith, and D.J. Schanzlin, *Surv. Ophthalmol.* **29**, 335–348 (1985).
124. A.R. Tall, V. Hogan, L. Askinazi, and D.M. Small, *Biochemistry* **17**, 322–326 (1978).
125. R.E. Stratford, D.C. Yang, M.A. Redell, and V.H.L. Lee, *Curr. Eye Res.* **2**, 377–386 (1982).
126. F.J. Holly, *J. Colloid Interface Sci.* **49**, 221–231 (1974).
127. G. Smolin, M. Okumoto, S. Feiler, and D. Condon, *Am. J. Ophthalmol.* **91**, 220–225 (1981).
128. H.E. Schaeffer and D.L. Krohn, *Invest. Ophthalmol. Visual Sci.* **22**, 220–227 (1982).
129. P. Fitzgerald, J. Hadgraft, and C.G. Wilson, *J. Pharm. Pharmacol.* **39**, 487–490 (1987).
130. M. Mezei and D. Meisner, in P. Edman, ed., *Biopharmaceutics of Ocular Drug Delivery*, CRC Press, Boca Raton, Fla., 1993, pp. 91–104.
131. D. Meisner and M. Mezei, *Adv. Drug Delivery Rev.* **16**, 75–93 (1995).
132. N.M. Davies, I.W. Kellaway, J.L. Greaves, and C.G. Wilson, in A.K. Mitra, ed., *Ophthalmic Drug Delivery Systems*, Dekker, New York, 1993, pp. 289–306.
133. P.N. Shek and R.F. Barber, *Biochim. Biophys. Acta* **902**, 229–236 (1987).
134. S.G. Norley, D. Sendele, L. Huang, and B.T. Rouse, *Invest. Ophthalmol. Visual Sci.* **28**, 591–595 (1987).
135. D. Meisner, J. Pringle, and M. Mezei, *Int. J. Pharm.* **55**, 105–113 (1989).
136. K. Taniguchi et al., *J. Pharmacobio-Dyn.* **11**, 39–46 (1988).
137. I. Henriksen et al., *Int. J. Pharm.* **145**, 231–240 (1996).
138. R.E. Stratford, D.C. Yang, M.A. Redell, and V.H.L. Lee, *Int. J. Pharm.* **13**, 263–272 (1983).
139. S.K. Dharma, P.H. Fishman, and G.A. Peyman, *Acta Ophthalmol.* **64**, 298–301 (1986).
140. S. Benita et al., *J. Microencapsul.* **1**, 203–216 (1984).

141. K. Singh and M. Mezei, *Int. J. Pharm.* **16**, 339–344 (1983).
142. N.M. Davies, S.J. Farr, J. Hadgraft, and I.W. Kellaway, *Pharm. Res.* **9**, 1137–1144 (1992).
143. K. Taniguchi et al., *J. Pharmacobio-Dyn.* **11**, 607–611 (1988).
144. H. Tanaka et al., *J. Eye* **2**, 1127–1129 (1985).
145. R.I. Juliano, in R.I. Juliano, ed., *Drug Delivery Systems: Characteristics and Biomedical Applications*, Oxford University Press, New York, 1980, pp. 189–236.
146. S.E.G. Nilsson and S. Latkovic, *6th Congr. Eur. Soc. Ophthalmol.*, 1981, pp. 21–22.
147. K. Singh and M. Mezei, *Int. J. Pharm.* **19**, 263–269 (1984).
148. A. Zimmer and J. Kreuter, *Adv. Drug Delivery Rev.* **16**, 61–73 (1995).
149. A. Joshi, in I.K. Reddy, ed., *Ocular Therapeutics and Drug Delivery*, Technomic Publishing, Lancaster, Pa., 1996, pp. 441–460.
150. J. Kreuter, in A.K. Mitra, ed., *Ophthalmic Drug Delivery Systems*, Dekker, New York, 1993, pp. 275–287.
151. A. Duc-Mauger, J. Benoit, and F. Puisieux, *Pharm. Acta Helv.* **61**, 119–124 (1986).
152. U.S. Pat. 4,666,641 (1987), R. Fickat, S. Benita, and F. Puisieux.
153. J.J. Marty and R.C. Oppenheim, *Aust. J. Pharm. Sci.* **6**, 65–76 (1977).
154. U.S. Pat. 4,107,288 (1978), R.C. Oppenheim, J.J. Marty, and P. Speiser.
155. G.V. Taplin, D.E. Johnson, E.K. Dore, and H.S. Kaplan, *J. Nucl. Med.* **5**, 259–275 (1964).
156. J. Kreuter, *Pharm. Acta Helv.* **58**, 196–209 (1983).
157. J. Kreuter, in J.S. Boylan and J.C. Boylan, eds., *Encyclopedia of Pharmaceutical Technology*, Dekker, New York, 1994, pp. 165–190.
158. J. Kreuter, in *Colloidal Drug Delivery Systems*, Dekker, New York, 1994, pp. 219–342.
159. I. Genta et al., *J. Pharm. Pharmacol.* **49**, 737–742 (1997).
160. M.J. Alonso et al., *5th Congr. Int. Technol. Pharm.*, APGI, 1989, Paris, pp. 77–83.
161. L. Marchal-Heussler et al., *S. T. P. Pharmacol. Sci.* **2**, 98–104 (1992).
162. L. Marchal-Heussler et al., *Int. J. Pharm.* **58**, 115–122 (1990).
163. P. Maincent et al., *Proc. Int. Symp. Controlled Release Bioact. Mater.* **19**, 226–227 (1992).
164. U.S. Pat. 4,001,388 (January 4, 1977), J.W. Shell (to ALZA Corporation).
165. A.K. Zimmer, P. Maincent, P. Thouvenot, and J. Kreuter, *Int. J. Pharm.* **110**, 211–222 (1994).
166. V. Masson et al., *Proc. Int. Symp. Controlled Release Bioact. Mater.* **19**, 423–424 (1992).
167. P. Calvo, J.L. Vila-Jato, and M.J. Alonso, *Int. J. Pharm.* **153**, 41–50 (1997).
168. P. Calvo, J.L. Vila-Jato, and M.J. Alonso, *Proc. Int. Symp. Controlled Release Bioact. Mater.* **24**, 97–98 (1997).
169. S.E. Leucuta, *Int. J. Pharm.* **54**, 71–78 (1989).
170. A.K. Zimmer, J. Kreuter, M.F. Saettone, and H. Zerbe, *Proc. Int. Symp. Controlled Release Bioact. Mater.* **18**, 493–494 (1991).
171. A.K. Zimmer, H. Zerbe, and J. Kreuter, *J. Controlled Release* **32**, 57–70 (1994).
172. A.K. Zimmer et al., *J. Controlled Release* **53**, 31–46 (1995).
173. T. Harmia, P. Speiser, and J. Kreuter, *J. Microencapsul.* **3**, 3–12 (1986).
174. T. Harmia, P. Speiser, and J. Kreuter, *Int. J. Pharm.* **33**, 45–54 (1986).
175. T. Harmia et al., *Int. J. Pharm.* **33**, 187–193 (1986).
176. J. Kreuter, in M.F. Saettone, M. Bucci, and P. Speiser, eds., *Ophthalmic Drug Delivery*, Liviana Press Springer-Verlag, Padua and Berlin, 1987, pp. 101–106.
177. A. Zimmer et al., *Pharm. Res.* **11**, 1435–1442 (1994).
178. V. Vidmar, S. Pepeljnjak, and I. Jalsenjak, *J. Microencapsul.* **2**, 289–293 (1985).
179. C. Andermann, G. de Burlet, and C. Cannet, *J. Fr. Ophthalmol.* **5**, 499–504 (1982).
180. H.Z. Klein et al., *Am. J. Ophthalmol.* **99**, 23–26 (1985).
181. U. Ticho et al., *Br. J. Ophthalmol.* **63**, 45–47 (1979).
182. M.E. Evans, N.E. Richardson, and D.A. Norton, *J. Pharm. Pharmacol.*, 19 p. (1981).
183. M. Beal, N.E. Richardson, B.J. Meakin, and D.J.G. Davies, in Davis, Illum, McVie, and Tomlinson, eds., *Microspheres and Drug Therapy: Pharmaceutical Immunological and Medical Aspects*, 1984, pp. 347–348.
184. J. Kreuter et al., *Proc. Int. Symp. Controlled Release Bioact. Mater.* **12**, 304–305 (1985).
185. V.H.K. Li et al., *J. Microencapsul.* **3**, 213–218 (1986).
186. T. Harmia-Pulkinnen, A. Ihantola, A. Tuomi, and E. Kristoffersson, *Acta Pharm. Fenn.* **95**, 89–96 (1997).
187. W.R. Vezin and A.T. Florence, *J. Pharm. Pharmacol.* **30**, 5P (1978).
188. V. Lenaerts et al., *Biomaterials* **5**, 65–68 (1984).
189. J. Kreuter, in V. Lenaerts and R. Gurny, eds., *Bioadhesive Drug Delivery Systems*, CRC Press, Boca Raton, Fla., 1990, pp. 203–212.
190. J.W. Sieg and J.W. Triplett, *J. Pharm. Sci.* **69**, 863–864 (1980).
191. R.W. Wood, V.H.K. Li, J. Kreuter, and J.R. Robinson, *Int. J. Pharm.* **23**, 175–183 (1985).
192. R. Diepold, J. Kreuter, P. Guggenbuhl, and J.R. Robinson, *Int. J. Pharm.* **54**, 149–153 (1989).
193. P. Fitzgerald, J. Hadgraft, J. Kreuter, and C.G. Wilson, *Int. J. Pharm.* **40**, 81–84 (1987).
194. A. Zimmer, J.R. Robinson, and J. Kreuter, *Pharm. Res.* **7**, S114 (1990).
195. A. Zimmer, J. Kreuter, and J.R. Robinson, *J. Microencapsul.* **8**, 497–504 (1991).
196. P. Calvo et al., *Int. J. Pharm.* **103**, 283–291 (1994).
197. M.F. Saettone, in P. Edman, ed., *Biopharmaceutics of Ocular Drug Delivery*, CRC Press, London, 1993, pp. 61–79.
198. R. Bawa, in A.K. Mitra, ed., *Ophthalmic Drug Delivery Systems*, Dekker, New York, 1993, pp. 223–260.
199. M.F. Saettone and L. Salminen, *Adv. Drug Delivery Rev.* **16**, 95–106 (1995).
200. M.A. Khan and M.J. Durrani, in I.K. Reddy, ed., *Ocular Therapeutics and Drug Delivery*, Technomic Publishing, Lancaster, Pa., 1996, pp. 405–439.
201. J.W. Shell, *Drug Dev. Res.* **6**, 245–261 (1985).
202. J.W. Shell, *Surv. Ophthalmol.* **29**, 117–128 (1984).
203. F. Gurtler and R. Gurny, *Drug Dev. Ind. Pharm.* **21**(1), 1–18 (1995).
204. M.F. Saettone et al., *Acta Pharm. Technol.* **36**(1), 15–19 (1990).

205. M.F. Saettone et al., *Int. J. Pharm.* **86**, 159–166 (1992).
206. M.C. Richardson and P.H. Bentley, in A.K. Mitra, ed., *Ophthalmic Drug Delivery Systems*, Dekker, New York, 1993, pp. 355–367.
207. L. Salminen, A. Urtti, H. Kujari, and M. Juslin, *Graefe's Arch. Clin. Exp. Ophthalmol.* **221**, 96–99 (1983).
208. S.P. Loucas, M. Heskel, and M. Haddad, *Metab. Ophthalmol.* **1**, 27–34 (1976).
209. A. Urtti, L. Salminen, and O. Miinalainen, *Int. J. Pharm.* **23**, 147–161 (1985).
210. G.M. Grass, J. Cobby, and M.C. Makoid, *J. Pharm. Sci.* **73**, 618–621 (1984).
211. L. Sendelbeck, D. Moore, and J. Urqhart, *Am. J. Ophthalmol.* **80**, 274–283 (1975).
212. Y.T. Maddox and H.N. Bernstein, *Ann. Ophthalmol.* **4**, 789–802 (1972).
213. Eur. Pat. 219-207-A2 (April 22, 1987), R. Bawa (to Bausch and Lomb, Inc.).
214. Eur. Pat. 219-207-B1 (April 22, 1987), R. Bawa (to Bausch and Lomb, Inc.).
215. U.S. Pat. 4,190,642 (February 26, 1980), R.M. Gale, M. Ben-Dor, and N. Keller (to ALZA Corporation).
216. U.S. Pat. 5,145,884 (September 8, 1992), Y. Yamamoto, Y. Kaga, T. Yoshikawa, and A. Moribe (to Menicon Co.).
217. V.H.L. Lee et al., *J. Ocul. Pharmacol.* **10**, 421–429 (1994).
218. V.H.L. Lee et al., *Proc. Int. Symp. Controlled Release Bioact. Mater.* **18**, 291–292 (1991).
219. H. Sasaki, C. Tei, K. Nishida, and J. Nakamura, *J. Controlled Release* **27**, 127–137 (1993).
220. S. Hosaka, H. Ozawa, and H. Tanzawa, *Biomaterials* **4**, 243–247 (1983).
221. H. Ozawa, S. Hosaka, T. Kunitomo, and H. Tanzawa, *Biomaterials* **4**, 170–174 (1983).
222. R.B. Phinney, D. Schwartz, D.A. Lee, and B.J. Mondino, *Arch. Ophthalmol. (Chicago)* **106**, 1599–1604 (1988).
223. S.E. Bloomfield et al., *Arch. Ophthalmol. (Chicago)* **96**, 885–887 (1978).
224. D.H. Slatter, N.D. Costa, and M.E. Edwards, *Aust. Vet. J.* **59**, 4–6 (1982).
225. F. Gurtler, V. Kaltsatos, B. Boisramé, and R. Gurny, *J. Controlled Release* **33**, 231–236 (1995).
226. V. Baeyens et al., *J. Ocul. Pharmacol. Ther.* **14**, 263–272 (1998).
227. P.I. Punch, D.H. Slatter, N.D. Costa, and M.E. Edwards, *Aust. Vet. J.* **62**(3), 79–82 (1985).
228. V. Baeyens et al., *J. Controlled Release* **52**, 215–220 (1998).
229. V. Baeyens, E. Varesio, J.-L. Veuthey, and R. Gurny, *J. Chromatogr. B* **692**, 222–226 (1997).
230. J.K. Milani et al., *Am. J. Ophthalmol.* **116**, 622–627 (1993).
231. K.K. Assil, S.R. Zarnegar, B.D. Fouraker, and D.J. Schanzlin, *Am. J. Ophthalmol.* **113**, 418–423 (1992).
232. R. Praus, I. Brettschneider, L. Krejci, and D. Kalvodova, *Ophthalmologica* **165**, 62–70 (1972).
233. M.A. Attia, M.A. Kassem, and S.M. Safwat, *Int. J. Pharm.* **47**, 21–30 (1988).
234. D.G. Hwang, W.H. Stern, P.H. Hwang, and L.A. MacGowan-Smith, *Arch. Ophthalmol. (Chicago)* **107**, 1375–1380 (1989).
235. D.S. Hull, H.F. Edelhauser, and R.A. Hyndiuk, *Arch. Ophthalmol. (Chicago)* **92**, 413–416 (1974).
236. M.R. Sawusch, T.P. O'Brien, and S.A. Updegraff, *J. Cataract Refract. Surg.* **15**, 625–628 (1989).
237. Ger. Offen. P-26-33-987.7 (February 10, 1977), R.M. Gale (to ALZA Corporation).
238. D. Pavan-Langston, R.H.S. Langston, and P.A. Geary, *Arch. Ophthalmol. (Chicago)* **93**, 1349–1351 (1975).
239. J.R. Gussler, P. Ashton, W.S. VanMeter, and T.J. Smith, *J. Cataract Refract. Surg.* **16**, 719–722 (1990).
240. U.S. Pat. 4,913,904 (April 3, 1990), S.N. Fyodorov et al.,
241. M.L. Friedberg, U. Pleyer, and B.J. Mondino, *Ophthalmology* **98**, 725–732 (1991).
242. M.R. Sawusch, T.P. O'Brien, J.D. Dick, and J.D. Gottsch, *Am. J. Ophthalmol.* **106**, 279–281 (1988).
243. J.M. Hill, R.J. O'Callaghan, J.A. Hobden, and H.E. Kaufman, in A.K. Mitra, ed., *Ophthalmic Drug Delivery Systems*, Dekker, New York, 1993, pp. 261–273.
244. R.S. Shofner, H.E. Kaufman, and J.M. Hill, *Ophthalmol. Clin. North Am.* **2**, 15–23 (1989).
245. B.J. Mondino, *Am. J. Ophthalmol.* **112**, 587–590 (1991).
246. R.J. Harwood and J.B. Schwartz, *Drug Dev. Ind. Pharm.* **8**(5), 663–682 (1982).
247. J.W. Shell and R.W. Baker, *Ann. Ophthalmol.* **6**, 1037–1045 (1974).
248. F. Gurtler et al., *Pharm. Res.* **12**, 1791–1795 (1995).
249. D.W. Lamberts, D.P. Langston, and W. Chu, *Ophthalmology* **85**, 794–800 (1978).
250. J.R. Robinson, *S.T.P. Pharmacol. Sci.* **5**(12), 839–846 (1989).
251. B.G. Clerc and C. Robberechts, *Recl. Med. Vet.* **168**, 97–103 (1992).
252. S.M. Drance, D.W.A. Mitchell, and M. Schulzer, *Can. J. Ophthalmol.* **10**, 450–452 (1975).
253. M.F. Armaly and K.R. Rao, *Invest. Ophthalmol. Visual Sci.* **12**(7), 491–496 (1973).
254. I.P. Pollack, H.A. Quigley, and T.S. Harbin, *South Med. J.* **69**(10), 1296–1301 (1976).
255. R.L. Friederich, *Ann. Ophthalmol.* **6**, 1279–1284 (1974).
256. U.S. Pat. 4,014,335 (March 29, 1977), R.K. Arnold (to ALZA Corporation).
257. Eur. Pat. 262-893-A2 (December 18, 1988), S. Darougar (to Merck and Co., Inc.).
258. U.S. Pat. 5,147,647 (September 15, 1992), S. Darougar.
259. M.F. Refojo, *Curr. Eye Res.* **4**(6), 719–723 (1985).
260. P.I. Punch, D.H. Slatter, N.D. Costa, and M.E. Edwards, *J. Vet. Pharmacol. Ther.* **8**, 335–338 (1985).
261. T.J. Nicholls et al., *Int. J. Pharm.* **138**, 175–183 (1996).
262. T. Loftsson and E. Stefansson, *Drug Dev. Ind. Pharm.* **23**, 473–481 (1997).
263. N.M. Davies, G. Wang, and I.G. Tucker, *Proc. Int. Symp. Controlled Release Bioact. Mater.* **24**, 547–548 (1997).
264. H. Guo, G. De Witt, M. Wu, and P. Ashton, *Proc. Int. Symp. Controlled Release Bioact. Mater.* **24**, 617–618 (1997).

See also BIOADHESIVE DRUG DELIVERY SYSTEMS; MUCOSAL DRUG DELIVERY, BUCCAL; MUCOSAL DRUG DELIVERY, INTRAVITREAL; MUCOSAL DRUG DELIVERY, NASAL; MUCOSAL DRUG DELIVERY, VAGINAL DRUG DELIVERY AND TREATMENT MODALITIES.

MUCOSAL DRUG DELIVERY, VAGINAL DRUG DELIVERY AND TREATMENT MODALITIES

JONATHAN D. EICHMAN
University of Michigan Medical School
Ann Arbor, Michigan
MICHAEL J. RATHBONE
InterAg
Hamilton, New Zealand
JOSEPH R. ROBINSON
University of Wisconsin
Madison, Wisconsin

KEY WORDS

Animal vagina
Bioadhesives
Contraception
Drug delivery
Estrus cycle control
Hormones
Human vagina
Inserts
Vagina
Vaginal dryness

OUTLINE

Introduction and Overview
Vaginal Anatomy and Physiology
  Premenopausal State
  Peri- and Postmenopausal State
Desirable Features of a Vaginal Drug Delivery System
Reproductive System Pathologies and Treatment
  Vaginal Dryness
  Menopausal Stress Incontinence
  Bacterial Vaginosis
  Sexually Transmitted Diseases
  Endometriosis
Topical Contraceptives
Other Vaginal Drug Delivery Systems
Veterinary Applications
  Brief History
Design Factors in Controlled Release Intravaginal Veterinary Drug Delivery Systems
Intravaginal Veterinary Drug Delivery Systems
Future Demands and Requirements of Intravaginal Veterinary Drug Delivery Systems
Bibliography

INTRODUCTION AND OVERVIEW

Products for women are on the rise in part because of gender equality issues and in part because of new drugs and/or delivery systems. Given the convenience of the oral route of administration, this is still the preferred route of drug delivery. However, many drugs are intended for local treatment and still other drugs are susceptible to first-pass metabolism; hence, the vaginal route of drug delivery is a more common site of drug application today than it was in the recent past.

Vaginal delivery of treatment modalities for local conditions is both understandable and expected whereas using the vaginal portal for systemic drug delivery carries with it both cultural and therapeutic issues. As will become clear in this article, the vaginal route is a very attractive route for drug delivery despite the presence of significant biological barriers.

A cartoon depiction of the reproductive organs is shown in Figure 1. Note the location of the vagina leading to the cervix. Dimensions of the vaginal cavity vary with age and tissue thickness and also varies with hormonal status. These changes present a challenge in the design of an appropriate drug delivery system that is effective across all age patients irrespective of their hormonal status.

VAGINAL ANATOMY AND PHYSIOLOGY

Premenopausal State

The vagina is a thin-walled, fibromuscular tube extending from the body exterior to the uterus. In the adult premenopausal female, the vagina is approximately 7 to 10 cm in length and 2 cm in width. The vagina may be segmented into the anterior wall (8 cm) and the posterior wall (11 cm), which combine to form two ridges of folds imparting a cross-sectional H-shaped appearance (1).

The vaginal wall consists of three principal layers: the epithelial layer, the muscular coat, and the tunica externa (adventitia). The inner mucosal layer may be further subdivided into the epithelium and lamina propria (2). The outermost epithelium is situated above the basement membrane and consists of noncornified, stratified squamous epithelium subdivided into four distinct layers: (*1*) a superficial layer consisting of large, flat cells with pyknotic nuclei; (*2*) an intermediate layer of larger and flatter nucleated cells; (*3*) a parabasal layer of polyhedral cells; and (*4*) a monolayer of cuboidal basal cells closely apposed to the basement membrane (3,4). A depiction of vaginal cell histology is shown in Figure 2. The first three cell categories are frequently exfoliated. Cuboidal cells are typically not sloughed off the vaginal wall unless undergoing extensive trauma. The epithelium overlies and is supported by the lamina propria, a region of dense connective tissue intertwined with a network of elastic fibers. The epithelium is drawn into numerous longitudinal and transverse muscular folds called rugae serving to increase the vaginal surface area (5). The vaginal wall does not contain mucus glands, but is continuously covered by a thin layer of protective moisture, some of which is obtained from Skene's and Bartholin's glands located near the vaginal orifice.

MUCOSAL DRUG DELIVERY, VAGINAL DRUG DELIVERY AND TREATMENT MODALITIES

JONATHAN D. EICHMAN
University of Michigan Medical School
Ann Arbor, Michigan
MICHAEL J. RATHBONE
InterAg
Hamilton, New Zealand
JOSEPH R. ROBINSON
University of Wisconsin
Madison, Wisconsin

KEY WORDS

Animal vagina
Bioadhesives
Contraception
Drug delivery
Estrus cycle control
Hormones
Human vagina
Inserts
Vagina
Vaginal dryness

OUTLINE

Introduction and Overview
Vaginal Anatomy and Physiology
  Premenopausal State
  Peri- and Postmenopausal State
Desirable Features of a Vaginal Drug Delivery System
Reproductive System Pathologies and Treatment
  Vaginal Dryness
  Menopausal Stress Incontinence
  Bacterial Vaginosis
  Sexually Transmitted Diseases
  Endometriosis
Topical Contraceptives
Other Vaginal Drug Delivery Systems
Veterinary Applications
  Brief History
Design Factors in Controlled Release Intravaginal Veterinary Drug Delivery Systems
Intravaginal Veterinary Drug Delivery Systems
Future Demands and Requirements of Intravaginal Veterinary Drug Delivery Systems
Bibliography

INTRODUCTION AND OVERVIEW

Products for women are on the rise in part because of gender equality issues and in part because of new drugs and/or delivery systems. Given the convenience of the oral route of administration, this is still the preferred route of drug delivery. However, many drugs are intended for local treatment and still other drugs are susceptible to first-pass metabolism; hence, the vaginal route of drug delivery is a more common site of drug application today than it was in the recent past.

Vaginal delivery of treatment modalities for local conditions is both understandable and expected whereas using the vaginal portal for systemic drug delivery carries with it both cultural and therapeutic issues. As will become clear in this article, the vaginal route is a very attractive route for drug delivery despite the presence of significant biological barriers.

A cartoon depiction of the reproductive organs is shown in Figure 1. Note the location of the vagina leading to the cervix. Dimensions of the vaginal cavity vary with age and tissue thickness and also varies with hormonal status. These changes present a challenge in the design of an appropriate drug delivery system that is effective across all age patients irrespective of their hormonal status.

VAGINAL ANATOMY AND PHYSIOLOGY

Premenopausal State

The vagina is a thin-walled, fibromuscular tube extending from the body exterior to the uterus. In the adult premenopausal female, the vagina is approximately 7 to 10 cm in length and 2 cm in width. The vagina may be segmented into the anterior wall (8 cm) and the posterior wall (11 cm), which combine to form two ridges of folds imparting a cross-sectional H-shaped appearance (1).

The vaginal wall consists of three principal layers: the epithelial layer, the muscular coat, and the tunica externa (adventitia). The inner mucosal layer may be further subdivided into the epithelium and lamina propria (2). The outermost epithelium is situated above the basement membrane and consists of noncornified, stratified squamous epithelium subdivided into four distinct layers: (*1*) a superficial layer consisting of large, flat cells with pyknotic nuclei; (*2*) an intermediate layer of larger and flatter nucleated cells; (*3*) a parabasal layer of polyhedral cells; and (*4*) a monolayer of cuboidal basal cells closely apposed to the basement membrane (3,4). A depiction of vaginal cell histology is shown in Figure 2. The first three cell categories are frequently exfoliated. Cuboidal cells are typically not sloughed off the vaginal wall unless undergoing extensive trauma. The epithelium overlies and is supported by the lamina propria, a region of dense connective tissue intertwined with a network of elastic fibers. The epithelium is drawn into numerous longitudinal and transverse muscular folds called rugae serving to increase the vaginal surface area (5). The vaginal wall does not contain mucus glands, but is continuously covered by a thin layer of protective moisture, some of which is obtained from Skene's and Bartholin's glands located near the vaginal orifice.

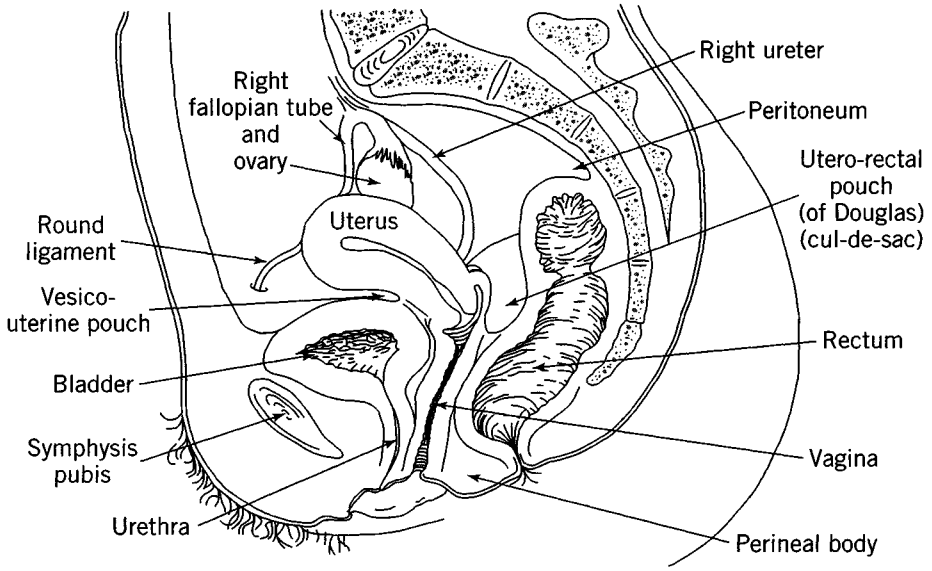


Figure 1. A depiction of the human reproductive system.

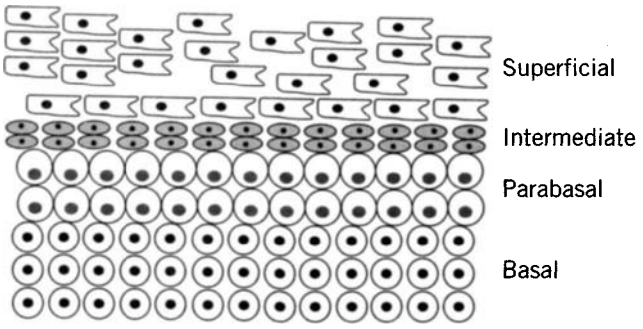


Figure 2. Depiction of vaginal histology.

Most vaginal secretions originate from cervical mucus glands and/or exuded fluid from the highly vascularized lamina propria (transudation) as well as cells sloughed off from the vaginal mucosa (3,6). Cervical mucus is a primary source of vaginal moisture and acts as a barrier layer protecting the underlying epithelium. During a woman's reproductive years, approximately 1 to 3 g/day of total fluid is secreted. Increased blood vessel dilation due to sexual stimulation leads to enhanced blood flow to the vaginal region and increases the production of this vaginal fluid. The volume and viscosity of cervical mucus undergoes significant changes during the menstrual cycle. Estrogen dominates during the first half of the cycle, which at ovulation induces large quantities of mucus secretion and is characteristically thin and alkaline. During the luteal phase, in which progesterone levels are high, mucus secretion decreases and is more viscous.

The muscular layer, lying distal to the epithelium, consists of smooth muscles and elastic fibers. The latter are primarily arranged in longitudinal fashion with a small inner portion of fibers arranged circularly. This organization imparts great elasticity to the vagina. The outer tunica adventitia consists of dense, loose connective tissue and provides a region of attachment of the vagina to surrounding organs.

Vaginal blood perfusion is supplied from uterine and pudendal arteries, which branch from the internal iliac arteries. Subsequently, these arteries form the cervicovaginal artery supplying the cervix and vaginal surfaces. The vaginal, uterine, and vesicle veins allow drainage of the rich plexus surrounding the vagina with eventual emptying into the internal iliac veins (3,7). Suffice it to say that the vagina is well endowed with a blood supply.

Vaginal fluid is acidic due to the presence of Döderlein's lactobacilli, which convert luminal carbohydrates such as glycogen secreted from exfoliated epithelial cells into lactic acid (8). A newborn child's vaginal pH ranges from 5.5 to 5.8, which is attributable to alkalinity of the amniotic fluid. During the first week of life, Döderlein's bacilli appear within the vaginal cavity dropping the pH to approximately 5.0. This value rises to neutrality within the first month and persists until puberty (9). During the years between the initial menstrual period (i.e., menarche) and menopause, pH for a healthy vagina drops to 4.0 to 5.0 with considerable fluctuation, dependent upon the menstrual cycle. The lowest pH values occur midcycle, whereas higher values are obtained during the period immediately prior to or preceding menstruation (9,10). A pH gradient also exists within the vagina, in which the lowest and highest values are obtained as one moves towards the cervix and vaginal vestibule, respectively (9). Sexual stimulation or enhanced blood flow stimulate an increase in vaginal pH.

The vaginal mucosa has been observed to undergo cytological changes influenced by the level and type of hormones present. Thus, due to a high concentration of maternal estrogen within the neonate, the vaginal epithelium is quite thick. Within three weeks, the epithelium flattens and remains relatively thin until puberty, at which time the epithelium thickens to normal levels ranging from 200 to 300 μm depending upon estrogen levels during the menstrual cycle.

Vaginal fluid consists primarily of cervical secretions and transudation from blood vessels through intercellular channels into the vagina. Thus, these secretions are dependent on blood flow rate. The weight of vaginal discharge in premenopausal women is 3–4 g/4 hours, whereas estrogen-deprived postmenopausal women have discharges that are 50% less. Table 1 shows typical vaginal discharges for women.

Peri- and Postmenopausal State

Perimenopause is the 3 to 5 years preceding menopause during which there is a reduction in estrogen levels. The perimenopause period typically begins during the midforties and is characterized by menstrual cycle irregularity (12). During a normal menstrual cycle, 6 to 12 follicles mature and proliferate in response to follicle-stimulating hormone (FSH) and luteinizing hormone (LH), but only a single follicle releases an ovum (13). The remaining follicles degenerate and by inception of menopause, a limited number of follicles are present in the ovary. During perimenopause, the reduction in functional follicles precipitates an alteration in ovary hormone secretion. Typically, the ovaries secrete high concentrations of estrogen during the follicular phase of the menstrual cycle. The menstrual cycle depends upon the presence of estrogen for development of theca and granulosa cells, which are involved in the production of estrone, estradiol-17 β, and also induce an LH surge required for ovulation (13,14). As the menstrual cycle becomes more irregular, the ovaries become unresponsive to higher FSH levels. By the end of perimenopause, estrogen production has declined 70–80% of its original concentration, leading to a subsequent decrease in estradiol production and thus removing an important negative feedback control to FSH production. The decline in estrogen levels also prevents LH production necessary for ovulation. Therefore, the initial clinical evidence of perimenopause is a shortened menstrual cycle precipitated by high FSH secretion creating rapid follicular development (14).

Menopause is defined as the last spontaneous episode of uterine bleeding in which the ovaries stop producing hormones (15). Histologically, the vaginal epithelium changes and returns to conditions similar to prepuberty. The epithelium thickness is reduced, corresponding to a shedding of the outer superficial and intermediate cell layers, in which vaginal smears of menopausal women primarily show the presence of basal cells and leukocytes (16). In premenopausal women, the vaginal mucosa may be as thick as 45 cell layers during the first half of the menstrual cycle. In comparison, the vaginal mucosa of postmenopausal women becomes fragile and may be composed of only three to four cell layers. Figure 3 represents a section of normal vaginal tissue compared with estrogen-deficient tissue. Along with epithelial thinning, there is a subsequent drop in glycogen and Döderlein's bacilli levels precipitating alterations in bacterial flora and an increased alkalinity to pH 7.0 (4). The pH change leads to an enhanced opportunity for bacterial and fungal infections due to the loss of acidic organisms within the vaginal cavity.

In postmenopausal women, there is a decrease in the size of the vagina in comparison to menstruating women. The average vaginal length and width decrease to 6.0 and 1.0 cm, respectively. The vagina also loses its elasticity and vascularity, the latter of which precipitates a reduction in vaginal secretions, which become increasingly watery after menopause (1).

Table 1. Vaginal Discharge Rates

Subjects	Rate of Discharge	Refs.
Reproductive Age		
Including cervical secretions	3–4 g/4 h	11
Without cervical secretions	2.7 g/24 h	10
Postmenopausal, no estrogen supplement	1.7 g/4 h	11
Hysterectomized		
Ovarectomized	1.56 ± 0.05 g/24 h	10
Intact ovaries	1.89 ± 0.12 g/24 h	10
Ovarectomized with estrogen supplement	1.97 ± 0.05 g/24 h	10

DESIRABLE FEATURES OF A VAGINAL DRUG DELIVERY SYSTEM

An ideal vaginal drug delivery system must be functionally effective and aesthetically pleasing to the patient. From a functional point of view, its purpose is to deliver drug at an effective rate over a predefined period of time. Because of patient compliance issues for every route of administration, the dosing interval should be as long as possible and preferably not less than once daily. A longer interval would be preferable provided it is not so unusual as to be confusing to the patient. Drug metering from the vaginal delivery system is determined by the pharmacodynamic response but minimally the drug delivery system must be sufficiently flexible to accommodate different drugs and different rates of release.

The aesthetic or patient-related issues can be prominent and must be considered. Such factors as vaginal leakage of the system and staining of undergarments are important concerns. It also goes without saying that the

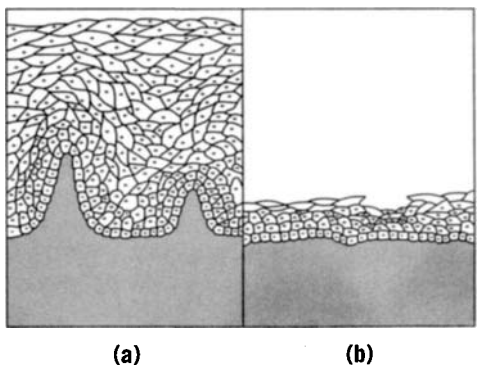


Figure 3. (**a**) Normal vaginal mucosa and (**b**) estrogen-deficient mucosa.

system must not be irritating or interfere with normal physiological processes.

A significant issue for chronically administered drugs is whether or not the system interferes with sexual intercourse. To this end, insoluble inserts, or bulky erodible systems, are likely to be less well accepted by the patient. Gels and creams must be odorless and not create a sticky sensation during sexual intercourse.

A concern for any product to be commercialized is the ease and cost of manufacturing. A unit dose system does not need a preservative but the microbial bioburden must be low. Methods to process the drug delivery system to ensure low bioburden are often limited by the physical nature of the system or the physicochemical stability of the system to sterilizing techniques. A multidose system does require a preservative, and this can require substantial development effort to find a suitable chemical preservative.

REPRODUCTIVE SYSTEM PATHOLOGIES AND TREATMENT

Vaginal Dryness

As the estrogen level begins to decline at the onset of menopause, subsequent vaginal anatomical and physiological changes occur such as vaginal atrophy and a lack of tissue hydration. A reduction in circulating estrogen levels precipitates vasoconstriction leading to less blood flow and consequently less fluid transudation to the vaginal tissue (6). Five years after the last menstrual period, only 25% of women complain of vaginal dryness, with the percentage of complaints increasing to 65% by 60 years of age. Vaginal dryness is more commonly a problem for postmenopausal women who are not sexually active or not undergoing drug therapy. The reduction of the epithelium to 4 or 5 cell layers and the lack of tissue hydration results in the vagina becoming predisposed to a greater likelihood of irritation with subsequent inflammation. Common complaints caused by vaginal dryness include a burning sensation, postcoital bleeding, purulent discharge, a decrease in lubrication with sexual arousal, and dyspareunia (6).

Vaginal dryness is typically not a serious problem and can often be treated with either hormone replacement therapy or topical lubricants. Estrogen replacement therapy has been shown to increase vaginal hydration to levels of the premenopausal state, but may be contraindicated in certain patients such as breast cancer patients who are likely also taking tamoxifen, an estrogen blocker. Therefore, the development of a nonhormonal therapeutic would be advantageous. A microparticulate system called Replens®, which incorporates a cross-linked bioadhesive polymer, polycarbophil, was introduced into the market. The topical moisturizer remains within the vagina for 3 to 4 days and has been shown to impart greater lubrication efficacy in comparison with other lubricants (17).

A study on breast cancer patients, a group for which estrogen replacement therapy is contraindicated, found that vaginal dryness was relieved with use of Replens as well as returning vaginal pH to premenopausal levels (6). Of 25 postmenopausal patients, the vaginal dryness index as described in Table 2 improved after the first month of treatment ($P < .001$). Other studies have also indicated the safety and efficacy of Replens compared with local estrogen therapy. Nachtigall showed that in a randomized study of 30 women, over one year past their last menstrual period, Replens was an alternative therapy to estrogen vaginal cream (18). This therapy induced significant enhancement in vaginal moisture, lubrication, and vaginal elasticity with concomitant reduction in pH to premenopausal levels.

Bioadhesive gels induce tissue hydration by increasing localized vaginal blood flow by 25%, leading to an increase in vaginal fluid transudation. Estrogen induces similar vaginal blood flow enhancement when used alone. If combined with a bioadhesive gel, an increase in vaginal blood flow of 50% has been exhibited. The exact mechanism for the blood flow increase is unknown, but it has been postulated that the bioadhesive polyelectrolyte on the tissue surface creates ion movement into the tissue. Subsequently, greater blood flow is observed. This is similar to the mechanism of tissue hydration induced by the mucus layer lining epithelial surfaces (6).

Menopausal Stress Incontinence

Given that both vaginal and urethral blood flow increased following application of Replens, it is expected that the same product might be useful to treat patients with menopause-related stress incontinence. As with vaginal dryness, there are a number of women, such as breast cancer patients, who cannot use estrogen replacement therapy and thus a nondrug alternative is attractive.

The lower urinary tract contains the urethra, a tubular structure that allows urine to exit from the urinary bladder. The urethra is composed of estrogen-sensitive tissues similar to those found in the vagina, due to the presence of estrogen receptors located in the mucosa and connective tissue (20). Urethral cells, like vaginal mucosa, mature and proliferate upon estrogen exposure. During menopausal and postmenopausal years, the reduction in estrogen levels lead to marked changes in the urinary system such as the inability for effective urine control. Urinary stress incontinence is a condition resulting in urine leakage due to physical stress such as heavy lifting, coughing, or laughing. In postmenopausal years, the urethral mucosa atrophies to a state in which the urethra is primarily lined with immature parabasal cells (19). Additionally, the lack of estrogen promotes a weakening and relaxation of urethra musculature and ligaments, while also diminishing the level of blood flow to the region. These three factors combine to contribute to the loss of urinary continence inducing a 30% drop in urethral closure pressure in postmenopausal women (19). Studies have shown a significant correlation between menopause and the onset of urinary stress incontinence with 70% of postmenopausal women in one study suffering from incontinence due to the initiation of menopause (20,21).

Estrogen replacement therapy is the most common form of treatment for urinary stress incontinence. Increased estrogen levels cause thickening of the mucosa, increased blood supply, and enhanced muscle tone to the urethra. Recently, it has been shown that bioadhesive gels may provide not only an enhancement in vaginal blood flow, but

Table 2. Vaginal Health Index

	1	2	3	4	5
Elasticity	None	Poor	Fair	Good	Excellent
Fluid volume (pooling of Secretions)	None	Scant amount, vault not entirely covered	Superficial amount, vault entirely covered	Moderate amount	Normal amount
pH	6.1 or above	5.6–6.0	5.1–5.5	4.7–5.0	4.6 or below
Epithelial integrity	Petechiae noted before contact	Bleeds with light contact	Bleeds with scraping	Not friable-thin epithelium	Normal
Moisture (coating)	None, surface inflamed	None, surface not inflamed	Minimal	Moderate	Normal

Source: From Ref. 19.

also induce a doubling of suburethral blood flow leading to the elimination of urinary stress incontinence (6). This result has been substantiated in double-blind cross-over studies.

Bacterial Vaginosis

Trichomoniasis, candidiasis, and bacterial vaginosis are several forms of vaginitis that commonly occur within the female population. Bacterial vaginosis, formerly named nonspecific vaginosis or *Gardnerella*-associated vaginitis, is the most prevalent vaginal infection among women of childbearing age, 16–48 years (22,23). Bacterial vaginosis is not a true infection but a condition in which there is an alteration in the balance of vaginal bacteria without inflammation. Under normal conditions, the vagina is heavily populated with lactobacilli bacteria, which help to maintain vaginal acidity. Bacterial vaginosis is characterized by a reduction in lactobacilli concentration with subsequent increases in aerobic and anaerobic bacteria including, *Gardnerella vaginalis*, *Mycoplasma hominis*, *Ureaplasma urealyticum*, and *Bacteroides* species (24,25).

Women with bacterial vaginosis often have a fish-like vaginal odor, a thin milky-grey homogenous vaginal discharge, vaginal pH > 4.5, and a positive test for clue cells in the vaginal fluid. An increase in vaginal pH liberates amines such as putrescine, trimethylamine, and cadaverine leading to the fish-like odor. Because semen is also slightly alkaline, women with bacterial vaginosis commonly complain of an enhanced odor following sexual intercourse (26).

Bacterial vaginosis commonly occurs in sexually active women with no convincing evidence that it should be categorized as a sexually transmitted disease. It is more common in women who use nonbarrier contraceptive methods but less common in postmenopausal women and prepubescent girls (27,28). These observations led to the theory that hormonal factors play a role in the condition. However, hormones have never been associated with the disease, and in many cases, there are no obvious factors predisposing women to bacterial vaginosis.

Since 1978, metronidazole has been the treatment of choice for bacterial vaginosis. Various studies have shown that oral metronidazole (500 mg twice daily for 7 days) is the preferred treatment (24,29,30) but other regimens consisting of single-dose metronidazole (2 g), 2% clindamycin vaginal cream, and oral clindamycin are effective treatments (31). Other alternatives to metronidazole delivery systems are needed due to unpleasant side effects and contraindications during the first trimester of pregnancy.

Recently, increased interest in the development of localized drug delivery systems within the vaginal cavity has been shown due to the advantage of localized drug levels, which reduces dosing frequency, drug administration, and side effects (32). Treatment of bacterial vaginosis with bioadhesive gels with pH-reducing properties would be expected to eliminate the characteristically fishy odor within a short time period due to the conversion of polyamines to nonvolatile salt forms. Additionally, the return of the vaginal environment to acidic pH would favor a higher lactobacilli population (6).

In a double-blind, placebo, crossover study consisting of women with vaginal odor, the bioadhesive gel product was locally applied every third day. The study showed two effects upon application: (*1*) a reduction in vaginal pH and (*2*) a concomitant decrease in vaginal odor when compared with the placebo group. The bioadhesive gel is not an antimicrobial gel but it potentiates an unfavorable condition for continued microbial growth (6).

Recently, there has also been interest in the development of a metronidazole bioadhesive tablet. Studies were performed to determine the efficacy of treatment between a localized metronidazole bioadhesive and oral tablets for the treatment of bacterial vaginosis (32). In a double-blind study, patients were randomly given a bioadhesive tablet with or without 100 mg metronidazole. The bioadhesive consisted of a modified starch–polyacrylic acid combination. The two groups were compared with patients given two 500 mg doses of oral metronidazole for 7 days. Similar cure rates were obtained with the metronidazole bioadhesive tablet and oral treatment groups with only one-seventh of the dose given with localized treatment.

Sexually Transmitted Diseases

There are an estimated 333 million new cases of sexually transmitted diseases (STDs) that occur worldwide each year. The United States leads the industrialized world with an STD rate that is 50–100 times greater than other industrialized countries with an estimated 10 to 12 million new cases annually (33). Women, adolescents, young children, and substance abusers are most susceptible to the

spread of STDs. Of the new cases, greater than 3 million occur in children and young adults 13 to 19 years of age. A recent Centers for Disease Control and Prevention (CDC) report indicated that of the common U.S. infectious diseases, 85% originated from sexual transmission (34).

Some of the most common STDs include chlamydia, gonorrhea, syphilis, human papillomavirus, genital herpes, and human immunodeficiency virus (HIV). Chlamydia is ranked by the CDC as the most prevalent with an estimated 4 million new cases annually. Gonorrhea is the next most prevalent with new cases occurring at a rate of 800,000 per year. In 20–40% of women who obtain inadequate treatment of chlamydia and gonorrhea, the disease leads to a more serious disease state, namely pelvic inflammatory disease. Inadequate treatment may also result in fatal ectopic pregnancies (34).

HIV infection has been reported in over 160 countries with 75% of the population infected via sexual transmission of the virus (35). Estimations are anywhere between 40,000 to 80,000 new HIV infections per year in the U.S. with an average of 500,000 to 2.3 million adult AIDS deaths worldwide between 1992 and 2000 (36).

Overcoming STDs is one of the greatest concerns and challenges facing the world today due to the health impact on infected individuals and the tremendous economic consequence associated with treatment. In the U.S. alone, STDs add between 15 and 18 billion dollars annually to the cost of the nation's health care system (34).

One potential method for controlling the spread of STDs is preventing the transmission of the infecting organism. Nonoxynol-9 (N-9) is a nonionic surfactant that exerts both spermicidal and antiviral/antibacterial activities by damaging cell membranes of spermatozoa and microorganisms. This agent is the only chemical currently used in the U.S. as the active substance in topically applied contraceptives. In vitro, N-9 has been shown to have activity against organisms responsible for STD pathogenicity such as *Neisseria gonorrhoeae*, *Trichomonas vaginalis*, *Treponema pallidum*, herpes simplex, *Chlamydia trachomatis*, and HIV (37–39). In vitro studies have indicated that 0.1–1.0% N-9 inactivates cell-free and cell-associated HIV (40). In concentrations of 5% or greater, N-9 kills lymphocytes containing the HIV virus. Because gonococcal, chlamydial, and trichomonal infections have been correlated with an increased risk of HIV transmission, the reduction in the spread of these diseases would also indirectly reduce the number of HIV infections.

Clinical trials have established that N-9 preparations can decrease the transmission of STDs such as gonococcal, chlamydial, and trichomonal infections (41–43). An N-9 film, when used in combination with condoms, in a single-blind randomized study of 343 women reduced the rate of cervical infections of *Chlamydia trachomatis* and *Neisseria gonorrhoeae* by 25% (40% if used in >75% coital acts). In a study by Rosenberg et al., N-9 (1.0 g) in a contraceptive sponge decreased the prevalence of gonorrhea and chlamydia infection in Thai women by 70% and 30%, respectively (36).

There is some controversy whether N-9 used in vivo is effective in HIV inactivation. A contraceptive vaginal sponge containing N-9 (1.0 g) did not protect women prostitutes against being infected with HIV (10). However, in a second study using an N-9 suppository with a lower N-9 dose (150 mg), there was evidence of a protective effect against HIV infection among women prostitutes (44).

One of the problems associated with N-9 administration is the potential for N-9 toxicity to the genital tract epithelium when frequently administered or used in high doses. Under these conditions, the vaginal mucosa may become irritated increasing the risk for women to be infected with HIV due to small lesions or disruptions within the vaginal lining.

The use of a bioadhesive gel in combination with N-9 would be advantageous particularly due to the fact that the spermicide would remain localized within the vaginal cavity for 1 to 3 days providing localization of N-9 for greater time periods in addition to a reduced N-9 concentration within the vaginal cavity. The gel allows intimate contact with the tissue with preferential binding to damaged tissue enabling an additional use as a barrier to systemic invasion of HIV viruses. The complex of N-9 and bioadhesive polymer has also been shown to increase N-9's antiviral and spermicidal activity. The Today Sponge and other nonbioadhesive topical spermicidal preparations contain anywhere between 1.0 g and 100–200 mg N-9, respectively. The combined bioadhesive spermicidal preparation contains a lower concentration of N-9 preventing cervical or vaginal epithelial ulceration while still having spermicidal, antiviral, and antimicrobial activity (45).

In studies at the Pasteur Institute in Paris, France, researchers have shown that N-9 can kill the free AIDS virus, but not when the virus is attached to a lymphocyte. If N-9 is combined with a bioadhesive, the bioadhesive attaches to the lymphocyte for a period of time allowing N-9 to kill the lymphocyte and subsequently the AIDS virus (44). However, clinical studies have yet to be performed that confirm these results.

Advantage 24, a topical contraceptive, contains N-9 in a bioadhesive gel composed of polycarbophil. The product adheres to the epithelium and remains localized allowing for once-a-day application. Advantage 24 forms a temporary barrier over the cervix and contains the lowest dose of N-9 (52.5 mg) of any product on the U.S. market (46). The frequency of sexual intercourse does not affect localization of the delivery system nor the dosing interval.

A randomized, placebo-controlled, double-blind crossover study of 60 female prostitutes in Mombasa, Kenya, was conducted to establish the safety and toxicity of Advantage 24 administration (47). Advantage 24 or a placebo gel was applied vaginally once daily for 2 weeks. The study concluded that Advantage 24 did not induce epithelial toxicity.

The Joint United National Programme on HIV/AIDS has recently announced that Advantage 24 was shown to inhibit STD transmission (HIV included) during intercourse (46). Due to the prospect that women may want to increase the N-9 dose or possibly decrease the potential for condom usage, the CDC will not accept N-9 as an alternative method for combating or preventing HIV/STD infection. Currently, additional Phase III studies of Advantage 24 for HIV are underway in Thailand and South Africa (46).

Endometriosis

The inner portion of the uterus is lined with endometrial tissue that responds to hormonal stimulation by proliferating prior to each menstrual period with subsequent shedding as menstrual flow during the latter portion of the menstrual cycle. Endometriosis is a benign disease in which the endometrial tissue migrates to areas outside the uterine cavity such as the ovaries, fallopian tubes, pelvic cavity, vagina, and large bowel (48). The invasive tissue is sensitive to hormonal stimulation with resultant breakdown and bleeding confined to a localized area with no outlet, leading to tissue irritation and inflammation (22,49). This may initiate scar tissue development with subsequent lesion, nodule, or growth formation resulting in pain or sexual discomfort.

Menstrual cramping (i.e., dysmennorrhea), an important diagnostic symptom, is the most frequently experienced pain associated with endometriosis. Endometriosis is found in 10–15% of menstruating women between the ages of 25 and 44 (50). Women may also experience pain associated with sexual activity (i.e., dyspareunia) and chronic midline pelvic pain (48,51). Bladder and large bowel lesions may cause pain upon defecation or abdominal bloating, or produce rectal bleeding (50). In 30–40% of cases, endometriosis may be severe enough to cause infertility (49). For women under 35 years of age, surgery may restore or maintain fertility in 25–50% of the cases. For women over 35, removal of the ovaries and uterus may be recommended.

There are various treatment options depending on the age, symptoms, desire for pregnancy, and disease extent. Typically, treatments include either drug therapy to suppress the growth and differentiation of the displaced tissue, surgery, or abdominal hysterectomy (50).

Drug therapy is used as a means for palliation and is very often not a cure. The standard for drug therapy is danazol, a drug that decreases estradiol concentration by reducing the frequency of estradiol pulses. Disease recurrence occurs between 20 and 30% per year and side effects include nausea, weight gain, and hot flashes (51). Gonadotropin-releasing hormone agonists (e.g., nafarelin, leuprolide) are used to control the release of anterior pituitary hormones producing a state of reversible hypoestrogenemia (50). There are concerns over the long-term usage of these medications due to an increase in low density lipoprotein (LDL) levels and/or a greater chance of developing osteoporosis.

Progestin agents have been shown to decrease the risk of estrogen-precipitated endometrial hyperplasia by promoting the transformation of the endometrium into a secretory mucosa, but their use has been limited due to promotion of irregular vaginal bleeding, depression, and enhanced LDL levels (52).

In order to reduce these unwanted side effects, strategies were developed aimed at looking toward new delivery routes and using natural progesterone to reduce side effects. Natural progesterone is problematic when administered orally due to rapid prehepatic and hepatic metabolism leading to insufficient endometrial effects (53). The production of metabolites also leads to symptomatic side effects, in particular, drowsiness. Vaginal administration of natural progesterone induced higher plasma concentrations reached later after dosing and reduced side effects than when administered orally due to a reduction in prehepatic metabolism (21).

Crinone®, a biocompatible bioadhesive gel incorporating natural progesterone (90 mg), was developed as a delivery system to circumvent oral delivery problems. The bioadhesive gel adheres to the vaginal epithelium imparting prolonged release properties. The gel may be administered once daily with peak progesterone plasma levels occurring 6 hours after application (29). Crinone given every 48 hours induced an effective secretory endometrial transformation usually encountered with oral progesterone (300 mg) administration or with 150–600 mg vaginal tablets (37). The explanation for the effectiveness of Crinone is the bioadhesive vehicle allows for greater absorption of progesterone by promoting enhanced contact time with vaginal epithelium. Although not approved for endometriosis at this time, but approved for in vitro fertilization patients, Crinone has shown the potential for use of a vaginal bioadhesive delivery system providing prolonged release of progesterone at lower doses which results in fewer side effects, reduced dosing frequency, and improved patient compliance and acceptance.

TOPICAL CONTRACEPTIVES

Prevention of pregnancy, i.e., population control, is a global problem. Oral contraceptives have been the treatment of choice since their introduction in the 1950s. However, for many individuals, because of their inability to use hormone products, or the cost of such products, topical contraceptives are a reasonable alternative. For a topical contraceptive to be effective, its active ingredient, usually N-9, must be placed in the vaginal cavity to immobilize or destroy the approximately 40 million sperm in a typical ejaculate. If not destruction of these sperm then elimination of those sperm prevents them from the cervical canal (Figure 4). This is a formidable challenge.

Present topical contraceptives have label instructions to the patient that the product must be inserted 10 minutes before sexual intercourse. Presumably the clearing mechanisms of the vagina are sufficiently robust to remove applied material, which is a strong argument for using a bioadhesive product that may keep the product in place for 3–4 days.

The more difficult issue is how to place and maintain the spermicidal product at the opening of the cervical canal both during and after sexual intercourse. At midcycle, when the egg is available for fertilization, there is a change in consistency of cervical mucus and subsequent leakage of this material out through the opening of the cervical canal, i.e., the os. This flow of mucus will hinder retention of a liquid or semisolid material from remaining at the site of expected maximal need.

Current topical contraceptives are reasonably unreliable, as compared with oral contraceptives. The need to use the product 10 minutes before sexual intercourse and thus no overnight protection is a significant liability. A bioadhesive polymer can indeed provide extended duration of action and thus elevate the reliability of bioadhesive-

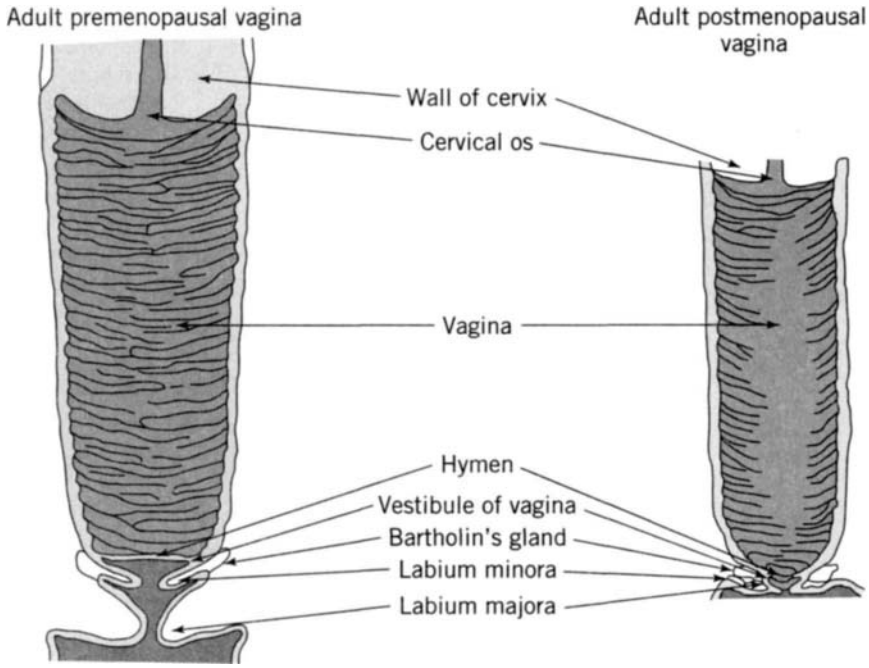


Figure 4. Depiction of vaginal anatomy.

based topical contraceptives. However, until a product can be made that will remain at the opening of the os, to serve as both a physical and chemical barrier, topical contraceptives will remain less reliable than oral contraceptives.

OTHER VAGINAL DRUG DELIVERY SYSTEMS

Many dosage forms have been used for vaginal drug delivery with the most common being pessaries (suppositories), gels, and foams. Early work by Masters and Johnson showed that vaginal distribution of these dosage forms varied considerably with the nature of the system and method of instillation.

Table 3 gives a summary of vaginal delivery systems using hydrogel polymers. The forms of these vaginal products include rod-shaped monolithic devices (54), gels (20), and discs.

VETERINARY APPLICATIONS

Current commercially available controlled release drug delivery systems intended for intravaginal use in animals are restricted to the delivery of compounds used to control the estrus cycle (55–57). These compounds include progesterone, fluorogestone acetate, and methyl acetoxy progesterone (55–57). A further drug, estradiol benzoate, is also administered intravaginally in a commercially available product (58,59); however, it is administered to cattle as a 10 mg hard gelatin capsule that does not include any controlled release component. Following administration and release, the estradiol is immediately available for absorption (58,59).

Table 3. Hydrogen-Based Vaginal Delivery Systems

Drug	Hydrogel[a]	Test animal	Refs.
Bleomycin	HPC/C-934	Human	15
Insulin	PAA	Rats/rabbits	20
Progesterone	MEEMA/HEMA/MEMA	Not tested	54
Progesterone	Noveon AA1/C-934	Human	35
Prostaglandin E_2	HEMC	Human	31
Prostaglandin E_2	Unspecified	Human	31
Prostaglandin E_2	Cross-linked PEG	Human	43,44

[a]HPC, hydroxypropyl cellulose; PAA, poly(acrylic acid); MEEMA, (methyl ethyl)ethyl methacrylate; HEMA, hydroxyethyl methacrylate; MEMA, methyl ethyl methacrylate; HEMC, hydroxy ethyl methyl cellulose; PEG, poly(ethylene)glycol.

Possible reasons for the area of controlled release intravaginal drug delivery focusing on compounds for the control of the estrus cycle include (*1*) the demand for improved herd or flock management techniques coupled with the need to control the estrus cycle for more economic animal production, which was confounded by the inability of the compounds used to control the estrus cycle to be effective orally (due to extensive hepatic metabolism) and therefore the need for an alternate route of administration; (*2*) the need for rapid termination of drug delivery to allow a sharp decline in progestagen plasma levels to induce an estrus response, which requires a route of administration that allows ready access and easy removal of a delivery system; (*3*) the inabilities of other routes of administration to achieve these requirements (the one exception being the ear flap for which a small subcutaneous ear implant containing norgestomet was developed) (60–69); (*4*) the ideal physicochemical properties of the compounds that control the estrus cycle, which was reflected in their ability to be rapidly absorbed across the vaginal mucosa; and (*5*) the conductive pharmacokinetic properties of the compounds that control the estrus cycle, i.e., the small minimum effective concentrations that are associated with these compounds to maintain control over follicular growth, coupled with their rapid elimination kinetics, which facilitate the sharp drop in plasma levels which is needed to induce estrus.

Several commercially available intravaginal veterinary drug delivery systems have been marketed. These include PRID, CIDR-S (no longer available), CIDR-G, CIDR-B and polyurethane sponges of various sizes and densities (Fig. 5). None of these delivery systems impart a true controlled release over the drugs they contain; all simply allow the incorporated drug to slowly leach out with time. Recently a sophisticated microchip-controlled intravaginal drug delivery system was introduced onto the New Zealand market. This delivery system was designed to allow a constant daily release of a progesterone for 10 days, and a pulsed release of estradiol and prostaglandin 1 hour and 6 days, respectively, after insertion. In addition to commercially available products, several conceptual intravaginal veterinary drug delivery systems have also been described in the literature (17–24). These include Rajamahendrans Rubber Tubing device (cattle) (70–72), the Plasthyd Device (sheep) (73), and Kabadi and Chiens silicone sheets (sheep) (74–77).

Animals species in which these intravaginal drug delivery systems are used are currently limited to cattle, sheep, and goats. This is a reflection of several reasons including the conducive management practices associated with these animals; the needs and demands of the end user; the economics associated with the unit cost of the intravaginal drug delivery system versus the value of the animal concerned; the high progestagen requirements that are needed to control the estrus cycle of some animals, e.g., pigs; and the laws governing artificial insemination procedures in some animals (e.g., until recently artificial insemination in horses was banned). The availability of cheaper technologies and delivery systems, changes to artificial insemination laws, and innovative delivery systems that can deliver greater quantities of progestagen may see an expansion in the types of animals in which intravaginal veterinary drug delivery systems are developed and used.

Other species have been investigated for the potential application of intravaginal drug delivery. These include deer (78–95), horses (96–103), and buffalo (104–109). The commercially available sponges designed for use in sheep and goats have been investigated in deer (78–81) and horses (96–99). The probable reasons for these delivery

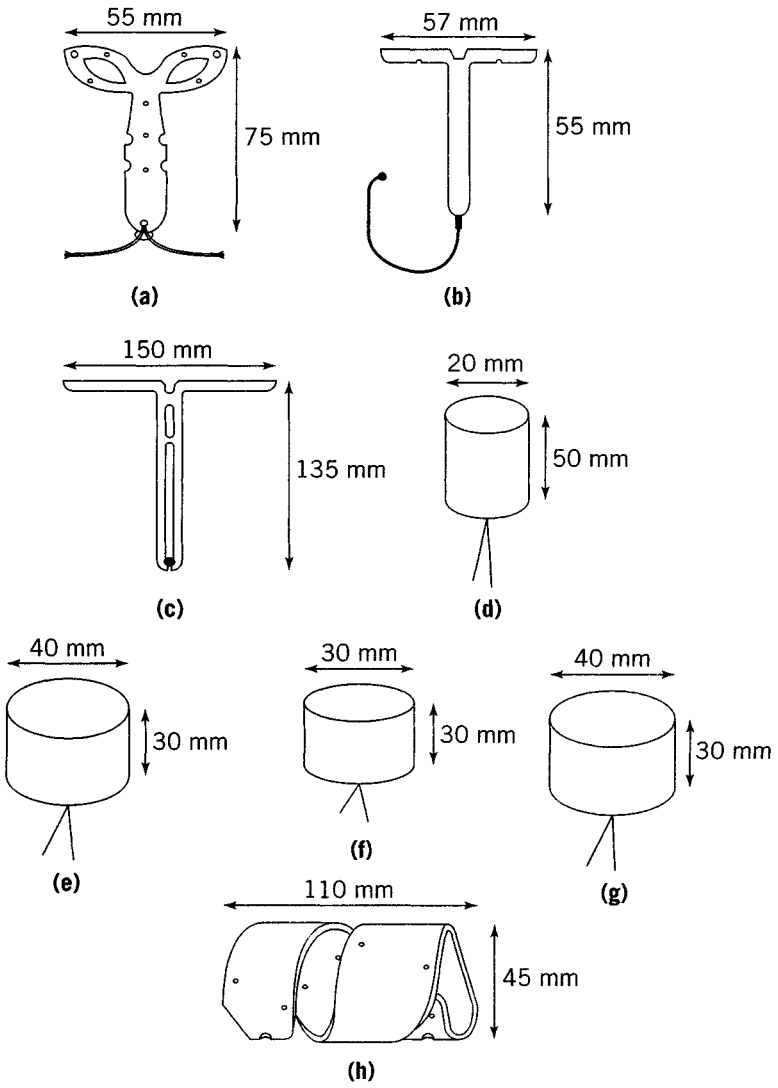


Figure 5. Commercially available estrus-synchronizing controlled release intravaginal drug delivery systems used in cattle, sheep, and goats. (**a**) CIDR-S (0.465 g progesterone; sheep) (no longer commercially available); (**b**) CIDR-G (0.33 g progesterone; sheep and goats); (**c**) CIDR-B (1.9 g progesterone; cattle); (**d**) Repromap sponge (60 mg methyl acetoxy progesterone; sheep); (**e**) Chronogest sponge (30 mg fluorogestone acetate; sheep); (**f**) Chronogest sponge (40 mg fluorogestone acetate; goats); (**g**) Chronogest sponge (45 mg fluorogestone acetate; goats); and (**h**) PRID (1.55 g progesterone; cattle). Delivery systems E and G are manufactured from sponges of different density.

Table 4. Factors To Consider When Designing an Intravaginal Veterinary Drug Delivery System for Estrus Control

Factor	Objective	Reason
Size	Optimize: Length Diameter Width	Animal comfort Ease of insertion Ease of removal
Shape	Optimize: Overall spatial geometry	Impel retention characteristics Prevent animal discomfort and damage Impel a means for insertion and removal
Retention	Maintain device inside vagina for entire treatment period	Ensure continuity of drug delivery over required insertion period
Release characteristics	Meet clinical requirements	Maintain sufficiently high progestagen plasma levels to prevent ovulation
Removal	Ability to: Terminate delivery at will Remove easily	Impel sudden drop in progestagen levels to induce estrus
Adverse effects	Avoidance of: Damage to mucosa Damage to cervix Irritation to vaginal mucosa	Reduce discharge formation Eliminate membrane perforation

Table 5. Polymers, Drugs, Manufacturing Methods and in vitro and in vivo Release Characteristics of Commercially Available Controlled Release Intravaginal Veterinary Drug Delivery Systems

Delivery system	Drug	Polymer	Manufacturing technique	Type of delivery system	Release characteristics	
					in vitro	in vivo
Sponge	FGA[a] MAP[b]	Polyurethane	Single application of drug dissolved in ethanol	Matrix	$t^{1/2}$ (21)	$t^{1/2}$ (142–144)
PRID	Progesterone	Silicone	Low temperature injection molding[c]	Matrix	$t^{1/2}$ (94)	$t^{1/2}$ (145)
CIDR-S	Progesterone	Silicone	High temperature (190°C) injection molding[d]	Matrix	Not reported	Not reported
CIDR-G	Progesterone	Silicone	High temperature (190°C) injection molding[d]	Matrix	$t^{1/2}$ (Personal results)	Not reported
CIDR-B	Progesterone	Silicone	High temperature (190°C) injection molding[d]	Matrix	$t^{1/2}$ (146)	Not reported

[a]PGA, Fluorogestone acetate
[b]MAP, Methyl acetoxy progesterone
[c]Progesterone/silicone mixture around a stainless steel sheet
[d]Progesterone/silicone mixture around a nylon spine

systems not being successful in these animals may include the excessive amount of discharge associated with sponges (which may be acceptable by sheep and goat farmers but not by owners of these other species) and poor retention rates. CIDR-G have been inserted into deer with success both in terms of estrus synchrony and suitability of the delivery system design with respect to animal comfort, retention, etc. (86–95). Both PRID and CIDR-B have been investigated in horses (100–103) and buffalo (104–109). The probable reason for these delivery systems not being completely successful in these animals is the inappropriate design for these species (i.e., overall dimensions), which results in either straining following insertion (100,101) or the need to adapt the dimensions of the device before insertion to improve retention characteristics (103).

Brief History

Controlled drug delivery has a long history in the animal reproduction field. Polyurethane sponges were first investigated in sheep in the early 1960s as a delivery system for the administration of synthetic progestagens to control the estrus cycle (110–112). T.J. Robinson successfully demonstrated the worth of this delivery system in large sheep trials under Australian farming conditions (110–112). Shortly afterwards, D.F. Wishart demonstrated that the sponge was equally effective in sheep farmed under British conditions (113–124). In the 1970s, J.F. Roche in collaboration with Abbott Laboratories developed the PRID device for use in cattle (116–123). In the 1980s, R.A.S. Welsh in collaboration with D. Miller developed the CIDR-S (124,125) and shortly afterwards the CIDR-G (for sheep and goats) (126–130). Rapid development resulted in the CIDR-G technology being extended to the design and development of a device for use in cattle called the CIDR-R (131–141). Interdispersed with these developments were conceptual approaches of Rajamahendran (cattle) (70–72), the Plasthyd Device (sheep) (73) and Kabadi and Chiens silicone sheets (sheep) (74–77).

DESIGN FACTORS IN CONTROLLED RELEASE INTRAVAGINAL VETERINARY DRUG DELIVERY SYSTEMS

A number of factors should be considered when designing a controlled release intravaginal veterinary drug delivery system (M.J. Rathbone et al., unpublished data, 1998). These are summarized in Table 4. Ease of insertion, retention characteristics, ease of removal, animal comfort, and achievement of clinical objectives (through release rates) are the key aspects that need to be considered and tailored to a particular animal species if an intravaginal veterinary drug delivery system is to be successfully developed.

INTRAVAGINAL VETERINARY DRUG DELIVERY SYSTEMS

Currently available intravaginal veterinary drug delivery systems are shown in Figure 5 together with their dimensions. A brief description of the delivery system, polymer used to manufacture it, and the type of release characteristics are given in Table 5.

FUTURE DEMANDS AND REQUIREMENTS OF INTRAVAGINAL VETERINARY DRUG DELIVERY SYSTEMS

The future demands for intravaginal veterinary drug delivery for animal health and production are dependent upon the perception in some circles for the need to eliminate the adverse and unwanted effects which intramuscular and subcutaneous injection cause on administration such as ulcer formation and hide damage. Alternate routes for drug administration may be necessary to limit the occurrence of these problems and the intravaginal route offers advantages for some compounds. Future demands on the intravaginal veterinary drug delivery scientist will be influenced by the extent to which this concept is pursued and the suitability of the physicochemical and pharmacokinetic properties of the drugs which need to be delivered. In addition intravaginal veterinary drug delivery system design will be influenced by the requirements of the reproductive physiologists and endocrinologists who are currently defining the types of drugs and their delivery patterns for "ideal" synchrony programs (55–58).

BIBLIOGRAPHY

1. D.G. Ferris et al., *J. Fam. Pract.* **41**, 443–449 (1995).
2. A. Forbes, *Crit. Pathol. AIDS Proj.* **31**, 19–20 (1996).
3. D.A. Grimes and W. Cates, Jr., in K.K. Holmes, P.A. Mardh, and P.F. Sparting, eds., *Sexually Transmitted Diseases*, McGraw-Hill, New York, 1990, pp. 1087–1099.
4. A.C. Guyton and J.E. Hall, *Textbook of Medical Physiology*, Saunders, Philadelphia, 1996, pp. 1017–1032.
5. L.H. Hill, H. Ruperalia, and J.A. Embil, *Sex. Transm. Dis.* **10**, 114–118 (1983).
6. C.S. Iosif and Z. Bekassy, *Acta Obstet. Gynecol. Scand.* **23**, 257–260 (1984).
7. M.R. Joesoef and G.P. Schmid, *Clin. Infect. Dis.* **20**, S72–S79 (1995).
8. R.W. Kistner, in E.S.E. Hafez, and T.N. Evans, eds., *The Human Vagina*, Elsevier/North-Holland Biomedical Press, Amsterdam, 1978, pp. 109–120.
9. K. Knuth, M. Amiji, and J.R. Robinson, R., *Adv. Drug Delivery Rev.* **11**, 137–167 (1993).
10. J. Kreiss et al., *J. Am. Med. Assoc. JAMA*, **268**, 477–482 (1992).
11. C. Landau, M.G. Cyr, and A.W. Moulton, *The Complete Book of Menopause*, The Berkley Publishing Group, New York, 1994, pp. 23–41.
12. P.-G. Larsson, *Int. J. STD AIDS* **3**, 239–247 (1992).
13. W.C. Louv et al., *J. Infect. Dis.* **158**, 518–523 (1988).
14. R.I.J. MacDermott, *Br. J. Obstet. Gynaecol.* **102**, 92–94 (1995).
15. Y. Machida et al., *Chem. Pharm. Bull.* **27**, 93–100 (1979).
16. H.L. Martin et al., *Sex. Transm. Dis.* **24**, 279–283 (1997).
17. S.M. McKinlay, *Maruritas* **23**, 137–145 (1996).
18. H. Moi, *Int. J. STD AIDS* **1**, 86–94 (1990).
19. L.E. Nachtigall, *Fertil. Steril.* **61**, 178–180 (1994).
20. K. Morimoto, T. Takeeda, Y. Nakamoto, and K. Morisaka, *Int. J. Pharm.* **12**, 107–111 (1982).
21. K. Nahoul, L. Dehennin, M. Jondet, and M. Roger, *Maturitas* **16**, 185–202 (1993).
22. M.E. Niatas, *U.S. Pharmacist* **21**, 6 (1996).
23. S. Niruthisand, R.E. Roddy, and S. Chutivongse, *Lancet* **339**, 1371–1375 (1992).
24. M. Nisolle and J. Donnez, *Peritoneal, Ovarian, and Rectovaginal Endometriosis. The Identification of Three Separate Diseases*, Parthenon Publishing Group, New York, 1997.
25. T. O'Dowd, *Practitioner* **239**, 538–541 (1995).
26. E.W. Page, C.W. Villee, and D.B. Villee, *Human Reproduction; Essentials of Reproductive and Perinatal Medicine*, Saunders, Philadelphia, 1981.
27. W. Platzer, S. Poisel, and E.S.E. Hafez, in E.S.E. Hafez and T.N. Evans, eds., *The Human Vagina*, Elsevier/North-Holland Biomedical Press, Amsterdam, 1978, pp. 39–53.
28. B. Polsky et al., *Lancet*, **1**, 1456 (1988).
29. J.L. Pouly et al., *Hum. Reprod.* **11**, 2085–2089 (1996).
30. C.J.F. Priestley and G.R. Kinghorn, *Br. J. Clin. Pharmacol.* **50**, 331–334 (1966).
31. W.F. Rayburn et al., *Obstet. Gynecol.* **79**, 374–379 (1992).
32. H. Rekers, A.C. Drogendijk, H.A. Valkenburg, and F. Riphagen, *Maturitas* **15**, 101–111 (1992).
33. J.L. Richardson and L. Illum, *Adv. Drug Delivery Rev.* **8**, 341–366 (1992).
34. J.R. Robinson and W.J. Bologna, *Drug Store News / Inside Pharm.* (1990).
35. J.R. Robinson and W.J. Bologna, *J. Controlled Release* **28**, 87–94 (1994).
36. M.J. Rosenberg, W. Rojanaopithayakorn, P.J. Feldblum, and J.E. Higgins, *JAMA, J. Am. Med. Assoc.* **257**, 2308–2312 (1987).
37. D. Ross et al., *Am. J. Obstet. Gynecol.* **177**, 937–941 (1997).
38. M.M. Shaaban, *Maturitas* **23**, 181–192 (1996).
39. D. Sokai and P.L. Hermonat, *Am. J. Public Health* **85**, 737–738 (1995).
40. S.Z. Song, J.R. Cardinal, S.H. Kim, and S.W. Kim, *J. Pharm. Sci.* **70**, 216–219 (1981).
41. R.W. Steger and E.S.E. Hafez, in E.S.E. Hafez and T.N. Evans, eds., *The Human Vagina*, Elsevier/North-Holland Biomedical Press, Amsterdam, 1978, pp. 95–106.

42. P. Stratton and N.J. Alexander, *Infect. Dis. Clin. North Am.* **7**, 841–859 (1993).
43. A.V.G. Taylor, J. Boland, A.L. Bernal, and I.Z. MacKenzie, *Prostaglandins* **41**, 585–594 (1991).
44. C.A. Temple, *Nurs. Times* **90**, 42–43 (1994).
45. A.V.G. Taylor, J. Boland, and I.Z. MacKenzie, *Prostaglandins* **40**, 89–98 (1990).
46. R.W. Tureck, Ph.D. Thesis, University of Pennsylvania Health System, Philadelphia, 1997.
47. G. Wagner and R.T. Levin, in E.S.E. Hafez and T.N. Evans, eds., *The Human Vagina*, Elsevier/North Holland Biomedical Press, Amsterdam, 1978, pp. 121–138.
48. M.E. Watanabe, *Scientist* **11**, 1–4 (1997).
49. L. Zekeng, P.J. Feldblum, R.M. Oliver, and L. Kaptue, *AIDS* **7**, 725–731 (1993).
50. R. Berkow, *Endometriosis: The Merck Manual*, Merck Research Laboratories, Rahway, NJ, 1992, pp. 1809–1813.
51. L. Fedele et al., *Fertil. Steril.* **53**, 155–173 (1990).
52. F. Casanas-Roux et al., *Hum. Reprod.* **11**, 357–363 (1996).
53. H. Adlercreutz and F. Martin, *J. Steroid Biochem.* **13**, 231–244 (1980).
54. S.Z. Song, J.R. Cardinal, S.H. Kim, and S.W. Kim, *J. Pharm. Sci.* **70**, 216–219 (1981).
55. M.J. Rathbone, K.L. Macmillan, C.R. Bunt, and S. Burggraaf, *Adv. Drug Delivery Rev.* **28**, 363–392 (1997).
56. M.J. Rathbone et al., *J. Controlled Release* **53**, 274–282 (1998).
57. M.J. Rathbone et al., *Crit. Rev. Ther. Drug. Carrier Sys.* **15**, 285–380 (1998).
58. J.F. Roche, *Anim. Rep. Sci.* **1**, 145–154 (1978).
59. J.F. Roche and D.J. Prendiville, *Vet. Rec.* **102**, 12–14 (1978).
60. S.E. Curl, W. Durfey, R. Patterson, and D.W. Zinn, *J. Anim. Sci.* **27**, 1189 (1968).
61. J.N. Wiltbank et al., *J. Anim. Sci.* **33**, 600–606 (1971).
62. C.O. Woody and R.A. Pierce, *J. Anim. Sci.* **39**, 903–906 (1974).
63. C. Burrell, J.N. Wiltbank, D.G. LeFever, and G. Rodeffer, *J. Anim. Sci.* **34**, 915 (1972).
64. R.W. Whitman, J.N. Wiltbank, D.G. LeFever, and A.H. Denham, *Proc. West. Sect. Am. Soc. Anim. Sci.* **23**, 280–282 (1972).
65. C. Burrell, J.N. Wiltbank, D.G. LeFever, and G. Rodeffer, *Proc. West. Sect. Am. Soc. Anim. Sci.* **23**, 547–551 (1972).
66. C.O. Woody and F.B. Abenes, *J. Anim. Sci.* **41**, 1057–1064 (1975).
67. J.C. Spitzer, D. Miksch, and J.N. Wiltbank, *J. Anim. Sci.* **43**, 305 (1976).
68. J.C. Spitzer, D.L. Jones, E.D. Miksch, and J.N. Wiltbank, *Theriogenology* **10**, 223–227 (1978).
69. E.D. Miksch et al., *Theriogenology* **10**, 201–221 (1978).
70. R. Rajamahendran, P.C. Laguë, and R.D. Baker, *Anim. Reprod. Sci.* **3**, 271–277 (1980/1981).
71. R. Rajamahendran, P.C. Laguë, and R.D. Baker, *J. Anim. Sci.* **49**, 554–559 (1979).
72. R. Rajamahendran, L. Forgrave, P.C. Laguë, and R.D. Baker, *Can. J. Anim. Sci.* **55**, 787 (1975).
73. S.M.N. Mandiki, J.L. Bister, and R. Paquay, *Small Rumin. Res.* **15**, 265–272 (1995).
74. M.B. Kabadi and Y.W. Chien, *J. Pharm. Sci.* **73**, 1464–1468 (1984).
75. M.B. Kabadi and Y.W. Chien, *Drug Dev. Ind. Pharm.* **11**, 1271–1312 (1985).
76. M.B. Kabadi and Y.W. Chien, *Drug Devel. Ind. Pharm.* **11**, 1313–1361 (1985).
77. Y.W. Chien, in *Novel Drug Delivery Systems: Fundamentals, Developmental Concepts, Biomedical Assessments*, Y.W. Chien, ed., Marce Dekker, New York, 1982, pp. 413–463.
78. R.W. Kelly, K.P. McNatty, G.H. Moore, and M. Gibb, *J. Reprod. Fertil.* **64**, 475–483 (1982).
79. R.W. Kelly and G.H. Moore, *N. Z. Agric. Sci.* **11**, 179–181 (1977).
80. J.C. Haigh, M. Cranfield, and R.G. Sasser, *J. Zoo Anim. Med.* **19**, 202–207 (1988).
81. G.W. Asher et al., *J. Zool.* **215**, 197–203 (1988).
82. G.W. Asher, *J. Reprod. Fertil.* **75**, 521–529 (1985).
83. H.N. Jabbour et al., *Proc. N. Z. Soc. Anim. Prod.* **51**, 147–151 (1991).
84. H.N. Jabbour, G.W. Asher, J.F. Smith, and C.J. Morrow, *J. Reprod. Fertil.* **94**, 353–361 (1992).
85. G.W. Asher et al., *N. Z. Vet. J.* **40**, 8–14 (1992).
86. K.L. Macmillan and G.W. Asher, *Proc. N. Z. Soc. Anim. Prod.* **50**, 123–133 (1990).
87. G.H. Moore and G.M. Cowie, *Proc. N. Z. Soc. Anim. Prod.* **46**, 175–178 (1986).
88. M.W. Fisher et al., *Proc. N. Z. Soc. Anim. Prod.* **46**, 171–173 (1986).
89. G.W. Asher, J.L. Adam, R.W. James, and D. Barnes, *Anim. Prod.* **47**, 487–492 (1988).
90. C.J. Morrow, G.W. Asher, J.F. Smith, and F.A. Veldhuizen, *Proc. N. Z. Soc. Anim. Prod.* **53**, 417–421 (1993).
91. G.W. Asher et al., *Anim. Reprod. Sci.* **33**, 241–265 (1993).
92. H.N. Jabbour, F.A. Veldhuizen, G. Green, and G.W. Asher, *J. Reprod. Fertil.* **98**, 495–502 (1993).
93. G.W. Asher et al., *J. Reprod. Fertil.* **89**, 761–767 (1990).
94. G.W. Asher and J.G.E. Thompson, *Anim. Reprod. Sci.* **19**, 143–153 (1989).
95. C.J. Morrow, G.W. Asher, and K.L. Macmillan, *Anim. Reprod. Sci.* **37**, 159–174 (1995).
96. D.L. Thompson, S.I. Reville, D.J. Derrick, and M.P. Walker, *J. Anim. Sci.* **58**, 159–164 (1984).
97. J.E. Dinger, E.E. Noiles, and M.J.L. Bates, *Theriogenology* **16**, 231–237 (1981).
98. D.L. Thompson, R.A. Goodke, and T.M. Nett, *J. Anim. Sci.* **56**, 668–677 (1983).
99. M.A. Draincort and E. Palmer, *J. Reprod. Fertil.* **32**, 283–291 (1982).
100. M. Lübbecke, E. Klug, H.O. Hoppen, and W. Jöchle, *Reprod. Domest. Anim.* **29**, 305–314 (1994).
101. W. Jöchle, D. Hamm, H. Sieme, and H. Merkt, *Reprod. Domest. Anim.* **26**, 183 (1991).
102. K. Arbeiter, U. Barth, and W. Jöchle, *J. Equine Vet. Sci.* **14**, 21–25 (1994).
103. D.R. Rutten et al., *Vet. Rec.* **119**, 569–571 (1986).
104. A.R. Rao and C. Rao, *Vet. Rec.* **113**, 623–624 (1983).
105. R. Rajamahendran and M. Thamotharam, *Anim. Reprod. Sci.* **6**, 111–118 (1983).
106. R. Rajamahendran, K.N. Jayatilaka, J. Dharmawardena, and M. Thamotharam, *Anim. Reprod. Sci.* **3**, 107–112 (1980).
107. G. Singh, G.B. Singh, R.D. Sharma, and A.S. Nanda, *Theriogenology* **21**, 859–867 (1983).

108. G. Singh, G.B. Singh, R.D. Sharma, and A.S. Nanda, *Theriogenology* **19**, 323–329 (1983).
109. F.I. Hill et al., *Proc. N. Z. Soc. Anim. Prod.* **52**, 25–27 (1992).
110. T.J. Robinson, *Proc. Aust. Soc. Anim. Prod.* **5**, 47–52 (1964).
111. T.J. Robinson, *Nature (London)* **206**, 39–41 (1965).
112. T.J. Robinson, *The Control of the Ovarian Cycle in the Sheep*, Sydney University Press, Sydney, 1967.
113. D.F. Wishart, *Vet. Rec.* **79**, 356–357 (1966).
114. D.F. Wishart, *Vet. Rec.* **80**, 276–287 (1967).
115. D.F. Wishart and B.D. Hoskin, *J. Reprod. Fertil.* **17**, 285–289 (1968).
116. R.E. Mauer, S.K. Webel, and M.D. Brown, *Ann. Biol. Anim. Biochim. Biophys.* **15**, 291–296 (1975).
117. J.F. Roche, *J. Reprod. Fertil.* **43**, 471–477 (1975).
118. J.F. Roche, *Ann. Biol. Anim. Biochim. Biophys.* **15**, 301–302 (1975).
119. J.F. Roche, *J. Reprod. Fertil.* **43**, 471–477 (1975).
120. J.F. Roche, *J. Reprod. Fertil.* **46**, 253–255 (1976).
121. J.F. Roche, *J. Reprod. Fertil.* **46**, 341–345 (1976).
122. J.F. Roche, *Vet. Rec.* **99**, 184–186 (1976).
123. J.F. Roche, D.J. Prenderville, and W.D. Davis, *Vet. Rec.* **101**, 417–419 (1977).
124. R.A.S. Welch, Annual Report of Agricultural Research Division, New Zealand Ministry of Agriculture and Fisheries, 1982–1983, p. 64.
125. R.A.S. Welch et al., *Proc. 10th Int. Congr. Anim. Reprod. Artif. Insem.* 1984, p. 354.
126. A.J. Ritar, P. Ball, T.M. Black, and R.B. Jackson, *Proc. Aust. Soc. Reprod. Biol.* **19**, 26 (1987).
127. A.J. Ritar et al., *Proc. Aust. Soc. Reprod. Biol.* **19**, 27 (1987).
128. A.J. Ritar et al., *Proc. Aust. Soc. Reprod. Biol.* **19**, 28 (1987).
129. N.A. Holt, *Proc. Aust. Soc. Reprod. Biol.* **19**, 34 (1987).
130. D.R. Barnes, A.P. Oakley, K.L. Macmillan, and T.J. Braggins, *Proc. Aust. Soc. Reprod. Biol.* **19**, 62 (1987).
131. R.A.S. Welch, *Proc. Ruakura Farmers' Conf.* **37**, 105–107 (1985).
132. K.L. Macmillan, A.J. Peterson, D.R. Barnes, and S.M. Duncan, *Proc. Endocrinol. Soc. Aust.* **29**, E3 (1986).
133. K.L. Macmillan, V.K. Taufa, D.R. Barnes, and A.M. Day, *Proc. Asian / Aust. Assoc. Anim. Prod.* **4**, 220 (1987).
134. G.F. Duirs et al., *Proc. Aust. Soc. Reprod. Biol.* **19**, 59 (1987).
135. K.L. Macmillan et al., *Proc. Aust. Soc. Reprod. Biol.* **19**, 61 (1987).
136. K.L. Macmillan, V.K. Taufa, and A.M. Day, *Proc. 11th Int. Congr. Anim. Reprod.*, 1988, vol. 4, p. 444.
137. K.L. Macmillan and J.G.E. Pickering, *Proc. 11th Int. Congr. Anim. Reprod.*, 1998, vol. 4, p. 442.
138. S.P. Washburn, H.G. Howard, W. Jöchle, and K.L. Macmillan, *J. Anim. Sci.* **67**, 382 (1989).
139. A.J. Peterson and H.C. Henderson, *J. Reprod. Fertil. Suppl.* **43**, 315 (1990).
140. K.L. Macmillan, S.P. Washburn, H.V. Henderson, and S.F. Petch, *Proc. N. Z. Soc. Anim. Prod.* **50**, 471–472 (1990).
141. K.L. Macmillan and A.J. Peterson, *Anim. Reprod. Sci.* **33**, 1–25 (1993).
142. T.J. Robinson, *Aust. J. Agric. Res.* **21**, 783–792 (1970).
143. A.J. Allison and T.J. Robinson, *J. Reprod. Fertil.* **22**, 515–531 (1970).
144. J. Morgan, R.E. Lack, and T.J. Robinson, in T.J. Robinson, ed., *The Control of the Ovarian Cycle in the Sheep*, Sydney University Press, Sydney, 1967, pp. 195–207.
145. V.W. Winkler, S. Borodkin, S.K. Webel, and J.T. Mannebach, *J. Pharm. Sci.* **66**, 816–818 (1977).
146. C.R. Bunt, M.J. Rathbone, S. Burggraaf, and C. Ogle, *Proc. Int. Symp. Controlled Release Bioact. Mater.* **24**, 145–146 (1997).

See also BIOADHESIVE DRUG DELIVERY SYSTEMS; MUCOSAL DRUG DELIVERY, BUCCAL; MUCOSAL DRUG DELIVERY, INTRAVITREAL; MUCOSAL DRUG DELIVERY, NASAL; MUCOSAL DRUG DELIVERY, OCULAR.

NANOPARTICLES

FANNY DE JAEGHERE
ERIC DOELKER
ROBERT GURNY
University of Geneva
Geneva, Switzerland

KEY WORDS

Applications in therapeutics
Biodistribution
Drug carrier
Drug targeting
Freeze-drying
Long-circulating nanoparticle
Nanocapsule
Nanoparticle
Nanosphere
Physicochemical characterization
Polymer
Preparation methods
Purification
Sterilization
Surface modification

OUTLINE

Manufacture of Nanoparticles
- In Situ Polymerization
- Dispersion of a Preformed Polymer
- Pharmaceutical Aspects

Modulation of the in Vivo Fate of Nanoparticles
- Mechanisms Regulating Body Distribution of Nanoparticles
- Surface Engineering of Nanoparticles
- Targeting Strategies

Characterization of Nanoparticles
Applications of Nanoparticles
- Parenteral Administration
- Peroral Administration
- Other Routes of Administration

Conclusion
Bibliography

The challenge of modern drug therapy is the optimization of the pharmacological action of drugs coupled with the reduction of their toxic side effects in vivo. One response is the use of colloidal drug carriers that can provide site-specific or targeted drug delivery combined with optimal drug release profiles. Among these carriers, liposomes and nanoparticles have been the most extensively investigated. In the late seventies, because liposomal formulations started to face some technological limitations including poor stability and low drug entrapment efficiency, polymeric nanoparticles were proposed as alternative drug carriers. Nanoparticles are solid colloidal particles ranging in size from 10 to 1,000 nm. They are made of a macromolecular material which can be of synthetic or natural origin. Depending on the process used for their preparation, two different types of nanoparticles can be obtained, namely nanospheres and nanocapsules. Nanospheres have a matrix-type structure in which a drug is dispersed, whereas nanocapsules exhibit a membrane-wall structure with an oily core containing the drug. Because these systems have very high surface areas, drugs may also be adsorbed on their surface. The general structure and drug association modes of nanoparticles are illustrated in Figure 1 (1).

MANUFACTURE OF NANOPARTICLES

Numerous methods exist for the manufacture of nanoparticles, allowing extensive modulation of their structure, composition, and physicochemical properties. The choice of the manufacturing method essentially depends on the raw material intended to be used and on the solubility characteristics of the active compound to be associated to the particles. Regarding the raw material, criteria such as biocompatibility, the degradation behavior, choice of the administration route, desired release profile of the drug, and finally, the type of biomedical application determine its selection. From these considerations, it is clear that nanoparticle formulation requires an initial and very precise definition of the needs and objectives to be achieved.

Historically, the first methods used to produce nanoparticles were derived from the field of latex engineering developed by polymer chemists. These methods were based on the in situ polymerization of a monomer in various me-

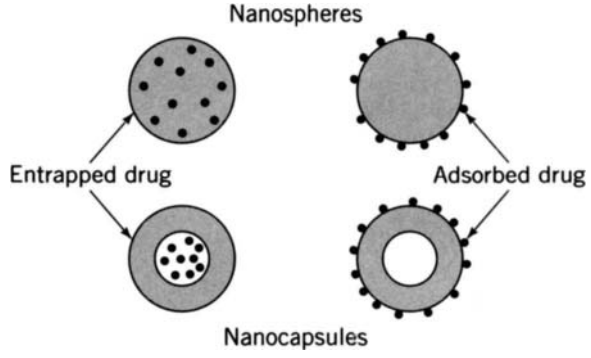


Figure 1. Various types of drug-loaded nanoparticles. *Source:* From Ref. 1.

dia. Pioneers in this field were Birrenbach and Speiser (2) who produced in the early seventies the very first polymerized nanoparticles for pharmaceutical use. Since that time, in situ polymerization-based methods have been widely developed, allowing a great diversity of nanoparticulate formulations to be obtained, as well as a better understanding of the mechanisms involved in these processes. In spite of real technological advances realized in this field, polymerization-based methods may present some drawbacks and limitations, which have made the development of new methods necessary. Thus, alternative methods based on the dispersion of well-characterized preformed polymers or natural macromolecules have been proposed, enlarging the field of possibilities for nanoparticulate formulations. As with polymerization-based methods, these new techniques allow the production of both nanospherical and nanocapsular systems. The most important milestones in the development of nanoparticulate systems are summarized in Table 1 (2–13).

In Situ Polymerization

Nanospheres. Two different approaches have been considered for the preparation of nanospheres by in situ polymerization, depending on whether the monomer to be polymerized is emulsified in a nonsolvent phase (emulsification polymerization), or dissolved in a solvent that is a nonsolvent for the resulting polymer (dispersion polymerization).

General Aspects of Emulsification Polymerization. Depending on the nature of the continuous phase in the emulsion, it is traditional to distinguish conventional emulsification polymerization from inverse emulsification polymerization. In the former case, the continuous phase is aqueous (o/w emulsion), whereas in the latter process it is organic (w/o emulsion). In both cases the monomer is emulsified in the nonsolvent phase with surfactant molecules, leading to the formation of monomer-swollen micelles and stabilized monomer droplets. The polymerization reaction (consisting of a nucleation and a propagation stage) takes place in the presence of a chemical or physical initiator. The energy provided by the initiator creates free reactive monomers in the continuous phase which then collide with the surrounding unreactive monomers and initiate the polymerization chain reaction. The reaction generally stops once full consumption of monomer or initiator is achieved. The drug to be associated to the nanospheres may be present during polymerization or can be subsequently added to the preformed nanospheres, so that the drug can be either incorporated into the matrix or simply adsorbed at the surface of the nanospheres.

Table 1. Milestones in the Field of Nanoparticle Manufacture

Year	Milestone	Refs.
	Nanoparticles formed by polymerization	
1976	Polyacrylamide nanospheres	2
1976	Poly(methyl methacrylate) nanospheres	3
1979	Poly(alkyl cyanoacrylate) nanospheres	4
1986	Poly(alkyl cyanoacrylate) nanocapsules	5
	Nanoparticles from preformed polymers	
1972	Albumin nanospheres by heat denaturation	6
1978	Gelatin nanospheres by desolvation	7
1979	Albumin nanospheres by cross-linking	8
1981	Poly(lactic acid) nanospheres by emulsification-solvent evaporation	9
1986	Poly(lactic acid) nanospheres by direct precipitation	10
1987	Poly(lactic acid) nanocapsules by interfacial deposition	11
1988	Poly(lactic acid) nanospheres by salting-out process	12
1995	Poly(lactic acid) nanospheres by emulsification-diffusion	13

Far from being totally elucidated, the mechanism by which the polymeric particles are formed during emulsification polymerization is not as simple as it was first believed, being initially described as a simple polymerization within the stabilized monomer droplets (14). Indeed, it is well established that the particles obtained by emulsification polymerization are generally much smaller (100–300 nm) than the original stabilized monomer droplets in the continuous outer phase (1–10 μm) (15). Other mechanisms, involving sites of nucleation other than the monomer droplets, have been considered to explain the particle formation process (16–19). First, the so-called micellar polymerization mechanism was proposed, involving the swollen-monomer micelles as the site of nucleation and polymerization. Swollen micelles exhibit sizes in the nanometer range and thus have a much larger surface area in comparison with that of the monomer droplets. It was assumed that, once generated in the continuous phase, free reactive monomers would more probably initiate the reaction within the micelles. Being slightly soluble in the surrounding phase, the monomer molecules reach the micelles by diffusion from the monomer droplets through the continuous phase, thus allowing the polymerization to be pursued within the micelles. So, in this case, monomer droplets would essentially act as monomer reservoirs (Fig. 2).

A second mechanism, called the homogeneous nucleation and polymerization process, has been proposed (16–19). If the monomer is sufficiently soluble in the continuous outer phase, the nucleation and polymerization stages can occur directly in this phase, leading to the formation of primary polymer chains called oligomers. In this case, throughout polymer chain growth, both the micelles and the droplets play the role of monomer reservoirs (Fig. 3). When the oligomers have reached a certain length, they precipitate and form primary particles which are stabilized by the surfactant molecules provided by the micelles and the droplets. Depending on the bulk conditions and system stability, the end-product nanospheres are formed either by additional monomer input into the primary particles or by fusion of the primary particles.

Whatever the mechanism involved (droplet, micellar, or homogeneous polymerization) each terminal nanosphere formed by emulsification polymerization usually consists of a large number of polymeric chains (18,19).

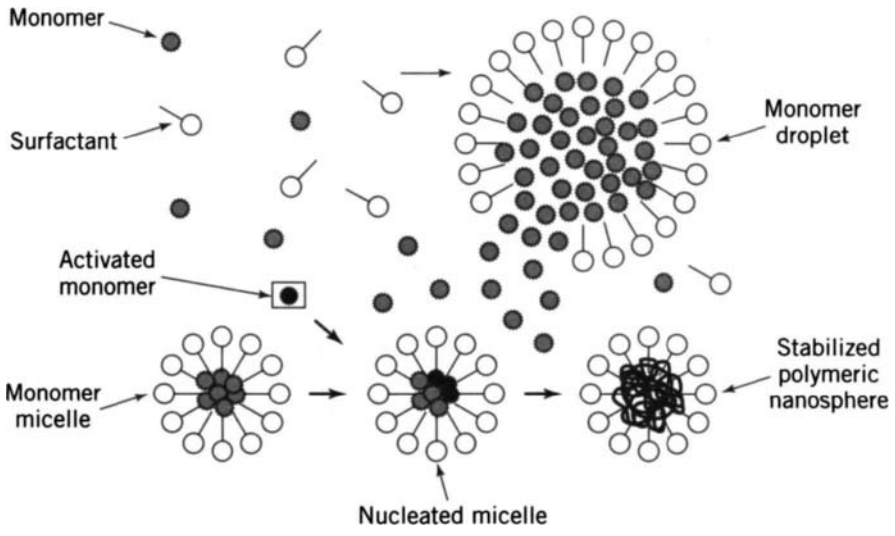


Figure 2. Micellar polymerization mechanism. *Source:* Adapted from Ref. 18.

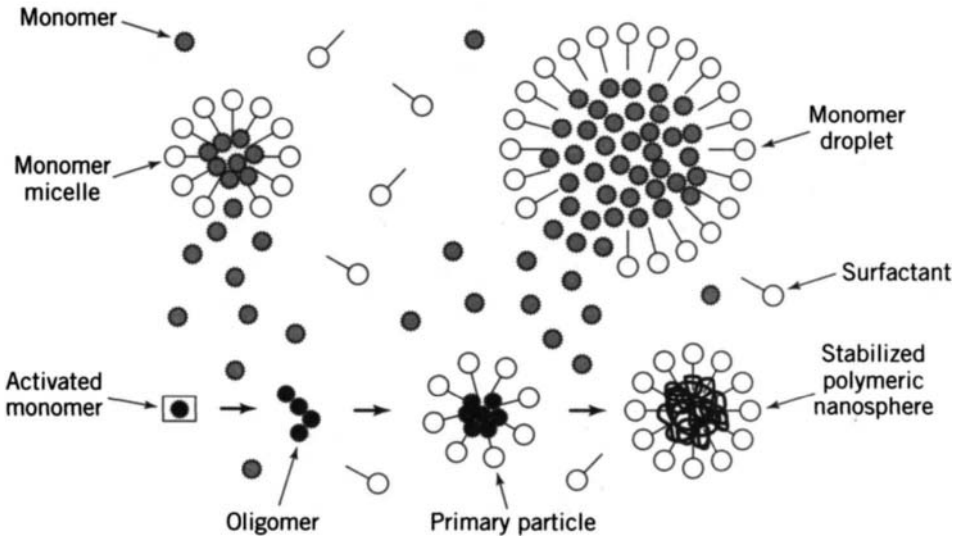


Figure 3. Homogeneous nucleation mechanism. *Source:* Adapted from Ref. 18.

Emulsification Polymerization in an Organic Continuous Phase. According to certain authors (2,20–22), the previously described mechanisms are only applicable when the polymerization process involves an aqueous continuous outer phase. It was assumed that in the case of inverse emulsification polymerization, in which the continuous phase is an organic one, the very water-soluble monomers used in this system cannot diffuse from the micelles through the organic phase because of their very low partition coefficient. As a result, particle formation would only result from the fusion of small nucleated micelles of constant size (Fig. 4). For this reason, this process is generally mentioned as an inverse "microemulsification" polymerization. The resulting nanospheres would contain fewer polymeric chains and a narrower distribution size, in contrast to the particles obtained by conventional emulsification polymerization (20–22). This theory has been debated by Kreuter (16) assuming that, whatever the partition coefficient of the monomer, the latter should still be slightly soluble in and diffuse through the organic phase. According to this author the mechanism of polymerization in an inverse emulsion is not qualitatively different from that in a conventional emulsion.

As previously mentioned, the first report concerning the use of nanoparticles for pharmaceutical applications was made by Birrenbach and Speiser in the seventies (2). These earliest nanoparticles were polyacrylamide nanospheres prepared by inverse emulsification polymerization and were intended to incorporate water-soluble antigenic material for vaccination purposes. Typically, water-soluble acrylamide monomers and human immunoglobulin G (IgG) were emulsified in *n*-hexane in the presence of a crosslinker (*N*,*N*′-methylene bisacrylamide) and large amounts of anionic surfactants (bis-(2-ethylhexyl)-sodium sulfosuccinate and poly(oxyethylene)-4-lauryl ether). The polymerization was initiated by γ-, ultraviolet, or visible light ir-

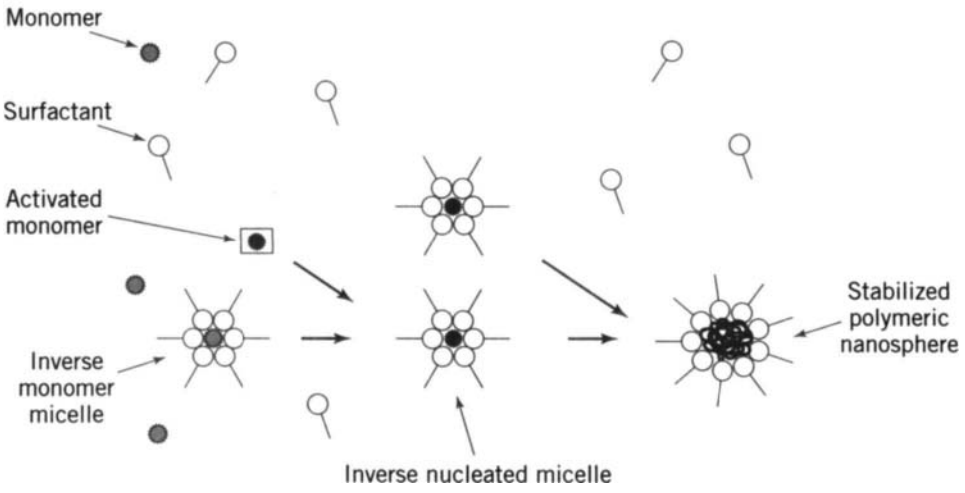


Figure 4. Mechanism of inverse emulsification polymerization. *Source:* Adapted from Ref. 18.

radiation, leading to the formation of IgG-loaded polyacrylamide nanospheres in the organic phase. Subsequently, several authors (20–25) used variants of this technique for the production of polyacrylamide nanospheres, but only a few produced nanospheres containing an active substance. Kopf et al. (23) succeeded in entrapping 96% of norephedrine HCl in polyacrylamide nanospheres. Labhasetwar and Dorle (25) produced polyacrylamide nanospheres incorporating metronidazole and primaquine but in this case the entrapment efficiency was low (<6%). In fact, these formulations have not been further developed for medical purpose, due, in particular, to the nonbiodegradable nature of this acrylic material. The use of polyacrylamide nanospheres as vaccine adjuvants is still being considered, but the large amounts of solvents and surfactants required for their production limit somewhat the interest of this application. However, these initial nanoparticle formulations allowed a better understanding of polymerization processes and opened up new prospects in the field of drug targeting.

The inverse emulsification polymerization process was rapidly adapted for the production of biodegradable poly(alkyl cyanoacrylate) (PACA) nanospheres (26–30). In these studies, the drug was dissolved in a small volume of water or hydrophilic solvent (methanol) and emulsified in an organic phase (e.g., isooctane, cyclohexane-chloroform, hexane) in the presence of large amounts of surfactants. Alkylcyanoacrylate monomers were then added directly or dissolved in an organic solvent to the preformed w/o emulsion under stirring. It was initially claimed that due to this subsequent addition of the monomers, particles with a shell-like wall (nanocapsules) were formed, resulting from the interfacial polymerization of monomers at the surface of the water-swollen micelles containing the drug. In fact, on the basis of transmission electron microscopy observations, it was later shown that the presence of nanocapsules was only occasional in the final nanoparticulate suspension and that most of the particles formed during this process were true nanospheres (19,26). Hydrophilic compounds such as doxorubicine (27,29,30), fluorescein (27), and methylene blue (28), as well as lipophilic compounds such as triamcinolone acetonide (26), were efficiently incorporated into PACA nanoparticles using this technique. As with former polyacrylamide nanospheres, PACA nanoparticles were finally obtained in the form of an organic dispersion containing large amounts of potentially toxic surfactants. In view of their therapeutic use, a tedious and extensive washing of the particles was required, making the overall manufacturing procedure long and difficult. This drawback has placed this process at a disadvantage with respect to polymerization in an aqueous phase for the production of PACA nanospheres.

Emulsification Polymerization in an Aqueous Continuous Phase. A major improvement was the preparation of nanospheres by emulsification polymerization in an aqueous continuous phase using no, or very little, surfactant. In this process, the surfactant acts mainly as stabilizer of the polymerized particles rather than emulsifier. Emulsification polymerization in a continuous aqueous phase is actually the most important method for the production of nanospheres.

A simple emulsification polymerization procedure was proposed in 1982 by Couvreur et al. (4) for the production of biodegradable PACA nanospheres. Since that time, these nanospheres have been the object of the most extensive investigations in the field of submicroscopic polymeric carriers. PACA nanospheres are produced by emulsifying water-insoluble alkylcyanoacrylate monomers in an acidic aqueous phase containing the drug and nonionic surfactants (e.g., poloxamer 188, polysorbate 20) or steric stabilizers (e.g., dextran 70). An anionic micellar polymerization takes place after diffusion of the monomer molecules through the aqueous phase. Once the polymerization is fully completed, the particle suspension is neutralized with NaOH, brought to isotonicity by glucose, and filtered. In contrast to other polymerization systems requiring an energy input that can affect the stability of the incorporated drug, the polymerization here is spontaneously initiated at room temperature by the hydroxide ions present in water, under vigorous stirring. The pH of the medium determines

the polymerization rate. The pH has to be acidic in order to prevent excessively rapid polymerization and enable the formation of monodispersed (nonagglomerated) nanoparticles. At pH values below 3, the size of the nanospheres obtained is approximately 200 nm with a narrow size distribution. Nanospheres with diameters as small as 30 nm can be produced by increasing the concentration of the surfactant or the pH of the polymerization medium in the pH range from 1 to 3 (31). Even smaller nanospheres can be obtained using sulfur dioxide as polymerization inhibitor (32). Among other parameters, the pH of the polymerization medium also has a major influence on the molecular weight of the polymer forming the nanospheres. This effect is generally described as being complex and is related to the antagonist action of initiator (OH^-) and terminator (H^+) during the polymerization process. As a result of the termination mechanism by H^+ ions, the molecular weights after anionic polymerization are generally very low and decrease with decreasing pH (33,34). To control the molecular weight of the polymer forming the nanospheres is important given the great influence of this parameter on the degradation rate of the particle, on the resulting drug release kinetic, as well as on the biodistribution of the particles. Consequently, optimization of the polymerization conditions (pH, temperature, stirring rate, type and concentration of monomer, surfactant, stabilizer, and acidifying agent) has been the object of very extensive investigations (33–36). It has been shown that such formulations were very reproducible in term of size and drug content, even after preparation at a semiindustrial level. Since the early patent of Couvreur et al. (4), a wide variety of drugs have been efficiently incorporated into PACA nanospheres. Most of them are hydrophilic and display cytostatic or antibiotic activities (1).

A major advantage of PACA nanospheres is their very rapid elimination from the body, within a few days, as a result of their very rapid degradation in vivo (37). The degradation mechanism of PACA nanospheres in biological conditions is complex. It involves at least two pathways, a chemical process (the so-called formaldehyde-producing pathway) and an enzymatic process, which was shown to be dominant and to occur through the hydrolysis of the ester side chains of the polymer (37–39). The incidence of the resulting degradation products (specially formaldehyde) in vivo is still a matter of debate. Toxic effects have been shown to occur toward a number of cells in vitro, with a clear relationship between the toxicity graduation and the alkyl chain length of the polymer (39–41). PACA nanospheres with long side chains (butyl, isobutyl, and isohexyl cyanoacrylates) generally exhibit a lower toxicity, which is attributed to their slower degradation, compared with nanospheres with short side chains (methyl and ethyl cyanoacrylates) (39,40). In addition, nanospheres with long alkyl chains are generally characterized by higher entrapment efficiencies and, as a result of slower degradation, slower drug release profiles (39). Although the bioacceptability of PACA nanospheres has to be considered carefully, they are actually considered as one of the most promising candidates for drug delivery in humans. A Phase I clinical trial using doxorubicin-loaded PACA nanospheres has been performed and revealed an improvement of the doxorubicin therapeutic index, illustrating the potential of these formulations as drug delivery systems (42).

The acidic nature of the polymerization medium can represent a major drawback when the drug intended to be incorporated into PACA nanospheres is labile at low pH. This problem can be overcome by using slightly different monomers such as the methylidene malonate derivatives. Those monomers have been proposed for the production of nanospheres in polymerization media having higher pH values. Developed on the same basis as alkylcyanoacrylates, alkyl methylidene malonic acid esters present an alkyl oxycarbonyl group instead of a cyano group, which is less electrophilic and thus less reactive in the presence of nucleophilic hydroxide ions (43). Diethyl methylidene malonate monomers were successfully used for the production of nanospheres by anionic polymerization in aqueous media (pH 6.7 to 8.7) (43,44). Unfortunately, poly(diethyl methylidene malonate) nanospheres could not be considered as suitable systemic drug carriers given their demonstrated nonbiodegradability both in vitro and in vivo (43). A new methylidene malonate derivative, methylidene malonate 2.1.2. was designed to overcome the lack of degradation of the former polymeric derivative. Poly(methylidene malonate 2.1.2.) (PMM 2.1.2.) nanospheres could be produced through anionic polymerization at pH values from 4 to 9, with an excellent batch to batch reproducibility in the pH range from 5 to 6 (45,46). In addition to the fact that these newly developed nanospheres may be useful for the incorporation of acid labile drugs, they have also been shown to exhibit satisfactory degradability and erodability (46,47), low in vitro (46,47), and in vivo (48) toxicity as well as a satisfactory shelf life (49). Although the production of drug-loaded PMM 2.1.2. nanospheres has not been described yet, these formulations appear to be promising alternative tools for the intravenous delivery of drugs, as well as good candidates for targeting purposes (50).

Numerous other derivatives have been used to prepare polymerized nanospheres in situ. The production of polyglutaraldehyde, poly(vinyl pyridine), poly(acroleine) and polystyrene nanospheres has been described by different authors (19). Although the lack of biodegradability of these systems compromises their clinical use as drug carriers, they could be potentially useful as adjuvants in vaccines (19).

Dispersion Polymerization in Water for Production of Polymethacrylic Nanospheres. The term *emulsification polymerization* is used when the monomer is emulsified in a nonsolvent by mean of surfactants. In the case of dispersion polymerization, the monomer is no more emulsified but dissolved in an aqueous medium which acts as a precipitant for the polymer to be formed. The nucleation is directly induced in the aqueous monomer solution and the presence of stabilizers or surfactants is not absolutely necessary for the formation of stable nanospheres. This method was developed in the mid-seventies by Kreuter and Speiser (3) for the production of very slowly biodegradable poly(methyl methacrylate) (PMMA) nanospheres. The aim of these authors was to propose a simplified manufacturing procedure based on the method previously developed by Birrenbach and Speiser (2) but avoiding the use of large

amounts of organic solvents and surfactants. In this method, water-soluble methyl methacrylate monomers are dissolved in an aqueous medium and polymerized by γ-irradiation (3,51) or by chemical initiation (ammonium or potassium peroxodisulfate) combined with heating to temperatures above 65°C (52,53). In the case of chemical initiation, the aqueous medium must be previously flushed with nitrogen for 1 h in order to remove its oxygen content, which could inhibit the polymerization by interfering with the initiated radicals. Whatever the type of initiation used, oligomers are formed and above a certain molecular weight precipitate in the form of primary particles which may or may not be stabilized by surfactant molecules. Finally, nanospheres are obtained by the growth or the fusion of primary particles in the aqueous phase (Fig. 5).

The possible production of PMMA nanospheres by surfactant-free polymerization is very advantageous because, as previously mentioned, the removal of detergents is generally very cumbersome. Being very slowly biodegradable and biocompatible (54), PMMA nanoparticles have been shown to be an optimal material for vaccination purposes. For this application, initiation by γ-irradiation can be useful for the production of PMMA nanospheres by polymerization in the presence of antigenic material, because it can be carried out at room temperature or below, thus preventing the destruction of these heat-sensitive substances (51). Antigens may be present during polymerization (3,55) but can also be added to the preformed nanospheres (3,53,55,56). The antigenic materials used to produce nanoparticulate PMMA adjuvants were influenza virions (3,55), influenza subunit antigens (53), bovine serum albumin (52,53), and more recently HIV-1 and HIV-2 antigens (56,57). For the particles produced in the presence of influenza virions, a shell-like structure was proposed (55,58). Because of their large dimension (~80 nm), the virions are more probably coated by a shell of polymerized monomers initially adsorbed at their surface, than strictly incorporated in a polymeric matrix.

Besides PMMA nanospheres, copolymer methacrylic nanospheres can also be produced by the dispersion polymerization process using blends of methyl methacrylate with one or several other acrylic acid derivatives (e.g., hydroxyethyl methacrylate, methacrylic acid, ethylene glycol dimethacrylate, sulfopropylmethacrylate) (53,59–61). These copolymer nanospheres were developed with the intention of modifying the surface properties of the nanospheres, namely the hydrophilicity but also the charge (61) which are important parameters governing the body distribution of the particles.

Various types of drugs have been linked to PMMA and polymethacrylic nanospheres (1). Rolland (62) performed extensive investigations with doxorubicin-loaded polymethacrylic nanospheres suggesting that, in spite of their very low biodegradability, these particles could be used in humans for cancer treatment using a monthly intravenous injection protocol. Nevertheless, compared with some other colloidal systems, the use of such practically nonbiodegradable particles appears to be very limited, if not precluded when regular therapeutic administration is desired. Essentially suitable as adjuvants for vaccination purpose, PMMA and polymethacrylic nanospheres are also of great value for fundamental studies on the in vitro and in vivo behavior of particles remaining intact in biologic media over extended time periods (59,63–66). In providing general information about the interactions of the nanospheres with cells or opsonins, their biodistribution and bioelimination, these studies allow a better understanding of the mechanisms regulating the biological fate of nanoparticulate drug carriers.

Nanocapsules

PACA Nanocapsules. On the basis of the method proposed by Couvreur et al. (4) for preparing PACA nanospheres, Al Khouri-Fallouh et al. (5) developed a new method leading to the production of nanocapsules, a new type of colloidal carrier with a capsular structure consisting of a polymeric envelope surrounding an oily central cavity. The aim was to produce a nanoparticulate formulation with high entrapment efficiency for lipophilic drugs. This could be hardly achieved with PACA nanospheres prepared by anionic emulsion polymerization because this method required dissolution of the drug in an aqueous polymerization medium, precluding the incorporation of poorly water-soluble compounds.

In the procedure described by Al Khouri-Fallouh et al. (5), the monomer (isobutyl cyanoacrylate) and a lipophilic drug (lomustine, progesterone) are dissolved in an ethanolic phase containing an oil (Myglyol®, Lipiodol®) or a non-

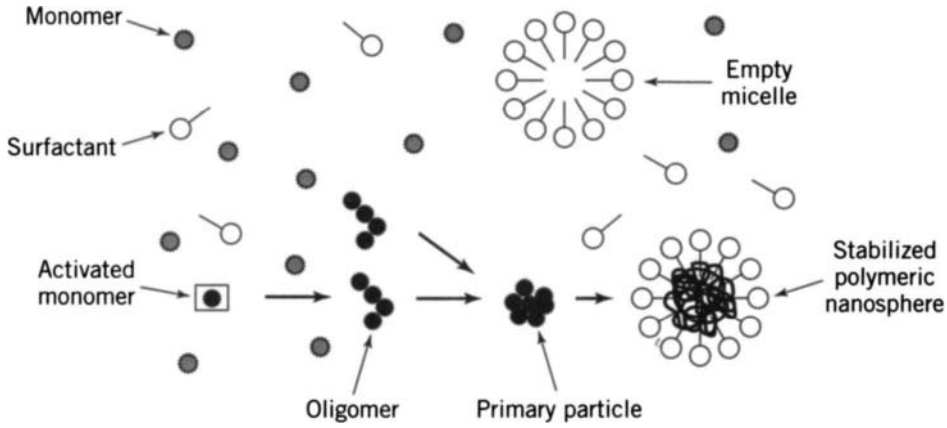


Figure 5. Mechanism of dispersion polymerization. *Source:* Adapted from Ref. 18.

miscible organic solvent (benzylic alcohol). This mixture is slowly injected through a needle into a magnetically stirred aqueous phase (pH 4–10) containing a nonionic surfactant (poloxamer 188). The mixture immediately becomes milky and nanocapsules with a mean diameter of 200–300 nm with a narrow polydispersity are formed. The colloidal suspension can then be concentrated by evaporation under reduced pressure and filtered through sintered glass before redilution with a physiological buffer. Examination by transmission electron microscopy, after negative staining of the particles, demonstrated the existence of a polymeric wall with a mean thickness of about 3 nm (5,67). On the basis of these observations, it was assumed that formation of nanocapsules resulted from the so-called interfacial polymerization mechanism. This mechanism was described as a spontaneous and rapid process: upon mixing with the aqueous phase, ethanol rapidly diffuses out of the organic phase giving rise to spontaneous emulsification of the oil/monomer/drug mixture. Due to their interfacial properties (67), the monomer molecules spontaneously locate at the surface of the oil nanodroplets and, upon contact with aqueous hydroxide anions, immediately polymerize at the water–oil interface, leading to the formation of solid wall-structured particles. The speed of magnetic stirring has no influence on the particle size, which depends solely on the nature and the volume of the oil, and on the volume of the diffusing organic phase (68). The presence of surfactant in the aqueous phase is not necessary for the successful formation of nanocapsules but does guarantee the physical stability of the preparation. For efficient encapsulation, the lipophilic drug must have a partition coefficient which favors its location in the oil, and the oil must then be chosen accordingly (68). Since the early description of this new process, numerous workers have used it as such or with slight modifications to produce nanocapsules incorporating a wide variety of lipophilic drugs with high entrapment efficiencies (1).

Extensive investigations have been performed to determine the influence, on PACA nanocapsule morphology and structure, of parameters such as the nature and pH of the aqueous phase, composition of the organic phase (solvent, oil, monomer), surfactant and emulsification conditions (67,69–72). In particular, in a very interesting study employing freeze-fracture electron microscopy, Fresta and Puglisi (71,72) showed that, depending on the type of organic solvent used for the nanocapsule preparation, heterogeneous systems consisting of a mixture of nanocapsules and nanospheres could be obtained. When protic water-miscible organic solvents such as ethanol, *n*-butanol, or isopropanol were used in the preparation, both types of particles were formed in the suspension, whereas when aprotic water-miscible organic solvents such as acetone and acetonitrile were used, only true nanocapsules were obtained. It was assumed that protic solvents, with a certain nucleophilic character, could give rise to the polymerization of the monomer molecules initially in the organic mixture, before emulsifying it in the aqueous phase. Evidence of initial polymerization in an organic protic phase was supported by the fact that when the monomer was dispersed, for example, in pure ethanol, cloudy suspensions were observed, whereas when it was added to acetone or acetonitrile the resulting solutions remained absolutely clear. On the basis of these observations, Fresta and Puglisi (71,72) assumed that upon contact with the aqueous phase, oligomers, preformed in the protic organic phase, may precipitate and lead to the formation of nanospheres in the final suspension. As to the nanocapsules, they may be formed according to two different mechanisms: (*1*) by normal polymerization of the monomers at the water–oil interface and (*2*) by deposition at the interface of the preformed oligomers present in the organic phase (interfacial deposition of a preformed polymer theory). When an aprotic solvent is used, only interfacial polymerization may occur, allowing the production of true nanocapsule suspensions. Accordingly, the use of acetone was shown to provide high-quality nanocapsules, with regular wall thickness and homogeneous size distribution (32).

Slightly different theories have been proposed by other investigators to explain the presence of both nanospheres and nanocapsules in the suspensions prepared with nucleophilic solvents (73,74). Whatever the real nature of the mechanism involved, it clearly appears that when the production of a true nanocapsule formulation is desired, the most suitable conditions of preparation have to be established, especially with regard to the organic solvent to be chosen. In addition, a selective characterization of the resulting particles should be systematically conducted in order to assess the real homogeneity of the system. In good accordance with these considerations, Chouinard et al. (69) described the preparation of poly(isohexyl cyanoacrylate) nanocapsules using an ethanolic oily phase. In order to prevent immediate polymerization in ethanol, the monomer was initially saturated with a polymerization inhibitor (sulfur dioxide) prior to mixing with the ethanolic oily phase. Upon contact with the aqueous phase, sulfur dioxide rapidly diffuses into water, allowing interfacial polymerization to occur and nanocapsules to be formed. Evidence of the homogeneous capsular morphology of the particles was assessed by freeze-fracture microscopy, as well as by density measurements (69).

Several authors have reported the production of nanocapsules by interfacial polymerization of cyanoacrylate monomers using a inverse emulsification polymerization procedure. This technique was used to encapsulate hydrophilic compounds such as doxorubicin (27,29,30), fluorescein (27), or methylene blue (28), as well as the lipophilic drug triamcinolone acetonide (26). In this procedure, the drug was dissolved in a small volume of water (or methanol in the case of triamcinolone acetonide) and emulsified in an organic external phase (e.g., isooctane, hexane) containing a surfactant. Then, an organic solution of cyanoacrylate monomers was added to the preformed w/o emulsion. It was generally assumed that, using this procedure, nanocapsules were formed, resulting from an interfacial polymerization process around the nanodroplets. However, it was showed by Krause et al. (26) by transmission electron microscopy that, in fact, following this procedure, a mixture of nanospheres and nanocapsules was formed, with a predominance of nanospheres. A rational explanation for the formation of nanocapsules is that the polymerization process in some cases is so rapid that an impermeable poly-

mer wall may be formed at the interface, preventing the diffusion of further monomers into the interior of the particles. However, in most cases, the interior of the particles is also polymerized and solid monolithic nanospheres are formed (19). For this reason, this particular technique is sometimes classified in the literature with other related methods allowing the preparation of PACA nanospheres by inverse emulsification polymerization (1,19).

Poly(N^{α},N^{ϵ}-L-lysinediethylterephthaloide) Nanocapsules by Interfacial Polycondensation Using Electrocapillarity Emulsification. Arakawa and Kondo (75) proposed an original technique for the preparation of blood hemolysate–loaded nanocapsules. These hemoglobin containing nanoparticles were intended to be used as artificial red blood cells. Poly(N^{α},N^{ϵ}-L-lysinediethylterephthaloide) nanocapsules containing sheep hemolysate are prepared by interfacial polycondensation of L-lysine with terephthaloyl dichloride in an emulsion made by electrocapillarity. A water phase containing the hemolysate and L-lysine is slowly injected into an organic solution of terephthaloyl dichloride containing a surfactant. During the injection, an electrical potential difference is applied between the two phases. When this potential reaches a certain value (850 V), the interfacial tension is reduced to zero and spontaneous emulsification occurs. The polycondensation between the monomers should be expected to occur exclusively at the water–oil interface, leading to the formation of wall-type nanoparticles. However, formation of true nanocapsules still remains to be proven by electron microscopy analysis (19). In addition, as for other preparation methods implying a w/o emulsion, these particles must be subsequently transferred to an aqueous phase by successive washings.

Dispersion of a Preformed Polymer

As described already, since the early description of polymerization processes for the production of latex in the polymer industry, extensive efforts have been made to adapt this technology for the production of polymeric colloids that meet pharmaceutical requirements. Although real technological advances have been achieved, allowing for example the fulfillment of the submicroscopic size criteria, most of the polymeric carriers prepared by polymerization still encounter major drawbacks (74). With the exception of PACA and recently developed PMM 2.1.2. nanoparticles, most of the carriers produced by polymerization have inadequate biodegradability properties precluding their use for regular therapeutic administration. Only for vaccination purposes can very slowly biodegradable PMMA systems be considered as being suitable adjuvants when achievement of a very prolonged immune response is desired. In addition, due to the multicomponent nature of the polymerization media, it is generally very difficult to predict the molecular weight of the resulting polymerized material. This is a major drawback because the molecular weight greatly influences the biodistribution and release behavior of the polymeric carrier. Another drawback is the possible inhibition of drug activity due to interactions with activated monomers or with the numerous H^+ ions present in anionic polymerization processes. Finally, the main limitation to the use of polymerized carriers is related to the presence of toxic residues, namely the unreacted monomer, initiator, and surfactant molecules whose elimination requires time-consuming and not always efficient procedures.

In order to circumvent those limitations and extend the manufacturing possibilities for the achievement of biodegradable, well-characterized, and nontoxic nanoparticles, new methods involving the use of already polymerized materials have been developed. These materials include natural macromolecules (biopolymers) and synthetic polymers.

Nanospheres Prepared From Natural Macromolecules. Among the natural macromolecules available for the manufacture of nanospheres, proteins such as albumin, gelatin, legumin, or vicilin, as well as polysaccharides like alginate or agarose have been evaluated (Table 2). These macromolecules have attracted wide interest as biomaterials due to their intrinsic properties of biodegradability and biocompatibility. Of the previously mentioned macromolecules, albumin and gelatin have been the most extensively used. Two main manufacturing techniques have been reported to produce nanospheres from natural macromolecules. The first technique is based on the formation of a w/o emulsion and subsequent heat denaturation or chemical cross-linking of the macromolecule. The second approach involves a phase separation process in an aqueous medium that may be followed by chemical cross-linking (see Table 2). The term cross-linking is used to describe the formation of covalent bonds between the lysine amino groups of proteins and an aldehydic compound, leading to the hardening and stabilization of the formed particles.

Emulsification-Based Methods. The emulsification technique was initially introduced by Scheffel et al. (6) for the production of albumin nanospheres and was later optimized by Gallo et al. (76). In this process, an aqueous solution of albumin is emulsified at room temperature in a vegetal oil (cottonseed oil) and homogenized either by mean of a manual (6) or mechanical high pressure homogenizer (77) or by mean of ultrasonication (76). Once a high degree of dispersion is achieved, the emulsion is added dropwise to a large volume of preheated oil (>120°C) under stirring. This leads to the immediate vaporization of the water contained in the droplets and to the irreversible denaturation of the albumin which coagulates in the form of solid nanospheres (18) (Fig. 6). The suspension is then allowed to cool down at room temperature or in an ice bath. Subsequently, the particles are submitted to several washings using large amounts of organic solvent (e.g., ether, ethanol, acetone) for complete removal of the oil. This purification step represents a main drawback in terms of manufacturing wastes, especially in view of large scale particle production. In addition, the hardening step by heat denaturation may be harmful to heat-sensitive drugs. To circumvent this latter problem, the use of a cross-linking agent was proposed by Widder et al. (8) for the chemical hardening of the albumin nanodroplets. Surprisingly, although the cross-linking agent (2,3-butanedione or formaldehyde) was added only after the washing and resuspension of the system in ether, no coalescence of the soft

Table 2. Main Methods for the Production of Nanospheres from Natural Macromolecules

Macromolecule	Production principle	Hardening procedure[a]	Reference
Albumin	w/o emulsification	HD	6,76
	w/o emulsification	CL	8,78,79
	Phase separation in an aqueous medium		
	By addition of a desolvating agent	CL	7
	By modification of the pH	CL	83
Gelatin	w/o emulsification	CG + CL	80
	Phase separation in an aqueous medium		
	By addition of a desolvating agent	CL	7
	By modification of the temperature	CL	84
Vicilin, legumin	Phase separation in an aqueous medium by modification of the pH	CL	85,86
Alginate	Phase separation in an aqueous medium by addition of divalent cations	PC	82
Agarose	w/o emulsification	CG	81

[a]HD, heat denaturation; CL, cross-linking; CG, cold gelation; PC, polyelectrolytic complexation.

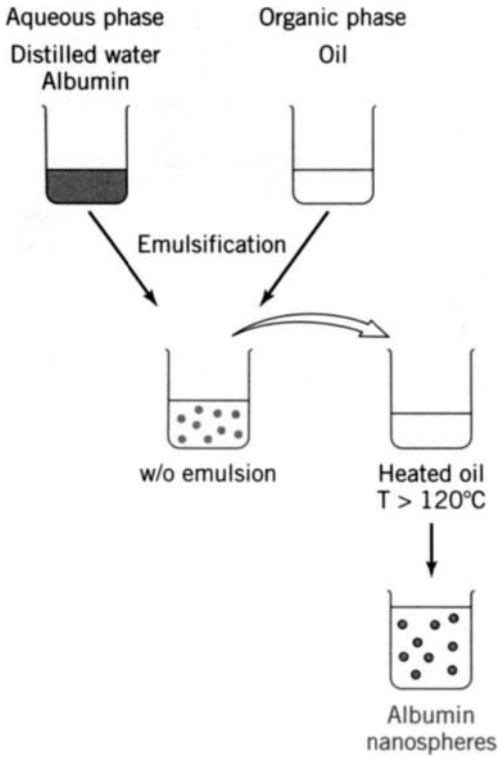


Figure 6. Preparation of nanospheres by thermal denaturation of albumin.

non-cross-linked albumin droplets was reported during these experiments (16).

Another method for preparing cross-linked albumin nanospheres has been proposed using a polymeric phase (ethylcellulose in toluene or hydroxypropylcellulose in chloroform) instead of an oily dispersing phase (78,79). It was asserted that, after purification and drying, the resulting particles were more easily redispersed and also exhibited narrower size distributions compared with particles produced with an oily dispersing phase (79). Nevertheless, with this particular method, the elimination of the polymeric dispersing agent still remains a problem, requiring several washings with large amounts of organic solvent (78,79), and thus it does not offer any advantage over the previously described techniques.

Gelatin and, more recently, polysaccharidic agarose nanospheres have been produced using an emulsification-based method involving the gelation of the macromolecule (80,81). In this process, the w/o emulsion was cooled (0–5°C) below the gelation temperature of the macromolecule, leading to the complete gelation of the macromolecule droplets. The resulting hydrogel nanospheres were further stabilized by cross-linking (80) or directly washed with an organic solvent (81).

Phase Separation-Based Methods in an Aqueous Medium. As previously mentioned, the main disadvantage of emulsification methods is that large amounts of organic solvents are required to obtain nanospheres free of any oil or dispersing agent residues. Another disadvantage is that it is very difficult to produce small nanospheres (<500 nm) with narrow-size distributions, due to the intrinsic instability of the emulsion prior to hardening by heat or cross-linking (19). Coacervation or controlled desolvation methods have been developed to circumvent these problems. In this case, the particles are formed in an aqueous medium by a phase separation process and are subsequently stabilized by cross-linking with glutaraldehye.

A now traditional method was proposed by Marty et al. (7), based on the desolvation and resolvation properties of proteins. In this process, gelatin and albumin nanospheres can be produced by the slow addition of a desolvating agent (neutral salt or alcohol) to the protein solution. Upon this addition, a progressive modification of the protein tertiary structure is induced leading, when a certain degree of desolvation is obtained, to the formation of protein aggregates. The nanospheres are obtained by subsequent cross-linking of these aggregates with glutaraldehyde. To obtain small and monodispersed particles, it is important to maintain the system at a point just before coacervation is initiated (7,16). The addition of the desolvating agent is monitored by turbidimetry measurements of the system and must be stopped as soon as the turbidity increases, otherwise aggregates that are too large will be formed. Alternatively and for optimal monitoring of the process, the system can be desolvated until the coacervation state is reached, and then rapidly reverted to the precoacervated

state by adding a very small amount of resolvating agent (7,16) (Fig. 7).

Other phase separation-based methods have been developed in recent years for the production of other protein and polysaccharide nanospheres, as shown in Table 2 (82–86). In these processes, phase separation could be induced by changes in the pH or temperature, or by addition of appropriate counterions in the protein or polysaccharide aqueous solution. In the latter case, for example, alginate nanospheres were formed by controlled gelation of an alginate solution. The alginate gelation was induced by divalent cations (calcium chloride) and the resulting gelated nanospheres were subsequently stabilized by polyelectrolytic complexation with a polyamine (poly(L-lysine)) (82).

Several drugs or tracers have been successfully combined with natural macromolecular nanospheres, either by incorporation (codissolution with the macromolecule), chemical coupling on the surface (reaction with free functional groups of the cross-linking agent), or by simple adsorption on preformed nanospheres (1). The emulsification-based methods can be considered especially suitable for the incorporation of hydrophilic drugs in term of loading capacity. With regard to the phase separation-based techniques, the entrapment efficiency for hydrophilic drugs can be strongly affected depending on the drug affinity which is partitioned between the macromolecular particle and the aqueous environment (87). In general, highly water-soluble drugs are less well incorporated by these methods, because they interact more strongly with water than with the macromolecule and are readily washed out of the particles (7). Nevertheless, the major concerns with techniques involving natural macromolecules lie in the necessity for using hardening agents (most frequently glutaraldehyde) that may react with the drug and may also confer some toxicity to the nanoparticle formulations (87).

Nanospheres Prepared From Synthetic Polymers. Among the numerous synthetic polymers available for the preparation of nanospheres, the most commonly used are poly(lactic acid) (PLA), poly(glycolic acid) (PGA), poly(lactic-*co*-glycolic acid) (PLGA), poly(ϵ-caprolactone) (PCL), and poly(β-hydroxybutyrate) (PHB). Belonging to the family of polyesters, these polymers are known to exhibit adequate biodegradability and biocompatibility. Under physiological conditions, polyesters are generally degraded by hydrolysis into products which are well tolerated by various tissues. For example, the degradation products of PLA, PGA, and PLGA, namely glycolic acid and lactic acid, are physiologic substances easily eliminated through the Krebs cycle (41,88). The safety of polyesters is illustrated by their extensive use as sutures and orthopedic implants for approximately two decades, and more recently by their use as controlled delivery devices for drugs. At present, a number of microparticle and implant formulations composed of PLGA copolymers are available on the market, for human use (e.g., Decapeptyl retard®, Zoladex®). Being directly related to the rate of degradation, the drug release capabilities of polyesters can be easily tailored, depending on the monomer composition and the polymerization conditions (88,89). Consequently, polyesters make possible the preparation of delivery systems from which the drug is released in a controlled way, over days to months. Polyesters nanoparticles can be produced using two different approaches. The first approach is based on the emulsification of an organic solution of the polymer in an aqueous phase containing surfactants, stabilizers, or electrolytes, and subsequent precipitation of the polymer by removal of the organic solvent. A second approach is based on the direct precipitation of the solubilized polymer upon addition of a nonsolvent.

Emulsification-Based Methods. Different emulsification-based methods have been described depending on the miscibility of the organic solvent in the aqueous phase. Some methods involves volatile and water-immiscible solvents which can be extracted by simple evaporation, leading to polymer precipitation (emulsification-solvent evaporation method). In other methods, partially or fully water-miscible organic solvents are used and polymer precipitation occurs as a result of controlled diffusion processes (salting-out and emulsification-diffusion methods).

The emulsification-solvent evaporation method was first used by Gurny et al. (9) in the early eighties for the preparation of PLA nanospheres, based on a patent filed by Vanderhoff et al. (90). This method was later adopted for the production of nanospheres with a wide range of polymers including PLGA, PCL, and PHB, as well as methacrylic acid copolymers and cellulose derivatives (1,19,87). The preformed polymer is dissolved in a volatile organic solvent (e.g., chloroform, methylene chloride, ethyl acetate), and the organic solution is dispersed in an aqueous phase to form an o/w emulsion, in the presence of a surfactant (e.g., polysorbate, poloxamer, sodium dodecyl sulfate) or a stabilizer such as poly(vinyl alcohol) (PVA). Continuous emulsification under stirring prevents coalescence of the organic droplets and can be further improved by sonication or microfluidization with a high pressure homogenizer. The extraction of the solvent from the nanodroplets

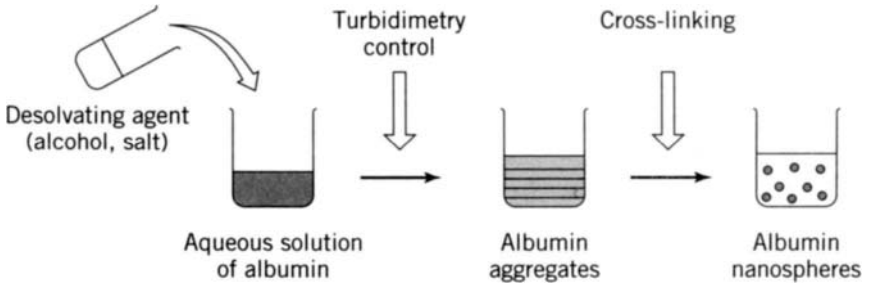


Figure 7. Preparation of nanospheres by desolvation of albumin.

is achieved by evaporation at room temperature under stirring or in a rotary evaporator under reduced pressure. As a consequence of this extraction, the polymer precipitates, leading to the formation of nanospheres (Fig. 8). The technique was later optimized by Julienne et al. (91), who investigated the influence of various parameters on the resulting particle size, such as the nature and concentration of the surfactant and stabilizer, the conditions of emulsification, the polymer concentration, and the phase volume ratio.

The emulsification-solvent evaporation method generally allows efficient entrapment of lipophilic compounds (e.g., testosterone, indomethacin), which can dissolved in the polymer solution (1). Recently, the encapsulation of a model amphiphilic protein, bovine serum albumin, was achieved by a slight modification of the technique (92). An aqueous solution of bovine serum albumin and poloxamer 188 was emulsified in a solution of PLGA in ethyl acetate by sonication. Then, this pre-emulsion was added to an aqueous phase containing PVA as stabilizer, resulting in a (w/o)/w emulsion which was sonicated again, diluted, and finally introduced in a rotavapor to eliminate the solvent. Entrapment efficiencies up to 70% could be achieved using this procedure (92).

Another modification of the technique was proposed to achieve the entrapment of water-soluble compounds in PLGA nanospheres, based on the use of a mixture of a chlorinated solvent and polar solvents (acetone, methanol) to dissolve the polymer and the drug (93). Due to their polarity and water miscibility, the admixed polar solvents were shown (*1*) to improve the dissolution of a water-soluble drug (5-fluorouracil) in the organic phase and (2) to promote the emulsification of the system by rapid diffusion out of the nanodroplets upon addition of the aqueous phase (93).

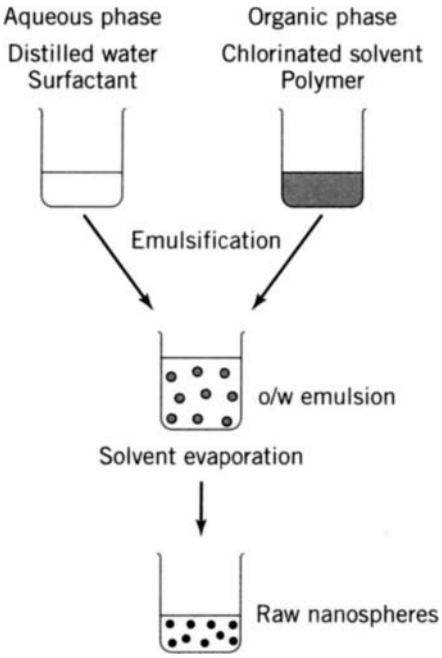


Figure 8. Emulsification-solvent evaporation method.

Although less toxic solvents such as ethyl acetate can be used, the emulsification-solvent evaporation method generally requires the use of toxic chlorinated solvents and surfactants, which constitute a major drawback for this method. In addition, the possibility to efficiently entrap water-soluble compounds remains very limited.

The salting-out procedure was proposed by Bindschaedler et al. (12) in the late eighties. This technique makes use of acetone, a water-miscible solvent, instead of the chlorinated solvents previously used and, furthermore, avoids the use of surfactants. An aqueous phase saturated with electrolytes (e.g., magnesium acetate, magnesium chloride) and containing PVA as a stabilizing and viscosity increasing agent is added under vigorous stirring to an acetone solution of polymer. In this system, the miscibility of both phases is prevented by the saturation of the aqueous phase with electrolytes, according to a salting-out phenomenon. The addition of the aqueous phase is continued until a phase inversion occurs and an o/w emulsion is formed. Then, a sufficient amount of pure water is added to disrupt the equilibrium between the two phases and to allow complete diffusion of acetone into water, leading to polymer precipitation in the form of spherical nanospheres (Fig. 9). Optimization of the method was performed by Allémann et al. (94) and the influence of various manufacturing parameters on the particle size was investigated. Furthermore, it was shown in this study that solvents other than acetone (e.g., tetrahydrofuran) as well as nonelectrolytic salting-out agents (e.g., sucrose) could be also used to produce nanospheres, demonstrating the relative versatility of the method (94). A wide variety of polymers can be used with this technique including PLA, methacrylic acid copolymers, and cellulose derivatives (1). High

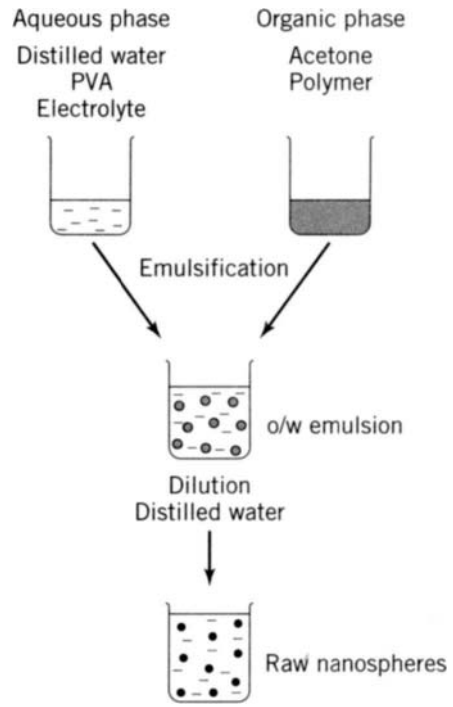


Figure 9. Salting-out process.

drug loadings can be achieved, depending on the solubility of the drug in acetone and on the nature of the salting-out agent used. For instance, savoxepine, a neuroleptic drug (pK_a 8.3), was loaded in PLA nanospheres either in the form of a free base or as a salt, the salt being much less soluble in acetone. Two different salting-out agents, magnesium chloride and magnesium acetate, were used, providing an acidic or a basic aqueous phase, respectively (95). The highest entrapment efficiency (95%) was achieved with the formulation involving savoxepine base and a basic aqueous phase (pH 8). Having minimal affinity for the aqueous phase under these conditions, the drug remains within the organic phase, leading to very efficient entrapment in the resulting nanospheres.

Although the salting-out process has proved suitable for the production of large quantities of highly drug-loaded nanospheres, the use of acetone and large amounts of salts may raise some concern about recycling of the salts and about compatibility with active compounds. Recently, Leroux et al. (13) developed a new method called emulsification-diffusion, which involves the use of benzyl alcohol as organic solvent. The originality of this method is based on the partial miscibility of benzyl alcohol with water. An aqueous phase containing a stabilizing agent (PVA or gelatin) is added to a solution of polymer in benzyl alcohol under mechanical stirring. Because benzyl alcohol is only miscible at a ratio of 1:25 (m/v) with water, a two-phase system is formed and an o/w emulsion is obtained upon complete addition of the aqueous phase. Then, the emulsion is diluted with a large amount of pure water in order to overcome the 1:25 miscibility ratio of benzyl alcohol. The precipitation of the polymer occurs as a result of the diffusion of benzyl alcohol into water, leading to the formation of nanospheres. By increasing the percentage of PVA in the external phase, it was possible to produce nanoparticles as small as 70 nm in diameter, whereas with gelatin the smallest nanoparticles obtained had an average size of 700 nm. The polymers used were PLA, PLGA, PCL, and methacrylic acid copolymer Eudragit® S100. Chlorambucil, a cytostatic drug with a very slight water solubility, was successfully entrapped into PLA nanospheres (13). In a recent study, the potential use of other partially water-soluble solvent and stabilizing agents was investigated, and a mechanism based on interfacial phenomena was proposed to explain the formation of nanospheres (96).

Direct Precipitation-Based Method. This technique, proposed by Fessi et al. (10), involves the use of an organic solvent that is completely miscible with the aqueous phase, typically acetone, but ethanol or methanol can also be used. This method allows nanospheres to be obtained without prior emulsification. In this case, the polymer precipitation is directly induced in an aqueous medium (containing or not a surfactant) by progressive addition under stirring of the polymer solution (Fig. 10). After nanoparticle formation, the solvent is removed by vaporization under reduced pressure. The usefulness of this method is limited to drugs that are highly soluble in polar solvents, but only slightly soluble in water (e.g., indomethacin), to avoid extensive loss of the drug during the solvent diffusion (87). In fact, the main limitation of this method is that it is not easy to choose a polymer/drug/solvent/nonsolvent system allowing high entrapment efficiencies and production yields. In general, this method has to be carried out with low concentrations of polymer in the organic phase. In this case, polymer dispersion and small particle size can be obtained easily. In contrast, when it is necessary to increase the amount of polymer in the organic phase (e.g., for the preparation of large-scale batches), large aggregates tend to form, resulting in poor production yields (97). Recently, it was shown that changing the nature of the organic phase could reduce the polymer loss. For example, the use of mixtures of acetone and water instead of acetone alone was shown to favor the dispersion of the polymer and to increase the production yield (97).

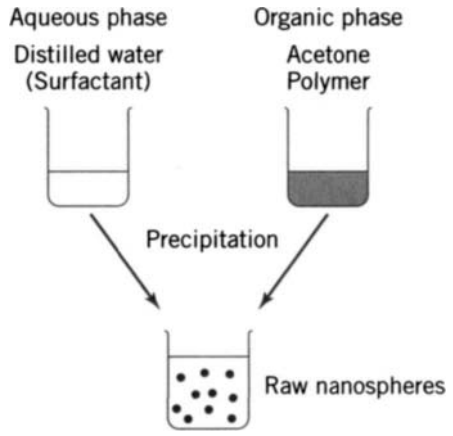


Figure 10. Direct precipitation method.

Nanocapsules Prepared From Synthetic Polymers. Nanocapsules can be produced from synthetic polymers by a very similar procedure to that already described. This method was also proposed by Fessi et al. (11) and is generally called the interfacial deposition technique. It differs from the nanosphere preparation method by the introduction of an oily component into the polymer organic solution. First, the polymer is dissolved in acetone, then a phospholipid mixture (e.g., Epikuron®) and benzyl benzoate are added to this solution. The resulting organic solution is poured into an aqueous phase containing a surfactant (e.g., poloxamer 188) under moderate stirring. Acetone diffuses immediately into the aqueous phase, inducing the deposition and the precipitation of the polymer around the oily droplets (Fig. 11). Once the nanocapsules are formed, acetone is eliminated under reduced pressure. Drugs intended to be encapsulated by this method must have a high solubility in the organic-oily phase, otherwise they diffuse from the oily solution and precipitate in the aqueous medium during particle formation (11,98). For example, as a result of the poor solubility of indomethacin in organic-oily phases, very poorly loaded PLA nanocapsules (0.25% w/v) could be produced with this drug (11). The production of cyclosporin A–loaded nanocapsules made of PCL was recently reported (98). Under optimized conditions, drug loadings as high as 50% could be obtained, but because no data about production yields were provided, it is not clear

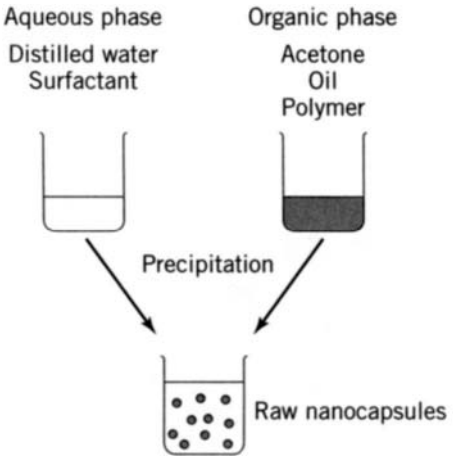


Figure 11. Interfacial deposition technique.

whether this procedure is suitable for the production of large-scale batches.

Pharmaceutical Aspects

Because nanoparticles are intended to be used as pharmaceutical dosage forms in humans, among other requirements, they are required (*1*) to be free of any potentially toxic impurities, (*2*) to be easy to store and to administer, and finally (*3*) to be sterile if parenteral use is envisaged.

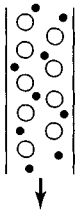
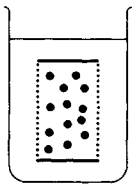
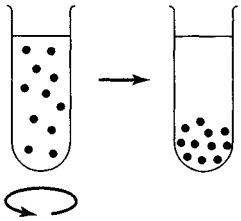
Purification. Depending on the preparation method, various potentially toxic impurities can be found in the nanoparticulate suspensions including organic solvents, residual monomers, polymerization initiators, electrolytes, surfactants, stabilizers, and large polymer aggregates. The necessity for and degree of purification are dependent on the final purpose of the formulation developed. For example, the stabilizer PVA, frequently used to prepare polyester nanoparticles, is not acceptable for parenteral administration, whereas it is not so critical for oral and ocular administration (87). Although polymer aggregates can be easily removed by simple filtration through sintered glass filters, the removal of other impurities requires more sophisticated procedures. The most commonly reported procedures are gel filtration, dialysis, and ultracentrifugation (7,69,99–101). However, these methods are not entirely satisfactory because they are restricted to the laboratory scale or they are incapable of eliminating molecules with high molecular weight (Table 3). The necessity of finding an efficient purification technique that can be scaled up from an industrial standpoint led to the development of the cross-flow filtration method. In this technique, first used by Allémann et al. (99), the nanoparticle suspension is filtered through membranes, with the direction of the fluid being tangential to the surface of the membranes. In contrast to perpendicular filtration modes, the clogging of the filters is thereby avoided (Fig. 12). Depending on the type of membrane used, either microfiltration or ultrafiltration can be performed. The suspension is submitted to several filtration cycles, while the filtrate, containing components smaller than the pores of the membrane as well as soluble impurities, is discarded. First, concentration of the suspension is achieved. Then, pure water is added to the system at the same rate as the filtration rate, thus allowing the circulation volume to remain constant (diafiltration step). Simple to use, this technique allows the fast purification of large amounts of nanoparticles with no alteration of their size. For example, it was shown that by using a microfiltration membrane (porosity of 100 nm), approximately 6 g of PLA nanoparticles produced by the salting-out process could be purified in less than 3 hours, with complete removal of the salts and PVA macromolecules (99). In addition, scale-up is feasible by enlarging the filtering surface.

Freeze-drying. If nanoparticles are stored as aqueous suspensions, degradation and/or solubilization of the polymer, drug leakage, drug desorption, and/or drug degradation may occur. Freeze-drying (lyophilization) probably represents one of the most useful methodologies to ensure the long-term conservation of polymeric nanoparticles (102). This technique involves the freezing of the suspension and the subsequent elimination of its water content by sublimation under reduced pressure. After complete desiccation, nanoparticles are obtained in the form of a dry powder that is easy to handle and to store. Freeze-dried nanoparticles are usually readily redispersible in water without modification of their physicochemical properties (1). Because nanoparticles are usually produced with surfactants or stabilizers (e.g., polysorbate, poloxamer, PVA), the residual presence of these compounds generally favors the redispersion of the particles. However, in some specific cases, full redispersion of the system may be difficult to achieve. For example, nanocapsules composed of an oily core surrounded by a tiny polymeric wall tend to aggregate during the freeze-drying process (67,102). Similarly, aggregation problems have been reported with nanospheres made of various materials (102–104). This problem can be circumvented by desiccating these systems in the presence of an appropriate lyoprotective agent such as mono- or disaccharides (e.g., trehalose, sucrose, glucose) (102,104). The mechanisms by which sugars protect nanoparticles during freeze-drying are frequently referred to as "poorly understood" in the literature. However, very detailed and useful information about these mechanisms can be found in a number of articles dealing with lyoprotection and cryoprotection of liposomes and proteins (105,106). In these studies, it is commonly suggested that during freeze-drying sugars may interact with the solute of interest (e.g., liposome, protein) through hydrogen-bonding. As a result, the solute might be maintained in a "pseudo-hydrated" state during the dehydrating step of freeze-drying, and would therefore be protected from damage during dehydration and subsequent rehydration. Such a protective interaction is made possible by the ability of sugars to remain amorphous during freeze-drying (105,106). It has to be kept in mind that the addition of sugar may affect the isotonicity of the final nanoparticulate suspension, and that a subsequent step of tonicity adjustment may be required prior to any parenteral or ocular administration.

Sterilization. Nanoparticles intended to be used parenterally are required to be sterile and apyrogenic. Surpris-

Next Page

Table 3. Main Methods for the Purification of Nanoparticles on the Laboratory Scale

Method (Reference)	Schematic principle	Drawback
Gel filtration (7,100)		Removal of high molecular weight impurities difficult
Dialysis (101)		Removal of high molecular weight impurities difficult Time consuming Scaling-up difficult
Ultracentrifugation (69,99)		Aggregation of the particles Time consuming Scaling-up difficult

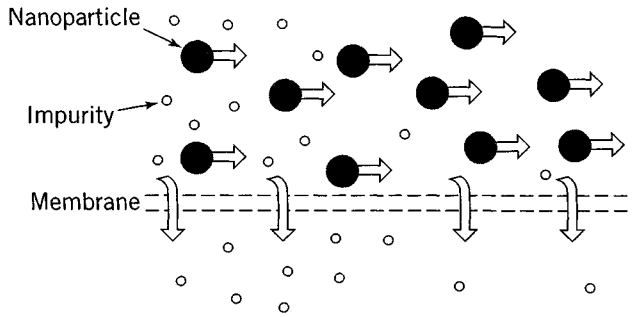


Figure 12. Cross-flow filtration technique.

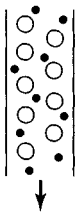
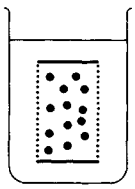
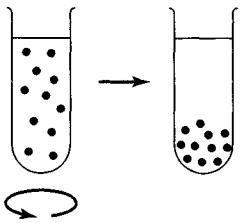
ingly, few authors have addressed this question. Sterile filtration on 0.22 μm filters is not adequate for nanoparticle suspensions because microorganisms and nanoparticles are generally similar in size (0.25–1 μm). Sterilization may be achieved, as for other microparticulate systems, either by using aseptic conditions throughout formulation, or by subsequent sterilizing treatments such as autoclaving or γ-irradiation (1,87). Production under aseptic conditions is possible but not very realistic, because it is complex, expensive, and inherently not safe. A terminal sterilization step will always be required to ensure the microbiological safety of the finished product. The choice of the sterilizing treatment depends on the physical susceptibility of the system. Autoclaving (moist heat sterilization) and γ-irradiation were shown to have an impact on the physicochemical properties of the particles in several systems, as illustrated by modification of the particle size, stability, and drug release characteristics (1,107). Most of the time, these modifications occur as a consequence of the cleavage or cross-linking of the polymeric chains, but can also result from alterations of other constituents such as the surface agents or the drug itself (107,108). It is apparent from these considerations that the sterilization of nanoparticulate formulations is a very critical step that should be systematically investigated early in the development program for an eventual optimization of the formulation. For example, the chemical stability of the polymeric matrix may be markedly improved by optimization of the polymer molecular weight (108). The final formulation would therefore result from a rational balance between conditions maintaining the formulation integrity upon sterilization and the final purpose of the formulation.

MODULATION OF THE IN VIVO FATE OF NANOPARTICLES

There are many ways to administer colloidal drug carriers including the intravascular, oral, ocular routes as well as intramuscular and subcutaneous injections. The main challenge for administering nanoparticles into the vascular compartment is the targeting of active compounds to the desired organs or cells, allowing a site-selective action of the compound and minimization of side effects. Another aim is related to the sustained delivery of drugs, in particular the increase of the therapeutic availability of drugs normally rapidly degraded or excreted in their free form, for various administration routes.

Previous Page

Table 3. Main Methods for the Purification of Nanoparticles on the Laboratory Scale

Method (Reference)	Schematic principle	Drawback
Gel filtration (7,100)		Removal of high molecular weight impurities difficult
Dialysis (101)		Removal of high molecular weight impurities difficult Time consuming Scaling-up difficult
Ultracentrifugation (69,99)		Aggregation of the particles Time consuming Scaling-up difficult

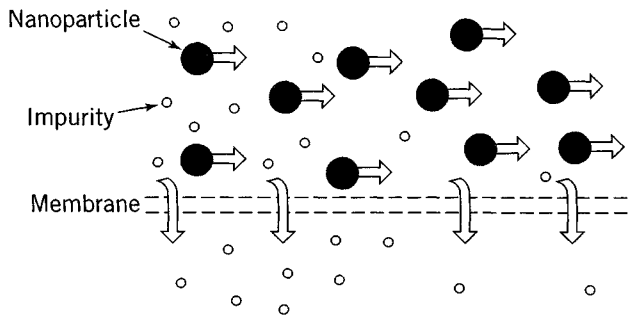


Figure 12. Cross-flow filtration technique.

ingly, few authors have addressed this question. Sterile filtration on 0.22 μm filters is not adequate for nanoparticle suspensions because microorganisms and nanoparticles are generally similar in size (0.25–1 μm). Sterilization may be achieved, as for other microparticulate systems, either by using aseptic conditions throughout formulation, or by subsequent sterilizing treatments such as autoclaving or γ-irradiation (1,87). Production under aseptic conditions is possible but not very realistic, because it is complex, expensive, and inherently not safe. A terminal sterilization step will always be required to ensure the microbiological safety of the finished product. The choice of the sterilizing treatment depends on the physical susceptibility of the system. Autoclaving (moist heat sterilization) and γ-irradiation were shown to have an impact on the physicochemical properties of the particles in several systems, as illustrated by modification of the particle size, stability, and drug release characteristics (1,107). Most of the time, these modifications occur as a consequence of the cleavage or cross-linking of the polymeric chains, but can also result from alterations of other constituents such as the surface agents or the drug itself (107,108). It is apparent from these considerations that the sterilization of nanoparticulate formulations is a very critical step that should be systematically investigated early in the development program for an eventual optimization of the formulation. For example, the chemical stability of the polymeric matrix may be markedly improved by optimization of the polymer molecular weight (108). The final formulation would therefore result from a rational balance between conditions maintaining the formulation integrity upon sterilization and the final purpose of the formulation.

MODULATION OF THE IN VIVO FATE OF NANOPARTICLES

There are many ways to administer colloidal drug carriers including the intravascular, oral, ocular routes as well as intramuscular and subcutaneous injections. The main challenge for administering nanoparticles into the vascular compartment is the targeting of active compounds to the desired organs or cells, allowing a site-selective action of the compound and minimization of side effects. Another aim is related to the sustained delivery of drugs, in particular the increase of the therapeutic availability of drugs normally rapidly degraded or excreted in their free form, for various administration routes.

Mechanisms Regulating Body Distribution of Nanoparticles

Mononuclear Phagocytic System. At the present time, the ideal aims mentioned earlier have still not been adequately achieved with nanoparticles. As every other colloidal systems (e.g., liposomes, niosomes, microemulsions), intravascularly injected nanoparticles are rapidly detected as foreign products and quickly removed from blood circulation by the action of the mononuclear phagocytic system (MPS), which is also known as the reticuloendothelial system. The MPS is a collective name for a group of highly phagocytic mononuclear cells found throughout the body, either at fixed sites (tissular macrophages) or free in the bloodstream (circulating monocytes). Large concentrations of these cells are found in the liver (macrophages called Kupffer cells), spleen, and to a lesser extent, in the bone marrow. Because of the rich blood supply and specialized architecture of these organs, intravenously injected nanoparticles are extensively taken up by the liver (up to 90%) and the spleen (2–5%) within minutes or seconds following administration (109,110). Phagocytosis of particles by macrophages involves two steps: attachment of the particles to the cell membrane and ingestion of the particles. The attachment of the particles to macrophages is generally mediated through the action of serum proteins, called opsonins, which after adsorption onto the surface of the particles make any foreign material (immune complex, microorganisms, or particulate drug carrier) recognizable to the phagocytic cells of the MPS. Opsonization is a dynamic, complex and not fully elucidated process involving a great diversity and number of serum proteins, among which immunoglobulins and components of the complement system (particularly C3 and C5) have been shown to play a predominant role (111). Short half-lives are commonly observed whatever the chemical composition of the injected particles (e.g., albumin, polystyrene, PLA, PLGA, PACA). Therefore, using these types of systems, site-specific or sustained delivery of drugs is not readily achievable using the intravascular route, except in the MPS organs where the sequestration of these systems may be of clinical value. The exploitation of such "passive targeting" has led to some therapeutic advantages as illustrated by the use of nanoparticles for the treatment of some MPS-located diseases and intracellular infections, especially in the liver. This aspect will be developed in more detail in the section entitled "Parenteral Administration." However, for targeting to organs other than those of the MPS, the natural homing of nanoparticles to elements of the MPS is a serious obstacle which must be overcome. One of the earliest strategies was through suppression of the MPS phagocytic function by saturating it with high amounts of colloidal particles (e.g., plain polystyrene nanoparticles) or by use of phagocytosis depressants such as dextran sulfate, methyl palmitate, or gadolinium chloride (112). However, the concept of MPS blockage is not clinically acceptable, because it would rapidly lead to impaired MPS function and suppress the essential defense system of the body.

Factors Affecting the Biodistribution of Nanoparticles. It is now well established that the extent and nature of opsonin adsorption at the surface of colloidal particles depend on the physicochemical properties of the particles such as the size, surface charge, and surface hydrophobicity (111,113). In general, the adsorption of opsonins preferentially occurs onto hydrophobic rather than hydrophilic surfaces. The higher the particle hydrophobicity, the faster the particles are removed from the circulation and taken up by the cells of the MPS. The charge carried by the colloidal particles can also have an important role in determining the clearance and fate of the particles. It is generally accepted that negative surface charge increases the clearance of particulates, relative to neutral or positively charged surfaces. Together with the surface characteristics, the size of the nanoparticles also greatly influences their biological fate. Particles larger than 5,000 nm are normally entrapped in the capillary network of the lungs, whereas nanoparticles less than 100 nm may be able to leave the circulation through gaps or fenestrations in the endothelial cells lining the blood vessels.

Surface Engineering of Nanoparticles

The development of colloidal carriers with appropriate size and protein-resistant surfaces such that opsonization is minimized is currently the subject of great interest. Several approaches have been proposed during the last decade to achieve long-circulating nanoparticles, based on appropriate modifications of the nanoparticle surface.

Biomimetic Nanoparticles. The biomimetic approach is illustrated by the coating of a nanoparticles by sialic acids or plasma proteins such as albumin or inactivated complement moieties. Such surface modification was proposed as an elegant way to mimic the biological environment and make the foreign surface invisible to the MPS (66,114–116). The rationale for using albumin and complement moieties are the following: albumin is the main protein present in the blood (40 g/L), whereas complement moieties are among the most important opsonins involved in clearance mechanisms. As to the sialic acids, they may be components that are able to prevent the drug carrier surface from being recognized by the MPS, by imitating the sialylated cell surface. Human orosomucoid, a sialic acid-rich serum glycoprotein, has been used recently to coat PACA nanoparticles (116). The nanoparticles are generally coated by simple incubation (12 to 24 h) with a solution of the protein (66,116) or by direct incorporation of the protein during the production process (114,115). Unfortunately, so far none of these biomimetic coatings has provided adequate protection against opsonin adsorption and MPS phagocytosis, presumably due to rapid desorption of the coat (114–116) or insufficient mimetic ability (66).

Sterically Stabilized Nanoparticles. Most of the previously described polymeric materials forming nanoparticles are relatively hydrophobic with regard to opsonin adsorption. Creation of a new surface by coating the particle with a hydrophilic and nonionic macromolecule was suggested to be an efficient means to prevent recognition of the particles by the cells of the MPS and prolong their systemic circulation time. The concept of surface hydrophilization was rapidly extended to the concept of steric stabilization

when it was shown that hydrophilicity alone could not provide antiphagocytic effect. Indeed, highly hydrophilic macromolecules or polymers such as dextran, gelatin, or PVA failed to prevent the massive capture of colloidal carriers by phagocytic cells of the MPS (110). It has been proposed that besides hydrophilicity, high flexibility of the coating chains is another major requirement to provide effective protection against opsonization. Among the nonionic hydrophilic polymers fulfilling this criteria, poly(ethylene oxide) (PEO), also commonly named poly(ethylene glycol), has been the most successful synthetic materials used to alter the opsonization process. The protein-resistant nature of PEO chains is attributed to their unique solution properties and molecular conformation in aqueous solutions. Highly hydrated PEO chains produce a surface which is in a liquid-like state and thereby minimizes the tendency to make hydrophobic interactions (117). The considerable flexibility and mobility of the chains result in the sampling of a large number of possible conformations at the particle surface. This highly dynamic state may prevent interactions with approaching opsonins (111,117).

The surface modification of particles using PEO derivatives has been achieved using two main approaches. In a first attempt, preformed particles were modified by physical adsorption of amphiphatic PEO-based compounds including commercially available ethoxylated surfactants and, more recently, new block copolymers with a tailored composition and a R-PEO structure (where R is a synthetic polymer similar to the polymer forming the particle core). In this first approach the PEO moieties are maintained around the particle through intermediate hydrophobic interactions of noncovalent nature. The main concern was to ensure the coating stability, which through the adsorption process was shown to be somewhat limited. As a result, a second approach was recently developed involving use of the previously mentioned R-PEO copolymers and leading to PEO-grafted nanoparticles.

PEO-Coated Nanoparticles. The adsorption approach was initially based on the use of commercially available PEO-based surfactants, such as ethoxylated nonyl phenol (Antarox®), polysorbates (Tween®), PEO-24-laurylether (Brij® 35), perethoxylated castor oils (Cremophor®) (110,118), or different PEO homopolymers (119,120).

However, during the last decade, the most popular and promising coating surfactants have been ethylene oxide (EO) and propylene oxide (PO)-based copolymers, the so-called poloxamers and poloxamines. In contrast to the previously mentioned compounds, these surfactants are available in a very wide range of molecular weights and hydrophilicity, allowing a real modulation of the surface modification and an optimal efficacy in terms of steric stabilization. Poloxamers are linear ABA block copolymers with the general structure $(EO)_n$-$(PO)_m$-$(EO)_n$, where n and m are the numbers of (EO) and (PO) units, respectively. Poloxamines are also ABA block copolymers, but instead of being linear, they present a branched tetrafunctional structure with a central ethylene diamine bridge: $\{(EO)_n$-$(PO)_m\}_2$-N-CH_2-CH_2-N-$\{(EO)_n$-$(PO)_m\}_2$. Due to their original structure, these amphiphatic surfactants attach themselves onto the surface of nanoparticles through their central hydrophobic portion (i.e., $(PO)_m$ or $(PO)_m$ ethylene diamine, respectively), whereas the hydrophilic $(EO)_n$ portions protrude into the surrounding medium, forming a brush-like coat around the particle. The adsorption of surfactant molecules onto the particles is generally performed by 24 hours' incubation of equal volumes of nanoparticle suspension (2.5%) with a coating solution of the relevant surfactant (0.05–2.5% w/w) (121).

Within the poloxamer and poloxamine series, only polymers with a certain optimal molecular weight and n/m ratios have an ability to provide efficient protection against phagocytosis (121,122). The length of the protruding $(EO)_n$ chains determines the coating layer thickness around the particle and their ability to cover the hydrophobic $(PO)_m$ anchoring parts. Another prerequisite is a sufficient length of the anchoring $(PO)_m$ block to preclude the desorption/displacement of the coat upon contact with dynamic biological environments. In this respect, poloxamer 407 (69 PO and 2 × 98 EO), poloxamer 338 (54 PO and 2 × 128 EO) and poloxamine 908 (4 × 17 PO and 4 × 119 EO) were shown to be the most efficient products in diverting model polystyrene or PMMA nanoparticles from the liver and in providing extended circulation times after intravenous administration in different animal models (112,122). In some cases, the foregoing polymers led not only to the decrease of particle uptake by liver macrophages but also to the redirection of the nanoparticles to other organs such as the bone marrow, spleen, and lymph nodes (112,122). In addition to the intrinsic properties of the coating material, other parameters such as the particle size (curvature) and the surface characteristics have been shown to strongly influence the final conformation of the adsorbed polymer and thereby its ability to alter the biological fate of the particles (111,121,122). Although the correlations between these different factors have not been clearly established yet, particle size has been shown to affect the adsorbed amount of polymer, the coating layer thickness, as well as the mobility of the protruding PEO chains (111,121,122). Together with the particle size, the nature of the surface to be coated also determines the final conformation of the coating polymer. Until recently, the promising in vivo results achieved with poloxamer- and poloxamine-coated polystyrene and PMMA particles could not be transferred to biodegradable drug carriers. In general, the surface of biodegradable particles is distinctly less hydrophobic than that of nonbiodegradable model particles, leading to no or weak adsorption of poloxamer and poloxamine surfactants to the particle surface (110). In the latter case, a rapid desorption of the coating layer can be expected to occur upon contact with biological media, or even before when a washing procedure is performed to remove excess of free surfactant molecules prior to biological testing. In addition, the production of biodegradable nanoparticles frequently involves the use of a hydrophilic stabilizer (e.g., dextran or PVA) whose residual presence on the particle surface can further inhibit surfactant adsorption (123,124). As a result, attempts to provide a steric protection to biodegradable particles using poloxamers and poloxamines have usually failed (111,123,124). Recently, these surfactants were used to stabilize PLGA nanoparticles prepared by a emulsifier-free nanoprecipitation method (125,126). In vitro, different particle uptake and protein resistance abil-

ities were observed between PLGA and polystyrene model nanoparticles modified in the same manner. This was attributed to distinct conformations of the coating layer on the two different surfaces. However, following intravenous administration to rats, PLGA-coated nanoparticles were shown to exhibit slightly prolonged circulation times and reduced accumulation in liver and spleen, comparable, surprisingly, to that obtained with polystyrene nanoparticles tested in parallel that had been modified in the same manner. Furthermore, when the PLGA-coated particles were washed of excess surfactant before intravenous administration, prolonged circulation times, although slightly reduced, were still observed. A relative stability of the coatings could obviously be achieved in this study. Although this point was not discussed by the authors, this might be partly explained by the absence of emulsifier in the preparation process.

New amphiphilic R-PEO diblock copolymers were recently proposed for the advantageous replacement of the surfactants previously used. The advantage of the R-PEO copolymers over the poloxamers and poloxamines is in replacing the poly(propylene oxide) (POP) moiety of the latter polymers with a biodegradable and biocompatible R chain. Indeed, the R moiety can be chosen among the family of the hydrophobic polymers generally used to produce biodegradable nanoparticles. In addition to its safe nature, the R part of the R-PEO copolymers is expected to be a better anchor group when adsorbed onto a surface of a similar nature. These polymeric materials are generally synthesized by ring-opening polymerization or by melt condensation, with tailored molecular weights and R/PEO ratios (127,128). In a recent study, a PLA-PEO block copolymer was adsorbed onto both PLGA and polystyrene nanoparticles (129). Following intravenous administration into rats, the PLGA modified particles were shown to exhibit extended circulation levels, whereas the coated polystyrene particles, after one hour of effective blood circulation, were suddenly massively taken up by the MPS. These distinct behavior patterns of the two systems have been attributed to a difference in the stability of the PLA-PEO coatings on polystyrene and PLGA nanoparticles, the affinity of the PLA anchor moity presumably being higher for the PLGA surface than for that of polystyrene.

PEO-Grafted Nanoparticles. It is evident from results with both model nonbiodegradable and biodegradable systems that the stability of the coating layer is an essential feature in modifying particle interaction with the biological environment. Although the adsorption approach undoubtedly provided information on the in vivo behavior of sterically stabilized nanoparticles, the relative unreliability of the resulting steric barrier was soon considered a limitation, especially in terms of interpreting the results. Theoretically, whatever the affinity between the surface and the coating material, the desorption of the latter is always possible in vivo.

The introduction of novel R-PEO block copolymers provided a very interesting alternative to the adsorption approach for surface modification. As a matter of fact, due to their peculiar amphiphatic structure and composition, these copolymers can be used as the main material to produce, in a single-step procedure, nanoparticles with the R blocks forming the central core and the PEO blocks forming a hydrophilic shell covalently linked to the core. Recently, several authors reported the production of PEO-grafted nanoparticles using emulsification-solvent evaporation, direct precipitation, or the salting-out process. In these procedures, the R-PEO copolymer is dissolved in an organic phase which is subsequently mixed with an aqueous phase. Due to their high affinity for the aqueous phase, the PEO blocks are presumed to migrate to the water interface, whereas the hydrophobic R blocks remain within the nanodroplets and subsequently form the solid core of the particles after organic solvent removal. So far the copolymers used have been PLA-, PLGA-, PCL- and poly(sebacic acid)-PEO diblock copolymers (104,115,128,130–136). The resulting PEO-grafted nanoparticles exhibited sizes between 100 and 300 nm. It has to be emphasized that, in most studies, the particle size was determined directly after purification of the raw nanoparticle suspensions, avoiding the possible effects of a freeze-drying step on the resuspension ability of the PEO surface-modified nanoparticles. It was shown recently that the presence of PEO at the nanoparticle surface could severely impair the redispersion of the freeze-dried particles after rehydration (104). This effect may be attributed to the well-known tendency of PEO to crystallize during freeze-drying (106,137) and can be circumvented using an appropriate lyoprotectant additive (e.g., trehalose) (104,106,137). It appears that the use of a lyoprotectant additive should be systematically considered when PEO surface-modified nanoparticles are intended to be freeze-dried.

The blood clearance and biodistribution of the R-PEO based systems have been studied (Table 4). It was demonstrated that the protective effect of PEO depends on both the chain length and the surface density of the PEO chains, although it is still not clear which parameter is the most dominant (104,111). Nevertheless, results from the literature indicate that, above a certain threshold, increase of the PEO density no longer prevents phagocytosis (111,133). Similarly, there appears to be an optimal chain length (around 2,000 Da) that is necessary to achieve efficient protection (111,129). To further improve the performance of PEO-coated nanoparticles, new copolymers presenting more than one PEO block have been recently proposed (128,138). These so-called R-$(PEO)_n$ multiblock copolymers would allow the production of nanospheres with optimal PEO surface-densities.

Various drugs were successfully entrapped into PEO-grafted nanospheres such as lidocaine (128,131), prednisolone (128), ibuprofen (115), as well as oligonucleotides (139). The entrapment efficiency and in vitro drug-release patterns were shown to depend strongly on the chemical nature of the hydrophobic core, as well as the molecular weight and surface density of the hydrophilic PEO chains (128). The fact that the PEO chains might be involved in the release process was unexpected for the authors. However, some studies performed on various PLA/PLGA-PEO copolymers have shown that the PEO segments can greatly influence the physical properties of the polymer, such as its degradation behavior and its degree of swelling and permeability in water (140,141). Therefore, depending

Table 4. In vivo Studies with R-POE–Based Nanoparticles

Copolymer	Method[a]	Size (nm)	Animal	Comment	Reference
PLGA-PEO	ESE	<200	Mouse	Significant increase of AUC vs. control	130,131
PLA-PEO	DP	60–200	Rat	Significant increase of AUC vs. control	115,133
PLA-PEO	DP	<200	Rat	No particle-induced inflammatory response contrary to control	134

[a]ESE, emulsification-solvent evaporation; DP, direct precipitation.

on the copolymer composition, a more or less pronounced modification of the release can be expected in the presence of PEO segments (140,141). From this outcome, it appears that tailor-made PEO-polyester copolymers have great potential as nanoparticulate delivery systems. Illustrating this consideration, the kinetic profile and biodistribution of a labeled drug (^{14}C-ibuprofen) were investigated after intravenous administration of 20% loaded PLA-PEO nanoparticles in rats. A sustained release profile was reported for the drug (plasma half-life of 2 h 30 min) as well as a widespread body distribution 6 h post injection, demonstrating that in addition to their long-circulating ability, the PLA-PEO nanoparticles tested could also behave as sustained delivery dosage forms in vivo (115).

Nanoparticles made of R-PEO preformed block copolymers are actually among the most extensively investigated systems for the achievement of prolonged circulation following intravenous administration (104,115,128,130–136). As previously mentioned, the possible tailoring and easy characterization of R-PEO block copolymers allow a rational modulation of nanoparticle physicochemical properties and thereby a more precise understanding of the relationship between the surface properties and the in vivo behavior of the particles. However, other types of PEO-grafted nanoparticles can be produced, based on in situ copolymerization reactions. Polystyrene-PEO (PS-PEO) nanoparticles were produced by copolymerizing styrene monomers with various amounts of methoxyPEO (142). These nonbiodegradable PS-PEO nanoparticles were designed as model particles to study the influence of surface density of PEO on the in vitro and in vivo behavior of the particles. In rats, the blood circulation time was shown to be increased with increasing surface densities of PEO (142). More recently, biodegradable PACA-PEO nanospheres were produced by emulsion polymerization of cyanoacrylate monomers in water, in the presence of homopolymer PEO 4,000 (143). The authors hypothesized that, in this process, the OH groups of PEO act as polymerization initiators. In addition, it was shown that the presence of PEO in the polymerization medium avoided the need for surfactant or stabilizer such as polysorbate or dextran. Data obtained from chemical analysis suggested that a covalent bond was formed between PEO and PACA during the anionic polymerization process (143). So far, the ability of these systems to avoid MPS recognition has not been reported.

Direct attachment of protective PEO chains onto the surface of preformed albumin nanospheres has been described (144). PEO grafting could be achieved through the carboxylic acid and amino functionalities of the chemically cross-linked albumin surface. The PEO protective effect against phagocytosis was demonstrated in vitro, as well as the clear influence on this effect of both the length and surface density of the PEO chains (144).

Targeting Strategies

Although PEO surface-modified nanoparticles can partially avoid the MPS and exhibit extended circulation times in the bloodstream, they are not able to target a specific site in vivo. Over the last decades, two main approaches have been investigated to provide a targeting ability to nanoparticulate systems.

External Magnetic Guidance. The concept of magnetically controlled targeting for particulate systems emerged in the seventies. It was proposed as a means to minimize nanoparticle uptake by the MPS and to enhance their access to extravascular sites, particularly to tumors. Nanoparticles are rendered magnetic by incorporating Fe_3O_4 particles (10–20 nm) simultaneously to the drug during the preparation process. The magnetic nanoparticles are then injected through the artery supplying the tumor tissue and are guided externally with a magnet to the target. This technique has been investigated with magnetic nanoparticles made of albumin but the production and testing of polyglutaraldehyde, PACA, and PMMA magnetic nanoparticles was also reported (1,19). The efficacy of this technique has been demonstrated by using readily accessible target areas with an abundant blood supply, such as the tail or the kidneys of rodents, and therefore should be considered with caution. In fact, the usefulness of this technique in treating dispersed metastatic neoplasms appears to be limited. Moreover, the feasibility of using magnetic nanoparticulate systems in humans strongly depends on the possibility of using low-strength magnetic fields which would not be harmful for the patient in case of prolonged treatment.

Nanoparticles Coated With Antibodies. Several authors have investigated the possibility of attaching antibodies to the nanoparticle surface to facilitate their direction to specific sites. The underlying rationale is the possibility of using monoclonal antibodies (MAb) with unique antigen specificity. MAb can be fixed on nanoparticles by direct adsorption or via a spacer molecule (protein A) as well as by covalent linkage (e.g., carbodiimide, cyanogen bromide, and glutaraldehyde reactions) (145). Whatever the procedure used, MAb must bind to the particle via their Fc part with their antigen binding site Fab protruding into the medium, free to interact with the antigenic target site. This technique has been applied to a wide variety of nanopar-

ticles including PACA, polymethacrylic, albumin, and recently PMM 2.1.2. nanoparticles (50,78,146,147). Some authors demonstrated the capacity of these immunospecific nanoparticles to bind specifically tumor cells in vitro, but failed to demonstrate a significant accumulation of the carriers in targeted tumors in vivo (78,146). A number of reasons for this failure have been proposed including the competitive displacement of the MAb by blood components, secondary coating processes where the MAb-coated particles receive an opsonic layer, and also insufficient access of the immunospecific nanoparticles to the target site (145). It clearly appears that the success of immunospecific targeting strongly depends on the potential of the drug carrier to overcome MPS recognition. Future strategies will probably be based on the development of nanoparticles combining long-circulating properties (surface modification with PEO surfactant or polymer) and targeting abilities (attachment of MAb) (112,148).

CHARACTERIZATION OF NANOPARTICLES

As any other dosage form intended to be use in medicine, nanoparticulate formulations are usually characterized in term of size, morphology, drug content, and in vitro drug release. The determination of these properties is of great relevance for quality control as well as for evaluating the influence of process parameters on the resulting formulation. In addition to these pharmaceutical considerations, a major challenge is to establish a correlation between the physicochemical properties of the systems and their interaction with blood components and resulting site deposition. Recently, the design of surface-modified nanoparticles for the avoidance of the MPS has promoted the development of sophisticated methods for surface chemical analysis, allowing, for example, the identification of specific chemical groups on the surface of the particles. A wide range of techniques is available for a comprehensive physicochemical examination of nanoparticle properties. The most widely used techniques are listed in Table 5. Detailed descriptions of each technique can be obtained in the references, which are either very complete review articles (19,110,149,150) or recent specific reports focusing on these techniques (60,72,126,128,131,143,151–155).

APPLICATIONS OF NANOPARTICLES

Parenteral Administration

Delivery of Anticancer Drugs. One of the most promising application of nanoparticles is their use as parenteral carriers for anticancer drugs. Interestingly, nanoparticles exhibit a significant tendency to accumulate in a number of tumors after intravenous administration. This particular behavior has been related to the frequently observed high endocytic activity of cancer cells. In addition, some tumors have been shown to exhibit an increased vascular permeability which may favor the accessibility of nanoparticles to extravascular tumoral cells (19,156,157). The binding of a variety of anticancer drugs (e.g., doxorubicin, 5-fluorouracil, dactinomycin, methotrexate), immunomodulators (muramyl dipeptide-L-analyl-cholesterol) or antisense oligonucleotides mainly to PACA or albumin nanoparticles enhanced their efficacy against experimental tumors in comparison to free compound (157). In a number of cases, a reduction of the general toxicity of anticancer drugs was also demonstrated. This is usually attributed to the modification of the drug pharmacokinetic parameters that correlate with the distribution profile of the carrier itself. When associated with nanoparticles, drugs concentrate mainly in liver and spleen and are precluded to exert their acute toxicity in other organs (156,157). One of the most promising applications of anticancer drug-loaded nanoparticles may be their use in the treatment of hepatic metastases. Intravenously injected nanoparticles are mainly taken up by the Kuppfer cells. These latter may act as a reservoir for the drug, allowing its massive and prolonged diffusion into the neighboring neoplastic cells (156,157). Besides the use of this passive targeting, the incorporation of magnetic particles into albumin nanoparticles and subsequent electromagnetic guidance has been shown to improve the antimetastatic potential of the anticancer drug carrier by facilitating the access to extravascular tumors (19,157). A different approach to achieve tumor-specific targeting was made using MAb-coated nanoparticles. These formulations should be able to recognize specific cell determinants belonging only to tumor cells. Unfortunately, contrary to the very promising results obtained in vitro, the MAb-coated nanoparticles did not exhibit any increased tumor location after intravenous administration and were rapidly cleared by the MPS (157). New and attractive possibilities have recently become available with the development of PEO surface-modified nanoparticles (see "Surface Engineering of Nanoparticles"). In a recent study involving PLA nanoparticles loaded with a photoactivable sensitizer ($ZnPcF_{16}$) (120), coating the nanoparticles with PEO 20,000 by adsorption was shown to significantly increase their blood circulation time and in turn their tumor accumulation in mice. Efficient photodynamic therapy could be performed, as demonstrated by significant tumor regression following light treatment (120).

Delivery of Antiinfectious Agents. Intracellular infections are another field of interest for the use of nanoparticles. Infectious diseases are caused by obligate or facultative intracellular pathogens which can be bacterial, parasitic, fungal, or viral in nature. Most antiinfectious agents display limited efficacies against intracellular infections. For example, antibiotics usually exhibit either a poor ability to penetrate the infected cells or a decreased activity in intracellular compartments. Antiparasitic agents have a limited efficacy due to their lack of selectivity for the infected cells, resulting in a poor therapeutic index. Finally, antiviral agents generally display very short plasma half-lives. Because most of the cells that are frequently infected include phagocytic cells, it was suggested that nanoparticles should be of great interest to improve antiinfectious chemotherapy. This approach has been extensively investigated with PACA nanoparticles loaded with ampicillin as a model of acidic antibiotic. The efficacy of this formulation against *Listeria monocytogenes*

Table 5. Principal Techniques for the Physicochemical Characterization of Nanoparticles

Parameter	Technique	Reference
Particle size and morphology	Transmission electron microscopy	19,110,149
	Scanning (electron, force, tunneling) microscopy	19,131,149,151
	Freeze-fracture electron microscopy	19,72,128,149
	Photon correlation spectroscopy	19,110,149
Drug content		19,149
In vitro drug release		19,149,150
Molecular weight	Gel permeation chromatography	19,149,152
Crystallinity	X-ray diffraction	19,131,149
	Differential scanning calorimetry	19,128,131,149
Surface charge	Zeta potential measurement	19,60,110,143,149
Surface hydrophobicity	Hydrophobic interaction chromatography	19,60,110,143
	Contact angle measurement	19,110,153
	Rose Bengal binding	60,110
Surface chemical analysis	Secondary ion mass spectrometry	19,110,149
	X-ray photoelectron spectroscopy	19,128,149,152
	Nuclear magnetic resonance	128,143,152
	Fourier transform infrared spectroscopy	143
Protein adsorption	Two-dimensional polyacrylamide gel electrophoresis	126,154,155

and *Salmonella typhimurium* infections has been demonstrated in numerous studies, both in cell cultures and in mouse models (19,156). The effective uptake of ampicillin-loaded nanoparticles was demonstrated in murine macrophages by confocal and transmission electron microscopy studies. In addition, the authors reported that the nanoparticles were localized in the same vacuoles as the infecting bacteria (158).

Nanoparticles also hold promise as drug carriers for the treatment of parasitic infections such as visceral leishmaniasis. This infection is caused by *Leishmania donovani*, an intracellular parasite of the MPS. Most of the drugs usually used to treat this infection (e.g., primaquine, dehydroemetine) exert, apart from the desired activity, very toxic and adverse side effects. The binding of these drugs to various types of nanoparticles was shown to significantly increase their therapeutic index as a result of passive targeting to the MPS (19,159). Surprisingly, it was shown that unloaded PACA nanoparticles exhibited a significant antileishmanial activity on their own. In fact, it appeared that PACA nanoparticles could induce an activation of the respiratory burst in macrophages leading to the production of toxic oxygen metabolites (19,156). It is reasonable to think that this immunomodulation activity of plain nanoparticles may open interesting perspectives not only in the field of parasitic infections, but also in the treatment of other infectious or tumoral diseases.

In the field of viral infections, a very important challenge is the targeting of human immunodeficiency virus (HIV)-infected macrophages. Indeed, it is now well established that macrophages of the MPS play an important role in the immunopathogenesis of HIV infection by acting as a reservoir for the virus and its dissemination throughout the body (19). Therefore, nanoparticles represent an interesting system for the specific transport of antiviral agents displaying poor selectivity and/or short plasma half-life. Recently, PACA nanoparticles loaded with the protease inhibitor saquinavir were shown to be effective in HIV-infected human macrophage cultures (160). In another study, azidothymidine bound to PACA nanoparticles was successfully targeted into macrophage-rich organs in rats (161). These initial promising results suggest that new perspectives in the treatment of HIV-related diseases may be open. Substances whose development has been halted because of their unfavorable pharmacokinetic properties could be made efficient and available, using nanoparticulate technology.

Peroral Administration

Delivery of Poorly Absorbed Drugs. Some authors have supported the idea that nanoparticles may improve the bioavailability of peptide or protein drugs administered orally. The rationale for this approach is that nanoparticles can protect these labile drugs from extensive enzyme degradation in the gastrointestinal tract (GIT) and enhance their absorption (*1*) by optimizing their interaction with the absorption site in the gut wall or (*2*) by directly transporting them through the intestinal mucosa to the systemic circulation.

Precursors in this field, Maincent et al. (162) reported that the relative peroral bioavailability of vincamine in rabbits was considerably increased when this drug was associated with PACA nanoparticles. Later, Michel et al. (163) found that insulin encapsulated in PACA nanocapsules reduced glycemia by 50–60%, whereas free insulin did not affect glycemia when administered orally to diabetic rats. This effect was attributed to the protection of insulin from proteolytic degradation. It was also suggested that this effect could result from the retarded passage of intact nanocapsules through the rat mucosa (163). Although experimental evidence of such a mechanism was found in rodents, whether or not it plays a significant role in increasing the bioavailability of drugs is still a controversial issue. In fact, in many studies, the passage of nanoparticles across the gastrointestinal mucosa was shown to be very low (2–3% of the injected dose), leading to the conclusion that only very potent drugs would be able to exert

their activity by this specific route (1,164). In fact, the most probable mechanisms by which nanoparticles increase the oral bioavailability of drugs is by protecting them against degradation and by releasing them in the GIT in a way that favors their absorption. For example, in a study by Lenaerts et al. (165), the peroral efficacy of PACA nanoparticles loaded with vincamine was attributed to the bioadhesive behavior of the particles, allowing the slow release of the drug close to its absorption window and its subsequent diffusion into the vascular compartment. Similarly, Mathiowitz et al. (166) reported enhanced oral bioavailability for model proteins and gene (insulin, dicumarol, plasmid DNA) encapsulated into biologically adhesive nanoparticles made of polyanhydride copolymers of fumaric acid and sebacic acid. The latest developments in the field of bioadhesive particulate systems, involving for example the use of lectins as specific bioadhesive moieties, are described in the literature (167,168). Recently, it was demonstrated by our group that pH-sensitive nanoparticles could significantly increase the bioavailability of poorly water-soluble HIV-protease inhibitors in mice and dogs (169). These formulations are made of polymethacrylic copolymers which rapidly dissolve and release the poorly water-soluble drug at a specific level of the GIT. It was suggested that this rapid and specific release, combined with the very high level of dispersion provided by the nanoparticulate formulation, favored the solubilization of the drug in the intestinal fluid, resulting in a positive impact on drug absorption.

Delivery of Vaccines. As previously mentioned, although restricted, particulate uptake does take place in the intestinal mucosa (164). This uptake was shown to occur mainly in the lymphoid regions of the intestine called the Peyer's patches, through the action of specialized epithelial cells, called M cells. These cells play a determining role in the sampling and transport of luminal antigens into lymphoid tissues for immunologic surveillance and initiation of appropriate immunologic response. It is generally accepted that limited doses of antigen are sufficient to induce an efficient immunization. Thus, it has been postulated that the use of nanoparticles would be profitable for the oral delivery of antigens, because of their ability to control the release of proteins and to protect them from enzymatic degradation in the GIT. Biodegradable PACA nanoparticles have been shown to enhance the secretory immune response after their oral administration in association with ovalbumin in rats (170). PMMA nanoparticles appear to be promising nanoparticulate systems for this application. The very slow degradation rate (30–40% per year) of these particles seems to be particularly appropriate for vaccine purposes, because prolonged contact between the antigen and the immunocompetent cells favors the persistence of immunity. Factors affecting the efficacy of the immunoparticles include particle size, hydrophobicity, and the presence or absence of surface ligands. Indeed, by associating targeting agents such as MAb specific from M cells, it may be possible to increase the levels of absorption of nanoparticle vaccines and therefore the immune response (171). Coupled with advances in molecular biology, immunology, and virology, controlled delivery nanoparticulate systems may be the next generation of effective vaccines in the field of oral immunization.

Other Routes of Administration

Besides the previously described main applications, nanoparticles can be considered for the intramuscular and subcutaneous routes. Although these routes have been so far rarely employed with nanoparticles, they may present some advantages in the attempt to prolong the plasma level of drugs, to protect them from enzymatic degradation or to reduce their irritant effect when applied intramuscularly. Depending on the rate of release which is desired for the drug, PACA or polylactide (PLA, PLGA) nanoparticles appear to be particularly suitable for these routes, due to their particular and controllable degradation properties (1,172–174). Due to their very slow biodegradation rate, PMMA nanoparticles are very attractive for vaccine purposes using the intramuscular or subcutaneous routes. These nanoparticles were shown to exhibit very powerful adjuvant properties for a number of antigens either trapped in the polymer or adsorbed onto the particle surface (175) (see also "Dispersion Polymerization in Water for Production of Polymethacrylic Nanospheres").

Another possible route of administration for nanoparticles is their topical application to the eye. The use of nanoparticles by the ocular route has been investigated for the treatment of chronic diseases such as glaucoma, following the observation that various types of nanoparticles tend to adhere to the ocular epithelial surface. As a result, several authors have tried to take advantage of this prolonged residence time of nanoparticles, because most of the conventional ophthalmologic formulations failed so far in providing sufficient drug bioavailability (176). The polymers that seem to have the best potential for this application are PACA, PLGA, and PCL. They have been used in the form of either nanospheres or nanocapsules. Because of their low viscosity in suspension, these systems can be administered as easily as eye-drops with the advantage of having a reservoir-like behavior, that is, able to deliver the drug progressively (176–178, as well as MUCOSAL DRUG DELIVERY, OCULAR).

CONCLUSION

Nanoparticles represent very promising drug delivery systems which can be considered for a very wide range of applications. Optimization of earlier polymerization procedures combined with the development of new procedures using well-characterized and biodegradable polymeric materials has enabled the development of nanoparticulate systems with increased acceptance and potential. Although the entrapment of hydrophilic compounds (e.g., proteins, DNA, oligonucleotides) still faces some limitations, the many possible variations in structure and type of nanoparticles allow the efficient entrapment of a great number of molecules. The technology of nanoparticles being now quite well mastered, the main objective is the improvement of their targeting properties following intravenous administration. Although the massive uptake of nanoparticles by the MPS can be very advantageous for

the treatment of diseases associated to this system, the targeting to sites other than the MPS remains an exciting and major challenge. Several strategies have been developed to achieve this goal, relying on the considerable progress made in the field of nanoparticle characterization and the growing understanding of their in vivo behavior. The strategy that is actually gaining a widespread interest is based on the design of nanoparticules with tailored surface characteristics. More than ever, the achievement of pharmaceutical nanoparticle formulations for human use depends on the successful exploitation of multidisciplinary knowledge.

BIBLIOGRAPHY

1. E. Allémann, R. Gurny, and E. Doelker, *Eur. J. Pharm. Biopharm.* **39**, 173–191 (1993).
2. G. Birrenbach and P.P. Speiser, *J. Pharm. Sci.* **65**, 1763–1766 (1976).
3. J. Kreuter and P.P. Speiser, *Infect. Immun.* **13**, 204–210 (1976).
4. U.S. Pat. 4,329,332 (May 11, 1982), P. Couvreur, M. Roland, and P. Speiser.
5. N. Al Khouri-Fallouh et al., *Int. J. Pharm.* **28**, 125–132 (1986).
6. U. Scheffel, B.A. Rhodes, T.K. Natarajan, and H.N. Wagner, *J. Nucl. Med.* **13**, 498–503 (1972).
7. J.J. Marty, R.C. Oppenheim, and P. Speiser, *Pharm. Acta Helv.* **53**, 17–23 (1978).
8. K. Widder, G. Flouret, and A.E. Senyei, *J. Pharm. Sci.* **68**, 79–82 (1979).
9. R. Gurny, N.A. Peppas, D.D. Harrington, and G.S. Banker, *Drug Dev. Ind. Pharm.* **7**, 1–25 (1981).
10. Fr. Pat. 2,608,988 (December 31, 1986), H. Fessi, J.P. Devissaguet, F. Puisieux, and C. Thies (to Centre National de la Recherche Scientifique).
11. H. Fessi et al., *Int. J. Pharm.* **55**, R1–R4 (1989).
12. U.S. Pat. 4,968,350 (November 6, 1990), C. Bindschaedler, R. Gurny, and E. Doelker (to the inventors).
13. J.C. Leroux, E. Allémann, E. Doelker, and R. Gurny, *Eur. J. Pharm. Biopharm.* **41**, 14–18 (1995).
14. D.P. Durbin, M.S. El-Aasser, G.W. Poehlein, and J.W. Vanderhoff, *J. Appl. Polym. Sci.* **24**, 703–707 (1979).
15. J.W. Vanderhoff and S. El-Aasser, in H.A. Lieberman, M.M. Rieger, and G.S. Banker, eds., *Pharmaceutical Dosage Forms: Dispersed Systems*, Dekker, New York, 1988, pp. 93–149.
16. J. Kreuter, *Pharm. Acta Helv.* **58**, 196–208 (1983).
17. J.W. Vanderhoff, *J. Polym. Sci., Polym. Symp.* **72**, 161–198 (1985).
18. C. Vauthier-Holtzscherer et al., *S. T. P. Pharma. Sci.* **1**, 109–116 (1991).
19. J. Kreuter, in J. Kreuter, ed., *Colloidal Drug Delivery Systems*, Dekker, New York, 1994, pp. 219–343.
20. F. Candeau and Z. Zekhnini, *Macromolecules* **19**, 1895–1902 (1986).
21. C. Holtzscherer, J.P. Durand, and F. Candeau, *Colloid Polym. Sci.* **265**, 1067–1074 (1987).
22. M.T. Carver et al., *J. Phys. Chem.* **93**, 4867–4873 (1989).
23. V.H. Kopf, R.K. Joshi, M. Soliva, and P. Speiser, *Pharm. Ind.* **39**, 993–997 (1977).
24. I. Sjöholm and P. Ekman, *J. Pharmacol. Exp. Ther.* **211**, 656–662 (1979).
25. V.D. Labhasetwar and A.K. Dorle, *J. Controlled Release* **12**, 113–119 (1990).
26. H.-J. Krause, A. Schwarz, and P. Rohdewald, *Drug Dev. Ind. Pharm.* **12**, 527–552 (1986).
27. M.S. El-Samaligy, P. Rohdewald, and H.A. Mahmoud, *J. Pharm. Pharmacol.* **38**, 216–218 (1986).
28. M.R. Gasco and M. Trotta, *Int. J. Pharm.* **29**, 267–268 (1986).
29. R. Carpignano, M.R. Gasco, and S. Morel, *Pharm. Acta Helv.* **66**, 28–32 (1991).
30. M.R. Gasco, S. Morel, and I. Viano, *Pharm. Acta Helv.* **66**, 47–49 (1991).
31. B. Seijo, L. Roblot-Treupel, and P. Couvreur, *Int. J. Pharm.* **62**, 1–7 (1990).
32. V. Lenaerts et al., *J. Pharm. Sci.* **78**, 1051–1052 (1989).
33. S.J. Douglas and S.S. Davis, *Br. Polym. J.* **17**, 339–342 (1985).
34. G. Puglisi et al., *J. Microencapsul.* **10**, 353–366 (1993).
35. S.J. Douglas, L. Illum, S.S. Davis, and J. Kreuter, *J. Colloid Interface Sci.* **101**, 149–158 (1984).
36. L. Vansnick, P. Couvreur, D. Christiaens-Leyh, and M. Roland, *Pharm. Res.* **1**, 36–41 (1985).
37. L. Grislain et al., *Int. J. Pharm.* **15**, 335–345 (1983).
38. V. Lenaerts et al., *Biomaterials* **5**, 65–68 (1984).
39. P. Couvreur and C. Vauthier, *J. Controlled Release* **17**, 187–198 (1991).
40. S. Maassen, E. Fattal, R.H. Müller, and P. Couvreur, *S. T. P. Pharma. Sci.* **3**, 11–22 (1993).
41. R. Zange and T. Kissel, *Eur. J. Pharm. Biopharm.* **44**, 149–157 (1997).
42. J. Kattan et al., *Invest. New Drugs* **10**, 191–199 (1992).
43. J. De Keyser, J.H. Poupaert, and P. Dumont, *J. Pharm. Sci.* **80**, 67–70 (1991).
44. T.K.M. Mbela, J.H. Poupaert, and P. Dumont, *Int. J. Pharm.* **79**, 29–38 (1992).
45. F. Lescure et al., *Proc. Int. Symp. Controlled Release Bioact. Mater.* **18**, 325–326 (1991).
46. F. Lescure et al., *Pharm. Res.* **11**, 1270–1277 (1994).
47. P. Breton et al., in G. Gregoriadis, ed., *Targeting of Drugs*, Plenum, New York, 1994, pp. 161–172.
48. P. Breton et al., *Proc. Int. Symp. Controlled Release Bioact. Mater.* **21**, 608–609 (1994).
49. D. Roy et al., *Int. J. Pharm.* **148**, 165–175 (1997).
50. P. Breton et al., *Eur. J. Pharm. Biopharm.* **43**, 95–103 (1996).
51. J. Kreuter and H.J. Zehnder, *Radiat. Eff.* **35**, 161–166 (1978).
52. J. Kreuter et al., *Vaccine* **4**, 125–129 (1986).
53. J. Kreuter et al., *Vaccine* **6**, 253–256 (1988).
54. J. Kreuter, *Methods Enzymol.* **112**, 129–138 (1985).
55. J. Kreuter and P.P. Speiser, *J. Pharm. Sci.* **65**, 1624–1627 (1976).
56. F. Stieneker, J. Kreuter, and J. Löwer, *AIDS* **5**, 431–435 (1991).
57. J. Kreuter, F. Stieneker, and J. Löwer, *Proc. Int. Symp. Controlled Release Bioact. Mater.* **18**, 277–278 (1991).
58. J. Kreuter, *Pharm. Acta Helv.* **58**, 242–250 (1983).
59. A. Rolland, B. Collet, R. Le Verge, and L. Toujas, *J. Pharm. Sci.* **78**, 481–484 (1989).

60. G. Lukowski, R.H. Müller, B.W. Müller, and M. Dittgen, *Int. J. Pharm.* **84**, 23–31 (1992).
61. K. Langer et al., *Int. J. Pharm.* **137** 67–74 (1996).
62. A. Rolland, *Int. J. Pharm.* **54**, 113–121 (1989).
63. A. Rolland et al., *J. Immunol. Methods* **96**, 185–193 (1987).
64. J.-Y. Cherng et al., *Pharm. Res.* **13**, 1038–1042 (1996).
65. S.D. Tröster et al., *J. Controlled Release* **20**, 247–260 (1992).
66. G. Borchard and J. Kreuter, *Pharm. Res.* **13**, 1055–1058 (1996).
67. N. Al Khouri et al., *Pharm. Acta Helv.* **61**, 274–281 (1986).
68. F. Puisieux et al., S. Dumitriu, ed., *Polymeric Biomaterials*, Dekker, New York, 1994, pp. 749–794.
69. F. Chouinard et al., *Int. J. Pharm.* **72**, 211–217 (1991).
70. F. Chouinard, S. Buczkowski, and V. Lenaerts, *Pharm. Res.* **11**, 869–874 (1994).
71. G. Puglisi, M. Fresta, G. Giammona, and C.A. Ventura, *Int. J. Pharm.* **125**, 283–287 (1995).
72. M. Fresta et al., *Biomaterials* **17**, 751–758 (1996).
73. M. Gallardo et al., *Int. J. Pharm.* **100**, 55–64 (1993).
74. P. Couvreur, G. Couarraze, J.P. Devissaguet, and F. Puisieux, in S. Benita, ed., *Microencapsulation, Methods and Industrial Applications*, Dekker, New York, 1996, pp. 183–211.
75. M. Arakawa and T. Kondo, *J. Pharm. Sci.* **70**, 354–357 (1981).
76. J.M. Gallo, C.T. Hung, and D.G. Perrier, *Int. J. Pharm.* **22**, 63–74 (1984).
77. S. Winoto-Morbach and W. Müller-Ruchholtz, *Eur. J. Pharm. Biopharm.* **41**, 55–61 (1995).
78. Y. Akasaka et al., *Drug Des. Delivery* **3**, 85–97 (1988).
79. M. Roser and T. Kissel, *Eur. J. Pharm. Biopharm.* **39**, 8–12 (1993).
80. T. Yoshioka, M. Hashida, S. Muranishi, and H. Sezaki, *Int. J. Pharm.* **81**, 131–141 (1981).
81. N. Wang and X.S. Wu, *Pharm. Dev. Technol.* **2**, 135–142 (1997).
82. M. Rajaonarivony et al., *J. Pharm. Sci.* **82**, 912–917 (1993).
83. W. Lin et al., *J. Drug Target.* **1**, 237–243 (1993).
84. M.S. El-Samaligy and P. Rohdewald, *J. Pharm. Pharmacol.* **35**, 537–539 (1983).
85. I. Ezpeleta, J.M. Irache, J. Gueguen, and A.M. Orecchioni, *J. Microencapsul.* **14**, 557–565 (1997).
86. T. Mirshahi, J.M. Irache, J. Gueguen, and A.M. Orecchioni, *Drug Dev. Ind. Pharm.* **22**, 841–846 (1996).
87. M.J. Alonso, in S. Cohen and H. Bernstein, eds., *Microparticulate Systems for the Delivery of Proteins and Vaccines*, Dekker, New York, 1996, pp. 203–242.
88. S.J. Holland, B.J. Tighe, and P.L. Gould, *J. Controlled Release* **4**, 155–180 (1986).
89. A. Göpferich, *Eur. J. Pharm. Biopharm.* **42**, 1–11 (1996).
90. U.S. Pat. 4,177,177 (December 4, 1979), J.W. Vanderhoff, M.S. El-Aasser, and J. Ugelstadt (to the inventors).
91. M.C. Julienne, M.J. Alonso, J.L. Gómez Amoza, and J.P. Benoit, *Drug Dev. Ind. Pharm.* **18**, 1063–1077 (1992).
92. M.D. Blanco and M.J. Alonso, *Eur. J. Pharm. Biopharm.* **43**, 287–294 (1997).
93. T. Niwa et al., *J. Controlled Release* **25**, 89–98 (1993).
94. E. Allémann, R. Gurny, and E. Doelker, *Int. J. Pharm.* **87**, 247–253 (1992).
95. E. Allémann, J.C. Leroux, R. Gurny, and E. Doelker, *Pharm. Res.* **10**, 1732–1737 (1993).
96. D. Quintanar-Guerrero, H. Fessi, E. Allémann, and E. Doelker, *Int. J. Pharm.* **143**, 133–141 (1996).
97. O. Thioune, H. Fessi, J.P. Devissaguet, and F. Puisieux, *Int. J. Pharm.* **146**, 233–238 (1997).
98. P. Calvo et al., *Pharm. Res.* **13**, 311–315 (1996).
99. E. Allémann, E. Doelker, and R. Gurny, *Eur. J. Pharm. Biopharm.* **39**, 13–18 (1993).
100. K. Langer, E. Seegmüller, A. Zimmer, and J. Kreuter, *Int. J. Pharm.* **110**, 21–27 (1994).
101. A. Rolland, D. Gibassier, P. Sado, and R. Le Verge, *J. Pharm. Belg.* **41**, 94–105 (1986).
102. M. Auvillain, G. Cavé, H. Fessi, and J.P. Devissaguet, *S.T.P. Pharma. Sci.* **5**, 738–744 (1989).
103. P. Sommerfeld, U. Schroeder, and B.A. Sabel, *Int. J. Pharm.* **155**, 201–207 (1997).
104. F. De Jaeghere et al., *Pharm. Res.* **16**, 864–871 (1999).
105. G. Strauss, P. Schurtenberger, and H. Hauser, *Biochim. Biophys. Acta* **858** 169–180 (1986).
106. J.F. Carpenter, S.J. Prestrelski, and T. Arakawa, *Arch. Biochem. Biophys.* **303**, 456–464 (1993).
107. V. Masson, F. Maurin, H. Fessi, and J.P. Devissaguet, *Biomaterials* **18**, 327–335 (1997).
108. C. Volland, M. Wolff, and T. Kissel, *J. Controlled Release* **31**, 293–305 (1994).
109. R.L. Juliano, *Adv. Drug Delivery Rev.* **2**, 31–54 (1988).
110. R.H. Müller, *Colloidal Carriers for Controlled Drug Delivery and Targeting*, CRC Press, Boca Raton, Fla., 1991.
111. S. Stolnik, L. Illum, and S.S. Davis, *Adv. Drug Delivery Rev.* **16**, 195–214 (1995).
112. G. Storm, S.O. Belliot, T. Daemen, and D.D. Lasic, *Adv. Drug Delivery Rev.* **17**, 31–48 (1995).
113. S.J. Douglas, S.S. Davis, and L. Illum, *Crit. Rev. Ther. Drug Carrier Syst.* **3**, 233–261 (1987).
114. D.V. Bazile et al., *Biomaterials* **13**, 1093–1102 (1992).
115. T. Verrecchia, G. Spenlehauer, and D.V. Bazile, *J. Controlled Release* **36**, 49–61 (1995).
116. J.-C. Olivier et al., *J. Controlled Release* **40**, 157–168 (1996).
117. J.H. Lee, J. Kopecek, and J.D. Andrade, *J. Biomed. Mater. Res.* **23**, 351–368 (1989).
118. J.C. Leroux et al., *Life Sci.* **57**, 695–703 (1995).
119. J.C. Leroux et al., *J. Controlled Release* **39**, 339–350 (1996).
120. E. Allémann et al., *Int. J. Cancer* **66**, 821–824 (1996).
121. R.H. Müller, D. Rühl, and K. Schulze-Forster, *Eur. J. Pharm. Sci.* **5**, 147–153 (1997).
122. S.M. Moghimi, *Adv. Drug Delivery Rev.* **16**, 183–193 (1995).
123. S.J. Douglas, S.S. Davis, and L. Illum, *Int. J. Pharm.* **34**, 145–152 (1986).
124. R.H. Müller and K.H. Wallis, *Int. J. Pharm.* **89**, 25–31 (1993).
125. S.E. Dunn et al., *J. Controlled Release* **44**, 65–76 (1997).
126. T.I. Armstrong, M.C. Davies, and L. Illum, *J. Drug Target.* **4**, 389–398 (1997).
127. R. Gref, Y. Minamitake, M.T. Peracchia, and R. Langer, in *Microparticulate Systems for the Delivery of Proteins and Vaccines*, Dekker, New York, 1996, pp. 279–306.
128. M.T. Peracchia et al., *J. Controlled Release* **46**, 223–231 (1997).
129. S. Stolnik et al., *Pharm. Res.* **11**, 1800–1808 (1994).
130. R. Gref et al., *Proc. Int. Symp. Controlled Release Bioact. Mater.* **20**, 131–132 (1993).
131. R. Gref et al., *Science* **263**, 1600–1603 (1994).

Next Page

132. D. Labarre et al., *Proc. Int. Symp. Controlled Release Bioact. Mater.* **21**, 91–92 (1994).
133. D. Bazile et al., *J. Pharm. Sci.* **84**, 493–498 (1995).
134. R. Fernàndez-Urrusuno et al., *Pharm. Res.* **12**, 1385–1387 (1995).
135. M. Vittaz et al., *Biomaterials* **17**, 1575–1581 (1996).
136. H. Sahli et al., *Biomaterials* **18**, 281–288 (1997).
137. K.-I. Izutsu, S. Yoshioka, and S. Kojima, *Pharm. Res.* **12**, 838–843 (1995).
138. R. Gref et al., *Adv. Drug Delivery Rev.* **16**, 215–233 (1995).
139. C. Emile et al., *Proc. 1st World Meet. APGI/APV*, 1995, vol. 1, pp. 461–462.
140. K.J. Zhu, L. Xiangzhou, and Y. Shilin, *J. Appl. Polym. Sci.* **39**, 1–9 (1990).
141. P. Ferruti et al., *Biomaterials* **16**, 1423–1428 (1995).
142. S.E. Dunn et al., *Pharm. Res.* **11**, 1016–1022 (1994).
143. M.T. Peracchia, C. Vauthier, F. Puisieux, and P. Couvreur, *J. Biomed. Mater. Res.* **34**, 317–326 (1997).
144. B.G. Müller and T. Kissel, *Pharm. Pharmacol. Lett.* **3**, 67–70 (1993).
145. L. Illum, P.D.E. Jones, and S.S. Davis, in S.S. Davis, L. Illum, J.G. McVie, and E. Tomlinson, eds. *MIcrospheres and Drug Therapy*, Elsevier, Amsterdam, 1984, pp. 353–363.
146. L. Illum, P.D.E. Jones, R.W. Baldwin, and S.S. Davis, *J. Pharmacol. Exp. Ther.* **230**, 733–736 (1984).
147. A. Rolland, D. Bourel, B. Genetet, and R. Le Verge, *Int. J. Pharm.* **39**, 173–180 (1987).
148. V.P. Torchilin and V.S. Trubetskoy, in S. Cohen and H. Bernstein eds., *Microparticulate Systems for the Delivery of Proteins and Vaccines*, Dekker, New York, 1996, pp. 243–277.
149. B. Magenheim and S. Benita, *S. T. P. Pharma. Sci.* **1**, 221–241 (1991).
150. C. Washington, *Int. J. Pharm.* **58**, 1–12 (1990).
151. M. Skiba, F. Puisieux, D. Duchêne, and D. Wouessidjewe, *Int. J. Pharm.* **120**, 1–11 (1995).
152. S.K. Das, I.G. Tucker, J.T. Hill, and N. Ganguly, *Pharm. Res.* **12**, 534–540 (1995).
153. S.D. Tröster and J. Kreuter, *J. Microencapsul.* **9**, 19–28 (1992).
154. J.C. Leroux et al., *J. Biomed. Mater. Res.* **28**, 471–481 (1994).
155. T. Blunk et al., *Eur. J. Pharm. Biopharm.* **42**, 262–268 (1996).
156. P. Couvreur and C. Vauthier, in A.G. de Boer, ed., *Drug Absorption Enhancement, Concepts, Possibilities, Limitations and Trends*, Harwood Academic Publishers, Chur, Switzerland, 1994, pp. 457–486.
157. J.C. Leroux, E. Doelker, and R. Gurny, in S. Benita, ed., *Microencapsulation Methods and Industrial Applications*, Dekker, New York, 1996, pp. 535–575.
158. H. Pinto-Alphandary et al., *Pharm. Res.* **11**, 38–46 (1994).
159. J.M. Rodrigues, Jr. et al., *Int. J. Pharm.* **126**, 253–260 (1995).
160. A.R. Bender et al., *Antimicrob. Agents Chemother.* **40**, 1467–1471 (1996).
161. R. Löbenberg, J. Maas, and J. Kreuter, *Proc. Int. Symp. Controlled Release Bioact. Mater.* **23**, 657–658 (1996).
162. P. Maincent et al., *J. Pharm. Sci.* **75**, 955–958 (1986).
163. C. Michel et al., in T.L. Whateley, ed., *Microencapsulation of Drugs*, Harwood Academic Publishers, Chur, Switzerland, 1992, pp. 233–242.
164. A.T. Florence, *Pharm. Res.* **14**, 259–266 (1997).
165. V. Lenaerts, P. Couvreur, L. Grislain, and P. Maincent, in V. Lenaerts and R. Gurny, eds., *Bioadhesive Drug Delivery Systems*, CRC Press, Boca Raton, Fla., 1990, pp. 93–104.
166. E. Mathiowitz et al., *Nature (London)* **386**, 410–414 (1997).
167. G. Ponchel et al., *Eur. J. Pharm. Biopharm.* **44**, 25–31 (1997).
168. E. Haltner, J.H. Easson, and C.-M. Lehr, *Eur. J. Pharm. Biopharm.* **44**, 3–13 (1997).
169. J.C. Leroux et al., *J. Pharm. Sci.* **84**, 1387–1391 (1995).
170. D.T. O'Hagan, K.J. Palin, and S.S. Davis, *Vaccine* **7**, 213–216 (1989).
171. J. Pappo and T.H. Ermak, *Clin. Exp. Immunol.* **76**, 144–148 (1989).
172. S.S. Guterres et al., *Proc. 1st World Meet. APGI/APV*, 1995, vol. 1, pp. 515–516.
173. C. Tasset et al., *J. Controlled Release* **33**, 23–30 (1995).
174. A. Sanchez and M.J. Alonso, *Eur. J. Pharm. Biopharm.* **41**, 31–37 (1995).
175. J. Kreuter, *Vaccine Res.* **1**, 93–98 (1992).
176. C.A. Le Bourlais et al., *Drug Dev. Ind. Pharm.* **21**, 19–59 (1995).
177. T. Harmia, P. Speiser, and J. Kreuter, *Pharm. Acta Helv.* **62**, 322–331 (1987).
178. A. Joshi, *J. Ocul. Pharmacol.* **10**, 29–45 (1994).

See also LIPOSOMES; MICROENCAPSULATION; MICROENCAPSULATION FOR GENE DELIVERY.

NONDEGRADABLE POLYMERS FOR DRUG DELIVERY

ROLAND BODMEIER
JÜRGEN SIEPMANN
Freie Universität Berlin
Berlin, Germany

KEY WORDS

Acrylic polymers
Aquacoat®
Cellulose esters
Coating
Ethyl cellulose
Eudragit®
Hydroxypropylmethyl cellulose
Implantable systems
Intravaginal systems
Matrix systems
Microencapsulation
Ocular systems
Poly(ethylene oxide)
Poly(ethylene vinyl acetate)
Silicones

OUTLINE

Ethyl Cellulose
  Coated Systems and Films
  Matrix Systems
  Microencapsulation
Cellulose Esters: Cellulose Acetate, Cellulose Acetate Butyrate, and Cellulose Acetate Propionate

132. D. Labarre et al., *Proc. Int. Symp. Controlled Release Bioact. Mater.* **21**, 91–92 (1994).
133. D. Bazile et al., *J. Pharm. Sci.* **84**, 493–498 (1995).
134. R. Fernàndez-Urrusuno et al., *Pharm. Res.* **12**, 1385–1387 (1995).
135. M. Vittaz et al., *Biomaterials* **17**, 1575–1581 (1996).
136. H. Sahli et al., *Biomaterials* **18**, 281–288 (1997).
137. K.-I. Izutsu, S. Yoshioka, and S. Kojima, *Pharm. Res.* **12**, 838–843 (1995).
138. R. Gref et al., *Adv. Drug Delivery Rev.* **16**, 215–233 (1995).
139. C. Emile et al., *Proc. 1st World Meet. APGI/APV*, 1995, vol. 1, pp. 461–462.
140. K.J. Zhu, L. Xiangzhou, and Y. Shilin, *J. Appl. Polym. Sci.* **39**, 1–9 (1990).
141. P. Ferruti et al., *Biomaterials* **16**, 1423–1428 (1995).
142. S.E. Dunn et al., *Pharm. Res.* **11**, 1016–1022 (1994).
143. M.T. Peracchia, C. Vauthier, F. Puisieux, and P. Couvreur, *J. Biomed. Mater. Res.* **34**, 317–326 (1997).
144. B.G. Müller and T. Kissel, *Pharm. Pharmacol. Lett.* **3**, 67–70 (1993).
145. L. Illum, P.D.E. Jones, and S.S. Davis, in S.S. Davis, L. Illum, J.G. McVie, and E. Tomlinson, eds. *MIcrospheres and Drug Therapy*, Elsevier, Amsterdam, 1984, pp. 353–363.
146. L. Illum, P.D.E. Jones, R.W. Baldwin, and S.S. Davis, *J. Pharmacol. Exp. Ther.* **230**, 733–736 (1984).
147. A. Rolland, D. Bourel, B. Genetet, and R. Le Verge, *Int. J. Pharm.* **39**, 173–180 (1987).
148. V.P. Torchilin and V.S. Trubetskoy, in S. Cohen and H. Bernstein eds., *Microparticulate Systems for the Delivery of Proteins and Vaccines*, Dekker, New York, 1996, pp. 243–277.
149. B. Magenheim and S. Benita, *S. T. P. Pharma. Sci.* **1**, 221–241 (1991).
150. C. Washington, *Int. J. Pharm.* **58**, 1–12 (1990).
151. M. Skiba, F. Puisieux, D. Duchêne, and D. Wouessidjewe, *Int. J. Pharm.* **120**, 1–11 (1995).
152. S.K. Das, I.G. Tucker, J.T. Hill, and N. Ganguly, *Pharm. Res.* **12**, 534–540 (1995).
153. S.D. Tröster and J. Kreuter, *J. Microencapsul.* **9**, 19–28 (1992).
154. J.C. Leroux et al., *J. Biomed. Mater. Res.* **28**, 471–481 (1994).
155. T. Blunk et al., *Eur. J. Pharm. Biopharm.* **42**, 262–268 (1996).
156. P. Couvreur and C. Vauthier, in A.G. de Boer, ed., *Drug Absorption Enhancement, Concepts, Possibilities, Limitations and Trends*, Harwood Academic Publishers, Chur, Switzerland, 1994, pp. 457–486.
157. J.C. Leroux, E. Doelker, and R. Gurny, in S. Benita, ed., *Microencapsulation Methods and Industrial Applications*, Dekker, New York, 1996, pp. 535–575.
158. H. Pinto-Alphandary et al., *Pharm. Res.* **11**, 38–46 (1994).
159. J.M. Rodrigues, Jr. et al., *Int. J. Pharm.* **126**, 253–260 (1995).
160. A.R. Bender et al., *Antimicrob. Agents Chemother.* **40**, 1467–1471 (1996).
161. R. Löbenberg, J. Maas, and J. Kreuter, *Proc. Int. Symp. Controlled Release Bioact. Mater.* **23**, 657–658 (1996).
162. P. Maincent et al., *J. Pharm. Sci.* **75**, 955–958 (1986).
163. C. Michel et al., in T.L. Whateley, ed., *Microencapsulation of Drugs*, Harwood Academic Publishers, Chur, Switzerland, 1992, pp. 233–242.
164. A.T. Florence, *Pharm. Res.* **14**, 259–266 (1997).
165. V. Lenaerts, P. Couvreur, L. Grislain, and P. Maincent, in V. Lenaerts and R. Gurny, eds., *Bioadhesive Drug Delivery Systems*, CRC Press, Boca Raton, Fla., 1990, pp. 93–104.
166. E. Mathiowitz et al., *Nature (London)* **386**, 410–414 (1997).
167. G. Ponchel et al., *Eur. J. Pharm. Biopharm.* **44**, 25–31 (1997).
168. E. Haltner, J.H. Easson, and C.-M. Lehr, *Eur. J. Pharm. Biopharm.* **44**, 3–13 (1997).
169. J.C. Leroux et al., *J. Pharm. Sci.* **84**, 1387–1391 (1995).
170. D.T. O'Hagan, K.J. Palin, and S.S. Davis, *Vaccine* **7**, 213–216 (1989).
171. J. Pappo and T.H. Ermak, *Clin. Exp. Immunol.* **76**, 144–148 (1989).
172. S.S. Guterres et al., *Proc. 1st World Meet. APGI/APV*, 1995, vol. 1, pp. 515–516.
173. C. Tasset et al., *J. Controlled Release* **33**, 23–30 (1995).
174. A. Sanchez and M.J. Alonso, *Eur. J. Pharm. Biopharm.* **41**, 31–37 (1995).
175. J. Kreuter, *Vaccine Res.* **1**, 93–98 (1992).
176. C.A. Le Bourlais et al., *Drug Dev. Ind. Pharm.* **21**, 19–59 (1995).
177. T. Harmia, P. Speiser, and J. Kreuter, *Pharm. Acta Helv.* **62**, 322–331 (1987).
178. A. Joshi, *J. Ocul. Pharmacol.* **10**, 29–45 (1994).

See also LIPOSOMES; MICROENCAPSULATION; MICROENCAPSULATION FOR GENE DELIVERY.

NONDEGRADABLE POLYMERS FOR DRUG DELIVERY

ROLAND BODMEIER
JÜRGEN SIEPMANN
Freie Universität Berlin
Berlin, Germany

KEY WORDS

Acrylic polymers
Aquacoat®
Cellulose esters
Coating
Ethyl cellulose
Eudragit®
Hydroxypropylmethyl cellulose
Implantable systems
Intravaginal systems
Matrix systems
Microencapsulation
Ocular systems
Poly(ethylene oxide)
Poly(ethylene vinyl acetate)
Silicones

OUTLINE

Ethyl Cellulose
  Coated Systems and Films
  Matrix Systems
  Microencapsulation
Cellulose Esters: Cellulose Acetate, Cellulose Acetate Butyrate, and Cellulose Acetate Propionate

Coated Systems
Matrix Tablets
Microencapsulation
HPMC
Uncoated Matrix Systems
Coated Matrix Systems
Polymer Blends
Acrylic Polymers
Coated Systems
Films
Matrix Tablets
Microencapsulation
Silicones
Implantable Systems
Intravaginal Systems
Ocular Systems
Miscellaneous
EVA
Implantable Systems
Intravaginal Systems
Ocular Systems
Miscellaneous
Poly(ethylene oxide)
Matrix Systems
Miscellaneous
Bibliography

Polymers play a dominant role as carrier materials in drug delivery systems. The selection of a particular carrier is primarily determined by the intended use and the desired release profile. The polymer should be inexpensive, readily available, and easily processed on a large scale. When applied to an animal or human, it must be biocompatible and nontoxic. The route of administration also plays a decisive role: Polymers for parenteral use have to satisfy different requirements than polymers for oral use. This article reviews the most important nondegradable polymers used in drug delivery systems. They include the cellulose derivatives ethyl cellulose, cellulose acetate, cellulose acetate butyrate, cellulose acetate proprionate, and hydroxypropylmethyl cellulose; various acrylic polymers; silicones; poly(ethylene vinyl acetate); and poly(ethylene oxides). The physicochemical properties of the polymers are briefly discussed, followed by a review of various drug delivery systems in which the polymers have been incorporated.

ETHYL CELLULOSE

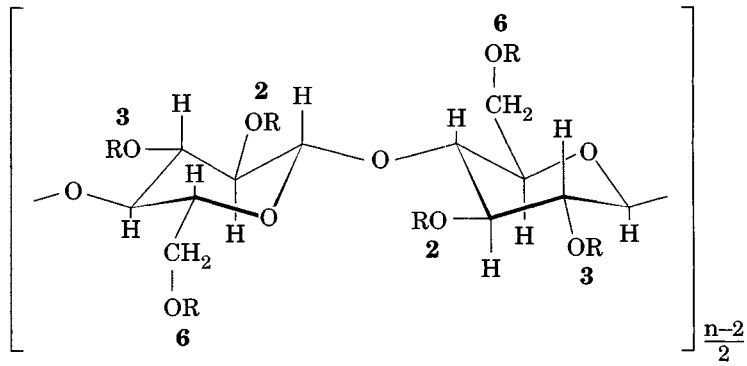
Ethyl cellulose is a cellulose ether prepared by the reaction of alkali cellulose with ethyl chloride; its chemical structure is shown in Figure 1. Its properties and applications have been reviewed recently (1). Its glass transition temperature is 120°C (2). It is characterized by the degree of ethoxy substitution and the solution viscosity. Commercial grades of ethyl cellulose have a degree of substitution between 2.25 and 2.58 (44 to 50% ethoxyl content) per anhydroglucose unit. Ethyl cellulose polymers are sold under the trade name Ethocel® by the Dow Chemical Company. Ethocel is available in six grades from standard 4 to 100, the numbers representing the viscosity of 5% w/v solutions in toluene ethanol (80:20) in cP, with the 7 and 100 grades also being offered with a fine particle size for applications in which the polymer is not dissolved in organic solvents but is used as a dry powder. A similar range of ethyl cellulose products is also offered by Hercules. Ethyl cellulose is water insoluble but soluble in a variety of organic solvents/solvent mixtures (3). The desired use of ethyl cellulose will determine the choice of a particular grade, for example, lower-molecular-weight grades are used for coating, and higher-molecular-weight grades are used for microencapsulation. Different grades can also be blended to obtain films with special properties. The polymer is tasteless and odorless, physiologically inert, stable in a pH range between 3 and 11, and, because of its nonionic character, compatible with most drug substances.

Ethyl cellulose has been used by the pharmaceutical industry for almost 40 years for the coating of solid dosage forms (tablets, pellets, granules); in matrix systems, which are prepared by wet granulation or direct compression; or in microencapsulation processes. It has excellent film-forming properties. Besides the predominant use as controlled-release barriers, thin films have been used as a moisture barrier to improve the stability of hydrolytically unstable drug substances or for taste-masking purposes.

Coated Systems and Films

Ethyl cellulose is one of the most widely used water-insoluble polymers for the coating of solid dosage forms. It can be applied as an organic solution or as an aqueous colloidal polymer dispersion. Many studies have been performed with ethyl cellulose films to predict properties of the coatings, for example, mechanical or permeability properties.

Various factors of the spraying process with organic polymer solutions, such as spraying distance, flow rate, and atomizing air pressure, affected the mechanical and release properties of ethyl cellulose films (4). It was pointed out that the variables governing solvent evaporation and spreading of the organic polymer solution droplets during the coating process are very important to obtain films with the desired properties. The selection of a suitable organic solvent system has been facilitated through the determination of the dilute solution properties of ethyl cellulose, namely the intrinsic viscosity and the interaction constant (5). Methylene chloride and ethanol in a ratio of 60:40% w/w were found to be optimal. Water concentrations in excess of 10% resulted in uncontrolled situations (e.g., polymer precipitation) during solvent evaporation. Based on tensile tests and thermal analysis, dibutyl sebacate and Myvacet were the most efficient plasticizers for ethyl cellulose films cast from ethanolic solution (6). The permeability of the polymeric films can be controlled by the molecular weight of the polymer or polymer blends or by the inclusion of additives like plasticizers or pore formers. The mechanical stability of the polymeric films increases with



Cellulose derivative	Substituent R (other than H)
Ethyl cellulose	$-CH_2CH_3$
Cellulose acetate	$-COCH_3$
Cellulose acetate propionate	$-CH_2CH_3$, $-COCH_2CH_3$
Cellulose acetate butyrate	$-CH_2CH_3$, $-COCH_2CH_2CH_3$
Hydroxypropylmethyl cellulose	$-CH_2CH(CH_3)OH$, $-CH_3$

Figure 1. Structure of a section of two anhydroglucose units (cellobiose) in a cellulose derivative. *Source:* Adapted from Doelker (117) with permission from Springer-Verlag.

increasing molecular weight. The release of drug from ethyl cellulose/hydroxypropylmethyl cellulose (HPMC) (9:1)–coated pellets decreased with increasing molecular weight of ethyl cellulose and increasing diethyl phthalate (plasticizer) concentration for the lower-molecular-weight ethyl cellulose grades (7). Above a molecular weight of 35,000 Da, the addition of a plasticizer had no effect on the drug release. The rapid release with the lower-molecular-weight grades was attributed to the weak mechanical properties of the coating, reflected by cracks and flaws in the film.

A porous ethyl cellulose film was obtained by spraying an ethyl cellulose–ethanol–water ternary mixture (8–10). The film porosity increased with increasing water content of the coating solution as a result of a phase separation process. The film porosity was also affected by the temperature and the relative humidity but was only slightly affected by the concentration of the polymer and its molecular weight. The increased film porosity resulted in increased permeation rates.

Although coating with organic polymer solutions is still widespread, aqueous ethyl cellulose dispersions have been developed to overcome problems associated with organic solvents (11). Two aqueous ethyl cellulose pseudolatexes are commercially available, namely Aquacoat®, manufactured by FMC, and Surelease®, by Colorcon®. Aquacoat® (30% solids content) is prepared by a direct emulsification–solvent evaporation method (12), whereby an organic polymer solution is emulsified into water to form an emulsion. The pseudolatex is obtained after homogenization and solvent removal. Sodium lauryl sulfate and cetyl alcohol are used as emulsifier and coemulsifier. The polymer dispersion must be plasticized to reduce its minimum film formation temperature (MFT). For coating purposes, 20–30% plasticizer is added, and the dispersion is diluted to a solids content between 10 and 25%. Surelease® (25% solids content) is a fully plasticized dispersion and is prepared by a phase inversion–in situ emulsification technique (13). Ethyl cellulose, dibutyl sebacate or fractionated coconut oil (plasticizer), and oleic acid (secondary plasticizer) are hot-melt extruded under pressure into water containing ammonia. Initially, a water-in-polymer dispersion is formed, which then inverts into a polymer-in-water dispersion. Ammonium oleate forms in situ as a stabilizer. Upon drying and film formation, ammonia evaporates, leaving oleic acid as an additional plasticizer within the film.

Various additives, which are present in the ethyl cellulose dispersions, will also be present in the final film or coating and can therefore affect film properties, such as mechanical properties or the permeability. Surfactants are necessary to physically stabilize the dispersion during preparation and storage. Plasticizers and antitacking agents or additives, which affect the permeability of the ethyl cellulose film (e.g., hydrophilic polymers such as HPMC), are added shortly before the application of the polymer dispersion.

Although a pH-independent drug release is expected with ethyl cellulose, several studies with Aquacoat®-coated beads showed a faster drug release in simulated intestinal fluid when compared to simulated gastric juice (14–17). This was caused by the presence of the anionic surfactant, sodium lauryl sulfate, which resulted in better wetting of the coated pellets in pH 7.4 buffer as indicated by contact-angle measurements (18) and not by residual acid/base groups in the ethyl cellulose polymer (19). Later, it was reported that the pH-dependent release could be circumvented by curing the coated dosage form above the glass-transition temperature of the plasticized polymer coating (20,21). During storage, sodium lauryl sulfate and cetyl alcohol were squeezed from the film, possibly changing the permeability (22). In addition, charged surfactants such as sodium lauryl sulfate could form insoluble complexes with cationic drugs present in the core (23,24).

Although the drug release from ethyl cellulose–coated multiparticulates such as pellets or granules is adequate, the release from tablets is often too slow. Water-soluble additives have therefore been incorporated into ethyl cellulose coatings to modify the drug release. They include low-molecular-weight materials including various sugars (e.g., sucrose, lactose, and sorbitol); salts (e.g., sodium chloride and calcium phosphate); surfactants such as sodium lauryl sulfate; or hydrophilic polymers including polyethylene glycol, polyvinyl pyrrolidone and, in particular, cellulose ethers (e.g., HPMC) (15,25–32). During dissolution studies, these additives leach from the coating membrane, or hydrate in the coating in the case of high-molecular-weight polymers, resulting in more permeable membranes and generally in a faster drug release. In addition, with thin coatings, hydrophilic polymers are added to increase the quantity of the coating to achieve a more uniform coating distribution on the pellet. Slight variations in the coating level will then not affect the release rate significantly.

The water-soluble high-molecular-weight polymers are usually not considered true pore-forming agents because they do not completely leach out from the coating to leave a well-defined pore structure. Ethyl cellulose/HPMC blends have shown phase separation with a limited degree of mixing between the polymers (33). Film studies revealed that HPMC-rich macroscopic polydispersed domains were dispersed within the ethyl cellulose–rich matrix. Complete leaching of HPMC was only observed at HPMC concentrations above 60% w/w; otherwise, some HPMC retention was observed. A critical HPMC concentration was identified below which very little polymer leached from the coating and no pores are formed. Above 24% HPMC, the polymer leaches from the ethyl cellulose films, resulting in pore formation and an increase in drug release (34,35). For the development of an osmotic system, the water permeability of pure ethyl cellulose was only about one-tenth of cellulose acetate but increased with HPMC in the film. At higher HPMC content, the initially semipermeable ethyl cellulose/HPMC film also became permeable for the drug (34). In an interesting experimental setup developed by the same research group, the permeability of ethyl cellulose/HPMC increased with increasing HPMC content as was shown with a pressurized cell device in which the permeability was measured in dependence to an applied tensile stress (36). Pellets coated with an aqueous ethyl cellulose dispersion containing HPMC initially formed water-filled pores after extraction of the HPMC at the beginning of the release process in the aqueous medium (37). However, after 2 h, these pores closed irreversibly as a result of fusion at temperatures above the MFT. The release was then as slow as without HPMC. A decrease in acetaminophen release with increasing HPMC concentration was contributed to the lower solubility of the drug in the HPMC-containing Aquacoat® film (38).

During coating with the HPMC-containing ethyl cellulose dispersion (Aquacoat®), a sediment formed in the colloidal dispersion upon standing, indicating destabilization of the colloidal ethyl cellulose particles by HPMC (39,40). The addition of HPMC to the ethyl cellulose pseudolatex resulted in the flocculation of the colloidal polymer particles above a critical HPMC concentration. The observed flocculation phenomena could interfere with the film formation of the colloidal polymer dispersion upon removal of water and thus could affect the drug release from the polymer-coated dosage forms.

A pore-forming agent, urea, was dissolved in the ethyl cellulose pseudolatex, Aquacoat®, to increase the release rate of drugs from coated osmotically active tablets (41). The release rates varied as a function of coating thickness, pore-former level and plasticizer type, and concentration. Scanning electron microscopy revealed that the urea was eluted from the coating, leaving a porous coating.

The drug release could also be increased by incorporating drug powder in the coating formulation (30). Theophylline was incorporated in the coating and resulted in faster drug release due to an increase in film porosity after dissolving from the coating. A gradient matrix system has been developed that consisted of an ethyl cellulose film with acetaminophen and xylitol coated on a core (42,43). A constant release could be obtained by increasing the drug concentration toward the core and having an inverse concentration gradient for xylitol. The drug release occurred through water-filled pores. Both compounds were soluble in the polymer, with acetaminophen acting as a plasticizer. Above a critical concentration, both the drug and xylitol crystallized, and the plasticizing effect disappeared.

Besides water-soluble additives, insoluble ingredients such as magnesium stearate or talc help reduce agglomeration or sticking of the coated particles during the coating process (15). The pigment concentration has a strong influence on the final film properties such as mechanical strength and permeability. Care must be taken when incorporating coloring agents into Surelease®, an aqueous dispersion of high pH value, because the basicity of the dispersion will destroy the dye–substrate complex (44). Colorants such as aluminum lakes should be replaced with inorganic pigments such as titanium dioxide.

With aqueous colloidal polymer dispersions, the addition of plasticizers is required for polymer dispersions having an MFT above the coating temperature. Water-soluble plasticizers are dissolved in the aqueous dispersions, whereas water-insoluble plasticizers are emulsified. Iyer et al. determined the uptake of the water-insoluble plasticizer, dibutyl sebacate, into Aquacoat® by using an alkaline partition column to separate the unbound plasticizer and gas chromatography for the plasticizer assay (45). The uptake of dibutyl sebacate was found to be complete within 30 min irrespective of the amount used; the uptake rate was faster with increasing solids content of the pseudolatex or when smaller quantities of plasticizer were incorporated. However, a previous study reported the presence of visible dibutyl sebacate droplets in Aquacoat® after 1 week of mixing, indicating incomplete plasticization after such a long plasticization time (17). Factors influencing the rate and extent of the plasticizer uptake by the colloidal particles, such as type and concentration of the plasticizer and type and solids content of the polymer dispersion, were investigated with Aquacoat® (46–48). The distribution behavior of the water-soluble plasticizers, triethyl citrate and triacetin, within Aquacoat® was virtually not affected by the mixing time or degree of agitation. The water-insoluble plasticizers were not completely taken up by the colloidal

polymer particles within a 24-h period. This may have important implications for the coating with aqueous polymer dispersions when compared to organic polymer solutions in which the plasticizer is completely dissolved. During coating, in addition to the plasticized polymer particles, the emulsified plasticizer droplets will be sprayed onto the solid dosage forms. This could result in an uneven plasticizer distribution within the film, potentially causing changes in the mechanical and especially release properties upon aging.

Plasticizers do not only affect the film formation from colloidal polymer dispersions or the mechanical properties of the resulting films; their choice will also affect the drug release from the coated dosage form (14,15,49). Increasing the concentration of dibutyl sebacate or triethyl citrate decreased the drug release from Aquacoat®-coated dosage forms (15), probably because of better fusion of the colloidal polymer particles. In general, water-insoluble plasticizers retard the drug release more than water-soluble plasticizers.

Process variables such as spray rate, droplet size, bed temperature, spray mode, chamber geometry, and so on can have a significant impact on the drug release (12–14,50). Dissolution data and morphological studies indicated differences in the nature of the coating, which was attributed to differences in particle motion in the bed, in particle distribution and density in the coating zone, and in the direction and distance the droplets had to travel prior to impinging on the particles (51). The coating temperature should be sufficiently high to achieve efficient water removal and subsequent particle coalescence. In general, it should be 10–20°C higher than the MFT of the polymer dispersion (52). The drug release with Surelease®-coated theophylline pellets decreased with increasing the product temperature from 32 to 48°C because of a more complete film formation. Coating at low product-bed temperatures prevents sufficient coalescence of the colloidal particles and promotes drug diffusion in the coating, resulting in a rapid release (53). Excessive temperatures resulted in porous films and poorly coalesced particles because of the high evaporation rate of water. Smaller nozzle diameters resulted in better coatings with fewer imperfections (54).

The coalescence of the colloidal ethyl cellulose particles into a homogeneous film is often incomplete after coating with aqueous polymer dispersions. As a consequence, changes in the drug release from the coated dosage form caused by further coalescence during storage have been observed as a function of storage temperature and time (12,16–18,55–57). A curing step or thermal treatment (storage of the coated dosage forms at elevated temperatures for short time periods) is often recommended to accelerate the coalescence of the ethyl cellulose particles prior to long-term storage. The storage temperature should be about 10°C above the MFT (16). Higher curing temperatures could cause excessive tackiness and agglomeration of the solid dosage forms. Curing was reported to be required with Aquacoat®-coated pellets but not with Surelease®-coated pellets (57).

Although curing at 40°C for 24 h was insufficient curing at either 50 or 60°C resulted in a significant reduction in drug release with Aquacoat®-coated pellets (18). The limiting drug-release pattern was approached after curing the beads for 1 h at 60°C. This value was also found by other authors (58). As an alternative to oven curing, Aquacoat®-coated beads have been cured directly in the fluidized bed after the coated beads have been applied with a thin layer of hydroxypropylmethyl cellulose (59). The hydrophilic overcoat prevented the sticking and agglomeration of the beads without altering the release profiles of the original coated pellets. The curing temperature had a more dramatic effect than curing time with Aquacoat®-coated pellets (60). An increase in drug release was observed with dibutyl sebacate, while a decrease was observed with tributyl citrate. The decrease was explained with a further gradual coalescence, while the increase was explained by either the plasticizer being squeezed from the coating or by drug being solubilized in the plasticizer at higher curing times. Although curing of the Aquacoat®-coated chlorpheniramine maleate beads produced a retarding effect in drug release, curing of ibuprofen beads coated with a comparable coating system resulted in more complex drug-release patterns (61). At curing times in excess of 4 h, the drug release increased. The increase in drug release (curing periods in excess of 4 h) could be explained by the migration of ibuprofen from the bead interior to the bead surface through the ethyl cellulose coating during the curing step. Large drug crystals could be observed throughout the coated surface by scanning electron microscopy. The drug–polymer affinity, coupled with the drug's low melting point, could thus serve as an explanation for the phenomenon of drug migration, a process that was accelerated at elevated temperatures. The diffusion of guaifenesin, another low-melting drug, through the vapor phase across the Aquacoat® coatings during storage of the coated beads has also been observed (17).

The ethyl cellulose pseudolatexes Aquacoat® and Surelease® resulted in very brittle films in the dry state and weak films in the wet state with low values for puncture strength and elongation (<5%) in both cases (62). In contrast, acrylic-based polymeric films were stronger and more flexible. Curing did not improve the mechanical properties of the Aquacoat® films. Ethyl cellulose films, when cast from organic solutions, were stronger (had higher puncture strength) in both the dry and wet state when compared with Aquacoat® films. However, the elongation values were still low. Interestingly, triethyl citrate leached almost completely from the pseudolatex-cast film, while more than 75% of the original plasticizer was still present in films cast from organic solutions. The higher leaching of triethyl citrate could have been the result of the anionic surfactant, sodium lauryl sulfate, being present in Aquacoat® films. The pseudolatex-cast films took up almost 43% water, compared with only 12% with the solvent cast films.

Most studies on the compaction of pellets coated with ethyl cellulose revealed a damage to the coating with a loss of the sustained release properties (63–69). This is not surprising because of the weak mechanical properties of ethyl cellulose.

Several articles discussed possible mechanisms by which drug release from multiparticulate dosage forms coated with water-insoluble polymers and in particular

ethyl cellulose might occur (70,71). The mechanism of drug release will be determined by the physicochemical properties of the drug, the polymer, and the dosage form. The possible mechanisms included solution/diffusion through a continuous polymer phase, solution/diffusion through plasticizer channels, diffusion through aqueous pores, and release driven by osmotic effects (70). Ozturk reported the release from ethyl cellulose–coated dosage forms to be a combination of osmotically driven release and diffusion through the polymer and or aqueous pores. To determine if the drug release was driven by osmosis or occurred primarily by diffusion through the polymer, the drug release from pellets and the drug diffusion across cast films was measured in diffusion cells (62). Ibuprofen had a significantly higher solubility in ethyl cellulose films than chlorpheniramine maleate. Ibuprofen, the water-insoluble drug, was released from the coated beads and diffused across free films, while chlorpheniramine maleate, the water-soluble drug, was released from the beads but did not diffuse across the polymeric film. Ibuprofen was released primarily by solution/diffusion through the hydrophobic polymer. On the other hand, chlorpheniramine maleate, the water-soluble drug, was not released by a solution/diffusion mechanism from the beads because of its negligible diffusion across cast films. Chlorpheniramine maleate was released through aqueous (micro)channels caused by osmotic effects with subsequent rupturing of the weak polymeric membrane. As described earlier, Aquacoat® films were extremely weak in the wet state (% elongation <1%).

The mechanism of release was reported to be different with pellets with lower coating levels and pellets with higher coating levels coated with Aquacoat® or Surelease® from diffusion through water-filled pores to diffusion of the drug through the membrane (57). Drug release from incompletely coated beads at low coating levels followed the square-root-of-time model, whereas the drug release at higher coating levels was best described with zero-order release kinetics (72). As with a typical reservoir system, three phases, an initial lag time, a constant-release phase, and a final declining-release phase, were observed (73). The major mechanism for release was reported to be diffusion and not osmotic pumping. The constant-release rate was proportional to the size (surface area) of coated pellets for metoprolol salts of different solubility. The zero-order release phase was shorter for more water-soluble drugs from Aquacoat®-coated pellets (74). Free films were not permeable for the water-soluble drugs, while the drugs were released from pellets through water-filled channels. The channels were attributed to artifacts of the coating process and not to the formation during contact with dissolution media. Each pellet was described to work like a mini–osmotic pump with multiple orifices (pores).

In addition to the colloidal ethyl cellulose dispersions, a micronized ethyl cellulose powder with an average particle size of a few μm is available in Japan from Shin-Etsu (54,75). The polymeric powder is dispersed in water with the addition of relatively large amounts of plasticizer prior to use. A comparative coating study of aqueous ethyl cellulose suspensions and pseudolatex dispersion revealed that the pseudolatex required less plasticizer for film formation than the aqueous polymer suspension. The average diameter of the ethyl cellulose particles in the suspension was 5.6 μm.

Matrix Systems

Ethyl cellulose can be incorporated as a carrier material into matrix preparations either by solution granulation or direct compression. Ethyl cellulose solutions were used for the preparation of granules by wet granulation, whereby the drug release was controlled by the amount of ethyl cellulose or the addition of a hydrophilic polymer (e.g., HPMC) to the granulation fluid. Ethyl cellulose has been used for solvent granulation of water-sensitive drugs. The resulting tablets have good physical properties. Controlled release theophylline tablets were prepared by fluid bed granulation of the drug and excipients with the aqueous dispersion, Surelease®, followed by compression of the granules (13). Because of its thermoplastic nature, ethyl cellulose can also be used for extrusion granulation.

Various studies have evaluated ethyl cellulose as a directly compressible excipient (76–81). The compressibility of ethyl cellulose has recently been reported (80). With directly compressible systems, the particle size of ethyl cellulose affected the release rate and the tablettability. Ethyl cellulose matrix controlled release tablets containing pseudoephedrine HCl were prepared by direct compression of different viscosity grades of ethyl cellulose (76). The lower viscosity grades produced harder tablets. Compared to HPMC matrix systems, matrix systems based on ethyl cellulose will release the drug faster at higher drug loadings because of a diffusion/erosion vs leaching drug release mechanism.

Microencapsulation

Ethyl cellulose microparticles can be prepared by various microencapsulation processes (see MICROENCAPSULATION). Depending on the microstructure of the microparticles, microcapsules (reservoir system) or microspheres (matrix system) can be distinguished.

Ethyl cellulose was one of the first polymers used for the microencapsulation of water-soluble drugs by the classical organic phase separation process (82). Phase separation can be induced by a temperature change in a cyclohexane system, whereby the drug is dispersed in a heated ethyl cellulose solution in cyclohexane at 80°C followed by gradual cooling of this solution to form the polymer coacervate to enclose the drug particles. In addition to the temperature change, the coacervation can be further induced by the addition of incompatible polymers, such as low-molecular-weight polyethylene or polyisobutylene. Polyisobutylene also acts as a protective colloid. As with aqueous phase separation techniques, the phase separation of ethyl cellulose can also be induced by the addition of nonsolvents, for example, in an ethyl cellulose–dichloromethane (solvent)-*n*-hexane (incompatible solvent) system.

Although microcapsules are formed primarily with the organic phase separation techniques, ethyl cellulose microspheres have been prepared with the solvent evaporation method, whereby the polymer is dissolved in an organic solvent followed by emulsification of this polymer–

drug solution into an external phase (83,84). The microspheres are obtained after solvent diffusion in the external phase and solvent evaporation. Depending on the solubility of the drug, either an external aqueous or oily phase can be used. Various modifications of this method have been developed, including multiple-emulsion (water-in-oil-in-water, W/O/W) and cosolvent methods. Water-soluble drugs were entrapped, whereby an alcoholic ethyl cellulose solution containing the active drug was emulsified into liquid paraffin followed by solvent evaporation (85).

Indomethacin polymeric nanoparticles were prepared by microfluidization, whereby the drug-containing solution was emulsified into an aqueous phase followed by microfluidization (86). The nanoparticles formed after solvent diffusion in the aqueous phase and solvent evaporation. For the drug to be encapsulated, it had to have a high solubility in the polymeric matrix. Otherwise, unwanted drug crystallization was observed in the aqueous phase.

Ethyl cellulose microparticles can also be prepared by spray-drying of organic polymer solutions or aqueous polymer dispersions. With organic polymer solutions, the drug is dissolved or dispersed in the organic ethyl cellulose solution, followed by spray-drying and removal of the organic solvent. The drug can be either dissolved or dispersed in a crystalline or amorphous state in the polymeric matrix. With aqueous polymer dispersions, the drug is dissolved or dispersed in the polymer dispersion; with plasticizer-free ethyl cellulose dispersions, a plasticizer has to be included to reduce the MFT of the dispersion, followed by spray-drying. The coalescence of the colloidal particles into microparticles has to be ensured.

Two microencapsulation methods that used the coalescence of colloidal particles into microparticles were recently developed. In the first method, the colloidal polymer particles were coalesced into microparticles by using the ionotropic gelation of polysaccharides with oppositely charged counterions as a process for the microparticle formation (87). In the second method, a drug-containing aqueous polymer dispersion was emulsified into a heated external oil phase to form a water-in-oil (W/O) emulsion. The colloidal polymer particles then coalesced into microparticles within the internal aqueous phase (88).

Naproxen microcapsules were prepared by a coacervation phase separation technique, and ibuprofen–ethyl cellulose microspheres were prepared by the solvent evaporation process (89). Both microparticles were compressed into tablets; the matrix-structure ibuprofen particles were intact after tabletting, whereas the coatings of the naproxen microcapsules were ruptured to some extend.

CELLULOSE ESTERS: CELLULOSE ACETATE, CELLULOSE ACETATE BUTYRATE, AND CELLULOSE ACETATE PROPIONATE

Cellulose acetate (CA), cellulose acetate butyrate, and cellulose acetate propionate are pharmaceutically used cellulose esters that are insoluble in physiological fluids. Their chemical structures are shown in Figure 1. Commercially available grades of the cellulose esters vary in their molecular weight, their degree of esterification, and their type of alcohol substitution, resulting in a wide range of polymers with different physicochemical properties, such as melting temperature, glass-transition temperature, mechanical properties, permeability characteristics, and solubility (90). A major supplier of these polymers is the Eastman Chemical Company; detailed information about important properties of the different polymer grades is given in the product literature (91).

CA is obtained by the controlled esterification of purified cellulose with acetic acid and anhydride. The acetylation of CA is carried out to completion followed by hydrolysis to obtain CAs with lower acetyl contents. Cellulose triacetate has the highest acetate content and the highest melting point of the cellulose esters and is therefore soluble in fewer organic solvents. It has only limited compatibility with plasticizers. Decreasing the acetyl content increases the hydrophilicity of CAs. The water or moisture permeability can therefore be controlled through the acetyl content. Cellulose acetate butyrate is soluble in a variety of organic solvents; it has a low water permeability and good mechanical properties. It is compatible with a wide number of plasticizers.

Cellulose esters have been used as coating materials, particularly in osmotically driven coated drug-release systems, as carrier materials in matrix systems, and in the area of microencapsulation.

Coated Systems

CA coatings have been used for many years in osmotically controlled drug delivery systems. A review of the patent literature on osmotic drug delivery systems has been recently published (92). The Theeuwes elementary osmotic pump consists of an osmotically active drug-containing core surrounded by a semipermeable membrane, usually CA, having an orifice (93). The polymeric membrane is impermeable for the drug but permeable for aqueous fluids. Water is osmotically attracted through the membrane into the core and dissolves the drug, which is then released through the orifice at a constant rate as long as solid excess drug and a constant osmotic pressure gradient are maintained. The CA coating is rigid and does not expand during the drug release. The drug release from the elementary osmotic pump depends on the surface area, the water permeability of the membrane, its wall thickness, and the osmotic pressure gradient.

CA coatings with a controlled porosity were formed by including water-soluble agents (e.g., sorbitol) in concentrations between 10 and 50% based on the polymer into the polymer solution (27,28,94). After contact with dissolution fluids, the water-soluble additives leached from the film, leaving a membrane with controlled porosity. The spongelike porous membrane was substantially permeable to both water and the drug. The drug is not released through a prefabricated orifice, as with the elementary osmotic pump, but through a porous network. Zero-order drug release was obtained, with the drug release being dependent on the level of pore former, the wall thickness, the drug loading, the solubility of the core, and the osmotic pressure difference across the membrane but being independent of the agitation and the pH of the medium. A microporous CA

coating was also prepared from CA pseudolatexes containing urea as the pore former (95). The tablets had to be cured to promote the coalescence of the polymer particles in a film.

Tablets were coated with an asymmetric CA membrane by first dip-coating the tablets in a solution of the polymer in acetone and a nonsolvent (formamide or glycerol), followed by air-drying the tablets 5 s and then immersing the coated tablets for 3 min in a water quench bath (96). The coatings have an asymmetric structure, similar to membranes used for reverse osmosis. The new membranes have several unique characteristics when compared with conventional osmotic tablets. Higher water fluxes can be obtained, allowing the release of low-solubility drugs or higher release rates. The permeability can be controlled by the membrane structure.

A multiparticulate delayed-release system consisting of an osmotically active core and a CA coating was developed (97,98). The membrane was initially semipermeable and then also became permeable for the drug after expansion of the osmotically active core and creation of pores in the coating induced by the osmotic pressure gradient and the water influx. The drug release could be controlled by the properties of the coating and the core.

CA is normally applied from organic solutions to the solid dosage forms. To avoid organic solvents, aqueous colloidal CA dispersions have been prepared and evaluated (99–101). The problems with aqueous CA dispersions are their high MFT, requiring high amounts of plasticizer, and the hydrolytic instability in aqueous media, requiring storage at low temperatures. Plasticizer levels between 160 and 320% based on the polymer were required to form adequate films. Volatile plasticizers, which evaporated to some extent during the coating process, gave stronger films when compared with films prepared with nonvolatile plasticizers. The water permeability of the membranes was strongly dependent on the type of plasticizer and the processing conditions. A high-performance liquid chromatography (HPLC) method was developed to determine the acidic degradation products, acetic, propionic, and butyric acid in aqueous pseudolatexes (102). The preparation of a redispersible polymer dispersion would overcome the stability and inconvenient storage problems.

With a CA pseudolatex, 150% triacetin and 120% triethyl citrate had to be used as plasticizers to obtain dense and homogeneous films after coating propranolol HCl tablets (103). The permeability of the coating was too low, and 40% sucrose and 10% polyethylene glycol (PEG) 8,000 were included as flux enhancers to provide macroporous membranes with adequate release characteristics. The thermal and mechanical properties of films cast from a CA latex were evaluated by thermal mechanical analysis by the FMC Corporation, the manufacturer of the dispersion. Various plasticizers in the range of 0–160% were evaluated, with glyceryl diacetate, glyceryl triacetate, and triethyl citrate being the most effective. The water permeability of CA decreased with increasing plasticizer concentration to a minimum and then increased at higher concentrations (104). An antiplasticization effect was responsible for the decreased water permeability. This effect disappeared at temperatures above the glass-transition temperature.

Matrix Tablets

Powdered cellulose esters have been evaluated as matrix materials for both immediate- and slow-release preparations (105,106). The tablets were prepared by direct compression, wet granulation with aqueous binders, and solvent wet-granulation processes. All three cellulose esters were directly compressible. Sustained release was especially obtained with the solvent granulation method, whereby the polymer partially dissolved in the organic solvent. Plasticized CA powder has been used as a direct compression vehicle to form sustained-release theophylline matrix delivery systems. The drug release decreased with increasing polymer/drug ratio and the inclusion of a plasticizer, triethyl citrate. The release was not strongly affected by the polymer molecular weight and the particle size distribution. In a related study, the plasticizer triacetin was incorporated into CA by film casting, particles were then prepared by grinding the film with dry ice. Blending the plasticizer with the polymer resulted in wet powders that had poor flow properties.

Microencapsulation

The water-insoluble cellulose esters have also been used as carrier materials for microparticles. A review of the different methods is given in the product literature of Eastman (107). The major methods used are organic phase separation and solvent evaporation techniques. Cellulose acetate butyrate microcapsules were formed by organic phase separation by the addition of heptane to a cellulose acetate butyrate solution in heptane/chloroform (108). Theophylline–cellulose acetate proprionate microspheres were formed by the solvent evaporation method, whereby a drug suspension in the acetonic polymer solution was emulsified into mineral oil followed by solvent evaporation and microsphere formation (109,110). The drug release from the microspheres depended on the type of polymer, its molecular weight, the particle size of the microspheres, and the drug loading. Cellulose acetate butyrate microspheres were prepared by a similar technique, whereby hexane was added to the oil to precipitate the polymer (111,112). The drug release could be accelerated through the inclusion of PEG. Drug-loaded ion-exchange resins were encapsulated from an acetonic cellulose acetate butyrate solution by the nonaqueous solvent evaporation method (113,114). Overcoating dried gelatin beads with cellulose acetate butyrate by the nonaqueous solvent evaporation reduced the drug release rate (115).

HPMC

The chemical structure of HPMC is given in Figure 1. The physicochemical properties of this substance strongly depend on the following parameters: (*1*) methoxyl content, (*2*) hydroxypropyl content, and (*3*) molecular weight. HPMC 2208 is a well-defined U.S. Pharmacoreial Convention (USP) type with a nominal methoxyl and hydroxypro-

pyl content of 22 and 8%, respectively. Dahl et al. (116) found broad variations concerning important characteristics of seven batches of HPMC 2208 provided by two different manufacturers. As can be seen in Table 1, three batches violated the USP specification with respect to the required methoxyl content (19–24%). Although all products were within the specified hydroxypropyl content limits of 4–12%, Dahl and coworkers presented relevant differences concerning the naproxen release rates from HPMC 2208 matrix tablets within this range (116). The observed differences (up to more than 100%) are of significant practical importance for the application of potent drugs. In conclusion, the USP specification concerning the hydroxypropyl content is insufficient and should be reinforced.

Grafting and cross-linking HPMC are common methods to achieve desired properties of the resulting polymer. To study these modifications in more detail, the reader is referred to numerous reviews and publications (117–120). A good summary of the work that has been done to determine the glass-transition temperature (T_g) of HPMC has been written by Doelker (117). He compares the results of various researchers and lists values ranging from 154 to 184°C (Table 2). Various techniques have been used to determine the T_g: differential scanning calorimetry (DSC), differential thermal analysis (DTA), thermomechanical analysis (TMA), torsional braid analysis (TBA), and dynamic mechanical analysis (DMA). Different techniques often lead to different T_g values, and usually only the results achieved with one special method can be compared directly. In addition, the variation of the degree of substitution and of the molecular weight (as discussed earlier) play a role in the observed variance of the T_g. Furthermore, a 57°C value was reported by Conte et al. (129), which seems to correspond to a low-energy secondary transition. The relevance of this low-temperature transition is unknown but could be of significance in the diffusion of oxygen and water.

The swelling and solubility behavior of HPMC strongly depends on the molecular weight, degree of substitution, cross-linking, and grafting. Non-cross-linked polymers absorb water, swell, and dissolve (erode); cross-linked HPMC swells to some equilibrium state, at which the retractive force of the network balances the swelling force. Recently, an excellent review concerning the quantitative treatment of these swelling processes has been written by Narasimhan and Peppas (130).

Talukdar and coworkers (131) investigated the rheological properties of HPMC by oscillatory as well as by steady shear measurements. The dynamic moduli, that is, storage modulus (G′) and loss modulus (G″), have been determined.

The formation of a gel layer is of evident importance for the drug release from HPMC systems. Initially, the polymer is in a glassy state. Upon exposure to the respective biological fluid, water penetrates into the device and decreases the T_g of HPMC (acting as a plasticizer). With increasing water concentration, this reduction of the T_g also increases. At a critical concentration of water, the T_g equals the temperature of the system, and the polymer undergoes the transition from the glassy to the rubbery state. The increasing mobility of the macromolecular chains results in drug-diffusion coefficients orders of magnitude higher than those in the glassy state. The kinetics of water penetration, swelling, and drug release have been studied extensively by Colombo and Peppas (132–135). Figure 2 shows the experimental as well as the theoretical concentration profiles of KCl (as a model drug), water, and HPMC 2208 in the gel phase of compressed tablets, 5 h (a) and 6 h (b) after exposure to water. The thickness of the swollen polymer changed from 1.75 mm at 4 h to 3 mm at 5 h and 5.25 mm at 6 h. In case of relevant dissolution of the polymer, the kinetics of this process must also be taken into account (136). In 1987 Lee and Peppas presented an appropriate model (137). The equilibrium swelling behavior of porous and nonporous hydrogels as well as their characterization has been reviewed by Brannon-Peppas and Peppas (138,139).

Table 1. Physicochemical Characteristics of Various Batches of HPMC 2208 15,000 mPa s

Batch number	Viscosity (mPa s)	Methoxyl content (%)	Hydroxypropyl content (%)
1[a]	15,200	23.7	8.7
2[a]	14,000	22.5	10.9
3[a]	14,200	25.9	11.1
4[a]	15,000	26.4	7.2
5[a]	15,000	25.5	5.3
6[b]	15,600	22.7	10.7
7[b]	12,491	23.4	9.5

Source: Adapted from Dahl et al. (116) with permission from Elsevier Science Publishers B. V.
[a]From manufacturer a.
[b]From manufacturer b.

Table 2. Reported T_g for HPMC

Material	Method	T_g (°C)	References
	Type 2910		
Methocel® E15	TMA	172–175[a]	121
Pharmacoat® 606	DSC	177	122
Pharmacoat® 606	DSC	155	123
Pharmacoat® 606	DSC	180	124
Pharmacoat® 606	DTA	169–174	124
Pharmacoat® 606	TBA	153.5, 158.5	124
Pharmacoat® 606	DSC	155.8	125
Pharmacoat® 606	TMA	163.8, 174.4	125
Pharmacoat® 603	DMA	160	126
Pharmacoat® 606	DMA	170	126
Pharmacoat® 615	DMA	175	126
Pharmacoat® 606	DMA	154	127
	Type 2208		
Methocel® K4M	DSC	184	128
Methocel® K4M	DSC	(57)	129

Source: Adapted from Doelker (117) with permission from Springer-Verlag.
[a]The values obtained by TMA in the penetration mode have been reported by the authors as softening temperatures.

Uncoated Matrix Systems

A newly developed antihistaminergic drug, TA-5707F, has been released from HPMC matrix tablets by Yamakita et

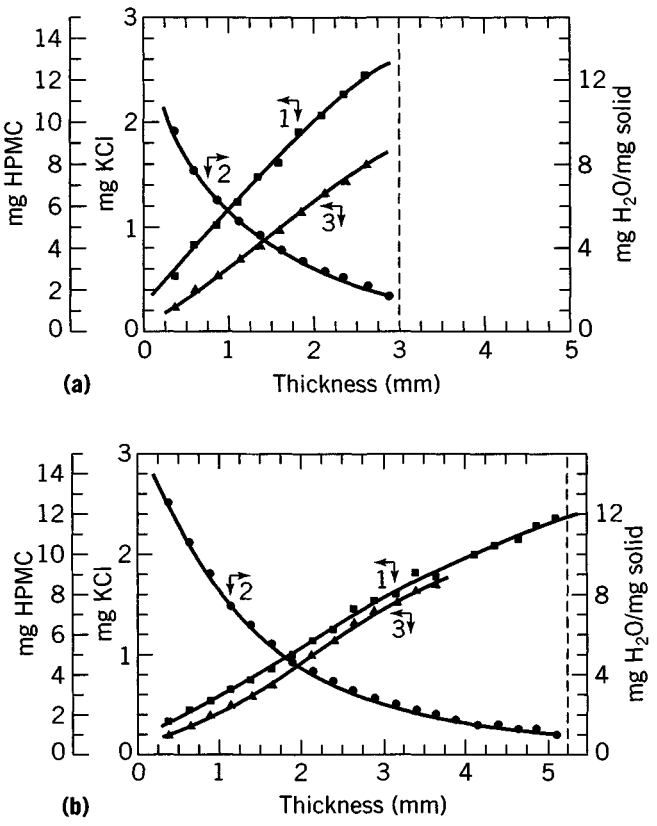


Figure 2. Concentration profiles of KCl (1), water (2), and HPMC 2208 (3) in the gel phase of compressed tablets after (**a**) 5 h and (**b**) 6 h. The dashed line corresponds to the swelling front. *Source:* Reprinted from Peppas et al. (132) with permission from Elsevier Scientific Publishing Company.

al. (140). They studied the in vitro as well as the (canine) in vivo kinetics. Liu and coworkers (141) presented the influence of the viscosity grade of HPMC on the release of diclofenac sodium in matrix tablets, performing in vitro and in vivo studies. The release mechanism of indomethacin containing HPMC matrix tablets in dependence on the initial drug loading and specific additives (e.g., starch) has been investigated by Xu and Sunada (142).

Pham and Lee (143) measured the transient dynamic swelling and dissolution behavior of HPMC matrices during drug release using a new flow-through cell (providing well-defined hydrodynamic conditions) and fluorescein as model drug. Studies of Ahlskog and Koller (144,145) deal with the treatment of Parkinson's disease, using a novel, potent, and selective dopamine D-2 agonist: MK-458 (PHNO; [+]-4-propyl-9-hydroxynaphthoxazine). The drug was administered in controlled-release devices (using HPMC matrices) as monotherapy in a double-blind, placebo-controlled, 12-week investigation.

Coated Matrix Systems

To achieve constant drug-release rates, Colombo and coworkers (146–148) covered different surface portions of an HPMC matrix tablet with an impermeable coating as can be seen in Figure 3. Systems prepared were uncoated matrix (Case 0), matrix with one base coated (Case 1), matrix with two bases coated (Case 2), matrix with lateral surface coated (Case 3), and matrix with one base plus lateral surface coated (Case 4). The applied coating modifies the relaxation rate of the polymer by affecting the dimension of the swelling of the plain matrix while leaving the diffusion characteristics of the active agent practically unchanged. The resulting drug release behavior is shown in Figure 4, for the case of diltiazem as active agent and Methocel® K100M as polymer. The release curves of cases 2–4 are nearly linear, except for a short period at the beginning of the experiment. These multilayer matrix systems for the controlled release of drugs have been patented by Colombo et al. (149) and are known as Geomatrix® systems. To facilitate the industrial production, the manual film-coating process can be avoided using press-coating techniques (150).



Figure 3. Schematic drawing of the matrix tablet (Case 0) and of the four coating designs investigated: Case 1, Case 2, Case 3 and Case 4. *Source:* Reprinted from Conte et al. (150) with permission from Elsevier Science Publishers B. V.

Polymer Blends

Perez-Marcos et al. (151) investigated the influence of the pH on the release of propranolol hydrochloride from matrices containing HPMC K4M and Carbopol® 974. At pH 1, the HPMC predominantly controlled the release of the drug, whereas at higher pH values, the Carbopol® became ionized and interacted with the active agent. In addition,

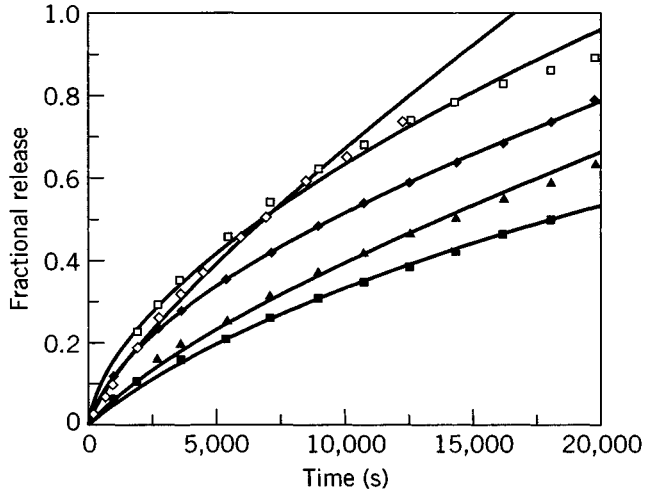


Figure 4. Fractional diltiazem release from five systems prepared by coating versus time. Case 0 (□), Case 1 (♦), Case 2 (▲), Case 3 (◇), and Case 4 (■). The straight lines have been calculated theoretically. *Source:* Reprinted from Colombo et al. (135) with permission from Elsevier Science Publishers B.V.

Next Page

the interaction of the two polymers was significantly dependent on the pH. A controlled-release formulation for the α-MSH analog melanotan-I was developed by Bhardwaj and Blanchard (152) using HPMC and poloxamer 407. They characterized the release kinetics in vitro as well as in vivo (guinea pigs, intraperitoneal administration). Buccoadhesive morphine sulfate tablets have been developed and tested (in vitro and in vivo) by Anlar et al. (153). Carbomer (CP) served as the bioactive adhesive compound. The release behavior of systems containing 30 mg morphine sulfate and various amounts of HPMC and CP was found to be non-Fickian. The adhesion force was weakest at a ratio of 1:1 of the two polymers because of the formation of an interpolymer complex between HPMC and CP.

Poly(ethylene-vinyl acetate) (EVA) needle-shaped polymeric devices containing antitumor drugs may be applicable as drug carriers in cancer chemotherapy. Lin et al. (154) investigated the in vivo antitumor activity of adriamycin hydrochloride (ADH) in C3H mice bearing mammary carcinoma and nude mice bearing brain tumor. HPMC was used as a release rate regulator. Tumor growth was markedly inhibited by treatment with needle devices after being locally inserted into the solid tumor. Recent studies of Chowdary and Sankar (155) deal with solid dispersions of nifedipin in HPMC and microcrystalline cellulose (MCC). These systems gave a fast dissolution of the drug. However, when the dispersions were microencapsulated with Eudragit® RL PM, controlled, slow release was observed. The kinetics depended on the proportion of HPMC–MCC in the solid dispersion used as a core, on the coat/core ratio, and on the size of the microcapsules. The release was found to be independent of pH and ionic strength.

ACRYLIC POLYMERS

Besides cellulose derivatives, acrylic polymers are a popular choice for controlled-release dosage forms (156,157). Several derivatives of poly(methyl methacrylate) with different solubility properties were developed, predominantly for oral use. Enteric polymers were obtained by copolymerization of methyl methacrylate with methacrylic acid; polymers soluble at low pH by introducing dimethylaminoethyl methacrylate and water-insoluble but permeable polymers for diffusion-controlled drug delivery systems by the copolymerization of methyl methacrylate, ethyl acrylate, and small amounts of trimethylammonioethyl methacrylate chloride as monomers. The chemical composition of the commercially available poly(meth)acrylates, which are sold by Röhm under the trade name Eudragit®, is shown in Table 3. This review is limited to polymers insoluble in gastrointestinal fluids and used in controlled-release formulations and does not cover enteric polymers.

The poly(meth)acrylates were initially applied from organic solutions in alcohols, acetone, or solvent blends (156). Problems associated with the use of organic solvents led to the development of aqueous polymer dispersions. The water-insoluble methacrylate ester copolymers are neutral (Eudragit® NE 30D) or weekly cationic polymers (Eudragit® RS or RL 30D), which are insoluble in gastrointestinal fluids. The aqueous dispersions have a solids content of 30%. The residual monomer content in the Eudragit® products for pharmaceutical applications is below 0.1%. The shelf-life specifications for aqueous polymer dispersions do usually not exceed 1 year.

Eudragit® NE 30D (a copolymer of ethyl acrylate and methyl methacrylate in a ratio of 2:1) is produced by emulsion polymerization. It has an MFT around 5°C and does not require plasticizers. The latex forms soft and highly flexible films upon drying. Eudragit® NE 30D could be blended with Eudragit® L 30D (an aqueous dispersion of an enteric polymer) to form enteric coatings without the use of additional plasticizer.

The cationic polymers, Eudragit® RL 100 or RS 100, are obtained by bulk polymerization of ethyl acrylate, methyl methacrylate, and trimethylammonioethyl methacrylate chloride. RL 100 contains twice as many quaternary ammonium groups than RS 100 and is therefore more hydrophilic and more permeable. The commercially available aqueous polymer dispersions are prepared by directly emulsifying the solid polymer into hot water at 80°C, which is above its T_g of 55°C. The dispersion process and the stability of the resulting polymer dispersion is positively affected by the positive charges of the polymer. No emulsifier is needed for the emulsification process. 0.25% sorbic acid is added as preservative. Eudragit® RL 30D and Eudragit® RS 30D require the addition of plasticizer to reduce the MFT below the coating temperature. The most frequently used plasticizers for the polymers are triethyl citrate, triacetin, and acetyltributyl citrate. The polymer dispersions are compatible with additives such as talc, titanium dioxide, and pigments. A colorimetric ion-pair complexation method has been developed to rapidly quantify RS and RL in pharmaceutical dosage forms (158).

RL and RS pseudolatexes were also prepared by a solvent change technique, whereby the polymer was dissolved in a water-miscible organic solvent (e.g., acetone) or solvent system followed by dispersion of this polymer solution in deionized water under mild agitation (159). The pseudolatex formed spontaneously after the diffusion of the organic solvent in the aqueous phase and solvent evaporation.

In Table 4, the mechanical and thermal properties of films from methacrylic ester copolymer latexes are summarized.

Coated Systems

Methacrylates have been used in the coating of pharmaceutical dosage forms for several decades. They can be applied either as an organic solution or as an aqueous colloidal dispersion.

The permeability of Eudragit® NE 30D films can be increased by adding water-soluble substances, such as sugars or water-soluble polymers: (PVP), poly(vinyl alcohol) (PVA), and PEGs (156). The addition of water-soluble cellulose ethers, such as HPMC, is not recommended because they can result in flocculation. Theophylline tablets have been coated with NE 30D latexes containing dispersed pore formers (160). Normally, microporous coatings are

Previous Page

the interaction of the two polymers was significantly dependent on the pH. A controlled-release formulation for the α-MSH analog melanotan-I was developed by Bhardwaj and Blanchard (152) using HPMC and poloxamer 407. They characterized the release kinetics in vitro as well as in vivo (guinea pigs, intraperitoneal administration). Buccoadhesive morphine sulfate tablets have been developed and tested (in vitro and in vivo) by Anlar et al. (153). Carbomer (CP) served as the bioactive adhesive compound. The release behavior of systems containing 30 mg morphine sulfate and various amounts of HPMC and CP was found to be non-Fickian. The adhesion force was weakest at a ratio of 1:1 of the two polymers because of the formation of an interpolymer complex between HPMC and CP.

Poly(ethylene-vinyl acetate) (EVA) needle-shaped polymeric devices containing antitumor drugs may be applicable as drug carriers in cancer chemotherapy. Lin et al. (154) investigated the in vivo antitumor activity of adriamycin hydrochloride (ADH) in C3H mice bearing mammary carcinoma and nude mice bearing brain tumor. HPMC was used as a release rate regulator. Tumor growth was markedly inhibited by treatment with needle devices after being locally inserted into the solid tumor. Recent studies of Chowdary and Sankar (155) deal with solid dispersions of nifedipin in HPMC and microcrystalline cellulose (MCC). These systems gave a fast dissolution of the drug. However, when the dispersions were microencapsulated with Eudragit® RL PM, controlled, slow release was observed. The kinetics depended on the proportion of HPMC–MCC in the solid dispersion used as a core, on the coat/core ratio, and on the size of the microcapsules. The release was found to be independent of pH and ionic strength.

ACRYLIC POLYMERS

Besides cellulose derivatives, acrylic polymers are a popular choice for controlled-release dosage forms (156,157). Several derivatives of poly(methyl methacrylate) with different solubility properties were developed, predominantly for oral use. Enteric polymers were obtained by copolymerization of methyl methacrylate with methacrylic acid; polymers soluble at low pH by introducing dimethylaminoethyl methacrylate and water-insoluble but permeable polymers for diffusion-controlled drug delivery systems by the copolymerization of methyl methacrylate, ethyl acrylate, and small amounts of trimethylammonioethyl methacrylate chloride as monomers. The chemical composition of the commercially available poly(meth)acrylates, which are sold by Röhm under the trade name Eudragit®, is shown in Table 3. This review is limited to polymers insoluble in gastrointestinal fluids and used in controlled-release formulations and does not cover enteric polymers.

The poly(meth)acrylates were initially applied from organic solutions in alcohols, acetone, or solvent blends (156). Problems associated with the use of organic solvents led to the development of aqueous polymer dispersions. The water-insoluble methacrylate ester copolymers are neutral (Eudragit® NE 30D) or weekly cationic polymers (Eudragit® RS or RL 30D), which are insoluble in gastrointestinal fluids. The aqueous dispersions have a solids content of 30%. The residual monomer content in the Eudragit® products for pharmaceutical applications is below 0.1%. The shelf-life specifications for aqueous polymer dispersions do usually not exceed 1 year.

Eudragit® NE 30D (a copolymer of ethyl acrylate and methyl methacrylate in a ratio of 2:1) is produced by emulsion polymerization. It has an MFT around 5°C and does not require plasticizers. The latex forms soft and highly flexible films upon drying. Eudragit® NE 30D could be blended with Eudragit® L 30D (an aqueous dispersion of an enteric polymer) to form enteric coatings without the use of additional plasticizer.

The cationic polymers, Eudragit® RL 100 or RS 100, are obtained by bulk polymerization of ethyl acrylate, methyl methacrylate, and trimethylammonioethyl methacrylate chloride. RL 100 contains twice as many quaternary ammonium groups than RS 100 and is therefore more hydrophilic and more permeable. The commercially available aqueous polymer dispersions are prepared by directly emulsifying the solid polymer into hot water at 80°C, which is above its T_g of 55°C. The dispersion process and the stability of the resulting polymer dispersion is positively affected by the positive charges of the polymer. No emulsifier is needed for the emulsification process. 0.25% sorbic acid is added as preservative. Eudragit® RL 30D and Eudragit® RS 30D require the addition of plasticizer to reduce the MFT below the coating temperature. The most frequently used plasticizers for the polymers are triethyl citrate, triacetin, and acetyltributyl citrate. The polymer dispersions are compatible with additives such as talc, titanium dioxide, and pigments. A colorimetric ion-pair complexation method has been developed to rapidly quantify RS and RL in pharmaceutical dosage forms (158).

RL and RS pseudolatexes were also prepared by a solvent change technique, whereby the polymer was dissolved in a water-miscible organic solvent (e.g., acetone) or solvent system followed by dispersion of this polymer solution in deionized water under mild agitation (159). The pseudolatex formed spontaneously after the diffusion of the organic solvent in the aqueous phase and solvent evaporation.

In Table 4, the mechanical and thermal properties of films from methacrylic ester copolymer latexes are summarized.

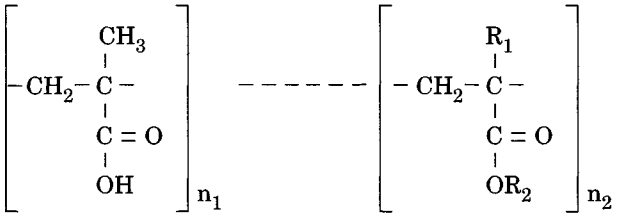
Coated Systems

Methacrylates have been used in the coating of pharmaceutical dosage forms for several decades. They can be applied either as an organic solution or as an aqueous colloidal dispersion.

The permeability of Eudragit® NE 30D films can be increased by adding water-soluble substances, such as sugars or water-soluble polymers: (PVP), poly(vinyl alcohol) (PVA), and PEGs (156). The addition of water-soluble cellulose ethers, such as HPMC, is not recommended because they can result in flocculation. Theophylline tablets have been coated with NE 30D latexes containing dispersed pore formers (160). Normally, microporous coatings are

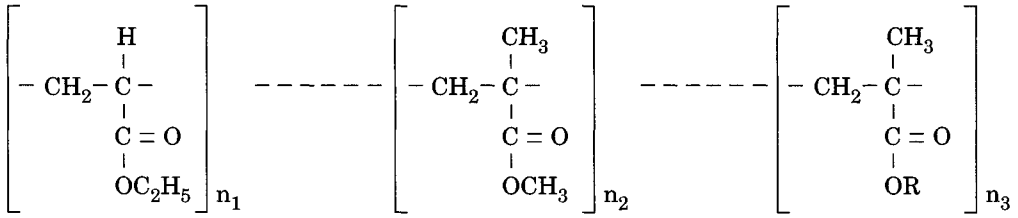
Table 3. Methacrylic Acid and Methacrylic Ester Copolymers

Methacrylic acid copolymers



Scientific name	n_1:n_2	M_W	USP/NF type	R_1	R_2	Behavior in digestive juices	Eudragit® type	Marketed form
Poly (methacrylic acid, ethyl acrylate)	1:1	250,000	C	H	C_2H_5	Soluble, pH > 5.5	L 30D L 100-55	30% aqueous dispersion powder
Poly(methacrylic acid, methyl methacrylate)	1:1	135,000	A	CH_3	CH_3	Soluble, pH > 6.0	L 100	Powder
Poly(methacrylic acid, methyl methacrylate)	1:2	135,000	B	CH_3	CH_3	Soluble, pH > 7.0	S 100	Powder

Methacrylate ester copolymers



Scientific name	n_1:n_2:n_3	M_W	Behavior in digestive juices	Eudragit® type	Marketed form
Poly(ethyl acrylate,methyl methacrylate)	2:1	800,000	Insoluble films of medium permeability	NE 30D	30% aqueous dispersion
Poly(ethyl acrylate, methyl methacrylate) trimethylammonioethyl methacrylate chloride R: CH_2-CH_2-$N^+(CH_3)_3Cl^-$	1:2:0.2	150,000	Insoluble films of high permeability	RL 30D RL 100	30% aqueous dispersion Granules
Poly(ethyl acryate, methyl methacrylate)trimethylammonioethyl methacrylate chloride R: CH_2-CH_2-$N^+(CH_3)_3CL^-$	1:2:0.1	150,000	Insoluble films of low permeability	RS 30D RS 100	30% aqueous dispersion Granules

Table 4. Mechanical and Thermal Properties of Films from Methacrylic Ester Copolymer Latexes

	Tensile stress at break (N/mm^2)	Elongation (%)	T_g (°C)
	Eudragit® NE 30D		
	8	600	−8
	Eudragit® RS 30D		
+ 10 % triacetine	5	40	–
+ 20% triethyl citrate	2	300	20
	Eudragit® RL 30D		
+ 10% triacetine	5	22	35
+ 20% triethyl citrate	4	300	30

Source: Adapted from K. Lehmann (156) with permission from Marcel Dekker, Inc.

prepared by dispersing water-soluble pore formers in organic polymer solutions followed by the coating step. The pore formers then leach from the coating into aqueous fluids, forming a microporous coating. With this novel system, a microporous membrane could be prepared without organic solvents by using pore formers with pH-dependent solubility properties (e.g., calcium salts), which were insoluble at the pH of the latex but were soluble in gastric juice. The pore former was dispersed in the coating and leached in aqueous media to form a multiporous coating through which the drug was released in a zero-order fashion.

Although the release from RS or RL-coated systems has been described to be pH-independent, a "pH-dependent" drug release was observed (161–163). This was actually caused by the presence in the release media of different anionic buffers species, which acted as counterions for the quaternary ammonium groups and replaced the chloride ion. The drug release correlated well with the hydration of the polymer films in different buffers (161). In another study, the release of theophylline from pellets coated with RS also showed a great dependence on the composition of the buffer solution. In contrast, the drug release from pellets coated with NE and the swelling of NE films was not significantly affected by the buffer species (162). Although the influence of buffer species can be diminished by the addition of NaCl (163), anionic species in the gastrointestinal tract, such as bile salts, have also been shown to have a dramatic effect on the drug release (164).

RS and RL 30D dispersions can be mixed in any ratio, with the coatings showing intermediate permeability properties (165,166). The addition of silica or talcum increased the drug release (166). The permeability of the films can also be influenced by the choice of plasticizer (167). An overcoat with the enteric polymer, Eudragit® S 100, eliminated the agglomeration of RS-coated pellets (167,168). Otherwise, talc or glycerol monostearate are used as antitacking agents (157).

The lag time prior to the diltiazem HCl release from RS-coated pellets could be controlled by varying the thickness of the coating (169). The drug release had a pattern of a lag period followed by an instantaneous release phase. A linear relationship was reported between the lag time and the square of the amount of polymer coated. High drug solubility was required for the rapid drug release after the lag period, which was caused by the time necessary for the polymeric film to hydrate. A sigmoidal release system (time-controlled drug delivery system) was developed, which consisted of a prolonged lag time followed by a rapid release phase (170–172). Because of the low water permeability of the RS film, the lag time could be varied by varying the thickness of the film. The drug release phase after the lag period could be enhanced by electrostatic or other physicochemical interactions between the polymer and organic acids such as succinic acid. The organic acid affected the hydration of the polymeric film. The drug release from beads coated with NE 30D, which has no quaternary ammonium group in the polymer chain, was not affected by succinic acid. Ion-exchange experiments revealed that organic acids interacted with the quaternary ammonium groups of RS by an ion-exchange mechanism.

A wide range of release rates can be obtained by adding additives to a single polymer or by blending different polymers. The membrane permeability of film-coated theophylline pellets was controlled by using blends of different aqueous acrylic polymer dispersions (173). A film with pH-dependent permeability was obtained by blending the neutral acrylic polymer, NE, with the enteric polymer, L, showing higher release rates at intestinal pH values. A wide range of dissolution profiles was obtained by blending the more permeable RL with the less permeable RS to obtain pH-independent permeabilities. Heterogeneous film structures were obtained by blending RS 30D and ND 30D, as indicated by two individual glass-transition temperatures. Enteric polymers can be incorporated into the water-insoluble polymers to develop pH-dependent systems for the linearization of release profiles or to adjust the drug release with drugs with pH-dependent solubility.

A model was developed that permitted the quantitative correlation of the release kinetics from coated pellets with the permeation properties of free films (174). The film data allow the prediction of the drug release from coated pellets, under the condition that the manufacturing process was kept constant and the cores of the coated pellets were identical.

Coated particles or pellets have also been compressed into tablets. Various formulation and process parameters have to be optimized to obtain tabletted reservoir-type pellets having the same properties, and, in particular, release properties as the original, uncompacted pellets. The most important variable is the type of polymer selected for the coating of the pellets. The polymer coating must remain intact during compaction. When compared to ethyl cellulose films, films prepared from acrylic polymers are more flexible and therefore more suitable for the coating of pellets to be compressed into tablets (62). Films of Eudragit® NE 30D were very flexible. The elongation was in excess of the elongation limit of 365% achievable with the puncture test device. With plasticized Eudragit® RS and RL 30D, flexible films were obtained with elongation values in excess of 125%. Crystals, granules, and pellets were coated with various aqueous acrylic polymer dispersions (Eudra-

git® NE 30D, RS/RL 30D, and L 30D-55) and compressed into fast-disintegrating tablets (156,175). Multiparticulates coated with flexible polymers (Eudragit® NE 30D and plasticized Eudragit® RS/RL 30D) could be compressed without significant damage to the coating. No or only small changes in drug release were found with coatings with elongation values in excess of 75%. These films have enough elasticity to deform on coated pellets during compression without rupture. Very little difference in drug release was observed between the compressed granules and the noncompressed granules, which contained theophylline and were coated with an Eudragit® RL/RS dispersion. Enteric coatings based on Eudragit® L 30D-55, a methacrylic acid–ethylacrylate copolymer, were brittle, and the compression of the pellets resulted in film damage. This damage could be avoided by mixing the enteric polymer with the flexible Eudragit® NE 30D. Heterogeneous films, which retained their enteric properties, were obtained after the addition of Eudragit® NE 30D.

The effect of compression force on the dissolution from Eudragit® NE 30D–coated theophylline pellets was evaluated in a range of 6–20 kN (176). The compaction-induced pellet deformation was practically complete at 6 kN, and no change in dissolution rate was observed upon increasing the compression force to 20 kN. The increase in drug-release rate was not attributed to rupturing of the polymeric film but to a thinning of the flexible film because of stretching. A recent review provides an update on the tabletting of coated pellets and discusses important formulation and process parameters necessary to obtain pellet-containing tablets, which, ideally, have the same properties—in particular, drug-release properties—as the individual coated pellets (177).

Films

Various release, permeability, and mechanical properties of drug-containing or drug-free films have been determined to predict primarily the properties of film-coated dosage forms. The films can be prepared either from organic polymer solutions or from the aqueous polymer dispersions. The drug has to be compatible with the polymer dispersion; for example, the addition of anionic drugs to the cationic polymer dispersion, RS 30D, results in flocculation.

The choice of organic solvents affected the permeability of cast Eudragit® RL and RS films. Including ethanol in the acetonic casting solution resulted in a greater permeability, which was caused by a decrease in pore size but an increase in pore number. The microstructure of the film was therefore strongly affected by the composition of the solvent mixture (178). Differences in the solute diffusion were also observed between the lower and upper surface of polymeric films (179,180). The lower film surface, which was in contact with the mold during casting, was more permeable than the upper surface.

The partition coefficients and diffusion coefficients of progesterone and a synthetic progestin were determined with drug-loaded Eudragit® RL films. The partition coefficients showed that both steroids were dissolved in the polymer films, and the values of the diffusion coefficients revealed that the mechanism of diffusion was a solution-diffusion and not a pore-diffusion mechanism (181).

RL and RS films containing salicylic acid and chlorpheniramine maleate were prepared by organic solvent casting (182,183). The drugs were soluble in the polymers and acted as plasticizers for the polymers, as shown by a decreased T_g. The addition of hydrophilic adjuvants increased the release rate. Salicylic acid interacted with the cationic groups of the polymers via electrostatic interactions. Increasing the ionic strength of the dissolution media increased the drug release from the matrix films (184).

Drug-containing films have been prepared by casting the aqueous colloidal polymer dispersions followed by drying. The propranolol HCl release from RS films increased with increasing RS-RL ratio (185). The drug-release rate was high at low plasticizer concentrations because of incomplete coalescence of the colloidal particles and film formation and then was constant in a plasticizer range between 10 and 30% and then increased at higher plasticizer concentrations because of the leaching of the plasticizer. The drug release from latex-cast films was faster when compared with that from solvent-cast films of the same composition. Films cast from organic polymer solution were less porous and denser than the comparable latex-cast films, as observed with scanning electron microscopy.

Depending on the solubility of the drug, it could be either dissolved or dissolved/dispersed in the polymeric NE matrix (186). Depending on the drug loading, the drug release was a combination of diffusion through the polymer and diffusion through pores or channels. The drug release increased with increasing drug loading and increasing amount of HPMC in the NE film. Zero-order drug release could be achieved by laminating a second drug-free latex film onto the first reservoir layer (187).

The mechanical properties of RS 30D films were tested in the dry and in the wet state by a puncture test (188). The water-soluble plasticizer triethyl citrate leached into the dissolution medium, while the water-insoluble plasticizer acetyltributyl citrate remained in the film. While films were quite flexible with both plasticizers in the dry state (the elongation values at normally used plasticizer concentrations were in excess of 100%), the elongation values of wet triethyl citrate–containing films were significantly lower than the elongation values of wet acetyltributyl citrate–containing films. The choice of the plasticizer therefore strongly affects the mechanical properties of the resulting films in the wet and therefore in the gastrointestinal media. NE films were highly flexible in both the dry and wet state.

Eudragit® NE 30D and RL and Eudragit® RS 30D have also been used in dermal and transdermal systems. They form clear and transparent films that are insoluble in water but hydrate. Films for transdermal therapeutic systems have been prepared from organic polymer solutions, aqueous polymer dispersions, and by a hot-melt extrusion technique (156,157). Matrix films can be prepared by incorporating the drug in the polymer phase followed by casting/drying or extrusion. Forty to sixty percent plasticizer are used for the hot-melt extrusion of RS and RL at 80–120°C. Films of Eudragit® NE 30D have shown good

skin tolerance; they are flexible and permeable to water vapor.

Matrix Tablets

Poly(meth)acrylate powders have also been used as retarding materials in matrix tablets (156,157). The polymer can be directly compressed or wet granulated. The necessary amount of polymer to obtain controlled release was in the range of 10 to 50% of the tablet weight. It is mainly affected by the solubility and dose of the drug. The polymer can also be incorporated by granulating the drug and excipients with the aqueous colloidal polymer dispersions. Eroding sustained-release tablets have been formulated by granulating Emcompress® and diprophylline with NE 40D. RS 100 and salicylic acid were directly compressed into tablet cores (189). The drug release was further retarded by a coating with aqueous RS–sucrose mixtures of varying ratios.

Microencapsulation

Micro- or nanoparticles based on the acrylic polymers as carriers have been prepared by various microencapsulation techniques including organic phase separation, solvent evaporation, and spray-drying techniques (see MICROENCAPSULATION).

Paracetamol was encapsulated with RS by an organic phase separation process. The nonsolvent, cyclohexane, was added to a chloroformic solution of the polymer. Polyisobutylene was used as an antiaggregating agent. The drug release increased with increasing proportion of the core material and with a reduced coating thickness (190). A gradation of the microcapsule wall porosity could be obtained by depositing polymer mixtures of RL and RS on drug particles by the organic phase separation process (191). The release rates increased with increasing polar group content (RL content). Salicylic acid has been encapsulated by a coacervation process whereby the nonsolvent, water, was added to an ethanolic solution of the drug and polymer. Both drug and polymer precipitated after the addition of water (192).

Various antiinflammatory agents were encapsulated within RS- and RL-microspheres by the solvent evaporation method, whereby an organic drug containing polymer solution was emulsified into an external aqueous phase (83). Nanoparticles in the colloidal size range were obtained after microfluidization of the oil-in-water (O/W) emulsion (86). Ketoprofen–RS microspheres were formed by a nonaqueous solvent evaporation method by emulsifying a drug–polymer solution in liquid paraffin (193). Aluminium tristearate was used as a stabilizing agent.

Multiple-unit hollow microspheres (microballoons) were prepared by an emulsion solvent-diffusion method (194). The drug and acrylic polymer were dissolved in an ethanol–methylene chloride mixture. This solution was poured into an aqueous PVA solution to form emulsion droplets followed by polymer precipitation. The volume of the internal cavity of the microballoons increased at higher polymer ratios. Floatable microballoons could be prepared. Ibuprofen–RS microspheres and microsponges with different intraparticle porosities were prepared by a similar method (195–197). The internal porosity of the microsponges could be controlled by changing the concentration of the drug and the polymer in the ethanolic emulsion droplet. The formation of the microspheres with ethanol, a water-miscible solvent, was possible because of the quaternary ammonium groups in polymer chain, which stabilized the emulsion.

Nanoparticles containing the water-insoluble drugs ibuprofen, indomethacin, or propranolol were formed spontaneously after the addition of solutions of the drugs and RS or RL 100 polymers in the water-miscible solvents acetone or ethanol to water without homogenization (198). The nanoparticle dispersion was stabilized by the quaternary ammonium groups of the polymer and did not require the addition of external stabilizers. Other water-insoluble polymers require the use of water-immiscible organic solvents (e.g., methylene chloride) and a homogenization step to form nanoparticles. The cationic acrylic polymers allowed the formation of nanoparticles without homogenization or toxic organic solvents. RS or RL nanoparticles could also be formed by the melt method. The drug containing acrylic nanoparticles could be transformed into films by including plasticizers. This could be useful for dermal applications of nanoparticle dispersions. The release from the resulting films could be controlled by the ratio of RS to RL or the inclusion of water-soluble polymers to the nanoparticle suspensions prior to casting.

Acetyl salicylic acid–RS microspheres were prepared by a falling-drop process (solvent-partition method) whereby a solution of the polymer in methylene chloride and acetone (9:1) was injected into a flowing mineral oil stream (199). The solvent was extracted, and drug–polymer microspheres were formed. This method is in principle very similar to a nonaqueous solvent evaporation method.

Microparticles containing diltiazem HCl were prepared by spray-drying RS and RL polymer solutions (200). The choice of the solvent affected the structure of the resulting microparticles; either microspheres or microcapsules could be obtained. When compared with other encapsulation methods, spray-drying has many attractive features. It is a rapid, single-operation procedure suitable for large-scale production. Most microencapsulation methods are based on two immiscible phases, and drug loss to the external phase resulting in low encapsulation efficiencies is often a problem. With spray-drying, the external phase is air, and drug loss is therefore not an issue. Alternatively to organic RS or RL solution, drug-containing aqueous polymer dispersions were used to form the microparticles by spray-drying (201–205). The drug was either dissolved (chlorpheniramine maleate) or suspended (ibuprofen, naproxen) in the aqueous phase of the polymeric dispersion (164). Under optimal spray-drying conditions, the colloidal polymer particles coalesced into microparticles within the atomized droplets. Spherical microparticles with drug loadings between 10 and 50% were obtained with an average particle size in the range of 5–20 μm. The yield decreased with increasing drug loading and plasticizer level because of sticking and agglomeration. Chlorpheniramine maleate and ibuprofen acted as plasticizers for the polymer. Although ibuprofen was suspended in the polymer disper-

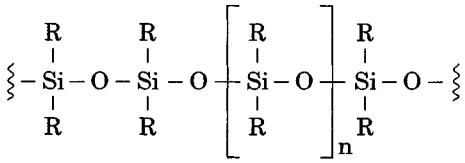


Figure 5. Structure of Si–O polymer chains; R is an organic substituent.

sion, it was dissolved in the microparticles, as indicated by X-ray diffraction studies.

Coprecipitates of ibuprofen and various acrylic polymers were prepared by adding a drug–polymer solution in acetone to water, followed by drying and milling of the precipitate (206). The coprecipitates had improved flow properties when compared with ibuprofen and are useful for the preparation of sustained-release tablets. Coevaporates of dipyridamole and the Eudragit® S, L, RL, or RS were prepared by dissolving the drug and polymer in an ethanol/methylene chloride (1:1) mixture, followed by removal of the solvent in a rotary evaporator and pulverization of the residue. Depending on the processing conditions, either a solid solution or dispersion was formed, as determined by X-ray and DSC. pH dependence and a variety of release profiles could be obtained by blending the different polymers (207).

SILICONES

Most silicones used in pharmaceutical applications consist of cross-linked Si–O polymer chains (shown in Fig. 5). R is an organic substituent, for example, CH_3 (in polydimethylsiloxane [PDMS]). There are several commonly used methods of synthesis, such as two-component condensation cures, one-component moisture cures, and two-component vinyl cures (208), resulting in different kinds of chemical cross-linking (Fig. 6a and b). Depending on the average chain length, type of substituent, and type and degree of cross-linking, the resulting polymers have significantly different properties (fluids, resins, elastomers). Generally, silicones are inert, poor conductors of electricity and hydrophobic.

The synthesis of drug-containing silicone systems is often very convenient. Before cross-linking, the adequate prepolymers are usually in a liquid state. The fluid components are mixed with the drug, and a cross-linking agent and/or a catalyst are/is added. This mixture is subsequently cast into a mold of the desired shape. After a few hours the formation of the polymer network (cross-linking reaction) hardens the device (209).

Owing to the ease of fabrication and high permeability for many drugs (e.g., steroids) silicones are often used for controlled drug delivery. The exceptionally high diffusion coefficients result from the high chain mobility of the Si–O backbones (210). The possibility of heat sterilization and remarkable biocompatibility make them favorable for parenteral systems.

As most silicones are physically weak, silica fillers are usually added to increase the mechanical stability of the resulting controlled-release system. The effective diffusion coefficient of the active agent is lowered by this addition of silica because the latter is usually not permeable for the drug and thus increases the diffusion pathways (211). Drug-release rates in these controlled-release systems are also significantly dependent on the amount and type of free polymer chains (that have not been cross-linked to the network during the synthesis of the device). Mazan et al. (211) used two different unreactive PDMS oils, $MD_{25}M$ and $MD_{75}M$, to produce well-defined systems (M represents a terminal block with three methyl groups; D is an SiO group with two methyl groups). Not only the diffusion coefficient of the drug but also the swelling extent of the system is a function of these components. The dependencies of the progesterone diffusion coefficient (D) and swelling extent (Q) of the silicone network on the amount and type of free polymer chains is illustrated in Figure 7 (nomenclature: relative amount of free chains F = [mass of cross-linked sample − mass of dry sample after elution in hexane]/mass of cross-linked sample). Moreau et al. (212) studied the effect of grafting an organic pendent segment along the PDMS chains. They evaluated the impact of this modification on the drug solubility, diffusivity, and elastomer properties. Thermal analysis and measurements of the swelling ratio have been used to characterize the influence of vulcanization conditions and chemical modifications on the network mesh size and subsequently on the diffusion of an active agent (213). An excellent review has been written by Baker

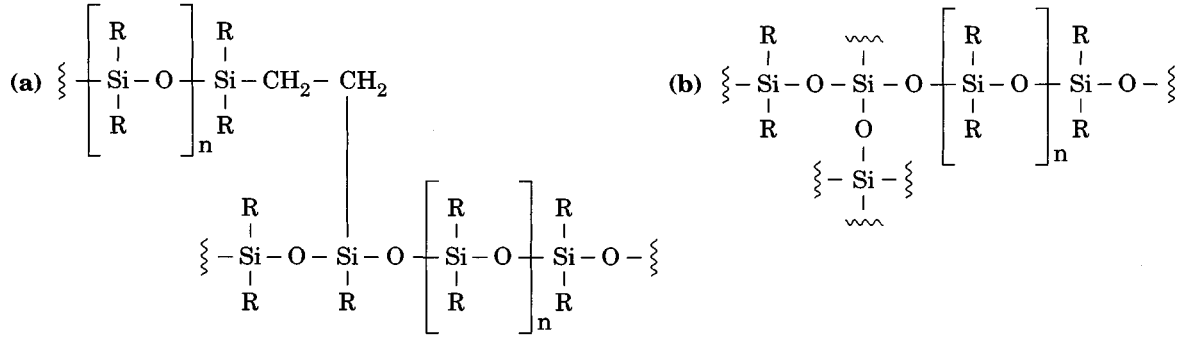


Figure 6. (**a**) and (**b**): Different types of cross-linkings in silicone networks.

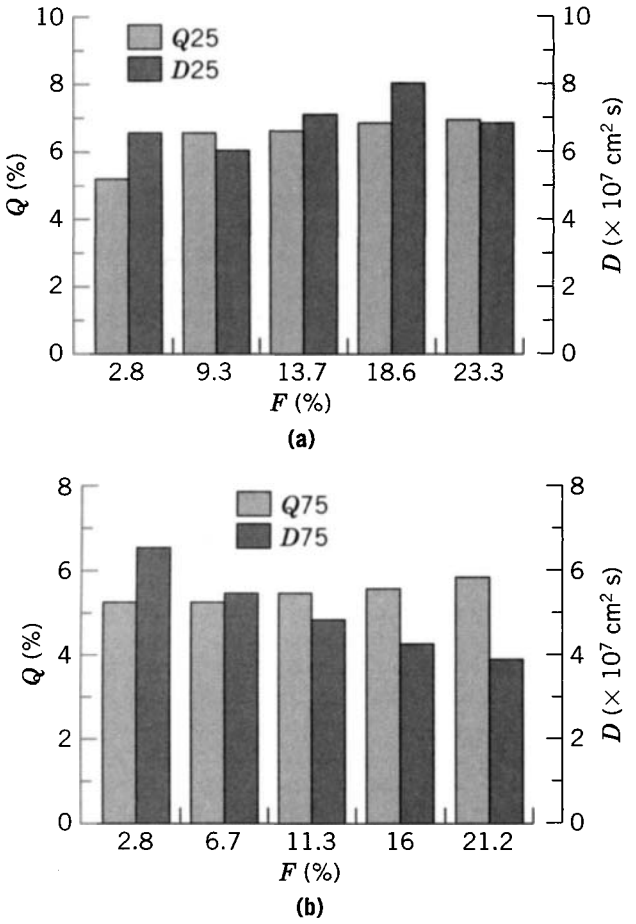


Figure 7. Variation of the swelling extend (Q) and the progesterone diffusion coefficient (D) as a function of the relative amount of free chains: (**a**) network loaded with $MD_{25}M$; (**b**) network loaded with $MD_{75}M$. *Source:* Reprinted from Mazan et al. (211) with permission from Pergamon Press.

(214) concerning the role of silicones in controlled drug delivery systems.

Implantable Systems

Norplant® (Leiras) is a contraceptive subdermal implant system consisting of six hollow PDMS cylinders filled with levonorgestrel crystals (215–217). Figure 8 shows schematically the design of this device, which is implanted in the inner aspect of the woman's upper arm. The drug-release rate is controlled by the total surface area and thickness of the silicone cylinders. Because of the excess of drug at the inner surface, approximately constant release rates are achieved over a period of 5 years (216). Compared to oral contraceptives, implantable long-term systems have two main advantages: (*1*) owing to the elimination of the hepatic first-pass effect, the applied doses can be reduced significantly; and (*2*) avoiding daily application, the compliance and safety of the system are markedly increased.

The utility of controlled-release norgestomet/silicone implants in synchronizing estrus and diagnosing pregnancy in ewes has been investigated by Kesler and Favero (218). The overall estrus and lambing responses were 90 and 67%, respectively; the accuracy of the diagnosis of the pregnancy status was 100%. Refillable and implantable devices containing the anticancer drug 1,3-bis(2-chloroethyl)-1-nitrosourea (BCNU) were investigated by Ueno et al. (219). The release kinetics of various kinds of silicone and silicone–nylon-based systems were studied in dependence of the surface area and wall thickness of the device. Reversible chemical castration is one of the possible applications of RS-49947 ([D-Nal^6, aza-Gly^{10}]-luteinizing hormone-releasing hormone)–silicone elastomer implants, investigated by Burns et al. (220,229). In vitro and in vivo studies have been performed, investigating the effect of drug loading, γ-irradiation, and particle and implant size. The sustained behavioral recovery from unilateral nigrostriatal damage produced by the controlled release of dopamine from a silicone polymer pellet placed into the denervated striatum of rats was studied by Becker et al. (222). Studies of Hirsch et al. (223) deal with the synergistic inhibition of the calcification of glutaraldehyde-pretreated bovine pericardium by $FeCl_3$ and calcium ethanehydroxydiphosphonate (CaEHDP) containing silicone–rubber matrices. Calcification is a frequent cause of the clinical failure of bioprosthetic heart valves fabricated from glutaraldehyde-pretreated porcine aortic valves or glutaraldehyde-pretreated bovine pericardium (GPBP). Twenty-one-day subdermal implants in 3-week-old male rats showed 1% $FeCl_3$–20% CaEHDP silicone–rubber matrices to be most effective for inhibiting GPBP mineralization.

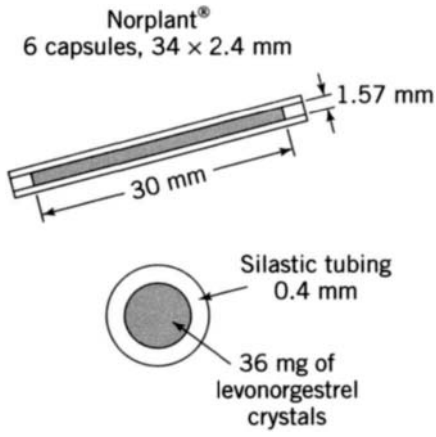


Figure 8. Design and dimensions of the contraceptive system Norplant®. *Source:* Reprinted from Sam (215) with permission from Elsevier Science Publishers B.V.

Intravaginal Systems

Silicone-based intravaginal devices (diaphragms and discs) have been developed by Lee et al. (224,225). They optimized the loading dose of the spermicide Nonoxynol-9 and studied the effect of an additional cosolvent (optimizing drug release) and of storage time.

Ocular Systems

Ocular drug delivery systems based on silicones were developed and tested in vitro and in vivo by Urtti et al. (226–228). Timolol inserts were compared to conventional eyedrops and were found to give similar decreases in intraocular pressure in open-angle glaucoma patients but to produce lower drug concentrations in the blood. Thus, the unwanted absorption of timolol into the systemic circulation could be reduced significantly. Dissolving or dispersing various prodrugs of 5-fluorouracil in silicone oil for ocular drug delivery has been studied by Steffansen et al. (209). The effect of γ-irradiation and exposure to heat on the physicochemical properties of novel silicone-based gentamicin sulfate ocular drug delivery systems has been presented by Bawa and Nandu (230). The mechanical properties were found to be unchanged, whereas the drug-release rates were affected by γ-irradiation as well as exposure to heat. In addition, a certain degradation of the active agent was caused by long-term heat treatment.

Miscellaneous

Li et al. published various articles concerning the preparation and testing of silicone-based matrix tablets (e.g., 231–234). They investigated, for example, the effect of additives like PEG or colloidal silica as well as different shapes and methods of fabrication. Planar dimethylsiloxane matrix systems containing 10 different substituted pyridines at their solubility limit were presented by Chen and Matheson (235) with respect to the drug–polymer interactions. Hydrogen bonding between the pyridines and the polymer matrix was found to be one of the factors governing the release rate. Numerous studies were performed by Sutinen et al. concerning silicone reservoir systems (of various shapes) with different additives to manipulate the release kinetics (236–238). Osmotic (e.g., sodium chloride) and buffering (e.g., Tris buffer) additives are excellent tools to achieve a desired release profile (239,240). Zero-order release kinetics during a considerable time interval were observed for cinnamyl alcohol from spherical PDMS beads in pentane by Lee and Lum (241). In water, however, the corresponding release was completely Fickian. Veterinary controlled-release systems have been developed by Brochart et al. (242). Reservoir devices of different composition were tested and constant release rates were achieved over a period of 22 days.

The use of aqueous silicone latex for the coating of tablets and pellets as well as the impact of heat treatment and the addition of the pore former PEG 8,000 on the mass transport in these systems were presented by Dahl and Sue (56,243). pH-sensitive hydrogels, releasing the drug at enteric pH but not at gastric pH, have been synthesized by γ-irradiation of solutions of *N*-isopropylacrylamide (NIPAAm), acrylic acid (AAc), and bis-vinyl-terminated polydimethylsiloxane (VTPDMS) and tested by Dong and Hoffman (244,245). This property is especially interesting for stomach-irritating active agents like indomethacin. An in vitro study has shown that only a negligible amount of indomethacin is released at pH 1.4 within 24 h, while at pH 7.4 more than 90% of the total drug in the gel is gradually released over 5 h. The effect of propranolol on the prevention of ventricular tachycardia/fibrillation due to acute coronary ischaemia using polyurethane–silicone copolymers was studied in dogs by Siden et al. (246). Loth and Euschen investigated liquid-crystalline side-chain silastomers (247). The type of polysiloxane main chain and the chain length of the PDMS cross-linker as well as the mesogenic group determine the structure and properties of the resulting silastomer. The relationship between the drug-release rate particle size, and swelling of PDMS matrices was studied by Golomb et al. (248). Controlled polymer cracking (osmotically induced) to promote macromolecular release (bovine serum albumin) was presented by Carelli et al. (249). Recent studies of Sheppard and coworkers (250) deal with a new class of controlled-release devices based on micromachined silicone structures. Processes developed for integrated circuit fabrication are used to produce three-dimensional networks that can be loaded with drugs. The advantage of this method is the possibility to gain well-defined pore structures instead of random pore size and shape distributions.

EVA

The general structure of the copolymer EVA is shown in Figure 9. EVA is chemically stable, nontoxic, and biocompatible. Owing to its thermoplasticity, it can be processed by extrusion and injection molding. Two other main advantages of this polymer are (*1*) its high flexibility (which allows avoiding plasticizers) and (*2*) its ability to be sterilized by radiation.

The physicochemical properties of EVA (and thus its permeability properties) are strongly dependent on the comonomer ratio. Not only the *Tg* but also the crystallinity of the resulting copolymer is determined by the relative vinyl acetate content. Generally, both the *Tg* as well as the crystallinity significantly influence the diffusion coefficient (*D*) of a drug (251). In crystalline regions, *D* is several orders of magnitude smaller than in amorphous regions (owing to the reduced chain mobility); in rubbery domains, *D* is higher than in glassy ones (for analogous reasons). Desired permeabilities can easily be achieved by varying the relative vinyl acetate content. Johnson and Nachtrab (252) investigated the influence of the vinyl acetate content on the crystallinity of the resulting copolymer. Pure polyethylene has a crystallinity of 70%. The addition of vinyl acetate into this structure destroys the regularity of the polymer chains, thus reducing crystallinity. Above 50 wt % vinyl acetate content, the copolymer is almost completely amorphous. On the other hand, the *Tg* of EVA varies sig-

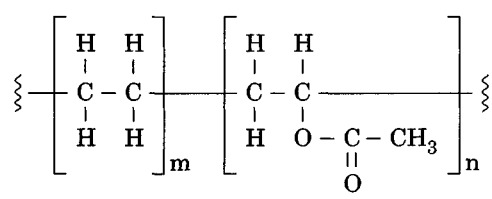


Figure 9. Chemical structure of the copolymer EVA [Poly(ethylene-vinyl acetate)].

nificantly with increasing vinyl acetate content (Fig. 10). This dependence is biphasic: The *Tg* remains constant (approximately −25°C) for 0 wt % up to 50 wt % vinyl acetate and then linearly rises up to 38°C at 100 wt % vinyl acetate (253,254). There are two contrary influences on the diffusion coefficient of a drug with increasing vinyl acetate content: (*1*) a rising *Tg* generally lowers *D*, whereas (*2*) the decreasing crystallinity increases *D*. The resulting permeability properties for the model drug camphor have been studied by Gale and Spitze (255,256). As a result of the two competitive processes, the limiting flux of camphor through EVA goes through a maximum.

Recently, Shin and Byun (257) investigated the permeation of ethinylestradiol through EVA membranes as a function of the drug concentration, vinyl acetate content, membrane thickness, and temperature. Benzocaine was chosen as a model drug by Chen and Lostritto (258) to study the effect of ethanol in EVA membranes. As ethanol leads to significant swelling of the copolymer, the permeability of the drug was markedly increased. The release mechanism from drug containing EVA films was elucidated by Miller et al. (259). Considerable pore collapse was observed during the release process.

Implantable Systems

In 1976 Langer and Folkman opened the door for the controlled release of proteins and other macromolecules from polymeric systems (260). They presented a simple method for incorporating large molecules into noninflammatory polymers (like EVA) and demonstrated sustained release of biologically active agents for periods exceeding 100 days. In that study, pellets were prepared by casting a mixture of an EVA solution and the macromolecular drug into glass molds. No inflammation was observed after implantation into the eyes of rabbits. The in vitro and in vivo release of soybean trypsin inhibitor and tumor angiogenesis factor was investigated. Langer and coworkers studied the use of EVA in various different controlled drug delivery systems. For example, they developed a new fabrication technique (261), leading to more uniform drug distributions in the EVA matrices and higher reproducibilities of the release kinetics. A mixture of powdered protein and polymer solution is cast at −80°C and dried at −20°C and subsequently 20°C. The effect of drug particle size, drug loading, and matrix coating has also been investigated. They observed three phases: (*1*) an initial burst, (*2*) a period of approximately $t^{1/2}$ release, and (*3*) a final period when release tapered off. The initial burst effect presumably is due to protein dissolution on the surface. As the macromolecules are too large to diffuse through a pure polymer film, it is possible that sustained release occurs via diffusion through channels in the matrix. The incorporation of the macromolecules during casting may introduce such channels through which the dissolved drug can diffuse. Thus, matrix characteristics (e.g., porosity and tortuosity) are very important for the resulting release rate. Figure 11 shows that the release rate increases with increasing drug particle size, probably due to the formation of larger channels or pores within the polymer matrix. Similarly, increased loadings may provide simple pathways (lower tortuosity) and greater porosity for diffusion, both of which facilitate the movement of water into and proteins out of the matrix (Fig. 12). The exposure to organic solvent can be avoided when mixing drug and EVA powders below the *Tg* of the polymer and compressing the mixture at a temperature above the glass-transition point (262). The mechanism of drug release (dissolution/diffusion) was studied in more detail 1989 by Saltzman and Langer (263). They developed predictive models using percolation concepts to describe pore topology and continuum models of diffusion/dissolution to describe protein movement at each single pore, and they measured pore size distributions. Up to 10-fold reversible increases in the release rate of incorporated molecules within EVA copolymers were observed when ap-

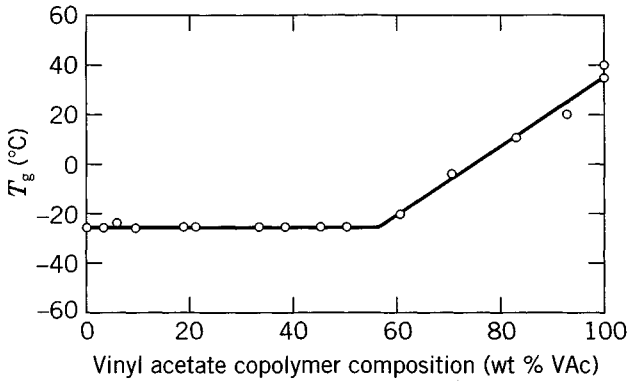


Figure 10. Glass-transition temperature of EVA, depending on the copolymer composition. *Source:* Reprinted from Baker (214) with permission from John Wiley & Sons.

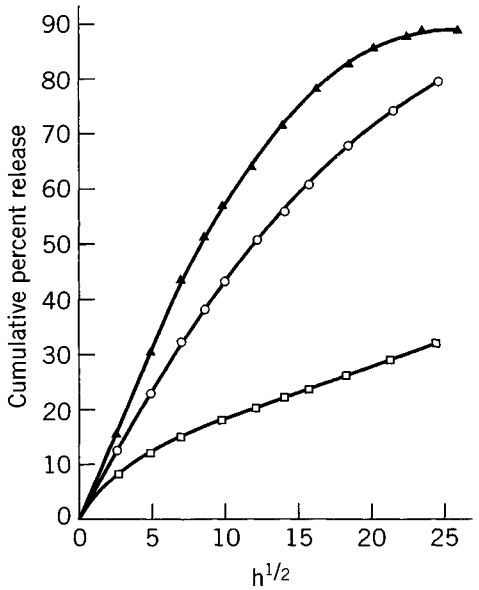


Figure 11. Particle size effect on cumulative release. Bovine serum albumin particles of three size ranges (<75 μm [empty squares], 75–250 μm [empty circles], and 250–425 μm [filled triangles]) were incorporated into EVA matrices. *Source:* Reprinted from Rhine et al. (261) with permission from APhA and ACS.

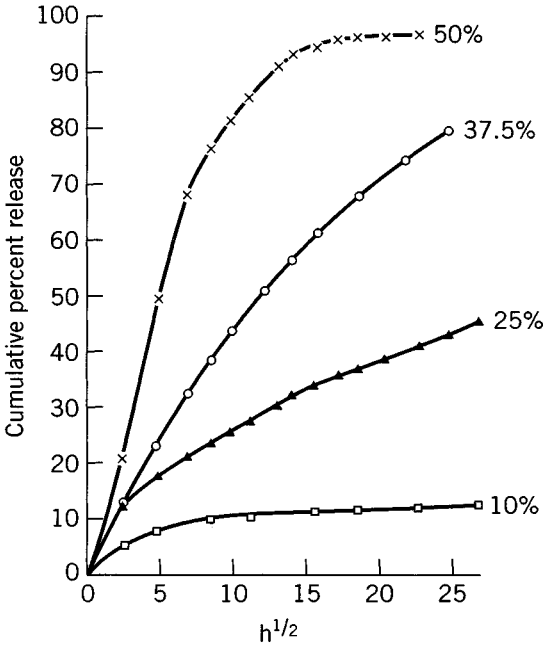


Figure 12. Loading effect on cumulative release. EVA matrices with four different loadings of bovine serum albumin (by weight) have been investigated. *Source:* Reprinted from Rhine et al. (261) with permission from ACS.

plying ultrasound, the increase being in proportion to the intensity of ultrasound (264). The treatment of Parkinson's disease is a potential application of a system releasing dopamine from EVA matrix discs for up to 65 days following stratial implantation. Drug release occurs through a single cavity present on one side of the disc, which is otherwise fully coated with an additional, impermeable layer of EVA (265). Langer and coworkers also embedded a drug and a small magnet into an EVA matrix and applied a magnetic field on this system (266). The presented drug release was increased up to 30 times above baseline levels. Using DSC and TMA, they studied the release of proteins from different types of EVA matrices over a wide range of temperatures. The observed effects could be related to the temperature-dependent diffusivity of the drug and elastic modulus of EVA (267). Another important system Langer et al. studied is an implantable, glucose-sensitive device releasing insulin. Feedback control is mediated by the glucose oxidase enzyme immobilized to Sepharose beads, which are incorporated along with insulin into an EVA matrix. When glucose in solution enters the device, gluconic acid is produced, causing a drop in the microenvironmental pH of the matrix. This fall in pH results in a rise in insulin solubility and consequently a rise in the insulin release rate from the matrix (268). Recently, they elucidated the role of the burst effect in an essentially zero-order controlled-release coated hemispherical EVA device (269). The macromolecular active agent bovine serum albumin (BSA) leaves the system through a single, small orifice.

The prevention of calcification of aortic walls using implants based on EVA and the calcium salt of ethanehydroxybisphosphonate (CaEHBP) and ferric chloride ($FeCl_3$) have been studied by Vyavahare et al. (270). They developed films releasing the drugs continuously over 60 days without any rapid burst phase. Calcification of the aortic walls was inhibited synergistically by the two active agents. Studies of Lesser et al. (271) investigate the in vitro and in vivo release of subcutaneous hydromorphone implants designed for the treatment of cancer pain. They developed and tested an implantable opioid delivery device capable of releasing the potent drug subcutaneously at a constant rate for 4 weeks. The treatment of Alzheimer's disease might be an application of the EVA discs prepared by Krewson et al. (272), releasing a protein (nerve growth factor [NGF]).

Intravaginal Systems

A very well known application of EVA in controlled-release devices is the intravaginal release of steroidal contraceptives, as in Progestasert® (marketed by ALZA Corporation). A liquid silicone oil serves as inert carrier medium for progesterone, surrounded by a controlling barrier of EVA (T-shaped reservoir device) (273–276). Barium sulfate is added to render the system radiopaque. Figure 13 shows a scheme of the device. The in utero release rate of the drug in humans remains approximately constant over a period of 400 days: 65 ± 10 μg/day (277). This is due to the constant progesterone concentration at the inner surface of the EVA copolymer membrane. Drug molecules leaving the reservoir are replaced due to the excess of progesterone in the silicone oil (initial concentration > solubility). Compared with conventional contraceptives, the decisive advantage of this system is the protection from pregnancy for more than 1 year without the need of daily self-medication or other regular patient action.

Ocular Systems

Another well-known system using EVA membranes is the Ocusert® (ALZA Corporation). It is placed in the conjunc-

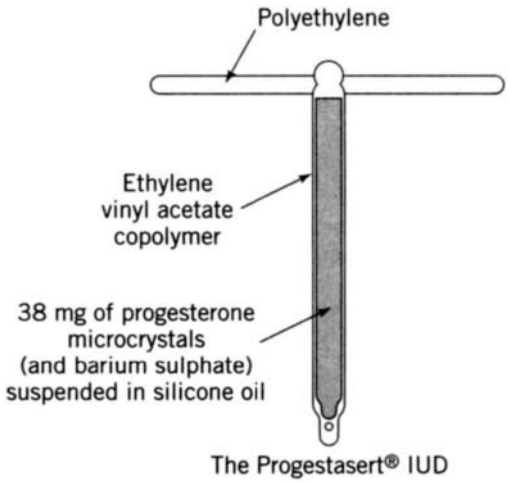


Figure 13. Scheme of Progestasert®, an intrauterine progesterone contraceptive system. *Source:* Reprinted from Sam (215) with permission from Elsevier Science Publishers B.V.

tival cul-de-sac to release pilocarpine during 1 week. The drug is dispersed in alginic acid and surrounded by two EVA membranes, controlling the release rate (278–281). As in Progestasert®, excess of drug (11.0 mg in Pilo-40, 5.0 mg in Pilo-20) leads to a constant drug concentration at the inner membrane surface of this reservoir system and subsequently to constant release rates, as shown in Table 5.

Miscellaneous

Miyazaki et al. (283) investigated the factors affecting the release patterns of 5-fluorouracil from EVA matrices. The influence of the surface area, temperature, pH, and an additional coating on the release characteristics of the devices has been studied. Blends of EVA and the bioerodable poly(D, L-lactic acid) (PLA) for controlled-release applications have been presented by Dollinger and Sawan (284). The PLA mass loss was evaluated as a function of blending technique employed, incubation media, and molecular weight of the polymer. Spherical devices composed of a core and a shell have been studied by David et al. (285). The core was made of a polymer able to absorb the agent to a large extent (more than 100%), while the shell exhibited both low diffusivity and low capacity. The release rate of an active agent was significantly influenced by the shell properties, such as thickness, nature of polymer, and capacity of absorption for the drug. A one-step preparation method of double-walled microspheres with layers made of PLA and EVA was described by Pekarek et al. (286). This technique takes advantage of the phenomenon of phase separation and can be used to produce spheres of diameters less than 20 μm and up to 1,000 μm. A completely different kind of release system containing EVA was developed by Amsden and Cheng (287). These devices consist of particles of intimately mixed sodium chloride and a protein dispersed in EVA. Protein and NaCl release results from osmotically induced membrane rupture subsequent to water inhibition.

POLY(ETHYLENE OXIDE)

PEG and poly(ethylene oxide) (PEO) are terms for materials containing a multiplicity of connected units of the structure [-CH_2CH_2-O-]. PEG is one subspecies of PEO that contains a hydroxyl group on each end of the chain: HO[-CH_2CH_2-O-]$_n$H.

The physicochemical properties of PEO have been described in detail by Graham (288). Depending on the molecular weight, PEO is a liquid, a waxy solid, or a solid. PEO has a very regular backbone structure, free of sidechains. In the absence of crystallinity, the amorphous material is a rubber with a low Tg, typically -60°C and exhibiting a maximum of Tg at molecular weights in the region of 4,000 Da. Having no chiral centers in the structure and no sidegroups, the polymer is normally highly crystalline, with melting points up to 65–68°C. The crystalline structure of linear PEO has been determined by X-ray diffraction as a 7_2 helix (289). This is a coil containing 3.5 -[CH_2CH_2-O]- groups per turn and a repeat unit of seven such groups. The non-cross-linked polymer swells in water and subsequently dissolves, but it can also be made insoluble by cross-linking.

One major advantage of PEG is its low toxicity: It is approved by the U.S. Food and Drug Administration (FDA) for use in foodstuffs and in pharmaceutical products via injection, topical, or oral routes.

Table 5. Average In Vitro Release Rates of Pilo-20 and Pilo-40

Time (h)	Release rate for Pilo-20 (μg/h)	Release rate for Pilo-40 (μg/h)
0–7	57.6 ± 2.2	108.0 ± 5.0
7–24	25.3 ± 0.6	54.4 ± 2.5
24–168	19.4 ± 0.3	40.4 ± 4.2

Source: Adapted from Ocusert® (Pilocarpine) Ocular Therapeutic System (282) with permission from ALZA Corporation.

Matrix Systems

The drug-release mechanism from monolithic PEO devices depends strongly on the molecular weight (M_w) and the degree of cross-linking of the polymer. Low-M_w PEO dissolves fast, leading to an erosion (polymer dissolution) controlled process. On the contrary, high-M_w PEO swells owing to penetrant uptake and either dissolves (non-cross-linked polymer) or swells until an equilibrium state is reached. Depending on the diffusion characteristics of the incorporated drug, the entire release kinetics will be governed by diffusion, swelling, dissolution, or a combination of these. Apicella et al. (290) investigated the release of etofylline from compression-molded tablets of semicrystalline PEG with M_w of 600,000 and 4,000,000 Da, respectively. While the low-molecular-weight polymer dissolves at a constant rate (continuously delivering the practically immobilized drug), the release from the slowly dissolving high-molecular-weight polymer is exclusively driven by the drug diffusion. Similar results were found by Kim (291). He studied the release kinetics from compressed tablets manufactured with a powder mixture of PEO, a drug, and magnesium stearate. Several factors such as molecular weight, drug loading, drug solubility, the pH of the dissolution medium, and stirring rate were investigated. To provide a constant drug release over a long period of time (>20 h), Kim also produced tablets with a central hole (donut-shaped) (292). The release of theophylline was observed to be zero order for the first 80–90% of the drug. Semicrystalline, cross-linked PEG was used by McNeill and Graham (293) to prepare and study prostaglandin E_2 (PGE_2)–containing vaginal pessaries. To avoid drug degradation during the fabrication process of the device, the PEG hydrogel was swollen with a solution of PGE_2 in an organic solvent and not in water. Approximately zero-order release was achieved for the first 45% of drug from a dry slab in vitro. Laboratory pessaries have been stored at 4°C for more than a year with no significant change in the release profile or degradation of PGE_2.

Miscellaneous

Graham and McNeill (294) studied hydrogels based on PEG with a number average molecular weight of 3,000 to

8,000 Da. Drugs have been classified into five groups showing different release profiles. They also developed and tested morphine-loaded PEG suppositories, showing zero-order release. Urquhart and Theeuwes (ALZA Corporation) have a patent (295) on an orally administrable dispersing device for controlled delivery of drugs, comprising a matrix of nonhydrated PEO and a number of tiny pills dispersed through the polymer matrix. A cellulose–polymer coating controls the release rate. An oral capsule utilizing an aqueous polymer (like PEO) and an oil to control gastrointestinal transit time has been patented by Uemura et al. (Fujisawa Pharmaceutical Co.) (296). The capsule is filled with a substantially anhydrous mixture being in solid or semisolid form consisting of (*1*) a drug or a drug treated by a conventional manner, each of which is in solid form; and (*2*) a drug carrier that is a semisolid mixture comprising an aqueous polymer (e.g., PEO) and a liquid oil (e.g., arachis oil or medium-chain triglyceride). The ratio of the aqueous polymer to the liquid oil by weight is 2:1 to 1:40.

BIBLIOGRAPHY

1. G.S. Rekhi and S.S. Jambhekar, *Drug Dev. Ind. Pharm.* **21**(1), 61–77 (1995).
2. M.R. Harris and I. Ghebre-Sellassie, in J.W. McGinity, ed., *Aqueous Polymeric Coatings for Pharmaceutical Dosage Forms*, 2nd ed., Dekker, New York, 1996, p. 81.
3. Dow Chemical Product Information, *Ethocel® Premium Polymer*, Formular No. 198-1172-1095GW, Dow Chemical Company, Midland, Mich., 1995.
4. H. Arwidsson, *Acta Pharm. Nord.* **3**(1), 25–30 (1991).
5. H. Arwidsson and M. Nicklasson, *Int. J. Pharm.* **56**, 187–193 (1989).
6. R. Hyppölä, I. Husson, and F. Sundholm, *Int. J. Pharm.* **133**, 161–170 (1996).
7. R.C. Rowe, *Int. J. Pharm.* **29**, 37–41 (1986).
8. S. Narisawa, H. Yoshino, Y. Hirakawa, and K. Noda, *Chem. Pharm. Bull.* **41**(2), 329–334 (1993).
9. S. Narisawa, H. Yoshino, Y. Hirakawa, and K. Noda, *Int. J. Pharm.* **104**, 95–106 (1994).
10. S. Narisawa et al., *Chem. Pharm. Bull.* **42**(10), 2131–2134 (1994).
11. J.W. McGinity, ed., *Aqueous Polymeric Coatings for Pharmaceutical Dosage Forms*, 2nd ed., Dekker, New York, 1996.
12. *Aquacoat®—Aqueous Polymeric Dispersion*, technical literature, FMC Corp., Philadelphia, Pa., 1997.
13. *Surelease®—The Aqueous Sustained Release Coating System*, technical literature, Colorcon Ltd., West Point, Pa., 1997.
14. R.K. Chang, C.H. Hsiao, and J.R. Robinson, *Pharm. Technol.* **11**(3), 56–68 (1987).
15. F.W. Goodhart, M.R. Harris, K.S. Murthy, and R.U. Nesbitt, *Pharm. Technol.* **8**(4), 64–71 (1984).
16. B.H. Lippold, B.K. Sutter, and B.C. Lippold, *Int. J. Pharm.* **54**, 15–25 (1989).
17. B. Sutter, Ph.D. Dissertation, University of Düsseldorf, Germany, 1987.
18. R. Bodmeier and O. Paeratakul, *Int. J. Pharm.* **70**, 59–68 (1991).
19. G.M. Derbin, J.B. Dressman, D.C. Heldsinger, and T.A. Wheatley, *Proc. Int. Symp. Controlled Release Bioact. Mater.* **21**, 754–755 (1994).
20. J.B. Dressman et al., *J. Controlled Release* **36**, 251–260 (1995).
21. G.M. Derbin et al., *Pharm. Technol.*, **9**, 70–80 (1996).
22. B.C. Lippold, B.H. Lippold, B.K. Sutter, and W. Gunder, *Drug Dev. Ind. Pharm.* **16**, 1725–1747 (1990).
23. U. Kositprapa, J. Herrmann, and R. Bodmeier, *Pharm. Res.* **10**, S-153 (1993).
24. U. Kositprapa and R. Bodmeier, *Pharm. Res.* **11**, S-235 (1994).
25. U.S. Pat. 4,138,475 (February 6, 1979), J. McAinsh and R.C. Rowe (to idi, Ltd.).
26. M.R. Harris and I. Ghebre-Sellassie, in J.W. McGinity, ed., *Aqueous Polymeric Coatings for Pharmaceutical Dosage Forms*, Dekker, New York, 1989, pp. 63–79.
27. G. Källstrand and B. Ekman, *J. Pharm. Sci.* **72**, 772–775 (1983).
28. G.N. Zentner, G.S. Rork, and K.J. Himmelstein, *J. Controlled Release* **2**, 217–229 (1985).
29. G.S. Rekhi, R.W. Mendes, S.C. Porter, and S.S. Jambhekar, *Pharm. Technol.* **13**, 112–125 (1989).
30. S.P. Li et al., *Pharm. Technol.* **14**(3), 20–24 (1990).
31. R.U. Nesbitt, *Drug Dev. Ind. Pharm.* **20**(20), 3207–3236 (1994).
32. D. Wong and R. Bodmeier, *Eur. J. Pharm. Biopharm.* **42**(1), 12–15 (1996).
33. P. Sakellariou and R.C. Rowe, *Int. J. Pharm.* **125**, 289–296 (1995).
34. B. Lindstedt, M. Sjöberg, and J. Hjärtstam, *Int. J. Pharm.* **67**, 21–27 (1991).
35. B. Lindstedt, G. Ragnarsson, and J. Hjärtstam, *Int. J. Pharm.* **56**, 261–268 (1989).
36. J. Hjärtstam, K. Borg, and B. Lindstedt, *Int. J. Pharm.* **61**, 101–107 (1990).
37. W. Gunder, B.H. Lippold, and B.C. Lippold, *Eur. J. Pharm. Sci.* **3**, 203–214 (1995).
38. G.H. Zhang et al., *Proc. Int. Symp. Controlled Release Bioact. Mater.* **17**, 194–195 (1990).
39. D. Wong, Ph.D. Dissertation, University of Texas at Austin, 1994.
40. R. Bodmeier and D. Wong, *Eur. J. Pharm. Biopharm.* **42**, 12–15 (1996).
41. L.E. Appel and G.M. Zentner, *Pharm. Res.* **8**, 600–604 (1991).
42. E.M.G. van Bommel, J.G. Fokkens, and D.J.A. Crommelin, *J. Controlled Release* **10**, 283–292 (1989).
43. E.M.G. van Bommel, J.G. Fokkens, and D.J.A. Crommelin, *Acta Pharm. Technol.* **35**(4), 232–237 (1989).
44. S.C. Porter, *Controlled Release Symposium*, Colorcon Inc., West Point, Pa., 1990, p. I-1-54.
45. U. Iyer, W.H. Hong, N. Das, and I. Ghebre-Sellassie, *Pharm. Technol.* **14**(9), 68–87 (1990).
46. R. Bodmeier and O. Paeratakul, *J. Liq. Chromatogr.* **14**, 365–375 (1991).
47. R. Bodmeier and O. Paeratakul, *Int. J. Pharm.* **103**, 47–54 (1994).
48. R. Bodmeier and O. Paeratakul, *Int. J. Pharm.* **152**, 17–26 (1997).
49. G.S. Banker and G.E. Peck, *Pharm. Technol.* **5**, 55–61 (1981).
50. N.H. Parikh, S.C. Porter, and B.D. Rohera, *Pharm. Res.* **10**, 525–534 (1993).

51. S.T. Yang, G.V. Savag, J. Weiss, and I. Ghebre-Sellassie, *Int. J. Pharm.* **86**, 247–257 (1990).
52. Y. Fukumori et al., *Chem. Pharm. Bull.* **36**, 4927–4932 (1988).
53. S.T. Yang and I. Ghebre-Sellassie, *Int. J. Pharm.* **60**, 109–124 (1990).
54. M. Hossain and J.W. Ayres, *Pharm. Technol.* **14**, 72–82 (1990).
55. H. Nakagami, T. Keshikawa, M. Matsumura, and H. Tsukamoto, *Chem. Pharm. Bull.* **39**, 1837–1842 (1991).
56. T.C. Dahl and I.T. Sue, *Drug Dev. Ind. Pharm.* **16**, 2097–2107 (1990).
57. N.H. Shah et al., *Pharm. Technol.* **18**(10), 140–149 (1994).
58. C.A. Gilligan and A. Li Wan Po, *Int. J. Pharm.* **73**, 51–68 (1991).
59. M.R. Harris, I. Ghebre-Sellassie, and R.U. Nesbitt, *Pharm. Technol.* **10**(9), 102–107 (1986).
60. D. Hutchings, B. Kuzmak, and A. Sakr, *Pharm. Res.* **11**(10), 1474–1478 (1994).
61. R. Bodmeier and O. Paeratakul, *Drug Dev. Ind Pharm.* **20**, 1517–1533 (1994).
62. R. Bodmeier and O. Paeratakul, *Pharm. Res.* **11**(6), 882–888 (1994).
63. P. Bansal, S. Vasireddy, F. Plakogiannis, and D. Parikh, *J. Controlled Release* **27**, 157–163 (1993).
64. N. Sarisuta and K. Punpreuk, *J. Controlled Release* **31**, 215–222 (1994).
65. L. Maganti and M. Celik, *Int. J. Pharm.* **103**, 55–67 (1994).
66. L. Maganti and M. Celik, *Proc. 6th Int. Conf. Pharm. Technol.*, 1992, pp. 117–125.
67. R.-K. Chang and E.M. Rudnic, *Int. J. Pharm.* **70**, 261–270 (1991).
68. S.R. Béchard and J.C. Leroux, *Drug Dev. Ind. Pharm.* **18**(18), 1927–1944 (1992).
69. S.A. Altaf, S.W. Hoag, and J.W. Ayers, *Proc. Int. Symp. Controlled Release Bioact. Mater.* **22**, 290–291 (1995).
70. A.G. Ozturk et al., *J. Controlled Release* **14**, 203–213 (1990).
71. J.B. Dressman, B.O. Palsson, A.G. Ozturk, and S.S. Ozturk, in I. Ghebre-Sellassie, ed., *Multiparticulate Oral Drug Delivery*, Dekker, New York, 1994, pp. 285–306.
72. G. Zhang, J.B. Schwartz, and R.L. Schnaare, *Pharm. Res.* **8**(3), 331–335 (1991).
73. G. Ragnarsson et al., *Int. J. Pharm.* **79**, 223–232 (1992).
74. R.U. Nesbitt, M. Mahjour, N.L. Mills, and M.B. Fawzi, *J. Controlled Release* **32**, 71–77 (1994).
75. *Ethylcellulose*, technical information, Shin-Etsu Chem. Inc., Tokyo, Japan, 1991.
76. P.R. Katikaneni, S.M. Upadrashta, S.H. Neau, and A.K. Mitra, *Int. J. Pharm.* **123**, 119–125 (1995).
77. J.D. Bonny and H. Leuenberger, *Pharm. Acta Helv.* **68**, 25–33 (1993).
78. A. Stamm and J.C. Tritsch, *Drug Dev. Ind. Pharm.* **12**, 2337–2353 (1986).
79. S.M. Upadrashta, P.R. Katikaneni, G.A. Hileman, and P.R. Keshary, *Drug Dev. Ind. Pharm.* **19**, 449–460 (1993).
80. S.M. Upadrashta et al., *Int. J. Pharm.* **112**, 173–179 (1994).
81. G. Shlieout and G. Zessin, *Drug Dev. Ind. Pharm.* **22**(4), 313–319 (1996).
82. P.B. Deasy, *Microencapsulation and Related Drug Processes*, Dekker, New York, 1984, pp. 97–117.
83. R. Bodmeier and H. Chen, *J. Controlled Release* **10**, 167–175 (1989).
84. R. Bodmeier, H. Chen, P. Tyle, and P. Jarosz, *J. Controlled Release* **15**, 65–77 (1991).
85. H.-P. Huang and I. Ghebre-Sellassie, *J. Microencapsul.* **6**(2), 219–225 (1989).
86. R. Bodmeier and H. Chen, *J. Controlled Release* **12**, 223–233 (1990).
87. R. Bodmeier and J. Wang, *J. Pharm. Sci.* **82**(2), 191–194 (1993).
88. C.M. Chang and R. Bodmeier, *Int. J. Pharm.* **130**, 187–194 (1996).
89. S.J. Sveinsson, T. Kristmundsdóttir, and K. Ingvarsdóttir, *Int. J. Pharm.* **92**, 29–34 (1993).
90. J. Wallace, in J. Swarbrick and J.C. Boylan, eds., *Encyclopedia of Pharmaceutical Technology*, vol. 2, Dekker, New York, 1990, pp. 319–337.
91. Eastman Chemical Company, *Cellulose Esters for Pharmaceutical Drug Delivery*, Publ. EFC-223A, 2, Eastman Chemical Company, Kingsport, Tenn., 1995.
92. G. Santus and R.W. Baker, *J. Controlled Release* **35**, 1–21 (1995).
93. F. Theeuwes, *J. Pharm. Sci.* **64**, 1987–1991 (1975).
94. G.M. Zentner, G.S. Rork, and K.J. Himmelstein, *J. Controlled Release* **1**, 269–282 (1985).
95. L.E. Appel, J.H. Clair, and G.M. Zentner, *Pharm. Res.* **9**(12), 1664–1667 (1992).
96. M. Herbig, J.R. Cardinal, R.W. Korsmeyer, and K.L. Smith, *J. Controlled Release* **35**, 127–136 (1995).
97. P. Schultz, I. Tho, and P. Kleinebudde, *J. Controlled Release* **47**, 191–199 (1997).
98. P. Schultz and P. Kleinebudde, *J. Controlled Release* **47**, 181–189 (1997).
99. C. Bindschaedler, R. Gurny, E. Doelker, and N.A. Peppas, *J. Colloid Interface Sci.* **108**, 75–82, 83–94 (1985).
100. C. Bindschaedler, R. Gurny, and E. Doelker, *J. Pharm. Pharmacol.* **39**, 335–338 (1986).
101. C. Bindschaedler, R. Gurny, and E. Doelker, *J. Pharm. Sci.* **76**(6), 455–460 (1987).
102. R. Bodmeier and H. Chen, *Drug Dev. Ind. Pharm.* **17**(13), 1811–1822 (1991).
103. M. Kelbert and S.R. Béchard, *Drug Dev. Ind. Pharm.* **18**(5), 519–538 (1992).
104. J.-H. Guo, *Drug Dev. Ind. Pharm.* **19**(13), 1541–1555 (1993).
105. S.H. Wu, W. Hopkins, R. Fengl, and D. Wyatt, *Proc. Int. Symp. Controlled Release Bioact. Mater.* **23**, 53–54 (1996).
106. Eastman Chemical Company, *Cellulose Esters*, technical literature, Eastman Chemical Company, Kingsport, Tenn., 1993.
107. Eastman Chemical Company, *Cellulose Esters and Oxidized Cellulose*, Publ. No. EFC-216, Eastman Chemical Company, Kingsport, Tenn., 1991.
108. D.L. Gardner and D.J. Fink, *Polym. Prepr.* **21**(1), 102–103 (1980).
109. A.J. Shukla and J.C. Price, *Pharm. Res.* **6**(5), 418–421 (1989).
110. A.J. Shukla and J.C. Price, *Pharm. Res.* **8**(11), 1396–1400 (1991).
111. Y. Pongpaibul and C.W. Whitworth, *Int. J. Pharm.* **33**, 243–248 (1986).
112. Y. Pongpaibul and C.W. Whitworth, *Drug Dev. Ind. Pharm.* **12**, 2387–2402 (1986).
113. O.L. Sprockel et al., *Drug Dev. Ind. Pharm.* **15**, 1393–1404 (1989).

114. W. Prapaitrakul and C.W. Whitworth, *Drug Dev. Ind. Pharm.* **15**, 2049–2053 (1989).
115. C.S.L. Chiao and J.C. Price, *Pharm. Res.* **6**, 517–520 (1989).
116. T.C. Dahl et al., *J. Controlled Release* **14**, 1–10 (1990).
117. E. Doelker, *Polym. Sci.* **107**, 199–265 (1993).
118. K.D. Belfield and G. Garcia, *Proc. Am. Chem. Soc. Polym. Mater. Sci. Eng.* **76**, 383–384 (1997).
119. A. Hebeisch and J.T. Guthrie, *The Chemistry and Technology of Cellulosic Copolymers*, Springer-Berlin, New York, 1981.
120. Y. Tabata and Y. Ikada, *Biomaterials* **9**, 356–362 (1988).
121. F.C. Masilungan and N.G. Lordi, *Int. J. Pharm.* **20**, 295–305 (1984).
122. C.A. Entwistle and R.C. Rowe, *J. Pharm. Pharmacol.* **31**, 269–272 (1979).
123. A.O. Okhamafe and P. York, *Pharm. Res.* **2**, 19–22 (1985).
124. P. Sakellariou, R.C. Rowe, and E.F.T. White, *Int. J. Pharm.* **27**, 267–277 (1985).
125. A.O. Okhamafe and P. York, *J. Pharm. Sci.* **77**, 438–443 (1988).
126. T.T. Kararli, J.B. Hurlbut, and T.E. Needham, *J. Pharm. Sci.* **79**, 845–848 (1990).
127. K. Johnson, R. Hathaway, P. Leung, and R. Franz, *Int. J. Pharm.* **73**, 197–208 (1991).
128. E. Doelker, in L. Brannon-Peppas and R.S. Harland, eds., *Absorbent Polymer Technology*, Elsevier, Amsterdam, 1990, pp. 125–146.
129. U. Conte et al., *Biomaterials* **9**, 489–493 (1988).
130. B. Narasimhan and N.A. Peppas, in K. Park, ed., *Controlled Drug Delivery*, American Chemical Society, Washington, D.C. 1997, pp. 529–558.
131. M.M. Talukdar, I. Vinckier, P. Moldenaers, and R. Kinget, *J. Pharm. Sci.* **85**, 537–540 (1996).
132. N.A. Peppas, R. Gurny, E. Doelker, and P. Buri, *J. Membr. Sci.* **7**, 241–253 (1980).
133. P. Colombo, *Adv. Drug Delivery Rev.* **11**, 37–57 (1993).
134. P. Colombo et al., *J. Pharm. Sci.* **84**, 991–997 (1995).
135. P. Colombo et al., *Int. J. Pharm.* **88**, 99–109 (1992).
136. B. Narasimhan and N.A. Peppas, *Adv. Polym. Sci.* **128**, 157–207 (1997).
137. P.I. Lee and N.A. Peppas, *J. Controlled Release* **6**, 207–215 (1987).
138. L. Brannon-Peppas and N.A. Peppas, in L. Brannon-Peppas and R.S. Harland, eds., *Absorbent Polymer Technology*, Elsevier, Amsterdam, 1990, pp. 67–102.
139. L. Brannon-Peppas, in L. Brannon-Peppas and R.S. Harland, eds., *Absorbent Polymer Technology*, Elsevier, Amsterdam, 1990, pp. 45–66.
140. H. Yamakita, T. Maejima, and T. Osawa, *Biol. Pharm. Bull.* **18**, 1409–1416 (1995).
141. C.H. Liu et al., *J. Pharm. Pharmacol.* **47**, 360–364 (1995).
142. G. Xu and H. Sunada, *Chem. Pharm. Bull.* **43**, 483–487 (1995).
143. A.T. Pham and P.I. Lee, *Pharm. Res.* **11**, 1379–1384 (1994).
144. J.E. Ahlskog, M.D. Muenter, P.A. Bailey, and P.M. Miller, *Clin. Neuropharmacol.* **14**, 214–227 (1991).
145. W.C. Koller et al., *Clin. Neuropharmacol.* **14**, 322–329 (1991).
146. P. Colombo et al., *Acta Pharm. Technol.* **33**, 15–20 (1987).
147. P. Colombo et al., *Int. J. Pharm.* **63**, 43–48 (1990).
148. R. Bettini et al., *Eur. J. Pharm. Sci.* **2**, 213–219 (1994).
149. Eur. Pat. EP 598 309 A2 (June 25, 1994), P. Colombo et al. (to Inverni della Beffa S.p.A.).
150. U. Conte, L. Maggi, P. Colombo, and A. La Manna, *J. Controlled Release* **26**, 39–47 (1993).
151. B. Perez-Marcos et al., *J. Pharm. Sci.* **85**, 330–334 (1996).
152. R. Bhardwaj and J. Blanchard, *J. Pharm. Sci.* **85**, 915–919 (1996).
153. S. Anlar et al., *Pharm. Res.* **11**, 231–236 (1994).
154. S.Y. Lin et al., *Biomater. Artif. Cells Artif. Organs* **17**, 189–203 (1989).
155. K.P.R. Chowdary and G.G. Sankar, *Drug Dev. Ind. Pharm.* **23**, 325–330 (1997).
156. K. Lehmann, in J.W. McGinity, ed., *Aqueous Polymeric Coatings for Pharmaceutical Dosage Forms*, 2nd ed., Dekker, New York, 1996, pp. 101–176.
157. *Röhm Eudragit®*, Technical Literature Folder, Röhm, Darmstadt, Germany, 1996.
158. C.D. Melia, B.R. Hansraj, K.A. Khan, and I.R. Wilding, *Pharm. Res.* **8**(7), 899–902 (1991).
159. R.-K. Chang, J.C. Price, and C. Hsiao, *Drug Dev. Ind. Pharm.* **15**(3), 361–372 (1989).
160. R. Bodmeier and O. Paeratakul, *J. Pharm. Sci.* **79**(10), 925–928 (1990).
161. R. Bodmeier, X. Guo, R.S. Sarabia, and P.F. Skultety, *Pharm. Res.* **13**, 52–56 (1996).
162. K. Knop, *Eur. J. Pharm. Sci.* **4**, 293–300 (1996).
163. T.E. Beckert, E. Lynenskjold and H.-U. Petereit, *Proc. Int. Symp. Controlled Release Bioact. Mater.* **24**, 1031–1032 (1997).
164. X. Guo, Ph.D. Dissertation, University of Texas at Austin, 1996.
165. S.S. Jambhekar, P.J. Breen, and Y. Rojanasakul, *Drug Dev. Ind. Pharm.* **13**(15), 2789–2810 (1987).
166. R.-K. Chang and C. Hsiao, *Drug Dev. Ind. Pharm.* **15**(2), 187–196 (1989).
167. S.P. Li, K.M. Feld, and C.R. Kowarski, *Drug Dev. Ind. Pharm.* **17**(12), 1655–1683 (1991).
168. S.P. Li, K.M. Feld, and C.R. Kowarski, *Drug Dev. Ind. Pharm.* **23**(7), 623–631 (1997).
169. C.-C. Kao, S.-C. Chen, and M.-T. Sheu, *J. Controlled Release* **44**, 263–270 (1997).
170. S. Narisawa et al., *Pharm. Res.* **11**(1), 111–116 (1994).
171. S. Narisawa et al., *J. Pharm. Sci.* **85**(2), 184–188 (1996).
172. S. Narisawa et al., *J. Controlled Release* **33**, 253–260 (1995).
173. K. Amighi and A.J. Moes, *Drug Dev. Ind. Pharm.* **21**(20), 2355–2369 (1995).
174. I. Husson et al., *J. Controlled Release* **17**, 163–174 (1991).
175. K. Lehmann, H.-U. Petereit, and D. Dreher, *Drugs Made in Germany* **37**, 53–60 (1994).
176. M.-P. Flament et al., *Pharm. Technol. Eur.* **6**, 2–5 (1994).
177. R. Bodmeier, *Eur. J. Pharm. Biopharm.* **43**, 1–8 (1997).
178. S.A.M. Abdel-Aziz and W. Anderson, *J. Pharm. Pharmacol.* **28**, 801–805 (1976).
179. S.A.M. Abdel-Aziz, W. Anderson, and P.A.M. Armstrong, *J. Appl. Polym. Sci.* **19**, 1181–1192 (1975).
180. R.S. Okor, *J. Appl. Polym. Sci.* **39**, 43–48 (1990).
181. S. Blanchon et al., *Int. J. Pharm.* **72**, 1–10 (1991).
182. M.R. Jenquin, S.M. Liebowitz, R.E. Sarabia, and J.W. McGinity, *J. Pharm. Sci.* **79**(9), 811–816 (1990).
183. M.R. Jenquin, R.E. Sarabia, S.M. Liebowitz, and J.W. McGinity, *J. Pharm. Sci.* **81**(10), 983–989 (1992).

184. M.R. Jenquin and J.W. McGinity, *Int. J. Pharm.* **101**, 23–34 (1994).
185. R. Bodmeier and O. Paeratakul, *Int. J. Pharm.* **59**, 197–204 (1990).
186. R. Bodmeier and O. Paeratakul, *Pharm. Res.* **6**(8), 725–730 (1989).
187. R. Bodmeier and O. Paeratakul, *J. Pharm. Sci.* **79**(1), 32–36 (1990).
188. R. Bodmeier and O. Paeratakul, *Int. J. Pharm.* **96**, 129–138 (1993).
189. R.S. Okor, S. Otimenyin, and I. Ijeh, *J. Controlled Release* **16**, 349–354 (1991).
190. S. Benita, A. Hoffman and M. Donbrow, *J. Pharm. Pharmacol.* **37**, 391–395 (1985).
191. M. Donbrow, A. Hoffman, and S. Benita, *J. Microencapsul.* **12**(3), 273–285 (1995).
192. R.S. Okor, *J. Controlled Release* **12**, 195–200 (1990).
193. M. Kawata, M. Nakamura, S. Goto, and T. Aoyama, *Chem. Pharm. Bull.* **34**(6), 2618–2623 (1986).
194. Y. Kawashima et al., *J. Controlled Release* **16**, 279–290 (1991).
195. Y. Kawashima et al., *J. Pharm. Sci.* **78**(1), 68–72 (1989).
196. Y. Kawashima et al., *Chem. Pharm. Bull.* **40**(1), 196–201 (1992).
197. Y. Kawashima et al., *Chem. Pharm. Bull.* **41**(1), 191–195 (1993).
198. R. Bodmeier, H. Chen, P. Tyle, and P. Jarosz, *J. Microencapsul.* **8**(2), 161–170 (1991).
199. M.G. Vachon and J.G. Nairn, *J. Microencapsul.* **12**(3), 287–305 (1995).
200. T. Kristmundsdóttir, Ó.S. Gudmundsson, and K. Ingvarsdóttir, *Int. J. Pharm.* **137**, 159–165 (1996).
201. J. Traue and H. Kala, *Pharmazie* **39**, 233–237 (1984).
202. J. Traue and H. Kala, *Pharmazie* **39**, 331–333 (1984).
203. H. Takeuchi, T. Handa, and Y. Kawashima, *Drug Dev. Ind. Pharm.* **15**, 1999–2016 (1989).
204. S.Y. Lin and Y.H. Kao, *Pharm. Res.* **8**, 919–924 (1991).
205. G.F. Palmieri, P. Wehrle, and A. Stamm, *Drug Dev. Ind. Pharm.* **20**, 2859–2879 (1994).
206. M.S. Kislalioglu et al., *J. Pharm. Sci.* **80**(8), 799–804 (1991).
207. D.B. Beten and A.J. Moes, *Int. J. Pharm.* **103**, 243–251 (1994).
208. U.V. Banakar, in M.A. Kohudic, ed., *Advances in Controlled Delivery of Drugs*, Technomic Publishing, Lancaster, Pa., 1994, pp. 134–138.
209. A.G. Thombre and J.R. Cardinal, in J. Swarbrick and J.C. Boylan, eds., *Encyclopedia of Pharmaceutical Technology*, vol. 2, Dekker, New York, 1990, pp. 71–72.
210. J. Crank and G.S. Park, *Diffusion in Polymers*, Academic Press, London and New York, 1968, pp. 54–58.
211. J. Mazan et al., *Eur. Polym. J.* **28**, 1151–1154 (1992).
212. J.C. Moreau, B. Leclerc, J. Mazan, and G. Couarraze, *J. Mater. Sci.: Mater. Med.* **2**, 243–247 (1991).
213. J.C. Moreau et al., *J. Mater. Sci.: Mater. Med.* **5**, 177–180 (1995).
214. R. Baker, *Controlled Release of Biologically Active Agents*, Wiley, New York, 1986, pp. 156–161.
215. A.P. Sam, *J. Controlled Release* **22**, 35–46 (1992).
216. S. Diaz et al., *Contraception* **25**, 447–456 (1982).
217. S. Diaz et al., *Contraception* **35**, 551–567 (1987).
218. D.J. Kesler and R.J. Favero, *Drug Dev. Ind. Pharm.* **23**, 217–220 (1997).
219. N. Ueno, M.F. Refojo, and L.H. Liu, *J. Biomed. Mater. Res.* **16**, 669–677 (1982).
220. R. Burns, K. Peterson, and L. Sanders, *J. Controlled Release* **14**, 221–232 (1990).
221. R. Burns, G. McRae, and L. Sanders, *J. Controlled Release* **14**, 233–241 (1990).
222. J.B. Becker et al., *Brain Res.* **508**, 60–64 (1990).
223. D. Hirsch et al., *Biomaterials* **14**, 705–711 (1993).
224. C.-H. Lee, P.P. Bhatt, and Y.W. Chien, *J. Controlled Release* **43**, 283–290 (1997).
225. C.-H. Lee, R.E. Bagdon, P.P. Bhatt, and Y.W. Chien, *J. Controlled Release* **44**, 43–53 (1997).
226. A. Urtti, H. Rouhiainen, T. Kaila, and V. Saano, *Pharm. Res.* **11**, 1278–1282 (1994).
227. A. Urtti, J.D. Pipkin, G. Rork, and A.J. Repta, *Int. J. Pharm.* **61**, 235–240 (1990).
228. A. Urtti et al., *Int. J. Pharm.* **61**, 241–249 (1990).
229. B. Steffansen, P. Ashton, and A. Buur, *Int. J. Pharm.* **132**, 243–250 (1996).
230. R. Bawa and M. Nandu, *Biomaterials* **11**, 724–728 (1990).
231. L.C. Li and G.E. Peck, *Drug Dev. Ind. Pharm.* **17**, 27–39 (1991).
232. L.C. Li and Y.-H. Tu, *Drug Dev. Ind. Pharm.* **17**, 2197–2214 (1991).
233. L.C. Li and G.E. Peck, *Drug Dev. Ind. Pharm.* **18**, 333–343 (1992).
234. L.C. Li, *Int. J. Pharm.* **87**, 117–124 (1992).
235. Y. Chen and L.E. Matheson, *Int. J. Pharm.* **94**, 153–160 (1993).
236. R. Sutinen, A. Kovanen, A. Urtti, and P. Paronen, *Int. J. Pharm.* **57**, 149–154 (1989).
237. R. Sutinen, O. Bilbao-Revoredo, A. Urtti, and P. Paronen, *Int. J. Pharm.* **57**, 155–161 (1989).
238. R. Sutinen, A. Urtti, P. Raatikainen, and P. Paronen, *Int. J. Pharm.* **92**, 177–181 (1993).
239. R. Sutinen, A. Urtti, R. Miettunen, and P. Paronen, *Int. J. Pharm.* **62**, 113–118 (1990).
240. R. Sutinen, V. Laasanen, P. Paronen, and A. Urtti, *J. Controlled Release* **33**, 163–171 (1995).
241. P.I. Lee and S.K. Lum, *J. Controlled Release* **18**, 19–24 (1992).
242. H. Brochart, P. Ehret, P. Goldbach, and A. Stamm, *Int. J. Pharm.* **91**, 95–101 (1993).
243. T.C. Dahl and I.T. Sue, *Pharm. Res.* **9**, 398–405 (1992).
244. L.-C. Dong and A.S. Hoffman, *J. Controlled Release* **15**, 141–152 (1991).
245. L.-C. Dong and A.S. Hoffman, *J. Controlled Release* **13**, 21–31 (1990).
246. R. Siden, W.E. Flowers, and R.J. Levy, *Biomaterials* **13**, 764–770 (1992).
247. H. Loth and A. Euschen, *Drug Dev. Ind. Pharm.* **16**, 2077–2095 (1990).
248. G. Golomb, P. Fisher, and E. Rahamim, *J. Controlled Release* **12**, 121–132 (1990).
249. V. Carelli, G. Di Colo, C. Guerrini, and E. Nannipieri, *Int. J. Pharm.* **50**, 181–188 (1989).
250. N.F. Sheppard, Jr., D.J. Mears, and S.W. Straka, *J. Controlled Release* **42**, 15–24 (1996).

251. L.T. Fan and S.K. Singh, *Controlled Release*, Springer-Verlag, Berlin and New York, 1989, pp. 20–44.
252. U. Johnson and G. Nachtrab, *Angew. Makromol. Chem.* **7**, 134–146 (1969).
253. L.E. Nielsen, *J. Polym. Sci.* **42**, 357–366 (1960).
254. F.P. Reding, J.A. Faucher, and R.D. Whitman, *J. Polym. Sci.* **57**, 483–498 (1962).
255. R.M. Gale, M.Sc. Thesis, San Jose State University, San Jose, CA, 1973.
256. R. Gale and L.A. Spitze, *Proc. Int. Symp. Controlled Release Bioact. Mater.* **8**, 183–184 (1981).
257. S.C. Shin and S.Y. Byun, *Int. J. Pharm.* **137**, 95–102 (1996).
258. S.X. Chen and R.T. Lostritto, *J. Controlled Release* **38**, 185–191 (1996).
259. E.S. Miller, N.A. Peppas, and D.N. Winslow, *J. Membr. Sci.* **14**, 79–92 (1983).
260. R. Langer and J. Folkman, *Nature (London)* **263**, 797–800 (1976).
261. W.D. Rhine, D.S.T. Hsieh, and R. Langer, *J. Pharm. Sci.* **69**, 265–270 (1980).
262. J. Cohen, R.A. Siegel, and R. Langer, *J. Pharm. Sci.* **73**, 1034–1037 (1984).
263. W.M. Saltzman and R. Langer, *Biophys. J.* **55**, 163–171 (1989).
264. J. Kost, K. Leong, and R. Langer, *Proc. Natl. Acad. Sci. U.S.A.* **86**, 7663–7666 (1989).
265. M.J. During et al., *Ann. Neurol.* **25**, 351–356 (1989).
266. E.R. Edelman, A. Fiorino, A. Grodzinsky, and R. Langer, *J. Biomed. Mater. Res.* **26**, 1619–1631 (1992).
267. N.F. Sheppard, M.Y. Madrid, and R. Langer, *J. Appl. Polym. Sci.* **46**, 19–26 (1992).
268. L.R. Brown, E.R. Edelman, G.F. Fischel, and R. Langer, *J. Pharm. Sci.* **85**, 1341–1345 (1996).
269. B. Narasimhan and R. Langer, *J. Controlled Release* **47**, 13–20 (1997).
270. N.R. Vyavahare et al., *J. Controlled Release* **34**, 97–108 (1995).
271. G.J. Lesser et al., *Pain* **65**, 265–272 (1996).
272. C.E. Krewson, R. Dause, M. Mak, and W.M. Saltzman, *J. Biomater. Sci., Polym. Ed.* **8**, 103–117 (1996).
273. B.B. Pharriss et al., *Fertil. Steril.* **25**, 915–921 (1974).
274. G. Zador et al., *Contraception* **13**, 559–569 (1976).
275. M. Mall-Haefeli, *Gynaekol. Rundsch.* **18**, 253–262 (1978).
276. K.W. Schweppe, D. Tenhaeff, and D. Rache, *Fortschr. Med.* **96**, 1685–1690 (1978).
277. Alza Corporation, *The Progestasert® Intrauterine Progesterone Contraceptive System*, monograph, ALZA Corporation, Palo Alto, Ca., 1976, pp. 6–7.
278. R.L. Friederich, *Ann. Ophthalmol.* **6**, 1279–1284 (1974).
279. F. Ros, E. Greve, C. Dake, and W. Miller, *Ophthalmologica* **175**, 38–39 (1977).
280. K. Heilmann, *Klin. Monatsbl. Augenheilk.* **170**, 109–119 (1977).
281. K. Heilmann, *Fortschr. Med.* **96**, 1101–1106 (1978).
282. Alza Corporation, *Ocusert® (Pilocarpine) Ocular Therapeutic System*, Alza Corporation, 1984, pp. 1–6.
283. S. Miyazaki, S. Takeuchi, M. Takada, and K. Ishii, *Chem. Pharm. Bull.* **32**, 1633–166 (1984).
284. H.M. Dollinger and S.P. Sawan, *Polym. Prepr.* **31**, 429–430 (1989).
285. H. David, J. Bouzon, and J.M. Vergnaud, *Plast. Rubber Process. Appl.* **11**, 9–16 (1989).
286. K.J. Pekarek, J.S. Jacob, and E. Mathiowitz, *Adv. Mater.* **6**, 684–687 (1994).
287. B. Amsden and Y.-L. Cheng, *J. Controlled Release* **33**, 99–105 (1995).
288. N.B. Graham, in N.A. Peppas, ed., *Hydrogels in Medicine and Pharmacy*, vol. 2, CRC Press, Boca Raton, Fl., 1987, pp. 96–113.
289. J.L. Koenig and A.C. Angood, *J. Polym. Sci.* **8**, 1787–1796 (1970).
290. A. Apicella, M.A. Del Nobile, G. Mensitieri, and L. Nicolais, in R.M. Ottenbrite and E. Chiellini, eds., *Polymers in Medicine*, Technomic Publishing, Lancaster, Pa., 1992, pp. 23–37.
291. C.-J. Kim, *J. Pharm. Sci.* **84**, 303–306 (1995).
292. C.-J. Kim, *Pharm. Res.* **12**, 1045–1048 (1995).
293. M.E. McNeill and N.B. Graham, *J. Controlled Release* **1**, 99–117 (1984).
294. N.B. Graham and M.E. McNeill, *Biomaterials* **5**, 27–36 (1984).
295. U.S. Pat. 4,649,043 (March 10, 1987), J. Urquhart and F. Theeuwes (to Alza Corp.).
296. U.S. Pat. 4,690,822 (September 1, 1987), T. Uemura et al. (to Fujisawa Pharmaceutical Co.).

OLIGONUCLEOTIDE DELIVERY

C. RUSSELL MIDDAUGH
University of Kansas
Lawrence, Kansas

KEY WORDS

Antisense
Cationic lipids
Delivery
Liposomes
Membrane fusion
Microparticles
Oligonucleotide
Peptides
Polymers
Targeting

OUTLINE

Bibliography

One of the immediate consequences of the late twentieth century revolution in molecular biology was the availability of biological macromolecules and their analogues as potential drug substances. The first of these were the recombinant and synthetic proteins and peptides, which can be used as agonists and antagonists of their natural homologues. Recently, polynucleotides have moved to center stage in a similar manner. Thus, the coding regions of entire genes can be used to produce proteins or peptides of therapeutic consequence in situ. Furthermore, shorter oligonucleotides and oligonucleotide analogues can be employed to alter gene expression and, consequently, the in vivo levels of specific proteins. The utility of all four of these macromolecules, proteins, peptides, large polynucleotides, and oligonucleotides, is severely limited by delivery problems that include instability as a consequence of enzymatic, chemical, and conformational processes, as well as targeting, passage across the cytoplasmic membrane, and intracellular processing and targeting. A general consensus seems to be that delivery is in many if not most cases the limiting step in the ultimate therapeutic efficacy of these agents. Not surprisingly, work on the delivery of small molecules as well as proteins, peptides, and DNA plasmids has had a major influence on early attempts to deliver oligonucleotides. In this regard, the reader is referred to the article POLYMERIC SYSTEMS FOR GENE DELIVERY, CHITOSAN AND PINC™ SYSTEMS, in which many of the same problems are addressed with a molecule of related physical properties but of much greater size.

A discussion of oligonucleotide delivery presents several problems due to the embryonic state of the field. For example, a wide variety of different types of oligonucleotide analogues have already been synthesized and examined, with varying degrees of characterization. Besides the prototypic phosphodiester type, forms that have been modified in their backbone, termini, sugar base, and stereochemistry have all been produced (1,2). Because of their increased nuclease resistance (and therefore potentially longer half-life), the backbone-modified analogues have been most intensively studied. These include thiolated forms and the methylphosphonates, as well as the peptide nucleic acids, in which the phosphodiester linker is replaced by an amide moiety (3). For simplicity, here we will primarily consider the phosphodiester and phosphorothiolate forms because up to this point they have received the most extensive examination from a delivery perspective. Both have the property of being polyanions, which is the physical characteristic that might be expected to dominate their chemical and biological properties. These molecules are usually 15–25 nucleosides in length, although both larger and smaller chains are sometimes encountered.

Although not the subject of this review, the potential mechanisms of action of oligonucleotides need to be understood to rationally prepare them as pharmaceuticals (4). In fact, multiple mechanisms of action are recognized, and knowledge of the one (or more) involved in a specific case will usually be helpful. The one most often postulated to be involved in the reduction of expression of specific genes involves complementary binding to mRNA molecules (5). Changes in translation of these hybrids can be due to simple steric effects or result from activation of the enzyme RNase H, which specifically degrades the mRNA component of the complex (potentially releasing the pharmaceutical oligonucleotide for further activity). Alternatively, the oligonucleotide can bind directly to nuclear double-stranded DNA, forming a triple-helical structure that blocks transcription (6). It is a matter of semantics whether we consider such triple-helix-forming oligonucleotides as true "antisense" agents, but from a delivery perspective this is relatively unimportant with the exception of potential nuclear-targeting issues. A third class of oligonucleotides is the RNA-based ribozymes, which themselves manifest enzymatic activity (7,8). These molecules have primarily been used to target mRNA, but they also have the potential to attack nonnucleic acid targets (e.g., proteins) with therapeutic effects. Finally, a fourth type of oligonucleotide with potential therapeutic utility has recently been developed, the so-called aptamers (9,10). These are single- or double-stranded oligonucleotides that bind to sites on proteins that perturb their activity. These molecules are usually selected through combinational approaches and may contain specific tertiary structure that is involved in their biological activity. Extensive discussion of the mechanism of action of oligonucleotides can be found in the references already cited. Although the specific delivery method employed for a particular oligonucleotide will be dependent on the unique situation in which each will be employed, the basic principles of delivery will probably

be similar among the various classes, at least in terms of organ and cellular targeting and entry.

It is convenient to begin our discussion of the oligonucleotide delivery process itself in the middle, at the cellular entry stage, and then consider earlier stages (e.g., pharmacokinetics and tissue targeting), followed by final elements of the delivery pathway (intracellular). It is perhaps somewhat surprising that highly negatively charged oligonucleotides are able to enter cells, but this is certainly the case. Without the assistance of transport facilitators this process is rather inefficient, but it is clear that incubation of cells in culture or administration to animals of phosphodiester or phosphorothiolate oligonucleotides at many sites will result in transport of these molecules into cells. It is fair to say, however, that the mechanism by which this is accomplished is currently unclear. Several non–mutually exclusive hypotheses can be advanced to explain such phenomena. Most postulate the existence of some type of receptor on the cell surface that can mediate entry. This is, of course, the mechanism used by viruses that are able to transfer very large oligonucleotides into cells with high efficiency. Attachment of oligonucleotides to such receptors could then facilitate entry by a number of well-recognized different processes including receptor-mediated endocytosis, pinocytosis, and phagocytosis. What is not known is the identity of the attachment size of oligonucleotides and oligonucleotide complexes on the outer surface of the plasma membrane (11).

Attractive candidates for this binding site are the cell surface proteoglycans. These molecules contain polyanionic polysaccharide side chains attached to proteins that are cycled into cells and back onto the cell surface at a rate commensurate with that seen for cellular entry of oligonucleotides (12). Thus, this can be viewed as one natural ingress pathway for polyanions. Oligonucleotide attachment to these similarly charged entities would presumably be mediated by a cross-linking mechanism through normally present cationic molecules (e.g., divalent metal cations, cationic peptides, proteins) or synthetically produced cationic sites on delivery vehicles (e.g., cationic lipids, polymers, peptides; see later). In support of this pathway, enzymatic removal of the heparan sulfate side chains of cell surface proteoglycans or inhibition of their sulfation produces a dramatic decrease in the passage of oligonucleotides into cells (13,14).

A second potential site of entry is the specialized structures known as caveolae, which have been implicated in transcytotic events. Studies of intramuscular delivery of polynucleotides have specifically identified these cell surface invaginations as potential sites of entry of "naked" polynucleotides (15). These membrane microdomains are enriched in cholesterol and various sphingolipids and are thus regions of positive charge concentration (16). It is therefore possible that they could be involved in direct electrostatic interactions with polynucleotides, although this has yet to be experimentally demonstrated. Certain proteins are also commonly found in these regions, including many involved in signal transduction events (17). These proteins could also provide potential polyanion binding sites and serve as vectors to "piggy-back" polynucleotides into cells. In this regard, it is still entirely possible that one or more unknown proteins located elsewhere in the plasma membrane play a role in cellular entry (e.g., see Ref. 18), but no strong evidence in support of this idea as a general mechanism has yet been presented. Obviously if such proteins exist, efforts could be made to directly target these molecules. Because cell surface proteins are generally recycled from the cell surface into the interior, these molecules potentially provide a facile point of entry. Thus, as will be discussed later, by construction of artificial targeting vehicles, it is possible to attempt to target any cell surface molecule that eventually reenters the cell.

Once inside a cell, an oligonucleotide must be transported to an appropriate site of action. In the case of antisense or catalytic activity, this could be either the cytoplasm or the nucleus. If the target is DNA itself, then nuclear transport will be required. Aptamers, on the other hand, would need to be present at the specific intra- or extracellular location of the target protein. Most evidence suggests that oligonucleotides will initially be found in endosomal compartments (14), although this has been disputed (e.g., see Ref. 19). Thus it may be necessary to provide some active mechanism to release oligonucleotides from these membrane-bound vesicles. In general, the transport of oligonucleotides into the nucleus does not present the problem encountered with DNA plasmids because they are small enough to passively diffuse through nuclear pores. Nevertheless, it is at least possible in principle to either increase the efficiency of this process or enhance nuclear retention. In general, attempts to stimulate endosomal release or nuclear entry have been peptide or lipid based and will be considered below in that light.

By what routes might oligonucleotide-based pharmaceuticals be initially delivered? The major approach has been intravenous infusion, although numerous other routes such as direct injection into specific sites or oral, nasal, or bronchial administration have been examined with some limited success (20,21). Most pharmacokinetic information has been obtained from the intravenous route. In general, it is found that negatively charged oligonucleotides are rapidly distributed throughout the body, with most accumulation in organs such as the kidneys, liver, and spleen, with extensive secretion in the urine over a 24-h period (22–24). Extensive degradation of phosphodiester oligonucleotides is seen, but phosphorothiolate analogues are much more stable at all sites examined (22,23). Equilibration is slower upon intraperitoneal injection and much slower with subcutaneous administration. It should be noted that in many cases oligonucleotides rapidly become protein bound with serum albumin and immunoglobulins, the major binding proteins so far identified (25). Conjugation of oligonucleotides to cholesterol appears to retarget them to low-density lipoproteins and extend their circulation time (26). The exact role of oligonucleotide–protein complexes in oligonucleotide delivery is poorly understood but will be critical to the ultimate design and use of these pharmaceutical agents.

Informative comparative studies of the delivery of oligonucleotides by noninvasive methods have been performed (25). Somewhat surprisingly, direct introduction of 5′-^{32}P-labeled phosphodiester oligonucleotides into the nose, vagina, or rectum or onto the skin of mice resulted

in significant levels of labeled compounds in the blood. Intranasal and oral administration resulted in serum levels 5–20% of those seen with intraperitoneal injection, and levels 5–10 times less than those seen with intravaginal and rectal application. The ocular route was also found to be about 10% as effective as i.p. administration. Interestingly, longer oligonucleotides seems to be more effective when introduced through the eye. The skin route was much less effective. The relative distribution of the oligonucleotide among the various organs examined was very similar.

Although oligonucleotides have some ability to pass through the circulation and enter cells, it is not clear that they will be able in most cases to do this with sufficient efficacy to be effective pharmaceuticals. Thus, efforts are actively underway to design vehicles that better target and more effectively enter and ultimately act at desired sites. Because the mechanisms by which oligonucleotides enter cells are still obscure, most efforts at designing novel vehicles have been semiempirical in nature. We therefore focus on a select number of approaches that currently appear most promising. In general, the design of oligonucleotide delivery vehicles is based on the following criteria. First, one wishes to protect the potentially labile oligonucleotide to the maximum extent possible from destructive processes; enzymatic digestion is probably the chief concern. Secondly, it is usually thought (although see earlier) that the polyanionic character of the oligonucleotide should be reduced or even eliminated. This is usually accomplished by some type of charge neutralization or shielding mechanism, although later-generation oligonucleotide analogues have this built directly into their intrinsic structure. Third, the surface characteristics of any resulting complex should be such that some degree of intrinsic targeting resides in the vehicle. Fourth, some type of endosomal release property might be incorporated. Fifth, nuclear targeting may or may not be included. In some cases, it is thought that creating a particle that could range from submicron to many microns in size might be advantageous. We consider here a number of examples in which one or, usually, more of these properties are included in oligonucleotide delivery vehicles. We discuss only representative examples in which more extensive citations to other examples are included, and the reader is referred to these for more extended considerations.

A potentially very powerful approach to the oligonucleotide delivery problem employs viral vectors. In this method, the nucleic acid sequence of interest is inserted into a viral genome where it can then be expressed as part of the normal viral infection and maturation process. This approach has the great advantage that it avails itself of the natural ability of certain viruses to infect specific cells with high efficiency. The virus particles may also possess intrinsic effective endosomal release mechanisms that further enhance their utility. The most common viruses usually considered for such use are the retro-, adeno-, and adeno-associated viruses. Unfortunately, this technology manifests several serious shortcomings. These include toxic effects often involving potential insertional mutagenesis, immunogenicity (especially upon repeat usage), and the complexity of the vehicle, which introduces major problems in analysis, reproducibility, and manufacturing. For these reasons, unlike the case in gene therapy, viral delivery systems are not generally pursued for oligonucleotide administration if a more classic chemical pharmacological approach seems possible.

By far, the area in which the most effort has been expended has involved the use of liposomes. Two somewhat different approaches have been undertaken. In the first, oligonucleotides are entrapped within anionic lipid vesicles of varied size, structure, and composition. In the second, the oligonucleotides are complexed to cationic lipids of various structural and assembly types. Most recently, the latter approach has received the most attention. We begin with the former.

Employing what is usually considered the "conventional" liposomal approach, several research groups have had some success in enhancing the uptake of oligonucleotides into cells. In an early report, Loke et al. (27) used phosphatidylserine-based liposomes to deliver oligonucleotides into cells in tissue culture. This required polyethylene glycol (PEG) to induce liposomal cell fusion, as well as calcium to enhance loading of the oligonucleotide. Using specially designed minimal volume entrapment approaches, Thierry et al. (28,29) have employed cardiolipin-based liposomes to enhance entry of oligonucleotides 10- to 20-fold into different types of cancer cells, resulting in measurable biological response. Biologically active ribozymes have been successfully delivered in a similar manner using a dipalmitoylphosphatidylglycerol-based system. Several important observations can be made from these and related studies. First, oligonucleotides are substantially protected by the anionic lipid barrier created. Secondly, uptake is enhanced, and activity is detectable. Thirdly, the oligonucleotides seem to be concentrated in the nucleus soon after administration. The efficiency of delivery, however, is not as high as desired for optimal therapeutic effects.

Although evidence exists that even unmodified anionic liposomes can enhance endosomal release to some extent, pH-sensitive liposomes have been designed with the intent of avoiding lysosomal destruction (30,31). The lipid most commonly used for the construction of pH-sensitive liposomes is dioleylphosphatidylethanolamine (DOPE). In bilayers, DOPE can be present in a lamellar form at neutral pH. Under certain conditions of temperature, salt concentration, and pH, however, an inverted hexagonal phase can be induced, which leads to fusogenic behavior. Most importantly from our perspective, low pH leads to protonation of DOPE headgroups, which removes their stabilizing repulsive interactions and induces hexagonal phases. Almost always, however, a second molecule (usually a fatty acid) is necessary to prevent premature formation of fusogenic hexagonal phases under physiological conditions. Examples of such agents include cholesterol hemisuccinate, palmitoylhomocysteine, and oleic acid. Alternatively, as described later, peptides or proteins that undergo pH-dependent conformational changes to structures that can insert into lipid bilayers or create pores can be employed; this latter approach more closely simulates the mechanism used by viruses to escape endosomal degradation, with actual viral proteins sometimes inserted

into a synthetic lipid-based delivery system to achieve this end.

It is clear that such systems work in protein-based systems, at least to a limited extent in that cytoplasmic localization is enhanced. For example, delivery of the diphtheria toxin A fragment by DOPE–oleic acid liposomes results in significant inhibition of protein synthesis, an effect normally prevented by endosomal encapsulation (32). Even more dramatic effects are seen when the diphtheria toxin A fragment is presented in DOPE–cholesterol hemisuccinate liposomes (33). Nevertheless, more than 90% of the protein is still undelivered to the cytoplasm.

Several studies have shown that oligonucleotides can also be delivered in a biologically active form by pH-sensitive liposomes. Inhibition of the replication of retroviruses by oligonucleotides complementary to envelope proteins has been demonstrated, with free polynucleotide unable to induce any effect (34). This area remains relatively undeveloped, however, with few reports of successful in vivo delivery. This seems to reflect, at least in part, the relative instability of pH-sensitive liposomes in a biological milieu including serum. Initial attempts at increasing stability by the inclusion of compounds such as cholesterol have been promising, but at some cost of release efficiency. This should remain an active area of investigation.

Attempts have also been made to deliver oligonucleotides by various types of anionic multilamellar vesicles, which are complexes that contain many lipid bilayers that may or may not be separated by an aqueous space. Cellular delivery can be significantly increased by such structures, and they can provide dramatic protection from nuclease digestion (reviewed in Ref. 35). The fusogenic properties of both unilamellar and multilamellar anionic vesicles has been enhanced by the inclusion of viral proteins into the bilayers. This should in principle permit direct introduction of oligonucleotides into the cytoplasm, bypassing the endosomal degradation route already discussed. Most effort has focused on the Sendai virus fusion proteins (e.g., protein F), although a wide variety of proteins is potentially available for such uses (36) (see later). This method does result in the increase in entry of polynucleotides, but problems of increased structural complexity and immunogenicity are apparent.

By far, the currently most promising liposome-based approach involves the use of cationic lipids (37–39). In this case, preformed cationic liposomes are induced to spontaneously form electrostatic complexes with polynucleotides. Recent structural studies suggest that oligonucleotides are adsorbed between cationic bilayers in these complexes (40,41). Although perhaps not true liposomes, the retention of the bilayer structure in cationic lipid–nucleic acid complexes has resulted in use of the liposome designation. It is clear that some fusion of the original liposomes occurs upon complex formulation (42). The effectiveness of cationic lipids as delivery agents appears to be a complex function of the nature of the lipid itself (headgroup, headgroup charge, fatty acid side chains), absolute concentration, and perhaps most importantly the charge ratio (lipid headgroup to oligonucleotide phosphate). Attempts to establish clear structure–function relationships, however, have so far been unsuccessful, and final formulations are normally based on empirical studies of the aforementioned variables. Several investigations suggest that (1) cationic lipid–nucleic complexes are readily taken up into cells by an ill-defined endocytotic pathway, (2) some enhancement of endosomal release is seen, and (3) nuclear entry and dissociation of complexes may be rate limiting steps in oligonucleotide (and plasmid) activity (43–47). A further accumulation of data will be necessary, however, for a consensus to be reached about the mechanism of transport and activity of these complexes.

Although most work with cationic lipid–nucleic acid complexes has focused on DNA plasmids for gene delivery, a variety of studies of oligonucleotide delivery have appeared. It is apparent that the uptake of cationic lipid–oligonucleotide complexes is usually markedly enhanced relative to both pure oligonucleotides and oligonucleotides encapsulated in conventional anionic lyposomes (37–39). Most work has focused on commercially available cationic lipids such as *N*-[1-(2,3-dioleoyloxy)propyl]-*N*,*N*,*N*-trimethylammonium chloride (DOTMA), dioctadecylamidoglycyl spermine (DOGS), 1,2-dioleoyl-3-trimethylammonium propane (DOTAP), and dimethyldioctadecylammonium bromide (DDAB) (which also often include a helper lipid such as dioleylphosphatidylethanolamine [DOPE] or cholesterol), but as second-generation cationic lipids become increasingly available, we can expect to see a reemphasis on these improved delivery vehicles. It is also clear that cationic lipid–oligonucleotide complexes provide some protection against nuclease digestion, although the relative contribution of this effect to their observed enhanced cellular delivery efficiency is unknown. Perhaps most importantly, cationic lipid–oligonucleotide complexes have demonstrated improved efficacy in some in vivo animal systems. For example, inhibition of tumor growth in nude mice by a phosphorothiolate oligonucleotide complimentary to an untranslated region of the 3′ end of human nucleolar antigen mRNA is significantly improved by complexation to DOTMA (48). Importantly, no toxicity was observed in these studies. In another instance, intracerebroventricular injection of antisense DNA complexed to DOTAP was able to inhibit expression of a potassium channel in mice, resulting in impaired memory (49). At least one situation has been described, however, in which cationic-lipid antisense-mediated inhibition of expression in cultured cells was not reflected in in vivo activity because the lipid was not required to produce the biological response in the animal (50). Thus, actual studies in animals are still necessary to ensure the utility of cationic-lipid-mediated delivery. In general, effects in cell culture of complexes composed of cationic lipids and oligonucleotides do not correlate well with in vivo results. This seems to be due to a combination of reasons including interaction of complexes with plasma components and variable bioavailability, especially involving uptake by the liver and reticuloendothelial system (51).

Both conventional liposomes and cationic lipids clearly have the potential to be used to enhance oligonucleotide delivery (36,52). Both can protect oligonucleotides as well as enhance cellular uptake, but differ significantly in their bioavailability and intrinsic localization properties in situ. Both can potentially be further targeted; this is discussed

later under the general approaches available to cellular targeting.

An alternative attractive approach from a pharmaceutical perspective involves the use of synthetic polymers to facilitate oligonucleotide delivery. Behr et al. have described the use of polyethyleneimine to markedly enhance the uptake of oligonucleotides into embryonic neurons (53). They postulate that this polymer can act as a "proton sponge," which can buffer lysosome interiors, thereby protecting DNA from nuclease digestion. A pH-sensitive polymer, poly(α-ethylacrylic acid), however, had only minor effects compared with fusogenic peptides, a pH-dependent surfactant, or dendrimers (54). The latter polymeric substances, of the cascade polyamidoamine type, have shown some promise in several laboratories. Transfection of antisense agents into several cell lines significantly inhibited luciferase expression (55), and increased uptake of oligonucleotide–dendrimer complexes as well as enhanced metabolic stability have been directly demonstrated (56). The effectiveness of dendrimer complexes is a function of the generation of the dendrimer as well as pH and ionic strength (57). Further studies of these well-defined cationic polymers are clearly warranted.

Peptides provide a second class of polycationic polymer that has been preliminarily examined. This work involves several different ideas including (*1*) the creation of neutralized oligonucleotide–peptide complexes, (*2*) the use of fusogenic sequences, and (*3*) nuclear translocation signals (58). In general, the simple use of nonspecific peptide–polynucleotide complexes has not been particularly promising and is not discussed further here. More promising is the use of sequences that possess pH-dependent activity that leads to membrane destabilization. Such peptides are usually based on the structure of natural sequences found in viral surface proteins. More than a hundred natural and synthetic peptide sequences have been described that possess fusogenic and/or lytic activity (59). These sequences can be complexed to oligonucleotides electrostatically, covalently, or as part of purified proteins or viral particles (59–62). In many cases, dramatically improved antisense activity is observed, presumably due to facilitated exit of oligonucleotides from endosomes (59,63,64). In several instances, enhanced uptake into cells of oligonucleotides as well as ribozymes has been obtained by combining liposomes and the hemagglutinating virus of Japan (65–68). In a somewhat analogous manner, nuclear entry has been facilitated by peptides containing nuclear localization sequences. The transport of nuclear proteins from the cytoplasm through the nuclear membrane pore complex is mediated by short, basic sequences. Preliminary studies suggest that the inclusion of such sequences can indeed facilitate the nuclear transport of oligonucleotides and even of plasmids (69), but their utility as components of oligonucleotide vectors has yet to be convincingly demonstrated. It is attractive to imagine peptide-based vectors that contain cellular entry, endosomal release, and nuclear entry facilitation sequences (58), but potential problems of immunogenicity, interference between activities, and overall complexity compared to naked oligonucleotides must currently temper enthusiasm for this approach.

Other combined approaches have been described. For example, well-defined poly(ethylene glycol)–poly(L-lysine) (70) and polyspermine–PEG (71) block copolymers have been created, with the latter manifesting antisense activity in cultured cells. Oligonucleotides have been complexed to leucine- and lysine-containing peptides and then entrapped in PEG–polylactic acid "stealth" liposomes (72). Although biological experiments have yet to be reported in this system, the physical properties of these particles make them interesting candidates for oligonucleotide delivery vehicles. Enhanced oligonucleotide cellular entry as well as improved polynucleotide stability have been obtained with synthetic 30-nm particles created from an internal core of cross-linked polysaccharide, a middle covalently attached fatty acid layer, and an external lipid bilayer (73). These complexes were passaged at least 10-fold more efficiency than free oligonucleotides. We can expect that increasing numbers of vectors containing multiple components will be constructed, but this approach is in its infancy.

The well-known method of encapsulation of drugs into bioerodable microparticles has also been attempted with oligonucleotides (74). Although there are many different polymers that have been employed to this end, initial studies with oligonucleotides have been primarily confined to the polylactide–coglycolide type. Both poly(L-lactic acid) (75,76) and lactic acid–glycolic acid matrices (77,78) have been tested and found to release oligonucleotides in a controllable, biphasic manner as well as protect them from degradation. A novel type of microsphere has recently been described that can bind to intestinal mucus and transverse both mucosal absorptive and follicle-associated epithelium (79). Polynucleotides have been successfully delivered to the circulation by this method, suggesting the potential for oral delivery. Compared to peptides and proteins, systems of this type have only been fleetingly examined for oligonucleotides, and their promise remains uncertain but provocative.

We conclude this discussion of delivery complexes by noting that small molecules can also be used to facilitate oligonucleotide delivery. For example, under certain conditions, a cell permeabilizer such as streptolysin O can be used to enhance uptake of RNA into living cells without cell death (80). Perhaps more promisingly, cyclodextrin analogues have been prepared than can stimulate oligonucleotide cellular entry (81,82). Interestingly, cyclodextrin analogues were able to specifically inhibit the immunostimulatory activity of a phosphorothiolate oligonucleotide in mice (83). Further exploration of small molecules in formulations of oligonucleotides seems in order. Finally, we mention that electroporation, ultra- and low-frequency sonic energy, and shock waves have been briefly explored as delivery facilitators, but it is too early to judge the potential utility of such external energy-based approaches. The reader is referred to the article POLYMERIC SYSTEMS FOR GENE DELIVERY, CHITOSAN AND PINC SYSTEMS for a discussion of the "gene-gun" approacn and related methods.

Lastly, we turn to the question of targeting; in this case the term indicates the localization of oligonucleotides to specific cell types after systemic administration. In some

ways this is the "holy grail" of oligonucleotide as well as gene delivery because many of the potential problems of oligonucleotide therapy could be overcome if we could limit the delivery of oligonucleotides to specific sites (84,85). It will probably often be the case that the inherent selectivity of oligonucleotides will not be sufficient from either a toxicity, bioavailability, or efficacy perspective for optimum pharmaceutical use. The availability of numerous specific receptors on the surface of all cells seems to offer such an opportunity. Ligands can be attached to oligonucleotide delivery vehicles in any number of ways. This includes covalent attachment to a component of the vehicle, including the oligonucleotide itself, electrostatically through ionic complexes with the polyanionic component or through apolar interactions, perhaps by insertion into lipid bilayers. The choice of ligand is really limited only by the presence of an appropriate receptor and its intracellular pathway, the latter generally seeming to permit at least some limited release into the cytoplasmic compartment without the use of further mechanisms to stimulate endosomal membrane breakdown. Ligands that have so far been successfully employed to deliver oligonucleotides into cells with some degree of selectivity include carbohydrates (to the asialoglycoprotein and mannose scavenger receptors) (86–89), monoclonal antibodies and associated antigen-binding fragments (85,90), folic acid (91–93), and growth factors (94). The reader is referred to the article on gene therapy in this encyclopedia as well as reviews for further discussion of this topic (84).

We conclude by what is perhaps a statement of the obvious. Oligonucleotides will not be successfully developed as therapeutic agents unless they can be delivered to their site of action in a stable form and gain entry into the proper regions of a cell where they can exert their biological effects. An understanding of the biology necessary to accomplish this is still primitive, and current efforts at delivery thus remain semiempirical at best. Because current clinical studies of pure oligonucleotides hint at some activity (95–97), more complex delivery systems will be required to demonstrate a significant improvement on these simpler, more convenient formulations. Although much of the work described here would seem to offer some leads in this regard, much more extensive work including radically novel developments will probably be necessary to produce pharmaceutically acceptable delivery methods for oligonucleotide drugs.

BIBLIOGRAPHY

1. J.F. Milligan, M.D. Matteucci, and J.C. Martin, *J. Med. Chem.* **36**, 1923–1937 (1993).
2. D. Kregenow, M.Z. Ratajczak, and A.M. Gewirtz, in S. Akhtar, ed., *Delivery Strategies for Antisense Oligonucleotide Therapeutics*, CRC Press, Boca Raton, Fla., 1995, pp. 1–15.
3. D.R. Corey, *Trends Biotechnol.* **15**, 224–229 (1997).
4. M.D. Matteucci and R.W. Wagner, *Nature (London)* **384** (Suppl.), 20–22 (1996).
5. H. Lönnberg and E. Vuorio, *Ann. Med.* **28**, 511–522 (1996).
6. N. Chaudhary, J.S. Bishop, K. Jayaraman, and J.K. Guy-Caffey, in S. Akhtar, ed., *Delivery Strategies for Antisense Oligonucleotide Therapeutics*, CRC Press, Boca Raton, Fla., 1995, pp. 39–60.
7. D.A. Elkins and J.J. Rossi, in S. Akhtar, ed., *Delivery Strategies for Antisense Oligonucleotide Therapeutics*, CRC Press, Boca Raton, Fla., 1995, pp. 17–38.
8. H. Kijima et al., *Pharmacol. Ther.* **68**, 247–267 (1995).
9. L.C. Bock et al., *Nature (London)* **355**, 564–566 (1992).
10. J. Feigon, T. Dieckmann, and F.W. Smith, *Chem. Biol.* **3**, 611–617 (1996).
11. R.M. Bennett, *Antisense Res. Dev.* **3**, 235–241 (1993).
12. M. Yanagishita and V.C. Hascall, *J. Biol. Chem.* **267**, 9451–9454 (1992).
13. K.A. Mislick and J.D. Baldeschwieler, *Proc. Natl. Acad. Sci. U.S.A.* **93**, 12349–12354 (1996).
14. A.M. Gewirtz, C.A. Stein, and P.M. Glazer, *Proc. Natl. Acad. Sci. U.S.A.* **93**, 3161–3163 (1996).
15. J.A. Wolff et al., *J. Cell Sci.* **103**, 1249–1259 (1992).
16. K. Simons and E. Ikonen, *Nature (London)* **387**, 569–572 (1997).
17. J. Couet et al., *Trends Cardiovasc. Med.* **7**, 103–110 (1997).
18. P. Rockwell et al., *Proc. Natl. Acad. Sci. U.S.A.* **94**, 6523–6528 (1997).
19. P. Zamecnik et al., *Proc. Natl. Acad. Sci. U.S.A.* **91**, 3156–3160 (1994).
20. Y. Rojanasakul, *Adv. Drug Delivery Rev.* **18**, 115–131 (1996).
21. E. Wickstrom, *Trends Biotechnol.* **10**, 281–287 (1992).
22. R. Zhang et al., *Clin. Chem. (Winston-Salem, N.C.)* **41**, 836–843 (1995).
23. R. Zhang et al., *Biochem. Pharmacol.* **50**, 545–556 (1995).
24. R. Zhang et al., *Biochem. Pharmacol.* **49**, 929–939 (1995).
25. V.V. Vlassov et al., in S. Akhtar, ed., *Delivery Strategies for Antisense Oligonucleotide Therapeutics*, CRC Press, Boca Raton, Fla., 1995, pp. 71–83.
26. P.C. Shmidt, T.L. Doan, S. Falco, and T.J.C. van Berkel, *Nucleic Acids Res.* **19**, 4695–4702 (1991).
27. S.L. Loke et al., *Curr. Top. Microbiol. Immunol.* **141**, 282–289 (1988).
28. A.R. Thierry and A. Dritschilo, *Nucleic Acids Res.* **20**, 5691–5698 (1992).
29. A.R. Thierry, A. Rahmann, and A. Dritschilo, *Biochem. Biophys. Res. Commun.* **190**, 952–960 (1993).
30. C. Ropert, P. Couvreur, and C. Malvy, in S. Akhtar, ed., *Delivery Strategies for Antisense Oligonucleotide Therapeutics*, CRC Press, Boca Raton, Fla., 1995, pp. 233–245.
31. P. Couvreur, E. Fattal, C. Malvy, and C. Dubernet, *J. Liposome Res.* **7**, 1–18 (1997).
32. D. Collins and L. Huang, *Cancer Res.* **47**, 735–739 (1987).
33. C.J. Chu et al., *Pharm. Res.* **7**, 824–834 (1990).
34. C. Ropert et al., *Biochem. Biophys. Res. Commun.* **183**, 879–885 (1992).
35. A.R. Thierry and G.B. Takle, in S. Akhtar, ed., *Delivery Strategies for Antisense Oligonucleotide Therapeutics*, CRC Press, Boca Raton, Fla., 1995, pp. 199–211.
36. O. Zelphati and F.C. Szoka, Jr., *J. Controlled Release* **41**, 99–119 (1996).
37. C.F. Bennett, in S. Akhtar, ed., *Delivery Strategies for Antisense Oligonucleotide Therapeutics*, CRC Press, Boca Raton, Fla., 1995, pp. 223–232.

Next Page

38. O. Zelphati and F.C. Szoka, Jr., *J. Liposome Res.* **7**, 31–49 (1997).
39. R.I. Mahato, A. Rolland, and E. Tomlinson, *Pharm. Res.* **14**, 853–859 (1997).
40. J.O. Radler, I. Koltover, T. Salditt, and C.R. Safinya, *Science* **275**, 810–814 (1997).
41. D.D. Lasic et al., *J. Am. Chem. Soc.* **119**, 832–833 (1997).
42. H. Gershon, R. Ghirlando, S.B. Guttman, and A. Minsky, *Biochemistry* **32**, 7143–7151 (1993).
43. J. Zabner et al., *J. Biol. Chem.* **270**, 18997–19007 (1995).
44. M.E. Dowty et al., *Proc. Natl. Acad. Sci. U.S.A.* **92**, 4572–4576 (1995).
45. F. Labat-Moleur et al., *Gene Ther.* **3**, 1010–1017 (1996).
46. Y. Xu and F.C. Szoka, Jr., *Biochemistry* **35**, 5616–5623 (1996).
47. O. Zelphati and F.C. Szoka, Jr., *Proc. Natl. Acad. Sci. U.S.A.* **93**, 11493–11498 (1996).
48. L. Perlaky et al., *Anti-Cancer Drug Des.* **8**, 3–14 (1993).
49. N. Meiri et al., *Proc. Natl. Acad. Sci. U.S.A.* **94**, 4430–4434 (1997).
50. N. Dean, *Proc. Natl. Acad. Sci. U.S.A.* **91**, 11762–11766 (1994).
51. D.C. Litzinger, *J. Liposome Res.* **7**, 51–61 (1997).
52. T. Boulikas, *Oncol. Rep.* **3**, 989–995 (1996).
53. O. Boussif et al., *Proc. Natl. Acad. Sci. U.S.A.* **92**, 7297–7301 (1995).
54. J.A. Hughes, A.I. Aronsohn, A.V. Avrutskaya, and R.L. Juliano, *Pharm. Res.* **13**, 404–410 (1996).
55. A. Bielinska et al., *Nucleic Acids Res.* **24**, 2176–2182 (1996).
56. S.W. Poxon, P.M. Mitchell, E. Liang, and J.A. Hughes, *Drug Delivery* **3**, 255–261 (1996).
57. M.X. Tang, C.T. Redemann, and F.C. Szoka, Jr., *Bioconjugate Chem.* **7**, 703–714 (1996).
58. L.C. Smith et al., in A.M. Gotto, Jr. et al., eds., *Drugs Affecting Lipid Metabolism*, Kluwer Academic Publishers, Dordrecht, The Netherlands, 1996, pp. 337–345.
59. B. Oberhauser, C. Plank, and E. Wagner, in S. Akhtar, ed. *Delivery Strategies for Antisense Oligonucleotide Therapeutics*, CRC Press, Boca Raton, Fla., 1995, pp. 247–266.
60. S. Soukchareun, G.W. Tregear, and J. Haralambidis, *Bioconjugate Chem.* **6**, 43–53 (1995).
61. J.-P. Bongartz, A.-M. Aubertin, P.G. Milhaud, and B. Lebleu, *Nucleic Acids Res.* **22**, 4681–4688 (1994).
62. M. Wilke et al., *Gene Ther.* **3**, 1133–1142 (1996).
63. E. Tomlinson and A.P. Rolland, *J. Controlled Release* **39**, 357–372 (1996).
64. V.J. Dzau, M.J. Mann, R. Morishita, and Y. Kaneda, *Proc. Natl. Acad. Sci. U.S.A.* **93**, 11421–11425 (1996).
65. M. Aoki et al., *Biochem. Biophys. Res. Commun.* **231**, 540–545 (1997).
66. I. Kitajima et al., *J. Biol. Chem.* **272**, 27099–27106 (1997).
67. R. Morishita et al., *Proc. Natl. Acad. Sci. U.S.A.* **90**, 8474–8478 (1993).
68. K. Yamada et al., *Am. J. Physiol.* **271**, R1212–R1220 (1996).
69. T. Boulikas, *Int. J. Oncol.* **10**, 301–309 (1997).
70. K. Kataoka et al., *Macromolecules* **29**, 8556–8557 (1996).
71. V.A. Kabanov, S.V. Vinogradov, Y.G. Suzdaltseva, and V.Y. Alakhov, *Bioconjugate Chem.* **6**, 639–647 (1995).
72. C. Emile et al., *Drug Delivery* **3**, 187–195 (1996).
73. M. Berton et al., *Biochim. Biophys. Acta* **1355**, 7–19 (1997).
74. P.Y.P. Kuo and W.M. Saltzman, *Crit. Rev. Eukaryotic Gene Expression* **6**, 59–73 (1996).
75. K.J. Lewis, W.J. Irwin, and S. Akhtar, *J. Controlled Release* **37**, 173–183 (1995).
76. A.J. Hudson, K.J. Lewis, M.V. Rao, and S. Akhtar, *Int. J. Pharm.* **136**, 23–29 (1996).
77. R.L. Cleek et al., *J. Biomed. Mater. Res.* **35**, 525–530 (1997).
78. I. Yamakawa et al., *Biol. Pharm. Bull.* **20**, 455–459 (1997).
79. E. Mathiowitz et al., *Nature (London)* **386**, 410–414 (1997).
80. S. Paillasson, M. Robert-Nicoud, and X. Ronot, *Cell Biol. Toxicol.* **12**, 359–361 (1996).
81. I. Habus, Q. Zhao, and S. Agrawal, *Bioconjugate Chem.* **6**, 327–331 (1995).
82. Q. Zhao, J. Temsamani, and S. Agrawal, *Antisense Res. Dev.* **5**, 185–192 (1995).
83. Q. Zhao, J. Temsamani, P.L. Iadarola, and S. Agrawal, *Biochem. Pharmacol.* **52**, 1537–1544 (1996).
84. C.R. Middaugh, M. Chastain, and C.T. Caskey, in N.R. Lemoine and D.N. Cooper, eds., *Gene Therapy*, Bios Sci. Publ., Oxford, 1996, pp. 11–32.
85. C.S.R. Gooden and A.A. Epenetos, in S. Akhtar, ed., *Delivery Strategies for Antisense Oligonucleotide Therapeutics*, CRC Press, Boca Raton, Fla., 1995, pp. 283–293.
86. Y. Rojanasakul et al., *J. Biol. Chem.* **272**, 3910–3914 (1997).
87. J.C. Perales et al., *J. Biol. Chem.* **272**, 7398–7407 (1997).
88. J. Madon and H.E. Blum, *Hepatology* **24**, 474–481 (1996).
89. E.P. Carmichael et al., in S. Akhtar, ed., *Delivery Strategies for Antisense Oligonucleotide Therapeutics*, CRC Press Boca Raton, Fla., 1995, pp. 267–282.
90. M.P. Selvam et al., *Antiviral Res.* **33**, 11–20 (1996).
91. S. Wang et al., *Proc. Natl. Acad. Sci. U.S.A.* **92**, 3318–3322 (1995).
92. P. Ginobbi, T.A. Geiser, D. Ombres, and G. Citro, *Anticancer Res.* **17**, 29–36 (1997).
93. S. Li and L. Huang, *J. Liposome Res.* **7**, 63–75 (1997).
94. B.A. Sosnowski et al., *J. Biol. Chem.* **271**, 33647–33653 (1996).
95. A.M. Gewirtz, *Mt. Sinai J. Med.* **63**, 372–380 (1996).
96. S. Akhtar and S. Agrawal, *Trends Pharmacol. Sci.* **18**, 12–18 (1997).
97. Antisense '97, *Nat. Biotechnol.* **15**, 519–524 (1997).

See also MICROENCAPSULATION FOR GENE DELIVERY; POLYMERIC SYSTEMS FOR GENE DELIVERY, CHITOSAN AND PINC SYSTEMS.

ORAL DRUG DELIVERY, SMALL INTESTINE & COLON

JOSEPH FIX
Yamanouchi Shaklee Pharmaceutical Research Center
Palo Alto, California

KEY WORDS

Absorption window
Bioadhesive
Enteric coating
Enzymatic activity
Gastrointestinal tract
Microspheres
Osmotic systems
pH
Pharmacokinetics
Prodrugs
Time-specific controlled release systems
Zero-order release

OUTLINE

Small Intestine
  Time Specificity
  Bioadhesives
  pH Sensitivity
  Prodrugs
Colon
  Time Specificity
  Enzymatic Control
Bibliography

Oral administration has been the traditionally preferred route of administration for most therapeutic agents and is, in general, the first avenue investigated in the discovery and development of new drug candidates and formulations. Owing to patient acceptance, convenience of administration, cost-effective manufacturing that does not require sterile processing, and a generally long product shelf-life that is often dictated more by the stability of the active drug itself rather than the formulation components, a continued emphasis on development of oral formulations will persist. For many drugs and therapeutic indications, conventional immediate-release formulations provide effective therapy. The required balance of pharmacokinetic and pharmacodynamic profiles with an acceptable level of safety to the patient can be achieved, and the often costly and complex development of specially designed controlled-release formulations is neither necessary or justified.

Oral controlled-release formulations for the small intestine and colon have, however, received considerable attention in the past 20–25 years for a variety of reasons, including pharmaceutical superiority and clinical benefits derived from the drug-release pattern that are not achieved with traditional immediate- or sustained-release products (1). The necessity for frequently repeated administration to maintain therapeutically effective plasma drug levels can present problems for both patient compliance and fluctuating pharmacodynamic responses. Obviously, drugs that are susceptible to acid hydrolysis or enzymatic degradation in the stomach require a delayed-release mechanism, most often accomplished with stable coatings that prevent drug release in the stomach and thereby postpone release until the formulation is in the more favorable environment of the small intestine. This technology, commonly referred to as enteric coating, is rather routinely employed and will not be discussed in any detail in this section. Some examples of oral formulations employing coating technology to delay drug release until the formulation exits the gastric environment are given in Table 1. Another relatively common problem requiring development of controlled-release formulations is peak-associated side effects that have the potential to be reduced or minimized if a formulation can provide lower, but effective, constant plasma levels of the active drug. The ultimate goal has been to develop true zero-order-release formulations that provide a constant rate of drug release that is independent of remaining drug content in the formulation. Although this approach has certainly proved effective for some drugs and has been utilized to prolong drug absorption or achieve a more stable pharmacodynamic response, the varying absorption rates and drug stability in different regions of the gastrointestinal (GI) tract has meant that a zero-order release pattern will not necessarily achieve constant plasma drug levels. Controlled-release systems that achieve pseudo-zero-order or first-order release can also achieve effective pharmacokinetic and pharmacodynamic results. Another factor that occasionally justifies the development of controlled-release formulations for the small intestine and colon is the apparent presence of drug absorption "windows" that can dictate the regions of the GI tract from which a potential drug candidate can be effectively absorbed (3–5). When an absorption window exists for a drug candidate, a time- or location-directed formulation may be required to achieve the necessary driving force in the proper region of the GI tract to effect adequate drug absorption. In some cases, particularly for drugs that are susceptible to enzymatic degradation in the small intestine, such as peptides and proteins, designed formulations that release the drug in the lower small intestine or colon are thought to present potential advantages by minimizing enzymatic degradation and achieving higher local concentrations of the drug at the absorptive surface (6,7). The relatively more quiescent state of the lower small intestine and colon, as well as reduced fluid content, have also been cited as rationales for developing controlled-

Table 1. Examples of Enteric-Coated Oral Products

Product Name	Drug	Company
Ery-Tab	Erythromycin	Abbott
Prilosec	Omeprazole	Astra Merck
Pancrease	Pancrelipase	McNeil Pharmaceutical
Easprin	Aspirin	Parke-Davis
Eryc	Erythromycin	Parke-Davis

Source: Ref. 2.

release formulations for the lower small intestine and colon. In addition to designing formulations to achieve specific release profiles, modifying the drug itself through complexes or conjugates, that is, prodrugs, can be utilized as a controlled-release technology to achieve specific delivery profiles. For the reasons previously cited as well as others specific to individual drug candidates, the interest in controlled-release formulations for the small intestine and colon remains high and is the target of major pharmaceutical research and development efforts.

By definition, oral controlled-release products refer to those formulations in which a "controlling technology or component" is incorporated that is critical to modulating the drug-release pattern in a predictable fashion or that controls the timing, and subsequently the location, of drug release within the GI tract. Also included in the category of controlled-release formulations are strategies that are conceived and design to improve the pharmacokinetic profile, often by improving the performance or stability of the oral formulation in the dynamic and often hostile environment of the GI tract, in other words, by utilizing bioadhesive technologies to localize the drug and formulation components in close spatial and temporal proximity at the epithelial barrier membrane of the GI tract and, hence, increase the driving force for drug absorption. Table 2 provides examples of some marketed products that have employed sustained- or controlled-release technologies to provide a product with therapeutic or marketing alternatives. To provide an organized discussion of various approaches to small intestine and colon controlled-release technology, the subject matter is divided into pharmaceutical approaches as indicated below:

- Small intestine
  1. Time specificity
  2. Bioadhesives
  3. pH sensitivity
  4. Prodrugs
- Colon
  1. Time specificity
  2. Enzymatic control

It is important to bear in mind that with the exception of the transition from the stomach to the duodenum, there are few, if any, dramatic changes in physiology. Rather, the changes that occur in the physiology of the GI tract are more truly characterized as a continuum or gradual change, with decreasing enzymatic activity, decreasing motility and fluid content, and increasing pH. The presence of specific bacterial populations in the colon and an apparent transient, small reversal in the otherwise increasing pH gradient (8) are exceptions that have been targets for pharmaceutical strategies. These gradually changing physiological parameters means that few "triggering" elements can be utilized to effect a sudden and dramatic change in the performance or release characteristics of an oral controlled-release formulation. As a result, many of the same principles have applied to developing technologies for the small intestine and colon, and in some cases, the duration or timing of the controlling factor has been modified to achieve the desired end result. As such, the performance of controlled-release formulations can often be precisely regulated only in an in vitro environment but becomes subject to the vagaries of GI physiology and its resultant impact on controlling elements in the formulation itself.

SMALL INTESTINE

Time Specificity

Time-specific controlled-release systems are engineered formulations that are designed to release the active drug(s) in a specific temporal pattern. The technology, which can be applied to both continuous and pulsatile release systems, is generally utilized to deliver the active drug to a specific region of the absorptive GI surface. In this section, a variety of time-specific controlled-release systems are reviewed to provide the reader an appreciation for the range of applications for which these technologies might be useful.

The performance of time-specific controlled-release systems for drug delivery to the small intestine can be dra-

Table 2. Examples of Marketed Oral Controlled-Release Products

Product Name	Drug	Form	Company
Tegetrol-XR	Carbamazepine	ER tablet	CibaGeneva
Procardia XL	Nifedipine	ER tablet (osmotic)	Pfizer
Glucotrol XL	Glipizide	ER tablet (osmotic)	Pfizer
Sinemet CR	Carbidopa-Levodopa	CR tablet	DuPont Pharmaceuticals
Indocin SR	Indomethacin	Pellets in capsule	Merck & Co.
Dilacor XR	Diltiazem	ER capsule	Rhone-Poulenc Rorer
Cardene SR	Nicardipine	SR capsule	Roche
Calan SR	Verapamil HCl	SR caplets	Searle
Covera-HS	Verapamil HCl	ER tablet (osmotic)	Searle
Theo-24	Theophylline	ER capsule	UCB Pharmaceuticals
Inderal AL	Propranolol HCl	ER capsule	Wyeth Ayerst
Toprol-XL	Metoprolol succinate	ER tablet	Astra USA
Isoptin SR	Verapamil HCl	SR tablet	Knoll Laboratories
Slow-K	KCl	ER tablet	CibaGeneva
Cardizem SR	Diltazem HCl	SR capsule	Hoechst Marion Roussel

Source: Ref. 2.

matically affected by residence time in the stomach. In the fasted state, the physiologic mechanisms responsible for emptying nondigestible solids from the stomach will generally ensure that a dosage form will exit the stomach within 15–120 min of administration as a result of the "housekeeper" wave of contractile activity (9). Drugs that are susceptible to acid hydrolysis or enzymatic degradation in the stomach will potentially, therefore, exhibit lower-than-desired absorption during residence of the formulation in the stomach environment. This can be overcome by applying specific coating technologies (as represented in Table 1) that prevent activation of the controlling mechanism until the dosage form exits the stomach. As a result, however, initiation of drug absorption will be delayed by a factor proportional to gastric residence time and may not be appropriate for therapeutic indications where an immediate pharmacological effect is necessary. The same issue of gastric residence times applies to time-specific bolus-release systems, that is, controlled-release systems where the drug is released in a manner similar to an immediate-release formulation except that the initiation of drug release is delayed by the controlling mechanism of the delivery system. These factors must be evaluated in the development of any oral controlled-release formulation designed for delivery of the therapeutic agent to the small intestine.

Of the variety of approaches that have been employed to incorporate a time-specific element to oral controlled-release systems, perhaps the most widely used approach has been designing technologies based on generation of osmotic pressure as the driving force. The rationale for this approach is that the presence of water in the GI tract is relatively constant, at least in terms of the amount required for activating and controlling osmotically-based technologies, and provides a more constant regulating parameter than does enzyme activity, pH, bacterial activity, or any other physiological or biochemical parameter. Not surprisingly, a rather incredible number of patent applications have been submitted and approved based on osmotic technologies. In a review published in 1995 (10), Santus and Baker identified 240 U.S. patents that have been approved in the past 20 years covering various applications of osmotic technology. Obviously, it is not possible to review and discuss all of the various osmotic technologies that have been evaluated and, in some cases, developed into commercialized products. The discussion here will deal with the basic concept of osmotically based time-specific drug delivery technologies and a presentation of representative examples that are in various stages of research and development.

In general, osmotic systems incorporate a drug core that contains an osmotically active drug and a semipermeable membrane coating that serves to regulate the influx of water into the device in response to the osmotic core (Fig. 1). In some cases, the drug core also contains an osmotically active salt, for example, NaCl, to assist in establishing the necessary osmotic driving force. Pressure developed as a result of the influx of water serves as a driving force to control the rate of drug release, which can be in either solution or suspension form. A port for drug release is normally created in the device through an orifice engineered

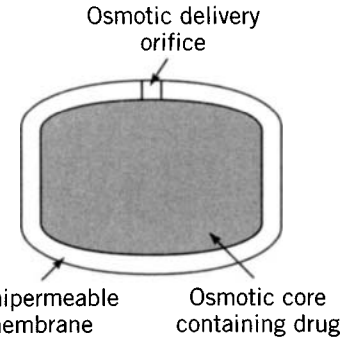


Figure 1. Osmotic pressure-controlled drug delivery system. *Source:* Reprinted from Ref. 11, with kind permission from Marcel Dekker, Inc., New York.

during manufacturing or created in the in situ environment of the GI tract. As long as the concentration of osmotically active agent(s) remains above saturation solubility, zero-order drug release can be achieved in which the rate of drug release $(Q/t)_z$ can be described as shown in the following equation (12):

$$(Q/t)_z = \frac{P_w A_m}{h_m(\Pi_s - \Pi_e)S_D} \quad (1)$$

where P_w, A_m, and h_m are water permeability, effective surface area, and thickness of the semipermeable membrane, respectively. S_D, Π_s, and Π_e are drug solubility, osmotic pressure of the saturated solution of osmotic drug and salt core, and osmotic pressure of the GI fluids, respectively. The mathematical description of the osmotically driven device permits calculation of a desired release rate based on such parameters as osmotic load (Fig. 2) and thickness of

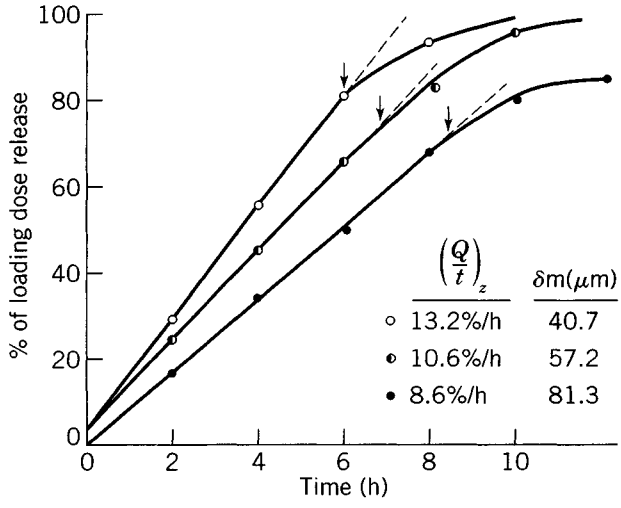


Figure 2. Effect of coating membrane thickness on the rate and duration of zero-order release of indomethacin from osmotic pressure-controlled gastrointestinal delivery system. *Source:* Reprinted from Ref. 11 with kind permission from Marcel Dekker, Inc., New York.

the rate-controlling membrane (Fig. 3) that modulates water influx (11). Several examples of employing osmotic technology to achieve time-controlled release of therapeutic agents are described in the following sections.

The absorption of metoprolol from conventional tablets, an osmotic OROS system (Ciba Geigy, lot No. L 001), and a multiple-unit coated pellet formulation (CR/ZOK) was evaluated in 18 healthy volunteers (13). The OROS design was a single-unit tablet coated with a semipermeable membrane according to principles of the elementary osmotic pump. The CR/ZOK formulation utilized metoprolol succinate as coated pellets in a disintegrating tablet. The CR formulations contained 95 mg metoprolol, while the conventional immediate-release formulation contained 100 mg. Both the OROS and CR/ZOK formulations afforded linear drug release for 2–3 h and continuous, nearly linear release for up to 6 h (Fig. 4). An analysis of the in vivo pharmacokinetics demonstrated that the CR and OROS formulations were essentially bioequivalent on the basis of C_{max} and AUC, and both resulted in a relatively constant maintenance of the plasma metoprolol profile (Fig. 5). The 24-h absorption profile for nifedipine was examined in 12 volunteers given a commercially available nifedipine GI therapeutic system (GITS, Adalat® XL, Miles Canada, Inc.) (14). The GITS system is a push–pull design that can be utilized for delivery of insoluble or poorly soluble drug suspensions and provides essentially zero-order release for 24 h following an initial 2-h hydration period, which is typical of these osmotically based systems (15,16). Measurable nifedipine levels were not observed in the first 2 h postadministration, which is expected based on the initial hydration period required for the GITS. Both 30-mg and 60-mg formulations were evaluated and showed that, as expected, the C_{max} and AUC were approximately doubled with the 60-mg dose compared with the 30-mg dose. The observed T_{max} value frequently occurred at 24 h in spite of the fact that a number of volunteers had total GI transit times considerably less than 24 h (6–32 h). The authors suggest that nifedipine chronopharmacokinetics might account for this observation based on previously reported data that suggest a lower absorption of nifedipine when dosed in the evening versus the morning (17). Regardless of the underlying cause for the specific pharmacokinetic profile with nifedipine, this study points out a common concern with controlled- or sustained-release oral dosage forms, particularly those with release profiles approaching 24 h, in that total GI transit may occur in a significantly shorter time frame than the time required for total drug release from the formulation (i.e., the formulation is eliminated from the body prior to complete absorption). An obvious outcome is that less than the total dose is absorbed, which may have therapeutic implications.

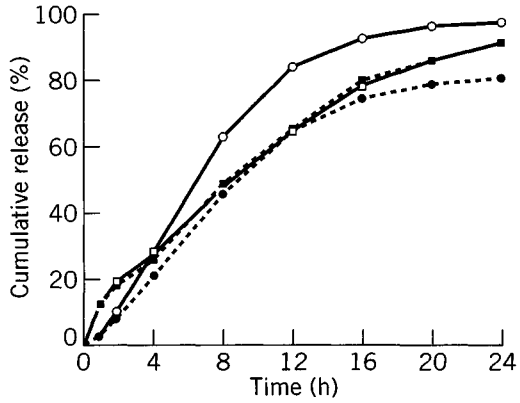


Figure 4. Cumulative in vitro dissolution profiles for metoprolol CR (95 mg metoprolol succinate; squares) and metoprolol OROS (95 mg metoprolol fumarate; circles). Mean of six tablets, determined at a paddle speed of 50 rpm in simulated gastric juice, pH 1.2 (open symbols), and in a phosphate buffer solution, pH 6.8 (filled symbols). *Source:* Reprinted from Ref. 13 with kind permission of Plenum Publishing Corporation, New York.

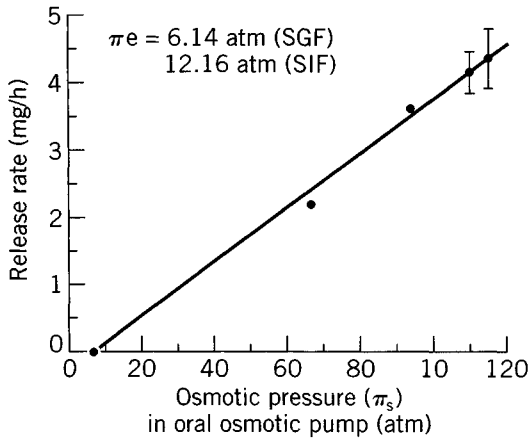


Figure 3. Effect of osmotic pressure Π_s in the osmotic pressure-controlled gastrointestinal delivery system on the rate of release of phenylpropanolamine. *Source:* Reprinted from Ref. 11 with kind permission from Marcel Dekker, Inc., New York.

Both OROS and GITS systems employ an engineered (i.e., laser-drilled) port for drug exit from the device. Other systems have been designed that do not require prefabrication of the exit port. Pore-forming agents can be employed in the coating process to effect in situ pore generation (18–20). Potassium chloride–core tablets were coated with a cellulose acetate–latex formulation containing a plasticizer (triacetin) and urea as a pore-forming agent (19). Coated tablets required high-temperature (60 or 80°C) curing to coalesce the latex beads into a film on the tablet surface. Urea content was found to be the most important variable in terms of the resultant release profile. Cure time did not affect performance. Excellent agreement was observed between in vitro release rates (14.6 ± 0.87%/h in U.S. Pharmacopeial Convention (USP) method 2) and in vivo release rates (12.04 ± 1.18%/h as determined after necropsy retrieval of devices from fasted dogs). The release profile, both in vitro and in vivo (Fig. 6), approximated linearity over 6–8 h. Controlled-porosity osmotic pumps (MODS) were also evaluated for their applicability to the sustained delivery of simvastatin, an HMG–CoA reductase inhibitor for controlling plasma cholesterol levels (20). Core tablets of 105 mg drug-free base, 25.4 mg tromethammonium II, 100 mg mannitol, 45 mg Dowex 50 × 8–100,

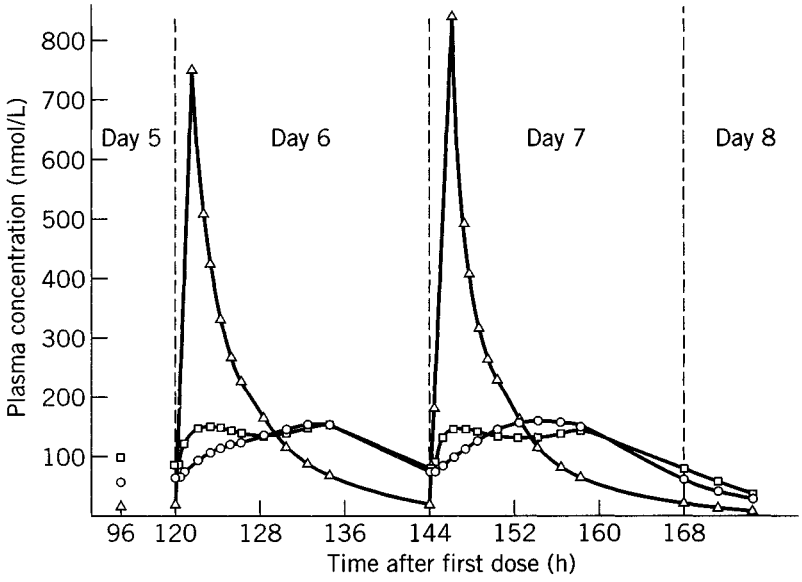


Figure 5. Mean plasma concentrations of metoprolol on treatment days 5 (predose) through 8 following once-daily dosing of (□) metoprolol CR (95 mg metoprolol succinate), (○) metoprolol OROS (95 mg metoprolol fumarate), and (△) conventional metoprolol tablets (100 mg metoprolol tartrate) in 18 healthy subjects. *Source:* Reprinted from Ref. 13 with kind permission of Plenum Publishing Corporation, New York.

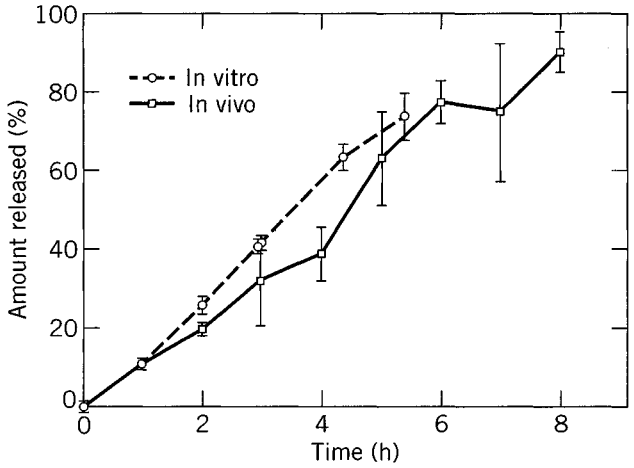


Figure 6. Comparison of in vitro (dashed lines) and in vivo (solid lines) release profiles. *Source:* Reprinted from Ref. 19 with kind permission of Plenum Publishing Corporation, New York.

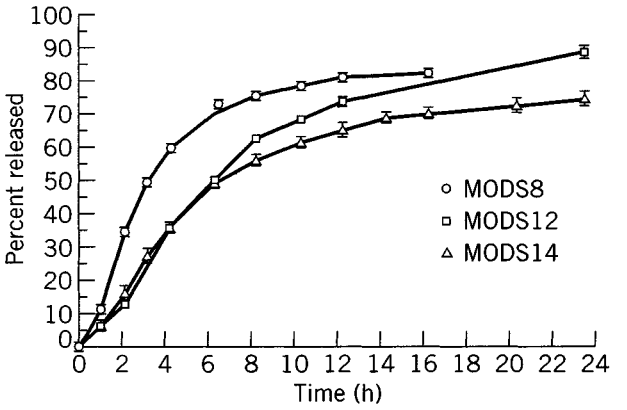


Figure 7. Mean (± SD) in vitro release profiles from simvastatin MODS8 (n = 6), MODS12 (n = 3), and MODS14 (n = 6) devices. *Source:* Reprinted from Ref. 20, with kind permission of Plenum Publishing Corporation, New York.

25 mg Povidone 29–32 K, and 0.06 mg BHA were formulated by aqueous granulation. Magnesium stearate (1.5 mg per core tablet) was used as the lubricant, and 3/8-in.-round standard concave tablets were compressed. The controlled-porosity coat was applied to the core tablets by fluidized-bed spray-coating techniques with a coating solution of CA-398-30, CA-320S, sorbitol, and poly(ethylene glycol) (PEG) 400 dissolved in a water/methanol/methylene chloride (1:10:15) solvent blend. Simvastatin systems (8-, 12-, and 14-h release profiles) were prepared and evaluated in dogs and humans. The in vitro release profile for the 12-h system (Fig. 7) exhibited approximately zero-order release kinetics over the initial 6 h (55% release), with 74% release in 12 h and 90% released in 24 h. The 8- and 14-h MODS systems provided 76% release in 8 h and 70% release in 14 h, respectively. Comparing the MODS12 system with conventional tablets in a single-dose dog study, 4-fold reduction in AUC and 13-fold reduction in C_{max} for MODS was observed compared with the conventional tablet. Similar results were observed in a phase I human study in which a 14-h 20-mg simvastatin MODS system afforded a 54% reduction in AUC and 73% reduction in C_{max} compared with conventional tablets. Given that the pharmacodynamic effects on cholesterol lowering were similar between MODS and conventional tablets in the dog study, the data indicate that the MODS controlled-porosity system could be utilized to afford lower but constant plasma simvastatin levels that provided the same therapeutic potential without wide fluctuations in plasma drug levels.

Other osmotically based systems have been reported that are designed to release drugs in a pulsed or bolus fashion rather than the continuous profile achieved by OROS or GITS. The PORT System (Fig. 8) comprises a gelatin capsule, a semipermeable membrane coating, an insoluble

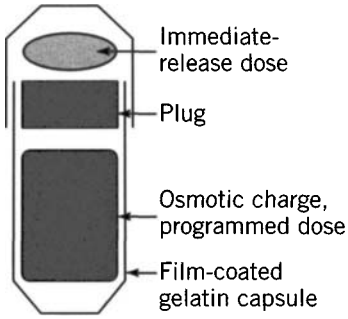


Figure 8. Design of PORT Systems. *Source:* Reprinted from Ref. 21, with kind permission of Elsevier Science–NL, Sara Burgerhartstraat 25, 1055 KV Amsterdam, The Netherlands.

plug, and an osmotic charge that can be balanced to achieve the desired drug-release time (21). A drug-osmotic core was placed in #-elongated hard gelatin capsules and overlayed with melted Gelucire 50/02 (Gattefosse). Following cooling, solidification of the Gelucire layer, and coating of the capsules with an acetone solution of 0.7% w/v triacetin and 2.1% w/v cellulose acetate, the release time was proportional to the number of coats applied. In vitro release times in simulated intestinal fluid (pH 7.5) of 0.23 ± 0.03 h, 1.68 ± 0.04 h, 2.96 ± 0.31 h, and 8.53 ± 0.28 h were observed for capsules with one, three, five, and seven coating layers. Combined with an understanding and estimate of GI transit times, one could envision utilizing these time-delayed systems to target relatively specific regions of the GI tract for drug release.

Not all controlled- or sustained-release technologies are based on underlying osmotic principles as the main driving force. A wide variety of other strategies have been employed and are being evaluated and developed with the goal of providing predictable, time-controlled oral drug delivery. The following sections, although not totally inclusive, describe a variety of technologies that may be appropriate for achieving time-controlled drug delivery.

TIME CLOCK, developed by Zambon Group SpA (Milano, Italy), is a pulsed-release system manufactured with conventional film-coating techniques and uses common pharmaceutical excipients (22). The principle behind TIME CLOCK involves applying a hydrophobic surfactant layer (as an aqueous dispersion) containing a water-soluble polymer onto a tablet or capsule core. The dried coating dispersion can then rehydrate and redisperse in an aqueous environment (e.g., GI tract fluids), and the time for rehydration/redispersion is proportional to the coating thickness (Fig. 9). A typical tablet core consisted of 74.5 mg lactose, 3 mg poly(vinylpyrrolidone), 13.5 mg corn starch, and 1 mg magnesium stearate. The compression mixture is prepared by granulating lactose with an aqueous solution of poly(vinylpyrrolidone), drying and sieving, and adding additional components by blending. The mixture was compressed to a theoretical weight of 100 mg with convex, 5.5-mm-diameter punches. The dispersion coating consisted of 3.5% carnauba wax, 1.5% beeswax, 0.5% poly(oxyethylene) sorbitan monooleate, 1.0% hydroxypropylmethyl cellulose (HPMC), and 93.5% deionized water and was applied with fluid-bed techniques with inlet air at 75°C. Tablet weight increases due to the coating process were in the range of 45% (B45 batch) to 60% (B60 batch). Mean lag times for in vivo disintegration in human volunteers after a light breakfast for the two batches were 204 ± 18 min and 345 ± 54 min, reflecting the impact of the coating thickness on disintegration times. Uncoated tablets showed complete disintegration in less than 20 min. Lag and disintegration times were unaffected by pH. Scintigraphic evaluation indicated that the in vivo behavior of TIME CLOCK did not influence the absorption of a model drug, salbutamol.

Dry-coated wax matrix tablets comprised of a table core with disintegrator and an outer layer compressed from pentoxifylline and behenic acid provided sigmoidal drug-release profiles with the high rate of drug release occurring during core tablet disintegration (23). The disintegration time decreases with increasing tablet core weight due to the concomitant reduced outer layer. A linear relationship was shown for time for 50% dissolution versus disintegration time for tablet cores ranging from 31 to 63% drug content, indicating that drug-release rate was controlled by tablet disintegration. Tablets composed of 70% amylodextrin and 30% paracetamol exhibited constant in vitro drug release in pH 6.8 buffer for approximately 8 h and relatively constant plasma paracetamol levels for 14 h in human volunteers (24). The amylodextrin tablets were apparently not hydrolyzed in vivo by α-amylase. Plasma levels on repeated dosing tended to decrease, apparently due to excretion of tablets prior to complete drug release and absorption. Wax microspheres of ibuprofen were examined, and it was shown that modifiers such as stearyl alcohol and glyceryl monostearate significantly increased the in vitro dissolution rate (20% w/w optimal) (25). Drug concentrations of 17% could be achieved in these microsphere formulations. Approximately 80–90% of the drug load was released within 12 h, indicating the potential application of wax microspheres for drug candidates with physicochemical properties similar to ibuprofen. Multiparticulate sustained-release theophylline formulations (26) comprised of spherical pellets (ethylcellulose–methylcellulose) coated with rate-controlling membranes of two different thicknesses (4.1 and 2.3% weight gain) afforded in

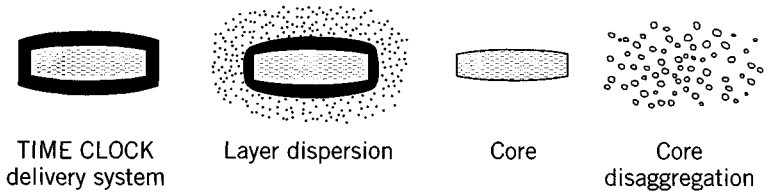


Figure 9. The working principle of the TIME CLOCK system. *Source:* Reprinted from Ref. 22, with kind permission of Elsevier Science–NL, Sara Burgerhartstraat 25, 1055 KV Amsterdam, The Netherlands.

vitro theophylline drug release that was independent of pH between pH 1 and pH 7. In vitro release was nearly complete within 5–8 h, while in vivo release was extended to 8–10 h. Although the rates of release varied with the two coating thickness, the extent of release was comparable and complete for both formulations, and the extent of theophylline absorption equated with that seen in solution dosing. Hydrophilic matrix tablets of felodipine, composed primarily of hydroxypropyl methylcellulose, were examined in human volunteers (27). In vitro disintegration and dissolution were linear over 8–10 h. In the human evaluation, felodipine absorption was related to tablet erosion as evinced by similarity between the in vivo erosion (as determined by γ-scintigraphy) and pharmacokinetic profiles.

Hydrophilic matrix tablets of zileuton, a 5-lipoxygenase inhibitor, were prepared by directly compressing hydroxypropyl methylcellulose and 50–60% zileuton (28). Wet granulations with water and low shear force were also used to compress tablets with magnesium stearate. In vitro release in USP I, II, and III methods was linear for 8 h. Sustained in vivo absorption in dogs was observed, which correlated with the in vitro release profiles although in vivo release was more rapid (release complete in approximately 4 h) than that noted in vitro. Prodan, a fluorescent marker, release from poly (D,L-lactic acid) (PLA) nanospheres coated with albumin or poly(vinyl alcohol) (PVA) was examined in vitro (29). In simulated gastric fluid where polymer degradation did not occur, release kinetics typified diffusion through the intact polymer matrix, with complete release within 120 min. In simulated intestinal fluid, release was dependent on the coating applied to the nanospheres. With PVA coating, the marker was released by diffusion through the PLA matrix, with only 44% released due to the marker's poor affinity for water. With an albumin coating, marker release was both matrix erosion and diffusion controlled with 100% release in 480 min.

A soluble oral controlled-release formulation regulated by both pulsatile and zero-order release kinetics has been described (30) that utilizes poly(ethylene oxide) and HPMC excipients with diclofenac in a three-layer matrix system (Fig. 10). In vitro dissolution studies suggested that both biphasic release and zero-order release kinetics up to 24 h could be achieved with this system. Dissolution and swelling/erosion are proposed to account for the linear portion of drug release, while disintegration and dissolution are mechanistically suggested for the burst phase. Hydroxyethylcellulose (HEC) has been utilized as a gel-forming matrix to prepare delayed release tablets of diltiazem hydrochloride (31). The tablets are cores of diltiazem surrounded by an outer shell of HEC of different viscosity grades. Diltiazem was rapidly released from all tablets after an initial lag phase, which was a function of the HEC coating. Lag time increased as the HEC viscosity increased. The lag time was not greatly affected by pH between pH 1.2 and pH 6.8. In a human volunteer study, T_{max} and mean residence time increased with increasing HEC viscosity with small intersubject variability. In vitro and in vivo lag times appear to exhibit a reasonable correlation. The diltiazem AUC did, however, decrease as the lag time increased. This approach for time delaying could represent a useful approach for drug candidates where an initial delay is appropriate.

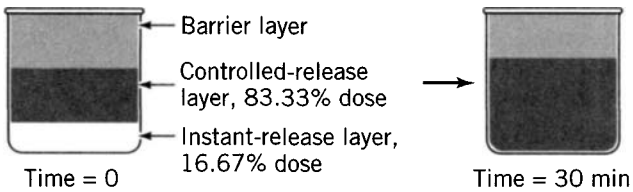


Figure 10. Schematics of diclofenac sodium asymmetric configuration delivery system. (**a**) Delivery system at time zero, (**b**) complete dissolution of one layer and gradual swelling of the system. *Source:* Reprinted from Ref. 30, with kind permission of Elsevier Science–NL, Sara Burgerhartstraat 25, 1055 KV Amsterdam, The Netherlands.

Although it has clearly not been possible to elucidate and discuss the tremendous number of approaches that have been, and continue to be, developed for oral time-controlled drug delivery, the examples presented here should at least provide a sampling of the varied approaches that can be considered. Inherent in the selection of any time-controlled release technology has to be the physicochemical properties of the drug candidate, as this can determine or modify drug release from a given formulation, depending on the release mechanism. The intended therapeutic regimen is also critical in the selection process because the duration of drug release is obviously dependent on residence in the GI tract, and the absorption profile of a given drug may be different depending on the location within the GI tract.

Bioadhesives

The use of mucoadhesive polymers to improve oral drug absorption or the performance of oral controlled-release drug delivery systems has received considerable attention in the past 10–15 years and has been the subject of previous review articles (32,33). This interest has been generated with several goals in mind, including increasing local drug concentrations to improve absorption, retarding the transit of controlled-release dosage forms to take advantage of upper-GI absorption windows, or targeting drugs or dosage forms to specific regions of the GI tract for specific applications, such as antigen sampling by the M-cells of the Peyer's patches in the lower small intestine and colon. In every case, the successful application of bioadhesive technology is a balancing act between the creativity and expertise of the pharmaceutical scientist and the physiologic mechanisms of the GI tract that function to dilute, mix, and propel food substances in a proximal to distal direction in the GI tract.

In one potential application for bioadhesive polymers, the intrinsic permeability of the drug candidate is too low or the drug is susceptible to hydrolytic or enzymatic degradation in the lumen of the GI tract, either of which results in insufficient absorption of the drug candidate. In both instances, it has been felt that the ability to localize high concentrations of the drug candidate at the absorptive epithelial surface would increase the driving force and

thereby lead to increased levels of drug absorbed into the systemic circulation. The approach here has been attempting to link a mucoadhesive polymer to a drug candidate such that a selective attachment to the epithelial cells occurs and presents the drug candidate in high concentration and close proximity to the absorptive surface. To be therapeutically effective, the attached bioadhesive polymer must not interfere with the absorption or activity of the parent drug, or the linkage of the polymer to the active drug must be reversible such that the active parent drug is efficiently released, either at the epithelial surface or after absorption, and can exert its pharmacologic effect.

Another area of interest for bioadhesive polymers has been to retard the GI transit of controlled-release dosage forms for those drugs whose absorption is restricted to the upper regions of the GI tract, that is, absorption-window drug candidates. Some drugs have been clearly shown to be absorbed in specific regions of the upper GI tract, including chlorothiazide (33), riboflavin (34), and furosemide (35), and other drugs are likely to have specific preferred regions of absorption there. Additionally, for most drugs examined to date, it is generally felt that absorption in the colonic region is significantly lower than in the small intestine, probably because of differences in the lumenal contents of the colon that either impair the dissolution and diffusion of drugs from the lumen to the epithelial cell wall or impose additional degradative pathways, such as bacterial enzyme activity, that also decrease drug absorption. With this apparently common problem, controlled-release dosage forms whose release times exceed 5–6 h will likely exhibit a significant deviation in zero- or first-order kinetics owing to poor colonic absorption. To overcome this problem and extend the effective release time of controlled-release dosage forms, major interest has evolved in ways to prolong the upper GI residence time of controlled-release dosage forms such that a greater proportion of the drug load is released in an environment where reliable absorption can occur. Owing to the very high fluid content and mixing activity in the stomach, attempts to prolong gastric residence times via adhesive technologies have not been successful and will not be covered here. Rather, the focus will be on approaches that are being investigated to retard the small-intestine transit of small particulates where the balance of bioadhesion and physical forces in the GI tract offers some promise for success.

A final area of interest for bioadhesive technology has emerged from the advances in the biotechnology arena where biopharmaceuticals directed toward the gut-associated lymphoid tissues (M-cells in the Peyer's patches) are being developed for vaccination, immunization, and tolerance therapies. The M-cells are known as a preferred site for particulate uptake in the GI tract, and this mechanism has been proposed as a possible avenue for improving the absorption of particulate formulations, although it is not clear yet how effective this route will be for systemic delivery of drug candidates because the primary function of these cells is macromolecular sampling and degradation to feed the antigen-processing cells of the immune system. Regardless, bioadhesive polymers specific for M-cells, particularly lectins, have been evaluated as candidates for this approach.

A variety of bioadhesive molecules, particularly polymers, have been evaluated with varying results in terms of in vitro adhesive forces and in vivo efficacy. Polyanions with a high charge density, particularly those containing carboxylic acid groups, appear to exhibit the highest degree of bioadhesive properties. Mucoadhesive hydrogels have received the major share of attention and effort, from which polymers of poly(acrylic acid) derivatives (35), hyaluronic acid (36), and some chitosans (37) have demonstrated adhesive properties (Fig. 11). Linear cellulose polymers have not demonstrated effective in vivo bioadhesive properties, probably due to a lack of rigidity and structural integrity seen in hydrated, non-cross-linked polymers (38).

Akiyama and coauthors (39) reported on the preparation and evaluation of 177- to 500-μm-diameter polyglycerol ester fatty-acid microspheres composed of tetraglycerol pentastearate and tetraglycerol monostearate in which Carbopol 934P was either applied as a coating (CPC) or dispersed into the matrix of the microspheres (CPD). Carbopol 934P was chosen because of previously demonstrated bioadhesive properties (38,40). In an in vitro bioadhesion assay, more than 90% of the CPD microspheres adhered to gastric and small intestinal tissue, whereas only <10% of CPC and PGEF (similar composition without Carbopol 934P) microspheres showed adhesion. In an in vivo evaluation in conscious rats each receiving 100 PGEF and 100 CPD microspheres, the CPD microspheres showed significantly longer gastric retention time (T_s 50 = 1.8 h) and

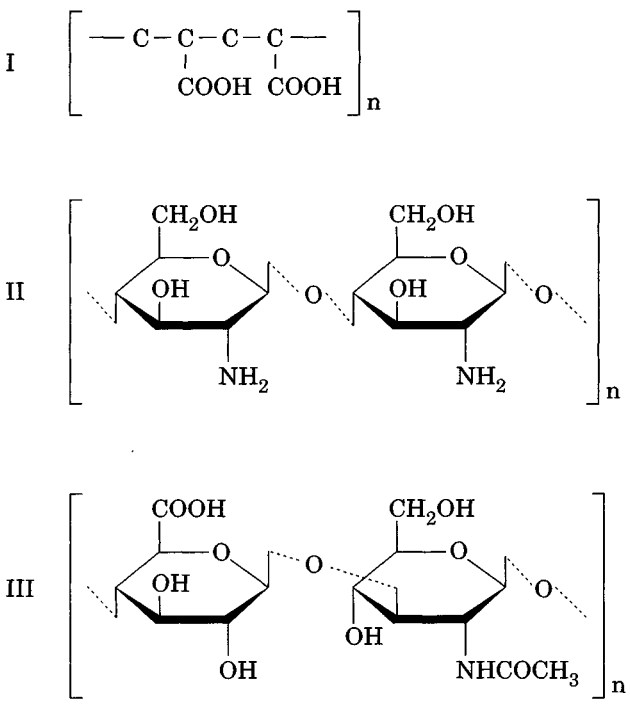


Figure 11. Polymers forming mucoadhesive hydrogels: I, poly(acrylic acid); II, chitosan (poly[D-glucosamine]); III, hyaluronic acid (poly[D-glucuronic acid-*N*-acetylglucosamine]). *Source:* Reprinted from Ref. 32, with kind permission of Begell House, Inc., New York.

a longer transit time to the colon ($T50$ = 7.3 h) than that observed with PGEF microspheres (T_s50 = 0.5 h and $T50$ = 4.9 h). The mean residence times of the CPD microspheres in the stomach and three sequential small-intestine regions were also significantly greater for CPD microspheres than for PGEF microspheres, although small-intestine transit was not delayed as significantly as gastric residence time. The potential mechanism proposed by the authors (Fig. 12) suggests that the bioadhesive properties of CPD microspheres (when compared with PGEF or CPC microspheres) are caused by the partial extrusion of gelled polymer from the matrix dispersion, which allows the bioadhesive properties of Carbopol 934P to "anchor" the microspheres to the mucosa. PGEF microspheres did not contain a bioadhesive polymer, and the coated CPC microspheres formed an overhydrated surface gel that separated from the microsphere and would not serve to anchor the microsphere to the mucosal surface. Regardless of the mechanism, the in vitro and in vivo characterizations of the dispersed Carbopol 934P polyglycerol ester fatty-acid microspheres suggest this approach may provide limited advantages in terms of increasing the residence time of a microsphere formulation in the upper small intestine.

Hosny (41) evaluated polycarbophil diclofenac sodium tablets and compared their in vitro and in vivo performance to a commercially available enteric-coated preparation (Voltaren). Directly compressed tablets were prepared from polycarbophil (0.2- to 0.3-mm or 0.5- to 0.8-mm particle size) and diclofenac sodium. Release testing was conducted with USP dissolution apparatus I. Voltaren tablets did not release measurable drug during 2 h at pH 1.2 owing to the enteric coating. The bioadhesive tablets released approximately 9–12% of the drug content under similar conditions. On increasing the pH of the dissolution media to 6.8, complete drug release was seen in approximately 1 h for Voltaren and 0.5 and 2.0 h for small- and large-particle-size bioadhesive tablet formulations, respectively. Comparing the in vivo performance of Voltaren tablets and the bioadhesive tablets in a fasted dog model (n = 6) indicated no significant differences between any of the formulations in terms of C_{max}, T_{max}, and AUC. The equivalent pharmacokinetic performance of the bioadhesive tablets to enteric-coated Voltaren shows that the bioadhesive tablets may be a reasonable alternative to the enteric-coating approach. Previous work (42,43) had shown that a similar formulation with indomethacin was less irritant to gastric and intestinal mucosa, presumably owing to cross-linking between the polycarbophil and the mucosal surface, which creates a protective environment on the underlying cell layers.

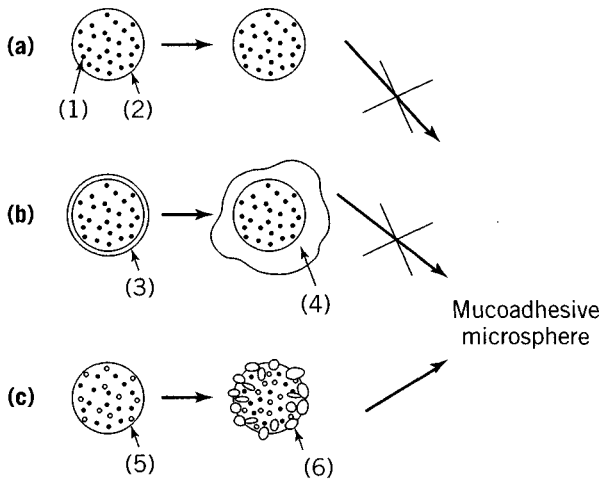


Figure 12. Schematic description of the mucoadhesion process with microspheres. (**a**) PGEF microsphere, (**b**) CPC microsphere, (**c**) CPD microsphere; (1) drug, (2) PGEF, (3) coated CP layer, (4) swollen CP layer, (5) dispersed CP, (6) swollen CP. *Source:* Reprinted from Ref. 39, with kind permission of Plenum Publishing Corporation, New York.

Eudragit RL-100 (ERL) has been shown to be able to affect the swelling property, mechanical properties, and bioadhesive nature of polycarbophil compressed tablets (44). All compositions of ERL and polycarbophil exhibited a lower degree of swelling in pH 5 buffer as compared to pH 7.4 buffer, but in all cases, increasing amounts of ERL significantly decreased swelling relative to pure polycarbophil films. As the amount of ERL increased relative to polycarbophil, the mechanical properties (torsion force and modulus of elasticity) also increased, indicating that it was possible to formulate ERL–polycarbophil mixtures with acceptable mechanical properties for withstanding the external forces present in the GI tract and provide sufficient physical integrity to tablets in vivo. By balancing the ratios of ERL and polycarbophil, it was possible to achieve linear and comparable in vitro release rates for sodium cefazolin (highly water soluble) and ibuprofen (poorly water soluble). Sodium cefazolin could be expected to possess a significant diffusive component to its release profile given its high water solubility, while the release of poorly soluble ibuprofen would necessitate an erosion process because little aqueous diffusion would be expected. The fact that the sodium cefazolin and ibuprofen releases were nearly identical (Fig. 13) demonstrated that balancing the ratios of ERL and polycarbophil could be achieved in such a manner that the release profiles were identical for two compounds of very different physicochemical properties. The bioadhesive properties of ERL–polycarbophil tablets were evaluated with an in vitro model utilizing intestinal tissue from various regions of the rat GI tract and indicated a preferential bioadhesion to tissue from the cecum (Fig. 14). The combination of ERL and polycarbophil evaluated in this study indicated that tablets could be obtained that allowed designed control of release rates for both water-soluble and water-insoluble compounds, had adequate mechanical properties, and exhibited a preferential bioadhesive potential for cecal tissue of the rat. The potential of this application, particularly the bioadhesive activity and specificity for cecal tissue, requires confirmation in large animal models or human clinical studies.

Lectins are proteins that possess an affinity for binding to specific sugars and therefore have been shown to bind to the mucous and epithelial cells layer of the GI tract (45,46). Irache and colleagues have covalently coupled various lectins to latex particles (826–956 nm diameter) and evaluated their mucoadhesive properties with an in

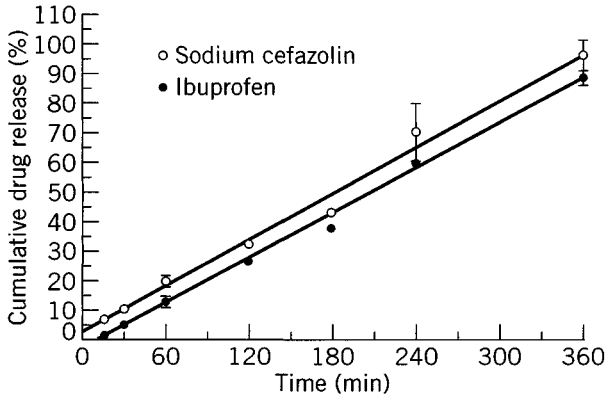


Figure 13. The release kinetics of sodium cefazolin and ibuprofen from CEF/IBU tablets, demonstrating similar release rates of the highly soluble (sodium cefazolin) and the sparingly soluble (ibuprofen) drug molecules from the erodible matrices. The mean values of six measurements ± SD are shown. *Source:* Reprinted from Ref. 44, with kind permission of Elsevier Science–NL, Sara Burgerhartstraat 25, 1055 KV Amsterdam, The Netherlands.

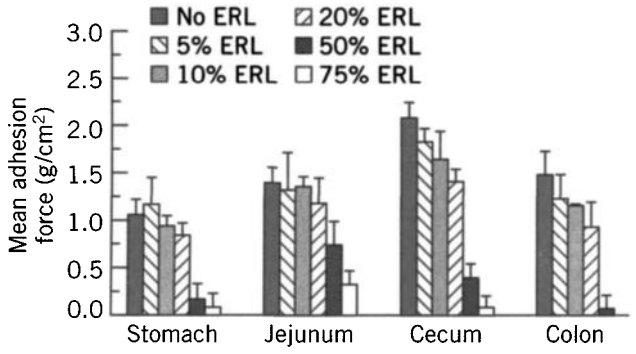


Figure 14. The mucoadhesion properties of polycarbophil–ERL discs with elevated amounts of ERL as measured on the epithelium of four regions in the GI tract of rats. The mean values of four measurements ± SD are shown. *Source:* Reprinted from Ref. 44, with kind permission of Elsevier Science–NL, Sara Burgerhartstraat 25, 1055 KV Amsterdam, The Netherlands.

vitro intestinal tissue model (47). Control BSA–conjugated latex particles possessed only minimal bioadhesive properties. The results obtained with tomato lectin (TL), asparagus pea lectin (AL), and bacterial adhesin (ML) demonstrated tissue specific responses. Latexes prepared with TL showed greater affinity than AL or ML for the mucous glycoproteins of non–Peyer's patch tissue. In contrast, both AL– and ML–latex conjugates demonstrated higher affinity for the Peyer's patch region of the intestine than did TL–latex conjugates. This difference could form the basis for selection of lectin-targeted formulations to target different regions of the GI tract. With all latex conjugates, the mucoadhesive properties decreased with distal distance down the GI tract, probably reflecting decreasing amounts of mucous glycoproteins in the direction from duodenum to ileum. Additional studies with tomato lectins confirmed these observations by demonstrating a specificity of tomato lectin–conjugated nanoparticles for absorptive epithelial cells rather than cells of the gut-associated lymphoid tissue (48). Fluorescent 500-nm polystyrene nanoparticles were covalently coupled with tomato lectin through a carbodiimide reaction and administered to rats on a daily oral gavage regimen. The results of this study (Fig. 15) clearly demonstrate a significant increase in tomato lectin–nanoparticle uptake when compared to uptake of control nanoparticles.

A high degree of species and intestinal site specificity has been shown in the binding of lectins to tissues from mouse and rabbit intestine. M-cells from mouse Peyer's patches have been shown to have a binding affinity for α-L-fucose–specific lectins (49). This specific binding was not found in Peyer's patches from rabbit small intestine, although strong binding was seen in rabbit cecal lymphoid patches. Sugar specificities between mouse and rabbit tissue were also observed for peanut agglutinin, wheat germ agglutinin, and *Bandeiraea simplicifolia* agglutinin II. These observations, although not involving pharmaceutical preparations, indicate that a concern must be noted when extrapolating experimental results from one species to another and from one tissue type to another in the same species.

Mathiowitz and coworkers have prepared and evaluated a number of polymeric approaches to bioadhesive oral formulations. Initial evaluations included developing and utilizing a microbalance-based system to quantitate the bioadhesive forces of various polymeric microspheres (50,51). The results from these early in vitro evaluations indicated that (poly)fumaric-*co*-sebacic anhydride polymers, which rapidly degrade, afforded the strongest bioadhesive interactions with rat small intestinal tissue of the polymers tested. The proposed mechanism of adhesion is the generation of carboxylic acid groups during degradation, which increases the potential for hydrogen bonding to mucus and epithelial glycoproteins. Alginate microspheres were also shown to possess significant in vitro adhesive properties. Subsequent to the in vitro selection of

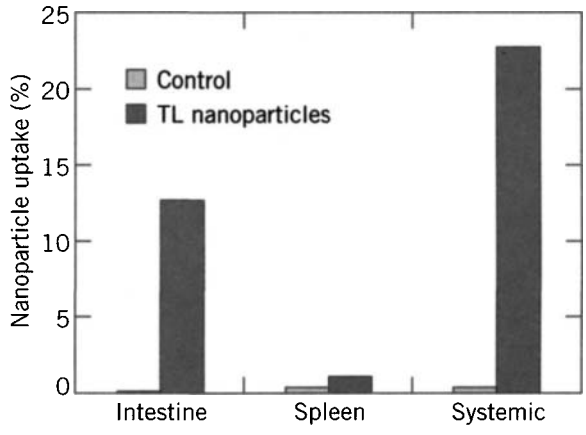


Figure 15. Oral uptake of tomato lectin–conjugated (TL) and blocked nanoparticles (500 nm) as a function of total dose administered and organ weight. *Source:* Reprinted from Ref. 48, with kind permission of Plenum Publishing Corporation, New York.

these two polymers, in vivo evaluations were carried out in a rat model to determine whether the in vitro adhesive properties translated into an advantage that could be exploited in vivo in the development of oral drug delivery systems (52). Alginate microspheres were prepared by blending dissolved alginate and dicumarol or radioopaque marker and pumping droplets into a calcium chloride bath. Microsphere size range from 600 to 850 μm for radioopaque-loaded microspheres and <212 μm for dicumarol-containing microspheres. A phase inversion microencapsulation technique was used to prepare polyanhydride microspheres. Briefly, polymer and dicumarol were dissolved in an appropriate solvent (methylene chloride), and the solution was poured into a strong nonsolvent (petroleum ether) that was miscible with the solvent. Microspheres were spontaneously formed whose size ranged from 0.5 μm to 5 μm. The phase inversion microencapsulation techniques avoided the need to utilize a hot-melt procedure (with temperatures around 100°C), which can have significant limitations in terms of drug stability. Compatibility with an organic solvent, for example, methylene chloride, still has to be taken into consideration. The polyanhydride microspheres were at a fumaric acid/sebacic acid ratio of 20:80, P(FA:SA)20:80. The GI transit of barium-loaded microspheres was evaluated in a rat model in which fasted rats received approximately 200 mg of barium-loaded microspheres by stomach gavage in 0.9% sodium chloride. Transit of particles was quantitated by X-ray techniques, and the results (Fig. 16) indicated the P(FA:SA)20:80 microspheres had a significantly slower GI transit than the alginate microspheres. Pharmacokinetic analysis of dicumarol (6.5 dicumarol in 40-mg microspheres) plasma levels also demonstrated that improved absorption of dicumarol was achieved with the P(FA:SA)20:80 microspheres relative to spray-dried dicumarol (Fig. 17). The plasma AUC for P(FA:SA)20:80 dicumarol microspheres was 363 ± 100.3 μg/h/mL compared to 232 ± 38.4 μg/h/mL and 211 ± 30.3 μg/h/mL for spray-dried dicumarol and alginate dicumarol microspheres, respectively. These data are highly encouraging with respect to potential utility for developing effective oral delivery technologies based on bioadhesive principles. However, it should be noted that the dose of microspheres employed in the GI transit studies, 200 mg per rat, is quite high and may or may not be reproducible in larger animal models or humans where the formulation mass relative to GI dimensional parameters may not favor such an intimate and highly concentrated contact of bioadhesive microspheres with the GI mucosal cell layer.

In addition to their potential utility in localizing drug or particulate formulations at the mucosal surface of the GI tract, several bioadhesive polymers have also been shown to possess activity with regard to inhibiting degradative enzyme activity and modifying the barrier function of the epithelial cell layer. This mixed function activity of the bioadhesive polymers offers an opportunity to coordinate both formulation localization and biological effects of a single formulation component.

Polycarbophil and carbomer have been shown to inhibit trypsin enzymatic activity in a calcium-dependent manner (53). Both poly(acrylic acid) derivatives are known to bind divalent cations in the undissociated state. Utilizing 0.35% (w/v) polycarbophil or 0.25% (w/v) carbomer in an in vitro incubation experiment, trypsin activity was inhibited approximately 93%, calcium was depleted to 10–15% of its original content, and free protein concentration was decreased approximately 30–40% (indicating the bioadhesive potential of polycarbophil and carbomer toward proteins).

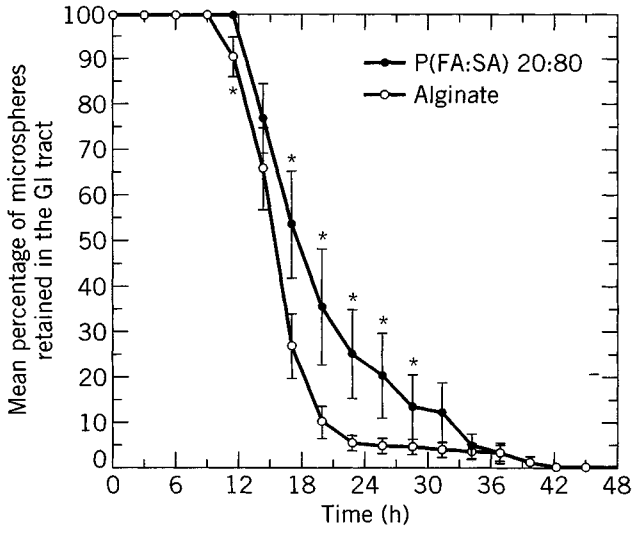


Figure 16. Percentage of microspheres retained over time. Paired, one-tailed *t*-tests were performed on the raw data, and those time points with percentages statistically different ($P \leq 0.05$) from each other are represented by asterisks (*). Reprinted from Ref. 52, with kind permission of Elsevier Science–NL, Sara Burgerhartstraat 25, 1055 KV Amsterdam, The Netherlands.

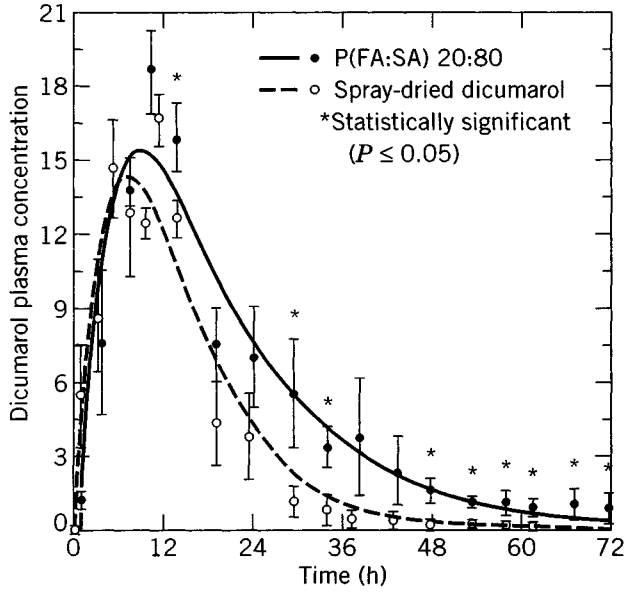


Figure 17. Dicumarol plasma concentration versus time (P[FA:SA] 20:80 versus spray dried). *Source:* Reprinted from Ref. 52, with kind permission of Elsevier Science–NL, Sara Burgerhartstraat 25, 1055 KV Amsterdam, The Netherlands.

Carbomer, which has a higher binding affinity for calcium than polycarbophil, also was able to inhibit trypsin activity at lower concentration than polycarbophil, indicating a relationship between calcium-binding activity and enzyme inhibition. This is consistent, considering the important role of calcium in maintaining the thermodynamic stability of trypsin (54).

The enzyme inhibitory activity of polycarbophil and carbomer were also examined with a variety of peptide substrates (55). Employing brush-border membrane vesicles (BBMVs) obtained from the entire small intestine of rats, the capacity of polycarbophil (0.1–0.5%) and carbomer (0.1–0.5%) to inhibit the enzymatic degradation of buserelin, 8-arginine vasopressin (DGAVP), metkephamid, L-pyroglutamic acid *p*-nitroanilide (PGNA), hippuryl-L-arginine (Hipp-Arg), and insulin was determined. Because BBMVs were utilized as the biological system, only enzymes associated with brush-border membranes are evaluated by this method. Buserelin degradation was not affected by either carbomer or polycarbophil. Polycarbophil and carbomer were only weakly effective in inhibiting degradation of DGAVP and Hipp-Arg at the highest concentration (0.5%) tested. Insulin, which only exhibited an approximate 10% degradation by BBMV enzymes with 240 min, was slightly protected by 0.25% carbomer. Overall, the data indicate that carbomer and polycarbophil are only very weakly protective against brush-border enzyme activity isolated from rat GI tissue. Polymers with a stronger affinity for divalent cations could afford an advantage in terms of inhibiting BBMV enzyme activity.

In addition to the bioadhesive and enzyme inhibitory potential of some of the polymers utilized in the aforementioned studies, there are also data to indicate that these polymers may also be capable of modifying the barrier properties of epithelial cells in a manner that increases drug flux. Carbomer (0.5 and 1.5% w/v) and chitosan (0.5, 1.0, and 1.5% w/v) were evaluated for their effects on electrical resistance (TEER) and drug flux utilizing an in vitro Caco-2 cell monolayer derived from a human colon carcinoma cell line (56). TEER was significantly decreased to approximately 40–50% of the original resistance by both polymers but only at the highest concentration tested. If the polymer solutions were replaced with fresh buffer, TEER recovery was observed to occur (65% for carbomer and 88% for chitosan of original TEER), indicating that the change in resistance was not due to irreversible damage to the cell layer. Chitosan–glutamate at 1.5% did not increase mannitol flux over a 150-min incubation period, whereas 1.0% carbomer afforded a 2.7% flux of mannitol over a 120-min period. It should be noted that drug flux in this in vitro model is not directly proportional to what could be anticipated in vivo. In fact, an in vitro flux of 2.7% in 120 min would likely translate into a rather more significant in vivo absorption level. Carbomer was also found to significantly enhance the in vitro flux of FD-4 (FITC-dextran, M_W 4,000). Confocal fluorescence microscopy provided evidence that carbomer was loosening the tight junction structure of the epithelial cell layer and providing an aqueous pathway for molecule movement between cells of the monolayer. The affinity of carbomer for divalent calcium may account for its effect on tight junction structure because calcium depletion has been shown to open tight junctional pathways of epithelial cell monolayers.

Several polymers and polymer systems have been described that possess varying degrees of bioadhesive potential. Most of the data generated to date has involved in vitro evaluations and, in some instances, evaluation in small animal models, for example, rats. The practical utility of bioadhesive approaches for oral drug delivery will obviously depend on demonstrating a similar performance and efficacy in larger animal models and human clinical studies. The particular intriguing feature of some of the polymers employed, particularly the polyacrylate types as carbomer, is that they possess multiple functional capabilities, including a bioadhesive potential, enzyme inhibitory activity, and some membrane permeation–enhancing activity. These multiple effects may afford particular advantages to utilizing these systems for oral controlled drug delivery. Finally, the data and interpretations from several investigators would suggest that the potential for bioadhesive properties may be optimal in the lower GI tract where the epithelial mucus layer is thinner and there is at least a somewhat reduced state of fluid content and muscle contractility. It remains to be demonstrated that the mucoadhesive approaches evaluated here will have a practical utility in the upper GI tract.

pH Sensitivity

Controlled-release technologies based on pH-sensitive control mechanisms are designed to release acidic or basic drugs in the GI tract at a rate that is not dependent on the pH of the GI fluids, which can vary from pH 1.2–3.5 in the stomach to pH 6.0–7.5 in the lower small intestine. The general principle underlying this technology is the incorporation of an acidic (or basic) drug and appropriate buffering agents as a core granulation. These particles can then either be coated with a fluid-permeable membrane that allows influx of GI fluids, or the particles can be uniformly dispersed in a tablet core that serves a similar function. In either application, the influx of fluid from the GI tract dissolves the buffering agents and provides a microclimate pH within the formulation that regulates the rate of drug release. Ideally, the rate of drug release should be independent of the pH of the GI fluid being imbibed.

Sutinen et al. have reported on the development of pH-controlled silicone microspheres for controlled drug delivery (57). Silicone microspheres were prepared with an amine-resistant Dow Corning X7-3012 silicone elastomer. Monosodium phosphate, disodium phosphate, trisodium phosphate, and tris(hydroxymethylaminomethane) were used as potential buffering agents. Using timolol maleate as a model drug, spray-dried mixtures of timolol with and without varying compositions of buffering agents were prepared and mixed with the silicone elastomer. Spray-drying timolol and buffers together proved most effective, as opposed to mixing timolol and buffer that had been spray-dried separately, because the drug and buffer were localized in the same particle within the silicone elastomer microsphere. Spray-dried timolol particles were approximately 3 μm and incorporated into the silicone microspheres at a 30 wt % loading (loaded microsphere diame-

ter, 143–301 μm). Without added buffering agents, timolol release was relatively slow, showing less than 20% release in 11 h. When trisodium phosphate was incorporated in the microsphere preparation, the timolol release rate was increased 3.3–8.2 times greater than nonbuffered microspheres. Release of timolol from the silicone microspheres followed square-root-of-time kinetics, which is typical of a matrix-controlled dissolution process (58). The rate of timolol release was directly proportional to timolol loading (wt %), basic nature of the added buffer, and the loading level of the buffer (10–25%). This reflected a higher proportion of timolol in the unionized state, which could more readily partition through the silicone matrix and be released in the dissolution medium. As the strength of the buffering agent increased, not only did the timolol release rate increase but the release rate also became independent of the pH of the dissolution medium (Fig. 18). These studies indicated the potential utility of silicone-type elastomers as components for developing pH-sensitive oral controlled-release systems.

Methacrylic acid copolymers (Eudragit, Rohm GmbH) have been utilized as pH-sensitive polymers in oral drug delivery. A peptide analog inhibitor of HIV-1 protease (CGP 57813) has shown increased bioavailability in mice when administered as a pH-sensitive polymeric nanoparticle formulation (59). Similar results have been recently reported in a dog oral bioavailability study (60). Nanoparticles (245–264 nm) were prepared from poly(methacrylic acid-*co*-ethylacrylate) with a 1:1 molar monomer ratio (Eudragit L100-55) or poly(methacrylic acid-*co*-methylmethacrylate) with a 1:2 molar monomer ratio (Eudragit S100). The Eudragit L100 nanoparticles were soluble above pH 5, and the Eudragit S100 nanoparticles were soluble above pH 7. Aqueous suspensions of CGP 57813 in an amorphous form were used as controls for oral dosing studies in dogs and showed no detectable plasma levels of the drug. Significant increases in CGP 57813 bioavailability were observed in the dog oral dosing study (Fig. 19) that were both polymer and food dependent. With both polymers, bioavailability

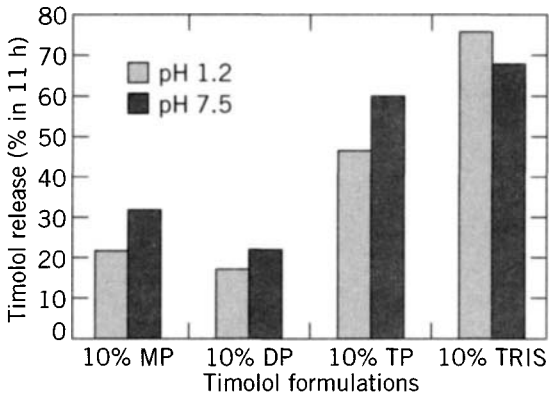


Figure 18. Effect of the pH of dissolution medium on the release of timolol from pH-controlled silicone microspheres (100 mg) at 37°C. Means ± SE of 3–5 experiments are presented. *Source:* with kind permission of Elsevier Science–NL, Sara Burgerhartstraat 25, 1055 KV Amsterdam, The Netherlands.

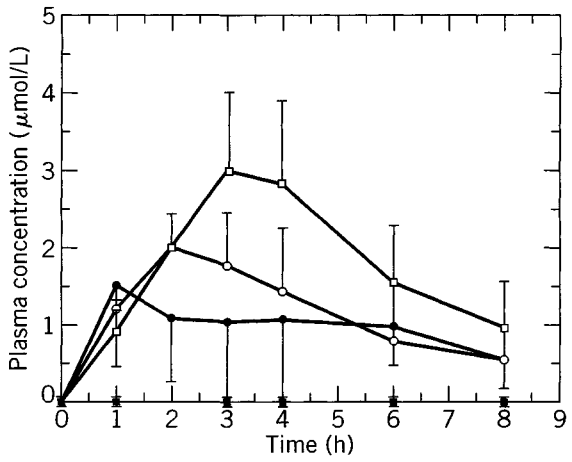


Figure 19. Plasma concentration profiles following oral administration of CGP 57813 from Eudragit L100-55 (● fasted dogs, ○ fed dogs) and S100 (■ fasted dogs, □ fed dogs) nanoparticles; mean ± SEM (n = 4). In vitro, the IC90 against HIV-1/LAV in MT-2 cells is 0.1 umol l^{-1}. *Source:* Reprinted from Ref. 60, with kind permission of Plenum Publishing Corporation, New York.

was greater in the fed state than the fasted state, possibly reflecting a slowing of GI transit, allowing more efficient nanoparticle dissolution and drug absorption. S100 nanoparticles showed a greater effect on CGP 57813 bioavailability in dogs than did L100 nanoparticles, which is in contrast to results previously observed in mice. This discrepancy in results may be related to species-specific differences in GI pH and is a factor that requires further evaluation to predict the performance of these systems in a human clinical application. The results of this study do indicate, however, that pH-sensitive polymers that dissolve above pH 5.5 may be useful as controlled-release polymers for oral administration.

Narisawa et al. also employed Eudragit coatings in a pH-sensitive bead formulation to develop a sigmoidal release system (SRS) (61). Uncoated drug beads were prepared from a powder mixture of drug and sucrose or drug and succinic acid using a CF granulator. After applying the powder mixture to nonpareil seeds with continuous binder spray, the resultant beads were spray-coated with Eudragit RS 30D, talc, triethylcitrate, and water. The beads were approximately 1,100 μm in diameter, with a 90-μm coating film. Utilizing sucrose instead of succinic acid in the initial bead preparation led to beads from which the release of a model drug was dependent on the coating thickness and followed first-order (10% coating) or zero-order (15% or 20% coating) kinetics without a significant lag period. At 30% coating, there was little or no drug release. Conducting the dissolution studies in various organic acid media demonstrated that drug release was significantly increased in the presence of an acidic medium, with succinic acid providing the most dramatic increase in drug release. Incorporation of succinic acid into the bead formulation converted the release profiles to a sigmoid shape characterized by an initial lag phase that was followed by a rapid increase in drug release. The duration of the lag phase

could be controlled by the thickness of the applied coating, but the release phase at a fixed succinic acid level was extremely constant after the lag delay. An evaluation of this bead formulation with acetaminophen as a model drug was evaluated in an oral dosing study in dogs (Fig. 20) and indicated that the lag and release phases observed in vitro were confirmed in vivo.

Polymer beads that are pH sensitive and thermally responsive have also been studied. The strategy employed with these systems is based on the fact that the polymer blends will not solubilize at gastric pH levels and the incorporated drug will be protected during residence time in the stomach. Linear terpolymers of (poly[*N*-isopropylacrylamide-*co*-butylmethacrylate-*co*-acrylic acid]) were fabricated into beads loaded with human calcitonin, an enzymatic labile peptide (62). The polymer becomes soluble in the vicinity of neutral pH and can thus release drug once in the small intestine. Higher loading of calcitonin was attained with increasing content of acrylic acid (hydrophilic polymer). Polymer beads with 7 and 10% acrylic acid achieved approximately 50% calcitonin loading with 85% drug release in 4 h at pH 4.5 (compared with 15% calcitonin loading and 15% drug release under similar conditions). The released calcitonin was apparently not aggregated into fibrillar structures because it could be isolated from the dissolution media and used in a rat intramuscular injection study to show the expected changes in plasma calcium levels. The ability to achieve high loading capacity and rapid release in a pH-responsive manner could provide a useful basis for developing this system into an effective oral controlled-release system. A somewhat similar system has been reported using theophylline as a model drug with polymeric nanobeads prepared from poly(*N*-isopropylacrylamide-*co*-methacrylic acid) with *N,N'*-methylenebisacrylamide as the cross-linking agent (63). Particle size ranged from 114 to 413 nm depending on polymer composition and experimental temperature (decreasing size with increasing temperature at a fixed polymer composition). Volume-phase transitions of polymer lattices demonstrated clear dependence on polymer composition, temperature, and ionic strength. Regulation of volume changes and drug loading can be achieved by varying these parameters and can be envisioned to provide a rational basis for designing pH-sensitive controlled-release strategies for oral administration.

Gelling polymers have also been utilized with or without rate-controlling coatings to effect controlled release of active agents. Typically, water-soluble drugs are released by diffusion of dissolved drug across the gel layer, whereas poorly soluble drugs are primarily released via a surface erosion mechanism. Matrices incorporating alginate salt or a combination of salts have been utilized with several drugs (64–66). Sodium alginate is a high-molecular-weight linear random copolymer of D-mannuronic acid and L-guluronic acid residues. Below pH 3, alginic acid is insoluble but forms a swellable polymer. At or above neutral pH, sodium alginate is soluble and hydrates to form viscous solutions. Because of the pH dependence of alginate hydration and rheology, pH-dependent controlled-release formulations can be designed that afford varying release rates depending on the water solubility of the incorporated drug. Tablets prepared from 49% sodium alginate, 20% drug, 30% lactose, and 1% magnesium stearate can be manufactured by direct compression of the blend and have been shown to provide pH-dependent drug release (67). When chlorpheniramine maleate, a highly water-soluble drug, was prepared in this matrix, the release rate was significantly higher in simulated gastric fluid (pH 1.2) than in simulated intestinal fluid (pH 7.5). Incorporation of hydrochlorothiazide, a poorly soluble drug, afforded the opposite results, that is, release was faster at pH 7.5 than at pH 1.2. The differences in release rates for very soluble and poorly soluble drugs at different pH levels were attributed to differences in the internal microscopic structure of the

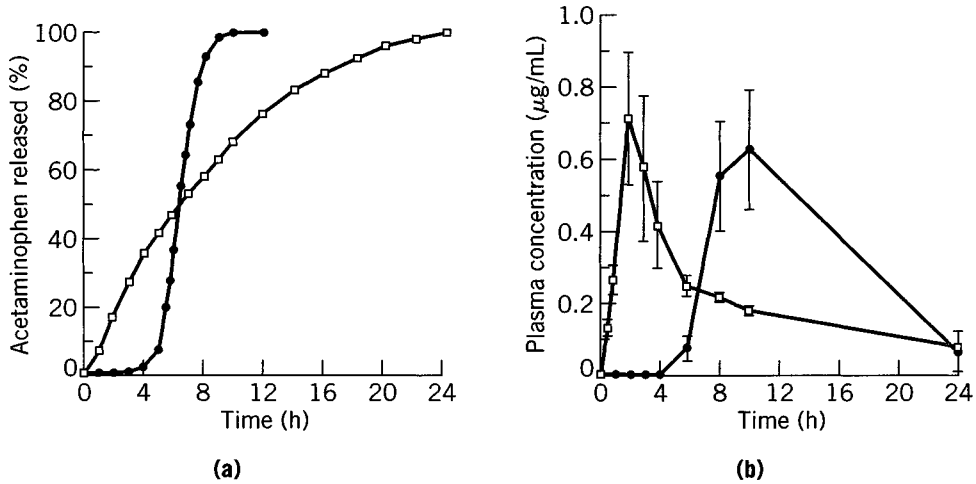


Figure 20. Release profiles in water (**a**) and plasma concentration-time profiles (**b**) of acetaminophen following oral administration to beagles of EC-coated beads or SRS with the same T_{50}. Preparations: (□) EC-coated beads (4% coating); (●) SRS (70% coating). *Source:* Reprinted from Ref. 61, with kind permission of Plenum Publishing Corporation, New York.

hydrated surface layer and the different hydration kinetics in the two pH conditions. At low pH, alginate matrices formed a particulate and porous gel medium, which could account for the very rapid release of highly water-soluble drugs through aqueous pathways. This same particulate hydrated layer observed at low pH, however, also exhibited strong mechanical properties that were much more resistant to surface erosion than the continuous gel that is formed at pH 7.5. The resistance to surface erosion at low pH can explain the slow release of poorly soluble drugs at low pH because the release of poorly water-soluble drugs from a hydrated gel matrix generally relies on surface erosion processes rather than diffusion.

pH-responsive gelatin microspheres have also been prepared by coating glutaraldehyde–cross-linked gelatin and applying either alginate or chitosan coatings (68). Chitosan is deacylated chitin and a linear, cationic polymer of 2-amino-2-deoxy-β-D-glucan that is soluble in dilute acid. Alginate is a linear, anionic polymer that is soluble at higher pH values. Cross-linked methotrexate gelatin microspheres of various particle sizes were prepared and coated with either alginate or chitosan. Nearly zero-order methotrexate release could be obtained that was inversely proportional to particle size and coating thickness. Alginate-coated microspheres afforded slower release rates in simulated gastric fluid than in simulated intestinal fluid, whereas chitosan coated microspheres gave the opposite result. As such, alginates coatings could be utilized to prolong drug release in acidic environments (for example, the stomach), whereas chitosan coatings could provide the same control in neutral or basic environments (for example, the intestine). The results from these studies, however, were of questionable utility because the release profiles generally extended over a period of days rather than hours. Although microsphere coatings that exhibited pH selectivity could be selected, the eventual practicality of the approach requires developing particles and coatings that provide release rates more consistent with the gastric and intestinal residence times that oral formulations normally experience.

The examples provided in the preceding paragraphs indicate the potential utility of pH-sensitive controlled-release systems. As indicated, the performance of these systems is determined by the effects of GI pH changes on the components of the dosage form and the incorporated active drug. Further optimization and development of this approach is required to lead to effective oral controlled-release systems that can be manufactured to perform in a reliable fashion.

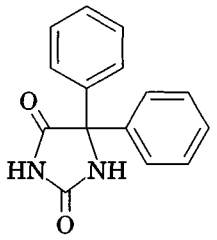
Prodrugs

Many potential therapeutic candidates do not possess satisfactory physicochemical properties to be viable candidates for oral drug delivery, either as immediate-release formulations or through controlled-release technology. The limitations can be related to solubility, stability, aggregation tendency, and intrinsic membrane permeability. These factors, either alone or in combination for some drug candidates, can render the candidate ineffective as an orally administered drug. The general strategy of prodrug technology, which has been known and practiced for decades, is to synthesize a chemically modified version of the parent drug that overcomes the inherent problem in the ability of the drug to be adequately absorbed. For instance, a drug may be too hydrophilic to partition into biologic membranes. If a prodrug can be synthesized that modifies the parent drug partitioning behavior appropriately, then flux across a biologic membrane can be achieved. Inherent in this whole approach is the aspect that the prodrug must be readily reversible to the parent drug, either by hydrolytic or enzymatic mechanisms, and that the regenerated parent drug must retain its intrinsic pharmacologic activity. An additional item that has to receive careful attention is the potential pharmacologic or toxicological activity of the prodrug moiety. Because the prodrug moiety will be released in the in vivo setting after cleavage of the prodrug to the parent drug and prodrug moiety, the potential exists for either unwanted pharmacologic effects or undesired adverse effects due to the prodrug moiety itself. If the prodrug moiety is a chemical entity that has not been proven to be safe, then regulatory issues concerning additional required safety studies also become a factor. The prodrug itself, given that it will likely have to exist in the prodrug form for a discreet amount of time after administration, will also be subject to both pharmacologic and toxicological scrutiny in the development and regulatory cycles. Prodrug strategies have been frequently attempted to improve the absorption of poorly absorbed drug candidates. In some cases, such as sulindac sulfide, poor water solubility has limited absorption from oral formulations. Sulindac, which is a prodrug of sulindac sulfide with improved water solubility compared to sulindac sulfide, was developed to reduce GI toxic reactions but also demonstrated improved bioavailability (69,70). Improving aqueous solubility does not, however, ensure improved bioavailability of drug candidates. Absorption across biological membranes requires a certain degree of lipophilicity and the creation of very aqueous soluble prodrugs can, in fact, reduce membrane transport if a proper hydrophile/lipophile balance is not attained. In many cases, in fact, lipophilic prodrugs have been created to improve absorption of polar drug candidates including clindamycin (71), erythromycin (72), cefotiam (73), and ampicillin (74). The ester prodrugs of ampicillin, namely bacampicillin, pivampicillin, and talampicillin, show improved bioavailability compared to ampicillin and rapid reconversion via ester hydrolysis. Within the scope of this text, it is not practical to review all of the prodrug approaches that have been evaluated for a rather long list of potential drug candidates to which they have been applied. What will be attempted is a review of several approaches to provide a background for what may be achievable with prodrug approaches to oral controlled-release technology.

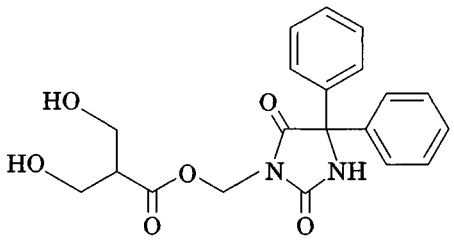
Phenytoin is an anticonvulsant with poor bioavailability that is most often attributed to poor water solubility. A number of investigators have evaluated various prodrugs of phenytoin, including fosphenytoin, which increased water solubility nearly 5,000-fold (75). A glyceride-derived prodrug of phenytoin has also been synthesized (76) and evaluated both in vitro (77) and in vivo (78) for its applicability as a phenytoin prodrug that can overcome the in-

herent poor oral bioavailability of phenytoin itself. Direct esterification of 3-hydroxy-2-hydroxymethylproprionic acid (bis-hydroxyisobutyric acid) with 3-hydroxymethylphenytoin yielded the test prodrug, phenytoin-bis-hydroxyisobutyrate as shown in Figure 21. The pharmacokinetic profile and pharmacologic activity of phenytoin-bis-hydroxyisobutyrate were evaluated in rat models. Both phenytoin and the phenytoin prodrug were orally administered to rats as oral suspensions in 0.5% methyl cellulose. Pharmacokinetic analysis based on plasma phenytoin levels indicated that the prodrug afforded an earlier T_{max} (0.74 ± 0.1 h versus 1.25 ± 0.5 h), a higher C_{max} (5.25 ± 0.99 μg/mL versus 1.90 ± 0.11 μg/mL), and a larger AUC (28.5 ± 4.2 μg.h/mL versus 10.0 ± 1.1 μg/h/mL) than that observed following administration of the parent drug, phenytoin. The plasma half-life of phenytoin was not significantly altered. Measurable quantities of the prodrug were not identified in the plasma samples. Phenytoin-bis-hydroxybutyrate was found to be equipotent with phenytoin following ip administration but more active than phenytoin following oral dosing in rats (based on the maximal electroshock test). Toxicity was not observed for the prodrug. The temporal profile of the anticonvulsant activity of phenytoin-bis-hydroxybutyrate was consistent with its pharmacokinetic profile, suggesting that the improved pharmacologic activity of the prodrug is due to its improved bioavailability relative to phenytoin itself.

Morpholinoalkyl esters (HCl) salts of naproxen and indomethacin (Fig. 22) were synthesized and evaluated with both in vitro and in vivo models (79). Both parent compounds are poorly water soluble ($<5.9 \times 10^{-5}$ M/L in simulated gastric fluid and $<6.7 \times 10^{-3}$ M/L in pH 7.4 phosphate buffer) and are known to present issues with regard to a tendency to cause local tissue irritation. Aqueous solubility of prodrugs of both naproxen and indomethacin increased over 2,000-fold in both simulated gastric fluid and phosphate buffer. The pK_a values increased from a range of 4.2–4.5 for the parent drugs to 6.9–8.6 for the prodrugs. The prodrugs were more lipophilic at pH 7.4 but less lipophilic at pH 1.3 when compared with the parent drugs. As the carbon chain length was extended between the ester function and the morpholino function, stability in pH 7.4 buffer increased, while stability in pH 1.3 buffer decreased. The prodrugs of naproxen and indomethacin had half-lives in rat plasma of 1.1–4.1 min and 20.4–31.5 min, respectively. Based on an analysis of in vitro properties, naproxen and indomethacin prodrugs with a 4-carbon spacer were evaluated in a rat model for absorption kinetics and tissue irritation. When dosed to rats as an equimolar gavage solution, prodrugs of naproxen and indomethacin were 33.73 ± 8.4% and 34.3 ± 3.4% more bioavailable, respectively, than the corresponding parent drug. Using a ranked recording scale for tissue irritation or damage, both prodrugs were found to be less damaging than the parent drugs on both acute and chronic dosing regimens. These data indicated that the morpholino prodrugs of naproxen and indomethacin showed improved stability in gastric fluid, improved solubility at small-intestine pH, rapid in vivo conversion to the parent drug, and were more bioavailable and less irritating than the parent compounds. As such, this prodrug approach may be applicable to compounds similar to naproxen and indomethacin for oral delivery systems.



Phenytoin



Phenytoin-bis-hydroxyisobutyrate

Figure 21. Structures of the compounds. *Source:* Reprinted from Ref. 78, with kind permission of Plenum Publishing Corporation, New York.

Another prodrug approach to indomethacin has utilized a triethylene glycol indomethacin ester (TIE) (80,81). The plasma half-life of TIE was 11.55 min in rat plasma with complete reversion to the parent drug, but it should be pointed out that this is significantly shorter than the half-life observed in human plasma, which was 3.8 h. Pharmacokinetic analysis of TIE prodrug indicated that in contrast to that observed with the morpholino ester prodrug (79), the relative bioavailability and time to C_{max} for TIE was less than that observed with indomethacin alone. The plasma profile was, however, significantly extended over that seen with indomethacin itself, which could indicate slower and more prolonged absorption or a partitioning into and slow release from a tissue compartment. Although the plasma profile of indomethacin was lower and more prolonged than indomethacin itself, the prodrug did not show an ulcerogenic potential, which could make this approach useful in spite of a lack of improvement in systemic bioavailability.

Phosphomonoester products of primary alcohols and unhindered phenols have shown good chemical stability and rapid enzymatic hydrolysis in vivo but exhibit a slow rate of conversion with sterically hindered secondary and tertiary alcohols (82,83). In an attempt to overcome this problem, an oxymethyloxycarbonyl spacer group has been utilized as a less sterically hindered spacer group between the hydroxyl group and phosphate functionality (84). Phosphoryloxymethyloxycarbonyl derivatives should be converted by phosphatase-mediated hydrolysis to an intermediate with subsequent rapid decomposition to the parent drug. The reconversion reaction scheme for these prodrugs is shown in Figure 23. Prodrugs of alcohols

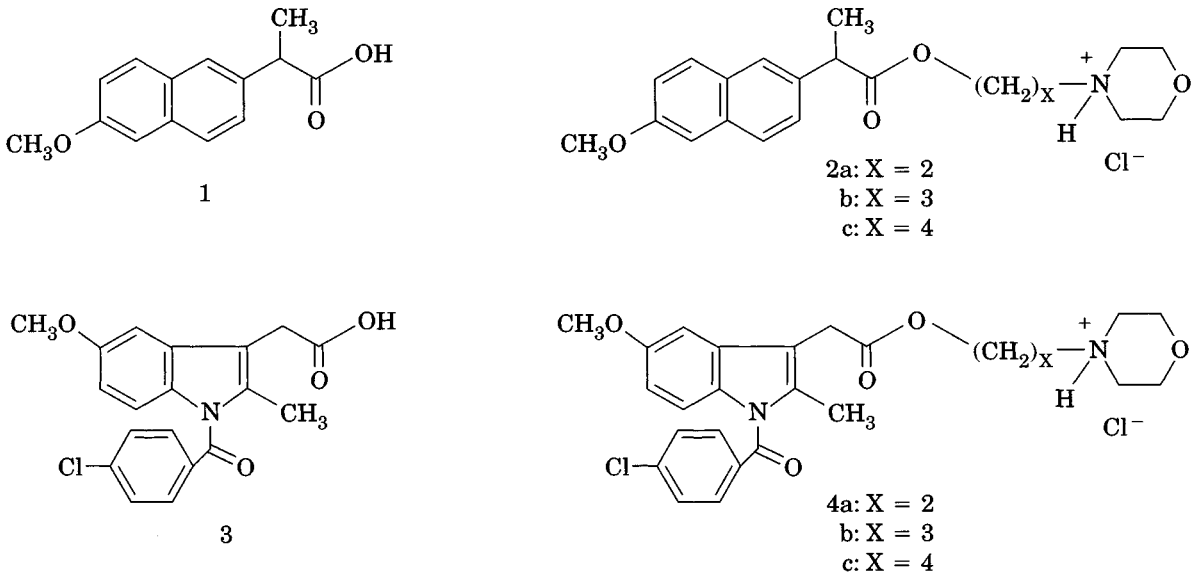


Figure 22. Chemical structures of naproxen 1, indomethacin 3, and their hydroxyalkylmorpholine (HCl) ester prodrugs. *Source:* Reprinted from Ref. 79, with kind permission of Plenum Publishing Corporation, New York.

(2-indanol), aliphatic amines (β-[3,4-dimethoxyphenyl]ethylamine), and aromatic amines (benzocaine) were synthesized but all exhibited unacceptable chemical stability, at least with regard to potential for utility in formulation processes. Even though the chemical stability of the prodrugs was not as great as needed, the phosphoryloxymethyloxycarbonyl prodrug of benzocaine was shown to have an approximately 10-fold greater catalytic constant for dephosphorylation by isolated human placental alkaline phosphatase at 25 C and pH 10.4 when compared with the constants for *p*-nitrophenyl phosphate. The other two prodrugs were not evaluated for enzymatic reactivity owing to either their very poor chemical stability (2-indanol) or low interest in water-soluble prodrugs (β-(3,4-dimethoxyphenyl)ethylamine. Therefore, even though chemical stability is not fully adequate with the current prodrug forms and requires further evaluation of alternate spacer groups, the basis for rapid enzymatic reconversion of the prodrug appears to be present, at least for the one benzocaine prodrug that was evaluated.

PMEA (9-[2-phosphonylmethoxyethyl]adenine) is an acyclic nucleoside phosphonate analog with antiviral activity that exhibits relatively poor permeation of biological membranes due to ionization of the phosphonate group at physiologic pH (pK_{a1} = 2.0 and pK_{a2} = 6.3). Measured oral bioavailability ranges from less than 1% in rhesus monkeys (85) to 7.8% in rats (86). A bis(pivaloyloxymethyl)-ester prodrug of PMEA (bis[POM]PMEA) was synthesized and evaluated in an in vitro cell culture model (Caco-2) to determine its transport, uptake, and metabolism (87). The bis(POM)PMEA prodrug was rapidly hydrolyzed by purified carboxylesterase with K_m = 87 μM and V_{max} = 9.5 μM/min values. Incubation of bis(POM)PMEA with homogenates of Caco-2 cells produced a similar profile. Transport studies in the human colon adenocarcinoma cell line, Caco-2, showed that 8.8% of the prodrug was transport in 3 h versus 0.1% of PMEA itself, which is consistent with the octanol–water partition coefficients (log P) of −4.11 and 2.48 for PMEA and bis(POM)PMEA. Because mono(POM)PMEA showed negligible transport across Caco-2 cells (<0.1% in 3 h), the increased flux seen with bis(POM)PMEA could not be attributed to the monoester. The ester was rapidly hydrolyzed with 23% appearing in the receiver compartment as intact bis(POM)PMEA, 33% as free PMEA, and 44% as mono(POM)PMEA. No intact bis(POM)PMEA was found intracellularly after a 3-h incubation, indicating rapid hydrolysis within the epithelial cells themselves. High levels of PMEA were found in the intracellular compartment, however, probably reflecting entrapment of the negatively charged PMEA.

The charge-related entrapment of PMEA intracellularly could account for slow release to the basolateral side of the cell monolayer. These results demonstrate an important point with regard to prodrug strategies for oral drug absorption. Unlike simplified lipid bilayer models that treat the GI mucosal as a single-lipid barrier membrane, the pathway for drug flux actually involves traversing two lipid bilayers (apical and basolateral) separated by a largely aqueous compartment (cytosol). For prodrugs that are absorbed via transcellular pathways and rapidly hydrolyzed in the aqueous intracellular compartment, the rate-controlling element in total drug flux can be the rate of release of the reconverted parent drug from the aqueous cytosol across the basolateral barrier membrane rather than the apparent transport of the prodrug across the apical membrane. The kinetics of prodrug absorption must also take into account the pathway of absorption as well as the hydrolytic or enzymatic lability of the prodrug in various cellular compartments to explain, or predict, the observed pharmacokinetic profile.

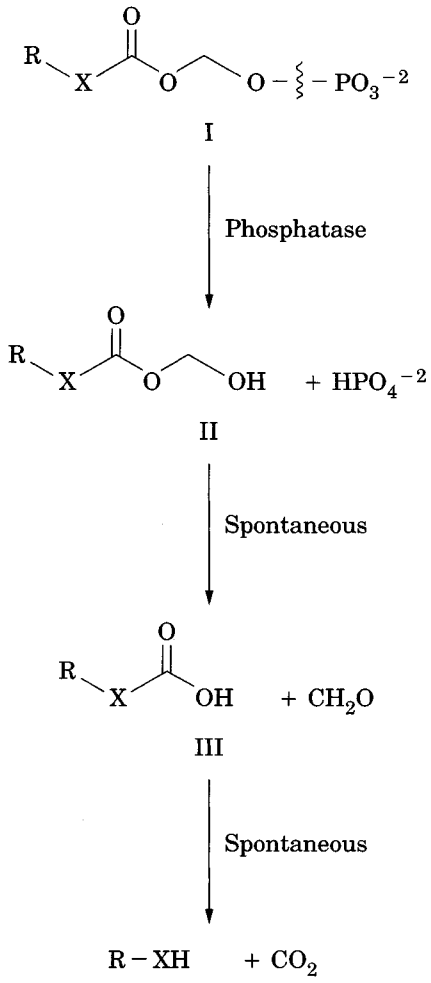


Figure 23. Enzymatic and nonenzymatic catalyzed steps involved in the generation of the parent drug from the phosphoryloxymethyloxycarbonyl prodrug system. *Source:* Reprinted from Ref. 84, with kind permission of Plenum Publishing Corporation, New York.

The potential utility of the bis(POM)PMEA prodrug was further evaluated in a nonhuman primate oral bioavailability study (88). The prodrug was orally administered to *Cynomolgus* monkeys as a solution in one of three formulations: hydroxypropyl-β-cyclodextrin complex, PEG-based cosolvent solution, and an aqueous suspension. The resulting plasma PMEA profiles are shown in Figure 24. Although PMEA itself showed only 4 ± 1% oral bioavailability, the three formulations tested in this study afforded bioavailabilities in the range of 22.2–24.7%. These data confirmed and extended the earlier in vitro data and demonstrated the potential utility of this prodrug approach.

Didanosine (2′,3′-dideoxyinosine, ddI) is an approved antiviral for HIV infection that exhibits relatively low and variable oral absorption that appears to be membrane permeability-limited (89). Adenosine deaminase (ADA)-activated 6-halo-dideoxypurine prodrugs (90,91) showed improved CNS penetration and were evaluated for oral bioavailability (92). Utilizing a conscious, chronically cannulated rat model, it was shown that the prodrug 6-Cl-ddP

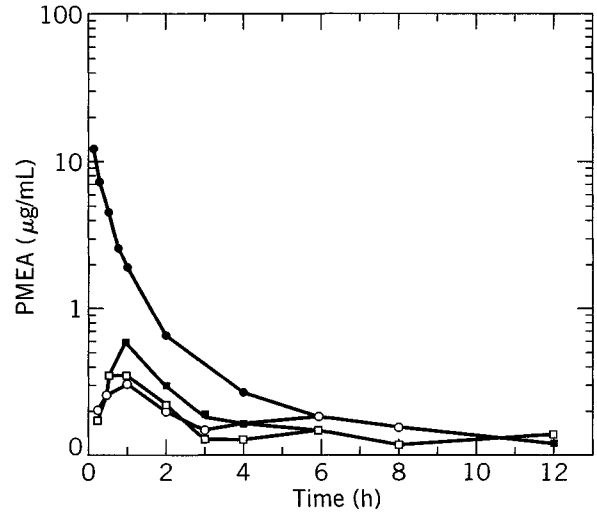


Figure 24. Mean PMEA concentrations in plasma following administration of intravenous ^{3}H-PMEA and three oral formulations of ^{3}H-bis(POM)-PMEA to *Cynomolgus* monkeys (n = 4). (●), intravenous PMEA; (○), oral HPBCD complex; (■), oral PEG solution; (□) aqueous suspension. *Source:* Reprinted from Ref. 88, with kind permission of Plenum Publishing Corporation, New York.

(6-Cl-2′,3′-dideoxypurine) had poor oral bioavailability (7 ± 3%) but high bioavailability (97 ± 11%) after portal administration, indicating that hepatic metabolism was not limiting. Greater than 50% of an oral dose of 6-Cl-ddp appeared in the systemic circulation as parent drug (ddI), indicating that the prodrug significantly improved the systemic availability of ddI and that prodrug absorption was not rate limiting. The data additionally demonstrated that the prodrug was extensively converted to the parent compound via ADA activity in the gut mucosa. These data suggest that lipophilic adenosine deaminase–activated prodrugs may have utility for improving the oral bioavailability of highly polar dideoxynucleosides such as ddI or related compounds.

Not all prodrug approaches for small molecules are directed toward improving bioavailability of the parent compound. An example is utilizing a glucuronide prodrug of menthol to provide stability in the small intestine with release of the parent drug upon arrival at the cecum or colon (93). Menthol-β-D-glucuronide stability was evaluated in contents isolated from various regions of the rat intestinal tract. The data (Fig. 25) demonstrated that the prodrug was stable in the stomach and small intestine but exhibited a fairly rapid hydrolytic rate in contents from the cecum and colon. Additionally, the change in octanol/water partition coefficient (log K = −1.61 and 3.07 for menthol-β-D-glucuronide and menthol, respectively) should minimize the absorption potential of the prodrug from the GI tract. This prodrug approach with menthol indicated, at least under in vitro conditions, how a strategy could be developed to synthesize a prodrug that is stable in the small intestine, has a log K value that should minimize absorption in the colon to effect local delivery of a therapeutic agent, and hydrolyzes to release the parent drug in the cecum or colon milieu.

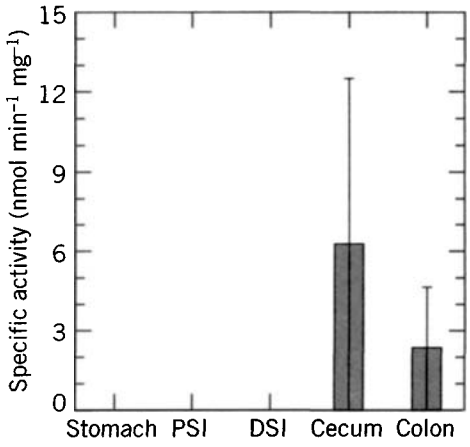


Figure 25. Hydrolysis of the prodrug menthol-β-D-glucuronide (nmoles of substrate hydrolyzed per min per mg of luminal contents) measured from various locations in the rat gastrointestinal tract. There was no menthol detected over the 1-h experiment in the luminal contents of the stomach, PSI, or DSI. Error bars are mean ±SD (n = 6). *Source:* Reprinted from Ref. 93, with kind permission of Plenum Publishing Corporation, New York.

Although most of the early prodrug efforts were directed toward traditional, organic drug candidates, the emergence of peptide and peptidelike drug candidates has spurred an interest in developing peptide prodrug strategies to improve their oral delivery. Unlike prodrug strategies for nonpeptidic drug candidates, where the goal is often to either modify solubility in the GI environment or alter the permeation properties of the parent drug in a favorable direction, prodrug strategies for peptides most often focus on providing increased protection against proteolytic enzymes in the GI tract because enzymatic degradation is generally a major barrier to effective oral formulation efforts. Several examples are provided to illustrate this approach.

A tripeptide prodrug of L-dopa was synthesized in an effort to develop a prodrug that overcame the decarboxylation of L-dopa in the gut wall and afforded acceptable oral bioavailability. Many prodrugs of L-dopa have been generated and evaluated, including esters, with varying degrees of success. In this study, the pGlu-L-Dopa-Pro prodrug was synthesized, and the proposed enzymatic pathway for reconversion to the parent drug in vivo is shown in Figure 26 (94). The prodrug structure effectively prevents L-dopa decarboxylation, which is the major intestinal degradative pathway for L-dopa. The conversion to parent drug involves two enzyme catalyzed steps, pyroglutamyl aminopeptidase I and prolidase. Evaluations with in vitro Ussing chambers with rat jejunal tissue and with an in situ single-pass intestinal perfusion model demonstrated that the prodrug was readily absorbed via an intestinal peptide transport that could be inhibited by captopril and various dipeptide competitors. The tripeptide was readily converted, both in vitro and in vivo, to the parent drug L-dopa, thereby demonstrating the potential utility of this approach.

Desmopressin (dDAVP), a synthetic analog of antidiuretic hormone, is normally administered nasally or orally, although the oral availability is quite low (<1%). The poor oral bioavailability is generally attributed to low lipophilicity, but susceptibility to enzymatic degradation, particularly by α-chymotrypsin, probably also plays a role (95). In an attempt to address these issues with the oral bioavailability of dDAVP, a series of ester prodrugs were synthesized at the tyrosine phenolic group of dDAVP (96). Several aliphatic carboxylic acid esters and a carbonate ester were made as shown in Figure 27. The octanol/aqueous buffer pH 7.4 log P of dDAVP is < -3.5. The log P values for the various prodrugs ranges from < -3 for proprionyl to 0.41 for octanoyl. All prodrugs were essentially stable in pH 7.4 buffer (half-lives ranged from 66 to 4,460 h) but exhibited half-lives from <1 min (hexanoyl and octanoyl) to 40 min (pivaloyl) in the presence of α-chymotrypsin. In 80% human plasma, the prodrug half-lives were basically similar except for pivaloyl (5.9 h) and 2-ethylhexanoyl (14.1 h). Utilizing the Caco-2 cell culture model, all the prodrugs except isobutyloxycarbonyl showed increased permeability relative to the parent dDAVP. There was, however, no correlation between permeability and lipophilicity. Regardless, the data indicated that this prodrug approach led to ester prodrugs of dDAVP that were stable in a buffer environment but readily converted to the parent drug in the presence of enzyme or plasma and generally afforded improved permeability characteristics.

A final example of prodrug strategy for developing oral formulations for peptide drug candidates involves recent efforts to develop intramolecular cyclic prodrugs to provide prodrug candidates with improved absorption characteristics as well as reduced susceptibility to metabolic degradation via intestinal enzymes (97,98). A phenylproprionic acid prodrug of a model hexapeptide (H-Trp-Ala-Gly-Gly-Asp-Ala-OH) was prepared and evaluated. Previous work (99) had demonstrated that a cyclic acyloxyalkoxycarbamate prodrug of the same model hexapeptide gave enhanced membrane-permeation properties and increased stability to metabolic enzymes. The proposed scheme for metabolic breakdown of the phenylproprionic prodrug is shown in Figure 28 and involves a relative slow esterase-catalyzed step followed by a rapid chemical hydrolysis to regenerate the linear hexapeptide plus lactone. The permeability of the prodrug (P_{app} = 1.21 ± 0.12 × 10^{-7} cm/s) across Caco-2 cell monolayers was approximately 70 times greater than that for the parent hexapeptide (P_{app} = 0.17 × 10^{-8} cm/s) and showed greater stability for the prodrug than the parent peptide. Enzymatic cleavage and hydrolysis of the prodrug to the parent compound was significantly faster in 90% human plasma, rat intestinal homogenate, or Caco-2 cell homogenate than in pH 7.4 aqueous buffer. The intramolecular cyclization prodrug strategy for peptides offers another novel approach to developing peptide drugs as oral formulation candidates that possess improved stability to enzymatic degradation (of the parent peptide) and improved absorption characteristics across epithelial cell layers.

In the scope of the text here, it has obviously not been possible to cover all the diverse prodrug strategies that have been evaluated in attempts to develop oral formulations for both traditional, organic drug candidates and peptide or peptidelike drug candidates. Hopefully, the exam-

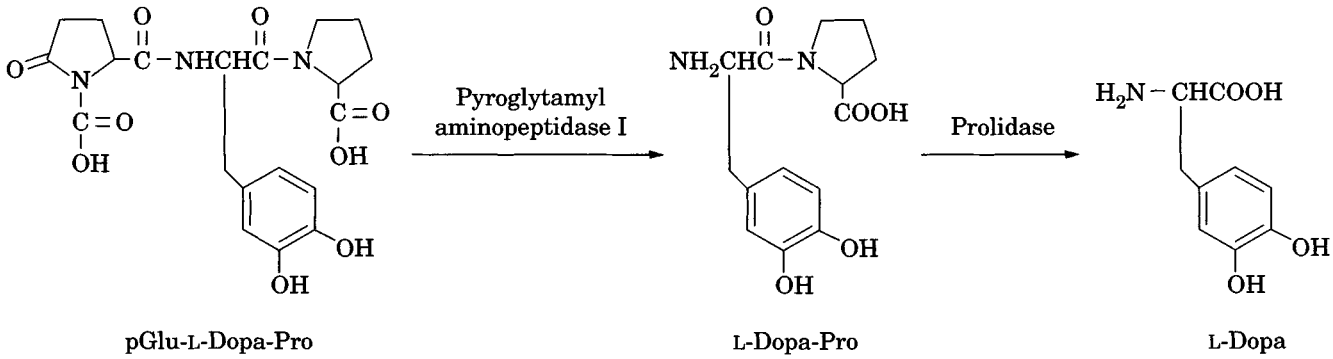


Figure 26. Release of L-dopa from pGlu-L-Dopa-Pro by successive actions of proteolytic enzymes. *Source:* Reprinted from Ref. 94, with kind permission of Plenum Publishing Corporation, New York.

ples given exemplify the varied approaches that can be considered and provide a basis for development and utilization of prodrug strategies toward drugs that would otherwise be unsuitable candidates for oral drug delivery systems.

COLON

Although it is generally felt that the small intestine is the primary site of drug absorption and therefore the preferred area of the GI tract to target with various controlled-release technologies, a major interest has developed in directing drugs and dosage forms to effect primary drug release in the colon region (100–102). The reasons for this interest are varied, but include (*1*) reduced proteolytic activity in the colon region, which may be helpful in effecting reasonable absorption of certain drugs that are enzymatically labile in the small intestine, particularly peptides and proteins; (*2*) reduced fluid and motility in the colon when compared with the small intestine, which could afford advantages in terms of incorporating multiple components in a formulation, such as permeation enhancers, that must reach the epithelial absorptive layer in a high concentration and in close spatial proximity to the each other; and (*3*) treatment of local pathologies of the colon such as carcinomas and inflammatory bowel disease.

Regardless of the therapeutic strategy justifying efforts to develop systems for drug release in the colon, some basic elements will apply from a therapeutic standpoint regarding drugs that are reasonable candidates for this approach. Because the arrival time of a drug or dosage form in the colon is subject to the vagaries of gastric emptying and small-intestine transit, drugs that require an immediate onset of action or a very specific time of onset after oral administration are not reasonable candidates. As an extension of this—and the fact that under normal conditions a patient is on a daily meal regimen—it can be assumed that the transit time to the colon will likely exceed 6–8 h on average. Therefore, twice-a-day dosing is the maximum frequency that can be expected from colon controlled-release systems, and, more likely, controlled-release systems for the colon will most commonly have to be once-a-day dosing therapies. This is particularly true if the controlled-release system is a sustained-release formulation where a drug release profile of 6–8 h is superimposed on an average transit time of 6–8 h to the colonic region. In this case, the overall time from administration to completion of drug release will probably approach 12–16 h, thereby restricting applications to those where once-a-day dosing without a specific time of onset is an acceptable therapeutic regimen.

There have been three basic approaches to designing drugs or dosage forms for delivery of therapeutic agents specifically to the colon: (*1*) utilizing pH changes that occur in the upper colon (103); (*2*) timed-release capsules with sufficient delay to allow transit to the colon before activating significant drug release (104); and (*3*) polymeric carriers that are degraded by bacterial enzyme activity specific to the colon region (105). With all of these approaches, effectiveness will be limited by the capability of the dosage form to resist the hydrodynamic and enzymatic forces present during transit from the stomach to the colon and to protect the active drug from premature release or degradation prior to arriving in the colon. Another general concern, which will not be directly addressed here, is the viscous contents of the colon region. As food stuffs are digested and absorbed, nonabsorbed materials pass from the small intestine to the colon where water is gradually reabsorbed and the intestinal contents become more viscous, eventually reaching a semisolid state. The presence of this material in the colon can present significant problems to the effective performance of drugs or dosage forms in the colon. The viscosity of the contents can present a formidable barrier to release and diffusion of drugs from a controlling dosage form to the wall of the colon where absorption occurs. Additionally, a potential for significant nonspecific adsorption to colonic contents can reduce the effective amount of drug available for absorption. A third potential problem is that although bacterial contents can be utilized to effect drug release in the colon, these same bacteria may present a degradative pathway for the drug itself, again reducing the amount of drug available for absorption. This potential interference in drug release and absorption will not be evaluated here in any quantitative sense, but it is critical that the research and developer of colon controlled-release technologies be aware of this po-

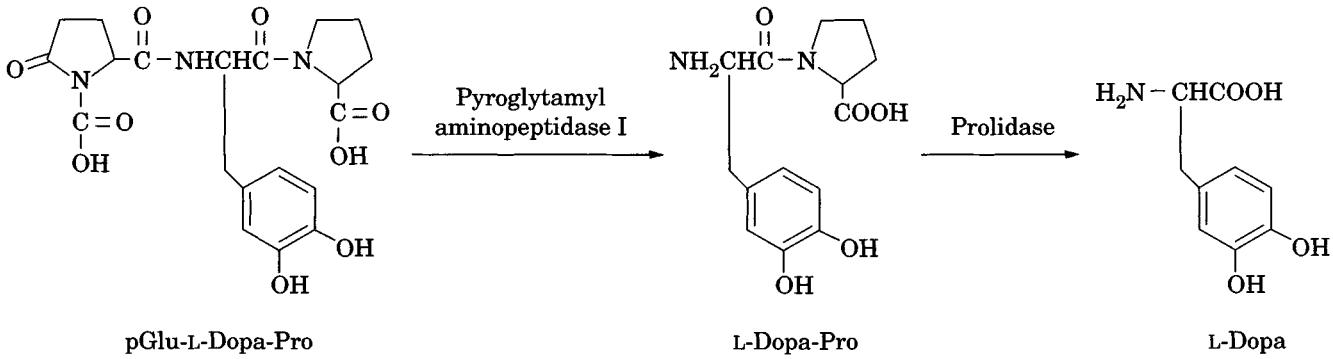


Figure 26. Release of L-dopa from pGlu-L-Dopa-Pro by successive actions of proteolytic enzymes. *Source:* Reprinted from Ref. 94, with kind permission of Plenum Publishing Corporation, New York.

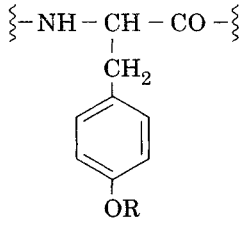
ples given exemplify the varied approaches that can be considered and provide a basis for development and utilization of prodrug strategies toward drugs that would otherwise be unsuitable candidates for oral drug delivery systems.

COLON

Although it is generally felt that the small intestine is the primary site of drug absorption and therefore the preferred area of the GI tract to target with various controlled-release technologies, a major interest has developed in directing drugs and dosage forms to effect primary drug release in the colon region (100–102). The reasons for this interest are varied, but include (*1*) reduced proteolytic activity in the colon region, which may be helpful in effecting reasonable absorption of certain drugs that are enzymatically labile in the small intestine, particularly peptides and proteins; (*2*) reduced fluid and motility in the colon when compared with the small intestine, which could afford advantages in terms of incorporating multiple components in a formulation, such as permeation enhancers, that must reach the epithelial absorptive layer in a high concentration and in close spatial proximity to the each other; and (*3*) treatment of local pathologies of the colon such as carcinomas and inflammatory bowel disease.

Regardless of the therapeutic strategy justifying efforts to develop systems for drug release in the colon, some basic elements will apply from a therapeutic standpoint regarding drugs that are reasonable candidates for this approach. Because the arrival time of a drug or dosage form in the colon is subject to the vagaries of gastric emptying and small-intestine transit, drugs that require an immediate onset of action or a very specific time of onset after oral administration are not reasonable candidates. As an extension of this—and the fact that under normal conditions a patient is on a daily meal regimen—it can be assumed that the transit time to the colon will likely exceed 6–8 h on average. Therefore, twice-a-day dosing is the maximum frequency that can be expected from colon controlled-release systems, and, more likely, controlled-release systems for the colon will most commonly have to be once-a-day dosing therapies. This is particularly true if the controlled-release system is a sustained-release formulation where a drug release profile of 6–8 h is superimposed on an average transit time of 6–8 h to the colonic region. In this case, the overall time from administration to completion of drug release will probably approach 12–16 h, thereby restricting applications to those where once-a-day dosing without a specific time of onset is an acceptable therapeutic regimen.

There have been three basic approaches to designing drugs or dosage forms for delivery of therapeutic agents specifically to the colon: (*1*) utilizing pH changes that occur in the upper colon (103); (*2*) timed-release capsules with sufficient delay to allow transit to the colon before activating significant drug release (104); and (*3*) polymeric carriers that are degraded by bacterial enzyme activity specific to the colon region (105). With all of these approaches, effectiveness will be limited by the capability of the dosage form to resist the hydrodynamic and enzymatic forces present during transit from the stomach to the colon and to protect the active drug from premature release or degradation prior to arriving in the colon. Another general concern, which will not be directly addressed here, is the viscous contents of the colon region. As food stuffs are digested and absorbed, nonabsorbed materials pass from the small intestine to the colon where water is gradually reabsorbed and the intestinal contents become more viscous, eventually reaching a semisolid state. The presence of this material in the colon can present significant problems to the effective performance of drugs or dosage forms in the colon. The viscosity of the contents can present a formidable barrier to release and diffusion of drugs from a controlling dosage form to the wall of the colon where absorption occurs. Additionally, a potential for significant nonspecific adsorption to colonic contents can reduce the effective amount of drug available for absorption. A third potential problem is that although bacterial contents can be utilized to effect drug release in the colon, these same bacteria may present a degradative pathway for the drug itself, again reducing the amount of drug available for absorption. This potential interference in drug release and absorption will not be evaluated here in any quantitative sense, but it is critical that the research and developer of colon controlled-release technologies be aware of this po-



Tyr (dDAVP)

R

I —C(=O)—C_2H_5

II —C(=O)—$C(CH_3)_3$

III —C(=O)—$(CH_2)_4CH_3$

IV —C(=O)—$(CH_2)_6CH_3$

V —C(=O)—$CH(C_2H_5)—(CH_2)_3CH_3$

VI —C(=O)—$O—CH_2CH(CH_3)_2$

Figure 27. Scheme I. *Source:* Reprinted from Ref. 96, with kind permission of Plenum Publishing Corporation, New York.

tential and factor these parameters into any analysis of the effectiveness of a given drug or dosage form.

Time Specificity

Attempting to predict the time required for a dosage form to transit from the stomach to the colon has been tenuous at best. Some reasonably reproducible data have been generated indicating that, in humans, the small intestinal transit time generally falls in the range of 2–4 h (106). These data seem to be reasonably consistent, at least in the fasted dog model, regardless of the size or density of the formulation or the fed/fasted state of the volunteer (107). With multiparticulate dosage forms, data in dogs indicated that there is little spreading of multiparticulates after exit from the stomach, (108) whereas in the fed state, considerable spreading and dilution of multiparticulate dosage forms might be expected due to mixing with food contents and variable gastric emptying (106). Although this 3- to 4-h time window of small intestinal transit can be argued as to its validity and reproducibility in humans, it is well accepted that the major variable in overall intestinal transit is residence time in the stomach and that this plays the predominant role in determining the average time it would take a dosage form of any size or geometry to traverse the stomach and small intestine en route to the colon. In humans with normal GI physiology, dosage forms exceeding approximately 2 mm in diameter are not readily emptied from the stomach during the fed state. Rather, these dosage forms are most typically emptied during the interdigestive phase, which is generally initiated somewhere in the range of 3–4 h after meal consumption, depending on the mass, volume, and caloric content of the meal. The interdigestive contractile activity, which is physiologically divided into several phases, has a repeating cycle of motility with each overall cycle lasting approximately 3–4 h. Therefore, it can be expected that a dosage form >2 mm in size might reasonably be expected to exit the stomach somewhere in the range of 4–8 h after ingestion with a meal. Obviously, the normal physiologic motility patterns of the stomach and small intestine can be affected by an individual's health, presence of GI pathologies, and any concomitant medications being taken. The net result of all these factors is that transit time from mouth to colon is very difficult to estimate in humans with any great deal of reliability. For the sake of discussion, it can be assumed that the overall transit time to the colon will be approximately 3–5 h in the fasted state and 6–10 h in the fed state. Given these rather wide ranges of overall transit times, it is apparent that predicting arrival of dosage forms in the colon, and targeting drug release to be dependent on a timing mechanism, is complicated at best. In spite of these normal variabilities that must be factored into any design of an oral controlled-release dosage form for delivery of drug to the colon, significant efforts have been directed toward achieving such goal.

The most well-studied and well-published time-based delivery system for targeting drug delivery to the colon has been the Pulsincap capsule of R.P. Scherer (109–111). The Pulsincap capsule consists of a water-insoluble body and a water-soluble cap. The drug formulation is contained and protected within the capsule body and separated, inside the water soluble cap, by a hydrogel polymer plug. After a predetermined lag due to dissolution of the cap, the hydrogel swelling rate controls the time of release. After reaching a critical swelling stage, the hydrogel plug is ejected, and the drug formulation is released. In theory, by designing the hydrogel plug with specific swelling and ejection times, the Pulsincap capsule can be made to deliver its contents to any site along the GI tract, including the colon. The additional apparent advantage is that the formulation itself is relatively protected from the GI environment prior to release, thereby affording advantages in terms of drug stability. Toxicologic evaluation of the polymeric hydrogel plug and components indicated no safety issues (R.P. Scherer data on file). The maximum size of the Pulsincap

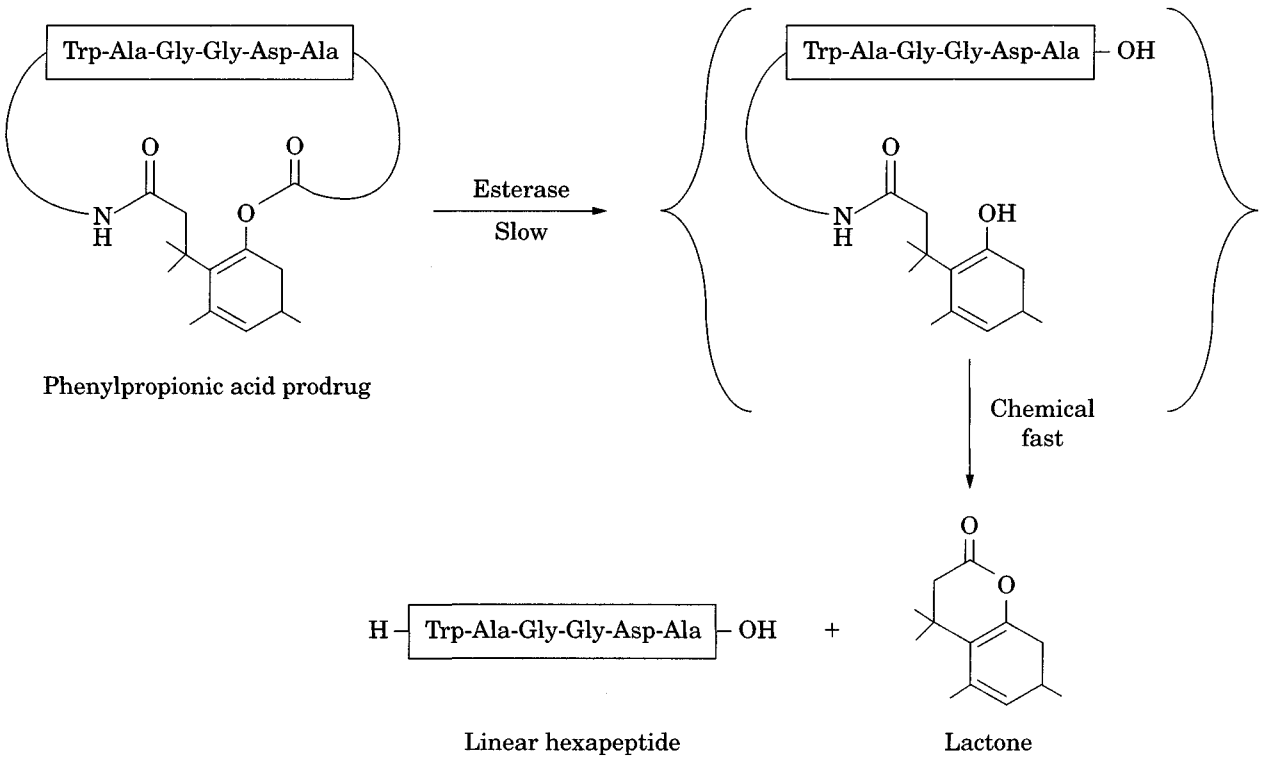


Figure 28. Proposed mechanism for the release of the linear hexapeptide from the cyclic phenylpropionic acid prodrug. *Source:* Reprinted from Ref. 98, with kind permission of Plenum Publishing Corporation, New York.

capsule approximates a size #0 standard gelatin capsule. In vitro studies indicated that the system maintained its integrity in pH 1.2 conditions for 5 h (simulating residence in the stomach) and exhibited a mean pulse-release time of 195 min after switching to pH 6.8 conditions. The mean 195-min lag time would represent the time interval over which the capsule must transit the small intestine to deliver formulation components to the colon. In an in vivo scintigraphic imaging confirmation study in humans (109), the Pulsincap capsule demonstrated integrity maintenance for 197–414 min in the stomach of fed volunteers with evidence of water-soluble cap dissolution within 29–70 min after exiting the stomach and entering the small intestine. A second phase of this study in fasted volunteers showed that the Pulsincap capsule hydrogel plug ejected at a mean time of 230 min postadministration, with a range from 208 to 275 mins. At the time of hydrogel plug ejection, all devices were shown to reside in the ascending colon. These data confirmed that, at least in the fasted state where gastric residence is not overly prolonged, the Pulsincap capsules successfully reached the colon prior to formulation release. The Pulsincap capsules were also evaluated in a double-blind placebo-controlled parallel group study evaluating the tolerability of a 28-day regimen of twice-daily dosing (no active drug agent). The incidence of reported adverse events was comparable between Pulsincap and placebo, with no indication of their being causally related to the formulation. This tolerability study indicated that this designed formulation for time-delayed drug release to the colon holds promise as a technology that can be effective without significant tolerability issues.

Limited information has been presented on a somewhat similar time-delayed drug delivery system named Chronset from ALZA Corporation (112). This device contains the drug formulation within an impermeable capsule configuration in which the driving force is an osmotic engine contained in the base of the capsule. By controlling the rate of water imbibition with the osmotic load and a semipermeable membrane coating, a swelling polymer is utilized to expand the capsule over a preengineered time frame resulting in the release of active components at either 2 or 6 h. In the fasted state where residence time in the stomach could be expected to be less than 2 h, the 6-h systems hold promise for delivery of therapeutic agents specifically to the ascending colon region. Pharmacokinetic data, with acetaminophen as a model compound, demonstrated that the formulation was released in a bolus fashion (simulating an immediate-release profile) after the predetermined lag time designed into the system.

Niwa and coworkers have reported on the development and evaluation of a novel ethylcellulose (EC) capsule that releases drug in a time-controlled fashion (113). The capsule, shown in Figure 29, has four-components comprising a drug container, swellable polymer, capsule body, and cap. The cap, body, and drug container were made of EC. The capsule body was a #00 gelatin capsule coated internally with EC, with the gelatin capsule subsequently dissolved to yield an EC capsule body. Four micropores, each ap-

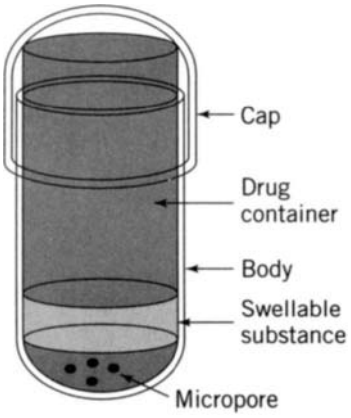


Figure 29. Schematic representation of the release time-controlled capsule used in this study. *Source:* Reprinted from Ref. 114, with kind permission of G+B Publishing Group, Lausanne.

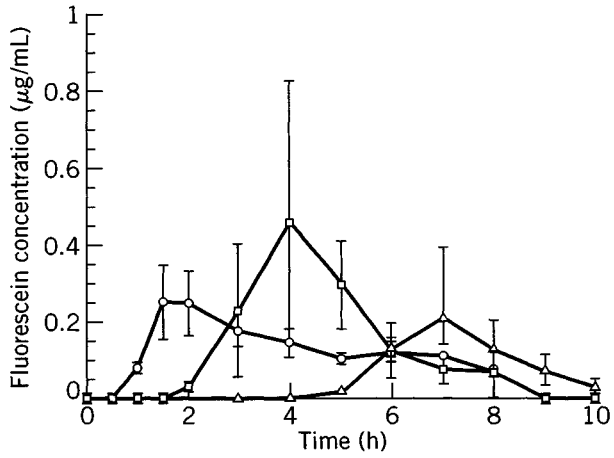


Figure 30. Plasma fluorescein concentrations versus time curves after oral administration of three kinds of EC capsules of which mean cap thicknesses are 39.1 ± 2.3 (SE) μm (○), 63.1 ± 5.0 μm (□), and 75.6 ± 4.1 μm (◇). Each point is the mean of three individual determinations and is expressed as the mean ±SE. *Source:* Reprinted from Ref. 113, with kind permission of G+B Publishing Group, Lausanne.

proximately 400 μm in diameter, were mechanically drilled in the bottom of the body capsule. The drug container was made from an EC film. When assembled, the drug container is separated and placed above a swellable polymer (i.e., a low-substituted hydroxypropylcellulose) in the capsule body and sealed with the cap. The proposed mechanism controlling the timing of drug release is a balance between the swelling pressure of the polymeric material and the strength of the capsule cap. Utilizing the same swelling-polymer composition, it was shown that the time of in vitro drug release (or rupture of the EC cap) was dependent on the thickness of the cap. The mean times at which 50% of a model compound, fluorescein, was released were 2.4 ± 0.15 h, 3.39 ± 0.09 h, and 6.21 ± 0.15 h for caps with thickness of 44.1 μm, 65.7 μm, and 76.7 μm, respectively. In vivo, these same capsule designs performed comparably in fasted beagle dogs, with respective T_{max} values at 2.0 h, 4.0 h, and 7.0 h (Fig. 30). These data suggest the potential utility of this design, although lag times in excess of 7 h will most likely be required to ensure effective delivery to the colon, particularly in the fed condition. Additional studies examining the effects of food on these time-release capsules were conducted and suggested that in the postprandial study leg, the capsules actually disintegrated in the stomach rather than the colon (114). The mean residence time (MRT) of fluorescein in these capsules was not statistically different in the postprandial state (6.43 h) and fasted state (4.76 h). Simple enteric coating of capsules with either hydroxypropylmethylcellulose phthalate or Eudragit S afforded MRTs of 11.30 h and 12.83 h, respectively, in the fed state. These data suggested that the time-controlled capsule, which did not have an enteric coating, probably dissolved in the stomach. To effectively delivery a drug formulation to the colon with these time-controlled systems, an enteric coating is necessary to delay the initiation of the timing cycle until the capsule exits the stomach. Not only does this eliminate the variability due to gastric residence times but it also increases the likelihood that a 6- to 8-h time delay will be sufficient to deliver the formulation to the colon region prior to drug release.

In addition to the bolus or delayed-release systems just described for targeting drug delivery to the colon, more traditional or conventional sustained-release technology can also be considered as a means to provide continuous drug release in the colonic environment. Essentially any of the systems described in the section on time-controlled drug release for the small intestine could be extended to colonic applications. If a sustained- or continuous-release dosage form was enteric coated, then initiation of the release profile would not commence until the device empties from the stomach and the enteric coating dissolves. Given this circumstance and under normal GI physiological conditions, any sustained drug release beyond approximately 3 to 4 h will most likely occur in the colon. Therefore, an enteric-coated 12-h sustained-release system could be expected to release drug for approximately 8 h in the colon. Technical strategies for designing time-controlled, sustained-release formulations will not be repeated here (see "Time Specificity"). Obviously this approach is simply an attempt to utilize a general sustained-release delivery profile and time the release such that a significant portion of the dose is released after the formulation traverses the small intestine and enters the colon.

Enzymatic Control

A major share of the effort in designing and developing controlled-release technology for colon delivery has attempted to utilize the presence of colonic bacteria as a triggering element to initiate or control drug release on arrival of the drug or dosage form in the ascending colon. Although there is a significant population of bacteria in the lower small intestine (10^5–10^7 cfu/mL), there is a rather abrupt and dramatic increase in bacterial density (10^{11}–10^{12} cfu/mL) immediately distal to the ileocecal junction. The en-

zymes produced by these bacteria are the targets of controlled-release technology efforts. As with any other physiologic parameter, the specific strains and densities of bacteria resident in the ascending colon can be affected by numerous factors, including age, diet, pathological states, concomitant drug administration, general health, and normal interindividual variability. Although there is certainly variability in bacterial content, all individuals have very high resident populations of bacteria in the ascending colon, and this ubiquitous presence can justify efforts to target these bacterial enzymes as potential triggers for controlled-release technology. Additionally, the successful use of sulphasalazine and olsalazine, which depend on bacterial azoreductases for activity, strongly indicate that the bacterial enzymes of the colon are capable of providing the desired effect.

The vast majority of work in this field has been directed toward developing drugs or dosage-form technologies as substrates for bacterial enzymes and evaluating these approaches in either simulated in vitro environments or in small-animal studies. Simulated in vitro models are difficult to establish and validate, particularly because the colonic bacteria are primarily anaerobic, but they represent the first method of choice for comparing different substrates and strategies. Studies in small animals, while useful for verifying results observed in vitro, must be interpreted with a certain degree of caution because there may be considerable species-to-species variability in bacterial enzymes between selected animal models and humans. Enzymes produced by colonic bacteria can hydrolyze a wide variety of substrates, including glycosides, sulphates, nitrates, esters, amides, and sulphonates. They have also been shown to reduce double bonds, nitro groups, azo groups, aldehydes, sulphoxides, ketones, alcohols, *N*-oxides, and arsonic acids. Other metabolic processes affected by colonic bacterial enzymes include dealkylation, deamination, decarboxylation, ring fission, nitrosamine formation, acetylation, and esterification. Although obviously a very large number of metabolic process could be chosen as potential controlling elements in controlled-release drugs or dosage forms for colon delivery, the focus has been on azoreductases, which reduce azo bonds, and polysaccharides, which are represented by glycosidic enzymes.

Significant efforts have been directed toward utilizing the azoreductase capacity of colonic bacterial enzymes. Saffran and coworkers (115,116) synthesized various polymers that were cross-linked with aromatic azoaromatic groups. The polymer films developed in these studies were resistant to degradation or dissolution in the upper GI tract and could be utilized as tablet or capsule coatings that were substrates for bacterial azoreductase activity in the colon. Vasopressin and insulin were effectively delivered to the colon in animal studies utilizing this approach.

Van den Mooter et al. (117) investigated the release of a model compound, ibuprofen, from capsules coated with azopolymers. Gelatin capsules containing 20 mg of ibuprofen were dip coated in an ethanolic solution of azopolymers (20% w/w). PEG 400 (20% w/w) was utilized as a coating plasticizer, and the coating level on the capsules was 9.7% (w/w). The azopolymers employed in this study were copolymers of 2-hydroxyethyl methacrylate (HEMA) and methyl methacrylate (MMA) and terpolymers of HEMA, MMA, and methacrylic acid (MA). *N,N'*-bis-(methacryloyloxyethyloxycarbonylamino)azobenzene (B-[MOEOCA]AB) was used as the azoreductase substrate in the polymers. An in vitro dissolution medium was prepared from isolated rat cecal contents to which cofactors were added to create an electron-generating system capable of significant reducing activity that simulated the environment of the colonic milieu. Because ibuprofen has low water solubility, diffusion through the polymer coating prior to enzymatic degradation of the azopolymer coating is minimal. Copolymers of HEMA/MMA at ratios of 4:1 or 5:1 did not demonstrate in vitro drug release rates that were statistically different in buffer or reducing medium, indicating that the release most likely reflected diffusion of the drug through the polymer coating over extended time periods (34 h). Although a HEMA/MMA coating at a 6:1 ratio did demonstrate statistically faster drug release in the reducing medium compared to buffer, the lag phase exceeded 24 h, which is not practical for in vivo applications given the estimated residence time of dosage forms in the colon. The effectiveness of azopolymer coatings is based on a balance between the hydrophilic HEMA, which ensures good hydration and availability of azo bonds for enzymatic attack, and the hydrophobic MMA, which retards polymer swelling and prevents early drug release in the stomach and small intestine. Because neither of these components contains an ionizable group, swelling is pH independent. Incorporation of a small amount of methacrylic acid as a terpolymer with HEMA and MMA increases the degree of swelling when going from acidic to neutral or alkaline conditions owing to neutralization of the carboxylic acid group of MA while still retaining the generally water-insoluble nature of the polymer. As shown in Figure 31, a terpolymer of HEMA/MMA/MA 9:2:0.1 provided a coating that exhibited significant ibuprofen release beginning as early as 8–10 h after initiation of incubation

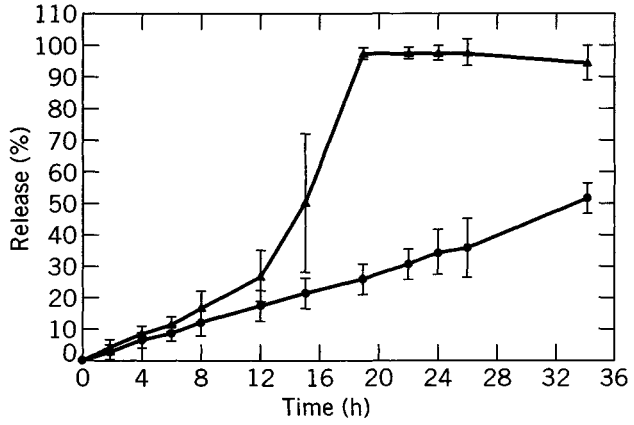


Figure 31. Release of ibuprofen from capsules coated with azopolymer P12 in RCCRM (▲) and phosphate buffer (●). $n = 6$; error bars indicate the standard deviation. *Source:* Reprinted from Ref. 117, with kind permission of Plenum Publishing Corporation, New York.

in simulated rat cecal content–releasing medium. Total release was achieved by 18 h, indicating the effectiveness of this coating composition.

Van den Mooter and colleagues (118) extended their in vitro characterization of azopolymer-coated capsules for colonic delivery by examining their performance in vivo. Theophylline was used as a model compound for measuring plasma concentrations and gelatin minicapsules were coated with azopolymers as described previously (117). Given the small size of the rat model, the minicapsules were surgically placed in either the upper small intestine or cecum. With the three polymer compositions evaluated, none showed significant theophylline absorption when administered to the small intestine of rats, indicating that drug release and subsequent absorption were primarily controlled by diffusion through the polymer coating rather than dissolution or degradation of the coating. Placement of the capsules in the cecum demonstrated the apparent effectiveness of the azopolymer coatings in initiating drug release in the colonic environment (Fig. 32). Significant plasma levels of theophylline were measurable as early as 6–8 h with the terpolymers containing HEMA/MMA/MA. The copolymer of HEMA and MMA also showed a significant increase in the absorption rate of theophylline, although the onset was significantly later (16–20 h postadministration) than that seen with the more rapidly swelling terpolymers. The data obtained in vivo are in general agreement with the previously reported in vitro release data, although less discrimination was seen in vivo with the terpolymers. The results obtained in the two studies by Van den Mooter et al. (117,118) were encouraging, but as currently formulated, the azopolymer coatings are unlikely to be effective in a normal, human dosing application. A residence time in the reductive environment of at least 10–12 h was required to initiate polymer degradation, and complete degradation and drug release were not achieved for nearly 24 h. With a transit time to the colon of approximately 6–8 h, one could not expect full absorption prior to 24 h, which would severely limit the applicability at this stage. In addition, the capsules would not be static in the ascending colon as they were in the cecal administration model evaluated in these studies but rather continue to transit through the colon, where enzymatic activity may be lower. This would most likely even further prolong drug release and absorption. This technology, therefore, requires further evaluation and optimization before it can be considered a viable approach for controlled release of therapeutic agents to the colon, where systemic absorption is the primary target.

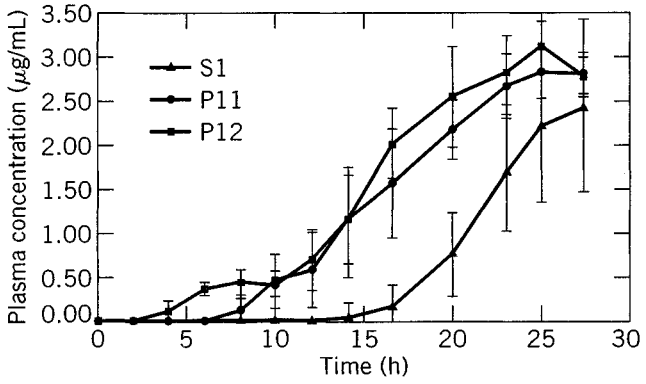


Figure 32. Theophylline plasma concentration after cecal administration of capsules coated with S1, P11, and P12. Error bars indicate SD, n = 5–6, except for P12 after 25 h, where n = 3. *Source:* Reprinted from Ref. 118, with kind permission of Plenum Publishing Corporation, New York.

A different variation on the azopolymer composition theme was investigated by incorporating poly(ether-ester)s (119). Azopolymers were synthesized from 4-(2-(2-(2-hydroxyethoxy)ethoxy)ethoxy)benzoic acid (HEEEBA) and 4-(2-(2-(2-hydroxyethoxy)ethoxy)ethoxy)phenylazobenzoic acid (HEEEPABA) with either 12-hydroxydodecanoic (C-12) or 16-hydroxyhexadecanoic (C-16) acid. The degradation of the various azopolymers was determined in a cell-free extract prepared from the cecal content of male rats (118). Various compositions of HEEEBA, HEEEPABA, and the C-12 or C-16 acids were evaluated and indicated that HEEEBA concentration from 20 to 33% did not modify degradation rates, and there was no difference in utilizing the C-12 or C-16 acid in the formulation. All polymers without HEEEBA, however, showed slower degradation rates, indicating the importance of the hydrophilic properties of HEEBA in promoting accessibility of the polymer bonds to the azoreductase in the dissolution medium. The addition of small amounts of polysorbate 80 further accelerated the degradation rate, probably by a similar mechanism of increasing the wettability of the polymer matrix and hence the access of azoreductase to the polymer bonds. The measured reduction in azo bonds, however, was still only approximately 50% in 48 h of incubation, so the practical use of these systems also remains in contention given the normal in vivo residences times in the cecum or colon.

Shantha et al. have prepared and evaluated azo groups containing polymeric hydrogels for targeting to the colon (120). Methacryloyloxy azobenzene (MAB) was copolymerized with hydroxy thylmethacrylate (HEMA) as hydrogels containing 5-fluorouracil (5-FU) as a model drug. When drug release was determined in simulated gastric fluid or simulated intestinal fluid, releases were in the range of 20–30% in 3 h, with approximately 50% released in 12 h. The release rate decreased as the concentration of the azopolymer increased, possibly reflecting a higher crosslinking density in the copolymer hydrogel. When the same compositions were tested for in vitro 5-FU release in a dissolution medium made from a culture of intestinal flora obtained from human fecal samples under anaerobic conditions, the release rate was nearly zero-order over 4 h, with approximately 80% of the drug released over the interval. Complete release was achieved by 6 h, with the rate of release slower from 4 to 6 h than the zero-order release seen in the first 4 h of the in vitro incubation. Although a significant amount of drug (20–30%) would be expected to be released during transit through the stomach and small intestine on the basis of the results discussed in this article, a significant increase in release rate would appear likely in the colonic region, probably due to the higher pH and azoreductase activity. This polymer composition could

appear promising for colonic controlled release, although the very slow drug release in the small-intestine environment observed with some of the other azopolymer compositions is not likely to be obtained with this system.

Azo compounds have also been utilized to deliver active agents as prodrugs to the colon with the goal of releasing the active agent as a result of bacterial azoreductase activity. Various low-molecular-weight and macromolecular prodrugs of 5-aminosalicylic acid (5-ASA) have been prepared for colonic delivery (105,121). Schacht et al. (122) have prepared azo-linked polymeric prodrugs of 5-ASA wherein the drug is linked to a polymeric carrier via an azo-containing spacer. Drug carriers evaluated included dextran, poly(*N*-[2-hydroxyethyl]-D,L-aspartamide), and poly(1-vinyl-2-pyrrolidone-*co*-maleic anhydride). A continuous simulated human intestinal microbial ecosystem (SHIME) reactor was utilized to assess the degradation of various 5-ASA azo prodrugs in simulated sections of the human GI tract. Evaluation of the azo-linked prodrugs indicated that the major degradation occurred in the reactors simulating proximal colon medium (approximately 60% in 6 h). Little or no parent drug was released in reactors simulating the duodenum and jejunum (approximately 15% in 6 h). The amount of drug released with the most favorable macromolecular prodrugs approached that seen with low-molecular-weight prodrugs. The disadvantage of this prodrug approach is that specific chemistry needs to be developed and applied for each individual drug candidate and therefore lacks the potential general applicability that could potentially be achieved with the use of azopolymer controlled-release formulations that could be applicable to a variety of drug candidates.

Although azopolymers have received a significant share of the research and development effort targeting bacterial enzyme substrate–based delivery technologies, they are certainly not the only technologies that have been evaluated. In fact, given the unknown safety and toxicity issues that may become a factor with some of the substrates for azoreductase activity, the use of more commonly occurring substrates, particularly polysaccharides, may offer important development advantages. Table 3 lists polysaccharides that are known to be degraded by colonic bacteria (123–133). It is obvious from the list that a large number of polysaccharide-based substrates could be utilized for delivering drugs and dosage forms to the colon. Many of the compounds, however, are too soluble in water to survive transit through the stomach and small intestine, and the films created from these polymers often do not have the necessary physical properties. In spite of these limitations, a number of groups have successfully demonstrated the potential utility of these polysaccharides as substrates for colon bacterial enzyme activity.

A double-coated system has been tested in which the outer coat is a traditional enteric coat and the inner coat is an insoluble microcrystalline cellulose polymer subject to colonic degradation (134). X-ray evaluation of the performance of these systems in human volunteers indicated that the dual-coating system afforded protection in the small intestine, with apparent disintegration in the colon. A similar dual-coating system comprised of chitosan as the inner coat and chitosan/Eudragit L as the outer coat disintegrated in the large intestine of beagle dogs (135).

Table 3. Polysaccharides Degraded by Colon Bacteria

Polysaccharide	Reference
Alginate	11
Amylose	11
Arabinogalactan	11–13
Arabic gum	13
Arabinoxylan	14
Cellulose	15–17
Condroitin sulphate	13,14
Dextran	11
Guar gum	13,14,18,19
Heparin	13
Laminarin	14
Locust bean gum	14,19
Mucin	13
Pectin	11
Polygalacturonic acid	11–14
Starch	13,20
Tragacanth gum	11,14,19
Xylan	12–14,19

Source: Ref. 12.

One polysaccharide that has received some considerable attention as a potential substrate for colonic bacterial enzymes in a controlled-release formulation is pectin (polygalacturonic acid). Some early studies with pectin have suggested its possible usefulness (136), although certain limitations also were apparent. Pectin itself is very water soluble and unlikely to serve as a resistive coating or barrier during transit through the stomach and small intestine. Rubinstein et al. have attempted to address the problems associated with pectin solubility by utilizing a less water-soluble salt, calcium pectinate (137). Pectin and calcium pectinate tablets were prepared with indomethacin, a water-insoluble drug. Sieved pectin or calcium pectinate was mixed with indomethacin at 1% or 10% (w/w), respectively, and compressed into tablets at 7 kP. Each tablet weighed 200 mg and contained either 2 mg indomethacin (pectin tablets) or 20 mg indomethacin (calcium pectinate tablets). Pectin tablets showed complete indomethacin release in 2 h when incubated with a pectinolytic enzyme preparation at pH 3.5 but essentially no release over 8 h if the degradative enzymes were not present. Reducing the concentration of pectin-degrading enzymes by 10-fold significantly reduced indomethacin release (100% release in about 7 h), but the release profile now approximated linearity. When the studies were conducted at pH 6.2 in the presence of the anaerobic bacterium *B. ovatus*, cumulative indomethacin release ranged from 5 to 20% over 4 h, with an initial burst phase that can likely be explained by diffusion from the tablet surface. Calcium pectinate tablets exhibited a somewhat similar profile of indomethacin release with little or no release in the absence of pectinolytic enzymes and a fairly rapid zero-order release when incubated in the presence of these enzymes (~100% release in 6 h). As with the pectin tablets, incubation of calcium pectinate tablets in the presence of rat cecal contents at pH 7.0 exhibited greater indomethacin release when com-

pared to incubation without rat cecal contents (Fig. 33). These results indicated that calcium pectinate, as well as pectin itself, can be degraded by bacterial enzyme activity. In addition, because indomethacin has very poor water solubility, it is unlikely that diffusion of indomethacin from the tablet could account for the observed release; more likely, an erosion process initiated by bacterial enzymes is responsible for initiating and controlling drug release.

The initial in vitro work with pectin and calcium pectinate tablets was subsequently confirmed in human clinical studies utilizing α-scintigraphy to visualize the performance of tablets in volunteers (138). Either CaP/P tablets (calcium pectinate and pectin) or CaP/GG tablets (calcium pectinate and guar gum) were evaluated in 10 fasted, healthy volunteers. Both tablet formulations were enteric coated with Eudragit L. Guar gum was added to CaP/GG tablets to slow the disintegration. External imaging of the physical state of the CaP/P and CaP/GG tablets indicated only slight disintegration of either formulation in the small intestine, with tablets reaching the cecum in a relatively intact condition. Both formulations reached the cecum in approximately the same time frame (CaP/P: 272 ± 48 min; CaP/GG: 223 ± 47 min). With the CaP/P tablets, complete disintegration was observed in the ascending colon for 7 of 10 tablets and in more distal colonic regions for 2 of 10; 1 did not totally disintegrate during colonic transit. With CaP/GG tablets, total disintegration was seen for 3 of 10 in the ascending colon and 3 of 10 in more distal colonic regions; 4 of 10 did not fully disintegrate during transit of the colon. The data from this human volunteer study indicate that CaP/GG tablets appear to disintegrate more slowly, as predicted, than CaP/P tablets, but that both may be potential candidates for controlled delivery of therapeutic agents to the colonic region.

Although compressed tablets as reported by Rubinstein et al. (137) indicated a potential utility for pectin and calcium pectinate to direct drug delivery to the colon, this approach may not be suitable for all applications. As with the azopolymers, the ability to develop a film-coating process that would protect the components of the formulation prior to arrival in the colon and then degrade to release the active drug in the colonic environment could be a significant advantage. Due to its high water solubility, pectin alone is not a good candidate for a film-coating process. Wakerly et al. investigated the potential utility of combining pectin with EC in a film coat intended for colon-specific drug delivery (139). Paracetamol tablets were compressed with a hardness of 8 KP and disintegration times of less than 15 min. The paracetamol tablets were film coated in a fluid-bed spray granulator with a coating solution of 2% w/v pectin in water blended with distilled water and Surelease S (EC). Three different film coats were prepared and evaluated: 60S:40P, 50S:50P, and 40S:60P. The amount of paracetamol release was significantly higher in pH 7.4 buffer than 0.1 N HCl for both compositions with the lower concentrations of EC (40S and 50S). Increasing levels of EC reduced drug release at both pH levels, and only marginal paracetamol release (≤5% in 6 h) was observed with the 60S coating under both pH conditions. The 50S:50P coating was tested in a system utilizing pectinolytic enzymes and shown to release paracetamol at a higher rate in the presence of enzymes than in the absence of enzymes. The difference (37% versus 23% in 400 min) was, however, not particularly dramatic, and the release curves did not begin to separate until after approximately 170 min of incubation in the presence of the pectinolytic enzymes. These data appear to suggest that although the pectin/EC coatings do provide some degree of control based on bacterial enzyme activity, the effect may not be rapid enough or the effect large enough to utilize in a practical sense. However, these studies do show a potential utility of pectin in film-coating processes if the solubility can be reduced by coformulation with other less soluble components. Additionally, it is not really possible to predict how these coatings would perform in an in vivo environment, particularly that encountered in the human colon.

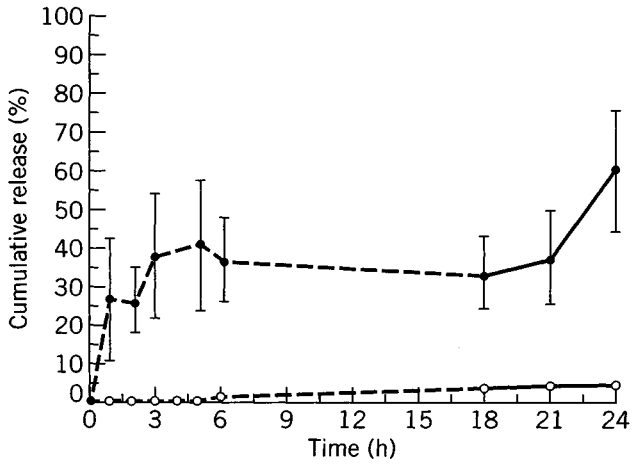


Figure 33. Percentage cumulative amounts of indomethacin released from CaP tablets in PBS medium, pH 7.0; (●) with rat cecal content, (○) without rat cecal content. Data are the mean of three experiments ± SD. *Source:* Reprinted from Ref. 137, with kind permission of Plenum Publishing Corporation, New York.

Pectin-based multiparticulates have also been evaluated as potential formulations for specific delivery to the colon (140). Control of release from a multiparticulate systems requires tighter regulation because the large surface-to-volume ratio of beads relative to tablets increases the probability that a gel or swelling system will become diffusion controlled, particularly for very water-soluble compounds, rather than degradation controlled by enzymatic activity in the colon. Amidated pectin/indomethacin and amidated pectin/sulphamethoxazole beads (2 mm) were prepared either with or without a chitosan coating. Drug levels were 20, 33, and 50% w/w based on theoretical loadings of dry beads. Swelling increased as a function of increasing pH, and chitosan reduced the degree of drug release. In the presence of pectinolytic enzymes, complete bead degradation was observed with 135 min. Although significant drug release occurred in enzyme-free media, especially with the more water-soluble sulphamethoxazole, the presence of calcium and/or chitosan did reduce this release aspect. The results indicated that a particulate formulation for delivery to the colon may be feasible. The particularly attractive feature of the multiparticulate

approach is that total degradation can occur in a much shorter time frame (i.e., 135 min) because of the large surface-to-volume ratio of multiparticulates compared to the much longer time (typically 15–24 h) required for total degradation of tablet formulations. If the early drug-release phase during transit through the stomach and small intestine can be adequately controlled with a particulate formulation, this approach offers promise for a delivery system that can effect more rapid and hopefully more complete drug release shortly after arrival of the dosage form in the colonic region.

Amylose is a linear α-D-glucan polymer composed of α(1→4)-linked D-glycosyl units and is comprised of approximately 20% starch. Films of amylose have been prepared that are resistant to pancreatic α-amylase (141) but are degraded by colonic bacterial enzymes (142,143). If used alone, amylose swelling in aqueous media is too rapid to be effective as a controlling coating because water-soluble drugs can diffuse through the coating membrane and would be released during transit through the stomach and small intestine. Milojevic et al. (144) have combined amylose with pharmaceutical polymers to decrease the swelling properties of amylose alone and provided a significant change in the resultant drug-release profile. Pellets (1.4–1.7 mm) containing 60% 5-ASA were prepared and coated in a fluidized bed coater with either a single coat comprised of mixed dispersions of amylose with acrylate polymer or with EC or as multiple coats with an inner amylose coat and an outer layer of either EC or acrylic polymer. During in vitro dissolution testing, uncoated pellets exhibited complete drug release in 2–3 h, while pellets coated with amylose alone showed complete release in 6 h. EC-coated pellets did not release drug over a 24-h period. Coatings comprised of amylose and EC showed a release rate that was dependent on the ratio of the two components. With low ratios of amylose to EC (e.g., 1:2.5 w/w), release was rapid and accompanied by cracking of the coating. An amylose/EC ratio of 1:4 appeared optimal for retarding drug release in simulated intestine fluid and was employed to further show a direct dependence of release rate on coating thickness. While release from the amylose/EC-coated pellets was significantly retarded in simulated intestinal fluid, dissolution studies conducted in a fermenter simulating bacterial flora (Fig. 34) showed a dramatic increase in 5-ASA release after approximately 2–5 h of incubation. A variety of other coating mixtures were evaluated, including Eudragit RS/RL30D and Aquacoat ECD30 in both mixed coatings and multilayer coatings. With Aquacoat ECD30, release was too rapid regardless of plasticizer or coating thickness. Eudragit RS/RL 30D was also ineffective in retarding amylose swelling and drug release, presumably because of pores formed by the dissolution of the soluble PEG plasticizer present in the coating formulation. The overall conclusion from this in vitro study was that an amylose/EC coating at a ratio of 1:4 provided the most promising formulation for coating tablets whose release rate could be initiated and controlled by colonic bacterial enzyme activity.

The potential utility of the amylose/EC coating technology was evaluated further in a human clinical setting (145). Pellets (1.4–1.7 mm) were prepared that contained

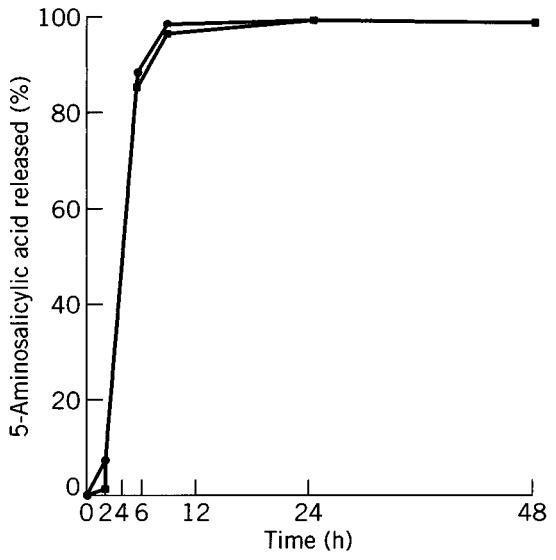


Figure 34. Release profile of 5-aminosalicylic acid in fermenter (simulated colon) system from pellets coated with (■) amylose-Ethocel (ratio 1:4 w/w) TWG 4.8% and (●) amylose TWG 4.8%. *Source:* Reprinted from Ref. 144, with kind permission of Elsevier Science–NL, Sara Burgerhartstraat 25, 1055 KV Amsterdam, The Netherlands.

50% [^{13}C]-glucose and coated with a 1:4 ratio of amylose:EC. Nine fasted subjects received a capsule containing 300 mg of the formulation and exhalation of $^{13}CO_2$ was monitored as a measure of pellet disintegration and release. A coadministered capsule of identical size and density containing a ^{99m}Tc marker was used to monitor GI transit and location by external scintigraphy techniques. The data obtained in this study (Fig. 35) indicated that less than 1% of the dose was recovered in the initial 6 h, followed by a steady increase in $^{13}CO_2$ recovery through 15 h, indicating degradation of the amylose/EC pellets over this time frame. The percent of dose recovered decreased from 15 to 24 h. External imaging of the second marker indicated that the pellets resided in the ascending, transverse, and descending colon during the rapid phase of $^{13}CO_2$ recover. These results in a human study confirmed the potential of the amylose/EC coatings as a colon-targeting technology that was previously demonstrated in the in vitro incubation studies.

A final approach to utilizing colon-specific bacteria as "triggering elements" for colon drug delivery involves the potential application of dextran-based hydrogels (146). Dextran-based prodrugs of naproxen have previously been shown to be specifically degraded in the presence of colon bacterial enzymes. In applying dextran to hydrogel technology, hydrogels were prepared that varied in dextran molecular weight (40,000 to 2,000,000), length of cross-linking agent (HDI: 1,6-hexamethylenediisocyanate; DDI: 1,12-dodecamethylenediisocyanate), cross-linking density from 2.9 to 17.5 mol %, and amount of DMSO (80–90% v/v) in the reaction mixture. The degree of hydrogel swelling in vitro was inversely related to dextran molecular weight and cross-linking density and directly related to the level

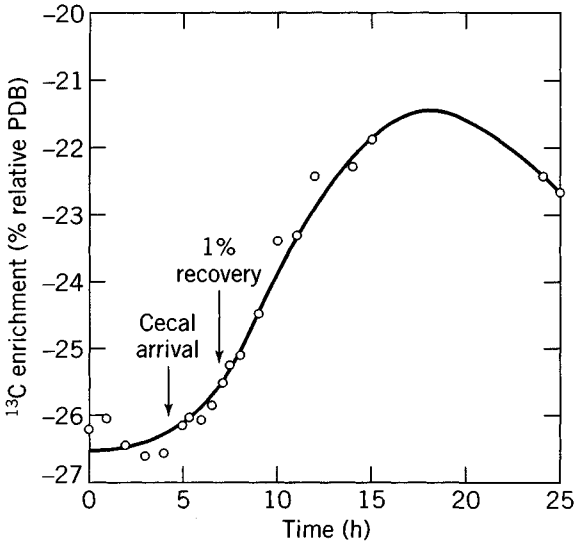


Figure 35. The time course of ^{13}C enrichment of breath CO_2 following the ingestion of pelleted ^{13}C-labeled glucose. The time at which >5% of the total observable activity was first recorded in the cecum and the time at which 1% of the dose given had been recovered in the breath are shown. *Source:* Reprinted from Ref. 145, with kind permission of Elsevier Science–NL, Sara Burgerhartstraat 25, 1055 KV Amsterdam, The Netherlands.

of DMSO in the reaction mixture. In general, both dextran molecular weight and cross-linking density were felt to increase the level of entanglement of dextran strands, thereby decreasing swelling. At the highest dextran molecular weight (2,000,000), however, hydrogel swelling actually increased, which may be related to interference with the cross-linking reaction. In vitro hydrocortisone release was determined with hydrogel discs (Dex-70, 85% DMSO, 11.6% cross-linking with HDI) in the absence and presence of dextranase. The observed release was approximately 32 and 100% in 120 min in the absence and presence, respectively, of dextranase. The in vitro performance of cross-linked dextran-based hydrogels appear promising as a potential technology for colon delivery of active agents.

Clearly, a variety of approaches have been evaluated with regard to identifying and optimizing a colon drug delivery system utilizing the endogenous bacterial enzyme activity as a site-specific triggering mechanism for drug release. Although considerable progress has been made at a research level, these approaches have not yet been commercialized. The primary advantage of utilizing colonic bacterial enzyme activity is that the relatively unique bacterial activity in the colon (both strain and density) represents a noncontinuous event that could serve as a mechanism relatively specific to the colon that has the potential of being independent of GI transit time. This potential benefit could be a major factor in practical utility because GI transit, which has to include the highly variable gastric residence time component, can be quite variable both between individuals and within the same individual depending on a variety of factors such as age, diet, pathology, and concomitant medications. The major drawback to the use of bacterial enzyme activity would appear to be the kinetics of the degradation process. In general, degradation of polymer coatings or tablet matrices by pectinolytics, dextranases, amylases, and the like is relatively slow, generally necessitating 12–24 h for complete degradation. As such, this approach is unlikely to be useful in attempts to deliver therapeutic agents to the colon in a bolus or pulsed fashion. For similar reasons, the slow release of active agents in the colon over prolonged time periods may be less than optimal in effecting adequate systemic drug absorption. Attempts to increase the rate of degradation by utilizing thinner coats or particulates will have to balance changes in degradation rate with stability of the formulation in the upper GI tract. The most apparent application of these types of colon delivery formulations may be for local application of therapeutic agents to treat pathologies of the colon itself. In this case, a prolonged, slower release over a number of hours while the dosage form is traversing toward the distal colon may be an effective means to spread the therapeutic agent over the maximal colon surface area. Obviously, a great deal of additional work is needed to develop formulations based on these strategies, but the early data offer a hope for success and warrant further investigation.

BIBLIOGRAPHY

1. Y.C. Chien, *Med. Prog. Technol.* **15**, 21–46 (1989).
2. *Physicians' Desk Reference*, Medical Economics Data Production Company, Montvale, N.J., 1997.
3. M.A. Longer, H.S. Ch'ng, and J.R. Robinson, *J. Pharm. Sci.* **74**, 406–411 (1985).
4. G. Levy and W.J. Jusko, *J. Pharm. Sci.* **55**, 285–289 (1966).
5. L.L. Boles Ponto and R.D. Schoenwald, *Clin. Pharmacokinet.* **18**, 381–408 (1990).
6. V.H.L. Lee and A. Yamamoto, *Adv. Drug Delivery Rev.* **4**, 171–207 (1990).
7. J.F. Woodley, *Proc. Int. Symp. Controlled Release Bioact. Mater.* **18**, 337–338 (1991).
8. D.F. Evans et al., *Gut* **29**, 1035–1041 (1988).
9. J.N. Hunt and M.T. Knox, *Handbook of Physiology*, American Physiology Society, Washington, D. C., 1968.
10. G. Santus and R.W. Baker, *J. Controlled Release* **35**, 1–21 (1995).
11. Y.W. Chien, *Novel Drug Delivery Systems*, 2nd ed., Dekker, New York, 1992, pp. 139–196.
12. F. Theeuwes, *Drug Dev. Ind. Pharm.* **9**, 1331–1357 (1983).
13. A. Sandberg et al., *Pharm. Res.* **10**, 28–34 (1993).
14. J.S. Grundy, D.W. Grace, and R.T. Foster, *J. Controlled Release* **44**, 247–254 (1997).
15. J.S. Grundy and R.T. Foster, *Clin. Pharmacokinet.* **30**, 28–51 (1996).
16. D.R. Swanson, B.L. Barclay, P.S. Wong, and F. Theeuwes, *Am. J. Med.* **83** (1987).
17. B. Lemmer, G. Nold, S. Behne, and R. Kaiser, *Chronobiol. Int.* **8**, 485–494 (1991).
18. G.M. Zentner, G.S. Rork, and K.J. Himmelstein, *J. Controlled Release* **1**, 269–282 (1985).
19. L.E. Appel, J.H. Clair, and G.M. Zentner, *Pharm. Res.* **9**, 1664–1667 (1992).

20. H. Cheng et al., *Pharm. Res.* **10**, 1683–1687 (1993).
21. J.R. Crison, P.R. Siersma, M.D. Taylor, and G.L. Amidon, *Proc. Int. Symp. Controlled Release Bioact. Mater.* **22**, 278–279 (1995).
22. F. Pozzi et al., *J. Controlled Release* **31**, 99–108 (1994).
23. M. Otsuka and Y. Matsuda, *Pharm. Res.* **11**, 351–354 (1994).
24. J. Van der Veen, A.C. Eissens, and C.F. Lerk, *Pharm. Res.* **11**, 384–387 (1994).
25. C.M. Adeyeye and J.C. Price, *Pharm. Res.* **11**, 575–579 (1994).
26. K.H. Yuen, A.A. Desmukh, and J.M. Newton, *Pharm. Res.* **10**, 588–592 (1993).
27. B. Abrahamsson et al., *Pharm. Res.* **10**, 709–714 (1993).
28. Y. Qiu, H. Cheskin, J. Briskin, and K. Engh, *J. Controlled Release* **45**, 249–256 (1997).
29. F.B. Landry et al., *J. Controlled Release* **44**, 227–236 (1997).
30. L. Yang and R. Fassihi, *J. Controlled Release* **44**, 135–140 (1997).
31. K. Murata, H. Yamahara, and K. Noda, *Pharm. Res.* **10**, 1165–1168 (1993).
32. C.M. Lehr, *Crit. Rev. Ther. Drug Carrier Syst.* **11**, 119–160 (1994).
33. V.M. Lenaerts and R. Gurney, *Bioadhesive Drug Delivery Systems*, CRC Press, Cleveland, Ohio, 1990.
34. H.O. Alpar, W.N. Field, R. Hyde, and D.A. Lewis, *J. Pharm. Pharmacol.* **41**, 194–196 (1989).
35. J.M. Gu, J.R. Robinson, and H.S. Leung, *Crit. Rev. Ther. Drug Carrier Syst.* **5**, 21–67 (1988).
36. M.F. Saettone et al., *Int. Pharm.* **51**, 203–207 (1989).
37. C.M. Lehr, J.A. Bouwastra, E.H. Schacht, and H.E. Junginger, *Int. J. Pharm.* **78**, 43–48 (1992).
38. J.D. Smart, I.W. Kellaway, and H.E.C. Worthington, *J. Pharm. Pharmacol.* **36**, 295–299 (1984).
39. Y. Akiyama et al., *Pharm. Res.* **12**, 397–405 (1995).
40. K. Satoh et al., *Chem. Pharm. Bull.* **37**, 1366–1368 (1989).
41. E.A. Hosny, *Int. J. Pharm.* **133**, 149–153 (1996).
42. E.A. Hosny and M.A. Al-Meshal, *Pharm. Ind.* **56**, 71–73 (1994).
43. E.A. Hosny and M.A. Al-Meshal, *Drug Dev. Ind. Pharm.* **20**, 2715–2720 (1994).
44. B. Tirosh et al., *J. Controlled Release* **45**, 57–64 (1997).
45. D.C. Kilpatrick et al., *FEBS Lett.* **185**, 299–305 (1985).
46. T.P. King, A. Pusztai, and E.M.N. Clarke, *Histochem. J.* **12**, 201–208 (1980).
47. J.M. Irache, C. Durrer, D. Duchene, and G. Ponchel, *Pharm. Res.* **13**, 1716–1719 (1996).
48. N. Hussain, P.U. Jani, and A.T. Florence, *Pharm. Res.* **14**, 613–618 (1997).
49. M.A. Jepson et al., *J. Drug Target.* **3**, 75–77 (1995).
50. D.E. Chickering and E. Mathiowitz, *J. Controlled Release* **34**, 251–261 (1995).
51. D.E. Chickering, J.S. Jacob, and E. Mathiowitz, *Reac. Polym.* **25**, 189–206 (1995).
52. D.E. Chickering et al., *J. Controlled Release* **48**, 35–46 (1997).
53. H.L. Leussen et al., *Pharm. Res.* **12**, 1293–1298 (1995).
54. M.K. Delaage and M. Lazdunski, *Biochem. Biophys. Res. Commun.* **28**, 390–394 (1967).
55. H.L. Luessen et al., *Int. J. Pharm.* **141**, 39–52 (1996).
56. G. Borchard et al., **39**, 131–138 (1996).
57. R. Sutinen, V. Laasanen, P. Paronen, and A. Urtti, *J. Controlled Release* **33**, 163–171.
58. R.W. Baker and H.K. Lonsdale, in Tanquaray and R.E. Lacey, eds., *Controlled Release of Biologically Active Agents*, Plenum, New York, 1974, pp. 15–71.
59. J.C. Leroux et al., *J. Pharm. Sci.* **84**, 1387–1391 (1995).
60. J.C. Leroux et al., *Pharm. Res.* **13**, 485–487 (1996).
61. S. Narisawa et al., *Pharm. Res.* **11**, 111–116 (1994).
62. A. Serres, M. Baudys, and S.W. Kim, *Pharm. Res.* **13**, 196–201 (1996).
63. X.Y. Wu and P.I. Lee, *Pharm. Res.* **10**, 1544–1547 (1993).
64. M. Nakano and A. Ogata, *Chem. Pharm. Bull.* **32**, 782–785 (1984).
65. H.E. Huber, L.B. Dale, and G.L. Christenson, *J. Pharm. Sci.* **55**, 974–976 (1966).
66. M. Bamba, F. Puisieux, J.P. Marty, and J.T. Carstensen, *Int. J. Pharm.* **2**, 307–315 (1979).
67. A.C. Hodsdon, J.R. Mitchell, M.C. Davies, and C.D. Melia, *J. Controlled Release* **33**, 143–152 (1995).
68. R. Narayani and K.P. Rao, *J. Appl. Polym. Sci.* **58**, 1761–1769 (1995).
69. T.S. Shen and C.A. Winther, *Adv. Drug Res.* **12**, 89–246 (1977).
70. D.E. Duggan et al., *Clin. Pharmacol. Ther.* **21**, 326–335 (1977).
71. A. Sinkula, W. Morozowich, and E.L. Rowe, *J. Pharm. Sci.* **62**, 1106–1111 (1973).
72. A.A. Sinkula, *J. Pharm. Sci.* **63**, 842 (1974).
73. Y. Yoshimura, N. Hamaguchi, and T. Yashiki, *Int. J. Pharm.* **38**, 179–190 (1987).
74. P. Bolme et al., *Eur. J. Clin. Pharmacol.* **10**, 237–243 (1976).
75. S.A. Varia, S. Schuller, K.B. Sloan, and V.J. Stella, *J. Pharm. Sci.* **73**, 1068–1073 (1984).
76. G.K.E. Scriba, *Arch. Pharm. (Weinheim, Ger.)* **326**, 477–481 (1993).
77. G.K.E. Scriba, *Pharm. Res.* **10**, 1181–1186 (1993).
78. G.K.E. Scriba and D.M. Lambert, *Pharm. Res.* **14**, 251–253 (1997).
79. V.K. Tammara, M.M. Narurkar, M.M. Crider, and M.A. Khan, *Pharm. Res.* **10**, 1191–1199 (1993).
80. P. De Caprariis et al., *J. Pharm. Sci.* **83**, 1578–1581 (1994).
81. F.P. Donina et al., *J. Controlled Release* **41**, 187–193 (1996).
82. A. Williams and R.A. Naylor, *J. Chem. Soc. B*, pp. 1973–1979 (1971).
83. A.S. Kearney and V.J. Stella, *Pharm. Res.* **9**, 497–503 (1992).
84. M. Safadi, R. Oliyai, and V.J. Stella, *Pharm. Res.* **10**, 1350–1355 (1993).
85. J. Balzarini et al., *AIDS* **5**, 21–28 (1991).
86. J.E. Starrett et al., *J. Med. Chem.* **37**, 1857–1864 (1994).
87. P. Annaert et al., *Pharm. Res.* **14**, 492–496 (1997).
88. K.C. Cundy et al., *Pharm. Res.* **11**, 839–843 (1994).
89. P.J. Sinko, N.R. Patel, and P. Hu, *Int. J. Pharm.* **109**, 125–133 (1994).
90. B.D. Anderson et al., *J. Controlled Release* **19**, 219–230 (1992).
91. M.E. Morgan, S.C. Chi, K. Murakami, and B.D. Anderson, *Antimicrob. Agents Chemother.* **36**, 2156–2165 (1992).
92. B.D. Anderson, M.E. Morgan, and D. Singhal, *Pharm. Res.* **12**, 1126–1133 (1995).

Next Page

93. H.W. Nolen and D.R. Friend, *Pharm. Res.* **11**, 1707–1711 (1994).
94. J.P.F. Bai, *Pharm. Res.* **12**, 1101–1104 (1995).
95. K. Morimoto et al., *Pharm. Res.* **8**, 1175–1179 (1991).
96. A.H. Kahns, A. Buur, and H. Bundgaard, *Pharm. Res.* **10**, 68–74 (1993).
97. D. Shan, M.G. Nicolaou, R.T. Borchardt, and B. Wang, *J. Pharm. Sci.* **86**, 765–767 (1977).
98. G.M. Pauletti, S. Gangwar, B. Wang, and R.T. Borchardt, *Pharm. Res.* **14**, 11–17 (1997).
99. G.M. Pauletti et al., *Pharm. Res.* **13**, 1615–1623 (1996).
100. M. Saffran, C. Bedra, G.S. Kumar, and D.C. Neckers, *J. Pharm. Sci.* **77**, 33–38 (1988).
101. T.N. Tozer et al., *Pharm. Res.* **8**, 445–454 (1991).
102. Friend, *Oral Colon-Specific Drug Delivery*, CRC Press, Boca Raton, Fla., 1992.
103. M. Ashford, J.T. Fell, D. Attwood, and P.J. Woodhead, *Int. J. Pharm.* **91**, 241–245.
104. S.S. Davis, J.G. Hardy, and J.W. Fara, *Gut* **27**, 886–892 (1986).
105. J.P. Brown et al., *J. Med. Chem.* **26**, 1300–1307 (1983).
106. P.K. Gupta and J.R. Robinson, in A. Kydoneius et al., eds., *Textbook on Controlled Release Technologies*, Dekker, New York, 1991, Chapter VI.
107. P. Gruber et al., *J. Pharm. Sci.*, 76–83 (1986).
108. G.A. Digenis, *Proc. Int. Symp. Biol. Mater.* **13**, 115 (1986).
109. J.S. Binns, H.N.E. Stevens, M. Bakhshaee, and C.G. Wilson, *Proc. Int. Symp. Controlled Release Bioact. Mater.* **21**, 260–261 (1994).
110. I.R. Wilding et al., *Pharm. Res.* **9**, 654–657 (1992).
111. J. Binns et al., *J. Controlled Release* **38**, 151–158 (1996).
112. J.A. Fix et al., *213th Natl. Meet. Am. Chem. Soc.*, 1997.
113. K. Niwa, T. Takaya, T. Morimoto, and K. Takada, *J. Drug Target.* **3**, 83–89 (1995).
114. K.I. Matsuda et al., *J. Drug Target.* **4**, 59–67 (1996).
115. M. Saffran et al., *Science* **233**, 1081–1084 (1986).
116. M. Saffran et al., *Pharm. Weekb. Sci. Ed.* **10**, 43–44 (1988).
117. G. Van den Mooter, C. Samyn, and R. Kinget, *Pharm. Res.* **11**, 1737–1741 (1994).
118. G. Van den Mooter, C. Samyn, and R. Kinget, *Pharm. Res.* **12**, 244–247 (1995).
119. C. Samyn, W. Kalala, G. Van den Mooter, and R. Kinget, *Int. J. Pharm.* **121**, 211–216 (1995).
120. K.L. Shantha, P. Ravichandran, and K.P. Rao, *Biomaterials* **16**, 1313–1318 (1995).
121. U. Klotz, K. Maier, C. Fischer, and K. Heinkal, *N. Engl. J. Med.* **303**, 1499–1502 (1980).
122. E. Schacht et al., *J. Controlled Release* **39**, 327–338 (1996).
123. M. Ashford and J.T. Fell, *J. Drug Target.* **2**, 241–258 (1994).
124. A.A. Salyers et al., *Appl. Environ. Microbiol.* **33**, 319–322 (1977).
125. H.N. Englyst, S. Hay, and G.T. MacFarlane, *FEMS Microbiol. Ecol.* **95**, 163–171 (1987).
126. J.H. Cummings, G.T. Macfarlane, and B.S. Drasar, in R. Whitehead, ed., *Gastrointestinal and Oesophageal Pathology*, Churchill-Livingstone, Edinburgh, 1989, pp. 201–219.
127. A.A. Salyers, S.E.H. West, J.R. Vercellotti, and T.D. Wilkins, *Appl. Environ. Microbiol.* **34**, 529–533 (1977).
128. D.A.T. Southgate and J.V.G.A. Durnin, *Br. J. Nutr.* **24**, 517–535 (1970).
129. J.L. Slavin, P.M. Braver, and J.A. Marlett, *J. Nutr.* **111**, 287–297 (1981).
130. J.H. Cummings, *Gut* **25**, 805–180 (1984).
131. J. Tomlin, N.W. Read, C.A. Edwards, and B.I. Duerden, *Br. J. Nutr.* **55**, 481–486 (1986).
132. C.M. Lancaster and M.A. Wheatley, *Polym. Prepr.* **30**, 480–481 (1989).
133. G.T. Macfarlane and H.N. Englyst, *J. Appl. Bacteriol.* **60**, 195–201 (1986).
134. U.S. Pat. 4,432,966 (1984).
135. EPO 460 921 A2 (1991), T. Suzuki, K. Hahiudo, T. Matumoto, and T. Fujii.
136. P. Zeitoun et al., *J. Controlled Release* **26**, 213–220 (1993).
137. A. Rubinstein et al., *Pharm. Res.* **10**, 258–263 (1993).
138. D.A. Adkin et al., *Pharm. Res.* **14**, 103–107 (1997).
139. Z. Wakerly, J.T. Fell, D. Attwood, and D. Parkins, *Pharm. Res.* **13**, 1210–1212 (1996).
140. O. Munjeri, J.H. Collett, and J.T. Fell, *J. Controlled Release* **46**, 273–278 (1997).
141. V.M. Leloup, P. Colonna, and S.G. Ring, *Biotechnol. Bioeng.* **38**, 127–135 (1991).
142. H.N. Englyst and G.T. Macfarlane, *J. Sci. Food Agric.* **37**, 699–706 (1986).
143. S.G. Ring et al., *Food Chem.* **28**, 97–109 (1988).
144. S. Milojevic et al., *J. Controlled Release* **38**, 75–84 (1996).
145. J.H. Cummings et al., *J. Controlled Release* **40**, 123–131 (1996).
146. L. Hovgaard and H. Brondsted, *J. Controlled Release* **36**, 159–166 (1995).

See also BIOADHESIVE DRUG DELIVERY SYSTEMS; CARRIER-MEDIATED TRANSPORT, ORAL DRUG DELIVERY; ORAL DRUG DELIVERY, TRADITIONAL.

ORAL DRUG DELIVERY, TRADITIONAL

KANJI TAKADA
Kyoto Pharmaceutical University
Kyoto, Japan

HIROSHI YOSHIKAWA
Toyama Medical and Pharmaceutical University
Toyama, Japan

KEY WORDS

Absorption enhancement
Beads
Capsules
Chemical modification
Emulsion
Liposome
Microgranules
Microparticles
Nanoparticles
Pellets
Spheroids
Stabilization of drugs
Tablets

Previous Page

93. H.W. Nolen and D.R. Friend, *Pharm. Res.* **11**, 1707–1711 (1994).
94. J.P.F. Bai, *Pharm. Res.* **12**, 1101–1104 (1995).
95. K. Morimoto et al., *Pharm. Res.* **8**, 1175–1179 (1991).
96. A.H. Kahns, A. Buur, and H. Bundgaard, *Pharm. Res.* **10**, 68–74 (1993).
97. D. Shan, M.G. Nicolaou, R.T. Borchardt, and B. Wang, *J. Pharm. Sci.* **86**, 765–767 (1977).
98. G.M. Pauletti, S. Gangwar, B. Wang, and R.T. Borchardt, *Pharm. Res.* **14**, 11–17 (1997).
99. G.M. Pauletti et al., *Pharm. Res.* **13**, 1615–1623 (1996).
100. M. Saffran, C. Bedra, G.S. Kumar, and D.C. Neckers, *J. Pharm. Sci.* **77**, 33–38 (1988).
101. T.N. Tozer et al., *Pharm. Res.* **8**, 445–454 (1991).
102. Friend, *Oral Colon-Specific Drug Delivery*, CRC Press, Boca Raton, Fla., 1992.
103. M. Ashford, J.T. Fell, D. Attwood, and P.J. Woodhead, *Int. J. Pharm.* **91**, 241–245.
104. S.S. Davis, J.G. Hardy, and J.W. Fara, *Gut* **27**, 886–892 (1986).
105. J.P. Brown et al., *J. Med. Chem.* **26**, 1300–1307 (1983).
106. P.K. Gupta and J.R. Robinson, in A. Kydoneius et al., eds., *Textbook on Controlled Release Technologies*, Dekker, New York, 1991, Chapter VI.
107. P. Gruber et al., *J. Pharm. Sci.*, 76–83 (1986).
108. G.A. Digenis, *Proc. Int. Symp. Biol. Mater.* **13**, 115 (1986).
109. J.S. Binns, H.N.E. Stevens, M. Bakhshaee, and C.G. Wilson, *Proc. Int. Symp. Controlled Release Bioact. Mater.* **21**, 260–261 (1994).
110. I.R. Wilding et al., *Pharm. Res.* **9**, 654–657 (1992).
111. J. Binns et al., *J. Controlled Release* **38**, 151–158 (1996).
112. J.A. Fix et al., *213th Natl. Meet. Am. Chem. Soc.*, 1997.
113. K. Niwa, T. Takaya, T. Morimoto, and K. Takada, *J. Drug Target.* **3**, 83–89 (1995).
114. K.I. Matsuda et al., *J. Drug Target.* **4**, 59–67 (1996).
115. M. Saffran et al., *Science* **233**, 1081–1084 (1986).
116. M. Saffran et al., *Pharm. Weekb. Sci. Ed.* **10**, 43–44 (1988).
117. G. Van den Mooter, C. Samyn, and R. Kinget, *Pharm. Res.* **11**, 1737–1741 (1994).
118. G. Van den Mooter, C. Samyn, and R. Kinget, *Pharm. Res.* **12**, 244–247 (1995).
119. C. Samyn, W. Kalala, G. Van den Mooter, and R. Kinget, *Int. J. Pharm.* **121**, 211–216 (1995).
120. K.L. Shantha, P. Ravichandran, and K.P. Rao, *Biomaterials* **16**, 1313–1318 (1995).
121. U. Klotz, K. Maier, C. Fischer, and K. Heinkal, *N. Engl. J. Med.* **303**, 1499–1502 (1980).
122. E. Schacht et al., *J. Controlled Release* **39**, 327–338 (1996).
123. M. Ashford and J.T. Fell, *J. Drug Target.* **2**, 241–258 (1994).
124. A.A. Salyers et al., *Appl. Environ. Microbiol.* **33**, 319–322 (1977).
125. H.N. Englyst, S. Hay, and G.T. MacFarlane, *FEMS Microbiol. Ecol.* **95**, 163–171 (1987).
126. J.H. Cummings, G.T. Macfarlane, and B.S. Drasar, in R. Whitehead, ed., *Gastrointestinal and Oesophageal Pathology*, Churchill-Livingstone, Edinburgh, 1989, pp. 201–219.
127. A.A. Salyers, S.E.H. West, J.R. Vercellotti, and T.D. Wilkins, *Appl. Environ. Microbiol.* **34**, 529–533 (1977).
128. D.A.T. Southgate and J.V.G.A. Durnin, *Br. J. Nutr.* **24**, 517–535 (1970).
129. J.L. Slavin, P.M. Braver, and J.A. Marlett, *J. Nutr.* **111**, 287–297 (1981).
130. J.H. Cummings, *Gut* **25**, 805–180 (1984).
131. J. Tomlin, N.W. Read, C.A. Edwards, and B.I. Duerden, *Br. J. Nutr.* **55**, 481–486 (1986).
132. C.M. Lancaster and M.A. Wheatley, *Polym. Prepr.* **30**, 480–481 (1989).
133. G.T. Macfarlane and H.N. Englyst, *J. Appl. Bacteriol.* **60**, 195–201 (1986).
134. U.S. Pat. 4,432,966 (1984).
135. EPO 460 921 A2 (1991), T. Suzuki, K. Hahiudo, T. Matumoto, and T. Fujii.
136. P. Zeitoun et al., *J. Controlled Release* **26**, 213–220 (1993).
137. A. Rubinstein et al., *Pharm. Res.* **10**, 258–263 (1993).
138. D.A. Adkin et al., *Pharm. Res.* **14**, 103–107 (1997).
139. Z. Wakerly, J.T. Fell, D. Attwood, and D. Parkins, *Pharm. Res.* **13**, 1210–1212 (1996).
140. O. Munjeri, J.H. Collett, and J.T. Fell, *J. Controlled Release* **46**, 273–278 (1997).
141. V.M. Leloup, P. Colonna, and S.G. Ring, *Biotechnol. Bioeng.* **38**, 127–135 (1991).
142. H.N. Englyst and G.T. Macfarlane, *J. Sci. Food Agric.* **37**, 699–706 (1986).
143. S.G. Ring et al., *Food Chem.* **28**, 97–109 (1988).
144. S. Milojevic et al., *J. Controlled Release* **38**, 75–84 (1996).
145. J.H. Cummings et al., *J. Controlled Release* **40**, 123–131 (1996).
146. L. Hovgaard and H. Brondsted, *J. Controlled Release* **36**, 159–166 (1995).

See also BIOADHESIVE DRUG DELIVERY SYSTEMS; CARRIER-MEDIATED TRANSPORT, ORAL DRUG DELIVERY; ORAL DRUG DELIVERY, TRADITIONAL.

ORAL DRUG DELIVERY, TRADITIONAL

KANJI TAKADA
Kyoto Pharmaceutical University
Kyoto, Japan

HIROSHI YOSHIKAWA
Toyama Medical and Pharmaceutical University
Toyama, Japan

KEY WORDS

Absorption enhancement
Beads
Capsules
Chemical modification
Emulsion
Liposome
Microgranules
Microparticles
Nanoparticles
Pellets
Spheroids
Stabilization of drugs
Tablets

OUTLINE

Tablets
- Matrix-Type Tablets
- Film-Coating Tablets
- Multiple-Unit Tablets

Capsules
- Hard Capsules
- Soft Elastic Capsules
- Floating Capsules

Microgranules/Spheroids

Beads

Pellets

Stabilization of Drug
- Stability in Liquid Preparation
- Factors Affecting Drug Stability and Method of Stabilization

Control of the Absorption Process
- Enhancement of Absorption
- Micro- and Nanoparticles

Bibliography

Before the advance of drug delivery systems (DDSs), tablets and capsules were the principal oral preparations for drugs. However, with the development of drug delivery technology, many novel oral DDSs have been invented in the last two decades. Although these oral DDSs are prepared in traditional dosage forms as tablets, capsules, suspensions, emulsions, and solutions, they are superior to the conventional oral preparations. Oral DDSs are divided into two categories: controlled-release preparations and targeting preparations. Targeting preparations such as colon delivery systems are described in the next section; oral DDSs having controlled-release characteristics as shown in Table 1 are described in this section.

Table 1. Traditional Oral DDS

1. Tablets
   - 1.1 Matrix type
     - Hydrophobic and hydrophilic matrices
     - Plastic matrices
     - Ion-exchange resins
     - Coprecipitates and solid dispersions
   - 1.2 Film-coating tablets
     - Diffusion-controlled membranes
     - Osmotic pumps
     - Enteric coating
     - Floating tablets
     - Swellable tablets
     - Mucoadhesive tablets
     - Complexation
       - Cyclodextrins
       - Pharmaceutical additives
   - 1.3 Multiple-unit tablets
2. Capsules
   - 2.1 Hard capsules
   - 2.2 Soft elastic capsules
   - 2.3 Floating capsules
3. Microgranules/spheroids
4. Beads
5. Pellets
6. Stabilization of drug
   - 6.1 Stabilization in liquid preparation
   - 6.2 Factors affecting drug stability and method of stabilization
7. Control of absorption process
   - 7.1 Enhancement of absorption
     - Absorption promoters
     - Chemical modification
     - Classical suspensions
     - Emulsions
       - Classification of emulsions
       - Application of emulsions to gastrointestinal absorption
     - Liposomes
     - Employment of liposomes in gastrointestinal absorption
   - 7.2 Micro- and nanoparticles
     - Particulates for gastrointestinal delivery
     - Intestinal uptake of particulates

TABLETS

Controlled-release technologies have been studied for a long time, and many preparations have been supplied on the market. The drug release-time is prolonged according to one of the following mechanisms (*1*) changing the physical properties such as solubility and stability of the drug molecules, (*2*) forming a complex of drug molecules with ion-exchanging resins, (*3*) incorporating drug molecules in slowly disintegrating or inert porous matrices, (*4*) coating drug molecules with pharmaceutical polymers that have a barrier function for the diffusion of drug molecules, and (*5*) osmotic pumps. In addition, new additives such as linear short-chain starches can be used to make sustained-release tablets (1). Delivery from this nonporous tablet is based on a swelling-controlled solvent-activated mechanism. In oral DDSs, this mechanism is used by itself or in combination with others (2).

Matrix-Type Tablets

Hydrophobic and Hydrophilic Matrices. To prepare a sustained-release tablet of water-soluble drugs, the drugs are mixed with hydrophobic matrices. With hydrophobic materials like fatty alcohols, acids, and esters, slow-release drug particles are prepared and are compressed into tablets. Voltaren SR is a commercial product of sodium diclofenac and is a hydrophobic matrix tablet consisting of a cetyl alcohol matrix. Ethylcellulose (EC), an inert and hydrophobic polymer that has been widely used in a number of dosage forms, was used as a matrix substance to prepare a sustained-release tablet of a water-soluble drug, pseudoephedrine HCl, by direct-compression technology (3). The lower-viscosity grades of EC are more compressible than the higher-viscosity grades, resulting in harder tablets and slower release rate. To prepare sustained-release tablets of a highly water-soluble drug, ABT-089, a cholinergic channel modulator for treatment of cognitive disorders, a hydrophobic matrix composed of carnauba wax and partially hydrogenated cottonseed oil were used as the rate-controlling materials (4).

Cellulose ether polymers such as hydroxypropylmethylcellulose (HPMC) in hydrophilic matrices are also used

to prepare oral controlled-release tablets (5). In particular, high-viscosity grade of HPMC (≈1,000–1,500 cps) is used to prepare matrix tablets by a dry-granulation method. The combination of high- and low-viscosity grades of HPMC was shown to be applicable as the matrix base to prepare diclofenac sodium (6) and zileuton (7) sustained-release tablets. A new ternary polymeric matrix system composed of pectin, HPMC, and highly water-soluble drugs such as diltiazem HCl was developed by direct-tablet compression (8). Further adjustments in the drug-release rate can be accomplished by two external layers (caps). This system, the Geomatrix trilayered tablet, was applied to develop a once-a-day formulation of diltiazem HCl (9). Diltiazem is contained in the hydrophilic polymer core, and two external layers serve to control the rate of hydration of the core, thereby restricting the surface area available for drug diffusion. Xanthan gum was also used as a hydrophilic matrix for sustained-release ibuprofen tablets (10). MSContin tablets, a controlled-release system for morphine, is a combination matrix consisting of a hydrophilic granular system inserted in a hydrophobic matrix. Theo-Dur is a controlled-release tablet of theophylline. As shown in Figure 1, it consists of 2 components: a matrix of compressed theophylline crystals and coated theophylline granules embedded in the matrix (11). One-third of the dose is in the matrix, and the remainder is in the pellets. In contact with fluid, the theophylline matrix disintegrates and dissolves. Next, theophylline diffuses slowly through the wall of the free granules. Finally, the granules dissolve completely. After oral administration of Theo-Dur 300-mg tablets to human subjects, serum theophylline concentrations over 1 mg/L were maintained over 24 h (12). A new melt-extrusion method for manufacturing matrix DDSs for theophylline was proposed (13). The powder mixture, drug, and polymerlike polyethylene and polycaprolactone were melted at 100–120°C for 30–45 s in a melt extruder. Thereafter, the mass was extruded into a disk mold (3 × 12 mm), and the polymer disk containing the drug was removed by cooling. Three-layer matrix tablets of diclofenac sodium have been reported in which poly(ethylene oxide) (PEO) and HPMC together with diclofenac sodium were directly compressed into a three-layer matrix system (14).

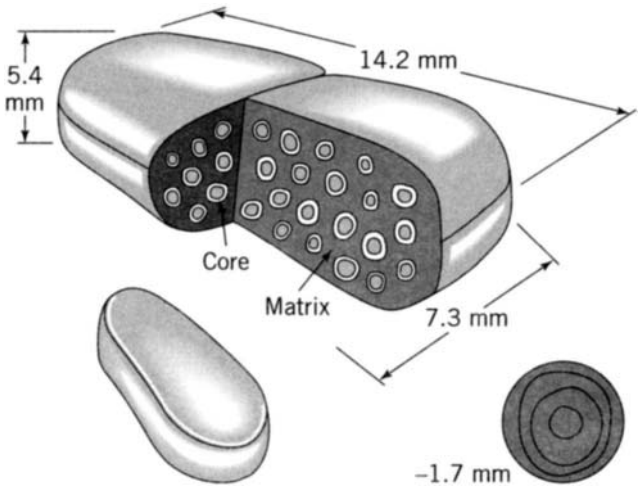


Figure 1. Structure of Theo-Dur.

Plastic Matrices. Sustained-release tablets can be also prepared by formulating an inert pharmaceutical polymer such as poly(vinyl chloride), poly(vinyl acetate), and methyl methacrylate. These polymers protect the tablet from disintegration due to the effects of peristalsis and turbulence and also reduce the dissolution rate of the drug inside the tablet. This technology was applied to theophylline (Theograd), sodium valproate, and iron. Theograd tablets consist of a matrix of a methylacrylate/methylmethacrylate copolymer that is mixed with theophylline and compressed into 250- and 350-mg tablets. In human studies, the extent of bioavailability increased about 1.4 times in fasting conditions (15,16). Therefore, it is recommended that Theograd sustained-release tablets be taken after a meal.

Owing to the shape of an average tablet (biconvex or disc), it is theoretically improbable for these tablets to release active drugs at a zero-order rate. Whether the matrix releases drug via swelling control or erosion (or both), it is almost impossible to attain a zero-order release. To solve this problem, core-in-cup tablets that release drug from a single, stable eroding surface of constant surface area were developed (17). As shown in Figure 2, the cup tablets were prepared by directly compressing the mixture of EC and carnauba wax, and the resultant cups were compressed with core tablets containing ibuprofen.

Ion-Exchange Resins. Drug molecules are formulated inside the tablets so as to be bound to ion-exchange resins and coated with a semipermeable water-insoluble polymer membrane made of EC or a similar substance. The merits of the ion-exchange resin–drug complex are (*1*) that sustained-release preparations can be made by formulating a gel-forming ion-exchange resin, (*2*) there is reduction of the degradation of drug molecules in the gastrointestinal tract by complexation, (*3*) the flavor is masked. Among the ion-exchange resins, divinylbenzenesulfonate is most commonly used because of its safety. This technology was applied to drugs with unpleasant flavors and strong effects on the stomach walls that, hence, need sustained-release characteristics. Phenylpropanolamine, codeine, dextromethorphan, acetaminophen, ephedrine, and chlorpheniramine are representative drugs to which cationic ion-exchange polymer matrices technology has been applied. For example, divinylbenzenesulfonate was used to prepare

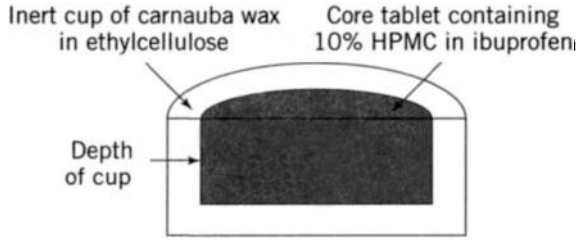


Figure 2. Schematic diagram of the core-in-cup tablet. *Source:* Ref. 17.

a sustained-release oral preparation of phenylpropanolamine by coating the tablet with EC (18). A problem associated with this approach is that drug release can be very rapid in the presence of an excess of ions, and dose dumping can occur. This can be prevented by impregnating the ion-exchange resin with an agent to impart plasticity and then coating it with a permeable membrane such as EC so that diffusion through the coating becomes the rate-limiting step (19).

Coprecipitates and Solid Dispersions. To modify the dissolution characteristics of drugs, coprecipitation involving the dissolution of ibuprofen and Eudragit S 100 in alcohol followed by the addition of cold water under agitation was developed (20). The release of oxazepam, a poorly water-soluble drug, was enhanced from tablets containing dispersions with a carrier, Gelita collagel (molecular weight 18,300), an enzymatically produced collagen hydrolysate, where the solid dispersion was prepared by a spray-drying method using the mixture of oxazepam, carrier, and lactose in 70% ethanolic solution (21). The bioavailability of cyclosporin A, a water-insoluble drug, was improved by solid dispersion with enteric coating polymer and surfactant (22).

Film-Coating Tablets

The dissolution rate of drug molecules from the tablet can be controlled by coating the tablet with a polymer membrane. For this purpose, EC and enteric-coating polymers such as Eudragit L and S (methacrylic acid copolymer) and hydroxypropylmethylcellulose phthalate (HPMCP) have been used.

Diffusion-Controlled Membranes. The dissolution rate of drug molecules can be modified by selecting the coating materials. Cellulose derivatives are generally used for this purpose. When a water-insoluble polymer such as EC is homogeneously used, the dissolution rate is dependent on the membrane thickness. However, when both water-insoluble and soluble polymers are used for the coating, the drug-release rate is accelerated. The addition of large amount of plasticizers such as triethyl citrate and tripropyl citrate to the coating polymer solution also increases the release rate of drug molecules. For example, drugs such as captopril, diltiazem, or ranitidine are blended with HPMCP, microcrystalline cellulose, poly(vinylpyrrolidone) (PVP), and magnesium stearate, wetted with anhydrous ethanol, and then compressed into tablets after drying. When these tablets were coated with a semipermeable membrane made from a mixture of microcrystalline cellulose acetate, PVP, and tripropyl citrate, satisfactory sustained-release tablets were obtained.

A gastrointestinal diffusion system (GDS) is a typical example of a DDS and consists of a soluble core including drug and tablet excipients. The porous membrane composed from arabic gum, dextrin 40,000, sodium chloride, sucrose, and cellulose acetate covering the core controls the diffusion rate of the drug (23). GDS was applied to metoprolol, diltiazem, lithium acetate, and disopyramide. As a new coating material, cross-linked amylose was developed and gave a sustained drug delivery (24).

Osmotic Pumps. The osmotic pump consists of a drug contained in a rigid, semipermeable membrane in which an orifice of approximately 300 μm has been created by a laser beam. This system is applicable to a drug having a suitable aqueous solubility, such as indomethacin and metoprolol (25). These drugs are formulated within the system with hydrogel polymers. After water is drawn into the capsule by osmosis, osmotic pressure increases within the capsule, and as a result the saturated drug solution is forced out through the orifice. The factors affecting the drug-release rate from the system are (*1*) quality and quantity of the hydrogel polymer and (*2*) permeability of the membrane. As semipermeable membrane substances, cellulose acetate ethylcarbamate, polyamide, and polyurethane are used. When drug molecules are dispersed within the tablet in a hydrogel, controlled release is obtained. Among the hydrogel polymers, ionic materials such as carboxymethyl cellulose (CMC) were useful because the ionizable groups provide most of the osmotic pressure required to draw water through the semipermeable membrane. These polymers can be compressed into tablets with conventional machinery when dry. There are three representative products: (*1*) The generic osmotic pump, supplied as OSMET, in which antipyrine or theophylline was contained. These pumps were applied to human subjects as rectal delivery systems for antipyline and theophylline (26). (*2*) The elementary osmotic pump, which is called OROS, was applied to metoprolol. The merit of OROS is the capability of obtaining a zero-order release rate, and the release rate is independent of the gastrointestinal pH and food intake. (*3*) The push–pull osmotic pump, which was developed to overcome the shortcomings of the osmotic pump system, namely, to produce small tablets in large quantities with high reliability and low cost for clinic application.

The technology has been applied to nifedipine, phenylpropanolamine, prazosin, and salbutamol. The GITS (gastrointestinal therapeutic system) tablet is a representative one (27). This tablet consists of a push layer and a pull layer. After oral administration, drug molecules are suspended within the water owing to the gastrointestinal fluid, and the polymer in the push layer swells. Because of this pressure, nifedipine molecules stream through the micropores on the surface of the tablet.

The first drug to which the osmotic pump was applied was indomethacin, which is a representative nonsteroidal antiinflammatory drug. However, severe gastric irritation occurred because of the concentrated indomethacin solution liberated from the small hole. To overcome this problem, bilayered osmotic tablets were applied to atenolol (28).

These osmotic tablet formulations are well suited for soluble drugs and core excipients with high osmotic pressures. However, osmotic delivery of moderate- to low-solubility drugs is limited because the dense coatings have relatively low permeabilities. To improve this problem, asymmetric-membrane tablet coating was developed (29).

Enteric Coating. To protect the drug molecules from the gastric degradation, as can occur with digoxin or erythromycin, and to reduce the side effects by protecting the gas-

tric mucosa from attack by drugs, such as can occur with indomethacin, enteric-coating tablets are used (30). The polymers used for enteric coating are acid-impermeable polymers. Commonly used enteric-coating materials and their threshold pH are as follows: cellulose acetate trimellitate (CAT), 4.8; HPMCP, 4.5–4.8; poly(vinyl acetate)phthalate (PVAP), 5.0; HPMCP 50, 5.2; HPMCP 55, 5.4; Eudragit L30D, 5.6; cellulose acetate phthalate (CAP), 6.0; Eudragit L, 6.0; and Eudragit S, 6.8. The use of CAP has been decreased because the phthalate ester group in CAP is known to be susceptible to hydrolysis during storage, with the gradual formation of phthalic acid and a reduction in acid resistance of the polymer film (30). Eudragit contains free carboxyl groups and is impermeable at low pH but disintegrates at a pH of about 7. According to the dissolution characteristics, several types of polymers are available. Eudragit S dissolves at pH 6.8, and two types of Eudragit L dissolve at pH 5.5 and 6.0 HPMCP dissolves at pH 5.5. These enteric-coating polymers were designed based on the assumption that the pH of the stomach is acidic, pH 1–3, while that of the intestine is neutral, pH 6–7. The reported ranges of the gastrointestinal pH values in healthy human subjects are 0.5–0.8 (stomach), 5.0–6.5 (jejunum), 6.0–7.5 (ileum), and 6.0–8.0 (colon). Although the normal gastric pH of human subjects is 1–3, the higher gastric pH was reported in the case of geriatric patients. Patients with achlorhydria also have higher gastric pH. In addition, the gastric acid is completely buffered by food in the case of postprandial administration. Therefore, considerable amounts of drug may be released into the stomach in these cases. The proximal jejunum usually lies within pH 5.0–6.5. The pH rises slowly along the length of the small intestine to reach only pH 6 to 7 in most subjects, although high values in the range 7 to 9 have occasionally been found. Therefore, the enteric coat should be soluble at a pH slightly lower than 7.

Enteric coating was applied to tablets using a solution of polymer dissolved with alcohol, acetone, methylene chloride, and similar substances. Usually, 6–8% of the tablets' weight is necessary to obtain acid resistance and impermeability. However, owing to environmental concerns, aqueous-based latex suspensions are used nowadays. In these cases, a much more precise coating technique is needed to eliminate the possibility of pinholes. Therefore, a higher quantity of coating material is required, approximately 10–12% of the tablet weight (30).

The evidence that enteric-coated drugs lessen or eliminate local side effects such as gastric irritation is conflicting. Enteric-coated aspirin is reported to be less likely to produce injury to the gastric or duodenal mucosa than plain or buffered aspirin. Enteric-coated potassium chloride tablets, however, are no longer used because of the risk of intestinal ulceration.

Erythromycin (EM) is rapidly degraded by gastric acid. Therefore, EM is administered as a stable ester prodrug or in enteric-coated tablets. However, the high pH (6.5–7.0) required for the dissolution of the enteric coating delayed the release of EM beyond its principle absorption site in the proximal small intestine. Therefore, choosing the right enteric-coating polymer is critical to produce efficacy. To obtain good reproducibility and less intersubject variation, enteric-coated tablets with diameters of less than 5 mm or so are preferable.

Floating Tablets. A floating dosage unit is useful for drugs acting locally in the proximal gastrointestinal tract. These systems are also useful for drugs that are poorly soluble or unstable in intestinal fluids. The floating properties of these systems help to retain these systems in the stomach for a long time. Various attempts have been made to develop floating systems, which float on the gastric contents and release drug molecules for the desired time period. After the release of a drug, the remnants of the system are emptied from the stomach. As a floating tablet, the hydrodynamically balanced system (HBS) is representative (31). This system is based on the principle that an object of less specific gravity than the gastric fluid will float on the gastric fluid in the stomach and thus keep the tablet in the stomach for a long period. Consequently, gastrointestinal residence time will increase. This system is applicable to drugs that suffer degradation in the intestine, have a higher pH than the stomach, and are poorly absorbed from the lower part of the small intestine. Diazepam, captopril, and morphine are suitable drugs for this system. These drugs are mixed with gel-forming hydrocolloids such as HPMC and fillers of low density in a tablet. Therefore, the hydrocolloids also retain drug molecules inside the tablet by decreasing the diffusion rate of drug molecules in the gel matrix.

The developing theory of gastric floating systems is based on the assumption that the subject is always upright. However, if the subject lies on his or her left side, this assumption breaks down. This point is the shortcoming of the floating system.

Intragastric floating diltiazem HCl tablets were prepared from chitosan and its HCl salt, polyvinyl alcohol (PVA) and PVP (32). Chitosan, a natural polysaccharide, has mucoadhesive properties. Therefore, the residence time of the chitosan-based tablets in the stomach was thought to be increased.

Swellable Tablets. It is possible to retain tablets in the stomach by increasing their size. The stomach discharges its contents through the pylorus into the small intestine. If the tablets are larger than the pylorus, they can stay in the stomach for a long time. For the sake of ease of swallowing, the tablets must swell in the stomach and attain a large size quickly. If not, the tablets are emptied through the pylorus. In addition, the swelled tablet should not block the pylorus. The physical characteristics of tablets such as size, shape, and flexibility also affect gastric emptying. The cloverleaf-, disk-, string-, and pellet-shaped tablets shown in Figure 3 were prepared from a silastic elastomer, and their gastric retain was studied (33). The tetrahedron made with low-density polyethylene remained in the stomach for longer periods than other shapes of similar size. Gastric retention of rigid rings was affected by their size. Disk and cloverleaf shapes showed poor gastric retention. The stomach eliminated strings and pellets fairly rapidly. As swellable gel-forming polymer retain drug molecules within the tablet, sustained-release tablets can be prepared. A tablet composed of a pH-independent

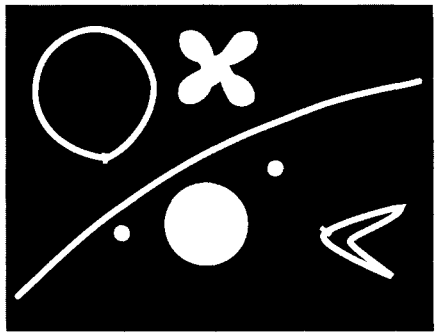


Figure 3. Shapes tested in the in vivo size/shape study. *Source:* Ref. 33.

hydrocolloidal gelling agent, a pH-dependent polymer such as sodium alginate, and a binder showed a sustained-release pattern of incorporated basic drugs.

The effect of fasted and fed conditions on gastric retention of balloon dosage forms were studied by comparing the gastric emptying time of the balloon dosage forms and the uncoated nondisintegrating tablets. The balloon tablet was 3–6 times larger than the plain tablet (34). The balloon type and nondisintegrating types of tablets were emptied from stomach under fasted conditions quite quickly. However, the balloon tablets remained in the stomach for a longer time than the plain tablets under fed conditions. The balloon tablets remained in the stomach for about 6 h more than the plain tablets. The balloon tablets floated more quickly in fasted condition than in fed condition. This could be due to the presence of high-viscosity gastric contents during fed condition.

Mucoadhesive Tablets. Oral cavities such as the buccal and sublingual sites have advantages for drug administration, for example, rapid onset of action, high blood levels, avoidance of the first-pass effect, and no exposure of the drug to the gastrointestinal tract. Drugs are also applied, localized, and removed easily. Several synthetic polymers including cellulose derivatives, plant gums, and polyacrylic acid are bioadhesive. For the treatment of aptha and oral *Candida* infections, bioadhesive tablets containing steroids or miconazole have been studied (35). Mucoadhesive, erodible buccal tablets containing clotrimazole have also been reported (36). Alternatively, mucoadhesive films composed of the highly water-soluble drug lidocaine HCl, EC, and HPC were reported as controlled-release preparations (37). To achieve high bioavailability and extended absorption time for nitroglycerin and isosorbide dinitrate, a slowly disintegrating plain tablet and a film-covered tablet in which disintegration was controlled by a hole in the film coating were developed (38).

Complexation ***Cyclodextrins.*** Hydrophobic drugs must be dissolved in the gastrointestinal tract to cross the membrane of the enterocytes. To accelerate the dissolution of water-insoluble drugs, traditional formulation systems involved a combination of organic solvents, surfactants, and extreme pH conditions. However, these systems often cause the irritation to the gastrointestinal tract. To solve this problem, cyclodextrins (CDs) have been included in tablets to improve the dissolution rate of drugs (39). CDs of pharmaceutical relevance are cyclic oligosaccharides composed of dextrose units joined through a $1 \rightarrow 4$ bond. CDs form complexes with hydrophobic drugs and increase the water solubility of drugs. Six types of CDs are now commercially available: α-, β-, and γ-CDs and three modified derivatives of β-CD-methyl, hydroxypropyl, and sulfobutylether (40). However, β-CD is the most popular pharmaceutical additive of these. The commercial pharmaceuticals with β-CD–based formulations are piroxicam as a plain tablet, prostaglandin (PG) F_2, and nitroglycerin as a sublingual tablet. CDs are capable of forming inclusion complexes with drugs. These noncovalent, inclusion complexes can have physical, chemical, and biological properties that are dramatically different from those of either the parent drug or CD. The safety evaluation of CDs have been reviewed (41). These complexes can be used to increase solubility (42,43) and dissolution rate, decrease volatility, alter release and dissolution rates, modify local irritation, and increase the stability of drugs. A complex formation of oxazepam and β-CD by the spray-drying method gave the most efficient dissolution characteristics (44). Solubility of ketoconazole was increased with β-CD complexation (45,46). In addition, sustained-release tablets were prepared by incorporating drug within the matrix in the form of a hydrophobic complex with β-CD. This technology was applied to diltiazem HCl using ethylated β-CD, and pH-dependent release of diltiazem was obtained. β-CD was also applied to salbutaine release preparations (47).

Pharmaceutical Additives. Polymeric complexes based on the interaction between Eudragit L and naltrexone HCl gave a significant reduction in the release rate of drug from the complex used as a naltrexone controlled-release system (48). New water-soluble polycations were synthesized and used as oral carriers (tablet) of diclofenac sodium and sulfathiazole sodium (49).

Multiple-Unit Tablets

The term *multiple-unit tablets* refers to tablets containing subunits that may be either the same (homogeneous) or different (heterogeneous). Multiple-unit tablets give much diversity in achieving dissolution profiles by combining various types of subunits in a tablet. Usually, by combining the immediate-release portion and controlled-release portion, sustained-release tablets are prepared. This system has been recently applied to nifedipine. The Adalat CR tablet is composed of two portions; the core is a immediate release, and the coat is a controlled release layer in which a gel-forming polymer is formulated with nifedipine. After oral administration, the coat tablet forms a gel by the permeation of gastrointestinal fluid. Thereafter, constant-rate drug release occurs according to the erosion of the matrix gel. In contrast to the finish of the drug release from the coat matrix gel, the core tablet releases drug at a comparatively fast rate. This nifedipine is a once-a-day tablet. After oral administration of an Adalat CR 40-mg tablet, plasma nifedipine concentration was maintained between 20 and 50 ng/mL for 24 h (50).

A sustained-release tablet formulation of naproxen (Naprelan) disintegrates to release discrete pellets that act as individual sustained-release units (51). A delayed-release tablet system that consists of a core containing diltiazem and an outer shell of CM-type hydroxyethylcellulose (HEC), a gel-forming polymer, has been designed. This system is useful for treating time-related symptoms that require time-controlled or site-specific delivery in the gastrointestinal tract (52).

CAPSULES

Hard Capsules

Gelatin capsules are the most popular hard capsules. Except for gelatin, which is a protein, carbohydrate and synthetic polymers are used as capsular materials. These are Capill capsules, HPMC (hydroxypropylmethylcellulose) capsules, poly(ethylene glycol) (PEG) capsules, and LSSM (liquid and semisolid matrix) capsules (53). The composition of HPMC capsules are HPMC/carrageenan/NaCl/water = 93.3:1.1:0.6:5.0 and have the following merits: (*1*) low water content, about one-third as much as gelatin capsules; and (*2*) applicability to drugs that are unstable with water. PEG capsules are produced by adding PEG 4,000 (5%) to gelatin; the resulting capsules have much tolerance to water loss. LSSM capsules can contain water-insoluble drugs that are dissolved with solvent. By using LSSM capsules, the bioavailability of water-insoluble drugs is improved. LSSM capsules were applied to oral sustained-release captopril, which was suspended in a semisolid oily base and filled inside LSSM capsules. After the gelatin layer dissolved, a sustained-release profile of captopril was obtained from the oily base matrix. Capill is made from potato starch and is an alternative to hard gelatin capsules. Capill capsules represent a robust dosage form with a reduced susceptibility to changes in storage conditions (54).

The solid-dispersion technique was applicable to prepare sustained-release gelatin capsules of dipyridamole and indomethacin, where enteric and insoluble acrylic polymers such as Eudragit S, RS, and RL were used (55). As compared with the conventional method of preparing solid dispersion by the melting-carrier method, the spray-drying method gives much better dissolution rates of low-solubility drugs (55). The bioavailability of a poorly water-soluble drug, a novel leukotriene B_4 antagonist, was further improved by the addition of a surfactant, Labrasol (a defined combination of mono-, di-, and triglyceride and mono- and difatty acid, C_8–C_{10}, esters) (56). Enteric solid dispersion was applied to nifedipine and enhanced release was reported (57). Solid dispersion of piroxicam in PVP K-30 was prepared to increase the solubility (58). The mixture of HPC and PEO was used to prepare solid dispersion of flurbiprofen (59).

However, in the field of sustained-release preparations, hard gelatin capsules have been generally used. As the contents composed of multiple units can elucidate the function of sustained-release preparation, hard gelatin capsules are used merely as a container. In these preparations, gelatin capsules are made of subunits such as granules or spheroids, beads, or beadlets and pellets. Hard gelatin capsules can be also filled with molten formulations of drug substances that solidify on cooling. The carriers are PEGs and macrogol esters such as Gelucires. However, recent study suggests that rapid cooling will leave material that is not fully solidified and is liable to change on storage (60). Modification of gelatin capsules with enteric coating is possible (61,62). Microporous EC capsules were prepared for the sustained release of cisplatin, an extremely hydrophilic and low-molecular-weight anticancer drug (63). To improve the bioavailability of peptide that undergoes degradation by proteolytic enzymes, capsules with fast gel-forming and fast drug-releasing properties were developed by formulating neutralized freeze-dried carbomer inside the capsule (64,65). The bioavailability of the water-insoluble drug KNI-272, a protease inhibitor for HIV, was improved by dissolving with propylene glycol and filling a gelatin capsule whose inside surface was coated with EC (66). Sustained-release of diclofenac sodium was achieved from several minimatrices enclosed in a hard gelatin capsule containing locust bean, xanthan, and karaya gums (67).

Soft Elastic Capsules

To solve many problems associated with tableting, including poor compaction, lack of content or weight uniformity, and other powder-flow or mixing problems, formulation of drugs into soft gelatin capsules has been performed. Soft elastic capsules are made of gelatin, glycerin, ethylparaben, propylparaben, and water. The representative composition of capsule film is gelatin/glycerin/*p*-hydroxybenzoate esters/tar color = 100:30:0.2:q.s. As a plasticizer, sorbitol is added to this formula to decrease the permeability of water vapor through the soft capsule. Usually drug liquid or paste is contained inside the capsule. However, the drug and the base must be inert to the gelatin layer. Both oily and aqueous bases are available in soft capsules. The formers are vegetable oil, medium-chain fatty-acid triglyceride, lecithin, paraffins, and higher alcohols. The later are PEG, propylene glycol, and polyhydric alcohols such as sorbitol, glycerin, and so on. Soft capsules are applicable to oily drugs and drugs whose clinical dose is extremely low, for example, prostaglandins. The drug content of these preparations is less than 1 mg. With the recent implementation of drug-development systems such as computer-aided drug design (CAD), extremely hydrophobic compounds are identified. However, these compounds suffer from low bioavailability because of their low solubility. To improve the dissolution rate of these compounds, soft capsules are used as delivery systems (68). Nifedipine is an example of this type. By formulating nifedipine into soft capsules after being dissolved with PEG, the bioavailability of nifedipine was improved. Ibuprofen soft capsules are another example. On the other hand, soft capsules also have several problems, namely, (*1*) hydrophilic base cannot be used; (*2*) drugs that need high clinical doses are not suitable, because the percentage of the formulated base is high compared with the amount of the drug; and (*3*) the stability of drug molecules must be considered because of the water remaining in the gelatin capsule film.

The most successful soft gelatin capsule is the new oral cyclosporin formulation Sandimmune Neoral. As cyclosporin is extremely hydrophobic and a poorly water soluble drug, it has low bioavailability, limited dose proportionality, and highly variable systemic plasma drug concentrations. Neoral is a microemulsion formulation of cyclosporin. Microemulsions are thermodynamically stable, isotopically clear dispersions of two immiscible liquids, oil and water, stabilized by an interfacial film of surfactant molecules (69). When the water is absent, mixtures of oil and nonionic surfactant form clear solutions that are known as self-emulsifying drug delivery systems (SEDDSs) (70,71). In Neoral, cyclosporin A, surfactant, a hydrophilic cosolvent, and a blend of lipophilic and hydrophilic solvent are contained in a soft gelatin capsule. Neoral showed reduced inter- and intrapatient variability in the bioavailability of cyclosporin A compared with the original preparation (72).

Solid-state water-in-oil-in-water (w/o/w) emulsion was applied to vancomycin. The primary emulsion (w/o) comprised sesame oil, monoglycerol stearate, and water (73.5:1.5:25). Vancomycin was contained in the aqueous phase, which was isotonized with NaCl. By using sucrose as a matrix material at a ratio of 3.5:1 sucrose/primary emulsion, w/o/w solid-state emulsion was obtained. Although vancomycin is not normally absorbed, it was significantly absorbed, and sustained-release characteristics were obtained after administration to rats in solid-state w/o/w emulsion (73). Enteric-coated soft gelatin capsules containing ibuprofen in either PEG 400 or Miglyol can also improve the bioavailability of hydrophobic drugs (74). Microemulsion is a useful delivery system for the improvement of bioavailability of RGD peptide, a fibrinogen-receptor antagonist of tetrapeptide, after oral administration in rats, where microemulsions were prepared by formulating Captex 200 (C_8/C_{10} diesters of propylene glycol), Capmul MCM (C_8/C_{10} mono-/diglycerides), and Cremophor EL (polyoxyl 35 castor oil) (75). Lipid-based vehicles for the oral delivery of poorly water soluble drugs have been reviewed recently (76). A list of natural and synthetic lipids and formulations using lipid-based vehicles is described in relation to the dissolution and digestion processes occurring in the intraluminal circumstance. Inversely, solubilization of hydrophilic drugs in oily formulations gives rise to new possibilities for peptide delivery via the intestine (77). For the oral delivery of calcitonin, Bridgelock formulation, a w/o emulsion system, was proposed (78). In an alternative approach to improve the bioavailability of a low-water-solubility drug, DMP 329, a protease inhibitor for HIV, an amphiphilic material such as Gelucire 44/14 (a mixture of glycerides and PEG esters) was shown to be useful (79).

Floating Capsules

A billeted floating capsule was developed for misoprostol. There were two layers in a capsule: a release layer and a floating layer. The floating layer consisted of Methocel K4M, lactose, Aerosil 200, and magnesium stearate. The release layer consisted of various combinations of Methocel K4M, K100, drug, HPMC, and Pharmacoat 606 and 603. Large quantities of high-viscosity polymer were incorporated to form a strong viscous layer. This helped in maintaining the integrity of the floating layer for a long time. The drug-release layer consisted of a gelling agent. This helped avoid disintegration and prevented delivery of large particles containing drug into the intestine, thus reducing side effects (30). HALO delivery capsules consists of a biphasic rapid- and sustained-release formulation contained a lipophilic drug such as propranolol dissolved in oleic acid. Initial rapid release of the drug–oleic acid solution is followed by the subsequent sustained release of those components from a solid erodible matrix containing a Gelucire of low hydrophilic lipophilic balance (HLB) and melting point above 37°C (80,81). A novel in vitro dissolution test method for a floating-dosage form with biphasic releasing characteristics was proposed (82).

MICROGRANULES/SPHEROIDS

Wet-granulating drugs or incorporating them into inert granules that are then coated to control the release pattern are two common approaches in preparing controlled-release oral preparations. The majority of published work on spheronization relates to idealized aqueous-based systems, which contain high concentrations of microcrystalline cellulose and lactose. With respect to the organic solvent-based systems, which have potential applications for many drugs that are moisture and/or heat sensitive, extruders and spheronizers fitted with flame-proof motors and specialized drying equipment are used (83). As pharmaceutical additives that regulate the release rate of drug molecules from the granules, cross-linked β-CD, crospovidone (a water-insoluble but swellable nonionic polymer), Eudragit RS (a slightly water-soluble polymer), Eudragit NE 30D, and EC are used. In addition, wax or waxlike pharmaceutical additives such as cetostearyl alcohol are used. These technologies were applied to diltiazem and hydrochlorothiazide.

BEADS

Small beads prepared from various polymers and other pharmaceutical additives are used as carriers to prepare oral sustained-release capsules of water-soluble drugs by filling gelatin capsules. Rapid- and slow-release beads were obtained by coating the central cores of beads with different amounts of Eudragit RS and RL. By adjusting the ratio of these two types of beads in a hard gelatin capsule, a once-a-day diltiazem preparation can be obtained. A sigmoidal drug-release pattern can be obtained by preparing the beads from Nonpareil (sugar spheres) layered with drug molecules and coated with a swellable polymer layer and a water-insoluble polymer layer. The most representative of these is the time-controlled explosion system (TES) (84). The most important point is that a swellable layer is formed between the drug layer and the water-insoluble layer. The sigmoidal drug-release pattern is obtained by the following processes: (*1*) permeation of fluid into the system through the water-insoluble polymer layer (membrane), (*2*) creation of pressure by expansion of swellable material, (*3*) pressure causing drug to break out of the

water-insoluble layer, and (3) drug release to the outside. By adjusting the thickness of the water-insoluble layer, beads having any release lag time can be prepared. By formulating several kinds of beads with different release lag times, sustained-release capsules have been prepared in which EC was used as a water-insoluble coating polymer. Granules were prepared by a centrifugal fluidizing (CF) granulator (83). As a variation of TES, a sigmoidal release system and pulsatile-release tablet were also designed (85,86). Flowable-bead cellulose (BC) coprecipitates consisting of spherical BC as carrier, the film former HPMC, the hydrophilic solubilizer PEG 6000, the plasticizers dimethyl phthalate and dioctyl phthalate, and the model drugs prednisolone and griseofulvin were prepared for controlled release (87). Chitosan was used to prepare controlled-release beads containing piroxicam by gelling the cationic polysaccharide with an anionic counterion, tripolyphosphate, solutions (88). Swellable porous hydrogel beads were loaded with diclofenac sodium, and sustained release was obtained (89).

PELLETS

Multiple-unit dosage forms are also known to have less variance in transit time through the gastrointestinal tract than single-unit dosage forms. Sustained-release diltiazem HCl pellets were prepared simply by coating inert diltiazem HCl pellets with soluble Eudragit L and S film-forming polymers (90). Alternatively, similar diltiazem pellets capable of controlling the drug release over 24 h were possible. Diltiazem HCl, fumeric acid, and talc were blended, mixed, and applied to Nonpareil using a coating solution of PVP to prepare the pellet core. The core was then coated by spraying solutions of Eudragit RS and Eudragit RL. The ratio of the two polymers could be optimized to get a controlled-release profile over 24 h. A comparative bioavailability study using two types of sustained-release oral isosorbide dinitrate (ISDN) showed that pellets had higher bioavailability than tablets (91). Two reasons are possible: One is the lower dissolution rate of ISDN from the tablet, as ISDN received high hepatic first-pass effect, and another is that ISDN was absorbed from the larger area of the gastrointestinal tract as pellets received wide distribution there. Moreover, to prevent the effect of gastric emptying or the change of the transit of the preparation through the gastrointestinal tract, pellets are preferred because the gastric emptying time for pellets is faster than that for tablets. For this purpose, sustained-release oral pellets of ISDN and propranolol have been developed. To prepare pellets, the mixture of drug, organic acid, and polymer was coated on the core substance. Organic acids like citric acid and tartaric acid have the role of accelerating the release rate of drug even in the high-pH environment of the gastrointestinal tract. As a polymer, HPMC, PVP, Eudragit RL and RS, methylcellulose, and EC are used. As a coating material that was used to control the release rate of drug molecules, EC, sometimes with a small amount of HPC, was used. In the case of sustained-release propranolol pellets, a mixture of 20% PVP in isopropanol/33% shellac in ethanol (19:1) was used as a polymer solution. Sustained release from pellets is conventionally achieved by polymeric coating. However, versatile matrix pellet formulation based on the combination of a hydrophobic material and a starch derivative using a melt pelletization technique is possible (92).

Another method for the production of enteric beads using a purely aqueous system composed of HPMCP and riboflavin has been developed (93). Pellets containing enteric coprecipitates of nifedipine formed by nonaqueous spheronization have also been reported (57). Calcium pectinate was used as a coating material to prepare sustained-release theophylline pellets (94).

On the other hard, prolonged gastric residence was obtained by increasing the density of pellets. The critical density to achieve prolonged gastric residence was reported to lie between 2.4 and 2.8 g/cm^3 (95). For the manufacture of sustained-release pellets for highly dosed, freely soluble drugs such as diltiazem HCl, the hot-melt extrusion method was shown to be suitable (96). Figure 4 shows the extruder used in this study. The volume and viscosity of coadministered fluid also affect the gastrointestinal distribution of small particles (97). Recently, an extrusion–spheronization method was developed to prepare sustained-release indomethacin pellets whose shape and size are shown in Figure 5 (98).

STABILIZATION OF DRUG

Examinations of drug stability using chemical kinetics gives us clues to how to stabilize the drug and helpful suggestions for its preservation requirements as well as a determination of its validation date.

Stability in Liquid Preparation

In liquid preparations of drugs, hydrolysis, oxidation, racemization, decarboxylation, or ring-opening reactions are usually observed; however, the majority of drugs in liquid phase are disintegrated according to hydrolysis or oxidation (99). The most popular order of reaction observed in liquid preparation is first order due to a large excess of medium compared with drug, which is called pseudo-first-order reaction.

Factors Affecting Drug Stability and Method of Stabilization

Temperature, pH, and other factors such as kind of medium, concentration, ionic strength, or permittivity are major factors that affect stabilities of drugs in liquid phase (99). To investigate the effect of temperature, which is one of the strongest factors affecting the rate of drug degradation, an analysis using the Arrhenius equation should be performed. When this Arrhenius plot is linear, the reaction rate of the drug at normal temperature can be estimated by the results under a higher temperature; this relation is applicable when activation energy is 10–30 kcal/mol unless chemicals are separated or melted (99). In general, Arrhenius plotting is done at several temperatures. The statistical evaluation of accelerated stability can be determined for a single temperature, and by this method it was reported that a reasonable prediction of the expected

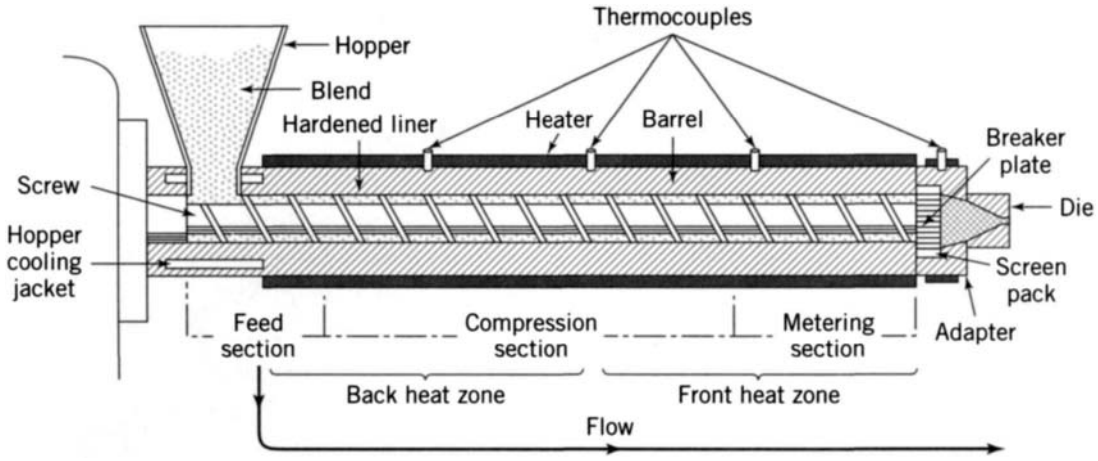


Figure 4. Cross-section of the single screw extruder. *Source:* Ref. 96.

shelf life as a function of activation energy may be possible (100). When we design a liquid preparation, the effect of pH on drug stability is also a frequently encountered problem. In pH analysis, the reaction rate of the pH profile can indicate the most stable pH range of the drug. There are three types of pH profiles: the so-called V type, the sigmoid type, and the bell type (101,102). Specific acid–base catalysis, an action of a single dissociation group, and that of two dissociation groups affecting reaction rate is a major cause of drug degradation according to the pH profile of the V type, sigmoid type, and bell type, respectively. From this information we can determine how to stabilize a drug in liquid preparation, that is, we can select a pH at which a drug is most stable, storage at lower temperature, blocking of oxygen in air, and preservation in a shaded container. In addition to these countermeasures, which sound like passive stabilization, various active stabilizations have also been attempted (Table 2). Stabilization of ampicillin in aqueous solution using a base formation with benzaldehyde and furfural has been reported (103). With an increase of added benzaldehyde and furfural, the degradation rate of ampicillin decreased, which is caused by binding of both chemicals to form a Schiff base, which is relatively insoluble in aqueous solution and thus leads to drugs being excluded from a degradation system. This stabilization by aldehyde is also observed in cephalexin, a β-lactam antibiotic that possesses an amino group at the α-

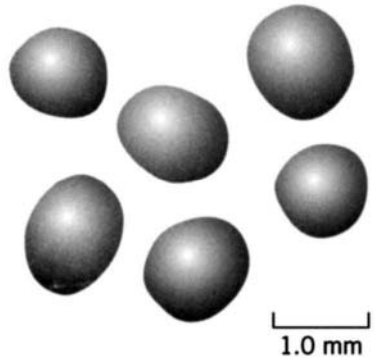


Figure 5. Shape and size of indomethacin pellets.

position (103). Inclusion compounds such as cyclodextrin can also stabilize drugs that are disintegrated by hydrolysis. In these attempts, bencyclane (104), prostacyclin (105), and a nonsteroidal antiinflammatory agent (106) were stabilized by an addition of cyclodextrin. In these chemicals' hydrolysis, sites are considered to be protected from reaction by means of cyclodextrin. Dissolved oxygen contributes to oxidative degradation that is accelerated by metal ions as catalists, and an attempt to protect isoniazid in aqueous solution from oxidative degradation has been

Table 2. Factors Affecting Drug Stability in Solution and Methods for Stabilization

Major ways of degradation	Factors affecting degradation	Methods for stabilization	
		Passive methods	Active methods
Hydrolysis	Temperature pH Ionic strength Permittivity Polarity	Storage under suitable conditions	Formation of complex or base Chemical modification Addition of solvent or surfactant
Oxidation	Oxygen Metal ions Light	Protection from air and light	Addition of chelating agents and antioxidants

made using chelating agents. In this report, chelating agents such as ethylenediaminetetraacetic acid or nitrilotriacetic acid, which trap metal ions in liquid preparation, stabilized high-isoniazid solutions (107). Whereas the components of containers for liquid preparations sometimes decrease drug stability owing to adsorption of drugs to the container wall or evaporation of medium through the wall, comparative stability was reported with cimetidine, furosemide, and theophylline in glass and polypropylene containers (108). After 30 days of storage, the residual rate of furosemide in glass containers was approximately 80%, but only 70% in polypropylene containers. With cimetidine and theophylline, a significant difference of stability was not observed between the containers. This study suggests that container materials should also be considered as a factor leading to degradation of drugs.

CONTROL OF THE ABSORPTION PROCESS

Enhancement of Absorption

Many important therapeutic agents, such as peptide drugs, are not absorbed sufficiently through gastrointestinal tissue barriers. In pharmaceutical research, efficient drug delivery of poorly absorbable medicines from the gastrointestinal tract has been of major interest. A series of compounds with very different structures has been proposed as effective absorption promoters for drugs after gastrointestinal administration in recent years (109). According to their ability of promotion and their adverse reaction with the mucosal membrane of the gastrointestinal tract, these promoting agents are classified into four groups (109). Middle-acyl-chain saturated fatty acids (110), long-chain unsaturated fatty acids (111,112), and Azone (1-dodecylazacycloheptan-2-one) (113) promote drug absorption with strong, fast reactivity and also with a rapid recovery of barrier function. The next group exerts a moderately fast reactivity at absorption enhancement and also has fast recovery. In this class, salicylates (114) and bile salts (115) are representative examples. Relatively effective at enhancing the absorption of chemicals but with a slow recovery rate is a third group of agents in which various chelating agents and powerful surfactants such as sodium lauryl sulfate (SLS) are categorized (116,117). Group four is a category of moderate reactivity as miscible solvents on absorption promotion: ethanol (118), dimethylsulfoxide (119), dimethylformamide (120), and so on. Structurally, in these enhancing agents the most promising have mutual peculiarities: (*1*) hydrophobic moieties such as C_{10}–C_{20} acyl chain or steroid skeleton and (*2*) hydrophilic groups such as hydroxy, carboxyl, glyceryl, or sulfate groups (109).

Chemical Modification. Attempts to modify preexisting drugs chemically and improve their physicochemical characteristics, thus gaining more valuable derivatives, have been systematized as a drug design strategy. These chemically modified drug derivatives are divided into two classes: prodrugs and analogs (121). A promoiety is added chemically to the parent drug, and when the new drug expresses its pharmacological effect after separation from the parent drug, the derivative is called a prodrug. On the other hand, if the derivative exerts a pharmacological activity without disintegration, it is called an analog. In absorption enhancement of drugs from the gastrointestinal tract, efforts using prodrugs for promotion have also been performed. Generally, gastrointestinal absorption of most drugs depends on simple diffusion, which is controlled by the lipid membrane of epithelial cells, and therefore increasing lipophilicity of drugs to raise their permeability across the biomembrane barrier is one of the most important purposes of prodrugs (121). Among attempts to improve gastrointestinal absorption of medicines, antibiotics have been target drugs for long time. Ampicillin is a typical drug for such targeting its absorption from the intestine is not good owing to a poor oil–water partition. As prodrugs for increasing lipophilicity of ampicillin, bacampicillin (122) or talampicillin (123) were synthesized. These are stable in aqueous solution at neutral pH; however, in the presence of a hydrolysis enzyme, an ester site is rapidly hydrolyzed and reverts to ampicillin. For both prodrugs, oral administration to humans indicated higher blood levels compared with ampicillin, which is sufficient for therapy. Also for cephalosporin, same esterification increased its lipophilicity and thereby improved its gastrointestinal absorption (124). Despite the importance of peptides and protein drugs for various therapies, their oral bioavailability is not good usually because of their poorly absorbabilities and enzymatic degradation in the gastrointestinal tract (125). Thus, in the absorption promotion of peptides and proteins, enhancement of absorption as well as protection from proteolysis should be addressed. For peptides and proteins, it has been pointed out that chemical modification may be a potential method for fulfilling these requirements in their gastrointestinal absorption (126). Consequently, the advantages of chemical modification of peptide drugs are (*1*) protection from degradation by peptidase or other enzymes in the lumen or the mucosae of gastrointestinal tract and (2) increasing their permeability through the membrane when lipophilic residues are added. Recently, derivatives of insulin (127,128), calcitonin (129), tetragastrin (130,131), and thyrotropin-releasing hormone (132,133) were synthesized in which acyl-chain residues of aliphatic fatty acids were added. In these, acylated insulins such as dicaproyl and lauryl insulin still possessed moderately high pharmacological activities (over 60% compared with that of native insulin), and their half-lives in the small-intestine mucosa in vitro increased 1.2- to 3.4-fold in monoacylated derivatives (128). However, the absorption of insulin after small-intestine administration could barely be improved. In contrast, its absorption after large-intestine administration was enhanced by increasing the number of caproic acid molecules attached to insulin (128). These in situ results indicated that the chemical modification of insulin with fatty acids was a beneficial approach for improving insulin absorption from the large intestine. Similar results have been obtained with other peptide drugs (129,131). Thus, these findings indicate that lipophilicity is an important factor for enhancing the permeation of peptides through the intestine; however, the small intestine is a more powerful degradation barrier in

vivo, probably because of potent enzymes, than the large intestine.

Classical Suspensions. Usually suspensions are chosen for administering drugs for the following reasons: insolubility or instability of drugs, difficulty of correction of taste, and adjustment of overly rapid absorption when dissolved in medium. A crystal polymorphism is a frequent problem in absorption using the suspension form. In spite of the same chemical composition, different crystal structures yield various physical differences, for example, the dissolution rate is sometimes greatly affected by polymorphism, which causes the absorption fluctuation (134).

Emulsions. Emulsion is a heterogeneous system that finely disperses a liquid into another one using a third material such as an emulsifying agent. This formula is suitable for liquid preparation of lipid-soluble drugs as well as water-soluble drugs; however, few products use emulsion for oral administration.

Classification of Emulsions. A dispersed phase, that is, an inner phase of emulsion, usually ranges from 0.1 to 1.0 μm in its diameter (135). When the diameters of emulsions are under 0.1 μm, they are called microemulsions, which appear translucent or transparent, and compared with conventional emulsions, microemulsions are thermodynamically stable (136). Emulsions consist of at least three components, the inner phase (dispersed phase), outer phase (dispersion medium), and emulsifying agent. Oil-in-water (o/w) emulsion includes a lipid in inner phase, and inversely, the same phase of water-in-oil (w/o) emulsion is an aqueous solution. In addition to these simple emulsions, there are so-called multiple-phase emulsions such as w/o/w type and o/w/o type.

Application of Emulsions to Gastrointestinal Absorption. Conventional emulsions are physically unstable heterogeneous mixture systems, which limits their broad application to medicine. However, many investigators have recently attempted to use emulsions as dosage forms in gastrointestinal absorption for the purpose of improving absorption and retaining drugs in the alimentary canal. Lipid-soluble drugs are the main target for improved absorption, especially immunosuppressive drugs such as cyclosporins, which are clinically administered as microemulsions, resulting in a more enhanced absorption of the drug compared with marketed oily formulations (137,138). A multiple emulsion (w/o/w type) has also been reported useful for promotion of drug absorption; it was reported that intestinal absorption of a poorly absorbable model fluorescein chemical by this emulsion using oleic acid as an oily phase was almost equal to that of solubilized mixed micelles (139).

Liposomes. Liposomes are vesicles that consist of a double-layer membrane of phospholipid. Liposomes have fundamentally the same structures as natural biomembranes, and thus they have been investigated as model membranes. The reasons why liposomes have been highlighted as drug carriers are their ability to encapsulating drugs inside themselves like microcapsules and their susceptibility to endocytosis or fusion with cell membranes. By devising the proper preparation methods, various kinds of liposome shapes and sizes are available, such as multiple liposomes or unilamellar liposomes (140). Additionally, incorporating basic lipids or acidic lipids into membranes can change the surface charge of liposomes. From these characteristics, we can expect to use them as controlled-release media, or to stabilize or target drugs in the body.

Employment of Liposomes in Gastrointestinal Absorption. On application of liposomes for gastrointestinal absorption, the oral administration of liposome-encapsulated insulin was reported to reduce the blood sugar level of rats with diabetes (141). Since this report, many others have been submitted on the improvement of gastrointestinal absorption of drugs such as glucose oxidase (142), cytarabine (143), gentamicin (144), erythropoietin (145), and amphotericin B (146). However, there are many problems regarding the application of liposomes to improve gastrointestinal absorption of drugs: (*1*) less reproducibility of absorption enhancement, (*2*) low rate of entrapment of water-soluble drugs, and (*3*) unclear mechanism of absorption enhancement. Regarding the mechanism of liposome's absorption enhancement, it has been argued that liposomes might reach through the cell membrane to circulation or that drugs are released from liposomes and then transfer to the blood or lymph. On this point, an experiment of permeability of liposome through rat everted sac using encapsulated macromolecular dextran as a marker revealed that a little bit of intact liposome was taken up into the epithelial cells (147,148). However, any clear mechanism on absorption enhancement by liposomes has been not submitted, and thus further investigations are necessary for clinical use of them in gastrointestinal absorption. Most drugs that are employed with liposomes are hydrophilic, but some investigators reported that the intestinal uptakes of lipophilic drugs such as vitamin K (149) and dolichol (150) are being considered to locate at the membrane of liposome were enhanced.

Micro- and Nanoparticles

Microparticles are polymeric particles ranging in size from 1 to 1,000 μm, and nanoparticles are similar, ranging in size from 1 to 1,000 nm (151). Both consist of natural or synthetic macromolecular materials in which drugs are encapsulated, entrapped, or dissolved or to which they are adsorbed (151).

Particulates for Gastrointestinal Delivery. In peroral administration, particulates have been employed for carriers to enhance the absorption of drugs (152). An enhanced oral absorption of vincamine was reported in rabbits using nanoparticles of adsorbed type (153). Using the same type of nanoparticles, the oral absorption of insulin was enhanced in diabetic rats (154). In this attempt, a reducing effect on blood sugar level was sustained for 20 h after administration. Additionally, the absorption of tomato lectin in rats has been shown to be enhanced by nanoparticles (155), whereas microparticles have been reported to also be useful for sustainment or enhancement of gastrointestinal absorption. Sustained release of zidovudine (AZT)

was shown in vivo using EC microspheres after oral administration in dogs (156). Encapsulated AZT showed significantly lower maximum concentration (C_{max}) values and longer times to C_{max} (t_{max}) values. And longer mean residence time (MRT) was also observed compared with AZT powder. In rats an oral delivery of γ-interferon was attempted in which it was encapsulated in polylacetate microspheres (157). In this report, a quite different distribution of interferon level was observed in vivo at 15 and 240 min after oral administration, in contrast to the control group, which received equivalent doses of unencapsulated interferon. These findings would suggest the tentative conclusion that microencapsulation of proteins markedly affects oral uptake and possibly postabsorption pharmacokinetic parameters as well. This experiment stands on the hypothesis that particulate material itself could be absorbed from the gastrointestinal tract.

Intestinal Uptake of Particulates. Despite many findings in the past 20 years of the uptake of micro- or nanoparticles through the intestine after peroral administration, there is much difference of opinion as to the site of absorption and its mechanism. In 1977, so-called persorption of large starch microspheres (5–150 μm) via the intestinal villae tips was reported in animals including humans (158). It was pointed out that this persorption was an infrequent occurrence and also a rather pathological phenomenon (159). Several investigators examined cytosis of particulates by the intestinal epithelial cells. In these examinations, phagocytic transport of 1-μm polystyrene microspheres in the intestines of rats and dogs was found (160). The uptake of polystyrene nanospheres up to 100 nm with the aid of endocytosis was also reported histologically (161). However, it was insisted that 2-μm microspheres of polystyrene could be taken up through the epithelial cells of the intestine (162). In addition to these convenient routes of intestinal absorption, recent studies have revealed a predominant contribution of M cells on uptake of particulates at the Peyer's patch. Peyer's patch localizes in duodenum, jejunum, and ileum spottily and originally constructs a gut-associated lymphoid tissue in which there are M cells being specially compared with normal absorption cells (163). These M cells possess a high activity of endocytosis that is performed by specific receptors at the surface of its cell membrane. Macromolecules or particulates absorbed by M cells are released into extracellular space, being included by lymphocytes or macrophages, and thus appear in the intestinal lymph nodes (163). The effect of particulate size on their uptake through M cells has been argued by many investigators. In their research, various upper-limit sizes of particulates for uptake into Peyer's patch were reported: 15 μm (164), 10 μm (165), and 3 μm (161). It was also found that although particulates under 5 μm were transferred into the lymphatics, larger particles of 5–10 μm remained in the Peyer's patch (165). Recently, the usefulness of biologically erodable and adhesive particulates (0.1–10 mm) composed of a copolymer of fumaric acid with sebacic acid or lactide-*co*-glycotide was reported for potential oral drug delivery systems (166). These particulates were recognized microscopically to traverse both the intestinal absorptive cells as well as Peyer's patches and to reach the spleen and liver tissues after lengthy contact with gastrointestinal mucosa. An enhanced exertion of pharmacological effects of three model chemicals (dicumarol, insulin, and plasmid DNA) with widely different molecular weights loaded in these particulates was observed inside the intestinal tissue, in the liver and in the blood. As just mentioned, despite the very limited area of Peyer's patch, microparticles or nanoparticles probably enable the absorption of loaded drugs through M cells. Thus, for drugs designed for lymphatic absorption, uptake through the Peyer's patch is surely significant; however, further examinations are necessary for drugs that require a transfer into systemic circulation. Additionally, the route as well as mechanism of particulate uptake in the intestine is not completely clear, and thus such examinations also should be continued for clinical usage of micro and nanoparticles.

BIBLIOGRAPHY

1. G.H.P. Te Wierik et al., *J. Controlled Release* **45**, 25–33 (1997).
2. L.F. Prescott and W.S. Nimmo, *Novel Drug Delivery and its Therapeutic Application*, Wiley, Chichester, England, 1989.
3. P.R. Katikaneni, S.M. Upadrashta, S.H. Neau, and A.K. Mitra, *Int. J. Pharm.* **123**, 119–125 (1995).
4. Y. Qiu et al., *Int. J. Pharm.* **157**, 43–52 (1997).
5. T. Salsa, F. Veiga, and M.E. Pina, *Drug Dev. Ind. Pharm.* **23**, 929–938 (1997).
6. C. Liu et al., *J. Pharm. Pharmacol.* **47**, 360–364 (1995).
7. Y. Qiu, H. Cheskin, J. Briskin, and K. Engh, *J. Controlled Release* **45**, 249–256 (1997).
8. H. Kim and R. Fassihi, *Pharm. Res.* **14**, 1415–1421 (1997).
9. I.R. Wilding et al., *J. Controlled Release* **33**, 89–97 (1995).
10. J.D. Ntawukulilyayo et al., *Int. J. Pharm.* **139**, 79–85 (1996).
11. A.L. Golub, R.W. Frost, C.J. Betlach, and M.A. Gonzalez, *J. Allergy. Clin. Immunol.* **78**, 689–694 (1986).
12. A.P. Sips et al., *Eur. J. Clin. Pharm.* **26**, 405–407 (1984).
13. O.L. Sprockel, M. Sen, P. Shivanand, and W. Prapaitrakul, *Int. J. Pharm.* **155**, 191–199 (1997).
14. L. Yang and R. Fassihi, *J. Controlled Release* **44**, 135–140 (1997).
15. M. Lagas and J.H.G. Jonkman, *Eur. J. Clin. Pharm.* **24**, 761–767 (1983).
16. M. Lagas and J.H.G. Jonkman, *Int. J. Clin. Pharm. Ther. Toxicol.* **23**, 424–426 (1985).
17. M.P. Danckwerts and J.G. van der Watt, *Int. J. Pharm.* **123**, 85–94 (1995).
18. Y. Raghunathan, L. Amsel, O. Hinsvark, and W. Bryant, *J. Pharm. Sci.* **70**, 379–384 (1981).
19. N.W. Read and K. Sugden, *Crit. Rev. Ther. Drug Carrier Syst.* **4**, 221–263 (1987).
20. M.A. Khan et al., *J. Controlled Release* **37**, 131–141 (1995).
21. R. Jachowicz and E. Nürnberg, *Int. J. Pharm.* **159**, 149–158 (1997).
22. K. Takada et al., *Chem. Pharm. Bull.* **37**, 471–474 (1989).
23. P. Arnaud, I. Guillard, D. Brossard, and J.C. Chaumeil, *Int. J. Pharm.* **129**, 279–282 (1996).
24. I.S. Moussa and L.H. Cartilier, *Int. J. Pharm.* **149**, 139–149 (1997).

25. G. Santus and R.W. Baker, *J. Controlled Release* **35**, 1–21 (1995).
26. L.G.J. de Leede, A.G. de Boer, and D.D. Breimer, *Biopharm. Drug Dispos.* **2**, 131–136 (1981).
27. J.S. Grundy, D.W. Grace, and R.T. Foster, *J. Controlled Release* **44**, 247–254 (1997).
28. S.V. Sastry, I.K. Reddy, and M.A. Khan, *J. Controlled Release* **45**, 121–130 (1997).
29. S.M. Herbig, J.R. Cardinal, R.W. Korsmeyer, and K.L. Smith, *J. Controlled Release* **35**, 127–136 (1995).
30. J.N.C. Healey, in J.G. Haedy, S.S. Davis, and C.G. Wilson, eds., *Drug Delivery to the GastroIntestinal Tract*, Ellis Horwood, Chichester, England, 1989, pp. 83–96.
31. A.A. Deshpande, C.T. Rhodes, N.H. Shah, and A.W. Malick, *Drug Dev. Ind. Pharm.* **22**, 539–547 (1996).
32. W. Hou, S. Miyazaki, and M. Takada, *Yakuzaigaku* **51**, 93 (1991).
33. R. Cargill et al., *Pharm. Res.* **5**, 533–536 (1998).
34. G.A. Agyilirah, M. Green, R. duCret, and G.S. Banker, *Int. J. Pharm.* **75**, 241–247 (1991).
35. S. Bouckaert, L. Vakaet, and J.P. Remon, *Int. J. Pharm.* **130**, 257–260 (1996).
36. R. Khanna, S.P. Agarwal, and A. Ahuja, *Int. J. Pharm.* **138**, 67–73 (1996).
37. Y. Kohda et al., *Int. J. Pharm.* **158**, 147–155 (1997).
38. K. Iga and Y. Ogawa, *J. Controlled Release* **49**, 105–113 (1997).
39. D.O. Thompson, *Crit. Rev. Ther. Drug Carrier Syst.* **14**, 1–104 (1997).
40. E. Albers and B.W. Müller, *Crit. Rev. Ther. Drug Carrier Syst.* **12**, 311–337 (1995).
41. T. Irie and K. Uekama, *J. Pharm. Sci.* **86**, 147–162 (1997).
42. R.A. Rajewski and V.J. Stella, *J. Pharm. Sci.* **85**, 1142–1169 (1996).
43. T. Loftsson and M.E. Brewster, *J. Pharm. Sci.* **85**(10), 1017–1025 (1996).
44. J.R. Moyano, J.M. Ginés, M.J. Arias, and A.M. Rabasco, *Int. J. Pharm.* **114**, 95–102 (1995).
45. M.T. Esclusa-Díaz et al., *Int. J. Pharm.* **142**, 183–187 (1996).
46. M.T. Esclusa-Díaz et al., *Int. J. Pharm.* **143**, 203–210 (1996).
47. V. Lemesle-Lamache, D. Wouessidjewe, M. Chéron, and D. Duchêne, *Int. J. Pharm.* **141**, 117–124 (1996).
48. J. Alvarez-Fuentes et al., *Int. J. Pharm.* **148**, 219–230 (1997).
49. N. Konar and C. Kim, *J. Pharm. Sci.* **86**, 1339–1344 (1997).
50. M. Ishii and T. Tanaka, *Clin. All-Round* **46**, 2336–2342 (1997).
51. C.J. Kenyon et al., *J. Controlled Release* **34**, 31–36 (1995).
52. M. Matsuo, K. Arimori, C. Nakamura, and M. Nakano, *Int. J. Pharm.* **138**, 225–235 (1996).
53. T. Yamamoto and S. Matsuura, *Pharm Tech Jpn.* **8**, 1257–1260 (1992).
54. S.J. Burns et al., *Int. J. Pharm.* **134**, 223–230 (1996).
55. M.J. Arias et al., *Int. J. Pharm.* **123**, 25–31 (1995).
56. P. Sheen, V.K. Khetarpal, C.M. Cariola, and C.E. Rowlings, *Int. J. Pharm.* **118**, 221–227 (1995).
57. P.B. Deasy and M.P. Gouldson, *Int. J. Pharm.* **132**, 131–141 (1996).
58. V. Tantishaiyakul, N. Kaewnopparat, and S. Ingkataowornwong, *Int. J. Pharm.* **143**, 59–66 (1996).
59. T. Ozeki, H. Yuasa, and Y. Kanaya, *Int. J. Pharm.* **155**, 209–217 (1997).
60. S.K. Dordunoo, J.L. Foad, and M.H. Rubinstein, *J. Pharm. Pharmacol.* **48**, 782–789 (1996).
61. M.E. Pina, A.T. Sousa, and A.P. Brojo, *Int. J. Pharm.* **133**, 139–148 (1996).
62. M.E. Pina, A.T. Sousa, and A.P. Brojo, *Int. J. Pharm.* **148**, 73–84 (1997).
63. T. Houjou et al., *J. Pharm. Pharmacol.* **48**, 474–478 (1996).
64. Y. Akiyama et al., *Int. J. Pharm.* **136**, 155–163 (1996).
65. Y. Akiyama et al., *Int. J. Pharm.* **138**, 13–23 (1996).
66. A. Kiriyama et al., *Biopharm. Drug Dispos.* **17**, 125–134 (1996).
67. J. Sujja-Areevath, D.L. Munday, P.J. Cox, and K.A. Khan, *Int. J. Pharm.* **139**, 53–62 (1996).
68. M. Takahashi, *Pharm Tech Jpn.* **8**, 1263–1268 (1992).
69. J.M. Sarciaux, L. Acar, and P.A. Sado, *Int. J. Pharm.* **120**, 127–136 (1995).
70. N.H. Shah et al., *Int. J. Pharm.* **106**, 15–23 (1994).
71. L. Halbaut, C. Barbé, and A. del Pozo, *Int. J. Pharm.* **130**, 203–212 (1996).
72. K.K.C. Tan, A.K. Trull, J.A. Uttridge, and J. Wallwork, *Eur. J. Clin. Pharm.* **48**, 285–289 (1995).
73. M.L. Shively and D.C. Thompson, *Int. J. Pharm.* **117**, 119–122 (1995).
74. L.A. Felton et al., *Int. J. Pharm.* **113**, 17–24 (1995).
75. P.P. Constantinides et al., *J. Controlled Release* **34**, 109–116 (1995).
76. A.J. Humberstone and W.N. Charman, *Adv. Drug Delivery Rev.* **25**, 103–128 (1997).
77. R.R.C. New and C.J. Kirby, *Adv. Drug Delivery Rev.* **25**, 59–69 (1997).
78. R. New et al., *Int. J. Pharm.* **156**, 1–8 (1997).
79. B.J. Aungst et al., *Int. J. Pharm.* **156**, 79–88 (1997).
80. S.G. Barnwell et al., *Int. J. Pharm.* **128**, 145–154 (1996).
81. S.J. Burns et al., *Int. J. Pharm.* **141**, 9–16 (1996).
82. S.J. Burns et al., *Int. J. Pharm.* **121**, 37–44 (1995).
83. P.B. Deasy, *Crit. Rev. Ther. Drug Carrier Syst.* **8**, 39–89 (1991).
84. T. Hata and S. Ueda, *Pharm Tech Jpn.* **4**, 1415–1422 (1988).
85. S. Narisawa et al., *J. Controlled Release* **33**, 253–260 (1995).
86. S. Narisawa et al., *Int. J. Pharm.* **148**, 85–91 (1997).
87. B. Wolf, *Int. J. Pharm.* **156**, 97–107 (1997).
88. A.D. Sezer and J.A. Kbugă, *Int. J. Pharm.* **121**, 113–116 (1995).
89. Y. Sun, C. Chang, W. Huang, and H. Liang, *J. Controlled Release* **47**, 247–260 (1997).
90. K. Vasilevska, Z. Djurić, M. Jovanović, and A. Simov, *Drug Dev. Ind. Pharm.* **18**, 1649–1655 (1992).
91. V. Gladigau et al., *Arzneim-Forsch.* **31**, 835 (1981).
92. F. Zhou, C. Vervaet, and J.P. Remon, *Int. J. Pharm.* **133**, 155–160 (1996).
93. H.C. Zaniboni, J.T. Fell, and J.H. Collett, *Int. J. Pharm.* **125**, 151–155 (1995).
94. P. Sriamornsak, S. Prakongpan, S. Puttipipatkhachorn, and R.A. Kennedy, *J. Controlled Release* **47**, 221–232 (1997).
95. G.M. Clarke, J.M. Newton, and M.B. Short, *Int. J. Pharm.* **114**, 1–11 (1995).
96. N. Follonier, E. Doelker, and E.T. Cole, *J. Controlled Release* **36**, 243–250 (1995).

97. P.K. Gupta and J.R. Robinson, *Int. J. Pharm.* **125**, 185–193 (1995).
98. P.B. Deasy and M.F.L. Law, *Int. J. Pharm.* **148**, 201–209 (1997).
99. A. Martin, J. Swarbrich, and A. Cammarata, *Physical Pharmacy*, 3rd ed., Lea & Febiger, Phyladelphia, 1983, pp. 352–398.
100. S. Yoshioka, Y. Aso, and Y. Takeda, *Chem. Pharm. Bull.* **38**, 1760–1762 (1990).
101. K.A. Connors, G.L. Amidon, and L. Kennon, *Chemical Stability of Pharmaceuticals*, Wiley, New York, 1979, pp. 33–62.
102. K.A. Connors, *J. Parenter. Sci. Technol.* **35**, 186–208 (1981).
103. H. Fujiwara, *Seiyaku-koujou* **4**, 853–859 (1984).
104. K. Fujioka et al., *Chem. Pharm. Bull.* **31**, 2416–2423 (1983).
105. K. Uekama et al., *J. Pharm. Sci.* **68**, 1059–1060 (1979).
106. Y. Hamada, N. Nambu, and T. Nagai, *Chem. Pharm. Bull.* **23**, 1205–1211 (1975).
107. H.O. Ammar, S.A. Ibrahim, and M.G. Abd EI-Mohsen, *Pharmazie* **37**, 270–271 (1982).
108. J.M. Christensen, *Am. J. Hosp. Pharm.* **40**, 612–618 (1983).
109. S. Muranishi, *Crit. Rev. Ther. Drug Carrier Syst.* **7**, 1–33 (1990).
110. T. Sawada et al., *Pharm. Res.* **8**, 1365–1371 (1991).
111. S. Muranishi, Y. Tokunaga, K. Taniguchi, and H. Sezaki, *Chem. Pharm. Bull.* **25**, 1159–1161 (1977).
112. H. Fukui et al., *J. Pharmacobio-Dyn.* **10**, 236–242 (1987).
113. M. Murakami, K. Takada, and S. Muranishi, *Int. J. Pharm.* **31**, 231–239 (1986).
114. T. Nishihata et al., *Int. J. Pharm.* **21**, 239–248 (1984).
115. E.J. Van Hoogdalem et al., *J. Pharmacol. Exp. Ther.* **251**, 741–748 (1989).
116. K. Nakanishi, S. Miyazaki, M. Masada, and T. Nadai, *Yakugaku Zasshi* **102**, 1133–1144 (1982).
117. Y. Sancho-Chust et al., *Arzneim. Forsch.* **45**, 595–601 (1995).
118. T. Kurihara-Bergstrom, K. Knutson, L.J. DeNoble, and C.Y. Goates, *Pharm. Res.* **7**, 762–766 (1990).
119. R.S. Geary, N.F. Swynnerton, S.F. Timmos, and D.J. Mangold, *Biopharm. Drug. Dispos.* **12**, 261–274 (1991).
120. P. Hadad, I. Moran, and E. Cid, *Ann. Pharm. Fr.* **5**, 265–271 (1975).
121. A.A. Sinkula and S.H. Yalkowsky, *J. Pharm. Sci.* **64**, 181–210 (1975).
122. N.O. Bodin et al., *Antimicrob. Agents Chemother.* **8**, 518–525 (1975).
123. K.H. Jones, P.F. Langley, and L.J. Lees, *Chemotherapy (Basal)* **24**, 217–226 (1978).
124. A.A. Sinkula, *Ann. N.Y. Acad. Sci.* **507**, 281–288 (1987).
125. V.H.L. Lee and A. Yamamoto, *Adv. Drug Delivery Rev.* **4**, 171–207 (1990).
126. H. Bundgaard, *Adv. Drug Delivery Rev.* **8**, 1–38 (1992).
127. M. Hashimoto, K. Takada, Y. Kiso, and S. Muranishi, *Pharm. Res.* **6**, 171–176 (1989).
128. H. Asada et al., *J. Pharm. Sci.* **84**, 682–687 (1995).
129. T. Fujita et al., *Int. J. Pharma.* **134**, 47–57 (1996).
130. T. Tenma et al., *Pharm. Res.* **10**, 1488–1492 (1993).
131. E. Yodoya et al., *J. Pharmacol. Exp. Ther.* **271**, 1509–1513 (1994).
132. S. Muranishi et al., *Pharm. Res.* **8**, 649–652 (1991).
133. K. Yamada et al., *J. Pharm. Pharmacol.* **44**, 717–721 (1992).
134. R. Li, P.T. Mayer, J.S. Trivedi, and J.J. Fort, *J. Pharm. Sci.* **85**, 773–780 (1996).
135. H.D. Goff, *Adv. Exp. Med. Biol.* **415**, 137–148 (1997).
136. M. Borkovec, *Adv. Colloid Interface Sci.* **37**, 195–217 (1992).
137. S. Friman and L. Backman, *Clin. Pharmacokinet.* **30**, 181–193 (1996).
138. D.I. Min, *J. Transplant. Coord.* **6**, 5–8 (1996).
139. N. Oba et al., *Lipids* **27**, 701–705 (1992).
140. F. Szoka and D. Papahadjopoulos, *Annu. Rev. Biophys. Bioeng.* **9**, 467–476 (1980).
141. H.M. Patel and B.E. Ryman, *FEBS Lett.* **62**, 60–63 (1976).
142. G. Dapergolas, E.D. Nurunjun, and G. Gregoriadis, *FEBS Lett.* **63**, 235–249 (1976).
143. Y.M. Rustum, C. Dave, E. Mayhew, and D. Papahadjopoulos, *Cancer Res.* **39**, 1390–1395 (1979).
144. J.R. Morgan and K.E. Williams, *Antimicrob. Agents Chemother.* **17**, 544–548 (1980).
145. Y. Maitani et al., *J. Pharm. Sci.* **85**, 440–445 (1996).
146. A.C. Leenders et al., *AIDS* **11**, 1463–1471 (1997).
147. T. Kimura, K. Higaki, and H. Sezaki, *Pharm. Res.* **5**, 221–224 (1984).
148. T. Kimura, *Saishin Igaku* **40**, 1818–1824 (1985).
149. M. Nagata, T. Yotsuyanagi, M. Nonomura, and K. Ikeda, *J. Pharm. Pharmacol.* **36**, 527–533 (1984).
150. T. Kimura et al., *Chem. Pharm. Bull.* **37**, 463–466 (1989).
151. J. Kreuter, *Pharm. Acta Helv.* **58**, 196–204 (1983).
152. D.T.O. Hagan, *Adv. Drug Delivery Rev.* **5**, 265–285 (1990).
153. P. Maincent et al., *J. Pharm. Sci.* **75**, 955–958 (1986).
154. C. Damge, C. Michel, M. Aprahamian, and P. Couvreur, *Diabetes* **37**, 246–251 (1988).
155. N. Hussain, P.U. Jani, and A.T. Florence, *Pharm. Res.* **14**, 613–618 (1997).
156. K. Abu-Izza, L. Tambrallo, and D.R. Lu, *J. Pharm. Sci.* **86**, 554–559 (1997).
157. J.E. Eyles, H.O. Alpar, B.R. Conway, and M. Keswick, *J. Pharm. Pharmacol.* **49**, 669–674 (1997).
158. G. Volkheimer, *Adv. Pharmacol. Chemother.* **14**, 163–187 (1977).
159. B.J. Freedman, *Med. Hypotheses* **35**, 85–87 (1991).
160. C.L. Wells, M.A. Maddaus, S.L. Erlandsen, and R.L. Simmons, *Infect. Immun.* **56**, 278–282 (1988).
161. P.U. Jani, A.T. Florence, and D.E. MaCarthy, *Int. J. Pharm.* **84**, 245–252 (1992).
162. G.M. Hodges, E.A. Carr, R.A. Hazzard, and K.E. Carr, *Dig. Dis. Sci.* **40**, 967–975 (1995).
163. R.L. Owen, *Gastroenterology* **72**, 440–451 (1977).
164. M.E. Le Febre, D.C. Hancock, and D.D. Joel, *J. Toxicol. Environ. Health* **6**, 691–704 (1980).
165. J.H. Eldridge et al., *J. Controlled Release* **11**, 205–214 (1990).
166. E. Mathiowitz et al., *Nature (London)* **386**, 410–414 (1997).

See also BIOADHESIVE DRUG DELIVERY SYSTEMS; CARRIER-MEDIATED TRANSPORT, ORAL DRUG DELIVERY; ORAL DRUG DELIVERY, SMALL INTESTINE & COLON.

PARENTERAL DRUG DELIVERY SYSTEMS

M.J. GROVES
University of Illinois at Chicago
Chicago, Illinois

KEY WORDS

Albumin
Antigens
Aseptic processing
Chitosan
Emulsions
Gelatin nanoparticles
Implants
Microbial death
Nanoparticles
Sterility
Sterilization

OUTLINE

Introduction
- Some General Considerations
- Essential Requirements of Parenteral Products
- The Importance of Scale-up and Reproducibility

Methods of Sterilization of Parenteral Drug Delivery Systems
- Introduction
- The "Death" of Microorganisms
- Sterilization Methods
- The Effect of Heat
- Conditions for the Application of Heat
- Use (and Abuse) of the Sterility Assurance Level
- Sterilization Using Gases
- Other Methods Used To Sterilize Surfaces
- Sterilization by Filtration
- The Concept of "Size" Applied to the Filtration Process
- Sterilization by Ionizing Radiation
- Pulsed Light Sterilization
- Aseptic Processing

Sterile Implants
- Protein Compacts
- Effects Produced by Compaction of Proteins
- Sterilization of Protein Compacts
- Polymeric Implants
- Sterilization of Polymeric Implants

Production of Macro-, Micro- and Nanoparticulate Systems
- Introduction and Definitions
- Production Methods for Solid Particles
- Emulsions
- Mixed Micelles
- Spraying Processes
- Antigens and Adjuvants
- Other Current Formulation Issues
- Albumin
- Collagen
- Gelatin and Gelatin Vehicles
- Chitosan

Conclusions
Bibliography

INTRODUCTION

Some General Considerations

Gregordiadis in 1978 (1) noted that the ideal dosage form in cancer chemotherapy was one that provided a sufficient amount of an antineoplastic drug or anticancer agent—not necessarily the same thing—to the tumor site in a sufficient amount for an adequate period of time without adverse interaction on normal, healthy tissue. This definition implies that the delivery system is capable of targeting the tumorous tissue, and it is easier to envisage small particles being able to specifically target tumors, tissues, or organs. However, the definition applies equally well to devices that are implanted or inserted in close proximity to the target tissue. These devices may consist of a drug dispersed in a slab or rod of suitable polymer that can be implanted into the tissue or a pump that infuses controlled amounts of drug into the vicinity of the target.

Nevertheless, as Illum and Davis (2) suggested, targeting of microparticulate drug carriers to extravascular tumors required particles in the submicrometer size range, by implication in the colloidal region. Colloidal drug carriers have been described by others (3,4). More recently colloidal microspheres as sustained release targeting agents for antitumor drugs have received a considerable amount of attention, reviewed by Donbrow (5) and Kreuter (6,7). Microparticulate vehicles prepared from albumin, gelatin, or polymers such as poly(lactic acid) (PLA) have been evaluated (8,9) and, in some cases, have become pharmaceutical products, although for the most part these have been diagnostic agents. Other colloidal systems such as liposomes and emulsion products are also now appearing in the pharmaceutical marketplace after extensive development and scientific exploration of their properties. One is always reminded, after reading about a new "development" or drug delivery system, that it took roughly 25 years for liposomes to be developed to marketable, realistic products. The initial excitement evident in the early research papers describing the possibility of using liposomes

as drug delivery systems makes for interesting reading today. These early pioneering authors were apparently unaware that there are huge differences between making an ill-defined suspension of liposomes on a 5 mL scale in the laboratory and to manufacturing a 5,000 liter (or more) batch of a well-defined and well-characterized material suitable for administration to patients with efficacy, safety, and reproducibility. Moreover, these pioneers did not seem to be aware that before patients could receive these complex systems, the systems themselves had to have other basic requirements. Thus, knowledge of the reproducibility of the state of dispersion—not only the mean particle diameter itself but also the way in which the distribution of size was spread around the mean—were essential requirements for any product specification. In addition, because many of these laboratory-scale products were going to be injected directly into the patient, they had to be sterile and apyrogenic, requirements that were evidently of low priority to many of these early workers. Indeed, one early review on parenteral products failed to even mention sterility (10). Eventually, when it became necessary to scale-up these laboratory-scale experiments to make sufficient of a product for sale, issues such as particle size changes associated with chemical degradation of components on autoclaving or thermal effects produced on dispersions became evident and proved to be difficult to resolve for several years. These requirements resulted in significant delays in the development of some liposomal products, in some cases having profound economic consequences on their developers.

These issues have now become evident on hindsight for liposomal products; in fact, they are applicable to any controlled release product intended for parenteral delivery. A general review of issues associated with scale-up has recently appeared and can be strongly recommended as an introduction to the topic (11).

Essential Requirements of Parenteral Products

All parenteral products are designed to bypass the body's natural defenses against microorganism invasion associated with skin and mucosal tissues. Irrespective of the physical nature of the product, be it a simple solution of the drug in water or a complex insertable pump, all parenteral products have some basic requirements to which must be added the general requirements associated with all pharmaceutical products:

1. Sterility
2. Apyrogenicity
3. Reproducibility in performance
4. Safety
5. Efficacy

Methods of achieving *sterility* are reviewed in a later section, but it makes sense not to introduce a pathogenic microorganism into a body that is most likely already debilitated by disease and therefore has lower resistance to bacterial invasion. *Apyrogenicity* is closely associated with the need for sterility because, under some conditions, bacteria or products associated with dead bacteria can produce febrile reactions that are rarely fatal but can be unpleasant for the patient. Moreover, pyrogens can be measured with some precision and accuracy, and low levels of pyrogen infer a low bioburden in the product being tested. *Reproducibility* of the product implies that there is uniformity of drug content, not only in each item produced in a batch but also from batch to batch. The same implication applies to the rates of drug release from the device or system so that ultimately there is a reproducible effect produced on the target tissues over a sufficient and reproducible length of time. *Safety* is also clearly necessary, and even the Hippocratic Oath required that doctors (and their associated medications) do no harm. *Efficacy* is also implied—there would be little point in administering the system otherwise.

Over the past two decades or more, many elegant and ingenious methods for obtaining the controlled release of a wide variety of drugs have been described in the literature; few products based on these methods have actually achieved commercial success. Obviously, one could argue that much of this ingenuity was expended in what were, for the most part, academic exercises designed to train, learn, and stimulate. However, it could also be argued that the intellectual effort expended in this area may have been substantially dissipated by a failure to realize that parenteral products must have these five essential requirements before proceeding to test the devices or systems in humans. Nevertheless, some groups of workers still persist in making impressive claims for potential applications based on experiments involving laboratory experiments on a scale of 5–10 mL or less. Naturally, beginnings have to be made somewhere but one might suggest that these initial claims could have been somewhat muted.

The Importance of Scale-up and Reproducibility

Most of the five essential requirements have been covered by textbooks that are readily available. However, scale-up and reproducibility are generally not covered and the following section provides some pointers.

Parenteral sustained release products are usually dispersions of one phase, often a solid, or a liquid in another liquid phase, usually water. Exceptions are the implanted solid products, which are themselves macroscopic and therefore relatively easy to produce with precision and accuracy. In the same way, characterization in terms of dimensions and performance prior to administration is also straightforward. This is less true for dispersed systems, which are generally much more difficult to make reproducible and characterize with precision and accuracy. Although it is not appropriate to go into this area in more detail, it should be noted that regulatory authorities such as the U.S. FDA rightly demand that production and characterization methods used for human-use products must be validated. The scientific challenge is to prove (and validate) claims made for the product. If the specification calls for a product containing particles 200 nm in diameter, the key question to be answered by the validation process is just how true is that statement? How do different batches of the product compare; are they always 200 nm in diam-

eter (as measured by an appropriate method itself validated as precise and accurate), and how does any batch-to-batch variation in the diameter, if detected, affect performance as measured by a suitable method, preferably in human patients? Scale-up and, to a large degree, reproducibility go hand in hand and should be considered together.

METHODS OF STERILIZATION OF PARENTERAL DRUG DELIVERY SYSTEMS

Introduction

Any material introduced into the body (human or animal) parenterally (that is, *para enteron* or "beyond the gut") should be sterile, because the body defenses have been bypassed. Philosophically, sterilization is quite absolute in concept and means (e.g., *The Concise Oxford Dictionary*) "rendered free of microorganisms"). Certainly it is important that any parenteral "should do no harm." The production of disease or even death by injection of contaminated product is not unknown, and it is certainly not acceptable. Even the production of abscesses following injection, which may ultimately heal, is not acceptable. Many patients receiving parenteral products are doing so because they have a disease or condition that impairs their natural defense mechanisms through the immune system. What would be easily dealt with by a healthy individual often cannot be tolerated by a sick person.

The absolute need for sterility is therefore easy to understand and one can appreciate why regulatory authorities insist on regarding sterility as an absolute concept. Nevertheless, there have been reasons to raise questions about this rigidity of definition because situations have arisen that ultimately lead to confusion. Sterility as such is easy to conceive but, in reality, microorganisms are ubiquitous in the environment and difficult to remove. In a closed system they can be killed by the application of heat or irradiation, but exposed to the environment once again, the product will become contaminated with more viable and therefore equally potentially dangerous microorganisms. The dictionary definition of sterilization, "rendering free of living microorganisms," can be carried out, but now we are becoming more aware of peripheral issues. For example, if we apply some environmental stress to a closed system containing living microorganisms (e.g., heat), how do we know just how much stress we need to apply to kill, or render nonviable, *all* of the microorganisms present? In practice a manufacturer uses a traditional overkill approach, such as autoclaving for 15 minutes at 121°C. These conditions are generally recognized as being sufficient to produce a "sterile" product. But what if the exposure time was only 14 minutes; does that mean the product is no longer sterile and therefore safe to use? How about only 10 minutes exposure to the stress or only 5 minutes?

The issue here is the rigidity of the thinking process and the attitude of regulatory authorities reviewing processing proposals. The absolute approach—15 minutes safe, 14 minutes unsafe—is safe from a regulatory standpoint but scientifically it is unlikely to be valid. A modern solution of a drug, filtered repeatedly through porous membranes down to 100 nm pore size, is "almost sterile," i.e., the bioburden is very low, before it is put into the autoclave, and a much lower heat insult is required to achieve "absolute sterility." To be fair, parametric release is now allowed by some regulatory authorities, and this process takes these considerations into account. There are additional issues if the drug itself is labile and is adversely affected by heat. In that situation it is likely that the solution would need to be "sterile filtered" and filled into a presterilized container in an "aseptic process." However, a filtration process is anything but absolute, and there are issues associated with running a truly satisfactory aseptic process. Here the absolute certainty associated with an overkill heating process is diminished considerably, and one has to start thinking in terms of an acceptable element of risk.

Some of the issues of this dilemma have recently been discussed by Gilbert and Allison (12) and their arguments expanded by Groves (13). The essential point of the argument is that a filtration process is certainly not an absolute process in the sense that, perhaps, a few microorganisms may not have been removed so the filtrate may not be truly sterile. Issues now arise, such as how can such small numbers of microorganisms per unit volume be measured or even detected. Gilbert and Allison pointed out that, in fact, not all microorganisms are pathogenic and are easily dealt with by the body's defense mechanisms or are simply not able to survive in a physiological environment. Moreover, even most pathogens require a sufficient number of organisms to produce some manifestation of disease. There are some interesting exceptions to this point but essentially their argument is that, if we remove most organisms from a product, that product can be regarded as aseptic and is therefore *safe* to use.

As already noted, in practice absolute sterility cannot be achieved in many situations because of the lability of the drug. In addition, because degrees of sterility of a product cannot be measured—it is either sterile or not—we have to start using statistical concepts to estimate the effectiveness of the sterilization process. Many of these concepts were proposed at the turn of the twentieth century with especial reference to foodstuffs, where levels of contamination were often very high and product lethality was a major concern. One must therefore question just how valid these earlier concepts are now when applied to modern pharmaceutical products that, by any standards, are exceptionally clean, so that the initial numbers/unit volume of contaminating microorganisms are very low. A real difficulty is that concepts or probabilities are not scientific *measurements* and many attempts to understand and explain modern ideas on the subject have simply become confused. Judgments are being made based on poor science, and one must suspect that nobody benefits, especially the patient who ultimately pays for all of this confusion.

It is also ironic that novel processes and ideas being used or explored in the food industry today are proving very difficult to translate into what is already a very conservative and economically driven pharmaceutical industry. It is also true that the death rate today due to microbiologically contaminated foodstuffs is finite although small, due to heavy regulation, the death rate in the pharmaceutical industry is infinitely small.

Many of these issues have been discussed in detail elsewhere by this author (13), and only a summary is necessary in this article.

The "Death" of Microorganisms

Because of the labile nature of so many of the new biotechnological drug entities such as proteins, genes, or DNA fragments, it has become necessary to explore sterilization procedures that lack the overkill approaches associated with older, more stable drugs. With heat or radiation it may be more feasible to apply a graded approach, using the minimum amount of energy sufficient to kill likely microbial contaminants without producing loss of product. The issue has now become about how to define bacterial "death." Dictionaries are of little help, because they just define *death* as a state of annihilation or ceasing to exist. For a bacterial cell, there is generally a clear relationship between form and function that is essential for "life" or conversely "death." Vegetative bacterial cells are relatively easy to kill by exposure to modest temperatures; the cell stops metabolizing and is unable to divide to form other bacterial cells. The metabolic processes by which the cell generates, uses, and stores energy in order to synthesize cellular components and allow replication of genetic material are complex but, individually, are dependent on a series of sequential reactions that can be blocked or broken when, perhaps, the conformation of just one essential protein is subtly changed. This process in itself is unlikely to require much external energy to accomplish. However, bacteria have developed survival mechanisms designed to resist environmental stresses, and generally, if one enzymatic pathway is disrupted, it is replaced by another. Damage to DNA sequences can be repaired over time, so it is possible that bacterial cells that shut down after the application of a mild heat stress would, over a period of time, recover their functionality. Bacterial death is therefore not very easy to define or to measure. Some bacteria have an interesting defense mechanism in that, when exposed to extreme environment changes such as desiccation, they form endospores that are nonfunctional cells in the usual sense but are quite capable of resisting applied environmental stress. When subsequentially exposed to a milder, favorable environment, the endospores rapidly revert to the usual metabolizing (vegetative) dividing cell forms. Endospores can be killed by exposure to extreme heat conditions such as those encountered in an autoclave or hot air oven, and it is for this reason that otherwise overkill conditions are employed. Part of the problem is judging the total amount of energy required to inactivate a mixed culture of different bacterial species in suspension. A typical but exaggerated situation in a nonsterile situation is that not only do the different individual species have inherently different susceptibilities to an applied stress but that individual organisms of the same species also have different sensitivities, mainly because they are inevitably at different points of their growth cycles. Some, for example, have just divided and others would be just on the point of dividing, with other cells at various stages in between. In order to inactivate (sterilize) such a broad cellular mixture, it would be necessary to apply enough stress to kill the least susceptible (or most resistant) organisms present, and it is usually assumed that in practice these are the endospores noted already. However, not all microorganisms produce endospores, and this is apparently also true for some of the extreme thermophilic organisms recently reported (14).

Historically, this type of rationalization has been derived from studies on foodstuffs where the bacterial burdens are usually much heavier than those of pharmaceutical solutions, quite apart from the fact that the latter are generally less hospitable and, therefore, less favorable for growth. Working on the survival of the spore-forming botulism organism *Clostridium botulinum* in canned foods, the highest concentration of endospores that could be harvested, cleaned, and suspended in phosphate buffer was approximately 10^{11} organisms/mL. It was therefore reasonable to apply enough heat to kill every organism in the system. Because one-tenth of the organisms could be killed in 0.21 minutes at 250°F (121°C), (D, the decimal reduction value) it is not difficult to calculate that $12 \times 0.21 = 2.52$ minutes, under the same conditions, would be sufficient to kill all the spores in the system and more (i.e., 10^{12}/mL). This is the basic logic that most of the pharmaceutical regulatory authorities are using to control sterilization processes. Enough energy is required to be applied in order to produce a reduction of 12 logs in the bacterial count to ensure that a pharmaceutical solution is sterile. In the case of a foodstuff consisting almost entirely of *Clostridium* spores, 2.52 minutes autoclaving would be sufficient heat exposure; any additional heating time would be an unnecessary overexposure and would most likely result in spoilage of the food due to a loss of quality or flavor. Applying the same logic to a pharmaceutical solution, likely to be less hospitable and certainly containing far fewer viable organisms or endospores in the first place, one can begin to realize why exposure to 12D values is an anachronism which could result in a deteriorated product. Unfortunately, regulatory authorities are going to need to be convinced that less heat (or energy trauma) is acceptable. The arguments of Gilbert and Allison (12) are very persuasive at this time but their gospel needs to be disseminated more widely and pondered on longer. Heat sterilization conditions may well destroy bacteria but, at the same time, the product is also destroyed. If the product could be manufactured with very few bacteria (per unit volume) it would mean that the applied stress could be much lower, and consequentially, there would be less resultant deterioration of the product.

Sterilization Methods

Killing or inactivation processes are limited to applied physical environmental stresses or the application of chemicals that irreversibly damage the bacterial cell functionality. In addition, filtration is used to physically remove all bacteria present, although this is an assumption that needs to be evaluated more closely.

Physical means of sterilization include:

- Dry heat
- Moist heat

- Ionizing radiation
- Intense light
- Filtration

Chemical means of sterilization include:

- Aldehydes
- Ethylene oxide
- β-propriolactone
- Peroxides
- Chlorine dioxide
- Iodine
- Ozone
- Alcohols/phenols
- Quaternary ammonium compounds
- Chlorine, chlorate

In its very helpful review of the current technicalities of sterilization in a General Information Chapter (⟨1211⟩ Sterilization and Sterility Assurance of Compendial Articles), the United States Pharmacopeia 23 (15), notes, as discussed earlier, that the absolute definition of sterility cannot realistically be demonstrated because of limitations in testing. In other words, every container in a lot would need to be tested in order to demonstrate that the lot had been made sterile. The emphasis of the USP 23 chapter then turns to the sterility of a product in probabilistic terms, the *chance* of a container being contaminated or not. Since probabilities cannot be *measured*, the importance of properly validated procedures and equipment becomes dominant. This requires, of course, total reliance on documented good manufacturing procedures (GMPs), which is outside the scope of this present review. Nevertheless, it serves to emphasize when working in a modern pharmaceutical plant just how important are properly validated and documented procedures. The USP 23 lists five methods for sterilization, which are briefly reviewed here, together with a more recent procedure currently under development.

The Effect of Heat

Heat sterilization processes are divided into moist heat and dry heat conditions. Because these conditions vary considerably both in the temperature and time of application required to achieve sterilization, it seems that there may be a fundamental difference in the mechanism by which loss of functionality is achieved.

As the environmental temperature around a microorganism is raised, enzymatic processes increase in tempo to a plateau temperature that may be at or only slightly above that of the normal environment of the organism. Indeed, some organisms are now known to be at their optimal activity at temperatures approaching that of boiling water (14), although most other vegetative bacteria are killed under those same conditions. The rate processes decline after plateauing until the main enzymes associated with cell functionality have effectively stopped. Initially, the slowing of the processes may be due to some enzymatic proteins changing conformation but, at higher temperatures, the hydrogen bonding affecting the overall protein structure becomes unable to hold it together, and it comes out of solution as more and more hydrophobic groups are exposed to the aqueous environment around the molecule. Ultimately, the protein becomes completely denatured, unable to function, and unable to recover functionality. This process affects all of the proteins within the cell as well as DNA and RNA, but some of these are more readily affected than others, thereby becoming key or limiting reactions. Applying heat to a mixed bacterial suspension does not affect all bacteria equally, and as noted earlier, some may be more resistant to the stress than others. In any mixed population it is the most heat-resistant organism that is the crucial element in determining the success of a heat sterilizing process. In a suspension of a single species or organism the key reaction is the enzymic process that is the most heat-sensitive, resulting in complete and irreversible damage. In the application of heat—moist or dry—the process is deliberately designed to produce an overkill, mainly in order to kill endospores that are very resistant to heat and may be presumed to be present in a system. The point of the previous discussion was to emphasize that it might be possible to design an effective sterilization process in which a minimal amount of heat could be applied for a sufficient time to achieve the same endpoint. This becomes more feasible if there are very small numbers of viable bacteria present in the system in the first place. The kinetics of this process are examined later in this article.

One essential difference between moist heat (e.g., 121°C for 15 minutes) and dry heat (e.g., 150°C for 60 minutes) sterilization conditions may simply lie in the efficiency with which heat is applied. Beyond desiccation, however, dry heat probably also destroys some, if not all, functionality by oxidation of proteins as well as inflicting irreversible structural damage to the cellular DNA.

Conditions for the Application of Heat

The conditions noted for sterilization (121°C moist heat for 15 minutes or 150°C dry heat for 1 hour) were applied in a time when sterilization was regarded as a cookery book exercise without necessarily taking into account the bacteriology involved. Today, any sterilization process is designed to kill the most resistant organism that could conceivably be present in a system, using it as a "marker" or test species. For example, *Bacillus stearothermophilus* and *B. subtilis* endospores are both used as markers for the moist heat and dry heat sterilization processes, respectively, by the United States Pharmacopeia, although it does not follow that these microorganisms are guaranteed or even likely to be present in any pharmaceutical system prior to sterilization. They simply represent species of heat-resistant spores that are considered to have an above average degree of resistance to the chosen heating process, a worst case situation, and are therefore markers to indicate the likelihood of success.

The interesting thing about this USP chapter is that it has moved away from the classical cookery book approach to sterilization and places emphasis on the design and validation of a particular system or set of circumstances. In

other words, if it works (i.e., if it can be validated to demonstrate effectiveness), that should be sufficient. The chapter actually states that with an article where extensive heat exposure may produce damage, the development of the sterilization process (Chapter ⟨1211⟩ uses the word *cycle*) depends heavily on the knowledge of the microbial burden over a suitable time period of a *substantial* number of lots of the presterilized product. The inference is there; the actuality is not. This means it is up to the manufacturer to present sufficient evidence to the regulatory authorities that any new process is satisfactory for its purpose.

Use (and Abuse) of the Sterility Assurance Level

The sterility assurance level (SAL) is defined (16) as the probability of the nonsterility of a unit from a batch of product in the final container. This author then goes on to explain that it is assumed throughout the parenterals industry and by regulatory authorities such as the FDA that where a process appears to have an SAL of 10^{-3}, approximately 1 vial per 1,000 could be contaminated with microbes.

There are two problems with this. The first is that SAL cannot be measured; it is a concept or probability. The second issue is that, as a concept, it applied to each and every vial in the batch—each vial, for example, has a *chance* of 1:1,000 of being contaminated. It is certainly not acceptable to produce a single contaminated vial in any batch of product, irrespective of the lot size. So where does this concept come from and how may it be used correctly?

It should be noted that D values for any microorganism are characteristics of the applied heat stress. A typically resistant endospore-forming organism such as *Bacillus stearothermophilus* has a D value of 1.5 minutes at 121°C, much longer at lower temperatures, and, typically, vegetative organisms have D values well below 1 minute at a temperature of 100°C. If we set the sterilization criteria at 6D and the actual, measured, D value is 4.5 minutes, and, if the initial solution contains 100 organisms mL, it will take $4.5 \times 6 = 27$ minutes at 121°C to reduce the count to one-millionth of the original count. The SAL is 100/1,000,000 or 10^{-4}. Under the same conditions, if the initial viable count in the product was 1 organism/mL, and, assuming a worst-case scenario, the SAL then drops to 1/1,000,000 or 10^{-6}. Sterility assurance is therefore a direct function of the number or organisms initially present in the product to be sterilized.

Again, SAL values cannot be measured directly, even in a heat sterilization process, and when talking about SALs for aseptic processes or other less dramatic sterilization processes, one is strictly speaking talking about a concept, not a precise entity. The concept has become abused, with "experts" speaking of the numbers of contaminated containers to be found in a production process. If there is a SAL of 10^{-6}, in principle one of the containers in a batch size of one million could be contaminated. Should the batch size be higher than a million, this implies that the lot has one or more contaminated units in it. The issue becomes more personal when considering that aseptically assembled products are required to have an SAL of 10^{-3} or better and are made in batch sizes that might suggest several containers could be contaminated. This concept has encouraged regulatory authorities to insist on media fills to "validate" a particular aseptic process. If more than one "contaminated" sample appears in a run of 3,000, the process is considered to be unsatisfactory. One could argue that any contaminated sample in any run, irrespective of the size, is unacceptable and the fact that these guidelines have been written at all is an indication of just how far away the technology is from the older overkill situation of terminal heat sterilization. Application of the same concept to totally different and dissimilar processes would appear to be poor science and is certainly not justified.

Nevertheless, what the SAL is effectively doing is to suggest that there is a *chance* that every single vial in the batch has a *possibility* of being contaminated; it does not mean that there are going to be x vials in the batch that are contaminated. Nevertheless, the principle of a complete, validated process designed to reduce the presterilization bioburden to its lowest feasible level, together with a worst-case scenario in terms of the thermal resistance of any possible microbial contaminant is quite scientifically reasonable, but there must be emphasis on validation. Although the discussion here has tended to be concerned with a heat-stress situation, the same broad concepts apply to any other sterilization process.

Sterilization Using Gases

An attractive alternative to the application of heat stress is the use of reactant gases that are able to permeate a product and sterilize *surfaces*. The commonest gaseous sterilant at present is ethylene oxide, which is extremely effective, albeit a little slow compared with heat stress. The gas itself is highly flammable and must be mixed with suitable inert carrier gases such as nitrogen. Moreover, the mode of action depends on the humidity, concentration of sterilant, and time of exposure. The gas is also harmful to humans because of its mutagenic properties. The process, usually carried out in a sealed pressurized chamber, essentially similar to an autoclave, is designed to ensure that the product is exposed to the ethylene oxide without at the same time exposing the operators to even small residues of gas. After the sterilization process has been carried out in the presence of the required level of humidity for the requisite amount of time, often for 16 hours overnight at ambient room temperature, the residual gas must be removed by pulling a vacuum and passing sterile nitrogen through the system, again for the necessary amount of time. Sterilized product is often allowed to stand under atmospheric conditions to ensure that the last traces of gas have been removed, because even small amounts can be toxic or irritant. This is especially true for surgical dressing materials.

Again, the USP 23 emphasizes the need for adequate validation of the designed process, placing emphasis on using appropriate biological indicators such as *Bacillus subtilis* spores. Other gases have been evaluated, including β-propriolactone, but toxicity to equipment operators was unacceptably high and better alternatives are being sought.

Again, gases are useful for sterilizing surfaces, although the gas may permeate into some polymeric materials. In

these cases this permeation through and below the surface only makes it even more difficult to remove gaseous residues.

Other Methods Used To Sterilize Surfaces

The surfaces of containers and the interior of barriers where sterilized components are aseptically assembled also need to be sterilized. Containers made of glass can be heat sterilized, often in hot air tunnels through which the containers pass on their way into the aseptic assembly area. Stoppers or seals, often made of natural rubber or suitable polymers, cannot be dry-heat sterilized but can be washed and autoclaved, often in smaller quantities enclosed in plastic bags to enable them to be more readily transported to the assembly area. An alternative is ethylene oxide gas, but this is more rarely used because of the associated difficulty of removing residual gas after exposure.

Barrier technology has been developed over the past decade for aseptic processes. It effectively places a barrier between the human operators, who are the main source of bacterial and particulate contamination, and the product being assembled by providing a blanket of sterile filtered air moving under laminar flow conditions. More and more computer-controlled robotic assembly processes are being employed inside the barrier but all of these surfaces need sterilization. Where robotic arms are moving this becomes more difficult because moving surfaces must have lubrication and the lubricants may react with some if not most of the chemically reactive materials used to sterilize the internal environment. Foremost amongst current sterilants are sprays or mists generated with steam of concentrated hydrogen peroxide, which is an extremely effective material but is equally a strong oxidizing agent. Surfaces under barriers are generally composed of stainless steel, poly(methyl methacrylate), or other transparent polymers. All materials used to construct barrier and isolates must be able to withstand hydrogen peroxide and, in the case of steam-generated mists, temperatures in excess of 100°C for at least the period required during the clean or sterilize in place cycle. Not only are moving surfaces of, for example, fans and pumps affected by the sterilants but sensors, and flexible materials such as rubber or latex gloves, may be affected. In addition, barrier systems require transfer ports. The evident complexity of an effective barrier system requires an integrative approach to its design and construction. Some of the issues involved are described by Melgaard and Haas (17), and this can be considered to be a rapidly developing subject.

Other sterilant gases are probably unsuitable for plastic and stainless steel constructions because chlorine and chlorides are known to attack stainless steel surfaces. Sprays of alcohols, phenols, and detergent bactericides, although less corrosive, are also less effective. The main advantage of steam or peroxide is that no residue is left, and the degradation products are environmentally acceptable water and oxygen.

Formaldehyde and glutaraldehyde are effective sterilants for surfaces but may leave residues. However, these materials are also used as cross-linking agents in the preparation of some particulate drug delivery systems such as those involving albumin, gelatin, or chitosan. It is tempting to suggest that bacterial bioburden during processing with these materials would most likely be reduced but this does not appear to have been demonstrated in practice.

The use and effectiveness of other chemical sterilant systems was recently reviewed by Olson (18).

Sterilization by Filtration

Because many drugs, especially those produced by the new biotechnology, are heat-labile, cold sterilization through appropriate filters has been widely employed. Many microorganisms can be physically removed from liquid products, and gases may also be filtered free of microorganisms. An assembly for filtration usually incorporates a porous matrix, sealed or clamped into a suitable nonporous holder, but the assembly needs to be considered as a whole. Groves (19) noted that the criteria for an ideal filter depends on the nature of the product to be filtered, but the following attributes are generally desirable:

1. A filter should be absolute in the sense that there should be a known limit to the size of the particles in the filtrate.
2. There should be an independent means of checking the efficiency of the filter.
3. The filtration process should not be materially affected by the pressure differential across it or pressure fluctuations produced by the pumping of fluids through it.
4. The filtration medium should not affect the product.
5. The filtration system as a whole should be capable of being sterilized by heat or gas.
6. It should be economical in use.

Unfortunately, there is no ideal filtration medium and, as described by Groves (19) and Olson (20), the whole area has been confused by overenthusiastic sales personnel for the various media, not by any means confined to one commercial source. The novice reader is therefore enjoined to use much caution when reviewing sales literature in this area.

Physically one can envision the passage of suspended particles through a porous matrix until the particles become trapped when the pore becomes smaller than the particle, a sieving mechanism. Although broadly true, some filters have a surface charge that also helps to trap particles carrying an opposite charge. Asbestos fiber filters, for example, carry a strong electropositive charge that helps to collect microorganisms, which often have an electronegative charge, depending to some degree on the pH of the continuum. Asbestos fiber filters are not used today because of concerns about possible toxicity, but the same type of charge–charge interaction may well help modern membrane filters to remove particles that are much smaller than the nominal size of the filter.

Membrane matrices are now available in a wide variety of materials, including cellulose derivatives and polymers, and have different porosities. Selection of a filter depends

on the requirements of the process and compatibility with the product. Some membranes are claimed to be "absolute" in the sense already discussed, but this term is probably best avoided because the underlying science remains, even today, somewhat uncertain. Even very carefully regulated and controlled production processes result in filtration matrices with a range of pore sizes, although the range in some cases may be narrow. So-called anisotropic membranes, with coarser pores on the face of the filter decreasing in size to very small pores at the exit, are useful in effectively behaving like a staked pair of filters, one coarse and the other fine, but *all* filters have a range of pore sizes. To talk of a membrane filter with a pore size of 200 nm is misleading in an absolute sense because, in reality, the pores probably range in size from 100 to 300 nm diameter. One absolute sense would be to demonstrate that there was no pore larger than 200 nm present in the membrane, but it is not likely that a filter manufacturer would make that claim today. Instead, manufacturers have taken to claiming, again absolutely, that the filtrate will not contain particles larger than the 200 nm diameter, or whatever size is being claimed. This now becomes a performance issue that, in the case of 200-nm membranes, can be validated by challenging the sterilized filter with a suspension of 60 or fewer cm^2 filter area *Pseudomonas diminuta* organisms. This microorganism, when grown in unstirred saline–lactose broth, grows to a diameter of around 250–300 nm and is, as noted earlier, a worst-case scenario. Nevertheless, as discussed by Olson (20), if the filter is challenged with more than 60 organisms/cm^2 of filter, passage usually occurs. The use of filtration as an absolute sterilization procedure is therefore affected by the conditions of use. As noted by Olson (20), passage of particulate through a porous medium can almost certainly be considered as a probalitistic process, the higher the challenge the more likely particles are going to pass through. The success or otherwise of a terminal sterilization process therefore depends on the degree of the challenge, and this means that the bioburden prior to sterilization must be reduced to very low levels before the sterilization process is applied. This is a situation that will be familiar when considering heat sterilization, and the analogy is probably reasonably close.

These issues apart, some microorganisms are very likely to pass through filtration matrices, especially viruses. Although it may be true that many are removed by adsorption onto the medium surface as they pass across the charged surface of the matrix, this cannot be quantitated or relied on. Filtration is therefore anything but an absolute process and needs to be carefully designed into any cold sterilization process.

The Concept of "Size" Applied to the Filtration Process

Most bacteria have sizes somewhat larger than 1 μm, but spherical forms, with an unique dimension (diameter) defining size with precision, are generally only found in endospores which have diameters varying from 400 nm to 1 μm. Viruses are considerably smaller, with diameters of 50–100 nm, and fungi are often larger than 20 μm. The range of size to be removed from the system being filtered is therefore at least three orders of magnitude, varying from, say, 50 nm to 50 μm. This immediately suggests that the solid phase separation needs to be carried in stages, removing first the large particles with coarse screens, followed sequentially by smaller and smaller screens. Conventional wisdom suggests that final screens with pore sizes of 0.2 μm (200 nm) or even better 100 nm are required to remove most, if not all, of the biological particulate matter. When sterilizing a solution by this method, this size must be regarded as being a *maximum* size as determined by some externally applied physical test such as measurement by a mercury intrusion test or gaseous or liquid flow method. This consideration is important because in any filter surface a range of pore sizes is present, some large and some small, and obviously, it is the largest pore diameter that determines which is the smallest size of particle that will be retained on or in the surface. Very few membranes have uniformally sized pores, which may also vary in size as one passes from the front of the membrane to the rear. An exception to this may be found in the Nuclepore™ membranes made by weakening the structure of a polycarbonate film by etching the track left by exposure to neutron particles to remove damaged polymer. Another exception are glass membranes made by stacking bundles of acid-resistant and acid-soluble glass rods together. The acid-soluble glass is dissolved out to leave parallel and uniform pores in the sheets. In practical terms, although the maximum pore sizes represent a limit to the performance of the filter, in fact there are other considerations that affect the performance, including environmental factors such as pH and electrolyte concentration. These factors influence the electrical charge on the surface of the membrane or on the bacteria themselves, and electrostatic adsorption, quite apart from physical screening, is a mechanism by which particles much smaller than the nominal opening or pore size can be retained by the membrane.

Practical use of these types of membranes is substantially limited by the support equipment. Large filter surfaces can be wound onto cartridge-type filters that are connected to other filters or to other equipment. Flat filters made of cellulose or plastics need to be carefully supported by metal perforated screens, and a single hole in the entire system is a source of contamination because bacterial particles pass onto the product filtrate or are drawn in from the surrounding atmosphere. For this reason, performance tests designed to detect unusually large holes in a complete filtration system (filtration surfaces and supports) have been designed. These include bubble testing, in which gas is forced under pressure through the system wetted with product, the pressure at which bubbles are first detected being a measure of the largest hole.

Some microorganisms are capable of growing through or insinuating themselves through the porous filtration medium. This is especially true of protoplasts, which lack the rigid walls of most bacteria. Currently, a recommended pore size of 200 nm for a sterilizing filter is being advocated because there are forms of *Pseudomonas diminuta* that grow under certain conditions to be around 250 nm in diameter, thereby providing a useful challenge for the system. Nevertheless, it is noticeable that newer filters of 100-nm nominal diameter are being employed for sterilization of biotechnological products, in part because virus

removal at this level becomes more efficient. However, an important requirement is to use stacked or sequential filters, passing the solution through the coarsest first back down to the finest. Nevertheless, there must always be doubts that filtration is an absolute sterilization process. The best that can be said is that the process is aseptic, following the argument put forward by Gilbert and Allison (12).

Sterilization by Ionizing Radiation

Although it was rapidly realized that ionizing radiation reduced bacterial counts, there was some uncertainty about the dose needed to achieve sterility. Two types of ionizing radiation are in use, γ irradiation from radioisotope decay and electron beam radiation. γ radiation is usually carried out by exposing the product to a source of ionizing radiation such as cobalt 60 (^{60}Co) or cesium 137 (^{137}Cs). Electron beam sources are usually Van de Graaff generators in some form, and X-rays may also be used. The same amount of energy is delivered slowly by a ^{60}Co source but very rapidly as an electron beam, and it is important to validate the product for a specific type of radiation to be used. Reed and Fairand (21) noted that when ^{60}Co radiation was first introduced there was general agreement that high absorbed doses of at least 25 kGy were necessary, but these became associated with color and viscosity changes, and in some cases undesirable chemical changes were also observed. As experience developed, it became evident that much smaller doses could achieve sterility without degradation. Taken with current advances in aseptic processing and the reduction of bioburden before sterilization, smaller radiation doses are likely to be required, but validation on a case-by-case basis is still required.

Radiation has a large number of advantages over other methods of sterilization. It is operated in the cold and radiation penetrates both product and container, so sealed containers and their bulk packages can be treated as one. The process does require investment in significant capital equipment, but it has a long and effective life, it is quiet and environmentally acceptable, and minimal maintenance is required, unlike that required for steam autoclaves. The process is now accepted as being cost-effective and experience gained in the treatment of foodstuffs and cosmetics has been successfully applied to pharmaceutical products.

Pulsed Light Sterilization

As part of a technology developed during the Star Wars initiative, the use of very short pulses of high-intensity, broad-spectrum white light is a technology that may become more widespread. The light has approximately the same spectrum width as sunlight but is actually richer in ultraviolet light since same ultraviolet light is usually filtered out by the earth's atmosphere. However, the intensity is 20,000 times brighter than sunlight but the pulse may only last a few milliseconds. Produced by condenser discharge through appropriate lamps, the light is a form of nonionizing radiation and appears to be very effective at rapidly sterilizing surfaces contaminated with vegetative and spore-forming organisms. One advantage of light is that the intensity may be increased by focusing with mirrors to a point or target of the application. This means that individual containers in a production line may be sterilized as they pass through an appropriately designed tunnel, which is readily incorporated into a production line. The cost of incorporation of this type of device would therefore be minimal.

If the container is translucent to the ultraviolet radiation, the technique can be used to sterilize the contents. For example, plastic ampoules are transparent, and the method is being applied to automated filling lines associated with blow, fill, and seal methods. However, it may not work with glass ampoules because the appropriate ultraviolet wavelengths are filtered out, but development work in this area is ongoing. The Pure Bright® technique was reviewed in more detail by Dunn (22) and may be a valuable technique for sterilization of some types of packaging materials on a continuous basis.

Aseptic Processing

Aseptic processing is the assembly of a product using components sterilized by different methods in a suitable aseptic environment designed to minimize or totally eliminate contamination of the product. There is no final sterilization of the sealed container; it is assumed that sterility has been designed into the product. Now very widely used in the pharmaceutical industry, Groves and Murty (23) suggested that as many as 87% of parenteral products were being aseptically assembled. The likelihood is that, as more and more thermolabile products enter the marketplace, this number will increase. Regulatory agencies went on record a decade ago, requiring terminal sterilization unless the product was demonstrated to be labile. This was not a particularly timely move although the FDA still does not allow a large volume parenteral (100 mL or more in volume) to be assembled aseptically.

An aseptic process usually consists of filling a thoroughly filtered solution of a drug, the final filtration being regarded as a sterilization process, into glass or plastic vials sterilized by dry heat or gas and sealing these containers with rubber plugs sterilized batchwise using moist heat. A series of steps are required to bring the components to the assembly area, put them together in an aseptic environment, and remove the final product to the open environment. The success of an aseptic filling operation critically depends on the successful operation of the individual steps but must be considered as a whole. The entire operation needs careful and consistent planning and operation, with constant monitoring. Final and ongoing validation represents an essential stage that is often extremely difficult to carry out satisfactorily. The complete operation is operator-dependent, which means that the operators not only have to be properly trained but also have to know how to apply methodologies thoroughly documented in standard operating procedures that are such a critical element in GMP. It can be seen that an aseptic process is where all of these regulatory requirements come together. Nevertheless, some agencies, including the FDA, require validation to be carried out using media fills in which sterile growth media instead of actual product is passed through the sys-

tem. In some ways it can be seen that this might be a proof of concept; to actually validate the process itself is an exercise in futility. First of all, the final product, with some exceptions, is unlikely to resemble a fluid culture medium. Secondly, the growth medium does not necessarily demonstrate a failure or breakdown in the system, because the level of contamination may be very low, and contaminating microorganisms may not grow rapidly enough to be visibly evident in the medium after only a few days incubation. Finally, it seems ludicrous to suggest that 1 contaminated vial in a media fill of 3,000 is satisfactory, because it indicates a SAL of less than 1 in 1,000. Surely *any* contamination is unsatisfactory, and SALs, being a statistical concept, are not measurable directly.

Improvements in system design, especially those involving the use of robotic and barrier technologies designed to eliminate human contact, have certainly increased confidence in the effectiveness of aseptic processing. Nevertheless, it is probably time to reexamine the concepts of Gilbert and Allison (12) and attempt to *measure* the risks involved in aseptic processing. Given the very low incidence of microbiological issues associated with the parenteral administration of millions of aseptically prepared products worldwide over 80 years or more, the issue may have become more remote.

STERILE IMPLANTS

Protein Compacts

One of the oldest drug delivery systems is the pellet or tablet produced by compaction or extrusion of powdered drug together with appropriate excipients. Tabletting technology is not confined to the pharmaceutical industry but the technology is exceptionally well developed and is both simple and inexpensive in its basic form. Generally applied to low molecular weight drugs for oral administration, tabletted proteins are also employed in a number of nonpharmaceutical industries. Compacted proteinaceous materials such as enzymes are used in dairying, fermentation, brewing, fruit processing, wine making, milling, baking, starch production, and detergent applications. All have been prepared as tablets as a convenient form for handling and ensuring accurate dosage as well as improved storage and transportation. With the advent of the newer highly biologically active proteinaceous drugs, this pharmaceutical presentation has assumed a major challenge. This is especially true for proteins or polypeptides for oral administration. For example, Saffran et al. (24,25) claimed that vasopressin or insulin in enteric-coated gelatin capsules were active orally, although these observations do not appear to have been confirmed. Nevertheless, compaction of dried proteins appears to allow them to retain much of their native conformation and, therefore, biological activity. They are readily protected from moisture when suitably packaged. Azain et al. (26) described prolonged release devices for parenteral administration of somatotropins and Oppenheim et al. (27) suggested that protein compacts could be used for subdermal administration. In both cases the final product must be sterilized using an appropriate procedure.

Effects Produced by Compaction of Proteins

During compaction the protein molecule is subjected to both pressure and shear (and possibly heat) that could result in reversible or irreversible denaturation. Most studies of denaturation have been carried out on protein solutions. Tirrel and Middleman (28), for example, showed that the jack bean urease-catalyzed urea hydrolysis reaction was both reversible and irreversible, depending entirely on the rate of shear and the presence or absence of additives such as glycerol or ethylene diamine tetra acetic acid. Similar results have been reported for lactic hydrogenase, peptidases, and rennet, and amongst the genetically engineered proteins, human growth hormone is known to be denatured by mild shearing conditions. These are all believed to be due to the hydrodynamic induction of conformational changes at the molecular level. There are relatively few published studies of dried protein compacts and the effects induced by the compaction process or the complex three-dimensional structure of a protein, especially as measured by the changes produced on subsequent biological activity. Graf and co-workers (29–31) studied the effect of compactional pressure on pancreatin and showed that a slight loss of activity occurred at 500 MPa, the minimum pressure needed to form a compact. However, this loss of activity was mitigated by incorporation of pharmaceutical adjuvants such as lubricants and diluents normally employed to make acceptable tablets. These observations would suggest, in retrospect, that solid-state shear caused loss of activity in an analogous fashion to that observed in the solution state. However, most authors agreed that compactional pressure produced some degree of adverse effects on biologically active proteins. Groves and Teng (32) reviewed earlier work and described their own investigations on the compaction of four enzymes with widely disparate molecular weights and functionalities. Working over a much wider range of compactional pressures, urease, lipase, α-amylase, and β-glucuronidase were all shown to be affected by pressure, although to different extents. More to the point, the mechanism of loss of biological activity was evidently different in each case. For example, α-amylase and β-glucuronidase both lost their α-helix structures, whereas the secondary structures of urease and lipase were unaffected. The molecular weight of urease showed an increase, suggesting effects on both tertiary and quaternary structures. The 30% loss of activity observed with lipase could not be correlated with any structural changes measured by sodium dodecyl sulfate-polyacrylamide gel electrophoresis (SDS-PAGE) or circular dichroism (CD) methods, indicating that, whatever structural changes had actually occurred were too subtle to be detected directly. In all cases limiting compactional densities were observed. This lead to the proposal that the mechanism of activity loss was due to a reduction of the space in between the molecules or particles, irrespective of the source of the protein. Compacting at different rates or holding pressures for different times had no measurable effect on activity loss, showing in these cases that thermal energy inactivation was not responsible for activity loss. Water adsorption onto dried proteins was also shown to be influential on the subsequent properties of compacts, es-

Next Page

pecially the rate of release of the active component into an aqueous environment.

As noted, the range of pressures tested were in excess of pressures normally required to make serviceable compacts, and the additional of appropriate pharmaceutical adjuvants was not evaluated. Activity losses ranged from 50% (urease) at 190 MPa to 15% (β-glucuronidase) at 290 MPa, pressures well inside the approximately 500 MPa required to form a compact. Nevertheless, one can be optimistic about the issue because if a loss of activity of a biologically active protein is detected it would appear that the effect can be minimized by judicious selection of diluents and lubricants making up the rest of the tablet composition. However, it should be noted that if a compressed protein was required for parenteral use, the usual pharmaceutical diluents and formulation adjuvants used for orally administered tablets would be unlikely to be suitable. This may apply to fatty acid derivates, such as magnesium stearate, and certainly applies to the talc when used as a lubricant. Alternative adjuvants and diluents are available but should be selected with care. Indeed, in some cases, they may not be needed.

If a protein was to be compressed and a loss of biological activity was demonstrated, it would be necessary to totally evaluate the mechanism of degradation, to find methods of minimizing the effect, and to carry out a complete investigation of the influence of the presence of resultant degradation products on the biological behavior of the compact. Appropriate analytical methodologies are certainly more widely available today, and this type of investigation would be a normal part of providing a complete characterization of what is likely to be a complex drug entity.

Sterilization of Protein Compacts

The safest way of producing a sterile protein drug implant would be to operate the entire process aseptically, starting with sterile filtration of a solution of the drug and aseptic lyophilization to provide a sterile solid. If a diluent were needed, this could be added to the solution of the drug prior to the sterile filtration process. Suitable diluents such as lactose or mannitol are unlikely to be available as bulk sterile products so it would be necessary to go through the same process, especially if the diluent was required to be added as a separate entity. The compaction equipment would need to have metal surfaces cleaned and sterilized, which could be achieved with a gaseous sterilant such as ethylene oxide. The use of halogen oxides or hydrogen peroxide as gas or mist is likely to be corrosive to most metal surfaces and therefore unsuitable for sterilization of the compaction surfaces. Aseptic manipulation using barrier technology has certainly become more widely accepted in recent years, and providing the equipment was dedicated to this function, it should be an acceptable procedure. Shangraw (33) suggested that a dedicated single punch tablet machine was likely to be used but, more recently, extrusion of the material has been preferred, using poly(ethylene glycol) 6,000 as an external lubricant. Direct sterilization of the compact by heat is unlikely to be effective or acceptable but γ-radiation is a possibility, providing the drug itself is not damaged or the vehicle affected in terms of its performance such as release/time pattern.

Polymeric Implants

Polymeric implants are commonly prepared from hydrogels, silicone rubbers, or other biocompatible materials. Hydrogels generally have an advantage in that they are able to swell in an aqueous medium without necessarily dissolving. This capacity for water is useful in that it promotes or improves compatibility with body tissues but it has been suggested that incorporated low molecular weight drug substances are able to diffuse out of the device without necessarily being rate-controlled.

Implants are usually introduced subcutaneously using a surgical procedure. The need for surgery is an obvious disadvantage but, conversely, the device can also be removed when required or when exhausted of drug, which is an advantage. Numerous shapes have been explored, from plates, long rods, and short rods to spheres, and newer bioerodable matrixes are coming into use. For example, poly(lactide-co-glycolide) (PLGA) was originally developed as an absorbable suture so that it has obvious advantages as an implant containing a drug. The Norplant device has been introduced in which silicon rubber rods containing levonorsgestrel have been implanted under the skin with the aid of a local anesthetic. For additional information see the chapter FERTILITY CONTROL.

Subdermal injection of small rods or cylinders or even spheres through a cannula has some advantages, and these devices have also been evaluated clinically.

Sterilization of Polymeric Implants

Polymeric implants are readily made by extrusion of powdered components but application of heat would melt the polymer and affect the release properties of the device, assuming that the drug itself was stable enough for the purpose. γ-irradiation is effective and commonly used for this purpose because of the great deal of experience in the sterilization, for example, of PLGA suture threads. Oxidizing gases such as peroxides are not suitable for sterilization of surfaces because, with a bioerodable implant, there is a need to sterilize throughout the structure of the implant, not just its surface. Moreover, there is a real danger that these reactive chemicals produce chemical changes at the interface of both the biopolymer and its incorporated drug. One group has suggested that a volatile sterilant such as chlorbutanol be incorporated in the matrix, which is then removed by exposing the final product to a temperature of 80°C, preferably for a long time and under vacuum (34).

Implants, being introduced under the skin and exposed to a biological environment, must not irritate the tissues surrounding them or produce an infected or sterile abscess. Sometimes this may be due to the polymer alone. For example, PLGA hydrolyzes to lactic and glycolic acids, which in the high concentration immediately adjacent to the surface of the dissolving implant, may become irritating. However, one possibility here would be to insert the implant into muscle where the tissue environment is normally acidic due to lactic acid production.

Previous Page

PRODUCTION OF MACRO-, MICRO- AND NANOPARTICULATE SYSTEMS

Introduction and Definitions

It has to be realized that sterile drug delivery systems have to be produced by close attention to the preparation process, with appropriate modifications being made to achieve sterility. Particulate systems have been used as drug delivery vehicles, probably since at least ancient Egyptian times, but more recently they have become of interest to the pharmaceutical sciences in a rather more sophisticated form. Defined by size rather than constitution, macroparticles can be considered to be larger than 100 μm, microparticles are 1–100 μm, and nanoparticles are less than 1 μm in diameter. Approximately rounded in shape, these systems can be employed according to their size, macroparticles being too large to pass down an hypodermic needle but being suitable for controlled release implants or, in some cases, as artificial cells or organs. Micro- and nanoparticulate solids, on the other hand, can pass through hypodermic needles and be employed for targeted drug delivery. An example here would be passive targeting of the lung, which can be achieved by intravenous administration of particles around 7–10 μm diameter or larger. In a similar manner, nanoparticles of 100 nm or less can escape through the fenestrations (or holes) of the lining of the blood vessels and reach hepatocytes in the liver. These small particles also accumulate in the mononuclear phagocytic system (MPS). As pointed out by Wright and Illum (35), particle size is a major factor in determining the sites of lodgment but also, to a lesser degree, so are the particle surface characteristics in terms of identity, hydrophilicity, and especially electrical charge. Foreign particles in the bloodstream are removed through phagocytosis by MPS components, especially macrophages. This process is initiated by recognition of opsonins. These are proteins that precipitate onto the particle surface, which are then recognized by specific receptors on the macrophage surface. It is possible to interfere with this process by adsorbing or incorporating competitive high molecular weight surfactants or polymers such as poly(ethylene glycol) onto the particle surface, and this is the principle underlying the new generation of surface or sterically modified liposomes (Stealth™ liposomes) (36).

It is a matter of semantics as to whether or not one should define surface-modified microparticles as microcapsules (that is, particles that are encapsulated or covered in a material that differs from the core). Chemically core materials reported for macro- and microparticulate systems vary widely from starches and celluloses to polymers such as PLA and polymethacrylates. One essential requirement is that the core material should be metabolizable or biodegradable. This is obviously likely to be true for albumin and gelatin particles, and PLA dissolves slowly by hydrolysis of the polymer.

Release of incorporated material—a drug or guest molecule—has been discussed by Jalšenjak (37) in theoretical terms. Although he regarded microcapsules as a general case, strictly speaking, they are core materials surrounded by another medium. He did, however, admit that the rate-controlling solution stage could be affected by the presence of a stagnant aqueous layer at the microcapsular surface. Other than this, three stages were identified in the release process:

1. Solvent penetration to the core
2. Solution of the core material(s)
3. Solute removal by a diffusional process into the bulk aqueous phase

Jalšenjak (37) then explored the case of release from microspheres where the drug was not concentrated in a core but rather distributed throughout the particular matrix. There is no reason, a priori, to assume that the particles are indeed spherical although this is a convenient approximation that is adequate for most purposes. The constitution, preparation, and properties of injectable nanoparticles and microparticles are reviewed in several texts, including Donbrow (38). However, rarely if ever in these texts is the sterilization of the intended product discussed, although this remains a prime requirement for any parenteral product. Accordingly, methods of production are reviewed here to allow interpolation of points in the process where sterilization can be introduced or where the process could be improved to ensure sterility.

Production Methods for Solid Particles

For the most part, it will be presumed that macroparticles and particles with a mean diameter $\approx$50–100 μm would not be suitable for parenteral administration for the simple reason that a suspension of these particles would be less likely to pass smoothly through, say, a 20-gauge hypodermic needle, depending on the concentration of the particles, their shape, and the presence of larger particles in the system (39). Nevertheless, although the administration system is different, large rods or granules have been used as sustained drug delivery systems for subcutaneous or even intramuscular implantation.

This limitation on the size of the particulate, although not absolute, limits the application of some technologies involving growth of primary systems such as granulation, spray-drying, or spray-chilling, because the resultant products tend to be too large in size to be suitable for the purpose. For the most part, this may also be true for many of the microencapsulation processes that have been described in the literature. Methods suitable for the preparation of micrometer and submicrometer (nano-) particulate systems are:

1. Grinding
2. Phase changes (solvent precipitation)
3. Emulsification process, with or without solvent removal
4. Spontaneous liposome and emulsion processes
5. Polymer emulsification

Grinding. Until recently grinding solids was associated with manufacturing processes involving ores and rocks, and relatively few grinding processes have survived into

current pharmaceutical production processes. However, in recent years this perception has changed with development of a grinding process originally developed by Kodak for production of submicrometer pigments used in photographic processes. An offshoot of this process has been adapted for pharmaceutical use by Nano Systems, Inc. Details of the processing are proprietary but involve ball-milling insoluble drugs in the presence of stabilizing agents in water. In this process a solid dispersion is ground by rolling in a closed pot with steel or ceramic balls. One must assume that the stabilizing agents are viscous materials with surfactant properties. As crystalline and bonding forces are exposed during the grinding process, fundamental properties of the particulate change as the nanoparticles are generated, including solubility. Some impressive claims have been made for this process and a number of major pharmaceutical companies are exploring the potential application of the technology. Ball-milling is certainly not a new process and traditionally has had some well-recognized problems, including the time taken to grind to a specific size, the generation of heat, and the presence of significant quantities of fragments of the grinding balls and container walls that inevitably contaminate the product.

Preparation of Sterile Product. Although ball-milling is carried out in a closed vessel, this vessel has to be opened and closed during the process, and even if sterile components were added to the mill it would be difficult to maintain sterility. Terminal heat sterilization of the final product is likely to be counterproductive, because solubility would be increased at higher temperatures and the particle size therefore increased on cooling. However, with modern heat-resistant ceramic materials, this may be one option in the final process stage, with additional grinding and handling the mill and its contents under aseptic conditions thereafter. Regulatory authorities traditionally have had problems with aseptic processes operated without adequate controls, but, although not impossible, production of a sterile product with this process has considerable difficulties.

Phase Changes. The formation of small particles can sometimes be achieved by mixing a solution of the drug in one solvent with another miscible solvent, thereby precipitating out the drug. An example would be the precipitation of gelatin particles by cold alcohol in the process described by Öner and Groves (40) (Fig. 1). Gelatin is readily soluble in water but is insoluble in ethanol. Many systems described in the literature involve precipitating a component out of an aqueous solution with water-miscible solvents such as acetone, ethanol, or dimethylsulfoxide. Careful control of the relative amounts of the two solvents, temperature, rates of stirring, and rate of addition of one component to another help to control the resulting size of the precipitate. In some cases the addition of the wetting agents may help to stabilize the size of the precipitated particles, and for most purposes this is an essential requirement.

Preparation of Sterile Product. Because the process involves adding two liquids together, it should be feasible to sterile-filter both components separately and carry out the processing and collection of product under aseptic conditions.

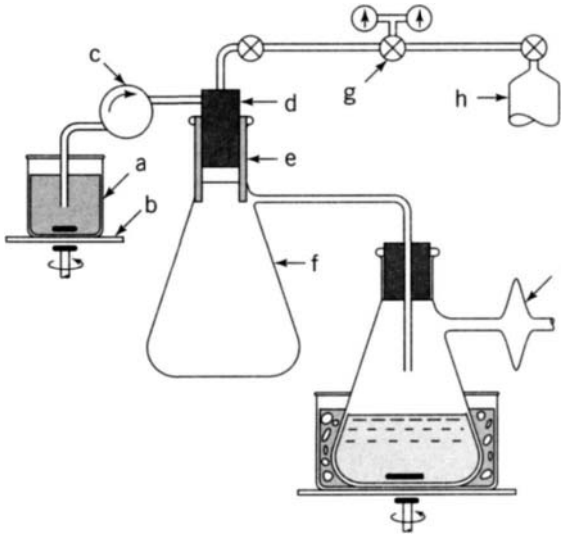


Figure 1. Precipitation of gelatin by cold alcohol using a two-stage carbon dioxide-activated spray system. a, Hot protein solution; b, magnetic stirrer; c, peristaltic pump; d, Turbotak; e, sleeve cut from Masterflex tubing, 1.5 cm below base of Turbotak; f, empty 2-L glass conical flask; g, gas regulator; h, CO_2 tank; i, 0.45-μm membrane filter. *Source:* By permission of the editor, *Pharmaceutical Research*, from Ref. 40.

Emulsions

Introduction: Essential Requirements. Emulsions, defined as dispersions of one immiscible liquid in another liquid, are intrinsically thermodynamically unstable and therefore require interfacial stabilizing agents. Because of the physical complexity of emulsion systems, they have received relatively little attention as parenteral drug vehicles with one exception, the vehicle and system originally marketed as Intralipid® (Pharmacia-Upjohn and, more recently, Fresenius-Kabi), which appeared in Sweden in the 1960s after a great deal of original research by Wretlind (41) and Håkansson (42). Earlier attempts to develop injectable emulsions as nutritional supplements were rather less than successful due to toxicological issues associated with raw materials and degradation products, as well as long-term stability concerns. Some principles were established early on, because it became quite clear that only oil-in-water emulsions, which had to mix quickly with blood, were suitable for intravenous administration. On the other hand, it should be noted that water-in-oil emulsions would form depot drug delivery systems, suitable for subcutaneous or intramuscular administration, and these have been used since the turn of the twentieth century.

Wretlind (41) demonstrated that, ideally, particles in intravenous lipid emulsions should mimic the small triglyceride emulsion droplets—chylomicra—that carry lipids throughout the body after a fatty meal. These chylomicra vary in diameter from 200 to 3,000 nm and consist of a

lipid core surrounded by phospholipids, together with adsorbed protein. He envisaged an artificial chylomicron made of natural triglycerides, obtained from soybean oil, as an example, emulsified and stabilized with phospholipids purified from avian egg yolks. Wretlind went to a great deal of trouble to obtain and specific highly purified materials, and it was even rumored that he specified eggs from one particular source collected at the same time of the year to ensure that the natural and therefore variable constitution of the separated egg phospholipids were reproducible. The importance of storage conditions for the system was established and it was shown that these homogenized emulsions, with mean droplet diameters of 200–400 nm, were stable enough to be sterilized by autoclaving without the catastrophic destabilization that is characteristic of most other emulsions when heated. Indeed, it was later shown that the particle size of a heat-sterilized emulsion actually decreased, suggesting that structural changes were occurring in the emulsion or at the oil–water interface as a result of the application of heat (43). These considerations resulted in the realization that injectable emulsions can be terminally heat-sterilized, and this observation has contributed to confidence in their clinical application.

Phospholipid-stabilized emulsions have been used clinically for almost 40 years as nutritional supplements, for the most part without serious clinical problems. Their clinical usage is clearly understood, and limitations in their application are well recognized. Moreover, other manufacturers have marketed similar systems with artificial short-chain triglycerides, safflower or olive oils, and phospholipids obtained from soybean. The potential for the use of these emulsions as drug delivery systems is considerable, and a number of emulsion-based products are now in the marketplace.

For successful clinical application as a nutritional product or drug delivery system, an emulsion must be:

1. Miscible with blood and body tissues
2. Compatible with both blood and body tissues
3. Sterile
4. Nonpyrogenic
5. Prepared with droplets small enough not to pose a potential for forming embolisms
6. Fully metabolizable
7. Isotonic
8. Stable, both physically and chemically

For the most part, the aqueous phase does not provide a problem if it is Water for Injection (USP) or, more accurately, Water for Injections (BP). The tonicity is provided by adding a small amount of glycerol, and the initial pH is adjusted to around 8.0 with sodium hydroxide.

The oil phase, coming as it does from a natural source such as soybean oil, can vary in composition, and the Swedish workers associated with Wretlind (41) found that soybean oil could be fractionated and purified by cooling and filtration to remove the waxes, unsaponifiable matter, and higher-molecular weight entities usually found in the expressed oil. Oils with aliphatic unsaturated centers are prone to air oxidization so precautions have to be taken to avoid degradation. Natural oils usually contain antioxidants such as tocopherols, and either these are allowed to remain or are added after purification (44). Triglycerides are readily metabolizable and the differences between commercial products tend to lie on the distribution and degree of unsaturation of the various fatty acids. In Table 1, the Intralipid soy oil and Liposyn safflower and soy oil formulae are compared; the linolenic acid, deficient in the Liposyn II brand, was later determined to be an essential fatty acid. As noted, emulsions are intrinsically unstable, and a stabilizer, surfactant, or emulsifier is required to stabilize the dispersion. Most surfactants commercially available are unsuitable for parenteral administration because they have a potential to cause hemolysis and other direct manifestations of toxicity. Moreover, most stabilized emulsions break when heated, often due to significant movement of the interfacial material into one phase or another as the solubility characteristics change with temperature. Phospholipid stabilizers, on the other hand, are unusual in that the interface between the oil and water phases becomes more stable after heating. This effect was investigated by Groves and Herman (45,46). When freshly prepared, an emulsion system stabilized with an egg phospholipid containing phosphatidylcholine (PC), phosphatidylethanolamine (PE), and their respective lysoderivatives had the phosphatides roughly equally distributed in the aqueous bulk phase and at the oil interface. On heating there was an irreversible movement of the PE and PC toward the oil phase and from the aqueous compartment. It was suggested that this could have been due to the heat-induced formation of an interfacial cubic liquid crystalline phase. There is some parallel evidence for this type of reaction in isolated systems although, in a true emulsion, this has proven difficult to investigate. Cubic phase material, forming a mesophase at the oil–water interface, would then revert to a semiviscous mesophase lamellar liquid crystal, and indeed the two may coexist as an equilibrium mesophasic composition. This organization of interfacial material was held to account for the unexpected enhanced stability of sterilized phospholipid stabilized emulsions during sterilization. When investigating the stability of freshly prepared emulsions to lysine, a known water structure-modifier, stability was markedly enhanced when the emulsion was heated even under relatively mild conditions for a sufficiently long period (47,48).

Emulsification. Direct emulsification involves application of shear energy to two separate immiscible liquids (for

Table 1. Distribution of Fatty Acids From the Triglycerides of Intralipid and Liposyn Intravenous Emulsions

Fatty acid	Intralipid (g/100 g)	Liposyn (g/100 g)
Linoleic acid (C18:2)	54	77
Oleic	26	13
Palmitic (C16)	9	7
Linoleic acid (C18:3)	8	—
Stearic (C18)	3	2.5

example, oil and water) in order to produce small droplets of one phase dispersed in the continuous phase. Inevitably a stabilizing agent is required to prevent (or at least minimize) coalescence of the dispersed drops back to their preferred condition for minimal energy (i.e., as a completely separated layer, one floating on top of the other). Properties of the stabilizing agents employed as systems used for parenteral administration vary widely although for the most part purified egg or soy phospholipids are considered suitable. Because phospholipids are not truly soluble in either oil or water, forming dispersions in both phases, they are often to be found at the oil–water interface. This interface is structurally complex, and these properties are essential for the stability of the dispersion, although at present knowledge and understanding of this arena is less than perfect. Application of shear forces to dispersed droplets often has the effect of decreasing the droplet size, probably down to the limiting surface coverage of the emulsifier. Below this monolayer (or even multilayer) coverage, the droplets are not stable and quickly coalesce to the minimum size of particle under the conditions of manufacture. Other factors are involved, in particular the interface surface tension between the disperse and continuous phases. In addition, relative viscosity of the two phases is most probably involved, as is the relative density.

Shear forces can be applied by a number of methods, including simple stirring, high speed stirring, and pumping through small orifices.

One factor that needs to be mentioned is the phase behavior of the dispersed droplets. Usually these are assumed to be liquids, capable of demonstrating internal fluidity or movement. In point of fact, as droplets get smaller internal circulation becomes limited, and the droplets start to behave as if they were solid. This behavior is facilitated by the properties of the external mesophasic stabilizing layers, which are often viscous to the point of being semisolid, and these properties also inhibit internal circulation inside the liquid droplet. For all practical purposes, therefore, dispersed droplets, especially in the submicrometer region, behave like solid spheres or particles. This has not prevented some authors from claiming special properties for systems made of waxes or high melting point oils. From a manufacturing perspective, at elevated temperatures these systems consist of molten waxes or liquid oil droplets dispersed in water, and these liquid droplets cool to solid particles at room temperature after dispersion. Known and widely used in the cosmetic industry for many years, these systems undoubtably have potential as drug delivery systems. A recent paper (44) has demonstrated that high melting point trilaurin nanoparticles formulated with phospholipids were effectively similar in composition to phospholipid-stabilized emulsions with phospholipid bilayers wrapped around the central lipid core. Like the liquid lipid emulsions, these solid lipid systems have the potential to trap hydrophobic guest molecules in the phospholipid bilayers, with hydrophilic materials being held in the aqueous spaces.

Surface-Modified Emulsions. The physiological compatibility, together with their optimal chemical and physical stability profiles, make phospholipid-stabilized emulsions valuable parenteral drug delivery systems (49). It is inevitable that these systems should be compared with liposomes, and indeed the analogy is close when considered from the external surface view of the two systems. However, the interior structure differs, and it is the liquid triglyceride droplet that is the characteristic feature of the more stable emulsions systems. Some authors have claimed that solid lipid dispersions differ from liquid–liquid emulsions (44). This is not likely from a physical perspective because, as noted earlier, small liquid droplets behave physically as solid particles in the same size range. In addition, since the interfacial mesophase of phospholipid-stabilized systems is almost certainly very viscous if not solid in nature, the underlying liquid droplets would effectively behave like solid particles, and the similarities become quite evident.

Surface-modified systems have become available as modified liposomes or emulsions. One characteristic of both phospholipid-stabilized systems is the rapidity with which they are coated with apoproteins after coming in contact with blood as part of the opsonization process. Recently, liposomes surface-modified with poly(ethylene glycol) have appeared, sometimes referred to as Stealth® liposomes (36). These surface modifications, likened to disguising the surface with bound water, have effects on protein binding and, therefore, on physiological behavior and clearance. The net effect of surface modifications has been to extend the effects observed in the body produced by injected liposomes and, incidentally, to enhance the stability and commercial viability of these drug products (49).

Preparation of Sterile Product. Depending on the properties of the stabilizing entity used in the formulation, usually to be found at the interface of the dispersed droplets, it might be feasible to sterile-filter each of the components before processing under aseptic conditions. However, as noted earlier, most surfactants are too toxic to be employed as parenteral stabilizers and for the most part suitably purified egg or soy phospholipids are used. These have some curious properties in that phospholipid-stabilized emulsion systems can be terminally heat sterilized, thereby avoiding many of the issues associated with handling product under aseptic conditions. This, of course, presupposes that the drug entity itself is stable enough to be heat sterilized. If it is not, then presterilized emulsion would be aseptically manipulated to allow subsequent incorporation of the drug prior to packing. Nevertheless, it is extremely unlikely that any regulatory authority would approve an aseptically assembled large volume (>100 mL) parenteral and would insist on terminal sterilization of the product.

The Chemical Stability of Phospholipids. Phospholipids are heat-labile and hydrolyze in aqueous dispersion. Strictly speaking phospholipids are not truly soluble in water but readily form dispersions that could be recognized as liposomes. Groves et al. (50) reported the presence of liposomal-like material in phospholipid-stabilized emulsions, so aggregates of phospholipids readily form but a true solution of these materials, consisting of single molecular entities, does not.

Dispersions of pure PC or PE in water when heated, for example, in a sterilization process, hydrolyze to their cor-

responding monoacyl derivatives, called lyso-lecithins (51,52). These materials are also found in some snake venoms and have lytic properties on red blood cells (53). In principle, these might appear to be undesirable degradation products in an intravenous system, and this may also be true for the free fatty acids that are produced by hydrolysis of both the phospholipids and the triglycerides present in the starting material. However, no toxicity has ever been noted since the intact emulsions were first introduced into clinical practice over 30 years ago. It has been suggested that this may be a direct result of complexation within the intact emulsion so that the degradation products are not available in the free state. The general schema of degradation is shown in Figure 2. Degradation rates of phospholipids in liposomes have been measured (54). Similarly, Herman and Groves (45,46) determined degradation rates of these stabilizers in emulsions. Generally speaking, both groups found broadly similar results and consideration of the kinetics demonstrated that relatively small amounts of lyso-compounds are actually produced under the conditions necessary for heat sterilization. In the case of emulsions, it is likely that any small amounts of lyso-compound produced in the reaction would be held within the droplet mesophase, as noted earlier.

This cannot be entirely true for the free fatty acids produced by autoclaving because the pH does drop during sterilization (46). However, the amount of free fatty acid as determined by titration with potassium hydroxide or measurement of pH did not correlate well. It was therefore suggested that residual oxygen dissolved in the triglyceride oil phase was capable of reacting with some of the acyl unsaturated centers. There was evidence that the involvement of oxygen in the heat-induced lowering of the pH and emulsions made with saturated phospholipids did not show the same disparity.

Emulsification With Solvent Removal. It has been recognized for many years that dispersive emulsification processes often generate submicrometer droplets. A method widely employed to make polymer microparticles is to dissolve the polymer such as PLGA, in chloroform or methylene chloride, emulsify this solution in aqueous poly(vinyl alcohol) (PVA) or carboxymethycellulose in order to produce small droplets. The solvent is then effectively removed by adding the concentrated emulsion to an excess of water, allowing the microspheres to be collected by centrifugation or over a filter and dried under vacuum to remove both the water and the residual solvent. Drugs for controlled release purposes can be incorporated into the polymer system as an aqueous solution before making the polymer/water dispersion, effectively making a water/polymer/water double emulsion, analogous to an w/o/w double emulsion system. Thus, these are encapsulation procedures in some senses, using polymers to encapsulate an aqueous dispersion, and this is described as such in a recent patent (55). One major advantage of this process is that it is readily scaled-up using a static mixer fitted with continuous flow through.

An emulsification process has also been used to prepare micro- and nanoparticulate forms of albumin, a protein that is readily denatured by heat. This process has to be handled in different ways according to whether or not the incorporated drug is labile or not. If the drug is heat-stable, it can be incorporated in an aqueous solution of an appro-

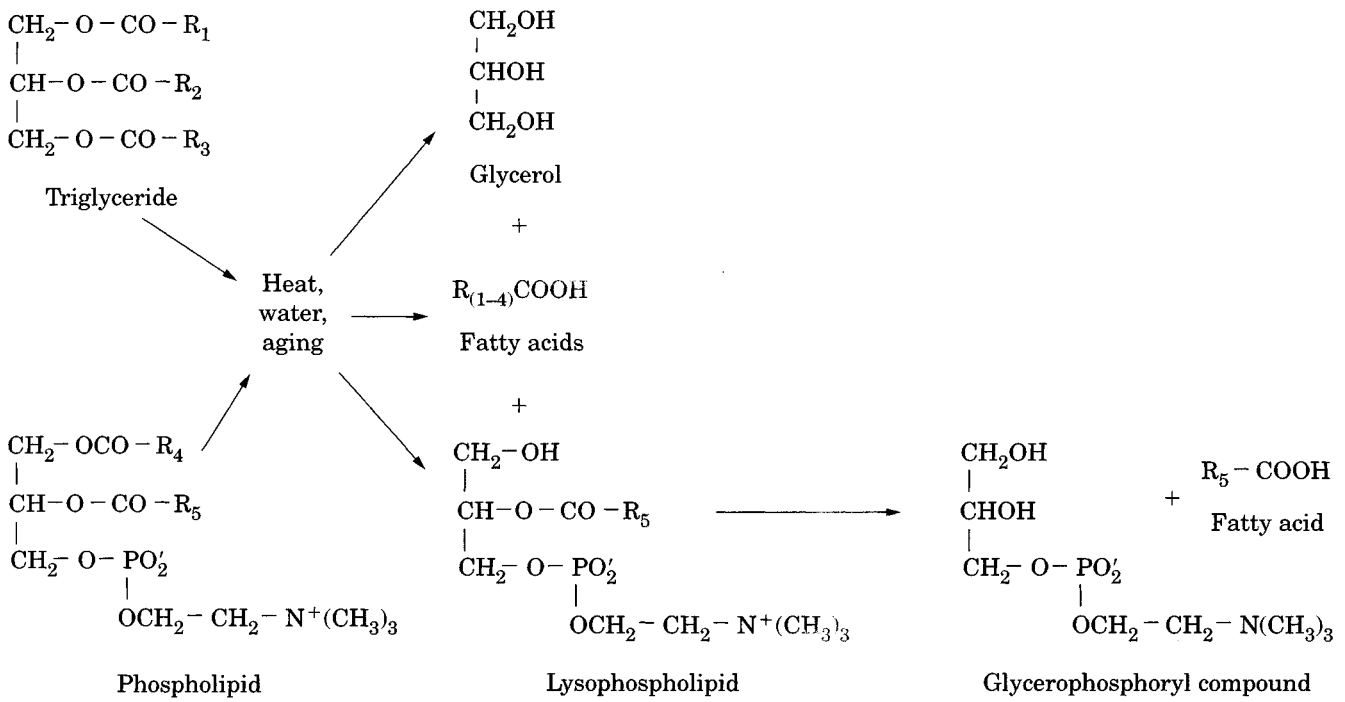


Figure 2. Degradation pathways for phospholipids and triglycerides in phospholipid-stabilized emulsions.

priate albumin (human is preferred for human administration), which is then emulsified in a suitable oil such as arachis or even mineral oil. A water-in-oil emulsion is prepared, usually requiring a suitable emulsifier such as Span®, and the system is heated up to 120°C or higher whilst stirring when adding the initial emulsion into an excess of hot oil. The albumin solution solidifies as the protein is denatured and comes out of solution. By maintaining the heat above 100°C the water is evaporated, leaving the albumin particles suspended in the oil. The dried particles are then collected and the residual oil removed with a solvent, often petroleum ether or diethyl ether. Both of these solvents are highly flammable, and this process is basically unsuitable for industrial application, although this consideration has not inhibited claims being made for the resulting product based on small-scale laboratory processes. Denaturation of a dispersed protein aqueous solution can be achieved by other methods, including addition of cross-linking agents such as glutaraldehyde or even formaldehyde. The issue of oil removal remains, especially as available solvents for this purpose are flammable and are often not acceptable from a toxicity standpoint. Once prepared, however, these microparticles can be loaded with a drug, and it does not matter if the drug is labile or not. Loading may have to be achieved by adding a solution of the drug in an acceptable solvent such as alcohol to the dried proteinaceous particles and stirring under reduced pressure until the solvent has evaporated. Unfortunately, alcohol and water from constant composition boiling point mixtures and the process may have to be modified accordingly, perhaps by using an alternative solvent.

Polymers such as PLGA, PLA, or poly(acrylamide) are acceptable physiologically and are generally soluble in organic (or water-immiscible) solvents. Ciftci et al. (56) described a simple process in which a PLAGA copolymeric system (containing drug) in methylene chloride was stirred in an aqueous PVA solution until the methylene chloride had evaporated. No evidence of the residual levels of methylene chloride was provided and, clearly, on a large scale this would be an essential element of information required for subsequent regulatory approval. However, the process is undoubtably simple and should be readily scaled up. Without the use of added surfactant the particles had mean sizes between 2 and 5 μm in diameter; with surfactant it might be anticipated that the resultant size would be in the nanometer region.

An earlier process described for the preparation of gelatin nanoparticles involved emulsifying gelatin aqueous solutions containing the drug in a vegetable oil such as sesame and cooling below the gelation point using an ice bath (57). Because the oil is soluble in acetone, the cold droplets were passed through a filter and cross-linked with formaldehyde in acetone before final collection, acetone washing, and air-drying. The particles were claimed to be between 100 and 600 nm in diameter, and apart from the use of a flammable solvent, the basic process is obviously more acceptable. As Kreuter (6) commented, it is a bit surprising that the nascent emulsion passed through a 50-nm pore size membrane filter, but once the acetone was removed the resulting particles had an average size of 280 nm. This suggested the small droplets of the initial emulsion were sufficiently fluid to change their shape and pass through the 50 nm filter. Nevertheless, based on a developing knowledge of the properties and structure of gelatin, it should be possible to produce gelatin microparticles by careful attention to the type of gelatin, pH, temperature, and concentration of the solution. Marty et al. (58) claimed that addition of ethanol or sodium sulfate to gelatin solutions enabled nanoparticles to be precipitated. This work has proved difficult to replicate with materials now available 20 years later, and the formation of microparticulates from gelatin solutions may depend on factors not yet completely evaluated (see later discussion). In both Kreuter's 1992 chapter and his more recent book (6,7) the subject of nanoparticle formation is dealt with in considerable detail with appropriate references, but the methodologies remain basically the same. The core materials, on the other hand, vary widely.

Preparation of Sterile Product. The very complexity of these processes does not prevent the need for sterility of the end-product. However, some processes may lend themselves to sterility being achieved inadvertently. For example, where a hot oil at temperatures up to 180°C is used to precipitate a proteinaceous vehicle such as albumin or to dry a gelatin system, it is evident that the product, under carefully controlled conditions, has effectively been heat sterilized. In processes in which glutaraldehyde or formaldehyde are used, these are sterilizing agents in their own right, and again, the process could be designed to ensure that the final product was sterile. Additional design changes would be needed to ensure that the sterility was maintained, if necessary operating under aseptic conditions for the final stages of production.

Spontaneous Liposome and Emulsion Processes. One well-recognized characteristic of liposome formation is the spontaneous formation of these vesicles when a thin lipid/phospholipid layer is placed in contact with an excess of water. This is due to the marked ability of phospholipids to form curved surfaces. The resulting vesicles may not have the desired properties in terms of size or the required lamellar structure, which can be designed into the process by application of additional shear (extrusion through small orifices) or heat. What is perhaps less well recognized is the fact that anhydrous oil systems containing appropriate oil-soluble surfactants, when added to water, or, preferably, aqueous solutions of other surfactants, also spontaneously and rapidly form oil-in-water emulsions. These emulsions are usually submicrometer in dispersion and are remarkably stable. Familiar examples are seen in domestic products such as insecticidal sprays or antiseptic solutions where a "concentrate" is added to water, forming an immediate emulsion. Spontaneous systems have been explored for pharmaceutical application although the number of suitable (i.e., nontoxic surfactants) suitable for this purpose are somewhat limited (59). The speed of the emulsification process is a function of the temperature and oil viscosity as well as the properties of the surfactants employed. The advantage of an anhydrous system is that it can be stored as an oily paste in gelatin capsules which, when administered orally, spontaneously forms small droplets in the stomach and upper gastrointestinal tract

once the capsule wall is broken. For injection, the system would be packed as an oil to which water or electrolytes would be added immediately prior to injection. Pouton (59) has found that 30% Tagat OT(poly(oxyethylene-(25)glyceryltrioleate) with 70% medium chain triglycerides (Miglyol 812) was a suitable system for oral administration but there appear to be no reports of similar systems being suitable for parenteral use.

Preparation of Sterile Product. Because both systems are effectively made by adding one liquid to another, it should be feasible to sterile-filter both components and operate under aseptic conditions for the rest of the process. Heat sterilization of liposomes has been attempted but this may cause considerable changes in the state of dispersion and generally redistribution of guest drug molecules (60). γ-irradiation has also been investigated for the sterilization of liposomes (60), but was found to be limited in application because of phospholipid degradation. Frozen liposomes in the presence of effective antioxidants may be an alternative application for sterilization by γ-irradiation, but this possibility requires further evaluation.

Polymer Emulsification. The production of polymer emulsions, especially nanoparticulate systems, is carried out by an emulsification process that is physically different from those processes used for the usual pharmaceutical processes. Polymers are usually derived from monomeric systems by providing an appropriate stimulus or catalyst. Some reaction initiators are heat or high-energy radiation and catalysts are often heavy metal salts or, in the case of methyl methacrylate, potassium peroxidisulfate. However, greater control over the polymerization process is exerted if the liquid monomer is emulsified in water and the catalysts added to the system. The polymerization process itself does not occur in the oily or dispersed droplets but rather to the monomer molecules that have dissolved in the aqueous continuous phase from the disperse phase. The polymerization or chain-growth process is maintained by more monomer molecules diffusing out of the dispersed phase. Because the polymerization process is always slower than the monomer diffusion process, polymerization continues in the continuous aqueous phase until the droplet reservoir is exhausted. The monomer droplets can be reasonably coarse by comparison with the dispersed polymer particles and, as noted by Kreuter (6), some systems do not require an interfacial stabilizer, although addition of casein (e.g., to a methyl methacrylate suspension) results in a finer, more monodispersed, polymer particles.

Preparation of Sterile Product. Although many of the monomeric compounds used are unfavorable for bacterial growth, this cannot be relied upon to sterilize the system prior to or during the polymerization process. In addition, the effect of a terminal heat-sterilization process on the polymer would be to change equilibrium conditions and, therefore, properties of the final product. Because the reactants are liquids, in a liquid medium, this would suggest that a process could be designed as an aseptic process in which components and reactants are sterile-filtered together into a sterile reaction vessel, and aseptic precautions maintained throughout.

Mixed Micelles

Mixed micelles, consisting of mixtures of phospholipids, especially PC, and bile salts have recently been advocated as solubilization systems for sparingly soluble drugs such as teniposide and paclitaxel (Taxol®) (61,62). Phospholipids are insoluble in both oil and water, forming swollen suspensions in both. In water these dispersions are better known as liposomes because they form spherical molecular aggregates with aqueous centers. Bile salts, on the other hand, are water-soluble and readily form micellar aggregates. When added together, bile salts and phospholipids form complex structures, most likely rod-like aggregates that have a significantly higher capacity for guest molecules (63). These structures are readily formed as transparent aqueous dispersions, and this transparency is maintained as the system is diluted (although the actual structure changes from rods to spheres, in other words to liposome-like structures). Both components are amphiphilic in nature and both can be used to solubilize water-insoluble (i.e., with aqueous solubilities of below 0.01%) drugs. Individually these materials can be employed to solubilize drugs although handling phospholipids on their own is not easy (see "Emulsions") and bile salts can manifest toxicities on administration principally due to their detergent properties. However, when mixed, the new structures vastly increased the solubilization capacity of the individual systems, and the incorporated "guest" molecules were not precipitated on further aqueous dilution. This was because the bile salt molecules were effectively disaggregated by dilution, but the phospholipids form curved bilayer structure-liposomes that retained the associated hydrophobic guest molecules.

These mixed micellar solutions therefore have a number of advantages:

1. Precipitation is eliminated when injected or diluted for injection.
2. The vehicle is aqueous throughout and can be adjusted for pH and osmolarity.
3. The solutions are clear, isotropic, and have low viscosities, which make them ideal for injection.
4. Mixed micelles form spontaneously by the internal energy of the system, which effectively means that they are thermodynamically stable and reproducible at defined compositions and temperature.
5. Technically these systems are readily made by solution in a mutual solvent such as isopropanol, which can then be removed.
6. These solutions can be easily sterilized by filtration. Terminal heat sterilization, often demanded by regulatory authorities, has not been evaluated but under carefully controlled conditions, may not represent a serious problem, depending critically on the properties of the incorporated drug.
7. Unlike liposomal formulations there is no problem with vesicle leakage and mixed micellar systems are readily lyophilized, spontaneously recovering their original properties on reconstitution with water.

8. In some cases pain on injection has been shown to be reduced.
9. The chemical stability of some labile molecules has been shown to be improved, hydrolysis being reduced or prevented altogether when the drug is incorporated into mixed micelles.

A number of other drugs have been explored in mixed micellar systems, including diazepam and steroids (63). A systematic evaluation of steroidal structures on solubilization by simple and mixed micelles has recently been published by Cai et al. (64) although here the emphasis was on oral absorption of these drugs. Ayd (65) demonstrated that linear increases in solubilized drug concentration with increased total lipid concentration were often observed. A critical lipid concentration was defined as a specific mixed micelle composition that existed over a limited range, showing a linear relationship between the phospholipid: bile salt molar ratio. Measurement of the particle size suggested that a molar ratio of $\approx$ 1.0 was optimal. Beyond this range the systems appear to react more until they restructured to form a gel-like state consisting of associated rods. Ayd (65) concluded that mixed micellar solubilization was a multifactorial event, with different types of aggregated structures contributing to the entire solubilization process.

Yet to be used in a commercial product, this approach to an old issue associated with poorly soluble drug substances would appear to be exceptionally promising and may well be investigated further.

Preparation of Sterile Product. The effect of terminal heat sterilization conditions on the final mixed micellar product remains to be explored. The use of filtration to sterilize components in an aseptic process may be necessary but the point of application may need careful selection because, often, the component solutions have high viscosities that renders any filtration process difficult to carry out.

Spraying Processes

Kwok et al. (66,67) were able to demonstrate that 5–15-μm diameter particles of alginate-poly(lysine) particles suitable for encapsulating microorganisms such as bacillus Calmette-Guérin (BCG) vaccine could be made by spraying solutions of the polymer system through a suitable atomizer. Later, this system was adapted to preparing gelatin or albumin microparticles (40). The process consisted of atomizing aqueous 1% gelatin or [human albumin] solutions through a Turbotak atomizer, Turbotak Ltd., Waterloo, Ontario, Canada) with a 1 mm orifice. Two sets of apparatus were used (Figs. 1 and 3). The gas inlet to a Turbotak was connected to a compressed carbon dioxide tank at an inlet pressure of 20 psi. The inlet solutions were sprayed into anhydrous ethanol (95% ethanol, 5% isopropanol) held at a temperature of -15°C. The droplets were then hardened by the addition of glutaraldehyde for 24 hours, followed by sodium metabisulfite to stop the crosslinking reaction. The particles were collected and washed before lyophilization in the presence of mannitol as a diluent. The process was improved by adding a second stage

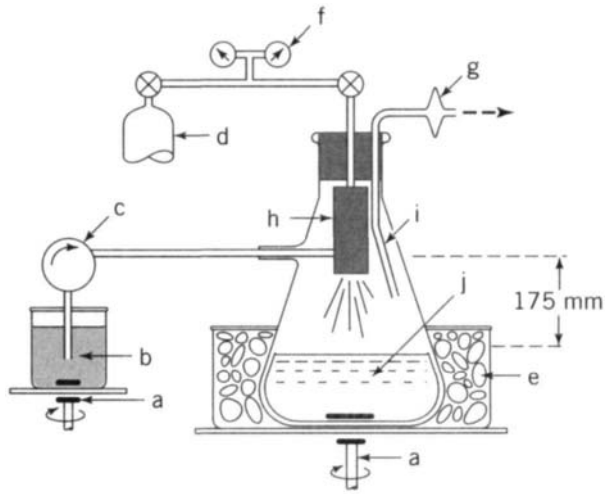


Figure 3. A closed system for making gelatin microparticles using a single-stage carbon dioxide-activated spray system. a, Magnetic stirrer; b, hot gelatin solution; c, peristaltic pump; d, carbon dioxide tank; e, solid carbon dioxide pellets; f, gas regulator; g, 0.45-μm membrane filter venting to atmosphere; h, Turbotak; i, vent tube; j, cold stirred anhydrous ethanol. *Source:* By permission of the editor, *Pharmaceutical Research*, from Ref. 40.

vessel designed to trap the larger droplets also produced by the Turbotak. This proved to be somewhat less effective and gave a much lower yield, most probably because it had already been shown that direct mixing of the aqueous gelatin and anhydrous ethanol was effective in producing gelatin particles (68). Nevertheless, the spraying technique did produce significantly smaller particles with an average size of 0.86 μm as opposed to an average of 1.18 μm made by the direct mixing process. Although relatively large volumes of flammable alcohol are required, one advantage of using the inexpensive carbon dioxide gas is that it is a flame retardant, suggesting that the process might have some potential for scale-up to an industrial process.

Preparation of Sterile Product. Refreshingly, Burgess and her co-workers (66,67,69) have continued work on sterile or axenic product (i.e., containing only one, predetermined microbiological species), and this has recently culminated in a detailed description of how sterile microparticles of alginate/poly(L-lysine) could be made (70). The process was described in detail, producing sterile particles from 3 to 16 μm diameter (volume weighted mean) according to the spraying conditions. The method involves using a Turbotak atomizer operating inside a bioreactor chamber and was shown to be robust enough for major changes in operating conditions to have insignificant effects on the product properties. Attention needs to be drawn to this important pioneering contribution to the subject of sterile microcapsules; it is likely that other processes could be designed in a similar fashion.

Preparation of Poly(L-lactide) Particles by Carbon Dioxide Precipitation Solutions. Müller and his colleagues (71) have recently described an aerosol solvent extraction system for

preparing microparticles by spraying solutions of polymers in organic solvents, usually methylene chloride, into liquid carbon dioxide under supercritical conditions. The apparatus is described in Figure 4, and poly(L-lactide) microparticles were prepared in order to determine solvent residues in the final particles. Varying the conditions of particle production produced little change in the mean/particle size (~2.0 μm diameter), although residual solvent levels were affected. This suggested that microparticle production was by a precipitation process rather then one associated with spray-drying. More to the point, it indicates that this product is also robust enough not to be significantly affected by slight changes in the process.

Preparation of Sterile Product. Ruchatz et al. (71) also referred to their particles as being "sterile." No evidence for this was provided, and an adequate validation of this supposition would be required, although the supposition would appear to be not unreasonable. However, the lack of viability or otherwise of microbacterial spores and other viable contaminants in liquid carbon dioxide has not been established and would certainly make an interesting study.

Homogenization. Calvör and Müller (9) have recently demonstrated that polymers such as PLA can be heated above their glass-transition temperatures and dispersed to nanoparticle sizes by high-pressure homogenization without the need for organic solvents. This process may be potentially important since it is readily scaled up.

Antigens and Adjuvants

Vaccination is by far the most efficient and cost-effective means for preventing a wide variety of infectious diseases. The effective use of what we can now recognize as a vaccine was known to the ancient Chinese as a means of preventing the spread of smallpox, a disease that has been eliminated from the world within living memory. Vaccines have been used to minimize polio, measles, diphtheria, tetanus, and pertussis in most areas of the world, and a tuberculosis vaccine, BCG, has been available since the 1920s. More recently, subunit vaccines against hepatitis A, B, and C have been developed, and vaccines against malaria and HIV have been explored and are currently on trial.

The use of vaccines, although originally empirically derived, follows from the way in which the immunological system of the body responds to the invasion of a foreign microorganism such as a virus or bacterium. Small amounts of foreign protein can stimulate a protective immune response, producing two types of immunity to subsequent infections. The first, called humoral immunity, develops after the invading pathogenic organisms have been destroyed by the immune system. The damaged bacterial cells are ingested by macrophages, which then present some of the foreign proteins to antibody-secreting cells called B lymphocytes. These cells then produce proteinaceous antibodies that recognize and bind strongly to the foreign protein. If these antigenic proteins are encountered again, the B lymphocytes carrying the appropriate antibodies are able to neutralize them or mark them down for destruction by other elements of the immune system. The second type of response, cellular immunity, occurs when invading cells penetrate cells in the body and make them produce more of the pathogen. The infected cells then display fragments of the pathogen proteins at the surface. This time the immune system responds by producing specific activated T lymphocytes that can recognize these fragments and bind directly to the infected cell surface. Antibodies are not produced by the T cells; they bind to the infected cells and destroy them, often by making the cell wall porous so that the cellular contents are lost.

For the most part, antigens are proteinaceous in nature. However, from the central dogma of biology, in which it is held that protein production in the cell is controlled and coded by DNA sequences through matching RNA fragments, it has now become clear that specific proteins antigens can be produced by administering so-called naked plasmid DNA sequences. Naked DNA has been used to generate antibodies to HIV proteins, and a naked-DNA influenza vaccine is currently in human clinical trial. Some workers have felt that liposomal-encapsulated DNA se-

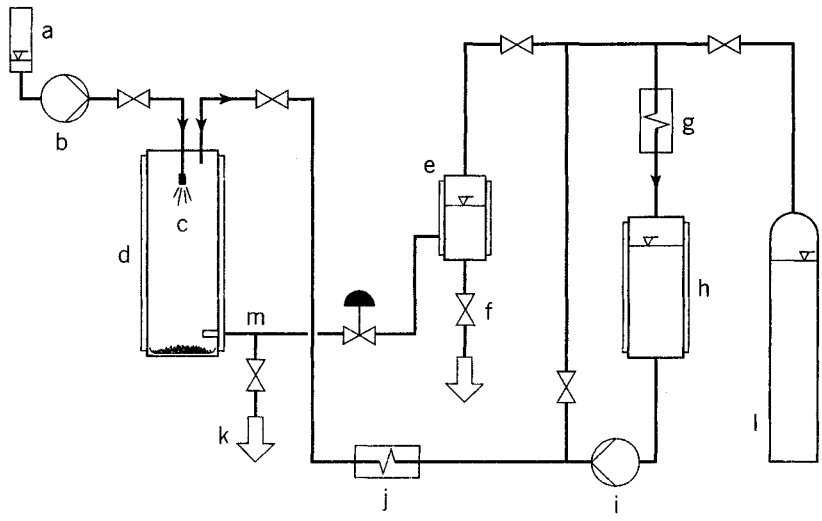


Figure 4. Supercritical production of poly(L-lactide) particles. a, Solution of poly(L-lactide) in methylene chloride; b, pump; c, nozzle; d, high pressure vessel with collecting pan kept at 40°C and 90 bar; e, separation vessel to collect methylene chloride through f; g, condenser; h, CO_2 supply; i, pump; j, temperature equilibration unit; k, sampling tube; l, CO_2 reservoir used for start-up; m, metal sintered filter to collect microparticle contamination of flowing CO_2 stream. *Source:* By kind permission of the authors and the editor, *Pharmaceutical Science*, from Ref. 71.

quences may offer better prospects for cellular delivery than naked DNA (72).

For the most part, earlier vaccines consisted of heat-inactivated or attenuated viral or bacterial cultures. These systems contained numbers of unwanted proteins or portions of proteins, epitopes, that interacted not only with the antibodies for the disease but also with other receptors throughout the body. It should not, therefore, be surprising that unwanted side effects were often experienced on administration of a whole organism. The mildest of these side effects might vary from a mild to severe fever or, as in smallpox, a low-caliber manifestation of the disease. The attenuated tuberculosis vaccine, BCG, is a living organism, *Mycobacterium bovis*, which has to be administered orally or intradermally. Given intravenously, either deliberately or inadvertently during clinical treatment of superficial bladder cancer, it becomes disseminated throughout the body, producing a tuberculosis-like reaction that may require intensive isoniazid treatment for six months. There is little information about the oral administration of BCG, although it was by this route that the early vaccine was administered. Today, the preferred route is by superficial intradermal administration where it has become evident that the living organism is effectively behaving like a controlled release system, delivering on a continuous basis small amounts of cell wall proteins as antigens and stimulating production of the appropriate antibodies after administration, in some cases for several years (73).

Use of monoclonal antibodies, with very specific epitopes that react with exquisite specificity to other proteins, have demonstrated that the target site may be moveable. An excellent example of this is HIV, which is capable of changing its surface proteins, making the development of an epitopic vaccine exceptionally difficult. Although epitopic vaccines are attractive from a manufacturer's point of view because they are chemically well defined, generally free of the side effects associated with older vaccines, and relatively straightforward to manufacture, they are exquisite in the sensitivity and specificity of their antibody reactions. Thus, if the antibody shifts its epitopic identification center slightly the reaction may not take place at all. There are, therefore, advantages to using the older types of vaccine because they contain a much broader range of required epitopic sites even though, for the same reason, they are also capable of producing toxicity. A compromise may therefore be necessary.

Another disadvantage with these subunit antigens is that they are almost, without exception, poorly immunogenic. In order to induce an effective protective immunity, these vaccines require boosting with agents called adjuvants. The most effective adjuvant is probably Freund's complete adjuvant, consisting of BCG cells dispersed in a oily matrix, but the reaction produced on injection is so severe that it is not acceptable in human practice, and ideally should not be used in animal testing either.

The only adjuvants approved by the FDA for human use are aluminum hydroxide and aluminum phosphate in the form of alum. More effective adjuvants are currently being evaluated, including liposomal phospholipids, Lipid A, muramyl dipeptide (MDP), and various forms of quillaia saponins, including a purified form in a construct with cholesterol and phospholipids termed ISCOMS. Part of the issue associated with adjuvant use is how they work. Recent investigations have indicated that the immune system is controlled and coordinated by local excretion of cytokines such as interleukins, tumor necrosis factors, and interferons. An alternative strategy to the use of adjuvants might be to use controlled and targeted delivery of cytokines to specific sites of action. These materials are now available in significant quantities through the application of genetic engineering, although when administered in bulk, almost inevitably these compounds produce additional and unacceptable side effects.

In a recent review Zhao and Leong (74) suggested that advances in controlled release technology could improve immune responses by altering the spatial and temporal presentation of both antigens and adjuvants. The rate of delivery and the duration could be manipulated to generate an optimal immune response. Other evident advantages would be to protect the vaccine from degradation until it was released, and by combining slow release and depot effects, the amounts of antigens and the required adjuvants could be reduced, thereby reducing toxicity. It was suggested that by providing a continuous supply of antigen, progressive maturation of the neutralizing antibodies may be promoted. Unfortunately, as these authors admit, the exact mechanism by which an adjuvant is effective is poorly understood at present. The use of single epitopic vaccines may not be the best approach to vaccination in all cases but at least controlled release matrices do allow the possibility of encapsulating multiple antigenic epitopes as well as a number of adjuvants in a single carrier. At present in an exploratory phase, this approach might be feasible when a great deal more information is available about the mode of action of adjuvants, the number of subunit epitopes that are required, and the optimal quantities and type of cytokines. Nevertheless, the future development of prophylactic vaccines in the future is almost certain to involve controlled release formulations for both humoral and cellular responses. Selkirk (75) suggested that what was needed was the development of vectors that enabled both the target antigen and regulatory cytokines to be secreted simultaneously, taking care to minimize toxicity. He noted that delivery systems were needed that would target specific tissues and antigen-presenting cells. Some ideas and approaches will undoubtably disappear into the mists of history but, from the present perspective, many appear to be very promising.

Current Vaccine Delivery Systems. Although systems now used for antigen and adjuvant delivery have been discussed elsewhere, it might be helpful to summarize some of the more useful systems.

Liposomes. Liposomes and their recent derivatives, lipoplexes, have advantages in that they are hollow spherical constructs formed by phospholipids when dispersed in water. The constructs consist of one or more lipid bilayers that have aqueous spaces between them, thus allowing entrapment of either hydrophilic or hydrophobic moieties. By the addition of cholesterol the fluid lipid bilayers can be rendered rigid at ambient room temperature, and by changing the phospholipid constitution, the liposomes can

have an electropositive surface charge instead of the natural negative charge. Liposomes act as potent nontoxic immunological adjuvants and can be made to incorporate many antigens expressed at the surface. The versatility of the liposome as a drug delivery system is well recognized (76).

Adjuvants such as MDP and its analogues have been added to liposomes containing an antigen, and interleukin-2 has also been incorporated, confirming the versatility of the delivery system. Liposomes have another advantage in that the phospholipid bilayer is capable of fusing to cell walls. For this reason, they tend to get incorporated into elements of the reticuloendothelial system quite rapidly after administration. The recent introduction of surface-modified liposomes (sometimes called sterically stabilized or Stealth® liposomes) has produced a new generation of liposomes that are physiologically more stable. This has been achieved by covalently bonding poly(ethylene glycol) to the PE found in the lipid layer, producing a strongly hydrophilic surface that is not opsonized by proteins (36). This development appears to be exceptionally promising and may make the clinical application of liposomal products more realistic in the immediate future. Moreover, by attaching appropriate antibodies to the terminus of the liposome-attached poly(ethylene glycol) (77,78), the targeting of liposomes has been vastly improved.

Solid Particulate Systems. Biodegradable polymers, in particular PLGA, previously used as a surgical implant and suture material, have proved popular as particulate drug delivery systems. The polymer can be tailored to a specific purpose and has been explored as a matrix antigen delivery system. The polymer degrades by an aqueous hydrolytic process, producing acids and therefore low pH conditions close to the surface, which may be detrimental to any incorporated protein. In addition, as noted by Davis recently (79), storage of PLGA immunological systems can result in loss of immunogenicity, and "conventional" sterilization systems can cause damage, suggesting the need for aseptic processing. Davis also noted that scale-up of PLGA systems was proving to be difficult. According to Zhao and Leong (74), there have been vast differences between various workers in terms of vaccine preparation, immunization, and challenge protocols, as well as the assay methods. However, some general conclusions may be drawn. For example, the antigens need to be encapsulated in microspheres to elicit an enhanced antibody production and humoral protective immunity. The effect of particle size was evident, especially if the antigen dose was low. Because of the larger surface-to-mass ratio, release was faster from small particles compared with larger ones, and it seems that small ($<10\ \mu m$) microspheres are capable of facilitating extracellular delivery of antigens to the phagocytic accessors cells that infiltrate the administration site, leading to enhanced antigen processing and processing.

Indeed, larger particles could not be phagocytosed by the macrophages until they had disintegrated into smaller debris. In principle it was suggested that a combination of large and small particles might produce a pulsatile pattern of antigen release, mimicking an immunization process that involved a primary dose followed by booster shots. Other particulate systems can be made from cross-linked albumin or gelatin, as noted earlier. Interestingly, empty gelatin microparticles produce only a mild inflammatory response at the injection site, suggesting that gelatin itself has only a minimal immunogenic activity.

However, gelatin on its own does have adjuvant activity and this probably arises from the ability of macrophages to phagocytose the microparticles. Poly(phosphazenes) are a class of polymers with a simple -P=N- backbone with physicochemical properties strongly influenced by side chain attachments to the phosphorus atom. Some can be rendered water-soluble, allowing the antigen to be encapsulated in the aqueous state at low temperature. Addition of ionic cross-linking agents such as calcium can then render the system insoluble, allowing sustained release from the precipitated solid. Further control is obtained by coating the solid surface with the cationic polymer, poly(lysine), and this approach has been used to control the release of antibacterial drugs in a controlled-release string made from calcium alginate, which was designed for impaction into dental periodontal cavities (80).

Other Current Formulation Issues

Pain on Injection. Injectable products are administered by various routes according to the physiological requirements of the product. The main routes are

1. *Intravenous* directly into the intravenous blood supply
2. *Subcutaneous* into the soft tissues just underneath the skin
3. *Intramuscular* directly into the muscles of the arm or gluteal region

Other routes include the *intrathecal* (subarachnoid space), *intraarticular* (directly into joints), *intracardial* (directly into the heart), *intraperitoneal* (used for kidney dialysis), and *intracutaneous* (just under the stratum corneum of the epidermis). However, all routes of parenteral administration require professional medical skills for successful delivery of the drug, and this can sometimes be stressful for the patient, contributing to pain. Nevertheless, although it is basically true that no parenteral administration is without pain, some drugs or their vehicles themselves produce pain. It is generally recognized that painful injections should be administered by intramuscular injection because there are few nervous receptors in these tissues. Nevertheless, this site is not always feasible and pain experienced by administration of a pain-causing drug can be difficult by the subcutaneous route or, due to drug residues along the needle-track, by the intravenous route. Some factors producing pain on injection, reviewed by Fransson and Espander-Jansson (81) include:

- Injection volume (the subcutaneous route should not exceed 1.0 mL and the intramuscular 2.0 mL)
- Speed of injection
- Injection site
- Size and quality of the hypodermic used (is it sharp or blunted?)

- Temperature of injection
- Presence of irritating substances (e.g., citrates)
- pH
- Osmolality

Fransson and Espander-Jansson (81) were concerned about severe pain experienced by patients receiving subcutaneous injections of human insulin-like growth factor. This protein is most stable at a pH of 6.0, which although not physiological, should have been acceptable. Morphine sulfate injections have a pH of 3.0, although these are administered into muscles where the ambient pH is often lower. These authors were able to demonstrate that the pain was not due to the drug itself but was caused by the concentration of the phosphate buffer used. Although lower concentrations of phosphate (10 mM compared with 50 mM) had lower buffer capacity, this was judged to be acceptable in view of the reduced pain experienced. In addition, it is probable that dilution to physiological pH occurred more rapidly around the administration site.

Pain is a subjective sensation and therefore difficult to measure. However, there are statistically valid methods of measuring it, and other sensations such as muscle damage, redness, paleness, and edema at the injection site can also be used to supplement the measurements (82,83).

Needleless or Jet Injectors. Alexander Wood invented the graduated glass syringe fitted with a hollow reed in Edinburgh around 1853, although syringes as such were widely employed in early Tudor times, to judge by artifacts found on the warship Mary Rose, which sank off Portsmouth in the early 1500s. After over a century of needle injections, the technology is well understood, although some issues have become evident, such as the associated dangers of needle sticks to health care personnel and cross-contamination during administration. A needleless injector, the Porton injector, was developed in the 1930s and used for routine mass inoculations in both military and veterinary applications. The principle was straightforward: a high-pressure liquid flow from a pressurized container penetrated the skin and deposited material in the dermis and subdermal layers. The equipment was heavy and required a compressor, which made it unsuitable for routine individual use. Various attempts to improve the technology have appeared in recent years and at least one of these, the Intraject® system, Weston Medical (United Kingdom), is one of several recently developed systems that have considerable promise as a technology for the immediate future. The Weston device uses a preloaded gas or coil spring-activated piston to force the liquid through an orifice that does not come into direct contact with the skin. The drug can be supplied in the type of filled cartridges already in wide use for dental syringes. The two are coupled together, and when activated, the spring-powered ram accelerates and strikes a piston with viscoelastic properties. This causes the formation of a liquid pulse in what is described as a "liquid nail," and this has sufficient energy to penetrate the skin, depositing a predetermined volume of fluid. The volume of liquid that can be deposited is limited to 0.2 to 1.0 mL, optimally 0.5 mL, but analysis of the hydrodynamics of the administration process has demonstrated that viscosity of the solution is relatively unimportant. In addition, if the orifice is very short, shear forces are minimized. This is relevant because many proteinaceous injections such as antigens are readily denatured by shearing. The advantages of the Intraject system is that it is light, readily portable, and allows individual patients to administer their own intradermal or subcutaneous injections. Intramuscular injections may also be possible, depending on the obesity of the patient. These may be more painful because of the speed with which liquid is introduced into the muscles, the individual fibers having insufficient time to displace and allow the injected fluid to penetrate into the tissues. In addition, because of the way the liquid pulse splays out on administration, some of the drug may be deposited into adipose tissue, potentially altering the pharmacokinetics. However, individual patients would be likely to adjust dosage according to their requirements, and this has been observed with diabetics using the system. The injector is automatically fired when the device is pressed lightly on the skin. This means that the amount of skill required for administration is minimal, and medical personnel are not required, thereby significantly reducing the associated costs. The device itself is also claimed to be inexpensive, below 20 cents (U.S.) in 1997 money. Obvious advantages of this system is the small size, speed of administration, and insignificant pain levels experienced on intradermal injection. It is therefore entirely possible that this type of device and others being commercially developed will provide a valuable means of administering sterile nanoparticulate systems subdermally for controlled drug delivery.

Albumin

Albumins are a group of proteins widely found in nearly all living body tissues. They are characterized by solubility in dilute salt solutions and precipitation at relatively low temperatures, heating at 55–65°C being sufficient to denature most albumins. Commercially they are obtained from egg white, bovine serum, and human serum, although significant quantities are also available from soybeans, milk, and some grains. Egg white albumins, for example, are usually called *albumins*, and the Latin for egg white is *albumen*. Pharmaceutical materials are generally from bovine or human serum and the remainder of the nonpharmaceutical albumins are widely used for baking although, as noted by Teng and colleagues (84), soy albumins are potentially valuable tablet excipients. Human serum albumin separated from whole human blood is employed as a plasma volume expander, and iodinated (^{131}I) albumin is used as a diagnostic in the measurement of blood volume. This protein has a relatively low molecular weight (~69 kDa) and comprises about 60% of the plasma proteins. Although it denatures and comes out of solution at temperatures below 65°C, the protein is carbohydrate-free and is stable at higher temperatures. The denaturation process in this case is reversible, and commercially available dried albumin, as an example, goes back into solution at lower temperatures, forming as much as a 40% solution at pH 7.4. Ovalbumin, on the other hand, is denatured at

61°C and, when dried, swells initially before it returns back into solution. Both bovine and human albumins could be potentially contaminated in vivo, the bovine with bovine spongiform encalphalopathy (BSE) organism and the human with the AIDS virus. Both contaminants are of concern to regulatory bodies, suggesting care be taken in sourcing the starting material.

Particulate Forms of Albumin. Because albumins readily come out of solution under mild heating conditions, they are suitable for preparing spherical nanoparticles or microparticles. Nanoparticles were first prepared by Zolle et al. (85) as vehicles for nuclear medicines, with the process effectively being repeated by others as general pharmaceutical formulations. The process involved dissolving albumin in water, together with the drug dissolved or suspended in water, and then emulsifying this mixture in oil to produce a water-in-oil emulsion. The size of the droplets was decreased using an homogenizer or by applying ultrasonics, and this system was slowly added to a bulk preheated oil phase and held at elevated temperatures (from 100° to 180°C) for 10 minutes. This was more than sufficient to denature and harden the albumin in the submicrometer water droplets. The overall system was then cooled, filtered, or centrifuged to collect the droplets, and the excess oil was removed with diethyl ether. Because of the hazard of this solvent, the process was not suitable for industrial scale-up, but has since been widely employed in the laboratory. Gallo et al. (86) evaluated factors that influenced the particle size, finding that nanoparticles between 400 and 800 nm in diameter were produced with relatively little effect being seen when manufacturing parameters were changed. Kreuter (6,7) commented in his review that a critical preparation parameter was the rate at which the primary emulsion was added to the bulk heated oil. Others have also demonstrated the inverse relationship between the subsequent release rate and the denaturation temperatures (7).

An alternative process, readily applicable to albumins, is desolvation of the dissolved protein followed by cross-linking. Desolvation can be carried out with ethanol or acetone as shown by Öner and Groves (40) or by using sodium or ammonium sulfates, the latter being preferred because an appreciably higher saturation concentration can be obtained. Wetting agents such as polysorbate 20 appear to help the process, perhaps by inducing interfacial changes in the protein configuration or by acting as a stabilizer (6). Cross-linking reagents such as formaldehyde or glutaraldehyde are then added and allowed sufficient time to react before being removed or neutralized with sodium metabisulfite.

In terms of the sterility of the final product, the heating process and certainly the presence of cross-linking reagents must have a major influence because they are potent chemical sterilants in their own right. Handled under aseptic conditions, it would appear very likely that particles treated with aldehydic cross-linking reagents would be "sterile" at the end of the process. However, this supposition does not appear to have been tested experimentally.

Although it is relatively easy to prepare submicrometer albumin particles by emulsification methods and low micrometer-range particles by desolvation procedures, the release properties of the resultant core matrix systems (i.e., where there is no outer skin or shell) appear to depend on the cross-linking conditions such as concentration of reagent and time of exposure. Anhydrous particles added to water appear to swell first as water is imbibed, hydrating the proteins, and this phase is followed by a slower solution or erosion process. In vivo the process would most likely be accelerated by the presence of proteases, which are ubiquitous throughout the body. In vitro the release of drugs from albumin microspheres is considerably slower than that from other materials, occurring in two fairly separate phases, an initial rapid phase being followed by a slow phase (37). Each phase was characterized as a first-order reaction, with the actual release rate being proportional to the remaining drug concentration in the particles. Jalšenjak (37) suggested a simple biexponential function to describe the release profile:

$$Q = \text{amount remaining in the microspheres at time } t = A \exp(-\alpha t) + B \exp(-\beta t) \quad (1)$$

where A and B are constants and α and β the rate constants. There is no physical explanation for the faster initial process unless it is analogous to the burst phase observed with other types of controlled release products in which the incorporated drug is present as superficial crystals or some other form that is readily available to the penetrating solvent. As noted, the release mechanism in vivo is likely to be activated by enzymes and should therefore be somewhat different both in the form of the release curve and the actual release rate. This does not appear to have been evaluated experimentally.

Preparation of Albumin Microparticles by Atomization. Although albumin microparticles are readily prepared by the application of heat (>55°C) to suspensions or emulsions containing aqueous solutions of the protein, these methods all require removal of oils and emulsifying agents from the precipitated protein. Many authors have employed solvents such as diethyl ether, chloroform, or methylene chloride to remove oils from the product, which for the most part are considered to be environmentally and toxicologically undesirable. Moreover, removal of solvent residues is by no means complete, and the net effect is that albumin microparticles in the final product are often less than ideal.

These considerations led to the exploration of alternative processes involving chilled dehydrating solvents such as anhydrous ethanol or acetone. Öner and Groves (40) described a relatively simple process in which aqueous solutions of albumin or gelatin were mixed into anhydrous ethanol at −15°C. The microparticles produced were hardened for collection by exposure to glutaraldehyde for a prolonged period before collection by filtration and extensive washing. Particles of albumin in the range of 2 to 5 μm in diameter were readily prepared, the size being controlled to some extent by the time of exposure and concentration of glutaraldehyde (40). Later, the process was refined by

Next Page

atomization of albumin solutions through a Turbotak atomizer and allowing the droplets to impinge into the chilled ethanol. This process reduced the mean size of microparticles produced by the mixing process from 3 to 1.8 μm by the atomization process, although the overall yield was obviously lower (85% vs. 67%). The use of carbon dioxide as a propellant was considered to be an advantage because the gas behaves as a flame retardant (87). The equipment used for this purpose is shown in Figures 1 and 3.

Properties of Albumin Microparticles. There have been relatively few studies of the properties of albumin microparticles, although they may be presumed to be porous assemblies of insoluble proteinaceous molecules formed by either heat or aldehyde cross-linking. Factors involved in the formation of albumin beads by the emulsification process have been evaluated. However, studies of factors involved in the in vitro disintegration of albumin microparticles are relatively limited. One advantage of insoluble microparticles made of proteins such as albumin is that the surfaces can be eroded by digestion with a nonspecific proteolytic enzyme such as trypsin. This was the method used to evaluate albumin microparticles (68). These authors found that both the size and the rate of in vitro disintegration of albumin microparticles (made by the chilled desolvation technique) were affected by both the concentration of the cross-linking agent (glutaraldehyde) and the time of exposure (Fig. 5). This strongly suggested that the cross-linking process itself was essentially a dynamic process, with particles becoming larger with both time and exposure and concentration of the cross-linking agent (Fig. 6). This observation was very different from that observed by the same authors for the formation of gelatin microparticles where, once formed, the particle remained constant

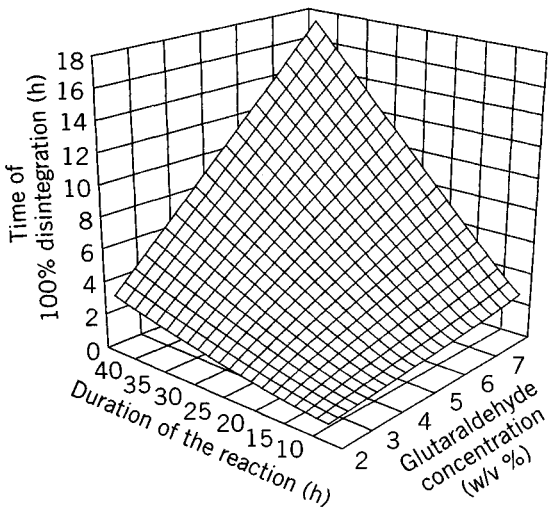


Figure 5. Response surface diagram, for 100% enzymic disintegration of albumin microparticles prepared by variation of the glutaraldehyde concentration and duration of cross-linking. *Source:* By permission of the editor, *Journal of Pharmacy and Pharmacology*, from Ref. 37.

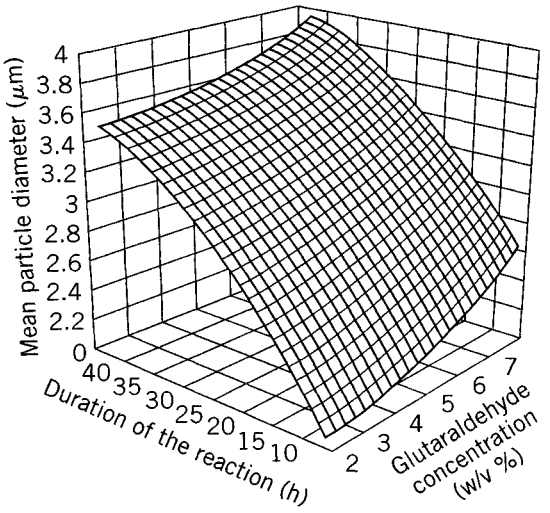


Figure 6. Response surface diagram for the mean particle diameter of albumin microparticles prepared by variation of glutaraldehyde concentration and duration of cross-linking. *Source:* By permission of the editor, *Journal of Pharmacy and Pharmacology*, from Ref. 37.

in size (40). This was considered to be due to the higher molecular weight of the globular albumin molecules and subsequent greater sensitivity to structural changes induced by the cross-linking agent. In the case of the linear gelatin molecules, unless particles had been hardened for a sufficient length of time they simply swelled and dissolved on exposure to water. On the other hand, microparticles formed very rapidly at low concentrations of reagent, and the size increased as reagent concentration and exposure time were increased.

Enzymic disintegration of hardened microparticles and, presumably, release of any incorporation drug was affected by a number of associated factors, especially particle size. Because the molecular size of the digesting enzyme is sufficiently large to inhibit diffusion into the particle interior, the attack and subsequent solution of the matrix would be anticipated to occur at the surface of the particles. The disintegration of the microparticle could be treated as a square root of time relationship commonly observed with Fickian transport phenomena. The release (disintegration) surface diagram (Fig. 5) is substantially but not completely the reverse of the formation surface (Fig. 6). However, the relationship between initial size of the microparticles and time for the solution process to go to completion was clearly more complex than a simple root time function would suggest, as is readily seen by comparing the two surface diagrams, and by the fact that the relationship between particle size and complete disintegration time was not linear. This may indicate that the process is going faster than might be anticipated because enzyme is capable of penetrating to the interior surfaces of the microparticles, thereby increasing the rate of the disintegration process. Involvement of particle interior surfaces was also suggested when investigating loading of thiotepa or low and high molecular weight sugars onto preformed gelatin microparticles (87,88).

Previous Page

Collagen

Collagen is widely used, especially in Europe, as a base material for a wide variety of drug carrier systems. In general, it is considered to be biocompatible and biodegradable, allowing, for example, its exploitation as lenses for ophthalmic delivery. Collagen sponges impregnated with antibiotics have been employed in surgery to improve wound healing and prevent diseases such as osteomyelitis (89). For the most part, parenteral collagen systems have been developed as matrices and are claimed to offer better alternatives to synthetic polyester of polyanhydride devices. However, most of the systems described to date are monomolecular collagen (atelocollagen) in which the nonhelical telopeptides are removed enzymatically (see "Gelatin and Gelatin Vehicles" for a discussion of the structure of collagen and its degradation products). This soluble product requires chemical cross-linking to prevent or delay the devices from dissolving at body temperature, 37°C. Using glutaraldehyde increases the danger of side reactions that can occur on incorporated sensitive drugs, such as proteins, and reduces the biocompatibility. Friess and colleagues (90) suggested that an alternative method was to use the higher molecular weight soluble collagens as a drug carrier. This insoluble material comes about from the natural tendency of the collagen triple helix structure to aggregate, eventually forming fibers and bundles of fibers that were stabilized by inter- and intramolecular cross-links. Commercially, the insoluble collagen is available as a slurry after milling, purification, and enzyme treatment designed to remove the noncollagenous materials. Friess and Lee (89) lyophilized this slurry for storage but could rehydrate it by swelling in water followed by homogenization. Devices were easily prepared by casting films of hydrated suspensions and punching out discs after air-drying. Properties were modified by adding glutaraldehyde to induce cross-linking.

Differential scanning calorimetry demonstrated that denaturation occurred at relatively high temperatures, 80–103°C, higher than the 43°C recorded for aqueous solutions of the same material. Cross-linking caused some controlled slow release from the devices but, correspondingly, increasing amounts of drug were entrapped in the matrix. This entrapped material was shown to be released by enzymatic digestion (90). This observation suggests that implanted devices would release incorporated drugs, especially those of high molecular weight, under the influence of locally available enzymes such as collagenases.

Because chemical cross-linking is required to obtain controlled release, it was found to be important to load the devices after preparation and initial lyophilization by soaking and swelling in a solution of the drug, followed by a second lyophilization. Proteins were readily loaded by this method (90) as were polysaccharidic glycans (91). In this latter case the drug, PS1, as a known immunostimulant, stimulated the in vivo degradation of the devices, apparently by macrophage attack. The mechanism involved here was not clearly defined but any unexpected in vivo effect similar to that observed here would obviously negate the purpose of using this type of controlled release system.

Gelatin and Gelatin Vehicles

Constitution of Gelatin. Gelatin is a biopolymer obtained commercially by the controlled hydrolysis of collagens from a number of animal sources. Native collagen consists of rods formed from triple helices that are held together by covalent bonds. During the denaturation process, which usually consists of heating in the presence of acid or alkali, the covalent bonds are destroyed and the helical structure disrupted. Above 37°C solutions of gelatin in water are liquids, and the molecules behave effectively as random polymeric coils. However, when cooled to ambient room temperature in excess of 1% concentrations by weight, gelatin solutions change to gels and the random chains partially revert back to triple helix structures. The bulk of the gelatin chain is made up of glycine, proline, and hydroxyproline (≅58%), which are weakly hydrophobic. Their periodicity along the chain, combined with the structural flexibility of the glycine molecule, provides a vehicle for the formation of helical structures (92).

At around neutral pH the gelatin chain is amphoteric and groups such as lysine and arginine (≅7.5% of residues) are positively charged, and others such as glutamic and aspartic acids (≅11.8%) are negatively charged. These entities provide centers for electrostatic binding. Light, small angle neutron and x-ray scattering all provided evidence of the persistent length and stiffness of the chain as approximately 20 nm, with a radius of gyration R_G of ≃35 nm. As the concentration was increased, two regions became evident by quasielastic light scattering. The fast mode was evidently due to cooperative movements of the entangled network of chains, and this appeared to persist over a range of concentrations and temperatures. The second mode was associated with the diffusion coefficient being inversely proportioned to the bulk Newtonian viscosity of the solution. This has been interpreted as being due to the self-diffusion of clusters of chains that have a constant hydrodynamic radius $R_C \cong 75$ nm. Contrary to the properties of the chains themselves, the clusters are affected by the molecular weight of the individual chains, the temperature and the presence of salts or surfactants such as sodium dodecyl sulfate. Herning et al. (93) concluded that clusters were stabilized by hydrophobic interactions between apolar lateral groups of the protein. Gelatin as such is not a single entity but behaves like a model protein. The bulk material is deficient in some amino acids, having only 18 constituent units, of which the principal constituents are glycine (32–35%), proline (11–13%), alanine (10–11%), hydroxyproline (9–19%), glutamic acid (7–8%), aspartic acid (4–5%), and arginine (5%). The parent collagen, for the most part, consists of three subunits of approximately equal molecular weight (95 kDa). When denatured to form gelatin, the collagen is broken down to a single chain α-fragment (M_w 95 kDa) and β-fragments (M_w 190 kDa), together with branched γ-chains of M_w 285 kDa which actually consist of three α-chains joined near the center point. As might be anticipated, there are also low molecular weight oligomeric degradation products (Table 2).

Using high-performance liquid chromatography and gel electrophoresis, Zavlin et al. (95) have examined the constitutional difference of gelatins from various sources al-

Table 2. Oligomers of Gelatin Showing the Relationship of the Basic α-chain to Other Components

Molecular weight class	Molecular weight range (kDa)	Possible composition (α-chains)	Approximate % w/w in B225 gelatin
Subalpha	<80	Low molecular weight fragments	20
Alpha (α)	80–125	1-α	14
Beta (β)	125–225	2-α	18
Gamma (γ)	225–340	3-α	8
Epsilon (ε)	340–700	6-α (or 2γ)	15
Zeta (ζ)	700–1,000	9-α (or 3γ)	5
Delta (δ)	1,000–1,800	12-α (or 4γ)	9
Microgel	>1,800	high molecular weight aggregates >12-α	11

Source: Ref. 94.

though with photographic film processing in mind. Skin or bone gelatins were basically similar one to another, β-chains being substantially missing from skin gelatins. Differences between acid and alkaline processed gelatin were noted, the former apparently containing more degradation products. The authors suggested that desired properties for any particular gelatin could be obtained by blending various samples to give the desired low molecular (α) or high molecular (γ) fractions according to the end product usage. What is certainly missing at the present point in time is evidence that the gelatin-producing industry is prepared to carry out this blending process for the pharmaceutical industry, in part because pharmaceuticals represent a relatively small section of the total economic requirement and in part because there have been relatively few pharmaceutical studies that have helped to define the essential requirements for pharmaceutical gelatins.

Phase Relationships. Although gelatin is proteinaceous, comprising linear assemblies of covalently bonded amino acids, in many ways it has atypical behavior because it shows no tertiary structure and is not denatured by heating up to temperatures of 100°C. Albumin, for example, is denatured at 55–60°C and is readily precipitated out of aqueous solution by the addition of ethanol or sodium or ammonium sulfate. Gelatin, on the other hand, is slowly precipitated by the addition of either of these desolvating components, resulting in a complex phase diagram that is influenced by the temperature of the system. Gelatin is a mildly hydrophobic protein, and the addition of solutes results in two-phase liquid systems, today called coacervates, and it is the creation of coacervate structures that is the key step in the production of many encapsulated gelatin products. Although this has been known for many years, it is only recently that attempts have been made to systematically, experimentally determine the effect of temperature and solutes on the transition between various constituent phases of what is an exceptionally complex system (96). Ternary phase diagrams are often used to depict the effect of a third component on the phase behavior of a particular compound in aqueous solution. More commonly used for inorganic systems, the ternary diagrams have proved to be invaluable for defining the phase behavior of surfactants and spontaneous emulsions. Effectively, defining points or boundaries between incompatible systems or components, interpretation of ternary phase diagrams requires care and are rarely precise or exact. The first studies of the effects of salts on gelatin go back to the 1930s (97) but recently a systematic study of the effects of ammonium sulfate or ethanol on the solubility or constitution of Gelatin B (Bloom 225) has been published (96). These authors found after the inspection of several hundred gelatin–water combinations that a total of seven morphologies could be distinguished visually (Table 3) although only six were seen with the ethanolic systems. It must be assumed that the states described by these authors are stable and that the equilibrium phase boundaries are also stable, although these assumptions are not always justified. At least 33% water is needed to break apart and hydrate the gelatin in order to form a solution (Fig. 7). Interestingly, the addition of ethanol did not appear to change this situation, suggesting that the compact gelatin powder showed little preference for either water or ethanol and, as noted earlier, can therefore be defined as being relatively hydrophobic. It should be noticed that water-structure promoters such as sodium chloride destabilize gelatin structure, and almost 50% water is required to form a solution in the presence of 5% sodium chloride. This can be interpreted as indicating that both the gelatin and the salt compete for water of hydration. However, the question not answered by these authors is the nature of the structure of the opaque sols and gels described. It was pointed out that below 40°C, gelatin molecules began to interact with each other to form linkages stabilized by hydrogen bonds, which accounted for ethanol encouraging gel formation, as shown in morphology I, Figure 7. Herning et

Table 3. Gelatin Morphologies on Addition of Ethanol or Ammonium Sulfate

Morphology	Description
I	Transparent clear colorless liquid
II	Opaque liquid (small aggregates)
III	Coacervate region
IV	Transparent or opaque lower gel, upper liquid
V	Homogeneous transparent gel
VI	Powdery aggregates
VII	Transparent lower gel, upper, liquid phase with solid salt

Source: Adapted from Ref. 96.

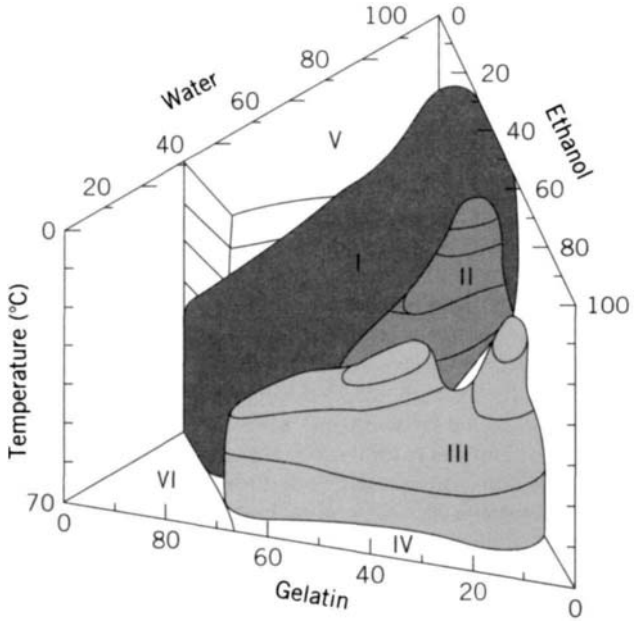


Figure 7. Phase diagram for water-gelatin-ethanol as a function of temperature (Morphologies I–VI defined in Table 3). *Source:* By permission of the authors and the editor, *Journal of Agriculture and Food Chemistry*, from Ref. 96.

al. (93) suggested that stable clusters of gelatin chains formed with hydrodynamic radii of 75 nm at concentrations in excess of 1% w/w, the radii being even smaller at around 60 nm for lower molecular weight samples. Electron microscopy of gelatin nanoparticles and microparticles (94) suggest that these consist of aggregates of small spherical primary particles of around 100–200 nm diameter, quite consistent with the clusters of molecular chains with diameters of ~150 nm postulated by Herning et al. (93).

The nature of the process involved with gel characteristic of gelatins remains unclear in details but must involve chains of the amino acids forming the primary structure to develop associations, most probably involving triple helix structures. Native collagen consists of triple helixes covalently bound to form a solid structure. These are broken by hydrolysis to allow triple helices that reform in the gelatin solution when favored by the presence of large numbers of glycine and proline molecules along the length of the chain. These helices can form along different segments of adjacent chains, thus producing a linked three-dimensional structure as a gel. Dimensions of these systems have been measured by various methods. Chains are approximately 16–20 nm long and a 5% gel has a three-dimensional structure, with "mesh" sizes of approximately 5 nm, the size of which are affected by the presence of salts or surfactants (92).

These parameters may be considered to be fundamental to the structure of the gels, being only determined by the nature and constitution of the primary gelatin molecules. Other parameters involving the gel structure are conditioned by environmental factors, especially temperature and constitution of the medium. Coacervates that form, such as morphology states II, III, or IV (see Table 3), are actually diphasic and consist of separated particles and a liquid. The real questions are, what is the size of these precipitated particles and how can they be made and preserved for use as drug delivery systems?

The Preparation of Gelatin "Nanoparticles". In what has proved to be an influential paper, Marty and her colleagues (58) pointed out that colloidal drug delivery systems lend themselves to parenteral administration and may have uses as sustained release products. It was noted that the ideal colloidal delivery system would transport the bound drug to its desired site of action and release it at an appropriate rate. The carrier itself was required to be nontoxic and to degrade in vivo so it did not accumulate indefinitely in the tissues. Somewhat optimistically, these authors also suggested that the colloidal product should have pharmaceutical stability and ease of administration, such as the ability to pass through an hypodermic syringe and needle. The preparations for parenteral use were also required to be sterilized although, as noted, this may not always be necessary if the production process is adequately designed. The systems, called "nanoparticles" by Speiser, were considered to be the closest approach to being ideal because particles with diameters 200–500 nm in diameter were prepared from materials such as gelatin, human serum albumin, ethylcellulose, or casein. Marty et al. described a process for preparing gelatin microparticles because gelatin was readily available, had low antigenicity, and had previously been used in parenteral formulations. However, although this paper has often been cited, the actual process described by these authors has proved exceptionally difficult to replicate (94) and clearly materials available 20 years later as well as the actual methods themselves are not precisely reproducible.

Gelatin Precipitation. The process described by Marty et al. (58) involved adding ethanol slowly with stirring to a 1–3% w/v solution of gelatin in water containing surfactant (e.g., polysorbate 20) and buffering salts at 37°C until a permanent turbidity was visible. A small amount of ethanol (or isopropanol) was then added until the turbidity was lost and aqueous glutaraldehyde added to cross-link (harden) the gelatin particles. Excess glutaraldehyde was then removed with sodium sulfite or sodium metabisulfite and the entire system lyophilized to remove both the water and the ethanol. The particles were claimed to be spherical, fairly uniformally sized at approximately 200 nm diameter, and a column chromatographic process was employed to separate out the salts and smaller molecular weight components. In fact, looking more closely at the electron photomicrographs these authors published, it may be that they were being somewhat optimistic in their estimates of size. Hydrated particles shrink considerably when exposed to the hard vacuum required for scanning electron microscopy, and associations between particles were evident in their published electron photomicrographs.

Over the years various groups have reevaluated this pioneering work and developed the concept further. Öner

and Groves (40) demonstrated that it was possible to produce micrometer-range sized particles by effectively reversing the process described by Marty et al. (58), in that warm 1% gelatin solutions were added to stirred dehydrating solvents such as anhydrous ethanol (95% ethanol plus 5% isopropanol) at −15°C obtained by surrounding the mixing vessel with solid carbon dioxide (see Fig. 1). In this case the generated particles are likely to be in the Morphology Region I (see Table 3) described by Elysée-Collen and Lencki (96), moving rapidly to Region II as the local concentration of ethanol is increased at the surface of the precipitated and frozen water (aqueous solution of gelatin) droplet. At this stage the solidified water would be removed by the excess of ethanol, leaving the gelatin solid behind. These authors found that considerably longer periods of glutaraldehyde contact than have been previously reported in the literature were necessary to effectively cross-link the gelatin particles. The particle size was found to be significantly affected by the pH, volume, and the concentration of the initial solution as well as the type of gelatin and temperature used (Figs. 8 and 9). The described process involved extensive washing to remove extraneous electrolytes, which meant that the microparticles, 2–5 μm in diameter, could not be preloaded with drug. However, later work by Lou and Groves (88) showed that highly water-soluble sugars and polysaccharides could be loaded by adsorption onto the surface of preformed gelatin microparticle using a lyophilization process, desorption (release) occurring by a reverse of this process. In addition, these authors demonstrated the sensitivity of the process to the temperature at which the dehydrating solvent was maintained. Here scanning electron micrographs suggested that the cross-linked microparticles were aggregates of small primary particles of ≈200 nm diameter, inviting comparison with size estimates of particles reported by Marty et al. (58) and the measurements of stable gelatin

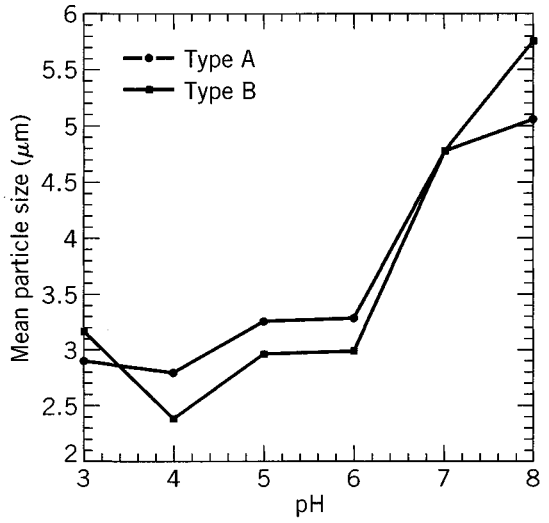


Figure 9. The relationship between pH of gelatin solutions and particle size. Type A, Bloom 60; Type B, Bloom 225. *Source:* By permission of the editor, *Pharmaceutical Research*, from Ref. 69.

chain clusters by Herning et al. (93). Lou and Groves (88) showed that the resultant size of particles was only modestly affected by the origin of the gelatin but was significantly affected by the pH of the system (Fig. 9). Moreover, systems prepared at high pH were shown to have bimodal size distributions, the small size (~2.5 μm) at low pH (≤6.0) being conserved. A second population developed with a diameter of ~5.0 μm as the pH was increased. The response surface demonstrated environmental influences for systems made at −15°C (Fig. 10).

The Toxicity of Gelatin. Although widely perceived as being innocuous, intravenous gelatin solutions adminis-

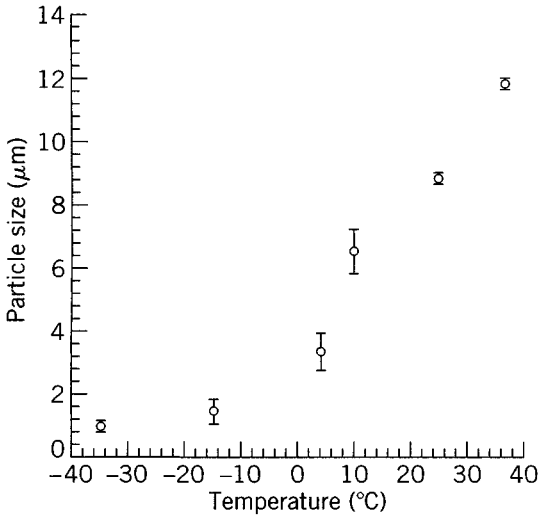


Figure 8. Effect of precipitation temperature on the size (dvn) of the resulting gelatin microparticle (lime-cured Type B, Bloom number 225). Bar = s.e., n = 3. *Source:* By permission of the editor, *Journal of Pharmacy and Pharmacology*, from Ref. 93.

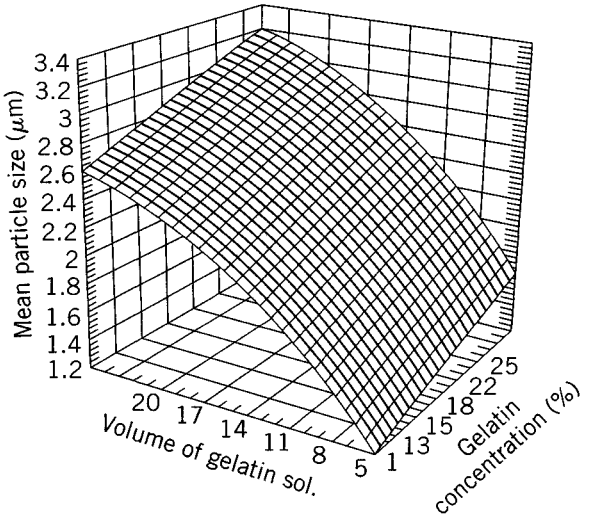


Figure 10. Response surface of the mean particle size of gelatin microparticles prepared with variation in concentration and volume of Type B, Bloom 225 gelatin solutions. *Source:* By permission of the editor, *Pharmaceutical Research*, from Ref. 69.

tered as blood expanders proved to have unexpected toxicities. Accordingly, gelatin microparticles, although perhaps less likely to suffer from the same effects, should not be viewed as being entirely without potential harm. As discussed in the following section, gelatin (and collagen) bind to fibronectin with a high affinity (98–102). By specifically binding to fibronectin, gelatin could interfere with the cell binding interactions that are characteristic of cancers but are also required in the healthy body. Infusion of gelatin-based plasma substitutes produced severe side effects due to depletion of plasma fibronectin, and this obviously limits the widespread use of gelatin solutions. Nevertheless, side effects due to the injection of gelatin microparticles, for example, would not be anticipated to be so severe or widespread. However, in human use the investigator should at least be aware of the previously observed manifestations of toxicity and anticipate possible side effects associated with the therapy. Two other more problematic issues also need to be raised here. One is the slow release of aldehydic cross-linking agents, as the cross-linked polymer disassociates in vivo. Although obviously at low levels and probably over a prolonged time, the long-term effects of local administration of glutaraldehyde have not been evaluated. The second issues of contamination of bovine sources gelatins with BSE or mad cow disease, which appears to have originated in the United Kingdom and is therefore of more immediate concern to European regulators. Although some politicians have attempted to ban all products derived from cows, including leather, gelatin products have also been somewhat irrationally targeted. Although it is true that much needs to be learned about prions, the causative agents of BSE, it is difficult to imagine anything surviving the processes used to produce pharmaceutical gelatin. Other nonbovine sources of gelatin are available, although porcine sources are not acceptable in some cultures. Moreover, at the time of writing no pharmaceutical gelatin products have been found to contain prions, so the issue is obviously a remote one that can probably be ignored.

Sterilization of Gelatin Products. Gelatin as such does not have a precise chemical structure, and solutions of gelatin are readily heat sterilized. Obvious heat damage to the general structure occurs, in particular a loss of viscosity induced by hydrolytic destruction of covalent and hydrogen beads. But, as noted earlier, gelatin has a tendency to attempt to revert to its original collagen-type structure. The structures effectively heals or reforms, and the properties for which gelatin is so widely used can be restored. However, irreversible damage undoubtably occurs, suggesting that aseptic filtration is probably required for most, if not all, injectable gelatins.

Tissue Targeting With Gelatin Microparticles. As noted in the previous section, gelatin binds avidly to fibronectin and by analogy to fibronectin-enriched surfaces. This interaction has been studied extensively starting with Engvall and Ruoslahti in 1977 (103). Fibronectin is an ubiquitous asymmetric glycoprotein or, more accurately, a family of at least 100 glycoproteins with structural homology (104). They have two similar but not identical polypeptide chains joined near their c-termini that are held together with disulfide bridges. The protein has a high molecular weight (~440 kDa) and is a normal constituent of blood plasma besides being widely deposited in connective tissues, blood vessel walls, and basement membranes. Excreted on the surface of a cell, fibronectin functions as a cell-to-cell or cell-to-basement membrane adhesive (Fig. 11). The free plasma fibronectin is considered to be the main opsonic protein modulating the functional capacity of the reticuloendothelial system. However, it is as a factor involved in the propensity of tumor cells to spread or metastasize from their site of origin to other body sites that fibronectin is of interest in the present context. As is well known, the high rate of death following diagnosis of cancer is due principally to the biological consequences of tumor cells disseminating from their original site. About half of all diagnosed cancer patients survive at least five years when treated by conventional means, involving surgery, chemotherapy, or radiotherapy alone or in combination. The failures are almost always due to metastases that removal of the primary tumor site has failed to eradicate.

The dissemination of malignant cells from a primary to a secondary site involves a complex sequence of biological events that are linked in both time and space, and although basically a very inefficient process in that thousands of cells may be detached from the tumor but only a few survive, malignancies can occur at sites well removed from the original tumor. The invasive process is assisted by the expression or recognition of a group of proteins called adhesins in the endothelial or subendothelial extracellular matrix; fibronectin is considered to have a key role in the metastatic process as an adhesion.

Because of the complexity of its function in a biological system, fibronectin has been shown to have areas or domains along its molecule that can be identified to specific binding functions. For example, as indicated in Figure 11, there are at lease two domains with direct cellular binding activity, another binds to DNA, and yet others to fibrin and to heparin. However, one domain has been specifically identified as being responsible for the binding to collagen or, in its degraded form, to gelatin.

A clear distinction need to be made between altered adhesive behavior that may come about because of a direct or indirect consequence of the neoplastic process and the exploitation by abnormal cells of the normal adhesion process. Tumor cells may need to adhere in order to proliferate or migrate through tissues but to do so may not necessarily require alternations to their normal adhesive machinery. Humphries (100) recognized this process and found that a simple peptide sequence, RGD (arginine-glycine-aspartic acid), actually in the form of a pentapeptide GRGDS, could interfere with the adhesion process. Although this peptide proved to be only effective with frequent administrations of high doses, because it had an exceptionally short half-life and it was not pharmaceutically stable, the work on RGD analogues and derivatives is still being developed a decade later. Nevertheless, the concept itself was of interest and has resulted in the development of the type of targeted drug delivery system implied in Gregordiadis's (1) definition.

Fibronectin-Targeted Gelatin Particles. In the treatment of human superficial bladder cancer with cellular suspen-

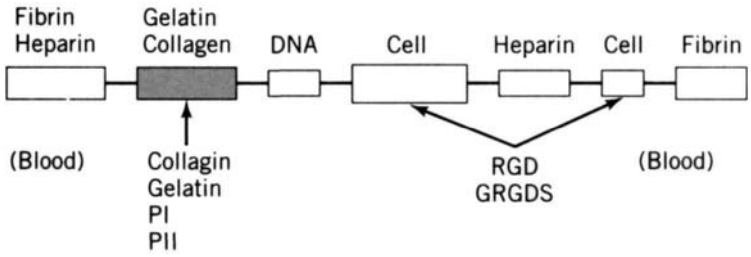


Figure 11. Schematic model of binding domains of the fibronectin molecule. *Source:* After Refs. 104–106.

sions of BCG vaccine, an attenuated living *Mycobacterium bovis*, it has become evident that the bacterial cells actually target and adhere to the tumor cells (99,100,102, 103,107). The mechanism of adhesion involves fibronection at or on the tumor cell surface and a specific fibronectin receptor on the bacterial wall thought to be cell wall proteins of the Antigen 85 homologous complex and other similar proteins of higher molecular weight. Because fibronectin has an affinity for collagen, Lou and her colleagues (99) hypothesized that gelatin would have much the same activity and measured the avidities of gelatin and gelatin microparticles for fibronectin-bearing surfaces as well as murine S180 sarcoma cells. This supposition was confirmed, and it was suggested that it might be feasible to load gelatin particles with suitable antineoplastics and substitute them for the viable microorganisms in the treatment of bladder cancer. It should be pointed out that although BCG treatment is clinically effective and the treatment of choice, most side effects associated with this treatment are due to the fact that a living organism is used and occasionally produces a form of septicemia and mild fever-like reactions as side effects. Lou later demonstrated that high molecular weight, highly water-soluble antineoplastics and thiotepa could be loaded onto gelatin microparticles and were effective in vivo (88). However, the clinical potential of this idea has not been evaluated.

Targeting of Macrophages Using Gelatin Microspheres. In a recent review by Tabata and Ikada (108) attention was drawn to the possibility of activating macrophages (Mφ) against neoplasms by incorporating biological response modifiers (BRMs). They suggested that the Mφ phagocytosed the biodegradable microspheres, in this case gelatin, digested them, and released any incorporated drug. In the case of BRMs these would be presented at the Mφ surface. These authors demonstrated that micrometer-range gelatin microparticles (mean ~1–5 μm) could be made by the water-in-oil method described for albumin. The drug, recombinant human α interferon (α-IFN), was incorporated in the initial aqueous gelatin solution so the subsequent glutaraldehyde treatment must have affected the α-IFN as well as the gelatin. Of interest was a figure in their paper showing spherical particles from approximately 200 nm to 2.0 μm diameter, suggesting a wide size distribution. The authors demonstrated the effect of glutaraldehyde on the solubility of the gelatin in the presence of collagenase. Using ^{125}I-labelled IFN demonstrated that the label was released slowly with time, although it is by no means clear if unmodified IFN was released at the same time, because it could be argued that this would be made available as the gelatin was digested by the environmental collagenase. Later, in vivo experiments involving injection into the peritoneal cavity of mice demonstrated Mφ activation by gelatin microspheres containing IFN. The authors noted that IFN-loaded gelatin particles were not always effective in preventing or suppressing tumor growth in the mouse peritoneal cavity. One must therefore ask if the IFN incorporated into the cross-linked gelatin microparticles was also affected by the glutaraldehyde treatment. No evidence was offered either way but in vitro data based on a radiolabeled release in vivo data on antineoplastic activity are not necessarily the same thing. Indeed, these authors then went on to produce a covalently bonded IFN–gelatin conjugate that was water-soluble and superior in in vivo performance to the particulate forms of the drug. It would have been interesting to determine what would have happened if the α-IFN had been loaded into preformed gelatin microparticles, thus avoiding the likely glutaraldehyde-induced structural modification of the drug.

Chitosan

The availability of chitosan, its biocompatibility, and its unique chemical and biological properties make it an attractive biomaterial for a variety of pharmaceutical applications, especially in the areas of wound dressing and drug delivery. It has been used or tested in different forms, such as tablets, matrix, and microparticles for the purpose of sustained release, controlled drug delivery, mucosal formulations and, more recently, drug absorption enhancement protein and peptide drug delivery and vaccine development (109).

Chitosan is a biocompatible and biodegradable natural biopolymer consisting of β-1→4 linked 2-amino-2-deoxy-glucopyranose (Fig. 12). It is currently manufactured commercially on the large scale by alkaline *N*-deacetylation of chitin, an abundant biopolymer isolated from the outer shells of crustaceans such as crabs and shrimps. Commercial chitosans have average molecular weights between 3.8 and 2,000 kDa and are from 66% up to 95% deacetylated (110). Chitosan has rather specific solution properties. It is only soluble at acidic pH when the free amino group ($-NH_2$) becomes protonated to form cationic amine group ($-NH_3^+$). At these pHs, chitosan has been identified as a linear polycation with an intrinsic pKa value of 6.5, independent of the degree of acetylation (111). The polycationic chitosan molecules have been found to readily adhere to negatively charged surfaces, such as skin, mucus, and proteins (112,113). Recent studies indicate that the binding of chitosan onto epithelial membranes resulted in cellular

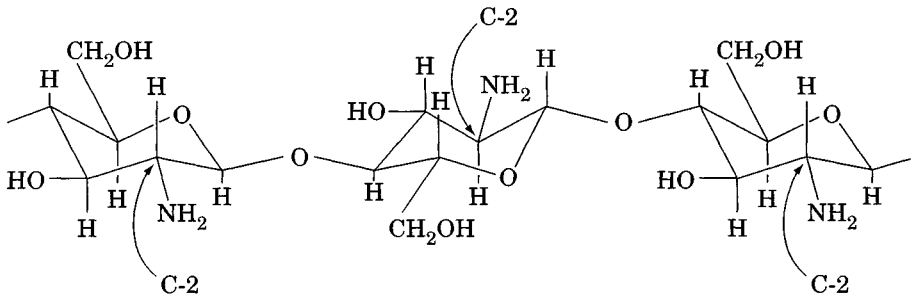


Figure 12. The repeating structural unit of chitosan.

F-actin depolymerization and disbandment of the tight junction protein ZO-1. This property is currently considered to be the major mechanism by which chitosan enhances drug adsorption (114). In vivo, chitosan is degraded by several glycosidases, primarily lysozyme and *N*-acetylglucosaminidase (115). Chitosan also has stimulatory effects on macrophages and this activity was suggested as being mainly attributable to the remaining *N*-acetylglucosamine groups (116). Activated macrophages were found to be able to accelerate the in vivo degradation of chitosan (116).

Preparation of Chitosan Micro-and Nanoparticles. High molecular weight chitosans have a low solubility at normal physiological pH, and until recently this factor may have inhibited pharmaceutical application of this otherwise attractive natural polymer. Conversion of the polymer to small particles is, however, readily achieved. Surprisingly, some authors (117,118) have described emulsification methods that, as noted earlier, require organic solvents and strong mechanical shearing forces. Apart from environmental concerns these factors are likely to be detrimental to any incorporated biological molecules and would not appear to be promising for future application. Fortunately, the solution to this problem is much simpler.

Recent studies demonstrated that chitosan nanoparticles could be formed spontaneously through ionic interaction between the positively charged amino group and negatively charged multivalent counterions, such as tripolyphosphate and sulfate groups. Novel precipitation methods based on this unique chitosan property have been developed and proved efficient in preparing chitosan nanoparticles (110,113). The attractive features of these techniques include: (*1*) the chitosan nanoparticles could be formed spontaneously through a relatively mild process, (*2*) the resultant particle size was homogenous and adjustable, and (*3*) there was no need for any organic solvents (113). Tian (119) has recently demonstrated that nanoparticles of low molecular weight chitosan are readily prepared by sonicating and stirring a solution of chitosan in aqueous acetic acid containing Tween 80 as a wetting agent while a 20% aqueous solution of sodium sulfate was added dropwise. Tian discovered that the resulting nanoparticles (diameter ~700 nm) could be stabilized for washing by cross-linking with glutaraldehyde, excess reagent being neutralized with sodium metabisulfite (Fig. 13). The lyophilized product was suitable for loading with drug by soaking the dried chitosan nanoparticles in an aqueous solution of the drug, followed by a second lyophilization process. He demonstrated the utility of the process by loading with bovine serum albumin. A adsorption/desorption process was demonstrated and information learned applied to the formulation and delivery of chitosan nanoparticles containing a bacterially derived immunostimulant, PS4. From this admittedly limited evaluation, chitosan nanoparticles appear to be an exceptionally interesting drug delivery system, with considerable potential for further application.

Sterilization of Chitosan Nanoparticles. Although effectively chitosan is a high molecular weight polymer, dilute solutions of this material can be sterilized by passing through a 200-nm filter (X.X. Tian, private communication). This would require operation of an aseptic process, with all its attendant complications and precautions. It would be unwise to attempt to heat-sterilize drug-loaded nanoparticles, especially if the drug is labile, but it is just possible that unloaded nanoparticles could be. Tian also used ethylene oxide to sterilize his nanoparticles, apparently without damage.

CONCLUSIONS

In a recent summary of the current and future status of controlled release technologies, Guy and his colleagues (120) pointed out that significant advances have been made over the past 25 years. One could not argue with this statement. However, they listed topics on current status and future possibilities without necessarily discussing the need for the technical advances needed to take the subject out of the laboratory and into the patient on a large or commercial scale. Powell (72) discussed the issues in greater depth, but the emphasis would appear to be the more immediate problem of getting vaccines (and related systems) to work on the small scale. The need to optimize sterilization procedures is, indeed, mentioned but there is no further consideration. It is true that one must run before walking. However, consideration of this essential requirement at any early stage of development may influence the design of initial experiments because, if the production process is evidently not realistic, it will be necessary to reconsider and redesign the approach being taken. Too many really innovative and impressive ideas may have died on the vine because, ultimately, production on a realistic scale as a "product" was simply impossible. Fortunately this issue is beginning to gain attention and progress is undoubtably being made. The subject is being

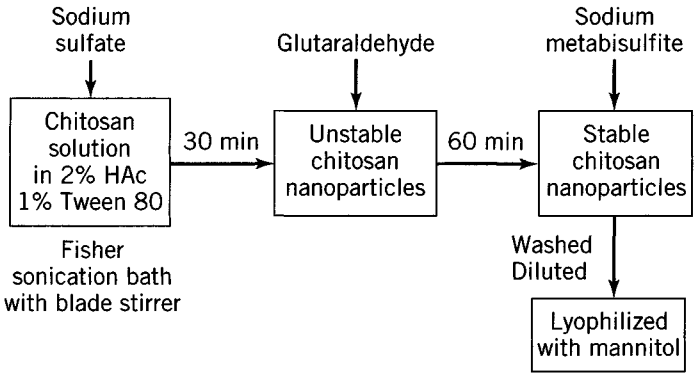


Figure 13. Preparation of chitosan nanoparticles. *Source:* From Ref. 119.

brought out into the light for deeper discussion. However, the discussion must be broad-ranged because not only is the technology of parenteral controlled release products changing and developing so also is understanding of the meaning of the word *sterility* and how it may be achieved and interpreted. The future will always be interesting!

BIBLIOGRAPHY

1. G. Gregordiadis, *Ann. N.Y. Acad. Sci.* **308**, 325–342 (1978).
2. L. Illum and S.S. Davis, *FEBS Lett.* **167**, 79–82 (1984).
3. S. Cohen and H. Bernstein, *Microparticulate Systems for the Delivery of Proteins and Vaccines*, Dekker, New York, 1996.
4. L.S.C. Wan, P.W.S. Heng, and L.W. Chan, *J. Microencapsul.* **9**(3), 309–316 (1992).
5. M. Donbrow, ed., *Microparticles and Nanoparticles in Medicine and Pharmacy*, CRC Press, Boca Raton, Fla., 1992.
6. J. Kreuter, in M. Donbrow, ed., *Microparticles and Nanoparticles in Medicine and Pharmacy*, CRC Press, Boca Raton, Fla., 1992, pp. 125–148.
7. J. Kreuter, ed., *Colloidal Drug Delivery Systems*, Dekker, New York, 1994.
8. J.L. Cleland and A.J.S. Jones, *Pharm. Res.* **13**(10), 1464–1475 (1996).
9. A. Calvör and B.W. Müller, *Pharm. Dev. Technol.* **3**(3), 297–305 (1998).
10. J.R. Robinson, ed., *Sustained and Controlled Release Drug Delivery Systems*, Dekker, New York, 1978.
11. L.L. Block, in H.A. Lieberman, M.M. Rieger, and G.S. Banker, *Pharmaceutical Dosage Forms: Disperse Systems*, 2nd ed., vol. 3, Dekker, New York, 1998, pp. 363–394.
12. P. Gilbert and D.G. Allison, *Eur. J. Parenter. Sci.* **1**, 19–23 (1996).
13. M.J. Groves, in F.M. Nordhauser and W.P. Olson, eds., *Sterilization of Drugs and Devices*, Interpharm Press, Buffalo Grove, Ill., 1998, pp. 5–44.
14. M.I. Madigan and B.L. Marrs, *Sci. Am.* **276**(4), 82–87 (1997).
15. *The United States Pharmacopeia 23*, U.S. Pharmacopeia Convention, Rockville, Md., 1995, Chapter ⟨1211⟩.
16. W.P. Olson, in F.M. Nordhauser and W.P. Olson, eds., *Sterilization of Drugs and Devices*, Interpharm Press, Buffalo Grove, Ill., 1998, pp. 471–486.
17. H.L. Melgaard and P.J. Haas, in F.M. Nordhauser and W.P. Olson, eds., *Sterilization of Drugs and Devices*, Interpharm Press, Buffalo Grove, Ill., 1998, pp. 267–310.
18. W.P. Olson, in F.M. Nordhauser and W.P. Olson, eds., *Sterilization of Drugs and Devices*, Interpharm Press, Buffalo Grove, Ill., 1998, pp. 235–265.
19. M.J. Groves, *Parenteral Products: Preparation and Quality Control of Products for Injection*, Heinemann, London, 1973.
20. W.P. Olson, in F.M. Nordhauser and W.P. Olson, eds., *Sterilization of Drugs and Devices*, Interpharm Press, Buffalo Grove, Ill., 1998, pp. 197–234.
21. B.D. Reid and B.P. Fairand, in F.M. Nordhauser and W.P. Olson, eds., *Sterilization of Drugs and Devices*, Interpharm Press, Buffalo Grove, Ill., 1998, pp. 311–392.
22. J. Dunn, in F.M. Nordhauser and W.P. Olson, eds., *Sterilization of Drugs and Devices*, Interpharm Press, Buffalo Grove, Ill., 1998, pp. 393–431.
23. M.J. Groves and R. Murty, eds., *Introduction: Aseptic Pharmaceutical Manufacturing II Applications for the 1990's*, Interpharm Press, Buffalo Grove, Ill., 1995.
24. M. Saffran et al., *Science* **233**, 1081–1084 (1986).
25. M. Saffran, C. Bedra, G.S. Kumar, and D.C. Neckers, *J. Pharm. Sci.* **77**, 33–38 (1988).
26. Eur. Pat. Appl. 0283458 (1988), M.J. Azain, T.R. Kasser, K.E. Elgenberg, and M.J. Sabacky,
27. R.C. Oppenheim et al., *Proc. Int. Symp. Controlled Release Bioact. Mater.* **15**, 54–55 (1988).
28. M. Tirrell and S. Middeman, *Biophys. J.* **23**, 121–128 (1978).
29. E. Graf and A. Nada, *Arch. Pharm. (Weinheim, Ger.)* **319**, 808–814 (1986).
30. E. Graf and A. Sakr, *Pharm. Ind.* **41**, 86–91 (1979).
31. E. Graf, A. Sakr, and A. Nada, *Pharm. Ind.* **42**, 282–286 (1981).
32. M.J. Groves and C.D. Teng, in T.J. Ahern and M.C. Manning, eds., *Pharmaceutical Biotechnology*, vol. 2, Part A, Plenum, New York, 1992, pp. 311–359.
33. R.F. Shangraw, in G.S. Banker and C.T. Rhodes, eds., *Modern Pharmaceutics*, 2nd ed., Dekker, New York, 1990, pp. 427–440.
34. P.H. Cox and F. Spanjers, *Pharm. Weekbl.* **105**, 681–687 (1970).
35. J.J. Wright and L. Illum, in M. Donbrow, ed., *Microcapsules and Nanoparticles in Pharmacy and Medicine*, CRC Press, Boca Raton, Fla., 1992, pp. 281–297.
36. D. Lasic and F. Martin, eds., *Stealth Liposomes*, CRC Press, Boca Raton, Fla., 1995.
37. I. Jalšenjak, in M. Donbrow, ed., *Microcapsules and Nanoparticles in Pharmacy and Medicine*, CRC Press, Boca Raton, Fla., 1992, pp. 193–218.

38. M. Donbrow, in M. Donbrow, ed., *Microcapsules and Nanoparticles in Medicine and Pharmacy*, CRC Press, Boca Raton, Fla., 1991, pp. 17–45.
39. J.C. Boylan, A.L. Fites, and S.L. Nail, in G.S. Banker and C.T. Rhodes, eds., *Modern Pharmaceutics*, 3rd ed., Dekker, New York, 1998, p. 459.
40. L. Öner and M.J. Groves, *Pharm. Res.* **10**(4), 621–626 (1993).
41. A. Wretlind, *Acta Chir. Scand.* **325** (Suppl.), 31–42 (1964).
42. I. Håkansson, *Acta Chem. Scand.* **20**, 2267–2281 (1966).
43. P.K. Hansrani, S.S. Davis, and M.J. Groves, *J. Parenter. Sci. Technol.* **37**, 145–150 (1983).
44. H. Heiati, N.C. Phillips, and R. Tawashi, *Pharm. Res.* **13**(9), 1406–1410 (1996).
45. M.J. Groves and C.J. Herman, *J. Pharm. Pharmacol.* **45**, 592–596 (1993).
46. C.J. Herman and M.J. Groves, *Pharm. Res.* **10**(5), 774–776 (1993).
47. O. Lutz, M. Vrachopoulou, and M.J. Groves, *J. Pharm. Pharmacol.* **46**(9), 698–703 (1994).
48. O. Lutz and M.J. Groves, *J. Pharm. Pharmacol.* **47**, 566–570 (1995).
49. M. Rosoff, in H.A. Lieberman, M.M. Rieger, and G.S. Banker, eds., *Pharmaceutical Dosage Forms: Disperse Systems*, 2nd ed., vol. 3, Dekker, New York, 1998, pp. 1–42.
50. M.J. Groves, M. Wineberg, and A.P.R. Brain, *J. Dispersion Sci. Technol.* **6**(2), 237–243 (1985).
51. M. Grit, Ph.D. Thesis, University of Utrecht, The Netherlands, 1991.
52. M. Grit, J.H. de Smidt, A. Struijke, and D.J.A. Crommelin, *Int. J. Pharm.* **50**, 1–6 (1989).
53. H.V. Weltzien, *Biochim. Biophys. Acta* **559**, 259–287 (1979).
54. M. Grit and D.J.A. Crommelin, *Pharm. Res.* **7**, suppl., Abstr. 6060 (1990).
55. M. Blanko-Pieto et al., *Pharm. Res.* **13**(7), 1127–1129 (1996).
56. K. Ciftci et al., *Int. J. Pharm.* **131**, 73–82 (1996).
57. T. Yoshioka, M. Hashiba, S. Muranishi, and K. Sezaki, *Int. J. Pharm.* **8**, 131–135 (1981).
58. J.J. Marty, R.C. Openheim, and P. Speiser, *Pharm. Acta Helv.* **53**, 17–25 (1978).
59. M.G. Wakerly, C.W. Pouton, B.J. Meakin, and F.S. Morton, *ACS Symp. Ser.* **311**, 242–255 (1986).
60. M. Cherian and J.B. Portnoff, in H.A. Lieberman, M.M. Rieger, and G.S. Banker, eds., *Pharmaceutical Dosage Forms: Disperse System*, 2nd ed., vol. 3, Dekker, New York, 1998, pp. 395–422.
61. H. Alkan-Onyuksel and K. Son, *Pharm. Res.* **9**, 1556–1560 (1992).
62. H. Alkan-Onyuksel, S. Ramakrishnan, H.P. Chai, and J.M. Pezzuto, *Pharm. Res.* **11**, 206–210 (1994).
63. R.P. Hjelm, P. Thiyagarajan, and H. Alkan-Onyuksel, *J. Phys. Chem.* **96**, 8653–8661 (1992).
64. X. Cai, D.J.W. Grant, and T.S. Wiedmann, *J. Pharm. Sci.* **86**(3), 372–377 (1997).
65. S. Ayd, Ph.D. Thesis, University of Illinois at Chicago, 1998.
66. K.K. Kwok, M.J. Groves, and D.J. Burgess, *Pharm. Res.* **8**(3), 341–344 (1991).
67. K.K. Kwok, M.J. Groves, and D.J. Burgess, *Pharm. Res.* **9**, 410–413 (1992).
68. L. Öner and M.J. Groves, *J. Pharm. Pharmacol.* **45**, 866–870 (1993).
69. S.M. Abraham, R.F. Vieth, and D.J. Burgess, *Pharm. Res.* **11**(10), S-135 (1994).
70. S.M. Abraham, R.F. Vieth, and D.J. Burgess, *Pharm. Dev. Technol.* **1**(1), 63–68 (1996).
71. F. Ruchatz, P. Kleinbudde, and B.W. Müller, *J. Pharm. Sci.* **86**(1), 101–105 (1997).
72. M.F. Powell, *Pharm. Res.* **13**(12), 1777–1785 (1996).
73. M.J. Groves, *J. Pharm. Pharmacol.* **49**(Suppl. 1), 7–15 (1997).
74. Z. Zhao and K.W. Leong, *J. Pharm. Sci.* **85**(12), 1261–1270 (1996).
75. M.A. Selkirk, *Vaccine* **14**, 668–671 (1996).
76. L.B. Lachman et al., in M.F. Powell and M.J. Newman, eds., *Vaccine Design: The Subunit and Adjuvant Approach*, Plenum, New York, 1995, pp. 659–671.
77. T.M. Allen and E.H. Moase, *Adv. Drug Delivery Rev.* **21**, 117–133 (1996).
78. J.M.J. Marjan and T.M. Allen, *Biotechnol. Adv.* **14**(2), 151–175 (1996).
79. S.S. Davis, *Vaccine* **14**, 672–676 (1996).
80. U.S. Pat. 5,290,559 (March 1, 1994), M.J. Groves (to Illinois Board of Trustees).
81. J. Fransson and A. Espander-Jansson, *J. Pharm. Pharmacol.* **48**, 1012–1015 (1996).
82. S.C. Sutton, L.A.F. Evans, M.T.S. Rinaldi, and K.A. Norton, *Pharm. Res.* **15**, 1514–1518 (1998).
83. H. Park and K. Park, *Pharm. Res.* **13**(12), 1770–1776 (1996).
84. C.D. Teng, M.H. Alkan, and M.J. Groves, *Drug Dev. Ind. Pharm.* **12**(11–13), 2325–2336 (1986).
85. I. Zolle, F. Hosain, B.A. Rhodes, and H.N. Wagner, *J. Nucl. Med.* **11**, 379–382 (1970).
86. J.M. Gallo, C.T. Hung, and D.G. Perrier, *Int. J. Pharm.* **22**, 63–68 (1984).
87. Y. Lou and M.J. Groves, *Pharm. Sci.* **1**, 355–358 (1995).
88. Y. Lou and M.J. Groves, *J. Pharm. Pharmacol.* **47**, 97–102 (1995).
89. W. Friess and G. Lee, *Biomaterials* **17**, 2289–2294 (1996).
90. W. Friess, G. Lee, and M.J. Groves, *Pharm. Dev. Technol.* **1**(2), 185–193 (1996).
91. W. Friess, W. Zhou, and M.J. Groves, *Pharm. Sci.* **2**, 121–124 (1996).
92. D.J. Prockop and D.J.S. Hulmes, in: D. Yurchenco, D. Birk, and R. Mechan eds., *Extracellular Matrix Assembly and Structure*, 1994, pp. 95–104.
93. T. Herning, M. Djabourou, J. Leblond, and G. Takerkart, *Polymer* **32**(17), 3211–3217 (1991).
94. C.A. Farrugia, Ph.D. Thesis, University of Illinois, Chicago, 1998.
95. P.M. Zavlin et al., *Anal. Ind. Gelatins High-Perform. Liq. Chromatogr. Gel Electrophoresis*, 1993.
96. B. Elysée-Collen and R.W. Lencki, *J. Agric. Food Chem.* **44**, 1651–1657 (1996).
97. H.G. Bundenberg de Jong, in H.R. Kruyt, ed., *Colloid Science*, Elsevier, New York, 1949, pp. 250–258.
98. W.P. Olson, Ph.D. Thesis, University of Illinois at Chicago, 1992.
99. Y. Lou et al., *J. Pharm. Pharmacol.* **47**, 177–181 (1995).
100. M.J. Humphries, *J. Cell Biol.* **103**, 2637–2647 (1990).
101. K. Nakamura, S. Kashiwagi, and K. Takeo, *J. Chromatogr.* **597**, 351–356 (1992).
102. T.L. Ratliffe, L.R. Kavoussi, and W.J. Catalonia, *J. Urol.* **139**, 410–414 (1988).

103. R. Engvall and K. Ruoslahti, *Int. J. Cancer* **28**, 1–5 (1977).
104. S.E. Carsons, in S.E. Carsons, ed., *Fibronectin in Health and Disease*, CRC Press, Roca Baton, Fla., 1989, pp. 1–22.
105. M.J. Humphries et al., *J. Clin. Invest.* **81**, 782–790 (1988).
106. S. Akiyama et al., *Cancer Metast. Rev.* **14**, 173–189 (1995).
107. Y. Lou, M.J. Groves, and M.E. Klegerman, *J. Pharm. Pharmacol.* **46**, 863–866 (1994).
108. Y. Tabata and Y. Ikada, *J. Pharm. Pharmacol.* **39**, 698–704 (1987).
109. L. Illum, *Pharm. Res.* **15**(9), 1326–1331 (1998).
110. A. Berthold, K. Cremer, and J. Kreuter, *J. Controlled Release* **39**, 17–25 (1996).
111. A. Domard, *Int. J. Biol. Macromol. Mol.* **9**, 98–104 (1987).
112. C.M. Lehr, J.A. Bouwstra, E.H. Schacht, and H.E. Jüninger, *Int. J. Pharm.* **78**, 43–48 (1992).
113. P. Calvo, R. Remuñan-López, C.J.L. Vila-Jato, and M.J. Alonso, *Pharm. Res.* **14**, 1431–1436 (1997).
114. N.G.M. Schipper et al., *Pharm. Res.* **14**, 923–929 (1997).
115. R.A.A. Muzzarelli, *Cell. Mol. Life Sci.* **53**, 131–140 (1997).
116. G. Peluso et al., *Biomaterials* **15**, 1215–1220 (1994).
117. B.C. Thanoo, M.C. Sunny, and A. Jayakrishnan, *J. Pharm. Pharmacol.* **44**, 283–286 (1992).
118. J. Akbuga and G. Darmaz, *Int. J. Pharm.* **111**, 217–222 (1996).
119. X.X. Tian, Ph.D. Thesis, University of Illinois at Chicago, 1998.
120. R. Guy, M. Powell, J. Fix, and K. Park, *Pharm. Res.* **13**(12), 1759 (1996).

PATENTS AND OTHER INTELLECTUAL PROPERTY RIGHTS IN DRUG DELIVERY

PATREA PABST
Arnall Golden & Gregory, LLP
Atlanta, Georgia

KEY WORDS

Copyright
Enablement
Infringement
Intellectual property
Inventor
Nonobviousness
Novelty
Patent
Trademark
Trade secret

OUTLINE

Patents
  Patentability Requirements
  Patent Term and Provisional Applications
  Patent Procedure and its Implications to Inventors
  Infringement
  Trade Secrets, Copyrights, and Trademarks
    Trade Secrets
    Copyrights
    Trademarks
  Exploiting Intellectual Property Rights
  Summary
  Bibliography

Advancements in drug delivery technology often are achieved only through substantial investment of industrial, academic, and governmental resources. Patenting of these technological advancements is frequently employed to recoup that investment, to create profits that are used in part to develop new or improved products, and to enhance a competitive commercial edge. Other forms of intellectual property protection, such as trade secrets, copyrights, and trademarks, may also be used to further protect and exploit drug delivery processes, products, and services.

One of the most frequently asked questions is, why do we need to go to the trouble and expense of patenting a composition or method? The most common reason is that protecting a new composition or method of manufacture or use provides a means for obtaining the revenue required to develop a new drug or medical treatment. With the cost of developing and obtaining regulatory approval for a new drug approaching $200 million dollars in the United States, patent rights are essential to recovering expenses. For small companies that spend more time raising money then selling products, patents and patent applications represent the only tangible assets that they can show to potential investors. For universities and other nonprofit research institutions, patents and associated know-how and, in some limited cases, trade secrets, can be used to obtain royalties from license agreements, sponsored research funding in many cases, and equity in new companies started for the purpose of exploiting the technology.

Patents and other intellectual property are valued in many different ways. For example, a process for manufacture would typically be licensed for 2–3% of the gross selling price of a product of the process. This price would be decreased if multiple licenses had to be obtained to use the process. Patents claiming compositions tend to have a greater market value, for example, between 5 and 10% of the gross selling price, owing to the perception that these patents are easier to enforce than process patents.

Enforcement, however, is a risky business. A good patent strategy is to obtain patents that claim a product, methods of manufacture, and methods of use, broadly and specifically, so that a patentee is able to assert multiple patents against an alleged infringer. Patents with broad claims will generally be easier to invalidate than more specific patents. Faced with the prospect of fighting several patents, most parties will opt for settlement. The alternative, litigation, is extraordinarily expensive for both parties and can result in the patents being invalidated or the infringer being liable not only for damages for infringement but also attorney's fees and punitive damages.

103. R. Engvall and K. Ruoslahti, *Int. J. Cancer* **28**, 1–5 (1977).
104. S.E. Carsons, in S.E. Carsons, ed., *Fibronectin in Health and Disease*, CRC Press, Roca Baton, Fla., 1989, pp. 1–22.
105. M.J. Humphries et al., *J. Clin. Invest.* **81**, 782–790 (1988).
106. S. Akiyama et al., *Cancer Metast. Rev.* **14**, 173–189 (1995).
107. Y. Lou, M.J. Groves, and M.E. Klegerman, *J. Pharm. Pharmacol.* **46**, 863–866 (1994).
108. Y. Tabata and Y. Ikada, *J. Pharm. Pharmacol.* **39**, 698–704 (1987).
109. L. Illum, *Pharm. Res.* **15**(9), 1326–1331 (1998).
110. A. Berthold, K. Cremer, and J. Kreuter, *J. Controlled Release* **39**, 17–25 (1996).
111. A. Domard, *Int. J. Biol. Macromol. Mol.* **9**, 98–104 (1987).
112. C.M. Lehr, J.A. Bouwstra, E.H. Schacht, and H.E. Jüninger, *Int. J. Pharm.* **78**, 43–48 (1992).
113. P. Calvo, R. Remuñan-López, C.J.L. Vila-Jato, and M.J. Alonso, *Pharm. Res.* **14**, 1431–1436 (1997).
114. N.G.M. Schipper et al., *Pharm. Res.* **14**, 923–929 (1997).
115. R.A.A. Muzzarelli, *Cell. Mol. Life Sci.* **53**, 131–140 (1997).
116. G. Peluso et al., *Biomaterials* **15**, 1215–1220 (1994).
117. B.C. Thanoo, M.C. Sunny, and A. Jayakrishnan, *J. Pharm. Pharmacol.* **44**, 283–286 (1992).
118. J. Akbuga and G. Darmaz, *Int. J. Pharm.* **111**, 217–222 (1996).
119. X.X. Tian, Ph.D. Thesis, University of Illinois at Chicago, 1998.
120. R. Guy, M. Powell, J. Fix, and K. Park, *Pharm. Res.* **13**(12), 1759 (1996).

PATENTS AND OTHER INTELLECTUAL PROPERTY RIGHTS IN DRUG DELIVERY

PATREA PABST
Arnall Golden & Gregory, LLP
Atlanta, Georgia

KEY WORDS

Copyright
Enablement
Infringement
Intellectual property
Inventor
Nonobviousness
Novelty
Patent
Trademark
Trade secret

OUTLINE

Patents
  Patentability Requirements
  Patent Term and Provisional Applications
  Patent Procedure and its Implications to Inventors
  Infringement
  Trade Secrets, Copyrights, and Trademarks
    Trade Secrets
    Copyrights
    Trademarks
  Exploiting Intellectual Property Rights
  Summary
  Bibliography

Advancements in drug delivery technology often are achieved only through substantial investment of industrial, academic, and governmental resources. Patenting of these technological advancements is frequently employed to recoup that investment, to create profits that are used in part to develop new or improved products, and to enhance a competitive commercial edge. Other forms of intellectual property protection, such as trade secrets, copyrights, and trademarks, may also be used to further protect and exploit drug delivery processes, products, and services.

One of the most frequently asked questions is, why do we need to go to the trouble and expense of patenting a composition or method? The most common reason is that protecting a new composition or method of manufacture or use provides a means for obtaining the revenue required to develop a new drug or medical treatment. With the cost of developing and obtaining regulatory approval for a new drug approaching $200 million dollars in the United States, patent rights are essential to recovering expenses. For small companies that spend more time raising money then selling products, patents and patent applications represent the only tangible assets that they can show to potential investors. For universities and other nonprofit research institutions, patents and associated know-how and, in some limited cases, trade secrets, can be used to obtain royalties from license agreements, sponsored research funding in many cases, and equity in new companies started for the purpose of exploiting the technology.

Patents and other intellectual property are valued in many different ways. For example, a process for manufacture would typically be licensed for 2–3% of the gross selling price of a product of the process. This price would be decreased if multiple licenses had to be obtained to use the process. Patents claiming compositions tend to have a greater market value, for example, between 5 and 10% of the gross selling price, owing to the perception that these patents are easier to enforce than process patents.

Enforcement, however, is a risky business. A good patent strategy is to obtain patents that claim a product, methods of manufacture, and methods of use, broadly and specifically, so that a patentee is able to assert multiple patents against an alleged infringer. Patents with broad claims will generally be easier to invalidate than more specific patents. Faced with the prospect of fighting several patents, most parties will opt for settlement. The alternative, litigation, is extraordinarily expensive for both parties and can result in the patents being invalidated or the infringer being liable not only for damages for infringement but also attorney's fees and punitive damages.

PATENTS

Patents are used to exclude competition, not to "protect" a product. A patent is a limited monopoly granted by a government entity to an inventor in exchange for public disclosure of the invention. The limited monopoly permits the inventor to exclude others from making, using, selling, or importing into a geographical area (such as the United States) the invention, which may be a composition, method of manufacture, or method of use, defined by the claims in the patent, in exchange for teaching the public how to make and use what is claimed. The patent system is based on the public policy objective of fostering the collective advancement of technology and science through the sharing of individual achievements. The limited monopoly conferred by a patent provides the incentive for the inventor to publicly reveal his technological development.

Patentability Requirements

Patents have basically the same requirements throughout the world. In the United States, the requirements for obtaining and asserting a patent are defined by chapter 35 of the United States Code (U.S.C.). Patents are governed exclusively by federal law.

In the late 1990s, this law in the United States has been subject to a considerable number of changes. When the United States entered into the General Agreement on Trade and Tariffs (GATT) in December 1994, major changes in effective U.S. patent term resulted. Ongoing efforts to change the U.S. Patent and Trademark Office from a prominent agency to a governmental corporation, primarily to avoid further diversion of patent office fees to other government agencies, may result in even more changes to the U.S. patent law.

Further changes to the requirements for obtaining a patent, and in the enforceability of method of medical treatment claims, have resulted from reactionary changes in the laws following unpopular court decisions. Especially in the biotechnology area, the late 1990s are becoming known for the swift and drastic decisions by the U.S. Court of Appeals for the Federal Circuit, invalidating patents on the grounds that the claims are not enabled by the specifications.

Patentable Subject Matter. In general, patentable subject matter includes compositions, methods of manufacture, and methods of use (1). Compositions may include, for example, biodegradable polymeric microparticles containing a therapeutic agent or a bioadhesive compound useful for targeted drug delivery within the body. Methods of manufacture may be directed to, for example, a process for creating a unique drug delivery device. Methods of use may entail methods for administration of therapeutic compositions or surgical implantation of, for example, a synthetic tissue matrix containing implanted isolated cells that secrete insulin.

Although the law provides for patenting of compositions, methods of manufacture, and methods of use, biotechnology can present a problem under U.S. patent law when the subject matter moves away from the realm of the artificial or "things engineered by the hand of man" to a blend or chimera of "artificial" and "natural" (2). An example is when one blends cells and a matrix to form a cell matrix structure that is then implanted in a patient. Then the matrix degrades to leave only implanted cells and/or the patient's own tissue grows into an implanted matrix structure, which then degrades. At what point do these materials become the patient and cease to be patentable subject matter? Ethical issues may arise due to overlap between patient material and traditional subject matter, particularly in those cases involving dissociated isolated cells, biodegradable matrices for implantation, and polymeric materials for altering cell/cell interaction (such as adhesion or restenosis) as well as materials for implantation that are designed to remain in the body, such as stainless steel hip replacements or cryopreserved pig valves.

Outside of the United States, methods of treatment of humans or other animals is generally not patentable subject matter. For example, although surgical instruments, drugs, or devices used in surgery are patentable, surgical treatments are not patentable subject matter. Therefore, one cannot obtain a patent on a method for surgically treating a patient. Typically, while this subject matter is not patentable, the compositions and methods of manufacture for use in treating patients are patentable subject matter. Claims may be obtained to the composition per se that is to be implanted. In Europe, claims can be obtained to a first, or even a second, use of the material when the material itself is known. However, the patentability is quite limited in individual countries and in the European Patent Office for policy and ethical reasons. Generally, patent offices in Asian countries are far less flexible than the European Patent Office in this matter. As a result, patent attorneys have adopted a number of strategic approaches to obtain protection equivalent to that which is available in the United States. For example, one may draft claims directed to methods of manufacture of such materials as well as to methods of use that are defined by the composition rather than the method of use steps.

Novelty. The second requirement for patentability is novelty (3). Novelty, in its simplest terms, means that no one, including the applicant for the patent, has publicly used or described that which is being claimed prior to filing an application for patent. In the United States, there is an exception when the publication is made less than 1 year prior to filing of the patent application. The publication can be "removed" as prior art if the applicants are able to demonstrate that prior to the publication, they conceived and diligently reduced to practice what they are claiming.

What constitutes a publication? Generally, a publication is any oral, written, or physical description that conveys to the public that which applicant would like to claim. It may be a talk at the proceedings of a society (including any slides presented), an article in a scientific journal, a grant application that is awarded, a thesis, or even an offer for sale or a press release. A critical requirement is that the publication must be enabling, that is, it must convey to one of ordinary skill in the art how to make and use that which is being claimed. Public use means more than using the composition or method in one's laboratory. However, it

can include even a one-patient study that is reported during clinical rounds or at a presentation at which a drug company or surgical supply representative is present. The courts, in many cases, have had to interpret what it means to be publicly available. A frequent question is when is a student's thesis available as prior art. Courts have now held that once the thesis is cataloged, it is publicly available, because it has been entered into a computer database that one searching the database will be able to access (4). Accordingly, the publication date of a thesis is the date on which the thesis is cataloged, not the date on which it is defended or signed by the thesis committee. Slides that are not distributed but that are shown at an oral presentation are considered to be publications, particularly if the meeting is attended by those skilled in the art who would be able to understand and use the information in the slides.

Disclosures to another party under the terms of a confidentiality agreement are not publications. Uses that are strictly experimental may not be public disclosures, if, among other aspects, they are designed to determine if that which is to be claimed will work and if any other parties who are involved are clearly informed that the studies are experimental in nature. If something is an announcement that does not enable one of ordinary skill in the art to use or make that which is claimed, then the disclosure is not a publication. For example, an announcement could be a statement made to the press that researchers X and Y have discovered a cure for cancer. Because the announcement does not tell one of ordinary skill in the art how to cure cancer, it is not enabling. However, enablement can be difficult to prove, and standards may change over time. A recent court case in which the question of whether a publication was enabling related to the development of a transdermal patch for delivery of nicotine (5). The court found that a prior publication referring to transdermal patches for drug delivery mentioned that the drug in the transdermal patch for treatment of heart disease could be replaced with nicotine for assisting patients in quitting smoking. The court held that the article disclosed or made obvious the transdermal patch for delivery of nicotine claimed by the applicant because the applicant merely took the transdermal patch described in the article, put nicotine in it, and demonstrated that the nicotine was delivered and would work exactly as predicted based on delivery of the drug for treatment of heart disease. Even though there was no information relating to the exact dosage or schedule or how the drug was to be incorporated into the transdermal patch, the publication was enabling because those of ordinary skill in the art would have been able to determine the dosage and how to put the nicotine in the transdermal patch without undue experimentation.

Nonobviousness or Inventive Step. The third requirement for patentability is that the claimed method or composition must be nonobvious to those of ordinary skill in the art from what is publicly known (6). This is usefully referred to outside of the United States as a requirement for an inventive step. In the 1960s, the U.S. Supreme Court carefully analyzed nonobviousness and those factors that are to be considered in determining whether that which is claimed is obvious from the prior art (7). This analysis is a fact-based determination, involving not only the elements that are claimed but also the level of skill in the art and the expectation or predictability that the claimed method or composition would perform as predicted, actual success in the marketplace, long-felt need, and whether there are unexpected results. If one has no better than a 50–50 chance that a particular method may work and the method works, it is arguably not obvious, although it may be obvious to try. If one tries something and the results are vastly different from what was expected, then the results are not obvious. For example, if one administered two drugs each in the dosage known to yield a particular effect and the combination results in a substantially greater effect than the sum of the individual effects of the two drugs, resulting in the ability to use a much lower dosage of each drug than expected, then one would have unexpected results, or synergy. If the prior art teaches away from what the applicant has done, this result would support a finding of nonobviousness. For example, if the prior art states that one cannot administer drugs transdermally using ultrasound except at a very high frequency, then it may be nonobvious if the applicant for a patent finds that the same or better results are obtained using a very low frequency. Many other considerations factor into whether a claimed composition or method is obvious in view of the prior art.

Enablement and Best Mode. The fourth requirement for patentability is enablement and, in the United States only, disclosure of the best mode for practicing the invention (8). A written description is also required, but enablement and the written description requirement usually are considered together. To obtain a patent, the applicant must describe that which is claimed in sufficient detail and with appropriate methods and sources of reagents or other materials or equipment to enable one of ordinary skill in the art to make and use that which is claimed. This sounds far simpler than it actually is in practice. In many cases, particularly when coming out of a university study or a start-up company, the invention that applicants would like to claim is that which the applicant intends to develop over the next several years, based on a limited amount of data available at the time of filing. Particularly in the case of universities, where the applicant must publish or has submitted grant applications (which in and of themselves constitute prior art once they are awarded), the difficulty is in describing that which has not yet been done. The application must not only describe a specific limited example but must also describe the various ways in which one intends to practice that which is claimed.

The purpose of a patent is to exclude the competition from making and using that which is claimed, not to "protect" a product—a frequent misconception of patents. To exclude competition, one must describe and claim not only that which one intends to practice but also that which another party could practice in competition with the patentee. What does this mean in real terms? It means that the applicant for a patent must describe her preferred method, which is known as of the date of filing, the preferred embodiments that she or her company intends to market, and any embodiments that a competitor could make and use in competition with the applicant's product.

Invention usually consists of two steps: conception and reduction to practice. There are two kinds of reduction to practice: actual and constructive. Constructive practice means that the applicant has described in the application for patent *how* to make and use that which is claimed but has not actually made and used what is claimed. This may be as simple as stating that although a biodegradable polymer such as poly(lactic acid-*co*-glycolic acid) is preferred for making a matrix for drug delivery, other biodegradable polymers such as poly(orthoesters)s or poly(anhydride)s could also be used. It may be less obvious that other drugs may be used when only one example showing reduction to practice of a type of drug is available. The rule of thumb in this case is the level of predictability. Therefore, in stating what kind of drugs one could deliver using the claimed technology, one might list a wide variety of drugs based on the data available with one type of drug. However, delivery of a peptide or a very hydrophobic compound, which usually are viewed as difficult to deliver, may or may not be possible to list based on data obtained with a drug that is relatively easy to delivery, such as a sugar or low-molecular-weight dye. Being too predictive (i.e., engaging in extensive constructive reduction to practice), which includes "nonenabling" or non-enabled technology, may in some cases be a detriment during prosecution of subsequently filed applications because the examiner may cite the earlier work as making obvious the applicant's subsequent work. Patent attorneys frequently must play a balancing game in determining how far to go with constructive reduction to practice to exclude competitors while not eliminating the applicant's own ability to obtain additional, subsequent patent protection.

In the United States, there is a requirement to disclose the best mode for practicing that which is claimed at the time of filing the application. No similar requirement exists outside of the United States. Because most applicants file the same application in the United States as outside of the United States, U.S. applicants frequently disclose their best mode in foreign-filed applications. Furthermore, U.S. applications are not published until they are issued as a patent, whereas applications filed in other countries are published 18 months after their earliest priority date. Thus, it may be desirable in some cases to omit the preferred embodiment as of the date of the foreign filing to prevent one's competitors from knowing the best mode for practicing the invention until the U.S. patent is issued, which may be many years after publication of the corresponding foreign application. However, this strategy may create a problem, as patent laws vary from country to country. In particular, Japan has, in the past, required one to provide examples of that which one intends to claim, thus limiting available protection.

Patent Term and Provisional Applications

A patent is awarded by individual government entities for a defined period of time. In most cases that period of time will run 20 years from the initial date of filing an application for patent. In some cases, the term can be shortened, for example, by disclaimers of patent term in view of earlier issued patents, or lengthened, owing to delays relating to appeals or regulatory approval. Provisional applications are useful for delaying the filing of a utility patent application while simultaneously serving to establish priority over subject matter disclosed within the provisional application.

Patent Term. Under the revised U.S. patent law that was enacted as a result of implementation of GATT, the term of a patent is 20 years from the original date of filing or the filing date of the earlier application to which priority is claimed. Applicants therefore have more incentive to prosecute all claims in a single application to minimize costs for prosecuting and maintaining the patent. Under the law in effect prior to June 8, 1995, the patent term was 17 years from the date of issue in the United States. Divisional applications were a commonly used method to extent patent protection to encompass different aspects of the technology over a period of time much greater than 17 years. For example, an application would be filed in 1990, and a single inventive concept (e.g., the composition) would be prosecuted in the first application. Three years later, when those claims were allowable and a patent was to issue, a divisional application would be filed with another set of the claims that had been restricted out of the original application. This divisional application would be prosecuted for another 2 to 3 years, the claims would be determined to be allowable, the second patent would issue with a 17-year term, and a third divisional application would be filed. The result is that patents on related technology would issue sequentially over several years, increasing the effective term of patent protection beyond 20 years. Under the new law, this mechanism to extend patent protection is not possible.

GATT was signed into law in the United States on December 7, 1994, and the initial provisions affecting U.S. patent practice were implemented June 8, 1995. The most significant changes arising from enactment of that agreement, now called the Uruguay Round Act, were changes in the patent term in the United States, the implementation of provisional patent applications, and the broadening of what constitutes infringement in the United States. The change in patent term has already been discussed. For those applications filed before June 8, 1995, the term of any issuing patent is 17 years from the date of issue or 20 years from the filing date, whichever is longer. The term of any patent issued on an application filed June 8, 1995 or later is 20 years from the earliest claimed priority date. Extensions of terms are available upon delays in issuance arising from appeals or interferences. Additional extensions of terms are available for delays in obtaining regulatory approval by the U.S. Food & Drug Administration (FDA) for a device or a drug. Legislation is currently pending that would further revise patent terms in the United States.

Because biotechnology is a complex field, especially in the areas of patentable subject matter and enablement, many of the general observations relating to patents may not be as directly applicable to more conventional patentable subject matter. For example, the U.S. Patent Office has consistently maintained that the change from a 17-year term from the date of issue to a 20-year term from

the earliest priority date will not result in a significant loss of patent right. However, because the Patent Office applies such a stringent examination proceeding under §112 (enablement) in the biotechnology area, its assertion is likely untrue. Issue time in these cases typically has been considerably longer, not uncommonly taking as many as 5 to 7 years from the original priority date. The result is that these complex biotechnology patents will have a substantially shortened term as compared with many other types of patents. Because a patent extension can still be obtained for delays due to regulatory issues involving the FDA, as well as for appeals to the Board of Patent Appeals and Interferences, those in the United States who believe that their patent rights will be limited in term due to delays in prosecution should avail themselves of the Patent Extension Act if at all possible. One must bear in mind, however, that an extension for regulatory delays can only be obtained on *one* patent for any particular product or process; thus, the inventor or licensee with multiple, related patents clearly should choose the most important patent or the patent subject to the greatest increase in patent term when facing such a situation. The patent that is to be extended must be brought to the attention of the FDA. Following FDA approval of the claimed product or process, the extension must be applied for in a timely fashion.

Provisional Patent Applications. Provisional patent applications, while new to the United States, have been utilized for many years in other countries, such as the United Kingdom and Australia. These applications are a mechanism for obtaining a filing date at minimal cost and with fewer requirements for completeness of the application and determination of the inventive entity for a period of 1 year. The provisional application ceases to exist 12 months after the date of filing. If an application is filed as a provisional application, it can be converted to a standard utility application at any time during the 12-month period after filing. Alternatively, it can serve as a basis for a claim to priority in a subsequently filed utility application if the utility application is filed prior to the expiration of the 1-year life of the provisional application.

Although touted as a great benefit to the small entity or individual applicant, provisional applications have the same requirements for disclosure as a standard utility application. Failure in the provisional application to completely disclose and enable that which is subsequently claimed in an utility application can result in a loss of the claim to priority to the provisional application if that which is claimed is not enabled. Merely filing an article that will be published or presented to avoid loss of foreign rights usually will not comply with the enablement requirements and therefore will not serve as an adequate basis for priority. It is essential that applicants who file provisional applications based on an article amplify the description to encompass other embodiments and to provide the basis by which one of ordinary skill in the art can practice that which is claimed. Application sections that are not required for enablement but that are typically included in a utility application include the background of the invention, the problems that the claimed invention addresses, and the claims. These sections can be omitted from the provisional application, thus saving time and money in preparing the application. In many cases, fairly standard language can be used to expand or broaden the description in an article to meet the enablement requirements, providing a means for those with limited amounts of time or money to protect that which they are disclosing with minimum risk and expenditure.

The World Intellectual Property Organization (WIPO), which implements the provisions of the Patent Cooperative Treaty (PCT) and the European Patent Office, has confirmed that U.S. provisional applications serve as an adequate basis for a claim to priority in corresponding foreign file applications. However, under the Patent Convention, all foreign applications that claim priority from a previously filed application must still be filed within 1 year of the U.S. filing date or the filing date of the country in which the first application is originally filed.

Patent Procedure and its Implications to Inventors

An elaborate, detailed body of law and regulations has evolved to govern the granting of patents. These laws and regulations define, among other things, (*1*) the procedural steps that the Patent Office and applicant may undergo, (*2*) which individuals actually are the inventors of a particular claimed invention, and (*3*) the number of inventions or embodiments of an invention that properly can be claimed in a single patent. These laws and regulations also suggest certain beneficial habits, such as record keeping, that research scientists and other would-be inventors should undertake to facilitate issuance and enforcement of their patents.

Application Procedure. When a patent application is filed in the United States, it will be assigned to an examiner for review of the relevant prior art and for prosecution. The examiner may restrict the claims into more than one group, if, in his view, the claims are directed to patentably distinct inventions (see "Restriction Practice/Unity of Invention"). The nonelected claims can then be filed in divisional applications, which have the same effective filing date but issue as separate patents. The examiner likely will issue one or more office actions, objecting to the specification or rejecting the claims as lacking novelty, being obvious, not enabling the breadth of the claims, being indefinite, or a combination thereof. The applicant can amend the claims and present arguments and supporting data to overcome the rejections. The specification, or description, cannot be amended to add new matter once the application is filed. In many cases, an agreement will be reached as to what claims are allowable, and a patent will issue. In the event that the examiner finally rejects the claim and the applicant has exhausted her opportunities to respond to the rejections, an appeal to the Board of Patent Appeals and Interferences can be filed. A decision by the Board, which can be based not only on argument and data submitted during the prosecution of the application but also an oral hearing, typically will require 3 to 6 years. The applicant's only recourse following a negative decision by the Board is to file an appeal in the U.S. Court of Appeals for the Federal Circuit.

In the United States, patent applications are typically examined by a single examiner. In the European Patent Office, examination may be conducted by an examiner other than the one who conducted the initial search and issuance of a search report. If the applicant in the European Patent Office requests oral proceedings, at which oral arguments may be presented, the oral proceedings are held before a panel of three examiners, not just the original examiner. In contrast, the U.S. proceedings are between the applicant and the examiner, although the examiner's supervisor or a quality control specialist may be asked to attend if an in-person interview is held. In all cases, there are appeal procedures if an examiner maintains his rejection of the claims, asserting that the claims lack novelty, are obvious, or are insufficiently enabled.

Inventorship. The U.S. Constitution provides that inventors have the exclusive right to their discoveries (9). An application for patent must be made by the inventor, or under certain circumstances (such as when the inventor is dead) by persons on behalf of the inventor (10). When more than one person made the invention, the inventors are required to file jointly "even though they did not physically work together or at the same time, each did not make the same type or amount of contribution, or each did not make a contribution to the subject matter of every claim of the patent" (11). A patent may be invalidated if it names one who is not an inventor or if it fails to name an inventor, however, these errors may be corrected if they were not committed with an intention to deceive (12).

In a nutshell, an inventor is one who conceives and/or reduces to practice the claimed invention on his own and not at the direction of another. University settings are somewhat unique when it comes to determining what is prior art and what is the invention of another because it is often difficult to determine who is the inventor. When one attempts to remove prior art by demonstrating that one has conceived and reduced practice prior to the publication, one must first determine who the inventors are and whether the publication is in fact a publication by another entity. If the publication is the inventors' own, then it is easier to swear behind because they must have conceived and reduced to practice prior to that publication. Merely because a publication is coauthored by one of the inventors does not mean that the publication is the inventors' own work. There must be complete identity between the named authors and the inventors for the publication to be the inventors' own work. Publications typically will include coauthors who do not meet the legal definition of an inventor.

To determine who the inventors are, one must first ascertain that which is claimed. Second, one must determine what is already in the prior art; one is not an inventor if the claimed matter is already in the prior art. For example, if one is claiming a polymeric drug delivery device and the claim defines the matrix structure as formed from biodegradable polymer, then this particular element is probably already in the prior art, and that element alone would not be the invention of any named inventor upon the application for patent. However, if the polymeric matrix were defined as having a particular structure or shape or composition that has not previously been defined, then the individual (or individuals) who determines that shape or structure or composition would be an inventor. In methods for manufacture, the person who is in the laboratory using the method may or may not be an inventor. If this person has been told by another to go and make composition X using steps A, B, and C, then the person who performs the method is not an inventor—even if there is some optimization of the concentration or selection of reagents or conditions under which they are combined. If, however, that person determines that it is essential to use a concentration 10 times greater than what she has been told to make it work, then she may be an inventor of the method of use. A patent may name multiple parties as inventors. They do not all have to be inventors of each and every claim that defines the invention. One person may be an inventor of composition claims, another the method of manufacture claims, and yet another the method of use claims. Inventorship may need to be corrected following a restriction requirement or after cancellation or amendment of the claims.

The definition of *inventor* elicits questions about the definitions of *conception* and *reduction to practice*. In a university research laboratory, has a graduate student participated in the conception of his professor's invention if he conducted the experiments under her direction that resulted in the reduction to practice, that is, the synthesis of the claimed protein? Did the professor conceive the invention if she thought of the general idea and desired result but left it to the graduate student to figure out how to synthesize the protein? Is the professor's conception of a protein and the detailed steps of producing it an invention if she has not yet actually reduced her idea to practice by synthesizing the protein? And in a different laboratory, is a technician an inventor if he added bearings to the design that the supervising engineer told him to build? In each case, who, if anyone, is an inventor?

Conception is "the formation in the mind of the inventor of a definite and permanent idea of the complete and operative invention as it is thereafter to be applied in practice," such that a person of ordinary skill in the art would be enabled to convert the idea to tangible form without extensive research or experimentation (13). Usually, one who conceives the inventive idea, or part of it, is an inventor, while those who perform the ordinary interim experimentation under the direction of the inventor in reducing the inventive concept to practice are not defined as inventors. Conception followed by reduction to practice is a common sequence during invention, but invention may result from other sequences of events. For example, conception and reduction to practice may occur together, or unexpected discovery coupled with recognition of the discovery as something new and useful may occur without previous conception. For invention to be complete, the inventor's conception must include a clear idea of how the new product, process, or machine can be reduced to practice, or put into a tangible form. Reduction to practice may be done by persons other than the inventor if they work under his or her direction. In both university and commercial laboratories, an invention may occur through discovery without any previous conception. This type of invention is not formulated by conception of the inventive idea followed by

reduction to practice, as described earlier. Rather, the invention occurs through discovery coupled with recognition that the product, process, machine, or combination is new and useful. Experimentation involved in reduction to practice may also be part of conception.

Although coauthors may choose not to be named on a paper, the law requires that every person who contributes any part of what is claimed in a patent application must be named. If, in the course of prosecution of the patent application, all claims that reflect the contribution of one inventor are cancelled or rejected, that inventor's name must also be removed. There is an implicit lack of equality in coauthorship. Generally, the first or last listed author is considered to be the primary originator of the new ideas and data in the paper, and the others are assumed to be secondary collaborators. Joint inventors, however, are equal in the rights of patent that accrue to them, having a joint and undivided interest, unless they agree otherwise (14). Even though they did not conceive exactly the same idea together or each created a different part of the whole invention or the contribution of one was only a small but essential part of the invention, all are joint inventors and share an equal right to exclude others from making, using, or selling the claimed invention. In practice, university policy usually dictates that joint inventors assign ownership of the patent to the university, while the royalties that may accrue if the patent is licensed and the invention is marketed are allocated between the university and the inventors. The inventors' share of the royalties is distributed equally among them, unless they have contracted otherwise.

Ownership of the technology claimed in a patent is contractual. Unlike inventorship, ownership can be transferred by one or all of the inventors to one or more other entities merely by executing an agreement. Rights to use the technology can be granted by licensing of the patent to an entity by the owner of the technology. Once ownership is transferred from the inventors, they no longer have the right to allow a third party to make, use, sell, offer to sell, or impart that which is claimed. In fact, if a patent is exclusively licensed, or assigned, to another party, then the inventor and/or the assignee transferring the rights away will no longer be able to use the technology. In many cases, it may be important to retain the right to use the technology for noncommercial purposes (i.e., further research and development).

Provisional applications differ from standard utility applications in that there is no requirement to name all, or even the correct, inventors; neither do the inventors have to file a disclaimer of inventorship stating they believe they are the correct inventors of the claimed technology. This is in keeping with the absence of a requirement for having claims defining what applicants think constitutes their invention.

Outside of the United States, patent applications frequently are filed by the assignee rather than by the inventors. Inventorship is not usually a basis for challenging a foreign patent, and declarations of inventorship are not always required. A patent applicant may not even need an assignment to file and prosecute the foreign patent application.

Restriction Practice/Unity of Invention. A patent must have claims directed solely to a single invention (15). Guidelines for determining what constitutes a single invention in the United States are published in the *Manual of Patent Examining Procedures* (MPEP). For example, if the applicant has claims to a composition, a method of making that composition, and the method for using the composition, an examiner in the U.S. Patent Office may determine that multiple inventions are defined by the claims in the application as filed, and the examiner will require cancellation of the claims to all but the method of manufacture or use or composition from the application. The applicant would then be allowed to prosecute the elected claims in that application and file what are referred to as divisional applications with the nonelected claims, which may ultimately issue as a second or third patent. The effective priority date would still be the original filing date.

The standards for "unity of invention" are highly variable even within the United States, and U.S. standards are at wide variance with the standards of most foreign patent offices. One advantage of prosecuting PCT applications (discussed later) in the European Patent Office is the lower cost owing to far fewer restrictions being made.

Duty of Disclosure. Another unique requirement of the U.S. patent law is the duty of disclosure, described by Chapter 37 of the Code of Federal Regulations (C.F.R.), § 1.56. Applicants are required to submit to the examiner in the U.S. Patent Office copies of all publications or other materials that may be determined by an examiner to be material to examination of the claimed subject matter (16). Foreign publications must be accompanied by an English translation if they are not in English, although in some cases this may be limited to an abstract. Failure to cite relevant prior art to the Patent Office can result in a subsequent finding by an appropriate court of jurisdiction that the patent is invalid for fraud and violation of the duty of disclosure. Under the current standard, the applicant is not required to describe the relevance of the cited publication but may merely cite the publication and provide a copy to the examiner for the examiner's review. When many publications are being cited to the Patent Office, it may facilitate review to group the publications or even distinguish those that the applicant believes are most relevant. As discussed earlier, prior art includes oral or written publications made prior to applicant's filing date by applicant or any other entity. Relevance of material is more difficult to define. This requirement is in the process of again being revised and may soon change.

Record Keeping. It is extremely important in the intellectual property area that proper records be maintained. Laboratory notebooks should be completed and maintained in chronological order. Notebook pages should be consecutively numbered, entries should be recorded in ink, and each page should be signed and dated by the party making the entry. Furthermore, it is preferred that each page be witnessed at a time contemporaneous to the date the entries are made by one who is qualified to understand what is being entered on the page. The party does not have

to completely understand every aspect of the entry; he or she merely must be qualified to say, with some degree of certainty, what the entries on that page were.

Laboratory notebooks are used to show the origin of an invention. This may be important if there is a dispute as to ownership, if there is a dispute as to inventorship, or to prove priority of inventorship where, in the United States, patent rights are awarded to the first party to invent as opposed to the first party to file a patent application. Proceedings conducted by the U.S. Patent Office to determine priority of inventorship are referred to as *interferences*. The laws and regulations governing interferences were changed following enactment of GATT to allow parties other than those residing and inventing in the United States to obtain a patent in a dispute with another party also claiming the same subject matter by demonstrating that they were the first to conceive and reduce to practice. Interference law is very complicated. In the biotechnology area, the dates of inventorship are frequently within weeks of each other. Moreover, the courts have increasingly altered the law regarding what is conception and reduction to practice as applied to the biotechnology field (17). As a result, it has become much more difficult to predict what acts ultimately will be critical in showing priority of inventorship. Accordingly, accurate record keeping by all members of a research group is extremely important.

Infringement

In addition to changes in patent term and creation of provisional patent applications, passage of GATT changed the definition of infringement in the United States. One who, without authority, makes, uses, offers to sell, or sells any patented invention within the United States or imports into the United States any patented invention during the term of the patent therefor infringes the patent (18). In the United States, a claim for infringement cannot be made until after issuance of the patent. In some other countries, including the European Patent Convention countries, translated claims can be filed prior to issuance of the patent, and damages can be backdated to the date of filing the translated claim once the patent issues. In the United States, a patent application is secret until it is issued as a patent, at which point it is published and can be asserted against parties whom the patent owner or exclusive licensee of the patent believes are infringing the claims, that is, against those they believe are making, using, selling, or importing subject matter falling within the scope of the issued patent's claims.

A party who believes that an issued U.S. patent is not valid may file a request for reexamination, citing art that was not made of record during the prosecution of the patent. If the patent is asserted against the party, that party may go into federal district court and ask for a declaratory judgment that the patent claims are invalid or that they are not infringed. In Europe, and in many other countries, there is a postgrant opposition proceeding available. In the European Patent Office, there is also a process whereby one may file observations during the prosecution of an application, which is public, unlike in the United States. Third-party observations can be used as a means to bring relevant prior art, mischaracterized prior art, or problems relating to enablement to the attention of the European patent examiner and may result in revocation of the patent or narrowing of the claims.

TRADE SECRETS, COPYRIGHTS, AND TRADEMARKS

Other types of intellectual property that may have applicability to drug delivery technology include trade secrets and, to a lesser degree, copyrights and trademarks. Trade secret protection of an invention may be an appropriate alternative to patent protection for an invention or discovery in certain competitive circumstances. Copyrights and trademarks, which do not protect ideas or inventions, may have value in protecting other facets of a business related to the drug delivery technology. These three types of intellectual property are only briefly described in the following sections.

Trade Secrets

Trade secrets can be compositions or methods of manufacture or even uses that are maintained in secrecy. Most companies that have optimized methods for manufacture (e.g., methods for processing polymers to impart the most desirable physical and chemical properties) keep them secret. Trade secrets are unlimited in term but must be actively protected; they are lost if another party independently derives the same method or composition that is being maintained as a trade secret. Unlike patents, trade secrets are defined by and enforced pursuant to state laws. Trade secrets may be protected by asserting laws relating specifically to trade secrets as well as unfair competition and business practices.

To maintain the process or product as a secret, one must (*1*) not disclose the process or product in public and (*2*) take affirmative steps to protect the information from public disclosure. This duty includes informing parties who may accidentally become aware of the technology, as well as those who are intentionally informed regarding the technology, that the material is a trade secret and is to be maintained in confidence. Laboratory notebooks describing processes or products that are considered proprietary should be maintained in designated areas labeled "confidential" or "restricted access." Employees involved in the use of the trade secrets should be informed that the material is to be maintained as confidential and that breach of any agreement with the company by disclosing the trade secrets to a third party could result in irreparable harm and therefore be subject to injunctive relief. Trade secrets cease to be trade secrets upon public disclosure, as already discussed, or when they are independently developed by another party. If a third party independently develops the trade secret, the original holder of the trade secret has no recourse unless she can prove that the secret was acquired by theft, fraud, or other improper means. Unlike patents, which have a defined term during which the patentee can exclude others from competition, trade secrets are subject to no similar limitation. One of the most famous trade secrets is the formula for the original Coca-Cola®, which has been kept in secret for decades and is enormously valuable,

demonstrating that it is not just patents that have value as an asset to a company.

Copyrights

Copyright protects original works of authorship fixed in any tangible medium of expression (19). Unlike patent and trade secret law, however, copyrights do not protect an idea but only the expression of that idea. Copyright protection may extend, for example, to visual depictions of products or to advertising material associated with the use and sale of products. Also, copyright may protect computer software programs, publications, protocols, or other materials. In many cases where the author is employed or engaged as a consultant, the copyrights will be owned by the party contracting with the author, the journal publishing the work, or the employer. Copyrights, which also can be extremely valuable, are transferable and enforceable under U.S. law and in many foreign jurisdictions as a result of international agreements relating to copyrights.

Trademarks

Trademarks are typically associated with the sale of goods or services and are used to denote the origin of the goods or services. Advantages of trademarks are that they are not limited in term, and rights arise upon use in either intra- or interstate commerce. One very well-known trademark is Coca-Cola®, which has been in continuous use since before the turn of the century. The company has used the trademark in combination with retaining the formula as a trade secret to create enormous value for itself. A company name, as well as a product name, can be a trademark. A trademark can be a name design or combination thereof. The trademark cannot be generic or totally descriptive of the product, and it must be distinct enough from other trademarks in a similar field of use or similar good or service to avoid any likelihood of confusion as to the origin of the good or service among the consumers of the trademark good or service. Trademarks can be protected under either state or federal law. An applicant for a trademark registration must show that the trademark has been used in *intra*state commerce for a state registration and *inter*state commerce for a federal registration. A federal "intent to use" application can be used to preserve the right to use a trademark prior to actual use in commerce. This provides for an initial determination of the registerability of the trademark, in other words, that the mark is not already in use by another in a way that would be confusingly similar to the applicant's use and that the mark is not generic or descriptive and not contrary to the public interest.

EXPLOITING INTELLECTUAL PROPERTY RIGHTS

As is now evident, intellectual property rights help increase the value of technology. This is easiest to place in perspective and understand in relation to patents. Patents give the patent owner the right to exclude competition. This is accomplished by asserting the patent against third parties who are marketing a product or service that falls within the scope of the claims. Referred to as *infringement*, the criteria are totally different from the criteria for obtaining a patent, referred to as *patentability*. In simple terms, a patent claim consists of elements in a defined relationship. Certain phrases expand or limit the scope of the claim. For example, the term *comprising* can be translated as "including at least," whereas *consisting* means "including only." If a claim reads as follows: "Composition comprising: A, B, and C," then the claim would cover any composition including A, B, C, and any other component. Use of the term *consisting* would restrict the claim to a composition including *only* A, B, and C.

In determining infringement, one must look to the claims of the patent. Claims may be clear on their face or require reference to the specification, or description, of the patent. Claims may also be limited by agreements made during prosecution, a doctrine referred to as "file wrapper estoppel." For example, if the prosecuting attorney argues that the claims distinguish over the prior art on the basis that the prior art does not disclose a particular feature that the attorney argues is essential to the claims in the patent, then the claims will be construed to require that limitation, even if not explicitly recited in the claims as issued.

Asserting a patent allows the alleged infringer to file an action for declaratory judgment in a federal district court, asking the judge to declare the patent invalid or noninfringed. Litigation is very expensive and especially detrimental to small companies, thus providing a great deal of incentive to license the technology on terms favorable to both parties.

SUMMARY

Intellectual property rights provide a means for the owners of technology to recover their investment in the technology and, in some cases, to make a profit. More importantly, intellectual property rights provide a means for financing the incredibly expensive research and development and testing required for commercialization of new products and processes in the medical and biotechnology field. When the intellectual property rights have been lost or given away by publication, many times it is not possible to obtain the money required to see a product or process reach the clinic and benefit those for whom it is intended. It is only by protecting the technology that it can be used to help those who need it the most.

BIBLIOGRAPHY

1. U.S. Code, Title 35, Section 101, 1988.
2. See *Diamond v. Chakrabarty*, 447 U.S. 303,206 U.S. Patent Quarterly 193 (1980).
3. U.S. Code, Title 35, Section 102, 1988.
4. *Philips Elec. & Pharmaceutical Indus. Corp. v. Thermal & Elec. Indus., Inc.*, 450 F.2d 1164, 1169–1172, 171 U.S. Patent Quarterly 641 (3d Cir., 1971); *Gulliksen v. Halberg*, 75 U.S. Patent Quarterly 252 (Pat. Off. Bd. Int'f., 1937).
5. *Ciba-Geigy Corp. v. ALZA Corp.*, 864 F. Supp. 429, 33 U.S. Patent Quarterly 2d 1018 (D.N.J., 1994).
6. U.S. Code, Title 35, Section 103, 1998.
7. *Graham v. John Deere Co.*, 383 U.S. 1,148 U.S. Patent Quarterly 459 (1966).

Next Page

8. U.S. Code, Title 35, Section 112, 1988.
9. U.S. Constitution, Article 1, Section 8, Clause 8.
10. U.S. Code, Title 35, Section 111, 1988.
11. U.S. Code, Title 35, Section 116, 1988.
12. U.S. Code, Title 35, Section 256, 1988.
13. *In re Tansel*, 253 F.2d 241, 242 (C.C.P.A. 1958); *Mergenthaler v. Scudder*, 1897 C.D. 724, 731 (D.C. Cir., 1897).
14. U.S. Code, Title 35, Section 262, 1988.
15. U.S. Code, Title 35, Section 121, 1988.
16. *Code of Federal Regulations*, Title 37, Sections 1.56, 1.97, 1.98, 1996.
17. *Fiers v. Revel*, 984 F.2d 1164 (Fed. Cir. 1993); *Amgen, Inc. v. Chugai Pharmaceutical Co.*, 927 F.2d 1200 (Fed. Cir., 1991); *Colbert v. Lofdahl*, 21 U.S.P.Q.2d 1068 (Bd. Pat. App. & Int'f., 1995).
18. U.S. Code, Title 35, Section 271, 1988.
19. U.S. Code, Title 17, Sections 101–1101, 1996, Suppl. 1997.

PENDENT DRUGS, RELEASE FROM POLYMERS

STEVE BROCCHINI
RUTH DUNCAN
University of London
London, United Kingdom

KEY WORDS

Active targeting
Anticancer agent
Biodegradable polymers
Covalent linkage
Hydrolytically labile linkers
Passive targeting
Poly(ethyleneglycol)
Polymer
Polymer carrier
Polymer micelles
Polymer–protein conjugate

OUTLINE

Introduction
Biological Rationale for Design
  Lysosomotropic Delivery
  Passive and Active Targeting of Polymer–Drug Conjugates
Soluble Polymeric Carriers
  Nondegradable Synthetic Polymers
  Potentially Biodegradable Polymers
  Polymer Micelles
Pendent Chain Linkers
  Preparation and Characterization of Polymer–Drug Conjugates
  Pendent Chain Linkers
  Peptidyl Linkers
  Hydrolytically Labile Pendent Chain Linkers
  Other Linkers
Clinical Progress
Conclusions
Bibliography

INTRODUCTION

The term *polymer therapeutics* has been coined to encompass polymeric drugs (in which the polymer backbone itself displays biological activity), polymer–drug conjugates, polymer–protein conjugates, and polymeric micelles that include a covalent polymer–drug linker (1) (Fig. 1). These compounds are considered as "new chemical entities" by regulatory authorities, and this is the basis for using the term polymer therapeutics to describe this family of polymeric drugs, prodrugs, and drug delivery systems. Being synthetic, hybrid macromolecular systems polymer therapeutics constitute an innovative opportunity to design novel pharmaceuticals that have real potential to improve efficacy in life-threatening diseases such as cancer. Additionally, they may provide the multicomponent technologies needed to assist delivery of other macromolecular drugs such as peptide, protein, and gene therapeutics. The last decade has seen the emergence of the first polymer therapeutics into routine clinical use as anticancer agents, and many more are now in the clinical development pipeline. Development of the first compounds as anticancer agents is understandable because cancer (in its many forms) has last year for the first time become the major cause of mortality in the United Kingdom (2). It is predicted that "cancers" will also become the leading cause of mortality in the United States within 5 years. Statistically in the United States and Europe 1 in 3 people will have

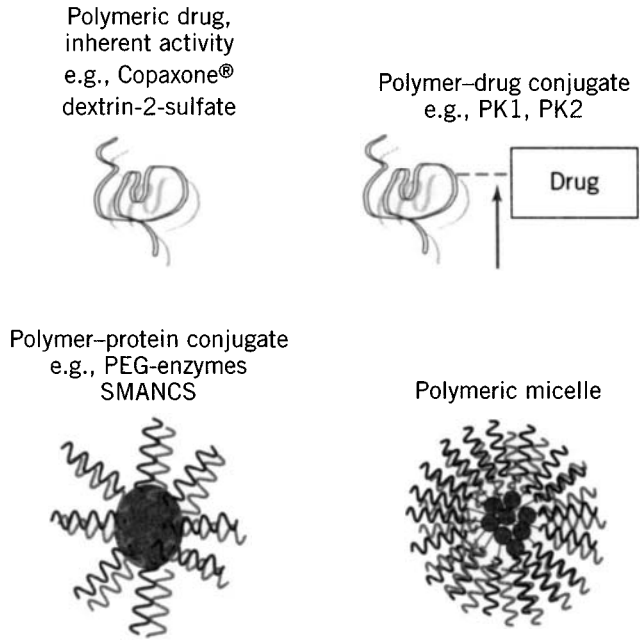


Figure 1. Polymer therapeutics.

Previous Page

8. U.S. Code, Title 35, Section 112, 1988.
9. U.S. Constitution, Article 1, Section 8, Clause 8.
10. U.S. Code, Title 35, Section 111, 1988.
11. U.S. Code, Title 35, Section 116, 1988.
12. U.S. Code, Title 35, Section 256, 1988.
13. *In re Tansel*, 253 F.2d 241, 242 (C.C.P.A. 1958); *Mergenthaler v. Scudder*, 1897 C.D. 724, 731 (D.C. Cir., 1897).
14. U.S. Code, Title 35, Section 262, 1988.
15. U.S. Code, Title 35, Section 121, 1988.
16. *Code of Federal Regulations*, Title 37, Sections 1.56, 1.97, 1.98, 1996.
17. *Fiers v. Revel*, 984 F.2d 1164 (Fed. Cir. 1993); *Amgen, Inc. v. Chugai Pharmaceutical Co.*, 927 F.2d 1200 (Fed. Cir., 1991); *Colbert v. Lofdahl*, 21 U.S.P.Q.2d 1068 (Bd. Pat. App. & Int'f., 1995).
18. U.S. Code, Title 35, Section 271, 1988.
19. U.S. Code, Title 17, Sections 101–1101, 1996, Suppl. 1997.

PENDENT DRUGS, RELEASE FROM POLYMERS

STEVE BROCCHINI
RUTH DUNCAN
University of London
London, United Kingdom

KEY WORDS

Active targeting
Anticancer agent
Biodegradable polymers
Covalent linkage
Hydrolytically labile linkers
Passive targeting
Poly(ethyleneglycol)
Polymer
Polymer carrier
Polymer micelles
Polymer–protein conjugate

OUTLINE

Introduction
Biological Rationale for Design
  Lysosomotropic Delivery
  Passive and Active Targeting of Polymer–Drug Conjugates
Soluble Polymeric Carriers
  Nondegradable Synthetic Polymers
  Potentially Biodegradable Polymers
  Polymer Micelles
Pendent Chain Linkers
  Preparation and Characterization of Polymer–Drug Conjugates
  Pendent Chain Linkers
  Peptidyl Linkers
  Hydrolytically Labile Pendent Chain Linkers
  Other Linkers
Clinical Progress
Conclusions
Bibliography

INTRODUCTION

The term *polymer therapeutics* has been coined to encompass polymeric drugs (in which the polymer backbone itself displays biological activity), polymer–drug conjugates, polymer–protein conjugates, and polymeric micelles that include a covalent polymer–drug linker (1) (Fig. 1). These compounds are considered as "new chemical entities" by regulatory authorities, and this is the basis for using the term polymer therapeutics to describe this family of polymeric drugs, prodrugs, and drug delivery systems. Being synthetic, hybrid macromolecular systems polymer therapeutics constitute an innovative opportunity to design novel pharmaceuticals that have real potential to improve efficacy in life-threatening diseases such as cancer. Additionally, they may provide the multicomponent technologies needed to assist delivery of other macromolecular drugs such as peptide, protein, and gene therapeutics. The last decade has seen the emergence of the first polymer therapeutics into routine clinical use as anticancer agents, and many more are now in the clinical development pipeline. Development of the first compounds as anticancer agents is understandable because cancer (in its many forms) has last year for the first time become the major cause of mortality in the United Kingdom (2). It is predicted that "cancers" will also become the leading cause of mortality in the United States within 5 years. Statistically in the United States and Europe 1 in 3 people will have

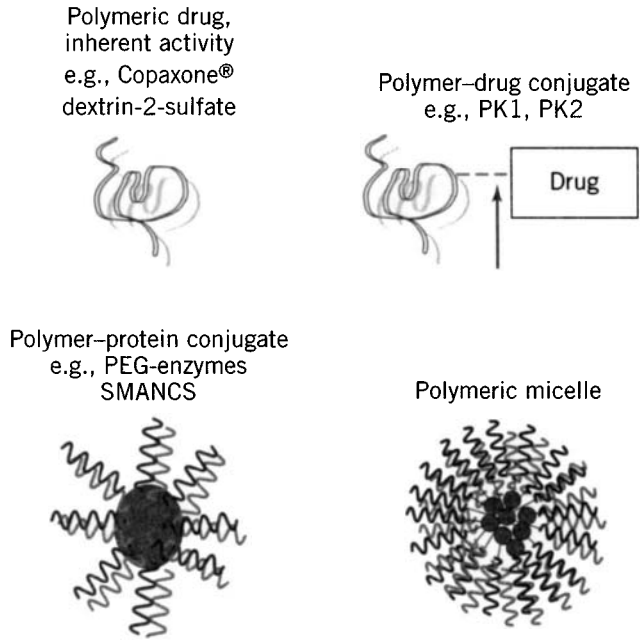


Figure 1. Polymer therapeutics.

some form of cancer at some stage in their lifetime and 1 in 4 will die from these diseases. Therefore the need for improved therapies is evident.

Covalent conjugation of a therapeutic agent to a polymer can improve its therapeutic index if biodistribution is beneficially altered compared with that of the unconjugated pharmacophore. Conjugation provides the opportunity for cell- or organ-specific targeting. By judicious selection of the polymer–drug linker it is possible to control both the site and rate of drug liberation in vivo. Historically polymer–drug conjugation has been achieved by either linking the drug using pendent chains along the polymer backbone (this allows several drug molecules to be conjugated per polymer chain) or by conjugation to one or both endgroups of the polymer chain (Fig. 2). The latter method has been preferred for binding monomethoxy poly(ethylene glycol) to proteins, where several polymer chains are conjugated per protein molecule in order to "coat" the protein surface. Elsewhere in this volume poly(ethylene glycol) (PEG) prodrugs and PEG-protein conjugates are described in detail, and several reviews discuss this topic (3–9).

Many excellent reviews have already described the evolution of polymer–drug conjugates and micellar drug carriers (1,3,4,10–21). Here we describe the basic rationale for the design of pendent chain polymer–drug conjugates. Experience suggests that careful selection of all the components of the polymer–drug conjugate; the polymer itself, the pendent chain linker, and the drug is required for development of a construct with increased efficacy and that is also amenable to industrial scale-up and clinical development. Examples are largely drawn from the field of polymeric anticancer agents and those compounds which are furthest in development, i.e., in vitro and in vivo observations correlate.

BIOLOGICAL RATIONALE FOR DESIGN

Whereas cellular uptake of low molecular weight molecules usually occurs by rapid transmembrane passage, the uptake of soluble macromolecules occurs almost exclusively by endocytosis (Fig. 3). The mechanism of endocytosis has been reviewed elsewhere (22,23). Endocytosis is a constitutive process common to all cell types and results in membrane invagination leading to the capture of extracellular fluid and all macromolecules contained therein.

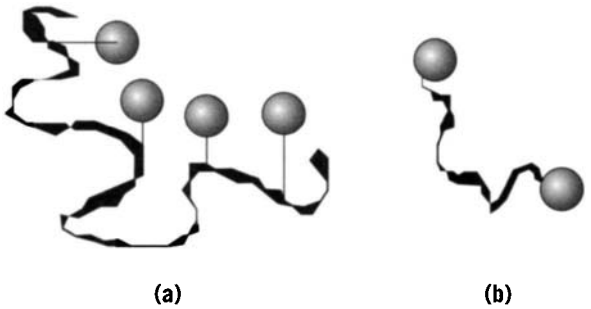


Figure 2. Polymer–drug conjugates: (**a**) pendent chain and (**b**) endgroup conjugation.

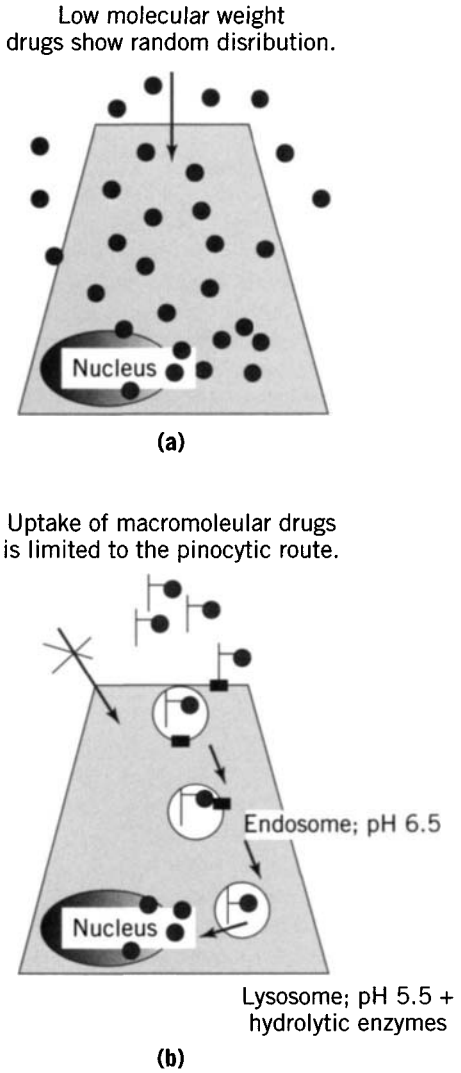


Figure 3. Mechanisms of cellular uptake of (**a**) low molecular weight anticancer agents and (**b**) polymer–drug conjugates.

Uptake of macromolecular solutes is referred to as fluid-phase pinocytosis (23). If a macromolecule is also internalized after binding to specific receptors on the plasma membrane or by binding through nonspecific hydrophobic or electrostatic membrane interactions, capture is designated adsorptive-pinocytosis. This results in rapid uptake and often significant concentration of macromolecules within the cell. After their formation at the plasma membrane, pinocytic vesicles migrate into the cytoplasm and, by a series of fusion events, enter the endosomal compartment of the cell where the pH falls to 6.5. Further fusion events lead to transfer of the vesicles' contents into the secondary lysosomal compartment. There pH falls to approximately 5.5. Furthermore, lysosomes contain a vast array of hydrolytic enzymes including proteases, esterases, glycosidases, phosphates, and nucleases (24). Internalized macromolecules that are substrates for these enzymes are degraded within the lysosomes to their constituent molecular fragments which, if small enough, subsequently dif-

fuse through the lysosomal membrane into the cytoplasm for cellular metabolism or removal. Macromolecules which are not degraded accumulate in the secondary lysosomes and can only be released slowly by exocytosis or upon cell death.

Lysosomotropic Delivery

De Duve and colleagues first suggested that macromolecules, particularly proteins, might be used to conjugate drugs and therefore restrict drug uptake by cells to the pinocytic route. This ensures that the secondary lysosomal compartment acts as a gateway for drug entry into the cell. They coined the term "lysosomotropic drugs" to describe compounds that exhibit pharmacological properties after internalization and delivery via this route (25).

Possessing the knowledge that macromolecular uptake by cells is limited to the pinocytic route (25,26), and that soluble synthetic polymers could be used as blood expanders (27,28), as prophylactics against radiation exposure (29), and as pharmacologically active agents (30–33), Ringsdorf proposed that polymers could also be systematically developed into targetable drug carriers (21,34,35), and that hydrophilic polymeric carriers could be used to solubilize poorly water-soluble drugs. His now famous model described how a polymer–drug linker might be used to allow controlled drug liberation at the target site. The model also proposed the coconjugation of targeting moieties capable of mediating cell-specific targeting.

The change in milieu during cellular internalization and the presence of specific lysosomal hydrolases provides the opportunity to design polymer–drug linkers from which drug is cleaved from the polymer only in the environment of the endosome or lysosome. This has allowed the design of polymeric anticancer conjugates that are essentially nontoxic in the extracellular environment (18). Ultimate antitumor activity is dependent on the efficient liberation of an active form of the drug from the polymer which can then permeate through the lysosome membrane into the cytoplasm to reach the pharmacological target. Structural characteristics of the released molecules including charge and hydrophobicity can influence the permeation rate of these molecules out of the lysosome; however, diffusion from the lysosome readily occurs at molecular weights below 200–220 Da (36–38).

Passive and Active Targeting of Polymer–Drug Conjugates

As conjugation of low molecular weight drugs to polymeric carriers restricts cellular uptake to the endocytic route, the biodistribution of conjugated drug is significantly changed. Increasingly, unequivocal evidence has shown that solid tumors exhibit enhanced or hyperpermeability of the tumor vasculature (39–44), and this, combined with the decreased lymphatic drainage of tumor tissue compared with healthy tissue (39,45), can produce significant tumor targeting of polymer–drug conjugates and particulate carriers that have a lengthy plasma residence time. Maeda and coworkers termed the passive targeting of polymer conjugates to solid tumor tissue the "enhanced permeability and retention" (EPR) effect (Fig. 4) (39,45).

Many macromolecules (39,46,47) passively accumulate within solid tumors, including albumin (48–55), antibodies (56,57), polymers (58,59), and polymer–drug conjugates (60,61). Tumor to blood ratios of the polymer–protein conjugate styrene maleic anhydride-neocarzinostatin (SMANCS) of up to 2,500 were measured in a rabbit tumor model (62,63) and *N*-(2-hydroxypropyl)methacrylamide (HPMA) copolymer–doxorubicin conjugates have shown tumor accumulation ranging from 2 to 20% dose/g in a B16F10 tumor model (64,65). Observations that tumor blood vessels are permeable to liposomes and particles in the size range 200 to 600 nm (44,66), and that neither the human colon xenograft LS174T (44), B16F10, or sarcoma 180 tumors (60) exhibited differences in tumor uptake of macromolecules in the 10,000 to 800,000 Da molecular weight range are indicative that passive tumor targeting by the EPR effect can be accomplished using polymeric and micellar carriers across a wide molecular weight and size range. Tumor accumulation of polymer–drug conjugates begins immediately after intravenous (i.v.) administration and the plasma concentration of polymer is the main driving force controlling the extent of tumor capture observed (47).

After i.v. administration polymers that do not bind to blood proteins display a plasma clearance that is primarily governed by the rate of kidney glomerular filtration and the rate of liver uptake. Macromolecules of molecular weight of 40,000–70,000 Da readily pass through the kidney glomerulus and are excreted. However, as the solution size of a molecule increases with molecular weight (or by forming supramolecular aggregates), extended blood clearance times result. Structural features including polymer flexibility, charge, and hydrophobicity affect the renal excretion threshold for macromolecules within this size range (67). Neutral, hydrophilic polymers including HPMA copolymers, poly(vinylpyrrolidone) (PVP) and PEG have flexible, loosely coiled solution structures, whereas proteins tend to be charged and exhibit more compact solution structures. For example, the molecular weight threshold limiting glomerular filtration of HPMA copolymer-tyrosinamide in the rat was approximately 45,000 Da (68) and the threshold for proteins is approximately 60,000 Da.

In addition to passive targeting, polymeric–drug conjugates can be targeted to specific cells by incorporation of targeting moieties into the polymer backbone (15,18). This process is termed *active targeting*. Although receptor-mediated endocytosis is highly efficient, particularly when cells display a high density of ligand-specific receptors, localization of a significant percentage of the dose of drug within the target in vivo by active targeting has not been very successful. Many candidate receptors proposed for tumor targeting have broad cellular distribution. For example, transferrin, low density lipoprotein, and growth factor receptors, which display elevated levels on tumor cells, have ubiquitous distribution. Many so-called tumor-specific receptors are actually only tumor-enhanced in terms of numbers of receptors per cell (69–74). Cell-specific receptors are present in the liver (75–78), and these have been used successfully to target polymer–drug conjugates after i.v. administration. For example, HPMA copolymer-doxorubicin containing additionally galactosamine (PK2,

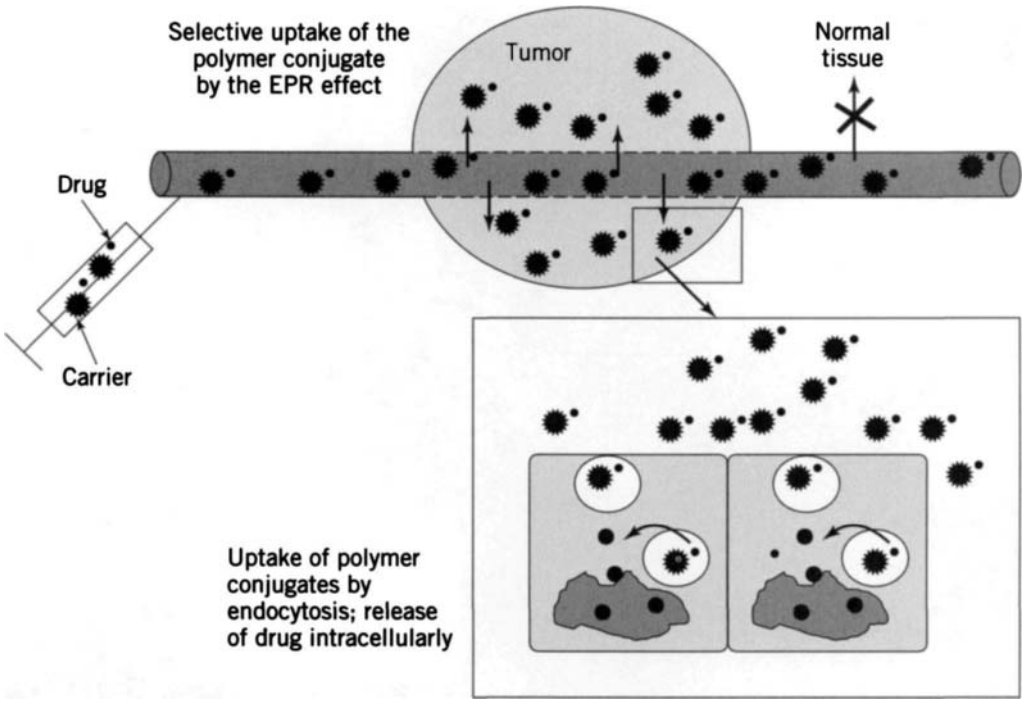


Figure 4. Passive tumor targeting by the EPR effect.

FCE 28069) localizes selectively in the liver due to uptake by the hepatocyte asialoglycoprotein receptor (79,80).

To be effective, it is important that polymer–drug conjugates are designed to improve drug localization in the target tissue, diminish drug exposure in potential sites of toxicity, and optimize drug release rate. Incorporation of a polymer–drug linker that only releases drug at the target site can reduce peak plasma concentrations, thus reducing drug-mediated toxicity. If the drug release rate is optimized, exposure at the target can be tailored to suit the mechanism of action of the pharmacophore being used (e.g., use of cell-cycle dependent antitumor agents) and to prevent the induction of resistance.

SOLUBLE POLYMERIC CARRIERS

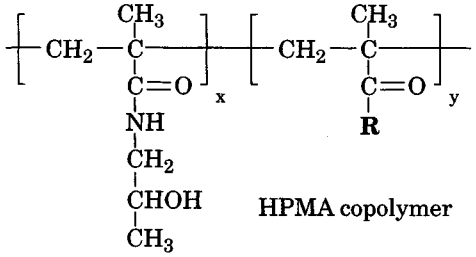
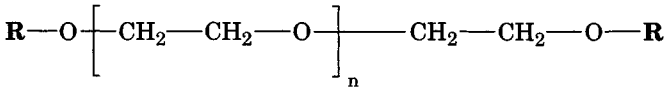
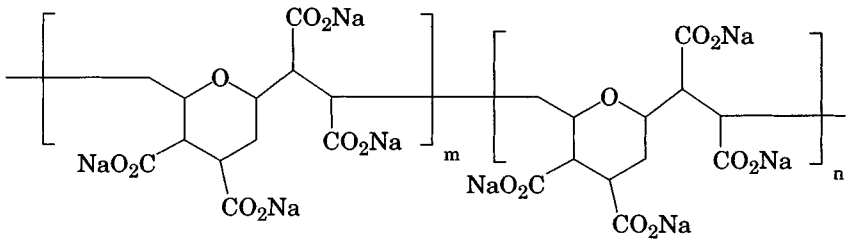
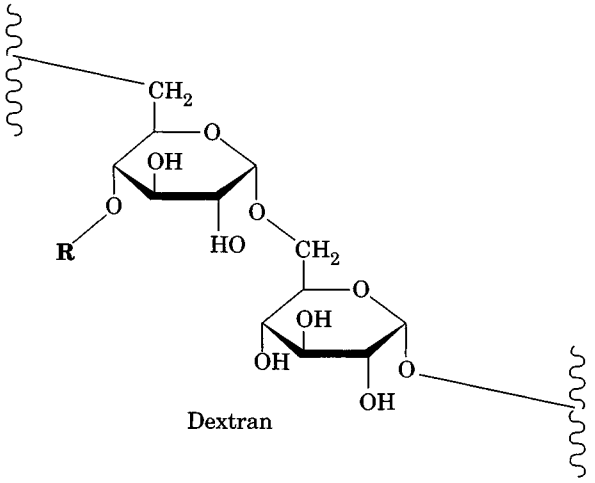
An increasing number of soluble polymers have been used as macromolecular partners for pendent chain drug conjugation. Shown in Table 1 are representative examples of several polymers that have been used to prepare polymer–drug conjugates. Many of these polymers have been extensively studied and can be organized into two broad classes: (*1*) nondegradable synthetic polymers and (*2*) potentially degradable synthetic polymers and natural polymers. Although several polymers with intrinsic therapeutic activity (81) have been used to conjugate drugs, e.g., copolymers derived from divinylether and maleic anhydride (DIVEMA) and some polysaccharides (82,83), many polymers used for conjugation were selected because they were water-soluble and biocompatible (e.g., did not bind blood proteins and were nonimmunogenic).

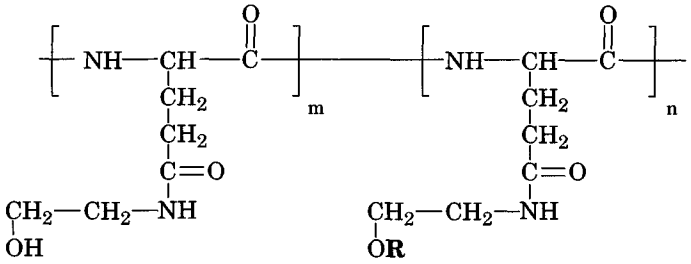
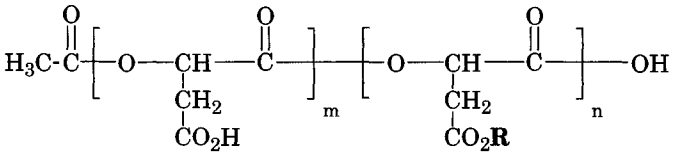
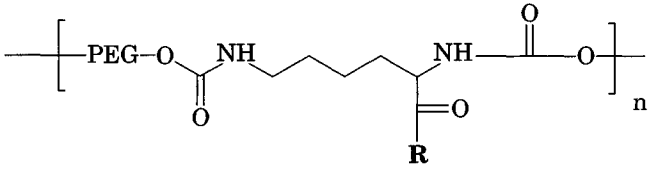
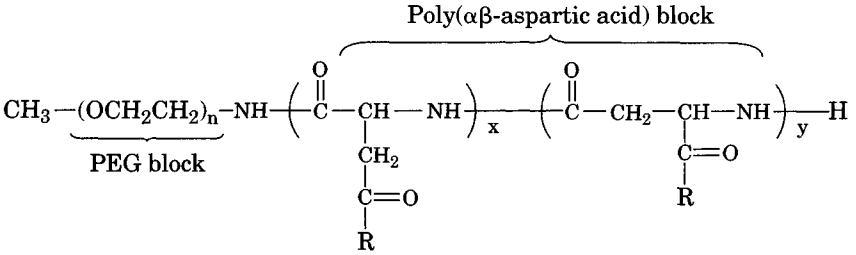
Nondegradable Synthetic Polymers

The synthetic polymers PEG and HPMA copolymers have been extensively studied as polymeric drug carriers. They are hydrophilic and are well tolerated in man, but their main disadvantage is that the polymer backbone is not biodegradable in vivo. Only polymers of molecular weight lower than the renal threshold can be used for systemic administration.

Poly(ethylene glycol). PEG is generally recognized as safe and is used in a wide range of pharmaceutical and consumer products (7,84–86). Monodisperse PEG is commercially produced in a range of molecular weights from 200 to over 100,000 Da with various endgroup chemical functionality and morphology, i.e., linear, graft, and star. Although PEG has been widely used to prepare polymer–protein conjugates it is only now being used more widely to conjugate anticancer drugs such as doxorubicin (87), camptothecin (88–90), and paclitaxel (Fig. 5) (91,92). PEG–drug conjugates can be prepared by linking via one terminus or both termini of an end functionalized PEG (see Fig. 5). Usually the PEGs selected for protein conjugation have a molecular weight of 3,400 or 5,000 Da, but for preparation of drug conjugates a wider range of molecular weights has been explored (91,93). Many conjugation strategies have been described (3,4,86). One potential disadvantage is the extent of polymer drug loading, which is limited by the availability of only two reaction sites at the termini of the linear PEG molecule. However, branched PEG polymers (87), alternating PEG polymers [e.g., PEG-lysine (94,95)] and copolymers [e.g., PEG-oligopeptide-PEG (96,97)] with pendent chains capable of conjugating

Table 1. Polymers Used for Pendant Drug Conjugation

Polymer	Linker	Example polymer structures[a]
	Nondegradable synthetic polymers	
HPMA copolymers	Pendent chain; peptidic or acid labile for lysosomal release of covalently conjugated drugs. Pendent chains can be derivatized to chelate metals.	 HPMA copolymer
PEG	Typically endgroup (terminal) drug conjugation. Both peptidic and acid labile linkers have been used, but PEG also directly conjugated to drug (i.e., via an ester bond).	 PEG
DIVEMA	Metals (e.g., platinum) can be conjugated by chelation directly to the polymer side chains, which are carboxylates.	 DIVEMA
	Potentially degradable polyers	
Polysaccharides Dextran Chitosan Carboxymethyl chitin Carboxymethyl pullulan Alginate	Most of these polymers are naturally occurring or can be synthesized from natural metabolites. Polymer usually derivatized to have caboxylate, amine, aldehyde, or reactive moiety on side chain, which is then conjugated with the drug. Can be conjugated with an appropriately derivatized drug to give either peptidic or acid labile pendent chain for lysosomal drug release. Pendent chains are also used to conjugate ligands for multivalent binding onto a cellular membrane surface.	 Dextran

Poly(amino acids) Poly[^{5}N-(2-hydroxyethyl)-L-glutamine) (PHEG) β-Poly(2-hydroxyethyl aspartamide) (PHEA) Poly(glutamic acid) Poly(aspartic acid) Polylysine	Polymer side chains tend to be derivatized analogous to polysaccharides to give pendent chain conjugation that can be either peptidic or acid labile. Pendent chains also used to conjugate ligands for multivalent ligand binding on the membrane surface.	 Poly[^{5}N-(2-hydroxyethyl)-L-glutamine]
Polyesters Poly(α or β-malic acid)	Pendent chain options are similar to poly(amino acids).	 Poly(α-malic acid)
Alternating polymers PEG-lysine	Provides practical means to incorporate pendent chains in a polymer which is predominantly PEG.	
Block copolymers Poly(ethylene glyco-aspartate)	Formation of polymeric micelles capable of both drug conjugation and entrapment. Linker potential similar to poly(amino acids).	

[a]**R** denotes a pendent chain linker with a conjugated drug.

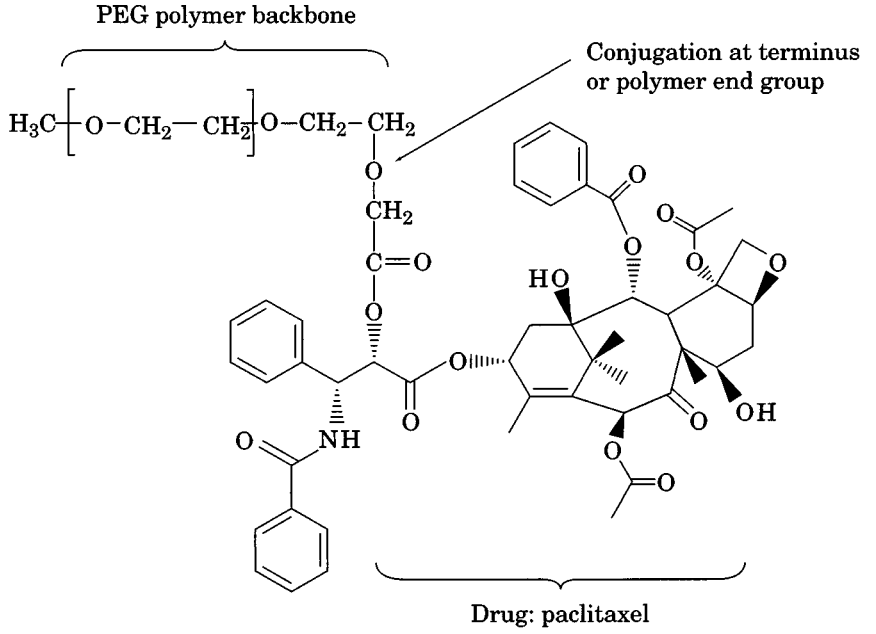


Figure 5. PEG–paclitaxel conjugate (91,92), an example of drug conjugation only at the polymer terminus.

a drug along the polymer backbone, and PEG block copolymers that can form polymeric micelles have recently been prepared (10,11,98–100).

***N*-(2-Hydroxypropyl)methacrylamide Copolymers.** Many synthetic hydrophilic polymers used for drug conjugation are derived from methylacrylamides (e.g., HPMA copolymers). These polymers have generally been prepared by free radical polymerization. HPMA homopolymer is nontoxic up to 30 g/kg, does not bind blood proteins, and is not immunogenic. It was initially developed as a plasma expander (101,102), and copolymers derived from HPMA have been widely used for drug conjugation using pendent chain attachment (Fig. 6) (12,15,18). Early confirmation of low protein binding (103), low complement activation (104), and low immungencity (105–108) was instrumental in establishing the potential of HPMA homo- and copolymers to be used for drug conjugation. Although HPMA copolymers of molecular weight less than 40,000 Da are readily excreted, HPMA copolymers of molecular weight above the renal threshold remain in circulation for long periods and are retained in the body, typically exhibiting accumulation in the reticuloendothelial system (RES) and skin (68). It is imperative that the systemic use of nondegradable polymers such as HPMA copolymers, PEG, and PVP is limited to molecules of a molecular weight that is readily cleared, otherwise long-term deleterious accumulation in healthy tissue could result (68,109–112).

Potentially Biodegradable Polymers

Polysaccharides. Some polysaccharides have the advantage of being enzymatically biodegradable, e.g., dextran, and can therefore be administered over a wider molecular weight range without the fear of prolonged accumulation in the body. However, polysaccharides lack structural uniformity and exhibit the propensity upon chemical modification (i.e., drug conjugation) to become immunogenic or nondegradable (113,114). Dextran is used safely as a blood plasma substitute (115) and has been investigated for use as polymeric carrier (14,116–123). The dextran backbone is composed of glucose repeat units. These hydroxylated, cyclohexyl units result in a more rigid polymer compared with many synthetic polymers (e.g., HPMA copolymers, PEG, and PVP), so dextran tends to exhibit a more compact solution structure than these polymers. Consequently, it has a higher renal threshold for excretion [55,000 Da (124) to 70,000 Da (46)]. Chemical modification of dextran by introduction of anionic moieties (carboxylates) reduces its rate of clearance (46), and addition of other substituents such as fluorescein isothiocyanate or sugar residues (113,125) promotes liver capture. Other polysaccharides that have been investigated include chitosan (126), alginate (127,128), hyaluronic acid (129), 6-*O*-carboxymethyl chitan (130) and 6-*O*-carboxymethyl pullulan (131). Typically, commercially available coupling agents have been routinely used to bind drugs to polysaccharides by direct conjugation to the polymer.

Polymers Derived From Natural Metabolites. Often hydrophilic polymers have been prepared from amino acids (e.g., poly(glutamic acid), poly[^{5}*N*-(2-hydroxyethyl)-L-glutamine) (PHEG), β-poly(2-hydroxyethyl aspartamide) (PHEA), poly(L-glutamic acid), and polylysine. Other polymers and copolymers including pseudo-poly(amino acids) (132) and polyesters such as poly (α or β-malic acid) (133,134), and alternating polymers such as PEG-lysine (94,95) and poly(lysine citramide) (133) have also been investigated for drug conjugation. These polymers can be prepared by condensation or ring opening (135) polymerization reactions.

In principle, proteins can also be used to conjugate drugs, and albumin has been a popular candidate. Albumin with a molecular weight of approximately 66,000 Da is the most abundant protein in the circulatory system. It

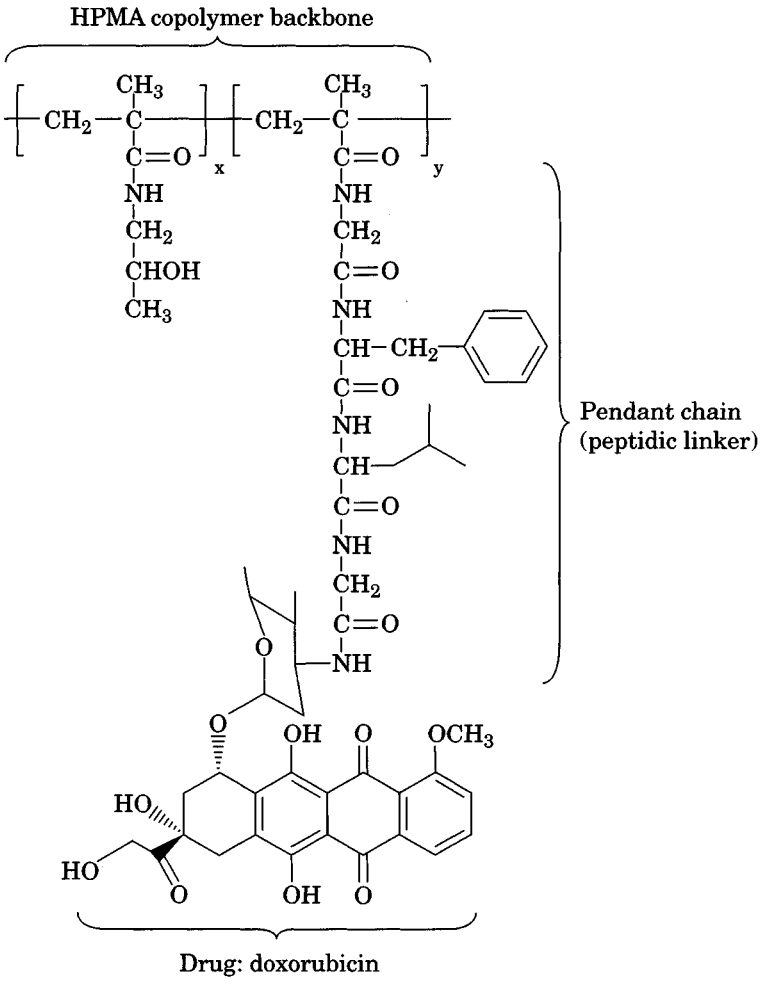


Figure 6. HPMA copolymer-doxorubicin conjugate (PK1, FCE 28068), an example of pendent chain drug conjugation using a peptidic linker (12,15). The conjugate has a M_W of approximately 30,000 Da and a doxorubicin content of approximately 8 wt %.

exhibits a circulation half-life of 19 days (only 2.2 days in the rat) and is found in every tissue and bodily secretion (136). Albumin continues to be actively investigated as a macromolecule candidate for drug conjugation (137–144), but the major limitations of proteins when compared with synthetic polymers as drug carriers are their increased propensity for inducing immunogenicity, denaturation, and nonspecific degradation. Other proteins such as transferrin [which binds to the transferrin receptor and thus have the potential to undergo receptor-mediated uptake (145,146)], and various immunoconjugates (57,147–158) have also been investigated. Narrow molecular weight distribution is often claimed to be a significant advantage for using proteins to conjugate drugs, but this can only be useful if a single species of the protein–drug conjugate can be created that is stable on storage. This has frequently been difficult to achieve in practice.

Polymer Micelles

Block copolymers, comprising hydrophilic and hydrophobic blocks, form polymeric micelles in solution (98,100,159–162) and self-assembling micellar delivery systems are receiving increasing attention (10,163–165). A significant advantage of these systems is the ability to design higher molecular weight micellar aggregates that display prolonged circulation times that can maximize tumor capture by the EPR effect. Upon micelle disassociation, the individual block copolymer molecules are safely excreted, and as long as they are of low enough molecular weight these polymers can be nonbiodegradable. For example, poly(ethylene glycol-aspartate) block copolymer doxorubicin conjugates form micelles ranging in size from 20 to 60 nm that accumulate in solid tumors and exhibit antitumor activity (11,98,160,161,166). The doxorubicin is conjugated by its free amine directly to either the α- or β- pendent carboxylates in the poly(aspartic acid) block. Details of this conjugate are further described in the section entitled "Other Linkers." Frequently physical entrapment of drug has accompanied conjugation (167), and with stable block copolymer micelles drug entrapment has become a viable strategy to deliver cytotoxic drugs to tumors (10,99,167–169). This aspect of block copolymer micelles is beyond the scope of this review (10).

PENDENT CHAIN LINKERS

Preparation and Characterization of Polymer–Drug Conjugates

Three distinct strategies have been employed to prepare polymer–drug conjugates incorporating pendent chain linkers.

1. Reaction of the linker or drug with functional groups already present in the polymer main chain. Generally, polymer side chains are activated using coupling reagents or by prior reaction. In this way, for example it is possible to derivatize -NH_2 groups in poly-L-lysine or -OH groups in polysaccharides.
2. Preparation of reactive polymeric intermediates by copolymerization using a monomer with a reactive pendent chain to which drugs or targeting groups can subsequently be bound (for example, conjugation of drugs to HPMA copolymers bearing pendent side chains containing reactive esters).
3. During polymerization use of a monomer containing the linker drug to produce the homopolymer or copolymer bearing linker and drug as pendent chains.

A significant amount of methodology for the conjugation of drugs to polysaccharides (170–172) has been developed using dextran as the model because this polysaccharide has been developed clinically as a blood plasma substitute (113,173) (for example, (*1*) partial periodate oxidation to give reactive aldehyde groups (113,174–177), (*2*) succinoylation (Fig. 7) or analogous derivatization (120,127) to give free carboxylates that can be conjugated, and (*3*) chloroformate (113,174) or cyanogen bromide (178) activation followed directly by reaction with a drug or drug derivative). Polymers derived from amino acids such as PHEG (179–181) and poly(L-glutamic acid) (182) have been directly conjugated to drugs using a commercial coupling agent (Fig. 8).

The majority of HPMA copolymer conjugates have been prepared by synthesis of polymeric precursors derived from free radical copolymerization of HPMA monomer and methacryolyated peptides terminating in *p*-nitrophenol. Subsequent aminolysis of the polymer precursor has been used to introduce covalently bound drug, drug analogue, or targeting ligand (183–192). This procedure for the preparation of polymer–drug conjugates is known as a polymer analogous reaction (101,102,108,184,193,194), and it has the significant advantage of allowing preparation of a common polymeric intermediate that can then be used to prepare different conjugates all having the same molecular weight characteristics (195). In the case of HPMA copolymers the polymeric precursor is prepared under very mild conditions by free radical precipitation polymerization (193). During aminolysis of the pendent chain terminal *p*-nitrophenol ester, the drug loading can be varied simply by using different drug stoichiometries (Fig. 9). The major limitations of the polymer analogous reaction are (*1*) incomplete removal of all free drug, which in the case of potent anticancer agents is essential to minimize potential toxicity associated with systemic administration, and (*2*) the difficulty in fully characterizing a complex polymer–drug conjugate.

Polymer–drug conjugates can also be prepared by copolymerization of underivatized and drug derivatized monomers (Fig. 10) (15,20). Copolymerization of such comonomers often requires optimization of the polymerization chemistry to maintain molecular weight characteristics, comonomer incorporation, and conversion (yield) at different drug loadings.

Whatever the route of synthesis, it is essential that polymer–drug conjugates developed for clinical evaluation be carefully characterized. HPMA copolymer conjugates destined for clinical use have been characterised by detailed NMR (to confirm identity), gel permeation chromatography, and viscosimetry (to describe molecular weight averages and distribution) (195) and by high-performance liquid chromatography (HPLC) techniques to quantify total and free drug in the preparation (196,197). Typically an acceptable level of free drug in a polymeric conjugate produced on a commercial scale is approximately 1% of the total drug in the preparation, although laboratory synthesis can frequently yield compounds with $\leq$0.1% free drug.

In the case of conjugates containing potent anticancer agents it is important to note that such traces of free drug can contribute significantly to the observed in vitro cytotoxicity. This limits the opportunity to use a simple in vitro bioassay to confirm activity/toxicity of polymeric drugs. Whereas the free drug generally diffuses rapidly through the plasma membrane into the cell, the polymer conjugate is taken up slowly by endocytosis and, if a peptidyl linker is used, liberation of active agent is also a lengthy process. Thus in vitro cytotoxicity assays are frequently inappropriate for predicting the in vivo potential of candidate anticancer polymer conjugates; they often simply give an indication of the free drug content of a preparation or reflect a fast rate of release of drug from the conjugate during incubation in tissue culture medium. For example, the in vitro cytotoxicity testing of HPMA copolymer-doxorubicin conjugates showed that toxicity was caused by the unconjugated doxorubicin impurity (Fig. 11) (198). This was corroborated by HPLC analysis (196). If the biological reproducibility of commercial batches of a polymer conjugate are to be determined, carefully designed in vitro and in vivo tests are required depending on the therapeutic target of the bound drug.

The molecular weight distribution or polydispersity of a polymer is defined as a ratio of molecular weight averages, specifically, M_w/M_n (weight average molecular weight/number average molecular weight). If all molecules of a polymer sample have the same size (e.g., proteins), this ratio is 1. The higher this ratio (it is never less than 1), the broader the distribution of molecular weights. Polymer therapeutics must be rigorously characterized with respect to their molecular weight and polydispersity because biodistribution and pharmacological activity are known to be molecular-weight-dependent. For example, blood circulation half-life (199), renal clearance, deposition in organs (27), rates of endocytic uptake (200,201), and biological activity can depend on polymer molecular weight characteristics (81,202–206). If a polymer analogous reaction is used for drug conjugation, determination of polymer molecular

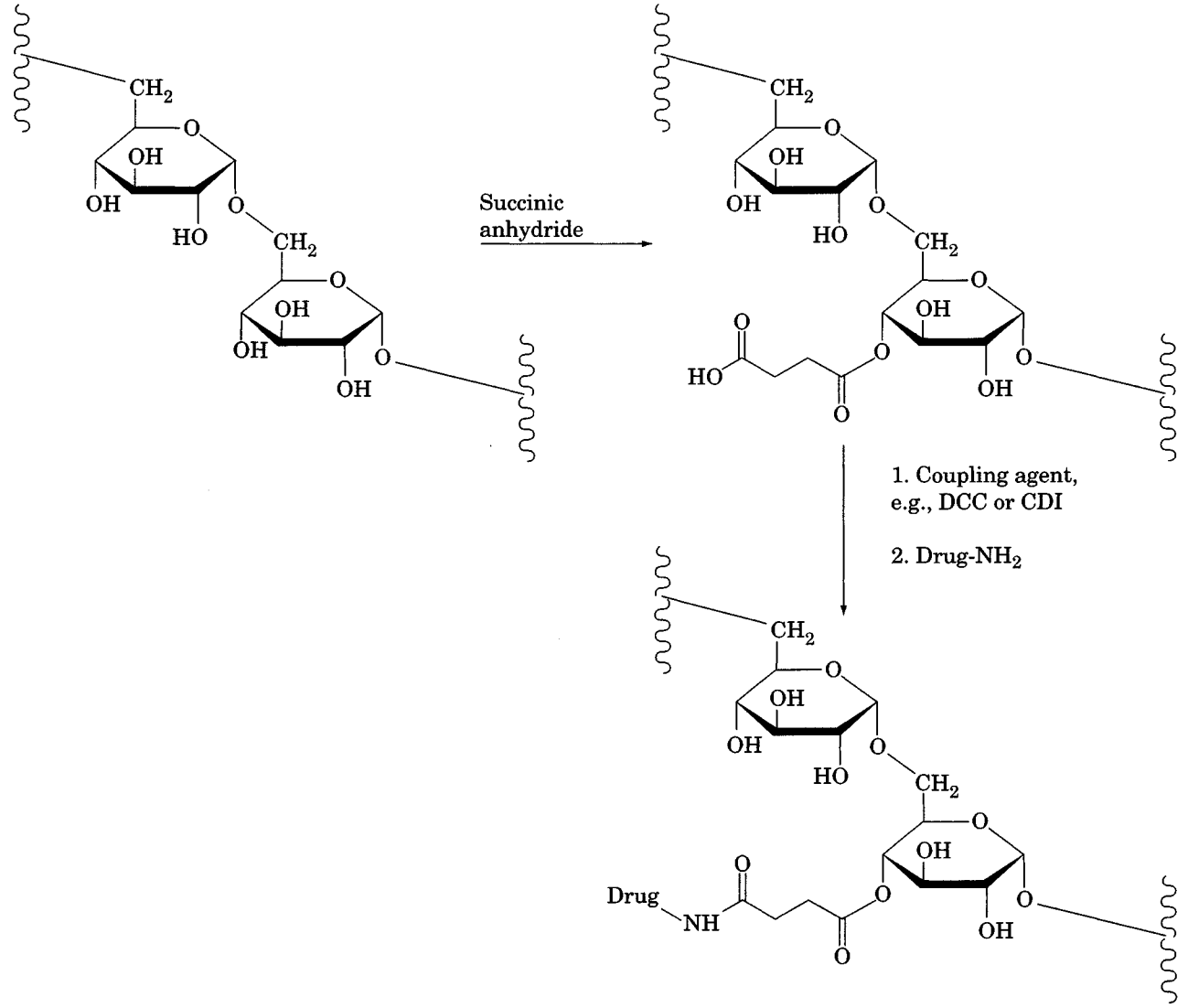


Figure 7. Succinylation of dextran, an example of polysaccharide derivatization often required prior to drug conjugation (113,173).

weight before and after the reaction ensures there has been no significant increase in molecular weight due to cross-linking.

Pendent Chain Linkers

A wide variety of linkages have been used to covalently bind a drug to the polymeric carrier (12,13,15,20). Several examples are illustrated in Table 2. Conjugation of metals to polymers by chelation has also been investigated (e.g., platinate anticancer conjugates (129,207–214; E. Gianas et al., unpublished data) and chelated conjugates for imaging (215–219)). Following the concept of lysosomotropic drug delivery (25,138) two broad classes of pendent chain linkers have emerged as the main focus of research over the last two decades.

1. Peptidyl linkers designed to be stable in the bloodstream but degradable by lysosomal enzymes and thus able to release the drug intracellularly (38,138,183,220–223).
2. Acid-labile, pH-dependent linkers designed to remain stable in plasma at neutral pH (7.4) but release drug intracellularly by hydrolysis in the more acidic environment of the endosome and lysosome (pH 5.5 to 6.5) (127,149,224).

Peptidyl Linkers

Early studies involving albumin-peptide-daunorubicin conjugates demonstrated that peptide linkers are able to mediate lysosomotropic drug delivery (138,225,226). It has become apparent that the best control of the rate and location of drug release from pendent chain polymers have occurred when a drug is bound to the polymer backbone via a peptidyl side chain, and the largest body of infor-

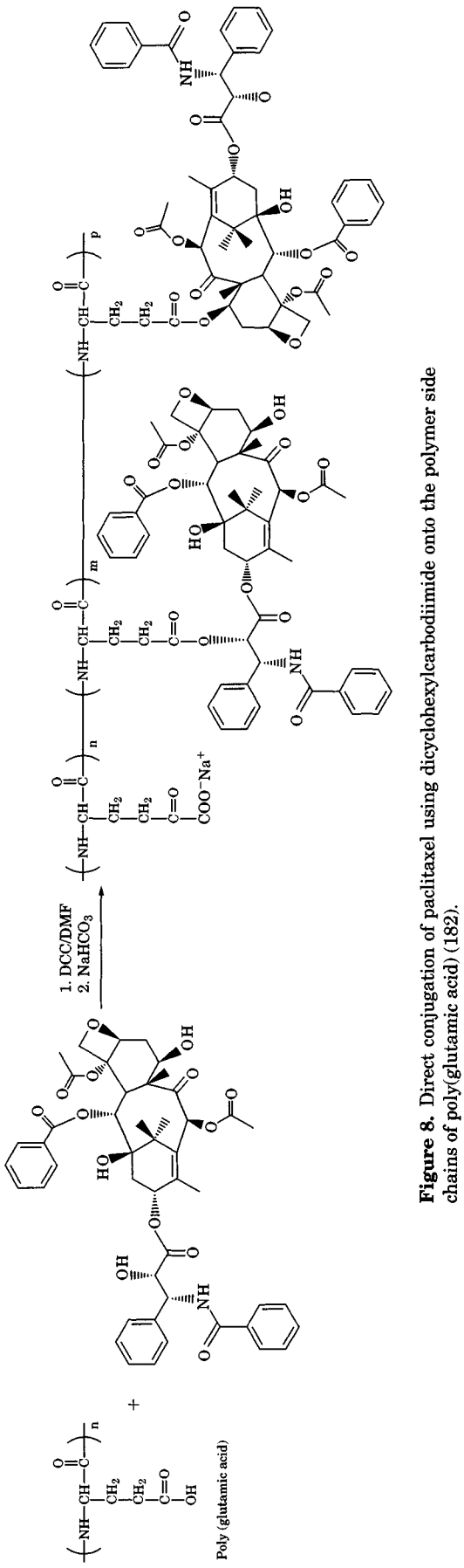


Figure 8. Direct conjugation of paclitaxel using dicyclohexylcarbodiimide onto the polymer side chains of poly(glutamic acid) (182).

mation has been collected thus far using HPMA copolymers synthesized to contain pendent peptide side chains for drug conjugation.

Since the discovery that peptidyl side chains in HPMA copolymers could be designed for cleavage by model enzymes such as chymotrypsin, trypsin, and papain (183,220,227–232), the last two decades have seen the systematic development of HPMA copolymer–anticancer conjugates containing peptidyl linkers tailored for cleavage by lysosomal proteases (15,18). Such linkers have now become more widely used in many different polymer conjugates (12,13,15). Initial studies using HPMA copolymers containing peptidyl pendent side chains terminating in *p*-nitroanilide (NAp) as a model compound found that mixtures of lysosomal enzymes (tritosomes) were not able to cleave many sequences in the absence of the reducing agent (reduced glutathione; GSH) (233), and indeed under these conditions the rate of NAp release was very slow (Table 3). In most cases, addition of GSH increased the rate of NAp release significantly (Table 3), and this, coupled with the observation that leupeptin inhibited degradation, indicated that the lysosomal thiol–dependent proteases (cathepsins B, H, and L) were particularly important for the degradation of such tri- and tetrapeptide sequences (220,222,230,231). It is preferable that a polymer–drug linker does not degrade in plasma and serum. Using similar HPMA copolymer conjugates, it was shown that release of NAp in rat serum was less than 5% in 5 h, varying to some extent depending on the exact structure of the peptide linker used (Table 4) (221).

Later studies sought to optimize the design of peptidyl linkers in HPMA copolymer conjugates as a means to control the site and rate of liberation of antitumor agents, particularly doxorubicin (223,227,228,232–234). As HPMA copolymer-Gly-Phe-Leu-Gly-doxorubicin (PK1, FCE 28068) (see Fig. 6) liberated doxorubicin over approximately 48 h when incubated with tritosomes (Fig. 12), this conjugate showed the ability to localize in solid tumors by the EPR effect (235–237) and demonstrated antitumor activity against a panel of solid tumor models including M5076 (237), Walker sarcoma (238), human colon xenograft LS174T (236,237), and established subcutaneous P388 (198) and B16 melanoma models (239). This compound was selected for clinical development.

HPMA copolymer-Gly-Phe-Leu-Gly-doxorubicin is stable in human serum, in vitro (223) and does not lead to liberation of drug in the circulation in vivo (240). The rate of anthracycline (doxorubicin and epirubicin) release from HPMA copolymers correlates with in vivo efficacy and toxicity (18,236,237). When doxorubicin conjugates with the slower releasing tripeptide linkers P-Gly-Phe-Gly-Dox and P-Gly-Leu-Gly-Dox were administered intraperitoneally (i.p.) to treat mice bearing an i.p. L1210 ascitic tumor model they proved more effective than conjugates with the faster-releasing tetrapeptide spacers. The slower release kinetics of the tripeptide linkers maintained a more sustained and relatively lower level of doxorubicin for a longer period of time in vivo. HPMA copolymer-doxorubicin conjugates containing a nondegradable linkers (e.g., P-Gly-Gly-Dox) did not display antitumor activity (241,242), confirming the need for lysosomotropic delivery with drug liberation.

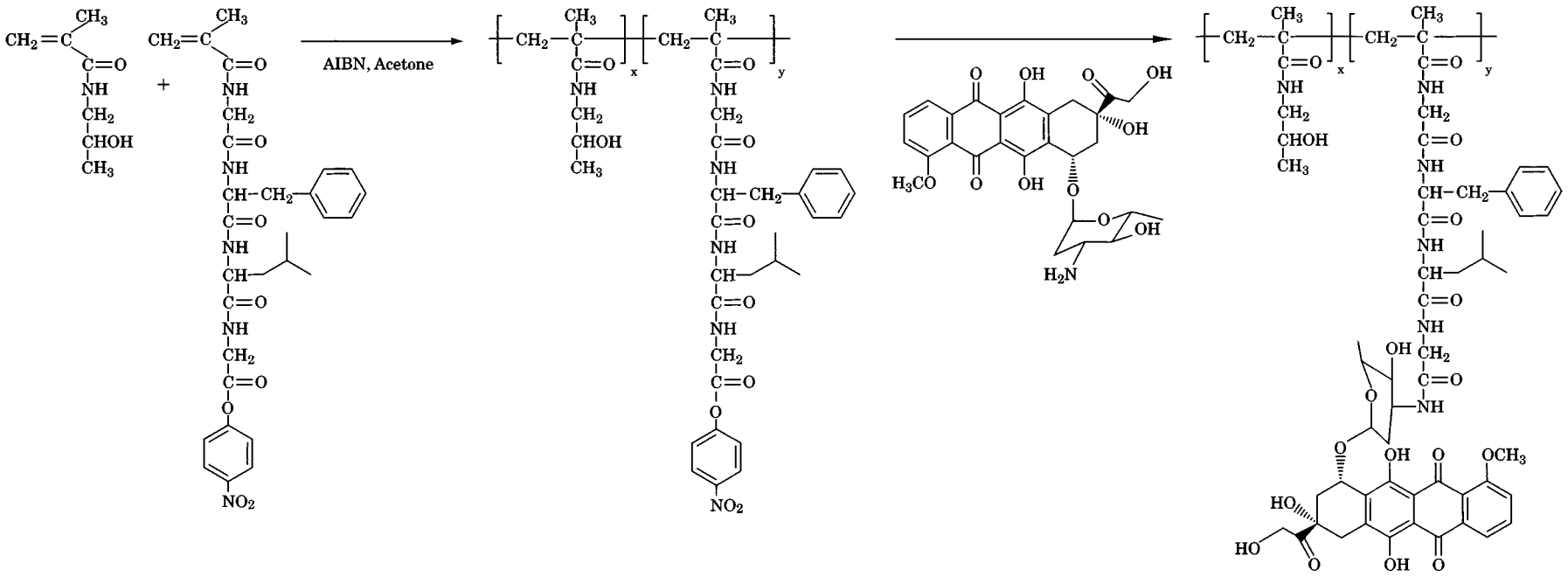


Figure 9. Aminolysis of a HPMA copolymer, an example of the polymer analogous reaction (184).

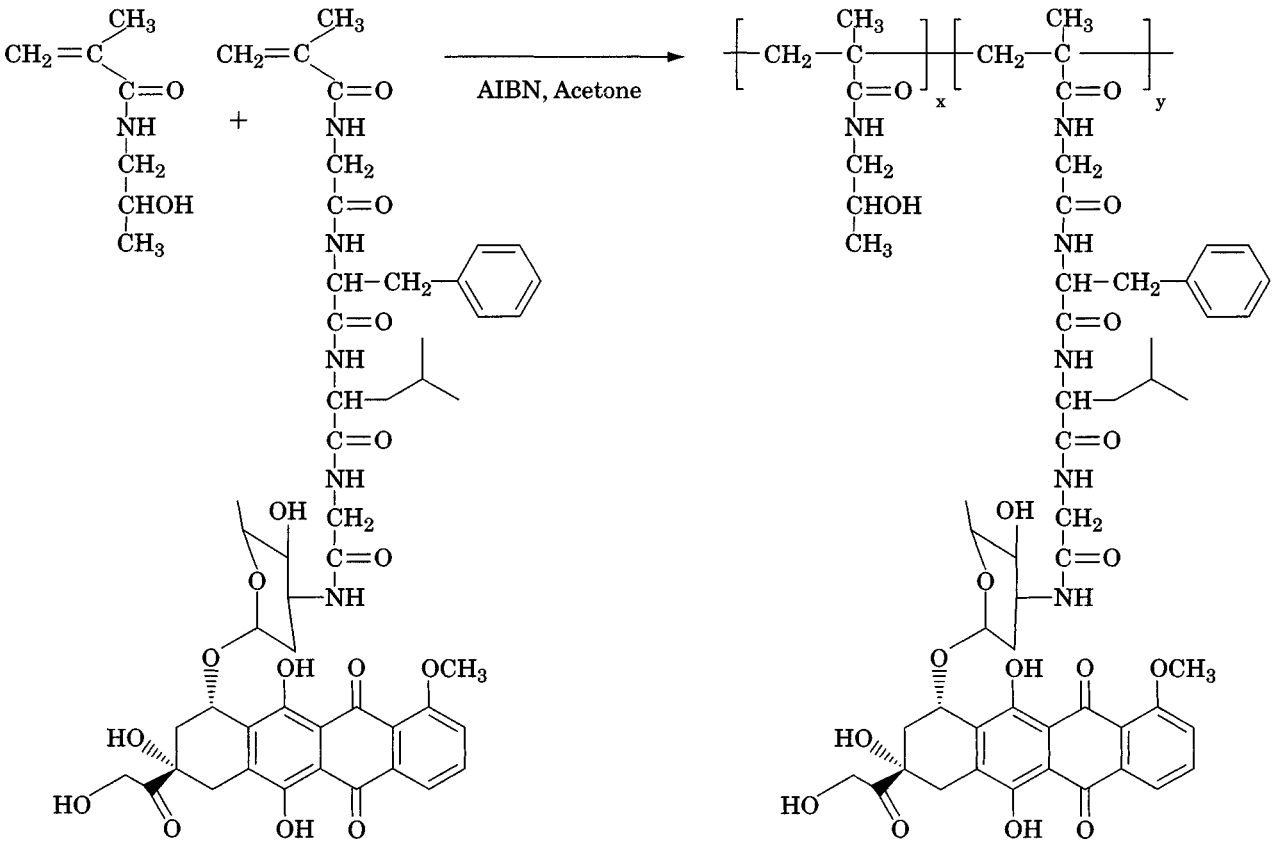


Figure 10. Preparation of HPMA copolymer-doxorubicin conjugate by the copolymerization of hydroxyproplymethacrylamide and a methacrylated doxorubicin tetrapeptide derivative (20).

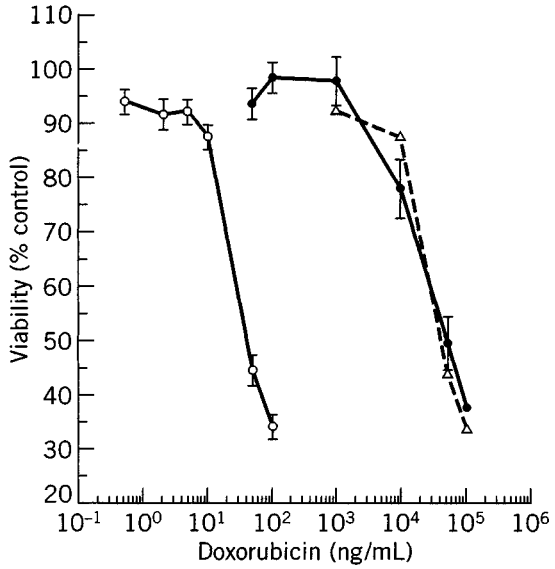


Figure 11. In vitro cytotoxicity of HPMA copolymer doxorubicin (PK1) during incubation with L1210 cells. Cytotoxicity of doxorubicin (○), PK1 (●), and the free doxorubicin present in the PK1 preparation (△) as measured by the MTT assay (72h) are shown (198).

Alkylating agents have also been conjugated to HPMA copolymers using peptidyl linkers (234). For example, HPMA copolymer–melphalan conjugates prepared with a variety of peptidyl linkers were less toxic than free melphalan and exhibited improved antitumor activity against Walker sarcoma (subcutaneous). Again, the peptidyl linker structure influenced drug release in vitro and this release rate correlated with anticancer activity seen in vivo. No antitumor activity was observed when melphalan was conjugated to HPMA copolymers via a nondegradable linker (P-Gly-Mel), again confirming that drug liberation was required for antitumor activity to be observed.

The rate of drug release from the polymer chain can also vary according to the polymer molecular weight and the amount of drug conjugated to the polymer. As greater amounts of hydrophobic drug are conjugated onto a hydrophilic polymer, the possibility to form polymeric micelles increases (243). Micellar conjugate structures may hinder access of the lysosomal enzymes to degrade the linker and release the conjugated drug. Additionally, hydrophilic polymers conjugated to hydrophobic drugs can exhibit a lower critical solution temperature where phase separation occurs and the conjugate becomes insoluble. Simple turbidometric assays (244) have been used as a preliminary screen to determine the propensity for phase separation of various HPMA copolymer-doxorubicin conjugates of different molecular weight and drug loading (245). As a

Table 2. Bonds Used to Conjugate Drugs to Polymer Pendent Chains

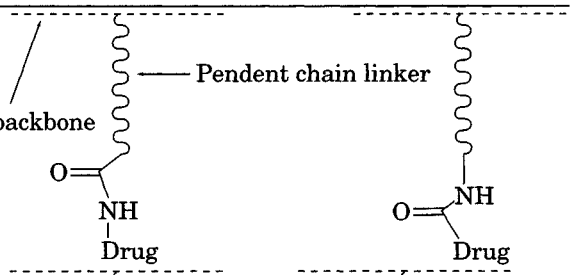
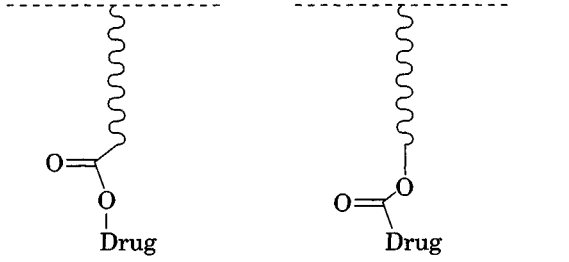
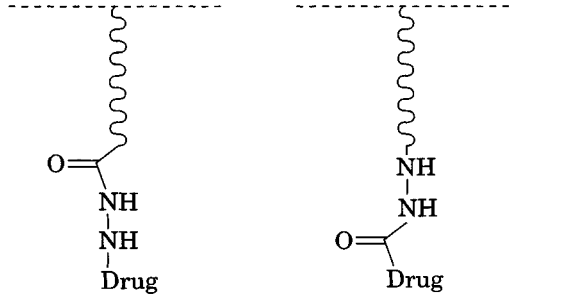
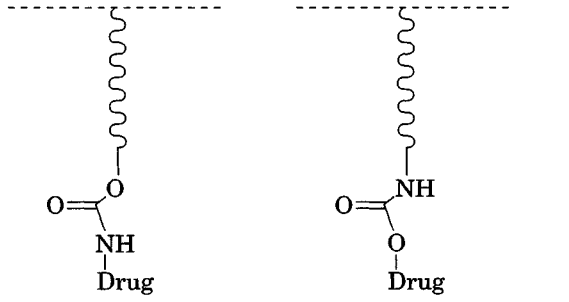
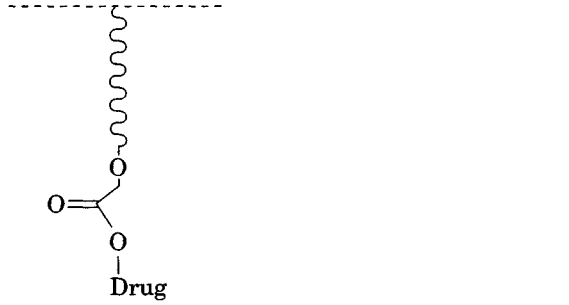
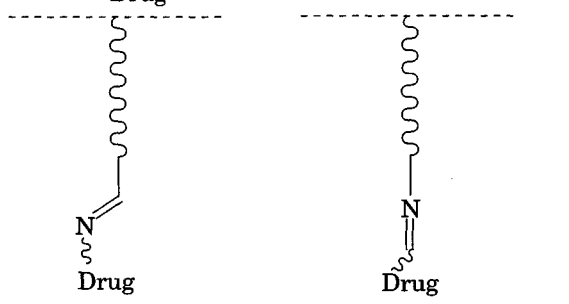
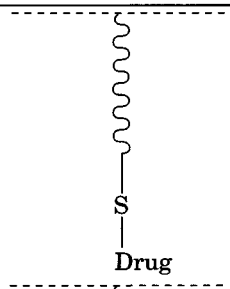
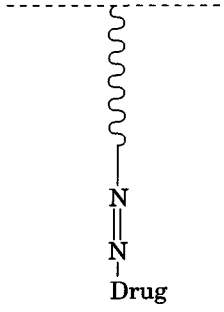
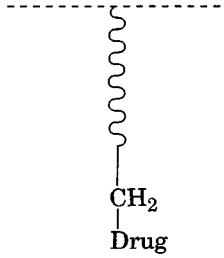
Bond linking drug to pendent chain	Structure
Amide	
Ester	
Hydrazide	
Urethane (carbamate)	
Carbonate	
Imine (Schiff base)	

Table 2. Bonds Used to Conjugate Drugs to Polymer Pendent Chains *(continued)*

Bond linking drug to pendent chain	Structure
Thioether	
Azo	
Carbon-carbon	

drug is released from a polymer conjugate, it would be expected that changes in polymer conformation will occur that might also lead to differences in drug release rate with time (246,247) and therefore pharmacological properties. The extent of drug loading and its influence on polymer solution properties is an important and yet poorly understood phenomenon and may well have a fundamental effect on the in vivo properties of therapeutic polymer conjugates.

A second HPMA copolymer conjugate containing the Gly-Phe-Leu-Gly-doxorubicin side chain has entered clinical testing, PK2 FCE 28069 (Fig. 13) (79,248–251). This conjugate benefits from the liver targeting mediated by introduction of galactosamine into the PK2 structure and demonstrated antitumor activity in two liver metastatic models: i.v. administered M5076 (237) and B16 melanoma (252).

A variety of anticancer agents have now been conjugated to other macromolecules using peptidyl linkers (12). For example, doxorubicin has been conjugated to poly(L-glutamic acid) (19,253,254), carboxymethylpullulan (131) and 6-*O*-carboxymethylchitin (130) via peptidyl linkers. Other anticancer agents including mitomycin (180) and paclitaxel (255–257) have also been conjugated to different polymers using peptidyl linkers (12,13,130,180,181). These cytotoxic compounds are potent and, when administered to patients, share similar problems as observed with doxorubicin, e.g., high toxicity and low solubility. The stability of mitomycin C (MMC) conjugated to PHEG (M_w~20,000 Da) (Fig. 14) (180,258) using peptidyl linkages has been systematically studied by measuring drug release in the presence of lysosomal enzymes (tritosomes, cathepsins B and D) and type IV collagenase in vitro. As expected, release characteristics were dependent on the structure of the peptide linker used (13,181).

The longer length spacers such as the hexapeptide (P-Gly-Phe-Leu-Gly-Phe-Leu-MMC) and the tetrapeptide (P-Gly-Phe-Ala-Leu-MMC) were readily degraded by tritosomes to release up to 80% of the conjugated MMC in 5 h, whereas tripeptide linkers released <10% MMC in the same time period (259). However, it was noted that the PHEG-hexa- and PHEG-tetrapeptide-MMC conjugates released Leu-MMC and Gly-MMC as well as free drug. These single amino acid–mitomycin derivatives were hydrolyzed (95%) in buffer (3 h) to give free MMC and were considerably less stable than the PHEG–MMC conjugates. This increased stability was attributed to the formation of polymeric intramolecular micelles with the MMC localized within the micellar core and thus making it less accessible for hydrolytic release (13,181). The in vivo antitumor activity of PHEG–MMC conjugates against P388 leukemia and C26 colorectal carcinoma solid tumors was highest for

Table 3. Stability of HPMA Copolymers Bearing Peptidyl Side Chains Terminating in NAp During Incubation with Lysosomal Enzymes

Peptidyl Side Chain	NAp release by Tritosomes (−GSH) Rate of degradation (nmol/h)	NAp release by Tritosomes (+GSH) Max. linear rate of release (%h)	NAp release by cathepsin B (%h)
	Dipeptides		
P[a]-Gly-Leu-NAp	0	0	—
P-Gly-Phe-NAp	0	0	—
P-Acap-Phe-NAp	15.6	0.6	—
P-Acap-Leu-NAp	0	0	0
	Tripeptides		
P-Gly-Ala-Phe-NAp	0	—	0.2
P-Gly-Ala-Tyr-NAp	0	0	—
P-Gly-Gly-Phe-NAp	0	0.4	0
P-Gly-Ileu-Ala-NAp	—	—	5.8
P-Gly-Ileu-Phe-NAp	0	1.4	—
P-Gly-Ileu-Tyr-NAp	0	6.0	—
P-Gly-Leu-Ala-NAp	—	—	7.8
P-Gly-Leu-Phe-NAp	7.8	3.0	—
P-Gly-Phe-Ala-NAp			10.6
P-Gly-Phe-Phe-NAp	0	3.0	—
P-Gly-D,Phe-Phe-NAp	0	3.6	—
P-Gly-Phe-Tyr-NAp	0	2.4	—
P-Gly-Val-Phe-NAp	0	3.7	2.2
	Tetrapeptides		
P-Ala-Gly-Val-Phe-NAp	0	12.6	2.4
P-Gly-Gly-Phe-Phe-NAp	4.3	1.8	—
P-Gly-Gly-Phe-Tyr-NAp	8.3	—	—
P-Gly-Gly-Val-Phe-NAp	0	3.1	—
P-Gly-Phe-Gly-Phe-NAp	—	—	0.2
P-Gly-Phe-Tyr-Ala-NAp	—	—	17.0
	Others		
P-Gly-Phe-Leu-Gly-Phe-NAp	—	NL[b]	0.2
P-Gly-Gly-Phe-Leu-Gly-Phe-NAp	—	NL	—

[a]HPMA copolymer backbone.
[b]NL, nonlinear.
Source: From Refs. 220, 228, 231, 233.

Table 4. Stability of HPMA Copolymers Bearing Peptidyl Side Chains Terminating in NAp During Incubation with Rat Plasma and Serum

Peptide linker	Percentage NAp released/5 h	
	Plasma	Serum
P[a]-Gly-Leu-Ala-NAp	0.9	0.9
P-Gly-Phe-Ala-NAp	0.0	0.9
P-Ala-Gly-Val-Phe-NAp	0.0	0.5
P-Gly-Phe-Phe-Ala-NAp	1.0	2.2
P-Gly-Phe-Phe-Leu-NAp	1.5	2.1
P-Gly-Phe-Leu-Gly-NAp	1.5	1.7
P-Gly-Phe-Tyr-Ala-NAp	1.3	1.3
P-Gly-Phe-Leu-Gly-Phe-NAp	3.3	3.8
P-Gly-Gly-Phe-Leu-Gly-Phe-NAp	3.5	5.1

[a]HPMA copolymer backbone.
Source: From Ref. 221.

the linkers with the best hydrolytic stability, e.g., P-Gly-Phe-Leu-Gly-Phe-Leu-MMC and P-Gly-Phe-Ala-Leu-MMC.

Peptidic linkers have also been used to bind the antimetabolite 5-fluorouracil (5-FU) to a variety of different polymers (259–263). The clinical dose of 5-FU is relatively high (often more than 500 mg/m^2), thus, this anticancer agent may not be the best candidate for polymer conjugation unless high levels of polymer substitution can be achieved, or the tumor targeting mediated by the EPR effect results in significantly increased therapeutic benefit. 5-FU is, however, an interesting candidate, as unlike other commonly used anticancer agents such as doxorubicin and mitomycin, 5-FU is not polycyclic nor is lipophilic. These structural differences might allow the higher polymer loading of 5-FU needed while maintaining favorable physicochemical characteristics of such conjugates, e.g., plasma solubility, low blood protein binding, and the relatively open polymer conformation needed for enzymatic lysosomal degradation and drug liberation.

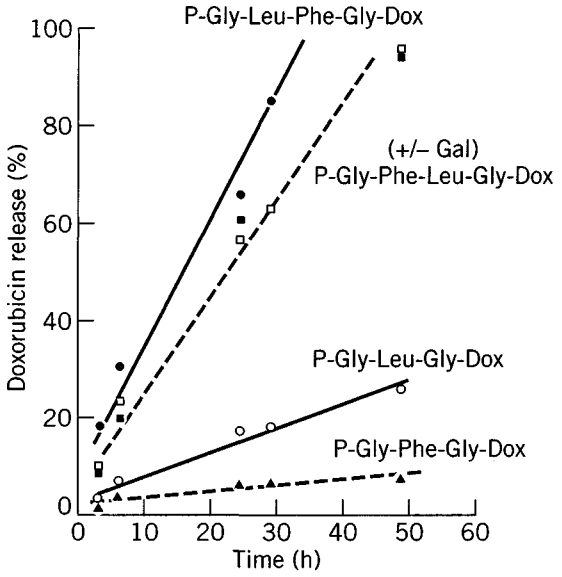


Figure 12. Release of doxorubicin from HPMA copolymer-peptide-doxorubicin conjugates during incubation with rat liver lysosomal enzymes (tritosomes). *Source:* Ref. 223.

PEG-, dextran- and PHEG-5-FU conjugates with about 1–4 wt % loading exhibited in vitro release of 5-FU that was dependent on the linker amino acid sequence (259,260). The peptide linkers chosen to bind 5-FU to these polymers had the structure P-Gly-Phe-X-Gly(5-FU)OEt (OEt is an ethyl moiety; on an acid denotes an ethyl ester) where P is the polymer backbone and X was Gly, Ala, Leu or Phe (Fig. 15). 5-FU was conjugated at the α-position of the glycine ethyl ester at the linker terminus. Initially cleavage by lysosomal enzymes gave X-Gly(5-FU)OEt (13), which then underwent further hydrolysis to produce free 5-FU. The release rate due to hydrolysis was slower in buffer at pH 5.5 (maximum drug release was 3% in 24 h) than at pH 7.4. (Maximum release ranged between 10 and 20% in 24 h depending on the structure of the peptide linker.) The degree of 5-FU liberation was greatest in the order PEG>PHEG>dextran and decreased with increased 5-FU content in the polymer.

Similar studies have been conducted using HPMA copolymers possessing peptidyl linkers terminated with an α-glycine derivative of 5-FU (2–3 mol %) (Fig. 16). These conjugates also exhibited release profiles that were a function of linker structure (261,262), and 5-FU was released as a dipeptide 5-FU derivative (261). The total length of the oligopeptide sequence (tetra- vs. hexapeptide), the stereochemistry of 5-FU substitution at the α-position of glycine (L or D) and the hydrophobicity of the penultimate

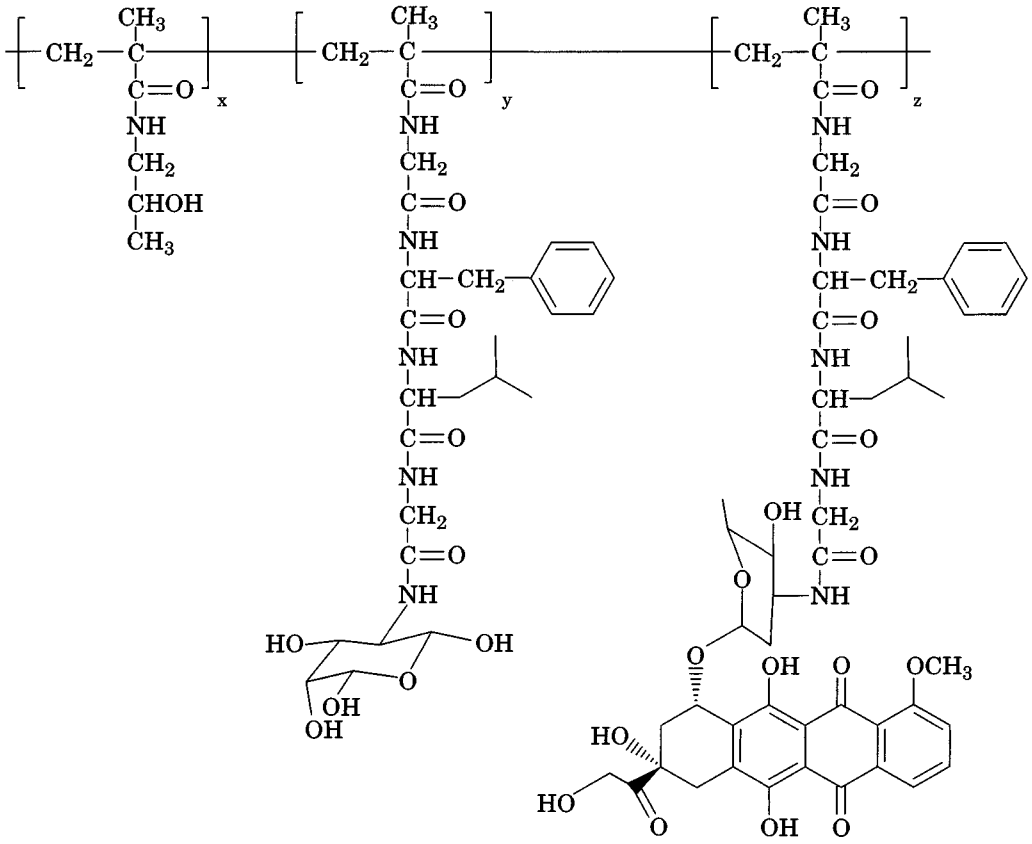


Figure 13. Structure of PK2. The conjugate has a molecular weight of approximately 28,000 Da, a doxorubicin content of approximately 7 wt %, and approximately 4 mol % galactosamine.

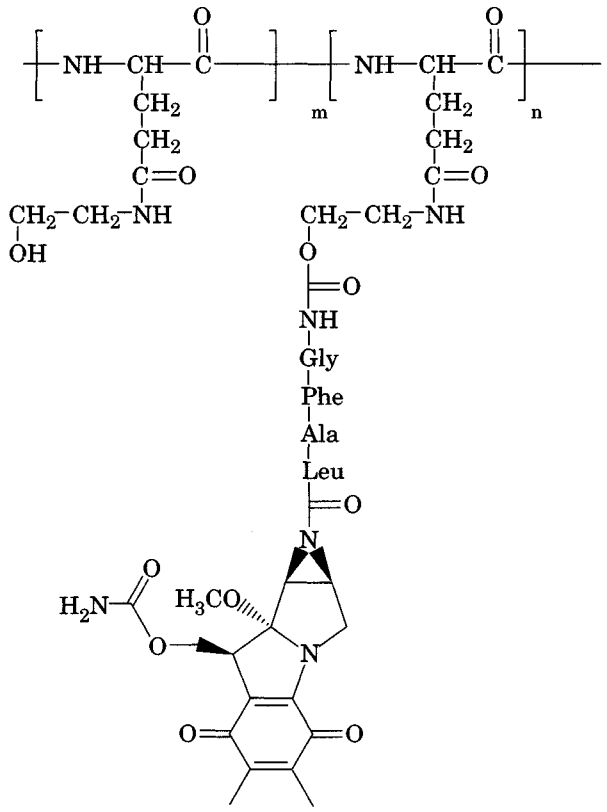


Figure 14. Structure of a PHEG conjugate of MMC using peptidic pendent chains (179,180,258).

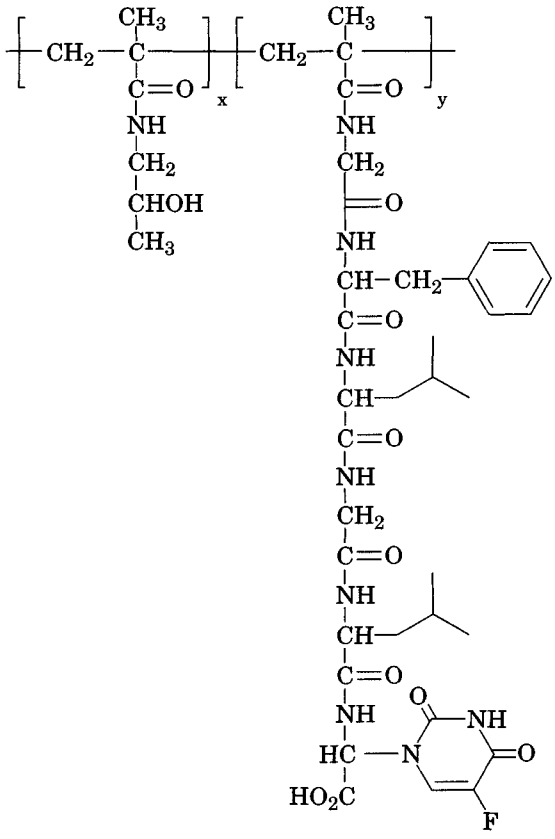


Figure 16. Structure of a HPMA copolymer–5-FU conjugate using peptidic pendent chains (261–263).

amino acid (Ala or Leu) all influenced the in vitro enzymatic release of 5-FU from HPMA copolymers, but in contrast with the studies mentioned already where tetrapeptide linkers in PEG, PHEG, and dextran resulted in 5-FU release, only the hexapeptide linkers in the HPMA copolymers underwent in vitro enzymatic cleavage to release 5-FU (261).

HPMA copolymers containing the -Gly-Phe-Leu-Gly linker used to prepare PK1 and PK2 have recently been used as a platform for conjugation of other antitumor agents. HPMA copolymer–paclitaxel conjugates (Fig. 17) contain an ester bond between a paclitaxel hydroxyl (C-2′) and the amino acid carboxylate at the terminus of the pen-

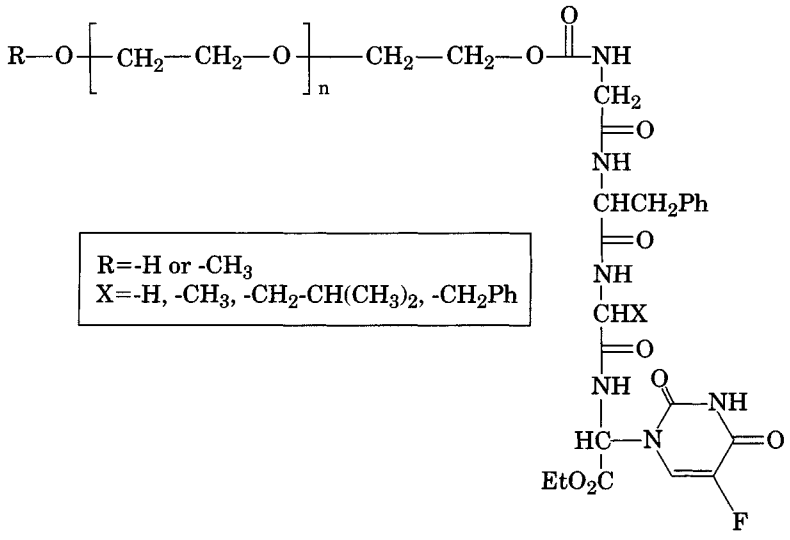


Figure 15. Structure of a PEG-5-FU conjugate. End-group conjugation (259,260).

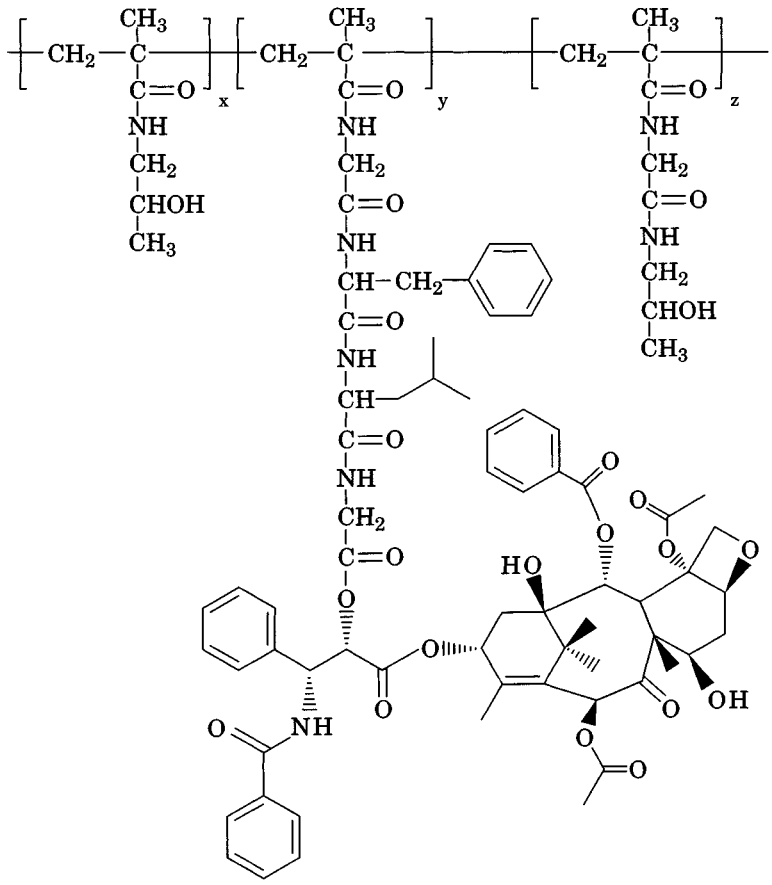


Figure 17. Structure of a HPMA copolymer–paclitaxel conjugate using peptidic pendent chains that are covalently bonded to the paclitaxel by an ester bond (255).

dent chain (255–257,264). In this case, the terminal bond linking the drug to the peptide pendent chain is not a hydrolytically stable amide bond (265,266). This may give rise to other possible hydrolytic mechanisms for drug liberation. These HPMA copolymer–paclitaxel conjugates were prepared to create a water-soluble paclitaxel conjugate that would slowly release free paclitaxel as the ester bond underwent hydrolysis, and in vivo studies (B16F10, M109, and M5076 murine models) showed that the conjugate exhibited greater efficacy of the conjugate compared to free paclitaxel.

Recently two types of HPMA copolymer–platinum chelates have been described. HPMA copolymers containing peptidyl side chains (Gly-Gly or Gly-Phe-Leu-Gly) terminating in carboxylate groups were allowed to react with cisplatin (E. Gianasi et al., unpublished data), or alternatively the same HPMA copolymers containing peptidyl sequences terminating in a diamine were allowed to react with potassium tetrachloroplatinate (Fig. 18) (E. Gianasi et al., unpublished data). The resultant HPMA copolymer platinates had a M_w of 25,000–31,000 Da with a platinum loading of 3–10 wt %. In vitro the HPMA copolymer platinates displayed a range of platinum release rates at pH 7.4 and 5.5; from <5%/24 h in the case of the diamino species, which requires lysosomal enzymatic degradation, up to >80%/24 h in the case of the carboxylate, which is a relatively poor hydrolytically labile ligand. Cisplatin and not surprisingly the fast-releasing carboxylate species displayed IC_{50} values of ~10 μg/mL Pt-equivalent against B16F10 cells in vitro, whereas the slow-releasing conjugates were not cytotoxic over the dose range studied. When conjugates were administered i.p. to treat i.p. L1210 tumors, the antitumor activity seen was within the range for free cisplatin. However, when conjugates were administered i.v. to treat subcutaneous (s.c.) B16F10 tumors grown to palpable size, free cisplatin was not active, but the HPMA copolymer platinates bearing carboxylate and diamine platinates showed significant antitumor activity. Activity in the solid tumor model was attributed to the tumor targeting by the EPR effect; a ~60-fold increase in Pt AUC in B16F10 tumor tissue than was achieved after administration of cisplatin (E. Gianasi et al., unpublished data).

Hydrolytically Labile Pendent Chain Linkers

The relatively low pH within the endosomal and lysosomal compartments and the observation that the extracellular, interstitial environment in some tumors is also acidic (267,268) has inspired the development of pendent chain linkers that hydrolytically degrade more quickly at pH values less than 7.4. *Cis*-aconityl acid and Schiff base derivatives are the two predominant types of hydrolytically labile linkers that have been explored. An advantage of conjugating a drug via an acid-labile linker is that free drug alone can be released from the pendent chain rather than amino acid or peptide drug derivatives, which can occur with peptidyl linkers.

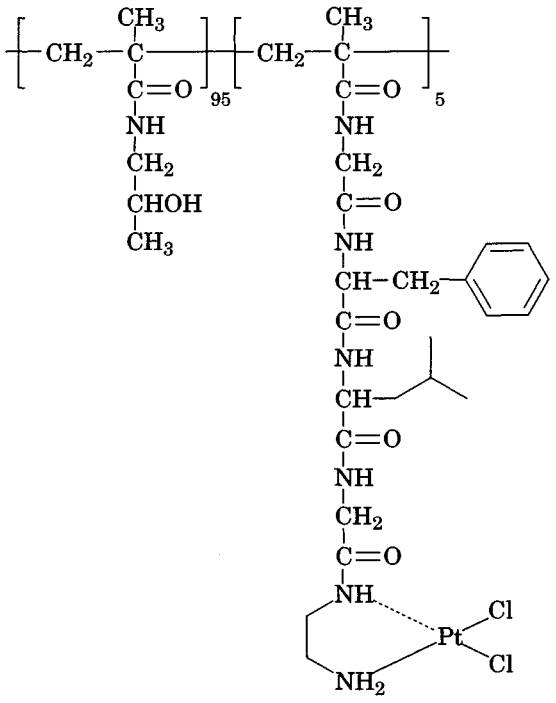


Figure 18. Structure of a HPMA copolymer-platinate (E. Gianasi et al., unpublished data).

The first example employing *cis*-aconityl linkers was the conjugation of daunomycin to poly(D-lysine) and Affi-Gel 701 (amionethyl polyacrylamide beads) (224). Poly(L-lysine) was not selected because it was thought in vivo degradation of this polymer would compete with release of daunomycin (269). When linked to Affi-Gel the *cis*-aconityl linker had a half-life for hydrolysis of 96 h at pH 6 but only 3 h at pH 4. The *cis*-aconityl linker has subsequently been used to conjugate anthracyclines to other synthetic poly(amino acids) (147,270), egg-white lysozyme (271), polysaccharides (127), lectins (272), alginates (synthesis shown in Figure 19) (127) and to monoclonal antibodies (Fig. 20) (149,158,273,274). Daunomycin release from alginate-*cis*-aconityl conjugates (127) incubated in buffers of different pH increased with lowering pH (Fig. 21). It has been pointed out that in some studies uncertainty exists as to which carboxylate is conjugated to the macromolecule (13). However, improved synthetic strategies have been developed so the *cis*-aconityl moiety can be unambiguously conjugated to the polymer at the requisite carboxylate to ensure pH-dependent drug release (272,273). Two possible mechanisms for *cis*-aconityl hydrolysis (275) are based on neighboring group interactions of the *cis*-carboxylic acid at lower pH values that accelerate the hydrolytic release of the conjugated drug (Fig. 22) (11,13).

Hydrazone-derived Schiff base bonds linking doxorubicin [and other drugs (276)] to polymers (277) have been prepared. These adducts may have slowly released doxorubicin while both in circulation and upon endocytosis (277). Analogous doxorubicin-immunoconjugates have also been studied (153,154,278). Doxorubicin conjugated via a Schiff base to oxidized dextran (176,177,279–281) has undergone Phase I evaluation (282). The Schiff base was prepared first by the mild periodate oxidation of dextran to generate aldehyde functionality then by reaction of the amino moiety on doxorubicin.

Other Linkers

Linkers which are not lysosomally degradable peptides or pH-labile moieties have been used to prepare soluble polymer–drug conjugates. As with the aforementioned polymer–drug conjugates, circulation times tend to be increased compared to the free drug. Slow release of drug may occur resulting in prolonged drug action (21,34). Typically the drug can be conjugated directly to an existing pendent chain or endgroup as, for example, the conjugation of paclitaxel to the side chains of poly(L-glutamic acid) (182) or the endgroups of PEG (91–93,283). Drug can also be conjugated by chelation (Figs. 18 and 23) (129,207–214; E. Gianasi et al., unpublished data).

Sometimes an amino acid (e.g., ϵ-aminocaprioticacid or lysine) or an aliphatic spacer serves as a conjugating linker. Amide or ester bonds are generally the limiting degradable bonds in these linkers (i.e., the bond expected to be cleaved to release drug), but carbonate, iminocarbonate, urea, and dithiol moieties along with metal chelates have also been used (12,13,15,20). Pendent chain degradation to release the drug in these conjugates is probably a combination of both enzymatic and hydrolytic release mechanisms. For example, conjugation of *cis*-hydroxy proline to PEG–lysine copolymers (Fig. 24) (284–286) by an amide bond resulted in higher activity compared to conjugates bound by a more hydrolytically labile ester bond (285). Such observations may be due to a combination of release mechanisms or by multivalent interactions. This example also illustrates the possibility for direct conjugation of a drug to an existing polymer side chain.

Conjugates of 5-FU with poly(α-1,4-galactosamine) and *N*-acetyl-α-1,4-polygalactosamine linked with a hexamethlene spacer via urea bonds had drug loadings ranging from 17 to 58 mol % (126). Unfortunately these conjugates were poorly water soluble. Hydrolysis of the urea bonds was faster than the degradation of the glycosidic bonds of the polysaccharide backbone. Administration of the conjugates to animals bearing P388 lymphocytic leukemia resulted in life span increases greater than seen with free 5-FU. This prolongation in survival correlated with increased 5-FU loading and dose of the conjugate. To improve solubility, 5-FU was conjugated to another polysaccharide, 6-*O*-carboxymethyl chitin (287). Conjugation was via amide and ester bonds through pentamethylene linkers and produced 5-FU loading of up to 35.2 mol %. Release from the chitin was slower (6% over 20 h) compared to the chitosan conjugates (25% over 20 h). Again with the P388 lymphocytic leukaemia model (i.p. tumor and i.p. treatment), life span increased with increasing dose of the chitin conjugate. Conjugates of 5-FU via amide, ester, and carbamoyl bonds to poly(α-malic acid) have also been investigated (134).

As mentioned previously, the micelle-forming properties of macromolecules comprised of both hydrophobic and hydrophilic domains can influence the rate of drug release in the lysosome. This property can be exploited to carry

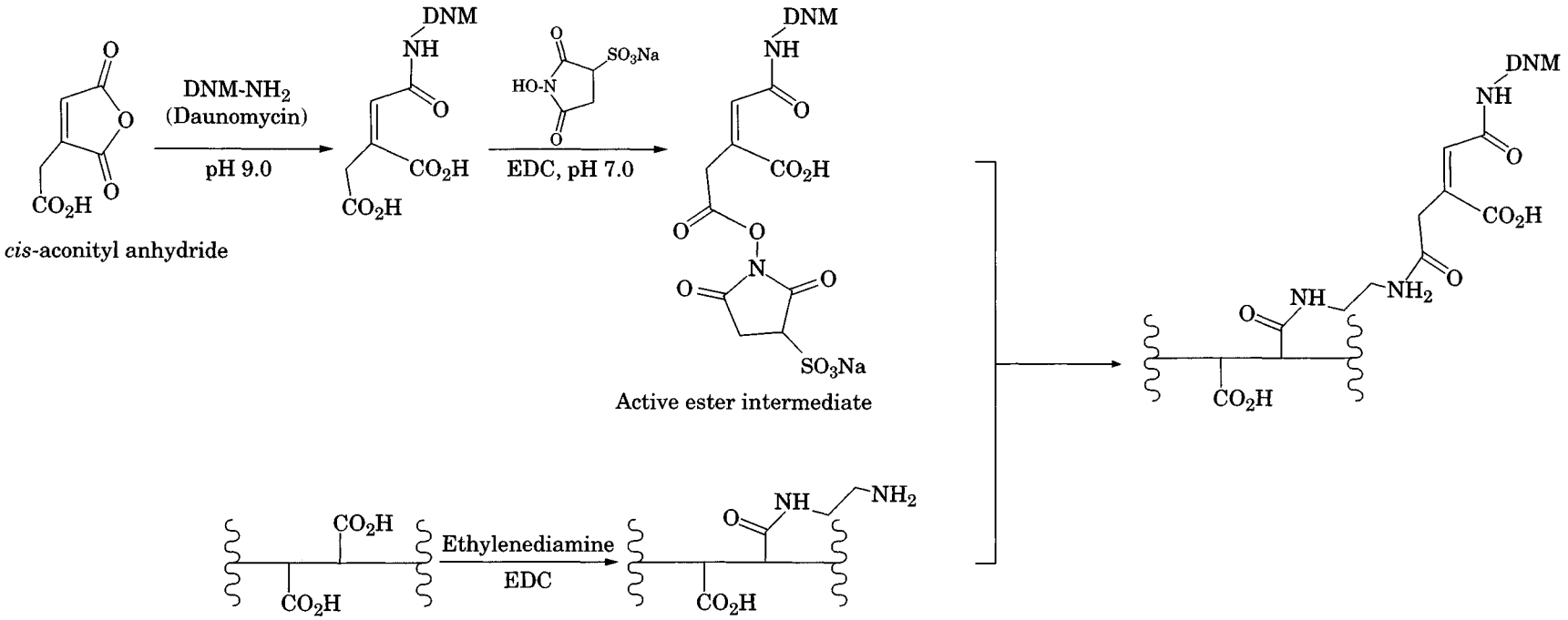


Figure 19. Preparation of alginate conjugates containing *cis*-aconityl-daunomycin (127).

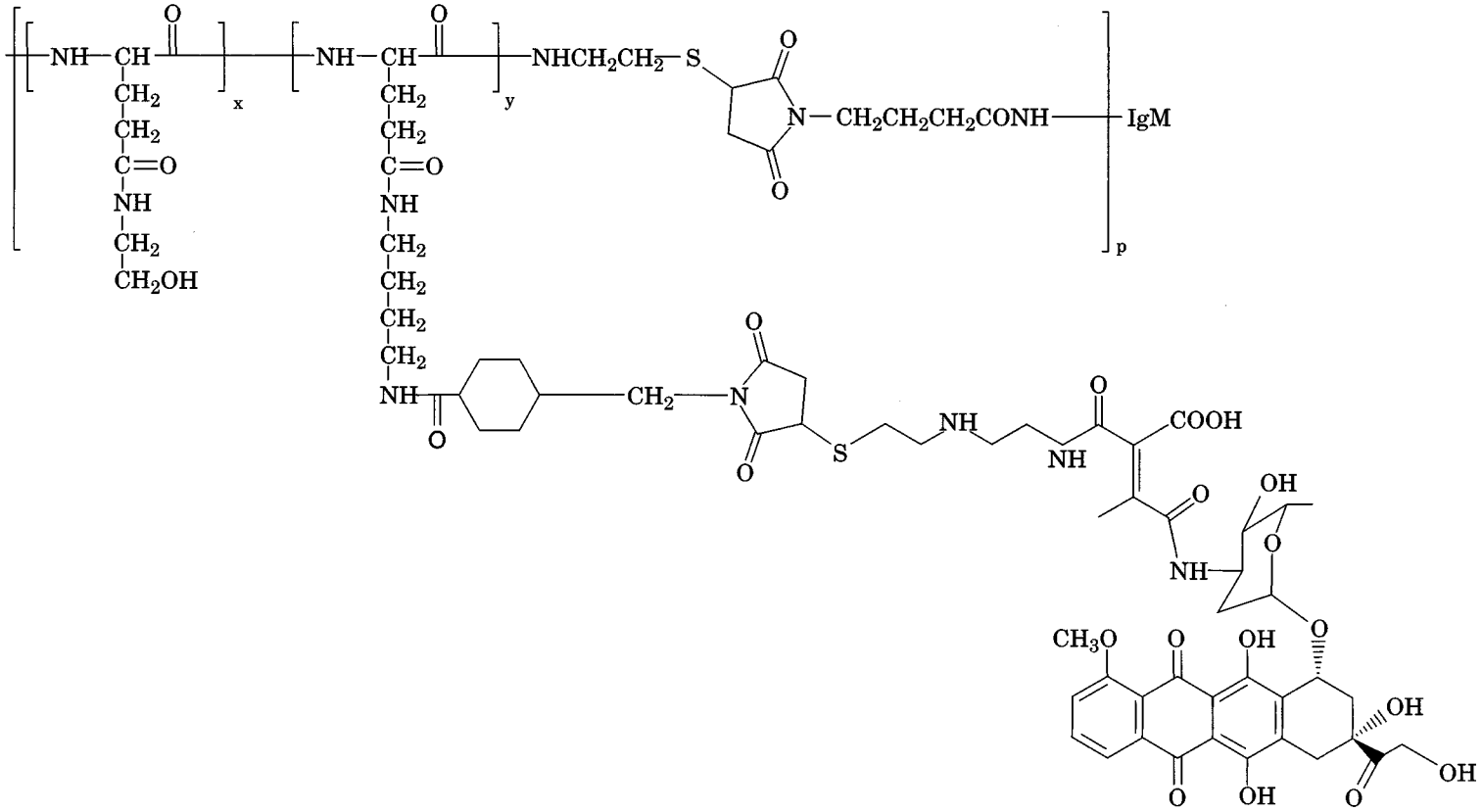


Figure 20. Structure of a PHEG-doxorubicin maleamic acid derived conjugate that is also conjugated to a human IgM (149).

Next Page

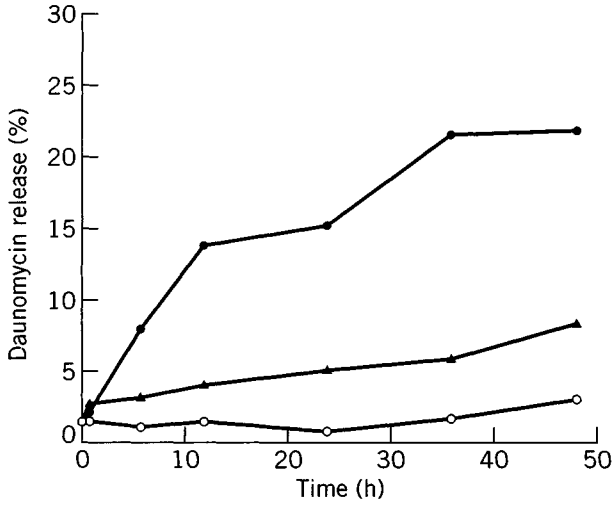


Figure 21. Release of daunomycin from alginate *cis*-acontinyl-daunomycin incubated in buffers of different pH. Release at pH 7 (○), pH 6 (▲) and pH 5 (●) is shown. *Source:* Ref. 127.

large amounts (up to 37 mol %) of doxorubicin within micelles which spontaneously form with PEG-poly(α,β-aspartic acid) AB-block copolymers (11,100,161,162,165,166, 289,290). Doxorubicin was conjugated by an amide bond directly to the pendent carboxyl moieties of the block copolymer (Fig. 25). Although the M_w of the block copolymer was approximately 14,000 Da and would have been expected to clear relatively quickly from circulation, these conjugates did exhibit increased tumor uptake. Micelle formation involved aggregation of several polymer chains to give constructs with an effective molecular weight exceeding 10^6 Da with a diameter of 50 nm. The hydrophilic PEG existed predominantly on the outer shell and the more hydrophobic poly(aspartic acid)-doxorubicin blocks existed within the micelle structure. The micelle remained stable in the presence of serum proteins (165) with low RES accumulation and prolonged circulation with 10% of the conjugate still in the blood after 24 h (160). These observations were attributed to minimal interaction of the PEG micellar surface with circulating proteins and with PEG-induced micellar stabilization. Biodistribution was dependent on micelle stability because with less stable micelles, free polymer was readily excreted. There was lowered toxicity (1/20 compared with free doxorubicin) and reduced nonspecific accumulation in major organs including heart, lung, and liver. In vivo studies with several murine and human solid tumor models (C 26, C 38, M 5076, and MX-1) resulted in higher antitumor activity compared with free doxorubicin.

It is increasingly evident that multivalent interactions (290) of polymeric molecules at cell surfaces can cause important biological effects (291,292); therefore, it is not necessary to rely on lysosomal delivery to exhibit pharmacological activity. Hence in this case, it is necessary to design linkers that do not degrade specifically in the lysosome. For example, the amino acid lysine has been used to link a carbohydrate, lysoganglioside GM_3 (a sialyl moiety), sphingosine, and a fluorescent probe to poly(glutamic acid) (Fig. 26) (293). This conjugate was designed to act as a multivalent inhibitor of influenza hemagglutinin at receptors on the cell surface. Affinities for carbohydrate–receptor interactions may potentially be increased using polymers conjugated with monomeric carbohydrate ligands to act as multivalent ligands. In vitro studies indicated that this conjugate inhibited the influenza virus by a dual mechanism: (*1*) by the action of the sialyl moieties binding hemagglutinin proteins on the surface of the virus and (*2*) by hydrophobic interactions at the membrane caused by the conjugated sphingosine.

CLINICAL PROGRESS

Although the literature contains many examples of polymeric anticancer conjugates only dextran-doxorubicin (AD-70, DOX-OXD) (282) and three HPMA copolymer conjugates (of molecular weight approximately 30,000 Da) incorporating the peptidyl (Gly-Phe-Leu-Gly) side chain (PK1, PK2, and PNU 166945) have so far entered controlled Phase I/II clinical trials.

In Phase I studies HPMA copolymer-Gly-Phe-Leu-Gly-doxorubicin (PK1, FCE 28068) (see Fig. 6) given once every 3 weeks displayed greatly reduced toxicity compared with free doxorubicin and showed evidence of activity in chemotherapy refractory patients (240,294,295). The maximum tolerated dose (MTD) of PK1 was 320 mg/m^2 (doxorubicin equivalent), and this is 4–5 times higher than the usual clinical dose of free doxorubicin. There was no evidence of the PK1-related cardiotoxicity (despite individual cumulative doses of up to 1,680 mg/m^2 doxorubicin-equivalent), and the dose limiting toxicity was bone marrow suppression. No polymer-related toxicity was observed, and PK1 is currently undergoing Phase II trials. In contrast, the dextran-doxorubicin conjugate (AD-70, DOX-OXD) of molecular weight of approximately 70,000 Da also administered on a thrice-weekly schedule had an MTD of 40 mg/m^2 doxorubicin-equivalent (282), somewhat lower than that seen for doxorubicin alone (60–80 mg/m^2). The severe hepatotoxicity seen after administration of AD-70, DOX-OXD was attributed to uptake of the conjugate by the RES. This could have been simply caused by the choice of dextran as a carrier and/or the fact that doxorubicin was conjugated to dextran via a Schiff base. Although a structural study of a doxorubicin-oxidized dextran conjugate was published after the clinical trial (177), no details of the preparation or properties of the conjugate used in this Phase I study (e.g., loading of doxorubicin, amount of free unconjugated doxorubicin) are available. Further information relating to the formulation used and the kinetics of doxorubicin release might help establish exactly why the increased toxicity was observed. Observations from one study suggest that doxorubicin might be released from dextran prior to tumor cell uptake of the conjugate (176). Reduction of the Schiff base in the dextran–doxorubicin conjugates to give a nonhydrolytic (and presumably nondegradable) amine bond (296–298) did show increased therapeutic indices compared with free doxorubicin, but the antitumor activities were not high enough to warrant continued development (176).

Previous Page

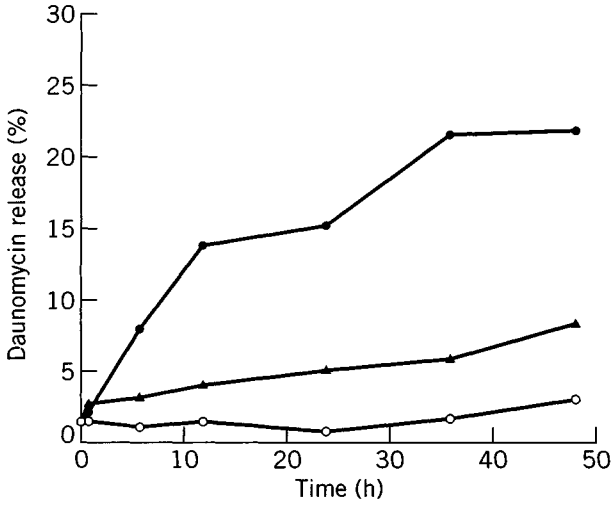


Figure 21. Release of daunomycin from alginate *cis*-acontinyl-daunomycin incubated in buffers of different pH. Release at pH 7 (○), pH 6 (▲) and pH 5 (●) is shown. *Source:* Ref. 127.

large amounts (up to 37 mol %) of doxorubicin within micelles which spontaneously form with PEG-poly(α,β-aspartic acid) AB-block copolymers (11,100,161,162,165,166, 289,290). Doxorubicin was conjugated by an amide bond directly to the pendent carboxyl moieties of the block copolymer (Fig. 25). Although the M_w of the block copolymer was approximately 14,000 Da and would have been expected to clear relatively quickly from circulation, these conjugates did exhibit increased tumor uptake. Micelle formation involved aggregation of several polymer chains to give constructs with an effective molecular weight exceeding 10^6 Da with a diameter of 50 nm. The hydrophilic PEG existed predominantly on the outer shell and the more hydrophobic poly(aspartic acid)-doxorubicin blocks existed within the micelle structure. The micelle remained stable in the presence of serum proteins (165) with low RES accumulation and prolonged circulation with 10% of the conjugate still in the blood after 24 h (160). These observations were attributed to minimal interaction of the PEG micellar surface with circulating proteins and with PEG-induced micellar stabilization. Biodistribution was dependent on micelle stability because with less stable micelles, free polymer was readily excreted. There was lowered toxicity (1/20 compared with free doxorubicin) and reduced nonspecific accumulation in major organs including heart, lung, and liver. In vivo studies with several murine and human solid tumor models (C 26, C 38, M 5076, and MX-1) resulted in higher antitumor activity compared with free doxorubicin.

It is increasingly evident that multivalent interactions (290) of polymeric molecules at cell surfaces can cause important biological effects (291,292); therefore, it is not necessary to rely on lysosomal delivery to exhibit pharmacological activity. Hence in this case, it is necessary to design linkers that do not degrade specifically in the lysosome. For example, the amino acid lysine has been used to link a carbohydrate, lysoganglioside GM_3 (a sialyl moiety), sphingosine, and a fluorescent probe to poly(glutamic acid) (Fig. 26) (293). This conjugate was designed to act as a multivalent inhibitor of influenza hemagglutinin at receptors on the cell surface. Affinities for carbohydrate–receptor interactions may potentially be increased using polymers conjugated with monomeric carbohydrate ligands to act as multivalent ligands. In vitro studies indicated that this conjugate inhibited the influenza virus by a dual mechanism: (*1*) by the action of the sialyl moieties binding hemagglutinin proteins on the surface of the virus and (*2*) by hydrophobic interactions at the membrane caused by the conjugated sphingosine.

CLINICAL PROGRESS

Although the literature contains many examples of polymeric anticancer conjugates only dextran-doxorubicin (AD-70, DOX-OXD) (282) and three HPMA copolymer conjugates (of molecular weight approximately 30,000 Da) incorporating the peptidyl (Gly-Phe-Leu-Gly) side chain (PK1, PK2, and PNU 166945) have so far entered controlled Phase I/II clinical trials.

In Phase I studies HPMA copolymer-Gly-Phe-Leu-Gly-doxorubicin (PK1, FCE 28068) (see Fig. 6) given once every 3 weeks displayed greatly reduced toxicity compared with free doxorubicin and showed evidence of activity in chemotherapy refractory patients (240,294,295). The maximum tolerated dose (MTD) of PK1 was 320 mg/m^2 (doxorubicin equivalent), and this is 4–5 times higher than the usual clinical dose of free doxorubicin. There was no evidence of the PK1-related cardiotoxicity (despite individual cumulative doses of up to 1,680 mg/m^2 doxorubicin-equivalent), and the dose limiting toxicity was bone marrow suppression. No polymer-related toxicity was observed, and PK1 is currently undergoing Phase II trials. In contrast, the dextran-doxorubicin conjugate (AD-70, DOX-OXD) of molecular weight of approximately 70,000 Da also administered on a thrice-weekly schedule had an MTD of 40 mg/m^2 doxorubicin-equivalent (282), somewhat lower than that seen for doxorubicin alone (60–80 mg/m^2). The severe hepatotoxicity seen after administration of AD-70, DOX-OXD was attributed to uptake of the conjugate by the RES. This could have been simply caused by the choice of dextran as a carrier and/or the fact that doxorubicin was conjugated to dextran via a Schiff base. Although a structural study of a doxorubicin-oxidized dextran conjugate was published after the clinical trial (177), no details of the preparation or properties of the conjugate used in this Phase I study (e.g., loading of doxorubicin, amount of free unconjugated doxorubicin) are available. Further information relating to the formulation used and the kinetics of doxorubicin release might help establish exactly why the increased toxicity was observed. Observations from one study suggest that doxorubicin might be released from dextran prior to tumor cell uptake of the conjugate (176). Reduction of the Schiff base in the dextran–doxorubicin conjugates to give a nonhydrolytic (and presumably nondegradable) amine bond (296–298) did show increased therapeutic indices compared with free doxorubicin, but the antitumor activities were not high enough to warrant continued development (176).

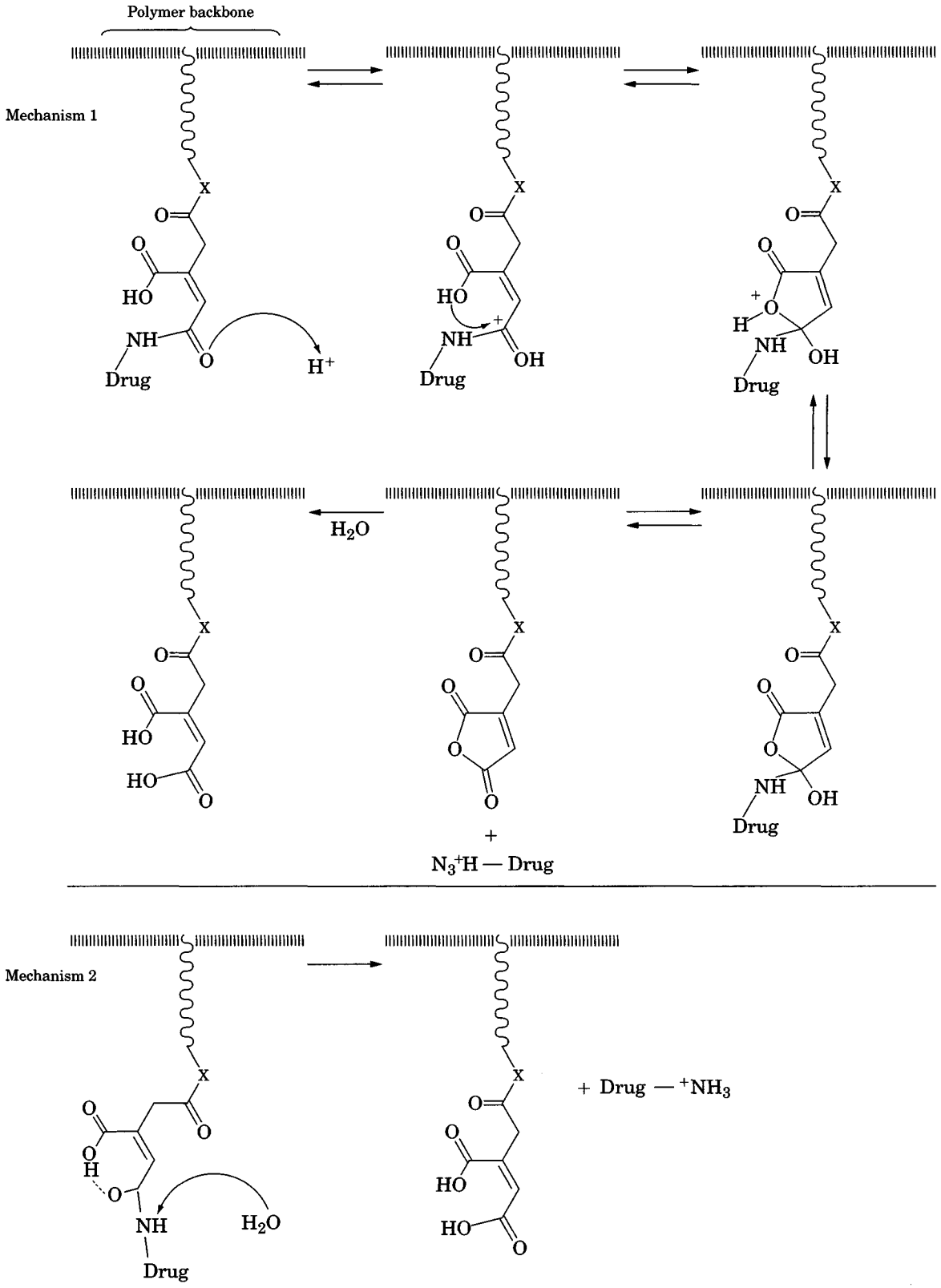


Figure 22. Possible mechanisms for acid-assisted hydrolysis of a *cis*-aconityl linker (11,13,275).

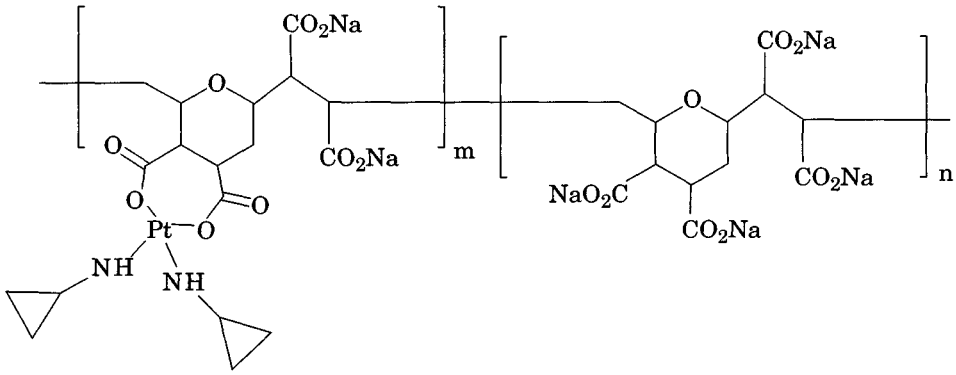


Figure 23. Chelation of platinum to the side chains of DIVEMA (129).

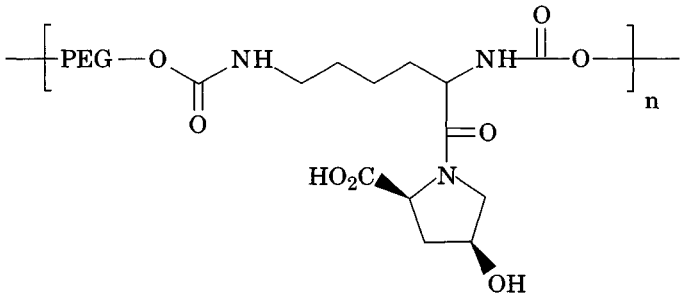


Figure 24. Structure of a PEG–lysine copolymer–hydroxyproline conjugate. Direct conjugation to a polymer side chain (284–286).

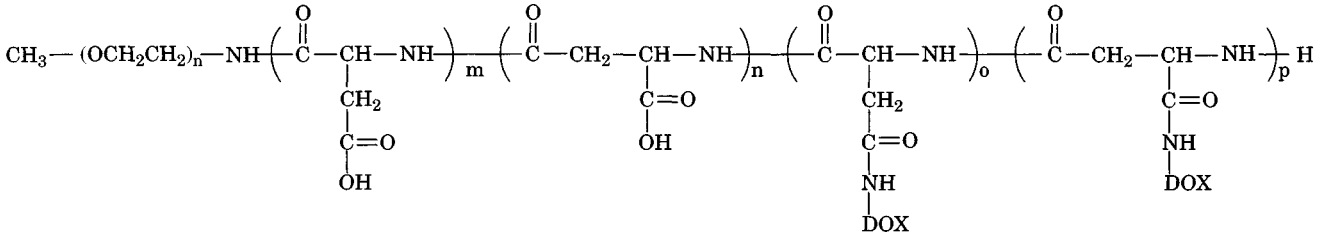


Figure 25. Structure of a PEG/poly(α,β-aspartic acid) AB-block copolymer–doxorubicin conjugate that can form polymeric micelles (11,98).

In Phase I/II trials of the HPMA copolymer doxorubicin–galactosamine conjugate, PK2 (see Fig. 13) (79,248–251), which is currently ongoing, the MTD for bolus (short infusion) administration of PK2 was found to be 160 mg/m^2 doxorubicin-equivalent with a dose limiting toxicity of neutropenia. Using an imaging analogue of PK2, γ camera imaging in humans verified that liver targeting of the conjugate occurred in patients having primary or secondary liver cancer. Liver targeting is now being maximized using a 24 h infusion rather than a rapid infusion.

During Phase I evaluation of an HPMA copolymer–paclitaxel conjugate (PNU 166945, see Fig. 17) (257) 13 patients were treated every 3 weeks with a 1 h infusion of conjugate at paclitaxel-equivalent doses of 80, 100, 140, and 196 mg/m^2. No significant myelosupression was observed up to the highest doses used, but grade 3 neurotoxicity was observed at 146 mg/m^2 paclitaxel-equivalents in one patient. Antitumor activity was observed (refractory breast cancer [1 patient] and disappearance of sigmoid cancer ascites [1 patient]), but the trial was interrupted due to concerns about neurotoxicity.

There are currently several other polymer–drug conjugates in preclinical development, and these compounds will soon to be evaluated clinically as anticancer compounds. They include an HPMA copolymer–camptothecin analogue, an HPMA copolymer platinate (see Fig. 18), poly(glutamic acid)-paclitaxel (see Fig. 8) (182), and a polymeric micelle containing noncovalently bound doxorubicin (168,169).

The two HPMA copolymer conjugates, like their previous relatives, contain the -Gly-Phe-Leu-Gly polymer–drug linkage. Although it is too early to draw definitive conclusions concerning the optimum means of polymer–drug conjugation, it is clear from the clinical experience emerging with PK1 and PK2 that drug conjugation via a peptidyl linker can only liberate anticancer agent after cleavage by lysosomal proteases is able to reduce the toxicity of the bound drug and may produce increased efficacy. Early

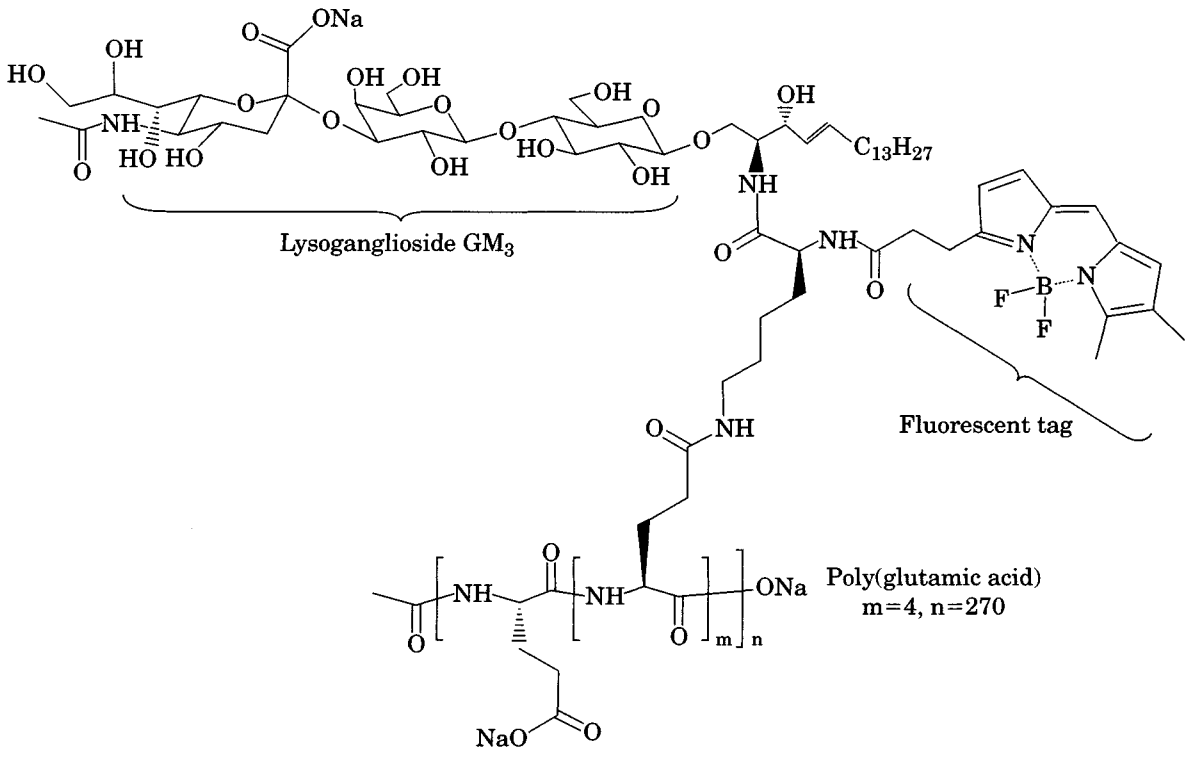


Figure 26. Structure of a multivalent poly(glutamic)–lysoganglioside conjugate designed for multivalent inhibition of influenza hemagglutinin at receptors on the cell surface (293).

clinical trials in oncology are designed to evaluate the safety of the therapy and determine the optimum dose (and schedule) for the later efficacy studies, not antitumor activity. However, the anticancer activity observed with PK1, PK2, and PNU 166945 is very encouraging, particularly as there is still an opportunity to maximize tumor targeting of such conjugates by the EPR effect with the aid of an optimal dosing schedule or polymer conjugate administration. There is also an opportunity to tailor further the rate of drug liberation from HPMA copolymer conjugates to suit the mechanism of action of the individual antitumor agent used in each case.

Most of the polymer–anticancer conjugates thus far described contain a relatively low drug payload (typically 5–10 wt % drug). Higher loading is often prohibited by loss of solubility. The clinical data emerging with the use of HPMA copolymer conjugates would advocate selection of more potent (than doxorubicin) anticancer agents for conjugation. Alternatively there is an obvious need for more hydrophilic carriers with greater solubilizing capacity.

CONCLUSIONS

It is evident from the early studies with anticancer compounds that polymer–drug conjugates have the potential to provide improved chemotherapy. The three basic components of a polymer–drug conjugate (i.e., polymer, linker, and drug) must be optimally matched to maximize therapeutic potential. Although the sophistication of synthetic chemistry can provide a plethora of structures, design based on the biological rationale and incorporating cost and simplicity is imperative if compounds of real clinical value are to emerge. There is a need for continued basic research in chemistry to produce novel, preferentially biodegradable, polymers and to examine the effects of polymer architecture (e.g., dendrimers and hyperbranched polymers) on pharmacokinetics at the whole organism and cellular level. Further effort is needed to understand the details of the biological fate of polymer–drug conjugates. Although considerable progress has been made with peptidyl linkers, there is the possibility that research could fall into the "Me too" trap. New families of linkers designed with a clear rationale for bioactivation are required. Each polymer–drug conjugate is a unique molecule, so increased effort will be needed to prepare uniform conjugates. Systematic and improved analytical methods are required to correlate structure–property relationships required to optimize the biological profile of preclinical candidates.

Undoubtedly polymer–drug conjugates will progress from clinical trials in cancer patients to use in treatment of other diseases. These compounds will only succeed if designed to accommodate the pathophysiology of a chosen disease. Future success in developing polymer–drug conjugates will hinge upon the ability of people in the disciplines of pharmaceutical science (e.g., chemistry, biology, and medicine) to look at drug development with a new perspective focused on the properties of large molecules.

BIBLIOGRAPHY

1. R. Duncan, *Chem. Ind. (London)*, pp. 262–264 (1997).
2. P. Mason, *Pharm. J.* **260**, 382–385 (1998).

3. C. Monfardini and F. Veronese, *Bioconjugate Chem.* **9**, 418–450 (1998).
4. S. Zalipsky, *Adv. Drug Delivery Rev.* **16**, 157–182 (1995).
5. C. Delgado, G. Francis, and D. Fisher, *Crit. Rev. Ther. Drug Carrier Syst.* **9**, 249–304 (1992).
6. M.L. Nucci, D. Shorr, and A. Abuchowski, *Adv. Drug Delivery Rev.* **6**, 133–151 (1991).
7. G. Francis et al., *J. Drug Target.* **3**, 321–340 (1996).
8. S. Herman, G. Hooftman, and E. Schacht, *J. Bioact. Compat. Polym.* **10**(2), 145–187 (1995).
9. G. Hooftman, S. Herman, and E. Schacht, *J. Bioact. Compat. Polym.* **11**(2), 135–159 (1996).
10. V. Alakhov and A. Kabanov, *Expert Opin. Invest. Drugs* **7**(9), 1453–1473 (1998).
11. K. Kataoka, in K. Park, ed., *Controlled Drug Delivery: Challenges and Strategies*, American Chemical Society, Washington, D.C., 1997, pp. 49–71.
12. R. Duncan, S. Dimitrijevic, and E. Evagorou, *S.T.P. Pharma. Sci.* **6**, 237–263 (1996).
13. H. Soyez, E. Schacht, and S. Vanderkerken, *Adv. Drug Delivery Rev.* **21**, 81–106 (1996).
14. M. Nishikawa, Y. Takakura, and M. Hashida, *Adv. Drug Delivery Rev.* **21**, 135–155 (1996).
15. D. Putnam and J. Kopecek, *Adv. Polym. Sci.* **122**, 55–123 (1995).
16. H. Maeda, in A.J. Domb, ed., *Polymer Site-Specific Pharmacotherapy*, Wiley, New York, 1994, pp. 95–116.
17. R. Duncan and F. Spreafico, *Clin. Pharmacokinet.* **27**, 290–306 (1994).
18. R. Duncan, *Anti-Cancer Drugs* **3**, 175–210 (1992).
19. C. Hoes and J. Feijen, in F. Roerdink and A. Kroon, eds., *Drug-Carrier Systems*, Wiley, England, Chichester, 1989, pp. 57–109.
20. R. Duncan and J. Kopecek, *Adv. Polym. Sci.* **57**, 51–101 (1984).
21. H. Ringsdorf, *J. Polym. Sci. Polym. Symp.* **51**, 135–153 (1975).
22. I. Mellman, *Annu. Rev. Cell Dev. Biol.* **12**, 575–625 (1996).
23. R. Duncan and M. Pratten, in R. Dean and W. Jessup, eds., *Mononuclear Phagocytes: Physiology and Pathology*, Elsevier Biomedical Press, Amsterdam, 1985, pp. 27–51.
24. A. Barret and M. Heath, in J. Dingle, ed., *Lysosomes: A Laboratory Handbook*, 2nd ed., North-Holland, New York and Oxford, 1977, pp. 19–147.
25. C. deDuve et al., *Biochem. Pharmacol.* **23**, 2495–2531 (1974).
26. A. Trouet, D. Campeneere, and C. deDuve, *Nat. (London), New Biol.* **239**, 110–112 (1972).
27. L. Sprincl, J. Exner, O. Sterba, and J. Kopecek, *J. Biomed. Mater. Res.* **10**, 953–963 (1976).
28. L. Sprincl, J. Vacik, J. Kopecek, and D. Lim, *J. Biomed. Mater. Res.* **5**, 197–205 (1971).
29. H. Ringsdorf et al., in T. Sugahara and O. Hug, eds., Igaku Shoin, Tokyo, 1971, p. 138.
30. I. Iliev, M. Georgieva, and V. Kabaivanov, *Russ. Chem. Rev. (Engl. Transl.)* **43**(1), 69–75 (1974).
31. W. Regelson, *Adv. Chemother.* **3**, 303–371 (1968).
32. W. Regelson, in N. Bikales, ed., *Water Soluble Polymers II*, Plenum, New York, 1973, pp 161–177.
33. W. Regelson et al., in A. Rembaum and E. Seligny, eds., *Polyelectrolytes and their Application*, Reidel Publ., Dordrecht, The Netherlands, 1974, pp. 131–144.
34. H. Batz, H. Ringsdorf, and H. Ritter, *Makromol. Chem.* **175**(8), 2229–2239 (1974).
35. B. Weiner, M. Tahan, and A. Zilkha, *J. Med. Chem.* **15**(4), 410–413 (1972).
36. S. Foster and J. Lloyd, *Biochim. Biophys. Acta* **947**, 465–491 (1988).
37. P. Goddard and K. Petrak, *J. Bioact. Compat. Polym.* **4**, 372–402 (1989).
38. H. Chiu, P. Kopeckova, S. Deshmane, and J. Kopecek, *J. Biomed. Mater. Res.* **34**, 381–392 (1997).
39. Y. Matsumura and H. Maeda, *Cancer Res.* **6**, 6387–6392 (1986).
40. H. Maeda, L. Seymour, and Y. Miyamoto, *Bioconjugate Chem.* **3**, 351–362 (1992).
41. H. Maeda, *J. Controlled Release* **19**, 315–324 (1992).
42. R. Jain, *Cancer Res.* **48**, 2641–2658 (1988).
43. R. Jain, *J. Nat. Cancer Inst.* **81**, 570–576 (1989).
44. F. Yuan et al., *Cancer Res.* **55**, 3752–3756 (1995).
45. H. Maeda and Y. Matsumura, *CRC Crit. Rev. Ther. Drug Carrier Sys.* **6**(3), 193–210 (1989).
46. Y. Takakura, T. Fujita, M. Hashida, and H. Sezaki, *Pharm. Res.* **7**, 339–436 (1990).
47. Y. Noguchi et al., *Jpn. J. Cancer Res.* **89**, 307–314 (1998).
48. E. Day, J. Palnisek, and M. Pressman, *J. Natl. Cancer Inst. (U.S.)* **23**, 799–805 (1959).
49. H. Peterson and K. Appelgren, *Eur. J. Cancer* **9**, 543–548 (1973).
50. H. Dvorak, V. Harvey, and J. McDonagh, *Cancer Res.* **44**, 3348–3354 (1984).
51. A. Babson and T. Winnick, *Cancer Res.* **14**, 606–611 (1954).
52. J. Hradec, *Br. J. Cancer* **12**, 290–294 (1961).
53. C. Andersson, B. Iresjo, and K. Lundholm, *J. Surg. Res.* **50**, 156–162 (1991).
54. G. Stehle et al., *Crit. Rev. Oncol. Hematol.* **26**, 77–100 (1997).
55. A. Wunder et al., *Int. J. Oncol.* **11**, 497–507 (1997).
56. R. Jain and L. Baxter, *Cancer Res.* **48**, 7022–7032 (1988).
57. T. Shockley et al., *Cancer Res.* **52**, 357–366 (1992).
58. L. Nugent and R. Jain, *Am. J. Physiol.* **246**, H129–H137 (1984).
59. Y. Tabata, Y. Murakami, and Y. Ikada, *J. Controlled Release* **50**, 123–133 (1998).
60. L. Seymour et al., *Eur. J. Cancer* **31A**(5), 766–770 (1995).
61. P. Steyger et al., *J. Controlled Release* **39**, 35–46 (1996).
62. K. Iwai, H. Maeda, and T. Konno, *Cancer Res.* **44**, 2114–2121 (1984).
63. H. Maeda et al., *J. Med. Chem.* **28**, 455–461 (1985).
64. L. Seymour et al., *Br. J. Cancer* **70**, 636–641 (1994).
65. R. Duncan and Y. Sat, *Ann. Oncol.* **9**(S2), 149 (1998).
66. S. Hobbs et al., *Proc. Natl. Acad. Sci. U.S.A.* **95**, 4607–4612 (1998).
67. R. Duncan et al., *Biochim. Biophys. Acta* **840**, 291–293 (1985).
68. L. Seymour, R. Duncan, J. Strohalm, and J. Kopecek, *J. Biomed. Mater. Res.* **21**, 1341–1358 (1987).
69. C. Hopkins and I. Trowbridge, *J. Cell Biol.* **97**, 508–521 (1983).
70. I. Trowbridge and D. Domingo, *Nature (London)* **294**, 171–173 (1981).
71. P.D. Smidt and J.V. Berkel, *CRC Crit. Rev. Ther. Drug Carrier Syst.* **7**, 99–120 (1990).

72. C. King, *Cancer Biol.* **1**, 329–337 (1990).
73. C. Robinson, *Trends Biotechnol.* **9**, 147–148 (1991).
74. G. Ghanem *Int. J. Cancer* **41**, 248–255 (1988).
75. D. Vera, R. Stadalnick, and K. Krohn, *J. Nucl. Med.* **26**, 1157–1167 (1985).
76. R. Fallon and A. Schwartz, *Adv. Drug Delivery Rev.* **4**, 49–63 (1989).
77. P. Dragsten, D. Mitchell, G. Covert, and T. Baker, *Biochim. Biophys. Acta* **926**, 270–279 (1987).
78. F. Ceulemans et al., *Pathol. Biol.* **35**, 61–68 (1987).
79. R. Duncan et al., *Biochim. Biophys. Acta* **880**, 62–71 (1986).
80. L. Seymour et al., *Br. J. Cancer* **63**, 859–866 (1991).
81. L. Seymour, *J. Bioact. Compat. Polym.* **6**, 178–216 (1991).
82. M. Otterlei et al., *J. Immunother.* **10**, 286–291 (1991).
83. W. Regelson, *J. Natl. Cancer Inst.* **81**, 1920–1930 (1989).
84. N. Burnham, *Am. J. Hosp. Pharm.* **51**, 210–218 (1994).
85. N. Katre, *Adv. Drug Delivery Rev.* **10**, 91–114 (1993).
86. J. Harris, ed., *Poly(ethylene glycol) Biotechnical and Biomedical Applications*, Plenum, New York, 1992.
87. P. Senter et al., *Bioconjugate Chem.* **6**(4), 389–394 (1995).
88. R. Greenwald et al., *J. Med. Chem.* **39**, 1938–1940 (1996).
89. C. Conover et al., *Anticancer Res.* **17**(5A), 3361–3368 (1997).
90. R. Greenwald et al., *Bioorg. Med. Chem.* **6**(5), 551–562 (1998).
91. R. Greenwald et al., *J. Med. Chem.* **39**(2), 424–431 (1996).
92. C. Li et al., *Anticancer Drugs* **7**, 642–648 (1996).
93. R. Greenwald, *Expert Opin. Ther. Patents* **7**(6), 601–609 (1997).
94. A. Nathan et al., *Bioconjugate Chem.* **4**, 54–62 (1993).
95. A. Nathan, S. Zalipsky, and J. Kohn, *J. Bioact. Compat. Polym.* **9**(3), 239–251 (1994).
96. M. Pechar, J. Strohalm, K. Ulbrich, and E. Schacht, *Macromol. Chem. Phys.* **198**, 1009–1020 (1997).
97. M. Pechar, I. Strohalm, and K. Ulbrich, *Collect. Czech. Chem. Commun.* **60**, 1765–1780 (1995).
98. K. Kataoka et al., *J. Controlled Release* **24**, 119–132 (1993).
99. T. Inoue, G. Chen, K. Nakamae, and A. Hoffman, *J. Controlled Release* **51**, 221–229 (1998).
100. G. Kwon and T. Okano, *Adv. Drug Delivery Rev.* **21**, 107–116 (1996).
101. J. Kopecek and H. Bazilova, *Eur. Polym. J.* **9**, 7–14 (1973).
102. J. Kopecek, *Makromol. Chem.* **178**, 2169–2183 (1977).
103. V. Chytry et al., *Makromol. Chem., Rapid Commun.* **3**, 11–15 (1982).
104. J. Simeckova, D. Plocova, B. Rihova, and J. Kopecek, *J. Bioact. Compat. Polym.* **1**, 20–31 (1986).
105. B. Rihova, K. Ulbrich, J. Kopecek, and P. Mancal, *Folia Microbiol.* **28**, 217–297 (1983).
106. B. Rihova, J. Kopecek, K. Ulbrich, and V. Chytry, *Makromol. Chem., Suppl.* **9**, 13–24 (1985).
107. B. Rihova, I. Riha, *CRC Crit. Rev. Ther. Drug Carrier Syst.* **1**, 311–374 (1985).
108. B. Rihova et al., *Biomaterials* **10**, 335–342 (1989).
109. P. Schneider, T. Korolenko, and U. Busch, *Microsc. Res. Tech.* **36**, 253–275 (1997).
110. C. Hall and O. Hall, *Experientia* **17**, 544–545 (1961).
111. C. Hall and O. Hall, *Experientia* **18**, 38–40 (1962).
112. P. Goddard et al., *J. Bioact. Compat. Polym.* **6**, 4–24 (1991).
113. J. Vercauteren, D. Bruneel, E. Schacht, and R. Duncan, *J. Bioact. Compat. Polym.* **5**, 4–15 (1990).
114. W. Shalaby and K. Park, in S. Shalaby, ed., *Biomedical Polymers. Designed-to-Degrade Systems*, Hanser Publishers, New York, 1994, pp. 213–258.
115. P. Labrude and C. Vigneron, *Lyon Pharm.* **26**(6), 629–646 (1975).
116. L. Moteni, in G. Gregoriadis, ed., *Drug Carriers Biology and Medicine*, Academic Press, London, 1979, pp. 107–125.
117. T. Fujita et al., *J. Controlled Release* **11**, 149–156 (1990).
118. M. Hashida et al., *Proc. Int. Congr. Chemother.*, Kyoto, 1985.
119. H.S.Y. Imoto et al., *Cancer Res.* **52**, 4396–4401 (1992).
120. T. Nomura et al., *J. Controlled Release* **52**, 239–252 (1998).
121. H. Sezaki, Y. Takakura, and M. Hashida, *Adv. Drug Delivery Rev.* **3**, 247–266 (1989).
122. Y. Yasuda et al., *Chem. Pharm. Bull.* **38**(7), 2053–2056 (1990).
123. Y. Takakura, R. Atsumi, M. Hashida, and H. Sezaki, *Int. J. Pharm.* **37**, 147–154 (1987).
124. K. Granath and B. Kvist, *J. Chromatogr.* **28**, 69–81 (1967).
125. S. Vansteenkiste et al., *J. Controlled Release* **16**, 91–100 (1991).
126. Y. Ohya et al., *J. Controlled Release* **17**, 259–266 (1991).
127. A. Al-Shamkhani and R. Duncan, *Int. J. Pharm.* **122**, 107–119 (1995).
128. S. Morgan et al., *Int. J. Pharm.* **122**, 121–128 (1995).
129. B. Schechter, A. Neumann, M. Wilchek, and R. Arnon, *J. Controlled Release* **10**, 75–87 (1989).
130. Y. Ohya, K. Nonomura, and T. Ouchi, *J. Bioact. Compat. Polym.* **10**, 223–234 (1995).
131. H. Nogusa et al., *Chem. Pharm. Bull.* **43**, 1931–1936 (1995).
132. K. James and J. Kohn, in K. Park, ed., *Controlled Drug Delivery: Challenges and Strategies*, American Chemical Society, Washington, D.C., 1997, pp. 389–403.
133. K. Abdellaoui et al., *Eur. J. Pharm. Sci.* **6**, 61–73 (1998).
134. T. Ouchi, A. Fujino, K. Tanaka, and T. Banba, *J. Controlled Release* **12**, 143–153 (1990).
135. T. Deming, *Nature (London)* **390**, 386–389 (1997).
136. D. Carter and J. Ho, *Adv. Protein Chem.* **45**, 153–203 (1994).
137. P. Balboni et al., *Nature (London)* **264**, 181–183 (1976).
138. A. Trouet, M. Masquelier, R. Baurain, and D. Campaneere, *Proc. Natl. Acad. Sci. U.S.A.* **79**, 626–629 (1982).
139. Y. Kaneo, T. Tanaka, and S. Iguchi, *Chem. Pharm. Bull.* **38**, 2614–2626 (1990).
140. K. Ohkwada et al., *Cancer Res.* **53**, 4238–4242 (1993).
141. F. Dosio et al., *J. Controlled Release* **47**(3), 293–304 (1997).
142. T. Yasuzawa and K. Tomer, *Bioconjugate Chem.* **8**, 391–399 (1997).
143. A. Wunder et al., *Int. J. Cancer* **76**, 884–890 (1998).
144. T. Tanaka, Y. Kaneo, M. Miyashita, and S. Shiramoto, *Biol. Pharm. Bull.* **18**(2), 1724–1728 (1995).
145. T. Tanaka, Y. Kaneo, and M. Miyashita, *Biol. Pharm. Bull.* **21**(2), 147–152 (1998).
146. T. Tanaka, Y. Kaneo, and M. Miyashita, *Biol. Pharm. Bull.* **19**(5), 774–777 (1996).
147. D. Gaal and F. Hudecz, *Eur. J. Cancer* **34**(1), 155–161 (1998).
148. V. Omelyanenko et al., *J. Drug Target.* **3**, 357–374 (1996).
149. C. Hoes et al., *J. Controlled Release* **38**, 245–266 (1996).
150. E. Eno-Amooquaye et al., *Br. J. Cancer* **73**, 1323–1327 (1996).

151. R. Duncan, *Contrib. Oncol.* **48**, 170–180 (1995).
152. P. Trail, D. Willner, and K. Hellestrom, *Drug Dev. Res.* **34**, 196–209 (1995).
153. P. Trail et al., *Science* **261**, 212–215 (1993).
154. D. Willner et al., *Bioconjugate Chem.* **4**, 521–527 (1993).
155. P. Flanagan et al., *J. Controlled Release* **18**, 25–38 (1992).
156. C. Springer et al., *Eur. J. Cancer* **11**, 1362–1366 (1991).
157. M. Magerstadt, *Antibody Conjugates and Malignant Disease*, CRC Press, Boca Raton, Fl., 1990.
158. H. Yang and R. Reisfeld, *Proc. Natl. Acad. Sci. U.S.A.* **85**, 1189–1193 (1988).
159. L. Gros, H. Ringsdorf, and H. Schupp, *Angew. Chem., Int. Ed. Eng.* **20**, 301–323 (1981).
160. G. Kwon et al., *Pharm. Res.* **10**, 970–974 (1993).
161. G. Kwon and K. Kataoka, *Adv. Drug Delivery Rev.* **16**, 295–309 (1995).
162. M. Yokoyama, *Crit. Rev. Ther. Drug Carrier Syst.* **9**, 213–248 (1992).
163. P. Calibresi and B. Chabner, in J.G. Hardman and L.E. Limbird, eds., *The Pharmacological Basis of Therapeutics*, McGraw-Hill, New York, 1996, pp. 1225–1288.
164. A. Kabanov and V. Alakhov, *J. Controlled Release* **28**, 15–35 (1994).
165. M. Yokayama, T. Okano, Y. Sakurai, and K. Kataoka, *J. Controlled Release* **32**, 269–277 (1994).
166. M. Yokoyama et al., *Cancer Res.* **51**, 3229–3236 (1991).
167. M. Yokoyama et al., *J. Controlled Release* **50**, 79–92 (1998).
168. E. Batrakova et al., *Br. J. Cancer* **74**(10), 1545–1552 (1996).
169. A. Venne et al., *Cancer Res.* **56**(16), 3626–3629 (1996).
170. D. Bruneel and E. Schacht, *Polymer* **34**(12), 2628–2632 (1993).
171. D. Bruneel and E. Schacht, *Polymer* **34**(12), 2633–2637 (1993).
172. D. Bruneel and E. Schacht, *Polymer* **35**(12), 2656–2658 (1993).
173. R. Vercauteren, E. Schacht, and R. Duncan, *J. Bioact. Compact. Polym.* **7**, 346–357 (1992).
174. D. Bruneel and E. Schacht, *J. Bioact. Compat. Polym.* **10**(4), 299–312 (1995).
175. Z. Brich et al., *J. Controlled Release* **19**, 245–258 (1992).
176. K. Munechika et al., *Biol. Pharm. Bull.* **17**(9), 1193–1198 (1994).
177. Y. Ohe et al., *Drug Delivery Syst.* **9**(5), 351–356 (1994).
178. Y. Takakura, S. Mastsumoto, M. Hashida, and H. Sezaki, *Cancer Res.* **44**, 2505–2510 (1984).
179. A. deMarre and E. Schacht, *Makromol. Chem. Macromol. Chem. Phys.* **193**, 3023–3030 (1992).
180. A. deMarre et al., *J. Controlled Release* **36**, 87–97 (1995).
181. H. Soyez, E. Schacht, A. Demarre, and L. Seymour, *Macromol. Symp.* **103**, 163–176 (1996).
182. C. Li et al., *Cancer Res.* **58**, 2404–2409 (1998).
183. J. Drobnik et al., *Makromol. Chem.* **177**, 2833–2848 (1976).
184. P. Rejmanova, J. Labsky, and J. Kopecek, *Makromol. Chem.* **178**, 2159–2168 (1977).
185. H. Batz, G. Franzmann, and H. Ringsdorf, *Angew. Chem., Int. Ed. Engl.* **11**(12), 1103–1104 (1972).
186. P. Ferruti, A. Bettelli, and A. Fere, *Polymer* **13**, 462–464 (1972).
187. J. Labsky and J. Kalal, *Eur. Polym. J.* **15**, 603–605 (1979).
188. J. Labsky and J. Kalal, *Eur. Polym. J.* **15**, 167–171 (1979).
189. C. Su and H. Morawetz, *J. Polym. Sci., Polym. Chem. Ed.* **15**, 185–196 (1977).
190. C. Su and H. Morawetz, *J. Polym. Sci., Polym. Chem. Ed.* **16**, 1059–1062 (1978).
191. J. Frechet et al., *Makromol. Chem.* **178**(8), 2159–2168 (1988).
192. C. Pitt and S. Shah, *J. Controlled Release* **39**, 221–229 (1996).
193. J. Strohalm and J. Kopecek, *Angew. Makromol. Chem.* **70**, 109–118 (1978).
194. J. Kopecek, *J. Controlled Release* **11**, 279–290 (1990).
195. R. Mendichi, V. Rizzo, M. Gigli, and A.G. Schieroni, *J. Liq. Chromatogr. Relat. Technol.* **19**(10), 1591–1605 (1996).
196. E. Configliacchi, G. Razzano, V. Rizzo, and A. Vigevani, *J. Pharm. Biomed. Anal.* **15**, 123–129 (1996).
197. V. Pinciroli et al., *Magn. Reson. Chem.* **35**(1), 2–8 (1997).
198. S. Wedge, Ph.D. Thesis, Keele University, England, 1990.
199. S. Cartlidge et al., *J Controlled Release* **4**, 253–264 (1986).
200. R. Duncan et al., *Biochem. J.* **196**, 49–55 (1981).
201. S. Cartlidge et al., *J. Controlled Release* **3**, 55–66 (1986).
202. A. Kaplan, in L. Donaruma, R. Ottenbrite, and O. Vogl, eds., *Anionic Polymeric Drugs*, Wiley, New York, 1980, pp. 227–254.
203. R. Ottenbrite et al., in L. Donaruma and O. Vogl, eds., *Polymeric Drugs*, Academic Press, New York, 1978, pp. 263–304.
204. G. Butler, in L. Donaruma, R. Ottenbrite, and O. Vogl, eds., *Anionic Polymeric Drugs*, Wiley, New York, 1980, pp. 49–142.
205. K. Mueck, H. Rolly, and K. Burg, *Makromol. Chem.* **178**, 2773–2784 (1977).
206. K. Mueck, O. Christ, and H. Keller, *Makromol. Chem.* **178**, 2785–2797 (1977).
207. B. Schechter, R. Pauzner, R. Arnon, and M. Wilchek, *Cancer Biochem. Biophys.* **8**, 277–287 (1986).
208. M. Filiova-Vopralova, J. Drobnik, B. Ramed, and J. Kvetina, *J. Controlled Release* **17**, 89–98 (1991).
209. E. Neuse, G. Caldwell, and A. Perlwitz, *J. Inorg. Organomet. Polym.* **5**, 195–207 (1995).
210. E. Neuse, *Macromol. Symp.* **80**, 11–128 (1994).
211. C. Mbonyana, E. Neuse, and A. Perlwitz, *Appl. Organomet. Chem.* **7**, 279–288 (1993).
212. M. Han et al., *J. Bioact. Compat. Polym.* **9**, 142–151 (1994).
213. Y. Sohn et al., *Preclinical Studies of a Water Soluble Polyphosphazene-Pt(DACH) Conjugate*, EORTC/NCI, Amsterdam, 1996.
214. A. Bogdanov et al., *Bioconjugate Chem.* **7**, 144–149 (1996).
215. A. Muhler, *Magma* **3**, 21–33 (1995).
216. A. Bogdanov, R. Weissleder, and T. Brady, *Adv. Drug Delivery Rev.* **16**, 335–348 (1995).
217. L. Harika et al., *Magn. Reson. Med.* **33**, 88–92 (1995).
218. A. Bogdanov et al., *J. Nucl. Med.* **35**, 1880–1886 (1994).
219. M. Wendland et al., *Magn. Reson. Med.* **32**, 319–329 (1994).
220. R. Duncan et al., *Biosci. Rep.* **2**, 1041–1046 (1983).
221. P. Rejmanova, J. Kopecek, R. Duncan, and J. Lloyd, *Biomaterials* **6**, 45–48 (1985).
222. V. Subr, J. Kopecek, and R. Duncan, *J. Bioact. Compat. Polym.* **1**, 133–146 (1986).
223. V. Subr et al., *J. Controlled Release* **18**, 123–132 (1992).
224. W. Shen and H. Ryser, *Biochem. Biophys. Res. Commun.* **102**, 1048–1054 (1981).
225. M. Masquelier, R. Baurain, and A. Trouet, *J. Med. Chem.* **23**, 1166–1170 (1980).

226. R. Baurain, M. Masquelier, D.D.-D. Campeneere, and A. Trouet, *J. Med. Chem.* **23**, 1171–1174 (1980).
227. J. Kopecek, *Biomaterials* **5**, 19–25 (1984).
228. P. Rejmanova et al., *Makromol. Chem.*, **184**, 2009–2020 (1983).
229. P. Rejmanova et al., *Makromol. Chem.* **182**, 1899–2010 (1989).
230. K. Ulbrich, E. Zacharieva, B. Obereigner, and J. Kopecek, *Biomaterials* **1**, 199–204 (1980).
231. R. Duncan et al., *Makromol. Chem.* **184**, 1997–2008 (1984).
232. V. Subr et al., *J. Controlled Release* **8**, 133–140 (1988).
233. R. Duncan, J. Lloyd, J. Kopecek, *Biochem. Biophys. Res. Commun.* **94**, 284–290 (1980).
234. R. Duncan et al., *J. Controlled Release* **16**, 121–136 (1991).
235. L. Seymour et al., *Biochem. Pharmacol.* **39**, 1125–1131 (1990).
236. R. Duncan et al., *Eur. J. Cancer* **27**(3), S52 (1991).
237. R. Duncan et al., *J. Controlled Release* **19**, 331–346 (1992).
238. J. Cassidy et al., *Biochem. Pharmacol.* **38**, 875–879 (1989).
239. K. O'Hare et al., *J. Drug Target.* **1**, 217–230 (1993).
240. P. Vasey et al., *Ann. Oncol.* **7**, 97 (1996).
241. R. Duncan et al., *Br. J. Cancer* **57**, 147–156 (1988).
242. R. Duncan et al., *J. Controlled Release* **10**, 51–63 (1989).
243. K. Ulbrich, C. Konak, Z. Tuzar, and J. Kopecek, *Makromol. Chem.* **188**, 1261–1272 (1987).
244. V. Chytry, M. Netopilik, M. Bohdanecky, and K. Ulbrich, *J. Biomater. Sci., Polym. Ed.* **8**(11), 817–824 (1997).
245. F. Uchegbu, H. Ringsdorf, and R. Duncan, *Proc. Int. Symp. Controlled Release Bioact. Mater.* **23**, 791–792 (1996).
246. C. Pitt, J. Wertheim, C. Wang, and S. Shah, *Macromol. Symp.* **123**, 225–234 (1997).
247. S. Shah, J. Werthim, C. Wang, and C. Pitt, *J. Controlled Release* **45**, 95–101 (1997).
248. K. O'Hare, I. Hume, L. Scarlett, and R. Duncan, *Hepatology* **10**, 207–214 (1989).
249. L. Seymour, K. Ulbrich, J. Strohalm, and R. Duncan, *Br. J. Cancer* **63**, 859–866 (1991).
250. L. Seymour et al., *Proc. Int. Symp. Recent Adv. Drug Delivery Syst.* **8**, 132–135 (1997).
251. D. Kerr, et al., *Proc. 3rd Int. Symp. Polym. Ther.*, London, January 7–9, 1998.
252. L. Seymour et al., *Br. J. Cancer* **63**, 859–866 (1991).
253. C. Hoes et al., *J. Controlled Release* **2**, 205–218 (1985).
254. C. Hoes et al., *J. Controlled Release* **23**, 37–53 (1993).
255. E. Pesenti et al., *Proc. Am. Assoc. Cancer Res.* **36**, 1824 (1995).
256. U.S. Pat. 5,362,831 (1994), N. Mongelli, E. Pesenti, A. Suarato, and G. Biasoli, (to Farmtalia Carlo Erba S.r.l.).
257. W.B. Huniunk et al., *Proc. 3rd Int. Symp. Polym. Ther.*, London, January 7–9, 1998.
258. A. deMarre, L. Seymour, and E. Schacht, *J. Controlled Release* **31**, 89–97 (1994).
259. M. Nichifor, V. Coessens, and E. Schacht, *J. Bioact. Compat. Polymer.* **10**, 199–222 (1995).
260. M. Nichifor, E. Schacht, and L. Seymour, *J. Controlled Release* **39**, 79–92 (1996).
261. D. Putnam and J. Kopecek, *Bioconjugate Chem.* **6**, 483–492 (1995).
262. D. Putnam, Ph.D. Thesis, University of Utah, Salt Lake City, 1996.
263. D. Putnam, J. Shiah, and J. Kopecek, *Biochem. Pharmacol.* **52**, 957–962 (1996).
264. R. Mendichi et al., *J. Liq. Chromatogr. Relat. Technol.* **21**(9), 1295–1309 (1998).
265. F. Angelucci, D. Ballinari, and M. Farao, *Proc. 13th Int. Symp. Med. Chem.*, Paris, September 1994.
266. M. Ripamonti et al., *Br. J. Cancer* **65**, 703–707 (1992).
267. I. Tannock and D. Rotin, *Cancer Res.* **49**, 4373–4384 (1989).
268. A. Kuin et al., *Cancer Res.* **54**, 3785–3792 (1994).
269. W. Shen and H. Ryser, *Proc. Natl. Acad. Sci. U.S.A.* **75**(4), 1872–1876 (1978).
270. F. Hudecz et al., *J. Controlled Release* **19**, 231–244 (1992).
271. E. Franssen et al., *J. Med. Chem.* **35**, 1246–1259 (1992).
272. M. Wirth et al., *Pharm. Res.* **15**(7), 1031–1037 (1998).
273. R. Dillman, D. Johnson, D. Shawler, and J. Koziol, *Cancer Res.* **48**, 6097–6102 (1988).
274. E. Diener et al., *Science* **231**, 148–150 (1986).
275. A. Kirby and P. Lancaster, *J. Chem. Soc. Perkin Trans. 2*, pp. 1206–1214 (1972).
276. M. Sato et al., *Biol. Pharm. Bull.* **19**(2), 241–245 (1996).
277. E. Hurwitz, M. Wilchek, and J. Pitha, *J. Appl. Biochem.* **2**, 25–35 (1980).
278. B. Mueller, W. Wrasidlo, and R. Reisfield, *Bioconjugate Chem.* **2**, 325–330 (1990).
279. Y. Ueda et al., *Proc. Int. Symp. Controlled Release Bioact. Mater.* **16**, 142–143.
280. Y. Ueda et al., *Chem. Pharm. Bull.* **37**, 1639–1641 (1989).
281. A. Kikukawa et al., *Drug Delivery Syst.* **5**, 255–260 (1990).
282. S. Danauser-Reidl et al., *Invest. New Drugs* **11**(2–3), 187–195 (1993).
283. Y. Ohya, H. Kuroda, K. Hirai, and T. Ouchi, *J. Bioact. Compat. Polym.* **10**(1), 51–66 (1995).
284. G. Poiani et al., *Am. J. Respir. Crit. Care Med.* **155**(4), 1384–1390 (1997).
285. G. Poiani et al., *Bioconjugate Chem.* **5**, 621–630 (1994).
286. M. Greco et al., *Am. J. Respir. Crit. Care Med.* **155**(4), 1391–1397 (1997).
287. Y. Ohya, K. Inosaka, and T. Ouchi, *Chem. Pharm. Bull.* **40**, 591–561 (1992).
288. N. Yokoyama et al., *Bioconjugate Chem.* **3**, 295–301 (1992).
289. M. Yokoyama et al., *Cancer Res.* **50**, 1693–1700 (1990).
290. M. Mammen, S. Choi, and G. Whitesides, *Angew. Chem., Int. Ed. Engl.* **37**, 2754–2794 (1998).
291. E. Gordon, L. Strong, and L. Kiessling, *Bioorg. Med. Chem.* **6**, 1293–1299 (1998).
292. D. Mann, M. Kanai, D.J. Maly, and L. Kiessling, *J. Am. Chem. Soc.* **120**(41), 10575–10582 (1998).
293. H. Kamitakahara et al., *Angew. Chem., Int. Ed. Engl.* **37**(11), 1524–1528 (1998).
294. P. Vasey et al., *Clin. Cancer Res.* **5**, 83–94 (1999).
295. P. Vasey, R. Duncan, S. Kaye, and J. Cassidy, *Eur. J. Cancer* **31A**, S193 (1995).
296. A. Bernstein, E. Hurwitz, and R. Arnon, *J. Natl. Cancer Inst. (U.S.)* **60**, 379–384 (1978).
297. E. Abound-Pirak et al., *Proc. Natl. Acad. Sci. U.S.A.* **86**, 3778–3781 (1989).

Next Page

298. H. Onishi and T. Nagai, *Chem. Pharm. Bull.* **34**(6), 2561–2567 (1986).

See also CANCER, DRUG DELIVERY TO TREAT—PRODRUGS.

PEPTIDE AND PROTEIN DRUG DELIVERY

OLUFUNMI L. JOHNSON
MARK A. TRACY
Alkermes Incorporated
Cambridge, Massachusetts

KEY WORDS

Biodegradable polymers
Controlled delivery
Drug delivery
Microspheres
Particles
Peptide
Pharmaceutical development
Polymers
Process development
Process scale-up
Protein
Stability
Sustained delivery
Sustained release

OUTLINE

Introduction
Protein and Peptide Stability
  Protein Degradation Pathways
  Protein Formulation Strategies
  Protein Stability within a Delivery Matrix
Protein Release from Polymeric Delivery Systems
  Strategies for Obtaining a Desired Release Profile
  Characterization of Release from Delivery Systems
Processes for Making Polymeric Delivery Systems
  Emulsification
  Coacervation
  Extrusion and Spraying Methods
Process Scale-Up, Manufacturing, and Regulatory Considerations
  Scale-Up Considerations
  Manufacturing Considerations
  Regulatory Considerations
Administration of Microsphere Delivery Systems
Sustained-Release Formulations of Peptides and Proteins
  Lupron Depot®
  Zoladex®
  De-Capeptyl® SR
  Posilac®
  Nutropin Depot®
Conclusions
Acknowledgments
Bibliography

INTRODUCTION

Efficacious delivery of protein and peptide drugs is taking on increasing significance as biotechnology companies mature and begin commercializing their products. As a result, there has been increasing interest in the development of protein and peptide delivery systems. The high level of interest is attributable to several factors. As the pharmaceutical and biotechnology industries consolidate and mature, there is an interest in value-added technologies, which drug delivery systems can provide. There is also an impending stream of patent expirations, which is fueling the demand for the rapid development of new products that may be realized by drug delivery technologies.

Drug delivery systems provide a number of advantages, including one or more of the following:

- Improved patient convenience
- Improved patient compliance
- Cost reduction
- Reduced frequency of administration
- Reduced adverse effect profile
- Patent protection extension
- Potential to reduce product development time and costs
- Possible new and broader therapeutic applications

However, to realize these advantages, it is critical to define clearly why a drug delivery technology is being sought and understand thoroughly the advantages and disadvantages of each delivery system, the unique physicochemical and biological properties of the protein or peptide of interest, and the requirements of the therapeutic indication.

The production of proteins by recombinant technology was an important milestone in the development of this new class of therapeutic agents. Proteins and peptides are poorly suited to the standard oral delivery route for administering small-molecule drugs because of the enzymatic and absorption barriers posed by the gastrointestinal tract; therefore, virtually all protein and peptide drugs are administered parenterally by subcutaneous or intramuscular injection (the immunosuppressant cyclosporine, a cyclic polypeptide, is a rare exception). However, the half-life of these drugs injected parenterally is only a few hours in most cases, necessitating multiple injections per week (typically 3–7) for therapeutic effectiveness. As a result, parenterally administered drugs generally have lower compliance levels than orally administered drugs. One way of improving compliance and minimizing discomfort arising from frequent injections is to couple protein and peptide drugs with sophisticated parenteral delivery systems that reduce the frequency of injection by providing a sustained release of the drug over time. Alternatively, these advantages may be achieved by immediate or sustained delivery to the systemic circulation via nonoral

Previous Page

298. H. Onishi and T. Nagai, *Chem. Pharm. Bull.* **34**(6), 2561–2567 (1986).

See also CANCER, DRUG DELIVERY TO TREAT—PRODRUGS.

PEPTIDE AND PROTEIN DRUG DELIVERY

OLUFUNMI L. JOHNSON
MARK A. TRACY
Alkermes Incorporated
Cambridge, Massachusetts

KEY WORDS

Biodegradable polymers
Controlled delivery
Drug delivery
Microspheres
Particles
Peptide
Pharmaceutical development
Polymers
Process development
Process scale-up
Protein
Stability
Sustained delivery
Sustained release

OUTLINE

Introduction
Protein and Peptide Stability
  Protein Degradation Pathways
  Protein Formulation Strategies
  Protein Stability within a Delivery Matrix
Protein Release from Polymeric Delivery Systems
  Strategies for Obtaining a Desired Release Profile
  Characterization of Release from Delivery Systems
Processes for Making Polymeric Delivery Systems
  Emulsification
  Coacervation
  Extrusion and Spraying Methods
Process Scale-Up, Manufacturing, and Regulatory Considerations
  Scale-Up Considerations
  Manufacturing Considerations
  Regulatory Considerations
Administration of Microsphere Delivery Systems
Sustained-Release Formulations of Peptides and Proteins
  Lupron Depot®
  Zoladex®
  De-Capeptyl® SR
  Posilac®
  Nutropin Depot®
Conclusions
Acknowledgments
Bibliography

INTRODUCTION

Efficacious delivery of protein and peptide drugs is taking on increasing significance as biotechnology companies mature and begin commercializing their products. As a result, there has been increasing interest in the development of protein and peptide delivery systems. The high level of interest is attributable to several factors. As the pharmaceutical and biotechnology industries consolidate and mature, there is an interest in value-added technologies, which drug delivery systems can provide. There is also an impending stream of patent expirations, which is fueling the demand for the rapid development of new products that may be realized by drug delivery technologies.

Drug delivery systems provide a number of advantages, including one or more of the following:

- Improved patient convenience
- Improved patient compliance
- Cost reduction
- Reduced frequency of administration
- Reduced adverse effect profile
- Patent protection extension
- Potential to reduce product development time and costs
- Possible new and broader therapeutic applications

However, to realize these advantages, it is critical to define clearly why a drug delivery technology is being sought and understand thoroughly the advantages and disadvantages of each delivery system, the unique physicochemical and biological properties of the protein or peptide of interest, and the requirements of the therapeutic indication.

The production of proteins by recombinant technology was an important milestone in the development of this new class of therapeutic agents. Proteins and peptides are poorly suited to the standard oral delivery route for administering small-molecule drugs because of the enzymatic and absorption barriers posed by the gastrointestinal tract; therefore, virtually all protein and peptide drugs are administered parenterally by subcutaneous or intramuscular injection (the immunosuppressant cyclosporine, a cyclic polypeptide, is a rare exception). However, the half-life of these drugs injected parenterally is only a few hours in most cases, necessitating multiple injections per week (typically 3–7) for therapeutic effectiveness. As a result, parenterally administered drugs generally have lower compliance levels than orally administered drugs. One way of improving compliance and minimizing discomfort arising from frequent injections is to couple protein and peptide drugs with sophisticated parenteral delivery systems that reduce the frequency of injection by providing a sustained release of the drug over time. Alternatively, these advantages may be achieved by immediate or sustained delivery to the systemic circulation via nonoral

or transmucosal routes such as the nasal, pulmonary, vaginal, rectal, and, in some cases, the transdermal routes (e.g., iontophoretic delivery of insulin). Thus, the availability of these new biopharmaceuticals has made their formulation and delivery an important part in the treatment of various disease states.

To address the challenges of protein and peptide delivery, a number of approaches are being pursued. One approach involves providing a controlled or sustained release of the drug by the parenteral route. Controlled delivery implies the incorporation of one or more elements of control on the release of an active ingredient from a dosage form to obtain a well-defined pharmacokinetic profile. A major advantage of controlled-release formulations over conventional dosage forms is the ability to manipulate the components of the dosage form to obtain a particular release profile. Sustained-release formulations are controlled-release dosage forms that have been engineered to release the active ingredient over an extended time period in a well-defined and reproducible fashion (1). As noted earlier, advantages include fewer injections and perhaps a therapeutic benefit for a sustained drug-release profile. For example, a short half-life may be increased either by chemically modifying the protein by coupling it to a moiety such as poly(ethylene glycol) (PEG) or by developing a degradable polymeric sustained-release formulation that would release therapeutic concentrations of the drug over an extended time period as the device degrades. A good example where a sustained drug serum concentration is actually required for therapeutic benefit is the sustained delivery of synthetic analogues of gonadotropin. It was demonstrated that the serum concentration of the drug needed to be above a certain threshold to produce a pharmacodynamic response, testosterone suppression in males and suppression of estrus in females.

Another delivery approach involves using nonparenteral routes for immediate or sustained release. A wide variety of dosage forms have been developed for the delivery of conventional small-molecule drugs for delivery via the oral, parenteral, buccal, transdermal, ocular, intravaginal, intrauterine, pulmonary, and nasal routes. Each of these routes of delivery has its own unique advantages and challenges that are a function of the physiology of the sites. The delivery of proteins via any of these routes requires special considerations that must be borne in mind in the development of protein formulations.

There are several sustained-release formulations of peptides on the market and, to our knowledge, there are no commercialized long-acting formulations containing a protein for humans; however, one long-acting protein-containing parenteral product is available for enhancing milk production in dairy cattle. Also, though there are a number of products for the delivery of proteins and peptides by nonparenteral routes in various stages of preclinical and clinical development, none (except cyclosporine), to our knowledge, have been commercialized for oral administration. One of the key reasons for the absence of novel protein formulations is their fragility and the need for suitable process and formulation approaches to maintain the protein structure while achieving desirable release characteristics. This article reviews the technical considerations in developing delivery products for proteins and peptides, focusing on injectable polymeric delivery systems as an example. Major stability, release, and manufacturing challenges in developing these products are discussed along with approaches to overcome them. Though we focus on polymeric delivery systems here, many of the principles presented are broadly applicable to a variety of peptide and protein drug delivery systems.

PROTEIN AND PEPTIDE STABILITY

Proteins differ from conventional small-molecule drugs in several respects, including size, but one of the most important differences affecting delivery and biological effectiveness is the complexity of protein structure. The full biological activity is dependent on preserving the integrity of this complex structure. The body has evolved ways of maintaining the specificity of action of proteins. This is controlled to a large extent by the different levels of organization within each molecule, that is, the primary, secondary, tertiary, and quaternary structure. Because of the close correlation between protein efficacy and the molecular three-dimensional structure, it is essential to maintain the structural integrity through all the formulation steps of a delivery system and while the drug is released from the dosage form at the site of delivery; otherwise, the activity of the protein or peptide drug may be reduced or lost entirely. Because of the fragile nature of proteins and peptides, the processes involved in the fabrication of the drug delivery systems may damage the protein and therefore, reduce its biological activity or render the protein immunogenic. For example, aggregated human growth hormone has less biological activity than the native monomeric form (2). The issues associated with ensuring the stability of a protein or peptide drug in various matrices have been discussed by several authors (3,4).

Strategies for stabilizing the protein in sustained-delivery systems are often more complex than those for proteins in solution for several reasons. First, the protein must survive the matrix fabrication process steps. It must also remain biologically active in the delivery system for an extended period in vivo where the protein may be subjected to pH, concentration, and temperature conditions conducive to degradation. In fact, overcoming the propensity for proteins to undergo degradation processes during incorporation into the delivery system or after injection into the body awaiting release is one of the key hurdles in bringing delivery systems for these drugs to market. It is therefore important to understand the degradation processes and the effects of protein stability on the biological response and release to devise formulation strategies to preserve protein stability. These approaches may include the addition of stabilizing excipients and the development of fabrication processes for delivery systems that are benign to proteins.

This section provides an overview of protein degradation pathways and discusses protein stability issues associated with the fabrication and delivery of protein drugs in sustained-release systems. Armed with this information, a variety of formulation approaches for developing stable formulations for delivery systems are presented.

Protein Degradation Pathways

The degradation mechanisms that proteins undergo can be divided into two classes, physical and chemical. Chemical degradation results in the modification of the protein's primary structure. In physical degradation, the native structure of the protein is modified by changes to its higher-order structure, that is, the secondary, tertiary, or quaternary structure. Degradation may be facilitated by environmental conditions such as pH, concentration, temperature, and the proximity of surfaces or chemically reactive groups. Examples of protein degradation pathways are shown in Table 1. Chemical degradation processes are usually preceded by a physical process such as unfolding, which then makes usually inaccessible amino acid residues available for chemical reactions.

Physical Instability. Proteins, because of their polymeric nature and ability to form higher-order structures, can undergo nonchemical changes (i.e., changes to the secondary, tertiary, or quaternary structure) that can alter their biological activity. The primary structure of a protein determines the native secondary and tertiary (and higher-order) conformation. In general, in globular proteins, hydrophobic residues are buried in the interior and hydrophilic residues are available near the surface for interaction with the aqueous solvent. Denaturation refers to the loss of the native globular structure and leads to protein unfolding. Once unfolded, newly exposed amino acid residues may interact with their surroundings by adsorbing to surfaces or aggregating with other protein molecules (5).

Denaturation may be reversible or irreversible and is caused by changes in the environment of the protein such as an increase or decrease in temperature, pH changes, the introduction of liquid interfaces by the addition of organic solvents, or the introduction of hydrophobic surfaces. In reversible denaturation, the protein refolds once the denaturing stimulus is removed, for example, unfolding when the temperature is increased and refolding correctly once the temperature is reduced. In irreversible denaturation, the native conformation is not regained by the removal of the stimulus (5). Precipitation often is the final result of self-association or aggregation of protein molecules. The aggregation of insulin has been well characterized and is thought to depend on unfolding of the insulin molecule (6).

Chemical Instability. Chemical degradation processes may occur at several points during the formulation and delivery of an encapsulated protein drug. It is important to be aware that the manifestation of a degradation process may occur sometime after the initial triggering step. For example, the pH of the buffer before freeze-drying can affect the stability of the lyophilized protein formulation (7).

Oxidation. Tryptophan, methionine, cysteine, histidine, and tyrosine amino acid side chains contain functionalities that are susceptible to oxidation. Methionine and cysteine can be oxidized by atmospheric oxygen and fluorescent light (2). Oxidation has been observed both in solution (8) and in the solid state (9). Oxidation of the methionine residues may cause a loss of bioactivity and, in the case of cysteine residues, the formation of nonnative disulphide bonds. Oxidation by atmospheric oxygen or auto-oxidation can be accelerated in the presence of certain metal ions such as copper and iron. Methionine residues under acidic conditions are especially prone to oxidation by reagents such as hydrogen peroxide, producing methionine sulphoxide. Oxidation by peroxide may be a concern if the protein is processed in a manufacturing area that is sterilized using hydrogen peroxide vapor or using equipment that is so treated (10). In this case, experiments must be performed and procedures put in place to ensure that the protein is not oxidized during manufacturing. A procedure for manufacturing sterile microspheres in an environment that was sterilized using vaporized hydrogen peroxide without oxidizing a protein has been described (11). Under conditions of higher pH, other groups, such as disulphide and phenol groups, may undergo oxidation reactions.

Deamidation. Deamidation is the hydrolysis of a side-chain amide on glutamine and asparagine residues to yield a carboxylic acid. The deamidation reaction has been extensively studied and is widely observed in therapeutic proteins and peptides (12). Some protein delivery system processing and formulation conditions that result in an increase in temperature or pH have been shown to facilitate deamidation. The deamidation process is important because of the potential loss in protein activity or function. Deamidation contributes to the reduction in catalytic activity of lysozyme (5) and ribonuclease at high temperatures (13).

Peptide Bond Hydrolysis. Aspartic acid residues have been implicated in the cleavage of peptide bonds, which have led to a decrease in biological activity. When lysozyme was heated to 90–100°C at pH 4, the loss in biological activity was attributed to hydrolysis of Asp-X bonds (5).

Disulphide Exchange. Many therapeutic proteins contain cysteine residues that form disulphide bonds. These bonds are important components of the structural integrity of proteins (14). Incorrect linkages of these disulphide bonds often lead to a change in the three-dimensional structure of the protein and therefore its biological activity. The reaction proceeds in both acidic and alkaline media, but the mechanisms are different. In neutral and alkaline media, the reaction is catalyzed by thiols. Thiols may be introduced during formulation (e.g., mercaptoethanol as an antioxidant) or by degradation of existing disulphide bonds via beta elimination of cysteine residues (15). The aggregation of lyophilized formulations of bovine serum albumin, ovalbumin, β-lactoglobulin, and glucose oxidase was attributed to disulphide interchange (16).

Table 1. Examples of Protein Degradation Pathways

Physical	Chemical
Noncovalent aggregation	Oxidation
	Deamidation
	Peptide bond hydrolysis
	Disulphide exchange
	Covalent aggregation

Protein Formulation Strategies

There is a large body of literature on protein-stabilizing excipients (especially for proteins in lyophilizates and solutions) including a number of excellent reviews on the subject (14,17,18). Some general approaches are reviewed in this section that are useful in developing stable protein formulations for incorporation in sustained-release systems (19,20).

Additives for Protein Stabilization. Stabilizing additives used in the formulation of proteins are diverse and include proteins, sugars, polyols, amino acids, chelating agents, and inorganic salts. These additives can stabilize the protein in solution and also in the frozen and dried states, although not all the additives confer stability under all three conditions. The stabilization mechanism in the solution or frozen state is different from that which occurs in the dried state. For example, carbohydrates in particular have the ability to stabilize proteins in the dried state (18,21). Thus, for many delivery systems that involve a number of formulation and processing steps, multiple additives may be required to produce a stable formulation (18). For example, a stable liquid protein formulation is a usually prerequisite because it will often form the starting bulk material for processing. If subsequent processing steps involve the transformation of the protein from a liquid to a powder by, for example, lyophilization or spray-drying, additional stabilizers may be needed for the dry state (22). Also, additives may be required for maintaining protein stability in a powder upon hydration to ensure stability during release and perhaps long-term storage (16). Approaches have been described to stabilize protein powders during hydration to prevent aggregation in lyophilizates and in polymeric microspheres (7,23–25).

Many additives used in protein formulations (e.g., sugars, salts, amino acids, and polyols) stabilize proteins by a similar mechanism (26–28). Sugars such as trehalose, sucrose, maltose, and glucose have been used as protein stabilizers. Their addition causes an increase in the glass-transition temperature of a number of proteins including collagen, ribonuclease, and ovalbumin (29). Similarly, salts such as potassium phosphate, sodium citrate, and ammonium sulphate have also been shown to increase the glass-transition temperature of proteins, thereby imparting thermal stability. All these additives increase the self-association of protein molecules and reduce their solubility. It has been proposed that these cosolvent stabilizers are preferentially excluded from the surface of the protein, thereby imparting stability (29). On the other hand, stabilizers such as magnesium chloride bind to the protein surface. Cyclodextrins have also been used as stabilizing excipients in protein and peptide formulations (30,31). Hydroxypropyl cyclodextrin (HPCD) stabilized formulations of porcine growth hormone against thermal and interfacial denaturation (32). The mechanism is poorly understood but is thought to involve changes in the properties of the solvent. Cyclodextrins have been found to complex with peptides, resulting in enhanced solubility of the drug (30,31). The addition of heparin, a polyanion, stabilized acidic fibroblast growth factor by increasing the unfolding temperature by 15–30°C by a direct interaction between the polyanion and the protein (33).

Surfactants are frequently added as stabilizers to protein formulations (34). They serve various useful functions in sustained-release formulations. Several commercial preparations of proteins, for example, Nutropin® (recombinant human growth hormone, Genentech Inc.), contain surfactants such as the polysorbates (2). Because of the amphipathic nature of proteins, they have a tendency to adsorb and accumulate at interfaces. This interfacial adsorption may lead to unfolding and eventually loss of solubility, aggregation, and biological activity (35). The addition of surfactants may be an important step in stabilizing the three-dimensional structure of a protein during incorporation into a delivery device, for example, during emulsification processes (36). The surfactant, polysorbate 20, was found to be useful in stabilizing human growth hormone incorporated in a poly(lactide-*co*-glycolide) (PLG) polymer matrix (37). Sustained-delivery devices having relatively hydrophobic surfaces may induce unfolding of the protein by adsorption. In this instance, the addition of a surfactant with a high hydrophilic–lipophilic balance (HLB) would reduce protein adsorption because the surfactant itself would adsorb to the device surface via its hydrophobic moieties, leaving the hydrophilic moieties exposed to the surrounding milieu (34). The ability of a surfactant to stabilize a protein upon rehydration has also been demonstrated (38). Therefore, the addition of a surfactant can stabilize a protein against denaturation during several stages from incorporation to release at the site of delivery.

The addition of certain metals has been shown to confer stability on proteins (39). Cunningham et al. showed that certain transition metals stabilized human growth hormone (hGH) against urea induced denaturation (40). They hypothesized that the presence of zinc in the secretory granules of the anterior pituitary (where growth hormone is secreted) stabilizes the hormone during storage before it is released into the circulation. Johnson et al. showed that an hGH–Zn complex was a viable formulation for encapsulation into a sustained-release formulation of PLG microspheres (25). The hGH–Zn complex was more stable in PLG microspheres compared with hGH in the uncomplexed form. The authors demonstrated in primates (rhesus monkeys) that biologically active protein was released over a 1-month period as determined by measuring sustained serum hGH levels and elevated levels of insulinlike growth factor I (IGF-I), a pharmacodynamic marker for hGH. Although the addition of metals may stabilize some proteins, the presence of metals may also catalyze the oxidation of cysteine residues. To overcome this, chelating agents such as ethylenediaminetetraacetate (EDTA) were added to stabilize a formulation of acidic fibroblast growth factor (33). Under accelerated storage conditions at 45°C, it was shown that the addition of EDTA stabilized a freeze-dried formulation of ribonuclease A (41). Where there is evidence that the presence of trace amounts of metals accelerate protein degradation, the addition of chelating agents should be considered.

Protein Stabilization in the Solid State. Changing the state of a protein or peptide from the liquid to the solid

state by lyophilization or spray-drying increases the storage stability of proteins (17). However, in addition to this obvious advantage, incorporation of the protein into a delivery device in the form of a lyophilized powder may also significantly reduce the potentially damaging stresses to which a protein solution would be subjected. For example, proteins in the solid state would be less susceptible to shear forces that occur during emulsification or atomization steps or denaturation at oil-water interfaces because the protein would not be in solution. These processes are described more fully in the later in this article.

Special precautions should be taken during freeze-drying because the drying process itself will expose the protein to destabilizing stresses; therefore, suitable excipients are often included in formulations for stability during freeze-drying (36). Additives that are normally added to stabilize a formulation that will be lyophilized may include a bulking agent (sucrose, dextrose, mannitol) to prevent collapse of the freeze-dried cake (18). Cryoprotectants are also added to lyophilized formulations to stabilize the protein to freezing (37). Some of the salts, polyhydric alcohols, and sugars described earlier stabilize a protein to withstand the effects of freezing, but additional stabilizers may be required to impart stability during the drying and rehydration steps. Carbohydrates, disaccharides in particular, stabilize proteins during drying (21). Using infrared spectroscopy, it was shown that hydrogen bonding occurs between these dissacharides and the proteins (bovine serum albumin and lysozyme). As the protein becomes dehydrated during the lyophilization process, these disaccharides are thought to act as water substitutes and are able to hydrogen bond to the proteins, thereby maintaining the integrity of the protein. The physical state of the carbohydrate stabilizer is also thought to be important (9,42). A surfactant is often added to facilitate dispersion of the protein and reduce adsorption (and unfolding) of the protein to the walls of the dissolution vessel.

It should be borne in mind that a lyophilized formulation is not stable indefinitely. Over time the protein may become denatured and lose activity. The effect of excipients on moisture-induced aggregation of human serum albumin under conditions designed to simulate the environment within sustained-delivery devices has been investigated (7,19,23,43). The authors showed that the aggregation could be induced via both covalent and noncovalent routes and suggested some rational solutions based on an understanding of the underlying aggregation mechanisms. These approaches included the effect of the buffer pH before lyophilization, the addition of high-molecular-weight polymers such as dextran and carboxymethyl cellulose, the modification of the hydrophilic properties of the delivery matrix to reduce water uptake, and manipulation of the protein molecule itself to chemically alter the residues involved in the degradation pathway. The studies described underline the importance of understanding the underlying degradation process. The more information there is on these degradation pathways, the more likely a rational approach can be successfully applied. Finally, in developing products with commercial potential, the U.S. FDA *Inactive Ingredients Guide* serves as an invaluable resource in identifying additives that have a history of use in approved pharmaceutical products (44).

Protein Stability within a Delivery Matrix

In addition to the considerations given to protein stabilization during the formulation and incorporation processes, the environment that the protein encounters within the delivery device should be considered in the formulation development. For sustained-release or depot formulations, the objective is to have a reservoir of the protein or peptide drug that is released over a period of days to months. Potential interactions between the protein and its surroundings over this prolonged period of time should be investigated during protein formulation. In addition to interactions between protein molecules discussed earlier, important interactions to consider include those between the protein and the matrix such as adsorption and those due to the changing internal environment of the device as, for example, polymer degradation occurs. The nature of these interactions are described in the following section along with formulation approaches to minimize them.

Interactions between the Delivery Matrix and the Protein. The incorporation of protein pharmaceuticals into solid delivery matrices exposes them to a high surface-to-volume environment, creating ample opportunity for adsorption to the delivery device. One obvious drawback of adsorption is that it may severely limit the amount of free unadsorbed protein that is available for release. It has been shown that salmon calcitonin adsorbs to the surface of PLG matrices (45). Another consequence of adsorption may be surface-induced changes in the three-dimensional structure of the protein that could result in a loss of biological activity. A number of factors affect the adsorption of proteins to a solid interface. These include the charges on both the protein and the surface and the effect of the environment, that is the pH, ions present, specificity of adsorption, surface area, and temperature (46). The surface activity of a protein depends on its amino acid composition and three-dimensional structure. The primary structure determines which amino acid residues are exposed to the surface in the three-dimensional structure and are therefore available for interaction with its surroundings. Because proteins are ampholytes, the pH and ionic strength of the surrounding medium will determine the net surface charge and therefore affect the nature of the interaction with the surface. Consequently, there will be a stronger interaction between the matrix surface and the protein when both possess opposite charges.

In aqueous solution, the three-dimensional structure of a protein in its native conformation results in more hydrophobic residues being buried within the interior and more hydrophilic amino acid residues exposed to the aqueous solution. However, when the same protein comes into contact with a hydrophobic surface, there will be an entropic driving force for the hydrophobic residues that are normally buried within the three-dimensional structure to interact with the surface, perhaps causing unfolding or other structural rearrangements. Conformational changes in the protein at a surface may also be driven by electrostatics. The adsorption of a hard protein (characterized by a low adiabatic compressibility, greater hydrophilicity, and high thermal stability) often occurs owing to electrostatics and

thus is less likely to adsorb to a similarly charged surface. A soft protein (characterized by a high adiabatic compressibility), however, can often adsorb to a similarly charged surface because it may experience greater conformational changes in the adsorption process (47,48). The extent and effect of adsorption on the biological activity of a protein is thus protein specific. The adsorption of antibodies on solid matrices in immunoassays suggests that interactions with solid matrices do not automatically result in a loss of activity.

The adsorption isotherms of proteins to solid surfaces display a saturation phenomenon. There is an initial rapid phase of adsorption in a particular medium that eventually reaches a plateau at a given protein concentration and temperature. The saturation point approximates a monolayer, suggesting that there is a fixed number of adsorption sites. The kinetics of adsorption may be controlled by either the transport of the protein to the surface (transport-limited adsorption) or by the intrinsic kinetics of adsorption at the surface (surface-limited adsorption). For example, bovine serum albumin (BSA) adsorption to PLG films was found to be surface-limited (S.M. Butler, M.A. Tracy, and R.D. Tilton, unpublished data).

Adsorption in a sustained-delivery system may be reduced by several formulation approaches. One of the most effective ways of formulating a protein to reduce adsorption to the delivery matrix or surface is the incorporation of a surface-active agent or the addition of another protein to compete for adsorption sites. Addition of albumin to insulin solution was found to reduce adsorption of the latter to solid surfaces. Addition of surfactants such as polysorbate or sodium dodecyl sulphate reduces the interfacial tension at the solid–liquid interface and therefore the driving force for the protein to adsorb (34).

Internal Environment of the Delivery Matrix. Many sustained delivery system matrices utilize biodegradable materials. Therefore, the protein is exposed to a changing environment as the delivery matrix degrades over time. For example, a number of implantable devices have been fabricated from polyesters made from lactide and glycolide monomer units that degrade ultimately to lactic acid and glycolic acid when exposed to water. It is feasible that the generation of acidic oligomers as these materials degrade could cause an increase in the acidity of the interior of the delivery device. The degree of isolation between the interior of the device and exterior will depend on the porosity and geometry of the device (49). There have been few studies to investigate the internal pH of PLG-based devices (50,51), but once implanted, it is unlikely that the interior of a porous device is totally isolated from the perfusion and buffering capacity of physiological fluids. It seems intuitive that if a large molecule such as a protein is able to exit the matrix (by diffusion through polymer networks or pores), then small molecules such as buffer salts or the soluble monomeric or oligomeric degradation products of biodegradable matrices should also be able to diffuse out of the matrix. If transport of acidic degradants out of a device is limited (due to perhaps a low porosity or a large size), it may be necessary to employ formulation approaches to overcome an acidic microclimate within the device. For example, basic salts may be incorporated as a buffering system into the matrix to counteract the increase in acidity produced by the degradation of the polymer into lactic and glycolic acids (52,53).

PROTEIN RELEASE FROM POLYMERIC DELIVERY SYSTEMS

In addition to maintaining the drug stability during processing and release, another key obstacle in producing protein and peptide sustained delivery systems is developing processing and formulation approaches to achieve a target release profile and duration. Developing such approaches begins with an understanding of the microstructure of the delivery system and the mechanism of release of macromolecules from the device.

Sustained release of biologically active macromolecules from biocompatible polymer matrices was first described by Langer and Folkman in 1976 (54). Prior to this discovery, it had been shown that small molecules (<600 Da) could be released slowly from polymeric materials (3,55). However, it was thought that macromolecules such as proteins and peptides were too large to slowly diffuse through polymeric materials because of their low porosity even after swelling. Langer and Folkman (54) showed that by solvent casting normally impermeable hydrophobic polymers in volatile solvents containing powdered macromolecules, molecules of nearly any size could be released for periods of greater than 100 days. The encapsulation of macromolecules in this manner resulted in the formation of a series of interconnecting channels within the polymer matrix that were large enough to permit macromolecular release and sufficiently tortuous to allow release in a controlled, prolonged fashion. A variety of polymers have been used to demonstrate macromolecular sustained release including nondegradable ethylene-vinyl acetate copolymers, degradable lactide–glycolide copolymers, and even hydrogels such as poly(vinyl alcohol) (3,54,56,57). Hydrogels typically release proteins for shorter periods than more hydrophobic polymers (3,54).

It has been found from microscopy that matrices produced by the processes described here consist of two major phases distributed throughout the device, one consisting of the macromolecule drug and the other consisting of the polymer (58). The drug release from nondegradable polymers occurs by dissolution and diffusion through interconnecting pores formed by the macromolecules themselves (54,55,58–66). Thus, the size of the drug powder and loading are important factors affecting the release rate. Saltzman and Langer (61) presented a detailed model for macromolecule release from nondegradable systems in which release by diffusion was due to the following variables: drug physical properties such as the drug concentration in the pores, its solubility, its aqueous diffusion constant, and the effect of the pore geometry and connectivity, including the porosity and the size distribution and shapes of the pores. Release from biodegradable matrices is determined by the polymer degradation and erosion rates in addition to diffusion (Fig. 1). Drug stability also may influence release because the solubility of nonnative forms, such as protein or peptide aggregates, is often reduced.

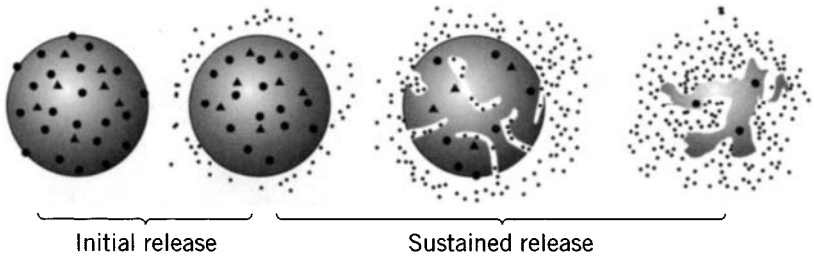


Figure 1. Mechanism of release from PLG microspheres. The initial release phase is controlled by diffusion of drug molecules that are on the surface or have access to the surface via pores in the microsphere matrix. The sustained-release phase is determined by the erosion of the polymer. As the polymer erodes, entrapped drug molecules are released from the delivery matrix. *Source:* Ref. 25.

Interactions between the drug and the polymer may also impact release whether or not there is an affect on drug stability. For example, the sustained release of leuprolide from biodegradable PLG microspheres (Lupron® Depot) is thought to be due, in part, to a charge interaction between the peptide and the carboxylic acid endgroup of the PLG used in the formulation (67,68).

Strategies for Obtaining a Desired Release Profile

The effects of various process and formulation variables on drug release and pharmacokinetics from biodegradable systems have been studied extensively by several authors (56,57,62,68). One of the most commonly used biodegradable polymers is PLG because of its biocompatibility and history of use in pharmaceutical products. The release profiles from PLG microspheres are usually described by two exponential curves attributed to drug diffusion and polymer erosion. After injection, there is an initial release phase, or "burst," that is thought to be dependent on dissolution and diffusion of drug at or near the surface of the microspheres. There may or may not be a lag period of little or no drug release depending on the characteristics of the polymer. The secondary release phase depends on erosion of the polymer, thereby exposing remaining encapsulated drug for dissolution and release (69). The onset and duration of the secondary release phase is modulated by polymer molecular weight, lactide glycolide ratio, and endgroup chemistry.

The initial release phase is affected by factors such as drug loading, drug particle size, drug solubility, microsphere diameter, and porosity. When the microsphere is hydrated after injection, for example, any entrapped drug that is present on the surface or that has unconstrained access to the surface via microscopic pores and channels will dissolve and diffuse out of the microspheres. This process usually occurs within 24–48 h after hydration. The proportion of encapsulated drug that is released during the initial phase is important for a number of reasons. Firstly, a large burst may pose safety and clinical concerns for narrow-therapeutic-index drugs. Secondly, if a significant proportion of the entrapped drug is released in the initial phase, there may be insufficient drug available for release later to provide a therapeutic benefit. Finally, there is also an economic imperative to reduce the burst and therefore, minimize drug wastage. Thus, formulation and processing approaches have been developed to minimize the initial burst. Formulation approaches for proteins and peptides include reducing drug solubility by complexing the drug for example with metal ions such as zinc (25). Alternatively, processing approaches may be used, for example, utilizing additional processing steps such as sonication or homogenization to reduce the encapsulated drug particle size (11,70). Finally, particles may be coated to reduce the fraction of drug immediately soluble.

The sustained-release phase is controlled by polymer erosion, and this phase is therefore controlled by the factors that affect polymer degradation (53,71–76). PLG polymers degrade by hydrolytic chain scission. This degradation process is affected by factors such as water sorption and solubility, the polymer morphology (crystalline or amorphous), device geometry (monolithic implants or microspheres), glass-transition temperature, molecular weight, chemistry (e.g., lactide glycolide monomer ratio, presence of residual monomer, and endgroup chemistry), the nature of encapsulated drug (acidic, basic), additives to the polymer phase, and the site of implantation (77). If polymer degradation and therefore erosion is delayed significantly (for example, for a high-molecular-weight, high-lactide-content polymer) so that the diffusion and erosion phases do not coincide, there is a lag phase with little or no drug release. Okada (67) showed that the addition of a hydrophilic surfactant, monoleic acid, had no impact on the lag phase but reducing the molecular weight of the PLG from 22 to 14 kDa eliminated the lag phase. Pulsatile release may be desirable for vaccine formulations but for most protein applications, a continuous-release profile is preferred. Vert et al. (78) demonstrated that in microspheres, degradation proceeds via a homogeneous hydrolytic process in which the degradation rate is the same throughout the microspheres. In monolithic implants, however, there is a heterogeneous process where the polymer degradation rate is faster within the core than it is on the outside (49). It has been suggested that the difference in degradation rate may be due to a buildup of self-catalyzing acidic monomers or oligomers within the core of the device. Also, certain additives have been found to affect the degradation rate of some PLGs (79). For example, the incorporation of slightly soluble basic salts such as zinc carbonate decreased the degradation rate of PLG microspheres in vitro and in vivo, probably because of the neutralization of acidic oligomers (52,53).

Characterization of Release from Delivery Systems

In addition to understanding the in vitro physical and chemical characteristics of the protein and the delivery system, it is important to understand and characterize drug release from a delivery system in vivo as part of the development of a sustained-delivery product for proteins

and peptides. This is invaluable in the development and selection of formulations with desirable release kinetics. It has been reported that in vivo release in small animal models such as rats was more predictive of release in primates and humans than in vitro release tests for proteins (11). As a result, microsphere formulations of rhGH were evaluated with respect to release in vivo. Once formulations with desirable release kinetics were identified, an in vitro release method was developed that correlated with in vivo release for quality control purposes. Kamijo et al. (80) also used in vivo models to confirm release of leuprolide from PLG microspheres and developed an in vitro release test to mimic in vivo release data as a quality control method for clinical samples. Variables that they investigated to develop a suitable in vitro test included the buffer pH, buffer salt concentration, the addition of additives such as mannitol or sodium chloride, and the mass of microspheres.

Drug release in vivo is affected by the physiology of the site of delivery because for systemic delivery, the drug, after being released from the delivery system, must be transported through the tissue at the site of administration before being absorbed into the bloodstream. Thus, before evaluating release from the delivery system, it is important to first characterize the drug absorption from the administration site and systemic clearance as a function of concentration and time by administering the drug as a solution bolus injection. Because the process of drug absorption from the administration site may depend on the kinetics of drug release, evaluating the pharmacokinetics of sustained delivery of the drug via osmotic pumps implanted in animals is useful in interpreting results from a new formulation of a delivery system.

In interpreting in vivo release data from sustained-delivery systems, it is important to characterize the expected biological responses. Parenteral introduction of any dosage form will induce a tissue response in vivo as a natural consequence of injection and the body's recognition of the presence of a foreign body (77,81,82). Release from the device may be affected by this response, so it is important to characterize its time course to aid in interpretation of release data (53,75). Also, a human protein or peptide is a foreign one to animals. Thus, they are expected to elicit an antibody response to the drug. The presence of antibodies (which reach measurable levels as soon as a couple of days after administration for IgM and about 7–10 days for IgG antibodies) may limit or prevent the ability to measure human protein levels. Antibodies may either impact the circulating levels of the drug or interfere with the assay (such as radioimmunoassays or ELISAs) used to quantify the drug in serum. Procedures have been developed to suppress antibody formation allowing the study of release from animal models beyond 7 days (83). Transgenic animal models may also be used to assess release and formulation immunogenicity in an animal producing circulating levels of a human protein (83).

PROCESSES FOR MAKING POLYMERIC DELIVERY SYSTEMS

A variety of processes have been developed to encapsulate drugs to produce biocompatible drug-containing polymeric matrices for sustained release that are capable of being implanted or injected. These processes most often involve the preparation of a drug solution, suspension, or emulsion with the polymer in solution followed by an extrusion or compression molding step for implants or a droplet formation step for microspheres. Processing solvents are removed by extraction and/or drying to produce the final microsphere or implant product. The fabrication steps must be performed under carefully controlled conditions of temperature, pH, and mixing to preserve the integrity of fragile proteins and peptides (84). Emulsion, coacervation, and extrusion/spray methods are described in the following sections with an emphasis on the protein stability implications of processing via these approaches.

Emulsification

Most microsphere fabrication processes are based on emulsification. Briefly, the water-soluble drug is dissolved in an aqueous solution (or water), and the polymer is dissolved in an organic solvent such as ethyl acetate or methylene chloride. A key characteristic is that the protein is processed in solution. The two solutions are mixed in the appropriate ratio to create a water-in-oil (w/o) emulsion. This primary emulsion is then again emulsified into a second aqueous solution containing an emulsifier such as poly(vinyl alcohol). The final product is a water-in-oil-in-water (w/o/w) emulsion (85). The organic solvent is then removed from the emulsion by evaporation under reduced pressure, filtration, or a moderate increase in temperature. The microspheres are then harvested and dried. There are variations on this basic approach where a range of aqueous and organic solvents and a range of aqueous phase emulsifiers are used. Alternatively, a single emulsion may be used for drugs that are dissolved or suspended in the polymer solution by forming an oil (containing dissolved polymer with dissolved or suspended drug) in water emulsion to create the microsphere droplet that is hardened as just described.

A commercial microsphere formulation of the peptide leuprolide acetate called Lupron® Depot is manufactured using a w/o/w double-emulsion method (56,68). Briefly, as depicted in Figure 2, the leuprolide acetate (Luprorelin) and gelatin are dissolved in water and added to a solution of the PLG polymer (in methylene chloride). The mixture is emulsified to produce a water-in-oil emulsion. This primary emulsion is then emulsified in an aqueous solution of poly(vinyl alcohol). The resulting w/o/w emulsion is stirred gently until the methylene chloride solvent evaporates and the wet microspheres are washed, collected, and freeze-dried. During the washing process, mannitol is added as an anticaking agent to prevent microsphere aggregation during drying and storage of the vialed commercial product.

The formation of an emulsion and its associated interfaces can create the potential for denaturation of fragile proteins and some peptides resulting from the use of mechanical agitation to facilitate formation of the droplets, exposure to organic solvent interfaces, and significant fluctuations in temperature, concentration and pH. There are a number of reports on the damaging effects on proteins of emulsification and exposure to organic solvent/aqueous in-

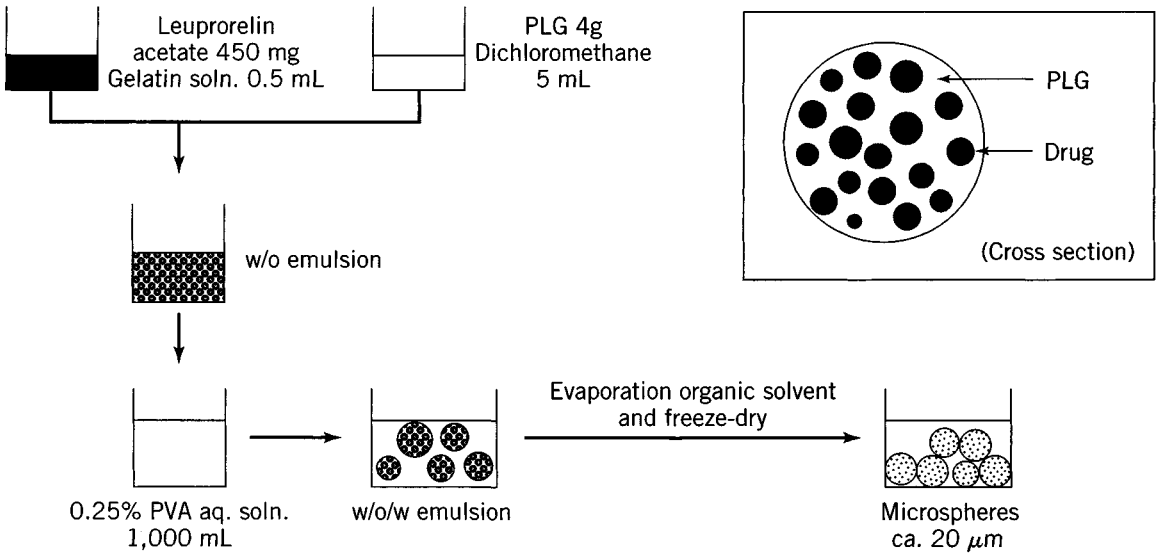


Figure 2. Schematic diagram of the double-emulsion process used to manufacture Lupron Depot®. The primary emulsion consists of leuprorelin acetate in an aqueous solution containing gelatin dispersed in a solution of PLG in methylene chloride. The water-in-oil emulsion is then emulsified in a solution of poly(vinyl alcohol) (surfactant and stabilizer). The microspheres are formed by evaporation of the methylene chloride, which is the continuous phase of the primary emulsion.

terfaces (86–88). In some cases, though, proteins have retained most of their biological activity after incorporation by an emulsion process (66,89). Emulsification is achieved by disrupting a mixture of the aqueous solution that contains the protein drug with other water soluble excipients and the organic water-immiscible phase that contains the polymer or matrix material. Emulsion droplets are formed by the input of energy, which may be mechanical, as with a homogenizer, or ultrasonic, with the use of an ultrasonic probe.

Formation of emulsion droplets is an energy-intensive process. It is initiated by film formation, generation of surface waves, deformation of the aqueous/organic solvent interface, and cavitation. Turbulence created by high-speed homogenization can cause the disruption of the interface and droplet formation. Cavitation is the main process by which ultrasonic waves form emulsion droplets, and it is the sudden formation and collapse of bubbles containing vapor that results in the generation of high pressures on the order of 10^{10} Pa and shock waves. It is the combination of high pressures, intense shock waves, and the dissipation of both over a short period that causes the formation of droplets. The energy that is generated is accompanied by an increase in temperature. Although these conditions may be short-lived, damage can still be done to the protein (90). Loss of protein activity or potency is often observed after encapsulation using these steps. The high shear rates that are generated during emulsification may be enough to cause foaming (adsorption of the protein at the air–water interface or at the aqueous–nonaqueous interface of the emulsion droplets) (9). As a result, emulsion processes are best suited for peptides and proteins that are sufficiently stable to these conditions. One advantage of an o/w versus a w/o/w emulsion process is that the protein may be encapsulated starting with a suspension rather than a solution of the drug in the polymer solution. Proteins in the solid state are less sensitive than proteins in solution to many mechanisms of degradation that may occur during emulsion, such as shear-induced denaturation.

Also, owing to the high cost of protein and peptide drugs, a high efficiency of incorporation of the protein or peptide into microspheres during processing is an important objective. This is particularly a concern for emulsion processes utilizing solvents for the protein or peptide during the last emulsion step. For example, proteins are soluble in water, which is the solvent used in the second emulsion of the w/o/w process. Thus, the process must be optimized to minimize loss of the protein during this process step.

Coacervation

Microparticles containing a protein may also be formed by coacervation. In simple coacervation, a hydrocolloid containing the protein is desolvated by the addition of another substance (such as a salt or an alcohol) that competes for the solvent by virtue of its higher hydrophilicity, solubility, or concentration. In complex coacervation, the charge of the hydrocolloid is opposite to that of the competing substance so that on addition of the latter, a complex of the two is formed, and the mixed coacervate is separated by dilution (91). The microcapsules formed are then "cured" by the addition of a cross-linking agent such as glutaraldehyde. Hydrocolloids that are used in pharmaceutical formulations include gelatin, acacia, and chondroitin sulphate (92). For example, cytokines have been encapsulated in gelatin–chondroitin sulphate microspheres. The cytokine IL-2 (interleukin 2) was dissolved in chondroitin sul-

phate solution, and a solution of gelatin was added to form microspheres. The microspheres were then cross-linked using glutaraldehyde. In addition to the stresses that the protein molecules undergo as a result of pH changes during the coacervation process, the cross-linking step with glutaraldehyde is indiscriminate and cross-links the microsphere matrix as well as the encapsulated protein or peptide drug. This lack of selectivity accounts for some of the loss in bioactivity of protein drugs encapsulated in microspheres that utilize a chemical cross-linking process.

Another coacervation method for preparing PLG microspheres was described by Cleland and is shown in Figure 3 (93). In this process, the PLG polymer is dissolved in an organic solvent, and the drug is either dissolved in an aqueous medium and added to the polymer solvent or dispersed as a solid in the polymer solvent. The emulsion or dispersion is then added to a nonsolvent for both phases

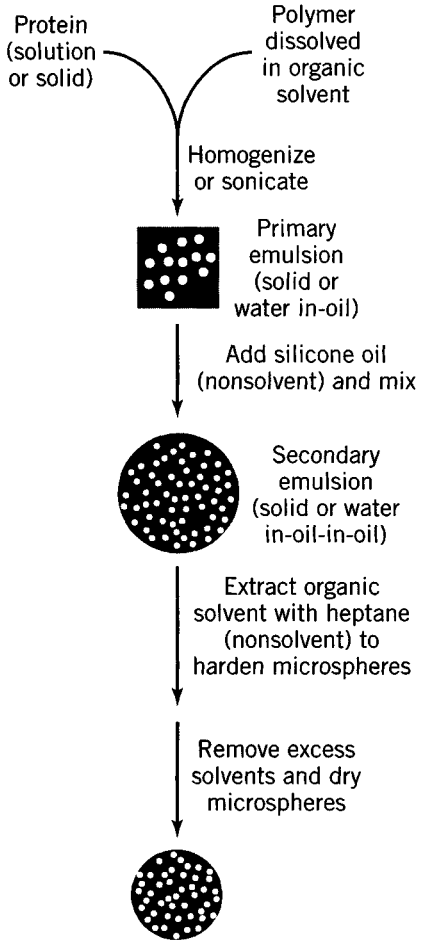


Figure 3. Schematic diagram of a coacervation process for the production of PLG microspheres. Silicone oil is a nonsolvent for methylene chloride; therefore, the primary emulsion can be emulsified in silicone oil to form a water-in-oil(methylene chloride)-in oil (silicone oil) emulsion. The microspheres are formed by extracting the methylene chloride from the primary emulsion droplets. This is achieved by the addition of heptane, which is a solvent for methylene chloride but a nonsolvent for silicone oil. *Source:* Reproduced from Ref. 93.

(e.g., silicone oil) and emulsified to give a water-in-oil-in-oil emulsion or a solid dispersion-in-oil-in-oil. A second nonsolvent for the outer oil phase (e.g., heptane) is then added to the double emulsion to extract the organic polymer solvent (e.g., methylene chloride) to harden the microspheres, and the silicone oil is then removed and the microspheres are dried. As discussed in the section on emulsions, steps in which immiscible phases are mixed must be carefully evaluated for their effects on the stability of the drug being encapsulated. In general, higher efficiencies of drug incorporation compared to w/o/w or w/o emulsions are expected from this coacervation approach because the last water phase is replaced with silicone oil and heptane, both nonsolvents for proteins and peptides.

Extrusion and Spraying Methods

Extrusion or spraying methods may be used in the fabrication of drug delivery systems to form droplets or in the formation of monolithic injectable delivery devices (85). In the former case, where extrusion or spraying is employed to form microspheres, the core material or matrix containing the protein drug, incorporated as a solution or particulate, is ejected from the orifice of a fine tube, syringe, or nozzle to form microdroplets. For example, in spray-drying, microspheres are produced by atomizing the polymer solution containing the drug at an elevated temperature to evaporate the solvent. The size of the droplets and, therefore, the final dosage form depends on the properties of the liquid (melt, solution, or suspension) to be sprayed and on the operating conditions of the extruder such as orifice diameter and jet velocities (94). The main considerations as far as the stability or integrity of protein is concerned are the processing conditions such as the melting temperature if a melt extrusion method is employed (84), the temperature for spray-drying processes, and the effect of the high shear forces that may be generated from the orifice at high jet velocities. Processes for producing sustained-release implants that maintain peptide and protein activity have been described in the literature. For example, Fujioka et al. (95,96) describe a low-temperature process for preparing an injectable rod implant containing α-interferon.

The ProLease® process, a spray method of producing microparticles containing proteins using a cryogenic process, has also been described (70). In this method, as depicted in Figure 4a and 4b, the protein drug is incorporated as a lyophilized powder, and all manipulations involving the matrix polymer (PLG) and the protein are performed at low temperatures ($\leq -80°C$). The fabrication process may be divided into two distinct processes. In the first process, the protein is formulated to form a stable, lyophilized product. During the protein-formulation process, stabilizing excipients such as surfactants or sugars may be incorporated. In the case of Nutropin Depot, hGH is complexed to zinc to form a Zn–hGH complex with reduced solubility. The encapsulation of this complexed form was demonstrated to stabilize hGH against aggregation postencapsulation (25). In the second part of the fabrication process, the protein powder is dispersed in a solution of the polymer in a solvent such as ethyl acetate, acetone, or methylene

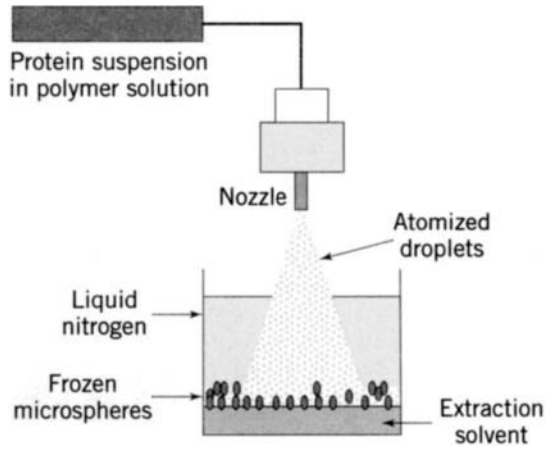


Figure 4. (**a**) Schematic diagram of the ProLease® encapsulation process (laboratory scale). The lyophilized protein formulation is dispersed in a solution of the PLG polymer and then atomized into a vessel containing frozen ethanol overlaid with liquid nitrogen. The droplets freeze as they travel through the cold nitrogen gas and liquid nitrogen and settle on top of the bed of frozen ethanol. As the ethanol melts, it extracts the methylene chloride (which is miscible with ethanol), and the microspheres harden. (**b**) Process steps in the production of ProLease® microspheres. The bulk protein may be formulated by the addition of stabilizing excipients or release modifiers or exchanged into a compatible buffer, spray-frozen, and lyophilized. The spray-freezing is performed with liquid nitrogen, and freezing occurs very rapidly. This rapid freezing may arrest degradation processes. The lyophilized drug is encapsulated as described in (**a**), and the dried microspheres are collected as a white or off-white, free-flowing powder and vialed. *Source:* Ref. 25.

chloride. The polymer and protein powder dispersion is homogenized to give a uniform suspension and then atomized over a bed of frozen ethanol overlaid with liquid nitrogen. The suspension droplets freeze as they travel through the liquid nitrogen and settle on the bed of frozen ethanol. The temperature of the frozen ethanol is increased, and the ethanol melts. Ethanol is miscible with the polymer solvents, so the polymer precipitates as the ethanol extracts the polymer solvent from the droplets. This solvent extraction process causes the microspheres to set and harden, and the microspheres are harvested by filtration. The wet microspheres are vacuum dried and vialed as a white or off-white free-flowing powder.

This fabrication process has several important benefits; first, the protein is in the more stable dry form, and any degradation processes that it is liable to undergo even in the dry state are hindered by the very cold temperatures. Additionally, stabilizing excipients may be included in the formulation during the lyophilization process. Because there are no aqueous phases, the protein is not subjected to freeze–thaw stresses or organic–aqueous solvent interfaces (which are present in emulsion-based processes) where some proteins may denature. This process effectively solves the issue of protein denaturation during incorporation or fabrication, provided a stable lyophilized formulation is available. It has been used to produce a stable microsphere formulation for hGH (25).

PROCESS SCALE-UP, MANUFACTURING, AND REGULATORY CONSIDERATIONS

The previous sections discuss approaches for stabilizing proteins, making polymeric sustained-delivery systems, and obtaining desirable release kinetics. Another major hurdle in developing a product is establishing the capability to produce the product in sufficient quantities for clinical testing and commercialization. This section reviews scale-up, manufacturing, and regulatory considerations in developing delivery systems for proteins and peptides, with a focus on polymeric microsphere systems for parenteral administration.

Scale-Up Considerations

The processes described in the previous sections are scalable. As noted in earlier sections, commercial products for peptides produced by emulsion and extrusion processes are on the market. Herbert et al. (97) described the scale-up of a cryogenic spray process for making microspheres. An effective scale-up effort begins with a detailed understanding at the laboratory scale of the effects of process unit operations on product characteristics and performance. Based on this knowledge and an estimate of the commercial scale batch size, suitable scalable unit operations can be selected and the operation conditions optimized to achieve the desired product characteristics. The equip-

ment used at the small scale may not be suitable at larger scales owing to, for example, higher throughput requirements. For example, sonicating probes often used to produce microspheres are not easily scalable to the batch sizes usually required; therefore, it is prudent to select equipment scalable to commercial scale at the initial process scale-up stage (98). Table 2 compares unit operations used for the ProLease® process at the small, laboratory scales and at the large scale (11). In scaling up the process from the lab scale, unit operations that were scalable to commercial scale were selected and combined to produce a sterilizable, enclosed process suitable for producing sterile microspheres with the characteristics of the lab scale batches. Selecting scalable unit operations as early as possible in development will help minimize unforeseen effects of processing variables on microsphere performance. For example, adding, removing, or changing a unit operation may cause a subtle change in the porosity or surface characteristics of microspheres affecting release.

One of the prerequisites of successful scale-up and process development is having a comprehensive microsphere characterization scheme in place. It is essential to understand the effects of various fabrication variables on the physicochemical properties of the microspheres and, if possible, to relate these physicochemical properties to a biological performance criterion. Some physical properties that should be characterized include particle composition (drug load, residual solvents), particle size (volume and number mean or median, polydispersity or other measure of diameter distribution), microsphere morphology (by, for example, microscopy), particle density, particle porosity, polymer glass-transition temperature, molecular weight, and encapsulated protein integrity. It is often valuable to relate one or more of these physical attributes to microsphere performance characteristics such as in vitro release kinetics or in vivo pharmacokinetic or pharmacodynamic criteria. For example, the effect of various process variables on C_{max} (the maximum serum protein concentration) may be evaluated. With leuprolide acetate microspheres, it was shown that a reduction in particle size had an effect on initial release although the effect was small and not directly proportional to the surface area of the microspheres (68).

The use of statistical experimental design during the scale-up of microsphere fabrication processes is useful in optimizing process operating parameters. One of the advantages of this approach is that key fabrication variables and relationships between them can be identified with a relatively small number of experiments (99). This approach is ideal for troubleshooting complex processes where there are a large number of variables to study with limited time and drug supply. For example, important process variables in emulsion processes include the polymer and drug concentrations, the emulsifying agent, processing temperature, volumes of the oil and water phases, the mixing rate and time, the extraction solution composition, filtration device, and drying method (100). Key variables for spray methods include the mixer speed, homogenization and atomization pressures, the atomization nozzle type, and the extraction solvent and drying temperature/time profiles. Figure 5 shows the results of optimizing processing parameters for two unit operations of the ProLease process using experimental design methods (11). C_{max} was a sensitive variable reflecting improvements in the amount of protein initially released from the microspheres as the process conditions were optimized.

Manufacturing Considerations

For commercial manufacture, the fabrication process for parenterally administered polymeric protein and peptide delivery systems must be performed under well-controlled aseptic conditions to produce a sterile product because the final product cannot be sterilized by autoclaving or γ-irradiation after manufacturing and vialing (called *terminal sterilization*). Either terminal sterilization process may degrade both the drug and the polymer. A common approach for aseptic manufacturing in the pharmaceutical industry is to produce the drug product in a Class 100 clean room. A concern with this approach is the challenge of ensuring sterility in an environment where personnel can come in direct contact with the product during manufacturing.

A new approach to resolving the issue of sterile microsphere production is to couple isolation (or barrier) technology to the microsphere fabrication process (11). Isolation technology has been used extensively in microbiological testing and it is an effective way of maintaining the sterility of a drug product while providing handling access. An isolator is a soft- or hard-walled enclosure in which the environment may be controlled for particulate count, sterility, temperature, and humidity. The enclosure provides a barrier between personnel handling the product and the product itself, providing increased sterility assurance compared to a traditional clean room. Asepsis is maintained within the isolator by the use of vapor-phase hydrogen peroxide (VHP). Filters and various air treatment devices are attached to control the particulate count, temperature, and humidity. Reaction vessels may be autoclaved and transferred aseptically to the isolator using transfer ports. So-

Table 2. Microsphere Process Development and Scale-Up

Unit operation	Laboratory-scale process	Large-scale process
Protein spray freeze-drying	Ultrasonic spray nozzle/lyophilizer	Air atomizer/lyophilizer
Protein particle size reduction	Probe sonicator	High-pressure homogenizer
Microsphere droplet formation	Ultrasonic spray nozzle	Air atomizer
Solvent extraction	Frozen ethanol bed at $-80°C$	Temperature-controlled stirred tank containing liquid ethanol
Residual solvent removal	Vacuum dryer	Vacuum dryer

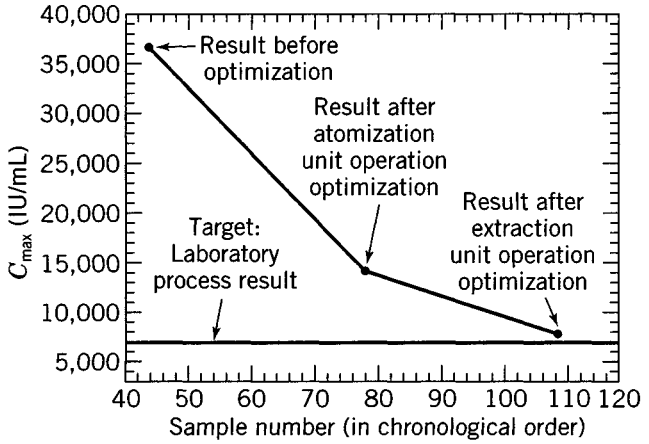


Figure 5. ProLease® process optimization. A target level of a critical performance characteristic (C_{max} in an animal model) was set based on the laboratory scale process. Samples 42–79 show the effect of varying atomization conditions on the C_{max}, and samples 80–110 show the effect of optimizing the extraction conditions combined with the optimized atomization settings. The optimization process was performed using a statistical design approach. *Source:* Ref. 11.

lutions may be sterile-filtered directly into the reaction vessels within the isolator.

Additionally, equipment such as lyophilizers, filter dryers, and filling machines may be coupled directly to the isolator, ensuring that the sterility of the microsphere product is maintained. The use of isolation technology enables the operation of complex, multistep microsphere production processes with a high degree of sterility assurance. Figure 6 shows a schematic of a manufacturing suite in which a microsphere production process is coupled to an isolator for aseptic manufacturing (11).

Regulatory Considerations

One of the considerations in manufacturing microspheres is minimizing the residual solvent and residual polymer monomer content in the microspheres. It has been suggested that bulk PLG polymers should be treated after manufacture to remove residual monomer or oligomers that may catalyze chain scission and, therefore, polymer erosion. Virtually all microsphere fabrication processes require the use of an organic solvent such as methylene chloride or ethyl acetate for polymer dissolution. Acceptable residual amounts of these solvents are determined by the regulatory agencies. For example, the International Conference on Harmonization (ICH) guideline for permissible methylene chloride content is 6 mg per day (101); unless it can be shown that the residual solvent is released in a sustained fashion over several days, the effective limit is <6 mg of methylene chloride per dose. Other solvents such as ethanol or other alcohols may not pose a direct safety hazard but may have a significant impact on the stability of the microsphere product. For example, high residual ethanol levels may reduce the glass-transition temperature of the polymer, which could impact the physical stability of the microspheres, causing them to agglomerate or clump either immediately or under long-term storage, and may result in poor injectability. Additionally, the presence of residual solvents at high levels may have a direct impact on encapsulated protein stability. Key regulatory issues in developing peptide products were reviewed by Niu and Chiu (102).

ADMINISTRATION OF MICROSPHERE DELIVERY SYSTEMS

The microspheres are vialed as a free-flowing powder and need to be resuspended in an aqueous medium before injection. To ensure that the microspheres do not sediment when dispersed in the injection vehicle, it is usually necessary to use a viscous medium. One of the most widely used suspending agents is a soluble, substituted cellulose, carboxymethyl cellulose. It is soluble in aqueous media at physiological pH. It is often necessary to add a wetting agent such as a hydrophilic surfactant to the vehicle to facilitate microsphere dispersion. Additionally, inclusion of a tonicifier and buffer are advisable to ensure that the microsphere suspension is isotonic and at (or close to) physiological pH upon injection. Successful injection of the microsphere dispersion is affected by factors such as microsphere diameter, microsphere concentration, and needle gauge. Large microspheres, or a high microsphere concentration, may cause clogging of the needle; therefore, it is important to conduct the appropriate studies to determine the optimum combination of microsphere diameter, concentration, vehicle, and needle gauge for successful injection.

SUSTAINED-RELEASE FORMULATIONS OF PEPTIDES AND PROTEINS

There are several sustained-release formulations of peptides (luteinizing hormone–releasing hormone [LH-RH] analogs) on the market. However, there is only one long-acting protein formulation, Posilac® (bovine somatropin), for increasing milk production in dairy cattle. Incorporating proteins into sustained-delivery systems has been a significant challenge compared to smaller peptide drugs because of the relative instability of proteins and the need to maintain their fragile three-dimensional structure for biological activity. Alkermes, Inc., in collaboration with Genentech, Inc., are in late-stage clinical trials with a protein sustained-release formulation for humans of rhGH (Nutropin Depot®). This section describes several products. More details on these and others can be found in the literature or directly from the companies producing them or their Web sites (103).

Lupron Depot®

One of the first peptide sustained-delivery products on the market was Lupron Depot®, a sustained-release formulation of leuprorelin acetate (Des-Gly-(d-Leu)–LH-RH ethylamide acetate) (56,67,68,103). Leuprorelin acetate is an LH-RH superagonist with a 10-fold higher biological activ-

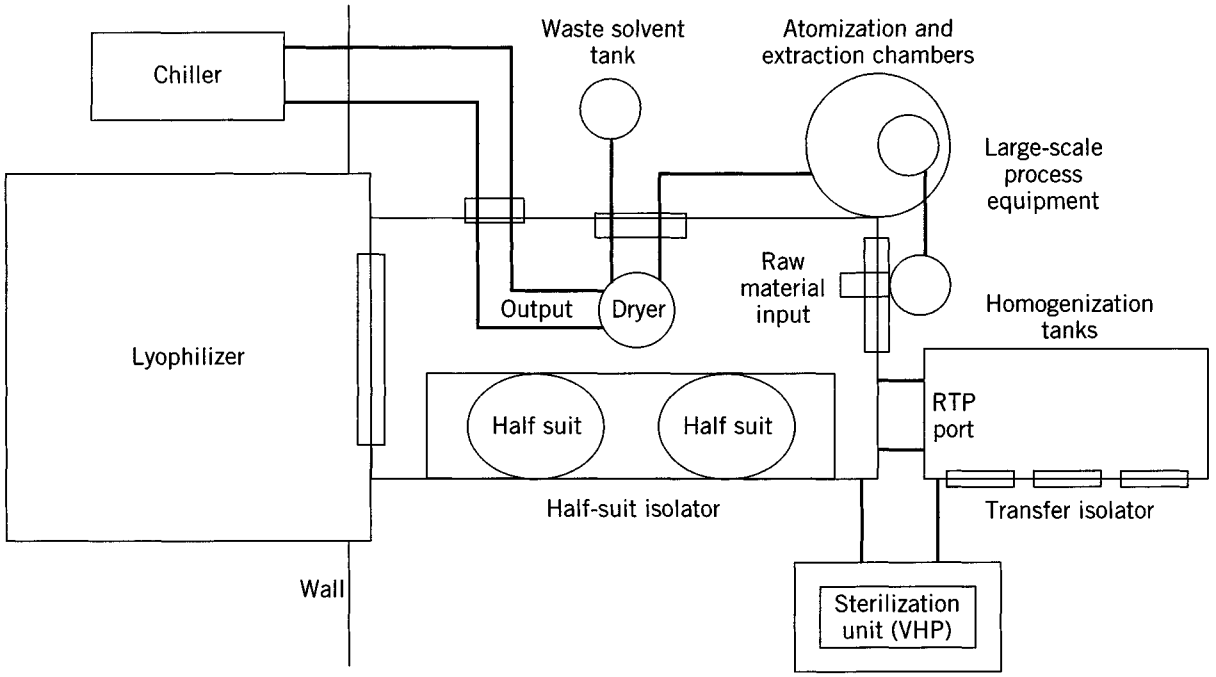


Figure 6. Isolator technology coupled with ProLease® microsphere production. Combining isolator technology with microsphere production enables the production of microspheres under controlled conditions (temperature, humidity, and Class 100 environment) and ensures the sterility of the product. The inside of the isolator is sterilized with vapor-phase hydrogen peroxide, and the non-autoclavable materials (protein and PLG polymer) are introduced into the isolator as sterile-filtered solutions. All subsequent processing, such as atomization, lyophilization, and extraction, occurs within the isolator or in equipment that is connected to the isolator and may be presterilized with VHP or steam. The operators are completely separated from the product being processed, but the half suits are comfortable and provide the dexterity required for the various manipulations. RTP = rapid transit port. *Source:* Ref. 11.

ity than native LH-RH. LH-RH and its analogs have a variety of effects on the gonads depending on the administered dose. At acute doses, the peptides stimulate gonadotropin production by the pituitary gland and production of the sex hormones in the genitals. Chronic administration at a higher dose causes "chemical castration," or an inhibition of testicular and ovarian production of the sex hormones. In this chronic administration regimen, LH-RH agonists are used in the treatment of endometriosis, uterine fibroids, and prostate and ovarian cancers. The chronic administration regimen required for these indications was an excellent opportunity to try and develop a long-acting formulation of the peptide. Okada (68) describes the problems associated with oral and transmucosal delivery (nasal, vaginal, rectal). The problem was poor absorption and, therefore, low bioavailabilities, which ranged from <0.1 to 1–5% for the transmucosal routes. In the presence of absorption enhancers, the bioavailability was increased to 5–10% for nasal and vaginal delivery. It was observed that sustained levels of the hormone produced a stronger castrating effect, suggesting that a sustained-release formulation might offer therapeutic benefits.

The microsphere formulations were based on the biodegradable polymers of lactic and glycolic acid, polylactic acid (PLA), and poly(lactic/glycolic acid). These polymers had long been used in biomedical applications such as suture and orthopedic implants and were known to be biocompatible and nonimmunogenic and could be easily synthesized to give different physicochemical properties, so they seemed to be ideal candidates for the development of implantable drug delivery devices. The scientists at Takeda Industries in the early 1980s synthesized the polymers in their laboratories and evaluated the effect of various physicochemical properties of the PLA and PLG family of polymers on the encapsulated drug-release properties in vitro and in vivo. Figure 7 shows leuprolide release over time from the microsphere formulation.

Zoladex®

Zoladex is a long-acting formulation of a synthetic decapeptide analogue of LH-RH called goserelin acetate. Goserelin acetate is dispersed in a matrix of D, L-lactic and glycolic acid copolymers and is presented as a sterile, white- to cream-colored, 1-mm-diameter cylinder. The implantable device comes preloaded in a special single-use syringe with a 16-gauge needle and is administered by subcutaneous injection to give continuous release of goserelin over 1–3 months. The encapsulated drug is released by a combination of diffusion and erosion-controlled mechanisms (104). However, because the delivery device is a monolith, heterogeneous hydrolysis is thought to be the predominant erosion process.

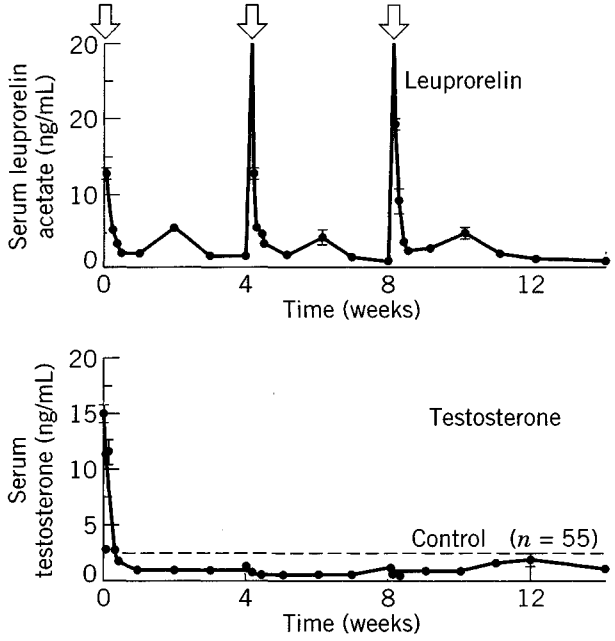


Figure 7. Serum levels of leuprorelin and testosterone following monthly im administration of Lupron Depot® in rats. The pharmacodynamic response, testosterone suppression, is achieved as long as the serum leuprorelin concentrations are above a threshold level. *Source:* Ref. 68.

De-Capeptyl® SR

De-capeptyl® SR is a long-acting formulation of triptorelin, another LH-RH agonist. Triptorelin is a decapeptide that functions in a manner similar to leuprorelin. The formulation contains microspheres made from a lactide–glycolide copolymer along with mannitol, polysorbate 80, and carboxymethyl cellulose sodium. For injection, the formulation is reconstituted using a vehicle containing mannitol in water. Injections are to be given every 4 weeks, usually in the buttocks.

Posilac®

Bovine somatotropin (bST), or bovine growth hormone, is secreted by the anterior pituitary gland and has growth-stimulating effects by direct stimulation of receptors or via mediators such as IGF-I. Posilac® is a sustained-release formulation of recombinant bST, sometribove, and is manufactured by Monsanto to increase milk production in dairy cattle. The formulation consists of the protein complexed to zinc and an oily base of aluminum stearate (5% w/w). The Zn–bST solid is dispersed in a hydrophobic gel matrix (semisolid at room temperature) of aluminum stearate and sesame oil. Oil-based formulations typically contain a vegetable-based oil such as sesame oil, a viscosity-imparting agent, and an antihydration substance. The increased viscosity is required for drug particle stability and injectability, and the antihydration agent is added to minimize moisture-induced degradation of the protein.

The development of oil-based injectable formulations for veterinary applications was appealing for several reasons. Firstly, the oil-based formulations are easier and usually cheaper to manufacture aseptically than microsphere-based systems because there are fewer fabrication steps. Secondly, because the formulations can be prepackaged in a syringe and because of the low moisture content, the formulations are stable, and administration and storage on the dairy farm is convenient. For these reasons, oil-based formulation approaches are attractive for cost-sensitive veterinary applications. Several companies including Upjohn and Elanco have evaluated these formulations, although only Monsanto has a formulation, Posilac, that is commercially available. Posilac is administered subcutaneously to dairy cows in the tailhead or shoulder at a dose of 500 mg of bST (36 mg of bST per day). The dose is administered every 14 days and consists of 1.4 cc of injectate in a prepacked 2-mL syringe with a 16-gauge needle. The drug is administered to healthy cows from the ninth week after lactation begins, and the increase in milk production is rapid, with the maximum increase observed after three to four injections. Figure 8 shows the effect of Posilac on milk production.

Nutropin Depot®

Recombinant growth hormone is used to treat short stature in children resulting from growth hormone deficiency, and the current treatments are daily or thrice weekly injections. It is therefore a suitable candidate for a sustained-release formulation. Although the endogenous secretion of hGH follows a pulsatile pattern, clinical studies have shown that continuous infusion via pumps gives serum hGH and IGF-I comparable with that obtained by daily injections. The protein is stabilized and encapsulated in a PLG microsphere matrix (25). The microsphere fabrication process (ProLease®) involves formulation of the protein into a stable lyophilized powder; then the solid protein particles are dispersed in a solution of the polymer in methylene chloride and atomized over liquid nitrogen into cold or frozen ethanol. The ethanol acts as a curing solvent and removes the methylene chloride, and the microspheres harden. The wet microspheres are collected and dried under vacuum and vialed as a white, free-flowing powder. Immediately before subcutaneous administration, the microspheres are suspended in an aqueous vehicle and injected.

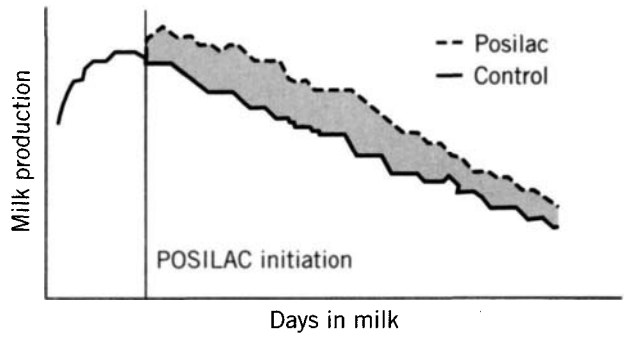


Figure 8. Effect of Posilac® on milk production in dairy cattle. Administration of Posilac to dairy cattle results in increased milk production compared with a control group of animals.

Preclinical studies in juvenile rhesus monkeys showed that a formulation that contained hGH in the complexed form, Zn–hGH, resulted in elevated serum hGH concentration for about 3 weeks, and serum IGF-I levels were elevated for 3–4 weeks. Four groups of animals each received 24 mg of hGH as a single, daily subcutaneous bolus injection for 28 days in a subcutaneously administered microsphere formulation or in a continuous-release osmotic pump. To mimic the expected release pattern from the microspheres, the pump group received 15% of the 24-mg dose as a single injection to mimic the initial, burst release phase, and the rest was delivered by the pump continuously. The serum hGH profiles for the microsphere formulation and the osmotic pump groups showed sustained hGH levels for 28–30 days (Fig. 9). The microsphere formulation group showed an initial release with a C_{max} of 260 ng/mL, and then the serum hGH concentration was maintained at about 10 ng/mL up to 30 days and then dropped to 4–5 ng/mL until 60 days. The animals that received the pump maintained serum hGH concentrations at ~16 ng/mL until day 28, when the pump was excised. A pharmacodynamic marker for hGH, IGF-I, was also measured. The serum IGF-I concentrations followed the serum hGH profile, with IGF-I levels above baseline for 1 month. The study demonstrated that it was possible to encapsulate a protein within a microsphere delivery system and obtain sustained release of the protein and biological activity of the released protein. This formulation is currently undergoing evaluation in phase III clinical trials.

CONCLUSIONS

Since it was first reported in the mid-1970s that sustained release of proteins and peptides from polymers was feasible, significant developments have occurred in the field to the point where there are now several peptide and protein sustained-release products on or close to market. The purpose of this article is to review the key research results and considerations in developing delivery systems for proteins and peptides, with emphasis on polymeric injectable delivery approaches. Both the challenges in formulating products for the marketplace and the achievements to date are emphasized. Unfortunately, there is not a single, simple approach to ensure the successful formulation of protein or peptides for sustained delivery. Rather, successful formulation and product development result from a thorough understanding of protein and peptide degradation processes, the diverse environments that the drug will encounter during processing and release, the mechanism of release from the delivery system, and an understanding of scale-up, manufacturing, and regulatory issues in developing pharmaceutical products.

Key obstacles in developing protein and peptide delivery products include stabilizing the drug, obtaining desirable release kinetics, and scaling up the fabrication process to support clinical testing and commercialization. In general, though suitable for many peptides, incorporation processes, such as emulsion and coacervation processes, that involve interfaces may not be suitable for proteins that are susceptible to denaturation at aqueous–organic interfaces. Because proteins are generally more stable in the solid state than in solution, it is advantageous to incorporate proteins into delivery systems in a solid form, such as a lyophilized powder. If, as in the case of human growth hormone, the protein can be encapsulated in a stable form with reduced aqueous solubility, then the potential for degradation during release at the site of delivery is greatly reduced owing to decreased protein molecular mobility. Also, the mechanism of release must be well understood to develop formulation or processing approaches to achieve a target release profile. For polymeric delivery systems, the polymer chemistry and degradation characteristics are very important as is the ability to process the drug to achieve a desired particle size prior to encapsulation. In addition, approaches for scaling up and manufacturing sustained polymeric delivery systems were presented. Thus, with the examples presented here, we have demonstrated that sustained protein and peptide delivery is commercially feasible and offers significant therapeutic advantages. This reality, coupled with the development of an increasing number of injectable, macromolecular drugs (which require chronic administration), suggests that the future is indeed bright for improved delivery technologies.

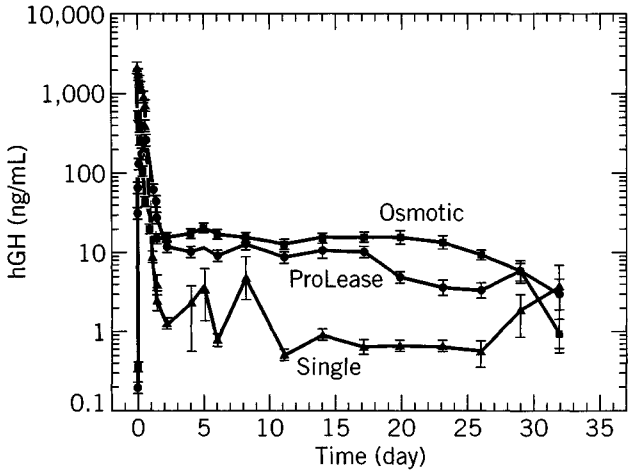


Figure 9. Serum hGH concentration from Nutropin Depot—juvenile rhesus monkeys. The ProLease® group show sustained serum hGH levels for about 28 days. The serum hGH profile was similar to the osmotic pump group that was preprogrammed to release hGH for 28 days.

ACKNOWLEDGMENTS

We would like to thank our colleagues at Alkermes for their insightful comments in the preparation of this manuscript.

BIBLIOGRAPHY

1. R. Langer, *Acc. Chem. Res.* **25**(10), 537–542 (1993).
2. R. Pearlman and T.A. Bewley, in Y.J. Wang and R. Pearlman, eds. *Stability and Characterization of Protein and Peptide Drugs: Case Histories*, Plenum, New York, 1993, pp. 1–57.
3. C.G. Pitt, *Int. J. Pharm.* **59**, 173–196 (1990).

4. W. Lu and T.G. Park, *J. Pharm. Sci. Technol.* **49**(1), 13–19 (1995).
5. M.C. Manning, K. Patel, and R. Borchardt, *Pharm. Res.* **6**(11), 903–918 (1989).
6. D.B. Volkin and C.R. Middaugh, in T.J. Ahern and M.C. Manning, eds., *Stability of Protein Pharmaceuticals. Part A: Chemical and Physical Pathways of Protein Degradation*, Plenum, New York, 1992, pp. 109–134.
7. H.R. Costantino, R. Langer, and A. Klibanov, *J. Pharm. Sci.* **83**(12), 1662–1669 (1994).
8. G.W. Becker et al., *Biotechnol. Appl. Biochem.* **10**, 326–337 (1988).
9. M.J. Pikal et al., *Pharm. Res.* **8**(4), 427–436 (1991).
10. A. Bardat, R. Schmitthaeusler, and E. Renzi, *J. Parent Pharm. Sci. Technol.* **50**(2), p. 83–88 (1996).
11. M. Tracy, *Biotechnol. Progr.* **14**(1), 108–115 (1998).
12. K. Patel and R. Borchardt, *Pharm. Res.* **7**(7), 703–711 (1990).
13. S.E. Zale and A.M. Klibanov, *Biochemistry* **25**(19), 5432–5443 (1986).
14. Y.-C.J. Wang and M.A. Hanson, *J. Parenter. Sci. Technol.* **42**(Suppl.), S3–S25 (1988).
15. D.B. Volkin and C.R. Middaugh, in T.J. Ahern and M.C. Manning, eds., *Stability of Protein Pharmaceuticals. Part A: Chemical and Physical Pathways of Protein Degradation*, Plenum, New York, 1992, pp. 215–248.
16. W.R. Liu, R. Langer, and A. Klibanov, *Biotechnol. Bioeng.* **37**, 177–184 (1991).
17. M.A. Hanson and S.K.E. Rouan, in T.J. Ahern and M.C. Manning, eds., *Stability of Protein Pharmaceuticals. Part B: In Vivo Pathways of Degradation and Strategies for Protein Stabilization*, Plenum, New York, 1992, pp. 209–233.
18. J.F. Carpenter, et al., *Pharm. Res.* **14**(8), 969–975 (1997).
19. S.P. Schwendeman et al., in S. Cohen and H. Bernstein, eds., *Microspheres / Microparticles: Characterization and Pharmaceutical Application*, Dekker, New York, 1996, pp. 1–49.
20. S.D. Putney and P.A. Burke, *Nat. Biotechnol.* **16**, 1–6 (1998).
21. J.F. Carpenter and J.H. Crowe, *Biochemistry* **28**, 3916–3922 (1989).
22. H.R. Costantino et al., *J. Pharm. Sci.* **87**(11), 1406–1411 (1998).
23. H.R. Costantino, R. Langer, and A.M. Klibanov, *Pharm. Res.* **11**(1), 21–29 (1994).
24. H.R. Costantino et al., *Int. J. Pharm.* **166**, 211–221 (1998).
25. O.L. Johnson et al., *Nat. Med.* **2**(7), 795–799 (1996).
26. T. Arakawa and S.N. Timasheff, *Biophys. J.*, **47**, 411–414 (1985).
27. T. Arakawa, *Biopolymers* **28**, 1397–1401 (1989).
28. K. Gekko and H. Ito, *J. Biochem. (Tokyo)* **107**, 572–577 (1990).
29. T. Arakawa, Y. Kita, and J.F. Carpenter, *Pharm. Res.* **8**(3), 285–291 (1991).
30. T. Loftsson and M.E. Brewster, *J. Pharm. Sci.* **85**(10), 1017–1025 (1996).
31. R.A. Rajewski and V.J. Stella, *J. Pharm. Sci.* **85**(11), 1142–1169 (1996).
32. S.A. Charman, K.L. Mason, and W.N. Charman, *Pharm. Res.* **10**(7), 954–962 (1993).
33. P.K. Tsai et al., *Pharm. Res.* **10**(3), 649–659 (1993).
34. H. Thurow and K. Geisen, *Diabetologia* **27**, 212–218 (1984).
35. T.A. Horbett, in T.J. Ahern and M.C. Manning, eds. *Stability of Protein Pharmaceuticals. Part A: Chemical and Physical Pathways of Protein Degradation*, Plenum, New York, 1992, pp. 195–214.
36. M.S. Hora, R.K. Rana, and F.W. Smith, *Pharm. Res.* **9**(1), 33–36 (1992).
37. J.L. Cleland and A.J.S. Jones, *Proc. Int. Symp. Controlled Release Bioact. Mater.* **21**, 514–515 (1995).
38. M. Mumenthaler, C.C. Hsu, and R. Pearlman, *Pharm. Res.* **11**(1), 12–20 (1994).
39. I. Gonda, *Adv. Drug Delivery Rev.* **19**(1), 37–46 (1996).
40. B.C. Cunningham, M.G. Mulkerrin, and J.A. Wells, *Science* **253**, 545–548 (1991).
41. M.W. Townsend, P.R. Byron, and P.P. Deluca, *Pharm. Res.* **7**(10), 1086–1091 (1990).
42. K-I. Izutsu, S. Yoshioka, and S. Kojima, *Pharm. Res.* **11**(7), 995–999 (1994).
43. S.P. Schwendeman et al., *Dev. Biol. Stand.* in press.
44. Food and Drug Administration, *Inactive Ingredients Guide,* Division of Drug Information Resources, Center for Drug Evaluation and Research, FDA, Washington, DC, 1996
45. S. Calis et al., *Pharm. Res.* **12**(7), 1072–1076 (1995).
46. W. Norde and J. Lyklema, *J. Colloid Interface Sci.* **71**(2), 350–366 (1979).
47. K. Gekko and Y. Hasegawa, *Biochemistry* **25**, 6563–6571 (1986).
48. T. Arai and W. Norde, *Colloids Surf.* **51**, 1–15 (1990).
49. I. Grizzi et al., *Biomaterials* **16**, 305–311 (1995).
50. P.A. Burke, *Proc. Int. Symp. Controlled Release Bioact. Mater.* **23**, 133–134 (1996).
51. K. Mäder, B. Gallez, K.J. Liu, H.M. Swartz, *Biomaterials* **17**, 457–461 (1996).
52. Y. Zhang, S. Zale, and H. Bernstein, *J. Biomed. Mater. Res.* **34**, 531–538 (1997).
53. M.A. Tracy et al., *Biomaterials*, in press.
54. R. Langer and J. Folkman, *Nature (London)* **263**, 797–800 (1976).
55. R. Langer, *Chem. Eng. Commun.* **6**, 1–48 (1980).
56. Y. Ogawa et al., *Chem. Pharm. Bull.* **36**, 2576–2581 (1988).
57. H. Okada et al., *J. Pharmacol. Exp. Ther.* **244**(2), 744–750 (1988).
58. R. Bawa et al., *J. Controlled Release* **1**, 259–267 (1985).
59. R. Langer, *Science*, **249**, 1527–1533 (1990).
60. T. Hsu and R. Langer, *J. Biomed. Mater. Res.* **19**, 445–460 (1985).
61. W.M. Saltzman and R. Langer, *Biophys. J.* **55**, 163–171 (1989).
62. S.S. Shah, Y. Cha, and C.G. Pitt, *J. Controlled Release* **18**, 261–270 (1992).
63. R.A. Siegel, *Pharm. Res.* **1**, 1–10 (1983).
64. M. Sefton, L. Brown, and R. Langer, *J. Pharm. Sci.* **73**, 1859–1869 (1984).
65. E.S. Miller, N.A. Peppas, and D.N. Winslow, *J. Membr. Sci.* **14**, 79–92 (1983).
66. S. Cohen et al., *Pharm. Res.* **8**(6), 713–720 (1991).
67. H. Okada et al., *J. Controlled Release* **28**, pp. 121–129 (1994).
68. H. Okada, *Adv. Drug Delivery Rev.* **28**(1), 43–70 (1997).
69. R.A. Batycky et al., *J. Pharm. Sci.* **86**(12), 1464–1477 (1997).
70. U.S. Pat. 5,019,400 (1991), W.R. Gombotz, M.S. Healy, and L.R. Brown (to Enzytech: United States).
71. A. Gopferich, *Macromolecules* **30**, 2598–2604 (1997).

Next Page

72. R.A. Kenley et al., *Macromolecules* **20**, 2398–2403 (1987).
73. G. Spenlehauer et al., *Biomaterials* **13**, pp. 594–600 (1992).
74. N.S. Mason, C.S. Miles, and R.E. Sparks, in C.G. Gebelein and F.F. Koblitz, ed., *Biomedical and Dental Applications of Polymers*, Plenum, New York, 1981, pp. 279–291.
75. P. Flandroy et al., *J. Controlled Release* **47**, 153–170 (1997).
76. E.A. Schmitt, D.R. Flanagan, and R.J. Linhardt, *Macromolecules* **27**, 743–748 (1994).
77. G.E. Visscher et al., *J. Biomed. Mater. Res.* **19**, 349–365 (1985).
78. M. Vert, S.M. Li, and H. Garreau, *J. Biomater. Sci. Polym.* **6**, 639–649 (1994).
79. S. Li, S. Girod-Holland, and M. Vert, *J. Controlled Release* **40**, 41–53 (1996).
80. A. Kamijo et al., *J. Controlled Release* **40**, 269–276 (1996).
81. F.D. Anderson et al., *Pharm. Res.* **10**(3), 369–380 (1993).
82. J.M. Anderson and M.S. Shive, *Adv. Drug Delivery Rev.* **28**(1), 5–24 (1997).
83. H.J. Lee et al., *J. Pharmacol. Exp. Ther.* **281**, 1431–1439 (1997).
84. D.H. Lewis, in M. Chasin and R. Langer, eds. *Biodegradable Polymers as Drug Delivery Systems*, Dekker, New York, 1990, pp. 1–41.
85. H. Jeffrey, S.S. Davis, and D.T. O'Hagan, *Pharm. Res.* **10**(3), 362–368 (1993).
86. Y. Hayashi et al., *Pharm. Res.* **11**(2), 337–339 (1994).
87. Y. Tabata, S. Gutta, and R. Langer, *Pharm. Res.* **10**(4), 487–496 (1993).
88. M. Morlock et al., *Eur. J. Pharm. Biopharm.* **43**, 29–36 (1997).
89. M.S. Hora et al., *Pharm. Res.* **7**(11), 1190–1194 (1990).
90. Y. Tabata and R. Langer, *Pharm. Res.* **10**(3), 391–399 (1993).
91. M. Donbrow, ed., *Microparticles and Nanoparticles in Medicine and Pharmacy*, CRC Press, Boca Raton, Fl., 1992, pp. 1–14.
92. Z. Zhao et al., *Proc. Int. Symp. Controlled Release Bioact. Mater.* **21**, 51–52 (1995).
93. J.L. Cleland et al., *Adv. Drug Delivery Rev.* **28**(1), 71–84 (1997).
94. E. Mathiowitz and R. Langer, in *Microparticles and Nanoparticles in Medicine and Pharmacy*, CRC Press, Boca Raton, Fl., 1992, pp. 100–123.
95. K. Fujioka et al., *J. Controlled Release* **33**, 317–323 (1995).
96. K. Fujioka et al., *J. Controlled Release* **33**, 307–316 (1995).
97. P. Herbert et al., *Pharm. Res.* **15**(2), 357–361 (1998).
98. J.L. Cleland, in L.S. Sanders and W. Hendren, eds. *Protein Delivery: Physical Systems*, Plenum, New York, 1996, pp. 1–43.
99. R.G. Launsby and D.L. Weese, *Straight Talk on Designing Experiments*, 2nd ed., Launsby Consulting, Colorado Springs, Co., 1995.
100. J.L. Cleland, *Biotechnol. Progr.* **14**, 102–107 (1998).
101. International Conference on Harmonization, *Fed. Regist.*, **62**, 24302–24309 (1997).
102. C.H. Niu and Y.Y. Chiu, *J. Pharm. Sci.* **87**(11), pp. 1331–1334 (1998).
103. *Physician's Desk Reference*, Medical Economics Data Production Company, Montvale, N.J., 1998, pp. 2907–2918, 3194–3198.
104. F.G. Hutchinson and B.J.A. Furr, in *Drug Delivery Systems*: Fundamentals and Techniques, P. Johnson and J.G. Lloyd, eds., Ellis Horwood/VCH Verlag., Chichester, England, 1987, pp. 106–119.

PHARMACOKINETICS

PRAVIN R. CHATURVEDI
Vertex Pharmaceuticals
Cambridge, Massachusetts

KEY WORDS

Bioavailability
Biopharmaceutics
Clearance
Compartmental analysis
Deconvolution
Drug input rate
Half-life
Loo-Riegelman method
Noncompartmental analysis
Pharmacodynamics
Pharmacokinetics
Toxicokinetics
Volume of distribution
Wagner-Nelson method

OUTLINE

Introduction
Background
  Fundamental Pharmacokinetic Parameters
Overview of the Theoretical Principles of Pharmacokinetics
  Laplace Transforms
  Linear Mammillary Models
  Method of Residuals
  Method of Estimating Areas Under the Curve
  Principle of Superposition
  General Principles of Pharmacokinetics
  Compartmental Analysis Approach
Classic Linear Compartmental Models
  One-Compartment Open Models with Linear Elimination
  One-Compartment Open Model with Michaelis-Menten Elimination
  Two-Compartment Open Models with Linear Elimination from Central Compartment
  Linear Two-Compartment Open Model with Peripheral Compartment Elimination
  Noncompartmental Analysis
  Physiologically Based Pharmacokinetic Models
  Population Pharmacokinetics
Assessment of Drug Input Rate from Controlled Drug Delivery Systems
  Mass Balance Methods for the Assessment of Input Rate

Previous Page

72. R.A. Kenley et al., *Macromolecules* **20**, 2398–2403 (1987).
73. G. Spenlehauer et al., *Biomaterials* **13**, pp. 594–600 (1992).
74. N.S. Mason, C.S. Miles, and R.E. Sparks, in C.G. Gebelein and F.F. Koblitz, ed., *Biomedical and Dental Applications of Polymers*, Plenum, New York, 1981, pp. 279–291.
75. P. Flandroy et al., *J. Controlled Release* **47**, 153–170 (1997).
76. E.A. Schmitt, D.R. Flanagan, and R.J. Linhardt, *Macromolecules* **27**, 743–748 (1994).
77. G.E. Visscher et al., *J. Biomed. Mater. Res.* **19**, 349–365 (1985).
78. M. Vert, S.M. Li, and H. Garreau, *J. Biomater. Sci. Polym.* **6**, 639–649 (1994).
79. S. Li, S. Girod-Holland, and M. Vert, *J. Controlled Release* **40**, 41–53 (1996).
80. A. Kamijo et al., *J. Controlled Release* **40**, 269–276 (1996).
81. F.D. Anderson et al., *Pharm. Res.* **10**(3), 369–380 (1993).
82. J.M. Anderson and M.S. Shive, *Adv. Drug Delivery Rev.* **28**(1), 5–24 (1997).
83. H.J. Lee et al., *J. Pharmacol. Exp. Ther.* **281**, 1431–1439 (1997).
84. D.H. Lewis, in M. Chasin and R. Langer, eds. *Biodegradable Polymers as Drug Delivery Systems*, Dekker, New York, 1990, pp. 1–41.
85. H. Jeffrey, S.S. Davis, and D.T. O'Hagan, *Pharm. Res.* **10**(3), 362–368 (1993).
86. Y. Hayashi et al., *Pharm. Res.* **11**(2), 337–339 (1994).
87. Y. Tabata, S. Gutta, and R. Langer, *Pharm. Res.* **10**(4), 487–496 (1993).
88. M. Morlock et al., *Eur. J. Pharm. Biopharm.* **43**, 29–36 (1997).
89. M.S. Hora et al., *Pharm. Res.* **7**(11), 1190–1194 (1990).
90. Y. Tabata and R. Langer, *Pharm. Res.* **10**(3), 391–399 (1993).
91. M. Donbrow, ed., *Microparticles and Nanoparticles in Medicine and Pharmacy*, CRC Press, Boca Raton, Fl., 1992, pp. 1–14.
92. Z. Zhao et al., *Proc. Int. Symp. Controlled Release Bioact. Mater.* **21**, 51–52 (1995).
93. J.L. Cleland et al., *Adv. Drug Delivery Rev.* **28**(1), 71–84 (1997).
94. E. Mathiowitz and R. Langer, in *Microparticles and Nanoparticles in Medicine and Pharmacy*, CRC Press, Boca Raton, Fl., 1992, pp. 100–123.
95. K. Fujioka et al., *J. Controlled Release* **33**, 317–323 (1995).
96. K. Fujioka et al., *J. Controlled Release* **33**, 307–316 (1995).
97. P. Herbert et al., *Pharm. Res.* **15**(2), 357–361 (1998).
98. J.L. Cleland, in L.S. Sanders and W. Hendren, eds. *Protein Delivery: Physical Systems*, Plenum, New York, 1996, pp. 1–43.
99. R.G. Launsby and D.L. Weese, *Straight Talk on Designing Experiments*, 2nd ed., Launsby Consulting, Colorado Springs, Co., 1995.
100. J.L. Cleland, *Biotechnol. Progr.* **14**, 102–107 (1998).
101. International Conference on Harmonization, *Fed. Regist.*, **62**, 24302–24309 (1997).
102. C.H. Niu and Y.Y. Chiu, *J. Pharm. Sci.* **87**(11), pp. 1331–1334 (1998).
103. *Physician's Desk Reference*, Medical Economics Data Production Company, Montvale, N.J., 1998, pp. 2907–2918, 3194–3198.
104. F.G. Hutchinson and B.J.A. Furr, in *Drug Delivery Systems*: Fundamentals and Techniques, P. Johnson and J.G. Lloyd, eds., Ellis Horwood/VCH Verlag., Chichester, England, 1987, pp. 106–119.

PHARMACOKINETICS

PRAVIN R. CHATURVEDI
Vertex Pharmaceuticals
Cambridge, Massachusetts

KEY WORDS

Bioavailability
Biopharmaceutics
Clearance
Compartmental analysis
Deconvolution
Drug input rate
Half-life
Loo-Riegelman method
Noncompartmental analysis
Pharmacodynamics
Pharmacokinetics
Toxicokinetics
Volume of distribution
Wagner-Nelson method

OUTLINE

Introduction
Background
  Fundamental Pharmacokinetic Parameters
Overview of the Theoretical Principles of Pharmacokinetics
  Laplace Transforms
  Linear Mammillary Models
  Method of Residuals
  Method of Estimating Areas Under the Curve
  Principle of Superposition
  General Principles of Pharmacokinetics
  Compartmental Analysis Approach
Classic Linear Compartmental Models
  One-Compartment Open Models with Linear Elimination
  One-Compartment Open Model with Michaelis-Menten Elimination
  Two-Compartment Open Models with Linear Elimination from Central Compartment
  Linear Two-Compartment Open Model with Peripheral Compartment Elimination
  Noncompartmental Analysis
  Physiologically Based Pharmacokinetic Models
  Population Pharmacokinetics
Assessment of Drug Input Rate from Controlled Drug Delivery Systems
  Mass Balance Methods for the Assessment of Input Rate

Assessment of Absorption Rate by Deconvolution Techniques
Conclusions
Bibliography

INTRODUCTION

The pharmacological response of drugs can be better correlated with the concentration of the drug (or its active metabolite) in blood or in some other biophase than with the dose administered. The concentration of the drug in blood or the biophase depends on disposition factors including distribution, metabolism, excretion, and on the efficiency and design of the drug delivery system. The drug delivery system is the sequence of events that provides the drug to the site of action. The pharmacological action of a drug is determined by its intrinsic activity, and drug delivery to the site of action is governed by physicochemical properties of the drugs.

The study of the relationship between the physicochemical properties of a drug in a dosage form and the pharmacologic, toxicologic, or clinical response of the drug after its administration is termed biopharmaceutics. Advancement in biopharmaceutics has primarily resulted from a better understanding of a descriptive discipline called pharmacokinetics (1).

Pharmacokinetics is a theoretical framework of the principles for determining the time course of drug absorption, distribution, metabolism, and excretion, as well as the study of the relationship of these processes to the intensity and time course of therapeutic and adverse effects of these drugs (2). Pharmacokinetics involves the application of mathematics and biochemistry in a physiologic and pharmacologic context. Two related disciplines have emerged from better understanding of pharmacokinetics. Clinical pharmacokinetics deals with the application of pharmacokinetics to safe and effective therapeutic management of patients. Toxicokinetics encompasses the study of the kinetics of absorption, distribution, metabolism, and elimination of large (toxic) doses of drug in the body, and the safety evaluation and assessment of adverse reactions caused by the excessive drug dose (3). The assessment of how drugs exert their therapeutic and toxic effects on the body by studying the relationship of drug concentration in a biophase to its therapeutic or toxic effect is called pharmacodynamics. Thus pharmacokinetics may be described as "what the body does to the drug," and pharmacodynamics can be described as "what the drug does to the body" (4).

Application of pharmacokinetics is critical to the development of various drug delivery technologies. The process of drug delivery includes the administration of the dosage form, the release of the drug from the dosage form, and transport of the drug across biological membranes to the site of action. Thus, increasing the rate and extent of drug delivery would improve the efficiency of the system leading to earlier onset of action and better intensity of pharmacological response. Administration of different formulations of the same drug does not necessarily produce the same response (5). The availability of the drug from different dosage forms may be affected. The term bioavailability is used to describe the rate and extent of drug absorption from a dosage form.

The goal of drug therapy is to produce therapeutic drug concentrations to produce the pharmacological effect without producing toxicity (6). This requires the maintenance of drug concentrations at effective levels while maintaining a reasonable dosing frequency such as once or twice daily. Conventional dosage forms are rapidly absorbed, producing rapid peak concentration and then declining as a function of the drug half-life. Drugs from such dosage forms usually require more frequent dosing due to half-life and duration of pharmacological effect requirements. A drug with a short half-life requires more frequent dosing than drugs with long half-life. The frequency of dosing is also affected by the therapeutic index of the drug. The therapeutic index of a drug is defined as the ratio of the concentration producing a toxic effect to that producing a safe and effective pharmacological effect. Thus, conventional dosage forms are significantly dependent on the pharmacokinetics of the drug (6). The rate and extent of drug absorption can be altered to produce controlled drug delivery via concepts such as sustained release, prolonged release, and delayed release. The discussion of various principles of controlled drug delivery is described in several other articles and is beyond the scope of this article. The goal of this article is to familiarize oneself with the fundamental principles of pharmacokinetics and its role in designing controlled drug delivery systems.

BACKGROUND

Currently four different approaches are used to describe the pharmacokinetics of drugs. The traditional approach is called compartmental analysis, which considers the rates of absorption, distribution, and elimination in terms of rate constants, usually of first-order. This approach is sometimes also called model-dependent approach to pharmacokinetic analysis. The main advantage of this traditional pharmacokinetic analysis is the ability to simulate and predict blood drug concentrations during altered physiological or pathological conditions and during chronic medication. The major disadvantage of the compartmental approach is the mathematical complexity of equations and the difficulty in obtaining reliable estimates of rate constants (2).

A second approach to describe pharmacokinetics is termed noncompartmental analysis. The parameters used to describe the pharmacokinetics of the drug are determined using statistical moments and are derived from relationships involving the area under the zero moment curve (AUC) and the area under the first moment curve (AUMC) of the blood drug concentration-time curve. The advantage of this approach is the ease of determination of these parameters and the lack of requirements of detailed description of the disposition of the drug (hence sometimes referred to as model-independent approach). However, knowledge of noncompartmental pharmacokinetic parameters is insufficient to predict or simulate blood drug concentration profiles in the body (2).

The third major approach to pharmacokinetic analysis focuses on the fundamental anatomical and physiological factors that influence drug uptake and disposition and is referred to as physiological pharmacokinetics. Individual organ systems are studied with respect to partitioning of drug between blood and the organ, the binding of drug in blood and tissues, and blood flow through the organ. Mass balance equations are developed to describe the rate of change in each organ system. The equations for all organs are solved simultaneously and change in drug concentration over time is predicted. The advantage of this approach is that the effects of changes in real physiological variables such as blood flow can be evaluated. This approach also provides reasonable predictions for human pharmacokinetics based upon preclinical animal data. However, the requirements of extensive computing power and unavailability of partitioning or tissue binding data for all species results in limited application of this approach for clinical studies (2).

Recently, with the availability of faster and better computers, a new approach termed population pharmacokinetics has been developed. The major advantage of this approach is the ability to collect sparse data from many subjects in clinical studies and predict the concentration-time profile in a population of patients. This approach allows one to understand inter- and intraindividual variability and is able to determine the role of different factors such as age, sex, and disease in the altered disposition of drugs. Thus, it is rapidly becoming more popular in the design and analysis of clinical studies. A major disadvantage of this approach is the requirement of a good understanding of statistics and mathematics and the need for powerful computers to perform the analysis of data.

Fundamental Pharmacokinetic Parameters

Although the pharmacokinetic approaches are different in the process, they are not mutually exclusive. Two fundamental parameters of pharmacokinetics are drug clearance and its volume of distribution (2). These two parameters can be estimated using any of these approaches and are invaluable to the understanding of pharmacokinetics. Furthermore, noncompartmental analysis can be used to determine some of the parameters for compartmental approaches, and the two approaches are often combined in pharmacokinetic analysis. Similarly, population pharmacokinetic analysis primarily provides an estimate of the drug clearance and its volume of distribution. A physiological pharmacokinetic approach requires the determination of organ clearance and volume of distribution, which can again be used to predict or simulate drug concentration-time profile in the body.

It has been suggested that for any pharmacokinetic analysis, 10 critical pharmacokinetic and pharmacodynamic parameters should be determined (7). These 10 parameters are (*1*) clearance, (*2*) effective drug concentrations, (*3*) extent of availability from a dosage form, (*4*) fraction of dose excreted unchanged, (*5*) blood/blood concentration ratio, (*6*) half-life, (*7*) toxic concentrations, (*8*) protein binding, (*9*) volume of distribution, and (*10*) rate of availability from a dosage form.

The estimates of clearance, effective drug concentration, and extent of availability are necessary to define the appropriate dosing rate (amount/day) of the drug by a particular route of administration (7). The knowledge of the fraction of the dose excreted unchanged in the urine allows one to estimate the nonrenal clearance of the drug (which may be assumed to represent the hepatic clearance). The ratio of blood to blood concentration ratio allows one to convert the more easily measured blood concentrations into blood concentrations. The ratio of hepatic blood clearance to hepatic blood flow subtracted from one allows an estimate of maximum oral bioavailability.

Half-life and toxic concentrations are very important in drug development. Half-life of the drug defines its dosing interval. Half-life is a derived parameter from clearance and volume of distribution of the drug. Hence, it should not be used as a tool to determine the disposition of the drug (7). The knowledge of toxic concentrations is important because the dosing frequency results in accumulation of drug, and the goal of drug therapy is to maintain effective and safe drug concentrations without entering the toxic concentration range. The knowledge of protein binding of the drug is important in the determination of drug clearance, and it is presumed that the unbound drug is responsible for pharmacological action of the drug because it is able to cross biological membranes.

The knowledge of volume of distribution is important in understanding drug distribution. The volume of distribution allows one to predict steady-state trough and maximum drug concentrations. Of most importance is the use of volume of distribution to determine whether disease states have affected the drug distribution rather than drug clearance (7). For this purpose, the estimation of the volume of distribution at steady-state, which relates the concentration of the drug in systemic circulation to the amount of drug in the body following multiple dosing of the drug. The rate of drug availability from a dosage form is considered a formulation parameter because it can be modified by a change in the formulation from a conventional dosage form to a controlled drug delivery system.

OVERVIEW OF THE THEORETICAL PRINCIPLES OF PHARMACOKINETICS

Several textbooks and review articles are available to provide a more detailed and thorough understanding of the fundamental concepts and mathematical principles of pharmacokinetics (8–10). This overview intends to provide the basis for the use of pharmacokinetics in the development of dosage forms. A brief description of different methods used in developing the mathematical basis for pharmacokinetics is provided in this section. These methods are generally applicable to the evaluation of pharmacokinetics regardless of whether compartmental, noncompartmental, physiological, or population pharmacokinetic methods are used in data analyses.

This review also intends to provide the reader with a general understanding of various methods available to allow the estimation of the fraction of the dose absorbed following extravascular administration for the assessment of

in vivo absorption kinetics. For a more detailed understanding on assessment of drug input rate from a controlled drug delivery system, the reader is referred to reviews of this subject (11–14).

Laplace Transforms

Rate equations that describe apparent zero-order or first-order processes are termed linear equations. The Laplace transform is used for solving linear differential equations. Hence, the Laplace transform is applicable to the solution of many equations used in pharmacokinetic analysis. The basic idea of the Laplace transform is to replace the time domain of a rate expression by the complex domain of the Laplace operators. This is achieved by eliminating the independent variable (in pharmacokinetics that being time). The Laplace transform enables complex rate expressions to be manipulated easily by conventional algebraic techniques. The transformed expression can be rearranged into a form that is commonly found in tables of Laplace transforms (15–17). Upon transformation of the Laplace domain into time domain, the complete solution of the linear differential equation is obtained. A table of Laplace transforms of common pharmacokinetic functions is provided in *Pharmacokinetics* (8).

Linear Mammillary Models

A method has been developed using simple treatments to derive equations for any linear mammillary compartment model with any first- or zero-order, or bolus input process. This is accomplished by the use of general input and disposition functions, a method for solving partial fractions to obtain solutions to Laplace transforms, and a multiple dosing function. The input function and the disposition function are defined such that the product of these two functions yields the Laplace transform of the equation describing the time course of a drug in a model compartment. A disposition function defines the model necessary to describe the levels of the drug in the body or a compartment and includes all distribution and elimination processes. Input functions describe the processes needed to get the drug into the body. The following general equation has been empirically derived to describe the Laplace transform for the disposition function of the central compartment in a linear N-compartment mammillary model, where elimination of the drug from any compartment is allowed:

$$d_{s,c} = \frac{\prod_{i=2}^{N} (s + E_i)}{\prod_{i=1}^{N} (s + E_i) - \sum_{j=2}^{N} \left[(k_{lj}k_{jl} \prod_{\substack{m=2 \\ m \neq j}}^{N} (s + E_m) \right]} \quad (1)$$

wherein $d_{s,c}$ is the disposition function for the central compartment (#1); it is a function of the Laplace operator, s, Π is the continued product where any term is defined as equal to 1 when the index takes a forbidden value, i.e., i = 1 in the numerator or m = j in the denominator, Σ is the continued summation where any term is defined as equal to zero when the index takes a forbidden value, $k_{ij} \cdot k_{jl}$ are the first-order intercompartmental transfer rate constants, E_i, E_m are the sum of the exit rate constants out of compartments i or m; and N is the number of driving force compartments in the disposition model (i.e., compartments having exit rate constants).

Various input function rates for different processes of input such as instantaneous bolus input, continuous intravenous infusion, or first-order extravascular administration are described (18). The product of the input and disposition function yields the Laplace transform for the amount of drug in the central compartment, $a_{s,c}$.

$$a_{s,c} = in_s \cdot d_{s,c} \quad (2)$$

One can use either the anti-Laplace of the resulting transform or use the general partial fraction theorem (19) to solve for the amount of drug in the central compartment.

Method of Residuals

The method of residuals is a commonly used technique in pharmacokinetics for resolving a curve into its various exponential components (8). This method is sometimes also referred to as feathering, peeling, or stripping the curve. The residual method entails the logarithmic representation of the blood concentration-time curves, followed by the subtraction of the observed blood concentrations from the extrapolated log-linear curves, yielding a series of residual values. A log-linear plot of residual concentrations versus time allows one to estimate rates of absorption, distribution, etc.

Method of Estimating Areas Under the Curve

The estimation of areas under the curve are required for pharmacokinetic analysis by compartmental or noncompartmental analysis. These areas are usually determined by using an approximate integration formula. The trapezoidal rule is one such formula used for estimating the AUC. This particular method involves the description of a given blood concentration-time curve by a function that depicts the curve as a series of straight lines, thereby enabling the area under the curve to be divided into a number of trapezoids. The area of each trapezoid is determined, and the sum of all the areas of trapezoids yield an estimate of the true AUC. The area under each trapezoid for a given segment of a blood concentration-time curve is given by:

$$AUC(t_1, t_2) = (t_2 - t_1) \cdot (C_1 + C_2)/2 \quad (3)$$

The accuracy of the approximation of AUC by this method is dependent on the number of blood concentration-time points sampled within the time interval from 0 to t. Yeh and Kwan (20) have shown that the area under the curve is overestimated by linear interpolation between data points using the trapezoidal rule. In cases where there are long intervals between samples, or changes in curvature, the linear interpolation of the logarithmically transformed data has been suggested. In the log trapezoidal method, the area under a given segment is obtained as:

$$AUC(t_1, t_2) = (C_1 - C_2)(t_2 - t_1)/(\ln C_1 - \ln C_2) \quad (4)$$

Two alternative algorithms based on known interpolating functions have been described in the literature. These include the Lagrange interpolation, in which the linear interpolation is replaced by a cubic polynomial function, and the spline method, in which the cubic functions are modified so that the fitted curves are smooth. The advantages and disadvantages of these interpolation techniques, relative to trapezoidal or log-trapezoidal methods, are discussed in detail by Yeh and Kwan (20).

Principle of Superposition

Fitting the blood concentration-time data requires some assumptions regarding the absorption kinetics of the drug. An alternative approach that requires no assumptions regarding the pharmacokinetic model or absorption kinetics is based upon the principle of superposition, and it employs the overlay technique (21,22). This method requires the following assumptions:

1. Each dose of the drug acts independently of every other dose.
2. The rate and extent of absorption and average systemic clearance are the same for each dosing interval.
3. Linear pharmacokinetics apply so that a change in dose during the multiple dosing regimen can be accommodated.

The overlay technique requires that the concentration-time profile of the drug should be completely characterized following a single dose.

The in vivo performance of controlled drug delivery systems can be influenced by various factors, which may be physiological, biochemical, and/or pharmacological (6). Physiological factors influencing the performance of controlled drug delivery systems include prolonged gastrointestinal absorption, variability in gastrointestinal emptying and motility, gastrointestinal blood flow, and presence or absence of food. Biochemical (or pharmacokinetic) factors influencing controlled delivery systems include dose dumping, first-pass metabolism, variability in excretion organs, and enzyme induction or inhibition following multiple dosing of the drug. The pharmacological factors affecting controlled drug delivery systems include the changes in drug effect following multiple dosing and tolerance or sensitization to the drug following repeated dosing. In order to minimize the influence of such factors, one normally selects drugs with long half-lives to minimize the frequency of dosing and/or develops sustained or controlled release dosage forms. The ultimate purpose of the latter approach is to maintain uniform blood concentrations through reducing the ratio of maximum to minimum concentrations and improving the therapeutic management of patients.

General Principles of Pharmacokinetics

It is important to note that following drug administration (by any route) there are dynamic processes reflecting drug absorption, distribution, and elimination (1). The amount of drug at the absorption site decreases with time as the drug is absorbed into the systemic circulation and distributed throughout the body. As soon as the drug reaches the systemic circulation, various elimination processes are initiated and the excretion of the drug (as parent or metabolite) in urine and other excretory fluids occurs. Thus the amount of the drug in the body continually changes as a function of these absorption and elimination processes.

In case the drug is administered directly into the systemic circulation (such as with an intravenous bolus injection), there is no absorption process and the dynamics of the drug in the body are simply a function of the elimination processes. Hence, some basic concepts of pharmacokinetics are discussed here assuming intravenous bolus injection administration. For purposes of simplicity, the distribution of the drug following intravenous administration is assumed to be instantaneous (i.e., one-compartment kinetics), and only elimination processes are considered. The reader is referred to an excellent book on pharmacokinetics (8) for more details on any of the following concepts.

Elimination Rate Constant. A simple first-order elimination process usually describes the elimination of most drugs. Thus, the rate of elimination of a drug from the body following intravenous administration is described by

$$-dA/dt = dA_e/dt = k_e A \quad (5)$$

where A is the amount of drug in the body at time t, A_e is the amount of drug eliminated from the body (by all routes) at time t, k_e is the apparent first-order elimination rate constant, and $-dA/dt$ and dA_e/dt are the rates of change in the amount of drug in the body and the elimination rate, respectively, at time t. Integrating equation 5 describes the amount of the drug in the body at any time t as,

$$A = A_0 e^{-ket} \quad (6)$$

where A_0 is the intravenous dose and equal to the initial amount of drug in the body.

The elimination rate constant can be estimated from equation 6 by simple transformation of drug amounts to their natural logarithm values. Thus, equation 6 can be rewritten as

$$\ln A = \ln A_0 - k_e \cdot t \quad (7)$$

This equation assumes the properties of a straight line and the slope of the line is equal to the elimination rate constant of the drug. Because common logarithms are used more frequently, equation 7 can be described in common logarithms as

$$\log A = \log A_0 - k_e \cdot t/2.303 \quad (8)$$

Thus, the elimination rate constant can be obtained by multiplying the slope of the line obtained from a semilogarithmic plot of A versus time by 2.303.

Half-life. A more commonly used term in clinical studies to describe the rate of elimination of drug from the body is the half-life. The half-life of a drug ($t_{1/2}$) is the time required for the amount in the body to decline to one-half its initial amount. The half-life is related to the elimination rate constant and can be obtained as

$$t_{1/2} = 0.693/k_e \tag{9}$$

Bioavailability. The fraction of an oral dose that reaches the systemic circulation is termed oral bioavailability (F). It is defined as the rate and extent of absorption of a drug. Bioavailability can be estimated as the ratio of the area under the blood concentration-time curve (AUC) following oral administration, to that obtained following an intravenous dose of the drug, corrected for the dose levels.

$$F = D_{iv}AUC_{oral}/D_{oral}AUC_{iv} \tag{10}$$

When the intravenous AUC is used as the reference, the bioavailability is termed *absolute* bioavailability. However, other routes of administration can be used as the reference, and an estimate of "relative" bioavailability can be obtained for any drug.

Volume of Distribution. Because there is a relationship between the amount of drug in the body and the drug concentration in the blood, we can rewrite the differential equation describing the rate of change of drug in the body as

$$-d(VC)/dt = -VdC/dt = k_e \cdot (VC) \tag{11}$$

or

$$-dC/dt = k_e \cdot C \tag{12}$$

where V is the apparent volume of distribution of the drug and is the ratio of the amount of drug in the body to the concentration of drug in the blood (C_b) at time t, i.e.,

$$V = A/C_b \tag{13}$$

The apparent volume of distribution is calculated by modifying equation 13 as

$$V = A_0/C_b^0 \tag{14}$$

where A_0 is the intravenous dose and C_b^0 refers to the initial drug concentration in the blood obtained by back extrapolating the semilogarithmic plot of blood concentration versus time to obtain the y-intercept. It is important to note that the volume of distribution varies from extremely low to extremely high values and does not correspond to any anatomical or physiological space. Instead, the principal factors that govern the volume of distribution are the blood and tissue binding of the drug. This can be better understood from the following:

$$A = A_b + A_t \tag{15}$$

where A is the amount of drug in the body, A_b is the amount of drug in the blood, and A_t is the amount of drug in the tissue compartment. By substituting the amount with the product of volume of distribution and concentration we get

$$V \cdot C_b = V_b \cdot C_b + V_t \cdot C_t \tag{16}$$

where V, V_b, and V_t are the apparent volume of distribution, physiological volume occupied by blood, and physiological space occupied by the tissues, respectively, and C_b and C_t refer to the drug concentrations in blood and tissue, respectively. Dividing equation 16 by the blood concentration (C_b), we obtain

$$V = V_b + V_t \cdot (C_t/C_b) \tag{17}$$

It should be noted that the total drug concentration in blood represents the sum of the bound and unbound fractions of the drug, and it is the free (unbound) fraction of drug that is able to freely diffuse out of blood into tissue spaces. Thus,

$$C_b^u = fu \cdot C_b \tag{18}$$

$$C_t^u = fu_t \cdot C_t \tag{19}$$

where C_b^u and C_t^u represent the unbound drug concentrations in blood and tissue compartments, respectively. Because the free concentration of drug is the same between blood and tissue, it is understood that

$$C_u^u = C_t^u \tag{20}$$

By substituting the relationships for C_b^u and C_t^u in equation 20, we get

$$C_t/C_b = fu/fu_t \tag{21}$$

Substituting this relationship in the relationship for volume of distribution in equation 21, we obtain

$$V = V_b + (fu/fu_t) \cdot V_t \tag{22}$$

Equation 22 shows that the volume of distribution is determined by the physiological spaces into which the drug distributes and the relative affinity of binding of the drug to blood and tissue components (2). As seen from this relationship, drugs with a high binding affinity to blood and plasma components have low volumes of distribution, whereas drugs with high tissue binding have high volumes of distribution.

Systemic (Total Body) Clearance. The most important pharmacokinetic parameter of a drug is its systemic blood clearance (Cl_s). Clearance is defined as the volume of fluid from which the drug is completely removed in a given period of time (volume/time). The clearance of drugs can be obtained at a total body level (systemic) or for individual organs. By definition, the total body (systemic) clearance

is the ratio of the overall rate of elimination (dA/dt) to the drug concentration in blood (C_b) (2,8)

$$Cl_s = (dA/dt)/C_b \quad (23)$$

Integrating the right hand side of the equation from time $t = 0$ to $t = \infty$, yields

$$Cl_s = \int_0^\infty (dA/dt)dt \Big/ \int_0^\infty C_b \cdot dt \quad (24)$$

It is seen that the term $\int_0^\infty (dA/dt)dt$ is equal to the total amount of drug that is ultimately eliminated, i.e., the intravenous dose administered (D_{iv}), whereas the term $\int_0^\infty C_b \cdot dt$ is equivalent to the total area under the curve of the drug concentration in blood versus time curve (AUC). Thus,

$$Cl_s = D_{iv}/AUC \quad (25)$$

By analogy, we can also prove that the systemic clearance of a drug is equal to the rate of intravenous infusion of a drug (k_0) divided by its steady-state blood concentration (C_{ss}^b),

$$Cl_s = k_0/C_{ss}^b \quad (26)$$

It can be also shown that systemic clearance can be estimated as the ratio of the dosing rate (in amount/time) to the average steady-state blood concentration of the drug

$$Cl_s = \text{Dosing rate/Avg } C_{ss}^b \quad (27)$$

Renal Clearance. Following drug administration, polar drugs and metabolites are removed from the body by the kidney. The rate of drug excretion by the kidney can be estimated as

$$dA/dt = Cl_r \cdot C_b \quad (28)$$

where Cl_r is the renal clearance of the drug, and C_b is the concentration of drug in the blood. Renal clearance is determined by three factors: glomerular renal filtration (Cl_{GFR}), active tubular secretion (Cl_{TS}), and passive tubular reabsorption (Cl_{TR}), of the drug. Thus, Cl_r can be represented as

$$Cl_r = Cl_{GFR} + Cl_{TS} - Cl_{TR} \quad (29)$$

If the drug is not bound in the blood, its renal filtration rate is equivalent to the glomerular filtration rate (measured as inulin or creatinine clearance). Protein-bound drugs are unable to cross the glomerular membrane, and their renal filtration rate is expressed as fu · GFR (2). Thus, equation 29 becomes

$$Cl_r = \text{fu} \cdot \text{GFR} + Cl_{TS} - Cl_{TR} \quad (30)$$

Renal clearance can be determined by dividing the total amount of the unchanged (unmetabolized) drug excreted in the urine (A_u^∞) with the area under the blood concentration versus time curve (AUC).

$$Cl_r = A_u^\infty/\text{AUC} \quad (31)$$

Following administration of an intravenous dose, the systemic clearance can be determined as described in equation 31, and difference between the systemic and renal clearance is referred to as nonrenal clearance of the drug.

$$Cl_{nr} = Cl_s - Cl_r \quad (32)$$

Hepatic Clearance. The difference between the systemic and renal clearance estimates is termed nonrenal clearance. For certain drugs, we can assume that the nonrenal clearance is the hepatic clearance, which is defined as the clearance of the drug from the body by the liver. For drugs that are completely metabolized (i.e., negligible renal clearance), the systemic clearance can be assume to be equal to the hepatic clearance. Under the latter assumption, hepatic clearance can be defined as the product of the hepatic blood flow (Q_h, about 1.5 L/min in humans) and the hepatic extraction ratio (E_h, ranging from 0 to 1). Thus,

$$Cl_h = Q_h \cdot E_h \quad (33)$$

The extraction ratio is defined as fraction of the drug removed by any organ and can be estimated from the difference in the arteriovenous concentration of the drug as

$$E = (Ca - Cv)/Ca \quad (34)$$

where Ca represents the concentration entering the organ (arterial blood) and Cv represents the concentration leaving the organ (venous blood). Because the extraction ratio is a fraction, it varies between 0 and 1 for all drugs. The extraction ratio is related to the fraction of drug escaping removal by the organ (F) by

$$F = 1 - E \quad (35)$$

This relationship is very important for highly extracted drugs, because orally administered drugs must pass through the liver before entering the systemic circulation. For drugs that are highly extracted by the liver, a much smaller fraction of the orally administered dose reaches the systemic circulation. This phenomenon of removal of the drug prior to its entering the systemic circulation is termed a first-pass effect.

The extraction ratio of the drug is dependent on the fraction of the drug bound in the blood and the intrinsic clearance (Cl_{int}) of the drug by the liver. Intrinsic clearance is defined as the maximal ability of any organ to irreversibly remove the drug in the absence of any blood flow limitations to the organ (2). In case of the liver, intrinsic clearance is directly related to the ratio of Vmax to Km (Michaelis-Menten kinetic parameters for drug metabolism). An equation that relates the extraction ratio of any drug to its intrinsic clearance and binding in blood is

$$E_h = (\text{fu} \cdot Cl_{int})/(Q_h + \text{fu} \cdot Cl_{int}) \quad (36)$$

Substituting this term for Eh in equation 36 for hepatic clearance, we obtain

$$Cl_h = Q_h \cdot [(\text{fu} \cdot Cl_{int})/(Q_h + \text{fu} \cdot Cl_{int})] \quad (37)$$

Equation 37 has two limiting conditions. For highly extracted drugs, $Cl_{int} \gg Q_h$, which results in the elimination of the Q_h term in the denominator. Thus, equation 37 is reduced to

$$Cl_h = Q_h \quad (38)$$

In case of drugs which are poorly extracted by the liver, $Q_h \gg Cl_{int}$, which results in the elimination of the Cl_{int} term in the denominator. For such drugs,

$$Cl_h = \text{fu} \cdot Cl_{int} \quad (39)$$

As seen from the last two equations, highly extracted drugs are limited by blood flow to the liver, and poorly extracted drugs are limited by drug binding in blood and its intrinsic clearance.

First-Pass Effect. For some drugs with high extraction, a significant portion of an oral dose is removed by the liver and/or the gut, resulting in a reduced fraction of the oral dose reaching systemic circulation. This phenomenon is referred to as first-pass effect. The extraction phenomenon is sometimes called first-pass metabolism or presystemic elimination. Assuming complete gastrointestinal absorption, the fraction of an oral dose reaching the circulation (bioavailability, F) is given by

$$F = 1 - E \quad (40)$$

where E is the extraction ratio of the drug. As defined earlier, bioavailability can be estimated as the ratio of AUC_{oral} to AUC_{iv} (assuming same intravenous and oral dose levels). Substituting the AUC ratio for F and expanding the relationship for E, we obtain

$$AUC_{oral}/AUC_{iv} = 1 - [(\text{fu} \cdot Cl_{int})/(Q_h + \text{fu} \cdot Cl_{int})] \quad (41)$$

Rearranging equation 41 and multiplying both sides of the equation by the administered dose, we obtain

$$D(Q_h + \text{fu} \cdot Cl_{int})/Q_h AUC_{iv} = D/AUC_{oral} = Cl_{oral} \quad (42)$$

Because D/AUC_{iv} is defined as the systemic clearance, and substituting for clearance as

$$Cl_h = Q_h \cdot [(\text{fu} \cdot Cl_{int})/Q_h + \text{fu} \cdot Cl_{int})] \quad (43)$$

we obtain

$$Cl_{oral} = \{Q_h \cdot [(\text{fu} \cdot Cl_{int})(Q_h + \text{fu} \cdot Cl_{int})]\} \div \{(Q_h)(Q_h + \text{fu} \cdot Cl_{int})\} \quad (44)$$

Upon canceling terms, we find that

$$Cl_{oral} = \text{fu} \cdot Cl_{int} \quad (45)$$

Thus, one can obtain an estimate of the intrinsic hepatic clearance of a drug of a drug from the area under the blood concentration-time curve following oral administration.

The extent to which a drug may be subject to first-pass effects can be estimated from either the oral or intravenous area under the blood concentration-time curve as follows:

$$F = 1 - E_h = 1 - (Q_h \cdot E_h)/Q_h = 1 - D/(Q_h \cdot AUC_{iv}) \quad (46)$$

Multiplying equation 46 with AUC_{oral}, we obtain

$$F \cdot AUC_{oral} = AUC_{oral} - [(D \cdot AUC_{oral})/(Q_h \cdot AUC_{iv})] \quad (47)$$

or

$$F \cdot AUC_{oral} = AUC_{oral} - FD/Q_h \quad (48)$$

Rearranging equation 47, the bioavailability of highly extracted drugs can be determined as

$$F = Q_h/\{[Q_h + (D_{oral}/AUC_{oral})]\} = Q_h/(Q_h + Cl_{int}) \quad (49)$$

Thus the systemic bioavailability of a drug (subject to first-pass metabolism) can be estimated by determining the AUC_{oral} and substituting an appropriate value for hepatic blood flow. As evident from equation 49, the higher the intrinsic hepatic clearance of any drug, the lower the anticipated oral bioavailability of the drug.

Gut Wall Clearance. The systemic availability of drugs subject to both first-pass hepatic and intestinal mucosa metabolism can be estimated as described by Gibaldi and Perrier (8). These authors have shown that the oral bioavailability (F) can be estimated as

$$F = (Q_h \cdot Q_{pv})/\{(Q_h + Cl_{hint})(Q_{pv} + Cl_{giint})\} \quad (50)$$

where Q_h is the hepatic blood flow (sum of hepatic arterial blood flow and portal venous blood flow), Q_{pv} is the portal venous blood flow, Cl_{hint} is the hepatic intrinsic clearance, and Cl_{giint} is the intrinsic intestinal mucosal clearance.

Lung Clearance. The lung is an important extrahepatic route of elimination of drugs. As already described, in the absence of significant lung clearance, systemic clearance is estimated as the ratio of the intravenous dose and the AUC_{iv}. Because of the unique anatomical position of the lungs, the true systemic clearance should be estimated from the intraarterial area under the blood concentration-time curve (AUC_{ia}). The fraction of a dose escaping the lung can be estimated as the ratio of AUC_{iv} to AUC_{ia}. Because the gastrointestinal mucosa, the liver, and the lungs are anatomically presented in series, the oral bioavailability of any drug (F) is the product of the fractions escaping first-pass metabolism by each of these organs, i.e.,

$$F_{oral} = f_{gi} \cdot f_h \cdot f_l \quad (51)$$

where f_{gi} is the fraction escaping first-pass metabolism by the gastrointestinal mucosa, f_h is the fraction escaping the first-pass metabolism by the liver, and f_l is the fraction escaping the first-pass metabolism by the lungs.

Multiple Dosing. Repeated administration of a drug results in accumulation in the body, particularly if the drug has a long half-life. When the drugs reach steady-state, the maximum and minimum concentrations of the drug fluctuate in a fixed manner. The peak concentration at steady-state should be (ideally) maintained below the toxic level, whereas the trough (minimum) concentration should be in an effective range. For drugs with narrow therapeutic index, this range has to be carefully maintained to avoid toxicity or therapeutic failure. It has been shown that the maximum and minimum concentrations (C^n_{max} and C^n_{min}) in the blood after n repeated doses are given by

$$C^n_{max} = (\mathrm{D/V})\{(1 - e_{-nke}{}^{T})/(1 - e^{-keT})\} \quad (52)$$

$$C^n_{min} = (\mathrm{D/V})\{(1 - e_{-nke}{}^{T})/(1 - e^{-keT})\}e^{-keT} \quad (53)$$

where T is the dosing interval of the drug.

Equations 52 and 53 also describe the peak and trough concentrations achieved at steady-state following repeated administration. Under steady-state conditions, the product of $n \cdot \mathrm{ke} \cdot T$ becomes very large, resulting in e-$n$ke$T$ approaching zero. Thus,

$$C^{max}_{ss} = (\mathrm{D/V})\{1/(1 - e^{-keT})\} \quad (54)$$

$$C^{min}_{ss} = (\mathrm{D/V})\{1/(1 - e^{-keT})\}e^{-keT} \quad (55)$$

And the average concentration at steady-state is obtained as the ratio of the dosing rate to the drug clearance.

$$C^{avg}_{ss} = \{(\mathrm{Dose}/T)\}/Cl \quad (56)$$

It should be noted that the time taken to reach steady-state is usually at least four to five half-lives of the drug. About seven half-lives of the drug are required to reach 99% of the steady-state drug concentration in the blood.

As mentioned earlier, repeated dosing results in accumulation of the drug in the body (R). Accumulation can be estimated by dividing the minimum concentration in blood at steady-state by the minimum concentration of the drug following a single dose, i.e.,

$$R = (C^{min}_{ss})/(C^{min}_{l}) \quad (57)$$

If one assumes that all the doses were administered in the postdistributive phase of the drug, or if the drug concentration profile can be described by one-compartment model, the accumulation factor (R) can be obtained from

$$R = 1/(1 - e^{-keT}) \quad (58)$$

Thus accumulation of the drug can be predicted by knowing the half-life and dosing interval of the drug.

Compartmental Analysis Approach

The most common approach in pharmacokinetics is to represent the body as a system of compartments, although these compartments have no anatomical or physiological reality. Further, one assumes that the transfer between compartments and the rate of drug elimination from these compartments follow first-order or linear kinetics. Thus, the one-compartment model represents the body as a single, kinetically homogenous unit. This model is useful for drugs that rapidly distribute throughout the body, and the plasma is usually the anatomical reference to the compartment. The assumption is that the rate of change in the blood concentration quantitatively reflects the change in drug concentration throughout the body.

However, most drugs entering the systemic circulation require a finite amount of time to distribute throughout the body into various tissues. This is usually seen following intravenous bolus injection of drugs. During this distributive phase, the drug concentration in plasma declines more rapidly than that observed in the postdistributive phase. Assuming that drug distribution is blood flow–dependent, the highly perfused tissues such as liver and kidney achieve rapid equilibrium with blood. Hence, conventionally the blood and all accessible fluids and tissues are represented as a kinetically homogenous unit and are referred to as the central compartment. On the other hand, poorly perfused tissues show an increase, followed by a decrease during the distribution phase and achieve a pseudodistribution equilibrium with the central compartment. Because the rates of transfer to the poorly perfused tissues are different but cannot be distinguished from blood concentration-time data, the poorly perfused tissues are lumped into a single peripheral compartment. Such representation of the body as multiple, kinetically homogenous units is referred to as multicompartment analysis (e.g., two-compartment, three-compartment). Drug elimination from multicompartment models is assumed to occur in a first-order (linear) fashion. Transfer of drug between body compartments is also assumed to occur by first-order processes. The mathematical basis and details of compartmental analysis are reviewed in great detail in several books and chapters (1,2,8,10).

CLASSIC LINEAR COMPARTMENTAL MODELS

One-Compartment Open Models with Linear Elimination

The blood concentration-time data for a one-compartment open model following a bolus intravenous dose are described by:

$$C = (\mathrm{D_{iv}}/V)e^{-ket} \quad (59)$$

Similarly, the blood concentration-time data for a one-compartment model with zero-order input (such as continuous intravenous infusion) are described by

$$C = (\mathrm{k_0}/V\mathrm{k_e})(1 - e^{-ket}) \quad (60)$$

The data for a one-compartment open model following first-order input (such as oral or other extravascular routes of administration) are described by:

$$C = (FD/V)\{(k_a/(k_a - k_e)\}\{e^{-ket} - e^{-kat}\} \quad (61)$$

One-Compartment Open Model with Michaelis-Menten Elimination

The blood concentration-time data for drugs showing one-compartment characteristics with nonlinear elimination (Michaelis-Menten) can be described by

$$dC/dt = V'_m C/(K_m + C) \quad (62)$$

where V'_m is the ratio of the maximum velocity of metabolism (V_m, mass/time) and the apparent volume of distribution (V); K_m refers to the Michaelis constant.

The integration of equation 62 yields:

$$C_1 - C_2 + K_m(\ln C_1 - \ln C_2) = V'_m(t_1 - t_2) \quad (63)$$

where C_1 and C_2 are any two points on the blood concentration-time curve corresponding to times t_1 and t_2, respectively, and $V'_m = V_m/V$.

Two-Compartment Open Models with Linear Elimination from Central Compartment

For drugs with two-compartment kinetics with central compartment elimination, the blood concentration-time data following intravenous bolus input are described by

$$C = [(D_{iv}/V_c(\lambda_2 - \lambda_1)]\{(k_{21} - \lambda_1)e^{-\lambda 1t} - (k_{21} - \lambda_2)e^{-\lambda 2t}\} \quad (64)$$

For a two-compartment open model with central compartment elimination, following zero-order input such as continuous intravenous infusion, the blood concentration-time data are described by

$$C = k_0/V_c\{[(k_{21} - \lambda_1)(e^{+\lambda 1t} - 1)e^{-\lambda 1t}/\lambda_1(\lambda_2 - \lambda_1)] + [(k_{21} - \lambda_1)e^{+\lambda 2t} - 1)e^{-\lambda 2t}/\lambda_2(\lambda_1 - \lambda_2)]\} \quad (65)$$

The postinput equation corresponding to equation 65 is simply obtained by replacing $e^{+\lambda 1t}$ by $e^{+\lambda 1T}$ and $e^{+\lambda 2t}$ by $e^{+\lambda 2T}$, where T is the zero-order input time and t remains the time from the beginning of the zero-order input.

The blood concentration-time profile of drugs following two-compartment open model with first-order input (extravascular administration such as oral) and central compartment elimination are described by:

$$C = (kaFD/V_c)\{[(k_{21} - \lambda_1)e^{-\lambda 1t}/(\lambda_2 - \lambda_1)(ka - \lambda_1)] + [(k_{21} - \lambda_2)e^{-\lambda 2t}/(\lambda_1 - \lambda_2)(k_a - \lambda_2)] + [(k_{21} - k_a)e^{-kat}/(\lambda_2 - k_a)(\lambda_1 - k_a)]\} \quad (66)$$

In equation 66, $\lambda_1 < \lambda_2$, and $\lambda_1 + \lambda_2 = k_{12} + k_{21} + k_{10}$, and $\lambda_1\lambda_2 = k_{21}k_{10}$.

Linear Two-Compartment Open Model with Peripheral Compartment Elimination

For drugs displaying two-compartment kinetics with elimination from the peripheral compartment, the blood concentration-time data following a bolus intravenous injection are given by

$$C = (D_{iv}/(V_c(\lambda_2 - \lambda_1)))\{(k_{20} + k_{;21} - \lambda_1) \cdot e^{-\lambda 1t}(k_{20} + k_{21} - \lambda_2)e^{-\lambda et} \quad (67)$$

where $\lambda_1 + \lambda_2 = k_{12} + k_{21} + k_{20}$, and $\lambda_1\lambda_2 = k_{12}k_{20}$

Noncompartmental Analysis

Noncompartmental methods are sometimes referred to as model-independent methods of data analysis. These methods do not require any assumptions regarding a specific compartmental model, but do assume linear pharmacokinetics. The noncompartmental approach for the determination of absorption, distribution, and elimination parameters is based on the theory of statistical moments (23,24). The zero moment of drug concentration in plasma versus time is referred to as the AUC from time zero to infinity. The AUC from time zero to time t is estimated using standard methods such as trapezoidal rule, whereas the area under tail of the curve from time t to infinity is estimated as:

$$AUC_{(t-\infty)} = C/k_e \quad (68)$$

Estimates of AUC are useful in calculating not only bioavailability but also drug clearance, which of all the pharmacokinetic parameters is the most useful for clinical application. Noncompartmental methods have also been used in estimating the apparent volume of distribution, the fraction of dose converted to a specific metabolite, the average steady-state concentration of a drug or a metabolite, and the time required to reach a given fraction of the steady-state concentration.

The first moment of a blood concentration-time profile is the area under the curve of a plot of the product of concentration and time versus time from zero to infinity (AUMC). As with AUC, the area under the moment curve from time zero to time t can be estimated using the trapezoidal rule. The area under the tail (time t to infinity) of the first moment curve can be estimated from:

$$AUMC_{(t-\infty)} = (C \cdot t)/k_e + C/k_e^2 \quad (69)$$

The AUM assumes that the sampling has been conducted such that the last sample is in the postabsorptive and where applicable, in the postdistributive phase of the curve.

Statistical Moments. The time course of drug concentration can usually be regarded as a statistical distribution curve (25). Irrespective of the route of administration, the first three (zero to second) moments are defined as follows:

$$AUC = \int_0^\infty C dt \quad (70)$$

$$MRT = \int_0^\infty t \cdot C dt \Big/ \int_0^\infty C dt = AUMC/AUC \quad (71)$$

$$\text{VRT} = \int_0^\infty t^2 \cdot C\mathrm{d}t \Big/ \int_0^\infty C\mathrm{d}t = \int_0^\infty (t - \text{MRT})^2 C\mathrm{d}t/\text{AUC} \tag{72}$$

where MRT is the mean residence time of the drug in the body and VRT is the variance of the mean residence time of the drug in the body. The AUC, MRT, and VRT are termed zero, first and second moment, respectively, of the drug blood concentration-time curve (8). As already noted, the area under the curve of the plot of the product of concentration and time versus time from zero time to infinity is called the area under the (first) moment curve (AUMC) (26).

Bioavailability (F) refers to the fraction of an oral dose of a drug that reaches the systemic circulation. In statistical moments, bioavailability is the ratio of the zero moments after oral and intravenous administration of the drug, adjusted for the dose levels. Thus,

$$F = \text{D}_{\text{iv}}\text{AUC}_{\text{oral}}/\text{D}_{\text{oral}}\text{AUC}_{\text{iv}} \tag{73}$$

The fraction of the oral dose reaching systemic circulation can be compared to other routes of administration (F_r) using similar equations.

Clearance of a drug can be estimated by noncompartmental methods as the reciprocal of the zero moment of a blood concentration-time curve normalized for dose, i.e.,

$$Cl_s = \text{D}_{\text{iv}}/\text{AUC}_{\text{iv}} \tag{74}$$

Clearance is usually estimated after an intravenous dose, but sometimes may be calculated after an intramuscular dose of the drug. Following oral administration, an apparent clearance can be estimated as,

$$Cl/F = \text{D}_{\text{oral}}/\text{AUC}_{\text{oral}} \tag{75}$$

The first moment of a blood concentration-time profile (MRT) is the statistical moment equivalent of half-life of drugs. MRT refers to the time required for 63.2% of the dose to be eliminated from systemic circulation. If the drug follows first-order elimination, MRT_{iv} would represent the reciprocal of the elimination rate constant (k_e)

$$\text{MRT}_{\text{iv}} = 1/\text{k}_\text{e} \tag{76}$$

$$\text{Half-life } (t_{1/2}) = 0.693\text{MRT}_{\text{iv}} \tag{77}$$

MRT is a function of the route of administration and is always greater than the MRT observed for intravenous administration. Thus the mean residence time after oral administration can be used to estimate the mean absorption time (MAT). In general,

$$\text{MAT} = \text{MRT}_{\text{oral}} - \text{MRT}_{\text{iv}} \tag{78}$$

When drug absorption can be described by first-order process, MAT represents the reciprocal of the absorption rate constant, i.e.,

$$\text{MAT} = 1/\text{k}_\text{a} \tag{79}$$

According to the statistical moments theory, the apparent volume of distribution at steady-state (V_{ss}), is a product of clearance and MRT after a single intravenous bolus dose. Thus,

$$V_{ss} = Cl \cdot \text{MRT} = \text{D}_{\text{iv}} \cdot \text{AUMC}/\text{AUC}^2 \tag{80}$$

Following an intravenous infusion, equation 80 can be amended to represent

$$V_{ss} = [\text{Infused Dose} \cdot \text{AUMC}/\text{AUC}^2] - [\text{Infused dose} \cdot T/2 \cdot \text{AUC}] \tag{81}$$

For extravascular administration (e.g., oral), the volume of distribution at steady-state is estimated as

$$V_{ss} = [(F \cdot \text{D}_{\text{oral}} \cdot \text{AUMC})/\text{AUC}^2] - [(F \cdot \text{D}_{\text{oral}})/(\text{k}_\text{a} \cdot \text{AUC})] \tag{82}$$

Nonlinear events cannot be described by noncompartmental methods. Furthermore, most noncompartmental parameters assume central compartment input, elimination, and sampling and thus may be considered to be a derivative of a compartmental mammillary model (10,27).

Physiologically Based Pharmacokinetic Models

A physiological pharmacokinetic model is composed of a series of lumped compartments (body regions) representing organ or tissue spaces whose drug concentrations are assumed to be uniform. The model requires that the volume, blood flow, and other properties of the lumped compartments be physiologically meaningful. An important consideration in the development of physiological pharmacokinetic model is the selection of which organs or tissues should be included in the model. An initial choice is made based upon the pharmacokinetic, pharmacodynamic, and physicochemical properties of the drug, as well as the anatomy and physiology of the body. The kind of information required for the model to be physiologically meaningful include (*1*) anatomical (e.g., organ or tissue volume), (*2*) physiological (e.g., blood flow rates and enzyme reaction parameters), (*3*) thermodynamic (e.g., protein binding isotherms), and (*4*) transport (e.g., membrane permeability of the drug). The models may be simplified to fit the information available because it is very likely that transport parameters may not be available, and the protein binding and enzyme reaction parameters may be available in simplified terms.

The concept of flow-limited conditions is used for all body regions. Mass balance equations are written for each lumped compartment. It is important to understand that physiologically based pharmacokinetic models are used to simulate the concentration data, not fit the concentration-time data. The degree of closeness of the simulation to real data can be quantitated using statistical parameters such as coefficient of determination (r^2). Some drugs require membrane-limited transport conditions. In such models,

all concentrations represent the free drug concentrations, and mass balance equations are written to describe drug in the extracellular and intracellular spaces and various tissues. These models are even more cumbersome than the blood flow-limited models because simple diffusion is usually not sufficient to describe membrane-limited uptake into certain tissues. However, membrane-limited models have been used to describe data for certain drugs including methotrexate and actinomycin D.

Because the correlation between simulated and real data is sparse in the literature, and because these models simulate an average concentration given that the models are based on average blood flows and average tissue partition coefficients, it is difficult to obtain any information on inter- or intrasubject variability using these models. However, these models are good tools to predict changes in disposition kinetics due to altered physiological or pathological conditions and provide a good mechanism to scale-up the data from preclinical studies to humans (28). The reader is referred to more detailed reviews of physiologically based pharmacokinetic models by Gibaldi and Perrier (8), Bischoff and Dedrick (29), and Bischoff (30).

Population Pharmacokinetics

The principles of population pharmacokinetics have been extensively studied, particularly by Sheiner, Beal, and others (31–35). Population pharmacokinetic parameters quantify population mean kinetics, interindividual variability, and residual variability including intraindividual variability and measurement error (35). An important issue in population kinetics is the identification of which pathophysiologic factor(s) influence the dose-concentration relationship and the degree to which they do so (34). Population kinetics are also popular because they require a fewer samples than traditional pharmacokinetic studies, thus making them amenable during the clinical use of the drug. Population pharmacokinetic studies are normally conducted during the clinical evaluation of a drug. They provide additional information regarding the drug but cannot be used to substitute the classic pharmacokinetic characterization of a drug.

NONMEM (Nonlinear Mixed Effects Model) is a software program developed for estimating population pharmacokinetic parameters from routine patient data (36). It is able to simultaneously determine all parameters including variance parameters, estimate intra- and interpatient variability, and using the extended least squares method, is able to take care of inadequate pharmacokinetic modeling, analytical error, and residual error. However, the use of NONMEM requires the specification of a model for the population being evaluated, and the individual data may be significantly different from the population mean. Although the use of NONMEM and population pharmacokinetics is increasing slowly, it is not yet used in the development of strategies for controlled drug delivery, although it has been used in the evaluation of data following administration of different dosage forms to patients.

ASSESSMENT OF DRUG INPUT RATE FROM CONTROLLED DRUG DELIVERY SYSTEMS

The measurement of the extent of absorption from a controlled drug delivery system provides useful but incomplete information of the absorption process. Additional information on the rate of absorption (i.e., rate of delivery to the systemic circulation) is needed to obtain a better understanding of the drug input (14). The pharmacokinetic principles described earlier provide simple measures such as maximum blood concentration (C_{max}) or time needed to reach the maximum blood concentration (t_{max}). Some more information can be obtained from statistical moments approach regarding the absorption rate. This is achieved via the estimation of mean absorption (input) time. However these single-parameter approaches are inadequate to provide an understanding of drug input rate. Hence more informative approaches involving the characterization of the full time course of the input process such as mass balance and deconvolution methods are used for assessment of drug input rate from controlled drug delivery systems. These methods require the assumption that the drug disposition should follow linear pharmacokinetics.

Mass Balance Methods for the Assessment of Input Rate

The estimation of the amount of the drug in the body at time t, $A(t)$, is determined via the measurement of blood concentrations of the drug following extravascular administration. The estimate of $A(t)$ requires the assumptions of one-compartment or two-compartment models for the disposition of the drug. The Wagner-Nelson method (37) assumes a one-compartment disposition of the drug, whereas the Loo-Riegelman method (38) is applicable to a drug following two-compartment disposition.

Wagner-Nelson Method. Assuming one-compartment disposition, the mass balance equation for the total amount absorbed up to time t is given by

$$A_{abs}(t) = V \cdot C(t) + Cl \int_0^t C(T)\mathrm{d}T \tag{83}$$

where $\int_0^t C(T)\mathrm{d}T$ is the area under the blood concentration-time curve up to time t, i.e., (AUC_{0-t}), V is the volume of distribution and $C(t)$ is the concentration at time t. Thus equation 83 may also be written as

$$A_{abs}(t) = V \cdot C(t) + Cl \cdot \mathrm{AUC}_{0-t} \tag{84}$$

The total amount of drug ultimately absorbed (at time infinity), noting that the drug concentration in the body at time infinity is zero, is given by

$$A_\infty = Cl \int_0^\infty C(T)\mathrm{d}T \tag{85}$$

where $\int_0^\infty C(T)\mathrm{d}T$ at time infinity is the area under the blood concentration-time curve ($\mathrm{AUC}_{0-\infty}$). The fraction of drug absorbed up to time t can be estimated from the ratio

$$A_{abs}(t)/A_\infty = (V \cdot C(t) + Cl \cdot \mathrm{AUC}_{0-t})/(Cl \cdot \mathrm{AUC}_{0-\infty}) \quad (86)$$

It should be noted that the Wagner-Nelson method makes no assumptions for the absorption process. However, if a semilogarithmic plot of percent drug remaining to be absorbed (i.e., $100(1 - [A_{abs}(t))/A_\infty])$ versus time yields approximately a straight line, it suggests an apparent first-order absorption process and the apparent first-order rate of absorption, k_a, can be estimated from the slope of the line. Similarly, a straight line from the plot of percent remaining to be absorbed versus time on rectilinear coordinates suggests zero-order absorption of the drug.

In order to analyze data from microsphere systems used in sustained or prolonged release controlled drug delivery systems, one may not be able to sample the plasma samples until the entire dose has been released from the delivery system. Recognizing that the product of the systemic clearance and the area under the blood concentration-time curve at time infinity is equal to the total amount of dose administered, the amount absorbed at time t is given by

$$A_{abs}(t)/A_\infty = [V \cdot C(t) + Cl \cdot \mathrm{AUC}_{0-t}]/\mathrm{Dose} \quad (87)$$

The fraction of the drug absorbed at time t may also be estimated from the urinary excretion data as discussed by Gibaldi and Perrier (8). The blood concentration at time t, $C(t)$ may be estimated from the urinary excretion data as

$$C(t) = [dA_u/dt]/[k_e \cdot V] \quad (88)$$

where k_e is the apparent first-order excretion rate constant, and dA_u/dt is the rate of excretion of the drug. Following substitution and rearrangement of the resulting equation, the amount of the drug in the body at time t, is given by

$$A_{abs}(t) = [(dA_u/dt)_T]/k_e + (k/k_e)(A_u)_T \quad (89)$$

where k is the first-order elimination rate constant from the body, and $A_{u(T)}$ is the amount recovered unchanged in the urine following administration of the controlled drug delivery system. At time infinity, the amount of the drug excreted in the urine is given as

$$A_{abs\infty} = [k/k_e] \cdot A_{u\infty} \quad (90)$$

Multiplying both sides by $V \cdot k_e$ (i.e., renal clearance Cl_r) in equations 89 and 90, yields

$$Cl_r \cdot A_{abs}(t) = V \cdot [(dA_u/dt)_T] + Cl \cdot (A_u)_T \quad (91)$$

and

$$Cl_r \cdot A_{abs\infty} = Cl \cdot A_{u\infty} \quad (92)$$

The ratio of equations 91 and 92 yields the fraction of the drug absorbed at any time t as

$$A_{abs}(t)/A_{abs\infty} = \{V \cdot [(dA_u/dt)_T] + Cl \cdot (A_u)_T\}/(Cl \cdot A_{u\infty}) \quad (93)$$

In theory, the fraction of the dose absorbed following administration can be solely calculated from the urinary excretion data. However, the collection of urine over an adequate period to allow the estimation of the pharmacokinetic parameters may not be practical in case of some controlled drug delivery systems.

The most serious limitation of the Wagner-Nelson method is that it is applicable only to drugs displaying one-compartment disposition. In all other cases, it is shown to be an approximation. For drugs displaying multicompartment disposition, the Wagner-Nelson method results in an underestimation of the time at which absorption ceases, and an overestimation of the absorption rate (8). One approach to overcoming this problem is to use the Loo-Riegelman method (38), described later. However, the application of the latter method requires concentration-time data, following both intravenous and the intended route of administration of the drug, which may or may not be available at all times. For this reason, the Wagner-Nelson method serves as a valuable approximation method for the determination of the input rate following administration of pharmaceutical controlled drug delivery systems.

Cohen et al. (39) presented a modified version of the Wagner-Nelson method for the assessment of in vivo release rate from liposomal formulations intended for sustained release over a month, following subcutaneous (s.c.) administration. These investigators determined the input rate into the surrounding tissues (s.c. space) and in the plasma following drug absorption. Based upon the mass balance equation, the concentration of the drug in the plasma can be obtained from

$$dA_p/dt = F \cdot k_a \cdot V_s \cdot C_s - k_{el} \cdot V_d \cdot C_p \quad (94)$$

where F is the extent of absorption of the drug from a solution of the drug administered subcutaneously, k_a and k_{el} are the absorption and elimination rate constants, V_s and V_d are the volume of the subcutaneous space and the volume of distribution, respectively, and C_s and C_p are the concentrations of the drug in the subcutaneous space and plasma, respectively. Rearranging and integrating equation 94 yields the following relationship between the plasma and subcutaneous drug concentration:

$$F \cdot V_s \cdot k_a \cdot \int_0^t C_s(T)dT = V_d C_p(t) + k_{el} V_d \int_0^t C_p(T)dT \quad (95)$$

The amount of drug in the subcutaneous space can be estimated from

$$V_s dC_s/dt = R_0 - k_a V_s C_s \quad (96)$$

where R_0 is the instantaneous release rate of the drug from the controlled drug delivery system into the s.c. space. The rate of release from the controlled drug delivery system into the s.c. space can be obtained by rearrangement and integration of equation 96 to yield

$$\int_0^t R_0(T)\mathrm{d}T = V_s C_s + k_a V_s \int_0^t C_s(T)\mathrm{d}T \qquad (97)$$

Dividing equation 97 by the total dose of the drug administered, the fraction of the dose released from the controlled drug delivery system can be estimated as

$$A_{abs}(t)/A_{abs\infty} = [V_d/F \cdot \text{Dose}] \cdot \{C_p \cdot (1 + k_{el}/k_a) + k_{el} \int_0^t C_p(T)\mathrm{d}T + (1/k_a)(\Delta C_p/\Delta t)\} \qquad (98)$$

This method is again restricted to compounds with one-compartment disposition and assumes that the estimates for the rates of absorption and elimination remain constant among studies. Furthermore, depending upon the error in the estimation of the absorption rate constant, an error is introduced in the fraction of the dose absorbed, usually leading to an overestimation of the fraction of the dose absorbed. Nevertheless, this method allows a reasonable first approximation of the in vivo release rate of the drug from prolonged release microsphere controlled drug delivery systems.

Loo-Riegelman Method. The Loo-Riegelman method (38) is applicable to a drug following two- or multicompartment disposition. It requires the blood concentration-time data following intravenous administration to assess the fraction of the dose absorbed at time t. The mathematical basis for a drug with two-compartment disposition is based upon the mass balance equation

$$A_{abs}(t) = A_1(t) + A_2(t) + A_{el}(t) \qquad (99)$$

where $A_1(t)$ and $A_2(t)$ are the amounts of the drug in the central and peripheral compartments, and $A_{el}(t)$ is the total amount eliminated from the body by all pathways. Assuming elimination from the central compartment only, the amount in the central compartment is given by

$$A_1(t) = V_1 \cdot C_1(t) \qquad (100)$$

where V_1 and $C_1(t)$ are the volume of the central compartment and the measured blood or blood concentration, respectively. The differential equation for the rate of change of the amount of drug in the peripheral compartment is given by

$$\mathrm{d}A_2/\mathrm{d}t = k_{1.2}A_1 - k_{2.1}A_2 \qquad (101)$$

where $k_{1.2}$ and $k_{2.1}$ are the first-order intercompartmental transfer rate constants. Loo and Riegelman (38) used a linear approximation for $C_1(t)$ over each data interval, and the amount of the drug absorbed at time t was estimated as

$$A_{abs}(t) = V_1 C_1(t) + V_2 C_2(t) + Cl \int_0^t C(T)\mathrm{d}T \qquad (102)$$

where

$$C_2(t) = C_2(t-1)e^{-k_{2.1}\Delta t} + [k_{1.2}/k_{2.1}]\{C_1(t-1)(1 - e^{-k_{2.1}\Delta t})\} + [k_{1.2}/(k_{2.1})^2]\{[C_1(t) - C_1(t-1)]/\Delta t\} \cdot (e^{-k_{2.1}\Delta t} - k_{2.1}\Delta t - 1) \qquad (103)$$

Loo and Riegelman assumed that the sampling period was relatively short so that the term $k_{2.1}\Delta t$ was less than or equal to 0.5; thus allowing the third term in the expression for $C_2(t)$ to be reduced using a Taylor expansion (i.e., $e^{-x} = 1 - x + x^2/2$) to

$$\{k_{1.2} \cdot [(C_1(t) - C_1(t-1))/\Delta t] \cdot (\Delta t)^2\}/2 \qquad (104)$$

Boxenbaum and Kaplan (40) have shown that this approximation is a potential source of error and should be avoided. Although the Loo-Riegelman approach is limited due to the requirement of intravenous concentration-time data, it is a very useful approach for the evaluation of absorption kinetics. Furthermore, the method can be used for drugs that distribute in any number of compartments, provided elimination occurs from the central compartment. Wagner (41) has shown that the Loo-Riegelman method can also be applied when the elimination occurs from the peripheral compartment. Expressions analogous to that presented for the estimation of $C_2(t)$ must be written for each peripheral compartment and the amount of drug absorbed in the body at time t can be estimated from the mass balance equation. A modification of the Loo-Riegelman approach without the need for intravenous reference data is presented by Gerardin et al. (42). However, this approach requires the unrealistic condition that distribution occurs much more slowly than the input (13).

Cutler (43) has also shown that both the Wagner-Nelson and Loo-Riegelman methods are applicable to compounds showing a variable clearance and/or nonlinear disposition. Although the mass balance approaches provide a reasonable approximation of the input rate, they are still restricted by assumptions and are "model-dependent." These limitations may be overcome by "model-independent" methods termed deconvolution, which are described in the next section.

Assessment of Absorption Rate by Deconvolution Techniques

The process of determination of the drug input rate from a measured response (for example, blood concentration-time profile) is referred to as deconvolution. The prediction of a response from drug input is known as convolution. It is reported that the deconvolution process is very sensitive to noise in the output data, and the error is amplified in the estimation of the drug input rate. On the other hand, the variation in the drug input rate is dampened when estimating the output. The methods used for deconvolution of output data for microsphere systems is similar to the available methods for other traditional controlled drug delivery systems. Several methods have been proposed in the literature for estimating the drug input rate using deconvolution from pharmaceutical controlled drug delivery systems (13,43–45).

Deconvolution techniques are used to analyze the pharmacokinetics of drug input following administration of the controlled drug delivery system. These methods arise from considering the body as a linear system with respect to drug disposition. It is a model-independent approach and uses two fundamental properties of linear response systems. First is the property of superposition, i.e., the sum or superposition of any two inputs, $f_1(t) + f_2(t)$, results in a response that is the superposition, $c_1(t) + c_2(t)$, of the individual responses for their respective input rates. The second property of linear response systems used in analysis using deconvolution techniques is the convolution integral property. This convolution integral property defines the relationship between the input function and the observed response following the input and is given by the following equation:

$$G(t) = \int R(I)G_\partial(t - T)\mathrm{d}T \tag{105}$$

where $R(t)$ is the input rate of the drug into the body, and $G(t)$ is the resulting response from the input. $G_\partial(t)$ is the response following a unit dose impulse input (such as an intravenous bolus dose). Excellent reviews on the mathematical basis of deconvolution are available in the literature (43–45). The major assumptions underlying the convolution integral property are that the response is linearly related to the input, and the system is time-invariant, i.e., the unit impulse response, $G_\partial(t)$, is independent of the time of administration. The limitations of the deconvolution approaches include its applicability to noninteracting inputs only (14). Prior to applying deconvolution techniques to assess the input rate, the system should be evaluated for the principle of superposition and interaction.

The convolution integral defined in equation 105 can be evaluated either analytically or numerically, when $R(t)$ and $G_\partial(t)$ are known, to predict the response (such as drug concentration) following drug input. This operation is termed *convolution*. When $G(t)$ and $G_\partial(t)$ are known, equation 105 serves as the basis for the estimation of the input rate. This procedure of estimating $R(t)$ from the convolution integral is termed *deconvolution*. Many methods have been proposed for numerical deconvolution. These include the finite difference methods, the least-squares methods, and Fourier analysis (14). The objective of this section is to define some of the mathematical basis for these approaches.

Rationale for the Development of Methods for Numerical Deconvolution. Vaughan and Dennis (46) discuss the need for numerical evaluation of data to determine the input function. They have shown that even if $G(t)$ and $G_\partial(t)$ are known analytically in the convolution integral

$$G(t) = \int R(T)G_\partial(t - T)\mathrm{d}T \tag{106}$$

the integral function defined by equation 106 cannot be solved, except in certain cases, because the Laplace transform of the equation

$$g(s) = r(s)\, g_\partial(s) \tag{107}$$

with solution

$$r(s) = g(s)/g_\partial(s) \tag{108}$$

cannot be transformed back into time space by the convolution theorem, because $1/g_\partial(s)$ is not a Laplace transform (47). In general, numerical evaluation of $g(s)$ and $g_\partial(s)$, with subsequent numerical calculation of $r(s)$ and inversion, is unsuccessful because of instability (48,49). Although Coulam et al. (49), have shown that Fourier transform methods are reasonably accurate, these methods are cumbersome, and the use of simple numerical methods would be advantageous in the deconvolution of blood concentration-time data to assess the input rate (46).

Finite Difference Methods for Numerical Deconvolution. The application of the finite difference method for deconvolution was initially introduced by Rescigno and Segré (50) as the area-area method. The deconvolution method requires no assumptions regarding the number of compartments or the kinetics of absorption. However, this method needs data following intravenous administration in addition to that following the intended route of administration. Furthermore, the concentrations must be measured at the same times following both routes of administration. However, the concentrations do not need to be measured at equally spaced intervals.

The mathematical basis for the area-area method is somewhat ambiguous. It approximates the absorption rate by a constant over a time interval. Essentially this method approximates the absorption rate as an equal pulse length "staircase" function (14). Upon deconvolution, Vaughan and Dennis (46) have shown that this product of the pulse lengths and exact output is interpreted as the actual area of the output function itself. These investigators have also shown that via simulations that the area-area method results in large and unpredictable errors in the estimation of the 'staircase' input function.

Benet and Chiang (51) have suggested that the area-area method is only appropriate when the characteristic response is a single exponential function. Vaughan and Dennis (46) have shown that the response to a 'staircase' input function can be derived for both, equal and unequal pulse lengths, by the application of the Laplace transformation methods. If $Y(p_j)$ is the concentration (exact output) at time point p_j, then the response can be obtained from

$$Y(p_j) = \sum_{i=1}^{j} I_i\left\{\int_0^{p_j - p_{i-1}} G_\partial(T)\mathrm{d}T - \int_0^{p_j - p_i} G_\partial(T)\mathrm{d}T\right\} \tag{109}$$

where $j = 1, 2, 3 \ldots$, $p_0 = 0$, and $Y(0) = 0$, and $\int G_\partial(T)\mathrm{d}T$ is the AUC following intravenous bolus administration over the defined time interval.

If all the staircase pulse lengths are equal, i.e., $p_j - p_{j-1} = a$ for all j, then the substitution of $p_j = ja$ and $p_i = ia$ into equation 110 yields:

$$Y(ja) = \sum_{i=1}^{j} I_i \int_{(j-i)a}^{(j-i+1)a} G_\partial(T)\mathrm{d}T \qquad (110)$$

where $j > 0$, $Y(0) = 0$, and $\int G_\partial(T)\mathrm{d}T$ is the AUC following intravenous bolus administration over the time interval.

Vaughan and Dennis (46) have shown that once the exact output, $Y(p_j)$ at time point p_j, or $Y(ja)$ at time point ja, and the response to a unit impulse dose are known, a particular staircase input function can be obtained from either equations 109 or 110, for unequal or equal pulse lengths, respectively.

Proost (52) proposed a general numerical deconvolution equation for drug concentration-time data with unequal lengths, applying model-independent methods. It was demonstrated that it is not necessary to know the response to a unit impulse input as an analytical function, i.e., curve fitting, and the drug concentration-time data from the unit impulse dose could be used directly. This method is an approximation of the method proposed by Vaughan and Dennis (46), with the exception that the integrals for $G_\partial(t)$ are obtained by the application of either linear or log-trapezoidal rule, and the concentration at time zero following an intravenous dose is estimated by logarithmic extrapolation. Proost (52) showed that the staircase approximation of the input rate, I_n, obtained by the trapezoidal approximation of the unit impulse data or an analytical solution for the integral of $G_\partial(t)$ yielded similar input rates. The cumulative fraction of the dose absorbed was estimated by the numerical integration of I_n as:

$$F_n = \sum_{i=1}^{j} [(I_{i-1 \text{ to } i})(T_i - T_{i-1})] \qquad (111)$$

where T_i is the ith sampling time point, and $I_{i-1 \text{ to } i}$ is analogous to the staircase input function of Vaughan and Dennis (46) in equation 111, with the exception that the integral of $G_\partial(t)$ is replaced by the trapezoidal approximation of the integral. The method of Proost (52) only assumes that the pharmacokinetics of the drug are linear.

A numerical deconvolution method has been derived for the determination of the in vivo input rates based upon the linear interpolation of the observed drug concentrations and deconvolution of the resulting trapezoidal function (53). The derived in vivo input functions are discontinuous and a general expression for the cumulative drug input is also derived. The expression for cumulative drug input was shown to be a generalization of the Loo-Riegelman equation, and it yielded similar results to the point-area method using the staircase approximation for input functions.

Wagner (54) has shown that the fraction of the drug remaining to be absorbed at the site of administration can be obtained from a similar expression. In terms of the sampling interval (Δt), the fraction unabsorbed (FR) can be obtained from:

$$FR_{n\Delta t} = [H_{(n+1)\Delta t}/H_{n\Delta t}] - \sum_{i=2 \text{ to } n+1}^{j=1 \text{ to } n} \{[F_{i\Delta t}/F_{\Delta t}][FR]_{(j-1)\Delta t}\} \qquad (112)$$

where $n\Delta t$ is the time after n sampling intervals equal to Δt, H is a function describing the drug concentration-time curve following the intended route of administration, and F is a function describing the drug concentration-time curve following intravenous bolus administration. $F_{n\Delta t}$ may be expressed as the drug concentration at time $n\Delta t$, or as the area under the curve between $n\Delta t$ and $(n-1)\Delta t$. $H_{n\Delta t}$ can only be expressed in terms of drug concentration. When both, H and F are expressed in terms of drug concentrations, the method is referred to as the point–point method (8). Benet and Chiang (51) recommended the use of the point–area method, in which F should be expressed as the area under the drug concentration-time curve following intravenous administration, and H should be expressed in terms of drug concentration in equation 112. Vaughan and Dennis (46) also designate their method of deconvolution as the point–area method, because specific output data points, $Y(p_j)$, and the integral of $G_\partial(t)$, is used to derive the staircase input function.

Chiou (55) proposed a finite difference method for numerical deconvolution using an instantaneous midpoint-input principle. This assumes that all the drug absorbed during a given interval, regardless of the complexity of the absorption kinetics, is absorbed instantaneously at the midpoint of the interval. This assumption is based upon the finding that the blood concentration for a one-compartment model system following an intravenous infusion can be approximated by assuming that the entire dose was administered as a bolus at the midpoint of the infusion period (56). This approximation is valid when the infusion period is much shorter than the half-life of the drug. The deconvolution method proposed by Chiou (55) requires no assumptions regarding the pharmacokinetic models or the site of drug elimination. The fraction of the dose absorbed at time $t(F)$ can be calculated from:

$$F_1 = C_{t1}/C_{\text{i.v.}(0.5t1)} \qquad (113)$$

where C_{t1} is the blood drug concentration at time $t1$ after dosing, and $C_{\text{i.v.}(0.5t1)}$ is the blood drug concentration at time $0.5t1$, following an intravenous bolus dose. The amount of drug absorbed between times $t1$ and $t2$ can be estimated by a similar comparison, provided the drug concentration is corrected for the contribution from the drug absorbed prior to $t1$ (C_{p1}). To estimate C_{p1}, it is assumed that all drug prior to time $t1$ is instantaneously absorbed at time $0.5t1$, and the contribution is estimated as

$$C_{p1} = F_1 C_{\text{i.v.}(t2-0.5t1)} \qquad (114)$$

where $C_{\text{i.v.}(t-0.5t1)}$ is the theoretical blood concentration at time $(t2 - 0.5t1)$, when the same extravascular dose is administered as an intravenous bolus dose. This principle is used to estimate the fraction absorbed during other sampling intervals as follows:

$$F_n = \left[C_{tn} - \sum_{i=1}^{n-1} C_{pi}\right] \Big/ C_{\text{i.v.}0.5(tn-tn-1)} \qquad (115)$$

Vaughan (57) has shown that the method described by Chiou (55) is an approximation of the point–area method (53). Furthermore, the midpoint–input method is similar

to the approximation of the area–area method (50), which uses rectangular functions to approximate the integrals of $G_\partial(t)$ centered about the midpoint of integration. Vaughan (57) cautions against the use of approximations of the point–area method for the estimation of staircase input, because it leads to large errors in the cumulative drug input functions.

The finite difference methods for numerical deconvolution provide a simple method to estimate the drug input rates without assumptions regarding the pharmacokinetic models or absorption kinetics. Their main drawback is the instability in presence of data noise, which may require smoothing procedures (58). Cutler (43) has pointed out that the smoothing procedures may yield errors in the estimates of the input functions. Because the finite difference methods are computationally simple, they can be used without the use of complex algorithms and computers, needed for the more complex, but stable, deconvolution methods such as the least-squares (11,12).

Least-Squares Method for Numerical Deconvolution. The least-squares method provides the determination of the best estimate of the true input rate. The criteria for determining the best estimate for the input function relies on the accuracy of the prediction of the response $G(t)$. Thus the proximity of the predicted $G(t)$ values with the observed $G(t)$ values determine the accuracy of the estimated input rate. The least-squares deconvolution method requires assumptions and specifications regarding the mathematical form of the input function. Once the function describing the input function is specified, it is introduced into the convolution integral and the observed response, $G(t)$, is compared with the predicted response, $G'(t)$.

When little or no information is available regarding the nature of the input function, Cutler (43) has proposed the use of polynomial functions to describe the input function. Cutler (11) has shown that an exponential input function and the cube-root dissolution law represent adequate approximations of the input rate with simulated data. Cutler (12) proposed the use of orthogonal functions to derive the polynomial functions for approximations of the input function. This approach was proposed based upon the difficulty in estimating the input function using a polynomial approximation by Gamel et al. (58), which was attributed to the ill-conditioned set of polynomial equations. The least-squares approach is more stable to data noise, but is computationally more complex and requires the use of fairly extensive and specialized programs to determine the drug input functions.

Veng-Pedersen (44,45,59) has also proposed a least-squares deconvolution method for estimating the drug input rate using both a polynomial and a polyexponential approximation of the input rate. This approach has led to the development of a method using an adaptive least-squares cubic spline function for the approximation of the input rate. Based upon simulated data, this method is reported to have significant advantages over the method proposed by Cutler (12). These include the superiority of fitting the bolus input response by a polyexponential expression which is a smoothing function and does not oscillate between the data points as a polynomial expression does. Furthermore, the Veng-Pedersen (44) approach provided a simple and explicit mathematical function for the rate and extent of drug input rate, which alleviates the complexity of the back-transformation and summation of terms in the Cutler approach (12). Because the input function is calculated directly by linear regression in the Veng-Pedersen method, it is purported to be computationally simpler and does not require the extensive and specialized methods for deconvolution.

The least-squares method for deconvolution are considered model-independent even though they require the determination of the unit impulse response parameters by fitting the data to some function (e.g., polyexponential). The unit impulse response parameters require their determination by nonlinear regression. However, these estimated parameters do not require any uniqueness, and their actual values have no influence on the accuracy of the determination of the input function (60). The input function is approximated by a polynomial expression that uses these estimated parameters collective rather than individually. Hence, the least-squares method is not affected by the individual errors in the estimation of the parameters. Furthermore, because the input function is determined by linear rather than nonlinear regression, it is computationally simpler, and the problems of multiple minima are eliminated with this approach (60).

Despite the advantage of the stability of the least-squares deconvolution methods in presence of data noise, these methods require complex algorithms to determine the input functions. A simpler algorithm for easier implementation of this deconvolution technique has been provided (61). It is based upon a polyexponential approximation of the absorption response and the the response from intravenous bolus or infusion administration. The absorption response is represented by:

$$c(t) = \sum_{i=1}^{m} b_i e^{-\beta_i t_+} \tag{116}$$

where $t_+ = (t - t_{lag})_+$ and $c(0) = 0$; t_{lag} is the estimated lag time prior to appearance of the drug into systemic circulation following extravascular administration. The characteristic response from a unit impulse dose $c\partial(t)$ is obtained from the polyexponential approximation of the intravenous bolus response:

$$c_{iv}(t) = \sum_{i=1}^{n} a_i e^{-\alpha_i t} \tag{117}$$

where $\alpha_i > 0$. Thus, $c_\partial(t)$ can be obtained as:

$$c_\partial(t) = c_{iv}(t)/D_{iv} \tag{118}$$

where D_{iv} is the intravenous bolus dose.

The cumulative amount of drug absorbed, expressed as a percentage of the dose (PCT) has been shown to be:

$$\mathrm{PCT}(t) = [100/\mathrm{D}] \int_0^t f(t)\mathrm{d}t \tag{119}$$

where $f(t)$ is the rate of direct input. This expression has been shown to be equivalent to:

$$\mathrm{PCT}(t) = u_0 + \sum_{i=1}^{m+n-1} u_i e^{-v_i t} + \quad (120)$$

The absorption rate has been shown to be

$$f(t) = [\mathrm{D}/100] \sum_{i=1}^{m+n-1} u_i(-v_i)e^{-v_i t} + \quad (121)$$

where $v_i = \beta_i$ for $i = 1, 2, 3 \ldots, m$; and $v_i = -\gamma_{i-m}$ for $i = (m + 1), (m + 2), \ldots, (m + n - 1)$. u_i is defined as:

$$u_i = \mathrm{K}_4 b_i \left\{ \mathrm{K}_1 - (\mathrm{K}_3/\beta_i) - \sum_{j=1}^{n-1} (g_j/\gamma_j(\gamma_j + \beta_i)) \right\} \quad (122)$$

for $i = 1, 2, 3, \ldots, m$; and

$$u_i = \mathrm{K}_4(g_{i-m}/\gamma_{i-m}) \sum_{j=1}^{m} (b_j/(\gamma_{i-m} + \beta_j)) \quad (123)$$

for $i = (m + 1), (m + 2), \ldots, (m + n - 1)$. u_0 is obtained as:

$$u_0 = - \sum_{i=1}^{m+n-1} u_i \quad (124)$$

The parameters $\{g_i, \gamma_i\}_1^{n-1}$ are obtained from the parameters $\{a_i, \alpha_i\}_1^n$. The γ parameters are $(n - 1)$ roots of the $(n - 1)$th polynomial and can be obtained by conventional numerical methods (61). The remaining parameters in the expression for PCT have been described by Veng-Pedersen (61).

This approach to deconvolution is purported to be computationally easier and Veng-Pedersen (61) has provided a computer subroutine for easy implementation of the algorithm. Although the use of least-squares deconvolution approach has been simplified by the use of more user-friendly algorithms, they still require the use of fairly extensive and specialized computer programs to estimate the input functions. These requirements, along with the a priori assumptions regarding the approximation of the input function, limit the routine use of this approach for deconvolution of data from extravascular administration of controlled drug delivery systems.

Miscellaneous Methods for Deconvolution of Extravascular Data. Berman (62) proposed a deconvolution scheme for the calculation of input function given a system and its response. It is based upon the conversion of the convolution integral equation to an initial value problem. This technique is particularly simple and advantageous when dealing with compartmental systems. Foster et al. (63) have illustrated the use of this deconvolution approach, using compartmental analysis, with commonly available numerical integration software. The scheme can be used to determine an unknown input over time, from the measured response and the impulse response of the system. These investigators report that this method requires the solution of two systems of differential equations; those specifying the compartmental systems for the response function and the impulse response of the system. The input function can be calculated using simulations of these compartmental models. The accuracy of the simulations is determined from the goodness-of-fit of the function to the observed response data from the system.

A novel approach for deconvolution based upon the principle of maximum entropy has been introduced by Charter and Gull (64). The resulting input functions have been shown to be physiologically realistic and smooth, blood samples are not required to be taken at equally spaced intervals, and no preliminary smoothing or interpolation of data is required. The maximum entropy approach is conceptually complex, and it is proposed that the maximum entropy may offer the most reliable deconvolution for drugs exhibiting nonlinear kinetics (13).

CONCLUSIONS

This article has provided an overview of the mathematical basis and applications of pharmacokinetic principles in the design and analysis of drug from various dosage forms, with a particular emphasis toward controlled drug delivery systems. The choice of the appropriate pharmacokinetic models for the analysis of data depends on the availability of data from intravenous and extravascular routes of administration. The pharmacokinetic evaluation of any drug usually entails the determination of the pharmacokinetics of the drug following intravenous and/or the extravascular (intended) route of administration. Model-dependent and model-independent pharmacokinetic parameter estimates should be obtained from in vivo experiments to obtain a proper handle on the bioavailability (extent of absorption), systemic clearance, volume of distribution, and half-life of the drug.

In addition to the information on the extent of absorption from controlled drug delivery systems, mass balance and deconvolution techniques allow the estimation of in vivo input of drug into the biological system. Using the method of preference, one calculates the input rates from the controlled drug delivery system. The input rates allow the estimation of the fraction of the dose absorbed as a function of time. Cumulative amount of drug absorbed (in vivo) versus time plots are constructed, and are compared with in vitro dissolution rate plots to establish meaningful in vitro–in vivo correlation. Such correlation precludes the need for the conduct of expensive and time-consuming pharmacokinetic experiments during formulation development and/or optimization and provides a tool for quality control purposes. Thus, the appropriate understanding of pharmacokinetic principles leads to considerable advancement in the development of better controlled drug delivery systems for various drugs.

BIBLIOGRAPHY

1. M. Gibaldi, ed., *Biopharmaceutics and Clinical Pharmacokinetics*, 3rd ed., Lea & Febiger, Philadelphia, 1984, pp. 1–28.
2. P.R. Gwilt, in C.R. Craig and R.E. Stitzel, eds., *Modern Pharmacology*, 2nd ed., Little, Brown, Boston, 1986, pp. 75–95.

Next Page

3. M. Leal, A. Yacobi, and V.K. Batra, in A. Yacobi, J.P. Skelly, V.P. Shah, and L.Z. Benet, eds., *Integration of Pharmacokinetics, Pharmacodynamics and Toxicokinetics in Rational Drug Development*, Plenum, New York, 1993, pp. 55–67.
4. G. Hochhaus and H. Derendorf, in H. Derendorf and G. Hochhaus, eds., *Handbook of Pharmacokinetic / Pharmacodynamic Correlation*, CRC Press, Boca Raton, Fla., 1995, pp. 79–120.
5. P.R. Gwilt, in C.R. Craig and R.E. Stitzel, eds., *Modern Pharmacology*, 2nd ed., Little, Brown, Boston, 1986, pp. 96–110.
6. B.M. Silber, M. Bialer, and A. Yacobi, in J.R. Robinson and V.H.L. Lee, eds., *Controlled Drug Delivery: Fundamentals and Applications*, 2nd ed., Dekker, New York, 1987, pp. 213–251.
7. L.Z. Benet, in A. Yacobi, J.P. Skelly, V.P. Shah, and L.Z. Benet, eds., *Integration of Pharmacokinetics, Pharmacodynamics and Toxicokinetics in Rational Drug Development*, Plenum, New York, 1993, pp. 115–123.
8. M. Gibaldi and D. Perrier, eds., *Pharmacokinetics*, Dekker, New York, 1982.
9. P.G. Welling and F.L.S. Tse, eds., *Pharmacokinetics: Regulatory, Industrial, Academic Perspectives*, Dekker, New York, 1988.
10. J.G. Wagner, in P.G. Welling and F.L.S. Tse, eds., *Pharmacokinetics: Regulatory, Industrial, Academic Perspectives*, Dekker, New York, 1988, pp. 1–56.
11. D.J. Cutler, *J. Pharmacokinet. Biopharm.* **6**, 227–242 (1978).
12. D.J. Cutler, *J. Pharmacokinet. Biopharm.* **6**, 243–263 (1978).
13. G.T. Tucker and P.R. Jackson, in L.F. Prescott and W.S. Nimmo, eds., *Novel Drug Delivery and Its Therapeutic Application*, Wiley, New York, 1989, pp. 113–120.
14. P.R. Chaturvedi, in S. Cohen and H. Bernstein, eds., *Microparticulate Systems for the Delivery of Proteins and Vaccines*, Dekker, New York, 1996, pp. 321–347.
15. N.F. Nixon, *Handbook of Laplace Transformation: Fundamentals, Application, Tables and Examples*, 2nd ed., Prentice-Hall, Englewood Cliffs, N.J., 1965.
16. N.F. Nixon, *Handbook of Laplace Transformation: Fundamentals, Application, Tables and Examples—Workbook (with answers)*, 2nd ed., Prentice-Hall, Englewood Cliffs, N.J., 1965.
17. H.S. Bear, Jr. *Differential Equations*, Addison-Wesley, Reading, MA, 1962.
18. L.Z. Benet, *J. Pharm. Sci.* **61**, 536–541 (1972).
19. L.Z. Benet and J.S. Turi, *J. Pharm. Sci.* **60**, 1593–1594 (1971).
20. K.C. Yeh and K.C. Kwan, *J. Pharmacokinet. Biopharm.* **6**, 79–98 (1978).
21. W.J. Westlake, *J. Pharm. Sci.* **60**, 883–885 (1971).
22. J.G. Wagner, (1974): *Med. Clin. North Am.* **58**, 479–492 (1974).
23. K. Yamaoka, T. Nakagawa, and T. Uno, *J. Pharmacokinet. Biopharm.* **6**, 547–558 (1978).
24. D.J. Cutler, *J. Pharm. Pharmacol.* **30**, 476–478 (1978).
25. D.M. Himmelblau and K.B. Bischoff, *Deterministic Systems*, Wiley, New York, 1968.
26. L.Z. Benet and R.R. Galeazzi, *J. Pharm. Sci.* **68**, 1071–1074 (1979).
27. J.J. Stefano, III, *Am. J. Physiol.* **243**, R1–R6 (1982).
28. R.L. Dedrick, *J. Pharmacokinet. Biopharm.* **1**, 435–461 (1973).
29. K.B. Bischoff and R.L. Dedrick, *J. Pharm. Sci.* **57**, 1347–1357 (1968).
30. K.B. Bischoff, *Cancer Chemother. Rep.* **59**, 777–793 (1975).
31. L.B. Sheiner, (1984): *Drug Metab. Rev.* **15**, 153–171 (1984).
32. L.B. Sheiner and S.L. Beal, *J. Pharmacokinet. Biopharm.* **8**, 553–571 (1980).
33. L.B. Sheiner and S.L. Beal, *J. Pharmacokinet. Biopharm.* **9**, 635–665 (1981).
34. L.B. Sheiner and L.Z. Benet, *Clin. Pharmacol. Ther.* **38**, 481–487 (1985).
35. L.B. Sheiner, B. Rosenberg, and V.V. Marathe, *J. Pharmacokinet. Biopharm.* **5**, 441–479 (1977).
36. S.L. Beal and L.B. Sheiner, *NONMEM Users Guide Part I. Users Basic Guide*, University of California, Division of Clinical Pharmacology, San Francisco, 1979.
37. J.G. Wagner and E. Nelson, *J. Pharm. Sci.* **52**, 610–611 (1963).
38. J. Loo and S. Riegelman, *J. Pharm. Sci.* **57**, 918–928 (1968).
39. S. Cohen et al., *Proc. Natl. Acad. Sci. U.S.A.* **88**, 10440–10444 (1991).
40. H. Boxenbaum and S. Kaplan, *J. Pharmacokinet. Biopharm.* **3**, 257–264 (1975).
41. J.G. Wagner, *J. Pharmacokinet. Biopharm.* **3**, 457–478 (1975).
42. A. Gerardin, D. Wantiez, and A. Jaouen, *J. Pharmacokinet. Biopharm.* **11**, 401–424 (1983).
43. D. Cutler, *Pharmacol. Ther.* **14**, 123–160 (1981).
44. P. Veng-Pedersen, *J. Pharm. Sci.* **69**, 298–305 (1980).
45. P. Veng-Pedersen, *J. Pharm. Sci.* **69**, 305–312 (1980).
46. D.P. Vaughan and M. Dennis, *J. Pharm. Sci.* **67**, 663–665 (1978).
47. G. Doetsch, *Guide to the Applications of Laplace Transforms*, Van Nostrand, New York, 1961, Chapter 7.
48. R.E. Bellman, B.E. Kalaba, and J. Lockett, *Numerical Inversion of the Laplace Transform*, Elsevier, New York, 1966.
49. C.M. Coulam, H.R. Warner, H.W. Marshall, and J.B. Bassingthwaighte, *Comp. Biomed. Res.* **1**, 124–138 (1967).
50. A. Rescigno and G. Segré, *Drug and Tracer Kinetics*, Blaisdell, Waltham, Mass., 1966.
51. L.Z. Benet and C.-W.N. Chiang, *Abstr. Pap., 13th Nat. Meet. Am. Acad. Pharma. Sci.*, 1972, vol. 2, p. 169.
52. J.H. Proost, *J. Pharm. Sci.* **74**, 1135–1136 (1985).
53. D.P. Vaughan and M. Dennis, *J. Pharmacokinet. Biopharm.* **8**, 83–98 (1980).
54. J.G. Wagner, *J. Pharmacokinet. Biopharm.* **3**, 51–57 (1975).
55. W.L. Chiou, *J. Pharm. Sci.* **69**, 57–62 (1980).
56. W.L. Chiou, G.W. Peng, and R.L. Nation, *J. Clin. Pharmacol.* **18**, 266–271 (1978).
57. D.P. Vaughan, *J. Pharm. Sci.* **70**, 831–832 (1981).
58. J. Gamel, W. Rousseau, C. Katholi, and E. Mesel, *Circ. Res.* **32**, 516–523 (1973).
59. P. Veng-Pedersen, *J. Pharm. Sci.* **69**, 312–318 (1980).
60. P. Veng-Pedersen, *J. Pharm. Sci.* **69**, 318–324 (1980).
61. P. Veng-Pedersen, *J. Pharmacokinet. Biopharm.* **8**, 463–481 (1980).
62. M. Berman, *Math. Biosci.* **40**, 319–323 (1978).
63. D.M. Foster, D.G. Covell, and M. Berman, *Comput. Biol. Med.*, **18**, 253–266 (1988).
64. M.K. Charter and S.F. Gull, *J. Pharmacokinet. Biopharm.* **15**, 645–655 (1987).

Previous Page

POLY(ORTHO ESTERS)

JORGE HELLER
Advanced Polymer Systems
Redwood City, California

ROBERT GURNY
University of Geneva
Geneva, Switzerland

KEY WORDS

Biotolerance
Bovine serum albumin
Cancer treatment
Diabetes
5-Fluorouracil
Glaucoma
Insulin
Levonorgestrel
Malaria
Naltrexone
Ocular delivery
Periodontal disease
Poly(ortho ester)
Protein delivery

OUTLINE

Poly(ortho ester) I
- Polymer Erosion
- Drug Release
- Typical Synthetic Procedure

Poly(ortho ester) II
- Polymer Erosion
- Polymer Physical Properties
- Drug Release
- Typical Synthetic Procedures

Poly(ortho ester) III
- Polymer Erosion
- Polymer Characterization
- Drug Release
- Typical Experimental Procedures

Acknowledgments
Bibliography

The development of bioerodible drug delivery implants has now been an area of great importance for a number of years. A major driving force in developing such implants is the ability to deliver therapeutic agents directly to the systemic circulation, which is important with drugs that undergo significant inactivation by the liver. Two major areas of application deserve special mention. These are the development of bioerodible drug delivery devices for protein delivery and site-specific delivery for the improved treatment of cancer.

At the present time, there are three major classes of totally synthetic bioerodible polymers under active development. These are polyesters, polyanhydrides, and poly(ortho esters). Poly(ortho esters) have been under development since 1970, and three major families have been described. These are shown in Scheme 1.

Because the history of their development and applications prior to 1992 has been comprehensively reviewed (1,2), it is not the purpose of this article to again comprehensively review all past work. Rather, we concentrate on significant developments that have taken place since the last review, but for the sake of completeness, for each polymer system we present a brief, updated review with pertinent references and refer the reader to the original literature for additional details.

POLY(ORTHO ESTER) I

Poly(ortho ester) I, the first such polymer prepared, has been developed at the Alza Corporation and described in a series of patents by Choi and Heller (3–7). This polymer was originally designated as Chronomer™ but the name was later changed to Alzamer®. The polymer is prepared as shown in Scheme 2. However, the Alza Corporation has now discontinued all work with poly(ortho ester), and because the polymer is no longer available, collaborative efforts have also been discontinued.

Polymer Erosion

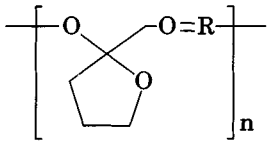
When placed in an aqueous environment, the polymer hydrolyzes as shown in Scheme 3. Because ortho ester linkages are acid sensitive and hydrolysis of this polymer produces γ-butyrolactone, which rapidly opens to γ-hydroxybutyric acid, the polymer must be stabilized with a base such as Na_2CO_3 to avoid an uncontrolled, autocatalytic hydrolysis reaction.

Drug Release

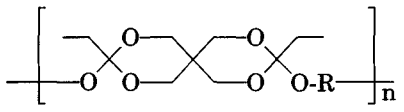
Even though a considerable amount of work with this polymer has been carried out at Alza, there is little detailed published information available, Alza publications do not specifically disclose the structure of the polymer, and only code names are used. However, it is now known that the code name of C111 represents a polymer prepared using 1,6-hexanediol, and C101ct is a polymer prepared using *cis/trans* cyclohexanedimethanol. The polymer has been used in the treatment of burns (8), in the delivery of the narcotic antagonist naltrexone (9), and in the delivery of the contraceptive steroid levonorgestrel (10). The polymer has also been investigated by Sudmann in a number of orthopedic applications (11–19).

Typical Synthetic Procedure

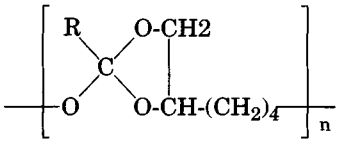
To 45 g (0.312 mole) of anhydrous *cis/trans*-1,4-cyclohexanedimethanol and 0.05 g polyphosphoric acid in a commercially available polymerization reactor is added with constant stirring under an inert nitrogen environment and normal atmospheric pressure 50 g (0.312 mole) of anhydrous 2,2-diethoxytetrahydrofuran. Next, the mixture is heated to 110–115°C and held at that temperature for 1.5 to 2 h with slow distillation of ethanol. Then, while main-



Poly (ortho ester) I

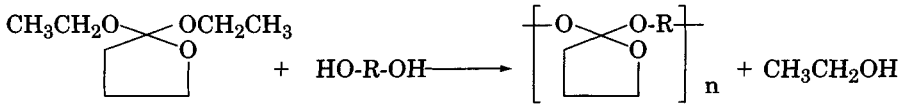


Poly (ortho ester) II

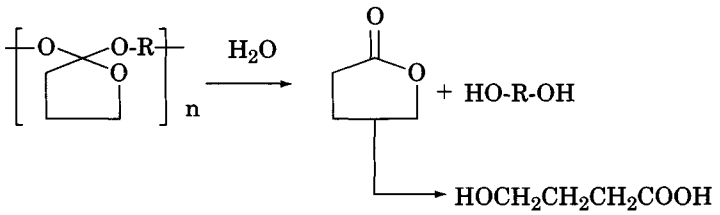


Poly (ortho ester) III

Scheme 1.



Scheme 2.



Scheme 3.

taining the temperature, the pressure is gradually reduced to 0.01 mm Hg, and at this reduced pressure the temperature is slowly increased to 180°C. The reaction is continued at this temperature for 24 h. The polymer is isolated by extrusion from the reactor.

POLY(ORTHO ESTER) II

Poly(ortho ester) II was developed at the Stanford Research Institute, now known as SRI International, under contract with the National Institute of Child Health and Human Development, and was prepared as shown in Scheme 4. A history of the development of this polymer has been published (1).

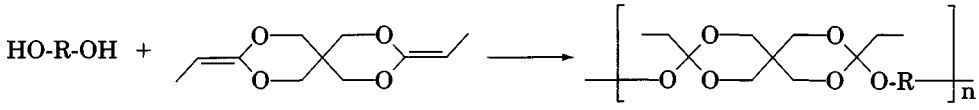
The diketene acetal, 3,9-diethylidene-2,4,8,10-tetraoxaspiro [5.5] undecane is not commercially available, but can be readily synthesized as shown in Scheme 5 (20).

Because a condensation between a diketene acetal and a diol, just like that between a diisocyanate and a diol, proceeds without the evolution of volatile by-products, dense, cross-linked materials can be produced by using reagents having a functionality greater than two (21). To prepare cross-linked materials, a molar excess of the diketene acetal is used, and the resulting prepolymer with ketene acetal end-groups is reacted with a triol or a mixture of diols and triols. This synthesis is shown in Scheme 6.

Polymer Erosion

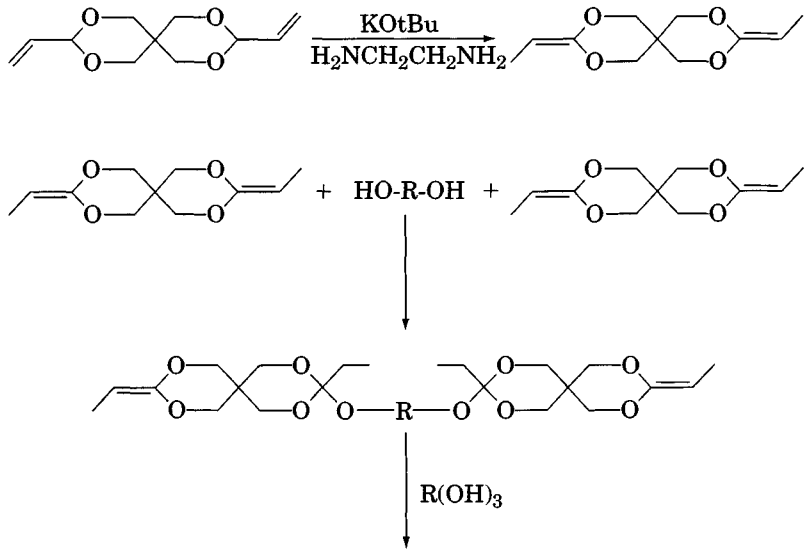
Use of Excipients. As shown in Scheme 7, this polymer hydrolyzes to initially neutral products so that it is not necessary to use bases to neutralize acidic hydrolysis products. Details of the hydrolysis mechanism have been published (22).

Even though ortho ester linkages are quite labile, polymers belonging to this family are extremely hydrophobic, and uncatalyzed poly(ortho esters), as shown in Figure 1, are very stable. Therefore, in order to achieve shortened erosion times, it is necessary to use small amounts of acidic excipients that are physically incorporated into the polymer (23,24). Then, rate of hydrolysis can be manipulated

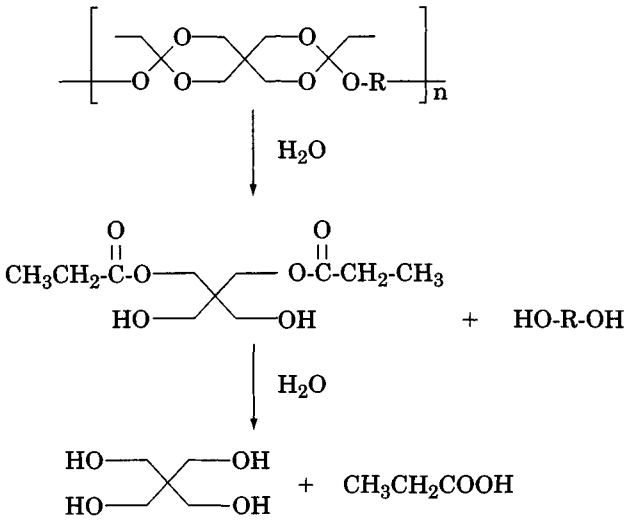


Scheme 4.

Scheme 5.



Scheme 6.



Scheme 7.

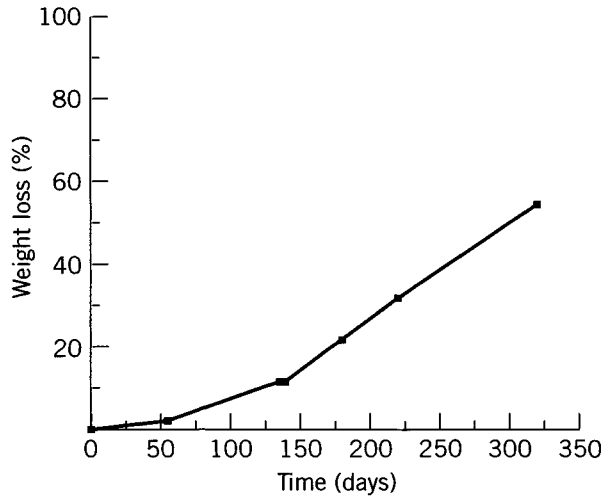


Figure 1. Weight loss as a function of time for a polymer prepared from 3,9-dimethylene-2,4,8,10-tetraoxaspiro [5.5] undecane and 1,6-hexanediol. 0.05 M phosphate buffer, pH 7.4, 37°C.

by varying the pKa and/or concentration of the acidic excipient. Although a number of different acidic excipients have been used with poly(ortho esters) (25), good results can be achieved by using suberic acid. When long delivery rates are desired, bases such as $Mg(OH)_2$ have been used to retard polymer erosion (21).

When the hydrophobic polymer with a physically dispersed acidic excipient is placed into an aqueous environment, water diffuses into the polymer, dissolves the acidic excipient in the surface layers, and the lowered pH accelerates hydrolysis of the acid-sensitive ortho ester bonds. This process is shown schematically in Figure 2, where it has been analyzed in terms of the movement of two fronts, F_1, the movement of a hydrating front, and F_2, the movement of an erosion front (26). The ultimate behavior of a device is then determined by the relative movement of these two fronts. If $F_1 > F_2$, the thickness of the reaction zone gradually increases, and at some time, the matrix is completely permeated by water. At that point, all ortho ester linkages hydrolyze at comparable rates and bulk hydrolysis takes place. However, if $F_1 = F_2$, then hydrolysis is confined to the surface layers and only surface hydrolysis takes place. In this latter case, rate of polymer erosion is completely determined by the rate at which water intrudes into the polymer.

Water sorption by poly(ortho esters) II has been found to be relatively small, about 0.30 to 0.75%, with a diffusion coefficient ranging from a high of 4.07×10^{-8} cm$^2 \cdot$ s^{-1} for a polymer based on 1,6-hexanediol (T_g 22°C) to a low of 2.11×10^{-8} cm$^2 \cdot$ s^{-1} for a polymer based on *trans-*

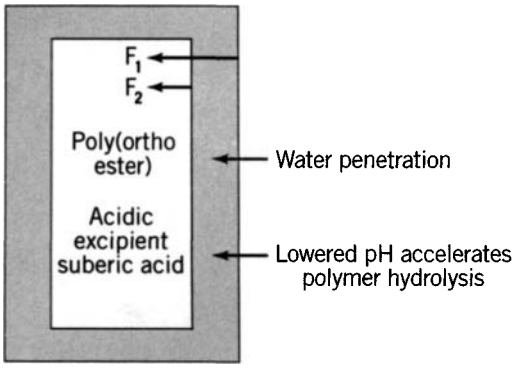


Figure 2. Erosion of a poly(ortho ester) containing dispersed suberic acid. F_1 is movement of eroding front, F_2 is movement of hydration front.

cyclohexanedimethanol (T_g 122°C) (27). Assuming a disk thickness of about 2 mm and using the lowest diffusion coefficient, the disk would be completely permeated by water in about 20 days if water penetrates only from one side of the disk and in about 10 days if water penetrates from both sides of the disk. Thus, the use of acidic excipients limits the design of surface-eroding devices to lifetimes that do not exceed 2–4 weeks, depending on the actual device size.

However, because ortho ester linkages are stable in base, very long time surface erosion is possible if the polymer is stabilized with a base that prevents hydrolysis even though the matrix is completely permeated by water. A plausible mechanism for erosion of devices that contain the base $Mg(OH)_2$ is shown in Figure 3. According to this mechanism, $Mg(OH)_2$ stabilizes the interior of the device, and erosion can only occur in the surface layers where the base has been eluted or neutralized. This is believed to occur by water intrusion into the matrix and diffusion of the slightly water-soluble $Mg(OH)_2$ out of the device where it is neutralized by the external buffer. Polymer erosion then occurs in the $Mg(OH)_2$-depleted layer (23).

Self-Catalyzed Polymers. Although the use of excipients represents a useful means of controlling rate of polymer erosion, when acidic excipients are used, diffusion of the excipient from the polymer is a serious problem that not only complicates kinetics of drug release, but more importantly, eventually leads to an excipient-depleted polymer

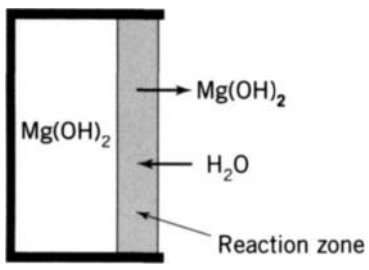


Figure 3. Water intrusion, $Mg(OH)_2$ diffusion, and erosion for one side of a bioerodible device containing dispersed $Mg(OH)_2$.

that remains in the tissues for a significant time. This residual polymer has been referred to as *ghosts*, and its formation has been mathematically modeled (28,29).

To eliminate complications inherent in using a low molecular weight excipient, the use of macromolecular excipients could be considered. However, a better approach is to incorporate into the polymer backbone a short segment that readily hydrolyzes to an acidic product that acts as the acidic excipient and catalyzes the hydrolysis of ortho ester linkages in the polymer. Then, by controlling the concentration of such a segments in the polymer, rate of erosion can be accurately controlled without complications arising from excipient diffusion (30).

We have found that a useful segment is one based on glycolic acid or lactic acid. Because the natural metabolite is L-lactic acid, this is the preferred segment. Lactic acid or glycolic acid segments can be readily incorporated into the polymer by first preparing a diol containing a hydroxy-acid segment, as shown in Scheme 8, by reacting a diol with either a cyclic lactide or glycolide. By controlling stoichiometry, the diol contains either mono or dilactic acid, or mono or diglycolic acid segments.

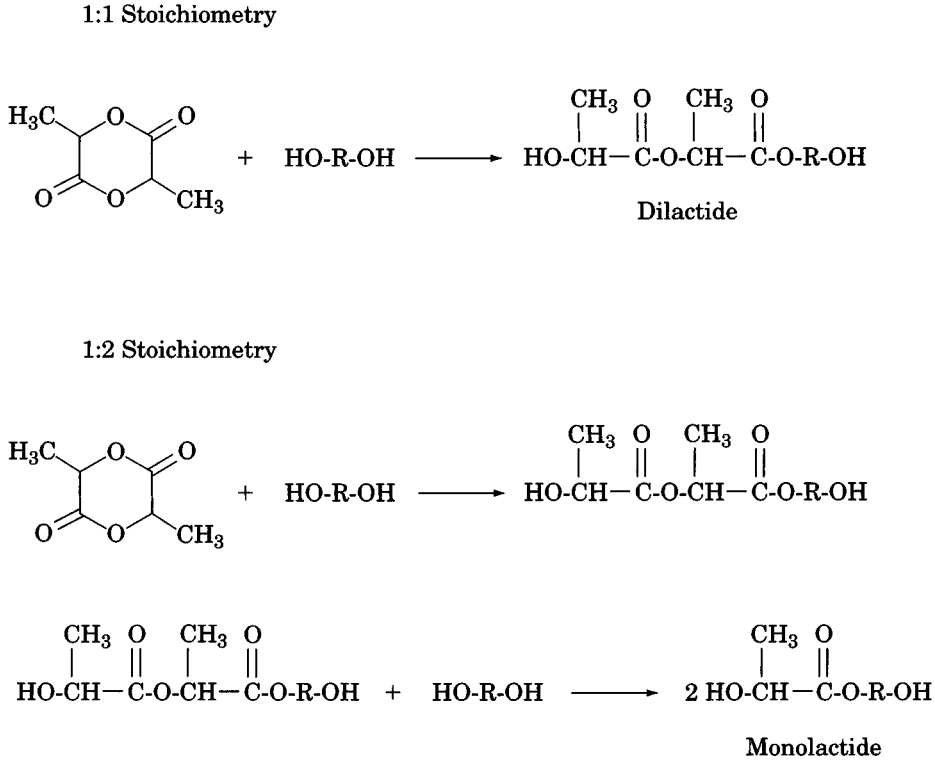
A polymer is then prepared, as shown in Scheme 9, and by varying the relative amounts of the two diols, polymers containing varying amounts of mono or dilactic acid, or mono or diglycolic acid segments can be prepared.

Hydrolysis of a polymer containing a diglycolic acid segment proceeds, as shown in Scheme 10, where the most labile segment, the diglycolic acid segment, hydrolyzes first, liberating glycolic acid, which then catalyzes erosion of the acid-labile ortho ester linkages. A similar hydrolysis can also be written for a polymer containing dilactic acid segments.

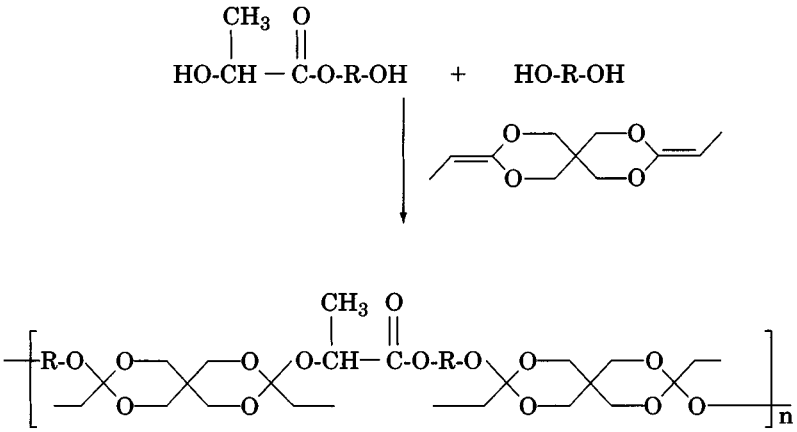
Weight loss of a polymer prepared from *trans*-cyclohexanedimethanol and *trans*-cyclohexanedimethanol diglycolide, shown in Scheme 11, are presented in Figure 4 (30). Clearly, incorporation of diglycolic acid segments into the polymer not only results in excellent erosion control, which proceeds by close to zero-order kinetics to completion, but also allow an accurate control over erosion rates, which range from days to many months.

Figure 5 shows weight loss and changes in number average molecular weight as a function of time for a 50/50 copolymer of *trans*-cyclohexanedimethanol and *trans*-cyclohexanedimethanol diglycolide (30). The points represent weights of remaining polymer and molecular weights of the remaining polymer. There is a slight induction period of about 2 days where no weight loss nor molecular weight decrease is detected, after which the molecular weight decreases steadily until about day 20, after which it remains relatively constant at about one-half of the original value. Rate of weight loss remains relatively constant throughout the entire study carried out over 60 days.

In view of the relatively high concentration of glycolic acid dimer segments in the polymer backbone, it is clear that these segments hydrolyze gradually because rapid hydrolysis of all glycolic acid dimer segments in the polymer would result in a decrease of polymer molecular weight to a value of about 350. Thus, the linearity of weight loss and the slow changes in molecular weights are consistent with a process that occurs predominantly in the surface layers



Scheme 8.



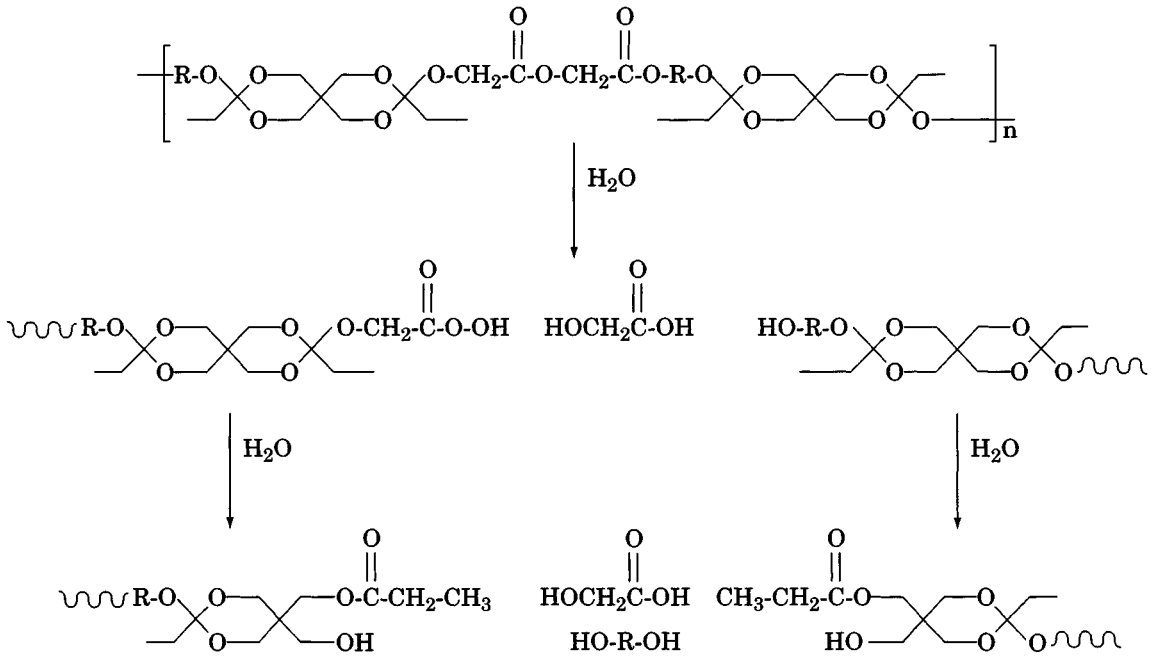
Scheme 9.

of the device with a gradual production of glycolic acid. At this point the discontinuity in the rate of molecular weight change that occurs at day 20, and details of the process are not yet fully understood. However, these preliminary results are encouraging and suggest that with this system, long-term surface erosion may perhaps be possible.

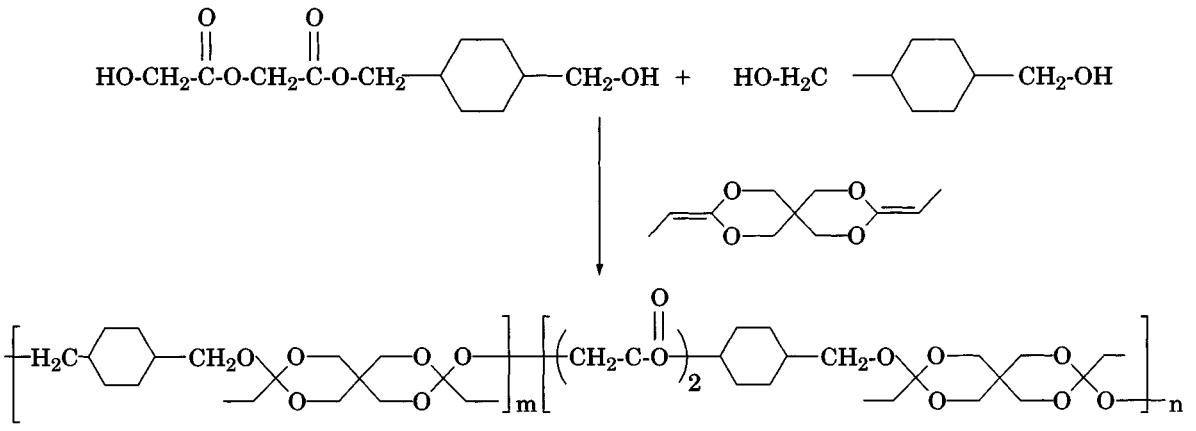
Polymer Physical Properties

The usefulness of a drug delivery system depends not only on an ability to control erosion rate and kinetics of drug release, but also depends on an ability to vary mechanical properties so that devices that have physical properties tailored to a specific application can be prepared. Poly(ortho esters) II are unique among all biodegradable polymers in that mechanical properties can be readily varied by choosing appropriate diols, or mixtures of diols in their synthesis. Thus, materials can be prepared that are rigid, flexible, or low melting solids, or that at room temperature are semisolids. The semisolid materials can either be fluid enough so that they can be injected at room temperature, or at the body temperature of 37°C are so viscous that little deformation takes place, even when pressure is applied, but at temperatures below 45°C soften enough so that the warm polymer can be injected.

Polymers Without the α-Hydroxyacid Segment. Figure 6 shows glass-transition temperatures for materials prepared from 3,9-diethylidene-2,4,8,10-tetraoxaspirol[5.5]-undecane and a mixture of *trans*-cyclohexanedimethanol and 1,6-hexanediol (31). The data show an excellent cor-



Scheme 10.



Scheme 11.

relation between mole ratios of the diols and glass-transition temperature and materials having glass-transition temperatures between 115 and 20°C can be readily prepared.

Materials having very low glass-transition temperatures can be prepared by using α,ω-diols. In Figure 7 is shown a correlation between the number of carbons in the diol and the glass-transition temperature (32).

Self-Catalyzed Polymers. The same variation in mechanical properties can also be achieved with polymers that incorporate an α-hydroxyacid segment. Depending on the desired mechanical properties, the α-hydroxyacid segment is incorporated into either the rigid or flexible diol.

Of particular interest are polymers that at room temperature are either fluid, ointment-like materials, or that can be converted to such materials by gentle heating. Because therapeutic agents can be incorporated by a simple mixing procedure in the absence of solvents, at very low temperatures, and without an organic solvent–water interface, such materials offer significant benefits for the delivery of sensitive therapeutic agents such as peptides and proteins. Although not yet verified, such delivery devices should be able to deliver peptides and proteins without loss of activity.

Semisolid materials can be prepared by using the triethylene glycol glycolide/triethylene glycol monomer pair, shown in Scheme 12. By varying the ratio of the two components, it is possible to prepare materials that at the body temperature of 37°C are so viscous that they do not show significant flow even when moderate pressure is applied, but at temperatures no higher than about 45°C are suffi-

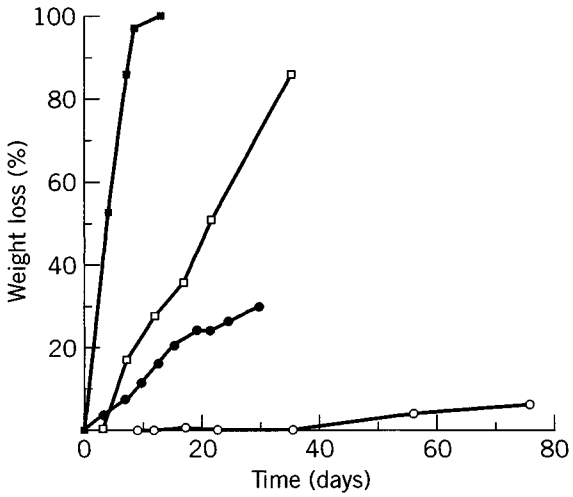


Figure 4. Weight loss as a function of diglycolic acid content for a polymer prepared from 3,9-diethylidene-2,4,8,10-tetraoxaspiro [5.5] undecane, *trans*-cyclohexanedimethanol glycolide (tCDM/Gly) and *trans*-cyclohexanedimethanol (tCDM). 25/75 tCDM-tCDM/Gly (■), 50/50 tCDM-CDM/Gly (□), 75/25 tCDM-tCDM/Gly (●), 90/10 tCDM-tCDM/Gly (○). 0.05 M phosphate buffer, pH 7.4, 37°C. *Source:* Reprinted with permission from Ref. 30. Copyright 1997 American Chemical Society.

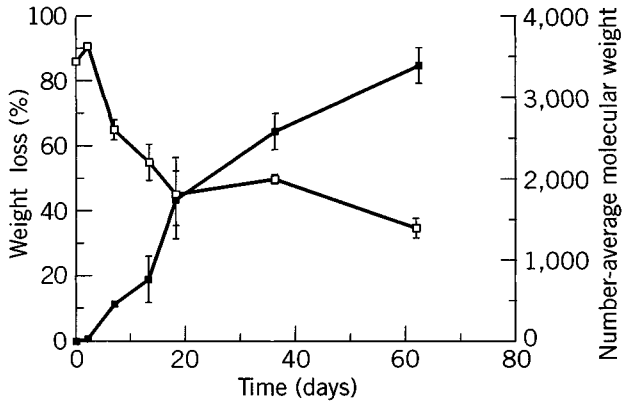


Figure 5. Weight loss (■) and changes in number average molecular weight (□) as a function of time for a polymer prepared from 3,9-diethylidene-2,4,8,10-tetraoxaspiro [5.5] undecane and a 50/50 mixture of *trans*-cyclohexanedimethanol glycolide and *trans*-cyclohexanedimethanol. 0.05 M phosphate buffer, pH 7.4, 37°C. *Source:* Reprinted with permission from Ref. 30. Copyright 1997 American Chemical Society.

ciently fluids so that they can be injected with a hypodermic syringe. Table 1 shows the effect of monomer ratios on polymer softening temperatures. However, injection of such materials requires a large needle, and the whole injection assembly must be heated prior to injection. This is clearly not an optimal means of administration, and for this reason, a high-pressure, heated injector has been developed at the University of Geneva.

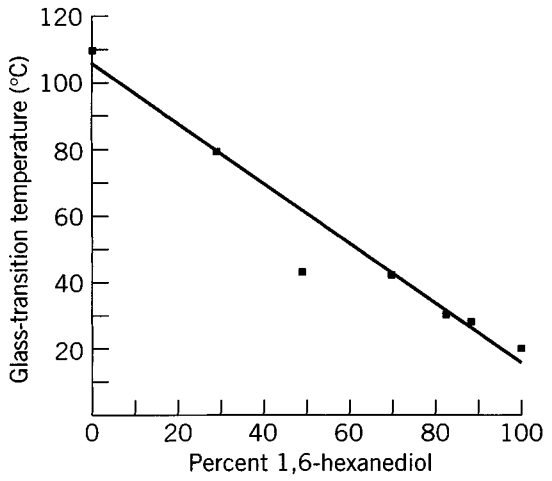


Figure 6. Glass-transition temperature of 3,9-diethylidene-2,4,8,10-tetraoxaspiro [5.5] undecane/*trans*-cyclohexanedimethanol/1,6-hexanediol polymer as a function of mole % 1,6-hexanediol. *Source:* Reprinted from Ref. 31, with permission of Elsevier Science.

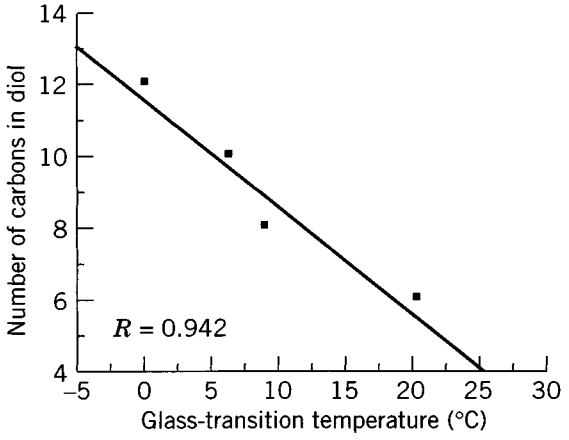
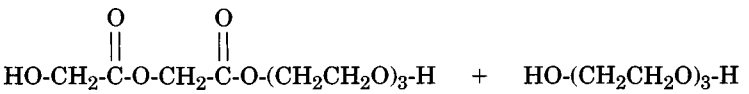


Figure 7. Effect of diol chain length on the glass-transition temperature of polymers prepared from 3,9-diethylidene-2,4,8,10-tetraoxaspiro [5.5] undecane and α,ω-diols. *Source:* Reprinted from Ref. 32, with permission.

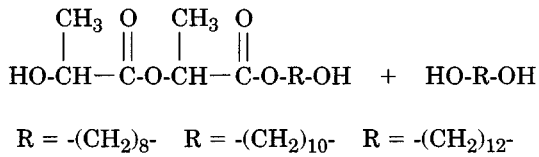
By using the long-chain aliphatic diols shown in Scheme 13, it is also possible to prepare materials that are soft, low melting solids (33). Some properties of such materials are shown in Table 2.

Drug Release

Polymers Without the α-Hydroxyacid Segment. Because as already mentioned, these materials erode at rates that



Scheme 12.



Scheme 13.

Table 1. Softening Points of Self-Catalyzed Poly(ortho esters) Prepared from Triethylene Glycol Monoglycolide (TEG/GLY) and Triethylene Glycol (TEG)

TEG/GLY	TEG	Softening point (°C)
100	0	35
50	50	40
10	90	45

Table 2. Properties of Self-Catalyzed Poly(ortho esters) Prepared from C8, C10, and C12 Diols

Diol	Mole Ratio Diol/Lactide Diol (%)	M_w (kDa)	M_w/M_n	T_g (°C)
C8	80/20	20.9	1.93	—
C10	95/5	66.5	1.82	−0.02
C10	90/10	57.6	1.68	−0.03
C10	80/20	30.9	1.77	−3.77
C12	95/5	49.8	1.85	−9.77
C12	90/10	40.7	1.80	−11.31
C12	80/20	17.0	1.67	−18.76

are too low for useful drug delivery, it is necessary to accelerate rate of hydrolysis by using acidic excipients.

Short-Term Delivery. In a preliminary study (34), 10 wt % 5-fluorouracil (5-FU) was incorporated into a polymer prepared from 3,9-diethylidene-2,4,8,10-tetraoxaspiro-[5.5]undecane and 1,6-hexanediol containing 0.15 wt % of the acidic excipient suberic acid, and release of 5-FU and polymer erosion determined. During this short release time, and as shown in Figure 8, 5-FU was released at a constant rate, and because release occurred concomitantly with polymer erosion, surface erosion was the dominant mechanism of release.

Subsequent to that study, two studies designed to test the effectiveness of such a device in the treatment of leukemia and colorectal carcinoma were carried out. In the first study (35), DBA_2 mice were inoculated with L1210 leukemia and the 5-FU containing polymer disks administered intraperitoneally. As shown in Figure 9, untreated mice, or those treated with polymer placebos, all died within two weeks, but those treated with the 5-FU–containing polymer showed a significant increase in survival time. When this study was compared with one where free 5-FU was administered, animals receiving a dose of 500 mg/kg did not survive longer than 10 days due to acute toxicity problems. Animals receiving free 5-FU at doses of 200 mg/kg and 100 mg/kg showed increased survival, but significantly less so than that with the intraperitoneally administered 5-FU–containing polymer.

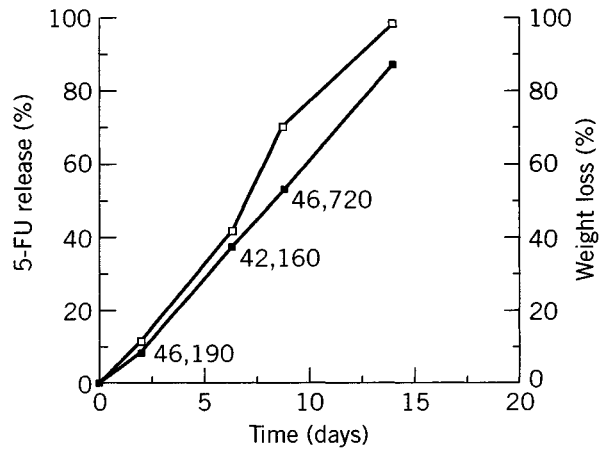


Figure 8. Cumulative weight loss (■) and cumulative release of (5FU) (□) from polymer disks prepared from 3,9-diethylidene-2,4,8,10-tetraoxaspiro [5.5] undecane and 1,6-hexanediol at pH 7.4 and 37°C. Devices contain 10 wt % 5FU and 0.15 wt % suberic acid. Numbers indicate weight average molecular weight of residual polymer. *Source:* Reprinted from Ref. 34, with permission of Elsevier Science.

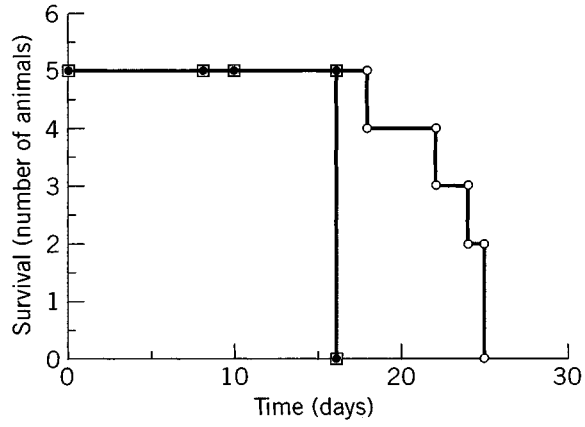


Figure 9. Survival times of DBA_2 mice inoculated with L1210 tumor. (□) control, (●) polymer alone, (○) polymer with 5-FU. Reprinted from Ref. 35, p. 7, with permission of Elsevier Science.

In view of these encouraging results, a more detailed study using LS174T human colorectal carcinoma in a subcutaneous xenograft in nude mice was carried out (36). Before 5-FU–containing polymers were administered, the potential toxicity of the polymer was investigated. In this study, 1, 2, 3, and 4 polymer disks, each weighing approximately 70 mg, were implanted intraperitoneally and animal weight loss determined. Results are shown in Figure 10. All animals survived for 60 days, but 2 of 3 mice that received four implants did exhibit some toxic effects, manifested by acute lethargy and slight trembling. The third animal receiving 4 implants survived with no signs of toxicity for 60 days. Based on these data, the polymer can be considered to be nontoxic.

The effect of implants, each containing approximately a 5-FU dose of 280 mg/kg, on tumor size is shown in Figure 11. In animals receiving 2 implants, average tumor size

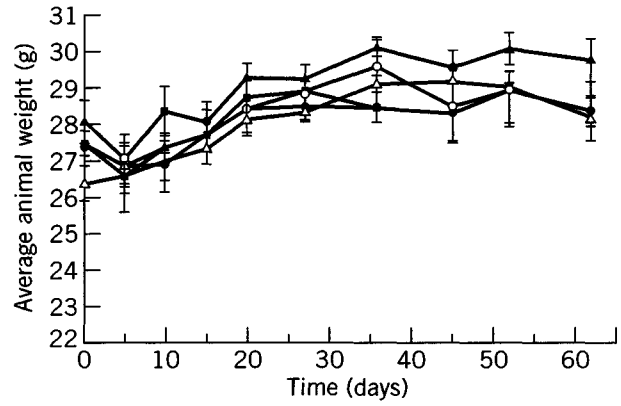


Figure 10. Effect of implantation of drug-free poly(ortho ester) matrices on animal weight. One (▲), two (○), three (△), or four (■) matrices were implanted i.p. in DBA_2 mice, and animal weights were compared with those of sham-operated control mice (●). Results are shown as mean ± S.E. *Source:* Reprinted from Ref. 36, p. 203, with permission of Elsevier Science.

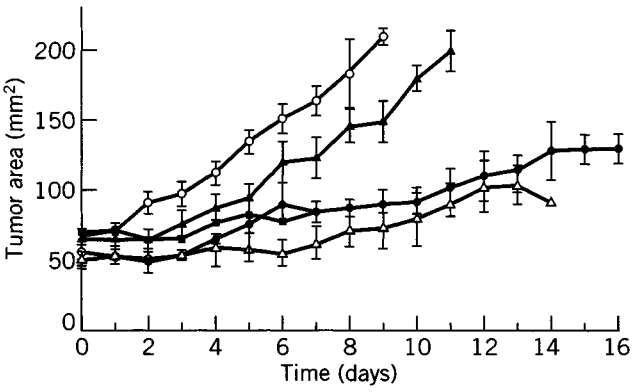


Figure 11. Effect of 5FU administration on the growth of LS174T xenografts in nude mice. Tumor size was measured as the product of two orthogonal diameters. One (▲), two (●), three (△), or four (■) matrices were implanted i.p. in DBA_2 mice, and tumor area was compared with that of sham-operated control mice (○). Results are shown as mean ± S.E. *Source:* Reprinted from Ref. 36, p. 204, with permission of Elsevier Science.

never exceeded 130 mm^2. In animals that received 3 implants, tumor growth was inhibited by more than 70%, and there were no overt signs of toxicity in the first days, but at day 6 they suffered substantial weight loss. Animals that received 4 implants showed very little tumor growth, but due to acute toxicity median survival was only 7 days.

These data suggest that a single dose intermediate between 260 and 580 mg/kg would be optimal for antitumor activity. However, this dose must be released at constant kinetics so as to avoid overdosing. Although the devices described here released 5-FU by excellent zero-order kinetics in vitro, we believe that in vivo 5-FU was not released at a constant rate. Additional work is in progress.

One of the current treatments of opiate addiction is to use narcotic antagonists, which generally have a chemical structure similar to those of opiates and which can preferentially occupy the body's opiate receptors and thus block the opiate's euphoric effect. This makes opiate intake pleasureless and removes the addict's incentive for continuing use (37,38). A commonly used narcotic antagonist is naltrexone, but a single oral dose is only effective for about two days. Thus, long-term therapy depends on continuing oral naltrexone intake. Because discontinuing naltrexone therapy produces no withdrawal effects, significant patient motivation is required and a much improved therapy could be achieved if the decision to continue naltrexone treatment is removed from the patient. Clearly, development of an implant that could release naltrexone for at least one month is desirable.

Because naltrexone is a base with a pK_a of 8.13, a saturated aqueous solution has a pH of about 10. Thus naltrexone exerts a stabilizing effect on poly(ortho esters). For this reason, the neutral naltrexone pamoate was used. An additional benefit is that naltrexone pamoate has a water solubility of only 0.5 mg/mL, about eight times less than naltrexone, which has a water solubility of 4 mg/mL.

Although the exact therapeutically effective blood plasma concentration of naltrexone is not known with certainty, it has been estimated that it is in the range of 0.5 to 1 ng/mL (39). To achieve this blood plasma level, a minimum 3.0 mg/day delivery is required. Thus, a very high drug loading is necessary if reasonably sized devices are to be used. For this reason, a soft polymer prepared from 3,9-diethylidene-2,4,8,10-tetraoxaspiro[5.5]undecane and 1,6-hexanediol was used with a naltrexone pamoate loading of 50 wt % (40).

Figure 12 shows release of naltrexone pamoate from polymer slabs from an uncatalyzed polymer and as a function of suberic acid concentration. Good correlation between suberic acid concentration and release has been achieved. It is interesting that the uncatalyzed device released naltrexone pamoate at reasonably linear kinetics at about 1 mg/day for 50 days. The best device was one containing 1 wt % suberic acid because it released naltrexone

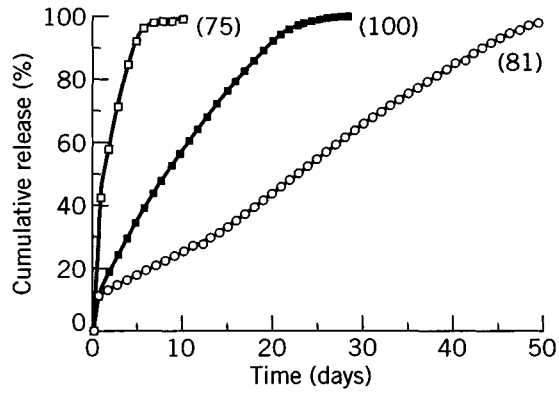


Figure 12. Cumulative release of naltrexone pamoate from polymer slabs (25 × 4 × 1.25 mm) prepared from 3,9-diethylidene-2,4,8,10-tetraoxaspiro [5.5] undecane and 1,6-hexanediol at pH 7.4 and 37°C. Numbers in parentheses indicate percent weight loss. Devices contain 50 wt % drug and varying amounts of suberic acid (SA). (□) 3 wt % SA, (■) 1 wt % SA, (○) no SA. *Source:* Reprinted from Ref. 40, p. 26, with permission of Elsevier Science.

pamoate at the desired 3 mg/day and because in this particular device drug depletion coincided with total polymer erosion.

Unfortunately, attempts to fabricate devices using a transfer molding procedures to produce rod-shaped devices for animal studies were not successful because at the temperatures and times necessary to produce devices, a naltrexone pamoate–induced polymer decomposition took place. Injection molding studies that could minimize heating times were not carried out because suitable small volume injection molding equipment was not available.

Malaria, dengue, yellow fever, and filiarisis are caused by stings of mosquitoes that introduce parasites into the body. Every year several hundred million people are infected (41). To this day, chemoprophylaxis remains the principal means of prevention, but because weekly administration of agents such as quinazoline, sulfadiazine, or pyrimethamine are necessary, poor compliance is responsible for one to two million deaths a year. Clearly, if an implant could be developed that would reduce the frequency of dosing, a significant improvement in prophylaxis could be achieved.

Pyrimethamine has been incorporated into a polymer prepared from 3,9-diethylidene-2,4,8,10-tetraoxaspiro-[5.5]undecane and a 40/60 mole ration of 1,6-hexanediol and *trans*-cyclohexanedimethanol. Disks containing 21 wt % pyrimethamine and varying amounts of suberic acid were then prepared and pyrimethamine release at pH 7.2 and 37°C investigated. Results are shown in Figure 13 (42). There is a very good correlation between amount of suberic acid, and good release kinetics have been achieved. Because pyrimethamine is a basic drug that stabilizes the polymer, fairly high amounts of suberic acid were needed.

Blood plasma levels of rabbits with implanted devices containing 5 wt % pyrimethamine are shown in Figure 14

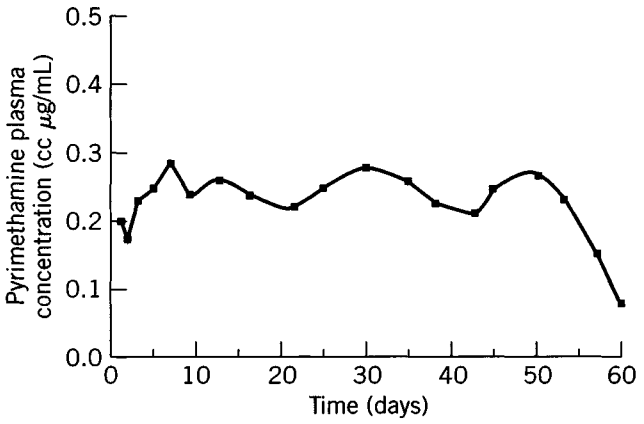


Figure 14. Plasma concentration of pyrimethamine in rabbits after administration of a disk, 25 × 3.0 mm containing 21 wt % pyrimethamine and 5 wt % suberic acid. *Source:* Reprinted from Ref. 42, p. 212, with permission of Elsevier Science.

(42). The values vary between 0.2 μg/mL and 0.3 μg/mL for 50 days after which they decline to zero, indicating that the implants have probably bioeroded, or at least have released their drug content. These results are highly encouraging because they demonstrate that constant blood plasma levels can be achieved for at least 50 days. Based on these results, development of delivery devices that could release pyrimethamine for 6 months at therapeutically useful levels should be possible.

The ability of the implants to protect mice injected with *P. berghei* is shown in Figure 15 (42). When pyrimethamine crystals were used, protection of the mice was limited to 3 weeks. However, when polymer implants with pyrimethamine and 5 wt % suberic acid were used, good chemoprophylaxis of malaria for 7–9 weeks was achieved, a very significant improvement.

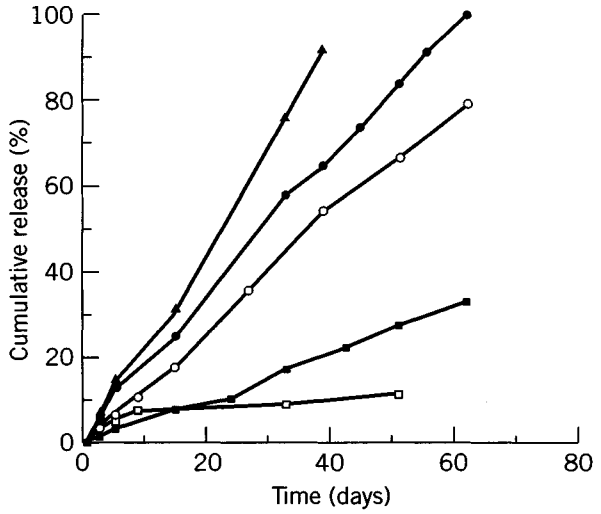


Figure 13. Release of pyrimethamine as a function of amount of incorporated suberic acid (SA). (□) no SA, (■) 1 wt % SA, (○) 3 wt % SA, (●) 5 wt % SA, (▲) 10 wt % SA. Disks, 25 × 3.0 mm. at pH 7.4 and 37°C. Pyrimethamine loading 21 wt %. *Source:* Reprinted from Ref. 42, p. 212, with permission of Elsevier Science.

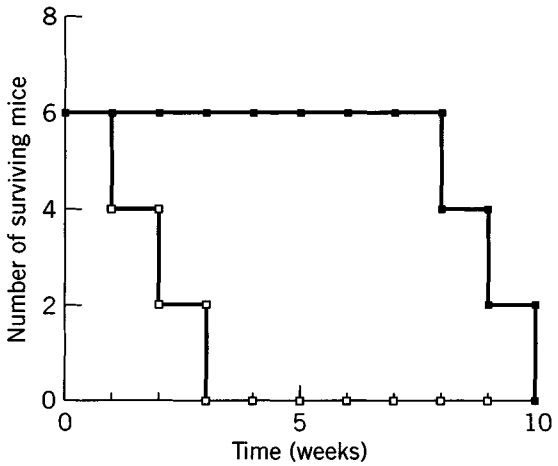


Figure 15. Mean survival time of *P. berghei* infected mice. (□) pyrimethamine base crystals, (■) disks, 25 × 3.0 mm containing 21 wt % pyrimethamine and 5 wt % suberic acid. *Source:* Reprinted from Ref. 42, p. 213, with permission of Elsevier Science.

Tobramycin sulfate has been used in the treatment of osteomyelitis and its in vitro release from poly(ortho esters) has been investigated (43). After an initial burst (20 wt %), reasonably constant release kinetics for up to 25 days were achieved with lactic acid or oleic acid excipients.

Long-Term Delivery. Long-term in vivo surface erosion using $Mg(OH)_2$ has been documented with cross-linked polymers prepared as shown in Scheme 5 (21). In these studies, devices were fabricated by first preparing a ketene acetal terminated prepolymer derived from two equivalents of the diketene acetal 3,9-diethylidene 2,4,8,10 tetraoxaspiro [5.5] undecane and one equivalent of 3-methyl-1,5-pentanediol. Then, 30 wt % micronized levonorgestrel, 7 wt % micronized $Mg(OH)_2$, and a 30 mole % excess of 1,2,6-hexanetriol were mixed into the semisolid prepolymer, and this mixture then was extruded into rods and cured. Erosion and drug release from these devices was studied by implanting the rod-shaped devices subcutaneously into rabbits, explanting at various time intervals and measuring weight loss and residual drug (21). Levonorgestrel blood plasma levels were also determined (44).

The explanted devices were also examined by scanning electron microscopy, and results are shown in Figure 16 (26). The pictures clearly show a progressive diminution of a central uneroded zone and the development of voids around the periphery of the rod-shaped device. The presence of voids suggest that once erosion starts, generation of hydrophilic degradation products at that location accelerates further polymer hydrolysis.

Modified Polymer. The need for a better therapy to control diabetes is now well recognized, because it is evident that simple replacement of insulin by periodic injections is unable to prevent the serious consequences of the disease (45). Consequently, the development of an implantable insulin delivery system that can meter out insulin in response to blood glucose levels is an important area of research.

Poly(ortho esters) have been used in the construction of a self-regulated insulin delivery device. In this approach, insulin was dispersed in an acid-sensitive polymer surrounded by a hydrogel containing immobilized glucose oxidase (46). When glucose diffuses into the hydrogel, it is oxidized by the enzyme glucose oxidase to gluconic acid, and the consequent lowered pH accelerated polymer erosion and concomitant insulin release.

Because poly(ortho esters) based on 3,9-diethylidene 2,4,8,10 tetraoxaspiro [5.5] undecane and ordinary diols are not sufficiently acid sensitive to adequately respond to the small pH changes caused by the gluconic acid generated by the glucose/glucose oxidase reaction, polymers containing a tertiary amine in the backbone were developed. By using a tertiary amine in the backbone, pH sensitivity was significantly increased. The structure of a polymer from 3,9-diethylidene 2,4,8,10 tetraoxaspiro [5.5] undecane and *N*-methyldiethanolamine is shown in Scheme 14.

When disks containing insulin dispersed in the polymer were subjected to well-controlled low pH pulses and the cumulative amount of insulin released during each pulse determined by radioimmunoassay, results shown in Figure 17 were obtained (46). The progressive decrease with repeated stimulation represents a gradual depletion of insulin from the device.

Self-Catalyzed Polymers. Because one of the more important applications of bioerodible polymers is in the treatment of cancer, where a bioerodible device containing an antineoplastic agent is used to deliver the agent systemically, or where the implant is located at the site from which a tumor has been excised, studies with devices containing 5-FU have been carried out. 5-FU release from a polymer constructed from *trans*-cyclohexanedimethanol glycolide and *trans*-cyclohexanedimethanol, used at varying ratios, is shown in Figure 18 (47).

These data show that excellent linear release has been achieved. Most importantly, when all drug has been delivered, only traces of polymer remain. Further, rate of release can be controlled by the concentration of the glycolic acid dimer segment in the polymer. Although devices containing 15 and 20 wt % of monomer with a glycolic acid dimer segment erode at about the same rate, release rates of 1, 2 and 3 weeks have been achieved. These are therapeutically useful release rates.

Release of 5-FU from the low melting polymers prepared from diols shown in Scheme 13 are shown in Figures 19 and 20 (48).

Figure 19 shows the effect of increasing amounts of a dilactide diol incorporated into a polymer prepared from 1,12-dodecanediol and 1,12-dodecanediol dilactide. As shown, only the polymer containing 20 mole % dilactide eroded completely. However, 70% of the polymer containing 10 wt % dilactide eroded at a time when 80% of the drug has been released. Because this experiment was stopped before release was complete, it is possible that this polymer would also have eroded to completion. At the time the experiment was stopped, the polymer containing 5 wt % dilactide had released about 80% of the drug, but only about 35% weight loss was observed. Thus, it is unlikely that this polymer would have eroded to completion. Clearly, complete erosion requires a certain minimum dilactide content.

Figure 20 shows release of 5-FU from polymers prepared from the C8, C10, and C12 diols, all containing 20 wt % dilactide. In this series, all polymers eroded to completion, and 5-FU release rate was a function of diol chain length, suggesting that polymer hydrophobicity is an important factor.

Release of 5-FU from an ointment-like material prepared from 50 mole % triethylene glycol, 40 mole % decanediol, and 1 mole % triethylene glycol monolactide is shown in Figure 21. This materials is highly viscous at body temperature, but at temperatures below about 45°C it can be injected with a hypodermic syringe. Release occurs after an induction period of about 10 days, after which time excellent linear kinetics for about 30 days are noted. Such kinetics are of interest because no burst of drug occurs and good control over amount of drug administered with repeated injections is achieved, provided such injections are appropriately spaced to take into account the lag time.

Some initial result of bovine serum albumin (BSA) release from an ointment-like material prepared from 99

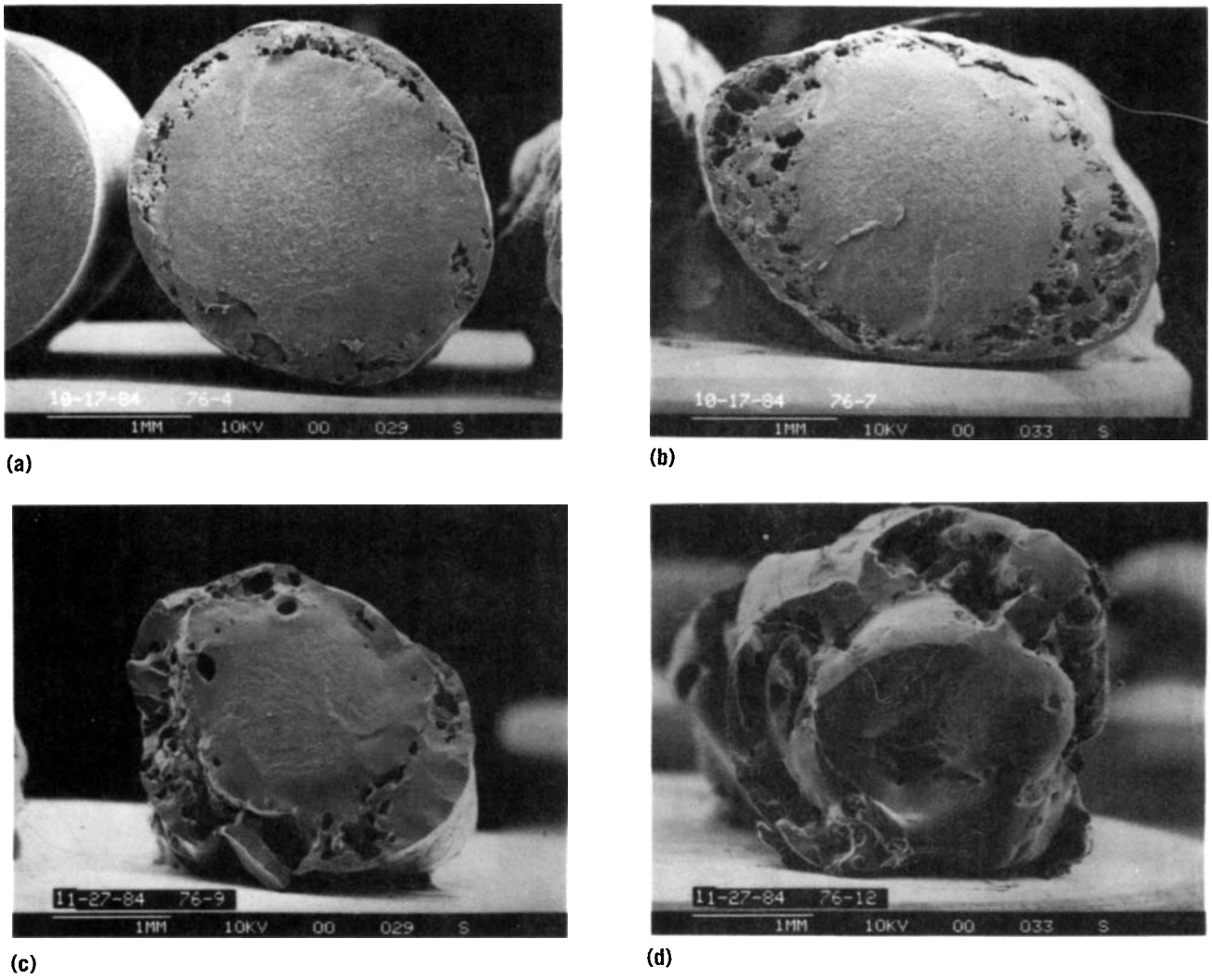


Figure 16. Scanning electron micrographs of cross-linked polymer prepared from 3,9-diethylidene-2,4,8,20-tetraoxaspiro [5.5] undecane/3-methyl-1,5-pentanenediol prepolymer cross-linked with 1,2,6-hexanetriol. Prepolymer contains 1 mole % copolymerized 9,10-dihydroxystearic acid. Polymer rods 2.4 × 20 mm containing 30 wt % levonorgestrel and 7.1 mole % $Mg(OH)_2$. Devices implanted subcutaneously in rabbits. (**a**) after 6 weeks, 30X; (**b**) after 9 weeks, 30X; (**c**) after 12 weeks, 25X; (**d**) after 16 weeks, 25X. *Source:* Reprinted from Ref. 26, p. 176, with permission of Elsevier Science.

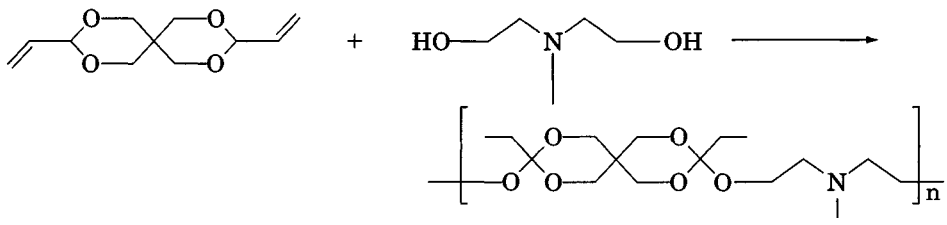
mole % triethylene glycol and 1 mole % triethylene glycol mono L-lactide is shown in Figure 22. These initial encouraging results indicate that ointment-like materials can release proteins at close to zero-order kinetics.

Typical Synthetic Procedures

Preparation of 3,9-diethylidene-2,4,8,10-tetraoxaspiro [5.5] undecane. In a 3-L three-necked flask filled with a mechanical stirrer, argon inlet tube, thermometer, and rubber septum is placed 1.2 L of ethylene diamine. The flask is cooled with ice water, and the contents kept at about 8°C under an argon atmosphere. A hexane solution of 130 g (2 moles) on *n*-butyllithium is added via a stainless steel hypodermic U-tube pushed through the rubber septum using carefully controlled argon pressure over a period of 1 h.

Next, a mixture of 530 g (2.5 moles) of 3,9-divinyl-2,4,8,10-tetraoxaspiro [5.5] undecane and 0.5 L of ethylenediamine is cooled to 8°C and added to the three-necked flask. After stirring at 8°C for 3 h, the reaction mixture is poured into 3 L of ice water with vigorous stirring. The aqueous mixture is extracted twice with 1-L portions of hexane. The combined hexane extracts are washed three times with 1-L portions of water, dried over anhydrous magnesium sulfate, and filtered under suction. The filtrate is evaporated to dryness on a rotary evaporator to give 413 g (78%) of crude material containing 90% of 3,9-diethylidene 2,4,8,10-tetraoxaspiro [5.5] undecane.

The crude product is dissolved in 2 L of hexane containing 10 mL of triethylamine, and the solution placed in a 4-L filter flask, sealed, and stored in a freezer at −20°C for 2 days. The crystals thus formed are collected by basket



Scheme 14.

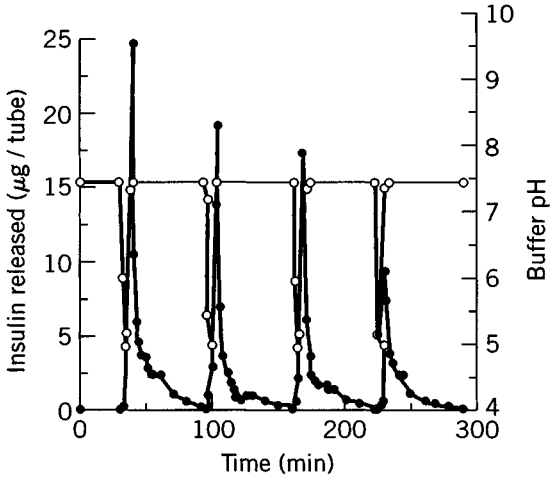


Figure 17. Release of insulin from a linear polymer prepared from 3,9-diethylidene-2,4,8,10-tetraoxaspiro [5.5] undecane and *N*-methyldiethanolamine as a function of external pH variations between pH 7.4 and 5.0 at 37°C. Buffer was continuosly perifused at a flow rate of 2 mL/min and total effluent collected at 1–10 min intervals. (○) buffer pH, (●) insulin release. *Source:* Reprinted from Ref. 46, with permission of Elsevier Science.

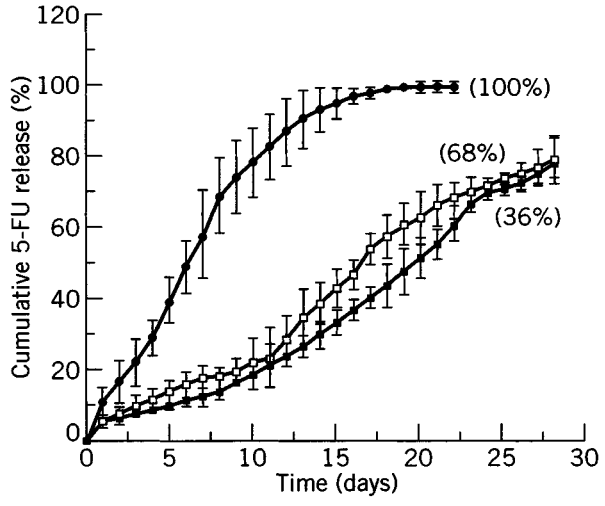


Figure 19. Cumulative release of 5-FU from a polymer prepared from 3,9-diethylidene 2,4,8,10-tetraoxaspiro [5.5] undecane and a C12 diol as a function of diol/lactide content. (■) 50 kDa, C12/5, (□) 41 kDa, C12/10, (●) 17 kDa, C12/20. Phosphate buffer, pH 7.4, 37°C. Drug loading 10 wt %. Percentage in parentheses indicate weight loss. *Source:* Reprinted from Ref. 48, with permission of Elsevier Science.

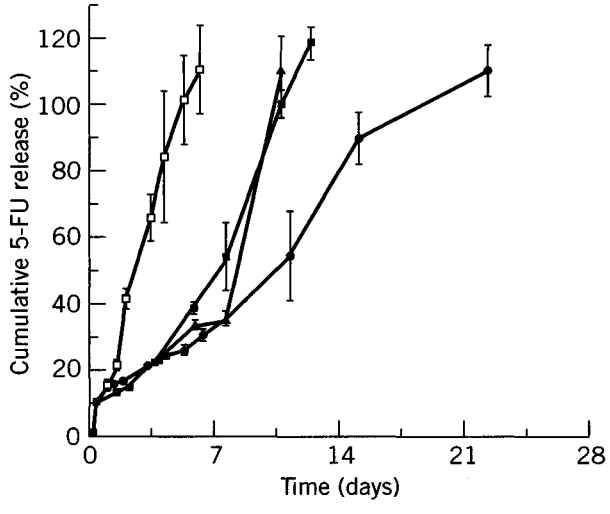


Figure 18. 5-FU release from a polymer prepared from 3,9-diethylidene-2,4,8,10-tetraoxaspiro [5.5] undecane, *trans*-cyclohexanedimethanol glycolide (tCDM/Gly), and *trans*-cyclohexanedimethanol (tCDM) as a function of diol ratios. (□) 75/25 tCDM-CDM/Gly, (■) 80/20 tCDM-tCDM/Gly, (▲) 85/15 tCDM-tCDM/Gly, (●) 90/10 tCDM-CDM/Gly. 0.05 M phosphate buffer, pH 7.4, 37°C. Drug loading 10 wt %. *Source:* Reprinted with permission from the New York Academy of Sciences.

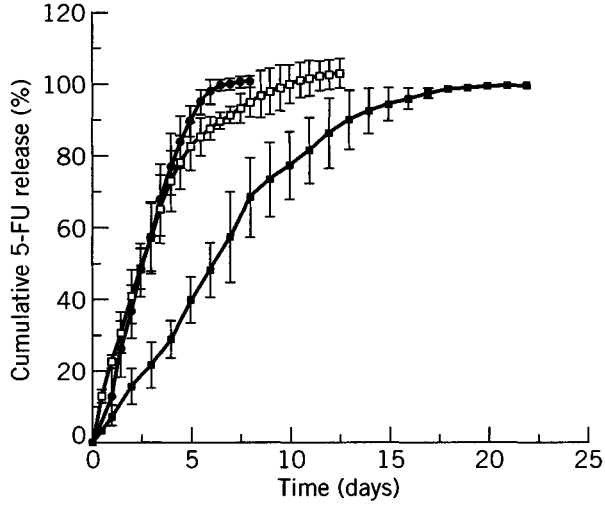


Figure 20. Cumulative release of 5-FU from a polymer prepared from 3,9-diethylidene 2,4,8,10-tetraoxaspiro [5.5] undecane and various diols as a function of diol chain length. (●) 21 kDa C8/20, (□) 31 kDa C10/20, (■) 17 kDa C12/20. Phosphate buffer, pH 7.4, 37°C. Drug loading 10 wt %. *Source:* Reprinted from Ref. 48, with permission of Elsevier Science.

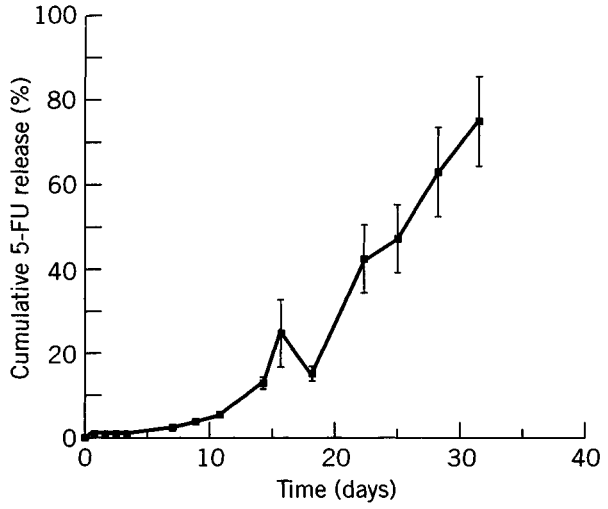


Figure 21. 5-FU release from a polymer prepared from 3,9-diethylidene 2,4,8,10-tetraoxaspiro [5.5] undecane, 50 mole % triethylene glycol, 49 mole % *n*-decanediol, and 1 mole % triethylene glycol DL-dilactide at pH 7.4 and 37°C. Drug loading 10 wt %.

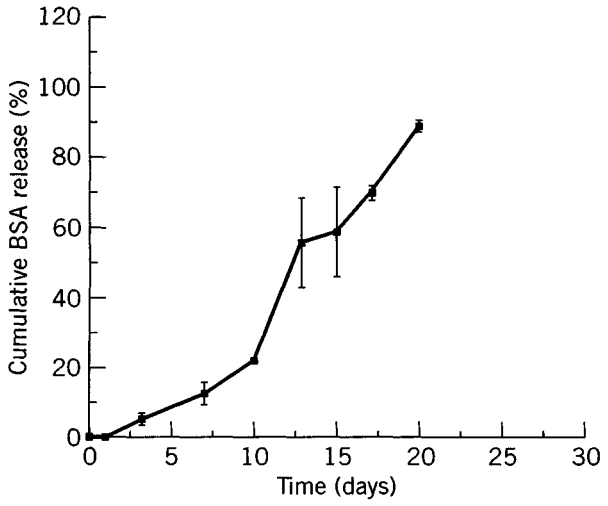


Figure 22. BSA release from a polymer prepared from 3,9-diethylidene 2,4,8,10-tetraoxaspiro [5.5] undecane, 99 mole % triethylene glycol, and 1 mole % triethylene glycol mono-DL, lactide at pH 7.4 and 37°C. Drug loading 10 wt %.

centrifugation at −5°C under an argon atmosphere. Distillation of the brownish product through a 12-inch vigreaux column at reduced pressure gives 313 g (61%) of 3,9-diethylidene 2,4,8,10-tetraoxaspiro [5.5] undecane as a colorless liquid, b.p. 82°C (0.1 torr), which crystallizes at room temperature, m.p. 30°C; characteristic IR band at 1700 cm^{-1}.

Preparation of Linear Polymers. Into a 5-L, three-necked flask equipped with an overhead stirrer, an argon inlet tube, and a condenser are placed 89.57 g (0.621 mole) of *trans*-cyclohexanedimethanol, 39.52 g (0.334 mole) of 1,6-hexanediol, and 1.8 L of distilled tetrahydrofuran. The mixture is stirred until all solids have dissolved; then, 200 g (0.942 mole) of 3,9-diethylidene 2,4,8,10-tetraoxaspiro [5.5] undecane is added. The polymerization is initiated by the addition of 2 mL of a solution of *p*-toluenesulfonic acid (20 mg/mL) in tetrahydrofuran.

The polymerization temperature rapidly rises to the boiling point of tetrahydrofuran and then gradually decreases. Stirring is continued for about 2 h, 10 mL of triethylamine stabilizer added, and the reaction mixture then very slowly poured with vigorous stirring into about 15 gallons of methanol containing 100 mL of triethylamine. The precipitated polymer is collected by vacuum filtration and dried in a vacuum oven at 60°C for 24 h. The weight of the dried polymer is 325 g (98.8% yield).

Preparation of Cross-Linked Polymers. To a solution of 31.84 g (0.159 mole) of 3,9-diethylidene 2,4,8,10-tetraoxaspiro [5.5] undecane in 200 mL of distilled tetrahydrofuran is added 10.42 g (0.100 mole) of 2-methyl-1,4-butanediol. The solution is stirred under argon and 0.5 mL of *p*-toluenesulfonic acid solution in tetrahydrofuran (20 mg/mL) is added to initiate the reaction. After the heat of reaction has subsided, the solution is stirred until the temperature returns to ambient and then concentrated on a rotary evaporator followed by heating in a vacuum oven at 40°C to remove residual solvent.

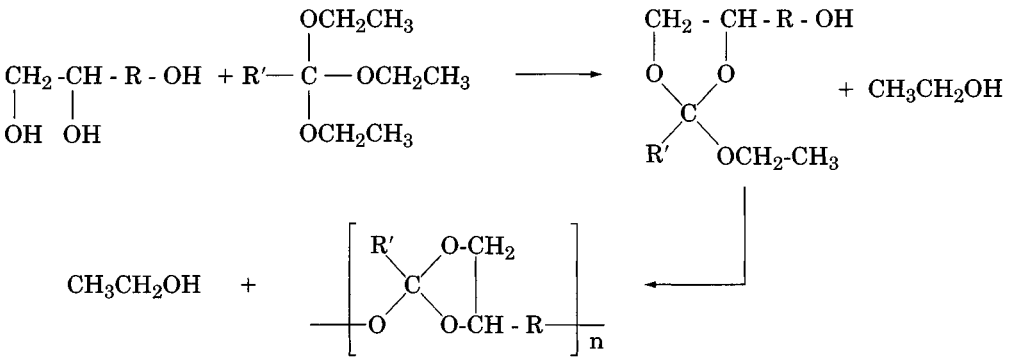
Devices are then prepared by mixing into the prepolymer an excess of 1,2,6-hexanetriol and the desired excipients and curing the mixture in a mold at 75°C for 5 h. Best results are obtained when the mole ratio hydroxyl to ketene acetal is about 1:3.

Synthesis of Diols Containing a Glycolide Segment. The following represents a typical preparation. In a dry-box, 15.07 g (100 mmoles) of triethylene glycol and 11.06 g (100 mmoles) of glycolide were weighed into a 50 mL flask. The flask was sealed with a rubber septum and heated overnight at 180°C in an oil bath. Similar reactions were also conducted with *trans*-cyclohexanedimethanol and with 1,10-decanediol. The resulting oils were not purified and used directly in the polymerization reactions.

Polymerization. The following represents a typical preparation. Under anhydrous conditions 13.515 g (90 mmoles) of triethylene glycol and 2.663 g (10 mmoles) of the triethylene glycol monoglycolide described earlier were weighed into a 250 mL flask, and the mixture dissolved in 50 mL of tetrahydrofuran. Then 19.103 g (90 mmoles) of 3,9-diethylidene-2,4,8,10-tetraoxaspiro [5.5] undecane were added. After the exothermic reaction subsided, the solution was first concentrated on a roto-evaporator and the remaining solvent removed in a vacuum oven at 40°C.

POLY(ORTHO ESTER) III

The third family of such polymers was originally developed at SRI International (49) and is also under active development at the University of Geneva (50). It is prepared as shown in Scheme 15. The intermediate does not have to be isolated, and continuing reaction produces the final polymer.



Scheme 15.

When R is $-(CH_2)_4-$, the polymer is a semisolid at room temperature even though molecular weights can exceed 35 kDa. This semisolid consistency provides a number of unique advantages. Dominant among these is the ability to incorporate into the polymer therapeutic agents by a simple mixing procedure without the need to use solvents or elevated temperatures. The semisolid consistency also allows some unique means of administration of the polymer.

The general synthetic procedure shown in Scheme 15 can also be used to prepare solid polymers. To do so, it is only necessary to replace the flexible triol, such as 1,2,6-hexanetriol, with a rigid one, such as 1,1,4-cyclohexanetrimethanol, as shown in Scheme 16 (51). As before, the intermediate does not have to be isolated, and continuing reaction produces a polymer.

The triol, 1,1,4-cyclohexanetrimethanol can be prepared as shown in Scheme 17 (51).

Unfortunately, even though small-scale preparations proceeded with no difficulties, attempts to scale-up the synthesis were unsuccessful, and large amounts of the monomer remained elusive. Thus, it was deemed unlikely that a viable commercial product could be developed, and further work with this polymer has been discontinued. Nevertheless, this is an interesting system, and one member of this family where R = CH_3 is highly crystalline, whereas polymers where R = CH_3CH_2 and higher, are totally amorphous. To this date, the methyl homologue remains the only crystalline poly(ortho ester) ever prepared. X-ray diffraction of the methyl and *n*-propyl homologues are shown in Figure 23.

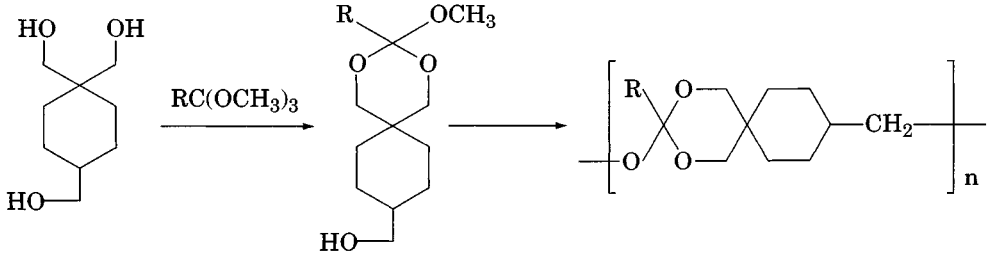
Polymer Erosion

Polymer hydrolysis occurs as shown in Scheme 18 for a polymer prepared from 1,2,6-hexanetriol (49). However, a similar scheme can also be written for the solid form (51). As with poly(ortho ester) II, initial hydrolysis occurs at the labile ortho ester bonds to generate one or more isomeric monoesters of the triol. This initial hydrolysis is followed by a much slower hydrolysis of the monoesters to produce a carboxylic acid and a triol. Thus, as with the poly (ortho ester) II, no autocatalysis is observed. Details of the hydrolysis mechanism for polymers based on 1,2,6-hexanetriol and 1,1,4-cyclohexanetrimethanol have been published (51,52).

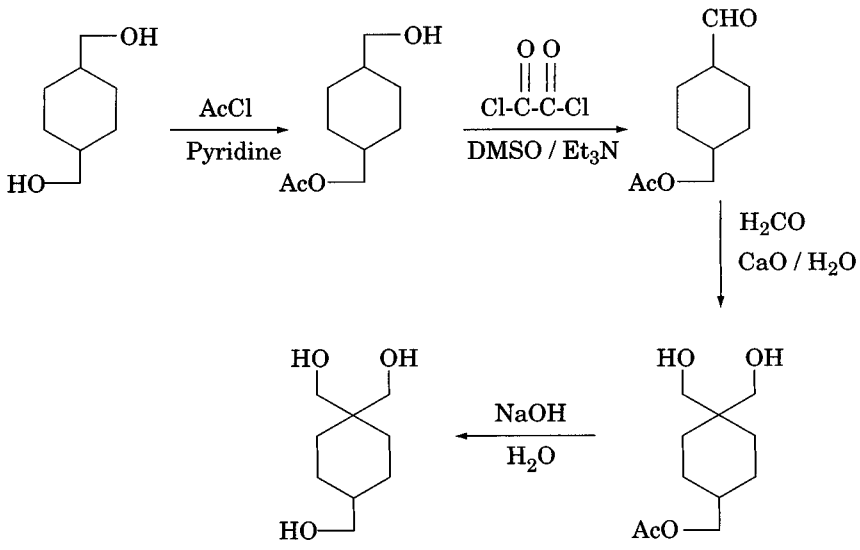
Unlike poly(ortho esters) II, which are extremely hydrophobic (27), poly(ortho esters) III prepared from alkyl orthoacetates and 1,2,6-hexanetriol are quite hydrophilic, and water uptake at a relative humidity of 80% is shown in Figure 24 (53). For this reason, and as will be shown later, the uncatalyzed erosion of this polymer proceeds at a relatively rapid rate.

Polymer Characterization

Radiation Sterilization. Due to the moisture sensitivity of poly(ortho esters) and their susceptibility to degradation at elevated temperatures, conventional methods such as dry heat or steam sterilization cannot be used. Although poly(ortho esters) can been successfully sterilized with ethylene oxide (54), there is the possibility that residues can remain in the polymer despite rigorous outgassing. This is clearly not desirable because mutagenic and possibly car-



Scheme 16.



Scheme 17.

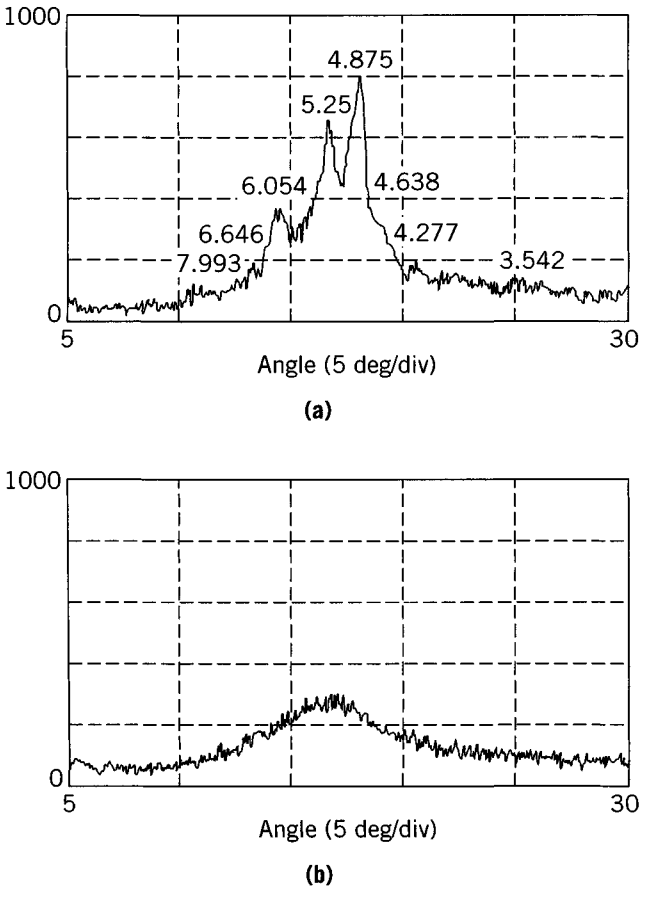


Figure 23. X-ray diffractometer traces of a polymer prepared from (**a**) trimethyl orthoacetate and 1,1,4-cyclohexanetrimethanol and (**b**) triethyl orthopropionate and 1,1,4-cyclohexanetrimethanol. Phillips 3KVA full-wave generator, Phillips "copper" 1800-W long-fine-focus tube, Phillips goniometer, and Bicron scintillator. *Source:* Reprinted with permission from Ref. 51. Copyright 1997 American Chemical Society.

cinogenic properties of such residues have been reported (55). Thus, γ-radiation sterilization was used. However, the use of radiation sterilization can lead to changes in polymer molecular weight, and polymer structure and the magnitude of such changes is largely determined by the structure of the polymer and by the radiation dose used. For γ-sterilization, depending on the dose, two different mechanisms have been observed (56). For doses lower than 2.0 Mrad the dominant degradation mechanism is scission of the polymer chain. As shown in Figure 25, such cleavage leads to a decrease in polymer molecular weight and a consequent decrease of dynamic viscosity. At doses higher than 2.0 Mrad, chemical changes begin to take place, as evidenced by an increase in the peak at 1750 cm^{-1} noted in the fourier transform infrared spectrum (56). The exact nature of the chemical changes is not clear, but a degradation mechanism similar to polymer hydrolysis seems to occur, even in the rigorous absence of moisture.

Purity and Stability. Poly(ortho esters) III prepared from alkyl orthoacetates and 1,2,6-hexanetriol contain residual monomer and low molecular weight oligomers and have a polydispersity (M_w/M_n) of about 3. After dissolution in tetrahydrofuran and precipitation into methanol, the low molecular weight components can be virtually eliminated, and two more precipitations reduce the polydispersity to about 2.1 (53). Residual solvent can be removed by drying at 40°C and 5 mbar for 24 h. Drying temperature must be selected so as to avoid thermal degradation, which, as shown in Figure 26, starts at about 45°C.

Preferred storage conditions are in sealed glass bottles under an argon atmosphere. Under these conditions, the average molecular weight remained virtually unchanged for 180 days (53).

Drug Release

This polymer has been used in a number of applications (2). The two most recent applications are the development of devices for the treatment of periodontal disease and as an adjunct for glaucoma filtration surgery.

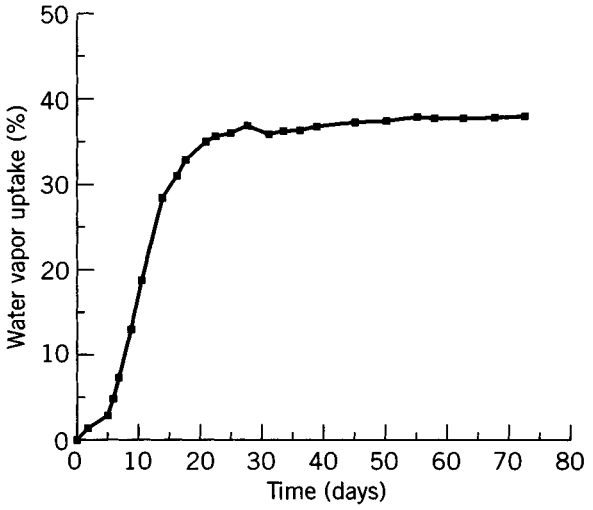


Figure 24. Water vapor uptake of a 21.5 kDa polymer prepared from a trimethyl orthoacetate and 1,2,6-hexanetriol at 80% relative humidity. *Source:* Reprinted from Ref. 53, p. 900, with permission of Elsevier Science.

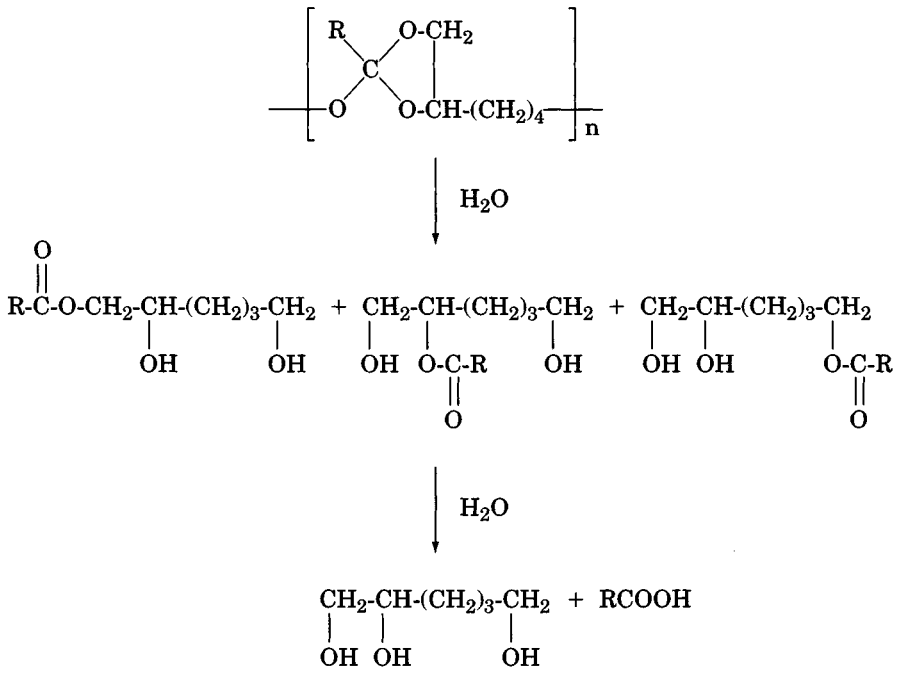
Treatment of Periodontal Disease. Periodontitis is a group of dentoalveolar infections that are one of the major causes of teeth loss. These infections are caused by a pathogenic flora, established within the gingival sulcus, which later deepens to form a periodontal pocket. Treatments are based on strategies that shift the microflora within the periodontal pocket to that observed around healthy teeth and gingiva, and a widely used treatment is to mechanically remove plaque and calculus followed by local treatment with antimicrobial agents. Clearly, controlled release devices that would maintain a therapeutically effective concentration of an antimicrobial agent within the pocket for the desired length of time would significantly improve treatment (57).

Ointment-like poly(ortho esters) III have been investigated as a tetracycline delivery device for the treatment of periodontal disease (58). In this application the ointment-like polymer with incorporated tetracycline was injected into the periodontal pocket using a blunt needle. Then if the polymer is dentoadhesive, it would reside in the periodontal pocket for 7 to 10 days, gradually releasing tetracycline. And because total erosion would take place, no removal of an expended polymer would be required.

Tetracycline Release. Figure 27 show release of tetracycline from a propionate polymer (R = CH_3CH_2) as a function of amount of $Mg(OH)_2$ dispersed in the polymer matrix (58). Release of tetracycline in the absence of $Mg(OH)_2$ was very rapid, but the addition of as little as 0.5 wt % $Mg(OH)_2$ resulted in a sustained release over about 10 days. Addition of 1 wt % Mg(OH)2 prolonged the release to about 25 days and addition of 2 wt % $Mg(OH)_2$ produced a release estimated to last about 75 days. In all cases drug depletion coincided with total polymer erosion so that satisfactory control over device lifetime and rate of tetracycline release should be possible.

Dentoadhesiveness. To test dentoadhesiveness, a microload cell was developed, and because the adhesiveness of human and bovine teeth are not significantly different (59,60), extracted bovine anterior teeth were used as adhesive substrates (56). It was found that for the pure polymer, the required force of detachment was 392 mN cm^{-2}. However, because the detachment occurred by cohesive failure of the polymer and not by failure of the bond between the polymer and the bovine tooth, this value was a minimal value, and the true value of the adhesive bond is very likely significantly higher.

However, this test was carried out with the neat polymer with no incorporated drug and excipient. Further, it



Scheme 18.

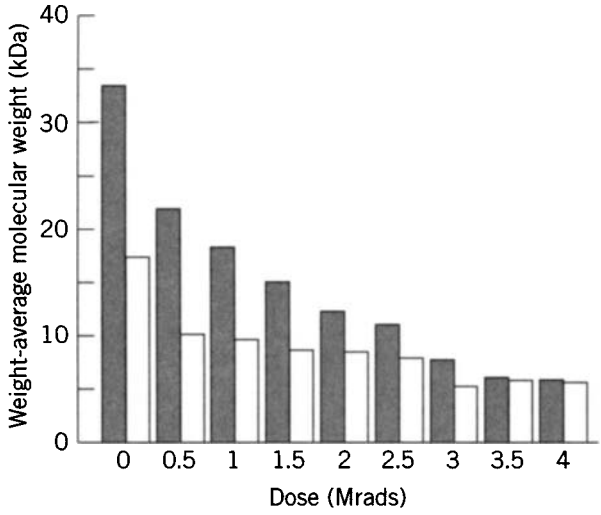


Figure 25. Influence of γ-radiation on the gel permeation chromatography average molecular weight of two different molecular weight polymers prepared from trimethyl orthoacetate and 1,2,6-hexanetriol as a function of radiation dose. (■) 33.3 kDa, (□) 17.4 kDa.

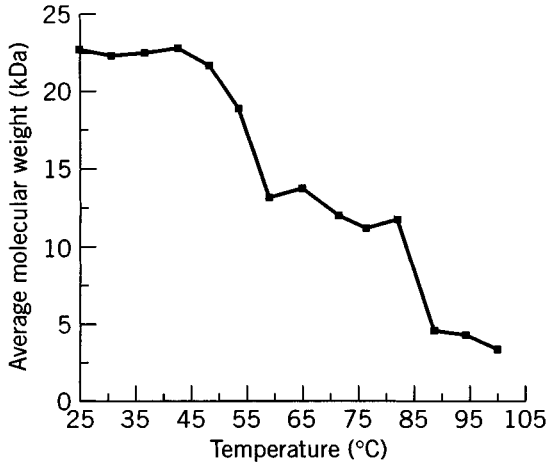


Figure 26. Gel permeation chromatography determination of the molecular weight of a polymer prepared from trimethyl orthoacetate and 1,2,6-hexanetriol after 24 hours of storage at different temperatures under anhydrous conditions (n = 3). *Source:* Reprinted from Ref. 53, p. 899, with permission of Elsevier Science.

was carried out on teeth surfaces that have not been exposed to proteins normally present in the oral environment. When the adhesion study was repeated using a formulation containing 10 wt % tetracycline and 1.0 wt % $Mg(OH)_2$ using teeth that had been exposed to dog serum (Sigma), rinsed with saline, and kept wet with saline, the detachment force decreased to 118 mN cm^{-2}. Again, as with the pure polymer, separation occurred by cohesive failure of the polymer and not between the bond between the specimen and polymer. The lower value indicates that polymer integrity has been weakened by the incorporation of tetracycline and $Mg(OH)_2$. However, it is clear that the

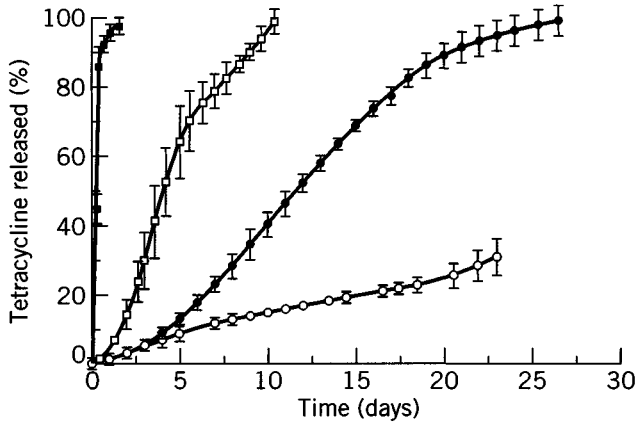


Figure 27. Cumulative release of tetracycline from a 27 kDa polymer prepared from trimethyl orthoacetate and 1,2,6-hexanetriol at pH 7.4 and 37°C as a function of $Mg(OH)_2$ content. 0.1 M phosphate buffer, flow rate 1 ml h^{-1}, drug loading 10 wt %. (○) 0%, (●) 0.5%, (□) 1.0%, (■) 2.0%. Error bars are standard deviation, n = 3. *Source:* Reprinted from Ref. 58, p. 316, with permission of Elsevier Science.

final formulation is also capable of strongly adhering to teeth. Thus, as judged from these in vitro studies, adequate residence time in the periodontal pocket should be possible.

Toxicology. Because there is the potential for ingestion of the polymer during treatment, acute and chronic feeding studies were carried out (61). Further, during bioerosion of the polymer, systemic absorption of hydrolysis products takes place so that acute intravenous toxicity studies using polymer hydrolysate were also carried out. All toxicological studies were carried out using adult Sprague Dawley rats using a doubly precipitated polymer that was then irradiated at 2.5 Mrad and stored in a dry-box at room temperature until use.

1. *Acute oral toxicity of intact polymer.* The intact polymer was emulsified in a vehicle consisting of 2 w/v % aqueous methyl cellulose solution with the aid of 1.6 w/v Tween 80 and administered to rats at a dose level of 3.3 g/kg. No deaths or adverse clinical signs were observed during the study, and no gross abnormalities were observed during necropsy. Thus, the polymer is nontoxic when administered as a single dose of 3.3 g/kg to rats.
2. *Chronic oral toxicity (28-day) of intact polymer.* The emulsified polymer prepared as already described was administered daily to rats at doses of 0.76, 1.64 or 3.27 g/kg for 28 days. At necropsy, no gross abnormalities were observed in the tissues or external features.

   Histopathologic examination revealed no significant microscopic findings and no target organs for poly(ortho esters) toxicity. All hematology and clinical chemistry parameters were in the normal range. Thus, the polymer is nontoxic when administered daily at a maximum oral dose of 3.3 g/kg for 4 weeks.
3. *Acute intravenous toxicity of polymer hydrolysate.* Sterile polymer was hydrolyzed by placing a known

weight of the polymer in sterile buffered saline, pH 7.4 at 37°C for 15 days. The hydrolyzed polymer was filtered through sterile 0.2 μg filters and diluted as necessary. Rats were given 10 ml/kg of sterile phosphate buffered saline containing hydrolyzed polymer equivalent to 0.5, 1.0, or 1.5 g/kg, based on the weight of starting polymer. Rats given doses greater than 1.0 g/kg had ataxia immediately following dosing, but recovered within 30 seconds and exhibited no other adverse clinical symptoms. The rats were kept under observation for 15 days. No gross abnormalities were observed following necropsy.

4. *In vivo studies.* The polymer with incorporated tetracycline has been investigated for effectiveness in the treatment of beagle dogs with naturally occurring periodontitis. These studies failed to show effectiveness due to rapid loss of polymer from the periodontal pocket. However, it is likely that this failure is due to anatomical differences between beagle dogs and humans, in that beagle dogs only develop a very shallow periodontal pocket, whereas humans develop a deep periodontal pocket. The shallowness of the periodontal pockets in beagle dogs makes placement of the polymer very difficult. Further, dentoadhesiveness only takes place if the tooth can be dried, which was not possible due to the presence of a great deal of blood and pus. Plans to carry out a study with human volunteers are currently being formulated.

5-FU Delivery as an Adjunct for Glaucoma Filtering Surgery. ***Drug Release.*** Postoperative subconjunctival 5-FU injection is used to increase the success in glaucoma filtering surgery in patients with poor surgical prognoses. These include glaucoma in aphakia or pseudophakia and previously unsuccessful filtering procedures (62–64). The antimetabolite 5-FU, a water-soluble pyrimidene analogue, acts by suppressing fibroblast proliferation and subsequent scarring following trabeculectomy (65,66). The application of 5-FU as an adjunct to glaucoma surgery has been investigated in animal studies and in human clinical trials (64,67,68). In order to maintain an effective concentration of the drug, daily injections of 5.0 to 7.5 mg of 5-FU for up to 7 days are used (67–69). This postoperative therapy has the disadvantage of frequent administration, patient discomfort associated with the injection, conjunctival incision, and needle track leaks. Other side effects frequently reported include corneal epithelial erosion, hypotonia, and endophthalmitis (64,70). For these reasons, development of an injectable polymer that could deliver 5-FU for the desired length of time and at the desired kinetics and rate is of considerable importance.

Figure 28 shows in vitro release of 5-FU from an acetate polymer of five different molecular weights (69). The data show one-day release from the lowest molecular weight polymer and one-week release from the highest molecular weight polymer. Thus, it is possible to control drug delivery times without the use of excipients by simply controlling polymer molecular weight.

Figure 29 shows a comparison between 5-FU release and polymer weight loss (50). These data are consistent

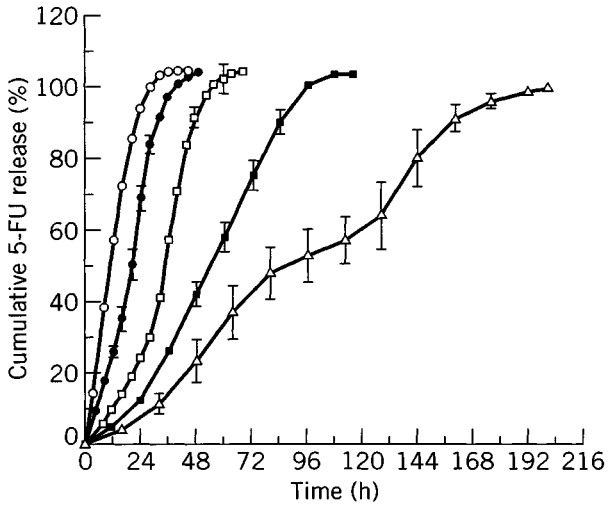


Figure 28. 5-FU release from a polymer prepared from trimethyl orthoacetate and 1,2,6-hexanetriol as a function of polymer molecular weight. Phosphate buffer, pH 7.4 at 37°C. (○) 3.5 kDa, (●) 5.8 kDa, (□) 10.1 kDa (■) 15.2 kDa (△) 33.3 kDa. Mean ± SD (n = 6). *Source:* Reprinted from Ref. 50, p. 109, with permission of Elsevier Science.

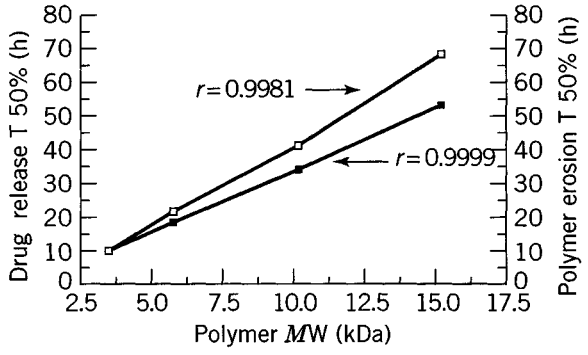


Figure 29. Comparison between 5-FU release (□) and polymer weight loss (■) for a polymer prepared from trimethyl orthoacetate and 1,2,6-hexanetriol as a function of polymer molecular weight using T50% for both parameters. *Source:* Reprinted from Ref. 50, p. 109, with permission from Elsevier Science.

with a combination of erosion-controlled and diffusion-controlled 5-FU release. For a low molecular weight polymer, where erosion is relatively rapid, the diffusional contribution is minimal, but as the erosion times increase, diffusion becomes progressively more important. However, even for the highest molecular weight polymer, total erosion occurs soon after drug depletion. This is highly desirable in glaucoma filtering surgery where lack of encapsulation of residual polymer is important.

Biocompatibility. Initial biocompatibility studies (71) have shown that the subcutaneous injection of a γ-ray sterilized ointment in rats induced a mild local inflammation at 3 days, which could be due to the large injection volume that stretched the tissues. At 7 days, granulation-type tissue was present, with focal zones of more intense inflammation. Mild chronic inflammation remained at 14 days

and was very minimal at 21 days. However, when subconjunctivally injected into rabbits, the same polymer triggered a marked hyperemia at day 3, which confirmed the high sensitivity to irritation of rabbit eyes (72,73).

For this reason, the polymer was further purified and the subconjunctival biocompatibility of a γ-ray sterilized polymer and one prepared under aseptic conditions compared (74). Because local tissue response depends not only on the biocompatibility of the polymer, but with biodegradable polymers, also on its hydrolysis products, an attempt was made to determine which, if any, of the hydrolysis products was responsible for the transient inflammatory reaction.

Figure 30 compares the effect of a 200 μL subconjunctival injections of γ-ray sterilized polymer and one prepared aseptically on hyperemia. Clearly, the significant hyperemia noted with the γ-ray sterilized polymer is markedly reduced.

Because it has been shown (53) that after reprecipitation a very pure polymer with only traces of monomers and oligomers is obtained, the observed transient irritation may be due to the isomeric monoesters of 1,2,6-hexanetriol intermediate hydrolysis products. When these were synthesized and injected subconjunctivally at 50 wt % in phosphate-buffered saline as well as neat, an immediate inflammatory reaction was noted. Because 1,2,6-hexanetriol has been shown to be nontoxic (75) and evoked no reaction when injected subconjunctivally, the irritation is almost certainly due to hydrolysis of the ester, accelerated by esterases, to produce acetic acid that can induce intense local irritation. Although acetic acid is not considered to be systemically toxic because it is eliminated via the Krebbs cycle as CO_2 and H_2O, in large enough amounts it can overwhelm the buffering capacity of the eye.

Attempts to improve biocompatibility by using buffers to neutralize the acetic acid released as a consequence of polymer hydrolysis are currently underway (M. Zignani et al., unpublished data). In this work, salts such as sodium acetate or magnesium hydroxide are incorporated into the polymer. Preliminary results shown in Figure 31 indicate that by using these excipients, it is indeed possible to control pH.

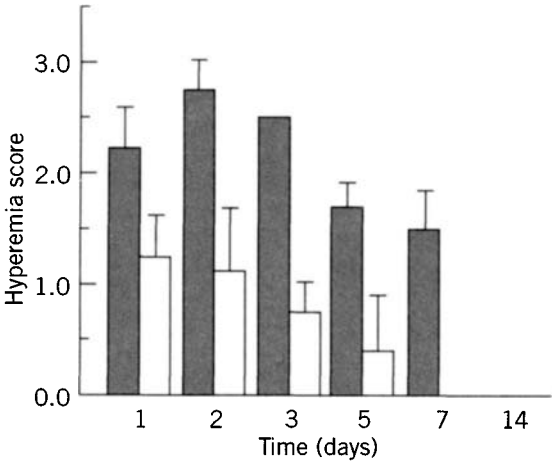


Figure 30. Comparative clinical evaluation of hyperemia induced by subconjunctival injection of a polymer prepared from trimethyl orthoacetate and 1,2,6-hexanetriol. (■) 200 μl of γ-ray sterilized polymer, (□) 200 μl of aseptically prepared polymer. *Source:* Reprinted from Ref. 74, with permission of John Wiley & Sons, Inc.

Typical Experimental Procedures

Semisolid Material. Under anhydrous conditions 48.67 g (0.30 mole) of triethyl orthoacetate, 40.25g (0.30 mole) of 1,2,6-hexanetriol, and 20 mg of *p*-toluenesulfonic acid were weighed into a 500 mL round-bottom flask equipped with a magnetic stirring bar. Next, 300 mL of cyclohexane was added and the flask adapted to a 60 cm spinning band column. The reaction flask was heated to 100°C with vigorous stirring, and the ethanol-cyclohexane azeotrope was rapidly removed at 55°C. Throughout the procedure, strictly anhydrous conditions were maintained. When the boiling point began to climb above 55°C, the take-off ratio of the column was reduced to 1/20 distillation/reflux ratio until the boiling point reached 81°C, where the take-off was set for total reflux. After heating for an additional 4 h, the solution was cooled to room temperature. Five drops of triethylamine were then added to stabilize the product and the solvent removed by distillation. The product was a viscous, ointment-like material with an average molecular weight of 29,000 as determined by gel permeation chromatography using a Waters 150-C instrument with Waters ultrastyrogel 10^3 and 10^4 columns, with tetrahydrofuran solvent at 30°C with a small amount of triethylamine stabilizer. Polystyrene was used for calibration.

Monomer Synthesis.

1. *1,4-Cyclohexanedimethanol monoacetate.* A mixture of *cis* and *trans* 1,4-cyclohexane dimethanol, (930 g, 6.448 moles) was dissolved in 3 L of tetrahydrofuran, and 550 mL of pyridine (7.69 moles) was added. The solution was cooled in an ice bath and stirred under argon. An acetyl chloride solution (506.4 g, 6.45

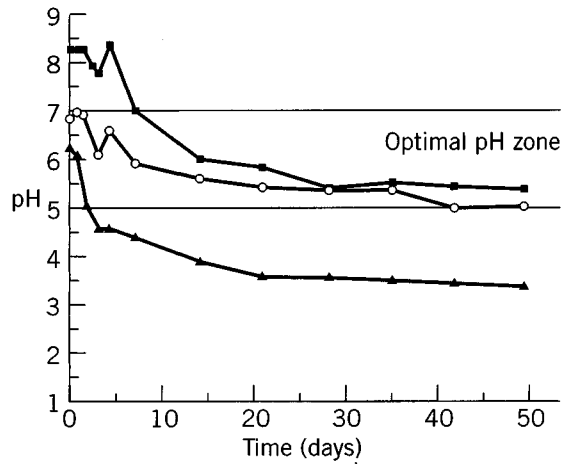


Figure 31. Changes in pH induced by hydrolysis of a polymer prepared from trimethyl orthoacetate and 1,2,6-hexanetriol. 1 g polymer placed in 10 ml 0.9% sodium chloride maintained at 37°C. (▲) neat polymer, (○) 1 wt % sodium acetate, (■) 0.25 wt % magnesium hydroxide.

moles) in 500 mL of tetrahydrofuran was added dropwise over a 2-h period. The ice bath was removed and the reaction mixture stirred for 2 h at room temperature. It was then filtered to remove the pyridine HCl salt and evaporated to remove the tetrahydrofuran. The residue was dissolved in 2 L of ethyl acetate and the solution extracted with diluted aqueous HCl (2 × 300 mL), warm water (2 × 300 mL), and aqueous $NaHCO_3$ solution (2 × 300 mL). The ethyl acetate solution was dried over anhydrous $MgSO_4$, and the ethyl acetate removed on a rotoevaporator. Vacuum distillation of the residue yielded 335 g of product. Gel chromatographic analysis showed that the product contained 59% cyclohexanedimethanol monoacetate and 41% cyclohexanedimethanol diacetate. The overall yield of the monoacetate was 16.5%.

2. *4-Acetoxymethyl-1-cyclohexanecarboxaldehyde.* Under anhydrous conditions, oxalyl chloride (358 g, 2.82 moles) was dissolved in 2.5 L of methylene chloride and the solution cooled to −40°C. Dimethylsulfoxide (407 g, 5.2 moles) dissolved in 200 mL of methylene chloride was then added via a dropping funnel while the reaction mixture was vigorously stirred and the temperature maintained between −40°C and −20°C. Next, a solution of cyclohexanedimethanol monoacetate (600 g, 59% pure, 1.9 moles) in 200 mL of methylene chloride was added dropwise while the reaction temperature was kept below −20°C. After the addition of cyclohexanedimethanol monoacetate solution was completed, the reaction mixture was stirred for an additional 15 min and triethylamine (658 g, 6.5 moles) added. The cooling bath was removed and the reaction mixture stirred for 2 h. It was then extracted successively with diluted aqueous HCl, aqueous $NaHCO_3$, and aqueous NaCl. After drying over anhydrous $MgSO_4$, the methylene chloride solution was distilled under argon to remove the solvent. The residue was distilled at 80°C at 0.4 mm to give the aldehyde (248 g, 70.8% yield).
3. *4-Acetoxymethyl-1,1-cyclohexanedimethanol.* A mixture of 4-acetoxymethyl-1-cyclohexanecarboxaldehyde, (248 g, 1.46 moles), a 37 wt % formaldehyde solution (700 mL, 8.6 moles), and tetrahydrofuran (200 mL) was cooled in an ice water bath. Calcium oxide was then added in small portions while the mixture was vigorously stirred with an overhead mechanical stirrer. After the addition of CaO was completed, the ice bath was removed and the mixture stirred for 2 h. It was then evaporated to dryness and the product extracted into acetone. Evaporation of the acetone solution produced a viscous oil.
4. *1,1,4-cyclohexanetrimethanol.* The crude 4-acetoxymethyl-1,1-cyclohexanedimethanol was added 1 L of an aqueous 2N NaOH solution and the mixture heated at 100°C for 2 h. After cooling to room temperature, the reaction mixture was neutralized with aqueous HCl and extracted with methylene chloride. The aqueous solution was evaporated to dryness, and the residue extracted with acetone. After drying over anhydrous $MgSO_4$, the acetone solution was evaporated to dryness. Distillation of the crude product from the acetone solution at 175°C and 0.1 mm yielded a viscous liquid. Repeated trituration with methylene chloride produced a solid product (150 g, 59% yield, 98.8% purity by gel chromatography).

Polymerization. Under anhydrous conditions, 1,1,4-cyclohexanetrimethanol (3.524 g, 20 mmoles), trimethyl orthoacetate (2.403 g, 20 mmoles), *p*-toluenesulfonic acid (~3 mg), and distilled cyclohexane (80 mL) were added to a predried flask. The flask was fitted with a spinning band column and heated at 100°C under argon. Methanol was removed azeotropically at 56°C at a fast rate, and as the boiling point began to rise, the distillation rate was reduced to 4 drops/min and heating continued for 15 h. The polymer thus prepared precipitated out of cyclohexane. The powdery polymer is crystalline with a melting point (DSC) of 212°C. It is insoluble in the usual organic solvents such as methylene chloride, chloroform, ether, tetrahydrofuran, ethyl acetate, acetone, dimethylformamide, and dimethylsulfoxide.

In a similar manner, 1,1,4-cyclohexanetrimethanol (3.524 g, 20 mmoles) was allowed to react with triethyl orthopropionate (3.634 g, 20 mmoles). This reaction produced a polymer which remained in the cyclohexane solution. Precipitation into methanol yielded a polymer having a M_W of 51,000 (gel permeation chromatography using polystyrene standards) and a T_g of 67.8°C. The polymer was soluble in organic solvents with low or medium polarities such as methylene chloride, chloroform, ether, tetrahydrofuran, and ethyl acetate.

ACKNOWLEDGMENTS

This work was started in 1970, and a great number of individuals have contributed to the development of the three families of poly(ortho esters), both in the United States and in Switzerland. Although they all deserve coauthorship, their sheer number makes this impractical. The following individuals have made major contributions: Dr. Nam Suk Choi, Mr. Donald W. H. Penhale, Mr. Robert F. Helwing, Mr. Bruce K. Fritzinger, Mr. John E. Rose, Dr. Kenneth J. Himmelstein, Dr. Randall V. Sparer, Dr. Gaylen M. Zentner, Dr. Chung Shi, Dr. S. S. Bhosale, Dr. Andrea W. Chow, Dr. Kathleen V. Roskos, Dr. A. C. Chang, Dr. Yu Fu Maa, Dr. Patrick Wuthrich, Dr. Ann France Rime, Dr. Sue S. Rao, Dr. Michelle S. Taylor, Dr. Tierry Vandamme, Dr. Alain Merkli, Dr. Monica Zignani, Dr. Martina B. Sintzel Dr. S. F. Bernatches and Dr. Cyrus Tabatabay.

One of us (JH) wants to especially acknowledge the contributions of Mr. Steven Y. Ng without whose creativity and superb laboratory work this review would have been much shorter. And finally, one of the authors (JH) also wishes to thank Dr. Henry L. Gabelnick, then at the National Institutes of Health, for providing the initial funding for the development of poly(ortho ester) II. Without his patience and understanding of the difficulties in developing a useful monomer and polymer synthesis, this polymer would probably not exist today.

The following funding sources are gratefully acknowledged: NIH Contract N01-HD-7-2826, NIH Contract N01-HD-8-2905, NIH Grant DA 05726, NIH Grant GM 27164, NIH Grant DE 10461, FNSRS Grant 32.35925.92, and FNSRS Grant 32.46795.96. In addition to the government funding, funds were

also provided by ComTech International and by the Finish funding agency TEKES.

BIBLIOGRAPHY

1. J. Heller, *Biomaterials* **11**, 659–665 (1990).
2. J. Heller, *Adv. Polym. Sci.* **107**, 41–92 (1993).
3. U.S. Pat. 4,079,038 (March 14, 1978), N. S. Choi and J. Heller (to ALZA Corporation).
4. U.S. Pat. 4,093,709 (June 6, 1978), N. S. Choi and J. Heller (to ALZA Corporation).
5. U.S. Pat. 4,131,648 (December 26, 1978), N.S. Choi and J. Heller (to ALZA Corporation).
6. U.S. Pat. 4,138,344 (February 6, 1979), N.S. Choi and J. Heller (to ALZA Corporation).
7. U.S. Pat. 4,180,646 (December 25, 1979), N.S. Choi and J. Heller (to ALZA Corporation).
8. L.M. Vistnes et al., *Surgery* **79**, 690–696 (1976).
9. R. C. Capozza, L. Sendelbeck, and W. J. Balkenhol, in R. J. Kostelnik, ed., *Polymeric Delivery Systems*, Gordon & Breach, New York, 1978, pp. 59–73.
10. B.B. Pharriss, V.A. Place, L. Sendelbeck, and E.E. Schmitt, *J. Reprod. Med.* **17**, 91–97 (1976).
11. E. Solheim, E.M. Pinholt, G. Bang, and E. Sudmann, *J. Neurosurg.* **76**, 275–279 (1992).
12. E. Solheim, E.M. Pinholt, G. Bang, and E. Sudmann, *J. Bone J. Surg. Am. Vol.* **74A**, 705–712 (1992).
13. E. Solheim, E.M. Pinholt, G. Bang, and E. Sudmann, *J. Biomed. Mater. Res.* **26**, 791–800 (1992).
14. E. Solheim et al., *J. Bone J. Surg. Am. Vol.* **74A**, 1456–1463 (1992).
15. E.M. Pinholt, E. Solheim, G. Bang, and E. Sudmann, *J. Oral Maxillofacial Surg.* **50**, 1300–1304 (1992).
16. B. Sudmann et al., *Acta Orthop. Scand.* **64**, 336–339 (1993).
17. M. Aaboe et al., *Clin. Oral Implant. Res.* **4**, 172–176 (1993).
18. E. Solheim et al., *J. Biomed. Mater. Res.* **29**, 1141–1146 (1995).
19. O. Bush, E. Solheim, G. Basng, and K. Tornes, *Int. J. Oral Maxillofacial Implants* **11**, 498–505 (1996).
20. S.Y. Ng, D.W.H. Penhale, and J. Heller, *Macromol. Synth.* **11**, 23–26 (1992).
21. J. Heller, B.K. Fritzinger, S.Y. Ng, and D.W.H. Penhale, *J. Controlled Release* **1**, 233–238 (1985).
22. J. Heller et al., *J. Controlled Release* **6**, 217 (1987).
23. J. Heller, in E. Chielini, P. Giusti, C. Migliaresi, and L. Nicolais, eds., *Polymers in Medicine II*, Plenum, New York, 1986, pp. 357–368.
24. R.V. Sparer, C. Shi, C.D. Ringeisen, and K.J. Himmelstein, *J. Controlled Release* **1**, 23–32 (1984).
25. C. Shi, S. Lucas, and G.M. Zentner, *J. Controlled Release* **15**, 55–63 (1991).
26. J. Heller, *J. Controlled Release* **2**, 167–177 (1985).
27. T.H. Nguyen, K.J. Himmelstein, and T. Higuchi, *Int. J. Pharm.* **25**, 1–12 (1985).
28. A.G. Thombre and K.J. Himmelstein, *AIChE J.* **31**, 759–766 (1985).
29. A. Joshi and K.J. Himmelstein, *J. Controlled Release* **15**, 95 (1991).
30. S.Y. Ng, T. Vandamme, M.S. Taylor, and J. Heller, *Macromolecules* **30**, 770–772 (1997).
31. J. Heller et al., *Contraception Delivery Syst.* **4**, 43–53 (1983).
32. J. Heller et al., in V.H.L. Lee, M. Hashida, and Y. Mizushima, eds., *Trends and Future Perspectives in Peptides and Protein Drug Delivery*, Harwood Academic Publishers, Chur, Switzerland, 1995, pp. 39–56.
33. M.B. Sintzel et al., *Biomaterials* **19**, 791–800 (1998).
34. Y.F. Maa and J. Heller, *J. Controlled Release* **13**, 11–19 (1990).
35. J. Heller et al., *J. Controlled Release* **16**, 3 (1991).
36. L.W. Seymour et al., *J. Controlled Release* **31**, 201–206 (1994).
37. G.M. Milne, Jr. and M.R. Johnson, *Annu. Rep. Med. Chem.* **11**, 23–32 (1976).
38. C.P. O'Brien, R. Greenstein, J. Ternes, and G.E. Woody, *Ann. N. Y. Acad. Sci.* **31**, 232–240 (1978).
39. C.N. Chiang, L.E. Holister, A. Kishimoto, and G. Barnett, *Clin. Pharmacol. Ther.* **36**, 704–708 (1984).
40. Y.F. Maa and J. Heller, *J. Controlled Release* **14**, 21–28 (1990).
41. J.M. Crampton, R. Galler, R.E. Sinden, and A. Crisanti, *Recherche* **259**, 1218–1227 (1993).
42. T.H. Vandamme and J. Heller, *J. Controlled Release* **36**, 209–213 (1995).
43. J. Du, B. Jasti, and R.C. Vasavada, *J. Controlled Release* **43** 223–233 (1997).
44. J. Heller, R.V. Sparer, and G.M. Zentner, in M. Chasin and R. Langer, eds., *Biodegradable Polymers as Drug Delivery Systems*, Dekker, New York, 1990, pp. 121–160.
45. R.H. Unger, *Diabetes* **31**, 479–483 (1982).
46. J. Heller, A.C. Chang, G. Rodd, and G.M. Grodsky, *J. Controlled Release* **13**, 295–302 (1990).
47. S.Y. Ng, T. Vandamme, M.S. Taylor, and J. Heller, in A. Prokop, D. Hunkeler, and A. Cherrington, eds., *Bioartificial Organs: Science, Medicine and Technology*, New York Academy of Sciences, Vol. 831, 1997, pp. 168–178.
48. M.B. Sintzel et al., *J. Controlled Release* **55**, 213–218 (1998).
49. J. Heller, S.Y. Ng, B.K. Fritzinger, and K.V. Roskos, *Biomaterials* **11**, 235–237 (1990).
50. A. Merkli, J. Heller, C. Tabatabay, and R. Gurny, *J. Controlled Release* **29**, 105–112 (1994).
51. J. Heller, S.Y. Ng, and B.K. Fritzinger, *Macromolecules* **25**, 3362–3364 (1992).
52. P. Wuthrich et al., *J. Controlled Release* **21**, 191–200 (1992).
53. A. Merkli, J. Heller, C. Tabatabay, and R. Gurny, *Biomaterials* **17**, 897–902 (1996).
54. A.U. Daniels et al., *J. Appl. Biomater.* **5**, 51–64 (1994).
55. J. Hoborn, *J. Pharm. Technol.* **6**, 34–35 (1985).
56. A. Merkli, J. Heller, C. Tabatabay, and R. Gurny, *Pharm. Res.* **11**, 1485–1491 (1994).
57. J. Urquhart, *Drugs* **23**, 207–226 (1982).
58. K.V. Roskos et al., *Biomaterials* **16**, 313–317 (1995).
59. I. Nakamitchi, M. Iwaku, and T. Fusayama, *J. Dent. Res.* **62**, 1076–1081 (1983).
60. D.E. Caldwell and B. Johannessen, *J. Dent. Res.* **50**, 1517–1525 (1971).
61. J. Heller et al., in T. Okano, N. Ogata, J. Feijen, and S.W. Kim, eds., *Advances in Biomedical Engineering and Drug Delivery Systems*, Springer-Verlag, Tokyo, 1996, pp. 106–110.
62. A.R. Bellows and A. Johnson, *Ophthalmology* **90**, 807–813 (1983).
63. P.H. Madsen, *Acta Ophthalmol., Suppl.* **120**, 88–91 (1973).
64. D.K. Heuer, R.K. Parish, II, and M.G. Gressel, *Ophthalmology* **91**, 384–394 (1984).
65. M.M. Tahery and D.A. Lee, *J. Ocular Pharmacol.* **5**, 155–179 (1989).
66. K.S. Mallick, A.S. Hajek, and R.K. Parish, II, *Arch. Ophthalmol.* **103**, 1398–1402 (1985).

67. M.G. Gressel, R.K. Parish, II, and R. Folberg, *Ophthalmology* **91**, 378–383 (1984).
68. D.K. Heuer, R.K. Parish, II, and M.G. Gressel, *Ophthalmology* **93**, 1537–1546 (1984).
69. The Fluorouracil Filtering Surgery Group, *Am. J. Ophthalmol.* **108**, 625–635 (1989).
70. D.A. Lee, P. Hersh, D. Kersten, and S. Melamed, *Ophthalmic Surg.* **18**, 187–190 (1987).
71. S.F. Bernatchez et al., *J. Biomed. Mater. Res.* **27**, 677–681 (1993).
72. S.F. Bernatchez et al., *J. Biomed. Mater. Res.* **28**, 1037–1046 (1994).
73. C.M. Hutak and R.B. Jacaruso, in I.K. Reddy, ed., *Ocular Therapeutics and Drug Delivery*, Technomic Publishing, Basel, 1996, pp. 489–525.
74. M. Zignani et al., *J. Biomed. Mater. Res.* **39**, 277–285 (1998).
75. H.F. Smyth, Jr. et al., *Toxicol. Appl. Pharmacol.* **15**, 282–286 (1969).

See also BIODEGRADABLE POLYMERS: POLY(PHOSPHOESTER)S; BIODEGRADABLE POLYMERS: POLYANHYDRIDES; BIODEGRADABLE POLYMERS: POLYESTERS.

POLYMERIC SYSTEMS FOR GENE DELIVERY, CHITOSAN AND PINC SYSTEMS

FIONA C. MACLAUGHLIN
ALAIN P. ROLLAND
Valentis, Inc.
The Woodlands, Texas

KEY WORDS

Chitosan
Complexation
Condensation
Controlled gene delivery
DNA plasmid
Gene delivery
Gene therapy
Muscle
Nonviral gene therapy
PINCs™
Polymers
Poly(*N*-vinyl pyrrolidone)

OUTLINE

Protective Interacting Noncondensing Systems
Chitosan
Bibliography

The concept of using DNA as a predrug for the prevention, correction, or modulation of genetic and acquired diseases is becoming increasingly promising with the advent of the human genome project and the resulting greater understanding of diseases. By controlling gene expression, it is possible to act on diseases at their genetic origin, thus minimizing nonspecific side effects that conventional therapies often induce. In essence, gene therapy involves the replacement or correction of a defective gene in somatic cells and is not necessarily a permanent means of treatment. For a therapeutic gene to be effective, it must be carefully selected and cloned in a plasmid-based expression system, efficiently delivered to the target cells in sufficient copy numbers, produce sufficient amounts of the required protein over a reasonable time-frame, and furthermore, must not induce any undesirable side effects. The determinants of a gene delivery system can be described by the acronym DART: it must control distribution (D) of the plasmid, access (A) to the cell, or recognition by a cell-surface receptor (R) with intracellular trafficking, and final nuclear translocation (T). The essential components of a plasmid expression system are the gene to be expressed, coupled with necessary control sequences (ART). The protein must be produced in controlled amounts (A) and regulated in a cell- or disease-specific manner (R), with controlled timing (T). Delivery and expression elements have to be rationally designed and assembled together to address the key limiting steps in gaining access from the site of administration to the nucleus of the target cell. The question of delivery is challenging from the fact that a plasmid is a negatively charged hydrophilic macromolecule with a large hydrodynamic size (up to 200 nm); for it to be effective, it must cross a negatively charged surface, the cell membrane. Additionally, after systemic administration, other barriers include opsonization and clearance by the reticuloendothelial system (RES), and rapid degradation by extra- and intracellular nucleases. Because viruses possess sophisticated mechanisms that allow for their effective access to many cells, nonviral gene delivery systems and artificial viruslike structures have been developed using synthetic or semisynthetic materials to mimic some of the viral functions. Nonviral delivery systems have a number of advantages over viral systems. For instance, the plasmid in a nonviral delivery system rarely integrates into the host chromosome, persisting instead as an episome. Few limitations are also placed on the type and size of gene construct. The delivery systems are generally safe, effective in animal models, and can be repeatedly administered. However, it is not yet possible in most cases to meet the high transfection efficiencies demonstrated with viral vectors. Attractive targets for nonviral therapies include directly accessible tissues such as the lungs, skin, solid tumor, and muscle, as well as normal and proliferating endothelia by systemic administration.

Microinjection and calcium phosphate precipitation are well-established techniques for transferring DNA into cells in vitro but are not applicable for in vivo gene therapy. Recent methods shown to enhance transfection include electroporation (1,2), sonoporation (3), and needle-free jet injection (4). Suitable delivery systems include liposomes and cationic lipids (5,6), and cationic (7,8) and uncharged polymers (9), poly(peptides), or lipo(polypeptides) (10). A plasmid is not efficiently encapsulated within liposomes, nonetheless, detectable levels of human α-1 antitrypsin were measured in plasma after intravenous administration in mice (11). Cationic lipids and lipopolyamines were

67. M.G. Gressel, R.K. Parish, II, and R. Folberg, *Ophthalmology* **91**, 378–383 (1984).
68. D.K. Heuer, R.K. Parish, II, and M.G. Gressel, *Ophthalmology* **93**, 1537–1546 (1984).
69. The Fluorouracil Filtering Surgery Group, *Am. J. Ophthalmol.* **108**, 625–635 (1989).
70. D.A. Lee, P. Hersh, D. Kersten, and S. Melamed, *Ophthalmic Surg.* **18**, 187–190 (1987).
71. S.F. Bernatchez et al., *J. Biomed. Mater. Res.* **27**, 677–681 (1993).
72. S.F. Bernatchez et al., *J. Biomed. Mater. Res.* **28**, 1037–1046 (1994).
73. C.M. Hutak and R.B. Jacaruso, in I.K. Reddy, ed., *Ocular Therapeutics and Drug Delivery*, Technomic Publishing, Basel, 1996, pp. 489–525.
74. M. Zignani et al., *J. Biomed. Mater. Res.* **39**, 277–285 (1998).
75. H.F. Smyth, Jr. et al., *Toxicol. Appl. Pharmacol.* **15**, 282–286 (1969).

See also BIODEGRADABLE POLYMERS: POLY(PHOSPHOESTER)S; BIODEGRADABLE POLYMERS: POLYANHYDRIDES; BIODEGRADABLE POLYMERS: POLYESTERS.

POLYMERIC SYSTEMS FOR GENE DELIVERY, CHITOSAN AND PINC SYSTEMS

FIONA C. MACLAUGHLIN
ALAIN P. ROLLAND
Valentis, Inc.
The Woodlands, Texas

KEY WORDS

Chitosan
Complexation
Condensation
Controlled gene delivery
DNA plasmid
Gene delivery
Gene therapy
Muscle
Nonviral gene therapy
PINCs™
Polymers
Poly(*N*-vinyl pyrrolidone)

OUTLINE

Protective Interacting Noncondensing Systems
Chitosan
Bibliography

The concept of using DNA as a predrug for the prevention, correction, or modulation of genetic and acquired diseases is becoming increasingly promising with the advent of the human genome project and the resulting greater understanding of diseases. By controlling gene expression, it is possible to act on diseases at their genetic origin, thus minimizing nonspecific side effects that conventional therapies often induce. In essence, gene therapy involves the replacement or correction of a defective gene in somatic cells and is not necessarily a permanent means of treatment. For a therapeutic gene to be effective, it must be carefully selected and cloned in a plasmid-based expression system, efficiently delivered to the target cells in sufficient copy numbers, produce sufficient amounts of the required protein over a reasonable time-frame, and furthermore, must not induce any undesirable side effects. The determinants of a gene delivery system can be described by the acronym DART: it must control distribution (D) of the plasmid, access (A) to the cell, or recognition by a cell-surface receptor (R) with intracellular trafficking, and final nuclear translocation (T). The essential components of a plasmid expression system are the gene to be expressed, coupled with necessary control sequences (ART). The protein must be produced in controlled amounts (A) and regulated in a cell- or disease-specific manner (R), with controlled timing (T). Delivery and expression elements have to be rationally designed and assembled together to address the key limiting steps in gaining access from the site of administration to the nucleus of the target cell. The question of delivery is challenging from the fact that a plasmid is a negatively charged hydrophilic macromolecule with a large hydrodynamic size (up to 200 nm); for it to be effective, it must cross a negatively charged surface, the cell membrane. Additionally, after systemic administration, other barriers include opsonization and clearance by the reticuloendothelial system (RES), and rapid degradation by extra- and intracellular nucleases. Because viruses possess sophisticated mechanisms that allow for their effective access to many cells, nonviral gene delivery systems and artificial viruslike structures have been developed using synthetic or semisynthetic materials to mimic some of the viral functions. Nonviral delivery systems have a number of advantages over viral systems. For instance, the plasmid in a nonviral delivery system rarely integrates into the host chromosome, persisting instead as an episome. Few limitations are also placed on the type and size of gene construct. The delivery systems are generally safe, effective in animal models, and can be repeatedly administered. However, it is not yet possible in most cases to meet the high transfection efficiencies demonstrated with viral vectors. Attractive targets for nonviral therapies include directly accessible tissues such as the lungs, skin, solid tumor, and muscle, as well as normal and proliferating endothelia by systemic administration.

Microinjection and calcium phosphate precipitation are well-established techniques for transferring DNA into cells in vitro but are not applicable for in vivo gene therapy. Recent methods shown to enhance transfection include electroporation (1,2), sonoporation (3), and needle-free jet injection (4). Suitable delivery systems include liposomes and cationic lipids (5,6), and cationic (7,8) and uncharged polymers (9), poly(peptides), or lipo(polypeptides) (10). A plasmid is not efficiently encapsulated within liposomes, nonetheless, detectable levels of human α-1 antitrypsin were measured in plasma after intravenous administration in mice (11). Cationic lipids and lipopolyamines were

designed to overcome some of the problems associated with liposomal delivery and were shown to condense DNA into small particulates (12–14). Neutral lipids such as dioleoylphosphatidylethanolamine (DOPE) and cholesterol are often included in such complexes, either to stabilize the complex or affect plasmid intracellular trafficking. High levels of cellular uptake and subsequent expression have been measured in vitro (6,15) and in vivo, for example, after aerosol administration into the lung (16). The only nonviral delivery systems currently used in clinical settings are cationic lipids (17,18). Polymers that can be classified as either condensing or noncondensing polymers have been used recently with increasing success, resulting in positive gene expression in vivo (Table 1). Condensing polymers such as poly(vinyl pyridinium), hydroxylated nylons, polybrene, polyethyleneimine, and linear and cascade polyamidoamine dendrimers (Fig. 1) typically compact DNA via electrostatic interaction between the DNA phosphates and the positively charged groups present in the polymer. Polyamidoamine dendrimers are examples of cascade polymers that evolve from a central core by controlled chemical reaction to produce a molecule with a defined number of generations. They possess multiple terminal amine groups that have pK_a's of 6.9 and 3.9, so that at physiological pH these polymers are only partially protonated. The successful use of these polymers was first described by Haensler and Szoka who showed that in vitro transfection using a sixth-generation polymer was 1,000-fold and 100-fold higher than when using poly-L-lysine and a DOTMA-based system, respectively (7). Polyethyleneimine (PEI) was also selected on the basis that it had a large reservoir of cationic charge, because at physiological pH every sixth amine is protonated. PEI was shown to condense DNA into particulates of 0.1–1 μm in size. Boussif et al. injected such complexes into the brains of newborn mice, and luciferase expression was observed in the brain fractions of the mice at 24 h (8). Transfection was also observed in adult brain; the highest expression was measured when formulations of charge ratios closest to neutral, using a 25-kDa molecular weight polymer, had been administered (19). Expression was observed up to 3 months after injection. Kabanov et al. have described the use of polyvinylpyridinium-based polymers for plasmid delivery, and proposed that, upon complexation with plasmid, hydrophobic interpolyelectrolyte complexes form (20). Only complexes with an excess of positive charges were efficiently transfected in NIH3T3 cells. The correlation between complex charge and transfection efficiency was later described (21). One limitation in the use of these complexes is their instability under physiological conditions. Their use in vivo has not been described to date. Such cationic polymer-based systems can also provide the basis for introduction of other agents including endosomolytic molecules and ligands. Ligand-based systems have been synthesized in which transferrin (22–24) and asialoorosomucoid (25–26) have been chemically conjugated to DNA plasmid/poly-L-lysine complexes, and specific uptake in vitro and in vivo has been observed. Endosomolytic agents such as heat-inactivated adenoviruses or synthetic viral peptides have also been conjugated to the complexes and shown to enhance expression (27–29).

This article focuses on the noncondensing PINC™ polymeric systems and the condensing polymer chitosan. The physical characteristics of both polymers are extremely different, and the use of these delivery systems has provided some promising results and an increased understanding of the properties required for enhanced in vivo gene transfer.

PROTECTIVE INTERACTING NONCONDENSING SYSTEMS

In skeletal muscle, the poor bioavailability of unformulated plasmid together with low and highly variable levels of expression are thought to be due to rapid degradation of plasmid by extracellular nucleases, which potentially occurs within minutes (30–33). Typically, less than 0.1% of the injected dose is taken up by muscle cells, and gene expression is limited to the myotubes located in the vicinity of the needle tract (30). By condensing the plasmid with cationic agents, such a stability problem might be overcome. However, in muscle, condensed plasmid does not diffuse easily through the extracellular matrix and gain access to the caveolae and T tubules (33). Protective interactive noncondensing polymers (PINCs), typically polyvinyl derivatives, were first reported for use as gene delivery agents in muscle by Mumper et al. (9,34). They have low toxicity, are biologically and chemically inert, and have the ability to stabilize proteins (35). PINCs are amphiphilic molecules that possess hydrophilic and hydrophobic regions (36–38). Among such PINC polymers, poly(vinylpyrrolidone) (PVP) is an example of a hydrogen-bond acceptor, and poly(vinyl alcohol) (PVA) is a hydrogen-bond donor. Potentially the hydrophilic portion interacts with DNA by Van der Waals or by hydrogen bonding, because DNA can function as either a hydrogen bond donor or acceptor. Such polymers have been shown by isothermal microtitration calorimetry, Fourier transform infrared spectroscopy, and dynamic dialysis to interact with DNA via hydrogen bonding, allowing the DNA to be maintained in a flexible form that can diffuse readily through muscle (39).

Molecular modeling showed that by placing PVP in a minimized conformation at pH 4 in the vicinity of DNA, PVP aligned itself in the major groove of the DNA model, permitting H bonds to form (Fig. 2). The vinyl portion of the PVP forms a hydrophobic shield around the DNA helix that may protect the plasmid from nuclease degradation and render the plasmid surface more hydrophobic (40). Similar hydrophobic regions were proposed by Kabanov et al. to form upon complexing pyridinium-containing polymers with plasmid (20,41). It was suggested that this enhanced hydrophobicity enabled adsorption to the cell membrane and hence facilitated uptake and gene expression. Zeta potential measurements showed that changes in the surface charge properties of the plasmid occurred upon complexation (40). In water, the zeta potential of PVP only decreased from +8.7 mV at pH 4 down to −5.8 mV at pH 7, indicating a small positive charge at lower pH due to the protonation and resonance between carbonyl groups of adjacent pyrrolidone monomers. Despite this slight positive charge, there was no evidence by laser light scattering that PVP condensed plasmid into particulates. The zeta potential of PVP only did not change over the pH range 4.5–7.5 in the presence of salt, supporting the fact that in a

Table 1. Polymers for Nonviral Gene Delivery

Polymer	Gene	In vitro	In vivo	Route	Species	References
Polyethyleneimine (PEI)	pCMV-*Luc*		Brain	Intracerebral	Adult rat	Abdallah et al. (19)
	Luciferase		Brain	Intracerebral	Newborn rat	Boussi et al. (8)
	Luciferase	3T3, HepG2, Cos-7, HeLa, MRC5, K562				Boussif et al. (8)
PEI/transferrin/antiCD3	Luciferase	Neuro 2A neuroblastoma, K562, Jurkat E6.1				Kircheis et al. (119)
pHPMA-pTMAEM	pCMV-β-*gal*	A2780, 293				Wolfert and Seymour (86)
pDMAEMA	pCMV-*lacZ*	Cos-7 cells				Cherng et al. (120)
pDMAEMA	pCMV-*lacZ*	Cos-7, OVCAR-3				van de Wetering et al. (121)
PEVP/PEVP-C	pBC16	*Bacillus subtilis*				Kabanov et al. (20)
	pCAT-*4XB*	NIH3T3, MDCK, Jurkat				Kabanov et al. (21)
PEVP/Pluronic P85	pRSV-CAT	NIH3T3, MDCK, Jurkat				Astafieva et al. (122)
Dendrimers	Luciferase	CV-1				Haensler and Szoka (7)
	Luciferase	Rat2				Kukowska-Latello et al. (123)
	pCAT		SCCVII tumor	Intratumoral	Mice	R. J. Mumper et al. (unpublished)
Fractured dendrimers		CV-1				Tang et al. (124)
Hydroxylated nylons/PolyCAT57	Luciferase	Human sarcoma HT-1080				Goldman et al. (125)
Chitosan	Luciferase	Cos-1				MacLaughlin et al. (84)
	pGFP	HEK293				Roy et al. (91)
Gelatin	pSA306 CFTR	3THE				Walsh et al. (126)
	pSA306 CFTR		Lungs	Bronchoscopy	New Zealand rabbits	Walsh et al. (126)
	pRSVLuc	HEK 293				Truong-Le et al. (127)
PINCs (PVP)	hIGF-I		Muscle	Intramuscular	Rats	Alila et al. (45)
	hGH, hFIX		Muscle	Intramuscular	Rats	Anwer et al. (44)
	INF-α		SCCVII tumor	Intratumoral	Mice	Coleman et al. (46)
Polybrene	β-*gal*	HUVEC				Sipehia and Martucci (128)

Note: Polyethyleneimine (PEI), poly-*N*-(-2-hydroxypropyl)methacrylamide-co-poly(trimethylammonioethyl methacrylate chloride) (pHPMA-pTMAEM); poly(2-dimethylamino)ethyl methacrylate (pDMAEMA); poly(*N*-ethyl-4-pyridinium) bromide (PEVP); poly(*N*-ethyl-4-pyridinium)-co-vinyl(*N*-cetyl-4-pyridinium) bromide (PEVP-C), protective interactive noncondensing (PINCs) polymers; polyvinyl pyrrolidone (PVP).

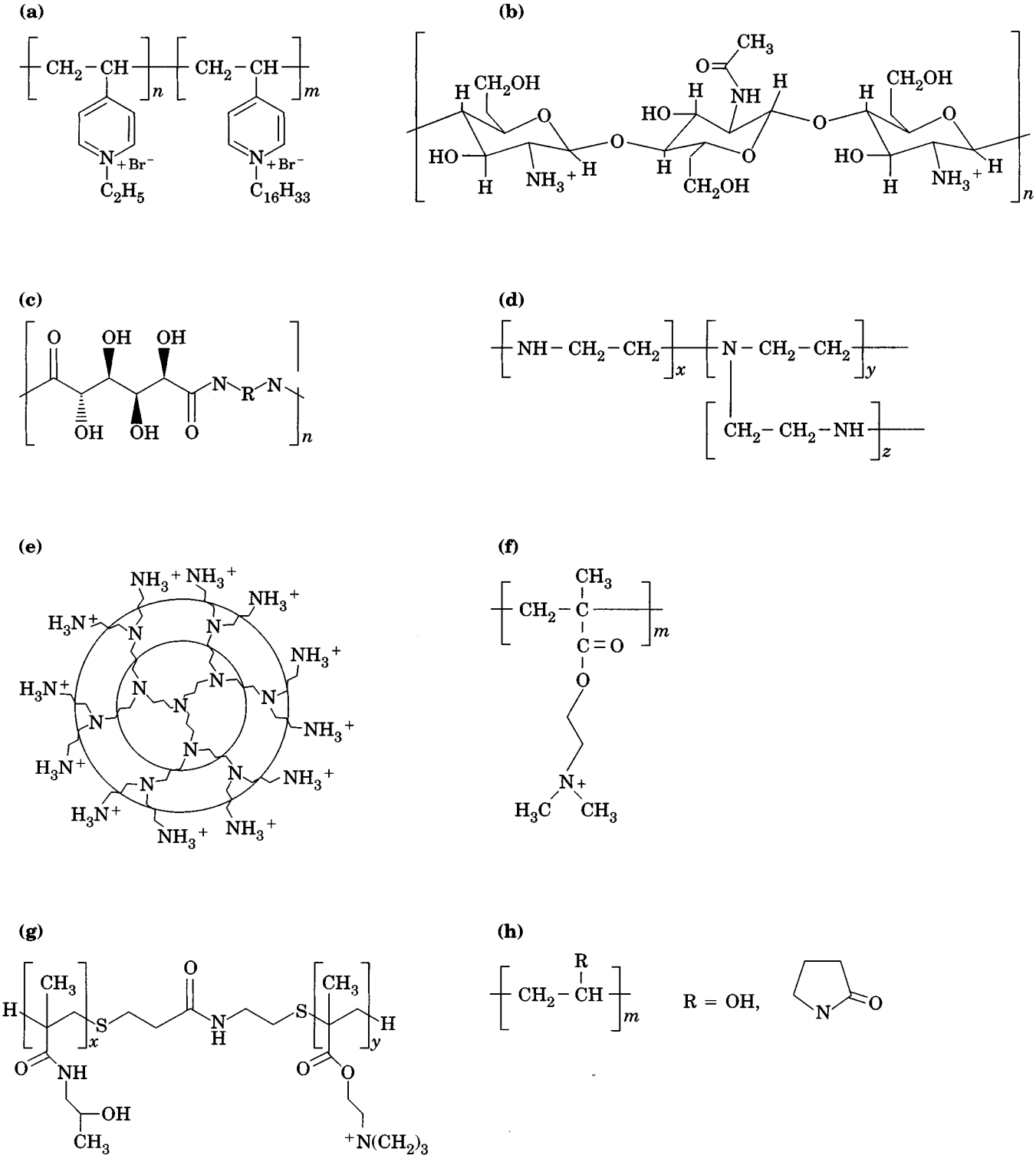


Figure 1. Structure of polymeric gene delivery systems: (**a**) poly(*N*-ethyl-4-vinylpyridinium)-covinyl(*N*-cetyl-4 pyridinium) bromide (PEVP-C); (**b**) chitosan; (**c**) hydroxylated nylons where R is linear alkylenediamines, branched alkylenediamines, arylalkylenediamines, or diamines with oxygen or nitrogen atoms in the alkylene chain; (**d**) polyethyleneimine; (**e**) polyamidoamine dendrimers; (**f**) poly(2-dimethylamino)ethyl methacrylate (pDMAEMA); (**g**) poly-*N*-(2-hydroxypropyl)methacrylamine-co-poly(trimethylammonio ethyl methacrylate chloride) (pHPMA-pTMAEM); (**h**) polyvinyl-based polymers where R is OH (polyvinyl alcohol [PVA]) or pyrrolidone (polyvinyl pyrrolidone [PVP]).

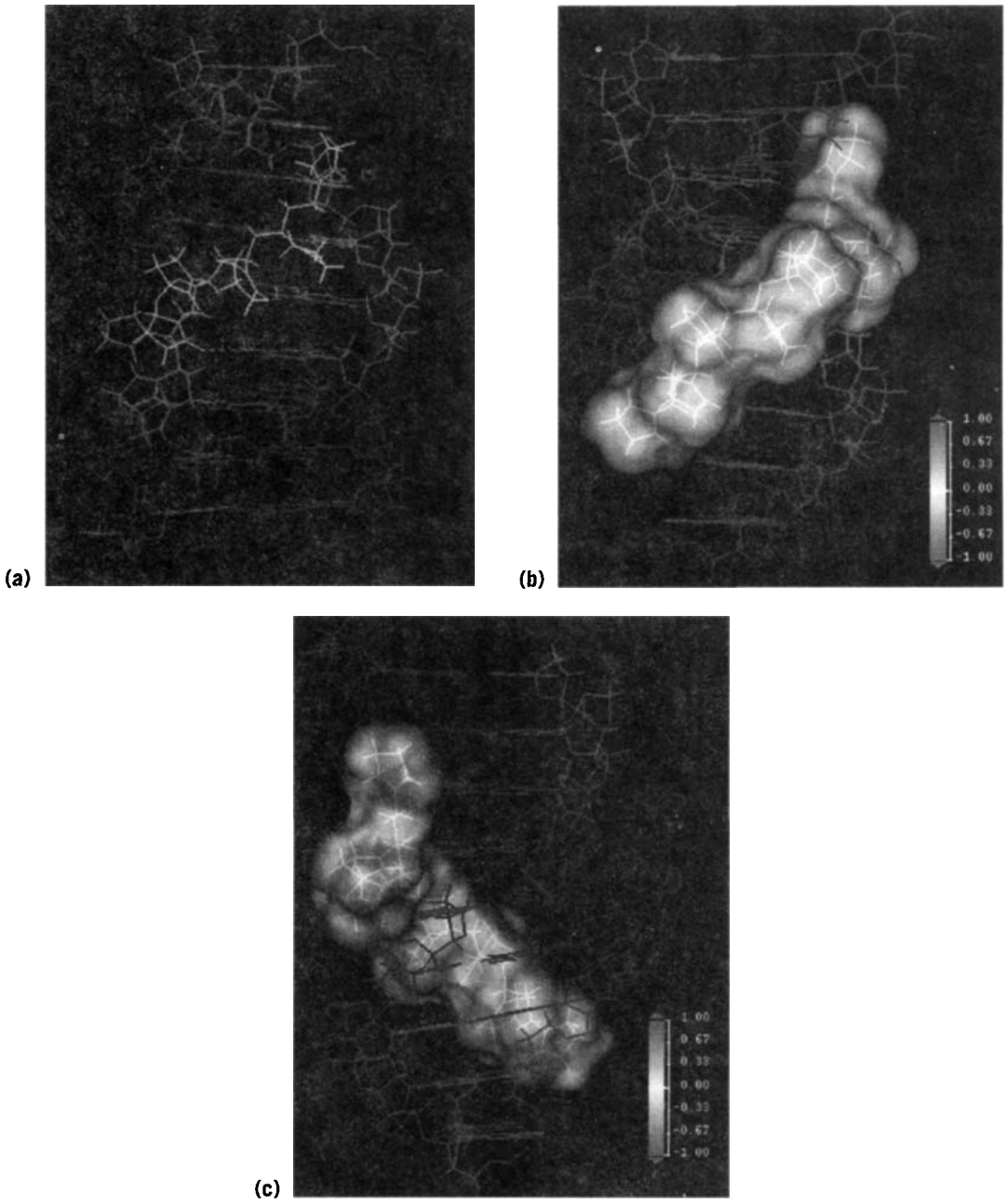


Figure 2. Molecular modeling of PVP–DNA interactions. (**a**) An oligomer of PVP (white) was minimized in the major groove of a plasmid at pH 4.0. The conformation of DNA was fixed, and the PVP was allowed to adopt a low energy conformation at pH 4.0. A number of hydrogen-bonding interactions can occur (hydrogen-bonding distances shown). (**b**) Connelly surface of PVP looking at a PVP coating of DNA. (**c**) Connelly surface of PVP looking through DNA with a coating of PVP. The surface has been colored to approximate the hydrophobic nature of the atoms, with dark gray being hydrophilic and white being more hydrophobic.

salt-containing medium, hydrophobic bonds potentially contribute to the complexation with plasmid. As increasing quantities of PVP were added to the plasmid in water, the zeta potential became increasingly neutral, indicating that the anionic phosphates were shielded. An ethidium bromide assay also indicated that PVP did not tightly condense plasmid. Upon adding increasing amounts of PVP to preformed or postformed complexes in water, an exponential inhibition of fluorescence was observed, suggesting quenching of the fluorescence rather than inhibition of intercalation of ethidium bromide. The reduction in fluorescence was much less when the complexes were formed in water initially and then made isotonic (150–500 mM) by the addition of 5 M NaCl, and was completely abolished

when the complexes were formed in HEPES buffer at pH 7.3.

As well as protecting the plasmid from nuclease degradation in vitro (39), PINCs have been shown to enhance the extent and levels of gene expression in a reproducible manner in muscle. Comparison of β-galactosidase expression in rat tibialis showed that upon administration of plasmid in saline (so-called naked DNA) (150 μg/50 μL), expression appeared to be low and localized around the needle tract, agreeing with previous studies (42,43). When plasmid was formulated with PVP in 150 mM saline (1:17 w/w), the number of fibers that expressed β-galactosidase was significantly higher (approximately 1 log), as was the distribution of expression. This could be due to increased protection against nuclease degradation as well as to hyperosmotic effects of the formulation. Variables shown to influence the extent of gene expression in muscle include PVP molecular weight and concentration, formulation pH and osmolality, and method of formulation. Maximal gene expression (typically 10-fold higher than with saline) was achieved using a 5% (w/v) polymer concentration (at 3 mg/mL DNA). Expression levels decreased as the polymer concentration increased (39). Formulations containing 5% PVP (50 kDa) produced higher expression than those formulations containing 10-kDa PVP (39). This was thought to be due to the ability of higher molecular weight PVP to bind plasmid more efficiently, as also observed with other drugs. Higher expression was observed using formulations of pH 3.75 rather than pH 5.8 or higher, and similarly with formulations of 500 mM osmolality compared with formulations of 150 mM osmolality.

The use of poly(vinyl pyrrolidone) to deliver a muscle-specific gene medicine for long-term secretion of human growth hormone (hGH) from muscle into the systemic circulation has been reported (44). Skeletal muscle is a convenient and useful site of administration for gene therapy because some proteins expressed in muscle can be secreted into the systemic circulation. In addition, intramuscular administration of gene medicines also provides a useful approach for the treatment of local neuromuscular disorders or, alternatively, for the administration of a genetic vaccine. A plasmid with a muscle-specific promoter encoding human growth hormone was injected into the tibialis muscle of normal rats (150 μg/50 μL). In comparison with naked DNA in saline, the plasmid formulated with PVP (1:17 w/w) produced over a 10-fold increase in the levels of hGH protein detected in muscle. The plasmid expression system was shown to be muscle specific, with no detectable expression after administration in the lung or in the liver. The influence of the same formulation in hypophysectomized rats was also determined after intramuscular administration. In tibialis muscle, mRNA was detectable by RT-PCR 7 days postinjection. The levels of mRNA remained the same for 14 days and then decreased to lower levels at day 21. A statistically significant increase in growth rate was observed in those rats treated with the PVP-formulated plasmid. The inclusion of a chicken skeletal α-actin 3′-UTR in the plasmid further enhanced expression of hGH. The low levels of hGH in serum were difficult to detect, although it was evident that the expressed hGH was biologically active, because elevated levels of endogenous IGF-I and an increase in growth of the animals was observed. Difficulty in detecting levels of hGH protein may have been caused by the rapid clearance of the plasmid, its short half-life in blood, and/or the production of antibodies. For instance, it was evident that the administration of hGH plasmid resulted in production of serum hGH antibodies at day 14 that increased and plateaued at day 21 up to day 35 (Fig. 3a). Cyclosporin A was administered as an immunosuppressant once every other day for 10 days after plasmid administration (Fig. 3b). The antibody response was then totally inhibited, and increased levels of hGH mRNA were correspondingly detected. PINCs have also been used for delivering human

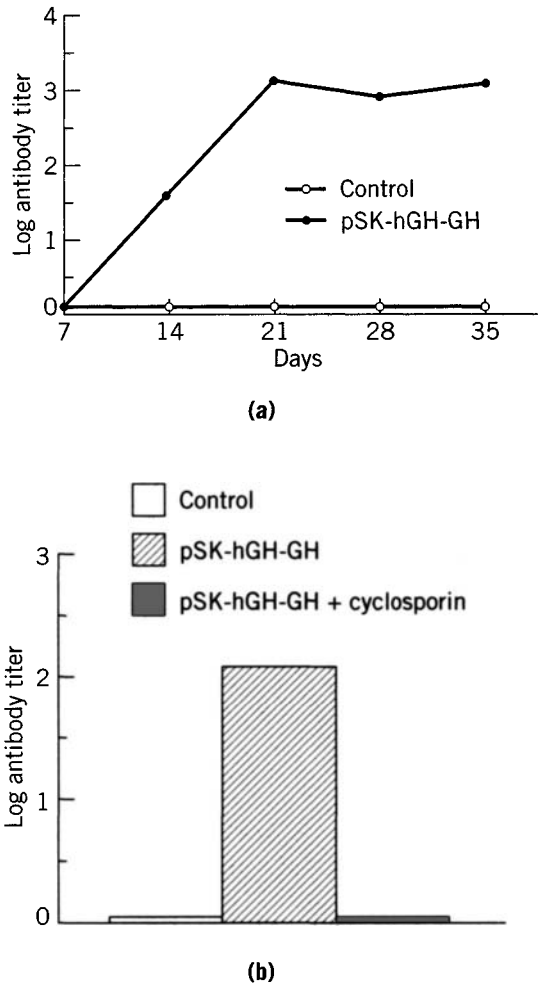


Figure 3. Production of serum anti-hGH antibodies after intramuscular administration of pSK-hGH-GH complexed with PVP. (**a**) Levels of anti–hGH antibodies 0, 7, 14, 21, 28, and 35 days after a single intramuscular injection of pSK-hGH-GH or control plasmid. Values are the average of two separate experiments; in each experiment the antibody titer was determined in pooled sera samples from five individual animals. (**b**) Effect of cyclosporin (5 mg/kg) on antibody response at day 35. Cyclosporin was given intramuscularly once every second day for 10 days (a total of five injections) after plasmid injection. The antibody titer was determined in pooled sera samples from five individual animals in each group.

factor IX gene, whose protein has a longer half-life than hGH. Detectable plasma levels of factor IX were measured at day 21 and increased up to day 29. Expression levels were 10- to 100-fold lower when this plasmid was injected in saline only (45).

An IGF-I gene medicine with reduced systemic toxicity was also developed based on a muscle-specific gene expression system formulated with a PINC polymer (45). The intent was to increase the therapeutic index of IGF-I by restricting local expression. When the human IGF-I plasmid was formulated with PVP, IGF-I protein and mRNA were measured in muscle for at least 28 days. The replacement of the skeletal α-actin 3′-UTR with an hGH 3′-UTR enhanced the secretion of IGF-I, thus improving biological activity. IGF-I plasmid, formulated with PVP, was administered to mice subjected to sciatic nerve crush injury. The formulations were administered intramuscularly every 7 days after nerve crush (E.D. Rabinovsky et al., unpublished data). Treated animals showed an increase and full recovery in gastrocnemius muscle mass, and the nerve conduction velocity in the muscle showed remarkable improvement. Expression of IGF-I plasmid peaked 7–14 days after injection and started to decrease at day 28.

Owing to the success achieved in muscle with PINC systems, such polymers have also been investigated for plasmid delivery to other solid tissues with a dense extracellular matrix, such as solid tumors (46). PINC polymers have been shown to enhance the extent and levels of expression in various mouse solid tumors as compared with naked DNA (Fig. 4).

Renca (murine renal cell carcinoma) and TS/A (differentiated mammary adenocarcinoma) tumors (10 mm^3) implanted in mice were treated using a plasmid encoding IFN-α. The tumors were harvested at 24 h, made into a single-cell suspension, and the supernatants were assayed. Tumors treated with the IFN-α/PVP formulation expressed active IFN-α; however, those that were treated with a control "empty" plasmid did not. The treatment regimen for measuring antitumor activity involved injecting the tumors eight times (four times per week), starting 7 days after challenging Balb/c mice with Renca or TS/A cells. The inhibition of tumor growth increased as the dose of administered plasmid increased (Fig. 5). In those animals implanted with Renca cells, inhibition of tumor growth was observed in 100% of the cases, with a 30% remission of tumors in those animals treated with the IFN-α/PVP formulation. When rechallenged 40–50 days later with the same cell line, all the mice that rejected the primary tumors were protected against this challenge, indicating a systemic immune response. Naïve mice were not protected. These results indicate that PINC systems can also be successfully applied to deliver expression plasmids to other target tissues such as solid tumors.

The uses of PVP as a gene delivery system have been well described, but it is necessary to determine if it is possible to improve its activity by replacing or substituting some of the polymer backbone. By substituting some of the vinyl pyrrolidone units with vinyl acetate groups, a decrease in hydrogen-bonding ability was accompanied by a decrease in gene expression. All formulations were formulated at the same pH and had similar viscosities. The structure–activity relationship (SAR) is shown in Figure 6 as the relationship between polymer structure and expression of β-galactosidase in the tibialis muscle of rats (47). Interestingly, when PVA, a hydrogen bond donor, was formulated with plasmid, higher levels of expression than with PVP were attained in skeletal muscle. A potential "interactive window of opportunity" was defined, such that by enhancing the interaction between the plasmid and the polymer, gene expression would be enhanced, but a point would be reached where the strength of interaction would

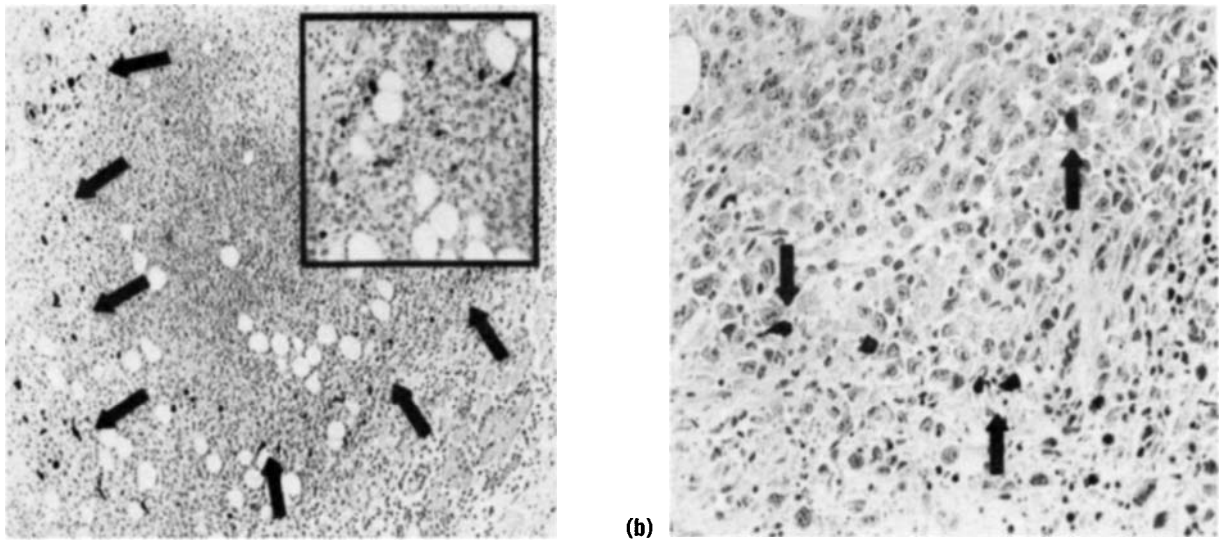


Figure 4. Immunohistochemical staining of paraffin cross sections (4 μm) for CAT in SCCVII tumors in C3HN mice, 24 h after intratumoral injection. (**a**) CMV-CAT (140 μg/50 μL) complexed with 3% PVA in 150 mM NaCl (4× magnification). Insert (40× magnification). (**b**) CMV-CAT (140 μg/50 μL) in saline (20× magnification).

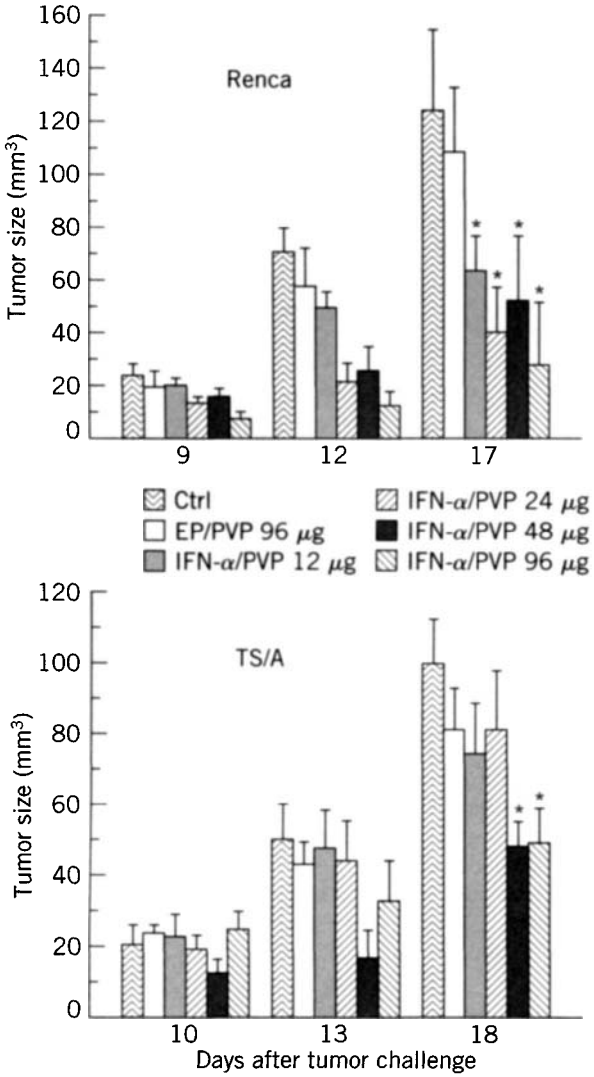


Figure 5. Induction of tumor growth inhibition following intratumoral injection of IFN-α/PVP. Renca and TS/A tumors were initiated by subcutaneous injection of 7×10^5 and 1×10^5, respectively, in BALB/c mice. Tumors were treated with scalar doses of IFN-α/PVP (from 12–96 μg) or empty plasmid (EP)/PVP (96 μg). Treatments started 7–8 days after tumor challenge when tumor size was approximately 10 mm^3, and repeated at 1- 2-day intervals four times per week for 2 weeks (total of eight treatments). Representative experiments are shown (five mice per group). Each experiment has been reproduced twice. ($^*p < 0.05$).

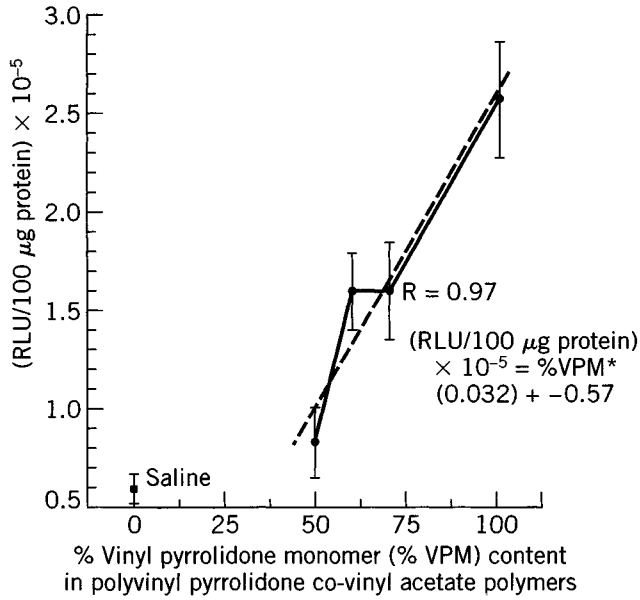


Figure 6. β-Galactosidase expression in rat tibialis muscle at 7 days after intramuscular injection of plasmid (150 μg/50 μL) complexed with copolymers (1:17 w/w) and formulated in 150 mM NaCl. β-Galactosidase expression is plotted as a function of the percentage vinyl pyrrolidone monomer (% VPM) content in the poly(vinyl pyrrolidone-covinyl acetate) polymers (●). The pH values (pH 3.7–4.0) of copolymer formulations and their viscosities were identical. These data are compared to β-galactosidase expression with a saline formulation at pH 6.5 (■). Results reported as mean ± S.E.M. (n = 10 rats).

inhibit gene expression (40,47). This SAR is being used at Valentis, Inc. (The Woodlands, Texas) to further design and synthesize novel PINCs that potentially will enhance gene expression. By enhancing the interaction between the plasmid and the polymer, it is envisaged that plasmid will remain protected from nuclease degradation but will promote more efficient gene transfer in vivo.

CHITOSAN

The concept of using chitosan and its derivatives as DNA delivery systems was introduced by Mumper et al. (9). Chitosan is a polysaccharide composed of two subunits, D-glucosamine and *N*-acetyl-D-glucosamine, linked together by $\beta(1,4)$ glycosidic bonds (Fig. 1). Chitosan is derived from chitin, a constituent of crustacean shells and the second most universally abundant biopolymer, next to cellulose. The potential availability of the raw material chitin therefore does not pose a problem, and over 1 billion tons of chitin is produced annually at low cost. The extraction process of chitin involves crushing the shells and removing proteins and minerals. Chitosan is formed upon deacetylation of chitin by treatment with sodium hydroxide at high temperature (48). Chitin and chitosan are copolymers: chitin is poly-*N*-acetylglucosamine with a small amount of deacetylation. Chitosan is the partially deacetylated derivative that is not polyglucosamine. Chitosan of 10,000–1 million Da can be readily made, with typical degrees of deacetylation in the 70–90% range. It is insoluble in water, alkalis, and organic solvents and requires the aid of select organic acids, such as acetic or formic acids, for solubilization. Other organic acids, for example, sulphuric and phosphoric acids, fail to dissolve chitosan. Due to its high molecular weight and integration of long unbranched chains, chitosan solutions are extremely viscous. Once in solution, chitosan behaves as a linear polyelectrolyte and a weak base; the amino groups present in the N-deacetylated subunits confer a highly positive charge density. A typical polyelectrolyte will exist in an extended conformation in the absence of salts due to the natural repulsion

of like charged groups, in this case the amino groups. Once salt is introduced into the media, the ions neutralize the charged groups and thus reduce repulsion, which allows the polyelectrolyte to exist in a more random coil-type orientation. If too much salt is added, the polymer will precipitate out of solution by a salting-out mechanism.

Chitosan has been used as a drug delivery system (49–51), an excipient in controlled release systems (52–55), a biological membrane (56), and wound dressings (57), and for potential cell targeting (58). Chitosan microspheres have been formulated using different preparation techniques for the controlled release of drugs such as prednisolone sodium phosphate (53) and anticancer agents (52,54). Chitosan has been indicated in preventing and treating peptic ulceration while also acting as a demulcent (57). The gastric mucosa was protected by chitosan after oral administration of ethanol in rats. Also used as a thickening, suspending, and stabilizing agent (59), a chelating agent for removal of harmful metals in industrial and chemical wastes (60), and as a support for ion exchange and affinity chromatography (61), this agent appears to have extreme diversity. By coating liposomes with polymers such as chitosan, their stability can be improved (62–64). Potentially, such liposomes can be used topically for treating wounds and burns (63) and for cell targeting (62). Takeuchi et al. demonstrated that by increasing the presence of chitosan on the surface of liposomes, they became increasingly mucoadhesive in rat intestinal mucosa (62). The liposomes were loaded with insulin and administered orally in rats. Relative to uncoated liposomes, a prolonged reduction in the basal blood glucose levels was achieved (62).

Chitosan is an approved food additive in Japan and in the United States, and it is generally considered to be nontoxic (57,59,65). It is degraded by lysozymes (enzymes present in serum, saliva, and other body fluids) into oligomers, which are further hydrolyzed to *N*-acetyl glucosamine, a common amino acid sugar in the body used in glycoprotein synthesis or else excreted as CO_2 (66,67). Because other drug absorption enhancers have histologically damaged the nasal epithelia (68) it might be assumed that chitosan would induce similar problems. To the contrary, chitosan did not induce any damage when applied to the nasal epithelium of rats (49), and only slight toxicity was observed when administered orally to mice at doses of 18 g/kg for a 19-day period (48). Another study in mice showed a weight loss upon intraperitoneal administration of 5 mg chitosan for 12 weeks (69), but when dosed with 1 mg chitosan, a normal increase in body weight was observed. When orally treated, all mice suffered a weight loss. Richardson et al. administered radiolabeled chitosan systemically and showed accumulation within 5 min in lungs (<10 kDa) and in liver (>10 kDa), and at 60 min, both polymers were found in the liver (70). In the frog palate model, a transient decrease in the mucociliary transport velocity (MTV), measured as the time to clear graphite particles (71), and in human turbinates (51) ex vivo suggested no permanent damage to the nasal surface. Minimal epithelial damage, which may have occurred upon tissue preparation, was observed in turbinates removed from volunteers after treatment with chitosan (51). Aspden et al. used a nasal perfusion technique in vivo to measure release of proteins that act as indicators of damage (50). Chitosan produced only minimal changes in comparison with laureth-9, a surfactant known to induce epithelial damage. In vitro toxicity of chitosan determined in erythrocytes and in a murine melanoma cell line (B16F10) displayed a concentration and salt dependency, the hydrochloride salt being most toxic (72). Chitosan was less toxic than poly-L-lysine but more toxic than DEAE-dextran. Red blood cell lysis was time and molecular weight dependent and occurred within 24 h, but not upon short-term exposure. Richardson et al. showed no toxicity of chitosan in rat red blood cells and L132 cells by the MTT (3-(4,5-dimethylthiazol 2-yl)-2,5-diphenyl tetrazolinium bromide) assay (70). Caco-2 cells were exposed to chitosan solution for 1 h, and discontinuities as well as a reduction in the number of microvilli were observed, but tight junctions appeared to be normal. Intracellular enzyme activity was not as greatly affected as with other absorption enhancers such as bile salts (65). Toxicity appears to be related to the degree of deacetylation and is higher with an increasingly positive charge density.

Chitosan has been used to enhance the absorption of poorly bioavailable drugs such as proteins and peptides across the nasal and intestinal epithelia in vivo (49,73) and in vitro (65,74). Enhanced plasma insulin levels and correspondingly reduced blood glucose levels after intranasal administration of insulin–chitosan solutions have been shown in sheep (49) and in rats (50). Chitosan is an example of a mucoadhesive agent, because at acidic pH, it becomes viscous and adhesive and binds sialic residues in mucus or on cell surfaces, due to its positive charge (49). Two explanations have been given to explain why chitosan works as an enhancing agent: the bioadhesive system is not cleared as efficiently by the mucociliary clearance system in the nose, permitting the drug to maintain a longer contact time with the nasal epithelium, and it is also thought to promote the opening of the tight junctions between cells, allowing larger molecules to pass through the membrane in a paracellular manner. A transient opening in the tight junctions between Caco-2 cells has actually been demonstrated using confocal laser scanning microscopy (75).

The amino groups on the glucosamine subunits have an intrinsic pK_a value of 6.5, and thus chitosan behaves as a polycation at acidic and neutral pH (65). It is these positively charged amino groups that make chitosan readily available for interaction with indomethacin (76), sodium hyaluronate (77), pectin and acacia polysaccharides (78), and polyacrylic acid (79). Such interactions have been well characterized in the literature. Variables shown to influence these electrostatic interactions include molecular weight, molecular size (particularly for controlled release), pH, weight and molecular ratios, and polymer concentration.

It also appears that chitosan possesses some of its own natural targeting ability. Structurally, chitosan resembles glycosaminoglycans, found in many tissues as cell membrane components (67), and is thought to mimic their behavior. It has also been shown to strongly associate with a number of mammalian and bacterial cells (80,81). Werner

and Kissel have also described binding sites on ciliated cells in human nasal epithelium for *N*-acetyl-glucosamine (58). A mannose receptor (a 170-kDa glycoprotein) that has been indicated in receptor-mediated phagocytosis of certain bacteria mediated through a terminal sugar residue such as *N*-acetylglucosamine has reportedly been found on the surface of dendritic cells (82).

Chitosan is commercially available at low cost, is nontoxic, and possesses amino groups for interaction with polyanionic molecules such as plasmid. The concept of allowing DNA to interact with chitosan, in the form of either an oligonucleotide or a plasmid, was thus conceived (9,34). It was demonstrated that condensation occurred upon charge neutralization by electrostatic interaction between the positively charged amino groups present in chitosan and the negatively charged plasmid phosphates. Chitosan has been shown to stabilize calf thymus DNA to melting (83), and prevent nuclease degradation (70). Condensation of DNA plasmid by an 8-kDa chitosan was shown by transmission electron microscopy (TEM) to produce toroids and rod-shaped particles, the size and shape of which suggest a relatively tight interaction (84). Similarly shaped complexes have been observed previously upon interaction of plasmid with condensing peptides or polymers (85,86). The heat of interaction between chitosan and plasmid was measured using isothermal titration microcalorimetry, an extremely sensitive technique used to measure the heat of interaction between two species (84). Aliquots of a ligand are added to a macromolecule, and the heat changes are measured as a series of peaks. Initially, the heat flow is large, as are the number of available sites for binding, but as these sites become bound, heat flow reduces. The initial heat flow was exothermic, representing the electrostatic interaction between the plasmid and chitosan that decreased to an approximate 1:1 (−/+) charge ratio. An endothermic heat flow was then measured, indicating a conformational change in the complexation process, perhaps representative of the condensation phenomenon. No more heat flow changes occurred at higher charge ratios, indicating completion of the interaction. Unfortunately the shape of the heat flow profile is complex, so that information including the binding constant and enthalpy of interaction cannot readily be obtained. In terms of changes to the secondary structure of DNA, circular dichroism has shown that, upon binding chitosan oligomers, a transition from the highly hydrated B-form to the dehydrated A-form of DNA occurred (83).

A number of research groups have now prepared chitosan particulates using different methods for the delivery of DNA, such as plasmid, to endothelial (lung vasculature) or epithelial surfaces (intestine, vagina, nose, and lung) (87,88). Illum proposed that DNA could be adsorbed onto the surface of a chitosan microsphere; however, significant expression was not measured in vitro (87). Particles (10^6) formed by first condensing DNA with chitosan to an ideal size of less than 1 μm, then adsorbing the condensate onto a charged particle, were shown to be embedded deeply in the lungs only 3 h after i.v. administration to rabbits (87). Alternatively, Alexakis et al. have shown the successful encapsulation of calf thymus DNA within cross-linked chitosan membranes or within chitosan-coated alginate microspheres (89). Such microspheres were used for oral delivery in rats. Illum et al. have also described the preparation of chitosan particulates of size less than 1 μm by simple mixing of plasmid and chitosan (88), following the method previously described by Mumper et al. (9,34). The rate of mixing influenced the sizes of the complexes formed at a 1:5 (100–300 nm) or 1:10 (170–470 nm) w/w ratio. Equal in vitro transfection of the macrophage RAW 264 and rat glial tumor cell lines by such formulations (3-μg plasmid dose) was reported; however the error bars were large, and no positive control was included for comparison. Further, a 1:10 w/w complex (100 μg/100 μL) was administered into the nasal cavity of rats, and 72 h later, tissues were harvested and analyzed for chloramphenicol acetyl transferase (CAT) activity. A positive Lipofectin™ control (1:2 w/w) (61.4 μg/100 μL) produced little if any expression in the harvested tissues. In contrast, the chitosan-formulated plasmid was highly expressed in the mandibular lymph nodes, but less so in the nasal mucosa and esophageal and lung tissues.

The complex coacervation of plasmid and chitosan was demonstrated by Mao et al. (90). Complexes were formed upon mixing chitosan (0.2% w/v) with plasmid (100 μg/mL) in acetate buffer, and particulates in the size range 200–500 nm were observed by transmission electron microscopy (TEM). Such complexes demonstrated low toxicity in HEK 293 cells relative to poly-L-lysine and Lipofectin™ complexes, and they produced lower transfection than the positive Lipofectamine™ control in 293, IB3 (bronchial epithelial cells), and THE cells (human tracheal epithelial cells) (91). Such a trend in transfection was also shown in Cos-1 cells (84). In this study, complexes (10 μg/well) made with chitosan with a range of molecular weights at a 1:2 (−/+) charge ratio were formulated in saline and incubated with Cos-1 cells in the presence or absence of serum. Cells were harvested at 72 h. If the affinity of complexation was critical in the transfection procedure, then transfection efficiency would be influenced by complexing plasmid with different molecular weight chitosan oligomers and polymers. The results showed that chitosan molecular weight had little influence on the transfection efficiency. Maximum expression was obtained using the complex containing the 102-kDa chitosan, the level of which was 250-fold less than that achieved using the Lipofectamine™ control. In the presence of serum, the complex formulated with the 540-kDa chitosan was most readily expressed. In contrast, plasmid–chitosan "polyplexes" of charge ratios greater than 1:1.2 (−/+) were transfected in 293 cells with comparable efficiency to a positive control plasmid–PEI (−/+ 1:5) at 6 days (92). CAT expression was observed for 3 weeks. Interestingly, the presence of serum somewhat hindered expression of complexes bearing lower charge ratios compared with higher ratios or even PEI complexes. Köping-Höggård proposed that this occurred because the negatively charged proteins could not neutralize the highly positively charged complexes, which were also more stable to degradation by nucleases (92).

It was conceived that by altering the molecular weight of the chitosan, it might be possible to control the size of the complexes, hence formulating particles of a specific size for targeting. In a method developed by Peniston and John-

son, chitosan was chemically depolymerized by deaminative cleavage to produce chitosan oligomers of reduced chain length (93). The free aliphatic amino groups are deaminated by reaction with nitrous acid formed in situ by the presence of sodium nitrite and 6% acetic acid. A stoichiometric amount of nitrogen is produced, which can be used to measure the extent of reaction, and thus the extent of deamination. Treatment with concentrated acid at high temperature (94) or with dilute acid (95) yields oligomers with low degrees of polymerization. The former method was not particularly selective, but the oligomers made were very pure although difficult to separate and costly to process. Other methods for depolymerization employing enzymes, including chitosanase (96), wheat germ lipase (97), or papain (98), have been described. Dependent on the method of depolymerization, the level of deacetylation will vary, which subsequently influences physical, chemical, and biological properties of the oligomer. Deacetylation can be measured enzymatically (99) or chemically (100). MacLaughlin et al. (84) described the depolymerization of chitosan using the method of Peniston and Johnson (93). As the added amount of sodium nitrite increased, the molecular weight of each oligomer decreased, but the degree of deacetylation and nitrogen content did not change. These observations agreed with those previously made by Peniston and Johnson (93). To efficiently interact with DNA plasmid, it is essential that as many amino groups as possible be available, so that a high positive charge density and the ability to condense DNA can be retained. The amine content was determined using a modified ninhydrin assay (100) but showed differences between the theoretical and experimental amine content (84). This was explained by the fact that the experimental amine content of Seacure 143 (a commercially available medium-grade chitosan, Natural Biopolymer, Inc., Raymond, WA) did not match that stated by the supplier. Once depolymerized, the influence of reduced oligomer molecular weight on the size of the complexes formed with DNA was determined. A proportional decrease in the size of the complexes was observed as the molecular weight of the chitosan decreased (Fig. 7). Although it might be expected that a higher molecular weight chitosan can interact and condense plasmid more efficiently than lower molecular weight chitosan, this is outweighed by the fact that the high molecular weight chitosan has reduced solubility, which may produce an increase in particle diameter or even aggregation. Other factors such as plasmid concentration and charge ratio were also shown to influence complex size. In general, as the plasmid concentration increased, the diameter of the complex increased. Using a 32-kDa chitosan oligomer, the 1:6 (−/+) complexes were only slightly larger than the 1:2 (−/+) complexes at all plasmid concentrations; however, using a 102-kDa oligomer, the 1:6 (−/+) complexes were larger than the 1:2 (−/+) complexes, and this difference became more defined as the plasmid concentration increased.

The stability of complexes in the biological milieu is desired; however, the release of plasmid within the cell is also essential for expression to be achieved. A balance of these two characteristics needs to be maintained. Colloidal stability of the complex to salt and serum challenge was very

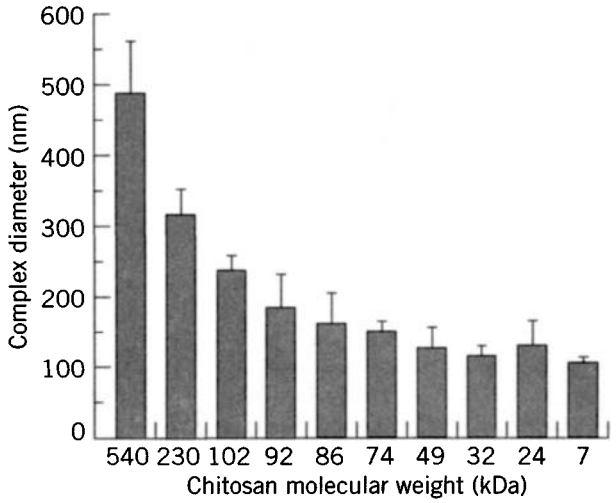


Figure 7. Factors influencing the size of chitosan–plasmid complexes. Complexes were made at 1:6 (−/+) with a plasmid concentration of 100 μg/mL.

much dependent upon the chitosan oligomer molecular weight and the charge ratio of the resultant complex (84). For example, when challenged with normal saline, the 1:0.5 (−/+) and 1:1 (−/+) complex prepared with a 7-kDa oligomer were stable, but the 1:2 (−/+) and 1:6 (−/+) complexes aggregated. The 1:2 (−/+) complex made with a 32-kDa oligomer was unstable, whereas the rest were stable. All complexes made with the 102- and 540-kDa oligomers were stable to salt challenge. The low molecular weight chitosan in positively charged complexes, which is only weakly associated with the plasmid, competes with the salt ions, but as the molecular weight of the oligomer increases, it will associate with plasmid more strongly. When challenged with a solution comprising 10% serum in normal saline, all complexes made with the 7-kDa chitosan dissociated over the 15-min challenge period. With the 32-kDa oligomer complexes, all complexes fell apart except the 1:6 (−/+) complex, which aggregated. Both the 102-kDa (Fig. 8) and the 540-kDa complexes behaved similarly to serum challenge. The 1:0.5 (−/+) and 1:1 (−/+) complexes fell apart, the 1:6 (−/+) complexes aggregated, but interestingly the 1:2 (−/+) complexes remained stable. It would appear that some component of the serum directly competes with the chitosan for association with the plasmid. Such 1:2 (−/+) complexes were also highly stable to challenge with sodium dodecyl sulfate and heparin. Other groups have observed high plasmid–chitosan complex stability. For instance, an insoluble polynucleotide–chitosan complex was formed that was highly stable in solution at 37°C for over 24 h (101). This very high stability may also become a rate-limiting step in the overall transfection process. Cos-1 cells were incubated with complexes containing fluorescently labeled plasmid, and by fluorescence microscopy, the 1:6 (−/+) complexes were observed to adhere to the cell surface in an aggregated manner, and the 1:2 (−/+) complexes adhered in a punctate manner. It was not possible to decipher the exact location of these complexes, and if they were intracellular.

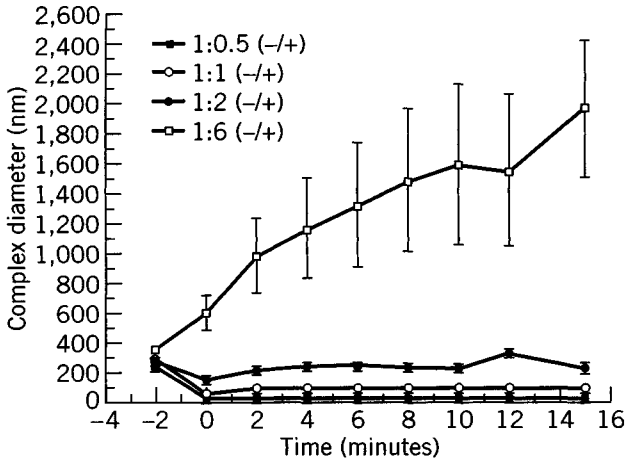


Figure 8. Stability of complexes made at a plasmid concentration of 200 μg/mL to serum challenge (10% v/v fetal bovine serum and 90% v/v normal saline). Complexes made with a 102-kDa chitosan were challenged. The complex diameter measured at −2 min is the diameter of the complex before challenge. The diameter at 0 min refers to the particle diameter measured upon immediate challenge. Where no error bands are shown, the particle distribution is considered to be broad.

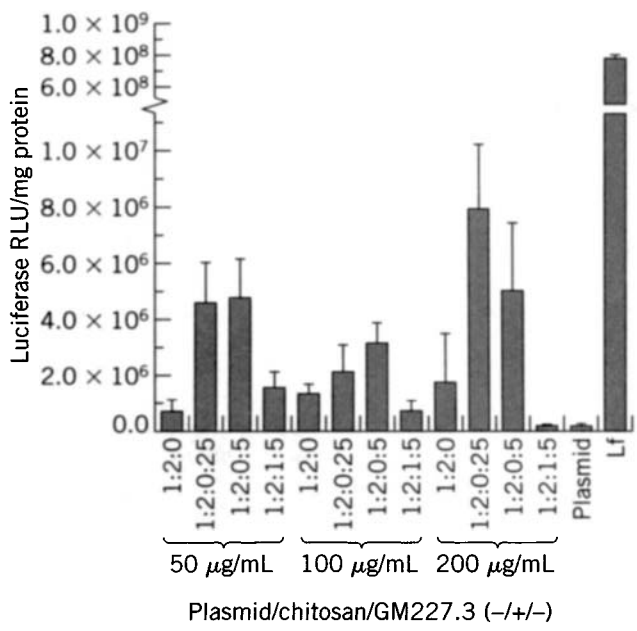


Figure 9. Transfection of Cos-1 cells with complexes containing the lipophilic endosomolytic peptide GM227.3 and chitosan (102 kDa). Complexes were made at a plasmid concentration of either 50, 100, or 200 μg/mL, with charge ratios (−/+/−) of 1:2:0, 1:2:0.25, 1:2:0.5, and 1:2:1.5. A 10-μg dose of plasmid was added to each well. The transfection levels obtained were compared with those obtained with 2.5-μg plasmid–Lipofectamine™ (Lf) (1:6 w/w).

One localization study using confocal microscopy has shown that, 1 h after transfection, particles made with fluorescently labeled plasmid and chitosan were localized in the vicinity of the cell membrane (91). In situ hybridization showed multiple copies of plasmid taken up into cells after 1 h, but after 4 h, some plasmid was observed in the cytoplasm and nucleus, while aggregates had formed outside the cells. At 24 h, most of the plasmid was observed in the nucleus. The researchers postulated that complete degradation or exocytosis of internalized plasmid may be one of the rate-limiting steps in the uptake process. In B16F10 cells, scanning electron microcopy showed that chitosan microspheres were taken into cells. The cell membrane was disrupted as the cell became laden with microspheres (72).

A reduction in the molecular weight of the chitosan did not influence expression, thus it was postulated that endosomal release might be a critical rate-limiting step (84). The influence of incorporating pH-sensitive lytic peptides in the plasmid–chitosan complex by electrostatic interactions was thus investigated. The lytic peptides GM225.1 (GLFEALLELLESLWELLLEA-OH) and GM227.3 (GLFEALEELWEAK(ϵ-G-dipalmitoyl)) were added to preformed plasmid–chitosan complexes and left to incubate at room temperature for 30 min. The presence of the lytic peptide was determined by zeta potential measurement and showed that, as more peptide was added, the zeta potential became electronegative. The presence of GM227.3 was shown to enhance the level of expression fourfold in Cos-1 cells for a 1:2:0.25 (−/+/−) complex formulated at a 200 μg/mL, compared with a complex containing no peptide (Fig. 9). Transfection efficiency was not improved by formulating complexes at different plasmid concentrations and thus different complex diameters. Some plasmid was taken into the cell and expressed, and the presence of the pH-sensitive lytic peptide enhanced the levels of expression slightly. The authors postulated that a small number of DNA plasmid–chitosan complexes were endocytosed and subsequently expressed, whereas the remainder of the complexes stuck to the cell surface (as suggested by fluorescence microscopy), thus explaining the low levels of expression achieved.

A formulation containing GM225.1 in 10% lactose (1:6:0.5 −/+/−) (100 μg/mL) was subsequently administered in the upper small intestines or the colons of female New Zealand white rabbits, and higher levels of expression were measured at 72 h compared with naked DNA or a plasmid–DOTMA:DOPE (1:3 −/+) formulation (84). This is in contrast with the results obtained in vitro where the lipid formulation gave higher levels of expression than the chitosan–lytic peptide formulation. When treated in the upper small intestine with the chitosan–lytic peptide formulation, all animals showed expression in at least two of the four tissues examined (Peyer's patches, enterocytes, colon, and mesenteric lymph nodes). CAT expression in the colon was not observed. When dosed in the colon, only two of the four animals expressed CAT in the colon, but three out of four animals expressed CAT in the mesenteric lymph nodes. Naked DNA was not expressed after administration via either route. MacLaughlin et al. also reported no expression after dosing via the intranasal, intramuscular, or subcutaneous routes (84). Koping-Hoggard et al. administered 1:3 (−/+) complexes via the trachea and lungs (102). Gene expression of formulated plasmids descended

in the following order: PEI > chitosan > naked plasmid. Interestingly, after nasal administration, unformulated plasmid produced the highest expression; however, orally administered plasmid–chitosan complexes were expressed more than unformulated plasmid. This data suggests that along with the fact that chitosan is an immunostimulant, it can be used as a potential carrier for oral nucleic acid–based vaccines. For example, upon rejection of chitosan a humoral response has been demonstrated in mice (103). Upon infection with Sendai virus, interferon levels were enhanced 1 day following infection, after treating with chitosan 1 day prior to infection (57). Chitosan was shown to activate a nonspecific immune response by stimulating the cell-killing abilities of peritoneal macrophages and NK cells. The mode of action for the stimulation of the immune response by chitosan was by enhancing production of lymphokines by NK and T helper cells, in response to stimulation by activated peritoneal macrophages but not spleen cells (57). Shibata et al. showed that intravenously injected chitin particles (1–10 μm) prime alveolar macrophages within 3 days, probably due to the production of interferon γ (IFN-γ), but neither soluble chitin nor chitosan induced an effect (104). Neither T nor B lymphocytes were involved. Chitosan was also shown to stimulate IgM production within 48 h in vitro in human lymphocytes, but did not promote the production of IgA or IgG (105). Deacetylated chitin (30% and 70%) was shown to induce antibody formation as well as cell-mediated immunity in guinea pigs and mice at 28 days (106). Roy et al. described how chitosan could be used as a delivery system for a DNA-based vaccine expressing a peanut antigen (107). The different dosing regimens were not described in detail. IgG (4 and 6 weeks) and IgA (3 and 4 weeks) responses were measured in those mice that were administered the formulations and then boosted. A weak antibody but no cellular immune responses were measured. When sensitized mice were challenged with the antigen, a delay in anaphylaxis and response was apparent. R.J. Mumper et al. (personal communication, 1998) measured the humoral response to expressed β-galactosidase following administration of plasmid/chitosan complexes in mice, 28 days after initial administration. Animals were boosted at day 14. Higher quantities of antigen-specific IgG were determined in sera with the plasmid–chitosan complex than with DNA plasmid alone. No cellular or mucosal effects were determined in this study.

The properties of the plasmid–chitosan complexes are intriguing thus far; however, they still have the potential for improvement. Fortunately, chitosan is an extremely versatile macromolecule possessing amino and hydroxy groups that can readily be modified to produce a molecule with improved properties, yet still retaining basic physical characteristics. For example, a new surface effective in reducing protein adsorption, platelet adherence, and activation was made by permanently immobilizing methoxypoly(ethylene glycol) sulfonate on a chitosan surface by polyelectrolyte interaction (108). Esters of amino acids were conjugated to chitosan via an intermediate glyoxylic acid–substituted chitosan. The removal of heavy metal ions was enhanced independently of the amino acid sequence (109). Krysteva et al. covalently conjugated enzymes by oxidizing the amino group and treating with urea and formaldehyde (110). By derivatizing the amino group with a highly positively charged group, the potential of chitosan for anion exchange was demonstrated. Schatzlein et al. described an interesting new biocompatible delivery system where unilamellar vesicles formed upon mixing acylated glycol chitosan in the presence of cholesterol. These vesicles were loaded with a hydrophilic water-soluble drug such as bleomycin (111). These micelles remained stable for 28 days at room temperature, and over 24 h in plasma. Due to the low solubility of chitosan at neutral intestinal pH values, a soluble derivative, trimethylchitosan chloride, was synthesized and shown to enhance permeability of intestinal layers at neutral pH values relative to chitosan (112) and in vitro in Caco-2 cells (113). A higher degree of substitution results in higher levels of transport. Enhanced uptake of hydrophilic drugs was observed in rats after nasal or rectal administration of the *N*-trimethyl chitosan chloride formulation at pH 7.4 in comparison with chitosan. The chitosan backbone has also been grafted with pluronics (114). Hofmann et al. conjugated Pluronic L122 polyol to chitosan by activating the OH group of the polyol and interacting it with the amino groups of chitosan at different pH values (114). Not surprisingly, the interaction was more efficient at higher pH values, but chitosan is not soluble at pH >7. The reaction still occurred with somewhat reduced efficiency at pH 6. The polymer gelled on increasing the temperature from 4°C to 37°C, probably by physical cross-linking of the hydrophobic polypropylene oxide groups and the chitosan backbone. In the future, it might be possible to evaluate controlled release of plasmid from that type of gel, because plasmid can interact with cationically charged chitosan (115). Chitosan has also been modified with deoxycholic acid to increase its hydrophobicity (116), and the formation of stable complexes with plasmid was indicated by agarose gel electrophoresis. No evidence of colloidal stability was described.

As well as modifying chitosan to improve its properties, a ligand such as transferrin or asialoorosomucoid, or saccharide residues such as galactose can be conjugated to exploit receptor-mediated endocytosis. An *N,N,N,*-trimethyl-chitosan–galactose conjugate was synthesized (117), and the ability to form polyelectrolyte complexes with plasmid was determined. The aminochitosan functionality was protected with a trimethyl group; the CH_2OH group was derivatized with monochloroacetic acid and was mixed with a galactose residue overnight in vitro. Toxicity of the plasmid complexes was similar to DEAE-dextran. Chitosan nanospheres derivatized with transferrin or mannose-6-phosphate using succinimidyl chemistry have also been prepared (118). Interestingly, in HEK293 cells (2-μg plasmid dose) the presence of either targeting ligand did not significantly enhance transfection relative to plain nanospheres, although transfection was still at least 10-fold less than with the positive Lipofectamine™ control. The transferrin conjugates were further derivatized with polyethylene glycol (PEG), and the excess hydrophilicity did not appear to inhibit transfection efficiency in any way. These PEGylated transferrin particles remained stable for 1 month in solution, as did the plain nanospheres and the PEGylated transferrin particles after lyophilization.

So far, the results using chitosan to produce gene medicines or gene-based vaccines appear promising. Many of the ideal characteristics of a gene delivery system are provided. Chitosan is readily available, cost-effective, and relatively nontoxic. Complexes of controllable sizes and high colloidal stability can be readily formulated, that have the potential for further modification for more specific cell targeting. The high stability and low expression achieved in vivo suggest that uptake and/or decomplexation, but to a lesser extent endosomal release, may be critical rate-limiting steps. These issues will have to be addressed to optimize that type of polymeric delivery system.

Potentially, gene therapy offers a useful and efficient option for preventing, correcting, or modulating diseases that typically have no other methods of treatment. In order to design and produce an ideal delivery system, the uptake and fate of the plasmid and barriers to expression need to be further understood. The ideal nonviral delivery system should produce controllable and reliable levels of protein upon in vivo administration and have minimal side effects. The polymers described here offer potential as gene delivery systems, but they still present some limitations. Future goals must involve identifying the location of the gene and controlling levels of expression upon delivery. It is understood that each disease and gene will require a rationally designed delivery and expression system enabling targeting of the gene, yet retaining plasmid functionality.

BIBLIOGRAPHY

1. T. Suzuki et al., *FEBS Lett.* **425**, 436–440 (1998).
2. M.-P. Rols et al., *Nat. Biotechnol.* **16**, 168–171 (1998).
3. J.A. Wyber, J. Andrews, and A. D'Emanuele, *Pharm. Res.* **14**(6), 750–756 (1997).
4. S.A. Johnston and D.C. Tang, *Methods Cell Biol.* **43**(A), 353–365 (1994).
5. P.L. Felgner et al., *Proc. Natl. Acad. Sci. U.S.A.* **84**, 7413–7417 (1987).
6. L. Vitiello, A. Chonn, J.D. Wasserman, and R.G. Whorton, *Transfus. Sci.* **17**(1), 63–69 (1996).
7. J. Haensler and F.C. Szoka, Jr., *Bioconjugate Chem.* **4**, 372–379 (1993).
8. O. Boussif et al., *Proc. Natl. Acad. Sci. U.S.A.* **92**, 7297–7301 (1995).
9. R.J. Mumper, J. Wang, J.M. Classpell, and A.P. Rolland, *Proc. Int. Symp. Controlled Release Bioact. Mater.* **22**, 178 (1995).
10. V. Escriou et al., *Biochim. Biophys. Acta* **1368**, 276–288 (1998).
11. S.F. Alino et al., *Biochem. Biophys. Res. Commun.* **204**, 1023–1030 (1994).
12. E. Tomlinson and A. Rolland, *J. Controlled Release* **39**, 357 (1996).
13. P.L. Felgner et al., *Ann. N. Y. Acad. Sci.* **772**, 126–139 (1995).
14. B. Sternberg, F.L. Sorgi, and L. Huang, *FEBS Lett.* **356**(2–3), 361–366 (1994).
15. P. Felgner, *Adv. Drug Delivery Rev.* **5**, 163–187 (1990).
16. R. Stribling et al., *Proc. Natl. Acad. Sci. U.S.A.* **89**, 11277–11281 (1992).
17. G.J. Nabel et al., *Proc. Natl. Acad. Sci. U.S.A.* **90**, 11307–11311 (1993).
18. N.J. Caplen et al., *Gene Ther.* **1**(2), 139–147 (1994).
19. B. Abdallah et al., *Hum. Gene Ther.* **7**, 1947–1954 (1996).
20. A.V. Kabanov et al., *Biopolymers* **31**, 1437–1443 (1991).
21. A.V. Kabanov et al., *Bioconjugate Chem.* **4**, 448–454 (1993).
22. E. Wagner et al., *Proc. Natl. Acad. Sci. U.S.A.* **87**, 3410–3414 (1990).
23. E. Wagner et al., *Bioconjugate Chem.* **2**, 226–231 (1991).
24. M. Zenke et al., *Proc. Natl. Acad. Sci. U.S.A.* **87**, 3655–3659 (1990).
25. C.H. Wu and G.Y. Wu, *J. Biol. Chem.* **262**(10), 4429–4432 (1987).
26. G.Y. Wu and C.H. Wu, *J. Biol. Chem.* **263**(29), 14621–14624 (1988).
27. E. Wagner et al., *Proc. Natl. Acad. Sci. U.S.A.* **89**, 7934–7938 (1992).
28. E. Wagner et al., *Proc. Natl. Acad. Sci. U.S.A.* **89**, 6099–6103 (1992).
29. D.T. Curiel, S. Agrawal, E. Wagner, and M. Cotton, *Proc. Natl. Acad. Sci. U.S.A.* **88**, 8850–8854 (1991).
30. M. Manthorpe et al., *Hum. Gene Ther.* **4**, 419–431 (1993).
31. S. Jiao et al., *Hum. Gene Ther.* **3**, 21–33 (1992).
32. M.Y. Levy, L.G. Barron, K.B. Meyer, and F.C. Szoka, *Gene Ther.* **3**, 201–211 (1996).
33. J.A. Wolff et al., *J. Cell Sci.* **103**, 1249–1259 (1992).
34. R.J. Mumper et al., *Pharm. Res.* **12**, 80 (1995).
35. U.K. Pat. WO 97 04122 (February 6, 1997) J.M. Lee, N.S. Magnuson, G. An, and R. Reeves (to Washington State University Research Foundation).
36. T. Hosono, S. Tsuchiya, and H. Matsumaru, *J. Pharm. Sci.* **69**(7), 824–826 (1980).
37. D. Horn and W. Ditter, *J. Pharm. Sci.* **71**(2), 1021–1026 (1982).
38. T.L. Lebedeva, V.E. Igonin, M.M. Feldstein, and N.A. Plate, *Proc. Int. Symp. Controlled Release Bioact. Mater.* **24**, 447 (1997).
39. R.J. Mumper et al., *Pharm. Res.* **13**, 701–709 (1996).
40. R.J. Mumper et al., *J. Controlled Release* **52**, 191–203 (1998).
41. A.V. Kabanov and V.A. Kabanov, *Bioconjugate Chem.* **6**, 7–20 (1995).
42. H.L. Davis et al., *Hum. Gene Ther.* **4**, 733–740 (1993).
43. R.A. Winegar et al., *Hum. Gene Ther.* **7**, 2185–2194 (1996).
44. K. Anwer et al., *Hum. Gene Ther.* **9**, 659–670 (1998).
45. H. Alila et al., *Hum. Gene Ther.* **8**, 1785–1795 (1997).
46. M. Coleman et al., *Hum. Gene Ther.* **9**, 2223–2230 (1998).
47. R.J. Mumper and A.P. Rolland, *Adv. Drug Delivery Rev.* **30**, 151–172 (1998).
48. R.A.A. Muzzarelli, *Natural Chelating Polymers: Alginic Acid, Chitin and Chitosan*, Pergamon, Oxford, 1973, pp. 144–176.
49. L. Illum, N.F. Farraj, and S.S. Davis, *Pharm. Res.* **11**, 1186–1189 (1994).
50. T.J. Aspden, L. Illum, and O. Skaugrud, *Eur. J. Pharm. Sci.* **4**, 23–31 (1996).
51. T.J. Aspden et al., *J. Pharm. Sci.* **86**(4), 509–513 (1997).
52. Y.M. Wang, H. Sato, I. Adachi, and I. Horikoshi, *J. Pharm. Sci.* **85**(11), 1204–1210 (1996).
53. A. Berthold, K. Cremer, and J. Kreuter, *J. Controlled Release* **39**, 17–25 (1996).
54. S.R. Jameela and A. Jayakrishnan, *Biomaterials* **16**, 769–775 (1995).
55. I. Henriksen, O. Skaugrud, and J. Karlsen, *Int. J. Pharm.* **98**, 181–188 (1993).

56. S. Hirano, K. Tobetto, M. Hasegawa, and N. Matsuda, *J. Biomed. Mater. Res.* **14**, 477–486 (1980).
57. R. Muzzarelli, in S. Dumitriu, ed., *Polymeric Biomaterials*, Dekker, New York, 1994, pp. 179–197.
58. U. Werner and T. Kissel, *Pharm. Res.* **13**, 978–988 (1996).
59. E.S. Lower, *Manuf. Chem.* **55**(10), 47–52 (1984).
60. DE Pat. 19544455, (June 5, 1997), P. Horlacher and J. Schad (to Henkel KGAA).
61. JP Pat. 62-288601 (December 15, 1987), A. Seiichi (to Japanese Agency of Industrial Science and Technology).
62. H. Takeuchi et al., *Pharm. Res.* **13**(6), 896–901 (1996).
63. I. Henriksen, G. Smistad, and J. Karlsen, *Int. J. Pharm.* **101**, 227–236 (1994).
64. I. Henriksen et al., *Int. J. Pharm.* **146**, 193–204 (1997).
65. N.G.M. Schipper, K.M. Vårum, and P. Artursson, *Pharm. Res.* **13**, 1686–1692 (1996).
66. K.M. Vårum, M.M. Myhr, R.J.N. Hjerde, and O. Smidsrød, *Carbohydr. Res.* **299**, 99–101 (1997).
67. T. Chandy and C.P. Sharma, *Biomater. Artif. Cells Artif. Organs* **18**(1), 1–24 (1990).
68. S.G. Chandler, L. Illum, and N.W. Thomas, *Int. J. Pharm.* **76**, 61–70 (1991).
69. Y. Tanaka et al., *Biomaterials* **18**, 591–595 (1997).
70. S. Richardson, H.V.J. Kolbe, and R. Duncan, *Proc. Int. Symp. Controlled Release Bioact. Mater.* **24**, 649 (1997).
71. T.J. Aspden et al., *Int. J. Pharm.* **122**, 69–78 (1995).
72. B. Carreño-Gómez and R. Duncan, *Int. J. Pharm.* **148**, 231–240 (1997).
73. H.L. Luessen et al., *Pharm. Res.* **13**(11), 1668–1672 (1996).
74. P. Artursson, T. Lindmark, S.S. Davis, and L. Illum, *Pharm. Res.* **11**, 1358–1361 (1994).
75. G. Borchard et al., *J. Controlled Release* **39**, 131–138 (1996).
76. T. Imai, S. Shiraishi, H. Saitô, and M. Otagiri, *Int. J. Pharm.* **67**, 11–20 (1991).
77. K. Takayama et al., *Chem. Pharm. Bull.* **38**(7), 1993–1997 (1990).
78. M.M. Meshali and K.E. Gabr, *Int. J. Pharm.* **89**, 177–181 (1993).
79. V. Chavasit and J.A. Torres, *Biotechnol. Prog.* **6**, 2–6 (1990).
80. K.D. Vorlop and J. Klein, *Methods Enzymol.* **135**, 259–268 (1987).
81. T. Ouchi and T. Banba, *Trans. Soc. Biomater.* **11**, 232 (1988).
82. Y. Shibata, W.J. Metzger, and Q.N. Myrvik, *J. Immunol.* **159**, 2462–2467 (1997).
83. T. Motomura and Y. Aoyama, *Bull. Chem. Soc. Jpn.* **65**, 1755–1760 (1992).
84. F.C. MacLaughlin et al., *J. Controlled Release* **56**, 259–272 (1998).
85. Y.Y. Vengerov and T.E. Semenov, *Electron Microsc. Rev.* **5**, 193–207 (1992).
86. M.A. Wolfert and L.W. Seymour, *Gene Ther.* **3**(3), 269–273 (1996).
87. U.K. Pat. WO 98/01161 (January 15, 1998), L. Illum (to Danbiosyst U.K. Ltd.).
88. U.K. Pat. WO 98/01160 (January 15, 1998), L. Illum (to Danbiosyst U.K. Ltd.).
89. T. Alexakis et al., *Appl. Biochem. Biotechnol.* **50**, 93–106 (1995).
90. H.-Q. Mao et al., *Proc. Int. Symp. Controlled Release Bioact. Mater.* **23**, 401 (1996).
91. K. Roy, H.-Q. Mao, and K.W. Leong, *Proc. Int. Symp. Controlled Release Bioact. Mater.* **25**, 673 (1997).
92. M. Köping-Höggård, M. Nilsson, K. Edwards, and P. Artursson, *Proc. Int. Symp. Controlled Release Bioact. Mater.*, **25**, 368 (1998).
93. U.S. Pat. 3,922,260 (November 25, 1975), Q.P. Peniston and E.L. Johnson.
94. A. Domard and N. Cartier, *Int. J. Biol. Macromol.* **11**, 297–302 (1989).
95. G.G. Allan and M. Peyron, *Carbohydr. Res.* **277**, 257–272 (1995).
96. RU Pat. 2073016 (February 10, 1997) V.P. Varlamov, K.O. Stoyachenko, and M.V. Budanov.
97. R.A.A. Muzzarelli, W. Xia, M. Tomasetti, and P. Ilari, *Enzyme Microb. Technol.* **17**, 541–545 (1995).
98. R.A.A. Muzzarelli, M. Tomasetti, and P. Ilari, *Enzyme Microb. Technol.* **16**(2), 110–114 (1994).
99. F. Nanjo, R. Katsumi, and K. Sakai, *Anal. Biochem.* **193**, 164–167 (1991).
100. E. Curotto and F. Aros, *Anal. Biochem.* **211**, 240–241 (1993).
101. H. Hayatsu, T. Kubo, Y. Tanaka, and K. Negeishi, *Chem. Pharm. Bull.* **45**(8), 1363–1368 (1997).
102. M. Köping-Höggård et al., *Am. Assoc. Pharm. Sci.* **1**, S278 (1998).
103. J. Knapczyk et al., *Archives Immunol. Ther. Exp.* (Warsz) **1–2**, 127–132 (1991).
104. Y. Shibata, L.A. Foster, W.J. Metzger, and Q.N. Myrvik, *Infect. Immun.* **65**(5), 1734–1751 (1997).
105. M. Maeda, H. Murakami, H. Ohta, and M. Tajima, *Biosci. Biotech. Biochem.* **56**(3), 427–431 (1992).
106. K. Nishimura et al., *Vaccine* **3**, 379–384 (1985).
107. K. Roy et al., *Proc. Int. Symp. Controlled Release Bioact. Mater.* **25**, 348 (1998).
108. M.M. Amiji, *Carbohydr. Polym.* **32**(3–4), 193–199 (1997).
109. H. Ishii, M. Minegishi, B. Lavitpichayawong, and T. Mitani, *Int. J. Biol. Macromol.* **17**(1), 21–23 (1995).
110. M. Krysteva, E. Naidenova, A. Andreeva, and N.D. Huyen, *Biotech. and Biotech. Eq.* **8**, 66–70 (1994).
111. A.G. Schatzlein et al., *Proc. Int. Symp. Controlled Release Bioact. Mater.* **25**, 435 (1998).
112. M. Thanou et al., *Proc. Int. Symp. Controlled Release Bioact. Mater.* **25**, 14 (1998).
113. A.F. Kotzé et al., *Pharm. Res.* **14**(9), 1197–1202 (1997).
114. A.S. Hoffman et al., *Proc. Int. Symp. Controlled Release Bioact. Mater.* **24**, 563 (1997).
115. R. Dagani, *Chem. Eng. News*, 26–37 (June 1997).
116. K.Y. Lee et al., *Proc. Int. Symp. Controlled Release Bioact. Mater.* **24**, 651 (1997).
117. J. Murata, Y. Ohya, and T. Ouchi, *Carbohydr. Polym.* **29**(1), 69–74 (1996).
118. H.-Q. Mao et al., *Proc. Int. Symp. Controlled Release Bioact. Mater.* **24**, 671 (1997).
119. R. Kircheis et al., *Gene Ther.* **4**, 409–418 (1997).
120. J.-Y. Cherng et al., *Pharm. Res.* **13**(7), 1038–1042 (1996).
121. P. van de Wetering, J.-Y. Cherng, H. Talsma, and W.E. Hennink, *J. Controlled Release* **49**, 59–69 (1997).
122. I. Astafieva et al., *FEBS Lett.* **389**, 278–280 (1996).
123. J.F. Kukowska-Latello et al., *Proc. Natl. Acad. Sci. U.S.A.* **93**, 4897–4902 (1996).
124. M.X. Tang, C.T. Redemenn, and F.C. Szoka, *Bioconjugate Chem.* **7**, 703–714 (1996).
125. C.K. Goldman et al., *Nat. Biotechnol.* **15**, 462–466 (1997).

Next Page

126. S.M. Walsh et al., *Proc. Int. Symp. Controlled Release Bioact. Mater.*, **23**, 73 (1996).
127. V.L. Truong-Le, S.M. Walsh, J.T. August, and K.W. Leong, *Proc. Int. Symp. Controlled Release Bioact. Mater.* **22**, 466 (1995).
128. R. Sipehia and G. Martucci, *Biochem. Biophys. Res. Commun.* **214**(1), 206–211 (1995).

PROTEIN THERAPEUTICS FOR SKELETAL TISSUE REPAIR

HYUN D. KIM
Genetics Institute
Andover, Massachusetts
ROBERT F. VALENTINI
Brown University
Providence, Rhode Island

KEY WORDS

Bone
Bone morphogenetic protein
Carrier
Cartilage
Gene therapy
Growth factor
Matrix
Polymer drug delivery system

OUTLINE

Introduction
Growth and Morphogenetic Factors for Bone Repair
Mesenchymal Stem Cells
Mechanisms of Bone Repair
Carriers for Growth and Morphogenetic Factors
  Protein Delivery in Orthopedics
  Direct Gene Therapy
  Cell Based Gene Delivery
Summary
Bibliography

INTRODUCTION

Defects in bone that result from trauma (e.g., fractures), malformation, or disease processes such as cancer or osteoarthritis can cause significant morbidity. Current therapies for bone replacement rely on the use of allograft transplants from bone banks or autologous bone grafts. Frozen or freeze-dried allografts from human cadavers have been used clinically but are problematic due to potential for disease transmission, rejection, and resorption (1). The autograft involves direct transfer of viable bone-derived cells, inductive factors, and growth factors from the transplanted bone matrix, usually taken from the corticocancellous bone of the anterior iliac crest. Although trabecular autografts have ample osteogenic cells and good revascularization capabilities, it is often difficult to obtain a sufficient quantity of bone from the patient (2). Cortical autografts are more easily obtained and provide greater stability, but they often exhibit poor vascularity, a lower content of osteogenic cells, and a high rate of fatigue fractures occurring 6–8 months following operation (3). Autografts also subject the patient to surgery at a second site, which may lead to additional pain, risk of infection, nerve and vessel damage, and a prolonged hospital stay. Thus, the search for alternatives to autograft and allograft remains an important topic in medical research.

In recent years, considerable research has focused on improving bone repair through the use of various growth (e.g., platelet-derived growth factor [PDGF], transforming growth factor [TGF], fibroblast growth factor [FGF], epidermal growth factor [EGF], insulin-like growth factor [IGF]) and morphogenetic factors (e.g., bone morphogenetic proteins [BMP]). For example, initially isolated from demineralized bone matrix (DBM), partially purified BMP was found to be osteoinductive, inducing bone formation by causing host mesenchymal stem cells (MSCs) to migrate to the repair site and differentiate into bone-forming cells (4,5). The key difference between these two classes of molecules is that growth factors affect cell growth and function (e.g., proliferation and differentiation), whereas morphogenetic factors are involved in cell commitment and induction from an undifferentiated state to a specific cell type. Recombinant techniques are now used to isolate, identify, clone, and express different types of BMPs as well as other growth factors (PDGF, TGF, FGF, IGF) normally present in bone matrix, which may operate in complex synergy. At least two of these proteins, BMP-2 and BMP-7, induce significant bone formation in the absence of other BMPs when implanted into ectopic (non-bony) sites (6,7) as well as orthotopic (bony) sites (8–12), and will likely be the first available therapeutics for bone repair in the clinic. The exact role of other growth factors in the complex cascade of molecules involved in bone formation and maintainance is not well understood.

Many basic research and developmental challenges remain in protein- and gene-based therapeutics for skeletal tissue repair. Perhaps the most basic are the identification and understanding of the complex cascade of genes and proteins that regulate skeletal growth and repair, in both normal and diseased states. Significant progress is being made in this area. With regard to product development, one of the major challenges limiting clinical availability has been the issue of delivery. Traditional systemic delivery of these proteins has not been feasible for a variety of reasons, including short biological half-lives of proteins as well as lack of drug localization to the target injury site. Oral delivery of therapeutic proteins, on the other hand, has been limited by breakdown of proteins by digestive enzymes and challenges with proteins crossing the intestinal wall intact and active. Progress is being made to protect proteins in the digestive tract using encapsulation systems, and this route of drug delivery would be appropriate for certain proteins that have systemic effects. Delivery of proteins and genes for skeletal tissue repair are founded

Previous Page

126. S.M. Walsh et al., *Proc. Int. Symp. Controlled Release Bioact. Mater.*, **23**, 73 (1996).
127. V.L. Truong-Le, S.M. Walsh, J.T. August, and K.W. Leong, *Proc. Int. Symp. Controlled Release Bioact. Mater.* **22**, 466 (1995).
128. R. Sipehia and G. Martucci, *Biochem. Biophys. Res. Commun.* **214**(1), 206–211 (1995).

PROTEIN THERAPEUTICS FOR SKELETAL TISSUE REPAIR

HYUN D. KIM
Genetics Institute
Andover, Massachusetts
ROBERT F. VALENTINI
Brown University
Providence, Rhode Island

KEY WORDS

Bone
Bone morphogenetic protein
Carrier
Cartilage
Gene therapy
Growth factor
Matrix
Polymer drug delivery system

OUTLINE

Introduction
Growth and Morphogenetic Factors for Bone Repair
Mesenchymal Stem Cells
Mechanisms of Bone Repair
Carriers for Growth and Morphogenetic Factors
  Protein Delivery in Orthopedics
  Direct Gene Therapy
  Cell Based Gene Delivery
Summary
Bibliography

INTRODUCTION

Defects in bone that result from trauma (e.g., fractures), malformation, or disease processes such as cancer or osteoarthritis can cause significant morbidity. Current therapies for bone replacement rely on the use of allograft transplants from bone banks or autologous bone grafts. Frozen or freeze-dried allografts from human cadavers have been used clinically but are problematic due to potential for disease transmission, rejection, and resorption (1). The autograft involves direct transfer of viable bone-derived cells, inductive factors, and growth factors from the transplanted bone matrix, usually taken from the corticocancellous bone of the anterior iliac crest. Although trabecular autografts have ample osteogenic cells and good revascularization capabilities, it is often difficult to obtain a sufficient quantity of bone from the patient (2). Cortical autografts are more easily obtained and provide greater stability, but they often exhibit poor vascularity, a lower content of osteogenic cells, and a high rate of fatigue fractures occurring 6–8 months following operation (3). Autografts also subject the patient to surgery at a second site, which may lead to additional pain, risk of infection, nerve and vessel damage, and a prolonged hospital stay. Thus, the search for alternatives to autograft and allograft remains an important topic in medical research.

In recent years, considerable research has focused on improving bone repair through the use of various growth (e.g., platelet-derived growth factor [PDGF], transforming growth factor [TGF], fibroblast growth factor [FGF], epidermal growth factor [EGF], insulin-like growth factor [IGF]) and morphogenetic factors (e.g., bone morphogenetic proteins [BMP]). For example, initially isolated from demineralized bone matrix (DBM), partially purified BMP was found to be osteoinductive, inducing bone formation by causing host mesenchymal stem cells (MSCs) to migrate to the repair site and differentiate into bone-forming cells (4,5). The key difference between these two classes of molecules is that growth factors affect cell growth and function (e.g., proliferation and differentiation), whereas morphogenetic factors are involved in cell commitment and induction from an undifferentiated state to a specific cell type. Recombinant techniques are now used to isolate, identify, clone, and express different types of BMPs as well as other growth factors (PDGF, TGF, FGF, IGF) normally present in bone matrix, which may operate in complex synergy. At least two of these proteins, BMP-2 and BMP-7, induce significant bone formation in the absence of other BMPs when implanted into ectopic (non-bony) sites (6,7) as well as orthotopic (bony) sites (8–12), and will likely be the first available therapeutics for bone repair in the clinic. The exact role of other growth factors in the complex cascade of molecules involved in bone formation and maintainance is not well understood.

Many basic research and developmental challenges remain in protein- and gene-based therapeutics for skeletal tissue repair. Perhaps the most basic are the identification and understanding of the complex cascade of genes and proteins that regulate skeletal growth and repair, in both normal and diseased states. Significant progress is being made in this area. With regard to product development, one of the major challenges limiting clinical availability has been the issue of delivery. Traditional systemic delivery of these proteins has not been feasible for a variety of reasons, including short biological half-lives of proteins as well as lack of drug localization to the target injury site. Oral delivery of therapeutic proteins, on the other hand, has been limited by breakdown of proteins by digestive enzymes and challenges with proteins crossing the intestinal wall intact and active. Progress is being made to protect proteins in the digestive tract using encapsulation systems, and this route of drug delivery would be appropriate for certain proteins that have systemic effects. Delivery of proteins and genes for skeletal tissue repair are founded

on local use, and various strategies are being developed to deliver these therapeutics to the local injury site. The emergence of polymeric drug delivery systems and biomaterials has contributed significantly to the challenges of local delivery of proteins and genes. These carriers of therapeutics serve to provide a reservoir that can maintain a local concentration of drugs as well as provide a controlled, sustained release of these drugs for extended therapeutic effect.

Three strategies exist when considering delivery of therapeutics for local skeletal tissue repair. Perhaps the simplest is protein delivery in which the recombinant protein itself is incorporated within a carrier system such as polymer microspheres or biomaterial matrices. Another method is direct gene therapy, whereby the goal is to deliver the naked genes themselves into the target site and have the genes incorporate into the host cells that can produce the gene products. A third option is cell-based delivery, in which the gene of interest is inserted into a specific cell line, usually autogenous or allogeneic, so that the cells become delivery systems for gene products. Active research is being carried out in all three areas with promising results that may become successful therapies in the clinic.

The ideal carrier for bone growth and morphogenetic factors and the genes encoding them is still under investigation. Various bioderived materials such as bone matrix collagen and DBM as well as synthetic materials including ceramics and degradable polymers (e.g., poly(lactic acid) (13), poly(lactide-*co*-glycolide) (PLGA) (10), poly(phosphazene) (14)) have been studied as suitable bone graft substitutes. Allogeneic DBM, which contains a cocktail of osteoinductive proteins, has been shown to form bone in vivo (15), but when the matrix proteins are extracted with guanidinium hydrochloride to yield insoluble collagenous bone matrix (ICBM), bone does not form. When ICBM is combined with this protein extract (containing various BMPs), the osteoinductive activity is restored. However, the use of ICBM or DBM in the clinical setting has serious drawbacks, including potential immunogenicity, potential pathogen transmission, sterility assurance, supply problems, and lack of structural integrity.

Consequently, growth and morphogenetic factors require a suitable matrix or carrier serving as an effective delivery system by localizing and creating a high concentration of protein at the injury site, preventing loss of protein into neighboring sites (i.e., when using scaffolds for local bone formation), providing a sustained release of protein for local or systemic delivery (i.e., when using polymer drug delivery systems), and maximizing the interaction between the protein and the target host cells. Ideally, the bone repair scaffolds should be biocompatible and biodegradable to minimize local tissue response and should resorb as new bone is formed. On the other hand, polymer drug delivery systems should provide a sustained, controlled release of therapeutics for either local or systemic action. Sustained, controlled delivery of growth and morphogenetic factors using polymer delivery systems, scaffolds, or other matrices are advantageous over conventional injection of these therapeutics in solution form due to the clearance or elimination of injected drug by the systemic circulation as well as the inconvenience and necessity for multiple or repeated injections for effective treatment. In this article, proteins and genes involved in skeletal tissue repair as well as novel strategies for delivering them are introduced.

GROWTH AND MORPHOGENETIC FACTORS FOR BONE REPAIR

Serious skeletal defects result from diverse causes including trauma, birth defects, oncologic resections, and disease pathosis (e.g., periodontitis, degenerative osteoarthritis, and osteomyelitis). To restore lost tissue or prevent fracture nonunion, orthopaedic, plastic, and oral surgeons perform more than 250,000 bone grafts annually in the U.S. (8). As currently practiced, bone grafting predominantly uses autogenous corticocancellous bone taken from a donor site such as the anterior iliac crest. Although highly effective, autologous bone grafting is limited by such issues as donor site morbidity and pain, donor site infection, blood loss, and limited supply of donor site material. Allogeneic human cadaver bone graft is the most common alternative to the bone graft, but allografts suffer from the potential for disease transmission, rejection, and resorption.

Urist first observed in 1965 that implanting DBM in extraskeletal sites generated osseous tissue in rats (4). This process has been termed osteoinduction, that is, bone formation from MSCs that have differentiated down the osteoblastic lineage. Osteoconduction, on the other hand, refers to the ability of a material to support bone ingrowth from surrounding bone and depends on the material itself, its biocompatibility, porosity, surface charge, surface texture, and biodegradability. Later studies demonstrated that extracting the DBM with aqueous guanidinium hydrochloride yielded ICBM that is not osteoinductive. Reconstituting ICBM with the aqueous extract, which Urist called BMP, restored the osteoinductive activity as in DBM. However, the use of ICBM or DBM in the clinical setting has serious drawbacks, including potential immunogenicity, potential pathogen transmission, sterility assurance, supply problems, and lack of structural integrity.

More recently, modern biotechnology techniques have been used to isolate, identify, clone, and express more than 15 individual BMPs, which are all members of the transforming growth factor-beta (TGF-β) superfamily. New molecules continue to be identified and cloned. These recombinant human BMPs (rhBMPs) are present in bone extracellular matrix in trace amounts and probably operate in complex synergies. However, at least two of the individual proteins, namely rhBMP-2 and rhOP-1 (osteogenic protein-1, also known as BMP-7), are potential candidates for clinical use because they induce bone formation in the absence of other BMPs when implanted into bony and nonbony sites (6,7). The rhBMP-2, which is expressed in Chinese hamster ovary cells, contains an aminoterminal propeptide of 40–45 kDa, a mature active 30 kDa homodimer consisting of 18 and 22 kDa subunits, and a small amount of uncleaved 60 kDa precursor protein (16).

In vitro, rhBMP-2 induces pluripotent MSCs to differentiate into bone, cartilage, and fat lineages in a dose- and time-dependent manner (17). When combined with ICBM fragments or polyester carriers (e.g., PLGA, PLLA), rhBMP-2 or rhOP-1 regenerates osseous tissue in various species and anatomic sites, including rat muscle (18), rat calvarium (8,11,12), rat subcutaneous tissue (6,7), rat femur (10,19), sheep femur (9), and canine maxillary cleft (20).

TGF-β (25 kD molecular weight) is another factor important in the regulation of cell proliferation and differentiation and has been implicated in bone and cartilage formation and maintenance (21). There are three isoforms (β1, β2, β3), which have the ability to influence the mesenchymal cell differentiation pathway to bone and cartilage in a dose-dependent manner (22). TGF-β is found in macrophages and other inflammatory cells, platelets during degranulation in hematoma formation, and bone matrix, where it is most abundant (23). TGF-β is converted to its active form under acidic conditions, such as those produced by macrophages or osteoclasts during bone resorption (24). There have been a number of studies that suggest that TGF-β is involved in cartilage differentiation and bone repair, although its exact role is not well understood. TGF-β has been shown to induce chondrocytic differentiation from micromass cultures of pluripotent C3H10T1/2 (T1/2) cells (25), chick limb bud mesenchymal cells (26), and periosteal cells (27). TGF-β has also been implicated in the process of endochondral ossification (22,27) (i.e., when TGF-β1 was injected subperiosteally into uninjured bone, it induced a cartilagenous mass that underwent endochondral ossification). Consequently, TGF-β has been shown to have both stimulatory and inhibitory effects on the differentiation of bone cells depending on the maturation stage of the cells used, cell density, and growth factor concentration (25,28).

PDGF is a polypeptide dimer of 30 kDa that is unrelated to the TGF-β superfamily but acts as a mitogen for a variety of cell types. PDGF was found to increase DNA synthesis in cultured rat calvariae and fibroblasts but did not stimulate collagen synthesis or organized bone formation (29). It exists as a homodimer or heterodimer comprising A or B subunits, although the BB homodimer is more effective than AA or AB in stimulating bioactivity in bone cells in vitro (29). Similar to TGF-β, the exact role of PDGF in bone repair is not clearly understood. Marden et al. (30) reported that PDGF inhibited bone regeneration in a rat cranial defect model, whereas Bolander (23) reported that PDGF subperiosteal injections resulted in stimulation of MSC proliferation and subsequent bone mass increase in rat femurs. Other proteins such as FGF and IGF have also been linked to bone cell function (23). In addition, many other types of factors have been identified to influence skeletal tissue development, repair, and maintenance (Fig. 1). Hormones (e.g., parathyroid hormone [PTH], estrogen, calcitonin), vitamins (e.g., vitamin A, C, D, etc.), and glucocorticoids (e.g., dexamethasone, cortisol, etc.) also have specific effects on mesenchymal stem cells, cartilage cells (chondrocytes), and bone cells (osteoblasts) as do growth and morphogenetic factors. The key difference between growth (e.g., PDGF, TGF-β) and morphogenetic (e.g., BMP) factors is that growth factors affect cell growth and function, whereas morphogenetic factors are involved in cell commitment and induction from an undifferentiated state to a specific cell type (Table 1). This will likely influence how they are used in the clinic and suggests that two or more proteins may be necessary for some treatments.

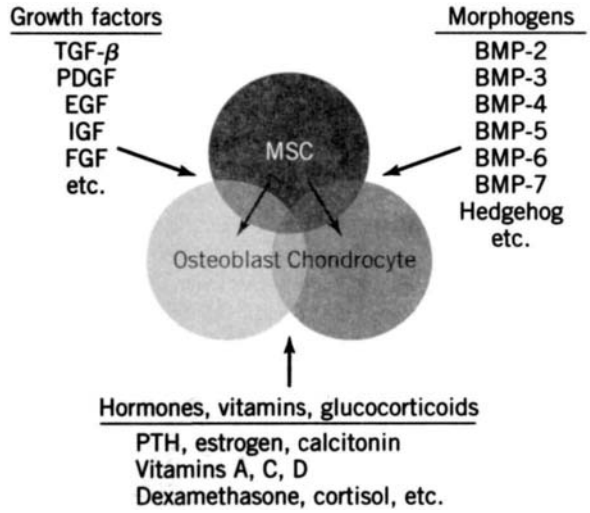


Figure 1. Skeletal tissue development, repair, and maintenance factors that affect MSC, osteoblasts, and chondrocytes.

MESENCHYMAL STEM CELLS

MSCs are undifferentiated, pluripotent cells capable of differentiating into cells that form into various connective tissues such as bone, cartilage, tendon, ligament, muscle, and fat. During development, multipotential stem cells progressively become committed to specific paths. This process, called determination or commitment, irreversibly alters the cells so that the progeny inherits this more limited potential. Once committed or determined, the precursor cell may exist in this state until it differentiates. Differentiation is defined as the expression of one or more markers of the functionally mature cell and may be reversible or terminal. The environment of the progenitor cells (i.e., protein factors, extracellular matrix, cellular contact, and other unknown factors) may influence commitment and differentiation (31). Compared with hematopoietic stem

Table 1. Role of Growth and Morphogenetic Factors on MSCs, Cartilage Cells (Chondrocytes), and Bone Cells (Osteoblasts)

	MSCs	Chondrocyte	Osteoblast
PDGF	Proliferation	Proliferation	Proliferation
TGF-β	Proliferation	Proliferation Differentiation	Differentiation
BMP	Commitment Proliferation Differentiation	Differentiation	Differentiation

cells, much less is known about multipotential progenitor cells of mesodermal origin (also referred to as MSCs). Like hematopoietic factors, BMPs influence the commitment of MSCs.

Bone marrow is a complex tissue comprised of red and white blood cells, their precursors, and a connective tissue network or stroma. Bone marrow stromal cells have a close structural and functional relationship with bone cells, and it is generally believed that osteoblast precursors are derived from the mesenchymal stromal cell lineage. In vitro, typical bone phenotypic markers such as alkaline phosphatase activity, cAMP response to parathyroid hormone, osteocalcin synthesis, collagen I production and gene expression, osteonectin gene expression, and mineralized nodules are expressed by cultured human bone marrow stromal cells (32). The existence of cells in marrow that have osteochondrogenic potential has been demonstrated with whole marrow and cultured marrow stromal cells from a variety of animal species including humans (33). Additional evidence of in vivo osteochondrogenic potential of marrow stroma has been derived from experiments using grafts of whole marrow or cultured marrow stromal cells with calcium phosphate ceramics (34,35).

C3H10T1/2 cells are an established murine MSC line originally isolated as embryonic limb-derived fibroblasts, which differentiate into muscle, fat, and cartilage cells when treated with azacytidine. BMP-2 causes a dose-dependent differentiation of these cells into fat, cartilage, and bone cells; low concentrations favor adipocytes and high concentrations result in chondrocytes and osteoblasts (17). Osteogenic cell markers such as alkaline phosphatase activity have been used to demonstrate stem cell differentiation into osteoblastic cells by BMP-2 (36). Therefore, C3H10T1/2 cells serve as a simple in vitro cell culture system to characterize the osteogenic potential of BMPs and other proteins.

MECHANISMS OF BONE REPAIR

Ectopic bone formation refers to bone formation in a non-bony site, such as in subcutaneous or intramuscular sites. These sites have been mainly used to test the osteoinductive ability of bone morphogenetic proteins in an environment that is surrounded by tissue of mesodermal origin. On the other hand, because bone is a self-repairing tissue (limited by the defect size), a model to test bone formation in a bony site has also been established. A critical size defect is defined as the smallest intraosseous wound that does not heal by bone formation during the lifetime of the animal (37–39). A critical size defect heals by fibrous connective tissue formation and the actual critical size varies in different species, often increasing with animal size. For example, an 8-mm diameter skull defect has been characterized as a critical size defect in a rat, whereas a 4 mm heals eventually. The traditional bony sites involved in testing defects or nonunions (fractures that do not heal) have been the skull and the femur. Calvarial critical defects have been extensively characterized and established as a site to test bone repair materials (37). It is important to note that the calvarium develops and heals by intramembranous ossification (direct formation of bone by osteoblasts) and is a non-weight-bearing bone. In contrast, femoral bone heals by endochondral ossification (bone formation through a cartilage intermediate), which is weight bearing (Fig. 2). BMP-2 has been shown to stimulate endochondral but not intramembranous bone formation.

CARRIERS FOR GROWTH AND MORPHOGENETIC FACTORS

Considerable effort has been dedicated to developing delivery systems for proteins targeted for bone repair. Oral administration presents difficulty for peptide-based drugs, which are rapidly digested by gastric and intestinal enzymes. Intravenous delivery results in alteration and clearance by the liver. Drug delivery vehicles facilitate the sustained, controlled delivery of growth factors and minimize the fluctuating levels achieved with single or multiple doses. A variety of delivery systems or carriers for peptides and proteins have been investigated (40–45) and are illustrated in Figure 3. For example, PDGF (40), basic FGF (46), EGF (47), and TGF-β (48) have been incorporated into various degradable (PLGA films, microspheres, rods, etc.) or nondegradable (mechanical pumps, diffusion

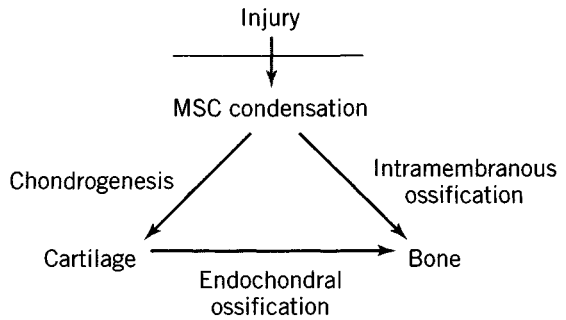


Figure 2. Bone and cartilage development and repair pathways.

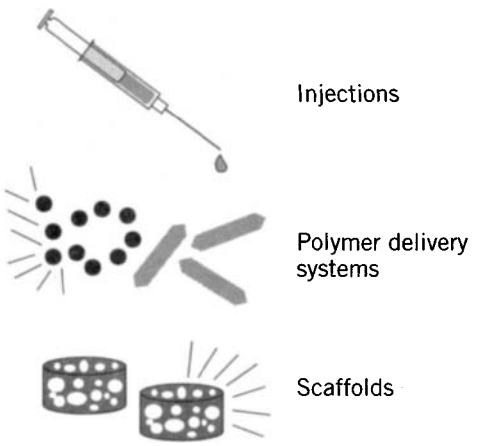


Figure 3. Strategies for delivering protein-, gene-, and cell-based therapeutics for local bone and cartilage repair.

based polymer matrices) delivery systems for controlled release. Ethylene vinyl acetate (EVA) copolymer is a nondegradable elastomer that has been used to deliver a host of small and large molecules (45). Bovine serum albumin (BSA) has been used extensively as carrier for EVA systems and EVA/BSA release has been shown to parallel growth factor release (45). Release kinetics for EVA systems can be controlled by varying drug loading, choice of carrier, device geometry, or by polymer surface coating (45). In one study, controlled, sustained release of bioactive PDGF and TGF-β was demonstrated from EVA polymer rods (40).

New tissue engineering approaches for bone and cartilage repair leverage the ability of growth and morphogenetic factors to control cell growth, differentiation, and new tissue formation at the site of injury or defect. Porous, degradable polymer scaffolds have been identified to be suitable bone or cartilage repair materials because they can be carriers for these tissue-inducing molecules and also allow the seeding of culture-expanded cells (i.e., chondrocytes, osteoblasts, MSCs) in vitro or host cell and tissue ingrowth in vivo. A wide variety of synthetic (e.g., PLGA) or natural polymers (e.g., collagen) have been explored as delivery vehicles for cells or growth/morphogenetic factors. These three-dimensional polymeric scaffolds have been fabricated using a variety of methods and used for a variety of applications such as cartilage repair, nonunion fracture defects, oral and maxillofacial defects, and spinal fusion. Various degradable polymer carriers or scaffolds containing BMPs have been used for local bone and cartilage formation (8,12,20,41,49–51).

Some semisynthetic polymers (e.g., chemically natural polymers) are also being explored. For example, derivatized hyaluronic acid is a class of semisynthetic biopolymer that can be fabricated into porous scaffolds for tissue reconstruction and repair. It is a benzyl ester derivative of the polysaccharide hyaluronic acid, which exists naturally in extracellular matrix and plays an important role in proteoglycan organization, cell hydration, cell differentiation, and wound healing (52). The benzyl esterification of the glucuronic acid residue of hyaluronic acid renders the polymer insoluble in aqueous conditions and significantly decreases the rate of degradation in vivo by hydrolysis and hyaluronidases (53). Hyaluronic acids are attractive choices for tissue repair scaffolds because biocompatibility has been well established (53). In addition, degradation can be controlled by altering the amount of esterification, and complex three-dimensional shapes with various porosities and pore sizes can be achieved (53).

Only a few formulations have been actively pursued for skeletal tissue repair. They include injectable formulations (such as microspheres, depots, and gels) and implantable matrices or scaffolds. Injectables can work as minimally invasive delivery systems by providing sustained release of a protein at the repair site. In open, surgical procedures, implantable scaffolds provide the opportunity for cells to migrate into the carrier, adhere, proliferate, and differentiate while also providing sustained release of protein. Scaffolds for tissue engineering should meet several design criteria: (*1*) the surface should permit cell adhesion and growth, (*2*) neither the polymer nor its degradation products should provoke inflammation or toxicity when implanted in vivo, (*3*) the material should be reproducibly processable into three-dimensional structures, (*4*) porosity should be high in order to provide a large surface area for cell migration, adhesion, and matrix regeneration, and (*5*) the scaffold should resorb in concert with new tissue formation.

Protein Delivery in Orthopedics

New advances are being made in the field of protein-, gene-, and cell-based therapeutics for skeletal tissue repair. Protein drug delivery is the direct delivery of already synthesized proteins using a specific carrier to the local tissue. Proteins are usually encapsulated or admixed within a polymer matrix and are released to the local site in a controlled, sustained fashion in the order of hours up to years (45). The simplicity of drug delivery systems and the ability to control dose and release rate remain the major advantages of this delivery strategy. However, drug stability and bioactivity must be carefully characterized within a particular carrier system.

Of all the growth and differentiation factors discovered to date, only a few have shown significant potential for skeletal tissue repair. These include human recombinant proteins of BMP-2, BMP-7 (or osteogenic protein-1, rhOP-1), basic FGF (bFGF), and TGF-β1. BMP-2 and rhOP-1 are currently in preclinical and clinical studies for a range of bone-specific indications such as fracture healing, oral and maxillofacial defects, spinal fusion, and cartilage repair. bFGF is also in clinical studies for accelerated fracture repair, whereas TGF-β1 is in preclinical studies for cartilage and bone repair. All of these proteins have been delivered in association with an appropriate drug delivery carrier (e.g., collagen), although simple injections of these proteins alone at high doses can still induce some level of efficacy (6). The presence of a matrix or carrier either enhances the volume of new repair tissue formed, decreases the amount of protein needed to induce efficacy, and prolongs residence of protein at the local repair site to allow sufficient time for responsive cells to migrate and react.

In the area of fracture and bone defect repair, BMP-2 and rhOP-1 have shown to be most effective when delivered in association with a carrier, which have mainly been collagen based to date. For example, BMP-2 loaded onto absorbable collagen sponges has shown good efficacy in accelerating healing in a fracture model (54). In another study, rhOP-1 incorporated with another type of implantable collagen matrix was shown to heal large segmental bone defects (55). Both of these devices performed equally or better than the traditional clinical standard of using autogenous bone graft for nonunion defects or immobilization for union fractures. Other carriers such as ceramic-based calcium phosphates containing BMP (56) have been shown to be effective for bone defect repair. More recently, injectable gels such as bFGF-containing hyaluronic acid have shown efficacy for accelerated fracture repair (57). Injectable gels that deliver the protein for the duration of the healing period and contribute to fracture callus formation would be ideal carriers. Polymer, ceramic, or com-

posite matrices that can withstand soft tissue pressure or bear weight may represent the next generation of bone defect repair materials.

Other bone-specific indications for protein delivery include spinal fusion and oral and maxillofacial surgery. In one study, BMP-2 loaded onto absorbable collagen sponges has been shown to enhance fusion in nonhuman primate lumbar interbody spinal fusion models (58). In oral and maxillofacial surgery, collagen matrix/BMP-2 was shown to be successful in repairing mandibular defects in a canine model (59), alveolar ridge augmentation procedures in human clinical trials (60), osseointegration of titanium dental implants in nonhuman primates (61), and maxillary sinus floor augmentation procedures (62).

Cartilage, tendon, and ligament repair are also being using protein therapeutics. Recent studies using BMP-2 in combination with absorbable collagen sponges has shown success in repairing articular cartilage defects in a rabbit model (63). Injection of TGF-β1 encapsulated within liposomes was shown to accelerate the repair of articular cartilage defects in rabbits (64). New members of the TGF-β gene family, the growth and differentiation factors 5, 6, and 7 (GDF-5, 6, 7) have been shown to induce neotendon and ligament when implanted in association with a collagen matrix in rat models (65).

Direct Gene Therapy

An alternative to delivering proteins is to directly deliver the genes encoding these proteins to the host cells as naked plasmid DNA injections, or using nonviral transfection or viral transduction methods. Potential advantages of gene therapy over direct protein delivery include (*1*) no need for manufacturing or purification facilities, (*2*) constant production of fresh protein in bioactive form, and (*3*) lower dose requirements for achieving efficacy. Limits of gene therapy include poor long-term gene expression, inefficient transfection of genes to target cells, and the inability to control or cease expression as needed. Nevertheless, significant progress is being made in orthopedic preclinical studies. In one study, plasmid DNA encoding for either BMP-4 or a fragment of PTH (amino acids 1–34) alone resulted in new bone formation when implanted into segmental bone defects in the rat femur (66). When BMP-4 and the parathyroid fragment were implanted together, acceleration of bone formation was observed compared with either factor alone, suggesting synergy. Adenovirus containing the β-galactosidase reporter gene injected into the synovium of cartilage joints was able to infect the cells lining the synovium and express the marker gene for at least 8 weeks after injection (67). Expression of marker genes using an adenoviral vector injected into segmental defect sites for 6 weeks has also been reported (68).

Cell Based Gene Delivery

An alternative approach for delivering proteins is to use genetically engineered cells as carriers for genes encoding the proteins of interest. This strategy is a novel concept in orthopedic drug delivery and limited literature exists. The basic concept is to generate, in vitro, cells or tissues that are implantable protein factories. The cell-based factories are injected at the local tissue repair site and produce the protein of interest over time. Cells can be injected as a cell suspension or in association with a carrier such as a scaffold or gel. They can also be formed into organized tissue in vitro and subsequently implanted as a discrete structure (69). The advantages of this system are (*1*) the ability to control the dose of protein delivered (by controlling expression levels, cell numbers, etc.), (*2*) the ability to retrieve the cells as needed (if implanted in a defined scaffold such as a cell-occlusive membrane), (*3*) the ability to control transfection or transduction in only the desired cells, and (*4*) the ability to treat acute or chronic conditions. The cells that are transfected or transduced ex vivo can be autologous, allogeneic, or xenogeneic (if protected by a immunoisolatory membrane). Autologous cells are the currently preferred choice as they eliminate any immune response, but they must be harvested from the donor as a separate procedure. Preliminary studies for bone and cartilage repair are encouraging. In one study, a bone marrow stromal cell line infected with an adenovirus expressing recombinant human BMP-2 was able to form ectopic bone when injected into rat muscle (70). In another study, chondrocytes that were infected with adenovirus expressing a marker gene β galactosidase remained in the joint space and expressed the reporter gene for at least 45 days when injected into cartilage explants (71). Additionally, bone marrow cells transfected with a gene encoding for a new osteoinductive protein (LIM mineralization protein-1) and seeded onto a collagen matrix supported successful spinal fusion following implantation into rats (72). Despite promising results, further research is needed to develop cell-based approaches into viable therapies.

SUMMARY

Protein-, gene-, and cell-based systems offer powerful new approaches for skeletal tissue repair. Applications range from fracture healing, bone defect repair, spinal fusion, and oral and maxillofacial surgery to cartilage, tendon, and ligament repair. These approaches require the development of novel delivery systems. Delivery systems have several requirements and must (*1*) serve as effective carriers for therapeutic agents, (*2*) provide localization of the protein to the target repair site, (*3*) maintain bioactivity in vivo, (*4*) provide controlled, sustained release to the surrounding tissue, and (*5*) in some instances, concurrently serve as scaffolds for tissue ingrowth.

BIBLIOGRAPHY

1. G.D. Bos et al., *J. Bone J. Surg., Am. Vol.* **65-A**, 239–246 (1983).
2. D. Prolo and J. Rodrigo, *Clin. Orthop. Relat. Res.* **200**, 322–341 (1985).
3. W.F. Enneking, J.L. Eady, and H. Burchardt, *J. Bone J. Surg., Am. Vol.* **62-A**, 1039–1058 (1980).
4. M.R. Urist, *Science* **150**, 893–899 (1965).

5. M.R. Urist et al., *Clin. Orthop. Relat. Res.* **162**, 219–232 (1982).
6. E.A. Wang et al., *Proc. Natl. Acad. Sci. U.S.A.* **87**(6), 2220–2224 (1990).
7. T.K. Sampath et al., *J. Biol. Chem.* **267**(28), 20352–20362 (1992).
8. R. Kenley et al., *J. Biomed. Mater. Res.* **28**, 1139–1147 (1994).
9. T.N. Gerhart et al., *Clin. Orthop. Relat. Res.* **293**, 317–326 (1993).
10. S.C. Lee et al., *J. Biomed. Mater. Res.* **28**, 1149–1156 (1994).
11. L.J. Marden, N.C. Quigley, A.H. Reddi, and J.O. Hollinger, *Calcif. Tissue Int.* **53**, 262–268 (1993).
12. L.J. Marden et al., *J. Biomed. Mater. Res.* **28**, 1127–1138 (1994).
13. A.G. Mikos et al., *Polymer* **35**, 1068–1077 (1994).
14. C.T. Laurencin et al., *J. Biomed. Mater. Res.* **27**, 963–973 (1993).
15. T.A. Einhorn et al., *J. Bone J. Surg., Am. Vol.* **66-A**, 274–279 (1985).
16. D.I. Israel et al., *Growth Factors* **7**, 139–150 (1992).
17. E.A. Wang, D.I. Israel, S. Kelly, and D.P. Luxenberg, *Growth Factors* **9**, 57–71 (1993).
18. P.A. Lucas, G.T. Syftestad, V.M. Goldberg, and A.I. Caplan, *J. Biomed. Mater. Res.* **23**(A1), 23–29 (1989).
19. A.W. Yasko et al., *J. Bone J. Surg., Am. Vol.* **74-A**(5), 659–670 (1992).
20. M. Mayer, J. Hollinger, E. Ron, and J. Wozney, *Plast. Reconstr. Surg.* **98**, 247–259 (1996).
21. M. Centrella, M.C. Horowitz, J.M. Wozney, and T.L. McCarthy, *Endocr. Rev.* **15**, 27–39 (1994).
22. M.E. Joyce, S. Jingushi, and M.E. Bolander, *Orthop. Clin. North Am.* **21**, 199–209 (1990).
23. M.E. Bolander, *Proc. Soc. Exp. Biol. Med.* **200**, 165–170 (1992).
24. D.A. Lawrence, R. Pircher, and P. Jullien, *Biochem. Biophys. Res. Commun.* **133**, 1026–1034 (1985).
25. A.E. Denker, S.B. Nicoll, and R.S. Tuan, *Differentiation (Berlin)* **59**, 25–34 (1995).
26. E.F. Roark and K. Greer, *Dev. Dyn.* **200**, 103–116 (1994).
27. M.E. Joyce, A.B. Roberts, M.B. Sporn, and M.E. Bolanders, *J. Cell. Biol.* **110**, 2195–2207 (1990).
28. P.V. Hausckha, T.L. Chen, and A.E. Mavrakos, *Ciba Found. Symp.* **136**, 205–207 (1988).
29. J.M. Hock and E. Canalis, *Endocrinology (Baltimore)* **134**, 1423–1428 (1994).
30. L.J. Marden et al., *J. Clin. Invest.* **92**, 2897–2905 (1993).
31. A.I. Caplan, *J. Orthop. Res.* **9**(5), 641–650 (1991).
32. R.W. Zhang et al., *Calcif. Tissue Int.* **56**, 283–291 (1995).
33. S.P. Bruder, D.J. Fink, and A.I. Caplan, *J. Cell. Biochem.* **56**, 283–294 (1994).
34. J. Goshima, V.M. Goldberg, and A.I. Caplan, *Clin. Orthop. Relat. Res.* **262**, 298–311 (1991).
35. S.E. Haynesworth, J. Goshima, V.M. Goldberg, and A.I. Caplan, *Bone* **13**, 81–88 (1992).
36. T. Katagiri et al., *Biochem. Biophys. Res. Commun.* **172**(1), 295–299 (1990).
37. J.O. Hollinger and J.C. Kleinschmidt, *J. Craniofacial Surg.* **1**(1), 60–68 (1990).
38. J.P. Schmitz and J.O. Hollinger, *Clin. Orthop. Relat. Res.* **205**, 299–308 (1986).
39. J.P. Schmitz, Z. Schwartz, J.O. Hollinger, and B.D. Boyan, *Acta Anat.* **138**, 185–192 (1990).
40. H.D. Kim and R.F. Valentini, *Biomaterials* **18**, 1175–1184 (1997).
41. J.O. Hollinger and K. Leong, *Biomaterials* **17**, 187–194 (1996).
42. M. Isobe et al., *J. Biomed. Mater. Res.* **32**, 433–438 (1996).
43. J. Hollinger, *J. Craniofacial Surg.* **4**, 135–141 (1993).
44. J. Hollinger, *J. Craniofacial Surg.* **4**, 102–108 (1993).
45. R. Langer, *Science* **249**, 1527–1533 (1990).
46. E.R. Edelman, E. Mathiowitz, R. Langer, and M. Klagsburn, *Biomaterials* **12**, 619–626 (1991).
47. J.B. Murray, L. Brown, R. Langer, and M. Klagsburn, *In Vitro* **19**, 743–748 (1983).
48. W.R. Gombotz et al., *J. Biomater. Sci. Polym. Ed.* **5**, 49–63 (1993).
49. B.P. Robinson, J.O. Hollinger, E.H. Szachowicz, and J. Brekke, *Otolaryngol. Head Neck Surg.* **112**, 707–713 (1995).
50. J.H. Schimandle, S.D. Boden, and W.C. Hutton, *Spine* **20**, 1326–1337 (1995).
51. H.S. Sandhu et al., *Spine* **21**, 2115–2122 (1996).
52. B. Toole, *In* E. Hay, ed, *Cell Biology of Extracellular Matrix*, Plenum, New York, 1991, pp. 305–341.
53. L. Benedetti et al., *Biomaterials* **14**, 1154–1160 (1993).
54. R.D. Welch et al., *J. Bone Miner. Res.* **13**, 1483–1490 (1998).
55. S.D. Cook et al., *J. Orthop. Trauma* **12**, 407–412 (1998).
56. M.R. Urist et al., *Clin. Orthop.* **214**, 295–304 (1987).
57. M.L. Radomsky, A.Y. Thompson, R.C. Spiro, and J.W. Poser, *Clin. Orthop.* **355**, S283–S293 (1998).
58. S.D. Boden et al., *J. Spinal Disord.* **11**, 95–101 (1998).
59. D.M. Toriumi et al., (1991) *Arch. Otolaryngol. Head Neck Surg.* **117**, 1101–1112 (1991).
60. T.H. Howell et al., *Int. J. Periodont. Restorative Dent.* **17**, 124–139 (1997).
61. O. Hanisch et al., *Int. J. Oral Maxillofacial Implants* **12**, 785–792 (1997).
62. C.A. Kirker-Head et al., *Int. J. Oral Maxillofacial Implants* **12**, 403–411 (1997).
63. R.S. Sellers, D. Peluso, and E.A. Morris, *J. Bone J. Surg., Am. Vol.* **79-A**, 1452–1463 (1997).
64. T. Abe et al., *Proc. 44th Ann. Meet., Orthop. Res. Soc.*, 1998, p. 380.
65. N.M. Wolfman et al., *J. Clin. Invest.* **100**, 321–330 (1997).
66. J. Fang et al., *Proc. Natl. Acad. Sci. U.S.A.* **93**, 5753–5758 (1996).
67. B.J. Roessler et al., *J. Clin. Invest.* **92**, 1085–1092 (1993).
68. C. Niyibizi et al., *Clin. Orthop.* **355**, S148–S153 (1998).
69. H. Vandenburgh et al., *Hum. Gene Ther.* **7**, 2195–2200 (1996).
70. J.R. Lieberman et al., *J. Orthop. Res.* **16**, 330–339 (1998).
71. P.J. Doherty et al., *Osteoarthritis Cartilage* **6**, 153–159 (1998).
72. S.D. Boden et al., *Spine* **23**, 2486–2492 (1998).

PUMPS/OSMOTIC

Introduction
ALZET® System
VITS Veterinary Implant
DUROS™ Osmotic Implant for Humans
Ruminal Osmotic Bolus

PUMPS/OSMOTIC—INTRODUCTION

JEREMY C. WRIGHT
CYNTHIA L. STEVENSON
ALZA Corporation
Palo Alto, California

KEY WORDS

Diaphragm
Osmosis
Osmotic system theory
Semipermeable membrane
Sodium chloride
Zero-order

OUTLINE

Early Osmotic Systems
Characteristics of Osmotic Systems
Osmotic System Theory
System Design Considerations
Current Osmotic Pump Applications
Bibliography

Historically, pharmaceutically active agents have been chosen based on biological activity, with absorption, efficacy, and side effect profiles determined by metabolic processes. The effectiveness of the therapeutic agent can be enhanced by sophisticated drug delivery systems that actively control the delivery rate and site of drug action (1–8). Over the past 30 years, drug delivery systems based on the principles of osmosis have shown themselves to be reliable and adaptable to an impressive variety of uses, ranging from oral dosage forms that deliver for less than 24 hours to implantable systems that precisely deliver exquisitely small amounts of potent agents over periods of a year or more.

EARLY OSMOTIC SYSTEMS

The Rose–Nelson osmotic pump is generally recognized as the forerunner of most modern osmotic systems (9). This pump, developed in 1955 for pharmacologic research, consisted of a water compartment, an osmotic agent compartment, and a drug compartment (Fig. 1) (10). The water and osmotic agent compartments were separated by a semipermeable membrane, and the osmotic agent and drug compartments were separated by an elastic diaphragm. In operation, water was drawn into the osmotic agent compartment, resulting in volume displacement of the diaphragm and pumping of the drug solution from the drug compartment. If the osmotic agent compartment was filled with sufficient osmotic agent to maintain a saturated solution, zero-order delivery would be observed.

In 1971, Stolzenberg was issued the first patent for an osmotic pump, which incorporated pistons between the osmotic agent compartment and the drug compartment and between the water compartment and the exterior of the pump (11). Higuchi and Leeper proposed a variation of the Rose–Nelson pump in 1973 in which the internal water compartment was eliminated, placing the membrane in direct contact with the surrounding aqueous environment (12). In the mid-1970s, researchers at ALZA designed a capsular osmotic pump, in which the drug compartment was almost fully surrounded by an osmotic layer and a semipermeable membrane (this design was used in the ALZET® osmotic pump) (13). In 1975, Theeuwes developed the "elementary osmotic pump," which further simplified the design by combining the osmotic agent compartment and drug compartment into one (14). A subsequent variation on this design was the Push-Pull™ osmotic pump, which consisted of an osmotic layer and a separate drug layer (15,16). The development of these systems has been described in numerous articles (14,17–21). This article reviews the ALZET® osmotic pump and several newer applications of osmotic technology.

CHARACTERISTICS OF OSMOTIC SYSTEMS

Osmotic systems exhibit good correlation between in vitro and in vivo release; with proper system design, performance tends to be unaffected by in vivo variables. Therefore, these systems can be engineered to provide a variety of drug-release profiles such as increasing, decreasing, or zero order. The delivery rate can also be biochemically triggered (22) or patterned to mimic a periodic event, such as a circadian rhythm (23–25). Depending on the design, osmotic systems can deliver drug orally into the gastrointestinal tract or parenterally into the systemic circulation. Drug delivery also can be targeted via a catheter into the venous, arterial, or central nervous system or directly to an organ, such as the cerebrum, spleen, or liver. In general, bioavailability issues may be circumvented with osmotic pumps by selection of the optimum delivery site for drug delivery. Dosing is less frequent, and plasma drug concentrations are maintained within the therapeutic window, providing a dose-sparing effect, improved patient compliance, and minimized side effects for extended periods.

The osmotic systems described in this article release a therapeutic agent at a predetermined, typically zero-order, delivery rate based on the principle of osmosis. Osmosis is the natural movement of a solvent through a semiperme-

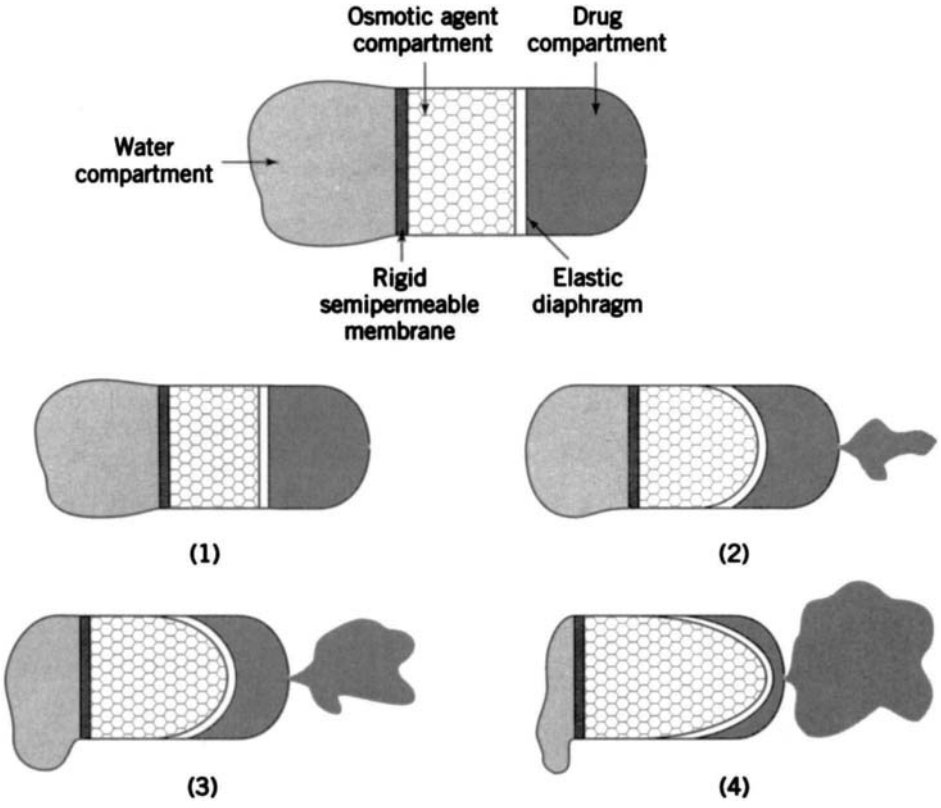


Figure 1. Principle of the Rose–Nelson osmotic pump. *Source:* Ref. 10.

able membrane into a solution of higher solute concentration, leading to equal concentrations of the solute on both sides of the membrane. Osmotic systems imbibe water from the body through a semipermeable membrane into an osmotic material, which swells, resulting in slow and even delivery of drug formulation.

In comparison with drug delivery systems based on diffusion and erosion, osmotic systems tend to be less volume efficient and more complex in design. However, osmotic systems also tend to provide better zero-order delivery and to deliver a greater percentage of the drug loading at a zero-order delivery rate.

OSMOTIC SYSTEM THEORY

Figure 2 illustrates the function of a semipermeable membrane (26). The semipermeable membrane (**a**) is permeable to water (compartment **c**) but impermeable to the solute (osmotic agent, e.g., NaCl) in compartment **b**. When the pressure is equal between compartments **b** and **c** ($P^0 = P$), water (solvent) will permeate through the semipermeable membrane from compartment **c** to compartment **b**, reflecting the gradient in chemical potential of the solvent between the two compartments. As the pressure is increased in compartment **b**, the chemical potential of the solvent increases in this compartment. When the pressure in compartment **b** reaches the osmotic pressure of the solution, the chemical potential of the solvent in the two compartments becomes equalized, and net transport of the solvent through the membrane stops.

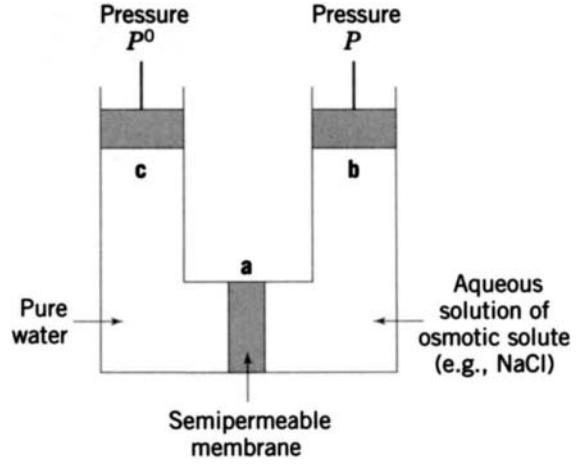


Figure 2. Diagram of a semipermeable membrane (**a**) separating an aqueous solution of an osmotic solute (**b**) from pure water (**c**). *Source:* Ref. 26.

The greater the gradient in chemical potential, the greater will be the rate of transport of solvent through the membrane. Considering the relationship between chemical potential and osmotic pressure, the rate of water transport through the membrane can be written as follows (14):

$$dV/dt = (A/h)L_P(\sigma \Delta\pi - \Delta p) \quad (1)$$

where dV/dt is the volume flow of solvent through the membrane, A is the cross-sectional area for transport, h is

the membrane thickness, L_p is the hydraulic permeability of the membrane, σ is the reflection coefficient, $\Delta\pi$ is the osmotic pressure difference across the membrane, and Δp is the hydrostatic pressure difference across the membrane.

Table 1 presents the osmotic pressures of saturated aqueous solutions of common pharmaceutical solutes (27). Hydrostatic pressure inside most osmotic drug delivery systems is generally less than 1 atm, although some systems may attain pressures as high as several atmospheres. Hence, in comparison with the osmotic pressures reported in Table 1, the hydrostatic pressure differential is negligible:

$$\Delta\pi \gg \Delta p$$

Equation 1 can then be written as follows:

$$dV/dt = (A/h)k\Delta\pi \quad (2)$$

where $k = L_p\,\sigma$. Therefore, k can be taken as the effective permeability of the membrane. (Reflection coefficients for membranes used in osmotic systems are generally quite close to 1.)

A cross-sectional diagram of a generic osmotic pump illustrates the semipermeable membrane and water influx into the pump (Fig. 3) (28). Water permeates through the membrane and enters compartment V_s, causing it to expand; this expansion compresses compartment V_d, pushing drug out through the orifice. In equation 2, dV/dt represents the volume rate of change of the compartment indicated by V_s. If the compartment V_d is filled with a drug solution or suspension at concentration c and if the movable partition readily transmits displacement from compartment V_s to compartment V_d, the rate of drug delivery (dm/dt) from the generic osmotic pump is given by the following equation:

$$dm/dt = (dV/dt)c \quad (3)$$

Substituting in equation 2 for dV/dt, we get the following:

$$dm/dt = (A/h)k\Delta\pi c \quad (4)$$

Depending on the design of the system, A, h, k, $\Delta\pi$, and c may vary with time:

$$dm/dt = [A(t)/h(t)]k(t)\Delta\pi(t)c(t) \quad (5)$$

For some applications, equation 5 can be written in terms of the degree of hydration of the system (H):

$$dm/dt = (A_H/h)k\Delta\pi_H c \quad (6)$$

Consideration of equations 4 through 6 reveals that a variety of delivery rate profiles—increasing over time, decreasing over time, zero order, or some combination of these—are possible depending on the specific design of the osmotic system.

Table 1. Osmotic Pressures of Saturated Aqueous Solutions of Selected Pharmaceutical Solutes

Solute	Osmotic pressure (atm)
Sodium chloride	356
Fructose	355
Potassium chloride	245
Sucrose	150
Dextrose	82
Potassium sulfate	39
Mannitol	38
Sodium phosphate dibasic · 7 H_2O	31

Source: Ref. 27.

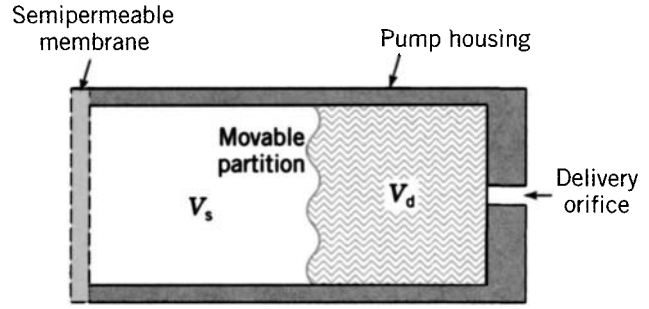


Figure 3. Schematic representation of a generic osmotic pump. *Source:* Ref. 28.

SYSTEM DESIGN CONSIDERATIONS

Osmotic drug delivery technology is based primarily on semipermeable membranes—membranes that are permeable to water but impermeable to ionic compounds and higher-molecular-weight compounds. For example, cellulosic ester membranes are permeable to water but reject sodium chloride. The water content of these membranes varies linearly with acetyl content (Fig. 4), and the hydraulic permeability varies exponentially with acetyl content (Fig. 5) (29). Typical membrane permeabilities range from 10^{-7} to 10^{-6} g/cm/s. Permeabilities can also be altered by incorporating additives into the membrane during processing (30).

For most pharmaceutical applications, the osmotic agent of choice is sodium chloride. Usually the system design provides for sufficient sodium chloride to maintain a saturated solution throughout the delivery period. In some applications, gellants are mixed with the osmotic agent; the resulting osmotic interactions can be complex and difficult to predict from theory.

CURRENT OSMOTIC PUMP APPLICATIONS

The following articles discuss four representative osmotic technologies: the ALZET® osmotic pump, an implant used in preclinical and basic research; the VITS veterinary im-

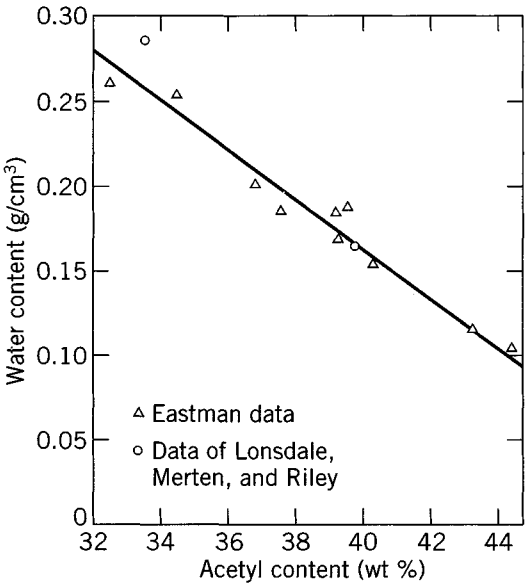


Figure 4. Water content of cellulose acetate at 100% relative humidity and 25°C versus acetyl content. *Source:* Adapted from Ref. 29, p. 112.

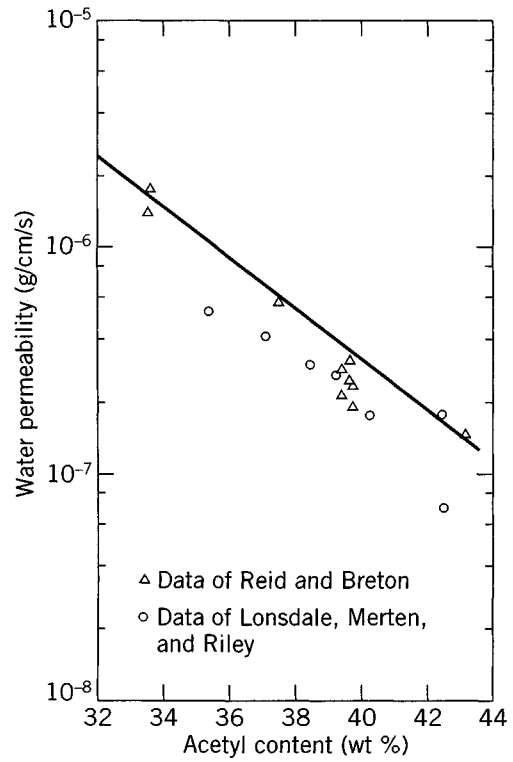


Figure 5. Water permeability as a function of acetyl content of normal cellulose acetate membranes. *Source:* Adapted from Ref. 29, p. 106.

plant, a tiny osmotic system for delivery of water-labile proteins and peptides; the DUROS™ implant, a miniature osmotic implant for use in humans; and the RUTS Push-Melt™ system, an osmotic ruminal bolus. Each article provides information on comparable technologies, design and function of the systems, and relevant applications of the technology.

BIBLIOGRAPHY

1. A. Zaffaroni, *Abstr. 31st Int. Cong. Pharma. Sci.*, Washington, D.C., 1971, pp. 19–20.
2. J.E. Shaw and F. Theeuwes, *Aust. J. Pharm. Sci.* **7**(2), 49–53 (1978).
3. A. Zaffaroni, *Drug Metab. Rev.* **8**(2), 191–221 (1978).
4. J. Urquhart, *Fed. Proc. Fed. Am. Soc. Exp. Biol.* **39**, 2460–2464 (1980).
5. J. Urquhart, in J. Urquhart, ed., *Controlled-Release Pharmaceuticals*, American Pharmaceutical Assoc., Washington, D.C., 1981, pp. 1–48.
6. F. Theeuwes, in F.G. McMahon, ed., *Principles and Techniques of Human Research and Therapeutics*, Futura, New York, 1985, pp. 63–85.
7. J. Urquhart, in L.F. Prescott and W.S. Nimmo, eds., *Rate Control in Drug Therapy*, Churchill-Livingstone, New York, 1985, pp. 19–29.
8. D. Edgren, H. Leeper, K. Nichols, and J. Wright, in *Kirk-Othmer Encyclopedia of Chemical Technology*, 4th ed., vol. 7, Wiley, New York, 1993, pp. 274–300.
9. S. Rose and J.F. Nelson, *Aust. J. Exp. Biol.* **33**, 415–420 (1955).
10. R. Baker, *Controlled Release of Biologically Active Agents*, Wiley, New York, 1987, pp. 132–155.
11. U.S. Pat. 3,604,417 (September 14, 1971), S.J. Stolzenberg (to American Cynamid Company).
12. U.S. Pat. 3,732,865 (May 15, 1973), T. Higuchi and H. Leeper (to ALZA Corp.).
13. F. Theeuwes and S.I. Yum, *Ann. Biomed. Eng.* **4**(4), 343–353 (1976).
14. F. Theeuwes, *J. Pharm. Sci.* **64**, 1987–1991 (1975).
15. D.R. Swanson, D.L. Barclay, T.S.L. Wong, and F. Theeuwes, *Am. J. Med.* **83**(6B), 3–9 (1987).
16. F. Theeuwes, in L.F. Prescott and W.S. Nimmo, eds., *Drug Absorption*, ADIS Press, New York, 1981, pp. 157–176.
17. F. Theeuwes, in A.F. Kydonieus, ed., *Controlled Release Technologies: Methods, Theory, and Applications*, CRC Press, Boca Raton, Fla., 1977, pp. 195–205.
18. F.E. Yates et al., *Adv. Biomed. Eng.* **5**, 1–34 (1975).
19. K. Chandrasekaran, F. Theeuwes, and S.I. Yum, in E.J. Ariëns, ed., *Drug Design*, Academic Press, New York, 1979, pp. 133–167.
20. F. Theeuwes, *Pharm. Ther.* **13**, 149–191 (1981).
21. F. Theeuwes, S.I. Yum, R. Haak, and P. Wong, *Ann. N. Y. Acad. Sci.* **168**, 428–440 (1991).
22. R.A. Siegel and B.A. Firestone, *J. Controlled Release* **11**, 181–192 (1990).
23. U.S. Pat. 4,723,958 (February 9, 1988), D.G. Pope and A.E. Royce (to Merck & Co., Inc.).
24. U.S. Pat. 5,017,381 (May 21, 1991), F. Maruyama and R. Cortese (to ALZA Corp.).
25. U.S. Pat. 4,957,494 (September 18, 1990), P.S.L. Wong, F. Theeuwes, and J.B. Eckenhoff (to ALZA Corp.).

26. K. Heilman, *Therapeutic Systems, Rate-Controlled Drug Delivery: Concept and Development*, 2nd ed., Thieme-Stratton, New York, 1984, p. 29.
27. U.S. Pat. 4,077,407 (March 7, 1978), F. Theeuwes and A.D. Ayer (to ALZA Corp.).
28. B. Eckenhoff, F. Theeuwes, and J. Urquhart, *Pharm. Technol.* **11**(6), 96–105 (1987).
29. H.K. Lonsdale, in U. Mertens, ed., *Desalination by Reverse Osmosis*, MIT Press, Cambridge, Mass., 1966, pp. 93–160, citing (1) C.E. Reid and E.J. Breton, *J. Appl. Polym. Sci.* **1**, 133 (1959); (2) Eastman Chemical Products, Inc., *Circular Cellulose Acetate*; and (3) H.K. Lonsdale, U. Merten, and R.L. Riley, *J. Appl. Polym. Sci.* **9**, 1341 (1965).
30. U.S. Pat. 4,160,020 (July 3, 1979), A.D. Ayer and F. Theeuwes (to ALZA Corp.).

See also PUMPS/OSMOTIC—ALZET® SYSTEM; PUMPS/OSMOTIC—VITS VETERINARY IMPLANT; PUMPS/OSMOTIC—DUROS™ OSMOTIC IMPLANT FOR HUMANS; PUMPS/OSMOTIC—RUMINAL OSMOTIC BOLUS.

PUMPS/OSMOTIC—ALZET® SYSTEM

LORRI PERKINS
CLARISA PEER
VIRGINIA FLEMING
ALZA Corporation
Palo Alto, California

KEY WORDS

Cellulose ester blend
Delivery rate
Drug reservoir
Osmotic sleeve
Semipermeable membrane
Therapeutic concentration range

OUTLINE

Background
System Design and Function
Applications
Conclusions
Bibliography
Additional Reading

ALZET® osmotic pumps are miniature, implantable research tools that deliver drug formulations at controlled rates in laboratory animals. Designed for preclinical and basic research, the ALZET® pump offers researchers enhanced control over drug levels in plasma and tissues. The capsule-shaped pumps (ranging from 1.5 to 5.1 cm in length and 0.6 to 1.4 cm in diameter) consist of a cylindrical, elastic reservoir for the drug solution surrounded by an osmotic layer, which is encased in a rigid, semipermeable membrane. Because of the osmotic gradient, water diffuses into the pump through the membrane and swells the osmotic layer, which collapses the reservoir and pushes the drug solution out of the pump at a controlled rate.

Although ALZET® pumps are most commonly implanted subcutaneously or intraperitoneally for systemic administration, they can be used with a catheter for intracerebral, intravenous, or intraarterial infusion. Specific regions can be targeted, such as the spinal cord, spleen, liver, gastrointestinal tract, and tissue transplantation or wound-healing sites. Table 1 lists the major routes of administration as reported in the literature.

Ten models of ALZET® osmotic pumps offer a range of delivery rates (from 0.25 to 10 μL/h) and durations (from 1 day to 4 weeks) (Fig. 1). The pumping rate is fixed at manufacture, but the dosage of drug delivered can be adjusted by varying the concentration of the drug solution placed in the pump. Multiple pumps can be implanted simultaneously to achieve higher delivery rates. For more prolonged delivery, pumps can be serially implanted.

Over 5,200 publications illustrate the use of osmotic pumps to deliver more than 1,600 compounds in 40 animal species, including rats, mice, cats, cattle, chickens, dogs, fish, frogs, guinea pigs, hamsters, iguanas, monkeys, pigs, sheep, and squirrels.

BACKGROUND

The ALZET® osmotic pump was originally developed by ALZA as an in-house research tool. In the mid-1970s, it became available for investigational use, and in 1977, the first commercial product was introduced. Alternatively, animals were connected to heavy infusion pumps, or homemade devices were implanted that were made from Silastic tubes in which a drug, typically a steroid, was packed. Other common administration schemes included dosing in food or water or repeated injection.

With ALZET® osmotic pumps, the typical peak and trough serum profile often seen with repeated injection dosing is replaced with a constant, continuous flat curve,

Table 1. Major Routes of Administration (As Reported in the Literature)

Subcutaneous	Intraruminal
Intraperitoneal	Local tissue microperfusion
Intracavity	Arterial wall
Articular cavity	Bone
Bladder	Brain
Cerebral ventricles	Eye
Intestine	Muscle
Spinal cord	Ovary
Stomach	Peripheral nerves
Uterus	Spleen
Intravenous	Testes
Intraarterial	

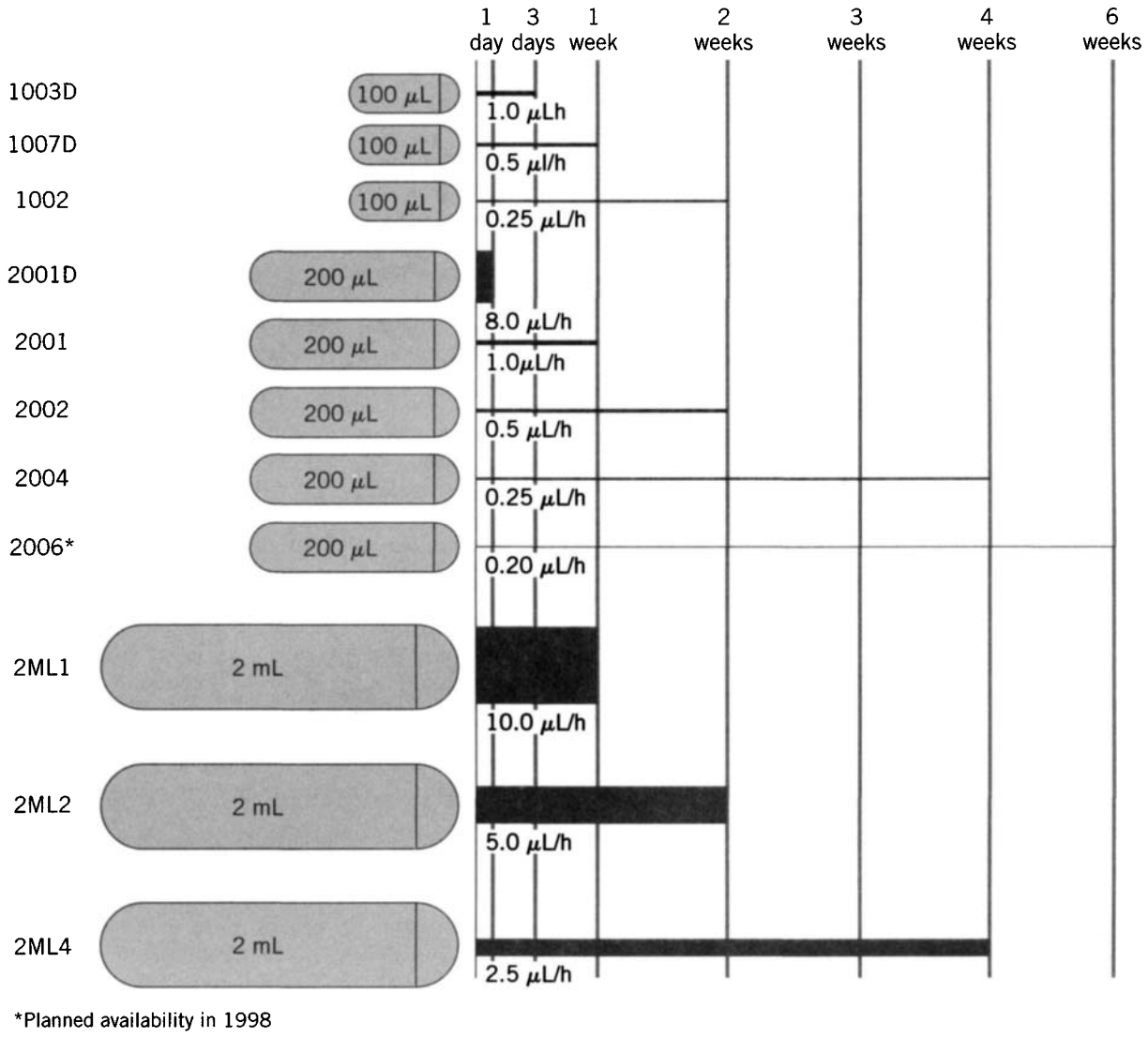


Figure 1. Comparison of delivery rates, durations, and reservoir capacities of ALZET® osmotic pumps.

which can stay in the therapeutic concentration range. This avoids spike concentrations, when adverse effects are more likely, and troughs, when drug effects may dwindle (Fig. 2). ALZET® pump infusion is much more predictable than dosing in food or water. With Silastic tubes, rate control is imprecise because the diffusion rate across the tube wall is not constant and differs by compound (1), whereas with the ALZET® pump, the delivery rate is precise and is not dependent on the physical or chemical properties of the drug. With ALZET® pumps, animal handling and stress are minimized, and repeated nighttime and weekend dosing is not necessary. The ALZET® pump is tamperproof. It does not require any external connections, so animals need no restraint.

SYSTEM DESIGN AND FUNCTION

ALZET® osmotic pumps are composed of three concentric layers: the drug reservoir, the osmotic sleeve, and the rate-controlling, semipermeable membrane (Fig. 3). The drug reservoir is a cylindrical cavity molded from a synthetic elastomer. The reservoir walls are impermeable, blocking any exchange of material between the drug reservoir and the surrounding osmotic sleeve. Outside the reservoir wall is the osmotic sleeve, which contains a concentrated solution of sodium chloride. The difference in osmotic pressure between this solution and the surrounding fluid at the implantation site constitutes the osmotic gradient, which drives the delivery of the drug solution. The outermost layer of the system is a semipermeable membrane made of a cellulose ester blend. An additional component, the flow moderator, is a 21-gauge stainless steel tube that is inserted into the body of the osmotic pump after filling. It minimizes passive diffusion of the drug out of the reservoir, reduces the effect of air bubbles trapped in the drug solution, and prevents accidental spillage. It also provides a convenient attachment point for a catheter.

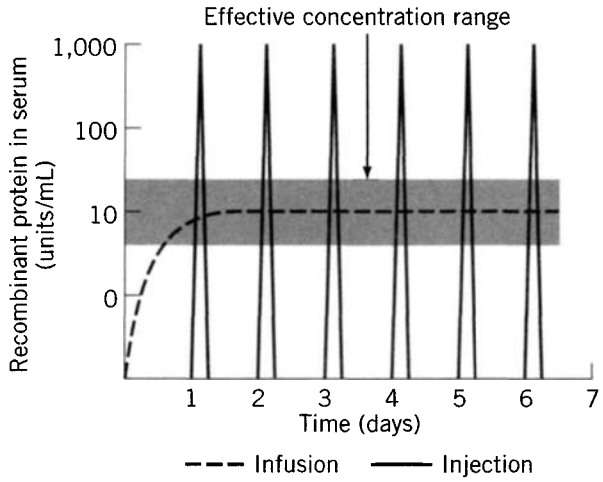


Figure 2. Comparison of serum protein levels over time with infusion versus injection therapy.

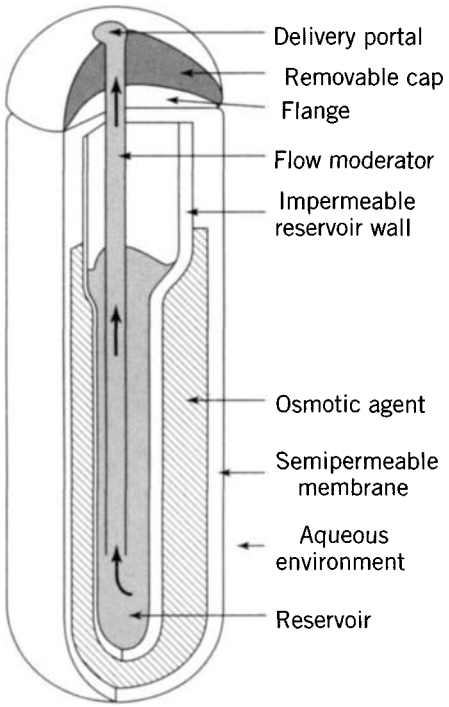


Figure 3. Cross section of a functioning ALZET® osmotic pump.

Before implantation, drug solution is injected into the drug reservoir, and the flow moderator is inserted. Once implanted, the pump imbibes water into the osmotic sleeve along the osmotic gradient. This causes compression of the flexible drug reservoir, which displaces the drug solution through the flow moderator at the same rate that water enters the semipermeable membrane of the pump.

Care is necessary when formulating the drug. The optimal solvent readily dissolves the drug and is compatible with both the interior reservoir of the pump and the tissues or fluids at the site of administration. Using the solvent that best dissolves the drug increases its maximum potential administration rate. ALZET® pump reservoirs are compatible with aqueous solutions, dilute acids and bases, dilute concentrations of dimethyl sulfoxide (DMSO) or ethanol, and up to 100% propylene or poly(ethylene glycol). Table 2 lists the most commonly used solvents.

ALZET® osmotic pumps are not compatible with aliphatic and aromatic hydrocarbons such as heptane, toluene, and natural oils. Standard parenteral fluids such as Ringer's solution (nonlactated form) are ideal for water-soluble drugs given subcutaneously, intraperitoneally, or intravenously. For infusions into the brain, artificial cerebrospinal fluid is recommended. The solution should be at room temperature when the pump is filled and should not generate gases, which would make the pumping rate unpredictable. Solutions with precipitated solute particles should be filtered before use. Homogeneous, viscous solutions of less than 100,000 cP can be administered. Suspensions can be delivered if they do not precipitate and if they remain homogeneous throughout the infusion period. Solvents can be tested for compatibility with the ALZET® pump using a test kit available from ALZA. Tissue compatibility at the implantation site may be an issue with nonaqueous solvents or aqueous solutions that are strongly alkaline or acidic. In addition, care is necessary during preparation and handling of the drug solution to ensure its sterility and isotonicity; microbial contamination can result in local fibrosis and inflammation around the pump and in degradation of some agents, especially peptides.

When filled at room temperature, most ALZET® pumps can reach steady-state delivery in 4 to 6 h (Fig. 4). For immediate in vivo pumping, the prefilled pumps can be placed in sterile saline at 37°C for at least 4 to 6 h (preferably overnight) before implantation. This procedure is mandatory when the pump is to be used with a catheter, when viscous solutions are being delivered, or when the dose of the drug may have acute toxic effects.

After the initial start-up period, the pump operates at a constant rate until 95% of its contents has been delivered; then the pumping rate falls rapidly to zero. The coefficient of variation for the pumping rate of an individual

Table 2. Common Solvents Compatible with the ALZET® Reservoir Material

Artificial cerebrospinal fluid
Bacteriostatic culture media
Dextrose, 5% in water or NaCl
Dilute acids (pH > 1.8)
Dilute bases (pH < 14)
Distilled water or any aqueous solution
DMSO, up to 50% in water
Ethanol, up to 15% in water
Glycerol
Isotonic NaCl or other salt solution
Poly(ethylene glycol) (PEG) 300, neat or in water
Propylene glycol, neat or in water
Rat serum
Ringer's solution
Tween, 2% in water

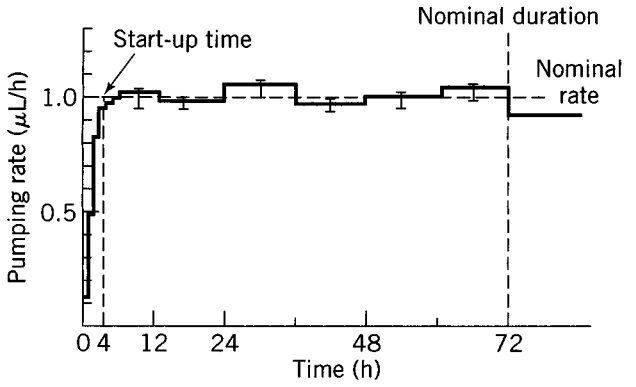


Figure 4. The pumping rate of the Model 1003D ALZET® osmotic pump in 0.9% NaCl at 37°C (±0.5°C).

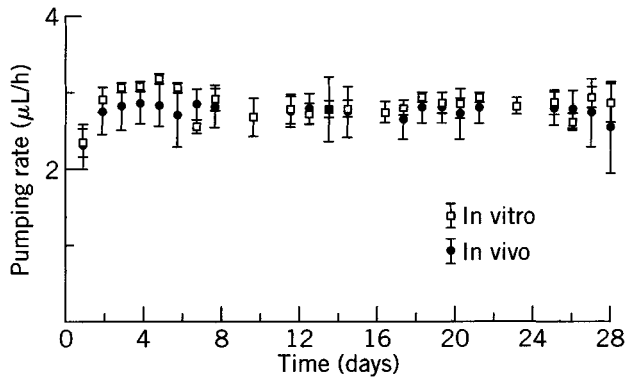


Figure 5. The in vitro versus in vivo pumping rates of the Model 2ML4 ALZET® osmotic pump (in vitro in 0.9% NaCl at 37°C [±0.5°C]; in vivo in Sprague Dawley rats after subcutaneous implantation).

pump and among a group of ALZET® pumps is less than 10% over the pumping duration. At the end of the infusion period specified for each pump model, the pump becomes an inert object for a period roughly equivalent to half the length of its pumping duration. Then, because of continued osmotic attraction of water into the pump, it may swell and leak a concentrated salt solution, which can cause local tissue irritation. Thus explantation is suggested before this point (1.5 times the system's lifetime).

As expressed in the standard osmotic equation (equation 4 from the PUMPS/OSMOTIC—INTRODUCTION), the delivery rate of an ALZET® pump is determined by the rate at which water enters the osmotic sleeve, which in turn depends primarily on the permeability and dimensions of the semipermeable membrane. The rate is also affected by the osmotic pressure difference across the membrane and the temperature, which become considerations when working with nonmammalian species. The osmotic driving agent is designed to maintain a constant osmotic gradient during the lifetime of the pump. Note that the delivery rate of the pump is independent of the physical and chemical properties of the drug formulation dispensed. Thus, agents of various molecular configurations, including ionized drugs and macromolecules, can be dispensed continuously in a variety of vehicles at a constant rate. Continuous, zero-order release allows the effects of drugs to develop fully and reproducibly, which is particularly useful for compounds with short half-lives, such as recombinant proteins or peptides.

ALZET® pump models are available with fixed delivery rates between 0.25 and 10 μL/h and delivery durations between 1 day and 4 weeks. The exact pumping rate and reservoir volume are measured in 0.9% saline at 37°C (±0.5°C) for each lot of ALZET® osmotic pumps, and this information is provided with the product. This in vitro pumping rate is expected to be within 5% of the pumping rate in homeothermic animals for which 0.9% saline is isotonic. Figure 5 illustrates that the release rate profiles for ALZET® osmotic pumps tested in vivo were within 5% of the analogous systems tested in vitro.

The average duration of pumping can be estimated by dividing 95% of the average reservoir fill volume (μL) by the average pumping rate (μL/h). A 5% residual cannot be displaced from the pump. Although the volume delivery rate of the pump is fixed, different dosages of drug can be achieved by varying the concentration of the drug solution using the following formula:

$$k_0 = Q(C_d)$$

where k_0 is the mass delivery rate (μg/h), Q is the pumping rate (μL/h), and C_d is the concentration of drug solution (μg/μL). Temperature and osmolality affect the rate at which water crosses the semipermeable membrane; thus, they affect the pumping rate. For heterothermic animals or for animals whose body fluids are hypertonic relative to mammals, the following equations can be used to predict the pumping rate:

For models with 100- and 200-μL reservoirs:

$$Q_T = Q_0(0.135e^{(0.054T)} - 0.004\pi + 0.03)$$

For models with 2-mL reservoirs:

$$Q_T = Q_0(0.141e^{(0.051T)} - 0.007\pi + 0.12)$$

where Q_T is the pumping rate at temperature T (μL/h), Q_0 is the specified pumping rate at 37°C (μL/h), T is the temperature (°C), and π is the osmolality of the solution outside the pump (atm). These equations are useful in the range of π = 0–25 atm and T = 4°–42°C, and they are predictive within ±10%. At normal mammalian osmolality of 310 mOsm/L, the osmotic pressure is 7.5 atm. ALZET® pumps have been used at body temperatures up to 42°C (2,3).

Frequently, researchers verify the operation of ALZET® osmotic pumps in their experimental application by monitoring the blood or plasma levels of the infused drug. They can detect when levels reach steady state and whether variables unrelated to pump functionality (e.g., clearance) influence experimental results. When the pump is explanted, the actual pumping rate can be estimated by assaying for the remaining drug in the reservoir. This is done by aspirating the solution from the reservoir using a syringe and a filling tube (provided with each box of pumps) and dividing the calculated volume of drug delivered by the

elapsed time to give the average pumping rate. The weight of an explanted pump cannot be used to determine the quantity of drug delivered because the pump imbibes water during operation.

The component materials of the ALZET® osmotic pump are highly compatible with tissue. When assembled units have been implanted in laboratory animals for the functional lifetime of the system, examination of the implantation site has shown minimal adverse tissue reaction.

ALZET® osmotic pumps are used most extensively in rats and mice. Animals that weigh at least 10 g tolerate subcutaneous implantation of the 100-μL-volume pumps. These pumps can be implanted intraperitoneally in animals weighing at least 20 to 25 g. Animals that weigh at least 20 to 25 g tolerate subcutaneous implantation of the 200-μL-volume pumps without deviation from their normal weight values. However, the same pumps are too large for intraperitoneal implantation in mice. Local tissue damage typically is not seen with subcutaneous, intraperitoneal, intravenous, or intraarterial administration and generally is not seen with local tissue microperfusion. For example, ALZET® osmotic pumps caused no noteworthy hydraulic damage or edema when used to perfuse the renal artery in rats at flow rates of 0.50 to 1.0 μL/h (4).

ALZET® osmotic pumps can be used for systemic or localized delivery. By use of a catheter, a drug can be targeted to discrete locations distant from the pump's implantation site, thereby maximizing local effects of the drug while limiting adverse systemic effects. For example, Ruers and colleagues (5) found that intrarenal infusion of prednisolone via the suprarenal or testicular artery prolonged graft survival time to a median of 26 days. In comparison, intraperitoneal injection, intravenous infusion, and intraperitoneal infusion sustained grafts for only 7, 8.5, and 9 days, respectively.

Direct access to the central nervous system (CNS) via a cannula implanted in the cranium is useful when a drug has effects in the CNS but does not cross the blood–brain barrier appreciably (6). Significant doses can be administered directly to the brain, eliminating the uncertainty of systemic pharmacokinetic variables. Drug can be infused into the cerebrospinal fluid via the cerebral ventricles for delivery to many brain regions or directly microperfused into specific regions of solid brain tissue to target discrete structures.

Although ALZET® pumps are designed to provide zero-order delivery, they can be adapted for pulsatile administration. This is accomplished by thermoforming a coil of polyethylene tubing around the pump (7) and filling the pump's reservoir with an appropriate solvent, such as Ringer's or saline solution. The drug solution is placed in the coiled external tubing in segments alternated with vehicle; each segment is separated with an immiscible barrier such as a small air bubble, mineral oil, or silicone oil. Once implanted, the constant flow of solvent from the pump into one end of the tubing forces the segments of the coil to flow out in sequence. For example, Lynch and colleagues (8) experimentally induced rhythms in plasma melatonin levels in pinealectomized rats using a 6-h-on, 18-h-off periodicity with an ALZET® pump. Additionally, Cronan and colleagues (9) infused nicotine with an 8-h-on, 16-h-off periodicity in rats to mimic drug use in humans.

Detailed descriptions of various techniques for surgically implanting ALZET® osmotic pumps are available from ALZA Corporation (6,10).

APPLICATIONS

Thousands of publications document the use of ALZET® osmotic pumps in over 40 species with more than 1,600 compounds (see Table 3). Key disciplines include neuroscience, cancer and immunology, toxicology, biotechnology, endocrinology, pharmacology, physiology, and cardiology. For a complete bibliography, categorized by drug, route of administration, research discipline, and special interests, see the ALZET website at *http://www.alza.com/alzet*. A bibliography of review articles at the end of this article also provides a good perspective on the literature.

The ALZET® pump has enabled neuroscientists to manipulate the central and peripheral nervous systems of unrestrained animals, permitting simultaneous study of behavioral, motor, and sensory functions. Researchers have administered drugs directly to discrete brain structures, the ventricles, and the spinal cord to bypass the blood–brain barrier. Delivery to peripheral nerves has also been conducted. Using these techniques, ALZET® pumps have contributed to the study of learning and behavior, nerve regeneration, neuronal plasticity, neurodegenerative diseases, drug dependence and tolerance, and neural regulation.

In immunology/cancer research, the ALZET® pump has been used to administer cytokines, target chemotherapeutic agents to a specific organ, and evaluate dosing regimens. Toxicologists have used ALZET® pumps to achieve chronic drug exposure and to conduct teratology research.

Table 3. Classes of Drugs Delivered by ALZET® Osmotic Pumps (As Reported in the Literature)

Anesthetics	Heavy metals
Antibacterials	Hormones
Antibiotics	Immunologic agents
Antibodies	Indicator substances
Anticancer agents	Macromolecules
Anticoagulants	Metabolites
Antiepileptics	Nerve growth factors
Antihypertensives	Neurotransmitters and neuromodulators
Antiparkinson agents	Oligonucleotides
Antivirals	Opiates
Barbiturates	Peptides
Benzodiazepines	Prostaglandins
Catecholamines	Proteins
Chelators	Radioisotopes
Cholinergics	Renin–angiotensin system components and inhibitors
Cytokines	Steroids
Drugs of abuse	Thyroid and thyroid-related hormones
Enzymes	Toxic substances
Gastrointestinal motility modulators	Vitamins and minerals
Growth factors	
Growth hormones	

ALZET® pumps have proved useful in biotechnology for characterizing novel proteins and peptides, such as growth factors, while also facilitating exciting new research in which antisense oligonucleotides have selectively blocked expression of a specific protein product. In endocrinology, applications have included research on diabetes, growth and development, and hormone replacement. Targeted delivery using ALZET® pumps has proved helpful in pharmacokinetic studies, where it has allowed the characterization of local effects without the obfuscating effects of rapid drug metabolism and clearance. The pump has been used in pharmacologic studies investigating receptor modulation and animal models of human disease. In cardiology, the ALZET® pump has been used to evaluate novel antihypertensive agents and to stimulate angiogenesis in the arterial wall via adventitial delivery of growth factors.

Although ALZET® pumps are frequently used in preclinical research, they are also used in basic research or in other specialized studies. Some notable examples include studies in space, work with endangered species, and oceanographic measurements. ALZET® pumps have been used to dispense fresh medium in a prototype study of a cell cultivation instrument for Spacelab (11), to test the delivery of recombinant human growth hormone (rhGH) in rats on board the space shuttle *Discovery* (11), and to test the effects of rhGH on the atrophic response of the soleus muscle in space (12).

Endangered species have benefited from ALZET® pumps. The green iguana (*Iguana iguana*), native to Central and South America and once abundant in the rain forest, is now threatened throughout most of its natural habitat. Researchers at the Center for Reproduction of Endangered Species (CRES) have bred iguanas in captivity using infused gonadotrophin-releasing hormone (GnRH) to improve the survival potential of this species (13). CRES has also used the ALZET® pump to infuse GnRH in a previously infertile female cheetah at the San Diego Zoo, resulting in the birth of twins. Infertile for nearly 2 years, the cheetah received 10-min pulses of GnRH every 3 h, a regimen calculated to induce ovulation (14).

ALZET® osmotic pumps have also been adapted by oceanographers at the Monterey Bay Aquarium Research Institute and Moss Landing Marine Laboratories to create a self-contained, continuous flow analyzer that measures nitrate concentrations in seawater during long-term, deep-sea deployment (15).

CONCLUSIONS

For more than 20 years, the ALZET® osmotic pump has provided researchers from many scientific disciplines with continuous, zero-order delivery of drugs for basic and preclinical research. Currently these pumps can deliver drugs at volumes of 0.25–10 μL/h, systematically or targeted to specific tissues, for periods up to 1 month. Further work is planned to add additional volumes and durations and to offer a wider range of add-on delivery devices.

BIBLIOGRAPHY

1. J.W. Fara and N. Ray, in P. Tyle, ed., *Drug Delivery Devices, Fundamentals and Applications*, Dekker, New York, 1988, pp. 137–174.
2. K.T. Rodrigues and J.P. Sumpter, *J. Endocrinol.* **101**, 277–284 (1984).
3. T.F. Davison, B.M. Freeman, and J. Rea, *Gen. Comp. Endocrinol.* **59**, 416–423 (1985).
4. J.F.M. Smits et al., *Am. J. Physiol.* **244**, H304–H307 (1983).
5. T.J.M. Ruers et al., *Transplantation* **41**(2), 156–161 (1986).
6. ALZA Corporation, *ALZET® Osmotic Pumps, Technical Information Manual*, ALZA Corp., Palo Alto, Calif., 1996.
7. N. Ray and F. Theeuwes, in P. Johnson and J.G. Lloyd-Jones, eds., *Drug Delivery Systems: Fundamentals and Techniques*, Ellis Horwood, Chichester, England, 1988, pp. 120–138.
8. H.J. Lynch, R.W. Rivest, and R.J. Wurtman, *Neuroendocrinology* **31**, 106–111 (1980).
9. T. Cronan, J. Conrad, and R. Bryson, *Pharmacol., Biochem. Behav.* **22**(5), 897–899 (1985).
10. ALZA Corporation, *ALZET® Osmotic Pumps Surgical Implantation Techniques*, videotape, ALZA Corp., Palo Alto, Calif., 1986.
11. F.K. Gmünder et al., *J. Biotechnol.* **7**, 217–228 (1988).
12. M. Cronin et al., *Physiologist* **35**(1), S51–S52 (1992).
13. J.A. Phillips et al., *J. Exp. Zool.* **234**, 481–482 (1985).
14. ALZA Corporation, *Special Delivery*, March, p. 2. ALZA Corp., Palo Alto, Calif., 1986.
15. K.S. Johnson, K.H. Coale, and H.W. Jannasch, *Anal. Chem.* **64**(22), 1065A–1075A (1992).

ADDITIONAL READING

Amkraut A.A., Fara J.W., Nichols K.C., and Ray N.P., *The Pharmacology and Toxicology of Proteins*, UCLA Symp. Mol. Cell. Biol., New Ser., Liss, New York, 1987, pp. 131–148.

Amkraut A., Eckenhoff J.B., and Nichols K., *Adv. Drug Delivery Rev.* **4**, 255–276 (1990).

Chandrasekaran S.K., Capozza R., and Wong P.S.L., *J. Membr. Sci.* **3**(3), 271–286 (1978).

Chandrasekaran S.K., Theeuwes F., and Yum S.I., in E.J. Ariëns, ed., *Drug Design*, Academic Press, New York, 1979, Chapter 3, pp. 133–167.

Clarke D.O., *Toxicol. Methods* **3**(4), 223–251 (1993).

Collins J.M., Leyland-Jones B., and Grieshaber C.K., in F.M. Muggia, ed., *Concepts, Clinical Developments, and Therapeutic Advances in Cancer*, Martinus Nijhoff, Boston, 1987, pp. 129–140.

Daemen M.J.A.P., Thijssen H.H.W., and Struyker-Boudier H.A.J., *Adv. Drug Delivery Rev.* **6**, 1–18 (1991).

Eckenhoff B., in S.K. Chandrasekaran, ed., *Controlled Release Systems*, vol. 77, Am. Inst. Chem. Eng., New York, 1981, pp. 1–9.

Eckenhoff B., and Yum S.I., *Biomaterials* **2**, 89–97 (1981).

Eckenhoff B., Theeuwes F., and Urquhart J., *Pharm. Technol.* **5**(1), 35–44 (1981).

Fara J., *J. Parenter. Sci. Technol.* **37**(1), 20–25 (1983).

Fara J.W., *Methods Enzymol.* **112**, 470–484 (1985).

Fara J., and Mitchell C., in H.A.J. Struyker-Boudier, ed., *Rate-Controlled Drug Administration and Action*, CRC Press, Boca Raton, Fla., 1986, Chapter 5, pp. 115–142.

Fara J., and Urquhart J., *Trends Pharmacol. Sci.* **5**(1), 21–25 (1984).
Goldsworthy T.L., Morgan K.T., Popp J.A., and Butterworth B.E., *Prog. Clin. Biol. Res.* **369**, 253–284 (1991).
Hagg T., in T.R. Flanagan, D.F. Emerich, and S.R. Winn, eds., *Methods in Neurosciences, Providing Pharmacological Access to the Brain: Alternate Approaches*, vol. 21, Academic Press, San Diego, Calif., 1994, pp. 201–213.
Lee V.H.L., *Pharmacokinet. Pharmacodyn.* **3**, 80–92 (1991).
Nau H., Trotz M., and Wegner C., in D.D. Breimer and P. Speiser, eds., *Topics in Pharmaceutical Sciences*, Elsevier, Amsterdam 1985, pp. 143–157.
Neckers L., and Whitesell L., *Am. J. Physiol.* **265**(9), L1–L12 (1993).
Nieschlag E., Akhtar F.B., Schurmeyer T.H., and Weinbauer G., in F. Labrie and A. Bélanger, eds., *LHRH and Its Analogues, Basic and Clinical Aspects*, Elsevier, Munster, Germany, 1984, pp. 277–286.
Pilowsky P.M., Suzuki S., and Minson J.B., *Clin. Exp. Pharmacol. Physiol.* **21**, 935–944 (1994).
Shaw J.E., and Theeuwes F., *Aust. J. Pharm. Sci.* **1**(2), 49–53 (1978).
Sikic B.I., and Carlson R.W., in H.A.J. Struyker-Boudier, ed., *Rate-Controlled Drug Administration and Action*, CRC Press, Boca Raton, Fla., 1986, Chapter 8, pp. 205–218.
Struyker-Boudier H.A.J., *Trends Pharmacol. Sci.* **3**(4), 162–164 (1982).
Theeuwes F., in A.F. Kydonieus, ed., *Controlled Release Technologies: Methods, Theory, and Applications*, vol. II, CRC Press, Boca Raton, Fla., 1980, Chapter 10, pp. 195–205.
Theeuwes F., in L.F. Prescott and W.S. Nimmo, eds., *Drug Absorption*, ADIS Press, New York, 1981, Chapter 16, pp. 157–176.
Theeuwes F., *Pharmacol. Ther.* **13**, 149–191 (1981).
Theeuwes F., and Eckenhoff B., in R. Baker, ed., *Controlled Release of Bioactive Materials*, Academic Press, New York, 1980, pp. 61–82.
Theeuwes F., and Yum S.I., *Ann. Biomed. Eng.* **4**(4), 343–353 (1976).
Theeuwes F., Eckenhoff B., and Urquhart J., *Pharm. Technol.* **11**(6), 96–105 (1987).
Urquhart J., *AAMI Technol. Assess. Rep.* **5**(83), 45–50 (1983).
Urquhart J., in L.F. Prescott and W.S. Nimmo, eds., *Rate Control in Drug Therapy*, Churchill-Livingstone, New York, 1985, pp. 19–29.
Urquhart J., Fara J., and Willis K.L., *Annu. Rev. Pharmacol. Toxicol.* **24**, 199–236 (1984).
Waynforth H.B., and Flecknell P., *Experimental and Surgical Technique in the Rat*, Academic Press, New York, 1980, pp. 49–50.
White J.D., and Schwartz M.W., in T.R. Flanagan, D.F. Emerich, and S.R. Winn, eds., *Methods in Neurosciences, Providing Pharmacological Access to the Brain: Alternate Approaches* vol. 21, Academic Press, San Diego, Calif., 1994, pp. 187–200.
Zaffaroni A., *Drug Metab. Rev.* **8**(2), 191–221 (1978).

See also PUMPS/OSMOTIC—INTRODUCTION; PUMPS/OSMOTIC—VITS VETERINARY IMPLANT; PUMPS/OSMOTIC—DUROS™ OSMOTIC IMPLANT FOR HUMANS; PUMPS/OSMOTIC—RUMINAL OSMOTIC BOLUS.

Next Page

PUMPS/OSMOTIC—VITS VETERINARY IMPLANT

JUDY MAGRUDER
ALZA Corporation
Palo Alto, California

KEY WORDS

Bovine somatotropin (BST)
Intraperitoneal
Porcine somatotropin (PST)
Pulsatile delivery
Steroids
Subcutaneous
Zero-order delivery

OUTLINE

Background
System Design and Function
Applications
Conclusions
Bibliography

The Veterinary Implantable Therapeutic System (VITS) is a small, implantable drug delivery system designed to provide controlled drug delivery in production animals and companion animals for periods of 1 day to 1 year. Typical VITS release is constant and zero order, but declining or pulsatile release profiles are possible by design. A wide spectrum of compounds ranging from small molecules such as steroids to larger, water-labile molecules such as peptides and proteins can be delivered. Because of the VITS pump design and its materials, VITS formulations are completely isolated from potentially damaging in vivo fluids. Because of the small pump size, dosages from μg/day to mg/day are possible, making VITS ideal for the delivery of potent molecules. VITS can be implanted subcutaneously or intraperitoneally. When used in food-production animals, the VITS is removed during slaughter. Possible candidates for VITS delivery include somatotropins, parasiticides, hormones such as estrus suppressants and growth promotion agents, β-agonists, nutritional supplements, and antibiotics.

BACKGROUND

Implants have been used commercially in animals for many years, typically for growth enhancement using steroids. For example, since the 1950s compressed tablets containing estrogenic anabolic steroids have been inserted subcutaneously in and at the base of the ears in cattle,

Previous Page

Fara J., and Urquhart J., *Trends Pharmacol. Sci.* **5**(1), 21–25 (1984).
Goldsworthy T.L., Morgan K.T., Popp J.A., and Butterworth B.E., *Prog. Clin. Biol. Res.* **369**, 253–284 (1991).
Hagg T., in T.R. Flanagan, D.F. Emerich, and S.R. Winn, eds., *Methods in Neurosciences, Providing Pharmacological Access to the Brain: Alternate Approaches*, vol. 21, Academic Press, San Diego, Calif., 1994, pp. 201–213.
Lee V.H.L., *Pharmacokinet. Pharmacodyn.* **3**, 80–92 (1991).
Nau H., Trotz M., and Wegner C., in D.D. Breimer and P. Speiser, eds., *Topics in Pharmaceutical Sciences*, Elsevier, Amsterdam 1985, pp. 143–157.
Neckers L., and Whitesell L., *Am. J. Physiol.* **265**(9), L1–L12 (1993).
Nieschlag E., Akhtar F.B., Schurmeyer T.H., and Weinbauer G., in F. Labrie and A. Bélanger, eds., *LHRH and Its Analogues, Basic and Clinical Aspects*, Elsevier, Munster, Germany, 1984, pp. 277–286.
Pilowsky P.M., Suzuki S., and Minson J.B., *Clin. Exp. Pharmacol. Physiol.* **21**, 935–944 (1994).
Shaw J.E., and Theeuwes F., *Aust. J. Pharm. Sci.* **1**(2), 49–53 (1978).
Sikic B.I., and Carlson R.W., in H.A.J. Struyker-Boudier, ed., *Rate-Controlled Drug Administration and Action*, CRC Press, Boca Raton, Fla., 1986, Chapter 8, pp. 205–218.
Struyker-Boudier H.A.J., *Trends Pharmacol. Sci.* **3**(4), 162–164 (1982).
Theeuwes F., in A.F. Kydonieus, ed., *Controlled Release Technologies: Methods, Theory, and Applications*, vol. II, CRC Press, Boca Raton, Fla., 1980, Chapter 10, pp. 195–205.
Theeuwes F., in L.F. Prescott and W.S. Nimmo, eds., *Drug Absorption*, ADIS Press, New York, 1981, Chapter 16, pp. 157–176.
Theeuwes F., *Pharmacol. Ther.* **13**, 149–191 (1981).
Theeuwes F., and Eckenhoff B., in R. Baker, ed., *Controlled Release of Bioactive Materials*, Academic Press, New York, 1980, pp. 61–82.
Theeuwes F., and Yum S.I., *Ann. Biomed. Eng.* **4**(4), 343–353 (1976).
Theeuwes F., Eckenhoff B., and Urquhart J., *Pharm. Technol.* **11**(6), 96–105 (1987).
Urquhart J., *AAMI Technol. Assess. Rep.* **5**(83), 45–50 (1983).
Urquhart J., in L.F. Prescott and W.S. Nimmo, eds., *Rate Control in Drug Therapy*, Churchill-Livingstone, New York, 1985, pp. 19–29.
Urquhart J., Fara J., and Willis K.L., *Annu. Rev. Pharmacol. Toxicol.* **24**, 199–236 (1984).
Waynforth H.B., and Flecknell P., *Experimental and Surgical Technique in the Rat*, Academic Press, New York, 1980, pp. 49–50.
White J.D., and Schwartz M.W., in T.R. Flanagan, D.F. Emerich, and S.R. Winn, eds., *Methods in Neurosciences, Providing Pharmacological Access to the Brain: Alternate Approaches* vol. 21, Academic Press, San Diego, Calif., 1994, pp. 187–200.
Zaffaroni A., *Drug Metab. Rev.* **8**(2), 191–221 (1978).

See also PUMPS/OSMOTIC—INTRODUCTION; PUMPS/OSMOTIC—VITS VETERINARY IMPLANT; PUMPS/OSMOTIC—DUROS™ OSMOTIC IMPLANT FOR HUMANS; PUMPS/OSMOTIC—RUMINAL OSMOTIC BOLUS.

PUMPS/OSMOTIC—VITS VETERINARY IMPLANT

JUDY MAGRUDER
ALZA Corporation
Palo Alto, California

KEY WORDS

Bovine somatotropin (BST)
Intraperitoneal
Porcine somatotropin (PST)
Pulsatile delivery
Steroids
Subcutaneous
Zero-order delivery

OUTLINE

Background
System Design and Function
Applications
Conclusions
Bibliography

The Veterinary Implantable Therapeutic System (VITS) is a small, implantable drug delivery system designed to provide controlled drug delivery in production animals and companion animals for periods of 1 day to 1 year. Typical VITS release is constant and zero order, but declining or pulsatile release profiles are possible by design. A wide spectrum of compounds ranging from small molecules such as steroids to larger, water-labile molecules such as peptides and proteins can be delivered. Because of the VITS pump design and its materials, VITS formulations are completely isolated from potentially damaging in vivo fluids. Because of the small pump size, dosages from μg/day to mg/day are possible, making VITS ideal for the delivery of potent molecules. VITS can be implanted subcutaneously or intraperitoneally. When used in food-production animals, the VITS is removed during slaughter. Possible candidates for VITS delivery include somatotropins, parasiticides, hormones such as estrus suppressants and growth promotion agents, β-agonists, nutritional supplements, and antibiotics.

BACKGROUND

Implants have been used commercially in animals for many years, typically for growth enhancement using steroids. For example, since the 1950s compressed tablets containing estrogenic anabolic steroids have been inserted subcutaneously in and at the base of the ears in cattle,

releasing drug through slow erosion or matrix diffusion. These growth enhancers are given for 2- to 3-month periods to improve the rate of weight gain and feed conversion, and their economic benefits have been well documented. Commercial examples of these growth promoters include Compudose® (estradiol-17β), Synovex® (progesterone and others), and Ralgro® (Zeranol) (1). These systems are not explanted. Similar implants have also been evaluated for delivery of parasiticides (2,3).

Although these systems have been suitable for the delivery of steroids and other water-stable agents, adaptation has proved necessary for newer biotechnology products. Larger peptides and proteins are extremely water labile, degrading rapidly in an aqueous environment. They are also very potent agents, given in very small doses. To satisfy these requirements, VITS was developed as a small system in which the active drug is kept isolated from the body's aqueous environment until release.

The VITS implant is much smaller than the Ruminal Therapeutic System (RUTS) ruminal bolus and can be implanted in any ruminant, nonruminant, companion, or production animal. In the VITS implant, drug is isolated from any contact with body fluids in the in vivo environment. Unlike the RUTS ruminal bolus system, in which the semipermeable membrane cup almost fully surrounds the entire system, the VITS absorbs water only at the membrane cup end; hence, the drug formulation is completely isolated from water inside the impermeable drug reservoir.

Compared with repeat-injection dosing, VITS reduces animal stress resulting from restraint, handling, and dosing. With its zero-order delivery, VITS minimizes the adverse effects often associated with the elevated drug serum levels seen shortly after injection dosing. VITS is more convenient to administer than repeat-injection dosing; it eliminates the need for procedures that are often costly, difficult, and labor intensive. With VITS, the amount of drug administered is known, in contrast to the administration of drug in drinking water or food. VITS is efficient in administering therapeutic dosages of potent, expensive compounds that otherwise would have to be given frequently and in large doses because of biological clearance processes. Controlled parenteral administration of therapeutic agents by VITS increases the range of usable veterinary compounds, because many potentially useful products, such as peptides and proteins, cannot be administered by feed or bolus owing to their water lability. Controlled-release dosage forms such as VITS can also reduce human exposure to those veterinary compounds that are unsafe for humans to handle.

SYSTEM DESIGN AND FUNCTION

As shown in Figure 1, the VITS system is a narrow cylinder that consists of an impermeable drug reservoir containing the drug formulation and a rate-controlling semipermeable membrane cup that contains the osmotic engine and a piston. The membrane cup subassembly is tightly coupled with the filled drug reservoir. At the time of implantation, the break-off tab is removed so that drug can be delivered. (An alternative design uses a microcrystalline wax plug, which prevents any backflow of body fluids into the system during start-up.) VITS systems can be designed at various sizes ranging from 2 to 10 mm in diameter, depending on the dosage requirements and the size of the animal.

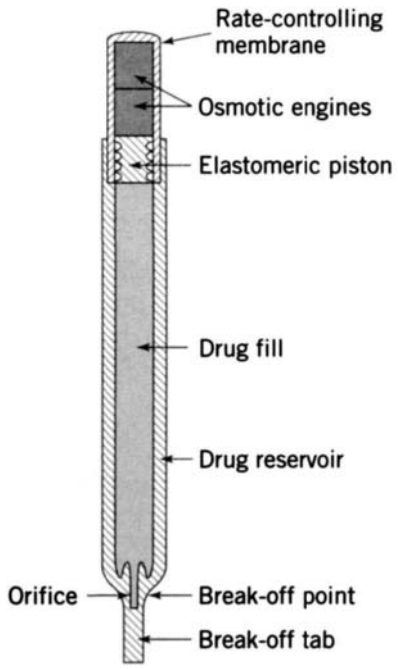


Figure 1. Cross section of VITS.

After implantation, water from the animal's tissues moves across the membrane wall at a constant rate governed by the thickness and composition of the wall. The osmotic material swells, which pushes the piston forward into the drug reservoir. This forces drug formulation through the orifice into the surrounding tissues. The rate of drug delivery is the same as the rate of water influx into the system, based on the basic osmotic equation (equation 4) described in PUMPS/OSMOTIC—INTRODUCTION. System design is described in detail in the patent literature (4–20).

VITS has a predictable start-up profile and a rapid shutdown profile that minimizes drug residues in tissue. At shutdown time, the piston reaches the end of the drug fill area, guaranteeing a complete cutoff of drug delivery at that point.

The dosage, duration, and delivery profile of a VITS system can be adjusted by design within the ranges of 1-week to 1-year duration and μg/day to mg/day dosage. For example, by altering the permeability of the membrane, the resulting dosage and duration of the system can be changed. For a fixed system size and drug reservoir volume, a more permeable membrane results in an increased delivery rate with a shorter delivery lifetime. The inverse holds true as well: A less permeable membrane results in a decreased delivery rate over a longer delivery lifetime. Decreasing the concentration of sodium chloride in the osmotic engine produces a declining release profile (as the osmotic engine solution falls below saturation, the release slows), as shown in Figure 2 (porcine somatotropin [pST]

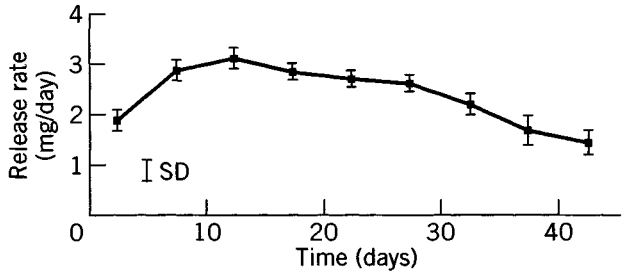


Figure 2. In vitro release profile of pST from a VITS system.

at 37°C). Pulsatile delivery can also be achieved through system design alteration.

In vivo data in finishing hogs show a good dose–response relationship, as demonstrated in Figure 3. For more than 40 days, pST plasma concentrations were maintained for the three dosages (1.2, 3.6, and 4.8 mg/day).

APPLICATIONS

One extensively studied application of VITS technology is the administration of bovine somatotropin (bST) to cattle and pST to pigs. For example, Baile and colleagues showed that administration of a 42-day VITS bST implant (17 mg/day) increased the growth rate by 16% for subcutaneous implantation and 25% for intraperitoneal implantation. Increases in growth rate were sustained with an 84-day VITS intraperitoneal implant when compared with two successive 42-day implants, suggesting that the formulation retains biological efficacy even when the delivery duration is extended to commercially significant time periods (21).

Another study by Kasser and colleagues compared a control group with a group that received bST from two consecutive 42-day intraperitoneal VITS implants at dosages of 6, 12, and 15 mg/day. Body weight and carcass weight were significantly ($P < .05$) higher in treated animals than in controls. Feed conversion was significantly ($P < .05$) better in treated animals than in controls (22).

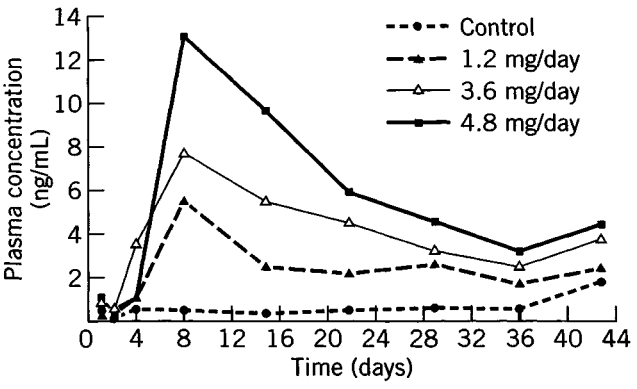


Figure 3. Comparison of plasma concentrations of VITS agent (pST) as a function of its dosage.

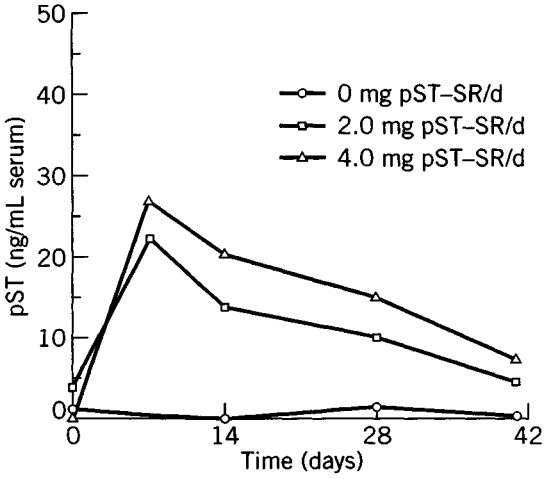


Figure 4. Comparison of serum concentrations of pST in lean gilts as a function of dosage. *Source:* Adapted from Ref. 24.

Armstrong and colleagues found that multiparous beef cows receiving an 84-day subcutaneous VITS bST implant had significantly ($P < .05$) higher milk yields and calf weaning weights than did cows that received vehicle only (23).

Subcutaneous VITS implants containing pST were compared with controls in a 6-week study in genetically lean and obese barrows and gilts (24). Administration of pST by VITS implant significantly increased efficiency of gain and lean deposition while decreasing fat deposition. Serum pST levels, measured each week, remained significantly higher in treated pigs than in controls throughout the study (Fig. 4) (24).

CONCLUSIONS

VITS is an osmotic implant specifically tailored for subcutaneous or intraperitoneal administration of small amounts of potent substances to animals. The drug reservoir completely isolates drug formulations from the surrounding environment, thus protecting proteins and other water-labile compounds for long periods. VITS is typically designed for zero-order release of agents, but other delivery profiles can be obtained through system design alternatives. VITS has been studied extensively in the release of bovine and porcine somatotropins. Demonstration of its feasibility for zero-order delivery of small amounts of potent molecules in animals has led to its adaptation for use in humans—the DUROS™ technology.

BIBLIOGRAPHY

1. P.R. Klink, T.H. Ferguson, and J.L. Magruder, in G.E. Hardee and J.D. Baggot, eds., *Development and Formulation of Veterinary Dosage Forms*, 2nd ed., Dekker, New York, 1998, pp. 145–229.
2. C. Shih, J. Fix, and R.L. Seward, *J. Controlled Release* **25**, 155–162 (1993).
3. S. Geerts et al., *Vet. Parasitol.* **50**, 15–21 (1993).

4. U.S. Pat. 4,959,218 (September 25, 1990), J.B. Eckenhoff et al. (to ALZA Corp.).
5. U.S. Pat. 5,034,229 (July 23, 1991), J.A. Magruder et al. (to ALZA Corp.).
6. U.S. Pat. 5,037,420 (August 6, 1991), J.A. Magruder et al. (to ALZA Corp.).
7. U.S. Pat. 5,057,318 (October 15, 1991), J.A. Magruder et al. (to ALZA Corp.).
8. U.S. Pat. 5,059,423 (October 22, 1991), J.A. Magruder et al. (to ALZA Corp.).
9. U.S. Pat. 5,110,596 (May 5, 1992), J.A. Magruder et al. (to ALZA Corp.).
10. U.S. Pat. 5,135,523 (August 4, 1992), J.A. Magruder et al. (to ALZA Corp.).
11. U.S. Pat. 5,137,727 (August 11, 1992), J.B. Eckenhoff (to ALZA Corp.).
12. U.S. Pat. 5,174,999 (December 29, 1992), J.A. Magruder et al. (to ALZA Corp.).
13. U.S. Pat. 5,180,591 (January 19, 1993), J.A. Magruder, J.R. Peery, and J.B. Eckenhoff (to ALZA Corp.).
14. U.S. Pat. 5,209,746 (May 11, 1993), S.M. Balaban, J.B. Pike, J.P. Smith, and C.A. Baile (to ALZA Corp.).
15. U.S. Pat. 5,234,692 (August 10, 1993), J.A. Magruder, J.R. Peery, and J.B. Eckenhoff (to ALZA Corp.).
16. U.S. Pat. 5,234,693 (August 10, 1993), J.A. Magruder, J.R. Peery, and J.B. Eckenhoff (to ALZA Corp.).
17. U.S. Pat. 5,234,694 (August 10, 1993), J.A. Magruder, J.R. Peery, and J.B. Eckenhoff (to ALZA Corp.).
18. U.S. Pat. 5,238,687 (August 24, 1993). J.A. Magruder, J.R. Peery, and J.B. Eckenhoff (to ALZA Corp.).
19. U.S. Pat. 5,320,616 (June 14, 1994), J.A. Magruder et al. (to ALZA Corp).
20. U.S. Pat. 5,443,461 (August 22, 1995), L.E. Atkinson, J.T. Dunn, R.M. Gale, and D.L. Rivera (to ALZA Corp.).
21. C.A. Baile et al., *J. Anim. Sci.* **71**(1), 131 (1993).
22. T.R. Kasser et al., *J. Anim. Sci.* **71**(1), 131 (1993).
23. J.D. Armstrong et al., *J. Anim. Sci.* **72**(1), 182 (1994).
24. J. Klindt, F.C. Buonomo, and J.T. Yen, *J. Anim. Sci.* **70**, 3721–3733 (1992).

See also PUMPS/OSMOTIC—INTRODUCTION; PUMPS/OSMOTIC—ALZET® SYSTEM; PUMPS/OSMOTIC—DUROS™ OSMOTIC IMPLANT FOR HUMANS; PUMPS/OSMOTIC—RUMINAL OSMOTIC BOLUS.

PUMPS/OSMOTIC—DUROS™ OSMOTIC IMPLANT FOR HUMANS

JEREMY C. WRIGHT
CYNTHIA L. STEVENSON
GREGORY R. STEWART
ALZA Corporation
Palo Alto, California

KEY WORDS

Biocompatibility
Osmosis
Recombinant technology
Semipermeable membrane
Site-specific delivery
Sodium chloride
Systemic delivery
Zero-order delivery

OUTLINE

Background
System Design
System Performance
Formulation Capabilities
DUROS™ Leuprolide Implant
Disease State
Formulation Stability
In Vitro Performance
In Vivo Performance
In Vivo–In Vitro Release Rate and Stability Correlation
Implantation and Explanation
Clinical Experience
Conclusions
Acknowledgments
Bibliography

The DUROS™ implant is a miniature, osmotically driven drug delivery system designed for the long-term, parenteral, zero-order delivery of potent therapeutic agents to humans. The DUROS™ implant consists of an impermeable titanium alloy cylinder capped on one end by a rate-limiting, semipermeable membrane and on the other end by a plug with an orifice for drug delivery. The interior of the DUROS™ implant contains a polymeric piston that separates the osmotic engine from the drug reservoir (Fig. 1). These single-use DUROS™ implants are sterile, nonpyrogenic, and nonbiodegradable.

The DUROS™ implant functions according to the same osmotic principles as described for other, similar pumps in

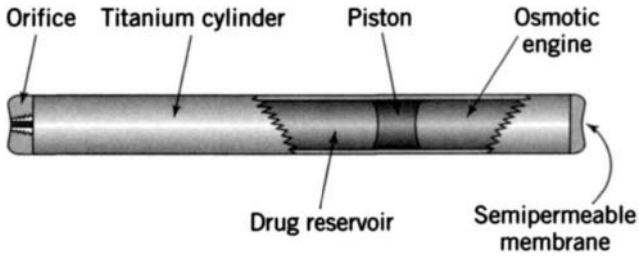


Figure 1. Cross section of a DUROS™ Implant.

this encyclopedia. The osmotic engine, a concentrated salt mixture, establishes a very steep osmotic gradient between the interior of the DUROS™ implant and the surrounding interstitial fluid. In response to this osmotic gradient, water flows into the DUROS™ implant at a rate governed by the permeation characteristics of the semipermeable membrane. As water flows into the DUROS™ implant, drug is delivered from the reservoir via the orifice at the same rate and volume.

A unique feature of the DUROS™ implant, compared with other implantable pumps, is its small size (4 mm × 45 mm), allowing implantation virtually anywhere in the body; the resultant drug reservoir volume is less than 200 μL. (DUROS^{SM} implants with drug reservoir volumes of 50 to 500 μL have been designed.) For systemic administration, the DUROS™ system is implanted under the skin in an outpatient setting with local anesthesia. Explantation at the end of the delivery period is accomplished by a similar, simple surgical procedure. In addition to subcutaneous administration, intravenous, intrathecal, intratumoral, and other forms of targeted drug delivery can be accomplished with the attachment of a catheter.

BACKGROUND

As of 1997, more than 40 biotechnology drug products have been approved, and more than 270 new biotechnology drugs are currently in human clinical trials. Most of these agents are proteins produced by recombinant technology (1). Because of rapid degradation within the stomach and poor absorption from the gastrointestinal tract, proteins and other complex biomolecules cannot be given orally. Drug therapy must therefore rely on parenteral administration via acute injection or preferably through a continuous delivery system. In response to this growing need from the biotechnology sector, researchers designed the DUROS™ implant for the delivery of proteins and peptides.

More than 15 years of research, development, and widespread industry use of osmotic pump technology in animals (the ALZET® osmotic pump, the Push-Melt™ ruminal bolus, and the VITS veterinary implant technology) has demonstrated the potential clinical utility of an implantable osmotic pump suitable for use in humans. In particular, the ALZET® pump has been used in more than 5,200 studies to deliver proteins in nonclinical studies (see PUMPS/OSMOTIC—ALZET® SYSTEM). The widespread use of ALZET® pumps further highlights the need for a human implantable osmotic pump.

The use of a continuous drug delivery system such as the DUROS™ implant offers several pharmacokinetic, pharmacoeconomic, and quality-of-life benefits over traditional bolus dosing methods. Unlike dosing by injection, where blood levels (and clinical efficacy) of the drug vary widely with an initial peak and subsequent trough pattern, the DUROS™ implant delivers drug at a precisely controlled, constant rate within the therapeutic range for long periods. In some therapeutic indications or when using drugs with short half-lives, less drug may be required to achieve the desired effect than with conventional injections, providing substantial dose savings. The DUROS™ implant therapy may offer other pharmacoeconomic advantages in today's health care environment because it requires no maintenance after implantation. The type of "silent therapy" provided by the DUROS™ implant is not only convenient to the patient but also ensures compliance.

SYSTEM DESIGN

The most important design considerations for the DUROS™ implant were biocompatibility; delivery of stable, active drug molecules; and extended zero-order delivery. All tissue-contacting materials were chosen for their biocompatibility and history of use in human implants. Likewise, the components in contact with the drug formulation (e.g. reservoir, orifice, and piston) had to be compatible with a variety of solvents and excipients used to solubilize or suspend the drug. Additionally, the implant components could not adversely affect the drug stability. Design issues based on these considerations will now be discussed for each of the components of the DUROS™ implant.

The rugged titanium reservoir design possesses sufficient mechanical strength to maintain the system configuration despite possible mechanical stresses, such as impact at the implant site. Additionally, the titanium reservoir is impermeable to water, ensuring drug stability and continual zero-order release.

The DUROS™ implant has a polymeric, semipermeable membrane that is permeable to water but essentially impermeable to the osmotic solutes in the osmotic engine. The membrane may include cellulose esters, polyamides, and polyurethanes, depending on the desired characteristics of the membrane, such as system duration. Testing of polyurethane membranes has shown that the membrane material does not change permeability following implantation. Membrane function is not influenced by extracellular fluid, and the membrane remains chemically stable under physiological conditions.

The osmotic engine of the DUROS™ implant can utilize any number of osmotically active solutes but typically contains a combination of sodium chloride (more than 50% by weight) and other excipients, including gelling polymers such as poly(vinylpyrrolidone) (PVP) or sodium carboxymethyl cellulose. The osmotic engine is produced as one or more tablets.

The elastomeric piston seals the drug formulation from the osmotic engine, thus preventing leakage of osmotic solutes into the drug formulation, which could cause significant loss of drug formulation stability and deviations from zero-order delivery. In addition, the piston is compatible with the osmotic engine and moves with relatively little resistance.

The orifice was designed with a small inner diameter and a suitable length to minimize diffusion of drug from the system. Otherwise, diffusion could represent a significant and uncontrolled contribution to the overall rate of delivery at low pumping rates. The drug formulation is not exposed to the surrounding tissue environment until it is released through the orifice. These features also help to prevent back-diffusion of extracellular components when

the system is implanted. Such design features are particularly important for the delivery of biotechnology drugs because proteins, peptides, and other macromolecules are easily rendered inactive by biological processes.

The DUROS™ implant packaging maintains sterility and provides a moisture barrier to prevent premature system start-up. The assembled DUROS™ implant is sterile and nonpyrogenic. Because most peptides and proteins will not withstand conventional sterilization methods (e.g., irradiation or autoclaving), a sterile DUROS™ implant can be produced by irradiating a partially assembled system and performing the remaining filling and assembly steps under aseptic conditions.

SYSTEM PERFORMANCE

When the system is implanted, water is osmotically drawn from the body tissue surrounding the implant (osmotic pressure, π = ~7 atm) through the membrane into the sodium chloride–containing osmotic engine (π = 356 atm). The release rate of the DUROS™ implant is given by equation 4 in PUMPS/OSMOTIC—INTRODUCTION, where A is the membrane cross-sectional area for water transport, h is the membrane thickness, k is the effective permeability of the membrane, and $\Delta\pi$ is the osmotic pressure difference across the membrane.

$$dm/dt = (A/h)k\Delta\pi c \quad (1)$$

If A, h, k, and $\Delta\pi$ are held constant, then a constant rate of drug delivery will result. In the DUROS™ implant, A and h are constant by design and manufacture, and k has been shown to remain constant over time, both in vitro and in vivo. The osmotic engine is manufactured with excess sodium chloride to maintain saturation, ensuring that $\Delta\pi$ will remain constant for the intended duration of drug delivery. Hence, a continuous zero-order release profile is expected for the DUROS™ implant.

The release rate and duration of a DUROS™ implant depend on the overall system size, membrane design, osmotic engine design, drug reservoir size, and concentration of the drug in the reservoir. Figure 2 shows the effect of changing the membrane permeability on release rate and duration while keeping the other parameters constant in the 4 mm × 45 mm device. For a particular reservoir size, the higher the release rate, the shorter the duration of drug delivery.

In vitro studies have demonstrated constant zero-order delivery from DUROS™ implants. DUROS™ implants were placed in test tubes containing phosphate-buffered saline (PBS) and held at 37°C. The implants were placed in fresh PBS weekly, and the remaining PBS was assayed for drug content. In one study with a target duration of 3 months, the delivery rate performance of five systems was measured by sampling at approximately weekly intervals. The systems exhibited zero-order delivery at 1.0 μL/day for 100 days, with coefficients of variation averaging 3% for days 7 to 104 (data not shown). In another study, 30 DUROS™ implants maintained a target of 0.38 μL/day release of blue dye solution for 360 days with a coefficient of variation of less than 9% among the implants (Fig. 3). A zero-order release profile was obtained from the data when assaying on a weekly basis by reversed-phase high-performance liquid chromatography (RP-HPLC). Sampling of cumulative implant output by ultraviolet (UV) spectrophotometry with a flow cell at 6-min intervals for 24 h demonstrated a continuous zero-order release rate (Fig. 4).

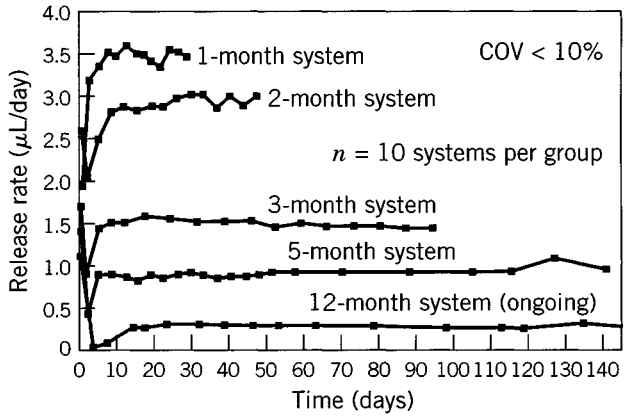


Figure 2. Comparison of release rates in DUROS™ Implants as a function of system duration.

FORMULATION CAPABILITIES

DUROS™ implants with diameters up to 7 mm have been designed, resulting in drug formulation volumes of 50 to 500 mL. The reservoir volume of the 4 mm × 45 mm implant has a total volume of less than 200 μL. Given the limited formulation volume in a single implant, concentrated drug formulations are usually required. Formulation parameters such as saturation solubility and chemical and physical (aggregation) stability are important. For example, in a 150-mL drug reservoir, a 2-month system delivers 2.5 μL/day. Given a 400-mg/mL solution drug formulation, the implant delivers 1.0 mg/day (60 mg/implant). Similarly, a 500-mL drug reservoir (7 mm × 45 mm) lasting 12 months delivers 1.4 mL/day. In this system, a drug formulation at 400 mg/mL delivers 560 mg/day (200 mg/implant).

Important formulation considerations for the DUROS™ implant include stability, solubility, and compatibility. For example, adequate drug stability and potency for a 2-year shelf life plus the implant life are desired. The formulated peptide or protein must be structurally stable and not unfold, gel, or precipitate with loss of activity or production of large particulates capable of clogging the orifice. The formulation must either chemically withstand terminal sterilization or possess sufficient physical stability for sterile filtration, if not aseptically processed. Generation of suspensions in an aseptic environment is often an important factor. The formulation must also be compatible with the pump components in terms of peptide adsorption characteristics and vehicle leachates.

Biotechnology drug moieties can be formulated in aqueous (up to 400 mg/mL) or nonaqueous (up to 500 mg/mL)

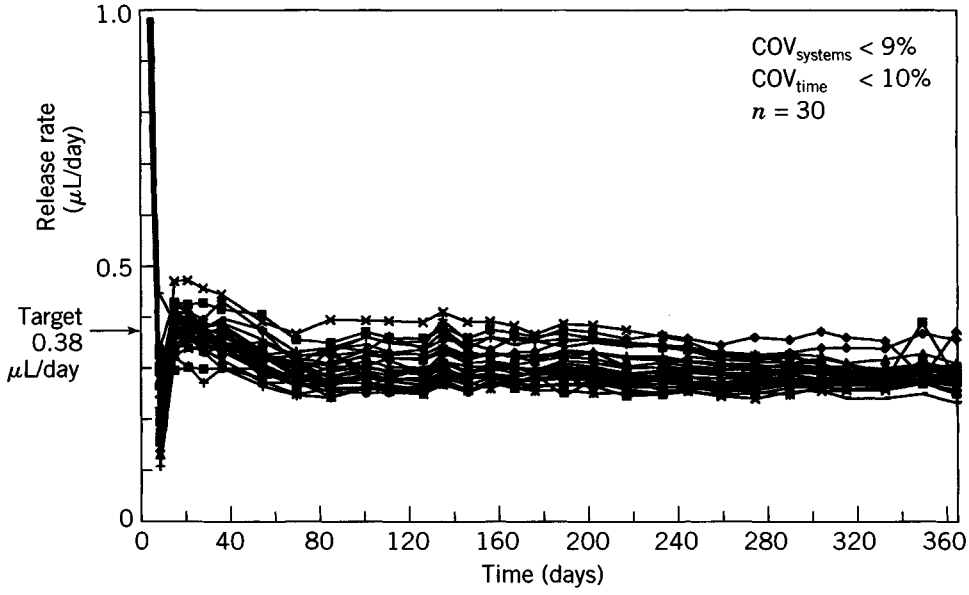


Figure 3. In vitro release rates in the DUROS® Implant as compared with the 0.38-μL/day target.

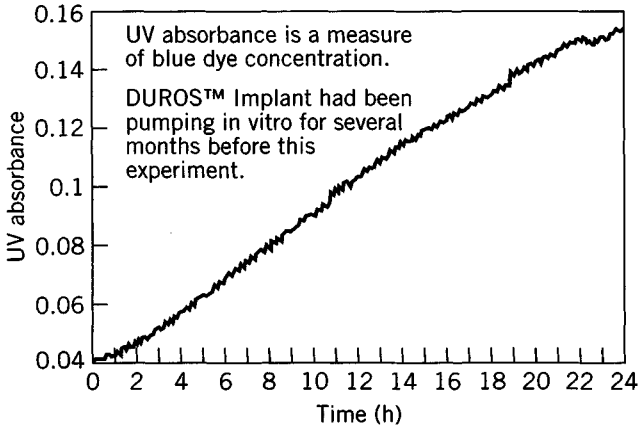


Figure 4. In vitro release rate in the DUROS® Implant, plotted in 6-min intervals.

solutions or in aqueous or nonaqueous suspensions (up to 500 mg/mL), depending on the solubility and stability of the specific molecule. Many times nonaqueous vehicles offer enhanced stability for biomolecules, such as proteins and peptides, by minimizing hydrolytic degradation pathways (2). For drug molecules with solubility or stability limitations, nonaqueous suspensions provide an alternative. For example, stable nonaqueous protein suspensions (e.g., α interferon) in excess of 30% weight in volume (w/v) for 3 to 6 months at 37°C have been reported (3).

DUROS® LEUPROLIDE IMPLANT

The DUROS® Leuprolide Implant is designed to deliver leuprolide continuously at a nominal rate of 125 μg/day over 1 year for the palliative treatment of prostate cancer. It is implanted subcutaneously in the upper arm and explanted after 1 year. The bioactive peptide for the DUROS® Leuprolide Implant is formulated as a stable nonaqueous solution. This implant is designed to provide an alternative to periodic injections of leuprolide, with the goals of long-term patient compliance and improved quality of life.

DISEASE STATE

Because of the dependence of prostate cancer on circulating androgen levels, testicular androgen ablation (i.e., lowering of circulating testosterone levels) has been the standard for primary therapy of advanced prostate cancer for more than 50 years (4). Continuous administration of luteinizing hormone–releasing hormone (LH-RH) agonists, such as leuprolide acetate, results in the decrease of serum testosterone levels to castrate levels. Since the 1980s, LH-RH agonist therapy has been the primary treatment strategy for androgen ablation (5–7). LH-RH therapies are associated with 80% to 90% stabilization of the disease for 10 to 18 months on average, and 2-year survival is approximately 60% (8,9).

Uninterrupted drug administration is essential to the efficacy of LH-RH agonist therapy, so compliance is critical for prostate cancer patients. Unfortunately, compliance is often a problem, where 44% of patients failed to present for one or more monthly Lupron Depot® injections, and 24% of patients were more than 2 weeks late in obtaining a monthly injection in the U.S. Veterans Administration system (10).

FORMULATION STABILITY

Highly concentrated leuprolide solutions have demonstrated good chemical and physical stability when stored in sealed DUROS® implants at 37°C for the functional lifetime of the implant (2,11,12). Excipients used for the early screening of formulations included solution vehicles such

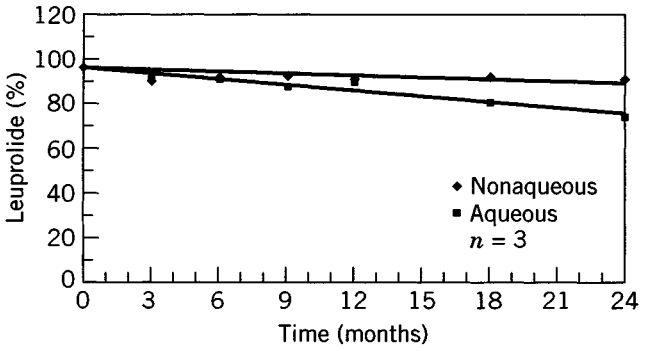


Figure 5. Comparison of the stability of aqueous and nonaqueous formulations in the DUROS® Leuprolide Implant (370 mg/mL at 370°C).

as propylene glycols, poly(ethylene glycols), ethanol, glycofurol, dimethyl sulfoxide, and water. Both aqueous and nonaqueous solution formulations demonstrated 80% to 95% leuprolide remaining after 12 months at 37°C (12). For example, a 370-mg/mL aqueous leuprolide formulation was stable for up to 6 months and then dropped off to slightly below 90% stability, whereas a nonaqueous formulation showed greater than 90% stability for more than 12 months (Fig. 5). The major degradation pathways for the nonaqueous formulation were hydrolysis, racemization, oxidation, and aggregation. Similar degradation pathways were observed for the aqueous formulation. However, in the nonaqueous formulation, the proportion of leuprolide degrading to hydrolytic products decreased while aggregation products increased, resulting in a more stable formulation. In general, no aggregates larger than a trimer were observed. The final formulation used for clinical trials was a 370-mg/mL nonaqueous formulation that provided 92% stability for 2 years at 37°C, which is adequate for a 2-year shelf life (25°C) in addition to a 1-year implant life (37°C).

IN VITRO PERFORMANCE

When in vitro device release rates were measured (n = 6), a zero-order release rate was seen for up to 1 year (Fig. 6). In addition, RP-HPLC analysis revealed greater than 95% in vitro drug stability on average over the test duration.

IN VIVO PERFORMANCE

A 14-month canine study evaluated the DUROS® Leuprolide Implant for serum testosterone concentrations. In the control group, serum testosterone levels fluctuated widely up to 600 ng/dL through the year. Conversely, for every dog that received a DUROS® Leuprolide Implant, testosterone levels were suppressed to castrate levels (below 50 ng/dL) by day 25 and remained completely suppressed (Fig. 7). After 365 days, the first implant was replaced, and blood levels of testosterone remained suppressed to the end of the study (14 months). Histological evaluation of the implantation site did not reveal any unusual changes in the tissue, and neither was any systemic toxicity seen in the study.

Local tissue reactions to the DUROS® Leuprolide Implant were further investigated in rats and Hanford miniature swine. In rats, no unexpected local tissue reactions were observed with the implants over the 38-week study, and in general, tissue reaction scores were equal to or better than those of historical controls receiving control implant material (high-density polyethylene). In miniature swine, no infections or system expulsions occurred over the 12 weeks, and no macroscopic or microscopic evidence of untoward local tissue reactions was seen.

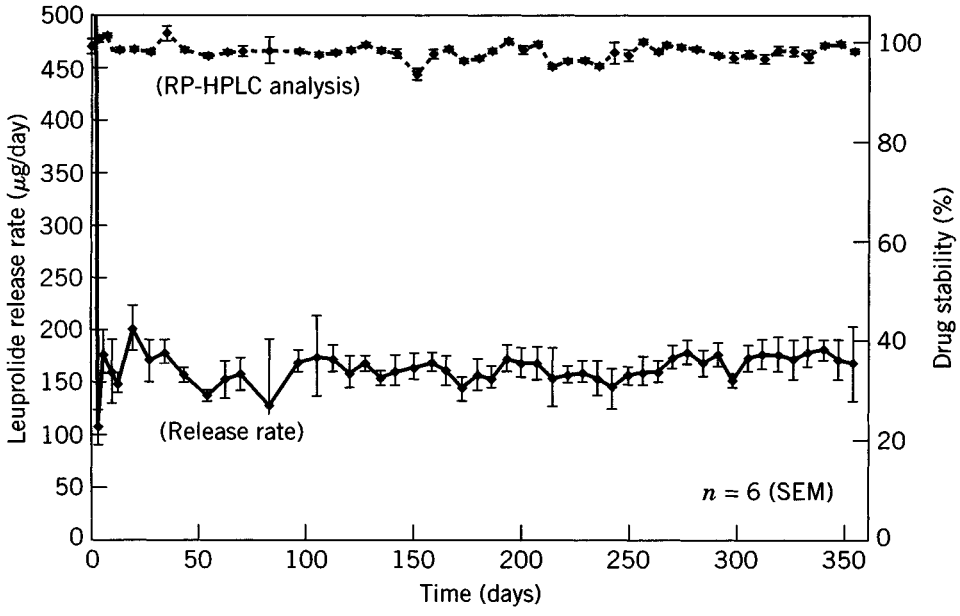


Figure 6. In vitro release rate and drug stability of the DUROS® Leuprolide Implant.

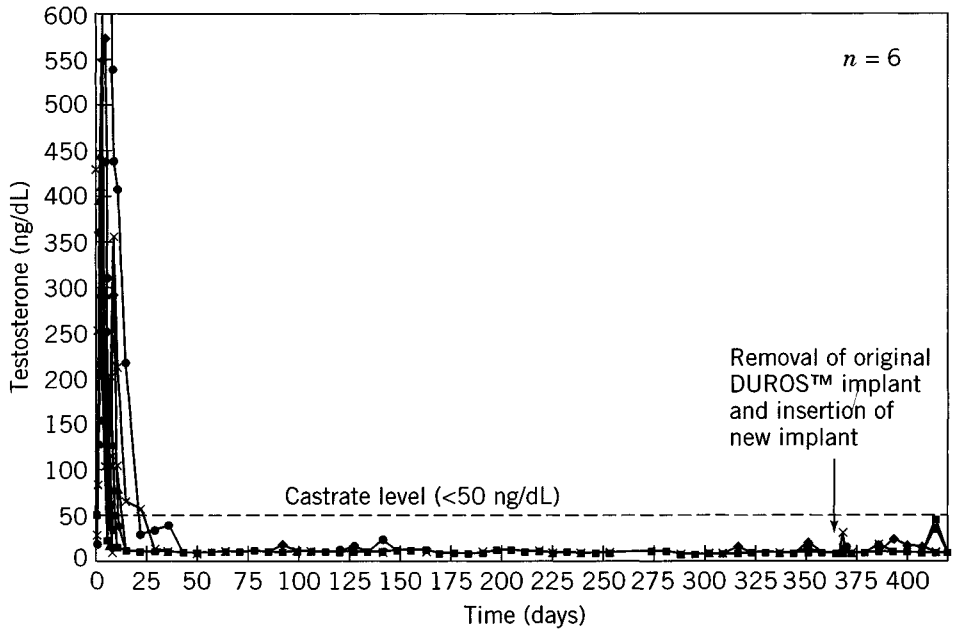


Figure 7. Testosterone concentrations in dogs with the DUROS™ Leuprolide Implant.

IN VIVO–IN VITRO RELEASE RATE AND STABILITY CORRELATION

The in vivo performance of the DUROS™ Leuprolide Implant has been characterized in both dogs and rats, and the results have been compared with the performance of the same batch of implants evaluated in vitro. Cumulative drug delivery was estimated from analysis of residual drug in the reservoir (Table 1). Comparison of in vivo cumulative drug delivery with in vitro cumulative drug delivery shows agreement to within 5%.

Analysis of the residual drug formulation (370 mg/mL) also permitted comparison of in vivo and in vitro stability values using RP-HPLC and SEC (Table 2). Stability was more than 96% for RP-HPLC and SEC measurements, both in vivo and in vitro, at the 6-month timepoint. At the 1-year timepoint, good stability was also observed, both in vitro and in vivo, reflecting the stability of the leuprolide formulation and the design of the orifice in preventing back diffusion of aqueous fluids and extracellular components. Taken together, the close correlation of the in vitro and in vivo release rates and of the in vitro and in vivo stability values for the DUROS™ Leuprolide Implant indicates that these attributes are essentially independent of in vivo conditions and can be predicted from in vitro testing results.

IMPLANTATION AND EXPLANATION

The DUROS™ Leuprolide Implant is implanted subcutaneously in the upper inner aspect of the nondominant arm. The implantation is an outpatient procedure requiring local anesthesia. After normal antiseptic preparation of the site, a local anesthetic is injected along a 5-cm track. A 4- to 5-mm incision is made with a scalpel through the skin at one end of the anesthesized area. The DUROS™ system is inserted through the incision and advanced subcutaneously along the anesthesized track. The incision site is closed with a Steristrip® and a sterile bandage.

Table 1. In Vivo–In Vitro Pumping Rate Comparison (Nonaqueous Formulation)

Species	Time of explant (weeks)	In vivo cumulative delivery (mg leuprolide)	In vitro cumulative delivery (mg leuprolide)	Difference (%)
Rat	24	28.7 ± 5.8 (n = 3)	29.2 ± 2.8 (n = 5)	1.6%
Dog	52	60.5 ± 3.2 (n = 6)	63.5 ± 2.3 (n = 9)	4.8%

Table 2. In Vivo–In Vitro Drug Stability Comparison (Nonaqueous Formulation)

Species	Time of explant (weeks)	Method	In vivo stability	In vitro stability	Difference (%)
Rat	24	RP-HPLC	97.0 ± 0.1% (n = 3)	96.6 ± 0.3% (n = 5)	0.4%
		SEC	97.3 ± 0.1% (n = 3)	97.2 ± 0.7% (n = 5)	0.1%
Dog	52	RP-HPLC	96.5 ± 0.1% (n = 6)	96.0 ± 0.4% (n = 4)	0.5%
		SEC	93.8 ± 2.4% (n = 4)	97.2 ± 0.7% (n = 4)	3.6%

Explanation is accomplished by external palpation and localization of the implant followed by incision and removal. After normal antiseptic preparation of the site, local anesthetic is injected at one end of the implant, and a 4- to 5-mm incision is made, perpendicular to the implant. Finger pressure is applied to the other end of the implant to elevate the removal end. A small slit is then made through any surrounding fibrotic tissue to expose the implant. The implant is then popped out by continued finger pressure on the opposite end, and the incision site is closed with a Steristrip® and a sterile bandage.

CLINICAL EXPERIENCE

A human clinical study (six male volunteers, aged 18–65 years) showed that the DUROS™ implant and explant procedures were well tolerated (13,14). The placebo implant utilized in the study consisted of a sterile titanium alloy DUROS™ reservoir and membrane and orifice components; no drug formulation or internal components were used. No adverse effects were reported during the 8-week study. Additionally no "wearing" sensation was reported by the volunteers. Each implant was explanted in an outpatient surgery area in approximately 3 min.

A 1-year human phase I/II clinical study, begun in March 1997, examines the feasibility, functionality, and efficacy of one versus two DUROS™ Leuprolide Implants (3.75 mg/month with one implant versus 7.5 mg/month with two) in patients with advanced prostate cancer. Preliminary data show that testosterone was suppressed to castrate levels (below 50 ng/dL) by the fourth week of the trial for both the patients who received one implant and the patients who received two implants.

CONCLUSIONS

The DUROS™ implant represents an emerging application of osmotic technology for the delivery of biomolecules for human therapy. The technology reflects recent advances in biotechnology and in stabilization of peptides and proteins formulated as aqueous and nonaqueous solutions and suspensions. The DUROS™ implant design is adaptable for many other compounds and sites of administration. Typically the delivery is systemic, but it can be made site specific by replacing the orifice with a catheter directed to the desired location—for example, into the intrathecal or epidural cerebrospinal fluid. The DUROS™ implant has demonstrated biocompatibility and functionality in animal studies. The first therapeutic application of this technology, currently in clinical trials, is the 1-year DUROS™ Leuprolide Implant for the treatment of prostate cancer.

ACKNOWLEDGMENTS

We thank Corinne Falender, Sally Tao, Paul Johnson, Jim Brown, Joe Leonard, and Keith Dionne for their contributions. We also thank the Implant Research and Development, Biopharmaceutical Development, and Toxicology departments at ALZA Corporation.

BIBLIOGRAPHY

1. Biotechnology Industry Organization, *1996 BIO Editors' and Reporters' Guide to Biotechnology*, 2nd ed., BIO, Washington, D.C., 1996.
2. C.L. Stevenson et al., *Proc. Int. Symp. Controlled Release Bioact. Mater.* **23** (1996).
3. J.E. Brown, *Pharm. Res.* **13**(9), S-79 (1996).
4. E.D. Crawford et al., *J. Clin. Endocrinol. Metab.* **80**, 1062–1078 (1995).
5. A. Kaisary, C.J. Tyrell, and W.B. Peeling, *Br. J. Urol.* **67**, 502–508 (1991).
6. M.S. Soloway, G. Chodak, and N.J. Vogelzang, *Urology* **37**, 46–51 (1991).
7. R.P. Huben and G.P. Murphy, *Cancer (Philadelphia)* **62**, 1881–1887 (1988).
8. N. Bruchovsky, in J.F. Holland et al., eds., *Cancer and Medicine*, 3rd ed., vol. 1, Lea & Febiger, Philadelphia, 1993, pp. 885–896.
9. P. Chrisp and E.M. Sorkin, *Drugs Aging* **1**, 487–509 (1991).
10. J.A. Shaheen, M. Amin, and J.I. Harty, *Urology* **42**, 533–535 (1993).
11. C.L. Stevenson et al., *Pharm. Res.* **13**(9), S-110 (1996).
12. C.L. Stevenson et al., *Program Abstr., 1997 Am. Pep. Symp.* Nashville, Tenn., June 14–19, 1997.
13. J.E. Brown, *Abstr. Pap. 213th Meet., Am. Chem. Soc.*, 1997, p. 271.
14. J.C. Wright et al., *Proc. Int. Symp. Controlled Release Bioact. Mater.* **24**, 59–60 (1997).

See also PUMPS/OSMOTIC—INTRODUCTION; PUMPS/OSMOTIC—ALZET® SYSTEM; PUMPS/OSMOTIC—VITS VETERINARY IMPLANT; PUMPS/OSMOTIC—RUMINAL OSMOTIC BOLUS.

PUMPS/OSMOTIC—RUMINAL OSMOTIC BOLUS

JEREMY WRIGHT
ALZA Corporation
Palo Alto, California

KEY WORDS

Hydration
Parasitic larvae
Rumen
Ruminants
Selenium deficiency
Semipermeable membrane

OUTLINE

Background
System Design and Function
Products
IVOMEC SR® Bolus (Ivermectin)
Dura SE® Bolus (selenium)
Conclusions
Bibliography

The Ruminal Therapeutic System (RUTS) Push-Melt™ technology is designed to provide controlled delivery of a drug for up to 1 year in the rumen of cattle and sheep. After oral administration, each capsular system is retained in the rumen, delivering drug for an extended duration. Drug is absorbed through the ruminal or lower intestinal mucosa into the systemic circulation. For cattle, RUTS systems are generally 2 to 3 cm in diameter and up to 10 cm in length. Larger dimensions are possible, depending on the particular application. Up to 10 g of drug can be administered. The RUTS Push-Melt™ technology is applicable to the delivery of parasiticides, insecticides, nutritional supplements, antibiotics, growth promoters, repartitioning agents, and estrus suppressants.

BACKGROUND

In the mid-1980s, the RUTS Push-Melt™ technology was developed to meet the need for drug-dedicated osmotic systems for use in ruminant production animals (1,2). Ruminants such as cattle and sheep have a complex digestive system that includes a large four-chambered stomach; the chambers are the rumen, the reticulum, the omasum, and the abomasum (Fig. 1) (3). In the rumen, ingested cellulose is broken down by microorganisms into simple mono- and disaccharides suitable for digestion. Orally administered, sustained-release delivery systems are typically limited by the target animal's gastrointestinal transit time, but in ruminants (cattle, goats, and sheep) the transit time can be controlled by using a device with sufficient density or a geometrical configuration that keeps it in the rumen for an indefinite period. Objects are retained in the rumen if they are suitably dense (density greater than 2.0 g/cm^3, preferably 2.7 to 3.0 g/cm^3) or large enough to prevent passage to the lower portions of the gastrointestinal tract or upward through the esophagus in regurgitation. In addition to the RUTS system, density-based systems include a system with two semipermeable membranes attached to a stainless steel cylinder that delivers morantel tartrate (4), a system described by Conrad and Skinner that consists of a high-density cylinder containing monensin dispersed in a biodegradable matrix of polylactic acid (5), and a completely degradable corrosion-based Panacur SR bolus that releases 12 g of fenbendazole over 4 to 5 months (6). Geometry-based systems usually have a mechanism for unfolding to a larger size once in the rumen; before administration, the system is secured in a compact configuration by a degradable tape or closure. The Laby device has "wings" (polymeric strips held in place by a water-degradable tape) that expand in the rumen (7,8); this device has been used to deliver albendazole (Captec Proftril™, SmithKline Beecham) by dissolution from tablets in contact with ruminal fluids (9). Another system, consisting of a rolled trilaminate sheet, uncoils in the rumen and releases morantel tartrate (10).

SYSTEM DESIGN AND FUNCTION

The RUTS Push-Melt™ osmotic system consists of an injection-molded semipermeable membrane that encapsulates an osmotic tablet, a partition layer, drug formulation, and an iron densifier. An exit port screen can be included (Fig. 2). Systems can vary in size from 2 to 3 cm in diameter and up to 10 cm in length, with overall drug loading capacity of up to 10 g.

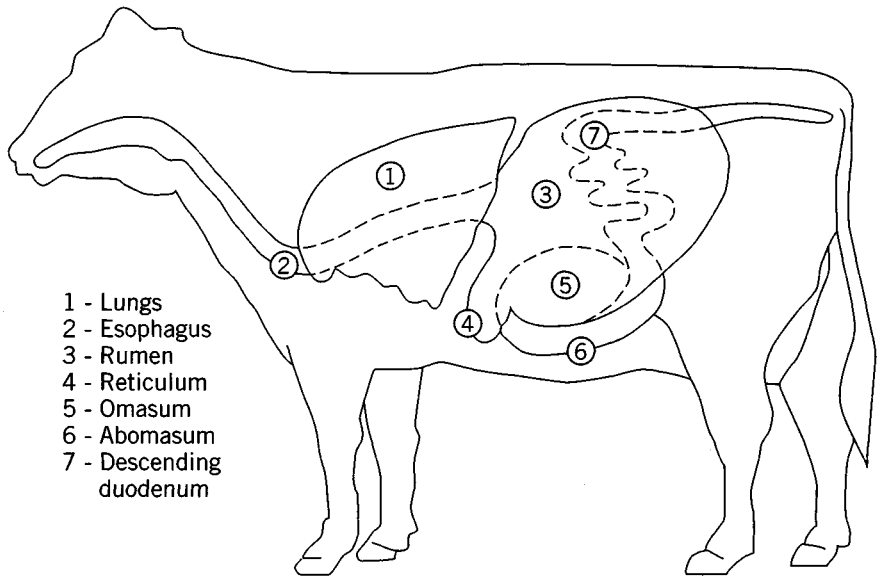


Figure 1. Bovine digestive system. *Source:* Ref. 3.

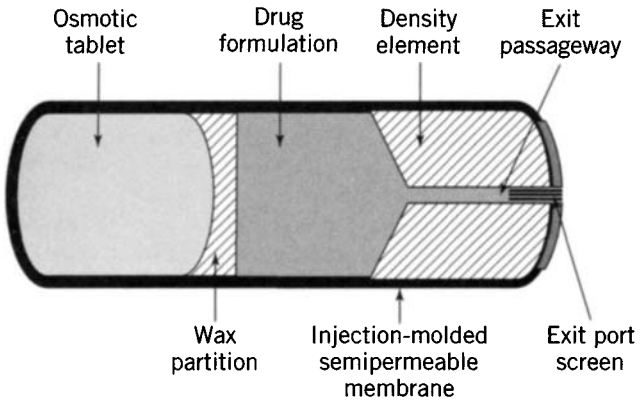


Figure 2. Cross section of the Push-Melt™ Ruminal Therapeutic System (RUTS).

In the aqueous environment of the rumen, water is imbibed through the semipermeable membrane into the osmotic tablet, which swells and pushes against the partition layer. The partition layer forces the thermoresponsive drug formulation through the orifice in the densifier and through the exit port screen if it is present.

The semipermeable membrane controls the rate of water imbibition and therefore the pumping rate of the system. This membrane, composed of cellulosic esters and plasticizers, must be rigid enough to ensure device integrity. The osmotic tablet consists of a swelling hydrogel (e.g., sodium carbomer) and an inorganic, osmotically active salt (e.g., sodium chloride), which provides a high osmotic gradient (more than 300 atm) across the membrane. Between the osmotic tablet and the drug formulation layer is the partition layer, which acts like a plunger in a syringe to ensure a smooth response to the swelling of the osmotic tablet. It consists of a compound with a higher melting point or a higher viscosity than the drug formulation layer. By altering the size of the partition layer, researchers can change the duration of the system while keeping the total dosage constant.

A RUTS Push-Melt™ system can deliver one or more drugs up to 50% by volume in a solution or a suspension. In the drug formulation, drug is suspended or dissolved in a thermoresponsive vehicle that is easily stored as a solid at room temperature. The drug formulation softens to form a viscous, flowable solution or semisolid in the 40°C ruminal environment. Microcrystalline waxes have proved useful as such vehicles (11); drugs can be suspended in these waxes at concentrations in excess of 30% by weight. Because many drugs are essentially insoluble in the wax, such formulations have minimal osmotic activity and high stability. Preparing the drug formulation as a solid improves the stability of compounds with limited solubility and increases the shelf life of the systems. Drugs can be hydrophobic or hydrophilic; if hydrophilic, they are prepared in a hydrophobic vehicle.

The densifier, made of sintered iron, adds sufficient weight to the system so that it will not be regurgitated; the amount of weight required varies with the species. At the end of the exit passageway, the optional exit port screen provides the system with additional protection from ruminal debris.

Although ruminal boluses are typically removed by magnets during slaughter, all system components are designed to be fragmentable and compatible with rendering equipment in the event that they are not completely removed (12).

The basic mathematical expressions that describe drug release from osmotic systems are given in PUMPS/OSMOTIC—INTRODUCTION. The drug delivery rate equation is

$$dm/dt = (A/h)k\Delta\pi c$$

where $\Delta\pi$ is the osmotic pressure gradient between the osmotic engine and the ruminal environment.

For Push-Melt™ systems, the membrane surface area (A) and the osmotic pressure gradient ($\Delta\pi$) change over time as the degree of hydration (H) increases (2). The effective membrane surface area increases over time as the osmotic tablet swells, but the osmotic engine itself is diluted, decreasing the osmotic pressure gradient. To reflect these time dependencies, the equation is modified as follows:

$$dm/dt = (A_H/h)k\Delta\pi_H c$$

where the subscript H represents the dependence of A and $\Delta\pi$ on osmotic engine hydration. The osmotic pressures of the drug formulation and of the partition layer are assumed to be negligible.

The mechanism of RUTS Push-Melt™ drug delivery is independent of in vivo environmental conditions, mainly because of the low osmotic pressures in the in vivo environment. Because of this, in vivo and in vitro system performance are closely correlated, and in vitro assessment is predictive of in vivo performance and therapeutic outcome.

RUTS Push-Melt™ systems can be designed for a variety of drug delivery profiles such as zero-order, pulsatile, ascending, or descending. They are typically designed for zero-order drug delivery of up to 5 g/day for durations ranging from 1 day to 1 year. With zero-order drug delivery, the RUTS Push-Melt™ system prevents drug plasma concentrations from attaining toxic levels or declining to subtherapeutic levels. Drug can be delivered in pulses by alternating the drug and placebo layers in the formulation layer (13). Ascending and descending release profiles can be designed into the system: Creating an increase in the membrane surface area (through choice of appropriate membrane materials and osmotic agents) results in an ascending profile, whereas providing a subsaturated solution in the osmotic tablet gives a descending profile.

PRODUCTS

Two commercial products have been developed and marketed using the RUTS Push-Melt™ technology. Dura SE®, introduced in 1989, delivers sodium selenite to selenium-deficient cattle for up to 4 months. IVOMEC SR® (ivermectin), released in 1992, delivers the parasiticide iver-

mectin to cattle for 135 days, controlling parasitic bronchitis and parasitic gastroenteritis for the entire grazing season when used at turnout. It is also effective in the treatment and control of sucking lice, mange mites, and warbles for 135 days after administration.

IVOMEC SR® Bolus (Ivermectin)

Ivermectin is a unique chemical entity discovered and developed by scientists at Merck Research Laboratories. Its broad-spectrum efficacy and wide margin of safety make it an ideal anthelmintic agent (14). Ivermectin acts by paralyzing parasitic nematodes, arachnids, insects, and warbles; this result is attributed to ivermectin's effect on the central nervous system of these parasites, specifically its effect on the mediation of neurotransmission by γ-aminobutyric acid (GABA) (15). At therapeutic doses, ivermectin has no effect on cattle because it does not readily penetrate the bovine central nervous system. For a discussion of the pharmacokinetics of ivermectin, see Baggot and McKellar (16).

Ivermectin can be given orally, parenterally, or topically. Continuous release is advantageous because animals are susceptible to reinfection when grazed on infected pastures. When ivermectin is given as a continuous-release ruminal bolus, steady-state levels of ivermectin can be ensured with minimal stress to the animal and minimal handling by the producer.

When ivermectin was delivered ruminally by a weighted ALZET® osmotic pump, mean plasma levels of ivermectin were predictable over a 0- to 40-μg/kg/day dosage range; bioavailability was 40% (17). Using the same method of administration, Egerton and colleagues showed that ivermectin was effective in preventing the establishment of nine nematode parasite species in cattle (18). A daily dose of up to 40 μg/kg/day, delivered intraruminally, was effective in protecting grazing calves against these parasites. This work helped establish the target delivery rate for ivermectin in fully grown cattle (300 kg) at 12 mg/day (2).

The IVOMEC SR® Bolus for cattle contains 1.72 g ivermectin as a 22% (w/w) suspension dispersed in a white, microcrystalline wax. The system includes an exit port screen (Fig. 2), which prevents ingress of ruminal matter into the system and increases the internal operating pressure of the system. The IVOMEC SR® Bolus is 9 cm long and 2.5 cm in diameter. Delivering 12 mg/day of ivermectin for 135 days, it is effective for the treatment and season-long control of parasitic bronchitis (lungworm), gastrointestinal nematodes, sucking lice, mange mites, and warbles.

Administration of the IVOMEC SR® Bolus is accomplished by using a balling gun of appropriate size to deliver the bolus into the pharynx just beyond the back of the animal's tongue (Fig. 3) (19). Once administered, the IVOMEC SR® Bolus has sufficient density to be retained in the rumen for an extended duration. Biting or regurgitation of the system occurs infrequently. In the few reported cases of biting, system integrity was not compromised, and the system could be readministered.

Because of the homogeneous nature of the drug formulation (a hydrophobic suspension), ivermectin delivery in an IVOMEC SR® Bolus can be directly calculated from the weight of the pumped drug formulation (2). Hence, when systems were immersed in a fixed volume of water or phosphate-buffered saline maintained at ruminal temperature (40°C), in vitro system performance could be determined from assayed ivermectin delivery or gravimetric measurements of the formulation delivered. For in vivo measurement, ruminants were fistulated so that the system could be removed periodically for analysis, then returned to the ruminal environment. In this case, the IVOMEC SR® Bolus was placed in a metal canister with perforations on one end to permit ruminal fluid access to the osmotic tablet; the other end was not perforated, and entry of water was prevented by means of O-rings. Drug formulation was released into this latter end of the collection vessel and analyzed on periodic removal (2).

IVOMEC SR® Start-up and Shutdown Delivery Profiles. Rapid, reproducible, and predictable drug delivery start-up is important with ruminal boluses for immediate prophylaxis, especially in the spring when animals are sent to fresh pastures, where an increase of parasitic larvae is typical. With prototype IVOMEC SR® boluses, drug delivery was not instantaneous; a time lag was associated with water permeation into the osmotic tablet and pressurization of the drug formulation. To minimize this start-up time, the IVOMEC SR® Bolus is prehydrated by adding a fixed amount of water to the packaged system, causing an increase in the internal hydrostatic pressure as water is imbibed into the osmotic tablet. Once in the 40°C ruminal environment, the thermoresponsive drug formulation softens, with rapid onset of osmotic pumping. Zingerman and colleagues (2) have shown that the onset of drug delivery for hydrated (1.3 g of water added) IVOMEC SR® boluses is rapid (2–3 days). Steady-state delivery is reached in 7 to 10 days. Anhydrous systems took 2 to 3 weeks to reach steady-state delivery (Fig. 4) (2).

Reproducible and predictable delivery termination for the IVOMEC SR® bolus is critical to establish the optimum withdrawal period so that drug residues are minimized to safe levels before slaughter. For the IVOMEC SR® Bolus, the withdrawal period (period since last drug administration in which the animal cannot be slaughtered for human consumption) is 180 days. As shown in Figure 4 (2), termination occurred rapidly at approximately 135 days for both in vivo and in vitro systems; within 14 days, shutdown was complete (2).

IVOMEC SR® In Vivo–In Vitro Release-Rate Correlation. Good agreement has been shown between the in vitro and in vivo release profiles for the IVOMEC SR® Bolus (2). Figure 5 (2) demonstrates this agreement, which has also been verified with seven large, commercial-scale batches. The cumulative coefficient of variation at the time when all the drug formulation was expelled was 4% for in vivo systems and 4.2% for in vitro systems.

IVOMEC SR® Efficacy. In a study by Yazwinski and colleagues, calves treated with the IVOMEC SR® Bolus had significantly fewer fecal egg counts and significantly fewer nematodes at necropsy than did the untreated calves; both

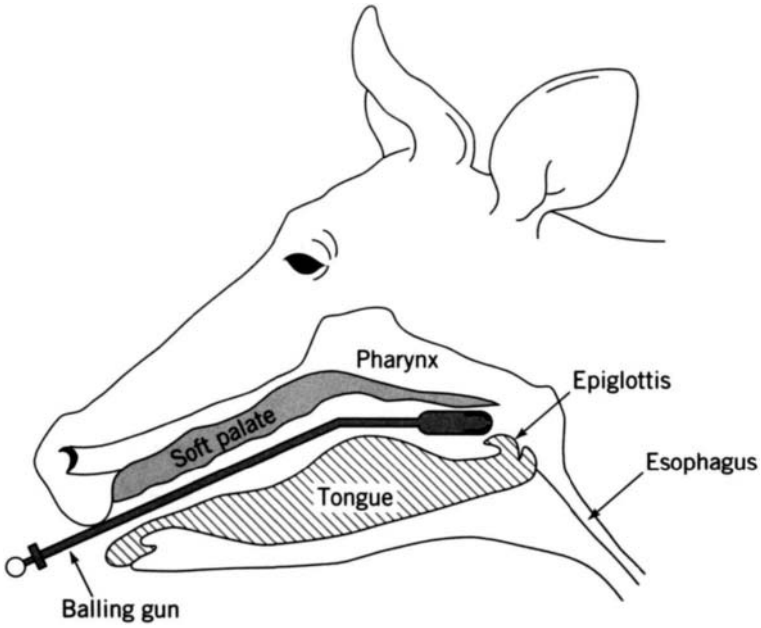


Figure 3. Bolus administration technique for controlled-release boluses. *Source:* Ref. 19.

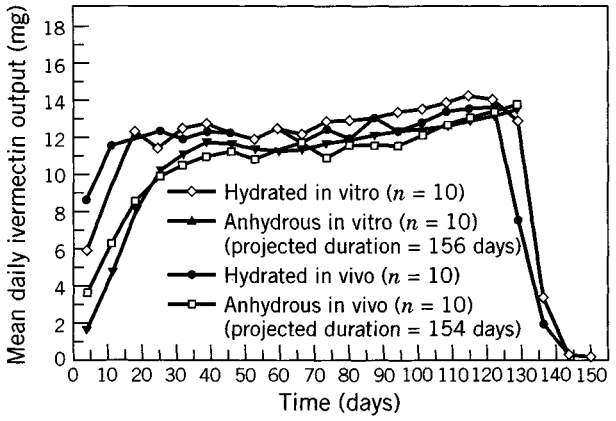


Figure 4. Comparison of anhydrous and hydrated (1.3 g) in vitro and in vivo ivermectin output profiles of IVOMEC SR® Bolus samples. *Source:* Ref. 2.

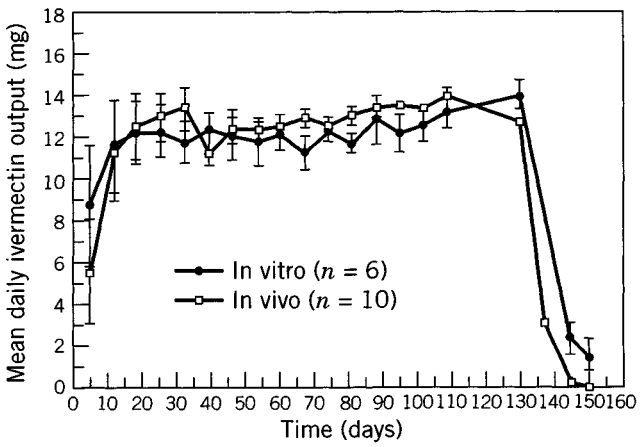


Figure 5. Comparison of in vitro and in vivo release profiles of ivermectin (bolus samples hydrated at 1.3 g). *Source:* Ref. 2.

groups were given infective larvae inoculum and grazed on an infected pasture. The ivermectin bolus prevented the establishment of not only actively developing parasitic nematodes but also arrested larvae (e.g., *Ostertagia* EL_4). No adverse reactions were seen, and all IVOMEC SR® boluses remained in the rumen throughout the study (20).

Dura SE® Bolus (selenium)

Selenium deficiency in cattle is a problem in many areas of the world, including parts of the United States. A Push-Melt system, the Dura SE® Bolus has been developed to deliver sodium selenite at the rate of 3 mg of selenium per day to cattle for 120 days. The system does not include the optional exit port screen; otherwise, the design is as shown in Figure 2. The drug formulation consists of sodium selenite dispersed in a microcrystalline wax. Figure 6 shows the in vitro, zero-order release profile obtained for

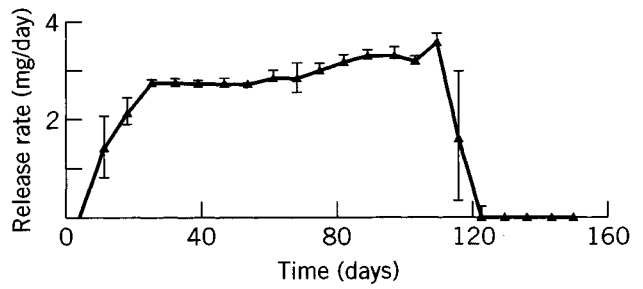


Figure 6. In vitro release profile of selenium delivered from a Dura-SE® bolus.

the Dura SE® Bolus. Adair and colleagues examined the in vivo behavior of Dura SE® Bolus and found that release reached a steady state within 4 weeks, continued at steady-state levels for 16 weeks, and dropped to less than 1% of steady-state levels in the final 2 weeks. Mean in vivo release was 3.1 mg/day, with a range of 2.4 to 4.1 mg/day. Excellent in vivo–in vitro correlation was obtained (21). Figure 7 shows selenium blood levels from selenium-deficient cattle treated with the Dura SE® Bolus. Selenium has a relatively long half-life, which is reflected in the slowly rising selenium levels. Nevertheless, selenium levels were in the normal range (more than 0.08 ppm) by day 35 (22).

In a 220-day study, Campbell and colleagues assigned 150 selenium-deficient, pregnant beef cattle to one of four treatment groups: one Dura SE® Bolus at day 0, two Dura SE® Boluses (one administered on day 0 and the second one on day 119), two selenium pellets at day 0, and control. The Dura SE® Bolus is designed to release 3 mg/day for 120 days; the 30-g pellets contain 10% elemental selenium and are designed to provide selenium supplementation for up to 18 months. At the end of the study, blood levels of selenium were significantly ($P < .01$) higher in the two-Dura SE® Bolus group than in any other group. Calves from cattle in the selenium-supplemented groups had significantly ($P < .001$) higher blood selenium levels, both before and after suckling, than did controls (23).

Maas and colleagues administered the Dura SE® Bolus to selenium-deficient beef heifer calves and found that mean blood selenium was maintained at more than 0.10 μg/mL for 188 days. No untoward effects were seen in the treatment group (24).

CONCLUSIONS

The RUTS Push-Melt™ osmotic system is an innovative adaptation of osmotic technology for the delivery of agents to ruminants. It extends the delivery duration beyond the 28-day lifetime of the ALZET® pump to 4 months or longer. Formulation options include suspensions as well as solutions. Commercialized applications of this technology have been developed for the delivery of ivermectin, a potent parasiticide, and sodium selenite, a nutritional supplement.

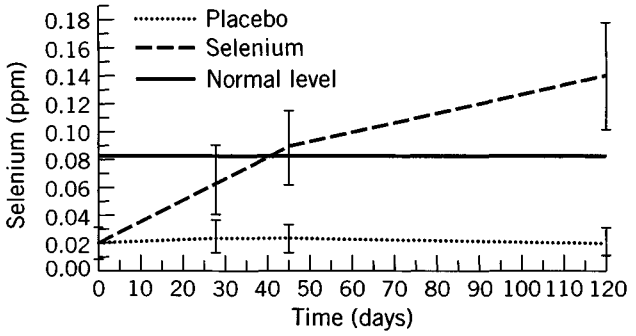


Figure 7. Selenium blood levels in cattle administered a Dura-SE® bolus. *Source:* Ref. 22.

BIBLIOGRAPHY

1. U.S. Pat. 4,595,583 (June 17, 1986), B. Eckenhoff, R. Cortese, and F.A. Landrau (to ALZA Corp).
2. J.R. Zingerman et al., *J. Controlled Release* **47**(1), 6 (1997).
3. G.L. Zimmerman and E.P. Hoberg, *Parasitol. Today* **4**(2), 55 (1988).
4. R.M. Jones, *Vet. Parasitol.* **12**, 223–232 (1983).
5. J.M. Conrad and D.S. Skinner, *J. Controlled Release* **9**, 133–147 (1988).
6. P. Berghen et al., *Vet. Q.* **16**, 161–164 (1994).
7. U.S. Pat. 3,844,285 (October 29, 1974), R.H. Laby (to Commonwealth Scientific and Industrial Research Organization).
8. N. Anderson, R.H. Laby, R.K. Prichard, and D. Hennessey, *Res. Vet. Sci.* **29**, 331–341 (1980).
9. M.Y.K. Ho, D.W. Gottschall, and R. Wang, in D.H. Hutson, ed., *Xenobiotics and Food-Producing Animals: Metabolism and Residues*, American Chemical Society, New York, 1992, pp. 149–157.
10. W.A. Boettner et al., *J. Controlled Release* **8**, 23–30 (1988).
11. J.B. Tuttle, in A. Standen, ed., *Kirk-Othmer Encyclopedia of Chemical Technology*, 2nd ed., Interscience, New York, 1963–1970, pp. 92–112.
12. U.S. Pat. 5,206,024 (April 27, 1993), B. Eckenhoff (to ALZA Corporation).
13. U.S. Pat. 4,723,958 (February 9, 1988), D.G. Pope and A.E. Royce (to Merck & Co. Inc.).
14. W.C. Campbell, *Ivermectin and Abamectin*, Springer-Verlag, New York, 1989.
15. W.C. Campbell et al., *Science* **221**, 823–828 (1983).
16. J.D. Baggot and Q.A. McKellar, *J. Vet. Pharmacol. Ther.* **17**, 409–419 (1994).
17. D.G. Pope, P.K. Wilkinson, J.R. Egerton, and J. Conroy, *J. Pharm. Sci.* **74**(10), 1108–1110 (1985).
18. J.R. Edgerton, D. Suhayda, and C.H. Early, *Vet. Parasitol.* **22**, 67–75 (1986).
19. R.J. Gyurik, in P. Tyle ed., *Drug Delivery Devices, Fundamentals and Applications*, Dekker, New York, 1988, p. 569.
20. T.A. Yazwinski, H. Featherston, and C. Tucker, *Am. J. Vet. Res.* **56**(12), 1599–1602 (1995).
21. D. Adair et al., *J. Pharm. Sci.* **76**(11), S253 (1987).
22. G.J. Sumner, *Proc. Acad. Vet. Consult. Meet.*, August 11–12, Kansas City, Kans., 1988.
23. D.T. Campbell et al., *Am. J. Vet. Res.* **51**(5), 813–817 (1990).
24. J. Maas, J.R. Peauroi, D.W. Weber, and F.W. Adams, *Am. J. Vet. Res.* **55**(2), 247–250 (1994).

See also PUMPS/OSMOTIC—INTRODUCTION; PUMPS/OSMOTIC—ALZET® SYSTEM; PUMPS/OSMOTIC—VITS VETERINARY IMPLANT; PUMPS/OSMOTIC—DUROS™ OSMOTIC IMPLANT FOR HUMANS.

RELEASE KINETICS, DATA INTERPRETATION

BALAJI NARASIMHAN
Rutgers University
Piscataway, New Jersey

SURYA K. MALLAPRAGADA
Iowa State University
Ames, Iowa

NICHOLAS A. PEPPAS
Purdue University
West Lafayette, Indiana

KEY WORDS

Drug release kinetics
Mathematical models
Polymer carriers
Release mechanisms

OUTLINE

Diffusion in Drug Delivery Systems
Release Kinetics from Diffusion-Controlled Systems
  Reservoir (Membrane) Systems
  Matrix (Monolithic) Systems
Swelling-Controlled Systems
Chemically Controlled Systems
  Pendent Chain Systems
Other Aspects of Release Kinetics Modeling
  Osmotic Systems
  Dissolution-Controlled Systems
Conclusions
Bibliography

Controlled release of drugs, proteins, and other bioactive agents can be achieved by incorporating them either in dissolved or dispersed form in polymers (1,2). During the design stage of these formulations or during experimental verification of their release behavior, it is desirable to develop and use simple and sophisticated mathematical models to describe the release kinetics (3). Although these models are clearly based on transport (diffusion) equations, they are commonly known in the pharmaceutical or drug delivery field as kinetic models or kinetic expressions, because they describe a time-dependent behavior of the drug release.

From a mathematical-modeling point of view, controlled-release systems may be classified according to the controlling physical mechanism(s) of release of the incorporated drug. We have proposed a convenient method (4) based on the mechanism of transport for categorizing them as diffusion-controlled, swelling-controlled, osmotically controlled, and chemically controlled systems.

Mathematical modeling of the release kinetics of specific classes of controlled-release systems may be used to

1. Predict drug release rates from and drug diffusion behavior through polymers, thus avoiding excessive number of experiments
2. Elucidate the physical mechanisms of drug transport by simply comparing the release data to mathematical models

Here we present a critical summary of important mathematical models for the description of drug release from controlled-release systems. In this article we have tried to incorporate only models that accurately depict the physical situation of the problems modeled. Unfortunately, the pharmaceutical literature includes a variety of inappropriately simplified, semiempirical or pseudo–steady-state models. The validity of these models is questionable, and their utility in analysis of drug diffusion data is doubtful. Most of these models have been ignored, except for one (the Higuchi equation), which has been included for historical reasons.

Mechanistic aspects of the diffusion phenomena observed in drug delivery systems are by necessity related to an accurate mathematical model and to the structural characteristics of the polymeric material under consideration. However, very few reviews address these two aspects of controlled-release systems (3–6). Here, we critically evaluate existing mathematical models for drug release from polymeric systems. Unfortunately, lack of a systematic analysis and classification is responsible for the use of inappropriate models, not necessarily describing the experimental conditions of the work of many investigators.

DIFFUSION IN DRUG DELIVERY SYSTEMS

With the exception of a number of swelling-controlled release systems, most polymeric formulations for drug release may be described by the two forms of Fick's law of diffusion, which can be written as equations (1) and (2) for one-dimensional diffusion:

$$j_i = D_{ip} \frac{dc_i}{dx} \tag{1}$$

$$\frac{\partial c_i}{\partial t} = D_{ip} \frac{\partial^2 c_i}{\partial x^2} \tag{2}$$

In these equations, c_i and j_i are the concentration and mass flux of drug I, respectively; x and t are position and time

of release; and D_{ip} is the drug diffusion coefficient through the polymer.

Several assumptions have been made in describing drug diffusion through polymers by equations 1 and 2. First, as one-dimensional diffusion is appropriate for treatment of drug release from thin, planar systems, application of this analysis to thick slabs or short cylinders is incorrect. Then, the drug diffusion coefficient D_{ip} is usually assumed to be independent of drug concentration. Finally, j_i is the drug flux with respect to the mass average velocity v of the system.

Fickian diffusion equations can be solved by standard mathematical techniques (7), provided that sufficient information about initial and boundary conditions of the pharmaceutical experimental situation is provided.

Solution of equations 1 or 2 provides the following information about drug release through polymers:

1. Determination of concentration profiles from the normalized drug concentration, c/c_o, versus dimensionless position, x/δ, as a function of dimensionless Fourier time, $D_{ip}t/\delta^2$. Here, c_o is a reference drug concentration, and δ is the slab thickness.
2. Drug release rates, dM_t/Adt, can be determined by differentiating the previous expressions with respect to position and evaluating the derivative at the water– or dissolution–medium interface. Here, A is the diffusional cross-sectional area.

$$\frac{dM_t}{Adt} = \left[D_{ip}\frac{\partial c_i}{\partial x}\right]_{x=\text{surf}} \tag{3}$$

3. The total amount of drug released per cross-sectional area, M_t/A, can be determined by integrating the previous expression over release time.

$$\frac{M_t}{A} = \int_0^t \frac{dM_t}{Adt}\,dt = \int_0^t \left[D\frac{\partial c_i}{\partial x}\right]_{x=\text{surf}} dt \tag{4}$$

Application of these equations to experimental data of drug release is often conveniently achieved with the use of the semiempirical equations 5 and 6 describing the fractional release, M_t/M_∞, and release rate, dM_t/Adt, as functions of release time, t. Here M_∞ is the amount of drug released at long times, which may or may not be equal to the total drug incorporated in a device (8,9).

$$\frac{M_t}{M_\infty} = kt^n \tag{5}$$

$$\frac{dM_t}{Adt} = nkt^{n-1} \tag{6}$$

The importance of this analysis is easily understood (Fig. 1) because most mathematical solutions of equation 2 for Fickian drug diffusion give release kinetics described by equation 5 with $n = 0.5$. Consequently, the release rate is proportional to $t^{-1/2}$.

A special case of release kinetics with $n = 1$ can be obtained when describing drug release from membrane-type diffusion-controlled systems, some geometrical shapes of matrix systems (e.g., hemispheres), or swelling-controlled release systems. This type of release kinetics is commonly known as zero-order release kinetics because it is characterized by constant drug-release rates (10–13).

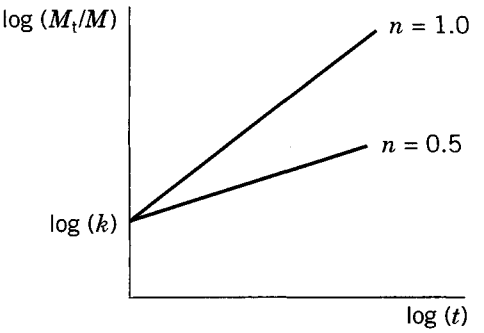


Figure 1. Schematic representation of log (normalized drug released) as a function of log (release time).

RELEASE KINETICS FROM DIFFUSION-CONTROLLED SYSTEMS

In diffusion-controlled release systems, drug diffusion through the polymer is achieved by molecular diffusion due to concentration gradients. Depending on the molecular structure of the polymer, these systems may be classified as porous or nonporous. Porous controlled-release systems contain pores that are large enough that diffusion of the drug is accomplished through water that has filled the pores of the polymer (14). These pores are usually of size greater than 200–500 Å.

Nonporous systems contain meshes of molecular (drug) dimensions. Molecular diffusion occurs effectively through the whole polymer, and the drug diffusion coefficient refers to the polymer phase (14). The macromolecular structure of the polymer affects drug diffusion according to theoretical analyses discussed elsewhere (15). Some of the polymer parameters controlling the drug diffusion coefficient are degree of crystallinity and size of crystallites, degree of cross-linking, degree of swelling, and molecular weight of the polymer. Many swollen, porous polymer systems retain the main characteristics of the porous structure so that drug diffusion occurs simultaneously through water-filled pores and through the swollen polymer per se.

The study of controlled release actually requires the study of diffusion, or transport through a particular medium. There are several types of transport mechanisms that can occur, with the most important being ordinary diffusion. The gradient that produces this diffusional behavior is due to a concentration gradient. It is only one of the forms of gradients that can be responsible for the drug release. In fact, it should be referred to as chemical potential gradient rather than concentration gradient. We are writing here for one dimension, but the actual system will be in three dimensions. The true type of release is a result of a gradient of activity, where the activity has incorporated in it the true nonideal behavior of the drug or solutes that is being released at the same time. The nonideal be-

havior is expressed in terms of the activity coefficient. By multiplying the activity coefficient by the mole fraction, we obtain the activity that leads to the gradient. In addition to this transport mechanism, one should expect to see convection when the pores of the carrier are large. In that case, there will be a flux of drug due to the drug being carried along with the solvent itself.

Another type of transport we may sometimes see is facilitated transport, otherwise known as carrier-mediated transport. It effectively involves one or more components being transported relatively quickly because they have reacted or formed a complex with another chemical agent that has a higher solubility in the phase through which it is diffusing. These are the three main mechanisms of transport, and within these there are unusual transport processes like osmotic transport. There is also relaxation-controlled mechanism, which is a significantly different mechanism. It happens in only one type of controlled-release device, which will be discussed separately. Many of the situations that will be discussed involve transport and reaction at the same time. This may be a reaction into the polymer or into the drug being released, so the equation will have this included in the expression.

The classical equation by which one expresses drug transport through a carrier is Fick's law. Fick's first law describes the flux of the drug, peptide, or protein that is diffusing as a function of a concentration gradient in one direction. This is the simplest form of the equation and can be written in three dimensions or in different coordinate systems. It is important to note that in the simplest possible form that is found in the literature (7), the equation is given in terms of a concentration gradient, not an activity or chemical potential gradient. The equation is modified somewhat if it is in terms of a chemical potential gradient. It must be noted that the concentration units are usually in moles/cm^3, and that gives a flux of moles/cm^2/s. This is the difference between a flux and a rate, where the rate of transport of a drug is expressed in units of mol/s. The flux is expressed per area of release, whereas a rate is expressed simply per time.

For release from a thin film or tablet, the flux per area includes two areas, the upper and lower surface, whereas the rate doesn't have an area at all. As the equation is written here, it is assumed that the diffusion coefficient is constant. Several assumptions are made. The first one is that whether it is a controlled-release device with a large or a small amount of drug in it, the drug exhibits a constant rate. This assumes that the diffusion coefficient does not depend on the concentration of drug, a major hypothesis that is unfortunately incorrect. However, traditionally in the field of controlled release, it has been difficult to express the diffusion coefficient in terms of more sophisticated theories. The diffusion coefficient does not remain constant with concentration. Typical values of the drug diffusion coefficients in polymers range from 10^{-6} to 10^{-7} cm^2/s for diffusion in rubbery polymers and from 10^{-10} to 10^{-12} cm^2/s for diffusion in glassy polymers.

In the Eyring analysis (16), the diffusion coefficient, which is the ease of transport through the polymer carrier system, can be easily calculated as

$$D = \lambda^2 \nu / 6 \tag{7}$$

Here λ is the diffusional jump through the polymer or the specific system being studied. This diffusional jump is related to the polymer and the drug studied. The second parameter, ν, is the frequency of jumping. Thus, in the Eyring theory, diffusion is not a continuous process, and we can distinguish specific jumps. The parameter λ, which is the diffusional jump parameter, is a function of the diffusing species, v_i, the available volume space, V_p, and other characteristics of the system.

Mathematical modeling of such situations has been a major problem in physical chemistry and has been addressed over the last 40 years by many investigators. One of the earliest published studies is that of Ogston (17) involving transport of spheres in stochastic networks.

In 1961, Fujita (18) introduced the idea of free volume in diffusional problems. He defined the free volume, v_f, and came up with a free-volume theory with the drug diffusion coefficient having an exponential dependence on the free volume.

$$D = D_o \exp(-k/v_f) \tag{8}$$

The Fujita theory was modified in the late 1960s by Yasuda and Lamaze (19). This was the first exact free-volume theory in which the diffusion coefficient of the diffusing species through a polymer structure is described in a rather accurate way. This approach is based on the molecular level and tries to explain how diffusion occurs in a controlled-release device. Unfortunately, our field has been marred with improper expressions and incorrect definitions.

Transport through these systems is the classical solute transport in porous media that one would find in any chemical engineering textbook (20). The classical way of describing the diffusion coefficient in such a system is as an effective diffusion coefficient related to the diffusion coefficient of the drug through the pores filled with a solution of drug, D_{iw}.

$$D_{eff} = D_{iw}\varepsilon/\tau \tag{9}$$

In reality, it is not water that occupies these pores but a solution of the drug. As the release occurs, more of the drug is dissolved, and the solution becomes more and more dilute. The porosity is the fraction of pores in the system that are open ($0 < \varepsilon < 1$). The tortuosity, τ, indicates the tortuous path of transport of a drug through this particular porous network structure. For example, in the case of a straight cylindrical pore, the tortuosity is 1 because the diffusion path is straight. If, however, the pores are tilted at 45°, the tortuosity becomes $\sqrt{2}$, or 1.41. As the path becomes more tortuous, τ becomes 3–5. This is the simplest way to describe a situation in a controlled-release system with large pores.

Faxén (21) proposed the following equation for diffusion of spheres through porous media:

$$D/D_b = (1 - \lambda)^2(1 + \alpha\lambda + \beta\lambda^3 + \gamma\lambda^5) \quad (10)$$

Here λ is the ratio of the drug radius, r_s, to the pore average radius, r_p. The diffusion coefficient of the sphere through the pore, D, relative to the diffusion coefficient in bulk solution, D_b, is equal to the semiempirical relation just shown that has been proven for a variety of systems. The diffusion in this porous system is very much dependent on the size of the drug and the size of the pore. We should expect the parameter D/D to attain a limit of one.

A swelling mechanism requires that the water come to the surface and start swelling the polymer itself. In such situations, the diffusion coefficient is very much dependent on the concentration of water that is incorporated into the system. It is interesting that this process takes effectively place in "layers," so that in the case of a controlled-release device in the form of a thin disk or tablet, we expect that the layers on the surface will have swollen first whereas the center will still be a solid. The diffusional behavior of water into the drug-containing system can be described by the following Fujita equation:

$$D_{drug} = D_{do} \exp\{-\alpha(\beta - c_w)\} \quad (11)$$

The diffusion coefficient of the drug is equal to a preexponential term multiplied by an exponential relation, where α and β are two characteristic constants of the polymeric system and c_w is the water concentration of the system. Hence, the higher the concentration of water, the higher the diffusion coefficient of the drug. The terms α and β can be determined by the free-volume theory or the Duda–Ventas theory (22), where several terms appear that are known for specific polymer systems and can be evaluated to give α and β.

Reservoir (Membrane) Systems

In reservoir (membrane) systems, the bioactive agent is usually enclosed at relatively high concentrations between two semipermeable membranes and is placed in contact with a dissolution medium (water or other biological fluid). The bioactive agent may be solvent free or in the form of a concentrated solution.

Equation 1 may be used to describe drug release through reservoir systems. However, because the concentration c_i in this equation refers to drug concentration in the membrane and because this value is difficult to determine experimentally, it is customary to relate drug concentrations in the membrane through the partition (distribution) coefficient, K.

The partition coefficient describes thermodynamic rather than structural characteristics of the drug/polymer/solvent system. It is rather easy to determine experimentally, and it is a measure of drug solubility in a swollen polymer.

When the concentration of the released bioactive agent in the phase external to the system is maintained at a constant low level of concentration, for example, by good agitation and continuous removal of the released drug, equation 1 may be integrated over the thickness of the membrane (for plane sheet geometry) to give equations 12 and 13, where c_{i1}, c_{i2} are drug concentration in the two sides of a membrane:

$$\frac{dM_t}{Adt} = \frac{D_{ip}K}{\delta}(c_{i2} - c_{i1}) \quad (12)$$

$$M_t = \frac{D_{ip}KA(c_{i2} - c_{i1})}{\delta} t \quad (13)$$

Clearly drug release from these systems is zero order, that is, the release rate of drug does not depend on time. The amount of drug released from such a device for the case of two specific drugs as a function of time is shown in Figure 2.

Similarly, for cylindrical devices it is readily shown that

$$\frac{dM_t}{dt} = \frac{D_{ip}KA}{\ln(r_e/r_i)}(c_{i2} - c_{i1}) \quad (14)$$

and

$$M_t = \frac{D_{ip}KA(c_{i2} - c_{i1})}{\ln(r_e/r_i)} t \quad (15)$$

where r_e and r_i are the external and internal radii of the cylinder, respectively, and A is the length of the cylinder. In both situations of slabs and cylinders, one-dimensional diffusion is assumed. This assumption requires that these equations be applied only for analysis of release from thin membranes or long cylindrical systems. Corrections for edge effects due to violation of the one-dimensional diffusion assumption are available (23), if thick membranes are used. However, the preferable method of modeling would be numerical solution of the three-dimensional diffusion problem.

For spherical reservoir systems, the corresponding equations for drug release are

$$\frac{dM_t}{dt} = \frac{4\pi D_{ip}K}{(r_e - r_i)/r_e r_i}(c_{i2} - c_{i1}) \quad (16)$$

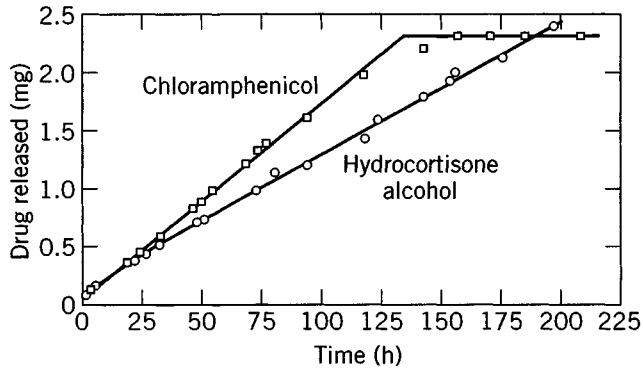


Figure 2. Zero-order release as obtained from a constant-activity reservoir source for chloramphenicol and hydrocortisone alcohol. *Source:* Reproduced with permission from Ref. 1. Copyright 1974 Plenum.

and

$$M_t = \frac{4\pi D_{ip} K(c_{i2} - c_{i1})}{(r_e - r_i)/r_e r_i} t \quad (17)$$

Therefore, drug-release rates from conventional reservoir systems are time independent. However, they depend on the concentration difference, geometry of the device, thermodynamic characteristics of the system (solubility, through the partition coefficient), and structure of the polymer (through the diffusion coefficient).

Situations of drug release from membrane systems at low initial drug concentration or to experimental vessels of finite volumes cannot be modeled with the equations given previously. Instead, equation 18 has been derived (23) for the drug release rate from these systems.

$$\frac{dM_t}{dt} = \frac{M_\infty D_{ip} KA}{V_1 \delta} \exp\left[\frac{-D_{ip} KA(V_1 + V_2)}{\delta V_1 V_2} t\right] \quad (18)$$

Here V_1 and V_2 are the volumes of the device and the vessel, respectively, and M_∞ is the initial loading of the device. The release rate in this situation is an exponential function of release time.

Special release problems observed with reservoir devices include time lag and burst effects. These effects are related to the time history of the device, and they have been mathematically analyzed in previous reviews (1).

The time lag and burst effects alter the initial release kinetics of the expected steady-state release behavior of membrane systems due to accumulation of drug (burst effect) or due to the induction period for drug diffusion (time-lag effect).

It has been previously shown (1) that for membrane devices exhibiting time-lag effects, the steady-state expression (at long times) for fractional drug release is given by equation 19:

$$M_t = \frac{AD_{ip} c_{i1}}{\delta}\left[t - \frac{\delta^2}{6D_{ip}}\right] \quad (19)$$

Here c_{i1} is the initial drug concentration in the membrane.

In a similar manner, one can derive equation 20 for the fractional drug release of membrane devices exhibiting burst effects.

$$M_t = \frac{AD_{ip} c_{i1}}{\delta}\left[t + \frac{\delta^2}{3D_{ip}}\right] \quad (20)$$

The second terms in the parentheses of equations 19 and 20 are known as the characteristic time lag and burst time, θ_l and θ_b, respectively, and they are useful in determining drug-diffusion coefficients in membranes by simple release experiments. More recently, the role of the burst effect in drug-release kinetics from matrix systems has been analyzed, and we discuss this in detail in the section on matrix systems.

Porous Reservoir Systems. Release from porous reservoir systems of hydrophobic polymers may be modeled by equations 9 to 11 where the diffusion coefficient is replaced by the effective diffusion coefficient, D'_{eff}. This parameter describes diffusion through water-filled pores (14,24) and incorporates the porosity (void fraction), ε, and tortuosity, τ, in the drug-diffusion coefficient through water, D_{iw}, according to equation 21:

$$D'_{eff} = D_{iw} \frac{\varepsilon}{\tau} \quad (21)$$

It is sometimes desirable to incorporate into this expression a partition coefficient, K_p, for possible adsorption of the drug on the walls of the pores, and a restriction coefficient, K_r, which accounts for hindered diffusion and is described according to equation 22, where λ is the ratio of the drug radius, r_s, to the pore average radius, r_p:

$$K_r = (1 - \lambda)^2 \text{ with } \lambda = r_s/r_p \quad (22)$$

Then, the effective diffusion coefficient of drug through the pores may be written as

$$D_{eff} = D_{iw} K_p K_r \frac{\varepsilon}{\tau} \quad (23)$$

The well-known theoretical analyses of Anderson and Quinn (25) and Colton et al. (23) are often used to predict the parameters K_p and K_r for drug-release systems with fine pores. Very often, diffusion through porous membranes is accompanied by osmotic effects as a result of which equations 9–11 and 21–23 do not fully describe phenomena occurring in porous reservoir systems.

Matrix (Monolithic) Systems

In matrix (monolithic) systems, the bioactive agent is incorporated in the polymer phase either in dissolved or in dispersed form. Therefore, the solubility of the drug in the polymer becomes a controlling factor in the mathematical modeling of these systems. When the initial drug loading is below the solubility limit, release is achieved by simple molecular diffusion through the polymer. However, when the drug loading is above the solubility limit, dissolution of the drug in the polymer becomes the limiting factor in the release process.

Solutions of the transient diffusion equation 2 can be obtained for a variety of initial and boundary conditions (7), which represent appropriate experimental situations. Some of these solutions are presented here. However, the reader is warned that unusual experimental conditions of release will require solution of equation 2 under the boundary conditions that best describe one's experimental situation.

It is also important to note that most mathematical models for controlled-release kinetics presented in the literature have been derived with the assumption of an experimentally rather unattainable boundary condition of zero (and constant) drug concentration at the interface of the device. This condition requires complete elimination of boundary layer effects, probably by high agitation during the release experiment.

In this section we include, in addition to the conventional solutions of the diffusion equation 2 widely used in

controlled-release technology, new models and mathematical solutions with boundary conditions affected by drug mass transfer from the surface of the polymer to the liquid phase. These models do not require that the concentration at the polymer interface be constant or zero, although previous determination of the mass transfer coefficient is needed. The mass transfer coefficient can be determined by a variety of expressions or experimental techniques discussed in standard mass transfer monographs (26), if the flow characteristics of the release experiment are known.

Dissolved Drug, Nonporous Systems. In these systems the drug is loaded uniformly at initial concentration c_{io}. Several models may be readily developed for plane sheet matrix devices under different boundary conditions (27).

When the surface concentration of the drug in the dissolution medium is kept constant at c_i, we can derive

$$\frac{M_t}{M_\infty} = 1 - \sum_{n=0}^{\infty} \frac{8}{(2n+1)^2\pi^2} \exp\left[\frac{-D_{ip}(2n+1)^2\pi^2}{\delta^2} t\right] \tag{24}$$

Important simplifications of this equation may be used if one is interested in avoiding the lengthy calculations of this series solution. For example, for long release times ($M_t/M_\infty > 0.6$), this equation may be written as

$$\frac{M_t}{M_\infty} = 1 - \frac{8}{\pi^2} \exp\left[-\frac{D_{ip}\pi^2}{\delta^2} t\right] \tag{25}$$

For small release times ($M_t/M_\infty > 0.6$), equation 2 has an alternative solution in the form of equation 26:

$$\frac{M_t}{M_\infty} = 4\left[\frac{D_{ip}t}{\delta^2}\right]^{1/2}\left[\frac{1}{\sqrt{\pi}} + 2\sum_{n=1}^{\infty}(-1)^n \text{ierfc}\,\frac{n\delta}{\sqrt{D_{ip}t}}\right] \tag{26}$$

Equation 26 can be further simplified to give

$$\frac{M_t}{M_\infty} = 4\left[\frac{D_{ip}t}{\pi\delta^2}\right]^{1/2} \tag{27}$$

It is clear that when slabs of monolithic devices are kept at constant external drug concentration, the fractional release is proportional to the square root of release time. However, equation 27 is valid only for the early portion of a release experiment and only under the boundary conditions and assumptions discussed before. By differentiation, we can obtain

$$\frac{dM_t}{dt} = 2M_\infty\left[\frac{D_{ip}}{\pi\delta^2 t}\right]^{1/2} \tag{28}$$

This equation shows that the drug-release rate drops considerably during the release experiment and that it is dependent on $t^{-1/2}$. This observation is important for design of zero-order release systems because it shows that it is not possible to obtain constant drug release rates from "simple" matrix-type devices.

In many experimental studies, the drug concentration at the surface c_i cannot be kept constant. Instead a constant drug concentration, c_o, can be obtained far enough from the surface (28). Therefore a boundary condition for equation 2 can be written as

$$\left[-D\frac{\partial c}{\partial x}\right]_{surf} = k(c_o - c_i) \tag{29}$$

where k is the mass transfer coefficient. Then equation 2 can be solved to give

$$\frac{M_t}{M_\infty} = 1 - \sum_{n=1}^{\infty} \frac{\frac{1}{2}\left[\frac{\delta k}{D_{ip}}\right]^2 \exp\left[-\frac{4\beta_n^2 D_{ip}}{\delta^2} t\right]}{\beta_n^2\left[\beta_n^2 + \left[\frac{\delta k}{2D_{ip}}\right]^2 + \frac{\delta k}{2D_{ip}}\right]} \tag{30}$$

where β_n are the positive roots of equation 31.

$$\beta \tan \beta = \delta k/2D_{ip} \tag{31}$$

Experiments can be also performed with surface concentration c_i of drug varying in a specific way. For example, when

$$c_i = k't \tag{32}$$

the corresponding expression of the released drug is

$$\frac{M_t}{A} = k'\delta t - \frac{k'\delta^3}{12D_{ip}} + \frac{8k'\delta^3}{\pi^4 D_{ip}} \sum_{n=0}^{\infty} \frac{\exp\left[-\frac{D_{ip}(2n+1)^2\pi^2}{\delta^2}\right]}{(2n+1)^4} \tag{33}$$

When the surface concentration increases according to equation 34,

$$c_i' = c_i[1 - \exp(-\gamma t)] \tag{34}$$

the corresponding expression for the released drug is

$$\frac{M_t}{A} = \delta c_i - \exp(-\gamma t)\left[\frac{4D_{ip}}{\gamma\delta^2}\right]^{1/2} \tan\left[\frac{\gamma\delta^2}{4D_{ip}}\right]^{1/2} - \frac{8}{\pi^2}\sum_{n=0}^{\infty} \frac{\exp\left[\frac{-(2n+1)^2\pi^2 D_{ip}}{\delta^2} t\right]}{(2n+1)^2\left[1 - \frac{(2n+1)^2 D_{ip}\pi^2}{\gamma\delta^2}\right]} \tag{35}$$

Models for drug release from devices with other geometries can also be derived by appropriate solution of equation 2 in cylindrical or spherical coordinates (7).

For example, for cylindrical devices of radius r kept at constant surface concentration c_i, the amount released can be calculated by equation 36:

$$\frac{M_t}{M_\infty} = 1 - 4\sum_{n=1}^{\infty} \frac{\exp(-D_{ip}\alpha_n^2 t)}{r^2\alpha_n^2} \tag{36}$$

Here α_n are positive roots of a Bessel function of the first kind of zero order. For long times, only the first term of the

summation of equation 36 is necessary. For short times, this equation can be approximated by equation 37:

$$\frac{M_t}{M_\infty} = 4\left[\frac{D_{ip}t}{\pi r^2}\right]^{1/2} - \left[\frac{D_{ip}t}{r^2}\right] - \frac{1}{3}\left[\frac{D_{ip}t}{\pi^{1/3}r^2}\right]^{3/2} \quad (37)$$

For spherical devices, the early term approximation is going to be again for $M_t/M < 0.4$ and is going to look something like that. Figure 3 shows a comparison of the fractional release and the release rate as a function of release time for slabs, cylinders, and spheres. This equation here is very useful because pharmacists often work with microparticulate systems. The only problem is that it is written for one-size particles. Basically, we have a dependency of $t^{1/2}$ and the first power at the same time. The rate is a function of $t^{-1/2}$. The rate drops with time, and this is why we need to have other particles to keep the rate constant.

Based on this idea, researchers started thinking that perhaps what they could create is a distribution of particle sizes. A design where one particle-size distribution working from the beginning is in contact with the physiological fluid, and a second particle-size distribution, which is much smaller, is brought into contact with the physiological fluid a little bit later, yields approximately zero-order release.

Solutions for other boundary conditions are available in standard references (7). For example, for cylindrical systems with boundary condition described by equation 29, the fractional drug release is

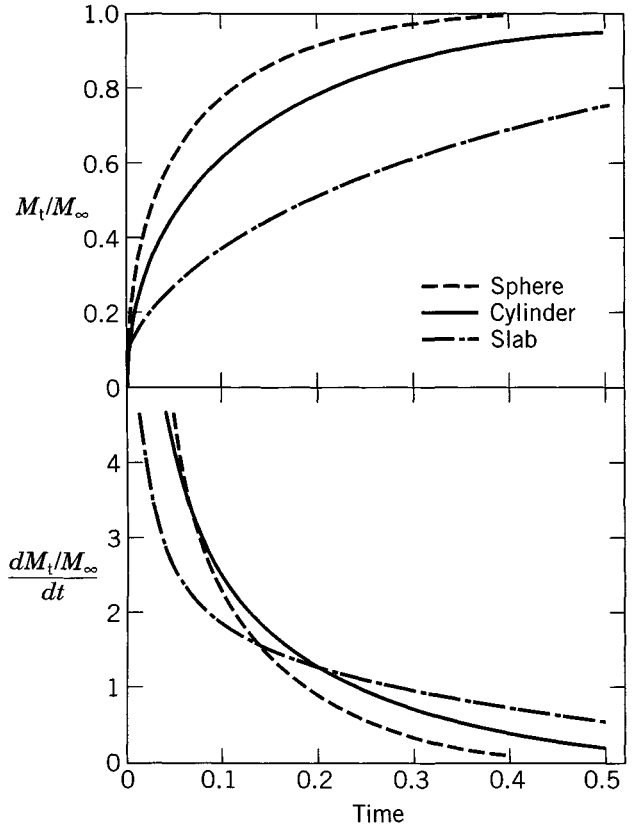


Figure 3. Fractional release and release rate as a function of time for slabs, cylinders, and spheres. *Source:* Reproduced with permission from Ref. 1. Copyright 1974 Plenum.

$$\frac{M_t}{M_\infty} = 1 - \sum_{n=1}^{\infty} \frac{4\left[\frac{kr}{D_{ip}}\right]^2 \exp\left[-\frac{\beta_n^2 D_{ip}}{r^2}t\right]}{\beta_n^2\left[\beta_n^2 + \left[\frac{kr}{D_{ip}}\right]^2\right]} \quad (38)$$

where β_n are the roots of equation 39:

$$\beta D_{ip} J_1(\beta) - krJ_0(\beta) = 0 \quad (39)$$

where $J_0(\beta)$ and $J_1(\beta)$ are Bessel functions of zero and first order, respectively.

An appropriate solution suitable for small times is

$$\frac{M_t}{M_\infty} = \left[\frac{2kt}{r}\right] - \left[\frac{8k^2t^{3/2}}{3D_{ip}^{1/2}\pi^{1/2}r}\right] - k^2\left[\frac{1}{2} - \frac{kr}{D_{ip}}\right]t^2 \quad (40)$$

For spherical matrix devices, equation 2 can be solved with spherical coordinates and constant surface concentration to give

$$\frac{M_t}{M_\infty} = 1 - \frac{6}{\pi^2}\sum_{n=1}^{\infty}\frac{1}{n^2}\exp\left[-\frac{D_{ip}n^2\pi^2}{r^2}t\right] \quad (41)$$

For long times, only the first term in the summation need be retained. For short times of release ($M_t/M_\infty < 0.6$) an approximate solution may be obtained in the form of equation 42:

$$\frac{M_t}{M_\infty} = 6\left[\frac{D_{ip}t}{\pi r^2}\right]^{1/2} - 3\frac{D_{ip}t}{r^2} + 12\left[\frac{D_{ip}t}{r^2}\right]^{1/2}\sum_{n=1}^{\infty}\text{ierfc}\frac{nr}{\sqrt{D_{ip}t}} \quad (42)$$

which may be further simplified for $M_t/M_\infty < 0.4$ by retaining only the first two terms of the right hand side (rhs) of this equation.

Solutions for other boundary conditions are available (27,28). For example, when using spherical devices in conjunction with the boundary condition of equation 29, the fractional drug release is given by equation 43:

$$\frac{M_t}{M_\infty} = 1 - \sum_{n=1}^{\infty}\frac{6\left[\frac{kr}{D_{ip}}\right]^2\exp\left[-\frac{\beta_n^2 D_{ip}}{r}t\right]}{\beta_n^2\left[\beta_n^2 + \frac{kr}{D_{ip}}\left[\frac{kr}{D_{ip}} - 1\right]\right]} \quad (43)$$

where β_n are the roots of equation 44:

$$\beta_n D_{ip}\cot\beta_n + kr - D_{ip} = 0 \quad (44)$$

In general, description of drug-release kinetics from matrix-type systems under different boundary conditions and different geometries can be achieved by selecting an appropriate model from the ones described by Crank (7). Consequently, unnecessary assumptions and gross simplifications, such as unfortunate use of equation 27 where it does not apply, can be avoided.

Dispersed Drug, Nonporous Systems. Monolithic devices may contain drug uniformly distributed at a loading, c_{io}, which is significantly higher than the drug solubility in the polymer, c_{is}. In these systems, dissolution of the drug may be the rate-limiting step of this release process. Therefore, several models have been proposed to describe this phenomenon.

A simple pseudo–steady-state model, the Higuchi model, has attained popularity among researchers working in this area (29). It is based on Fickian diffusion according to equation 1, with zero surface concentration, and it gives the amount of drug released and its release rate according to equations 45 and 46, respectively:

$$M_t = A[D_{ip}c_{is}(2C_{io} - c_{is})t]^{1/2} \tag{45}$$

$$\frac{dM_t}{dt} = \frac{A}{2}[D_{ip}c_{is}(2c_{io} - c_{is})]^{1/2}t^{-1/2} \tag{46}$$

Similar expressions have been developed for cylindrical and spherical devices (1,30). For cylindrical devices and for $c_{io} \gg c_{is}$, one obtains

$$\frac{M_t}{M_\infty} + \left[1 - \frac{M_t}{M_\infty}\right]\left[\ln\left[1 - \frac{M_t}{M_\infty}\right]\right] = \frac{4D_{ip}c_{is}}{r^2c_{io}}t \tag{47}$$

For spherical devices, the corresponding expression for the fractional drug release is

$$\frac{3}{2}\left[1 - \left[1 - \frac{M_t}{M_\infty}\right]^{2/3}\right] - \frac{M_t}{M_\infty} = \frac{3D_{ip}c_{is}}{r^2c_{io}}t \tag{48}$$

Solutions of the Higuchi model with finite external mass transfer resistance according to equation 44 have been presented by Paul and McSpadden (28) using pseudo–steady-state approximation and the boundary condition described by equation 29, with $c_i = 0$. For example, the amount of drug released as a function of release time is expressed by equation 49:

$$M_t = A\left[c_{io} - \frac{c_{is}}{2}\right]\left\{\left[\left[\frac{D_{ip}}{k}\right]^2 + \frac{2D_{ip}c_{is}t}{\left[c_{io} - \frac{c_{is}}{2}\right]}\right]^{1/2} - \frac{D_{ip}}{k}\right\} + \frac{Ac_{is}}{2}\left\{\frac{\left[\frac{D_{ip}}{k}\right]^2}{\left[\left[\frac{D_{ip}}{k}\right]^2 + \frac{2D_{im}c_{is}t}{\left[c_{io} - \frac{c_{is}}{2}\right]}\right]^{1/2}} - \frac{D_{ip}}{k}\right\} \tag{49}$$

Clearly as the mass transfer coefficient increases to infinity (no mass transfer limitations), this equation reduces to the Higuchi model (equation 45). The pseudo–steady-state analysis is the only approximate modeling effort that is included in this contribution because of historical reasons and its wide acceptability by researchers working in this area.

However, exact solutions of this problem are available through the work of Paul and McSpadden (28). The total amount of drug released can be calculated by equation 50, where x^* is the position of the dissolution front of the dissolving drug, which can be determined by solving equation 51 either numerically or using tabulated values from Crank's monograph (7):

$$\frac{M_t}{A} = \frac{2c_{is}}{\operatorname{erf}\left[\frac{x^*}{2\sqrt{D_{ip}t}}\right]}\left[\frac{D_{ip}t}{\pi}\right]^{1/2} \tag{50}$$

$$x^*\left[\frac{\pi}{D_{ip}t}\right]^{1/2}\exp\left[\frac{x^{*2}}{4D_{ip}t}\right]\operatorname{erf}\left[\frac{x^*}{2\sqrt{D_{ip}t}}\right] = \frac{c_{is}}{c_{io} - c_{is}} \tag{51}$$

Equation 50 corresponds to equation 45 for slabs under the boundary conditions of the Higuchi model. If in addition to this model, mass transfer limitations are taken into consideration (equation 29), an asymptotic solution may be obtained in the form of equation 52:

$$\frac{M_t}{A} = \frac{2c_{is}}{\operatorname{erf}\left[\frac{x^*}{2\sqrt{D_{ip}t}}\right]}\left[\frac{D_{ip}t}{\pi}\right]^{1/2} - \frac{D_{ip}c_{io}}{k} \tag{52}$$

Once again, x^* can be estimated from equation 51.

Mathematical problems of drug release from matrix systems initially loaded at concentrations above the solubility limit of the drug in the polymer are problems of moving boundaries, because the front of dissolved drug/undissolved drug clearly moves into the polymer as release proceeds. These problems are known as Stefan or Stefan–Neumann problems (31). Alternative solutions using moving coordinate systems may be obtained by analogy to mathematical solutions discussed by Danckwerts (32).

Certain problems require numerical or approximate solutions. For example, Lee (33) has recently discussed a variety of diffusional release problems for slabs, spheres, and cylinders using Stefan-type analysis, and he has offered some approximate solutions.

Narasimhan and Langer (34) have recently studied the role of the burst effect in an essentially zero-order, controlled-release, coated hemispherical polymeric device containing a single, small orifice in its center face. Asymptotic solutions of their model show that the burst effect is controlled by the solubility of the drug in the release medium and by the drug-diffusion coefficient. The rates of drug release during the burst effect ($t \to 0$) and the steady state ($t \to \infty$) are related by

$$\frac{[dM/dt]_{t\to 0}}{[dM/dt]_{t\to\infty}} = \frac{16}{B(6 + B)} \tag{53}$$

Here B is given by c_s/c_0. The parameter c_0 is the initial drug loading, and c_s is the solubility of the drug in the release medium. From equation 53, it can be concluded that the burst effect is significant for systems where $B \sim O(1)$. It was shown that as drug solubility increased, the drug released faster, and the velocity of the interface between dissolved and dispersed drug is higher. The model solutions established that the burst behavior could be manipulated by using different initial drug distributions. Using the model, conditions under which the burst effect could be

minimized/maximized were established. Figure 4 shows a plot of the fraction of bovine serum albumin released from an inwardly releasing ethylene-vinyl acetate (EVAc) hemisphere as a function of time, where the release as well as the burst period is zero order.

Porous Matrix Systems. Modeling of the drug-release kinetics of porous matrix systems is still at a rather primitive stage, despite significant developments in recent years. Before using existing models, one has to consider several aspects of the physics of this diffusion phenomenon.

1. If the polymer phase is hydrophobic, swelling is negligible, and the problem can be treated as a constant-volume diffusion problem. However, if the polymer phase is hydrophilic, two modeling routes may be considered.
2. If the pores are large enough to be thought of as "channels" for diffusion (pore diameter greater than 150 Å), diffusion occurs predominantly through these water-filled pores and the effective diffusion coefficient, D'_{eff}, of equation 21 must be used. However, if the pores are smaller than 100 Å, then the diffusion coefficient, D_{ip}, through the swollen polymer can be used without corrections for porosity and tortuosity.
3. Phenomena related to drug partition in the pore walls and hindered diffusion due to the relative size of the drug with respect to the pores can be addressed by including the parameters K_{p} and K_{r} in the diffusion coefficient through water and using the effective diffusion coefficient, D_{eff}, described by equation 23.
4. Phenomena related to elastically changing pore walls must be taken into consideration.

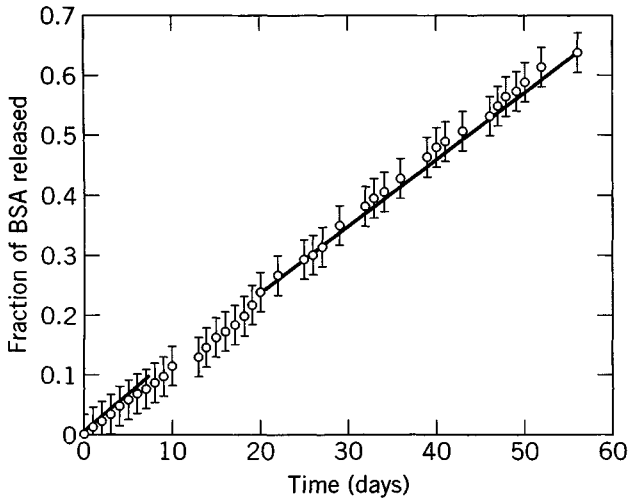


Figure 4. Fraction of bovine serum albumin released as a function of time from coated EVAc hemispheres. The open circles represent experimental data (37) while the line represents model predictions. *Source:* Reproduced with permission from Ref. 34. Copyright 1997 Elsevier.

Therefore, the models developed in "Reservoir (Membrane) Systems" and "Dissolved Drug, Nonporous Systems" may be used for porous systems, with D_{ip} for porous hydrophilic systems of pore size smaller than 100 Å or with D_{eff} for porous hydrophilic systems of pore size larger than 100 Å or with all types of porous hydrophobic systems. Release kinetics for porous systems containing drug at concentrations higher than the solubility limit are somewhat more difficult to model, and equations cannot be written by simple analogy to the models given in "Dispersed Drug, Nonporous Systems."

A traditional pseudo–steady-state model for these systems was developed by Higuchi (35) and predicts drug release according to equation 54, where D_{eff} is given by equations 21 or 23:

$$M_{\text{t}} = A[D_{\text{eff}}c_{\text{is}}(2c_{\text{io}} - \varepsilon c_{\text{is}})t]^{1/2} \tag{54}$$

These models may be unable to describe many experimental results with porous systems loaded with drug above its solubility limit in water.

Two alternatives have been proposed to explain the experimental results. The first model (36) assumes that dissolution of the drug in the pores is the controlling mechanism of release and describes overall diffusion in terms of a modified diffusion equation where the term $k(c_{\text{is}} - c_{\text{i}})$ is a dissolution-dependent contribution to diffusion:

$$\frac{\partial c_{\text{i}}}{\partial t} = D_{\text{eff}}\frac{\partial^2 c_{\text{i}}}{\partial x^2} + k(c_{\text{is}} - c_{\text{i}}) \tag{55}$$

This model can be used under the assumptions of pseudohomogeneous dissolution and of initially unfilled pores in the matrix system, as is the case with tablets and other pharmaceutical systems produced by compression of solids. For finite slabs of thickness δ and zero surface concentration, the amount of drug released is expressed by equation 56, where α_{n} is defined as in equation 57:

$$\frac{M_{\text{t}}}{A} = \left[c_{\text{is}}\sqrt{D_{\text{eff}}k}\tanh\left[\frac{\delta}{2}\sqrt{\frac{k}{D_{\text{eff}}}}\right]\right]t - \frac{c_{\text{is}}D_{\text{eff}}}{\delta}\sum_{n=0}^{\infty}\frac{1 - \exp[-D_{\text{eff}}\alpha_{\text{n}}^2 + k)t]}{(D_{\text{eff}}\alpha_{\text{n}}^2 + k)^2} \tag{56}$$

$$\alpha_{\text{n}} = \frac{(2n + 1)}{\delta}\pi \tag{57}$$

It is interesting to note that at long times, the last term of equation 56 is small, and zero-order release is predicted.

The second modeling effort assumes (11) that solid drug fills completely the pores and dissolution occurs. This phenomenon can be modeled as an unsteady-state, moving-boundary (Stefan-type) problem. For this case, it can be shown that the released drug can be determined by equation 58:

$$\frac{M_{\text{t}}}{A} = \frac{2\varepsilon^{2/3}c_{\text{is}}}{\text{erf}\left[\dfrac{x^*}{2\sqrt{D'_{\text{iw}}t}}\right]}\left[\frac{D'_{\text{iw}}t}{\pi}\right]^{1/2} \tag{58}$$

The position of the front x^* can be determined by equation 59:

$$x^*\left[\frac{\pi}{D'_{iw}t}\right]^{1/2}\exp\left[\frac{x^{*2}}{4D'_{iw}t}\right]\mathrm{erf}\left[\frac{x^*}{2\sqrt{D'_{iw}t}}\right] = \frac{c_{is}}{\rho_i M_i} \quad (59)$$

The diffusion coefficient, D'_{iw}, is defined by equation 60; ϵ is the porosity upon complete dissolution, ρ_i is the density of the drug, and M_i is its molecular weight.

$$D'_{iw} = D_{iw}/\tau \quad (60)$$

Because of the assumptions made, this model can be used to describe the unexpected release behavior of drugs from dense, hydrophobic matrix systems such as those studied by Langer and co-workers (10,37).

SWELLING-CONTROLLED SYSTEMS

Swelling-controlled release systems are rather difficult to model owing to complex macromolecular changes occurring in the polymer during release. These systems consist of water-soluble drugs that are initially dispersed in solvent-free glassy polymers. If a slab is placed in contact with water, diffusion of water into the polymer will be observed depending on the thermodynamic interactions between the polymer and the solvent. This dynamic swelling phenomenon may lead to considerable volume expansion of the original slab. Two fronts (interfaces) are characteristic of the swelling behavior:

1. The swelling interface that separates the rubbery (swollen) state from the glassy state and that moves inward with velocity v
2. The polymer interface that separates the rubbery state from water and moves outward

Swelling of glassy polymers is accompanied by macromolecular relaxation, which become important at the swelling interface (38). This relaxation, in turn, affects the drug diffusion through the polymer, so that Fickian or non-Fickian diffusion may be observed. In these systems, drug release is controlled by the velocity of the water penetration front, v, because drug diffusion through the glassy polymer is negligible.

Mathematical modeling of this type of diffusion behavior clearly belongs to a category of mathematical problems known as Stefan, Stefan–Neumann, or moving-boundary problems. The Fickian diffusion equation 2 is solved with concentration-dependent or concentration-independent drug-diffusion coefficients and moving-boundary conditions (at the two fronts). If, in addition, one imposes problems of non-Fickian diffusion due to macromolecular relaxation, then the mathematical analysis becomes rather complicated (39). Some attempts to describe this behavior have been discussed by Peppas et al. (40), and a more complete literature review is given elsewhere (31).

A common procedure for analyzing experimental data of drug release from swelling-controlled release systems is by fitting them to equation 5 and determining the exponent n. As discussed before (9), the value of this exponent is characteristic of the Fickian or non-Fickian diffusion behavior of swelling-controlled release systems. It is possible to derive sufficient and necessary conditions for obtaining zero-order release from swelling-controlled release systems (41) by examining the dimensionless number, Sw, the so-called swelling interface number, defined according to equation 61:

$$Sw = \frac{v\delta(t)}{D_{ip}} \quad (61)$$

When $Sw \ll 1$, zero-order release should be expected, whereas for values of $Sw \gg 1$, Fickian diffusion is observed.

Kou et al. (42) proposed a model for drug diffusion through swellable cylinders with Fickian equations and concentration-dependent diffusion coefficients. Cohen and Erneux (43,44) presented a treatment of free boundary problems that had fundamental ideas in solving drug delivery problems in swellable systems.

The first detailed model of drug transport with concentration-dependent diffusion coefficients and swelling was proposed by Korsmeyer et al. (45). Lustig and Peppas (46) proposed a free-volume–based model with three-dimensional swelling beyond the point where the fronts meet. Lustig et al. (47) proposed a mathematical model for drug release based on rational thermodynamics, containing a full viscoelastic description of the polymer and concentration-dependent transport of the drug, with three-dimensional swelling.

Drug release from environmentally responsive polymeric systems has also been studied in great detail. Peppas and Brannon-Peppas (48) studied the drug-release rates in a system that responded to changes in temperature. The time-dependent response of the drug was also studied by Brannon-Peppas and Peppas (49) and by Bell and Peppas (50). Models for drug delivery from polymeric systems that responded to changes in the pH and ionic strength of the surrounding medium were proposed by Hariharan and Peppas (51,52).

In addition to these important modeling efforts, researchers have sought to analyze non-Fickian transport with relatively simple equations. One such effort relating the fractional release of the drug to time uses the so-called swelling area number (53). The swelling area number was defined as

$$Sa = \frac{1}{D}\frac{dA}{dt} \quad (62)$$

Here, A is the area available for drug release, and D is the drug-diffusion coefficient. The swelling area number, Sa, has been used to describe systems with varying area (see Fig. 5) due to swelling (specifically the Geomatrix® systems).

CHEMICALLY CONTROLLED SYSTEMS

Chemically controlled release systems include all polymeric formulations where drug diffusion is controlled by the dissolution of the polymer matrix. Modeling of these systems is similar to that followed for swelling-controlled release systems, because mass erosion replaces the phase

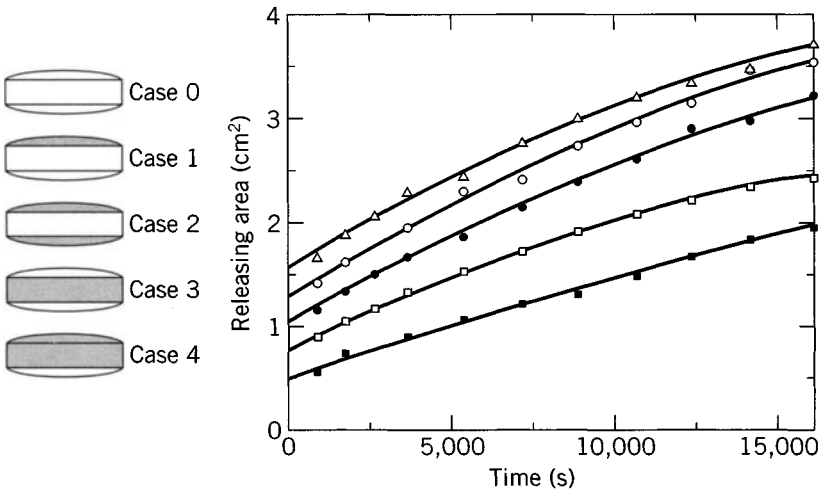


Figure 5. Releasing area as a function of time for the five systems shown. *Source:* Reproduced with permission from Ref. 53. Copyright 1988 Elsevier.

erosion (moving front) observed in swelling-controlled systems. Within this category, there are systems where a chemical reaction triggers the release. That reaction may be induced by hydrolysis, whether enzymatic or biochemical.

The difference between bioerosion and biodegradation is that the latter is the actual degradation, the breaking down of the polymer due to a chemical reaction that is taking place. The polymer will break down into small-molecular-weight materials. A matrix like that would be a polymeric material with the drug molecularly distributed throughout. In the case of biodegradable materials, the drug does not have to be molecularly dispersed; it can also be microscopically dispersed with large particles. The release process is controlled by a surface chemical reaction that will break down the polymer, giving oligomers and small-molecular-weight compounds. As time elapses, the geometry is unchanged but smaller, and the drug that was incorporated in the lost portion is free to dissolve and diffuse. That is why biodegradable systems, with a first-order biodegradation reaction with respect to the area, yield zero-order release for a planar device where the area remains constant.

Bioerosion is a process whereby a phase of the carrier is lost, not by chemical reaction but by dissolution. When bioerodible polymers are brought in contact with physiological fluids, the fluids simply dissolve the polymer rather than break it down. The definition is blurred, and people speak of bioerodible systems when they mean biodegradable systems.

In most chemically controlled systems, the geometric shape of the device controls drug release. The controlling mechanism may be either polymer dissolution or reaction and degradation at the polymer surface. Depending on the type of degradation reaction, these systems may be classified as chemically degradable (e.g., by hydrolysis) or biodegradable (e.g., by enzymatic reaction) controlled-release systems.

Shrinking-core models provide the most accurate description of this release. Cooney (54,55) developed simple expressions for drug release from cylindrical, spherical, and cylindrical devices.

Hopfenberg (56) derived expressions for drug release from erodible slabs, cylinders, and spheres. If one recognizes that the erosion rate is proportional to the continuously changing area of the device, A_e, one may write

$$\frac{dM_t}{dt} = k_e A_e \tag{63}$$

Solution of this equation for various geometries gives the following general expression

$$\frac{M_t}{M_\infty} = 1 - \left[1 - \frac{k_e t}{c_{io} l}\right]^n \tag{64}$$

Here $n = 1$ for a slab of thickness $\delta = 2l$, $n = 2$ for a cylinder of radius $r = l$, and $n = 3$ for a sphere of radius $r = l$.

Mathematical models of erodible systems where drug release from the surface is also important have been recently discussed by Lee (57) and further analyzed elsewhere (58). In order to obtain zero-order release from such erodible devices, the drug distribution was studied (57,58). It was found that a sigmoidal type of initial drug distribution gave almost zero-order release (58). This effect is represented in Figure 6.

Thombre and Himmelstein (59) developed models to describe drug release from poly(orthoester)s. The boundary condition used to solve the transport–reaction problem is given by equation 29, where k_i now represents the reaction constant of species i. The diffusion–reaction model was solved in terms of typical Thiele moduli, φ_i, to describe the reaction–diffusion ratio and Biot numbers, Bi_i, to describe the mass transfer–diffusion ratio. The solutions were reported as fractional amount of each species as a function of time as shown in Figure 7.

$$\varphi_i = a\sqrt{\frac{k_i c_i}{D_i}} \qquad Bi_i = \frac{k_i a}{D_i} \tag{65}$$

where D_i is the diffusion coefficient of the ith species and a is the half thickness of the polymer film.

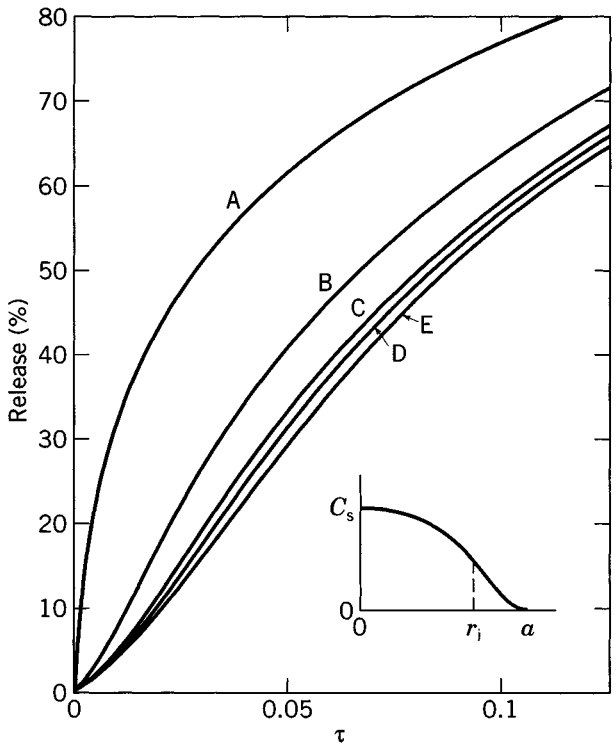


Figure 6. Effect of sigmoidal initial drug concentration distribution on the cumulative release from spherical matrices. Curves A through E represent different values of ξ_i. ξ_i is the initial position of the inflection point in the concentration profile. *Source:* Reproduced with permission from Ref. 58. Copyright 1986 Butterworth. The distribution function is

$$f(\xi) = \frac{1 - \exp\left[-0.5\left(\frac{1-\xi}{1-\xi_i}\right)^2\right]}{1 - \exp\left[-0.5\left(\frac{1}{1-\xi_i}\right)^2\right]}$$

Computer-aided methods (60,61) have also been used to model bioerosion. In these approaches, the polymer matrix is represented as the sum of individual matrix parts, and the erosion of each part is regarded as a random event. Comparisons with experiment yielded good agreement. This analysis was later extended (62) to describe the release of a monomer from an eroding polymer. The model predicts parameters like the porosity of the eroding polymer, the matrix weight, and amount of monomer released. The analysis could be extended to model drug release from such systems (63,64).

Pendent Chain Systems

Models have been proposed by Anderson and his coworkers (65) to describe cortisol hydrolysis from bound PGA systems. The hydrolysis starts at the surface, giving hydrophilic polymer. The rate of water permeation, R_w, in the hydrophobic zone and the rate of hydrolysis, R_h, are important parameters in tuning the release kinetics.

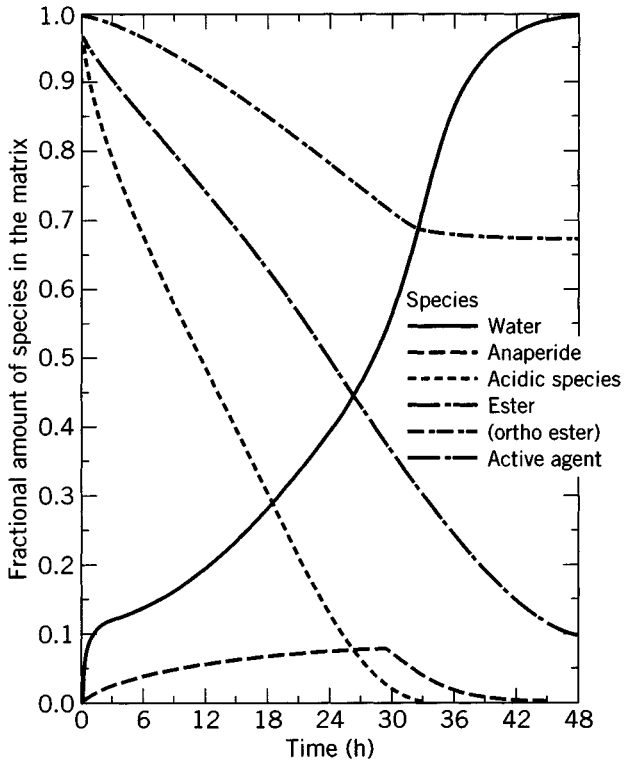


Figure 7. Fractional amount of species in the matrix as a function of time. *Source:* Reproduced with permission from Ref. 59. Copyright 1985 AIChE.

OTHER ASPECTS OF RELEASE KINETICS MODELING

Osmotic Systems

Osmotic systems for drug delivery are designed by applying irreversible thermodynamics and the Kedem–Katchalsky (66) analysis. The total volume flow, J_u, and the total exchange flow, J_D, are respectively given by

$$J_u = L_p \Delta p + L_{pD} \Delta \pi_s \qquad (66)$$
$$J_D = L_{Dp} \Delta p + L_D \Delta \pi_s$$

Here, L_i ($i = p, pD, Dp, D$) represents Onsager coefficients, Δp is the hydrostatic pressure, and $\Delta \pi_s$ is the osmotic pressure of the solvent.

The systems under consideration may also be defined by the reflection coefficient, σ, and the permeability coefficient, L_p. The term σ is defined as

$$\sigma = -\frac{L_{pD}}{L_p} \qquad (67)$$

The osmotic pressure is given by

$$\Delta \pi_s = NRT/V = cRT \qquad (68)$$

where N is the number of moles of the solvent, V is the solvent volume, R is the universal gas constant, and T is the temperature.

The volume flux, dV/dt, for a membrane of thickness δ and cross-sectional area A is given by

$$\frac{dV}{dt} = \frac{A}{\delta}(\sigma \Delta\pi_s - \Delta p) \tag{69}$$

The value $\sigma = 0$ represents a coarse filter, and $\sigma = 1$ represents an impermeable drug. For large orifices,

$$\Delta\pi_s \gg \Delta p \tag{70}$$

Hence,

$$\frac{dV}{dt} = \frac{A}{\delta} L_p \sigma \Delta\pi_s = \frac{A}{\delta} k \Delta\pi_s \tag{71}$$

Using $dM/dt = cdV/dt$, we have

$$\frac{dM}{dt} = \frac{A}{\delta} kc\Delta\pi_s \tag{72}$$

Hence, the drug-release rate in osmotically controlled systems can be tuned to achieve zero-order kinetics.

Dissolution-Controlled Systems

Dissolution-controlled systems have the additional characteristic that in addition to polymer swelling and drug diffusion through the continuously changing phase, they are accompanied by slow disentanglement of the polymer chains, leading to complete dissolution of the carrier. Obviously, this mechanism will occur only in un-cross-linked polymer carriers.

Harland et al. (67) formulated for a model for drug release in a dissolving polymer–solvent system. The transport was assumed to be Fickian, and mass balances were written for the drug and the solvent at the glassy–rubbery interface and at the rubbery–solvent interface. The important parameters identified in the phenomenon were the polymer volume fraction c^* at the glassy–rubbery transition, the polymer volume fraction c_d for disentanglement of the chains, and the dissolution–mass transfer coefficient, k. The expression for drug release as a function of time was obtained as

$$\frac{M_d}{M_{d,\infty}} = \frac{c_b}{ac_{cd}} \cdot \left(\sqrt{\frac{2[-D_s(c^* + c_s - c_d - c_b) + D_d(c_s - c_b) + D_d/c_b]^2(1 - c^* - c_s)t}{D_s(2 - c^* - c_s)(c^* + c_s - c_d - c_b) + D_d(c^* + c_s)(c_s - c_b)}} + kc_b t \right) \tag{73}$$

Here, D_s is the diffusion coefficient of the solvent in the polymer, and D_d is the diffusion coefficient of the drug in the polymer. The parameter c_b is the volume fraction of the drug in the bulk. This model can predict both Fickian as well as non-Fickian behavior. It is to be noted that front synchronization leads to zero-order release in dissolution-controlled systems. The predicted normalized drug release as a function of time is shown in Figure 8.

The previous model was modified by Narasimhan and Peppas (68) by accounting for macromolecular chain disentanglement. An expression for the fraction of the drug released was derived as

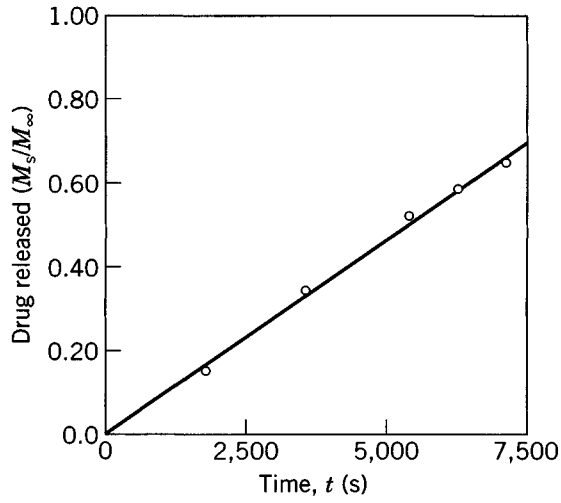


Figure 8. Normalized drug release as a function of time for drug–polymer tablet dissolution system. *Source:* Reproduced with permission from Ref. 67. Copyright 1985 Plenum.

$$\frac{M_d}{M_{d,\infty}} = \frac{v_{d,eq} + v_d^*}{2l}(\sqrt{2At} + Bt) \tag{74}$$

Here, A and B are given as

$$A = D(v_{1,eq} - v_1^*)\left(\frac{v_{1,eq}}{v_{1,eq} + v_{d,eq}} + \frac{1}{v_1^* + v_d^*}\right) + D_d(v_d^* - v_{d,eq})\left(\frac{v_{d,eq}}{v_{1,eq} + v_{d,eq}} + \frac{1}{v_1^* + v_d^*}\right) \tag{75}$$

$$B = \frac{k_d}{v_{1,eq} + v_{d,eq}} \tag{76}$$

Here, l is the half-thickness of the polymer, D is the diffusion coefficient of the solvent, and D_d is the diffusion coefficient of the drug. v_1^* and v_d^* are equilibrium concentrations of solvent and drug, respectively. The parameter k_d is the disentanglement rate of the polymer chains and is calculated using reptation theory (69–71). Figure 9 shows the fraction of drug released as a function of α ($\alpha = A/B$) and dimensionless time τ ($\tau = Bt/l$). It is observed that the model captures Fickian behavior, anomalous transport, as well as zero-order release.

For the drug-release rate to be zero order (see equation (74)), $B^2/A \gg 1$. Hence, choosing a polymer–drug–solvent system such that this inequality is satisfied would result in a zero-order drug release. This model also captures the transition between Fickian and non-Fickian type behavior.

When the polymer carrier is semicrystalline, the process of carrier dissolution is preceded by a process of phase erosion of the crystalline region to an amorphous region. Under certain conditions, this transition may lead to relaxation-controlled conditions of drug transport. Drug release from a new class of such systems—crystal dissolution–controlled-release systems—was modeled by Mallapragada and Peppas (72). In the presence of a thermodynamically compatible solvent, polymer crystals may start dissolving by crystal unfolding and disentanglement. In these dissolving phase-erosion systems, the drug-

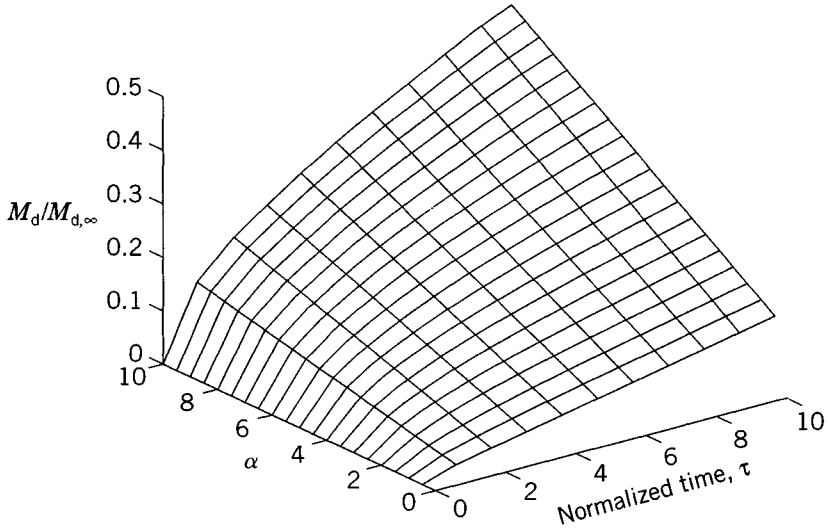


Figure 9. Predicted normalized drug released, M_d/M_d, as a function of normalized time, τ ($\tau = Bt/l$), for different values of α ($\alpha = A/B$). *Source:* Reproduced with permission from Ref. 68. Copyright 1997 ACS.

release rate is controlled by the transformation of the crystalline phase of the polymer to the amorphous phase. The crystalline regions are modeled as impermeable structures that do not permit drug diffusion. Therefore, as the polymer swells and drug is released, the concentration gradient for drug diffusion decreases, but simultaneously, disappearance of part of the crystalline phase causes an increase in the overall drug diffusion coefficient from the polymer. If these two effects compensate for each other, then zero-order drug release can be obtained.

A mathematical model was proposed by coupling crystal-unfolding theories with free-volume–based drug-diffusion theories (18) to predict conditions under which zero-order drug release can be obtained. Expressions were written for changes in the volume fractions of the crystalline polymer, amorphous polymer, and the drug as functions of time. The coupled partial differential equations were solved with the appropriate boundary conditions to yield drug-release profiles as functions of time under various conditions (Fig. 10). Factors affecting the drug-release rate were found to be the polymer degree of crystallinity, crystal size distribution, molecular weight of the polymer, the polymer–water interaction parameter, and the crystal-unfolding rate. The release from these systems was found to be non-Fickian.

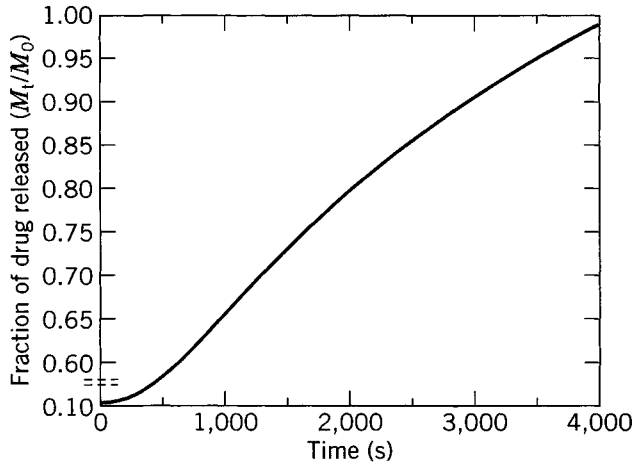


Figure 10. Predicted fraction of metronidazole released as a function of time from a poly(vinyl alcohol) sample with degree of crystallinity = 30% and drug loading of 2%. *Source:* Reproduced with permission from Ref. 72. Copyright 1997 Elsevier.

CONCLUSIONS

Drug release through controlled-delivery polymeric systems has been modeled predominantly by steady-state and transient description of drug diffusion by use of Fick's law. The correct interpretation of release kinetics from such drug-release models depends on the mechanism of the release itself, the polymer microstructure, and the conditions of the experiment (in other words, the boundary conditions). More accurate mathematical descriptions are necessary in modeling drug release in swellable and porous polymeric systems. Consideration of aspects such as countercurrent solvent diffusion, chain disentanglement, polymer state transitions, degree of crystallinity, and porous structure will enhance understanding and interpretation of release kinetics data from existing models. The advent of codelivery polymeric systems has necessitated the need for models incorporating interacting and noninteracting multicomponent diffusion through polymers.

BIBLIOGRAPHY

1. R.W. Baker and H.K. Lonsdale, in A.C. Tanquarry and R.E. Lacey, eds., *Controlled Release of Biologically Active Agents*, Plenum, New York, 1974, pp. 15–72.
2. R. Langer, *Chem. Eng. Commun.* **6**, 1–8 (1980).
3. B. Narasimhan and N.A. Peppas, in K. Park, ed., *Controlled Drug Delivery*, American Chemical Society, Washington, D.C., 1997, pp. 529–557.
4. R.S. Langer and N.A. Peppas, *J. Macromol. Sci., Rev. Macromol. Chem. Phys.* **C23**(1), 61–126 (1983).

5. C.E. Rogers, *ACS Symp. Ser.* **33**, 15 (1976).
6. N.A. Peppas, in V.H.L. Lee, M. Hashida, and Y. Mizushima, eds., in *Peptide and Protein Drug Delivery*, Harwood Academic Publishers, Chur, Switzerland, 1995, p. 23.
7. J. Crank, *The Mathematics of Diffusion*, 2nd ed., Oxford University Press, New York, 1975.
8. R.W. Korsmeyer and N.A. Peppas, in S.Z. Mansdorf and T.J. Roseman, eds., *Controlled Release Delivery Systems*, Dekker, New York, 1983, p. 77.
9. P.L. Ritger and N.A. Peppas, *J. Controlled Release* **5**, 23–36 (1987).
10. W.D. Rhine, V. Sukhatme, D.S.T. Hsieh, and R.S. Langer, in R. Baker, ed., *Controlled Release of Bioactive Materials*, Academic Press, New York, 1980, p. 177.
11. R. Gumy, E. Doelker, and N.A. Peppas, *Biomaterials* **3**, 27–32 (1982).
12. S.K. Chandrasekaran and D.R. Paul, *J. Pharm. Sci.* **71**, 1399–1402 (1982).
13. N.A. Peppas and R.W. Korsmeyer, in N.A. Peppas, ed., *Hydrogels in Medicine and Pharmacy*, vol. 3, CRC Press, Boca Raton, Fla., 1987, p. 109.
14. R.A. Siegel, in M. Rosoff, ed., *Controlled Release of Drugs*, VCH, New York, 1989, p. 1.
15. N.A. Peppas, in R.S. Langer and D. Wise, eds., *Medical Applications of Controlled Release Technology*, vol. 2, CRC Press, Boca Raton, Fla., 1984, p. 169.
16. H. Eyring, *J. Chem. Phys.* **4**, 283 (1936).
17. A.G. Ogston, *Trans. Faraday Soc.* **54**, 1754 (1958).
18. H. Fujita, *Fortschr. Hochpolym.-Forsch.* **3**, 1–47 (1961).
19. H. Yasuda and C.E. Lamaze, *J. Macromol. Sci., Phys.* **B5**, 111–120 (1971).
20. E.N. Lightfoot, *Transport Phenomena and Living Systems*, Wiley, New York, 1974.
21. H. Faxén, *Ark. Mat. Astron. Fys.* **17**, 27 (1923).
22. J.M. Vrentas and J.L. Duda, *J. Polym. Sci., Polym. Phys. Ed.* **17**, 1085–1092 (1979).
23. C.K. Colton, K.A. Smith, E.W. Merrill, and P.C. Farrell, *J. Biomed. Mater. Res.* **5**, 459–488 (1971).
24. R.S. Harland and N.A. Peppas, *Colloid Polym. Sci.* **267**, 218–225 (1989).
25. J.L. Anderson and J.A. Quinn, *Biophys. J.* **14**, 130 (1974).
26. T.K. Sherwood, R.L. Pigford, and C.R. Wilke, *Mass Transfer*, McGraw-Hill, New York, 1975.
27. J.C. Fu, C. Hagemeier, and D.L. Moyer, *J. Biomed. Mater. Res.* **10**, 743–758 (1976).
28. D.R. Paul and S.K. McSpadden, *J. Membr. Sci.* **1**, 33–48 (1976).
29. T. Higuchi, *J. Pharm. Sci.* **50**, 874–875 (1961).
30. T.J. Roseman and W.I. Higuchi, *J. Pharm. Sci.* **59**, 353–357 (1970).
31. J. Crank, *Free and Moving Boundary Problems*, 2nd ed., Oxford University Press, New York, 1975.
32. P.V. Danckwerts, *Trans. Faraday Soc.* **46**, 701 (1950).
33. P.I. Lee, *J. Membr. Sci.* **7**, 255–275 (1980).
34. B. Narasimhan and R. Langer, *J. Controlled Release* **47**, 13–20 (1997).
35. Higuchi, T., *J. Pharm. Sci.* **52**, 1145 (1963).
36. E.A. Swan and N.A. Peppas, *Proc. Symp. Controlled Release Bioact. Mater.* **8**, 18–19 (1981).
37. W. Rhine, D. Hsieh, and R. Langer, *J. Pharm. Sci.* **69**, 265–270 (1980).
38. N.A. Peppas and R. Korsmeyer, *Polym. News* **6**, 149 (1980).
39. J.C. Wu and N.A. Peppas, *J. Polym. Sci., Polym. Phys. Ed.* **31**, 1503 (1993).
40. N.A. Peppas, J.C. Wu, and E.D. von Meerwall, *Macromolecules* **27**, 5626 (1994).
41. N.A. Peppas and N.M. Franson, *J. Polym. Sci., Polym. Phys.* **21**, 983 (1983).
42. J.H. Kou, D. Fleisher, and G.L. Amidon, *J. Controlled Release* **12**, 241 (1990).
43. D.S. Cohen and T. Erneux, *SIAM J. Appl. Math.* **48**, 1451 (1988).
44. D.S. Cohen and T. Erneux, *SIAM J. Appl. Math.* **48**, 1466 (1988).
45. R.W. Korsmeyer, S.R. Lustig, and N.A. Peppas, *J. Polym. Sci., Polym. Phys.* **24**, 395 (1986).
46. S.R. Lustig and N.A. Peppas, *J. Appl. Polym. Sci.* **33**, 533 (1987).
47. S.R. Lustig, J.M. Caruthers, and N.A. Peppas, *Chem. Eng. Sci.* **47**, 3037 (1992).
48. N.A. Peppas and L. Brannon-Peppas, *J. Membr. Sci.* **48**, 281 (1990).
49. L. Brannon-Peppas and N.A. Peppas, *Int. J. Pharmacol.* **70**, 53 (1991).
50. C.L. Bell and N.A. Peppas, *Polym. Prepr.* **34**(1), 831–832 (1993).
51. D. Hariharan and N.A. Peppas, *J. Membr. Sci.* **78**, 1 (1993).
52. D. Hariharan and N.A. Peppas, *J. Controlled Release*, **23**, 123 (1993).
53. P. Colombo et al., *Int. J. Pharmacol.* **88**, 99 (1992).
54. D.O. Cooney, *AIChE J.* **17**, 754 (1971).
55. D.O. Cooney, *AIChE J.* **18**, 446 (1971).
56. H.B. Hopfenberg, *ACS Symp. Ser.* **33**, 222 (1976).
57. P.I. Lee, *Polymer* **25**, 973 (1984).
58. P.I. Lee, *J. Controlled Release* **4**, 1–6 (1986).
59. A.G. Thombre and K.J. Himmelstein, *AIChE J.* **31**, 759 (1985).
60. A. Gopferich and R. Langer, *Macromolecules* **26**, 4105–4112 (1993).
61. K. Zygourakis and P.A. Markenscoff, *Biomaterials* **17**, 125–135 (1996).
62. A. Gopferich and R. Langer, *J. Controlled Release* **33**, 55–69 (1995).
63. A. Gopferich, *Biomaterials* **17**, 103–114 (1996).
64. A. Gopferich, *Macromolecules* **30**, 2598–2604 (1997).
65. N. Tani, M. Van Dress, and J.M. Anderson, in D.H. Lewis, ed., *Controlled Release of Pesticides and Pharmaceuticals*, Plenum, New York, 1981, p. 79.
66. O. Kedem and A. Katchalsky, *Biochim. Biophys. Acta* **27**, 229 (1958).
67. R.S. Harland et al., *Pharm. Res.* **5**, 488 (1988).
68. B. Narasimhan and N.A. Peppas, *J. Pharm. Sci.* **86**(3), 297–304 (1997).
69. B. Narasimhan and N.A. Peppas, *J. Polym. Sci., Polym. Phys. Ed.* **34**, 947–961 (1996).
70. B. Narasimhan and N.A. Peppas, *Macromolecules* **29**, 3283–3291 (1996).
71. P.G. de Gennes, *Scaling Concepts in Polymer Physics*, Cornell University Press, Ithaca, N.Y., 1979.
72. S.K. Mallapragada and N.A. Peppas, *J. Controlled Release* **45**, 87–94 (1997).

RESPIRATORY SYSTEM DELIVERY

DAVID A. EDWARDS
Advanced Inhalation Research (AIR)
Cambridge, Massachusetts

KEY WORDS

Aerodynamic size
Asthma
Dry powder
Estradiol
Insulin
Lungs
Macrophage
Mass density
Porosity
Respiratory

OUTLINE

Introduction
Lung Morphology and Physiology
Aerosol Delivery to the Respiratory Tract
Fast-Acting Inhalation Therapies
Sustained Drug Delivery
Summary
Bibliography

INTRODUCTION

Inhalation therapies have until now primarily provided fast-acting treatment for respiratory illnesses such as asthma and chronic obstructive pulmonary disease (COPD). Relative to oral delivery, inhalation of bronchodilators, corticosteroids, and other antiinflammatory agents to the airways often produces therapeutic levels in the respiratory tract while maintaining low systemic concentrations and thereby minimizing side effects (1–6). More recently, inhalation therapies for the systemic delivery of proteins and peptides to the body have made important advances in human clinical trials, notably owing to the success with which many macromolecules permeate the alveolar/blood barrier once inhaled (7). For these newer inhalation therapies, inhalation systems are often required that achieve high reproducibility and efficiency; this need has propelled active research and development in the inhalation drug delivery field (8).

The heightened scientific and industrial attention paid to inhaled drug delivery has exposed an unmet need for the controlled release of inhaled drugs (9). Controlled release of drugs in the respiratory system can benefit a variety of existing and future therapies whose success depends critically on multiple daily dosing. Examples include sustained release of bronchodilators and corticosteroids for asthma or drugs such as insulin for diabetes. A logical strategy to achieve sustained release of drugs in the respiratory tract involves encapsulating drugs in slowly degrading particles that can be inhaled. This strategy can, however, be foiled by the relatively rapid (less than a day) natural clearance of insoluble particles from the respiratory system. Efforts are therefore underway to create sustained-release particles that safely avoid respiratory clearance mechanisms, thereby permitting the development of practically useful controlled drug release in the lungs (10–15).

LUNG MORPHOLOGY AND PHYSIOLOGY

The human lung is often conceptually divided into conducting and respiratory zones. The conducting zone serves as the relatively long channel for inhaled air and consists of trachea, bronchus, bronchioles, and terminal bronchioles (Table 1). Insoluble particles deposited in this zone are propelled upward by means of cilia action within the mucus layer residing on the surfaces of the conducting zone. Eventually the insoluble particles reach the pharynx, where they are swallowed. The clearance of insoluble particles from the conducting airways by mucociliary activity is usually complete in 12–24 h (16–19). Respiratory bronchioles are located beyond the terminal bronchioles, followed by alveolar ducts and alveolar sacs; together they comprise the respiratory zone, where primary gas exchange occurs between the air spaces and the blood (Table 1). Insoluble particles deposited in this zone are quickly engulfed by alveolar macrophages, whose ability to chemically break down engulfed material makes them the nemesis of inhaled drugs.

The average alveolar surface area in human lungs (20) is 102 ± 21 m^2, corresponding to 95% of the total surface area in the lungs. The total surface area of alveoli in contact with blood capillaries is approximately 75 m^2 (roughly 40 times greater than the external body surface area) (21). This broad area facilitates the lung's function as the primary gas exchange organ (the lung receives all the blood circulated through each of the peripheral organs and tissues, whereas the abdominal organs receive about 24% of body blood [22]). The epithelial lining of the alveolar spaces, the most significant absorption barrier separating blood from the alveolar lumen (23), has an average thickness of only 0.2 μm—approximately 34 times smaller than the diameter of an average red blood cell (23). The thinness of this barrier and its extensive surface area permits a high accessibility of inhaled drugs to the blood stream. This makes the alveolar region a natural target for inhaled drugs destined for the systemic circulation.

AEROSOL DELIVERY TO THE RESPIRATORY TRACT

To possess a high likelihood of depositing in the alveolar zone of the lungs, inhaled particles must exhibit an aerodynamic diameter in the range of 1–3 μm (25–28). The aerodynamic diameter of a spherical particle (d_a) can be expressed as the product of the geometric diameter (d) and the square root of the particle mass density ρ (R. Vanbever et al., unpublished data) (appropriately normalized to give the proper units). It can be shown that a spherical particle

Table 1. Approximate Dimensions of the Human Lung.

Generation	Length (cm)	Diameter (cm)	Number	Cross-sectional area (cm^3)
Trachea (0)	12.0	1.80	1	2.54
Bronchi (1)	4.8	1.22	2	2.33
Bronchi (2)	1.9	0.83	4	2.13
Bronchi (3)	0.8	0.56	8	2.00
Bronchioles (4–16)	1.3–0.12	0.45–0.06	16–60,000	2.48–180.0
Respiratory bronchioles (17–19)	0.12–0.10	0.06–0.05	60,000–500,000	180–1,000
Alveolar ducts (20–22)	0.10–0.05	0.05–0.04	5×10^5–8×10^6	10^3–10^4
Alveolar sacs (23)	0.05	0.04	8×10^6	10^4

Source: Ref. 24.

of any mass density, in flight, will settle with a velocity that depends only on its aerodynamic diameter (R. Vanbever et al., unpublished data). The concept can thus be used to predict a particle's expected lung deposition performance following inhalation. Numerous experimental (25–28) and theoretical (29–32) studies have shown that particles with aerodynamic diameters in the 1- to 3-μm-range deposit minimally in the mouth and throat and maximally in the lung's alveolar region. Tracheobronchial deposition, generally not desired for inhalation therapy, is maximized for mean d_a between approximately 8–10 μm owing to inertial impaction, whereas central airway deposition by gravity occurs maximally for $3\mu m < d_a < 5\mu m$. Particles possessing d_a less than 1 μm are mostly exhaled, and particles larger than about 10 μm have little chance of making it into the mouth.

For these reasons, inhalation therapies today rely on liquid or dry-powder aerosols comprised of particles with mean diameters in the range of 1–5 μm. Therapeutic particles in this size range are found to produce optimal therapeutic (whether systemic or local) effect.

However, aerosols formed of 1–5 μm particles, in addition to rapidly clearing from the lungs, can aggregate prior to delivery (33). This produces poor efficiency of delivery from standard inhaler devices; hence, devices on the market deliver only about 10% of an inhaled dose into the lungs (34,35). This inefficiency magnifies patient-to-patient variability and can lead to patient discomfort, as manifested in coughing or bronchospasm.

One way to address this problem involves adjusting inhalation procedures. An optimal inhalation maneuver appears to involve a slow, deep inhalation to reduce impaction losses in the orapharynx, with about 10 s of breath hold to allow particles that enter the lung to settle by gravity (36–41). Pulmonary deposition can also be greatly affected by patient inspiratory flow rate, as inertial impaction of particles in the mouth and throat increases sharply with increasing flow rate (42,43).

Greater progress has been achieved by modifications to the inhaler device. Inhalation devices broadly fall into three categories: pressurized metered-dose inhalers (MDIs), nebulizers, and dry-powder inhalers (DPIs). The most commonly used inhalers on the market are MDIs; they contain active ingredient as a solution or as a suspension of fine particles in a liquefied propellant (often a chlorofluorocarbon, CFC) held under high pressure. The drug is emitted through an orifice from a metering valve. Droplets of a MDI tend to exit the orifice at a high velocity, potentially causing extensive orapharyngeal deposition. New breath-activated devices (44,45) now address this problem, and new non-CFC propellants address the CFC concern.

The typical maximum drug dose delivered by a single actuation of a MDI is around 1 mg (46). Nebulizers do not require propellants and can generate large quantities of small droplets capable of penetrating into the lung. As in the case of MDIs, new nebulizer systems avoid the problems of older generation nebulizers (bulk, excessive mouth–throat deposition) though they continue to be considered impractical for daily portable use. Given the concern about CFC's negative effects on the ozone layer, a great deal of work has been done to develop DPI systems. Although DPIs are sold widely in Europe, their use is still limited in other parts of the world, such as the United States. Current developments in the field may change this situation. DPIs have the attraction of storing the inhaled drug in a dry state, which often carries with it advantages of long-term stability and sterility. New generation DPIs modulate flow rate dependence and deaggregate powder, leading to significant improvements in device performance (8). Depending on the device, DPIs deliver either quantities of drug similar to MDIs (1–3 milligrams or less) or in certain cases considerably more.

DPIs may be most useful for controlled-release applications, as they can be maintained on the shelf in a dry state prior to delivery. On the other hand, MDIs might prove useful as well upon appropriate choice of propellant.

FAST-ACTING INHALATION THERAPIES

The mainstay of asthma treatment is the inhalation of a bronchodilator, such as albuterol, for fast-acting relief from bronchoconstriction and a corticosteroid, such as beclamethasone or fluticasone, for antiinflammation protection (1–6). Other bronchodilators and corticosteroids are commonly inhaled, as are anticholinergics. All these inhalation therapies involve fast action and delivery from either a MDI, DPI, or both. Nebulization is the preferred route of delivery in the clinic for a variety of substances, including lung surfactant for surfactant-replacement therapy and DNase for cystic fibrosis (46). DNase is the sole inhaled protein currently on the market, although other proteins are being tested in the clinic, including insulin, salmon cal-

citonin, parathyroid hormone, and LHRH (7). Each of these clinical therapies involves fast delivery of protein to the systemic circulation, with a delivery profile similar to intravenous injection.

SUSTAINED DRUG DELIVERY

Notwithstanding the rapid clearance of inhaled insoluble particles from the lungs, many efforts have been made to achieve sustained drug delivery from an inhalation aerosol. Primarily inhaled drugs have been encapsulated inside liposomes and biodegradable polymers (47,48), though the most successful long-acting inhaled drug (salmeterol, or Serevent) was developed by chemical modification of a fast-acting drug (salbutamol) (49).

Liposomal systems, delivered to the lungs by nebulization, are among the most commonly used methods for sustained pulmonary drug delivery. Liposome-encapsulated drugs have been released over many hours following inhalation in animals and humans; these drugs include, for local delivery, cytotoxic agents, bronchodilators, and antimicrobial agents (50–56); for systemic delivery, drugs such as insulin (57,58) have been released slowly from liposomes as well. Drawbacks to the inhalation of liposomes include (*1*) their relatively short action owing to clearance (they can be eliminated rapidly by alveolar macrophages [59–62]); (*2*) their poor stability during storage and use (63); and (*3*) their apparent need for delivery by nebulization.

Biodegradable polymer microspheres as drug carriers have also been extensively investigated. Albumin (59–62) and polylactide-*co*-glycolide (PLGA) microspheres (64–67) have repeatedly been used to achieve the sustained release of drugs in the lungs (9). Both biodegradable materials appear to be nontoxic and nonimmunogenic, although few if any chronic toxicity studies appear in the literature (9). Another approach to obtaining sustained release from inhaled drug particles involves incorporating macromolecules such as dextran (68,69) or poly(ethylene glycol) (70,71) to reduce particle hydrophilicity. One of the primary drawbacks to this approach for lung delivery is the possibility of accumulation of macromolecular materials within the lung over an extended administration period owing to the relatively slow removal of these materials from the lungs (9).

These techniques, among others, have achieved little success at maintaining therapeutic action following a single inhalation for more than several hours (9) (Fig. 1). To overcome this limitation posed by the lungs' natural clearance mechanisms, a new method to achieve sustained release in the lungs has involved preparing insoluble particles with aerodynamic diameter in the 1- to 5-μm range yet with very low mass density so that particles possess geometric diameters significantly greater than 5 μm (10). This permits the penetration of particles deep into the lungs (owing to small aerodynamic diameter) yet lowers the degree of clearance, because (geometrically) large particles tend to be cleared less by phagocytosis than particles in the size range of 1–5 μm (72–74).

Several studies have now appeared in the literature demonstrating the ability to achieve sustained release of

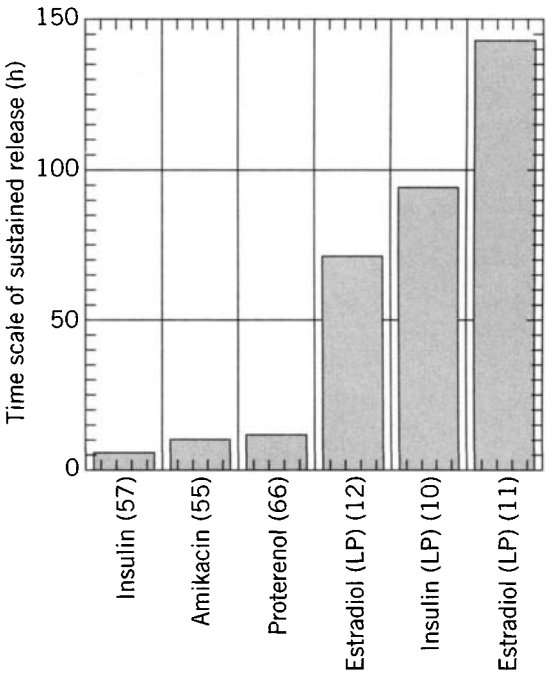


Figure 1. Approximate times of release in vivo from various controlled-release carriers following inhalation. The rightmost columns, indicated by the symbol LP, denote results from large porous particles in humans (12) and animals (10,11).

drugs from the lungs following a single inhalation of large porous particles for up to several days (10–15). In a first study, large, porous particles were prepared using PLGA biodegradable polymers and containing either insulin or testosterone for systemic delivery (10). For comparison purposes, small nonporous particles of similar composition and identical aerodynamic size were prepared. Both types of particles were aerosolized into the lungs of rats. In the case of the insulin aerosols, exogenous insulin appeared in the bloodstream for up to 96 h following inhalation of the porous particles, compared with 4 h for the nonporous particles. Given that the presence of insoluble particles in the lungs beyond 24 h indicates deep lung deposition and that bronchoalveolar lavage demonstrated that the large porous insulin particles were less avidly taken up by alveolar macrophages than the small nonporous insulin particles, the long release (>24 h) of insulin into the systemic circulation appears to owe to lower particle phagocytosis of large porous particles in the deep lungs. In another study, estradiol was formulated in large porous particles comprised of dipalmitoyl phosphatidyl choline (DPPC) as well as particles comprised of other soluble excipients (11). Particles were prepared with large size (approximately 10 μm) and low mass density (approximately 0.1 g/cc) as well as with small size (approximately 3 μm) and standard mass density. Both porous and nonporous powders were aerosolized into the lungs of rats. For two different formulations of the large porous estradiol particles, estradiol released into the systemic circulation following inhalation for 3 days or more. On the other hand, estradiol appeared in the systemic circulation following administration of two

different small nonporous particle formulations for a day or less. As porous and nonporous subcutaneously injected estradiol formulations acted therapeutically for several days, the short action of the small nonporous inhaled estradiol formulation appears again to relate to the more rapid clearance of small nonporous particles from the lungs. Sustained release in the estradiol study (11) was achieved by the use of both a relatively water-insoluble drug (estradiol) and insoluble surfactant (DPPC) rather than by biodegradable polymers.

One of the DPPC/estradiol formulations (Fig. 2) that achieved several-day delivery in rats has recently been inhaled in a human subject study using a simple DPI system (Fig. 3) (12). Inhalation of the porous dry powder at 30 L/min led to systemic estradiol absorption for 72 h, with estimated absolute bioavailability of 47%. The systemic absorption profile obeyed a two-phase model, with an initial fast elimination of estradiol from the body consistent with rapid absorption of estradiol from the lungs and systemic clearance and a secondary slow elimination phase, reflecting slow release from inhaled particles (Fig. 4). This study confirms that inhalation of large porous particles can produce sustained (>24 h) release of drugs into the lungs of humans as previously demonstrated in animals.

An example of sustained release of drugs from large porous particles for the treatment of respiratory disease has recently been described involving albuterol sulfate for asthma therapy (13). Albuterol sulfate particles were prepared using DPPC, human serum albumin, and lactose. Large porous and small nonporous albuterol particles were delivered as inhalation aerosols to the lungs of guinea pigs. To induce bronchoconstriction, immediately prior to measuring airway resistance (at selected intervals following inhalation of albuterol particles), carbachol was intramuscularly delivered. The small nonporous particles provided significant bronchodilatory effect for approximately 5 h following inhalation at a dose of 200 μg. The large porous albuterol particles produced sustained bronchodilation for at least up to 15 h (13).

As the porous-particle and other new sustained-release technologies emerge in the inhalation drug delivery arena, the possibility of several-day, or even several-week, sustained-release inhalation therapies arises. Clearly the desire (and ability) to achieve long drug release times in the lungs will place demands on drug dosing by inhalation. The current limitation of most inhalation systems (other than nebulizers) to inhaled doses of a few milligrams or less will need to be removed so that several tens of milligrams of drug can be inhaled in a single breath, a feat that does not appear too difficult even given currently emerging technologies (75). Another challenge will be to design sustained-release inhalation formulations that comprise materials that are safe for inhalation. Given the slow absorption of very large macromolecules in the lungs, standard sustained-release additives used to achieve oral sustained release (for example, methyl cellulose) may not be

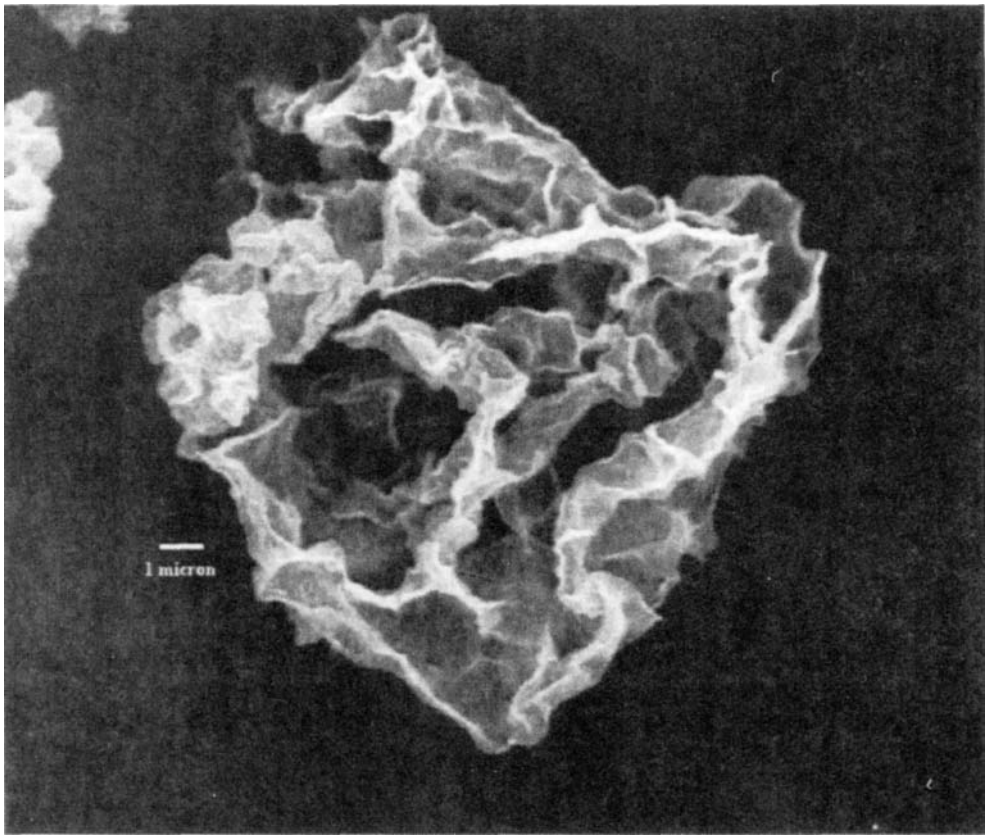


Figure 2. A large porous estradiol particle (12).

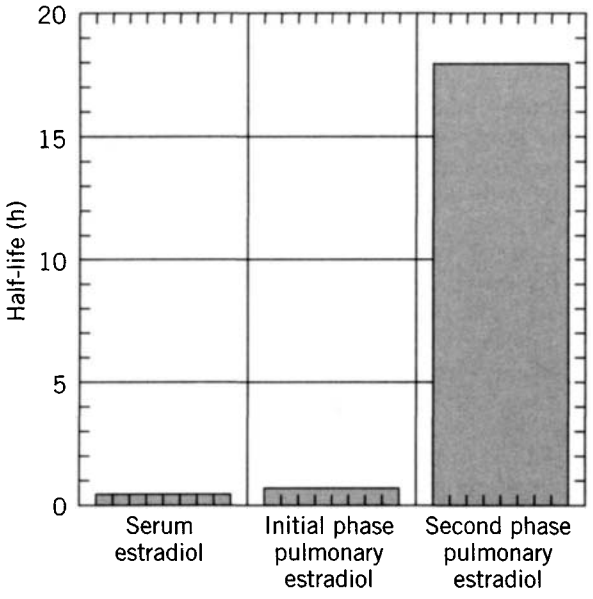


Figure 3. Approximate systemic half-lives of estradiol following intravenous injection and inhalation in humans. The second and third columns refer to clearance of estradiol following inhalation of a large porous particle formulation.

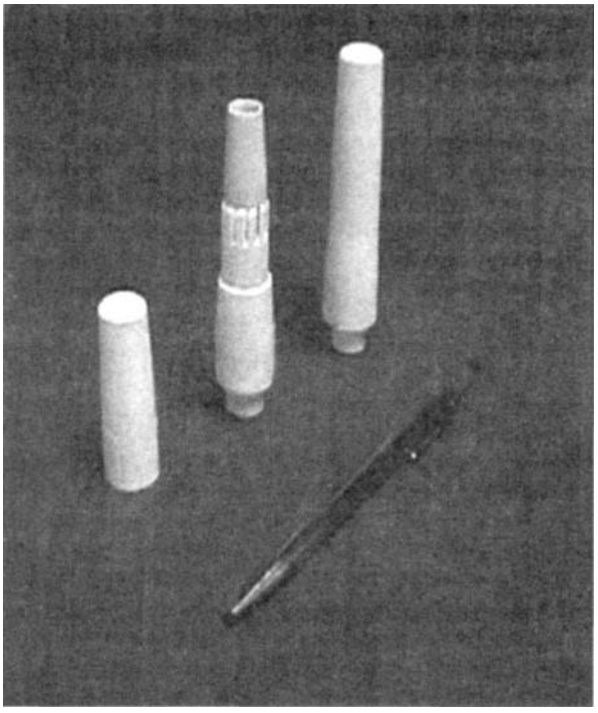


Figure 4. The AIR dry-powder inhaler.

appropriate for inhalation formulations. The search for excipients suitable for frequently dosed inhaled sustained-release formulations will play an important role in the practical success of sustained drug delivery in the respiratory tract.

SUMMARY

Efforts to achieve sustained drug delivery in the respiratory tract have been hindered in the past owing to the rapid clearance of insoluble drug particles in the lungs by mucociliary and phagocytic clearance processes, which remove or engulf particles within approximately 12–24 h after inhalation. Standard size and mass density liposomal and biodegradable polymer sustained-release systems have achieved drug release for modest periods, up to several hours. A new technique involving the production of large porous particles that display an ability to escape lung clearance has led to longer sustained release of drugs in the lungs, up to several days. One of the challenges of this technology will be to formulate sustained-release systems that do not lead to accumulation of materials in the lungs over time.

BIBLIOGRAPHY

1. T.J.H. Clark, *Lancet* **6**, 1361–1367 (1972).
2. S.D. Anderson et al., *Am. Rev. Respir. Dis.* **114**, 493–502 (1976).
3. A. Neville et al., *Br. Med. J.* **1**, 413–419 (1977).
4. S.P. Newman and S.W. Clarks, in F. Moren, M.T. Newhouse, and M.B. Dolovich, eds., *Aerosols in Medicine: Principles, Diagnosis and Therapy*, Elsevier, Amsterdam, 1985, pp. 289–301.
5. N. Svedmyr and G.-G. Lofdahl, in J.W. Jenne and S. Murphy, eds., *Drug Therapy for Asthma: Research and Clinical Practice,* Dekker, New York, 1987, pp. 177–185.
6. R.G. Taylor, in D. Ganderton and T. Jones, eds., *Drug Delivery to the Respiratory Tract*, Ellis Horwood, Chichester, England, 1987, pp. 27–32.
7. R.F. Service, *Science* **279**, 1631–1633 (1998).
8. C.A. Dunbar, A.J. Hickey, and P. Holzner, *KONA* **16**, 7–44 (1998).
9. X.-M. Zeng, G.P. Martin, and C. Marriott, *Int. J. Pharm.* **124**, 149–164 (1995).
10. D.A. Edwards et al., *Science* **276**, 1868–1871 (1997).
11. J. Wang, A. Ben-Jebria, and D.A. Edwards, *J. Aersol. Med.* **12**, 27 (1999).
12. D.A. Edwards et al., *Int. Symp. Recent Adv. Drug Delivery Syst.*, Salt Lake City, Utah, February 22–25, 1999.
13. A. Ben-Jebria, D. Chen, R. Langer, and D.A. Edwards, *Pharm. Res.* **16**, 555–561 (1998).
14. D.A. Edwards, D. Chen, J. Wang, and A. Ben-Jebria, *6th Respir. Drug Delivery Conf.*, Hilton Head, S.C., 1998, p. 187.
15. D.A. Edwards, A. Ben-Jebria, and R. Langer, *J. Appl. Physiol.* **84**(2), 379 (1998).
16. D.J. Gore and G. Patrick, *Phys. Med. Biol.* **23**, 730–737 (1978).
17. G.C. Smaldone et al., *J. Aerosol Med.* **1**, 1–20 (1988).
18. W. Stahlhofen, J. Gebhart, G. Rudolf, and G. Scheuch, *J. Aerosol Sci.* **17**, 333–338 (1986).
19. P. Gehr et al., *Microsc. Res. Tech.* **26**, 423–436 (1993).
20. K.C. Stone et al., *Am. Respir. Cell Mol. Biol.* **6**, 235–243 (1992).
21. A.J. Vander, J.H. Sherman, and D.S. Luciano, *Human Physiology*, 6th ed., McGraw-Hill, New York, 1994, pp. 473–514.
22. A.J. Vander, J.H. Sherman, and D.S. Luciano, *Human Physiology*, 6th ed., McGraw-Hill, New York, 1994, pp. 393–472.
23. J. Patton, *Adv. Drug Delivery Rev.* **19**, 3–36 (1996).

24. E.R. Weibel, in H.K. Chang and M. Paiva, eds., *Respiratory Physiology: An Analytical Approach*, Decker, New York, 1989, pp. 1–56.
25. B. Altschuler, L. Yalmus, E. D. Palmes, and N. Nelson, *AMA Arch. Ind. Health* **15**, 293–303 (1957).
26. D.C.F. Muir and C.N. Davies, *Ann. Occup. Hyg.* **10**, 161–174 (1967).
27. C.N. Davies, J. Heyder, and M. C. Subba Ramu, *J. Appl. Physiol.* **32**, 591–600 (1972).
28. J. Heyder et al., *J. Aerosol Sci.* **6**, 311–328 (1975).
29. T.R. Gerrity et al., *J. Appl. Phys.* **47**, 867–873 (1979).
30. J. Heyder and R. Rudolf, *J. Aerosol Sci.* **13**, 697–707 (1984).
31. A.R. Clark and M. Egan, *J. Aerosol Sci.* **25**, 175–186 (1994).
32. I. Gonda, *J. Pharm. Pharmacol.* **33**, 692–696 (1981).
33. D. French, D.A. Edwards, and R.W. Niven, *J. Aerosol Sci.* **27**, 769–780 (1996).
34. I. Gonda, in A.J. Hickey, ed., *Pharmaceutical Inhalation Aerosol Technology*, Dekker, New York, 1992, pp. 61–82.
35. M.P. Timsina et al., *Int. J. Pharm.* **101**, 1–13 (1994).
36. J.D. Brain and R.A. Valberg, *Am. Rev. Respir. Dis.* **120**, 1325–1373 (1979).
37. J. Heyder, J. Gebliard, and W. Statilofen, in K. Willeke, ed., *Generation of Aerosols and Facilities for Exposure Experiments*, Ann Arbor Sci. Publ., Ann Arbor, Mich., 1980, pp. 135–152.
38. D. Pavia, J.R.M. Bateman, and S.W. Clarke, *Bull. Eur. Physiopathol.* **16**, 335–366 (1980).
39. T.T. Mercer, *Chest* **80**, 813–818 (1981).
40. G.C. Smaldone et al., *J. Aerosol* **2**, 81–87 (1989).
41. M. Dolovich, *J. Aerosol Med.* **2**, 171–186 (1989).
42. R.M. Auty, K. Brown, M.G. Neale, and P.D. Snashall, *Br. J. Dis. Chest* **88**, 371–378 (1987).
43. R. Richards, S.F. Simpson, A.G. Renwick, and S.T. Holgate, *Eur. Respir. J.* **1**, 896–901 (1988).
44. D. Genderton and N.M. Kassem, *Adv. Pharm. Sci.* **6**, 165–191 (1992).
45. K. Masters, *Spray Drying Handbook*, 5th ed., Lonmans, New York, 1991.
46. R. Langer, *Nature (London)* **392**, 5–11 (1998).
47. Int. Pat. Appl. No. PCT/WO96/09814 (1996), A.D. Sutton and R.A. Johnson.
48. S.S. Davis and L. Ilium, *Biomaterials* **9**, 111–115 (1983).
49. D.M. Hammerbeck et al., *J. Aerosp. Med.* **10**, 41–54 (1997).
50. R.L. Juliano and H.N. McCullough, *J. Pharmacol. Exp. Ther.* **214**, 381–387 (1980).
51. A. Kamarel, A. Wong, and T. McCalden, *Proc. West. Pharmacol. Soc.* **32**, 32–35 (1989).
52. R.M. Fielding, *Proc. West. Pharmacol. Soc.* **32**, 103–106 (1939).
53. K.M.G. Taylor, G. Taylor, I.W. Kellaway, and B. Stevens, *Pharm. Res.* **6**, 633–636 (1959).
54. I.W. Kellaway and F. Farr, *Adv. Drug Delivery Rev.* **5**, 149–161 (1990).
55. P. Couvreur, E. Fattal, and A. Andrernont, *Pharm. Res.* **8**, 1079–1086 (1991).
56. R.S. Gonzalez-Rothi, S. Cacace, L. Straub, and H.E. Schreier, *Lung Res.* **17**, 687–705 (1991).
57. P. Clothorpe et al., *Pharm. Res.* **9**, 764–768 (1992).
58. F.-Y. Liu, Z. Shao, D.O. Kildsig, and A.K. Mitra, *Pharm. Res.* **10**, 228–232 (1993).
59. P.K. Gupta and C.T. Hung, *J. Microencapsul.* **4**, 427–462 (1989).
60. M. Haghapanab, G.P. Martin, and C. Marriott, in J. Hadgraft, I.W. Kellaway, and G.D. Parr, eds., *Proceedings of the Second United Kingdom Association of Particle Scientists Annual Conference*, STS, Cardiff, Wales, 1993, p. 74.
61. X.-M. Zeng, G.P. Martin, and C. Marriott, *Int. J. Pharm.* **109**, 135–145 (1994).
62. X.-M. Zeng, C.P. Martin, and C. Marriott, *Eur. J. Pharm. Sci.* **3**, 87–93 (1995).
63. R.S. Langer, *Science* **249**, 1527–1533 (1990).
64. Int. Pat. Appl. No. PCT/GBS7/00566 (1988), R.N. Boyce, T.R. Tice, R.M. Gilley, and K.L. Pledger.
65. T.R. Tice, D.W. Mason, and R.M. Gilley, in L.F. Prescott and W.O. Nirruno, eds., *Novel Drug Delivery and its Therapeutic Application*, Wiley, New York, 1989, pp. 223–235.
66. L. Masinde and A.J. Hickey, *Pharm. Res.* **8**, 5–12 (1991).
67. Y.L. Lai et al., *Pharm. Res.* **10**, 119–125 (1993).
68. L. Molteni, *Methods Enzymol.* **112**, 285–299 (1985).
69. A.S. Williams and G. Taylor, *Int. J. Pharm.* **83**, 233–239 (1992).
70. E. Tomlinson, in L.F. Prescott and W.S. Nimino, eds., *Novel Drug Delivery and its Therapeutic Application*, Wiley, New York, 1989, pp. 257–259.
71. D.H.W. Ho et al., *Drug Metab. Dispos.* **16**, 27–29 (1988).
72. H. Kawaguchi et al., *Biomaterials* **7**, 61–66 (1986).
73. Y. Tabata and Y. Ikada, *Biomaterials* **9**, 356–362 (1988).
74. S. Rudt and R.H. Muller, *J Controlled Release* **22**, 263–272 (1992).
75. D.A. Edwards et al., *ACS Symp. Drug Delivery 21st Century*, Annaheim, Calif, March 23, 1999.

SYNTHETIC VASCULAR GRAFTS AND CONTROLLED-RELEASE TECHNOLOGY

MARK R. KREITZ
Brown University
Providence, Rhode Island

KEY WORDS

Amikacin
Antibiotic
Controlled-release drug delivery
Expanded poly(tetrafluoroethylene) (ePTFE)
Heparin
Microsphere
Poly(ethylene terephthalate) (Dacron)
Polyurethane
Teflon
Vascular graft

OUTLINE

Introduction
Early Investigations
The Introduction of Synthetic Vascular Grafts
Small-Diameter Synthetic Graft Success or Failure
  Biology of Small-Diameter Vascular Graft Failure
  Materials
  Porosity
  Compliance Matching and Blood Flow Patterns
Cell Seeding and Other Graft Modifications
Polymeric Controlled Release
  Vascular Grafts and Controlled Release
Tissue-Engineered Vascular Grafts
Summary
Bibliography

INTRODUCTION

The design of artificial organ systems typically incorporates those functions necessary for successful organ substitution and, if technology and circumstance permits, those of less critical value. Synthetic vascular grafts are replacements for organs of some chemical and physiologic complexity, but as a vessel substitute, their primary function is to provide a durable, relatively nonthrombogenic conduit for blood. Current larger-diameter vascular grafts accomplish this design goal remarkably well with simple synthetic materials. In smaller-diameter synthetic grafts, where the same synthetic materials perform less well, the absence of complex function may predispose them to failure. The abilities of controlled-release technologies may be able to compensate for the lack of some functions in smaller-diameter synthetic vascular grafts. This article will provide a limited review of the history of vascular grafts, the achievements of synthetic grafts of the past few decades, and some specific applications of controlled-release technology to synthetic grafts.

EARLY INVESTIGATIONS

In 1906 substitutive medicine made its debut into the emerging field of vascular surgery when, during a procedure to remedy a popliteal aneurysm, J. Goyanes replaced the degenerate vessel with a segment of autologous popliteal vein (1). The following year E. Lexer used this approach to repair an axillary artery gap defect with a saphenous vein (2). It could not have been known at the time but this seemingly intuitive resolution, the substitution of an autologous vein for a diseased or damaged artery, would become a preferred and commonplace solution in thousands of annually performed vascular surgeries many decades later. In part, such bold procedures owed their success to the endeavors in vessel repair of many surgeons of the prior three decades (3), but especially to Alexis Carrel, whose defining techniques on vascular anastomoses and philosophies concerning minimal trauma, meticulousness, and asepsis would illuminate the field and win him the Nobel Prize.

The following years witnessed radical and often disastrous attempts at vascular restitution. During World War I, desperate repairs of British soldiers' vascular injuries were sometimes attempted with silver tubes lined with paraffin while, across the battlefield, fresh cadaveric arterial and venous homografts were sutured into wanting German soldiers (2). Though patency of the silver tubes persisted in a few rare instances, the great majority of these and the homografts failed after thrombus formation. The use of paraffin-lined silver tubes as vascular substitutes was not as unconventional as would first appear because "foreign material" implant precedents, such as paraffined and gold-plated aluminum (4), glass (5), and even ivory (3) did exist.

During the following decades, novel vascular surgical concepts and practices were advanced but were concerned more with suture technique and repairing rather than replacing defects. It was not until the post–World War II era that as a result of many factors, vascular substitution again became a popular avenue of investigation. These factors—a growing need for an adequate vascular replacement, the proliferation of surgical research laboratories, the advent of arteriography, the expansion of blood banks, anticoagulant therapy, and the sudden abundance of military surgeons eager to return to career pursuits—invited vascular surgical discovery (3,6).

In 1947, Hufnagel reported on the use of methyl methacrylate (Lucite™) conduits in the "permanent intubation"

of aortas of mongrel dogs, citing the material's strength, smoothness, ready availability, low cost, low tissue response, and its delaying of coagulation times as justifications for its selection (7). These arterial prostheses, 1–3 cm in length, remained patent until the scheduled dates of sacrifice and autopsy, this being from 6 h to 6 months. In 1948, homografts again emerged as though the reasons for past failures were no longer applicable. This time, however, experimental processing was performed on the harvested vessels in hopes of improving the results. After storage in a chilled, isotonic saline solution containing 10% human serum, Gross et al. implanted arterial homografts in humans and dogs in an attempt to correct cardiovascular defects (8,9). In 1952 and 1953, Dubost et al. (10) and Oudot (11), respectively, performed and reported on homograft replacements in human subjects, and others soon followed (12–14).

THE INTRODUCTION OF SYNTHETIC VASCULAR GRAFTS

The replacement of natural vessels with synthetic fabric conduits began somewhat serendipitously in 1947 after Voorhees noted the formation of a "glistening" coat on a silk suture that had remained in the ventricle of the heart of a dog for months (3). From this he reasoned that a fabric mesh formed into a tube and implanted as an arterial replacement would be similarly coated. Shortly thereafter, scraps of a parachute were fashioned into tubes on a home sewing machine and implanted. Following this, tubes fabricated from what was a more biologically preferred material, Vinyon N (vinyl chloride-acrylonitrile), were implanted into 15 mongrel dogs (15). In 1954 18 patients with aneurysms had defective vascular segments replaced with synthetic grafts (2). This experimentation, suggesting a new direction in vascular prosthesis exploration, came a few years prior to reports highlighting the less-than-adequate long-term performance of arterial homografts. Degeneration of the homograft, rather than progression of the patient's disease, was believed responsible for the 70% occlusion rate observed (2). In 1955, Szilagyi had reported on the treatment of arterial occlusion by resection and replacement with arterial homografts (14), but in 1957, after 2 years of experimentation in close to 400 dogs, his group had abandoned such homografts in favor of poly(ethylene terephthalate) (PET), or Dacron®, grafts (16). In a 1957 report on the fate of human arterial homografts, Szilagyi et al. predicted that degenerative changes and diminishing tensile strengths in aortic homografts would begin to endanger patients' lives after 5 years (17). In the following year, Linton noted a 40% failure rate in 38 patients during the first 2–3 postoperative years (2).

Now surgeons, harboring a growing dissatisfaction with long-term biologic graft performance and acknowledging the recent success of the implanted synthetic grafts, began viewing synthetic fabrics as a serious alternative for graft manufacture and implementation. This is not to say that biologic grafts were abandoned, but these factors, combined with the often unsuitable state of potential autograft vessels; advancements in surgical technique; and refinements in anticoagulation, antimicrobial therapy, and angiography, invited exploration.

The early explorations, not surprisingly, focused on the choice of material. However, even in the beginning, other graft characteristics were recognized to influence success or failure. After preliminary investigations, Harrison observed a correlation between graft diameter and occlusion and conducted a comparative study on smaller-diameter grafts (<9 mm) of nylon, Dacron, Orlon® (polyacrylonitrile, PAN), Ivalon® (formalized poly[vinyl alcohol], PVA), and Teflon® (poly[tetrafluoroethylene], PTFE), of varying porosities (18). Following implantation into the abdominal aorta and carotid and femoral artery positions of 133 dogs, he witnessed occlusion rates of up to 92% in periods of 6 weeks. He concluded that because none of the grafts satisfactorily maintained patency, these materials would not serve adequately as small-diameter replacements. However, the contributions of unrefined surgical techniques, crude graft constructions, and harsh preparations (e.g., concentrated acid and base washes, bleaching, and melting of cut ends to prevent unraveling) toward the failure rate should be acknowledged. Also, in retrospect, it is easy to recognize the difficulty of maintaining successful grafts in high-resistance/low-blood-flow positions. Even with modern sterilization techniques and surgical procedures, it is difficult to speculate on whether such poor results would be obtained today with similar graft materials.

In the same month and using the same materials, Harrison published results from a similar comparative study, this time on larger-diameter grafts (>9 mm, with 6–7 cm length) as replacements for thoracic aortas in 84 dogs (19). These results were remarkably different, with only 1 of the 84 grafts failing from occlusion. It was determined that Teflon, Orlon, and Dacron performed equally, well but nylon and Ivalon were not suitable graft materials, as some had extensively degraded during the study period. This study was extended to 2–3 years in 10 of these animals with patent nylon, Dacron, Orlon, and Teflon grafts (20). Of the four nylon grafts observed, only one remained patent at 36 months, though subsequent testing revealed an 80% loss of tensile strength in this graft. Again the Teflon, Orlon and Dacron grafts were viewed as superior, having lost no more than 25% of their tensile strength.

In a report the following year on the fate of human aorta replacements, knitted Dacron grafts were found to be superior to those of nylon and Orlon and to homografts as well (21). In 1964, this emerging trend of positive results was reinforced in an analysis by DeBakey et al. (22) of 67 Dacron grafts removed from 58 patients. After thorough visual, histological, and electron microscopy examinations and demonstrated sustained patency and function for many years, his group was convinced that Dacron could serve as an effective arterial substitute. However, it should be noted that many—if not most or all—of these grafts were in medium- to high-flow positions, primarily serving as aortoiliac and femoropopliteal bypasses. This doesn't lessen the significance of these findings concerning the suitability of Dacron, especially because DeBakey's investigations made this fabric an industry standard, but serves only to place them in perspective. The potential of Dacron as small-diameter replacements in humans was illustrated in a clinical note documenting the patency of a small-diameter Dacron graft (3 mm) as a coronary artery bypass

graft at 17 months (23). But as exemplified in a report by Darling and Linton (24) that showed lower-extremity Dacron graft patency rates of less than 10% at 8 years compared with 65% for reversed saphenous vein, prolonged patency of synthetic grafts of this diameter are the exception, not the rule.

The other synthetic fabric that rose to the status of industry standard for vascular grafts, Teflon, was first used with some success in dogs in the early 1950s by Daniel (25). A few years later, Deterling and Bhonslay (26) obtained satisfactory function with a Teflon graft after some initial blood loss. In 1957 Harrison conducted a 6-month trial of Teflon grafts in the thoracic and abdominal aortas in dogs for which he witnessed an average occlusion rate of 8% (27). He noted that the inner surface layer was thinner and that the grafts healed faster than other grafts. Harrison's 1958 investigations with Teflon as material for larger-diameter grafts gave positive results (19,20), while the smaller-diameter Teflon grafts fared poorly (18).

While these results of Teflon grafts are near those of Dacron, there is one characteristic in the healing of Teflon grafts that sometimes lowers its success. Researchers have noted that the neointima formed on Teflon grafts does not always attach strongly and may be displaced with some ease, even after a year (28). This type of dissection would readily facilitate thrombus and emboli formation, originating not just from the loose intima but possibly from the newly exposed biomaterial surface as well.

In 1969, Robert Gore invented expanded poly(tetrafluoroethylene) (ePTFE) (29), a Teflon that when shaped is simultaneously stretched. The stretching, or expansion, produces a microscopic node–fibril–node pattern throughout the material, the lateral spaces between the fibrils forming the pores. This material, which was introduced in vascular grafts a few years later, can be stretched to varying degrees during fabrication, providing control over the degree of porosity in the graft (30).

The initial results with ePTFE were very favorable. Soyer et al. observed the presence of pannus ingrowth at the anastomoses but also noted its poor attachment (31). The following year Matsumoto et al. obtained extremely positive results of 100% patency in femoral artery replacements in dogs when using high-porosity ePTFE grafts in contrast to the 100% occlusion of ultralightweight woven Teflon grafts in the same study (32). These results were difficult to replicate, and as subsequent investigations indicated, the results were still good, though typically not as good as those of Matsumoto et al. The excitement about ePTFE was soon tempered however, as longer-term results began to be reported. Hobson et al. (33) published 30-month patency results of only 45%, compared with 54% for autogenous saphenous vein, in femoropopliteal, femorotibial, and femoroperoneal replacements. In 250 patients who had ePTFE grafts implanted as femoropopliteal artery reconstructions, a patency rate of 74% at 1 year dropped to 56% at 2 and 3 years (34,35).

The years of experimentation with different fabrics and modifications, by virtue of their poorer performance, reinforced these materials and made them the synthetic graft standards. But along the way, the characteristics to which success was attributed were noted, analyzed, and often integrated into general, but not necessarily universal, acceptance. This resulted in part from varying experimental results and in part from the poor results obtained from small-diameter grafts of fabrics that typically yielded good results when used in a larger-diameter graft. Today, the desired features of successful synthetic vascular grafts are, for the most part, standardized.

SMALL-DIAMETER SYNTHETIC GRAFT SUCCESS OR FAILURE

Synthetic vascular graft characteristics thought to be desirable haven't so much changed over the years as they have been refined. It was apparent early on that porosity, hemocompatibility, biocompatibility, sterility, flexibility, compliance, and durability were vital components of a successful graft (2). Today, little in the fundamental requirements has changed. Abbott et al. have recently published a list of preferable characteristics including optimal biomechanical properties, cosmetic acceptability, handling characteristics, sterility, reasonable cost, production consistency, durability, infection resistance, strength, and a thromboresistant flow surface (36). A comparison of preferred characteristics then and now are outlined and matched in Table 1. It is apparent that the major requirements have changed little and that the later additions reflect contemporary capabilities and realities.

Biology of Small-Diameter Vascular Graft Failure

Before exploring and enumerating the features of synthetic fabric grafts that contribute to success, it is appropriate to highlight and understand the mechanisms of graft failure. Beyond the obvious considerations of vascular graft failure attributable to infections, mechanical degradation, preexisting vascular disease progression, and technical errors are those related to the tissue and blood reactions to the implanted material, specifically the hyperproliferative cellular events occurring in and near the graft.

Upon exposure to a foreign material such as a polymer graft, specific blood components respond as if the integrity of a native vessel has been compromised and the endothelium denuded. These components recognize the material as foreign, become activated, and initiate a series of events

Table 1. Comparison of Preferred Synthetic Vascular Graft Characteristics of the 1950s and 1990s

1950s	1990s
Compliance	Biomechanical properties
Durability	Durability
Flexibility	Handling characteristics
Porosity	Porosity
Proper tissue reactivity	Flow surface, biocompatibility
Sterility	Cleanliness and sterility
	Consistency
	Cost
	Cosmetic attributes
	Infection resistance

in an attempt to repair the perceived damage. The first event is the immediate adsorption of multifarious plasma proteins to the entire graft surface, which may remain attached or desorb under the influence of other proteins or blood flow. It is thought that the graft surface can denature the proteins (37) and that these bound, altered protein configurations may bind platelets and initiate their activation. Additionally, direct contact with a foreign surface alone is sufficient to provoke platelet activation (38). Surface fibrin, platelet debris, and red blood cells (RBCs) comprising the newly formed layer, called *pseudointimal hyperplasia*, can lead to clot and thrombus formation, the progression of which could be the short-term failure of a vascular graft.

Subsequent to platelet coverage and activation upon the graft, specific substances are released from the platelets (e.g., platelet-derived growth factor [PDGF], transforming growth factor β1 [TGF-β1], and thrombin) that are chemoattractants and/or growth factors for smooth muscle cells (39). As a component of the vascular tunica media, the smooth muscle cells begin to migrate from the anastomotic vessel wall and progress into the synthetic graft via chemotaxis. On the graft lumen surface, the sustained proliferation of smooth muscle cells with attendant deposition of cellular matrix, collectively termed *intimal hyperplasia*, can develop substantially and narrow or eventually occlude the graft lumen (40). This mode of graft failure typically occurs more frequently at the anastomoses, reflected in the adjusted designation anastomotic hyperplasia.

In as much as synthetic vascular grafts are viewed as foreign surfaces and can effect compliance mismatches and therefore immediately approximate two components of Virchow's triad (endothelial injury, stasis, and hypercoagulability) (41) with the third not far behind, it would seem appropriate that modifications to the graft that eliminate one or more elements of the triad would improve its potential for success.

Materials

As was discovered very early, an unfortunate choice in graft material will doom the fate of the graft and probably the patient. Thus, in the quest for the best synthetic graft fabric, it was realized that not all implanted graft materials and constructs would behave equally. This opened the door to experimentation, and over the past few decades a variety of different synthetic fabrics (usually polymer derived), constructions, textures, and modifications have been evaluated.

Teflon and Dacron grafts remain the most durable ones available and are fabricated in a variety of sizes and constructions, including weaves and knits (42). Primarily because of their durability and stability and secondarily because of their ease of handling and relative lack of thrombogenicity, they are the only synthetic grafts in clinical use today. Their patency rates are fairly good, but they still suffer higher failure rates in low-flow, small-diameter situations.

Many synthetic graft materials have been investigated over the past few decades, and unfortunately, most either exhibited poorer performance than the available (and well entrenched) grafts or demonstrated success based on difficult-to-reproduce fabrication or preparation techniques. Other synthetic grafts appear in the literature with limited claims of success, typically in small animals, and then disappear after failure in larger animals or after long-term studies reveal failures not foreseen in shorter-term studies.

In 1989, Chaikof et al. examined cross-linked poly(ethylene oxide) (PEO)/polysiloxane as a material for small-diameter vascular grafts (4 mm) based on PEO's low protein and cellular adsorption levels (43). Their results confirmed their predictions of low fibrinogen and platelet deposition, but unfortunately, no grafts were implanted. Subsequent research by this group, again without implantation into animals, alternately confirmed these results with similar-molecular-weight PEO (44) and contradicted the original expectations with low-molecular-weight PEO (45).

A few years later, Greisler et al. implanted 5-cm-long, 4-mm-diameter, woven polypropylene grafts in the aortoiliac position in dogs (46). The selection of polypropylene was based on its physical properties of high tensile strength, degradation resistance, and low platelet adhesion. Excellent results were demonstrated with a one-year patency of 92%, compared with 69% for Dacron and 20% for Teflon, but apparently no subsequent investigations were performed.

The genesis of grafts of bioresorbable materials began in the early 1960s when, as a means to control hemorrhaging at the time of implantation, degradable materials were incorporated into existing grafts (47). In subsequent investigations, significant reductions in hemorrhage with comparable patency rates were obtained for gelatin-treated Dacron and Teflon (48), bovine collagen–impregnated Dacron (49), and gelatin-impregnated Dacron (50). This method of preventing postsurgical graft hemorrhage was superseded by the preclotting of grafts with autogenous blood at the time of surgery.

The goal of bioresorbable grafts was, in principle, to provide a temporary scaffold for the ingrowth and permanent structural establishment of native tissues. In 1985, van der Lei et al. studied partially bioresorbable small-diameter grafts composed of mixtures of polyurethane (PU) and poly(L-lactic acid) (PLLA) in rats (51). Of the four PU/PLLA compositions investigated, the 19:1 PU/PLLA mixture yielded the best results, displaying regeneration of neointima and neomedia similar to the native and no aneurysm formation. However, this was virtually a polyurethane graft, which, if fabricated with porosity introduced by another method, would probably have yielded similar results and obviated the need for the degradable polymer.

Greisler et al. took the idea of bioresorption to the limit in 1985 when they constructed grafts solely of polyglycolic acid (PGA) and implanted these and Dacron controls into rabbit aortas for up to 12 months (52). Inflammatory reactions in each were equal, but the neointima that developed in the PGA grafts was three times thicker than that of the controls. Aneurysmal dilation was also observed in 15% of the PGA grafts, while none was seen in the controls. Two years later, as a means to prevent aneurysmal dila-

tion, Greisler et al. (53) constructed woven grafts from yarns of bioresorbable polyglactin 910 (PG910) and nonresorbable polypropylene in a 69:31 ratio. Forty-two grafts were implanted into the infrarenal aorta position in rabbits and were explanted from 2 weeks to 12 months later. These grafts fared better than the completely bioresorbable grafts, showing 100% patency, no aneurysm formation, and stenosis in only one graft.

In 1988, Galletti et al. (54) experimented with fully bioresorbable Vicryl prostheses that were coated with either of two blends of bioresorbable polymers, which were included to retard the Vicryl fabric degradation time. Eighteen grafts were implanted in the infrarenal aorta position in dogs and were explanted from 3 days to 24 weeks later. Upon explanation, 14 of the 18 grafts were patent, though generally a neointimal thickness of 2–3 times that seen in similarly implanted Dacron grafts was observed. Resembling previous studies of Greisler et al. (52,55) and Bowald et al. (56,57), no elastin was found in the grafts, a consequence thought to be due to the graft rigidity inhibiting elastin expression (54). Aneurysm formation was observed in two of the animals.

Though a completely bioresorbable graft is an ideal, it was an optimistic assumption that the eventual tissue content and arrangement would resemble natural blood vessels in form and function. Unfortunately, these newly formed quasi vessels instead often possessed discordant tissue compositions and failed to maintain the necessary mechanical integrity. Frequent tissue degradation and aneurysm formation were commonly the reason for failure of these grafts.

In the search for an optimal small-diameter graft material, polyurethanes have generated tremendous excitement. These polymers can possess outstanding strength, flexibility, and fatigue resistance (58). Their consideration as a small-diameter graft material arose from concerns of compliance matching and investigations into polymers that preferentially bound albumin instead of fibrinogen, the binding of the latter correlating to thrombogenesis (47). In very early research, Dryer et al. implanted polyurethane foam grafts as aorta replacements in 16 dogs and obtained patency in 13 of the 16 for up to 6 months (59). Using the same polyurethane, Marinescu et al. implanted grafts in canine aortas that lasted for up to 10 years (60). Though minor, this inconsistency in patency results of different researchers could be attributable to surgical experience. In later earliest investigations, Lyman et al. (61) prepared porous, 4-mm-i.d. *co*-polyether-urethane-urea (PEUU) grafts that were implanted in the femoral artery position of 20 dogs. Upon removal, from 10 to 111 days later, 45% of the grafts were patent, comparing favorably with 6-mm-i.d. Dacron and solid-wall, noncompliant PEUU grafts that demonstrated almost zero patency in similar implant situations. These results are appreciably different from those of Dryer et al. and Marinescu et al. and could be due to polyurethane composition, which can vary tremendously between different polyurethanes. Alternately, the smaller graft diameter or the different surface morphology of the grafts could have been the determining factor.

Polyurethane grafts have been fabricated by a variety of unique methods other than the typical weaving or knitting. Annis et al. used an electrostatic spinning method to produce 10-mm-i.d. fibrous, porous poly(ether urethane) grafts, which were implanted in the thoracic aorta position in 42 minipigs (62). Of the 42 grafts, 4 failed due to "faults in the material," and the others remained patent for up to 12 months with no observed aneurysm formation. Hiratzka et al. (63) created polyurethane grafts with a replamineform process whereby machined, microporous, 6-mm-diameter sea urchin spines (tubes) of calcite acted as a templates into which polyurethane was injected. The calcite was dissolved away, leaving a microporous polyurethane tube as a form inversion of the template. These 3-cm-long grafts were implanted in the infrarenal position of dogs and explanted from 1 to 32 weeks later. At the time of removal, all grafts were patent with complete tissue ingrowth and no aneurysmal dilation, though complete endothelial coverage of the lumen was not observed in grafts explanted prior to 16 weeks.

It is believed by many that complete endothelial coverage would render synthetic vascular grafts nonthrombogenic and therefore greatly improve their chances for long-term patency. For unknown reasons, in humans the endothelial pannus ingrowth into the graft from the anastomoses almost always ceases after progressing a few centimeters. Because complete graft endothelialization usually occurs in nonhuman animals but not in humans, incomplete endothelialization of an experimental graft in animals *may* suggest potential failure for this graft in humans.

In 1983, Hess et al. published their results about implanted small-diameter, fibrous polyurethane prosthesis in the abdominal aorta of rats, focusing on the endothelialization process (64). Forty-seven of these 1.6-mm-i.d. grafts were implanted in place of abdominal aorta segments in rats and were explanted after 1 to 25 days and at 6 and 9 months with a patency rate of 91%. Endothelialization began at 5 days and progressed at 0.3 mm per day until day 21, when coverage was complete. In a similar investigation published the same year, Hess et al. (65) described the cells comprising the pannus ingrowth as a combination of layers of smooth muscle cells covered by a continuous endothelium.

The experimental successes of polyurethanes as small-diameter grafts has encouraged their commercial development. Physical and chemical comparisons of a novel microporous polyurethane graft (Vascugraft®) to another microporous polyurethane graft (Mitrathane® prosthesis) and to a microporous ePTFE graft (Gore-tex®) were made by Zhang et al. (66). The resulting favorable analyses and conclusions prompted larger-diameter graft (10 mm i.d.) implantations as thoracoabdominal bypasses in dogs, which yielded mostly positive results (67,68). With awareness of minor concerns raised in the canine studies, 15 femoropopliteal and femoroperoneal Vascugraft bypasses were performed in humans (69). Unfortunately, 8 of the 15 grafts failed during the first year, and the research program was ended by the manufacturer.

Porosity

Even in the first application of synthetic fabric grafts, Voorhees hypothesized on the benefit that porosity would contribute to healing. By 1964, vascular surgeons and researchers believed that the fate of a synthetic graft would be resolved, for better or worse, by its porosity (70). It was and is thought that anchoring of the neointima to the lumen surface would sustain the health of the neointima. Tissue and capillary ingrowth into the external graft surface are believed to stabilize the graft in situ and to supply the tissue ingrowth, and possibly the neointima, with oxygen and nutrients, respectively (71,72). Improved performance of porous synthetic grafts over nonporous grafts was observed early on (73).

In 1964 Fry et al. (74) reviewed case histories of patients who, after having received nonporous Teflon grafts in the aortoiliac position, suffered from complete occlusion of the grafts at 2 months to 3 years postimplantation. At reoperation it was discovered that the neointima of the Teflon grafts had separated from the prosthetic surface and caused thrombosis. Most of the patients then had woven, porous grafts implanted.

Hermansen et al. analyzed two types of Dacron grafts to assess the influence of their markedly different porosities on the viability of the neointima (71). Although dislodged neointima was attributed to the lower porosity in those grafts, no pronounced histological differences were seen. In a study on porosity and healing, White found minimal tissue ingrowth in grafts with pore sizes less than 15 μm, fibrohistiocytic tissue incorporation in grafts with pore sizes of 15–45 μm, and organized fibrous tissue incorporation in grafts with pore sizes greater than 50 μm (75).

Using the graft fabrication technique of Soldani et al. (76), which involves the phase inversion of polyurethane onto a rotating mandrel, Okoshi et al. (77) compared nonporous versus porous graft inner-surface morphologies. After explanation from rat abdominal aortas, the patency rates for the grafts with "skinned" and porous surfaces were 0 and 72% at 2 weeks, respectively, and 0 and 8% at 3 months, respectively. The lower-than-expected patency rate of the porous grafts prompted fabrication of grafts with highly porous inner surfaces, which showed a patency rate of 73% at 3 months.

An interesting and simple way of inducing custom pore sizes during the fabrication of polyurethane grafts was demonstrated by Fujimoto et al. in 1993 (78). Mixtures of polyurethane and monodisperse salt crystals were extruded as 3-mm-i.d. tubes, wrapped with Spandex yarn, and then coated with the same polyurethane/salt mixture. After evaporation of the solvent, the formed tubes were immersed in water to dissolve away the salt. Grafts with average pore sizes from 1.7 to 30 μm were fabricated and implanted into the common carotid arteries of dogs and explanted at 1, 2, and 6 months. All of the grafts with an average pore size of less than 5 μm were occluded by 1 month, while those with a 5- to 30-μm average pore size were patent at 2 months. All of the grafts with average pore size of 30 μm were patent at 6 months as well.

Compliance Matching and Blood Flow Patterns

When anastomotic hyperplasia was observed as a separate phenomenon from general neointimal hyperplasia, it was speculated that host artery/graft differences might have contributed to the failures (79). The difference in compliance between the artery and the graft was one factor thought to affect anastomotic blood flow patterns, which would induce higher shear stresses. This postulate, combined with animal data suggesting a relation between compliance and patency, led to experimentation with more elastic materials in the hope that similar compliances would avert the previously observed hyperplasia. Materials such as latex, Silastic, fluoroelastomers, and hydrocarbon rubbers were investigated, but any benefits derived from similarities in compliance were overshadowed by the thrombogenic effects of the materials, most of which failed (47). It was realized that one desired graft characteristic, however necessary it is thought to be, should not be sought at the expense of others.

Additionally, too often conclusions were drawn after comparisons between less compliant synthetic grafts and more compliant autografts (80). This was the case in a publication by Walden et al. that compared patency rates of various processed and unprocessed natural vessels with Dacron and ePTFE grafts (81). The attribution of an effect to one factor, in a comparison of grafts with multiple differences, is inappropriate. Regardless of the correlations, the conclusions derived from such flawed experimental schemata lack validity.

Lyman et al. examined the patency of otherwise similar small-diameter (4-mm-i.d.) copolyurethane compliant and noncompliant grafts in dogs (82). Although six of the nine compliant grafts were patent upon removal (at up to 77 days), most of the noncompliant grafts failed within 48 hours. In contrast to findings such as these, Annis et al. saw very little patency difference between polyurethane grafts with greater and lesser compliances (83). In this investigation it seems that the compliance of the less compliant grafts was sufficient for equal performance and was not low enough to effect a difference.

In consideration of compliance as a cause of vascular graft deficiency, as with any complex system, there is not always just one well-defined mode of failure. In a statistical investigation of reported vascular graft failures over a 30-year period, Pourdeyhimi et al. (84) concluded that the second leading cause of graft failure was compliance. However, the route to failure was not the expected compliance mismatch, inducing turbulent flow and leading to thrombosis path. Instead, suture line failure due to compliance mismatch, occurring mostly between 30 and 50 months, was the reason for the graft failures.

CELL SEEDING AND OTHER GRAFT MODIFICATIONS

With the incredible numbers of surface-modified vascular grafts and other experimental grafts studied and reported on every year, it may appear as though investigators have acknowledged the limitations of plain polymeric materials in their performance as synthetic vessels. This may be true, or there may be other reasons behind this growing direction in graft research. Possibly some biomaterials searches, now extending past those commonly available and inexpensive and in light of a looming biomaterials lit-

igation crisis, are simply too costly in time and money to pursue. Also, potential elements of a synthetic graft that were once assumed relatively inconsequential may now be thought significantly influential. Or it simply may be that new ideas for grafts appear as technologies progress. Each of these reasons may be the motivation pushing researchers in different directions, or more likely, it is a combination of all of these reasons.

Speculation may have been expressed that because endothelial cells wouldn't completely cover the inner surface of a synthetic vascular graft in a human after implantation, an application of cells prior to graft implantation might improve long-term cell coverage. Cell seeding is the application of endothelial cells in a physiologic medium such as whole blood to a vascular graft and was first attempted on microfiber scaffolds in vitro by Burkel and Kahn in 1977 (85). The popularity of endothelial cell seeding arose from Herring's single-staged method, published in 1978 (86). In his procedure, he scraped endothelial cells from veins of dogs, mixed them with whole blood, and preclotted Dacron prostheses with the mixture before implanting them. In his 1978 report, 12 6-mm-i.d. Dacron grafts were implanted into the infrarenal aortas of dogs, half of which were seeded. Upon explantation at 2, 4, and 8 weeks, the seeded grafts displayed a higher percentage of clot-free surface (76% versus 31%), and Herring concluded that the formed lining was biologically superior to that which developed in the unseeded grafts. As an extension of this technique, Graham used cultured endothelial cells for seeding (87) and in 1982 performed this procedure with 25-cm-long (6- and 10-mm-i.d.) ePTFE grafts in dogs (88). The seeded grafts showed 64 and 91% endothelial cell surface coverage at 2 and 4 weeks, respectively, while the endothelial cell surface coverage of unseeded grafts never exceeded 10%.

In 1987 Emerick et al. determined that up to 90% of the endothelial cells seeded onto a graft are washed away in the first 24 hours (89). Consequently, additional modifications to the cell-seeding procedure, aimed at better endothelial cell retention, have been developed. A few of these are fibronectin (90), Transglutine (a biological glue) (91), and short peptide sequence (92) coatings of grafts prior to seeding. However, these techniques are more modifications of the graft than of the seeding procedure itself.

Other graft modifications focused on changing the graft surface so as to reduce thrombogenicity, prevent infection, induce endothelial cell coverage and retain the cells after coverage, and inhibit specific cell growth. Many of these techniques involve the bonding or application of specific materials or drugs to graft lumen surface to achieve the desired effect, while others employ somewhat unconventional techniques.

Greisler et al. fabricated an interesting small-diameter graft that harnessed the desirable surface properties of Teflon and the bulk properties of Dacron (93). In this study, gaseous tetrafluoroethylene (TFE) monomer was covalently bound to Dacron grafts by radio-frequency plasma discharge, creating a compound graft. Sixty-six grafts, including controls, were implanted into canine aortas (6-mm-i.d. grafts) and carotid arteries (4-mm-i.d. grafts). However, the TFE-coated PET grafts did not demonstrate significantly better performance than the similarly implanted controls.

For a long time it has been thought that capillary ingrowth into the graft wall might be a source of the endothelial coverage on the lumen surface (94). In an effort to induce this ingrowth, Noishiki et al. infiltrated the graft walls with autologous bone marrow cells and implanted these grafts into dogs (95). At all time points past 3 weeks, the marrow-infiltrated grafts showed complete endothelialization and patency, whereas noninfiltrated control grafts demonstrated endothelial coverage only at the anastomoses.

Heparin bonding to the inner surfaces of vascular grafts has been attempted by different researchers hoping to reduce the incidence of thrombogenesis. Esquivel et al. (96) ionically and covalently bonded heparin to polyurethane (PU) and ePTFE grafts (6 cm long and 4 mm i.d.) and implanted these into the carotid arteries of sheep. The results showed reduced early thrombogenicity in both types of grafts with covalently bound heparin and in ionically bound heparin PU grafts though not in ionically bound heparin ePTFE grafts. Unfortunately, this method has shown only sporadic success in humans.

Synthetic graft infection carries far greater risk for the patient than focal infections in other areas of the body (97) and has resulted in limb amputation and patient death (98). The bacteria, which may be otherwise negligible in number at the beginning, can gain a foothold in the fabric interstices of grafts. There, protected from the reach of the immune system, the bacteria multiply virtually unchallenged. Today, infections of vascular grafts almost always necessitate their removal, an invasive procedure with unavoidable risks. Although some infections arise systemically, far past the date of implantation, others result from inadvertent contamination during implantation or the postoperative period. Short-term infection prevention would be welcome and may be possible.

Through methods similar to heparin bonding, antibiotics have been bonded to graft surfaces to prevent graft infections. Moore examined the effectiveness of amikacin bonded to 6-mm-i.d. Dacron grafts in preventing graft infection in dogs (99). After the grafts were implanted in the abdominal aorta, approximately 10^8 *Staphylococcus aureus* bacteria were administered intravenously. Infections were observed in only 8% of the experimental grafts versus 100% in the control grafts.

POLYMERIC CONTROLLED RELEASE

Conventional drug delivery methods are inherently inefficient. Typical bolus administrations often require repeated dosing to sustain drug levels within the therapeutic range, a waste of sometimes costly drugs. To ensure delivery of a sufficient quantity of drug to the intended organ(s), increased dosages can be required. Additionally, specific methods of administration (e.g., injections) can be painful. These combined factors can easily induce stress and avoidance behavior in patients, reducing their compliance and increasing their risk of prolonged illness or worse.

Through drug delivery systems, the controlled release of therapeutics offers significant advantages over conven-

tional delivery methods of drug administration. Controlled-release devices can deliver drugs at a steady rate for extended periods of time, minimizing deviations from the therapeutic range and the need for repeated administrations. Localized controlled-release devices serve to reduce the amount of drug necessary. Oral and topical controlled-release formulations obviate the need for injections. The advantages of controlled-release devices increase patient compliance, reduce drug wasting, and save money for the manufacturer and the patient.

Vascular Grafts and Controlled Release

If synthetic materials are to succeed as small-diameter grafts, then closer approximation to a natural vessel is required. One function of a vessel that could be simulated in a synthetic graft is the controlled release of chemicals that influence the vessel's environment. Cell seeding may loosely be considered a form of controlled drug release from a synthetic graft because the seeded cells invariably secrete specific chemicals. However, the definition, as it is applied here, will include only the release of drugs from nonliving constructs.

Sometimes a sustained presence of antibiotics around an implanted graft is desired. With or without parallel prophylactic systemic administration, localized controlled release of antibiotics to or from the synthetic graft is one option. Ney et al. investigated this method of therapy with grafts that had been intentionally infected with solutions containing *Escherichia coli* and *S. aureus* and then implanted into the infrarenal aorta position in dogs (100). Prior to closure of the surgical wound, low-dose (100 mg antibiotic) or high-dose (300 mg antibiotic) amikacin-loaded biodegradable microspheres were applied topically to the vascular grafts. When the grafts were explanted and analyzed 14 days later, 88% of the control grafts (no administration of antibiotics) manifested clinical infections, while none of the treated grafts demonstrated clinical infection. However, two of the eight grafts treated with the low-dose microspheres did test positive for cultures of *S. aureus*.

Also, growth factors and other drugs have been openly and loosely incorporated into vascular grafts although not specifically engineered as controlled-release devices. In 1991 Soldani et al. fabricated small-diameter polyurethane grafts with an incorporated mixture of nonencapsulated albumin and basic Fibroblast Growth Factor (bFGF) particles (101). After an initial burst, the graft showed fairly constant release for 2 weeks, although the cumulative levels never exceeded 20% of the total amount incorporated.

In an effort to facilitate endothelialization and maintain patency, Lado et al. applied a biodegradable carrier polymer containing platelet-derived angiogenesis fraction (PDAF) to the inner surfaces of 2-mm-i.d. PTFE grafts (102). Twenty-four grafts, 12 experimental and 12 control, were implanted. After a 3-week initial implant period in the retroperitoneum of rats, the grafts were in situ anastomosed, end to side, into the abdominal aorta. Though capillary and tissue ingrowth differences were seen, no significant differences were observed between the treated and untreated grafts. A similar investigation by Greisler et al. (103), with fibrin glue containing fibroblast growth factor (FGF) applied to ePTFE grafts, demonstrated release of the FGF to 30 days. Capillary ingrowth and endothelial cell proliferation promoting endothelialization of the graft was observed. Similar techniques involving the controlled release of therapeutics from tubular structures such as vascular grafts have been patented (104).

Richey and Harris (105) examined the effect on in vitro platelet adherence of controlled-release indomethacin (IM) and aspirin (ASA) from PLA/PLGA-blend microspheres present in the pores of ePTFE discs (1.5 cm diameter). The samples were placed into tissue culture dishes with phosphate-buffered saline for periods of 2 h, 4 days, and 14 days. After these periods of drug release, the samples were exposed to a platelet preparation for 1 h and rinsed, at which time platelet adherence was measured. After 2 h the platelet adherence of the four experimental samples (10 and 20% loaded IM and ASA) was less than that of the controls, though only the two samples with 20% loaded microspheres demonstrated significant differences. The other time points showed similar, though not significant, differences.

Kreitz et al. describe the construction and characterization of controlled-release synthetic vascular grafts without and with incorporated biodegradable polyester microspheres, as shown in Figure 1. Using a modification of the spray–phase inversion technique of Soldani et al. (76), microporous polyurethane grafts were fabricated with heparin-loaded poly(lactic-*co*-glycolic acid) (PLGA) microspheres incorporated into the walls of the grafts (106,107). The controlled release of heparin is intended to inhibit smooth muscle cell (SMC) proliferation in the vascular grafts. Characterizations revealed PLGA degradation over 2–3 months, but with a very rapid heparin release. This was thought to be due to the use of water as a nonsolvent in the graft fabrication process, the extreme water solubility of heparin, and pores in the microsphere coatings of the heparin. Subsequently, an alternate nonbiodegradable controlled-release system was devised for the same graft fabrication technique. Heparin release from these grafts observed over 1–2 months was adequate to effect inhibition of SMC proliferation in vitro.

Therapeutics other than solids have been employed for controlled release to the vascular graft environment. Pulfer et al. (108) used cross-linked polyethyleneimine microspheres to release nitric oxide (NO), a reported inhibitor of thrombus formation, from Gore-tex grafts in vitro. Release from microspheres alone demonstrated nearly linear release of NO over 1 week, whereas the microspheres incorporated into the graft released substantially lower amounts of NO in less time. Because a mixture of microspheres was used, some with lower NO loadings, the results of NO release from the grafts were not unexpected.

TISSUE-ENGINEERED VASCULAR GRAFTS

It is ironic that after so many years of pursuing perfection of small-diameter synthetic vascular grafts, investigation should again turn to natural vessels, albeit in a different way. Researchers may have recognized evolution's power

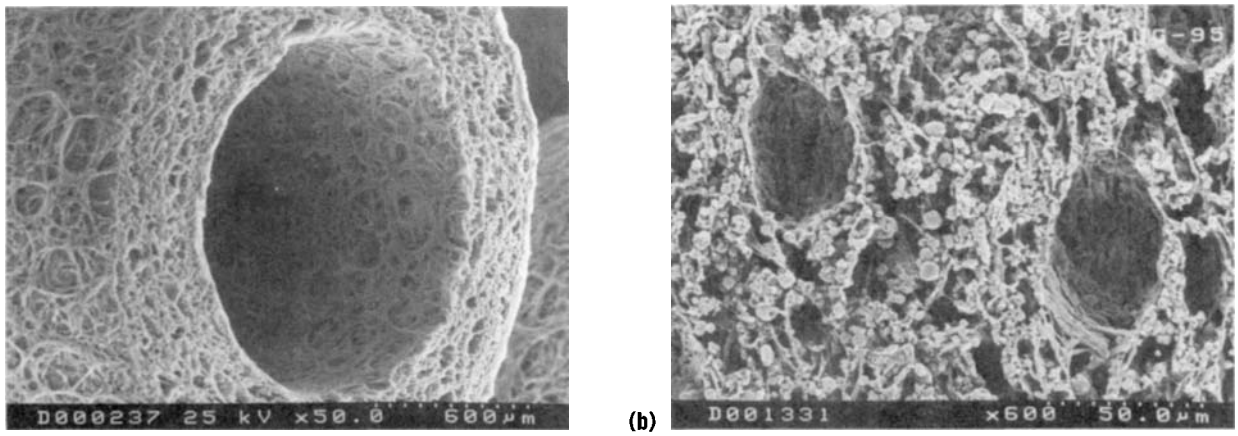


Figure 1. Scanning electron micrographs of vascular grafts produced by the spray–phase inversion process. (**a**) Micrograph shows the microfibrillar structure and porosity of the inner and outer surfaces (magnification 50×). (**b**) Micrograph of a cross section of a composite vascular graft fabricated with spray-dried polyester microspheres. The large quantity of spray-dried polyester microspheres are visible (magnification 150×).

to achieve what they yet cannot, and consequently have begun to focus on recreation instead of simulation. These new vessels are not harvested from animals or humans but rather engineered in the laboratory from human cells. L'Heureux et al. (109) produced tubular structures with three layers of cells, fibroblasts, smooth muscle cells, and endothelial cells, emulating in a natural vessel the adventitia, media, and intima, respectively. Positive indications of comparative function such as expression of von Willebrand factor, incorporation of acetylated low-density lipoprotein, and production of prostacyclin were observed in vitro. The burst strength capacity of this TEBV compared favorably with natural vessels, in contrast to a similar tissue-engineered blood vessel (TEBV) (110) previously constructed by others. In the L'Heureux TEBVs intended for implantation, the endothelial cell component was excluded to lessen the possibility of acute rejection. These human cell–derived TEBVs were implanted into the femoral artery position in dogs and when explanted 7 days later, they xenografts showed a 50% patency rate.

SUMMARY

With refinements in materials, surgical techniques, and related peripheral technologies, the performance of vascular grafts has improved since the initial trials in the 1950s. Though the currently used synthetic materials perform adequately as clinical larger-diameter vascular prostheses, their lack of sufficient antithrombogenicity becomes evident in smaller-diameter grafts. A variety of experimental materials and modifications to existing materials have resulted in limited successes, as have some novel biologically derived grafts. The application of controlled-release technology to smaller-diameter synthetic vascular grafts offers the possibility of emulating some of a natural vessel's functions, which may prove critical for maintaining patency.

BIBLIOGRAPHY

1. D.N. Ku and R.C. Allen, in J.D. Bronzino, ed., *The Biomedical Engineering Handbook*, CRC Press, Boca Raton, Fla., 1995, pp. 1871–1878.
2. A.D. Callow, in J.C. Stanley et al., eds., *Biologic and Synthetic Vascular Prostheses*, Grune & Stratton, New York, 1982, pp. 11–26.
3. A.B. Voorhees, Jr., *Arch Surg. (Chicago)* **120**(3), 289–295 (1985).
4. A. Carrel, *Surg Gynecol. Obstet.* **15**, 245–248 (1912).
5. R. Abbe, *N.Y. Med. J.* **59**, 33–40 (1894).
6. A.D. Callow, in A.D. Callow and C.B. Ernst, eds., *Introduction: Vascular Surgery: Theory and Practice*, Appleton & Lange, Stamford, Calif., 1995, pp. xxii–xxxv.
7. C.A. Hufnagel, *Arch. Surg. (Chicago)* **54**, 382–389 (1947).
8. R.E. Gross, E.S. Hurwitt, A.H. Bill, and E.C. Pierce, *N. Engl. J Med.* **239**, 578–579 (1948).
9. R.E. Gross, A.H. Bill, and E.C. Pierce, *Surg. Gynecol. Obstet.* **88**, 689–701 (1949).
10. C. Dubost, M. Allary, and N. Oeconomos, *Arch. Surg. (Chicago)* **64**, 405–408 (1952).
11. J. Oudot and P. Beaconsfield, *Arch. Surg. (Chicago)* **66**, 365–374 (1953).
12. M.E. DeBakey, O. Creech, and D.A. Cooley, *Ann. Surg.* **140**, 290–310 (1954).
13. O.C. Julian et al., *Ann. Surg.* **138**, 387–403 (1953).
14. D.E. Szilagyi, R.F. Smith, and P.R. Overhulse, *JAMA*, **157**, 426–433 (1955).
15. A.B. Voorhees, A. Jaretzki, and A.H. Blakemore, *Ann. Surg.* **135**(3), 332–336 (1952).
16. D.E. Szilagyi, *Ann. Vasc. Surg.* **1**(3), 357–363 (1986).
17. D.E. Szilagyi, R.T. McDonald, and R.F. Smith, *Arch. Surg. (Chicago)* **75**, 506–509 (1957).
18. J.H. Harrison, *Am. J. Surg.* **95**, 3–14 (1958).
19. J.H. Harrison, *Am. J. Surg.* **95**, 16–24 (1958).

20. J.H. Harrison, *Surg. Gynecol. Obstet.* **108**, 433–438 (1959).
21. B. Halpert, M.E. DeBakey, G.L. Jordan, and W.S. Henly, *Surg., Gynecol. Obstet.* **111**(6), 659–674 (1960).
22. M.E. DeBakey et al., *Arch Surg. (Chicago)* **89**, 757–782 (1964).
23. L.R. Sauvage, R. Schloemer, S.J. Wood, and G. Logan, *J. Thorac. Cardiovasc. Surg.* **72**(3), 418–421 (1976).
24. R.C. Darling and R.R. Linton, *Am. J. Surg.* **123**, 472–479 (1972).
25. W.W. Daniel, *Cancer (Philadelphia)* **5**, 1041–1048 (1952).
26. R.A. Deterling and S.B. Bhonslay, *Surgery* **38**(1), 71–91 (1955).
27. J.H. Harrison, *Surg. Gynecol. Obstet.* **104**, 81–87 (1957).
28. C.A. Kottmeier and M.W. Wheat, *Am. Surg.* **31**, 128–134 (1964).
29. B. Boyce, in J.C. Stanley et al., eds., *Biologic and Synthetic Vascular Prostheses*, Grune & Stratton, New York, 1982, pp. 553–561.
30. L.M. Graham and J.J. Bergan, in J.C. Stanley et al., eds., *Biologic and Synthetic Vascular Prostheses*, Grune & Stratton, New York, 1982, pp. 563–586.
31. T. Soyer, M. Lempinen, and P. Cooper, *Surgery* **72**, 864–872 (1972).
32. H. Matsumoto et al., *Surgery* **74**(4), 519–523 (1973).
33. R.W. Hobson, J.A. O'Donnell, and Z. Jamil, *Arch. Surg. (Chicago)* **115**, 833–837 (1980).
34. M. Haimov, F. Giron, and J.H. Jacobson, *Arch. Surg. (Chicago)* **114**, 673–677 (1979).
35. V. Echave, A.R. Koornick, and M.E.A. Haimov, *Surgery* **86**, 791–798 (1979).
36. W.M. Abbott et al., *J. Vasc. Surg.* **17**(4), 746–756 (1993).
37. J.D. Andrade and V. Hlady, in E.F. Leonard, V.T. Turitto, and L. Vroman, eds., *Blood in Contact with Natural and Artificial Surfaces*, N. Y. Acad. Sci., New York, 1987, pp. 158–172.
38. M.A. Gimbrone, in E.F. Leonard, V.T. Turitto, and L. Vroman, eds., *Blood in Contact with Natural and Artificial Surfaces*, N. Y. Acad. Sci., New York. 1987, pp. 5–11.
39. E.T. Choi and A.D. Callow, in A.D. Callow and C.B. Ernst, eds., *Vascular Surgery: Theory and Practice*, Appleton & Lange, Stamford, Calif., 1995, pp. 151–166.
40. A.W. Clowes, *Cardiovasc. Pathol.* **2**(3), 179S–186S (1993).
41. J.L. Halperin and P. Peterson, in V. Fuster and M. Verstraete, eds., *Thrombus in Cardiovascular Disorders*, Saunders, Philadelphia, 1992, pp. 215–236.
42. R. Guidon et al., in M. Szycher, ed., *High Performance Biomaterials: A Comprehensive Guide to Medical and Pharmaceutical Applications*, Technomic Publishing, Lancaster, Pa. 1991, pp. 449–474.
43. E.L. Chaikof et al., *J. Surg. Res.* **47**, 193–199 (1989).
44. S.L. Verdon et al., *Scanning Microsc.* **4**(2):341–349 (1990); discussion pp. 349–350.
45. E.L. Chaikof et al., *J. Biomed. Mater. Res.* **26**(9), 1163–1168 (1992).
46. H.P. Greisler, C.W. Tattersall, S.C. Henderson, and E.A. Cabusao, *J. Biomed. Mater. Res.* **26**, 1383–1394 (1992).
47. J.L. Cronenwett and G.B. Zelenock, in J.C. Stanley et al., eds., *Biologic and Synthetic Vascular Prostheses*, Grune & Stratton, New York, 1982, pp. 595–620.
48. J.U. Bascom, *Surgery* **50**, 504–512 (1961).
49. A.W. Humphries, W.A. Hawk, and A.M. Cuthbertson, *Surgery* **50**, 947–954 (1961).
50. G.L. Jordan, M.M. Stump, and J. Allen, *Surgery* **53**, 45–51 (1963).
51. B. van der Lei, H.L. Bartels, P. Nieuwenhuis, and C.R. Wildevuur, *Surgery* **98**(5), 955–963 (1985).
52. H.P. Greisler, D.U. Kim, J.B. Price, and A.B. Voorhees, Jr., *Arch. Surg. (Chicago)* **120**(3), 315–323 (1985).
53. H.P. Greisler et al., *J. Vasc. Surg.* **5**(4), 572–583 (1987).
54. P.M. Galletti et al., *Surgery* **103**(2), 231–241 (1988).
55. H.P. Greisler, *Arch. Surg. (Chicago)* **117**(11), 1425–1431 (1982).
56. S. Bowald, C. Busch, and I. Eriksson, *Surgery* **86**(5), 722–729 (1979).
57. S. Bowald, C. Busch, and I. Eriksson, *Acta Chir. Scand.* **146**, 391–395 (1980).
58. R.R. Kowligi and R.W. Calcotte, in M. Szycher, ed., *High Performance Biomaterials: A Comprehensive Guide to Medical and Pharmaceutical Applications*, Technomic Publishing, Lancaster, Pa., 1991, pp. 425–442.
59. B. Dryer, T. Akutsu, and W.J. Kolff, *J. Appl. Physiol.* **15**, 18–22 (1960).
60. V. Marinescu, E. Pausescu, and S. Carnaru, *Thorax* **26**(1), 108–111 (1971).
61. D.J. Lyman, D. Albo, R. Jackson, and K. Knutson, *Trans. Am. Soc. Artif. Intern. Organs* **23**, 253–261 (1977).
62. D. Annis et al., *Trans. Am. Soc. Artif. Intern. Organs* **24**, 209–214 (1978).
63. L.F. Hiratzka, J.A. Goeken, R.A. White, and C.B. Wright, *Arch. Surg. (Chicago)* **114**, 698–702 (1979).
64. F. Hess, C. Jerusalem, and B. Braun, *J. Cardiovasc. Surg.* **24**, 516–524 (1983).
65. F. Hess, C. Jerusalem, and B. Braun, *J. Cardiovasc. Surg.* **24**, 509–515 (1983).
66. Z. Zhang et al., *Biomaterials* **15**(7), 483–501 (1994).
67. Z. Zhang et al., *Biomaterials* **15**(13), 1099–1112 (1994).
68. Y. Marois et al., *Biomaterials* **17**(13), 1289–1300 (1996).
69. Z. Zhang et al., *Biomaterials* **18**(2), 113–124 (1997).
70. M. Krajicek, V. Zastava, and M. Chvapil, *Surg. Res.* **4**(7), 290–296 (1964).
71. C. Hermansen, K. Kraglund, E. Ludwigsen, and C. Mouritzen, *Eur. Surg. Res.* **12**(5), 349–362 (1980).
72. P. Misiuna, *Ann. Univ. Mariae Curie-Sklodowska, Sect. D* **19**, 1–12 (1964).
73. H. Lee and K. Neville, *Handbook of Biomedical Plastics*, Pasadena Technology Press, Pasadena, Calif., 1971, pp. 1–61.
74. W.J. Fry, M.S. DeWeese, R.O. Kraft, and C.B. Ernst, *Arch. Surg.* **88**, 836–842 (1964).
75. R.A. White, *Trans. Am. Soc. Artif. Intern. Organs* **34**, 95–100 (1988).
76. G. Soldani et al., *J. Mater. Sci. Mater. Med.* **31**, 106–113 (1992).
77. T. Okoshi, M. Goddard, P.M. Galletti, and G. Soldani, *Trans. Am. Soc. Artif. Intern. Organs* **37**(3), M480–M481 (1991).
78. K. Fujimoto et al., *J. Appl. Biomater.* **4**, 347–354 (1993).
79. D.E. Hokanson and D.E. Strandness, *Surg. Gynecol. Obstet.* **127**, 57–60 (1968).
80. W.M. Abbott and R.P. Cambria, in J.C. Stanley et al., eds., *Biologic and Synthetic Vascular Prostheses*, Grune & Stratton, New York, 1982, pp. 189–220.

81. R. Walden, G.J. L'Italien, J. Megerman, and W.M. Abbott, *Arch. Surg. (Chicago)* **115**, 1166–1169 (1980).
82. D.J. Lyman et al., *J. Biomed. Mater. Res.* **12**, 337–345 (1978).
83. D. Annis, A.C. Fisher, T.V. How, and L. deCossart, in E. Chiellini, P. Giusti, C. Migliaresi, and L. Nicolais, eds., *Polymers in Medicine II: Biomedical and Pharmaceutical Applications*, Plenum, New York, 1986, pp. 217–221.
84. B. Pourdeyhimi and D. Wagner, *J. Biomed. Mater. Res.* **20**, 375–409 (1986).
85. W.E. Burkel and R.H. Kahn, *Ann. N. Y. Acad. Sci.* **283**, 419 (1977).
86. M. Herring, A. Gardner, and J. Glover, *Surgery* **84**(4), 498–504 (1978).
87. S.P. Schmidt, W.V. Sharp, M.M. Evancho, and S.O. Meerbaum, in M. Szycher, ed., *High Performance Biomaterials*, Technomic Publishing, Lancaster, Pa., 1991, pp. 483–496.
88. L.M. Graham et al., *Surgery* **91**(5), 550–559 (1982).
89. S. Emerick et al., *J. Vasc. Surg.* **5**(2), 342–347 (1987).
90. J.M. Seeger and N. Klingman, *J. Surg. Res.* **38**(6), 641–647 (1985).
91. J.P. Mazzucotelli et al., *Int. J. Artif. Organs* **14**(8), 482–490 (1991).
92. S.K. Williams et al., *J. Biomed. Mater. Res.* **26**, 103–117 (1992).
93. H.P. Greisler et al., *Arch. Surg. (Chicago)* **124**(8), 967–972 (1989).
94. J.R. Mackenzie, M. Hackett, C. Topuzlu, and D.J. Tibbs, *Arch. Surg. (Chicago)* **97**, 879–885 (1968).
95. Y. Noishiki, Y. Tomizawa, Y. Yamane, and A. Matsumoto, *Nat. Med.* **2**(1), 90–93 (1996).
96. C.O. Esquivel et al., *Surgery* **95**, 102–107 (1984).
97. S.M. Lindenauer, W.J. Fry, G. Schaub, and D. Wild, *Surgery* **62**(3), 487–492 (1967).
98. R.B. Smith, K. Lowry, and G.D. Perdue, *Am. Surg.* **33**(9), 711–714 (1967).
99. W.S. Moore, in J.C. Stanley et al., eds., *Biologic and Synthetic Vascular Prostheses*, Grune & Stratton, New York, 1982, pp. 661–669.
100. A.L. Ney et al., *J. Surg. Res.* **57**, 698–705 (1994).
101. G. Soldani et al., *Clin. Mater.* **8**, 81–88 (1991).
102. M.D. Lado et al., *Int. J. Artif. Organs* **15**(12), 727–736 (1992).
103. H.P. Greisler et al., *Surgery* **112**(2), 244–255 (1992).
104. U.S. Pat. 5,290,271 (March 1, 1994), G.R. Jernberg (to Jernberg, G.R.).
105. T. Richey and F.W. Harris, *Proc. Int. Symp. Controlled Release Bioact Mater.* **23**, 391–392 (1996).
106. M.R. Kreitz, W.L. Webber, P.M. Galletti, and E. Mathiowitz, *Biomaterials* **18**, 597–603 (1997).
107. M.R. Kreitz, J.A. Domm, and E. Mathiowitz, *Biomaterials* **18**, 1645–1651 (1997).
108. S.K. Pulfer, D. Ott, and D.J. Smith, *J. Biomed. Mater. Res.* **37**, 182–189 (1997).
109. N. L'Heureux et al., *FASEB J.* **12**, 47–56 (1998).
110. C.B. Weinberg and E. Bell, *Science* **231**, 397–400 (1986).

TISSUE–IMPLANT INTERFACE, BIOLOGICAL RESPONSE TO ARTIFICIAL MATERIALS WITH SURFACE-IMMOBILIZED SMALL PEPTIDES

GEOFFREY MOODIE
ROBERT F. VALENTINI
Brown University
Providence, Rhode Island

KEY WORDS

Biomaterial
Cell
Extracellular matrix
Peptide
Surface modification

OUTLINE

Introduction
Integrins
Application to Bone-Contacting Prostheses
  Limitations of Total Joint Replacement
  Integrin-Mediated Control of Cell Function
  Osteoblast Adhesion and Integrins
Specific Immobilization Chemistries
  Sepharose
  Polyacrylamide
  Silicone
  Glass
  Polyurethanes
  Poly(ethylene terephthalate)
  Poly(ethylene acrylic acid)
  Polyacrylonitrile
  Hydrogels
  Silicon Dioxide
  Fluorinated Ethylene Propylene
  Gold
Bibliography

INTRODUCTION

The nature of the tissue–implant interface is a critical component in the success or failure of most medical implants. Investigators have sought to improve and control this interface by modifying surface chemistry, surface charge, and surface topography. This article focuses on a subset of approaches that immobilize bioactive peptides on a biomaterial surface to elicit a controlled tissue reaction, particularly for bone-contacting applications. Using small peptides has several practical and experimental advantages over the use of entire proteins:

1. Many extracellular matrix (ECM) proteins are not commercially available, are difficult to purify, and are difficult to work with chemically.
2. Synthetic peptides are widely available and pure, thus minimizing cost and the risk of infection.
3. Linear peptides do not require tertiary or quaternary structure.
4. Small peptides are more resistant than whole proteins to changes in pH and temperature (1) and are less susceptible to proteolysis and hydrolysis.
5. Bioactive peptides allow manipulation at the nuclear level. Specificity in cell stimulation can be gained through the use of sequences known to interact with certain receptors.

Peptides are referred to in this article by their single-letter amino acid sequences (Table 1). Peptides can be protected from proteolytic degradation by modifying the peptide bond, chemically blocking the termini, using NH_2 to COO-terminal cyclization, or using the D-forms of amino acids (which do not occur naturally in proteins) (2).

The Arg-Gly-Asp (RGD) sequence is the archetypal bioactive peptide, and many cells have receptors for it (2,3). Thus, RGD is an ideal model peptide and has been used widely to modify biomaterial surfaces. RGD and other peptides bind to a family of ECM receptors called *integrins* (described later). RGD is a promiscuous sequence that can bind to several integrin receptors. This tripeptide was first found in fibronectin (4). It has since been found to be in the integrin-binding sections of many proteins; of particular relevance to bones are bone sialoprotein (5) and osteopontin (6). Such a ubiquitous sequence may have the disadvantage of attracting undesirable cells such as fibroblasts to a bone implant. The presence of fibroblast-induced soft tissue versus hard tissue could, for example, lead to poor host–implant integration. Several types of bacteria also possess RGD receptors (7), which could lead to implant colonization, although this has not been studied in detail. For bone-contacting implants, the addition of flanking peptide sequences can increase receptor specificity. For example, the RGD-containing peptide CGGNGEPRGDTYRAY from bone sialoprotein has been used by Rezania et al. (5).

Ultimately, favorably controlling cell response is the goal of immobilizing bioactive peptides on biomaterial surfaces. In vitro properties such as cell adhesion, morphology, protein synthesis, and gene expression can be evaluated. In vivo cell and tissue response, cellular makeup, and degree of vascularization can be evaluated. Basic in vitro and in vivo approaches will be discussed, and specific immobilization schemes will be reviewed.

INTEGRINS

Integrins are heterodimeric cell surface receptors for extracellular proteins. The two subunits, designated α and β,

Table 1. Single-Letter Codes for Amino Acids

Amino Acid	Single Letter	Amino Acid	Single Letter	Amino Acid	Single Letter
Alanine (ala)	A	Isoleucine (ile)	I	Arginine (arg)	R
Cysteine (cys)	C	Lysine (lys)	K	Serine (ser)	S
Aspartate (asp)	D	Leucine (leu)	L	Threonine (thr)	T
Glutamate (glu)	E	Methionine (met)	M	Valine (val)	V
Phenylalanine (phe)	F	Asparagine (asn)	N	Tryptophan (trp)	W
Glycine (gly)	G	Proline (pro)	P	Tyrosine (tyr)	Y
Histidine (his)	H	Glutamine (gln)	Q		

are noncovalently associated. Both subunits are compact transmembrane glycoproteins with heavy disulfide binding and a single hydrophobic domain. Under electron microscopy, an integrin presents as a globular head with two stalks (one for each subunit) extending down into the lipid bilayer (8,9). Sixteen α- and nine β-chains have been identified, and they assemble to form the 24 distinct integrins currently identified (10). Each β-subunit can associate with multiple α subunits; however, of the α subunits only α_v can associate with multiple β-subunits (11).

Beyond simply adhering cells to the surrounding extracellular matrix, integrins are key components in many intracellular signaling pathways, and a number of functional changes occur when cells are in contact with ECM proteins. One example of this is mammary epithelial cells, which will not produce milk proteins until after they have attached to extracellular matrix proteins, even when milk-inducing hormones (prolactin and cortisone) are present (12). Synergies exist between integrins and growth factors. Vuori and Ruoslahti showed that insulin receptor substrate -1 (IRS-1) associates with the $\alpha_v\beta_3$-integrin in the presence of insulin. This association appears to increase DNA production in response to insulin, possibly by increasing the phosphorylation of IRS-1 and consequently enhancing intracellular signaling. When exposed to insulin, human pancreatic carcinoma (FG) cells transfected to overexpress $\alpha_v\beta_3$ showed a 250% increase in DNA synthesis versus nontransfected FG cells. When the transfected cells were plated on a non-$\alpha_v\beta_3$-binding substrate (collagen), DNA synthesis was similar to that seen in nontransfected cells (13). A similar association has been found between platelet-derived growth factor (PDGF) and α_v-integrins associating with a 190-kDa protein (14).

ECM–integrin binding can influence cell shape, migration, differentiation, and gene expression (9,15–19). Some integrins may, via cytoskeletal elements, connect directly with the nucleus and serve as mechanotransducers (20). Integrin expression can be regulated by external influences such as growth factors (most notably TGF-β), pharmacologic agents, mechanical stress, and infectious agents. Cells regulate integrin expression by transcriptional or postranscriptional mechanisms, alternative splicing of mRNA, conformation control, and mobilizing intracellular stores (11).

Most immobilized peptides reviewed in this article target integrins (YIGSR-containing sequences are noted exceptions). Integrin receptors recognize specific amino acid sequences within their target proteins, such as the RGD sequence and its variants mentioned earlier. As another example, type I collagen, the major bone protein, contains the DGEA sequence that binds to the $\alpha_2\beta_1$-integrin (21).

APPLICATION TO BONE-CONTACTING PROSTHESES

Limitations of Total Joint Replacement

Total joint replacement is widely used to relieve pain, improve function, and enhance the quality of life for patients with medical conditions caused by osteoarthritis, rheumatoid arthritis, posttraumatic degeneration, avascular necrosis, and other aging-related conditions. Almost 600,000 total joint replacements are performed in the United States alone each year. Current techniques to stabilize the interface between bone and prostheses are physical or geometric in nature. Most orthopedic prostheses are composed of alloys of titanium (Ti6A14V) or cobalt (CoCrMo) and rely on poly(methyl methacrylate) cements for attachment and fixation to bone. Loosening due to cement failure has been implicated in revision of hip, knee, and elbow implants (22–28). Perioperative allergic, hypotensive, and embolic events, although currently unusual, have also been related to the use of cements (29–31). An unacceptably high number of implant failures occur. With cemented total hip arthroplasty, for example, long-term studies indicate a combined (aseptic and radiographic) loosening rate of 20–30% in the acetabulum and 5–10% in the femur, with about a 10% overall revision rate (32). In total knee arthroplasty, for which over 200,000 procedures were performed last year alone, cemented knees also exhibit a 0.5–1% per year loosening rate and approach a 10% revision rate (33–35).

Cementless prostheses are designed to encourage bone ingrowth through the use of porous or sintered coatings (36–38). These implants have the potential advantages of stable long-term fixation, circumventing the issues surrounding the use of cement, and are more easily retrieved should revision become necessary. Tissue ingrowth into porous materials is influenced by several factors, including pore size and implant stability (37,39–41). Experience thus far suggests that using "press-fit" prostheses is problematic for two major reasons (36,38): First, minimal or inadequate ingrowth is observed in a significant number of patients, resulting in loosening and failure, and second, the process of ingrowth occurs over a period of weeks to months, such that weight bearing is necessarily limited early on in an effort to prevent micromotion and allow stable osseointegration. This can potentially increase expense and complication and may become particularly problem-

atic when addressing elderly patients, who comprise the greatest percentage of those needing arthroplasties performed today. Another approach is to coat prostheses with hydroxyapatite and tricalcium phosphate, but such implants have had difficulties with delamination and biodegradation and are still unable to demonstrate optimal bony ingrowth and biomechanical fixation (23,38,42).

Integrin-Mediated Control of Cell Function

The ability to enhance and accelerate ingrowth using biological factors with bone-promoting capabilities would be a significant advancement in implant technology. Bone-implant integration is regulated by numerous factors including extracellular matrix (ECM) elements and growth/morphogenic proteins. The development of orthopaedic devices incorporating bioactive surface molecules may improve our understanding of tissue repair mechanisms and enhance the design of bone-inducing substrates for clinical application. This may be done by stimulating integrin pathways (9,43,44).

Minimal peptide sequences that bind to integrins and mimic the action of much larger and insoluble ECM molecules have recently been identified (Table 2).

Small peptides can be used as agonist or antagonist drugs. In the latter case, soluble peptides can be used to occupy integrin receptors on migrating or blood-borne cells. Receptor occupancy blocks cell–ECM or cell–cell interactions. For example, metastatic melanoma and other tumor cell spreading can be decreased by injection of soluble RGD or laminin (e.g., YIGSR) peptides in animal models (59,74–77). Platelet aggregation has also been reduced by intravascular administration of soluble cyclic RGD peptides or RGD-containing analogs (51,78,79). Finally, osteoclastic resorption has been reduced by innoculation with RGD-containing peptides or analogs (80,81). Osteoclasts are known to express several integrin receptors (49,80). The fact that osteoclasts have RGD-binding integrins is relevant to the present work because activation of osteoclastic resorption at the bone interface is not favorable. Small peptides can be used as agonists to improve cell adhesion if they are immobilized on insoluble substrates (63,64,82,83). For example, endothelial cell and fibroblast adhesion to several biomaterials is enhanced by coatings of peptide ligands from fibronectin and laminin, RGD and YIGSR, respectively (52,63,64,84). YIGSR also supports nerve cell attachment, whereas a second laminin fragment, SIKVAV, supports neurite outgrowth (85). Certain peptides can act synergistically to enhance binding affinity. For example, two nonadjacent peptide sequences from fibronectin, including RGD and PHSRN, a so-called synergy sequence, exhibit such behavior (74,86). The conformation of peptide is important because small chemical changes can have profound effects on cell adhesion (87). Peptides can also effect cell and tissue function beyond cell adhesion.

Osteoblast Adhesion and Integrins

Bone cells are known to attach to tissue culture substrates via fibronectin and vitronectin molecules (88), although the effect of cell attachment peptides has not been widely studied. Osteoblast adhesion, ECM synthesis, and mineralization are influenced by the chemical nature and electrical charge of tissue culture substrates such as modified polystyrene and bioglass (89–93). Osteoblast adhesion on some biomaterials results in the formation of focal adhesion contacts, which entail clustering of integrin receptors (94,95).

Recently, it has been shown that human and rat osteoblasts/osteocytes express a range of integrins (Table 3). There are, however, conflicting data regarding the expression of certain integrins. Most studies report the expression of integrins a5b1, avb3, and a1b1 in rat osteoblasts.

SPECIFIC IMMOBILIZATION CHEMISTRIES

These entries are arranged in roughly chronological order. The level of detail dedicated to each method is not intended to indicate the importance of any particular immobilization chemistry. Rather, it is simply a reflection of the amount of literature available on each technique.

Sepharose

Pierschbacher and Ruoslahti pioneered work in pursuit of active protein sequences and immobilized peptides to sepharose beads using a carbodiimide coupler. Rat kidney fibroblast attachment was assessed by staining the cells with toludine blue and examining with microscopy. They found that only those peptides containing RGD promoted cell attachment, and this sequence is still widely used by investigators today (4).

Further experiments pointed to the importance of immobilization chemistry. Normal rat kidney cells do not rec-

Table 2. Small Peptide Ligands

ECM protein	Peptide ligand	Integrin receptors
Collagen I	cRGD, RGDT, DGEA, GTPGPQGIAGQRGVV	a1b1, a2b1, a3b1
Bone sialoprotein	EPRGDNYR	avb3
Osteopontin	RGD	avb3
Fibronectin	RGDS, EILDV, REDV	a3b1, a4b1, a5b1, avb1, avb3, avb5, avb6, a4b7
Laminin	YIGSR, SIKVAV, RGD	a1b1, a2b1, a3b1, a6b1, a7b1, a6b4
Thrombospondin	RGD	avb3
Vitronectin	RGDV, HRNRKGV	avb1, avb3, avb5
Osteonectin (SPARC)	KKGHK	?

This table includes reported extracellular matrix proteins, their peptide ligands, and their integrin receptors. This table is not intended to be exhaustive and focuses on molecules relevant to bone research. *Source:* Refs. 3,8,9,21,44–73.

Table 3. Bone Cell Interins

Rat calvarial osteoblasts	a1b1, a5b1, avb1, avb3, avb5
Human osteoblasts	a3b1, a4b1, a5b1, avb3

Source: Refs. 3,57,70,96,97.

ognize RGDC when it is linked directly to cyanogen bromide–activated sepharose beads, but RGDS was recognized when tethered with a six-carbon spacer (98). Interestingly, RGDC has been found to be active when linked by a gold–thiol bond (see "Gold").

Polyacrylamide

Among the first to covalently link peptides to artificial surfaces were Brandley and Schnaar. The polymer used was a polyacrylamide gel surface to which cells do not adhere in the absence of serum proteins. The N-terminus of the peptide used (YAVTGRGDS) reacted with N-succinimidyl ester groups in the polymer. A linear correlation between the amount of peptide in solution to the amount of peptide immobilized was established, with about 80% of the peptide in solution being bound to the surface (99).

Balb/c 3T3 mouse fibroblasts were used to test these peptide-treated surfaces (5.6 ± 0.3 nmol peptide/cm^2 in the reaction fluid). Cells adhered to the RGD peptide-treated material but not to polyacrylamide with a non-RGD control peptide or plain activated acrylamide. Using a lactate dehydrogenase proliferation assay, they found that the proliferation of cells on the peptide-treated polyacrylamide was about the same as that on tissue culture plastic, but on control surfaces growth was not supported. These effects could be seen with as little as 2 nmol/cm^2 of peptide (99).

Silicone

Another group that first immobilized peptides to artificial substrates was Imanshi et al. Silicone rubber film was exposed to aminoalkylated polydimethylsiloxane followed by oxalic acid, water-soluble carbodiimide, and polyallylamine. This provided a surface amino group density of 0.713 μmol/cm^2. Water-soluble carbodiimide was used again to couple RGDS to these amino groups. Cell attachment increased in a linear manner with peptide surface concentration, from about 11,000 cells/cm^2 with no immobilized peptide to about 26,000 cells/cm^2 with 41 mmol/cm^2 of peptide (1).

Glass

Massia and Hubbell covalently linked the peptides GRGDY, GYIGSRY, GPDSGRY, and GREDVY to glycophase glass (63,100,101). Briefly, glycophase glass is prepared by reacting glass with sodium hydroxide followed by immersion in (3-glycidoxypropyl)-trimethoxysilane. Oxyrane moieties are converted to glycol groups by treatment with acid and heat. Tresyl chloride was used to couple peptides through their N-termini (63).

Peptide surface concentration was measured by radiolabeling the *C*-terminal tyrosine groups on the peptides prior to immobilization. They found that peptide surface concentrations rose linearly with available peptide up to 12.1 ± 0.1 pmol/cm^2. A maximum surface concentration of 12.1 pmol/cm^2 corresponds to a surface spacing of 3.3 nm between peptides (63). 10 fmol/cm^2 was required for complete spreading, focal contact formation, and f-actin cytoskeletal organization in human fibroblasts (102).

Cell proliferation studies were performed with human foreskin fibroblasts by counting cells in 10 fields under a phase-contrast microscope with a 100 × objective. The media used was DMEM + 10% fetal bovine serum. This data showed no differences between the growth rate on surfaces with immobilized RGD and that on nonglycophase glass (63).

Cell spreading was analyzed with image analysis; results are summarized in Table 4. For the sake of comparison, a well-spread cell area on tissue culture plastic in serum-containing media is 2,100 μm^2; a nonspread cell area is about 355 μm^2.

As can be seen from Table 4, cell spreading increased with time on the RGD substrates with and without serum but failed to do so on glycophase glass, especially in the absence of serum (63).

Cell spreading was also noted on YIGSR-treated surfaces with and without serum, but it was not as rapid as RGD, taking over 6 h to occur. At 9 h the median cell area with serum was 2,333 μm^2, without serum it was 1,400 μm^2. Glycophase glass without peptide did not show cell spreading greater than 600 μm^2 at any time point. The effects were due primarily to the immobilized peptide, as cells seeded on an immobilized control peptide, GRGESP, and preincubated with soluble forms of the active peptides did not spread. The fraction of cells that spread on YIGSR or RGD was not effected by the addition of cycloheximide to the media to prevent cellular protein synthesis. Spreading of quiescent or active platelets was absent on all surfaces. Data from several Massia and Hubbell experiments is summarized in Table 5.

As can be seen from Table 5, cell selectivity was demonstrated using this system. Whereas human endothelial cells (HUVECs) showed a high avidity for a GREDVY-treated surface, human foreskin fibroblasts, vascular smooth muscle cells, and platelets did not. In the absence of serum, small focal contacts were present on the RGD-treated surfaces around the outer margins of the cells and at discreet locations on the cell body. Serum promoted the formation of larger, well-defined focal contacts. The YIGSR-treated substrates did not form focal contacts without serum. When serum was added, elongated focal adhesions formed around the periphery of the cells.

Cells on RGD in serum-free conditions showed an extensive actin network. This thickened in the presence of serum. Very few microfilament bundles were seen on the YIGSR in the absence of serum, but in serum thick microfilaments formed (63).

Further in vitro spreading tests were done on this substrate with human umbilical vein endothelial cells (HUVEC). Table 6 summarizes the spreading data obtained. This experiment was done in serum containing medium.

Table 4. Fibroblast Spreading

Time (min)	RGD–glass + serum: median cell area (μm^2)	RGD–glass − serum: median cell area (μm^2)	Glycophase glass + serum: median cell area(μm^2)	Glycophase glass − serum: median cell area (μm^2)
15	265	248	385	377
30	906	950	397	325
60	1113	864	448	388
120	2130	1207	453	388

Table 5. Cell Spreading on Immobilized Peptides

Peptide grafted to surface	Serum in medium (10% v/v)	Peptide in medium (200 μg/mL)	Spread HFF cells (%)	Spread HVSMC cells (%)	Spread HUVEC Cells (%)
GRGEY	−	−	0	Not tested	Not tested
	+	−	0	Not tested	Not tested
GRGDY	+	−	87 ± 8	Not tested	Not tested
	−	−	91 ± 4	93 ± 3	90 ± 9
	−	+(RGDS)	0	Not tested	Not tested
GYIGSRY	+	−	78 ± 7	Not tested	Not tested
	−	−	81 ± 12	88 ± 9	84 ± 10
	−	+(GYIGSRY)	0	Not tested	Not tested
GPDSGRY	−	−	59 ± 6	62 ± 4	66 ± 8
GREDVY	−	−	9 ± 4	7 ± 2	89 ± 6
Glycophase Glass	−	−	9 ± 2	10 ± 4	8 ± 1

Source: Refs. 63,101.

Table 6. Cell Spreading Time Curve

Time (min)	RGD–glass mean cell area (μm^2)	YIGSR–glass mean cell area (μm^2)	Glycophase glass mean cell area (μm^2)
15	1196 ± 1548	1027 ± 606	249 ± 136
30	1064 ± 780	1389 ± 1076	343 ± 228
60	1812 ± 1429	1825 ± 1233	211 ± 132
120	2449 ± 2196	2370 ± 1587	372 ± 99
240	2679 ± 667	2373 ± 1904	456 ± 570

Source: Ref. 100.

As may be inferred from Table 6, there was no statistically significant difference in cell spreading between RGD and YIGSR treated surfaces with this cell type. Focal contacts and large close-contact regions formed on RGD-treated glycophase glass, but focal contacts with minimal close-contact regions were noted on the YIGSR-treated surface. More extensive actin networks formed in cells on the RGD surface than the YIGSR (100).

The type of peptide immobilized affected cell function. HUVECs showed proper antithrombogenic activity on GRGDY, GYIGSRY, GREDVY, and gelatin. However, when these cells were plated on GPDSGR, the antithrombogenic activity was lost even though their morphology was normal (101).

It was also of consequence whether or not the peptide was covalently immobilized or simply adsorbed. Adsorption was done with 20 μg/mL of protein or peptide for 1 h followed by bovine serum albumin for 30 min. Cells were incubated on surfaces in serum-free media for 6 h. Human foreskin fibroblasts incubated with antisera against laminin receptors failed to spread, indicating that these events are receptor specific.

A variety of cells showed consistently that although attachment occurred, cells failed to spread on adsorbed peptide. Two possible explanations for the improved spreading are that covalent immobilization (*1*) helps to stabilize the YIGSR in an active conformation and (*2*) may present the YIGSR to the receptor in a more favorable way (fixed end forward rather than adsorbed on its side) (103).

Polyurethanes

Polyurethanes are currently used as biomaterials in blood-contacting applications. It may be possible to improve the performance of polyurethane implants by developing an endothelial cell layer on the blood-contacting surface. Toward this end, Imanishi began work in 1988 to link a peptide substrate for thrombin, Val-Pro-Arg, to the surface of carboxylated polyurethaneurea (1,104). Three configurations were used. (*1*) immobilizing by the amine terminis of

the peptide (P1), (2) immobilizing the carboxylic terminis at the end of a six-carbon spacer (P2), and (3) repeating P2 with a reversed amino acid sequence (Arg-Pro-Val) (P3).

When the polyurethaneurea samples were placed into solutions containing known amounts of thrombin, both the peptide P1–and nonpeptide-treated surfaces adsorbed the same amount of thrombin. However, the peptide-treated surface did so much more quickly (P1 required less than 30 min for 100% adsorption of 0.22 mg/mL thrombin, while plain polyurethaneurea needed more than 120 min). Thrombin was desorbed from the surfaces and tested for activity. The peptide P1 from the nonpeptide polyurethaneurea retained 73% of its original activity, while that from the peptide polyurethaneurea had only 12%, which would indicate a specific reaction between the thrombin and the immobilized peptide. In experiments using platelet-poor plasma from canine blood, it was found that increasing peptide P1 concentration yielded increasing time to clotting.

The other peptide attachment schemes (P2 and P3) failed to show as much antithrombogenic activity as P1 when incubated with canine platelet-poor plasma in a thromboplastin buffer solution activated with $CaCl_2$. Glass took 930 s; plain polyurethaneurea, 1,079 ± 10s; P1, 1,139 ± 7s; P2, 1,068 ± 11s; and P3, 1,077 ± 7s. It was theorized that the Arg side chain couldn't be blocked (1).

Lin et al. developed a method to carboxylate polyurethanes to facilitate peptide coupling. This was accomplished by grafting β-propiolactone to the polymer backbone using a bimolecular substitution reaction (105). Peptides were then coupled via their free N-termini to the carboxyl groups on the polymer using the coupling agent EDCI. Cold-stage and variable take-off–angle ESCA verified enhanced peptide presence at the surface of the polymer in aqueous environments, presumably due to its hydrophilicity and the ability of polyurethane surfaces to rearrange in response to their environment (106). In vitro tests for human umbilical vein endothelial cell (HUVEC) spreading and adhesion were performed with polyurethane grafted with GRGDSY, GRGDVY, and GRGESY. About 20,000 cells per cm^2 were plated onto glass coverslips coated with the experimental polymer. Four time points were taken for the adhesion experiments: 40 min, 80 min, 120 min, and 240 min. At each of these time points, nonadherent cells were rinsed away, and remaining cells were counted manually with the aid of a phase-contrast microscope. Cell spreading was measured using a combination of scanning electron microscopy and image analysis. These tests were done in both the presence and absence of serum (107). Cell growth on these surfaces was measured in serum with porcine pulmonary aortic endothelial cells. Twelve-millimeter-diameter glass coverslips coated with polymer were inserted into 24-well plates. Cells were seeded at 5,000 cells/well, and growth was quantified using an MTT (3-[4,5-dimethylthiazol-2-yl]-2,5-diphenyltetrazolium bromide; thiazolyl blue) assay (84).

The results of this experiment showed that after 4 h in serum-free conditions, the cell attachments on GRGDVY and GRGDSY were 50 and 23% of the original seeding density, respectively. On the control peptide GRGESY, plain polyurethane, and carboxylated polyurethane, the cell attachment was only 5%. In serum, the cell attachment numbers were higher on all substrates and did not change significantly after the 40-min time point. This is most likely because of the fact that serum contains adhesive proteins that adsorbed onto substrates. The pattern was similar to serum free, however. 65 and 40% attachment was observed on GRGDVY and GRGDSY, respectively. Control peptide, carboxylated, and plain polyurethane all showed a 22% attachment (107).

Cell spreading was not supported in serum-free conditions on control peptide, carboxylated, or plain polymer. Rounded cells on these substrates had an area of 92 ± 15 μm^2. On GRGDVY, cells spread to an area of 532 ± 159 μm^2, and on GRGDSY their mean area was 281 ± 107 μm^2. In serum, spreading occurred on the GRGESP (330 ± 35 μm^2), carboxylated (315 ± 50 μm^2), and plain samples (320 ± 30 μm^2), but not to the degree found on GRGDVY (603 ± 119 μm^2) and GRGDSY (549 ± 138 μm^2) surfaces. It was proposed that the greater effect of the GRGDVY peptide might have been due to a greater affinity for the endothelial cell receptors (107).

Cell growth was relatively poor on noncarboxylated polyurethane, as it had less than half the number of cells on it at 72 h than any other substrate. Unlike the other experiments, the difference between the other controls and the active peptides were not large. This is probably due to the growth factors and adhesive proteins in the serum used in the media (84).

In vivo experiments were performed by Yanagi et al. using modified polyurethane sponges. The polyurethane was carboxylated by graft polymerization with acrylic acids. Proteins and GRGDSP were immobilized via the coupling agent CDI. These sponges were modified with immobilized collagen, fibronectin, GRGDSP, apatite, and a collagen coating. Fibronectin-, GRGDSP-, and apatite-treated rat subcutaneous implants showed lower inflammatory response at 3 days and high or vascularization at 7 days than plain polyurethane or collagen-treated sponges. When these sponges were implanted to fill partial defects in canine tracheas, epithelization on GRGDSP was about the same as that of untreated sponges, which was better than collagen-treated but inferior to fibronectin- and apatite-treated implants (108).

Breuers et al. used plasma polymerization to graft vinylacetate onto bulk polyurethane. After hydrolysing the acetate groups with sodium methoxide glycine and GRGDS, peptide was linked to the film via benzoquinone (109).

Poly(ethylene terephthalate)

Poly(ethylene terephthalate) (PET, commonly called Dacron) is used for vascular grafts and other medical implants. In one study, PET was surface modified with poly(ethylene glycol) (PEG) to make it nonadhesive to cells and proteins. Briefly, the PET surface is partially solubilized in dilute trifluoroacetic acid (TFA). PEG was introduced into this partially solvated surface and then was sterically "locked" into place by removing the PET from the TFA and putting it into water. Peptides were then linked to the hydroxyl groups on the PEG with essentially the same technique used for glycophase glass (101,110).

When compared with data obtained from glycophase glass, two important differences stand out. First, unlike glycophase glass, there is no attachment to the PET + GPDSGR, and second, the HVSMCs failed to adhere on PET. Both may be due to the much lower peptide surface concentrations of the peptide (<20 fmol/cm^2 on the PET, compared with 10 pmol/cm^2 on the glass) (101).

Telios Pharmaceuticals, Inc., developed PepTite (Ac-G(dR)GRSPASSKGGGGS(dR)LLLLLL(dR)-NH_2, which binds via a hydrophobic interaction between its polyleucine domain and the underlying material. This has been shown to attach to a number of materials and promote the integrin-specific attachment of varied cell types (79). Experiments with PET and poly(tetrafluoroethylene) (PTFE) vascular patches modified with PepTite were preformed. Two 2-by-0.5-cm elliptical patches of plain PTFE, plain PET, PTFE + PepTite, and PET + PepTite were implanted into the carotid and femoral arteries of mongrel dogs. The animals were sacrificed at 3 weeks, and the arteries were opened opposite the patches and photographed. Portions of the patch were sectioned for histological analysis, while other parts were used for scanning electron microscopy.

Three of the four PepTite-treated patches showed coverage by endotheliallike cells, and only one of the four plain polymer grafts showed such development, most displaying instead a platelet–fibrin mesh containing macrophages and leukocytes. Foreign-body giant cells were reduced on PET + PepTite fibers compared with plain PET fibers. The neointimal thickness on PET + PepTite was about half of that of on plain PET, while there was little difference between plain PTFE and PTFE + PepTite (both between plain PET and PET + PepTite).

PepTite was also evaluated on the PET sewing cuffs of artificial heart valves in juvenile sheep. After the native mitral valves were removed, artificial valves with plain PET or PepTite + PET sewing rings were implanted and left in place for 3 or 4 weeks. After gross and histologic evaluation, it was found that the tissue growth on the PepTite-treated valves was significantly greater in extent, maturity, and thickness (111).

Poly(ethylene acrylic acid)

RGDS, RGDV, and RGDT are derived from fibronectin, vitronectin, and collagen, respectively. Hirano et al. coupled these peptides plus RGD to the surface of poly(ethylene acrylic acid) (EAA) via carbodiimide-mediated activation of the EAA's carboxylic acid groups.

Adhesion of a mouse epithelial fibroblast cell line (L-929) was evaluated on plain EAA and peptide-treated EAA. Cells were plated at 100,000 cells/cm^2 in serum-free media and allowed to adhere for 1 or 3 h. The peptide-treated surfaces supported two to four times more cell adhesion than plain EAA.

Surprisingly, these investigators found that the peptides solubilized at 2 mg/mL inhibited the attachment of cells to plain polystyrene in serum-free media over 3 h. It is interesting that adhesion to polystyrene is blocked by soluble peptides, and more analysis is required (55).

Polyacrylonitrile

Beer et al. did some investigative work on peptides with varying spacer lengths on polyacrylonitrile and human blood platelets. After rinsing polyacrylonitrile beads in sodium acetate, RGDF peptides with spacers containing 1, 3, 5, 7, 9, 11, 13, 15, 17, and 19 glycine residues in length were reacted with *N*-hydroxysuccinimide groups. Unreacted groups were quenched with glycine ethyl ester. Calculations based on high-performance liquid chromatography (HPLC) data from pre- and postreaction solutions and the surface area of the beads gave a spacing of approximately 4.6 Å.

Platelets were introduced to these beads. When the platelets recognized the immobilized peptides, agglutination would occur. Minimal reaction occurred with a single glycine spacer, but nine-glycine spacers promoted maximal agglutination. Three glycine spacers were most sensitive to outside agents, with no appreciable agglutination occurring with prostaglandin E_1 platelet inhibitor, delayed and incomplete platelet agglutination normally, and extensive agglutination with platelets activated with ADP. Prostaglandin E_1 inhibited but did not eliminate agglutination of surfaces with peptides having nine or more glycine spacers.

Platelet preincubation with soluble forms of the peptides containing one to nine glycine spacers was done to test for inhibition of agglutination. Shorter peptides had a more potent effect than longer peptides, indicating that the glycine spacers were not increasing binding generally. It was hypothesized that a spacer putting the peptide 11 to 32 Å from the surface of the bead is optimal for interaction with its receptor. However, the possibility that this spacer was more important in allowing the peptide to "escape" from the complex molecular geometry of the polymer's surface was also mentioned. Antibody studies indicated that the GPIIb/IIIa receptor is the one targeted by the RGDF peptide (112).

Hydrogels

Hydrogels are hydrophilic cross-linked polymer networks that swell in an aqueous environment. Their mechanical properties are similar to that of some biological tissues and are permeable to tissue metabolites, which makes them potentially useful as scaffolds for cells to grow into during tissue repair. Peptides can be grafted onto these hydrogels to enhance this activity (113,114).

Moghaddam and Matsuda began work on a peptide-modified photocurable hydrogel in 1993. 7-hydroxy coumarin was reacted with potassium carbonate. The excess potassium carbonate is removed, and 2-bromoethyl methacrylate is added. The result is a methacrylic acid-(7-coumaroxy)ethyl ester (MACEE). *N,N*-dimethylacrylamide (DMAAm), MACEE, and *N*-acryloxy succinimide (NASI) were copolymerized and reacted with GGGRGDSP.

Moghaddam and Matsuda mixed 0.5 mL of the polymer solution in phosphate-buffered saline with 0.5 mL of Dulbeco's modified Eagle medium (DMEM) containing 25,000 bovine aortic smooth muscle cells/mL. This mixture was exposed to ultraviolet light, causing the polymer to cross-link and form a hydrogel matrix. Cells entrapped within

this matrix took a few days to spread and proliferated slowly. It was suspected that either the 30 min of UV irradiation required to produce the gel damaged the cells, or the 3-D culture environment effected the proliferation rates (114).

Plant et al. created an *N*-(2-hydroxypropyl)methacrylamide (HPMA)–based hydrogel grafted with RGD. Incorporating glucosamine (NHGlc) or *N*-acetylglucosamine (AcNHGlc) into the polymer backbone enhances the biocompatibility of HPMA (115,116), and so RGD-modified HPMA was compared with these amino sugar–modified implants as well as unmodified HPMA. No control peptide was used.

Optic-tract lesions in 17- to 19-day-old PVG/c and Wistar rats were created and plugged with the experimental hydrogels. Nineteen-week-old PVG/c rats were given circular cortical lesions 500 μm in diameter that were again plugged with the hydrogels (all tested except AcNHGlc). Ten to 12 months after implantation, brains were excised and cryosectioned, and immunohistochemistry was performed. Positive staining for both glial fibrillary acidic protein and S100 marked astrocytes. Oligodendroglia could be identified with a stain against carbonic anhydrase II, and macrophages could be identified with a one against ED1. Antibodies against laminin (for evidence of neovascularization), neurofilaments, and myelin basic protein were also used.

Cortical Implant Results. Two unmodified HPMA plugs are implanted, but only one stayed in place for analysis. This showed no appreciable ingrowth. Macrophages were present outside the polymer, but not within it, and an astrocytic region surrounded the implant. Extensive integration was found around the two NHGlc-containing hydrogels, with 70% of the available hydrogel surface area attached to brain tissue. Laminin staining was evident throughout most of the hydrogel matrices. Astrocytes again surrounded the implant but the staining was only of low to moderate intensity, and unlike the unmodified HPMA a few astrocytes were present within the implant. There was evidence of a few ingrowing axons (average of 6 per section). Macrophage number and location were similar to unmodified HPMA, and here, too, no oligodendroglia could be seen in the implant.

One of the RGD-containing implants had become displaced, but of the remaining three, integration was very good, with about 90% of the available surface area attached to brain tissue. Laminin structures were evident throughout the hydrogels and were often associated with axonal ingrowth. The maximum number of axons found in one section was 78. An extensive matrix of astrocytes was also present within the implant, and there was little evidence of encapsulation by the surrounding tissue. Large numbers of macrophages were present, and no oligodendroglia could be located.

Optic Tract Implant Results. Four unmodified HPMA implants were used in these experiments. Only one of the four was found in the optic-tract lesion site after the brain was removed, and even this one was not attached to the host tissue. The surrounding tissue showed a low astrocytic response, and no astrocytes were found within the polymer matrix. There were no axons, oligodendroglia, or laminin in the polymer. Macrophages were present around the implant but not within.

The two NHGlc-modified implants showed attachment, with a good interface between host tissue and implant; however, a full bridge did not form across the lesion. Laminin staining indicated the presence of new blood vessels. A low number of astrocytes was found within the matrix. No oligodendroglia were present, and macrophages were present inside and outside the matrix. These appeared to be removing debris from the site, which would help explain these implants being a bit smaller than the unmodified HMPA. An average of six axons per section was found.

Three AcNHGlc implants were put into place. Only one of them was attached to host tissue. About 55% of available surface area on the implant was attached to tissue. Very little laminin and few astrocytes were seen in the matrix. No oligodendroglia and very few macrophages were seen in the implant. No axons had grown in.

Six of the seven RGD implants attached to host tissue, with about 75% of the available surface area attached. Laminin was present throughout the matrix and there were an extremely high number of astrocytes within the implant, with relatively little in the surrounding tissue. Many macrophages were present inside and outside of the implant and were in the same areas as astrocytes inside the implant. Five of the six implants showed axonal ingrowth, with an overall average of 36 axons per section. Once again axons were closely associated with laminin structures.

Poly(vinyl alcohol). GRGDSP were all immobilized to poly(vinyl alcohol) (PVA) by Matsuda et al. Hydroxyl groups on the surface of PVA films were activated with CDI, and the peptide in DMF was reacted with the surface. All unreacted active hydroxyl groups were reconverted to surface hydroxyls by treatment with a pH 8.1 solution.

Bovine aortic endothelial cells seeded on plain PVA surfaces in serum did not adhere, but cells seeded on peptide and fibronectin (covalently linked to the surface by the same method) did adhere and proliferate. In the absence of serum, cells on peptide-treated surfaces could be removed by soluble RGDS, indicating specificity for this reaction. The growth of cells at day 3 was greater on immobilized peptide than on fibronectin. Control over peptide density could be achieved by modifying the initial CDI reaction, and it was found that increasing the peptide density slightly enhanced cell growth (117).

Photocoupled Dimethacrylamide and PVA. Others have used coupling agents to covalently link peptides to polymers. Sugawara et al. immobilized an RGD-containing peptide (GGGRGDSP) to PVA and poly(*N*,*N*-dimethacrylamide-*co*-3-azidostyrene) (poly[DMAM]) using 4-azidobenzoyloxysuccimide. The succinimide reacted with the amine terminus of the RGD peptide and the azidobenzoyl bound to the polymer upon exposure to ultraviolet light. Photolysed phenyl-azido groups generate phenyl nitrenes, which are highly reactive (capable of addition to C=C bonds, insertion of C—H bonds, and abstraction of

protons from neighboring compounds). Even though the peptide was successfully immobilized to both polymers, the PVA also supported the nonspecific adsorption of the RGD peptide and was not used for most cell studies (118).

The poly(DMAM) alone did not support the adhesion and spreading of bovine aorta endothelial cells in serum-free medium, but once treated with photoimmobilized peptide, it did. These could be removed from the surface with soluble RGDS peptide, indicating a specific reaction between the cell and the immobilized peptide. A photomask was used to ensure peptide grafting to only specific areas of the polymer in a honeycomb or striped pattern. Cells were plated down in media without serum for a day and then switched to serum-containing media. Over the next few days, cells became confluent only in the peptide-grafted areas (118).

Silicon Dioxide

Rezania used this material to examine the morphology and attachment strength of cells to peptide-immobilized materials. Quartz surfaces were modified with an aminofunctional organosilane. A heterobifunctional cross-linker was used to link the terminal amines to the thiols of peptides with N-terminal cysteines. The experimental peptide was an RGD-containing sequence (CGGNGEPRGDTYRAY) derived from bone sialoprotein. A similar RGE-containing peptide was used as a control. Contact angle, ellipsometry, and ESCA were used to verify peptide attachment.

Cells used were isolated from neonate (6- to 12-day-old) rat calvaria and used at passage 2, 3, and 4. These were plated onto the test surfaces at 5,000 cells/cm^2 in DMEM with 1% bovine serum albumin (to block nonspecific binding).

To measure the strength of adhesion, a radial-flow apparatus (RFA) was used. This device is made of two parallel plates with a fluid jet in the center of one of the plates. The jet produces an axisymmetric flow pattern that in turn puts shear stresses on the surfaces of the plate. The shear stress at which 63.2% of attached cells would be expected to detach (Weibull characteristic strength) was significantly greater ($P < .05$) for RGD-grafted surfaces ($\approx 57 \pm 8$) than that of RGE-grafted surfaces ($\approx 37 \pm 4$).

Morphologically, cells were more spread ($P < .05$) on the RGD-grafted surfaces than on plain or RGE-grafted surfaces at 20 min and 2 h after plating. The spreading on the RGD was also significantly greater at 2 h than at 20 min (5). Fluorescent tagging of vinculin was also used to look at focal adhesion formation. RGE surfaces showed no focal adhesion formation even at 2 h. Though nothing was apparent at 20 min, at 2 h focal adhesions were present on the RGD-grafted surfaces. Focal adhesions were also present at 2 h when the substrate had been exposed to 15% serum-containing media. A major difference between RGD-grafted and serum-adsorbed surfaces was that the cells on the RGD showed many projections, while those on adsorbed serum were pancake shaped (5).

Fluorinated Ethylene Propylene

Vargo et al. developed a technique to immobilize peptides to the surface of a fluoropolymer without the use of coupling agents. Fluorinated ethylene propylene (FEP) was hydroxylated using radio-frequency glow discharge, forming FEP-OH. This material was immersed in DMSO containing YIGSR peptide and K_2CO_3. This was heated to 50°C and allowed to react for 72 h, and the peptide was linked to the surface via its *C*-terminus. Covalent attachment was verified with attenuated total reflection–fourier transform infrared spectrometry, and fluorescent microscopy of rinse solutions indicated against the presence of physisorbed YIGSR. The integrity of the immobilized peptide was verified by time-of-flight secondary-ion mass spectrometry (119).

It was found that increasing the time in the RFGD chamber increased the surface hydroxylation but that the optimal peptide incorporation was achieved between 0.5 to 1 min of plasma treatment (≈2% oxygen at 12-Å sampling depth). This may be due to a decrease in electron density at the surface or surface degradation with longer treatments. As would be expected, Vargo et al. found this technique to be applicable to a number of peptides (119,120).

FEP films were thus modified with the laminin-derived YIGSR and IKVAV sequences (IKVAV in the form of the peptide CSRARKQAASIKVAVSADR). NG108-15 neuroblastoma cell and PC12 pheochromocytoma cell attachment was evaluated.

Cell attachment was performed in serum-free media. All surfaces were preadsorbed with albumin to prevent nonspecific attachment. Quantification was done by randomly selecting a minimum of 300 cells per well under a Zeiss microscope equipped with Hoffman optics at 200× and developing a cells/area plot. To test for the specificity of attachment, soluble IKVAV-containing peptide or CDPYIGSR was used at 1 mg/mL concentration to block cell surface receptors in solution, preventing them from interacting with the immobilized peptide. As a further step, soluble CDPYIGSK was used as a soluble control peptide to ensure that a nonspecific reaction between cell and soluble peptide was not to blame for any decrease in adhesion.

The attachment of the NG108-15 cells to the YIGSR-modified surfaces in the absence of soluble peptide was statistically greater than that with soluble CDPYIGSR ($P < .05$). There was no statistical difference between no peptide and control peptide attachment ($P > .1$). Attachment of PC12 cells to IKVAV-modified surfaces showed a similar pattern, with attachment inhibited by soluble IKVAV peptide ($P < .001$) (120).

FEP surfaces have also been used to immobilize peptides for bone cell applications (121–123). Our lab has shown increased osteocalcin and osteonectin mRNA expression on RGD and RGE surfaces and increased osteocalcin mRNA and protein expression on RGD surfaces and has found that the cells successfully mineralized on all substrates. RAD-treated FEP did not show the same levels of protein and mRNA expression that RGD and RGE treated samples did (123).

Gold

With the exception of silane coupling agents and PepTite, the techniques described earlier, while effective, cannot be

directly applied to skeletal implant metals as they depend on covalent linkages with polymers. The gold–thiol bond has potential in this area.

Sulfur-containing molecules spontaneously form monolayers on gold surfaces. Gold interacts with ligands such as sulfur and phosphorous but remains inert to organic first-row elements (124). This makes this system especially useful for peptides, whose only non-first-row element is sulfur found in the amino acid cysteine.

The bond itself is not completely understood. Some call it covalent (125,126), while others refer to it as chemisorption (127). Basically, gold(I) (gold lacking one electron) thiolates ($RS^- Au^+$) are formed from gold(0) (gold lacking no electrons) and organosulfur species and adsorbed onto the gold(0) surface. This reaction requires the loss of a proton, possibly leaving as water or H_2. The bond energy is high: 40–45 kcal/mol (127).

Monolayers formed by this reaction tend to be close packed, resist the pooling of like molecules in a mixed surface, and require hours or days to exchange with thiols in solution to a significant degree (127,128).

Moodie et al. used cysteine-terminated peptides to evaluate bone cell responses to modified surfaces. Peptides were all solubilized in 50% ethanol at a concentration of 0.22 mM. Gold-coated substrates were exposed to this solution overnight to allow the thiols to react with the surface and the peptides to reach a stable arrangement. The resultant surface is diagrammed in Figure 1.

Cell attachment doubled in the first 20 min on RGDC-treated surfaces, even in the presence of serum (129), and an increased rate of spreading has been recorded over a 2-h time span (130). Alkaline phosphatase, a marker for bone cell maturation, was up-regulated on RGDC-treated gold as shown in Figure 2 (129).

Changes in mRNA expression for integrin subunits were also observed, with increasing α_5 and maintained β_1 expression over 19 days (decreased on plain gold or CG-immobilized surfaces) (129). As mentioned earlier, $\alpha_5\beta_1$ is a known RGD receptor.

Focal adhesions formed on RGDC-treated surfaces, and even after storage for 4 weeks in aqueous media, the percentage of cells showing focal adhesions remained high. This contrasts with adsorbed fibronectin, which lost its ability encourage focal adhesion formations under identical storage conditions during this time, eventually falling to the same level as plain gold surfaces (G. Moodie et al., unpublished data). In vivo bone formation was also increased around RGDC-treated rat femur intramedullary rods as compared to plain gold-coated rods (D. Ferris et al., unpublished data).

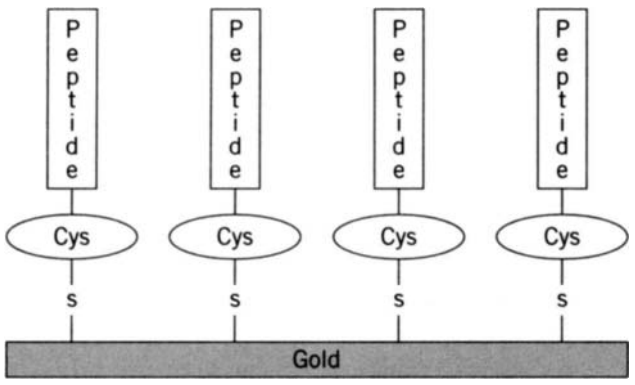


Figure 1. Peptide immobilized on gold through cysteine.

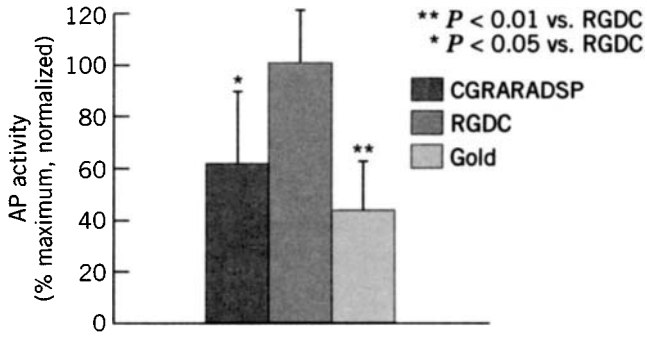


Figure 2. Alkaline phosphatase activity on peptide-modified gold surfaces.

BIBLIOGRAPHY

1. Y. Imanishi, Y. Ito, L. Liu, and M. Kajihara, *J. Macromol. Sci. Chem.* **A25**, 555–570 (1988).
2. M. Pierschbacher et al., *J. Cell. Biochem.* **56**, 150–154 (1994).
3. C. Brighton and S. Albelda, *J. Orthop. Res.* **10**, 766–773 (1992).
4. M. Pierschbacher and E. Ruoslahti, *Nature* **309**(3), 30–33 (1984).
5. A. Rezania et al., *Biomed. Mater. Res.* **37**, 9–19 (1997).
6. E. Ruoslahti, *J. Clin. Invest.* **87**, 1–5 (1991).
7. N. Sugano, H. Tanaka, K. Ito, and S. Murai, *J. Nihon Univ. Sch. Dent.* **39**(3), 154–155 (1997).
8. S. Vukicevic, F. Luyten, H. Kleinman, and A. Reddi, *Cell* **63**, 437–445 (1990).
9. R. Hynes, *Cell* **69**, 11–25 (1992).
10. G. Hannigan and S. Dedhar, *J. Mol. Med.* **75**, 34–44 (1997).
11. L. Kim and K. Yamada, *Proc. Soc. Exp. Biol. Med.* **214**, 123–131 (1997).
12. R. Juliano, *BioEssays* **18**, 911–916 (1996).
13. K. Vuori and E. Ruoslahti, *Science* **266**, 1576–1578 (1994).
14. N. Bartfeld, E. Pasquale, J. Geltosky, and L. Languino, *J. Biol. Chem.* **268**, 17270–17276 (1993).
15. N. Boudreau, C. Sympson, Z. Werb, and M. Bissell, *Science* **267**, 891–893 (1995).
16. R. Juliano and S. Haskill, *J. Cell Biol.* **120**(3), 577–585 (1993).
17. J. Meredith et al., *Endocr. Rev.* **17**(3), 207–213 (1996).
18. C. Roskelley, P. Desprez, and M. Bissell, *Proc. Nat. Acad. Sci. USA.* **91**(26), 12378–12382 (1994).
19. M. Schaller, *J. Endocrinol.* **150**, 1–7 (1996).
20. N. Wang, J. Butler, and D. Ingber, *Science* **260**, 1124–1127 (1993).
21. W. Staatz et al., *J. Biol. Chem.* **266**(12), 7363–7367 (1991).

22. S. Horowitz and M. Purdon, *J. Biomed. Mater. Res.* **29**, 477–484 (1995).
23. R. Friedman et al., *J. Bone Jt. Surg., Am. Vol.* **75-A**, 1086–1109 (1993).
24. L. Jones and D. Hungerford, *Clin. Orthop.* **225**, 192–206 (1987).
25. R. Austin and P. Stoney, *Injury* **13**(5), 414–418 (1982).
26. H.D. Huddleston, *J. Arthroplasty* **3**(4), 285–297 (1988).
27. J. Maguire, *Rheum. Dis. Clin. North Am.* **14**(3), 519–535 (1988).
28. J. Galante et al., *J. Orthop. Res.* **9**(5), 760–765 (1991).
29. A. Newens and R. Volz, *Anesthesiology* **36**(3), 298–300 (1972).
30. S. Bengston, K. Knutson, and L. Lidgren, *Clin. Orthop.* **245**, 173–178 (1989).
31. T. Kallos, J. Enis, F. Gollan, and J. Davis, *J. Bone Jt. Surg., Am. Vol.* **56-A**(7), 1363–1367 (1974).
32. K. Schulte, J. Callaghan, S. Kelley, and R. Johnston, *J. Bone Jt. Surg., Am. Vol.* **75-A**(7), 961–975 (1993).
33. D. Collins, S. Heim, C. Nelson, and P.I. Smith, *Clin. Orthop. Relat. Res.* **267**, 128–135 (1989).
34. K. Vince, J. Insall, and M. Kelly, *J. Bone Jt. Surg., Br. Vol.* **71**(5), 793–797 (1989).
35. G. Scuderi, J. Insall, R. Windsor, and M. Moran, *J. Bone Jt.J. Surg., Br. Vol.* **71B**(5), 798–803 (1989).
36. H. Cameron, *Clin. Orthop.* **208**, 81–83 (1986).
37. R. Pilliar, *J. Biomed. Mater. Res.* **21**(A1 Suppl.), 1–33 (1987).
38. M. Spector, *J. Arthroplasty* **2**, 163–177 (1987).
39. R. Haddad, S. Cook, and K. Thomas, *J. Bone Jt. Surg., Am. Vol.* **69-A**, 1459–1466 (1987).
40. P. Ducheyne et al., *Acta Orthop. Belg.* **40**(5–6), 799–805 (1974).
41. K. Soballe et al., *J. Orthop. Res.* **10**(2), 285–299 (1992).
42. C. Tisdel et al., *J. Bone Jt. Surg., Am. Vol.* **76-A**(2), 159–171 (1994).
43. A. Hoffman, *Artif. Organs* **16**(1), 43–49 (1992).
44. R. Hynes, *Cell (Cambridge, Mass.)* **48**, 549–554 (1987).
45. J. Bassuk et al., *Eur. J. Biochem.* **218**(1), 117–127 (1993).
46. P. Cardarelli et al., *J. Biol. Chem.* **267**(32), 23159–23164 (1992).
47. S. Cheng et al., *J. Med. Chem.* **37**(1), 1–8 (1994).
48. D. Cheresh and R. Mecham, eds., *Integrins: Molecular and Biological Responses to the Extracellular Matrix*, Academic Press, San Diego, Calif., 1994.
49. J. Clover, R. Dodds, and M. Gowen, *J. Cell Sci.* **103**, 267–271 (1992).
50. E. Danen, D. Ruiter, and G. Van-Muijen, *Biochem. Soc. Trans.* **23**(3), 403S (1995).
51. M. Ginsberg et al., *J. Biol. Chem.* **260**(7), 3931–3936 (1985).
52. J. Graf et al., *Cell* **48**(6), 989–996 (1987).
53. W. Grzesik and P. Robey, *J. Bone Miner. Res.* **9**(4), 487–496 (1994).
54. W. Grzesik, Y. Grzesik, and B. Ivanov, *17th Annu. Meet. Am. Soc. Bone Miner. Res.*, September 9–13, 1995, p. M268.
55. Y. Hirano et al., *J. Biomed. Mater. Res.* **25**, 1523–1534 (1991).
56. J. Hubbell, S. Massia, and P. Drumheller, *Ann. N.Y. Acad Sci* **665**, 253–258 (1992).
57. D. Hughes, D. Salter, S. Dedhar, and R. Simpson, *J. Bone Miner. Res.* **8**(5), 527–533 (1993).
58. K. Hultenby, F. Reinholt, and D. Heinegard, *Eur. J. Cell Biol.* **62**, 86–93 (1993).
59. Y. Iwamoto et al., *J. Cell. Physiol.* **134**(2), 287–291 (1988).
60. T. Lane, M. Iruela-Arispe, and E. Sage, *J. Biol. Chem.* **267**(23), 16736–16745 (1992).
61. T. Lane, M. Iruela-Arispe, R. Johnson, and E. Sage, *J. Cell Biol.* **125**(4), 929–943 (1994).
62. F. Maquart et al., *J. Clin. Invest.* **92**(5), 2368–2376 (1993).
63. S. Massia and J. Hubbell, *Anal. Biochem.* **187**, 292–301 (1990).
64. S. Massia and J. Hubbell, *Ann. N. Y. Acad. Sci.* **589**, 261–270 (1990).
65. A. Oldberg, A. Franzen, and D. Heingard, *J. Biol. Chem.* **263**, 19430–19432 (1988).
66. V. Pesakova, J. Novotna, and M. Adam, *Biomaterials* **16**(12), 911–915 (1995).
67. M. Pfaff et al., *J. Biol. Chem.* **269**(32), 20233–20238 (1994).
68. D. Puleo and R. Bizios, *Bone* **12**, 271–276 (1991).
69. E. Ruoslahti and M. Pierschbacher, *Science* **238**, 491–497 (1987).
70. T. Saito, S. Albelda, and C. Brighton, *J. Orthop. Res.* **12**(3), 384–394 (1994).
71. S. Van Dijk et al., *J. Bone Miner. Res.* **8**(12), 1499–1506 (1993).
72. B. Vogel et al., *J. Cell Biol.* **121**(2), 461–468 (1993).
73. J. Qian and R. Bhatnagar, *J. Biomed. Mater. Res.* **31**(4), 545–554 (1996).
74. S. Akiyama, K. Olden, and K. Yamada, *Cancer Metastasis Rev.* **14**(3), 173–189 (1995).
75. K. Gehlsen, W. Argraves, M. Pierschbacher, and E. Ruoslahti, *J. Cell. Biol.* **106**(3), 925–930 (1988).
76. I. Hart and N. Hogg, *Cell Adhesion and Cancer*, Cold Spring Harbor Lab. Press, Plainview, N.Y., 1995.
77. M. Humphries, K. Olden, and K. Yamada, *Science* **233**, 467–470 (1986).
78. M. Ginsberg, J. Loftus, and E. Plow, *Thromb. Haemostasis* **59**, 1–6 (1988).
79. W. Craig et al., *Biopolymers (Pept. Sci.)* **37**, 157–175 (1995).
80. M. Chorev, P. Dresner, Y. Eshel, and M. Rosenblatt, *Biopolymers* **37**(6), 367–375 (1995).
81. R. Dresner-Pollak and M. Rosenblatt,, *J. Cell. Biochem.* **56**(3), 323–330 (1994).
82. Y. Danilov and R. Juliano, *Exp. Cell Res.* **182**(1), 186–196 (1989).
83. M. Takatsuka, *ASAIO J.* **38**(3), M275–M278 (1992).
84. H. Lin et al., *J. Biomed. Mater. Res.* **28**, 329–342 (1994).
85. G. Sephel et al., *Biochem. Biophys. Res. Commun.* **162**(2), 821–829 (1989).
86. S. Aota, M. Nomizu, and K. Yamada, *J. Biol. Chem.* **269**(40), 24756–24761 (1994).
87. M. Pierschbacher et al., *Ciba Found Symp.* **136**, 131–141 (1988).
88. R. Howlett et al., *Biomaterials* **15**(3), 213–222 (1994).
89. B. Callen, R. Sodhi, R. Shelton, and J. Davies, *J. Biomed. Mater. Res.* **27**, 851–859 (1993).
90. J. Davies, *The Bone-Biomaterial Interface*, University of Toronto Press, Toronto, Ontario, Canada, 1991.
91. K. Healy et al., *Biomaterials* **17**(2), 195–208 (1996).
92. T. Matsuda and J. Davies, *Biomaterials* **8**, 275–284 (1987).
93. S. Peel, R. Sodhi, T. Duc, and J. Davies, *Mater. Res. Soc. Symp. Proc.* **252**, 71–77 (1992).
94. D. Puleo and R. Bizios, *J. Biomed. Res.* **26**, 291–301 (1992).

95. G. Schneider and K. Burridge, *Exp. Cell Res.* **214**, 264–269 (1994).
96. S. Cheng, S. Zhang, R. Civitelli, and L. Avioli, *17th Annu. Meet. Am. Soc. Bone Miner. Res.*, 1995, T223.
97. S. Dedhar, *J. Cell. Physiol.* **138**(2), 291–299 (1989).
98. R. Pytela et al., *Methods Enzymol.* **144**, 475–489 (1987).
99. B. Brandley and R. Schnaar, *Anal. Biochem.* **172**, 270–278 (1988).
100. S. Massia and J. Hubbell, *J. Biomed. Mater. Res.* **25**, 223–242 (1991).
101. J. Hubbell, S. Massia, N. Desai, and P. Drumheller, *Bio/Technology* **9**, 568–572 (1991).
102. S. Massia and J. Hubbell, *J. Cell Biol.* **114**(5), 1089–1100 (1991).
103. S. Massia, S. Rao, and J. Hubbell, *J. Biol. Chem.* **268**(11), 8053–8059 (1993).
104. Y. Ito, M. Sisido, and Y. Imanishi, *J. Biomed. Mater. Res.* **20**, 1157–1177 (1986).
105. H. Lin et al., *J. Biomater. Sci., Polym. Ed.* **3**(3), 217–227 (1992).
106. H. Lin et al., *J. Biomater. Sci., Polym. Ed.* **4**(3), 183–198 (1993).
107. H. Lin et al., *Biomaterials* **13**(13), 905–914 (1992).
108. M. Yanagi et al., *ASAIO J.* **40**(3), M412–M418 (1994).
109. W. Breuers, D. Klee, H. Hocker, and C. Mittermayer, *J. Mater. Sci. Mater. Med.* **2**, 106–109 (1991).
110. N. Desai and J. Hubbell, *Biomaterials* **12**, 144–153 (1991).
111. K. Tweden et al., *J. Heart Valve Dis.* **4**(Suppl. 1), S90–S97 (1995).
112. J. Beer, K. Springer, and B. Coller, *Blood* **79**(1), 117–128 (1992).
113. G. Plant, S. Woerly, and A. Harvey, *Exp. Neurol.* **143**, 287–299 (1997).
114. M. Moghaddam and T. Matsuda, *J. Polym. Sci., Part A: Polym. Chem.* **31**, 1589–1597 (1993).
115. S. Woerly et al., *Brain Res. Bull.* **30**, 423–432 (1993).
116. S. Woerly, Morassutti-DJ, *Cell Transplant.* **2**, 229–239 (1993).
117. T. Matsuda, A. Kondo, K. Makino, and T. Akutsu, *Trans. Am. Soc. Artif. Intern. Organs* **35**, 677–679 (1989).
118. T. Sugawara and T. Matsuda, *J. Biomed. Mater. Res.* **29**, 1047–1052 (1995).
119. T. Vargo et al., *J. Biomed. Mater. Res.* **29**, 767–778 (1995).
120. J. Ranieri et al., *J. Biomed. Mater. Res.* **29**, 779–785 (1995).
121. R. Valentini et al., *Trans. Soc. Biomater., 23rd Ann. Meet.*, April 30–May 4, 1997, Vol. 20, p. 55.
122. R. Valentini, L. Zou, and H. Kim, *Trans. Soc. Biomater., 21st Ann. Meet.*, March 18–22, 1995, Vol. 18, p. 65.
123. M. Sherling et al., *Artif. Organs* **21**(6), 497 (1997).
124. C. Bain and G. Whitesides, *Science* **240**, 62–63 (1988).
125. C. Duschl, M. Liley, and H. Vogel, *Angew. Chem., Int. Ed. Engl.* **33**(12), 1274–1276 (1994).
126. C. Duschl, M. Liley, G. Corradin, and H. Vogel, *Biophys. J.* **67**, 1229–1237 (1994).
127. G. Whitesides and P. Laibinis, *Langmuir* **6**(1), 86–96 (1990).
128. C. Bain and G. Whitesides, *J. Am. Chem. Soc.* **111**, 7164–7175 (1989).
129. G. Moodie et al., *Trans. Soc. Biomater., 24th Annu. Meet.*, April 22–26, 1998, Vol. 21, p. 116.

Next Page

TRANSDERMAL DRUG DELIVERY, ELECTRICAL

JANET TAMADA
Cygnus, Inc.
Redwood City, California

KEY WORDS

Electrical
Electroosmosis
Electroporation
Enhancer
Iontophoresis
Skin
Stratum corneum
Transdermal

OUTLINE

Introduction
Iontophoresis
- Transport Pathway
- Description and Mechanisms of Transport
- Factors Controlling Delivery Rate
- Toxicology
- Electrode Design
- Applications of Iontophoresis

Electroporation
- Basic Principles
- Comparison of Tissue Electroporation and Iontophoresis
- Applications of Skin Electroporation
- Physiological Effects

Bibliography

INTRODUCTION

Electrically assisted transdermal delivery uses electric fields to enhance transport of active agents across the skin. Iontophoresis and electroporation are the two major methods of electrically assisted transdermal delivery. These methods avoid the gastrointestinal degradation and hepatic first-pass metabolism found in oral administration. Both local delivery (e.g., lidocaine for topical anesthesia) and systemic drug administration (e.g., fentanyl for pain relief) are possible. Both methods can enhance drug flux up to several orders of magnitude above that allowed by passive diffusion (as in conventional skin patches), depending on the nature of the solute. Whereas the effective delivery range for passive diffusion across the skin is con-

95. G. Schneider and K. Burridge, *Exp. Cell Res.* **214**, 264–269 (1994).
96. S. Cheng, S. Zhang, R. Civitelli, and L. Avioli, *17th Annu. Meet. Am. Soc. Bone Miner. Res.*, 1995, T223.
97. S. Dedhar, *J. Cell. Physiol.* **138**(2), 291–299 (1989).
98. R. Pytela et al., *Methods Enzymol.* **144**, 475–489 (1987).
99. B. Brandley and R. Schnaar, *Anal. Biochem.* **172**, 270–278 (1988).
100. S. Massia and J. Hubbell, *J. Biomed. Mater. Res.* **25**, 223–242 (1991).
101. J. Hubbell, S. Massia, N. Desai, and P. Drumheller, *Bio/Technology* **9**, 568–572 (1991).
102. S. Massia and J. Hubbell, *J. Cell Biol.* **114**(5), 1089–1100 (1991).
103. S. Massia, S. Rao, and J. Hubbell, *J. Biol. Chem.* **268**(11), 8053–8059 (1993).
104. Y. Ito, M. Sisido, and Y. Imanishi, *J. Biomed. Mater. Res.* **20**, 1157–1177 (1986).
105. H. Lin et al., *J. Biomater. Sci., Polym. Ed.* **3**(3), 217–227 (1992).
106. H. Lin et al., *J. Biomater. Sci., Polym. Ed.* **4**(3), 183–198 (1993).
107. H. Lin et al., *Biomaterials* **13**(13), 905–914 (1992).
108. M. Yanagi et al., *ASAIO J.* **40**(3), M412–M418 (1994).
109. W. Breuers, D. Klee, H. Hocker, and C. Mittermayer, *J. Mater. Sci. Mater. Med.* **2**, 106–109 (1991).
110. N. Desai and J. Hubbell, *Biomaterials* **12**, 144–153 (1991).
111. K. Tweden et al., *J. Heart Valve Dis.* **4**(Suppl. 1), S90–S97 (1995).
112. J. Beer, K. Springer, and B. Coller, *Blood* **79**(1), 117–128 (1992).
113. G. Plant, S. Woerly, and A. Harvey, *Exp. Neurol.* **143**, 287–299 (1997).
114. M. Moghaddam and T. Matsuda, *J. Polym. Sci., Part A: Polym. Chem.* **31**, 1589–1597 (1993).
115. S. Woerly et al., *Brain Res. Bull.* **30**, 423–432 (1993).
116. S. Woerly, Morassutti-DJ, *Cell Transplant.* **2**, 229–239 (1993).
117. T. Matsuda, A. Kondo, K. Makino, and T. Akutsu, *Trans. Am. Soc. Artif. Intern. Organs* **35**, 677–679 (1989).
118. T. Sugawara and T. Matsuda, *J. Biomed. Mater. Res.* **29**, 1047–1052 (1995).
119. T. Vargo et al., *J. Biomed. Mater. Res.* **29**, 767–778 (1995).
120. J. Ranieri et al., *J. Biomed. Mater. Res.* **29**, 779–785 (1995).
121. R. Valentini et al., *Trans. Soc. Biomater., 23rd Ann. Meet.*, April 30–May 4, 1997, Vol. 20, p. 55.
122. R. Valentini, L. Zou, and H. Kim, *Trans. Soc. Biomater., 21st Ann. Meet.*, March 18–22, 1995, Vol. 18, p. 65.
123. M. Sherling et al., *Artif. Organs* **21**(6), 497 (1997).
124. C. Bain and G. Whitesides, *Science* **240**, 62–63 (1988).
125. C. Duschl, M. Liley, and H. Vogel, *Angew. Chem., Int. Ed. Engl.* **33**(12), 1274–1276 (1994).
126. C. Duschl, M. Liley, G. Corradin, and H. Vogel, *Biophys. J.* **67**, 1229–1237 (1994).
127. G. Whitesides and P. Laibinis, *Langmuir* **6**(1), 86–96 (1990).
128. C. Bain and G. Whitesides, *J. Am. Chem. Soc.* **111**, 7164–7175 (1989).
129. G. Moodie et al., *Trans. Soc. Biomater., 24th Annu. Meet.*, April 22–26, 1998, Vol. 21, p. 116.

Previous Page

TRANSDERMAL DRUG DELIVERY, ELECTRICAL

JANET TAMADA
Cygnus, Inc.
Redwood City, California

KEY WORDS

Electrical
Electroosmosis
Electroporation
Enhancer
Iontophoresis
Skin
Stratum corneum
Transdermal

OUTLINE

Introduction
Iontophoresis
- Transport Pathway
- Description and Mechanisms of Transport
- Factors Controlling Delivery Rate
- Toxicology
- Electrode Design
- Applications of Iontophoresis

Electroporation
- Basic Principles
- Comparison of Tissue Electroporation and Iontophoresis
- Applications of Skin Electroporation
- Physiological Effects

Bibliography

INTRODUCTION

Electrically assisted transdermal delivery uses electric fields to enhance transport of active agents across the skin. Iontophoresis and electroporation are the two major methods of electrically assisted transdermal delivery. These methods avoid the gastrointestinal degradation and hepatic first-pass metabolism found in oral administration. Both local delivery (e.g., lidocaine for topical anesthesia) and systemic drug administration (e.g., fentanyl for pain relief) are possible. Both methods can enhance drug flux up to several orders of magnitude above that allowed by passive diffusion (as in conventional skin patches), depending on the nature of the solute. Whereas the effective delivery range for passive diffusion across the skin is con-

strained to small, hydrophobic agents, electrically enhanced delivery can be used for larger, hydrophilic molecules, which is particular advantageous for peptide and oligonucleotide drug administration. Additionally, these methods can be programmed to varied levels for nonconstant delivery patterns, such as for pain management. However, there are practical constraints. The efficiency of transdermal delivery is low, so applications are limited to potent compounds. Irritation, metabolism, and interaction of the agent with the skin can also limit application. The literature on electrically enhanced delivery is extensive, particularly for iontophoresis, and the reader is directed to more complete reviews (1–8).

The skin functions as a physical, chemical, and microbial barrier to transport and is divided into the subcutaneous tissue, the dermis, and the epidermis. The outermost layer of the epidermis is the stratum corneum, which is generally the primary barrier to transport across the skin. In a classic description, the stratum corneum is described as being composed of dense, protein-rich, keratin "bricks" and a more fluid, lipid filled "mortar" (9), which is a multilamellar structure of lipid bilayers that forms a circuitous pathway around the keratinocytes. Additionally, structures such as hair follicles, sebaceous glands, and sweat ducts, collectively known as skin appendages, play a major role in electrically enhanced transport. The skin poses another barrier in that it can metabolize compounds, and the extent of drug loss prior to absorption by the blood stream will adversely affect its effective transport (10). Comprehensive reviews of skin physiology, particularly relating to transdermal delivery, are available (11,12).

IONTOPHORESIS

Iontophoresis involves application of a low-level electrical current across the skin. Iontophoresis uses two electrodes, the anode and the cathode, each of which is in contact with a reservoir containing an electrically conductive medium, which is, in turn, in contact with the skin (Fig. 1). The agent to be delivered is contained in one the reservoirs in an aqueous solution. An electrical potential is applied across the electrodes, causing current to flow across the skin and facilitating delivery of the therapeutic agent. The first well-documented experiments that reported using iontophoresis for delivery of an active agent were performed in 1900 by LeDuc, who demonstrated the delivery of positively charged strychnine sulfate into rabbits, causing convulsions when placed in the anode but no effect when placed in the cathode. Negatively charged cyanide caused poisoning when delivered from the cathode but no effect when delivered from the anode (13).

Transport Pathway

The transport pathway of molecules through skin under the influence of an electric field may be through the skin appendages, across the keratinocytes, or through the multilamellar lipid bilayers. For passive transdermal diffusion, it has been established that diffusion through the lipid layers is the dominant transport mechanism. However, for iontophoresis, substantial evidence indicates that most ion transport occurs through the pathways of lowest electrical resistance, which consist of hair follicles, sweat ducts, and skin imperfections (4). It has been shown in a number of studies that the route of ion transport is elevated in localized areas (14). Evidence includes methylene blue iontophoresis showing a pattern of blue dots on the skin (15), a vibrating-probe study showing locally high areas of current flow (16), and iontophoretic transport of $Fe(CN)_6^4$ coupled with scanning electrochemical microscopy (17) showing that areas of ion transport were associated with hair follicles. However, results also indicate that hair follicles alone do not account for the totality of transdermal flux (18), and some additional route may be present. Confocal microscopy of two dyes with different physicochemical properties indicated that the transport pathways can vary with the properties of the permeant (19). Evidence of transport through the lipid bilayer route has been found in studies of mercuric chloride iontophoresis through porcine skin. Transmission electron microscopy showed evidence of staining by the transported compound within the lipid bilayers (20).

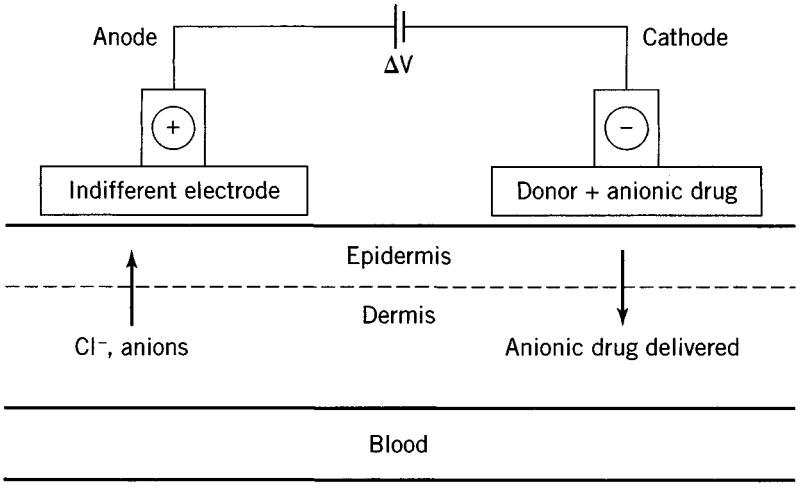


Figure 1. Schematic of iontophoretic drug delivery system. Example shows delivery of an anionic agent from the cathodal reservoir. The agent goes through the nonvascularized epidermis and into the dermis, where it can be transported into the blood through the capillary loops. The counter electrode is sometimes known as the indifferent electrode.

Description and Mechanisms of Transport

Mechanisms of Transport. Drug transport under the influence of iontophoretic current has three main contributions: electrophoretic, passive, and electroosmotic. The electrophoretic transport is caused by the electrical potential gradient applied to the charged species. Anionic (negatively charged) species are driven away from the cathode and towards the anode; cationic (positively) charged species are driven away from the anode and towards the cathode.

The electrophoretic transport for charged species is giving by the following equation:

$$J_{i,\text{electrophoretic}} = D_i C_i \frac{z_i F}{RT} \frac{dE}{dx}$$

where J_i is the flux of the ith species, D_i is its diffusion coefficient, C_i is its concentration, and z_i is its charge. F is Faraday's constant, R is the gas constant, T is absolute temperature, and E is the electric field.

Passive diffusion results from the concentration driving force. The passive diffusion contribution is described by the classic Fick's Law description:

$$J_{i,\text{positive}} = D_i\left(\frac{dC_i}{dx_i}\right)$$

The Nernst–Planck equation is the sum of the electrophoretic and passive diffusive contributions.

Electroosmotic transport is a convective flow of solvent induced by the application of a voltage gradient across a charged, porous medium (14,21). The transport pathways in the stratum corneum generally have a net negative charge. When an electric field is applied across the skin, cations, mostly sodium in the case of a physiological system, are preferentially passed through the skin due to the net negative charge. Volume flow toward the cathode is created by momentum transfer from the cations to the surrounding fluid (22,23). The magnitude of the flow is small, on the order of $\mu L/cm^2/h$, but for large or neutral molecules, it can have a substantial impact on skin flux (24,25). The electroosmotic effect can decrease the transport from the cathode compared with passive diffusion, because the molecule is moving against the direction of electroosmotic flow, impeding its progress (26).

Electroosmotic transport has the following form:

$$J_{i,\text{electroosmotic}} = C_i v$$

where v is the electroosmotic flow rate. In-depth mathematical descriptions and derivations are available (27–29).

Transport Number. An important concept in iontophoretic delivery is the transport, or transference, number. The transport number is a measure of how efficiently the agent of interest is transported relative to the other ions present in the system. It is an indicator of the permselectivity properties of the skin (30). A detailed description of the concept is give by Phipps and Gyory (31). The flux is characterized by

$$J_i = \frac{t_i I_i}{z_i F}$$

where t_i is the ion transport number and I_t is the total current density applied. F is Faraday's constant, and z_i is the charge on the ith ion. For example, for skin at physiological pH the transport numbers of sodium and chloride are approximately 0.66 and 0.33, respectively, indicating that for a given current, more sodium will flow across the skin than chloride and that the skin has a higher permselectivity for sodium than chloride. Therefore, the flux of the molecule of interest is controlled by its mobility *relative* to the other ions that undergo transport. Thus, increasing passive permeability of the skin does not necessarily lead to increased iontophoretic transport of the target molecule. If the mobility of permeants through the skin increases due to an increase in skin permeability, sodium and chloride are also more easily transported, and the applied voltage necessary to generate a current decreases, which may counteract any enhanced mobility of the target permeant.

Factors Controlling Delivery Rate

Experimental Methods. Skin flux of the drug of interest is commonly tested in vitro in diffusion cells with a layer of skin between the two reservoirs. Various configurations of diffusion cells are available (32–35). Common skin sources are cadaver skin; hairless mouse, rat, and guinea pig skin; pig skin; and shed snake skin (36). Animal models, such as hairless rat, mouse, and guinea pig and pigs, are used for in vivo studies, but studies on human subjects are limited to relatively few compounds. In vivo and in vitro results have been shown to correlate well (37,38), although the correlation may vary with the particular compound and drug of interest.

A novel model that is intermediate between a live animal and cadaver or animal skin is the isolated perfused porcine skin flap, developed by Riviere et al. This model uses excised tissue from the belly of the pig, which can be perfused to maintain tissue viability over the course of a 1-day experiment (39–41).

Drug Physicochemical Properties. Generally, smaller and more highly charged molecules will be delivered more effectively by iontophoresis than larger, neutral molecules (42–45). The isoelectric point of the skin is between 4 and 5, so molecules that are charged between the pI of the skin and physiological pH are most suitable (46). Under most conditions, the skin has a net negative charge, so cationic compounds are transported more readily than similar anionic compounds. Hydrophilic compounds transport more readily than similar hydrophobic compounds (47). There is no particular molecular weight cutoff for iontophoretic delivery; however, 1,000 to 3,000 Da is probably the highest molecular weight that could be effectively delivered with present technology. Analysis of a variety of compounds of various molecular weights have been reported (48,49), including an elegant study of various molecular weights of poly(ethylene glycol), an uncharged polymer (50).

Certain compounds can change the electroosmotic transport properties of the skin as they are delivered

(23,51,52). This was discovered from the observation that drug flux for certain peptides did not increase as expected with increasing peptide donor concentration. An investigation of the transport of mannitol, an uncharged compound commonly used to investigate electroosmosis, with the concurrent delivery of the peptides leuprolide and Nafarelin showed a decrease in electroosmotic flow in the presence of the peptide. The mechanism is proposed to be peptide binding to the transport pathway in the skin, with the positive charge of the peptide decreasing the permselectivity of the skin toward sodium and decreasing electroosmotic flow. Electroosmotic flow was increased slightly by using an anionic compound, poly-*l*-lysine, but the effect was less dramatic than the converse decrease for the cationic peptides (53).

The rational design of drug compounds to enhance their iontophoretic mobility, thereby increasing therapeutic efficacy, is an emerging development (54). Systematic modifications of insulin analogs, generated by recombinant DNA technology, have been studied. The delivery of monomeric insulin with two additional negative charges, created by substitute of aspartate and glutamate for uncharged residues, was 100 times more than regular, hexameric human insulin (55).

Current Application Protocol. The current levels used are low, typically in the mA to sub-mA range, with a typical maximum current density of 0.5 mA/cm^2 of skin. The practical current density maximum is primarily limited by the skin irritation that results from the current flow, although sensation associated with the current can be limiting for large application areas. Normally, current is applied across the skin in a constant, direct-current mode. Numerous studies have established the linearity of drug flux with current density for the vast majority of compounds (30,32,44,56,57).

Neutral molecules also show a linear flux relationship to current density because the electroosmotic flow is proportional to sodium transport, which is proportional to current density. The amount of drug delivered is proportional to the amount of delivery time, although there can be an onset period before flux stabilization occurs. However, as iontophoresis duration progresses, accumulation of ions in the reservoir, depletion in drug donor concentration, pH changes, or interaction of the drug with skin can cause a decrease in flux over long-duration experiments (58).

The application of the iontophoretic current has been shown to affect the subsequent passive diffusion of molecules, suggesting that the intrinsic permeability of the skin is increased by the applied current (24,25,27,59–62). Studies of electrical resistance indicate there are changes in the skin following iontophoresis (63,64), but the exact mechanism is unknown. There are no apparent changes in skin permselectivity, as evidenced by the linear relationship of drug flux to current and duration of application.

Constant-voltage, rather than constant-current, iontophoresis has also been used (65). There has also been work using pulsed, rather than constant-current, iontophoresis (5,66) showing enhanced transport from high-frequency pulsing. Interpretation of the effectiveness of these techniques relative to conventional iontophoresis can be complex. Constant-voltage iontophoresis is complicated by the decrease in skin resistance that occurs after application of current (63). From Ohm's Law, as the resistance decreases, current increases, which causes an increase drug transport. However, there is no evidence that the inherent efficiency of transport has been improved. The concept of rapid pulsing developed from the observed decrease in electrical skin impedance as pulse frequency increases. However, it is resistance, not impedance, that is related to ion transport across the skin. Several controlled studies of pulsing showed little or no effect of pulse frequency on ion transport (2,67,68).

Characteristics of the Reservoir Medium. The composition of the reservoir formulation can profoundly affect the delivery rate of the therapeutic agent (69). The concentration of the drug in the donor reservoir is one important parameter. Generally, the drug flux is linear with increasing concentration (47,70), although aggregation, interaction with the skin, and other factors can lead to nonlinear concentration effects (23). Maximum drug concentration is dictated by solubility, although self-aggregation, cost, and other factors affect optimal drug donor concentration.

The pH of the medium affects the drug charge, which, depending on the pK_a, affects its mobility. As stated earlier, charged, especially positively charged, drugs are transported more easily through the skin. A pH gradient between the donor formulation and physiological pH can cause the drug to get "stuck" in the middle of the skin. As the drug moves through different pH environments, it reverses charge and will be driven back in the direction from which it came (41,71). In addition to affecting the charge on the drug, the pH of the medium changes the relative charge on the skin, thus changing its permselectivity (72). As pH of the reservoir is decreased to less than 4.0–5.0, the skin undergoes a transition from being a net negatively charged membrane to a positively charged membrane, and it will become increasingly favorable to anion permeation. Conversely, as pH increases above 4.0–5.0, the skin becomes negatively charged, and cation and electro-osmotic delivery will be favored. The range of physiologically acceptable pH is usually considered to be pH 4.0–9.0.

Another important characteristic of the donor reservoir is the ionic strength and presence of competing ions in the formulation (70,73). Because the total amount of current delivered is constant, a high ionic strength donor and competing ions compete with the drug for the charge transfer and decrease the drug flux. Therefore, it is generally good practice to keep extraneous ions at an absolute minimum. However, the donor must be sufficiently buffered to prevent any side reactions from electrode reactions and to keep the drug in the appropriately ionized state.

Skin Pretreatment. Skin pretreatments have been used with varying effects. Some have reported successful synergistic enhancement over iontophoresis and passive enhancement alone for using oleic acid for AZT (74), ethanol for insulin (55,75,76), and depilatory lotion for insulin (77), whereas others report no enhancement effect (78) or varied enhancement (79). Vasomodulating agents can also alter drug flux. Co-iontophoresis of vasoconstrictors decrease

flux, whereas co-iontophoresis of vasodilators increase delivery (80). The application of proteolytic enzyme inhibitors to prevent the metabolism of peptides in the skin, thereby increasing the absorption efficiency, has been reported (81,82).

Toxicology

The application of the iontophoretic current can cause skin irritation and possibly affect the skin barrier function (83,84). Erythema (redness) and edema (swelling) can result to various degrees depending on formulation, duration, current density, and polarity. Generally, the irritation decreases within hours, although it may take a few days for complete resolution. Additionally, the active agent itself may cause irritation or sensitization of the skin. Studies of prostaglandin E2 (PGE2) release, by sampling using reverse iontophoresis, shows a difference in PGE2 release for several different active agents. PEG2 was correlated with erythema/edema scores (85). The effect of the pK_a of the transported species, among salicylic acid, salicylamide, *m*-nitrobenzoic acid, and *m*-anisic acid (pK_a range from 3.0 to 8.1) showed a sharp increase in irritation as the pK_a of the drug decreased to less than 4 (86). Irritation resulting from lidocaine and luteinizing hormone–releasing hormone (LH-RH) iontophoresis has been examined for gross changes (erythema and edema) and histologically, and the alteration caused by the iontophoresis resolved and had minimal toxicological significance (87,88). Studies using techniques such as measurement of transepidermal water loss, laser Doppler flowmetry, skin capacitance, and skin temperature postiontophoresis showed moderate response and no change in skin permeability or integrity (89,90).

Electrode Design

Electrode design is an important part of an iontophoretic device (33). A number of different types of electrodes have been used in iontophoresis, both for research and commercial applications, including platinum, stainless steel, and carbon. A widely used electrode system is the Ag/AgCl system (91) because it maintains the pH of the iontophoretic medium and has no negative toxicological implications. For Ag/AgCl electrodes, the following reactions occur stoichiometrically:

$$\text{Reaction on the anode: } Ag + Cl^- \rightarrow AgCl + e^-$$

$$\text{Reaction on the cathode: } AgCl + e^- \rightarrow Ag + Cl^-$$

These reactions maintain the pH of the reservoir at a constant level. Platinum and other metal electrodes can have an undesirable hydrolysis reaction, particularly at the cathode:

$$\text{Reaction on the cathode: } H_2O + e^- \rightarrow OH^- + 1/2H_2$$

The resultant high pH is not compatible with living skin tissue. Furthermore, the hydroxide ions formed from the reaction are driven into the skin by the negative charge on the cathode, which can cause a small, but relatively deep, localized skin injury. However, it is possible to circumvent the pH changes caused by water hydrolysis by buffering the medium sufficiently to prevent large pH swings (92).

Another aspect of electrode design is prevention of accumulation of unwanted ions as iontophoresis current accumulates. For example, if the drug is anionic and is being delivered from the cathode, for the Ag/AgCl system, the concentration of chloride ions in the medium will increase over time and will eventually compete with the drug for the available current flow. This would cause a steady decrease in drug transport over the duration of the iontophoresis application period.

Applications of Iontophoresis

Several local and subcutaneous conditions have been treated by iontophoresis. Lidocaine iontophoresis for localized analgesia is a common commercial application (93,94). The Iontocaine® (Iomed, Salt Lake City) is a U.S. FDA–approved combination drug–device system. Topical epinephrine (93), dexamethasone, hydrocortisone (95), and prednisolone has been reported. Antiinflammatory drugs (e.g., diclofenac and ketoprofen) have been given to relieve pain, and steroids and retinoids have been used to treat scarring (46). Other local applications include delivery of antivirals and corticosteroids for herpes infections (96). Irritation reduction by administration of antiflammin 1 peptide has been demonstrated (97). Iomed (Salt Lake City), Iontophor-PM (Life-Tech, Houston, TX), and other companies also produce commercial power supplies with multipurpose electrode reservoirs and electrodes for iontophoresis, which are marketed primarily for localized applications.

Systemic administration of drugs is also possible. Fentanyl is in clinical trials for pain relief (46). Apomorphine, for treatment of idiopathic Parkinson's disease, has been tested in human subjects (37,98). Peptide drugs have been a major target of iontophoresis, and various reviews are available (1,2,4,5,41,99–101). Peptides that have been tested include thyotropin release hormone (56), various series of amino acid derivatives and tripeptides (45,60,62), LH-RH and analogs (23,38,57), vasopressin (5,71,73,75), and calcitonin (102,103). Transdermal delivery of insulin has been reported in vitro and in animal models (41,54,55,77,104–110).

There are applications of iontophoresis in addition to transdermal delivery of a therapeutic agent, and in fact some of these have been the most commercially successful applications (111). Hyperhydrosis, excessive sweating, has been successfully treated with application of iontophoretic current and no additional therapeutic agent (112–116). The Drionic device (General Medical Products, Los Angeles) is a commercial example. Iontophoresis has been applied to the eye to deliver compounds intraocularly (117–121), to the teeth to reduce hypersensitivity (96,122,123), across the nail (124), and to the ear (125). One of the first commercial uses of iontophoresis was for a cystic fibrosis diagnostic test (126): Iontophoresis is used to deliver pilocarpine to the skin to induce sweating, and the sweat is collected and tested for chloride content, which is used as

a diagnostic marker for cystic fibrosis (127,128). This device is available from Wescor, Inc. (Logan, Utah). A newer application of iontophoresis is to extract substances from the body for diagnostic purposes (129–131). Proof of concept of this application for a noninvasive glucose-monitoring system for diabetics has been established. The electroosmotically extracted glucose flux was found to be proportional to the concentration of glucose in the blood (132).

ELECTROPORATION

Basic Principles

Electroporation involves the application of a short, high-voltage pulse across a lipid membrane, which creates transient pores in the lipid bilayers, a phenomenon sometimes known as reversible electrical breakdown (REB) (133). Electroporation has been used for a number of years in cell biology and biophysics, primarily as a method to introduce DNA into isolated cells (134–136). The idea of applying electroporation to whole tissues to increase permeability for drug delivery is a relatively recent development (137). Electropermeabilization of tissue has been used to deliver chemotherapy agents to tumors in vivo, increasing the efficacy of uptake of the agent into the tumors and thus improving effectiveness of the chemotherapy (138–143). Electroporation has also been used to deliver DNA into intact tissue in vivo (144,145). Pioneering work by Prausnitz et al. on transdermal electroporation demonstrated enhanced delivery of molecules through the skin after application of short, high-voltage pulses (146). Electroporation of mammalian skin was shown to increase flux by up to four orders of magnitude over passive delivery for three polar molecules with molecular weights up to slightly more than 1,000 Da. Studies on hairless rats showed similar increases in flux in vivo. After the pulsing was stopped, transdermal flux decreased by more than 99% within 1 or 2 h, indicating significant reversibility of the permeability increase. The transient nature of the permeability change is consistent with the proposal that there is reversible electric breakdown in the skin lipid layers.

There is strong evidence in the literature that in isolated cells, electroporation causes the molecules in the lipid bilayer of the cell membrane to reorient themselves to form a transient hydrophilic pore. After the pulse application is stopped, the pores can reseal over a period of milliseconds to hours, depending on the duration and magnitude of the applied pulse. This allows large molecules, such as DNA, to get into the cell but allows for resealing so that the cell retains viability. The lipid bilayer structure of the skin suggests that it could also be effectively electroporated. However, the skin lipid layers are multilamellar and are composed of different types of lipids than unilamellar cell membranes, so the conditions for skin and cell electroporation may differ. The required transdermal potential to create sufficient transbilayer potentials in the multiple lipid bilayers of the skin for electroporation is in the tens to hundreds of volts. The pulse duration can be a square or an exponentially decaying capacitive discharge, with time constants in the micro- to millisecond range.

Comparison of Tissue Electroporation and Iontophoresis

Although electroporation and iontophoresis both involve application of an electric current across the skin, the mechanism of transport enhancement is generally accepted to be different. Iontophoresis enhances transport through the electric field–gradient driving force. Electroporation enhances the permeability of the skin by altering skin structure. Any driving force—iontophoretic, passive, electroosmotic—can be applied postelectroporation to effect flux enhancement compared with nonelectroporated skin. At this time, the mechanism for electroporation of skin is not as well understood as for cell membranes. Actual visualization of the pores is difficult, owing to their small size and fluctuating nature, so lipid reorientation to form hydrophilic pores must be inferred.

There is mounting evidence that electroporation creates dramatic alterations of the skin structure, as shown from studies of skin permeability changes, skin electrical impedance, microscopic imaging, and mathematical modeling (147). Studies of calcein flux showed that there is a sharp increase in skin flux at a threshold of about 60 V across the skin, followed by linear transport increases and then a plateau. The flux rapidly decreases when pulsing is stopped. The sudden increase in permeability once a voltage threshold has been attained and the reversibility of the permeability increase suggest that the mechanism of enhanced transport in skin lipids may be similar to that of electroporation in individual cells. Studies of the electrical properties of the skin demonstrated that changes in the skin barrier properties from pore formation did occur during high-voltage pulsing and did not occur during low-voltage iontophoresis (148,149). Confocal microscopy, a technique that images fluorescent molecules within the skin, has shown localized transport regions associated with electroporation that are not present under iontophoretic conditions (150,151). These regions may be associated with altered skin structure resulting from electroporation. Modeling of theoretical flux under low- and high-field strengths has led to the hypothesis that electroporation causes a unique form of transport enhancement (152).

Examinations of the transport number to compare efficiency of transport between electroporated and nonelectroporated skin have been reported. The flux of calcein, a highly charged model compound, was compared under a series of high-voltage pulses versus low-voltage iontophoresis. Enhancement of transport efficiency for both small and large ions was demonstrated (153). Electroporation has been used in conjunction with iontophoresis, and studies of the effect of electroporation on iontophoretic transport number were performed. Transdermal skin flux under iontophoresis of LH-RH, vasopressin, and neurotensin were three to eight times greater after the application of a single electroporative pulse than the same iontophoretic current without the pulse. This suggests some modification of the skin transport properties due to the electroporative pulse (154).

Conversely, Higuchi et al. have hypothesized that traditional low-voltage iontophoresis induces pore formation

and that large-voltage pulses are not necessary (26,155,156). It is well documented that regular iontophoresis has been shown to increase passive skin permeability and change the electrical properties of the skin (61). However, it is uncertain whether this is actual electroporation of the lipid bilayers of the skin or some other phenomenon. In a combined theory, it has been proposed that application of voltages in the 1- to 5-V range, levels found in typical iontophoresis, causes electroporation through breakdown of the epithelial cells lining the walls of the skin appendages (sweat ducts and/or hair follicles). Further increases in voltage to tens of volts can cause the stratum corneum lipid lamellae to form pores, but the authors propose that such a pathway is not sufficient to provide a continuous pathway for effective transport. They suggest that a combination of passage through the keratinocytes and lipid bilayers is the transport pathway in high-voltage, pulsed electroporation (157).

Applications of Skin Electroporation

Practical application of electroporation is less advanced than for iontophoresis. A number of researchers have completed initial studies of potential applications of electroporation. Faster response has been suggested as an advantage of electroporation over iontophoresis and passive transdermal delivery, which could be an advantage for pain management applications (158). Vanbever et al. have studied the kinetics of transport of fentanyl, an analgesic therapeutic agent, both in vitro (159) and in vivo (160). Effective analgesia was achieved in hairless rats with rapid onset. Vanbever studied transport of metoprolol (161). Wang et al. have examined topical delivery of cyclosporin A for the treatment of psoriasis (162,163). Jadoul and Preat investigated electroporative and iontophoretic flux of domperidone (164). Delivery of various peptides are discussed by Potts et al. (165). Prausnitz et al. studied transdermal delivery of heparin, an anticoagulant. The anticoagulant activity of the delivered heparin was one-eighth of the donor heparin, indicating preferential transport of the small (less active) heparin molecules (166). The transport of DNA antisense oligonucleotides of 15 mer in length were demonstrated. Zewert et al. have proposed transdermal transport of anticancer nucleotides for treatment of melanomas (167).

Weaver et al. examined a method to increase the lifetime of the pathways created by electroporative pulses (168). It was hypothesized that long, highly charged molecules can act as separators, holding open the pathways in the lipid layers. Molecules such as heparin, dextran sulfate, neutral dextran, and polylysine were shown to enhance electroporation-assisted delivery of mannitol as a model compound. Postpulse skin permeability was higher and skin resistance was lower in the treated skin compared to control. The same molecules did not enhance passive or iontophoretic transport (169). Hofmann (170) and Zhang (171) have proposed enhancing the effect of electroporation of the skin by cocontacting the therapeutic agent with micron-sized particles, followed by the application of pressure. This method was studied for 2- to 20-μm Lupron Depot microspheres and the *lacZ* reporter gene. Additionally, the use of electroporation in conjunction with encapsulation of the agent into vesicles has been proposed (170). Electroporation has also been studied in conjunction with ultrasound to synergistically enhance the effects of both methods (172).

Physiological Effects

Sensation caused by the pulsed current would be expected to be an issue in practical application of the technology. There has not been any significant testing on human subjects under the conditions for transdermal delivery. Studies of transcutaneous electrical neural stimulation (TENS), a technique of applying electrical pulses across the skin to reduce pain, show significant sensation associated with the method (173,174). The applied charge in TENS units are typically less than 25 μC, produced by 30 to 60 V of 200-μs duration or 500 V of 15-μs duration. This is substantially less than those used in in vitro skin electroporation studies (100 to 300 V for millisecond to tens of millisecond duration). The electroporative pulses also cause muscle contraction, which may not be acceptable for some applications. However, there are engineering designs to mitigate the sensation and muscle contracts caused by the pulses. Theoretical work has been done in designing systems to take the electrodes and tissue physiology into account. Closely spaced electrodes could effectively localize the electric field to the stratum corneum, where there are no nerve endings. Such localization would reduce or eliminate sensation, muscle contraction, and damage to underlying viable epidermal tissue

Because the use of electroporation across the skin is a new development, the physiological effects of skin electroporation have not yet been studied extensively. Riviere et al. (88) studied changes in the skin toxicology following electroporation. Vanbever et al. compared the irritation caused by iontophoresis and electroporation (175). In these studies, there was no additional irritation associated with electroporation compared to iontophoresis. On the other hand, tissue injury above that created by thermal burns that occur in accidents involving high-voltage power lines has been related to tissue electroporation causing damage to cell membranes in the injured area (176,177). However, the voltages and currents are at a much higher level than that used in skin electroporation, and the relevance to skin electroporation may be limited. Tissue electropermeabilization has been use in preliminary studies on human subjects to enhance tumor cell permeability for the treatment of squamous cell carcinoma (178). Subjects reported some sensation and muscle contraction associated with the electrical pulses but completed the treatment. The demonstration of human use of tissue electroporation suggests that transdermal electroporation is feasible in human subjects. Ultimately, more work on living skin tissue is needed to assess the viability of electroporation for practical drug delivery.

BIBLIOGRAPHY

1. B.G. Amsden and M.F.A. Goosen, *AIChE J.* **41**, 1972–1997 (1995).

2. M. Pikal, *Drug Target. Delivery* **4**, 83–109 (1995).
3. J.E. Riviere and M.C. Heit, *Pharm. Res.* **14**, 687–697 (1997).
4. C. Cullander and R.H. Guy, *Adv. Drug Delivery Rev.* **8**, 291–329 (1992).
5. Y.W. Chien et al., *J. Controlled Release* **13**, 263–278 (1990).
6. P.G. Green, M. Flanagan, B. Shroot, and R.H. Guy, in K.A. Walters and J. Hadgraft, eds., *Pharmaceutical Skin Penetration Enhancement*, Dekker, New York, 1993, vol. 59, pp. 311–333.
7. R.H. Guy, *Pharm. Res.* **13**, 1765–1769 (1996).
8. P. Singh and H.I. Maibach, *Crit. Rev. Ther. Drug Carrier Syst.* **11**, 161–213 (1994).
9. A.S. Michaels, S.K. Chandrasekaran, and J.E. Shaw, *AIChE J.* **21**, 985–996 (1975).
10. I. Steinstrasser and H.P. Merkle, *Pharm. Acta Helv.* **70**, 3–24 (1995).
11. N.A. Monteiro-Riviere, in D.W. Hobson, ed., *Dermal and Ocular Toxicology Fundamentals and Methods*, CRC Press, Boca Raton, Fla., 1991, pp. 3–18.
12. N.A. Monteiro-Riviere, in F.N. Marzulli and H.I. Maibach, eds., *Dermatotoxicology*, Taylor & Francis, Washington, D.C., 1996, pp. 3–18.
13. S. LeDuc, *Ann. D'Electrobiol.* **3**, 545–560 (1900).
14. R.R. Burnette and B. Ongpipattanakul, *J. Pharm. Sci.* **77**, 132–137 (1988).
15. H.A. Abramson and M.H. Gorin, *J. Phys. Chem.* **44**, 1094–1102 (1940).
16. C. Cullander and R.H. Guy, *J. Invest. Dermatol.* **97**, 55–64 (1991).
17. R.D. Lee, H.S. White, and E.R. Scott, *J. Pharm. Sci.* **85**, 1186–1190 (1996).
18. E.R. Scott, A.I. Laplaza, H.S. White, and J.B. Phipps, *Pharm. Res.* **10**, 1699 (1993).
19. N.G. Turner and R.H. Guy, *J. Pharm. Sci.* **86**, 1385–1389 (1997).
20. N. Monteiro-Riviere, A.O. Inman, and J.E. Riviere, *Pharm. Res.* **11**, 251–256 (1994).
21. B.D. Bath, R.D. Lee, H.S. White, and E. Scott, R., *Anal. Chem.* **70**, 1047–1058 (1998).
22. M.J. Pikal, *Adv. Drug. Delivery Rev.* **9**, 201–237 (1992).
23. M.B. Delgado-Charro and R.H. Guy, *Pharm. Res.* **11**, 929–935 (1994).
24. M.J. Pikal and S. Shah, *Pharm. Res.* **7**, 213–221 (1990).
25. M. Pikal and S. Shah, *Pharm. Res.* **7**, 222–229 (1990).
26. S.M. Sims, W.I. Higuchi, and V. Srinivasan, *Int. J. Pharm.* **69**, 109–121 (1991).
27. G.B. Kasting, *Adv. Drug Delivery Rev.* **9**, 177–199 (1992).
28. R.R. Burnette, in J. Hadgraft and R.H. Guy, eds., *Transdermal Drug Delivery: Developmental Issues and Research Initiatives*, Dekker, New York, 1989, vol. 35, pp. 274–291.
29. M.J. Pikal, *Pharm. Res.* **7**, 118–126 (1990).
30. R.R. Burnette and B. Ongpipattanakul, *J. Pharm. Sci.* **76**, 765–773 (1987).
31. J.B. Phipps and J.R. Gyory, *Adv. Drug Delivery Rev.* **9**, 137–176 (1992).
32. N.H. Bellantone, S. Rim, M.L. Francoeur, and B. Rasadi, *Int. J. Pharm.* **30**, 63–72 (1986).
33. J.B. Phipps, R.V. Padmanabhan, and G.A. Lattin, *J. Pharm. Sci.* **78**, 365–369 (1989).
34. P. Glikfeld, C. Cullander, R.S. Hinz, and R.H. Guy, *Pharm. Res.* **5**, 443–446 (1988).
35. R. Van Der Geest, M. Danhof, and H. E. Bodde, *J. Controlled Release* **51**, 85–91 (1998).
36. R.L. Bronaugh, in R.L. Bronaugh and H.I. Maibach, eds., *Percutaneous Absorption: Mechanisms-Methodology, Drug Delivery* Dekker, New York, 1989, Chapter 16.
37. R. Van Der Geest et al., *Pharm. Res.* **14**, 1804–1810 (1997).
38. M.C. Heit et al., *J. Pharm. Sci.* **82**, 240–243 (1993).
39. J.E. Riviere et al., *Fundam. Appl. Toxicol.* **7**, 444–453 (1986).
40. J.E. Riviere and N.A. Monteiro-Riviere, *CRC Crit. Rev. Toxicol.* **21** (1991).
41. B.H. Sage, Jr., R. Bock, J.D. DeNuzzio, and R.A. Hoke, *Drug Target. Delivery* **4**, 111–134 (1995).
42. M.S. Roberts, P.M. Lai, S.E. Cross, and N.H. Yoshida, *Drugs Pharm. Sci.* **83**, 291–349 (1997).
43. C.R. Behl et al., *J. Pharm. Sci.* **78**, 355–360 (1989).
44. J.B. Phipps, R.V. Padmanabhan, and G.A. Lattin, *Solid State Ionics* **28–30**, 1778–1783 (1988).
45. P.G. Green et al., *Pharm. Res.* **8**, 1113–1119 (1991).
46. V. Merino, Y. Kalia, and R.H. Guy, *Trends Biotechnol.* **15**, 288–290 (1997).
47. S. Del Terzo, C.R. Behl, and R.A. Nash, *Pharm. Res.* **6**, 85–90 (1989).
48. N.H. Yoshida and M.S. Roberts, *J. Controlled Release* **25**, 177–195 (1993).
49. N. Turner et al., *Pharm. Res.* **14**, 1322–1331 (1997).
50. S.B. Ruddy and B.W. Hadzija, *Drug Des. Discovery* **8**, 207–224 (1992).
51. A.J. Hoogstraate, V. Srinivasan, S.M. Sims, and W.I. Higuchi, *J. Controlled Release* **31**, 41–47 (1994).
52. J. Hirvonen and R.H. Guy, *Pharm. Res.* **14**, 1258–1263 (1997).
53. J. Hirvonen and R.H. Guy, *J. Controlled Release* **50**, 283–289 (1998).
54. J. Brange, *Diabetologia* **40**, S48–S53 (1997).
55. L. Langkjaer, J. Brange, G.M. Grodsky, and R.H. Guy, *J. Controlled Release* **51**, 47–56 (1998).
56. R.R. Burnette and D. Marrero, *J. Pharm. Sci.* **75**, 738–743 (1986).
57. L.L. Miller, C.J. Kolaskie, G.A. Smith, and J. Riviere, *J. Pharm. Sci.* **79**, 490–493 (1990).
58. P.C. Panus et al., *Pharm. Sci.* **2**, 467–469 (1996).
59. V. Srinivasan, W.I. Higuchi, and M.-H. Su, *J. Controlled Release* **10**, 157–165 (1989).
60. P.G. Green et al., *J. Controlled Release* **20**, 209–217 (1992).
61. P.G. Green, in K.R. Brain, V.J. James, and K.A. Walters, eds., *Prediction of Percutaneous Penetration*, Vol. 36, STS Publishing, Cardiff, U.K., 1993.
62. P.G. Green et al., *Pharm. Res.* **8**, 1121–1127 (1991).
63. R.R. Burnette and T.M. Bagniefski, *J. Pharm. Sci.* **77**, 492–497 (1988).
64. Y.N. Kalia, L.B. Nonato, and R.H. Guy, *Pharm. Res.* **13**, 957–960 (1996).
65. V. Srinivasan et al., *J. Pharm. Sci.* **78**, 370–375 (1989).
66. K. Okabe, H. Yamaguchi, and Y. Kawai, *J. Controlled Release* **4**, 79–85 (1986).
67. T. Bagniefski and R.R. Burnette, *J. Controlled Release* **11**, 113–122 (1990).
68. M.J. Pikal and S. Shah, *Pharm. Res.* **8**, 365–369 (1991).
69. S.K. Gupta et al., *J. Controlled Release* **30**, 253–261 (1994).

70. P. Lelawongs, J.-C. Liu, O. Siddiqui, and Y.W. Chien, *Int. J. Pharm.* **56**, 13–22 (1989).
71. B.H. Sage, R.A. Hoke, A.C. McFarland, and K. Kowalczyk, in K.R. Brain, V.J. James, and K.A. Walters, eds., *Prediction of Percutaneous Penetration*, Vol. 36, STS Publishing, Cardiff, U.K., 1993.
72. P. Santi and R.H. Guy, *J. Controlled Release* **38**, 159–165 (1996).
73. W.H.M. Craane-van Hinsberg, et al., *Pharm. Res.* **11**, 1296–1300 (1994).
74. S.Y. Oh, S.Y. Jeong, T.G. Park, and J.H. Lee, *J. Controlled Release* **51**, 161–168 (1998).
75. V. Srinivasan, M.-H. Su, W.I. Higuchi, and C.R. Behl, *J. Pharm. Sci.* **79**, 588–591 (1990).
76. K. Bhatia and J. Singh, *J. Pharm. Sci.* **87**, 462–469 (1998).
77. C.A. Zakzewski, J. Wasilewski, P. Cawley, and W. Ford, *J. Controlled Release* **50**, 267–272 (1998).
78. L. Wearley and Y.W. Chien, *Pharm. Res.* **7**, 34 (1990).
79. C.L. Gay, P.G. Green, R.H. Guy, and M.L. Francoeur, *J. Controlled Release* **22**, 57–68 (1992).
80. J.E. Riviere, B. Sage, and P.L. Williams, *J. Pharm. Sci.* **80**, 615–620 (1991).
81. K. Morimoto, Y. Kwakura, E. Nakatani, and M. Miyazaki, *Int. J. Pharm.* **81**, 119–125 (1992).
82. K. Morimoto et al., *J. Pharm. Pharmacol.* **44**, 216–218 (1992).
83. P.W. Ledger, *Adv. Drug Delivery Rev.* **9**, 289–307 (1992).
84. N.G. Turner, Y.N. Kalia, and R.H. Guy, *Pharm. Res.* **14**, 1252–1257 (1997).
85. N.K. Mize et al., *Exp. Dermatol.* **6**, 298–302 (1997).
86. B. Berner et al., *Pharm. Res.* **5**, 660–663 (1988).
87. N.A. Monteiro-Riviere, *Fundam. Appl. Toxicol.* **15**, 174–185 (1990).
88. J.E. Riviere et al., *J. Controlled Release* **36**, 229–233 (1995).
89. R. Van Der Geest et al., *J. Controlled Release* **41**, 205–213 (1996).
90. E. Camel et al., *Fundam. Appl. Toxicol.* **32**, 168–178 (1996).
91. C. Cullander, G. Rao, and R.H. Guy, in K.R. Brain, V.J. James, and K.A. Walters, eds., *Prediction of Percutaneous Penetration*, Vol. 36, STS Publishing, Cardiff, U.K., 1993.
92. J.E. Sanderson, S. de Riel, and R. Dixon, *J. Pharm. Sci.* **78**, 361–364 (1989).
93. J.M. Maloney, *Arch. Dermatol.* **128**, 331–333 (1992).
94. T. Petelenz et al., *J. Clin. Pharmacol. Ther. Toxicol.* **22**, 152–155 (1984).
95. W. Murray, L.S. LKavine, and E. Seifter, *J. Am. Phys. Ther. Assoc.* **43**, 579 (1963).
96. L.P. Gangarosa, Sr. and J.M. Hill, *Int. J. Pharm.* **123**, 159–171 (1995).
97. N.K. Mize et al., *Exp. Dermatol.* **6**, 181–185 (1997).
98. R. Van Der Geest, M. Danhof, and H. E. Bodde, *Pharm. Res.* **14**, 1798–1803 (1997).
99. S. Singh and J. Singh, *Med. Res. Rev.* **13**, 569–621 (1993).
100. W. Hinsberg, H.M. Craane-Van, J.C. Verhoef, and H.E. Bodde, *Drug Target. Delivery* **3**, 199–220 (1994).
101. J.-C. Liu and Y. Sun, *Drugs Pharm. Sci.* **62**, 247–272 (1994).
102. P. Santi et al., *Farmaco* **52**, 445–448 (1997).
103. S. Thysman, C. Hanchard, and V. Preat, *J. Pharm. Pharmacol.* **46**, 725 (1994).
104. Y.W. Chien et al., *Ann. N. Y. Acad. Sci.* **507**, 32–51 (1988).
105. Y.W. Chien et al., *J. Pharm. Sci.* **78**, 376–383 (1989).
106. B. Kari, *Diabetes* **35**, 217–221 (1986).
107. O. Siddiqui, Y. Sun, J.-C. Liu, and Y.W. Chien, *J. Pharm. Sci.* **76**, 341–345 (1987).
108. R.L. Stephen, T.J. Petelenz, and S.C. Jacobsen, *Biomed. Biochim. Acta* **43**, 553–558 (1984).
109. J.-C. Liu et al., *Int. J. Pharm.* **44**, 197–204 (1988).
110. Y. Tomohira, Y. Machida, H. Onishi, and T. Nagai, *Int. J. Pharm.* **155**, 231–239 (1997).
111. A. Banga and K., Y.W. Chien, *J. Controlled Release* **7**, 1–24 (1988).
112. E. Holzle and N. Alberti, *Dermatologica* **175**, 126–135 (1987).
113. K. Sato et al., *J. Appl. Physiol.* **78**, 2258–2264 (1993).
114. J.B. Sloan and K. Soltani, *J. Am. Acad. Dermatol.* **15**, 671–684 (1986).
115. R.L. Dobson, *Arch. Dermatol.* **123**, 883–884 (1987).
116. L.P. Stolman, *Arch. Dermatol.* **123**, 893–896 (1987).
117. M.O. Yoshizumi, A. Dessouki, D.A. Lee, and G. Lee, *J. Ocul. Pharmacol. Ther.* **13**, 529–536 (1997).
118. D. Sarraf and D.A. Lee, *J. Ocul. Pharmacol.* **10**, 1 (1994).
119. D.M. Maurice, *Ophthalmology* **93**, 128–132 (1986).
120. M. Barza, C. Peckman, and J. Baum, *Ophthalmology* **93**, 133–139 (1986).
121. J.M. Hill, Y. Shimomura, B.S. Kwon, and L.P. Gangarosa, *Invest. Ophthalmol. Visual Sci.* **26**, 1299–1303 (1985).
122. W.D. Lutkins, G.W. Greco, and W.T. McFall, Jr., *J. Am. Dent. Assoc.* **111**, 761–765 (1985).
123. K.M. Brough, D.M. Anderson, J. Love, and P.R. Overman, *J. Am. Dent. Assoc.* **111**, 761–765 (1985).
124. M.P. James, R.M. Graham, and J. English, *Clin. Exp. Dermatol.* **11**, 54–61 (1986).
125. R.T. Ramsden, W.P.R. Bigson, and D.A. Moffat, *J. Laryngol. Otolaryngol.* **91**, 779–785 (1977).
126. L.E. Gibson and R.E. Cooke, *Pediatrics* **23**, 545–549 (1959).
127. W.H. Yeung et al., *Clin. Pediatr.* **23**, 603–607 (1984).
128. C.R. Denning, N.N. Huang, and L.R. Cuasay, *Pediatrics* **66**, 752–757 (1980).
129. G. Rao, P. Glikfeld, and R. Guy, *Pharm. Res.* **10**, 1751–1755 (1993).
130. G. Rao et al., *Pharm. Res.* **12**, 1869–1873 (1995).
131. P. Glikfeld, R.S. Hinz, and R.H. Guy, *Pharm. Res.* **6**, 988–990 (1989).
132. J.A. Tamada, N.J.V. Bohannon, and R.O. Potts, *Nat. Med.* **1**, 1198–1201 (1995).
133. J.C. Weaver, *J. Cell. Biochem.* **51**, 426–435 (1993).
134. E. Neumann, A.E. Sowers, and C.A. Jordan, eds., *Electroporation and Electrofusion in Cell Biology*, Plenum, New York, 1989.
135. D.C. Chang, B.M. Chassy, J.A. Saunders, and A.E. Sowers, *Guide to Electroporation and Electrofusion*, Academic Press, New York, 1992.
136. R. Chakrabarti, D.E. Wyle, and S.M. Schuster, *J. Biol. Chem.* **264**, 15494–15500 (1989).
137. K.T. Powell, A.W. Morgenthaler, and J.C. Weaver, *Biophys. J.* **56**, 1163–1171 (1989).
138. L.M. Mir, S. Orlowski, J. Belehradek, Jr., and C. Paoletti, *Eur. J. Cancer* **27**, 63–72 (1991).
139. L. Mir, S. Orlowski, B. Poddevin, and J. Belehradek, Jr., *Eur. Cytokine Network* **3**, 331–334 (1992).
140. J. Belehradek et al., *Eur. J. Cancer* **27**, 73–76 (1991).
141. M. Okino et al., *Jpn. J. Cancer Res.* **83**, 1095–1102 (1992).

Next Page

142. M. Okino and K. Esato, *Jpn. J. Surg.* **20**, 197–204 (1990).
143. M. Okino and H. Mohri, *Jpn. J. Cancer Res.* **78**, 1319–1321 (1987).
144. A. Titomirov, S. Sukharev, and E. Kistanova, *Biochim. Biophys. Acta* **1088**, 131–134 (1991).
145. R. Heller et al., *FEBS Lett.* **389**, 225–228 (1996).
146. M.R. Prausnitz, V.G. Bose, R. Langer, and J.C. Weaver, *Proc. Natl. Acad. Sci. U.S.A.* **90**, 10504–10508 (1993).
147. M.R. Prausnitz, *J. Controlled Release* **40**, 321–326 (1996).
148. U.L. Pliquett, R. Langer, and J.C. Weaver, *Biochim. Biophys. Acta* **1239**, 111–121 (1995).
149. U. Pliquett and J. Weaver, *J. Controlled Release* **38**, 1–10 (1996).
150. U. Pliquett et al., *Biophys. Chem.* **58**, 185–204 (1996).
151. M.R. Prausnitz *et al., J. Pharm. Sci.* **85**, 1363–1370 (1996).
152. D.A. Edwards, M.R. Prausnitz, R. Langer, and J.C. Weaver, *J. Controlled Release* **34**, 211–221 (1995).
153. M.R. Prausnitz et al., *J. Controlled Release* **38**, 205–217 (1996).
154. D.B. Bommannan, J. Tamada, L. Leung, and R.O. Potts, *Pharm. Res.* **11**, 1809–1814 (1994).
155. S.K. Li, A.-H. Ghanem, K.D. Peck, and W.I. Higuchi, *J. Pharm. Sci.* **87**, 40–48 (1998).
156. H. Inada, A.H. Ghanem, and W.I. Higuchi, *Pharm. Res.* **11**, 687–697 (1994).
157. Y.A. Chizmadzhev, V.G. Zarnitsin, J.C. Weaver, and R.O. Potts, *Biophys. J.* **68**, 749–765 (1995).
158. M.R. Prausnitz, U. Pliquett, R. Langer, and J.C. Weaver, *Pharm. Res.* **11**, 1834–1837 (1994).
159. R. Vanbever, G. Langers, S. Montmayeur, and V. Preat, *J. Controlled Release* **50**, 225–235 (1998).
160. R. Vanbever, E. Le Boulenge, and V. Preat, *Pharm. Res.* **13**, 559–565 (1996).
161. R. Vanbever, N. Lecouturior, and V. Preat, *Pharm. Res.* **11**, 1657–1662 (1994).
162. S. Wang, M. Kara, and T.R. Krishnan, *J. Controlled Release* **50**, 61–70 (1998).
163. S. Wang, M. Kara, and T.R. Krishnan, *Drug Dev. Ind. Pharm.* **23**, 657–663 (1997).
164. A. Jadoul and V. Preat, *Int. J. Pharm.* **154**, 229–234 (1997).
165. R.O. Potts et al., *Pharm. Biotechnol.* **10**, 213–238 (1997).
166. M.R. Prausnitz et al., *Bio/Technology* **13**, 1205–1209 (1995).
167. T.E. Zewert, U.F. Pliquett, R. Langer, and J.C. Weaver, *Biochem. Biophys. Res. Commun.* **212**, 286–292 (1995).
168. J.C. Weaver, R. Vanbever, T.E. Vaughan, and M.R. Prausnitz, *Biochem. Biophys. Res. Commun.* **234**, 637–640 (1997).
169. R. Vanbever, M.R. Prausnitz, and V. Preat, *Pharm. Res.* **14**, 638–644 (1997).
170. G.A. Hofmann, W.V. Rustrum, and K.S. Suder, *Bioelectrochem. Bioenerg.* **38**, 209–222 (1995).
171. L. Zhang et al., *Bioelectrochem. Bioenerg.* **42**, 283–292 (1997).
172. J. Kost et al., *Pharm. Res.* **13**, 633–638 (1996).
173. J.P. Reilly, *Electrical Stimulation and Electropathology*, Cambridge University Press, New York, 1992.
174. J.A. Balogun, *J. Sports Med. Phys. Fitness* **31**, 521–526 (1991).
175. R. Vanbever et al., *Skin Pharmacol. Appl. Skin Physiol.* **11**, 23–24 (1998).
176. R.C. Lee et al., *Proc. Natl. Acad. Sci. U.S.A.* **89**, 4524–4528 (1992).
177. R.C. Lee and M.S. Kolodney, *Plast. Reconstr. Surg.* **80**, 672–679 (1989).
178. L.M. Mir et al., *C.R. Sciences Acad. Sci.* **313**, 613–618 (1991).

See also TRANSDERMAL DRUG DELIVERY, PASSIVE.

TRANSDERMAL DRUG DELIVERY, PASSIVE

ROBERT GALE
JAMES HUNT
MARY E. PREVO
ALZA Corporation
Palo Alto, California

KEY WORDS

Absorption
In vitro
In vivo
Nonclinical toxicology
Permeation enhancement
Predictive models
Skin permeation
Transdermal

OUTLINE

Introduction
Structure, Composition, and Function of Skin
Permeability of Human Skin
  Mechanism of Permeation
  Techniques for Measuring Skin Permeation
  Regional Differences in Permeation
  Transepidermal Water Loss and Water Content of the Stratum Corneum
  Immature, Diseased, or Damaged Skin
Permeability Models for Stratum Corneum
  Effects of Stratum Corneum Lipids on Diffusivity
  Predictive Models
Animal Models for Percutaneous Absorption
Toxicology
  Skin Metabolism
  In Vivo Testing
  In Vitro Testing
  Other Preclinical Testing Requirements
Transdermal Drug Delivery
  Permeation Enhancement
  Pharmacokinetics
Marketed Transdermal Systems
  Types of Transdermal Systems

Previous Page

142. M. Okino and K. Esato, *Jpn. J. Surg.* **20**, 197–204 (1990).
143. M. Okino and H. Mohri, *Jpn. J. Cancer Res.* **78**, 1319–1321 (1987).
144. A. Titomirov, S. Sukharev, and E. Kistanova, *Biochim. Biophys. Acta* **1088**, 131–134 (1991).
145. R. Heller et al., *FEBS Lett.* **389**, 225–228 (1996).
146. M.R. Prausnitz, V.G. Bose, R. Langer, and J.C. Weaver, *Proc. Natl. Acad. Sci. U.S.A.* **90**, 10504–10508 (1993).
147. M.R. Prausnitz, *J. Controlled Release* **40**, 321–326 (1996).
148. U.L. Pliquett, R. Langer, and J.C. Weaver, *Biochim. Biophys. Acta* **1239**, 111–121 (1995).
149. U. Pliquett and J. Weaver, *J. Controlled Release* **38**, 1–10 (1996).
150. U. Pliquett et al., *Biophys. Chem.* **58**, 185–204 (1996).
151. M.R. Prausnitz *et al., J. Pharm. Sci.* **85**, 1363–1370 (1996).
152. D.A. Edwards, M.R. Prausnitz, R. Langer, and J.C. Weaver, *J. Controlled Release* **34**, 211–221 (1995).
153. M.R. Prausnitz et al., *J. Controlled Release* **38**, 205–217 (1996).
154. D.B. Bommannan, J. Tamada, L. Leung, and R.O. Potts, *Pharm. Res.* **11**, 1809–1814 (1994).
155. S.K. Li, A.-H. Ghanem, K.D. Peck, and W.I. Higuchi, *J. Pharm. Sci.* **87**, 40–48 (1998).
156. H. Inada, A.H. Ghanem, and W.I. Higuchi, *Pharm. Res.* **11**, 687–697 (1994).
157. Y.A. Chizmadzhev, V.G. Zarnitsin, J.C. Weaver, and R.O. Potts, *Biophys. J.* **68**, 749–765 (1995).
158. M.R. Prausnitz, U. Pliquett, R. Langer, and J.C. Weaver, *Pharm. Res.* **11**, 1834–1837 (1994).
159. R. Vanbever, G. Langers, S. Montmayeur, and V. Preat, *J. Controlled Release* **50**, 225–235 (1998).
160. R. Vanbever, E. Le Boulenge, and V. Preat, *Pharm. Res.* **13**, 559–565 (1996).
161. R. Vanbever, N. Lecouturior, and V. Preat, *Pharm. Res.* **11**, 1657–1662 (1994).
162. S. Wang, M. Kara, and T.R. Krishnan, *J. Controlled Release* **50**, 61–70 (1998).
163. S. Wang, M. Kara, and T.R. Krishnan, *Drug Dev. Ind. Pharm.* **23**, 657–663 (1997).
164. A. Jadoul and V. Preat, *Int. J. Pharm.* **154**, 229–234 (1997).
165. R.O. Potts et al., *Pharm. Biotechnol.* **10**, 213–238 (1997).
166. M.R. Prausnitz et al., *Bio/Technology* **13**, 1205–1209 (1995).
167. T.E. Zewert, U.F. Pliquett, R. Langer, and J.C. Weaver, *Biochem. Biophys. Res. Commun.* **212**, 286–292 (1995).
168. J.C. Weaver, R. Vanbever, T.E. Vaughan, and M.R. Prausnitz, *Biochem. Biophys. Res. Commun.* **234**, 637–640 (1997).
169. R. Vanbever, M.R. Prausnitz, and V. Preat, *Pharm. Res.* **14**, 638–644 (1997).
170. G.A. Hofmann, W.V. Rustrum, and K.S. Suder, *Bioelectrochem. Bioenerg.* **38**, 209–222 (1995).
171. L. Zhang et al., *Bioelectrochem. Bioenerg.* **42**, 283–292 (1997).
172. J. Kost et al., *Pharm. Res.* **13**, 633–638 (1996).
173. J.P. Reilly, *Electrical Stimulation and Electropathology*, Cambridge University Press, New York, 1992.
174. J.A. Balogun, *J. Sports Med. Phys. Fitness* **31**, 521–526 (1991).
175. R. Vanbever et al., *Skin Pharmacol. Appl. Skin Physiol.* **11**, 23–24 (1998).
176. R.C. Lee et al., *Proc. Natl. Acad. Sci. U.S.A.* **89**, 4524–4528 (1992).
177. R.C. Lee and M.S. Kolodney, *Plast. Reconstr. Surg.* **80**, 672–679 (1989).
178. L.M. Mir et al., *C.R. Sciences Acad. Sci.* **313**, 613–618 (1991).

See also TRANSDERMAL DRUG DELIVERY, PASSIVE.

TRANSDERMAL DRUG DELIVERY, PASSIVE

ROBERT GALE
JAMES HUNT
MARY E. PREVO
ALZA Corporation
Palo Alto, California

KEY WORDS

Absorption
In vitro
In vivo
Nonclinical toxicology
Permeation enhancement
Predictive models
Skin permeation
Transdermal

OUTLINE

Introduction
Structure, Composition, and Function of Skin
Permeability of Human Skin
  Mechanism of Permeation
  Techniques for Measuring Skin Permeation
  Regional Differences in Permeation
  Transepidermal Water Loss and Water Content of the Stratum Corneum
  Immature, Diseased, or Damaged Skin
Permeability Models for Stratum Corneum
  Effects of Stratum Corneum Lipids on Diffusivity
  Predictive Models
Animal Models for Percutaneous Absorption
Toxicology
  Skin Metabolism
  In Vivo Testing
  In Vitro Testing
  Other Preclinical Testing Requirements
Transdermal Drug Delivery
  Permeation Enhancement
  Pharmacokinetics
Marketed Transdermal Systems
  Types of Transdermal Systems

Summary
Bibliography

INTRODUCTION

The use of the skin as a route of drug delivery has a long history; throughout the ages, many types of plasters and poultices have been used to treat various local and systemic complaints. It is only within the last 30 years that increased understanding of the skin and its barrier properties has allowed the development of more reliable and efficacious means of safely delivering therapeutic agents through the skin.

The skin functions as the largest organ in the body and is comprised of several layers that protect the underlying tissues. Absorption of chemicals by the skin may have substantive local and systemic consequences, and a number of factors influence the rate and extent of chemical transport through human skin. A variety of qualitative and quantitative methods are used to determine percutaneous absorption of drugs, and the results of both in vitro and in vivo studies may be used to predict absorption in humans. It has been demonstrated that there are intraindividual and interindividual differences in percutaneous absorption; understanding these differences is key in the design of a reliable transdermal system. The use of predictive models is extremely important in preclinical testing of new transdermal formulations and drug delivery systems. These studies include assessment of transdermal drug permeability and the potential for drug toxicity; skin irritation, immunological responses, and systemic toxicity are also important testing parameters.

The simplest of today's transdermal or topical drug delivery systems incorporate a vehicle such as a liquid, gel, or cream for direct application to skin. Hydrocortisone lotions and acne treatments are prime examples of topical formulations. More recently, transdermal therapeutic systems have been introduced, offering a more sophisticated and more reliable means of administering drug through the skin. Greater understanding of the pharmacokinetics of percutaneously administered drugs has led to the development of rate-controlled systems with optimized delivery profiles, and the use of permeation enhancers has expanded the number of drugs that can be administered transdermally.

In the United States, transdermal systems are now used for analgesics (fentanyl), hormone replacement therapies (estradiol and testosterone), and for the treatment of angina (nitroglycerin), hypertension (clonidine), and motion sickness (scopolamine). Transdermal nicotine replacement therapy for smoking cessation is also available, and a number of other drugs are being studied for possible inclusion in transdermal systems. As compared with other means of drug administration, transdermal systems have been associated with improved bioavailability, sustained therapeutic effect, diminished side effects, and convenient, noninvasive use that allows easy termination of therapy.

In this article, a review of skin biology and permeability is provided, and a discussion of the predictive models and toxicology testing employed in the development of transdermal products is presented. An overview of marketed transdermal systems technology is also presented with an emphasis on product characteristics and the clinical performance measures of safety, efficacy, reliability, and acceptability of drug treatment.

STRUCTURE, COMPOSITION, AND FUNCTION OF SKIN

The skin and other tissues protect internal organs from heat, humidity, pollution, radiation, and other potential insults. Human skin is comprised of the unvascularized epidermis and the highly vascularized dermis just below it (Fig. 1). The external layer of the epidermis is called the stratum corneum, which in Latin means "horny layer." This layer of skin is considerably less permeable than the dermis itself and protects the more permeable skin layers beneath it. The human stratum corneum varies from 10 to 50 μm in thickness and is a heterogeneous structure of dead, flattened, interdigitated keratinocytes that are each 0.5–1.0 μm thick. The constituents of these cells are protein, water, and lipids, the latter are concentrated largely in the extracellular phase and serve to cement the structure together into a coherent membrane (1). The range of stratum corneum thickness varies depending upon anatomic location. On the palms of the hands and soles of the feet, the stratum corneum is adapted for friction and weight bearing, respectively, and is considerably thicker than at other locations. Below the stratum corneum, the living epidermis ranges from 50 to 100 μm and proliferates rapidly by cellular differentiation. Cells migrate from the basal layer toward the skin surface at a rate of one new cell layer per day and undergo keratinization as they approach the external skin surface; the stratum corneum is completely replaced every 15 to 30 days. The epidermis itself is capable of most biotransformation reactions that are seen in the liver; the specific enzyme activity of the skin sometimes surpasses that of the hepatic enzymes. Phase I reactions include oxidation, reduction, and hydrolytic reactions, and Phase II reactions are conjugation reactions such as methylation, glucuronidation, and sulfatation.

The dermis is relatively thick compared with the stratum corneum and epidermis, comprising approximately 2,000 μm and containing a matrix of connective tissue that is penetrated by nerves, blood vessels, and lymphatics. Localized structural features of the skin include the hair follicles, sweat glands, and sebaceous glands, which may serve as permeation pathways to the underlying vascular bed.

PERMEABILITY OF HUMAN SKIN

Although the skin serves as a barrier and was once thought to be virtually impermeable, it is now recognized as a permeable organ capable of local absorption that may have substantive systemic consequences. Many factors influence the rate and extent of drug transport through human skin.

Mechanism of Permeation

It has been clearly demonstrated that the mechanism of permeation through skin is a partition-diffusion process

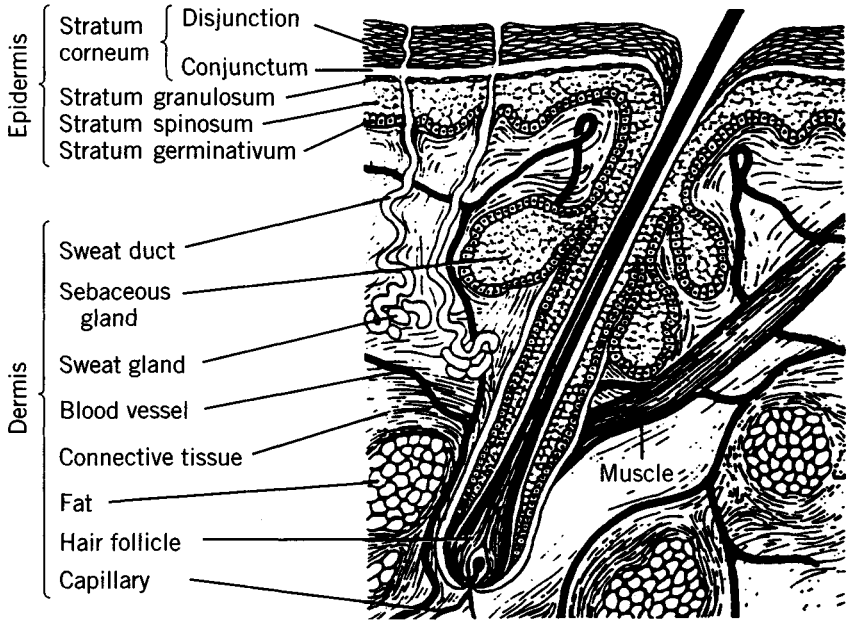


Figure 1. Structure of normal skin. *Source:* From *Casarett and Doull's Toxicology: The Basic Science of Poisons* 3rd C.D. Klaassen, M.O. Amdur, and J. Doull, ed., Macmillan, New York, 1986, p. 414.

rather than an active process (2–5) and, therefore, follows the diffusion principles described by Fick (6). In skin that is intact, the major barrier to drug penetration is the stratum corneum with its bilayer arrays of lipids. These well-organized and repetitive arrangements of lipids form "seals" such that material exchange between the skin surface and the layers beneath it is inefficient. There are various micro routes of drug permeation that have been suggested (Fig. 2) (7).

Techniques for Measuring Skin Permeation

There are a number of methods, both qualitative and quantitative, that may be used to determine the extent and rate of percutaneous absorption of drugs. Results of in vitro and in vivo study may be used to predict absorption in humans (Fig. 3) (8).

In vivo methods. In vivo permeation may be measured by determining what remains of a known amount of a sub-

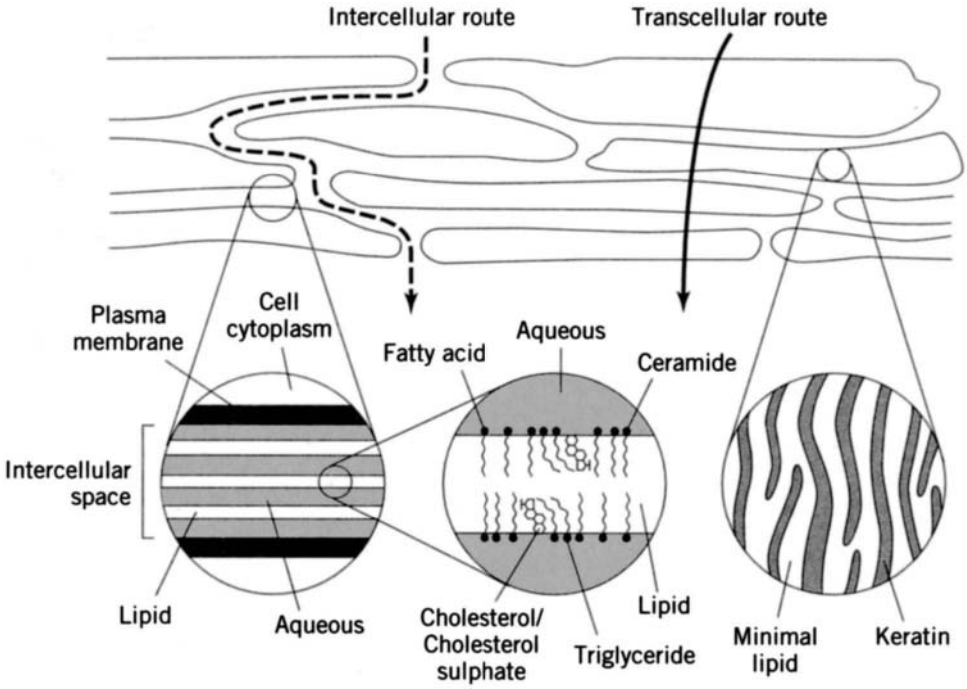


Figure 2. Possible microroutes of drug permeation through human skin—intercellular or transcellular pathways. *Source:* After Ref. 1.

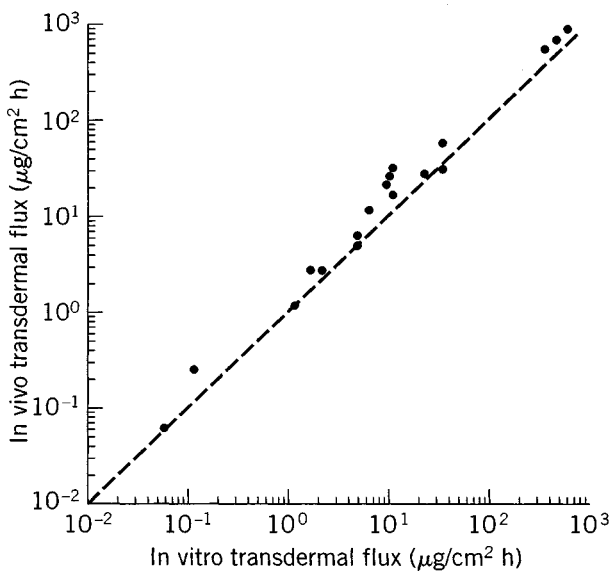


Figure 3. Correlation between in vivo and in vitro transdermal drug flux. Each data point represents a different drug. Dashed line indicates perfect correlation between in vivo and in vitro transdermal drug flux. *Source:* Ref. 8.

stance after it is applied to skin for a given time period. This "residual drug" method of determination is based on the assumption that the difference between the dose initially applied and the residual represents the amount of drug that permeated the skin and has been or will be absorbed by the underlying capillaries. In fact, the drug may have been absorbed in the epidermis or stratum corneum and metabolized in those structures. The "pharmacokinetic method" is an alternative and relies on measured serum or plasma concentrations and the predetermined clearance rate of the compound for calculation of the steady-state permeation rate. Variability in skin permeation between individuals or at different skin sites (Fig. 4) may confound these results.

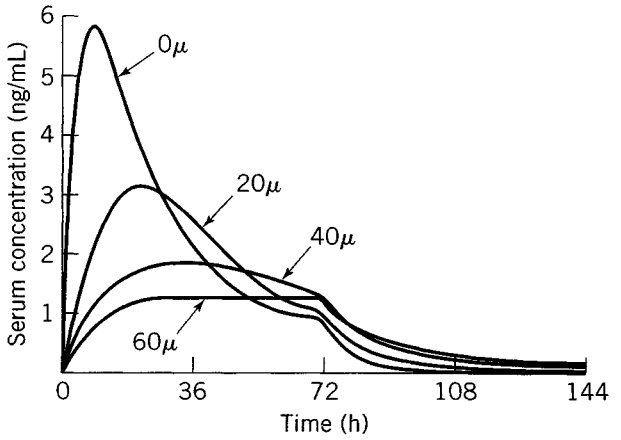


Figure 4. Effect of skin thickness on serum fentanyl concentrations (TTS (fentanyl)-100, 72h).

A number of other methods of determining skin permeation in vivo are also available. Topical application of a radiolabeled compound allows measurement of the amount of radioactivity in excreta, and the final amount of radioactivity is expressed as the percentage of the applied dose that was absorbed. Determination of percutaneous absorption by this method does not account for skin metabolism. Absolute bioavailability of a topically applied compound may be determined by measuring the compound by specific assay in blood or urine after topical and intravenous administration, but this is often difficult because drug plasma concentrations are frequently low after topical administration (9). Estimation of percutaneous absorption may also be determined by substituting a biological assay for a chemical assay and estimating (10); however, this method is only appropriate to use in studying compounds that elicit an easily measurable response.

Skin stripping may be used to determine the concentration of chemical in the stratum corneum after short-term topical exposure. The compound is applied to skin for a period of 30 minutes, and then the stratum corneum is removed by successive application and "stripping" of cellophane tape from the skin. Tape strippings are assayed for chemical content, and linear extrapolation predicts the percutaneous absorption of the chemical for longer application periods (11,12). This method eliminates the use of radiolabeled compounds and the need to measure absorption via excreta. More recently, a number of other methods for in vivo determination of percutaneous absorption have been reported, including infrared spectroscopy (13–15), microdialysis (16), and a laser-photoacoustic method for percutaneous absorptiometry (17).

In vitro methods. In vitro methods of determining the skin permeability of various substances may be more convenient; correlation of in vitro and in vivo flux of a variety of compounds has been described previously (8). In one method, skin specimens may be mounted as a membrane in a diffusion chamber with two compartments. The compound to be tested is placed in contact with the stratum corneum side of the skin at a relatively high concentration or level of activity, and an appropriate receptor vehicle is placed in the other compartment in contact with the dermal side of the skin. The diffusion chambers allow evaluation of mass-transport phenomena through the skin (18). Excised human or animal skin may be used, and the skin can be intact or separated from the epidermis (9). Apparent correlation of any of these data do, however, need to be verified with in vivo pharmacokinetic data. Another in vitro model that employs a partition coefficient of a drug or chemical in vehicle with powdered human stratum corneum has been used to determine the proportion of chemical bound to the skin particles (9).

Regional Differences in Permeation

Research has demonstrated the existence of both intraindividual and interindividual differences in percutaneous absorption. The extent of these differences varies considerably and is affected by the physiochemical nature of the penetrant (19). In evaluations of permeation rates that

have tested skin from the same and different donors, regional intraspecimen variability has been shown to be less than regional interspecimen variability (20). Explanations for these regional differences have been ascribed to a variety of factors, including differences in blood flow, the thickness and lipid content of the stratum corneum, and the number of sweat ducts and hair follicles at the skin site. Percutaneous absorption may also be influenced by other conditions such as temperature, friction, and hydration of the skin (19).

Dermal absorption studies of polycyclic aromatic hydrocarbons demonstrate low but variable regional differences in absorption. Skin at the shoulder is two times more permeable than skin on the forearm; the skin of the ankle and at the palm of the hand is two times less permeable than that on the forearm (19). In vivo permeation of caffeine, benzoic acid, and acetylsalicylic acid have also been demonstrated to be site dependent (12), as has the permeability of scopolamine (Fig. 5) (21). In the latter study, the postauricular epidermis was shown to be about twice as permeable as specimens from the trunk and was even more permeable than epidermis from the forearm and thigh. Scrotal skin has been shown to be considerably more permeable than skin at other anatomic locations; this phenomenon is thought to be the result of its superficial vascularity (22).

Study of in vitro permeation of fentanyl and sufentanil at different skin sites yielded results that contrasted with those of in vivo studies (23). The permeability coefficients obtained on skin from a single cadaver at the upper arm, thigh, abdomen, chest, and sole of the foot were all quite similar. Fentanyl, however, was less permeable at the sole of the foot than at other sites. Both drugs are quite permeable due to high lipophilicity (favoring partitioning in the stratum corneum), and thus their in vitro permeation rates through cadaver skin may not be influenced greatly by skin site. Differences in age and gender did not appear to affect the permeation of these drugs.

Skin permeability frequently differs among patients, leading investigators to study the effects of age, gender, and race on percutaneous absorption using a variety of chemical agents. Advancing age appears to compromise

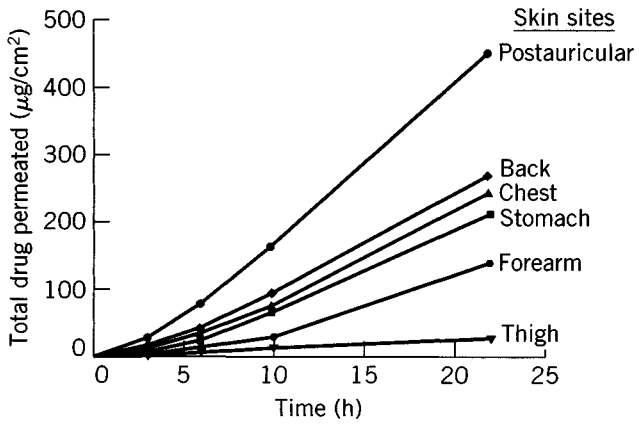


Figure 5. Variation in cumulative scopolamine flux as a function of skin site.

skin, causing the epidermis to atrophy, the dermoepidermal junction to flatten, and the dermis to thin. The majority of published literature indicates that irritant and allergic inflammatory reactions are weaker in older subjects. There is a lack of consensus, however, as to whether there are measurable differences in percutaneous absorption between young and old subjects (24). Gender differences in percutaneous absorption have been postulated, but in general, no significant gender-related differences in barrier integrity or barrier recovery have been found (25). Study of skin structure indicates that the thickness and lipid content of stratum corneum of men and women is similar (26).

The question of whether or not there are racial differences in percutaneous absorption is difficult to answer with complete certainty. Wester and colleagues (27) and Lotte and colleagues (28) studied the percutaneous absorption of benzoic acid, caffeine, and acetylsalicylic acid and found no significant differences in absorption between Asians, Blacks, and Caucasians (Fig. 6). However, a study of nitroglycerin absorption indicates Black subjects had lower systemic drug concentrations than Asians or Caucasians (29). Black skin also showed increased resistance to tape stripping as compared with Caucasian skin and has been thought to resist chemical irritation better than lighter skin. This general assumption, however, may be based primarily on differences in the appearance of erythema, which is far more difficult to detect in Black skin than in light-colored skin (9).

Transepidermal Water Loss and Water Content of the Stratum Corneum

The measurement of transepidermal water loss (TEWL) and the water content of the stratum corneum provide important information about skin function and integrity. The skin loses water as vapor, which evaporates from the skin surface. Occlusion of the surface prevents water loss and increases the water content of the stratum corneum. Healthy skin is characterized by direct proportionality of TEWL and hydration of the skin. Damage to the skin raises TEWL as compared with that of intact skin (30).

In its fully hydrated state, the permeability of the stratum corneum to water can be substantially higher than during its normal state. Occlusion of human skin with vinylidiene polymer film indicated skin was fully saturated with water within 24 hours and reverted to preocclusion values within 18 hours of film removal (31). The increasing permeability of skin under occlusion is attributed to an increasing fluidity of the stratum corneum that is induced by moisture.

Immature, Diseased, or Damaged Skin

Changes in the integrity of skin affect TEWL. The immature skin of infants with a gestational age of less than 36 weeks has significantly greater TEWL than that of a full-term infant (32). In infants over 37 weeks of gestational age, however, TEWL is lower than in adults, suggesting a more efficient stratum corneum. As the skin ages, TEWL and hydration decrease, maintaining their directly proportional relationship. In people over 60 years of age, a number of factors may contribute to decreased TEWL, includ-

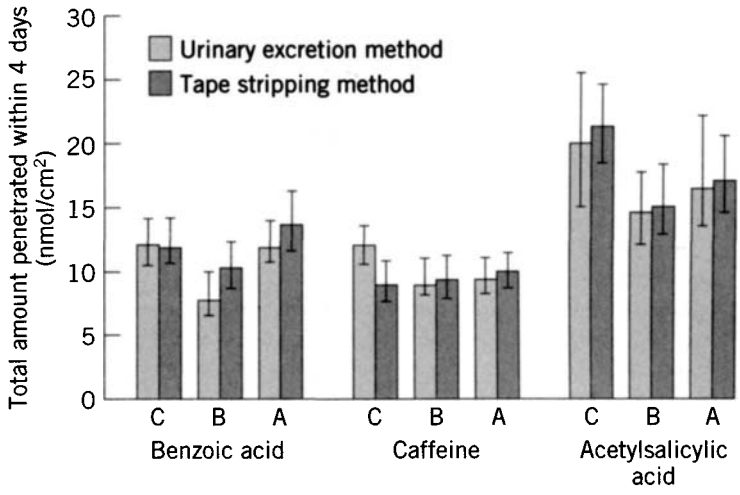


Figure 6. Influence of race on percutaneous absorption of benzoic acid, caffeine, and acetylsalicylic acid in Caucasian (C), Black (B), and Asian (A) subjects. *Source:* After Ref. 28.

ing increases in the size of corneocytes and in the thickness of stratum corneum, the latter is likely related to impaired desquamation of corneocytes (30).

In skin that is damaged or diseased, there is an inverse correlation between TEWL and the stratum corneum water content; the lower the skin hydration, the higher the TEWL (Fig. 7). Alteration of the skin barrier and/or the keratinization of cells are thought to be potential causes of defective stratum corneum water-holding capacity (30). Hyperproliferative diseases, such as psoriasis and exfoliative dermatitis, may lead to significant increases in TEWL due to weakening of the permeation barrier (33). Although this damaged skin is frequently thickened, increased percutaneous absorption is characteristic in patients with inflamed eczematous skin (34,35). Essential fatty acid deficiency or ultraviolet radiation damage may also induce epidermal hyperproliferation and increase TEWL and percutaneous absorption (36–38). TEWL may also be increased by tape stripping or abrading the skin surface; permeability is increased in these settings (36).

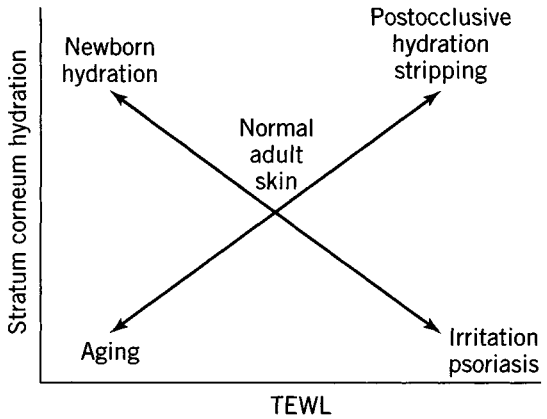


Figure 7. Relationship between TEWL and skin surface hydration. The quantification of hydration and transepidermal water loss may allow the differentiation between physiologic dry skin and pathologic dry skin. In the latter, damage to the water barrier is present. *Source:* After Ref. 30.

PERMEABILITY MODELS FOR STRATUM CORNEUM

The use of a model to predict skin permeability is important in determining the local and systemic characteristics of transdermal drug administration and in providing an understanding of the skin's barrier properties. Several types of models have proven useful in predicting skin permeability to penetrants.

Effects of Stratum Corneum Lipids on Diffusivity

The lipid components of skin appear to play a significant role in the permeability of the stratum corneum. Delipidizing the tissue with a solvent such as a chloroform–methanol mixture removes lipid components without discernible mechanical or morphological alteration of the membrane. The water permeability of the delipidized, hydrated stratum corneum is three to four times greater than that of the normal tissue, and its permeability to larger molecules may be as much as six times greater than that of normal tissue (5).

The importance of lipids as a primary permeability barrier is evidenced by the "brick and mortar" model in which lipids are envisioned as a mortar that holds keratinized stratum corneum cells together (39). Clinical evidence—such as abnormally high TEWL seen in patients with essential fatty acid deficiencies or abnormalities of keratinocytes related to lipid impairment in the stratum corneum—supports the idea that an intact lipid phase is crucial to the integrity of the stratum corneum (1). Permeability of a substance is determined by its solubility and diffusivity in the aqueous protein and lipid phases of the stratum corneum (40). Bearing these principles in mind, low rates of permeability are associated with substances that possess low aqueous or lipid solubility, whereas highly water- or lipid-soluble compounds exhibit relatively high permeation rates (41).

Predictive Models

Several predictive models for skin permeation have been developed. A two-compartment model employs a mineral oil–water partition coefficient and accounts for the water

solubility of penetrant molecules to generate a predicted maximum permeation rate through human epidermis in vitro (39). A stratum corneum diffusion model based on ion–dipole and lipid–lipid interactions resulted in drug flux equations that predicted a linear dependence of flux on the dipole moment of penetrant and on the solubility of penetrant models in a cosolvent system (Fig. 8) (42). The model assumes two separate diffusion pathways for polar and lipid-soluble compounds as follows: (*1*) the skin permeation rate of polar compounds decreases in a linear fashion with interactions between the penetrant dipole and ionized amino acids in the stratum corneum; and (*2*) the nonpolar penetrants interact with the van der Waals and other dispersion forces in tissue. Another skin permeation model, in which the stratum corneum is treated as a homogeneous, passive lipid membrane, indicates the maximum percutaneous absorption rate is a function of molecular weight and melting point. Molecular weight is assumed to affect diffusivity, whereas melting point is assumed to predict the solubility of the penetrant in the stratum corneum lipids (43).

In contrast to the phenomenological approaches used in the predictive models already described, Lien and Gao (44) pioneered a model based on a classic quantitative structure activity relationship. These authors considered as predominant permeability factors the octanol–water partition coefficient, hydrogen bonding characteristics, and the molecular weight of drug molecules. The former two properties are estimated from the structures of drugs. A good log-linear relationship between skin permeability and these three molecular properties was obtained for selected drugs (Fig. 9). Depending on the vehicles used, the optimum octanol–water partition coefficient of drug for a maximum skin permeability changes. However, the hydrogen-bonding has a negative effect on the skin permeability. As in the phenomenological models, the molecular weight always has a negative effect on the permeability.

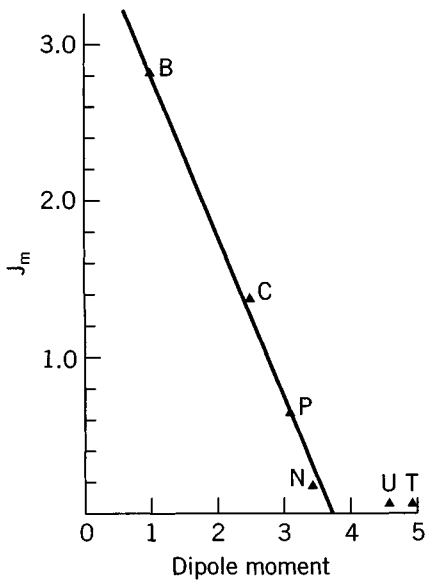


Figure 8. Regression of dipole versus absorption rate. J_m maximum percutaneous absorption rate (%/h); B. benzoic acid dipole moment; C, caffeine dipole moment; N, nicotinamide dipole moment; P, *p*-aminobenzoic acid dipole moment; U, urea dipole moment; T, thiourea dipole moment. *Source:* After Ref. 42. Reproduced with permission of the copyright owner, the American Pharmaceutical Association.

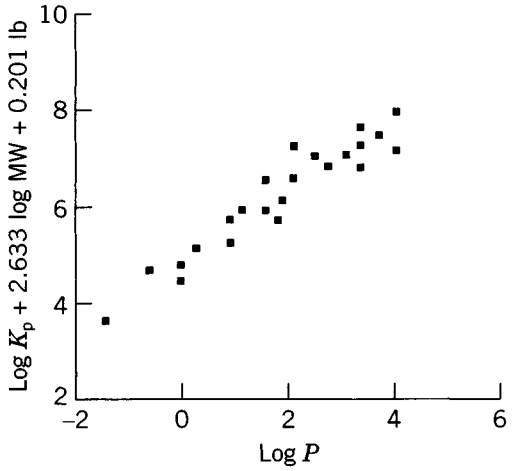


Figure 9. Log K_p after correcting for differences in log MW and H_6 vs log P (Equation 8, $n = 23$, $r = 0/965$, $s = 0.361$). *Source:* After Ref. 44.

ANIMAL MODELS FOR PERCUTANEOUS ABSORPTION

The use of animal models is less than ideal in predicting the percutaneous absorption of chemicals in man. However, many compounds are potentially toxic and must be tested first in vitro or in vivo in animals to determine relative safety for experimentation in humans. In general, primates and miniature pigs are thought to be relatively good models for human percutaneous absorption, whereas the smaller laboratory animals (rabbit, rat, mouse) are poor animal models (9). The Rhesus monkey and the marmoset have demonstrated particular usefulness as models for human skin permeability (9,45).

The skin permeability of certain compounds as tested in the guinea pig and hairless mouse were also comparable to that of human skin (36). Hairless animal skin has the advantage of not requiring any shaving prior to testing. Although it has been hypothesized that the hair follicle represents a cutaneous absorption pathway, the skin of hairless guinea pigs has been shown to be much more permeable to some compounds than the skin of haired guinea pigs (46).

Lipids extracted from skin have utility in the preparation of skin models and for study of the effects of various compounds on stratum corneum lipids (47). Simple in vitro skin models have been prepared by air-drying liposomal suspensions containing epidermal ceramides, cholesterol, free fatty acids, and cholesterol sulfate on hydrophilic filter disks (48). Water permeabilities through these filter-supported lipid lamellae were measured using a diffusion cell; the ultrastructure was characterized by scanning and thin-section electron microscopy. Water flux data and the

ultrastructure of the model were shown to be similar to that of the native human stratum corneum.

TOXICOLOGY

The assessment of the potential for drug toxicity is an important consideration in the evaluation of any transdermal drug candidate. Toxic consequences of percutaneous administration may include skin irritation, immunological responses, and systemic toxicity. Many factors influence absorption of and skin response to a compound; the dose, concentration, occlusion, vehicle, mode and site of application, frequency of use, skin physiology, and the nature of the compound are all important variables.

Skin Metabolism

The metabolic activity of the skin can alter the delivery profile and pharmacologic effects of substances that undergo percutaneous absorption. A topically applied drug can be transformed into either active or inactive metabolites that are capable of different levels of toxicity than the parent compound (27). For example, epidermal keratinocytes have the potential to metabolize propranolol via a pathway that includes formation of an aldehyde intermediate (49). Changes in the pharmacologic or toxicologic profile that result from skin metabolism may have local as well as systemic effects.

In Vivo Testing

Irritation. Reliable testing for skin irritation should provide a means for differentiating substances that produce different degrees of skin irritation. In this context, irritation is the local inflammatory response of normal living skin to direct injury by single, repeated, or prolonged contact with a chemical agent. Macroscopic manifestations of such irritation are erythema and edema. Acute and subchronic irritation testing is used to place compounds into general groups according to their irritant properties. The most standardized toxicological procedures are based on the methods described by Draize, Woodard, and Calvery (50). The primary irritation of the skin is measured by the skin patch technique on intact and intentionally abraded skin of albino rabbits. In contrast, the subchronic skin irritation test measures the cumulative irritation on intact skin that has been exposed to the chemical agent for an extended amount of time. The Draize rabbit skin irritancy test is valuable for its ability to distinguish between chemical agents that are moderate to severe irritants. This method of testing, however, does not allow accurate distinctions between mild and moderate irritants.

Sensitization. Toxicological study also includes evaluation of hypersensitivity. The guinea pig and, more recently, the hairless guinea pig strain, have been widely accepted as the animals of choice for studying this phenomenon because of their genetically based proclivities to sensitization (51). These animals may be used as predictive models to study mechanisms involved in contact sensitization to therapeutic agents. Compounds intended for cutaneous application that are capable of producing sensitization are readily identified by predictive testing (51). The hairless guinea pig has all the humoral and cellular components necessary for sensitization and is responsive to known sensitizers (52,53). A parallel does exist in the sense that the strong and weak sensitizers in man are, respectively, the strong and weak sensitizers of the guinea pig (54–56).

Contact sensitivity is characterized by cellular mediated (thymocyte) allergic reactions of the skin that may be induced by a single contact or may require repeated contacts with the sensitizer, with or without potentiation (57). Potentiation may be provided by physical or chemical irritants such as sodium lauryl sulfate (used in the Kligman Maximization Test) (58) or by immunopotentiators such as Freund's complete adjuvant. The ensuing sensitization response develops slowly on challenge and may require from 8 to 35 hours to appear; it generally persists for 24 hours or more.

Freund's complete adjuvant test is an appropriate method for screening single chemical substances for their immunogenic properties. It is a semiquantitative method for measuring the minimal concentration needed to elicit a response in sensitized animals. The test can establish the allergenicity of a chemical substance, but it cannot establish the actual risk of contact sensitization under conditions of use (51).

In Vitro Testing

Irritation. Organ and cell cultures can help predict whether or not application of some agents results in damage to keratinocytes or to other types of cells. Endpoints used to assess cytotoxicity include cell growth, which may be determined by protein analysis and cell counts. In addition, characteristics such as enzyme release, release of radioactive markers, exclusion of dyes, metabolism, and plating efficiency are all measurable endpoints of cell function. Because these endpoints involve active cellular processes, false-negative results are infrequent. In contrast, tests that interfere with passive structures such as the cell membrane may yield false negatives because testing agents that kill by fixation preserve structural components of the membrane (59). Other types of assays measure sublethal and lethal endpoints.

In vitro testing includes direct and indirect test methods. The latter involve testing individual components or combinations of chemicals as extracts. The types of characteristics not measured by in vitro assays are those that are time dependent or reversible; likewise, complex in vivo interactions are not measured by in vitro assays. The atypical pharmacokinetic profile seen with some compounds may produce changes in vitro that are normally not seen in vivo. It has been reported that the high in vitro toxicity associated with some agents is not representative of local irritation in vivo. When choosing a testing strategy, investigators are wise to select a battery of in vitro assays that assess both active and passive cellular processes.

The use of standard in vitro testing may link the study of toxicity and its mechanism (60). In vitro testing that employs standardized methods can determine a maximum tolerated concentration and the concentration that reduces

a study parameter by 50% of the control value. The neutral red uptake assay, for example, is a test in which the drug effects on the membrane or its ability to alter lysosomes then influences binding of the cationic dye to anionic sites in the lysosome matrix (61). In another similar assay, the metabolic reduction of 3-(4,5-dimethylthiozol-2-yl)-2,5-diphenyltetrazolium bromide (MTT) by cells results in formation of a blue formazon dye (62). Modification of this MTT assay has allowed its use for screening of compounds for their in vitro cytotoxicity in human keratinocytes (63). Inhibitory concentration values, such as the IC_{50}, represent the molar concentration of the drug compound required to kill 50% of fibroblast cells and are also used in screening of compounds for in vitro toxicity (64).

Sensitization. Evaluating the potential for sensitization may include assay of the lymphokines released by antigens from sensitized lymphocytes and lymphocyte proliferation assays (60). Another assay is the murine lymph node assay that studies lymphocyte proliferation and provides both objective and quantitative results. A modification of this procedure involves occluded application of the compound on the shaved abdomen of the animal for 24 hours. Another application is repeated on day 5 and on day 6; the animals are sacrificed, and the brachial and inguinal lymph nodes are removed. Measurement of the spontaneous proliferation capacity of cells seeded in the microtiter well is measured by incorporation of [^{3}H]thymidine. A percent stimulation index is calculated by dividing test-cell incorporation by control-cell incorporation. Results may be correlated with those obtained from in vivo guinea pig sensitization assays. The murine node lymph assay provides a relatively simple, rapid, and inexpensive way to identify agents that exhibit moderate to strong sensitizing potential.

Other Preclinical Testing Requirements

In addition to the determination of irritation and sensitization potential, drugs that are to be used in pharmaceutical products must undergo standardized preclinical testing as part of the requirements for marketing approval. The U.S. FDA considers transdermal drugs as if they were new drugs. Transdermal products that include approved drugs are likely to be approved more readily, however. It is widely accepted that transdermal systems generally produce plasma levels of drug that are considerably lower than those resulting from other administration methods; systemic safety may be less of a concern in such cases.

TRANSDERMAL DRUG DELIVERY

Since the introduction of the first transdermal therapeutic system, the field of transdermal drug delivery has advanced rapidly through greater understanding of the mechanisms, variables, and measurement of percutaneous absorption. Greater understanding of the pharmacokinetics of percutaneously administered drugs has led to the development of systems with optimized delivery profiles. Use of permeation enhancers has increased the number of drugs available for transdermal therapy. The potential advantages of rate-controlled transdermal therapy include the following:

- Improved bioavailability for many drugs
- Reliable blood levels of drug
- Sustained therapeutic effect, allowing use of drugs with short half-lives
- Diminished side effects
- Daily, multiday, or weekly dosing to improve patient compliance
- Simple, noninvasive administration, particularly important for patients who are unable to take medication orally
- Reduced overall treatment costs in many instances

These advantages of transdermal therapy may yield enhanced safety, efficacy, reliability, and acceptability of drug treatment.

Permeation Enhancement

Chemical Enhancers. The skin's physical structure provides a barrier that may limit the permeation of some agents. Skin permeation enhancers broaden the range of drugs that can be delivered transdermally by increasing the penetration of permeants through enhanced diffusion of the stratum corneum and/or by increasing the solubility of the penetrant. Protein denaturation may disrupt the barrier as may fluidization and randomization of intercellular lipids or intercellular delamination and expansion (65).

Ideally, a permeation enhancer functions only to reduce the barrier resistance of the stratum corneum and does not damage any viable cells. The necessary attributes of an enhancer have been reviewed by Barry (7); the ideal enhancer is:

- Pharmacologically inert
- Nontoxic
- Nonirritating
- Nonallergenic
- Rapid-acting with a duration of activity that is predictable and suited to its use
- Chemically compatible and easily formulated into a variety of systems
- Inexpensive
- Odorless
- Tasteless
- Colorless

The enhancer should not extract endogenous material out of the skin but should spread well on skin and have a suitable skin feel. If the substance is a liquid and is to be used at high volume fractions, it should be a suitable solvent for drugs (7).

There are numerous chemical permeation enhancers now being used to facilitate transdermal drug administration. Solvents are frequently used and include alcohol, di-

methyl sulfoxide, dimethylformamide, dimethylacetamide, propylene glycol, pyrrolidones, and water. Other enhancers include Azone® and its derivatives, surfactants, fatty acids, terpenes and their derivatives, alkyl sulfoxides, phosphine oxides, sugar esters, urea and its long chain analogues, *N,N*-diethyl-*m*-toluamide, calcium thioglycolate, and anticholinergic agents (7).

Ethanol has been used very successfully as a permeation enhancer in a variety of commercial transdermal systems (66), including those that deliver estradiol and fentanyl. Pure ethanol-enhanced permeation of solutes across the skin in vitro is thought to be a result of the extraction of skin lipids by ethanol, but apparent diffusivity has not been significantly altered in in vivo studies (67). For example, the flux of estradiol across viable human skin was shown to be increased in vivo only with saturated solutions of estradiol, indicating the increased solubility of estradiol in ethanol and an increased concentration gradient of estradiol across the skin. Knowledge of the apparent partitioning of the solute into the stratum corneum and the solute concentration in the vehicle allow prediction of the flux of estradiol across human skin in vivo.

More recently, use of composite lipidic agent-carriers such as liposomes and niosomes has been tried. These agents have been less successful than conventional enhancers because of their inability to pass through the narrow intracellular passages in the outer skin layers. A more deformable supramolecular aggregate known as the transfersome has been described and is thought to use the transepidermal gradient as a means of permeation enhancement. Successful use of transfersomes to achieve transcutaneous peptide and protein delivery in animals and in humans has been reported (Fig. 10) (47).

Epidermal enzymes have also been identified as potentially valuable permeation enhancers in transdermal drug delivery (68). It has been demonstrated that epidermal enzymes play an important role in the differentiation of keratinocytes, and that epidermal phospholipids undergo enzymatic conversion to nonpolar species and contribute to the barrier function of the stratum corneum. In vitro study of the role of these enzymes on the permeation of benzoic acid, mannitol, and testosterone in an excised human skin model reveal that enzymes may have remarkable effects on the permeation of topically applied compounds. Of the enzymes studies (phospholipase C, triacylglycerol hydrolase, acid phosphatase, phospholipase A_2), phopholipase C was the most effective in facilitating the transport of all solutes. The effects of these topical enzymes appear to be mediated through their influence on skin lipids.

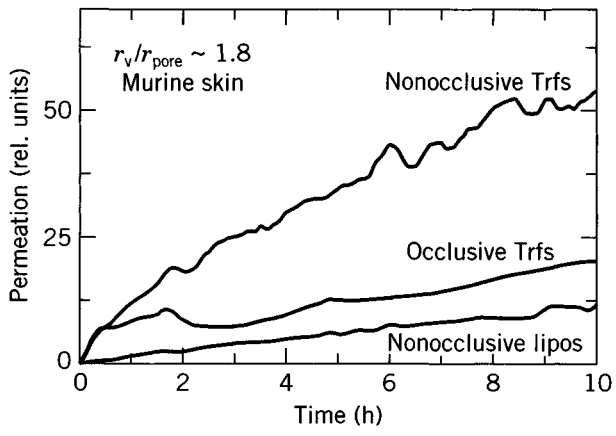


Figure 10. The penetration of standard liposomes (dotted curve) and of the highly deformable transfersomes (full curve) through the murine skin after an occlusive or nonocclusive application. Only an open suspension of transfersomes results in significant transfer of the fluorescently labeled lipids incorporated into the lipid vesicles through the intact murine skin. The small signals observed in the other cases are largely due to the permeation of the free label. *Source:* From Ref. 47.

Pharmacokinetics

The successful delivery of drugs through skin and into the systemic circulation may require four to five biological half-lives of a compound to transpire before steady-state blood levels are reached (41). Thus, the plasma half-life of a drug is a major consideration when selecting a drug for transdermal administration. Drugs with shorter half-lives are ideal, whereas agents with longer half-lives may interfere with the ability to achieve and maintain close control over drug levels in plasma. However, modifications in transdermal system design may allow the use of drugs with a less than ideal pharmacokinetic profile. Examples of two transdermal drugs, nicotine and fentanyl, are presented to illustrate differences in pharmacokinetic properties and, thus, system requirements.

Nicotine is an example of an agent that is highly soluble, readily penetrates the skin, and possesses a relatively short half-life. It is administered transdermally to aid in smoking cessation. Following intravenous (IV) administration of nicotine, the volume of distribution is approximately 2–3 L/kg and its half-life ranges from 1 to 2 hours. In one nicotine transdermal system (Nicoderm® CQ, SmithKline Beecham Consumer Healthcare, Pittsburgh, PA), approximately 68% of the nicotine released from the system enters the systemic circulation (69). Plasma nicotine concentrations rise rapidly when the system is applied, plateau within 2–4 hours, and slowly decline until the system is removed (Fig. 11) (69,70). Plasma nicotine concentrations achieved are proportional to system size (dose); linear kinetics are observed (70). Nicotine kinetics are similar for all sites of application on the upper body and upper outer arm, and no gender-related differences in nicotine kinetics have been observed. Removal of the nicotine transdermal system results in an exponential decline in plasma nicotine levels with an apparent mean half-life of 3–4 hours. The half-life of transdermally administered nicotine is longer than that seen with IV administration because of continued absorption from the skin depot (70).

Fentanyl is an opioid analgesic that has a longer IV half-life (3–12 hours) than nicotine and penetrates the skin slowly, requiring a permeation enhancer (ethanol) for adequate delivery (71,72). The drug's average volume of distribution is 6 L/kg, and the variability in reported ranges of distribution volumes is large (73). Transdermal absorption of fentanyl is generally characterized by a zero-order process. In the fentanyl transdermal system, a permeation

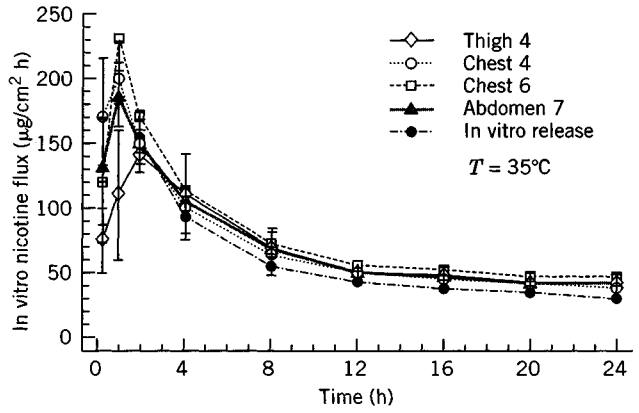


Figure 11. Mean (SD) in vitro nicotine flux for the Nicoderm® system.

enhancer increases the rate of drug flux through skin, resulting in effective blood concentrations for a prolonged period. Transdermal fentanyl is 92% bioavailable and, thus, does not appear to be metabolized by skin nor significantly degraded by the skin's bacterial flora (71). Following application of Duragesic® [fentanyl transdermal system] CII (ALZA Corporation, Palo Alto, CA, and Janssen Pharmaceutica, Titusville, NJ), the skin absorbs fentanyl and dissipates it into the systemic circulation (71,72). Absorption continues throughout the 72-hour dosing interval (Fig. 12). Low enhancer flux minimizes the skin drug depot (74). Serum fentanyl concentrations increase gradually following initial application of the system, generally leveling off between 12 and 24 hours and remaining relatively constant for the remainder of the 72-hour dosing period. Peak serum levels of fentanyl generally occur between 24 and 72 hours after initial application. Serum fentanyl concentrations are proportional to the delivery rate, and after several sequential 72-hour applications, patients reach and maintain a steady-state serum concentration that is determined by individual variation in skin permeability and body clearance of fentanyl (71,72).

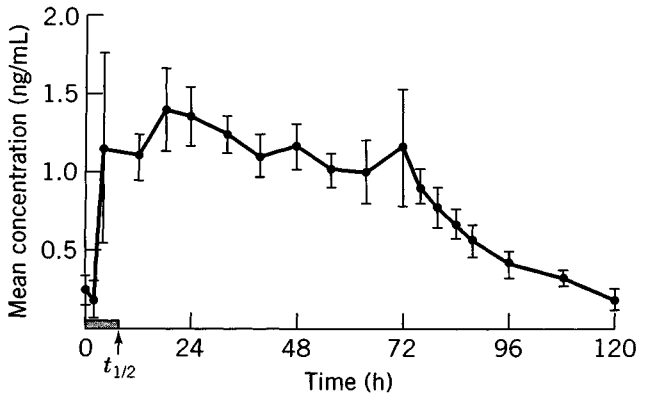


Figure 12. Fentanyl concentrations from TTS (fentanyl)-75 (72 h application).

MARKETED TRANSDERMAL SYSTEMS

There are a number of transdermal systems now available. Generally speaking, however, system design can be classified based on the type of rate control employed (skin-controlled vs. system-controlled drug delivery) and by the presence or absence of permeation enhancers in the delivery system. Skin-controlled drug delivery devices rely on the skin's barrier properties to control the rate of drug input to the body. These devices may include a matrix or multilaminate design to act as a carrier that maintains drug in contact with the surface of the skin. Drug diffuses through the skin at a rate dictated by the concentration of drug on the skin and by the permeability of the skin to the drug. Because rate control relies completely on the skin's diffusive properties, variations in skin permeability (e.g., at different sites) may have variable effects on the delivery rate of systems without built-in control mechanisms (75).

System-controlled drug delivery requires a rate-controlling element such as a polymeric membrane (Fig. 13). The membrane allows measured release of drug throughout the wearing period and provides more protection from potential drug overdose than skin-controlled delivery. Drug delivery with a system that incorporates a rate-controlling membrane produces less variability in drug input, yielding a more predictable and reproducible pharmacokinetic profile (75).

The need for permeation enhancers is determined by the nature of the drug intended for use in the transdermal delivery system. Highly skin-permeable drugs agents, such as nicotine, do not require a permeation enhancer. The transcutaneous flux of most hormones, however, is low, requiring the use of a permeation enhancer such as ethanol or triethanloamine. These solvents permeate the skin but without rate control or occlusion, their effectiveness is brief and limited. The use of certain types of permeation enhancers has been associated with skin irritation.

Types of Transdermal Systems

Worldwide, a variety of transdermal systems are available. In the United States, transdermal systems are used for delivery of analgesics (fentanyl), hormone replacement therapies (estradiol and testosterone) and medications for angina (nitroglycerin), hypertension (clonidine), and motion sickness (scopolamine) (Table 1). Transdermal systems that deliver nicotine for use in smoking cessation are also available. In Japan and in parts of Europe, systems that incorporate antiinflammatory drugs (flurbiprofen and

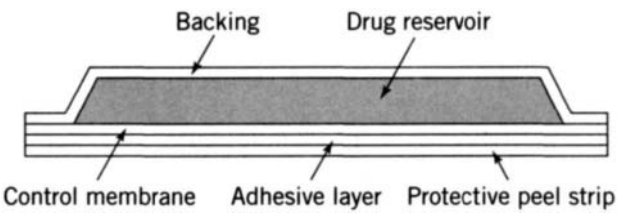


Figure 13. System-controlled drug delivery system.

Table 1. Advantages of Rate-Controlled Transdermal Drugs: Three Examples

Drug	Use	Dosing frequency via transdermal delivery	Dosing frequency via other means	Improved selectivity of action with transdermal delivery	Other advantages of transdermal delivery
Scopolamine	Motion sickness	Once every 3 days	4–6 times per day	CNS effects diminished or absent	May be used in the presence of nausea/ vomiting
Nitroglycerin	Prophylaxis of angina	Once daily	2–3 times per day		Prevents massive drug degradation in the liver
Clonidine	Treatment of hypertension	Once daily	2–3 times per day	Dry mouth, drowsiness, sexual dysfunction lessened or absent	

ketaprofen) and monoamine oxidase inhibitors such as selegiline have also been introduced. In this section, a review of a selected group of systems is provided with an emphasis on product characteristics and the clinical performance measures of safety, efficacy, reliability, and acceptability of drug treatment.

Fentanyl. The successful management of chronic pain frequently requires long-term administration of opioids such as fentanyl. Fentanyl is an opioid analgesic that has been used parenterally to treat chronic pain for more than 20 years and has been available in a transdermal delivery system (Fig. 14) (Duragesic® [fentanyl transdermal system] CII, ALZA Corporation, Palo Alto, CA, and Janssen Pharmaceutical, Titusville, NJ) since 1990. For patients who require continuous opioid analgesia for pain that cannot be managed by lesser means, the development of a transdermal system that delivers fentanyl over 72 hours confers a number of advantages over traditional IV administration, including prolonged dosing that does not require an indwelling catheter and maintenance of drug presence that may prevent breakthrough pain. The system comprises a peel-off protective liner and four functional layers: a backing of polyester film, a drug reservoir containing fentanyl base and alcohol, an ethylene–vinyl acetate copolymer membrane that controls the rate of drug delivery to the skin, and a fentanyl-containing adhesive layer. The impermeable outer layer prevents loss of drug from the system and entry of water into the drug reservoir. The inclusion of alcohol in the reservoir enhances drug flux through the rate-limiting membrane and increases the skin's permeability to fentanyl (Fig. 15); the amount of alcohol released during the 72-hour application period is small (<0.1 mL/10 cm^2). The adhesive layer, which contains a bolus of drug, allows initial administration of fentanyl with system application. The system is available in four strengths that deliver fentanyl at rates of 25, 50, 75, or 100 μg per hour. The amount of fentanyl released from each system is proportional to its surface area (2.5 $\mu g/h/cm^2$).

The analgesic activity of transdermal fentanyl has been demonstrated in a number of clinical trials (72,76–78). System functionality and a pharmacokinetic model have also been studied, and these results indicate the serum fentanyl profile for the transdermal system is a net result of system performance and drug absorption and elimination (79).

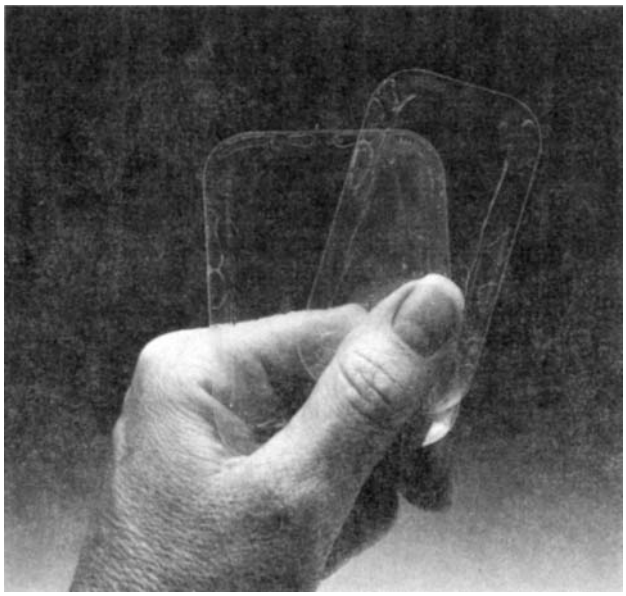


Figure 14. The Duragesic® (fentanyl transdermal system).

Estradiol. A variety of transdermal systems are available for use in hormone replacement therapy. Estraderm® (Ciba-Geneva Pharmaceuticals, Summit, NJ) is available in 0.05 mg and 0.1 mg dosage forms and incorporates a

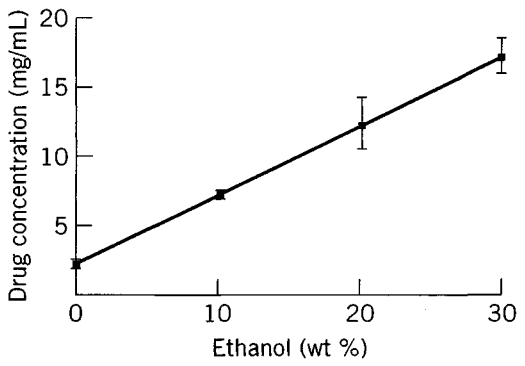


Figure 15. Fentanyl Concentration in Human Epidermis (room temperature).

rate-controlling membrane that allows controlled release of estradiol from a drug reservoir. Climara® estradiol transdermal system (Berlex Laboratories, Wayne, NJ), uses an acrylate adhesive matrix that contains estradiol in a 0.05 mg or 0.1 mg strength. The Vivelle® estradiol transdermal system (Ciba-Geneva Pharmaceuticals, Summit, NJ) is available in the following strengths: 0.0375 mg, 0.05 mg, 0.075 mg, and 0.1 mg of estradiol. The system contains estradiol in a multipolymeric adhesive and releases the hormone continuously upon application to the skin. FemPatch® (Parke-Davis, Morris Plains, NJ) is a self-adhesive matrix system that delivers estradiol at a rate of 0.025 mg/day for 7 days and contains a silicone-based contact adhesive. Alora® (Proctor and Gamble Pharmaceuticals, Cincinnati, OH) is another self-adhesive matrix system that incorporates an acrylate contact adhesive and delivers estradiol at rates of 0.05, 0.075, and 0.1 mg/day for 3–4 days.

Transdermal administration of estradiol has proven to be a very successful means of hormone replacement therapy, alleviating the vasomotor and other estrogen deficiency symptoms among postmenopausal women. These symptoms include hot flushes and other discomforts such as vaginal atrophy, vaginitis, and atrophic changes of the lower urinary tract. Hormone replacement therapy is also given to prevent osteoporosis. The transdermal route is associated with fewer adverse effects than oral regimens and allows serum estrogen levels of remain quite steady over the 3–4-day application period; daily peaks and troughs are minimized (Table 2). The direct absorption of estradiol into the circulation allows peripheral metabolization to estrone and achieves a premenopausal pattern of estrogen as well as premenopausal levels of the hormone (80).

Testosterone. Currently, two transdermal products are available for testosterone replacement therapy: a scrotal system (Testoderm® Testosterone Transdermal System, ALZA Pharmaceuticals, Palo Alto, CA) and a nonscrotal system (Androderm® Testosterone Transdermal System, SmithKline Beecham Pharmaceuticals, Philadelphia, PA) that may be applied to the torso or appendages. The efficacy of both products in establishing optimal levels of testosterone in hypogonadal males was demonstrated in clinical trials (22). Transdermal administration has several benefits over other routes of testosterone administration. It minimizes the nonphysiologic peaks and troughs associated with intramuscular (IM) or oral dosing, and avoids the inconvenience of frequent injections. Unlike absorption via the oral route, transdermal absorption is not affected by food intake or hepatic first-pass metabolism, which may increase dosage requirements, produce unusual metabolites, or possibly result in liver toxicity (81–84). Testosterone transdermal systems have demonstrated an ability to approximate the natural endogenous pattern of serum testosterone levels in normal males and have been shown to produce positive effects on fatigue, mood, and sexual function, as well as significant increases in sexual activity (85–88).

Table 2. Benefits of Transdermal Estradiol

Use of natural hormone
Effective treatment of hot flushes
Therapeutic hormone levels with low daily dose
Restoration of premenopausal ratio of estradiol to estrone
Avoidance of dose-related hepatic effects
Rapid initiation and termination of therapy

The Testoderm® testosterone transdermal system is designed for scrotal application to take advantage of the unique superficial vascularity and highly permeable nature of the scrotal skin. Application of the Testoderm® system at this site allows a high transfer rate of the hormone without the use of a permeation enhancer, adhesives, or preservatives. The scrotal system is designed to release controlled amounts of testosterone continuously upon application to dry-shaved scrotal skin. A single scrotal system delivers either 4 mg or 6 mg of testosterone over a 24-hour period in a pattern that approximates normal circadian rhythms of testosterone secretion. Data suggest testosterone delivery is negligible when the scrotal system is applied to nonscrotal skin (unpublished data, ALZA Corporation, 1991).

The Androderm® testosterone transdermal system is designed to deliver testosterone through intact nonscrotal skin—for example, on the back, abdomen, thighs, and upper arms. The system contains a drug reservoir gel that is surrounded by a peripheral adhesive area and relies on the barrier properties of the skin to control permeation. Testosterone flux is facilitated by permeation enhancers in the system that assist the transport of drug across the skin. Originally, two Androderm® systems (each 2.5 mg) were applied nightly to deliver approximately 5 mg of testosterone over a 24-hour period. Recently, however, a 5 mg Androderm® system has been developed to allow nightly application of a single system. Both the 2.5 and 5 mg systems produce hormone levels that mimic the daily pattern of testosterone release in healthy men.

In one study comparing the two marketed testosterone transdermal systems (89), the scrotal system was shown to be better tolerated. In those using the permeation-enhanced Androderm® system, allergic contact dermatitis and spontaneous flaring of prior application sites occurred in 7 (12%) subjects using Androderm® systems on day 12. In contrast, use of the Testoderm® testosterone transdermal system resulted in no confirmed cases of allergy ($P < 0.001$). For Testoderm® and Androderm® systems, respectively, moderately intense irritation was noted in 5% and 32% of subjects ($P < 0.001$) and in 1% and 7% of application sites ($P < 0.001$). The Testoderm® system produced no confirmed contact allergy and less topical irritation than the Androderm® system, and patients with contact allergy to Androderm® used the Testoderm® system without a reaction, suggesting testosterone was not the allergen.

Nitroglycerin. Nitroglycerin has been used in the treatment of angina pectoris for more than a century. Nitroglycerin ointment preceded the development of nitroglycerin patch systems and is still available (Nitro-Bid® Ointment 2%, Hoechst Marion Roussel, Kansas City, MO). Plasma concentrations of nitroglycerin with ointment treatment, however, are subject to a rapid rise following

application and a sharp decline after approximately 8 hours (90). There have been a number of nitroglycerin systems that have come to market, including Deponit® (Schwarz-Pharma, Milwaukee, WI) Nitrodisc® (Roberts Pharmaceutical Corp., Eatontown, NJ), Nitro-Dur® (Key Pharmaceuticals, Inc., Kenilworth, NJ), Minitran® (3M Pharmaceuticals, Northridge, CA) and Transderm-Nitro® (Ciba-Geneva). The rate of delivery of the drug from the inner surface of the patches is controlled either by dispersing it in a solid-nitroglycerin-impregnated polymer (Nitrodisc®), incorporating it in a gel-like matrix (Nitro-Dur®) or adhesive matrix (Deponit®, Minitran®), or by placing a permeability-modulating membrane between the drug and the skin (Transderm-Nitro®).

Studies have demonstrated clinical efficacy, indicating effectiveness over 24 hours or longer and decreased frequency, severity, and duration of anginal attacks and S-T segment depression during treadmill tests (91). A number of studies have also investigated patient preference, including factors such adhesion, incidence of local skin reactions, and cosmetic properties. In a comparison of Transderm-Nitro® and Nitro-Dur® systems, the former was associated with superior adhesive properties and a lower incidence of local reactions such that the patient preference was nearly 10 to 1 in favor of Transderm-Nitro® (92). In another comparison of the two systems, a preference for Transderm-Nitro® was also cited based on adhesion, a lower rate of local reactions, and better cosmetic properties (93). Comparison of Transderm-Nitro®, Nitrodisc®, and Nitro-Dur® revealed that patient preferences varied considerably and that use of Transderm-Nitro® was associated with significantly fewer intolerable skin reactions than Nitro-Dur® and caused less discomfort upon removal as compared with Nitrodisc® (94). Results of a later study by Chinoy and colleagues (95) indicate the Tranderm-Nitro® system showed better adhesion than Deponit® ($P < 0.0001$) and improved tolerability at the site of application ($P < 0.0588$).

Clonidine. Clonidine is a potent, central-acting hypotensive agent. The drug is widely used and normally administered orally two to three times daily. A transdermal therapeutic system with a rate-controlling membrane (Catapres®-TTS, Boehringer Ingelheim Pharmaceuticals, Inc., Ridgefield, CT) administers this drug over 7 days after a single application (Fig. 16). Following system application to intact skin, clonidine in the adhesive layer saturates the skin site below the system; clonidine from the drug reservoir then begins to diffuse through the rate-controlling membrane and through the skin for absorption by the capillaries beneath the skin. Therapeutic clonidine levels are achieved 2–3 days after application of the first system; application of a new system at weekly intervals maintains therapeutic drug levels. To ensure constant release over 7 days, the total drug content of the system is maintained at or above saturation. The mean plasma concentration of clonidine is proportional to the surface area of the system, demonstrating the linearity between the system size (dose) applied and associated plasma levels. A comparison of oral clonidine (three times daily) with once-weekly transdermal administration revealed that the former resulted in a seesaw pattern of drug concentration in plasma. Virtually steady plasma concentrations of clonidine are produced by transdermal dosing over 7 days (8). In a clinical trial of patients suffering from mild hypertension, 48 of the 69 subjects achieved long-term control of blood pressure with Catapres®-TTS. Side effects associated with orally administered clonidine, such as drowsiness and dry mouth were reduced by rate-controlled transdermal administration (41).

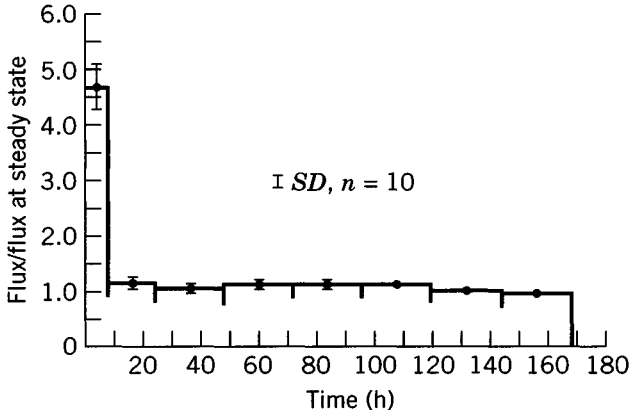


Figure 16. Mean in vitro drug release rate from Catapres-TTS® (Water receptor, $T = 32°C$).

Scopolamine. The first controlled-release transdermal dosage form was Transderm-Scop® (Ciba Self-Medication, Inc., Woodbridge, NJ). One application of the system, which incorporates a rate-controlling membrane, delivers 0.5 mg scopolamine over 3 days to prevent motion sickness. Transdermal administration allows reduction in the total dose required and is a clear improvement over the usual intramuscular injections that require four to six daily doses. A loading dose is released from the transdermal system in the first two hours of application, and then drug release declines rapidly to a constant rate designed to maintain steady-state levels. It has been demonstrated that when scopolamine is administered transdermally or intravenously at similar constant rates over 24 to 72 hours, the rates of urinary excretion of the drug are also similar (96). These results suggest blood levels via the two different administration methods are also similar. Rate-controlled transdermal delivery under steady-state conditions can be compared with continuous, controlled, IV infusion.

Clinical results with the Transderm-Scop® system indicate considerable success in the treatment of motion sickness. In one controlled trial, the system prevented motion sickness in 75% of the susceptible subjects and yielded a low incidence of side effects (Fig. 17) (97). Although the drug has a narrow therapeutic index, study of the general use of Transderm-Scop® indicates that the efficacy of the transdermal dosage form has been excellent and that the incidence of side effects of a parasympatholytic nature have been low (98). Clearly, the clinical performance of this dosage form is related to the rate-controlled delivery of the

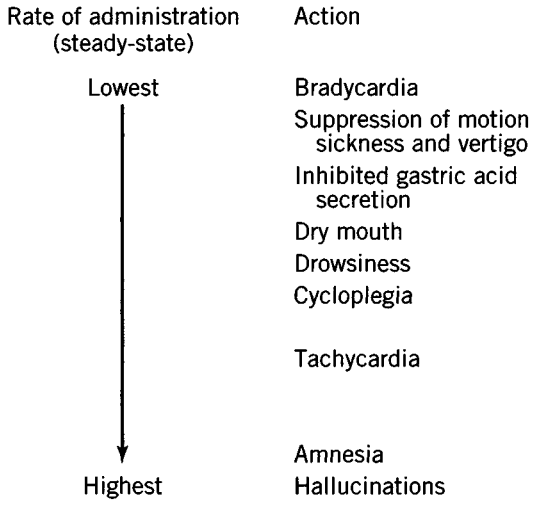


Figure 17. Zero-order pharmacology of scopolamine.

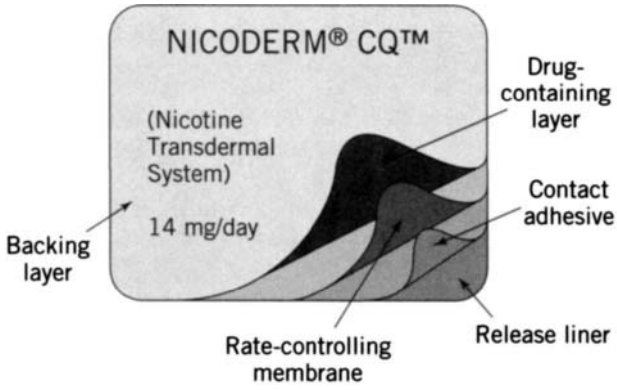


Figure 18. NicoDerm® CQ™ nicotine transdermal system.

Table 3. Nicotine Transdermal Systems: Comparative Functionality

Parameter	Nicoderm®	Habitrol®	Prostep®
Dose (mg/day)	21	21	22
C_{max} (ng/mL)	23	17	16
C_{avg} (ng/mL)	17	13	11
C_{min} (ng/mL)	11	9	5
T_{max} (hours)	4	6	9

system, which regulates systemic drug input in the therapeutic range.

Nicotine. The addictive properties of nicotine are well known, and its potential for abuse is well established (99). Withdrawal from nicotine causes physical complaints that are abated by smoking, and thus, smoking behavior is reinforced by the disappearance of these symptoms. The administration of nicotine to nicotine-dependent individuals is the most successful pharmacologic approach to smoking cessation (75), significantly decreasing the severity of nicotine withdrawal symptoms (100,101).

There are a number of nicotine transdermal systems now available worldwide, including Habitrol® (Ciba Self-Medication, Woodbridge NJ), Nicoderm® CQ (SmithKline Beecham Consumer Healthcare, Pittsburgh PA), Nicotrol® (McNeil Consumer Products Company, Fort Washington, PA), and Prostep® (Lederle Laboratories, Wayne, NJ). These systems have several features in common: they are self-adhesive, multilayered, and possess a removable protective liner. The patches vary in their methods of nicotine storage, mode of drug release, and degree of rate control. Habitrol® and Nicotrol® have a drug reservoir that equilibrates within the system after manufacture; neither possess any rate control features. Prostep® contains a nonadhesive drug gel, and the system is not self-adhesive,

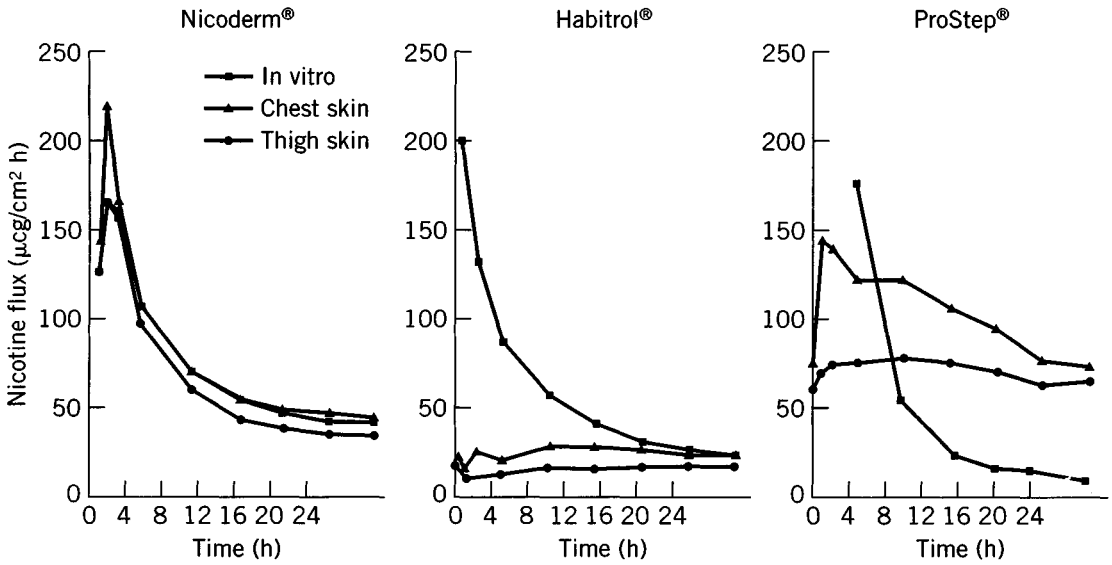


Figure 19. In vitro release of three transdermal nicotine products.

requiring a peripheral adhesive to adhere the product to the skin.

Habitrol®, Nicotrol®, and Prostep® are examples of products that depend on the rate-controlling properties of the skin to modulate nicotine input. In contrast, Nicoderm® (Fig. 18) possesses a membrane that controls the rate of drug input through the skin. This system provides several advantages over its non-rate-controlled counterparts, including rapid onset of therapeutic levels of nicotine in plasma, more consistent drug input among application sites (Fig. 19), greater control over absorption and drug-blood levels (Table 3), and improved protection from abuse and drug overdose (75,102,103).

Treatment with nicotine transdermal systems should be used as part of a comprehensive behavioral smoking-cessation program and has been shown to result in significantly higher "quit rates" than placebos (104).

SUMMARY

Transdermal therapy has advanced rapidly amid greater understanding of the skin's permeability characteristics. Techniques for measuring permeation of chemical agents and the development of appropriate predictive models have been extremely important in the design of safe and effective transdermal systems. A number of pharmacotherapeutic and pharmacoeconomic benefits have been realized with transdermal therapy, and research and development programs will undoubtedly reveal additional merits of this important technology.

BIBLIOGRAPHY

1. P.M. Elias, *J. Invest. Dermatol.* **80**(6), 44S–49S (1983).
2. R.J. Scheuplein, *J. Invest. Dermatol.* **45**, 334–346 (1965).
3. R.J. Scheuplein, *J. Invest. Dermatol.* **48**, 79–88 (1967).
4. R.J. Scheuplein, *J. Invest. Dermatol.* **60**, 263–269 (1973).
5. R.J. Scheuplein and I.H. Blank, *Physiol. Rev.* **51**(4), 702–747 (1971).
6. A. Fick, *Annln. Phys.* **170**, 59 (1855).
7. B.W. Barry, *Molec. Aspects. Med.* **12**, 195–241 (1991).
8. J.E. Shaw, M.E. Prevo, and A. Amkraut, *Arch. Dermatol.* **123**, 1548–1556 (1987).
9. R.C. Wester and H.I. Maibach, *Clin. Pharmacokinet.* **23**, 253–266 (1992).
10. A.W. McKenzie and R.B. Stoughton, *Arch. Dermatol.* **86**, 608–610 (1962).
11. A. Rougier et al., *J. Invest. Dermatol.* **81**, 275–278 (1983).
12. A. Rougier et al., *Arch. Dermatol. Res.* **278**, 465–470 (1986).
13. V.H. Mak, R.O. Potts, and R.H. Guy, *Pharm. Res.* **7**, 835–841 (1990).
14. B. Sennhenn et al., *Skin Pharmacol.* **6**, 152–160 (1993).
15. N. Higo et al., *Pharm. Res.* **10**, 1500–1506 (1993).
16. C. Anderson, T. Anderson, and M. Molander, *Acta. Derm. Venereol.* **71**, 389–393 (1991).
17. R. Takamoto, R. Namba, M. Matsuoda, and T. Sawada, *Anal. Chem.* **64**, 2661–2663 (1992).
18. S.K. Chandrasekaran, P.K. Campbell, and A.S. Michaels, *Am. Inst. Chem. Eng. J.* **23**, 810–816 (1977).
19. J.G. VanRooij, J.H. De Roos, M.M. Bodelier-Bade, and F.J. Jongeneelen, *J. Toxicol. Environ. Health* **38**, 355–368 (1993).
20. S. Southwell, B. Barry, and R. Woodford, *Int. J. Pharmacol.* **18**, 299–309 (1984).
21. J.E. Shaw and S.K. Chandrasekaran, in ed., *Drug Absorption, Proceedings of the International Conference on Drug Absorption*. ADIS Press, Edinburgh, Scotland, 1979, pp. 186–193.
22. *Physicians' Desk Reference*, 51st ed., Medical Economics Data Production Company, Montvale, New York, 1997.
23. S.D. Roy and G.L. Flynn, *Pharm. Res.* **7**, 842–847 (1990).
24. J.D. Harvell and H.I. Maibach, *J. Am. Acad. Dermatol.* **31**, 1015–1021 (1994).
25. J.T. Reed, R. Ghadially, and P.M. Elias, *Arch. Dermatol.* **131**, 1134–1138 (1995).
26. D. Weigand, C. Haygood, and G. Gaylord, *J. Invest. Dermatol.* **62**, 563–568 (1974).
27. R.C. Wester, A. Rougier, C. Lotte, and H. Maibach, *Pharm. Res.* **7**, S211 (1990).
28. C. Lotte, R.C. Wester, A. Rougier, and H.I. Maibach, *Arch. Dermatol. Res.* **284**, 456–459 (1993).
29. R.L. Williams et al., *Pharm. Res.* **8**, 744–749 (1991).
30. E. Berardesca, and H.I. Maibach, *Dermatosen* **38**, 50–53 (1990).
31. R. Aly, *Sem. Dermatol.* **1**, 137–142 (1982).
32. V.A. Harpin and N. Rutter, *J. Pediat.* **102**, 419–425 (1983).
33. W. Schalla, B. Lambrey, E. Lamand, and H. Schaefer, *Pharmacol. Skin* **1**, 190–200 (1987).
34. K. Arndt and R. Clark, in T.B. Fitzpatrick et al., eds., *Dermatology in General Medicine*, McGraw-Hill, New York, 1979, pp. 1753–1758.
35. I. Gigli and R. Baer, in T.B. Fitzpatrick et al., eds., *Dermatology in General Medicine*, McGraw-Hill, New York, 1979, pp. 520–528.
36. R. Bronaugh and R. Stewart, *J. Pharm. Sci.* **74**, 1062–1066 (1985).
37. A. Solomon and N. Lowe, *Arch. Dermatol.* **114**, 1029–1034 (1978).
38. H. Shaefer et al., *Pharmacol. Skin* **1**, 50–56 (1987).
39. A.S. Michaels, P.S.L. Wong, R. Prather, and R.M. Gale, *Am. Inst. Chem. Eng. J.* **21**, 1073–1080 (1975).
40. R.J. Scheuplein, in W. Montagna, E.J. Van Scott, and R.B. Stoughton, eds., *Advances in Biology of Skin*, vol. 12, Appleton-Century-Crofts, New York, 1972, pp. 135–148.
41. J.E. Shaw, M.E. Prevo, R.M. Gale, and S.I. Yum, in L.A. Goldsmith, ed., *Physiology, Biochemistry, and Molecular Biology of the Skin*, 2nd ed., Oxford University Press, New York, 1991, pp. 1447–1479.
42. H.Y. Ando, R.L. Schultz, R.L. Schaare, and E.T. Sugita, *J. Pharm. Sci.* **73**, 461–467 (1984).
43. G.B. Kasting, R.L. Smith, and E.R. Cooper, *Pharmacol. Skin* **1**, 138–153 (1987).
44. E.J. Lien and H. Gao, *Pharm. Res.* **12**(4), 583–587 (1995).
45. R.C. Scott, M.A. Corrigan, F. Smith, H. Mason, *J. Invest. Dermatol.* **96**, 921–925 (1991).
46. G. Hisoire and D. Bucks, *J. Pharm. Sci.* **86**(3), 398–400 (1997).
47. G. Cevc, *Critical Reviews in Therapeutic Drug Carrier Systems* **13**, 257–388 (1996).
48. W. Abraham and D.T. Downing, *J. Invest. Dermatol.* **93**, 809–813 (1989).

49. M. Cormier, P.W. Ledger, J.P. Marty, and A. Amkraut, *J. Invest. Dermatol.* **97**, 447–453 (1991).
50. J.H. Draize, G. Woodard, and H.O. Calvery, *J. Pharmacol. Exp. Ther.* **82**, 377–390 (1944).
51. G. Klecak, in F.N. Marzulli and H.I. Maibach, eds., *Dermatotoxicology*, 2nd ed. Hemisphere Publishing Corp., Washington, D.C., 1983, pp. 200–203.
52. D.F. Woodard et al., in H.I. Maibach and N.J. Lowe, eds., *Models in Dermatology*, Karger, New York, 1989, pp. 71–78.
53. A.E. Chester et al., *J. Toxicol.* **7**, 273–281 (1988).
54. H.C. Maguire, in H.I. Maibach, ed., *Animal Models in Dermatology*, Churchill-Livingstone, New York, 1975, pp. 67–75.
55. J.F. Griffith, *Toxicol. Appl. Pharmacol.* **3**, 90–102 (1969).
56. E.V. Buehler, *Arch. Dermatol.* **91**, 171–175 (1965).
57. E.V. Buehler, in K.E. Anderson and H.I. Maibach, eds., *Contact Allergy Predictive Tests in Guinea Pigs*, Karger, New York, 1985, pp. 39–44.
58. A.M. Kligman, *J. Invest. Dermatol.* **47**, 369–374 (1966).
59. B. Ekwall, *Ann. N.Y. Acad. Sci.* **407**, 64–77 (1983).
60. W.E. Parish, *Food Chem. Toxicol.* **24**, 481–494 (1986).
61. E. Borenfreund and J.A. Puerner, *J. Tissue Cult.* **9**, 7–9 (1984).
62. L. Green, J.L. Reade, and C.F. Ware, *J. Immunol. Methods* **70**, 257–268 (1984).
63. D.A. Swisher, J. Johnson, and P.W. Ledger, *J. Invest. Dermatol.* **88**, 520–524 (1987).
64. N.K. Mize, J.A. Johnson, C. Hansch, and M. Cormier, *Curr. Prob. Dermatol.* **23**, 224–229 (1995).
65. R.J. Scheuplein and L. Ross, *J. Soc. Cosmet. Chem.* **21**, 853–873 (1970).
66. S.I. Yum, E. Lee, and F. Theeuwes, in D.S. Hsieh, ed., *Drug Permeation Enhancement: Theory and Applications*, Marcel Dekker, New York, 1994, pp. 143–170.
67. L.K. Pershing, L.D. Lambert, and K. Knutson, *Pharm. Res.* **7**, 170–174 (1990).
68. S. Patil, P. Singh, C. Szolar-Platzer, and H. Maibach, *Am. Chem. Soc. Am. Pharm. Assoc.* **85**(3), 249–252 (1996).
69. J. Gorsline, *Health Values*, **17**, 20–24 (1993).
70. S.K. Gupta et al., *J. Clin. Pharmacol.* **33**, 169–174 (1993).
71. J.R. Varvel et al., *Anesthesiology* **70**, 928–934 (1989).
72. R.K. Portenoy et al., *Anesthesiology* **78**(1), 36–43 (1993).
73. K.A. Calis, D.R. Kohler, and D.M. Corso, *Clin. Pharm.* **11**, 22–36 (1992).
74. M.A. Southam, *Anti-Cancer Drugs* **6**(suppl 3), 29–34 (1995).
75. J.A. Hunt and D.J. Enscore, *Pharm. Res.* **10**, S-252 (1993).
76. R.A. Caplan et al., *JAMA, J. Am. Med. Assoc.* **261**, 1036–1039 (1989).
77. C. McLeskey and J. McRae, *Anesth. Analg.* **70**, S264 (1990).
78. D.J. Rowbotham et al., *Br. J. Anaesth.* **63**, 56–59 (1989).
79. S.K. Gupta, M. Southam, R. Gale, and S.S. Hwang, *J. Pain Symptom Manag.* **7**, S17–26 (1992).
80. Transdermal HRT Investigators Group, *Int. J. Fertil.* **38**, 5–11 (1993).
81. R.D. McClure, R. Oses, and M.L. Ernest, *Urology* **37**(3), 224–228 (1991).
82. J.C. Findlay, V. Place, and P.J. Snyder, *J. Clin. Endocrinol. Metab.* **64**(2), 266–268 (1987).
83. S. Bhasin, *J. Clin. Endocrinol. Metab.* **74**(6), 1221–1225 (1992).
84. H.M. Behre, F. Oberpenning, and E. Nieschlag, in E. Nieschlag and H.M. Behre, eds., *Testosterone: Action, Deficiency, Substitution*. Springer-Verlag, Berlin, Germany, 1990, pp. 115–135.
85. S.G. Korenman, S. Viosca, and D. Garza, *Am. J. Med.* **83**, 471–478 (1987).
86. R. Ahmed, A.E. Boucher, and A Manni, *J. Clin. Endocrinol. Metab.* **66**, 546–556 (1988).
87. A.W. Meikle et al., in S. Bhasin, ed., *Pharmacology, Biology, and Clinical Applications of Androgens*, Wiley Liss, New York, 1996, pp. 449–457.
88. A.W. Meikle, N.A. Mazer, J.F. Moellme, J.D. Stringham, K.G. Tolmar, S.W. Stencels, and W.D. Odel, *J. Clin Endocrinol. Metab.* **76**, 623–628 (1992).
89. W. Jordan, *Am. J. Contact. Derm.* **8**(2), 103–113 (1997).
90. A. McCallister, H. Mosberg, J.A. Settlage, and J.A. Steiner, *Br. J. Clin. Pharmacol.* **21**, 365–369 (1986).
91. *The Medical Letter on Drugs and Therapeutics* **26**, 59–60 (1984).
92. D. Chinoy, P. Breaux, and F. Ibrahim, *Clin. Ther.* **8**, 30–34 (1985).
93. K. Gatlin, *Curr. Ther. Res.* **38**, 733–737 (1985).
94. B.J. Schrader et al., *Pharmacother.* **6**, 83–86 (1986).
95. D. Chinoy et al., *Clin. Ther.* **11**(5), 678–684 (1989).
96. J.E. Shaw and J. Urquhart, *Trends Pharmacol. Sci.* **1**, 208–211 (1980).
97. N.M. Price et al., *Clin. Pharmacol. Ther.* **29**, 414–419 (1981).
98. J.E. Shaw, M.P. Cramer, and R.M. Gale, in A.F. Kyodenieus and B. Berner, eds., *Transdermal Delivery of Drugs*, vol. 1, CRC Press, Boca Raton, FL, 1987, pp. 101–116.
99. J.E. Henningfield and R.M. Keenan, *J. Consult. Clin. Psychol.* **61**, 743–750 (1993).
100. Transdermal Nicotine Study Group, *JAMA, J. Am. Med. Assoc.* **266**, 3133–3138 (1991).
101. D.M. Daughton et al., *Arch. Intern. Med.* **151**, 749–752 (1991).
102. S.K. Gupta, C.N. Rolf, and J. Gorsline, *J. Pharm. Res.* **8**, S-299 (1991).
103. J. Gorsline, S.K. Gupta, D. Dye, and C. Rolf, *J. Clin. Pharmacol.* **33**, 161–168 (1993).
104. *Physicians' Desk Reference for Non-Prescription Drugs*, 18th ed., Medical Economics Data Production Company, Montvale, New York, 1997, pp. 795–802.

See also TRANSDERMAL DRUG DELIVERY, ELECTRICAL.

VACCINE DELIVERY

GERARDO P. CARINO
Brown University
Providence, Rhode Island

KEY WORDS

Diphtheria vaccine
Hepatitis vaccine
HIV vaccine
Influenza vaccine
Liposome vaccine
Measles vaccine
Mucosal immunology
Oral vaccine
Particle uptake
Pertussis vaccine
Peyer's Patch
Polymer vaccine
Single shot vaccine
Tetanus vaccine
Tuberculosis vaccine

OUTLINE

Vaccine Immunology
  Types of Vaccines
  Mucosal Immunology
Particle Uptake by Intestinal M Cells
Liposome Uptake
Liposome-Based Vaccines
  Model Vaccines Delivered in Liposomes
  Specific Liposome Vaccines under Development
Polymer-Based Devices
  Adjuvant Effect of Degradation Products
  Model Vaccines
  Specific Vaccine Formulations
Comparison Between Liposomes and Microspheres
Future Directions
Bibliography

Immunization against infectious diseases is arguably the most effective intervention to improve public health. There are over 50 vaccine formulations currently available in the United States (1), but a great worldwide need for effective vaccines remains as this represents only a small minority of all infectious diseases. Also, there is still need for improvement among the existing vaccines. These needs are particularly evident in the developing world, where infectious diseases continue to be one of the leading causes of morbidity and mortality despite widescale vaccination programs (2). In addition, the emergence of a number of drug-resistant organisms, such as multidrug-resistant *Mycobacterium tuberculosis*, and pathogens for which a totally effective treatment has yet to be developed, most notably HIV, have also highlighted the need for improved preventative measures.

A number of authors have described the ideal vaccine and the various properties that it would have to possess. Most importantly, an ideal vaccine would have the ability to elicit the appropriate immune response for the pathogen under consideration. Many bacterial and viral infections can be successfully stopped by serum antibodies that confer immunity while intracellular microbes, like *M. tuberculosis*, require a cell-mediated response. Some pathogens, such as HIV, might be best controlled by a combination of both types of immunity. Ideally, the immune response would be long term, preferably for life. It should under no circumstances cause the disease that it is supposed to prevent and possess minimal side effects. To make the widespread use of the vaccine economically feasible, the vaccine should be easily administered in a single dose, preferably close to birth to initiate protection when people are most vulnerable, and production conditions should be well defined and reproducible. Finally, the vaccine itself must be stable enough to maintain immunogenicity before administration without the use of an expensive cold chain (3). None of the existing vaccines meet all of the requirements for being ideal. However, the use of controlled-release technology may allow for the development of vaccines that better approach all these criteria, which are summarized in Table 1.

This article concentrates on describing some of the work being conducted toward the development of controlled-release vaccines. After a brief description of some of the relevant concepts in immunology and current vaccines, descriptions of some of the existing research follow. The types of vaccines considered have been broken down into two types, either liposome- or polymer microsphere–based, as these have received the most attention. Special emphasis will be placed on mucosal immunology and the development of oral controlled-release formulations. This article is not meant to be exhaustive in its coverage of the work conducted so far but should serve as a good starting point in describing some of the key concepts and developments in controlled-release vaccine technology, with emphasis on liposome- and thermoplastic polymer–based systems.

Table 1. Properties of the Ideal Vaccine

Biologic considerations	Economic considerations
Confers lifelong immunity	Administered in a single dose
Never causes disease	Reproducible production conditions
Minimal side effects	Stable without a cold chain
Administered perinatally	Medically trained individuals not required for administration

Source: Modified from Ref. 3.

VACCINE IMMUNOLOGY

The immune response to natural infection is generally characterized by an initial antibody response to the pathogen followed by a prolonged memory response with continued exposure. Upon first exposure to an antigen, the immune system responds by an increase in serum antibody levels (within 2–4 weeks), followed by a relatively rapid drop-off of antibody levels. However, this initial exposure to the antigen enhances the body's ability to respond because of the proliferation of those lymphocytes specific for that particular antigen. The immune system becomes primed, and any further exposures to the same antigen are usually larger, more rapid, and longer lasting than the first (4). To take advantage of these natural immune responses, vaccines need to be presented once in an initial dose and then in booster shots to achieve long-lasting immunity. It is this natural limitation that presents one of the most difficult challenges in the development of an effective, widespread vaccination program. In fact, the World Health Organization (WHO) estimates that only 70% of people in developing countries receiving the initial dose of a vaccine return for the booster, leading to an extraordinary waste of limited resources and an undervaccinated population. Considering this, controlled-release technology has great promise in improving these numbers with the development of vaccines that would combine an initial immunization and boosters in a single shot or dose, thus hurdling this obstacle presented by the body's immune system.

Types of Vaccines

By definition, a *vaccine* is a material that induces an immunologically mediated resistance to a disease but not necessarily infection. It is important to understand this distinction when developing new vaccines as colonization by a pathologic organism would be acceptable if disease could still be controlled. The different types of vaccines include live or inactivated organisms as well as subunits or DNA. All of these forms of vaccines can potentially be delivered by controlled release.

Live Vaccines. Edward Jenner's smallpox vaccine of 1798 was based on the coxpox virus (bovine vaccinia virus), which was unable to produce clinical disease in humans but homologous enough to the human vaccinia virus to produce immunity. With this type of vaccine, a closely related organism of lesser virulence is administered, and the resulting immune response is sufficient to stop the virulent organism. This was certainly fortuitous in the case of smallpox, but even in cases where a naturally occurring attenuated organism does not exist, one can be produced in vitro by culturing under adverse conditions. This results in the selection of certain mutants that have adapted to grow well under these conditions but poorly in the human host. The BCG (for tuberculosis), oral polio (OPV), yellow fever, measles, and pertussis vaccines are all based on attenuated organisms produced in the laboratory. The immune response is usually good, producing both humoral and cell-mediated responses. Lifelong immunity is often achieved with a single dose. However, although much success has been achieved with attenuated organisms, they do possess major problems. These include the potential reversion of the vaccine to virulence especially in the immunodeficient, a huge group considering the world's aging population, the spread of HIV infection and the prevalence of diabetes mellitus and cancer. In fact, OPV, which has long been the preferred vaccine for the prevention of polio in the United States, is currently being replaced by the inactivated polio vaccine (IPV) for this reason because the chance of obtaining polio from the vaccine is actually becoming more likely than obtaining it from the general population! In addition to this, live vaccines need to be stored frozen, which is often prohibitively expensive.

Live recombinant vaccines have also been explored. Bacterial or viral vectors are genetically engineered to express an immunogenic protein of another organism. After administration, this recombinant would replicate and express the foreign antigen to induce an immune response to that protein. These systems are currently still only in the experimental phase.

Killed Vaccines. Entire viruses or bacteria can be killed and delivered as vaccines. These vaccines are not infectious, assuming that all the pathogens are actually killed in the fabrication process, and are therefore generally safe. Of course, they must be carefully monitored to ensure that all the infective organisms are indeed inactivated. This type of vaccine has the advantage of possessing all the necessary antigens, but immunogenicity is often reduced, leading to the need for repeated boosters. The inactivated polio vaccine is an example of this type and, as mentioned earlier, is regaining popularity.

Subunit Vaccines. In cases where protective immunity is known to be directed against one or two proteins of an organism, often surface proteins, purified antigens can be used as an effective, well-defined vaccine. For diseases that are caused by toxins produced by the infectious agent (such as diphtheria, tetanus, and cholera), the subunit can be inactivated toxoids of the bacteria. The subunits can also be surface polysaccharides (as used for the *Hemophilus influenzae* vaccine) or specific viral proteins (as in the hepatitis B vaccine.) There is great potential in this type of vaccine because the development of recombinant DNA technology can allow for the synthesis of desired antigenic epitopes in large and well-defined quantities. However, the greatest problem in the development of this type of vaccine lies in identifying the epitopes that possess sufficient antigenicity to produce long-term immunity. DNA vaccines, vaccines in which cells of the recipient are transfected to produce an immunogenic protein (often a subunit), have been proposed and are being worked on by many investigators.

Mucosal Immunology

Much of the early work on vaccine development has concentrated on the induction of antibody-based humoral immunity toward specific pathogens. This type of immunity is conferred within the bloodstream and is most effective against organisms that have a significant presence or portion of its life cycle within the bloodstream. However, a great deal of the recent work has focused on the develop-

ment of new vaccines that induce mucosal immunity. Mucosally delivered, most often by the oral route, controlled-release vaccines have been shown to be effective in inducing this type of immunity. An immune response focused at the mucosal surfaces may be sufficient to prevent the colonization of these surfaces and therefore help prevent the spread of the pathogen even before it enters the bloodstream. This mucosal immune response is characterized by a secretory immunoglobulin A (sIgA) response towards the antigen at mucosal surfaces (gastrointestinal, respiratory, rectal, vaginal, etc.). There is evidence that all these sites are linked so that vaccination at any mucosal surface, such as the gut wall after oral dosing, will induce secretory IgA responses at not only that specific mucosal site but also at the other mucosal sites (McGhee, 1993 #3). This property of the mucosal immune system, although somewhat oversimplified as stated, has great implications for the development of effective mucosal vaccines. More than 70% of the body's antibody-producing lymphocytes are part of this mucosal immune system and are located in the intestinal tract (5). Considering its size and pervasiveness and the fact that all vaccines currently available (except the oral polio virus) are given systemically and do not elicit a meaningful mucosal immune response, it is safe to say that mucosal immunology has yet to be exploited to its full potential. The greatest promise of controlled-release vaccine development lies in its potential of harnessing this powerful natural barrier to infection.

The mucosal immune system has evolved into a complex system to deal with the many foreign antigens presented at the mucosal surfaces. There are two areas of antigen processing where mucosal immune responses can be induced: the gut-associated lymphoreticular tissue (GALT) and the nasal-associated lymphoreticular tissue (NALT), both of which possess similar cell architecture. The GALT is made up of the Peyer's patches (collections of lymphoid tissue located in the small intestines, mostly in the terminal ileum), isolated lymphoid follicles of the appendix, and the mesenteric lymph nodes. The GALT is covered by a special epithelium, the follicle-associated epithelium (FAE), which is lined by M cells, which sample intestinal antigens and particulates and deliver them to the underlying lymphoid tissue (6). Here, antigen-presenting cells present the antigens to Th2 and B lymphocytes, which can then travel systemically to the mucosal effector sites. These effector sites include, but are not limited to, the lamina propria of gastrointestinal (GI), respiratory, and genitourinary tracts. At these sites, B cells are then stimulated to secrete IgA.

Most work on mucosal controlled-release vaccines has been focused on trying to immunize the GALT by delivering the antigen in either liposomes or thermoplastic microspheres directly to the M cells of the Peyer's patch following oral administration. Therefore, understanding the interactions between luminal particulates and the cells lining the FAE is critical to the design of vaccines meant to illicit a mucosal immune response. Some of the work at quantifying the uptake of liposomes and microspheres by the GALT is reviewed in this section and followed by a description of some of the controlled-release vaccines described in the literature.

PARTICLE UPTAKE BY INTESTINAL M CELLS

As early as 1961, it was known that the intestine is an imperfect barrier to small particulates. Polystyrene beads of 220-Å diameter were shown to cross gastrointestinal epithelial cells and appeared in the liver following oral administration to rats (7). Other work, 17 years later, showed that commercially available 2-μm polyvinyltoluene particles chronically fed to mice would accumulate in the Peyer's patches, intestinal villi, and mesenteric lymph nodes (8). However, the connection of this phenomenon to the potential development of oral vaccine delivery systems was yet to be made. A large body of work now exists in which investigators attempt to document the uptake of orally fed particulates, specifically by M cells lining the Peyer's patches, to establish the feasibility of an oral controlled-release vaccine. Such particles with an affinity for uptake by the Peyer's patch could be used to encapsulate an antigen and elicit a mucosal immune response.

Microscopy has been the most common method used to follow the uptake of microspheres or other particulates by the GI epithelium. In particular, light microscopy has been used extensively. Rabbits have been used frequently as the animal model in this type of research as they possess a relatively large number of Peyer's patches in their GI tracts when compared to other mammals. In one specific study, light microscopy was used to show the translocation of fluorescent, polystyrene microparticles through the intestinal wall of rabbits. The temporal movement of these 600- to 700-nm beads across the epithelial surface of the FAE was followed after intraluminal instillation. Translocation occurred within 10 min, approximately the same amount of time that soluble tracers needed to cross the epithelium. The authors estimated that 5% of the intraluminal dose entered the FAE. These results implied that translocation of thermoplastic microparticles did indeed quickly occur into the Peyer's patch and could potentially be utilized for vaccine delivery (9).

In another study, chronically fed polystyrene microspheres of different sizes (50 nm to 3 μm) were also shown to appear in rat Peyer's patches, villi, liver, spleen, and mesenteric lymph nodes. No spheres were seen in the heart, kidney, or lungs. Radiolabelling of the spheres with ^{125}I allowed quantification of spheres in tissues and demonstrated that, in general, smaller spheres had greater uptake than larger particles (Table 2). However, a few interesting observations, were made. In particular, the largest spheres examined (3 μm) appeared to show greater uptake

Table 2. Total Uptake of Various Sized Polystyrene Beads following Oral Administration

Polystyrene microsphere size	uptake (%)
50 nm	33.7 ± 3.7
100 nm	25.9 ± 3.2
300 nm	9.5 ± 1.25
500 nm	13.7 ± 1.2
1 μm	4.6 ± 0.7
3 μm	≈12

Source: Data from Ref. 10.

than the 1-μm spheres, but they were not observed in the bloodstream or in the liver as the smaller spheres were. This was explained by the authors as being due to a large number of 3-μm spheres that were adsorbed and immobile within the submucosal layer of the Peyer's patch and therefore not allowed into the circulation. The smaller spheres were quickly translocated into the serosal layer and appeared in the circulation (11). Histological work by the same group indicated that most of the uptake of these spheres did occur through the Peyer's patch and that particles in the liver were mainly in the Kupffer cells (macrophages) or endothelial cells lining the sinusoids, not the hepatocytes themselves.

Other methods of microsphere identification and/or quantification have also been used, including confocal microscopy (12), electron microscopy (13–15), extraction of the polymer from tissue followed by quantification by gel permeation chromatography (11), and flow cytometry (16). All of these studies came to similar conclusions: Polymer microparticulates of <10 μm in diameter indeed can enter the GALT, often within 1 h of oral administration, and have promise as antigen carriers for controlled-release vaccine applications.

Although particle uptake has been demonstrated using hard, nonbiodegradable microspheres, it is clear that biodegradable polymers would be more useful for the development of a controlled release system. Such a polymer, poly (D, L-lactic-*co*-glycolic acid) (PLGA), in the form of 1- to 10-μm microspheres, has also been shown to be transported into rabbit Peyer's patches following intraluminal instillation. This system has advantages over the other mentioned in that the PLGA is biodegradable and has already been studied and used extensively as the carrier in a number of controlled-release devices. Electron microscopy shows that microspheres of this copolymer are taken up by M cells and translocated toward the underlying lymphatic tissue within 1 h (17). This rapid uptake of PLGA microspheres and its biodegradative properties has led to extensive work with this polymer in vaccine applications. Many of these are discussed later in this section. Other degradable polymers, most notably polyanhydrides, have also been shown to exhibit uptake properties. Light and transmission electron microscopy studies with poly(fumaric-*co*-sebacic) anhydride fabricated into microspheres of 0.5–5 μm in diameter show translocation across the epithelium of the GI tract. The spheres were seen as early as 1 h postfeeding and were observed in the Peyer's patch at 3, 6, 12, and 24 h following oral administration (18).

LIPOSOME UPTAKE

In addition to thermoplastic microspheres, studies have also been conducted to determine the extent of uptake of orally administered liposomes. Significant uptake after intraluminal administration of a fluorescent marker, 6-carboxyfluorescein, was seen only when enclosed in negatively charged liposomes greater than 374 nm and made up of at least 25 mol % phosphatidylserine. The uptake was seen predominantly by the ileal Peyer's patches in rats as compared to those in the more proximal small intestine. The authors suggested that these findings indicate that these liposomes could therefore be used to specifically target the Peyer's patch (19). To address the issue of the stability of these liposomes in the harsh conditions of the GI tract, the same investigators demonstrated that liposomes made of distearoylphasphatidylcholine or dipalmatidyldiphosphaidylcholine, phosphatidylserine, and cholesterol were stable in simulated gastric, bile, and pancreatic fluids. These findings lend greater support to the belief that such liposomes could successfully deliver antigens to the Peyer's patch and indeed were seen to enter the Peyer's patch after oral administration (20). Further support to this hypothesis was provided by a study in which gold-labeled liposomes intraluminally administered to isolated intestinal loops of rats were seen within endocytic vesicles in M cells of the Peyer's patch with transmission electron microscopy (TEM) (21). Many other investigators, both before and after these findings, have used antigen-loaded liposomes to elicit immune responses. These will be addressed later in this section.

LIPOSOME-BASED VACCINES

As mentioned earlier, the greatest problem with subunit vaccines is their decreased immunogenicity. A large number of materials, known as adjuvants, can potentiate immune responses to weak antigens. These include Freund's incomplete antigen, a water-in-oil emulsion containing the antigen, Freund's complete adjuvant (FCA), the same water-in-oil emulsion including killed tubercule bacilli, aluminum hydroxide (alum), and others. However, alum is the only material approved for human use as the others are quite toxic; FCA causes undesirable granulomas at the site if injected. Alum has been shown to be inadequate in many situations because of variations in its adjuvant effect with different antigens and formulations. Despite their differences in structure, most adjuvants are believed to derive their ability to increase immune responses by forming emulsions or depots with the antigen and by slowly releasing it over a period of time. Controlled-release systems behave similarly and, in fact, it has been known for many years that liposomes act as immunological adjuvants.

Liposomes loaded with proteins or other antigens have been shown to slow the release of these antigens and act as immunological adjuvants. In the seminal work on liposome-based antigen presentation, mice immunized with diphtheria toxoid (DT) loaded in multilayered, negatively charged liposomes made of egg lecithin, cholesterol, and phosphatidic acid showed greater primary and secondary immune responses than mice administered free DT (22). These results were observed with all three different routes of administration tested, intravenous, subcutaneous, and intramuscular. Unlike the other types of adjuvants, the liposomes caused no granulomas or other undesired immune reactions at the site of injection.

This work was followed by many others exploring the possibility of taking advantage of this adjuvant property and the apparent safety of liposomes to produce liposome-based vaccines. There are certainly a great number of var-

iations possible when designing liposome-based vaccines. Vesicle size, lipid composition, antigen loading (including how much and where the antigen is loaded), lamellarity, and surface composition of the liposomes can all be modified to try to optimize the adjuvant effect on the desired antigen. However, a wide variety of liposomal formulations have shown increased immunogenicity, suggesting that specific liposomal properties such as size, composition, lamellarity, and charge may be less important to the systems adjuvanticity than the simple act of the antigen's release being slowed by its interaction with the lipids (23). Liposome technology has been applied to many different types of antigens—bacterial, protozoal, viral, protein, and others. In fact, there have been over 100 (and counting) international patents issued for variations on this type of technology (24). It would be impossible to describe all of the systems that have been explored, so only a few representative ones are discussed here. Table 3 shows just a few of the recent papers based on liposome-encapsulated vaccines and demonstrates the wide variety of antigens that have been attempted, including a description of some of these liposome-based vaccines.

Model Vaccines Delivered in Liposomes

Bovine Serum Albumin. In a search for easier routes of vaccine delivery, the intranasal route has received a large share of interest, especially when dealing with infectious agents that gain entry through the respiratory tract. In these cases, a local sIgA response on the nasopharyngeal mucosa would be extremely beneficial. This route of delivery targets the nasal-associated lymphoreticular tissue and thus may also induce a disseminated mucosal immune responses. Work with a model protein antigen, bovine serum albumin (BSA), showed that serum IgG and salivary IgA were significantly elevated after nasal administration of BSA-loaded liposomes (26). Antigen localization, whether within aqueous spaces in the liposomes or attached to the outer surfaces, did not seem to influence the systemic IgG response. However, salivary sIgA responses were noted to be significantly higher with antigen linked to the outer surface of the liposomes, hinting that the immune processing of the two types of liposomes may be different.

T-Independent Antigens. As is discussed in the following section on *Streptococcus mutans* vaccines, conjugated polysaccharide and protein antigens can be delivered by liposomes to elicit a long-term immune response to polysaccharide antigens. This conjugation of polysaccharide and protein antigens is a common immunological method used to induce T cell–dependent response (normal for protein antigens) to antigens that normally induce T cell–independent responses (polysaccharides). However, it has been shown that the conjugation of polysaccharide and protein

Table 3. Examples of Liposome-Based Vaccines

Antigen	Comments
Ascaris suum crude antigen	Slightly increased protection from nematode infection, especially when combined with levamisole (25)
BSA as a model antigen	Increased IgG and sIgA after nasal administration of liposomes in mice (26)
Conalbumin as model antigen	In vivo to in vitro comparing encapsulated antigen to surface-linked antigen (27)
Diptheria, tetanus, HAV, HBV, and influenza	Shows good immunogenicity and tolerance in humans; may lead to development of new combined vaccines (28).
Ferritin as a model antigen	Increased IgA responses to rectally administered vaccine, especially when combined with cholera toxoid and LPS (29)
Hepatitis A virus, formalin-inactivated	Protective antibody levels in clinical trials; currently marketed in Europe (30)
HIV-1, subunit from gp120	Antigen in "protein cochleates" induces humoral and cellular immunity after both oral and intramuscular administration (31).
HIV-1, subunit from gp120	Increased antibody and cytotoxic T cell lymphocyte responses in vaccinated mice (32)
Influenza virus, HA and NA	Phase 1 clinical trials showing slightly more adverse reactions than those receiving standard HA vaccine (33)
Influenza virus, HA3/NA2	Increased primary and secondary immune responses to HA3/NA2 in hamsters (34)
Influenza virus, LPS and HA2	Liposomes induce a T cell–dependent response to loaded LPS in mice (35).
Measles virus inactivated	Increased serum IgG and sIgA in respiratory tract in mice after intranasl administration (36)
Plasmodium falciparum circumsporozoite protein (Malaria)	The protein loaded into liposomes, but not unencapsulated protein, resulted in cytolytic T cell–lymphocytes and an antibody response. This reactant serum inhibited sporozoite invasion of hepatoma cells in vitro. [White, 1993 #259]
Streptoccocus mutans glucosyltransferase	Increased salivary IgA in humans after oral dosing; serum IgG not greatly increased (37)
Streptoccocus mutans, purified antigens	Oral liposomes induce salivary IgA and result in increased protection from dental caries (38).
Streptoccocus sobrinus ribosomal antigen	Orally immunized rats showed greater salivary IgA and were more protected from dental caries (39).
Vibrio cholerae cell-free lysate	Liposome vaccines were effective orally and parenterally. Polyester-loaded antigens were only effective parenterally (40).

is not actually necessary when delivering the antigens in a liposome formulation. Liposomes have been shown to provide T cell–dependent help to T cell–independent antigens by simply loading both polysaccharide and protein in the same liposome. DNP-aminocaproyl phosphatidylethanolamine (DNP-CapPE), a well-characterized T cell–independent antigen and influenza hemagluttinin A2 (HA2), a well-known T cell–dependent antigen, were loaded into phosphatidylcholine liposomes by the dehydration–rehydration technique. These liposomes elicited a memory response made up of all the IgG subclasses to DNP-CapPE after injection in mice. When liposomes containing just DNP-CapPE were used, an IgM response was observed. These results are very interesting in that one of the tenets of immunology, T cell–independent antigens can only elicit a T cell–dependent response when conjugated to a T cell–dependent antigen, can be circumvented by the delivery of both antigens, unconjugated to one another, in liposomes (41).

This work also illustrates another important concept: In addition to the desired antigen, other potentially helpful compounds or adjuvants can be encapsulated in or conjugated to the liposome formulation. For example, cholera toxin (CT) or the cholera toxin B (CTB) subunit, known mucosal adjuvants, can be incorporated to the liposome vaccine to produce a greater response after oral vaccination. The adjuvant effect of the CT and CTB may be due to its targeting of intestinal ganglioside on the epithelial cell surface or increasing cell permeability of the antigen. The coupling of biologically active CT or CTB to small unilamellar liposomes by a thioether bond retains their immunogenicity (42). The authors suggest that these formulations may be helpful in specifically targeting the liposomes to the Gm1 ganglioside receptors on the Peyer's patch M cells, resulting in greater uptake after oral delivery of the vaccine. These last two studies illustrate an important point about controlled-release formulations that deserves emphasis: In addition to the specific antigen, other desired agents (such as adjuvants, targeting molecules, or even other antigens) can be coadministered in the controlled-release system and potentially improve the response.

Effect of Antigen Association. Liposomal antigens have been shown to influence different immune responses depending on how the antigen is associated to the liposome and whether it is encapsulated within the aqueous portion inside the liposome or surface linked within the lipid bilayer (27). Encapsulation was performed by using a dehydration–rehydration technique, and surface linkage was accomplished by covalently attaching lipid to protein by using a heterobifunctional reagent. Mice intraperitoneally immunized with encapsulated antigen showed only a short-lived antibody response, while those immunized with surface-linked microspheres showed a longer-lasting effect. However, as stated earlier, a multitude of different liposome formulations have proven effective in the induction of long-lasting immune responses implying that generalizations about optimal liposome formulations for different antigens may not be possible to make. Further study is needed into how different liposome structure, size, lamellarity, and other properties lead to the activation of different immune pathways. The examples of just a few of the current vaccines under development for specific diseases shown in Table 3 demonstrate the diversity of liposomal formulations that can be used.

Specific Liposome Vaccines under Development

Dental Caries. The bacterium *Streptococcus mutans* has been identified as the major causative agent of human dental caries. The bacteria colonize the mouth, adhere to teeth, and, with sugar as a food source, produce acids that cause cavities. Increased salivary IgA responses to antigens from this bacteria are expected to control this colonization and potentially offer protection from dental cavities. As a result, a number of studies have attempted to present streptococcal antigens in a liposome vaccine. Purified surface polysaccharide and proteins (43), ribosomal proteins (38), and bacterial glucosyltransferase (37,38,44) have all been explored as potential antigens.

The adherence of *S. mutans* to teeth was found to be dependent on a complex mechanism that involves many of the bacteria's cell wall components, including certain polysaccharides, proteins, and lipoteichoic acids. Secretory IgA responses to any or all of these components would be expected to inhibit bacterial attachment. In general, polysaccharides are thymus-independent (TI) antigens that can induce short-term IgM responses but can not induce immunological memory. This problem can be overcome by conjugating the polysaccharide to a protein, a thymus-dependent (TD) antigen. This conjugate can then be used to elicit a long-term immunological response, as is done in the current *H. influenzae* vaccine. Such a protein–polysaccharide conjugate was associated with liposomes to produce both serum and salivary immune responses following oral administration (43). Briefly, conjugates were formed from polysaccharide and protein obtained from bacterial cell cultures and loaded into liposomes that were then administered orally to rats. Salivary IgA to the polysaccharide were evident in rats fed the conjugate liposome vaccine but not in rats fed vaccines containing only polysaccharide or protein. Salivary IgA responses to the more immunogenic protein occurred with both unconjugated and conjugated antigens. As demonstrated by some of the work with model antigens described earlier, this experiment demonstrated that although it is not able to produce an immune response to unconjugated polysaccharide, a liposome formulation could deliver a thymus-independent antigen when conjugated to a protein and produce an extended response.

It is well known that certain surface antigens of *S. mutans* can induce antibodies cross-reactive to the patient's own heart. The perceived danger of this cross-reactivity led to work on developing a vaccine based on a ribosomal preparation. These ribosomal vaccines have been shown to react to many strains of *S. mutans*, inhibiting adherence, acid production, and growth. Encapsulation of the ribosomal antigen into dipalmitoyl phosphatidylcholine, cholesterol, and dicetylphosphate was accomplished by a modified dehydration–rehydration procedure. All rats vaccinated with these liposomes elicited salivary IgA responses, but so did all rats fed just the ribosomal antigen.

No or low levels of salivary IgG, serum IgA, and IgG were seen in all cases. In bacterial challenge experiments, fewer adherent bacteria were found in rats given the liposome vaccine than in unvaccinated animals. In addition, there were significantly fewer carious lesions in liposome-vaccinated rats than in those that received only free ribosomes or no vaccine (39).

The final antigen to be discussed here that has been studied for the induction of sIgA to *S. mutans* after incorporation in a liposomal vaccine is the bacterial glucosyltransferase. This protein has been loaded into well-characterized dipalmitoyl phosphatidylcholine, cholesterol, and dicetylphosphate (16:7:1) unilamellar liposomes of uniform size (~100 nm) and loading. Administration of these liposomes to rats showed a 25–38% reduction in *S. mutans* colonization and a 30–40% reduction in caries (38). Human studies using similar liposomes that were dehydrated and loaded into gelatin capsules also showed increased levels of salivary IgA lasting for 56 days and minimal plasma immune responses. This was the first evidence that a dehydrated liposome preparation could rehydrate after oral dosing and still successfully elicit an immune response in humans (37,44).

Hemophilus influenza. The currently available *H. influenza* type B vaccine consists of a purified surface lipopolysaccharide (LPS) from the bacteria surface conjugated with a protein carrier, which allows the polysaccharide to achieve a T cell response. The necessity for a "carrier" protein has also been shown to be required when LPS is loaded into liposomes for vaccine applications. Incorporation of LPS and HA2 peptide from the influenza virus in liposomes resulted in anti-LPS-specific IgG responses following subcutaneous immunization (35). This response was characterized by IgG1, IgG2, and IgG3 subclasses, indicating that the normally T cell–independent antigen had been given a T cell–dependent quality, allowing for immune recognition by both T cell–helper and T cell–cytotoxic lymphocytes. Liposomes loaded with only LPS maintained their T cell–independent status and elicited only low levels of IgG3 responses.

Hepatitis A. A commercially available and very effective liposome-based hepatitis A vaccine is currently licensed and available in Europe. This vaccine is based on a specific type of liposome dubbed an immunostimulating reconstituted influenza virosome (IRIV); these are described as spherical, unilamellar vesicles of approximately 150 nm in size. The IRIVs are made of 70% egg yolk phosphatidylcholine, 20% phosphatidylethanolamine, and 10% envelope phospholipids from the H1N1 influenza virus. In addition, biologically active neuraminidase (NA) and hemagluttin (HA) glycoproteins from the influenza virus are located in the lipid bilayer of the virosome, forming short surface projections of 10–15 nm in size. These surface glycoproteins are meant to contribute to the effect of encapsulation within the virosome. HA is a major antigen of the influenza virus and thus a major constituent of its vaccine, and it is responsible for the fusion of the influenza virus with cell membranes. The presence of HA on the surface of the virosome is expected to lead to greater uptake and immune processing of the antigen by macrophages (30).

A number of variations have been made on the successful IRIV hepatitis A vaccine. As stated earlier, one of the properties of an ideal vaccine is the ability to confer immunity after a single dose, yet this vaccine is given as part of a recommended vaccination schedule of three doses of 0, 1, and 6 or 0, 1, and 12 months apart. In a human trial, three vaccine formulations were compared to determine the efficacy of a single-dose vaccine. One group received intramuscular injections of purified inactivated hepatitis A vaccine (HAV) in IRIVs, one received (HAV) absorbed to alum, and the other received soluble HAV. Although 100% of all the subjects showed responses to each of the formulations at 6 months, the mean antibody levels for the virosome vaccines were greater than the alum-associated and soluble vaccines at 14 days, 28, days and 6 months. However, owing to individual variability among the immune responses, the differences among antibody titers were only significant at 14 days (45). Work continued with this system until a safe and effective IRIV-based hepatitis A vaccine was produced (46). The IRIV system has also been used in an attempt to create a combination vaccine containing five commonly used inactivated vaccines that are usually delivered as alum-associated products: hepatitis A and B, diphtheria toxoid, tetanus toxoid, and two different strains of influenza. For diphtheria, tetanus, and influenza, the combined vaccine showed greater immune responses than single vaccines at almost all times tested (28, 90 and 180 days). The immune response at 28 days for the hepatitis A vaccine in the combined vaccine was statistically less than the response to a single vaccine; however, this difference disappeared at the other two time points. This work showed that a number of different antigenic could successfully be incorporated into the same IRIVs and that showed promise as combined vaccines (28).

Human Immunodeficiency Virus. Most of the examples considered thus far have concentrated on vaccination strategies designed to elicit a predominantly humoral immune response. However, both humoral immunity and cellular immunity are required for the effective prevention of a number of diseases, most notably AIDS. The human immunodeficiency virus (HIV) is blood borne, and thus potentially stoppable by serum antibodies, and takes up residence in T lymphocytes, thus requiring the presence of cell-mediated immunity. In addition, because HIV infects across mucosal membranes, a mucosal immune response is thought to also be beneficial. A vaccine that results in cellular, humoral, and mucosal immune responses to HIV has the potential to protect HIV-negative individuals and help stop the spread of the current pandemic of HIV infection.

A lipid-based HIV vaccine has been developed that successfully induces each of the three branches of the immune response. It possesses original structures called protein cochleates that are stable protein and phospholipid bilayers rolled up into a "jellyroll" shape. This rolled-up lipid structure is stabilized by the presence of calcium ions that cross-link successive layers. In a low-calcium environment or in the presence of chelating agents, the calcium is re-

moved, and the cochleates unroll and form unilamellar liposomes with the antigenic proteins incorporated in the lipid bilayers (31). When the envelope protein gp160 from HIV-1 is incorporated into protein cochleates and administered intramuscularly to mice, a strong anti-gp160 antibody response at 8 weeks was measured as well as a strong response (60–70% specific kill at 17 weeks) was observed (47). Following two oral administrations, this type of liposome has proven to induce both high sIgA and systemic antibodies. In addition to HIV, protein cochleate vaccines for influenza and parainfluenza viruses have been studied in experimental animals (47).

Influenza Virus. The vaccine for influenza changes from one year to the next. Based on epidemiological studies around the world, the strain of influenza virus most expected to spread the following year is identified, and the appropriate HA and NA proteins are incorporated into that year's vaccine. As a result, a great deal of work goes into the production of the influenza vaccine each year. In addition, a number of liposome-based strategies have been explored to improve on this current method. In one example, influenza (A/PR/8 strain) envelopes and influenza (A/Sichuan/87 [H3N2] strain) surface antigens were encapulsulated in phospholipid/cholesterol liposomes using a dehydration–rehydration technique. The liposomes produced had encapusulation efficiencies of approximately 40%, which is very good for liposome fabrication. These liposomes were administered to mice intramuscularly in a primary dose and booster dose after 4 weeks, which resulted in increased antibody responses to both HA and NA. This was compared with no response toward unencapsulated HA and NA, which are normally not very immunogenic. The authors concluded that such a system could be used to improve the efficacy of the influenza vaccine and could quite possibly be used for combination vaccines (34). Another liposome-based influenza vaccine has gone through phase I clinical trials in human volunteers showing that it was safe and did indeed produce greater anti-HA antibodies than the standard vaccine. The liposomes were made from B30-MDP, cholesterol, and octyl glucoside. As this was a phase I study, it concentrated on safety of the vaccine and not efficacy. Unfortunately, it was found to have slightly greater side effects than the standard vaccine (reddening at the injection site and deviations from the norm on blood and urine tests). Clearly, more work on this vaccine needs to be done (33).

Measles Virus. The current measles vaccine generally consists of a live, attenuated organism given parenterally, most often intramuscularly. Although these vaccines have been shown to be very effective, they do not induce a secretory IgA response, which may be of great importance in protecting from airborne virus particles. In addition, as discussed earlier, there are other advantages in developing inactivated whole virus or subunit vaccines. In work to this end, an inactivated whole virus vaccine mixed with phosphatidylcholine, dicetyl phosphate, and cholesterol (4:1:5) liposomes showed a significant increase in serum IgG and sIgA in the lungs and nasal cavity. Free inactivated virus was unable to induce an sIgA response. In addition, intramuscularly administered virus-containing liposomes elicited an IgG response but not an sIgA response. This is important as it shows that the route of administration is crucial in obtaining the desired immune response and that nasally administered liposomes can indeed present antigens to the nasopharyngeal lymphoid tissue (48).

POLYMER-BASED DEVICES

A great deal of work has also been conducted with polymer-based, controlled-release vaccine formulations. In the earliest application of this technology, an antigen released from a polymeric device made of nonbiodegradable ethylene-vinyl acetate copolymer (EVAc) enhanced antibody formation for more than 6 months in mice (49). In this work, a 1-mm EVAc pellet loaded with model antigens (albumin, gamma globulin, and ribonuclease) was implanted subcutaneously in mice; the immune response was comparable to antigen emulsified in FCA. The three different proteins used resulted in different antibody responses, which was considered to be due to the fact that larger proteins resulted in slower release, thus resulting in a greater adjuvant effect and immune response. These results were very encouraging and began a new field of inquiry into this type of antigen-loaded polymers.

Adjuvant Effect of Degradation Products

In addition to the adjuvant effect gained by the slow release of an antigen, a number of individuals have theorized that beyond the intrinsic adjuvant effects of controlled-release systems, other biodegradable systems can be engineered that possess added adjuvancy in the form of degradation products. A biodegradable polymer based on poly(CTTH-iminocarbonate) degrades into *N*-benzyloxycarbonyl-L-tyrosyl-L-tyrosine hexyl ester (CTTH), which is as potent an immunological adjuvant as FCA. It was hypothesized that an antigen delivered in a matrix of such a material would benefit by the adjuvant effects of the degradation products. BSA loaded into this polymer and delivered subcutaneously in mice did elicit a much greater immune response than BSA loaded into a comparable control polymer made of EVAc (50). This provides evidence for the idea that there is indeed difference between the adjuvancy of different polymers and that the effect can not solely be attributed to the slow release of antigen from these devices. Although this is a very interesting concept and one that should certainly be considered when selecting specific polymers for use in a vaccine formulation, not much more specific research along these lines has been published since this work.

Model Vaccines

Many of the early experiments conducted on controlled-release vaccines concentrated on illicting immune responses to model antigens loaded into thermoplastic matrices. The purpose of these studies was not to develop a specific protective immunity to a pathogen but to prove that antigens could successfully be included in a controlled-release device and retain immunogenicity. The

most popular of these model controlled-release vaccines incorporate ovalbumin (51–56) or BSA (49,57) as an antigen. Table 4 offers a brief description of some of these model controlled release vaccines.

Many of the important general characteristics of controlled-release vaccine systems were elucidated in these studies. However, only a few of these are discussed further, and the remainder of this section concentrates mainly on vaccines potentially effective for specific pathogens. Most work on controlled-release vaccines from biodegradable microspheres has been based on poly(lactide-*co*-glycolide) (PLGA), which is approved by the U.S. FDA for specific applications and is widely used in biodegradable sutures. The literature contains many examples of controlled-release formulations based on this system.

By far, the most common polymer used for the development of controlled release vaccines has been PLGA. Ovalbumin (OVA), a poorly immunogenic model antigen, when loaded into PLGA, is able to elicit a strong immune response after intraperitoneal or subcutaneous administration (61). Microspheres were prepared by solvent evaporation from an oil-in-water emulsion and had an average size of 5.3 μm and protein content of 1%. After 10 weeks, mice immunized by a single ip injection of encapsulated OVA showed significantly higher serum IgG levels than animals given an equivalent dose of OVA emulsified with FCA. However, after 12 weeks, the antibody levels were not significantly different. After sc booster doses, the secondary responses to OVA in microparticles remained higher than responses to unencapsulated OVA. Further experimentation yielded information on how the size of the microparticles effected immune response. Microspheres of 1.5 μm were significantly more immunogenic than 72.6-μm microspheres (54).

Positive results have also been obtained with model oral vaccines. Orally fed ovalbumin-loaded polyacrylamide microspheres of 2.55 μm in diameter were shown to induce a increase of IgA response when compared to a soluble control group (62). The rats were primed intraperitoneally 14 days before receiving oral doses of microspheres for 4 consecutive days. The primary and memory sIgA response in saliva were measured at 14 and 65 days postimmunization, respectively. Primary responses lower in encapsulated formulations, but memory responses were higher.

It is important to keep in mind, before discussing any specific formulations, that a major goal of controlled-release vaccines is to provide the initial immunization and booster doses in a single shot. Patients would no longer need to return for three or four doses to gain immunity, and medical personnel costs would be greatly reduced. Therefore, determinants of the release rates from various formulations are vital to the development of "single-shot" vaccines. Most of the examples in the literature address this issue and are careful to include good descriptions of the release characteristics of their specific formulation. These examples of microsphere-based vaccines are numerous, many more than can be fully presented here. A description of some, categorized by disease, follows.

Specific Vaccine Formulations

Again, most of the work on polymer-based vaccines, whether delivered parenterally to elicit systemic IgG immune responses or orally to elicit mucosal IgA responses, has been centered on PLGA microspheres. Table 5 summarizes some of the literature on polymer-based vaccines, including information about the specific antigen delivered, polymer used, route of delivery, and size of formulation. The section following Table 5 describes a few of these examples further.

Diphtheria. Diptheria is a localized infection of either mucous membranes (most often the oropharynx) or skin caused by *Corynebacterium diptheriae*. The infection causes pathology by means of DT produced by the bacteria. DT is currently included in the diphtheria–tetanus–pertussis (DTP) vaccine, commonly included in vaccination schedules worldwide, and is effective at preventing diph-

Table 4. Examples of Polymer-Based Vaccines Using Model Antigens

Model antigen	Comments
Bovine serum albumin	10- to 100-μm spheres made of PLGA showed greater adjuvanticity than both Alum and FCA when administered subcutaneously (57).
Bovine serum albumin	Poly(methyl methacrylate) and polystyrene particles between 62 and 306 nm possess adjuvant effect after intramuscular administration (58).
Bovine serum albumin, gamma globulin, and ribonuclease	First study to show that an antigen in a subcutaneously implanted polymer pellet (EVAc) elicited long-term antibody responses (49).
Human serum albumin	Intraperitoneal administration of polyacryl starch particles elicited both humoral and cellular response (59).
Ovalbumin	Antigen absorbed onto poly(butyl-2-cyanoacrylate) particles demonstrated increased oral immunogenicity in rats (53).
Ovalbumin	Intraperitoneal administration in poly(lactic acid) microspheres showed greater primary and secondary responses (60).
Ovalbumin	Oral administration in an acid-resistant acrylic polymer results in IgA and IgG responses (55).
Ovalbumin	Particle size study for subcutaneously administered PLGA microspheres showed better response with 3.5-μm spheres than 1.2-μm spheres (51).
Ovalbumin	Subcutaneously administered PLGA microspheres demonstrated antibody response. 1.5-μm spheres were more effective than 72.6-μm spheres (54).

Table 5. Examples of Polymer-Based Controlled Release Vaccines showing Antigen and Polymer Used, Microsphere Size and Route of Vaccine Delivery

Antigen	Polymer	Particle size	Route Delivery	Refs.
Bordatella pertussis fimbriae	PLGA	0.8–5.3 μm	ip	63
Bordatella pertussis hemagluttinin	PLGA	1 μm	in	64
Diphtheria toxoid	PLGA	30–100 μm	im	65
Escherichia coli, CFA/I	PLGA	10–200 μm	ig	66
Escherichia coli, CFA/II	PLGA	Not stated	po	67
Hepatitis B surface antigen	PGA	1–10 μm and 20–60 μm	ip	68
Human imunodeficiency virus, gp120	PLGA	Not stated	sc	69
Influenza virus, formalinized	PLGA	2.2–10.8 μm	sc and po	70
Malarial antigen	PLA and PLGA	1–10 μm and 10–100 μm	sc	71
Mycobacteria tuberculosis, 38-kDA antigen	PLGA	0.67 μm mean	ip	72
Simian immunodeficiency virus, formalinized	PLGA	Not stated	im, po, and it	73
Staphylococcal enterotoxin B	PLGA	1–10 μm	sc	74
Staphylococcal enterotoxin B	PLGA	1–10 μm	po	75
Staphylococcal enterotoxin B	PS, PMMA, PLA and PLGA	1–10 μm	po	76
Tetanus toxoid	PLA and PLGA	10–60 μm	sc	77
Tetanus toxoid	PLA and PLGA	1–10 μm and 10–100 μm	sc	71
Venezuelan equine encephalitis, formalinized	PLGA	<10 μm	sc	78
Vibrio cholerae cell-free lysate	PLGA	1–10 μm	po and ii	40

Note: PLA = polylactic acid, PLGA = poly(lactide-*co*-glycolide), PS = polystyrene, PMMA = poly(methyl methacrylate), ii = intraileal, im = intramuscular, in = intranasal, sc = subcutaneous, ip = intraperitoneal, it = intrathecal, po = oral.

theria. However, in an attempt to improve the delivery of this toxoid, it has been encapsulated in PLGA microspheres by the in-water encapsulation technique (65). In vitro drug release studies of this formulation show that 90% percent of the drug was released in 60 days. When mice were subcutaneously immunized once with these microspheres, antibody titers over 3 months were comparable to mice receiving the conventional three-injection schedule. It appears that the toxoid retained its antigenicity upon encapsulation, and its slow release from the microspheres allows for a boosting effect. This controlled release of the diphtheria toxoid certainly appears to show promise for the development of a single-dose vaccine, and further work needs to be conducted to determine the longevity of the immune response and whether the other vaccines traditionally given with diphtheria toxoid can also be incorporated.

Enterotoxigenic Escherichia coli. Vaccination of rabbits with entererotoxigenic *E. coli* colonization factor antigen (CFA/I), a surface fimbrial adhesion that is important for successful adhesion of the bacteria to the intestinal wall, induces intestinal mucosal responses and protects from colonization and disease (66). CFA/I fimbriae were purified and encapsulated into a 50:50 PLGA copolymer at 0.1% w/w. In vitro release of the encapsulated antigen began within 2 h and occurred for up to 72 h. Rabbits were intragastrically immunized with either encapsulated or soluble antigen, resulting in greater systemic immune responses in those fed encapsulated antigen. One of the animals also showed sIgA antibodies in its feces. In clinical trials, 10 human volunteers vaccinated with a prototype vaccine based on this work tolerated it well, and 5 developed IgA responses. When challenged by live enterotoxigenic bacteria, the vaccine showed a 30% efficacy, hardly overwhelmingly protective but still very promising. Work continues on variations of this vaccine, which is now in phase II clinical trials (67).

Hepatitis B. Recombinant Hepatitis B surface antigen (HBSA) has been shown to be effective as a hepatitis B vaccine. This vaccine has recently been added to the standard vaccinations administered to children and people at risk in the United States. However, to achieve a long-lasting immune response, one needs a minimum of three intramuscular injections. In order to improve this system, HBSA has also been encapsulated in polymer microspheres for sustained release. In one very interesting study, five different formulations of HBSA encapsulated in polyglycolic acid (PGA) microspheres were studied. Solvent evaporation and solvent extraction methods were used to produce microspheres of either 1–10 or 20–60 μm in size. In addition, formulations containing the known adjuvants MDP (*N*-acetyl-muramyl-L-alanyl-D-isoglutamin) and Alum were also fabricated and studied. The in vivo studies called for groups of guinea pigs to receive the equivalent of 20 μg of antigen or a negative control of blank microspheres intraperitoneally. Blood samples were obtained periodically, and a booster was given at 16 weeks. The smallest spheres, 1–10 μm, showed the best early response at 2 and 4 weeks; however, this decreased at 6 weeks when the 20- to 60-μm spheres showed the highest antibody response. A combination of these two formulations showed the longest immune response (16 weeks) and is possibly the more favorable formulation. Although the vaccine including Alum did not show any improved response, the greatest response by far was seen with the microspheres that were loaded with both MDP and HBSA. This demonstrates that known immunological adjuvants can indeed be coincorporated into microsphere formula-

tions with the antigen and still contribute to an increased immune response (68). With further work, such a system may be able to reduce the number of injections needed for immunity and therefore allow for a more effective vaccination program against hepatitis B.

Human and Simian Immunodeficiency Virus. A large number of possible vaccines for AIDS are currently under investigation. Many of them are focused at stopping the colonization of mucosal surfaces by the causative virus, HIV. PLGA microspheres loaded with formalin-treated simian immunodeficiency virus (SIV), the simian virus analogous to HIV, have been shown to induce effective protection from vaginal challenge of virus in female macaques (73). A number of immunization routes (oral, im, intrathecal) were used in a variety of schedules. Animals immunized orally showed IgM, IgG, and IgA responses after all doses, but none showed protection from intravaginal viral challenge. When intramuscular priming in the thighs was combined with oral boosting, systemic IgG levels were maintained, and transient increases in vaginal sIgA levels were seen. Five of six macaques immunized this way and vaginally challenged by SIV did not become infected. Although it is unclear whether the vaginal antibodies were the result of successful oral vaccination or intramuscular vaccination close to this site, these results have promise for the development of an HIV vaccine that protects at the vaginal mucosa level. This is incredibly important to help control the spread of HIV infection, as the male–female spread of the virus is currently its fastest-growing means of transmission.

Other PLGA-based vaccines for HIV are also under development. One is directed toward a peptide taken from the principal neutralizing determinant of HIV-1. The vaccine has been extremely well characterized, with good assessments of particle size and distribution, microsphere surface structure, antigen loading and efficiency, in vitro release rates, and measures of stability during storage. After oral administration and combined oral and subcutaneous administration to guinea pigs, the microspheres were shown to elicit high levels of serum IgG toward HIV. Future work will seek to combine this immunogen with approximately 15 other HIV peptides in an attempt to cover much of the worldwide variability of HIV and use the controlled-release vaccine in clinical trials (79).

Another single-shot HIV-1 vaccine based on PLGA microspheres is also in development (69). The HIV-1 subunit antigen, MN rgp120, is encapsulated by a double-emulsion technique. Release from the microspheres was studied to determine whether a release profile mimicking repeated administration could be engineered. An initial release of MN rpg120 occurred over a period of 2 days. This was followed by a lag phase; the microspheres began to release protein in a continuous manner over 4 weeks as part of the second burst. This second burst occurred due to the bulk erosion of the polymer matrix. The second burst has been successfully controlled by different formulations to occur at 1, 2, 3, or 4 months. Guinea pigs given a single injection of a microsphere formulation with a second burst that occurred at 6 weeks postinjection showed much greater immune responses than control animals immunized with MN rgp 120 and Alum. This work is promising in that it suggests that a common feature of controlled-release formulations, the burst effect, may actually be beneficial in the design of self-boosting, single-dose vaccines.

Influenza Virus. Biodegradable microspheres can also be used to encapsulate and orally deliver whole, inactivated pathogens. A good example of this exists with the influenza virus. Formalin-treated influenza virus was encapsulated in 2- to 10-μm PLGA microspheres. After systemic immunization, encapsulated vaccine induced antibody levels comparable to the virus in solution. When oral formulations were used as boosters for animals initially vaccinated systemically, mucosal antibodies were higher than and systemic antibodies were comparable with levels in animals vaccinated and boosted solely systemically. Again, this type of protection is important for pathogens such as influenza that generally infect through mucosal surfaces, specifically the nasal mucosa in this case. Animals challenged by active virus after this vaccination produced antibodies and were virtually completely protected (70).

Pertussis. Pertussis, or whooping cough, is a disease of the respiratory tract that, although under good control in the United States and other countries with widespread use of the combined DTP vaccine, is a major cause of worldwide morbidity and mortality. The existing vaccine has been based on a killed, whole-cell vaccine of the causative bacteria, *Bordatella pertussis*. However, because of some serious adverse effects to this killed vaccine, a new acellular pertussis vaccine has been developed and incorporated in the new combined vaccine, the DTaP (diphtheria–tetanus–acellular pertussis). One of the antigens included in this acellular vaccine, filamentous haemagglutinin (FHA), has been incorporated in biodegradable PLGA microspheres for delivery as a controlled-release vaccine. FHA, like CFA/I in *E. coli*, is important in the attachment of the bacteria to the mucosal surfaces of the host. Intranasal administration of FHA-loaded PLGA spheres showed both strong systemic IgG and pulmonary sIga, similar to that obtained with soluble FHA. Protection from intranasal challenge was very good, with improved clearance of bacteria from the respiratory tract in those animals vaccinated intranasally compared to those vaccinated intraperitoneally (64).

Staphylococcal Enterotoxin B. Staphylococcal enterotoxin B (SEB) is a toxin produced by *Staphylococcus aureus*, which causes food poisoning. SEB was encapsulated in 1- to 10-μm PLGA microspheres made from an emulsion-based solvent extraction technique and delivered both orally and subcutaneously. In the earlier oral study, the PLGA microspheres (<10 μm) were observed to be taken up by the Peyer's patch with "good" uptake and could therefore be useful in this application (76). Those that were >5 μm remained fixed in the lymphoid tissue for an extended period of time, but the smaller spheres were able to cross through, entering the mesenteric lymph nodes, systemic circulation, and eventually the spleen. The oral vaccination with these spheres resulted in disseminated sIgA immune responses at various sites including saliva,

gut, and bronchioles. Soluble enterotoxoid delivered orally showed no immune response (75). When injected subcutaneously, these microspheres induced an antibody response 500 times that of soluble SEB and approximately equal to that induced by the same amount of antigen administered with FCA. Another important finding included in this work was that vaccine-loaded microspheres $>10\,\mu m$ did not possess nearly as great a response as those 1- to 10-μm. This finding was explained by the fact that those spheres greater than $10\,\mu m$ could not enter draining lymph nodes and thus were less effective. Also, a mixture of blank microspheres and soluble toxin showed just the same response as the soluble antigen, thus indicating that the vaccine needs to be incorporated into a slow-release polymer device and not just presented together with it to obtain an adjuvant effect (74).

Tetanus. A different type of single-shot system has been studied to deliver tetanus toxoid. Instead of a single, extended release, pulsed-release formulations have been suggested based on different-sized PLGA microspheres (80). In such a system, the vaccine is a mixture of different-sized vaccine-loaded PLGA microspheres with various release times. Specifically, 2-μm spheres were engineered to release their contents over 1–14 days, followed by larger spheres that released at 1–2 months and 9–12 months for boosting purposes. This straightforward approach may prove to be more useful, as the pulsed formulation may be more effective in delivering a booster dose, which is necessary for a long-term humoral response. However, it is complicated by the fact that the vaccine is actually a combination of two (or more) different controlled-release formulations and would therefore involve more steps in manufacture.

Tuberculosis. An effective vaccine for tuberculosis still does not exist. The efficacy of the BCG vaccine used in Europe is questionable, considered somewhere between zero and total depending on which population study is considered. In addition to this, vaccination with the BCG vaccine causes people to that positive for purified protein derivative permanently, thus obscuring people who have been exposed to the mycobacteria. As a result, the vaccine has not gained worldwide acceptance, and the United States, in particular, has opted against its use in favor of being able to identify exposed individuals. PPD-positive individuals can then be entered into aggressive antibiotic therapy for 6 months. This option is obviously not ideal. And now, with the emergence of multidrug-resistant *M. tuberculosis* in various areas around the world and the strong association between HIV infection and tuberculosis, the need for an effective vaccine has never been greater.

A 38-kDa antigen from *M. tuberculosis* has been encapsulated in PLGA microspheres and tested for immunogenicity in vivo. When compared to antigen delivered subcutaneously and intraperitoneally with incomplete Freund's adjuvant (IFA) delivered similarly, the PLGA vaccine showed both increased systemic IgG and improved T cell responses (important for intracellular organisms such as *M. tuberculosis*). In another measure of improved cellular immune responses, in vitro antigen-induced gamma interferon (IFN-γ) levels in T cells from microsphere-administered animals were 10 times greater than those given the IFA vaccine. Unfortunately, challenge experiments comparing PLGA vaccine, IFA vaccine, the BCG vaccine, and a control of blank microspheres did not show any differences in the health of the animals (72). Still, these results, specifically the induction of cellular immune responses by microsphere formulations, is promising for the development of vaccines for intracellular organisms.

COMPARISON BETWEEN LIPOSOMES AND MICROSPHERES

This article has described quite a few examples of controlled-release vaccines based on either liposomes or thermoplastic microspheres; other systems are also being explored and may prove to be effective in the future. These include vaccines based on hydrogels (81,82) and starches (59,83), but they are not discussed further here. It is unclear which type of system is the most promising. Very few studies have been conducted comparing liposomes and microspheres with one another. One direct comparison between PLGA-encapsulated and liposome-encapsulated antigens from *Vibrio cholerae* has shown that a liposome-based vaccine induced the greater immune response (40). Antigenic proteins from lysed *V. cholerae* were collected and loaded into PLGA microspheres and liposomes. PLGA microspheres were made by a modified water-in-oil solvent extraction method. Multilamellar liposomes were made using the process known as dehydration–rehydration vesicles. Rabbits were immunized by multiple regimens, and systemic IgG and intestinal sIgA were measured. Immune protection was assessed by measuring the fluid volume in ileal loops. The greatest protection was offered by intraileally administered liposomes followed by intravenous boosters. Orally administered microspheres followed by oral boosters showed a 33% immunity to challenge. Although in this one case liposomes appeared to work better, it is unclear if any generalizations can be made. Of course, different investigators will have different opinions. Liposomes seem to be closer to widespread use (as stated earlier, there is already a liposome-based vaccine licensed in Europe), but this is probably just because liposome technology is a bit more established. As time passes, it is likely that a microsphere-based system will also be proven effective and used in humans. Both methods do have great promise and may have their own advantages and disadvantages depending on the specific antigen under consideration.

FUTURE DIRECTIONS

As mentioned, a large number of investigators are working on controlled-release vaccines, and only some of the current literature has been presented here. Many of the vaccines have made it to clinical trials and, as mentioned earlier, a liposome-based hepatitis vaccine is already licensed in Europe. Future work needs to concentrate on more fully understanding the interactions among polymer, antigen, and biological organism so that formulations best suited to

induce the type of immune response desired can be engineered. For example, the uptake of particulates by the GALT needs to be better understood, and materials other than PLGA, that may exhibit greater uptake by this tissue and greater potential to elicit immune responses need to be identified. Substantial advances in vaccine technology are likely to come using controlled-release technology, with the most exciting potentially being the development of oral vaccines that induce mucosal immunity.

As this article is being written, new directions and applications for controlled-release vaccines are being considered. With the development of better nonviral vectors for gene therapy, controlled-release DNA vaccines are likely sometime in the future. Very recent studies have shown that thermoplastics can indeed be used to deliver plasmid DNA both subcutaneously (84) and orally (18), resulting in transfection and protein production. Plasmid DNA encoding the insect protein luciferase has been successfully encapsulated in PLGA microspheres and delivered to mice orally successfully, eliciting both systemic and mucosal antibody responses to the luciferase (85). This is an extremely exciting development that opens up a new avenue of research toward the development of controlled-release vaccines.

BIBLIOGRAPHY

1. G.T. Keusch and K.J. Bart, *Harrison's Principles of Internal Medicine*, vol. 14, McGraw-Hill, New York, 1998, pp. 758–771.
2. P.P.H. Lambert, *Rev. Med. Suisse Romande* **113**, 193–198 (1993).
3. D.E. Helland and A.W. Hey, *Scand. J. Infect. Dis.* **76**, 32–38 (1990).
4. A.K. Abbas, A.H. Lichtman, and J.S. Pober, *Cellular and Molecular Immunology*, Saunders, Philadelphia, 1991.
5. W.S. Shalaby, *Clin. Immunol. Immunopathol.* **74**, 127–134 (1995).
6. D.F. Keren, *Semin. Immunol.* **4**, 217–226 (1992).
7. E. Sanders and C.T. Ashworth, *Exp. Cell Res.* **22**, 137–145 (1961).
8. M.E. LeFevre, J.W. Vanderhoff, J.A. Laissue, and D.D. Joel, *Experientia* **34**, 120–122 (1978).
9. J. Pappo and T.H. Ermak, *Clin. Exp. Immunol.* **76**, 144–148 (1989).
10. P. Jani, G.W. Halbert, J. Langridge, and A.T. Florence, *J. Pharm. Pharmacol.* **41**, 809–812 (1989).
11. P. Jani, G.W. Halbert, J. Langridge, and A.T. Florence, *J. Pharm. Pharmacol.* **42**, 821–826 (1990).
12. C. Porta et al., *Exp. Physiol.* **77**, 929–932 (1992).
13. M.A. Jepson et al., *Cell Tissue Res.* **271**, 399–405 (1993).
14. T. Landsverk, *Immunol. Cell Biol.* **66**, 261–268 (1988).
15. W. Sass, H.P. Dreyer, and J. Seifert, *Am. J. Gastroenterol.* **85**, 255–260 (1990).
16. J.P. Ebel, *Pharm. Res.* **7**, 848–851 (1990).
17. T.H. Ermak et al., *Cell Tissue Res.* **279**, 433–436 (1995).
18. E. Mathlowitz et al., *Nature (London)* **386**, 410–414 (1997).
19. H. Tomizawa et al., *Pharm. Res.* **10**, 549–552 (1992).
20. Y. Aramaki et al., *Pharm. Res.* **10**, 1228–1231 (1993).
21. N.K. Childers, F.R. Denys, N.F. McGee, and S.M. Michalek, *Reg. Immunol.* **3**, 8–16 (1990).
22. A.C. Allison and G. Gregoriadis, *Nature (London)* **252**, 252 (1973).
23. G. Gregoriadis, I. Gursel, M. Gursel, and B. McCormack, *J. Controlled Release* **41**, 49–56 (1996).
24. R. Glück, *Vaccine Design: The Subunit and Adjuvant Approach*, Plenum, New York, 1994, pp. 325–345.
25. S. Lukes, *Vet. Parasitol.* **43**, 105–113 (1992).
26. Y. Aramaki et al., *Vaccine* **12**, 1241–1245 (1994).
27. E. Shahum and H. Thérien, *Vaccine* **12**, 1125–1131 (1994).
28. B. Mengiardi, R. Berger, M. Just, and R. Gluck, *Vaccine* **13**, 1306–1315 (1995).
29. F. Zhou, J.P. Kraehenbuhl, and M.R. Neutra, *Vaccine* **13**, 637–644 (1995).
30. R. Glück, *Vaccine* **10**, 915–919 (1992).
31. S. Gould-Fogerite et al., *AIDS Res. Hum. Retroviruses* **10**, S99–S103 (1994).
32. W.I. White et al., *Vaccine* **13**, 1111–1122 (1995).
33. M. Kaji et al., *Vaccine* **10**, 663–667 (1992).
34. G. Gregoriadis, L. Tan, E.T.S. Ben-Ahmeida, and R. Jennings, *Vaccine* **10**, 747–753 (1992).
35. P.J.F. Pietrobon, N. Garcon, C.H. Lee, and H.R. Six, *Immunomethods* **4**, 236–243 (1994).
36. A. de Haan, J. Tomee, J. Huchshorn, and J. Wilschut, *Vaccine* **13**, 1320–1324 (1995).
37. N.K. Childers, S.S. Zhang, and S.M. Michalek, *Advances in Mucosal Immunology*, Plenum New York, 1995, pp. 1481–1484.
38. S.M. Michalek et al., *Genetically Engineered Vaccines*, Plenum, New York, 1992.
39. R.L. Gregory et al., *Infect. Immun.* **54**, 780–786 (1986).
40. U. Chandrasekhar, S. Sinha, H.R. Bhagat, V.B. Sinha, and B.S. Srivastava, *Vaccine* **12**, 1384–1387 (1994).
41. N.M. Garcon and H.R. Six, *J. Immunol.* **146**, 3697–3702 (1991).
42. E. Harokopakis et al., *J. Immunol. Methods* **185**, 31–42 (1995).
43. D. Wachsmann et al., *Infect. Immun.* **52**, 408–413 (1986).
44. N.K. Childers, S.S. Zhang, and S.M. Michalek, *Oral Microbiol. Immunol.* **11**, 146–153 (1994).
45. M. Just et al., *Vaccine* **10**, 737–739 (1992).
46. Y. Poovorawan et al., *Vaccine* **13**, 891–893 (1995).
47. R.J. Mannino, *Vaccine Design: The Subunit and Adjuvant Approach*, Plenum, New York, 1995, pp. 363–387.
48. A. de Haan et al., *Vaccine* **13**, 155–162 (1995).
49. I. Preis and R.S. Langer, *J. Immunol. Methods* **28**, 193–197 (1979).
50. J. Kohn et al., *J. Immunol. Methods* **95**, 31–38 (1986).
51. T. Uchida, S. Goto, and T.P. Foster, *J. Pharm. Pharmacol.* **47**, 556–560 (1994).
52. D.T. O'Hagan et al., *Advances in Mucosal Immunology*, Plenum, New York, 1995, pp. 1463–1467.
53. D.T. O'Hagan, K.J. Palin, and S.S. Davis, *Vaccine* **7**, 213–216 (1989).
54. D.T. O'Hagan, H. Jeffery, and S.S. Davis, *Vaccine* **11**, 965–969 (1993).
55. S.L. Jain, K.S. Barone, M.P. Flanagan, and J.G. Michael, *Vaccine* **14**, 42–48 (1996).
56. R. Kakaoka, Y. Tabata, and Y. Ikada, *J. Controlled Release* **37**, 215–224 (1995).
57. H. Sah, R. Toddywala, and Y.W. Chien, *J. Controlled Release* **37**, 137–144 (1995).

Next Page

58. J. Kreuter et al., *Vaccine* **4**, 125–129 (1986).
59. L. Degling and P. Stjarnkvist, *Vaccine* **13**, 629–636 (1995).
60. R. Nakaoka, Y. Tabata, and Y. Ikada, *J. Controlled Release* **37**, 215–224 (1995).
61. D.T. O'Hagan et al., *Immunology* **73**, 239–242 (1991).
62. D.T. O'Hagan et al., *Vaccine* **7**, 421–424 (1989).
63. D.H. Jones et al., *Infect. Immun.* **64**, 489–494 (1996).
64. E.S. Cahill et al., *Vaccine* **13**, 455–462 (1995).
65. M. Singh, A. Singh, and G.P. Talwar, *Pharm. Res.* **8**, 958–961 (1991).
66. R. Edelman et al., *Vaccine* **11**, 155–158 (1993).
67. C.O. Tacket et al., *Vaccine* **12**, 1270–1274 (1994).
68. R.V. Nellore, P.G. Pande, D. Yound, and H.R. Bhagat, *J. Parenter. Sci. Technol.* **46**, 176–180 (1992).
69. J.L. Cleland et al., *AIDS Res. Hum. Retroviruses* **10**, S21–S26 (1994).
70. Z. Moldoveanu et al., *J. Infect. Dis.* **167**, 84–90 (1993).
71. C. Thomasin et al., *J. Controlled Release* **41**, 131–145 (1996).
72. H.M. Vordermeier et al., *Vaccine* **13**, 1576–1582 (1995).
73. P.A. Marx et al., *Science* **260**, 1323–1327 (1993).
74. J.H. Eldridge et al., *Infect. Immun.* **59**, 2978–2986 (1991).
75. J.H. Eldridge et al., *Adv. Exp. Med. Biol.* **25**, 192–202 (1989).
76. J.H. Eldridge et al., *J. Controlled Release* **11**, 205–214 (1990).
77. M.A. Alonso et al., *Pharm. Res.* **10**, 945–953 (1993).
78. T.E. Greenway et al., *Vaccine* **13**, 1411–1420 (1995).
79. D.T. O'Hagan et al., *J. Controlled Release* **37**, 75–84 (1995).
80. M.T. Aguado and P.H. Lambert, *Immunobiology* **184**, 113–125 (1992).
81. T.L. Bowersock et al., *Am. J. Vet. Res.* **55**, 502–509 (1994).
82. G.B. Pier et al., *Infect. Immun.* **62**, 3972–3979 (1994).
83. D.T. O'Hagan, D. Rafferty, S. Wharton, and L. Illum, *Vaccine* **11**, 660–664 (1993).
84. Y.S. Jong et al., *J. Controlled Release* **147**, 123–134 (1997).
85. D.H. Jones et al., *Vaccine* **15**, 814–817 (1997).

VETERINARY APPLICATIONS

MICHAEL J. RATHBONE
InterAg
Hamilton, New Zealand

LEONORE WITCHEY-LAKSHMANAN
Schering-Plough Research Institute
Kenilworth, New Jersey

KADRIYE CIFTCI
Temple University
Philadelphia, Pennsylvania

KEY WORDS

Anithelmintics
Companion animal
Ectoparasites
Endoparasites
Estrous control
Growth enhancement
Intramammary
Intravaginal
Long-acting injectables and implants
Postruminal
Proteins and peptides
Ruminal
Steroids
Veterinary drug delivery
Veterinary gene therapy
Veterinary medicine
Veterinary vaccines

OUTLINE

Introduction
Factors Influencing Controlled Drug Delivery in Animals
Comparison of Human and Animal Controlled Drug Delivery
- Reasons for Producing Controlled Drug Delivery Systems
- Dosing Interval
- Drug Candidates
- Pharmacokinetics
- Physiology and Anatomy
- Delivery System Design
- Site of Absorption
- Means of Administration
- Storage Conditions
- Regulatory Considerations
- In Vivo/In Vitro Correlations

Veterinary Controlled-Release Drug Delivery and Delivery Systems
- Intraruminal Drug Delivery
- Postruminal drug delivery
- Intramammary Drug Delivery
- Steroid Hormone-Containing Growth Promotants
- Vaginal Drug Delivery
- Long-Acting Injectable Products Used in Food-Producing Animals
- Topical Dosage Forms for Food-Producing Animals
- Controlled-Release Technologies in Companion Animals
- Ophthalmic Drug Delivery
- Protein and Peptide Delivery

Recent Initiatives
- Vaccine Delivery
- Gene Therapy
- Trends and Future Directions of Vaccines and Gene Therapy

Concluding Remarks
Bibliography

Previous Page

58. J. Kreuter et al., *Vaccine* **4**, 125–129 (1986).
59. L. Degling and P. Stjarnkvist, *Vaccine* **13**, 629–636 (1995).
60. R. Nakaoka, Y. Tabata, and Y. Ikada, *J. Controlled Release* **37**, 215–224 (1995).
61. D.T. O'Hagan et al., *Immunology* **73**, 239–242 (1991).
62. D.T. O'Hagan et al., *Vaccine* **7**, 421–424 (1989).
63. D.H. Jones et al., *Infect. Immun.* **64**, 489–494 (1996).
64. E.S. Cahill et al., *Vaccine* **13**, 455–462 (1995).
65. M. Singh, A. Singh, and G.P. Talwar, *Pharm. Res.* **8**, 958–961 (1991).
66. R. Edelman et al., *Vaccine* **11**, 155–158 (1993).
67. C.O. Tacket et al., *Vaccine* **12**, 1270–1274 (1994).
68. R.V. Nellore, P.G. Pande, D. Yound, and H.R. Bhagat, *J. Parenter. Sci. Technol.* **46**, 176–180 (1992).
69. J.L. Cleland et al., *AIDS Res. Hum. Retroviruses* **10**, S21–S26 (1994).
70. Z. Moldoveanu et al., *J. Infect. Dis.* **167**, 84–90 (1993).
71. C. Thomasin et al., *J. Controlled Release* **41**, 131–145 (1996).
72. H.M. Vordermeier et al., *Vaccine* **13**, 1576–1582 (1995).
73. P.A. Marx et al., *Science* **260**, 1323–1327 (1993).
74. J.H. Eldridge et al., *Infect. Immun.* **59**, 2978–2986 (1991).
75. J.H. Eldridge et al., *Adv. Exp. Med. Biol.* **25**, 192–202 (1989).
76. J.H. Eldridge et al., *J. Controlled Release* **11**, 205–214 (1990).
77. M.A. Alonso et al., *Pharm. Res.* **10**, 945–953 (1993).
78. T.E. Greenway et al., *Vaccine* **13**, 1411–1420 (1995).
79. D.T. O'Hagan et al., *J. Controlled Release* **37**, 75–84 (1995).
80. M.T. Aguado and P.H. Lambert, *Immunobiology* **184**, 113–125 (1992).
81. T.L. Bowersock et al., *Am. J. Vet. Res.* **55**, 502–509 (1994).
82. G.B. Pier et al., *Infect. Immun.* **62**, 3972–3979 (1994).
83. D.T. O'Hagan, D. Rafferty, S. Wharton, and L. Illum, *Vaccine* **11**, 660–664 (1993).
84. Y.S. Jong et al., *J. Controlled Release* **147**, 123–134 (1997).
85. D.H. Jones et al., *Vaccine* **15**, 814–817 (1997).

VETERINARY APPLICATIONS

MICHAEL J. RATHBONE
InterAg
Hamilton, New Zealand

LEONORE WITCHEY-LAKSHMANAN
Schering-Plough Research Institute
Kenilworth, New Jersey

KADRIYE CIFTCI
Temple University
Philadelphia, Pennsylvania

KEY WORDS

Anithelmintics
Companion animal
Ectoparasites
Endoparasites
Estrous control
Growth enhancement
Intramammary
Intravaginal
Long-acting injectables and implants
Postruminal
Proteins and peptides
Ruminal
Steroids
Veterinary drug delivery
Veterinary gene therapy
Veterinary medicine
Veterinary vaccines

OUTLINE

Introduction
Factors Influencing Controlled Drug Delivery in Animals
Comparison of Human and Animal Controlled Drug Delivery
- Reasons for Producing Controlled Drug Delivery Systems
- Dosing Interval
- Drug Candidates
- Pharmacokinetics
- Physiology and Anatomy
- Delivery System Design
- Site of Absorption
- Means of Administration
- Storage Conditions
- Regulatory Considerations
- In Vivo/In Vitro Correlations

Veterinary Controlled-Release Drug Delivery and Delivery Systems
- Intraruminal Drug Delivery
- Postruminal drug delivery
- Intramammary Drug Delivery
- Steroid Hormone-Containing Growth Promotants
- Vaginal Drug Delivery
- Long-Acting Injectable Products Used in Food-Producing Animals
- Topical Dosage Forms for Food-Producing Animals
- Controlled-Release Technologies in Companion Animals
- Ophthalmic Drug Delivery
- Protein and Peptide Delivery

Recent Initiatives
- Vaccine Delivery
- Gene Therapy
- Trends and Future Directions of Vaccines and Gene Therapy

Concluding Remarks
Bibliography

INTRODUCTION

Veterinary medicine offers many challenges to the scientist developing controlled-release products (1). These challenges arise from the diverse nature of the field, which covers a multitude of animal species that differ in size, habits, social behavior, and so on; farm management practices in which farmers may not have any direct contact with their flock or herd for many weeks or even months; and anatomical and physiological constraints that are peculiar to an individual animal species. These factors present the formulation scientist with a unique opportunity to develop innovative solutions to challenging and demanding delivery problems (1).

The purpose of this article is to provide a comparison between human and veterinary controlled-release drug delivery, to highlight some of the factors that influence the development of controlled-release products for animals, to describe relevant issues pertaining to the design and development of controlled-release products for various routes/clinical conditions, and to describe the various conceptual and commercially available controlled-release drug delivery systems that are available for those routes or conditions.

Because the largest body of veterinary and controlled-release literature focuses on food-producing and companion animals, these two areas are also the focus of this article. However, it should be realized that there are other areas of minor market interest such as the fur industry, wildlife management, and zoological medicine that also present unique and interesting opportunities for controlled drug delivery. For example, consider the challenges within the area of wildlife management. Not only would it be desirable to have the formulation fulfill all the normal physical and chemical stability criteria associated with a controlled-release product, but there may also be the need for it to be designed to allow delivery through the barrel of a dart gun!

FACTORS INFLUENCING CONTROLLED DRUG DELIVERY IN ANIMALS

Controlled drug delivery to animals can be conveniently divided into two broad categories—those delivery systems developed for food-producing animals and those developed for companion animals. Food-producing animals consist primarily of cattle, sheep, swine, and poultry, together with fish and any other animal from which meat or other products such as eggs or milk are obtained. Companion animals are those that are considered pets, primarily dogs and cats, but animals such as horses, birds, lizards, rabbits, and so on can also be considered companion animals. Rabbits, birds, and lizards are sometimes classified as "exotic" animals. Because the latter species represent only a small proportion of the companion animal market, drug delivery systems that have been developed for the more mainstream species (e.g., dogs and cats) or indeed, for children, are often adapted for use in the exotic species because the markets are not usually large enough to warrant development of such specialized products.

In the food animal pharmaceutical business, many issues make the development of a controlled drug delivery system particularly challenging. For example, the profit margins associated with the raising and selling of farmed animals are rather slim. As a result, it is not atypical for only a few cents per dose to make a large difference to the farmer's overall profit. Therefore, the formulation scientist must produce a product under considerable cost constraints. In addition, the product manufacturers must also accept that their profit margins will be slim. However, this low profit margin can actually be used to the controlled release formulator's advantage because every visit of the veterinarian is associated with the cost of his or her time and expertise to the farmer as well as the cost of rounding up individual animals for treatment. Thus, the more frequently a product needs to be administered (e.g., once a day versus once a season), the more the cost of the treatment increases for the animal handler. Therefore, it behooves the formulation personnel to develop a controlled release product to reduce the number of times an administration procedure is required during the treatment period. Innovative adjustments in a once-a-day administration to make it a one-time-only administration can vastly improve the marketability of the product. Moreover, the development of a more complex controlled-release delivery system that delivers the active agent over an entire season has the potential to open huge areas of the market, allowing the handling of the animals only once, when they are turned to pasture.

In contrast, the companion animal market is somewhat different in that the potential cost and profit margins associated with a product developed for a companion animal can be much higher compared to one developed for the food animal market. First, the companion animal owner does not own, and therefore does not have to treat, several hundred animals in his or her herd or flock. Rather, the outlay is directed toward a single animal. Second, the price of the delivery system is not determined by the profitability of the animal but by the arbitrary value of the animal to the owner. Theoretically, therefore, the companion animal market will support the development of more complex and expensive dosage forms.

When one analyzes markets in the United States for both food and companion animals, one can divide the markets into three areas: pharmaceuticals, biologicals and feed additives. The breakdown of each of these U.S. markets is listed in Table 1, in which both the companion animal and food animal markets are combined. It is interesting to note that in contrast to human health, where one single drug formulation can accrue over $1 billion sales to a company, the entire animal health market in the United States has been estimated to be less than $3 billion total.

The highest yields (in market dollars) within the veterinary field are in the areas of antibiotics and endoparasiticides, each grossing over $500 million total in 1997. Biologicals offer the next largest portion, at nearly $500 million. This latter category includes items such as vaccine dosage forms of all kinds for all species. Insecticides and parasiticides account for the next largest category, while hormones and vitamin nutritionals account for

Table 1. Summary of Market Areas in the Animal Health Industry

Therapeutic area	1997 U.S. sales (millions of $)
Antibacterials	551.9
Biologicals	483.2
Hormones	266.6
Insecticides and parasiticides	414.1
Internal parasiticides	540.2
Vitamins and nutritionals	134.7
Other (analgesics, anesthetics, lab diagnostics, antiseptics, grooming aids)	415.3
Total	2,806

the remaining largest portions of the market. The remainder of the market still represents a large portion in total; however, these are the sum of several individual therapeutic areas, each of which represents only a fraction of total U.S. animal health sales.

In relation to the global economy, U.S. sales represent almost one-third of the entire world animal health industry. Table 2 shows that the next largest animal health products consumer is Russia, but it accounts for less than 10% of the entire world market. Japan follows closely behind Russia, with China and France each accounting for about 5–6% of the entire world market. The total contribution of all the other countries represents at most 5% of the global market. It should be noted, however, that with the establishment of the European Union, the numbers in Table 2 will inevitably change owing to the unification of the animal health market within this region. In addition, given the large Chinese population coupled with the small fraction of the world market, many have suggested that the most untapped potential for veterinary pharmaceuticals lies within China.

From Tables 1 and 2 it can be calculated that the total worldwide market is estimated to be approximately $9–10 billion. This offers many global opportunities worldwide, and therefore it is no wonder that several animal health companies have consolidated in the last several years to improve their efficiency in the light of the broad-reaching competitiveness of the industry.

Table 2. Market Share of Specific Countries in the World Animal Health Market

Country	Worldwide sales (%)
U.S.A.	28.7
Russia	8.8
Japan	7.6
China	5.4
France	5.4
Brazil	4.6
Germany	4.6
U.K.	2.9
Spain	2.8
Italy	2.5
Central Europe	2.2
South Korea	2.0
Others	22.5

COMPARISON OF HUMAN AND ANIMAL CONTROLLED DRUG DELIVERY

Reasons for Producing Controlled Drug Delivery Systems

In humans one reason for developing a drug into a controlled-release drug delivery system is to reduce the dose frequency to improve patient compliance (2–4). An additional reason is to improve the efficiency of therapy and thereby improve the health of the patient (2,3). In the veterinary field, the reason for developing a drug into a long-acting controlled-release drug delivery system is to minimize animal handling to reduce the stress to animals from repeated administration and to reduce the cost in terms of money and time spent by the end-user on drug administration.

Dosing Interval

The dosing interval of human and veterinary products differs widely. In humans it is common that an improvement in compliance and efficacy is obtained if the number of required doses is reduced twofold, resulting in (approximately) an 8- to 12-h duration of action of the drug (5). In a few cases the aim to decrease the number of required doses multifold to provide a very extended duration of drug action in the order of months also exists, as in Norplant (6). This contrasts markedly to the animal case, where an increase in drug action by only several hours would rarely be useful. In animals, in most cases, the duration of drug action though the development of a controlled-release product must be extended by at least several days, and in the vast majority of cases, in the order of months to cover an entire season (e.g., a flea or tick season for companion animals or a growing season for food-producing animals).

Drug Candidates

In humans, typical drug types that are incorporated into controlled-release products have short biological half-lives (2,7,8), which is the reason why a twofold increase in drug delivery can result in improvements over single-dose therapy. In contrast, drugs used in the veterinary field may possess half-lives that may be very short or very long. It is the need to deliver that drug over an entire season (for weeks or months) and not the short duration of biological activity of the drug, that dictates the need to incorporate it into a controlled-release formulation.

Pharmacokinetics

The pharmacokinetics of a given drug in humans differs between infants, children, and adults and may change as a function of disease status. The same applies to animals. In addition, in the veterinary field, the pharmacokinetics of a given drug differs markedly between different species. The pharmacokinetics of a given drug in a given animal is an important consideration when developing an animal health product and presents challenges when developing

the same drug product for different animal species. Commonly, more than one formulation of delivery device must be prepared based on species as well as the age of the animal.

Physiology and Anatomy

The physiological and anatomical characteristics of the human species differ only slightly between the young and adult of the species. However, the physiological characteristics of the different routes for drug delivery differ substantially between various animal species. The differences that exist in skin between animal species (e.g., thickness, composition, number of hair follicles, etc.) can influence the design of transdermal preparations where, for example, different mechanisms for absorption can be exploited. For instance, follicular penetration routes may be exploited in sheep but not in pigs. The differences in anatomy between species can also influence the design of a delivery system as is observed in ruminant versus monogastric animals. Because of the peculiarities of the ruminant gastrointestinal tract, delivery systems can be designed to be retained for months in a manner impossible to mimic in monogastrics.

Delivery System Design

There are vast differences between human and animal controlled drug delivery with respect to the scope and latitude associated with the geometry of the delivery system. For example, with human controlled-release drug delivery systems, dose size can be product limiting (8). For example, the physical size of a solid oral dosage form can limit its development because its size influences the ease of swallowing (8). A similar scenario applies to the development of implants for human use. The pain associated with too large a volume of an injection or too large an implant can prohibit the development of a controlled-release injection or implant in humans. In contrast, although there are constraints on the physical size of a delivery system, whether oral, implant or injection, in general in animals (particularly farmed animals), the overall size of a delivery system can be much larger such that dose size is not the limiting factor in the design of the delivery system. It should be noted, however, that because the animal is generally much larger than its human counterpart, it will require larger doses to be administered to produce the desired therapeutic effect. It should also be realized that this is not the case for all animals because the size of different species varies—for example, compare cattle with cats. The geometry of the delivery system for humans is in general defined by history and revolves around product shapes that humans are used to seeing, such as round flat tablets. In contrast, in animals the geometry of the delivery system is generally dictated by the administration devices that are available for that route for drug delivery, such as balling guns, intravaginal applicators, implanters, and so on.

Site of Absorption

In humans oral products would be expected to traverse the length of the gastrointestinal tract and release drug along its entire length. Subcutaneous or intramuscular injections or implants would be expected to release from the injection site. With veterinary products orally administered products to ruminant animals are often retained at a specific site within the gastrointestinal tract (the rumer) (9) for several months, as opposed to continuing along the length of the gastrointestinal tract. Injections are more preferably placed subcutaneously in animals. Intramuscular administration is less favored because it can decrease meat quality in food-producing animals.

Means of Administration

Administration is an interesting aspect in the development of a controlled-release product for animals. In the case of humans, self-administration is feasible, and orally administered products usually are easily swallowed with a glassful of water. Topical products are specifically designed to be easily placed on the skin. Factors such as size, shape, ease of administration, and safety to the person administering the product over a series of time intervals are built into the product. Injections or implants are often administered by a second person; however, a patient can be trained to self-administer an injection, or products may be designed to facilitate this process (e.g., insulin pens). In contrast, with a veterinary product, the means of administration must be carefully considered and be part of the product development process. The issues of safety, ease of use, and so on just outlined must still be thought through for animal products but in addition, so should a series of other additional considerations. These include

- How will the delivery system be administered?
- What will the handler safety be for one person administering to several hundred animals over several time intervals (e.g., feedlot cattle for every shipment that comes in)?
- Is the administration device easy to use, or has it the potential to cause repeated stress syndromes?
- Will it be easy to train nontechnical people in its use?
- Can standard equipment be used to administer the product?
- How does the required administration method of the product fit into to current animal-handling practices?
- Can the device withstand "downstream" operations (such as rendering) without harming the equipment used in those operations?
- Can the package it is presented in withstand the various field conditions it will be subjected to (e.g., plastic versus glass)?
- Can the administration device withstand several hundred administrations, severe weather conditions, rough handling, and large animals (i.e., what is the administration device's life expectancy?).

Storage Conditions

The required storage conditions for the product can also be contrasted between human and veterinary medicine. Human products can be refrigerated relatively easily if nec-

Next Page

essary and indeed some human products, for example, insulin and other biologicals, carry this provision on the label. However, this is not the case for veterinary pharmaceuticals. A veterinarian or other end-user would not typically have access to a refrigerator. Indeed, once the product has left the ideal storage conditions of the supply warehouse or surgery, most veterinary products are stored in the back of a car or in a non-temperature-controlled environment on the farm. Veterinary products are therefore required to be developed to withstand higher temperatures. This impacts heavily on the product's stability requirements, which must be addressed and overcome by the formulator during the development stages of the controlled-release product.

Regulatory Considerations

For human products, regulatory requirements include toxicity, safety, dosing intervals, therapeutic effect, stability, approved excipients, and the like. Veterinary products not only include all of the above but also require tissue residue and handler safety issues to be addressed, particularly for food-producing animals. This typically involves a full tissue-residue analysis to be performed, first with radiolabeled drug to determine the sites of deposition and then with nonradiolabled drug to prove it in the final formulation. From these data, a "tissue withdrawal" time is determined to inform the farmer of when the animal is fit for slaughter. Obviously, the shorter the withdrawal time is for the product, the more desirable the overall product profile.

In Vivo/In Vitro Correlations

In vivo/in vitro correlations for the purpose of product development, quality control, and so on are much more challenging for a product required to release over several months versus a few hours or a day. In animals, therefore, proof of control of the release to prevent dose dumping can be more challenging when the dose is for several months as opposed to a single day. Rarely do in vitro correlations exist to predict exact performance. The final determination is in the actual use.

VETERINARY CONTROLLED-RELEASE DRUG DELIVERY AND DELIVERY SYSTEMS

Intraruminal Drug Delivery

Intraruminal drug delivery systems are designed to be administered to, and retained in, the rumen of ruminant animals (e.g., cattle, sheep) and to deliver drugs over extended periods (months).

The anatomical and physiological characteristics of the stomach of ruminant animals are relatively complex. The stomach is large and composed of four compartments: the rumen, reticulum, omasum, and abomasum. The rumen is the largest compartment and may contain 80–200 L of ruminal fluid of pH 5–7 (9). The temperature of the rumen is in the range of 38–42°C and has a total internal gas pressure in the range of 1–1.1 atm arising from the conversion of foodstuffs into absorbable nutrients through microbial fermentation (9). This process is accompanied by the evolution of up to 600 L/day of gas. The composition and density of ruminal materials varies with the location (9). At the bottom of the rumen, the material is relatively well digested and mixed with copious amounts of fluid and is, therefore, of relatively high density. The upper layers of the rumen contain the newly ingested materials, which are much drier and of relatively low density (9).

A characteristic of the ruminant animal is that it spends much of its life grazing open pasture and is not extensively handled by the farmer. Consequently, the administration of pharmaceuticals is challenging, time-consuming, and costly because of the need to initially herd the animals into a convenient location to permit drug administration. The need to reduce handling of such animals on a regular basis for drug administration provides one of the biggest opportunities for the application of controlled-release technology to animal health and production.

Cardinal has recently outlined several key design features that are required of a controlled-release intraruminal drug delivery system (9). These include the inherent needs to (*1*) design the delivery system around a balling gun to allow for oral administration, (*2*) design the delivery system with a shape compatible with passage down the esophagus, (*3*) design the device with some mechanism that allows for long-term retention in the rumen of the animal (i.e., prevents regurgitation), and (*4*) incorporate some form of controlled-release technology that allows for the long-term delivery of the drug (up to 180 days) (8).

Several balling guns are commercially available (10). Regurgitation of the delivery system by the animal is prevented by either geometric design or density of the product. The literature suggests that a density of 1.8 or greater is required to prevent regurgitation of delivery systems from the rumen of cattle (11). When the density is less than 1.6, a significant number are not retained in cattle. The concept behind retention of the device in the rumen through geometry relies on creating a device that can be administered in a small enough size to allow for administration but will change its size or shape following administration to a form that is much greater in size than the esophagus.

Many controlled-release drug delivery systems have been developed for intraruminal administration over the last few decades (Table 3). For extensive reviews on intraruminal drug delivery, the reader is referred to Refs. 9, 36, 59, and 60.

Postruminal drug delivery

The process that allows the ruminant to utilize cellulose and nonprotein nitrogen is called rumen fermentation (61). Although this biological process is beneficial to the animal, it presents challenges to the drug delivery formulator because it also destroys or modifies bioactive materials (nutrients and drugs) that have been administered orally to prevent or treat disease (61). Thus, although ruminants could potentially benefit from the administration of bioactive materials (such as supplemental amino acids or saturated fatty acids), the administration of such materials orally through simple addition to feed is not practical. If the formulator wishes to persist with the administration

Previous Page

essary and indeed some human products, for example, insulin and other biologicals, carry this provision on the label. However, this is not the case for veterinary pharmaceuticals. A veterinarian or other end-user would not typically have access to a refrigerator. Indeed, once the product has left the ideal storage conditions of the supply warehouse or surgery, most veterinary products are stored in the back of a car or in a non-temperature-controlled environment on the farm. Veterinary products are therefore required to be developed to withstand higher temperatures. This impacts heavily on the product's stability requirements, which must be addressed and overcome by the formulator during the development stages of the controlled-release product.

Regulatory Considerations

For human products, regulatory requirements include toxicity, safety, dosing intervals, therapeutic effect, stability, approved excipients, and the like. Veterinary products not only include all of the above but also require tissue residue and handler safety issues to be addressed, particularly for food-producing animals. This typically involves a full tissue-residue analysis to be performed, first with radiolabeled drug to determine the sites of deposition and then with nonradiolabled drug to prove it in the final formulation. From these data, a "tissue withdrawal" time is determined to inform the farmer of when the animal is fit for slaughter. Obviously, the shorter the withdrawal time is for the product, the more desirable the overall product profile.

In Vivo/In Vitro Correlations

In vivo/in vitro correlations for the purpose of product development, quality control, and so on are much more challenging for a product required to release over several months versus a few hours or a day. In animals, therefore, proof of control of the release to prevent dose dumping can be more challenging when the dose is for several months as opposed to a single day. Rarely do in vitro correlations exist to predict exact performance. The final determination is in the actual use.

VETERINARY CONTROLLED-RELEASE DRUG DELIVERY AND DELIVERY SYSTEMS

Intraruminal Drug Delivery

Intraruminal drug delivery systems are designed to be administered to, and retained in, the rumen of ruminant animals (e.g., cattle, sheep) and to deliver drugs over extended periods (months).

The anatomical and physiological characteristics of the stomach of ruminant animals are relatively complex. The stomach is large and composed of four compartments: the rumen, reticulum, omasum, and abomasum. The rumen is the largest compartment and may contain 80–200 L of ruminal fluid of pH 5–7 (9). The temperature of the rumen is in the range of 38–42°C and has a total internal gas pressure in the range of 1–1.1 atm arising from the conversion of foodstuffs into absorbable nutrients through microbial fermentation (9). This process is accompanied by the evolution of up to 600 L/day of gas. The composition and density of ruminal materials varies with the location (9). At the bottom of the rumen, the material is relatively well digested and mixed with copious amounts of fluid and is, therefore, of relatively high density. The upper layers of the rumen contain the newly ingested materials, which are much drier and of relatively low density (9).

A characteristic of the ruminant animal is that it spends much of its life grazing open pasture and is not extensively handled by the farmer. Consequently, the administration of pharmaceuticals is challenging, time-consuming, and costly because of the need to initially herd the animals into a convenient location to permit drug administration. The need to reduce handling of such animals on a regular basis for drug administration provides one of the biggest opportunities for the application of controlled-release technology to animal health and production.

Cardinal has recently outlined several key design features that are required of a controlled-release intraruminal drug delivery system (9). These include the inherent needs to (*1*) design the delivery system around a balling gun to allow for oral administration, (*2*) design the delivery system with a shape compatible with passage down the esophagus, (*3*) design the device with some mechanism that allows for long-term retention in the rumen of the animal (i.e., prevents regurgitation), and (*4*) incorporate some form of controlled-release technology that allows for the long-term delivery of the drug (up to 180 days) (8).

Several balling guns are commercially available (10). Regurgitation of the delivery system by the animal is prevented by either geometric design or density of the product. The literature suggests that a density of 1.8 or greater is required to prevent regurgitation of delivery systems from the rumen of cattle (11). When the density is less than 1.6, a significant number are not retained in cattle. The concept behind retention of the device in the rumen through geometry relies on creating a device that can be administered in a small enough size to allow for administration but will change its size or shape following administration to a form that is much greater in size than the esophagus.

Many controlled-release drug delivery systems have been developed for intraruminal administration over the last few decades (Table 3). For extensive reviews on intraruminal drug delivery, the reader is referred to Refs. 9, 36, 59, and 60.

Postruminal drug delivery

The process that allows the ruminant to utilize cellulose and nonprotein nitrogen is called rumen fermentation (61). Although this biological process is beneficial to the animal, it presents challenges to the drug delivery formulator because it also destroys or modifies bioactive materials (nutrients and drugs) that have been administered orally to prevent or treat disease (61). Thus, although ruminants could potentially benefit from the administration of bioactive materials (such as supplemental amino acids or saturated fatty acids), the administration of such materials orally through simple addition to feed is not practical. If the formulator wishes to persist with the administration

of such bioactive materials orally, they must develop delivery systems that are stable in the rumen (i.e., that protect the drug from the harmful environment of the rumen) and that release their contents postruminally. Ideally, nutrients, drugs, and other active compounds incorporated into postruminal delivery systems should be fully protected from fermentation in the rumen and then be completely released and available for absorption or for performing their intended postruminal function (61). Many factors need to be considered when developing and designing a postruminal drug delivery system, including the typical retention times of particles and solids in the rumen and abomasum, pH of the rumen and abomasal fluid, the ruminant digestive process, the dynamics of ruminal motility, and the effects of rumination on particle degradation.

Several methods have been developed for protecting nutrients, drugs, and other active compounds from the environment of the rumen and are shown in Table 4 (61).

Intramammary Drug Delivery

The intramammary route for drug delivery is primarily used for the treatment of mastitis in cows and can be classified according to two main areas: lactating and dry (nonlactating). A once-only administration is beneficial to both these areas because it reduces handling of the animal. Each of these areas offers specific challenges to the delivery of an active agent. For example, the requirements for drug delivery to lactating cattle requires that the active ingredient be removed from the mammary gland or milk as soon as possible after the treatment period has elapsed so that there is no issue with regard to the presence of drug in the milk. In contrast, intramammary delivery in dry cows would allow for the formulation to be developed such that the drug persisted for a longer period of time after the treatment period had elapsed. Dry cow applications, therefore, lend themselves more readily to controlled drug delivery applications because the prolonged exposure of the infected site to drug improves the efficacy of treatment, and the concerns for drug residues in milk are not an issue.

A list of the various formulation types which have been explored for the intramammary route is shown in Table 5. Early developed formulations for intramammary drug delivery were aqueous based. Such formulations suffered from the disadvantage that they were short acting; however, they did distribute well over the infected areas (66). To overcome the problem of the short action, aqueous-based formulations have been developed that are coformulated with a water-soluble polymer such as poly(ethylene glycol). Oil-based formulations have also been investigated that allow for prolonged release of the active ingredient in the udder (66–71); however, they suffer from the disadvantage that they often irritate the udder mucosa (67) and distribute less homogeneously throughout the udder than aqueous preparations (66). Ointment-based products have also been studied and appear to offer an improvement over oil-based products. A further formulation type that has been investigated is the encapsulated drug product (68,69,72). Such formulations appear less irritating and more uniformly distributed around the udder. In addition, in some cases they also release drug over a prolonged period of time.

In recent years, with the rise of biotechnology, researchers have been investigating the use of vaccines and recombinant therapies to treat mastitis (73–78). These vaccines should offer the longest-term protection because they allow the animal to develop an immunity to the organisms that are causing the mastitis in the first place. However, because several types of organisms have been implicated in the cause of mastitis, the best vaccine would have to offer protection against a large spectrum of organisms and to date, no such vaccine exists.

Steroid Hormone-Containing Growth Promotants

Steroid hormone-containing implants improve the average growth of the animal. They contain either singularly or in combination estrogenic, androgenic, or progestegenic drugs (Table 6) (79). Growth response depends on the level and type of hormone incorporated into the delivery system, and commercially available controlled-release products differ in their hormone content, delivery matrix, and release pattern. Implants contain drugs incorporated into either lactose, cholesterol, polyethylene, or silicone rubber delivery matrix. Lactose-based implants are shorter acting (approximately 40 days) compared to cholesterol-based implants (approximately 80 days). Silicone rubber matrices provide the longest duration of release for estrogens (approximately 200–400 days). The amount of drug released from these delivery systems is greatest initially and slowly decreases with time, and release kinetics are typically described by either a first-order kinetics or a square-root-of-time mechanism (80). The most comprehensively described steroid hormone-containing implant is the Compudose delivery system (36,81,82). Compudose is a silastic implant composed of a drug-free silastic cylinder coated with a layer of silastic containing 20% dispersion estradiol. It has a surface area of 4.84 cm^2 and has been shown to release drug by a square-root-of-time mechanism.

Development of a steroid hormone-containing controlled-release implant requires that the implantation procedure is given consideration. Implants should not cause tissue irritation, and the administration site must be chosen such that it does not allow the delivery system to enter the food chain. Historically, the ear has been chosen as the site for administration because it represents an inedible portion of the carcass and is discarded on slaughter, accessible to the administrator, and well perfused with blood; as well, administration is relatively pain free and, therefore, provides minimal distress to the animal. The disadvantage of using this site is the need for restraint of the animal. Steroid hormone-containing controlled-release implants are not manufactured sterile, and therefore there is the need for an aseptic administration procedure. Implantation of commercially available implants into the subcutaneous tissue of the ear requires the use of a specially designed implanter.

The route of administration dictates the maximum size of the implant, which is an important consideration because modifying the surface area of the implant is an effective way of modifying release rate. The literature suggests that the optimum release profile for a steroid

Table 3. Intraruminal Drug Delivery Systems

Product name/ inventor	Description of delivery system	Drug	Retention mechanism	Animal and approximate release time	Mechanism of release
Paratect bolus	Hollow stainless steel cylinder about 4 in. in length and 1 in. in diameter that is filled with a drug reservoir comprising a paste of the drug/poly(ethylene glycol) 400. Each end of the cylinder is capped with rate-controlling membranes prepared from a microporous sintered polyethylene disk whose pores are filled with cellulose triacetate (12–15).	Morantel tartrate	Density	Cattle (90 days)	Diffusion through the water-filled channels of the two porous membranes at each end of the cylinder
Paratect Flex (16,17)	A central sheet of drug loaded a 50:50 mixture of ethyl vinyl-acetate coated on both sides with a layer of ethyl-vinyl acetate that renders each surface of the drug reservoir impermeable to drug to form a trilaminate structure. A series of holes is then punched in the device that transverse the complete trilaminate. The trilaminate sheet is then rolled into a cylinder and maintained as a roll with a water-soluble tape.	Morantel tartrate	Geometry trilaminate sheet that unrolls following administration to increase its dimensions	Cattle (90 days)	Moratal tartrate is a water-soluble salt and cannot permeate EVA. Drug is released from both the outer edges of the trilaminate and from the inner surface of each hole that was punched through the matrix. The kinetics of drug release from the outer edges follows the typical $t^{1/2}$ kinetics. The release from each hole is a function of increasing surface area at the receding drug boundary and increase in the diffusional pathlength over time within the depleted zone, which results in a net overall decrease in the release rate with time and thus a release rate that is relatively constant with time. The release rate is a function of the number and the diameter of the perforations and the usual parameters that control the rate of release from dispersed matrix devices.
Spanbolet II	Rectangular-shaped delivery systems approximately 3.5 in. by 0.5 in. by 0.5 in. in size. Manufactured by compressing drug, carnauba wax, barium sulphate, poly(ethylene glycol) and iron powder (18)	Oxytetracyclines	Density	Cattle (50 days)	Slow erosion of device within rumen

Laby	The device is composed of a hollow cylinder capped at both ends. One end is closed and serves to help constrain a spring that acts against a piston that in turn acts against an erodible composition containing drug or nutrient. The erodible composition comes in contact with the exterior environment via a portal in the second endcap. Attached to the cylinder are polymeric wings that are constrained to the side of the cylinder during administration by a water-soluble tape. This basic design has been subject of extensive work that has appeared in the patent literature, which describes improvements in device-retention mechanisms, core composition, piston/spring design, and delivery of multiple drugs with a single device (19–27).	This device design has been commercialized for the delivery of various compounds (e.g., albendazole and monensin) for sheep and cattle.	Geometry (expanding polyethylene wings that fold against the device on insertion but open within the rumen)	Sheep and cattle (100 or 135 days)	The drug/nutrient-release rate is controlled via erosion of the tablet formulations incorporated into the device via the portal in the second endcap.
Beecham I	A matrix device in the form of a large sheet that can be rolled up to form a cylinder and constrained by a water-soluble tape; the size of the sheet is such that its unrolled dimensions are greater than that of the diameter of the esophagus. The device utilized a trilaminate sheet in which the inner lamina was composed of a core matrix of drug dispersed in an ethylene-vinyl acetate copolymer. This inner lamina was coated with a layer that was either imprevious to fluid (and drug) or prepared with a filler such as starch or lactose to control the overall drug permeability properties in the coating (28).		Geometry; water-soluble tape dissolves and trilaminate unrolls.	Cattle (90 days)	Controlled release is achieved via two rate-limiting barriers containing a highly water-soluble compound that rapidly dissolves, leaving water-filled pores through which the drug leaches out.
Beecham II	A similar device configuration to the one above was also described by Griffin and Brewer but was composed of two lamina: One lamina was impermeable to drug, whereas the second lamina was an erodible dispersed matrix of drug plus ethylene-vinyl acetate (29).		Geometry; water soluble-tape dissolves and the laminate unrolls.	Cattle (90 days)	The drug-release rate was controlled via erosion of the erodible lamina.
Time capsule	A core containing zinc oxide and binding and releasing agents covered over all but one open end by a waxy coat (30)	Zinc oxide (± selenium and cobalt)	Density	Cattle (4 weeks) and sheep (6 weeks)	

Table 3. Intraruminal Drug Delivery Systems *(continued)*

Product name/ inventor	Description of delivery system	Drug	Retention mechanism	Animal and approximate release time	Mechanism of release
Pulsatile bolus (Hollaway device)	Cylindrical device loaded with a steel ball in its rounded base for retention; the inside of the cylinder is filled with a series of drug-containing compartments, each separated by layers of degradable cellulosic partitions (31).	Monensin	Density	Cattle	A dose of drug is delivered (pulsed) from each drug-loaded compartment following exposure after dissolution/ erosion of each of the cellulosic partitions. The dosage regimen can be controlled via the composition of each drug compartment and by the thickness and composition of the dividing layers.
IVOMEC SR Bolus	The device has recently been described by cardinal (9): The product is composed of a membrane cup that is extruded from cellulose acetate and various plasticizers. This cup is filled with an osmotic tablet that swells following the imbibement of water through the membrane cup. Placed above the tablet are a partition layer, a drug-containing layer, and a densifier. Both the partition layer and the drug layer are prepared from paraffin waxes and Cab-O-Sil. Drug is suspended at a concentration of 22% in the drug layer. The softening point of the partition layer is somewhat higher than the drug layer so that the partition layer will basically serve as a piston to help direct the flow of the drug-containing layer through the exit port channel located centrally in the densifier. The drug layer begins to soften in the range of 31–35°C. Under these conditions the drug is maintained as a suspension during storage and delivery without settling. At temperatures greater than about 35°C, the material has the requisite fluidity to flow through the exit channel and exit port screen. The densifier is made of sintered iron fillings designed such that it has a crush strength similar to that of bone (32,33). This is to ensure that the densifier will not harm the equipment utilized in rendering plants following slaughter of the animal. The central port in the densifier is covered with a capscreen made from plastic and designed such that the drug suspension is forced through a series of small openings in the capscreen (34).	Ivermectin	Density	Cattle (110 days)	Imbibement of water through the semipermeable membrane followed by expansion of the hydrogel that constantly forces a drug-containg vehicle through an exit port

Osmotic pressure–based ruminal bolus	Thombre et al. (35) describe a delivery device similar in overall design to that of the Paratect bolus but utilizing a novel osmotic technology suitable for the long-term delivery of drugs in which the drug is delivered as a solution in oil. This system utilized both the cylinder and membranes of the Paratect bolus as described above; however, the membranes and core formulations were suitably modified to convert the overall mechanism of drug delivery from diffusion control to an osmotic-based mechanism. In this system the core formulation was composed of an oil such as octanol, isopropyl myristate, or soybean oil and a swellable polymer such as PEG 600 or poly-vinyl alcohols dispersed as pellets within the oil. The drug was dissolved within the oil phase. One microporous polyethylene membrane was impregnated with cellulose triacetate and wetted with PEG 400. The other microporous membrane was either unimpregnated or treated with various other options to permit the membrane to be permeable to oil.	An ionophore with potential as a growth promotant	Density	Cattle	Osmotic-based release mechanism
Rumensin ABC	Consists of a plastic capsule about 16 cm long (utilizes Laby device technology) (36,37)	Monensin sodium	Geometry; following administration, two plastic wings unfold.	Cattle (100 days)	
Autoworm/Multidose 130	The delivery system is made up of a steel endweight connected to a magnesium alloy spindle. Around the spindle are placed five drug-loaded lifesaver-shaped tablets that are encased in PVC caps and separated by scaling washers (36,37).	Oxfendazole	Density	Multidose 130 delivers five doses of oxfendazole to grazing cattle over approximately 130 days. The first dose is delivered at about 21 days following administration.	Pulsed delivery at 23 days intervals as the drug-loaded lifesavers become exposed, following corrosion of the metal at a relatively constant rate
Marston erodible system	Erodible bolus containing cobalt oxide and other diluents (38)	Cobalt	Density		Erosion due to dissolution or abrasion due to the solution or mechanical action of the rumen

Table 3. Intraruminal Drug Delivery Systems *(continued)*

Product name/ inventor	Description of delivery system	Drug	Retention mechanism	Animal and approximate release time	Mechanism of release
Pierce et al. erodible bolus	An erodible bolus comprising 2% active in combination with 5% monostearin, 10% carnauba wax, and 83% barium sulfate (39)	*S*-methoprene		Cattle	Erosion
Wood et al.	A combination of glycerol monostearate, carnauba wax, and barium sulfate (40)	Potent antiparasitacides		Cattle (120–180 days)	The devices can be configured to deliver drug at rates that range from about 0.001 to about 0.075 mg/kg/day.
Hemingway et al.	An erodible device composed of a core matrix of compressed particles containing the drug or nutrient, which is then coated with a rigid polymeric coat (41)	Minerals and vitamins	Density		The coating is insoluble in rumen fluids and is brittle and progressively fractures off following erosion of the core matrix. The duration of activity of this device is a function of the composition of the core matrix.
Baker	The delivery system is a relatively rapidly acting bolus composed of a core layer and an outer layer. Each layer is composed of the therapeutic agent, a water-swellable polymer, and inert materials so blended as to create a rapidly acting outer layer and a slower-dissolving core matrix (42).	Antibacterials			Dissolution
Soluble glass bolus	Glass-based delivery systems formed by melting the glass and nutrient components at high temperatures (up to 700°C) and drawing the melt into the desired shape (43–49)	Trace nutrients, copper, cobalt, and selenium	Density	Sheep (365 days)	Drug is released by diffusion of drug and/ or dissolution of the glass.
Lilly	Comprises a stainless steel cylinder that is coated with a mixture of drug dispersed in a copolymer of lactic acid and glycolic acid (50–52)	Density	Monensin	Cattle (90 days)	Erosion of the drug-loaded polymer

Monensin RDD	The core matrix is a mixture of 40% drug and a biodegradable copolymer prepared from lactic and glycolic acids (80:20 w/w). The core matrix is adhered to the inner surface of a metal cylinder by hot-melt adhesives and then placed inside a plastic case that has openings in the end large enough to allow drug release but of sufficient dimensions to prevent solid foreign material from the rumen contents from entering the device and physically abrading the core (53–55).	Monensin	Density	Cattle (150 days)	Controlled hydrolysis and degradation of the low-molecular-weight copolymer
Bagnall and Gyuril device	The device is composed of a series of cylindrical drug reservoirs. The drug formulation is maintained within the cylindrical reservoir by a plug (56).	Oxfendazole	Density	Cattle (three pulses at 30-day intervals)	Expulsion of the plug through the generation of a gaseous internal pressure within the cylindrical reservoir; the timing of release is regulated by an electrical circuit and a chemical squib that generates the necessary pressure. The squib is activated via a current that is controlled by an electrical circuit that regulates the timing for the application of current. The whole system is activated by placement within the rumen fluids that acts to close the circuit.
Kwan and Steber	A system that is composed of several doses of drug held together using an adhesive; each dose is composed of a bilaminated core that contains a layer containing drug and a layer that is comprised of sufficient weight to retain the delivery system in the rumen. Each dose is coated with a hydrophobic polymer that controls the time that the drug is exposed to ruminal fluid. A delivery system is described that contains three doses, each coated with a different biodegradable polymer (57,58)		Density	Multiple pulses	Degradation of polymer matrix; the polymer coatings surrounding each dose degrade at different rates and control the time of release of drug.

Table 4. Methods for Protecting Nutrients, Drugs, and Other Active Compounds from the Environment of the Rumen

Approach	Method	Advantages	Disadvantages
Heat treatment	Heat treatment of proteins reduces their solubility and degradation in the rumen (62).	Low cost	Heat treatment promotes reaction of amino acids with carbohydrates and reduces their bioavailability. Predictability and control of rumen protection is poor. Postruminal release of the active material is generally inversely related to the degree of rumen protection.
Chemical treatment	Chemical treatment reduces protein solubility and increases the amount of protein escaping rumen fermentation. A variety of chemical agents have been evaluated including formaldehyde, other aldehydes, acetic acid, and tannins among others (63,64).	Generally low cost	Use of formaldehyde raised significant safety concerns and has been abandoned in some countries. Chemical treatment is unsuitable for amino acids and other nutrients or drugs. Rumen protection and postruminal availability are quite variable.
Low-solubility peptides, amino acid derivatives or analogs, and calcium salts; for example, peptides of lysine and/or lysine with other amino acids have been investigated.	Analogs tested include *N*-stearyl-methionine, *N*-hydroxymethyl-methionine (HMM-Ca), α-hydroxy-γ-methyl-mercapto butyrate calcium, and methionine hydroxy calcium (HMB-Ca) (65).		Poor bioavailability postruminally (e.g., lysine peptides); Limited protection from rumen degradation for methionine analogs (65)
Lipid-based formulations (embedding in a fatty matrix) (61)	To formulate a lipid-based product, active compounds are either embedded in a lipid matrix or are formulated in small spheres and coated with lipid. The low solubility of the formulation in the rumen allows a large part of these materials administered orally to reach the small intestine and be absorbed. For this reason, they are formulated as calcium salts or in lipids that have poor solubility in the rumen. Lipid-protected products rely on their inherent resistance to enzymes in the rumen to maintain the integrity of the protective coating and their digestion by enzymes postpostruminally to release the active component.	Embedding in a lipid matrix or the process of applying a lipid coating has the advantage of using low-cost food-grade materials compared with formulated polymeric coatings.	Lipid matrix systems exhibit low payloads. Postruminal release of the active material for absorption is usually low and generally inversely related to the degree of rumen protection. Amino acids and small peptides are readily water soluble and do not remain inside the lipid matrix and become released into the rumen.
Ruminally inert, pH-sensitive polymers (reverse-enteric coating system) (61)	The bioactive material is coated with a coating system composed of a basic polymer such as poly(2-vinylpyridine-*co*-styrene, 8020), a pigment material such as talc or aluminum, and a hydrophobic substance such as stearic acid at a typical ratio of 31.563.55.0 by weight.	Process can be applied to a variety of nutrients, drug, or other active compounds	The coating efficiency was shown to be highly dependent on the solubility of active ingredients, pellet size, and smoothness of pellet surfaces Because the polymeric coating is soluble in acid, the coating should not be in direct contact with acidic feed components such as silage. The coated particles should not be added along with other feed ingredients into a feed-pelleting machine because the coating cannot survive in a high-shear and abrasive pelleting process. Only a few polymers are suitable as the coating material.

Table 5. Delivery Systems for Intramammary Applications

Types of delivery formulations	Reference
Water- and ointment-based systems	66–69
Oil-based systems	66,68–71
Encapsulated systems	68,72
Polymeric aqueous systems	68,69,72
Vaccines and recombinant therapies	73–78

hormone-containing controlled-release implant is unknown (80). The literature is unclear as to whether an initial burst followed by a declining release rate, a constant release rate, or an increasing release rate is desirable (80).

The need to remove the implant is not a consideration because the delivery system will remain in the animal for its life span and be discarded at slaughter with the inedible portion of the carcass.

Vaginal Drug Delivery

The use of controlled-release drug delivery systems in estrous control has a history dating back to the early 1960s when polyurethane sponges were first investigated as a means to deliver synthetic progestagens to sheep (83). Both the intravaginal and subcutaneous route for drug delivery are used to administer controlled-release drug delivery systems for estrous control (Table 7). Compounds used to control the estrous cycle include progesterone, methyl acetoxy progesterone, fluorogestone acetate, and estradiol. Other drugs for example, melatonin, antibiotics, oxytocin, prostaglandins, GnRH, and a variety of other synthetic progestagens, have been shown to be systemically absorbed from the vagina of farmed animals. To date, polymers utilized for systemically delivering drugs via the vaginal cavity of animals in commercially available products have been limited to polyurethane and silicone (85).

Several factors that affect the design and development of an intravaginal veterinary drug delivery system have recently been identified and discussed by Rathbone et al. (87). These include applicator design, end-user acceptance, dimensions and geometry of delivery system, retention rate, retention mechanism, dimensions of the device, release rate, ease of use, animal comfort, irritation (mucopurrelant discharge production), polymer used to manufacture delivery system, drug properties, presence or absence of additives, ease of removal, damage to vaginal mucosa and cervix, applicator design, removal mechanism, and manufacturing process (87). A further valuable overview of this area has been published by Chien (88).

Long-Acting Injectable Products Used in Food-Producing Animals

Many of the various long-acting injectable drug delivery systems discussed elsewhere in this encyclopedia have also been explored in veterinary medicine. For example, biodegradable polymers, liposomes, and other microencapsulated materials have been investigated for use in animals; however, to date none have been commercialized (89–92). Carter et al. (93) provide an excellent overview of long-acting injectables in veterinary medicine. Implants containing steroids for growth promotion and those formulated for estrous control have already been presented, and injectables used in companion animals are discussed in a following section. Therefore, the focus of this section are the other applications for long-acting injectables for food-producing animals, such as antibiotics and antiparasiticides.

The use of the more technologically advanced systems, such as polylactide–glycolide polymers, has not been widely applied in the markets of veterinary injectables be-

Table 6. Controlled-Release Steroid Hormone-Containing Implants

Product	Estrogen	Androgen	Progesterone	Time to hormone concentration at which production is no longer enhanced (days)
Ralgro®	36 mg resorcyclic acid lactone (zeranol)			70
Ralgro Magnum	72 mg zeranol			Unpublished
Calfoid	10 mg estradiol 17β		100 mg	Unpublished
Synovex-C	10 mg estradiol 17β		100 mg	120
Synovex-S	20 mg estradiol 17β		200 mg	120
Synovex-H	20 mg estradiol 17β	200 mg testosterone		120
Synovex-Plus	28 mg estradiol benzoate	200 mg trenbolone acetate		Unpublished
Implus-S	20 mg estradiol 17β		200 mg	Unpublished
Implus-H	20 mg estradiol 17β	200 mg testosterone		Unpublished
Torevex-S	20 mg estradiol 17β		200 mg	
Finaplix-S		140 mg trenbolone acetate		105
Finaplix-H		200 mg trenbolone acetate		105
Revalor-G	8 mg estradiol 17β	40 mg trenbolone acetate		Unpublished
Revalor-H	14 mg estradiol 17β	140 mg trenbolone acetate		120 (estimated)
Revalor-S	24 mg estradiol 17β	120 mg trenbolone acetate		120
Compudose 200	24 mg estradiol 17β			200
Compudose 400	45 mg estradiol 17β			400

Source: Ref. 79.

Table 7. Controlled-Release Intravaginal Inserts and Subcutaneous Drug Delivery Systems Used for the Control of the Estrous Cycle in Cattle

Delivery system	Description of delivery system	Principle animal for which delivery system designed	Drug	Route
PRID	Comprises micronized progesterone (1.55 g) uniformly suspended throughout silicone rubber that is cured onto a stainless steel spiral coiled to produce a spiral-shaped cylinder approximately 4 cm in diameter and with a length of 12 cm; the delivery system has a hard gelatin capsule attached to its inner surface and a string to aid removal.	Cattle	Progesterone	Intravaginal
CIDR-B	Consists of a preformed T-shaped nylon spine over which is molded a silicone rubber skin containing 1.9 g of micronised progesterone; one end of the device has two flattened wings that are hinged to the body of the device. The wings retain the device in the vagina by gently exerting pressure against the walls of the anterior vagina. At the bottom end of the device is attached a plastic tail to aid removal.	Cattle	Progesterone	Intravaginal
Sponge	Cylindrical-shaped polyurethane sponges impregnated with varying amounts of synthetic progestagens	Sheep and goats	Fluorogestone acetate; methyl acetoxy progesterone	Intravaginal
Rajamehendran rubber tubing	The device contained progesterone and estradiol 17β and was manufactured by cutting silicone rubber tubing into 20-cm lengths, sealing one end with silicone medical adhesive, and then pouring in diethyl ether containing 1 g of progesterone. After the diethyl ether had evaporated, the open end of the tubing was sealed with more adhesive. Approximately 1 mL of adhesive containing 10 mg estradiol 17β was then coated around the end of each tube. Two of these tubes were then centrally tied together, and lengths of string were secured to each of the free ends to be pulled together and knotted to form the umbrella-shaped intravaginal device. Following insertion, the string was allowed to protrude from the vulva to enable removal of the device at the end of treatment.	Cattle	Progesterone/estradiol	Intravaginal
IBD	The Intelligent Breeding Device is a technologically advanced, controlled-release drug delivery system in which estradiol, prostaglandin, and progesterone are released at different rates and at specific times (estradiol, 1 h after insertion; prostaglandin, 6 days later; and progesterone, continuously for 10 days).	Cattle	Progesterone/estradiol/ prostaglandin	Intravaginal

SYNCRO-MATE-B	A small ear implant containing 6 mg norgestomet (= 5% load) in the polymer Hydron, which measures approximately 3 mm × 18 mm and weighs approximately 0.125 g. The implants come encased within a protective plastic sheath and are supplied in individually sealed foil packaging.	Cattle	Norgestomet	Subcutaneous (ear)
SYNCRO-MATE-C	An ear implant that utilized the Microsealed Drug Delivery® (MDD) technology. The ear implant was formed by dispersing crystalline norgestomet in microreservoirs of aqueous PEG 400 throughout a matrix of polymerized silicone. The resulting solid composition was then cut into tiny cylindrical forms for implantation in the ear of cattle.	Cattle	Norgestomet	Subcutaneous (ear)
Ear implant (Crestar)	An ear implant containing 3 mg norgestomet homogeneously dispersed throughout a silicone matrix	Cattle	Norgestomet	Subcutaneous (ear)
CIDR-S	CIDR-S was rabbit eared in shape, containing 9% w/w micronized progesterone homogeneously distributed throughout silicone cured over a nylon spine. The device had a string attached to its lower end to aid removal.	Sheep	Progesterone	Intravaginal
CIDR-G	The CIDR-G is a T-shaped intravaginal device comprising of a preformed nylon spine than has a filament of flexible nylon preformed onto it to aid its removal. The device is coated with silicone impregnated with 9% w/w USP-grade micronized progesterone	Sheep	Progesterone	Intravaginal
Sil-Estrus	Comprised a solid silicone rod containing 375 mg of progesterone (10% w/w initial load), which measured 0.9 cm in diameter and 5.0 cm in length	Sheep	Progesterone	Subcutaneous (in the wool-free area under the foreleg along the brisket)
C-shaped plasthyd device	Comprised of a C-shaped delivery system manufactured from the polymer Plasthyd	Sheep	Progesterone	Intravaginal
Lutamate Plus	Poly(D,L-lactide) microspheres	Horse	Progesterone/estradiol	Intramuscular
Ovuplant	A cylindrical implant 2.3 mm in diameter and 3.6 mm in length containing 2.1 mg of Deslorelin (as Deslorelin acetate) in an inert matrix	Horse	Deslorelin	Subcutaneous

Source: Refs. 84–86.

cause the development of such products for a veterinary market is not economically favorable. As a result, the development of a controlled-release injectable in veterinary medicine has been based on three approaches: reliance on the pharmacokinetics of the particular drug compound, the use of a nonaqueous vehicle, or the manipulation of drug and/or vehicle composition to create a suspension.

For example, Ivomec® injection (Merial) is a solution of 1% w/w ivermectin in propylene glycol and glycerol formal that is given subcutaneously at ~200 μg/kg in cattle and 300 μg/kg in pigs. This injection is given once a month for the treatment of endoparasites. The main reason the injection is so long lasting is that the half-life of ivermectin in cattle is long and the potency of the compound is high, allowing even trace levels of the drug in the blood to be effective (94). The half-life of the drug, combined with its formulation into a nonaqueous vehicle (which allows for the creation of a depot at the site of injection), prolongs the action of the drug for over a month. Similar results are also seen with the doramectin and moxidectin products because they are of the same drug classification and exhibit similar half-life profiles.

In the area of antibiotics, florfenicol and oxytetracycline have been developed as long-acting injectables, Nulfor® injection (florfenicol) was developed by Schering-Plough to replace a chloramphenicol product needed to be administered at frequent intervals to combat bovine respiratory disease, or shipping fever. The dose of florfenicol is approximately 20 mg/kg; however, its solubility is low in most solvents. Therefore, to improve the drug's solubility, the formulators devised a complex nonaqueous cosolvent system that allowed for sufficient drug to be administered to allow administration once every two days. The solvents added to the formulation included propylene glycol, poly(ethylene glycol) and *n*-methyl pyrrolidone (95). This system allows for dosing at 48-h intervals.

Similarly, oxytetracycline was also developed to combat shipping fever. The development of the Liquamycin® LA by Pfizer has been well documented in the literature (96). In this case, tetracyclines were well known to also be insoluble as well as irritating, upon injection. To alleviate this problem, the formulators identified 2-pyrrolidone as a solubilizer and developed methods of chelating the oxytetracycline with magnesium ion to reduce the irritation upon injection. The theory was to prepare a solution of drug that was close to saturation so that upon injection, the drug would slowly deposit a fine precipitate, creating in effect a drug suspension depot at the injection site. This depot formulation would reduce the irritation and necrosis that had been previously observed. The resulting formulation succeeded in reducing the irritation and provided release of drug over 2 to 3 days.

Topical Dosage Forms for Food-Producing Animals

Various classes of long-acting topical formulations have been used in food-producing animals (Table 8). Historically, the application of topicals for food-producing animals has been primarily for ectoparasite control. The short-term formulations were applied by hand as dusts, ointments, sprays, and/or liquids. Dips have also been used in which a vat is prepared containing the active ingredient, and the cattle is trotted down into the vat and run up a ramp on the other side. Each of these formulation types, however, would only provide treatment for a few days at the most, because they would inevitably be rubbed off by the animals or washed off by the rain. Therefore, it became necessary to develop methods for prolonging the delivery of active agents over longer periods of time so that the animals would not have to be handled frequently (97).

Table 8. Classes of Long-Acting Topical Formulations for Food Animals

Class of formulation	References
Oil-based liquids; spot-ons	97
Wax bars/cables/dust bags	97
Ear tags, e.g., PVC matrices	98
Ear tags, reservoir type	99,100
Microencapsulation formulations	101

The earliest controlled-release dosage forms for topical delivery were oil-based, which promoted the adhesion of the drug to the skin. Another early approach was to create a system in which the animals repeatedly dosed themselves. This was the principle behind the oil cables, wax bars, and dust bags that were impregnated with the active agents and left hanging near the locations in which the animals resided (97). The cattle would rub against the cable, bar, or bag and then rub itself or others, administering the active agent. The disadvantage of these systems was that the level of dosing could not be controlled and relied heavily on the behavior of the animal.

Eventually, people recognized the utility of placing the active ingredients into polymer matrices such as poly(vinyl chloride) (98). In these cases, the drug substances were blended into a monolithic structure and molded into a tag that was, for example, fixed on the ear. The tag then released the active agent over a prolonged period of time, such as several months. The active ingredient was transferred over the body of the animal by the natural rubbing motion of the animal on itself, as well as onto other animals. This dosage form is the most common in use today for the controlled release of topical ectoparasiticides.

In spite of its broad use, the monolithic tag concept does have disadvantages. For example, the tag delivers the largest portion of the active agent in the first part of the efficacious life span of the product. This is because the high concentrations of active agent provides a large driving force for delivery. In the latter half of the product life, the amount of drug substance delivered is greatly reduced because of the lower amount of active agent remaining in the matrix. Moreover, drug utilization is poor, and only a fraction of the active agent that is loaded into the matrix is actually released. Because of these limitations of the monolithic tag, a second generation of tag devices was developed in which the release profile was more zero-order, or more uniform, over the life of the product. This resulted in products that utilized a greater percentage of the total active agent loading (99–101). Such devices are based on reservoir technology rather than matrix technology. The tag is comprised of a depot of the active agent imbedded into

a drug reservoir within the tag, which is covered by a membrane whose properties control the release of the active ingredient. Because the active agent exists as a solid in the depot, the rate of release is governed by the vapor pressure of the active, its solubility in the membrane, and its diffusivity through the membrane. These types of tags can also release drug substance to the animal for several months (99).

Microencapsulation has also been explored for the prolonged delivery of topical ectoparsiticides. For example, Despins et al. (101) developed a microencapsulated formulation containing permethrin and compared it with an emulsifiable product. The authors found that the microencapsulation product prolonged its efficacy but only by a short period of time. The release of the active ingredient to the skin appeared to be limited by the residence time of the formulation on the skin.

In addition to those formulations just described, there exist pour-on or spot-on applications, such as IVOMEC pour-on. These dosage forms are low-volume products that are applied (poured) directly over the back of the animal. In the case of IVOMEC pour-on, the prolonged pharmacokinetics of the active ingredient, ivermectin, is the main reason for the long-acting efficacy. Ivermectin is efficacious in very low quantities, and at a dose of 5 mg/10 kg body weight, enough of the active agent is absorbed to be efficacious for up to 28 days (102). A similar duration length is observed for other avermectin-type pour-on products containing ingredients such as duramectin and moxidectin.

Controlled-Release Technologies in Companion Animals

The therapeutic applications for companion animal health are as diverse as those already discussed for the food animal species. Those areas that will be discussed in this section include parasite control technologies; chemotherapeutic parenteral systems such as antibiotics, insulin, and estrous control; and finally ophthalmics. Products available for dogs and cats will be primarily reviewed, with the understanding that similar technologies could be employed for the other species, and in fact the exact same products are typically used and adapted for use in more exotic species.

Parasite Control. One of the largest markets in companion animal drug delivery is in endo- and ectoparasite control and elimination. In ectoparasite control, the most popular compounds are included in the Interceptor (Norvartis) and Heartgard (Merial) products. These are milbemycin based and ivermectin based, respectively. The main reason for the long-acting nature of these orally administered dosage forms is the high potency of the compounds combined with their long biological half-lives. This allows for small dosages to be formulated into tablets that are easily given to companion animals, in particular dogs, at monthly intervals.

The most traditional mode of ectoparasite control is the ubiquitous flea collar. First developed in the late 1960s from vinyl resins containing dichlorvos, these collars have progressed to a variety of polymers containing an equally broad spectrum of active agents. The main basis of the technology of these collars is the incorporation of an active ingredient blended into the plastic matrix. The basic incompatibility between the plastic and the liquid and/or solid active agent forces the active to migrate to the surface of the collar, allowing it to be available to the fur of the animal, thereby eliminating the parasites.

Other technologies have also been explored for the release of ectoparasiticides. Reservoir systems in which the active agent is incorporated into a depot that is surrounded by a rate-controlling membrane have been explored, as have mechanical approaches (such as pumps) that release the active agent slowly over a long period of time. A history of ectoparasiticide collars has recently been published that discusses the development of the technologies used in this area from the vinyl collars to the recent technologies of today (L.C. Witchey-Lakshmanan, unpublished data).

The two most dramatic improvements in ectoparasite control have been in the development of spot-on products and orally active compounds, which provide protection for as long as 1 month per administration. Spot-on products can be applied with only a few milliliters of liquid along the back of the animal or at the base of the neck, and the duration of action of the active ingredient is sufficient to allow for control over approximately 30 days. Examples of these products include Frontline® TopSpot by Merial, Advantage® by Bayer, and Ex-Spot® by Schering-Plough (103). The staying power of these medications depends on the unique properties of the active agents and excipients with which they are compounded. For example, the active ingredient in Frontline is purported to remain unaffected by rain or washing because it sequesters into the sebaceous oils of the animal and releases slowly from there.

Program® and Sentinal® from Novartis also provide month-long protection; however, the initial presentations were in oral tablet form and are not effective against adult fleas. In this case, the long half-life of the drug substance allows for the long-acting control of the ectoparasites, similar to the mode discussed for the endoparasite products. More recently, Novartis has released an injection suspension in a prefilled syringe for which they claim 6-month efficacy against fleas. This is currently available for cats but is contraindicated for dogs due to injection site irritation.

Parenteral Chemotherapeutic Systems ***Antibiotics and Cancer Therapies.*** In companion animal medicine, it can be advantageous to formulate the therapeutic ingredient into a sustained-release injectable dosage form that would allow administration of the active ingredient by the veterinarian at the clinic and would obviate the need for the pet owner to have to administer tablets. The administration of tablets can be quite challenging for the owner of a companion animal, especially for those who own cats, because the animal will often spit the tablet or liquid out of its mouth if the flavor is not to its liking. Indeed, once an adverse taste or feel of an oral preparation has been established to the feline patient, the owner will most likely find the animal under the furniture or behind a cabinet at the next dosing time. Therefore, a long-acting injection can

improve the convenience to the owner, improve "patient compliance," and reduce the stress of the administrator.

As with long-acting injectable products used in food-producing animals, most of the long-acting injectable formulations discussed in other parts of this encyclopedia, such as implants, PLGA microspheres, liposomes, and so on, have also been investigated in companion animals. In contrast to human medicine, the use of advanced drug delivery approaches in animals is still primarily used only experimentally. For example, antimicrobial-laden poly(methyl methacrylate) beads have been used in human medicine since the 1970s for the treatment of internal infection. These beads are typically on a wire "string" and surgically implanted into the location of interest. Once the infection is eliminated, these beads are then surgically removed. A similar application can be found in experimental companion animal medicine for the treatment of osteomyelitis and other internal infections (104). Naturally, one would wish to avoid the second surgery for the removal of the polymer beads once they are spent. This would lead one to the development of a biodegradable system that would deliver the active agent and then be absorbed by the body. Examples of such work can be seen by Garvin et al. (105) and Gupta et al. (106). Here, polylactide–glycolide-type polymers were prepared as microspheres or compressed rods and administered to dogs. Although these studies were developed for eventual use in humans, these still demonstrate the feasibility of such drug delivery approaches in the canine itself.

Liposomes have also been used for a variety of infections and cancers in animals (107–110). Gentamicin can be encapsulated for injectable delivery (107), as can other chemotherapeutic agents (108). Kruth (109) has presented an interesting article on the delivery of various biologically active agents for treatment of infections and cancers in companion animals. Included in this review is the use of liposomes in small-animal practice. Collagen implants loaded with chemotherapeutic products have also been used in companion animals for intratumoral treatment of skin cancers in veterinary patients (110).

Insulin. The types of insulin used for the treatment of diabetes in dogs and cats are often those also used in humans. For example, diabetes can be treated in humans by using porcine or beef insulin. This is acceptable because human insulin is similar to bovine and nearly identical to porcine insulin, differing only by one amino acid. Similarly, dog insulin is identical to porcine insulin and cat insulin is nearly identical to bovine insulin, which also only differs by one amino acid group (111). Now that recombinate human insulin is available, companion animals can be treated with that as well.

The insulins currently available on the market for use in animals include short-, intermediate-, and long-acting insulins. Short-acting insulin is designed to be released for the immediate treatment of high glucose levels in the animal. Intermediate, or lente, insulin is typically given to the animal twice per day, with feedings scheduled according to the injection times. Long-acting, or ultralente, insulin can be used for once-a-day delivery. In addition, there are several combinations of insulin that have been specifically formulated to provide certain release profiles and are available on the market. Greco et al. (111) present an excellent table of the types of insulin that are available commercially for companion animal use.

For the most part, the pharmacokinetics of these three types of insulin is determined by the crystal size of the insulin itself. For example, lente insulin is composed of 30% prompt zinc–insulin crystals and 70% extended insulin zinc. The small zinc–insulin crystals allow for a slower release than what would be observed over a regular insulin preparation but still allows for fairly complete dissolution into the bloodstream. In contrast, ultralente insulin is compose of large zinc crystals that dissolve more slowly.

As in humans, research continues in the exploration of implanting islet cells into animals to produce insulin under more naturally modulated circumstances. In brief, the islets are generally encapsulated into a hydrophilic polymer that allows the glucose to migrate into the cells and allows the insulin to migrate out. In addition, implantable reservoirs containing insulin have been formulated in hydrogel-type materials to provide a similar effect. Various types of glucose-sensitive moieties are placed onto the polymer, which will cause the polymeric material to expand in the presence of glucose. The expansion in the polymer network allows for the unhindered diffusion of the insulin out of the reservoir. Once the glucose level decreases, the moieties respond by causing the contraction of the polymeric material, thereby trapping the remaining insulin within the reservoir and impeding its diffusion out of the hydrogel. Both of these approaches are in the experimental stage. Further reading on this topic can be found in Refs. 112–115.

Estrous Control. Estrous control in companion animals is important for many reasons, from controlling the numbers of the canine and feline population to synchronizing the estrous in a manner predictable for breeders. To this end, several products are available, but most of them are not long acting. Some research has explored the use of a medroxyprogesterone acetate product for canine population control. This product, known as Perlutex Leo® in Norway, has become popular in replacing surgery and has reduced the number of dogs in various locations (116). However, the use of the product has also been associated with the formation of uterine lesions and canine mammary tumors (116,117).

The potential use of testosterone implants has been examined in a few studies for the purpose of inhibition of estrous in dogs (118,119). For example, Vincent et al. (119) have examined the plasma concentrations of testosterone in castrated dogs following the administration of implants composed of poly(dimethylsiloxane) capsules that were filled with various amounts of testosterone.

Bone Growth Therapies. In the last 10 years the presence and activity of bone morphogenic proteins (BMP) have become known. These are biological factors whose function is to differentiate mesenchymal cells into chondroblasts and osteoblasts, inducing the formation of bone. Interestingly, these factors can be included into implants that can be placed into fractures to promote healing in instances that would not normally heal properly on their own.

A review of the development of delivery devices containing BMPr has been published (120). This review primarily discusses the patents issued that discover the BMPs as well as those regarding the delivery devices and methods. A review of BMP technology as it relates to veterinary medicine has also been published (121). Kirker-Head discusses the function of BMPs, the delivery devices, and other potential applications from bone graft replacement to soft tissue joining with bone.

Ophthalmic Drug Delivery

Historically, ophthalmic dosage forms have been ointments or drops that are cleared from the eye quite quickly, requiring that the medicine be delivered several times in a day. When the challenges of dosing ophthalmic drops to a 50- to 500-kg animal by holding it still enough to apply the medication and repeating this activity several times a day are considered, one can easily see the need for a long-acting ophthalmic dosage form.

A thorough review of ocular delivery in veterinary medicine has been presented recently by Baeyens et al. (122). They include a discussion of ocular diseases and the agents used to treat them, an excellent list of the available products currently on the market, and a disclosure of the technologies being explored to prolong the release of the active agents.

The typical excipient added to prolong the release of an ophthalmic product is a hydrophilic polymer, such as a cellulosic, which increases the viscosity of the ophthalmic solution and increases the duration of the solution in the conjunctival sac. Another method that has been used is to add gums such as gellan or carrageenan that cross-link in the presence of the calcium ions in the tear fluid. This cross-linking also increases the viscosity and thereby the residence time of the product in the eye. A final mechanism found in aqueous gels is to use poloxamers, which can be formulated as liquids at room temperature but will gel at body temperature.

Inserts and implants have also been developed for ophthalmic drug delivery. Soluble inserts are most desirable because they do not have to be removed. However, some of these inserts have been shown to be irritating to the eye (122). Gurtler et al. (123) discuss the development of a veterinary insert that releases gentamicin for the treatment of ocular infections. This device is prepared with a combination of ethylcellulose and carbomer (poly[acrylic acid]) and can provide efficacious drug levels for as long as 72 h. A silicone implant has also been used experimentally for the treatment of glaucoma in dogs (124). However, these implants required surgical removal once the therapy was complete.

Protein and Peptide Delivery

Somatotropins. Somatotropins (growth hormones) are protein hormones produced by the anterior pituitary that stimulate growth in virtually all vertebrate species (125) as a result of direct receptor stimulation and stimulation of insulinlike growth factor I (IGF-I), a related anabolic protein hormone (126).

The gastrointestinal tract is a hostile environment for somatotropins. Administration by this route results in extensive degradation. In addition, because of the size and physicochemical properties of somatotropins, they are poorly absorbed via this route. The administration route of choice is parenterally. However, somatotropins are relatively large water-soluble molecules with a molecular weight of approximately 21,000 comprising 191 amino acid residues and contain two disulphide linkages. In addition, these molecules have a tendency to form aggregates within both the delivery system and in the biological environment that are biologically inactive or poorly absorbed. As a result of these features, somatotropins present challenges to the formulation scientists developing controlled-release parenteral drug delivery systems. Several important factors must be considered when formulating somatotropins into controlled-release parenteral drug delivery systems. Such factors include the following (125,127–130):

Properties of the Somatotropin.

- Stability of the protein drug during drying, formulation, manufacturing, and postadministration must be ensured. Somatotropin degradation can occur through aggregation, deamination or oxidation.
- The inherent bioactivity of the somatotropin will dictate, amongst other things, its selection and dose size.
- Physiochemical properties of the protein such as isoelectric point, molecular weight, amino acid composition, aqueous solubility at different pHs, and salt concentrations and organic solubilities are also important.

Properties of the Formulation

- Shelf-life stability should be as long as possible. One method to prolong the chemical shelf-life of a somatotropin product is to manufacture and store the formulation in the dry state, for example, as a pellet or implant. Alternatively, oily preparations can be formulated. To increase the physical stability of liquid preparations, viscosity-inducing agents can be added to the formulation.
- Commercially feasible delivery systems must be small to be easily administered. Given the high level of active-agent loads in the delivery system required to achieve therapeutic levels over extended periods of time, the size of the delivery systems may becoming the rate-limiting factor in their success.
- A zero-order release profile seems preferable, but most drug delivery systems currently available release somatotropins through a pseudo-first-order process. Pulsed delivery offers an alternative and mimics the natural method by which somatotropins appear in the blood.
- The duration of delivery of somatotropins to farmed animals is at least 1–2 weeks and up to 6 weeks. Such extended times offer stability and efficacy challenges, given the other factors discussed in this section.
- Administration must be able to be integrated into different management practices. The administration

Next Page

procedure must also be relatively free from discomfort for the animal, and the delivery systems must not cause local irritation or a reaction while in the animal. For parenteral applications, solutions are easier to administer compared with implants, which may require specially designed implanters with large-bore needles.

- The bioactivity of the somatotropin needs to be considered and maintained throughout the shelf-life of the delivery system.
- The formulation needs to be such that aggregation of the somatotropin is avoided or minimized throughout the shelf-life of the sustained-release system.
- Interaction between the somatotropin and formulation should be considered and avoided to maximize shelf-life stability.
- The price of the controlled-release delivery system must be cost effective to realize commercial potential.
- The delivery system must be designed to efficiently utilize the incorporated dose.
- The delivery system must be reasonably aesthetic to appeal to the end-user. It must also be easily administered, offer improvements in control of therapy, adapt to farm management practices, be safe to the end-user and to the environment, and offer increased return on investment.

Considerations during Manufacture

- The bioactivity of the somatotropin needs to be considered and maintained during manufacture.
- Interaction between the somatotropin and formulation ingredients during the manufacture process should be identified and avoided.
- Issues such as method of drying the protein, storage conditions before and during processing, formulation processing conditions (e.g., light, time, heat, shear, etc.) and sterilization must be taken into consideration.

Considerations after Administration

- After administration, the formulation will absorb water from the surrounding environment and hydrate. This will result in the somatotropin existing at high concentrations in an aqueous environment and being exposed to elevated temperatures (37–39°C) for the duration of release. Thus, the aqueous stability of the somatotropin must be considered and known in the development of a controlled-release delivery system. Indeed, the in vivo stability of the somatotropins is the primary limitation for extending the duration of release, and formulators must investigate a variety of methods to improve to aqueous stability of somatotropins when their delivery system is exposed to condition typical of the in vivo environment.
- Because the animal enters the food chain, the level of somatotropin in the tissues must be evaluated so that none is left at the time of slaughter.
- The bioactivity of the somatotropin needs to be considered and maintained after implantation in the animal.
- The formulation needs to be designed such that aggregation of the somatotropin is avoided or minimized within the biological milieu.
- Interaction between the protein drug and formulation in the in vivo environment should be considered and investigated.

Table 9 documents various somatotropin drug delivery systems.

Other Peptides and Proteins. Many of the same controlled-release delivery systems that have been developed for somatotropins have been evaluated for the delivery of other proteins and peptides to animals. A prerequisite to the transfer of technologies between proteins is an inherent knowledge of the physicochemical properties of each individual protein or peptide prior to successful transposition of the technology. A delivery system and manufacturing process appropriate for the formulation of one protein or peptide may not be appropriate for a second. Table 10 documents delivery systems investigated for various protein and peptide compounds.

RECENT INITIATIVES

Vaccine Delivery

The market share for veterinary vaccines represents approximately 1% of the total world pharmaceutical market. With the increasing cost of research and development, production, licensing, and marketing of all medicinal products—including immunological veterinary products, their development, and clinical application—must be carefully considered. This section summarizes recent developments in the area of immunological veterinary products and discusses their potential applications. In addition, the specific application of molecular biology for the diagnosis, therapy, and basic investigation of diseases in animals is discussed.

The purpose of a vaccine is to protect a human or an animal against future exposure to an organism or pathogen that could potentially cause disease. Immunological veterinary products such as veterinary vaccines contribute greatly to the health of animals and reduced economic losses resulting from diseases, increase productivity, and ensure high-quality food for the customer.

There are two important issues that must be considered when formulating a veterinary vaccine: (*1*) the ability of the vaccine to protect against disease, that is, the need to identify what kind of immune response best controls the exposure to a particular pathogen and (*2*) the potential tissue damage that the vaccine may cause at the injection site. It is important to select the best vaccine for a particular pathogen or disease; the failure of the vaccine to protect against the particular disease for which it is administered results in animals that become ill later and therefore require additional treatment and costs. The dosage form, dose, route, and frequency of administration of a vaccine all play important roles in ensuring that an effective immune response is stimulated (186,187). The traditional means of evoking an immune response to an an-

Previous Page

procedure must also be relatively free from discomfort for the animal, and the delivery systems must not cause local irritation or a reaction while in the animal. For parenteral applications, solutions are easier to administer compared with implants, which may require specially designed implanters with large-bore needles.

- The bioactivity of the somatotropin needs to be considered and maintained throughout the shelf-life of the delivery system.
- The formulation needs to be such that aggregation of the somatotropin is avoided or minimized throughout the shelf-life of the sustained-release system.
- Interaction between the somatotropin and formulation should be considered and avoided to maximize shelf-life stability.
- The price of the controlled-release delivery system must be cost effective to realize commercial potential.
- The delivery system must be designed to efficiently utilize the incorporated dose.
- The delivery system must be reasonably aesthetic to appeal to the end-user. It must also be easily administered, offer improvements in control of therapy, adapt to farm management practices, be safe to the end-user and to the environment, and offer increased return on investment.

Considerations during Manufacture

- The bioactivity of the somatotropin needs to be considered and maintained during manufacture.
- Interaction between the somatotropin and formulation ingredients during the manufacture process should be identified and avoided.
- Issues such as method of drying the protein, storage conditions before and during processing, formulation processing conditions (e.g., light, time, heat, shear, etc.) and sterilization must be taken into consideration.

Considerations after Administration

- After administration, the formulation will absorb water from the surrounding environment and hydrate. This will result in the somatotropin existing at high concentrations in an aqueous environment and being exposed to elevated temperatures (37–39°C) for the duration of release. Thus, the aqueous stability of the somatotropin must be considered and known in the development of a controlled-release delivery system. Indeed, the in vivo stability of the somatotropins is the primary limitation for extending the duration of release, and formulators must investigate a variety of methods to improve to aqueous stability of somatotropins when their delivery system is exposed to condition typical of the in vivo environment.
- Because the animal enters the food chain, the level of somatotropin in the tissues must be evaluated so that none is left at the time of slaughter.
- The bioactivity of the somatotropin needs to be considered and maintained after implantation in the animal.
- The formulation needs to be designed such that aggregation of the somatotropin is avoided or minimized within the biological milieu.
- Interaction between the protein drug and formulation in the in vivo environment should be considered and investigated.

Table 9 documents various somatotropin drug delivery systems.

Other Peptides and Proteins. Many of the same controlled-release delivery systems that have been developed for somatotropins have been evaluated for the delivery of other proteins and peptides to animals. A prerequisite to the transfer of technologies between proteins is an inherent knowledge of the physicochemical properties of each individual protein or peptide prior to successful transposition of the technology. A delivery system and manufacturing process appropriate for the formulation of one protein or peptide may not be appropriate for a second. Table 10 documents delivery systems investigated for various protein and peptide compounds.

RECENT INITIATIVES

Vaccine Delivery

The market share for veterinary vaccines represents approximately 1% of the total world pharmaceutical market. With the increasing cost of research and development, production, licensing, and marketing of all medicinal products—including immunological veterinary products, their development, and clinical application—must be carefully considered. This section summarizes recent developments in the area of immunological veterinary products and discusses their potential applications. In addition, the specific application of molecular biology for the diagnosis, therapy, and basic investigation of diseases in animals is discussed.

The purpose of a vaccine is to protect a human or an animal against future exposure to an organism or pathogen that could potentially cause disease. Immunological veterinary products such as veterinary vaccines contribute greatly to the health of animals and reduced economic losses resulting from diseases, increase productivity, and ensure high-quality food for the customer.

There are two important issues that must be considered when formulating a veterinary vaccine: (*1*) the ability of the vaccine to protect against disease, that is, the need to identify what kind of immune response best controls the exposure to a particular pathogen and (*2*) the potential tissue damage that the vaccine may cause at the injection site. It is important to select the best vaccine for a particular pathogen or disease; the failure of the vaccine to protect against the particular disease for which it is administered results in animals that become ill later and therefore require additional treatment and costs. The dosage form, dose, route, and frequency of administration of a vaccine all play important roles in ensuring that an effective immune response is stimulated (186,187). The traditional means of evoking an immune response to an an-

tigens to achieve adequate and lasting immunity is to administer it at timed intervals (initial and booster shot[s]) (Table 11).

Conventional vaccine formulations possess inherent disadvantages, and as a result, researchers have recently been focusing on the development of more suitable vaccine formulations. One approach has been the delivery of an antigen from an oil-based vehicle such as Freund's adjuvant (188). Such an approach has resulted in the reduction of the number of doses needed; however, because of the toxicity of the oil-based adjuvants, the search for a safer and more potent adjuvant continues. This search has resulted in the formulation of antigens into delivery systems that administer the antigen in particulate form rather than as soluble molecules. This approach facilitates recognition by the phagocytic systems and results in presentation of the antigen to the lymphocyte (189). Several particulate systems have been studied as vaccine delivery systems. These include emulsions, liposomes, nanoparticles, and microparticles. Each of these approaches are discussed in more detail in the following sections. The advantages of such vaccine delivery systems is that they can provide the ability to deliver antigens in a continuous manner or result in more control over the production of antibodies (190).

Emulsions. The manufacturing procedure of vaccine emulsions is relatively simple: The antigens are dissolved in a water phase and then emulsified in the oil in the presence of an appropriate emulsifier. The physicochemical characteristics of the final emulsion play an important determinant in the efficacy and handling of the vaccine. The controlled-release characteristics of an emulsion and dependent on certain properties of the emulsion, such as the viscosity of the oil phase, the oil–water phase ratio, and the emulsion droplet size. For example, a high oil content can cause unnecessary injection site irritation, and too large a droplet size can result in a physically unstable product, thereby reducing its shelf-life. Some problems may be observed with the oil/water emulsion type, but these can be overcome with multiple emulsion formulations (water/oil/water).

Foot and mouth disease (FMD) is as a highly contagious disease of domesticated and wild animals. FMD outbreaks can have devastating effects on the agricultural economies of developed, particularly FMD-free, countries, owing to the direct cost of control and indirect cost of trade embargoes. Oil-based FMD vaccines have been used in the field for many years, particularly in cattle in South America (191). Two novel oil-based FMD vaccines (FMDVs) were investigated by Salt et al., who examined their protective ability in pigs (191). In this study, the FMDV was formulated with new-generation, ready-to-formulate, mineral oil–based adjuvants. Basically, type C1 Oberbayyern FMDV antigen concentrate was emulsified using ISA 206 (Seppic, Paris) or ISA 25 as a water/oil/water or oil/water emulsion. Both formulations were shown to protect pigs against FMD virus within 4 days of vaccination. However, reimmunization was shown to be necessary after 21–28 days because of the continued risk of challenge.

Similar emulsion formulations were developed to protect a wild population of elephants against a natural outbreak of diseases caused by encephalomyocarditis virus (EMC) (192). The economic concerns associated with a wild population of elephants contracting EMC is that if the EMC virus spreads to swine, it may result in high piglet mortality due to myocarditis and respiratory failure (192). The experimental vaccine developed by Hunter et al. was tested in elephants, mice, and pigs. Their results showed that elephants vaccinated with the EMC vaccine formulation developed high antibody titers, whereas controls developed fatal or subclinical myocarditis. Similar results were also observed in mice and pigs. The vaccinated animals showed persistent antibody responses after a single vaccination and a lack of reaction to the adjuvant used (192). Their results suggested that the vaccine may be useful in wildlife species in zoos.

Perhaps nowhere in veterinary medicine has the practical application of vaccinations been more visible and rewarding than in the development of vaccines and diagnostics to assist in the control and eradication of pseudorabies (PR). Pensaert et al. (193) developed an emulsion vaccine formulation for PR in pigs (Aujeszky's disease). In this study, Aujeszky's disease vaccines and their ability to induce an immune response, which suppresses virus excretion optimally upon infection, were compared. All the pigs were vaccinated with glycoprotein deletion vaccines suspended in phosphate-buffered saline (PBS). Two additional groups were vaccinated with a gI-deleted vaccine virus suspended in an oil/water emulsion–excreted vaccine 2–6 days after injection. A 100- to 1,000-fold reduction in excreted virus titers was observed in vaccinated pigs compared with unvaccinated ones. Some vaccines suppressed virus excretion better than others, but no correlation could be made between the type of deletion and the degree of reduction in virus excretion. Similar results were obtained with two applications of inactivated vaccines. The lowest number of excreting pigs, the lowest duration of excretion, and the lowest titers were obtained in groups vaccinated with the attenuated vaccine suspended in emulsion (194).

Gliding bacterial adjuvant (GBA) has been characterized as a potent immune modulator, stimulating the growth of murine B lymphocytes in mice, inducing murine natural killer-cell activity, and promoting the release of several murine cytokines. Zeidner et al. tested gliding GBA emulsion formulations for their ability to activate feline peripheral T cells to secrete cytokines and to potentiate specific antibody responses in cats against a well-characterized T cell–dependent antigen and a recombinant immunogen derived from *Dirofilaria immitis* (194). The results of the trial showed that GBA also appeared to be a potent stimulator of feline T cell proliferation and induced both IFN and IL-2 production in cats. GBA has relatively low local and systemic toxicity and exhibits potent activity, both in PBS or within an oil vehicle. These characteristics make GBA an attractive new adjuvant for use in feline vaccines (194).

Liposomes. A variety of lipids have been used to create bilayer liposomal structures. Phospholipids were among the first chemicals used to form bilayer structures to mimic

Table 9. Parenterally Administered Somatotropin Controlled-Release Drug Delivery Systems

Delivery system type	Formulation of delivery system	Drug	Factors affecting release and stability	Disadvantages
Nonaqueous gels	Biocompatible vegetable oil (e.g., sesame oil, peanut oil) containing a dispersion of the somatotropin and incorporating thickening agents (e.g., aluminium monostearate, white beeswax, yellow beeswax). Appropriate amounts of thickening agent need to be added to achieve a compromise between physical stability and ease of injectability (126). Examples of nonaqueous gels for the delivery of somatotropins can be found in references (131–134)	N-terminated bovine somatotropin zinc salt (135) Bovine somatotropin (136)	Absence of water within the formulation results in a relatively long-term shelf-life. Viscosity of formulation can be modified to increase duration of release; can be achieved by selecting an oil from the range of hydrophobicity of oils or addition of excipients (e.g., esters of glycerol) or thickening agents. Improvement of the shelf stability, drug loading, injectability, and injection site; chemical and physical stability of the somatotropins, once injected into the animals, can also be achieved by alteration of the viscosity of the formulation.	Injectable nonaqueous gels form variable-shaped depots, which may affect the release profile from animal to animal (125) Release profiles are not zero order.
Microparticles (microspheres or microcapsules)	Microsphere matrix prepared from lactide/glycolide copolymers (D,L-lactide 50:50) using an anatomization process in liquid nitrogen containing about 10% drug load (137) Microsphere matrix prepared from glyceryl tristearate or glyceryl distearate using a spray prilling technique; microspheres containing 24.5% were suspended in soybean oil/ Miglyol®812 and administered subcutaneously (138). Microspheres of polyglycholic acid (139).	Human growth hormone Bovine somatotropin Porcine somatotropin	Fat-based formulations provided better physical stability and shelf-life for glyceryl tristearate or glyceryl distearate microspheres when reconstituted in an oil vehicle (140). Aggregation of somatotropin reported to occur within the polymer	Animal growth-rate studies suggest that the release profiles from such formulations are not zero order.
Liposome	Egg phosphatidylcholine, ethanolomine, and α-tocopheryl hemisuccinate and Tris salt vescicles (141) Hydrogenated soy phosphatidylcholine–cholesterol hemisuccinate liposomes (142)	Bovine somatotropin Bovine somatotropin	Coformulation of liposomes with other delivery systems may provide opportunities to exploit liposomes as delivery systems for somatotropins, e.g., Refs. 143–145.	Low product loadings, difficulty and cost of manufacture, and stability issues are associated with the use of liposomes as delivery systems for somatotropins.
Emulsion (multiple water-in-oil-in-water type)	Appropriately buffered aqueous phases (e.g., carbonate-buffer) and oil phases (e.g., mineral oil) and stabilizing agents (e.g., sorbitan surfactants) (146,147)	Bovine somatotropin	Somatotropin was incorporated into the primary aqueous phase. Multiple emulsion was achieved using polyoxyethylene sorbitan surfactants.	
Aqueous solutions gelled with polymers	Aqueous injections using carbohydrate polymers such as dextrins, heteropolysaccharides, and various gums (148)	Bovine somatotropin		Injectable nonaqueous gels form, variable-shaped depots that may affect the release profile from animal to animal.

Aqueous conjugates (suspended complex)	HGH- and BST-prepared conjugates with bovine serum albumin using glutaraldehyde or with immunoglobulin using carboimide (149)	Bovine somatotropin	The conjugated molecule exhibited increased solubility over BST alone in solutions of pH less than 5 (149)	
Hydrogels	Somatotropins suspended in silicone oil and placed into hydroxyethyl methacrylate–methyl methacrylate copolymer and hydroxyethyl methacrylate homopolymer cross-linked with ethyene glycol dimethacrylate cylindrical reservoirs that acted as a rate-limiting membrane have been described (150) Small spheres of somatotropin–chitosin (60:40) coated with a hydrogel comprising poly(vinyl alcohol) have also been described (151) In a matrix system, biodegradable thermoplastic hydrogels consisting of ABA or AB block polymers, where the block A is a glycolide and block B is polyethylene oxide or in the case of an ABA block polymer, a glycolide and trimethylene carbonate (152) Delivery systems comprising polymers of D,L-lactide–glycolide containing poly(ethylene glycol) (153)	Ovine, equine, and bovine somatotropins Porcine somatotropin Bovine somatotropin Bovine somatotropin		
Implants	A variety of methods are described in the patent literature, which describe the formulation and manufacture of both uncoated (154–158) and coated implants (by either a spray technique (e.g., ethyl cellulose/poly(ethylene glycol), poly(vinyl alcohol), poly(ethylacrylate methylmethacrylates) (159–162) or dip coating (e.g., molten blend of beeswax, carnauba wax, and Mazol®) (163). Controlled release from implants have also been achieved by placing the implant inside silicone tubes which had their ends covered by microporous polyethylene disks each having a 70-μm pore. The release of somatotropin from silicone tube-covered implants was designed to occur from the ends of the tubes (164).	Porcine somatotropin Bovine somatotropin Silicone tube-covered implants were prepared containing 40 mg of porcine somatotropin alone or 40 mg porcine somatotropin with sucrose.	Factors affecting release from coated implants include thickness of coating, ratio of drug to excipients, type of excipients, degree of polymer cross-linking, surface area of the rate-limiting membrane, coating material, presence/absence of coating, and solubility of the somatotropin.	Implants contain somatotropins at much higher concentrations than injection formulations. This may impact on the stability of the somatotropin following administration. Implant administration requires a relatively large bore needle. Implantation requires the design of a more complex administration system than a hypodermic syringe. Implants generally require a more complex manufacturing process, particularly if an aseptic implant is required.
Osmotic devices	Several osmotic devices have been described in the patent literature. The constant delivery of drug from the devices relies on the incorporation of expandable excipients surrounded by a semipermeable wall into specially designed dispensers (165–169).	Porcine somatotropin		Cost of final product, final product size, administration difficulties, and delivery system recovery issues after slaughter limit the application of this technology to the administration of somatotropins.

Table 10. Delivery Systems for Various Protein and Peptide Compounds

Peptide or protein	Use	Formulation of delivery systems
Somatotropins	Increased milk yield Accelerated growth Increased feed conversion efficiencies Increase in lean-to-fat ratio Reduced fat deposition Increased ovulation	See Table 9.
Somatotropin releasing hormone (growth hormone–releasing hormone)	Increased milk production Accelerated growth Increased feed conversion efficiencies Increase in lean-to-fat ratio Reduced fat deposition Increased ovulation	Silicone rubber matrix (170) Collagen implant (171,172) Cholesterol acetate implants (173) 50:50 poly(D,L-lactide-*co*-glycolide pellets (174)
Luteinizing hormone–releasing hormone	Control of fertility Stimulation of spermatogenesis and ovulation	Compressed implants containing lactose and calcium phosphate and coated with Eudragit NE30 D (175–177); compressed core excipient ratios, percentage active present, and coating thickness affected rlease rate.
Luteinizing hormone–releasing hormone agonists (e.g., nafarelin acetate, leuprolide acetate)	Estrus suppression	Microspheres of various ratios of poly(D,L-lactide-*co*-glycolide (178–182) Silicone rubber implant (183) Crosslinked poly(orthoester) (184,185)

Table 11. Examples of Conventional Veterinary Vaccines on the Market

Vaccine	Animal	Disease
PHF-VAX-3	Horse	Tetanus, fever,
EWTF	Horse	Influenza, tetanus
MHB[a]	Pigs	Pneumonia
Prime Pac_R PRRS	Pigs	Respiratory viruses
Scourmune[R] CRT	Pigs	*Escherichia coli*
AR-Pac[R]	Pigs	Atropic rhinitis
Pliguard[R] *E. coli*-1	Calves	*E. coli*
Eclipse[R]3	Feline	Panleukopenia
Fevaxyn FeLV	Cats	Leukemia
Galaxy[R]D	Dogs	Distemper vaccine

cell membranes (195). Liposomes can induce both a humoral and cell-induced immunity, which is clearly an advantage when formulating a vaccine (196). In addition, liposomes can serve as carriers of antigens and adjuvants, as depots for the controlled release of antigens, and as targeting agents for the delivery of novel antigens and adjuvants to antigen-presenting cells (APCs). Although, liposomes have limited applications in veterinary medicine, the literature contains several encouraging experimental results that demonstrate their potential application in this field.

Nakanishi et al. showed that the pulsed administration of APCs with various antigens to mice resulted in the introduction of potent antigen-specific immune responses (197). These authors investigated the relationship between the liposome surface charge and the adjuvant action of liposomes in inducing immune responses to soluble antigen. Results revealed that the positive charge on the surface of the liposomes was important for enhancing their immunoadjuvancy in the induction of antigen-specific immune responses (197).

Enteric diseases remain one of the great causes of motility and morbidity in both human and veterinary species. However, mucosal surfaces are also the target of significant diseases. Although immunization strategies have been available for many years and have achieved significant success in the reduction of disease incidence and mortality when applied to diseases affecting organs, there has been a remarkable lack of success in vaccination to control mucosal disease (198). It has therefore become apparent that novel strategies are required to achieve effective defenses at such sites.

All mucosal surfaces, but particularly the intestine, represent a physiological dilemma whereby selective absorption of essential nutrients must occur with concomitant exclusion of pathogen (198). The oral route of immunization is a trustworthy way to induce mucosal IgA antibody responses. However, this immunization route has the problem of antigen degradation by gastric acidity and proteolytic enzymes in the intestinal lumen. The poor immunogenicity of ganglioside antigen such as ganglioside-GM1 is well documented (199). Therefore, the stability of ganglioside liposomes to acidic solution, bile, and pancreatic solution has been examined in the literature (200). Liposomes that contained the antigen ganglioside-GM1 demonstrated that their stability to acidic solution, bile, and pancreatin solution would permit them to effectively serve as an oral vaccine delivery vehicle for inducing mucosal immune response (200).

Saponin (201) and muramyldipeptide (MDP) (202) was used as an adjuvant to deliver ovalbumin (OVA) intraperitoneally (ip) in rats based on their availability, ease of preparation and previously demonstrated adjuvanticity in systemic immunization applications. The subsequent anti-OVA–containing cell response in the intestine was assessed in the study. The adjuvants were formulated in either vegetable oil emulsion or liposome vehicles, these formulations being biodegradable alternatives to the min-

eral oil component used in Freund's adjuvants. Results showed that both saponin and MDP exhibited adjuvant activity for IgA responses to OVA when administered ip. Although data showed that both MDP and saponin given in an emulsion provided an alternative to Freund's adjuvant for ip stimulation of IgA responses, the success of liposomes as a systemic antigen delivery system suggested their potential as an alternative vehicle for ip use. Although these alternatives have been developed for veterinary applications in which they have proved to be both effective and practical, they also show promise for the development of improved delivery systems for human mucosal vaccines (203).

Nanoparticles and Microspheres. Microspheres are defined as small particles typically no greater in size than 1 μm. Nanospheres are defined as colloidal particles with a diameter less than 1 μm. In contrast to liposomes, microspheres or nanospheres are prepared from polymers that can be manipulated according to the release requirements of the formulation. Preparation of these particles is discussed elsewhere in this encyclopedia.

The advantages of delivering vaccines in microparticles is that they may reduce the number of vaccinations required to give a prolonged protective response and/or that release of the vaccine can be controlled by a number of different mechanisms. Antigen is released from microparticles either by diffusion through pores or by erosion of the matrix. Among the acceptable polymers available to prepare microparticles, poly(lactic acid) and poly(lactide-*co*-glycolide) (PLGA) have been chosen the most often. These polymers are biodegradable, biocompatible, and FDA approved for use in therapeutic products (204). Veterinary applications of microparticulate vaccines are limited, but investigations in this area are increasing rapidly. For example, a two-bait delivery systems for oral immunization of dogs against rabies was tested in small-scale field trials in Tunisia (205). The bait consisted of a freeze-dried core unit containing a biomarker covered with a paraffin matrix. The baits were placed on transect lines, which offered the possibility to vaccinate certain categories of dogs that were not accessible via a dog owner–mediated approach. Unfortunately, the method offered less safety than other systems, was less specific, was not readily accepted by the human population, and was costly.

Immunization against luteinizing hormone–releasing hormone (LH-RH) may offer an interesting experimental tool and also a veterinary vaccine capable of increasing meat production by immunological castration. Production of antibodies against LH-RH has been reported in sheep, cattle, rats, rabbits, and primates (206). However, because this decapeptide is only a weak antigen, immunization has traditionally required repeated injections of the synthetic hormone conjugated to a carrier and emulsified in Freund's complete adjuvant. However, Carelli et al. investigated a more superior method of immunization by using the synthetic adjuvant MDP conjugated with polylysine (207). Results revealed that those synthetic haptens and the synthetic adjuvant MDP could be usefully coupled to the polymeric carrier. Moreover, LH-RH mixed with MDP or conjugated with MDP–lysine and injected in an aqueous medium produced a greater binding activity than that observed with Freund's adjuvant alone (207).

Yersinia pestis is the causative agent of pneumonic and bubonic plague. *Y. pestis* vaccine offers protection against bubonic plague; however, vaccinated animals acquired pneumonic plague (207). Therefore, the ability of the vaccine to confer protection against pneumonic plague is questionable. In addition, undesirable side effects are common immunity induced by the vaccine is short lived, and further doses (one given every 6 months) are required to maintain the same level of protection (208). Subunit vaccines using protective components from *Y. pertis* may avoid adverse effects but require adjuvants or appropriately formulated delivery systems to boost immunity (209). To achieve this, one approach is to encapsulate antigenic material within polymeric carriers such as PLGA. For example, F1 antigen from *Y. pestis* was encapsulated in PLGA microparticles, which induced high serum titers when injected ip in mice (209). In addition, mucosal IgA was also detected. The 1-μm-diameter PLGA microparticles gave effective protection against challenge with *Y. pestis* after only one dose, which may be due to the microspheres having depot-release properties; therefore, less antigen and fewer doses were necessary for protection (209).

It is known that small particles are able to cross the mucosal barrier and penetrate into the blood circulation when administered nasally. Animal experiments using microspheres induced significantly higher levels of serum antibodies to the antigen than when the free antigen was administered to the nasal mucosa. In a similar study, F1 and V subunits of *Y. pestis* were encapsulated in PLGA and administered intranasally to mice. Results revealed that encapsulated subunits induced significantly elevated serum antibody titers to F1 and V relative to free antigen, and served to protect 66% of the vaccinated animals from inhalation challenge (210).

Nonparenteral immunization, such as simple mucosal application of antigenic proteins (for example, in the gastrointestinal or respiratory tracts), is usually ineffective in terms of vaccination (211). This is a result of enzymatic or chemical destruction combined with poor absorption into subepithelial compartments. To overcome these problems, some form of an antigen delivery system needs to be formulated, for example, biodegradable microspheres that protect the antigen from enzyme degradation in the lumen. Several investigations suggest the applicability of such an approach. Atarki et al. (212) investigated the possibility of using an inert oral delivery system to stimulate mucosal antiphosphorylcholine immunity. Phosphorylcholine was noted to be a hapten present on different pathogenic bacteria such as *Streptococcus pnemoniae, Salmonella typhimurium, Proteus morganii*, and *Neisseria menengiditis* and on parasites such as *Ascaris suum* and *Trichinella spiralis*, which invade or colonize via the mucosa at different anatomical sites. Oral administration of biodegradable microspheres loaded with phosphorylcholine induced a specific IgA response in intestinal, pulmonary, and vaginal secretions as well as a strong specific immune response in female Balb/c mice (211).

Genetically Engineered Vaccines. Modern vaccine technology has now provided us, through genetic engineering,

the ability to use genetic material as a vector to protect animals and human against a variety of diseases (213). These vaccines, especially those constructed of genetically engineered proteins, are expensive. However, currently available (nongenetically engineered) vaccines are not cheap. In addition, many of them provide only temporary immunity, and the weaker the vaccine, the greater the dose necessary to stimulate an immune response and the greater the risk of overactivating the immune response, resulting in shock and death. Genetically engineered vaccines have the potential to overcome these latter problems; however, when the first genetically engineered hepatitis-B vaccine was developed, it cost $150 for three injections. The vaccine was safe and effective. Nevertheless, few farmers or pet owners would be willing to pay so costly a price for a vaccine. The issue surrounding the cost of genetically engineered vaccines is the current stumbling block in their acceptance and use in veterinary medicine.

The new generation of vaccines include subunit, synthetic peptide, and live recombinant vaccines, which contain only the most critical proteins involved in inducing protection, or live attenuated vaccines, in which specific genes involved in virulence have been deleted, with a low probability of back mutation and reservation to virulence. However, genetically engineered vectors offer the advantage of being able to carry multiple antigens from a variety of pathogens and therefore provide the opportunity for immunizing animals with delivery systems that would be adaptable to various species. Hence, the induction of various types of immune responses, depending on the agent and the animal being immunized, might be possible.

The first recombinant DNA-derived modified live vaccine was licensed for manufacture and sale in 1986. Gene-deleted PR vaccines (PRV) OMNIVAC-PRV and OMNIMARK-PRV were a major breakthrough for PR control and eradication (214). PR is caused by a herpes virus that induces acute or fetal infections of baby pigs and a variety of clinical symptoms in older animals. Cattle, sheep, dogs, cats, rodents, and raccoons are also susceptible to fetal PRV infections. The annual cost to the U.S. producer of a PR outbreak has been estimated at $30–72 million. Unfortunately, vaccination does not prevent latent infection by field strains. Neither modified live virus (MLV) or inactivated conventional PRV vaccines have prevented infection. To maximize safety, a purified clone of a Bucharest (BUK) vaccine strain of PRV was chosen as the starting material for the genetic engineering of OMNIVAC-PRV and OMNIMARK-PRV. Although total eradication of PRV may be unrealistic, previous studies have shown that a saturation vaccination program using OMNIVAC-PRV with culling is effective without having to resort to depopulation.

The forms of antigen and its formulation have a significant influence on vaccine efficacy and on the duration of immunity. This is particularly important if the immunity is cell mediated or mucosal. With viral infections, the major targets for immunity are often surface glycoproteins that are found in mucosa. Hence, the surface glycoproteins are important for the attachment and entry of the virus to host cells; consequently, a virus vaccine in one species might be used in another. Babik et al. tested this hypothesis using purified glycoprotein B and C of the herpes virus to use as an experimental vaccine in cattle (215). In all cases, the purified protein induced neutralizing antibodies, and more importantly, calves were protected from infection.

The other type of live recombinant vaccine uses the most studied poxvirus, vaccinia virus (VV), as a vector, by incorporating immunogenic genes of disease agents into the VV genome (216). Vaccinia was used for almost 200 years as a vaccine for smallpox. A large variety of genes have been expressed in vaccinia virus recombinants, including enzymes, clotting factors, hormones, and importantly, genes that encode for protective immunogens. These latter genes have been derived from other viruses, bacteria, and parasitic organisms. This can be exploited to produce a recombinant vaccine directed toward multiple pathogens pertinent to a specific population. One of the potential advantages of the poxvirus vector is its large volume, which has a large capacity available for the insertion of multiple foreign genes. In addition, unlike many live vaccines, the lyophilized form of VV is heat stable. This is a major advantage in carrying out successful vaccination programs in developing tropical countries. When the VV vector is introduced into an animal, the virus replicates in the host cell, and the foreign genes are expressed together with those of VV. For example, rinderpest is an acute, febrile, and highly contagious viral disease of ruminants with a rapid course and a mortality rate exceeding 90% (216). It is characterized by inflammation, hemorrhaging, necrosis, and erosion of the gastrointestinal tract, accompanied by bloody diarrhea, wasting, and death. Cattle vaccinated with a VV vaccine were shown to be completely protected from rinderpest and exhibited no detectable illness or clinical disease (216,217).

Panicali et al. constructed recombinant VVs containing the cloned hemagglutinin gene from the influenza virus (217). Immunization of rabbits with recombinant poxviruses resulted in the production of antibodies reactive with authentic influenza HA. The production of antibodies directed against influenza HA suggested that the HA gene expressed in vaccinia is immunogenic. These data indicate the potential of genetically engineered poxvirus for use in generic live vaccine vehicles that have veterinary or human application (217).

Marek's disease (MD) is a malignant T-lymphomatosis of chickens and is caused by Marek's disease virus type 1 (MDV1) (218). MD is the first cancer that was made preventable by vaccination and has been largely controlled by use of live attenuated or naturally avirulent vaccines since the early 1970s. To examine the protective efficacy of the recombinant MD vaccine, specific pathogen-free chickens were vaccinated with rMDV1. Almost all birds were protected from MDV challenge via intramuscular, ocular, intranasal, and intratracheal routes at 4 weeks after vaccination. In addition, the rMDV1 provided 100% protection against virulent MDV1 challenge in chickens. Antibody responses against MDV1 antigen were observed up to as long as 11 weeks after immunization (218).

In the case of bovine respiratory disease, management systems vary around the world, with economic losses often occurring following weaning, movement, and confinement of animals. Respiratory pathogens in cattle such as bovine

respiratory syncytial virus (BRSV) and bovine herpes virus are challenging targets for DNA vaccine development (219). These viruses are important pathogens in cattle for which various live and inactivated vaccines are currently used in the field (220). Schrijver et al. compared the protection afforded by three different DNA application methods against BRSV infection in cattle (220). Intradermal (id) administration with a needleless injector reduced BRSV excretion significantly better after BRSV challenge than when administered iv or id with a needle. Serum antibody levels against G protein were high and showed less variation in calves vaccinated with needleless injectors compared with those in id- and im-vaccinated calves. Parenteral DNA application was shown to be capable of inducing the priming of the immune response at the respiratory mucosa (220).

DNA plasmid vaccines can stimulate very specific and powerful long-term immune responses against virtually any pathogen. These vaccines can be delivered by either direct injection or by gene gun. Delivery of genes via a gene gun involves coating gold particles with the plasmid of interest (221). Direct injection of DNA into all species requires larger quantities of plasmid to induce an immune response than if administered by a gene gun. The reason for this may be degradation of the plasmids before they are taken up by the cells in vivo and transported to the nucleus. Lodmell et al. demonstrated that direct intracellular epidermal delivery of plasmid DNA–coated gold particles via a handheld helium-powered gene gun would elicit protective immune responses against a rabies virus (222). The gun system permitted a more simple and rapid delivery of DNA compared with the more typical needle injection, and more importantly, the force of the particle bombardment propulsion was thought to propel the DNA-coated beads through the plasma membrane of the cells. In another study using an AccellR gene gun, particle-mediated immunization with DNA encoding the glycoprotein gene of the standard strain of rabies virus was shown to elicit highly protective levels of rabies virus–neutralizing antibody in mice. At 315 days postprimary immunization, 100% of the mice survived intraplantar rabies virus challenge (223).

It has also been shown that plasmid DNA-encoding canine parvovirus (CPV) induced immunity may protect dogs against challenge with virulent virus (224). Nucleic acid (NA)–vaccinated dogs showed an increase of serum IgG titer starting 1 week postinjection, which peaked at 2 weeks and remained detectable for at least 14 weeks. All NA-accinated dogs were protected against infection after virulent CPV challenge regardless of dose, whereas the control dog was fully susceptible. This study demonstrated for the first time that NA can protect dogs against an infectious disease (224).

In addition to inducing immune responses to infectious diseases, DNA immunization has also the potential for the control of ectoparasites (225,226). Recently, investigators have used concealed antigens as vaccines. Concealed antigens are antigens that do not normally induce immune responses during ectoparasite infestations because they are rarely exposed to the immune system (225). However, if the host contains antibodies to these antigens in the blood, these antibodies interact with the concealed antigen in the gastrointestinal tract and in combination with complement may result in lysis or disruption of gastrointestinal tract cell function and death of the ectoparasite. These concealed antigens are glycoproteins; therefore, administration of genes encoding these glycoproteins in plasmid should induce very high levels of immune responses to the appropriate epitope (226). Although there is limited literature indicating that DNA immunization works with concealed ectoparasite antigens, some reported studies have been promising (226). For example, immunization of rabbits against the midgastrointestinal tract antigen of mosquitoes demonstrated a lower survival rate of mosquitoes in those fed on immunized rabbit versus those fed on normal (nonimmunized) rabbits (225).

Gene Therapy

The identification of underlying genetic disorders has recently made gene therapy an attractive treatment option for a wide variety of disorders in both humans and animals. Gene therapy offers new opportunities to treat these disorders both by restoring gene functions that have been lost through mutation and/or by introducing genes that can inhibit the replication of infectious agents. Genes used in such therapies are viewed as medicines, and their development as a therapeutic agent faces similar issues to those encountered during the development of other drugs and proteins such as bioavailability, toxicity, activity, and cost/risk/benefit (227). The ideal gene therapy vector should be easy to formulate, nonimmunogenic, and nontoxic and should have a low cost/risk ratio; it has to reach to target cells and then should be transported to the nucleus where gene expression takes place, and it must be expressed in predictable controlled fashion.

The development of gene delivery systems has included both nonviral and viral vector systems. Viral vectors can arise from viruses that are extensively modified to provide immune responses with increased cloning capacity to permit the incorporation of genes and complex regulatory elements. Other viral vectors emerge through the modification of existing, relatively inefficient, nonviral delivery systems. Therapeutic applications of gene therapy in animals are currently limited, except for the genetically engineered vaccines that have been previously discussed in this section. However, the number of applications of nucleic acid probes or recombinant DNA products for clinical or diagnostic use in veterinary medicine is increasing rapidly (228,229).

Hormones, growth-stimulating factors, enzymes, cytokines, and immunomodulating proteins have all been cloned from the human genome for use in veterinary medicine.

Only a small number of genes from species of veterinary importance have been cloned so far. Two immunomodulating cytokines have been cloned for the cat α-interferon and tumor necrosis factor. Human interferon can also be administered either orally or subcutaneously to cats for the treatment of feline leukemia virus infection. Recombinant interferon acts as immunomodulator and antiviral agent (230).

Hemaropeietic growth factor is a regulatory molecule essential for controlling blood cell differentiation and in vitro proliferation and survival. Potentially, this agent may be useful in prevention and treatment of chemotherapy- or radiation-induced cytopenia and treatment of suppression of bacterial infections associated with clinical feline panleukopenia virus infection of kittens (231).

Hemophilia is a bleeding disorder caused by a deficiency in the clotting factor VIII. A canine model was used to determine if an adenoviral vector expressing a human factor VIII cDNA could be used to correct the hemophilia A phenotype. Results showed that the disease in dogs could be treated effectively using the human factor VIII. However, further advances in vector design are needed to enable sustained expression. Correction of the coagulation defect in a large-animal model is a crucial step to verifying the feasibility of gene therapy for this disease (232).

The polymerase chain reaction (PCR) is particularly important for identification and diagnosis of parasites as well as for many other applications in veterinary medicine. The key to the development of a nucleic acid probe is to identify nucleotide sequences that are unique to the particular organism of interest. The application of molecular biology in veterinary parasitology requires the classification of parasites, the diagnosis of infection, the development of the antiparasitic vaccine, the development of antiparasitic drugs, and the selection of a host with genetic resistance (233). This reaction can be used to screen a cDNA or genomic DNA library for classification and diagnosis and many other purposes. PCR primers and a probe derived from a gene encoding an intraerythrocytic piroplasm surface protein of *Theileria sergenti* has used. *Babesia bovis* has been diagnosed in chronically infected cattle by using PCR for a merozoite surface protein. High sensitivity was achieved with a limit of detection of parasitemia (233,234).

Molecular biology is also being applied to the improvement of chemotherapy against veterinary parasites. The use of antisense nucleotides for therapy generally relies on the synthesis of an antisense oligonucleotide and the delivery to the target, which is the parasite's nucleic acid. Therefore, an antisense oligonucleotide has to be synthesized and delivered into the parasite's cells, where it must not be degraded too rapidly and must hybridize with the parasite's nucleic acid to prevent the protein expression, which is essential for the survival of the parasite. Adequate delivery systems remain a problem in the practical application of antisense therapeutics to parasites.

Trends and Future Directions of Vaccines and Gene Therapy

This section has considered some of the recent progress in the development of new vaccines and genetically engineered products for improving animal health and their veterinary application using by molecular biology and biotechnology techniques. Vaccines have played, and will continue to play, a critical role in presenting, controlling, and eliminating diseases in animals and humans. Although applications of genetically engineered products are presently limited, the use of recombinant products is increasing. We are confident that in the future we will have unlimited potential for the production of safer and more effective vaccines, therapeutic proteins, and recombinant products and more sensitive diagnostic reagents.

CONCLUDING REMARKS

The veterinary area offers unique opportunities to the formulation scientist that arise from the diverse nature of the field, the desire of the end-user to fit drug therapy around farm management practices, and the anatomical and physiological peculiarities of an individual animal species. Many technologies have been developed to overcome the challenges associated with the delivery of drugs to animals, and numerous examples of innovative controlled-release drug delivery systems exist in the literature.

BIBLIOGRAPHY

1. M.J. Rathbone, *Adv. Drug Delivery Rev.* **28**, 301–302 (1997).
2. P.G. Welling and M.R. Dobrinska, in J.R. Robinson and V.H.L. Lee, eds., *Controlled Drug Delivery: Fundamentals and Applications*, 2nd ed., Dekker, New York, 1978, pp. 253–291.
3. W.-Y. Kuu, R.W. Wood, and T.J. Roseman, in A. Kydonieus, ed., *Treatise on Controlled Drug Delivery: Fundamentals, Optimization, Applications*, Dekker, New York, 1992, pp. 37–154.
4. T.J. Roseman and N.F. Cardarelli, in A. Kydonieus, ed., *Controlled Release Technologies: Methods, Theory, and Applications*, CRC Press, Boca Raton, Fl., 1980, pp. 37–154.
5. V.H.K. Li, J.R. Robinson, and V.H.L. Lee, in J.R. Robinson and V.H.L. Lee, eds., *Controlled Drug Delivery: Fundamentals and Applications*, Dekker, New York, 1978, pp. 3–94.
6. Y.W. Chien, in Y.W. Chien, ed., *Novel Drug Delivery Systems*, 2nd ed., Dekker, New York, 1991, pp. 381–528.
7. B.M. Silber, M. Bialer, and A. Yacobi, in J.R. Robinson and V.H.L. Lee, eds., *Controlled Drug Delivery: Fundamentals and Applications*, 2nd ed., Dekker, New York, 1978, pp. 213–251.
8. P.K. Gupta and J.R. Robinson, in A. Kydonieus, ed., *Treatise on Controlled Drug Delivery: Fundamentals, Optimization, Applications*, Dekker, New York, 1992, pp. 255–313.
9. J.R. Cardinal, *Adv. Drug Delivery Rev.*, 303–322 (1997).
10. D.W. Cook, in G.E. Hardee and J.D. Baggott, eds., *Development and Formulation of Dosage Forms*, 2nd ed., Dekker, New York, 1998, pp. 305–356.
11. J.L. Riner, R.L. Byford, L.G. Stratton, and J.A. Hair, *Am. J. Vet. Res.* **43**, 2023–2030 (1982).
12. R.M. Jones, *Vet. Parasitol.* **12**, 223–232 (1983).
13. U.S. Pat. 4,220,153 (1980), D.S. Dresback.
14. H. Prosl et al., *Vet. Parasitol.* **12**, 251–260 (1983).
15. F.H.M. Borgsteed, *Vet. Parasitol.* **12**, 251–260 (1983).
16. W.A. Boettner et al., *J. Controlled Release* **8**, 23–30 (1984).
17. U.S. Pat. 4,601,893 (1986), J.R. Cardinal.
18. R.L. Byford, J.L. Riner, and J.A. Hair, *Bovine Pract.* **15**, 91–94 (1981).
19. U.S. Pat. 3,844,285 (1974), R.H. Laby.
20. U.S. Pat. 4,416,659 (1983), B.E. Simpson and N.A. Gervais.
21. U.S. Pat. 4,671,789 (1985), R.H. Laby.
22. U.S. Pat. 4,687,480 (1987), R.H. Laby and M.A. Lance.
23. U.S. Pat. 4,883,484 (1989), M.T. Shepard and S.R. Edwards.

24. U.S. Pat. 5,162,116 (1991), M.T. Shepard.
25. U.S. Pat. 5,198,222 (1993), M.O. Scully and D. Woodling.
26. U.S. Pat. 5,277,912 (1994), L.B. Lowe and T. McArthur.
27. U.S. Pat. 5,562,915 (1996), L.B. Lowe and C.J. McArthur.
28. U.S. Pat. 4,228,149 (1980), M.D. Brewer and G.J.L. Griffin.
29. U.S. Pat. 4,308,250 (1981), G.J.L. Griffin and M.D. Brewer.
30. U.S. Pat. 5,720,972 (1998), R. Munday.
31. E.P. 0,062,391 (1982), J.W. Hollaway.
32. P.K. Wilkinson and J.B. Eckenhoff, *Proc. Int. Symp. Controlled Release Bioact. Mater.* (1987).
33. U.S. Pat. 5,206,024 (1993), R.B. Eckenhoff.
34. U.S. Pat. 5,122,128 (1992), J.R. Cardinal, P.K. Wilkerson, and J.L. Zingerman.
35. A.G. Thombre, J.R. Cardinal, and L.A. Fournier, *J. Controlled Release* **18**, 221–234 (1992).
36. J.R. Cardinal and L.C. Witchey-Lakshmanan, in A. Kydonieus, ed., *Treatise on Controlled Drug Delivery*, Dekker, New York, 1992, pp. 465–489.
37. R. Duncan and L.W. Seymour, *Controlled Release Technologies*, Elsevier, Oxford, U.K., 1989.
38. U.S. Pat. 3,056,724 (1962), H.R. Marston.
39. R.C. Pierce, T.P. Bowman, J. McDaniel, and R. Winslow, *Proc. Int. Symp. Controlled Release Bioact. Mater.* **15**, 294–295 (1988).
40. U.S. Pat. 5,322,692 (1994), I.B. Wood, R.B. Toothill, and J.C. Dietz.
41. U.S. Pat. 4,732,764 (1988), R.G. Hemingway, N.S. Ritchie, and J.J. Parkins.
42. U.S. Pat. 5,190,760 (1992), R.C. Baker.
43. U.S. Pat. 4,350,675 (1982), C.F. Drake.
44. U.S. Pat. 4,482,541 (1984), S.B. Telfer, G. Zervas, and P. Knott.
45. B.F. Alger, *Proc. Int. Symp. Controlled Release Bioact. Mater.* **14**, 89–90 (1987).
46. U.S. Pat. 4,662,879 (1987), C.F. Drake and M. Tripp.
47. U.S. Pat. 4,793,997 (1988), C.F. Drake and A.J. Arch.
48. U.S. Pat. 4,851,225 (1989), C.F. Drake and J.O. Alfred.
49. W.M. Allen et al., *Vet. Rec.* **115**, 55–57 (1984).
50. E.P. 0,025,697 (1983), J.W. Kleber and B.E. Simpson.
51. E.P. 0,026,599 (1984), R.S. Nevin.
52. E.P. 0,062,391 (1982), B.E. Simpson.
53. J.M. Conrad and D.S.J. Skinner, *J. Controlled Release* **9**, 133–147 (1988).
54. J.M. Parrott, J.M. Conrad, R.P. Basson, and L.C. Pendlum, *J. Anim. Sci.* **68**, 2614–2621 (1990).
55. U.S. Pat. 4,649,042 (1985), R.C. Davis et al.
56. U.S. Pat. 4,564,363 (1983), B.G. Bagnall and R.J. Gyurik.
57. U.S. Pat. 5,110,598 (1992), L. Kwan and W. Steber.
58. U.S. Pat. 5,178,874 (1993), L. Kwan and W. Steber.
59. J.R. Cardinal, *J. Controlled Release* **2**, 393–403 (1985).
60. P.R. Klink, T.H. Ferguson, and J.A. Magruder, in G.E. Hardee and J.D. Baggott, eds., *Development and Formulation of Dosage Forms*, 2nd ed., Dekker, New York, 1998, pp. 145–229.
61. S.H.W. Wu and A. Papas, *Adv. Drug. Delivery Rev.* **28**, 323–334 (1997).
62. W.C. Bergen and F.N. Owens, *Anim. Health Nutr.* **40**, 32–35 (1985).
63. U.S. Pat. 3,988,480 (1976), S.R. Ames and C.D. Robeson.
64. W. Chalupa, in Y. Ruckebusch and P. Thivend, eds., *Digestive Physiology and Metabolism in Ruminants*, Avi Pub. Co., Westport, Conn., 1980, pp. 325–347.
65. A. Papas, G.A.B. Hall, E.E. Hatfield, and F.N. Owens, *J. Nutr.* **104**, 653–659 (1974).
66. I. Schipper, *Am. Vet. Med.* **50**, 111–113 (1955).
67. W.G. Huber, C.E. Lofgrin, W. Reynolds, and H.G. Luther, *Vet. Med.* **55**, 35–38 (1960).
68. G. Ziv, in D.C. Monkhouse, ed., *Animal Health Products, Design and Evaluation*, American Pharmaceutical Association, Washington, D.C., 1978, pp. 32–66.
69. S. Vangelov, *Vet. Med. Nauki* **18**, 84–90 (1981).
70. J.K. Pearson and C.L. Wright, *Vet. Rec.* **84**, 294–298 (1959).
71. W.D. Schultze and H.D. Mercer, *Am. J. Vet. Res.* **37**, 1281–1284 (1976).
72. U.S. Pat. 3,639,560 (1972), D.M. Moran, B. Regis, and J. Croucher.
73. J.M. Finch, A. Winter, A.W. Walton, and J.A. Leigh, *Vaccine* **15**, 1138–1143 (1997).
74. J.S. Hogan et al., *J. Dairy Sci.* **78**, 285–290 (1995).
75. G.M. Pighetti and L.M. Sordilio, *J. Dairy Sci.* **78**, 528–537 (1995).
76. D.E. Shuster and M.E. Kehrli, *Am. J. Vet. Res.* **56**, 313–320 (1995).
77. P.G. Reddy et al., *Cytokine* **4**, 227–231 (1997).
78. M.J. Daley and E.R. Oldham, *Vet. Immunol. Immunopathol.* **31**, 301–312 (1992).
79. F.D. Lehman and J.R. Rains, *Compendium*, August, S174–S177, S206 (1996).
80. R.L. Preston, *Adv. Drug Delivery Rev.*, in press.
81. I.H. Ferguson, G.F. Needham, R.R. Pfeiffer, and J.F. Wagner, *Proc. Int. Symp. Controlled Release Bioact. Mater.* **14**, 51–52 (1987).
82. U.S. Pat. 4,191,741 (1980). J.L. Hudson and J.F. Wagner.
83. T.J. Robinson, *The Control of the Ovarian Cycle in the Sheep*, Sydney University Press, Australia, 1967.
84. M.J. Rathbone, K.L. Macmillan, C.R. Bunt, and S. Burggraaf, *Adv. Drug Delivery Rev.*, in press.
85. M.J. Rathbone et al., *J. Controlled Release*, in press.
86. M.J. Rathbone et al., *Crit. Rev. Ther. Drug Carrier Syst.* (in press).
87. M.J. Rathbone et al., *Adv. Drug Delivery Rev.*, in press.
88. Y.W. Chien, in Y.W. Chien, ed., *Novel Drug Delivery Systems; Fundamentals, Developmental Concepts, Biomedical Assessments*, Dekker, New York, 1982, pp. 413–463.
89. Q.A. McKellar, *Vet. Parasitol.* **54**, 249–258 (1994).
90. Y.S. Yang and K.F. Fung, *Acta Vet. Scand.* **87**, 406–407 (1991).
91. M. Onuma et al., *Zentralbl. Veterinaermed, Reihe B* **36**, 139–147 (1989).
92. S. Trostle, D. Hendrickson, W. Stone, and A. Klohen, *J. Am. Vet. Med. Assoc.* **208**, 404–407 (1996).
93. D. Carter, M. Luttinger, and D. Gardner, *J. Controlled Release* **8**, 15–22 (1988).
94. *Veterinary Pharmaceuticals and Biologicals*, 8th ed., 1993, pp. 730–731.
95. U.S. Pat. 5,082,863 (1992), H.M. Apelian, D. Coffee-Beach, and A. Hug.
96. A. Aguiar, W.A. Armstrong, and S.J. Desai, *J. Controlled Release* **6**, 375–385 (1987).

97. R.O. Drummond, *Vet. Parasitol.* **18**, 111–119 (1985).
98. W.O. Haufe, *Can. J. Anim. Sci.* **62**, 567–573 (1982).
99. S.M. Herbig and K. Smith, *J. Controlled Release* **8**, 63–72 (1988).
100. E.P. 0,152,190 (1985), C.A. Speckman.
101. J.L. Despins, J.S. Hunter, R.B. Davey, and J.E. George, *J. Agric. Univ. P. R.* **79**, 93–98 (1995).
102. *Veterinary Pharmaceuticals and Biologicals*, 8th ed., 1993, p. 732.
103. J. Cunningham, R. Everett, P. Tanner, and P. Jeannin, *Proc. North Am. Vet. Conf.*, January, 1997.
104. K. Tobias, R. Schneider, and T. Besser, *J. Am. Vet. Med. Assoc.* **208**, 841–845 (1996).
105. K. Garvin et al., *J. Bone Joint Surg.* **76**, 1500–1506 (1994).
106. P.H. Gupta, H. Johnson, and C. Allexon, *J. Controlled Release* **26**, 229–238 (1993).
107. T. Hernandez-Caselles, A. Vera Crespo, F.J. Villalain, and J. Gomez-Fernandez, *Am. J. Vet. Res.* **50**, 1486–1488 (1989).
108. E. MacEwen et al., *J. Natl. Cancer Inst.* **81**, 935–938 (1989).
109. S. Kruth, *Vet. Clin. North Am.: Small Anim. Pract.* **28**, 269–295 (1998).
110. E. Orenbuer, E. Luck, D. Brown, and B. Kitchell, *Clin. Dermatol.* **9**, 561–568 (1991).
111. D. Greco, J. Broussard, and M. Peterson, *Vet. Clin. North Am.: Small Anim. Pract.* **25**, 677–689 (1995).
112. D. Church, *J. Small Anim. Pract.* **22**, 301–310 (1981).
113. E. Bertoy, R. Nelson, and E. Feldman, *J. Am. Vet. Med. Assoc.* **206**, 1729–1731 (1995).
114. S. Moise and T. Reimers, *J. Am. Vet. Med. Assoc.* **182**, 158–164 (1983).
115. P. Graham, A. Nash, and Q. McKellar, *J. Small Anim. Pract.* **38**, 434–438 (1997).
116. A. von Berky and W. Townsend, *Aust. Vet. J.* **70**, 249–250 (1993).
117. M. Stovring, L. Moe, and E. Glattre, *Acta Pathol. Microbiol. Immunol. Scand.* **105**, 590–596 (1997).
118. J. Simmons and C. Hammer, *Am. J. Vet. Res.* **34**, 1409–1419 (1973).
119. D. Vincent et al., *Am. J. Vet. Res.* **40**, 705–709 (1979).
120. L. Appel and L. Witchey-Lakshmanan, *Crit. Rev. Patol.* **10**, 30 (1994).
121. C. Kirker-Head, *Vet. Surg.* **24**, 408–419 (1995).
122. V. Baeyens et al., *Adv. Drug Delivery Rev.* **28**, 335–361 (1997).
123. F. Gurtler, V. Kaltsatos, B. Boisrame, and R. Gurny, *J. Controlled Release* **33**, 31–236 (1995).
124. T. Glover, M. Nasisse, and M. Davidson, *Am. J. Vet. Res.* **56**, 936–940 (1995).
125. S.M. Cady and W.D. Steber, in L.M. Sanders and P. Hendren, eds., *Protein Delivery: Physical Systems*, Plenum, New York, 1997, pp. 289–317.
126. I.C. Hart and I.D. Johnson, in P.J. Buttery, D.B. Lindsay, and N.B. Haynes, eds., *Control and Manipulation of Animal Growth*, Butterworth, London, 1986, pp. 135–159.
127. T.H. Ferguson, in K. Park, ed., *Controlled Drug Delivery*, American Chemical Society, Washington, D.C., 1997, pp. 289–308.
128. J.L. Cleland and R. Langer, *ACS Symp. Ser.* **567** (1994).
129. M.J. Hageman, J.M. Bauer, P.L. Possert, and R.T. Darrington, *J. Agric. Food Chem.* **40**, 348–355 1992.
130. T. Chen, *Drug Dev. Ind. Pharm.* **18**, 1311–1354 (1992).
131. U.S. Pat. 5,013,713 (1991), J.W. Mitchell.
132. U.S. Pat. 4,988,140 (1990), T.H. Ferguson, R.G. Harrison, and D.L. Moore.
133. U.S. Pat. 4,977,659 (1988), A.L. Thakkar, R.G. Harrison, and D.L. Moore.
134. Aust. Pat. 9,170,937 (1991), N.J. Kim, B.G. Rhee, and H.S.
135. U.S. Pat. 5,013,713 (1991), J.W. Mitchel.
136. U.S. Pat. 4,977,140 (1990) T.H. Ferguson, R.G. Harrison, and D.L. Moore.
137. WO 94/12158 (1994), H. Auer, M.A. Khan, and H. Bernstein.
138. U.S. Pat. 4,837,381 (1989), W.D. Steber, R. Fishbein, and S.M. Cady.
139. J.W. Wyse, Y. Takahashi, and P.P. DeLuca, *Proc. Int. Symp. Controlled Release Bioact. Mater.* **16**, 334–335 (1989).
140. U.S. Pat. 5,213,810 (1993), W. Steber.
141. U.S. Pat. 4,861,580 (1989), A.S. Janoff et al.
142. WO 89/05151 (1989), A.L. Weiner, L.F. Estis, and A.S. Janoff.
143. T.M. Feeser and M.A. Wheatley, *Proc. Int. Symp. Controlled Release Bioact. Mater.* **20**, 32–33 (1993).
144. T.M. Feeser and M.A. Wheatley, *Proc. Int. Symp. Controlled Release Bioact. Mater.* **21**, 196–197 (1994).
145. G. Gregoriadis and B. McCormack, *Proc. Int. Symp. Controlled Release Bioact. Mater.* **21**, 89–90 (1994).
146. U.S. Pat. 4,857,506 (1989), P. Tyle.
147. P. Tyle and S.M. Cady, *Proc. Int. Symp. Controlled Release Bioact. Mater.* **17**, 49–50 (1990).
148. U.S. Pat. 5,266,333 (1993), S.M. Cady et al.
149. U.S. Pat. 5,045,312 (1991), R. Aston, R. Bomford, and A.T. Holder.
150. U.S. Pat. 4,959,217 (1990), L.M. Sanders and A. Domb.
151. C. Younsik et al., *Proc. Int. Symp. Controlled Release Bioact. Mater.* **18**, 595–596 (1991).
152. U.S. Pat. 4,882,168 (1989), D.J. Casey and L. Rosati.
153. E.P. 809,482 (1983), J.R. Churchill and F.G. Hutchinson.
154. U.S. Pat. 5,198,422 (1993), M.T. Clark et al.
155. U.S. Pat. 5,015,627 (1991), T.O. Lindsay and M.T. Clarke.
156. U.S. Pat. 4,863,736 (1989), M.J. Azain, K.E. Eigenberg, T.R. Kasser, and M.J. Sabacky.
157. U.S. Pat. 5,328,697 (1994), S.N. Raman and M.W. Gray.
158. WO 91/05548 (1991), K.N. Sivaramakrishnan.
159. U.S. Pat. 5,015,627 (1991), T.O. Lindsay and M.T. Clarke.
160. E.P. 462,959A1 (1991), E.J. Castillo, K.E. Eigenberg, K.R. Patel, and M.J. Sabacky.
161. U.S. Pat. 5,213,810 (1993), W. Steber.
162. WO 92/07556 (1992), C.G. Pitt, Y. Cha, E.M. Donaldson, and E. McLean.
163. WO 90/11070 (1990), K.N. Sivaramakrishnan and L.F. Miller.
164. U.S. Pat. 4,917,685 (1990), R. Viswanathan and R.B. DePrince.
165. U.S. Pat. 5,023,088 (1991), P.S.L. Wong et al.
166. U.S. Pat. 5,110,597 (1992), P.S.L. Wong et al.
167. U.S. Pat. 4,959,218 (1990), J.B. Eckenhoff et al.
168. U.S. Pat. 5,110,596 (1992), J.A. Magruder et al.
169. U.S. Pat. 5,238,687 (1993), J.A. Magruder, J.R. Perry, and J.B. Eckenhoff.
170. E.P. 219,076 (1987), K. Fujioka, S. Sato, N. Tamura, and Y. Takada.

171. Aust. Pat. 8,655,983 (1986), K. Fujioka, S. Sato, and Y. Takada.
172. E.P. 326,151 (1989), K. Fujioka et al.
173. U.S. Pat. 5,039,660 (1991), R.J. Leonard and S.M. Harman.
174. B. Mariette et al., *J. Controlled Release* **24**, 237–246 (1995).
175. WO 90/11070 (1990), A.H. Williams et al.
176. R.C. Oppenheim et al., *Proc. Int. Symp. Controlled Release Bioact. Mater.* **15**, 54–55 (1988).
177. W.J. Theil and K.C. Tsui, *Proc. Int. Symp. Controlled Release Bioact. Mater.* **18**, 207–208 (1991).
178. L.M. Sanders, G.I. McRea, J.S. Kent, and B.H. Vickery, *Proc. Int. Symp. Controlled Release Bioact. Mater.* **10**, 91–96 (1983).
179. L.M. Sanders et al., *J. Pharm. Sci.* **73**, 1294–1297 (1984).
180. R. Burns and J. Sanders, *Proc. Int. Symp. Controlled Release Bioact. Mater.* **15**, 452–453 (1988).
181. H. Okada, *Proc. Int. Symp. Controlled Release Bioact. Mater.* **16**, 12–13 (1989).
182. J.R. Lawter, N.S. Brizzolara, M.G. Lanzilotti, and G.O. Morton, *Proc. Int. Symp. Controlled Release Bioact. Mater.* **14**, 99–100 (1987).
183. R. Burns, G. McRea, and L. Sanders, *Proc. Int. Symp. Controlled Release Bioact. Mater.* **15**, 64–65 (1988).
184. J. Heller, L.M. Sanders, P. Mishky, and S.Y. Ng, *Proc. Int. Symp. Controlled Release Bioact. Mater.* **13**, 69–70 (1986).
185. J. Heller et al., *J. Controlled Release* **6**, 217–224 (1987).
186. T.W.F. Pay and P.J. Hingley, *Vaccine* **5**, 60–65 (1987).
187. J.G. Hu, A. Ide, T. Yokoyoma, and T. Kitagava, *Chem. Pharm. Bull.* **37**, 3042–45 (1989).
188. S.J. Brett, L. Dunlop, F.Y. Liew, and J. Tile, *Immunology* **80**, 306–310 (1993).
189. C. Andre, J.F. Heremans, J.P. Vearmen, and C.L. Combiaso, *J. Exp. Med.* **142**, 1509–1519 (1975).
190. E.C. Anderson, R.C. Masters, and G.N. Mowat, *Res. Vet. Sci.* **12**, 342 (1971).
191. J.S. Salt, P.V. Barnett, P. Dani, and L. Williams, *Vaccine* **16**, 746–754 (1998).
192. P. Hunter et al., *Vaccine* **16**, 55–61 (1998).
193. M.B. Pensaert, K. Desmet, and K. Dewaele, *Vet. Microbiol.* **22**, 107–117 (1990).
194. N.S. Zeidner et al., *Vaccine* **14**, 1294 (1995).
195. H. Mizugichi et al., *Br. J. Cancer* **73**, 472–476 (1996).
196. C. Alving, *J. Immunol. Methods* **140**, 1–13 (1991).
197. T. Nakanishi et al., *Biochem. Biophys. Res. Commun.* **240**, 793–797 (1997).
198. D. Rowley, *Aust. J. Exp. Biol. Med. Sci.* **55**, 1–10 (1977).
199. A. Makita and N. Tanuguchi, *Glycosphingolipids*, Elsevier, Amesterdam, 1985, p. 1.
200. M. Han, S. Watarai, K. Kobayashi, and T. Yasuda, *J. Vet. Med. Sci.* **59**, 1109–1114 (1997).
201. A.A. MacColm, R. Bomford, and L. Dalton, *Parasite Immunol.* **4**, 455–461 (1982).
202. H. Kiyano, J.R. McGhee, J.F. Kearny, and S.M. Mealek, *Scand. J. Immunol.* **15**, 329–332 (1982).
203. M.L. Dunkley and A.J. Husband, *Immunology* **61**, 475 (1986).
204. J.H. Eldridge, J.K. Staas, J.A. Meulborek, and T.R. Tice, *Infect. Immunol.* **59**, 2978–2983 (1991).
205. H.C. Matter et al., *Vaccine* **16**, 657–665 (1998).
206. I.S. Robertson, J.C. Wilson, and H.M. Fraser, *Vet. Rec.* **105**, 556–557 (1979).
207. C. Carelli, F. Audibert, J. Gaillard, and L. Chédid, *Proc. Natl. Acad. Sci. U.S.A.* **79**, 5392–5395 (1982).
208. P. Bartelloni, J.D. Marshal, and D.C. Cavanaugh, *Mil. Med.* **138**, 720–722 (1973).
209. K.M. Reddin et al., *Vaccine* **16**, 761–767 (1998).
210. J.E. Eyles et al., *Vaccine* **16**, 698–707 (1998).
211. D.T. O'Hagan, *Novel Delivery System for Oral Vaccines*, CRC Press, Boca Raton, Fla., 1994, pp. 1–268.
212. K.A. Atarki et al., *Vaccine* **16**, 685–691 (1998).
213. J.J. Donnely, J.B. Ulmer, and M.A. Liu, *J. Immunol. Methods* **176**, 145–152 (1994).
214. S. Kit, *Vaccine* **8**, 420–425 (1990).
215. L.A. Babiuk et al., *DNA Vaccines*, N. Y. Acad. Sci., New York, 1995, pp. 50–56.
216. T. Yilma, *Dev. Biol. Stand.* **82**, 201–209 (1994).
217. D. Panicali, W.S. Davis, L. Weinberg, and E. Paoletti, *Proc. Natl. Acad. Sci. U.S.A.* **80**, 5364–5368 (1983).
218. M. Sakaguchi et al., *Vaccine* **16**, 472–479 (1998).
219. R.S. Schrijver, J.P.M. Langedijik, and G.M. Keil, *Vaccine* **15**, 1908–1916 (1997).
220. R.S. Schrijver, J. Langedijik, G. Keil, and F.A.M. Rijsewijk, *Vaccine* **16**, 130–134 (1998).
221. J.B. Ulmer, J.J. Donnely, and S.E. Parker, *Science* **259**, 1745–1749 (1993).
222. D.L. Lodmell, N.B. Ray, and L.C. Ewalt, *Vaccine* **16**, 115–118 (1998).
223. E. Fynan et al., *Proc. Natl. Acad. Sci. U.S.A.* **90**, 11478–11482 (1995).
224. W. Jiang et al., *Vaccine* **16**, 601–607 (1998).
225. G. Nogge, *J. Insect Physiol.* **24**, 299–304 (1978).
226. C.H. Eisemann and K.C. Ginnigton, *Int. J. Parasitol.* **24**, 15–26 (1994).
227. F.D. Ledley, *Hum. Gene Ther.* **6**, 1129–1144 (1995).
228. D. Gillespie, *Vet. Microbiol.* **24**, 217–233 (1990).
229. E.W. Collission et al., *Vet. Microbiol.* **24**, 261–271 (1990).
230. P. Jameson and M. Essex, *Antiviral Res.* **3**, 115–118 (1983).
231. M.L. Martinez and R.C. Weiss, *Vet. Clin. North Am.: Small Anim. Prac.* **23**, 213–226 (1993).
232. S. Connelly et al., *Blood* **88**, 3846–3852 (1996).
233. R. Prichard, *Vet. Prasitol.* **71**, 155–175 (1997).
234. W.C. Brown et al., *Infect. Immun.* **61**, 236–244 (1993).

Index

Index terms	Links
A	
ABCD. *See* AmB colloidal dispersion (ABCD)	
ABELCET®	485
ABLC	442
Abortifacients	379
Abrin	179
Absorption	
chemical modification and	738
enhancement	738
FDA study requirements	383
Absorption rate, by deconvolution	846
AccuSite Injectibel Gel	356
Acela-Cata	302
Acetylcholinesterase, ocular topical application	615
L-α-Acetylmethodol acetate, opioid maintenance with	5
Aclacinomycin A, intravitreal	566
Acrylic polymers	674
Activated soft drugs	287
Active targeting, cancer therapy	145
Acupaque	314
Acute retinal necrosis syndrome (ARN), treatment	567 586
Acyclovir, ocular topical application	615
Adaprolol	290
Addictive disorders, controlled drug delivery	1
Additives, for protein stabilization	819
Adhesins, carrier systems using	176
Adhesion, in controlled release systems	262
Adhesive bond formation, bioadhesion	11
ADR. *See* Adriamycin	
Adriamycin (ADR)	122 129 204
Adsorption theory, theory	12

This page has been reformatted by Knovel to provide easier navigation.

Index terms	Links			
Advantage®	1023			
Advantage 24	732			
Aerosol delivery, to respiratory tract	936			
Aerosol solvent extraction system (ASES)	531			
Aerosomes®	330			
AFM. *See* Atomic force microscopy				
Agarose, gelation	525			
Agricultural products				
delivery systems	350			
microencapsulation	543			
ail gene product	178			
Airvol™ PVA	511			
Albumin	765			
Albumin microspheres	522			
Albunex	323			
Alcohol dependence, treatments for	1	6		
Alginate				
encapsulated contrast agents	328			
pendent drug conjugation	790			
Alginates, gelation	523			
Aliphatic polyanhydrides	61			
Alora®	987			
ALZET® osmotic pump	896	900		
AmB. *See* Amphotericin B				
AmB colloidal dispersion (ABCD)	443			
AmBisome	441	483	485	
Amikacin, liposomal	439			
Aminoglycosides	437	439		
Amorphous pharmaceutical solids	218			
Amphocil	483			
Amphotec®	485			
Amphotericin B (AmB), liposomal	440	483	485	580
Ampicillin, liposomal	437			
Amylose	725			
Androderm®	987			
Angina pectoris, oral treatment	557			
Angioplasty	162			

This page has been reformatted by Knovel to provide easier navigation.

Index terms	Links			
Animal reproduction				
companion animals	1024			
controlled drug delivery to regulate	634			
Animals. *See* Veterinary drug delivery				
Annamycin	483			
Anthracycline antibiotics, intravitreal	566			
Anthracycline products, liposomal	482			
Antibodies				
cancer therapy	145			
drug delivery systems using	456			
localization in encapsulation	240			
nanoparticles coated with	658			
Antibody-drug conjugates				
cancer therapy	132			
targeted drug delivery	132	145		
Anticalcification drugs, controlled drug delivery	115			
Anticancer drugs				
liposomal delivery systems	133	140	482	484
local delivery systems	121			
nanoparticle delivery	136	659		
for pets	1023			
polymer-drug conjugates	143	810		
systemic delivery	131			
tumor targeting	143			
Anticholinergics, soft anticholinergics	287	291		
Antifungal agents				
intravitreal delivery	568	584		
liposomal	440	484		
Antigen binding, cancer therapy	145			
Antigens	762			
liposomal	998			
T-independent antigens	997			
Antiinflammatory agents, encapsulation	678			
Antimicrobial agents	437			
liposomal	437	484		
local delivery to the mouth	560			
nanoparticle delivery	659			
for pets	1023			

This page has been reformatted by Knovel to provide easier navigation.

Index terms	Links			
Antimicrobial agents *(Continued)*				
veterinary	1022			
vitreoretinal disease	568	579		
Antimycobacterial agents, liposomal	438			
Antiparasitic agents				
liposomal	444			
nanoparticles	659			
veterinary use	1023			
Antiproliferative drugs, intravitreal drugs	566	577	582	
Antiviral agents				
liposomal	443			
nanoparticles	659			
Aortic root calcification, preventing	116			
Aquacoat®	666	667	668	669
Area under the curve (AUC), pharmacokinetics	834	836		
Aromatic polyanhydrides	61			
Artificial organs	419	425		
Artificial pancreas	419	424		
Aseptic processing, parenteral drugs	751			
ASES. *See* Aerosol solvent extraction system				
Asialofetuin	478			
Atenolol	289	290		
Atomic force microscopy (AFM), controlled-release systems, surface analysis	262	265	266	
ATR. *See* Attenuated total reflectance (ATR) spectroscopy				
ATRIDOX™	355			
Atropine	291	615		
Attenuated total reflectance (ATR) spectroscopy	257	265		
Atypical mycobacteriosis	438			
AUC. *See* Area under the curve				
Auger electron spectroscopy, controlled-release systems, surface analysis	262	63		
Aujeszky's disease	1027			
Autoworm/Multidose 130	1015			
Avidin	478			
Azidothymidine	567			
Azo compounds	723			
AZT. *See* Zidovudine				

This page has been reformatted by Knovel to provide easier navigation.

Index terms	Links		
B			
Bacteria. *See also* Antimicrobial agents			
carrier systems using adhesins and invasins	176	178	
carrier systems using toxins	178		
Bacterial vaginosis, treatment	631		
Ball milling	755		
Balloon catheter, cardiovascular drug delivery	163		
Barrier technology, sterilization	749	827	
BBB. *See* Blood-brain barrier			
BBB disruption (BBBD)	190		
BCB. *See* Blood-cerebrospinal fluid barrier			
BCNU. *See* Carmustine			
Beads, oral drug delivery	735		
Beecham I and II	1013		
Benzyl benzoate	309		
Beta blockers	289		
Bile acids	174		
Bile acid transport system	174	176	177
Bioadhesion	10		
in controlled release systems	262		
evaluating	13		
mechanisms	11		
surface analytical studies	267		
theory	11		
Bioadhesive drug delivery	9		
bioadhesion mechanism	9		
bioadhesive polymers	14	24	
bioavailability study	33		
case study	16		
of dicumarol, study	33		
of insulin	40		
oral delivery	40		
of salicylic acid, study	33		
Bioadhesive gels	16		
nonoxynol-9	632		
vaginal use	630	631	633
Bioadhesive liposomes	16		
Bioadhesive measurements	19		

This page has been reformatted by Knovel to provide easier navigation.

Index terms	Links			
Bioadhesive microspheres	16			
Bioadhesive polymers	14	24		
drug delivery	15			
FTIR analysis	26			
morphological characterization	25			
nasal peptide drug delivery	599			
oral drug delivery	558	704		
Bioadhesive tablets	15			
Bioavailability	838			
carrier-mediated transport	173			
FDA study requirements	382	383	384	
Biochemical BBBD, central nervous system drug delivery	191			
Biocompatibility	72			
polyanhydrides	64			
poly(ortho ester) III	870			
poly(phosphoester)s (PPEs)	46	53		
surface properties	261			
Biodegradable polymers	352			
chemical composition	83			
classification	570			
configuration	83			
γ irradiation and	88			
implants	764			
intravitreal drug delivery	569	588		
ionic strength	88			
molar mass	86			
morphology	80			
pendent drug conjugation	790	792		
pH	88			
polyanhydrides	60	193	316	505
	532	572		
polyesters	71	316		
poly(ortho esters)	374	560	573	853
poly(phosphoester)s	45			
porosity	86			
size	86			
Biodegradable systems, female contraception	374			

This page has been reformatted by Knovel to provide easier navigation.

Index terms	Links			
Biodegradation				
PPEs	53			
SIMS studies	274			
Bioequivalence, FDA study requirements	383	384		
Bioerodible drug delivery implants	852			
Bioerodible ocular inserts	622			
Bioerodible polymers	852			
Bioerodible thermoplastic microspheres	20			
Biofunctionality	72			
Biomimetic nanoparticles	655			
Biomolecules, SIMS study	272			
Bioprosthetic heart valves (BPHVs), calcification	113			
Bioresorbability	71	72		
Bisphenol A-based poly(phosphoester)s	46			
Bisphosphonates	115			
Bleomycin	122			
Blood-brain barrier (BBB)	129	185	187	188
	190	293		
bacterial glycopeptides for penetration	324			
central nervous system drug delivery	188	190		
Blood-cerebrospinal fluid barrier (BCB)	186			
Blood-retinal barrier (BRB)	564			
Blood substitutes	94			
characteristics	95	96		
elective surgery and	101			
safety trials, healthy volunteers	95	97		
traumatic shock and	107			
Blood-tumor barrier	187			
Blood vessels, synthetic vascular grafts	943			
BMP. *See* Bone morphogenetic proteins				
Bone, integrins	955	967		
Bone-contacting prostheses	955			
Bone growth therapies, veterinary	1024			
Bone morphogenetic proteins (BMP)	562	889	890	1024
Bone repair	889			
See also Joint replacement				
gene therapy	894			

This page has been reformatted by Knovel to provide easier navigation.

Index terms	Links			
Bone repair *(Continued)*				
growth and morphogenetic factors for	890			
mechanisms	892			
mesenchymal stem cells (MSCs)	891			
Bovine respiratory disease	1032			
Bovine serum albumin (BSA)	997			
Bovine somatotropin (bST)	830			
BPHVs. *See* Bioprosthetic heart valves				
BR1	330	332		
Bragg equation	275			
Brain, drug delivery to	129	185	502	
Brain tumors	187	196		
Brazil wax	308			
BRB. *See* Blood-retinal barrier				
Bromocriptine, IVIVC study	431			
BSA. *See* Bovine serum albumin				
BST. *See* Bovine somatotropin				
Buccal drug delivery	553	555		
Buccal mucosa	555			
Buprenorphine	4	5	556	557
Butorphanol	4	600		
n-Butyl-2-cyanoacrylate	332			
BW-759U	567			
BY963	330			

C

Calcification. *See* Cardiovascular calcification				
Calcitonin, nasal administration	600			
Calcium alginate microspheres	524			
Calorimetry				
differential scanning calorimetry (DSC)	212	213	225	
differential thermal analysis (DTA)	212			
heat conduction calorimetry	222			
HSDSC	220			
isoperibol calorimetry	223			
micro-DSC	219	225		
modulated differential scanning calorimetry (MDSC)	221	225		
thermogravimetric analysis (TGA)	223			

This page has been reformatted by Knovel to provide easier navigation.

Index terms	Links			
Camptothecin (CPT)				
brain tumors	204			
conjugated with polyethylene glycol	152	154		
Cancer	119			
See also Anticancer drugs; Cancer treatment				
cause	144			
defined	144			
mortality statistics	143			
multiple-drug resistance (MDR)	120			
stages	144			
subtypes	144			
Cancer treatment	120	143		
antibody-drug conjugates	132			
chemoembolization	126			
depot systems	131			
drugs. *See* Anticancer drugs; Chemotherapy				
hydrogels	414			
immunotherapy	139			
liposome-encapsulated agents	133	140	482	484
magnetic localization	137			
microspheres	126	140		
nanoparticle delivery	136	659		
for pets	1023			
polymer-drug conjugates	143	810		
radiation therapy	120	143		
stealth liposomes	133	135		
surgery	120			
tumor targeting	132	145		
Candidiasis	631			
Canine parvovirus (CPV)	1033			
CAP. *See* Cellulose acetate phthalate				
ϵ-Caprolactone, synthesis	73	74		
Capronor®	365	374		
Capsules	734			
filling	359			
floating capsules	735			
gelatin capsules	359	734		
Carbopol®	16	609		

This page has been reformatted by Knovel to provide easier navigation.

Index terms	Links		
Carboxymethyl chitin, pendent drug conjugation	790		
Carboxymethyl pullulan, pendent drug conjugation	790		
Carcinoma	144		
See also Cancer; Cancer treatment			
Cardiovascular calcification, drug delivery to prevent	113		
Cardiovascular drug delivery systems	162		
catheter-based systems	162		
from polymer devices	169		
from stents	165		
Carmustine (BCNU)	122		
for brain tumors	196		
drug-impregnated polyanhydride wafers	196		
encapsulated delivery	130		
lipophilic analogs	188		
manufacture	357		
silicone oil	577		
systemic delivery	130		
Carnauba wax	308		
Carrier-mediated transport systems	173		
adhesins	176		
bile acid transport system	174	176	177
central nervous system drug delivery	189		
hemagglutinins	178		
immunoglobulin transport system	175		
intestinal peptide transporter	174		
invasins	177		
lectins	178		
toxins	178		
vitamin B_{12}-mediated transport	179	183	
Carriers			
for growth and morphogenetic factors	892		
polymeric	789		
Castor oil	308		
Catapres-TTS®	3	988	
Catheter-based delivery systems			
cardiovascular drugs	162		
central nervous system	192		
Cationic liposomes	480		

This page has been reformatted by Knovel to provide easier navigation.

Index terms	Links
CDDP. *See* Cisplatin	
CDS. *See* Chemical delivery systems	
Cellacephate	307
Cell based gene delivery	894
Cells, SIMS study	272
Cell seeding, synthetic vascular grafts	948
Cellulose acetate (CA)	670
Cellulose acetate butyrate	670
Cellulose acetate phthalate (CAP)	307 611
Cellulose acetate propionate	670
Cellulose compounds, as gastrointestinal contrast agents	332
Cellulose derivatives, ocular drug delivery	607 609
Cellulose embolization gel	314
Cellulose esters	670
Cellulosic enteric coatings	307
Cellulosic nonenteric coatings	308
Central nervous system, nonneoplastic diseases	208
Central nervous system drug delivery	184 209
blood-brain barrier	129 185 187 188 190
blood-cerebrospinal fluid barrier	186
blood-tumor barrier	187
carrier-mediated drug delivery	189
controlled-release polymer systems	193
enhancement strategies	188
interstitial delivery	192
intranasal route	191
intraventricular/intrathecal route	191
lipohilic analogs	188
prodrugs	188
receptor/vector-mediated drug delivery	189
redox chemical delivery systems	189
Cephalothin	437
Cerebrospinal fluid, blood-cerebrospinal fluid barrier	186
Cetyl alcohol	308
Channel catheter, drug delivery	163
Channeled balloon catheter, drug delivery	163

This page has been reformatted by Knovel to provide easier navigation.

Index terms	Links			
Characterization of delivery systems				
atomic force microscopy (AFM)	262	265	266	
attenuated total reflectance (ATR) spectroscopy	257	265		
Auger electron spectroscopy	262	263	264	
calorimetry	212			
contact-angle methods	262	263	264	
Coulter technique	252			
differential scanning calorimetry (DSC)	212	213	225	
differential thermal analysis (DTA)	212			
dynamic light scattering (DLS)	254			
electric sensing zone method	252			
electron paramagnetic resonance (EPR)	230			
electron spectroscopy for chemical analysis (ESCA)	262	263	266	270
FDA requirements	383			
gel permeation chromatography (GPC)	227			
heat conduction calorimetry	222			
infrared spectroscopy	256	265		
isoperibol calorimetry	223			
laser diffraction	253			
laser light scattering methods	252			
light scattering	252			
magnetic resonance imaging (MRI)	230			
microscopy	234	250		
modulated differential scanning calorimetry (MDSC)	221	225		
nuclear magnetic resonance (NMR)	229			
optical microscopy	234			
particle sizing techniques	250			
photon correlation spectroscopy (PCS)	254			
scanning electron microscopy (SEM)	235	242	262	
scanning probe microscopies (SPM)	265			
scanning tunneling microscopy (STM)	265			
secondary-ion mass spectrometry (SIMS)	262	270		
sieving methods	250			
staining	236			
static light scattering	253			
surface analysis	261			
thermogravimetric analysis (TGA)	223			
transmission electron microscopy (TEM)	234	236	249	
X-ray photoelectron spectroscopy (XPS)	263	270	274	

This page has been reformatted by Knovel to provide easier navigation.

Index terms	Links			
Characterization of delivery systems *(Continued)*				
X-ray powder diffractometry (XRD)	276			
Chelation, drug delivery system using	457			
Chemical bonds, bioadhesion	11			
Chemical delivery systems (CDSs)	291			
enzymatic physical-chemical-based CDS	292	293		
kinetics	930			
receptor-based CDSs	293	295	297	
site-specific, enzyme-activated CDSs	293	295		
Chemoembolization, cancer therapy	126			
Chemotherapy	120	143		
liposomal delivery systems	133	140	482	484
local delivery systems	121			
nanoparticle delivery	136	659		
systemic delivery systems	131			
Chimeric peptide, CNS drug delivery	189			
Chitosan	599	773		
beads	736			
gene delivery	877	881		
microspheres	520	522	525	
pendent drug conjugation	790			
Chlamydia	632			
Chloramphenicol, ocular inserts	618			
Chlorhexidine, local delivery	559			
Chlorobutanol	309			
Chlorpheniramine maleate, IVWC study	431			
Chromaffin cells, implants	422			
Chronic pain, implants	422			
Chronset	719			
Cidofovir	444	567	582	
CIDR-B	1020			
CIDR-G	635	636	1021	
CIDR-S	635	636	1021	
Cinnarizine, IVIVC study	430			
Ciprofloxacin, liposomal	439			
Cisplatin (CDDP)	122			
controlled release through microspheres	55	128		
implantable pump delivery	124			

This page has been reformatted by Knovel to provide easier navigation.

Index terms	Links			
Clarithromycin, liposomal	439			
Climara®	987			
Clinical studies, FDA requirements	382			
Clofazimine, liposomal	439			
Clonidine				
oral	3			
transdermal	1	3	4	988
Coacervation	358	494	513	543
	824			
Coatings	299			
acrylic polymers	674			
cellulose acetate	670			
for colonic delivery	305			
compression coating	303			
controlled release	301			
development	303			
enteric coating	731			
enteric coatings	305	307		
ethyl cellulose	665			
FDA evaluation	304			
fluidized-bed coating	303			
information sources on	300			
manufacture	302			
materials	306			
melt coating	303			
multilamellate	302			
optimization	304			
oral medicatons	731			
pan coating	302			
regulatory concerns	299			
scanning electron microscopy (SEM)	248			
silicone latex	681			
tablet coating	359			
trends	303			
validation	304			
Codrugs. *See also* Polymer-drug conjugates				
intravitreal	585	588		
Colchicine	567			

This page has been reformatted by Knovel to provide easier navigation.

Index terms	Links		
Collagen	328	768	
Collagen microspheres, cisplatin-loaded	128		
Collodian	500	520	
Colloidal particles	72		
Colon, oral drug delivery system to	698	717	
Colonic delivery, coatings for	305		
Compaction, proteins	752		
Companion animals, controlled-release technologies for	1023		
Compartmental analysis, pharmacokinetics	834	841	
Complexation, oral drugs	733		
Complex coacervation	494	502	512
Complexing hydrogels	409	413	
Composition analysis, infrared spectroscopy	259		
Compression coating	303		
Compression molding, polymer manufacture	355		
Computed tomography (CT), microencapsulated X-ray agents	314		
Concavalin A (Con A)	450		
Configuration, degradation and	83		
Confocal microscopy	235	971	
Conjugate drug. *See* Codrugs; Polymer-drug conjugates			
Conjugation			
PEG-conjugated proteins	148		
to vitamin B-12	180		
Consensus interferon, vitamin B-12-mediated transport	182		
Contaceptives. *See also* Female contraceptives; Male contraceptives			
history	365		
Contact angle methods, controlled-release systems, surface analysis	262		
Contact lenses, ocular drug delivery and	621		
Contamination			
SIMS studies	273		
surface analysis	262		
CONTIN analysis	254		
Contraceptive films	378		
Contraceptive vaginal ring (CVR)	365	367	371
Contrast agents			
magnetic resonance imaging (MRI)	317		
microspheres	313		

This page has been reformatted by Knovel to provide easier navigation.

Index terms	Links			
Contrast agents *(Continued)*				
ultrasound	325			
X-ray imaging	313			
Controlled drug delivery	72	261	349	381
See also Drug delivery systems				
addictive disorders	1			
agricultural products	350			
anticalcification drugs	115			
biodegradable polymers. *See* Biodegradable polymers				
cancer therapy	120			
capsule filling	359			
to central nervous system	193			
coatings	299			
complexing hydrogels	409	413		
controlled-release dosage forms	381			
cosmetics	351			
definitions	381			
delayed-release dosage form	382			
diffusion-controlled release systems	406			
drug-polymer conjugates	360			
economics of	341			
environmentally responsive systems	407			
enzymatic control	720			
erodible drug delivery systems	407			
extended-release dosage form	382			
fabrication of devices	351			
FDA requirements for	381			
in vivo-in vitro correlation (IVTVC)	425			
iontophoretic devices	360			
locally implanted	128			
magnetically responsive systems	409			
magnetic resonance techniques	230			
matrix systems	406			
modified-release dosage form	381			
pendent chain systems	407			
pharmacokinetics	844			
pH sensitivity	709			
polymer-controlled delivery systems	445			
polymeric materials	351			

This page has been reformatted by Knovel to provide easier navigation.

Index terms	Links
Contrast agents *(Continued)*	
regulatory issues	351
reservoir systems	406
surface characterization	261
swelling-controlled release systems	406
synthetic vascular grafts and	943
tablet coating	359
temperature-sensitive hydrogels	408
time-specific	699 718
to animals	1007
TOF-SIMS studies	272
transdermal devices	360
tumor targeting	143
veterinary Pharmaceuticals	350
Controlled-release dosage forms	381
Copper T 380A IUD	369
Copper T IUD	369
Coprecipitates	731
Copyright	785
Core ring	371
Coronary stents, cardiovascular drug delivery systems using	165
Correlation	
USP definition	426
in vivo-in vitro correlation (IVIVC)	425
Cortical implants	962
Cortienic acid	289
Cosmetics	351 542
Coulter technique, particle sizing	252
CPT. *See* Camptothecin	
Crestar ear implant	1021
Crinone®	633
Cromolyn sodium, nasal administration	602
Cryogenic solvent extraction, polymer manufacture	359
Cryosectioning	245
Cryoultramicrotomy	239
CT. *See* Computed tomography	
Cubosomes	463
Cusp calcification, cardiovascular calcification	115

This page has been reformatted by Knovel to provide easier navigation.

Index terms	Links			
CVR. *See* Contraceptive vaginal ring				
Cyclodextrins, complexation	283	733		
Cyclofem®	367	369		
Cyclohexane-1,4-dimethyl phosphate, PPE gels based on	52			
Cycloprovera	369			
Cyclosporin, intravitreal delivery	568			
CYDOT	556			
Cytokines, liposome-encapsulated	140			
Cytomegalovirus (CMV) retinitis	567	575	580	582
	584			
Cytotoxicity, PPEs	53			
D				
Dacron	48			
DADLE	294			
Danazol	633			
Daunomycin, intravitreal	566			
Daunorubicin (DAU)	122			
intravitreal	566			
liposome encapsulation	133	482	483	
Daunosome®	482			
DaunoXome®	133	483		
DBM. *See* Demineralized bone matrix				
DCLHb™	96	97		
in elective surgery	101	102	106	
in healthy volunteers	98			
in traumatic shock	107	108		
DDSs. *See* Drug delivery systems				
DDT	289	290		
De-Capeptyl® SR	830			
Deconvolution, absorption rate by	846			
Defect analysis, infrared spectroscopy for process control	259			
Definity	330	331		
Deformation, microspheres	23			
Deformation to failure	18			
Degradation				
configuration and	83			
and drug load	87			

This page has been reformatted by Knovel to provide easier navigation.

Index terms	Links		
Degradation *(Continued)*			
drug/polymer interactions	87		
γ irradiation and	88		
ionic strength and	88		
molar mass and	86		
molar mass distribution and	86		
pH and	88		
poly anhydrides	61	65	
polyesters	77		
porosity and	86		
PPEs	53		
proteins	818		
in vitro and in vivo behaviors, comparison	89		
Degree of crystallinity	277	283	
Dehydration/rehydration vesicles (DRV)	466		
Delayed-release dosage form	382		
Demineralized bone matrix (DBM)	889		
Dendrimers, gene delivery	877		
Dental caries, vaccine	998		
Dental drugs			
delivery systems	350		
local delivery	559		
poly(ortho ester) III	868		
Dentoadhesiveness	868		
Deponit®	988		
Depo-Provera®	365	367	368
Depotfoam™	472		
Depot injections	365	367	
Depot systems, cancer therapy	131		
Desmopressin	601	716	
Dexamethasone	122		
EVAc wafers	209		
intravitreal	566	584	586
ocular inserts	618		
ocular topical application	615		
Dextran			
microspheres, contrast agents attached to	315		
pendent drug conjugation	790		

This page has been reformatted by Knovel to provide easier navigation.

Index terms	Links		
Dextran-coated SPIO	321		
DHPG	567		
Diabetes treatment. *See* Insulin			
Diatrozoic acid, ethyl ester derivatives	316		
Dibutyl sebacate	309		
Dichlorvos	1023		
Diclofenac sodium	431	524	
Dicumarol, bioadhesive drug delivery	33		
Didanosine, prodrugs	715		
Diethyl phthalate	309		
Differential scanning calorimetry (DSC)	212	213	225
amorphous compounds	216	218	
calibration	215		
drug purity by	216		
freezing temperature by	216		
glass-transition temperature by	216	218	
melting temperature by	216		
micro-DSC	219	225	
phase transitions and	215		
polymorphism and	217		
power compensation DSC	214		
power flux DSC	213		
protein applications	219		
sample preparation	214		
Differential thermal analysis (DTA)	212		
Differential thermogravimetry (DTG)	223		
Diffraction, laser diffraction	253		
Diffusion			
in drug delivery systems	921		
in hydrogels	402		
theory	13		
Diffusional ocular inserts	620		
Diffusion barriers	261	267	
Diffusion-controlled membranes	731		
Diffusion-controlled release systems	406		
Dihydroergotamine, nasal administration	601		
Dihydrostreptomycin sulfate, ocular topical application	615		
1,25-Dihydroxyvitamin D3, brain tumors	204		

This page has been reformatted by Knovel to provide easier navigation.

Index terms	Links		
Diltiazem			
buccal delivery	556		
IVIVC study	431		
microparticles	678		
Diphtheria, polymer-based vaccine	1001		
Dispatch catheter, drug delivery	164		
Dispersed systems, ocular drug delivery	613		
Dispersion polymerization, nanosphere manufacture	645		
Disposition, FDA study requirements	384		
Dissolution-controlled release systems, kinetics	933		
Dissolution, IVIVC study	434		
Dissolution testing, FDA requirement	390		
Disulfiram	1	6	
DIVEMA, pendent drug conjugation	79		
DLS. *See* Dynamic light scattering			
DMP-115	330	331	
DNA. *See also* Gene delivery; Gene therapy			
liposome-entrapped DNA	487		
DNA vaccination	548	551	1033
Döderlein's bacilli	628		
Dogs, IVIVC study	431		
L-dopa, prodrug	716		
Dosage, multiple dosing	841		
Double-balloon catheter, cardiovascular drug delivery	162		
Double emulsion evaporation, liposome preparation	471		
Double-walled microspheres	537		
Doxil™	133	135	483
Doxorubicin (DOX)	122		
conjugated to HPMA	148		
controlled release through P(CHDM-HOP) gel	57		
encapsulated and locally implanted	129		
implantable pump delivery	124		
liposome encapsulation	134	483	
polymer-drug conjugates	808	810	
stealth liposomes	133	135	
targeted liposomes	135	136	
Doxycycline, local delivery to the mouth	560		

This page has been reformatted by Knovel to provide easier navigation.

Index terms	Links			
Droplet size, of emulsion	498			
Drug carriers	147	148		
Drug characteristics				
atomic force microscopy (AFM)	262	265	266	
attenuated total reflectance (ATR) spectroscopy	257	265		
Auger electron spectroscopy	262	263	264	
calorimetry	212			
contact-angle methods	262	263	264	
Coulter technique	252			
differential scanning calorimetry (DSC)	212	213	225	
differential thermal analysis (DTA)	212			
dynamic light scattering (DLS)	254			
electric sensing zone method	252			
electron paramagnetic resonance (EPR)	230			
electron spectroscopy for chemical analysis (ESCA)	262	263	266	270
gel permeation chromatography (GPC)	227			
heat conduction calorimetry	222			
infrared spectroscopy	256	265		
isoperibol calorimetry	223			
laser diffraction	253			
laser light scattering methods	252			
light scattering	252			
magnetic resonance imaging (MRI)	230			
magnetic resonance techniques	229			
microscopy	234	250		
modulated differential scanning calorimetry (MDSC)	221	225		
nuclear magnetic resonance (NMR)	229			
optical microscopy	234			
particle sizing techniques	250			
photon correlation spectroscopy (PCS)	254			
quasielastic light scattering (QELS)	254			
scanning electron microscopy (SEM)	235	242	262	
scanning probe microscopies (SPM)	265			
scanning tunneling microscopy (STM)	265			
secondary-ion mass spectrometry (SIMS)	262	270		
sieving methods	250			
static light scattering	253			
surface analysis	261			
thermogravimetric analysis (TGA)	223			

This page has been reformatted by Knovel to provide easier navigation.

Index terms	Links		
Drug characteristics *(Continued)*			
transmission electron microscopy (TEM)	234	236	249
X-ray photoelectron spectroscopy (XPS)	263	270	274
X-ray powder diffractometry (XRD)	276		
Drug concentration profiles	266		
Drug-cyclodextrin complexes, XRD studies	283		
Drug delivery systems (DDSs)	9	445	463
See also Drug characteristics; Drug design; Drug formulation; Drug reformulation; Pharmacokinetics			
abortifacients	379		
agricultural products	350		
bioadhesive. *See* Bioadhesive drug delivery			
for bone repair	889		
to the brain	129		
cardiovascular system. *See* Cardiovascular drug delivery systems			
carrier-mediated transport. *See* Carrier-mediated drug transport			
central nervous system. *See* Central nervous system drug delivery			
characterization	212		
chemical approaches to	285		
coatings	299		
colon, oral drug delivery system	698	717	
controlled delivery. *See* Controlled drug delivery			
cosmetics	351		
dental drugs	350		
diffusion barriers	261		
diffusion in	921		
female contraceptives	365		
implants	680		
for infectious diseases	435		
intelligent systems	445		
intestine, oral drug delivery system	698		
liposomal. *See* Liposomal drug delivery			
local. *See* Local drug delivery			
male contraceptives	378		
microencapsulation. *See* Microencapsulation			
modulated drug delivery systems	446		
mucosal. *See* Mucosal drug delivery			
nasal. *See* Nasal drug delivery			
nondegradable polymers for	665		

This page has been reformatted by Knovel to provide easier navigation.

Index terms	Links			
Drug delivery systems (DDSs) *(Continued)*				
oligonucleotides	691			
oral. *See* Oral drug delivery				
parenteral. *See* Parenteral drug delivery				
peptide and protein drugs	816			
polymer-controlled delivery systems	445			
polymeric. *See* Polymer-based delivery systems				
respiratory system delivery	936			
systemic. *See* Systemic drug delivery				
transdermal. *See* Transdermal drug delivery				
tumor targeting	145			
vaginal. *See* Vaginal drug delivery				
veterinary drugs	350			
Drug dependence, treatment	1	4		
Drug design	285			
chemical delivery systems (CDSs)	291			
soft drug design	285			
Drug formulation. *See also* Drug reformulation				
atomic force microscopy (AFM)	262	265	266	
attenuated total reflectance (ATR) spectroscopy	257	265		
Auger electron spectroscopy	262	263	264	
calorimetry	212			
contact-angle methods	262	263	264	
Coulter technique	252			
differential scanning calorimetry (DSC)	212	213	225	
differential thermal analysis (DTA)	212			
dynamic light scattering (DLS)	254			
electric sensing zone method	252			
electron paramagnetic resonance (EPR)	230			
electron spectroscopy for chemical analysis (ESCA)	262	263	266	270
gel permeation chromatography (GPC)	227			
heat conduction calorimetry	222			
infrared spectroscopy	256	265		
isoperibol calorimetry	223			
laser diffraction	253			
laser light scattering methods	252			
light scattering	252			
magnetic resonance imaging (MRI)	230			
magnetic resonance techniques	229			

This page has been reformatted by Knovel to provide easier navigation.

Index terms	Links		
Drug formulation. *See also* Drug reformulation *(Continued)*			
microscopy	234	250	
modulated differential scanning calorimetry (MDSC)	221	225	
nuclear magnetic resonance (NMR)	229		
optical microscopy	234		
particle sizing techniques	250		
photon correlation spectroscopy (PCS)	254		
quasielastic light scattering (QELS)	254		
scanning electron microscopy (SEM)	235	242	262
scanning probe microscopies (SPM)	265		
scanning tunneling microscopy (STM)	265		
secondary-ion mass spectrometry (SIMS)	262	270	
sieving methods	250		
static light scattering	253		
surface analysis	261		
thermogravimetric analysis (TGA)	223		
transmission electron microscopy (TEM)	234	236	249
X-ray photoelectron spectroscopy (XPS)	263	270	274
X-ray powder diffractometry (XRD)	276		
Drug load, degradation and	87		
Drug manufacture, infrared spectroscopy for process control	259		
Drug-polymer conjugates. *See* Polymer-drug conjugates			
Drug/polymer interactions, degradation	87		
Drug purity, by DSC	216		
Drug reformulation			
candidate drugs	343	346	
economic value of	341	344	
Drug release	821		
chemically controlled systems	930		
diffusion-controlled systems	921		
kinetics	70	511	
matrix systems	925		
microspheres and microcapsules	495		
modeling	932		
pendent chain systems	932		
pharmacokinetics	495	511	921
poly(ortho ester) I	852		
poly(ortho ester) II	858		

This page has been reformatted by Knovel to provide easier navigation.

Index terms	Links	
Drug release *(Continued)*		
poly(ortho ester) III	867	
reservoir systems	924	
stent delivery	167	
swelling-controlled systems	930	
Drug release profile	822	
Drugs. *See also* Drug characteristics; Drug delivery systems (DDSs); Drug design; Drug formulation; Drug reformulation; Pharmacokinetics		
absorption	738	
bioavailability. *See* Bioavailability		
copyrights	785	
dosage	344	
elimination rate constant	837	
FDA requirements	381	
first-pass effect	840	
generic	342	
gut wall clearance	840	
half-life	838	
hepatic clearance	839	
lung clearance of drugs	840	
lysosomatropic drugs	788	795
mode of administration	344	
multiple dosing	841	
patents	342	777
patient compliance	342	344
pendent chain polymer-drug conjugates	786	
pharmacokinetics. *See* Pharmacokinetics		
renal clearance	839	
side effects	344	
stabilization	736	
sterilization	653	745
systemic clearance	838	
trademarks	785	
volume of distribution	838	
DRV. *See* Dehydration/rehydration vesicles		
Dry eye syndrome	606	
DTA. *See* Differential thermal analysis		
DTG. *See* Differential thermogravimetry		
DTP vaccine	1001	1003

This page has been reformatted by Knovel to provide easier navigation.

Index terms		Links
Duragesic®	986	
Dura SE® Bolus	919	
Duros™ Leuprolide Implant	912	914
Duros™ osmotic implant	898	909
Dynamic DSC™	221	
Dynamic light scattering (DLS), particle size determination	254	
E		
Ear implant, veterinary	1021	
EC. *See* Ethylcellulose		
EchoGen®	328	
Echovist	328	
Ectoparasite control, for pets	1023	
EHBP. *See* Ethane hydroxybisphosphonate		
Elastomeric polymers	351	
Electrically regulated delivery systems	448	
Electrical sensing zone method, particle sizing	252	
Electrical transdermal drug delivery	966	
See also Electroporation; Iontophoresis		
Electrocapillarity emulsification, nanocapsule manufacture	648	
Electronic theory	12	
Electron paramagnetic resonance (EPR)	230	231
Electron spectroscopy for chemical analysis. *See* ESCA		
Electroporation	971	
Elimination rate constant	837	
Elvax® 40	514	
Embolization, microencapsulated X-ray agents	314	
Emulsification	756	
of polymers	760	
protein drugs	823	
with solvent removal	758	
Emulsification polymerization	642	643
Emulsion capacity	498	
Emulsions	739	755
classification	739	
evaluation of	468	
formation	497	823

This page has been reformatted by Knovel to provide easier navigation.

Index terms	Links			
Emulsions *(Continued)*				
gastrointestinal absorption and	739			
spontaneous formation	759			
stability	498			
sterilization	757	759	760	
surface-modified emulsions	757			
vaccines	1027			
Enantiotropy	218			
Encapsulation. *See also* Microencapsulation				
central nervous system drug delivery	209			
imaging agents	313			
localization by TEM	240			
oligonucleotides	695			
plasmid DNA	550			
processing techniques	356			
Encephalomyocarditis virus (EMC)	1028			
Endoglin	146			
Endoluminal paving	170			
Endometriosis				
leuprolide acetate therapy	407			
treatment	633			
Endophthalmitis	567	569	579	580
	584			
Enteric coatings	305	307	731	
Enterotoxigenic *Escherichia coli* vaccine	1002			
Entrapment, liposomes	473			
Environmentally responsive systems	407			
Environmental SEM	244			
Enzymatic control, controlled drug delivery	720			
Enzymatic degradation, polyesters	77			
Enzymatic physical-chemical-based CDS	292	293		
Enzyme localization, TEM	240			
Enzymes, drug delivery system using	451			
Epikuron®	652			
Epinephrine, ocular topical application	615			
Epithelium, of the gut	10			
EPO, vitamin B-12 transport system	182			
EPR. *See* Electron paramagnetic resonance				

This page has been reformatted by Knovel to provide easier navigation.

Index terms	Links			
Erodible drug delivery systems	407			
Erosion				
polyanhydrides	61	65		
poly(ortho ester) I	852			
poly(ortho ester) II	853			
Erythromycin, ocular inserts	618			
ESCA (electron spectroscopy for chemical analysis), controlled-release systems, surface analysis	262	263	266	270
Estraderm®	986			
Estradiol	365	986		
Estriol	365			
Estrogen replacement therapy	620			
Estrogens	365			
Estrone	365			
Estrus control, companion animals	1024			
Ethane hydroxybisphosphonate (EHBP), controlled release	115			
Ethinyl estradiol	365			
Ethisterone	365			
Ethylcellulose (EC)	308	664	719	729
Ethyl 4,4-dichlorobenzilate	289			
Ethylene vinylacetate copolymer (EVA copolymer)	309	574	681	
Ethyl ester, contrast agents attached to	316			
Etodolac, IVTVC study	431			
Eudragit®	307	674	677	706
	710	733		
EVA copolymer. *See* Ethylene vinylacetate copolymer				
EVAc wafers, dexamethasone impregnated	209			
Everted sac experiments	30			
Ex-Spot®	1023			
Extended-release dosage form	382			
Extrusion				
polymer manufacture	353			
protein drugs	825			
Eye, drug delivery to. *See* Intravitreal drug delivery; Ocular drug delivery				

This page has been reformatted by Knovel to provide easier navigation.

Index terms	Links		
F			
F127	511		
FAD:SA polymers, central nervous system drug delivery	206		
FDA. *See* Food and Drug Administration			
Female contraceptives			
contraceptive film	370	378	
Cyclofem	369		
Depo-Provera	365	368	
history	365		
implantable devices	373		
injectable devices	376		
intracervical device	377		
intrauterine devices (IUDs)	367	369	377
Norplant	365	367	
transdermal	377		
vaginal drug delivery	633		
vaginal rings	365	371	
FemPatch®	987		
Fentanyl, transdermal delivery	986		
Feret's diameter	251		
Ferromagnetic MRI contrast agents	317	319	
Fertility control	365	379	
abortifacients	379		
female contraceptives	365		
history	365	379	
male contraceptives	378		
Fibronectin-targeted gelatin particles	772		
Fick's law	402		
Film-coating tablets	731		
Films			
acrylic polymers	677		
ethyl cellulose	666		
First-pass effect, drugs	840		
FITC-BSA, controlled release through P(CHDM-HOP) gel	58		
Flea collar	1023		
Floating capsules	735		
Floating tablets	732		
Florfenicol	1022		

This page has been reformatted by Knovel to provide easier navigation.

Index terms	Links		
5-Floxuridine (FUDR)	123	124	
Fluconazole	443		
Fluid-bed coating, polymer manufacture by	357		
Fluidized-bed coating	303		
Fluorinated ethylene propylene, immobilization chemistry	963		
5-Fluorouracil (5-FU)			
conjugated with polyethylene glycol	154	156	
glaucoma treatment	870		
implant	124	859	862
intravitreal	566	586	
microsphere delivery	522		
5-Fluorouridine-51-monophosphate (FUMP)	582		
FMD vaccines	1027		
Food and Drug Administration (FDA)			
bioavailability studies requirement	382		
characterizing dosage form	384		
characterizing drug entity	383		
clinical studies, need for	382		
dissolution specifications	392		
dissolution testing	390		
New Drug Application (NDA)	383		
Foot and mouth disease	1027		
Foscarnet, CMV retinitis	567		
Fracture strength, microspheres	23		
Fracture theory, bioadhesion	13		
Freeze-drying, nanoparticle manufacture	653		
Freeze-etching	242		
Freeze-fracture	242		
Frontline® TopSpot	1023		
FTIC-BSA, controlled release	56		
FTIR			
membranes	517		
microspheres	535	539	
FTIR-ATR, controlled-release systems, surface analysis	262		
FUDR. *See* 5-Floxuridine			
FUMP. *See* 5-Fluorouridine-51-monophosphate			
Fungal endophthalmitis	568		

This page has been reformatted by Knovel to provide easier navigation.

Index terms	Links			
Fungal infection, liposomal antifungal agents	440	484	568	584

G

Galactose particles, encapsulated contrast agents	328			
γ Irradiation, degradation and	88			
Ganciclovir, CMV treatment	567	575		
Gastrointestinal system				
gut wall clearance of drugs	840			
oral drug delivery to	698	739		
GBA. *See* Gliding bacterial adjuvant				
G-CSF, vitamin B-12-mediated transport	179	182		
Gelatin	768			
complex coacervation	494	512		
encapsulated contrast agents	328			
gene delivery	877			
"nanoparticles"	770			
phase relationships	769			
precipitation	770			
pseudolatexes	611			
sterilization of	772			
toxicity	771			
Gelatin capsules	734			
filling	359			
Gelation				
gellan gum	612			
microencapsulation	494	523		
pseudolatexes	611			
Gelita collagel	731			
Gellan gum	612			
Gel paving	170			
Gel permeation chromatography (GPC)	227			
Gene delivery				
by microencapsulation	546			
cell-based	894			
chitosan	877	881		
polymeric systems for	874			
Generic drugs	342			

This page has been reformatted by Knovel to provide easier navigation.

Index terms	Links			
Gene therapy	193	546		
bioadhesive microspheres for oral delivery	40	41		
bone repair	894			
by microencapsulation	546			
immunoisolation	423			
as immunological adjuvants	486			
liposomes	485			
PINC system	875			
polymeric systems for	874			
veterinary	1033			
viral vectors	547			
Genetically engineered vaccines	1031			
Genetic immunization, liposomes	486			
Genetic therapy	193			
Gentamicin, ocular inserts	618			
Gentamicin-hydrogel, MRI	325			
Glass, immobilization chemistry	958			
Glass-transition temperature, by differential scanning calorimetry (DSC)	216	218		
Glaucoma treatment	606	870		
Gliadel®	130	202	357	359
Gliding bacterial adjuvant (GBA)	1027			
Glucose-sensitive systems	413	450	453	
Glycerin	309			
Glycerol	309			
Glyceryl trinitrate	555			
Glycolides, synthesis	73			
Glycophase glass, immobilization chemistry	958			
Gold, immobilization chemistry	963			
GPC. *See* Gel permeation chromatography				
Gum arabic, complex coacervation	512			
Gyne T 380 Slimline IUD	370			

H

Habitrol®	989	990		
Half-life	838			
Hard capsules	734			

This page has been reformatted by Knovel to provide easier navigation.

Index terms **Links**

HBOC-201 96 97
in elective surgery 101 103
in healthy volunteers 99
HBOCs. *See* Hemoglobin-based oxygen carriers
HBSE. *See* Recombinant hepatitis B surface antigen
HCG. *See* Human chorionic gonadotropin
HDSDC. *See* High sensitive differential scanning calorimeters
Heart valve bioprostheses, calcification, preventing 113
Heat conduction calorimetry 222
Heat flux DSC 213
Heat sterilization 747
HEC. *See* Hydroxyethylcellulose
HEMA. *See* Hydroxy thymethacrylate
Hemagglutinins, carrier systems using 178
HemAssist™ 96
Hemodialysis membranes 420
Hemoglobin, conjugated with polyethylene glycol 156
Hemoglobin-based oxygen carriers (HBOCs) 94
characteristics 95 96
elective surgery and 101
safety trials, healthy volunteers 94 97
traumatic shock and 107
Hemolink™ 96 97 100
Hemophilus influenza, liposomal vaccine 999
Hemopure® 96 97 98
Henderson-Hasselbalch equation 229
Hepatic clearance, drugs 839
Hepatitis A, liposomal vaccine 999
Hepatitis B, polymer-based vaccine 1002
Hepatocellular carcinoma (HCC), temporary occluding devices 126
Heroin 4
Hexasomes 463
Hi-Coater 302
High-pressure microfluidization 351
High sensitive differential scanning calorimeters (HDSDC) 220
HIV 660
HIV infections 444 632

This page has been reformatted by Knovel to provide easier navigation.

Index terms	Links			
HIV vaccine	999	1003		
HLB. *See* Hydrophilic-lipophile balance				
Hollaway device	1014			
Homogenization	762			
Homogenizer	497			
Hormone replacement therapy, transdermal delivery	986			
Hot melt encapsulation	494	525		
HPC. *See* Hydroxypropylcellulose				
HPMA				
doxorubicin conjugated to	148			
pendent drug conjugation	790	792	793	800
	810			
HPMC. *See* Hydroxypropyl methylcellulose				
HPMCP. *See* Hydroxypropylmethylcellulose phthalate				
HPMPC, CMV retinitis	567			
HRP 102	369			
HAS. *See* Human serum albumin				
Human chorionic gonadotropin (HCG)	457			
Human immunodeficiency virus. *See* HIV				
Human serum albumin (HSA)				
liposomal	443			
microencapsulation	524			
Hyaluronidase injectable microparticles	522			
Hydrocortisone				
metabolism	292			
ocular inserts	618			
Hydrocortisone hemisuccinate, buccoadhesive matrix tablets	559			
Hydrogel-coated balloon catheter, drug delivery	164			
Hydrogel microspheres	20			
Hydrogels	397			
applications	397	409		
cancer treatment	414			
classification	397	406	606	
complexing hydrogels	409	413		
contrast agents and	314			
defined	397			
diffusion-controlled release systems	406			
diffusion in	402			

This page has been reformatted by Knovel to provide easier navigation.

Index terms	Links			
Hydrogels *(Continued)*				
drug delivery systems	406			
environmentally responsive systems	407			
equilibrium swelling theories	398			
erodible drug delivery systems	407			
glucose-sensitive systems	413	453		
immobilization chemistry	961			
ionic hydrogels	399			
macroporous hydrogels	403			
magnetically responsive systems	409			
matrix systems	406			
microporous hydrogels	403			
network pore size calculation	401			
neutral hydrogels	398	409		
nonporous hydrogels	403			
ocular drug delivery	606	622		
oral insulin delivery systems	414			
pendent chain systems	407			
pH-sensitive hydrogels	412			
properties	397			
reservoir systems	406			
rubber elasticity theory	400			
spermicide delivery	378			
structure and properties	398			
swelling-controlled release systems	406			
temperature-sensitive hydrogels	408	412		
thermoreversible hydrogels	610			
vaginal drug delivery	634			
Hydrogenated vegetables	309			
Hydrolytic degradation, polyesters	78			
4-Hydroperoxycyclophosphamide (4HC)	130			
Hydrophilic-lipophile balance (HLB)	498			
Hydroxyethylcellulose (HEC)	308	607		
Hydroxypropylcellulose (HPC)	607			
Hydroxypropyl methylcellulose (HPMC)	308	555	607	666
	671	729	734	
Hydroxypropylmethylcellulosephthalate (HPMCP)	307			
Hydroxy thymethacrylate (HEMA)	722			

This page has been reformatted by Knovel to provide easier navigation.

Index terms	Links		
Hyperhydrosis, iontophoresis treatment	970		
Hypoxia, tumor cells and	126	144	
I			
IBD	1020		
Ibuprofen, nanoparticles	678		
ICBM. *See* Insoluble collagenous bone matrix			
ICD. *See* Intracervical device			
Idoxuridine	615	618	
IGF-1. *See* Insulin-like growth factor one			
Imagent US	330		
Imaging agents			
microencapsulation	313		
microspheres	313		
MRI contrast agents	317		
ultrasound contrast agents	325		
X-ray contrast agents	313		
Immunoglobulin transport system	175		
Immunoisolation	419		
Immunoisolatory implants	421		
Immunoliposomes	190	442	478
Immunology. *See* Vaccine delivery; Vaccines			
Immunostimulating reconstituted influenza virosome (IRIV)	999		
Immunotherapy, cancer treatment	139		
Immunotoxins, sustained release	132	146	
Implanon®	373		
Implantable drug delivery			
biodegradable polymers	764		
cancer therapy	121	124	
central nervous system drug delivery	192	209	
chromaffin cells	422		
EVA copolymers	682		
female contraception	368	373	
5-fluorouracil (5-FU)	859	862	
immunoisolatory implants	421		
osmotic pumps. *See* Osmotic pumps			
polyesters	76		
polymer-encapsulated drugs	128		

This page has been reformatted by Knovel to provide easier navigation.

Index terms	Links			
Implantable drug delivery *(Continued)*				
polymeric systems, MRI to characterize	232			
silicones	680			
Implant depots	355			
Implants				
polymeric	753	764		
sterility	752			
Inactive metabolite approach, soft drug design	288			
Indomethacin	670	678	713	
Indoxole, ocular topical application	615			
Infectious diseases	436			
antifungal agents	440	484	568	584
antimicrobial agents	437	484	560	568
	579	659	1022	1023
antimycobacterial agents	438			
antiparasitic agents	444	659	1023	
antiviral agents	443			
Inflammation-sensitive delivery systems	450			
Influenza virus				
liposomal vaccine	1000			
polymer-based vaccine	1003			
Infrared spectroscopy	256			
drug delivery research	258			
surface analysis with	265			
techniques	256			
Infusaid® pump	124	192		
Infusion pumps	124	192		
Infusion systems, cancer therapy	121	124		
Inhalation therapies	936			
Injectable drug delivery devices				
contraceptive delivery system	376			
polyesters	76			
Injection molding, polymer manufacture	354			
Injectors	765			
Inserts, ocular drug delivery	616			
In situ-forming implant depots	355			
Insoluble collagenous bone matrix (ICBM)	890			
Insufflator	593			

This page has been reformatted by Knovel to provide easier navigation.

Index terms	Links	
Insulin		
glucose-sensitive release system	451	452
glycosylated insulin	450	
implantable form	862	
microsphere delivery system	505	530
oral delivery	40	414
oral mucusal adhesive tablets	555	
for pets	1024	
Insulin-like growth factor one (IGF-1), dental use	562	
Integrins	955	967
Intellectual property rights, drug delivery systems	777	
Intelligent drug delivery systems		
antibody interaction	456	
chelation, systems using	457	
electrically modulated systems	448	
enzymes, systems utilizing	452	
glucose-responsive insulin delivery	452	
glucose-sensitive polymers	450	
inflammation-resonsive systems	450	
magnetically modulated systems	446	
morphine-triggered naltrexone delivery system	456	
photoresponsive systems	448	
pH-sensitive systems	449	
pulsatile systems	446	
responsive systems	449	
saccharide-sensitive polymers	450	
temperature-sensitive systems	449	
ultrasonically modulated systems	447	
urea-responsive system	451	
Interfacial coacervation	500	519
Interfacial phenomena, microencapsulation	503	
Interfacial polymerization	494	515
Interfacial polycondensation, nanocapsule manufacture	648	
Interleukin 2 (IL-2)		
controlled release through P(CHDM-HOP) gel	58	
liposome-encapsulated	140	
porous microspheres	524	
Internalin	177	

This page has been reformatted by Knovel to provide easier navigation.

Index terms	Links		
Internal radiation therapy	128		
Internal reflectance spectroscopy (IRS)	257		
International Pharmaceutical Excipient Council (IPEC)	300		
Interstitial delivery, central nervous system	192		
Intestinal peptide transporter	174		
Intestine			
M cells, particle uptake by	995		
oral drug delivery system to	698		
Intracervical device (IGD)	377		
IntraDose Injectable Gel	356		
Intramammary drug delivery	1011		
Intranasal route, central nervous system drug delivery	191		
Intraruminal drug delivery	1010	1012	
Intrathecal route, central nervous system drug delivery	191		
Intrauterine devices (IUDs)	367	369	377
Intrauterine Progesterone Contraceptive System (IPCS)	377		
Intravaginal drug delivery. *See* Vaginal drug delivery			
Intraventricular route, central nervous system drug delivery	191		
Intravitreal drug delivery	564		
biodegradable polymers	569	588	
codrugs	585	588	
iontophoresis	583	588	
liposomes	578	588	
nanoparticles	577	588	
non-biodegradable polymers	574	588	
prodrugs	585	588	
Inulin, ocular topical application	615		
Invasin	178		
In vivo-in vitro correlation (IVIVC)	425		
FDA requirement	390		
veterinary drugs	1010		
Iodipamide ethyl ester	332		
Iodixanol	314		
Iohexol	314		
Ion-exchange resins	730		
Ionic hydrogels	399		
Ionic strength, degradation and	88		

This page has been reformatted by Knovel to provide easier navigation.

Index terms	Links			
Ionizing radiation, sterilization using	751			
Iontophoresis	165	583	588	967
applications	970			
delivery rate in	968			
toxicology	970			
transport in	967			
Iontophoretic devices	360			
IPCS. *See* Intrauterine Progesterone Contraceptive System				
IRIV. *See* Immunostimulating reconstituted influenza virosome				
Iron(III) uptake, transferrin and	179			
IRS. *See* Internal reflectance spectroscopy				
ISDN. *See* Isosorbide dinitrate				
Isoniazid, liposomal	439			
Isoperibol calorimetry	223			
Isosorbide dinitrate (ISDN)	556	557		
Isothermal microcalorimeters	225			
ITG. *See* Polyiodinated triglycerides				
IUdR	205	509		
IUDs. *See* Intrauterine devices				
Ivermectin, osmotic pump	918			
IVIVIC. *See* In vivo/in vitro correlation				
Ivomec® injection	1022			
IVOMEC SR® Bolus	918	014		

J

Jet injectors	765			
Joint replacement. *See also* Bone repair				
immobilizing bioactive peptides at tissue-implant interface	955			
limitations of	955			

K

K4M, IVIVC study	432			
Kanamycin, liposomal	439			
Kelthane	289	290		
Keratoconjunctivitis sicca (KCS)	606			
Ketobemidone, buccal delivery	556			
Ketoconazole	584			

This page has been reformatted by Knovel to provide easier navigation.

Index terms	Links
3-Keto desogestrel	373
Killed vaccines	994
Kinetics, drug release kinetics	70
L	
Laby device	1013
Lactides	73 74
Lamellae (ocular)	616
Large neutral amino acids (LNAAs)	189
Large unilamellar vesicles (LUV)	465 470
Laser diffraction	253
Laser light scattering methods, particle size determination	252
Lateral force microscopy (LFM)	265
Lectins, carrier systems using	178
Leucovorin	123
Leukemia	144
Leukotriene C4 (LTC4), central nervous system drug delivery	191
Leuprolide	507 633
Leuprolide acetate	507
Leuprorelin	507
Levonorgestrel (LNG)	367
LFM. *See* Lateral force microscopy	
LHRH. *See* Luteinizing hormone-releasing hormone	
LH-RH analogs, vitamin B-12 transport system	181
Lidocaine, controlled release	55
Light microscopy. *See* Optical microscopy	
Linear attenuation coefficient	279
Linear mammillary models, pharmacokinetics	836
Lipid bilayers, infrared spectroscopy	258
Lipids	
polymorphism	462
self assembly	462
Lipiodol	314
Lipophilic analogs, CNS drug delivery	188
Liposomal-based vaccines	483 486 763 996 1027 1030

This page has been reformatted by Knovel to provide easier navigation.

Index terms	Links			
Liposomal drug delivery	461	463	482	
antifungal agents	440	484		
antimicrobial agents	437	484		
antimyobacterial agents	437			
antiparasitic agents	444			
antiviral agents	443			
cancer therapy	133	140	482	484
contrast agents	316			
gastrointestinal absorption of drug	739			
intravitreal agents	578	588		
microbubbles	331			
ocular drugs	613	622		
oligonucleotides	694			
vaccines	483	486	763	996
	1027	1030	739	
applications	482			
bioadhesive	16			
cationic liposomes	480			
characterization	474			
dehydration/rehydration vesicles (DRV)	466			
entrapment	473			
formation	462			
immunoliposomes	190	442	478	
industrial manufacture	472			
large unilamellar vesicles (LUV)	465	470		
ligand coupling strategies	478			
long-circulating liposomes	477			
manufacture	351			
morphology	465			
multilamellar reverse phase evaporation vesicles (MLV-REV)	470			
multilamellar vesicles (MLV)	465	471		
multivesicular liposomes	470			
nomenclature	465			
paramagnetic	323			
PEG and	482			
pH-sensitive	479			
polymerized	479			
polymerized liposomes	479			
preparation in laboratory	466			

This page has been reformatted by Knovel to provide easier navigation.

Index terms	Links		
Liposomes *(Continued)*			
resizing	468		
sizing	473		
small unilamellar vesicles (SUV)	323	465	470
spontaneous formation	759		
stability	474		
stable plurilamellar vesicles (SPLV)	469		
structure	474		
tailoring	477		
targeted liposomes	134	477	
temperature-sensitive	479		
vesicle clearance rates	475		
in vivo behavior	475		
Liquamycin® LA	1022		
Liquid paving	170		
Liquid and semisolid matrix capsules (LSSM)	734		
"Liquid whistle"	497		
Listeriosis	437		
Liver failure, implants	422		
Live vaccines	994		
LNAA carrier system	189		
LNAAs. *See* Large neutral amino acids			
LNG. *See* Levonorgestrel			
LNG Nova-T IUD	370		
Loaded microspheres	530		
Local delivery catheters, drug delivery	162		
Local drug delivery			
to brain	129		
cancer therapy	121		
chemoembolization	126		
implantable pumps	121	124	
locally implanted controlled-release systems	128		
microspheres	126		
to the mouth	553	558	
Localmed Infusion Sleeve, drug delivery	164		
Long-circulating liposomes	477		
Loo-Riegelman method, assessment of input rate	846		
Loteprednol etabonate	289		

This page has been reformatted by Knovel to provide easier navigation.

Index terms	Links		
LSSM. *See* Liquid and semisolid matrix capsules			
LTC4. *See* Leukotriene C4 (LTC4)			
Lubritab®	309		
Lungs			
clearance of drugs	840		
inhalation therapies	936		
morphology and physiology	936	937	
Lupron Depot®	131	510	823
Lutamate Plus	1021		
Luteinizing hormone-releasing hormone (LHRH), buccal delivery	556		
LUV. *See* Large unilamellar vesicles			
Lymphoma	144		
Lysosomatropic drugs	788	795	

M

MAB. *See* Methacryloyloxy azobenzene			
MAC. *See Mycobacterium avium-intracellulare* complex			
Macrocapsules	421		
Macrogol	309		
Macrolides	437		
Macromolecular contrast media (MMCM), for MRI	320		
Macromolecular prodrugs	72		
Macroporous hydrogels	403		
Macroporous membranes	495		
Magic angle spinning (MAS)	230		
"Magic bullet," cancer therapy	145		
Magnetically modulated delivery systems	446		
Magnetically responsive systems	409		
Magnetic guidance, targeting	658		
Magnetic localization, anticancer agents	137		
Magnetic resonance	292		
Magnetic resonance imaging (MRI)	230		
contrast agents	317		
drug analysis	232		
microcapsules for fluorine MRI	323		
principles	317		
with therapeutic modalities	364		

This page has been reformatted by Knovel to provide easier navigation.

Index terms		Links
Magnetic resonance techniques. *See* Electron paramagnetic resonance; Magnetic resonance imaging; Nuclear magnetic resonance		
Magnetic starch microspheres (MSM)	321	
Male contraceptives	378	
Malignant tumors	120	
immunotoxins	133	
micro vasculature	147	
oxygen deprivation	126	144
properties	143	
MALLS. *See* Multiple angle laser light scattering		
MALT. *See* Mucosal associated lymphoid tissue		
Marek's disease	1032	
Marston erodible system	1015	
Martin's diameter	251	
MAS. *See* Magic angle spinning		
Mass attenuation coefficient	279	
Massive vitreous retraction	565	
Mastitis therapy	1011	
Matrix systems		
controlled drug delivery	406	
ethyl cellulose	669	
plastic matrices	730	
poly(ethylene oxide)	684	
release kinetics	925	
Matrix tablets		
cellulose esters	671	
poly(meth)acrylate powders	678	
silicone-based	681	
Matrix-type tablets	729	
MBBB. *See* Metabolic blood-brain barrier		
MC. *See* Methylcellulose		
MDP. *See* Muramyldipeptide		
MDSC. *See* Modulated differential scanning calorimetry		
Measles virus, liposomal vaccine	1000	
Mechanical bonds, bioadhesion	11	
Medical implants, tissue-implant interface	955	
Melt coating	303	

This page has been reformatted by Knovel to provide easier navigation.

Index terms	Links		
Membranes			
diffusion-controlled membranes	731		
for immunoisolation	419		
osmotic drug delivery	898		
porosity	495		
Menopausal stress incontinence, treatment	630		
Menopause			
defined	629		
hormone replacement therapy, transdermal	986		
MENT	378		
Mesenchymal stem cells (MSCs)	891		
Metabolic blood-brain barrier (MBBB)	185		
Metaloporphyrins, MRI contrast agents	322		
Metal shadowing	241		
Metastases	120	144	
Methacrylates, coatings	307		
Methacrylic acid copolymers	710		
Methacryloyloxy azobenzene (MAB)	722		
Methadone	4		
Methadone maintenance	1	5	
Methocel®, IVIVC study	432		
Method of residuals, pharmacokinetics	836		
Methotrexate (MTX)	123	124	
Methylcellulose (MC)	308	607	
Metoprolol	289	290	701
Metrazol	190		
Metronidazole	562	631	
Micelles	760	793	
Miconazole, oral gel	558		
Microballoons	678		
Microbial degradation, polyesters	80		
Microbubbles	328	332	335
Microcapsules			
defined	495		
drug release characteristics	495		
for fluorine MRI	323		
protein microcapsules	329	824	

This page has been reformatted by Knovel to provide easier navigation.

Index terms	Links			
Micro-DSC	219	225		
Microencapsulation	356	493	670	
See also Encapsulation				
acrylic polymers	678			
agricultural products	543			
applications	541			
cellulose esters	671			
coacervation	358	494	513	543
complex coacervation	494	502	512	
cosmetics	542			
DNA vaccination	548			
double-walled microspheres	537			
emulsion formation	497			
ethyl cellulose	669			
gelation	494	523		
gene delivery by	546			
hot melt encapsulation	494	525		
hydrophilic-lipophile balance (HLB)	498			
imaging agents	313			
interfacial coacervation	500	519		
interfacial polymerization	494	515		
phase inversion microencapsulation (PIN)	541	550		
phase separation	358	494	500	669
plasmid DNA	550			
salting-out	494			
solvent evaporation	358	494	504	550
	669			
solvent removal	494	528		
spray-drying	356	494	531	543
thermal denaturation	494	520		
Microfluidization	351	468		
Microgranules, oral drug delivery	735			
Microparticles	72			
albumin	766			
cardiovascular drug delivery	171			
chitosan	774			
ethyl cellulose	669	670		
gastrointestinal delivery	739			
gelatin	772			

This page has been reformatted by Knovel to provide easier navigation.

Index terms	Links
Microparticles *(Continued)*	
manufacture 76	
ocular drug delivery 614	622
veterinary vaccines 1031	
Microporous hydrogels 403	
Microporous membranes 495	
Microscopy 234	
See also Optical microscopy; Scanning electron microscopy; Transmission electron microscopy	
particle size determination 250	
Microspheres 1031	
bioerodible thermoplastic 20	
brain tumor treatment 130	
cancer therapy 126	140
central nervous system drug delivery 206	
contrast agents 313	
denned 495	
diagnostic use of 313	
double-walled 537	
drug release characteristics 495	
ESCA and SIMS surface studies 266	
everted sac experiments 30	
hydrogel 20	
internal radiation therapy with 128	
intravitreal use 577	
loaded 530	
manufacture 356	
MRI contrast agents 317	
plasmid DNA 550	
porous 524	
PPE 55	
protein drug delivery 828	
SIMS studies 274	
ultrasound contrast agents 325	
vaccine delivery 996	
X-ray contrast agents 313	
Microtensiometer, bioadhesion 16	
Minitran® 988	
Minocycline, brain tumors 205	

This page has been reformatted by Knovel to provide easier navigation.

Index terms	Links	
MION-46. *See* Monocrystalline iron oxide		
Mirofluidization	670	
Mitomycin	123	
Mitomycin C (MMC)	123	127
Mixed agonist-antagonists	4	
Mixed micelles	760	
MLV. *See* Multilamellar vesicles		
MLV-REV. *See* Multilamellar reverse phase evaporation vesicles		
MMC. *See* Mitomycin-C		
MMCM. *See* Macromolecular contrast media		
Modeccin	179	
Modeling, drug release kinetics	932	
Modified-release dosage form	381	
Modulated differential scanning calorimetry (MDSC)	221	225
Modulated drug delivery systems	446	
Modulated DSC®	221	
Molar mass, degradation and	86	
Molar mass distribution, degradation and	86	
Molecular weight distribution (MWD)	351	
Monoclonal antibodies (MAb)		
cancer therapy	145	146
nanoparticles and	658	
Monocrystalline iron oxide (MION-46)	321	
Monotropy	218	
Morphine	4	
Morphology, biodegradable polymers	80	
MOTS. *See* Mucosal Oral Therapeutic System		
MOTT. *See* Mycobacterial infections other than tuberculosis		
Mouth, drug delivery. *See* Oral drug delivery		
MRI. *See* Magnetic resonance imaging		
MRX-408	334	
MSCs. *See* Mesenchymal stem cells		
MSM. *See* Magnetic starch microspheres		
MTX. *See* Methotrexate		
Mucins	10	
Mucoadhesion	11	
Mucoadhesive tablets	733	

This page has been reformatted by Knovel to provide easier navigation.

Index terms	Links
Mucosal associated lymphoid tissue (MALT)	603
Mucosal drug delivery	
intravitreal	564
nasal	593
ocular	605
oral	553
vaginal	627
Mucosal Oral Therapeutic System (MOTS)	558
Mucus	
contact angle measurements	31
in the gastrointestinal tract	10 31
Multilamellar reverse phase evaporation vesicles (MLV-REV)	470
Multilamellar vesicles (MLV)	465 471
Multilamellate coatings	302
Multiload IUD	369
Multiple angle laser light scattering (MALLS)	253
Multiple-dose, steady-state studies	385 388
Multiple-drug resistance (MDR), cancer	120
Multiple-unit tablets	733
Multivesicular liposomes	470
Muramyldipeptide (MDP)	1030
Mycobacterial infections, liposome-encapsulated antimyobacterial agents	437 485
Mycobacterial infections other than tuberculosis (MOTT)	438
Mycobacterium avium-intracellulare complex (MAC)	438

N

Nafarelin	633
Naloxone, receptor-based CDS for	295
Naltrexone	
alcoholism treatment with	1 6
morphine-triggered delivery systems	456
opioid antagonist therapy	1 5 860
Nanocapsules	543 646 652
Nanoparticles	72 441 577 641 1031
anticancer drugs	136 659
applications	659
biodistribution	655

This page has been reformatted by Knovel to provide easier navigation.

Index terms	Links		
Nanoparticles *(Continued)*			
biomimetic	655		
cancer treatment	136		
characterization	659	660	
chitosan	774		
cosmetics	543		
gastrointestinal delivery	739		
gelatin	770		
history	642		
manufacture	641		
ocular drug delivery	614	622	
PEO-coated	656		
SIMS studies	274		
sterically stabilized	655		
targeting with	658		
veterinary vaccines	1031		
vitamin B-12 uptake system	182	183	
in vivo action of	654		
Nanospheres, manufacture	642	648	
Nanosponges	332		
Naproxen	670	713	
Narcotic antagonists	1	5	860
Nasal aerosol	595	596	
Nasal drug delivery	593		
Nasal mucosa	598		
Natamycin	444		
NCS. *See* Neocarzinostatin			
NDA. *See* New Drug Application			
Near-field optical scanning microscopy (NFOSM)	265		
Needleless injectors	765		
Negative staining, transmission electron microscopy (TEM)	241		
Neocarzinostatin (NCS)	147		
Nestorone® implant	373		
NET-EN. *See* Norethindrone enanthate			
Neutral hydrogels	398	409	
New Drug Application (NDA), FDA requirement	383		
New Ophthalmic Delivery System (NODS®)	620		
NFOSM. *See* Near-field optical scanning microscopy			

This page has been reformatted by Knovel to provide easier navigation.

Index terms	Links		
NGF	208		
NicoDerm® CQ	989		
Nicotine			
gum	3		
health sequelae of chronic use	2		
inhaler	3		
nasal spray	3		
transdermal	2		
transdermal delivery	989		
Nicotrol®	3	989	990
Nifedipine, IVIVC study	432		
Nitrocellulose	500		
Nitrodisc®	988		
Nitro-Dur®	988		
Nitroglycerin			
buccal delivery	556		
sublingual delivery	557		
transdermal delivery	987		
NMR. *See* Nuclear magnetic resonance			
NODS. *See* New Ophthalmic Delivery System			
Noncellulosic enteric coatings	307		
Noncellulosic nonenteric coatings	308		
Noncompartmental analysis, pharmacokinetics	842		
Noncondensing PINC™ polymeric systems	875		
Nondegradable polymers			
acrylic polymers	674		
cellulose esters	670		
ethyl cellulose	664		
EVA	681		
HPMC	666	671	
pendent drug conjugation	790		
poly(ethylene oxide)	684		
silicones	679		
Nonlinear Mixed Effects Model (NONMEM)	844		
Nonoxynol-9	370	378	632
Nonporous hydrogels	403		
Nonporous membranes	495		
Nonspecific vaginosis	631		

This page has been reformatted by Knovel to provide easier navigation.

Index terms	Links			
Norethindrone	365	376		
Norethindrone enanthate (NET-EN)	369			
Norethindrone pellets	385			
Norethisterone	365			
Noristerat	369			
Norplant®	365	367	680	
Nose, anatomy and physiology	593			
See also Nasal drug delivery				
Nova-T IUD	369			
NS-718	442			
Nuclear magnetic resonance (NMR)				
drug analysis	231			
pulse field gradient (PFG) NMR	230			
solid-state NMR	230			
solution NMR	229			
Nulfor® injection	1022			
Nutropin Depot®	830			
Nystatin	440	443	483	558

O

Ocular drug delivery				
dispersed systems	613			
EVA copolymers	683			
hydrogels	606	622		
inserts	616			
liposomes	613	622		
microparticles	614	622		
nanoparticles	614	622	661	
silicones	681			
Ocular inserts	616			
Ocusert®	620	683		
Olfactory pathway, central nervous system drug delivery	191			
Oligonucleotides, delivery systems	691			
Ommaya reservoir	191	192		
OMNIMARK-PRV	1032			
Omnipaque	314			
OMNIVAC-PRV	1032			
One-compartment open models, pharmacokinetics	841			

This page has been reformatted by Knovel to provide easier navigation.

Index terms	Links			
Open-loop control systems	446			
Ophthalmic drug delivery				
intravitreal	564			
ocular	605			
veterinary	1025			
Ophthalmic hydrogels	606			
Ophthalmic inserts	616			
Ophthalmic pseudolatex	611			
Ophthalmology, vitreoretinal diseases	565			
Opioid dependence, treatment	1	4		
Opioid receptors	4			
Optical microscopy	234			
confocal light microscopes	235			
particle size determination	251			
polarized light microscopy	235			
sample preparation	235			
staining	235			
Optic tract implants	962			
Optison®	329			
Optro®	96			
Orabase system	558			
Oral contaceptives. *See also* Female contraceptives; Male contraceptives				
history	365			
Oral drug delivery	344	349	553	729
See also Capsules; Tablets				
beads	735			
bioadhesives	558	704		
buccal	553	555		
carrier-mediated transport	173			
drugs using	554			
local delivery to mouth	553	558		
microgranules	735			
pellets	736			
spheroids	735			
sublingual	553	557		
to colon	698	717		
to small intestine	698			
Oral mucosae, structure of	553			

This page has been reformatted by Knovel to provide easier navigation.

Index terms	Links		
Orthopedics			
bone repair	889		
joint replacement	955		
protein delivery in	893		
Osmotic BBBD, central nervous system drug delivery	190		
Osmotic drug delivery	898		
See also Osmotic pumps			
kinetics	932		
ocular inserts	620		
Osmotic pressure-based ruminal bolus	1015		
Osmotic pumps	731		
ALZET® system	896	900	
applications	898	904	908
characteristics of osmotic systems	896		
design	898		
Duros™ osmotic implant	898	909	
history	896		
ruminal osmotic bolus	916		
RUTS Push-Melt® System	899	916	
theory	897		
VITS veterinary implant	898	906	
Osteocalcin	114		
Osteopontin	114		
Ovuplant	1021		
Oxazepam	731		
Oxprenolol, IVIVC study	430	431	
Oxytetracycline, veterinary use	1022		

P

PAA. *See* Poly(acrylic acid)			
PAAm. *See* Polyacrylamide			
PACA nanoparticles	646	659	
Paclitaxel	123	152	
biodegradable paste	129		
conjugated with polyethylene glycol	152	153	154
controlled release through poly(terephthalate-co-phosphate) film	57		
controlled release through PPE microspheres	55		
encapsulated	129		

This page has been reformatted by Knovel to provide easier navigation.

Index terms	Links			
Paclitaxel *(Continued)*				
liposome encapsulation	134			
Pain, from injection	764			
Pan coating	302			
Pancreas, artificial	419	424		
Paracetamol, encapsulation	678			
ParaGard® T 380A IUD	370			
Paramagnetic MRI contrast agents	317	318		
Parasitic infection, antiparasitic agents	444	659	1023	
Paratect bolus	1012			
Paratect Flex	1012			
Parenteral drug delivery	350	743		
emulsions	468	497	739	755
micelles	760			
nanoparticles	659			
pain on injection	764			
sterile implants	752			
Parenteral products				
manufacturing	754			
requirements of	744			
sterilization	745			
Parkinson's disease, implant drug delivery for	192	208	422	
Particle sizing	250			
Passive targeting, cancer therapy	147			
Patents	342	777		
application procedure	781			
infringement	784			
term of	780			
Patient compliance	342	344		
PBA. *See* Phenylboronic acid				
P(BHET-EOP/TC)	48	51		
PBLG. *See* Poly(benzyl L-glutamate) microcapsules				
PCF. *See* Polysulfone capillary fiber				
P(*trans*-CHDM-HOP)	52			
PCL:PLA block copolymers, female contraception	375			
PCL. *See* Poly(ε-caprolactone)				
P(CPP)	61			

This page has been reformatted by Knovel to provide easier navigation.

Index terms	Links		
P(CPP-IPA)	61		
P(CPP-SA)	65	66	196
PCS. *See* Photon correlation spectroscopy			
PDEAEMA. *See* Poly(diethylaminoethyl methacrylate)			
PDGF. *See* Platelet-derived growth factor			
PDMAEMA. *See* Poly(dimethylaminoethyl methacrylate)			
PDMS. *See* Poly(dimethylsiloxane)			
PEG. *See* Poly(ethylene glycol)			
PEG-camptothecin	154		
PEG-5-fluorouracil	154		
PEG-hemoglobin (PEG-Hb)	96	100	156
PEG-paclitaxel-2'-glycinate	152	153	154
PEL *See* Polyethyleneimine			
Pellets, oral drug delivery	736		
Pendent chain polymer-drug conjugates	786		
Pendent chain systems	407	932	
Penicillin	437	615	
Pentazocine	4		
Pentylenetatrazol	190		
PEO. *See* Poly(ethylene oxide)			
Peptide and protein drugs			
delivery systems	816		
sustained-release formulations	828		
veterinary	1025		
Peptides			
buccal delivery	557		
immobilizing at tissue-implant interface	955		
ologonucleotide-peptide complexes	695		
protein stability	817		
vitamin B-12 transport system	181		
Peptide transport process	174		
Peptidyl linkers, polymer-drug conjugates	795	798	800
Percutaneous transluminal angioplasty (PTA)	162		
Perfluorochemical (PFC) emulsions	156		
Perfluorooctyl bromide, stabilized PFC emulsions	330		
Periodontitis	868		
Peroral administration, nanoparticles	660		

This page has been reformatted by Knovel to provide easier navigation.

Index terms	Links			
Pertussis vaccine	1003			
Pesticides, encapsulation	543			
PET. *See* Polyethylene terephthalate)				
Peudolatexes	668			
PEVAc. *See* Polyethylene vinyl-*co*-acetate)				
PEVP, gene delivery	877			
P(FAD-SA)	61			
PFG NMR. *See* Pulse field gradient NMR				
PGA. *See* Poly(glycolic acid); Propylene glycol alginate				
pH, degradation and	88	736		
Pharmaceuticals. *See under* Drugs				
Pharmacokinetics	833			
absorption	383			
bioavailability	383	384		
bioequivalency	384			
controlled drug delivery	844			
defined	834			
disposition	384			
dissolution	390			
drug release	495	511	921	
FDA requirements	383			
in vivo-in vitro correlation (IVIVC)	425			
liposomally encapsulated drugs	579			
noncompartmental analysis	842			
one-compartment open models	841			
population pharmacokinetics	844			
theory	834			
transdermal drug delivery	984			
two-compartment open models	842			
veterinary drugs	1008			
Phase diagrams, coacervation	514			
Phase inversion microencapsulation (PIN)	541	550		
Phase separation, microencapsulation	358	494	500	669
PHEMA. *See* Poly(2-hydroxyethyl methacrylate)				
Phenobarbitone, chitosan microsphere delivery	522			
Phenylboronic acid (PBA)	451			
Phenytoin, prodrug	712			
Phonophoresis	448			

This page has been reformatted by Knovel to provide easier navigation.

Index terms	Links		
Phospholipids, chemical stability	757		
Photon correlation spectroscopy (PCS)	254		
Photoresponsive delivery systems	449		
pH-sensitive delivery systems	449		
pH-sensitive hydrogels	412		
pH-sensitive liposomes	479		
Physical bonds, bioadhesion	11		
pIgR. *See* Polymeric immunoglobulin receptor			
Pili, carrier systems using	176		
Pilocarpine	615	617	
PIN. *See* Phase inversion microencapsulation			
PINC. *See* Protective interacting noncondensing systems			
Piperacillin, liposomal	437		
PLA. *See* Poly(L-lactic acid)			
PLAGA copolymers	72	78	128
Plant toxins, carrier systems using	179		
Plasmid-chitosan complexes	886		
Plasmid DNA	57	59	550
See also Gene delivery; Gene therapy			
Plasticizers	309		
Platelet-derived growth factor (PDGF)	562	889	891
PLGAs. *See* Poly(lactide-*co*-glycolide)s			
PLLA. *See* Poly(L-lactic acid-*co*-L-lysine)			
PMAA. *See* Poly(methacrylic acid)			
PMEA	714		
PMMA. *See* Poly(methyl methacrylate)			
PNAs. *See* Polyamide (“peptide”) nucleic acids			
PNIPAAm. *See* Poly(*N*-isopropylacrylamide)			
Pohlmann generator	497		
Polarized light microscopy	235		
Poloxamers	656		
Poloxamines	656		
Polyacrylamide (PAAm)	411	958	
Polyacrylate coatings	307		
Poly(acrylic acid) (PAA)	16	411	609
Polyacrylonitrile, immobilization chemistry	961		
Polyamide capsules	494		

This page has been reformatted by Knovel to provide easier navigation.

Index terms	Links			
Polyamide (“peptide”) nucleic acids (PNAs)	190			
Polyamines, contrast agents attached to	316			
Poly(amino acids), pendent drug conjugation	791			
Polyanhydrides	60	532	572	
aliphatic	61			
aromatic	61			
biocompatibility	64			
characterization	63			
contrast agents attached to	316			
crosslinked and branched	62			
degradation	61	65	532	
design of	193			
drug delivery systems	68	193		
erosion	61	65		
microspheres, preparation	505			
monomers	61			
synthesis	62	194		
Poly(benzyl L-glutamate) microcapsules (PBLG), contrast agents attached to	316			
Polybrene, gene delivery	877			
Poly(*t*-butyloxycarbonylmethyl glutamate)	332			
Poly(ϵ-caprolactone) (PCL)	72	75	374	572
Polycarbophil	16			
Poly(CPP-SA)	505	528	529	530
Poly(diethylaminoethyl methacrylate) (PDEAEMA)	411			
Poly(dimethylaminoethyl methacrylate) (PDMAEMA)	411	413		
Poly(dimethylsiloxane) (PDMS)	367			
Polydispersity	351			
Polyesters				
contrast agents attached to	316			
degradation	77			
drug delivery devices, manufacture	75			
enzymatic degradation	77			
hydrolytic degradation	78			
microbial degradation	80			
pendent drug conjugation	791			
synthesis	72			
Poly(ethylene acrylic acid), immobilization chemistry	961			
Polyethylene glyco-aspartate), pendent drug conjugation	791			

This page has been reformatted by Knovel to provide easier navigation.

Index terms	Links			
Polyethylene glycol) (PEG)				
camptothecin conjugated with	154			
as coating	309			
as drug carrier	148			
hemoglobin conjugated with	156			
hydrogels	411			
liposomes	482			
paclitaxel conjugated with	145	152	153	
polymer-drug conjugates with	789	790	791	
proteins, covalent linkage with	361			
Polyethyleneimine (PEI), gene delivery	875	877		
Poly(ethylene oxide) (PEO)	684			
drug delivery systems	411			
R-PEO diblock copolymers	657	658		
star polymers	415			
Polyethylene terephthalate) (PET), immobilization chemistry	960			
Poly(ethylene terephthalate)-based poly(phosphoester)s	47			
Poly(ethylene vinyl-co-acetate) (PEVAc), hydrogels	411			
Poly(glycolic acid) (PGA)	71	72	75	
PolyHeme®	96	97	108	
Poly(α-hydroxy acids)	570			
Poly(2-hydroxyethyl methacrylate) (PHEMA)	314	410	413	
Polyiodinated triglycerides (ITG)	316			
Poly(*N*-isopropylacrylamide)(PNIPAAm)	412			
Poly(L-lactic acid) (PLA)	72	75	128	129
female contraception	375			
microspheres	508	531		
synthesis	72	76		
Poly(L-lactic acid-*co*-L-lysine) (PLLA)	508			
Poly(L-lactide), preparation	761			
Polydactide-*co*-glycolide)s(PLGAs)	50	570		
characterization by NMR	231			
dexamethasone encapsulated by	171			
female contraceptives	376			
liposome-encapsulated	140			
microcapsules	332			
microspheres	508	512	531	535
	550			

This page has been reformatted by Knovel to provide easier navigation.

Index terms **Links**

Polydactide-*co*-glycolide)s(PLGAs) *(Continued)*
SIMS study 272
Polymer-based drug delivery. *See also* Polymer-controlled delivery systems; Polymer therapeutics
cardiovascular drugs 169
manufacture 823
protein release from 821
vaccines 1000
Polymer-controlled delivery systems. *See also* Polymer-based drug delivery; Polymer therapeutics
antibody interaction 456
chelation, systems using 457
electrically modulated systems 448
enzymes, systems utilizing 452
glucose-responsive insulin delivery 452
glucose-sensitive polymers 450
inflammation-resonsive systems 450
magnetically modulated systems 446
morphine-triggered naltrexone delivery system 456
photoresponsive systems 449
pH-sensitive systems 449
pulsatile systems 446
responsive systems 449
saccharide-sensitive polymers 450
temperature-sensitive systems 449
ultrasonically modulated systems 447
urea-responsive system 452
Polymer-drug conjugates 360
See also Codrugs; Prodrugs
cancer treatment 143 810
characterization 794
pendent chain conjugates 786
properation 794
targeting 788
Polymer erosion. *See* Erosion
Polymeric immunoglobulin receptor (pIgR) 176
Polymeric materials
biodegradable. *See* Biodegradable polymers
classification 352

This page has been reformatted by Knovel to provide easier navigation.

Index terms	Links	
Polymeric materials *(Continued)*		
compression molding	355	
drug carriers	147	
emulsification	760	
for encapsulation	499	
encapsulation techniques	356	
erosion. *See* Erosion		
extrusion	353	
implant depots	355	
implants	753	
injection molding	354	
intervitreal drug delivery	569	
manufacture	353	
molecular weight	351	
nondegradable. *See* Nondegradable polymers		
ocular inserts	617	
phase separation	500	
rheology	353	
SIMS	271	
solvent casting	355	
solvent processing	355	
structure	351	
synthetic vascular grafts	946	
Polymeric membranes, porosity	495	
Polymeric methacrylates, coatings	307	
Polymer implants	128	
Polymerization, nanoparticle manufacture	642	
Polymers. *See* Polymeric materials		
Polymer therapeutics	786	
See also Polymer-based drug delivery; Polymer-controlled delivery systems		
clinical progress	808	
design	787	
pendent chain linkers	793	
soluble polymeric carriers	789	
Poly(methacrylic acid) (PMAA)	411	
Poly(methyl methacrylate) (PMMA)	315	645
Polymorphism	217	462
Poly(ortho ester) I	852	

This page has been reformatted by Knovel to provide easier navigation.

Index terms	Links		
Poly(ortho ester) II	853		
drug release	858		
erosion	853		
physical properties	856		
synthesis	863		
Poly(ortho ester) III	865		
characterization	866		
drug release	867		
synthesis	871		
toxicity	869		
Poly(ortho ester)s	573	852	
chemical structure	574		
history	852		
for local delivery to mouth	560		
rod devices, female contraception	374		
Poly(phosphoester)s (PPEs)	45		
based on cyclohexane-1,4-dimethyl phosphate backbone	52		
based on oligomeric lactide chain extension	50		
based on poly(ethylene terephthalate)	47		
biocompatibility	46	53	
biodegradation	53		
with bisphenol A backbone	46		
cytotoxicity	54		
drug release properties	55		
poly(lactide-*co*-glycolides)s(PLGAs)	50		
properties	46		
stability	53		
sterilizability	53		
Polyrotaxanes	415		
Polysaccharides	315	790	792
Poly SFH-P	96	98	108
Polysulfone	576		
Polysulfone capillary fiber (PCF)	576		
Poly(terephthalate-co-phosphate), properties	49		
Polyurethane	316	959	
Polyurethane sponges	635		
Polyvinylacetate phthalate (PVAP)	308		

This page has been reformatted by Knovel to provide easier navigation.

Index terms	Links
Poly(vinyl alcohol) (PVA)	309 607
drug delivery systems	410
immobilization chemistry	962
intravitreal drug delivery	569
Poly(vinyl alcohol) coupled with quinaldic acid chelator (PVA-QA)	457
Poly(vinyl pyrrolidone) (PVP), gene delivery	875 879
Population pharmacokinetics	844
Porosity	
degradation and	86
polymeric membranes	495
synthetic vascular grafts	948
Porous balloon catheter, cardiovascular drug delivery	163
Porous matrix systems, release kinetics	929
Porous microspheres	524
Porous reservoir systems, release kinetics	925
Posilac®	830
Posterior uveitis	568
Postruminal drug delivery	1010
Powders, nasal	595 597
Power compensation DSC	213 214
PPEs. *See* Poly(phosphoester)s	
Prednisolone acetate, ocular inserts	618
Preformed hydrogels, ocular drug delivery	607
PRID	635 636 1020
Principle of superposition, pharmacokinetics	837
Process control, FVTVC study	434
Prodrugs	72 143
See also Polymer-drug conjugates	
CNS drug delivery	188
for intestinal drugs	712
intravitreal	585 588
Progestasert™ device	367 370 377
Progesterone	
buccal delivery	557
effect on female	365
Progestin	365 371 374 633
Program®	1023

This page has been reformatted by Knovel to provide easier navigation.

Index terms	Links	
Projected area diameter	251	
ProLease® process	825	826
Proliferative vitreoretinopathy (PVR)	565	580
Propranolol, nanoparticles	670	678
Propylene glycol alginate (PGA)	524	
Prostaglandin analogs	379	
Prostep®	989	990
Prostheses, immobilizing bioactive peptides at tissue—implant interface	955	
Protective interacting noncondensing systems (PINC)	875	
Protein microcapsules	329	
Proteins. *See also* Peptide and protein drugs		
albumin	765	
bioadhesive microspheres for oral delivery	40	
compaction	752	
covalent linkage with PEG	361	
degradation	818	
formulation strategies	819	
stability	817	
stabilization	819	
vitamin B-12 transport system	181	
Protein therapeutics, for skeletal tissue repair	889	
Pseudoephedrine, IVIVC study	431	
Pseudolatex, ethyl cellulose	667	
Pseudolatexes	611	
PTA. *See* Percutaneous transluminal angioplasty		
Pulsatile bolus	1014	
Pulsatile drug delivery systems	446	
Pulsed light sterilization	851	
Pulse field gradient (PFG) NMR	230	
Pulsincap capsule	718	
Pumps		
cancer therapy	121	124
nasal	595	
osmotic. *See* Osmotic pumps		
Purification, nanoparticle manufacture	653	
PVA. *See* Poly(vinyl alcohol)		
PVAP. *See* Polyvinylacetate phthalate		

This page has been reformatted by Knovel to provide easier navigation.

Index terms	Links		
PVA-QA. *See* Poly(vinyl alcohol) coupled with quinaldic acid chelator			
PVP. *See* Poly(vinyl pyrrolidone)			
PVR. *See* Proliferative vitreoretinopathy			
Pyrimethamine	861		
Q			
Qualitative analysis			
infrared spectra	257		
nasal dose delivery	595		
Quality assurance, infrared spectroscopy for process control	259		
Quality control, infrared spectroscopy for process control	259		
Quantison®	329		
Quantitative analysis			
infrared spectra	257		
nasal dose delivery	595		
X-ray powder diffractometry (XRD)	279		
Quasielastic light scattering (QELS)	254		
R			
Radiation, sterilization using	751	866	
Radiation therapy			
cancer treatment	120	143	
internal, using microspheres	128		
Radiopaque markers. *See* Contrast agents			
Rajamehendran rubber tubing	1020		
REB. *See* Reversible electrical breakdown			
Receptor-based chemical delivery system	293	295	297
Receptor-mediated transport			
cell models	180		
central nervous system drug delivery	189		
Recombinant hepatitis B surface antigen (HBSA)	1002		
Recombinant human BMPs (rhBMPs)	890		
Red cell substitutes. *See* Hemoglobin-based oxygen carriers			
REDOR. *See* Rotational-echo double resonance			
Redox chemical delivery systems, central nervous system drug delivery	189		
Reformulation. *See* Drug reformulation			
Release. *See* Drug release			

This page has been reformatted by Knovel to provide easier navigation.

Index terms	Links
Renal clearance, drugs	839
Renografin®	314
Replens®	630
Replica techniques, TEM	241
Reservoir systems	406
for ectoparasiticides	1023
release kinetics	924
Reservoir-type devices	360
Respiratory system, drug delivery to	936
Responsive delivery systems	449
Restenosis	162
Retinoic acid	483 577
Retinoids	567
Reverse phase evaporation, liposome preparation	471
Reversible electrical breakdown (REB)	971
rHb1.1	96
in elective surgery	102
in healthy volunteers	98 99
rhBMPs. *See* Recombinant human BMPs	
Ricin	179
Rifampin, liposomal	439
Rismorelin porcine	510
RMP7	191
Rose-Nelson osmotic pump	896
Rotary shadowing	241
Rotational-echo double resonance (REDOR)	230 231
R-PEO diblock copolymers	657 658
Rumensin ABC	1015
Ruminal osmotic bolus	916
RUTS Push-Melt® System	899 916

S

Saccharide-sensitive polymers	450
SAL. *See* Sterility assurance level	
Salbutamol, IVIVC study	432
Salicylic acid, bioadhesive drug delivery	33
Salting-out	494

This page has been reformatted by Knovel to provide easier navigation.

Index terms	Links
Saponin	1030
Sarcoma	144
Saturation transfer EPR (ST-EPR)	230
Scanning electrochemical microscopy (SECM)	265
Scanning electron microscopy (SEM)	234 242
advantages and disadvantages	243
coatings	248
controlled-release systems, surface analysis	262 265
drug delivery systems	248
microspheres	535 536 540
optics	243
particle size determination	251
sample preparation	245 248
Scanning probe microscopies (SPMs), surface analysis	265
Scanning tunneling microscopy (STM), surface analysis	265
Scopolamine	291 988
SD design. *See* Soft drug design	
SEB. *See* Staphylococcal enterotoxin B	
SEC. *See* Size exclusion chromatography	
SEC-HPLC. *See* Size-exclusion high performance chromatography	
SECM. *See* Scanning electrochemical microscopy	
Secondary-ion mass spectrometry (SIMS), controlled-release systems, surface analysis	262 263 264 266 270
SEM. *See* Scanning electron microscopy	
Sentinal®	1023
Sepharose, immobilization chemistry	957
Sera carnauba	308
Sex-hormone-binding globulin (SHBG)	457
Sexually transmitted diseases	631
SH. *See* Sodium hyaluronate	
Shadowing	241
SHBG. *See* Sex-hormone-binding globulin	
Shellac, as coating	308
Shell ring	372 373
SHIME reactor. *See* Simulated human intestinal microbial ecosystem (SHIME) reactor	
Sieving, particle size determination	250
Silastic	367 371

This page has been reformatted by Knovel to provide easier navigation.

Index terms	Links		
Sil-Estrus	1021		
Silicon-based polymers	309		
Silicon dioxide, immobilization chemistry	963		
Silicones	577	679	958
Simian immunodeficiency virus. *See* SIV			
SIMS. *See* Secondary-ion mass spectrometry			
Simulated human intestinal microbial ecosystem (SHIME) reactor	723		
Single-dose crossover study	385		
Site-specific enzyme-activated CDSs	293	295	
SIV, vaccine	1003		
Size exclusion chromatography (SEC)	253		
Size-exclusion high performance chromatography (SEC-HPLC)	248		
Skeletal tissue repair. *See* Bone repair			
Skin			
drug metabolism and	982		
drug testing on	982		
percutaneous absorption, animal models	981		
permeability of	976		
structure and composition	976	977	
transdermal drug delivery. *See* Transdermal drug delivery			
Slimline IUD	370		
SLS. *See* Static light scattering			
Small unilamellar vesicles (SUV)	323	465	470
SMANCS	147		
Smoking cessation	1	3	989
Sodium carboxymethylcellulose (NaCMC)	308	607	
Sodium hyaluronate (SH), ocular drug delivery	608		
Sodium selenite, veterinary use	919		
Sofisan®	309		
Soft analogues	287		
Soft anticholinergics	287	291	
Soft beta blockers	289		
Soft drug (SD) design	286		
Soft elastic capsules	734		
Soft quaternary salts	287		
Solid-state NMR	230		
Solution NMR	229		

This page has been reformatted by Knovel to provide easier navigation.

Index terms	Links			
Solvent casting, polymer films	355			
Solvent evaporation	358	494	504	550
	669			
Solvent extraction, polymer manufacture	358			
Solvent infusion, liposome preparation	471			
Solvent removal, microencapsulation	494	528		
Somatotropins, veterinary	1025	1028		
Sonovist	332			
Sonovue®	330	332		
Sorbitan trioleate	519			
Sorbitol	309			
Span® 85	519			
Spanbolet II	1012			
Spermicides	378			
SPIO. *See* Superparamagnetic oxide particles				
SPLV. *See* Stable plurilamellar vesicles				
SPMs. *See* Scanning probe microscopies				
Spray-drying, microencapsulation	356	494	531	543
Spraying processes	761	825		
Spray-polycondensation	357			
Sputter-coating	248			
SSIMS. *See* Static SIMS				
ST-1435	373			
Stability	72	736		
infrared spectroscopy	259			
liposomes	474			
poly(ortho esters) III	867			
proteins	817			
Stabilization	736			
Stable plurilamellar vesicles (SPLV)	469			
Staining				
characterization of drug delivery systems	236			
optical microscopy	235			
transmission electron microscopy (TEM)	236	240		
Stannous octoate, as initiator	73	75		
Staphylococcal enterotoxin B (SEE), vaccine	1003			
Starch microcapsules, contrast agents attached to	315	321		

This page has been reformatted by Knovel to provide easier navigation.

Index terms	Links
Star polymers	415
Static light scattering (SLS), particle size determination	253
Static SIMS (SSIMS)	265
Stealth liposomes, cancer treatment	133 135
Stents, cardiovascular drug delivery systems using	165
ST-EPR. *See* Saturation transfer EPR	
Sterility	
implants	752
parenteral products	745
Sterility assurance level (SAL)	748
Sterilization	
aseptic processing	751
ball milling	755
barrier technology	749 827
by filtration	749
by ionizing radiation	751 866
of chitosan nanoparticles	774
emulsions	757 759 760
with gases	748
of gelatin	772
heat sterilization	747
implants	753
nanoparticle manufacture	653
parenteral drugs	745
poly(ortho ester) III	866
protein compacts	753
protein drugs	827
pulsed light sterilization	851
spraying process	761
terminal sterilization	827
Sterilization stability, PPEs	53
Steroid drugs, nasal administration	602
Steroid hormone-containing growth promotants, veterinary	1011 1019
Sterotex®	309
STM. *See* Scanning tunneling microscopy	
Stokes-Einstein equation	254
Storage, drug degradation	222
Streptavidin	478

This page has been reformatted by Knovel to provide easier navigation.

Index terms	Links			
Streptomycin	438			
Subconjunctival injections	564			
Sublingual drug delivery	553	557		
Sublingual mucosa	555			
Substance abuse. *See* Opioid dependence				
Subunit vaccines	994			
Sumatriptan, nasal administration	601			
Superparamagnetic MRI contrast agents	319			
Superparamagnetic oxide particles (SPIO), encapsulated	321			
Surelease®	668			
Surface analysis				
AFM	262	265	266	
Auger electron spectroscopy	262	263		
contact angle method	262			
ESCA	262	263	266	270
FTIR-ATR	262			
SEM	262	265		
SIMS	262	263	265	266
	270			
Surface erosion	262	266		
Surface-modified emulsions	757			
Surfactant	497			
Surfactant-stabilized microbubbles	332			
Surgery, as cancer therapy	120			
Suspensions	739			
Sustained drug delivery, to respiratory system	938			
SUV. *See* Small unilamellar vesicles				
Swellable tablets	732			
Swelling-controlled release systems	406	930		
SychroMed Infusion System®	124			
Synchron	555			
SYNCRO-MATE	1021			
Synthetic vascular grafts, controlled drug delivery and	943			
Systemic clearance	838			
Systemic drug delivery				
antibody-drug conjugates	132			
cancer therapy	131			

This page has been reformatted by Knovel to provide easier navigation.

Index terms	Links			
Systemic drug delivery *(Continued)*				
depot systems	131			
liposomes	133			
magnetic localization	137			
nanoparticles	136	182	183	
polymer-drug conjugates (prodrugs)	72	143	188	585
	588	712		
targeted delivery	132			
T				
Tableting	359			
Tablets	729			
film-coating tablets	731			
floating tablets	732			
matrix-type tablets	729			
mucoadhesive tablets	733			
multiple-unit tablets	733			
swellable tablets	732			
Targeted drug delivery				
antibody-drug conjugates	132			
cancer therapy	132			
contrast agents	322	334		
magnetic localization	137			
nanoparticles	136	182	183	
polymer-drug conjugates (prodrugs)	72	143	188	585
	588	712		
Targeted liposomes	134	477		
Targeting				
with gelatin microparticles	772			
intranasal drug delivery	602			
magnetic guidance	658			
with nanoparticles	658			
oligonucleotides	695			
polymer-drug conjugates	788			
Taxanes, antitumor activity	152			
Taxol	123	203	566	567
TEC-11	146			
TEM. *See* Transmission electron microscopy				

This page has been reformatted by Knovel to provide easier navigation.

Index terms	Links		
Temazepam, sublingual delivery	558		
Temperature-sensitive delivery systems	449		
Temperature-sensitive hydrogels	408	412	
Temperature-sensitive liposomes	479		
Tensiometer, electrobalance-based	16		
Terminal sterilization	827		
Testoderm®	987		
Testosterone	378	556	987
Testosterone replacement therapy, transdermal delivery	987		
Tetanus vaccine	1004		
Tetracycline			
dental use	868		
local delivery to the mouth	560	561	
ocular inserts	618		
TEWL. *See* Transepidermal water loss			
TGA. *See* Thermogravimetry			
TGF-β. *See* Transforming growth factor-β			
Theeuwes elementary osmotic pump	670		
Theophylline			
ethylcellulose microcapsules	514		
IVIVC study	431	432	433
microsphere delivery	525		
Thermal denaturation, microencapsulation	494	520	
Thermogravimetry (TGA)	223	516	
Thermoplastic elastomers	352		
Thermoplastic polymers	352		
Thermoreversible hydrogels	610		
Thermosetting polymers	352		
Thyrotropin-releasing hormone (TRH), delivery to brain	293		
TILS. *See* Total intensity light scattering			
Time capsule	1013		
TIME CLOCK®	703		
Time-of-flight SIMS. *See* TOF SIMS			
T-independent antigens	997		
Tissue-engineered vascular grafts	950		
Tissue-implant interface, immobilizing bioactive peptides	955		

This page has been reformatted by Knovel to provide easier navigation.

Index terms **Links**

Tobramycin
  implants 862
  liposomal 437
  ocular inserts 618
TOF (time-of-flight) SIMS 265 271 272
Topical drugs
  for food-producing animals 1022
  ocular. *See* Ocular drug delivery
Total intensity light scattering (TILS) 253
Total joint replacement, limitations of 955
Toxins, carrier systems using 178
Trademarks 785
Trade secrets 784
Transcorneal iontophoresis 583
Transdermal drug delivery 350
  drug toxicology and 982
  electrical 966
  female contraceptives 377
  hormone replacement therapy 986
  passive 975
  pharmacokinetics 984
  skin, permeability 976
  types 985
Transdermal patches 360
Transderm-Nitro® 988
Transderm-Scop® 988
Transepidermal water loss (TEWL) 979
Transforming growth factor-β (TGF- β) 889 891
Transluminal angioplasty 162
Transmission electron microscopy (TEM) 234
  drug delivery systems, characterization 249
  enzyme and protein localization 240
  freeze-etch 242
  freeze-fracture 242
  membranes 517
  metal shadowing 241
  negative staining 241
  optics 236

This page has been reformatted by Knovel to provide easier navigation.

Index terms	Links		
Transmission electron microscopy (TEM) *(Continued)*			
replica techniques	241		
sample preparation	237		
staining	236	240	
Transmission spectroscopy	256		
Transplanted organs	419		
Transport coronary angioplasty catheter, drug delivery	163		
Transscleral iontophoresis	583	584	
TRH. *See* Thyrotropin-releasing hormone			
Triacetin	309		
Triamcinolone acetonide	566	586	615
Trichomoniasis	631		
Triethyl citrate	309		
Trifluorothymidine	582	618	
Tropicamide, ocular topical application	615		
Tuberculosis	438		
Tuberculosis vaccine	1004		
Tumors	144		
blood-tumor barrier	187		
central nervous system tumors	187		
controlled-release treatment	120		
immunotoxins	133		
malignant. *See* Malignant tumors			
oxygen deprivation	126	144	
properties	144		
Tumor targeting	144		
Two-compartment open models, pharmacokinetics	842		
Two-stage negative replica	241		

U

U-86983	511		
Ultrasonically modulated delivery systems	447		
Ultrasound			
cardiac and blood vessel imaging	327		
contrast agents	325		
gastrointestinal tract	328		
gynecology	328		
liver imaging	327		

This page has been reformatted by Knovel to provide easier navigation.

Index terms	Links			
Ultrasound *(Continued)*				
oncology	328			
principles	325			
with therapeutic modalities	335			
Uniplant	374			
Urea-responsive delivery system	452			
U.S. Food and Drug Administration. *See* Food and Drug Administration				
Uveitis	568	580	584	
V				
Vaccine delivery	763	993		
intranasal	502	602		
liposomal	483	486	763	
nanoparticles	661			
polymer-based systems	1000			
veterinary	1026			
Vaccines	762			
emulsions	1027			
genetically engineered vaccines	1031			
immunology of	994			
killed vaccines	994			
liposomal drug delivery	483	486	763	996
	1028	1030		
live vaccines	994			
subunit vaccines	994			
Vagina, anatomy	627	634		
Vaginal Contraceptive Film (VCF®)	370			
Vaginal drug delivery	629			
EVA copolymers	683			
implantable devices	680			
for pathologic conditions	630			
topical contraceptives	633			
veterinary pharmaceuticals	634	1019	1020	
Vaginal dryness, treatment	630			
Vaginal health index	631			
Vaginal ring	365	367	371	
Vaginosis	631			
Vancomycin, capsules	735			

This page has been reformatted by Knovel to provide easier navigation.

Index terms **Links**

Van't Hoff equation 216
Variable-temperature powder diffractometry (VTXRD) 271
Vascular grafts, controlled drug delivery and 943
VCF® 370
Vector-mediated drug delivery, central nervous system drug delivery 189
Vectors, gene therapy 547
Ventolin®, IVIVC study 432
Verapamil, buccal absorption 555
Vesicle clearance rates 475
Veterinary drug delivery 350 1007
  anticancer therapy 1023
  bone growth therapy 1024
  companion animals 1023
  compared with human drug delivery 1008
  emulsion vaccines 1027
  estrous control 1024
  food-producing animals 1019 1022
  genetically engineered vaccines 1031
  insulin 1024
  intramammary drug delivery 1011
  intraruminal drug delivery 1010 1012
  IVIVC study 431
  liposomal vaccines 1027 1030
  long-acting injectables 1019 1022
  microspheres 1031
  nanoparticles 1031
  ophthalmic drugs 1025
  parasite control 1023
  parenteral drug delivery 1023
  pharmacokinetics 1008
  postruminal drug delivery 1010
  protein and peptide delivery 1025
  RUTS Push-Melt® System 899 916
  somatotropins 1025 1028
  steroid-containing growth promotants 1011 1019
  vaccine delivery 1026
  vaginal drug delivery 634 1019 1020
  VITS veterinary implant 898 906

This page has been reformatted by Knovel to provide easier navigation.

Index terms	Links		
Veterinary Implantable Therapeutic System (VITS)	898	906	
Vinblastine	124		
Vincamine	660		
VincaXome	483		
Vincristine (VCR)	123	134	483
Viral infection, antiviral agents	443	659	
Viral vectors	547		
Viruses, carrier systems using hemagglutinins	178		
Visceral leishmaniasis	660		
Viscumin	179		
Vitamin B-12 (VB12), uptake system based on	179	183	
Vitreoretinal diseases	565		
VITS veterinary implant. *See* Veterinary Implantable Therapeutic System			
Vivelle®	987		
Volkensin	179		
Volmax®, IVIVC study	432		
Voltaren, buccal delivery	556		
Voltaren SR	729		
Volume of distribution	838		
VRC. *See* Vincristine			
VTXRD. *See* Variable-temperature powder diffractometry			

W

Wafers, BCNU-impregnated polyanhydride	196		
Wagner-Nelson method, assessment of input rate	844		
Wetting theory, theory	12		
Whey protein (WPI) microspheres	522		
Wilhelmy plate technique	14	264	
Women			
abortifacients	379		
contraceptives. *See* Female contraceptives			
drugs for	627		
estrogen replacement therapy	620		
estrogens	365		
vaginal anatomy	625	634	
vaginal drug delivery. *See* Vaginal drug delivery			
vaginal health index	631		

This page has been reformatted by Knovel to provide easier navigation.

Index terms	Links		
X			
Xenotransplantation	419		
X-ray imaging, contrast agents	313		
X-ray photoelectron spectroscopy (XPS)	263	270	274
X-ray powder diffractometry (XRD)	276		
crystallinity determination	277		
drug delivery systems and	282		
limitations	277		
membranes	517		
phase identification with	276		
phase transition studies	281		
quantitative analysis	279		
X-rays	274		
XRT	205		
Y			
Yttrium-90 (Y-90), microspheres loaded with	128		
Z			
Zidovudine, CMV retinitis	567		
Zileuton	704		
Zinc metal, as initiator	73	75	
Zoladex®	131	829	

This page has been reformatted by Knovel to provide easier navigation.